XI. INTERNATIONAL CONFERENCE ON PERMAFROST

POTSDAM, GERMANY

20-24 JUNE 2016

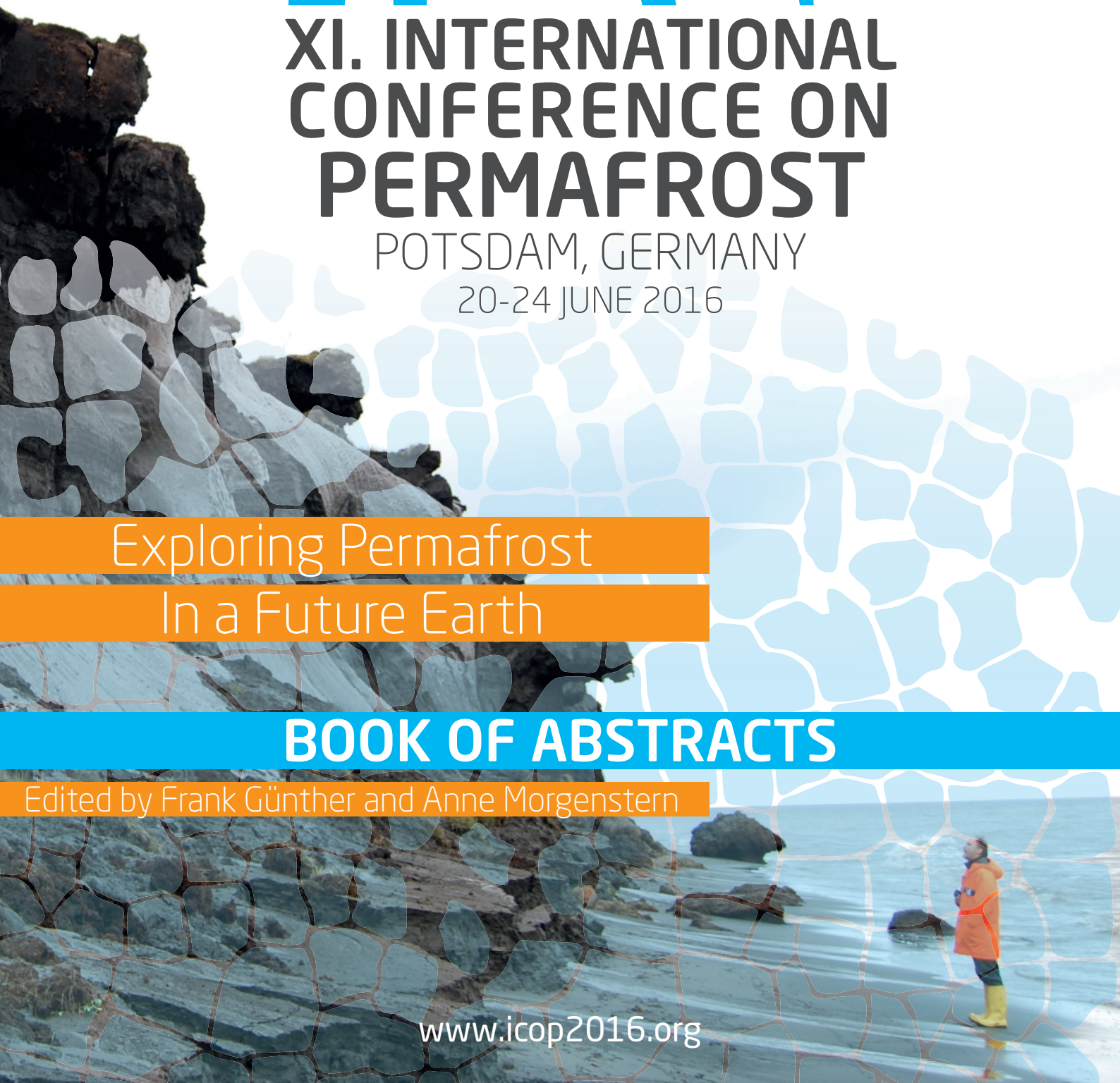

Exploring Permafrost In a Future Earth

BOOK OF ABSTRACTS

Edited by Frank Günther and Anne Morgenstern

www.icop2016.org

XI. International Conference on Permafrost
20 – 24 June 2016, Potsdam, Germany

XI. International Conference On Permafrost

Exploring Permafrost in a Future Earth

Book of Abstracts

Edited by Frank Günther and Anne Morgenstern

Co-editors:
Hans-Wolfgang Hubberten, Lydia Polakowksi, Matthias Fuchs, Ingmar Nitze, Samuel Stettner, Karina Schollaen, Hugues Lantuit, & Guido Grosse

Alfred Wegener Institute Helmholtz Centre for Polar and Marine Research
International Permafrost Association

Recommended citation
Günther, F. and Morgenstern, A. (Eds.) (2016): XI. International Conference On Permafrost – Book of Abstracts, 20 – 24 June 2016, Potsdam, Germany. Bibliothek Wissenschaftspark Albert Einstein, doi:10.2312/GFZ.LIS.2016.001

Disclaimer and Copyright
Each author is responsible for the content of his or her abstract and has the copyright for his or her figures.

Imprint

Publisher
Bibliothek Wissenschaftspark Albert Einstein
Telegrafenberg
14473 Potsdam
Published in Potsdam, Germany

Editors
Frank Günther
Anne Morgenstern
doi:10.2312/GFZ.LIS.2016.001

Preface

The Local Organizing Committee (LOC) of the Eleventh International Conference on Permafrost (ICOP2016) is excited about the breadth and the quality of the abstracts submitted for this conference.

It was the first time that ICOP topical sessions were not set by the organizing committee in a top-down manner. Instead, sessions were submitted from the bottom-up by groups of researchers and engineers from all over the world. This grassroots effort prompted the submission of many innovative topics covering the full range of modern permafrost research. It also facilitated not only the engagement of the core permafrost community, but also of science disciplines traditionally less involved in ICOPs. In total, 51 session proposals were received by the LOC. These were submitted by up to three conveners including at least one early career researcher from the Permafrost Young Researchers Network (PYRN). After the evaluation process by the International Scientific Committee (ISC) and the LOC, including the addition of strategic topics and the combination of sessions with thematic overlap, 40 topical sessions were eventually opened for abstract submission. There was yet another novelty compared to previous ICOPs: the submission of contributions was not divided into abstracts and papers, in favor of a quicker and uniform review process allowing for the submission deadline to be set closer to the conference. This opened the possibility for authors to present recent results in the rapidly evolving field of permafrost research. Abstracts of up to 3000 words were allowed, either plain or formatted with subheadings, and including one figure, table or equation.

We received the extraordinary number of 980 abstracts. This number varied between 79 and 0 among sessions, which led to a further consolidation into the final set of 32 sessions presented in this abstract volume. Abstract evaluation was placed in the hands of the session conveners. The vast majority of abstracts (97 %) was deemed eligible to be accepted for presentation during the conference, either immediately or after revision by the authors. The reduced number of abstracts presented in this volume is mostly due to the inability of travelling to the conference for some authors.

We are very delighted that the modified procedures for the compilation of the scientific conference program proved so successful and wish to extend our gratitude to the session conveners and ISC members for their tremendous efforts and great support in compiling such a high-quality program. We also wish to thank Hans-Wolfgang Hubberten, Lydia Polakowski, Matthias Fuchs, Ingmar Nitze, Samuel Stettner, Karina Schollaen, Hugues Lantuit, and Guido Grosse for their technical help in the final editing phase of this abstract volume.

Frank Günther and Anne Morgenstern

Contents

Preface i

Plenary Session 1

From 1D to 4D – recent developments in mountain permafrost research
I. Gärtner-Roer . . . 2

Livelihoods on frozen ground: Why permafrost matters to indigenous communities in Siberia and elsewhere
J. O. Habeck . . . 3

The Wiley-Blackwell Permafrost and Periglacial Processes Award Lecture: Permafrost-Ecosystem Interactions
M. T. Jorgenson . . . 4

Adaptation of transportation infrastructure built on degrading permafrost
F. Niu . . . 5

All fall down? Urban infrastructure and permafrost in the Russian Arctic
N. Shiklomanov . . . 6

Finding paths for future permafrost research
Y. Sjöberg . . . 7

Predicting thermokarst: detecting hot spot changes in ecosystems, fate of permafrost carbon, and infrastructure vulnerability
M. R. Turetsky . . . 8

Carbon fluxes of inland and coastal waters in permafrost regions
J. E. Vonk . . . 9

Reconstructing paleoenvironments from environmental DNA
E. Willerslev . . . 10

1 **Periglacial Geomorphology (co-organized by the International Association of Geomorphologists)** 11

Landscape evolution triggered by polycyclic thermokarst on Herschel Island, Yukon Territory
M. Angelopoulos, W. Pollard, M. Krautblatter, & H. Lantuit . . . 12

Late Pleistocene and Holocene topography evolution of the northern part of the Yamal and Gydan Peninsula, Russia
A.V. Baranskaya . . . 14

Assessing the genesis of periglacial ramparted depressions (PRDs) by characterising internal structures macroscopically and microscopically
S.S. Bromfield 16

Holocene landscape and permafrost history based on geomorphology and cryostratigraphy in the Zackenberg valley, NE-Greenland
S. Cable, H.H. Christiansen, G.L. Gilbert, C. Thiel, A. Kroon, A. Westergaard-Nielsen, & B. Elberling 18

Rapid micro-scale weathering of glacially abraded basalts in SE Iceland
M. Dąbski 20

Seasonal variations of rock glacier creep: time series observations from the Western Swiss Alps
R. Delaloye & B. Staub 22

Spatial and temporal snow cover variability and resulting thermal and mechanical response in a steep permafrost rock wall
D. Draebing, A. Haberkorn, M. Krautblatter, R. Kenner, & M. Phillips 24

Bridging periglacial geomorphology and ecology: a conceptual model of turf-banked solifluction lobe development
J. Eichel, D. Draebing, C. Eling, L. Klingbeil, M. Wieland, S. Schmidtlein, H. Kuhlmann, & R. Dikau 26

Cryo-conditioning of geomorphological processes in steep slopes
B. Etzelmüller, S. Westermann, & K.S. Myhra 28

Topographical conditions and geomorphological distribution of rock glaciers and protalus lobes in Aran valley (Central Pyrenees)
M.V. Fernandes, L.F. Lopes, & M. Oliva 29

Non-linearity of rockglacier flow law determined from geomorphological observations: A case study from the Murtèl rockglacier (Engadin, SE Switzerland)
M. Frehner, D. Amschwand, & I. Gärtner-Roer 30

Regional patterns and asynchronous onset of ice-wedge degradation in Arctic Alaska
G.V. Frost, T.C. Christopherson, A.K. Liljedahl, M.J. Macander, D.A. Walker, & A.F. Wells . . 32

Evolution of permafrost landscapes in an area of thermal suffosion processes development, Central Yakutia
L. Gagarin & I.I. Khristoforov 33

Rockglaciers in transition – recent results from longterm kinematic monitoring in the Swiss Alps
I. Gärtner-Roer & J. Müller 34

The complex pluri-decennial and multiphasic destabilization of the Jegi rock glacier (western Swiss Alps): historical development and ongoing crisis
A. Ghirlanda, L. Braillard, R. Delaloye, M. Kummert, & B. Staub 36

Recent evolution of mountain permafrost in the Southern Swiss Alps: The results of 2006 – 2015 period
E. Giaccone, S. Fratianni, C. Ambrosi, M. Antognini, R. Delaloye, C. Lambiel, S. Mari, & C. Scapozza 39

Ground thermal regime and geomorphological consequences in the Pyrenean high mountain.
M. González-García, E. Serrano, & J.J.González-Trueba 41

3D snow distribution and energy balance modelling in steep rock walls
A. Haberkorn, M. Lehning, M. Hoelzle, M. Bavay, N. Wever, R. Kenner, & M. Phillips 42

Rock glacier permafrost in the semi-arid Andes of Argentina
C. Halla, J.H. Bloethe, & L. Schrott 44

Reconstructing past extent of periglacial and glacial conditions in the NW of the Iberian Peninsula through micromorphometric analysis: the use of SEM techniques on geomorphology studies
J.F. Hall Riaza & M. Valcárcel 46

Rockfall in permafrost-affected cirque walls: New insights on spatial variability and potential causes derived from a 4-year LiDAR monitoring campaign, Kitzsteinhorn, Austria
I. Hartmeyer, M. Keuschnig, R. Delleske, & L. Schrott 47

Geomorphological implications of climate-driven permafrost change: The case of the Russian Altai Mountains
H. Hendrickx, J. Nyssen, B. Sannel, R. Goossens, F. Lehmkuhl, & V. Babin 49

Potential rock weathering by freeze-thaw processes in alpine cirques of Austria in 2006-2015 exemplified by the Hinteres Langtal Cirque, Austria
A. Kellerer-Pirklbauer & M. Wecht 50

Terrain sensitivity in northwestern Canada
S. Kokelj, J. Tunnicliffe, T. Lantz, R. Segal, D. Lacelle, R. Fraser, A. Rudy, & S. Lamoureux . . 52

Evidence of past permafrost features in the loess cover of eastern Poland and their relation to closed depression location
R. Kołodyńska-Gawrysiak, J. Adamczyk, L. Gawrysiak, L. Chabudziński, & G. Gajek 53

Spatial and temporal variability of the sediment transfer at the front of active rock glaciers, cases studies form the western Swiss Alps
M. Kummert, L. Braillard, B. Staub, & R. Delaloye 54

10-year kinematic monitoring of two destabilized rock glaciers in the Western Swiss Alps
C. Lambiel & R. Delaloye 57

Spatial distribution and morphometry of permafrost-related landforms in Boí valley (Central Pyrenees)
L.F. Lopes, M. Fernandes, & M. Oliva 59

Modelling three-dimensional distribution and evolution of rock wall permafrost in the Mont Blanc massif
F. Magnin, L. Ravanel, P. Deline, B. Pohl, J. Pergaud, & D. Joly 61

Snow control on active layer and permafrost in steep alpine rock walls (Aiguille du Midi, 3842 m a.s.l, Mont Blanc massif)
F. Magnin, S. Westermann, T. Barth, G.-M. Saulnier, P. Pogliotti, P. Philip Deline, & L. Ravanel 62

Imaging the transition from micro- to macro cracking of freezing rock using micro-computed tomography scanning
V. Maji & J.B. Murton 63

Towards a mechanical failure model for degrading permafrost rock slopes representing changes in rock toughness and infill
P. Mamot, M. Krautblatter, & R. Scandroglio 64

A multi-method approach to detecting high-mountain rockfall activity
N. Matsuoka 66

Slow, but steady movement of an Arctic rock glacier: 10 years of dynamics and thermal conditions
N. Matsuoka, T. Watanabe, A. Ikeda, H. H. Christiansen, & O. Humlum 68

Depth of seasonally frozen ground in the Karkonosze Mts (Sudetes, SW Poland) in the light of GIS modeling of topoclimate and geomorphic conditions
K. Migała & A. Traczyk 70

Geomorphic evolution in an ice-rich glaciated permafrost environment
B.J. Moorman 72

Rockglaciers on the move – A multi sensorial approach to rockglacier evolution
J. Müller, I. Gärtner-Roer, & A. Vieli 73

Short time changes of permafrost degradation triggered by anthropogenic impact and climatic events in Yamal Peninsula, Western Siberia 2010 – 2013/2015
C. Noerling, A. Morgenstern, M. Leibman, A. Bartsch, B. Widhalm, Y. Dvornikov, A. Khomutov, & B. Heim 75

Periglacial cirque analogs: regional trends of cryoplanation terrace elevation in Eastern Beringia
K. E. Nyland & F. E. Nelson 76

Subterranean periglacial landforms in Ledena jama pod Hrušico cave, Slovenia
J. Obu, J. Košutnik, P. Overduin, J. Boike, & S. Zwieback 78

The periglaction of the Iberian Peninsula
M. Oliva, E. Serrano, A. Gómez-Ortiz, M. J. González-Amuchastegui, A. Nieuwendam, D. Palacios, A. Pérez-Alberti, R. Pellitero-Ondicol, J. Ruiz-Fernández, M. Valcárcel, G. Vieira, & D. Antoniades 79

Deep-seated rock slope failure in mountain permafrost rock walls: Pizzo Cengalo and Piz Kesch, Swiss Alps
M. Phillips, F. Amann, A. Huwiler, R. Kenner, A. Kos, R. Luethi, & A. Wolter 80

Permafrost research collaboration between PYRN Iberian members (Spain and Portugal)
A. Pisabarro, N. Campos, M. Gómez-Lende, A. Molina, R. Pellitero, M. González-García, A. Merino, D. Gallinar, J. Ruiz-Fernández, C. García-Hernández, J. Hall-Riaza, P. Carrera, J. M. Fernández, A. Nieuwendam, G. Goyanes, A. S. David, I. Girao, M. Cardoso, A. Ferreira, J. Branco, L. Bandeira, & M. Lousada 82

Thermokarst landforms in Buckinghamshire, England
S. J. Price, S. Boreham, P. Gibbard, & T. Berry 83

GPR imaging of slope, fluvial and coastal sediments in high Arctic valley (Ebbadalen, Svalbard)
G. Rachlewicz & K.G. Rymer 84

Distribution and evolution of thermo-erosional drainage pathways between the 1950s and 2011 along the Yukon Coast, Canada
J.L. Ramage, A.M. Konopczak, A. Morgenstern, & H. Lantuit 85

Influence of periglacial conditions on the structure of Pleistocene glacial till (based on the example of Poland)
J. Rychel, M. Morawski, & L. Wachecka-Kotkowska 86

Solifluction and block streams activity in alpine area of Southern Carpathians, Romania
R.D. Şerban, A. Onaca, P. Urdea, & M. Popescu 87

Periglacial landforms and processes on a calcareous high mountain. Picos de Europa (Cantabrian Mountains, Northern Spain)
E. Serrano, A. Pisabarro, J.J. Sanjosé, M. Gómez-Lende, J.J. González-Trueba, & M. González-García 88

Siberia's glaciation as a specific component of permafrost characterizing a type of cryodiversity in the region
V. Sheinkman & V. Melnikov 90

Salix polaris growth responses to active layer detachment, solifluction, deflation and channel erosion processes in High Arctic
L. Siekacz 92

Floodstreams on coasts of the East Arctic seas at the Pleistocene-Holocene transition
V. V. Spektor, V. B. Spektor, Y. I. Torgovkin, A. A. Shestakova, G. T. Maksimov, & V. V. Andreeva 94

Rock glacier creep as a thermally-driven phenomenon: A decade of inter-annual observations from the Swiss Alps
B. Staub, C. Lambiel, & R. Delaloye 96

Fluvial and thermal: river bank erosion in permafrost regions
N. Tananaev 98

The Role of Cryogenesis in the Formation of Sand deposits in the Chara Basin (Transbaikalia)
N. Taratunina, A. Kurchatova, & E. Slagoda 99

Earth hummocks from Southern Carpathians: Morphometry, characteristics of internal structure and thermal behavior
P. Urdea, A. Onaca, A.C. Ardelean, & R.D. Serban 100

Distribution and Morphology of Sorted Circles and Polygons in the Northern Billefjorden, Central Svalbard
T. Uxa, P. Mida, & M. Křížek 101

Upper Pleistocene Geocryological evolution in Northwest of the Iberian Peninsula
M. Valcárcel, M. Costa-Casais, J.F. Hall-Riaza, & R. Blanco-Chao 103

Thermal erosion of ice-rich permafrost in the Lena River Delta / Siberia – Determining the decisive factors using logistic regression
G. Veh, A. Morgenstern, & F. Haas 105

Glacier-Permafrost interactions, debris transfer mechanisms and the development of distinctive sediment-landform associations in a High Arctic glacial environment: the case of Fountain Glacier, Bylot Island, Nunavut, Canada
R.I. Waller, M.J. Hambrey, & B.J. Moorman 106

High-resolution imaging of patterned ground features based on UAV photogrammetry
T. Watanabe, N. Matsuoka, & H.H. Christiansen 108

Reversible and irreversible movements in steep fractured bedrock permafrost
S. Weber, J. Beutel, J. Faillettaz, A. Hasler, & A. Vieli 109

Numerical modelling of convective heat transport by air flow in permafrost-rich talus slopes
J. Wicky & C. Hauck 111

Contrasting environments of sand wedge formation in discontinuous permafrost, Great Slave High Boreal Plains, Northwest Territories, Canada
S.A. Wolfe, P.D. Morse, S.V. Kokelj, C.M. Neudorf, & O.B. Lian 112

2 **Antarctic Permafrost, Soils and Periglacial Environments (co-organized by SCAR)** 115

The viable microorganisms from the Antarctic permafrost
A. Abramov, E. Rivkina, E. Karaevskaya, G. Wilson, & C. Cary 116

Distribution of frozen ground conditions in Byers Peninsula (Antarctica) based on electrical resistivity data
A. Correia, M. Oliva, & J. Ruiz-Fernández 117

PERMASNOW: Snow cover characterization and its effects on the thermal regime of permafrost and active layer in Deception and Livingston Islands, Antarctica
M.á. de Pablo, M. Ramos, A. Molina, J.J. Jiménez, M.á. Hidalgo, M. Prieto, S. Fernández, C. Recondo, J.F. Calleja, J.J. Peón, G. Vieira, C. Mora, K. Láska, F. Hrbáček, Z. Engel, & D. Nyvlt 119

Snow cover evolution at Livingston and Deception Islands, Antarctica, from 2006 to 2015
M.á. de Pablo, M. Ramos, A. Molina, G. Vieira, M. á. Hidalgo, M. Prieto, & J.J. Jiménez 121

The influence of inter-annual variations of snow cover on TTOP modelling in Hurd Peninsula (Maritime Antarctic)
A. Ferreira, G. Vieira, & M. Ramos 123

Permafrost thermal snapshot: Marble Point and Wright Valley, Ross Sea Region, Antarctica
M. Guglielmin, M. R. Balks, & C. Seybold 124

High resolution TanDEM-X imagery for mapping surface land cover features of Barton Peninsula (King George Island, northern Antarctic Peninsula region)
S. Guillaso, T. Schmid, J. López-Martínez, E. Serrano, A. Nieto, S. Mink, T. O'Neill, & M. Koch 126

Investigations into the ground thermal regime near Troll station, in the Jutulsessen of Antarctica: 2007–2016
C. D. Hansen, K. I. Meiklejohn, & W. Nel 127

Short-term changes observed in the ground thermal regime following the construction of a building: A case study from the Antarctic
C. D. Hansen & K. I. Meiklejohn 128

Active layer thickness variability on James Ross Island, Eastern Antarctic Peninsula
F. Hrbacek, K. Laska, D. Nyvlt, Z. Engel, & M. Oliva 129

Active layer thickness variability in two climatic settings of the Eastern and Western Antarctic Peninsula
F. Hrbacek, M. Oliva, M. Ramos, K. Laska, J. Ruiz-Fernández, M. A. de Pablo, G. Vieira, & D. Nyvlt 131

Seasonal snow cover characterization using field data and X-band radar imagery in Deception Island (Antarctica)
J. Jimenez, C. Mora, M. Ramos, G. Vieira, & M. A. de Pablo 133

Near-surface ground ice conditions in University Valley, McMurdo Dry Valleys of Antarctica
C. M. L. Lapalme, D. Lacelle, W. Pollard, D. Fisher, A. Davila, & C. McKay . . . 134

Influence of snow cover distribution on active-layer thermal regime on James Ross Island, eastern Antarctic Peninsula
K. Láska, F. Hrbacek, Z. Engel, & D. Nyvlt . . . 135

Characterization of soils related to periglacial processes on Fildes Peninsula and Ardley Island (Antarctic Peninsula region)
J. López-Martínez, T. Schmid, M. Pelayo, J. Díaz-Puente, T. O'Neill, E. Serrano, M. Rodríguez-Rastrero, M. J. Sierra, S. Mink, M. Lacal, R. Millán, & M. Balks . . . 137

Active Layer Monitoring in Western Dronning Maud Land, Antarctica since 2007
K. I. Meiklejohn, C. Kotzé, & C. D. Hansen . . . 138

Seasonal variability of discharge and sediment transport in two small streams in James Ross Island, Antarctic Peninsula
J. Ondruch, J. Kavan, D. Nývlt F. Hrbáček, & K. Láska . . . 139

Coupling in situ permafrost and active layer observations with Global Surface Temperatures from GISS: South Shetlands, Antarctica
M. Ramos, M. A. de Pablo, J. J. Jimenez, A. Molina, & G. Vieira . . . 141

Enthalpy method comparation between two different boreholes sites in Hurd Peninsula (Livingston Island)
M. Ramos, J. J. Jimenez, M. A. de Pablo, A. Molina, & G. Vieira . . . 142

Surface characteristics of rock glaciers in the Jutulsessen, Dronning Maud Land, Antarctica
E. M. Rudolph, K. I. Meiklejohn, & A. Bumby . . . 143

Mapping ice-free areas of King George Island (South Shetland Islands, Antarctica) using full polarimetric RADARSAT-2 data
T. Schmid, S. Guillaso, J. López-Martínez, A. Nieto, S. Mink, M. Koch, O. D'Hondt, A. Maestro, & E. Serrano . . . 145

Evidence of methane and *Archaeal* in permafrost of Antarctic oases
D. Shmelev, N. Demidov, E. Karaevskaya, & E. Rivkina . . . 146

3 **Ground Ice and Cryostratigraphy** 148

Relationship of Cryofacies, Surface and Subsurface Terrain Conditions in the Brooks Range and Foothills of Northern Alaska, USA
A. Balser, J. Jones, & T. Jorgenson . . . 149

Experimental ice wedge rejuvenation, Illisarvik drained lake, western Arctic coast, Canada
C. R. Burn . . . 150

Structure of wedge ice and massive ice: a comparative study
E. Galeeva, A. Kurchatova, V. Rogov, & E. Slagoda . . . 152

Ancient environments and climate of Central Siberia inferred from ice wedge at Cyuie village near Yakutsk
K. Kim, J. Ahn, E. Byun, H. Yoon, A. Fedorov, & J.-W. Yang . . . 153

Cryostratigraphy and sedimentology of the early Holocene Zackenberg delta (NE Greenland)
G. L. Gilbert, S. Cable, & H. H. Christiansen . . . 154

Ice-wedge stable isotopes at the Dmitry Laptev Strait (Northeast Siberian Arctic) – indications for Late Quaternary stratigraphy and paleoclimate
T. Opel, S. Wetterich, A. Y. Dereviagin, H. Meyer, M. C. Fuchs, & L. Schirrmeister . . . 155

Structure and distribution of ice lenses in artificial frozen soils and arctic-alpine permafrost
T. Saruya, T. Sueyoshi, T. Watanabe, A. Rempel, & H. Enomoto . . . 157

Radiocarbon dating, stable-isotope composition and pollen spectra of the Holocene ice wedge in the Chara depression, Northern Transbaikalia
A.C. Vasil'chuk, Y.K. Vasil'chuk, & J.V. Stanilovskaya . . . 158

Hydrogen and oxygen isotopes in ice wedges near Vorkuta town, north of East European Plain
Y. K. Vasil'chuk, N. A. Budantseva, J. N. Chizhova, & A. C. Vasil'chuk . . . 160

Assessing permafrost formation age by radium isotopes
Y. Weinstein, D. Rotem, H. H. Christiansen, J. Yechieli, Y. Niro, & H. Kooi . . . 162

4 **Arctic and Antarctic Cryosols: Frontier of Global Change and Human Action** 164

Variability of organic contaminants in the snowpack and soils near Arctic coal mining sites in Svalbard
A.S. Abramova, S.S. Chernyanskii, & N.A. Marchenko . . . 165

Active soil-landscape processes in the Ross Sea Region, Antarctica: two case studies
M.R. Balks, & T.A. O'Neill . . . 166

Warming enhance permafrost cryoturbation and deeper soil carbon store
R. Chang & G. Wang . . . 169

Mesoscale vegetation shift as a consequence of permafrost thawing in northern Siberia
A. Evgrafova, I. Haase, A. Otto, U. Bange, N. Tananaev, O. Shibistova, G. Guggenberger, L. Sauheitl, & S. Spielvogel . . . 170

Initial soil formation and soil carbon accumulation on King Georges Island (maritime Antarctica)
P. Kühn, D. Noses Spinola, & C.E.C.G. Schaefer . . . 172

Content of heavy metals in Arctic permafrost-affected soils of the Russian European Northeast
E. Lapteva, D. Kaverin, A. Pastukhov, E. Shamrikova, & Y. Kholopov . . . 174

The preliminary analysis of soil cover spatial structure of Fildes Peninsula, King-George Island (West Antarctica)
A. Lupachev & E. Abakumov . . . 175

Formation of suprapermafrost accumulative organo-mineral horizons in Turbic Cryosols
A. Lupachev & S. Gubin . . . 176

Heat line in permafrost – a large experiment of transformation of the Arctic ecosystems
G. Matyshak, O. Goncharova, A. Bobrik, D. Sukhova, N. Petrzhik, & R. Kireev . . . 177

Pedodiversity and Carbon storage of permafrost-affected soils in the Lena River Delta
E.-M. Pfeiffer & S. Zubrzycki . . . 179

Formation of microorganisms in tundra soils of the European North-East
J. Vinogradova, F. Khabibullina, & E. Lapteva 180

Cryosols of the Lena River Delta and its hinterland – genesis and diversity
S. Zubrzycki, L. Kutzbach, E. Abakumov, & E.-M. Pfeiffer 182

5 **Climate Change and the Permafrost Carbon Feedback: Past, Present and Future** 183

The biggest terrestrial tipping point or a potential carbon sink? 124 experts weigh in on the permafrost carbon feedback
B.W. Abbott, J.B. Jones Jr., J.R. Larouche, W.B. Bowden, S.E. Godsey, & A.W. Balser 184

Thawing permafrost carbon decomposition under aerobic and anaerobic conditions
C. Beer, C. Knoblauch, & E.-M. Pfeiffer 185

The sensitivity of carbon in Arctic permafrost soils to climate change
M. P. Björkman, P. Boeckx, J. Rethemeyer, F. Lindwall, B. Elberling, & R. G. Björk 186

Permafrost thaw - decadal responses to climate change
M. P. Björkman, C. Larose, J. Rethemeyer, B. Elberling, L. Klemedtsson, & R. G. Björk 187

Pan-arctic lakes: an important source of atmospheric methane during the last deglaciation?
L. Brosius, C. Treat, K. Walter Anthony, M. Jones, G. Grosse, & J. Lenz 188

Including permafrost carbon within the land surface scheme of the UK Earth System Model (JULES)
E. Burke, A. Ekici, & S. Chadburn 189

Trapped greenhouse gas in permafrost active layer: Methane peaks in the vertical profiles of frozen Alaskan soil cores
E. Byun, J.-W. Yang, Y. Kim, & J. Ahn 190

Active layer thickness and vegetation phenology as key factors affecting the variability of CO_2 fluxes in polar environments
N. Cannone, S. Ponti, M. Guglielmin, T. Christensen, F.-J. Parmentier, N. Pirk, & H. Christiansen 191

Measurement of carbon-dioxide fluxes from permafrost disturbances using eddy covariance in a high arctic tundra ecosystem
A. E. Cassidy, G. Henry, & A. Christen 193

Implications of shrub expansion on soil carbon dynamics and thaw depth in arctic Alaska
C. I. Czimczik, S. R. Holden, & J. M. Welker 194

Partitioning CO_2 net ecosystem exchange fluxes into photosynthesis, autotrophic and heterotrophic respiration in a polygonal tundra landscape
T. Eckhardt, C. Knoblauch, L. Kutzbach, G. Simpson, & E.-M. Pfeiffer 195

Closing the loop - the permafrost carbon feedback in a fully coupled system
A. Ekici, E. Burke, S. Chadburn, C. Huntingford, & P. Friedlingstein 196

Regional assessment of dissolved CH_4 and CO_2 sources (^{14}C age) from thaw lakes in Northern Alaska
C. D. Elder, X. Xu, K. Walter Anthony, A. Townsend Small, K. Hinkel, & C. I. Czimczik 197

Abiotic controls on permafrost C mineralization rates based on incubating samples from 4 contrasting arctic localities
S. Faucherre, I. Banyasz, C. J. Jørgensen, N. Weiss, G. Hugelius, P. Kuhry, & B. Elberling 198

New low-cost automated system of closed chambers to measure greenhouse gas emissions from the tundra
S. Gagnon, E. L'Hérault, M. Lemay, & M. Allard 199

Analysis of permafrost carbon release processes after 25 years of climate warming
S. Gagnon, & M. Allard 200

$\Delta^{14}C$ and $\delta^{13}C$ signatures of CH_4, CO_2 and Dissolved Organic Matter of Siberian peatland and thermokarst lake complexes in relation to permafrost degradation
L. Gandois, A. Hoyt, X. Xu, C. Hatté, R. Teisserenc, & N. Tananaev 201

Quantifying the impact of permafrost dynamics on soil carbon accumulation in response to climate change and wildfire intensification in Alaska
H. Genet, Y. He, A. D. McGuire, Q. Zhuang, Z. Zhu, N. Pastick, B. Wylie, & K. Johnson 203

Relevance of aggregation and chemisorption for carbon sequestration in thawing permafrost soils of Northern Siberia
I. C. Haase, A. Evgrafova, N. Tananaev, O. Shibistova, P. Kühn, G. Guggenberger, S. Spielvogel, & L. Sauheitl 204

Thermokarst-lake methanogenesis along a complete talik (thaw bulb) profile
J. K. Heslop, K. Walter Anthony, A. Sepulveda-Jauregui, K. C. Martínez Cruz, A. Bondurant, G. Grosse, & M. Jones 205

Relationships between organic matter quality and methane production in thermokarst lake sediments
J. K. Heslop, K. Walter Anthony, & M. Zhang 206

Changing Permafrost in the Arctic and its Global Effects in the 21^{st} Century (PAGE21): Final Results for a large-scale international and integrated project to measure the impact of permafrost degradation on the climate system
H.-W. Hubberten, H. Lantuit, J.Boike, & L.-K. Viitanen 207

Comparing permafrost soil carbon pools from earth system models to empirically derived datasets
G. Hugelius, A. D. McGuire, C. Beer, T. J. Bohn, E. J. Burke, S. E. Chadburn, G. Chen, X. Chen, D. J. Hayes, E. E. Jafarov, C. D. Koven, S. Peng, & K. M. Schaefer 208

More than Methane: Linking geomorphology and biogeochemistry to understand biogas emissions from two wetlands on Spitsbergen
E. L. Jones & A. Hodson 210

Permafrost thaw in boreal peatlands: the importance of permafrost formation processes in post-thaw carbon losses
M. C. Jones, K. Manies, C. Treat, J. Harden, J. O'Donnell, & M. Waldrop 211

Constraining the uncertainty of the Arctic CH_4 sink and its potential effects on permafrost carbon feedbacks to the global climate system
C. J. Jørgensen, J. R. Christiansen, T. Mariager, & G. Hugelius 212

Modelling carbon in permafrost soils from preindustrial to the future
T. Kleinen 213

Permafrost thawing as a possible source of abrupt carbon release at the onset of the Bølling/Allerød
P. Köhler, G. Knorr, & E. Bard . . . 214

Lability classification of soil organic matter in the northern permafrost region based on simple soil horizon and landscape unit criteria
P. Kuhry, J. Barta, D. Blok, B. Elberling, S. Faucherre, G. Hugelius, A. Richter, H. Santruckova, & N. Weiss . . . 215

Hydrolaccoliths of West Siberia – cold methane seeps in permafrost
A. N. Kurchatova & V. V. Rogov . . . 216

Net effects of drying experiment on permafrost stability through radiocarbon signals
M. J. Kwon, S. M. Natali, C. Hicks Pries, K. G. Crummer, E. A. G. Schuur, N. Zimov, S. A. Zimov, M. Heimann, & M. Goeckede . . . 217

LGM permafrost carbon stocks inferred from empirical paleodata and modern analogues
A. Lindgren, P. Kuhry, & G. Hugelius . . . 218

Permafrost and feedbacks to the atmosphere in an Arctic regional climate model: an evaluation
H. Matthes, A. Rinke, & K. Dethloff . . . 219

Tundra carbon dynamics in response to five seasons of experimental air warming and permafrost thaw
M. Mauritz, R. Bracho, G. Celis, S. Natali, J. Hutchings, V. Salmon, E. Webb, & E. Schuur . . . 221

The role of permafrost-dominated forest and tundra ecosystems in a changing climate, North-Eastern Russia
T. Maximov, H. Dolman, K. v. Huissteden, T. Ohta, & A. Sugimoto . . . 222

The temporal evolution of changes in carbon storage in the Northern Permafrost Region simulated by carbon cycle models between 2010 and 2300: Implications for atmospheric carbon dynamics
A. D. McGuire, D. Lawrence, E. Burke, G. Chen, E. Jafarov, C. Koven, A. MacDougall, D. Nicolsky, S. Peng, & D. Ji . . . 224

Early results simulating permafrost carbon processes in the coupled CLASS-CTEM model
J. Melton . . . 225

Simulating the carbon, water and energy budgets of arctic soils with the ISBA land surface model
X. Morel, C. Delire, B. Decharme, M. Lund, & F. Domine . . . 225

Using physical soil fractions to study small scale distribution and composition of soil organic matter in permafrost soils
C. W. Müller, J. Rethemeyer, S. Zubrzycki, S. Höfle, M. Molina Gamez, J. Kao-Kniffin, L. Zoor, S. Löppmann, K. M. Hinkel, & J. G. Bockheim . . . 226

A Pan-Arctic synthesis of carbon emissions during the nongrowing season
S. Natali, A. Selbmann, B.W. Abbott, M. Björkman, R. Commane, E. Cooper, C. Czimczik, S. Davydov, A. Davydova, B. Elberling, H. Genet, M. Goeckede, E. Jafarov, J. Jastrow, Y. Kim, M. Lara, M. Lupascu, W. Oechel, F. Rezanezhad, D. Risk, P. Semenchuk, C. Treat, M.P. Waldrop, Q. Zhuang, & D. Zona . . . 227

New estimates of soil organic carbon storage in the Zackenberg valley, NE Greenland by combining geomorphology and land cover
J. Palmtag, G. Hugelius, & P. Kuhry . . . 228

Carbon exchange in northern ecosystems influenced by sea ice decline
F.-J. W. Parmentier & T. R. Christensen . . . 229

The stable isotopes and C/N ratio as indicators of peat plateaus sustainability in the southern limit of East-European cryolithozone
A. Pastukhov, C. Knoblauch, D. Kaverin, I. Antcibor, & E.-M.Pfeiffer . . . 230

Greenhouse gas emissions from Arctic lakes and ponds as influenced by carbon lability and geomorphology
V. Prėskienis, I. Laurion, F. Bouchard, D. Fortier, & M. Rautio . . . 231

Degradability of organic matter in permafrost soils revealed by a comprehensive radiocarbon study: Clues from compound-specific to soil density fractions
J. Rethemeyer, S. Höfle, C. W. Müller, & S. Kusch . . . 232

The IsoGenie Project: Integrating high-resolution characterization of organic matter, isofluxes, and microbiota in a thawing permafrost peatland
V. I. Rich, S. Saleska, G. Tyson, J. Chanton, P. Crill, R. Varner, S. Frolking, W. Cooper, M. Sullivan, & The IsoGenie Consortium . . . 233

Holocene peatland development, carbon accumulation and permafrost history in Tavvavuoma, northern Sweden
A. B. K. Sannel, L. Hempel, A. Kessler, P. Kuhry, & V. Prėskienis . . . 234

Identifying circumpolar trends in greening versus browning of the Arctic
C. Schädel, H. Epstein, M. Loranty, S. Natali, & V. Salmon . . . 235

Observation-based modelling of CO_2 and CH_4 fluxes from newly thawed carbon
T. Schneider von Deimling, G. Grosse, J. Strauss, L. Schirrmeister, A. Morgenstern, & J. Boike . 236

The carbon balance of Alaskan tundra in response to long-term permafrost degradation
E. Schuur, R. Bracho, G. Celis, J. Ledman, & M. Mauritz . . . 237

High resolution maps of soil organic carbon and typical soil profiles
M. B. Siewert, P. Kuhry, & G. Hugelius . . . 238

Microbial lipid distribution and substrate potential of the organic matter in terrestrial Siberian permafrost deposits from NE Siberia
J. G. Stapel, K. Mangelsdorf, L. Schirrmeister, B. Horsfield, & D. Wagner . . . 239

Permafrost aggradation reduces peatland methane fluxes during the Holocene
C. C. Treat, M. Jones, G. Grosse, L. S. Brosius, & K. Walter Anthony . . . 241

Thermokarst terrains and carbon cycling: A circumpolar perspective
M. R. Turetsky, A. D. McGuire, D. Olefeldt, & Members of the Permafrost Carbon Network . . . 242

Assessment of climate driven dynamics of active layer, hydrological and vegetation status in Heilongjiang province, Northern China using dynamic global vegetation model
S. Venevsky, Y. Yang, & W. Chao . . . 244

Positive feedback of all three greenhouse gases (CO_2, CH_4, N_2O) to experimental warming in Russian subarctic tundra
C. Voigt, R. E. Lamprecht, M. E. Marushchak, P. J. Martikainen, & C. Biasi . . . 245

Ecosystem functional zonation approach to integrate multi-type multiscale datasets for scaling above and below-ground control on carbon cycling
H. M. Wainwright, B. Dafflon, N. Tas, Y. Wu, M. Torn, L. Smith, J. B. Curtis, C. Ulrich, J. E. Peterson, & S. S. Hubbard . . . 247

Present-day permafrost carbon feedback from thermokarst lakes
K. Walter Anthony, R. Daanen, P. Anthony, T. Schneider von Deimling, C.-L. Ping, J. Chanton, & G. Grosse . . . 249

Regulation of soil organic matter decomposition in permafrost-affected soils
J. Walz, C. Knoblauch, L. Böhme, & E.-M. Pfeiffer . . . 250

Subsoil carbon and nitrogen dynamics: Implications of deeper plant rooting for the arctic carbon balance
B. Wild, R. J. E. Alves, J. Bárta, P. Čapek, K. Diáková, N. Gentsch, A. Gittel, G. Guggenberger, G. Hugelius, C. Kaiser, A. Knoltsch, P. Kuhry, N. Lashchinskiy, R. Mikutta, J. Palmtag, J. Prommer, H. Šantrůčková, C. Schleper, J. Schnecker, O. Shibistova M. Takriti, V. L. Torsvik, T. Urich, M. Watzka, & A. Richter . . . 251

Linking geomorphology and biogeochemistry in dynamic permafrost environments
N. Weiss . . . 253

Mobilization of old carbon during deglacial permafrost retreat in East Asia
M. Winterfeld, W. Dummann, J. Hefter, L. Lembke-Jene, C. McIntyre, R. Tiedemann, & G. Mollenhauer . . . 254

Land cover and landform classification upscaling of soil organic carbon stocks in the Brøgger Peninsula, Svalbard
R. Wojcik, P. Kuhry, J. Palmtag, G. Hugelius, & N. Weiss . . . 255

Permafrost peatland dynamics during the last millennia in NE European Russia and Finnish Lapland
H. Zhang, M. Väliranta, S. Piilo, M. Amesbury, A. Gallego-Sala, & D. Charman . . . 256

The role of wetlands in projected future permafrost carbon-climate feedbacks: An ensemble simulation experiment with the land surface model LPJ-wsl
Z. Zhang, N. Zimmermann, & B. Poulter . . . 256

Net ecosystem exchange of CO_2 above alpine meadow in permafrost regions of the Qinghai-Tibetan Plateau
Y. Zhao, L. Zhao, Y. Xiao, G. Yue, G. Hu, Y. Qiao, & K. Jiao . . . 258

Variability in microbial Arctic soil carbon usage: Implications for climate feedback
L. A. Ziolkowski, C. Czimczik, S. Holden, H. Li, T. Onstott, G. Slater, A. Townsend Small, & L. Whyte . . . 259

Carbon and nitrogen storages of the Lena River Delta
S. Zubrzycki, L. Kutzbach, A. Desyatkin, E. Abakumov, & E.-M. Pfeiffer . . . 260

Carbon dioxide fluxes over larch permafrost stand in Central Siberia, Russia
V. Zyrianov, O. Zyryanova, Y. Matsuura, & A. Prokushkin . . . 261

6 **Towards Regional Assessments of Permafrost-Atmosphere Carbon Fluxes** 262

Evaluating the ecosystems' carbon uptake in Russian permafrost regions under current and projected for the 21st century climatic conditions
O. Anisimov, & Y. Ziltcova 263

Inter-annual variability and drivers of the carbon balance of a northeast Siberian tundra
L. Belelli Marchesini, J. van Huissteden, M. van der Molen, F.-J. W. Parmentier, T. Maximov, A. Budishchev, & H. Dolman 265

The carbon budget of Eurasian Arctic sites: a synthesis from the PAGE21 flux network
L. Belelli Marchesini, C. Wille, F.-J. W. Parmentier, M. Goeckede, J. van Huissteden, H. Dolman, M. Aurela, J. Boike, T. Christensen, T. Friborg, T. Laurila, M. Lund, M. Jammet, L. Kutzbach, T. Maximov, T. Sachs, & N. Shurpali 267

Use of spectrometer data to analyse the impact of fine-scale phenology patterns on CO_2 fluxes from an Arctic permafrost ecosystem
I. Burjack, A. Berninger, M. Heimann, & M. Göckede 269

Northeast Siberian methane fluxes from permafrost soils: First results from a regional land-vegetation model configuration
K. Castro-Morales, T. Kleinen, S. Kaiser, C. Beer, S. Zaehle, & M.Goeckede 270

Carbon stocks and fluxes in the high-latitudes: Using site-level data to evaluate earth system models
S. Chadburn, E. Burke, A. Ekici, C. Beer, P. Porada, G. Krinner, T. Wang, C. Brutel-Vuilmet, L. Belelli, K. Van Huissteden, L. Kutzbach, G. Hugelius, J. Boike, M. Langer, B. Elberling, M. Johansson, & S. Westermann 271

Regional carbon budget for Alaska: Response to seasonal and interannual temperature variations
R. Commane, S. Wofsy, J. Lindaas, K. Luus, J. Benmergui, R. Chang, N. Parazoo, C. Sweeney, A. Karion, C. Miller, & J. Henderson 272

Modeling and upscaling methane emission hotspots in the polygonal tundra
F. Cresto Aleina, B. R. K. Runkle, A. Winkler, C. Knoblauch, & L. Kutzbach 273

Upscaling of high-latitude CO_2 fluxes in NE Siberia based on a satellite data-driven model
M. Goeckede, K. Luus, T. Sachs, L. Kutzbach, M. Aurela, L. Belelli Marchesini, E. Euskirchen, K. van Huissteden, & A. Serafimovich 274

First assessment of methane emission during ice thaw from southern tundra lakes in Western Siberia
L. Golubyatnikov, V. Kazantsev, & M. Cherbunina 275

The Permafrost Regionalization Map (PeRM): How well do observations, models and experiments represent the circumarctic-scale spatial variability in permafrost carbon vulnerability?
D. J. Hayes, P. Kuhry, S. Goswami, G. Grosse, A. D. McGuire, & E. A. G. Schuur 276

Process-based modelling of methane emissions from a polygonal tundra at Samoylov, Lena Delta
S. Kaiser, C. Beer, & M. Goeckede 278

Seasonal patterns and annual budgets of CO_2 and CH_4 fluxes from a permafrost ecosystem based on year-round eddy-covariance measurements
F. Kittler, M. Goeckede, I. Burjack, N. Zimov, S. A. Zimov, & M. Heimann 279

Disproportional contribution of geological sources to Mackenzie Delta methane emissions revealed from airborne eddy-covariance measurements
K. Kohnert, A. Serafimovich, S. Metzger, J. Hartmann, & T. Sachs 280

Regional pattern of carbon emission from the Mackenzie Delta, Canada – Results from an airborne flux study
K. Kohnert, A. Serafimovich, S. Metzger, J. Hartmann, & T. Sachs 281

Temporal and spatial extrapolation of CO_2 fluxes of polygonal tundra by modeling ecosystem photosynthesis-respiration flux parameters with NDVI and reanalysis data
L. Kutzbach, C. Wille, A. J. Winkler, & B. R. K. Runkle 282

Interaction of fire, moss and permafrost in the land vegetation model JSBACH
G. Lasslop, P. Porada, C. Beer, & S. Kloster 283

Quantifying the biogeochemical processes and environmental controls that drive Arctic-Boreal ecosystem carbon fluxes
C. Miller, S. Biraud, A. Bloom, J. Budney, R. Chang, S. Chazanoff, R. Commane, B. Daube, Y. Fang, E. Gottlieb, S. Hardman, J. Henderson, S.-J. Jeong, A. Karion, J. Kimball, C. Koven, T. Kurosu, D. Lawrence, K. Luus, K. McDonald, K. McKain, A. Michalak, J. Miller, S. Miller, G. Mouteva, W. Oechel, N. Parazoo, J. Pittman, E. Podest, C. Potter, J. Randerson, T. Sachs, D. Schimel, A. Slater, N. Steiner, C. Sweeney, M. Torn, S. Veraverbeke, J.D. Watts, E. Wiggins, S. Wofsy, S. Wolter, D. Worthy, V. Yadav, & D. Zona 284

A multi-year estimate of methane fluxes in Alaska from the CARVE aircraft campaign
S. Miller, R. Commane, R. Chang, C. Miller, A. Michalak, S. Dinardo, E. Dlugokencky, S. Hartery, A. Karion, C. Sweeney, J. Lindaas, & S. Wofsy 285

Detecting Patterns of Changing CO_2 Flux in Alaska
N. C. Parazoo 285

Wintertime emissions of methane and carbon dioxide from permafrost-underlain Arctic tundra
N. Pirk, M. Mastepanov, M. Lund, S. H. Pedersen, M. R. Mylius, M. P. Tamstorf, H. H. Christiansen, & T. R. Christensen 286

Quantifying the effect of lichen and bryophyte cover on permafrost soil within a global land surface model
P. V. Porada, A. Ekici, & C. Beer 287

Constraining Arctic methane emissions through atmospheric methane signals at coastal sites
F. Reum, M. Goeckede, U. Karstens, C. Gerbig, J. Lavrič, S.A. Zimov, N. Zimov, O. Kolle, F.-T. Koch, & M. Heimann 288

Spatio-temporal variability of CH_4 fluxes and environmental drivers on a modern flood plain of the Siberian Lena River Delta
N. Rößger, C. Wille, L. Beckebanze, & L. Kutzbach 289

Mobilization of organic carbon and nitrogen in a retrogressive thaw slump on Herschel Island, Yukon Territory, Western Canadian Arctic
S. Ruttor, G. Tanski, & H. Lantuit 291

Low permafrost methane emissions from regional airborne flux measurements
T. Sachs, A. Serafimovich, S. Metzger, K. Kohnert, & J. Hartmann 292

The new field laboratory at the Samoylov Island observatory – possibilities of controlled high precision instrumentation to obtain new insights in environmental conditions of the high arctic lowland tundra.
P. Schreiber, M. Langer, N. Bornemann, & J. Boike . . . 293

Airborne measurements of greenhouse gas and energy fluxes in the Lena River Delta
A. Serafimovich, E. Larmanou, S. Metzger, & T. Sachs . . . 294

Variability of surface energy fluxes over high latitude permafrost wetlands
A. Serafimovich, S. Metzger, J. Hartmann, S. Wieneke, & T. Sachs . . . 295

Seida landscape heterogeneity and regional GHG modelling
N. J. Shurpali, C. Biasi, Y. Zhang, M. Marushchak, T. Virtanen, & P. Martikainen . . . 296

Monitoring a decade of change in Pan-Arctic CO_2 and CH_4 exchange through integrated satellite remote sensing
J. D. Watts & J. S. Kimball . . . 297

Studies on carbon dioxide fluxes of alpine meadows at non-growing season in the continuous permafrost zone of the Qinghai-Tibet Plateau
H. Yun, Q. Wu, J. Luo, & F. Niu . . . 299

Variability of methane and carbon dioxide fluxes at permafrost peatland in the European Northeast
S. Zagirova & M. Miglovets . . . 300

7 Reconstructing Past Permafrost: Spatial Distribution and Temporal Changes 301

The French Pleistocene permafrost database: GIS-based analysis and OSL dating of sand wedges
E. Andrieux, P. Bertran, & M. Bateman . . . 302

Permafrost and large ice wedge pseudomorphs in Last Glacial European loess series: a northern France perspective
P.L. Antoine, O. Moine, & G. Gilles . . . 302

Periglacial features and permafrost disappearance in the last glaciated area in N-Poland and NE-Germany
A. Börner & M. Blaszkiewicz . . . 304

Active and fossil permafrost in the glacier-permafrost system. Storglaciären, Kebnekaise, Northern Sweden
W. Dobiński & M. Glazer . . . 305

Tracking the southern boundary of the Late Pleistocene permafrost in the Ural Mountains using cryogenic cave carbonates: a feasibility study
Y. Dublyansky, O. Kadebskaya, M. Luetscher, H. Cheng, G. Koltai, & C. Spötl . . . 308

On ice-age glaciers and permafrost in connection with radioactive waste repositories in northern Switzerland
W. Haeberli, D. Cohen, & U. H. Fischer . . . 309

Formation Chronology of Arsain Pingo, Darhad Basin, northern Mongolia
M. Ishikawa & J. Yamkhin . . . 311

Extents of permafrost on the Qinghai-Tibet Plateau during the Last Glaciation Maximum (LGM) and Holocene Megathermal Period
H. Jin, X. Chang, & R. He . . . 312

Regional climatic significance of relict rock glaciers in the Eastern Alps
O. C. Kronig, J. M. Reitner, M. Christl, & S. Ivy-Ochs 313

Past permafrost and landscape dynamics in Central Beringia: Two case studies from drained thermokarst lake basin cores
J. Lenz, S. Wetterich, B. M. Jones, K. Walter Anthony, H. Meyer, A. Bobrov, S. Wulf, & G.Grosse 314

Reconstructing permafrost thaw events from alpine cave systems
M. Luetscher, D. Hoffmann, S. Frisia, B. Sattler, & C. Spötl 316

Broken stalagmites may be an indicator of permafrost thawing
L. Luhová., R. Milovský, M. Orvošová, S. Milovská, J. Šurka, P. Herich, Y.-C. Chou, & C.-C. Shen 317

Heterochronous populations of cryogenic cave calcite may reflect depth of permafrost thawing events
R. Milovský, M. Orvošová, S. Milovská, J. Šurka, P. Herich, A. Biroň, & T. Mikuš 319

Multi-proxy reconstruction of environmental changes and cryogenic processes in the Picos de Europa (Cantabrian Mountains, Northern Spain) since the Last Glaciation
A. Nieuwendam, J. Ruiz-Fernández, M. Oliva, V. Lopes, A. Cruces, & M. C.Freitas 320

Periglacially-induced versus earthquake-induced load structures - similarities and differences
M. Pisarska-Jamroży, B. Woronko, & A.J. Van Loon 322

Last Glacial palaeotemperatures in loess context from oxygen isotopes of earthworm calcite granules
C. Prud'homme, C. Lécuyer, P. Antoine, O. Moine, C. Hatté, F. Fourel, F. Martineau, & D.-D. Rousseau 323

Dry valley dynamics in periglacial conditions (a case study from NE Poland)
J. Rychel, B. Woronko, M. T. Karasiewicz, M. Kupryjanowicz, M. Fiłoc, & L. Marks 324

Paleo- permafrost and groundwater systems in the UK over the past 1 Million years
J. Scheidegger, J. Busby, C. Jackson, F. McEvoy, & S. Norris 325

Paleopedological cryotrassology: Tracers of former permafrost – the cases from the late pleistocene paleosol/sedimentary sequences of Europe and western Siberia
V. Sheinkman, S. Sedov, V. Melnikov, B. Terhost, & A. Rusakov 327

Permafrost as a background for development of ancient glaciation and the problem of bedded ice bodies in Northwestern Siberia
V. Sheinkman & V.Melnikov 329

The final disappearance of permafrost as a trigger for early Holocene landscape evolution in the southern Baltic lowlands
M. Słowiński, F. Ott, A. M. Noryśkiewicz, N. Dräger, M. Kramkowski, R. Tjallingii, C. Haas, M. Błaszkiewicz, J. Kordowski, I. Zawiska, M. Theuerkauf, E. Dietze, M. Rzodkiewicz, M. J. Schwab, & A.Brauer 332

The late Pleistocene episodes of permafrost aggradation in the Wielkopolska region, Poland – palaeoclimatological and palaeogeographical implications
R. J. Sokołowski, P. Zieliński, W. Wysota, S. Fedorowicz, K. Przegiętka, & A. Molodkov 333

Permafrost peatland succession in high latitudes: Regional trends in permafrost aggradation and thaw
C. C. Treat & M. C. Jones 335

Sedimentological evidence for stacked paleo-thaw (thermokarst) lake successions in Western Europe
J. van Huissteden, C. Berritella, & J. M. Warnsloh . . . 336

Thermokarst evidences in the Paris Basin
B. Van Vliet-Lanoe, J. Brulhet, P. Combes, C. Duvail, F. Ego, S. Baize, & I. Cojan . . . 337

The reconstruction of past permafrost: recent results, present-day gaps and future challenges
J. Vandenberghe . . . 338

Testing the accuracy of yedoma radiocarbon age
A. Vasil'chuk & Y.Vasil'chuk . . . 339

High temporal resolution winter air temperatures and permafrost maps at 40-12 ka BP using oxygen isotope data from Siberia yedoma
Y. K. Vasil'chuk & A. Vasil'chuk . . . 341

Micro-scale frost weathering of quartz sand grains
B. Woronko & M. Pisarska-Jamroży . . . 343

8 **Permafrost Mapping and Data** 344

Permafrost temperature and active-layer thickness of Yakutia with 0.5-degree spatial resolution for model evaluation
C. Beer, A. N. Fedorov, & Y. Torgovkin . . . 345

Dependency of C- and Ku-band backscatter on snow height and air temperature in permafrost areas
H. Bergstedt, A. Bartsch, & S.Zwieback . . . 346

Comparing models for mountain and lowland permafrost in British Columbia, Canada
A. R. Bevington, M. Geertsema, V. Foord, & A. G. Lewkowicz . . . 347

Electronic edition of the permafrost map of Russia 1: 2 500 000
A. Brouchkov & A.Falaleeva . . . 348

HyLab: Alaska's in-state capability for airborne imaging spectroscopy – Applications for permafrost
M. Buchhorn, A. Prakash, D. L. Hampton, J. Cristóbal-Rosselló, C. F. Waigl, M. Stuefer, P. Graham, & D. A. Walker . . . 349

Assessment of permafrost areas using characteristics of rock glaciers in the Himachal Himalaya, North-west part of India
P. Chand, S. Kumar, & M. Sharma . . . 351

The Barrow Area Information Database (BAID) and development of a wireless sensor network to provide near real-time climate data for the Barrow Peninsula area of Northern Alaska
R. P. Cody, C. E. Tweedie, S. Escarzaga, A. Kassin, M. Barba, A. Gaylord, W. Manley, F. Mazza Ramsay, S. Vargas, G. Tarin, C. Laney, L. R. Lestak, S. Villarreal, G. Ramirez, Q. Aiken, J. Collins, E. Green, & L. Nelson . . . 352

Characterization of sporadic discontinuous permafrost occurrences in Northeastern, British Columbia, Canada
T. L. Coultish, G. K. Claypool, & L. U. Arenson . . . 353

Analysis and mapping of mountain permafrost data: spatial modelling using machine learning algorithms
N. Deluigi, M. Kanevski, R. Delaloye, & C. Lambiel . . . 354

Feature selection algorithms for permafrost variable importance assessment: A support to efficient permafrost distribution mapping
N. Deluigi, C. Lambiel, R. Delaloye, & M. Kanevski 355

Data Publications – persistent and citable products of research
K. Elger, K. Lehnert, & D.Ulbricht 357

Experiences of contributions to an international monitoring network from an institutional data repository
J. Fiddes, N. Kryvych, C. Fierz, & Ø. Godøy 358

A new permafrost map for the Scandinavian Peninsula
K. Gisnås, B. Etzelmüller, G. Alm, H. H. Christiansen, J. Engström, A. Frampton2, J. Hjort, K. Isaksen, P. Kuhry, C. Lussana, A. B. K. Sannel, S. Westermann, & J. Åkerman 359

Measurement of subsurface ice content and temperature using broadband spectral induced polarization
R. Grimm & D.Stillman 360

Continental and global scale permafrost mapping: Persistent challenges and new directions
Stephan Gruber 361

Permafrost-related research data - their accessibility, visualization, and publication using GIS and WebGIS technology
A. Haas, B. Heim, S. Zubrzycki, K. Elger, & A. Morgenstern 361

The Arctic Permafrost Geospatial Centre (APGC): A new central platform for hosting and distributing geospatial permafrost datasets
S. Laboor, G. Grosse, A. Haas, B. Heim, & I. Nitze 362

Mapping polygonal tundra geomorphology across the Arctic Coastal Plain of Alaska
M. J. Lara, P. Martin, & A. D. McGuire 363

Mapping permafrost distribution using the remote sensing techniques and geophysical measurements in a characteristic watershed on the Qinghai-Tibet Plateau, China
D. Luo, H. Jin, X. Wang, S. Gao, & L. Lü 365

Permafrost map update for the Igarka region as a climate change and human impact tracking tool
E. Makarycheva, N. Tananaev, D. Sergeev, & A. Litovko 366

Permafrost distribution in the French Alps: Statistical modelling using rock glacier inventory
M. Marcer, X. Bodin, & P.Schoeneich 367

Applicability of the ecosystem type approach to model permafrost and ground temperature dynamics across the Alaska North Slope
D. Nicolsky, V. Romanovsky, S. Panda, R. Muskett, & S. Marchenko 368

Archeologically significant cold ice patches in southern Norway – an indicator of mountain permafrost
R. S. Ødegård, A. Nesje, K. Isaksen, L. M. Andreassen, & T. Eiken 370

Past, present and future permafrost distribution in national parks of Alaska: A high-resolution modeling investigation
S. K. Panda, V. E. Romanovsky, S. S. Marchenko, & D. K. Swanson 371

Permafrost distribution in the Aksu-Tarim Catchment (Central Tien Shan)
J. Peters & T. Bolch . . . 373

Grounds thaw subsidence and spatial analysis of landscape transformation
F. Rivkin, Y. Vlasova, S. Marchenko, & I. Parmuzin . . . 374

Method of assessing the significance of the factors contributing to the temporary temperature changes in the upper permafrost horizons using GIS tools
Y. Rumyantseva . . . 377

Permafrost Information in the Engineering Geological Map of the Republic of Sakha (Yakutia), Scale 1:1,500,000
A. A. Shestakova, V. B. Spektor, Y. I. Torgovkin, & V. V. Spektor . . . 378

GlobPermafrost – how space supports understanding of permafrost?
F. M. Seifert, A. Bartsch, G. Grosse, A. Kääb, S. Westermann, T. Strozzi, A. Wiesmann, & C. Duguay . . . 380

Cartographic analysis of the damage, associated with geocryological processes
D.O. Sergeev, I.V. Chesnokova, A. V. Morozova, & A. S. Voytenko . . . 381

Using Random Forest to model permafrost distribution
F. Sirbu, L. Dragut, & A. Onaca . . . 382

Development and degradation of permafrost in the source region of the Datong River, Qilian Mountains
S. Wang, S. Yu, J. Wu, J. Li, X. Hu, & Z. Feng . . . 383

Field and model-based characterization of permafrost conditions in mountainous terrain in western Labrador
R. G. Way & A. G. Lewkowicz . . . 384

Mapping the thermal state of permafrost through modeling and remote sensing
S. Westermann, M. Langer, K. Aalstad, J. Boike, K. Gisnås, M. Peter, T. Schuler, Torbjørn Østby, & B. Etzelmüller . . . 386

Application of logistic regression model and multi-criteria analysis methods to map permafrost distribution and assess its dynamics on the Qinghai-Tibetan Plateau
T. Wu, T. Wang, R. Li, & Y. Qin . . . 387

Reconstruction of MODIS LST data
G. Yadamsuren & J. Yamkhin . . . 388

Temporal and spatial variation analysis on land surface temperature over Qinghai-Xizang Plateau
C. Yang & T. Che . . . 390

Building tools to bridge scales: Permafrost data integration for easier reuse
L. Yarmey, K. Schaefer, E. Jafarov, H. Jóhannsson, & J.-P. Lanckman . . . 390

Geocryological Database of the Siberian Platform
M. Zhelezniak, V. Zhizhin, D. Sivtsev, L. Shipitsyna, & L. Gagarin . . . 391

9 **Results from GTN-P: Thermal State of Permafrost (TSP) and Circumpolar Active Layer Monitoring (CALM)** 393

Characteristics of permafrost at local and regional scales: the Altai and Khentii Mountains, Mongolia
D. Avirmed, I. Mamoru, I. Yoshihiro, J. Yamkhin, S. Natsagdorj, Y. Gansukh, K. Temuujin, Y. Amarbayasgalan, G. Tsogterdene, & T. Undrakhtsetseg 394

And it continues: A new borehole extends the longest mountain permafrost temperature record on rock glacier Murtèl, Swiss Alps
A. Bast, J. Noetzli, I. Gärtner-Roer, M. Hoelzle, C. Hauck, D. Vonder Mühll, J. Müller, M. Phillips, D. Wasser, & A. Vieli 396

A global snapshot on the thermal state of permafrost and active layer thickness
B. K. Biskaborn, V. E. Romanovsky, S. L. Smith, D. Streletskiy, J. Nötzli, G. Vieira, P. Schoeneich, J.-P. F. Lanckman, & H. Lantuit 398

Interactions between active layer thickness and soil properties of CALM sites in different permafrost zones (North West Siberia, Russia)
A. Bobrik, O. Goncharova, & G. Matyshak 400

Influence of coastal proximity on ground thermal regime in a High Arctic environment, Eureka, Nunavut, Canada
P. Bonnaventure, A. Lewkowicz, S. Smith, & M. Ednie 401

Measured two-dimensional ice-wedge polygon thermal dynamics
W. L. Cable, V. E. Romanovsky, & R. C. Busey 403

Best practices in permafrost temperature measurement
W. L. Cable & V. E. Romanovsky 405

Constraining global permafrost thaw in the future using models and observations
S. Chadburn, E. Burke, P. Cox, & P. Friedlingstein 407

Permafrost thermal state and active layer dynamics from various landforms in Svalbard
H. H. Christiansen, G. L. Gilbert, S. M. Strand, & O. Humlum 408

Permafrost temperature development in Norway and Iceland over the last decade
B. Etzelmüller, C Hauck, C. Hilbich, K. Isaksen, & S. Westermann 409

Changes to permafrost active-layer temperature after tall shrub expansion in low Arctic tundra
G. V. Frost, H. E. Epstein, D. A. Walker, & G. Matyshak 410

Preliminary analysis of ground temperatures in north and northeast Greenland
G. L. Gilbert & H. H. Christiansen 412

The influence of snow cover accumulation, snow fall intensity and air temperature on seasonal freezing and thawing depth
V. N. Golubev & D. M. Frolov 413

The Eco-Grid of Ny Alesund: A multidisciplinary approach to investigate the Climate Change effects in the Arctic
M. Guglielmin, S. Ponti, V. Vitale, & N. Cannone 414

Permafrost temperature measurements in the Okhotsk coastal area of the Verkhoyansk-Chukotka region
S.A. Gulyy & M.N. Zhelezniak 415

Thermal state of permafrost across the circumpolar permafrost regions – results from the latest assessment report, the SWIPA update
K. Isaksen, V. Romanovsky, S. L. Smith, & D. S. Drozdov 417

The influence of mountain climate, snow cover and vegetation on the ground surface temperature along environmental gradients in Norway
K. Isaksen, R. S. Ødegård, J. I. Holten, & A. Nesje 418

Compilation of ground temperature records in the Northwest Territories, Canada
K. Karunaratne, S. Kokelj, P. Morse, S. Smith, S.A. Wolfe, S. Gruber, M. Palmer, E. Hoeve, & T. Lantz 419

Ground temperature and active layer monitoring at southern permafrost limit (Northeast European Russia)
D. Kaverin & A. Pastukhov 421

Effect of vegetation and soil characteristics on thermal state of permafrost in Alaska
A. Kholodov, V. Romanovsky, S. Natali, M. Loranty, & K. Heard 422

Comparison of measured air and soil-surface temperatures with satellite trends of increasing phytomass in northern Alaska
A. E. Klene, N. I. Shiklomanov, F. E. Nelson, K. E. Nyland, D. A. Streletskiy, & Q. Yu 424

Surface temperature reconstructions in the Lena River Delta and in the Western Laptev Sea, Russia, from borehole data
F. Kneier, M. N. Grigoriev, M. Langer, J. Boike, & P. P. Overduin 426

A 18-year record (1998-2016) of surface and ground temperature and water content from a high permafrost Arctic site (Bayelva, Spitsbergen): evaluation of land surface, permafrost and snowpack models and remote sensing data
S. Lange, N. Bornemann, S. Muster, & J. Boike 428

Variability in active layer dynamics associated with stand density in an arctic Siberian larch forest
M. Loranty, H. Alexander, S. Natali, A. Kholodov, & S. Davydov 429

Borehole temperature data processing and analysis using data from the SLF permafrost monitoring network
R. Luethi & M. Phillips 431

Environmental and climatological monitoring at the Zackenberg Research Station, northeast Greenland
M. Lund, K. Skov, & J. Abermann 432

Thermal state of permafrost in disturbed and undisturbed cryogenic geosystems in the European North
G. Malkova, M. Sadurtdinov, A. Skvortsov, & A. Tsarev 433

High resolution soil temperature and active layer dataset for estimating rates of permafrost degradation and their impact on ecosystems, infrastructure, CO_2 and CH_4 fluxes and net C storage following permafrost thaw in Alaska and Northwest Canada
S. Marchenko, H. Genet, E. Euskirchen, D. McGuire, S. Rupp, W. R. Bolton, A. Breen, M. Waldrop, S. McAfee, F. Yuan, Y. Zhang, V. Romanovsky, J. Walsh, T. Kurkowski, M. Lindgren, A. Bennett, M. Leonawicz, T. Carman, A. Floyd, & K. Timm 435

Positive aspects of having GTN-P monitoring site in Eastern Chukotka
A. Maslakov, V. Ruzanov, O. Tregubov, G. Kraev, & D. Zamolodchikov 437

Russian contribution to the permafrost monitoring: Development of the State Geocryological Monitoring Research Sites
V. P. Melnikov, D. S. Drozdov, V. A. Dubrovin, V. E. Romanovsky, & V. V. Pendin 439

Site-specific terrestrial model intercomparison of subsurface thermal regime in circum-Arctic region
J. Mori, K. Saito, S. Miyazaki, H. Machiya, Y. Iijima, & Group GTMIP 441

Connection of climatic agents with active layer depth dynamics on the Central Yamal
D. R. Mullanurov, Y. A. Dvornikov, A. Khomutov, & A. Polukhin 442

The contribution of the 2015 heat wave to mountain permafrost warming in Switzerland
J. Nötzli, R. Delaloye, I. Gärtner-Roer, A. Hasler, C. Hauck, C. Hilbich, M. Hoelzle, C. Lambiel, M. Phillips, C. Scapozza, S. M. Springman, B. Staub, & D. Vonder Mühll 444

Thermal conditions of permafrost on Peel Plateau, Northwest Territories, Canada
B. O'Neill, C. Burn, & S. Kokelj 446

Absence of permafrost conditions at the top of the Veleta Peak (Sierra Nevada, Spain)
M. Oliva, A. Gómez-Ortiz, F. Salvador-Franch, M. Salvà-Catarineu, D. Palacios, L. M. Tanarro, M. Ramos, P. Pereira, & J. Ruiz-Fernández 448

Model assessment of influences of snow depth on pan-Arctic permafrost temperature
H. Park, A. N. Fedorov, & P. Y. Konstantinov 449

Analysis of ground temperature and active layer thickness monitoring results in relation to a number of climatic controls at Vaskiny Dachi research station, Yamal, Russia
A. N. Polukhin, Y. A. Dvornikov, A. V. Khomutov, M. O. Leibman, D. R. Mullanurov, & D. D. Perednya 450

Hoher Sonnblick: A super site for monitoring the cryosphere
C. Riedl, S. Reisenhofer, D. Binder, A. Bartsch, A. Flores-Orozco, G. Heinrich, W. Schöner, S. Pfeiler, R. Supper, & I. Hartmeyer 452

Past, present and future changes in permafrost temperatures in Alaska
V. E. Romanovsky, D. J. Nicolsky, S. S. Marchenko, W. L. Cable, A. L. Kholodov, S. K. Panda, & R. R. Muskett 453

Active layer temperature variations in Ebba valley (central Spitsbergen) in the years 2009 – 2015
K. G. Rymer & G. Rachlewicz 455

A Permafrost Benchmark System to evaluate permafrost models
K. Schaefer, E. Jafarov, M. Piper, C. Schwalm, & L. Yarmey 456

Ground thermal regimes of seasonal frost in the French Alps
P. Schoeneich, P. Choler, T. Morin, & D. Kenny 457

Soil moisture redistribution and its effect on active layer response to inter-annual temperature variations 2000-2014 in a dry loess terrace in Adventdalen, Svalbard
C. Schuh, A. Frampton, & H. H. Christiansen 458

Twenty years of active layer monitoring in Northern Alaska: Results and lessons learned
N. Shiklomanov, F. E. Nelson, A. E. Klene, K. E. Nyland, & D. A. Streletskiy 460

Investigations of effects of forest fires on the ground thermal regime and permafrost, Northwestern Canada
S.L. Smith & P. Bonnaventure . . . 461

Spatial and temporal variability in permafrost thermal state and active layer thickness along the Mackenzie Valley transect, NWT Canada
S. L. Smith, C. Duchesne, M. Ednie, & P. Bonnaventure . . . 463

Varied response of near-surface ground temperatures in Spitsbergen to mid-winter warming events
S. M. Strand & H. H. Christiansen . . . 465

Arctic permafrost thermal and active layer variability across an environmental gradient from continuous to sporadic permafrost
S. M. Strand, H. H. Christiansen, J. Boike, K. van Huissteden, B. Elberling, B. U. Hansen, M. Johansson, & G. Iwahana . . . 466

Thermal state of permafrost and recent active layer dynamics in the South Shetlands, Antarctica
G. Vieira, M. Ramos, M. A. de Pablo, G. Goyanes, M. Oliva, C. Schaefer, A. Ferreira, A. Abramov, A. Correia, A. Nieuwendam, & C. Mora . . . 467

The influence of increasing rainfall on permafrost on the Qinghai-Tibetan plateau
Z. Wen, M. Zhang, & M. Zhang . . . 468

Characteristics of permafrost at local and regional scales: The Khovsgol and Khangai Mountains, Mongolia
J. Yamkhin, I. Mamoru, I. Yoshihiro, D. Avirmed, S. Natsagdorj, G. Yadamsuren, T. Khurelbaatar, A. Yondon, T.-E. Gansukh, & U. Tsogtbaatar . . . 469

Estimating rainfall influence on the thermal regime of sandy soils
A. F. Zhirkov & M. Zhelezniak . . . 471

10 **Palaeoenvironments in Permafrost Affected Areas** 472

Environmental plant DNA (eDNA): To which degree does it represent the flora?
I.G. Alsos, P. Sjögren, N. Yoccoz, M.E. Edwards, L. Gielly, E. Coissac, M.K.F. Merkel, & P. Taberlet . . . 473

Modern spatial variability of limnoecology and sedimentary processes in a mountain lake at the permafrost margin of southern Yakutia (Russia)
B. K. Biskaborn, B. Diekmann, H. Meyer, B. Chapligin, A. Dressler, T. Löffler, L. Weniger, & L. Pestryakova . . . 474

Tree migration since the LGM in Siberia and the potential interaction with climate change and active layer depth development
X. Cao & U. Herzschuh . . . 475

Development and dynamics of ice-wedge polygons in NE Siberia revealed by interdisciplinary palaeoecological research
P. de Klerk, M. Gałka, & H. Joosten . . . 476

Patterns in vegetation and pollen deposition along surface sample transects in three ice wedge polygon
P. de Klerk & H. Joosten . . . 478

Holocene vegetation change and turnovers of treeline forming species
L. S. Epp, S. Kruse, N. J. Kath, L. Pestryakova & U. Herzschuh . . . 480

Resilience of plants communities to changes in climate, fire regime and carbon accumulation: Palaeoecological insights from arctic peatlands in Alaska
M. Gałka, G. Swindles, A. Gallego-Sala, M. Szal, & A. Feurdean 481

Macrophyte (Potamogeton sp.) and ancient DNA analyses from Lake Sediments - Lake Karakul, Tajikistan
L. Heinecke, S. Mischke, M. Reschke, L. Epp, K. Stoof-Leichsenring, I. Rajabov, & U. Herzschuh . 482

The emergence of permafrost as vegetation driver in Siberia from the Plio-Pleistocene Transition onwards
U. Herzschuh, J. Birks, A. Andreev, M. Melles, & J. Brigham-Grette 483

Last interglacial versus last cold stage: Palaeovegetation in North Yakutia's most continental part recorded in the Batagay permafrost sequence
F. Kienast, K. Ashastina, N. Rudaya, & K. Wesche 484

Siberian treeline dynamics in a warming climate - results from larch population genetics and vegetation modelling
S. Kruse, L. S. Epp, K. Stoof-Leichsenring, L. Pestryakova, & U. Herzschuh 487

Time-lagged response of siberian treeline forests revealed by individual-based modelling
S. Kruse, M. Wieczorek, F. Jeltsch, & U. Herzschuh 488

A biomarker-based paleoclimatic reconstruction of MIS1, MIS3 and MIS5e based on permafrost deposits from NE Siberia
J. Martens, S. Kusch, M. Winterfeld, G. Mollenhauer, G. Schwamborn, L. Schirrmeister, S. Wetterich, P. P. Overduin, & J. Rethemeyer 489

Climatic and environmental implications of millennial-scale phases of ice-rich permafrost active layer installation in western Europe between 35 and 20 ka evidenced by terrestrial mollusc fauna
O. Moine & P. Antoine 490

Modern and ancient DNA in lacustrine sediments – Vegetation signals unraveled
B. Niemeyer, L. S. Epp, L. Pestryakova, & U. Herzschuh 493

West Beringia bison population dynamics during the late Pleistocene and early Holocene
P. Nikolskiy & V. Pitulko 494

Impact of glacial climate on soil formation at the end of the Pleistocene, Ecuador
S. Opfergelt, P. Delmelle, C. Duhain, A. de Potter d'Indoye, R. Vera, Q. Yin, & A. Guevara . . . 496

Palaeoecology from permafrost deposits in Southwest Greenland - Inuit, Norse and their insect footprints
E. Panagiotakopulu 498

Paleoenvironment and paleoclimate at the end of the late Pleistocene – Early Holocene in the western part of the Yana-Indigirka lowland (based on palaeobotanical data)
E. Pavlova, M. Dorozhkina, & V. Pitulko 499

Late Pleistocene – Early Holocene paleoenvironment proxy record from the Yana RHS site (low Yana river, Arctic Siberia)
E. Pavlova, E. Zinovyev, O. Korona, & V. Pitulko 501

Environmental changes and the archaeological record of arctic West Beringia within last 50,000 years
V. Pitulko & E. Pavlova 503

Metagenomic analyses of the late Pleistocene permafrost – additional tools for reconstruction of environmental conditions
E. Rivkina 506

Simulated biome and permafrost distributions for the Late Quaternary Beringia
K. Saito, A. Hendricks, N. Bigelow, J. Walsh, S. Marchenko, V. Romanovsky, & K. Yoshikawa . . 508

Glacial and interglacial sediment history on Bol'shoy Lyakhovsky, New Siberian Archipelago, from multiple permafrost cores
G. Schwamborn, L. Schirrmeister, S. Wetterich, M. C. Fuchs, & H. Meyer 510

Past genetic patterns of arctic freshwater diatoms - a study on ancient sedimentary DNA elucidates diatom diversification at the treeline ecotone
K. Stoof-Leichsenring, L. Pestryakova, & U. Herzschuh 512

The climate and permafrost evolution since 6 ka BP recorded by peat in the source area of the Yellow River, Northeastern Qinghai-Tibet Plateau
Q. Wang, H. Jin, Q. Wu, T. Zhang, Y. Huang, Y. Yang, & M. Liu 513

Development of polygonal peatlands on the Yukon Coastal Plain, Canada, during the past 5000 years
J. Wolter, H. Lantuit, M. Fritz, & U. Herzschuh 514

Late Quaternary vegetation history of North-Eastern Siberia inferred from ancient DNA analyses of permafrost sediment cores
H. Zimmermann, L. Epp, P. Overduin, G. Schwamborn, L. Schirrmeister, & U. Herzschuh 515

11 **Microbial Ecology of Permafrost Ecosystems** 516

The impact of transcriptionally active microbial communities on soil greenhouse gas emissions in the Canadian High Arctic
I. Altshuler, J. Ronholm, T. Onstott, C. Greer, & L. Whyte 517

Methanotrophic population and methane oxidation around the Lena Delta, Siberia, Russia
I. Bussmann, S. Hackbusch, P. Schaal, & A. Wichels 518

Changing chemistry and aquatic microbial functioning of streams draining sub-arctic landscapes impacted by permafrost thaw
S. Cottingham, R. Giesler, R. A. Sponseller, F. Guillemette, R. G. M. Spencer, J. E. Vonk, D. A. Pearce, J. Woodward, & P. J. Mann 519

Linking microbial community activities to carbon turnover in Siberian sub-arctic permafrost-affected soils
S. Evgrafova, L. Mukhortova, D. Wagner, & G. Guggenberger 520

What kills permafrost microbes during Marssimulations? More new questions than answers
K. W. Finster, B. A. Lomstein, P. Nørnberg, J. Merrison, A. A. Hansen, % L. Liengaard 522

Denitrifiers limited by available organic carbon drive nitrous oxide production in peat circles of the arctic Tundra despite their capability for nitrous oxide consumption
S. Hetz & M. A. Horn 523

Diverse acid-tolerant denitrifier communities in arctic peatlands control nitrous oxide fluxes
M. A. Horn, K. Palmer, N. Roßbach, & S. Hetz 524

Distinct depth profile of bacterial and archaeal communities between four Alaskan soil cores
M. Kim, E. Byun, Y. Kim, J. Ahn, J.-W. Yang, & Y. K. Lee . . . 525

Bacterial community shifts along the chronosequence in the Austre Lovénbreen glacier foreland, Svalbard
Y. K. Lee, J. Y. Jung & M. Kim . . . 525

Development of cell numbers and microbial community composition along a natural temperature gradient in subsea permafrost
J. Magritz, M. Winkel, L. Mahler, F. Horn, P. P. Overduin, M. Thiele, C. Knoblauch, D. Wagner, & S. Liebner . . . 526

Frozen in time? Microbial strategies for survival and carbon metabolism over geologic time in a Pleistocene permafrost chronosequence
R. Mackelprang . . . 527

The Arctic 'enzymic latch': Regulation of organic matter decomposition by extracellular enzymes in peat-permafrost
A. S. Rose, C. Dunn, H. Kang, & C. Freeman . . . 528

Combined assessment of Archaeal and Bacterial communities in soil samples from Hornsund, Spitsbergen using Illumina Mi-Seq
E. S. A. Sia, N. Denis, A. Mujahid, J. Zhang, S. A. Alias, S. H. Ali, A. A. Samah, & M. Mueller 530

The Arctic methane oxidizer *Methylobacter tundripaludum* responds to changing temperatures by global transcriptional shifts
A. T. Tveit, A. Didriksen, S. L. Robinson, & M. M. Svenning . . . 531

Microbial activity in thermokarst soils: Mechanisms of carbon loss following permafrost thaw
M. Waldrop, M. Jones, K. Manies, J. McFarland, S. Blazewicz, M. Haw, R. Neumann, & J. Harden 532

Exploring the rare biosphere of methanogenic archaea in frozen ground affected soils of the Tibetan Plateau
S. Yang, D. Wagner, M. Winkel, & S. Liebner . . . 533

12 **Planetary Permafrost and Earth Analogues** 534

Rock glaciers as proxies for identifying terrestrial and analogous Martian permafrost
A. Bhardwaj, L. Sam, & F. J. Martín-Torres . . . 535

Investigation of cryobot movement through frozen structures
A. Butenko, S. Aksenov, & O. Erokhina . . . 538

Mapping the northern plains of mars: origins, evolution and response to climate change – a new overview of recent ice-related landforms in Utopia Planitia on Mars
F. Costard, A. Séjourné, Z. M. Swirad, & A. Losiak . . . 539

Towards reconstructing the very recent climate on Mars: Insights from terrestrial analogues in the Arctic and Antarctica
E. Hauber, J.-P. de Vera, N. Schmitz, D. Reiss, A. Johnsson, & H. Hiesinger . . . 541

Veiki-moraine-like landforms in Nereidum Montes on Mars: Insights from analogues in northern Sweden
A. Johnsson, D. Reiss, E. Hauber, M. D. Johnson, M. Olvmo, & H. Hiesinger . . . 543

Surface temperatures and thermal inertia in Coogoon Valles Mars
A. Molina, M. á. de Pablo, I. López, O. Prieto-Ballesteros, D. Fernandez-Remolar, & M. Ramos . 546

Observed present-day seasonal gully activity within three Martian years in a south polar pit (Sisyphi Cavi) on Mars
J. Raack, D. Reiss, T. Appéré, M. Vincendon, O. Ruesch, & H. Hiesinger 549

Ice caves as a target location for the first Human Mission to Mars: The case for a Hebrus Valles Landing Site
D. Schulze-Makuch, A. Davila, A. Fairen, A. Rodriguez, J. Rask, & J. Zavaleta 551

Constrain on the nature of polygons on Mars by studying thermokarst degradation in Utopia Planitia and comparison with Central Yakutia (Central Siberia)
A. Séjourné, F. Costard, J. Gargani, & A. Fedorov 553

High resolution geomorphological mapping of glacial and periglacial landforms at the lower NW flank of the HecatesTholus volcano, Mars: A contribution to the paleoenvironmental reconstruction
M. Valcárcel, J. F. Hall-Riaza, & M. á. de Pablo 555

Distribution and evolution of cold-climate landforms in a subpolar and hyperarid environment, Hellas Planitia, Mars
M. Voelker, E. Hauber, & R. Jaumann 556

13 **The Yedoma Region: Origin, Records and Future Projections in a Changing Arctic** 559

The Batagai Outcrop – window into the past of North Yakutia's most continental part
K. Ashastina, L. Schirrmeister, B. Diekmann, & F. Kienast 560

A 10,000-year record of atmospheric mercury deposition in northern Yukon, Canada
S. Bandara, D. Froese, C. Cooke, & V. St. Louis 562

Methane as a paleopermafrost indicator of Yedoma accumulation in Yakutia
M. Cherbunina & D. Shmelev 563

Past and possible future evolution of the Yukon Flats southern upland yedoma region, Alaska
M. Edwards, B. Jones, P. McDowell, G. Grosse, & J. Rose 565

Tracking the age of ice and the fate of carbon from yedoma thaw
S. A. Ewing, J. O'Donnell, J. Paces, G. Aiken, M. Kanevskiy, J. Koch, & R. Striegl 566

The ancient cryosphere: diverse evidence for relict Middle Pleistocene permafrost from northwestern Canada
D. Froese, B. J. L. Jensen, A. V. Reyes, J. A. Westgate, H. Poinar, B. Shapiro, & G. Zazula . . . 598

Soil organic carbon stocks along transects from Yedoma uplands into drained thaw lake basins on Sobo-Sise Island, Lena Delta, Siberia
M. Fuchs, G. Grosse, & F. Günther 599

Ice complex and Yedoma in Yakutia
V. Kunitskiy 601

Late Quaternary palaeo-environmental history of Muostakh Island, Northern Siberia based on sedimentological and geocryological studies
H. Meyer, T. Opel, A. Y. Dereviagin, M. Fritz, C. Manthey, C. Siegert, L. Schirrmeister, & M. N. Grigoriev 603

Reconnaissance palaeoenvironmental study of 90 m of permafrost deposits at Batagaika megaslump, Yana Uplands, northern Siberia
J. Murton, M. Edwards, P. Anderson, M. Cherepanova, T. Goslar, S. Gubin, J. Korzun, A. Lozhkin, A. Lupachev, G. Savvinov, A. Tikhonov, & O. Zanina 604

Characterization of organic matter stored in frozen Yedoma and thermokarst basin deposits on Sobo-Sise Island, Lena Delta
D. Neubauer, J. Strauss, K. Mangelsdorf, & G. Grosse 605

Holocene ice wedges in the Eurasian Arctic – review of stable-isotope based climate records
T. Opel, H. Meyer, T. Laepple, & A. Y. Dereviagin 607

The last 50,000 years of hydroclimate change revealed by stable water isotopes of relict permafrost in the Klondike goldfields, Yukon, Canada
T. Porter, D. Froese, & M. Mahony 608

The polygenetic hypothesis of Yedoma origin - comparing grain-size distributions of Alaskan and Siberian Yedoma
L. Schirrmeister, G. Grosse, J. Strauss, E. Dietze, & S. Wetterich 609

Paleopermafrost conditions during Ice Complex accumulation, Kolyma Lowland, Dyvanny Yar exposure
D. Shmelev, M. Cherbunina, V. Rogov, & V. Konishchev 611

The nitrogen inventory of the Yedoma permafrost region
J. Strauss, F. Beermann, C. Biasi, C. Fiencke, G. Grosse, L. Kutzbach, T. Sanders, L. Schirrmeister, T. Schneider von Deimling, S. Wetterich, & S. Zubrzycki 614

Ice-rich Yedoma permafrost: A synthesis of northern hemisphere distribution and thickness (IPA Action Group)
J. Strauss, A. N. Fedorov, D. Fortier, D. Froese, M. Fuchs, G. Grosse, F. Günther, J. Harden, G. Hugelius, M. Kanevskiy, A. Kholodov, V. Kunitskiy, G. Kraev, S. Laboor, L. Lapointe-Elmrabti, A. Lozhkin, E. Rivkina, J. Robinson, L. Schirrmeister, D. Shmelev, Y. Shur, C. Siegert, V. Spektor, M. Ulrich, S. Vartanyan, A. Veremeeva, K. Walter Anthony, & S.A. Zimov 616

Multi-proxy reconstruction of Holocene thermokarst dynamics in Central Yakutia
M. Ulrich, J. Schmidt, N. Rudaya, S. Wetterich, L. Frolova, L. Pestryakova, C. Siegert, B. Schneider, C. Zielhofer, P. Efremov, & A. N. Fedorov 619

Landscapes and thermokarst lake area changes in Yedoma regions under modern climate conditions, Kolyma lowland tundra
A. Veremeeva, N. Glushkova, F. Günther, I. Nitze, & G. Grosse 620

An isotopic tool to distinguish between Yedoma and topsoil organic carbon sources: compound-specific deuterium analysis
J. E. Vonk, T. Tesi, L. Bröder, G. Hugelius, P. Kuhry, & ö. Gustafsson 622

Reconciling carbon-stock estimates for the Yedoma region
K. Walter Anthony, G. Grosse, P. Anthony, M. Jones, S. Davydov, & S.A. Zimov 623

Ice Complex chronologies and environments in western Beringia
S. Wetterich, V. Tumskoy, N. Rudaya, A. A. Andreev, V. Kuznetsov, M. C. Fuchs, G. Schwamborn, T. Opel, H. Meyer, & L. Schirrmeister 627

14 **Permafrost Hydrology and Groundwater Systems** 629

Seasonal variability of groundwater discharge in a permafrost watershed, Ogilvie River, Yukon, Canada
N. Baranova & I.D. Clark 630

Assessing agricultural vulnerability in a snow- glacier-fed watershed in central Chile
A. Bellisario, J. Janke, & S. Ng 631

Towards an understanding of the impact of permafrost degradation on the hydrogeology of the Source Area of the Yellow River, Qinghai-Tibet Plateau, China
V. F. Bense, H. Jin, & D. Luo 632

Carbon outflow from the active layer of thermokarst lake catchments in the Lena River delta
O. Bobrova, I. Fedorova, A. Chetverova, A. Morgenstern, & A. Eulenburg 633

Quantification of a full year water balance of a thermokarst lake in East Siberia based on field measurements
N. Bornemann, S. Niemann, S. Stettner, A. Morgenstern, M. Langer, & J. Boike 634

Simulation and prediction of suprapermafrost groundwater level variation using Neural Networks model in permafrost response to climate change
J. Chang & G. Wang 635

Assessing groundwater dynamics in a discontinuous permafrost environment using hydrogeochemical tracers
M. Cochand, J. Molson, J.-M. Lemieux, J. A. Barth, R. van Geldern, R. Fortier, & R. Therrien . 637

Changing runoff pathways due to permafrost thaw in discontinuous permafrost terrains
R. F. Connon & W. L. Quinton 638

Laboratory simulation of river talik
F. Costard, N. Roux, & C. Grenier 639

Thermal algorithms in the water balance simulation model
R. Daanen, J. Schulla, & A. Liljedahl 641

Evaluation of the continental biosphere model (ORCHIDEE) over Siberia with remote sensing products
S. Dantec-Nédélec, C. Ottlé, F. Maignan, & N. Delbart 643

Modeling of pollutant transport in streams with riverbeds deformed due to thawing permafrost
E. Debolskaya, O. Maslikova, I. Gritsuk, & D. Ionov 644

Modeling permafrost and its impacts on subarctic watersheds hydrology using distributed hydrological model WaSiM
M. Debolskiy, R. Hock, V. Romanovsky, V. Alexeev, D. Nicolsky, & J. Shulla 645

Improved parametrization of a meso-scale hydrologic model in a discontinuous permafrost, boreal forest ecosystem
A. M. Endalamaw, W. R. Bolton, J. M. Young, D. Morton, & L. D. Hinzman 646

Spatial-temporal coherence of different scale hydrological processes in the Lena River delta
I. Fedorova, A. Chetverova, O. Bobrova, T. Skorospekhova, G. Nigamatzyanova, N. Shumskaya, A. Shadrina, A. Morgenstern, & V. Dmitriev 647

Permafrost contribution to streamflow under drought conditions in a river watershed of the extra tropical western Andes in central Chile
F. J. Ferrando Acuña & A. Bellisario 649

Mechanisms governing solute transport in the active layer of coupled permafrost-hydrogeological systems
A. Frampton, R. Pannetier, & G. Destouni 651

Processed-based hydrological modeling of a continuous permafrost catchment on the Arctic Coastal Plain, Alaska to evaluate how climate change will affect surface water runoff and connectivity
A. Gädeke, A. Liljedahl, C. Arp, R. Daanen, B. Jones, V. Alexeev, & L. Cai 653

Assessing watershed-scale linkages between glaciers, permafrost and hydrology in sub-arctic Interior Alaska using field observations and a process-based hydrological model
A. Gädeke, A. Liljedahl, T. Gatesman, T. Douglas, & J. Zhang 654

Investigating features of permafrost and talik in the peripheries of the Wanlong Worma Lake using electrical resistivity tomography (ERT) in the Source Area of the Yellow River (SAYR), NE Qinghai-Tibet Plateau, China
S. Gao, H. Jin, X. Wang, D. Luo, & L. Lü 655

Going with the flow: bank erosion versus floods on the Middle Lena River (Siberia)
E. Gautier, C. Virmoux, F. Costard, A. Fedorov, & P. Konstantinov 657

The InterFrost benchmark of Thermo-Hydraulic codes for cold regions hydrology – first inter-comparison phase results
C. Grenier, H. Anbergen, V. Bense, E. Coon, N. Collier, F. Costard, M. Ferry, A. Frampton, J. Frederick, J. Holmen, A. Jost, S. Kokh, B. Kurylyk, J. McKenzie, J. Molson, L. Orgogozo, R. Pannetier, A. Riviere, N. Roux, W. Rühaak, J. Scheidegger, J. Selroos, R. Therrien, P. Vidstrand, & C. Voss 659

Hydrology of arctic regions. Synergy of modelling and remote sensing
M. Haver, E.A. Zakharova, A. Kouraev, & I. Krylenko 662

The hydrological impact of rock glaciers in the Aconcagua river basin, Chile
J. Janke, A. Bellisario, & S. Ng 663

Hydrological and thermal modeling of Imnavait Cr. basin, Alaska, using WaSiM
M. Kaiser, A. Liljedahl, R. Daanen, A. Gädeke, & W. Rieger 664

Altered stream discharge, chemistry, ecosystem productivity, and fish habitat related to climate change and permafrost thaw at the boreal-arctic transition in Alaska
J. C. Koch, M. Carey, J. O'Donnell, C. E. Zimmerman, & G. Aiken 665

Permafrost and hydrological conditions of the Baikal Lake basin under the impacts of climate and land use changes
V. Kurovskaia, O. Semenova, & T. Vinogradova 666

Deciphering the impact of permafrost change and disturbance on catchment water quality
S. F. Lamoureux & M. J. Lafreniere 668

Interaction of permafrost and hydrological processes at a sandy permafrost hillslope in Central Yakutia: the observations and modelling results
L. Lebedeva, O. Semenova, A. Kolesnikov, & V. Ogonerov 669

Distribution of organic matter in sub-channel permafrost deposit within the Lena River Delta
G. T. Maksimov, M. N. Grigoriev, S. E. Zubrzycki, T. V. Khodzher, & T. V. Pogodaeva 670

Influence of seasonal conditions on the deformation of coastal slopes, occuring in the permafrost zone
O. Maslikova, E. Debolskaya, I. Gritsuk, & D. Ionov 671

Runoff modelling in the zone of frost mound bogs by the example of small watersheds of the Muravlenkovsky research station
A. S. Mysina & O. M. Semenova 673

Hydrological processes at the Suntar-Hayata ridge (Eastern Siberia): Analysis of historical data and modelling
N. Nesterova, O. Semenova, & L. Lebedeva 675

River routing over "Glass Surface" in permafrost regions
M. E. Norman, M. Brakebusch, & C. Beer 677

Preliminary studies of water, snow and ice in the Quebrada del Medio, Hans Stepanek rock glacier, Mendoza, Argentina
M. T. OConnor, M. B. Cardenas, B. T. Neilson, M. H. Kaufman, & George W. Kling 678

Transfers along slopes in a permafrost-dominated watershed of Central Siberia: A mechanistic 2D coupled thermo-hydrological modelling study
L. Orgogozo, A. S. Prokushkin, O. S. Pokrovsky, Y. Goddéris, C. Grenier, M. Quintard, J. Viers, D. Labat, & S. Audry 679

Process-rich projections of permafrost integrated surface/subsurface thermal hydrology in a warming climate
S. L. Painter, E. T. Coon, A. Atchley, & A. Jan 681

The seasonal dynamics of a hydrohalite tufa associated with a perennial hyper-saline spring in the Canadian high Arctic
W. H. Pollard & M. K. Ward 685

Mathematical Modeling of Climate – Permafrost – Groundwater Dynamics: A Study of Bestyakh Terrace, Lena River, Siberia
N. N. Romanovskii, G. S. Tipenko, S. N. Buldovich, D. O. Sergeev, A. V. Gavrilov, V. E. Romanovsky, N. S. Duxbury, & K. Yoshikawa 687

Thermal impact of a small alas-valley river in a continuous permafrost area - insights from field monitoring in Syrdakh (Central Yakutia) and 1D numerical analysis
N. Roux, C. Grenier, A. Fedorov, P. Konstantinov, A. Sejourne, & F. Costard 688

Watershed-scale hydrogeochemical impacts caused by permafrost thermal perturbation and physical disturbance, eastern Banks Island, NT, Canada
A. C. A. Rudy, S. F. Lamoureux, S. V. Kokelj, M. J. Lafrenière, & R. Smith 690

Runoff generation on hillslopes underlain by continuous permafrost
C. Rushlow, S. E. Godsey, C. Voss, & A. Sawyer 692

Recent changes of runoff characteristics in permafrost basins of Eastern Siberia
O. Semenova, N. Tananaev, L. Lebedeva, & N. Nesterova 693

Study of river runoff generation in continuous permafrost zone based on new field data from Cherskiy, Russian Arctic
A. Shiklomanov, I. Tokarev, S. Davydov, A. Davydova, & D. Streletskiy 694

Preliminary studies of water, snow and ice in the Quebrada del Medio, Hans Stepanek rock glacier, Mendoza, Argentina
N. R. Sileo, D. Trombotto Liaudat, C. Dapeña, X. Bodin, I. P. Marcosig, & N. A. Taboada 695

Small-scale evapotranspiration in the polygonal tundra of the Lena River Delta, northeastern Siberia
G. Simpson, T. Eckhardt, B. Runkle, & L. Kutzbach 697

Implications of ignoring permafrost in glacio-hydrological models in high mountains
S. Singh, A. Bhardwaj, & R. Kumar 698

Impact from groundwater flow on ground temperature dynamics – Observations and numerical simulations for a sporadic permafrost peatland environment
Y. Sjöberg, E. Coon, B. Sannel, R. Pannetier, D. Harp, A. Frampton, S. L. Painter, & S. Lyon . 700

Relationships between colored dissolved organic matter (CDOM), dissolved organic carbon (DOC) and dissolved mineral substances in different surface waters of the Lena River Delta
T. Skorospekhova, I. Fedorova, B. Heim, A. Chetverova, A. Morgenstern, O. Bobrova, A. Eulenburg, & Y. Dvornikov 701

Snowmelt water balance for a permafrost watershed: Case study from Alaska Arctic
S. Stuefer, D. Kane, & R. Gieck 702

The role of paraglacial and paraperiglacial cryoforms on the water balance of a changing watershed in the Chilean and Argentinean Andes
P. A. Wainstein, L. U. Arenson, & J. Umerez 704

Soil temperature-threshold based runoff generation processes in a permafrost catchment
G. Wang, T. Mao, & J. Chang 705

Climate change, permafrost decline and its hydrological impact in the Sheldrake catchment (Québec, Canada)
L. Wang, R. Ludwig, & M. Bernier 706

The influence of local factors on the seasonal freeze-thaw processes of the active layer in the alpine permafrost regions in the upper reaches of the Heihe River, in Qilian Mountains
Q. Wang, H. Jin, T. Zhang, Q. Wu, B. Cao, X. Peng, & K. Wang 707

Simulating the impacts of surface hyper-saline spring activity on thermal regimes of underlying permafrost on Axel Heiberg Island, Nunavut
M. K. Ward & W. H. Pollard 709

Isotope-tracing studies on impacts of degrading permafrost on hydraulic connections in the Source Area of Yellow River on SE Qinghai Plateau, SW China
P. Yi, H. Jin, V. Bense, & Y. Yang 710

Permafrost distribution and flow regime along a hill slope in West Greenland
S. F. Zastruzny, K. Høgh Jensen, B. Elberling, & L. Nielsen 711

15 **The Importance of Lakes and Ponds in Permafrost Regions** 712

Thermokarst lake changes between 1962 and 2008 in Mongolia
S. Adiya, I. Mamoru, & J. Yamkhin 713

Temporal variability of dissolved nutrients in lakes of Antarctic oases (Schirrmacher and Larsemann Hills)
N. Alekseeva, N. Lavinen, I. Fedorova, T. Skorospekhova, & E. Dobrotina 714

TerraSAR-X backscatter and interferometric coherence of thermokarst lake ice in the Lena River Delta
S. Antonova, C. Duguay, A. Kääb, S. Westermann, M. Langer, B. Heim, & J. Boike 715

Extreme sensitivity of shallow lakes and sublake permafrost to Arctic climate change
C.D. Arp, B. Jones, A. Bondurant, G. Grosse, A.D. Parsekian, V. Romanovsky, & K. Hinkel . . 717

Stable isotope climate records from drained thermokarst lake basins in northern Yukon, Canada
S. Bandara, D. Froese, T. Porter, F. Calmels, & P. Sanborn 719

Rates and mechanisms of expansion in thermokarst lakes with bedfast and floating ice regimes on the Arctic Coastal Plain of northern Alaska
A. C. Bondurant, C. Arp, B. Jones, & M. Engram 719

Thermokarst and kettle lakes in the eastern Canadian Arctic: A paleolimnological perspective
F. Bouchard, I. Laurion, & D. Fortier 721

New compilation of formation dates, origins and fates for lakes within the Last Glacial/Permafrost Maximum domain of the Northern Hemisphere
L. Brosius, C. Treat, J. Lenz, G. Grosse, K. Walter Anthony, & M. Jones 722

Lakes in the arctic carbon cycle: Long-term perspectives using a palaeolimnological approach
M. Edwards, S. McGowan, J. Anderson, P. Langdon, V. Jones, S. Turner, M. van Hardenbroek, E. Whiteford, & E. Wiik 723

Exchange of CO_2 and CH_4 between a Siberian thaw lake and the atmosphere
D. Franz, E. Larmanou, N. Bornemann, M. Langer, J. Boike, & T. Sachs 724

'Lake colour' in permafrost landscapes of the central Lena River Delta and central Yamal - case studies of Coloured Dissolved Organic Matter (cDOM) and turbidity regimes
B. Heim, A. Bartsch, & Dvornikov, Y. 725

Remote sensing and quantitative statistic methods applied to different theories of thermokarst lake occurrence
V. N. Kapralova, A. S. Viktorov, T. V. Orlov, O. N. Trapeznikova, M. V. Arkhipova, A. V. Zverev, E. G. Panchenko, & A. A. Sadkov 726

Regulation of methane fluxes from ponds of the northeast Siberian polygonal tundra
C. Knoblauch, O. Spott, S. Evgrafova, L. Kutzbach, & E.-M. Pfeiffer 727

Simulating the impact of water bodies on the thermal stability of permafrost using a coupled permafrost-lake model.
M. Langer, S. Westermann, J. Boike, G. Kirillin, G. Grosse, S. Peng, & G. Krinner 728

Landsat-based lake distribution and changes in Western Alaska Permafrost Regions between 1972 and 2014
P. R. Lindgren, G. Grosse, & V. Romanovsky 729

Impact of thermokarst lake expansion rate on ground thermal regime and talik development beneath thermokarst lakes on the Qinghai-Tibet Plateau
F. Ling 731

Analysis of Sediment Cores and Methane Fluxes from Alaskan and Siberian Thermokarst Lakes
O. H. Meisel . . . 732

Hungry ponds in a thawing world: variations in subarctic pond runoff quality and quantity depend on peatland moisture and frost conditions
M. Morison, M. Macrae, R. Petrone, & L. Fishback . . . 733

Temporal and seasonal variation in tundra pond seasonal biogeochemical trajectories in a permafrost landscape and implications for river export of solutes
M. Morison, M. Macrae, R. Petrone, & L. Fishback . . . 734

Multi-year landscape-gradient assessment of thermokarst lake hydrology in Nunavik (Quebec, Canada) using water isotope tracers
B. Narancic, R. Pienitz, & B. Wolfe . . . 735

A circumpolar dataset of bottom fast lake ice
G. Pointner & A. Bartsch . . . 736

Carbon mobilization through the expansion of thermokarst lakes in polygonal tundra of Old Crow Flats, northern Yukon
P. Roy-Leveillee, E. R. Humphreys, C. Z. Braul, & C. R. Burn . . . 737

Assessing the Contribution of Arctic Lakes to the Methane Budget via Upscaling and GOSAT Satellite Derived Flux Data
K. Reuss-Schmidt, J. Dash, & M. Edwards . . . 738

Structure from Motion (SfM) orthoimage generation for characterizing methane ebullition features in thermokarst lake ice
K. Schlobies, G. Grosse, & K. Walter Anthony . . . 739

Freshwater ostracods from ice-wedge polygon ponds in Adventdalen, Svalbard
A. Schneider, S. Wetterich, B. Sannel, & L. Schirrmeister . . . 742

Sediment-water interaction as an important factor of Arctic lake thermic regime
A. Shadrina, I. Fedorova, S. Golosov, J. Boike, A. Chetverova, & T. Skorospekhova . . . 744

Thermal Regime Caused by Difference of Freeze-Thaw processes between Lake and Permafrost Areas in Hovsgol Regions, Northern Mongolia
A. Sugita, K. Takeda, M. Kimura, & M. L. Lopez Caceres . . . 745

Solar energy input determines methane emissions on timescales of days to seasons from shallow subarctic lakes
B.F. Thornton, M. Wik, & P. Crill . . . 747

UAV surveying of thaw lake areas for the characterization of geomorphology, vegetation and water colour (Whapmagoostui-Kuujjuarapik and Umiujaq, Quebec, Canada)
G. Vieira, S. Girst, V. Paulo, J. Canário, A. Padeiro, & W. Vincent . . . 748

Surface Water and Ocean Topography (SWOT) satellite mission prototype data for study the Arctic lakes seasonal dynamic and water storage
E. A. Zakharova, A. V. Kouraev, D. Blumstein, & V. Elsakov . . . 749

16 **Where, when, and why will the Arctic become wetter or drier?** 750

Satellite-derived changes in the permafrost landscape of central Yakutia, 2000 – 2011: Wetting, drying, and fires
J. Boike, T. Grau, B. Heim, G. Frank, L. Moritz, M. Sina, G. Isabelle, & L. Stephan 751

Dynamical downscaling products to facilitate climatic impact research on hydrology, permafrost, and ecosystems on the Alaskan North Slope
L. Cai, V. A. Alexeev, C. D. Arp, & B. M. Jones 752

Massive thermokarst lake area loss in continuous ice-rich permafrost of the northern Seward Peninsula, Northwestern Alaska, 1949 – 2015
G. Grosse, B. M. Jones, I. Nitze, P. R. Lindgren, K. M. Walter Anthony, & V. E. Romanovsky . 753

Can wet summers trigger permafrost collapse at a Siberian lowland tundra site?
M. Heijmans, K. v. Huissteden, B. Li, P. Wang, J. Limpens, T. C. Maximov, & F. Berendse . . . 754

Increasing impacts of summer precipitation on permafrost environmental change in eastern Siberia
Y. Iijima, H. Park, T. Nakamura, Y. Tachibana, & A. N. Fedorov 755

Quantifying lateral and subsurface flow potential on the Arctic Coastal Plain of Alaska
J. C. Koch, J. A. Schmutz, M. T. Jorgenson, B. Uher-Koch, K. E. Gurney, & M. S. Wipfli 757

Parameterizing permafrost thaw induced wetland dynamics and its effects on CH_4 dynamics in the Community Land Model (CLM)
H. Lee, S. Swenson, & D. Lawrence 759

Active-layer soil moisture content regional variations in Alaska and Russia by ground-based and satellite-based methods, 2002 through 2014
R. R. Muskett, V. E. Romanovsky, W. L. Cable, & A. L. Kholodov 760

Investigating patterns of pond and lake distributions to enhance the modeling of future Arctic surface inundation
S. Muster, K. Roth, M. Langer, F. Cresto Aleina, W. Riley, C. Koven, G. Grosse, S. Lange, & J. Boike 761

Monitoring dynamic changes in Pan-Arctic land surface water coverage
J. D. Watts, J. S. Kimball, J. Du, & Y. Kim 762

17 **Integrating Hydrology and Biogeochemistry along the Land-to-Ocean Continuum** 764

Lateral and vertical fluxes of carbon and nitrogen from upland thermokarst
B. W. Abbott, J. B. Jones Jr., J. R. Larouche, W. B. Bowden, S. E. Godsey, & A. W. Balser . . 765

A macro-scale biogeochemical model to simulate carbon emissions from high-latitude and permafrost lakes
T.K. Bayer, M. Brakebusch, E. Gustafsson, & C. Beer 767

Fate of permafrost-released organic matter in the Laptev Sea: What is its lateral transport time from the Lena delta area to the deep sea of the Arctic interior?
L. Bröder, T. Tesi, I. Semiletov, O. Dudarev, & ö. Gustafsson 769

Permafrost draining rivers in the Canadian Arctic Archipelago: Biogeochemical properties and carbon export potential
K. A. Brown, B. Williams, E. Carmack, D. McLennan, A. Pedersen, A. Schimnowski, G. Fiske, R. Francois, V. Galy, Z. A. Wang, & B. Peucker-Ehrenbrink 770

Trace element cycles in permafrost thaw lakes
J. Canário, A. Padeiro, L. Castanheira, M. C. Santos, M. F. Araújo, T. Duarte, M. C. Oliveira, J. Ascenso, T. G. Nunes, S. S. Gomes, M. J. Ferreira, G. Vieira, & W. F. Vincent 772

Sulphur biogeochemistry in permafrost thaw lakes
J. Canário, A. Padeiro, L. Castanheira, M. C. Santos, G. Vieira, & W. F. Vincent 773

Hydro-geochemical characteristics and transformation processes of the Lena River Delta branches
A. Chetverova, I. Fedorova, A. Morgenstern, O. Bobrova, T. Skorospekhova, & S. Romanov 774

Investigating hydrology and related nutrient dynamics on Herschel Island, Yukon Territory, Canada
C. Coch, I. Eischeid, M. Fritz, S. Lamoureux, & H. Lantuit 775

Age and source of fluvial DOC, CO_2 and CH_4 in a carbon-rich landscape in the western Canadian Arctic
J. F. Dean, M. F. Billett, M. H. Garnett, Y. v. d. Velde, R. Baxter, K. J. Dinsmore, J. S. Lessels, L. E. Street, J. Subke, I. Washbourne, & P. A. Wookey 776

Modern and Holocene fluxes of sediment and organic matter into the Arctic Ocean
M. Fritz & H. Lantuit 778

Dissolved organic matter properties in arctic coastal waters are strongly influenced by fluxes from permafrost coasts and by local meteorology
M. Fritz, G. Tanski, & H. Lantuit 780

Dissolved organic matter export from forest-tundra ecotone of Siberia under discontinuous permafrost. Insights from high frequency acquisition in situ fluorescence of dissolved organic matter (fDOM)
L. Gandois, R. Teisserenc, T. Le Dantec, A. Prokushkin, S. Binet, & N. Tananaev 782

Dissolved Organic Matter export from forest-tundra ecotone of Siberia under discontinuous permafrost. Insights from high frequency acquisition in situ fluorescence of dissolved organic matter (fDOM)The formation of iron particles in the Lena River: Insights from iron isotopes (δ^{56}Fe), electron microscopy and X-ray spectroscopy
C. Hirst, L. Kutscher, S. Shaw, I. T. Burke, T. Maximov, M. Murphy, M. Schmidtt, C. Mörth, P. S. Andersson, & D. Porcelli 784

Contrasting sources of dissolved and particulate organic matter along 62N – 72N in the Lena River
E. S. Karlsson 785

Application of high resolution remotely sensed channel geometry to quantify lateral inflow gains through an arctic watershed
T. V. King, B. Neilson, A. Jensen, A. Torres-Rua, & M. Rasmussen 786

Large spatial variations in export and sources of organic carbon in the Lena River basin, Siberia
L. M. Kutscher, P. S. Andersson, C. Mörth, D. Porcelli, C. Hirst, & T. Maximov 787

Dissolved organic matter flux, characterization and dynamic in the Yenisei river
T. A. Le Dantec, R. Teisserenc, A. Myers-Pigg, P. Louchouarn, N. Tananaev, L. Gandois, & J. Probst 788

Arctic river organic carbon export through the ice-free season: isotopic and compositional analyses of DOM and POM collected in the Lena Delta between May and August 2014
G. Mollenhauer, M. Winterfeld, L. Bodenstab, C. Mörth, B. Koch, B. Heim, J. Hefter, A. Prokushkin, & J. Rethemeyer 790

Hydrochemical assessment of water quality characteristics in frost mound bogs impacted by gas industry
A. S. Mysina & T. M. Potapova 791

Contribution of permafrost degradation landforms to summer export of DOC from Yedoma-type Ice Complex to rivers, Lena Delta, Siberia
A. Morgenstern, L. Polakowski, A. Chetverova, A. Eulenburg, I. Fedorova, T. Skorospekhova, O. Bobrova, B. Heim, J. Boike, & P. Overduin 792

Summer surface water chemistry dynamics in different landscape units from Yedoma Ice Complex to the Lena River
L. Polakowski, A. Morgenstern, J. Boike, N. Bornemann, & P. Overduin 793

Contribution of retrogressive thaw slumps to the near shore carbon budget along the Yukon Coast, Canada
J. L. Ramage, A. M. Konopczak, A. Morgenstern, & H. Lantuit 794

Hydrological fluxes of carbon within the Yenisei River basin: A multi-scale study
A. S. Prokushkin, R. M. Amon, M. A. Korets, G. Mollenhauer, M. Winterfeld, M. P. Prokushkina, R. Teisserenc, L. Gandois, W. H. McDowell, L. S. Shirokova, J. Karlsson, O. S. Pokrovsky, & M. Heimann 795

Riverine carbon flux in permafrost terrains of Central Siberian Plateau
I. V. Tokareva, A. S. Prokushkin, R. A. Kolosov, S. V. Titov, L. S. Shirokova, O. S. Pokrovsky, & A. M. Rainer 796

Permafrost carbon degradation and transport pathways at thermokarst coasts in the Arctic
G. Tanski, S. Ruttor, H. Lantuit, C. Knoblauch, B. Radosavljevic, J. Ramage, G. Mollenhauer, J. Strauss, & M. Fritz 797

Erosion of ice-rich permafrost coasts and the release of dissolved organic carbon into the Arctic Ocean
G. Tanski, N. Couture, H. Lantuit, A. Eulenburg, & M. Fritz 798

A lignin phenol-based assessment of the provenance of organic matter discharged from a large permafrost affected watershed (Lena River, Siberia)
S. Trojahn, M. Winterfeld, J. Hefter, S. Zubrzycki, & G. Mollenhauer 799

Connecting aquatic biogeochemical spatial and temporal heterogeneity to hydrological processes and active layer dynamics within the Yukon River Basin
R. C. Toohey, E. Mutter, N. Herman-Mercer, & P. Schuster 800

Current and future thawing dynamics in a mega retrogressive thaw slump and resulting fresh water, sediment and carbon release to the nearshore zone on Herschel Island, Yukon Coast Territory, Canada
S. Weege & H. Lantuit 801

Organic matter deposition and preservation off the Lena Delta during the last 140 years
M. Winterfeld, D. Pittauer, P. Han, J. Rethemeyer, & G. Mollenhauer 803

18 **Submarine Permafrost, Arctic Gas Hydrate Deposits, and Greenhouse Gases in Arctic Coastal Waters** 804

Is submarine groundwater discharge a gas hydrate formation mechanism on the Circum-Arctic Shelf?
J. M. Frederick & B. A. Buffett 805

Lithogenetic types of offshore deposits of the Kara Sea
O. Kalashnicova, A. Kurchatova, E. Slagoda, & Y. Tikhonravova 806

Impact of glacial isostatic adjustment on shoreline migration and sea-level evolution in the Laptev Sea and the East Siberian Sea during the last glacial cycle
C. Klemann, B. Heim, H. A. Bauch, T. Opel, & S. Wetterich 808

Non-equilibrium simulation of hydrate formation and dissociation from CO_2 in the aqueous phase
K. Q. Nashaqi & B. Kvamme 809

Submarine permafrost map (SuPerMAP): a circum-arctic model of submarine permafrost distribution and state
P. Overduin, T. Schneider von Deimling, M. N. Grigoriev, & S. Westermann 810

Sub-sea permafrost modelling based on idealised laboratory experiment
M. Puglini, C. Brovkin, & D. Notz 811

Laboratory-based simulations of the microbial influence on permafrost-associated methane gas hydrate formation
J. M. Schicks, M. Luzi-Helbing, S. Liebner, E. Spangenberg, D. Wagner, & T. Wiersberg 812

Present and future gas release from degrading submarine permafrost regions
T. Schneider von Deimling, S. Westermann, & P. P. Overduin 813

How permanent is East Siberian Arctic Shelf permafrost?
M. Stendel, C. Rodehacke, V. E. Romanovsky, D. Nicolski, S. Marchenko, J. H. Christensen, R. Mottram, & M. Olesen 814

Controls on permafrost distribution within the near-shore zone of the Mackenzie Delta, Canada
C. Stevens & B. Moorman 815

Methane in tabular massive ground ice as a proxy of Late Pleistocene environmental conditions in western sector of Russian Arctic
I. D. Streletskaya, A. A. Vasiliev, G. E. Oblogov, & B. G. Vanshtein 816

Methane isotopologues and eddy covariance fluxes above the mid and outer Laptev and East Siberian Seas during SWERUS-C3
B. F. Thornton, P. M. Crill, K. Andersson, M. Wik, C. Sapart, J. Prytherch, I. M. Brooks, D. Salisbury, & M. Tjernström 818

Microbial activity mitigates the release of methane from degrading subsea permafrost
M. Winkel, J. Magritz, F. Horn, P. Overduin, C. Knoblauch, D. Wagner, & S. Liebner 819

Methane emission from the coastal retreat in the Western Yamal
N. Zadorozhnaia, V. Fedin, G. Oblogov, A. Vasiliev, & I. Streletskaya 820

19 **Polar Coastlines in Transition** 822

Analysis of coastal dynamics and permafrost conditions of the Yamal Peninsula using GIS
A.V. Baranskaya, S.A. Ogorodov, N.G. Belova, A.P. Vergun, N.N. Shabanova, D.E. Kuznetsov, O. Gosmant, E. Cauquil, N.N. Shabanova, A. Audibert-Hayet, P. Dauboin, & J.-B. Geldof . . . 823

Massive ice contribution to the coastal dynamics at Oyuyacha River mouth, west coast of Baydaratskaya Bay, Kara Sea
N.G. Belova, D.E. Kuznetsov, A.P. Vergun, & S.A. Ogorodov 825

Human-induced relief and permafrost dynamics at Yamal Coast of Baydaratskaya Bay, Kara Sea
N.G. Belova, S.A. Ogorodov, & O.S. Shilova 826

Arctic beach ridge morphology and Holocene sea-level fluctuations
M. Bendixen, & A. Kroon 828

Geomorphological features associated with coastal permafrost along an emerging coastline: Nunavik (Quebec), Canada
A. Boisson & M. Allard 829

Delta progradation and offshore sedimentary lobes in Kongsfjorden (western Spitsbergen, Svalbard)
M. Bourriquen, A. Baltzer, D. Mercier, J. Fournier, L. Perez, S. Haquin, E. Bernard, & M. Jensen 830

Applying a coastal erosion model at Tuktoyaktuk, Northwest Territories, Canada.
N. Couture, G. Manson, & D. Whalen 832

Comparing coastal dynamics between two geomorphologically distinct permafrost-affected coastlines in NW Alaska
L. M. Farquharson, D. H. Mann, G. Grosse, B. M. Jones, D. K. Swanson, & V. Romanovsky . . 833

Impact of storms on Arctic shorelines: Cases study
E. Guegan, A. Sinitsyn, & H. Christiansen 834

Permafrost coastal dynamics, a case study: Evaluating the coastal bluff in the Medynskiy sector (Varandey area), Barents Sea 2010 – 2015
L. C. Hyam, A. Sinitsyn, P. Hwang, & E. Guegan 835

The laboratory simulation of the deformation of the coastal slope under the wave action in the permafrost zone
D. Ionov, Y. Debolskaya, V. Debolsky, & I. Gritsuk 835

Dependencies of western Baydara Bay (Kara sea) coast retreat rate on lithology and height of coastal deposits
V. Isaev, S. Buldovich, A. Koshurnikov, R. Amangurov, D. Aleksyutina, N. Onischenko, O. Podchasov, E. Grishakina, I. Sokolov, & A. Usov 837

Controls of shoreline changes in Calypsostranda (Bellsund, Svalbard) over 1990 – 2015 period
K. Jarosz, P. Zagórski, L. Pawłowski, P. Lewińska, M.C. Strzelecki, & M. Jaskólski 839

Application of electrical resistivity tomography for monitoring of the state of coastal permafrost, SW Spitsbergen
M. Kasprzak, M.C. Strzelecki, K. Migała, M. Lim, M. Jaskólski, & L. Pawłowski 840

Modern rates of thermal denudation and thermal abrasion on western Kolguev Island
A. I. Kizyakov, M. V. Zimin, A. V. Sonyushkin, M. O. Leibman, N. V. Pravikova, & F. Günther 841

Coastal erosion and resulting impacts along the ice-rich permafrost coast of the Ivvavik National Park, Yukon Territory, Canada
A. M. Konopczak, H. Lantuit, & G. Manson 843

Polar beach-ridge systems: archives of a changing climate
S. Lindhorst . . . 844

Long-term local-scale study of coastal dynamics in Lorino, Chukotka
A. Maslakov & G. Kraev . . . 846

The role of shore ice in shaping the Calypsostranda shore (W Spitsbergen) in 2014/15 season
K. Męsdrek, J. Rodzik, & P. Zagórski . . . 847

Mass wasting and coastal erosion on Yukon Coast and Herschel Island
J. Obu, H. Lantuit, F. Günther, G. Grosse, T. Sachs, & M. Fritz . . . 849

The influence of climate change on the intensity of ice gouging at the Kara Sea bottom by hummocky formations
S. A. Ogorodov, V. A. Arkhipov, & O. V. Kokin . . . 850

POROCO – Mechanisms controlling the geomorphology and evolution of rocky coasts in polar climate – preliminary results
L. Pawłowski, M. C. Strzelecki, M. Lim, P. Migon, M. Kasprzak, Z. Swirad, M. W. Jaskolski, & P. Modzel . . . 853

Changes of High Arctic tidal flat systems as an indicator of climatic and sediment supply shifts in post-Little Ice Age period – examples from Svalbard
L. Pawłowski, M. C. Strzelecki, M. Lim, P. Migon, M. Kasprzak, Z. Swirad, M. W. Jaskolski, & P. Modzel . . . 854

Threats to coastal infrastructure from erosion and flooding: A case study from Herschel Island, Yukon Territory, Canada
B. Radosavljevic, H. Lantuit, W. Pollard, P. Overduin, N. Couture, T. Sachs, V. Helm, & M. Fritz 855

Thermo-erosion processes on the Marre Sale coast, Western Yamal
P. Schoeneich & A. Kurchatova . . . 856

Holocene deglaciation, sea-level changes and shifts in sediment supply recorded in High Arctic paraglacial coastal systems – Bjonapynten case study, Tempelfjorden, Central Spitsbergen
M. Strzelecki, S. Lindhorst, C. Hein, & J. Raff . . . 857

Hunting for Arctic tsunami - Impact of extreme waves on coastal evolution in western Greenland
M. Strzelecki, W. Szczucinski, A. Long, N. Rosser, A. Buchwal, & S. Dunning . . . 858

Patterns and controls of erosion along the Elson Lagoon coastline, Barrow, Alaska (2002–2015)
C. E. Tweedie, S. Escarzaga, R. P. Cody, B. Manley, A. Gaylord, Q. Aiken, & J. Brown . . . 859

20 **Permafrost-related Land Surface Subsidence and Frost Heave** 861

PermaSAR – Improving TanDEM-X D-InSAR techniques for the detection of small-scale vertical movements in arctic permafrost regions
I. Beck, J. Boike, S. Marx, M. Langer, & B. Höfle . . . 862

Using PSInSAR to detect thermokarst-induced subsidence in Eboling Mountain, China
J. Chen, L. Liu, H. Lin, T. Zhang, & B. Cao . . . 863

Dynamic slopes – spatio-temporal patterns and signals in permafrost related geometry changes
I. Gärtner-Roer, S. Weber, J. Müller, V. Wirz, & A. Vieli . . . 865

Modeling landscape vulnerability to thermokarst disturbance in boreal Alaska
H. Genet, M. Lara, W. R. Bolton, A. D. McGuire, V. Romanovsky, & M. Turetsky . . . 867

Surface kinematics of periglacial sorted circles over 8 years using SfM close-range photogrammetry
L. Girod, A. Kääb, & I. Berthling . . . 868

Ponding *vs.* baydzherakh formation on Yedoma uplands: Implications for modern thermokarst development and thaw subsidence in North Yakutia
F. Günther, G. Grosse, A. Veremeeva, & G. T. Maksimov . . . 869

Analysis of summer subsidence in Barrow, Alaska, using InSAR and hyperspectral remote sensing
M. Haghshenas Haghighi, M. Motagh, B. Heim, S. Chabrillat, D. Streletskiy, G. Grosse, T. Sachs, & K. Kohnert . . . 870

First measurements of permafrost-related surface movements using ground based SAR interferometry: A case study in the Eboling Mountain on the Qinghai-Tibet Plateau
L. Liu, L. Jiang, L. Liu, B. Gao, Y. Sun, H. Wang, & T. Zhang . . . 871

Study of frost susceptibility of normally consolidated clay using NGI frost heave cell
M. Kadivar, G. Grimstad, S. A. G. Amiri, H. P. Jostad, & E. Birkeland . . . 873

Geophysical forecasting of the formation of thermal suffosion depressions in Central Yakutia
I. I. Khristoforov, V. V. Olenchenko, L. Gagarin, & A. V. Omelyanenko . . . 874

ICESat GLAS elevation changes and ALOS PALSAR InSAR Line-Of-Sight changes on the continuous permafrost zone of the North Slope, Alaska
R.R. Muskett . . . 877

The potential of high resolution multi-scale monitoring of rockglacier kinematics using unmanned aerial vehicles (UAV) and terrestrial surveys
J. Müller, S. Dominik, I. Gärtner-Roer, V. Wirz, & A. Vieli . . . 878

Stochastic model of thermokarst within disturbed areas and its empirical verfication using high resolution images
T. Orlov, A. Victorov, S. Sadkov, E. G. Panchenko, & A. Zverev . . . 880

Realizing the full potential of Remotely Sensed Active Layer Thickness (ReSALT) Products
K. Schaefer, A. Chen, L. Liu, A. Parsekian, E. Jafarov, S. Panda, T. Zhang, & H. Zebker . . . 883

Thaw subsidence in undisturbed landscapes, Barrow, Alaska, U.S.A.
D. A. Streletskiy, N. I. Shiklomanov, F. E. Nelson, K. E. Nyland, A. E. Klene, J. Brown, & J. D. Little . . . 885

Differential interferometry for discontinuous permafrost monitoring with ALOS PALSAR data in Northern Quebec, Canada
L. Wang, R. Ludwig, M. Bernier, & P. Marzahn . . . 887

21 **Integrating Field and Remotely Sensed Measurements of Thaw-Driven Landscape Change in Permafrost Regions** 889

An ensemble-based snow data assimilation framework with applications to permafrost modeling
K. Aalstad, S. Westermann, J. Boike, L. Bertino, & K.S. Aas . . . 890

Identifying the amount and rate of forest-wetland cover change over the southern Taiga Plains discontinuous permafrost region in Canada using remote sensing
J. Adams, W. Quinton, A. Berg, & O. Carpino . . . 892

Towards circumpolar assessment of thaw lake dynamics
A. Bartsch, G. Pointner, & A.M. Trofaier . . . 893

Change of snow water equivalent in different arctic permafrost zones
S. Baumann . . . 894

Comparison of narrow, broad and visible band vegetation indices in a heterogeneous low Arctic ecosystem
A. L. Beamish, B. Heim, N. Coops, & M. Buchhorn . . . 894

Conceptualization and application of the Alaska Thermokarst Model
W. R. Bolton, M. Lara, H. Genet, V. Romanovsky, & A. D. McGuire . . . 895

Examining the ecosystem impacts of seismic lines in discontinuous permafrost from field and remotely sensed measurements
M. Braverman, W. L. Quinton, J. Adams, J. L. Baltzer, & R. F. Connon . . . 896

Airborne and field based measurements of thermokarst in pingos and adjacent collapse scar bogs in interior Alaska
T. A. Douglas, & M. R. Turetsky . . . 897

Colored dissolved organic matter in thermokarst lakes of Yamal Peninsula: sources, annual variations and connection to lake and catchment properties
Y. Dvornikov, M. Leibman, B. Heim, A. Bartsch, U. Herzschuh, A. Khomutov, B. Widhalm, T. Skorospekhova, & M. Mikhaylova . . . 899

Plant biomass, NDVI, and LAI along the Eurasian Arctic Transect
H. E. Epstein, D. A. Walker, G. V. Frost, M. K. Raynolds, & U. S. Bhatt . . . 900

Coupling soil field data with remote sensing to inventory permafrost soil carbon for two small Arctic river deltas, Alaska
M. Fuchs, G. Grosse, B.M. Jones, & I. Nitze . . . 902

User and Expert-supported Validation and Evaluation Experiments for high-latitude permafrost landscapes: ESA DUE PERMAFROST (2009-2012) and ongoing EnMAP, PAGE21, and HGF-EDA programs
B. Heim, A. Bartsch, A. Beamish, S. Stettner, M. Buchhorn, C. Duguay, H. Elin, B. Widhalm, K. Elger, & S. Walker . . . 904

Spatial characteristics of expanding water body and damaged boreal forest under permafrost degradation in central Yakutia by ALOS images
Y. Iijima, K. Abe, H. Ise, T. Masuzawa, & A. N. Fedorov . . . 905

The presence and degradation of residual permafrost plateaus on the western Kenai Peninsula Lowlands, southcentral Alaska
B. M. Jones, C. A. Baughman, V. E. Romanovsky, A. D. Parsekian, M. C. Jones, G. Grosse, & E. E. Berg . . . 906

Investigating the dynamics of a rock glacier using terrestrial laser scanning, time-lapse photography, in-situ GPS measurements and satellite SAR interferometry: Ritigraben rock glacier, Switzerland.
R. Kenner, M. Phillips, J. Beutel, P. Limpach, J. Papke, A. Hasler, & H. Raetzo 908

The rates of thermocirque development and driving factors of their activation on Central Yamal, Russia
A. V. Khomutov, Y. A. Dvornikov, M. O. Leibman, A. A. Gubarkov, & D. R. Mullanurov 910

Study of off-road vehicle trails impact on tundra landscapes by field and remote-sensing methods, Central Yamal, Russia
A. V. Khomutov, M. O. Leibman, Y. A. Dvornikov, & O. V. Khitun 912

Rapid palsa decay in Northern Finland interpreted from aerial photographs and RTK GPS field measurements
T. Kumpula, M. Verdonen, T. Tahvanainen, & A. Colpaert 914

Thermokarst rates intensify due to climate change and forest fragmentation in an Alaskan boreal forest lowland
M. J. Lara, H. Genet, A. D. McGuire, E. S. Euskirchen, Y. Zhang, D. R. Brown, M. Jorgenson, V. Romanovsky, A. Breen, & W. R. Bolton 915

Recent circum-Arctic ice-wedge degradation and its hydrological impacts
A.K. Liljedahl, J. Boike, R.P. Daanen, A.N. Fedorov, G.V. Frost, G. Grosse, L.D. Hinzman, Y. Iijima, J.C. Jorgenson, N. Matveyeva, M. Necsoiu, M.K. Raynolds, V. Romanovsky, J. Schulla, K.D. Tape, D.A. Walker, C.J Wilson, & H. Yabuki 917

Multi-sensor investigations of thermokarst development in Eboling Mountain, Heihe River Basin
L. Liu, L. Jiang, T. Zhang, J. Chen, B. Gao, J. Shang, Y. Nian, Y. Sun, B. Cao, & L. Liu 918

Quantifying the role of snow in soil thermal dynamics of the arctic terrestrial ecosystems
Z. Lyu & Q. Zhuang 919

Analysis of regional formation regularities of thermokarst processes on the basis of ground-field and remote monitoring data
E. Makarycheva 920

Measuring permafrost ground motion with Unmanned Aerial Systems
B. Moorman & A. Cully 922

A Landsat based monitoring framework for permafrost landscape dynamics
I. Nitze, G. Grosse, B. M. Jones, & D. J. Hayes 923

Distribution of thermokarst lakes and their area-frequency relations in Eastern Siberia
H. Saito, Y. Iijima, M. Ulrich, & A. N. Fedorov 925

Reconstruction of the development of retrogressive thaw slumps and controlling meteorological parameters in Central Yakutia (Central Siberia) using dendrochronology and remote-sensing
A. Séjourné, A. Decaulne, F. Costard, & A. Fedorov 926

Intra-annual dynamics of ice-rich riverbank erosion in the central Lena Delta
S. Stettner, H. Lantuit, A. Bartsch, B. Heim, G. Grosse, A. Roth, & B. Widhalm 928

Quantifying thermokarst and alas lake changes and influencing factors during the last 70 years in Central Yakutia
M. Ulrich, H. Matthes, Y. Iijima, H. Park, L. Schirrmeister, A. N. Fedorov, & J. Schütze 929

Stochastic models of lake thermokarst plain dynamics
A. Victorov & V. Kapralova 931

Eurasia Arctic Transect (Yamal Peninsula and Franz Josef Land, Russia): Relationships between climate, soil texture, vegetation, active-layer thickness, and spectral data
D. A. Walker, H. Epstein, M. Leibman, K. Ermokhina, A. Khomutov, N. Moskolenko, P. Orekhov, G. Matyshak, G. Frost, O. Khitun, S. Chasnikova, J. Šibík, E. Kaärlejarvi, & J. Kuss 933

Study on the method of building extraction based on the PolSAR images in permafrost regions
W. Pei, M. Zhang, Y. Lai, S. Li, W. Zhai, & X. Zhang 935

Using a mix-methods approach to monitor thermokarst activity in the Eureka Sound Lowlands, Ellesmere Island, Nunavut
M. K. Ward & W. H. Pollard 936

Thermokarst-induced landscape change in the Yukon Kuskokwim (YK) Delta, Alaska
M. A. Whitley, G. V. Frost, C. V. Maio, & M. T. Jorgenson 937

Combining remote sensing and field studies for assessment of landform dynamics and permafrost state on Yamal
B. Widhalm, A. Bartsch, M. Leibman, Y. Dvornikov, & B. Heim 938

Mapping landscape level changes in plant communities and impacts on permafrost dynamics in Siberia
Q. Yu, R. Engstrom, N. Shiklomanov, & D. Streletskiy 939

22 **Ground Based and Airborne Geophysical Applications in Permafrost** 941

Subsurface imaging with 3D ground-penetrating radar (GPR) in a permafrost landscape, Svalbard
N. Allroggen, B. Heincke, & W. Wheeler 942

Internal structure of a high arctic rock glacier based on quasi 3D electrical resistivity imaging and ground penetrating radar
I. Berthling, Alexander Bast, & I. Gärtner-Roer 944

Ground penetrating radar detection of visible and "hidden" ice wedges in the Chara Depression (Eastern Siberia, Russia)
S. Bricheva & J. Stanilovskaya 946

Monitoring and quantifying soil processes and interaction with vegetation and landscape properties in Arctic tundra using above- and below-ground imaging
B. Dafflon, A. P. Tran, J. Peterson, R. Oktem, C. Ulrich, H. Wainwright, J. B. Curtis, M. Torn, & S. Hubbard 948

Geophysical surveying of the Dempster Highway, Yukon, Canada
J. Dawson, L. Mitchell, & J. Henderson 950

Using electrical resistivity tomography, thermal and seasonal thaw depth measurements and airborne LiDAR to classify vegetation-geomorphology relationships in permafrost
T. A. Douglas, C. Hiemstra, K. Bjella, S. Newman, & J. Anderson 952

3D geoelectrical mapping of subarctic periglacial landforms
A. Emmert & C. Kneisel 954

Evidence of subglacial permafrost revealed by an electromagnetic study on the Greenland ice sheet in Central West Greenland
J. Engström, T. Ruskeeniemi, K. Korhonen, H. Vanhala, J. Lehtimäki, A. Lehtinen, L. C. Liljedahl, J. Näslund, & R. Pettersson 955

Electrical resistivity tomography in Polar Regions, field data and high performance GPU-based 3D numerical modeling
A.N. Fague, D.I. Fadeev, I.N. Yeltsov, V.A. Kashirtsev, D.E. Ayunov, & L.V. Tsibizov 957

Geophysical investigation of aquifers in a degrading permafrost environment in Northern Quebec, Canada
R. Fortier, D. Banville, J.-M. Lemieux, M. Ouellet, & R. Therrien 958

Resolution capacity of hydrological processes in ice-rich permafrost – results from geophysical monitoring and synthetic modelling
C. Hilbich, B. Mewes, R. Delaloye, & C. Hauck 960

Repeated ERT surveys to detect forest fire impacts on discontinuous permafrost, southwestern NWT, Canada
J.E. Holloway & A. Lewkowicz 961

Change in discontinuous permafrost in the Alaska Highway corridor examined by repeated electrical resistivity tomography and ground temperature monitoring, northwest Canada
A. G. Lewkowicz, O. Bellehumeur-Génier, C. Miceli, & S. L. Smith 963

Occurrence of large massive ground ice bodies buried under glacio-fluvial deposits along the Alaska Highway, Dry Creek area, south-western Yukon, Canada
B. Loranger, G. Doré, & D. Fortier 965

Using resistivity method to characterize water flow patterns in permafrost environment (Ilulissat, Greenland)
J. Malenfant-Lepage, G. Doré, T. Ingeman-Nielsen, & F. Daniel 966

Reconstructing the last century evolution of the Dérochoir rock glacier using a multi-approach monitoring
M. Marcer, X. Bodin, & P. Schoeneich 967

Long-term electrical resistivity tomography (ERT) monitoring of mountain permafrost in Switzerland – comparison of different sites and relevance for thermal modelling
C. Mollaret, C. Hilbich, S. Python, & C. Hauck 968

Delineation of permafrost and ice-rich terrain within fine-grained sediments using electrical resistivity, Yellowknife, Northwest Territories
G. Oldenborger, S.A. Wolfe, P.D. Morse, & A. Pugin 969

Geophysical evaluation of bedfast and floating ice lake talik, Alaska
A. Parsekian, A. Creighton, C. Arp, B. Jones, R. Dannen, A. Bondurant, & A. Gaedeke 971

Soil moisture data for the validation of permafrost models using direct and indirect measurement approaches at three alpine sites
C. Pellet, C. Hilbich, A. Marmy, & C. Hauck 973

Characterizing relict late Pleistocene permafrost valley fills along the Alaska Highway, southwest Yukon
J. Pumple, D. Froese, F. Calmels, & B. Minsley 974

Integration of seismic and GPR for study geocryological section in the floodplain of the Pechora river (the Nenets district, Russia)
M. Sadurtdinov, M. Sudakova, G. Malkova, A. Skvortsov, & A. Tsarev 975

The potential of ground-based 3D GPR imaging: 2D vs. 3D examples from the Yedoma region
S. Schennen, J. Tronicke, S. Wetterich, N. Allroggen, G. Schwamborn, & L. Schirrmeister 977

Optimizing electrode shapes for ERT monitoring in permafrost areas
S. Tomaskovicova, T. Ingeman-Nielsen, A. V. Christiansen, I. Brandt, T. Dahlin, & B. Elberling . 979

Automated long-term time lapse ERT monitoring of high-latitude permafrost – results of 3 years of monitoring and modeling study
S. Tomaskovicova & T. Ingeman-Nielsen 981

Magnetic studies in Lena river delta: the results of 2014-2015 fieldworks and future plans
L. Tsibizov, D. Ayunov, N. Semakov, P. Dyadkov, & D. Pavlova 983

Geophysical identification of hydrologic flow paths on arctic hillslopes
E. B. Voytek, C. R. Rushlow, S. E. Godsey, & K. Singha 984

23 **Hazards and Risks related to Changing Mountain, Low-Land and Coastal Permafrost** 985

GIS of the gas-emission crater area (Yamal Peninsula, Russia)
K. Ermokhina, A. Kizyakov, M. Leibman, & A. Khomutov 986

Measuring and modelling permafrost at local and regional scales in the Kazbek region, Russian Caucasus
R. Frauenfelder, C. Huggel, S. Zgraggen-Oswald, I. Galushkin, & S. Chernomorets 988

Ground thermal characteristics at a high-latitude rockslide site (Polvartinden, Northern Norway)
R. Frauenfelder & K. Isaksen 990

Root induced changes to soil hydrological properties and permafrost stability in Qinghai-Tibet Plateau, China
Z. Gao, F. Niu, Y. Wang, Z. Lin, & J. Luo 992

Historic movement analysis of frozen debris Lobes, Southern Brooks Range, Alaska
N.L. Gyswyt, M.M. Darrow, & R.P. Daanen 994

Evaluation of rock slope failures in steep permafrost slopes in Norway - first insights in the geological history of the Mannen unstable rock slope in Møre og Romsdal
P. Hilger, R.L. Hermanns, J.C. Gosse, B. Etzelmüller, S. Westermann, & M. Krautblatter 997

Svalbard coastal hazards and their impact on scientific and community infrastructure
M.W. Jaskólski, M.C. Strzelecki, & L. Pawłowski 998

Evaluation of risk of ice-wedge degradation, Prudhoe Bay Oilfield, AK
M. Kanevskiy, Y. Shur, D.A. Walker, M. Buchhorn, T. Jorgenson, G. Matyshak, M.K. Raynolds, J.L. Peirce, & L.M. Wirth 999

Gas-emission crater, geomorphological characteristics and relief dynamics on Yamal Peninsula, Russia
A.I. Kizyakov, M.O. Leibman, A.V. Sonyushkin, M.V. Zimin, & A.V. Khomutov 1002

Complex study of gas-emission crater in Central Yamal, Russia
M.O. Leibman, A.I. Kizyakov, I.D. Streletskaya, A.V. Khomutov, Y.A. Dvornikov, K.A. Ermokhina, & A.A. Gubarkov 1004

Temperature at bottom of thermokarst lakes and the relationship with lake depth along the Qinghai-Tibet Engineering Corridor
Z. Lin, F. Niu, & J. Luo . . . 1006

Characteristics of thaw-induced slope failures in permafrost regions of the Qinghai-Tibet Engineering Corridor, China
J. Luo, F. Niu, & Z. Lin . . . 1007

The effect of ground-ice on the mobility and behaviour of landslides: A case study in northern Iceland
C. Morino, S.J. Conway, Þ. Sämundsson, M.R. Balme, J.K. Helgason, J. Hillier, C. Jordan, & T. Argles . . . 1008

700 documented rockfalls in the Mont Blanc massif since 2003 validate the role of the permafrost warming in triggering
L. Ravanel, F. Magnin, & P. Deline . . . 1010

Landscape hazards mapping for climate change adaptation planning in the Yukon
L.-P. Roy, B. Benkert, K. Kennedy, D. Fortier, & A. Lewkowicz . . . 1011

Yamal Craters: State of knowledge and wished in-situ investigations
D.O. Sergeev, A. Khimenkov, G. Tipenko, A. Vlasov, E. Cauquil, E. Green, P. Dauboin, J. Stanilovskaya, & M. Mnushkin . . . 1013

Permafrost-related causes and consequences of the Sagavanirktok River flooding in spring 2015
Y. Shur, M. Kanevskiy, D.A. Walker, T. Jorgenson, M. Buchhorn, M.K. Raynolds, & H. Toniolo . 1014

24 **New Frontiers in Mountain Permafrost Research** 1017

Permafrost in the Indian Himalaya: A pilot Indo-Swiss study in Himachal Pradesh building new knowledge and scientific capacity
S.K. Allen, J. Fiddes, A. Linsbauer, S.S. Randhawa, B. Saklani, & N. Salzmann . . . 1018

Permafrost distribution modeling in the semi-arid Chilean Andes
G.F. Azócar, A. Brenning, & X. Bodin . . . 1021

The PermaSense Mountain Lab – Technology and infrastructure for an open permafrost data repository
J. Beutel, S. Weber, & T. Gsell . . . 1023

Multi-temporal mapping of rock glacier displacements: insights from SfM, ALS and TLS high-resolution datasets on the Laurichard rock glacier, French Alps
X. Bodin, O. Sanchez, S. Jaillet, A. Rabatel, & E. Thibert . . . 1025

Rock glacier activity and distribution in the semi-arid Andes of Chile and Argentina detected from dInSAR
X. Bodin, E. Thomas, D. Trombotto Liaudat, S. Vivero, & P. Pitte . . . 1027

Geomorphological characteristics, internal structures and hydrological importance of moraine–rock glacier landforms in Ak-Shiirak Range (Inner Tien Shan, Kyrgyzstan)
T. Bolch, N. Rohrbach, & A. Osmonov . . . 1029

Preliminary modelling of mountain permafrost on La Ramada Range. Central Andes, San Juan, Argentina
A.P. Forte, P. Pitte, & C.D. Villarroel . . . 1030

Morphometric characterization of cryogenic surfaces (Glacier Wedge) in the NW of the Iberian Peninsula and Argentinian Andes: applying a developed methology
J.F. Hall-Riaza, M. Valcárcel, R. Blanco-Chao, & R. Mikkan 1033

Recent speed-up of an Alpine rock glacier: An updated chronology of the kinematics of Outer Hochebenkar rock glacier based on geodetic measurements
L. Hartl, A. Fischer, J. Abermann, & M. Stocker-Waldhuber 1035

Assessing future water contents in permafrost soils by calibrating permafrost models with temperature and electrical resistivity monitoring data
C. Hauck, C. Hilbich, A. Marmy, C. Mollaret, C. Pellet, & S. Python 1036

Groundwater storage and flow pathways in a rock glacier complex in the Canadian Rockies
M. Hayashi, J. Harrington, A. Mozil, & L.R. Bentley 1037

Ground ice distribution and volumetric content in rock glaciers in the Chilean Andes – a comparison of geophysical data and ground truth from boreholes
C. Hilbich, C. Mollaret, J. Perrenoud, A. Wicki, J. Wicky, C. Hauck, L. Arenson, & P. Wainstein 1038

Long-term energy balance measurements at three different mountain permafrost sites in the Swiss Alps
M. Hoelzle & C. Hauck 1039

Variations in rockglacier speed in the Tien Shan and their significance
A. Kääb, T. Strozzi, A. Sorg, & M. Stoffel 1040

A regional signal of significant recent ground surface temperature warming in the periglacial environment of Central Austria
A. Kellerer-Pirklbauer 1041

Relations between vegetation and mountain permafrost along elevation gradients, Yukon Territory, Canada
Z.M.C.O. Kuntz & A. Lewkowicz 1043

Importance of the multidisciplinary approach in volcanic areas
E. Kuznetsova 1045

A rock glacier inventory of the Western and High Tatra Mountains, Western Carpathians
P. Mida & T. Uxa 1046

The effect of temporal variability of soil moisture on mountain permafrost: A combined model and monitoring approach
C. Pellet, C. Hauck, & M. Stähli 1047

Multi-disciplinary monitoring of rock glacier dynamic: the case study of Gran Sommetta (Valle d'Aosta, Italy)
P. Pogliotti, U. Morra di Cella, F. Diotri, C. Pellet, R. Delaloye, & C. Hauck 1048

Permafrost - Glacier interaction at the lower limit of mountain permafrost: A case study from Western Alps (Petit-Grapillon, Valle d'Aosta, Italy)
P. Pogliotti, U. Morra di Cella, M. Isabellon, & E. Cremonese 1049

Permafrost occurrence in the Himalayas - first results from an empirical model approach for area-wide estimates
M.-O. Schmid, N. Salzmann, A. Linsbauer, & A. Hasler 1050

New frontiers in detecting and quantifying mountain permafrost creep from radar interferometry
T. Strozzi, R. Caduff, U. Wegmüller, C. Werner, C. Barboux, R. Delaloye, & H. Raetzo 1051

Permafrost observation strategy in the Hindu Kush Himalayan region: A Proposal
D. Stumm, S. Gruber, C. Hauck, R. Kayastha, M.A. Khan, M.L. Rijal, N. Salzmann, R.J. Thayyen, & P. Wester 1053

Modelling of mean annual air temperature (1979-2010) for the study of mountain permafrost in the SW of San Juan
C.C. Tapia Baldis, D. Trombotto Liaudat, C. Villarroel, & F. Otero 1055

Inventory of landslides at the Santa Cruz river basin (San Juan, Argentina) and its relationship with the Andean cryogenic environment
C.C. Tapia Baldis & D. Trombotto Liaudat 1057

Data and permafrost frontiers in South America
D. Trombotto Liaudat, K. Saito, & I.P. Marcosig 1058

First results from thermal investigations of rock glaciers in the Slovak High Tatra Mountains, Western Carpathians
T. Uxa & A.W. Balser 1060

Permafrost detection through the use of geophysical methods in the Blanco River Basin, San Juan, Argentinia
C.D. Villarroel, A.P. Forte, & C. Tapia Baldis 1061

Soil moisture impacts on the thermal regime of mountain permafrost
A. Wicki, C. Hauck, C. Pellet, & C. Hilbich 1063

Short-term variability of rock glacier surface velocities in the Swiss Alps revealed by continuous GPS
V. Wirz, J. Beutel, R. Delaloye, T. Gsell, S. Gruber, I. Gärtner-Roer, A. Hasler, R. Kenner, P. Limpach, J. Müller, M. Phillips, H. Raetzo, C. Scapozza, A. Vieli, & S. Weber 1064

Isotope tracking of water sources and growth patterns of ground ice at the Kunlun Mountain Pass on northern Qinghai-Tibet Plateau
Y. Yang, Q. Wu, & H. Jin 1066

25 **Changing Permafrost and its Impacts across High Asia** 1067

Multi-time scale characteristics of climatic factors and its effects on permafrost in the Qinghai-Xizang Plateau
S. Gao, Q. Wu, & Z. Zhang 1068

Differences of the heat-moisture process in active layer among different ecosystems in Beiluehe basin of the Qinghai-Tibet Plateau, China
G. Jiang, Q. Wu, & Z. Zhang 1070

Permafrost-related Characteristics of vegetation in an inland watershed of the Qilian Mountains, northwestern China
J. Li, Y. Sheng, J. Wu, X. Zhang, Z. Feng, & S. Wang 1071

The soil thermal conductivity regime within active layer at different land surfaces in the northern Qinghai-Tibetan Plateau, China
R. Li, L. Zhao, T. Wu, C. Xie, Y. Xiao, G. Hu, & Y. Du 1073

Distribution characteristics of the depth of zero annual amplitude in permafrost regions on the Qinghai-Tibetan Plateau
G. Liu, L. Zhao, C. Xie, T. Wu, Q. Pang, & Y. Qiao . . . 1074

Temporal, Altitudinal and Spatial Variability of Permafrost in the Tian Shan Mountains during the Holocene
S. Marchenko, A.P. Gorbunov, & V. Romanovsky . . . 1075

Effects of stratified active layers on the high-altitude permafrost warming: A case study on the Qinghai-Tibet Plateau
X. Pan, Y. Li, Q. Yu, X. Shi, D. Yang, & K. Roth . . . 1077

Recent change in ground temperature in the east part of Qinghai-Tibet Plateau
Y. Sheng, J. Wu, J. Chen, J. Li, Z. Feng, X. Hu, & S. Wang . . . 1078

Seasonal variations of soil properties in a relic permafrost region on the eastern Qinghai-Tibet Plateau
L. Tian, L. Zhao, X. Wu, & C. Xie . . . 1079

Initial result of permafrost assess in Mongolia
U. Tsogtbaatar, D. Avirmed, J. Yamkhin, & T. Khurelbaatar . . . 1081

Mapping and inventorying active rock glaciers in northern Tien Shan (China) using satellite SAR interferometry
X. Wang, L. Liu, T. Wu, L. Zhao, Z. Li, & G. Liu . . . 1083

Diagnostic and model dependent uncertainty of simulated Tibetan permafrost area
W. Wang, A. Rinke, J.C. Moore, X. Cui, D. Ji, Q. Li, N. Zhang, C. Wang, S. Zhang, D.M. Lawrence, A.D. McGuire, W. Zhang, C. Delire, C. Koven, K. Saito, A. MacDougall, E. Burke, & B. Decharme . . . 1084

Comparison of climate and permafrost relations during recent years in mid-latitude alpine regions
T. Wu, L. Zhao, R. Li, & C. Xie . . . 1086

Evolutionary history and environmental information of permafrost on Mahan Mountain, Chinese Loess Plateau
C. Xie . . . 1087

Monitoring and modeling the thermal state of permafrost on the Tibetan Plateau
L. Zhao, Y. Sheng, Q. Pang, C. Xie, T. Wu, & Y. Qiao . . . 1088

26 **Frozen Ground Engineering** 1089

Improving the methodology for characterizing permafrost terrain for engineering
K. Bjella, J. Johnson, Y. Shur, M. Kanevskiy, J. Best, P. Duvoy, & K. Hinkel . . . 1090

An experimental investigation of the mechanical behavior of frozen loess
C. Cai . . . 1093

Influence of precipitation on the permafrost in the Fenghuo Mountain Region of Qinghai-Tibet Plateau
H. Cai, Z. Xiong, L. Jin, Y. Li, F. Li, L. Han, & L. Rong . . . 1094

Large-scale direct shear testing of compacted frozen soil under freezing conditions
E.M. De Guzman, M. Alfaro, L. Arenson, & G. Doré . . . 1095

Framework for the prediction of the hydraulic conductivity and of the compressibility of the fine-grained thawed permafrost
S. Dumais & J.-M. Konrad . . . 1096

Computer simulation of permafrost soil thermal regime under the thermal influence of engineering constructions
V. Gordiychuk & I. Gishkeluk . . . 1097

Thermal state dynamics of permafrost basement on engineering objects in cryolithozone of Russia
V.I. Grebenets, D.A. Streletskiy, N.I. Shiklomanov, A.G. Kerimov, E.A. Ostroumova, Y.V. Konovalov, & F.D. Andruschenko . . . 1098

Towards accurate measurement of soil freezing characteristic curves
S. Gruber, A. Adler, & H. Gagnon . . . 1101

Crack problems and causes of pavement and embankment in Qinghai-Tibet Plateau Permafrost Regions
D. Hu, X. Li, F. Han, W. Liu, Y. Lu, & W. Yu . . . 1102

The thermal influence analysis of The different distances between parallel pipelines on the foundation in permafrost region
X. Hu, Y. Sheng, J. Wu, & J. Li . . . 1104

Mitigation techniques to preserve permafrost under transportation infrastructures: Study case of the Alaska Highway, Yukon
X. Kong, G. Doré, F. Calmels, & C. Lemieux . . . 1106

Evaluation of the Norwegian gradation based regulations for frost susceptibility of aggregates in roads and railways
E. Kuznetsova, K.A. Skoglund, J. Aksnes, K. Rieksts, & I. Hoff . . . 1107

Study on the influence of pavement types to temperature transmission characteristics in permafrost regions
J. Li . . . 1108

Effects of using straw mulching as frost damage prevention measure for HSR under construction in deep seasonally frozen soil area in winter time
Z. Li, Y. Niu, & Q. Mu . . . 1109

The performance of direct driven piles in cold permafrost
T. Mayrberger, S. Baginski, M. Fenwick, & J. Cologgi . . . 1110

Design challenges of North America's first major bridge north of the Arctic Circle
T. Mayrberger, K. Braun, J. Brodie, & M. Fitzpatrick . . . 1111

Impacts of permafrost degradation on roadway engineering along the Qinghai-Tibet Engineering Corridor
W. Ma, Y. Mu, Q. Wu, F. Niu, & G. Li . . . 1112

Geotechnical hazards of embankments on sloping terrains in permafrost regions along the Qinghai-Tibet Railway
Y. Mu, W. Ma, F. Niu, & G. Li . . . 1112

Impact of permanent and seasonal thermal insulation in a ventilated crawl space on permafrost temperature under buildings
P.V. Perreault & Y. Shur . . . 1113

Overview of trunk pipeline practice in Russian permafrost
J. Stanilovskaya, D. Shmelev, E. Green, & P. Dauboin . . . 1114

Effects of warm, discontinuous permafrost on site response spectra at a site near Fairbanks, Alaska
J. Thornley & J. Yang . . . 1116

Dynamics of the seasonal thawing of frozen ground at the disturbed area, Alexandra Land, Franz-Joseph Land Archipelago
Y. Tikhonravova . . . 1117

Experimental study on mechanical properties of coarse-grained soil in cold regions
T. Wang, Z. Yue, T. Sun, & H. Song . . . 1119

Theoretical creep models of frozen soils
X. Yao, W. Ma, J. Qi, & F. Yu . . . 1119

Challenges and countermeasures of a power transmission line in permafrost regions – the Qinghai-Tibet Power Transmission Line
Q. Yu, Y. Xie, Y. You, L. Guo, & X. Wang . . . 1120

Investigation on the pore water pressures during soil freezing and thawing
L. Zhang, W. Ma, & C. Yang . . . 1121

Numerical analysis of the thermal characteristics and seismic response of bridges in permafrost regions
X. Zhang, M. Zhang, S. Li, & W. Pei . . . 1122

Relative vertical displacement of pile-soil under the freeze-thaw action
Z. Zhang, W. Ma, & W. Feng . . . 1123

27 **Infrastructure Stability in Permafrost Terrain** 1124

The decreasing of frozen foundations bearing capacity of Norilsk region buildings and structures associated with temperature changes
F. Andriushchenko & V. I. Grebenets . . . 1125

PIEVC vulnerability assessment for three airports in the Canadian North
L. Arenson, M. Telles-Langdon, J. Seto, J. Festa, & J. Craig . . . 1126

Assessment of embankments stability on the thawing base soil
E. Ashpiz & T. Vavrinyu . . . 1127

Quantifying probability of thaw settlement occurrence and vulnerability to climate warming – Iqaluit Airport, Nunavut
H.M. Brooks, G. Doré, M. Allard, A. Locat, & C. Lemieux . . . 1128

Experience in the assessment of long-term social-economic damage caused by the development of geocryological processes (Chara-China railway example)
I. Chesnokova, D. Sergeev, O. Borsukova, & A. Morozova . . . 1129

Performance of a reinforced highway embankment along the Inuvik-Tuktoyaktuk Highway, Northwest Territories, Canada
E.M. De Guzman, A. Piamsalee, M. Alfaro, L. Arenson, & G. Doré . . . 1130

The construction of Kangerlussuaq Airport - A case story from West Greenland
T. Ingeman-Nielsen & N. Foged . . . 1131

Longyearbyen port development - soil conditions and geotechnical challenges
A. Instanes 1134

Impact of the stationary thermal field on cryogenic processes in road embankments
V. A. Isakov & V. I. Grebenets 1135

Design procedure taking into account accumulation of snow along embankment built on permafrost
F. Lanouette, G. Doré, & D. Fortier 1137

Challenges emerging from climate change and urbanization in permafrost regions of Northeastern China
Y. Lu, W. Yu, F. Han, X. Yi, L. Chen, & W. Liu 1138

Effects in the active layer and permafrost of the spanish antarctic station "Gabriel De Castilla" (Deception Island)
A. Molina, M.á. de Pablo, M. Ramos, C. Blitz, M.á. Ropero, G. Goyanes, & M. Prieto 1140

Available flow rate for culverts built on permafrost and influence of the water source on thermal stability
L. Périer, & G. Doré 1143

Cone penetration testing for railways on permafrost
I. Sokolov, N. Volkov, & V. Isaev 1144

Investigation and management of permafrost and groundwater conditions at mining sites: Case studies in continuous permafrost of Alaska and Canada
E. Stephani, M. Angelopoulos, M. Musial, S. Anderson, P. Gince, & M. Kissiova 1146

Management strategies of slope stability geohazards near developments in permafrost areas – Current state-of-the-art
E. Stephani, G. Doré, & M. Darrow 1148

Cumulative economic damages in permafrost based on an example of a linear infrastructure (Railway Khanovey – Pesets)
A.S. Voytenko & D.O. Sergeev 1149

Cooling effects of highly porous media embankments constructed with ventilation ducts in permafrost regions
M. Zhang, W. Pei, X. Zhang, Z. Wu, & Z. Wen 1150

28 **Permafrost Engineering in Mountainous Terrain** 1151

Sonic drill for frozen core extraction in mountain permafrost in the dry Andes
L. Arenson, P. Wainstein, J. Umarez, & D. Welkner 1152

Risk assessment of infrastructure destabilization due to global warming in high mountain in the French Alps
P.-A. Duvillard, L. Ravanel, & P. Deline 1153

Thermal monitoring of pipe and permafrost beneath the China-Russia Crude Oil Pipeline
G. Li, W. Ma, H. Jin, Y. Wang, Y. Mu, S. Fan, & F. Wang 1154

Stability characteristics of a U-shaped crushed-rock embankment of the Qinghai-Tibet Railway in a warm permafrost region
F. Niu, M. Liu, & J. Wang 1155

Modelling internal deformation and slope stability of a protalus rampart: 'Estrecho B' at Pascua Lama in the high Andes of Chile
A.M. O'Sullivan, L.U. Arenson, & J.B. Murton . . . 1156

Challenges in construction of Europe highest cable car station at Klein Matterhorn (Switzerland)
D. Tobler, K. Graf, & P.D. Canassy . . . 1158

29 **Permafrost Problems in Mineral, Oil and Gas Exploration and Production** 1160

Application problems and potential for utilization of industrial outage of liquid natural gas cooling capacity for foundation soil thermostabilization as in the case of freezing of lenses of cryopegs with different salt content rage
D. Bek & K. Ilya . . . 1161

Study on recovery of permafrost and ecological environments after a strip-pit backfilling –A case study in the Da Xing'anling Mountains in Northeast China
R. He, H. Jin, L. Lu, & S. Wang . . . 1162

Changes of the engineering geocryogical conditions in the Yamburg settlement (Taz Peninsula)
A. Tolstogan, V. Grebenets, V. Pavlunin, & O. Kislov . . . 1163

Integrated geophysical monitoring as a basis for effective assessment of the influence of geocryological processes on slope stability in open pit mines
S. Velikin, D. Shesternev, I. Marchenko, & A. Yakimov . . . 1165

30 **Frozen Ground Properties: Field and Laboratory Testing** 1167

Effects of adsorbed cations and temperature on zeta potential of clay soils
H.A. Barnes & M.M. Darrow . . . 1168

The new test device for determining the frozen pressure and the strength of silty soils below the low temperature
A. Binal . . . 1170

Design and development of a test system for measuring ultrasonic wave of frozen soil
H. Bing, Y. Du, & X. Huang . . . 1170

The physical properties of permafrost soils of some mountain areas of Turkey
A. Binal, O. Karamut, B. Bas, & P. Adeli Ghareh Viran . . . 1171

Normalized stress-strain behavior of silty sand under the influence of freeze-thaw cycles
D. Chang, J. Liu, & X. Li . . . 1171

Comparison of methods to estimate methane content in permafrost
M. Cherbunina, A. Brouchkov, D. Shmelev, & V. Kazantsev . . . 1172

Thermal conductivity variations of gas bearing soils in permafrost during different conditions of hydrate accumulation
E. M. Chuvilin & B. A. Bukhanov . . . 1174

Change of gas permeability of frozen sandy soils during thawing
E.M. Chuvilin, S.I. Grebenkin, & M. Sacleux . . . 1175

Oil contamination influence on water phase composition and thermal conductivity of frozen soils
E.S. Grechishcheva & R.G. Motenko . . . 1177

Strength of frozen and unfrozen artificial rock joints depending on material porosity
F.K. Günzel . . . 1179

Express method for unfrozen water content in soils by using water potential
V.A. Istomin, E.M. Chuvilin, & B.A. Bukhanov . . . 1181

Regularities of cryogenic metamorphism of cryopegs with marine and continental quality of salinity
N. V. Kiyashko & I. A. Komarov . . . 1182

Forecasting technique of changing of phase and chemical composition for cryopegs in the act of changing of thermobaric conditions
I.A. Komarov, M.V. Mironenko, & N.V. Kiyashko . . . 1182

Refinement of pulse nuclear magnetic resonance (P-NMR) techniques for accurate determination of unfrozen water content in frozen soils
A. Kruse, M. Darrow, & S. Akagawa . . . 1183

Experimental research on acoustic wave propagation properties of frozen silt after freeze-thaw cycles
D. Li, X. Huang, F. Ming, Y. Zhang, & H. Bing . . . 1185

Frost heave property of saturated silty clay under one side freezing
H. Ma, F. Zhang, D. Feng, & B. Lin . . . 1186

Frost heave caused by formation of ice lenses in porous media
F. Ming & D. Li . . . 1187

Changes of moisture in soil freezing, Central Russia
V.S. Norkov, V.I. Grebenets, A.A. Maslakov, V.A. Tolmanov, & D.A. Streletskiy . . . 1188

Laboratory investigations of thermal properties of crushed rock materials
K. Rieksts, E. Kuznetsova, J. Cote, & I. Hoff . . . 1190

Using attribute of Electromagnetic wave to determine the water content and frost table in the permafrost area
Y. Shen, Y. Tian, & J. Liu . . . 1191

A coupled model for water, heat and solute transport in frozen soil: Evaluation with laboratory experiments
M. Wu, J. Huang, J. Wu, & X. Tan . . . 1191

Experimental study on anti-frost-heaving performance of screw pile foundations of photovoltaic stents in seasonal frozen soil region
T. Wang, J. Liu, Y. Shang, & H. Zhao . . . 1192

Model test on pore water pressure of soils subjected to freeze-thaw cycles
D. Xiao, W. Ma, S. Zhao, & Z. Zhang . . . 1193

Thermal, Electrical and Mechanical Properties of Permafrost from the North Slope, Alaska
Z. Yang, F. Zhang, B. Still, J. Wang, H. Li, & H. Zubeck . . . 1194

A review of physical and mechanical properties of saline frozen soil
Y. Lai, Z. Xiao, D. Wu, M. Liao, & X. Wan . . . 1195

Use of mercury intrusion porosity for microstructural investigation of silty clay with different contents of sodium sulfate
Z. You, Y. Lai, M. Liao, & Q. Ma . . . 1196

Experimental investigation on creep characteristics of artificial warm and ice-rich frozen sandy silt
F. Zhang, D. Feng, H. Ma, & L. Cai . . . 1197

31 **Permafrost in History and Culture** 1198

Urban livelihoods in past, present and future permafrost environments: Contrasting public perception of changes and instrumental data
O. Anisimov, Y. Zhegusov, Y. Ziltcova, & V. Kokorev . . . 1199

A database of participants attending the International Conferences on Permafrost (1963 – 2012)
J. Brown, M. McGraw, & J. Stanilovskaya . . . 1200

Effects of 45 years of heavy road traffic and climate change on the thermal regime of permafrost and tundra at Prudhoe Bay, Alaska
M. Buchhorn, M.K. Raynolds, M. Kanevskiy, G. Matyshak, Y. Shur, M.D. Willis, J.L. Peirce, L.M. Wirth, & D.A. Walker . . . 1203

Translation and contestation: Researching permafrost in the early cold war
P.-Y. Chu . . . 1205

The cautionary tales of the Alaska Highway and the Trans-Alaska Pipeline System
M.H. Cysewski & Y. Shur . . . 1207

Alas landscapes of Central Yakutia: Towards a periodization of land use and permafrost degradation
R.V. Desyatkin, J.O. Habeck, & A.I. Yakovlev . . . 1209

Permafrost in synthetic view of glacial and periglacial domain: New terms and definitions
W. Dobiński . . . 1210

Climate warming- and human-induced thermokarst activity in Central Yakutia and its social response
A.N. Fedorov, P. Konstantinov, N. Basharin, R. Desyatkin, Y. Iijima, H. Park, M. Ulrich, A. Sejournen, F. Costard, C. Grenier, T. Hiyama, & G. Iwahana . . . 1214

A methodological framework for the evaluation of climate change adaptation projects: A pilot study using the 'Terrain Analysis in Nunavut' project in Arviat, Canada
M.J. Flynn, J.D. Ford, & J. Labbé . . . 1215

Early investigations of permafrost in Siberia by Baltic-German and German scientists
D. Fritzsche & E. Tammiksaar . . . 1217

Changing permafrost-landscape conditions in an Arctic city experiencing urban decline (Igarka, Russia)
A.S. Gubanov, V.I. Grebenets, K.E. Nyland, & A.V. Litovko . . . 1220

Permafrost landscapes as objects of scientific tourism
R. Ivanova & A. Fedorov . . . 1222

Landscape and climate changes and their impacts to nenets reindeer herding in Yamal peninsula, Russia
T. Kumpula, M. Macias-Fauria, A. Skarin, M. Verdonen, T. Mikhailova, & B.C. Forbes . . . 1223

Permafrost Research Priorities, a roadmap for the future of permafrost research
H. Lantuit, M. Allard, M. Guglielmin, M. Johansson, G. Kraev, M. Krautblatter, G. Krinner, E. Schuur, Y. Sjöberg, J. Baeseman, & K.Schollän . . . 1224

Geocryological investigations in Louise Arner Boyd's 1933 and 1937 American Geographical Society Expeditions to East Greenland
F.E. Nelson & R.D. Lukens . . . 1225

Traditional and urban-industrial impacts on permafrost change
K.E. Nyland, N.I. Shiklomanov, F.E. Nelson, A.E. Klene, & D.A. Streletskiy . . . 1227

Evaluation of anthropogenic impacts on the thermal state of landscapes in Central Yakutia
P.N. Skryabin, S.P. Varlamov, & A.N. Fedorov . . . 1229

A study of the bottom variety of the cultural layer in urban landscapes of Yakutsk
I.I. Syromyatnikov & V. Kunitskiy . . . 1230

Alexander Theodor von Middendorff and permafrost study in the Russian empire in the second half of the 19^{th} century
E. Tammiksaar . . . 1232

Rapid Arctic Transitions due to Infrastructure and Climate (RATIC): An ICARP III initiative focusing on the cumulative effects of Arctic infrastructure and climate change
D.A. Walker, J. Peirce, T. Kumpula, M.O. Leibman, G. Matyshak, D. Streletskiy, M.K. Raynolds, Y.S. Shur, M. Kanevskiy, M. Buchhorn, G. Kofinas, K. Ambrosius, H.E. Epstein, V.E. Romanovsky, B.C. Forbes, A. Khomutov, O. Khitun, N. Shiklomanov, V. Grebenets, M. Lemay, M. Allard, W. Vincent, S. Lamoureux, T. Bell, D. Forbes, G. Fondahl, E. Kuznetsova, L.-P. Roy, A. Petrov, & P. Schweitzer . . . 1234

32 **Permafrost Education and Outreach: Students, Communities, and the World** 1237

A Frozen-Ground Cartoon: Explaining international permafrost research using comic strips
F. Bouchard, B. Deshpande, M. Fritz, J. Malenfant-Lepage, A. Nieuwendam, M. Paquette, A. Rudy, M. Siewert, Y. Sjöberg, A.Veillette, & J. Harbor . . . 1238

Hot times in cold places: Taking permafrost educational programs on the road
M.H. Cysewski, M. Sturm, L. Carsten-Conner, V. Coats, & A. Larson . . . 1239

Secrets in Ice: Interdisciplinary Summer Permafrost Science Education for Middle School and High School Students
R.A. Finger & M. Cysewski . . . 1243

The experience of the international field student courses on permafrost in northern Siberia
V.I. Grebenets, D.A. Streletskiy, N.I. Shiklomanov, K.E. Nyland, A.N. Kurchatova, A.V. Boycov, E.-M. Pfeiffer, A.E. Klene, & A.G. Kerimov . . . 1244

Frost depth outreach program in Japan
K. Harada, K. Yoshikawa, G. Iwahana, J. Stanilovskaya, & Y. Sawada . . . 1246

PermaModel new online tool on permafrost modeling
E. Jafarov, K. Schaefer, & L. Yarmey . . . 1247

Tandems 2 win
M. Kallfelz 1248

Permafrost as a topic in German schools
R. Lehmann 1249

The future of permafrost research: A contribution from early career researchers to ICARP III and beyond
A. Morgenstern, M. Fritz, B. Deshpande, F. Bouchard, E. Högström, J. Malenfant-Lepage, A. Nieuwendam, M. Oliva, M. Paquette, A. Rudy, M. Siewert, Y. Sjoberg, & S. Weege 1250

The International Permafrost Association: Current initiatives for cryospheric research
K. Schollaen, A.G. Lewkowicz, H.H. Christiansen, V.E. Romanovsky, H. Lantuit, L. Schrott, D. Sergeev, & M. Wei 1253

Field education in discontinuous permafrost region, Igarka Geocryology Lab
N. Tananaev, E. Makarycheva, A. Litovko, & D. Sergeev 1254

New approaches in climate science communication: an example from the field of permafrost research
R. Treffeisen, J. Borm, K. Grosfeld, P. Lemke, & R. Teigler 1256

Catching permafrost in the Zwickau classroom
M. Weidlich, L. Schirrmeister, & G. Schwamborn 1258

Author Index 1260

Plenary Session

Session Chair:

Vladimir E. Romanovsky, *University of Alaska Fairbanks, United States of America*

From 1D to 4D – recent developments in mountain permafrost research

Isabelle Gärtner-Roer

University of Zurich, Switzerland

Recent developments in mountain permafrost research can be approached at different levels or 'dimensions' and clearly indicate achievements as well as upcoming challenges.

The number of high-resolution data at single points (1D) has increased and delivers valuable data such as temperatures (underground, surface) or deformation (underground, surface), approving the occurrence of permafrost in many mountain areas. Very recently, the oldest rockglacier borehole at Murtél, Switzerland (running since 1987) was complemented by a new borehole to guarantee continuity (longterm monitoring) at this specific site. The 1D information can be used to prove the spatial extent of permafrost occurrence (2D) by mapping or modelling approaches. The availability of high resolution remote sensing data sets has improved for many mountain regions and builds an important base for mapping and modelling on different scales. Recently a first comprehensive map of permafrost distribution in the Himalaya was published. With the third dimension, the topography and the characteristics for mountains by definition (altitude, relief, steep slopes) become more important. In mountain areas, topographic as well as climatic parameters vary significantly within short distance and influence the energy balance very locally. Related geomorphological processes and landforms (e.g. rockglaciers) are highly dependent on these local conditions. The fourth dimension includes the changes in time, giving insight in ongoing processes of permafrost degradation or aggradation, as observable at single points (1D), over larger areas (2D) and entire landforms (3D). This dimension is relevant in observational time scales, but also in retrospective (palaeopermafrost evolution) and anticipatory (future evolution) modelling approaches.

With the increasing number of long-term information and high-resolution data on permafrost occurrence, thickness, temperature and dynamics in high mountain areas, the current changes become more and more respected and result in an improved process understanding. Geomorphic processes such as rock falls, detachment slides as well as rockglacier acceleration and destabilization indicate reactions to changes in the thermo-hydrological regime and hence demonstrate the sensitivity of mountain systems to recent climatic changes. Related impacts of degrading or vanishing permafrost affect human societies directly and indirectly from very local to global scales, from mountain regions down to the foothills and lowlands.

Livelihoods on frozen ground: Why permafrost matters to indigenous communities in Siberia and elsewhere

Joachim Otto Habeck

Universität Hamburg, Germany

Over the last years, scientific research and media coverage about the risks and consequences of permafrost degradation have been increasing. In particular, indigenous peoples in subarctic regions are considered to face serious difficulties in adapting to rapid environmental change. What has rarely been discussed, however, is the fact that pastoralism and other forms of renewable resource use in northern Eurasia had to grapple with rapid change in earlier periods too. This presentation will illustrate how past permafrost degradation has facilitated (rather than impeded) particular forms of Northern pastoralism. It also discusses the extent to which indigenous groups have exerted anthropogenic changes in permafrost-based landscapes. Finally, this keynote will sketch out how indigenous communities in different parts of northern Eurasia may be able to cope with and respond to future permafrost degradation.

The Wiley-Blackwell Permafrost and Periglacial Processes Award Lecture
Permafrost-Ecosystem Interactions

Mark Torre Jorgenson

Alaska Ecoscience, United States of America

Ecological processes affect permafrost aggradation and degradation by altering boundary-layer conditions, and in turn, changing permafrost conditions affect ecological development. The nature and distribution of permafrost can be conceptualized as a function of interacting state factors, such as climate, geology, topography, hydrology, soils, vegetation, disturbance and time, following Jenny's state-factor approach. To assess the effects of these ecological components on permafrost distribution, soil thermal regimes, and ground ice characteristics, we have explored five general approaches involving disturbance and experimental manipulations, integrated-terrain-unit classification, n-factors, chronosequence sampling at the landscape scale, and multivariate analysis of effects of landscape components on permafrost distribution at the region scale. Natural and human disturbance, as well as experiments involving canopy and ground cover removal, provide controlled conditions for assessing the sometimes dramatic effects of changing vegetation and soil conditions on permafrost stability under uniform climatic conditions. The terrain-unit approach has long been effective at relating the abundance and morphology of ground ice to surficial geology, and to a lesser extent to topography and vegetation. N-factors have been used as a simple integrator of the effects of ecological conditions on soil thermal regimes, and multiple-regression analyses have found topography, vegetation structure, snow depth, and soil organic thickness to be significant factors affecting soil temperatures. Sampling along chrono-sequences in landscapes with ecosystems in varying stages of successional development after disturbance, such as river channel migration, lake drainage, or fire, has shown that soil temperatures and ground ice are closely related to ecological changes that have occurred over periods of decades to millennium, and that ground-ice aggradation modifies the surface, causing feedbacks that lead to soil and vegetation changes. Disturbance related to fires and human activity, as well as climate change, can initiate permafrost degradation and loss of ground ice that leads to nearly complete reorganization of ecosystem patterns and processes. Immediately upon thawing, hydrologic shifts either through subsurface drainage in thaw-stable, course-grained soils, or from water impounding in collapsing depressions, to greatly alter vegetation and soil processes. Nutrient release, vegetation growth, and organic soil accumulation can lead to permafrost stabilization and recovery within decades to centuries. Finally, regression-tree analyses of large regional ground and remote sensing datasets have revealed nonlinear relationships among the state factors to control permafrost distribution. Overall, these permafrost-ecosystem interactions allow permafrost to degrade at mean annual air temperatures (MAAT) of −16 °C in the high Arctic and to persist at MAATs of 2 °C in boreal forests, greatly complicating our ability to predict the effects of climate change on permafrost.

Adaptation of transportation infrastructure built on degrading permafrost

Fujun Niu

Cold and Arid Regions Environmental and Engineering Research Institute, Chinese Academy of Sciences, People's Republic of China

During the second half of the 20^{th} century, the world has experienced a clear climate-warming trend. This warming is beginning to have significant impacts on infrastructures in perennial frost, permafrost, environments and it has already caused very expensive maintenance operations. Like most northern countries where permafrost is present, Canada, China and the United States of America have actively worked on the development of solutions to adapt the design of structures to degrading permafrost. This paper summarizes the key developments in the area of adaptation of transportation infrastructure to permafrost degradation associated with climate changes prevailing in the arctic. In this context, the paper presents a review of the permafrost degradation processes and their geotechnical impacts. It also describes the recent developments of technical and operational solutions, in order to recommend realistic adaptation scenarios, which will assure safe transportation services for the next 15 years.

All fall down? Urban infrastructure and permafrost in the Russian Arctic

Nikolay Shiklomanov

The George Washington University, United States of America

Planned socio-economic development during the Soviet period promoted migration into the Arctic and work force consolidation in urbanized settlements to support mineral resources extraction and transportation industries. These policies have resulted in very high level of urbanization in the Soviet Arctic. Despite the mass migration from the northern regions during the 1990s following the collapse of the Soviet Union and the diminishing government support, the Russian Arctic population remains predominantly urban. In five Russian Administrative regions underlined by permafrost and bordering the Arctic Ocean 66 to 82 % (depending on region) of the total population is living in Soviet-era urban communities. The political, economic and demographic changes in the Russian Arctic have coincided with climatic changes. One of the most significant impacts of climate change on arctic urban landscapes is the warming and degradation of permafrost, which negatively affects the structural integrity of buildings. There are numerous reports indicating an increase in urban infrastructure damage throughout Russian permafrost regions over the last two decades. In many instances it is difficult to differentiate between the effects of climate-induced permafrost changes and socioeconomic factors. However, while human-induced factors may or may not have contributed locally, climate change appears to be responsible for the broad patterns of the reported changes in infrastructure stability. This presentation provides a broad overview of urban development in Russian permafrost regions and focuses on potential changes in stability of Russian urban infrastructure built on permafrost in response to ongoing and future climatic changes.

Finding paths for future permafrost research

Ylva Sjöberg

Stockholm University, Sweden

How can we as a community identify the most pressing questions for permafrost research today? Inspired by the ICARPIII and SCAR Horizon Scan processes, IPA and CliC have joined forces to identify forward-looking permafrost research priorities through a community consultative process. The Permafrost Research Priorities (PRP) kicked off in 2014 with an on-line questionnaire open for permafrost researchers worldwide to submit their idea of the most pressing questions for permafrost research. In parallel to the PRP process, a similar project was launched among early-career permafrost researchers. As part of this effort, 71 questions were submitted from early career researchers in 15 countries. The ranking of these questions was made by 100 participants at an early-career workshop at the EUCOP in évora 2014 with the results published in The Cryosphere in 2015. The top five ranked research questions cover topics related to permafrost and landscape dynamics, the use of traditional knowledge, modeling, engineering, and ground ice. For the PRP, more than 600 questions were submitted by the community and these have now been processed by the PRP core group members to remove overlaps and questions not meeting the stated criteria. The top ranked questions from the early career parallel imitative were also included in this process. In a next step, the community will be asked to vote for their favorites among the submitted questions for a range of research themes. This will result in a ranking of research questions in each permafrost research theme, which will be presented as a short publication listing and putting into context research priorities. The document will be targeting policy-makers and funding agencies and is planned to become the benchmark against which permafrost research will be gauged in the near future.

Predicting thermokarst: detecting hot spot changes in ecosystems, fate of permafrost carbon, and infrastructure vulnerability

Merritt R. Turetsky

University of Guelph, Canada

While permafrost thaw can occur through the gradual deepening of the seasonally thawed layer, thermokarst development in some landscapes occurs rapidly and typically affects the entire soil profile. Thermokarst exposes previously-frozen carbon to microbial processes but also has dramatic consequences for vegetation, hydrology, and infrastructure due to subsidence and landscape change. With the goal of improving detection of thermokarst vulnerability at large scales, we developed a spatial modelling framework that assesses whether areas are predisposed to thermokarst or thermal erosion. The framework weighs the perceived relative importance of ground ice content, overburden thickness, permafrost zonation, terrestrial ecoregion, topographical roughness, and regional histel cover to the formation of wetland thermokarst features, thaw lakes, and hillslope features (retrogressive thaw slumps, active layer detachments, erosional gullies). Considering these multiple trajectories of change, approximately 20 % of the northern permafrost domain is vulnerable to thermokarst formation.

One application of this predisposition modeling is to better understand the relevance of hot spot processes like thermokarst to the overall permafrost carbon feedback. Carbon release from permafrost thaw and the microbial decomposition of previously frozen organic matter is considered one of the most likely positive feedbacks from terrestrial ecosystems to the climate system in a warmer world. While areas vulnerable to thermokarst tend to store a disproportionate amount of the total permafrost domain soil carbon, predicting the fate of this carbon requires an understanding of whether saturated conditions post-thaw will slow rates of microbial mineralization. Wetland thermokarst and the formation of collapse scar bogs and fens results in large losses of carbon to the atmosphere. This work shows that while thermokarst processes affect small portions of the landscape, they lead to carbon losses equivalent to those associated with more widespread active layer deepening. Ongoing efforts are focusing on how to use the thermokarst predisposition modeling in smaller scale applications to support infrastructure decisions in Alaska and the Northwest Territories, Canada.

Carbon fluxes of inland and coastal waters in permafrost regions

Jorien Elisabeth Vonk

VU University, The Netherlands

Circum-arctic frozen soils contain twice as much organic carbon as is currently present as greenhouse gases in the atmosphere. When permafrost thaws, the soil organic carbon within it becomes available for remobilization and introduction into inland and coastal aquatic systems. Here it can either be degraded, generating greenhouse gases, or be transported and buried in short and long-term reservoirs, attenuating greenhouse gas emissions. Here I present an overview of our current knowledge on riverine and coastal organic carbon fluxes in permafrost regions. I will also discuss the factors that determine the release and degradability of this carbon (i.e. potential greenhouse gas production), and will discuss how we expect this to change in the future.

Reconstructing paleoenvironments from environmental DNA

Eske Willerslev

Centre for GeoGenetics, Denmark

Reconstructing past ecosystems are traditionally done from pollen records and macrofossils. However, such approaches suffer from long distance dispersals, different preservation across taxa, and poor taxonomic resolution. In 2003 we discovered that DNA from higher plants and animals can be obtained directly from ancient sediments (permafrost and temperate soil) even in the absence of macrofossils and can be used as an efficient mean to reconstruct plant and animal life of the past. Since then we have explored how ancient environmental DNA can be used to reconstruct paleoenvironments using permafrost, contemporary sediments, lake cores and ice core. We have also tested the reliability of the approach on modern settings like surface soil, lakes, rivers, and sea water. In this talk I will provide an overview of the limitations and possibilities of environmental DNA and provide a number of examples where we have used environmental DNA for hypotheses driven research.

SESSION 1

Periglacial Geomorphology
(co-organized by the International Association of Geomorphologists IAG)

Convener:

Lothar Schrott, *University of Bonn, Germany*

Julian Murton, *University of Sussex, United Kingdom*

Florence Magnin, *Université de Savoie, France*

This session highlights the importance of periglacial and permafrost processes and landforms. In high-latitude and high-altitude environments intensive frost action produces a variety of periglacial phenomena, including weathering, mass movement, fluvial, aeolian, coastal and paraglacial features. Such periglacial processes and resulting geomorphologic changes play also an important role in the global warming debate. Major challenges are to understand the sensitivity of periglacial landforms and to address specific scientific values in relation to their societal relevance. Furthermore, periglacial geomorphology should maintain a bridging position between geomorphology, geocryology, Quaternary and engineering studies. We invite studies focusing on conceptual, empirical, experimental, and modeling approaches covering all spatial and temporal scales in periglacial and permafrost regions.

Landscape evolution triggered by polycyclic thermokarst on Herschel Island, Yukon Territory

Michael Angelopoulos[1], Wayne Pollard[2], Michael Krautblatter[4], & Hugues Lantuit[3]

[1] *Golder Associates, Montreal, Canada, Department of Geography, McGill University, Montreal, Canada*
[2] *Department of Geography, McGill University, Montreal, Canada*
[3] *Alfred Wegener Institute for Polar and Marine Research, Potsdam, Germany*
[4] *Technical University of Munich, Munich, Germany*

Retrogressive thaw slumps are a common thermokarst landform in areas of ice-rich continuous permafrost characterized by large massive ground ice bodies, often several metres thick and hundreds of metres in extent. These features can retreat inland by as much as 15 – 20 metres annually (Fig. 1) and are thus one of the most important carbon sources along Arctic coastlines. In locations like Herschel Island and the Yukon Coastal Plain, there are numerous active and stabilized thaw slumps (e.g. Lantuit and Pollard [2008]). In many cases, the new slumps form in the floor of a stabilized slump, leading to polycyclic thermokarst behaviour. Previous periods of thermokarst and retrogressive thaw slump activity can be identified morphologically and stratigraphically, as well as through changes in vegetation patterns (e.g. Cray and Pollard [2015]).

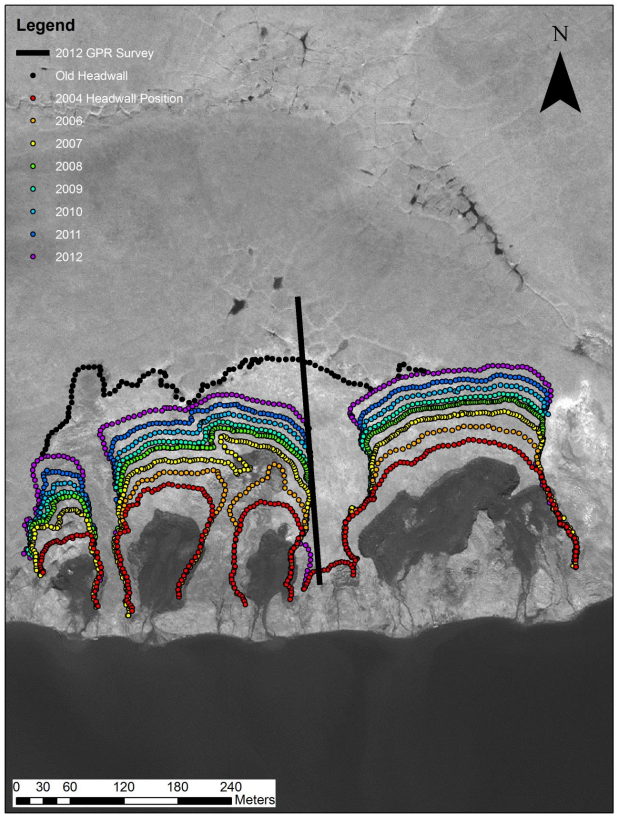

Figure 1: The retreat of polycyclic thaw slumps in the Thetis Bay region of Herschel Island from 2004-2012 superimposed on a 2001 IKONOS satellite image.

Former slumps are usually marked by open vegetated depressions with a well-defined (low) head scarp that faces downslope. The headwall of an active slump provides natural permafrost exposures from which considerable cryostratigraphic information can be obtained. In the case of a polycyclic retrogressive thaw slump, the previous cycle of thermokarst is marked by a well-defined thaw unconformity and truncated structures (e.g. ice wedges) overlain by massive debris flow deposits containing blocks of organic material. However, the polycyclic nature of slumps and how one episode may impact another are not fully understood. The objectives of this project are to:

1. visualize 3D landscape evolution changes related to polycyclic thermokarst for multiple slumps on Herschel Island from 2004 to 2013
2. investigate and compare the polycyclic thermokarst behaviour between the slumps using a combination of cryostratigraphic, ground-penetrating radar, electrical resistivity, and biogeographic datasets of vegetation succession following disturbance [Cray and Pollard, 2015].

The landscape evolution models are generated by comparing the annual headwall positions of the slumps (2004 – 2013) recorded using differential GPS to a LIDAR base image captured in 2013. The ground-penetrating radar and electrical resistivity surveys highlight the geomorphic details of a former slump's transition from an active to stabilized state, as well as provide insight into the thickness and extent of the debris flow deposits and ground ice units for different episodes of polycyclic thermokarst.

References

Cray, H.A. and Pollard, W.H. [2015] Vegetation recovery patterns following permafrost disturbance in a Low Arctic setting: case study of Herschel Island, Yukon, Canada. *Arctic, Antarctic, and Alpine Research*, 47(1):99–113, 2015.

Lantuit, H. and Pollard, W.H. [2008] Fifty years of coastal erosion and retrogressive thaw slump activity on Herschel Island, Southern Beaufort Sea, Yukon Territory, Canada. *Geomorphology*, 95(1): 84–102.

Late Pleistocene and Holocene topography evolution of the northern part of the Yamal and Gydan Peninsula, Russia

Alisa Vladislavovna Baranskaya

Lomonosov Moscow State University, Russian Federation

The northernmost part of Yamal and Gydan Peninsula is the heart of the central Russian Arctic. Studying the geomorphology and Quaternary geology of this region, as well as correlation with the neighbouring regions allows to reconstruct the evolution of topography in the Arctic during the Quaternary and to reveal the timing of the main palaeogeographic events. In spite of the long-term investigations which have been conducted during almost a century, many questions of the Pleistocene-Holocene history of the Western Siberia remain subjects to discussions. Researchers disagree on the presence and timing of glacial events in the Siberian Arctic, the altitude and sequence of marine transgressions, genesis of ground ice, etc. Even the most recent geologic times (Late Pleistocene-Holocene) leave a lot of questions open; one of them is the last marine transgression, its height and timing in the north of Yamal: some researchers [Astakhov and Nazarov, 2010] argue that the last transgression within Yamal and Gydan happened not later than the Kazantsevo time (MIS 5a); others [Bolshiyanov et al., 2008] suggest the presence of one or several Holocene transgressions in the whole Russian Arctic. Studying the Late Pleistocene and Holocene deposits of the low and medium terraces of the northern part of Yamal and Gydan can provide an insight into the history of the topography evolution of the region, giving an answer to these questions.

To investigate the least studied remote areas on the coasts of Yamal and Gydan, fieldwork was conducted during the expeditions 'Yamal-Arctic-2012, 2013' on Beliy Island and on Yavay Peninsula (Fig. 1). The objective was to describe and sample the youngest marine sediments in these key areas. Another goal was to determine when the lowlands of Beliy Island and Yavay Peninsula rose above sea level, and their stage of terrestrial development started.

The topography of Beliy island is relatively flat. Most of it is occupied by a low (4 – 6 m on the east, 2 – 3 m on the west) marine terrace reworked by aeolian processes. In the lowest parts of the island, swampy low laidas (1 – 2 m high) prevail.

In the coastal outcrop on the eastern side of Beliy Island, it can be seen that the section of the 4 – 6 m low terrace contains two units. In the lower part, up to the height of 1.5 – 2 m, bluish clays and loams outcrop. They are interbedded with sandy layers with flaser, lens-like and undulated lamination containing peat. The lamination, the presence of thin (1 – 4 cm) layers of peat, together with the alternation of clayey, loamy and sandy layers, allows to suggest that these are the sediments of a shallow sea, deposited in lagoons and on the littoral or laida, which was often flooded by this shallow sea.

The upper part of the section consists of dark yellow aeolian sands with lenses of embryonic palaeosoils up to 5 – 10 cm long. It is divided from the lower part by layers of peat of 10 – 20 cm thickness with occasional driftwood. The aeolian sands have probably been accumulating since the time when Beliy Island rose above sea level. The presence of peats indicates relatively warm conditions at the beginning of this time; however, after the peats were formed, severe conditions similar to the modern ones, were established.

Radiocarbon dating of the peat and driftwood between the two units provided the age between 35 and 36 radiocarbon years BP. Therefore, the latest marine sediments on Beliy Island are older than 35 – 36 ^{14}C kA BP, and the island rose above sea level at least in the third stage of the Late Pleistocene during the MIS 3. In the western part of Beliy island, the level of the surface is lower (2 – 3 m), and the border between the two units lies below the modern sea level. In the small coastal cliffs, only the upper, aeolian part of the section outcrops.

Yavay Peninsula is situated to the east of Beliy Island and is the northernmost tip of Gydan Peninsula. The surface of the terrace on Yavay Peninsula is more elevated (10 – 15 m); it is cut by thermoerosional gullies and small creeks. A large 10-km long coastal outcrop near Tirebiato Lake was studied.

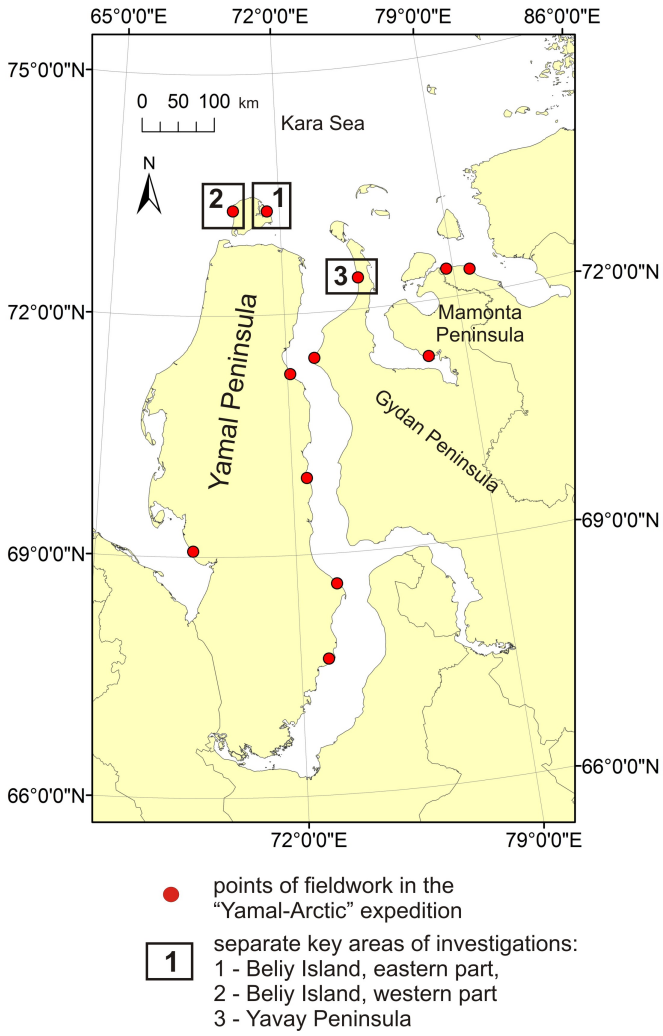

Figure 1: Points of fieldwork in Yamal and Gydan Peninsula

It is similar to the section of Beliy Island in many ways: up to 3 – 7 m a.s.l. within the sections on the south, deposits of marine (or, less probably, lacustrine) origin represented by loam and sand with flaser lamination, are observed. The sands often contain driftwood and small wood debris. Above this layer, sandy loams and fine-grained sands with parallel horizontal lamination outcrop. This parallel lamination, well extended along the strike, is occasionally disturbed by pseudomorphs formed in place of thawed ice wedges. Within this layer, thick lenses of peat (up to 1 – 2 m) are encountered; sometimes, they are situated at the bottom of the layer. Their radiocarbon dating provided ^{14}C ages between 24 and 30 kA BP. The layer of sandy loams with parallel lamination is supposed to have continental origin, most probably, aeolian. Therefore, at Yavay Peninsula, the transition from marine conditions to terrestrial ones happened not later than 30 kA BP (radiocarbon age), i.e. not later than MIS 3, similar to Beliy Island. The elevation of the lower, marine, sediments on Yavay Peninsula doesn't exceed 6 – 7 m above the modern sea level.

In other points of fieldwork to the south of Yavay and Beliy Island, no marine deposits of MIS3 age or younger were found. Older deformed marine sediments, corresponding to the Nyamsinskaya and Payutinskaya suites (MIS 5e) or Zverevskaya suite (MIS 5a) [Astakhov and Nazarov, 2010] and the glacial sediments supposedly attributed to MIS 4 are overlain by sands, sandy loams and loams of continental origin with peat, remnants of plants and bones of large mammals of the Late Pleistocene. No marine sediments of MIS3 or younger were described.

Therefore it has been established that, in the northernmost part of Yamal and Gydan the last marine transgression happened earlier than 30 – 37 kA BP, and the sea level was not higher than 6 – 7 m than the modern one for Yavay Peninsula, and even less (2 m) for Beliy Island. Such difference in the level of this shallow basin, together with the difference of the limit between marine and terrestrial sediments on both sides of Beliy Island, give evidence of small rate differentiated vertical block movements of the Earth's crust in this region, generally considered as tectonically stable. After this marine transgression, the topography was formed under the conditions

Fieldwork was executed in expeditions 'Yamal-Arctic-2012,2013' with the help of the RIF 'Yamal' and the Government of the Yamal-Nenets region. The reported study was funded by RFBR according to the research project No. 16-35-00453 мол_а.

References

Astakhov, V.I. and Nazarov, D.V. [2010] Stratigraphy of the upper Neopleistocene of the north of Western Siberia and its geochronometric determination. *Regionalnaya Geologiya i Metallogeniya*, (43):36–47. in Russian.

Bolshiyanov, D. Ju.; Makarov, A.S.; Gusev, E.A. and Schneider, W. [2008] The problems of origin of the Ice Complex and the existence of 'Sannikov Land' in the Laptev Sea in the past. *Problemy Arktiki i Antarktiki*, 78(1):151–160. in Russian.

Assessing the genesis of periglacial ramparted depressions (PRDs) by characterising internal structures macroscopically and microscopically

Samantha Susan Bromfield

University of Brighton, UK

Perennial frost mounds developed across northern Europe (>10 ka BP) following retreat of the Late Quaternary ice sheets. Their relict forms comprise depressions with surrounding ramparts (Periglacial Ramparted Depressions - PRDs). Although PRD surface geometry is well-documented, their genetic origin is less well-understood. In addition, relict PRDs are sometimes difficult to identify because they are geomorphologically similar to features formed by non-frost processes (e.g. solution hollows, iceberg gravity craters etc.). Various methods have been used to examine PRDs in the U.K. including macroscopic sedimentological analysis, geomorphological mapping, Electrical Resistivity Tomography (ERT) surveys, Ground Penetrating Radar (GPR) and seismic refraction surveys. However, there is still little agreement on:

- definitive identification of PRDs,
- PRD formation processes,
- the relationship between different frost mound types (e.g. pingo, palsa and lithalsa).

This research characterises PRDs by examining their internal structures at macro- (e.g. coring, logging) and micro-scales (thin sections) and contextualising this data with geomorphic mapping and remotely sensed data. Micromorphology is an innovative and original approach for characterising PRDs because frost processes create distinctive and resilient micro-scale features indicative of sediment deformation processes and environmental setting.

Internal sediment textures and structures at the micro-scale provide additional and detailed insights into sediment 'architecture', kinematics, deformation conditions, depositional and post-depositional processes, where macroscopic sediments cannot [van der Meer and Menzies, 2011]. The micromorphological approach adopted in this research examines the vertical profile of PRD ramparts to determine diagnostic suites of microstructures, particularly deformation structures, in different sediment types and thus grain size. This approach

i identifies the internal structure of PRDs,

ii considers the potential for change in deformation with depth within the rampart, and

iii considers the differences and similarities in micro-textures and structures in a variety of grain sizes across the sites where PRDs occur [van der Meer, 1993, Linch and van der Meer, 2014].

Further analysis will:

- provide a better understanding of the genesis of PRDs, potentially enabling classification of different types of ice-cored hills,
- inform palaeoenvironmental reconstruction, since ice-cored hills are diagnostic of former permafrost (frozen ground conditions),
- inform civil engineering projects where sediments are disturbed by PRD development (e.g. heave and subsidence).

Field sites include

1. Cledlyn Valley, west Wales;
2. Walton Common, Norfolk and
3. the Ardennes (Belgium-German border),
4. Temple Mills, the London Basin and
5. Damerham, the Wiltshire Basin.

Analysis confirms that despite differences in environmental setting, suites of deformation micro-structures can be identified in thin section indicative of PRD formation and/or collapse processes. By relating findings to sedimentological signatures observed at the macro-scale for currently decaying and relict frost mounds, as well as anticipated features at the micro-scale (based on field observations and evidence from previous investigations), it is possible to

i confirm the cryogenic origins of these landforms,

ii identify the prevailing stress regimes contributing to PRD growth and or decay and

iii consider characteristics common to all PRDs or diagnostic of specific PRDs e.g. pingo, lithalsa.

For example, rotational features (turbates etc.) and crude stratification are indicative of debris flow deposits found in collapsed ramparts. Consequently, this research identifies and characterises PRDs, which is particularly useful where surface features (e.g. ramparts) are missing due to burial or decay.

References

Linch, L.D. and van der Meer, J.J. [2014] Micromorphology of ice keel scour in pebbly sandy mud and fine-grained sands: Scarborough Bluffs, Ontario, Canada. *Sedimentology*, 62(1):110–129.

van der Meer, J.J.M. [1993] Microscopic evidence of subglacial deformation. *Quaternary Science Reviews*, 12(7):553–587.

van der Meer, J.J.M. and Menzies, J. [2011] The micromorphology of unconsolidated sediments. *Sedimentary Geology*, 238(3):213–232.

Holocene landscape and permafrost history based on geomorphology and cryostratigraphy in the Zackenberg valley, NE-Greenland

Stefanie Cable[1,2], Hanne H. Christiansen[2], Graham L. Gilbert[2,3], Christine Thiel[4,5], Aart Kroon[1], Andreas Westergaard-Nielsen[1], & Bo Elberling[1]

[1] *Center for Permafrost (CENPERM), Department of Geosciences and Natural Resource Management, University of Copenhagen, Øster Voldgade 10, 1350 Copenhagen, Denmark*
[2] *Arctic Geology Department, The University Centre in Svalbard, UNIS, P.O: Box 156, 9170 Longyearbyen, Norway*
[3] *Department of Earth Science, University of Bergen, Realfagbygget, Allegt. 41, 5007 Bergen, Norway*
[4] *Section S3: Geochronology and Isotope Hydrology, Leibniz Institute for Applied Geophysics, Hannover, Germany*
[5] *Nordic Laboratory for Luminescence Dating, Department of Geoscience, Aarhus University, Risø Campus, Roskilde, Denmark*

Permafrost degradation and aggradation in mountainous continuous permafrost landscapes is linked to geomorphological processes that determine the distribution of erosion and sedimentation. Assessing permafrost sensitivity, therefore, requires understanding the linkages between climate, the permafrost geocryological and geochemical conditions and the geomorphological dynamics in a landscape. Here, we combine geomorphological and geocryological investigations in the post-glacial landscape of the Zackenberg valley in NE-Greenland (74°N) to reconstruct the Holocene permafrost history. Detailed field and remote sensing based mapping in the 130 km^2 large study area was carried out during the summers of 2012 and 2013. In the eastern part of the valley, drilling of 13 boreholes to depths of up to 21 m was performed along a transect from the middle valley slope to the coast. In total, 10 shallow (1.8 – 4.6 m) and 3 deep (−14.5.0 m) frozen sediment cores were obtained from 11 sites covering three widespread landforms, solifluction sheets (2), different-size alluvial fans (7) and an exposed delta (4). The cores were analyzed with regard to cryostructures, ice-content, grain size distribution, carbon content, pore water electrical conductivity, and sediment age based on ^{14}C and OSL dating.

The geology of the valley creates a distinct geomorphological contrast between the eastern and western valley sides. The eastern valley side has sedimentary bedrock outcrops and periglacial landforms are widespread. The periglacial landforms develop on smoother slopes in more fine-grained allochthonous weathering material and lateral glacial moraines. Solifluction, debris flows, fluvial erosion, nivation and deflation are the most common processes on the upper and middle slope. These supply the lower slope with fine-grained sediment that accumulates on well-vegetated coalescing alluvial fans, which aggrade onto glacial landforms. The coastal lowlands are nowadays mostly cut-off from sediment supply due to river incision. Its relatively flat and stable surface exposes relict glacial, fluvial and deltaic landforms, locally overlain by a thin drape of aeolian or nival deposits. At the western valley side, in contrast, igneous and metamorphic bedrock is exposed and the slopes are overall steeper. The weathered bedrock and glacial deposits are coarser, often lacking a fine-grained matrix. The slopes show some solifluction, while debris cones and rock glaciers aggrade below free bedrock faces. In the lowlands, glacial moraines disintegrate in-situ creating an undulating surface. Additionally, the mapping area was classified into geomorphologically erosive, stable and aggrading areas, and a simplified surface stability map was created.

All permafrost cores contained high amounts of fine-grained frost-susceptible sediment. The ice content, however, differed between the slope and the delta. In ice-rich solifluction and alluvial deposits, lenticular and suspended cryostructures dominated. The excess ice content ranged between 15 – 54 %, on average, in the upper meter of permafrost. In alluvial deposits, alternating clastic and organic-rich sections have syngenetically aggraded during the past 9 ka. Sedimentation rates varied with time and among sites, from 0.1 to 5.1 m ka^{-1} reflecting shifts in drainage

patterns. The organic-rich sections, often 2-15 cm but up to 50 – 160 cm thick, had a total carbon content of up to 19.4%. The exposed delta, contrastingly, had low carbon contents and contained almost no excess ice; also no ice-rich transient layer was identified. The deltaic deposits were rapidly deposited onto glacial/glacio-fluvial deposits between 12.9 and 9.7 ka according to OSL-ages, and emerged due to relative sea-level fall. Thus, the permafrost is epigenetic, as is also indicated by an increasing solute-content with depth. By combining the cryostratigraphical data and ground ice estimates with the geomorphological map, a geocryological map of the estimated volumetric ice content in the upper permafrost was created.

We conclude that in the Zackenberg valley, the degree of post-glacial periglacial landscape transformation is highly linked to geological and hydrological conditions. High frost-susceptibility of the sediment and the high moisture availability on the gentler eastern slopes promotes periglacial processes leading to downslope sediment transport. Future thawing of the ice-rich upper permafrost on the slope could increase mass movement rates. The alluvial fans, covering 17 % of the mapping area, have been a sink for carbon throughout the Holocene due to continuous permafrost aggradation, also representing the largest permafrost carbon pool in the study area. Permafrost aggradation here seems to be less sensitive to climate variability and sediment yield than to snow conditions. Incoming melt-water from the entire slope seems promote aggradation of ice-rich permafrost both in times of high sedimentation, and during low sedimentation when vegetation establishes. Moreover, the high ice-content acts as thermal buffer against rapid permafrost degradation. In contrast, the emerged delta in the stable coastal lowlands is more sensitive to changes in the permafrost thermal regime where an ice-rich transient layer is absent and overall lower ice content and no or little sedimentation were detected. Increasing active-layer thickening at the delta may release solutes; however, the measured carbon contents were low. Relatively lower permafrost carbon and ice contents are also estimated for the coarsed-grained, well-drained, less vegetated western valley side.

The combination of detailed geomorphological and geocryological mapping with understanding landscape dynamics are important for understand permafrost dynamics. Moreover, this study offers relevant input data for permafrost modeling and helps identifying the significance of insights from other on-site ecological and carbon dynamics studies on-going in the Zackenberg area.

Rapid micro-scale weathering of glacially abraded basalts in SE Iceland

Maciej Dąbski

Faculty of Geography and Regional Studies, University of Warsaw, Poland

Abraded rocks, recently liberated from glacial ice, are subject to subaerial weathering leading to development of a weathering micro-relief and rock strength weakening. Recent studies of Dąbski [2014, 2015] and Dąbski and Tittenbrun [2013] showed rapid increase in levels of deterioration of basalts under cool temperate climatic conditions of SE Iceland.

The research area included sequences of moraines or abraded bedrocks spanning from the LIA glacier maxima to contemporary glacial termini of Hoffelsjökull, Fláajökull, Skálafellsjökull, and Virkisjökull which are developed in the Tertiary Basal Formation zone, older than 3.3 my, or within the Móberg Formation (a case of Virkisjökull), younger than 0.8 my. Chosen basaltic boulders found on moraines or basaltic whalebacks were dark-grey and fine-grained, hypocrystalline in places. Climate of the study area is cool temperate maritime with mean annual air temperature about 4.5 °C and mean annual precipitation, predominantly rain, between 1400 and 1800 mm. Snow cover is usually thin and fragmented, allowing for frequent but shallow freeze-thaw cycles. The cooling effect of the glaciers and katabatic winds decrease air temperature and influence duration of a snow cover. Frequent rains and strong winds facilitate wetting and drying of rock surfaces.

The electronic profilometer Handysurf E-35B was used to measure rock surface micro-roughness with micrometric precision. The measurements were performed parallel to visible striation in order to omit micro-erosional features on the run of the profilometer. On each dated test site thirty or forty-five measurements were done, each along a 4 mm profile. In the forelands of Hoffelsjökull, Fláajökull and Skálafellsjökull, the same rock surfaces were also tested with Schmidt hammer (N-type) and weathering rind thickness was measured. One hundred blows and thirty measurements of rind thickness per test site were performed. Optical as well as the scanning electron microscopy (SEM) with a microprobe were used to analyse rock texture and rock surface characteristics.

Initial rock surface deterioration and development of micro-relief in the proglacial environments occur relatively fast. Progressive development of micro-roughness of basaltic surfaces, expressed by increase in roughness parameters such as Ra, Rz and Rzmax, is visible on test sites deglaciated 80 to 100 years ago. For example, during this period average vertical distance between peaks and lows of the roughness profile (Rz) increased by 4.0 – 13.4 μm. Rock surfaces on older sites do not exhibit statistically significant progression of micro-roughness. Development of micro-relief in first 80 – 100 years after liberation from glacial ice is accompanied by a statistically significant increase in weathering rind (from 0.0 – 0.1 mm to 0.3 – 0.5 mm) and a decrease in Schmidt hammer R-values (from 67 – 65 to 64 – 61).

Within weathering rinds of rock samples taken from a site deglaciated hundred years ago numerous micro-fissures are seen between and within plagioclases, pyroxenes as well as different ferrous minerals (titanomagnetite, ilmenite). Surprisingly, some samples do not show signs of expected chemical weathering such oxidation or dissolution. Certain minerals, preferably plagioclases and pyroxenes, contain small sharp-edged voids or are shattered. Moreover, there is a characteristic orientation of micro-fissures parallel to the rock surface at depth of c. 20 μm. These features allow to infer micro-scale frost shattering leading to exfoliation and weakening of rock strength.

Due to abundance of abraded bedrock surfaces close to the margin of Skálafellsjökull it was possible to detect increase in micro-roughness parameters between the youngest test site (with no signs of wreathing discoloration), located just few meters away from the receding glacier margin, and the test site deglaciated 5 or 6 years earlier. Basalitc surfaces at the latter site were already oxidized and exhibited increase in micro-roughness parameters by 16 – 19 % and decrease by 1 unit in average R-values. Means, medians, maxima, minima as well as standard deviations of roughness parameters (Ra, Rz, Rzmax) increase in all of the studied glacier forelands within first 80 to 100 years since the onset of subaerial weathering. Progressive weathering is also registered by changes in Schmidt hammer R-values and weathering rind thickness.

References

Dąbski, M. [2014] Rock surface micro-roughness, Schmidt hammer rebound and weathering rind thickness within LIA Skálafellsjökull foreland, SE Iceland. *Polish Polar Research*, 35(1):99–114.

Dąbski, M. [2015] Application of the Handysurf E-35B electronic profilometr for the study of weathering micro-relief in glacial forelands in SE Iceland. *Acta Geologica Polonica*, 65(3):389–401.

Dąbski, M. and Tittenbrun, A. [2013] Time-dependant surface deterioration of glacially abraded basaltic boulders by Fláajökull, SE Iceland. *Jökull*, 63:55–70.

Seasonal variations of rock glacier creep: time series observations from the Western Swiss Alps

Reynald Delaloye & Benno Staub

University of Fribourg, Switzerland

The observed velocity of active rock glaciers, as well as other permafrost-related creep features (landslides), is changing from year to year in a relatively homogeneous and simultaneous way at the regional scale. The inter-annual changes may be large, exceeding sometimes 50 % of acceleration or deceleration in one year. They are often well congruent to changes in temperature of the creeping frozen ground particularly at the depth of the main shear horizon (> 15 m depth), except when a destabilization phase (dramatic change of velocity, opening of crevasses and/or scars) is occurring. Seasonal (intra-annual) variations of rock glacier surface velocity have also been observed and so far mainly attributed to the influence of hydrological (changing water content and/or pore pressure by snow melt or rain periods) and/or thermal factors (delayed response to seasonal changes of the ground surface temperature). This poster contribution aims at presenting and discussing results on the seasonal rhythm of creeping permafrost landforms based on observational data from the Western Swiss Alps.

Annual surface displacement rates have been measured by our group on about 30 active rock glaciers in the Swiss Alps for various monitoring purposes and since the early 2000s for the longest time series. On 8 rock glaciers, which are located in the Valais Alps (western Swiss Alps) and were moving between about 1 and 20 m a^{-1} in 2014/15, we dispose now of monitoring data which can be used to document and discuss seasonal variations of displacement rates. Considered seasonal time series are 2 to 10 years long, comprising at least 6 positions per year. They consist of either real-time kinematics GNSS measurements (10-year time series of the Becs-de-Bosson/Réchy rock glacier, 80 points surveyed 6 – 8 times per year), total station measurements (6-year time series for one point on the destabilized Grabengufer rock glacier) or permanent mono-frequency GNSS time series of hourly to monthly resolution depending on the site and the year (rock glaciers Becs-de-Bosson/Réchy, Tsavolires, Tsarmine, Gugla/Bielzug, Péterey, Tracuit, Jegi, Gruben). We investigate here the patterns (annual amplitude, type and time of changes, inter-annual regularities) of the seasonal variations of the observed velocities in order to detect possible responsible processes, especially a potential influence of the snow melt in early summer.

We can state on the basis of our observations that seasonal variations are occurring on all monitored rock glaciers. The seasonal velocity pattern roughly resembles a sinusoidal curve and is characteristic for each rock glacier or even for each rock glacier part. On all rock glaciers velocity minima were reached every year at the end of the winter (April-May) and acceleration occurred then during the snow melt season, with an onset between the end of April and the end of May (Fig. 1). The spring acceleration differed notably from a rock glacier to another, but not essentially from a year to the next one. It was either rapid and strong, or of medium intensity, or gentle. Moreover, the character of the spring acceleration did apparently not depend on the rock glacier velocity level. On most rock glaciers, velocity maxima were observed every year in autumn or early winter (September-December) and followed by a deceleration phase, which was often but not systematically stronger in the second half of the winter. The transition between the spring acceleration and the velocity maximum in autumn/early winter showed a large diversity among the different rock glaciers (Fig. 1). Some rock glaciers underwent an interim stagnation (e.g. Tsarmine) or deceleration (e.g. Becs-de-Bosson) in mid-summer after the snow melt period, whereas the velocities of other rock glaciers increased continuously until November (e.g. Grabengufer).

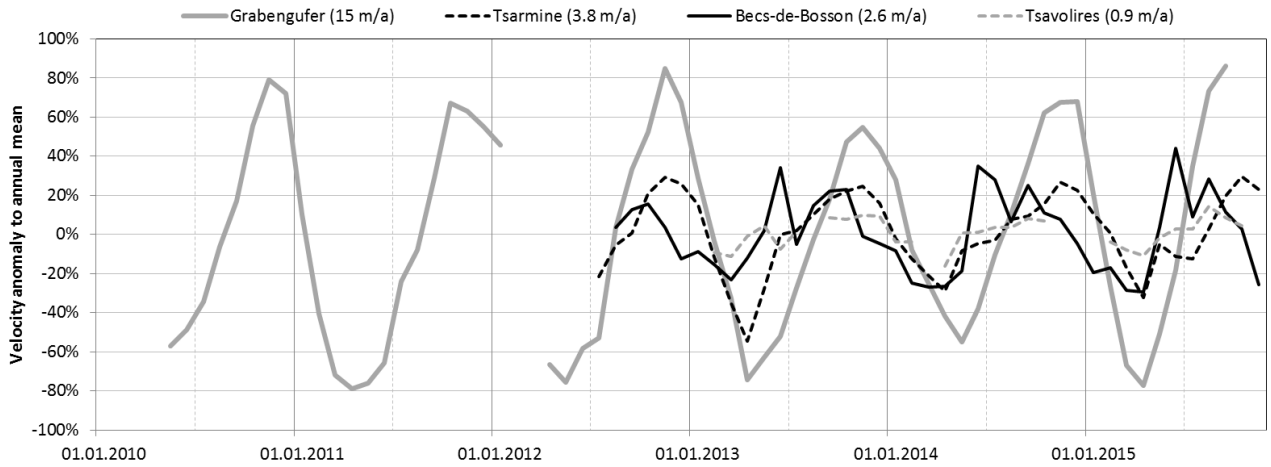

Figure 1: Various types of year-round surface velocity anomalies behavior observed at 4 rock glaciers in the Western Swiss Alps. Illustrated values are anomalies of the monthly velocity relative to the annual mean.

The behavior of the seasonal variations relatively to the annual mean velocity stayed almost similar over the years (rhythmic behavior), whereas the annual velocity amplitude varied strongly depending on the rock glacier (Fig. 1). The largest seasonal variations were observed on the extraordinary rapid Grabengufer rock glacier (1 : 9 ratio between minimal and maximal monthly values) and the smallest on the Tsavolires rock glacier (1 : 1.2). The longest time series measured on the Becs-de-Bosson rock glacier also showed that the intensity (amplitude) of the deceleration in winter time was depending on the intensity of the winter ground surface cooling (ground freezing index) and was usually following the behavior of the monthly mean surface temperature with a delay of 2 – 3 months.

The temporal regularity of the seasonal variations implies that the processes which control the kinematic behavior of the rock glaciers did not significantly change over the years, even though absolute creep velocities are in 2015 by factors (1.5 – 4) larger than during the slowest (and in the ground, coldest) period between 2005 and 2007. It appears that especially the wintertime may cause a significant inter-annual variability of the seasonal kinematic behavior, which nevertheless contributes only partly to observed changes in annual velocity. Significant summer acceleration phases have been occasionally observed on short term (a few hours to a few days, up to 30 cm total displacement) but only on steep, unstable and rapidly moving features. They were for most of them occurring in connection with strong rain events or intense snow melt phases and were obviously caused by the single movement of the boulder on which the GNSS device was installed or by movement affecting the active layer (or a part of it) in the surroundings. Significant behavior changes (from year to year) due to a possible influence of water (snow melt phase, rain events) have not been observed. Therefore, inter-annual variations in the water input during the summertime (including the snow melt phase) have not contributed significantly to the changes in annual velocities observed during the period of investigation.

In our point of view, two main questions are now rising up and require in-depth investigation:

1. the causes of the acceleration in spring, which are obviously connected to the snow melt, should be investigated at the process level;

2. the velocity maxima in late autumn/early winter and the effect of the ground cooling on the velocity decrease during winter time have to be explained.

For all these phenomena, seasonal temperature changes at the main shear horizon at > 15 m depth are certainly not the key controlling factor, because they may either not exist at all or occur with a timing which is different as those observed for the velocity changes.

Spatial and temporal snow cover variability and resulting thermal and mechanical response in a steep permafrost rock wall

Daniel Draebing[1], Anna Haberkorn[2,3], Michael Krautblatter[1], Robert Kenner[2], & Marcia Phillips[2]

[1] *Chair of Lanslide Research, Technische Universität München, Germany*
[2] *WSL Institute for Snow and Avalanche Research SLF, Switzerland*
[3] *Unit of Geography, University of Fribourg, Switzerland*

High-alpine rock walls generally have a highly structured micro-topography. The resulting highly variable temporal and spatial snow cover distribution is a key controlling factor of permafrost development and rock stability. We present the results of the German-Swiss project 'Influences of snow cover on thermal and mechanic processes in steep permafrost rock walls' (ISPR) derived on the Steintaelli rock wall, a NW to SE oriented ridge located between the Matter- and Turtmann valleys in the western Swiss Alps (3050–3150 m a.s.l.).

Based on an existing rock-ice-mechanical model, we developed a conceptual approach to explain the seasonal and long-term occurrence of permafrost-affected rock instabilities [Draebing et al., 2014]. To support the concept with data,

1. we combined remote sensing techniques such as terrestrial laser scanning and time-lapse cameras with near-surface rock temperature loggers and snow pits [Haberkorn et al., 2015] to estimate the spatial and temporal variation of snow cover distribution. Furthermore, we used
2. laboratory-calibrated seismic refraction tomography (SRT) [Krautblatter and Draebing, 2014] to monitor the thermal response of the rock wall and compared the SRT model to modelled rock temperatures using the 1D energy balance model SNOWPACK. This novel approach presents a cost-effective alternative to permafrost boreholes. To quantify the mechanical response,
3. we used continuous crackmeters for the monitoring of rock wall kinematics.

(1) Snow accumulation in steep rock walls depends on topographic factors such as aspect, slope angle, roughness and distance to ledges as well as meteorological factors such as wind and radiation. Our data demonstrate that snow accumulation evolves gradually upwards from flat terrain or ledges. Therefore, downslope areas are snow covered longer (8–9 months) than steep upslope areas (6 months). In addition, a snow cornice covered the ridge and only thinned at its edges. Snow ablation is controlled by net radiation and snow depth, thus, south-exposed rock walls ablate earlier. While snow distribution shows strong heterogeneity, distribution patterns are similar every year due to persisting micro-topographic and meteorological factors.

(2) The thermal regime is strongly controlled by the initial onset, depth and duration of snow cover. The SRT, as well as the rock temperature model show that ground cooling in downslope areas is prevented due to earlier onset of insulating snow. On the contrary, steeper upslope areas can cool efficiently due to delayed snow onset. Long-lasting snow cover prevents thawing in the rock, particularly on the NE slope. Early snow melt in steep rock sections enables deeper thaw depths, so the steep SW slope shows active layer thaw depths of over 10 m. The persistence of snow cover can change a cooling into a warming effect. The massive cornice on the ridge slows thawing to maximum 3.7 m in summer 2013, however, in summer 2014 active-layer thawed to maximum 5.8 m depth despite the existence of a thick snow cover.

(3) The mechanical regime responds to both snow cover and thermal regime. On the seasonal scale, the crackmeter data demonstrates that high-frequency thermal expansion and contraction occurs with highest magnitudes on the SW slope (up to 1 cm) during snow-free periods. Large temperature drops (−10 °C or below) may amplify thermal contraction by volumetric expansion (NE slope). In contrast, insulating snow enables ice segregation with highest crack opening magnitudes of 0.6 to 1.0 cm on the ridge. Despite this seasonal rock fracture oscillation, no persistent crack opening is observed. However, high-frequency high-magnitude thermal expansion and contraction

on the SW slope can lead to thermal stresses and thermal fatigue, reducing long-term rock stability.

References

Draebing, D.; Krautblatter, M. and Dikau, R. Interaction of thermal and mechanical processes in steep permafrost rock walls: A conceptual approach. *Geomorphology*, 226:226–235, 2014. doi:10.1016/j.geomorph.2014.08.009.

Haberkorn, A.; Hoelzle, M.; Phillips, M. and Kenner, R. Snow as a driving factor of rock surface temperatures in steep rough rock walls. *Cold Regions Science and Technology*, 118, 2015. doi:10.1016/j.coldregions.2015.06.013.

Krautblatter, M. and Draebing, D. Pseudo 3D – p-wave refraction seismic monitoring of permafrost in steep unstable bedrock. *Journal of Geophysical Research: Earth Surface*, 2014. doi:10.1002/2012jf002638.

Bridging periglacial geomorphology and ecology: a conceptual model of turf-banked solifluction lobe development

Jana Eichel[1], Daniel Draebing[1], Christian Eling[2], Lasse Klingbeil[3], Markus Wieland[3], Sebastian Schmidtlein[4], Heiner Kuhlmann[3], & Richard Dikau[1]

[1] *Department of Geography, University of Bonn, Germany*
[2] *Chair of Landslide Research, Technical University Munich, Germany*
[3] *Institute of Geodesy and Geoinformation, University of Bonn, Germany*
[4] *Department of Geography and Geoecology, Karlsruhe Institute of Technology, Germany*

Turf-banked solifluction lobes (TBLs) are widespread periglacial landforms in both high-latitude and high-altitude environments. Among soil texture, moisture, topography and climate, vegetation has been recognized as an important factor influencing solifluction processes and landform development. Vice versa, it has been shown that solifluction processes and landforms control vegetation patterns and properties. To understand these interactions becomes increasingly important in the context of global warming, as both solifluction and vegetation respond to rising temperatures. However, the role of vegetation for TBL development, and the reversed influence of TBL development for the lobe ecosystem, remains unclear. This gap between periglacial geomorphology and ecology can be bridged by biogeomorphology, which investigates feedbacks between geomorphic processes and vegetation. Recent biogeomorphic research suggested that TBLs are 'biogeomorphic structures', created to a significant extent by ecosystem engineering [Eichel et al., 2013, 2015]. In the ecosystem engineering processes, ecosystem engineers induce structural (e.g., geomorphometric), abiotic (e.g., thermal, material) and biotic changes (e.g., species composition) in their environments. In alpine environments, *Dryas octopetala L.* has been identified as ecosystem engineer and its role for the occurrence of solifluction processes has been stressed [Eichel et al., 2015]. Yet, the link between ecosystem engineering and the geomorphic and ecologic structure of TBLs is missing.

Here, our aim is to improve this understanding of TBL development and their geomorphic and ecologic properties by linking empirical results with biogeomorphic concepts. Based on an extensive geomorphic and ecologic survey at a TBL in the Turtmann glacier foreland (Switzerland), our objectives are to

1. identify the geomorphometric, material and vegetation properties, by which the TBL differs from its parent slope;
2. determine the geomorphic and ecologic properties of the lobe components;
3. develop a conceptual model of turf-banked solifluction lobe development through ecosystem engineering.

The field survey included an octocopter mission to derive a high resolution digital surface model (DSM) and orthophoto for terrain analysis, 2D and 3D Electric Resistivity Tomography (ERT) surveys of the TBL to identify material properties (soil texture, moisture), iButton temperature loggers (2014-2015), and a detailed geomorphic and vegetation mapping (1:50). In addition, the Normalized Difference Vegetation Index (NDVI) was derived from a multispectral image of the slope.

(1) Terrain analysis, geomorphic map, vegetation map, 2D ERT transects and NDVI calculation showed that the TBL differs from its parent slope in its geomorphometric (risers with higher slope gradient, tread with lower slope gradient), abiotic (finer soil texture, higher soil moisture at tread; coarse texture, low moisture at risers) and biotic (high vegetation cover, mostly *D. octopetala*) properties.

(2) The analysis of lobe elements (risers, tread, ridge) and their geomorphometric, abiotic and biotic properties reveals that high-gradient risers provide stable microhabitats with improved environmental conditions (e.g., less temperature fluctuation due to longer snow cover) for shrub species (e.g., *Salix hastata*). At the lobe tread, fine material with higher soil moisture is found below the dense *D. octopetala* mat, indicating the dominance of gelifluction movement, while a ridge-like feature at the origin of the

lobe tread is dominated by frost creep and mainly colonized by frost-tolerant *Silene exscapa*.

(3) Combining our results with knowledge from previous research, our conceptual model of turf-banked solifluction lobe development shows that feedbacks between engineer species and slope processes induce structural, abiotic and biotic changes on the parent slope. Through root stabilization and material accumulation, engineer species can initiate risers and promote their development, leading to a differentiation of slope gradient (riser, tread). The dense engineer cover at the tread reduces near-surface gelifluction movement due to root-derived increased shear strength, while accumulated fine material in the vegetation mat possesses a higher moisture storage capacity and favours a deeper movement. In addition, thermal differences between riser and tread occur due to a differential vegetation cover and snow distribution. These structural and abiotic changes lead to a vegetation differentiation on the lobe with shrubs colonizing the favourable microhabitats at the risers, while frost-adapted species colonize the ridge with active frost creep. As a consequence of these feedbacks, TBL lobe elements possess specific coupled geomorphic and ecologic properties, which need to be taken into account to understand TBLs and their future development.

Our conceptual model shows the importance of biogeomorphic approaches to periglacial environments. Furthermore, it highlights the need to integrate ecologic dynamics into solifluction research in order to understand biogeomorphic feedbacks and their role for solifluction movement and development.

References

Eichel, J.; Krautblatter, M.; Schmidtlein, S. and Dikau, R. [2013] Biogeomorphic interactions in the Turtmann glacier forefield, Switzerland. *Geomorphology*, 201:98–110.

Eichel, J.; Corenblit, D. and Dikau, R. [2015] Conditions for feedbacks between geomorphic and vegetation dynamics on lateral moraine slopes: a biogeomorphic feedback window. *Earth Surface Processes and Landforms*. doi:10.1002/esp.3859.

Cryo-conditioning of geomorphological processes in steep slopes

Bernd Etzelmüller, Sebastian Westermann, & Kristin S. Myhra

University of Oslo, Norway

The role of the ground thermal regime on geomorphological processes in settings associated to steep slopes has received little attention in the past. However, it is evident form recent studies that e.g. rock walls have a profound effect on the thermal regime in mountain sides, a.o. influencing glacier-permafrost interaction. Therefore, we introduced the concept of cryo-conditioning, which is Berthling and Etzelmuller [2011] defined as the 'interaction of cryotic surface and subsurface thermal regimes and geomorphic processes', and acts as a 'common control on processes, process interaction and landscape development'. The warming and degradation of mountain permafrost within alpine areas is an important process influencing the stability of steep slopes and rock faces. Further on, weathering processes and material transport is highly influenced by the thermal regime. The same is also valid for other environments, as e.g. coastal rock cliffs. This presentation conceptualize the importance of the thermal regime on geomorphological processes in steep slopes, and combines observations, measurements and numerical simulations using a 2D transient thermal model (CryoGRID 2D).

References

Berthling, I. and Etzelmuller, B. [2011] The concept of cryo-conditioning in landscape evolution. *Quaternary Research*, 75(2):378–384.

Topographical conditions and geomorphological distribution of rock glaciers and protalus lobes in Aran valley (Central Pyrenees)

Marcelo Vieira Fernandes, Luís Filipe Lopes, & Marc Franganillo Oliva

Instituto de Geografia e Ordenamento do Território – Univesidade de Lisboa, Portugal

In mid-latitude mountain regions such as the Pyrenees, rock glaciers and protalus lobes are the main indicators of permafrost conditions. The purpose of this contribution is to examine the spatial distribution of rock glaciers and protalus lobes in the Aran valley (Central Pyrenees). An accurate characterization of their topographic distribution and geomorphological setting will provide a better understanding of the environmental and climatic factors involved in the formation of these periglacial landforms.

The study area corresponds to the Aran valley, in the Central Pyrenees. The upper part of the Garona basin (550 km^2) shows a U-shaped glacial morphology with an orientation E-W. Annual precipitations range between 1200 and 1500 mm, with a mean annual temperature at 2270 m asl of 2.5 °C. Today, periglacial processes are active at elevations above 2300 – 2400 m.

The rock glaciers and protalus lobes existing in the Aran valley were mapped in a GIS environment through photointerpretation using high resolution imagery from the Cartographic and Geological Institute of Catalonia, the ESRI (Environmental Systems Research Institute) database and Google Earth pro 3D. Altimetry, aspect and slope gradient data of all landforms were obtained from the terrain model.

Up to 177 rock glaciers and 50 protalus lobes were identified in the area. Regarding the rock glaciers, most of them are distributed within the glacial cirques (74 %), with the rest located in valley bottoms and adjacent slopes. The fact that most of them are colonized by vegetation shows evidence of their inactivity pattern today. The southern tributary valleys of the Garonne river concentrate 81 % of all rock glaciers. They are distributed in a wide elevation range, between 1700 and 2800 m, and show an average size of 2.2 ha (between 0.2 and 23 ha). Up to 92 % of the rock glaciers are located in slopes between 10 to 30°, with 62% of them between 15 to 25°. They show a prevailing orientation to the north (35 %) and east (28 %).

Protalus lobes are always situated at the foot of slopes with high debris accumulation. Most of them are colonized by vegetation and landforms are degraded, showing signs of no activity today. Up to 71% of these landforms occur in the southern tributaries of Garonne. Protalus lobes occupy a mean surface of 1.5ha (between 0.1 and 6.5 ha) with an elevation range between 1900 and 2500 m. In general these landforms develop in slopes between 10 and 30°, mostly north (43 %) and east-exposed (18%).

The lowest elevation of rock glaciers suggests the altitudinal limit of local permafrost conditions in the area. However, this interpretation is not delineated by the distribution of protalus lobes, probably because of the low degree of preservation of these landforms. Ongoing geomorphological analysis of glacial and periglacial landforms in the area will provide the chronological framework for the formation of rock glaciers and protalus lobes in the Aran valley.

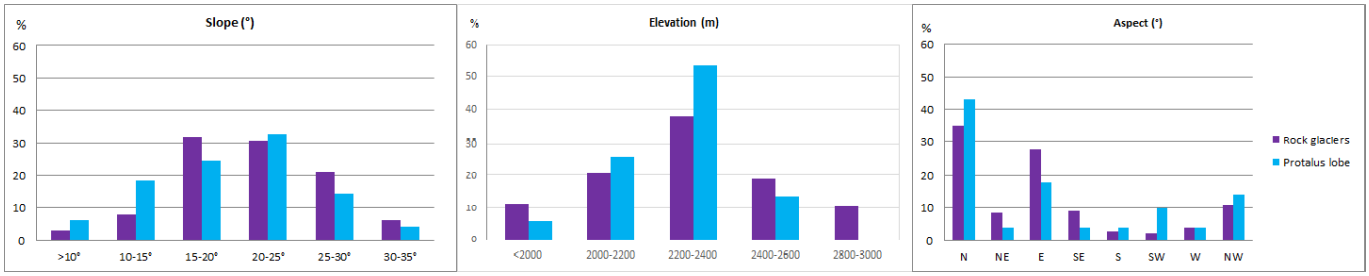

Figure 1: Topographical characterization of the distribution of rock glaciers and protalus lobes in the Aran valley.

Non-linearity of rockglacier flow law determined from geomorphological observations: A case study from the Murtèl rockglacier (Engadin, Switzerland)

Marcel Frehner[1], Dominik Amschwand[1], & Isabelle Gärtner-Roer[2]

[1] *Geological Institute, ETH Zurich, Switzerland*
[2] *Department of Geography, University of Zurich, Switzerland*

Rockglaciers are tongue-shaped permafrost landforms creeping downslope due to gravity. They consist of unconsolidated rock fragments (silt/sand–rock boulders) with interstitial ice. Therefore, their creep behavior (i.e., rheology) may deviate from the simple and well-known flow-laws for pure ice. Rockglaciers often feature a prominent furrow-and-ridge topography (Fig. 1A). The recent study of Frehner et al. [2015] identified viscous buckle folding as the dominant process forming this topography. Buckle folding is the mechanical response of layered viscous media to layer-parallel compression. For the Murtèl rockglacier (upper Engadin valley, SE Switzerland) as a case study, Frehner et al. [2015] were able to reproduce the wavelength, amplitude, and distribution of the furrow-and-ridge morphology using a linear viscous (Newtonian) flow model.

The Murtèl rockglacier is one of the best-studied rockglaciers in the world. Among others, high-resolution digital elevation models (DEM; Fig. 1A), time-lapse borehole deformation data (Fig. 1B), and geophysical soundings exist that reveal the exterior and interior architecture and dynamics of the landform. Arenson et al. [2002] presented borehole deformation data from the Murtèl rockglacier (Fig. 1B), which highlight the basal shear zone at about 30 m depth and a curved deformation profile above the shear zone. Similarly, the furrow-and-ridge morphology also exhibits a curved geometry in map view (Fig. 1A). Hence, the surface morphology and the borehole deformation data together describe a curved 3D geometry, which is close to, but not quite parabolic.

The study presented here uses this curved 3D geometry to constrain the viscous flow law that governs the creep of the Murtèl rockglacier. Linear viscous models result in perfectly parabolic flow geometries; non-linear creep leads to localized deformation at the sides and bottom of the rockglacier while the deformation in the interior and top are less intense. In other words, non-linear creep results in non-parabolic flow geometries.

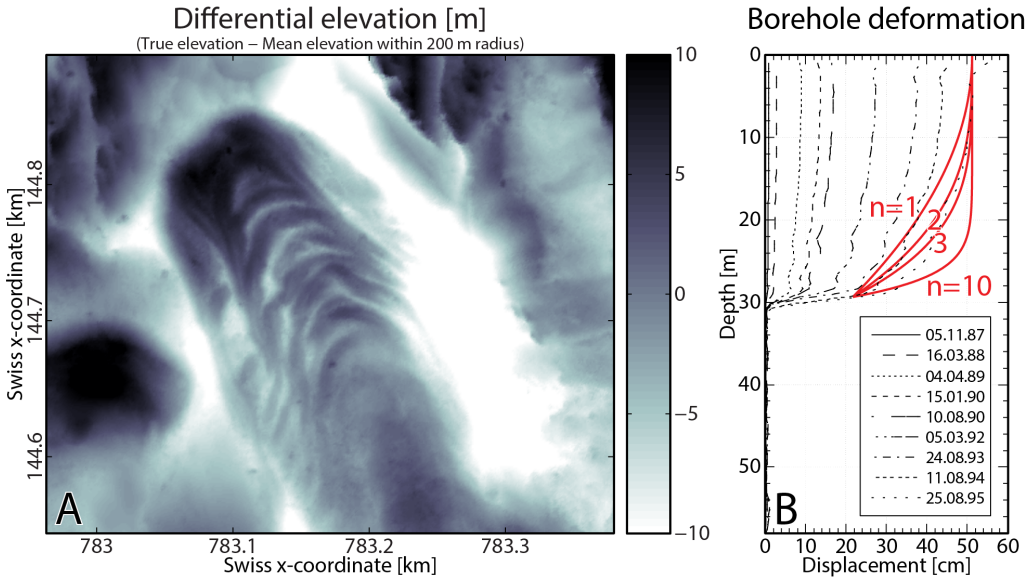

Figure 1: A) Differential DEM of Murtèl rockglacier [Frehner et al., 2015]. B) Time-lapse borehole deformation data [Arenson et al., 2002]. Red: theoretical flow geometries using different non-linear viscous flow laws ($n = 1$: linear viscous; $n = 10$: strongly non-linear).

Here we use a high-resolution DEM to quantify the curved geometry of the Murtèl furrow-and-ridge morphology. We then calculate theoretical 3D flow geometries using different non-linear viscous flow laws. By comparing them to the measured curved 3D geometry (i.e., both surface morphology and borehole deformation data), we can determine the most adequate flow-law that fits the natural data best.

Since this is a project in progress, we can only report preliminary data in this abstract. Fig. 1B presents the borehole deformation data of Arenson et al. [2002] together with four theoretical flow geometries using different non-linear viscous flow laws. It is clear that both the linear (power-law exponent, $n = 1$) and strongly non-linear models ($n = 10$) do not match the measured data well. However, the moderately non-linear models ($n = 2 - 3$) match the data quite well. Even though we did not perform a quantitative analysis yet, this preliminary result indicates that the creep of the Murtèl rockglacier is governed by a moderately non-linear viscous flow law, which has a power-law exponent close to the one of pure ice.

At the time of the conference, we will be able to present detailed quantitative results determining the most suitable flow law describing the Murtèl rockglacier creep. Our results are crucial for improving existing numerical models of rockglacier flow that currently use simplified (i.e., linear viscous) flow-laws.

References

Arenson, L.; M., Hoelzle and Springman, S. Borehole deformation measurements and internal structure of some rock glaciers in Switzerland. *Permafrost and Periglacial Processes*, 13:117–135, 2002. doi:10.1002/ppp.414.

Frehner, M.; Ling, A.H.M. and Gärtner-Roer, I. Furrow-and-ridge morphology on rockglaciers explained by gravity-driven buckle folding: A case study from the Murtèl rockglacier (Switzerland). *Permafrost and Periglacial Processes*, 26:57–66, 2015. doi:10.1002/ppp.1831.

Regional patterns and asynchronous onset of ice-wedge degradation in Arctic Alaska

Gerald V. Frost[1], Tracy C. Christopherson[1], Anna K. Liljedahl[2], Matthew J. Macander[1], Donald A. Walker[3], & Aaron F. Wells[1]

[1] *Alaska Biological Research, Inc., USA*
[2] *Water and Environmental Research Center, University of Alaska Fairbanks*
[3] *Alaska Geobotany Center, University of Alaska Fairbanks, USA*

Ice-wedge polygons are conspicuous and widespread in arctic landscapes, creating complex microtopography and strong, meter-scale contrasts in hydrology, soil, vegetation, and ground ice conditions. Thaw of the upper portion of ice-wedges results in ground subsidence (thermokarst), plant mortality and the formation of small, flooded pits along the polygon margins. Secondary impacts, such as changes in flowpaths, spatially-variable flooding and drainage of polygon centers, and thermal erosion of permafrost, extend well beyond the thermokarst pits themselves. Ice-wedge degradation is commonly triggered by surface disturbance, inundation, and other processes which alter the near-surface thermal regime, as observed near industrial infrastructure, coastlines, or after tundra fire. Observations of recent ice-wedge degradation in undisturbed landscape positions, however, have been increasing and many authors have pointed to recent (post-1980) climatic warming as a likely triggering mechanism. We sought to systematically assess ice-wedge degradation timing and extent across permafrost landscapes spanning climatic gradients across a large portion of Alaska's North Slope, including widespread geomorphic units that had not been previously studied and with a period-of-record dating to 1948. We delineated small waterbodies in historical airphotos and modern high-resolution satellite imagery and made ground observations across a network of 15 km^2 study areas in the National Petroleum Reserve-Alaska, spanning the western and central portions of Alaska's North Slope. The imagery archive covers three epochs: 1948 – 1955, 1979 – 1985, and 2009 – 2012. Our analysis focused on heretofore stable, residual upland surfaces dominated by Holocene-aged ice wedges in three distinct geomorphic units: alluvio-marine deposits (western coastal plain), eolian sand sheet (central coastal plain), and ice-rich loess (yedoma uplands). Analysis of ice-wedge dynamics was informed by field-based vegetation and soil observations and detailed mapping of geomorphic units and microtopography for the study areas. The total extent of flooded pits increased at eight of eleven landscapes since circa 1950. Relative changes in pit extent ranged from −65 % to > 7,000 % (i.e. virtually all pits appeared after circa 1950); across all landscapes, the median change in pit extent was +366 %. An intriguing regional pattern was evident, however; degradation of Holocene ice-wedges was already well underway by 1950 and is spatially much more extensive on alluvio-marine deposits on the Chukchi coastal plain (western North Slope) than at sites to the east. Degradation initiated much more recently on eolian sand and silt (yedoma) deposits prevalent to the east, but so far has affected much less of the landscape than on the Chukchi coastal plain. Our results indicate that recent degradation of Holocene ice wedges across northern Alaska cannot be explained by late-20th century warmth alone. Possible mechanisms for asynchronous onset include differences in recent climate history, snow regime, and thermal and physical properties of surficial materials, that influence local vulnerability to degradation during periods of warming after the Little Ice Age and in the late 20th century. These findings provide context for interpreting and predicting ice-wedge thermokarst processes, thresholds, and impacts in continuous permafrost of Alaska and elsewhere in the circumpolar arctic.

Evolution of permafrost landscapes in an area of thermal suffosion processes development, Central Yakutia

Leonid Gagarin & Ivan Ivanovich Khristoforov

Melnikov Permafrost Institute, Russian Federation

Central Yakutia is characterized by continental climate and presence of continuous permafrost, reaching 600 m in thickness. However, the region is non-uniform in terms of permafrost conditions, as exemplified by an unique natural system of IV terrace of the Lena river. The terrace consists of alluvial sands, and its surface is being reworked by aeolian processes. Modern structure of permafrost within the terrace differs from the surrounding territory, Here, intrapermafrost aquifers are widely present; the active layer depth reaches 3.0 to 3.5 m, and mean annual ground temperature is normally above −0.5 °C. Dominance of pine forest is indicative for such permafrost and hydrogeological conditions. Subaerial taliks are common features of the terrace surface. They serve as one of the major sources of intrapermafrost aquifers. In the valleys and inter-ridge depressions, in contrary, the active layer depth is 0.5 to 1.5 m, ground temperature decreases to −2.5 °C, and larch and dwarf birch are widespread in the landscape.

During the Holocene optimum, permafrost of the IVth Lena terrace had melted to a considerable depth, forming extensive aquifers (Shepelev, 1972). Permafrost aggradation at the following cold period led to partial freezing of the water-saturated aquifers and their spatial localization. Hydraulic gradient values in discharge area exceeded those in the transit area by 3-4 orders of magnitude. This was a major driver for the active development of thermal suffusion processes. The highest contemporary intensity of these processes is observed at the Ulakhan-Taryn spring area, where is poses hazard to the 'Lena' Federal Highway. Thermal suffosion development is associated with the formation of holes and ravines, and the rates of the process are extremely high. The terrace surface at one of the key observation sites at the Ulakhan-Taryn spring subsided after losing about 3,500 m^3 of material volume in one year, 2012 – 2013 period.

Thermal suffusion and associated surface subsidence alters significantly the land topography and subsequently transforms the permafrost landscapes. Formation of cracks in the frozen sand massifs, local surface depressions and vegetation disturbance all contribute to an increase in active layer depth, ground temperatures, and water storage in the active layer. Pine forest development is subdued in these areas, until a complete extinction. Increase in diameter and depth of thermal suffusion sinks leads to the development of ravines and gullies, where thermal conditions and humidity differ from the surrounding areas. Groundwater discharge at the thalweg has a quasi-constant temperature of 0 °C, causing soil moisture excess and lowering of amplitude of the active layer temperature fluctuations.

Gully entrainment and subsequent development leads to the plant succession at the gully outlet (alluvial fan). Grass and shrubs start to populate a bare surface of the fan, then birch and willow appear gradually on the moist soils. Spruce and larch species emerge after the birch and willow communities reach adulthood. The moss cover develops at this stage, leading to a decrease in the active layer depth and annual ground temperatures. The final phase of succession changes is characterized by increasing of larch forests with willow undergrowth.

In the Ulakhan-Taryn spring area, the full sequence of landscape and gullies' development was observed, and the results of the observations will be presented during the conference. The vegetation succession is argued to be one of the main causes of thermal-suffosion processes disappearance in Central Yakutia. Landscape development caused by thermal suffusion changes permafrost environment, gradually reducing groundwater discharge by its interception with gullies, hence the thermal suffusion process is self-restrained. However, it keeps emerging in new areas favourable for groundwater discharge, whence the described cycle is repeated.

Acknowledgements

The research was partially financed by Russian Foundation for Basic Research (grant 15-45-05053)

Rockglaciers in transition – recent results from longterm kinematic monitoring in the Swiss Alps

Isabelle Gärtner-Roer & Johann Müller

University of Zurich, Switzerland

Research on creeping permafrost bodies ranges from simple mapping approaches to elaborated borehole loggings and complex modelling approaches. Besides the research-driven investigations, longterm monitoring programs for subsurface temperatures, ground surface temperatures, geophysics and kinematics have been implemented on several rockglaciers in the Swiss Alps during the last decades (e.g. PERMOS). Most of the approaches are motivated by climate (change) related research, others account for geomorphological investigations including sediment budget approaches and hazard assessments. With the recognition of rockglaciers and their dynamics in the latest IPCC report these landforms have now been prominently respected as climate change indicators.

We apply remote sensing (different airborne sensors) and in situ methodologies to quantify rockglacier geometry changes and to derive horizontal movement rates and vertical changes. The combination of these observed surface dynamics, landform mapping and ground surface temperature data allow for the analysis of the general state of activity and has been documented since the 1970s. Our findings from three rockglaciers in the Valais (southern Switzerland) and five landforms in the Engadine (eastern Switzerland) indicate warming permafrost conditions and related process changes, such as increased horizontal velocities as well as signs of landform degradation. The horizontal velocities of the single landforms show different patterns: distinct interannual variations with single impact years or seasons (e.g., summer heat wave 2003 and 2015), overall synchronism with slight regional differences in magnitude as well as local characteristics. Such local characteristics are mainly due to topographic parameters (e.g., rockglaciers on steep slopes are generally faster than those on less inclined slopes), landform thickness, ice content and ice properties. Our findings indicate that warm rockglaciers show much stronger reactions to thermal forcing than colder ones. In addition, Ice rich landforms, such as the famous rockglacier Murtèl, nowadays depict low horizontal velocities (< 0.12 m a^{-1} at Murtèl), but with the enhanced warming and the possible thawing of subsurface ice, we expect to measure increasing horizontal velocities in the near future.

The vertical changes show distinct thinning in the rooting zone of several landforms, partly related to a change in sediment supply and transfer as well as to the thawing of subsurface ice. The findings underline the assumption that rockglaciers in the Alps are strongly influenced by increasing air temperatures. Despite their age of several hundred to several thousand years, we assume that rockglaciers are actually in transition. The creep process and geometrical landform evolution is strongly influenced by warming and thawing of subsurface ice, the latter also indicated by the observed subsidence. The related landform changes amplify the degradation and may lead to inactivation or destabilization of the respective landform (whether or not depends mainly on the slope inclination as well as the existence and amount of unfrozen water). Destabilization is observed on single landforms with strong geometric and topographic changes, which indicate the transition to sliding processes.

Our observations fit well with findings from other landforms in Switzerland and the entire European Alps [Delaloye et al., 2008, 2010, PERMOS, 2013] and confirm that the observed changes display local conditions that are strongly embedded in regional trends. Such trends can be important for the assessment of natural hazards as in recent years several rockglaciers within the Alpine belt have become instable and present – of course strongly depending on the topographic conditions of the landform – a danger for infrastructure as well as human beings in the Alpine valleys. A continuous monitoring of the permafrost evolution in general and the rockglacier development in particular is therefore of great importance.

References

PERMOS [2013]: Permafrost in Switzerland 2008/2009 and 2009/2010. In: Noetzli, J. (ed.) *Glaciological Report (Permafrost) No. 10/11 of the*

Cryospheric Commission of the Swiss Academy of Sciences. 80 pp.

Delaloye, R.; Perruchoud, E.; Avian, M.; Kaufmann, V.; Bodin, X.; Hausmann, H.; Ikeda, A.; Kääb, A.; Kellerer-Pirklbauer, A.; Krainer, K.; Lambiel, C.; Mihajlovic, D.; Staub, B.; Roer, I. and Thibert, E. [2008]. Recent interannual variations of rock glacier creep in the European Alps. In: Kane, D.L. and Hinkel, K.M.(eds.), *Proceedings of the Ninth International Conference on Permafrost*, Institute of Northern Engineering, University of Alaska Fairbanks, Fairbanks, USA, 29 June–3 July 2008, volume 1, pages 343–348. ISBN 978-0-9800179-2-2. URL http://ipa.arcticportal.org/publications/conference-proceedings.

Delaloye, R.; Lambiel, C. and Gärtner-Roer, I. [2010]. Overview of rock glacier kinematics research in the Swiss Alps. Seasonal rhythm, interannual variations and trends over several decades. *Geographica Helvetica*, 65(2):135–145.

The complex pluri-decennial and multiphasic destabilization of the Jegi rock glacier (western Swiss Alps): historical development and ongoing crisis

Alyssa Ghirlanda, Luc Braillard, Reynald Delaloye, Mario Kummert, & Benno Staub

Univeristy of Fribourg, Switzerland

The so-called destabilization of a rock glacier is characterized by a fast motion rate of the landform (usually more than 2 meters per year (m/y)) and the development of crevasse(s) or landslide-like scarp(s) on its surface. It may concern the entire of a rock glacier or only a part of it. Such a destabilization phase is generally considered to be the result of the varying and combined influence of factors related to

i the structure and composition of the rock glacier,

ii the thermal state of the permafrost,

iii the topography of the terrain,

iv the geometrical changes of the moving landform and

v a possible local overloading in debris [Delaloye et al., 2013].

In this context, our contribution presents the historical development of the Jegi rock glacier destabilization for the last 60 years and focuses on the ongoing crisis.

The 720 m long and 100 – 150 m wide Jegi rock glacier is located between 2750 and 2450 m a.s.l. on the western flank of the Jegihorn summit (3206 m a.s.l.) and on top of a deep-seated landslide moving 1 – 3 cm/y. Downwards its rooting zone, the rock glacier consists of an upper tongue ending with a first front (2550 m a.s.l.) superimposed on a 150 m long second tongue located below. The inclination of the slope is about 20° in the rooting zone, 15° in the median part of the first tongue, 30° or more above the upper front and 10 – 15° on the lower tongue (Fig. 1). In a regional study aimed at inventorying slope movements with satellite-borne DInSAR (synthetic aperture radar interferometry), the active Jegi rock glacier was presenting in 2008 morphological and kinematical evidences of an ongoing destabilization phase [Delaloye et al., 2008, Barboux et al., 2015].

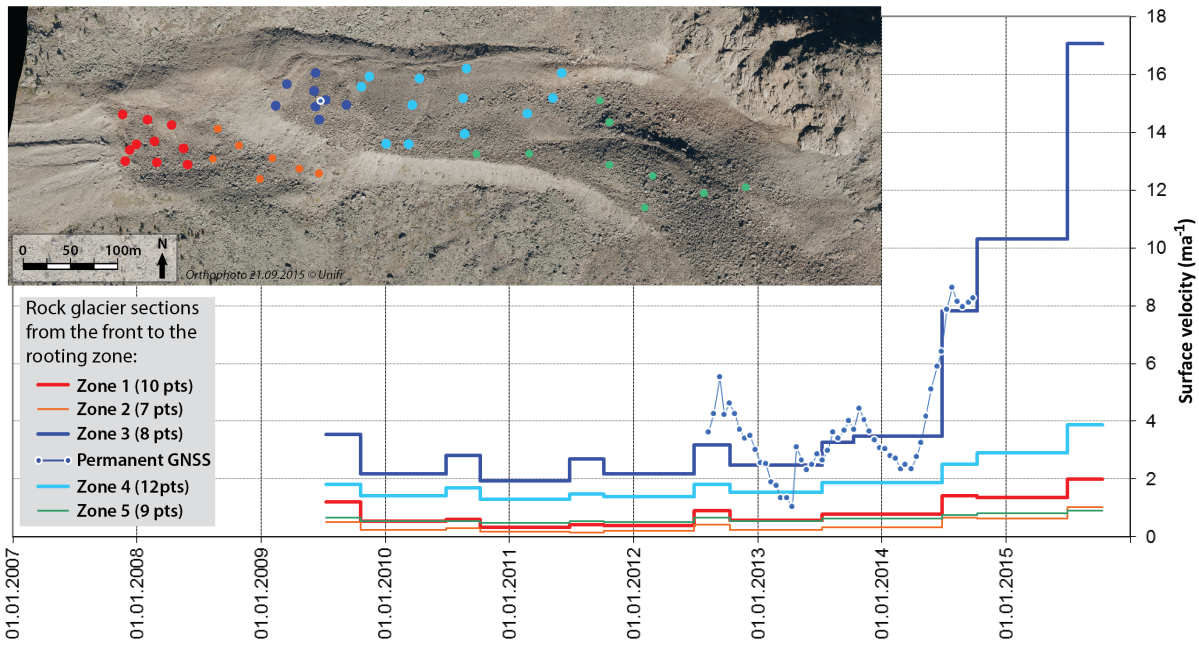

Figure 1: Surface velocities (m a^{-1}) of the 5 different zones of the Jegi rock glacier from 2009 to 2015 derived from GNSS measurements and from a permanent GNSS sensor located in the zone 3

More precisely, a steep section above the upper front was spotted moving in the order of 2 – 3 m/y since at least 1995, with larger velocities in summer than in winter [Delaloye et al., 2008]. Since then, its surface motion has been under investigation. First, in order to assess more precisely the pattern of the rock glacier flow field and its temporal evolution, GNSS measurements campaigns have been held twice a year since June 2009 (network of about 80 measurement points). Detailed investigations on the seasonal kinematical behavior of the rock glacier have also been conducted using DInSAR technologies between 2011 and 2013 [Barboux et al., 2015]. Moreover, a permanent GNSS sensor is installed in the center of the fast moving zone since July 2012. At the moment, aerial images available since 1958 are being photogrammetrically analyzed to recognize and reconstruct earlier stages of the destabilization development.

Our study points out so far that the Jegi rock glacier has suffered a minimum of two destabilization phases in his history. The first one already occurred before 1958, as indicated by the aerial image of that year showing morphological signs of a previous surge-like crisis: a longitudinal depression surrounded by two lateral levees is connecting the rooting zone to the median part of the upper tongue and an important transversal crevasse has developed on its frontal part. These morphological features witness the last stage of a formerly developed destabilization process, which affected the main part of the upper tongue.

This crisis was apparently caused by the pressure exerted by the rapid accumulation (overloading) of rock material collapsed from the headwall located above the rock glacier rooting zone. From 1958 to 1995, no further significant sign of destabilization is visible. Around 1995, a fast moving zone was detected on the terminal section of the upper rock glacier tongue. Between 2009 and 2013, the rock glacier flow field pattern was organized as follows: the rooting zone (zone 5, Fig. 1) was moving at a rate of 0.5 m/y; the median part of the upper tongue (zone 4), including the former depression and levees, was moving at a rate of 1 – 2 m/y, independently of the rock glacier surface morphology; the terminal part of the upper tongue (zone 3) was the fastest of the rock glacier with velocities of 2 – 3 m/y; finally the lower tongue (zones 1 and 2) was moving quite slowly (0.5 m/y).

Since the winter 2013/2014, dramatic changes of the rock glacier kinematical behavior have occurred. The landform has indeed entered into a new destabilization phase marked by a strong velocity increase in all zones: in comparison to the 2009 – 2013 mean, the annual velocity change reached in 2014/15 +50 % in the rooting zone, +100 % in zone 4, +200 % in zones 1 and 2 and +400 % in zone 3. At the time of writing this abstract (November 2015), the zone 3 was moving at a critical rate of about 5 centimeters per day (17 m/y). The new (and ongoing) destabilization phase can be considered as affecting this time only a smaller part of the rock glacier, namely the zone 3, whose area is about 0.01 square kilometers for a maximum volume of about 100'000 cubic meters. In less than 2 years, a 5 – 8 m high scarp has developed at the upper edge of the rapidly moving zone and rock falls from the destabilized frontal part have become frequent.

No specific meteorological or earthquake event has triggered the current destabilization phase and a sediment surcharge is excluded as a contributing factor. The ongoing destabilization has to be considered as resulting from the combination of

i the local steepness and convexity of the topographical slope (which in turn conducts to an extensive flow of the rock glacier),

ii the long-term geometrical changes of the moving mass (about 50-100 m advance of the upper tongue in 50 years), and

iii the pluri-decennial permafrost warming trend that has been particularly pronounced in the Swiss Alps for the 5 previous years (increasing rock glacier velocity values observed in most monitoring sites).

Thereby, one has to consider:

i that the destabilization of the Jegi rock glacier is a pluri-decennial, multiphasic and complex process, which is not always affecting the same section of the landform,

ii that the ongoing destabilization phase is in a preparation stage since 20 years at least (concomitance of the outline of the fastest zones in 1995 and 2015) and, because the whole rock glacier is simultaneously suffering a widespread and severe acceleration,

iii that the current phase has been doubtless thermally (climatically) triggered.

References

Barboux, C.; Strozzi, T.; Delaloye, R.; Wegmüller, U. and Collet, C. [2015]: Mapping

slope movements in Alpine environments using TerraSAR-X interferometric methods. *ISPRS Journal of Photogrammetry and Remote Sensing*, 109. doi:10.1016/j.isprsjprs.2015.09.010.

Delaloye, R.; Strozzi, T.; Lambiel, C.; Perruchoud, E. and Raetzo, H. [2008]: Landslide-like development of rockglaciers detected with ERS-1/2 SAR interferometry. In *Proceedings of the FRINGE 2007 Workshop* Frascati, Italy, 26–30 November 2007, (ESA SP-649, February 2008).

Delaloye, R.; Morard, S.; Barboux, C.; Abbet, D.; Gruber, V.; Riedo, M. and Gachet, S. [2013]: Rapidly moving rock glaciers in Matterthal. Mattertal – ein Tal in Bewegung. In: Graf, C.(ed.), *Publikation zur Jahrestagung der Schweizerischen Geomorphologischen Gesellschaft*, pages 21–31. 29. Juni – 1. Juli 2011, St. Niklaus. Eidg. Forschungsanstalt WSL.

Recent evolution of mountain permafrost in the Southern Swiss Alps: The results of 2006 – 2015 period

Elisa Giaccone[1,2], Simona Fratianni[2,3], Christian Ambrosi[4], Marco Antognini[5], Reynald Delaloye[6], Christophe Lambiel[1], Stefano Mari[6], & Christian Scapozza[4]

[1] *Institute of Earth Surface Dynamics, University of Lausanne, Lausanne, Switzerland*
[2] *Dipartimento di Scienze della Terra, Università degli Studi di Torino, Torino, Italy*
[3] *Centro di Ricerca sui Rischi Naturali in Ambiente Montano e Collinare (NatRisk), Grugliasco, Italy*
[4] *Institute of Earth Sciences, University of Applied Sciences and Arts of Southern Switzerland (SUPSI), Canobbio, Switzerland*
[5] *Museo cantonale di storia naturale, Lugano, Switzerland*
[6] *Department of Geosciences – Geography, University of Fribourg, Fribourg, Switzerland*

Rock glaciers are typical landforms related to the presence of permafrost and can be used as indicators of the influence of climate change on high mountain environments, especially under current global warming. Therefore, their study is essential to understand the Alpine cryosphere evolution. In recent decades, a systematic thermal and kinematics monitoring of active rock glaciers has started throughout the Alps in the framework of several national or transnational programs.

Since 2006 an important research network has been set up to study the permafrost in Southern Swiss Alps, with the aim to extend the Swiss permafrost monitoring network [2013, 2013] to the Southern part of the Alps. Nine rock glaciers in the Ticino Alps (Tab. 1), located between 2240 and 2800 m a.s.l., are subject to GST (Ground Surface Temperature) monitoring, using UTL-3 sensors.

In addition rock glacier surface velocities are measured each year or with plurennial frequency, depending on rock glacier kinematics, using dGPS (model GPS Leica SR530).

The collected data show that each rock glacier presents different horizontal surface velocities depending on morphostructural and topographical factors. The mean values for each rock glacier are comprised from a minimum of 0.02 m/y (at Alpe Pièi, 2009/2010 period) to a maximum of 1.39 m/y (Monte Prosa A, 2014/2015 period). A general increase in surface velocity was detected during the hydrological year 2014/2015 in all rock glaciers analysed, with maximal values for 2015 that are significantly higher than the maximal velocities mean for 2009 – 2014 (Tab. 1). Furthermore, the same trend was detected in GST maximum values, after the decrease of 2013/2014 period. Considering the period of rock glaciers analysis (2006 – 2015), the air temperatures show an evident warming due to the hot summer in 2015, combined with an increase in precipitation in Western and Eastern Ticino Alps. These results can explicate the rock glacier velocity increase during this year.

The annual velocity variations are significantly correlated with Mean Annual GST variations with a delay of some months. An increase of MAGST corresponds generally to an increase of velocity. In turn, MAGST is influenced not only by air temperature variations but also by snow depth and duration. This behavior is similar to what has been observed in several other regions of the Alps, and indicate a significant link between the increase of ice permafrost plasticity and the climate warming [Scapozza et al., 2015].

An analysis of climate data was conducted to understand how Ticino Alps climate has evolved during the last decades. The data from 16 automatic and manual stations of MeteoSwiss, located in the Cantons of Ticino and Graubünden between 273 and 2171 m a.s.l., were downloaded, homogenized with HOMER (HOMogenization softwarE in R) method [Venema et al., 2012] and analyzed for the 1981 – 2015 period. The maximum, mean and minimum values of temperature, rainfall and snow data were calculated to individuate the characteristics of climate. The trends of main climatic parameters were assessed and the Mann-Kendall test was applied to confirm the statistical significance. The results show a significantly increase of annual average temperatures, a not defined tendency for precipitation, because its heavy inter-annual variability, and a clearly decrease of fresh

snow and of snow cover duration, especially at middle altitudes (1000 – 1500 m a.s.l.).

Furthermore, an analysis of precipitation distribution with IDW method was performed using the 1981 – 2010 data, in according to current reference period of World Meteorological Organization. A clearly difference between Western and Eastern Ticino Alps was detected, with the highest precipitation values recorded in the western part and the lowest in the eastern part. This difference is one of the reasons which could explain why the rock glaciers of the Western Ticino Alps move more rapidly than the rock glaciers of the eastern part. A second reason is the larger influence of glacial processes, which allowed the formation in the Western Ticino Alps of greater number of debris and ice-core rock glacier, containing more ice and creeping more rapidly than the talus rock glaciers of the Eastern Ticino Alps.

Table 1: List and characteristics of the rock glaciers monitored in the Ticino Alps.

No. site	Site	Region	Elevation (m a.s.l.)	Aspect	GST No. logger	DGPS No. measures	PERMOS	Mean max velocity 2009-2014 (m/y)	Max velocity 2015 (m/y)
27	Monte Prosa A	Gotthard	2430-2600	N	3	Biennial	x	0.67	1.39
28	Monte Prosa B	Gotthard	2450-2520	WNW	1	Yearly	x	0.20	-
29	Pizzo Nero	Val Bedretto	2600-2700	S	-	Every five years	-	0.15	-
29b	Pizzo Gallina	Val Bedretto	2660-2760	SE	4	Yearly	-	0.11	-
30	Passo di Grandinagia	Val Bavona	2560-2800	NE	4	Biennial	-	0.30	-
31	Ganoni di Schenadüi	Val Cadlimo	2480-2640	N	4	Yearly	-	0.31	0.40
32	Piancabella	Val Malvaglia	2440-2550	NE	10	Yearly	x	0.44	0.45
33	Stabbio di Largario	Val Soi	2240-2550	N	4	Yearly	x	0.90	1.44
33b	Alpe Pièi	Valle di Blenio	2340-2500	S	-	Three yearly	-	0.05	-

References

PERMOS 2013. *Permafrost in Switzerland 2008/2009 and 2009/2010.* Glaciological Report (Permafrost) No. 10/11 of the Cryospheric Commission of the Swiss Academy of Sciences. 80 pp.

Scapozza, C.; Giaccone, E.; Mari, S.; Antognini, M.; Fratianni, S. and Ambrosi, C. [2015]: Il permafrost nelle Alpi Ticinesi: temperatura e movimenti dei ghiacciai rocciosi dal 2006 al 2014. *Dati - Statistiche e società*, 2. http://repository.supsi.ch/6809/.

Venema, V.K.C.; Mestre, O.; Aguilar, E.; Auer, I.; Guijarro, J.A.; Domonkos, P.; G. SzentimreyVertacnik, T.; Stèpànek, P.; Zahradnicek, P.; Viarre, J.; Müller-Westermeier, G.; Lakatos, M.; Williams, C.N.; Menne, M.J.; Lindau, R.; Rasol, D.; Rustemeier, E.; Kolokythas, K.; Marinova, T.; Andresen, L.; Acquaotta, F.; Fratianni, S.; Cheval, S.; Klancar, M.; Brunetti, M.; Gruber, C.; Prohom Duran, M.; Likso, T.; Esteban, P. and Brandsma, T. [2012]: Benchmarking homogenization algorithms for monthly data. *Climate of the Past*, 8. doi:10.5194/cp-8-89-2012.

Ground thermal regime and geomorphological consequences in the Pyrenean high mountain.

María González-García[1], Enrique Serrano[1], & Juan José González-Trueba[2]

[1] *PANGEA Research Group, University of Valladolid, Spain*
[2] *Department Cultural Studies, International Universiity Center CIESE-Comillas University of Cantabria, Spain*

The aim of this work is the ground thermal characterization and distribution, and the geomorphic processes of the Pyrenean high mountain related to the ground ice. The study focus on the analysis of three high mountain massifs of the Pyrenees in the Southern side, in the Aragonese Pyrenees. The study include the Infierno massif (3145 m; 42º46'59"N-0º15'49"W), in the Tena valley; Posets massif (3368 m, 42°39'29"N-0°26'15"E) and Maladeta massifs (3404 m, 42°38'51"N-0°38'30"E), in the Benasque valley. Under the summits are preserved the most extensive glaciers in the Pyrenees, but the high mountain is essentially a periglacial environment. The deglaciation of the high mountain has permitted the development of an environment where cold and snow are the main geomorphological processes.

The study has surveyed the ground thermal regime, using 21 thermal data loggers (ibutton DS1922L and DS1921G,and UTL-1 Datalog type 1-) since the year 2009 to 2011 at different altitudes and locations. 72 BTS measurements have been made between and 2220 and 3155 m a.s.l.. With the ground temperatures and BTS have been calculated different thermal parameters and using techniques GIS have been made three ground thermal maps. The geomorphological mapping to 1/10.000 scale of each massif has permitted correlations of the thermal conditions of ground and the geomorphological processes at different altitudes. The distribution of seasonal frozen ground, permafrost or activity not linked to the ice in the ground has been related to geomorphological processes at different altitudinal ranks.

The work has permitted us to establish a altitudinal zonation of the ground thermal regime where between 1700-1800 m and 2100-2150 m a.s.l. a nival-periglacial domain is dominated by the nival processes with a moderate presence of ice in ground. Between 2150-2200 and 2600-2700 m is developed a transitional ecotone where the seasonal frozen grounds exist and the geomorphic processes linked to the ice are dominant. From 2600-2700 m until the 3000-3100 m is developed the cryonival environment and above 3000-3100 m the glacial or supra-periglacial environment, where the mountain permafrost and seasonal frozen ground both are dominant and the geomorphic processes are directed by the ice ground.

3D snow distribution and energy balance modelling in steep rock walls

Anna Haberkorn[1,2], Michael Lehning[1,3], Martin Hoelzle[1], Mathias Bavay[2], Nander Wever[1,3], Robert Kenner[1], & Marcia Phillips[1]

[1] *WSL Institute for Snow and Avalanche Research SLF, Davos, Switzerland;*
[2] *Department of Geosciences, Unit of Geography, University of Fribourg, Fribourg, Switzerland;*
[3] *CRYOS, School of Architecture, Civil and Environmental Engineering, EPFL, Lausanne, Switzerland*

The effects of permafrost degradation on rock slope stability in high alpine regions affect the safety of local communities in the densely populated Alps. Modelling the spatial distribution and temporal evolution of permafrost is therefore of great importance and has been carried out for the Alps using statistically and numerically (e. g. Fiddes et al. [2015] based approaches at different scales, varying from tens of meters to kilometres. To investigate the ground thermal regime in heterogeneous terrain, this grid resolution is too coarse to simulate the spatial differentiation found in steep rock faces with complex micro-topography. In addition, the snow cover has generally not been taken into account in previous modelling studies of steep rock walls, based on the assumption that snow only has marginal effects in near-vertical compact rock. However, the most common type of rock slope in the Alps is heterogeneous, fractured and partly snow covered (Fig. 1), which seriously modulates the surface energy balance and consequently the ground thermal regime of such rock faces [Haberkorn et al., 2015].

We therefore present a spatially distributed study on the influence of the snow cover on the rock thermal regime of a steep NW and a steep SE facing rock wall using the physically based 3D atmospheric and surface process model Alpine3D, which provides distributed simulations using the 1D energy balance model SNOWPACK [Wever et al., 2014]. The model was applied to the rocky Gemsstock ridge (Swiss Alps) using a very high spatial resolution of 0.2 m. Alpine3D was then run for the period September 2012 to September 2014 with meteorological data provided from an on-site automatic weather station. The spatially and temporally heterogeneous snow cover in such steep terrain (up to 90°) was provided to the model using a precipitation scaling approach based on snow depth measurements from the on-site weather station and highly resolved spatial snow distribution data from a representative terrestrial laser scan (TLS) [Haberkorn et al., 2015].

We assess the potential of Alpine3D, with its highly resolved snow cover distribution to model the spatially and temporally heterogeneous rock temperatures in rugged, steep terrain. The single components of the surface energy balance were calculated to evaluate the dominant driving factors of the rock thermal regime close to the surface (0.1 m depth), which strongly vary over the course of the year and between the NW and SE facing rock walls. This is done for both a snow covered and a snow-free case. The bias between both cases is estimated and the error possibly made in recent permafrost distribution modelling is assessed. Additionally, the model performance was tested at different scales ranging from 0.2 m to 5 m.

The performance of Alpine3D, its limitations and uncertainties are discussed and evaluated against a dense network of 35 near-surface rock temperature measurements (0.1 m depth) distributed over the whole rock wall and high resolution (0.2 m) snow cover data derived from four independent TLS campaigns (Fig. 1). The model is able to simulate near-surface rock temperatures and snow depth reasonably well in the heterogeneous terrain. The correction of winter precipitation input using a precipitation scaling method based on TLS greatly improves simulations of snow depth and thus of the rock thermal regime. In addition, the fine-scale resolution of the model domain (0.2 m) and of the validation data allow to consider the strongly varying micro-topography occurring in the rock walls, such as aspect, slope, surface roughness and the distance to ledges (Fig. 1). Remaining errors in rock temperature simulations are explained by missing lateral heat fluxes in the rock and by errors due to wind interpolation, which is very complex in such terrain. Although ground temperature modelling over larger areas, such as the entire Alps is not feasible at such high resolution due to high computational effort, our site specific approach has the potential to reveal temperature variations for different snow cover

conditions and to discuss limitations of permafrost models running at coarse scales but being calibrated by point measurements. Model runs at coarser scales demonstrate the loss of information on aspect, slope and snow depth in this complex terrain.

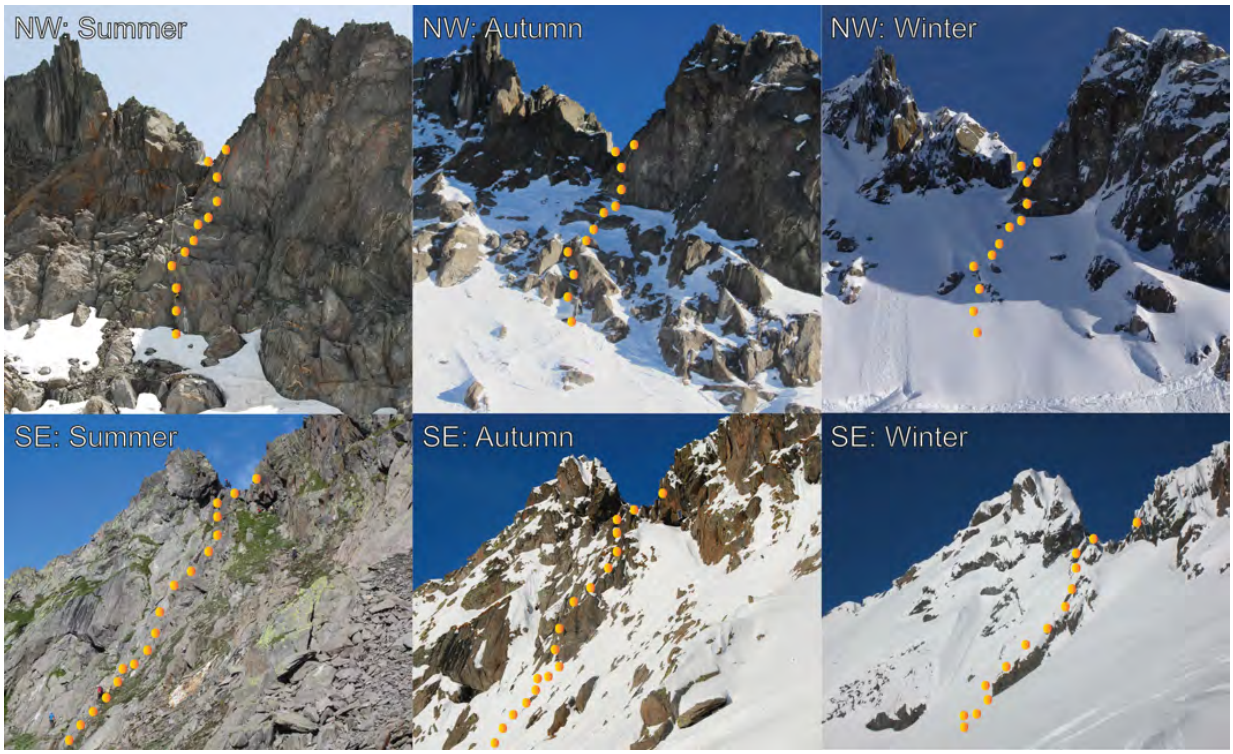

Figure 1: NW and SE facing study slopes on Gemsstock at different seasons, showing the strongly varying conditions in the rock walls with and without snow. Yellow dots: locations of NSRT validation data.

References

Fiddes, J.; Endrizzi, S. and Gruber, S. Large-area land surface simulations in heterogeneous terrain driven by global data sets: application to mountain permafrost. *he Cryosphere*, 9:411–426, 2015. doi:10.5194/tc-9-411-2015.

Haberkorn, A.; Phillips, M.; Kenner, R.; Rhyner, H.; Bavay, M.; Galos, S.P. and Hoelzle, M. Thermal regime of rock and ist relation to snow cover in steep alpine rock walls: Gemsstock, Central Swiss Alps. *Geografiska Annaler: Series A, Physical Geography*, 97, 2015. doi:10.1111/geoa.12101.

Wever, N.; Fierz, C.; Mitterer, C.; Hirashima, H. and Lehning, M. Solving Richards Equation for snow improves snowpack meltwater runoff estimations in detailed multi-layer snowpack model. *The Cryosphere*, 8:257–274, 2014. doi:10.5194/tc-8-257-2014.

Rock glacier permafrost in the semi-arid Andes of Argentina

Christian Halla, Jan Henrik Bloethe, & Lothar Schrott

University of Bonn, Germany

In the semiarid Andes, rock glaciers frequently develop impressive forms up to several kilometres in length covering surface areas up to 3 km^2, even outranging ice glaciers in size and number. Within the permafrost body and the seasonally frozen active layer rock glaciers potentially store large amounts of water. Due to their significant size and wide distribution, rock glaciers are assumed to be important water reservoirs and water sources for this part of the Andes and the foreland. However, our knowledge about their composition and ice content is very limited. In general, the internal rock glacier hydrology changes according to the thermal ground conditions. During frost periods (winter) the active layer sediments act as seasonal water storage due to interstitial ice contents. Whereas in thaw periods (summer), the active layer sediments become an aquifer and water is released and contributes to seasonal runoff. Beneath the active layer rock glacier permafrost features two hydrological functions: Ice-rich permafrost bodies and massive ground ice act as long-term water storage and as aquiclude. Furthermore, the ice content of rock glacier permafrost influences the permafrost degradation and its distribution due to latent heat effects.

The present study aims at assessing the hydrological significance of rock glacier permafrost in the semi-arid Andes of Argentina by combining the regional distribution with geophysical investigations of the internal structure. So far we created an inventory of 1174 rock glaciers, 154 debris-covered glaciers and 154 ice glaciers within the study area (30-33°S). Preliminary results indicate that the altitudinal range of intact rock glaciers varies between 3500 and 5000 m asl, with rock glacier density being lower in the dryer North (30-31°S) than in the South (31-33°). The highest rock glacier concentration is located between 32°S and 33°S. Intact rock glaciers (309 km^2) cover more surface areas as ice glaciers (240 km^2), and as debris-covered glaciers (104 km^2).

Two field sites were chosen for local permafrost investigations enframing the regional study area (between 30-33°S) towards their northern and southern edge. At both field sites, the distribution, dynamics and variability of rock glacier permafrost will be investigated in detail. A combination of field geophysics (electrical resistivity tomography (ERT), refraction seismic tomography (RST), ground penetrating radar (GPR)) and four phase modelling will be used to estimate the volumetric ice contents of the active layer and the permafrost bodies. Local investigations will be complemented by direct observations of sediment properties, thermal monitoring and field based mapping. The Morenas Coloradas catchment (Rio Vallecitos, 33°S) consists of a complex rock glacier system with several active, inactive and relict tongues in front of a large debris-covered glacier. Widespread thermokarst phenomena are indicating the transition (zone) between the rock glacier complex and the debris covered glacier. This field site is among the few locations in the study area where data from borehole temperatures [Trombotto and Borzotta, 2009] and geophysical properties of the active layer and rock glacier permafrost [Barsch and King, 1989, Otto and Keuschnig, 2009] are available in different altitudes. Geophysical prospections were carried out at the inactive rock glacier lobe "Balcón I" (3530 m asl), the active lobe "Balcon II" (3740 m asl) and close to the thermokarst (3810 m asl) in 1987 by [Barsch and King, 1989] and repeated in 2008 [Otto and Keuschnig, 2009]. The comparison of this geophysical data reveals that the permafrost body degraded at the inactive lobe Balcón I [Otto and Keuschnig, 2009]. This is consistent with results of the temperature logs that indicate an active layer thickening of 3.5 m between 1992 and 2007 at Balcón I [Trombotto and Borzotta, 2009]. During our field campaign in March 2016, we will survey these transects again in order to detect the current and changing state of the active layer and permafrost bodies in this part of the Andes.

References

Barsch, D. and King, L. [1989]: Origin and Geoelectrical Resistivity of Rock-Glaciers in Semi-Arid Sub-Tropical Mountains (Andes of Mendoza, Argentina). *Z Geomorphol*, 33(2):151–163.

Otto, J.C. and Keuschnig, M. [2009]: Geophysical prospection on a complex rock glacier system (morenas coloradas, mendoza, argentina). URL serc.carleton.edu/vignettes/collection/31903.html.

Trombotto, D. and Borzotta, E. [2009]: Indicators of present global warming through changes in active layer-thickness, estimation of thermal diffusivity and geomorphological observations in the Morenas Coloradas rockglacier, Central Andes of Mendoza, Argentina. *Cold Reg Sci Technol*, 55(3):321–330.

Reconstructing past extent of periglacial and glacial conditions in the NW of the Iberian Peninsula through micromorphometric analysis: the use of SEM techniques on geomorphology studies

Jonathan F. Hall Riaza & Marcos Valcárcel,

Departamento de Geografía, Universidad Santiago de Compostela, Spain

The area, object of this study, is located at Sierra do Xistral, on the NW of the Peninsula Ibérica. This mountain range is located at the north of the Lugo province and belongs to the mountain range known as Sierras Septentrionales. The highest altitudes are above 1000 m (Cuadramón 1062 m, Chao de lamoso 1047 m, Xistral 1036 m). However, the landscape lines aren't dominated by these elevations, but by the existence of flattened and smooth surfaces between the heights of 850 m and 950 m.

At Sierra do Xistral we have located a series of deposits, that due to their ubiequity, they were sampled and studied. These deposits present the aspect of having been generated in a glacial and permafrost ambient. The deposits appear at the summit of the range, and they have in their matrix rounded and subrounded clasts. These clasts are an indication of long distance transport as they are of hard quartzitic material.

We proceded to a classical morphometric analysis of the samples, following Folk and Ward method. The results showed that samples were not at all sorted. Further analysis will be applied using new technologies, such as SEM (scanning electron microscopy) and confocal laser scanning microscopy, using a diverse range of techniques and methodologies [Le Ribault, 1977, Torcal SáINZ and Tello Ripa, 1992, Mahaney, 2002]. Applying these techniques we will get to know how these deposits where formed and their micromorphometric characteristics.

All the results are being contrasted and compared whit the results of two deposits of near areas (Rio Boo, a periglacial deposit and Ancares, a glacial deposit) that also their genesis is under study by our group. The comparative analysis will allow us to check the micromorphometric differences between periglacial and glacial deposits using these methods.

Our hypothesis is that there were stronger glacial and periglacial conditions for the North West of the Península Ibérica that have been described previously, based, on our present data, the shape and ubiety of these deposits.

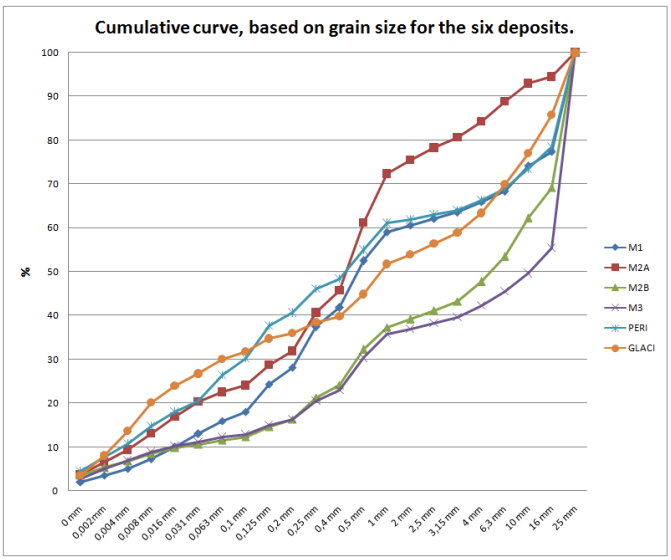

Figure 1: Folk and Ward analysis of the deposits.

References

Le Ribault, L. [1977]: *L'exoscopie des quarzt*. Masson, Paris.

Mahaney, W. [2002]: *Atlas of Sand Grain Surface Textures and Applications*. Oxford University Press, New York, 2002.

Torcal SáINZ, L. and Tello Ripa, B. [1992]: Análisis de sedimentos con microscopio electrónico de barrido: exoscopía del cuarzo y aplicaciones a la geomorfología. *Geoforma Ediciones, Logroño*.

Rockfall in permafrost-affected cirque walls: New insights on spatial variability and potential causes derived from a 4-year LiDAR monitoring campaign, Kitzsteinhorn, Austria

Ingo Hartmeyer[1,2], Markus Keuschnig[3], Robert Delleske[3], & Lothar Schrott[4]

[1] *alpS – Centre for Climate Change Adaptation, Grabenweg 68, 6020 Innsbruck, Austria*
[2] *University of Salzburg – Dept. of Geography and Geology, Hellbrunner Straße 34, 5020 Salzburg, Austria*
[3] *Geoconsult ZT GmbH, Hölzlstraße 5, 5071 Wals, Austria*
[4] *University of Bonn – Department of Geography, Meckenheimer Allee 166, 53115 Germany*

Thermal changes in permafrost-affected rock significantly alter the mechanical properties of rock and ice along potential failure planes. Within the context of recent climate warming the thermal state and stability of frozen rock walls have therefore become a key issue not only for rockfall risk considerations but also for high-alpine landscape evolution and periglacial geomorphology.

In the European Alps numerous, largely visual, observations indicate an increasing occurrence of rockfall events that may be connected to rising temperatures. However, long-term data on rockfall patterns and ground thermal conditions is scarce for these steep, inaccessible environments. Understanding of the controlling factors of climate-sensitive high-alpine rockfall has therefore remained elusive.

The presented study tackles the need for high-precision field data by analyzing a four-year terrestrial LiDAR time series from a high-alpine (peri)glacial environment. The study area is located in the summit region of the Kitzsteinhorn (3203 m a.s.l.), Hohe Tauern Range, Austria. LiDAR monitoring campaign was started in July 2011, since then six side- and backwalls of two glacial cirques were scanned at an interval of approximately two months during the snow-free summer season (June to October). The scanned rock faces predominantly consist of calcareous mica-schist and differ in terms of height, slope inclination, slope aspect, and discontinuity orientation. The rock faces are underlain by permafrost, their combined surface area is approximately 100000 m^2. All investigated rock faces are situated directly adjacent to the Schmiedingerkees cirque glacier, which has retreated and thinned significantly in recent decades (downwasting rate 1.5 m/a). The interpretation of the acquired terrestrial LiDAR data is supported by extensive in-situ borehole temperature measurements from depths of up to 30 m. LiDAR data acquisition was performed using a Riegl LMS-Z620i. For data acquisition a quick, flexible methodology was applied that does not require fixed installations and/or artificial, reflective markers. For data post-processing a procedure was developed which allows point cloud alignment by surface geometry matching and objective, automated discrimination between measurement errors und real surface changes.

From 2011 to 2014 a total number of 104 rock fall release zones were identified (LiDAR data of the 2015 summer season is currently analyzed, final results are not available yet). The total rockfall volume was 1130 m^3, the largest rockfall event reached a volume of about 250 m^3. The distribution of the rockfall release zones displays a distinct spatial pattern: Rock surfaces that were exposed by the thinning Schmiedingerkees glacier in recent years and decades show a significantly increased rockfall activity: 66 % of the detected rockfall release zones and 80 % of the detected rockfall volumes were triggered from areas located less than 20 m above the current glacier surface. The annual rockwall retreat rate within this 'active belt' (= 0–20 m above glacier) is approximately 7.5 mm. This clear correlation suggests that glacial thinning exerts a major destabilizing influence on the adjacent rock faces.

Permafrost degradation and glacial debuttressing, two frequently cited causes for high-alpine rockfall, do not provide conclusive explanations for most of the detected rockfall events. Maximum active layer thickness during the summer season (> 3 m) is larger than the depth of the failure plane for the majority of the detected rockfall events (95 %). Thus, permafrost degradation is an unlikely trigger for most events. While glacial debuttressing (i.e. loss of support at the base of a rock face due to glacial melting) certainly plays an

important role for some of the observed events there are two relevant counter-arguments: the existence of a distinctly opened randkluft at the base of most of the scanned rock faces necessarily implicates that there is no effective debuttressing impact at the time of the 'emergence' of a rock surface above the lowering glacier surface. The debuttressing effect, if relevant at all, should therefore occur subglacially in the bottom sections of the randkluft, which cannot be covered by LiDAR monitoring; (ii) glacial debuttressing fails to explain the observed high rockfall activity several meters above the glacier surface.

Frost cracking and thermo-mechanical forcing may provide alternative, more convincing explanations for the observed rockfall pattern. Sustained periods of subzero temperatures are likely to lead to intense frost cracking within the randkluft causing extensive fracturing of intact rock. When rock surfaces are exposed to atmospheric influences due to pronounced glacial thinning, ground thermal conditions are modified significantly. Newly exposed rock surfaces are subject to greater temperature amplitudes, leading to pronounced thermomechanical strain along critically stressed discontinuities and potentially to rockfall detachment.

Geomorphological implications of climate-driven permafrost change: The case of the Russian Altai Mountains

Hanne Hendrickx[1], Jan Nyssen[1], Britta Sannel[2], Rudi Goossens[1], Frank Lehmkuhl[3], & Valery Babin[4]

[1] *Ghent University, Belgium*
[2] *Stockholm University, Sweden*
[3] *RWTH Aachen University, Germany*
[4] *Gorno-Altaisk State University, Russia*

In cold regions, climate change driven permafrost thawing is causing geomorphic processes to intensify. This is especially true for mountain regions, where increased slope failures are in close relationship with the recent thawing of permafrost bodies. For both the intensity of geomorphic processes and permafrost dynamics, little information exists for mountain areas in the permafrost belt worldwide. The Russian Altai Mountains are marginally glaciated and house sporadic and discontinuous permafrost. Due to global warming, temperature and precipitation are changing rapidly in the area, at rates higher than the global average. This result in highly dynamic environmental processes, making the Altai Mountains a potential area to understand the interrelations between geomorphology and permafrost, as influenced by climate change. However, little information is available on geomorphic processes involved and their rates. Therefore, the objective of this paper is to understand the interrelationships between climate, permafrost and geomorphology in the climate sensitive Altai Mountains. Therefore, a geomorphological time-depth analysis will be done focusing on geomorphic permafrost indicators such as rock glaciers, solifluction, permafrost creep, polygon patterned ground, palsas and thermokarst. Mapping the present day situation will be based on fieldwork, existing maps, satellite imagery and ASTER Digital Elevation Models. A geomorphological map representing the geomorphology of the 1960s based on CORONA images will be prepared. In addition, 3D-photomodelling of rock glaciers and solifluction lobes will reveal short-term geomorphic dynamics. Spatio-temporal geomorphic dynamics will be linked to permafrost state and distribution using regional permafrost probability maps for the period 1960s–2010. By doing so, this study expects to contribute to the understanding of the geomorphological sensitivity of cold climate mountains to climate-driven permafrost degradation.

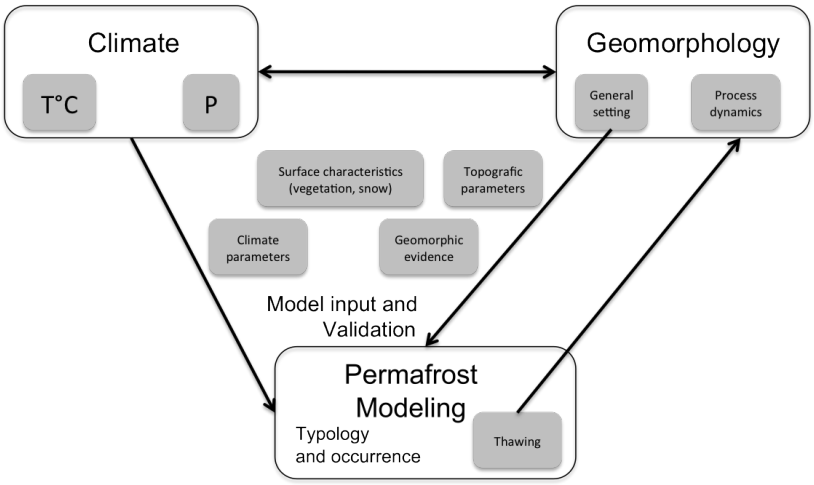

Figure 1: Conceptual model of this study

Potential rock weathering by freeze-thaw processes in alpine cirques of Austria in 2006-2015 exemplified by the Hinteres Langtal Cirque, Austria

Andreas Kellerer-Pirklbauer & Matthias Wecht

University of Graz, Austria

Rock temperature data give a good indication of the effects of air temperature anomalies on ground thermal conditions particularly if a long-lasting seasonal snow covers is absent. Such rock temperature data are furthermore useful to quantify the intensity and potential of near-surface physical weathering in bedrock and hence of potential rock shattering. In this contribution we present selected results from an ongoing bedrock-temperature monitoring program which is accomplished at fives study areas – 3 × cirques with rock glaciers (DOV, HLC, REI), 1 × valley walls overlooking a glacier (PAG), and 1 × a mountain pass location (HEV) – in the Austrian Alps (Fig. 1a).

The bedrock-temperature monitoring program itself is part of a comprehensive ground temperature monitoring network in alpine Central Austria initiated in 2006 aiming to understand the effects of present climate conditions and variability on the ground thermal regime of mountain environments in Austria. Regarding the bedrock-temperature monitoring, nine surface boreholes in vertical and near-vertical rockwalls with different slope orientations and two additional boreholes at flat rock sites were drilled and instrumented in summer/early autumn 2006. The eleven rock temperature sites (RTS) are located between latitude 46°55'N to 47°22'N and longitude 12°44' to 14°41'E at five different study areas (Fig. 1a). The RTS have been all installed in metamorphic rock (6 x gneiss, 5 × mica schist) and in the elevation range 1960-2725 m asl (mean 2491 m asl).

Three temperature sensors have been inserted at each RTS at vertical depths of 3, 10 and 30–40 cm. The three sensors are connected at each site to a 3-channel miniature temperature datalogger manufactured by GeoPrecision, Germany (accuracy of ±0.05 °C). Several temperature-derived parameters are calculated from the temperature data. These parameters form the basis of the assessment of the potential bedrock weathering and consist of: (a) the mean annual rock temperature at the rock surface and at different depths, (b) the number of freeze-thaw-cycles (FTC) and (c) effective freeze-thaw cycles for frost shattering (eFTC; Matsuoka [1990]), (d) the duration and intensity of freeze-thaw-cycles, and the number of days (e) and hours (f) within the so-called "frost-cracking-window" (hFCW; dFCW) using the two different temperature "windows"-3 °C to -6 °C and, respectively, 3 °C to -8 °C (cf. Fig. 5 in Hallet et al. [1991]). Therefore, both the volumetric-expansion model and the segregation-ice model for frost weathering were considered [Hallet et al., 1991, Matsuoka, 2008]. The effects of (g) aspect and (h) snow cover on the thermal regimes at the monitoring sites are additionally addressed. The temporal time frame was one hydrological year (HY 01.10.-30.09).

Results from all RTS sites show that the number of diurnal FTC and eFTC varied substantially during the observation period at all sensor depths. However, this variation differs from site to site related to snow cover condition, elevation and aspect. For instance, at one lower-elevated (2255 m asl) north-exposed RTS site (PAG-B) the number of FTC and eFTC was lowest during the hydrological year 06/07 (snow poor and warm winter) whereas highest in 11/12 (snow poor but rather cool winter). In contrast, results are completely different at two substantially higher-elevated but also north-exposed RTS (DOV-B; 2638 m; HLC-B; 2693 m asl) with highest FTC values in 06/07 and lowest in 11/12. Furthermore, at one flat bedrock site (HLC-C at 2650 m asl) the number of FTC and eFTC was highest in 06/07 related to the thin and short winter snow cover.

Exemplarily results regarding the duration of the frost cracking window in hourly resolution (hFCW) at the three different sites in the Hinteres Langtal Cirque (HLC) are depicted in Figure 1c-d. The cirque floor is almost completely covered by a highly-active rock glacier (Fig. 1b). The three RTS are located at different aspects (SW-, NE-, and W-facing slopes) and at different topographic positions (2 × near vertical rock face, 1 × flat surface of a boulder; Fig. 1b). All three sites are covered by seasonal snow for about half a year (estimated based on the temperature data).

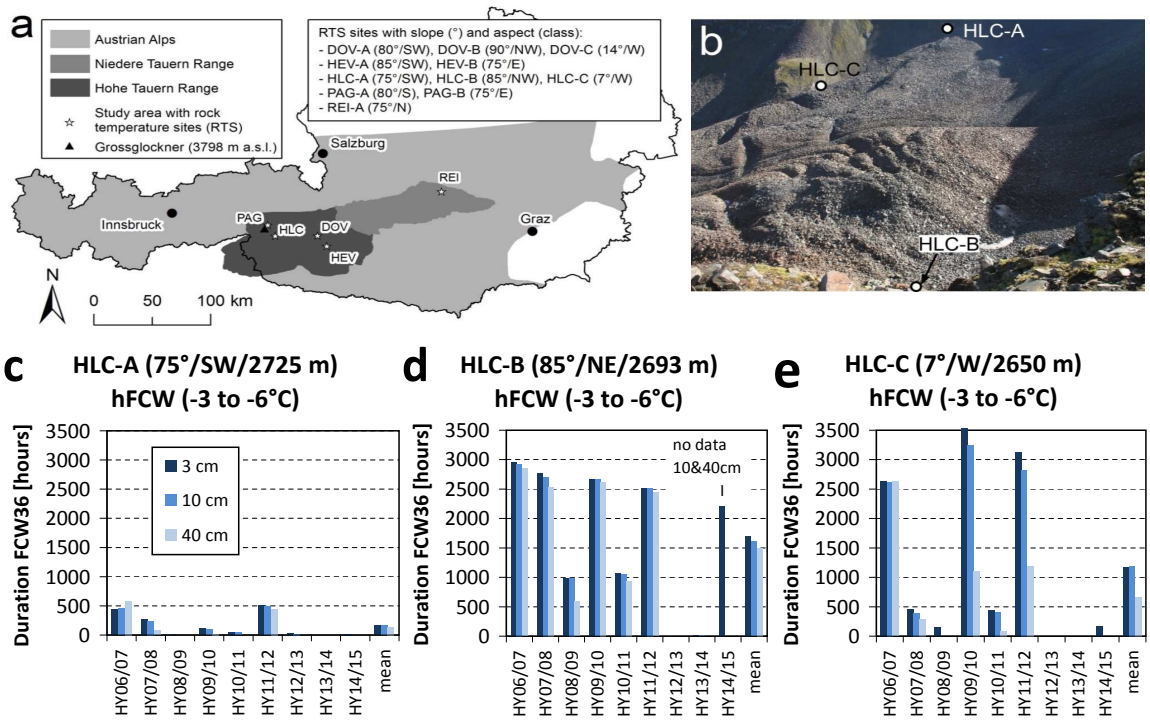

Figure 1: The five study areas with the eleven rock temperature sites (RTS) in Austria; (a) overview map; (b) field situation at the study area HLC with 3 RTS sites near a rock glacier;(c)-(d) duration of the frost cracking window (hours) at the HLC-sites.

The mean annual rock temperature of the sensor closest to the surface (3 cm) during the monitoring period was 2.8 °C at site HLC-A, 0.3 °C at site HLC-B, and 0.0 °C at site HLC-C. Results of hFCW indicate that aspect has a substantial effect. The duration of the FCW is 6 to 10 times longer (depending on sensor and year) at the north-exposed RTS compared to the south-exposed one. In some years the south-exposed RTS is not within the FCW at all. Furthermore, mild winter and/or snow-rich winter might cause almost a complete absence of hours within the frost-cracking window even at site HLC-B. The interannual change in this parameter-value varies substantially from year to year at all three sites. Particularly the boulder-rock site HLC-C has extreme variations from about 0 to >3500 hours/year.

Our observation suggests that predicted warmer and snow-poor winters in European Alps will enhance diurnal FTC and the intensity of near-surface physical weathering in the bedrock of the Austrian Alps. This seems to be feasible at least for north-facing slopes at elevations above c. 2600 m asl. The opposite is true for north-exposed slopes at elevations below 2200 m asl where the number of diurnal FTC might decrease. The duration of the FCW (in hours or days) is substantially longer at north-facing rockwalls compared to south-facing ones. However, plays a major role in the thermal regime of rockwalls even at near-vertical rock faces. Summarizing, our observations suggest that segregation ice formation is particularly important for rock weathering at north-facing rockwalls. In contrast, volumetric expansion during freezing might be the major control for rock weathering at the monitored south-facing rockwalls.

References

Hallet, B.; Walder, J. and Stubbs, C.W. [1991]: Weathering by segregation ice growth in microcracks at sustained sub-zero temperatures: Verification from an experimental study using acoustic emissions. *Permafrost and Periglacial Processes*, 2: 283–300.

Matsuoka, N. [1990]: The rate of bedrock weathering by frost action: Field measurements and a predictive model. *Earth Surface Processes and Landforms*, 15:73–90.

Matsuoka, N. [2008]: Frost weathering and rockwall erosion in the southeastern Swiss Alps: Long-term (1994–2006) observations. *Geomorphology*, 99:353–368.

Terrain sensitivity in northwestern Canada

Steven Kokelj[1], Jon Tunnicliffe[2], Trevor Lantz[3], Rebecca Segal[3], Denis Lacelle[4], Robert Fraser[5], Ashley Rudy[6], & Scott Lamoureux[6]

[1] *Northwest Territories Geological Survey, Canada*
[2] *School of Environment, University of Auckland, New Zealand*
[3] *School of Environmental Studies, University of Victoria, Canada*
[4] *Department of Geography, University of Ottawa, Canada*
[5] *Canada Centre for Remote Sensing, Natural Resources Canada, Canada*
[6] *Department of Geography and Planning, Queens University, Canada*

In circumpolar regions, the former margins of continental ice sheets are demarcated by extensive glacigenic land systems. These environments are particularly widespread across northwestern Canada. Thermokast and fluvial incision have modified these landscapes, but permafrost and cold climate conditions have constrained post-glacial landscape change. In northwestern Canada this terrain type has experienced a recent increase in rates and magnitudes of retrogressive thaw slumping. This dynamic form of thermokarst can rapidly degrade ice-rich permafrost tens of metres thick and mobilize large stores of sediments, reconfiguring slope and valley systems. In areas ranging from the forest-tundra transition on the Peel Plateau, lower Mackenzie Valley to polar desert on the Jesse Moraine of Banks Island there have been significant increases in thaw slump activity. The Jesse Moraine on eastern Banks Island is underlain by cold permafrost (MAGT -10 °C) and it has experienced a greater relative increase in thaw slump activity (>400 %) than any other ice-rich environment that we study. It is probably the most dynamic thermokarst region in the North American Arctic.

The fluvially incised, ice-rich terrain of the Peel Plateau, lower Mackenzie Valley hosts an abundance of very large retrogressive thaw slumps. Detailed investigations utilizing remote sensing and UAV technology indicate that individual disturbances displace on the order of 10^5 m^3 of ice-rich permafrost annually and multi-decadal slope sediment flux is on the order of 10^6 m^3. Localized permafrost degradation of this magnitude is comparable to a doubling of active layer thicknesses at the 10 km^2 catchment scale. The combination of air temperature-driven meltwater flux and an increase in the frequency and intensity of rainfall has induced significant flow events that evacuate slumped materials to downstream valley systems. This increased downslope sediment flux from slump scar zones has perpetuated slump activity and contributed to intensification of this disturbance regime. These disturbances are most common in low order catchments. The intense fluvial impacts have profoundly altered the stream sediment cascade such that downstream effects will persist for centuries.

The continental-scale influence of glacial legacy on the potential for climate-driven transformation of permafrost landscapes places into context the processes and impacts we describe above. We mapped the distribution and relative intensity of the thaw slump disturbance regime for a 1 250 000 km^2 area of northwestern Canada using SPOT imagery (10 m resolution) and a grid based classification scheme. These results are validated by fine-scaled mapping of thaw slump disturbances using high resolution imagery over selected study areas. Slump-impacted environments, bounded by the late Wisconsinan ice front comprise over 100,000 km^2 of the continuous permafrost zone in northwestern Canada. Our results indicate that areas of thick, relict ground ice are widespread. The great potential for thermokarst terrain modification of these landscapes provides focus for continued terrain monitoring and research.

Evidence of past permafrost features in the loess cover of eastern Poland and their relation to closed depression location

Renata Kołodyńska-Gawrysiak[1], Joanna Adamczyk[2], Leszek Gawrysiak[1], Lukasz Chabudziński[1], & Grzegorz Gajek[1]

[1] *Maria Curie-Sklodowska University in Lublin, Poland*
[2] *Warsaw University of Life Sciences, Poland*

Closed depressions are reported in various part of the European loess cover. They constitute the main characteristic landforms in loess areas but their origin is not fully understood. The study was conducted in eastern Poland (Nałęczów Plateau and Horodło Plateau). The study objective was to identify the relation between the location of the closed depressions and presence of the fossil polygonal network. During the study, the following were conducted:

i) a morphometric analysis of past polygonal network traces based on aerial and satellite photographs,

ii) an analysis of morphometric features and distribution of closed depressions based on topographic maps and LIDAR data,

iii) lithological and electrical resistivity profiles. The morphometric analysis was performed using GIS software.

Lithological and electrical resistivity profiles were conducted for the representative areas. The profiles were located in linear transects extending across the selected closed depressions and elements of the polygonal network.

Closed depressions are small landforms with peculiar morphometric features and distribution. The size of 70 % of all forms does not exceed 1500 m^2. The longer axis of more than half of the depressions (51.39 %) is within the narrow range from 25 to 50 m. The mean density here is 3–4 CDs/ km^2. Areas of concentration with 30–40 forms per km^2 can be clearly distinguished in the spatial arrangement.

The spatial distribution of closed depressions is correlated with the fossil polygonal network identified in the loess cover in aerial and satellite images. The location of the closed depressions is strongly linked with the nodal points of polygonal networks where large volumes of ice occurred in the past permafrost. The thaw-degradation of ice wedges was the cause of ground subsidence and formation of some closed depressions. Ice-wedge pseudomorphs observed under the bottom of some closed depressions suggest that the origin of the closed depressions can be related to the thawing of ice-wedges in Pleistocene permafrost. Permafrost-related structures are clearly visible in the lithological and electrical resistivity profiles.

The obtained results constitute an important contribution to the knowledge about the origin of closed depressions, which are typical features of loess plateau microrelief. The results of the study indicate the importance of Pleistocene permafrost degradation processes for the origin of the present microrelief of the loess cover.

Spatial and temporal variability of the sediment transfer at the front of active rock glaciers, cases studies form the western Swiss Alps

Mario Kummert, Luc Braillard, Benno Staub, & Reynald Delaloye

University of Fribourg, Switzerland

Permafrost creep is amongst the most important sediment transfer process in periglacial mountain environments. Large quantities of rock debris originating from weathering, talus slopes and moraine deposits are incorporated in the rooting zones of rock glaciers and slowly transferred by permafrost creep until their front. In some cases, the frontal part of the rock glacier is located on a steep slope and/or above a torrential channel. In such a configuration, the rock debris can be eroded from the front and transferred further downward by gravitational processes such as rock fall and debris flow (e.g. Lugon and Stoffel [2010], Delaloye et al. [2013]). In the current context of global warming, sediment transfer at the front of rock glaciers could become a more serious issue for torrential hazards assessment and mitigation. The warmer air temperature induces higher deformation rates of warming permafrost ice, resulting in an acceleration of rock glaciers (e.g. Roer et al. [2008]). Such acceleration could lead to an increase in the amount of sediment transferred into torrential channels and enhance rock fall and debris flow activity.

Results from observations and measurements carried out at three study sites in the western Swiss Alps (Dirru, Gugla, and Tsarmine; see Figure 1) are presented. Each of the investigated rock glaciers presents an effective sedimentary connection with a torrential gully and has been characterized by high displacement rates during the last three years at least (over 2 meters per year (m/y) and up to a maximum of 18 m/y measured locally at Gugla). The aim of our study is to determine the erosion mechanisms at the front of rock glaciers, to assess their variations both in time and space, and to quantify the sediment transfer into the torrents.

Besides the analysis of former aerial and terrestrial photographs dating back to the 1930's and the kinematic monitoring of the rock glaciers, a combination of methods has been applied during the last years. Webcams have been installed on each site to get high frequency images (1 image per hour). The first one was set up in 2009 and the last one in 2015. In addition, several terrestrial laser scanning (TLS) campaigns have been repeatedly conducted since 2013 to produce multi-temporal digital terrain models (DTMs). The computation of DTM differences has allowed to map and to quantify sediment transfer at the front of each studied rock glacier.

The variability of the erosion at the front of rock glaciers has been assessed at different time scales:

a) over decades,

b) over several years and

c) within one year:

a) Over decades, the erosion of the front is mainly driven by the rock glacier creep velocity and the topography on which the landform is advancing. This was deduced from the analysis of old aerial photographs, which shows that over long time periods, the position of the front line can either advance gradually or stay constant. In the first case, the erosion at the front is too low to balance the volume transferred by the creep and the topography allows the front line to advance over time (Dirru and Tsarmine between the 1960's and the mid-1990's). In the second case, the position of the front is constrained by topography and changes in creep velocity are directly related to changes in the amount of sediment eroded at the front (Dirru and Tsarmine since the mid-1990's, and Gugla since 1930). A long-lasting retreat of the front line position has not been observed at the studied sites.

b) Within the last years (June 2013 to October 2015), erosion rates at the front have been calculated for each rock glacier using a method based on the TLS-derived DTM differences and taking into account creep rate. The results are as follows: about 1500 cubic meters per year have been measured at Dirru, 2000 at Tsarmine and 8000 at Gugla. Differences between sites are related to the dimensions of the front and the creep velocity of the landforms. At each of the three rock glaciers, inter-annual variations in the erosion of the front have been identified by the observation of

webcam images and have been quantified since 2013 thanks to the TLS measurements.

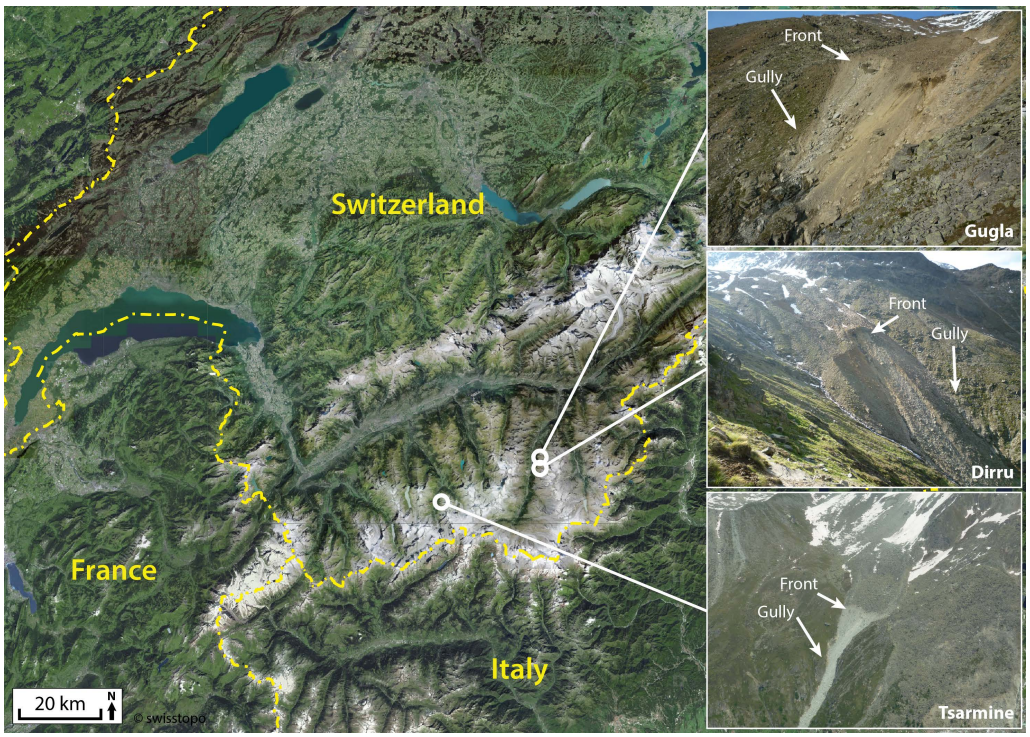

Figure 1: Location of the three investigated rock glaciers

They range in the order of several hundreds of cubic meters and are mainly related to the frequency of occurrence of erosion processes associated with specific groundwater and superficial water runoff conditions. These conditions are weather-dependent and can be met during

i) the snow-melt period, and

ii) important rainfall events occurring in summer or autumn.

Erosion induced by superficial water runoff is principally a consequence of rainfall events. It is usually widespread over the whole front but characterized by limited intensity. In addition, emergence of groundwater circulating either at the permafrost table or beneath the rock glacier frozen body may occur at the rock glacier front or downward in the gully. These temporary springs can be activated by rainfall or snow melt (at the scale of the whole catchment) and, depending on the water discharge and the position of the spring(s) in the gully, can generate significant linear regressive erosion along the water stream(s).

c) Within one year, three main periods can be distinguished in terms of erosion activity at the front. In winter (roughly 6 months between November and April), the rock glacier is advancing but the front is entirely frozen and covered with snow. Therefore, no erosion occurs. At the end of the winter, large volumes of sediments are potentially available for erosion as the mass transfer caused by the movement of the rock glacier has not been balanced by erosion. The second period, between winter and summer, corresponds to the melting of the snow covering the rock glacier and the progressive melt out of the active layer at the front. It is characterized by the frequent fall of small sediment volumes from the active layer and their progressive accumulation in the gully right under the front. This period can vary in time, length and intensity but usually lasts several weeks between April and May, or even sometimes June. During the summer (third period, lasting roughly 4 to 5 months), the erosion of the front is usually slow and continuous. It consists mostly in the fall of isolated boulders and rock debris from the edge of the front. During this period as well as during the snow melt, linear regressive erosion and/or superficial runoff erosion (cf. inter-annual variations) can temporary increase the erosion rate at the front.

To summarize, rock glaciers can act as important sediment conveyors and supply torrential channels with rock debris. The amount of sediments brought

into the torrents can however vary between sites depending on the morphology of the frontal area and the creep velocity. The sediments usually accumulate on the slopes a few meters/tens of meters under the front. Depending on the cases, more or less important parts of these sediments can be mobilized further downward by gravitational processes. Temporal variations have also been highlighted. Long term changes in the erosion at the front of rock glaciers are mostly dependent on creep velocity and topography, whereas variations occurring within one year or a couple of years are rather related to the occurrence of specific meteorological conditions. In terms of torrential hazards assessment and mitigation, the observations show that extensive linear regressive erosion related to the activation of springs with high discharge in the gully and/or at the front is the main process leading to the triggering of debris flows. Such torrential processes can therefore occur either during important rainfalls or during particularly intense snow-melt episodes at the scale of the catchment. Despite the steepness of the terrain and the high velocities measured on the investigated rock glaciers, no detachment and collapse of whole parts of the frontal areas have been observed so far.

References

Delaloye, R.; Morard, S.; Barboux, C.; Abbet, D.; Gruber, V.; Riedo, M. and Gachet, S. [2013]: Rapidly moving rock glaciers in mattertal. In *Mattertal – ein Tal in Bewegung, Publikation zur Jahrestagung der Schweizerischen Geomorphologischen Gesellschaft 29. Juni – 1. Juli 2011, St. Niklaus, Switzerland*, pages 113–124. Birmensdorf, Eidg. Forschungsanstalt WSL, Switzerland.

Lugon, R. and Stoffel, M. [2010]: Rock glacier dynamics and magnitude-frequency relations of debris flows in a high-elevation watershed: Ritigraben, Swiss Alps. *Global and Planetary Change*, 73:202–210.

Roer, I.; Haeberli, W.; Avian, M.; Kaufmann, V.; Delaloye, R.; Lambiel, C. and Kääb, A. [2008]: Observations and considerations on destabilizing active rock glaciers in the European Alps. In: Kane, D.L. and Hinkel, K.M.(eds.), *Proceedings of the Ninth International Conference on Permafrost*, Institute of Northern Engineering, University of Alaska Fairbanks, Fairbanks, USA, 29 June–3 July 2008, volume 2, pages 1505–1510. ISBN 978-0-9800179-3-9. URL http://ipa.arcticportal.org/publications/conference-proceedings.

10-year kinematic monitoring of two destabilized rock glaciers in the Western Swiss Alps

Christophe Lambiel[1] & Reynald Delaloye[2]

[1] *Institute of Earth Surface Dynamics, University of Lausanne, Lausanne, Switzerland*
[2] *Department of Geosciences, Geography, University of Fribourg, Fribourg, Switzerland*

Rock glacier creep velocities are controlled by several factors, such as ice content, liquid water content, slope gradient, sediment characteristics (eg. lithology, grain size) and ground temperatures. The latter explains why "warm" rock glaciers creep generally faster than colder rock glaciers and why rock glaciers speed up when ground is warming (Staub et al., this session). In particular, data on rock glacier velocities from the Western Swiss Alps show generally high and increasing values since 5-6 years, which is explained by warmer permafrost conditions.

About 10 years ago, several rock glaciers in the Western Swiss Alps were recognized as being destabilized. These landforms are characterised by unusual high velocities and by landslide-like morphologies, such as the presence of crevasses or transversal scarps. To better understand their dynamics, we initiated a kinematic monitoring with dGPS surveys of two of these rock glaciers: the Tsaté-Moiry (TM) and Petit Vélan (PV) rock glaciers.

TM is a 400 m long rock glacier located in a steep calcschists debris slope [Lambiel, 2011]. A first transversal scarp appeared at the roots in the late 1980's. Strong modifications of the surface appeared then, with the development of several scarps and a substantial advance of the front, which progressed of about 40 m downslope between 1988 and 2005. This fast moving body is delimited by two lateral stable crests, which suggests strong deformation at the shear horizon. Surprisingly, ground ice may be no more present in the first 60 meters uphill the front, as shown by geophysical surveys. PV is another 400 m long rock glacier, with complex morphology in the rooting zone, partly under the influence of a small glacier during the Little Ice Age. A transverse crevasse was observed in 1995 at the level of a step located 150 m above the front and evolved later in a landslide-like scarp. The destabilized terminal tongue is currently separated from the main body of the rock glacier, as attested by geophysical investigation carried out in 2007-09 [Delaloye and Morard, 2011].

DInSAR data shows that both rock glaciers moved at an unusually high rate in 1995 already and were doing so continuously until the start of our kinematic monitoring in August 2005. A network of around 50 GNSS points was marked on both rock glaciers. They have been measured 2x/year, in July and October. GST survey at five locations on each rock glacier fits well with longer time series in both regions.

The data collected display different behaviours across both rock glaciers (Fig. 1). From 2005 (year of the minimal velocities reached by most intact active rock glaciers studied in Switzerland since 2000), velocities strongly increased in the lower part, reaching values of 7 to 9 m/y in 2009. Since that period, the velocities decreased severely at Tsaté-Moiry, to reach values as low as 0.2 m/y in 2015. At Petit Vélan, the velocities decreased as well, but remained quite high, with values of 4 m/y in 2015, which are still 2x faster than in 2006. In the upper part of TM, the movements increased regularly from 2007 (0.6 m/y), to reach values of 2.8 m/y in 2015. In the intact part of PV, the velocities increased as well, from 0.25 m/y in 2005 to 1.3 m/y in 2015. Thus, whereas the upper, respectively intact parts display an evolution almost similar to what is measured on most of the rock glaciers, the destabilized parts show an opposite behaviour.

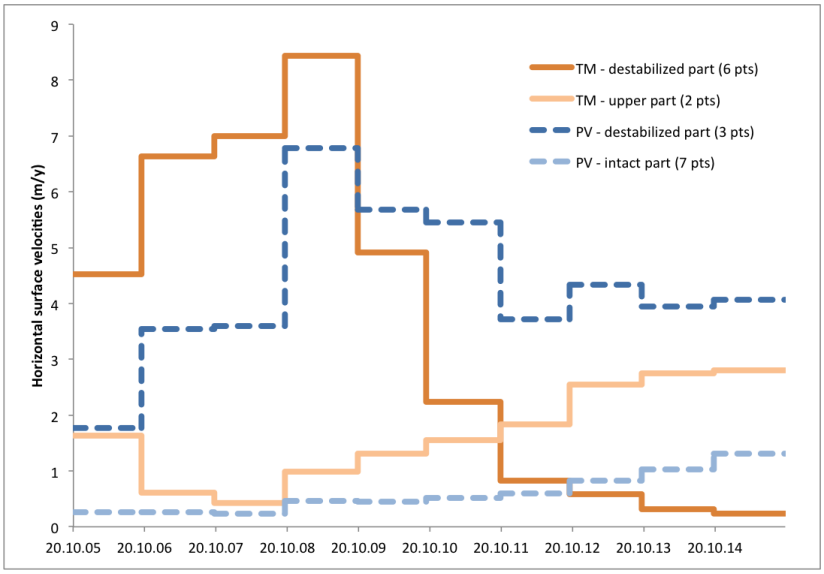

Figure 1: Horizontal surface velocities of the destabilized and upper/intact parts of the Tsaté-Moiry (TM) and Petit Vélan (PV) rock glaciers.

We interpret the initial increase of movements in the lower part of both rock glaciers by a response to rock glacier warming in the 80's. High deformation process at the shear horizon enhances extension, which can lead to the formation of transversal scarps. In turn, water can penetrate more easily at depth, which maintains high velocities. The decreasing strain rate consecutive to the size decrease of the rapidly moving part (by spreading and leaving sediments on its sides and by abandoning gradually debris behind it), the increasing friction due to lower slope angle, as well as ground ice melting are explanations for the following deceleration of the frontal part of the investigated rock glaciers. However, this slowing down appears to be partly compensated by the effects of the post-2011 warming at PV. In the upper/intact parts, the kinematical behaviour is well congruent with M2AGST (see approach proposed by Staub et al. [2016], this session on page 96).

This study shows that the rock glacier dynamics can be inhomogeneous at the scale of the landform: some parts can accelerate, whereas other can slow down. In particular, strong and rapid deceleration of former very active parts can occur, even in a period of a general increase of rock glacier velocities. This suggests that crisis in the rock glacier kinematics are time-limited.

References

Delaloye, R. and Morard, S. [2011]: Le glacier rocheux déstabilisé du Petit-Vélan (Val d'Entremont, Valais) : Morphologie de surface, vitesses de déplacement et structure interne. In: Lambiel, C.; Reynard, E. and Scapozza, C.(eds.), *La géomorphologie alpine: entre patrimoine et contrainte. Actes du colloque de la Société Suisse de Géomorphologie, 3-5 septembre 2009, Olivone (Géovisions n°36).* Institut de géographie, Université de Lausanne.

Lambiel, C. [2011]: Le glacier rocheux déstabilisé de Tsaté-Moiry (VS) : caractéristiques morphologiques et vitesses de déplacement. In: Lambiel, C.; Reynard, E. and Scapozza, C.(eds.), *La géomorphologie alpine: entre patrimoine et contrainte. Actes du colloque de la Société Suisse de Géomorphologie, 3-5 septembre 2009, Olivone (Géovisions n°36).* Institut de géographie, Université de Lausanne.

Staub, B.; Lambiel, C. and Delaloye, R. [2016]: Rock glacier creep as a thermally-driven phenomenon: a decade of inter-annual observations from the Swiss Alps. In Günther, F. & Morgenstern, A. (eds.) *XI. International Conference on Permafrost – Book of Abstracts*, 20–24 June 2016, Potsdam, Germany. Bibliothek Wissenschaftspark Albert Einstein, pages 95–96.

Spatial distribution and morphometry of permafrost-related landforms in Boí valley (Central Pyrenees)

Luis Filipe Lopes, Marcelo Fernandes, & Marc Oliva

Instituto de Geografia e Ordenamento do Território – CEG, Universidade de Lisboa

Present and past permafrost distribution in the Pyrenees is still under discussion. As in other mid-latitude mountain regions, rock glaciers and protalus lobes are the min indicators of permafrost conditions. In this study, we examine the distribution of these landforms in the Boí valley, a formerly glaciated U-shaped valley ranging from 850 to 3000 m a.s.l. The valley encompasses a surface of 247 km^2, mainly composed of granite and shales. At 2500 m a.s.l. the precipitation reaches 1200 mm and the mean annual temperature varies from 6.8 °C at 1500 m a.s.l. to -0. °C at 3000 m a.s.l., with negative monthly temperatures from November to April. The spatial distribution of rock glaciers and protalus lobes and their chronostratigraphic position within the valley allow a better understanding of the climatic and environmental conditions necessary for their development.

Geomorphological mapping of these landforms was built using high resolution imagery provided by the Institut Cartogràfic i Geologic de Catalunya, complemented with Basemap ESRI images and Google Earth Pro, and subsequently improved with field observations. The map was generated in a GIS environment following the RCP 77 mapping system of the Centre National de la Recherche Scientifique (CNRS) [Joly, 1997]. Several parameters of each landform have been measured (Tab. 1): area (ha), altitude (maximum, minimum, mean), length (L), width (W), aspect and slope. This information provides accurate characterization of the morphometric properties of these landforms as well as a detailed identification of their spatial distribution.

Only one rock glacier is active in this valley located at the foot of the highest peak [Chueca Cía and Julián Andrés, 2011], while the rest are inactive. Up to 121 permafrost-related landforms were identified in the Boí valley, including 84 rock glaciers and 37 protalus lobes. Most of the landforms (93 % for rock glaciers and 95 % for protalus lobes) are located inside the glacial cirques, while the rest is distributed in the valley bottom or slopes of the formerly glaciated valleys. The lowest elevation of both forms is situated at 2100 m a.s.l. Therefore, this altitude may be indicative of the lowest level recording permafrost conditions during the period in which these landforms formed. The maximum elevation of the landforms usually corresponds to the highest parts of the cirques, oscillating between 2700 m a.s.l. for protalus lobes and 2900 m a.s.l. for rock glaciers. Nevertheless, 77 % of the rock glaciers and 78 % of the protalus lobes are located in the elevation belt ranging from 2200 to 2600 m a.s.l., which is assumed to be the optimal elevation range for their development in the study area. Aspect does not show any prevailing orientation in the case of rock glaciers, though protalus lobe formed preferably on SW aspects (27 %), being almost absent in the S, SE and E aspects (only 5 %).

Table 1: Some physical parameters calculated for rock glaciers and protalus lobes, organized by altitudinal ranges.

	Elevation range	Nº of elements	Width	Length	W/L	Area (ha)	Slope (º)
Rock Glacier	< 2200	3	98	209	2.2	6.4	22
	2200 - 2399	18	84	187	2.4	5.4	21
	2400 - 2599	47	65	122	1.9	2.9	21
	2600 - 2799	14	72	120	1.7	3.6	21
	> 2800	2	50	76	1,7	1,2	22
Protalus Lobes	< 2200	2	179	41	0.2	2.2	24
	2200 - 2399	13	183	49	0.3	3.9	23
	2400 - 2599	16	217	46	0.2	4.0	19
	> 2600	6	145	33	0.2	1.8	23

Regarding morphometry, the average area occupied by the rock glaciers decreases with altitude (6.4 ha to 1.2 ha). This trend is not observed in the case of protalus lobes, which show the largest surfaces between 2200 and 2600 m a.s.l. The W/L ratio reveals that the rock glaciers distributed at lower altitudes are more elongated (W/L ratio > 2), while those at higher elevations are shorter. No clear patterns are observed when comparing the morphology of protalus lobes and the altitude. The average slope of both landforms lies between $21-22°$, with a maximum of 29° for rock glaciers and 31°for protalus lobes. The minimum slope necessary for the development of these two landforms is 11°.

The geomorphological mapping of the glacial landforms that is being now conducted will allow identifying the chronology of the development of these landforms based on its chronostratigraphic position within the valley and with respect to the four moraine complexes (glacial stages) identified in the area.

References

Chueca Cía, J. and Julián Andrés, A. [2011]: Besiberris glacigenic rock glacier (Central Pyrenees, Spain): Mapping Surface horizontal and vertical movement (1993-2003). *Cuadernos de Investigación Geográfica*, 37:7–24.

Joly, F. [1997]: *Glossaire de géomorphologie – Base de données sémiologiques pour la cartographie*. Armand Colin, Paris.

Modelling three-dimensional distribution and evolution of rock wall permafrost in the Mont Blanc massif

Florence Magnin[1], Ludovic Ravanel[1], Philip Deline[1], Benjamin Pohl[2], Julien Pergaud[2], & Daniel Joly[3]

[1] *EDYTEM Lab, Université de Savoie, France*
[2] *Centre de Recherches de Climatologie, Université de Bourgogne, France*
[3] *ThéMA, Université de Franche Comté, France*

Permafrost occupies about 65 % of the rock walls above 2500 m a.s.l. in the Mont Blanc massif. Multilateral heat transfers induced by the sharp topography with needles and ridges contribute to rapid temperature changes in steep alpine rock walls. Permafrost degradation could trigger mass movements bearing geomorphological and socio-economic issues as illustrated by the increase in rock fall activity observed over the past two decades, some rock falls having impacted infrastructure and human activities, and caused fatalities. The VIP Mont-Blanc project (VItesses des Processus contrôlant les évolutions morphologiques et environnementales du massif du Mont-Blanc, 2015-2019, funded by the french ANR) aims at gaining insight in the future changes of rock wall permafrost in the Mont Blanc massif.

Bi- and three-dimensional models of rock wall temperature will be implemented using the commercial software Feflow (Finite Element subsurface FLOW system). First, steady-state permafrost distribution for the present days will be simulated using statistically-derived mean annual rock surface temperature distributed over a high resolution DEM as upper boundary condition, and a heat conduction scheme. The subsurface temperature fields will be calibrated by the mean of measured temperature at three 10-m-deep boreholes installed on different aspects at the Aiguille du Midi (3842 m a.s.l.) since December 2009. Then steady state models will run for selected sites of the massif, some of them having been sounded in 2013 and 2013 by electrical resistivity tomography down to 25-m-depth, providing an independent data set to evaluate the model outputs. In a last step, transient simulations of future permafrost scenarios for the whole massif are forced by air temperature variables provided by the downscaling of General Circulation Models (GCMs).

Snow control on active layer and permafrost in steep alpine rock walls (Aiguille du Midi, 3842 m a.s.l, Mont Blanc massif)

Florence Magnin[1], Sebastian Westermann[1], Thierry Barth[3], Georges-Marie Saulnier[1,3], Paolo Pogliotti[4], Philip Deline[1], & Ludovic Ravanel[1]

[1] *EDYTEM Lab, Université de Savoie, France*
[2] *Department of Geosciences, University of Oslo, Norway*
[3] *TENEVIA, Meylan, France*
[4] *ARPA Valle d'Aosta,Saint Christophe, Italy*

Permafrost degradation through the thickening of the active layer and the rising temperature at depth is a crucial process of rock wall stability. The ongoing increase in rock falls observed during hot periods in mid-latitude mountain ranges is regarded as a result of permafrost degradation. However, the short-term thermal dynamics of alpine rock walls are misunderstood since they result of complex processes related to the interaction of local climate variables, heterogeneous snow cover and heat transfers. As a consequence steady-state and long-term changes that can be approached with simpler process mainly related to air temperature, solar radiations and heat conduction were the most common dynamics to be studied so far.

The effect of snow on the bedrock surface temperature is increasingly investigated and has already been demonstrated to be an essential factor of permafrost distribution. Nevertheless, its effect on the year-to-year changes of the active layer thickness and of the permafrost temperature in steep alpine bedrock has not been investigated yet, partly due to the lack of appropriate data.

We explore the role of snow accumulations on the active layer of steep rock walls of a high-elevated permafrost site, the Aiguille du Midi (AdM, 3842 m a.s.l, Mont Blanc massif, Western European Alps) by mean of a multi-methods approach. We first analyse six years of temperature records in three 10-m-deep boreholes. Then we describe the snow accumulation patterns on two rock faces by means of automatically processed camera records. Finally, sensitivity analyses of the active layer thickness and permafrost temperature towards timing and magnitude of snow accumulations are performed using the numerical permafrost model CryoGrid 3. The energy balance module is forced with local meteorological measurements on the AdM S face and validated with surface temperature measurements at the weather station location. The heat conduction scheme is calibrated with the temperature measurements in the S-exposed borehole. Results show that the snow is responsible for permafrost presence on the AdM South face. The long lasting of the snow during early or mid-summer has a delaying effect on the seasonal thaw, which contributes to the lowering of the active layer thickness. Summer snow falls may interrupt the thawing front propagation, especially if the snow stays several days on the rock surface. Early snow accumulations in September lead to the refreezing of the active layer meanwhile snow free rock faces can experience active layer thickening until mid-fall. The snow control is highly dependent on snow timing, thickness (due to the resulting melting time) and the sun-exposure on which it accumulates (due to its high albedo). Thus, this study encourages to better taking into account the local bedrock and snow conditions to improve the understanding of active layer formation and changes in steep rock walls.

Imaging the transition from micro- to macro cracking of freezing rock using micro-computed tomography scanning

Vikram Maji & Julian B. Murton

University of Sussex, United Kingdom

Fractures developed in rocks by prolonged exposure to cold climates are difficult to predict and of major concern for rock fall hazard prediction and prevention [Amitrano et al., 2010]. The objective of the present research is to monitor how flaws inherent within rocks (e.g., voids, sharp contrasting grain boundaries, discontinuities) develop first into microscopic cracks (microcracks) and then into larger cracks visible to the naked eye (macrocracks) as a result of freeze-thaw cycling. We defined a "connectivity index" as a ratio of the number of interconnecting flaws over the number of flaws per unit volume. We hypothesised that this index increases in value as the rock experiences stress (e.g. by thermal contraction, volumetric expansion of freezing water, or frost heave induced by ice segregation) and after an optimum value, macrocracking commences. We assumed that the rock specimen does not experience any other mechanical stress during the entire cooling period and reflects the changes only after experiencing sub-zero temperature.

We carried out freeze-thaw experiments on cylinders of rock and imaged crack development within them by micro-Computed Tomography (micro-CT) scanning. The freeze-thaw experiment was performed in a climate cabinet in the Sussex Permafrost Laboratory. Rock cylinders 2 cm in diameter and 2 cm in length were selected to maximize the resolution for imaging the transition from micro- to macrocracking. The rocks imaged were tuffeau (chalk) and Ardingly Sandstone, both types used in previous weathering experiments at Sussex, and the tuffeau known to be highly frost-susceptible and therefore subject to fracture by ice segregation. Micro CT scanning was carried out at Queen Mary University of London, using a maximum of 250 kV Tungsten target X-ray source, and a 1000 × 1000 pixel-sized detector. The detector measured the 3D distribution of the linear attenuation coefficient of an incident X-ray beam in order to visualise the internal structure of the rock specimens [Ketcham and Carlson, 2001]. Repeated scanning of the same rock cylinders before, during and after the freeze-thaw experiment recorded crack development through time. Micro-CT images were processed (using CT Pro, Fiji software) and analysed (using Drishti software) to quantify the micro- to macrocrack transition based on the connectivity index parameter.

This novel approach of quantifying the transition from micro to macrocracking in rocks due to natural freezing phenomena increases our understanding of rock fracture at small scales.

References

Amitrano, D.; Arattano, M.; Chiarle, M.; Mortara, G.; Occhiena, C.; Pirulli, M. and Scavia, C. [2010]: Micro-seismic activity analysis for the study of the rupture mechanisms in unstable rock masses. *Natural Hazards and Earth System Sciences*, 10:831–841.

Cnudde, V. and Boone, M.N. [2013]: High-resolution X-ray computed tomography in geosciences: A review of the current technology and applications. *Earth-Science Reviews*, 123(2013):1–17.

Ketcham, R.A. and Carlson, W.D. [2001]: Acquisition, optimization and interpretation of X-ray computed tomographic imagery: applications to the geosciences. *Computers & Geosciences*, 27(4):381–400.

Towards a mechanical failure model for degrading permafrost rock slopes representing changes in rock toughness and infill

Philipp Mamot, Michael Krautblatter, & Riccardo Scandroglio

Technical University of Munich, Germany

The climate-induced degradation of permafrost in mountain areas can reduce the stability of rock slopes. An increasing number of rockfalls and rockslides originate from permafrost-affected rock faces. Discontinuity patterns and their geometrical and mechanical properties play a decisive role in controlling rock slope stability. Under thawing conditions the shear resistance of rock reduces due to lower friction along rock-rock contacts, decreasing fracture toughness of rock-ice contacts, diminishing fracture toughness of cohesive rock bridges and altered creep or fracture of the ice itself. Compressive strength is reduced by 20 to 50 % and tensile strength decreases by 15 to 70 % when intact saturated rock thaws [Krautblatter et al., 2013]. Elevated water pressures in fractures can lead to reduced effective normal stresses and thus to lower shear strengths of fractures. Davies et al. [2001] show that joints filled with warm ice (up to -2 °C) reveal lower shear strength than ice-free joints. However, the impact of degrading permafrost on the mechanical properties of intact or fractured rock still remains poorly understood.

In this study, we develop a new approach for modeling the influence of degrading permafrost on the stability of high mountain rock slopes. Hereby, we focus on the effect of rock-mechanical changes along striking discontinuities onto the whole rock slope. We aim at contributing to a better rock-ice mechanical process understanding of degrading permafrost rocks.

For parametrization and subsequent calibration of our model, we chose a test site (2885 m a.s.l.) close by the Zugspitze summit in Germany. It reveals

i) a potential rockslide at the south face involving 10.000 m^3 of rock and

ii) permafrost occurrence due to ice-filled caves and fractures.

A combination of already conducted rock temperature measurements and a permafrost modeling of the Zugspitze summit area demonstrate that the test site is located at the lower permafrost extension limit. Further, permafrost conditions are found in the northern slope whereas positive rock temperatures are observed in the south slope.

We combine kinematic, geotechnical and thermal monitoring in the field with rock-mechanical laboratory tests and 2D numerical failure modeling (see table 1). Up to date, our following results underline the potential effects of thawing rock and fracture infill on the stability of steep rock slopes in theory and praxis:

1. ERT and SRT measurements confirm that the unstable area lies in a permafrost border zone. The south face of the Zugspitze crest is mainly thawed while the north face shows permanently frozen sections.

2. High-accuracy movement measurements along discontinuities reveal maximum rates of 73.8 mm/year and an average of 10.26 mm/year (median: 4.01 mm/year).

3. Brazilian lab tests on saturated Zugspitze limestone show that indirect tensile strength decreases by 30 % from frozen to unfrozen condition.

4. Saturated Zugspitze limestone shows a decrease by 15 % in P-wave velocity from frozen to unfrozen state.

5. Shear tests on fill material of discontinuities at the Zugspitze crest reveal that shear strength in frozen state is higher than in unfrozen state. Fine grained soil decreases by 5 – 45 % and coarse grained soil by 35 – 65 % after thawing.

Table 1: Applied methods and corresponding expected outcomes of the study.

Applied method	Expected results
Automatic continuous crackmeter + discontinuous extensometer (since 2009)	Fracture movements → Spatial and temporal assessment of rock instability
Electrical resistivity (ERT) + seismic refraction tomography (SRT)	Spatial assessment of rock temperatures / permafrost distribution
Rock temperature monitoring with iButton logger (since 2015)	Spatial assessment of rock temperatures / permafrost distribution, calibration of geophysical measurements
Discontinuity analysis and geomorphological mapping	Detection of geotechnical and geometrical factors influencing rock instability
F/u (frozen/unfrozen) rock strength of Zugspitze limestone: • f/u uniaxial compressive strength and tensile strength • f/u shear strength • f/u fracture toughness of intact rock bridges • f/u P-wave velocity and electrical resistivity Rock fatigue after repeated freeze-thaw cycles (JIA ET AL. 2015)	Identification of rock strength parameters for 2D numerical failure model
2D discontinuum mechanical modeling	Mechanical failure model

References

Davies, M.C.R.; Hamza, O. and Harris, C. [2001]: The effect of rise in mean annual temperature on the stability of rock slopes containing ice-filled discontinuities. *Permafrost and Periglacial Processes*, 12:137–144.

Jia, H.; Xiang, W. and Krautblatter, M. [2015]: Quantifying rock fatigue and decreasing compressive and tensile strength after repeated freeze-thaw cycles. *Permafrost and Periglacial Processes*, doi:10.1002/ppp.1857.

Krautblatter, M.; Funk, D. and Günzel, F.K. [2013]: Why permafrost rocks become unstable: a rock-ice-mechanical model in time and space. *Earth Surface Processes and Landforms*, 38:876–887.

A multi-method approach to detecting high-mountain rockfall activity

Norikazu Matsuoka

Faculty of Life and Environmental Sciences, University of Tsukuba, Japan

Recent technological advances have enabled accurate and high-spatial resolution monitoring of rockfall activity by 3D laser scanning and high-time resolution monitoring of bedrock micro-cracking that precursors rockfalls. Precise understanding of the triggering processes of each rockfall event, however, requires a combination of multiple methods for detecting cracking and falling processes, and their controlling environmental parameters. Long-term monitoring is also necessary to evaluate the contribution of each trigger to the rockwall retreat.

A combination of multiple methods has been applied to detect the timing and trigger of rockfall activity on an alpine rockslide cliff composed of Cretaceous sandstone and shale (Aresawa rock slide, 2900 m a.s.l., the Japanese Alps). The methodology includes time-lapse photography (daily) and thermography (yearly) of rockface, peeling from painted rockface and collection of fallen debris (4-5 times per year), monitoring of crack opening, rock temperature and moisture (3-4 hr intervals) and meteorological observations (air temperature and precipitation: 10-min intervals). A stereographic pair of sequential photographs allow us to visually detect the location of new erosion at daily resolution. The photographs also indicate the type of precipitation (rain or snow).

Five years (2010-2015) of debris trapping show that major rockfall activity occur in winter and occasional activity associated with heavy rains. The active parts of the rockwall experience retreat by >1 mm per year. Time-lapse photography displayed at least eight rockfall events within the shot area in the 2014-15 period (Fig. 1A). The combination of multiple data enables us to understand a sequence of natural processes towards rockfalls, suggesting that at least three types of rockfall processes recur annually. In summer and early autumn, heavy rainfalls (>100 mm/day) raise rock moisture content and often trigger significant rockfalls, probably due to water pressure or lubrication of rock joints (e.g., Event 2: Fig. 1B). In late autumn and late spring, light or intermediate rainfalls are sometimes followed by high moisture, shallow freezing, rapid thawing and eventually by small-scale rock peeling (e.g., Event 6: Fig. 1C). In early winter and early spring, rainfall in the second case is replaced by snowfall (e.g., Event 7: Fig. 1C).

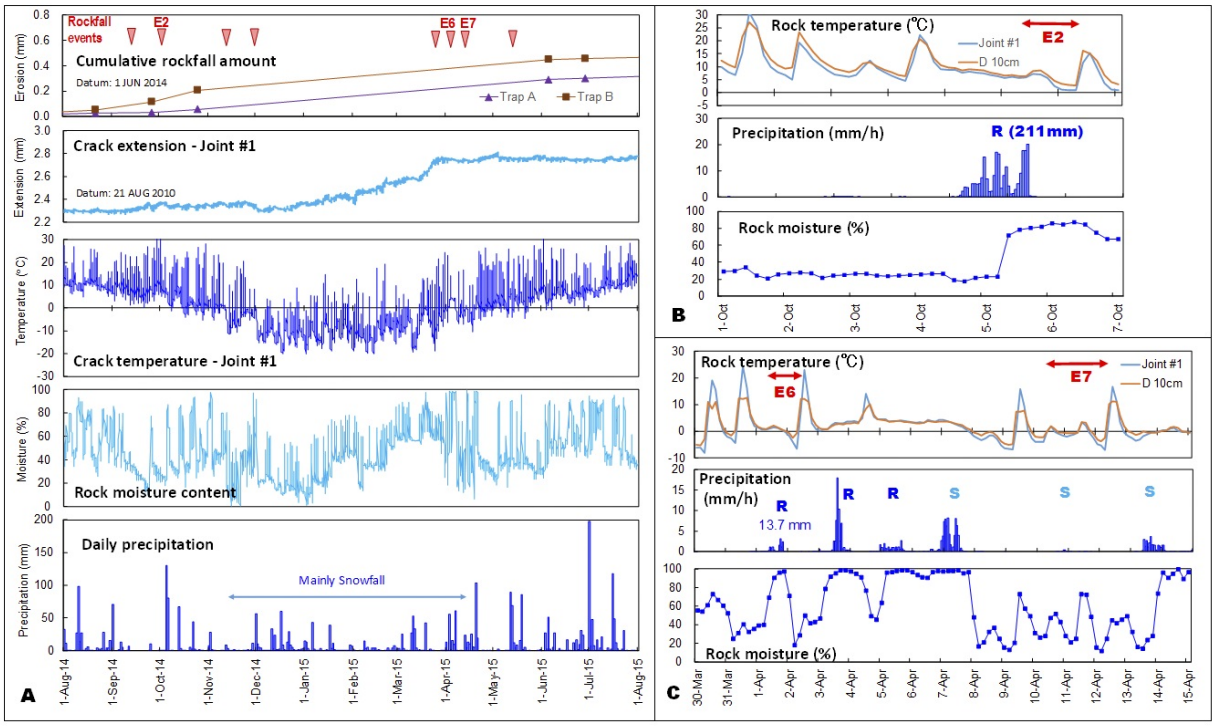

Figure 1: Annual and short-term variations in rockfall amount, crack width, rock temperature, moisture and precipitation monitored at a SE-facing rockwall, Japanese Alps. Rockfall events were detected from time-lapse photography. R=rainfall, S=snow.

Slow, but steady movement of an Arctic rock glacier: 10 years of dynamics and thermal conditions

Norikazu Matsuoka[1], Tatsuya Watanabe[2], Atsushi Ikeda[1], Hanne H. Christiansen[3], & Ole Humlum[4]

[1] *Faculty of Life and Environmental Sciences, University of Tsukuba, Japan*
[2] *Department of Civil and Environmental Engineering, Kitami Institute of Technology, Japan*
[3] *The University Centre in Svalbard, Norway*
[4] *University of Oslo, Norway*

Whereas recent studies have revealed the rates, processes and long-term evolution of active rock glaciers in mid-latitude and subpolar mountains, the dynamics of polar rock glaciers have rarely been observed, apart from remote sensing analysis of surface movements. This presentation summarizes 10 years'data (2005–2015) of thermal conditions and deformation of a small Arctic rock glacier (called Huset RG in the following) located within Longyear Valley, Svalbard. Huset RG (50 m long, 60 m wide) constitutes a basal bulge of U-shaped valley slope. In the summer of 2005, a 15-m deep borehole was drilled through the top surface of Huset RG. Thermal cables (at 0.02, 1, 2, 3, 5, 7, 9, 11, 13, 15 m depth) and inclinometers (at 5, 9, 13 m depth) were installed in the hole. In addition, ultra-sonic distance meter recorded the snow depth and a thermistor sensor provided air temperature data. All data were stored at 6-h intervals in a Campbell CR10X logger (Fig. 1).

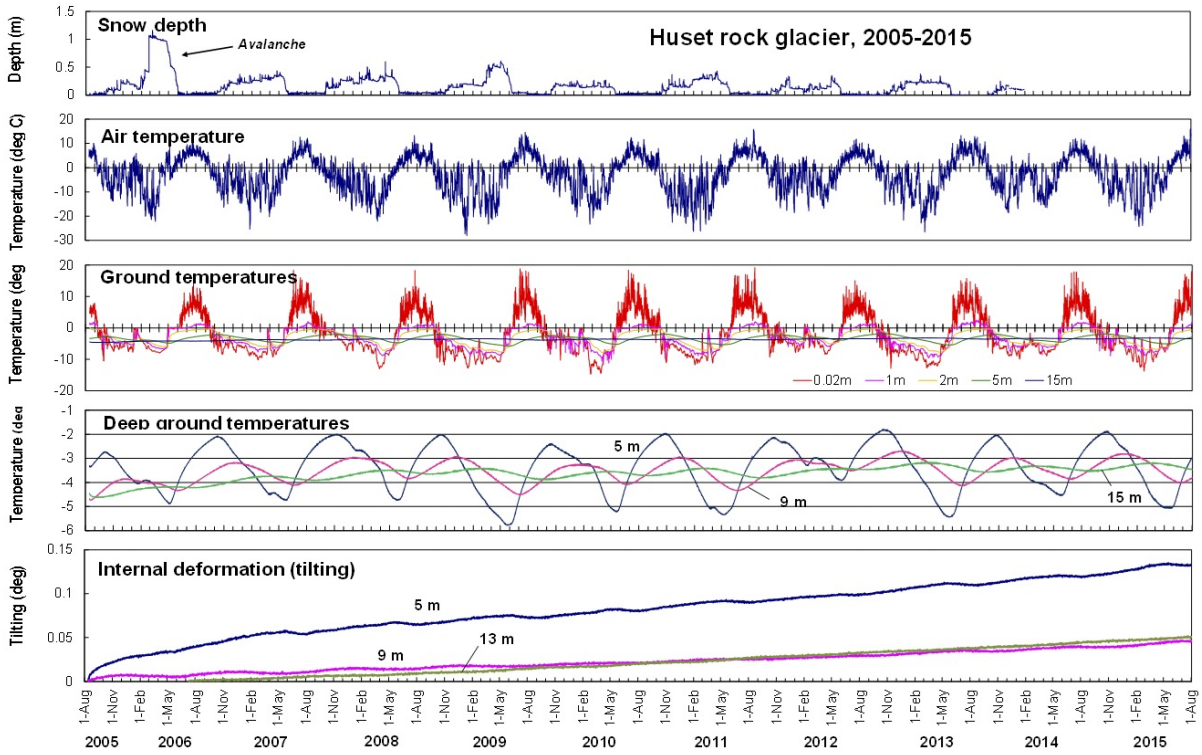

Figure 1: Ten years of ground thermal conditions and movements of Huset rock glacier.

During 10 years, annual mean air temperature fluctuated significantly, from -2.1 to -4.3 °C (average -2.9 °C). The top surface was covered with snow for about seven months in a year. Despite the long persistence, the thin snow cover (rarely in excess of 0.5 m thick) promotes intensive ground cooling. A blocky top layer of the rock glacier permits an active layer to reach about 2 m in depth. Annual mean ground temperatures at 5–15 m depth in permafrost was about -3.5 °C, with slight interannual fluctuation and overall warming by about 0.5 °C during the past 10 years. The inclinometers steadily tilted downslope by a rate of 0.005° to 0.01° per year, with the largest tilting at 5 m depth. The small but steady tilting was reflected by surface movements of 1–3 cm/yr, which were annually measured at 13 points with Realtime Kinematic GPS. The largest tilting at 5 m depth corresponded to the presence of an ice-rich layer at 5–10 m depth, which was confirmed by the electrical resistivity tomography. A noteworthy feature is that the annual rate of tilting generally increased with increasing annual mean ground temperature, which implies that further warming would promote gradual acceleration of movement.

Depth of seasonally frozen ground in the Karkonosze Mts (Sudetes, SW Poland) in the light of GIS modeling of topoclimate and geomorphic conditions

Krzysztof Migała & Andrzej Traczyk

University of Wrocław, Poland

The potential depth of seasonally frozen ground above tree line in the Karkonosze Mts (Giant Mountains) was estimated on the basis of long-term meteorological data (1961-2000) from the weather station located at 1325 m a.s.l. and geomorphometric parameters and spatial distribution of different cover deposits. Empirical formula proposed by Wiłun [1987] was used. The equation allows determining depth of frost penetration depending on the sum of mean monthly temperatures below zero. The relationship refers to clay and silty sediments but also can be applied to sandy-gravel deposits.

Frost penetration modeling assumed relationship between altitude and ground temperature specified by linear regression. The modeling also included geomorphometric parameters describing numerous landform shapes as well assumed spatial distribution and granulometric composition of Pleistocene periglacial cover deposits developed on granitic bedrock. System for Automated Geoscientific Analyses (SAGA GIS) was applied and potential frost depth was estimated for long-term daily values and for seasons with extremely warm and extremely cold winter. The impact of snow drift, decline of snow cover and variability of insolation was also taken under consideration.

Our study indicates that contemporary, seasonal freezing of the ground above tree line in Karkonosze Mts probably reaches a depth of 1.5-2.3 m and during extremely cold winters can exceed even 2.5 m. The zones of maximum depth of frost penetration coincide with areas of occurrence of slope block covers with "open-work" structure. In some places, where the depth of freezing exceeds 2 m the presence of active patterned grounds were identified on the basis of field mapping.

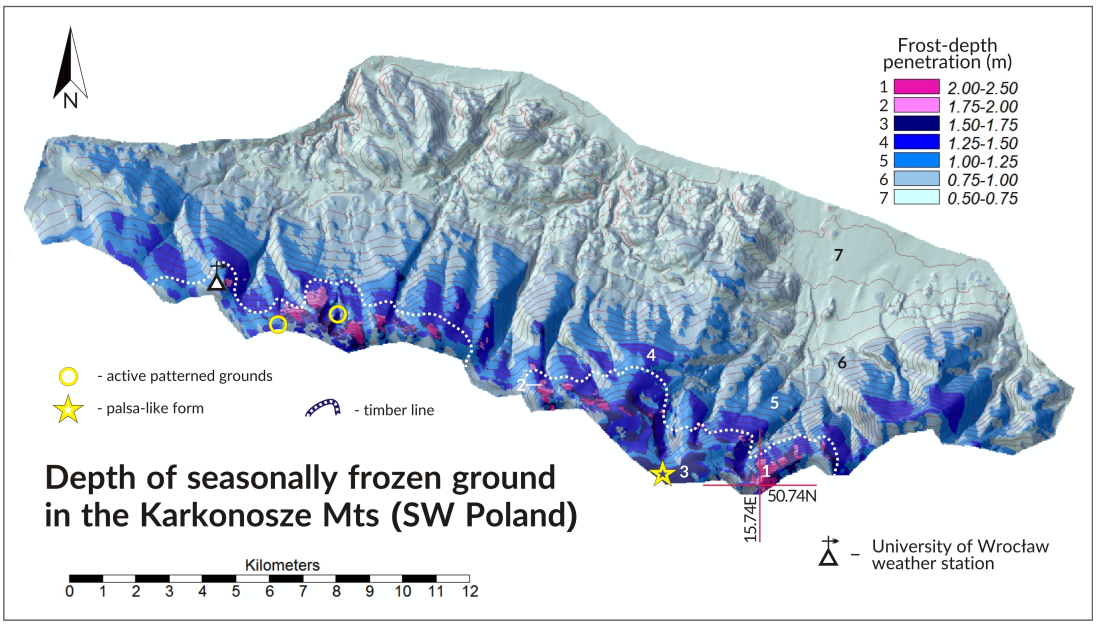

Figure 1: Depth of seasonally frozen ground in the Karkonosze Mountains (SW Poland)

Frost penetration reached the depth of 1.2-1.5 m in the area of summit and subslope flattenings with peat cover, which are located above 1100-1200 m a.s.l. High level of peat cover moisture creates an opportunity to develop the ground segregation ice bodies and structures of the "palsa" type. One of the "palsa" like-type form was described from the summit peat-bog lying in the eastern part of the Giant Mountains at the altitude 1425 m a.s.l. [Soukupová et al., 1995]. Spatial data analysis (GIS) and above mentioned observations suggest that in the highest part of Karkonosze Mts possibly occurred terms for contemporary seasonal activity of periglacial processes (e.g. frost heave and soil segregation, gelifluction), especially in places where on slopes exist fine-grained weathering and slope cover deposits or organic – peat deposits. The conditions favourable for deep ground freezing depend not only on extreme drops of temperature below 0 °C but also on decline of snow cover due to deflation and in the aftermath of small amount of winter precipitation. However, geomorphic manifestation of these periglacial processes in mid-latitude, Central European mountain massifs such like Karkonosze (Giant Mountains), depends on the global and long-term climate change.

References

Soukupová, L.; Kociánová, M.; Jeník, J. and Sekyra, J. [1995]: Arctic-alpine tundra in the Krkonoše, the Sudetes. In *Opera Corcontica (Yearbook of Scientific Papers from the Krkonoše National Park)*, volume 32, pages 5–88.

Wiłun, Z. [1995]: *Outline of the geotechnics*. Publishing House of Transportation and Telecommunication, Warsaw, 724 pp., (in Polish).

Geomorphic evolution in an ice-rich glaciated permafrost environment

Brian J. Moorman

University of Calgary, Canada

One of the unique elements of permafrost terrain is the presence of excess ice. This results in number of the geomorphic processes, and the resulting landforms, found in permafrost environments being different than anywhere else in the world. Pingos, rock glaciers and thermokarst lakes are three of the most dramatic examples of this. However, the presence and melt-out of excess ice in permafrost terrain has many more expressions. It also has wide-ranging implications to such things as animal habitat, hydrology and aquatic ecosystems, terrain stability for engineering development and the contribution of greenhouse gases to the atmosphere.

In this research project, the preservation and degradation of excess ice was examined with a specific focus on the rate and magnitude of change and the impact on the overall landscape. As we are currently experiencing rapid climatic change in the north, instead of looking at long-term broad landscape-scale changes, specific local change on the annual to decadal scale was examined.

The study area for this research was Bylot Island in the continuous permafrost zone of the Canadian Arctic Islands. It is home to many glaciers as well as recently deglaciated terrain and areas that have not been covered by glaciers for tens of thousands of years. It also contains a wide variety of buried ground ice types. At several locations across the south side of the island, the presence of excess ice in the permafrost and geomorphic activity on the surface were mapped and the rate of terrain change analysed over the last two decades.

The results of this study indicate that while there is appreciable differences in what controlled the rate of landscape evolution between different landforms (e.g. ice quantity and depth beneath the active layer), there was also some consistent variables across all terrain types (e.g. the impact of a warming climate and changing surface hydrology). Because the melt-out of excess ice can result in catastrophic landscape changes, the concept of "tipping points" is very applicable when studying these processes. For example, in some areas when the increase in the active layer thickness resulted in an active layer detachment and the exposure of massive ice, erosion rates could increase by several orders of magnitude. A number of unexpected geomorphic results were also identified. Events such as surface streams becoming subterrainian are very difficult to predict and yet can have dramatic implications on the overall environment. At the other end of the sectrum, there were some geomorphic processes that resulted in negative feed-back loops resulting in terrain stabilization (e.g. increase in active layer thickness leading to drainage and drying out of the near-surface soils, resulting in better thermal insulation and cooling of the ground.

In conclusion, it was revealed that studying short-term landscape evolution, in times of rapid environmental change, is important because this evolution can take on a very different character than the "smoothing" results produced by landscape evolution over the long term. This is especially true in ice-rich permafrost terrain where there is dramatic spatial variability. There was also an operational efficiency achieved where many different terrain types could be studied in a small area, while still providing representative examples of the broader landscape.

Rockglaciers on the move – A multi sensorial approach to rockglacier evolution

Johann Müller, Isabelle Gärtner-Roer, & Andreas Vieli

University of Zurich, Switzerland

Rockglaciers as a visually detectable feature of mountain permafrost have received considerable attention concerning their kinematics and thermal characteristics. The application of numerous terrestrial, airborne and spaceborne remote sensing techniques to acquire data on rockglacier kinematics and surface geometries have indicated an acceleration over the last decades of rockglacier velocity data and multitemporal geomorphometric analysis have shown destabilizing processes such as subsidence features and structural disintegration of alpine rockglaciers which can potentially become hazardous to alpine infrastructure and livelihoods. Statements about the current state and past/future evolution of permafrost landforms are mainly based on the analysis of subsurface temperature time series. As it does not directly capture all relevant properties, temperature alone, however, is insufficient to quantify and understand the geometric and kinematic responses of rockglaciers and other landforms as they occur in degrading permafrost systems in response to e.g., climate changes and other disturbances (such as ice aggregation and ice properties, sediment supply,...) .

It has been stated that various factors can lead to these signs of permafrost degradation and that a common thermal triggering for all the cases has not been identified. These factors are most likely connected to the complex combination of the local topography, the thermal state of permafrost (climate-induced response) and/or to variations in the sedimentation regime affecting the sediment load during long-term landform evolution.

In order to improve the understanding of the dynamics of rockglacier creep, there is a need to analyze the landform in a holistic setting, which includes its spatial and temporal long-term development. This study presents a modeling approach which assesses different types of rockglaciers concerning their position in a typical coarse debris process chain: rock wall ⇒ rock fall ⇒ talus slope ⇒ permafrost creep ⇒ rockglacier. Headwall recession, creep processes and sediment transport are quantified using a multi-method-approach combining remote sensing and terrestrial surveying methods. A numerical flow model based on the conservation of mass within the debris process chain is used to calculate the evolution of rockglacier surfaces. Variations in temperature and in the supply of sediment and ice show impacts on the rockglacier rheology and geometry. The flow model is used to generate observed rockglacier geometries and rheologies which are then subjected to variations in driving forces to induce degrading developments in the landforms.

Multitemporal digital terrain models developed during the last two decades allow the identification of changes in surface morphology, such as subsidence and acceleration, which can be identified as possible signs of degradation. The modelling helps to understand the driving forces of these degrading morphological changes and shows how sediment supply and temperature variations influence the morphological and rheological evolution of rockglaciers. Further, it elaborates to which degree changes in sediment/ice supply and temperature can be held responsible for signs of degradation.

The main objectives of this study are:

a) to present a holistic approach to the investigation of rockglacier dynamics which assesses the rockglacier as an integral part of a high mountain periglacial sediment transport system

b) to apply a numerical flow model to investigate rockglacier evolution and the role of temperature and sediment input variations and

c) to quantify and assess possible implications for rockglacier degradation and destabilization.

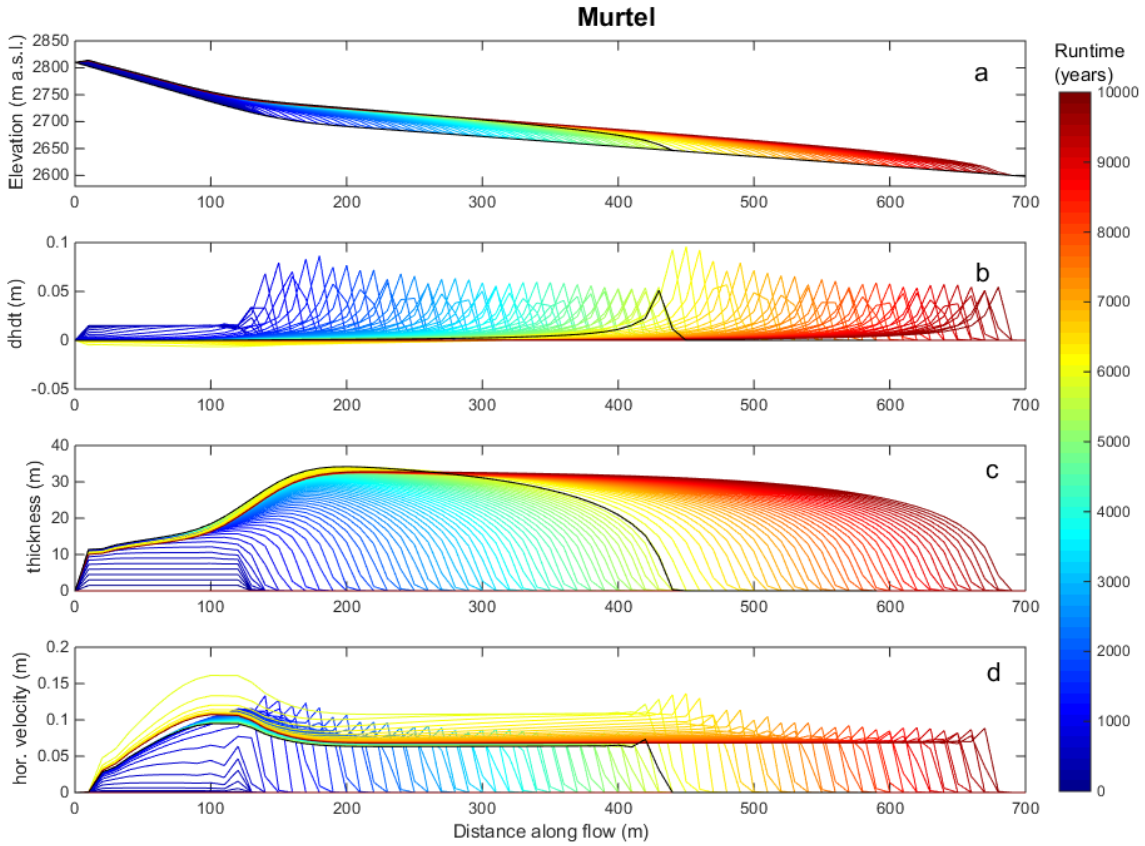

Figure 1: Results of the rockglacier evolution model for Murtel rockglacier in the Swiss Alps. Each line represents the surface information along flow every 250 years. After 6000yrs landform evolution (estimated age of Murtel rockglacier) a 1 °C increase in temperature

Short time changes of permafrost degradation triggered by anthropogenic impact and climatic events in Yamal Peninsula, Western Siberia 2010 – 2013/2015

Caroline Noerling[1], Anne Morgenstern[1], Marina Leibman[2], Annett Bartsch[3], Barbara Widhalm[3], Yuri Dvornikov[2], Artem Khomutov[2], & Birgit Heim[1]

[1] *Alfred Wegener Institute Helmholtz Institute for Polar and Marine Research, Germany*
[2] *Earth Cryosphere Institute Tyumen, Russia*
[3] *Technical University of Vienna, AT; Zentralanstalt fuer Meteorologie und Geodynamik, Vienna, AT*

The Arctic is affected by rapid climate change, which has substantial impact on permafrost regions and the world as a whole (Raynolds et al., 2014). In the last 30 years Arctic temperatures have risen 0.6 °C per decade, twice as fast as the global average (AMAP, 2011, Schuur et al., 2015). This in turn leads to the degradation of ice-rich permafrost (Grosse et al., 2011) and modifies drainage, increases mass movements and alters landscapes (Nelson et al., 2001; Anisimov et al., 2007, Romanovsky et al., 2010b).

Although permafrost regions are not densely populated, their economic importance has increased substantially in recent decades. This is related to the abundance of natural resources in the polar region and improved methods of hydrocarbon extraction, transportation networks to population centers and engineering maintenance systems (Nelson et al., 2002; Mazhitova et al., 2004, AMAP, 2011).

The Yamal Peninsula in North West Siberia is experiencing some of the most rapid land cover and land use changes in the Arctic due to a combination of climate change and gas development in one of the most extensive industrial complexes (Kumpula et al., 2006; Walker et al., 2011; Leibman et al., 2015). Specific geological conditions with nutrient-poor sands, massive tabular ground ice and extensive landslides intensify these impacts (Walker et al., 2011). The combination of high natural erosion potential and anthropogenic influence cause extremely intensive rates of erosion (Gubarkov et al., 2014). A considerable amount of recent work has focused on the effects of industrial development to ecological and social implications (Forbes, 1999; Kumpula et al., 2010; Walker et al., 2011). This study aims at exemplarily investigating a region that has been affected by natural and anthropogenic large-scale disturbances within a very short period. The construction of the world's northernmost railway for the Bovanenkvo Gas Field was finished in 2010. In addition the region experienced an extremly warm and wet summer in 2012.

The objectives of this study are

- to map surface disturbances of central Yamal between 2010 and 2013/2015 based on high-resolution satellite imagery and on the most recent SPOT5-TAKE-5 imagery in 2015,
- to quantify natural and anthropogenic impacts in terms of permafrost degradation,
- to use meteorological data from the nearest climate station (Marre Sale, Yamal) and from reanalyses climate data on air temperature and precipitation.

Periglacial cirque analogs: regional trends of cryoplanation terrace elevation in Eastern Beringia

Kelsey E. Nyland[1] & Frederick E. Nelson[1,2]

[1] *Michigan State University, USA*
[2] *Northern Michigan University, USA*

Cryoplanation terraces are large periglacial landforms incised into mountain- and hillsides in contemporary or past periglacial environments. The step-like terrace sequences are composed of alternating steep, rubble-covered risers and gently sloping treads culminating in extensive summit flats. Treads and summits are often covered with sorted patterned ground and sideslopes with solifluction lobes.

The formation of these features has been attributed to a suite of weathering and transport processes associated with late-lying snowbanks, referred to collectively by the shorthand term nivation. The snowpack provides moisture for weathering processes and facilitates transportation of material downslope. The postulated requirement of late-lying snowbanks implies that cryoplanation terraces are climatically controlled geomorphic features linked to the mass balance of persistent bodies of snow and hence to equilibrium-line altitude (ELA) and the positions of glacial cirques.

This study is focused on the uplands of eastern Beringia in central and western Alaska, a region with ubiquitous and well-developed cryoplanation landforms. Reger [1975] created an extensive and detailed inventory of cryoplanation terraces in this region. We performed a series of geostatistical analyses on Reger's data in conjunction with supplementary data obtained from Google Earth. Median cryoplanation terrace elevation rises from 100–300 m.a.s.l. from islands in the Bering Sea to greater than 1200 m in the Yukon-Tanana Upland near the Alaska-Canada border (Fig. 1). he regional trend of terrace elevation is similar to that of glacial cirques from western to eastern Alaska [Péwé and Reger, 1972], with gradients ranging from 0.74 to 1.2 m km^{-1}. The similarity of the trends of these two types of landforms indicates close genetic links between glacial cirques and cryoplanation terraces, involving topographic position, continentality gradients, and the mass balance of localized snow accumulation. These relations reinforce the analogy between cryoplanation terraces and glacial cirques [Nelson, 1989].

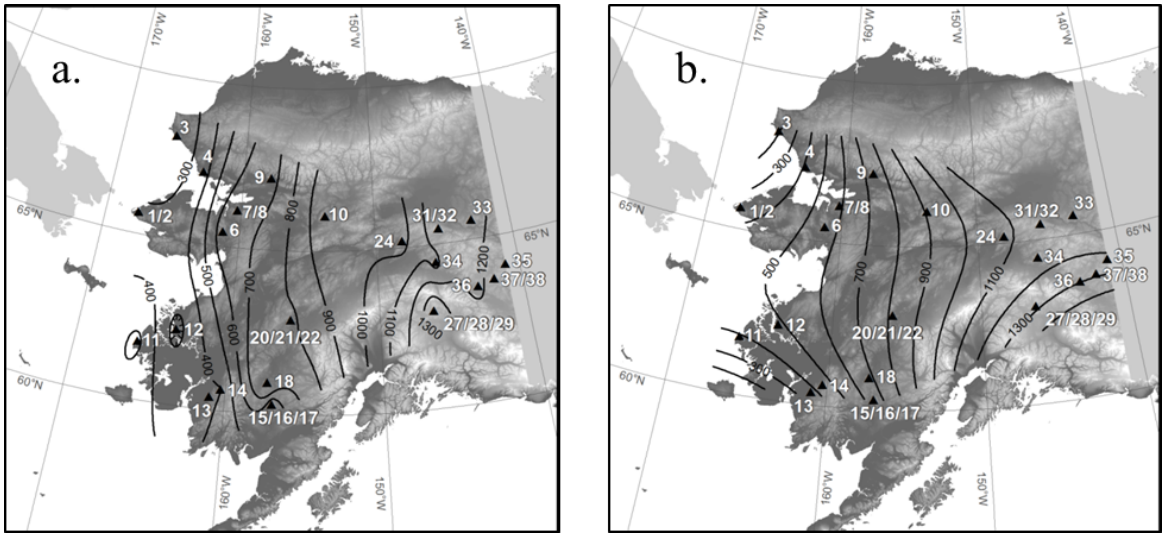

Figure 1: (a) Map of median terrace elevation (m.a.s.l.), created using a kriging interpolation algorithm. (b) Map generated by quadratic trend surface of median terrace elevation.

Cryoplanation landforms hold great potential as tools for reconstructing Quaternary environments. These features are unusual in this regard because they are less sensitive to short-term climatic variations than are smaller periglacial geomorphic features. This study will be continued with process-oriented investigations, age determinations, and high-resolution mapping aimed at identifying and quantifying the genetic processes responsible for the formation of cryoplanation terraces in high-latitude environments. Investigations involving multiple lines of evidence are necessary before the paleoenvironmental potential of cryoplanation landforms can be fully realized.

References

Nelson, F.E. [1989]: Cryoplanation terraces: periglacial cirque analogs. *Geografiska Annaler*, 71A(1–2): 31–41.

Péwé, T.L. and Reger, R.D. [1972]: Modern and Wisconsinan snowlines in Alaska. In *Proceedings of the 24th International Geological Congress*, volume 12, pages 187–197.

Reger, R.D. [1975]: *Cryoplanation Terraces of Interior and Western Alaska*. Ph.D. thesis, Arizona State University, 326 p.

Subterranean periglacial landforms in Ledena jama pod Hrušico cave, Slovenia

Jaroslav Obu[1], Jure Košutnik[2], Paul Overduin[1], Julia Boike[1], & Simon Zwieback[3]

[1] *Alfred Wegener Institute Helmholtz Institute for Polar and Marine Research, Germany*
[2] *University of Nova Gorica*
[3] *ETH Zürich*

Periglacial landscapes are characteristic for high latitudes or high elevations. Ice caves are environments where permafrost and periglacial conditions exist in milder climates due to specific microclimatic setting. Surface air is entering the cave only when its temperature drops below the cave air temperature. This results in a formation of cold air pool, which sustains a periglacial environment, permafrost and ice. Ice caves in karst can also contain a variety of sediments that were transported in a cave during its formation. These sediments can be subject to freeze-thaw cycles due to temperature fluctuations and form periglacial features.

Ledena jama pod Hrušico cave is situated on the Hrušica plateau on the elevation of about 800 m. It consists of spacious 20 m deep shaft, debris cone and two small passages. The ice is still present in the debris cone and is quickly disappearing. One of the passages contains silty sediments, which are mixed with limestone debris. Sorted stripes are present on an inclined slope of this passage.

Cave environment is less influenced by different subaerial processes thus cave environments are very suitable for controlled observations. Seven air temperature loggers were installed in order to monitor cave climate and identify processes responsible for periglacial conditions. Furthermore, we installed 12 soil temperature sensors in different parts of pattern ground to analyse the processes that lead to ground sorting. Ground movements and sorting are monitored with repeated photogrammetry. Results will help us to better understand dynamic responsible for ground sorting and soil movement processes in periglacial environments.

The periglaction of the Iberian Peninsula

Marc Oliva[1], Enrique Serrano[2], Antonio Gómez-Ortiz[3], María J. González-Amuchastegui[4], Alexandre Nieuwendam[1], David Palacios[5], Augusto Pérez-Alberti[6], Ramon Pellitero-Ondicol[7], Jesús Ruiz-Fernández[8], Marcos Valcárcel[6], Gonçalo Vieira[1], & Dermot Antoniades[9]

[1] *Institute of Geography and Spatial Planning – CEG, Universidade de Lisboa, Portugal*
[2] *Department of Geography, University of Valladolid, Spain*
[3] *Department for Physical and Regional Geography, University of Barcelona, Spain*
[4] *Department of Geography, Prehistory and Archaeology, University of the Basque Country, Spain*
[5] *Department for Regional and Physical Geography, Complutense University of Madrid*
[6] *Department of Geography, University of Santiago de Compostela, Spain*
[7] *Department of Geography and Environment, University of Aberdeen, UK*
[8] *Department of Geography, University of Oviedo, Spain*
[9] *Department of Géographie & Centre d'études Nordiques, Université Laval, Canada*

Periglacial processes in the Iberian Peninsula are currently active only in the highest mountain ranges. However, a wide variety of periglacial deposits and landforms occurs in low- and mid-altitude environments, which shows evidence of past periods with enhanced periglacial activity. This communication pretends to summarize the present-day knowledge on the distribution of periglacial phenomena in the Iberian Peninsula.

More than 300 scientific references dealing with past and present periglacial activity in Iberia have been consulted. The chronological framework has taken into account four main stages: Last Glaciation, deglaciation, Holocene and present-day processes (Fig. 1). This study focuses on the highest massifs (Pyrenees, Cantabrian Range, NW ranges, Central Range, Iberian Range, Sierra Nevada) as well as in other lower elevation environments, namely from the central Iberian Meseta.

During the Last Glaciation the periglacial belt extended to much lower altitudes than today, reaching current sea level in the NW corner of the Iberian Peninsula. A wide range of geomorphological landforms and sedimentary records is indicative of very active periglacial processes during that phase, in some cases related to permafrost conditions (i.e. block streams, rock glaciers). Most of the inactive landforms and deposits in low and mid elevations in Iberia are also related to these phase. The massive deglaciation of the Iberian massifs was accompanied by the gradual increase of temperatures. This phase was only interrupted by a short period with colder conditions (Younger Dryas) that reactivated periglacial processes in the formerly glaciated cirques of the highest lands, namely with the widespread development of rock glaciers. During the Holocene periglacial processes have been only active in the highest ranges, shifting in altitude according to the regime of temperature and moisture conditions. The Little Ice Age saw the reactivation of periglacial activity in lower elevations than today. Currently, periglacial processes are only active in elevations exceeding 2500 m a.s.l. in the southern ranges and above 2000–2200 m a.s.l. in the northern massifs, higher in Sierra Nevada, in the south of Iberian Peninsula.

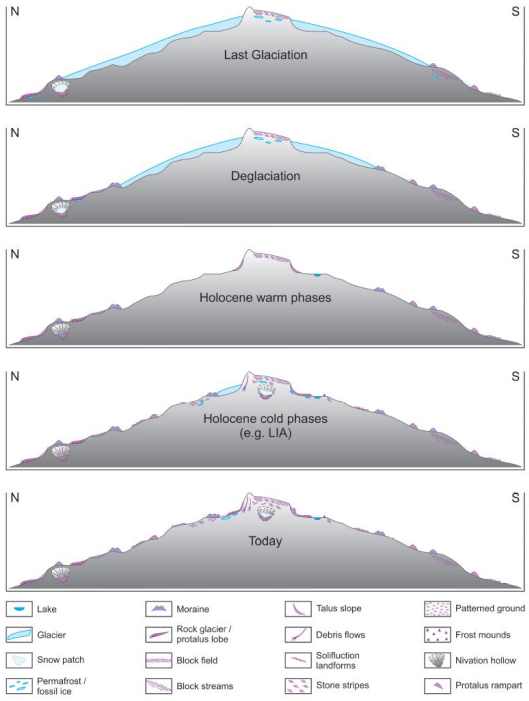

Figure 1: Geomorphological sketch of the periglacial activity in the highest Iberian mountain ranges since the Last Glaciation.

Deep-seated rock slope failure in mountain permafrost rock walls: Pizzo Cengalo and Piz Kesch, Swiss Alps

Marcia Phillips[1], Florian Amann[2], Andreas Huwiler[3], Robert Kenner[1], Andrew Kos[4], Rachel Luethi[5], & Andrea Wolter[2]

[1] *WSL Institute for Snow and Avalanche Research SLF, Switzerland*
[2] *Dept. of Earth Sciences, ETH Zurich, Switzerland*
[3] *Amt für Wald und Naturgefahren Graubünden, Switzerland*
[4] *Terrasense Switzerland AG, Switzerland*
[5] *Geotest, Davos Branch Office, Switzerland*

Two permafrost rock slopes at Pizzo Cengalo (Bergell, SE Switzerland) and Piz Kesch (Albula Alps, E Switzerland) are investigated using portable radar interferometric deformation measurements, terrestrial laser scans and time-lapse photography. Photogrammetric analyses were carried out to determine the role of structural controls on instabilities. The measurements were initiated after the occurrence of deep-seated failure at both sites in winter (approximately 1.5 million m^3 at Pizzo Cengalo, December 2011 and 150,000 m^3 at Piz Kesch, February 2014) and provide an overview of surface deformation. Our observations at Piz Kesch, Pizzo Cengalo and at other instrumented sites at elevations above 3000 m a.s.l. aim to investigate the role of permafrost in the predisposition and/or failure of these large rock slopes.

Post-failure observations can be used to determine the geological structure, the potential role of meteorological conditions prior to failure and to quantify the volume of the event. In addition, interferometric radar (Fig. 1) and laser scans can identify ongoing and new zones of instability and quantify surface deformation.

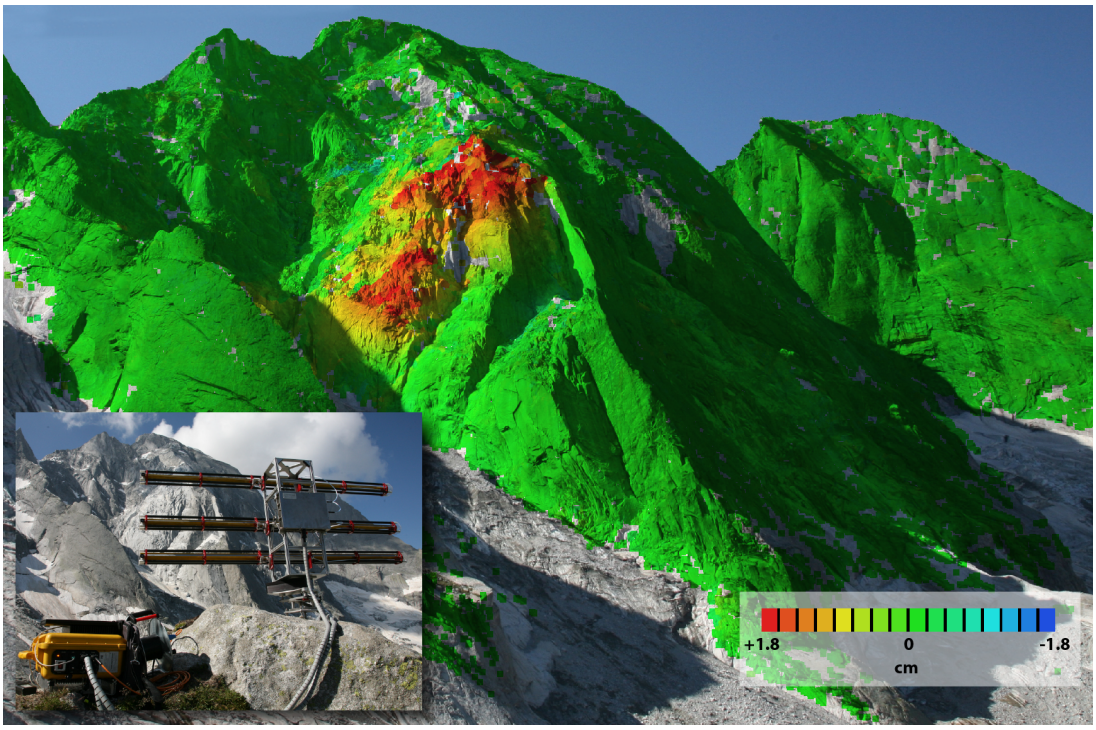

Figure 1: Total displacements on Pizzo Cengalo for a 2 year period (2012-2014) measured with a portable radar interferometer (Terrasense Switzerland). The instrument is shown in the lower left inset.

Only local meteorological data was available prior to these events and there was no in-situ data regarding rock temperature or crack movements. Thick fracture ice was present in the rock fall scars in both cases, revealing the presence of permafrost. At Piz Kesch organic matter in the ice was ^{14}C dated at 6000 years BP.

The SLF/PERMOS permafrost rockfall data base (290 events in the Alps, 1714-2015) indicates that whereas shallow rock slope failures within the active layer with volumes below 100,000 m^3 mainly occur in the summer months, deep-seated rock slope failures exceeding this size occur at any time of year - including winter. In the search for possible mechanisms leading to failure in winter, evidence from other permafrost sites in the Swiss Alps equipped with boreholes (e.g. the Jungfrau East ridge in the Bernese Alps or at Gemsstock in the central Swiss Alps) shows that there is a 6-month delay for summer heat to propagate to around 15 m depth. This is favourable for ice segregation in cracks in winter. In addition, crackmeter data (e.g. from the Kärpf ridge, Glarner Alps) display irreversible crack opening in winter.

In addition to geological structure, possible influencing factors leading to rock slope failure include glacier retreat and air temperature fluctuations. At Piz Kesch and Pizzo Cengalo ice segregation in winter resulting in ice wedging within tension cracks over several millennia most probably also contributed towards fracture propagation and failure.

Permafrost research collaboration between PYRN Iberian members (Spain and Portugal)

Alfonso Pisabarro[1], Nestor Campos[2], Manuel Gómez-Lende[1], Antonio Molina[3], Ramón Pellitero-Ondicol[4], María González-García[1], Alberto Merino[1], David Gallinar[5], Jesús Ruiz-Fernández[5], Cristina García-Hernández[5], Jonathan Hall-Riaza[6], Pedro Carrera[6], Jose M. Fernández[2], Alexandre Nieuwendam[7], Gabriel Goyanes[7], Ana S. David[7], Inês Girao[7], Miguel Cardoso[7], Alice Ferreira[7], Joao Branco[7], Lourenço Bandeira[8], & María Lousada[8]

[1] *Dpt. of Geography. University of Valladolid, Spain*
[2] *Dpt. of Geography. University Complutense of Madrid. Spain*
[3] *Dpt. of Dpt. of Geology, Geography and Environment. University of Alcalá de Henares. Spain.*
[4] *Dpt. of Geography and Environment. University of Aberdeen.Scotland.UK*
[5] *Dpt. of Geography. University of Oviedo. Spain*
[6] *Dpt. of Geography. University of Santiago de Compostela*
[7] *Centro de Estudos Geográficos/ IGOT, Universidade de Lisboa, Lisboa, Portugal*
[8] *Instituto Superior Técnico, Universidade de Lisboa*

The Iberian Peninsula is rich in past cryosphere evidences. However the studies of the past and present cold environments are done by a group of a few young researchers.

The Spanish young researchers have been focused in high mountain areas, related to the subjects of ground thermal regimes in High Mountain, glacial heritage, ice caves, periglacial processes, environmental changes and planetary cryosphere. The study of ground thermal regime in areas with more active periglacial processes is the subject that has involved more researchers from Spain, especially in massifs like Central and Occidental of Picos de Europa, Ubiñas massif, Alto Campoo and Cebolleda massifs and Posets and Maladeta in Central Pyrenees (North of Spain).

Paleoreconstruction of ELA's and postglacial landscape changes and cryogenic processes since the last Glacial Maximum have also been a main focuses of the Spanish young researchers in massifs like Galician mountains (NW Spain), Sierra de Gredos (Central Spain) and Sierra Nevada (South Spain), where some Portuguese members started collaborating in the last years.

Planetary cryosphere, specifically on Mars, is another of the collaborations between Spain and Portugal, together with mapping polygonal networks in the Arctic. Together, these two countries have also worked strongly on permafrost research in Antarctica, through the installation and maintenance of CALM sites and some deep permafrost boreholes. More innovated techniques are being used in Antarctica: Ground deformation assessment and snow cover detection using SAR and geoecological mapping and landscape dynamics using high resolution imagery. This approach will also be used in the Iberian Peninsula areas, strengthening the collaboration between Spanish and Portuguese young researchers.

Thermokarst landforms in Buckinghamshire, England

Simon J. Price[1,2], Steve Boreham[1], Philip Gibbard[1], & Tom Berry[3]

[1] *University of Cambridge, United Kingdom*
[2] *British Geological Survey, United Kingdom*
[3] *Ove Arup and Partners, United Kingdom*

Lowland southern Britain experienced multiple phases of cold-climate induced periglaciation during the Pleistocene. The recognition of periglacial features, including bedrock brecciation, involutions and ice-wedge pseudomorphs, are taken as evidence for the former presence of permafrost and palaeoactive layer development. Interpretation of the presence of past degradation of ground ice (thermokarst) is often lacking in studies of periglacial geomorphology [French, 2008] however.

This paper presents potential evidence for the occurrence of thermokarst landforms in part of Buckinghamshire, lowland southern Britain. Here the geological bedrock comprises interbedded mudstone, sandstone, siltstone and sandstone of middle to upper Jurassic age. Overlying superficial deposits comprise till, glaciofluvial sand and gravel, river terrace deposits and alluvium. Glacigenic sediments are present on interfluves to 130 m OD and are separated by fluvially incised valleys.

The tributary valleys of the rivers Great Ouse and Ray are characterised by near-circular and closed embayments with irregular-shaped boundaries. Glacigenic sediments in the depressions appear to be absent, but Holocene alluvium and river terrace deposits are common. Their distribution is restricted to the outcrop of the Oxford Clay Formation. Individual embayments reach 7 km wide and are characterised by an overflow channel on their northern margin. Some depressions appear to coalesce forming alas valleys. They form a series of bedrock strike-parallel basins constrained on their southern margins by northeast-southwest trending escarpments on their northern margins by gentle, southeast-facing bedrock dipslopes. In contrast, valleys, incised over limestone and sandstone-dominated Jurassic bedrock, are steeper and commonly flanked by glacigenic sediments.

Authors including Boreham [1996] and West [1991] interpreted small (1 km) near-circular depressions overlying clay or silt-rich bedrock of late Jurassic and Cretaceous age in the Fenlands of southern Britain as of thermokarst origin. They proposed that thermokarst develops through a combination of ground-ice melting, thermo-erosion, spring-fed surface water accumulation and poor-drainage over low permeability bedrock. Here it is proposed that genetically similar thermokarst features are present overlying low-permeability clay-rich bedrock in Buckinghamshire.

Evidence for the presence of thermokarst landforms in southern Britain is underestimated in periglacial geomorphological studies. The occurrence of multiple phases of past permafrost and active-layer development in regions that experienced periglaciation has important implications for future ground engineering and infrastructure design. Lithological variation, solifluction and differential weathering influence geotechnical properties and behaviour, including shear-strength and compressibility.

References

Boreham, S. [1996]: Thermokarst landforms in the Cambridge area. *Nature in Cambridgeshire*, (38): 16–22.

French, H. [2008]: Recent contributions to the study of past permafrost. *Permafrost and Periglacial Processes*, 194(2):179–194, doi:10.1002/ppp.614.

West, R.G. [1991]: On the origin of Grunty Fen and other landforms in southern Fenland, Cambridgeshire. *Geological Magazine*, 128(03):257.

GPR imaging of slope, fluvial and coastal sediments in high Arctic valley (Ebbadalen, Svalbard)

Grzegorz Rachlewicz & Krzysztof Grzegorz Rymer

Adam Mickiewicz University in Poznan, Poland

Sedimentary structures of post Last Glacial Maximum deposition architecture in high Arctic environment are evolving under conditions of continuous permafrost occurrence. Due to generally coarse granulation of sediments and lack of natural outcrops, the best imaging and spatial distribution of Quaternary geology is obtained by non-invasive methods, like ground penetration radar (GPR) techniques, in relation to point-like observations of rock properties and geomorphological mapping. During the spring expedition campaign 2014 we tested the application of GPR equipped with an unshielded 100 Mhz antenna performing over 6 km of profiles across the system of raised marine terraces, proglacial river accumulation planes and talus/alluvial cones along and across a post glacial valley Ebba (Norwegian: Ebbadalen) in central part of Spitsbergen (Svalbard, Billefjorden basin). The valley in its contemporary form is ca. 5 km long, from the coast of Petunia Bay to the front of Ebba Glacier and 3 km wide, between mountain ridges reaching above 800 m a.s.l. The best developed slope, fluvial and coastal sedimentary covers are occurring in the outer part of the valley. The hard rock geology in majority consist of sedimentary rocks of the late Carboniferous Campbellryggen Subgroup, including among others sandstone, dolomite, limestone, gypsum/anhydrite rocks as well as rocks of pre-Devonian metamorphic complex showing different resistance to weathering and denudational processes, that fragments are found within loose deposits. Slope sediments revealed by GPR profiling are showing vertical accretion with the thickness up to 5-7 m, with the sequence of inclined strata on overlapped conoidal landforms, that are different from horizontal bedding of valley bottom infill and over 7 m thick deposits of glacioisostatically uplifted coastal sediments. The whole sedimentary sequence is showing the continuous postglacial morphogenesis. In our works we were supported by the grant no. 2011/03/B/ST10/06172 from Polish National Science Centre.

Distribution and evolution of thermo-erosional drainage pathways between the 1950s and 2011 along the Yukon Coast, Canada

Justine L. Ramage[1,2], Anna M. Konopczak[1,2], Anne Morgenstern[1], & Hugues Lantuit[1,2]

[1] *Alfred Wegener Institute Helmholtz Centre for Polar and Marine Research, Potsdam, Germany*
[2] *University of Potsdam, Institute of Earth and Environmental Science, Potsdam, Germany*

Thermo-erosion, as a mechanism of rapid permafrost thaw, reshapes arctic landscapes and has a clear impact on the local topography and hydrology. Thermo-erosional drainage pathways – including gullies and valleys – are major components of permafrost environments and play an important role in redistributing materials, leading to a potential mobilization of soil organic carbon and nitrogen. However, the effects of these disturbances are at present not taken into account in the global climate models due to the limited amount of studies reporting on this topic.

This study provides an analysis of the thermo-erosional drainage pathways diversity along a ca. 105 km long coastal plain in the Yukon (Canada) and determines the prevailing factors accounting for their distribution and driving their expansion over the past 60 years.

We used a large set of high-resolution multispectral satellite images from 2011 (GeoEye and WorldView) for geocoding aerial photographs from the 1950s, using the software OrthoEngine (PCI Geomatica). This dataset was the basis for manually digitizing and classifying thermo-erosional drainage pathways according to morphological characteristics. We gathered additional observations on gullies and valley morphology during fieldwork (July-August 2015). Based on remote sensing, we computed and compared the changes in type, number and lengths of thermo-erosional drainage pathways over this time span. We used principal component analyses (PCA) to highlight the main environmental factors involved in the development of those landforms.

We observed a large variability in the spatial distribution of the landforms along the coast. On average, thermo-erosional drainage pathways decreased in length and did not significantly increase in number. Landform types showed different evolutions: thermo-erosional valleys were stable over the last 50 years, while thermo-erosional gullies were dynamic. We found a strong relationship between the decrease in thermo-erosional valley lengths and coastal erosion rates.

Those dynamics are related to the localisation of thermo-erosional drainage pathways within the coastal plain. The decrease in the length of thermo-erosional valleys occurs at the outlet of the streams and is due to high rates of coastal erosion along the coast. Most of the valleys have not developed further inland during the observation period. We suggest that thermo-erosional valleys formed after the last glacial maximum and are stabilized since then. Gully development heterogeneity might be related to increased soil subsidence in polygonal terrains and deepening of the active layer on slopes.

Influence of periglacial conditions on the structure of Pleistocene glacial till (based on the example of Poland)

Joanna Rychel[1], Marcin Morawski[3], & Lucyna Wachecka-Kotkowska[2]

[1] *Polish Geological Institute National Research Institute, Poland*
[2] *University of Lodz, Poland*
[3] *l'immeuble SarSaara Lot 124B-2 Yoff Toundoup Rya, Dakar, Senegal*

A periglacial zone developed in the extraglacial zone of each Pleistocene ice sheet, therefore some areas were affected by periglacial conditions several times, i.e. each time during transgression and recession of an ice sheet when a periglacial zone encroached on areas freed from the ice. Thus, glacial till deposited by successive Pleistocene ice sheets is a source of information about periglacial conditions. An attempt was undertaken to determine the effects of periglacial processes in the structure and texture of glacial till. Study sites were selected so as to reflect the potential longitudinal variability in the intensity of periglacial processes and to reveal the impact of climate continentalism on the development and the nature of these processes. The detailed research was conducted on the outcrops located successively in the foreland of the Pomeranian phase (Chobielin, 17.633°E; 53.104°N) and the Poznań phase (Szlachcin, 17.394°E; 52.198°N) – those two sites were situated within the periglacial zone only during the Last Glacial Maximum (LGM), and on the outcrops located in the area left by the Wartanian (MIS 6; Koczery, 22.706 E; 52.426 N) and Odranian ice sheets (MIS 8; Ochotnik, 19.814 E; 51.126 N) (Fig. 1). Each time lodgement till in the plateau position was examined.

Analysis of grain size composition, calcium carbonate content, morphoscopy of quartz grains from the sand fraction, analysis of thin sections and micromorphological surface of quartz grains as well as the determination of geomechanical parameters (compressibility and consolidation of deposits) were conducted under a scanning electron microscope (SEM-EDS).

The obtained results show that differences in the mechanical composition as well as in the geomechanical parameters at each site were not significant, which indicate a homogeneous type of deposit. At a depth of ca. 1 m, microstructures resulting from ground ice lenses were observed in thin sections from areas of older till. At similar depths, consolidation of till decreases and the content of cracked quartz grains increases. This also coincides with the complete decalcification of deposits. Such properties of deposits indicate the range of the active layer. On the other hand, no decalcification in the roof parts of the till accumulated by the Vistulian ice sheet or microstructures left by melted ground ice lenses were observed, or any decline in the consolidation of deposits within ca. 3 m thickness of the analysed profiles. Whereas a significant increase in the content of cracked grains was observed in the uppermost parts of the profiles (up to ca. 1 m depths). Quartz is less resistant to frost weathering compared to, for example, unweathered feldspars [Konishchev et al., 2005, French and Guglielmin, 2000]. The obtained data show large differences between properties of the Vistulian and older tills which were exposed to a much longer weathering in periglacial climate. No significant differences were found, however, between properties of till from the Wartanian and Odranian Glaciation, even though the latter were under the influence of periglacial conditions for a longer time.

Figure 1: Location outcrops on limits of the main Pleistocen glaciation in Poland [Marks, 2005] modified

References

French, H.M. and Guglielmin, M. [2000]: Cryogenic weathering of granite, Northern Victoria Land, Antarctica. *Permafrost and Periglacial Processes*, 11:305–314, doi:10.1002/1099-1530(200012)11:4<305::AID-PPP362>3.0.CO;2-T.

Konishchev, V.N.; Lebedeva-Verba, M.P.; Rogov, V.V. and Stalina, E.E. [2005]: *Cryogenesis of modern and Late Pleistocene deposits Altai and peryglacial region of Europe*. GEOS, Moscow. ISBN 5-89118-374-9 (in Russian).

Marks, L. [2005] Pleistocene glacial limits in the territory of Poland. *Przeg. Geol.*, 53/10/2:988–993.

Solifluction and block streams activity in alpine area of Southern Carpathians, Romania

Raul David Şerban, Alexandru Onaca, Petru Urdea, & Mihaela Popescu

West University of Timisoara, Romania

The aim of this approach is the quantification of present-day morphodynamic potential of solifluction in Southern Carpathians by identifying the current intensity of solifluction processes and determining the environmental controls on landforms morphometry. From all the solifluction features recognized in Southern Carpathians our attention is focused especially on turf-banked and stone-banked lobes, ploughing blocks and block streams which most often occur.

The methodology combines field and digital geomorphological mapping and measurements, with statistical and spatial analysis of terrain parameters. A landform inventory was created encompassing 2056 block streams, 70 turf-banked lobes and 182 ploughing blocks. Terrain parameters were derived from a Digital Elevation Model (DEM) with a 10 m cell resolution. To capture the connections between ground freezing and solifluction movements, both surface motion and thermal ground conditions were monitored for one to three consecutive years. Ground thermal regime within the solifluction landforms was assessed according to soil texture and sediments grain-size distribution. In order to identify the possible environmental controls on solifluction landforms morphometry and surface velocity, bivariate and multivariate statistical analyses were applied as: standard least-square linear regression and one-way analysis of variance (ANOVA).

Morphometry analysis of the solifluction related landforms place them in the category of medium sizes with slow dynamics of maximum 6 cm/year. The size and spatial variability of the block streams are influenced to a certain degree by the subjected variables as: lithology, slope aspect and elevation, but with a lower correlation factor (0.06 to 0.30). Significant negative correlation was identified between surface velocity of turf-banked solifluction lobes with altitude and slope. These relationships are explained in a proportion of 20 to 42 % by these variables. Significant correlations were observed also between lobes tread angle and riser angle with altitude, slope and coarse material content, explained in a proportion of 25 to 66 %. Additionally, it appears that the length of the solifluction lobes increases when the amount of coarse particles decreases.

Ground surface temperature (GST) reveals a higher number of freeze-thaw cycles in the substrate of the block streams than in the case of turf-banked solifluction lobes. It was found also that coarse blocks have a cooling influence on ground temperatures compared with fine-grained soils. Within a block stream the GST indicates an air circulation inside the block streams. This suggests that at the bottom side of the blocks stream could be present the chimney effect, where is the most suitable area for the occurrence of a ice layer for a longer period.

The analysis reveals that complex processes are involved in the evolution and downslope movement of solifluction structures, resulting from the interaction of multiple factors (e.g. topographic, climatic, soil moisture, uppermost layer texture, snow cover, freeze-thaw action, vegetation cover etc.). Solifluction structures also do not indicate permafrost occurrence in Southern Carpathians, but rather seasonal frost.

Periglacial landforms and processes on a calcareous high mountain. Picos de Europa (Cantabrian Mountains, Northern Spain)

Enrique Serrano[1], Alfonso Pisabarro[1], José Juan Sanjosé[2], Manuel Gómez-Lende[1], Juan José González-Trueba[3], & María González-García[1]

[1] *University of Valladolid, Spain*
[2] *University of Extremadura, Spain*
[3] *CIESE-UC, Spain*

Snow and seasonally frozen ground are the most representative thermal conditions of the cryosphere in the Picos de Europa, although ice patches and ice caves, both inherited from the Little Ice Age, are also important. Ice caves have a significant ice mass but they are disconnected from the surface.

Snow cover determines partially the periglacial processes due to its influence on the winter ground thermal regime, the water availability, the physical soil behaviour and the biogeochemical flows. Ground ice, mainly within seasonal frozen ground (SFG), is key to understand the periglacial processes and landforms in Picos de Europa.

Picos de Europa is divided in three massifs composed mainly of limestone, with some slates, conglomerate and turbiditic sandstone outcrops. It is the highest massif of the Cantabrian Mountains (Torre Cerredo, 2648 m a.s.l.), and it is located (43°10'N-4°50'W) just 20 km away of the sea coast. Its climate is a temperate oceanic one (annual precipitations are over 2500 mm/yr). Glacial and karstic landforms are ubiquitous, creating a high mountain glacio-karstic landscape. Quaternary deposits, such as till, decalcification deposits and colluvium are scattered on the dominant rocky valleys and cirques.

The aim of the study is to determine the presence or absence of ground ice, define the present-day periglacial processes and establish the altitudinal distributions of cold processes related to SFG.

Geomorphological mapping to a 1:25,000 scale enabled us to identify the types and distribution of periglacial landforms and active processes. The assessment of ground temperature regime and its statistical analysis is based on 12 thermal sensors and data-loggers (iButtons and UTL-Geotest AG) located between 1115 and 2535 m a.s.l., at 10 cm depth, between 2003 and 2007. Frost Index (FI), Frozen/Thawing cycles in the ground and the atmosphere (from OAPN meteorological Stations), and the number of days with temperatures below 0ºC and below -3 °C, have been calculated.

Partially active debris talus and cones are located mainly in S orientations above 1200 m a.s.l. and solifluction is very common at N, S, E, W orientations, always above 1400-1500 m a.s.l. Fine-grained solifluction lobes are located on shales and slates at N, S, E, W orientations, above 1500 m a.s.l. Ploughing boulders are common above 1700-1950 m a.s.l. Active debris talus and cones are located in S orientations above 1800-2000 and N orientations above 2000, related to rockfalls, snow avalanches, frost shattering, solifluction and debris flows. Nival landforms and processes are generated from 1000 m a.s.l., although they are dominant above 2100 m a.s.l. where stone pavement are frequent. Protalus ramparts are developed at northern orientations above 2400 m a.s.l.

SFG is present above 2200 m a.s.l. FI has values over 360-400, and between 2 and 65 days show ground temperatures below -2 °C, and between 120 and 138 days with ground temperatures below 0ºC. These thermal conditions are related to solifluction processes on N and NW slopes. Frost mounds and patterned ground are located above 2200 ma.s.l. in flat areas with a fine grained regolith. They are always small landforms occupying a very limited area. Both landforms are related to cryoturbation, but frost mounds are developed on sediments over buried ice patches, and they are related to topoclimatic factors. These landforms are located in marginal environments in disequilibrium with current atmospheric thermal conditions.

Solifluction processes are related to fine-grained regoliths on shales, slates or till. The ground thermal parameters of áliva area, where solifluxion processes are located, are: FI values lower than 360; between 0 to 8 freeze/thaw cycles; 0 to 63 days with ground

temperatures below -2 °C; and between 0 and 80 days with ground temperatures below 0 °C. Although SFG can exist over 1900 m a.s.l., the most active periglacial processes are located at high altitude, above 2200 m a.s.l. Below 1900 m.a.s.l. the dominant processes are solifluction and nival processes, and they are less active. Some landforms, as fine-grained lobes, solifluction sheets and ploughing boulders located below 1900 m a.s.l., might be inherited landforms of colder periods or induced by the anthropic action, such as overgrazing by sheep and cows. The absence or scarcity of ground ice has been confirmed.

Above 1100 m a.s.l. the nival processes are dominant, and the frozen ground exceptional. The most active periglacial processes (i.e. gelifluction and cryoturbation), are related to SFG above 2200 m a.s.l., always on till and colluvium deposits. Patterned ground is located at exceptionally low altitudes, between 2200 and 2430 m a.s.l., due to topoclimatic factors and the existence of sediments covering inherited ice-patches.

Table 1: Altitudinal distribution of environmental parameters.

Altitude m	AAMT °C	Month with $T^a \leq 0°C$	Winter snow cover	Processes	Frozen ground
2550	1,3	4-8	Unstable		SFG
2450	1,4			Cryoturbation,	
2400	1,7	7-9		Cryoreptation,	
2300	2,3		Stable	Gelifraction	
2200	2	6		Nivation.	Possible SFG
2150	3,2				
1900	6,3	3		Gelifraction,	SFG
1850			Unstable	Nivation	Altitudinal limit
1800	7	0		Solifluction,	Not probable
1700				Gravity, Nivation	
1200	11,7	0		Solifluction,	Not exist
1100			--	Gravity	

SFG, seasonal frozen ground

Siberia's glaciation as a specific component of permafrost characterizing a type of cryodiversity in the region

Vladimir Sheinkman & Vladimir Melnikov

Tyumen State Oil and Gas University, Russia; Tyumen State University, Earth Cryosphere Institute, SB RAS, Russian Federation

For a long time study of glaciation in Siberia had been carried out on the base of the predominantly Alpine scientific concept defining abundant snow supply and high ice turnover to form the glaciers. The glaciers have been then considered as so called warm ice bodies which lie on the ground outside of the permafrost area and are a result of primary snow sedimentary-metamorphic transformation. They must grow quickly under a cooling, since the snow supply is firstly enough against sharp ablation decrease yielded by the cooling. Such a process will go until the humid and cold (cryogygrotic) stage of the cooling will change by the dry and cold (cryoxerotic) stage.

So, under initial high moistening the glaciation can reach the sheet form over geologically short, relatively, Pleistocene cryochrones. This model is suitable in the regions with climate similar to the same that is in the Alpine area, in order to explain forming the past ice sheets in North-Western Europe moistened from the Atlantic. However such a model is not suitable in Siberia where dry and cold environments prevailed all over the Quaternary as an effect of cryoaridization (gradual increase in climatic continentality at a background of lowering in air temperature and permafrost promoting under cold and arid conditions). For this reason the glaciation in Siberia had been denied for a long time, whereas use of the Alpine rules and regularities yielded paleo-reconstructions of giant ice sheets alien to the Siberian terrain.

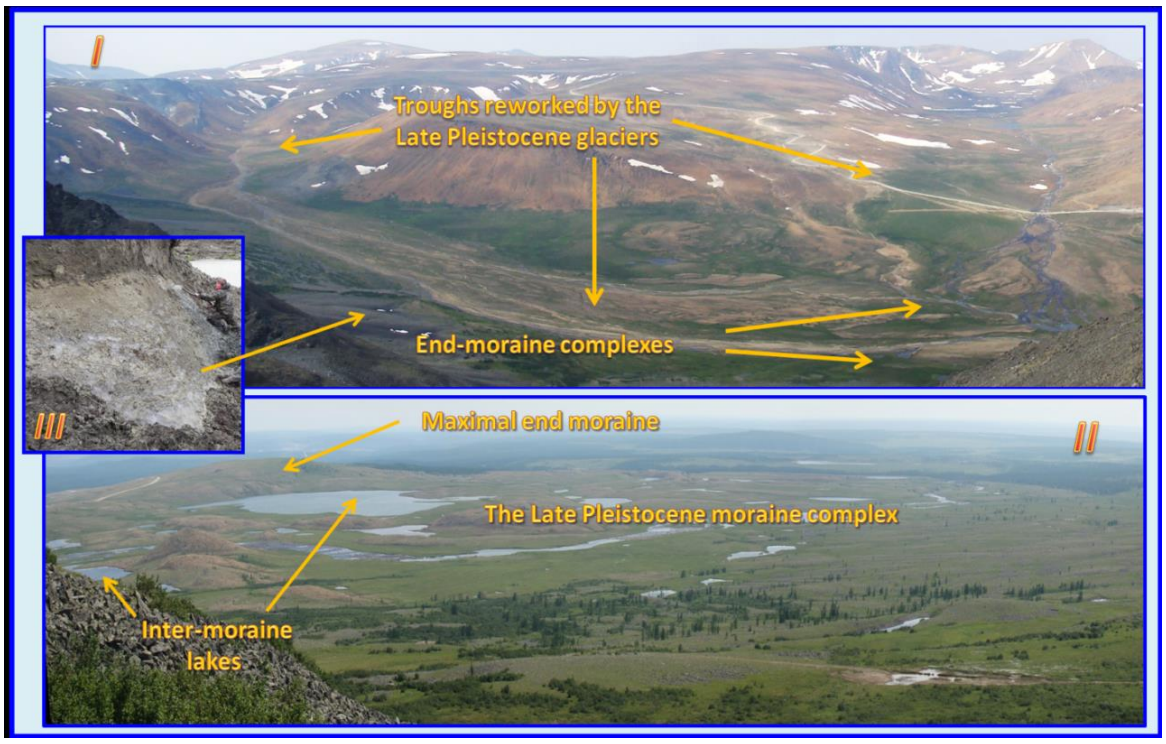

Figure 1: Central part of Rai-Iz Ridge, Polar Ural I – General view of its troughs reworked specifically by an element of cryodiversity, cold but not warm glaciers; II – a view down the valley from the high left-hand slope of the ridge to the Late Pleistocene moraine complex in the debouchments of the main trough (II), and an outcrop in the bottom of the trough with segregation ice (III).

Study of different modern glaciers all over Siberia, which have been developed under continental climatic conditions, was carried out and cleared up that there is not azonality in their development. In spite of low snow supply and active ablation (that is an attribute of Siberia's continental climate) the glaciers exist due to big cold storage in their bodies: it keeps additional ice feeding, when thawed water and snowy-hydrous mass can repeatedly freeze on the cold surface of the glaciers.

So, in Siberia, the glaciers, being under the initial developed cryoxerotic stage, had to react to the cooling during the Pleistocene cryochrones by slow growth. More so that their snow supply decreased as the cryoaridization was stronger, and during the cryochrones they, gradually absorbing their scanty supply, could reach the valley form only.

Cold continental climate in Siberia has made conditional on the particular environments to form glaciers and to determine their dynamics. The glaciers, interacted with permafrost, become a new element of cryodiversity – a set of objects and phenomena produced by cold – and differ from the glaciers which have been considered from the position of the Alpine glaciation model. Being cooled till enough low temperature (significantly lower than 0 °C), the glaciers in Siberia obtain properties which are more characteristic for permafrost, than for the Alpine-type glaciers. The obtained quality requires reckoning the formed combination of the glaciers with permafrost to the specific geosystems. We name such geosystems as permafrost-glacial systems.

Salix polaris growth responses to active layer detachment, solifluction, deflation and channel erosion processes in High Arctic

Liliana Siekacz

Adam Mickiewicz University, Poland

Dendrogeomorphology uses growth ring properties stored in woody plants to date back and interpret morphogenetic processes. It is established method in medium latitudes, where multiple research showed its usefulness and reliability in dating e.g. avalanches, landslides, fluvial erosion, tourist trail erosion. In high Arctic research woody plant material is very limited and restricted to small size, trailing shrub species and its preparation is much more time consuming. It is a relatively new method and at this stage it is very important to recognize and describe growth patterns of plants subjected to different morphogenetic processes to obtain information necessary to further processes interpretation.

Aim of this work is to demonstrate the potential of *Salix polaris* growth properties in the dendrogeomorphologic image, analyzing periglacially induced processes in the high Arctic. Observed anatomical and morphological plants responses to solifluction and active layer detachment processes as well as exposure of their roots by deflation and channel erosion are presented qualitatively and quantitatively as a summary of occurring features frequency. Mean vessel sizes, share of missing rings, partly missing rings, wedging rings, suppressed and released rings in plants from sites subjected to different morphogenetic processes in periglacial environment are presented. The results are discussed against the background of the other research results in this field. The investigations were performed in Ebba valley, in the vicinity of Petunia Bay, northernmost part of Billefjorden in central Spitsbergen (Svalbard). Environmental conditions are characterized by annual precipitation sum lower than 200 mm and average summer temperature of about 5 °C, with maximum daily temperatures rarely exceeding 10 °C.

Collected shrub material was prepared according to the methods presented by Schweingruber and Poschlod [2005]. Thin (approx. 15–20 μm) slices of the whole cross-section were prepared with a sledge microtome, stained with Safranine and Astra blue and finally permanently fixed on microslides with Canada balsam and dried. Snapshots were taken partially for each cross-section with digital camera (ColorView III, Olympus) connected to a microscope (Olympus BX41) and merged into one, high resolution image. Finally, ring widths were measured in 3-4 radii in every single cross-section using ImageJ software.

Contemporary progressive melting of glaciers, faster melting of snow patches, permafrost degradation etc., significantly affect the dynamics and temporal and spatial extent of water circulation in Arctic catchments and mobility of mineral matter. Released sediments can be easily subjected to intensified periglacial processes, such as slope processes, channel erosion, deflation etc. All of these can affect shrub growth by disturbance of their habitats, that can be recorded in rings parameters and wood properties. Observed permafrost degradation on neighboring slopes causes appearance of shallow landslides called active layer detachments. The aim of the study was to check how slope processes affect growth of *Salix polaris* dwarf shrub and if it is possible to use dendrochronological methods to date back their occurrence. *Salix polaris* specimens whose roots are exposed by deflation and channel erosion were also collected to check their growth reactions to these processes and dating possibilities.

Analyzed plants revealed extremely harsh environmental conditions of their growth. Buchwał et al. [2013] provided quantitative data concerning missing rings and partially missing rings in shrubs growing on Ebba valley floor. Mean ring width at the level of 79 μm represents one of the smallest values of yearly growth ever noted. The share of missing rings and partially missing rings was 11.2 % and 13.6 % respectively. Plants growing on Ebba valley slope affected by slope processes indicate almost twice smaller values of ring width (41 μm), and higher participation of missing and partially missing rings. Share of missing rings in shrubs growing within an active layer detachment on the valley slope reached 16.22 % and 15.36 %. Even higher variation is observed in partially missing rings which account for 31.07 % within detachment

and 23.39 % on surrounding slope. Those values are more than twice higher comparing to the valley floor. There is also noticeable difference between detachment and surrounding slope indicating that wedging rings are an effect of mechanical stress that is higher within the detachment. Comparing growth patterns in aboveground and belowground plant parts different growth allocation is noticed. Years of detachment event growth rings were present only in aboveground parts. It is supposed that mechanical stress delays the onset of the growing season similarly to low temperatures [Buchwał et al., 2013], resulting in not enough time to fully allocate resources for growth in the belowground parts. Growth pattern is extremely irregular, indicating that the slope is in constant movement, which disrupts growth conditions. Studied shrubs showed two possible event years: 2006 and 2008, with the highest participation of missing and partially missing rings. Air and ground temperature data were also analyzed and confirmed that active layer detachment happened in 2006. Specimens from deflation and channel erosion affected sites, showing variations in the occurrence of missing, partially missing rings and deformations in wood structure are also analyzed.

References

Buchwał, A.; Rachlewicz, G.; Fonti, P.; Cherubini, P. and Gärtner, H. [2013]: Temperature modulates intra-plant growth of Salix Polaris from a high Arctic site (Svalbard). *Polar Biology*, 36:1305–1318, doi:10.1007/s00300-013-1349-x.

Schweingruber, F.H. and Poschlod, P. [2005]: Growth rings in herbs and shrubs: life span, age determination and stem anatomy. *Forest Snow and Landscape Research*, 79(3):195–415.

Floodstreams on coasts of the East Arctic seas at the Pleistocene-Holocene transition

Valentin V. Spektor[1,2], Vladimir B. Spektor[1], Yaroslav I. Torgovkin[1], Alyona A. Shestakova[1], Georgiy T. Maksimov[1], & Varvara V. Andreeva[1]

[1] *Melnikov Permafrost Institute Siberian Branch Russian Academy of Sciences, Russian Federation*
[2] *Ammosov North-Eastern Federal University in Yakutsk*

For the first time, it has been established that the relief and sedimentary cover of the Laptev and East Siberian Seas coasts had been formed under the influence of catastrophic water flows – floodstreams. The similar features were not noted earlier in the well-known investigations of the Primorskaya Lowland [Grosswald et al., 1992, Grosse et al., 2007, Nagaoka et al., 1995]. Floodstreams on the coasts of the Laptev and East-Siberian Seas occurred at various times due to flowage of ancient (80-10 kyr BP) ice-dammed lake, which formed in front of the ice shelf. The reconstructed directions of floodstreams in the region are illustrated in Figure 1. The age of the floodstreams (in the interval 15-10 kyr BP) was refined. The separated floodstream deposits are represented by sand bodies of the Argaa-Muora-Sise Island in the Lena River Delta (Fig. 1B), sand ridges and outcrops of Sypnoi Yar in the Lower Indigirka River, sand ridges in vicinity of the Yana River mouth (Fig. 1C), sands of Khalerchinskaya Tundra in the Lower Kolyma River region (Fig. 1D), and others.

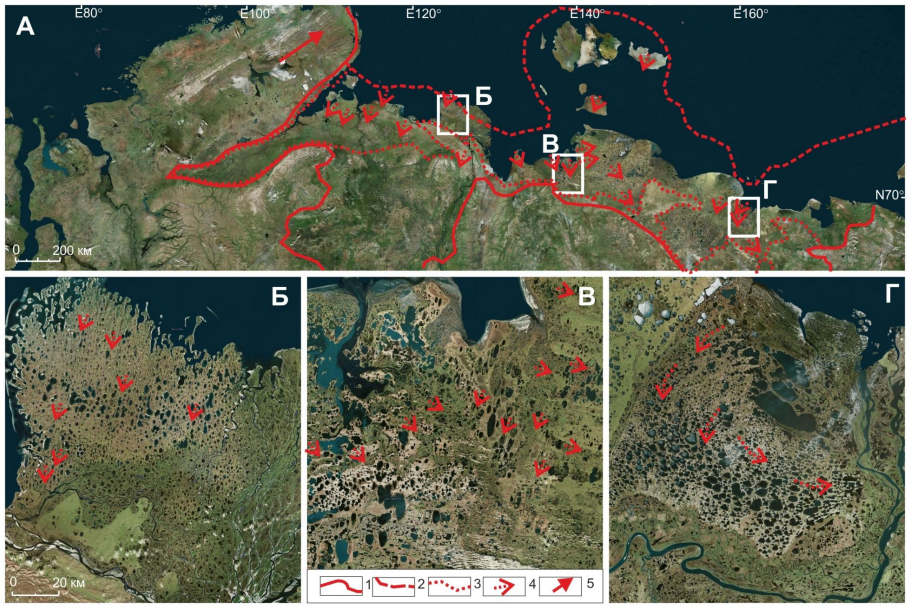

Figure 1: 1 А – The extent and directions of floodstreams on the coasts of the Laptev and East-Siberian Seas at the Late Pleistocene-Holocene transition. Б – on the Arga-Muora-Sise Island in the Lena River Delta. В – in the vicinity of the Yana River mouth. Г – in the Lower Kolyma region. Legend: 1 – northern limit of the continental (mountain and sheet) glaciers; 2 – northern limit of the periglacial shallow lake basin displaced by shelf ice and continental Taimyr glacier; 3 – southern limit of the periglacial dammed basin; 4 – directions of floodstreams; 5 – direction of the Taimyr glacier movement.

Landform analysis showed that linear-oriented forms of accumulative, erosional and exarational genesis occupy much of the coastal area of the Laptev and East-Siberian Seas. Catastrophic floodstreams and associated erosion formed much of lake basins in the Primorskaya Lowland, contributed to disintegration of coastal cryolithozone and substantially accelerated the subsequent permafrost degradation.

References

Grosse, G.; Schirrmeister, L.; Siegert, C.; Kunitsky, V.V.; Slagoda, E.A.; Andreev, A.A. and Dereviagyn, A.Y. [2007]: Geological and geomorphological evolution of a sedimentary periglacial landscape in Northeast Siberia during the Late Quaternary. *Geomorphology*, 86(1–2):25–51, doi:10.1016/j.geomorph.2006.08.005.

Grosswald, M.G.; Karlen, W.; Shishorina, Z. and Bodin, A. [1992]: Glacial Landforms and the Age of Deglaciation in the Tiksi Area, East Siberia. *Geografiska Annaler*, 74A(4):295–304, doi:10.2307/521428.

Nagaoka, D.; Saijo, K. and Fukuda, M. [1995]: Sedimentological environment of the edoma in high Arctic eastern Siberia. In *Proceedings of the Third Symposium on the Joint Siberian Permafrost Studies Between Japan and Russia, Tsukuba, Japan, Hokkaido Univ.*, pages 8–13, 1995.

Rock glacier creep as a thermally-driven phenomenon: A decade of inter-annual observations from the Swiss Alps

Benno Staub[1], Christophe Lambiel[2], & Reynald Delaloye[1]

[1]*Department of Geosciences, Geography, University of Fribourg, Fribourg, Switzerland*
[2]*Institute of Earth Surface Dynamics, University of Lausanne, Lausanne, Switzerland*

Many rock glaciers observed in the Alps show similar and synchronous relative inter-annual variations of surface velocities [Delaloye et al., 2008]. A common thermo-hydro-mechanical reaction to changes of the surface energy balance, mainly influenced by air temperature and the seasonal snow cover, is the most likely explanation for this phenomenon. To test the hypothesis of rock glacier creep rate variations being mainly a kinematic response to changes in ground temperature (GT), we analysed annual GPS data measured on 6 rock glaciers in the western and central Swiss Alps. The GPS data used for this study comprises about 200 surveying points followed over at least 10 years and covers both periods of velocity decrease between 2004 and 2006 and velocity increase since then. At most sites, new maxima were measured in the last one to three years surpassing prior velocity peaks of 2003 and 2004.

Based primarily on findings from Arenson et al. [2002] and Kannan and Rajagopal [2013] the displacement monitored at the ground surface is assumed to result mainly from deformation occurring in rather thin layer(s) of minimal viscosity within the permafrost at 10 to 30 m depth. But since the maintenance of boreholes is almost unfeasible for time periods longer than a few months to maximally a few years on fast moving landforms, active rock glaciers are usually lacking of GT time series measured within the permafrost and only ground surface temperature (GST) data are available. GST data have been used to characterise variations of the ground thermal state. Ground thermal state anomalies (GTSA) were arbitrary defined as average monthly GST anomalies over a specific time window and were validated using GT data measured in boreholes. The highest covariance between GTSA and GT data measured at 15 m depth was achieved with GST time windows of a length of ≈2 years and a delay of 2–6 months.

The relationship between relative variations of annual rock glacier velocities and GTSA has been systematically tested. A statistically significant solution was found for an ensemble of GPS points on each rock glacier or rock glacier zone in the form of an exponential regression function, as illustrated in Fig. 1 for the example of the Becs-de-Bosson rock glacier from the Valais Alps.

The comparison of different GPS points with GTSA time series clearly indicated that, within a decade, temperature changes at 10–30 m depth explain the largest part of inter-annual velocity variations. In addition, analysing the time series of the velocity residuals (namely the changes in velocity, which are not explained by the temperature function) may allow to evidence additional pluri-annual acceleration/deceleration trends. Such additional trends represent an alteration of the temperature/creep rate relationship with time as the 2010-2015 deceleration trend observed for the Aget rock glacier and could be caused for instance by the gradual change of the rock glacier geometry, a change of melt water infiltration rate at depth, or ice melt/aggradation and consecutive changing friction at the shear horizon.

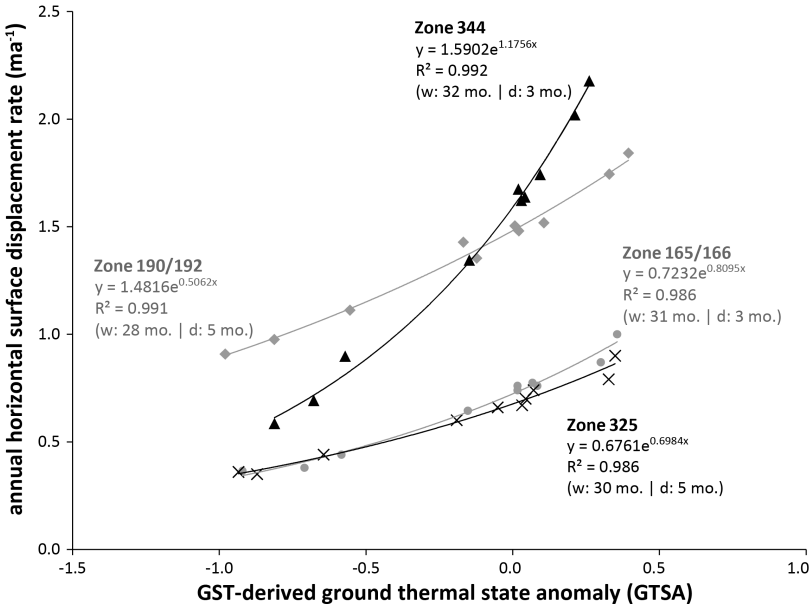

Figure 1: The influence of the ground thermal state on mean annual permafrost creep velocities illustrated using GPS and ground surface temperature (GST) monitoring data from the Becs-de-Bosson rock glacier in the Valais Alps measured between 2004 and 2014

Acknowledgements

The Swiss Permafrost Monitoring Network PERMOS and its partner institutions are highly acknowledged for providing borehole temperature data.

References

Arenson, L.; Hoelzle, M. and Springman, S. [2002]: Borehole deformation measurements and internal structure of some rock glaciers in Switzerland. *Permafrost and Periglacial Processes*, 13:117–135, doi:10.1002/ppp.414.

Delaloye, R.; Perruchoud, E.; Avian, M.; Kaufmann, V.; Bodin, X.; Hausmann, H.; Ikeda, A.; Kääb, A.; Kellerer-Pirklbauer, A.; Krainer, K.; Lambiel, C.; Mihajlovic, D.; Staub, B.; Roer, I. and Thibert, E. [2008]: Recent Interannual variations of rockglaciers creep in the European Alps. In: Kane, D.L. and Hinkel, K.M.(eds.), *Proceedings of the Ninth International Conference on Permafrost*, Institute of Northern Engineering, University of Alaska Fairbanks, Fairbanks, USA, 29 June–3 July 2008, volume 1, pages 343–348. ISBN 978-0-9800179-2-2. URL http://ipa.arcticportal.org/publications/conference-proceedings.

Kannan, K. and Rajagopal, K.R. [2013]: A model for the flow of rock glaciers. *International Journal of Non-Linear Mechanics*, 48:59–64, doi:10.1016/j.ijnonlinmec.2012.06.002.

Fluvial and thermal: river bank erosion in permafrost regions

Nikita Tananaev[1,2]

[1] *P.I. Melnikov Permafrost Institute, SB RAS, Russian Federation*
[2] *Ugra Research Institute of Information Technologies, Russian Federation*

Fluvial thermal erosion is supposed to be omnipresent in periglacial environment, where river flow has direct access to the frozen river banks. Nonetheless, in permafrost areas, rivers erode their banks largely in the same manner as their counterparts do elsewhere in the world. Periglacial river banks are not affected exclusively by fluvial thermal erosion, and whence the bank starts being eroded, it is not necessarily owing to fluvial and thermal erosion at once. It requires a thermal component (ablation) to exist and to precede mechanical washout. Sedimentary features, including ice content, and channel patterns' development are known to affect the thermal erosion process. Hydrological controls over the latter remain, however, largely understudied.

Water regime and sedimentary features of the middle Lena River reach near Yakutsk, central Yakutia, were studied to assess their control over fluvial thermal erosion. The Lena River floodplain in the studied reach has complex structure and embodies multiple levels varying in height and origin. Two key sites, corresponding to high and medium floodplain levels, were surveyed in 2008 to describe major sedimentary units and properties of bank material. Three units are present in both profiles, corresponding to topsoil, overbank (cohesive), and channel fill (noncohesive) deposits.

Fluvial activity occurs in all ranges of water levels. In a long-term perspective, however, some water levels are assumed to be more efficient in performing the geomorphic action, i.e., more frequent and implying higher stream energy. Thermoerosional activity is mostly confined to a basal layer of frozen channel fill deposits and in general occurs within an 'effective' water level interval. Effective water level interval was inferred from magnitude-frequency analysis, marking hydrological conditions under which the fluvial thermal erosion is active in a long-term perspective. For the studied middle Lena River section, it lies between 91.05 and 92.62 m asl, and corresponds, roughly, to water discharges between 21,000 and 31,000 $m^3\ s^{-1}$.

Effective water level represents the hydrological driver of fluvial erosion, but the erosional response of the river banks depends nonetheless on the mechanical features of the surface being eroded. Overlapping this effective water level with studied bank profiles allows drawing some conclusions on the differences between the sites and subsequently between various floodplain levels and banks in terms of processes involved in bank retreat. In high floodplain banks, effective water level corresponds to the noncohesive layer of sandy channel-fill deposits, remaining frozen during the spring peak discharges. Repeated thermoerosional niche failures and subsequent removal of collapsed material represent the dominant bank erosion process within this floodplain level. Medium floodplain level is significantly lower and is subject to mechanical washout, largely unaffected by thermal interactions. Bank retreat rate is argued to be positively linked with bank height under periglacial conditions.

The Role of Cryogenesis in the Formation of Sand deposits in the Chara Basin (Transbaikalia)

Natalia Taratunina[1], Anna Kurchatova[1,2], & Elena Slagoda[1,2]

[1] *Tyumen State Oil ang Gas University, Tyumen, Russian Federation*
[2] *Institute of the Earth Cryosphere of the Siberian Branch of the RAS, Tyumen, Russian Federation*

The study presents the transformation of sandy sediments of different lithogenetic types of Chara Basin. Sand deposits of the Chara Basin (708-740 m a.s.l.) located in the south of the Siberian Platform (Transbaikalia) were investigated. On the eastern side the basin is bounded by the Udokan Ridge (2515 m a.s.l.), on the western – by the Kodar Ridge (3073 m a.s.l.). The average annual air temperature was -7.6 °C during 1939–2004 according to the meteorological station'Old Chara'.

To determine the influence of cryogenic processes on the sand sediments of Chara Basin samples from the different areas were investigated:

1. the average flow of the river Middle Sakukan;
2. the icing field in the mouth of the river;
3. the first terrace of Chara River enclosing Holocene polygonal ice-wedges;
4. the dunes of "Chara Sands" area.

Grain size analysis of samples was made by particle size analyzer Mastersizer 3000 (Malvern). Mineral composition was determined by using X-ray diffractometer D2 PHASER (Bruker). Micromorphological analysis of mineral grains was made by SEM TM3000 (Hitachi).

The total content of the fine fraction in grain composition of modern alluvium is less than 10 %, and for aeolian deposits – less than 1 %. In the vertical section of Holocene terrace of Chara River, the content of silt increases from the bottom to up. According to the Ferre diagram, modern alluvium can be attributed to "sands" and "loamy sands", sediments enclosing the polygonal ice-wedges – "silty loam", dune deposits – "sands". Sediments are well sorted in according to the Track coefficient except for sediments of Holocene terrace of Chara River with a high silt content.

The morphology of quartz grains of alluvium differs with angularity, conchoidal fractures, striation, fracturing features. Quartz in sediments of Holocene terrace is characterized by cleavage face of grains. In dune deposits, grains differ with the most isometric form, smoothed surface, small-subrounded pits (cup-shaped hollows, crescentic grooves), clay coating but there are also angular quartz grains with cleavage face. Sediments of icing field and Holocene terrace are characterized by aggregation of grains by clay particles. There are also signs of primary moraine material in all lithogenetic types of sand sediments: angular shape of grains, subrounded pits and exarational grooves. Cryogenic processes are more expressed in sediments of icing field (predominance of "exploded" grains of quartz and feldspar) and sediments enclosing Holocene ice wedges (cryogenic weathering of quartz grains with the formation of cleavage face) [Konishchev and V.V., 1993, Rogov, 2009, Woronko and Pisarska-Jamrozy, 2015].

Acknowledgements

This study has been supported by Russian Science Foundation (Grant 14-17-00131).

References

Konishchev, V.N. and V.V., Rogov. [1993]: Investigation of cryogenic weathering in Europe and Northern Asia. *Permafrost and Periglacial Processes*, 4: 49–64, doi:10.1002/ppp.3430040105.

Rogov, V.V. [2009]: *Foundations of cryogenesis*. Novosibirsk: GEO Academic Publ., 236 pp.

Woronko, B. and Pisarska-Jamrozy, M. [2015]: Micro-Scale Frost Weathering of Sand-Sized Quartz Grains. *Permafrost and Periglacial Processes*, 27: 109–122, doi:10.1002/ppp.1855.

Earth hummocks from Southern Carpathians: Morphometry, characteristics of internal structure and thermal behavior

Petru Urdea, Alexandru Onaca, Adrian Cristian Ardelean, & Raul David Serban

West University of Timisoara, Romania

Earth hummocks are miniature cryogenic mounds widespread in the alpine domain of Southern Carpathians. These landforms result from the combined, but variable interaction of frost heave, cryoexpulsion of clasts, hydrostatic and cryostatic pressure and cellular circulation. Earth hummocks existence does not necessarily require permafrost conditions, being capable of forming due to seasonal frost penetration. The aim of our study was to examine the regional characteristics of these small dome-shaped hummocks and to better understand the relations between thermal regime, internal structure and actual evolution analyzing sites from Țarcu Mountains (1750 m asl) and Făguraș Mountains (2260 m asl). 100 mounds were measured at these sites, displaying an average of 31 cm in height and a mean length of 132 cm. Contrary to similar studies the earth hummocks from this sites become elongated and coalescent in a particular direction, as a consequence of the intense frost heave and more efficient frost action on northern aspects. This assumption was confirmed by thermal data recorded in the spring of 2013 on both northern and southern side of the earth hummock showing significant differences in the thermal regime.

The internal structure and its seasonal evolution was proved through electrical tomography investigations (ERT). On the other hand, the internal structure elements, some of them connected by cryogenic processes, are related to specific physico-chemical characteristics, such as granulometry, vertical and horizontal variation of thermal conductivity, magnetic susceptibility (Fig. 1), moisture and metal ions content, mineralogical content, density etc. For example, the variation in vertical profile of Fe content and specific oxides (limonite and hematite) and other neoformation minerals, especially clay minerals, is correlated with the specificity of the pedogenetical processes, that occur in natural environmental conditions of alpine domain. To find these characteristics were conducted XRF, FTIR, TGA, DTA /DSC, RMN investigations and computing tomography.

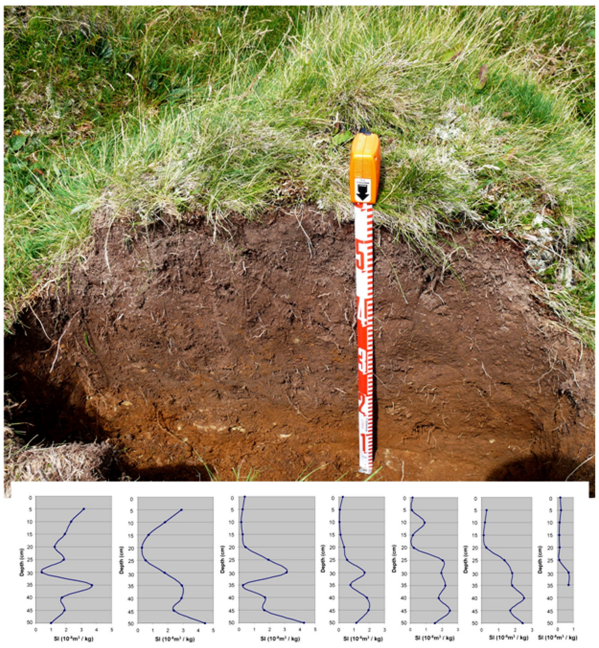

Figure 1: Earth hummock: magnetic susceptibility variation on the depth profiles.

The thermal regime inside one earth hummock was measured during two seasons at 5 different depths: 10, 20, 30, 40, 50 cm using 5 thermistors. The interval when the action of frost is efficient inside the earth hummock is December-May, and the maximum depth of frost penetration is between 30 and 40 cm. Therefore, at the beginning of cold season the frost penetrates progressively from the surface inside the earth hummock, but at 30 cm depth it occurs two months later. The thawing behavior is more complex, since the segregation ice starts to melt from the surface downward, but sometimes in spring during cold nights, the first 10-15 cm of soil refreeze. On the other hand, at 30 cm depth, the ice segregation is going to melt completely around the middle of May, when the temperature in the upper part of the soil is already above 5 °C.

Distribution and Morphology of Sorted Circles and Polygons in the Northern Billefjorden, Central Svalbard

Tomáš Uxa, Peter Mida, & Marek Křížek

Department of Physical Geography and Geoecology, Charles University in Prague, Czech Republic

Sorted patterned ground is a widespread and characteristic feature of the periglacial landscape in Svalbard archipelago or elsewhere on the Earth. Quantitative data about its morphology from both permafrost and seasonally frozen ground areas on a wider scale are, however, still surprisingly scarce. As a consequence, environmental controls over these periglacial landforms still remain poorly understood, which prevents their broader and more reliable use as palaeoenvironmental indicators.

Here, we describe distribution and morphology of well-developed large-scale sorted circles and polygons from the northern Billefjorden, central Svalbard (79°N), and we analyze their relation to environmental conditions. The bedrock at study sites composes mainly of Carboniferous sedimentary rocks (sandstones, shales, conglomerates, coal) and, to a lesser extent, of Mesoproterozoic metamorphic rocks (schists, amphibolites). The mean annual air temperature is around -6 °C at sea level and total annual precipitation is estimated around 200 mm [Rachlewicz and Styszyńska, 2007, Láska et al., 2012]. Extensive non-glaciarized areas are underlain by continuous permafrost with active-layer thickness generally reaching 30–160 cm [Gibas et al., 2005].

Sorted circles and polygons were investigated at sites where a continuous network of at least ten sorted features is developed on flat or gently inclined terrain up to 5°. In total, 290 sorted circles and polygons were examined at sixteen locations at elevations of 28 to 773 m asl. Length, width and height of ten or twenty randomly selected sorted patterned-ground features were measured at each study site, depending on the number of present landforms. At three sites, the sorting depth was determined by excavations as a maximum depth where a distinct boundary between the sediments located under fine centres and coarse borders is visible.

Well-developed large-scale sorted circles and polygons are found mainly on raised marine and kame terraces at elevations up to 200–250 m asl and on adjacent flat-topped mountain ridges above elevations of around 600 m asl. These two distinct regions are separated by steep, scree-covered slopes unfavourable for patterned-ground development. Glacier forelands deposited since the Little Ice Age are occupied only by rare small-scale and poorly-developed patterns. The diameters of the sorted circles and polygons range from several decimetres to up to 450 cm with an average of 198 cm and 154 cm for length and width, respectively. The average height is 16 cm, but it reaches up to 50 cm depending on the pattern diameter. For feature widths of 146 to 164 cm, sorting depths range between 44 to 64 cm giving width-to-sorting depth ratios from 2.41 to 3.73, which is roughly consistent with models of patterned-ground formation involving circulation mechanisms.

Generally, higher elevations host significantly smaller and less up-domed patterns than lower elevations do. Likewise, shallower sorting occurs at higher altitudes, though the sample is not representative. Accepting the premise that, in permafrost areas, sorting is confined to the base of the active layer and with respect to the linkage between the pattern diameter and the sorting depth, we explain these altitudinal changes in patterned-ground morphology by decrease of active-layer thickness towards higher elevations. Although statistically significant, the absolute differences in morphology between the lower- and the higher-elevated groups of features are not too large. However, this may be caused by complex interplay of site-specific factors, such as ground material, snow cover and/or drainage, which affect ground thermal regime at local scale, but are unable to completely override regional climate patterns. This suggests that large-scale sorted patterned ground can be an indicator of climate conditions. On the other hand, permafrost table was achieved only at one excavation site located near sea level and reached 36 cm below the sorting depth. At other two excavation sites, permafrost table was not encountered up to 10 cm below the sorting depth. Therefore, we believe that, at least in lower elevations, sorted circles and polygons are likely not in equilibrium with present-day climate conditions.

We also infer that patterned-ground development in the high-Arctic environment can take place on timescales of hundreds of years because well-developed large-scale sorted circles and polygons are absent on the Little Ice Age moraines and glacier forelands.

References

Gibas, J.; Rachlewicz, G. and Szczuciński, W. [2005]: Application of DC resistivity soundings and geomorphological surveys in studies of modern Arctic glacier marginal zones, Petuniabukta, Spitsbergen. *Polish Polar Research*, 26:239–258.

Láska, K.; Witoszová, D. and Prošek, P. [2012]: Weather patterns of the coastal zone of Petuniabukta, central Spitsbergen in the period 2008–2010. *Polish Polar Research*, 33:297–318.

Rachlewicz, G. and Styszyńska, A. [2007]: Porównanie przebiegu temperatury powietrza w Petuniabukta i Svalbard-Lufthavn (Isfjord, Spitsbergen) w latach 2001–2003. *Problemy Klimatologii Polarnej*, 17: 121–134.

Upper Pleistocene Geocryological evolution in Northwest of the Iberian Peninsula

Marcos Valcárcel, Manuela Costa-Casais, Jonathan F. Hall-Riaza, & Ramón Blanco-Chao

Universidade de Santiago de Compostela, Spain

During the Pleistocene cold stage, the palaeoclimatic conditions in the NW of Iberian Peninsula allowed the occurrence of nival and periglacial processes at present coastal line, and glacial dynamics in the mountain areas even at elevations below 1000 m. Intense cold climatic processes were developed, including permafrost evidences, that affected both non-glaciated and glaciated sectors during the progressive retreat of the glacial fronts [Valcárcel, 1998].

Today, the northwest of the Iberian Peninsula presents an oceanic wet climate with temperate winters [Martínez et al., 1999], more similar to the climates of Atlantic Europe than to the climates of Mediterranean type that dominate the most of the Iberian Peninsula. This condition of climatic border was maintained during the cold stages and was therefore very sensitive to global climatic variability, leaving an imprint of these oscillations in the sedimentary record in the present coastal areas that were affected by cold climate processes, and in the mountain sectors affected by glacial and periglacial dynamic. Therefore it is possible to establish a link of the Pleistocene climatic variations in the NW Iberian peninsula with the paleoclimatic evolution of northern Europe [Valcárcel, 1998].

On the other hand, the response to general climatic changes was probably faster in these local glaciers than in the inland ice located in the north of Europe. Their response to changes earlier and therefore apparently are not synchronous with the Fennoscandian ice cap. This would explain the early advance of the glaciers, but not the smaller extension during the Last Glacial Maximum (LGM). In this work we suggest that the explanation is not only their peripheral location, but also the Pleistocene paleoclimatic evolution at regional scale. Thus, an early local maximum glacial advance, possibly promoted by cold and wet climate conditions, allowed the succession of wet cold glacial and much colder and drier periglacial stages [Valcárcel, 1998]. This fact involves the change in the patterns of criologycal mountain types, as defined by Gorbunov [1978] to characterize different world cryospheres. The increasing elevation from the coast to the high mountains, of which Ancares Range is a good example, explains why the advance of these cold stages is expressed in the delimitation of mountain criologycal belts, first characterized by the occurrence of glacial conditions, and later by the occurrence of frozen grounds, especially the identification of altitudinal limit of mountain permafrost.

Consequently, the main focus in this work is to provide understanding of the geomorphological record in order to reconstruct the relationships between the glacial and periglacial phenomena in the different cold phases, or different mountain geocrilogycal types in the sense described by Gorbunov [1978], as well as to outline a chronological model of their evolution, using available absolute dating for the whole northwest of the Iberian Peninsula.

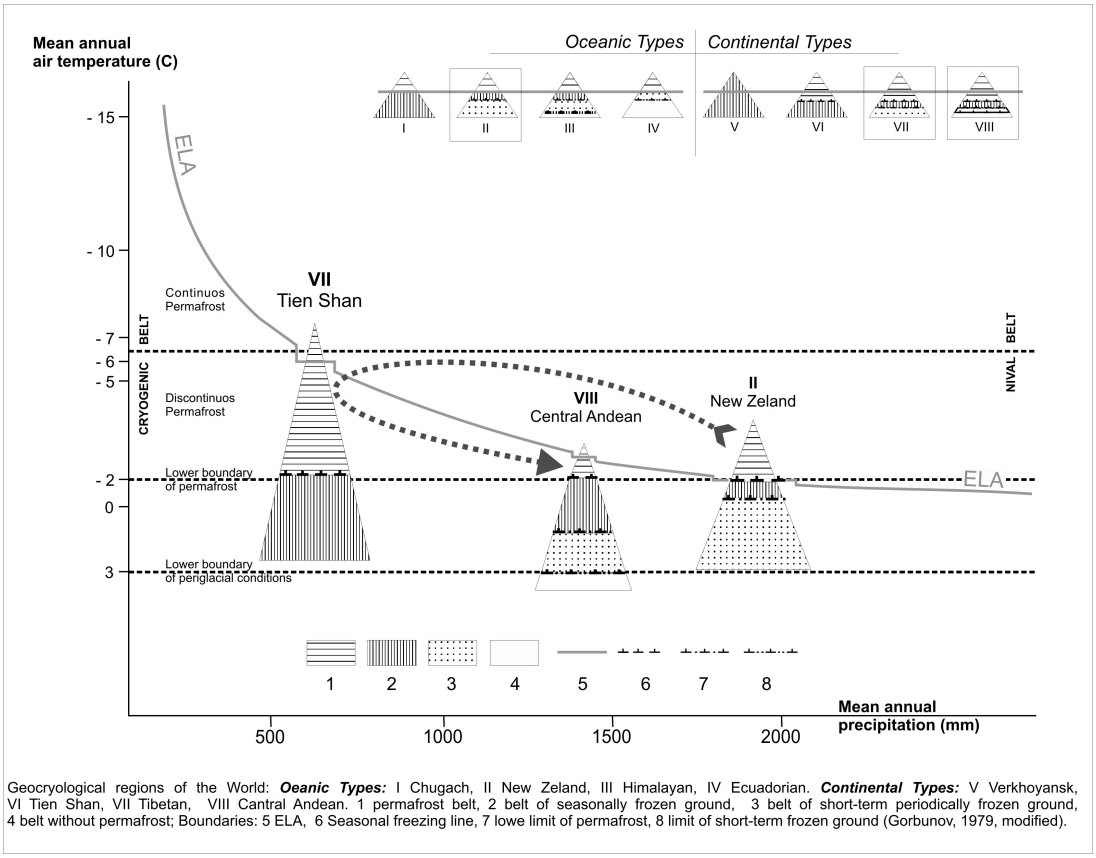

Geocryological regions of the World: ***Oeanic Types:*** I Chugach, II New Zeland, III Himalayan, IV Ecuadorian. ***Continental Types:*** V Verkhoyansk, VI Tien Shan, VII Tibetan, VIII Cantral Andean. 1 permafrost belt, 2 belt of seasonally frozen ground, 3 belt of short-term periodically frozen ground, 4 belt without permafrost; Boundaries: 5 ELA, 6 Seasonal freezing line, 7 lowe limit of permafrost, 8 limit of short-term frozen ground (Gorbunov, 1979, modified).

Figure 1: Geocryological evolution of Ancares Range along the Upper Pleistocene.

References

Gorbunov, A.P. [1978]: Permafrost investigations in high-mountain regions. *rctic and Alpine Research*, 10(2):283–294, doi:10.2307/1550761.

Martínez, A.; Pérez-Alberti, A.; Castillo, R.F.; Valcarcel, M. and Blanco, C.R. [1999]: *Atlas climático de Galicia*. Santiago de Compostela: Xunta de Galicia.

Valcárcel, M. [1998]: *Evolución geomorfológica y dinámica de las vertientes en el noroeste de Galicia*. Doctoral dissertation, tesis doctoral, Dpto de Xeografía. Universidade de Santiago.

Thermal erosion of ice-rich permafrost in the Lena River Delta / Siberia – Determining the decisive factors using logistic regression

Georg Veh[1,2,3], Anne Morgenstern[1], & Florian Haas[2]

[1] *Alfred Wegener Institute Helmholtz Center for Polar and Marine Research, Potsdam, Germany*
[2] *Catholic University of Eichstaett-Ingolstadt, Eichstaett, Germany*
[3] *Potsdam University, Potsdam, Germany*

Vast parts of Arctic Siberia are underlain by ice-rich permafrost, which is exposed to different processes of degradation due to global warming. Thermal erosion as a key process for landscape degradation in these regions causes the recent reactivation and formation of new landforms like thermo-erosional valleys and gullies. However, a statistical assessment about the decisive factors and the locations most susceptible to this phenomenon is still missing. We investigated the influence of different environmental parameters on the occurrence of recently observed thermal erosion using a GIS-based approach and statistical modeling by logistic regression. The study site is located on an island within the Arctic Lena River Delta and is mainly composed of ice- and organic-rich deposits of the Yedoma-type Ice Complex. Field surveys and mapping on the basis of high-resolution remotely sensed data revealed that thermal erosion occurs predominantly i) on very steep slopes along the margins of the island, ii) in the upper reaches of deeply incised valleys and iii) in gullies. In order to detect the regulation factors for those thermo-erosional landforms, we derived several environmental parameters using a high-resolution DEM and satellite imagery. We chose a stepwise logistic regression approach to reduce the full set of potential parameters. This approach allowed the selection of a parsimonious model, i.e. a best-fit model using as few parameters as possible. The parameters Contribution of warm open surface water, Relief ratio, Direct solar radiation and Snow accumulation turned out to be the decisive factors for thermal erosion. Uncertainties in the model due to sampling and model selection were evaluated both statistically and spatially through the generation of 100 models. Receiver Operating Characteristics (ROCs) were used to validate the spatial predictive capability of each model run. The consensus map as the median of all 100 susceptibility models represents the final susceptibility map. The agreement between mapped and predicted erosion turned out to be generally very high within the study site, confirmed by an Area under the ROC curve (AUC) of 0.957 for the consensus map. The variability of predicted erosion probabilities between the single models is about four percentage points per cell within the study site and thus, very low. We attributed the slight mismatches between observed and predicted erosion to the generation of the explanatory environmental parameters and the modeling approach. Model results seem promising for the spatial prediction of susceptible sites for thermal erosion and, thus, could be a tool to explain the geomorphic forming in this rapidly changing environment. As these results are based on a single case study, future investigation should focus on the transferability of the model by applying an external validation on other sites with comparable environmental conditions.

Glacier-Permafrost interactions, debris transfer mechanisms and the development of distinctive sediment-landform associations in a High Arctic glacial environment: the case of Fountain Glacier, Bylot Island, Nunavut, Canada

Richard I. Waller[1], Michael J. Hambrey[2], & Brian J. Moorman[3]

[1] *Keele University, United Kingdom*
[2] *Aberystwyth University, United Kingdom*
[3] *University of Calgary, Canada*

Detailed investigations of the sediment-landform associations being actively created in modern-day periglacial environments provide the opportunity to constrain the linkages between process and form that underpin palaeoenvironmental reconstructions. Glacial geomorphologists have commonly assumed that cold-based and polythermal glaciers underlain by permafrost are slow moving, geomorphologically inactive and therefore of limited research interest. However, recent research in both modern and ancient periglacial environments has illustrated the ability of glaciers and permafrost to couple and interact, leading to the operation of distinctive processes and the development of distinctive sediment-landform associations. Despite this, our knowledge and understanding of the mechanisms of debris transfer, the characteristics of the associated sediments and the diversity of geomorphic features associated with High Arctic glacial environments remain limited.

This research describes the distinctive landforms, lithofacies and sediment-landform associations characteristic of an Arctic outlet glacier on Bylot Island in the Canadian High Arctic. The island features a mountainous central icefield from which a series of outlet-glaciers flow towards the coastal lowlands. With a mean annual air temperature of approximately -15 °C, these glaciers terminate in an area of continuous permafrost estimated to be between 200-400 m in thickness. As such it constitutes an ideal location in which to examine the geomorphic processes and products associated with glacier-permafrost interactions. The observations reported were made primarily at the margin and foreland of Fountain Glacier, a polythermal glacier 16 km in length associated with a core of warm ice covered by a layer of cold ice that extends to the glacier margins.

Field observation and mapping showed the glacier margin to be characterised by a distinctive landform assemblage comprising boulder-dominated surfaces and moraine ridges (a number of which were ice-cored), areas of heavily weathered and shattered bedrock, incised lateral meltwater channels, outwash braidplains and large proglacial icings (Aufeis) (Fig. 1). In addition to these newly created landforms, recession of part of the margin has revealed an intact tundra surface complete with biologically-viable vegetation that showed little if any glacial modification associated with its inundation during the Little Ice Age. Significant glacial sediment transfer occurred through a prominent debris-rich basal ice layer dominated by sub-angular and angular material of up to boulder size.

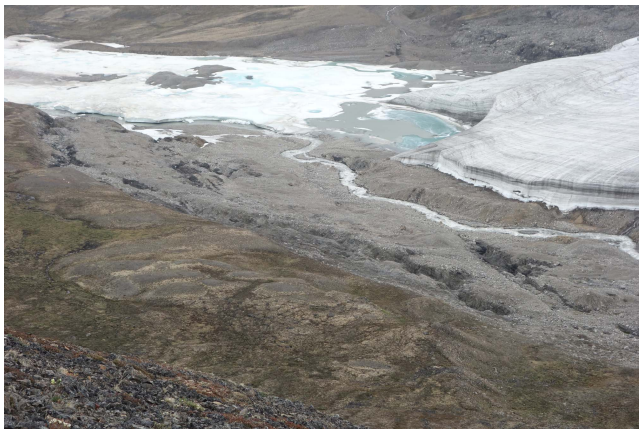

Figure 1: Ice margin and foreland of Fountain Glacier. This illustrates the boulder-dominated surfaces, incised lateral meltwater channels and large proglacial icing that are characteristic of this glacier.

The basal ice layer and ice margin as a whole displayed extensive evidence of glaciotectonic deformation intimately associated with the structural glaciology of the glacier as a whole. Thrusting was observed to elevate basal material from the basal ice to the glacier surface where the material contributed to a supraglacial sediment flux. Fluvial sediment transfer was associated primarily with a series of ice-marginal

meltwater systems producing the only lithofacies with a significant percentage of rounded clasts.

The glacial sediment-landform association at Fountain Glacier displays a number of distinctive elements illustrative of the specific geomorphic processes active in this environment. Bedrock shattering is predominant with there being little evidence of glacial abrasion, thereby leading to the development of glacigenic lithofacies with a surprising degree of angularity. In spite of the cold climatic conditions and limited meltwater production, fluvial processes remain important geomorphologically, leading to the erosion of lateral meltwater channels, the deposition of small outwash surfaces and the generation of large proglacial icings. The most enigmatic element however relates not to the new features being actively created but to the ability of the glacier to preserve delicate vegetated tundra surfaces during ice advance. The close proximity of these intact surfaces with more heavily modified areas suggests a spatial variability in process that merits further investigation and explanation.

High-resolution imaging of patterned ground features based on UAV photogrammetry

Tatsuya Watanabe[1], Norikazu Matsuoka[2], & Hanne H. Christiansen[3]

[1] *Department of Civil and Environmental Engineering, Kitami Institute of Technology, Japan*
[2] *Faculty of Life and Environmental Sciences, University of Tsukuba, Japan*
[3] *The University Centre in Svalbard, UNIS, Norway*

Periglacial processes give rise to a number of small-scale features of the permafrost landscape. Detailed mapping of small periglacial features over a wide range demands much time and effort. Recently, Structure from Motion (SfM) technique has been widely used to generate high-resolution 3D spatial models. This study applies SfM technique to map the microtopography of some patterned ground types in Adventdalen, Svalbard. Survey targets include ice-wedge polygons, small polygons and mudboils. The SfM technique requires multiple images of an object taken from different positions and simultaneously calculates camera parameters and orientations and a dense 3D point cloud representing the most prominent features in the images. To build 3D geometric models, ground surfaces were shot from 5–15 m high by a downward-view 4K video camera mounted on the phantom 3 professional, a small multi-rotor unmanned aerial vehicle (UAV). Several ground controlling points (GCP), increasing the accuracy of SfM analysis, were placed on the ground surface in shooting areas. The position of the GCP was measured using Real Time Kinematic GPS yielding absolute positions of 1–2 cm horizontal accuracy. Pictures for SfM analysis were captured from movie files every 1 or 2 seconds by a video editing software because accurate modelling requires 80 % of overlap between successive pictures.

In the ice-wedge polygon site, 321 images were captured from 11 minutes of the movie file taken at 15 m high from ground surface, covering an area of 9000 square meters. The 3D position error on the 16 GCP is about 10 cm on average. The SfM model faithfully reproduces microtopography such as polygon rims and troughs. The model can even delineate new generation ice-wedge cracks characterized by indistinctive lineaments. In the small polygon site, the flying height of the UAV was maintained at 5 m high from ground surface to image microrelief in detail. Total 1814 images were captured from 30 minutes of the movie file, covering an area of 440 square meters. The SfM process reproduces polygonal patterns as real, although the 3D position error on the 4 GCP is significantly large at the present stage. Huge position error might be due to the lack of images covering wide area from a higher altitude. In the mudboil site, the UAV took movies at 5 and 10 m high from ground surface. Total 740 images were captured from 25 minutes of the movie file, covering an area of 730 square meters. The SfM process images hummocky rough terrain with high resolution. The 3D position error on the 4 GCP is about 6 cm on average. Since all SfM processes have been done with medium accuracy so far, further improvements are expected in spatial position error. This study demonstrates that the combination of UAV shooting and SfM analysis is capable of drawing the high-resolution 3D images of small periglacial features in a short time.

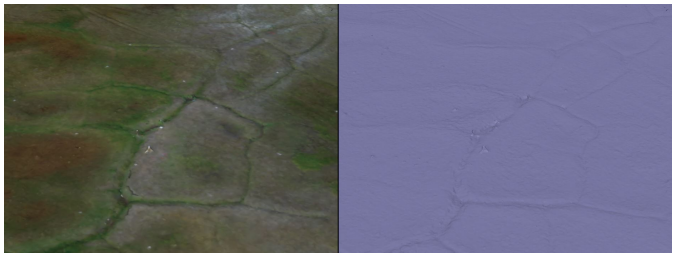

Figure 1: 3D terrain model of ice-wedge polygons produced by SfM analysis

Reversible and irreversible movements in steep fractured bedrock permafrost

Samuel Weber[1], Jan Beutel[2], Jérome Faillettaz[1], Andreas Hasler[3], & Andreas Vieli[1]

[1] *University of Zurich, Switzerland*
[2] *ETH Zurich, Switzerland*
[3] *SensAlpin, Switzerland*

Steep fractured rock slopes are common in alpine regions and the behavior of frozen zones is of fundamental importance in controlling slope stability as permafrost warms or thaws. Rising temperatures translate into slope destabilization in mountain permafrost areas globally, yielding increased hazard potential. A likely reason behind such phenomena is the presence of highly fractured zones containing ice (bedrock permafrost), acting as preferential failure planes as temperature increases. But identifying gravity-driven failure in rock is a complex task, mainly because the abrupt rupture is a highly nonlinear process sensitive to unknown heterogeneities present at all scales in rock. Thus, improved knowledge of processes and factors affecting slope stability is essential for detecting, monitoring and eventually assessing stability of potentially hazardous slopes.

Rock-slope creep may be a pre-failure deformation of rock fall or, at least, has similar controlling mechanisms. We have collected over seven years of fracture dilatation data at 3500 m a.s.l on Hörnligrat, Matterhorn, in steep fractured permafrost bedrock. The surface displacements measured using crackmeters include reversible and irreversible movement components resulting from a balance between driving and resistive forces in strongly fractured bedrock. As rupture is irreversible, we apply a linear regression model with rock temperature as input to remove the reversible movement component caused by thermal expansion and contraction of the rock (see Fig. 1).

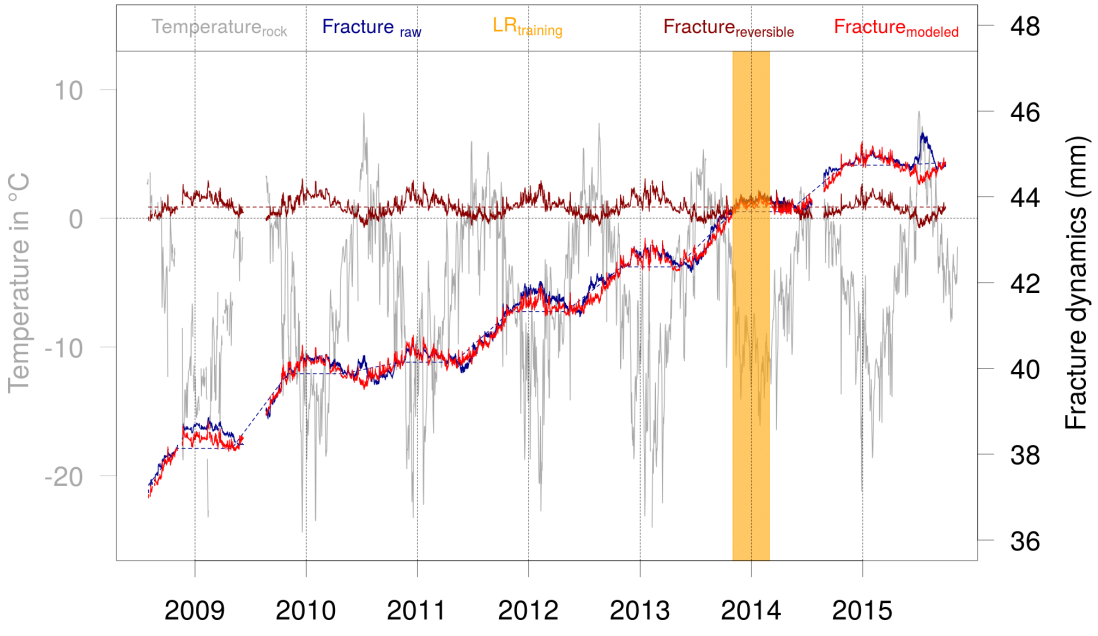

Figure 1: Result of raw dilatation measurements in tension (blue). The reversible component due to thermal expansion can get modeled by a linear regression model (LRM) with temperature as input data (darkgrey) and dilatation measurements during a several months training period (bright blue). Assuming there is a summer creep (blue dotted) that can be described by a one fracture dilatation measurement in winter and a defined winter period. The combination of the LRM and the summer creep results in modeled fracture dilatation (red).

The resulting movement pattern is strongly dominated by enhanced fracture dynamics during summer caused by a thawing related reduction in strength. The start of this summer creep correlates with the initiation of snow melt in early summer. The percolating water, mostly melted snow and ice, changes properties along friction zones in fractures. The inter annual variability and summer offsets show, in our seven years of data, no clear trend. Such surface displacement measurements strongly depend on the choice of the measurement location with obvious limitations in spatial coverage, temporal resolution and accuracy of the instruments used. As a complement to the initial external measurements, analysis and interpretation using a linear regression model, additional data describing the internal evolution of the bedrock is required.

The occurrence of rupture (macroscopic failure) proceeds in bursts of smaller internal failures prior rupture and does not appear instantaneously. These mechanical failures inside the rock mass, such as the evolution of the crack network through progressive damage accumulation or the frictional deformation of pre-fractured rock, release elastic energy that can be detected by the micro-seismic/acoustic emission (MS/AE) approach. Therefore, four different MS/AE sensors have been installed on Hörnligrat, profiling MS/AE activity across the whole frequency spectrum from 1 Hz to 80 kHz and measuring continuously from summer 2015. The initial data analysis and model development is currently ongoing. It is expected that in combination, surface displacement and MS/AE activity will allow to investigate the irreversible movement component in more detail. Here, the material's heterogeneity (anisotropic fractured bedrock) actually is seen as an advantage, because bursts of smaller cracks are expected to occur before major failures.

Numerical modelling of convective heat transport by air flow in permafrost-rich talus slopes

Jonas Wicky & Christian Hauck

University of Fribourg, Switzerland

Talus slopes are a widespread geomorphic phenomenon in the Alps. Due to their high porosity an internal air circulation can be established which is driven by the gradient between outside (air) and internal (talus) temperature. The thermal regime is different from the surrounding environment often leading to cold microclimates and permafrost occurrences [Delaloye and Lambiel, 2005]. So far this phenomenon has mainly been analysed by field studies. Numerical simulations of the ground temperature evolution in permafrost terrain often neglect the influence of convective heat transfer in air on the thermal regime, seldomly parameterizations of the process are included. In civil engineering many studies were carried out to investigate the thermal behaviour of blocky layers and to improve their passive cooling capacity [Goering and Kumar, 1996]. This study tries to use and adapt these concepts to model heat transfer in air flow also for alpine talus slopes. For this, a numerical model representing a schematical talus slope has been set up. In a first step the model takes into account heat conduction and convective heat transfer by air flow but neglects water flow and the formation of ice. Different configurations of the boundary conditions have been tested, and sensitivities of the model to important parameters such as slope angle or temperature gradient have been analysed. Modelling results show that convective heat transfer by airflow has the potential to develop a temperature difference between the lower and the upper part from about 0.5 °C (boundary closed to the atmosphere) to 2 °C (boundary open to the atmosphere). A seasonally alternating chimney-effect type circulation develops. Modelling results also show that this convective heat transfer leads to a cold reservoir in the lower part of the talus slope which can be crucial for maintaining the ground in frozen state under critical climate conditions. The key sensitivity factor seems to be the air velocity within the talus slope. The velocity depends mainly on the exchange potential with the atmosphere, angle of the slope and internal air conductivity. These factors are thus directly influencing the potential of convective heat transfer.

References

Delaloye, R. and Lambiel, C. [2005]: Evidence of winter ascending air circulation throughout talus slopes and rock glaciers situated in the lower belt of alpine discontinuous permafrost (Swiss Alps). *Norwegian Journal of Geography*, 59(2):194–203, doi:10.1080/00291950510020673.

Goering, D.J. and Kumar, P. [1996]: Winter-time convection in open-graded embankments. *Cold Regions Science and Technology*, 24(1):57–74, doi:10.1016/0165-232X(95)00011-Y.

Contrasting environments of sand wedge formation in discontinuous permafrost, Great Slave High Boreal Plains, Northwest Territories, Canada

Stephen A. Wolfe[1], Peter D. Morse[1], Steve V. Kokelj[2], Christina M. Neudorf[3], & Olav B. Lian[3]

[1] *Geological Survey of Canada, Natural Resources Canada*
[2] *Northwest Territories Geological Survey, Government of the Northwest Territories*
[3] *Department of Geography and the Environment, University of the Fraser Valley*

Introduction

In discontinuous permafrost, variations in surficial materials, vegetation, snow cover and moisture commonly dictate the presence or absence of frozen ground. Within this environment, the occurrence of ice-wedge polygons, palsas and lithalsas may be considered indicative of permafrost terrain. Similarly, the occurrence of sand wedges and sand veins are commonly considered to be associated with permafrost terrain although few, if any, studies of the environmental settings associated with these periglacial features have been undertaken. Herein, we examine three contrasting contemporary settings of sand wedges, sand veins and peatland terrain developed over sand within the extensive discontinuous permafrost environment of the Great Slave Lake region, southern Northwest Territories, Canada, where the mean annual (1980-2010) air temperature is approximately -4.1 °C. We document divergent thermal conditions between warm permafrost-bearing peatland terrain and unvegetated eolian sites without permafrost, but that experience extremely cold ground temperature conditions in winter, coupled with thermal contraction cracking.

Observations

The study area resides on a raised beach setting, with active and stabilized eolian surfaces, on the western shoreline of Great Slave Lake. Seasonal ground cracking, in linear and polygonal patterns, is observed on bare to sparsely vegetated active eolian surface (insets Fig. 1A) in the area. Sand wedges on a bare active eolian surface (Fig. 1A and B) are partially obscured by a surface cover of active eolian sand and surface lags of pebbles. They are tapered, extending to 1-m depth and up to 1-m wide at surface. These sand wedges have formed within a thin (up 40 cm) surface cover of sand-sheet sediments of variable thickness and within underlying beach sediments. The underlying beach sediments are optically dated to between 9.5 and 5.4 ka, and sand within a wedge is dated to between 5.0 and <1.0 ka (Fig 1D). Laminations in host eolian sand-sheet sediments are upturned adjacent to the wedges.

At a lichen-covered stabilized eolian site, numerous polygons, 6 - 12 m in diameter, are observed (Fig 1A and C). In contrast to the wedges at the bare active eolian site, these troughs are covered by a mat of live reindeer lichen and the underlying features extend to depths in excess of 1.2 m with maximum widths of 20 cm (Fig 1E and F). Their widths are relatively uniform below about 50-cm depth, but taper upwards from this depth towards the surface. These features are interpreted as sand veins, hosted by eolian sand-sheet sediments. Host sand-sheet sediments are optically-dated to about 3.0 ka at 80-cm depth, as are the sand vein sediments (Fig 1E). Overlying detrital charcoal within host eolian sediments dates to ca. 2.0 ka at 60-cm depth and to less than ca. 300 years at 30-cm depth (Fig 1F). Organic material infilling the trough 20 cm below the surface may be reworked organic debris, as it dates to ca. 1.1 ka (Fig 1F). Host eolian sand-sheet sediments are horizontal to upturned below 50-cm depth, but are downturned at 20- 40°within shallower adjacent sediments. In addition, overlying organic material from within the troughs extend downward into the underlying sand veins. Open voids, indicative of thermal contraction cracking, are apparent within the sand veins in the upper 50 cm.

Ground temperatures measured to 4.4-m depth, and augering to similar depths, indicate that permafrost is not currently present at the sand wedge or sand vein sites despite seasonal freezing to >3.0 m. However, a third site, which is in an open spruce forest peatland (Fig 1A) with peat extending to 90-cm depth, is underlain by permafrost. Ground temperatures recor-

ded for two years within the underlying sand at 1-m depth indicate that the active layer is contained entirely with the overlying peat. Although permafrost is sustained at this site, the seasonal variation in ground temperatures is less than at the non-permafrost eolian sites.

Significant differences are observed between the thermal regimes on the peatland and sand wedge sites. In 2014-15 annual mean, maximum and minimum air temperatures of the study area were -4.0, 25.2, -41.2 °C, respectively. Corresponding ground temperatures at 1-m depth for respective sites were: bare sand wedges -0.9 (mean), 11.2 (max), -12 °C (min); lichen-covered sand veins -0.2, 14.1, -14.7 °C; and peatland -0.9, -0.1, -2.8 °C. Ground temperatures at 50-cm depth within the permafrost peatland were no colder than -4.1 °C in either the winter of 2013 or 2014, whereas ground temperatures at both sand sites were colder than -20 °C. Snow cover on vegetated sites in this region typically exceeds 30 cm, but was less than 10 cm at these sand sites.

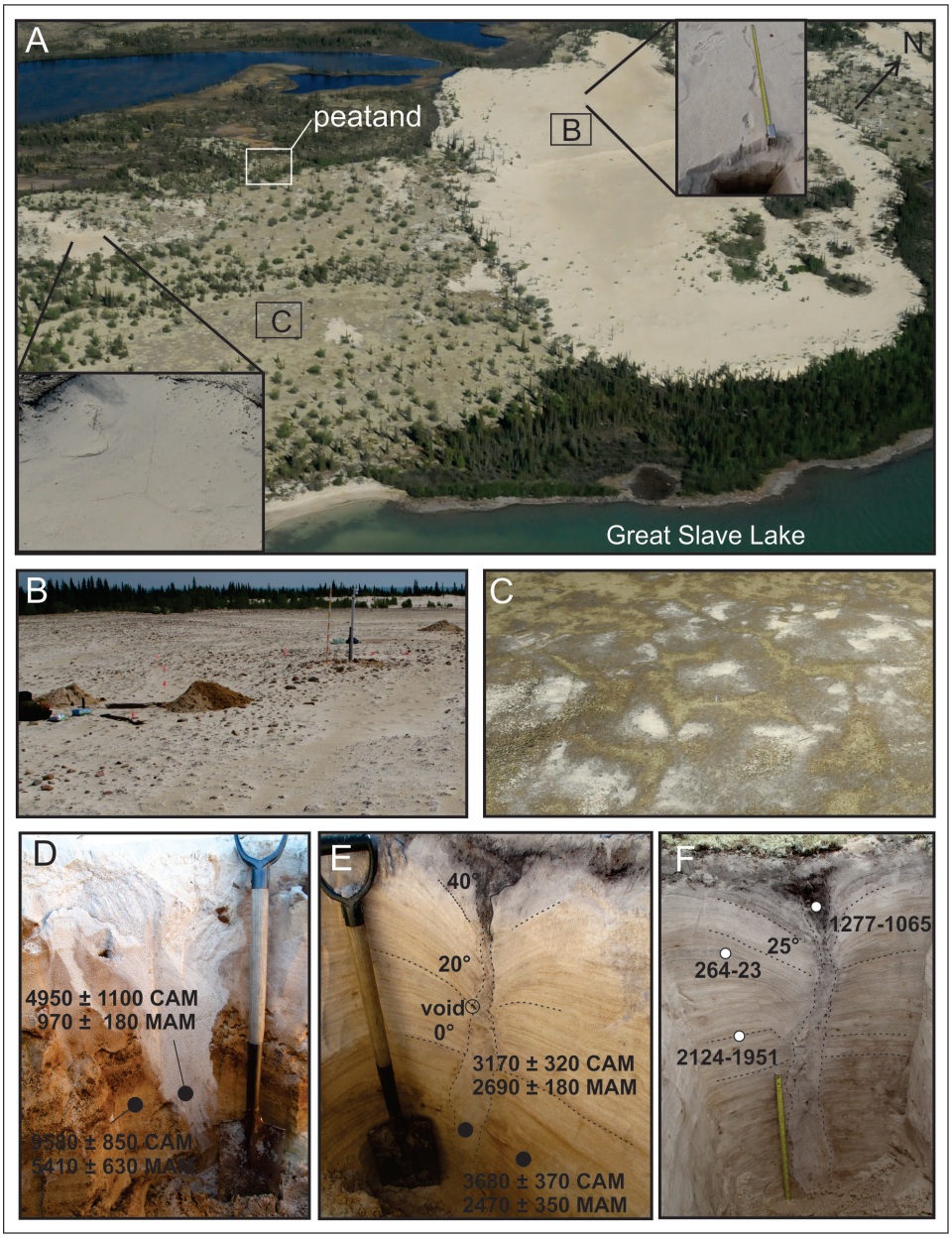

Figure 1: Study sites and profiles in sand wedges. A) Location of peatland, bare sand wedge (B) and lichen-covered sand wedge (C) sites. Profiles of sand wedges developed beneath the active eolian surface (D) and the lichen-covered stabilized eolian surface

Discussion

These observations reveal that divergent ground thermal conditions over short distances can yield contrasting geomorphic processes in discontinuous permafrost settings. Sand wedges on the active eolian surface are interpreted as having developed epigenetically within underlying beach sediments. However, the associated sand-sheet deposits, surface lag of pebbles and cobbles, as well as the broad width of the upper surface of the sand wedges suggests that these wedges may be presently developing anti-syngenetically. The shallow depth of these sand wedges suggest that they form from seasonal cracking, within less than 1-m depth where winter ground temperatures may be colder than -20 °C. Although it is uncertain if permafrost was present at the site in the past, the sand wedges are not presently developing within permafrost.

Sand veins on the lichen-covered stabilized eolian site are interpreted as having developed syngenetically within aggrading eolian sand-sheet deposits, as is apparent by their narrow width and their age relations with surrounding sediments. Upturning of adjacent host sediments at depth is indicative of infilling of the thermal contraction cracks by sand from the surface. However, significant downturning in upper host sediments, infilling of the veins by overlying organic material, and narrowing of the sand vein widths are indicative of the termination of sand infilling. This is most likely attributed to the stabilization of eolian activity and development of vegetation cover, which has occurred within the last few centuries.

Similar to the active eolian site, sand veins may have initially formed in permafrost terrain in the past, but cracking continues within seasonally frozen ground restricted to less than the upper metre of sediment based on the modern thermal regimes and the depth of observed downturning of host sediments adjacent to the upper sand vein sections. With a lack of sand input from the surface, open voids created by thermal contraction cracking are infilled from overlying organic material and by sand migrating from the sides. This process would account for downturning of adjacent sediments and infilling by reworked organic material within the polygon trough.

Within the upper few metres of sediment, these sand wedge and sand veins sites, which are not underlain by permafrost, are significantly colder in winter than adjacent permafrost peatland. Thus, the thermal regime within peatland terrain may be conducive to forming and sustaining permafrost but not to thermal contraction cracking, which occurs at the eolian site without permafrost but with strong seasonal variation in ground temperatures. Sand wedge and sand vein formation at these sites occurs within seasonally-frozen ground, typically at depths of less than 1 m. Although these sand wedges and sand veins are not directly associated with permafrost, they are presently found in association with discontinuous permafrost terrain.

SESSION 2

Antarctic Permafrost, Soils and Periglacial Environments (co-organized by SCAR)

Convener:

Gonçalo Vieira, *CEG/IGOT - University of Lisbon, Portugal*

Mauro Guglielmin, *University of Sussex, United Kingdom*

Christel Dorothee Hansen, *Rhodes University, South Africa*

The session is organized by the IPA Standing Committee and SCAR Expert Group on Permafrost, Soils and Periglacial Environments (ANTPAS). It aims at bringing together scientists working on the dynamics of the ice-free areas of Antarctica, and intends to serve as a forum for discussion and promotion of Antarctic permafrost research, within a highly interdisciplinary framework.

Research on Antarctic permafrost and periglacial environments has been subject to a recent rise of interest, especially following the International Polar Year core projects ANTPAS (SCAR/IPA) and TSP (IPA) and the new developments within GTN-P (WMO/GCOS/IPA). Permafrost, an Essential Climate Variable (ECV7) and the active layer are of central interest for the dynamics of Antarctic ice-free terrains, since their evolution shows impacts on climate (carbon cycle), soils, hydrology, geomorphic processes and on the terrestrial ecosystem. Permafrost is also known to contain biologically viable frozen microorganisms, widely increasing its scientifical interest and scope. Thermophysical conditions of permafrost and the active layer are very variable in the Antarctic and their better understanding is crucial for the assessment of the future fate of Antarctic terrestrial ecosystems.

Transdisciplinary contributions from permafrost, soils, geomorphology, microclimate, ecology, hydrology, geophysics and remote sensing are expected. Although not exclusively, the session also aims to contribute to the new questions from the SCAR Horizon Scan emphasising on the significance of the fast changing terrestrial environments, for example:

- #39. What are and have been the rates of geomorphic change in different Antarctic regions, and what are the ages of preserved landscapes?
- #42. How will permafrost, the active layer and water availability in Antarctic soils and marine sediments change in a warming climate, and what are the effects on ecosystems and biogeochemical cycles?

Other questions of significance to the periglacial environments are #20, 22, 23, 48, 49, 50, 53, 59 and 60.

The viable microorganisms from the Antarctic permafrost

Andrey Abramov[1], Elizaveta Rivkina[1], Ekaterina Karaevskaya[1], Gary Wilson[2,4], & Craig Cary[3]

[1] *Institute of Physico-Chemical and Biological Problems in Soil Science, Russian Federation*
[2] *New Zealand Antarctic Research Institute, New Zealand*
[3] *University of Waikato, New Zealand*
[4] *Department of Marine Science, University of Otago*

The first microbiological study of Dry Valleys permafrost have been done in Soil cryology laboratory leaded by David Gilichinsky on samples, collected at 1995 and 1999 expeditions, and included the cultivation of aerobic and anaerobic bacteria, yeasts, algae and total DNA analysis. Phylogenetic analysis of clones from total DNA by RDP database at that moment showed the presence of Gram-positive bacteria, Proteobacteria, Nitrospina, green nonsulfur bacteria, Fibrobacter, Acidobacterium and Flexibacter-Cytophaga-Bacteroides. In 2014, we returned to Dry Valleys with new ideas and technologies in collaboration with the University of Waikato and Otago. The main sampling technique was the same aseptic drilling without air or liquids. During the field season, we drilled several boreholes at Lower Wright Valley (300 m a.s.l., proposed permafrost age in the order of 10 000 years), Pearce Valley (700 m a.s.l., proposed permafrost age in the order of 1 000 000 years) and at Table Mountain (2000 m a.s.l., proposed permafrost age in the order of 10 000 000 years). The samples for exposure dating by the cosmogenic isotopes were collected in line with drilling. The viable bacterial communities have been found in frozen samples from all the sampling sites. The cultivated bacteria amount is up to 10^2 CFU/gram dry weight. The coldest and driest permafrost have been found in Dry Valleys, where ice content is close to 1 % at the surface, and 5 – 30 % at deeper layers. The total carbon content are very low, about 0.01 – 0.06 %. The mean annual ground temperature (MAGT) here are in range −15 – −25 °C (controlled by elevation). The 5 dominated cultures were found in the enriched cultures and prepared for PCR to the 16s rRNA gene and analyzed by Chromas and MEGA5. The cultures were attributed to phylums Beta-Proteobacteria Firmicutes, families Massilia, Bacillus, Paenibacillus and Sporosarcina.

From 2007, we have been investigating the permafrost on Russian Antarctic stations in the coastal regions around Antarctica. These areas are not so cold and dry, so the total count is higher and close to 10^6 cells/gram dry weight and cultivated bacteria amount is up to $10^3 – 10^6$ CFU/gram. The ice content is in range 10 – 50 %. The total carbon content – 0.4 – 1.5 %. The MAGT here are −7 – −11 °C (controlled by the distance from the coast), except of King George Island (KGI, sub Antarctica), where it close to −0.5 °C. Our bacterial cultures collection includes isolates of genera Bacillus, Cryobacterium, Frigoribacterium, Kocuria, Microbacterium, Micrococcus, Rhodococcus, Streptomyces, Pedobacter, Devosia, Delftia, Polaromonas, Acinetobacter. Clone libraries of v3-v5 site of 16S rRNA gene from KGI detect the members of sulfur reducing bacteria of class Desulfobacteriales and family Desulfobacteriaceae and methanogenic archaea of genera Methanosarcina, Methanobrevibacter, Methanogenium, Methanolobus and Methanoculleus and class Methanomicrobia.

The permafrost of Antarctica offers an opportunity to study the viable microorganism from a wide range of time scales and temperatures of cryopreservation. Combining the culture dependent approach with the recent advantages in molecular biology technologies can help us a fuller understand of the diversity of viable microorganisms in permafrost and optimum cryopreservation conditions. One of the possible future objectives from genomic approaches will be a reconstruction of depositional temperatures of the past.

Distribution of frozen ground conditions in Byers Peninsula (Antarctica) based on electrical resistivity data

Antonio Correia[1], Marc Oliva[2], & Jesus Ruiz-Fernández[3]

[1] *University of Evora, Evora, Portugal*
[2] *University of Lisbon, Lisbon, Portugal*
[3] *University of Oviedo, Oviedo, Spain*

Permafrost conditions in the South Shetland Islands (Antarctica) are considered to be marginal to discontinuous until ca. 20 – 40 m asl turning to continuous at higher elevations. However, the presence of permafrost in certain enclaves of this archipelago is yet to be better understood. This is the case of the Byers Peninsula, Livingston Island, the largest ice-free area in the South Shetland Islands. Some studies have shown the presence of permafrost conditions in the central plateau at elevations above 45 m asl in Byers, with an active layer thickness of 0.9 – 1.5 m.

Geophysical surveying and geoelectrical methods have been proven to be an effective method to unveil permafrost distribution and permafrost conditions in polar environments. With the purpose of better understanding the existence (or inexistence) of permanent frozen conditions in this area, a geophysical survey using an electrical resistivity tomography methodology was conducted in late January 2015. The snowy conditions during the cold season in 2014 in Byers Peninsula conditioned a late melting of snow in 2015, which must be taken into account when interpreting the data related to frozen conditions inferred from the geoelectrical survey.

Along the same direction three overlapping electrical resistivity tomographies (Byers 2, Byers 3, and Byers 4) of 7 m each were done along the same profile which ran from the coast (Byers 2) to the highest marine terraces (Byers 4). For each tomography 40 electrodes were used in a Wenner configuration; adjacent electrodes were 2 m apart. The software RES2DINV was used for inverting the apparent electrical resistivity values (apparent electrical resistivity pseudo-sections) into two-dimensional models of electrical resistivity of the ground (Fig. 1). The models are a representation of the distribution of the electrical resistivity of the ground to depths of about 13 m along the 78 m long profiles.

Several patches of high electrical resistivity are found along the three profiles done from the coast to the highest marine terraces, which are interpreted to be patches of sporadic permafrost. On average, electrical resistivities tend to increase inland. As observed in other polar maritime environments, electrical resistivity values as low as 1000 Ωm may be indicative of the presence of permanent frozen conditions in the area. This may suggest the lower limits of sporadic permafrost in the Byers Peninsula, significantly lower than in other ice-free environments in this archipelago.

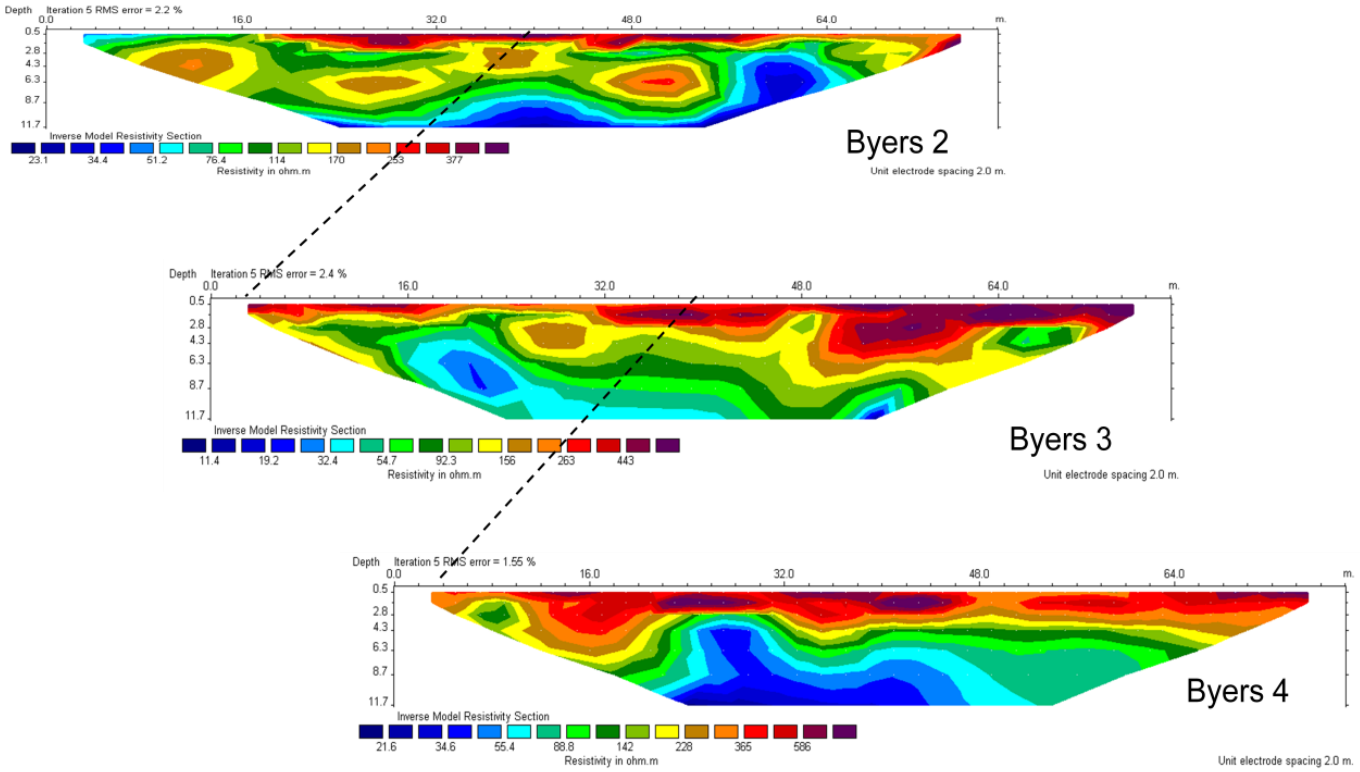

Figure 1: Geoelectrical models of the three ERTs described in the text. The points of overlapping for the three ERTs are represented by the dashed lines. Profile Byers 2 is the closest to the sea.

PERMASNOW: Snow cover characterization and its effects on the thermal regime of permafrost and active layer in Deception and Livingston Islands, Antarctica

Miguel ángel de Pablo[1], Miguel Ramos[2], Antonio Molina[1], Juan Javier Jiménez[2], Miguel ángel Hidalgo[2], Manuel Prieto[3], Susana Fernández[4], Carmen Recondo[5], Javier F. Calleja[6], Juan José Peón[5], Gonçalo Vieira[7], Carla Mora[7], Kamil Láska[8], Filip Hrbáček[8], Zbynek Engel[9], & Daniel Nyvlt[8]

[1] *Department of Geology, Geography and Environment, University of Alcalá, Madrid, Spain*
[2] *Department of Physics and Mathematics, University of Alcalá, Madrid, Spain*
[3] *Department of Automatics, University of Alcalá, Madrid, Spain*
[4] *Department of Geology, University of Oviedo, Oviedo, Spain*
[5] *Department of Mining Exploitation and Prospecting, University of Oviedo, Oviedo, Spain*
[6] *Department of Physics, University of Oviedo, Oviedo, Spain*
[7] *Center of Geographic Studies/IGOT, Universidade de Lisboa, Lisbon, Portugal*
[8] *Department of Geography, Masaryk University, Brno, Czech Republic*
[9] *Department of Physical Geography and Geoecology, Charles University, Prague, Czech Republic*

The study of the thermal properties of perennially frozen soils (permafrost) and its temporal evolution in Livingston and Deception Islands has been our research topic in the past two decades, within the TSP and CALM networks of the International Permafrost Association (IPA). Currently, we maintain six shallow boreholes and one CALM site (A16) in Deception Island at Crater Lake, near the Spanish Antarctic Station Gabriel de Castilla. In Livingston Island, we maintain eight monitoring sites in both Hurd and Byers peninsulas. In the former, we have seven monitoring sites, including the deepest borehole (25 meters) we have drilled in the region at the summit of Mount Reina Sofía (285 m a.s.l.). The other sites are distributed across an altitudinal gradient starting at 5 m a.s.l. in order to study the effects of elevation on the ground thermal regime. In Hurd Peninsula, there are not CALM sites due to the stony and rocky surface. However, in Byers Peninsula, we have installed one CALM site at the Limnopolar Lake basin (A25). At each site, we also measure air and ground surface temperatures, and snow temperature at different heights.

The data provided by the instruments (mainly iButtons and TinyTag temperature loggers) from 2006 to 2014 allowed to characterize thermally the soils of the study sites, as well as to understand the evolution of the air and ground temperatures, and the snow cover distribution. One remarkable observation is the increase in snow cover duration in selected sites resulting in a significant increase in the snow cover thickness during the monitored period (in one place over 3 meters). For that reason, PERMASNOW project (2015 – 2018) seeks to characterize the role of snow cover in the soil thermal regime and the active layer thickness, based on the preliminary observations of increased snow layer thickness and lifespan. The insulating effect of snow from a critical thickness could be the cause of the observed thermal evolution of permafrost and the active layer, and consequent degradation of the permafrost layer, at least at some of the monitored sites. However, depending on when the snow accumulates, it could cause the opposite effect contributing to the decrease of the ground temperatures observed in other of our monitoring sites.

This project, which brings together researchers from different universities of Spain, Portugal, and the Czech Republic, is based on this hypothesis. Its aim is to characterize the snow cover throughout the year at

a) high-resolution snow monitoring stations (thickness, density, water equivalent, duration) at a representative place of each CALM site;

b) thermal-snow-devices (thickness, length) distributed on each CALM site grid;

c) digital automatic cameras; and

d) field measurements of various parameters in each CALM site node (thickness, density, stratigraphy, texture, moisture, water equivalent).

These methods will result in the characterization and parameterization of the snow pack at each CALM site, in general, and the mesh nodes in particular, the spatial and temporal evolution of the snow cover is visualized on maps. These results are then compared with the thermal characteristics of the permafrost and thickness of the active layer obtained from the TSP stations and the measured thickness of the active layer, for possible correlation patterns. Moreover, we aim at identifying the minimum thickness of snow cover inducing a significant insulating effect. For comparison, we will analyze data from James Ross Island CALM sites. The interest of those sites is the lower snow precipitation during the winter compared to the South Shetland Islands, due to colder continental climate conditions in the Eastern Antarctic Peninsula.

Additionally, an approach was made to characterize snow cover and its evolution through the use of remote sensing. Firstly, multispectral satellite images with bands in the visible, infrared, and thermal regions at different spatial resolution (such as MODIS, Landsat and WorldView) will be used to characterize snow cover, surface color, albedo, and land surface temperature (LST). The accuracy of values derived from the images will be tested with the field data sets from the meteorological stations. MODIS images and field data sets will be also used to model thermal regimes of air cells and soils in the meteorological station and CALM sites surroundings.

Radar imaging data will be also analyzed to derive terrain features and snow type coverage. TerraSAR-X Spotlight products (X-band, 0.86 m azimuth × 0.90 m range resolution, HH or VV polarizations) and Sentinel 1: SAR L1 SLC or GRD products (C-band, 4.3 to 4.9 m azimuth × 1.7 to 3.6 m range, HH+HV, VH+VV, HH, VV polarizations) are the bases to conduct multitemporal studies, looking for seasonal melting patterns that allows snow classifications (wet snow/ dry snow) and bare soil conditions. Snow pits in CALM sites at close dates to Radar imaging to characterize the main physical factors of snow coverage (grain size, snow water equivalent, density and topo-climatic drivers) are the trial source to give the ground-true contrast to verify the accuracy of the backscattering results. This combination of radar data and terrain characterization will allow future projects to study the state of permafrost regarding the characteristics of snow cover at the regional scale.

In summary, PERMASNOW project aims to monitor in an accurate way the snow cover and its characteristics, establishing the real effect snow cover has on the thermal behavior of our CALM and GTN-P monitoring sites in Livingston and Deception Islands, Antarctica, using multidisciplinary approaches and comparative tasks with other locations in this polar region.

Acknowledgements

This work is being supported by funds from the Ministry of Economy of the Government of Spain by the Polar Research Program (CTM2014-52021-R) and an arrangement between the University of Alcalá, the Spanish Institute of Geology and Mining, and the Spanish Polar Committee for the maintenance of the monitoring stations in Deception and Livingston Islands. The work of the Czech team is funded by the Masaryk University project MUNI/A/ 1370/2014: Global environmental changes in time and space.

Snow cover evolution at Livingston and Deception Islands, Antarctica, from 2006 to 2015

Miguel ángel de Pablo[1], Miguel Ramos[2], Antonio Molina[1], Gonçalo Vieira[3], Miguel ángel Hidalgo[2], Manuel Prieto[4], & Juan Javier Jiménez[2]

[1]*Department of Geology, Geography and Environment, University of Alcalá, Madrid, Spain*
[2]*Department of Physics and Mathematics, University of Alcalá, Madrid, Spain*
[3]*Center of Geographic Studies/IGOT, Universidade de Lisboa, Lisbon, Portugal*
[4]*Department of Automatics, University of Alcalá, Madrid, Spain*

Permafrost, active layer evolution and their thermal behavior in Livingston and Deception Islands, has been our research topic in the last decades. In fact, different CALM and GTN-P sites has been established, mainly since 2006, at sites close to the Spanish Antarctic Stations 'Juan Carlos I' (Hurd Peninsula in Livingston Island) and 'Gabriel de Castilla' (Deception Island), as well as the International Antarctic refuge in Byers Peninsula (Livingston Island). We have, among other equipment, 14 boreholes (from 1.5 to 25 m deep), 11 surface and air temperature sensors, as well as 11 devices to measure air temperature to approach the snow cover thickness along the time in those locations. The last devices consist on a wood mast with miniature temperature loggers (DS1922L iButton model from Maxim) at different heights obtaining data each 3 hours.

We can observe an evident reduction in the active layer thickness as well as a slight increase in the temperature of the top of the permafrost since 2006, in spite the air temperatures were quite similar during this period. However, we have also witnessed an increase in the duration of snow cover during this same period. It is known the isolation effect of the snow cover when it reach a critic thickness, as well as the impact of the snow cover duration on the evolution of the temperatures of the surface and the ground. For that reason, in order to contribute to the understanding of the observed evolution of the active layer thickness (ALT) and ground temperatures, here we show our first detailed analysis of the snow cover thickness and duration evolutions in all our monitoring sites, including a comparative between both islands, as well as an analysis of the differences for each site at different elevations.

Despite the low resolution of the snow cover depth calculation from temperature data, and the underestimation of the thickness on this methods, the results (Fig. 1) are consistent with all the study sites, overlapping the local differences of each site (e.g., elevation, aspect, relief). Firstly, we could observe an interannual variation of the snow cover on each location, what clearly depends on the climatic conditions each winter. This variation is repeated on most of the sites, confirming the climatic origin. This is the case of the thinner snow cover in 2011 and 2012, with two exceptions: 'Limnopolar Lake' site in Byers Peninsula that shows more snow than in the other sites in 2012 and 'Crater Lake' site in Deception Island which also shows a thin snow cover in 2010.

In general, there is not a clear and pristine increase on the snow cover depth, although it is clear how the snow covers duration is slightly longer in the last years. Clear examples of this behavior occur at 'Sofia', 'Incinerador', 'Nuevo Incinerador', 'Limnopolar Lake' or 'Crater Lake' monitoring sites. Analyzing the results from 'Limnopolar Lake' site in Byers Peninsula, our instrumentation (installed in 2009) allowed to establish a similar snow depth each year, with an about constant snow onset in early March. However, the snow offset had substantial changes, increasing the snow cover duration in the last three years for more than 60 days (from 267 to 338 days).

The increase in the snow cover duration is relevant, even in very windy sites where normally there is not a significant snow accumulation. An example of this is 'Collado Ramos' site that also shows an elongation of the snow cover duration. In other cases, such as 'Glaciar' site (about one hundred meters away from 'Sofia' site and only about five meters lower in elevation), more than three meters of snow and ice does not disappear during the Antarctic summer in the last seven years. Unfortunately, we do not have instrumentation to measure snow depth at that site.

In summary, during the last few years, there is not a significant increase on the snow cover depth at our monitoring sites in Deception and Livingston Islands. However, we observed an increase in the snow cover duration, usually caused by a delay in the snow offset date. This behavior is quite similar for all the sites, despite differences in elevation, relief, aspect, and other geographical factors, that point to a climatic influence. This elongation on the snow cover could have significant effects on the thermal behavior of the ground and the thickness of the active layer.

Acknowledgements

This work has been supported by funds from the Ministry of Economy of the Government of Spain by the Polar Research Program (CTM2009-10165-E; CTM2011-15565-E; CTM2014-52021-R) and an arrangement between the University of Alcalá, the Spanish Institute of Geology and Mining, and the Spanish Polar Committee for the maintenance of the monitoring stations in Deception and Livingston Islands.

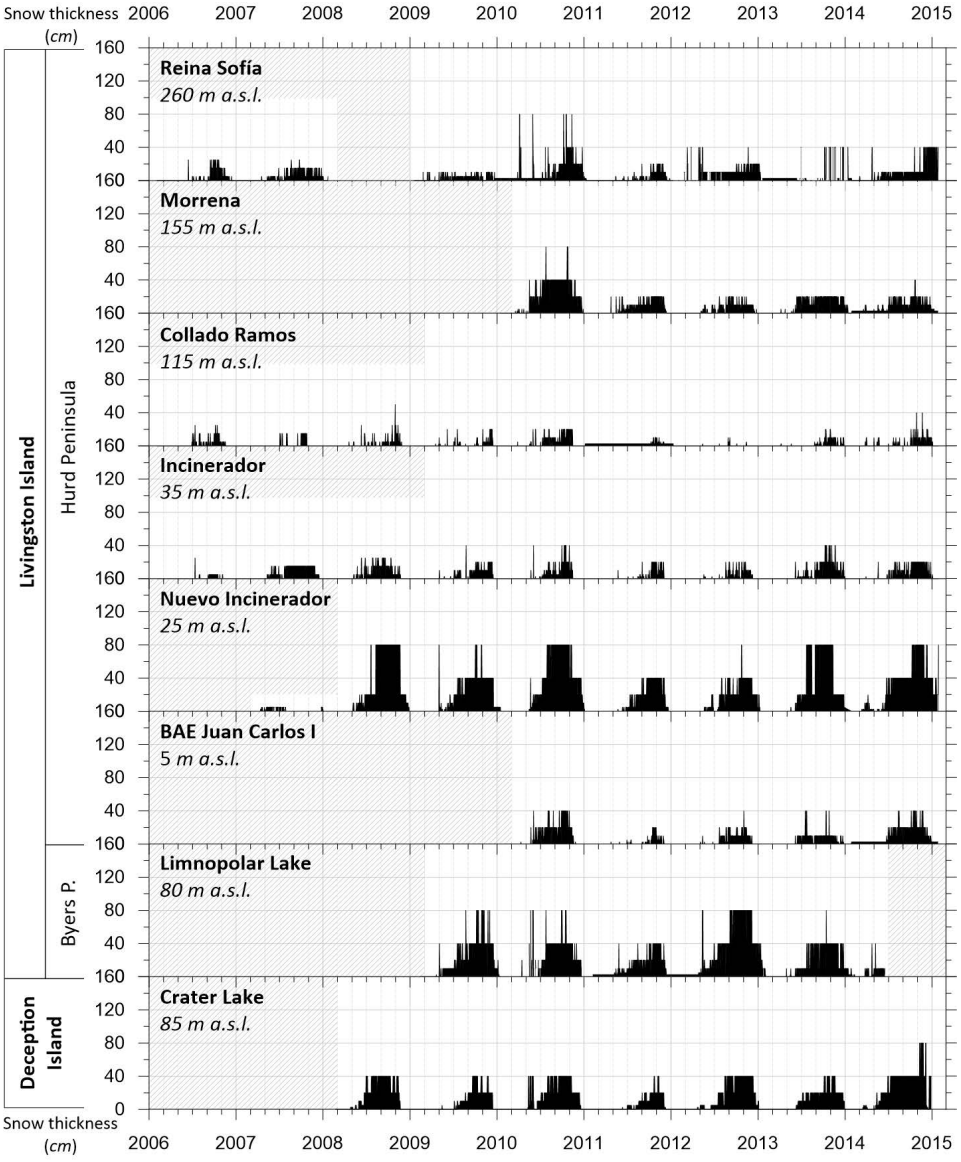

Figure 1: Snow depth derived from temperature data acquired at different sites in Deception and Livingston islands, Antarctica, by means of arrays of miniature temperature logger (iButtons from Maxim)

The influence of inter-annual variations of snow cover on TTOP modelling in Hurd Peninsula (Maritime Antarctic)

Alice Ferreira[1], Gonçalo Vieira[1], & Miguel Ramos[2]

[1]*Lisbon University, IGOT, Portugal*
[2]*Alcalá de Henares University, Physics Department, Spain*

The Western Antarctic Peninsula region shows mean annual air temperatures ranging from −4 to −2 °C and is close to the climatic threshold of permafrost. Freezing indexes and n-factors in key locations are used to understand the influence of snow cover on soil's thermal regime.

Permafrost, as a subsurface phenomenon is difficult to assess and monitor, and further, complex microclimatic factors such as snow, surface radiation budget, soil physical proprieties, moisture and vegetation determine its spatial distribution.

Snow pack duration, thickness and physical properties are crucial in determining the thermal characteristics of the ground. Using variables representing climate-ground interactions, the Temperature at the Top Of the Permafrost (TTOP) model provides a framework to understand permafrost conditions and limits in the South Shetland Islands. Eight sites in Hurd Peninsula with different geographical settings were studied to determine the site-specific surface ground thermal regime controls. Data was collected from 2009 to 2014 for air, surface and ground temperatures, as well as snow thickness. TTOP first results modeled and calculated values were very close to ground truth:, at the 275 m borehole difference from measured (−2.2 °C) was only 0.05 °C higher, at 160 m (−1.3 °C) 0.3 °C lower and at 140 m (−1.5 °C) difference was 0.15 °C lower. No permafrost was found below 36 m altitude and calculated thermal offset made for rock showed low values. This evaluation contributes to the understanding the spatial variability of GST and its controlling mechanisms and for the development of spatial models on the distribution of permafrost.

Permafrost thermal snapshot: Marble Point and Wright Valley, Ross Sea Region, Antarctica

Mauro Guglielmin[1], Megan R. Balks[2], & Cathy Seybold[3]

[1] *Dept. Theoretichal and Applied Sciences, Insubria University, Italy*
[2] *Waikato University, New Zealand*
[3] *Natural Resource Conservation Service, USDA, USA*

Two 30 m deep permafrost temperature-monitoring boreholes were installed, one at Marble Point and one in the Wright Valley, in the Ross Sea region of Antarctica in 2007. Flat areas located on the coast (Marble Point) and inland (Wright Valley floor), both with bedrock outcrops, were selected to avoid 3-D topographic effects and thermal offsets due to overlying till. At both sites the boreholes were instrumented with 16 thermistors calibrated to give a resolution of 0.1 °C at depths of 0.3, 0.6, 1, 2, 3, 5, 7, 10, 12, 14, 15, 16, 18, 20, 25 and 29.5 m. Both sites are near soil climate monitoring stations with the main climatic parameters (air temperature, solar incoming radiation etc,) monitored all year round. The first year of results (2008) was published [Guglielmin et al., 2011]. Now a new thermal snapshot is presented.

Since 2008 the air temperature has not shown any significant warming or cooling trend, at either site, following the general pattern known since 1960 in Continental Antarctica [Guglielmin and Cannone, 2012]. Active layer thickness (ALT) shows contrasting patterns. The ALT in the coastal (Marble Point) site ranges between 43 and 73 cm with a strong increasing trend (+ 5 cm/year for the period from 2008 to 2014) while in the inland (Wright Valley) site ranges between 54 and 80 cm apparently with no trend at all and larger inter-annual fluctuations (Fig. 1a). We considered the mean annual ground temperature at 1 m of depth as a proxy of the Mean annual permafrost temperature (MAPT). At the coastal site MAPT ranges between −17.8 °C and −16.1 °C while at the inland site between −20.3 °C and -18.1 °C. Within permafrost, mean daily temperatures at both sites at 10 and 20 m of depth show an increasing trend stronger at deeper depths (Fig. 1b).

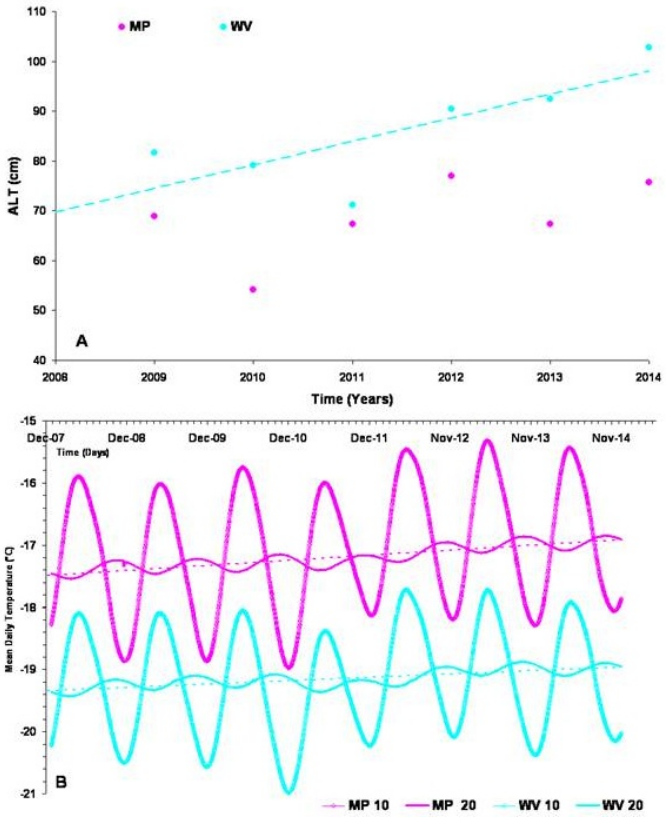

Figure 1: a) Active layer thickness trend at Wright Valley (WV) and Marble Point (MP); b) Mean daily temperatures at Wright Valley (light blue, WV) and Marble Point (violet, MP) at 10 (line with empty dots) and 20 m (solid line). The dashed lines represent t

The ALT pattern of increasing depth at Marble Point is stronger than that reported by Guglielmin and Cannone [2012] for another coastal site in Northern Victoria Land (Boulder Clay, close to the Italian station Mario Zucchelli at Terra Nova Bay) and similar to some coastal Arctic sites. In contrast, in the inland site in the Wright Valley where ALT is slightly thicker, no significant trends were observed emphasising the importance of the local conditions. The increasing trend of permafrost temperature at 20 m depth could reflect the changes in snow cover distri-

bution and/or non-conductive heat transfer processes, as the sublimation processes close to the surfaces, as already suggested by several authors. The increasing ALT in the coastal site can be correlated to some reported thermokarst development and the triggering of debris flows reported in the last few years in the McMurdo region [Fountain et al., 2014]. However with the low permafrost temperatures (about −18 °C) at both sites marked landscape or ecosystem changes are unlikely in the near future. Our results illustrate the complexity of the cryosphere because even with an almost stable atmosphere it is possible to have a thickening of the active layer and an increase in permafrost temperature, at least at Marble Point. This is important because the main feedbacks, such as changes in surface water and vegetation composition are primarily related to the thermal regime and moisture availability of the surface and of the active layer during the thawing season.

References

Fountain, AG.; Levy, JS.; Gooseff, MN. and D. Van Horn [2014]: The McMurdo Dry Valleys: A landscape on the threshold of change. *Geomorphology*, 225:25–35, doi:10.1016/j.geomorph.2014.03.044.

Guglielmin, M. and N. Cannone. [2012]: A permafrost warming in a cooling Antarctica? *Climatic Change*, 111:177–195, doi:10.1007/s10584-011-0137-2.

Guglielmin, M.; M.R., Balks; Adlam, L.S. and F. Baio [2011]: Permafrost Thermal Regime from Two 30-m Deep Boreholes in Southern Victoria Land, Antarctica. *Permafrost and Periglacial Processes*, 22(2): 129–139, doi:10.1002/ppp.715.

High resolution TanDEM-X imagery for mapping surface land cover features of Barton Peninsula (King George Island, northern Antarctic Pen. region)

Stéphane Guillaso[1], Thomas Schmid[2], Jerónimo López-Martínez[3], Enrique Serrano[4], Ana Nieto[3], Sandra Mink[3,5], Tanya O'Neill[6], & Magaly Koch[7]

[1] *Technische Universität Berlin, Germany*; [2] *CIEMAT, Madrid, Spain*;
[3] *Universidad Autónoma de Madrid, Spain*; [4] *Universidad de Valladolid, Spain*;
[5] *Instituto Geológico y Minero de España, Spain*;
[6] *Waikato University, Hamilton, New Zealand*; [7] *Boston University, USA*

Barton Peninsula, bordering Maxwell Bay on the western sector of King George Island (South Shetland Islands), has well developed and continuous series of raised beaches, moraines, and ancient marine platforms that extend from present sea level to as high as 275 m. There are also signs of intense recent and present periglacial activity, with the presence of a great diversity of periglacial landforms, that are affected by natural changes and, since 1988 influenced partially in some areas by human activities, including a permanent research station. In 2002, a detailed geomorphological map of the area, at 1:10,000 scale, was compiled by our group through field work and interpretation of aerial photography. Furthermore, a geological map from 2002 of the same area and at the same scale is also available. Nowadays, with the development of new radar sensors, bad weather conditions can be overcome by acquiring synthetic aperture radar (SAR) data over the region, with a spatial resolution of up to 0.25 cm. The objective of this study is to evaluate the potential of using very high resolution SAR data to map surface land cover features and to detect changes with features mapped in the field and interpreted with aerial photography, and to differentiate areas that are influenced by human activities. On the 3^{rd} of January 2015, two staring spotlight SAR data sets were acquired by the twin German satellites TerraSAR-X and TanDEM-X, with an interval of 10 seconds between acquisitions. The data have a ground resolution of 0.23×0.73 m (azimuth $\times$ ground range) and are in vertical polarized mode (emission and reception). Data have been ordered in SLC mode (single look complex) allowing the extraction of a very accurate digital elevation model (DEM) of the scene by combining the two data in an interferometric approach. The use of very high resolution SAR data enables 1) to identify soil surface characteristics; 2) to derive topographic parameters such as elevation, slope and aspect; and 3) to detect human impacts in surface features by identifying areas where activities have been carried out.

The existing geomorphological and geological maps were used as reference data, in order to determine training areas for classification purposes and for validation of the final mapping results. Data have been processed in two distinct approaches. On the one hand, statistical parameters (e.g. energy, entropy, contrast and homogeneity) are extracted from SAR amplitude data in order to perform a texture analysis (grey co-occurrence matrix) and to detect edges (edge-detector, variation coefficient, etc.). On the other hand, the extracted parameters are used for a supervised classification. This includes a series of segmentation classification cycles combining multi-resolution segmentation, histogram splitting and growing algorithms. Initial results show that different types of surfaces can be identified and at this resolution even small scale surface features can be differentiated. In this case, a change detection map of surface covers is developed by comparing results from the high-resolution SAR data and with the available reference maps. Additionally, with the 10 seconds difference between both acquisitions, the temporal effect is removed and a very accurate and up-to-date DEM is extracted. As a result, different geological and geomorphological characteristics of the surface are identified. Furthermore, human structures, such as individual buildings from the research station, are precisely located. The soil surface surrounding the station is characterized and compared to past reference data, identifying areas more influenced by human activities. From this study, a first map is produced to be progressively updated in future studies that could be used to monitor future changes on Barton Peninsula.

Investigations into the ground thermal regime near Troll station, in the Jutulsessen of Antarctica: 2007 – 2016

Christel Dorothee Hansen[1], Keith Ian Meiklejohn[1], & Werner Nel[2]

[1] *Rhodes University, South Africa*
[2] *University of Fort Hare, South Africa*

Periglacial landforms have been observed for the region around the Norwegian Antarctic research station of Troll (72°01'S, 02°32'E), located in the Jutulsessen of Dronning Maud Land (e.g. Dallmann et al. [1990], Lee et al. [2013], Hansen et al. [2014], Rudolph et al. [2014]). On moraine slopes of less than 15° thermal contraction polygon are observed [Dallmann et al., 1990] and similar features are found on the lower reaches of the rock glaciers at Grjotøyra and Vassdalen, as well as the southern slope of Nonshøgda [Hansen et al., 2014]. Within the larger area of Dronning Maud Land this area of the Jutulsessen has significant sediment cover present, having implications on frost processes and dynamics for the region. Similarly, the extreme aridity of the region, with soil moisture overall approaching zero percentage per volume, has implications on freeze-thaw events observed [Hansen et al., 2014].

Ground temperatures have been recorded for the area since early 2007. Temperatures are recorded at various levels in the ground, ranging from the near surface to 200 cm depths [Vieira et al., 2010]. Data show that ground temperatures stabilise with depth, with higher minimums recorded at 200 cm compared to 1 cm depths. In contrast, maximum temperatures steadily decrease with depth. At 50 cm depths only one continuous frozen event is recorded, indicating the presence of permafrost. The permafrost for this region has an average temperature of 17.3 °C and no thaw events are observed during the Austral winter period. During the Austral summer temperatures show greater variability, with thaw events recorded. Overall active layer depths and the number of thaw events observed during the summer months have increased with time. However, active layer depths are variable year-on-year, showing significant variation on an inter-annual scale. Annual active layer depths range from a depth of less than 10 cm in 2007 – 2009, to 38 cm for 2013, and a depth of 28 cm in 2015. Average temperatures for all measurement depths have remained approximately the same since records began in 2007, yet inter-annual variations observed for active layer depths are reflected for all recorded depths.

References

Dallmann, W.; Austrheim, H.; Bucher-Nurminen, K. and Ohta, Y. *Geology around the Norwegian Antarctic Station 'Troll', Jutulsessen, Dronning Maud Land*. Oslo: Norsk Polarinstitut, 1990.

Hansen; Dwight, R.A.; Kotze, C.; Rudolph, E.M. and Scott, D.A. [2014]: An investigation into the morphology and dynamics of thermal contraction crack polygons found at Mimelia in the Jutulsessen, Antarctica. *Paper presented to the XXXIII SCAR Biennial Meetings and Open Science Conference*, Auckland, August 25-28.

Lee, J.E.; Le Roux, P.C.; Meiklejohn, K.I. and Chown, S.L. [2013]: Species distribution modelling in low-interaction environments: Insights from a terrestrial Antarctic system. *Austral Ecology*, 38:278–299, doi:10.1111/j.1442-9993.2012.02401.x.

Rudolph, E.M.; Meiklejohn, K.I.; Bumby, A. and Hansen, C.D. [2014]: The Geomorphology of a rock glacier, near Troll Station in the Jutulsessen, Antarctica. *Paper presented to the XXXIII SCAR Biennial Meetings and Open Science Conference*, Auckland, August 25-28.

Vieira, G.T.; Bockheim, M.; Guglielmin, M.; Balks, M.; Abramov, A.; Boelhouwers, J.C.; Cannone, N.; L., Ganzert.; Gilichinsky, D.A.; Goryachkin, S.; López-Martínez, J.; Meiklejohn, K.I.; Raffi, R.; Ramos, M.; Schaefer, C.; Serrano, E.; Simas, F.; Sletten, R. and Wagner, D. [2010]: Thermal state of permafrost and active-layer monitoring in the Antarctic: Advances during the International Polar Year 2007 – 2009. *Permafrost and Periglacial Processes*, 21:182–197, doi:10.1002/ppp.685.

Short-term changes observed in the ground thermal regime following the construction of a building: A case study from the Antarctic

Christel Dorothee Hansen & Keith Ian Meiklejohn

Rhodes University, South Africa

Ground temperatures and ground moisture have been recorded in the area around the Norwegian research station of Troll, in the Jutulsessen, Antarctica, since early 2007 [Vieira et al., 2010] and the ground temperature regime for this region has been documented (e.g. Vieira et al. [2010], Hansen et al. [2014]). In the Austral summer of 2012/13 a permanent structure in the form of a large storage shed was erected in the vicinity of the existing logger. This logger consists of an XR5 logging unit and seven thermistors measuring ambient air temperature, temperatures at various depths within the ground (near surface, 50cm, 1m, 1.5m, 2m), as well as soil moisture sensor using a Decagon EC-5 sensor. Ground temperatures are affected by the physical properties of the ground, the climate-ground interaction, as well as the presence of surface cover such as vegetation or man-made structures. In particular the construction of buildings has been shown to alter the thermal dynamics of the ground [Kim et al., 2014], especially when no preventative measures, such as drainage and ventilated ducting for utility lines, are put in place to ensure the ground remains frozen [Porkhayev and Shchelokov, 1978]. This paper provides observations on changes in the observed temperature regimes recorded by the Troll logger following the construction of a permanent structure.

Thermal data show that the construction of the shed was accompanied by a change in the observed temperature regime. Average temperatures, as well as maximum and minimums recorded were higher during the year following the construction of the building. In contrast the variability of recorded data generally decreased. Two years after the construction of the building temperatures were observed to have stabilised to preconstruction levels. Freeze-thaw events using the 0 degree Celsius isotherm, as recorded during the Austral summer, increased by more than 40 from 2012-2013, decreasing by approximately 20 for 2013-2014. Warmer ambient temperatures were observed for 2013 yet cannot be applied as the sole driver for increased temperatures recorded. The removal of snow cover for construction is likely to have reduced permafrost temperatures and the building would also transmit heat directly into the ground. Furthermore, a temporary change in the local hydrology of the area in the vicinity of the logger is proposed as a potential reason for changes observed in the data.

References

Dallmann, W.; Austrheim, H.; Bucher-Nurminen, K. and Ohta, Y. *Geology around the Norwegian Antarctic Station 'Troll', Jutulsessen, Dronning Maud Land*. Oslo: Norsk Polarinstitut, 1990.

Hansen; Dwight, R.A.; Kotze, C.; Rudolph, E.M. and Scott, D.A. [2014]: An investigation into the morphology and dynamics of thermal contraction crack polygons found at Mimelia in the Jutulsessen, Antarctica. *Paper presented to the XXXIII SCAR Biennial Meetings and Open Science Conference*, Auckland, August 25-28.

Kim, H.K.; Ao, S-I. and Amouzegar, M.A.(eds.). [2014]: *Transactions on Engineering Technologies – Special Issue on the World Congress of Engineering and Computer Science 2013*. Springer: Dordrecht.

Porkhayev, G.V. and Shchelokov, V.K. [1978]: Evaluation of the variations of the temperature regime of permafrost in a built-up area. In: Sanger, F.J. and Hyde, P.J.(eds.), *Permafrost: Second International Conference, July 13-28, 1973*, USSR Contribution, National Academy of Sciences: Washington D.C.

Vieira, G.T.; Bockheim, M.; Guglielmin, M.; Balks, M.; Abramov, A.; Boelhouwers, J.C.; Cannone, N.; Ganzert, L.; Gilichinsky, D.A.; Goryachkin, S.; López-Martínez, J.; Meiklejohn, K.I.; Raffi, R.; Ramos, M.; Schaefer, C.; Serrano, E.; Simas, F.; Sletten, R. and Wagner, D. [2010]: Thermal state of permafrost and active-layer monitoring in the Antarctic: Advances during the International Polar Year 2007 – 2009. *Permafrost and Periglacial Processes*, 21:182–197, doi:10.1002/ppp.685.

Active layer thickness variability on James Ross Island, Eastern Antarctic Peninsula

Filip Hrbacek[1], Kamil Laska[1], Daniel Nyvlt[1], Zbynek Engel[2], & Marc Oliva[3]

[1] *Department of Geography, Masaryk University, Czech Republic*
[2] *Charles University in Prague, Department of Physical Geography and Geoecology*
[3] *Centre for Geographical Studies – IGOT, Universidade de Lisboa, Lisbon, Portugal*

Antarctic Peninsula (AP) region is considered the most rapidly warming part of Antarctica. Changes of air temperature have a significant effect on cryosphere components, including permafrost and active layer. From that perspective, AP region provides a unique environment to understand the impacts of climate change on permafrost and related ecosystems. Another important factor is represented by different climate conditions between western and eastern AP. Oceanic climate with mean annual air temperature (MAAT) around −2 to −3 °C and the mean annual precipitation above 500 mm prevail on the western AP coast; by contrast, the eastern AP part is colder (MAAT from −5 to −8 °C) and drier with annual precipitation < 500 mm [Bockheim et al., 2013]. Precipitation differences significantly affect the presence of snow cover and its thickness. Snow could persist for several months with thickness > 60 cm in western AP area, while irregular snow occurrence with thickness not exceeding 30 cm was observed at James Ross Island, eastern AP (Hrbáček et al. [2015], in press). This contribution brings results of active layer thermal regime and its thickness monitored in the period of 2006 to 2014 at the northern coast of James Ross Island, eastern AP.

Measurement of air temperature and ground temperature in a 75 cm deep profile started in January 2006 on a site near Johann Gregor Mendel Station elevated at 10 m a.s.l. (Fig. 1). Until December 2014, data for daily air and ground temperature and annual active layer thickness (ALT) determined as maximum depth of 0 °C isotherm are available. Our data reveal decreasing trend in air and ground temperatures as well as the ALT over the last decade. MAAT over period 2006 – 2014 reached −6.9 °C, while mean ground temperature at 5 cm reached −5.6 °C. The mean annual ALT was 61 cm. Maximum annual ALT varied between 61 and 85 cm in the period 2006 – 2009, while it ranged from 48 to 58 cm in the 2010 – 2014 period. The timing of maximum ALT detection in particular years varied between 16 January (2009) to 14 February (2006). Regression analysis showed a strong effect of the mean January air temperature on ALT ($R^2 = 0.73$), while the effect of MAAT on ALT was significantly lower ($R^2 = 0.23$). These results show the ALT is significantly affected by summer air temperatures, while the effect of ground thermal condition in winter, or the presence of snow cover was limited here.

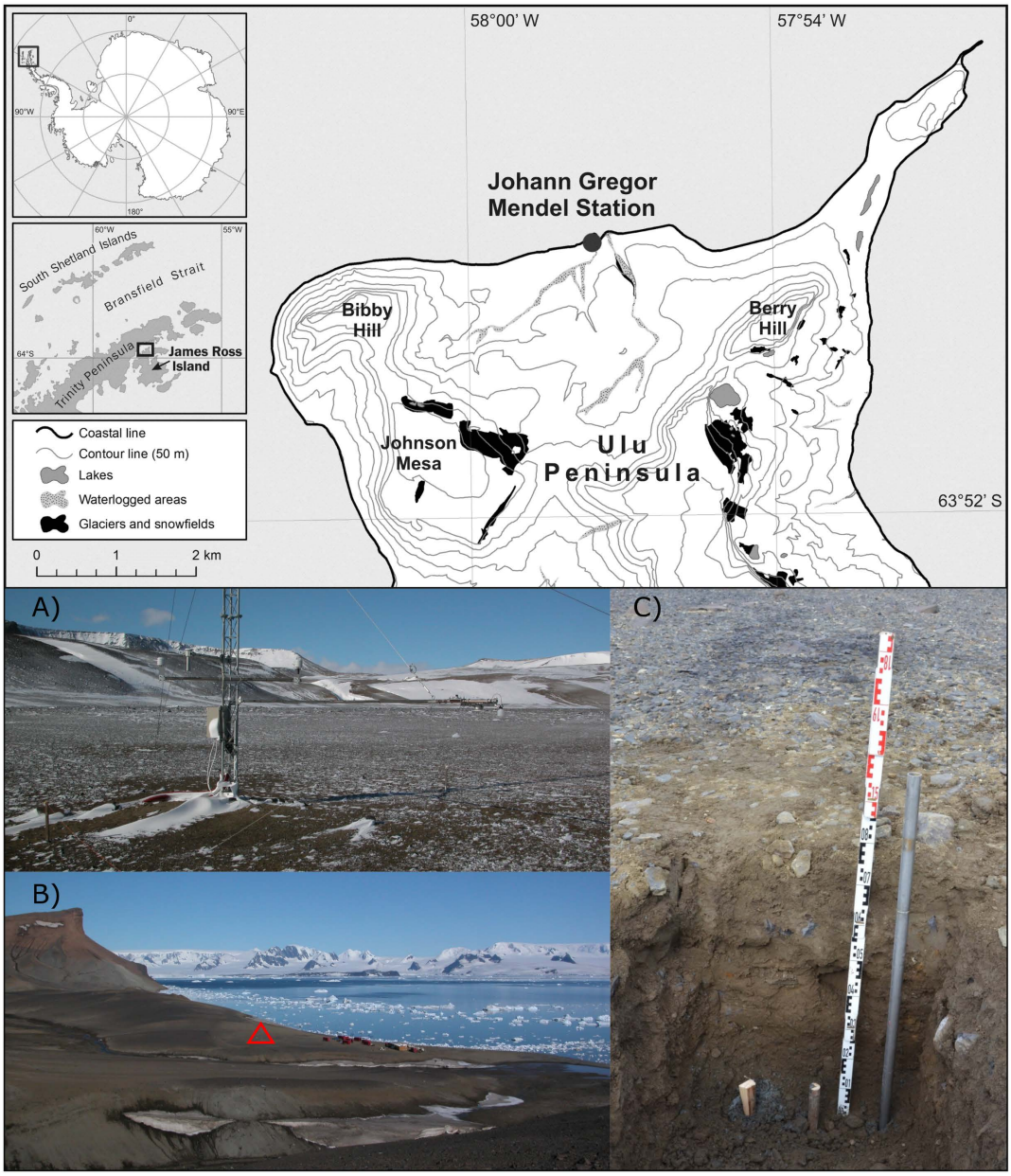

Figure 1: Map of northern part of James Ross Island and views on A) installation at study site, B) northern coast of James Ross Island, study site marked by red triangle C) surface and internal structure of active layer

References

Bockheim, J.; Vieira, G.; Ramos, M.; López-Martínez, J.; Serrano, E.; Guglielmin, M.; Wilhelm, K. and Nieuwendam, A. [2013]: Climate warming and permafrost dynamics in the Antarctic Peninsula region. *Global and Planetary Change*, 100:215–223, doi:10.1016/j.gloplacha.2012.10.018.

Hrbáček, F.; Láska, K. and Engel, Z. [2015]: Effect of Snow Cover on the Active-Layer Thermal Regime – A Case Study from James Ross Island, Antarctic Peninsula. *Permafrost and Periglacial Processes*, Early view, doi:10.1002/ppp.1871.

Active layer thickness variability in two climatic settings of the Eastern and Western Antarctic Peninsula

Filip Hrbacek[1], Marc Oliva[2], Miguel Ramos[3], Kamil Laska[1], Jesus Ruiz-Fernández[4], Miguel Angel de Pablo[5], Goncalo Vieira[2], & Daniel Nyvlt[1]

[1] *Department of Geography, Masaryk University, Czech Republic*
[2] *Centre for Geographical Studies – IGOT, Universidade de Lisboa, Lisbon, Portugal*
[3] *Department of Physics and Mathematics, University of Alcalá, Madrid, Spain*
[4] *Department of Geography, University of Oviedo, Oviedo, Spain*
[5] *Department of Geology, Geography and Environment, University of Alcalá, Madrid, Spain*

The Antarctic Peninsula region (AP) is one of the fastest warming regions on Earth. Mean annual air temperature (MAAT) locally increased by almost 3.0 °C over the last 60 years. However, there are significant differences in climate between

1. the western AP, typically with a cold oceanic climate and
2. the eastern AP under a cold polar-continental climate regime.

In the South Shetlands (western AP) MAAT are slightly below zero (−1 to −2 °C) at sea level and annual precipitation is 500 – 800 mm, whereas in James Ross Island (eastern AP) MAAT are −7 to −8 °C and precipitation is 200 – 400 mm. Continuous permafrost is present at James Ross Island, but discontinuous to continuous is found on the South Shetlands (Fig. 1). Therefore, based on climate conditions, significant differences in active layer thermal regime and its thickness are expected. The purpose of this study is to examine the patterns of soil thermal dynamics in the South Shetlands and James Ross Island for the period from January to December 2014.

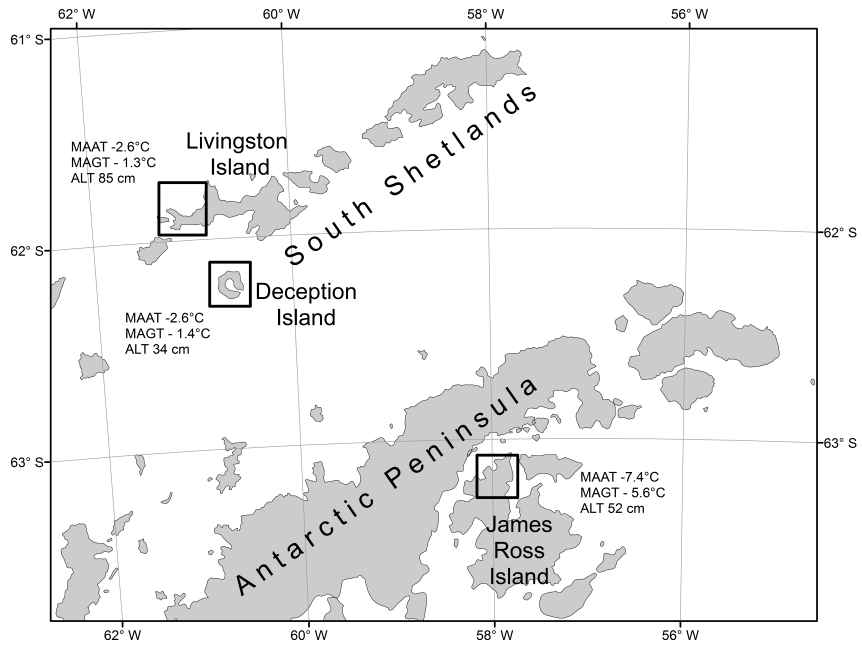

Figure 1: Mean annual air temperatures (MAAT), mean annual ground temperatures (MAGT) at 5 cm and maximum active layer thickness (ALT) at study sites of northern Antarctic Peninsula in 2014

One site in the eastern AP (Ulu Peninsula) and two sites in the western AP (Byers Peninsula, Crater Lake) have been chosen for this study. Site 1 is situated in Ulu Peninsula, northern James Ross Island. This site is located at 41 m a.s.l. in Abernethy Flats area and is composed of sandy regolith from fine grained calcareous sandstones and siltstones. Site 2, Byers Peninsula, is located on the western part of Livingston Island. The measuring site lies near Domo Lake at 45 m a.s.l., at a wind-exposed place with unconsolidated sediments mostly composed of sands and pebbles (sedimentary, volcanic and volcanoclastic). Site 3, Collado Irizar, is located in a flat terrain in Deception Island in an area composed of volcanic and volcanoclastic fragments near Crater Lake at 112 m a.s.l.

We analyse air temperatures, ground temperatures at 5 cm and maximum active layer thickness (ALT - estimated from the position of the 0 °C isotherm) from January to December 2014. Our results show significant differences in air and ground temperatures between eastern and western AP (Fig. 1). MAAT was identical in Domo Lake and Crater Lake (−2.6 °C) and reached −7.4 °C at Ulu Peninsula. Similar differences were also found when comparing mean annual ground temperatures (MAGT) at 5 cm depth, reaching −1.3 °C and −1.4 °C at Domo Lake and Crater Lake, respectively, and −5.6 °C at Ulu Peninsula. Although significant differences of air and ground temperatures were found, the maximum ALT was deeper at Domo Lake (85 cm) comparing to the 52 cm measured at Ulu Peninsula and 34 cm at Crater Lake.

These results show that climate regime is not the major factor controlling the maximum ALT in the AP region. Other factors, such as ground thermo-physical properties and snow distribution, its duration and thickness, must be also considered. In contrast to what happens in the Arctic, vegetation cover plays a minor role at these sites due its irregular occurrence with most ground been bare, with mostly patchy covers of lichens and mosses.

Seasonal snow cover characterization using field data and X-band radar imagery in Deception Island (Antarctica)

Javier Jimenez[1], Carla Mora[2], Miguel Ramos[1], Gonçalo Vieira[2], & Miguel Angel de Pablo[1]

[1] *University of Alcalá, Spain*
[2] *CEG/IGOT- Universidade de Lisboa*

The analysis of the thermal effects of snow cover on the active layer and permafrost due to its insulating properties affecting ground heat fluxes are a major focal point in recent studies about climatic change in Maritime Antarctica [Vieira et al., 2010].

Unraveling a solid and reliable remote sensing procedure to extract information on the seasonal variability of the snow cover and its impacts in melting process and water disponibility is a relevant approach to be covered. Radar imaging techniques, initially using C-band [Mora et al., 2013] and currently using X-band allow assessing surface properties even with high cloudiness and low sunlight conditions [Venkataraman et al., 2008], that limits the application of optical sensors.

The high spatial resolution of radar sensors and DEM covering CALM grids such as Crater Lake in Deception Island, allows jointly analysing data coming from observational sensors (snow-meters, air and soil temperature and time-lapse cameras), snow pit description (grain-size, SWE, density), together with backscattering features extracted from radar imagery in X-band (TerraSAR-X, Spotlight mode).

High spatial resolution (1.82 m azimuth $\times$ 2.51 m range) multitemporal studies of the backscattering are used to identify wet-snow, dry-snow and bare soil. Ground truthing to characterize snow stratigraphy is conducted in snow pits at image acquisition dates. Polarimetric studies aiming at discriminating types of snow cover are in an initial phase but promising to open new data sources for the accurate classification even at regional scale.

Acknowledgements

This work is supported by funds from the Project CTM2014-52021-R of Ministry of Economy of the Government of Spain in an arrangement between the University of Alcalá, the Spanish Institute of Geology and Mining, and the Spanish Polar Committee and from the Project PERMANTAR-3 (PTDC/AAG-GLO/3908/2012) of the Foundation for Science and Technology (FCT) of Portugal and the Portuguese Polar Program PROPOLAR.

References

Mora, C.; Viera, G. and Ramos, M. [2013]: Evaluation of Envisat ASAR IMP imagery for snow mapping at varying spatial resolution (Deception Island, South Shetlands-Antarctica). In: Hambrey, M.(ed.), *Antarctic Glacial and Periglacial Processes*. The Geological Society Publications, London (in press).

Venkataraman, G; Singh, G. and Kumar, V. [2008]: Snow cover area monitoring using multi-temporal TerraSAR-X data. In *Proc. 3rd TerraSAR-X Science Team Meeting*, Nov. 25–26, DLR–Oberpfaffenhofen. URL http://sss.terrasar-x.dlr.de/papers_sci_meet_3/poster/LAN0122_Venkataraman.pdf, Last access: 2015-04-09.

Vieira, G.T.; Bockheim, M.; Guglielmin, M.; Balks, M.; Abramov, A.; Boelhouwers, J.C.; Cannone, N.; L., Ganzert.; Gilichinsky, D.A.; Goryachkin, S.; López-Martínez, J.; Meiklejohn, K.I.; Raffi, R.; Ramos, M.; Schaefer, C.; Serrano, E.; Simas, F.; Sletten, R. and Wagner, D. [2010]: Thermal state of permafrost and active-layer monitoring in the Antarctic: Advances during the International Polar Year 2007 – 2009. *Permafrost and Periglacial Processes*, 21:182–197, doi:10.1002/ppp.685.

Near-surface ground ice conditions in University Valley, McMurdo Dry Valleys of Antarctica

Caitlin Maren Liette Lapalme[1], Denis Lacelle[1], Wayne Pollard[2], David Fisher[3], Alfonso Davila[4], & Christopher McKay[5]

[1] *Department of Geography, University of Ottawa, Ottawa, ON, Canada*
[2] *Department of Geography, McGill University, Montreal, QC, Canada*
[3] *Department of Earth Sciences, University of Ottawa, Ottawa, ON, Canada*
[4] *Carl Sagan Center at the SETI Institute, Mountain View, CA, USA*
[5] *NASA Ames Research Center, Moffet Field, CA, USA*

This study aimed to quantify ground ice content and describe the cryostructures and soil texture in 15 ice-bearing permafrost cores collected from nine sand-wedge polygons in University Valley located in the McMurdo Dry Valleys of Antarctica. The cores were taken from both the centers and shoulders of the polygons in order to investigate potential ground ice and soil texture variability within an individual polygon. Further, the polygons were sampled along a down-valley transect with the intent to quantify potential variability in ground ice and soil texture along the valley floor.

The objectives for this study were reached using the non-destructive technique of computed tomography (CT) scanning on five of the permafrost cores. The resulting images from the CT scan allowed a three dimensional visualization of the various components within the cores (i.e. sediment, ice and gas). Gravimetric water content (GWC), volumetric ice content (VIC), excess ice content and particle size distribution measurements of the permafrost cores were subsequently undergone using laboratory techniques.

The mineral soils in University Valley were predominantly classified as medium sand. In each polygon, little changes in particle size distribution were observed with depth. However, the gravel-sized sediment content (>2 mm) significantly increased in the shoulders of the investigated polygons with distance from the head of the valley.

Excess ice content ranged from 0 to 93 %, GWC ranged from 13 to 1881 % and VIC varied from 28 to 93 % in the 15 permafrost cores. Median excess ice, volumetric ice and gravimetric water contents significantly increased in the top 20 cm of the cores taken from the polygon shoulders with increasing distance from University Glacier (located at the head of the valley). Median excess ice and volumetric ice content significantly increased in the entire permafrost cores taken from the polygon shoulders with increasing distance from University Glacier. Ground ice was found to be preferentially stored in the centers of the investigated polygons where the ground surface remains cryotic throughout the year. Conversely, higher ground ice contents were measured in the shoulders of the investigated polygon where the ground surface is seasonally non-cryotic.

CT-scan image analysis allowed for the identification of cryostructures at a sub-mm scale, resulting in a more detailed description than would be possible when undergoing field-based cryostructural classification alone. The analysis of the CT scan images revealed four types of cryostructures in the five cores: structureless, suspended, crustal and porphyritic. The VIC of the cores derived from the CT scan images (CTVIC) under-represented the measured VIC. However, a statistically significant positive linear relation ($r^2 = 0.69$; $p = <0.02$) existed between CTVIC and the measured excess ice content for the cores. As such, the CT scan images reasonably assessed the distribution and presence of excess ice in the permafrost cores.

The results of this study provide the first comprehensive ground ice and cryostratigraphic study in the McMurdo Dry Valleys of Antarctica. These new findings, in addition to prior knowledge of ground ice in the region, can help contribute to a full and updated ground ice map for the McMurdo Dry Valleys of Antarctica.

Influence of snow cover distribution on active-layer thermal regime on James Ross Island, eastern Antarctic Peninsula

Kamil Láska[1], Filip Hrbacek[1], Zbynek Engel[2], & Daniel Nyvlt[1]

[1]*Department of Geography, Masaryk University, Czech Republic*
[2]*Department of Physical Geography and Geoecology, Charles University in Prague, Czech Republic*

Air temperature of the Antarctic Peninsula (AP) region has experienced significant increase over last 50 years [Turner et al., 2005]. However, magnitude and pattern of atmospheric warming differ significantly between the western and eastern side of the AP due to changes in sea surface temperatures, sea ice cover and atmospheric circulation. The permafrost response in both regions to this warming remains unclear due to high seasonal and interannual variability of local climate conditions and variety of mechanisms affecting permafrost distribution and active layer thickness. In contrast to western AP, there is little data along the eastern AP to support both thermal conditions of the active layer and its interactions with local meteorological factors. Therefore, James Ross Island (JRI) located near the eastern coast of the AP, represents a unique place to study the sensitivity of permafrost and active layer to regional atmospheric warming (Hrbáček et al. [2015], in press).

In this contribution, the influence of air temperature, global radiation and snow cover on active layer temperature in the northern part of JRI from March 2011 to February 2014 is presented. The study site is located on a Holocene marine terrace, approximately 100 m south of the Johann Gregor Mendel Station at 10 m a.s.l. Temperature conditions in the active layer were measured at depth of 5, 10, 20, 30, 50 and 75 cm by Pt100/Class A resistance probes (EMS Brno), while air temperature probe (EMS 33) was placed at 2 m above the ground. The occurrence of snow cover was estimated from surface albedo and measurements of incoming and reflected shortwave radiations using EMs-1 (EMS Brno) and CM6-B (Kipp & Zonen) radiometers. Snow depth was measured using an ultrasonic depth sensor (Judd Communication) at 2-h intervals. The other parameters were recorded at 30-min intervals to the EdgeBox V12 multichannel datalogger (EMS Brno) and allowed for calculation of daily and annual average values. In order to evaluate buffering effect of snow cover on ground temperature (GT) the freezing n-factors were used.

Correlation analysis indicated a significant effect of air temperature on GT regime. This effect was especially apparent under snow-free conditions at 5 cm depth with the correlation coefficients varying between 0.74 (2011) to 0.91 (2012). Conversely, the influence of global radiation was found less significant than air temperature forcing. Influence of snow depth on the ground thermal regime at the J. G. Mendel Station was found negligible due to mostly thin and irregularly distributed snow cover. This was confirmed by the total freezing n-factor value, which was higher than 0.9. The snow cover showed large day-to-day and seasonal variability with thickness rarely exceeding 10 cm. In general, the snow cover occurrence over the low-elevated coastal areas of JRI is highly variable in time, which was recently confirmed by both numerical models (e.g. Dethloff et al. [2010]) and in-situ observations [Hrbáček et al., 2015].

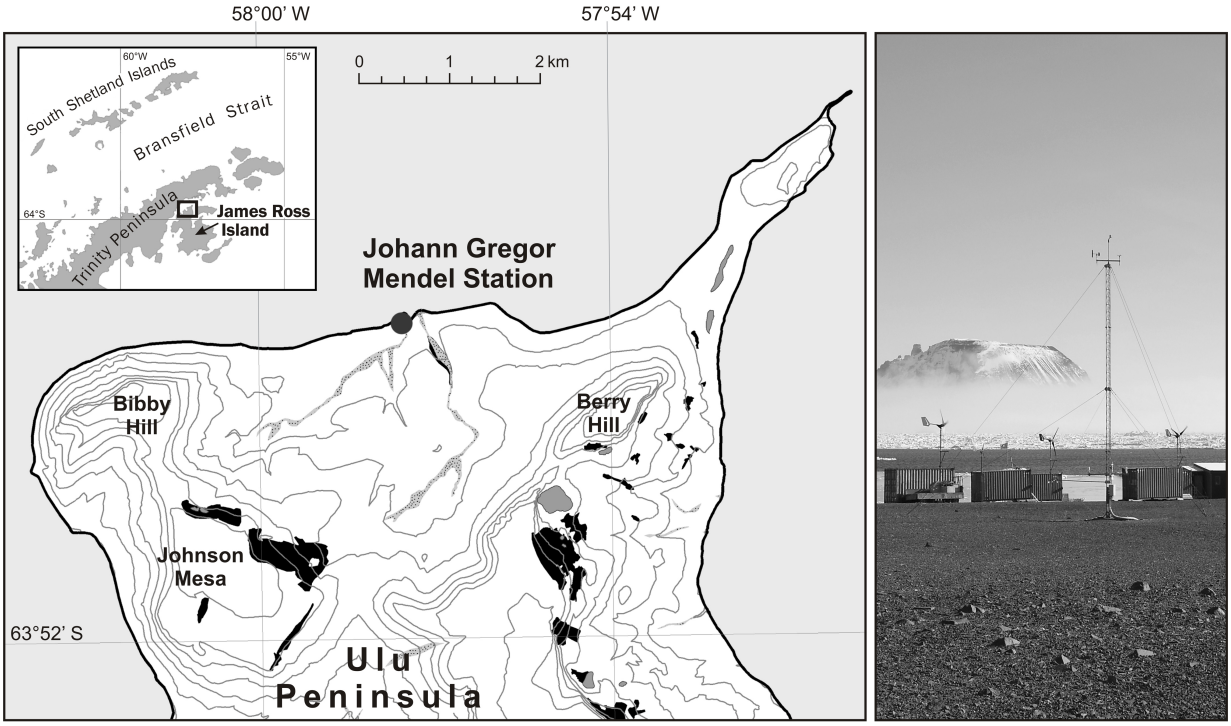

Figure 1: Northern part of James Ross Island with our study site located near the Johann Gregor Mendel Station. Modified map of James Ross Island-Northern part, Czech Geological Survey, 2009.

Acknowledgments

This research was supported by the project of Masaryk University MUNI/A/0952/2013 and project LM2010009 CzechPolar (MEYS CR).

References

Dethloff, K.; Glushak, K.; Rinke, A. and Handorf, D. [2010]: Antarctic 20^{th} Century Accumulation Changes Based on Regional Climate Model Simulations, *Advances in Meteorology*, 327172, doi:10.1155/2010/327172.

Hrbáček, F.; Láska, K. and Engel, Z. [2015]: Effect of Snow Cover on the Active-Layer Thermal Regime – A Case Study from James Ross Island, Antarctic Peninsula, *Permafrost and Periglacial Processes*, Early view, doi:10.1002/ppp.1871.

Turner, J.; Colwell, S.; Marshall, G.J.; Lachlan-Cope, T.A.; Carleton, A.M.; Jones, P.D.; Lagun, V.; Reid, P.A. and Iagovkina, S. [2005]: Antarctic climate change during the last 50 years, *International Journal of Climatology*, 25:279–294.

Characterization of soils related to periglacial processes on Fildes Peninsula and Ardley Island (Antarctic Peninsula region)

Jerónimo López-Martínez[1], Thomas Schmid[2], Marta Pelayo[2], Javier Díaz-Puente[2], Tanya O'Neill[3], Enrique Serrano[4], Manuel Rodríguez-Rastrero[2], María José Sierra[2], Sandra Mink[5], Margarita Lacal[2], Rocio Millán[2], & Megan Balks[3]

[1]*Dpto. Geología y Geoquímica, Facultad de Ciencias, Universidad Autónoma de Madrid*
[2]*Environment Department, Research Center for Energy, Environment and Technology - CIEMAT*
[3]*School of Science, Waikato University*
[4]*Dpt. Geografía, Universidad de Valladolid*
[5]*Instituto Geológico y Minero de España*

Fildes Peninsula together with Ardley Island are the most extensive ice-free area of King George Island (South Shetlands archipelago) with just over 30 km^2. These areas have a high biodiversity, which form the basis of the Antarctic Specially Protected Areas. They are also of geomorphological interest, where a total of fifteen individual periglacial landform types have been distinguished. Periglacial processes within ice-free areas are dominant in the most elevated areas and diminish in lowland areas and beaches of the South Shetland Islands. Such processes strongly influence soil characteristics and development. As shown in previous studies, soil properties vary widely within this dynamic region where, during the austral summer, freeze-thaw cycles are daily and permafrost is widely present.

The objective of this study is to determine the influence of periglacial processes and forms on a variety of soil characteristics within the study areas on Fildes Peninsula and Ardley Island. For this purpose, a field campaign was carried out during the 2012 – 2013 austral summer, in which different land covers were morphologically identified and associated soil profiles and surfaces were described and sampled according to pedological criteria. Chemical, physical and mineralogical laboratory analyses were carried out to determine the soil properties. Selected samples were further studied with a scanning electron microscope which enabled to obtain morphological, textural and chemical information of mineral phases, as well as to identify textural relationships between minerals which may affect physical properties of soils. Furthermore, a digital elevation model was used to further differentiate the topographic parameters such as elevation, slope, and slope aspect that can influence the processes. The results of these analyses were compiled into a georeferenced data base together with the field observations and characterizations of soil samples as well as associated auxiliary data such as conditions observed at the time of field work for the study areas. Field work shows that glacial deposits, patterned ground, pavements and slope debris, are among the most prevalent surfaces. Soil descriptions and laboratory results show substantial differences for soils sampled over the various landforms in terms of morphological and physiochemical properties such as pH, electrical conductivity organic carbon, texture and mineralogy. The soils show a general weak development, ranging from slightly acid to moderately alkaline and are non-saline. Organic carbon content shows some differences between the sampling points, although very low levels predominate. Soil texture is generally coarse with sandy loam and the structure is weakly developed. The mineralogical compositions of the soils contain very abundant phyllosilicates or a higher proportion of quartz and feldspars. There are traces of a minor content of calcite in some of the samples. The results show that soil drainage, the biologically active layer depth and the ongoing soil development are closely related to surface processes defining the land cover as well as the presence of permafrost. Further factors such as lithology, slope and distance from the coast have also shown an important influence on soil properties. Pavements and patterned grounds show more developed soil structure, unlike surfaces such as recent deposits, where soil structure is absent or very slightly developed. In this case, the soil properties are more clearly related to lithological or geomorphological factors. The study shows that geomorphology and in particular, periglacial processes, constitute a determining factor in various soil properties in the study areas.

Active Layer Monitoring in Western Dronning Maud Land, Antarctica since 2007

Keith Ian Meiklejohn, Camilla Kotzé, & Christel Dorothee Hansen

Rhodes University, South Africa

Temperature measurements of the active layer in Western Dronning Maud land commenced in 2007. Since then, the number of shallow boreholes monitored has increased from three to nine, the last seven being commissioned in the 2012/13 Austral Summer. While no definite longer term thermal trends are yet evident, the measured regimes are a function of a number of variables. With increasing distance from the edge of the ice shelf and increasing altitude, active layer and permafrost temperatures, the number of frost cycles and the period of thaw all decrease. However, local microclimatic and topographic influences may alter this trend. Intra-seasonal variability is largely influenced by synoptic scale weather, as well as Southern Ocean seasonal controls such as the Southern Annular Mode (SAM), and the Semi-Annual Oscillation (SAO). Thermal active layer monitoring is critical to understanding the impacts of climate change in the region as well as the role Geomorphology plays in providing a habitat for the colonisation of biodiversity from a microbial scale, increasing to microscopic invertebrates and avian fauna. Small depressions allow the accumulation of snow, which provides a habitat for microbial activity, algae and lichens. These species, in turn, support invertebrate detrital feeders. Landforms also provide habitats for nesting of pelagic bird populations on nunataks that are relatively close to the coast. The length of exposure of a nunatak following deglaciation is an additional influence on the observed Antarctic biodiversity. Initial results from almost a decade of exploration and monitoring are presented. It is argued that low-altitude nunataks near the ice shelf provide a proxy for the changes that are likely in the interior of the region.

Seasonal variability of discharge and sediment transport in two small streams in James Ross Island, Antarctic Peninsula

Jakub Ondruch[1], Jan Kavan[1,2], Daniel Nývlt[1,3], Filip Hrbáček[1], & Kamil Láska[1]

[1] *Masaryk University, Czech Republic*
[2] *Centre for Polar Ecology, Czech Republic*
[3] *Czech Geological Survey, Czech Republic*

The Antarctic Peninsula has experienced rapid warming in the last decades. Mean annual air temperature increased in Antarctic Peninsula by up to 3.5 °C since 1950's (Turner et al., 2005) and melt seasons have prolonged (Barrand et al., 2013), which resulted in the intensification of glacier-surface melt. This climate change has coincided with retreat and thinning of most of land-terminating glaciers around Antarctic Peninsula (e.g. Engel et al., 2012). Glacier dynamic directly influences catchment hydrology via control on meltwater entering proglacial fluvial system. When meltwater from glaciers and/or snowpacks is concentrated into streamflows, fluvial processes represent often one of the most important factors shaping deglaciated landscape. Moreover, they substantially control exchange of material, nutrients and organic matter and function as a habitat supporting the existence and evolution of living organisms.

Area of deglaciated surfaces in Antarctica reaches 44 890 km^2 (May 2005), which represents 0.32 % of the total area (BAS, 2005). In James Ross Island, 12.5 % of deglaciated surfaces is found on Ulu Peninsula. Our work aims to enhance the understanding of evolution of local landscape and thus contribute to the complex study of response of Antarctica to climate change. The purpose ofthis research isto comprehend links between surface runoff, meteorological and climatic conditions, suspended sediment transport, and geological settings in two small nearly deglaciated catchments in UluPeninsula.

Hydrological monitoring was conducted during period 8 January to 18 February 2015 on Bohemian and Algal Stream located in the vicinity of Johann Gregor Mendel Station. Air temperature and ground temperature in 5 cm below the surface and global radiation were obtained from automatic weather stations installed in the lower part of the Bohemian Stream catchment at 10 m asl. Discharge was measured in one profile set for each stream by Flowtracker Handheld ADV. Rating curve was constructed in order to acquire continuous discharge time series. Suspended sediment samples were taken on the discharge measurement sites. Provenance of suspended load was examined by utilizing X-ray fluorescence spectrophotometric approach.

Our results show that Bohemian Stream with the mean discharge of 0.19 m^3 s^{-1} (76 mm month^{-1}) for studied period belongs to relatively large streams in Antarctica in terms of discharge compared with streams in McMurdo Dry Valleys. Algal Stream is one order of magnitude smaller as the mean discharge reached 0.06 m^3 s^{-1} (60 mm month^{-1}) only. Longer melt-season and later occurrence of peak discharges were documented on James Ross Island in comparison with McMurdo Dry Valleys.

Daily discharge regime on both streams was affected mainly by air temperature and ground temperature in 5 cm below the surface. Global radiation effect on seasonal variation in discharge was negligible. Furthermore, runoff completely stopped only in periods with both air and ground temperatures dropped below 0 °C. This suggests active layer of permafrost to represent important source of water for streams' runoff. Moreover, time lag between discharge and ground temperature was shorter (2 – 3 hours) than for air temperature (4 – 4.5 hours), which could be explained by water from active layer in whole catchments to reach streams faster than surface meltwater from hanging glaciers/snowfields in upper part of catchments.

Suspended sediment concentrations reachedvery high values (up to 2927 mg l^{-1}), however the total sediment yield (46.53 t km^{-2} month^{-1}) is rather low. Observed anticlockwise hysteresis during diurnal manual sampling on 29/30 January followed by clockwise hysteresis week later on 6/7 February suggests seasonal depletion of available fine-grained material.

The sources of suspended load in both streams are mostly local Cretaceous strata, Mendel Formation

diamictites and laminites and Holocene marine and aeolian sediments. James Ross Island Volcanic Group rocks are not an important source for suspended load in studied streams. The high Rb/Sr ratios for some suspended load samples from Bohemian Stream point to chemical weathering of superficial rocks and regolith within this catchment. This has not been found important for Algal Stream catchment.

References

Barrand, N.E.; Vaughan, D.G.; Steiner, N.; Tedesco, M.; Kuipers Munneke, P.; Van Den Broeke, M.R. and Hosking, J.S. [2013]: Trends in Antarctic Peninsula surface melting conditions from observations and regional climate modeling. *Journal of Geophysical Research: Earth Surface*, 118:315–330, doi:10.1029/2012JF002559.

Engel, Z.; Nývlt D. and Láska K. [2012]: Ice thickness, areal and volumetric changes of Davies Dome and Whisky Glacier (James Ross Island, Antarctic Peninsula) in 1979–2006. *Journal of Glaciology*, 58: 904–914, doi:10.3189/2012JoG11J156.

Turner, J.; Colwell, S.; Marshall, G.J.; Lachlan-Cope, T.A.; Carleton, A.M.; Jones, P.D.; Lagun, V.; Reid, P.A. and Iagovkina, S. [2005]: Antarctic climate change during the last 50 years. *International Journal of Climatology*, 25:279–294, doi:10.1002/joc.1130.

Coupling in situ permafrost and active layer observations with Global Surface Temperatures from GISS: South Shetlands, Antarctica

Miguel Ramos[1], Miguel Angel de Pablo[2], Juan Javier Jimenez[1], Antonio Molina[2], & Gonçalo Vieira[3]

[1] *Depto. Física y Matemáticas. Universidad de Alcalá, Spain*
[2] *Unidad de Geología, Dpto. de Geología, Geografía y Medio Ambiente, Universidad de Alcalá, Spain*
[3] *Centro de Estudos Geográficos - Instituto de Geografía e Ordenamiento do Territorio, Universidade de Lisboa, Portugal*

Regional analysis of the Mean Annual Soil surface Temperatures (MAST) by means of the monthly mean air temperatures series developed by METeorologycal REference Antarctic Data for Environmental Research (MET-READER – SCAR, The Scientific Committee on Antarctic Research) and implemented by the Goddard Institute for Space Studies (GISS surface temperature analysis tool) [Hansen et al., 2010] in the Western Antarctic Peninsula, show a dispersion in the MAST values, resulting in a warming trend in the last 60 years. However, short time-series show periods in which the tendencies can be opposites.

One of the more interesting problems in the active layer thermal evolution is the soil and air energy balance effect and the ground propagation of the thermal wave. Some of the main parameters for studying this problem are air and soil surface temperatures and snow depth that affect directly to the soil surface isolation.

In this work, we present long-term regional Mean Annual Soil surface Temperatures (MAST) data in comparison with the maximum active layer thickness (ALT) and thermal regimes of the soil surface temperatures recorded in the experimental sites located in Livingston and Deception Islands during the same periods of time.

References

Giss surface temperature analysis. http://data.giss.nasa.gov/gistemp/station_data/

Hansen, J.; Ruedy, R.; Sato, M. and Lo, K. [2010]: Global surface temperature change. *Rev. Geophys.*, 48:RG4004. doi:10.1029/2010RG000345.

MET-READER. Meteorologycal reference antarctic data for environmental research. https://legacy.bas.ac.uk/met/READER/

Enthalpy method comparation between two different boreholes sites in Hurd Peninsula (Livingston Island)

Miguel Ramos[1], Juan Javier Jimenez[1], Miguel Angel de Pablo[2], Antonio Molina[2], & Gonçalo Vieira[3]

[1] *Depto. Física y Matemáticas. Universidad de Alcalá, Spain*
[2] *Unidad de Geología, Dpto. de Geología, Geografía y Medio Ambiente, Universidad de Alcalá, Spain*
[3] *Centro de Estudos Geográficos - Instituto de Geografía e Ordenamiento do Territorio, Universidade de Lisboa, Portugal*

The ground Enthalpy (energy exchange in a system without volume change) in the periods of cooling, during the frost season, corresponds to the heat loss through the ground surface in our systems. This Enthalpy parameter is a function of the thermodynamical processes of air-ground energy exchange (e.g. ground heat flux, sensible heat flux, turbulent fluxes, radiation balance and snow layer variability). In a similar way, the ground Enthalpy during the thaw season, in the period of warming, is the heat gained by the ground across its surface [Ramos and Vieira, 2009].

The ground surface heat flux exchange is a key parameter for studying the interactions between the ground and the atmosphere boundary layer and permit us evaluate the impact of the climate variability on the permafrost thermal evolution.

In this work we present the results of the application of the Enthalpy method in two different boreholes located close to the Juan Carlos I Spanish Antarctic Station (SAS JCI) in the period 2008 to 2012. Both boreholes are drilled on massive quartzite rock with very high thermal diffusivity and low porosity [Correia et al., 2012] but have differences in altitude, exposition and snow accumulation. Meanwhile 'Incinerador' borehole, 2.4 m deep and cased with a plastic cylinder 90 mm in diameter, is located very near to the SAS JCI (35 m a.s.l.), the 'Permamodel-Gulbenkian 1' borehole (PG1), 26 m deep and cased by plastic cylinder 42 mm in diameter, is located at the summit of Mount Reina Sofia (272 m a.s.l.) in both boreholes the sensor chain is composed by thermistors with a accuracy of 0.1 °C.

The absence of zero curtain effects in the temperature series supports the negligible effect of ground moisture. Moreover, in both cases, the bedrock is exposed to the surface and there is not vegetation or organic soils at the study site, neither in its vicinity [Ramos et al., 2009].

References

Correia, A.; Vieira, G. and Ramos, M. [2012]: Thermal conductivity and thermal diffusivity of cores from 26 meter deep borehole drilled in Livingston Island, maritime Antarctica, *Geomorphology*, 155–156, doi:10.1016/j.geomorph.2011.12.012.

Ramos, M. and Vieira, G. [2009]: Ground Surface Enthalpy Balance Based on Borehole Temperatures (Livingston Island, Maritime Antarctic). *The Cryosphere*, 3(1):133–145, doi:10.5194/tc-3-133-2009.

Ramos, M.; Hasler, A.; Vieira, G.; Gruber, S. and C., Hauck. [2009]: Drilling and Installation of Boreholes for Permafrost Thermal Monitoring on Livingston Island in the Maritime Antarctic, *Permafrost and Periglacial Processes*, doi:10.1002/ppp.635.

Surface characteristics of rock glaciers in the Jutulsessen, Dronning Maud Land, Antarctica

Elizabeth Magdalena Rudolph[1], Keith Ian Meiklejohn[1], & Adam Bumby[2]

[1] *Rhodes University, South Africa*
[2] *University of Pretoria, South Africa*

Rock glaciers are landforms that present downslope movement of debris under the influence of ice and gravity [Janke et al., 2013]. These landforms can be used as paleo-climate indicators as well as proxies for climate change [Wahrhaftig and Cox, 1959, Humlum, 1998]. Rock glaciers have been investigated in a variety of climates and landscapes, however continental Antarctica, Dronning Maud Land specifically, remains understudied [Humlum, 1998, Whalley and Martin, 1992, Bockheim et al., 2013]. This research aims to investigate and classify five rock glaciers observed in the Jutulsessen, Dronning Maud Land. The surface characteristics and geomorphology were assessed and used as generic classifiers. Size, shape and association was established by field surveying and GIS, whilst sediment and clast characteristics were determined from sampling. A surface temperature profile was created from short-term high frequency temperature measurements. All of the rock glaciers exhibit either undulating surfaces or patterned ground, or both, which suggests active-layer related processes. Sediment particle size analysis is inconclusive. The ^{137}Cs-content and fabric analysis suggest movement regimes similar to other rock glaciers with higher activity at the head, and variable movement directions at the toe. Relative activity is inferred from morphology: Grjotlia, Grjotøyra and Vassdalen were classified as lobate, spatulate and tongue-shaped respectively with Grjotlia the most stable. A new morphological classification of 'crown-shaped' is suggested for Bruggedalen and Jutuldalen, and they also appear most active. The control of local climate on rock glacier mechanics [Hassinger and Mayewski, 1983] is emphasised by the findings, and thus climatic interpolation from weather stations is not useful. Increased spatial and temporal coverage of sediment profiles, surface topography and active-layer characteristics could be used to elucidate the processes and controls of these landforms in the Antarctic.

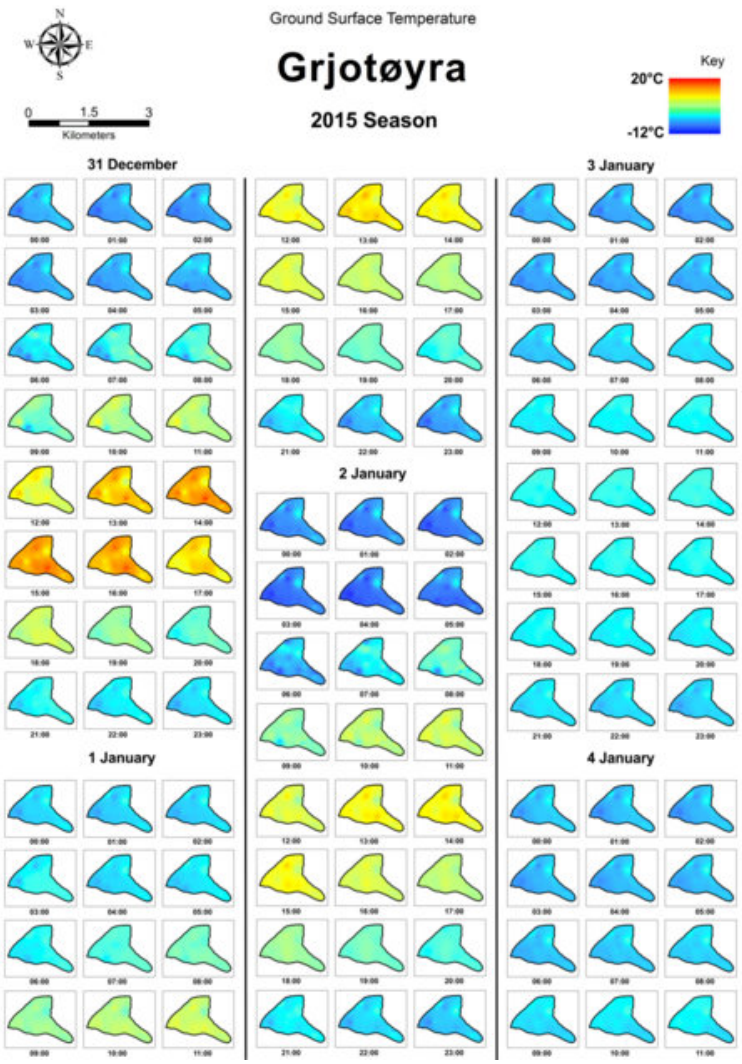

Figure 1: A snapshot of surface temperature change across a rock glacier, Grjotoyra, in the Jutulsessen

References

Bockheim, J.; Vieira, G.; Ramos, M.; López-Martínez, J.; Serrano, E.; Guglielmin, M.; Wilhelm, K. and Nieuwendam, A. [2013]: Climate warming and permafrost dynamics in the Antarctic Peninsula region. *Global and Planetary Change*, 100:215–223, doi:10.1016/j.gloplacha.2012.10.018.

Hassinger, J.M. and Mayewski, P.A. [1983]: Morphology and dynamics of the rock glaciers in Southern Victoria Land, Antarctica. *Arctic and Alpine Research*, 15:351–368.

Humlum, O. [1998]: The climatic significance of rock glaciers. *Permafrost and Periglacial Processes*, 9:375–395, doi:10.1002/(SICI)1099-1530(199810/12)9:4<375::AID-PPP301>3.0.CO;2-0.

Janke, J.R.; Regmi, N.R.; Giardino, J.R. and Vitek, J.D. [2013]: Rock glaciers. In: Shroder, J.F.(ed.), *Treatise on Geomorphology*, pages 238–273. San Diego: Academic Press.

Wahrhaftig, C. and Cox, A. [1959]: Rock glaciers in the Alaska Range. *Geological Society of America Bulletin*, 70:383–436.

Whalley, W.B. and Martin, H.E. [1992]: Rock glaciers: Ii models and mechanisms. *Progress in Physical Geography*, 16:127–186.

Mapping ice-free areas of King George Island (South Shetland Islands, Antarctica) using full polarimetric RADARSAT-2 data

Thomas Schmid[1], Stéphane Guillaso[2], Jerónimo López-Martínez[3], Ana Nieto[3], Sandra Mink[4], Magaly Koch[5], Olivier D'Hondt[2], Adolfo Maestro[4], & Enrique Serrano[6]

[1] *Environment Department, Research Center for Energy, Environment and Technology - CIEMAT*
[2] *Computer Vision and Remote Sensing Group, Technische Universität Berlin*
[3] *Dpto. Geología y Geoquímica, Universidad Autónoma de Madrid*; [4] *Instituto Geológico y Minero de España*
[5] *Center for Remote Sensing, Boston University*; [6] *Dpt. Geografía, Universidad de Valladolid*

Ice free areas within the South Shetland Islands are small compared to those covered by glaciers and ice fields. However, these regions are changing as these islands are the most rapidly warming places in the world over the past fifty years. Glacial and periglacial processes form a complex mosaic of glacial, periglacial, structural and coastal surfaces and together with the presence of permafrost, are the most relevant geomorphological features in the ice-free regions. Characterising these surface covers are an important step to associate changes that are occurring within these regions over the past decades. For this purpose remotely sensed data using Synthetic Aperture Radar (SAR) data are ideal for characterising the surface covers within these regions as Radar provide superior penetration capability through any type of weather condition, and can be used in the day or night time.

The objective of this work is to characterise and map the ice-free areas of King George Island using fully polarimetric SAR RADARSAT-2 data. A total of three Quad-pol fine and fine wide images as Single Look Complex data were acquired through the Canadian Space Agency within the framework of the Science and Operational Applications Research Program (Project SOAR-5169) during 2014 and 2015. An integrated methodology is established to exploit the SAR data together with a digital elevation model and field data containing reference sites with detailed observations and associated laboratory analyses and validation points. A first step is the preprocessing of the RADARSAT-2 data which includes radiometric correction, using a bilateral polarimetric speckle filter, terrain and geometric correction and a mosaicking of the images. A second step is for extracting and identifying polarimetric parameters of the different surface covers according to the backscattering characteristics. A next step is to implement a Support Vector Machine (SVM) algorithm as a supervised classification where the detailed field observations are used as reference for the classifier. A final step is the validation of the mapping results obtained for the entire ice-free regions of King George Island.

The results obtained show that individual scattering mechanisms are well identified with the polarimetric RADARSAT-2 data and can be associated to different surface cover features that are closely related to their physical properties and also to the different topography. Several groups of classes are distinguished that include:

1. gravel and sand deposits often associated to present day and Holocene beaches, and colluvium deposits;
2. different periglacial surfaces such as surface pavements, stone fields and patterned ground;
3. glacial deposits and rock outcrops; and
4. snow and ice cover as well as water bodies.

The distribution of the periglacial landforms are an indicator of the presence of permafrost as well as other dynamic surface features related to hydrological processes. Field data was mainly obtained from Fildes Peninsula where the overall accuracy obtained for the data is over 70 %. Therefore, the established methodology is considered adequate for extrapolation to all of King George Island. The characterisation of the these ice-free areas are regarded as very important for the future monitoring of geomorphological features affected by ongoing processes associated to climate change. Therefore future work would include further time series with this type of SAR data as well as extrapolating the methodology to the rest of the Northern Antarctic Peninsula region.

Evidence of methane and *Archaeal* in permafrost of Antarctic oases

Denis Shmelev, Nikita Demidov, Ekaterina Karaevskaya, & Elizaveta Rivkina

Institute of Physicochemical and Biological Problems in Soil Science, Russian Academy of Sciences, Pushchino, Russian Federation

The methane pool in the permafrost of Arctic landscapes has been studied by many research groups with a great deal of attention given to the estimation of greenhouse emissions from thawed permafrost [Rivkina et al., 2007]. Until recently greenhouse gases in the Antarctic have been discussed by a limited number of authors. Their interest focuses on greenhouse gas fluxes from lakes and modern soils. Numerical modelling suggests methane hydrate accumulation in sediments found under the Antarctic ice sheet [Wadham et al., 2012], yet methane distribution in permafrost has been characterized in few Antarctic oases by shallow core samples.

Ice-free oases occupy only 1 % of the Antarctic area and are underlain by permafrost with different age and genesis. Despite the severe modern landscape conditions, Antarctic permafrost contains greenhouse gases and viable bacteria [Gilichinsky et al., 2007, Rivkina et al., 2007]. Methane concentration and microbiological diversity are formed by palaeo-conditions of sedimentation and freezing. The goal of our investigation is the review of methane and methanogenic *Achaea* in permanently frozen deposits, which accumulated under severe climatic and permafrost conditions during the Miocene – Holocene.

Since the last century the Soil Cryology laboratory has researched frozen ground in ice-free oases of Antarctica. Samples were collected by drilling rig UKB-12/25 at four sites: King-George Island, Schirmacher, Larsemann and Bunger oases. The device uses no drilling fluid to prevent the contamination of the biogenic and sedimentologic characteristics of the core. Gas specimens were collected using headspace degassing in 150 mL syringes. Methane content was determined on a KhPM-4 gas chromatograph (Russia) equipped with a flame ionization detector. Dry combustion in O_2 was used to determine Total Carbon (TC) content in samples with determination of the produced CO_2 amount using the AN-7529U analyzer 'Izmeritel' (Belarus). In samples from King-George Island and Bunger Hills bacterial diversity has been studied by 16S RNA gene sequencing and metagenomic analysis [Karayevskaya et al., 2014].

The studied frozen deposits of Antarctic oases should mainly be dated as Holocene – Late Pleistocene. The moraine deposit is formed by coarse sand with boulders and rock during the Late Glacial Maximum and the Holocene. Lacustrine and marine deposits consist of ice-rich sand, silt and loam with gruss, rubbles and organic inclusions (mats) with a Late Pleistocene age (MIS 3 – MIS 2). The age and genesis of studied methane-content deposits are shown in table 1.

The methane content in Antarctic permafrost varies from several basis points to 200-300 mkmol/kg (see table 1). The isotopic composition (−78/−90 ‰ $\delta^{13}C$) from King George Island confirms the biological genesis of methane. High methane content has also been recorded in lacustrine-marine sediments of Larsemann Hills and the Schirmacher Oasis. Methane has not been found in moraine deposits. It should be noted that TC distribution in permafrost can be characterized in a similar way: mean TC is 0.0 – 0.5 %, but in silt and mats of Larsemann Hills 1.5 – 2.0 % TC concentrations have been found.

By molecular biological cloning data the marine permafrost of King George Island was characterized and showed a predominance of methanogenic *Archaea*, related to genera *Methanosarcina*, *Methanobrevibacter*, *Methanogenium*, *Methanolobus* and *Methanoculleus*. Archaeal diversity of Bunger Hills was very low and represented by only two phylotypes of class *Methanomicrobia*.

Despite the fact that TC content in the Antarctic permafrost is very low, methane has been found in sediments of lacustrine and marine origins. Genesis of the greenhouse gases is biogenic and caused by methanogenic *Achaea* activity. Within the methane containing sediments, we identified a wide diversity of *Achaea* bacteria for King George Island. In comparison the microbiological community of the Bunger Hills permafrost is limited.

Table 1 Methane content and microbiological diversity of the Antarctic permafrost.

Site	Deposits	Age	TC content, [%]	Methane content, [mkmol/kg]	Methanogene phulotypes by 16S rRNA data
King-George	Marine	<7.8 kyr	0.1 – 0.2	40 – 320	Genera *Methanosarcina*, *Methanobrevibacter*, *Methanobrevibacter*, *Methanolobus*, *Methanoculleus*, class *Methanomicrobia*
Schirrmacher Oasis	Lacustrine	$>$ 50 kyr		0 – 200	No data
Larsemann Hills	Moraine Lacustrine-marine Marine	0 – 11 kyr 29 – 38 kyr N2	0 – 0.2 0.5 – 1.7 1 – 1.5	0 10 – 120 5 – 90	No data
Banger Hills	Moraine Lacustrine	0 – 11 kyr $>$ 23 kyr	0 – 0.1 0.1 – 0.2	0 0 – 1	Class *Methanomicrobia*

References

Gilichinsky, D.A.; Wilson, G.S.; Friedmann, E. I.; McKay, C.P.; Sletten, R.S.; Rivkina, E.M.; Vishnivetskaya, T.A.; Erokhina, L.G.; Ivanushkina, N.E.; Kochkina, G.A.; Shcherbakova, V.A.; Soina, V.S.; Spirina, E.V.; Vorobyova, E.A.; Fyodorov-Davydov, D.G.; Hallet, B.; Ozerskaya, S.M.; Sorokovikov, V.A.; Laurinavichyus, K.S.; Shatilovich, A.V.; Chanton, J.P.; Ostroumov, V.E. and Tiedje, J.M. [2007]: Microbial populations in Antarctic permafrost: biodiversity, state, age, and implication for astrobiology. *Astrobiology*, 2(7):275–311, doi:10.1089/ast.2006.0012.

Karayevskaya, E.S.; Demchenko, L.S.; Demidov, N.E.; Rivkina, E.M.; Bulat, S.A. and Gilichinsky, D.A. [2014]: Archaeal diversity in permafrost deposits of Bunger Hills Oasis and King George Island (Antarctica) according to the 16S rRNA gene sequencing. *Microbiology*, 4(83):475–483, doi:10.1134/S0026261714040092.

Rivkina, E.; Shcherbakova, V.; Laurinavichius, K.; Petrovskaya, L.; Krivushin, K.; Kraev, G.; Pecheritsina, S. and Gilichinsky, D. [2007]: Biogeochemistry of methane and methanogenic archaea in permafrost. *FEMS Microbiology Ecology*, 1(61):1–15, doi:10.1111/j.1574-6941.2007.00315.x.

Wadham, J.L.; Arndt, S.; Tulaczyk, M.; Stibal, M.; Tranter, M.; Telling, J.; Lis, G.P.; Lawson, E.; Ridgwell, A.; Dubnick, A.; Sharp, M.J.; Anesio, A.M. and Butler, C.E.H. [2012]: Potential methane reservoirs beneath Antarctica. *Nature*, doi:10.1038/nature11374.

SESSION 3

Ground Ice and Cryostratigraphy

Convener:

Wayne Pollard, *McGill University, Canada*

Daniel Fortier, *University of Montreal, Canada*

Nataliya Belova, *Faculty of Geography, Moscow State University, Russia*

Many processes and landforms unique to permafrost regions are directly related to the aggradation and degradation of ground ice. Ground ice includes all types of ice formed in freezing and frozen ground and in some regions comprise over 50 % of the upper 10 m of continuous permafrost. It can range from disseminated ice crystals in a soil matrix (pore ice) to thick (10 – 20 m), horizontally layered bodies of nearly pure ice that extend for several km^2, or various forms of buried surface ice. The cryostratigraphic and geochemical analysis of permafrost materials containing ground ice provides valuable information about the nature, origin and age of ground ice deposits as well as its distribution and the environmental conditions under which they formed and have occurred since.

This session invites papers that examine the geocryologic significance of ground ice and permafrost systems containing ground ice. Papers may address any aspect of this topic from case studies about ground ice occurrence and its impact on landscape dynamics to regional paleoclimate reconstructions based on cryostratigraphy and ice chemistry. Detailed studies about ground ice detection and distribution, cryostratigraphic relationships, origin, geochemistry, dynamics, stability, and vulnerability to climate change are welcome.

Relationship of Cryofacies, Surface and Subsurface Terrain Conditions in the Brooks Range and Foothills of Northern Alaska, USA

Andrew Balser[1], Jeremy Jones[2], & Torre Jorgenson[3]

[1] *Oak Ridge National Laboratory, Oak Ridge, TN, USA*
[2] *Institute of Arctic Biology, University of Alaska Fairbanks, Fairbanks, AK, USA*
[3] *Alaska EcoScience, Fairbanks, AK, USA*

Permafrost landscape responses to climate change and disturbance impact local ecology and global greenhouse gas concentrations, but the nature and magnitude of response is linked with vegetation, terrain and permafrost properties which vary markedly across landscapes. As a subsurface property, permafrost conditions are difficult to characterize across landscapes, and modeled estimates rely upon relationships among permafrost characteristics and surface properties. While a general relationship among landscape and permafrost properties has been recognized throughout the arctic, the nature of these relationships is poorly documented in many regions, limiting modeling capability. We examined relationships among permafrost, terrain and vegetation within the Brooks Range and foothills of northern Alaska using field data from diverse sites within a multiple factor analysis ordination to identify and describe these relationships in this region, and to facilitate future modeling and ecological research. Terrain, vegetation and permafrost conditions were correlated throughout the region, with field sites falling into four statistically-separable groups based on ordination results. Our results identify index variables for honing field sampling and statistical analysis, illustrate the nature of relationships in the region, support future modeling of permafrost properties, and suggest a state factor approach for organizing data and ideas relevant for modeling of permafrost properties at a regional scale.

Experimental ice wedge rejuvenation, Illisarvik drained lake, western Arctic coast, Canada

Christopher Robert Burn

Department of Geography and Environmental Studies, Carleton University, Canada

Several of J. Ross Mackay's seminal contributions to permafrost science were made at Illisarvik, a lake near the western Arctic coast of Canada that was experimentally drained on 13 August 1978 [Mackay, 1997]. The development of ice wedges during permafrost aggradation in the drained-lake bed has been one of the principal areas of research [Mackay, 1984, 1986]. Three key results that Mackay obtained concern:

1. demonstration of upward cracking, originating from permafrost, towards the ground surface (Mackay 1984);

2. observation of continuous horizontal, seasonally directed movement of the active layer on either side of a new ice wedge [Mackay, 1986]; and

3. termination of thermal-contraction cracking several years after drainage when vegetation growth in the drained-lake bed led to deeper snow cover [Mackay and Burn, 2002].

A field experiment to rejuvenate thermal contraction cracking in the lake bed has been conducted at Illisarvik over two decades, beginning in 1996. The experimental hypothesis was that reduction in snow depth would lead to rejuvenation of ice-wedge cracking. The intention was to cut the annual crop of grass and hence reduce snow depth in an area of 75 m by 35 m, thereby lowering ground temperatures, and restarting thermal-contraction cracking of a 65 m-long ice wedge running through the centre of the area (Site 3 of Mackay and Burn [2002]). The wedge cracked for several years in the 1980s, and developed a width of about 22 cm at the top of permafrost [Mackay, 1986, Mackay and Burn, 2002].

Ground temperatures have been monitored by miniature data logger in the cut area, and in adjacent undisturbed ground. Snow and active-layer depths have been monitored in the two areas during field visits towards the end of winter, usually in April to collect snow depths, and in late August to measure active-layer thickness. Ground temperatures have also been measured at the bottom of the active layer in the ice-wedge trough, using thermistor cables tightly spread across the wedge. These cables have also acted as breaking cables to indicate the time of cracking. Miniature ground accelerometers have been used to time the cracking event, for comparison with time of cable breakage. The accelerometers have been buried in the active layer along the trough. Steel benchmarks with anti-heave rings were installed in permafrost on both sides of the wedge at three locations to monitor ground movement. The bench marks are in two pairs: one pair installed to 1-m depth (in 1996), the other pair to 2-m depth (in 1999). Hoop crackmeters, installed by Mackay [1986], have been used to measure movement of the active layer.

Ground temperatures have been recorded to ± 0.25 °C or better precision by the data loggers. Snow depths and active-layer depths have been measured to ± 5 mm with a steel probe. Horizontal separation of the tops of the benchmarks and of the hoop crackmeters have been measured with a tape to ± 1 mm. The tops of the benchmarks have been surveyed annually by optical levelling to ± 0.1 mm. Tilting of the benchmarks has been measured by an inclinometer placed on a level plate mounted on the benchmark, with a key to ensure consistent orientation of the instrument.

Ground temperatures and benchmark movements were measured for several years before late-summer cutting of vegetation began in August 2000. Subsequently, late winter snow depth declined from 40–60 cm to 10–30 cm. Active-layer thickness decreased from 95 to 60 cm.

Annual mean near-surface ground temperatures responded to reduced snow cover in the first and subsequent winters after cutting began. Before cutting, this index was -0.8 °C in the active layer and near-surface permafrost, but declined to -5.0 °C over four years. Similarly, minimum ground temperatures were ≥ -5 °C, but after cutting these declined to between -15 and -25 °C in the active layer and -10 to -15 °C in the active layer. Thermal contraction cracking was not initiated until winter 2004–05. The well-known

thermal threshold for ice-wedge cracking of −13 °C at the top of permafrost [Allard and Kasper, 1998, Fortier and Allard, 2005], was exceeded before cracking began. The threshold was not exceeded in some years when cracking occurred.

The benchmarks on either side of the trough that was established during ice-wedge growth in the 1980s decreased in separation until cracking began (1996–2005), but subsequently the separation has increased. Seasonal oscillation of the benchmarks has reflected movement of the active layer, as described above. The separation of benchmarks has been observed for both shallow (1 m) and deep (2 m) pairs, but the seasonal oscillation is pronounced in the nearer surface. Separation of the benchmarks, corrected for tilt, has indicated a steady expansion of about 0.5 cm/yr.

The accelerometers have indicated one event only each winter, between January 20 and February 14, for the period of measurement 2012 – 15. The acceleration was recorded by all loggers in the same time interval. The magnitude of the acceleration has ranged from 44 to 91 g. The shock is interpreted as the cracking event. The relative magnitudes of acceleration at points along the trough indicate that the point of crack initiation varies from year to year. Breakage of the thermistor cable in the ice-wedge trough has occurred a month or more after the cracking event, indicating crack widening [Mackay, 1989, Sarrazin and Allard, 2015].

Excavation of the rejuvenated ice wedge in 2014 indicated 25 cm of new ice wedge above the wedge that developed in the 1980s. The new ice had formed on one side of the wedge. The new ice was 3 to 4 cm wide, a size that is consistent with an increase in separation of benchmarks by about 0.5 cm/yr over 10 years. The top of the ice wedge now has a syngenetic form, but it has grown in an epigenetic environment. Reinitiation of cracking and growth of the wedge have been achieved by changing winter snow conditions.

The primary conclusions of this study are:

1. now depth has been the critical variable for controlling thermal contraction cracking at Illisarvik;
2. thresholds for crack initiation should be interpreted as guidelines, and not strict conditions;
3. active–layer movement on either side of the wedge may occur regardless of cracking;
4. ground acceleration occurs at the cracking event, but further widening of the crack is sufficiently gradual as to present no shock;
5. crack initiation in an ice wedge may occur from year-to-year at different points.

References

Allard, M. and Kasper, J.N. [1998]: Temperature conditions for ice-wedge cracking: field measurements from salluit, northern québec. In: Lewkowicz, A.G. and Allard, M.(eds.), *Permafrost, Seventh International Conference, Proceedings*. June 23–27, 1998, Yellowknife, NT.

Fortier, D. and Allard, M. [2005]: Frost-cracking conditions, Bylot Island, eastern Canadian Arctic archipelago. *Permafrost and Periglacial Processes*, 21:145–161, doi:10.1002/ppp.504.

Mackay, J.R. [1984]: The direction of ice-wedge cracking in permafrost: downward or upward? *Canadian Journal of Earth Sciences*, 21:516–524.

Mackay, J.R. [1986]: The first 7 years (1978-1985) of ice wedge growth, Illisarvik experimental drained lake site, western Arctic coast. *Canadian Journal of Earth Sciences*, 23:1782–1795.

Mackay, J.R. [1989]: Ice-wedge cracks, western Arctic coast. *The Canadian Geographer*, 33:365–368.

Mackay, J.R. [1997]: A full-scale field experiment (1978-1995) on the growth of permafrost by means of lake drainage, western Arctic coast: a discussion of the method and some results. *Canadian Journal of Earth Sciences*, 34:17–33.

Mackay, J.R. and Burn, C.R. [2002]: The first 20 years (1978/79 to 1998/99) of ice-wedge growth at the Illisarvik experimental drained lake site, western Arctic coast, Canada. *Canadian Journal of Earth Sciences*, 39:95–111, 2002.

Sarrazin, D. and Allard, M. [2015]: The thermo-mechanical behavior of frost cracks over ice wedges: new data from extensometer measurements. In *Proceedings, 7th Canadian Permafrost Conference and 68th Canadian Geotechnical Conference*, Quebec City, QC, 20–23 September 2015. Paper 248, 7 p.

Structure of wedge ice and massive ice: a comparative study

Elmira Galeeva[1], Anna Kurchatova[1,2], Victor Rogov[1,2], & Elena Slagoda[2,3]

[1] *Tyumen State Oil and Gas University, Russian Federation*
[2] *Earth Cryosphere Institute SB RAS, Tyumen, Russian Federation*
[3] *Lomonosov Moscow State University, Moscow, Russian Federation*

The ground ice structure was studied to identify the indicators of ice origin and metamorphism. It is necessary to distinguish the polygon ice wedges and the wedge-shaped massive ice bodies, for example diapirs, stocks at Cape Marresale (Yamal). Textural and structural analysis of ice microsections sampled from wedge ice (8 images) and massive ice (14 images) in various parts of Western and Eastern Siberia. To retrieve the following parameters, images of ice thin sections in polarized light were processed in computer:

- the mean crystal area (S, cm^2)
- the mean crystal area (S, cm^2)
- the mean crystal boundary length (L, cm)
- diameter of the mean crystal expressed as a diameter of circle having equal square(D, cm)
- the form-factor which is the ratio of the mean crystal boundary length to a boundary length of regular hexagon having equal square (K_F)
- the factor of crystal elongation which is the ratio of the number of ice crystals to the crystals on a circular area of 1 cm^2 (K_L)
- the mean angle between the maximal crystal diagonal and vertical (*a'*)
- the structure heterogeneity factor showing the range of crystal sizes in one slice (K_N).

Massive ground ice had layered structure of alternating layers of pure ice and ice soil 2 to 8 cm thick. The pure ice had large crystals (D = 4.5 cm^2) in contrast to the ice-soil with small crystals of 0.1–0.3 cm^2 and inclusions of mineral grains of sand-silt fraction as well as fragments of diatoms valves. The pure ice layers could be subdivided into the 2 cm wide zones having different crystal size. Additional to the layered structure, the massive ice had cracks underlined by offset crystal faces and allocation of gas bubbles. Moreover the massive ground ice characterized by the deformations – cracks that are distinguished by the dislocations of crystal faces and the location of gas bubbles. In these areas, there are some crystals that characterized by the internal cracks and twinning.

Ice wedges are characterized by the vertical orientation of ice layers or nearly that. The mean crystal size is changed from 1, 5 – 2, 5 cm^2 (D = 2 cm^2). The growing ice wedges is characterized by the crack zone in the central part with numerous elementary ice veins with small crystals of 0.01 – 0.1 cm^2. This foliated structure is distinguished by the distribution of mineral inclusions and chains of gas bubbles. The vertical orientation of the ice crystals is clearly expressed in polarized light.

Comparative analysis of samples of the massive ground ice and wedge ice from different areas of Western and Eastern Siberia is showed a significant difference in their structure. The elongated crystals (according to the layered structure of massive ice) reflect the deformation of viscoplastic flow of ice whereas the cracks represent the brittle failure. In the wedge ice with clear vertical texture, ice crystals become more isometric in according to the increasing of wedge width as a result of the processes of metamorphism and the development of the block brittle deformation due to the compressive and expand stresses in permafrost strata [Lokrantz and Ingólfsson, 2003, Rogov et al., 2003, Solomatin, 1986].

Acknowledgements

This study has been supported by Russian Science Foundation (Grant 14-17-00131).

References

Lokrantz, H.L. and Ingólfsson, ó. [2003]: Massive ground ice body of glacial origin at Yugorski Peninsula, Arctic Russia. *Permafrost and Periglacial Processes*, 14(3):199–295, doi:10.1002/ppp.455.

Rogov, V.V.; Perednya, D.D.; Leibman, M.O.; Vasiliev, A.A. and Kizyakov, A.I. [2003]: Tabular ground ice: cryolithological construction and crystalline structure. In: Phillips, M.; Springman, S.M. and Arenson, L.U.(eds.), *Permafrost. Proceedings of the Eighth International Conference on Permafrost*, 21–25 July 2003, Zürich, Switzerland.

Solomatin, V.I. [1986]: *Petrogenesis of ground ice*. Nauka, Moscow. in Russian.

Ancient environments and climate of Central Siberia inferred from ice wedge at Cyuie village near Yakutsk

Kyungmin Kim[1], Jinho Ahn[1], Eunji Byun[1], Hyunsuk Yoon[1], Alexander Fedorov[2], & Ji-Woong Yang[1]

[1]*Seoul National University, Republic of South Korea*
[2]*Melnikov Permafrost Institute, Yakutsk, Sakha Republic, Russian Federation*

In permafrost region, ice wedges are formed by refreezing of snow melt or hoarfrost densification in cracks that were made by contraction during extremely cold season. As ice wedges are preserved for thousands of years, they may preserve records for past environments and climate. Previously a few studies attempted to reconstruct paleoclimate with Siberian ice wedges, but the data interpretation remains unclear due to insufficient geographical coverage and understanding of ancient environments.

In the context, we sampled two ice wedges by a thermokarst lake in Cyuie village, near Yakutsk. So far we have analyzed ice crystal texture, gas composition ($\delta O_2/Ar$, $\delta N_2/Ar$, CH_4, CO_2, and $\delta^{15}N\text{-}N_2$) and water isotopes ($\delta^{18}O$, δD). The ice has relatively high air contents of 0.02 – 0.05 ml/g ice. The CO_2 mixing ratios of 7 – 13 % are greater than those of Siberian ice wedge in arctic coast (0.2~11 %), but CH_4 mixing ratios of 5 – 40 ppm are similar [Boereboom et al., 2013]. The O_2 content is nearly zero. We interpret that most of the CO_2 and CH_4 originated from microbiological activity within the ice wedges, and O_2 was eliminated by biological respiration. The ice crystals are equant with size of a few millimeters and the gas bubbles are spherical without any elongation. The $\delta Ar/N_2$ results are similar to that in the atmosphere. Thus, we interpret that the ice wedges were formed by hoarfrost/dry snow densification [St-Jean et al., 2011]. Our preliminary $\delta^{18}O$ data from 5 samples are $\approx -30‰$ and similar to the previous results for ice wedge which formed in LGM in central Yakutia [Vasil'chuk and Vasil'chuk, 2014]. To better constrain the ages and sources, we plan to analyze ^{14}C of the CO_2 and organic compounds in adjacent soil. We also plan to extensively analyze water isotopes ($\delta^{18}O$, δD) to better reconstruct ancient cold season temperature and precipitation sources.

References

Boereboom, T.; Samyn, D.; Meyer, H. and Tison, J. L. [2013]: Stable isotope and gas properties of two climatically contrasting (Pleistocene and Holocene) ice wedges from Cape Mamontov Klyk, Laptev Sea, northern Siberia. *The Cryosphere*, 7 (1):31–46, doi:10.5194/tc-7-31-2013.

St-Jean, M.; Lauriol, B.; Clark, I. D.; Lacelle, D. and Zdanowicz, C. [2011]: Investigation of ice-wedge infilling processes using stable oxygen and hydrogen isotopes, crystallography and occluded gases (O_2, N_2, Ar). *Permafrost and Periglacial Processes*, 22 (1):31–46, doi:10.1002/ppp.680.

Vasil'chuk, Y. and Vasil'chuk, A. [2014]: Spatial distribution of mean winter air temperatures in Siberian permafrost at 20–18 ka BP using oxygen isotope data. *Boreas*, 43(3):678–687, doi:10.1111/bor.12033.

Cryostratigraphy and sedimentology of the early Holocene Zackenberg delta (NE Greenland)

Graham L. Gilbert[1,2], Stefanie Cable[3], & Hanne H. Christiansen[1]

[1] *Arctic Geology Department, The University Centre in Svalbard, Norway*
[2] *Department of Earth Science, University of Bergen, Norway*
[3] *Center for Permafrost (CENPERM), Department of Geosciences and Natural Resource Management, University of Copenhagen, Denmark*

The Zackenberg Valley is located in northeast Greenland (74°30'N, 20°30'E). During the late Weichselian, the valley hosted an ice-stream, draining the Greenland ice sheet. Glaciation acted to remove much of the terrestrial record deposited during the previous interglacial. Immediately following deglaciation the low-laying areas (below ca. 90 m a.s.l.) were inundated by the sea. Landscape emergence occurred during the Holocene and attributed to glacio-isostatic rebound rates, which outpaced global eustatic sea level rise.

The deltaic fill at the mouth of the valley covers an area of ca. 4 km^2 and consists of a series of terraces – formed during relative sea level fall. To the west, the spatial extent of the paleo-delta is restricted by the Zackenberg Mountain. The eastern boundary is less easily defined and grades into glacial and glaciofluvial deposits. The modern Zackenberg River has incised through the paleo-deltaic deposits creating exposures (up to ca. 25 m in height) along the rivers banks. In addition, coastal processes have exposed sediments in ca. 10 – 20 m high coastal cliffs. In 2012, two 20 m deep ice-bonded sediment cores were retrieved from within the deltaic deposits. Samples from up to 70 % of the cored interval were recovered (i.e. 14 m of a possible 20 m). The combination of river and coastal exposures with the analysis of these cores permitted the reconstruction of the valley-fill succession and evaluation of the timing and nature of permafrost aggradation.

Ground ice, exposed in actively eroding sections and preserved in the frozen sediment cores, has been described using established cryostructure classification frameworks. Permafrost in the palaeodeltaic deposits is predominantly epigenetic, aggrading following the subaerial exposure of the delta plain. The pore-ice and layered cryostructures dominates in the sand-rich delta toe and delta slope facies. Pore ice forms due to the in situ freezing of water in the pore spaces. Formation of layered cryostructures is attributed to pore-water expulsion, occurring in sand-rich layers, during downward permafrost aggradation.

Where present, the uppermost syngenetic component is less than ca. three meters in thickness. The development of syngenetic permafrost is related to localized accumulation of aeolian and nival sediments and organic material. Cryostructures consists of pore, lenticular, reticulate, and ataxitic-types – reflecting changes in the sedimentation regime and sufficient moisture at the base of the active layer. Variations in cryostructures are tentatively attributed to temporal changes in sedimentation rates with ataxitic cryostructures forming during periods of reduced sedimentation.

Previous investigations and optically stimulated luminescence ages in this investigation indicate that the palaeo-deltaic fill was deposited during the early Holocene (ca. 12.5 – 6.0 kya). Sedimentological studies revealed an upwards coarsening succession reflecting the transition from the prodelta through to the delta-plain depositional environment – overlying a clast-rich diamicton. The diamicton is interpreted as having been deposited during the late Weichselian glaciation. The combination of sedimentology and cryostratigraphy indicate that permafrost aggradation was initiated following subaerial exposure. The exposed deposits in the Zackenberg Valley have provided a unique opportunity to investigate the ground ice characteristics of polygenetic permafrost deposits and the relationship between depositional environments and processes, grain-size properties, and cryostratigraphy.

Ice-wedge stable isotopes at the Dmitry Laptev Strait (Northeast Siberian Arctic) – indications for Late Quaternary stratigraphy and paleoclimate

Thomas Opel[1], Sebastian Wetterich[1], Alexander Yu. Dereviagin[2], Hanno Meyer[1], Margret C. Fuchs[3], & Lutz Schirrmeister[1]

[1] *Alfred Wegener Institute Helmholtz Centre for Polar and Marine Research, Periglacial Research Section, Potsdam, Germany*
[2] *Moscow State University, Faculty of Geology, Moscow, Russia*
[3] *Helmholtz-Zentrum Dresden-Rossendorf, Helmholtz-Institute Freiberg for Resource Technology, Freiberg, Germany*

Ice wedges are the most abundant type of ground ice in the ice-rich permafrost deposits of the Northeast Siberian Arctic. They form by repeated frost cracking and subsequent crack filling and refreezing in spring, mostly by melt water of winter snow. Ice wedges are studied by means of stable-water isotopes ($\delta^{18}O$, δD, d-excess). The isotopic composition is directly linked to atmospheric precipitation (i.e. winter snow) and, therefore, indicative of past climate conditions during the cold season. To a lesser extent also genetic aspects, such as the seasonality of precipitation, frost cracking and ice-vein formation, isotopic transformation of the snow cover by percolation (either by snow melt or rain water), or hoar frost prior to ice-wedge formation, may have an influence.

In this contribution we present stable-water isotope data of ice wedges from the mainland coast of the Dmitry Laptev Strait (Oyogos Yar, 72.7°N, 143.5°E). Ice wedges and surrounding sediments were studied and sampled in 2002 and 2007. Sediments ages were deduced using OSL dating and radiocarbon dating, while ice-wedge ages were deduced using ^{36}Cl/Cl dating [Blinov et al., 2009] and radiocarbon dating of ice-enclosed organic matter. Further cryostratigraphic correlation is based on ice-wedge stable isotope data.

Based on our chronology the studied ice wedges correspond to different stratigraphic units of the Late Quaternary. These are (1) Ice Complex deposits of MIS5 age [Wetterich et al., 2015], (2) flood plain deposits of MIS4 to MIS3 age, (3) Holocene themokarst deposits [Opel et al., 2011].

An ice wedge of the MIS5 Ice Complex exhibits mean $\delta^{18}O$ and d-excess values of −33 ‰ and 7 ‰, respectively, representing very cold winter temperatures. Smaller multi-stage ice wedges corresponding to the MIS4 to MIS3 flood plain deposits show two clusters of isotope values: (1) in their lower parts (composite sand-ice wedges or 'polosatics') $\delta^{18}O$ values of −31 to −28 ‰ (d-excess of 0 – 5 ‰) and (2) in their upper parts (classical ice wedge) $\delta^{18}O$ values of −34 ‰ (d-excess of 5 ‰), reflecting rather different formation conditions than climate variation under very cold winter climate conditions. The huge syngenetic ice wedges of the MIS3 Yedoma Ice Complex are characterized by mean $\delta^{18}O$ values of −33 ‰ to −29 ‰ and mean d-excess values between 4 and 8 ‰ corresponding to different altitude levels and reflecting cold to very cold winter temperatures. On top of the Ice Complex as well as predominantly in a thermokarst depression of Late Glacial origin Holocene ice wedges were found. Those formed predominantly in the Middle to Late Holocene and exhibit mean $\delta^{18}O$ values of about −25 ‰ and mean d-excess values of 8 ‰, mirroring distinctly warmer winter temperatures in the Holocene. Recently grown (modern) ice wedges of the last decades are characterized by mean $\delta^{18}O$ values of about −21 ‰ and mean d-excess values of 8 ‰, testifying the recent winter warming in the Arctic.

Ice wedge stable-water isotope data indicate substantial variations in Northeast Siberian Arctic winter climate conditions during the Late Quaternary, in particular between Glacial and Interglacial but also over the last centuries and decades. Hence, ice-wedge based reconstructions of shifts in winter air temperature ($\delta^{18}O$) as well as changes in moisture generation and transport patterns (d-excess) add substantial information to those derived from paleoecological proxies stored in permafrost and allow for differing between seasonal trends of past climate and environmental dynamics.

References

Blinov, A.; Alfimov, V.; Beer, J.; Gilichinsky, D.; Schirrmeister, L.; Kholodov, A.; Nikolskiy, P.; Opel, T.; Tikhomirov, D. and Wetterich, S. [2009]: Ratio of ^{36}cl/cl in ground ice of East Siberia and its application for chronometry. *Geochemistry Geophysics Geosystems*, 10, doi:10.1029/2009GC002548.

Opel, T.; Dereviagin, A.Y.; Meyer, H.; Schirrmeister, L. and Wetterich, S. [2011]: Palaeoclimatic Information from Stable Water Isotopes of Holocene Ice Wedges on the Dmitrii Laptev Strait, Northeast Siberia, Russia. *Permafrost and Periglacial Processes*, 22, doi:10.1002/ppp.667.

Wetterich, S.; Tumskoy, V.; Rudaya, N.; Kuznetsov, V.; Maksimov, F.; Opel, T.; Meyer, H.; Andreev, A.A. and Schirrmeister, L. [2015]: Ice Complex permafrost of MIS5 age in the Dmitry Laptev Strait coastal region (East Siberian Arctic). *Quaternary Science Reviews*, doi:10.1016/j.quascirev.2015.11.016.

Structure and distribution of ice lenses in artificial frozen soils and arctic-alpine permafrost

Tomotaka Saruya[1], Tetsuo Sueyoshi[1], Tatsuya Watanabe[2], Alan Rempel[3], & Hiroyuki Enomoto[1]

[1] *National Institute of Polar Research, Japan*
[2] *Kitami Institute of Technology, Japan*
[3] *University of Oregon, USA*

When the mixture of water and soil grains is cooled below the melting temperature, segregated ice layers of pure ice known as ice lens are formed by the migration and solidification of unfrozen water. Ice lenses can be formed in various porous media such as artificial glass beads in laboratory and natural soils in permafrost. Formation process of ice lens has been investigated by many researchers, however, the detailed observations of ice crystals in frozen soils are rarely performed even in laboratory. Not only the ice lens structures but also the internal structure of permafrost or active layer have still uncertainties.

We have conducted observations of frozen porous media obtained by unidirectional freezing experiments using glass beads in laboratory and permafrost core to investigate the structures of frozen soils and ice crystals. In laboratory experiments, we prepared various sizes of glass beads that are saturated with deionized water. Ice lenses are obtained by unidirectional freezing from bottom side of water-saturated glass beads. Beyond the artificial frozen porous media, we obtained natural permafrost cores in Adventdalen, Svalbard and summit area of Mt. Fuji. Boring site at Svalbard is typical tundra and covered with mud-boil and small polygons composed of fine-grained clay. On the other hand, alpine-volcanic permafrost at Mt. Fuji has peculiar properties such as pyroclastic materials surface. We measured the volume content and distribution of ice by X-ray computed tomography scan of frozen core. Svalbard core holds large amount of ice. In particular, periodic ice lenses are distributed throughout the core. Adventdalen permafrost is composed of fine-grained clay sediment that comes from adjacent river and has high water retention characteristics, which induces the high frost-susceptibility and ice-rich permafrost. On the other hand, Mt. Fuji permafrost core has minor amount of ice. Surface of summit area is covered with eruption-derived pyroclastic materials that have high porosity so that Mt. Fuji permafrost has high permeability and drainage.After non-destructive inspection, we manufactured the core sample and made ice slices to observe the crystal structures of segregated ice lenses. Figure 1 shows the polarized images of ice lens slices obtained in laboratory experiments. Host particle size is 0.6 micron. Left and right images correspond to horizontal and normal to heat flow direction. Left image indicates that ice lens is an assemblage of single crystals that grow along the heat flow direction. Cross-sectional image of ice lens normal to heat flow (right image) describes the hexagonal shape of single crystals with diameter of ≈1 mm. We could observe similar structures in permafrost core. In this presentation, we discuss the structures, distributions, characteristics of ice lenses and frozen soils, and relationship with environment.

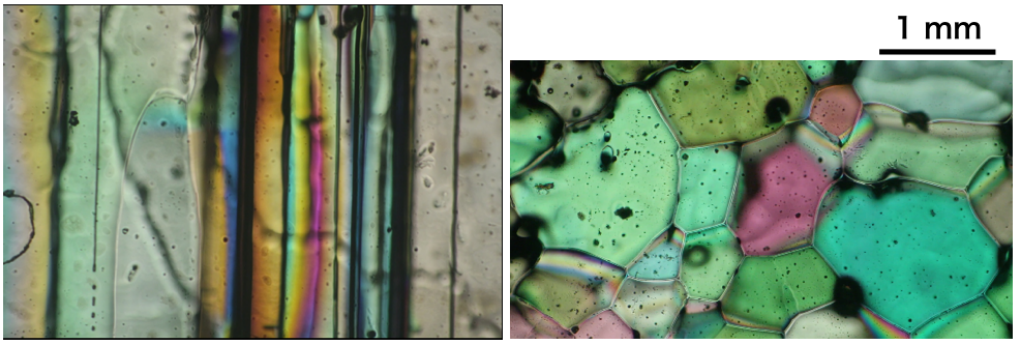

Figure 1: Polarized images of ice lens slices with horizontal and normal to heat flow direction.

Radiocarbon dating, stable-isotope composition and pollen spectra of the Holocene ice wedge in the Chara depression, Northern Transbaikalia

Alla Vasil'chuk[1], Yurij Vasil'chuk[1], & Julia Stanilovskaya[2]

[1]*Lomonosov Moscow State University, Russian Federation*
[2]*Sergeev Environmental Geoscience Institute of the Russian Academy of Sciences, Russian Federation*

Syngenetic and epigenetic ice wedges, their isotopic composition, radiocarbon age and pollen spectra of the surrounding deposits have been analyzed during long-term study of the 'Belenky' key site on the first (6 – 8 m high) terrace of Chara River (720 m a.s.l.) in Northern Transbaikalia. It has been revealed that the ice wedges are of Holocene age and were formed between 10 to 7.5 ka ^{14}C BP (Fig. 1).

This period is identified as the first half of the Holocene optimum for the south of East Siberia. The isotopic composition of ice wedges, segregated ice, blister ice, precipitations, river and lake waters has been specified. The isotopic composition ($\delta^{18}O$, δD) of relict ice wedges is the lightest and amounts to −23 ‰ and −185 ‰, respectively. The isotopic composition of structured ice from the sandy loam above the ice wedges is −15.7 ‰and −133 ‰; and of small ice wedges in peat and sand is −15.3 ‰ and −117.9 ‰, respectively.

Syngenetic ice wedges up to 7 m in height were actively formed during the Holocene (dated 10 – 7.5 ka BP) in sands interbedded with pebbles and gravel of the Chara River valley. The mean value of $\delta^{18}O$ is −23 ‰and of δD is −180 ‰. Comparison of the isotopic composition of Holocene and modern ice wedges showed that the $\delta^{18}O$ values of the Holocene were more negative by 1 – 3 ‰. Conversion of isotopic data to palaeotemperature showed that the average winter temperature of the cold stages of the Holocene optimum (10 – 7.5 ka BP) could be colder than today by 2 – 3 °C and for the average January by 3 – 4 °C. The sum of winter temperatures could drop to −5100 −5700 degree-days, i.e., it was even lower than the extremely cold modern winters by 300 – 600 degree-days. At warmer stages of 10 – 7.5 ka BP, winter temperatures were close to modern ones.

The three pollen phases can be divided by analyzing of pollen spectra.

The first one corresponds to the 2-meters of sand pack at the bottom. Conditions during the period of this horizon accumulation were the most favorable and characterized by relatively high temperatures and humidity. Likely larch forests were replaced with of pine and birch forests with spruce, larch and dwarf birch. According to the method of summer total temperature sums reconstruction on the composition of pollen spectra [A.Vasil'chuk, 2009], the sum of summer positive temperatures during the first period in the initial phase of the Holocene Optimum accounted as1600 – 1800 degree-day, i.e. they were slightly higher than today's total temperature (up to 200 degree-day higher than modern) or close to it.

The second pollen phase corresponds to a deterioration of vegetation conditions. Landscapes characterized by the maximum development of fens and birch-pine woodlands were formed during the end of the sand layer accumulation. It is possible to talk about decreasing of the total positive temperatures up to 1300 degree-day (i.e. 300 degree-day below modern).

Growth of wood pollen during the third pollen phase indicates the subsequent improvement of the conditions of vegetation and development of birch-pine forests with larch and spruce. This is evidenced by the appearance of Ericaceae and forest species of Lycopodiopsida in the spectra. The total positive temperatures were close to the modern and were about 1550 – 1600 degree-day.

The composition of pollen spectra at depths of 4.3 m, 2.7 m and 1.5 m fix the wide development of polygonal landscapes and possible growth of ice wedges (mostly in width). Indicators of the polygonal tundra development are the domination of *Sphagnum* and *Bryales* in these spectra with *Betula sect. Nanae, Caryophyllaceae, Artemisia.*

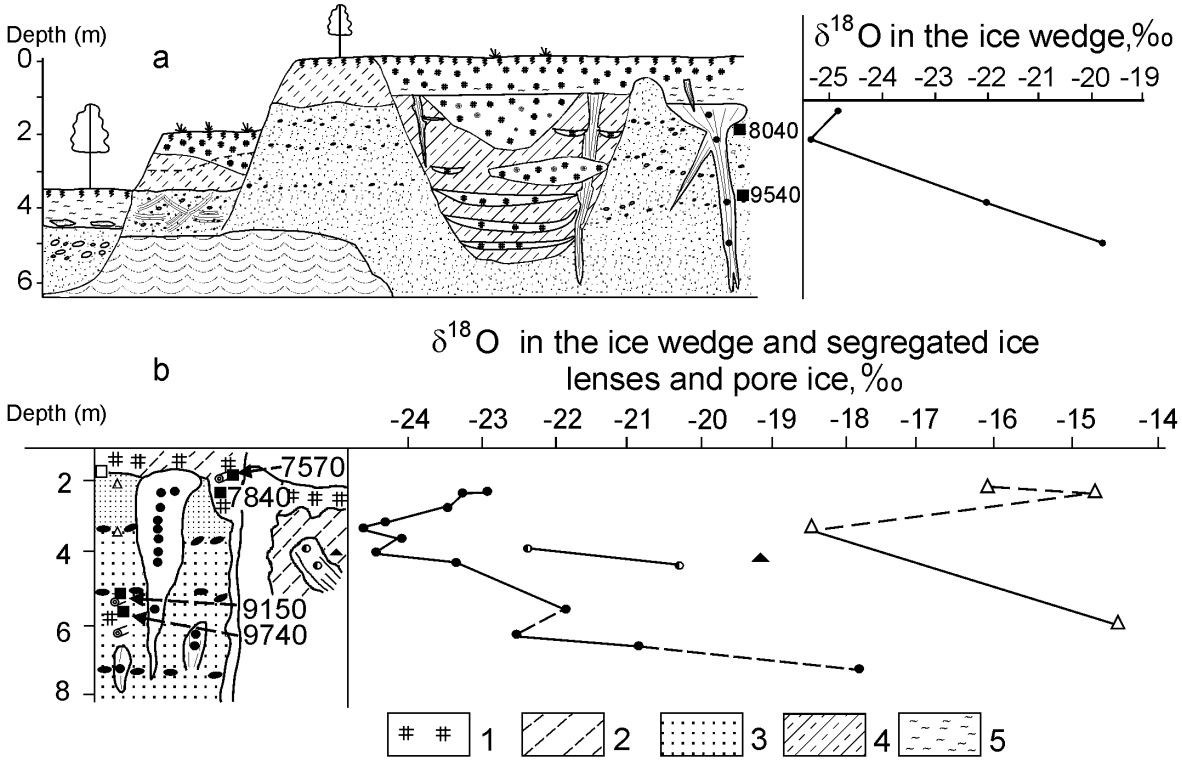

Figure 1: Radiocarbon dating and oxygen isotope ratios in ice wedges: a – ice wedge #4, 5 and 6; b – ice wedge #1, ice wedge #2 under peat and buried ice wedge #3: 1 – peat; 2 – sandy loam; 3 – sand; 4 – interbedded peat, loam and clay loam; 5 – silt

Hydrogen and oxygen isotopes in ice wedges near Vorkuta town, north of East European Plain

Yurij K. Vasil'chuk, Nadine A. Budantseva, Julia N. Chizhova, & Alla C. Vasil'chuk

Lomonosov Moscow State University, Russian Federation

We have obtained ^{14}C ages of polygonal peat and isotope composition of syngenetic ice wedges nearby Vorkuta town, north of East European Plain. It makes possible to reconstruct winter temperatures during ice wedge formation and deduce the temporal trend of the temperature. To establish the timing of ice wedge formation, a detailed sampling of various organic materials (peat and wood) from the ice wedges, surrounding peat and from the ground wedges was carried out. According to ^{14}C ages from the peat the timing of the ice-wedge, can be estimated at 9–5.5 ka BP. The ice wedges began to form within a drier part of the bog whereas ground wedges began to form in the more frequently flooded part. Under conditions of frequent changes in flooding environment, peat and twigs entered the thawing elementary ice wedges in the ground wedge. The subsequent drainage of this part of the swamp resulted in the formation of a new elementary ice wedge. Two or three such cycles produced the peat ice wedges. Later, this part of the swamp was substantially flooded. Consequently, ice began to thaw and replaced by loam, which now overlies the peat layer with the peat-loam wedge. The oxygen isotope and deuterium diagrams show stable winter conditions. In wedges, δD values varies from −119.1 to −111.6 ‰; $\delta^{18}O$ values varies from −16.35 to −15.45 ‰; and the deuterium excess, from 13.8 to 9.0 ‰. In the lens ice, δD values vary from −128.4 to −97.8 ‰; $\delta^{18}O$ values varies from −17.48 to −12.79 ‰; and the deuterium excess, from 11.4 to 4.5 ‰. In snow of an old snowfield, δD value is −134.4 ‰, $\delta^{18}O$ is −18.91 ‰, and the deuterium excess is 16.9 ‰. In water of a small interpolygonal pond, δD value is equal to −87.4 ‰, $\delta^{18}O$ is −11.31 ‰, and the deuterium excess is 3.1 ‰. The upper part of the wedge shows a sharper change at isotope plots: relatively sharp replacement of the positive shift of δD and $\delta^{18}O$ values by negative ones. A very perceptible increase of deuterium excess up to 13.8 ‰ (against the common value of 11-12 ‰). These data indicate relatively more contrast changes in winter climatic and, probably, geocryological conditions near the middle of the Holocene Optimum. For comparison, snow samples taken from fresh snow near stations Seida and Eletskaya near Vorkuta on December 24 yielded the following values: δD values varies from −203.6 to −189.4 ‰, $\delta^{18}O$ values varies from −27.22 to −25.93 ‰, and the deuterium excess from 14.2 to 18.0 ‰. Previously, $\delta^{18}O$ values were determined for ice wedges in recent sediments from Amderma (−15.2 ‰). It is evident that the oxygen-isotope ratio in ice wedges of the Vorkuta peat bog does not differ much from that of the Recent and Holocene varieties (usually 0.5–1 ‰ lighter than their Amderma counterparts). Judging from the isotopic composition of ice wedge, which is mainly characterized by its proximity to present-day isotope characteristics of Holocene ice wedges in this region, we can infer that winter conditions in the first half of the Holocene Optimum were similar in severity to current conditions (in any case, the Holocene winter was not warmer than the current one).

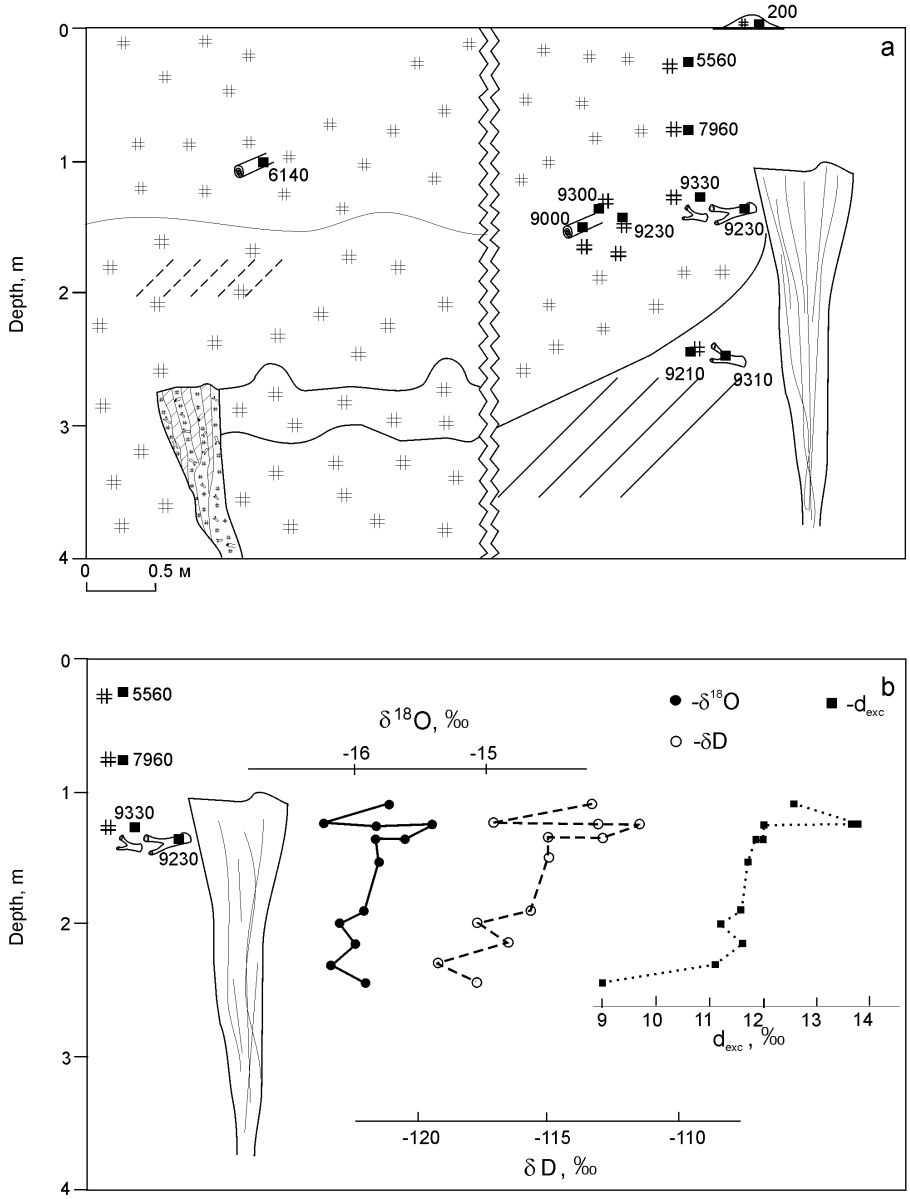

Figure 1: Radiocarbon dating (a) and b – hydrogen and oxygen isotope ratios and deuterium excess curve in ice wedges near Vorkuta town

Assessing permafrost formation age by radium isotopes

Yishai Weinstein[1], Dotan Rotem[1], Hanne H. Christiansen[2], Joseph Yechieli[3], Yael Niro[4], & Henk Kooi[5]

[1] *Bar-Ilan University, Israel*
[2] *University Centre of Svalbard (UNIS)*
[3] *Geological Survey of Israel*
[4] *Lamont-Doherty Earth Observatory, Columbia University*
[3] *Deltares*

While the methodology for soil age determination is well established (e.g. OSL), the age of permafrost formation (freezing) is often not so well defined, and it is mainly assessed based on the type of permafrost, the geomorphological development of the investigated landform and the age of the sediment. In this paper, we show that radium isotopes could be used for the determination of permafrost formation age, as well as for the geochemical characterization of the permafrost ice, which can then be used to trace the extent of active and the transient layers and the possibility of permafrost thawing.

Permafrost samples were collected from shallow cores (down to 3 m) in two lowland permafrost landforms at the Adventdalen valley, central Svalbard. In the first site, which is on a large fan with ice-wedge polygons, the top few meters of the sediment consist of relatively fine-grained loess. The second site is a loess-covered fluvial terrace, albeit the top loess is more sandy. In the ice-wedge polygons, the active layer is relatively thin (60 – 70 cm), while in the fluvial terrace site the active layer is around 1 m. Drilling was done in the late summers of 2014 and 2015, so active layer water was limited. Samples were thawed in small pieces, and water was immediately separated (centrifuged) from solids in order to minimize adsorption of the radium onto solids. Radium isotope analyses require relatively large volume of water (typically, 500 – 1000 ml), therefore depth intervals were relatively large (20 – 40 cm), and we had to combine similar depth intervals from several cores in the same landform (all, within 1 m from each other).

Radium has four naturally occurring isotopes, all radioactive, which span half lives between days (3.66 and 11.4 days for ^{224}Ra and ^{223}Ra, respectively) and 1,600 years (^{226}Ra). All isotopes are produced by alpha decay of thorium isotopes. While the short-lived isotopes get very fast to a steady state, the long-lived isotope (226Ra) will attain steady state only after 8,000 – 10,000 years. This allows the tracing of processes on the time range of hundreds to thousands of years.

The hypothesis of the current research is that the activity (concentration) of ^{226}Ra should buildup in the frozen pore space until recoil from the permafrost solids is balanced by its radioactive decay. We used ^{226}Ra/^{224}Ra and ^{226}Ra/^{223}Ra ratios in order to account for radium adsorption that might occur during permafrost thawing.

Preliminary results show that ^{226}Ra/^{224}Ra ratios in the permafrost were significantly higher than in the active layer water (Fig. 1), which supports the abovementioned hypothesis. In shallow (2 – 3 m) permafrost profiles, ^{226}Ra/^{224}Ra and ^{226}Ra/^{223}Ra ratios were higher at the topmost permafrost than 1 – 2 m deeper (Fig. 1). This suggests that the deeper permafrost is somewhat younger than the shallower one, which is not in accordance with the common interpretation of aggrading permafrost, and should be further studied. The high permafrost 'signal' (namely: high isotope ratios) at the topmost permafrost may also negate significant permafrost thawing.

Preliminary formation ages were calculated, based on the ^{226}Ra/^{223}Ra ratios in permafrost and the active layer, and assuming parent nuclide activity ratios of 21.7 (the ^{238}U/ ^{235}U ratio). The ages derived for the sampled profiles were between 500 – 3,000 years, in agreement with OSL ages of the sediments. Parent nuclide actual concentrations are still needed in order to further constrain the permafrost formation ages.

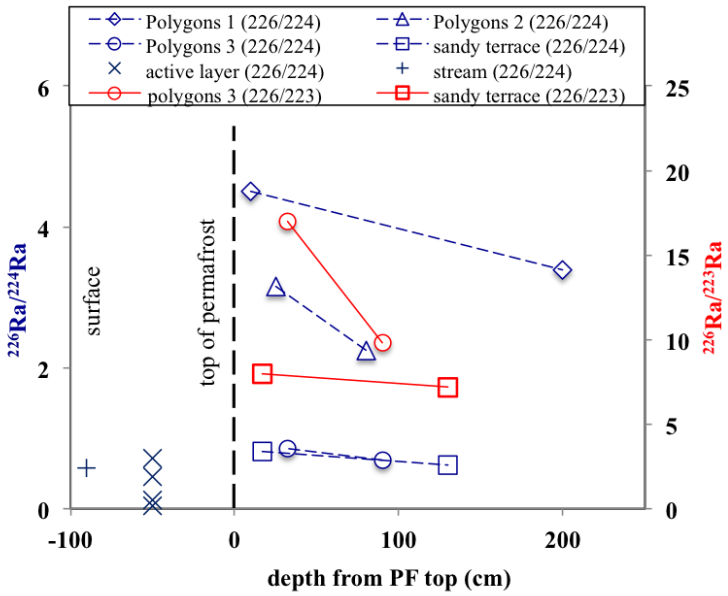

Figure 1: Ratios of long-lived to short-lived radium isotopes in permafrost and active layer water in two landforms at the Adventdalen valley and in a local stream. Note that active layer thickness actually ranges between 60 – 100 cm.

SESSION 4

Arctic and Antarctic Cryosols: Frontier of Global Change and Human Action

Convener:

Megan Balks, *Earth and Ocean Sciences University of Waikato, New Zealand*

Alexey Lupachev, *Institute of Physicochemical and Biological Problems of Soil Sciences, Russia*

Sebastian Zubrzycki, *Institute of Soil Science/Center for Earth System Research and Sustainability, Germany*

Polar regions of planet Earth are now becoming the focus of interest for humankind because of their great economic potential and indispensable role in sustainable functioning of the entire biosphere. Vulnerable ecosystems of high latitudes, fragile and complex cover of permafrost-affected soils and perennially frozen deposits themselves face the growing global pressure and become subjected to strong local human impacts. Arctic and Antarctic Cryosols may serve as sensitive indicators of changes in the thermal state of permafrost. Profound knowledge of Cryosols as a buffer zone of the human-environment interaction in terrestrial ecosystems is a must for the responsible management of natural resources in polar regions. Cryosols accumulate human footprints (contaminants, organic carbon, greenhouse gases etc.) even in the remotest areas far beyond the zones of current industrial activity and can contribute to their long-term cryoconservation. At the same time, Cryosols and upper permafrost layers being subjected to enhanced thawing can release ancient biogenic elements, greenhouse gases, and even viable biota into the modern ecosystems. Sustainable ecological functioning of the soil cover in such areas should be ensured to protect high-latitude ecosystems from irreversible degradation. It is important to find the keys for interpreting Cryosol records of the environmental evolution and predict its further development. The ecological functions of Cryosols allow high-latitude ecosystems to be both the source and sink of the organic carbon and greenhouse gases. The environmental role of cryogenic processes in permafrost-affected soils (in terms of matter and energy exchange with the environment) has to be studied more thoroughly.

Variability of organic contaminants in the snowpack and soils near Arctic coal mining sites in Svalbard

Anna Sergeevna Abramova[1,2,3], Sergey Stanislavovich Chernyanskii[2], & Nataliya Adolphovna Marchenko[3]

[1] *The George Washington University, USA*
[2] *Lomonosov Moscow State University, Moscow, Russia*
[3] *The University Centre in Svalbard*

Both residents and researchers of Svalbard, the one of world's most pristine areas, have expressed increasing concern about airborne contaminants originating from local and remote sources. Snow and soils in and around Longyearbyen and Barentsburg settlements was investigated in 2013 – 2015 for its particulates and associated highly-toxic trace elements and polycyclic aromatic hydrocarbons (PAHs). More than 54 sampling sites were positioned as transects across the most typical landforms of the studied areas with some of stations being associated with local sources of contamination (coal mining and transportation facilities, coal-fired power plant, etc.) and the others being used as reference.

By the end of snow season, the total supply of dust in snow cover varied from 0.001 g/m^2 at remote reference positions to 10 – 15 g/m^2 near operating mines and other coal-related facilities.

PAHs were identified in all of the dust samples. Levels and associations of individual hydrocarbons reflect contribution of local factors – coal dust and fuel combustion – and, to a much lesser extent, the effects of long-range transboundary air pollution.

Amongst the 16 individual PAHs, naphthalenes and phenanthrenes which are known to be typical microcomponents of the Svalbard's bituminous coals were found at the highest levels in snow particulates with their contribution varying from 60 to 90 %. Percentage of the other naturally occurring hydrocarbons like chrysene, fluoranthene, pyrene and benz(a)anthracene equals to 2 – 5 % for each compound.

The most harmful of technogenic PAHs, benzo(a)pyrene (BaP), was also detected in a majority of samples with minimum and maximum levels being 7 ng/g and 656 ng/g, respectively.

Fuel storages and other industrial and transport facilities stand out from the rest sites owing to high levels of BaP and associated PAHs as well.

Obtained results do not prove significant influence of remote sources on PAH distribution in Svalbard. Naphtalenes and phenanthrenes form a major part of PAH associations of both airborne particulates and local coal dust whose contribution in PAH level is apparently dominating. Another PAH association related to BaP and other fuel combustion products demonstrate a somewhat different distribution linked mostly to the local sources of emissions. At the same time, several locations have been revealed within the elevated remote areas of Svalbard where the snow cover showed the lowest PAH concentrations that can be further used as reference data for local environmental monitoring.

Active soil-landscape processes in the Ross Sea Region, Antarctica: two case studies

Megan Ruby Balks & Tanya Ann O'Neill

University of Waikato, New Zealand

Cryosols in the Ross Sea Region of Antarctica generally comprise a surface desert pavement and a seasonally thawed active layer over permafrost. The active layer ranges in depth from minimal in higher altitude, colder sites, to near 1 m deep at warmer coastal sites in the northern part of the region. Underlying permafrost may be ice-cemented, or dry with no ice cement. In some areas ice-cored moraine occurs where there is a large body of ice within the subsoil permafrost. The objectives of this paper are to describe two events where active landscape processes have occurred in the last decade as a result of interaction between surface events and the underlying permafrost and to discuss occurrence of such events and the possible response of permafrost-influenced landscapes to future physical environmental changes, both natural and human-induced.

We have observed two active fan-building events, one at Cape Evans in early January 2009, and one in the Wright Valley north wall near the eastern end of Lake Vanda which we observed at the end of December 2009 (Fig. 1). It was evident that the Cape Evans event had occurred in the weeks immediately prior to our visit and the Wright Valley event had most likely occurred in the summer prior to our visit (2008/09), possibly about the same time as the Cape Evans event.

The Cape Evans event serves as an example of the process that may occur. A small lake, one of several situated on a hummocky ice-cored moraine (at 77° 38' 16.2"S, 166° 26' 38.4"E) was underlain by a patterned ground crack. The water in the lake thawed and conducted heat and moisture into the underlying soil until it came in contact with the ice in the underlying patterned ground ice-wedge. The contact between the lake water and the ice-wedge caused the ice-wedge to melt, allowing the water to move about 15 m along the subsurface within the patterned ground crack until it emerged at the ground surface on the outer edge of the moraine. The extent of the gully erosion (that formed a straight gully about 40 m long and about 1 m deep), and deposition of material at the foot of the slope, suggests that this was a rapid event with all the water draining from the lake over a short time period once it broke through the moraine. The water from the drained lake would have also been added to by melt-water from the ice that it cut through. Once the ground-ice was exposed at the surface it continued to melt and ablate with the soil material from the sides of the gully slumping in. Gradually an insulating layer of soil material would be expected to accumulate on the surface, insulating the underlying ice from further melt-out and leaving only a gravel-covered gully visible. It is evident in more recent photos on Google Earth that the gully captures blowing snow. Periodic snow-melt and water erosion could be expected to continue the gradual process of melting of underlying ice and enlargement of the gully.

There are many fans visible on the walls of the Wright Valley, and it is often assumed that they are stable relict features. However in December 2009 we observed clear evidence for a fan-building event that we consider most likely occurred in the 2008/09 summer (Fig. 1). The material was deposited across a former trial site that was established in 1993/94 summer. The fan-building event had not occurred when the site was revisited in the 2000/01 summer. The transported materials were dried and stabilised so had not been deposited immediately prior to our visit. However they appeared 'fresh' with no evidence of wind erosion, thus our conclusion that they were most likely deposited in the previous summer. In contrast to the Cape Evans event the Wright Valley fan was a much larger scale, on a site that had evidence of numerous similar previous events. The feature was divided into seven zones covering a total horizontal distance of about 3 km and an altitudinal range of about 1400 m. The moisture source was the snow accumulation zone above about 1100 m altitude (Fig. 1). The snowmelt event must have led to a reasonably concentrated water flow but it was likely to have been sustained for a longer period than that observed at Cape Evans as there was a much larger potential

source area and the distributary channels in the lower part of the fan suggest stream flow that may have been sustained for hours or days. The flow was initially concentrated in a narrow gully which is snow-filled in the photos in figure 1, but is not perennial snow as evidenced in some photos on Google Earth. The flow changed from an erosive to depositional event as the slope dropped below about 13° and the number of distributary channels would have led to less intense flow in any one channel. The evidence of deposited material declined as the slope dropped below about 6°.

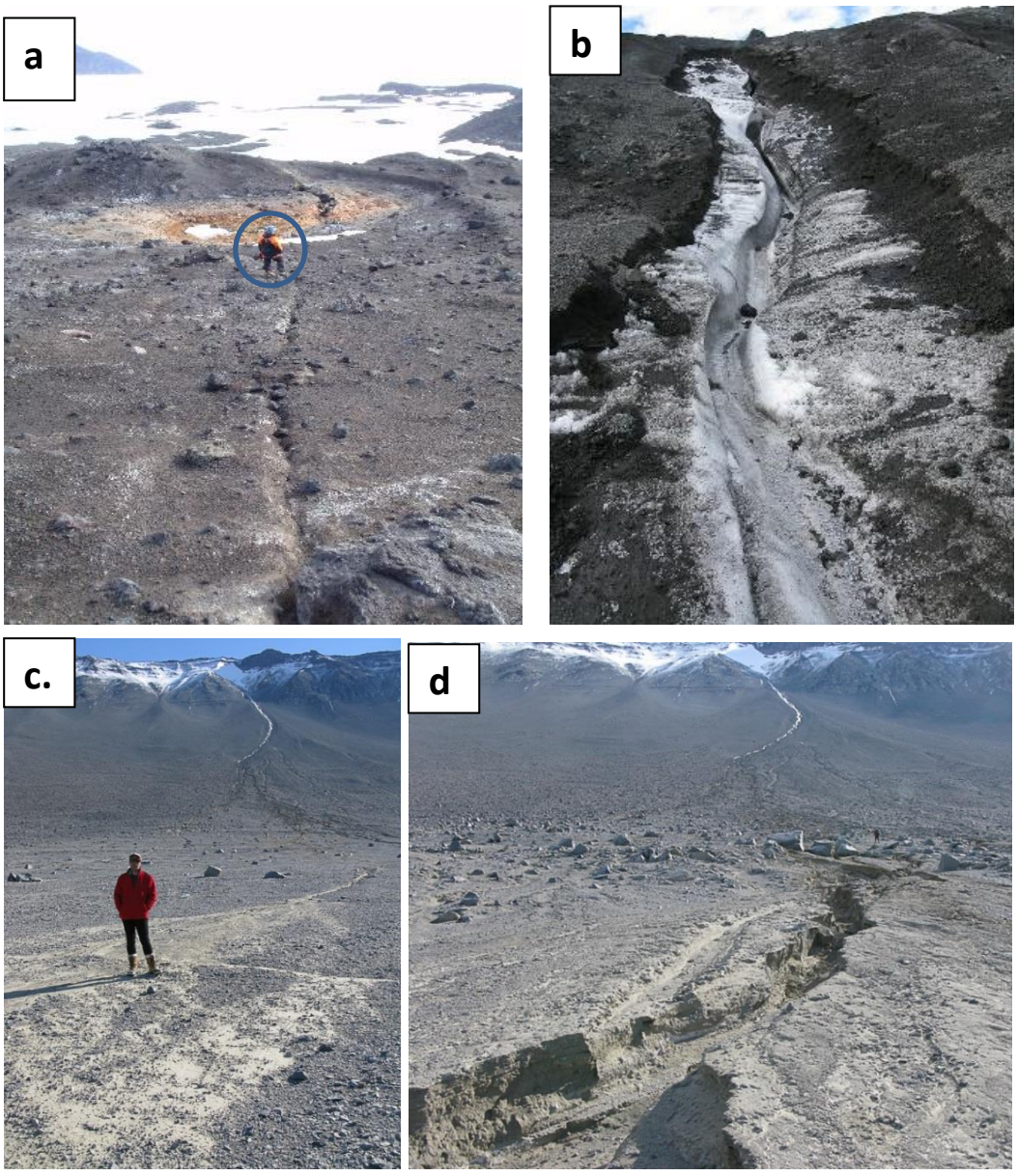

Figure 1: Active gully/fan forming events in the Ross Sea Region of Antarctica at Cape Evans, January 2009 (a & b), and on the north wall of Wright Valley, in December 2009 (c & d).

The two examples of erosion events shown here illustrate occasional events that occur within the Ross Sea Region. Evidence of previous gully-erosion and deposition on valley walls show that these are not unique events. Such occasional events, attributed to warmer than average summers, were described by Chinn [1979]. A warm summer with air temperature of 15 °C recorded at Lake Vanda in January 1974 resulted in extensive melting and water flow in the MDVs [Chinn, 1979]. A number of small lakes formed

in formerly dry depressions, one of which Chinn [1979] estimated would take 25 years to evaporate. Chinn [1979] also reports an exceptionally high snowfall event in 1977, which led to minimal flow in the Onyx River for two seasons, and variations of an order of magnitude in the flow of the Onyx River between seasons in the early 1970s. As Chinn [1979] observed, rare 'extreme' events in the MDVs can have lasting impacts on the landscape. The 2000/01 summer was notably warmer than average in the MDVs [Barrett et al., 2008] resulting in deeper than average penetration of the active layer at sites across the region and high meltwater flows with flooding and streambank erosion on the Onyx River and other streams. The pulse of meltwater impacted ecosystems in the Taylor Valley for several years afterwards [Barrett et al., 2008].

Fountain et al. [2014] describe increased occurrence of stream erosion and stream incision associated with erosion of surface soil material, and subsequent melting of underlying massive ice, over the previous decade in the Lower Wright, Taylor and Garwood Valleys which they found correlated with higher incoming solar radiation though no change in summer air temperatures.

Should there be an increase in temperatures and warming events in future the impacts will be most strongly evident in areas where there is ice-cored moraine, such as that illustrated here at Cape Evans. Once the insulating overlying soil material is removed then the melt-out of the underlying ice will continue until a new equilibrium is arrived at, either with a deeper overlying insulating layer of mineral material formed, or until erosion and melting reach the base of the ice body.

References

Barrett, J.E.; Virginia, R.A.; Wall, D.H.; Doran, P.T.; Fountain, A.G.; Welch, K.A. and Lyons, W.B. [2008]: Persistent effects of a discrete climate event on a polar desert ecosystem. *Global Change Biology*, 14:1–13, doi:10.1111/j.1365-2486.2008.01641.x.

Chinn, T.J.H. [1979]: Impacts of 'extreme' events on the Dry Valleys area. *New Zealand Antarctic Record*, 2(2):9–13.

Fountain, A.G.; Levy, J.S.; Gooseff, M.N. and Van Horn, D. [2014]: The McMurdo Dry Valleys: A landscape on the threshold of change. *Geomorphology*, 225:25–35, doi:10.1016/j.geomorph.2014.03.044.

Warming enhance permafrost cryoturbation and deeper soil carbon store

Ruiying Chang & Genxu Wang

Institute of Mountain Hazards and Environment, CAS, People's Republic of China

Permafrost soils in high altitudinal and latitudinal ecosystems store high soil organic carbon (SOC) stocks, especially in the subsurface layers inducing by cryoturbation. Also, the SOC in permafrost is generally suggested to be vulnerability to warming. However, the effect of warming on the cryoturbation in these soils and consequently the effects on the SOC is limited studied and unclear. The soils of a 8-year warming experiment with open-top chambers (OTCs, annual average air temperature increase by 3.6 °C) at Tibetan alpine meadow (4630 m asl) were samples and analyzed. In the control plots, the ^{137}Cs of the soils was general found to concentrate at top 5 cm layer and to decrease exponentially along the profiles and there was few ^{137}Cs in the 10 – 20 cm layer. In contrast, at warming plots, the ^{137}Cs concentration was found to be higher at 5 – 10 cm layer than top 5 cm and ^{137}Cs was detected in the 10 – 20 cm layer. These results indicated that warming may enhance the soil migrating from top layer to deeper layer due to a stronger cryoturbation. As a support, compared to the control, the SOC concentration under warming was found decrease in the upper layers (10 – 40 cm) but increase in the deeper layers (80 – 140 cm), and there was no difference in SOC stocks between warming and control. More interesting, the δ^{15}N of soil samples was significantly lower under warming compared to control in 0.25 – 2 mm, 0.053 – 0.25 mm and <0.053 mm fractions, respectively, but not in 2-8 mm fraction. Lower δ^{15}N under warming indicated a lower soil N loss from nitrification and denitrification and/or higher N input into soils. As an evidence, soil total nitrogen concentration was found significant higher under warming in the 0.25 – 2 mm, 0.053 – 0.25 mm, < 0.053 mm fractions and bulk soils, respectively. This result suggest that warming may increase N gain derived from enhanced N fixed other than C loss in this permafrost soils.

Mesoscale vegetation shift as a consequence of permafrost thawing in northern Siberia

Alevtina Evgrafova[1,2], Ina Haase[3], Alexander Otto[2], Ulli Bange[2], Nikita Tananaev[4], Olga Shibistova[3,5], Georg Guggenberger[3,5], Leopold Sauheitl[3], & Sandra Spielvogel[1]

[1] *Institute of Geography, University of Bern, Bern, Switzerland*
[2] *Geography Department, University of Koblenz-Landau, Koblenz, Germany*
[3] *Institute of Soil Science, Leibniz University of Hannover, Hannover, Germany*
[4] *Institute of Soil Science, Leibniz University of Hannover, Hannover, Germany*
[5] *VN Sukachev Institute of Forest, SB RAS, Krasnoyarsk, Russian Federation*

High-latitude soils have an important role in sequestering carbon to mitigate climate change. Nevertheless, permafrost thaw influences soil organic carbon (SOC) stocks, decomposition rates and nutrient availability by increasing soil temperature and, hence, microbial activity. An increased availability of macronutrients, such as nitrogen (N) and phosphorus (P), may leads to a possible shift in vegetation communities in high-latitude regions.

This study aimed to investigate the influence of changes in spatial distribution and variability of SOC, N and P stocks on vegetation communities due to permafrost thaw. Soil moisture, thickness of organic and active layers, and pH measurements were used to define their influence on the above-mentioned distributions at studied sites with discontinuous permafrost.

We studied six sites characterized by various active layers depths and located within the forest-tundra ecotone, precisely within the Little Grawijka Creek catchment (67°28.933' N, 86°25.682' E), Krasnoyarsk Krai, Russian Federation. Detailed vegetation descriptions, including species composition, were collected for each site. To obtain a high spatial resolution, we collected 122 spatially referenced soil samples per site; within a 4 m by 4 m grid with a 1 m mesh size from the depth increments 0 – 10 cm and 10 – 30 cm (Fig. 1). Also, the nested samples were obtained with a distance range of 0.2 to 0.7 m from previously mentioned grid samples in order to improve the performance of geostatistical models.

Furthermore, we determined the thickness of the active and organic layers for every 722 sampling points, as well as the soil moisture and pH. The SOC and total N concentrations were measured using a dry combustion method on a Vario EL cube (CHN mode) analyzer. Four P fractions, precisely $NaHCO_3$-P, NaOH-P, HCl-P and H_2SO_4-P fractions, were measured using the sequential P fractionation method according to Hedley et al. (1982) and modified by Kuo (1996), on a continuous-flow analyzer. The geostatistical approaches applied in R program were used to calculate the spatial distribution and variability of OC and N stocks, as well as of soil organic and inorganic P fractions.

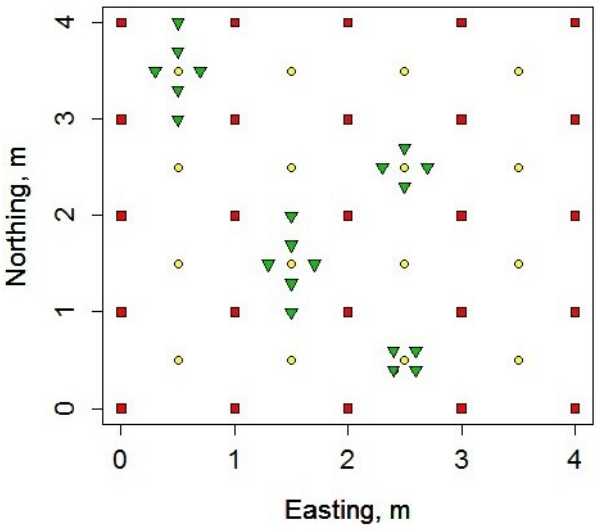

Figure 1: Sampling design, showing main (red), centered (yellow) and nested (green) sample locations.

We found that SOC and N stocks decreased with an increase in active layer depth and acidity, whereas P stocks increased with permafrost thaw. Soil moisture has a positive correlation with SOC and N stocks, $NaHCO_3$-P and NaOH-P fractions. The total P concentrations were lower in soils with a deeper active layer than with a shallow active layer. However, the amount of inorganic plant-available P was, in contrast, significantly higher in the former as compared to the latter. Therefore, permafrost thaw influences available P for plant uptake by releasing previously

bounded P.

Although permafrost thawing led to a decrease in the spatial variability of SOC, N and P stocks at the mesoscale, an abundance of site-specific vascular species at sites with a deeper active layer has increased, as was also confirmed by the vegetation analysis, due to an increased availability of macronutrients. However, the species diversity decreased at sites with a deeper active layer due to more homogenous distribution of macronutrients. To conclude, the changes in vegetation communities in high-latitude areas can be used as an indicator of permafrost degradation. In additional, the vegetation analysis in combination with a research on the total C ecosystem storage is a key approach to estimate C losses due to permafrost degradation and C sequestration potential in the northern regions in order to improve the climate models.

Initial soil formation and soil carbon accumulation on King Georges Island (maritime Antarctica)

Peter Kühn[1], Diogo Noses Spinola[1], & Carlos Ernesto C.G. Schaefer[2]

[1] *Universität Tübingen, Germany*
[2] *Universidade Federal de Viçosa (UFV), Brazil*

Many outlet glaciers showed a distinct retreat of the glacier front on King Georges Island (maritime Antarctica) during the last 40 years. Thus the margin of the Ecology Glacier is more than 500 m more inward than it was during the late 1970s. This gave us the opportunity to investigate juvenile soils on areas, which are subject to soil forming processes under periglacial climate conditions. We sampled three profiles (A, B, C) from well drained crest positions with slightly different leeside/windward positions in the present forefield of the Ecology Glacier and one soil profile (D) beyond the lateral moraine from around 1850 (Fig. 1).

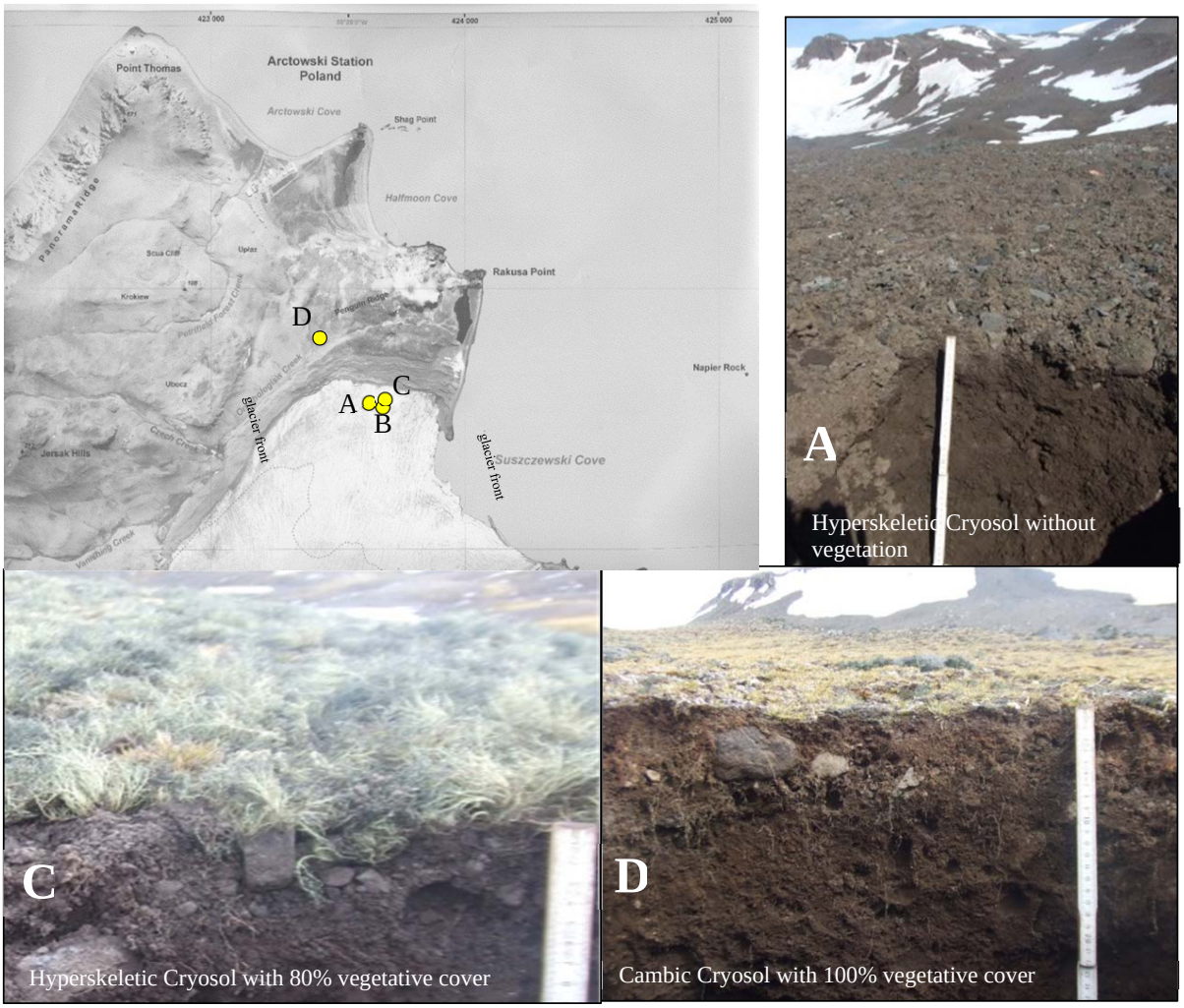

Figure 1: Different vegetation covers of three Cryosols in the forefield of the Ecology glacier on King Georges Island. Pedons B, C and D are in leeside position, Pedon A is exposed windward to the glacier. The area is deglaciated after 1979. Orthophotomap from Department of Antarctic Biology, Polish Academy of Sciences

Pedons A and B, classified as Hyperskeletic Cryosols, have a vegetative cover of 0 – 5 % and no significant accumulation of soil organic matter (Corg < 0.05 mass-%) from 0 – 1 cm depth. Pedon C with almost 80 % of the surface covered by vegetation (predominantly Usnea antarctica, Deschampsia antarctica, Colobanthus quitensis, Ochrolechia frigida) has significantly higher N and C contents with N = 0.09 and Corg 1.24 mass-% and lower soil pH[$CaCl_2$] of 5.4 within the first centimeter compared to A and B with 6.6 and 6.8. Whereas C and N contents correspond to the higher coverage by vegetation, the distinctly lower pH in pedon C may be predominantly caused by organic matter decomposition and microbial activity and additionally by percolating water. Pedon D, classified as a Cambic Cryosol has a vegetative cover of 100 % and is situated in a leeside position and has distinct accumulation of soil organic matter with 3.22 mass-% Corg from 0 – 3 cm (soil pH[$CaCl_2$] of 4.8) and 0.24 mass-% Corg from 3 – 15 cm with a soil pH[$CaCl_2$] of 5.0.

During the first four decades particularly microtopographic differences influence vegetation coverage even over short distances (meters) on juvenile substrates and thus are the main factor controlling the intensity of initial pedogenic processes. Time – as a soil forming factor – becomes more important after > 40 years and plays an increasing role after around 160 years (Pedon D) on recently deglaciated areas in maritime Antarctica.

Content of heavy metals in Arctic permafrost-affected soils of the Russian European Northeast

Elena Lapteva, Dmitry Kaverin, Alexander Pastukhov, Elena Shamrikova, & Yurii Kholopov

Institute of Biology Komi SC UrD RAS, Russian Federation

Exploration and development of raw hydrocarbon deposits sharply have increased technogenic load on the natural environment of Polar regions. In this sense, the Bolshezemelskaya tundra area (BZa) is of a special interest within the Arctic region of the European North. The area has numerous raw hydrocarbon deposits. Volumes of oil and gas extraction are forecasted to rise in the nearest decade. Accident oil spills contaminate above-ground tundra ecosystems both with organic pollutants (oil carbohydrates, polycyclic aromatic carbohydrates, organochlorids, and phenols) and heavy metals because heavy metals composite tarry asphaltene oil substances. Oil heavy metals include both non-toxic (Si, Fe, Al, Mn, Ca, Mg, P) and highly toxic (V, Ni, Co, Pb, Cu, U, As, Hg, Mo, etc.) elements. Natural oil carbohydrates of BZa deposits contain large amounts of vanadium, nickel, and iron. Heavy metals in accident oil spills possibly insert a negative effect on soil biota, vegetation cover, and migratory routes of heavy metals in BZa landscapes. But soil cover of BZa is largely understudied or studied very fragmentarily. Apart from BZa south part, soils of its north part are described very fragmentarily and have practically not been studied for heavy metals distribution.

The purpose of the present work was survey of heavy metals accumulation and profile distribution of permafrost affected soils of the Bolshezemelskaya tundra.

The studies were conducted on the territory of the Nenets Autonomous District (north tundra subzone) and the Komi Republic (south tundra subzone) with continuous permafrost. Permafrost-affected soils were assessed for background content of heavy metals (Cu, Pb, Cd, Zn, Ni, Co, V, Mn, Cr, Fe, Sr, Ba, Mo) and arsenic (As). Variation and profile distribution limits for elements in Podburs, Podsols, Cryosols, Histic Cryosols, Histosols and Fluvisols were identified. Content of principle pollutants (Hg, Pb, Cu, Ni, and Zn) in BZa soils was significantly less than the Russian norms on their approximate permissible concentrations. Single cases of high As, Co, Mn, and Cd content were related to specific composition of soil-forming rocks, as well as specific accumulation and migration of elements in cryolithozone. Generally, the majority of heavy metals corresponded to a low or mean regional soil concentration level. The specificity of BZa north tundra soils was a very low content of molybdenum.

South shrub tundra and north hypo-Arctic tundra soils were compared. Organic horizons of the soils contained different concentrations of heavy metals (Zn, Pb, Ni, Cu, Cd, Hg) and arsenic (As). From south to north tundra automorphic soils on watersheds (podburs, podzols), content of As, Zn, Ni, Pb, Cu increases. Soils in depressions and alluvial soils on river valleys, vice versa, tend to decrease in content of elements. Zinc was an exception. Its content in floodplain north tundra soils was higher than that in same south tundra soils. Cadmium content was higher by 2 – 3 times in every north tundra soil type than that in south tundra soil.

The obtained data are of an applied importance and can be used for the benefit of ecological monitoring in exploration and development areas of raw hydrocarbon deposits and for anthropogenic impact assessment on natural components of the Bolshezemelskaya tundra.

Acknowledgements

The work was partly financially supported by the Project of the Presidium of the Russian Academy of Sciences №15-15-4-46 'Interdependence of biodiversity and bioproduction potential of European Arctic aboveground ecosystems on formation of permafrost-affected soils and dynamic aspects of their transformation in modern climate'.

The preliminary analysis of soil cover spatial structure of Fildes Peninsula, King-George Island (West Antarctica)

Alexey Lupachev[1] & Evgeny Abakumov[2]

[1] *Institute of Physico-Chemical and Biological Problems in Soil Science, RAS, Russian Federation*
[2] *Applied Ecology Dept., Faculty of Biology, St-Petersburg State University, Russian Federation*

Fildes Peninsula is the second largest ice-free area of the South Shetland Islands and the largest on King George Island. Mosses, lichens, and algae are common here, along with two vascular plants (*Deschampsia antarctica* and *Colobanthus quitensis*). Penguins, seals, and seabirds are common in coastal areas and have significant effects on soil development. Major cryogenic surface-forming processes here are frost creep, cryoturbation, frost heaving and sorting, gravity and gelifluction [The Soils of Antarctica, 2014].

83 soil profiles of 6 soil groups [WRB, 2006] were studied during surveying the ice-free area of Fildes Peninsula. About two-thirds of described pedons belong to Leptosols (65.1 %): Hyperskeletic (27.7 %), Lithic and Nudilithic (22.9 % in total) and Histic (14.5 %) subgroups which is more or less coincide with the results of previous research [Bockheim et al., 2015]. Field survey of Antarctic Leptosols doesn't allow determining the certain presence of permafrost in solid rock, so authors intentionally did not use Gelic as suffix qualifier for these soils. About 14.5 % of soil pedons belong to Cryosols (with well-expressed features of cryoturbation and rock sorting and/or permafrost in the control section) of Hyperskeletic (7.2 %), Turbic (6.0 %) and Leptic (1.2 %) subgroups. These soils mainly occupy flat watersheds or gentle slopes with relatively thick cover of rock debris and water supply from snow patches. Fluvisols are locally expressed in the soil cover of the peninsula (about 7.5 %) and nearly equally presented by coastal (Tidalic) and inland (Gleyic and Histic) subgroups. Skeletic Regosols mainly occur in the zone of glacial retreat and moraine deposits (about 6.0 % of all pedons). A unique for Fildes Peninsula and locally expressed (few square meters) pedon of Fibric Histosol (Gelic) was also studied during the soil survey. Techosols (Leptic and Transportic) were presented with 6.0 % of pedons and occupy the surroundings of scientific stations. All of them are Skeletic and nearly half of them can be distinguished as Garbic and/or Toxic.

The initial processes of organic accumulation were identified in nearly half profiles of Leptosols (mainly of Hyperskeletic subgroup). Features of ornithogenic organic matter input were mainly observed in Leptosols of Lithic subgroup. Studied profiles of Cryosols here reveal both oxyaquic (on drained watersheds and slopes) and reductaquic features (in depressions or shallow slopes with poor drainage conditions). All of the Fluvisols and Regosols here have skeletic features. Some Technosols (in the oil-spill areas) can be distinguished as Toxic.

Acknowledgements

Study was partially supported by RFBR (15-04-06118a; 15-29-02629ofi_m; 16-04-01050a).

References

Bockheim, J.(ed.). [2014]: *The Soils of Antarctica.* 290 p. 201 illus., 144 illus. in color, ISBN 978-3-319-05496-4.

Bockheim, J.G.; Lupachev, A.V.; Blume, H.-P.; Bölter, M.; Simas, F.N.B. [2015]: and McLeod, M. Distribution of soil taxa in Antarctica: A preliminary analysis. *Geoderma*, 245–246, doi:10.1016/j.geoderma.2015.01.017.

WRB [2006]: *World Reference Base for Soil Resources.* 2^{nd} edition World Soil Resources Reports No. 103. FAO, Rome, 2006. 133 pp.

Formation of suprapermafrost accumulative organo-mineral horizons in Turbic Cryosols

Alexey Lupachev & Stanislav Gubin

Institute of Physico-Chemical and Biological Problems in Soil Science, RAS, Russian Federation

Suprapermafrost parts of about 40 % analyzed Turbic Cryosol profiles (n = 130) that form on watershed areas of Kolyma Lowland contain accumulative organo-mineral horizons with SOC content from 2,5 – 3,5 % up to 9 % (LOI = 8 – 10 % up to 30 %) which is comparable with uppermost horizons. Major conditions that determine the accumulation of coarse organic material over the permafrost border are the depth of the active layer, water/ice content of lowermost soil horizons, activeness of cryoturbation processes, permafrost table nanorelief. Two types of suprapermafrost accumulative organo-mineral horizons forming mechanisms now can be clearly distinguished in the profiles of Turbic Cryosols. First one is fully determined by downward cryoturbational movement of the fragments of surface organogenic and organo-mineral material and their accumulation in the over-permafrost part of the profile (cryoturbational accumulation of coarse organic material). Second one is determined by lateral redistribution of overmoistured histic material from the frost cracks to the lowermost parts of Cryosols over the surface of permafrost table during thawing (lateral accumulation of coarse organic material).

Beside these two described types of suprapermafrost accumulative organo-mineral soil horizons there are some other cases of significant accumulation of organic matter over the permafrost border. The abundant and polygenetical slope processes in permafrost zone (solifluction, creep, suffosion etc.) can also form different morphological types of buried organogenic horizons in Cryosols. After the transition of hydromorphic Histosols into the automorphous landscape positions the histic material of the upper and the middle parts of soil profile is mineralized much more intensively than the lowermost suprapermafrost parts, so the relict organic material can be preserved here.

More or less intensive effects of downward retinization of water-soluble organic substances can be obtained in the lowermost parts of Cryosols (from Lat. ‘retineo’ – to hold back). The field morphological characterization of such horizons enriched with organic matter is difficult because humus here is often colourless.

Acknowledgements

Study was supported by RFBR (15-04-03960a), RSF (14-14-01115).

Heat line in permafrost – a large experiment of transformation of the Arctic ecosystems

George Matyshak, Olga Goncharova, Anna Bobrik, Daria Sukhova, Natal'ja Petrzhik, & Roman Kireev

Lomonosov Moscow State University, Russian Federation

The last 50 years there is an active exploration of Russian permafrost zone, especially on north of West Siberia. The length of gas pipelines in Russia is more than 170 thousand kilometers. More than 10 % of them constructed on the territory of the permafrost zone. The most common method of gas pipelines construction in Russia is laying it on the soil surface or in a trench depth of 1.5 – 2 meters. The gas pipe is covered with mound up to 1.5 meters. An additional factor is the direct thermal influence of gas pipeline if 'warm' gas is transported. As a result there is a significant disturbance of the vegetation and soil cover and rapid permafrost degradation along the pipeline. Thus Kharionovsky VV in his observations showed that in the first years of Nadym-Punga gas pipeline operation permafrost thawed more than 6 meters in the palsa areas [Kharionovsky, 2000]. According to the literature, areas with transformed vegetation take at least 14 % (10 thous. km^2) of Taz Peninsula. These changes occurred during the period of Urengoy gas field development. One third of these areas relate to the construction facilities of gas pipelines [Kornienko et al., 2005]. Thus, the active transformation of ecosystems is observed over a large area in the Russian permafrost zone. The aim of this study is to evaluate the impact of the gas pipelines construction and operation on the frozen peatland ecosistems in northern taiga of West Siberia.

Field studies were carried out in August, 2013 and 2014, along the the Nadym-Punga gas pipeline, 40 km south-west from the Nadym city, Tyumen region, Yamal Nenets Autonomous District, Western Siberia, Russia (N 65°18'53.2" E 72°52' 52.1"). We investigated the properties of frozen peatland soils along the gas pipeline: the active layer thickness, soil moisture and temperature (soil surface and 20 cm), and the carbon dioxide effluxes. In the laboratory typical properties of soils, microbiological activity and the content of labile organic matter were measured.

Researches have been organized in the most typical areas of frozen peatlands using transect method. 100 m long transects with sampling points every 5 meters were made perpendicular to the pipeline (Fig. 1). Typical soils of study area are Turbic Cryosol, vegetation – dwarf-shrub and lichen community. The average depth of the permafrost is 60 cm. The pipeline was constructed through the frozen peatland by underground methods in 1977. The transported gas is 'warm' with temperature from 4 to 22 °C.

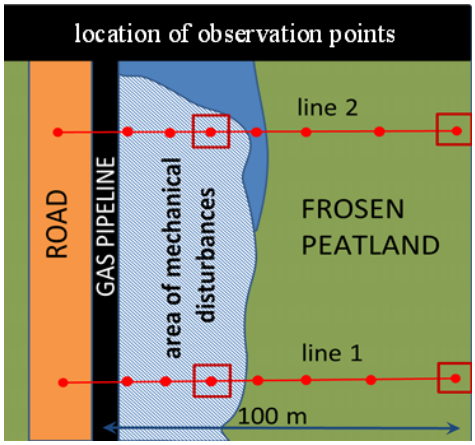

Figure 1: location of observation points

After 40 years of operation, the area along the pipeline is actively overgrowing with not specific vegetation communities for peatlands, there is an active expansion of tree species (birch, etc.). Significantly reduced cover of mosses and lichens and increasing proportion and size of vascular plants. Active layer thickness at distances up to 20 m from the pipeline is significantly increased (2 – 3 times) than on the control sites (40 m and more from pipeline). Soils near the pipeline are warmer. Average annual and daily mean temperatures at 20 cm depth near the pipeline are 2 – 3 times higher. These soils are unfrozen for 2 – 3 months longer. Summer temperatures of soils near the gas pipeline are higher by 5 – 10 °C. Soil moisture along the pipeline is reduced by 2 – 3 times. Change of hydrothermal regime is the cause of accelerating of soil transformation. In the peat soils the conditions for activation of microbiological activity are created. As a result, we are seeing changes in soil properties, a significant increase of the microbial

carbon and labile organic matter (WEOC, WEON). The CO_2 efflux of typical frozen peatlands are low (80 – 100 $mgCO_2$ m^{-2} h^{-1}) and indicating low biological activity of soils. But for soils near the pipeline we see an increase in CO_2 efflux in 3 – 6 times (500 – 600 $mgCO_2$ m^{-2} h^{-1}). Heightened values of CO_2 efflux are observed at distances up to 50 m from the pipeline. When flooding of the territory there is a significant increase in methane emission that exceeds the background value (for thermokarst depressions) in 5 – 10 times.

Thus, the pipeline is a kind of 'heater', providing year-round warming and drying effect on the surrounding ecosystem. The main result is permafrost degradation and changing ecosystem. The width of the pipeline influence up to 50 meters on each side. So – hundreds km^2 cryogenic landscapes along the gas pipeline system on Russian North are in the impact zone. Currently, it is a huge experiment whose results we are seeing in different natural zones. The long-term influence of the pipeline in the permafrost zone can be regarded as a model of warm effects on the ecosystem in the study of the climate change effects and the sustainability of Arctic ecosystems.

References

Kharionovsky, V.V. [2000]: *The reliability and service life of pipelines constructions*. Publishing House 'Nedra', Moscow. (in Russian).

Kornienko, S.G.; Jacobson, K.I. and Maslennikov, V.V. [2005]: A study of the transformations of natural complexes of oil and gas regions of the permafrost zone according to satellite imagery. *Science and Technology in the Gas Industry*, 3:71–77.

Pedodiversity and Carbon storage of permafrost-affected soils in the Lena River Delta

Eva-Maria Pfeiffer & Sebastian Zubrzycki

Universität Hamburg, Germany

Pedodiversity in Permafrost Regions means the variability of cryosols in different permafrost regions, as determined by its constitution, types, properties, functions and the conditions under which the different cryosols were formed in the cryosphere (completed after Ibáñez et al. [1998]).

With this accepted definition we choose for the given investigation the 'genetic pedodiversity' and 'taxonomic pedodiversity' as best ways for characterising of the soils forming in the Lena River Delta in North-East Siberia.

Using this approach we have defined the main soil types in the Lena River Delta. The soil complex of Glaci-Turbic Cryosols and Hapli-Histic Cryosols is dominating the Holocene river terrace of the delta whereas the Holocene active floodplain levels are dominated by sandy or gleyic Fluvi Gleyic Cryosols and Areni Fluvic Cryosols. The surfaces of the Arga-Muora-Sise Island are scarcely vegetated and dominated by cryoturbated and sand-rich soils with high moisture contents, e.g., various Areni-Turbic Cryosols and Aqui-Turbic Cryosols. The Pleistocene ice-complex plains consist of a soil complex of Glaci-Turbic Cryosols and Gleyi-Histic Cryosols. The widespread thermokarst depressions within the ice-complex are covered by Histi-Turbic Cryosols and Gleyi-Histic Cryosols, whereas the slopes are dominated by Aqui-Turbic Cryosols and Gleyi-Cryic Cryosols.

Using the information of properties of the investigated soils we have estimated the organic carbon stocks for the Holocene geomorphic units of the Lena River Delta to the depth of 100 cm. At the river terrace they were estimated at 29 $\pm$ 10 kg m^{-2} and on the floodplains at 14 $\pm$ 7 kg m^{-2}, respectively. For the depth of 100 cm, the total organic carbon storage of the Holocene river terrace (4,760 km^2) was estimated at 121 Tg $\pm$ 43 Tg, and the organic carbon storage of the active floodplains (8,830 km^2) was estimated at 120 Tg $\pm$ 66 Tg. About a half of these reported carbon storages is located in the perennially frozen ground below 50 cm soil depth and consequently excluded from intense biogeochemical exchange with the atmosphere today. However, these well conserved storages are likely to be mineralised in future due to the projected temperature increases in this region and thus, could be released to the atmosphere as a consequence of the climate change. To account for these changes and provide robust prognosis of the impact of climate change on cryosols we need proper and integrated field, lab and model analyses of relevant soil processes and their functions in permafrost-affected landscapes.

References

Ibáñez, J.J.; De-Alba, S.; Lobo, A. and Zucarello, V. [1998]: Pedodiversity and global soil patterns at coarser scales (with discussion). *Geoderma*, 83: 171–214, doi:10.1016/S0016-7061(97)00147-X.

Formation of microorganisms in tundra soils of the European North-East

Julia Vinogradova, Fluza Khabibullina, & Elena Lapteva

Institute of Biology Komi SC UrD RAS, Russian Federation

Soil formation in Polar regions proceeds in severe climatic conditions. This fact affects bacteria and microscopic fungi in soils of Arctic and sub-Arctic areas. Permafrost, low temperatures, excessive moisture content in seasonally-thawing soil layer during vegetation period, and poor plant waste respond for a low rate of biological and biochemical processes in tundra soils.

The purpose of the work was assessing composition of microbe complexes (bacteria and microscopic fungi) in tundra soils of the European North-East.

The studies were conducted on the territory of the Bolshezemelskaya Tundra area in the south tundra subzone (Komi Republic, Vorkuta region). The study materials were two soils, Histic Cryosol and tundra carbonate soil. Histic Cryosol forms in dwarf-shrub lichen-moss tundra on loams. Tundra carbonate soil forms on carbonate moraine outcrops in dwarf-shrub spotty tundra dominated by *Dryas octopetala*. Histic Cryosols, like tundra surface-gley soils, are very popular on watersheds in the southern part of the Bolshezemelskaya Tundra area. Tundra carbonate soils cover relatively small areas. By physical-chemical properties, tundra carbonate soils significantly differ from Histic Cryosols. Tundra carbonate soils have a neutral or basic reaction (pH = 6.8 – 8.1) and high content of exchangeable bases.

Microbiological analysis of tundra soils applied common methods. Soil samples were collected by horizons. Total amount of microorganisms was assessed by the luminescent microscopy method. One sample required 12 preparations. The preparations were colored with acridine orange solution (1:10000) for 2 – 3 minutes for identification of bacteria and *mycelium* of *actinomycetes* and with calcofluor white for 15 minutes for spores and *fungal mycelium*. Then, the preparations were analyzed using the Zeis microscope (Axiovert 200). Taxonomic attribution of micromycetes was identified after they were extracted as pure cultures. For that, we used manuals [Ramirez, 1982, Satton et al., 2001] and interactive 'keys' of Internet information site (http://www.indexfungarum.org).

Finally, microscopic fungi extracted from tundra non-carbonate and carbonate soils were divided into taxonomic groups. Microscopic fungi in Histic Cryosol belonged to only 10 and those in carbonate soils – to 9 species. Histic Cryosols was dominated by representatives of the *Penicillium genus*. Tundra carbonate soil included micromycetes of the *Paecelomyces*, *Acremonium*, *Aurobasidium*, and *Geomyces genera*. Alkaline-like (pH = 6.8 – 8) reaction of tundra carbonate soils responded for a decreasing number and species diversity of acid-forming micromycetes of the *Penicillium genus* and appearance of actinomycetes.

Microscopic fungi normally inhabited organic soil horizons. In organic horizon of Histic Cryosol, mycelium length of microscopic fungi attained 63 – 106 m g^{-1} soil, number of fungal spores 2.3 – 4.4 mill g^{-1} soil, number of yeast-like cells 4.0 – 7.9 mill g^{-1} soil. In tundra carbonate soil, the values were 41 – 63 m g^{-1} soil, 10 – 12 mill g^{-1} soil, 1.9 – 2.0 mill g^{-1} soil, correspondingly. Mineral horizons of Histic Cryosol were identified only for fungal spores (0.4 – 2.0 mill g^{-1} soil) and yeast-like cells (0.7 – 3.4 mill g^{-1} soil). In tundra carbonate soil, fungal mycelium was identified for mineral profile part as well. Mycelium length in mineral part possibly reached 10 – 62 m g^{-1} soil depending on organic carbon content and plant residues being available due cryoturbation.

The discussed soils largely differed by total biomass value. In tundra carbonate soil, total biomass of microorganisms comprised 0.2 – 2.0 mg g^{-1} soil depending on horizon. In Histic Cryosol it was 0.6 – 7.0 mg g^{-1} soil. This difference was because Histic Cryosol, in contrast to tundra carbonate soil, had high values of mycelium length for microscopic fungi in organic horizon and high number of yeast-like cells. High amount of yeast-like cells in Histic Cryosol could allow for mycelium of microscopic fungi at 0 – 8 % of total microbe biomass, fungal spores at 0.4 – 0.9 %, and yeast-like cells at 90 – 93 %. In tundra carbonate soil, ratio of fungal mycelium was 8 – 47 % of total microbe biomass, of fungal spores 0.4 – 17 %, and yeast-like cells 88 %.

Total number of bacteria in the study soils was generally similar and made 0.4 – 0.9 milliard cells 1 g^{-1}

soil. But differences in mycelium length of microscopic fungi, number of fungal spores and yeast-like cells, ratio of prokaryotes in biomass structure varied in dependence on soil type. In organic horizon of Histic Cryosol, it was 0.5 – 0.7 %. In same horizon of tundra carbonate soil, it comprised 1.2 – 1.7 %.

Thus, the decreasing acidity in tundra carbonate soils towards neutral and alkaline (pH = 6.8 – 8) reaction responds for appearance of actinomycetes which decompose plant waste along with micromycetes and changes biomass structure of microbe communities through decreasing total mycelium length of microscopic fungi and number of yeast-like cells.

The work was partly financially supported by the Project of the Presidium of the Russian Academy of Sciences №15-15-4-46 'Interdependence of biodiversity and bioproduction potential of aboveground ecosystems of the European Arctic area on formation of permafrost-affected soils and dynamic aspects of their transformation in modern climate'.

References

Ramirez, C. [1982]: *Manual and atlas of the Penicillia.* Elsevier Biomedical Press; Amsterdam; New York; Oxford, 1982. 874 p.

Satton, D.; Fotergil, A. and Rinaldi, M. [2001]: *Manual for identification of pathogenic and potentially pathogenic fungi.* Mir Publicity: Moscow, 486 p. (in Russian).

Cryosols of the Lena River Delta and its hinterland – genesis and diversity

Sebastian Zubrzycki[1], Lars Kutzbach[1], Evgeny Abakumov[2], & Eva-Maria Pfeiffer[1]

[1] *Universität Hamburg, Institute of Soil Science, Germany*
[2] *Saint-Petersburg State University, Department of Applied Ecology, Russia*

The North-Siberian Lena River Delta (LRD) is the largest Arctic delta and an important interface between the Arctic Ocean in the North and the large Siberian land masses in the South. LRD consists not only of Holocene deltaic sediment deposits as a river terrace and the modern active floodplains but also of remnants of the former Pleistocene mainland including large islands of ice-complex sediments and the Arga-Muora-Sise Island, which is composed of pure sand sediments of still debated origin. The highly diverse landscape structure of LRD is reflected by a great variety of permafrost-affected soils (cryosols). This study aims at describing this great cryosol diversity and at analysing the dominant soil-forming processes in this comparatively scarcely studied soil region. The soil development in the investigated continuous permafrost region is limited by the short thawing period of around three months (June to September) and takes place in the shallow (below 1 m) seasonally thawed active layer. The geological parent material plays an important role for the development of soils in the LRD region. The distribution of the various soil types closely follows the pattern of the geomorphic units characterised by differing sedimentation conditions. The properties and genesis of the soils on the Holocene river terrace and the modern floodplains are strongly affected by the enormous amounts of fluvial sediments (about 12×10^6 tons per year) brought by the Lena River into its delta. The fluvial sedimentation together with the also pronounced aeolian sedimentation results in a fast vertical growth of soils. The upward rise of the soil surface leads to an upward movement of the permafrost table resulting in fast incorporation of soil material formed in the supra-permafrost zone into the permafrost. Due to the morphodynamics of ice-wedge polygons and resulting formation of patterned ground with elevated rims and depressed and water-saturated centres, the Holocene river terrace of the delta is in its main extent covered by a soil complex of Glaci-Turbic Cryosols and Hapli-Histic Cryosols. The active floodplain levels are dominated by sandy or gleyic Fluvi Gleyic Cryosols or Areni Fluvic Cryosols. The surfaces of the Arga-Muora-Sise Island are frequently reshaped by aeolian sedimentation and erosion. The soils on these scarcely vegetated landscapes are dominated by cryoturbated and sand-rich soils with high moisture contents, e.g., various Areni-Turbic Cryosols and Aqui-Turbic Cryosols. The modern soils covering the older Pleistocene ice-complex plains are influenced by wide ice-wedge net structures and consist of a soil complex of Glaci-Turbic Cryosols and Gleyi-Histic Cryosols. The widespread thermokarst depressions within the ice-complex are covered by Histi-Turbic Cryosols and Gleyi-Histic Cryosols, whereas the slopes are dominated by Aqui-Turbic Cryosols and Gleyi-Cryic Cryosols. For the largely unexplored hinterland of LRD it can be assumed that the active genesis of the soils lasts longer than in the active delta regions due to a much lower sedimentation and more stable surface conditions. In these regions widespread cryoturbated and peat-rich soils like Histi-Turbic Cryosols and Histic Cryosols. An increased understanding of spatial variability and genesis of permafrost-affected soils is essential for meaningful predictions of climate change consequences in Arctic permafrost regions.

SESSION 5

Climate Change and the Permafrost Carbon Feedback: Past, Present and Future

Convener:

Christian Knoblauch, *Institute of Soil Science, Center for Earth System Research and Sustainability, Germany*

Christina Schädel, *Northern Arizona University, USA*

Yury A. Dvornikov, *Earth Cryosphere Institute, Tyumen, Russia*

Permafrost regions store twice as much carbon in frozen soils as is contained in the atmosphere. A warming climate can induce environmental changes leading to permafrost degradation, active layer deepening and subsequent microbial decomposition of newly thawed organic matter, but can also stimulate plant growth and increase carbon storage in vegetation and surface soils. Release of just a fraction of these frozen carbon pools as carbon dioxide and methane into the atmosphere could increase the rate of future climate change because of the heat-trapping properties of these trace gases. While increased permafrost carbon emissions in a warming climate are more likely to be gradual and sustained we need a better understanding of the magnitude and timing of greenhouse gas emissions from these remote regions to fully estimate the potential feedback from permafrost carbon to climate change.

This session invites papers that contribute to the understanding of losses and gains of carbon in permafrost regions dealing with the modern carbon cycle, the reconstruction of past carbon dynamics and simulations of future greenhouse gas fluxes relating to the questions: what is the magnitude, timing and form of carbon release from permafrost zone ecosystems in a changing climate, which are the parameters regulating permafrost organic matter formation and degradation and how will increasing atmospheric temperature and CO_2 concentrations affect soil organic matter dynamics? Papers may address any aspect of this topic from microbial communities to the global scale, using a range of measurements including laboratory analyses, field observations, ecosystem manipulation experiments and process-oriented modeling. Contributions applying new methods or combining different approaches (experiments, observations, modelling) are particularly welcome.

The biggest terrestrial tipping point or a potential carbon sink? 124 experts weigh in on the permafrost carbon feedback

Benjamin W. Abbott[1,3], Edward A.G. Schuur[2], Jeremy B. Jones Jr.[3], F. Stuart Chapin III[3], & Permafrost Carbon Network[4]

[1] *Université de Rennes 1, OSUR, CNRS, ECOBIO, France*
[2] *Northern Arizona University, Center of Ecosystem Science and Society, Flagstaff, Arizona, USA*
[3] *Institute of Arctic Biology and Department of Biology & Wildlife, University of Alaska Fairbanks, Fairbanks, Alaska, USA*
[4] *www.permafrostcarbon.org*

Arctic tundra and boreal forest contain approximately half of all terrestrial organic carbon. As the permafrost region warms, more of this immense carbon pool will be exposed to decomposition, combustion, and hydrologic export. This permafrost carbon feedback has been described as the largest terrestrial feedback to climate change as well as one of the most likely to occur; however, it is not included in current emissions negotiations and estimates of its strength vary by a factor of thirty. Models predict that some portion of this release will be offset by increased Arctic and boreal biomass, but the lack of robust estimates of net carbon balance increases the risk of further overshooting international emissions targets with serious societal and environmental consequences. Because precise empirical or model-based assessments of the critical factors driving carbon balance are unlikely in the near future, we collected expert judgments from 124 permafrost-region scientists of the response of high-latitude carbon balance to four warming scenarios. Experts provided quantitative estimates of CO_2 and CH_4 release, change in biomass, wildfire CO_2 emissions, and hydrologic carbon flux by 2040, 2100, and 2300. Results suggest that, contrary to current model projections, total permafrost-region biomass could decrease due to water stress and disturbance. Assessments indicate that end-of-the-century organic carbon release from Arctic rivers and collapsing coastlines could increase by 75 % while carbon emissions from wildfire could increase four-fold. For the business as usual scenario (RCP8.5), experts hypothesized that the permafrost zone could emit 14 to 40 % of the carbon necessary to push the climate system beyond the 2C threshold by the end of the century (140 to 240 Gt CO_2 equivalent) with cumulative net emissions reaching 320 to 510 Gt by 2300. However, because lower warming scenarios resulted in less carbon release from soils and more carbon uptake by Arctic and boreal biomass, results suggest that 65 to 85% of permafrost carbon release can still be avoided if human emissions are rapidly reduced.

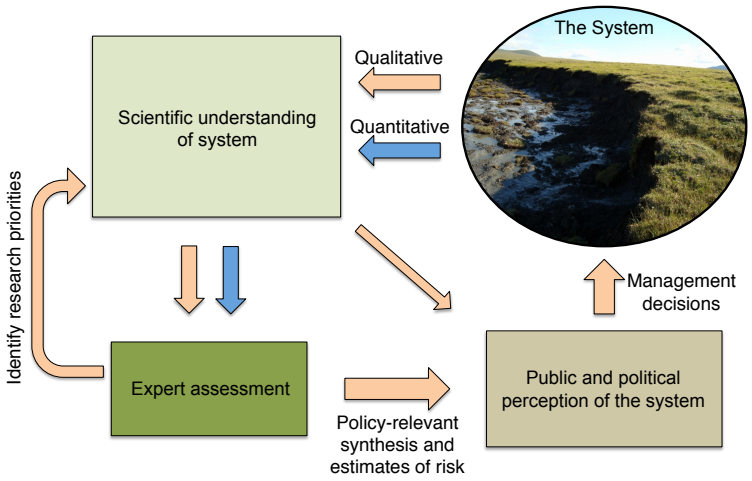

Figure 1: Conceptual model of expert assessment in generating and communicating scientific understanding

Thawing permafrost carbon decomposition under aerobic and anaerobic conditions

Christian Beer[1], Christian Knoblauch[2], & Eva-Maria Pfeiffer[2]

[1]*Department of Environmental Science and Analytical Chemistry, Bolin Centre for Climate Research, Stockholm University, Sweden*
[2]*Institute of Soil Science, University Hamburg, Germany*

Soil organic matter in permafrost deposits that has been frozen during many centuries may become subject to decomposition after thawing due to climate warming. Therefore, we need to increase our understanding about the potential decomposition rates of such material in order to inform global process-oriented models. To determine the rates of organic matter decomposition in thawing permafrost deposits, different permafrost cores have been taken at two locations in the Lena River Delta in Northeast Siberia representing organic matter from the Holocene and the late Pleistocene. Lab incubation experiments with permafrost samples of different ^{14}C age ($<$ 1ka to $>$ 30 ka) from both locations were conducted for more than 3 years. The data obtained from aerobic incubations have been used to calibrate a process-based two-pool organic matter decomposition model considering different periods of experiment time. The results show a large variation of initial aerobic mineralization rates which translates into a large standard deviation (1.6 years) of turnover time with a mean of 0.26 years of the so called 'fast pool'. However, turnover time standard deviation of the second more 'slow pool' is remarkable low (1.4) with a mean of 170 years. This second pool is dominating the long-term dynamics of soil organic matter in future and the small standard deviation rises confidence in using such long-term incubation studies to inform global models given that such results will be complemented by more locations around the Arctic region. Interestingly, uncertainty in turnover time estimation strongly increases when only using one or two years of incubation data for model calibration. This raises the question on what can be learned from short-term incubation experiments available at more locations. Based on the presented lab incubation experiments and process-based modeling, 15 ±5 % of permafrost organic matter that will be thawing until 2100 is projected to be lost as CO_2 into the atmosphere if mineralized under aerobic conditions. Anaerobic organic matter degradation was substantially slower than in the presence of oxygen. Due to complex interactions between several groups of microorganisms involved in anaerobic organic matter degradation, e.g. fermenters and methane producers, the formation of the trace gases CO_2 and methane did not follow the expected first order kinetic (Fig. 1). CO_2 formation was fastest at the beginning of the experiment but often almost ceased after about 1 year. In contrast, methane formation was often negligible at the beginning of the experiments and only started after a substantial lag phase of up to 3 years and even exceeded CO_2 production at the end of the incubations in several samples. With the onset of methane production also CO_2 formation increased again. These microbial interactions during the anaerobic degradation of organic matter yet cannot be simulated with current degradation models. Furthermore, the presented data demonstrate that the anaerobic production of trace gases from thawing permafrost may not be estimated from the currently available short time ($<$ 1 year) incubation studies, and hence the methane production potential from thawing permafrost is currently substantially underestimated.

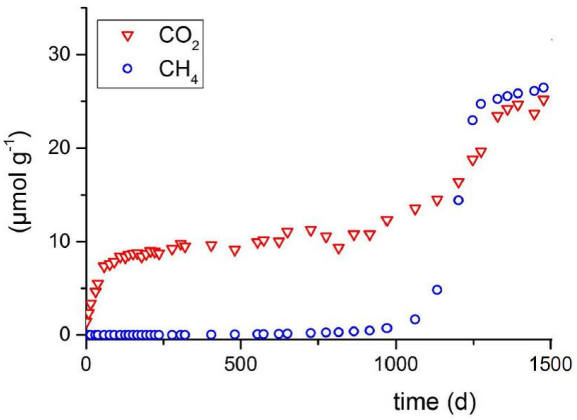

Figure 1: Carbon dioxide (CO_2) and methane (CH_4) production in a permafrost sample from the Pleistocene island Kurungnakh (4 m depth, ^{14}C age 19 ka)

The sensitivity of carbon in Arctic permafrost soils to climate change

Mats P. Björkman[1], Pascal Boeckx[2], Janet Rethemeyer[3], Frida Lindwall[4,5], Bo Elberling[4], & Robert G. Björk[1]

[1] *University of Gothenburg, Sweden*
[2] *Dep. of Applied Analytical and Physical Chemistry, Ghent University, Belgium*
[3] *Inst. of Geology and Mineralogy, University of Cologne, Germany*
[4] *Center of permafrost (CENPERM), University of Copenhagen, Denmark*
[4] *Dep. of Biology, University of Copenhagen, Denmark*

Arctic permafrost soils contain huge amounts of stored carbon (C), which upon thaw releases ancient organic matter that has been stored in the frozen soil for centuries. However, the critical role that the Arctic C stocks may come to play in the future of our climate system has not been adequately investigated. Particularly, there is a gap in our current knowledge as to which extent permafrost-protected C is available for microbial metabolism once the soils thaw.

During 2012 samples were obtained from permafrost soils at two Arctic locations; Adventdalen (Svalbard) and Zackenberg (Greenland). At both locations sites were chosen to represent Meadow and Heath communities. Soil-pits were established and the A, B and C soil horizons were collected, together with the upper 20 cm permafrost, with three replicates for each community. Homogenized soil sample where further divided into three sub-samples. Two of the sub-samples have been incubated at +5 °C with either Anaerobic or Aerobic conditions, with the third sub-sample sample working as a 'control' incubated at −5 °C.

The primary goal of this work is to understand the fate of carbon in Permafrost soils during altered environmental conditions. We would like to know if this carbon: is 'easy or hard to eat', 'how well packed the carbon is', 'how old the respired carbon is', 'who's eating the carbon', 'who is eating which part of the carbon stock' and 'how much faster/slower they will eat during changed environmental conditions'.

A preliminary result after 120 days incubation indicates that CO_2 emissions from drained soils (A, B and Permafrost horizons) are generally higher from Zackenberg meadow sites then the heath communities. No difference can so far be found between the Adventdalen communities. Generally the organic rich A horizon generates higher fluxes then the C (mineral soil) and Permafrost soils. First CH_4 production was detected after 56 days incubation (Zackenberg meadow A horizon) indicating that oxygen levels have dropped below the threshold for anaerobic decomposition. Full data from the 1.5 years incubation including radiocarbon analysis of the respired C will be available before the ICOP 2016.

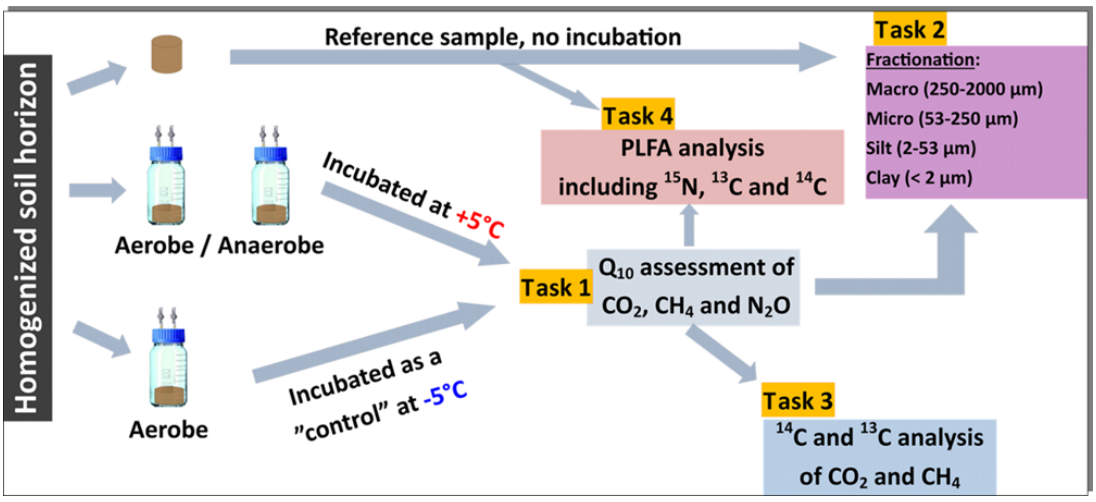

Figure 1: Incubation setup

Permafrost thaw - decadal responses to climate change

Mats P. Björkman[1], Catherine Larose[2], Janet Rethemeyer[3], Bo Elberling[4], Leif Klemedtsson[1], & Robert G. Björk[1]

[1] *Dep. of Earth Sciences, University of Gothenburg, Sweden*
[2] *Env. Microbial Genomics group, Laboratoire Ampère, University of Lyon*
[3] *Inst. of Geology and Mineralogy, University of Cologne, Germany*
[4] *Center of permafrost, University of Copenhagen, Denmark*

Permafrost soils contain approximately 1672 Pentagram carbon (C), twice the amount of the current atmosphere, and constitute 50 % of the world's belowground C pool. Along with the current change in climate these high latitudinal soils experience increased temperatures, with permafrost degradation as a result. This releases ancient organic matter where the following microbial degradation can release the previously stored C and nitrogen (N) to the atmosphere as carbon dioxide (CO_2), methane (CH_4) and nitrous oxide (N_2O), further influencing the climate systems. Thus, a changed climate leads to sever alterations of the C and N balance in Arctic and high altitude ecosystems.

This project (starting 2016) aims for understanding the future that lies ahead, following thaw and the establishment of new non-permafrost ecosystems, and how the predicted climate variability will influence these soils on a long-term timescale. By using a natural occurring permafrost degradation gradient in the northern part of Sweden, this project investigates: the change in C and N dynamics following thaw, the decomposability of ancient carbon (through radiocarbon dating), the chemical/physical protection of ancient C, and the microbial response following degradation and during the transit to new ecosystem types. Furthermore, by using laboratory incubation of soils from the gradient, the project will provide insights of how the C and N cycles at different stages of permafrost degradation will respond to the changing climate, giving a decadal perspective on permafrost thaw.

This project is currently under planning and collaborations and side projects are encouraged.

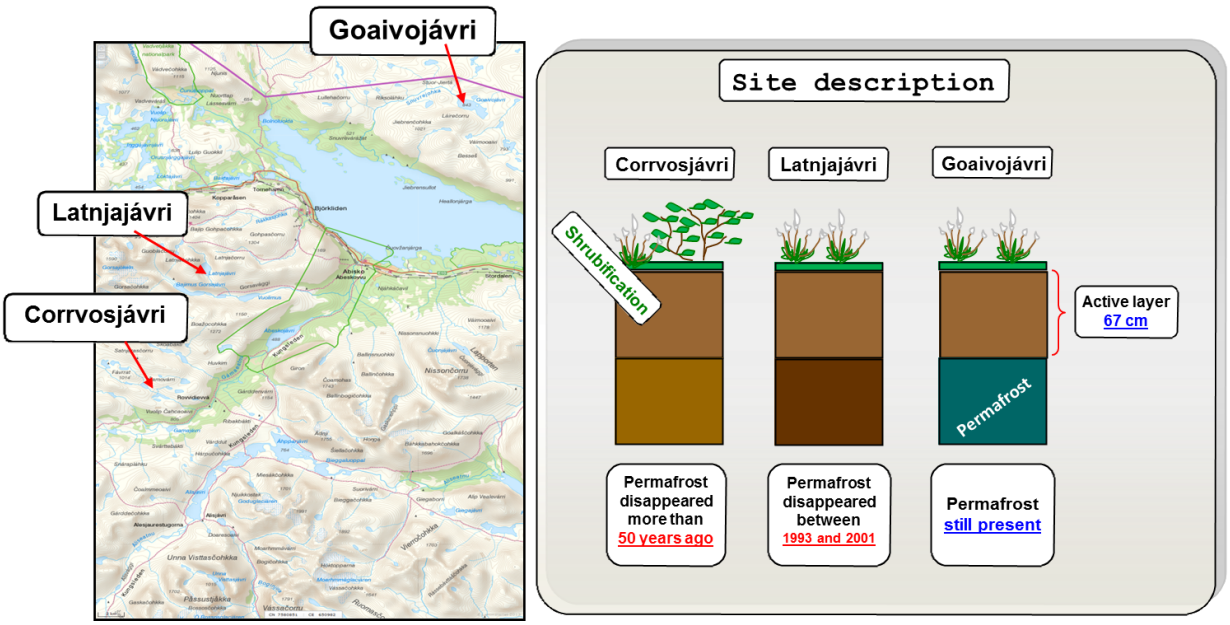

Figure 1: Map of area and site description

Pan-arctic lakes: an important source of atmospheric methane during the last deglaciation?

Laura Brosius[1], Claire Treat[2], Katey Walter Anthony[1], Miriam Jones[2], Guido Grosse[3], & Josefine Lenz[3]

[1] *University of Alaska, United States of America*
[2] *United States Geological Survey, United States of America*
[3] *Alfred Wegener Institute Helmholtz Centre for Polar and Marine Research, Potsdam, Germany*

Sources of atmospheric methane (CH_4) during the last deglaciation have yet to be reconciled with geological and paleoecological records. Greenlandic ice cores demonstrate that abrupt increases in North Atlantic temperature and precipitation were contemporaneous with an abrupt rise in atmospheric CH_4 concentration. Despite new evidence suggesting a more consistent difference between Greenlandic and Antarctic atmospheric CH_4 concentrations (the interpolar CH_4 gradient) than previously thought, a new boreal CH_4 source composing approximately 40 % of all new methane sources is still required to account for the abrupt increase in atmospheric CH_4 during the last glacial termination [Baumgartner et al., 2012]. The source of this increase in northern atmospheric CH_4 remains the subject of much debate. Previous work suggests that both thermokarst-lake formation in Beringia [Walter et al., 2007] and northern peatland expansion [MacDonald et al., 2006] likely contributed to the abrupt increase in atmospheric CH_4 following deglaciation. With the exception of thermokarst lakes in present day permafrost regions, lakes formed within the boundaries of past permafrost and glaciation extents by periglacial, glacial, and other processes during ice-sheet retreat have not been included in previous, region-specific estimates. Here, we compile an extensive dataset of 1154 unique lake basal and minimum ages from past and extant lakes of all origins to examine the timing and distribution of lake formation in the pan-arctic domain characterized by past permafrost or glaciations during the Last Glacial/Permafrost Maximum. Using this expanded dataset, we generate regional lake formation frequency curves and scale them by present day lake areas to obtain areal lake extent over time. We then apply methane emission rates and methane isotope values specific to each region and lake origin in order to put forth improved and expanded estimates of lake methane emissions and isofluxes from northern hemisphere lakes of all origins from 18 ka-present. Additionally, we reconcile bottom-up estimates with isotope mass balance constraints imposed by ice core records to assess the contribution of northern lakes to deglacial increases in atmospheric CH_4.

References

Baumgartner, M.; Schilt, A.; Eicher, O.; Schmitt, J.; Schwander, J.; Spahni, R.; Fischer, H. and Stocker, T.F. [2012]: High-resolution interpolar difference of atmospheric methane around the Last Glacial Maximum. *Biogeosciences*, 9(10):3961–3977, doi:10.5194/bg-9-3961-2012.

MacDonald, G.M.; Beilman, D.W.; Kremenetski, K.V.; Sheng, Y.; Smith, L.C. and Velichko, A.A. [2006]: Rapid early development of circumarctic peatlands and atmospheric CH_4 and CO_2 variations. *Science*, 314(5797):285–288, doi:10.1126/science.1131722.

Walter, K.M.; Edwards, M.E.; Grosse, G.; Zimov, S.A. and Chapin, F.S. [2007]: Thermokarst lakes as a source of atmospheric CH_4 during the last deglaciation. *Science*, 318(5850):633–636, doi:10.1126/science.1142924.

Including permafrost carbon within the land surface scheme of the UK Earth System Model (JULES)

Eleanor Burke[1], Altug Ekici[2], & Sarah Chadburn[3]

[1] *Met Office, United Kingdom*;
[2] *Exeter University, United Kingdom*;
[3] *Leeds University, United Kingdom*

Currently JULES uses a 4 pool soil carbon model with no vertical representation. This model uses only the physical conditions from the top soil layer and therefore cannot include stored permafrost carbon. However, the permafrost carbon stores represent a potentially significant climate feedback, so it is important to include this in Earth System Models.

A vertically discretised soil carbon scheme was implemented in JULES, where the soil vertical dimension was added into the carbon pools giving a set of pools in every soil layer. The respiration rate is determined for each soil layer depending on the temperature and moisture conditions in that layer. There is also a vertical mixing or diffusion term representing either cryoturbation or bioturbation. These vary with depth and depend on the presence or absence of permafrost. Both the litter inputs and the soil respiration are also a function of depth.

Global simulations show that the large scale distribution of soil carbon can be represented given an appropriate parameterisation of the inhibition of soil respiration at depth. However, the model is unable to simulate sufficient soil carbon in the tundra regions. Observed and modelled litter inputs are relatively low in these regions. Permafrost carbon is old carbon, some of which accumulated under previous climate states; therefore it is unlikely that a soil carbon model in equilibrium with the current climate can appropriately represent the permafrost carbon. A method was developed to initialize permafrost carbon within JULES in order to more appropriately represent the regions vulnerable to significant permafrost carbon loss.

Trapped greenhouse gas in permafrost active layer: Methane peaks in the vertical profiles of frozen Alaskan soil cores

Eunji Byun[1], Ji-Woong Yang[1], Yongwon Kim[2], & Jinho Ahn[1],

[1]*Seoul National University, Korea, Republic of (South Korea)*
[2]*International Arctic Research Center, University of Alaska Fairbanks, Alaska, U.S.A.*

Permafrost carbon degradation may be an additional source of atmospheric greenhouse gas (GHG) under climate warming. Multiple studies suggested that season-induced changes in gas-permeability of overlying active layers can temporarily prevent emission of methane in permafrost soils. However, production and transportation process of the methane in response to the seasonal freeze/thaw of active layer remain unclear, probably due to lack of chemical and physical analysis for the host soils in detail. To this end, we drilled five soil cores up to 90 cm depth at various latitudes in Alaskan permafrost during the early spring of 2013. We obtained vertical profiles of CO_2, CH_4 and other soil properties with 5 to 10-cm depth resolutions. Two cores from tundra and black spruce bog show sudden increases of methane concentration (up to 416 μmol/ L) at certain depths, which indicate excess CH_4 trapped in the gas impermeable soils. Temperature inversion (frozen surface and relatively warm interior) in late autumn might have promoted underground microbial activity and facilitate the CH_4 production, while the upward transport of the produced CH_4 was hampered by the frozen surface. Our results show that estimation on annual GHG efflux from permafrost regions can be more complicated by the irregular distribution of trapped methane along the soil columns.

Active layer thickness and vegetation phenology as key factors affecting the variability of CO_2 fluxes in polar environments

Nicoletta Cannone[1], Stefano Ponti[1], Mauro Guglielmin[1], Torben Christensen[2], Frans-Jan Parmentier[2], Norbert Pirk[2], & Hanne Christiansen[3]

[1] *Insubria University, Italy*
[2] *Lund University, Sweden*
[3] *UNIS, Norway*

Since the mid 20^{th}Century climate change has led to significant impacts in the Arctic, with increases in air and permafrost temperatures, snow cover decreases, and glacier retreat (IPCC 2013). The Arctic ecosystems play a key role in the global carbon cycle because northern permafrost soils account for approximately 50 % of the estimated global belowground organic carbon pool [Tarnocai et al., 2009]. Climate change may turn Arctic biomes from carbon sinks into sources and vice-versa, depending on the balance between Gross Ecosystem Photosynthesis (GEP), Ecosystem Respiration (ER) and the resulting Net Ecosystem Exchange (NEE).

Many environmental factors may affect the patterns of the CO_2 fluxes shifting the same ecosystem from a sink to a source. It has been emphasized that NEE shows large fluctuations in climatic regions dominated by snow, ice and permafrost [Lüers et al., 2014]. In particular, permafrost and active layer dynamics may be a key factor affecting the CO_2 fluxes.

At Adventdalen (Svalbard archipelago, Norway), a glacial valley near Longyearbyen, we analyzed the CO_2 fluxes under different vegetation and active layer conditions. We selected two transects along an active layer and moisture gradient, corresponding to different vegetation communities, ranging from the driest site dominated by *Cassiope tetragona* community (P3), to the mesic tundra dominated by *Luzula confusa*, *Poa arctica* and graminoids (P4, P6, P8), to the wettest site dominated by *Dupontia pelligera* with mosses (P1, P2, P5).

In 2013 we performed the measurements of NEE and ER and computed GEP, starting in late spring at the snowmelt (17^{th} June) and ending in early autumn when the soil was completely frozen (4^{th} October). We also measured soil temperature, soil moisture, PAR, active layer thickness (using a frost probe according to the CALM protocol, Circumpolar Active Layer Monitoring), species phenology (according to the ITEX protocol, International Tundra Experiment) and collected the most important climatic data (air temperature, precipitations).

We aimed to analyze and quantify the differences of CO_2 fluxes among the selected plots and identify which abiotic (soil temperature, soil moisture, PAR, active layer thickness) and biotic (vegetation community, phenological stage) factors affected NEE and ER. We hypothesized that

1. the CO_2 fluxes would be different among the selected plots both concerning NEE and ER;
2. the driving factors of NEE and ER would change during the growing season.

Our data showed differences of the abiotic factors characterizing our plots, with the wettest ones (dominated by *Dupontia pelligera*) exhibiting the lowest soil temperatures, thinner active layer and highest soil moisture, while the driest plot (dominated by *Cassiope tetragona*) had the lowest soil moisture, thicker (but not the thickest) active layer and higher soil temperature. The mesic graminoid tundra exhibited intermediate conditions relating to soil moisture, while showed thicker active layer and among the highest soil temperatures.

Analyzing the data concerning both the mean daily and cumulative values of NEE and ER, as well as their means across the entire season, we observed that during the entire season the wettest vegetation (corresponding to the thinner active layer) (P1, P2, P5) acted as sinks, performing a CO_2 uptake from the atmosphere as well as one of the graminoid tundra plot (P6). The mesic tundra plots (P4, P8) and the dry *C. tetragona* plots acted as sources, with a release of CO_2 from the ecosystems to the atmosphere. This patterns was the result of a very high ER measured

in the wettest plots (P1, P2, P5 all with *D. pelligera*) as well as in the driest one (P3, *C. tetragona*) but the former three exhibited also a much higher GEP, resulting in a negative NEE (sink effect).

We analyzed by General Regression Models (GRM) the factors influencing NEE and ER at inter-community level (i.e. analyzing together all the dataset of all the selected communities). Considering the entire growing season (from 17^{th} June to 4^{th} October), active layer thickness, vegetation community and soil temperature were the most important factors affecting NEE, while soil temperature and vegetation community were the key factors for ER.

Moreover, as from our data there were apparent different patterns of NEE and ER during the season in relation with the development of different phenological stages, we analyzed by GRM to assess if the factors affecting NEE and ER would change during the three main periods of the growing season. At the beginning of the growing season active layer thickness was the most important factor for NEE, followed by soil temperature. At the peak of the growing season active layer thickness and PAR were the most important factors, while soil temperature and soil moisture exerted a less important influence. At the end of the growing season PAR was the most important factor for NEE.

Concerning ER, soil temperature was the most important factor both at the beginning and at the peak of the growing season, while at the end of the growing season vegetation community and active layer thickness became the most important ones.

Our results confirm the importance of permafrost, and in particular of active layer thickness, as factor affecting both NEE and ER and useful to understand the patterns of their inter-annual variability. As the plots with the thinner active layer were the most efficient sinks among the studied vegetation communities, they represent an important component of the C cycle in the Arctic environments and their conservation deserves attention also in consideration of the ecological role they play. These data emphasize the sensitivity of high Arctic ecosystems to climate warming impacts as permafrost is one of the environmental components most vulnerable to climate warming.

References

IPPC [2013]: *Climate Change 2013: The Physical Science Basis. Contribution of Working Group I to the Fifth Assessment Report of the Intergovernmental Panel on Climate Change*. Cambridge University Press, Cambridge, United Kingdom and New York, NY, USA.

Lüers, J.; Westermann, S.; Piel, K. and Boike, J. [2014]: Annual CO_2 budget and seasonal CO_2 exchange signals at a high Arctic permafrost site on Spitsbergen, Svalbard archipelago. *Biogeosciences*, 11:6307–6322, doi:10.5194/bg-11-6307-2014.

Tarnocai, C.; Canadell, J.G.; Schuur, E.A.G.; Kuhry, P.; Mazhitova, G. and Zimov, S.A. [2009]: Soil organic carbon pools in the northern circumpolar permafrost region. *Global Biogeochemical Cycles*, doi:10.1029/2008GB003327.

Measurement of carbon-dioxide fluxes from permafrost disturbances using eddy covariance in a high arctic tundra ecosystem

Alison Elizabeth Cassidy, Greg Henry & Andreas Christen

Department of Geography, The University of British Columbia, Vancouver, BC, Canada

On the Fosheim Peninsula, Ellesmere Island, permafrost disturbances occur in the form of active layer detachment slides (ALDS) and retrogressive thaw slumps (RTS), which impact ecosystem structure and ecosystem functioning. We analyzed the impacts of retrogressive thaw slumps on carbon flux dynamics using the eddy covariance (EC) technique. Over the growing seasons of 2012 – 2014, we developed and tested three techniques for measuring carbon-dioxide fluxes. During the 2012 season, we deployed one EC tower adjacent to one RTS (extent: 2000 m^2). Over the measurement period, the undisturbed tundra acted as a small net sink and disturbance decreased sequestration ability. During the 2013 growing season, two EC towers were established adjacent to severely disturbed strings of RTS (extent: $>$ 30000 m^2). The impact of disturbance on CO_2 fluxes was dependent on vegetation community and differences were found in fluxes from different undisturbed communities. Over the 2014 growing season, two towers were established on either side of one isolated disturbance (extent: 12000 m^2). Disturbance shifted the system from a small net sink of carbon to a net source. Partitioning of fluxes indicate decreases in both productivity and respiration, with greater decreases found in productivity. Over these three periods, we contrast methods for measuring CO_2 fluxes to determine the impacts of permafrost disturbance on ecosystem function. Overall, during the measurement periods during the growing seasons of 2012 – 2014, undisturbed tundra acted as a minimal net sink of carbon while disturbed tundra decreased the amount of carbon sequestered. In all but one site, the degree of change shifted the tundra from a net sink to a net source of carbon. Fluxes from undisturbed tundra are up to four times greater in magnitude than those from disturbed tundra. Overall we find that vegetation composition acts to control the impacts of disturbance on CO_2 fluxes.

Implications of shrub expansion on soil carbon dynamics and thaw depth in arctic Alaska

Claudia I. Czimczik[1], Sandra R. Holden[1], & Jeffrey M. Welker[2]

[1] *Earth System Science, University of California, Irvine, United States of America*
[2] *Department of Biological Sciences, University of Alaska, Anchorage, United States of America*

Shrubs are increasing in abundance in some parts of the Arctic in response to climate warming, but the consequences of a shrubbier Arctic on the cycling of carbon (C) in tundra ecosystems are poorly understood. Greater shrub abundance on the tundra land surface may lead to a suite of complex changes, with both direct and indirect effects on biophysical and biogeochemical processes. For instance, greater productivity of shrubs may increase C fixation and C storage in vegetation and soils. But, labile C exudates from shrub roots and inputs of litter with lower carbon-to-nitrogen (N) ratios may stimulate the decomposition of existing soil C stocks. In addition, the presence of shrubs may influence snow accumulation, soil winter temperatures, and in turn rates of C and N mineralization and tundra-atmosphere C emissions.

We surveyed soils along natural gradients of increasing shrub cover in the Low Arctic near Toolik Lake, AK, USA. The vegetation ranged from graminoid tundra (moist acidic tussock-sedge, dwarf-shrub, moss tundra) to erect-shrub tundra (low to tall shrublands). We estimated shrub density and height, measured soil thaw depth, analyzed depth profiles of %C, %N, $\delta^{13}C$, and $\Delta^{14}C$, and inventoried active layer C stocks. We also analyzed depth profiles of %C, %N, $\delta^{13}C$, and $\Delta^{14}C$ in 1 m of permafrost underlying the graminoid tundra. In addition, we conducted a laboratory priming experiment with graminoid tundra soil. We incubated organic soil, the top 10 cm of mineral soil, and the lower 10 cm of active layer mineral soil with supplemental ^{14}C-labeled sucrose at 7 °C and 22 °C.

We found that mineral soils from shrub tundra had a significantly higher C content than graminoid tundra. Similarly, mineral soils from shrub tundra had more depleted $\delta^{13}C$ values compared to graminoid tundra, indicating that this soil has undergone less microbial processing. We also found that C under shrub tundra was on average older, and shrub tundra had significantly higher C stocks than graminoid tundra. Laboratory additions of labile C did not increase mineralization rates of existing C stocks. Furthermore, thaw depth decreased with increasing shrub cover, with a 40 % shallower thaw depth under shrub compared to graminoid tundra.

Our findings suggest that shrub expansion may augment soil C storage in the Arctic because a greater proportion of soil C is frozen in permafrost and existing C in mineral soil does not appear to be vulnerable to loss via priming. In addition to changing climate, we identify shrub cover as a key control on C cycling and thaw depth and thus for forecasting the C-climate feedback of the rapidly changing Arctic.

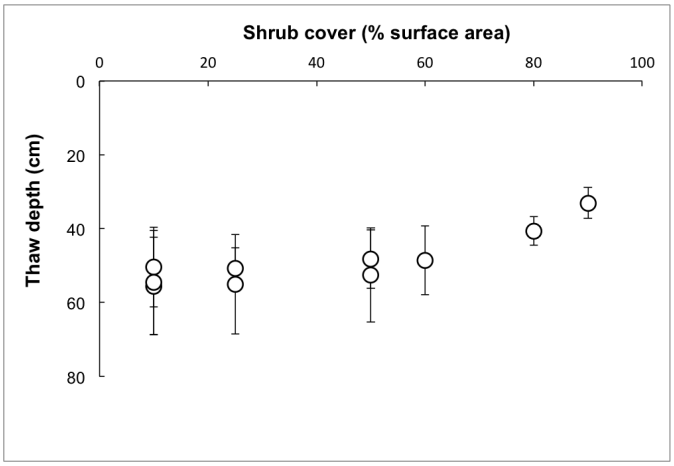

Figure 1: thaw depth

Partitioning CO_2 net ecosystem exchange fluxes into photosynthesis, autotrophic and heterotrophic respiration in a polygonal tundra landscape

Tim Eckhardt, Christian Knoblauch, Lars Kutzbach, Gillian Simpson, & Eva-Maria Pfeiffer

Institute of Soil Science, University of Hamburg, Germany

Warming of the Arctic will cause longer and deeper thawing of permafrost-affected soils. Hence, there will be a higher production of CO_2 due to the enhanced microbial mineralization of soil organic matter. However, it still remains unclear if changing climate conditions will turn permafrost-affected landscapes from a sink to a source of atmospheric carbon in the future. To estimate the effect of arctic warming on CO_2 fluxes, it is essential to gain a quantitative understanding of the underlying processes of net ecosystem exchange (NEE) fluxes on different time scales. Partitioning NEE into photosynthesis, autotrophic and heterotrophic respiration is necessary to identify the response of these basic ecophysiological processes to a changing climate. Furthermore, a better understanding of the environmental controls on these processes is needed to improve model simulations of future CO_2 fluxes.

Therefore, a total number of 4,400 closed chamber measurements of CO_2 fluxes have been made on Samoylov island in the Lena River Delta, northeastern Siberia (72°22'N, 126°28'E). The measurements were done during the vegetation period for two months in 2014 and for three months in 2015. Two different microsites were investigated; one characterized by water-saturated soils and densely vegetated by vascular plants and mosses in the center of an ice wedge polygon, and the second situated at a dryer polygon rim, with vegetation dominated by mosses. The soils in the polygon center were classified as Typic Historthels and in the polygonal rim as Glacic Aquiturbels. A combination of light and dark closed chamber measurements was used to partition NEE into photosynthesis and total ecosystem respiration. To partition total ecosystem respiration into autotrophic and heterotrophic respiration, a 'clipping experiment' was conducted. Here, living plant biomass was removed from a subset of the sampling plots, and fluxes from these plots were compared with measurements of total ecosystem respiration from another subset of plots with intact living plant biomass.

The averaged net CO_2 uptake was more than twice as high on the polygonal center than on the polygonal rim with daytime NEE fluxes of -76 ± 55 μg m^{-2} s^{-1} and -28 ± 23 μg m^{-2} s^{-1}, respectively. High temporal variability was also observed, with the highest CO_2 uptake rates seen at the beginning of August whereas at the end of arctic summer in September, both microsites were turning to small net sources of CO_2. The main drivers of the CO_2 flux dynamics were air temperature, hydrologic conditions and vegetation. Total ecosystem respiration fluxes were 32 ± 16 μg m^{-2} s^{-1} on the polygonal center and 38 ± 13 μg m^{-2} s^{-1} on the polygonal rim. Measurements on sampling plots where living plant biomass was removed showed high spatial variability: measured heterotrophic respiration fluxes were 12 ± 7 μg m^{-2} s^{-1} on the polygonal center and 23 ± 8 μg m^{-2} s^{-1} on the polygonal rim. Hence, heterotrophic respiration has a higher proportion to total ecosystem respiration on the polygonal rim than on the polygonal center (about 60 % and 40 %, respectively). This difference between the microsites might be explained by a lower plant/root density as well as the constrating hydrologic conditions on the polygonal rim compared to the polygonal center.

Closing the loop - the permafrost carbon feedback in a fully coupled system

Altug Ekici[1], Eleanor Burke[2], Sarah Chadburn[3], Chris Huntingford[4], & Pierre Friedlingstein[1]

[1] *University of Exeter, United Kingdom*
[2] *UK Met Office, United Kingdom*
[3] *Leeds University, United Kingdom*
[4] *Centre for Ecology and Hydrology, United Kingdom*

Any release of frozen, inert organic carbon within the permafrost soils has the potential to feedback onto the climate system and cause an additional warming. In this study, the potential magnitude of such a feedback was quantified in a fully coupled system. This system comprised a permafrost specific version of JULES, the land surface scheme of the UK Earth System Model, coupled with IMOGEN, an intermediate complexity climate model used to quantify the terrestrial feedbacks in a changing climate. IMOGEN is a computationally efficient modeling system, which uses a pattern scaling approach for the climate change. It can be driven by climate patterns from available climate models and so can readily represent uncertainties caused by different plausible model futures.

Simulations with the JULES-IMOGEN system are carried out until year 2300 under three emission scenarios, which represent RCPs 2.6, 4.5, and 8.5. After 2100, experiments driven with all emission scenarios show more release than uptake of carbon by land. In order to quantify the permafrost carbon feedback paired simulations were carried out, one which includes the permafrost carbon emissions and one which does not. Additionally, different versions of JULES soil carbon model are used to inspect the uncertainties arising from soil carbon formulation. Together with the scenarios and climate model range, our results show a full range of uncertainty analyses relating to the future experiments.

The key results include a consistent positive feedback from the loss of permafrost carbon in all cases. There is no slowing down of permafrost carbon emissions at 2300; however there is large uncertainty with the magnitude of permafrost induced temperature change between 0.05 to 0.4 K globally at year 2300. Interestingly, the lower emission scenarios RCP2.6 and RCP4.5 have greater percentage of permafrost induced temperature change than RCP8.5. Also, the results are observed to be highly sensitive to the structure of soil carbon model.

Regional assessment of dissolved CH_4 and CO_2 sources (^{14}C age) from thaw lakes in Northern Alaska

Clayton Drew Elder[1], Xiaomei Xu[1], Katey Walter Anthony[2], Amy Townsend Small[3], Kenneth Hinkel[3], & Claudia Isabel Czimczik[1]

[1] *University of California Irvine, United States of America*
[2] *University of Alaska Fairbanks, United States of America*
[3] *University of Cincinnati, United States of America*

Vast areas of the arctic land surface are covered by lakes, which are important conduits of terrestrial carbon (C) to the atmosphere. In ice-rich permafrost, expanding thaw lakes may rapidly re-introduce large quantities of ancient organic carbon (C) to the atmosphere as carbon dioxide (CO_2) or the more powerful greenhouse gas methane (CH_4). Future lake C emissions remain as large uncertainty in our understanding of the C-climate feedback from the Arctic and the global CH_4 budget.

We used two complementary approaches to characterize the sources and significance of dissolved CH_4 and CO_2 in Northern Alaska. First, we collected dissolved CH_4 and CO_2 along two 170 km north-south transects on the Arctic Coastal Plain of Alaska, USA. These arctic lakes represent a network monitored by the US-NSF funded project, Circum-Arctic Lakes Observation Network (CALON). In April 2013 and 2014, we collected samples from below ice in 40 lakes, two of which reside in active stream channels. These below ice samples represent integrated whole-lake estimates of CH_4 and CO_2 emitted by both diffusion and ebullition fluxes from the perennially thawed sub-lake sediments and within the water column. In August 2013 and 2014, we collected dissolved CH_4 and CO_2 from 8 CALON lakes using a mobile degasser (80 L of water/sample). Second, in May and August 2015, we collected CH_4 and CO_2 from 5 boreal lakes in interior Alaska. May samples, taken below ice, represent CH_4 and CO_2 emitted by both diffusion and up to 90 % total ebullition flux. In summer, we separately collected CH_4 and CO_2 from ebullition and dissolved CH_4 and CO_2 along gradients of increasing distance from visible ebullition. This sampling will test the extent to which ice-cover integrates isotope signatures over the winter months. All samples were analyzed for the ^{14}C and ^{13}C content and concentrations of CH_4 and CO_2.

We found that most arctic lakes were over-saturated and thus sources of CH_4 and CO_2 to the atmosphere. In arctic Alaska, dissolved CH_4 (average 836 years BP, modern to 2145 years BP) was older than dissolved CO_2 (480 years BP, modern to 1590 years BP). In a given lake, the mean age of CH_4 was correlated to the mean age of CO_2. Across the landscape, the mean age of CH_4 and CO_2 was best explained by surficial geology, with lakes and active steam channels in sandy deposits dominated by modern CH_4 and CO_2. May and August samples from the 5 interior Alaskan lakes are currently being analyzed.

This work provides the first regional-scale assessment of integrated whole-lake radiocarbon (^{14}C) ages of dissolved CH_4 and CO_2 as a proxy for C emission sources in northern Alaska. Our results imply that decomposing Holocene-age organic material is the primary source of CH_4 and CO_2 emissions from thaw lakes in Alaska and that currently generalized surface geology is a key predictor of CH_4 and CO_2 sources.

This baseline dataset provides the foundation for future regional lake monitoring in the rapidly warming Arctic. Our whole-lake proxy facilitates lake-to-lake comparison and regional up scaling, thereby strengthening quantitative understanding of how environmental drivers (water body size, climate, surficial geology) affect the magnitude and sources of biogenic CH_4 and CO_2 emissions. This dataset will reduce large uncertainties in the magnitude and timing of the C-climate feedback from the Arctic, and thus trajectories of climate change.

Abiotic controls on permafrost C mineralization rates based on incubating samples from 4 contrasting arctic localities

Samuel Faucherre[1], Imre Banyasz[1], Christian Juncher Jørgensen[1], Niels Weiss[2], Gustaf Hugelius[2], Peter Kuhry[2], & Bo Elberling[1]

[1] *Center for Permafrost (CENPERM), Department of Geosciences and Natural Resource Management, University of Copenhagen, Denmark*

[2] *Department of Physical Geography, Stockholm University, Sweden*

The vulnerability of the large carbon stocks stored in soils of the northern permafrost region is a key factor for understanding the potential warming climate feedback mechanism of greenhouse gas release to the atmosphere from thawing permafrost. It is widely accepted that the rate of carbon dioxide release is strongly related to soil temperature and water content, thus the overall environmental conditions given to microorganisms responsible for decomposing permafrost organic matter [Elberling et al., 2013]. Here we assess the controls on permafrost terrain carbon lability based on 240 samples from more than 100 sites at four contrasting arctic localities and diverse landscapes. All samples were incubated for 1 year at field water content levels under similar temperature and oxygen condition. Selected replicates of the samples were wet thieved into 3 different grain size fractions separately incubated. While [Kuhry et al., in prep.] studied the dataset for landscape-level carbon lability classification, this study shows the importance of abiotic physical sediment parameters such as the initial organic carbon content, the C/N ratio, the carbon age and the substrate grain size. We demonstrate that the single most important parameter controlling mineralization is the total carbon content but including nitrogen content and sediment ages provide improved understanding of the observed variability. Results also show that grain size distribution, and particularly the finest grain sizes, can significantly influence the observed greenhouse gas production rates. We describe permafrost carbon mineralization rate over time using 5 rate measurements over a year for each sample and project mineralization rates for 10 years of incubation – around 50 field years – using three-pool C dynamics model [Schädel et al., 2013]. We conclude that changes in observed rates decrease significantly over this time frame and need to be considered in future estimates of the permafrost carbon feedback to climate.

References

Elberling, B.; Michelsen, A.; Schädel, C.; Schuur, E.A.G.; Christiansen, H.H. and L. ... Sigsgaard-Berg, C. [2013]: Long-term CO_2 production following permafrost thaw. *Nature Climate Change*, 3 (10):890–894, doi:10.1038/nclimate1955.

Kuhry, P.; Barta, J.; Blok, D.; Elberling, B.; Faucherre, S.; Hugelius, G.; Richter, A.; Santruckova, H. and Weiss, N. [in prep.] Lability classification of soil organic matter in the northern permafrost region based on simple soil horizon and landscape unit criteria. *ICOP2016*.

Schädel, C.; Luo, Y.; David Evans, R.; Fei, S. and Schaeffer, S. M. [2013]: Separating soil $CO_2$2 efflux into C-pool-specific decay rates via inverse analysis of soil incubation data. *Oecologia*, 171(3):721–73, doi:10.1007/s00442-012-2577-4.

New low-cost automated system of closed chambers to measure greenhouse gas emissions from the tundra

Samuel Gagnon[1], Emmanuel L'Hérault[2], Mickaël Lemay[3], & Michel Allard[1]

[1] *Centre d'études nordiques and Université Laval, QC, Canada, G1V 0A6*
[2] *Centre d'études nordiques, QC, Canada, G1V 0A6*
[3] *Centre d'études nordiques and ArcticNet, QC, Canada, G1V 0A6*

The northern high latitudes represent the world's largest soil carbon reservoir. Due to the rapid warming in the Arctic, permafrost thawing is expected to lead to increased emissions of greenhouse gases (GHG). Therefore, quantifying these emissions has become very important in order to determine the feedback impacts of GHG release from permafrost on the global climate. However, permafrost GHG emissions are difficult to quantify because direct measurements with conventional methods are generally expensive and time-consuming, resulting in short-spanned experiments and limited number of measurements. In order to take continuous measurements of GHG emissions over long periods of time, we developed and tested an affordable automated system of four closed chambers equipped with low-cost sensors and open-source microcontrollers. We measured ecosystem respiration with a low-cost CO_2 sensor, which gave accurate results. The discrepancy between the sensor and the reference infrared gas analyzer was less than 5 % and was more apparent at low concentrations. Compared to a commercial chamber (SRC-1, PP Systems), ecosystem respiration measurements were more stable with our new automated chambers. We also measured methane emissions using gas sampling with syringes and laboratory analyses of the gas samples. The automated closed chambers were not sensitive enough to accurately detect CH_4 emissions, but this could be corrected by decreasing the volume of the chambers. This low-cost system shows high potential and represents a good alternative to existing methods and apparatuses to measure soil GHG emissions.

Analysis of permafrost carbon release processes after 25 years of climate warming

Samuel Gagnon & Michel Allard

Centre d'études nordiques and Université Laval, QC, Canada, G1V 0A6

Over the past 30 years, the Arctic regions have experienced a warming greater than anywhere else on Earth. This warming has led to important consequences such as the beginning of permafrost thaw. Permafrost (permafrost is a concept regrouping all grounds remaining below 0 °C over centuries and millennia) in the northern circumpolar region holds approximately half of the Earth's belowground organic carbon pool. This carbon, previously locked in permafrost, now threatens to be released into the atmosphere as Arctic average temperatures continue to rise. Despite the growing attention the northern regions are now receiving, studies spanning multiple decades are practically inexistent and consequence assessments of permafrost thawing over many years remain speculative, based on numerical models or limited to observations of short duration.

The first objective of this project is to revisit a site that was studied extensively in 1990 [Kasper and Allard, 2001] and to evaluate how the land evolved over the past 25 years. Using high-resolution satellite imagery analysis, we plan to measure how climate change affected the landscape and to determine at what rate such changes took place as warming only started around 1993 in the Nunavik region. This will allow quantifying the eroded volumes of the past 25 years. It will also allow elaborating mathematical models based on actual field measurements rather than estimates. We expect significant losses of eroded volumes due to the formation of erosion gullies and landslides.

The second objective is to study the different permafrost carbon release processes that took place in recent decades. We want to identify these processes and quantify the carbon losses that occurred in order to determine the relative importance of each mechanism leading to belowground carbon release. The quantification of these losses is very important because it allows estimating the vulnerability of permafrost and the carbon it contains to climate change. Although carbon release mechanisms are well documented individually for short periods of time, multi-decadal studies investigating simultaneously multiple processes remain fragmented and marginal. We expect to measure a larger amount of carbon available to interact with the environment and carbon depletion in the upper layers of permafrost.

To measure the impact of rising air temperatures on the landscape since 1990, we intend to revisit a dozen sites in the Foucault river valley near Salluit (Nunavik). With the Centre for Northern Studies (CEN), we will carry out several surveys and drillings of 2 – 3 m to compare the current depth of the active layer with that measured 25 years ago. We will also measure changes following the melting of the abundant networks of ice wedges mapped in this sector.

Laboratory analyses of the soil cores will provide more information about the content and properties of the carbon stored in the permafrost. By measuring the carbon content at different depths, we will be able to determine whether there was a decrease in belowground carbon in the upper layers, i.e. the areas most vulnerable to surface warming, in recent years. This analysis will allow us to assess how fast soil carbon depletion processes operated and with what magnitude. We will also collect gas samples from soil emissions and analyze the content of the samples to determine the proportion of old carbon emitted.

In short, we plan to conduct a research project that still has no equivalent in the field of climate change impact on permafrost by using a unique source of information and revisiting a research site with state-of-the-art analytical methods.

References

Kasper, J. and Allard, M. [2001]: Late-Holocene climatic changes as detected by the growth and decay of ice wedges on the southern shore of Hudson Strait, northern Québec, Canada. *The Holocene*, 11, doi:10.1191/095968301680223512.

$\Delta^{14}C$ and $\delta^{13}C$ signatures of CH_4, CO_2 and Dissolved Organic Matter of Siberian peatland and thermokarst lake complexes in relation to permafrost degradation

Laure Gandois[1], Alison Hoyt[2], Xiaomei Xu[3], Christine Hatté[4], Roman Teisserenc[1], & Nikita Tananaev[5,6]

[1]*ECOLAB, Université de Toulouse, CNRS, INPT, UPS, France*
[2]*Ralph M. Parsons Laboratory, Department of Civil& Environmental Engineering, Massachusetts Institute of Technology, Cambridge, MA 01239, USA*
[3]*Department of Earth System Science, University of California, Irvine, CA 92697-3100, USA*
[4]*Laboratoire des Sciences du Climat et de l'Environnement, UMR8212 CEA/CNRS/UVSQ, Domaine du CNRS, Gif-sur-Yvette, France*
[5]*Ugra Research Institute of Information Technologies, Khanty-Mansiysk, Russian Federation*
[6]*Melnikov Permafrost Institute, Siberian Branch, Russian Academy of Sciences, Yakust, Russia*

Global warming at high latitude alters the carbon cycle in terrestrial ecosystems and therefore carbon fluxes to surface water and atmosphere, in the form of Dissolved Organic Matter (DOM), CO_2 and CH_4. Permafrost stores half of the organic carbon stock worldwide [Tarnocai et al., 2009]. One of the main threats of permafrost degradation to climate change is the potential positive feedback it could induce, if the organic carbon stored in frozen soils and peatlands is transferred to the atmosphere. Determining the origin (permafrost or recent photosynthesis) and metabolic pathway of carbon which is released to surface waters and the atmosphere is therefore crucial to establish carbon budgets for northern ecosystems and assess their role in climate change.

A study was conducted in Siberia (Igarka (67°27'11"N, 86°32'07"E)), near the bank of the Ieniseï River. In the catchment of the Graviyka River, an tributary of the Ieniseï River un der discontinuous permafrost, two peatland-rich areas, shaped by different geomorphological and permafrost processes were investigated: on the North bank, palsas and glacier lakes and on the South bank, thermokarst lakes. In order to assess the impact of permafrost degradation on carbon release to surface water and the atmosphere, lakes, peatlands, and streams were sampled. Samples included surface water and bubbles from lake sediments, porewater collected in peatland profiles down to 2 m, as well as solid samples from palsa (active layer and melting fraction). In addition to classical geochemical analyses (major anions, cations and DOC concentrations), the samples were characterized for the $\delta^{13}C$ and $\Delta^{14}C$ of dissolved CO_2 and CH_4 and DOM. Dissolved organic carbon concentrations are higher and more heterogeneous in small palsa ponds (18.4 $\pm$6.8 mg L^{-1}) than in larger thermokast lakes (12.2 $\pm$2.5 mg L^{-1}). The isotopic composition of methane ($\delta^{13}C$-CH_4) covers a wide range of values: from -56.3 to -71.3 ‰ and the combined analysis of $\delta^{13}C$-CO_2 and of $\delta^{13}C$-CH_4 indicates that the methane production pathway depends on the area investigated. While CO_2 reduction is the dominant pathway in peatland porewater and small palsa ponds, acetate fermentation dominates in larger thermokarst lakes. In thermokarst lakes, strong methane oxidation is evidenced by heavy values of δD-CH_4 and a linear relationship between $\delta^{13}C$-CH_4 and δD-CH_4.

Radiocarbon analysis of dissolved gas (CO_2 and CH_4) reveals that in most places, they derive from recently fixed carbon. In two locations, methane in sediment bubbles have relatively low ^{14}C contents, with ages greater than 700 and 1000 yr BP, but till younger that what was previously reported in eastern Siberia [Walter et al., 2006]. In all samples $\Delta^{14}C$-CH_4 and $\Delta^{14}C$-CO_2 were strongly correlated, with CH_4 being consistently slightly more ^{14}C depleted than CO_2 ($\Delta^{14}C$-CO_2 = 0.74 $\times$ $\Delta^{14}C$-CH_4 + 0.44, r^2 = 0.97, n = 14, p < 0.001). The age of dissolved methane does not appear to be related to lake size, as previously hypothesized by [Nakagawa et al., 2002], who reported older methane in larger lakes. In our study, old methane is found in a small pond adjacent to palsa and a large thermokarst lake. In this case, bank erosion appears to be the main driver of mobilization of sequestered carbon, showing that some degree of permafrost degradation contributes to a pos-

itive feedback to global warming by methane emission. However, the majority of dissolved CO_2 and CH_4 analyzed from lakes and peatlands in region surrounding Igarka is modern and originates from recently fixed carbon.

Analyses are ongoing on solid and dissolved organic matter of the areas investigated. The complete data set that will be presented during the ICOP conference constitute a major contribution to carbon cycling knowledge in Siberian peatland complexes.

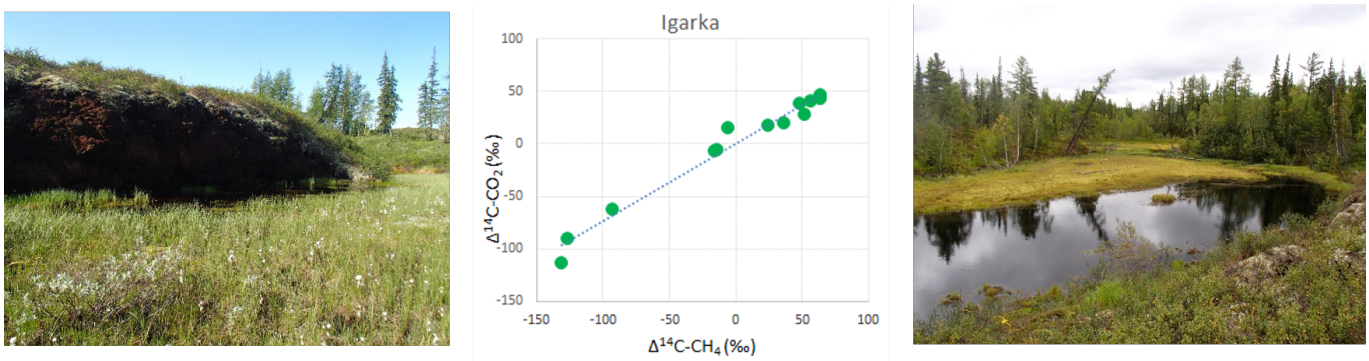

Figure 1: Palsa pound, Thermokarst lake and relation between D^{14}C-CO_2 and D^{14}C-CH_4 in bubbles, porewater and surface waters in the studied areas.

References

Nakagawa, F.; Yoshida, N.; Nojiri, Y. and Makarov, V.N. [2002]: Production of Methane from Alasses in Eastern Siberia: Implications from Its ^{14}C and Stable Isotopic Compositions. *Global Biogeochemical Cycles*, 16(août):1041, doi:doi:10.1029/2000GB001384.

Tarnocai, C.; Canadell, J.G.; Schuur, E.A.G.; Kuhry, P.; Mazhitova, G. and Zimov, S.A. [2009]: Soil organic carbon pools in the northern circumpolar permafrost region. *Global Biogeochemical Cycles*, doi:10.1029/2008GB003327.

Walter, K.M.; Zimov, S. A.; Chanton, J.P.; Verbyla, D. and Chapin, F.S. [2006]: Methane Bubbling from Siberian Thaw Lakes as a Positive Feedback to Climate Warming. *Nature*, 443(7107):71–75, doi:10.1038/nature05040.

Quantifying the impact of permafrost dynamics on soil carbon accumulation in response to climate change and wildfire intensification in Alaska

Hélène Genet[1], Yujie He[2], Anthony David McGuire[1,4], Qianlai Zhuang[3], Zhiliang Zhu[4], Neal Pastick[4], Bruce Wylie[4], & Kristopher Johnson[5]

[1] *University of Alaska Fairbanks, United States of America*; [2] *University of California, Irvine*
[3] *Purdue University*; [4] *U.S. Geological Survey*; [5] *U.S. Forest Service*

Nearly a third of the World's terrestrial carbon stock is located in boreal and arctic biomes, deep in permafrost soils where frozen organic matter is protected from decomposition. Therefore, the stability of soil carbon stocks in high latitudes depends largely on the resilience of permafrost to changing climate and disturbance regimes. The vulnerability of permafrost to increasing temperature and wildfire has been evaluated at local and regional scales through modeling studies that integrate local long-term field observations. However, the consequences of the deepening of the active layer and loss of permafrost on regional soil carbon stocks have not been well documented. Both climate warming and wildfire intensification (i.e. increase in fire frequency and severity) can be responsible for increasing active layer depth, talik formation and loss of permafrost, leading to increased amount of soil organic matter available for decomposition and release to the atmosphere through aerobic or anaerobic processes, depending on drainage conditions. Substantial carbon losses can also occur through pyrogenic emissions from soil organic horizons burning during wildfire. However, these losses may be offset to varying degrees by increased carbon input to the soil if vegetation productivity (and associated litterfall) would increase in response to climate warming and increased availability of the atmospheric CO_2. In addition, increases in litter input may contribute to the increases in organic horizon thickness that could insulate underlying permafrost and retard thaw (Fig. 1).

To better understand the impact of permafrost freeze and thaw dynamics on the vulnerability of soil carbon stocks, we used a process-based ecosystem model, the Terrestrial Ecosystem Model (TEM). TEM was coupled with a disturbance model and a model of biogenic methane dynamics to assess historical and projected soil carbon changes in Alaska, from 1950 to 2100. The uncertainties related to climate, fire regime and atmospheric CO_2 projections were quantified by running simulations using climate projections from two global climate system models, three fossil fuel emission scenarios. To quantify the relative effect of climate change, increasing fire frequency and severity and increasing atmospheric CO_2 on permafrost and its consequences on soil carbon accumulation, we used various combinations of detrended climate scenarios, constant fire regime and constant atmospheric CO_2.

During the historical period 1950 – 2009, soil carbon stocks increased by 4.7 Tg C/yr in Alaska, but decreased in the boreal region of Alaska due to substantial fire activity in the early 2000's. This loss was offset by net carbon accumulation in the arctic where the increase in active layer depth and associated CO_2 and CH_4 effluxes, were balanced by an increase in carbon input from the vegetation. Permafrost loss (below 1 m depth) from 2010 to 2099 would range from 25.4 and 40.5 % and changes in soil carbon stocks from 2010 to 2099 ranged from 8.9 to 25.6 Tg C/yr, depending on the climate projections. Soil carbon accumulation was less in lowlands than in uplands and less in boreal than in arctic regions of Alaska because of the negative effect of permafrost loss and fire activity on soil carbon stocks. Overall, this analysis illustrates the importance of accounting for permafrost dynamics and disturbance regimes in assessing responses of soil carbon in high latitude ecosystems.

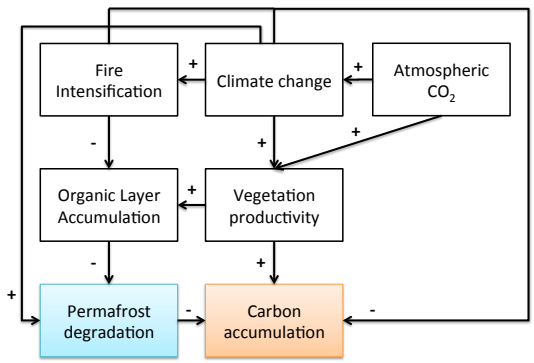

Figure 1: Diagram representing the interactions at play in the response of permafrost to climate change and its impact on carbon accumulation.

Relevance of aggregation and chemisorption for carbon sequestration in thawing permafrost soils of Northern Siberia

Ina Charlotte Haase[1], Alevtina Evgrafova[2,3], Nikita Tananaev[4], Olga Shibistova[1,5], Peter Kühn[6], Georg Guggenberger[1,5], Sandra Spielvogel[3], & Leopold Sauheitl[1]

[1] *Institute of Soil Science, Leibniz University Hannover, Hannover, Germany*
[2] *Geography Department, University of Koblenz-Landau, Koblenz, Germany*
[3] *Institute of Geography, University of Bern, Bern, Switzerland*
[4] *Igarka Geocryology Lab. of the Melnikov Permafrost Institute Yakutsk, SB RAS, Igarka, Russia*
[5] *VN Sukachev Institute of Forest, SB RAS, Akademgorodok, Krasnoyarsk, Russian Federation*
[6] *Lab. for Soil Science and Geoecology, Eberhard Karls University Tübingen, Germany, Tübingen, Germany*

One of major scientific focuses is a possible transition of permafrost soils from an important terrestrial carbon sink to a source due to climate change. In addition to the traditional view, global warming could lead not only to initial degradation of soil organic matter (SOM), but also to stabilization of SOM in the midterm at new developed mineral surfaces and via aggregation resulting from increased soil aeration while and after permafrost thaws.

To address the importance of SOM decomposition vs. stabilization and its temporal dynamics, a space-for-time approach was used. Soils with different active layer (AL) depths at a well-described Yenisei tributary catchment in Siberia (67°28.933' N, 86°25.682' E; Krasnojarsk Krai, Russian Federation) were investigated, representing different states of permafrost degradation. The catchment is part of the highly vulnerable high latitude forest tundra ecotone, which represents wide areas of northern Russia. We analyzed organic carbon (OC) content, aggregation, estimated via dry aggregate sieving, OC distribution and isotopic C- and N-signature in aggregate classes as well as in density fractions as site dependent variables.

First results show that the largest OC amounts are found in shallow AL profiles (AL between 20 to 40 cm below organic layer), thus holding a high potential of OC loss when thawing to an intermediate AL depth (AL between 40 to 60 cm below organic layer). Comparing the intermediate AL profiles with sites were no permafrost was found within a depth of up to 1 m below the organic layer, no distinct changes in OC stocks were found.

Concerning soil architecture, surprisingly, even soils with shallow AL having wet conditions in the thawed horizons exhibited a high intensity of aggregation, comparable to sites with no permafrost. According to these observations, we can conclude that the aggregate size distribution reacts in a non hierarchical way to thawing and soil aeration. Regarding C-sequestration in different aggregate classes, no clear trends were distinguished. In addition, micromorphological thin sections of selected profiles were evaluated to gain a deeper insight into in-situ soil architecture and processes. Here, first indications reveal features of high bioturbation even at sites with thinner ALs. This might have facilitated the aggregation of shallow AL sites.

Comparing ^{13}C signatures and C/N ratios of different density fractions from shallow AL to no permafrost sites, an advancing trend of retarded decomposition is recognized. While alterations of these signals were strong at the beginning (transition of shallow AL to intermediate stage), the change of degradation proxies was negligible at further stages. Mineral associated OC (MOM) plays a key role in C storage across all AL stages and upcoming ^{14}C dates of MOM may provide more understanding about the mean residence time of this pool under the current permafrost regime.

Regarding aggregation, statistical analysis will be performed to illustrate possible influences of other soil parameters such as pedogenic metaloxides or particle-size distribution.

We conclude that even though the main loss of OC in bulk soil may proceed fast after initial deepening of the AL, this is partly compensated by SOM stabilization. However, this process is dominated by SOC-sorption on mineral surfaces rather than sequestration in aggregates. Carbon storage in the form of MOM is already dominating in early stages of permafrost degradation. Moreover the high losses of C indicate that the sorption is still weak during initial MOM development.

Thermokarst-lake methanogenesis along a complete talik (thaw bulb) profile

Joanne Kathleen Heslop[1], Katey Walter Anthony[1], Armando Sepulveda-Jauregui[1], Karla Catalina Martínez Cruz[1,2], Allen Bondurant[1], Guido Grosse[3], & Miriam Jones[4]

[1] *University of Alaska, Fairbanks, United States of America*
[2] *Biotechnology and Bioengineering, Cinvestav, Mexico City, Mexico*
[3] *Alfred Wegener Institute Helmholtz Centre for Polar and Marine Research, Potsdam, Germany*
[4] *US Geological Survey, Reston, Virginia, USA*

Thermokarst (thaw) lakes emit methane (CH_4) to the atmosphere, with the carbon (C) originating from terrestrial sources such as the Holocene soils of the lakes' watersheds, thaw of Holocene- and Pleistocene-aged permafrost soil beneath and surrounding the lakes, and decomposition of contemporary organic matter (OM) in the lakes. However, the relative magnitude of CH_4 production in surface lake sediments versus deeper thawed permafrost horizons is not well understood. We assessed anaerobic CH_4 production potentials from 22 depths along a 590 cm long lake sediment core from the center of an interior Alaska thermokarst lake, Vault Lake, that captured the entire package of surface lake sediments, the talik (thaw bulb), and the top 40 cm of thawing permafrost beneath the talik. We also studied the adjacent Vault Creek permafrost tunnel that extends through ice-rich yedoma permafrost soils surrounding the lake and into underlying fluvial gravel. Our results show, in the center of a first generation thermokarst-lake, whole-column CH_4 production is dominated by methanogenesis in the organic-rich surface lake sediments [151 cm thick; mean ± SD 5.95 ± 1.67 μg C-CH_4 per g dry weight sediment per day (g dw^{-1} d^{-1}); 125.9 ± 36.2 μg C-CH_4 per g organic carbon per day (g C org^{-1} d^{-1})]. The organic-rich surface sediments contribute the most (67 %) to whole-column CH_4 production despite occupying a lesser fraction (26 %) of sediment column thickness. High CH_4 production potentials were also observed in recently-thawed permafrost (1.18 ± 0.61 μg C-CH_4 g dw^{-1} d^{-1}; 59.60 ± 51.5 μg C-CH_4 g C org^{-1} d^{-1}) at the bottom of the talik, but the narrow thicknesses (43 cm) of this horizon limited its overall contribution to total sediment column CH_4 production in the core. Lower rates of CH_4 production were observed in sediment horizons representing permafrost that has been thawed in the talik for longer periods of time.

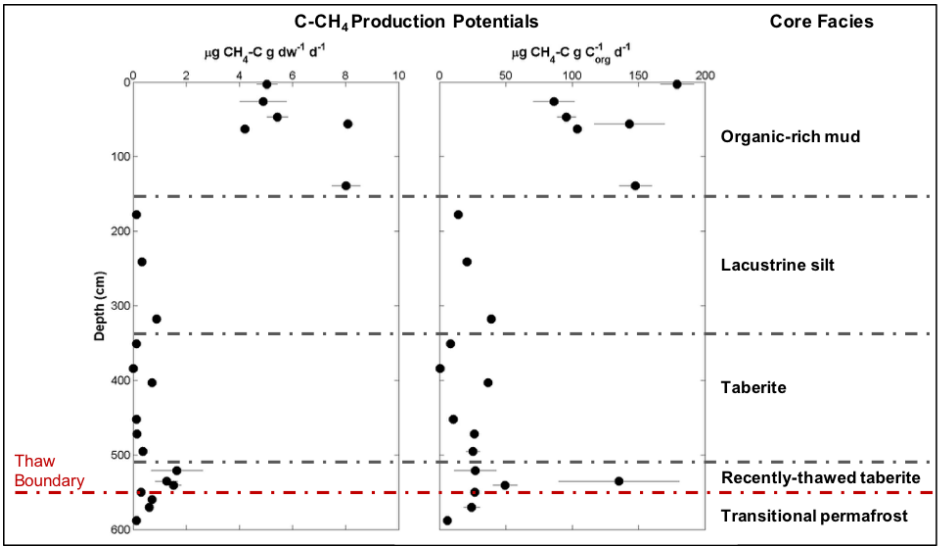

Figure 1: CH_4 production potentials in the Vault Lake core. Samples were anaerobically incubated at 3°C. CH_4 production potentials are represented as mean value ± SD among replicates normalized per gram dry weight sediment (left) and per gram organic carbon (right)

The thickest sequence in the Vault Lake core, which consisted of combined Lacustrine silt and Taberite facies (60 % of total core thickness), had low CH_4 production potentials, contributing only 21 % of whole sediment column CH_4 production potential. No CH_4 production was observed in samples obtained from the permafrost tunnel, whose sediments represent a non-lake environment. Our findings imply that CH_4 production is highly variable in thermokarst-lake systems and that both modern OM supplied to surface sediments and ancient OM supplied to both surface and deep lake sediments by in situ thaw, as well as shore erosion of yedoma permafrost, are important to lake CH_4 production. Knowing where CH_4 originates and what proportion of produced CH_4 is emitted will aid in estimations of how C release and processing in a thermokarst-lake environment differs from other thawing permafrost and non-permafrost environments.

References

Heslop, J.K.; Walter Anthony, K.M.; Sepulveda-Jauregui, A.; Martinez-Cruz, K.; Bondurant, A.; Grosse, G. and Jones, M.C. [2015]: Thermokarst lake methanogenesis along a complete talik profile. *Biogeosciences*, 12:4317–4331, doi:10.5194/bg-12-4317-2015.

Relationships between organic matter quality and methane production in thermokarst lake sediments

Joanne Kathleen Heslop, Katey Walter Anthony, & Mingchu Zhang

University of Alaska, Fairbanks, United States of America

Despite many thermokarst (thaw) lakes having exceptionally high methane (CH_4) emission rates, few studies have examined biodegradability of thawed permafrost organic carbon (Corg) in deep anaerobic environments, such as thermokarst lake sediments and taliks (thaw bulbs). We examined bulk sediment organic matter (SOM) and water-extractable organic matter (WEOM) composition in a full-talik lake core (590 cm) collected from the center of a thermokarst lake in interior Alaska. These properties were then correlated with CH_4 production measured on sediments from the same core. The surface organic-rich sediments horizon of our lake core (0-150 cm depth) had the highest CH_4 production potentials and rates. This section of the core also had: higher levels initial substrate, indicated by higher levels of total soil carbon (Ctot), Corg, and total soil nitrogen (Ntot); less decomposed OM, indicated by higher Corg:Ntot ratios and lighter $\delta^{13}C$org; and greater proportions of alkanes, lignin, and phenols and phenolic precursors in its bulk SOM compared to the remainder of the core. We observed statistically significant ($p < 0.05$) correlations between each of these bulk SOM parameters and anaerobic CH_4 production measured at an incubation temperature of 3 °C. Proportions of aromatic proteins and fulvic acid-like WEOM correlated with initial CH_4 production rates (t = 0-34 d) but not longer-term CH_4 production potentials (incubation length = 175 d), suggesting that initial WEOM composition influences short-term C mineralization rates but not longer term anaerobic C mineralization potentials. Some of the relationships we observed in our anaerobic incubations, such as a strong positive correlation ($r = 0.72$; $p=0.001$) between CH_4 production potentials and phenols and phenolic precursors, differed from previously observed relationships in aerobic incubations. This suggests OM is utilized differently in aerobic and anaerobic environments, emphasizing the importance of examining each of these environments separately to improve our estimates of potential C emissions from thawing permafrost soils.

Changing Permafrost in the Arctic and its Global Effects in the 21st Century (PAGE21): Final Results for a large-scale international and integrated project to measure the impact of permafrost degradation on the climate system

Hans-Wolfgang Hubberten, Hugues Lantuit, Julia Boike, & Leena-Kaisa Viitanen

Alfred Wegener Institute Helmholtz Centre for Polar and Marine Research, Potsdam, Germany

Our understanding of the physical and biogeochemical processes at play in permafrost areas has been greatly inadequate and significant gaps have existed in our current knowledge, hindering any accurate assessment of the vulnerability of Arctic permafrost to climate change, or of the implications of future climate change for global greenhouse gas (GHG) emissions. The PAGE21 project was designed to broaden our knowledge base by assessing the vulnerability of Arctic permafrost to climate change and by reducing the uncertainties in permafrost-related feedbacks to the global climate. In particular, the PAGE21 project has sought to answer the following questions:

- What are the key processes and parameters influencing and controlling the vulnerability of the carbon and nitrogen pools in Arctic permafrost to future climate change?
- How large an effect will Arctic climate change feedback (due to changes in the carbon and nitrogen pools contained in permafrost) have on anthropogenic global warming?

The concept of PAGE21 was to address these questions through a close interaction between monitoring activities, process studies and modeling on the pertinent temporal and spatial scales. Field sites were selected to cover a wide range of environmental conditions for the validation of large scale models, the development of permafrost monitoring capabilities, the study of permafrost processes, and for overlap with existing monitoring programs. Interaction between site-scale studies and large-scale modeling was designed to establish and maintain a direct link between these two areas for developing and evaluating, on all spatial scales, the land-surface modules of leading European global climate models taking part in the Coupled Model Intercomparison Project Phase 5 (CMIP5), designed to inform the IPCC process.

The PAGE21 results to date have highlighted that the amount of carbon released from permafrost over the 21st century may not be as large as previously claimed. The project has found an average loss of about 50 Gt C by 2100, which is at the lower end of the IPCC estimate of 50 to 250 Gt C. However, we have found that, in a much warmer world, this carbon loss would continue over hundreds of years leading to the severe degradation of permafrost ecosystems and a large cumulative loss of previously frozen carbon.

Comparing permafrost soil carbon pools from earth system models to empirically derived datasets

Gustaf Hugelius[1], A. David McGuire[2], Christian Beer[1], Theodore J. Bohn[3,4], Eleanore J. Burke[5], Sarah E. Chadburn[6], Guangsheng Chen[7], Xiaodong Chen[8], Daniel J. Hayes[7], Elchin E. Jafarov[9], Charles D. Koven[10], Shushi Peng[11,12], & Kevin M. Schaefer[13]

[1] *Stockholm University, Sweden*
[2] *US Geological Survey, Alaska Cooperative Fish and Wildlife Research Unit, University of Alaska Fairbanks, Fairbanks, AK, USA*
[3] *University of Washington, Seattle,WA, USA*
[4] *Arizona State University, Tempe, AZ, USA*
[5] *Met Office Hadley Centre, Exeter, UK*
[6] *University of Exeter, Exeter, UK*
[7] *Oak Ridge National Laboratory, Oak Ridge, TN, USA*
[8] *University of Washington, Seattle, WA, USA*
[9] *Institute of Arctic and Alpine Research, University of Colorado, Boulder, CO, USA*
[10] *Lawrence Berkeley National Lab, Berkeley, CA, USA*
[11] *Lab. des Sciences du Climat et de l'Environnement (LSCE CEA-CNRS-UVSQ), Gif-sur-Yvette, France*
[12] *Lab. de Glaciologie et Géophysique de l'Environnement, CNRS and Université Grenoble Alpes, Grenoble, France*
[13] *National Snow and Ice Data Center, University of Colorado, Boulder, CO, USA*

Permafrost region soils contain very large stocks of soil organic carbon, which has accumulated over long time periods. These large stocks are a result of environmental factors and soil forming processes that are particularly prevalent or unique in cold region soils, including, peat formation, cryoturbation and the presence of near-surface permafrost. The extent and detail to which these processes are represented in Earth System Models varies, but is typically very limited. Here we compare the soil carbon pools generated by spin-up runs of a suite of land surface models from the Permafrost Carbon Network model intercomparison [Koven et al., 2015, McGuire et al., in prep.] to the empirically based maps of soil carbon storage in the Northern Circumpolar Soil Carbon Database (NCSCD; Hugelius et al. [2014]. Circumpolar spatial correlations reveal very weak linear relationships between modeled and empirically mapped soil carbon stocks. Based on the mapped soil classification data in the NCSCD (following U.S.D.A Soil Taxonomy), we assigned the mapped soil carbon stocks to the following categories: permafrost peatlands (Histels), cryoturbated soils (Turbels), other permafrost soils (Orthels) non-permafrost peatlands (Histosols) and non-permafrost mineral soils (remaining soil orders). Following this scheme, we analyze regional-scale patterns of deviations between empirical and modelled soil carbon stocks. We place a particular emphasis on model benchmarking in regions where soil carbon storage is dominated by the particular soil forming processes affecting these different soil types. By focusing the spatial analyses to specific regions and soil types we can isolate which soil types are well represented in models and which are not. These types of comparisons reveal interesting trends that can provide semi-quantitative relationships between soil forming processes and observed model biases, which may in turn inform and improve future model development.

References

Hugelius, G.; Strauss, J.; S., Zubrzycki; Harden, J.W.; Schuur, E.A.G.; Ping, C.L.; Schirrmeister, L.; Grosse, G.; Michaelson, G.J.; Koven, C.; O'Donnell, J.; Elberling, B.; Mishra, U.; Camill, P.; Yu, Z.; Palmtag, J. and Kuhry, P. [2014]: Estimated stocks of circumpolar permafrost carbon with quantified uncertainty ranges and identified data gaps. *Biogeosciences*, 11, doi:10.5194/bg-11-6573-2014.

Koven, C.D.; Schuur, E.A.G.; Schädel, C.; Bohn, T.J.;

Burke, E.J.; Chen, G.; Chen, X.; Ciais, P.; Grosse, G.; Harden, J.W.; Hayes, D.J.; Hugelius, G.; Jafarov, E.E.; Krinner, G.; Kuhry, P.; Lawrence, D.M.; MacDougall, A.H.; Marchenko, S.S.; McGuire, A.D.; Natali, S.M.; Nicolsky, D.J.; Olefeldt, D.; Peng, S.; Romanovsky, V.E.; Schaefer, K.M.; Strauss, J.; Treat, C.C. and Turetsky, M. [2015]: A simplified, data-constrained approach to estimate the permafrost carbon–climate feedback. *Trans. R. Soc. A*, 373, doi:10.1098/rsta.2014.0423.

McGuire, A.D.; Koven, C.; Lawrence, D.M.; Clein, J.S.; Xia, J.; Beer, C.; Burke, E.; Chen, G.; Chen, X.; Delire, C.; Jafarov, E.; MacDougall, A.; Marchenko, S.; Nicolsky, D.; Peng, S.; Rinke, A.; Saito, K.; Zhang, W.; Alkama, R.; Bohn, T.J.; Ciais, P.; Decharme, B.; Hayes, D.J.; Ekici, A.; Gouttevin, I.; Hajima, T.; Ji, D.; Krinner, G.; Lettenmaier, D.P.; Luo, Y.; Miller, P.A.; Moore, J.C.; Romanovsky, V.; Schaedel, C.; Schaefer, K.; Schuur, E.A.G.; Smith, B.; Sueyoshi, T and Zhuang, Q. [in prep.]: A model-based analysis of the vulnerability of carbon in the permafrost region between 1960 and 2009. *manuscript intended for submission to Global Biogeochemical Cycles.*

More than Methane: Linking geomorphology and biogeochemistry to understand biogas emissions from two wetlands on Spitsbergen

Eleanor Louise Jones[1] & Andy Hodson[1,2]

[1] *Department of Geography, University of Sheffield, United Kingdom, S10 2TN*
[2] *Arctic Geology, University Centre in Svalbard, N-9171 Longyearbyen, Norway*

The coastal Arctic is very sensitive to oceanic warming, which makes it an important early warning system for the response of permafrost to climate change. The western coast of Spitsbergen, located in the zone of continuous permafrost, is kept relatively warm for its latitude [Romanovsky et al., 2010] by the north Atlantic current. Thawing of permafrost leads to the production of greenhouse gases, such as methane, carbon dioxide and nitrous oxide. The production of these gases is influenced by redox potential, which is linked to hydrology [Elberling et al., 2013]. Hence, understanding the links between geomorphology, hydrology and biogeochemistry is key to predicting the responses of ecosystems to climate change. The primary aim of the project presented here is to foster an improved understanding of biogas emissions from a changing permafrost landscape through an integrated study of sediment provenance, depositional history and in situ biogeochemical processes.

To achieve its aim, the project will focus on two locations in Western Spitsbergen, Svalbard, in conjunction with the EU-funded LowPerm project. Both sites were covered by warm-based ice during the Last Glacial Maximum, and so it was only after the deglaciation around 10,000 years ago that permafrost aggraded [Landvik et al., 1988]. Following the deglaciation, contrasting depositional environments developed. At Revneset, which is located ≈7 kilometres north of Longyearbyen, a sequence of raised beaches formed due to isostatic rebound. In Adventdalen, a delta prograded and was overlain by aeolian sediments. Ice-wedge polygons and wetlands formed at both sites. This study is the first to anticipate that depositional history and geomorphology have implications for biogas emissions.

This novel study will firstly involve coring the sites to a depth of 2 metres below the surface. Samples from the sediment cores will form the basis of manipulative microcosm experiments to quantify the response of microbial greenhouse gas production to different hydrological and nutrient/substrate conditions. Secondly, the sedimentology of both sites will be investigated by conducting analyses on the cores to determine particle size distribution, elemental composition, and mineralogy. The processes and rates of sediment accumulation will be ascertained; this will include dating of the sediment cores by optically stimulated luminescence. Finally, the feasibility of using microcosm experiments to predict landscape scale greenhouse gas emissions will be investigated by comparing the ratios of greenhouse gases produced in situ to those produced in the microcosm experiments.

References

Elberling, B.; Michelsen, A.; Schädel, C.; Schuur, E.A.G.; Christiansen, H.H. and L. ... Sigsgaard-Berg, C. [2013]: Long-term CO_2 production following permafrost thaw. *Nature Climate Change*, 3 (10):890–894, doi:10.1038/nclimate1955.

Landvik, J.Y.; Manderud, J. and Salvigsen, O. [1988]: Glacial history and permafrost in the svalbard area. In: Senneset, K.(ed.), *Proceedings of the 5th International Conference on Permafrost*, 2–5 August 1988, Trondheim, Norway. volume 1, pages 194–198. Trondheim: Tapir Publishers. ISBN 82-5 19-0863-9. URL http://ipa.arcticportal.org/publications/conference-proceedings.

Romanovsky, V.E.; Smith, S.L. and Christiansen, H.H. [2010]: Permafrost thermal state in the polar Northern Hemisphere during the International Polar Year 2007–2009: a synthesis. *Permafrost and Periglacial Processes*, 21(2): 106–116, doi:10.1002/ppp.689.

Permafrost thaw in boreal peatlands: the importance of permafrost formation processes in post-thaw carbon losses

Miriam C. Jones[1], Kristen Manies[1], Claire Treat[2], Jennifer Harden[1], Jonathan O'Donnell[3], & Mark Waldrop[1]

[1] *U.S. Geological Survey, United States of America*
[2] *University of Alaska Fairbanks, United State of America*
[3] *U.S. National Park Service, United States of America*

Permafrost peatlands are becoming increasingly vulnerable to thaw, as high latitudes warm faster than other regions and as disturbances such as wildfires become more frequent and intense. Peatlands have accumulated nearly 30 % of the soil organic carbon (C) within the northern high latitude permafrost region over the Holocene, storing roughly 275 Pg of organic C, which is equivalent to over one-third of the C currently in the atmosphere. However, the long term C balance may be affected by permafrost degradation, with uncertainty surrounding the timing, magnitude and controls on C losses. Here, we explore this concept using a chronosequence approach, a mass-balance modeling approach, and a synthesis of paleoecological reconstructions to show the timing of peatland development and permafrost aggradation and degradation over the Holocene. When permafrost thaws, carbon from the formerly frozen permafrost is released to the atmosphere on the order of years to decades, and long-term accumulation of post-thaw bog peat leads to carbon uptake over centuries to millennia. As much as two-thirds of the original forested permafrost plateau peat C is lost from boreal Alaskan peatlands following permafrost thaw, and the greatest losses are from the oldest peatlands. We also show that the permafrost formation process in peatlands can help explain the magnitude of C losses following thaw. Using the results of three Alaskan chronosequences, we show that peat that accumulates simultaneously with permafrost aggradation (syngenetic) will lose a greater fraction of C following thaw than peat that primarily accumulated prior to permafrost aggradation (epigenetic), because the syngenetic permafrost peat contains a higher fraction of labile C than epigenetic permafrost peat. In order to place these results into the context of permafrost peatlands across the northern high latitude region, we synthesized existing paleoecological peat core reconstructions and demonstrate that most peatlands containing permafrost today or that have experienced recent thaw (last few decades), formed permafrost epigenetically, with most permafrost aggradation occurring during Holocene Neoglacial cooling (< 4 kya) and the Little Ice Age (150 to 300 ya). When coupled with results from our Alaskan chronosequence studies, we find that boreal permafrost peatlands will lose a significant amount of C following permafrost thaw, but that because most permafrost aggradation in extant peatlands is relatively recent, C losses will be less than those in peatlands with syngenetic permafrost. We predict that over centuries to millennia, post-thaw bog C accumulation will eventually make up for the immediate C losses resulting from thaw.

Constraining the uncertainty of the Arctic CH_4 sink and its potential effects on permafrost carbon feedbacks to the global climate system

Christian Juncher Jørgensen[1], Jesper Riis Christiansen[1], Tue Mariager[1], & Gustaf Hugelius[2]

[1] *University of Copenhagen, Department of Geosciences and Natural Resource Management, Denmark*
[2] *Stockholm University, Department of Physical Geography, Sweden*

Using atmospheric methane (CH_4), certain soil microbes are able to sustain their metabolism, and in turn remove this powerful greenhouse gas from the atmosphere. While the process of CH_4 oxidation is a common feature in most natural and unmanaged ecosystems in temperate and boreal ecosystems, the interactions between soil physical properties and abiotic process drivers, net landscape exchange and spatial patterns across Arctic drylands remains highly uncertain. Recent works show consistent CH_4 consumption in upland dry tundra soils and sediments in Arctic and High Arctic environments [Christiansen et al., 2015, Jørgensen et al., 2015, Lau et al., 2015]. In these dominantly dry or barren soil ecosystems, CH_4 consumption has been observed to significantly exceed the amounts of CH_4 emitted from adjacent wetlands. These observations point to a potentially important but largely overlooked component of the global soil-climate system interaction and a counterperspective to the conceptual understanding of the Arctic being only an emitter of CH_4. However, due to our limited knowledge of spatiotemporal occurrence of CH_4 consumption across a wider range of the Arctic landscape we are left with substantial uncertainties and an overall unconstrained range estimate of this terrestrial CH_4 sink and its potential effects on permafrost carbon feedback to the atmospheric CH_4 concentration.

To address this important knowledge gap and identify the most relevant spatial scaling parameters, we studied in situ CH_4 net exchange across a large landscape transect on West Greenland. The transect represents soils formed from the dominant geological parent materials of dry upland tundra soils found in the ice-free land areas of Western Greenland, i.e.

1. granitic/gneissic parent material,
2. basaltic parent material and
3. sedimentary deposits.

Results show that the dynamic variations in soil physical properties and soil hydrology exerts an overriding control on the net CH_4 consumption both within and across these well-aerated soil systems. Quite surprisingly, we found high CH_4 sink rates in conditions when soils were both extremely thin ($<$ 10 cm to bedrock), very dry ($<$ 5 – 10 % soil moisture), weakly developed and highly exposed to harsh environmental conditions such as mountain tops, alpine tundra and abrasion plateaus, which are historically overlooked 'extreme soils' regarding CH_4 exchange. The results show that the physical areas and landforms where CH_4 oxidation and net CH_4 deposition occurs has not been delimited for the Arctic and calls for a revised understanding of the role of CH_4 consumption in natural drylands and extreme environments for the net CH_4 budget at the circumpolar scale. In these sensitive regions, changes towards warmer and drier soil conditions in some areas as a consequence of a warming Arctic could favor the activity of the CH_4 breathers, leading to future increase in net atmospheric CH_4 consumption in dry and barren land areas. This could have far-reaching implications for the permafrost carbon feedback to the global climate system and how we integrate the soil CH_4 consumption feedback in Earth Systems Model simulating the Arctic CH_4 budget.

References

Christiansen, J.R.; Romero, A.J.B.; N.O.G., Jørgensen; Glaring, M.A.; Jørgensen, C.J.; Berg, and Elberling, B. [2015]: Methane fluxes and the functional groups of methanotrophs and methanogens in a young Arctic landscape on Disko Island, West Greenland. *Biogeochemistry*, 122:15–33, doi:10.1007/s10533-014-0026-7.

Jørgensen, C.J.; Johansen, K.M.L.; Westergaard-Nielsen, A. and Elberling, B. [2015]: Net regional methane sink in High Arctic soils of north-

east Greenland. *Nature Geoscience*, 8:20–23, doi:10.1038/ngeo2305.

Lau, M.C.Y.; Stackhouse, B.T.; Layton, A.C.; Chauhan, A.; Vishnivetskaya, T.A.; Chourey, K.; Ronholm, J.; Mykytczuk, N.C.S.; Bennett, P.C.; Lamarche-Gagnon, G.; Burton, N.; Pollard, W.H.; Omelon, C.R.; Medvigy, D.M.; Hettich, R.L.; Pfiffner, S.M.; Whyte, L.G. and Onstott, T.C. [2015]: An active atmospheric methane sink in high Arctic mineral cryosols. *The ISME Journal*, 9:1–12, doi:10.1038/ismej.2015.13.

Modelling carbon in permafrost soils from preindustrial to the future

Thomas Kleinen

Max Planck Institute for Meteorology, Germany

The carbon release from thawing permafrost soils constitutes one of the large uncertainties in the carbon cycle under future climate change. Analysing the problem further, this uncertainty results from an uncertainty about the total amount of C that is stored in frozen soils, combined with an uncertainty about the areas where soils might thaw under a particular climate change scenario, as well as an uncertainty about the decomposition product since some of the decomposed C might result the release of CH_4 as well as CO_2.

We use the land surface model JSBACH, part of the Max Planck Institute Earth System Model MPI-ESM, to quantify the release of soil carbon from thawing permafrost soils. We have extended the soil carbon model YASSO by introducing carbon storages in frozen soils, with increasing fractions of C being available to decomposition as permafrost thaws. In order to quantify the amount of carbon released as CH_4, as opposed to CO_2, we have also implemented a TOPMODEL-based wetland scheme, as well as anaerobic C decomposition and methane transport.

We initialise the soil C pools for the preindustrial climate state from the Northern Circumpolar Soil Carbon Database to insure initial C pool sizes close to measurements. We then determine changes in soil C storage in transient model experiments following historical and future climate changes under RCP 8.5. Based on these experiments, we quantify the greenhouse gas release from permafrost C decomposition, determining both CH_4 and CO_2 emissions.

Permafrost thawing as a possible source of abrupt carbon release at the onset of the Bølling/Allerød

Peter Köhler[1], Gregor Knorr[1], & Edouard Bard[2]

[1] *Alfred Wegener Institute Helmholtz Centre for Polar and Marine Research, Bremerhaven, Germany*
[2] *CEREGE, Aix Marseille University, CNRS, IRD, College de France, Aix-en-Provence, France*

One of the most abrupt and yet unexplained past rises in atmospheric CO_2 (10 ppmv in two centuries in the EPICA Dome C [EDC] ice core) occurred in quasi-synchrony with abrupt northern hemispheric warming into the Bølling/Allerød, about 14.6 ka ago. In Köhler et al. [2014] we used a U/Th-dated record of atmospheric $\Delta^{14}C$ from Tahiti corals to provide an independent and precise age control for this CO_2 rise. We also used model simulations to show that the release of old (nearly ^{14}C-free) carbon can explain these changes in CO_2 and $\Delta^{14}C$. The $\Delta^{14}C$ record provides an independent constraint on the amount of carbon released (125 Pg C). We suggest, in line with observations of atmospheric CH_4 and terrigenous biomarkers, that thawing permafrost in high northern latitudes could have been the source of carbon, possibly with contribution from flooding of the Siberian continental shelf during meltwater pulse 1A. Our findings highlight the potential of the permafrost carbon reservoir to modulate abrupt climate changes via greenhouse-gas feedbacks. These calculations and conclusions were challenged by the new CO_2 data [Marcott et al., 2014] from the West Antarctic Ice Sheet Divide Ice Core (WDC), which have a higher temporal resolution. We therefore revised our carbon release experiments in order to meet these new WDC CO_2 data. We furthermore used a new age distribution during gas enclosure in ice which includes the most recent understanding of firn densification. We then can align EDC and WDC CO_2 data and propose a peak amplitude in atmospheric CO_2 of about 15 ppmv around 14.6 ka BP corresponding to a C pulse of 85 Pg C released in 200 years (0.425 Pg C per year). This is 68 % of the initial suggested strength of the C pulse of 125 Pg C, that then led to a peak amplitude in true atmospheric CO_2 of 22 ppmv. CO_2 data from other ice cores suggest that the amplitude in atmospheric CO_2 was in-between both these scenarios. The revised scenario proposes a carbon release that is still large enough to explain the atmospheric $\Delta^{14}C$ anomaly of – (50 – 60) ‰in 200 –250 years derived from Tahiti corals. However, in the revised scenario the released carbon needs to be essentially free of ^{14}C, while in the previously suggested scenario there was still the possibility that the released carbon still contained some ^{14}C and had a difference in the $\Delta^{14}C$ signature to the atmosphere $\delta(\Delta^{14}C)$ of −700 ‰. The previous scenario, therefore, contained a larger possibility that the released carbon might eventually been released from the deep ocean. The revised interpretation proposed here strengthens the idea that the carbon was released from permafrost thawing, since this had more likely a nearly ^{14}C-free signature than any other known source. We therefore conclude, that the new WDC CO_2 data are not in conflict with our permafrost thawing hypothesis, but indicate only that the magnitude of the released carbon might have been smaller than initially suggested.

References

Köhler, P.; Knorr, G. and Bard, E. [2014]: Permafrost thawing as a possible source of abrupt carbon release at the onset of the Bølling/Allerød. *Nature Communications*, 5, doi:10.1038/ncomms6520.

Marcott, S. A.; Bauska, T. K.; Buizert, C.; Steig, E. J.; Rosen, J. L.; Cuffey, K. M.; Fudge, T. J.; Severinghaus, J. P.; Ahn, J.; Kalk, M. L.; McConnell, J. R.; Sowers, T.; Taylor, K. C.; White, J. W. C. and Brook, E. J. [2014]: Centennial scale changes in the global carbon cycle during the last deglaciation. *Nature*, 514:616–619, doi:10.1038/nature13799.

Lability classification of soil organic matter in the northern permafrost region based on simple soil horizon and landscape unit criteria

Peter Kuhry[1], Jiri Barta[2], Daan Blok[3], Bo Elberling[3], Samuel Faucherre[3], Gustaf Hugelius[1], Andreas Richter[4], Hana Santruckova[2], & Niels Weiss[1]

[1] *Stockholm University, Sweden*
[2] *University of South Bohemia, Czech Republic*
[3] *University of Copenhagen, Denmark*
[4] *University of Vienna, Austria*

The large stocks of soil organic carbon (SOC) stored in soils and deposits of the northern permafrost region are sensitive to global warming and permafrost thawing (Hugelius et al., 2014). The potential release of this carbon pool as greenhouse gases to the atmosphere does not only depend on the quantity of soil organic matter (SOM) remobilized but also on its lability (rate at which it might decay following warming/thawing).

We aim to develop a pragmatic classification scheme of SOM lability based on simple soil horizon partitioning and landscape unit characteristics, useful for upscaling to the entire northern permafrost region. For this purpose, we focus on the relationship between a simple geochemical indicator (%C) and decomposition rates, based on an exhaustive analysis of abiotic controls on SOM decomposition derived from the laboratory incubation of ca. 250 soil samples from 4 study areas across the northern permafrost region [Faucherre et al., submitted].

Aerobic respiration rates after one year of incubation are expressed as C-CO_2 release per unit organic C and regressed against carbon content (%C in dry matter) of the incubated material. By expressing C-CO_2 production rates as a function of the organic C in the sample, inferred lability can be directly linked to SOC stocks as accounted for in the Northern Circumpolar Soil Carbon Database [Hugelius et al., 2014].

Decomposability-SOM quality relationships are statistically analysed for all samples combined, as well as for simple groupings into soil horizon type and soil formation environment. Preliminary results indicate that C-CO_2 respiration rates per unit organic C are higher in the organically-enriched top soil layer (O and O/A horizons) compared to the mineral subsoil layers (primarily B and C horizons). However, values are quite similar for the active layer and the upper permafrost layer suggesting that decomposition of older SOM at greater depths in the upper permafrost layer has been largely halted due to its frozen state. Peat shows a particularly low rate of C-CO_2 production. Substantial within-group variability remains following partitioning into these soil horizon types, but variability is greatly reduced when grouping samples according to general landscape units, with lability decreasing in the order alluvial > eolian > mineral upland > peatland.

Results are validated against an independent SOM incubation dataset from simple bioavailability assays performed on a large number of soil samples (ca. 475) from the Lower Kolyma region (NE Siberia). This comparison as well as other incubation experiments confirm the robustness and usefulness of the proposed lability classification scheme for widespread application. The aim is to add a measure of SOM quality to the current estimates of SOC quantity to define vulnerable carbon pools and regions across the northern circumpolar permafrost region.

References

Faucherre, S.; Banyasz, I.; Jørgensen, C.J.; Weiss, N.; Hugelius, G.; Kuhry, P. and Elberling, B. [submitted] Abiotic controls on permafrost C mineralization rates based on incubating samples from 4 contrasting arctic localities. *ICOP 2016*, page 198.

Hugelius, G.; Strauss, J.; S., Zubrzycki; Harden, J.W.; Schuur, E.A.G.; Ping, C.L.; Schirrmeister, L.; Grosse, G.; Michaelson, G.J.; Koven, C.; O'Donnell, J.; Elberling, B.; Mishra, U.; Camill, P.; Yu, Z.; Palmtag, J. and Kuhry, P. [2014]: Estimated stocks of circumpolar permafrost carbon with quantified uncertainty ranges and identified data gaps. *Biogeosciences*, 11, doi:10.5194/bg-11-6573-2014.

Hydrolaccoliths of West Siberia – cold methane seeps in permafrost

Anna N. Kurchatova[1,2] & Victor V. Rogov[1,3]

[1] *Earth Cryosphere Institute SB RAS, Russian Federation*
[2] *Tyumen State Oil and Gas University, Russian Federation*
[3] *Lomonosov Moscow State University, Russian Federation*

Hydrolaccoliths are ice-core mounds which are widespread in permafrost of West Siberia. They reach 30 – 40 m in height with diameter near the base up to 150 – 200 m. The area of elevated basement is usually in 2-3 times more than the area of the mound. Complex researches with using of drilling, seismic survey and remote sensing showed that hydrolaccoliths are located within the anticlinal structures where Paleogene clays had been raised to the surface from the depth of 100 – 150 m. Their formation is related to dislocations of sedimentary strata and is also caused by inversion of the rock density along the section: 0.8 – 1.0 g/cm^3 of diatomite in contrast to 1.8 – 2.0 g/cm^3 of the Oligocene–Pleistocene sediments.

Samples of the frozen core of hydrolaccolith located in the south of the Taz Peninsula were studied with SEM and EDX spectroscopy analysis. They were prepared by the replica method not to disturb the microstructure of the frozen sediments. Cryogenic structure (vertical shifts and zigzag curves of ice schlieren with crystal twinning in their knots) reflects the significant deformations of permafrost strata. At the depth of 30 m, the empty curved-faces spherical, caselike, and elongated ice crystallites of 100 – 500 μm in size were found in the textural ice. Their formation is related to the pulsating gas microbubbles and pore-water flow through the framework of the plastic-frozen clay due to shear stress. The residual methane content in nonhermetically stored core samples was 2.2 and 7.6 vol % in the ground and ice, respectively. Methane homologs and helium were also identified in the gas composition. Numerous destroyed quartz grains indicate the cryogenic weathering due to the cyclic freezing of pore water and also the destruction along the slip planes.

These phase transitions provide the required amount of water and oxygen for the oxidation of hydrocarbons by bacteria to form carbon dioxide or bicarbonate that eventually precipitates as siderite while calcium chloride accumulates in cryopeg lenses. When oxygen is depleted in pore fluid, other consortium reduces sulfate to produce hydrogen sulfide. The formation of secondary sulfides (pyrrhotite – marcasite – pyrite) depends on geology and pore-water geochemistry of the sedimentary sequence, and the nature of the bacterial degradation. Sources of iron include colloidal grain coatings, pore-filling clays, and rock fragments. Authigenic magnetite which is widely distributed in hydrocarbon-induced biogeochemical aureoles in non-permafrost regions was also found in the samples.

Characterization of 16S rRNA genes amplified from the frozen samples indicated that archaeal clones could be discretely grouped within the Euryarchaeota and Crenarchaeota domains. The bacterial clones exhibited greater overall diversity than the archaeal clones, with sequences related to the Proteobacteria, Firmicutes, Acidobacteria, Actinobacteria, Bacteroidetes, and green nonsulfur groups. The majority of the bacterial clones was either members of a novel lineage or most closely related to uncultured clones. The results of the analyses suggest that the microbial community in the permafrost permeability zone is close to those in previously characterized cold seep environment.

Acknowledgements

This study has been supported by Russian Science Foundation (Grant 14-17-00131).

Net effects of drying experiment on permafrost stability through radiocarbon signals

Min Jung Kwon[1], Susan M. Natali[2], Caitlin Hicks Pries[3], K. Grace Crummer[4], Edward A. G. Schuur[5], Nikita Zimov[6], Sergey A. Zimov[6], Martin Heimann[1], & Mathias Goeckede[1]

[1] *Max Planck Institute for Biogeochemistry, Germany*
[2] *Woods Hole Research Center, Falmouth, USA*
[3] *Earth Sciences Division, Lawrence Berkeley National Laboratory, Berkeley, USA*
[4] *Department of Biology, University of Florida, Gainesville, USA*
[5] *Center for Ecosystem Science and Society, Department of Biological Sciences, Northern Arizona Universty, Flagstaff, USA*
[6] *North-East science station, Cherskii, Russia*

Air temperatures within the Arctic have increased over the past century, and warming trends are expected to continue in the future. As a consequence of thawing ice-rich permafrost, soil hydrology patterns are anticipated to be modified and large parts of the Arctic will become drier. In this study, we investigate how drying manipulation affects the age of respired CO_2 in moist (DryPEHR, in Eight Mile Lake, Alaska) and wet (Chersky, in northeast Siberia, Russia) tundra ecosystems. Water table depth (WTD) was lowered effectively in both sites but the difference was more prominent in a wet tundra ecosystem because of originally high WTD. Respiration $\Delta^{14}C$ values were measured to estimate contributions of old carbon, with more negative $\Delta^{14}C$ values as more old carbon is decomposed. In the wet tundra in Northeast Siberia, $\Delta^{14}CO_2$ signals from drying plots were clearly higher compared to the wet control plots, which is mostly attributed to shifts in soil temperatures following drier conditions. Drying soils at this observation site lowered heat capacity and thermal conductivity, and therefore surface soil can be heated up easily during the daytime but this heat is not transferred to deeper soil layers. As a result decomposition rates at surface layer were significantly elevated whereas those at deeper soil layers decreased, and therefore, a larger amount of young carbon but a less amount of old carbon were released from dry sites. Similar patterns were observed in the moist tundra sites in Alaska, but the net effects were less pronounced than in Siberia. In summary, our results demonstrate that alterations in soil temperatures as a consequence of drying can significantly modify decomposition patterns in shallow and deep soil layers, with less contributions of old carbon. Therefore, shifts in soil hydrology need to be considered as a major control on future carbon decomposition and accumulation rates in tundra ecosystems.

LGM permafrost carbon stocks inferred from empirical paleodata and modern analogues

Amelie Lindgren[1,2], Peter Kuhry[1], & Gustaf Hugelius[1]

[1] *Stockholm University, Sweden*
[2] *Lund University, Sweden*

In light of ongoing and projected future changes in the northern permafrost region with thawing soils and emissions of greenhouse gases (Schuur et al. 2015), we aim to assess how past periods of climate change have impacted permafrost-carbon dynamics. Postglacial climate warming following the Last Glacial Maximum (LGM) has been linked to massive carbon release from degrading permafrost [Walter et al., 2007]. As part of the Swedish-French GAP project we are aiming for an improved understanding of the extent of the northern permafrost region and its soil organic carbon stocks at LGM times. During the LGM, permafrost covered vast areas across Eurasia, including areas of exposed sea shelves along the northern coast of Russia and across the Bering Strait. Since a large fraction of North America was covered by ice sheets it had less permafrost than today. A recent GIS-based study by Lindgren [2015] estimates a total permafrost terrain cover of 34.5 million km^2 at the LGM (see Fig. 1). Using this as a spatial base, we compile and analyze several different types of paleodata with the aim to update and revise estimates of LGM permafrost carbon stocks. By reviewing and compiling proxy data for reconstruction of LGM biome distribution, peatland extent, regions of cryoturbation, loess accumulation, and alpine conditions, we intend to calculate carbon storage through the use of carbon transfer functions. This revised empirical estimate can be compared to recent estimates of permafrost carbon stocks, providing information on the amount of carbon likely reallocated from permafrost to the atmosphere, ocean and biosphere following Postglacial warming.

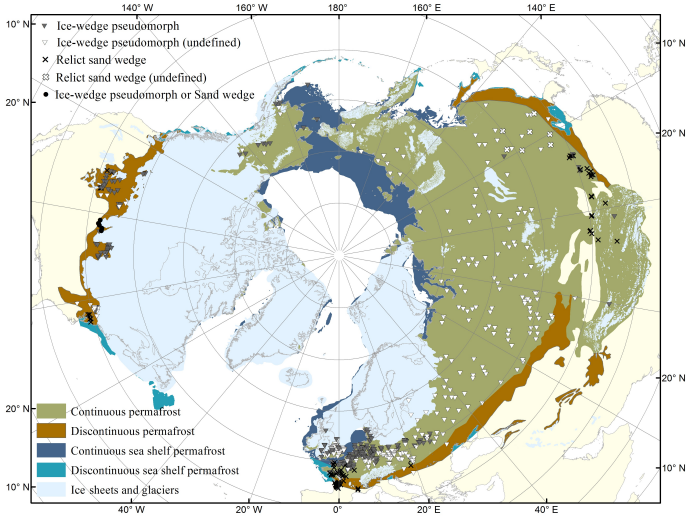

Figure 1: From Lindgren [2015] Speculative division between continuous and discontinuous permafrost

References

Lindgren, A. et al. GIS-based Maps and Area Estimates of Northern Hemisphere Permafrost Extent during the Last Glacial Maximum. *Permafrost and Periglacial Processes*, 2015. doi:10.1002/ppp.1851.

Schuur, E.A.G. et al. [2015]: Climate change and the permafrost carbon feedback. *Nature*, doi:10.1038/nature14338.

Walter, K.M.; Edwards, M.E.; Grosse, G.; Zimov, S.A. and Chapin, F.S. [2007]: Thermokarst lakes as a source of atmospheric CH_4 during the last deglaciation. *Science*, 318(5850):633–636, doi:10.1126/science.1142924.

Permafrost and feedbacks to the atmosphere in an Arctic regional climate model: an evaluation

Heidrun Matthes, Annette Rinke, & Klaus Dethloff

Alfred Wegener Institute Helmholtz Center for Polar and Marine Research, Potsdam, Germany

Frozen ground is an important component in the Arctic climate system as it influences the exchange of heat, moisture and gases between the land and the atmosphere. A good representation of permafrost and its coupling to the atmosphere is therefore essential for Arctic climate modelling. However, most climate models, both global General Circulation Models (GCMs) as well as Regional Climate Models (RCMs), have rather simplistic ground and land surface schemes which have strong limitations for frozen ground in the Arctic.

We use the RCM HIRHAM5 for the circum-Arctic domain. This model is based on the physical parameterizations of the GCM ECHAM5 including the ECHAM5 land model. The 10 m thick soil is divided into five vertical layers. Soil temperatures are calculated in each of those layers based on a vertically discretized thermal diffusion equation with a lower boundary condition of vanishing heat flux. Frozen soil is not adequately parameterized, i.e. latent heat of phase change of soil water (freezing/thawing) is not considered, soil heat capacity and conductivity do not depend on soil water/ice, and water permeability is not changed in frozen soils. Soil moisture is calculated based on a single-layer "bucket" approach. This simple soil scheme calculates climatological soil temperatures for present day which are up to −20 K too cold in winter and up to 15 K too warm in summer. However, the calculated permafrost extent of 11.3 Mio km^2 is rather close to observations (see Fig. 1).

In order to improve the representation of permafrost in our model, we coupled the NCAR land model CLM4 (Community Land Model Version 4) to the HIRHAM5 atmosphere via a flux coupling approach. The atmospheric forcing for the land model includes near-surface wind, temperature, pressure, precipitation and radiation, while the land feeds back to the atmosphere via the sensible and latent heat fluxes, short and long wave surface radiation and evaporation. The soil scheme in CLM4 consists of 11 soil layers up to 5.7 m depth plus 5 bedrock layers up to ≈45 m depth. Soil temperature is calculated similar to ECHAM5 but adjusted for phase changes. Soil moisture is calculated for each soil layer separately based on mass conservation. Heat conductivity and water permeability are different for unfrozen and frozen soils. This more advanced soil scheme calculates climatological soil temperatures more realistically; the bias in winter is reduced to −5 K, while the bias in summer is up to −8 K. Permafrost extent is however underestimated in this new coupled model with an estimated extent of 9.8 Mio km^2 (see Fig. 1). To arrive at a better understanding of the performance of both models, their differences and their biases to observations with respect to soil conditions, a comprehensive process- and climate-oriented model evaluation is necessary.

The new coupled model HIRHAM5-CLM4 includes also a more sophisticated snow model and a better representation of surface vegetation processes compared to HIRHAM5. It is therefore difficult to attribute the simulated feedbacks in the atmosphere to specific causes, such as e.g. the changed soil scheme. However, our analysis clearly indicates that the impact of the changed land-surface-soil component on the atmosphere is not restricted to land areas only. Atmospheric responses (e.g. in mean sea level pressure) also occur over the Arctic Ocean.

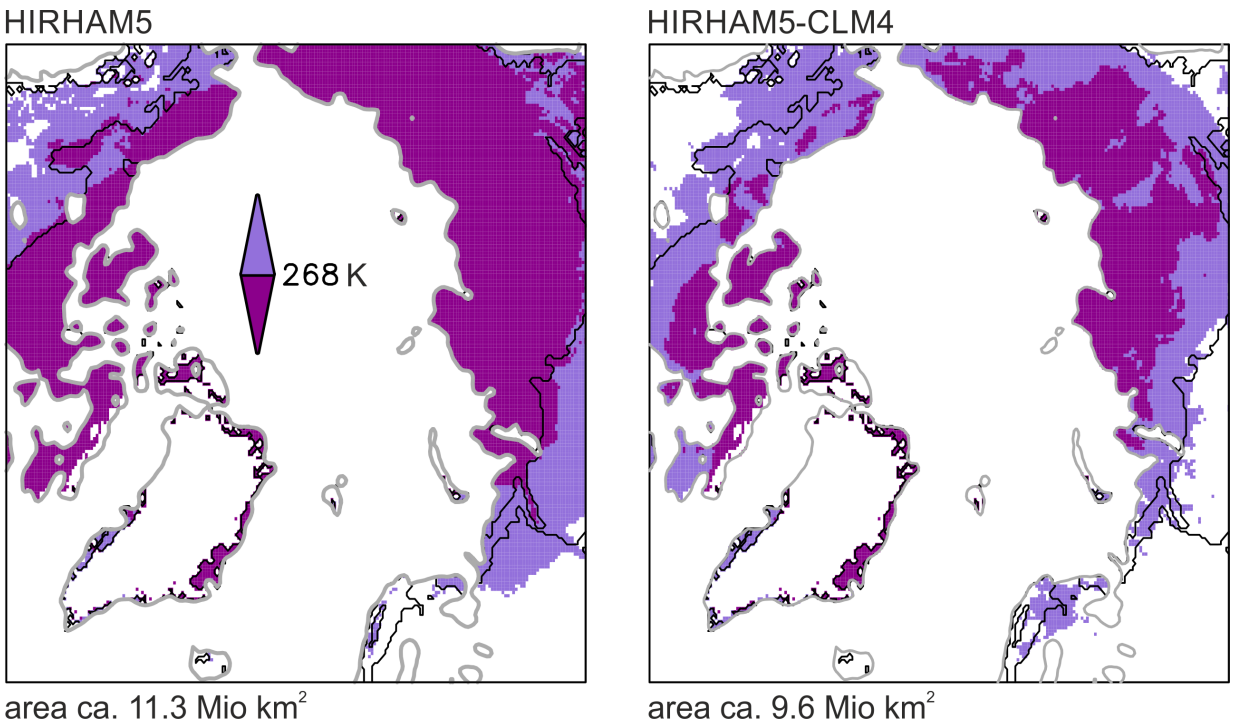

Figure 1: Permafrost extent calculated from HIRHAM5 (left) and HIRHAM5-CLM4 (right), based on the definition that permafrost exists where the ground is frozen for at least two consecutive years. The calculation is based on daily soil temperature data. The color scale refers to the maximum temperature in the uppermost continuously frozen layer of each grid cell. Black lines refer to observed permafrost extend after Brown et al. 2001 http://nsidc.org/data/ggd318.html. Observed permafrost extend based on the model domain and resolution is about 12.8 Mio km^2.

Tundra carbon dynamics in response to five seasons of experimental air warming and permafrost thaw

Marguerite Mauritz[1], Rosvel Bracho[2], Gerardo Celis[1], Susan Natali[3], Jack Hutchings[2], Verity Salmon[1,2], Elizabeth Webb[2], & Edward Schuur[1]

[1] *Northern Arizona University, United States of America*
[2] *University of Florida, United States of America*
[3] *Woods Hole Research Center*

Arctic permafrost soils store 1330 – 1580 Pg carbon (C), twice as much as current atmospheric C. For millennia permafrost soil C has been protected from decomposition by cold, waterlogged conditions. Warming temperatures will likely thaw permafrost, however the impact on Arctic and global C balance is uncertain. Nutrient availability is predicted to increase with thaw depth and promote plant growth, potentially creating an ecosystem C sink. However, deeper thaw could also increase microbial respiration and eventually soil C losses could exceed plant C gains.

We investigated spatial and temporal drivers of ecosystem C balance using data from a warming experiment in sub-arctic moist acidic tundra, designed to insulate soils in winter and stimulate permafrost degradation, and warm air temperatures in summer. Net ecosystem exchange (NEE) was measured continuously from May – September 2009 – 2013 using clear automated chambers; ecosystem respiration (Reco) was extrapolated from NEE under low light conditions, and gross primary productivity (GPP) was derived (GPP = NEE-Reco).

Five years of warming led to progressive increases in active layer depth. Active layer depth was positively correlated with cumulative growing season NEE, GPP and Reco. Although warming increased Reco the ecosystem remained a C sink during the growing season because plant biomass growth promoted GPP and offset the increases in Reco. *Eriophorum vaginatum* growth accounted for most of the increased plant biomass, and was positively correlated with both cumulative growing season GPP and Reco. Increases in NEE, GPP and Reco were largely due to higher mid-season amplitudes. In the shoulder seasons NEE and GPP were similar among years. In contrast, Reco increased at the end of the growing season each year, and high mid-season GPP was positively correlated with end season Reco. Thus, conditions that promoted plant growth also promoted C loss.

These results suggest plant responses to permafrost thaw are an important driver of C dynamics, and Reco associated with high biomass may result from greater autotrophic respiration as well as enhanced microbial soil decomposition. However, focusing only on the growing season may overestimate the C sink of the ecosystem because high uptake appears to enhance C losses at the end of the growing season, and C loss is likely to extend beyond the observation period.

The role of permafrost-dominated forest and tundra ecosystems in a changing climate, North-Eastern Russia

Trofim Maximov[1,2], Han Dolman[3], Ko v. Huissteden[3], Takeshi Ohta[4], & Atsuko Sugimoto[5]

[1]*Institute for Biological Problems of Cryolithozone, Siberian Branch of Russian Academy of Sciences, Russian Federation*
[2]*Institute for Natural Sciences of North Eastern Federal University (NEFU), Yakutsk, Russia*
[3]*Free University of Amsterdam, the Netherlands*
[4]*Nagoya University, Japan*
[5]*Hokkaido University, Japan*

Almost 65 % of Siberian forests and 23 % of tundra vegetation grow in permafrost zone. According to our estimate, carbon stocks in the soils of forest and tundra ecosystems of Yakutia (Eastern Siberia, Russia) amount to 17 billion tons (125.5 million hectares of forest and 37 million hectares of tundra in total) that is about 25 % of total carbon resource in forest soils of the Russian Federation.

Since the end of XIX century winter air temperatures in Arctic Siberia have risen by 10 °C, and average annual ones – by 2.0-3.5 °C. For the last 50 years in Eastern Siberia the average air temperature in January has grown by 7 °C, i.e. it was increasing 1.5-2 times faster compared to the first half of the century. Mean annual air temperature has increased by 1.0-2 °C. An increase in annual air temperature in the zone of permafrost development is able to cause the activation of biogeochemical processes, and speed up the release of greenhouse gases conserved in permafrost.

This report is compiled on the results of 14 year time series investigation conducted on the study of carbon and water cycles in permafrost-dominated forest and tundra ecosystems using flux towers and several micrometeorological, physiological and biochemical methods for the climatic and biogeochemical studies.

We were established transect SakhaFlux network of scientific monitoring stations ("Elgeeii", 60°N; "Spasskaya Pad", 62°N; "Kodac", 71°N; "Chokurdakh", 71°N) on studying climatic and biogeochemical cycles in a permafrost zone in the North-East of Russia.

For the first time in the conditions of Eastern Siberia an attempt has been made to ground the photosynthetic productivity of plants in terms of physiology, and quantitative parameters of the productive process were obtained. Original data on sink-source relations of plants are stated at the levels of integrity a plant organism and community. A number of specific results have been got:

1. conclusion was made about high depositing role of the root system of high latitude plants;
2. micrometeorological estimates of carbon balance were done;
3. quantitative dependence of CO_2 concentration on the season period, weather condition and forest fire intensity was shown;
4. carbon parameters of forest and tundra ecosystems were investigated;
5. attention was drawn to short growing season of plant development – this feature contributes to enrichment of the atmosphere of high latitudes by carbon dioxide;
6. carbon dioxide gas exchange of plants of different functional groups on a global scale is analysed.

Seasonal photosynthesis maximum of forest canopy vegetation in dry years falls into June, and in humid ones – into July. During the growing season the woody plants of Yakutia uptake from 1.5 to 4.0 t C ha^{-1} $season^{-1}$ depending on water provision. Night respiration is higher in dry and extremely dry years (10.9 and 16.1 % respectively). The productive process of tree species in Eastern Siberia is limited by endogenous (stomatal conductance) and exogenous (provision with moisture and nutrients, nitrogen specifically) factors.

The increase of an atmospheric precipitation after long 2-3 annual droughts accompanied with strong

surge in photosynthetic activity of forest plants is almost 2.5 times. To the contrary, the proceeding stabilization or increasing in precipitation has an adverse effect on photosynthetic function of forest plants and even to its inhibition.

The temperature of soil is a key factor influencing soil respiration in the larch forests. Average soil respiration for the growing season comes to 6.9 kg C ha^{-1} day^{-1}, which is a characteristic of Siberian forests in total. Annual average soil CO_2 emission is 4.5±0.6 t C ha^{-1} yr^{-1}.

Interannual variation of net ecosystem exchange (NEE) in permafrost forest makes 1.7–2.4 t C ha^{-1} yr^{-1} that results in the upper limit of annual sequestering capacity of 450-617 Mt C yr^{-1} at the total forest area in Russia of 257.1 Mha. In connection with climate warming there is a tendency of an increase in the volume of carbon accumulation by tundra and larch ecosystems in the result of prolongation of the growing season. This is also supported by changes in land use as well as by CO_2 sequestration in the form of fertilizer.

According our to long-term eddy-correlation obtained data, the annual uptake of carbon (NEE) in the larch forest of the Central Yakutia makes 2,12 ±0,34 t C ha^{-1} yr^{-1}, in the larch forest of Southeast Yakutia – 2,43 ±0,23 t C ha^{-1} yr^{-1}, and in a tundra zone – 0,75 ±0,14 t C ha^{-1} yr^{-1}.

For the two permafrost representative bioms, the following relevant factors are observed, over old mature of forests and changing of vegetation succession (shrubs and grasses) accelerated by growing of air temperature, summer precipitation and soil moisture.

Permafrost forest and tundra ecosystems at the present are estimated by carbon budget as areas of significant carbon sink. However, under predicted climate warming, their functions as carbon absorbers will essentially depend on the result of coordination of antagonistic processes.

The temporal evolution of changes in carbon storage in the Northern Permafrost Region simulated by carbon cycle models between 2010 and 2300: Implications for atmospheric carbon dynamics

A. David McGuire[1], David Lawrence[2], Eleanor Burke[3], Guangsheng Chen[4], Elchin Jafarov[5], Charles Koven[6], Andrew MacDougall[7], Dmitry Nicolsky[8], Shushi Peng[9], & Duoying Ji[10]

[1] *U.S. Geological Survey, Alaska Cooperative Fish and Wildlife Research Unit, University of Alaska Fairbanks, United States of America*
[2] *National Center for Atmospheric Research, United States of America*
[3] *Met Office Hadley Centre, United Kingdom*
[4] *Oak Ridge National Laboratory, United States of America*
[5] *University of Colorado, United States of America*
[6] *Lawrence Berkeley National Laboratory, United States of America*
[7] *University of Victoria, Canada*
[8] *University of Alaska Fairbanks, United States of America*
[9] *Laboratoire des Sciences du Climat et de l'Environment, France*
[10] *Beijing Normal University, China*

We conducted an assessment of changes in permafrost area and carbon storage simulated by 8 process-based models between 2010 and 2300. The models participating in this comparison were those that had joined the model integration team of the Vulnerability of Permafrost Carbon Network (see http://www.permafrostcarbon.org/). Each of the models in this comparison conducted simulations over the permafrost land region in the Northern Hemisphere driven by CCSM4-simulated climate for RCP 4.5 and 8.5 scenarios. Among the models, the area of permafrost (defined as the area for which active layer thickness was less than 3 m) in 2010 ranged between 8 and 19 million km^2. Between 2100 and 2300, models indicated the loss of permafrost area between 3 and 5 million km^2 for RCP 4.5 and between 6 and 16 million km^2 for RCP 8.5. Among the models, the density of soil carbon storage in 2010 ranged between 10 and 45 thousand g C m^{-2}; models that explicitly represented carbon with depth had estimates greater than 32 thousand g C m^{-2}. For the RCP 4.5 scenario, mean cumulative change in soil carbon between 2010 and 2300 was a gain of 10 Pg C (range: loss of 67 to gain of 70 Pg C; Fig. 1). For the RCP 8.5 scenario, the mean cumulative change in soil carbon was between 1960 and 2300 was a loss of 256 Pg C (range: losses of 7 to 652 Pg C; Fig. 1). Gains in vegetation carbon negated losses in the RCP 4.5 simulations for all but one of the models (mean change in total ecosystem carbon: 60 Pg C, range: loss of 14 Pg C gain of 244 Pg C; Fig. 1), but only for two of the RCP 8.5 simulations (mean: 148 Pg C, range: loss of 641 to gain of 167 Pg C; Fig. 1). For the RCP simulations that lost carbon between 2010 and 2300, substantial losses of carbon did not occur until after 2100. These results suggest that the permafrost carbon feedback would not have substantial consequences until after 2100, and that effective mitigation efforts during this century have the potential to prevent the negative consequences of the permafrost carbon feedback.

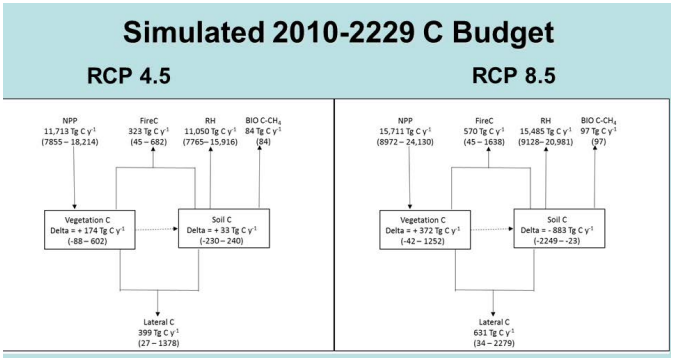

Figure 1: The future carbon budget from 2010 – 2300 for the permafrost region for the 4.5 and 8.5 Representative Concentration Pathways (RCP) scenarios 4.5 and 8.5 across the simulations by the models in this study

Early results simulating permafrost carbon processes in the coupled CLASS-CTEM model

Joe Melton

Environment and Climate Change Canada, Canada

The Canadian Land Surface Scheme (CLASS) and the Canadian Terrestrial Ecosystem Model (CTEM) form the land surface component of the Canadian Earth System Model (CanESM). To capture the feedbacks associated with the vast amount of carbon stored in permafrost regions I have developed a parameterization of permafrost C processes for CLASS-CTEM. The permafrost C processes scheme includes deeper soils with more soil layers and independently evolving soil C in each layer, direct addition of C by plant roots and root exudates into the soil layers, a parameterized form of cryoturbation, soil C respiration at depth, and accounting for Yedoma regions in model initialization. Early results demonstrate CLASS-CTEM, after deepening and increasing the number of soil layers, does a good job of simulating the areal extents of permafrost zones. Early analysis of the modelled distribution and quantity of C stored in the permafrost regions indicate the model performs adequately, albeit with some biases. The results presented are derived from offline simulations forced with historical observed meteorology, but this parameterization will eventually be incorporated into the CanESM framework.

Simulating the carbon, water and energy budgets of arctic soils with the ISBA land surface model

Xavier Morel[1], Christine Delire[1], Bertrand Decharme[1], Magnus Lund[3], & Florent Domine[2]

[1] *Centre National de Recherches Météorologiques (Meteo-France/CNRS), France*
[2] *Takuvik CNRS/University of Laval Joint Laboratory*
[3] *Aarhus University - Department of Bioscience*

Our aim is to be able to correctly represent the most important thermal, hydrologic and carbon cycle related processes in permafrost areas with our land surface model ISBA. This is particularly important since ISBA is part of the CNRM-CM Climate Model (Voldoire et al, 2012), that is used for projections of future climate changes.

To achieve this goal, we replaced the one layer original soil carbon module based on the CENTURY (Parton et al, 1987) by a multi-layer soil carbon module that represents C pools and fluxes, organic matter decomposition, gas diffusion according to Khvorostyanov et al (2008) and cryoturbation as proposed by Koven et al (2009, 2013). The soil carbon module is tightly coupled to the ISBA energy and water budget module that solves the one-dimensional Fourier law and the mixed-form of the Richards equation explicitly to calculate the time evolution of the soil energy and water budgets (Boone et al., 2000; Decharme et al. 2011). Snowpack processes are represented by a multi-layer snow model (Decharme et al, 2016).

We test this new model on a pair of monitoring sites in Greenland, one in a permafrost area (Zackenberg Ecological Research Operations, Jensen et al, 2014) and the other in a region without permafrost (Nuuk Ecological Research Operations, Jensen et al, 2013). We test the model's ability to represent the physical variables (soil temperature, water and ice profiles, snow height), the energy and water fluxes as well as the carbon fluxes. Comparing the model results on these two climaticaly distinct sites also gives a first insight on the sensitivity of the model to the forcing climate variables.

Using physical soil fractions to study small scale distribution and composition of soil organic matter in permafrost soils

Carsten W. Müller[1], Janet Rethemeyer[2], Sebastian Zubrzycki[3], Silke Höfle[2], Mercedes Molina Gamez[3], Jenny Kao-Kniffin[4], Lena Zoor[1], Sebastian Löppmann[5], Kenneth M. Hinkel[6], & James G. Bockheim[7]

[1] *TU München, Lehrstuhl für Bodenkunde, Freising-Weihenstephan, Germany*
[2] *University of Cologne, Institute of Geology and Mineralogy, Cologne, Germany*
[3] *University of Hamburg, Institut für Bodenkunde, Center for Earth System Research and Sustainability (CEN), Hamburg, Germany*
[4] *Cornell University, Department of Horticulture, Ithaca, NY, USA*
[5] *Georg August University of Göttingen, Soil Science of Temperate Ecosystems, Göttingen, Germany*
[6] *University of Cincinnati, Department of Geography, Cincinnati, Ohio, USA*
[7] *University of Wisconsin-Madison, Department of Soil Science, Madison, WI, USA*

A large number of studies predict changing organic matter (OM) dynamics in arctic soils due to global warming. In contrast to rather slowly altering bulk soil properties, single soil organic matter (SOM) fractions can provide a more detailed picture of the dynamics of differently preserved SOM pools in climate sensitive arctic regions. Although there is a large number of studies using physical soil fractionation for temperate soils to unravel the fate of soil organic matter and its stabilization within soil aggregates, there is only scarce information for permafrost affected soils. As especially the separation by means of density is used to differentiate between free particulate organic matter and such occluded in soil aggregates, it is questionable if aggregation is important at all in permafrost soils? Also only scarce information is available on the importance of the association of organic carbon (OC) with mineral surfaces for the sequestration of OC in arctic soils. Thus a mechanism known to play an important role for long term carbon sequestration in temperate soils is not well understood in arctic soils.

To study the importance of soil aggregation and organo-mineral associations in permafrost soils, we studied soils derived from the Alaskan and Siberian high arctic. Air dried soil samples from soil horizons of the active and permanently frozen layer were subjected to density fractionation in order to differentiate particulate OM and mineral associated OM. By the study of the chemical composition of distinctive SOM fractions using nuclear magnetic resonance spectroscopy (NMR) together with radiocarbon analyses and/or biomarker analyses it was possible to evaluate the stability of the major OM pools. Additional to bulk analyses we used microscopic techniques to evaluate soil aggregation and organo-mineral associations in-situ. Namely we analysed selected samples using a cascade of reflectance light microscopy, scanning electron microscopy (SEM) and nano-scale secondary ion mass spectrometry (NanoSIMS).

The study of microscale soil structures (SEM) and the elemental distributions (NanoSIMS) showed the initial formation of aggregates and organo-mineral interfaces in the studied permafrost soils. For the studied soils we can show that large amounts are stored mostly as probably labile particulate SOM rich in carbohydrates. To a lower extent OC was sequestered as presumably more stable mineral associated OC dominated by aliphatic compounds. Comparable to soils of temperate regions, we found small POM ($< 20\ \mu$m) occluded in aggregated soil structures which differed in the chemical composition from larger organic particles. This was clearly shown by increased amounts of aliphatic C in these small POM fractions. As revealed by ^{13}C CPMAS NMR, with advancing soil age increasing aliphaticity was also detected in occluded small POM fractions. By ^{14}C dating we could show the stabilization of younger more labile OM at greater depth in buried O horizons.

Although climatic stabilization due to reduced microbial decay at low temperatures is the most important factor in permafrost soils at the moment, in a warmer future this may change to other mechanisms, likely OC stabilization in aggregated soil structures and organo-mineral associations.

A Pan-Arctic synthesis of carbon emissions during the nongrowing season

Susan Natali[1], Anne Selbmann[2], Benjamin W. Abbott[3], Mats Björkman[4], Róisón Commane[20], Elizabeth Cooper[21], Claudia Czimczik[5], Sergei Davydov[6], Anna Davydova[6], Bo Elberling[7], Hélène Genet[8], Mathias Goeckede[9], Elchin Jafarov[10], Julie Jastrow[11], Yongwon Kim[8], Mark Lara[8], Massimo Lupascu[12], Walter Oechel[19], Fereidoun Rezanezhad[13], David Risk[14], Philipp Semenchuk[15], Claire Treat[8], Mark P. Waldrop[16], Qianlai Zhuang[17], & Donatella Zona[18]

[1] *Woods Hole Research Center*; [2] *University of Applied Sciences Mittweida*; [3] *Université de Rennes*; [4] *University of Gothenburg*; [5] *University of California Irvine*; [6] *Northeast Science Station*; [7] *University of Copenhagen*; [8] *University of Alaska Fairbanks*; [9] *Planck-Institute for Biogeochemistry*; [10] *University of Colorado Boulder*; [11] *Argonne National Laboratory*; [12] *National University of Singapore*; [13] *University of Waterloo*; [14] *St. Francis Xavier University*; [15] *Umeå University*; [16] *U.S. Geological Survey*; [17] *Purdue University*; [18] *The University of Sheffield*; [19] *San Diego State University*; [20] *Harvard School of Engineering and Applied Sciences*; [21] *The Arctic University of Norway*

Over the past few decades, surface air temperatures in the Arctic have increased at about twice the global rate. Climate models project that this rate of warming will continue through the century, with the greatest warming occurring during the winter months. Despite cold surface temperatures during the winter, microbial activity in the soil continues, releasing soil carbon during a critical period when plant uptake has ceased. Carbon dioxide (CO_2) and methane (CH_4) emissions during the winter and shoulder seasons (fall and spring) are an important component of annual respiratory carbon loss, yet there is large uncertainty in local and regional estimates of carbon emissions during the nongrowing season. Carbon dioxide emissions from microbial respiration during the snow-covered period vary from 10 – 40 % of annual CO_2 emissions. These nongrowing season CO_2 emissions may equal or exceed net growing season carbon uptake. Thus, nongrowing season respiration may shift arctic ecosystems from being carbon sinks during the growing season to net sources on an annual basis.

Cold temperatures during the winter affect soil physical properties, biogeochemistry, microbial activity, and rates of carbon cycling in soils. Not only can microbial activity occur at sub-zero temperatures, but soil freezing may even stimulate microbial activity by destroying soil aggregates, hence enhancing the availability of substrates and potentially leading to a pulse of CO_2 and CH_4 emissions during freezing conditions. However, current understanding of the microbial and biogeochemical functioning of soils derives primarily from studies carried out during the growing season. More attention needs to be drawn to the importance of sub-zero processes for global greenhouse gas budgets. Refining estimates of soil respiration and understanding the drivers of cold season respiration are critical for constraining estimates of current and future carbon emissions from the Arctic.

To address uncertainties in the drivers and magnitude of carbon emissions during the nongrowing season, we conducted a synthesis of respiration from northern high latitude regions. We examined differences in cumulative nongrowing season respiration among permafrost zones, biomes, ecosystem types, and effects of measurement method on nongrowing season respiration estimates. We also examined the effects of air temperature and precipitation on nongrowing season respiration, and synthesized data from winter warming (e.g., using snow accumulation) and vegetation removal experiments. We compiled a database containing more than 200 flux measurements from ≈50 studies at sites located throughout the permafrost region and that spanned a measurement timeframe from 1990 to 2015. We found that, on average, 20 % of annual ecosystem respiration occurs during the nongrowing season. Nongrowing season respiration was negatively related to latitude, with highest CO_2 emissions in the sporadic permafrost zone, and decreasing through the discontinuous and continuous zones. Additionally, nongrowing season CO_2 emissions were higher in boreal ecosystems than in tundra. Synthesized results from experimental studies show that CO_2 emissions were significantly higher when soils were warmed and lower when vegetation was removed, demonstrating the sensitivity of carbon release to rising temperatures and changes in vegetation

cover in northern high latitudes. These results suggest that permafrost degradation in southerly zones and increased soil temperature throughout the permafrost region will lead to greater carbon release, highlighting the importance of including nongrowing season respiration in current and future carbon assessments for high latitudes.

New estimates of soil organic carbon storage in the Zackenberg valley, NE Greenland by combining geomorphology and land cover

Juri Palmtag, Gustaf Hugelius, & Peter Kuhry

Department of Physical Geography, Stockholm University, Sweden

Recent estimates indicate that soils in the northern circumpolar permafrost region, which occupy an area of about 18.8 million km^2 (or c. 16 % of the global soil area), store substantial amounts of soil organic carbon (SOC). These soils are vulnerable to permafrost degradation under global warming and, if they thaw, soil organic matter (SOM) decomposition could release large amounts of carbon dioxide (CO_2) and/or methane (CH_4) into the atmosphere providing a positive feedback to climate warming. However, these soils have large regional and landscape-level variability depending on topographic, ecoclimatic and edaphic factors. Palmtag et al (2015) demonstrated how, in two contrasting continuous permafrost landscapes, land cover classifications could be used to provide local scale SOC storage estimates that account for some of these factors. The overall objective of this study is to further improve SOC storage estimates for Zackenberg, NE Greenland by including more of these local scale factors into the upscaling procedure. The first step is to improve the existing landscape classification and SOC stock upscaling product from Zackenberg by using a combination of geomorphological units and land cover classes. Especially in mountainous regions the same vegetation types show in some cases great differences in their SOC storage depending on their topographical position, which makes their further separation into landform units crucial for better upscaling estimates. In Zackenberg particularly grasslands and fens are present on the mountain slopes, at the foot of the slopes and in the central flat valley. Our data show large SOC variability between these landscape positions and a careful overlay analysis of geomorphology and land cover is expected to improve our SOC estimates. Second, with emphasis on organically enriched buried layers, we provide data on SOM burial history and its degree of decomposition based on carbon to nitrogen ratio (C/N) analyses and radiocarbon dates. Our results suggest that these layers represent periods of surface stability with normal vegetation/soil development where the SOM could undergo its normal decomposition pathway, before being only gradually buried by reactivated slope materials.

References

Palmtag, J.; Hugelius, G.; Lashchinskiy, N.; Tamstorf, M. P.; Richter, A. and Elberling, B. et al. [2015]: Storage, landscape distribution and burial history of soil organic matter in contrasting areas of continuous permafrost. *Arctic, Antarctic, and Alpine Research*, 47(1):71–88, doi:10.1657/AAAR0014-027.

Carbon exchange in northern ecosystems influenced by sea ice decline

Frans-Jan W. Parmentier & Torben R. Christensen

Lund University, Sweden

The Arctic is rapidly transitioning towards a seasonal sea ice-free state, perhaps one of the most apparent examples of climate change in the world. This dramatic change has numerous consequences, including a large increase in near-surface air temperatures, which in turn may affect the carbon exchange in terrestrial ecosystems [Parmentier et al., 2013]. Nonetheless, terrestrial and marine environments are seldom jointly analyzed.

By comparing satellite observations of Arctic sea ice concentrations to methane emissions simulated by three process-based biogeochemical models, we show that rising wetland methane emissions are associated with sea ice retreat [Parmentier et al., 2015]. Strong correlations with sea ice are apparent throughout the Arctic, with considerable variation through the seasons. Our analyses indicate that simulated high-latitude emissions for 2005 – 2010 were, on average, 1.7 Tg CH_4 yr^{-1} higher compared to 1981 – 1990 due to an autumn-focused sea ice-induced warming. These results suggest a continued rise in methane emissions with further warming from future sea ice decline, particularly in the autumn.

A similar connection may exist to CO_2 exchange, evidenced by previous studies that showed connections between sea ice and NDVI [Bhatt et al., 2014]. However, measurements of net ecosystem exchange by terrestrial flux stations have so far not shown the same connection due to incomplete data coverage, and the fact that net ecosystem exchange is composed of two large opposing fluxes – photosynthesis and respiration – both of which are stimulated by higher temperatures. We will therefore conclude by exploring connections to the warming pattern of sea ice decline, how this may affect net ecosystem exchange, and whether this has been detected by the current network of flux stations across the Arctic tundra biome.

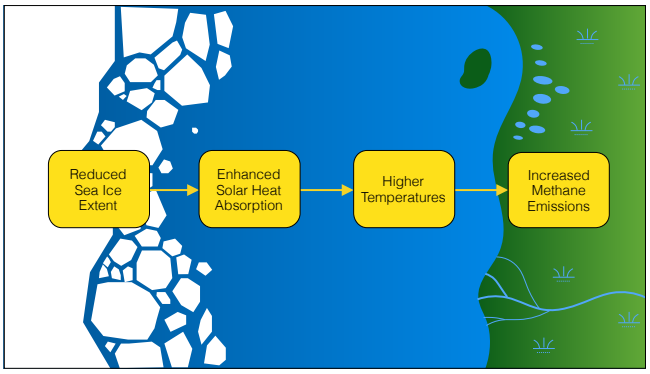

Figure 1: Schematic description of the connection between sea ice decline and increased methane emissions from northern wetlands [Parmentier et al., 2015].

References

Bhatt, U.S.; Walker, D.A.; Walsh, J.E.; Carmack, E.C.; Frey, K.E.; Meier, W.N.; Moore, S.E.; Parmentier, F.J.W.; Post, E.; Romanovsky, V.E. and Simpson, W.R. [2014]: Implications of Arctic Sea Ice Decline for the Earth System. *Annual Review of Environment and Resources*, 39,. doi:10.1146/annurev-environ-122012-094357.

Parmentier, F.J.W.; Christensen, T.R.; Sørensen, L.L.; Rysgaard, S.; McGuire, A.D.; Miller, P.A. and Walker, D.A. [2013]: The impact of lower sea-ice extent on Arctic greenhouse-gas exchange. *Nature Climate Change*, 3, doi:10.1038/nclimate1784.

Parmentier, F.J.W.; Zhang, W.; Mi, Y.; Zhu, X.; Huissteden, J.; Hayes, D.J.; Zhuang, Q.; Christensen, T.R. and David McGuire, A. [2015]: Rising methane emissions from northern wetlands associated with sea ice decline. *Geophysical Research Letters*, 42, doi:10.1002/2015GL065013.

The stable isotopes and C/N ratio as indicators of peat plateaus sustainability in the southern limit of East-European cryolithozone

Aleksandr Pastukhov[1], Christian Knoblauch[2], Dmitry Kaverin[1], Iulia Antcibor[2], & Eva-Maria Pfeiffer[2]

[1] *Institute of Biology Komi SC UB RAS, Russian Federation*
[2] *Universität Hamburg, Germany*

Permafrost degradation due to the climate warming is currently observed in the north-eastern part of the European Russia. Peat plateaus affected by permafrost extend only about 20 % of the territory and contain almost 50% of soil organic carbon (SOC) stocks which are considered to be very vulnerable to mineralization due to pronounced permafrost thaw. It is assumed that positive temperatures of thawed permafrost peat will increase SOC biodegradation rates (the same situation occurred during periods of Holocene climatic optimums). As a consequence, positive temperatures may also lead to a relative enrichment of the refractory SOC that are depleted in $\delta^{13}C$. Additionally, they may affect the C/N ratio and decomposition rates (high C/N ratio as an indicator of low decomposition rates and low ratio as an indicator of high decomposition rates).

The current study was performed in three key sites of peat plateaus located in the southern boundary of sporadic permafrost extension. All sites have similar morphology and do not differ from each other on satellite images but their geomorphological location, hydrological regime, nutrient status predefining their genesis as well as evolution during the Holocene are significantly different. Isotope ($\delta^{13}C$) and C/N ratios were measured and incubation experiments were conducted as essential indicators of SOC decomposition processes. The CO_2 production was measured in samples of peat of three key sites from the active layer (AL), the permafrost layer (PL), the transitional layer (TL), and the deep permafrost layer (DPL, in contact with mineral deposits in 3.7 m depth, only at the third key site) under aerobic and anaerobic conditions at 4 °C for 65 days.

Measurements of $\delta^{13}C$ showed the minor changes of stable isotopes values. The values ranged from −25 to −28 ‰$\delta^{13}C$ reflecting the different botanical origin (composition) and no degradation. The C/N ratio values ranged from 21 to 31 showing similar patterns as the $\delta^{13}C$ values.

During the experiment, the CO_2 respiration increased very rapidly in all samples of three key sites showing almost linear regression. At the first key site, the CO_2 production under anaerobic conditions was 1.06 ±0.18 mg CO_2-C g^{-1}C in peat samples from AL which was 5 times higher than in samples of PL and 3.5 times higher than in samples of TL. Under aerobic conditions, the CO_2 production amounted to 2.59 ±0.31 mg CO_2-C g^{-1}C in samples of AL which was 3.4 times higher than in PL and 5 times higher than in samples of TL. At the second key site, the results were completely opposite: a higher CO_2 production was observed in samples of PL in comparison with TL and AL, respectively. At the third key site, there was no significant difference between samples of AL, TL, and PL under both aerobic and anaerobic conditions. But, we also measured in the deep frozen peat which located just over mineral deposits in 3.7 m depth (DPL). The CO_2 production amounted to 2.09 ±0.31 mg CO_2-C g^{-1}C under aerobic conditions in DPL at the third key site which was 2.5 times higher than in other layers (AL, TL and PL). However, under anaerobic conditions, the production was 0.25 ±0.01 mg CO_2-C g^{-1}C which was significantly less than in other layers where CO_2 production varied from 0.33 to 0.35 mg CO_2-C g^{-1}C.

Our study showed that the C/N and $\delta^{13}C$ reflect the variability in origin and heterogeneity of three investigation sites but do not indicate peat vulnerability to SOC decomposition process. Debatable results of the incubation experiment still support the hypothesis about the sustainability of peat plateaus especially under anaerobic conditions. These results are in agreement with other studies performed for continuous and discontinuous permafrost areas suggesting that under the permafrost thawing conditions, water logging and the presence of anaerobic conditions would limit decomposition of organic matter of frozen peat deposits. It can be concluded that natural peat plateaus can be considered as stable ecological systems regardless the predicted climate warming.

Greenhouse gas emissions from Arctic lakes and ponds as influenced by carbon lability and geomorphology

Vilmantas Prėskienis[1,2], Isabelle Laurion[1,2], Frédéric Bouchard[1,2], Daniel Fortier[2,3], & Milla Rautio[2,4]

[1] *Centre Eau Terre Environment, Institut National de Recherche Scientific, Canada*
[2] *Centre for Northern Studies (CEN), Université Laval, Canada*
[3] *Département de Géographie, Université de Montréal, Canada*
[4] *Département des sciences fondamentales, Université du Québec à Chicoutimi, Canada*

The rapid warming in Arctic regions has induced extensive permafrost thaw and the mobilization of a large reservoir of organic carbon (C) that was frozen for millennia. Although the release of this old C to the atmosphere, either as carbon dioxide (CO_2) or methane (CH_4), may act as a positive feedback mechanism to global warming, little is known about the extent and rate of emissions by the wide range of ecosystems found in Arctic landscapes, and the biogeochemical processes involved as different C pools are becoming available upon thawing. As part of an interdisciplinary project investigating the influence of geomorphological and limnological factors on greenhouse gas (GHG) emissions from lakes and ponds on Bylot Island, in the Canadian Arctic Archipelago, the present study aims to determine the lability of the different C pools to microorganisms. Lability experiments were performed in 2014 and 2015 on six C pools collected from the organic-rich polygonal patterned landscape with syngenetic permafrost: active layer, permafrost, transient layer, and three different lacustrine sediments (from thermokarst lake, ice-wedge through pond, and coalescent polygonal pond with benthic mats). The soils were characterized in terms of their origin, age, C/N ratio, fatty acid, and % organic content. The different soils were incubated in one of the shallow tundra ponds under shaded conditions and after the addition of pond water as an inoculum. The incubations were repeated under controlled conditions in the laboratory. Leachates were also produced from the same soil samples and incubated similarly both in the field and laboratory. Dissolved oxygen (O_2) and headspace CH_4 and CO_2 concentrations were measured over a period of three weeks to calculate rates of gas consumption or production. Preliminary results show that both O_2 consumption and CO_2 production rates were higher in lacustrine sediments compared to terrestrial sediments, indicating the higher quality of freshly deposited aqautic material or living cells. Supporting these results, concentrations of polyunsaturated fatty acids (PUFAs) were highest in lake sediments (below gyttja), and lowest in terrestrial sediments (except in the transient layer). These results also suggest a previous decomposition of the organic matter through syngenetic permafrost formation, leaving behind less labile compounds before its incorporation into permafrost. Nevertheless, permafrost C was clearly used by microbes as shown from the old signature of the GHG emitted over this relatively short-term incubation. There is a clearly need to employ a wide array of indicators to assess the lability of Arctic soils to microbial decomposition, including a characterization of the source and age of the C being used for microbial production of GHG, in order to determine the feedback effects of GHG emissions by tundra lakes and ponds on future climate.

Degradability of organic matter in permafrost soils revealed by a comprehensive radiocarbon study: Clues from compound-specific to soil density fractions

Janet Rethemeyer, Silke Höfle, Carsten W. Müller, & Stephanie Kusch

University of Cologne, Germany

The release of organic carbon (OC) from Arctic permafrost soils due to global warming may significantly accelerate the rise in atmospheric carbon dioxide content. Predictions of the future development of this large OC pool are highly uncertain because of insecurities in the estimates of OC stocks and missing information on the organic matter composition and microbial degradability. Results of incubation experiments suggest that a relatively small fraction of the OC in permafrost soils is degradable on timescales of few years after thawing. The larger OC pool is supposed to turn over on timescale of several decades to hundreds of years thus consisting of older, potentially more resistant organic compounds. The number of field studies investigating OC turnover in permafrost is very limited, but such studies are urgently needed as incubations reduce the complexity of the Arctic carbon cycle to few parameters that are tested. The field studies performed so far equally point to rising portions of old OC release from permafrost soils upon longer or more intense thawing questioning the higher resistance to degradation of the larger old OC pool.

Radiocarbon analyses of bacterial membrane lipids give in-situ information on the microbial degradation of fresh and old organic components in permafrost soils. We thus analyzed radiocarbon contents of individual phospholipid fatty acids (PLFA) in the active layer and still frozen permafrost of the polygonal tundra in the Siberian Arctic. To obtain information on the degradation of different OC pool, we compare the radiocarbon contents of the PLFAs with those of potential OC sources including individual plant-derived lipids, dissolved OC, as well as free and occluded (in aggregates) organic matter separated by density fractionation.

Although total OC in the elevated rim above the ice wedges and in the depressed, water saturated polygon centre decline rapidly in the shallow active layer, organic matter composition and/or its turnover seems to be very different in both permafrost structures. In the rim the OC seems to be degraded slowly resulting in an accumulation of ca. 3000 years old OC near the permafrost table, while in the centre bulk OC is only few hundred years old in the near permafrost horizon. This however, does not necessarily imply a faster OC turnover in the centre but is caused more likely by the different redox conditions and vegetation on both structures, i.e. larger amounts of relatively fresh, little decomposed sedges at greater depth of the centre. The total PLFA concentration – indicative of the total bacterial biomass – increases with soil depth in the relatively dry, probably well aerated polygon rim (from 160 to 650 nmol per g DW). In the water-saturated polygon centre PLFA concentrations are highest near the soil surface (860 nmol per g DW) but decrease with depth (170 nmol per g DW) because of unfavourable conditions for aerobic soil bacteria. Individual PLFAs including i/a-C15:0, C16:0, C16:1, and C18:1 yield similar radiocarbon contents (within 1σ-uncertainty) in each horizons from which they were isolated in both polygon structures. In the near surface horizon of the rim the radiocarbon values of the PLFAs (107 – 111 pMC) are close to the atmospheric concentration (ca. 104 pMC in 2010), while bulk OC is significantly older (900 yrs BP, 90 pMC) indicating the preferential degradation of OC from recent photosynthesis. Surprisingly the long-chain n-carboxylic acids (C16:0, C24:0, C26:0, C28:0), one n-alkane (C27:0), and the free particular organic matter fraction commonly used as indictors for plant leaf waxes and plant debris, respectively show considerably lower radiocarbon values (93 – 103 pMC) than PLFAs. Apparently a fresher/younger substrate is the major source for soil bacteria living in the near surface horizon of the polygon rim. In the centre, the isolated PLFAs yield slightly higher values of 115 to 120 pMC, which are closely similar to that of the relatively fresh/young bulk OC (113 pMC) and of the isolated n-carboxylic acids and two n-alkanes (C23:0, C27:0: 118 – 122 pMC). In the deeper horizons near and below the permafrost table, respectively of both structures the PLFAs exhibit significantly higher radiocarbon concentration compared to the bulk OC and the deviation is more prominent in the rim than

in the centre. Again the relatively high radiocarbon values of the bacterial PLFAs in the rim (86 – 95 pMC; bulk OC: 68 pMC) and lower values of the long-chain n-carboxylic acids and n-alkanes (63 – 79 pMC) indicate the degradation of a fresher OC source in this structure. In the centre PLFA and plant-derived long-chain lipids yield very similar values between 100 and 108 pMC, which are close to that of bulk OC (96 pMC) suggesting that here the organic matter is composed of relatively fresh material that is microbially available. In summary, these results point to a preferential degradation of relatively fresh organic matter even at greater depth of the permafrost soils where bulk OC exhibits high apparent ages of up to 3000 yrs BP.

The IsoGenie Project: Integrating high-resolution characterization of organic matter, isofluxes, and microbiota in a thawing permafrost peatland

Virginia I. Rich[1], Scott Saleska[2], Gene Tyson[4], Jeff Chanton[5], Patrick Crill[6], Ruth Varner[3], Steve Frolking[3], William Cooper[5], Matthew Sullivan[1], & The IsoGenie Consortium[1]

[1] *The Ohio State University, United States of America*
[2] *The University of Arizona, United States of America*
[3] *The University of New Hampshire, United States of America*
[4] *Queensland University, Australia*
[5] *Florida State University, United States of America*
[6] *Stockholm University, Sweden*

The IsoGenie Project is investigating in situ changes in carbon cycling and microbiology across a thawing permafrost peatland mosaic landscape, at Stordalen Mire (68°21'N, 19°02'E) in Arctic Sweden. The Mire hosts palsas, bogs, fens, and post-glacial ponds and lakes, with total landscape methane emissions split approximately evenly between the wetlands and lakes. Over the last half-century of climate warming, the spatial extent of palsas has been decreasing while bogs and fens are increasing. Along the thaw gradient, vegetation shifts from ericaceous shrubs to mosses and sedges, and then aquatic plants. High-resolution characterization of organic matter using a range of methods (including Fourier transform ion cyclotron resonance mass spectrometry, UV/Vis absorbance, and excitation-emission matrix spectroscopy) has revealed that soil carbon becomes increasingly reduced and labile across the gradient, with evidence of greater humification rates and faster decomposition in the fen habitat. In the bog habitat, the Sphagnum moss is a key driver of dissolved organic matter characteristics, and acts as an inhibitor of rapid decomposition and methane release. The changes in substrate quality translate to shifting methane emissions, which peak in the fens, and which increase relative to carbon dioxide across the gradient. These emissions shift isotopically from ratios characteristic of hydrogenotrophic production in the bog habitat to a mixture with acetoclastic production in the fen. Microbes mediate carbon transformations and losses across this landscape, connecting substrates to emissions, but a mechanistic microbes-to-emissions scaling understanding is missing. The microbial communities mediating these processes are complex, and change dramatically across the landscape. Notable community shifts include high abundances of an undescribed group of Caldiserica in the early stages of palsa collapse, and of a recently-identified globally-distributed family of hydrogenotrophic methanogens (Methanoflorentaceae) in the bog and fen habitats. Metagenomic sequencing has been used to characterize more than two hundred samples spanning depths and habitat types at Stordalen Mire, and these metagenomes have allowed the assembly of several hundred high-quality population genomes. From these population genomes, we are gaining insights into the carbon-cycling metabolisms of previously-undescribed, novel, and abundant lineages within the Mire. Targeted metatranscriptomics and metaproteomics are helping identify which of these novel lineages are most metabolically active for the processes of interest. Unraveling the interconnections of microbial lineages and carbon transformations is ongoing.

Holocene peatland development, carbon accumulation and permafrost history in Tavvavuoma, northern Sweden

A. Britta K. Sannel[1], Liljen Hempel[1], Alexander Kessler[1], Peter Kuhry[1], & Vilmantas Prėskienis[1,2]

[1] *Stockholm University, Sweden*
[2] *Centre for Northern Studies, Canada*

Peatlands in the northern circumpolar permafrost region are important soil organic carbon reservoirs. Throughout the Holocene they have acted as carbon sinks, but under future warmer conditions deepening of the active layer and ground collapse as a result of permafrost thaw may, at least temporarily, turn these peatlands into carbon sources. In this study, analyses of plant macrofossils, bulk density, carbon and nitrogen content, and AMS radiocarbon dating have been performed for six profiles collected from peat plateaus and palsas in Tavvavuoma (68°28'N, 20°54'E), located in the sporadic permafrost zone in northernmost Sweden (Fig. 1). The preliminary results suggest that peatland development started around 10100 – 9600 cal yr BP, and that long-term net carbon accumulation rates are 8 – 17 gC/m^{2}yr. According to the macrofossil analyses the fen-bog transition and permafrost aggradation took place relatively recently, most likely during the Little Ice Age (additional radiocarbon dating is needed to confirm this). There are no indications of earlier permafrost aggradation in these peatlands around 2500 – 2700 cal yr BP, as suggested by other studies from nearby sites in Sweden and Finland [Oksanen, 2006, Kokfelt et al., 2010]. Today, the permafrost in Tavvavuoma is warm with temperatures just below 0 °C, and the warming trend in the ground temperature during the last decade is most likely a result of increases in winter precipitation and air temperature throughout the 20th century [Sannel et al., 2015]. If these peatlands thaw, the carbon that has been trapped in the permafrost for at least a few hundred years can become available for decomposition and be emitted to the atmosphere, as carbon dioxide from expanding active layers/taliks or as methane from thermokarst lakes and fens. A better understanding of long-term Holocene carbon and permafrost dynamics can improve our knowledge of permafrost peatland sensitivity to climate change, and help us make projections of future climate-carbon feedbacks from these ecosystems.

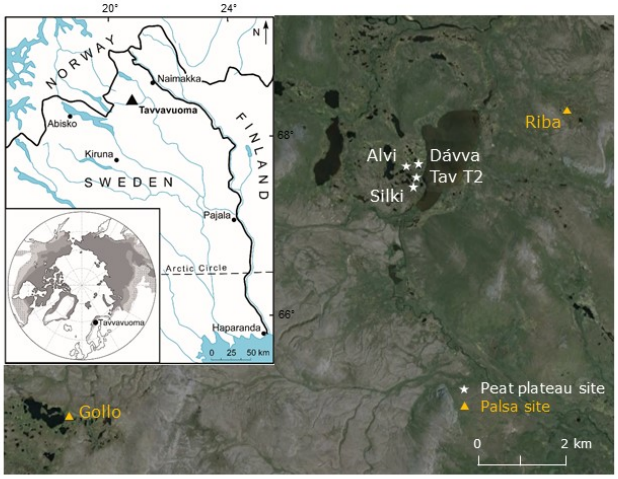

Figure 1: Peat profile sites in Tavvavuoma, northern Sweden. Inset map with circum-Arctic permafrost zonation, from continuous permafrost at high northern latitudes through discontinuous permafrost to sporadic and isolated permafrost at lower latitudes.

References

Kokfelt, U.; Reuss, N.; Struyf, E.; Sonesson, M.; Rundgren, M.; Skog, G.; Rosén, P. and Hammarlund, D. [2010]: Wetland development, permafrost history and nutrient cycling inferred from late Holocene peat and lake sediment records in subarctic Sweden. *J Paleolimnology*, 44:327–342.

Oksanen, P.O. [2006]: Holocene development of the Väisjeaggi palsa mire, Finnish Lapland. *Boreas*, 35: 81–95, doi:10.1111/j.1502-3885.2006.tb01114.x.

Sannel, ABK.; Hugelius, G.; Jansson, P. and Kuhry, P.[2015]: Permafrost warming in a subarctic peatland – which meteorological controls are most important? *Permafrost and Periglacial Processes*, doi:10.1002/ppp.1862.

Identifying circumpolar trends in greening versus browning of the Arctic

Christina Schädel[1], Howard Epstein[2], Mike Loranty[3], Sue Natali[4], & Verity Salmon[5]

[1] *Northern Arizona University, United States of America*
[2] *University of Virginia, United States of America*
[3] *Colgate University, United States of America*
[4] *Woods Hole Research Center, United States of America*
[5] *University of Florida, United States of America*

The Arctic is experiencing rapid increases in temperature, which have already stimulated carbon release from previously frozen permafrost carbon pools. Losses of permafrost carbon from these ecosystems may be partially offset by increased carbon uptake by plants due to extended growing season, CO_2 fertilization, and higher nutrient release associated with warming. However, other processes such as shifts in vegetation and increased frequency of disturbances (e.g. fire, drought, and permafrost degradation) could have the reverse impact and lead to a 'browning' of the Arctic as has been observed over the last few years. Multiple different approaches (such as remote sensing, modeling, and field measurements) are being used to estimate the magnitude and extent of 'greening' or 'browning' of the Arctic. While some studies show increases in vegetation productivity with warmer temperatures, other studies report decreasing trends in plant productivity. This could suggest large impacts of permafrost degradation and subsequent hydrological changes. This synthesis compares results from satellite data, field measurements and modeling approaches to develop a functional relationship (e.g. between soil moisture, permafrost thaw and vegetation responses) that can be used to predict areas in the circumpolar permafrost zone that will become greener or browner. We also compare the magnitude of the trends, which is a crucial step in estimating a potential offset of enhanced carbon release through decomposition with warming.

Observation-based modelling of CO_2 and CH_4 fluxes from newly thawed carbon

Thomas Schneider von Deimling[1,2], Guido Grosse[2], Jens Strauss[2], Lutz Schirrmeister[2], Anne Morgenstern[2], & Julia Boike[2]

[1] *Max Planck Institute for Meteorology, Germany*
[2] *Alfred Wegener Institute Helmholtz Centre for Polar and Marine Research, Potsdam, Germany*

Permafrost soils store vast amounts of old carbon which are currently locked under frozen conditions and thus are not contributing to the Arctic carbon flux budget. With projected strongly increased Arctic temperatures by end of this century, the deepening of the active layer will make available a growing portion of this permafrost carbon pool for microbial decomposition, which results in the release of carbon dioxide and methane The eventual increase in atmospheric greenhouse gas (GHG) concentrations accelerates global warming and describes a feedback loop, the so-called permafrost-carbon feedback.

In our modelling study [Schneider von Deimling et al., 2015] we describe the full cycle of permafrost degradation, soil microbial activity, carbon release and increase in atmospheric GHG concentrations to determine the strength of the additional temperature increase caused by newly thawed soil carbon.

For this purpose, we developed a simplified, two-dimensional multi-pool model, capturing latitudinal variations of surface climate, and vertical information on soil temperature profiles and carbon distributions. We use multiple lines of recent data sets (such as soil carbon inventories and incubation studies) for tuning our model parameters to observational evidence. The computational efficiency of our model allowed us to run large ensembles over many centuries. By considering differing scenarios of future warming, we describe the full spread of uncertainty in future permafrost degradation and GHG release inherent to simulations of the permafrost-carbon feedback.

Besides modelling the slow process of active layer deepening, we also describe fast thaw in sublake sediments resulting from increased future thermokarst activity. As we account for deep (below 3 meter depth) carbon inventories, we quantify the extent to which permafrost carbon fluxes are enhanced by the contributions from old soil carbon that has been removed from the active carbon cycle for multiple centuries to millennia. In our model description we consider two differing sub-reservoirs of deep soil carbon storage – Yedoma deposits (late Pleistocene ice- and organic-rich silty sediments) and deposits formed in thermokarst lake basins. Both environments differ in soil properties, such as ice content, carbon amount, lability, and age. By describing deposit-specific soil parameters, we simulate differing pathways of future carbon release. We analyse the timing and magnitude of individual carbon dioxide and methane fluxes from these deep carbon stores and discuss their role in enhancing circum-Arctic permafrost carbon release within this century and beyond. Our model simulates permafrost carbon fluxes which strongly increase with global temperatures. Under moderate warming (RCP2.6), we infer cumulated CO_2 fluxes from newly thawed permafrost until the year 2100 of 20 – 58 Pg-C. Under excessive warming (RCP8.5), our model suggests a carbon release of 42 – 141 Pg. When considering strongly enhanced thermokarst activity in a warmer climate, our simulated methane fluxes proved substantial, causing up to 40 % of total permafrost-affected radiative forcing in the 21^{st} century.

The additional global warming through the release from newly thawed permafrost carbon proved only slightly dependent on the pathway of anthropogenic emission and reached typical magnitudes of about a tenth of a degree by end of the 21^{st} century. The long-term, permafrost-affected global warming increased further in the 22^{nd} and 23^{rd} century, reaching a maximum of about 0.4 °C in the year 2300.

References

Schneider von Deimling, T.; Grosse, G.; Strauss, J.; Schirrmeister, L.; Morgenstern, A.; Schaphoff, S.; Meinshausen, M. and Boike, J. [2015]: Observation-based modelling of permafrost carbon fluxes with accounting for deep carbon deposits and thermokarst activity. *Biogeosciences*, 12(11):3469–3488, doi:10.5194/bg-12-3469-2015.

The carbon balance of Alaskan tundra in response to long-term permafrost degradation

Edward Schuur[1], Rosvel Bracho[2], Gerardo Celis[1], Justin Ledman[1], & Marguerite Mauritz[1]

[1] *Northern Arizona University, United States of America*
[2] *University of Florida*

New estimates place 1330 – 1580 billion tons of soil carbon in the northern circumpolar permafrost zone, more than twice as much carbon than in the atmosphere. Permafrost thaw and the microbial decomposition of previously frozen organic carbon is considered one of the most likely positive feedbacks from terrestrial ecosystems to the atmosphere in a warmer world. Understanding the magnitude, rate, and form of greenhouse gas release to the atmosphere is crucial for predicting the strength and timing of this carbon cycle feedback to a warming climate. Here we report results from eight years of eddy covariance measurements in a tundra landscape undergoing permafrost thaw at the Eight Mile Lake research watershed at Denali National Park, Alaska. This moist acidic tussock tundra site is located where permafrost temperatures are already close to zero and appear to be thawing due to regional changes in climate. Net carbon exchange was estimated using the eddy covariance approach starting in the growing season of 2008. This interval encompassed a range of climatic variability that included a 50 percent deviation from the long-term average in growing season precipitation, as well as record setting summer temperatures for the region. Active layer depth, the seasonal thaw depth measured from the soil surface to the permafrost at the end of the growing season, as well as ground subsidence that accompanies changes in soil ice volume, were used as indicators of permafrost degradation over time. Annual net ecosystem exchange of carbon ranged from a sink of 0.8 Mg carbon per hectare per year to a source of 0.6 Mg carbon per hectare per year, and summed together was a cumulative net loss of C over the time interval. Net ecosystem exchange during the growing season fluctuated from 1.1 to 1.8 Mg carbon per hectare per season representing net C uptake by growing vegetation. Parameters from the light response curve estimated by these measurements showed seasonal and interannual variation and varied among sectors of the tower footprint that differed in their extent of permafrost degradation. Annual net ecosystem exchange of carbon was strongly affected by winter respiration, which represented at least 30 % of the annual respiration even when air temperatures were sub-zero. Together these data point towards the importance of accurate and sustained winter measurements for understanding the net exchange of C from tundra, and also help constrain the magnitude of net C loss in a degrading permafrost ecosystem.

High resolution maps of soil organic carbon and typical soil profiles

Matthias Benjamin Siewert, Peter Kuhry, & Gustaf Hugelius

Stockholm University, Sweden

Soil pedon data and maps of soil organic carbon (SOC) storage are essential components to improve our understanding of the permafrost carbon climate feedback [Koven et al., 2015]. While high resolution satellite imagery is increasingly becoming available and improves the quality of land cover classifications significantly, there is still only a limited amount of soil pedons available from many remote study areas in the circum-polar permafrost region [Siewert et al., 2015]. Therefore, thematic mapping is usually performed as a mean of upscaling soil organic carbon data [Hugelius, 2012]. In this process the spatial distribution of soil properties, inferred from soil pedons, is upscaled based on its relation to vegetation cover, soil types or relevant land cover units. Further, in order to understand patterns in the spatial distribution of SOC and to assess different permafrost carbon vulnerability scenarios, detailed knowledge on several key variables of permafrost affected soils are necessary. These variables include among others soil parent material, bulk density, nitrogen storage, water and ice content. In addition to landscape-scale gradients and spatial variability of these properties, there are also significant trends with soil depth and substantial vertical variability. To further the understanding of these depth-specific trends and facilitate the use of field data in support of model improvement, we exemplify how typical soil profiles can be generated for different landscape types, soil classes and data sets.

We summarize findings from high-resolution studies of soil properties from four study areas. These study areas are one high-Arctic river delta (Lena river delta, Russia), one lowland tundra environment (Kytalyk, Russia), one taiga environment (Spasskaya Pad, Russia) and one sub-Arctic mountain environment (Abisko, Sweden). The advantages and limitations of thematic upscaling using land cover maps from satellite images are discussed and suggestions for future research directions with regard to mapping efforts are made. These include advanced classification methods and the inclusion of additional spatial datasets, such as digital elevation models, in a data-fusion approach. We also exemplify some key properties of permafrost affected soils and how they can be abstracted as typical soil profiles or datasets to project future permafrost carbon development.

References

Hugelius, G. [2012]: Spatial upscaling using thematic maps: An analysis of uncertainties in permafrost soil carbon estimates. *Global Biogeochemical Cycles*, doi:10.1029/2011GB004154.

Koven, C.D.; Schuur, E.A.G.; Schädel, C.; Bohn, T.J.; Burke, E.J.; Chen, G.; Chen, X.; Ciais, P.; Grosse, G.; Harden, J.W.; Hayes, D.J.; Hugelius, G.; Jafarov, E.E.; Krinner, G.; Kuhry, P.; Lawrence, D.M.; MacDougall, A.H.; Marchenko, S.S.; McGuire, A.D.; Natali, S.M.; Nicolsky, D.J.; Olefeldt, D.; Peng, S.; Romanovsky, V.E.; Schaefer, K.M.; Strauss, J.; Treat, C.C. and Turetsky, M. [2015]: A simplified, data-constrained approach to estimate the permafrost carbon–climate feedback. *Trans. R. Soc. A*, 373, 2015. doi:10.1098/rsta.2014.0423.

Siewert, M.B.; Hanisch, J.; Weiss, N.; Kuhry, P.; Maximov, T.C. and Hugelius, G. [2015]: Comparing carbon storage of Siberian tundra and taiga permafrost ecosystems at very high spatial resolution: ECOSYSTEM CARBON IN TAIGA AND TUNDRA. *Journal of Geophysical Research: Biogeosciences*, 1973–1994, doi:10.1002/2015JG002999.

Microbial lipid distribution and substrate potential of the organic matter in terrestrial Siberian permafrost deposits from NE Siberia

Janina Gabriele Stapel[1], Kai Mangelsdorf[1], Lutz Schirrmeister[2], Brian Horsfield[1], & Dirk Wagner[1]

[1] *GFZ German Research Centre for Geosciences, Germany*
[2] *Alfred Wegener Institute Helmholtz Centre for Polar and Marine Research, Potsdam, Germany*

The investigation of microbial ecosystems in permafrost sediments is an important approach to understand the role of microbial organic matter transformation in permafrost sediments for past and future climate changes, and is of high relevance in today's geoscience research (Wagner, 2008) due to the current debate on the temperature vulnerability of permafrost deposits. Especially, the interplay between the organic substrate and the distribution of the living and past microbial communities in Late Pleistocene (Yedoma) and Holocene permafrost deposits, as well as the substrate potential of the organic matter stored in potentially thawing permafrost deposits are in the focus of the current study.

Our investigation is part of the BMBF CarboPerm project an interdisciplinary Russian-German cooperation on the formation, turnover and release of carbon from Siberian permafrost landscapes. Sample material derived from terrestrial permafrost cores drilled at the coast of Bour Khaya in the North-Eastern Siberian Arctic. The gathered core material comprises Late Pleistocene to early Holocene deposits separated by an ice wedge.

The microbial life markers (intact phospholipids, PLs) prove the presence of currently living microorganisms in the entire permafrost sequence and show the highest concentration in the uppermost sample indicating an abundant microbial life in the active layer. In comparison, the PL profile is strongly decreased in the underlying permafrost deposits. Nevertheless, the inventory of the Phospholipid fatty acids (PLFAs) suggests that the cell membrane temperature adaptation to cold environmental conditions is mainly regulated via the ratio between iso- and anteiso-fatty acids (FAs) as well as the ratio between saturated and unsaturated FAs. The surface samples show higher proportions of anteiso and unsaturated FAs (adaptation to cooler conditions), which might derive from the fact that surface layers are more affected from the harsh Siberian winter conditions than the deeper constantly cold permafrost deposits, where the above-ground temperature extremes are buffered due to the overlying deposits. Indeed within the deeper permafrost sequence the variations of the ratios are rather small, indicating adaptation to similar constantly cold temperature conditions. Other microbial markers (GDGTs), already partly degraded and, therefore, not indicating microbial life, reveal similarities with the TOC content and an increase especially in Late Pleistocene deposits. This suggests increased microbial life during intervals in the Late Pleistocene presumably caused by periods of moisture and temperature increased environments.

Pore water analysis reveals the presence of low molecular weight organic acids (LMWOA) such as acetate, being excellent substrates for microbial metabolism. In the Late Pleistocene deposits below the ice wedge the substrate depth profiles show significant similarities to the TOC content. These points to a link between the organic matter and the LMWOA concentrations solved in the pore water and to the potential of those permafrost layers to provide substrates for microbial greenhouse gas production. In contrast, in the active layer the LMWOA concentrations are low, reflecting an active microbial turnover in the surface layers.

Ester cleavage experiments on the residual organic matter resulted in the release of ester linked LMWOAs forming a potential substrate pool when released in future. These bound LMWOA profiles are even better correlated to the TOC content suggesting that the deeper permafrost deposits (older organic material) are not significantly different from those in the surface sediment (fresh organic material). Overall this indicates that the organic matter stored in the permafrost deposits and, therefore, removed from the surface carbon cycle is not much different in terms of organic matter quality than the fresh surface organic material. Considering the discussed increase of permafrost thawing, this might imply a strong impact on

the generation of greenhouse gases from permafrost areas in future with its feedback on climate evolution.

In a second and ongoing study, four terrestrial permafrost cores spanning from the Eemian interglacial into the Holocene form Bol'shoy Lyakhovsky Island are investigated with the focus on the differences and potential of the organic matter by comparing Eemian, Late Pleistocene and Holocene deposits. First results already reveal similar relations between the living and dead microbial communities with respect to the availability of free substrates, and the quality and amount of the total organic carbon. The results on the future potential of these deposits will also be presented.

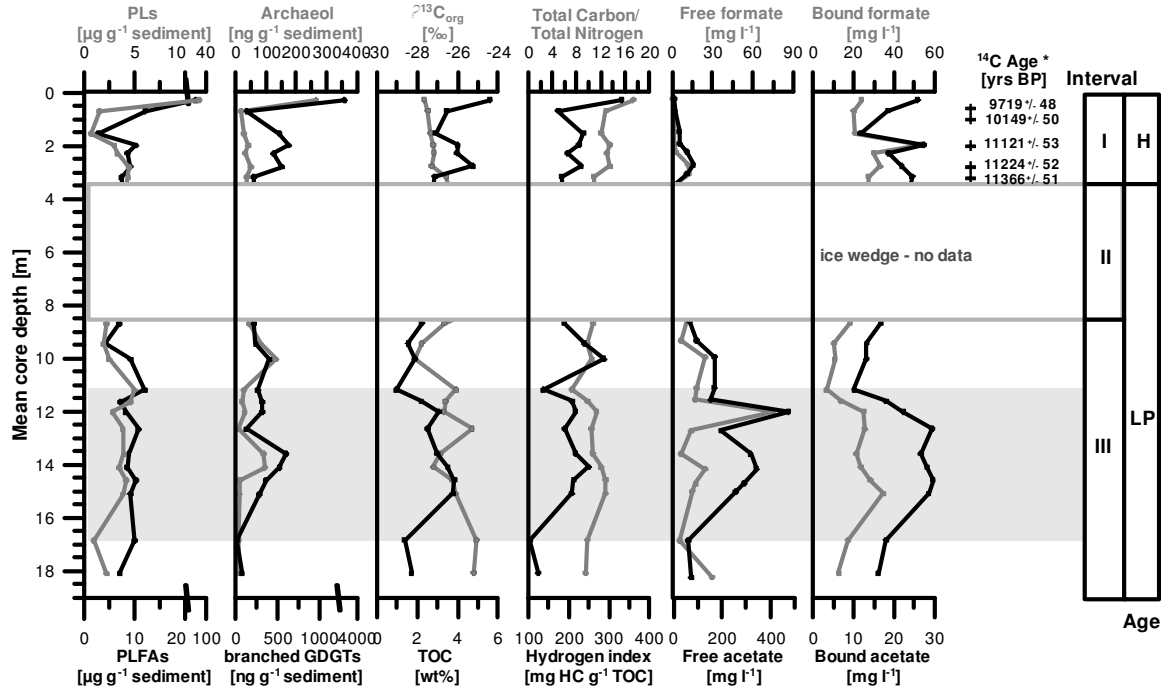

Figure 1: Microbial biomarker and geochemical profiles of Bour Khaya

Permafrost aggradation reduces peatland methane fluxes during the Holocene

Claire C. Treat[1], Miriam Jones[2], Guido Grosse[3], Laura S. Brosius[1], & Katey Walter Anthony[1]

[1] *University of Alaska Fairbanks, USA*; [2] *U.S. Geological Survey, Reston, VA, USA*
[3] *Alfred Wegener Institute Helmholtz Centre for Polar and Marine Research, Potsdam, Germany*

Methane emissions from northern high latitude wetlands are one of the largest natural sources of atmospheric methane, contributing an estimated 20 % of the natural terrestrial methane emissions to the atmosphere. Methane fluxes vary among wetland types and are generally higher in peatlands, wetlands with > 40 cm of organic soil, than in wetlands with mineral soils. However, permafrost aggradation in peatlands reduces methane fluxes through the drying of the peat surface, which can decrease both methane production and increase methane oxidation within the peat. We reconstruct methane emissions from peatlands during the Holocene using a synthesis of peatland environmental classes determined from plant macrofossil records in peat cores from > 250 sites across the pan-arctic. We find methane emissions from peatlands decreased by 20% during the Little Ice Age due to the aggradation of permafrost within peatlands during this period. These bottom-up estimates of methane emissions for the present day are in agreement with other regional estimates and are significantly lower than the peak in peatland methane emissions 1300 years before present. Our results indicate that methane emissions from high latitude wetlands have been an important contributor to atmospheric methane concentrations during the Holocene and will likely change in the future with permafrost thaw.

Thermokarst terrains and carbon cycling: A circumpolar perspective

Merritt R. Turetsky[1], A. David McGuire[2], David Olefeldt[3], & Members of the Permafrost Carbon Network[4]

[1] *University of Guelph, Canada*
[2] *University of Alaska Fairbanks and the Alaska Cooperative Fish and Wildlife Research Unit, USA*
[3] *University of Alberta, Canada*
[4] *Permafrost Carbon Network*

Carbon release from permafrost thaw and the microbial decomposition of previously frozen organic matter is considered one of the most likely positive feedbacks from terrestrial ecosystems to the climate system in a warmer world. Permafrost thaw can involve the gradual deepening of the seasonally thawed layer, but in certain landscape types also can occur via abrupt thermokarst development that potentially affects the entire soil profile. Both thermokarst and thermal erosion expose previously-frozen carbon to microbial processes but also alter hydrology. Critical for predicting carbon balance is understanding whether permafrost carbon, upon thaw, will be exposed to aerobic or anaerobic conditions. Changes in hydrology may cause permafrost carbon to be incorporated into a saturated zone, either as a result of subsidence or down-slope transport, where it may experience anaerobiosis. If saturated, overall rates of carbon mineralization and loss will be slower but permafrost carbon is more likely to released to the atmosphere in the form of methane, which has a stronger radiative forcing than carbon dioxide. Methane emissions typically are less than 8 % of carbon dioxide emissions during anaerobic laboratory incubations of soil, suggesting that permafrost carbon is likely to have a greater impact on climate if it thaws and decomposes in aerobic rather than anaerobic settings. However, some of the highest methane emissions in the Arctic have been observed in thermokarst wetlands and thaw lakes.

The main objective of this work is to explore how the potential magnitude of permafrost carbon losses resulting from thermokarst compares to carbon losses triggered by gradual deepening of the seasonally thawed layer. We are using mapping activities, data synthesis and simple land cover change modeling to better understand the relevance of abrupt thaw to the overall permafrost carbon feedback. First, we developed a spatial modelling framework that assesses whether areas are predisposed to thermokarst or thermal erosion (Fig. 1). The framework weighs the perceived relative importance of ground ice content, overburden thickness, permafrost zonation, terrestrial ecoregion, topographical roughness, and regional histel cover to the formation of wetland thermokarst features, thaw lakes, and hillslope features (retrogressive thaw slumps, active layer detachments, erosional gullies). Second, we are synthesizing process-level studies to parameterize a model to track the effects of thermokarst disturbance on changes in carbon storage and in carbon dioxide and methane emissions over the northern permafrost region. The book-keeping model is based state-and-transition conceptual models for generalized thermokarst trajectories in the northern permafrost region.

We estimate that thermokarst terrains cover 3.6×10^6 km^2, or 20 % of the northern permafrost domain. However, given disproportionally high soil organic carbon content, thermokarst terrains are estimated to store ≈30 % of the total permafrost domain soil organic carbon stored in the upper 3 meters of soil, and likely an even larger fraction when deeper carbon stocks are considered. Results from our book-keeping model suggests that wetland thermokarst and the formation of collapse bogs or fens causes the largest net releases of carbon to the atmosphere at circumpolar scales. Projections of net ecosystem carbon balance over two time periods (2010 – 2100 and 2010 – 2300) indicate that cumulative carbon losses from thermokarst are similar to estimates of permafrost carbon losses associated with widespread, gradual top-down thaw. We conclude that thermokarst and thermal erosion impacts a relatively small portion of the permafrost region, but has the potential to govern the overall magnitude of the permafrost carbon feedback to climate.

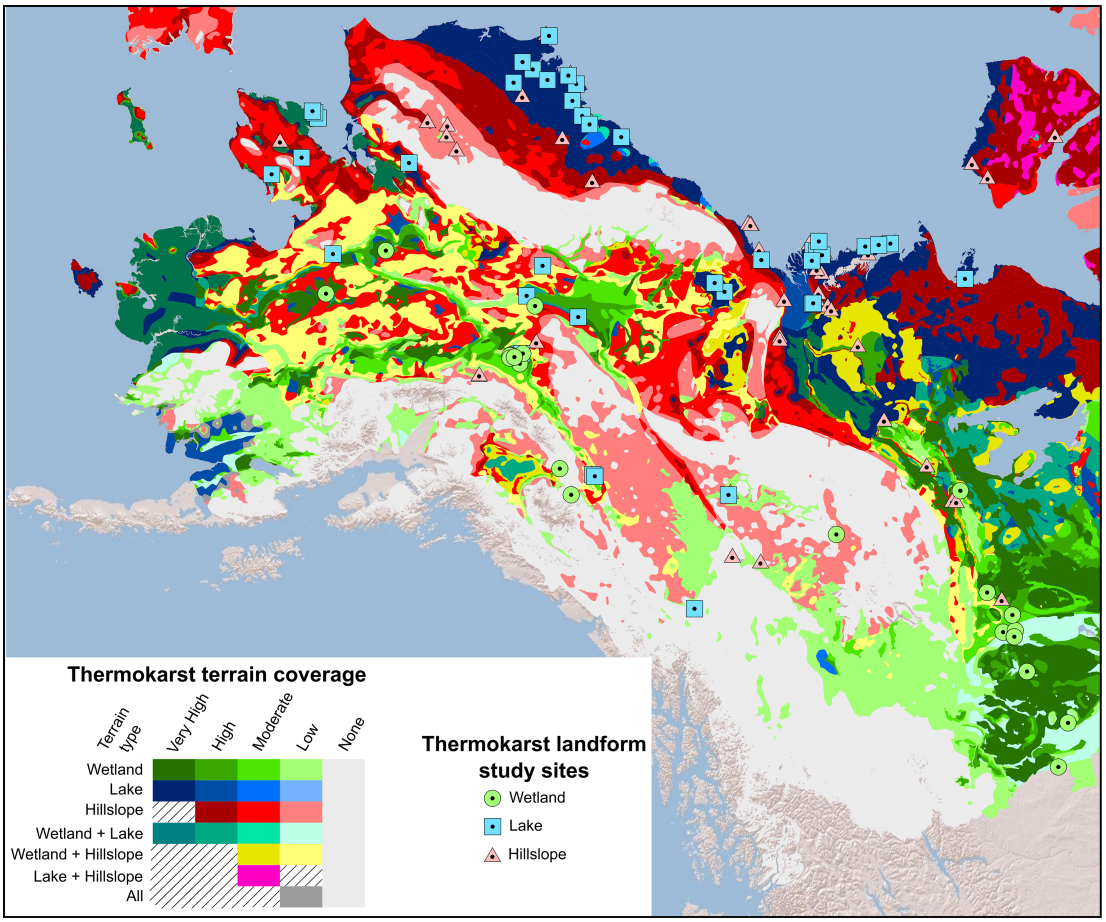

Figure 1: Dominant or co-dominant thermokarst terrain land cover in Alaska and western Canada, including the location of thermokarst study sites where field data are available.

Assessment of climate driven dynamics of active layer, hydrological and vegetation status in Heilongjiang province, Northern China using dynamic global vegetation model

Sergey Venevsky, Yang Yang, & Wu Chao

Tsinghua University, People's Republic of China

Extensive permafrost degradation starting from 1970s is observed near Heilongjiang (Amur) River, Northern China. Degradation is attributed to an increase in mean annual ground temperature 0.1 °–0.5 °C with mainly winter warming. Permafrost degradation caused negative environmental consequences in the area for infrastructure. The general pathway of future joint dynamics of permafrost, vegetation and hydrological status in Northern China is still poorly understood and foreseeable. Hydrology in the area is determined by heat-moisture dynamics of active layer. This dynamics is highly non-linear and depends as on external climatic variables temperature and precipitation, so on soil and rock properties (amount of sand against aeolian deposits in the Plateau) as well as vegetation cover, which determine thaw and freeze processes in the active layer and evaporation and run-off.

Global vegetation model SEVER DGVM was modified to include heat-moisture dynamics of active layer in the Heilongjiang province. SEVER DGVM is state of the art process oriented global vegetation model that imitates processes in 10 plant functional types (which represents plants from tropical to boreal area) in grid cells at coarse resolution of 0.5 degrees. This model imitates behavior of average individual of each plant type in each grid cell through simulation years. Each of those grid cells processed independently and not influences each other. First this model start from 'bare soil', place a bit of each plant type and gives them some time to grow and achieve equilibrium (of plant parameters and vegetation distribution), after this main simulation performed.

Inclusion of active layer thickness and soil moisture dynamics in this layer allowed assessment of potential environmental dynamics in Heilongjiang province.

Positive feedback of all three greenhouse gases (CO_2, CH_4, N_2O) to experimental warming in Russian subarctic tundra

Carolina Voigt, Richard E. Lamprecht, Maija E. Marushchak, Pertti J. Martikainen, & Christina Biasi

University of Eastern Finland, Finland

With climate change, global mean air temperature is predicted to increase and relative changes will be most pronounced in the Arctic region. Temperature is a key factor that regulates litter quantity and decomposition, microbial activity and respiration, nutrient dynamics, soil processes such as mineralization and (de-) nitrification as well as plant growth [Rustad et al., 2001]. The response of ecosystem processes to warming may differ largely across the landscape depending on soil type, vegetation cover, moisture conditions and permafrost condition. As arctic ecosystems are generally temperature limited, small changes in environmental settings have the potential to considerably impact on arctic ecosystem functioning and transform the system from a sink to a source of greenhouse gases (GHGs). This is especially the case in the subarctic region underlain by discontinuous permafrost, where permafrost temperatures are already close to zero and the ecosystem is particularly vulnerable to subtle changes in temperature. Typical landform types in subarctic tundra are upland mineral soils with a shallow organic layer, as well as peat plateaus, which are permafrost peatlands with vast peat deposits and carbon stocks that were uplifted above the surrounding tundra landscape by frost heave. While wetland areas are known to be a sink for carbon dioxide (CO_2) and at the same time a considerable source of methane (CH_4), upland tundra soils and peat plateaus are comparably dry and considered to be CH_4 neutral or small sinks for CH_4, while at the same time emitting CO_2. Moreover, bare patterned ground features on the peat plateaus have been identified as arctic hotspots for nitrous oxide (N_2O; Repo et al. [2009]. N_2O is a very potent greenhouse gas, which is almost 300 times more effective in its global warming potential than CO_2, but studies on arctic N_2O fluxes are rare.

In this study we examined how temperature increase reflects on the seasonal GHG balance (CO_2, CH_4 and N_2O) from three tundra surface types in the Russian Arctic (67°03' N 62°55' E), during the course of three growing seasons. Our study site is located close to the tree line on the southern extent of permafrost distribution in an area currently experiencing permafrost warming and thaw [Oberman and Mazhitova, 2001], which provides an ideal setting for assessing climate change impacts. We deployed open-top chambers (OTCs), inducing near-surface warming of air and soil temperature, thus mimicking predicted warming scenarios. GHG fluxes and soil profile concentrations of CO_2, CH_4 and N_2O as well as nutrient concentrations were linked to environmental parameters and major underlying biogeochemical processes.

Our results show that even gentle warming (0.5 – 2 °C) of the upper soil layer and air temperature close to the soil surface increases fluxes of CO_2, CH_4 and N_2O and thus drastically impacts on carbon (C) and nitrogen (N) dynamics in subarctic permafrost soils. We found increased ecosystem respiration rates from the warmed surfaces, while at the same time photosynthesis rates were lowered, significantly decreasing the sink function for CO_2 within all measured surface types. This suggests a stronger response of soil microbes than vegetation to warming and indicates that highly-adapted arctic plants in cold biomes might not be able to buffer increased microbial activity, at least in the short-term. Surprisingly, even though we studied comparably dry permafrost soils and not the typical wetland CH_4 emitters, CH_4 fluxes increased almost fivefold from patterned ground features. Though fluxes were still relatively low we found high potential for CH_4 production in the soil profile of the wetter, but still well-oxygenated deeper soil layers of the permafrost peatlands. While N_2O fluxes from arctic N_2O hotspots were found to increase with warming (mean seasonal flux of 0.46 mg N_2O m^{-2} d^{-1} and 0.62 mg N_2O m^{-2} d^{-1} from control and warmed surfaces, respectively), warming also generated some N_2O emissions from peat plateaus that did not emit N_2O prior to the warming treatment, and we observed N_2O production potential along the soil profile of those soils. Similarly to CH_4, N_2O fluxes from the dry peatlands were relatively low, but the abundance of peat plateau is with ca. 20 % of the Arctic relatively high, thus likely increasing the regional impact of N_2O on

the GHG budget in a future warmer world. Further, nitrate (NO3-) and ammonium (NH4+) pools got depleted in the warmed treatments and higher N_2O flux rates from warmed plots had a lower (i.e. more negative) $\delta^{15}N$ signal. $\delta^{15}N$ values of 1.6 ‰ and −2.1 ‰ from control and warmed surfaces, respectively, indicate that denitrification might be the main process controlling N_2O emissions. The overall seasonal GHG budget of the dominant surface types increased from −300 to 144 g CO_2-eq m^{-2} from the peat plateau and from −198 to 105 g CO_2-eq m^{-2} from mineral tundra surfaces, which together cover more than 80 % of the land area in the study region.

Our study set in subarctic tundra showed a strong and immediate response of the ecosystem to rising temperatures. While CO_2 remains the dominant trace gas regulating subarctic GHG budgets, we provide here first in-situ evidence for the potential of arctic soils to release increased amounts of N_2O with warming. Our results add to the growing body of evidence that interactions between warming, small-scale hydrological conditions as well as associated plant functions reduce the sink function of subarctic tundra ecosystems.

References

Oberman, NG. and Mazhitova, GG. [2001]: Permafrost dynamics in the north-east of European Russia at the end of the 20th century. *Norsk Geografisk Tidsskrift – Norwegian Journal of Geography*, 55, doi:10.1080/00291950152746595.

Repo, ME.; Susiluoto, S.; Lind, SE.; Jokinen, S.; Elsakov, V.; Biasi, C.; Virtanen, T. and Martikainen, PJ. [2009]: Large N_2O emissions from cryoturbated peat soil in tundra. *Nature Geoscience*, 189–192, doi:10.1038/ngeo434.

Rustad, L.; Campbell, J.; Marion, G.; Norby, R.; Mitchell, M.; Hartley, A.; Cornelissen, J.; Gurevitch, J. and GCTE-NEWS [2001]: A meta-analysis of the response of soil respiration, net nitrogen mineralization, and aboveground plant growth to experimental ecosystem warming. *Oecologia*, 126, doi:10.1007/s004420000544.

Ecosystem functional zonation approach to integrate multi-type multiscale datasets for scaling above and below-ground control on carbon cycling

Haruko M. Wainwright[1], Baptiste Dafflon[1], Neslihan Tas[1], Yuxin Wu[1], Margaret Torn[1,2], Lydia Smith[1,2], John Bryan Curtis[1], Craig Ulrich[1], John E. Peterson[1], & Susan S. Hubbard[1]

[1] *Lawrence Berkeley National Laboratory*
[2] *University of California, Berkeley*

A significant challenge associated with predicting ecosystem feedbacks to climate is the understanding and quantification of complex surface and subsurface interactions among permafrost, hydrology, vegetation, soil geochemistry, and microbiology. Although past studies identified correlations among various ecosystem functioning properties and landscape/topography controls on such properties, there was a significant uncertainty in identifying the scale at which such interactions (or co-variation) emerge in complex landscapes and how such interactions are related to ecosystem-climate feedbacks. By taking advantage of interdisciplinary team science in the Next Generation Ecosystem Experiment (NGEE) – Arctic project, we have led a comprehensive aboveground/belowground characterization of the Arctic tundra ecosystem to explore the spatial distribution of relevant ecosystem properties and their relationship to geomorphology, based on multi-type multiscale datasets including in situ measurements, core analysis, geophysics and remote sensing.

Working within an ice-wedge polygonal region near Barrow AK, we documented the strong co-variability of aboveground/belowground properties, and also identified 'ecosystem functional zones' to describe such co-variable ecosystem functioning in a large spatial extent, using spatially extensive geophysical and remote sensing datasets (Fig. 1; Hubbard et al. [2013], Wainwright et al. [2015]. Statistical analyses of various datasets showed that such functional zones have a larger explanatory power than fine-scale microtopographic features for describing the co-variations in the key properties (e.g., soil carbon contents, soil moisture, thaw depths, plant functional types, ice content, ice wedge density). Results suggested the importance of capturing a large-scale pattern emerged as a result of overall drainage, soil profile and also the transport of electron acceptors. The significance of such functional zones was further validated by detailed biogeochemical analyses. For example, we found that surface-water and pore-water chemistry showed significant differences among the functional zones. In Tas et al. [2013], 16S rRNA gene sequencing revealed a significant variation in microbial community structures among the functional zones.

These results reveal multiple lines of evidence suggesting the co-variability of above and below-ground properties, their influence on the Arctic ecosystem functioning, and the value of a functional-zone approach for characterizing a range of processes and properties in sufficient detail and from local to landscape scale relevant for climate models. Such approaches are particularly important to understand biological drivers and controls on greenhouse gas fluxes as well as their changes. The suite of controls on carbon decomposition is so tightly coupled and complex that it has been difficult to use mechanistic understanding for modeling greenhouse gas emissions accurately over a large area. Since the patterns of greenhouse gas fluxes and other biogeochemical properties – emerged as functional zones – are underlain by complex biological processes, such zonation could potentially be used as an emergent and scalable metric. Such co-variability and emergent functional zones can also be exploited to indirectly characterize important subsurface properties – such as microbial signature and biogeochemistry – over a large spatial scale, using remote-sensing datasets. This approach is expected to be very powerful to integrate remote sensing data with ground-based observations for upscaling surface and subsurface properties, and for parameterizing terrestrial ecosystem models used to predict feedbacks to climate.

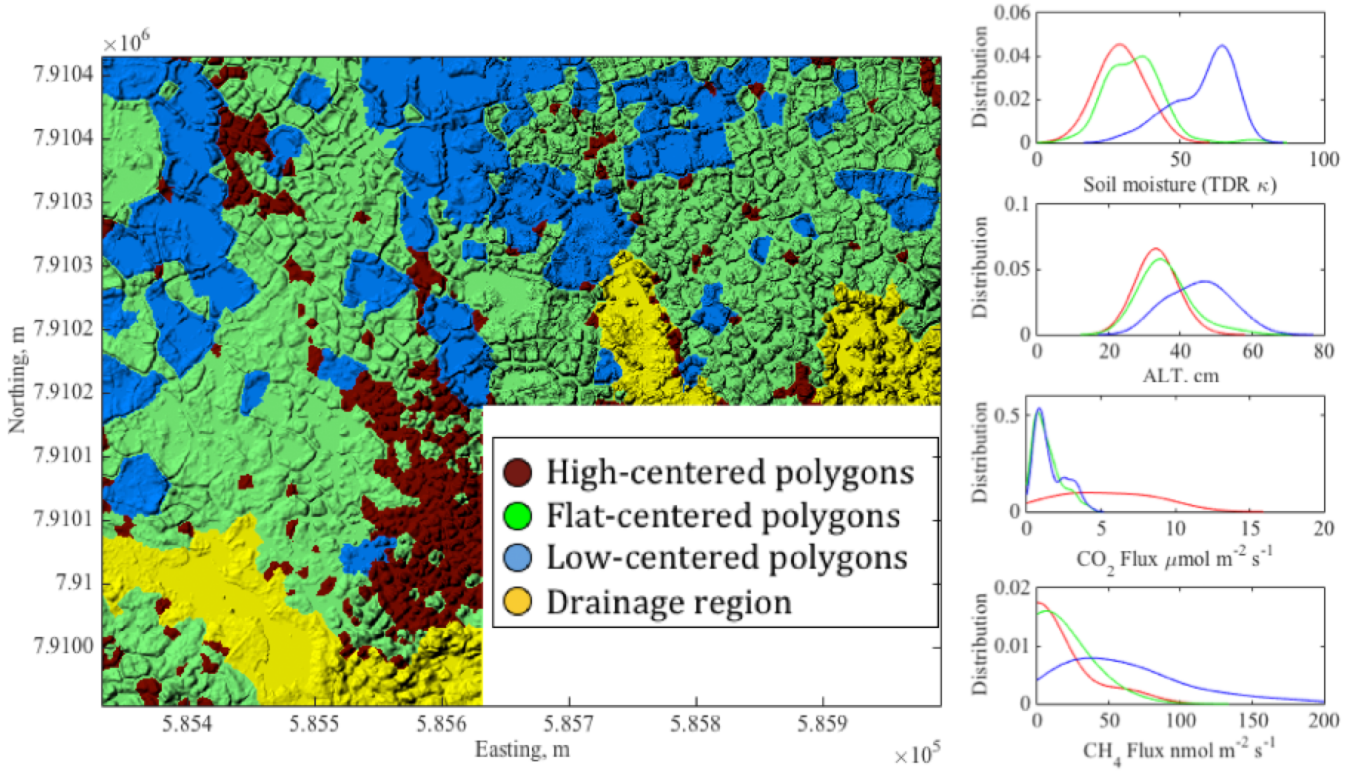

Figure 1: (Left) Distributed polygon types (i.e. ecosystem functional zones) over the study area. (Right) Examples of ecosystem property distributions in three zones. The color corresponds the one in the left panel (modified from Wainwright et al. [2015]

References

Hubbard, S.S.; Gangodagamage, C.; Dafflon, B.; Wainwright, H.M.; Peterson, J.E.; Gusmeroli, A.; Ulrich, C.; Wu, V; Wilson, C.; Rowland, J.; Tweedie, C. and Wullschleger, S.D. [2013]: Quantifying and relating land-surface and subsurface variability in permafrost environments using LiDAR and surface geophysical datasets. *Hydrogeology*, doi:10.1007/s10040-012-0939-y.

Tas, N.; Wu, Y.; Smith, L. J.; Ulrich, C.; Kneafsey, T. J.; Torn, M. S.; Hubbard, S. S.; Wullschleger, S. D. and Jansson, J. [2013]: Integrated metagenomics and field measurements of polygon features at the NGEE-Arctic Barrow site. In *AGU Fall Meeting Abstracts*, (Vol. 1, p. 0563).

Wainwright, H.M.; Dafflon, B.; Smith, L.J.; Hahn, M.S.; Curtis, J.B.; Wu, Y.; Ulrich, C.; Peterson, J.E.; Torn, M.S. and Hubbard, S.S. [2015]: Identifying multiscale zonation and assessing the relative importance of polygon geomorphology on carbon fluxes in an Arctic Tundra Ecosystem. *Biogeosciences*, doi:10.1002/2014JG002799.

Present-day permafrost carbon feedback from thermokarst lakes

Katey Walter Anthony[1], Ronald Daanen[2], Peter Anthony[1], Thomas Schneider von Deimling[3], Chien-Lu Ping[1], Jeffrey Chanton[4], & Guido Grosse[3]

[1] *University of Alaska Fairbanks*; [2] *Alaska Department of Natural Resources*
[3] *Alfred Wegener Institute Helmholtz Centre for Polar and Marine Research*; [4] *Florida State University*

Rapid temperature rise during recent decades (IPCC 2013) is causing permafrost in the Arctic to warm and thaw. This thaw exposes previously frozen soil organic carbon (SOC) to microbial decomposition, generating greenhouse gases methane (CH_4) and carbon dioxide (CO_2) in a feedback process that leads to further warming and thaw. A growing number of studies model the future permafrost carbon feedback (PCF) to climate warming [Koven et al., 2015, Schneider von Deimling et al., 2015]. However, despite observations of widespread permafrost thaw during recent decades and forecasts of thaw during the next 25-100 years [Koven et al., 2015], no research has quantified the PCF for recent decades. This is in part due to the difficulty of detecting the net movement of old carbon from permafrost to the atmosphere over years and decades amidst large input and output fluxes from ecosystem carbon exchange. In contrast to terrestrial environments, thermokarst lakes provide a direct conduit for processing and emission of old permafrost carbon to the atmosphere, and these emissions are more readily detectable. Results here are based on Walter Anthony et al. [submitted], whereby we quantified the permafrost SOC input to a variety of thermokarst and glacial lakes in Alaska and Siberia in thermokarst zones, defined as areas where land surfaces have transitioned to open lakes due to permafrost thaw during the past 60 years, the historical period most commonly covered by remote-sensing data sets. We also quantified the resulting methane emitted from these active thermokarst lake zones. Using field work, numerical modeling of thaw bulbs, remote sensing and spatial data analysis we will report on the relationship between methane emissions from thermokarst zones and SOC inputs to lakes across gradients of permafrost and climate in Alaska. We will also define the relationship between radiocarbon ages of methane and permafrost soil carbon entering into lakes upon thaw. We will report on the present-day PCF relationship between thaw of permafrost SOC and resulting greenhouse gas release.

An extrapolation of our results to the panarctic permafrost region will be presented and compared to permafrost carbon mass balance approaches. The fraction of the terrestrial permafrost carbon pool that has been released as methane from thermokarst along lake margins during the past 60 years will be evaluated relative to early Holocene thermokarst lake emissions and projected permafrost carbon emissions by year 2100. The data will be placed in the context of large regional temperature increases in the Arctic, up to 7.5 °C by 2100, and thicker, organic-rich Holocene-aged deposits subject to thaw and aerobic decomposition as active layer deepens. We will report on the inflection of large permafrost carbon emissions that is imminently expected to occur and whether or not it has commenced.

References

Koven, C.D.; Schuur, E.A.G.; Schädel, C.; Bohn, T.J.; Burke, E.J.; Chen, G.; Chen, X.; Ciais, P.; Grosse, G.; Harden, J.W.; Hayes, D.J.; Hugelius, G.; Jafarov, E.E.; Krinner, G.; Kuhry, P.; Lawrence, D.M.; MacDougall, A.H.; Marchenko, S.S.; McGuire, A.D.; Natali, S.M.; Nicolsky, D.J.; Olefeldt, D.; Peng, S.; Romanovsky, V.E.; Schaefer, K.M.; Strauss, J.; Treat, C.C. and Turetsky, M. [2015]: A simplified, data-constrained approach to estimate the permafrost carbon–climate feedback. *Trans. R. Soc. A*, 373, doi:10.1098/rsta.2014.0423.

Schneider von Deimling, T.; Grosse, G.; Strauss, J.; Schirrmeister, L.; Morgenstern, A.; Schaphoff, S.; Meinshausen, M. and Boike, J. [2015]: Observation-based modelling of permafrost carbon fluxes with accounting for deep carbon deposits and thermokarst activity. *Biogeosciences*, 12(11):3469–3488, doi:10.5194/bg-12-3469-2015.

Walter Anthony, K.; Daanen, R.; Anthony, P.; Schneider von Deimling, T.; Ping, C.-L.; Chanton, J. and Grosse, G. [submitted]: Ancient methane emissions from 60 years of permafrost thaw in arctic lakes.

Regulation of soil organic matter decomposition in permafrost-affected soils

Josefine Walz, Christian Knoblauch, Luisa Böhme, & Eva-Maria Pfeiffer

Inst. of Soil Science, Center for Earth System Research and Sustainability, Universität Hamburg, Germany

Permafrost-affected soils are an important sink for atmospheric carbon. But warming-induced environmental changes may strongly influence trace gas fluxes between thawing soils and the atmosphere. Soil organic matter (SOM) decomposition in the active layer and thawing permafrost is an important source of carbon dioxide (CO_2) and methane (CH_4). The large carbon pool in permafrost-affected soils may become a source of trace gases in a warmer Arctic, a fact that raises concerns of a positive climate feedback after permafrost thaw. However, regulating factors affecting SOM decomposition in permafrost landscapes is not well understood. Decomposability and potential CO_2 and CH_4 production are connected to the quality of SOM. SOM quality varies with vegetation composition, soil type, and soil depth. Furthermore, the decomposability of SOM under anaerobic conditions, which are characteristic for water-saturated soils, is generally lower than under aerobic conditions, causing less CO_2 being produced. However, under these conditions CH_4 can be formed, which has a substantially higher warming potential than CO_2.

Higher soil temperatures directly affect microbial activity, generally resulting in enhanced SOM decomposition. Indirectly, higher temperatures increase plant productivity, which results in a higher input of organic matter into the soil. On the one side, a higher allocation of below-ground carbon could increase the SOM pool. On the other side, the input of fresh organic matter could stimulate decomposition of older and more stable SOM (priming effect), resulting in further carbon losses. It still remains unclear, how fast SOM in permafrost-affected soils can be microbially decomposed and how much carbon will be released. Available data are scarce, but suggest a gradual, but prolonged release of carbon from permafrost regions [Schuur, 2015]. Here, we incubated permafrost-affected soils from a polygonal tundra landscape in the Lena Delta, Northeast Siberia, to examine the influence of depth, oxygen availability, temperature, and fresh organic matter addition on trace gas production.

CO_2 production in topsoil (0 – 10 cm) was up to three times higher than in subsoil (10 – 50 cm) and shallow permafrost (50 – 90 cm). In topsoil, about 3 % of the initial soil organic carbon (SOC) was aerobically decomposed and released as CO_2 within four months (approximate annual thaw period) at 4 °C (average summer soil temperature). Subsoil and permafrost carbon did not differ significantly in their decomposability. Anaerobic decomposition was two to six times lower than under aerobic conditions. Within the four-month incubation period, methanogenesis played only a minor role. CH_4 contributed 1 – 30 % to the total anaerobic carbon release. The ratio of anaerobically produced CO_2 and CH_4, however, decreased sharply during the incubation, indicating that CH_4 could be become an important trace gas in the long-term.

Temperature had a positive effect on SOM decomposition across all depths. Across a temperature gradient (1 – 8 °C) aerobic decomposition in topsoil was less sensitive to temperature than in subsoil or permafrost. The addition of labile plant organic matter (^{13}C-labelled *Carex aquatilis*, a dominant species in the region) significantly increased overall CO_2 production across all depths and temperatures. The amount of additional CO_2 production increased with depth and temperature. Partitioning the total amount of CO_2 in samples amended with *Carex* organic matter into SOM-derived CO_2 and *Carex*-derived CO_2, however, revealed that most of the additional CO_2 could be assigned to the organic carbon from the amendment. A significant increase in SOM-derived CO_2 (positive priming) was only evident in permafrost samples. Here, the relative priming effect was significantly weaker at 8 °C than at 1 °C or 4 °C. These results suggest that the release of fresh below-ground carbon from plants could accelerate the degradation of permafrost carbon upon thaw.

References

Schuur, E.A.G. et al. [2015]: Climate change and the permafrost carbon feedback. *Nature*, doi:10.1038/nature14338.

Subsoil carbon and nitrogen dynamics: Implications of deeper plant rooting for the arctic carbon balance

Birgit Wild[1,2,3], Ricardo J. E. Alves[3,4], Jiři Bárta[5], Petr Čapek[5], Kateřina Diáková[5], Norman Gentsch[6], Antje Gittel[7,8], Georg Guggenberger[6,9], Gustaf Hugelius[10], Christina Kaiser[2,3], Anna Knoltsch[2,3], Peter Kuhry[10], Nikolay Lashchinskiy[11], Robert Mikutta[6,12], Juri Palmtag[10], Judith Prommer[2], Hana Šantrůčková[5], Christa Schleper[3,4], Jörg Schnecker[2,13], Olga Shibistova[6,9], Mounir Takriti[2,14], Vigdis L. Torsvik[7], Tim Urich[4,15], Margarete Watzka[2], & Andreas Richter[2,3]

[1] *Department of Earth Sciences, University of Gothenburg, Sweden*
[2] *Department of Microbiology and Ecosystem Science, University of Vienna, Vienna, Austria*
[3] *Austrian Polar Research Institute, Vienna, Austria*
[4] *Department of Ecogenomics and Systems Biology, University of Vienna, Vienna, Austria*
[5] *Department of Ecosystems Biology, University of South Bohemia, České Budějovice, Czech Republic*
[6] *Institute of Soil Science, Leibniz Universität Hannover, Hannover, Germany*
[7] *Department of Biology, Centre for Geobiology, University of Bergen, Bergen, Norway*
[8] *Department of Bioscience, Center for Geomicrobiology, Aarhus, Denmark*
[9] *VN Sukachev Institute of Forest, Siberian Branch of Russian Academy of Sciences, Krasnoyarsk, Russia*
[10] *Department of Physical Geography, Stockholm University, Stockholm, Sweden*
[11] *Central Siberian Botanical Garden, Siberian Branch of Russian Academy of Sciences, Novosibirsk, Russia*
[12] *Soil Science and Soil Protection, Martin-Luther-University Halle-Wittenberg, Halle (Saale), Germany*
[13] *Dept. of Natural Resources and the Environment, University of New Hampshire, Durham, NH, USA*
[14] *Lancaster Environment Centre, Lancaster University, Lancaster, UK*
[15] *Institute of Microbiology, Ernst-Moritz-Arndt University, Greifswald, Germany*

Plant productivity in the Arctic, and thus the potential for ecosystem C sequestration, is often constrained by low soil N availability. This has been attributed to the slow breakdown of N-containing polymers such as proteins into units small enough for plant and microbial uptake under the cold and moist conditions in arctic soils. In addition, plant roots and plant N uptake are currently mostly confined to the organic layer, with more than 90 % of plant roots in the top 30 cm [Jackson et al., 1996]. Given that the organic layer is characterized by high C/N ratios of soil organic matter (SOM) and predominant N limitation of the soil microbial community, plants strongly compete with soil microorganisms for the small amounts of N available.

With active layer deepening, however, plants might increasingly access deeper, mineral soil horizons to meet their N demand. We here show that mineral soil horizons in the deep active layer harbour a large plant-available pool of N, as indicated by a comparison of gross rates of protein depolymerization (the breakdown of proteins into amino acids) and N mineralization (the microbial release of excess N as ammonium) across four horizons of the active layer (organic layer, mineral topsoil, mineral subsoil, cryoturbated material), and across five sites in the Siberian Arctic and Greenland. While protein depolymerization rates decreased with soil depth, we found the highest N mineralization rates per unit soil N in the mineral subsoil, indicating an increase in microbial N excess with depth. Our findings suggest that this increase in microbial N excess was driven by a shift of the microbial community from N to C limitation with depth, as indicated by a decrease in microbial N use efficiency. Considering the large N stocks in the mineral subsoil and the low microbial competition for N, we conclude that subsoil N might be increasingly accessed by plant roots if the active layer deepens and conditions in the subsoil become more favourable for root growth.

An increase in rooting depth, however, might not only increase plant CO_2 uptake in the Arctic by providing plants with additional N, but might also alter SOM decomposition in the subsoil. Plants allocate organic compounds into the soil (e.g., via root litter and root exudates) that can stimulate the microbial decomposer community and promote the de-

composition of native SOM. In a 25 week laboratory experiment comparing 119 soil samples from different horizons of active layer and permafrost and from four locations across the Siberian Arctic, we found that SOM decomposition in the mineral subsoil was particularly susceptible to such an increased input of plant-derived organic compounds, with a stimulation of native soil organic C mineralization by 31 ± 10 % after addition of cellulose and 120 ± 13 % after addition of protein (means ± standard errors).

Taken together, an increase in plant rooting depth with permafrost thaw can promote plant CO_2 uptake by reducing plant N limitation, but can also promote the release of CO_2 by stimulating SOM decomposition in the subsoil, beyond the direct temperature effect. Given that the majority of soil organic C and N in arctic permafrost soils is located below 30 cm [Hugelius et al., 2014, Gentsch et al., 2015], the balance between both mechanisms might have profound consequences for the ecosystem C balance, and alleviate or amplify the permafrost carbon feedback to global warming.

References

Gentsch, N.; Mikutta, R.; Alves, RJE.; Barta, J.; Čapek, P.; Gittel, A.; Hugelius, G.; Kuhry, P.; Lashchinskiy, N.; Palmtag, J.; Richter, A.; Šantrůčková, H.; Schnecker, J.; Shibistov, a O.; Urich, T.; Wild, B. and Guggenberger, G. [2015]: Storage and transformation of organic matter fractions in cryoturbated permafrost soils across the Siberian Arctic. *Biogeosciences*, 12:4525–2542, doi:10.5194/bg-12-4525-2015.

Hugelius, G.; Strauss, J.; S., Zubrzycki; Harden, J.W.; Schuur, E.A.G.; Ping, C.L.; Schirrmeister, L.; Grosse, G.; Michaelson, G.J.; Koven, C.; O'Donnell, J.; Elberling, B.; Mishra, U.; Camill, P.; Yu, Z.; Palmtag, J. and Kuhry, P. [2014]: Estimated stocks of circumpolar permafrost carbon with quantified uncertainty ranges and identified data gaps. *Biogeosciences*, 11, doi:10.5194/bg-11-6573-2014.

Jackson, RB.; Canadell, J.; Ehleringer, B.; Mooney, HA.; Sala, OE. and Schulze, ED. [1996]: A global analysis of root distributions for terrestrial biomes. *Oecologia*, 108:389–411, doi:10.1007/BF00333714.

Linking geomorphology and biogeochemistry in dynamic permafrost environments

Niels Weiss

Stockholm University, Sweden

Permafrost environments are known to contain immense amounts of soil organic carbon, and play an important role in the global carbon cycle. Increased greenhouse gas release upon thawing of carbon rich permafrost substrates is furthermore recognised as a potential positive climate feedback.

Understanding the likeliness of decomposition of soil organic matter (SOM) however remains a challenge. Potential decomposability, or quality, of SOM depends on many factors and characteristics of the material in question, such as botanical origin, degree of (previous) decomposition, and age.

We have investigated simple geochemical indicators for SOM quality, which have the potential to be used in a wide array of arctic environments. In this presentation we will highlight the results from several field studies.

Furthermore we will emphasise the importance of past, present, and future geomorphologic setting. Seemingly uniform landscapes can have developed in an inconsistent manner, for example caused by previous permafrost thaw events. Moreover, vegetation types on different landforms can appear similar in the field, as well as on satellite or aerial images, and because of it soil characteristics can be misinterpreted or misclassified.

In this presentation we will focus on the link between site-specific SOM characteristics, and the geomorphology of the landscape as a whole. In doing so, we aim to aid upscaling efforts and increase knowledge to translate detailed lab studies to real world implications.

Mobilization of old carbon during deglacial permafrost retreat in East Asia

Maria Winterfeld[1,2], Wolf Dummann[2,4], Jens Hefter[1], Lester Lembke-Jene[1], Cameron McIntyre[3,5], Ralf Tiedemann[1], & Gesine Mollenhauer[1,2]

[1] *Alfred Wegener Institute, Helmholtz Centre for Polar and Marine Research, Bremerhaven, Germany*
[2] *Department of Geosciences, University of Bremen, Bremen, Germany*
[3] *Department of Earth Sciences, Geological Institute, ETH Zürich, Zürich, Switzerland*
[4] *now at: Institute of Geology and Mineralogy, University of Cologne, Cologne, Germany*
[5] *now at: Scottish Universities Environmental Research Centre, University of Glasgow, Glasgow, UK*

During the last glacial the areas affected by permafrost were much larger, extending further to the south [Vaks et al., 2013], and storing substantially larger amounts of carbon than at present [Ciais et al., 2012]. In the course of deglacial and early Holocene warming some of this permafrost thawed, likely releasing large amounts of carbon stored within these soils. It remains unclear how this deglacial carbon redistribution from the terrestrial reservoir affected the global carbon cycle and contributed to atmospheric pCO_2 rise and $\Delta^{14}C$ decline, assuming that pre-aged or ancient carbon was released [Köhler et al., 2014].

Thawing permafrost likely has resulted in large amounts of terrigenous organic matter being exported to the ocean as well as in changes in vegetation and wetland extent. Records of these environmental changes may be found in sediments accumulated near the mouth of rivers draining permafrost-affected areas. The Amur River basin in East Asia was completely covered by permafrost during the last glacial and is basically permafrost-free today, with the southern boundary of modern continuous permafrost extent just to the north of the catchment [Vaks et al., 2013].

We investigated two sediment cores (LV28-4 and SO178-13-6) recovered from the Okhotsk Sea near the mouth of the Amur River to provide more insights on remobilized permafrost carbon and the dynamics of thaw-induced vegetation changes in the Amur catchment. Biomarker records from these two cores document increased discharge of terrigenous organic matter during the last deglaciation between 17 and 8 thousand years ago. Compound-specific radiocarbon dating of long-chain n-alkanoic acids reveals that the terrigenous organic matter was substantially older at deposition during this period than during the late Holocene. Throughout the deglaciation, $\Delta^{14}C$ of these leaf-wax lipids was similar to, or more depleted than, values observed off Siberian rivers draining discontinuous permafrost areas today (i.e., Ob and Yenisey), while modern values compare favorably with leaf-wax $\Delta^{14}C$ observed in sediments off the Danube, a large river at a similar latitude as the Amur. Furthermore, the deposition of old terrestrial carbon in the studied cores occurred primarily coevally with sea-level rise indicating that coastal erosion is the dominant process. In contrast, thermal degradation of permafrost areas and corresponding wetland development is slower and follows insolation driven changes in continental temperatures. Our results demonstrate that sea level rise bears the stronger potential to affect carbon mobilization on short timescales.

Most of the old permafrost-derived organic carbon is respired upon thawing and during transport, and only small amounts are preserved in marine sediments. Therefore, our deglacial records suggest the release of large quantities of old carbon to the atmosphere.

References

Ciais, P.; Tagliabue, A.; Cuntz, M.; Bopp, L.; Scholze, M.; Hoffmann, G.; Lourantou, A.; Harrison, S. P.; Prentice, I. C.; Kelley, D. I.; Koven, C. and Piao, S. L. [2012]: Large inert carbon pool in the terrestrial biosphere during the Last Glacial Maximum. *Nature Geosci*, 5(1):74–79, doi:10.1038/ngeo1324.

Köhler, P.; Knorr, G. and Bard, E. [2014]: Permafrost thawing as a possible source of abrupt carbon release at the onset of the Bolling/Allerod. *Nature Communications*, 5, doi:10.1038/ncomms6520.

Vaks, A.; Gutareva, O. S.; Breitenbach, S. F. M.; Avirmed, E.; Mason, A. J.; Thomas, A. L.; Osinzev, A. V.; Kononov, A. M. and Henderson, G. M. [2013]: Speleothems Reveal 500,000-Year History of Siberian Permafrost. *Science*, 340(6129):183–186, doi:10.1126/science.1228729.

Land cover and landform classification upscaling of soil organic carbon stocks in the Brøgger Peninsula, Svalbard

Robin Wojcik, Peter Kuhry, Juri Palmtag, Gustaf Hugelius, & Niels Weiss

Physical Geography department of Stockholm University, Sweden

Although interest in the soil organic carbon (SOC) pools of the northern circumpolar permafrost region has dramatically increased over recent years, certain areas such as the High Arctic, still remain substantially underrepresented in the Northern Circumpolar Soil Carbon Database (NCSCD). In addition, little work has been done to investigate SOC upscaling tools specifically suitable to the High Arctic, where traditional upscaling approaches used in other permafrost regions might fail to produce accurate results.

The present study aims to provide a quantitative estimate of the mean storage and landscape distribution of SOC for the Brøgger Peninsula, an area of continuous permafrost terrain in the High Arctic (Svalbard). In addition, this study investigates the use of geomorphological units for SOC upscaling in the High Arctic compared to more traditional approaches. To achieve this goal, soil samples from 31 profiles collected in various areas of Brøgger Peninsula were analysed for bulk density and loss on ignition in order to determine their SOC content. Next, the results of the field inventories were upscaled using both land cover (LCC) based on low resolution Landsat images, and landform (LFC) classification approaches. The SOC storage of each class was calculated for the top soil organic layer vs mineral horizons and for the reference depths 0 – 30 cm and 0 – 100 cm. Subsamples were analysed for C/N ratio as well as ^{14}C in order to characterize the degree of decomposition and age of soil organic matter. The LCC and LFC upscaling approaches have yielded to similar average SOC storages for the top meter of 1.24 and 1.12 kg C m^{-2}, respectively. Further, the results of both upscaling approaches indicate that ca. 65 % and 14 % of the total SOC storage in the study area occurs in the upper 30 cm of the soil and in the top soil organic layer, respectively.

SOC storage is largely dominated by the vegetated area in the LCC and by the solifluction and sandur landforms in the LFC, which store ca. 86 % and 77 % of the total SOC mass although they only represent 17 % and 18 % of the study area, respectively. The results of LCC an LFC upscaling approaches depict obvious vertical and spatial SOC distribution patterns. This lead to suggest that combining LCC and LFC schemes could enable to address the SOC variability among the classes and thus reveal an interesting potential to improve the SOC upscaling method in the High Arctic.

The estimates of the present study, validated by several other detailed studies, indicate that the SOC storage of Brøgger Peninsula and similar high arctic environments have typically been overestimated in large scale regional SOC estimates such as in the NCSCD. As Brøgger Peninsula holds little amount of SOC and most of it occurs in the active layer, it is estimated that permafrost thawing under climate warming would lead to insignificant SOC losses. In the future, Brøgger Peninsula and similar High Arctic environments are more likely to become carbon sink areas providing negative feedback to climate warming as a results of carbon uptake from increasing plant primary productivity and litter deposition.

Permafrost peatland dynamics during the last millennia in NE European Russia and Finnish Lapland

Hui Zhang[1], Minna Väliranta[1], Sanna Piilo[1], Matthew Amesbury[2], Angela Gallego-Sala[2], & Dan Charman[2]

[1] *Department of Environmental Sciences, University of Helsinki, Finland*
[2] *Geography, College of Life and Environmental Sciences, University of Exeter, UK*

Permafrost peatlands cover vast areas in circum-Arctic regions. Since the 1980s, annual temperatures in these areas have risen by ca. 2 °C and warming is projected to continue. Accordingly, the large carbon store in these peatlands may therefore be threatened. Alternatively, warming may increase productivity more than decomposition and peat accumulation rates may increase. To better understand how high latitude permafrost peatlands have responded to recent warming and what might be their future fate, we carried out detailed studies on two permafrost peatlands in NE Russia and two in Finnish Lapland. Our study methods included high resolution testate amoeba, plant macrofossil, C/N analyses, together with ^{210}Pb and radiocarbon dating. We reconstructed changes in hydrological conditions, plant composition, and peat and carbon accumulation rates. Our preliminary results showed large variations in peat accumulation rates even within a very small area. Furthermore, testate amoeba and plant macrofossil data suggest variations in hydrological conditions during the last millennia. In the future, we will compare our regional data derived from different peatlands to each other, to climate reconstructions and to measured meteorological data.

The role of wetlands in projected future permafrost carbon-climate feedbacks: An ensemble simulation experiment with the land surface model LPJ-wsl

Zhen Zhang[1,2], Niklaus Zimmermann[1], & Benjamin Poulter[2],

[1] *Dynamics Marcoecology, Swiss Federal Research Institute WSL*
[2] *Institute on Ecosystems and Department of Ecology, Montana State University*

Climate change is forecasted to trigger a large positive carbon-climate feedback in carbon-rich ecosystems of the northern latitudes. Wetlands (bogs, fens) currently store large amounts of organic carbon and emit methane (CH_4), yet their future footprint of net greenhouse gas emissions is uncertain. With projected permafrost thaw-induced transitions in soil hydrologic conditions, CH_4 emissions from wetlands will change both in spatial patterns and temporal variability. We apply a sustained pulse-response radiative forcing model, together with a prognostic global wetland dynamic model based on the hydrological TOPMODEL, which we coupled with the land surface model LPJ-wsl to quantify the role of wetlands under future atmospheric forcing. We ran LPJ-wsl under an ensemble of future RCP scenarios to generate a comprehensive assessment of wetland changes and related CH_4 emissions. Specifically, the LPJ-wsl model was used to run simulations for the period 1990 – 2099, forced with driving meteorological datasets from 36 CMIP5 climate models to comprehensively simulate CH_4 emissions and assess radiative forcing. Under stringent (RCP2.6) and medium warming (RCP4.5, RCP6.0) scenarios, CH_4 emissions from wetlands will cause 38 ±9 %, 56 ±11 %, and 62 ±12 %, respectively, of additional instantaneous radiative forcing (RF) by 2090 relative to current levels (0.35 W/m2). Yet, under a business-as-usual scenario (RCP8.5) it will cause a 195 ±15 % increase. Our results predict that the thawing of permafrost, together with the decay of permafrost carbon, will greatly affect the spatio-temporal variability of CH_4 emissions from

wetlands and will trigger an irreversible tipping point at mid-2040s, when CH_4 emission rates accelerate more dramatically than ever before under RCP8.5. Such a change in radiative forcing requires substantial climate mitigations to halt negative effects to the human society and to natural systems.

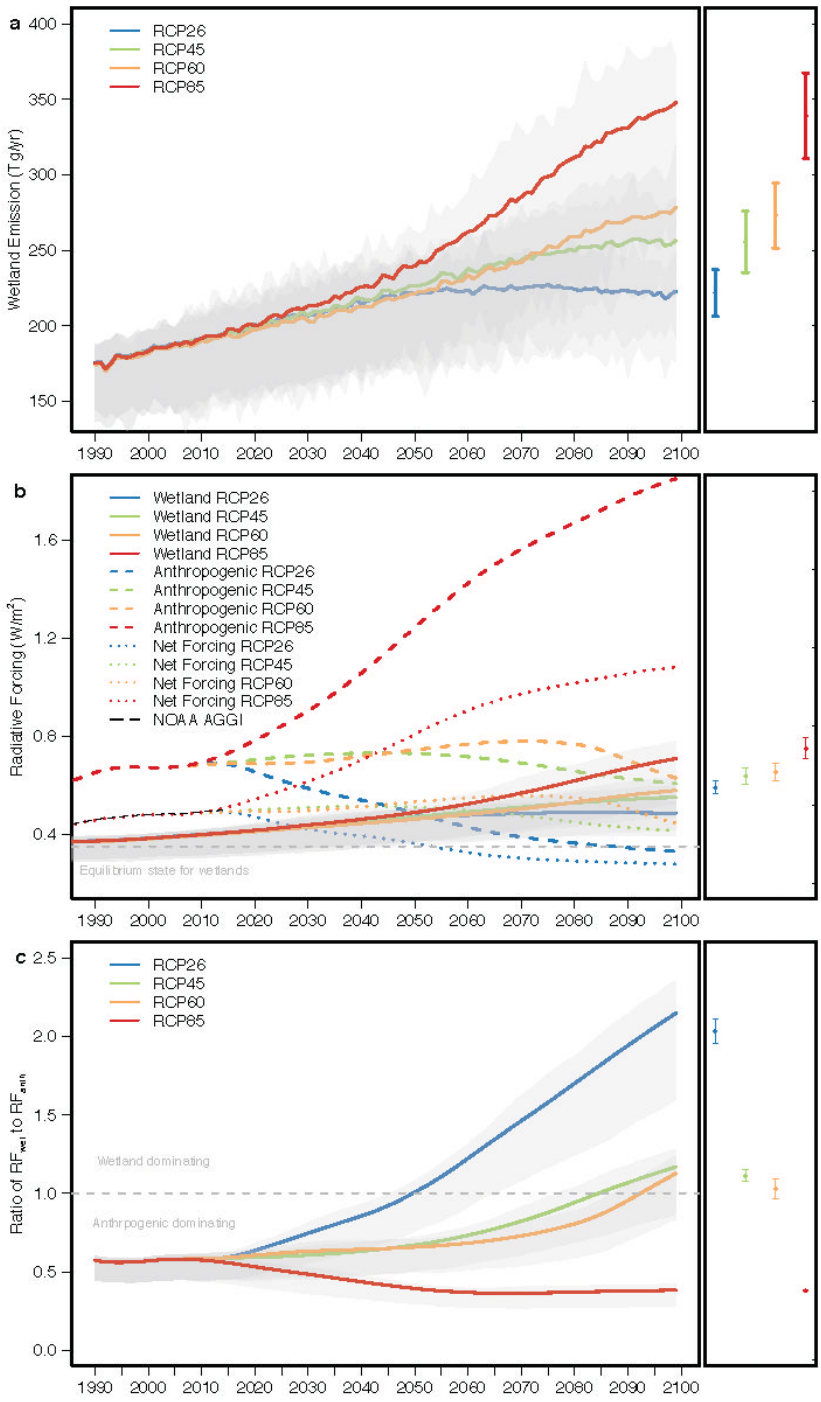

Figure 1: Future CH_4 emissions, radiative forcing and annual maximum extents of global wetlands

Net ecosystem exchange of CO_2 above alpine meadow in permafrost regions of the Qinghai-Tibetan Plateau

Yonghua Zhao, Lin Zhao, Yao Xiao, Guangyang Yue, Guojie Hu, Yongping Qiao, & Keqin Jiao

Cold and Arid Regions Environmental and Engineering Research Institute, Chinese Academy of Sciences, People's Republic of China

Alpine meadow is the dominant vegetation type in the continuous permafrost region of the Qinghai-Tibetan Plateau (QTP). To quantify the carbon budget, net ecosystem exchange (NEE) of CO_2 was examined above an alpine meadow in the continuous permafrost region of the QTP using the eddy covariance method in 2007. In each month, average daily NEE formed a unimodal curve, where the peak generally occurred at noon. Peak emission occurred in May, and the largest CO_2 uptake peak occurred in August. In most months, the daily variation of NEE was positive, but in July and August, atmospheric emission was negative. Peak daily variation of NEE was significantly lower than in surrounding areas of the continuous permafrost region in the QTP. Seasonal variations in NEE exhibited a bimodal pattern with high emission in both spring and autumn, weak CO_2 uptake in summer, and weak emission in winter. Total emission and CO_2 uptake were highest in May and August, respectively. The alpine meadow studied was a source of atmospheric CO_2, with an annual NEE of 271 g m^{-2} yr^{-1} in 2007. NEE in spring and early autumn was significantly positively correlated with the soil temperature and unfrozen moisture content at 5-cm depth, but significantly negatively correlated with soil temperature in summer and late autumn. NEE basically showed no response to the photosynthetic active radiation during the growth season.

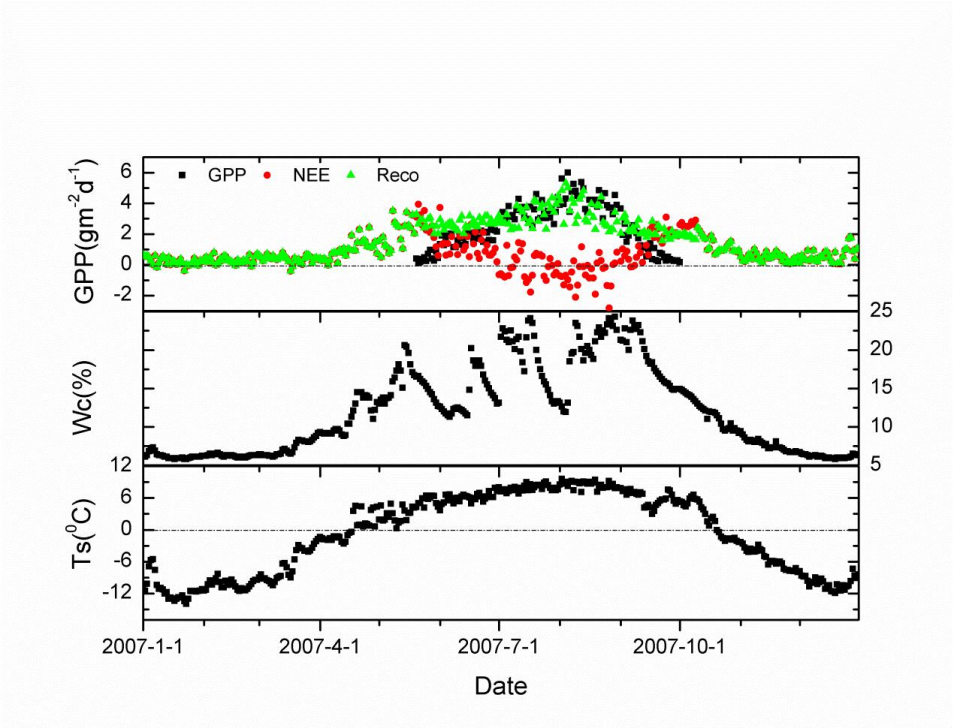

Figure 1: Seasonal variation in daily cumulative NEE and daily mean Ts and Wc, where Ts is the daily mean soil temperature at 5-cm depth, and Wc is the daily mean unfrozen soil water content at 5-cm depth.

Variability in microbial Arctic soil carbon usage: Implications for climate feedback

Lori Anne Ziolkowski[1], Claudia Czimczik[2], Sandra Holden[2], Hongyu Li[1], Tullis Onstott[3], Greg Slater[4], Amy Townsend Small[5], & Lyle Whyte[6]

[1] *University of South Carolina, United States of America*
[2] *University of California Irvine, United States of America*
[3] *Princeton University, United States of America*
[4] *McMaster University, Canada*
[5] *University of Cincinnati, United States of America*
[6] *McGill University, Canada*

Recent trends of increased global temperatures are amplified in the Arctic, where the soil contains twice as much carbon as is currently in today's atmosphere. This enhanced Arctic warming is projected to increase microbial activity and may release large quantities of soil carbon to the atmosphere. To examine soil carbon dynamics, we studied the in situ microbial carbon usage in mineral and organic soils from over a dozen locations in Svalbard, the Canadian high Arctic and various locations in Alaska. We measured the natural abundance radiocarbon in microbial biomarkers of the viable microbial community as phospholipid fatty acids (PLFA) and in different chemical fractions of the soils as it relates to the radiocarbon content of the bulk soil organic carbon. The premise of this technique is that membranes of the viable microbial community take on the isotopic value of the carbon the microbes are eating. We find that in general, microbes in surface mineral soils contained carbon consistent with atmosphere carbon even though the surface soil organic carbon was thousands of radiocarbon years old, while microbes in organic rich surface soils contained carbon that was more similar to the radiocarbon content of the surface soil organic carbon. Based on isotopic mass balance calculations, our findings demonstrate that microbes living in the low carbon, mineral surface soils are living along side geologic material but not interacting with it, while organic rich surface soil microbes are actively consuming some but not all of the soil carbon. Additionally, we will present data that compare the radiocarbon content of these biomarkers with that of respired carbon dioxide from microcosm experiments. Collectively, these findings suggest that only a portion of the soil carbon is readily accessible to soil microbes, which indicates that not all Arctic soils will respond uniformly to future warming and soil organic carbon quality must be incorporated into future climate models.

Carbon and nitrogen storages of the Lena River Delta

Sebastian Zubrzycki[1], Lars Kutzbach[1], Aleksey Desyatkin[2,4], Evgeny Abakumov[3], & Eva-Maria Pfeiffer[1]

[1] *Universität Hamburg, Institute of Soil Science, Germany*
[2] *Institute for Biological Problems of Cryolithozone, SB RAS, Russia*
[3] *Saint-Petersburg State University, Department of Applied Ecology, Russia*
[4] *Melnikov Permafrost Institute, SB RAS, Russia*

The Lena River Delta (LRD) is located in northeast Siberia and extends over a soil covered area of around 21,500 km^2. It is the largest delta in the Arctic and likely holds more than half of the entire soil organic carbon (SOC) mass stored in the seven major deltas in the northern permafrost regions. LRD consists of several geomorphic units different in size as well as in physical and chemical soil properties. Our recent studies showed that the spatial dominating Holocene units of the LRD (61 % of the area) store around 240 Tg of SOC and 12 Tg of nitrogen (N) within the first meter of ground. These units are a river terrace dominated by wet sedge polygons covered by a soil complex of Glacic Aquiturbels and Typic Historthels, and the active floodplains covered mainly by sand dominated soils as Psammentic Aquorthels and Typic Psammorthels. The mean SOC stocks for the upper 1 m of soils on both geomorphic units were estimated at 29 ±10 kg m^2 at the river terrace and at 14 ±7 kg m^2 on the floodplains, respectively. For the depth of 1 m, the total SOC storage of the Holocene river terrace was estimated at 121 ±43 Tg, and the SOC storage of the active floodplains was estimated at 120 ±66 Tg. The mean N stocks for the upper 1 m of soils were estimated at 1.2 ±0.4 kg m^2 for the Holocene river terrace and at 0.9 ±0.4 kg m^2 for the active floodplain levels, respectively. For the depth of 1 m, the total N storage of the river terrace was estimated at 4.8 ±1.5 Tg, and the total N storage of the floodplains was estimated at 7.7 ±3.6 Tg. About 50 % of these reported storages (SOC, N), are located in the perennially frozen ground below 50 cm soil depth and are excluded from intense biogeochemical exchange with the atmosphere today. However, these storages are likely to be mineralised in near future due to the projected temperature increases in this region.

A substantial part of the LRD (1,712 km^2) belongs to the so-called Yedoma region, which formed in Middle and Late Pleistocene. The area of this oldest unit of the LRD is characterised by extensive plains crossed by valleys, ice-cored pingos and is dominated by large thermokarst depressions. Such depressions are called Alases and cover around 20 % of the area. The modern soils covering the Pleistocene Yedoma plains are influenced by wide ice-wedge net structures and consist of soil complexes of Glacic Aquiturbels and Ruptic Historthels. The widespread thermokarst depressions within the ice-complex are covered by Ruptic Histoturbels and Ruptic Historthels, whereas the slopes are dominated by various Aquiturbels and Fluvaquentic Historthels. Yedoma deposits are known to store high amounts of SOC. However, within the LRD no detailed spatial studies on SOC and N were carried out so far.

With this work we present our 'investigation in progress' on these so important parts of this delta. Our first results show that the mean SOC stocks for the upper 30 cm of soils on both geomorphic units are high. They were estimated at 13.0 ±4.8 kg m^2 at the plains and at 13.1 ±3.8 kg m^2 in the Alas depressions, respectively. The stocks of N were estimated at 0.69 ±0.25 kg m^2 and at 0.70 ±0.18 kg m^2 at the plains and in the Alases, respectively. The estimated SOC and N storages for the depth of 30 cm within the investigated part of the LRD account to 20.9 Tg SOC and 1.1 Tg N, respectively. The Yedoma plains (1,313 km^2 soil covered area) store 17.1 ±6.3 Tg SOC and 0.9 ±0.3 Tg N, whereas the Alas depressions (287 km^2) store 3.8 ±1.1 Tg SOC and 0.2 ±0.05 Tg N within the investigated depth of 30 cm.

Carbon dioxide fluxes over larch permafrost stand in Central Siberia, Russia

Viacheslav Zyrianov[1], Olga Zyryanova[1], Yoijiro Matsuura[2], & Anatoly Prokushkin[1]

[1] *Institute of forest SB RAS, Russian Federation*
[2] *Forestry and forest product research institute, Tsukuba, Japan*

Systematic long-term annual eddy covariance measurements in mature Larix gmeilini larch ecosystem on permafrost in Central Siberia, Russia (64°16'N, 100°12'E) were initiated in 2004 by the Institute of Forest, Krasnoyarsk, Russia and FFPRI, Sapporo, Japan.

The larch forest was located near the settlement of Tura, 600 km east of the Yenisei River. This pure *Gmelin* larch forest was 105 yrs old, with mosses of *Pleurozium schreberi* and *Aulacomnium turgidum* as well as the dwarf-shrubs of *Vaccinium vitis-idaea*, *V. uliginosum*, and *Betula nana* dominating the ground vegetation. Moss cover formed a thick porous layer of 10-25 cm in depth above the mineral soil and functioned as a heat insulator. The stand structure was characterized by a stem density of about 5480 living trees ha-1, a LAI of 0.6 m^2 m^{-2}, a biomass (dry weight) of 1.14 kg m^{-2}, a mean diameter of the trees at breast height of 6.5 cm and a mean tree height of 7.1 m. Individual tree crowns rarely overlapped with one another.

The eddy covariance measurement system consisted of a three-dimensional sonic anemometer (R3; Gill Instruments) and an open-path infrared CO_2/H_2O gas analyzer (Li-7500; LiCor, Lincoln). The sensors were installed at a height of 20 meters in the larch stand. The open-path IRGA was 20 cm apart horizontally from the sonic anemometer. Meteorological variables were measured at the top of the tower to corroborate the flux measurements.

Eddy covariance fluxes of sensible heat, water vapor, and CO_2 were calculated for every 30-minute period. Quality-control procedures developed by LiCOR EddyPro software were used for the raw eddy data calculation.

Daily, seasonal and annual dynamics of energy (radiation and neat balance components) and mass (water and carbon dioxide) exchange between the atmosphere and Larch ecosystem was analyzed from measurements obtained during growing seasons of 2013, 2014 and 2015 (June–early September, approximately 90 days). Average daily net ecosystem exchange (NEE) was -6-8 μmol/m^2s. The daily uptake rates during mid-summer and thus the cumulative NEE during the growing season were considerably lower than in other mature boreal forests including the same species of larch reported in the literature. This may be due to the smaller LAI (< 0.6) of our *Gmelin* larch forest compared to other forests. Ecosystem was found to be a carbon sink up to -14 mol CO_2 m^{-2} season-1 increasing accordingly amount of precipitation.

Permafrost and cold soils of the larch site seemed to create a specific soil climate that was critical to the control of the carbon exchange: on one hand, it supports the forest existence in a dry climate over East Siberia delivering additional water from thawing permafrost; and on the other hand, much available energy, up to 30 – 50 %, is consumed in thawing ice. Thus, less energy remains for sensible heat and latent heat flux, warming the soil and ambient air and for physiological processes in ecosystems.

SESSION 6

Towards Regional Assessments of Permafrost-Atmosphere Carbon Fluxes

Convener:

Torsten Sachs, *GFZ German Research Centre for Geosciences, Germany*

Mathias Göckede, *Max Planck Institute for Biogeochemistry, Germany*

Jennifer D. Watts, *University of Montana, USA*

The Arctic is warming rapidly while storing vast amounts of organic carbon in permafrost that could potentially be released as carbon dioxide and methane, adding a new GHG source of unknown magnitude. Due to limited spatial and temporal data coverage on surface-atmosphere exchange processes, large uncertainties still exist in the contribution of Arctic permafrost areas to the global carbon dioxide and particularly methane budget. Moreover, a comprehensive assessment of carbon cycle processes for Arctic ecosystems is made difficult by a strong focus of existing databases on summertime observations, and a multitude of observational approaches across disciplines and scales that in part deliver inconsistent findings. The resulting high level of uncertainty is also projected on both bottom-up and top-down carbon flux estimates for high-latitude domains, limiting confidence in climate projections.

To reduce the uncertainties associated with current simulations of the sustainability of the permafrost carbon pool under future climate scenarios, pan-Arctic assessments of carbon cycle and related processes are required that are representative beyond individual sites. At the same time, observational and experimental findings on various temporal and spatial scales need to be assimilated into the frameworks of Earth System Models to improve process representation of permafrost landscapes.

For this session, observational and modeling studies relevant for regional carbon flux assessments are welcomed, and we highly encourage applications that combine both. We particularly invite contributions on:

1. the observational and/or experimental identification of key carbon cycle processes in permafrost ecosystems;

2. the incorporation of improved permafrost process representation into modeling frameworks such as e.g. land-surface schemes; and

3. the regionalization of local-scale processes or flux estimates by e.g. data-driven upscaling, model-data fusion, remote-sensing procedures or inverse modeling.

Evaluating the ecosystems' carbon uptake in Russian permafrost regions under current and projected for the 21st century climatic conditions

Oleg Anisimov & Yelena Ziltcova

State Hydrological Institute, Russian Federation

Currently the carbon balance between the photosynthetic uptake (atmospheric sink) and heterotrophic soil respiration (source) of Russian permafrost regions, excluding the forested zone, is estimated at ca. −618.8 Tg C/yr and +611.4 Tg C/yr [Dolman et al., 2012]. Both the sink and the source depend on the thermal state of permafrost, active-layer thickness, summer warmth and moisture conditions, distribution and productivity of biomes. In this study we access changes in these driving factors in the 21st century under the CMIP5 ensemble climatic projection with particular focus on the ecosystems' carbon uptake. Our study combines analysis of field observations at permafrost sites representing different ecosystem zones, satellite data on NDVI, and modelling.

We developed the statistical climate- and permafrost-driven model of the ecosystem zones that accounts for the key northern biomes, i.e. barrens, graminoids, prostrate-shrub, erect-shrub, pre-tundra, taiga, and alpine vegetation. The model was calibrated using contemporary data from the Russian vegetation map [Stolbovoi and McCallum, 2002] and circumpolar vegetation map [CAVM Team, 2003], and then used to calculate zonal shifts under projected for the 21st century climatic and permafrost conditions. To account for the pronounced gradient of the climatic and environmental conditions, we conducted model calibration and performed all further calculations separately in the four sectors in

1. the European permafrost regions
2. West Siberia
3. East Siberia, and
4. Russian Far East.

Several studies demonstrated that NDVI could be used as a proxy metric of biome productivity. Our analysis of NDVI data for the 1982-2014 period (STAR project by NASA) indicated positive trends of 4.7 – 7.0 % per decade over European permafrost region; 3.4 – 5.2 % per decade in West Siberia; 4.7 – 8.0% per decade in East Siberia, and 4.8 – 10.9 % per decade in the Russian Far East. Trends vary by ecosystem zones and generally are larger in the northernmost biomes. We applied a multifactorial regression analysis and developed statistical models linking NDVI-based estimates of productivity in each of the ecosystem zones with climatic predictive indexes characterizing summer warmth and moisture conditions derived from CRU TS 3.22 gridded temperature and precipitation data. The model indicated that summer warmth is the main factor governing the cumulative carbon uptake by permafrost ecosystems with the effect depending on the season. Throughout the entire study region we found strong positive correlation of biome productivity with June and August temperature sums, and mostly negative correlation with July temperature sums, which could be attributed to the suppression of photosynthesis in the driest and warmest month.

Predictive calculations under ensemble climatic projection are illustrated in figure 1. They suggest that by mid-21st century carbon uptake by permafrost ecosystems may increase by 12.4 – 30.6 % over European permafrost region; 16.3 – 32.5 % in West Siberia; 18.5 – 26.4 % in East Siberia, and 21.2 – 36.0% in the Russian Far East. This is likely to be a conservative estimate, since the overall changes will be further enhanced by the northward shifts in the ecosystem zones boundaries and advancement of the more productive biomes.

The ultimate conclusion of our study is that ecosystems are highly sensitive to the current and ongoing climatic and permafrost changes in Northern Eurasia, and are likely to offset the potential increase of the carbon flux to the atmosphere due to enhanced heterotrophic soil respiration in the 21st century. Differentiation between the carbon fluxes in the form of carbon dioxide and methane are needed for better understanding the effect on the global climate.

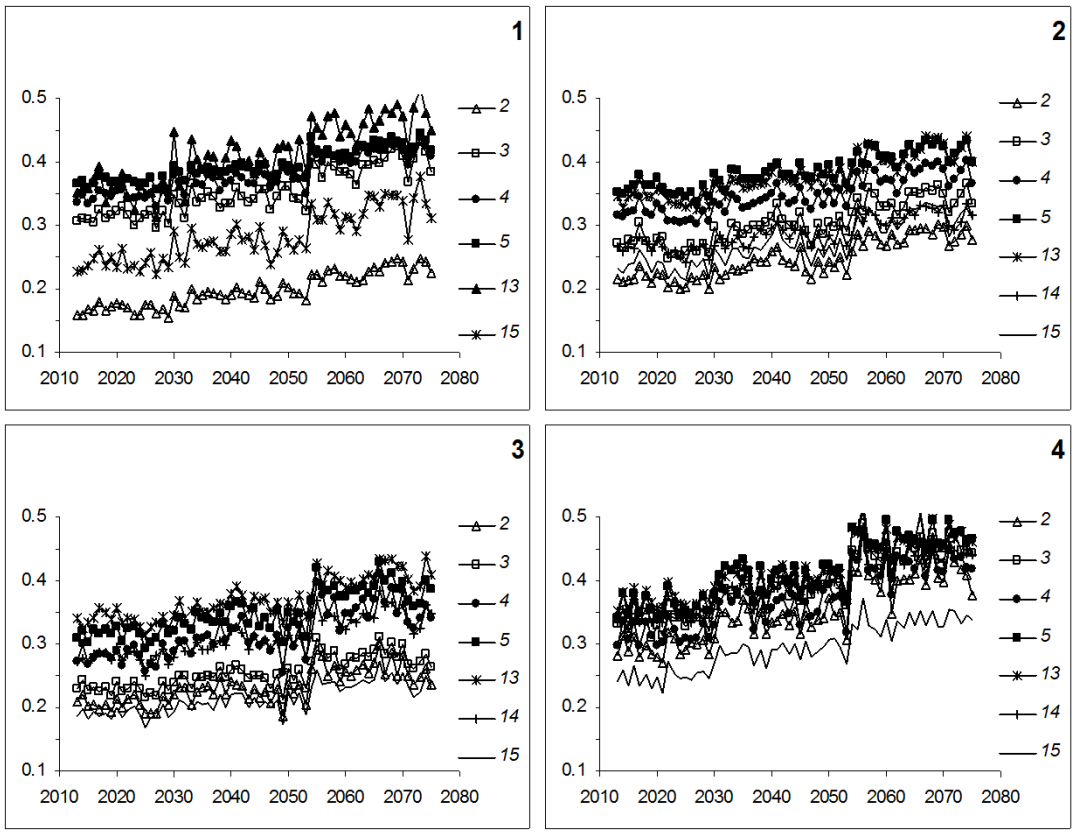

Figure 1: Projected changes of the photosynthetic carbon uptake (in relative units, as evaluated by NDVI). Panels 1–4 correspond to 4 sectors in (1) European permafrost region, (2) West Siberia, (3) East Siberia, (4) Russian Far East. Curves in each panel correspond to the following ecosystem zones: 2 – northern tundra; 3 – southern tundra; 4 – forest tundra; 5 – taiga; 13 – alpine taiga; 14 – alpine forest; 15 – alpine tundra.

References

Dolman, A.J.; Shvidenko, A.; Schepaschenko, D.; Ciais, P.; Tchebakova, N.; Chen, T.; van der Molen, M. K.; Belelli Marchesini, L.; Maximov, T. C.; Maksyutov, S. and Schulze, E.-D. An estimate of the terrestrial carbon budget of Russia using inventory-based, eddy covariance and inversion methods. *Biogeosciences*, 9:5323–5340, 2012. doi:10.5194/bg-9-5323-2012.

Stolbovoi, V. and McCallum, I. [2002]: Land resources of Russia. CD-ROM. Laxenburg, Austria: International Institute for Applied Systems Analysis and the Russian Academy of Science.

CAVM Team [2003]: *Circumpolar Arctic Vegetation Map.* 1:7,500,000 scale.

Inter-annual variability and drivers of the carbon balance of a northeast Siberian tundra

Luca Belelli Marchesini[1], Jacobus van Huissteden[1], Michiel van der Molen[2], Frans-Jan W. Parmentier[3,4], Trofim Maximov[5], Artem Budishchev[1], & Han Dolman[1]

[1] *Vrije Universiteit, Amsterdam, The Netherlands*
[2] *WUR - Wageningen University and Research Centre, Wageningen, The Netherlands*
[3] *Lund University, Lund, Sweden*
[4] *Arctic Research Centre, Aarhus University, Denmark*
[5] *Insitute for Biological Problems of Chryolithozone, Siberian Branch of Academy of Sciences, Yakutsk, Russia*

Climate has been warming over the Arctic region with the strongest anomalies occurred since the beginning of the XXI century, particularly in northern Eurasia. The quantification of the impact on climate warming on the degradation of permafrost and the associated potential release to the atmosphere of carbon stocked in the soil under the form of greenhouse gases (GHG), thus further increasing the radiative forcing of the atmosphere, is currently a matter of scientific debate [Schuur et al., 2015]. The positive trend in primary productivity in the last three decades inferred by vegetation indexes (NDVI), although not spatially homogeneous, and confirmed by observations of the enhanced growth of vascular plants [Elmendorf et al., 2012] represents indeed a contrasting process that, if prevalent, could mitigate the expected GHG emissions or even translate into a stronger carbon sink over the Arctic tundra. It appears however that the tundra greenness, as derived from remote sensing data, has been declining consistently in the last 2-4 years throughout the Arctic (Epstein, 2015) although in contrast field studies continue to report increased shrub growth in response to rising air temperatures.

At the tundra site of Kytalyk, in north-eastern Siberia, net ecosystem scale fluxes of CO_2 (NEE) have been monitored since 2003. Here we quantify the inter-annual variability (IAV) of NEE of the 2003-2013 decade, intended as the interplay between environmental (abiotic) drivers and biological response functions of ecosystems. We therefore test the role of air temperature and global radiation as controlling factors of NEE IAV in the last decade using a data oriented statistical approach [Marcolla et al., 2011].The impact of the timing and duration of the snow free period on the seasonal carbon budget is also considered. Finally, by assessing the seasonal methane budget based on the results of EC flux observations (FCH_4) in 2012, corroborated with results from previous campaigns, we evaluate the magnitude and stability of the greenhouse gas (GHG) balance.

The examined tundra ecosystem was found to sequester CO_2 during the snow free season with relatively small inter-annual variability (±12 %) during the last decade. Air temperature and global radiation explained between 78 % and 87 % of the 30 min NEE variability during the carbon uptake period, which resulted to be modulated consistently across the years by heat accumulation since the complete snowmelt (GDD, T_{base} >0). The carbon uptake period (CUP) tended to start earlier in the course of the year, potentially favoring a larger carbon sequestration; however the pronounced meteorological variability during the arctic summer controlled in turn the duration of the carbon uptake period and the flux rates with consequently no emerging trend in the carbon balance. The IAV of modelled NEE during the arctic summer (doy 180-230) driven solely by Ta and Rg was 66 % of the total observed IAV. We did not find significant trends in either modelled/observed NEE and functional parameters ecosystem with the exception of increasing maximum photosynthesis at light saturation. The carbon loss associated with seasonal CH_4 emissions and lateral dissolved organic carbon (DOC) export was similar for both terms and accounted for 6 % of the cumulative CO_2 balance. The Kytalyk tundra ecosystem was hence found to act so far as a steady carbon sink with a negative GHG balance, which could be potentially offset if seasonal methane emissions were threefold compared to the current levels.

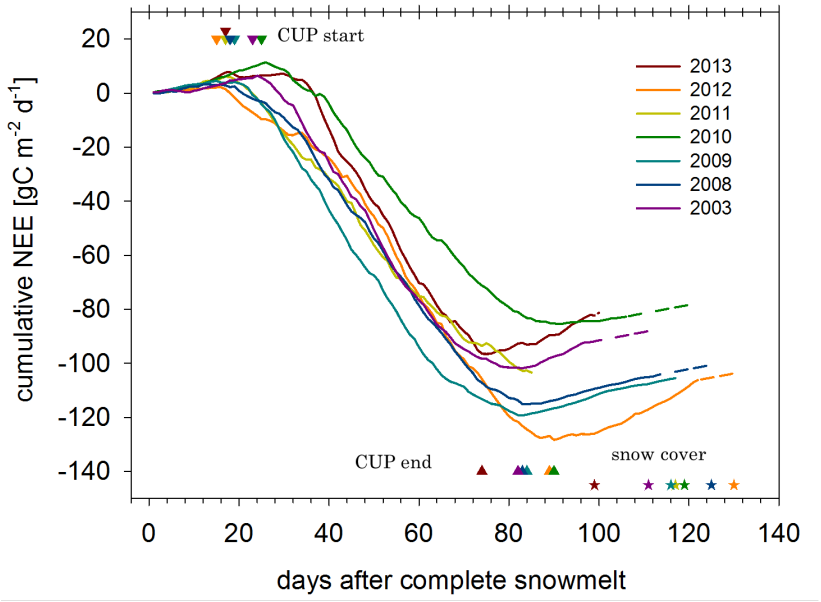

Figure 1: Cumulative NEE during the snow free period with indication of the dates of carbon uptake (CUP) start/end and snow cover start in late summer

References

Elmendorf, S.C.; Henry, G.H.R.; Hollister, R.D.; Björk, R.G.; Boulanger-Lapointe, N.; Cooper, E.J.; Cornelissen, J.H.C.; Day, T.A.; Dorrepaal, E.; Elumeeva, T.G.; Gill, M.; Gould, W.A.; Harte, J.; Hik, D.S.; Hofgaard, A.; Johnson, D.R.; Johnstone, J.F.; Jónsdóttir, I.S.; Jorgenson, J.C.; Klanderud, K.; Klein, J.A.; Koh, S.; Kudo, G.; Lara, M.; Lévesque, E.; Magnússon, B.; May, J.L.; Mercado-Díaz, J.A.; Michelsen, A.; Molau, U.; Myers-Smith, I.H.; Oberbauer, S.F.; Onipchenko, V.G.; Rixen, C.; Martin Schmidt, N.; Shaver, G.R.; Spasojevic, M.J.; Pórhallsdóttir, P.E.; Tolvanen, A.; Troxler, T.; Tweedie, C.E.; Villareal, S.; Wahren, C.-H.; Walker, X.; Webber, P.J.; Welker, J.M. and Wipf, S. [2012]: Plot-scale evidence of tundra vegetation change and links to recent summer warming. *Nature Climate Change*, 2(6):453–457, doi:10.1038/nclimate1465.

Marcolla, B.; Cescatti, A.; Manca, G.; Zorer, R.; Cavagna, M.; Fiora, A.; Gianelle, D.; Rodeghiero, M.; Sottocornola, M. and Zampedri, R. [2011]: Climatic controls and ecosystem responses drive the inter-annual variability of the net ecosystem exchange of an alpine meadow. *Agricultural and Forest Meteorology*, 151(9):1233–1243, doi:10.1016/j.agrformet.2011.04.015.

Schuur, E. A. G.; McGuire, A. D.; Schadel, C.; Grosse, G.; Harden, J. W.; Hayes, D. J.; Hugelius, G.; Koven, C. D.; Kuhry, P.; Lawrence, D. M.; Natali, S. M.; Olefeldt, D.; Romanovsky, V. E.; Schaefer, K.; Turetsky, M. R.; Treat, C. C. and Vonk, J. E. [2015]: Climate change and the permafrost carbon feedback. *Nature*, 520(7546):171–179, doi:10.1038/nature14338.

The carbon budget of Eurasian Arctic sites: a synthesis from the PAGE21 flux network

Luca Belelli Marchesini[1], Christian Wille[2], Frans-Jan W. Parmentier[3,4], Mathias Goeckede[5], Jacobus van Huissteden[1], Han Dolman[1], Mika Aurela[6], Julia Boike[7], Torben Christensen[3,4], Thomas Friborg[8], Tuomas Laurila[6], Magnus Lund[3,4], Mathilde Jammet[8], Lars Kutzbach[9], Trofim Maximov[10], Torsten Sachs[11], & Narasinha Shurpali[12]

[1] *Vrije Universiteit, Amsterdam, The Netherlands*
[2] *Hamburg University, Center for Earth System Research and Sustainability (CEN), Germany*
[3] *Lund University, Lund, Sweden*
[4] *Arctic Research Centre, Aarhus University, Denmark*
[5] *Max Planck Institute for Biogeochemistry, Jena, Germany*
[6] *Finnish Meteorological Institute, Helsinki, Finland*
[7] *Alfred Wegener Institute Helmholtz Centre for Polar and Marine Research, Potsdam, Germany*
[8] *Center for Permafrost, Department for Geosciences and Natural Resource Management, University of Copenhagen, Copenhagen, Denmark*
[9] *Universität Hamburg, Institute of Soil Science, Hamburg, Germany*
[10] *Insitute for Biological Problems of Chryolithozone, Siberian Branch of Academy of Sciences, Yakutsk, Russia*
[11] *GFZ German Research Centre for Geosciences, Potsdam, Germany*
[12] *University of Eastern Finland, Finland*

The large and potentially labile carbon pools currently stored at high latitudes in permafrost regions [Hugelius et al., 2013] may be released to the atmosphere under a warming climate in the form of greenhouse gases (CO_2, CH_4) which in turn would further contribute to an increase in the radiative forcing [McGuire et al., 2012].

Given the current predicament of rapid climate warming in the Arctic and the expectations that the area will experience the largest temperature increase over this century [Schuur et al., 2015], it is important to evaluate how these changes are impacting the land-atmosphere carbon exchange in terms of enhancing or mitigating the process of climate warming.

In this study, we present a synthesis of GHG flux observations from the site network of the PAGE21 project, which includes 10 eddy covariance sites distributed within the permafrost region among Greenland, Scandinavia and the Russian Federation. The analyzed CO_2 flux data consisted of 54 site-years collected in the period 2000-2014. Raw data were processed on the basis of a harmonized protocol and the resulting flux data underwent the same post-processing scheme including quality control, gap-filling and partitioning of net ecosystem fluxes (NEE) into photosynthetic (GPP) and respiratory (Reco) components. At the end of the workflow, 36 continuous time series of verified quality covering the whole warm season were obtained.

The magnitude of summer NEE showed inter-site differences in the CO_2 uptake rates up to a factor 6, with low productive heath ecosystems contrasting to wetlands (fens) with high net uptake. Considering the season between the start of the snowmelt and that of the freeze-up periods, nine sites were associated to a net sequestration of atmospheric CO_2 ranging between -226.5 and -10.2 gCm^{-2}, while only one Russian peatland was found to be a weak source (13.4 gCm^{-2}). Overall, cumulative warm season Reco consumed on average 65 % of GPP uptake (R^2=0.83).

Differences in NEE and GPP across sites were mostly explained by the season length (R^2=0.67), however this could not be related to the inter-annual variability at the respective sites. Relations between the carbon balance components and environmental drivers were also sought considering the summation of air temperature ($\sum T_a$), precipitation (P) and incoming short wave radiation (SW) during the thawing season. In the case of NEE and GPP the most robust (positive) correlations were found with $\sum T_a$ and P.

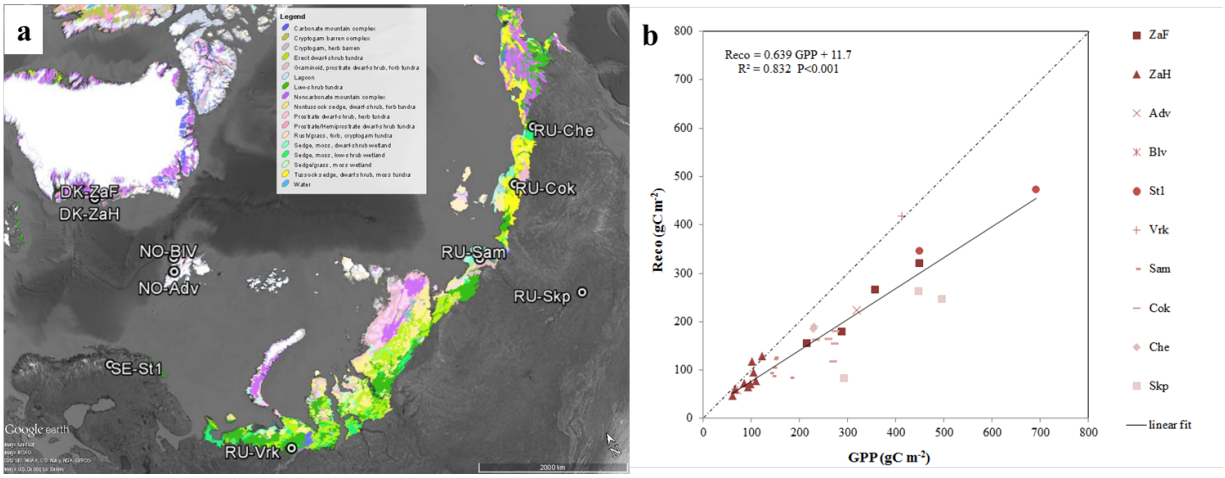

Figure 1: Location of the PAGE21 flux sites over the circumpolar Arctic vegetation map (a); Reco vs GPP cumulated during the warm season, linear regression (solid line) and 1:1 (dashed) line.

Interestingly the inter-site variability of Reco was best explained by the stock of decomposable soil carbon calculated for each site as the fraction of the soil carbon pool up to 1 m depth, multiplied by the average active layer depth (R^2=0.51).

After taking into account estimates of the methane budget (based on chambers or micrometeorological flux measurements) and lateral carbon fluxes, both when available in literature, the average carbon budget of all sites resulted in a sink of -61.9±67.4 g C m^{-2}.

References

Hugelius, G.; Bockheim, J. G.; Camill, P.; Elberling, B.; Grosse, G.; Harden, J. W.; Johnson, K.; Jorgenson, T.; Koven, C. D.; Kuhry, P.; Michaelson, G.; Mishra, U.; Palmtag, J.; Ping, C.-L.; O'Donnell, J.; Schirrmeister, L.; Schuur, E. A. G.; Sheng, Y.; Smith, L. C.; Strauss, J. and Yu, Z. [2013]: A new data set for estimating organic carbon storage to 3 m depth in soils of the northern circumpolar permafrost region. *Earth System Science Data*, 5 (2):393–402, doi:10.5194/essd-5-393-2013.

McGuire, A. D.; Christensen, T. R.; Hayes, D.; Heroult, A.; Euskirchen, E.; Kimball, J. S.; Koven, C.; Lafleur, P.; Miller, P. A.; Oechel, W.; Peylin, P.; Williams, M. and Yi, Y. [2012]: An assessment of the carbon balance of arctic tundra: comparisons among observations, process models, and atmospheric inversions. *Biogeosciences*, 9(8):3185–3204, doi:10.5194/bg-9-3185-2012.

Schuur, E. A. G.; McGuire, A. D.; Schadel, C.; Grosse, G.; Harden, J. W.; Hayes, D. J.; Hugelius, G.; Koven, C. D.; Kuhry, P.; Lawrence, D. M.; Natali, S. M.; Olefeldt, D.; Romanovsky, V. E.; Schaefer, K.; Turetsky, M. R.; Treat, C. C. and Vonk, J. E. [2015]: Climate change and the permafrost carbon feedback. *Nature*, 520(7546):171–179, doi:10.1038/nature14338.

Use of spectrometer data to analyse the impact of fine-scale phenology patterns on CO_2 fluxes from an Arctic permafrost ecosystem

Ina Burjack[1], Anna Berninger[1,2], Martin Heimann[1], & Mathias Göckede[1]

[1] *Max-Planck-Institute for Biogeochemistry, Germany*
[2] *Friedrich-Schiller University Jena, Germany*

Arctic permafrost covers about 25 % of the landmasses in the Northern hemisphere. Since surface based observational data coverage is sparse, remote sensing provides an important additional data source for the high latitudes, with coverage of all permafrost areas on a daily basis. Particularly linking remote sensing data with ground-based measurement of CO_2 and CH_4 fluxes to upscale these measurements to a larger area has the potential to provide new insight into spatiotemporal patterns of greenhouse gas fluxes and their net budgets for permafrost areas.

To gain new insight into the role of phenology patterns on Arctic carbon cycle processes, in summer 2015 we measured the reflectance of all dominant plant types in a wet tussock tundra ecosystem near Chersky in North-eastern Siberia for a period of six weeks using a small handheld spectrometer. In addition to continuous flux monitoring at this observation site based on two eddy-covariance towers, we performed chamber measurements to capture the fluxes of CO_2 and CH_4 at small scales for individual plant types. This dataset allows us to link plant phenology based on reflectance data to carbon fluxes both for isolated plant types and heterogeneous flux footprint areas of the eddy-systems.

Our spectrometer database reveals differences in the phenology between the two dominant local vegetation types, tussock forming sedges and cotton grasses: while the sedges display first signs of photosynthetically active biomass very early in summer, the cotton grasses are slower to develop in the early growing season.

This information can be used to improve interpretation of the mixed vegetation signal seen by the eddy-covariance towers, particularly when the data is to be used for upscaling the local fluxes to larger areas with a different vegetation distribution. Moreover, linking the CO_2 and CH_4 measurements to the reflectance of the plants facilitates an improved interpretation of the role of different environmental controls during different parts of the growing season on carbon flux patterns.

Northeast Siberian methane fluxes from permafrost soils: First results from a regional land-vegetation model configuration

Karel Castro-Morales[1], Thomas Kleinen[2], Sonja Kaiser[1], Christian Beer[3], Soenke Zaehle[1], & Mathias Goeckede[1]

[1] *Max Planck Institute for Biogeochemistry, Germany*
[2] *Max Planck Institute for Meteorology, Hamburg*
[3] *Stockholm University, Stockholm*

In the context of global warming, the potential high risk of methane emissions from thawing permafrost is well known. This is particularly relevant in the largest northern latitude permafrost region located in North Siberia. Due to its remote location and extreme weather conditions over autumn and winter, few on-site methane emission studies have been carried out in this region, most of them limited to the growing season. In this work, we use a soil-permafrost-vegetation model as a tool to evaluate the regional methane flux to the atmosphere from permafrost soils in Northeast Siberia. For this, we set up a regional configuration exclusive for Northeast Siberia (geographically limited by 158.25° to 164.75°E and 66.75° to 69.25°N) using the surface terrestrial component (Jena Scheme for Biosphere-Atmosphere Coupling in Hamburg, JSBACH) of the Max Planck Institute-Earth System Model. A permafrost soil model and a process-based methane emissions model are included. This model version contains a process-based representation of the active layer in each grid cell, i.e. the part of the soil column where methane is produced and respired. This comprises a highly resolved estimate of the ground water table (i.e. the soil column with water content). To dynamically constrain the wetland extent in our model configuration, we use the TOPogragphy MODel (TOPMODEL) hydrological framework in which the fraction of the grid cell that is inundated by water is determined by the statistics of the topography profile. Our model setup consists of 11 soil layers with thinner thicknesses in the top and deeper thicknesses toward the bottom of the soil column. The spatial resolution is 0.5° and it is driven by realistic atmospheric climate data. The model was spun up for equilibration of the soil carbon pools and the hydrological cycle, after that we performed a transient simulation with results analyzed for the period 2000 to 2014.

Once methane gas is produced within the soil active layer it can either dissolve in the water present in the soil column or it can oxidize above the water table (oxic soil portion). The dissolved portion can be then emitted to the atmosphere trough three main pathways: ebullition, diffusion and transport through the roots of plants. Our first results show that the dominating process of methane emission to the atmosphere in Northeast Siberia during the last decade is diffusion, with only very minor contributions from both ebullition and plant mediated-transport. The model output will be evaluated against recent on-site measurements at different spatial and temporal scales.

Carbon stocks and fluxes in the high-latitudes: Using site-level data to evaluate earth system models

Sarah Chadburn[1], Eleanor Burke[2], Altug Ekici[3], Christian Beer[4], Philipp Porada[4], Gerhard Krinner[5], Tao Wang[11], Claire Brutel-Vuilmet[5], Luca Belelli[6], Ko Van Huissteden[6], Lars Kutzbach[7], Gustaf Hugelius[4], Julia Boike[8], Moritz Langer[8], Bo Elberling[9], Margareta Johansson[10], & Sebastian Westermann[12]

[1] *University of Leeds, United Kingdom*; [2] *Met Office, UK*; [3] *University of Exeter, UK*
[4] *Stockholm University, Sweden*; [5] *Université Joseph Fourier-Grenoble, Grenoble, France*
[6] *VU University, Amsterdam, The Netherlands*; [7] *University of Hamburg, Germany*
[8] *Alfred Wegener Institute Helmholtz Centre for Polar and Marine Research, Potsdam, Germany*
[9] *CENPERM, University of Copenhagen, Denmark*; [10] *Lund University, Sweden*
[11] *Laboratoire des Sciences du Climat et de l'Environnement, France*; [12] *University of Oslo, Norway*

The high latitudes form an important component of the Earth's carbon cycle. It is therefore important to capture this in Earth System Models (ESM's). However, most carbon-cycle development and evaluation in ESM's focuses on lower latitudes, and therefore there is an urgent need to address Arctic carbon-cycle processes.

Here, we run land-surface schemes from ESM's at the site level at various Arctic sites, performing a detailed evaluation of the carbon dynamics in the models. They are process-based models, and therefore point-scale evaluations contribute directly towards improving the large-scale results.

The sites chosen for the simulations are the five principal field sites from the recently-concluded EU project PAGE21. This gives the distinct advantage that detailed data are available. In particular, data on the physical state of the climate and permafrost at these sites, and large datasets of soil carbon stocks and fluxes. The sites cover a range from low Arctic discontinuous permafrost to high Arctic desert, and a range of soil types from thick peat to mineral soils with little organic matter. The models involved are land surface schemes from three European ESM's: UKESM (UK), IPSL (France) and MPI-ESM (Germany). The models all have improved process representation as part of PAGE21.

The simulations are first compared with physical observations from the sites: specifically snow depth, soil temperature, soil moisture and maximum thaw depth. All models capture the physics with a reasonable accuracy, and certainly capture the major differences between sites, with a few exceptions. In particular, we see the importance of simulating the physical properties of the soil organic layer.

Comparing simulated soil organic carbon with observations shows the importance of including vertical soil carbon profiles. In one model this is not represented, which results in a failure to capture the differences in soil carbon in different physical conditions. Including cryoturbation mixing is key to simulating the vertical soil organic carbon profile. When vertical mixing is included, the profile of soil organic carbon at mineral soil sites matches very well with observations. However, none of the models are able to simulate the correct profile at sites with organic soils, highlighting the need for further process representation of peat accumulation.

Finally, the land-atmosphere carbon fluxes are assessed using different observations, and we discuss the meaning of these measurements in terms of the land surface model output and how they can be most usefully compared. The simulation of carbon fluxes depends on every aspect of the models: The physical state, the soil carbon stocks and most importantly, the vegetation. Large errors result from the models growing the wrong type of vegetation or no vegetation at all, as tundra vegetation types are not represented in two of the three models. Focussed work is required to better represent Arctic vegetation in such models, and our results highlight the next steps to take.

The observational datasets are more detailed than those used in past studies and this work will be used both to facilitate and to justify the development of Arctic carbon cycle processes in Earth system models.

Regional carbon budget for Alaska: Response to seasonal and interannual temperature variations

Roisin Commane[1], Steven Wofsy[1], Jakob Lindaas[1], Kristina Luus[2], Joshua Benmergui[1], Rachel Chang[3], Nicholas Parazoo[4], Colm Sweeney[5], Anna Karion[5], Charles Miller[4], & John Henderson[6]

[1]*Harvard University, Cambridge, MA, United States of America*
[2]*Dublin Institute of Technology, Dublin, Ireland*
[3]*Dalhousie University, Halifax, NS, Canada*
[4]*Jet Propulsion Laboratory, Pasadena, CA, USA*
[5]*CIRES, CU Boulder, Boulder, CO, USA*
[6]*AER, Lexington, MA, USA*

Determining the carbon budget of ecosystems in the arctic year-round is essential to understanding the response of arctic to increasing temperatures. We determined the regional fluxes of CO_2 using aircraft, tower, and eddy flux data collected in Alaska as part of the Carbon in the Arctic Reservoirs Vulnerability Experiment (CARVE) in 2012-2014. The towers and eddy flux see influence from either boreal or tundra ecosystems separately, while the aircraft sees influence from most of Alaska at various times.

We first developed a spatially and temporally detailed prior model for the regional carbon flux using a low-dimensional representation driven by remote sensing and assimilated meteorology (PVPRM, Luus& Lin, GMD, 2015), and then optimized the fluxes using our 3 years of data. The Alaska region was approximately carbon neutral in 2012, and a significant net source of carbon in the warmer years of 2103 and 2014. The strongest emissions of CO_2 occur in the dormant season (fall, early winter), highlighting the need for year-round observations. We found that the Enhanced Vegetative Index (MODIS EVI) estimates the start of the growing season almost two weeks too early and the end of the growing season two weeks too late, compared to the aircraft data and eddy flux towers; this extended growing season predicts that Alaska should be a significant carbon sink, when the atmospheric data show it is actually a source. Using Solar-induced Fluorescence (SIF) to represent the fraction of light absorbed by the vegetation results in the timing of model fluxes and the overall carbon budget that better match the observations.

Modeling and upscaling methane emission hotspots in the polygonal tundra

Fabio Cresto Aleina[1], Benjamin R. K. Runkle[2], Alexander Winkler[1,3], Christian Knoblauch[3], & Lars Kutzbach[3]

[1] *Max Planck Institute for Meteorology, Germany*
[2] *Department of Biological and Agricultural Engineering, University of Arkansas, Fayetteville, AR, USA*
[3] *Institute of Soil Science, Center for Earth System Research and Sustainability, Universitä Hamburg, Hamburg, Germany*

Local surface heterogeneities are important or even fundamental to better understand general and large scale properties of the climate system, since they often influence land-atmosphere fluxes of water and other greenhouse gases.

Because of their small scale, the underlying generating processes can be well explained and resolved only by local mechanistic models, which, on the other hand, fail to upscale these processes at the regional or global scale.

A challenging problem is how to deal with these interactions across different spatial scales, and how to improve our understanding of the role played by local soil heterogeneities in the climate system.

This is of particular interest in the northern peatlands, because of the large amount of carbon stored in these ecosystems.

Methane, carbon dioxide and water vapor fluxes vary largely within the environment, as an effect of the small scale processes that characterize the landscape. It is then essential to consider the local heterogeneous behavior of the system components, such as the water table level inside the polygon wet centers, to correctly capture these emission hotspots.

We developed a stochastic model for northern peatlands using Poisson-Voronoi diagrams, which is able to upscale statistical large scale properties of the system taking into account the main processes within the single polygons. This model, despite being a stochastic description of the ecosystem, provides an accurate description of the polygonal tundra hydrology if compared with in situ measurements. We used local measurements to tune and force the model, and to evaluate model output.

By coupling this surface hydrology model with a process-based model for methane emissions, we are able to upscale the effects of methane emission hotspots in the polygonal tundra.

We also developed a computationally inexpensive parameterization that takes into account the effect of the emission hotspots. This new parameterization can be potentially included in larger scale models and it is a first step towards bridging the scaling gap from the ecosystem to the regional and global scales.

Upscaling of high-latitude CO_2 fluxes in NE Siberia based on a satellite data-driven model

Mathias Goeckede[1], Kristina Luus[2], Torsten Sachs[3], Lars Kutzbach[4], Mika Aurela[5], Luca Belelli Marchesini[6], Eugenie Euskirchen[7], Ko van Huissteden[6], & Andrei Serafimovich[3]

[1] *Max-Planck-Institute for Biogeochemistry, Germany*; [2] *Dublin Institute of Technology, Ireland*
[3] *GFZ Potsdam, Germany*; [4] *University of Hamburg, Germany*
[5] *Finnish Meteorological Institute, Finland*; [6] *Free University of Amsterdam, The Netherlands*
[7] *University of Alaska, Fairbanks, USA*

Arctic ecosystems are characterized by pronounced gradients in ecosystem properties at various spatial scales. Even over short distances, systematic differences in e.g. vegetation community structure or water table depth can create mosaics of micro-sites where each unit displays an individual exchange pattern of carbon and energy with the atmosphere. To analyze the effect of high-resolution modeling on Arctic regional carbon budgets, we present CO_2 flux budgets that have been simulated based on a satellite-data driven model at high (0.1deg) resolution for a regional domain of 6 × 44 degrees in Northeast Siberia.

The model has been calibrated using eddy-covariance flux datasets from five sites within the region. Validation against independent datasets as well as comparison against MODIS reference flux fields demonstrates the good performance of this parsimonious modeling framework under the given conditions. On the other hand, comparison against helicopter-based flux transects over the Lena river delta indicate that the setup of the model domain would even need to be further refined to capture the observed spatial variability in flux rates. A direct comparison of model runs based on a model version trained on the regional flux sites against a version using North American observations sites representing similar biomes resulted in systematic differences between both versions, highlighting the importance of local reference datasets for model calibration. Moreover, the pronounced fine-scale variability and regional gradients due to vegetation and climate patterns partly creates strong deviations from coarser scale reference products, suggesting that aggregation errors can alter CO_2 budget simulations over the Arctic significantly.

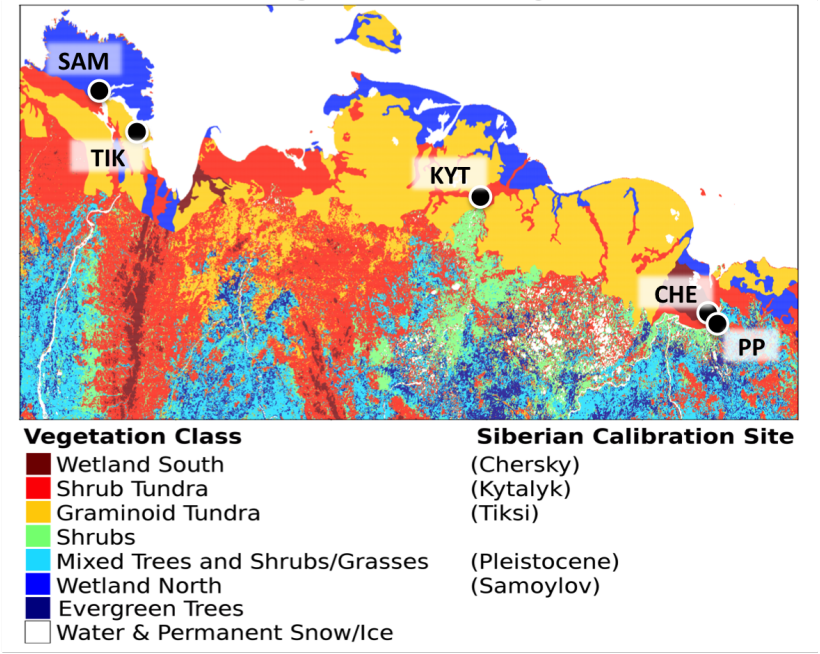

Figure 1: Vegetation map

First assessment of methane emission during ice thaw from southern tundra lakes in Western Siberia

Leonid Golubyatnikov[1], Vladimir Kazantsev[1], & Mariia Cherbunina[2]

[1] *A.M.Obukhov Institute of Atmospheric Physics, Russian Federation*
[2] *Lomonosov Moscow State University, Russian Federation*

Among natural sources of methane, lakes are second in its emission intensity into the atmosphere. Global methane emissions from lakes is estimated at 71.6 $MtCH_4$/year [Bastviken et al., 2011], which is about 35 % of global methane emissions from natural sources. During the open water season, a part of methane produced in lake sediments is released into the atmosphere by diffusion and ebullition. The production of methane in the lake sediments still continues during the winter season till the lake is completely frozen. The bottom sediments of many tundra lakes do not freeze in winter and methane is produced in these lakes all the year. The methane produced under the ice cover accumulates in the water column and partially freezes into ice. Methane produced during the winter subsequently releases to the atmosphere during ice break-up at spring. This early spring release of methane should be accounted for more realistic annual methane emission, especially in northern regions with a great number of lakes.

We have estimated the methane emission from tundra lakes in Western Siberia after early spring breakup of ice cover. Field experiments were carried out in June-July 2015 at two lakes located in the southern tundra zone of the Yamal-Nenets Autonomous District. In this region lakes are ice covered for about nine months (September-June). The presented lakes are typical thermokarst lakes for the northern part of Western Siberia: the small one (№1) with the area 6×10^3 m^2 up to 2.0 m depth, sapropel sediments, the biggest one (№2) is 97×10^3 m^2 up to 1.8 m depth, silty sediments. The lake water and ice were sampled for the measurement of methane content right before the ice thawing started.

Lake ice and water was sampled through a hole drilled in the lake ice. Sampling was made at depths with different intervals (0.15-0.4 m for the ice cover; for the water layer under the ice cover at the upper level right under the ice, and at the lower one, near the bottom). After ice thaws the lake water was sampled for the measurement of dissolved methane. Sampling was made at the water surface, in the middle of the water column for different depths. Calculation of methane emission during spring ice thawing was carried out as the difference in the mass of methane before and after ice melt, assuming that a slight part of the methane storage under ice was oxidized in the water column [Michmerhuizen et al., 1996].

According our field data and calculations methane store in the ice is about 0.0 μmol/l (median average) for the studied lakes. Data about concentrations in air bubbles and soil bottom layer were obtained (up to 96 μmol/l). The water under the ice is saturated with methane - methane concentration reaches 395 μmol/l. After ice melts the concentration of methane in water is sufficiently small, and varies from 0.11 to 4.71 μmol/l (№1) and 0.34-3.02 μmol/l (№2).

On the basis of experimental data we produced the calculations of methane release by diffusion during spring ice thawing: about 1 kg for the first lake and 40 kg for the second one.

Acknowledgements

This work was supported by the Russian Foundation of Basic Research (project 14-05-00193), the Basic Research Program (Department of Earth Sciences, Russian Academy of Sciences) “Integrated studies on actual problems of Earth Sciences” and FP7 Marie Curie Actions IRSES (grant 612642).

References

Bastviken, David; Tranvik, Lars J.; Downing, John A.; Crill, Patrick M. and Enrich-Prast, Alex. [2011]: Freshwater methane emissions offset the continental carbon sink, *Science*, 331(6013):50–50, doi:10.1126/science.1196808.

Michmerhuizen, C.M.; Striegl, R.G. and McDonald, M.E. [1996]: Potential methane emission from north-temperate lakes following ice melt. *Limnol. Oceanogr.*, 41:985–991.

The Permafrost Regionalization Map (PeRM): How well do observations, models and experiments represent the circumarctic-scale spatial variability in permafrost carbon vulnerability?

Daniel J. Hayes[1], Peter Kuhry[2], Santonu Goswami[3], Guido Grosse[4], A. David McGuire[5], & Edward A. G. Schuur[6]

[1] *University of Maine, USA*
[2] *Stockholm University, Sweden*
[3] *New York University, USA*
[4] *Alfred Wegener Institute Helmholtz Centre for Polar and Marine Research, Potsdam, Germany*
[5] *University of Alaska Fairbanks, USA*
[6] *Northern Arizona University, USA*

A large amount of organic carbon stored in permafrost soils across the high latitudes is vulnerable to thaw, decomposition and release to the atmosphere as a result of climate warming. Findings from observational, experimental and modeling studies all suggest that this process could lead to a significant positive feedback on future radiative forcing from terrestrial ecosystems to the Earth's climate system. With respect to the magnitude and timing of this feedback, however, observational data show large variability across sites, experimental studies are few, and different models result in a wide range of responses. These issues represent fundamental limitations on improving our confidence in projecting future permafrost carbon release and associated climate feedbacks. Recent studies have brought new insight into – and even quantitative estimates for – these issues through broader data synthesis and model-data integration approaches. But, how representative of the circumarctic-scale variability in permafrost carbon vulnerability are the data and models from these studies? To address this question, we developed a geospatial data synthesis and analysis framework designed to represent and characterize the variability in permafrost carbon vulnerability across the northern high latitudes. Here, we describe the rationale and methods used to develop the regionalization scheme, and then use the framework to assess the spatial representativeness of, and the variability described by, existing data sets defining the fundamental components and environmental drivers of permafrost carbon vulnerability.

The Permafrost Regionalization Map (PeRM, Fig. 1) considers the regional-scale environmental factors that generally determine the spatial variability in permafrost carbon vulnerability across the Arctic. The broadly-defined regional classification is based on a circumarctic spatial representation of the major environmental controls on

a) the rate and extent of permafrost degradation and thaw,

b) the quantity and quality of soil organic matter stocks, and

c) the form of permafrost carbon emissions as CO_2 and CH_4.

We chose a generalized, pragmatic approach that resulted in a feasible number of regional subdivisions (i.e., 'reporting units') based on an intersection of spatial data layers according to permafrost extent, permafrost distribution, climate regime, biome and terrain.

The utility of the PeRM framework is demonstrated here through areal density analysis and spatial summaries of existing data collections describing the fundamental components of permafrost carbon vulnerability. We use this framework to describe the spatial representativeness and variability in measurements within and across PeRM regions using observational data sets describing active layer thickness, soil pedons and carbon storage, long-term incubations for carbon turnover rates, and site-level monitoring of CO_2 and CH_4 fluxes from arctic tundra and boreal forest ecosystems. We then use these regional summaries of the observational data to benchmark the results of a process-based biogeochemical model for its skill in representing the magnitudes and spatial

variability in these key indicators. Finally, we discuss the on-going use of this framework as a basis for higher-resolution mapping of key regions of particular vulnerability to both press (active layer thickening) and pulse (thermokarst development) disturbances. This work is guiding on-going research toward characterizing permafrost degradation and associated vegetation changes through multi-scale remote sensing. Overall, this spatial data synthesis framework work provides a critical bridge between the abundant but disordered observational and experimental data collections and the development of higher-complexity process representation of the permafrost carbon feedback in geospatial modeling frameworks.

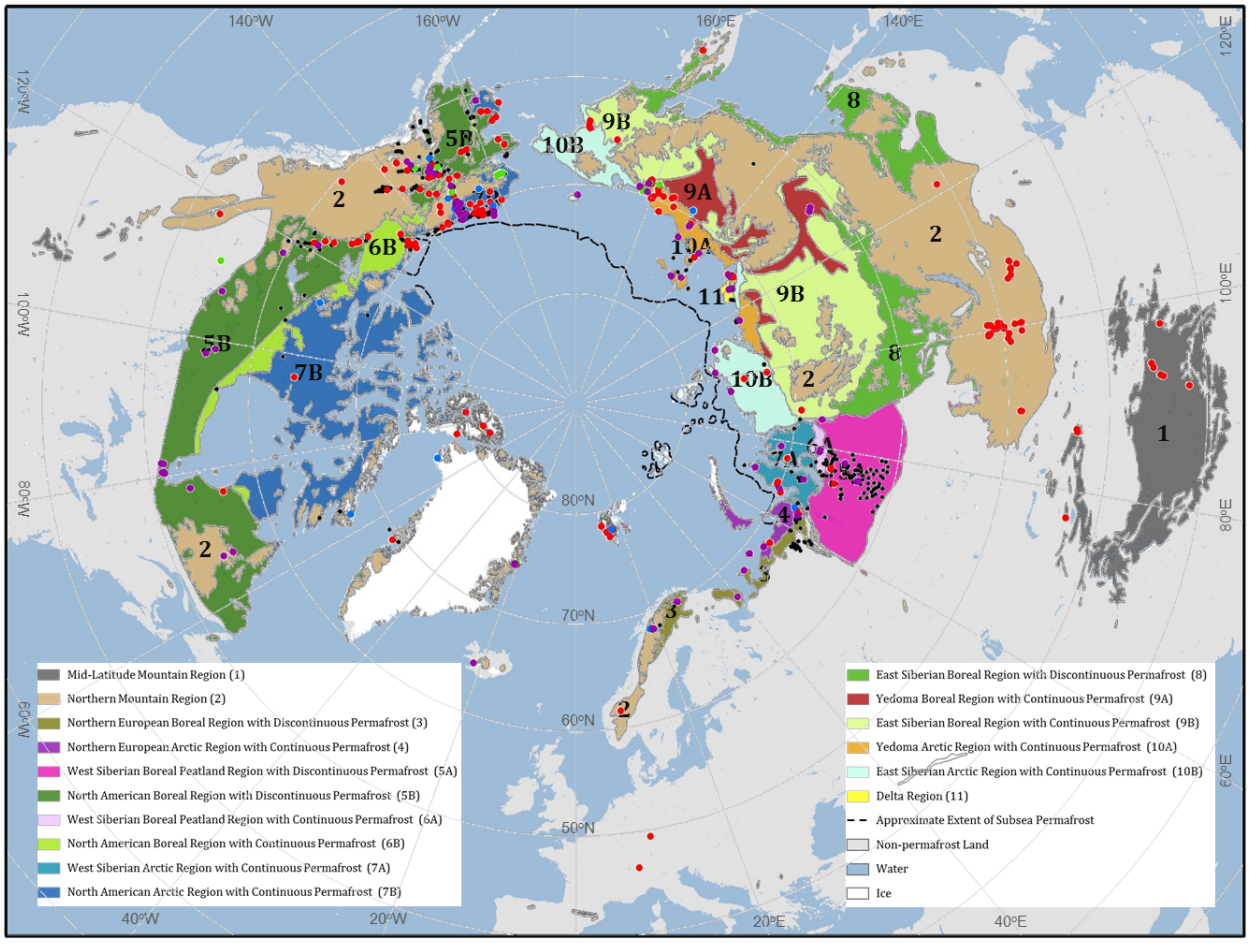

Figure 1: The Permafrost Regionalization Map (PeRM) showing the spatial intersection of a set of broadly-defined environmental controls on the circumarctic-scale variability in permafrost carbon vulnerability. Point locations are shown on the map representing data collections of thaw depth (red), soil carbon quantities (black), decomposability (green), and CO_2 (blue) and CH_4 (purple) fluxes.

Process-based modelling of methane emissions from a polygonal tundra at Samoylov, Lena Delta

Sonja Kaiser[1], Christian Beer[2], & Mathias Goeckede[1]

[1] *Max Planck Institute for Biogeochemistry, Jena, Germany*
[2] *Department of Environmental Science and Analytical Chemistry, Bolin Centre for Climate Research, Stockholm University, Sweden*

Permafrost regions show a large spatial variability of aerobic versus anaerobic conditions due to reduced percolation and pattern ground formation. Therefore, methane in addition to carbon dioxide is being released to the atmosphere in these regions. Process-based modelling of methane production, oxidation and soil gas transport is a powerful tool to assess the land-atmosphere exchanges of such greenhouse gases at large spatial scale and long time periods as a function of climate. In this paper we present a first version of a general methane model for the land surface scheme JSBACH which can in particular be applied at polygonal tundra. The comparison of first simulation results to observations at Samoylov, Lena Delta shows the general validity of the model. This development will be the basis for next studies on the future projection methane emissions from permafrost regions in response to climate change.

Seasonal patterns and annual budgets of CO_2 and CH_4 fluxes from a permafrost ecosystem based on year-round eddy-covariance measurements

Fanny Kittler[1], Mathias Goeckede[1], Ina Burjack[1], Nikita Zimov[2], Sergei A. Zimov[2], & Martin Heimann[1]

[1] *Max-Planck Institute for Biogeochemistry, Jena, Germany*
[2] *Northeast Scientific Station, Cherskii, Russia*

Permafrost landscapes in the Northern high latitudes are critically important for the global carbon cycle with their massive organic carbon stocks. Still large uncertainties in the sustainability of these carbon pools under future climate conditions persist, to a large part caused by limited understanding of the carbon cycle processes due to scarce observational databases for arctic permafrost ecosystems. To improve the understanding of mechanisms and controls dominating permafrost carbon cycling and allow to quantify reliable annual net carbon budgets, particularly data gaps in the non-growing seasons need to be closed.

In the context of the project presented here, a continuous monitoring program was established in a moist tussock tundra ecosystem near Cherskii in Northeastern Siberia (68.75°N, 161.33°E). Eddy-covariance measurements focus on the ecosystem-atmosphere exchange fluxes of carbon (CO_2 and CH_4), and an extensive suite of additional meteorological sensors provide insight into major environmental controls. With parallel observations over a disturbed (drained) area and a reference area nearby, respectively, we aim at evaluating the effect of a lowered water table on the carbon cycle budgets and its dominating biogeochemical mechanisms.

We present findings based on two full years of continuous eddy-covariance flux measurements using a closed-path gas analyser (LosGatos FGGA). Our year-round CO_2 and CH_4 flux measurements emphasize the importance of the non-growing season fluxes, where especially autumn and winter seasons contribute significantly to the annual budget and thus strongly alter the sink/source capacity of the ecosystem compared to growing season budgets alone. For methane, major contributions are observed during the freeze-in period (Oct/Nov) with 20 % of the annual budget, while the long winter season releases 50% of the summertime carbon dioxide uptake, resulting in an annual budgets of - 21 g C $m^{-2}$and + 8 gC m^{-2} for CO_2 and CH_4, respectively. Furthermore shifts in the relative influence of different environmental controls can be found between sub-seasons, highlighting the variability of the observed flux patterns and the underlying mechanisms that control net fluxes.

For the disturbance experiment, results show systematic shifts in the tundra ecosystem carbon cycle patterns, with decreased uptake rates for CO_2 and decreased emissions for CH_4 under drained conditions. Reduction in CH_4 emissions dominates global warming potential (GWP) at short timeframes, with both ecosystems acting as a strong net sources for atmospheric carbon (GWPref > GWPdrained) but for longer timeframes the GWP budget from both sites are near-neutral for atmospheric carbon, and shifts in the CO_2 budget dominate the differences between the disturbance regime.

Disproportional contribution of geological sources to Mackenzie Delta methane emissions revealed from airborne eddy-covariance measurements

Katrin Kohnert[1], Andrei Serafimovich[1], Stefan Metzger[2,3], Jörg Hartmann[4], & Torsten Sachs[1]

[1] *Helmholtz Centre Potsdam, GFZ German Research Centre for Geosciences, Potsdam, Germany*
[2] *National Ecological Observatory Network, Fundamental Instrument Unit, Boulder, CO, USA*
[3] *University of Colorado, Institute for Arctic and Alpine Research, Boulder, CO, USA*
[4] *Alfred Wegener Institute Helmholtz Centre for Marine and Polar Research, Bremerhaven, Germany*

Arctic wetlands associated with permafrost as well as thawing permafrost emit the greenhouse gas methane (CH_4). Two important contributors are recent microbial activity in the active layer or taliks (biogenic CH_4), and deeper fossil sources where pathways through the permafrost exist (geologic CH_4). Current emission estimates vary strongly between different models. Moreover, there is still disagreement between bottom-up estimates from local field studies, and top-down estimates from atmospheric measurements.

Here, we quantify permafrost CH_4 emissions directly on the regional scale, based on the Airborne Measurements of Methane Fluxes Campaigns (AIRMETH) in the Mackenzie River Delta region, Canada, in July 2012 and 2013 [Kohnert et al., 2014]. The Mackenzie Delta is the second largest Arctic delta (13,000 km^2). Our measurements covered an area extending 320 km from west to east (140°58'W to 133°22'W) and of 240 km from north to south (69°33'N to 67°26'N). The study area comprises the delta itself, the adjacent Yukon coastal plain, and Richards Island north east of the delta. The area surrounding the delta is described as continuous permafrost zone where the permafrost reaches a thickness of 300 m along the coastal plain and 500 m on Richards Island. In the delta itself the discontinuous permafrost reaches a maximum thickness of 100 m. The northern part of the study area is crossed by geological faults and underlain by oil and natural gas deposits.

We analyse the regional pattern of CH_4 fluxes and estimate the contribution of geologic emissions to the total CH_4 budget of the delta. CH_4 fluxes were calculated with a time-frequency resolved version of the eddy-covariance technique [Metzger et al., 2013], followed by the calculation of flux topographies [Mauder et al., 2008]. The result is a 100 m resolved gridded flux map within the footprints of the flight tracks. The results provide the first regional estimate of CH_4 release from the Mackenzie Delta and the adjacent coastal plain. We distinguish geological gas seeps from biogenic sources by their strength, and show that geologic sources contribute strongly to the annual CH_4 budget of the study area: One percent of the covered area contains the strongest geological seeps which contribute disproportionately to an annual emission estimate. The contribution of geological sources to CH_4 emission warrants further attention, in particular in areas where permafrost is vulnerable to increased geologic gas migration due to thawing and opening of new pathways. The presented map can be used as a baseline for future CH_4 flux studies in the Mackenzie Delta.

References

Kohnert, K.; Serafimovich, A.; Hartmann, J. and Sachs, T. [2014]: Airborne measurements of methane fluxes in alaskan and canadian tundra with the research aircraft "polar 5". In *Reports on Polar and Marine Research*, volume 673. Alfred Wegener Institue Bremerhaven, pp. 81.

Mauder, M.; Desjardins, R.L. and MacPherson, I. [2008]: Creating surface flux maps from airborne measurements: Application to the Mackenzie area GEWEX study MAGS 1999. *Boundary-Layer Meteorology*, 129:431–450, 2008.

Metzger, S.; Junkermann, W.; Mauder, M.; Butterbach-Bahl, K.; Trancón y Widemann, B.; Neidl, F.; Schäfer, K.; Wieneke, S.; Zheng, X. H.; Schmid, H. P. and Foken, T. [2013]: Spatially explicit regionalization of airborne flux measurements using environmental response functions. *Biogeosciences*, 10(4):2193–2217, 2013. doi:10.5194/bg-10-2193-2013.

Regional pattern of carbon emission from the Mackenzie Delta, Canada – Results from an airborne flux study

Katrin Kohnert[1], Andrei Serafimovich[1], Stefan Metzger[2,3], Jörg Hartmann[4], & Torsten Sachs[1]

[1] *Helmholtz Centre Potsdam, GFZ German Research Centre for Geosciences, Potsdam, Germany*
[2] *National Ecological Observatory Network, Fundamental Instrument Unit, Boulder, CO, USA*
[3] *University of Colorado, Institute for Arctic and Alpine Research, Boulder, CO, USA*
[4] *Alfred Wegener Institute Helmholtz Centre for Marine and Polar Research, Bremerhaven, Germany*

Among other regions of the world, the Arctic is strongly affected by climate change. Globally, it is the region with the most pronounced warming, leading to permafrost warming and thawing. Part of the 1,300 Pg soil organic carbon currently stored in the frozen ground is already and might be further released as carbon dioxide (CO_2) and methane (CH_4). CO_2 is released through aerobic soil respiration and from plant roots, but also sequestered through photosynthesis. CH_4 emission can be attributed to either recent microbial activity or to past microbial or thermal decomposition and is spatially heterogeneous. To our knowledge, regional assessments of the total carbon flux (CO_2 and CH_4) based on high frequency airborne measurements do not exist.

Here we determine the regional pattern of CO_2 and total carbon emissions (CO_2 + CH_4) of the Mackenzie Delta region, Canada, based on the Airborne Measurements of Methane Fluxes Campaign (AIRMETH) in July 2013 [Kohnert et al., 2014].

The Mackenzie Delta is the second largest arctic delta (13,000 km^2). Our measurements covered an area extending 320 km from west to east (140°58' W to 133°22'W) and of 240 km from north to south (69°33'N to 67°26'N). The study area is heterogeneous and comprises the delta itself, the adjacent Yukon coastal plain, and Richards Island north east of the delta. Part of the delta is located north of the treeline. The area surrounding the delta is described as continuous permafrost zone where the permafrost reaches a thickness of 300 m along the coastal plain and 500 m on Richards Island. In the delta itself the discontinuous permafrost reaches a maximum thickness of 100 m.

For the AIRMETH campaign we used the research aircraft Polar 5. Equipped with a 5-hole probe, the usual meteorological sensors, and a fast greenhouse gas analyser (GGA 24EP, Los Gatos Research Inc.) we flew at 30 - 60 m above ground at a true airspeed of 60 m s^{-1}.

CO_2 and CH_4 fluxes were calculated with a time-frequency resolved version of the eddy-covariance technique [Metzger et al., 2013]. We calculated flux topographies [Mauder et al., 2008] to resolve the fluxes along a linear flight track to the area within the footprint of the measurements. The result is a 100 m resolved gridded carbon flux map within the footprints of the flight tracks. Based on the flux topographies we produce a map of the regional pattern of peak growing season carbon fluxes.

References

Kohnert, K.; Serafimovich, A.; Hartmann, J. and Sachs, T. [2014]: Airborne measurements of methane fluxes in alaskan and canadian tundra with the research aircraft "polar 5". In *Reports on Polar and Marine Research*, volume 673. Alfred Wegener Institue Bremerhaven, pp. 81.

Mauder, M.; Desjardins, R.L. and MacPherson, I. [2008]: Creating surface flux maps from airborne measurements: Application to the Mackenzie area GEWEX study MAGS 1999. *Boundary-Layer Meteorology*, 129:431–450, 2008.

Metzger, S.; Junkermann, W.; Mauder, M.; Butterbach-Bahl, K.; Trancón y Widemann, B.; Neidl, F.; Schäfer, K.; Wieneke, S.; Zheng, X. H.; Schmid, H. P. and Foken, T. [2013]: Spatially explicit regionalization of airborne flux measurements using environmental response functions. *Biogeosciences*, 10(4):2193–2217, 2013. doi:10.5194/bg-10-2193-2013.

Temporal and spatial extrapolation of CO_2 fluxes of polygonal tundra by modeling ecosystem photosynthesis-respiration flux parameters with NDVI and reanalysis data

Lars Kutzbach[1], Christian Wille[1], Alexander J. Winkler[1], & Benjamin R. K. Runkle[1]

[1] *Universität Hamburg, Institute of Soil Science, Hamburg, Germany*
[2] *University of Arkansas, Department of Biological and Agricultural Engineering, Fayetteville, USA*

Permafrost-affected ecosystems are great reservoirs of organic carbon due to their function as long-term net carbon sinks. Within the projected climate and environmental changes in the Arctic, these ecosystems are vulnerable to switch to substantial net carbon sources in the Earth system. For the assessment of the atmospheric carbon flux balance of these landscapes, their inter-annual variability, and long-term trends, continuous flux data time series are desirable. However, measurements of atmospheric carbon fluxes in Arctic regions are sparse and the seasonal coverage is often incomplete, due to the logistical problems involved in working in these regions.

For the gap-filling and extrapolation of measured flux data, deterministic process models are needed which are based on meteorological and soil data, and information about the seasonal development of vegetation, i.e. a vegetation index (VI). Field-measured meteorological and VI data could drive a process model for a particular site. The use of re-analysis meteorological data and satellite VI data could allow the extrapolation of the process model in time and space.

Global soil-atmosphere process models are developed for this purpose, but so far they have been shown to not be able to reproduce site-scale measured fluxes well. Site-scale deterministic models of CO_2 exchange processes have been developed for gap-filling purposes (e.g. Lasslop et al. [2010], Runkle et al. [2013]. These models use only meteorological data as drivers and are usually not able to reliably extrapolate flux data outside the period covered by measured data. Moreover, these models often do not perform satisfactorily for arctic sites, especially outside the peak vegetation period, when fluxes are low.

These problems are addressed in the present study, which is based on Eddy-Covariance measurements of net Ecosystem CO_2 exchange (NEE) from polygonal tundra in the Lena River Delta, Northern Siberia (72°22' N, 126°28' E). The measured data covers the 13-year period 2002 - 2014, during which full growing season data was acquired in only 4 years. An ecosystem photosynthesis-respiration (EPR) model which had been used for this site's data before [Runkle et al., 2013] was refined to produce reliable parameters for photosynthesis fluxes (maximum photosynthetic capacity GPPmax, photon use efficiency α and respiration fluxes (basal respiration Rbase, temperature sensitivity Q10) for the entire data set.

The EPR parameters were found to be closely correlated with site-measured meteorological and VI data as well as re-analysis meteorological and MODIS NDVI data generated for the flux tower pixel (R2 of 0.66, 0.78, 0.83 for Rbase, α, and GPPmax, respectively). Based on the functional relationships found, the flux parameters will be modeled and used in the EPR model to gap-fill and extrapolate the measured fluxes for the complete vegetation periods 2002 - 2014.

This method will then be extended to estimate the seasonal CO_2 flux balance of the total polygonal tundra area in the Lena River Delta. Based on classified land cover maps [Zubrzycki et al., 2013], ECMWF ERA-interim re-analysis meteorological data, and MODIS NDVI data, the net ecosystem CO_2 exchange of the polygonal tundra in the Lena River Delta will be simulated on a high temporal and spatial resolution (three-hourly, 0.05°).

References

Lasslop, G.; Reichstein, M. and Papale, D. et al. [2010]: Separation of net ecosystem exchange into assimilation and respiration using a light response curve approach: critical issues and global evaluation. *Global Change Biology*, 16(1):187–208, doi:10.1111/j.1365-2486.2009.02041.x.

Runkle, B. R. K.; Sachs, T.; Wille, C.; Pfeiffer, E.-M. and Kutzbach, L. [2013]: Bulk partition-

ing the growing season net ecosystem exchange of CO₂ in Siberian tundra reveals the seasonality of its carbon sequestration strength. *Biogeosciences*, 10(3):1337–1349, doi:10.5194/bg-10-1337-2013.

Zubrzycki, S.; Kutzbach, L.; Grosse, G.; Desyatkin, A. and Pfeiffer, E.-M. [2013]: Organic carbon and total nitrogen stocks in soils of the Lena River Delta. *Biogeosciences*, 10(6):3507–3524, doi:10.5194/bg-10-3507-2013.

Interaction of fire, moss and permafrost in the land vegetation model JSBACH

Gitta Lasslop[1], Philipp Porada[2], Christian Beer[2], & Silvia Kloster[1]

[1] *Max-Planck Institute for Meteorology, Germany*
[2] *Department of Environmental Science and Analytical Chemistry (ACES) Bolin Centre for Climate Research Stockholm University*

Fire is a key process for vegetation structure and a long-term controlling factor on permafrost stability in the boreal zone. Fires potentially destroy surface layer vegetation, which serves as a protective, insulating layer for the underlying permafrost. Permafrost, in turn, impacts vegetation structure and fire activity through a strong hydrological control, as the frozen soil inhibits water drainage.

Both fire models and permafrost representations have been improved in Earth System models over the recent years. The MPI Earth system model (MPI-ESM) has been extended with the process-based fire model SPITFIRE (Lasslop et al., 2014), a permafrost scheme (Ekici et al., 2014) and most recently a dynamic bryophytes and lichens model (Porada et al., 2016). This study will, for the first time, couple these components in the MPI-ESM framework. The bryophytes and lichens layer will be explicitly burned in the fire model SPITFIRE, which will take into account moss specific biomass and moisture. This will impact insulation and active-layer thickness, which in turn will feedback on fire occurrence through changes in the hydrological cycle.

A set of artificial model experiments will be designed that include the different processes in a stepwise procedure, which will allow us to disentangle the contributions of the single processes to the overall fire-bryophytes and lichens-permafrost interaction. Spatial and temporal analyses of burned area and active-layer thickness will be presented.

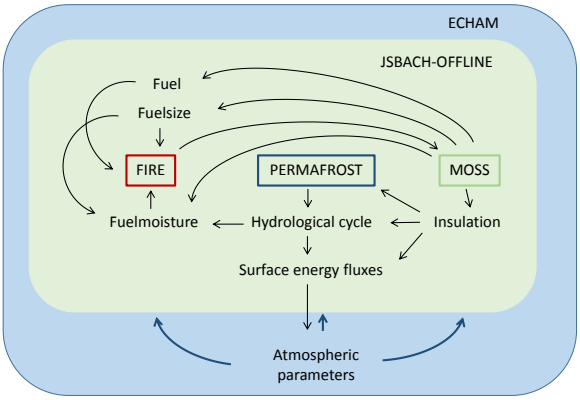

Figure 1: Interactions between fire, moss and permafrost in the JSBACH land surface model. The model may be coupled to the atmosphere model ECHAM

Quantifying the biogeochemical processes and environmental controls that drive Arctic-Boreal ecosystem carbon fluxes

Charles Miller[1], Sebastien Biraud[2], Anthony Bloom[1], John Budney[3], Rachel Chang[4], Seth Chazanoff[1], Roisin Commane[3], Bruce Daube[3], Yuanyuan Fang[5], Elaine Gottlieb[3], Sean Hardman[1], John Henderson[6], Su-Jong Jeong[1], Anna Karion[7], John Kimball[8], Charles Koven[2], Thomas Kurosu[1], David Lawrence[9], Kristina Luus[10], Kyle McDonald[11], Kathryn McKain[7], Anna Michalak[5], John Miller[7], Scot Miller[5], Gergana Mouteva[12], Walt Oechel[13], Nicholas Parazoo[1], Jasna Pittman[3], Erika Podest[1], Chris Potter[14], James Randerson[12], Torsten Sachs[15], Dave Schimel[1], Andrew Slater[7], Nick Steiner[11], Colm Sweeney[7], Margaret Torn[2], Sander Veraverbeke[12], Jennifer D. Watts[8], Elizabeth Wiggins[12], Steve Wofsy[3], Sonja Wolter[7], Doug Worthy[16], Vineet Yadav[1], & Donatella Zona[13]

[1] *Jet Propulsion Laboratory, Pasadena, CA, USA*
[2] *Lawrence Berkeley National Laboratory, Berkeley, CA, USA*
[3] *Harvard University, Cambridge, MA, USA*; [4] *Dalhousie University, Halifax, NS, Canada*
[5] *Carnegie Institution for Science, Stanford, CA, USA*; [6] *AER, Lexington, MA, USA*
[7] *CIRES, CU Boulder, Boulder, CO, USA*; [8] *The University of Montana, USA*
[9] *National Center for Atmospheric Research, Boulder, CO, USA*; [10] *Dublin Institute of Technology, Ireland*
[11] *The City College of New York, New York, NY, USA*; [12] *University of California, Irvine, CA, USA*
[13] *San Diego State University, San Diego, CA, USA*
[14] *NASA Ames Research Center, Moffett Field, CA, USA*
[15] *GFZ German Research Centre for Geosciences, Potsdam, Germany*
[16] *Environment Canada, Toronto, ON, Canada*

Vast stores of carbon are sequestered in the permafrost soils, peatlands and boreal forests of the pan-Arctic region. Dramatic increases in warming, permafrost thaw, fire severity and frequency, and other natural disturbances threaten to alter these Arctic-boreal ecosystems (ABEs) irreversibly, transforming the landscape and the ecosystem carbon balance as terrestrial carbon pools are released as atmospheric carbon dioxide (CO_2) and methane (CH_4).

Ecosystem dynamics in the ABR vary on meter scales due to microtopographic changes in permafrost, elevation, water table height, vegetation, microbial populations, etc., resulting in CO_2 and CH_4 fluxes that vary by orders of magnitude on these scales. It remains unclear how landscape scale processes and biogeochemical drivers impact meso-, regional- and pan-Arctic scale C fluxes or how diurnal to interannual variability of C exchange impacts decadal scale ABE C balance. What is the C balance of ABEs now and in the future? Are C flux scaling properties constant across the domain, or do they vary with ecosystem classification? What emergent properties or macroscopic variables characterize ABE C fluxes at intermediate space-time scales?

We will present geostatistical inverse model analyses that leverage recent atmospheric observations to evaluate the process-level representation of land-atmosphere carbon exchange inside terrestrial biospheric models (TBMs). Additionally, we will identify the environmental parameters that optimally explain the observed spatiotemporal variability in carbon flux patterns across western North America. We will use these observations to improve TBM skill, and then extrapolate our results to the pan-Arctic.

Figure 1: group photo

A multi-year estimate of methane fluxes in Alaska from the CARVE aircraft campaign

Scot Miller[1], Roisin Commane[2], Rachel Chang[3], Charles Miller[4], Anna Michalak[1], Steven Dinardo[4], Edward Dlugokencky[5], Sean Hartery[3], Anna Karion[6], Colm Sweeney[6], Jakob Lindaas[2], & Steve Wofsy[2]

[1]*Carnegie Institution for Science, Stanford*; [2]*Harvard University, Cambridge, USA*
[3]*Dalhousie University, Halifax, NS, Canada*; [4]*Jet Propulsion Laboratory, Pasadena, CA, USA*
[5]*NOAA GMD, Boulder, CO, USA*; [6]*CIRES, CU Boulder, Boulder, CO, USA*

We estimate methane fluxes across Alaska over a multi-year period using observations from a three-year aircraft campaign, the Carbon Arctic Reservoirs Vulnerability Experiment (CARVE). Existing estimates of methane from Alaska and other arctic regions disagree in both magnitude and distribution, and before the CARVE campaign, atmospheric observations in the region were sparse. We estimate surface fluxes at the model grid scale by combining CARVE observations with an atmospheric particle trajectory model and a geostatistical inversion. We first use this framework to estimate the spatial distribution of methane fluxes across the state. We find the largest fluxes in south-west and North Slope regions of Alaska. This distribution is consistent with several estimates of wetland extent but contrasts with the distribution in most existing flux models. These flux models concentrate methane in warmer or more southerly regions of Alaska compared to the estimate presented here. We next use the inversion framework to explore interannual variability in regional-scale methane fluxes for 2012-2014. We find some differences in the seasonal cycle of fluxes from one year to another, but total annual methane budgets show little year-to-year variability. These results indicate the possible sensitivity of regional-scale fluxes to short-term variability in climate.

Detecting Patterns of Changing CO_2 Flux in Alaska

Nicholas Cody Parazoo

UCLA, United States of America

Climate change in high northern latitudes has led to an intensification of the Arctic carbon cycle in recent years, with increased photosynthetic carbon uptake early in the growing season offset by increased carbon loss in early fall. As the Arctic carbon cycle continues to shift in response to climate warming, it is critical that we track carbon balance changes to avoid the risk of emerging carbon sources going unobserved. Here, we use satellite and airborne observations of atmospheric carbon dioxide (CO_2) with climate-induced CO_2 flux simulations to assess the detectability of Alaskan carbon cycle signals as future warming evolves. We find that current satellite remote sensing technologies have potential to detect changing uptake during the growing season but lack sufficient cold season coverage and near surface sensitivity to constrain annual carbon balance changes. Airborne strategies that target sustained vertical profile measurements within continental interiors present a viable option to constrain annual carbon balance changes, but currently don't measure at sufficient spatial resolution across the entire cold season. Due to limitations during the cold season, current CO_2 observing systems are unlikely to detect potentially dangerous carbon emission sources associated with deep permafrost thaw over the next 50 years. While continuity of these systems is vital, new strategies and technologies focused on dark season capability (active remote sensing, aircraft, tall towers, and flux towers) and systematic sampling across continental interiors over the full annual cycle are required to track changes over the long cold season.

Wintertime emissions of methane and carbon dioxide from permafrost-underlain Arctic tundra

Norbert Pirk[1,2], Mikhail Mastepanov[1,3], Magnus Lund[1,3], Stine H. Pedersen[3], Maria R. Mylius[4], Mikkel P. Tamstorf[3], Hanne H. Christiansen[2], & Torben R. Christensen[1,3]

[1] *Department of Physical Geography and Ecosystem Science, Lund University, Lund, Sweden*
[2] *Geology Department, The University Centre in Svalbard, UNIS, Longyearbyen, Norway*
[3] *Department of Bioscience, Arctic Research Centre, Aarhus University, Aarhus, Denmark*
[4] *Dept. of Geosciences and Natural Resource Management, University of Copenhagen, Copenhagen, Denmark*

The land-atmosphere exchange of the greenhouse gases methane (CH_4) and carbon dioxide (CO_2) in high Arctic tundra landscapes is particularly difficult to measure in wintertime. This means that there is large uncertainty about the flux magnitudes and the controlling factors when the ground is frozen.

Three winter campaigns were conducted to measure these gas dynamics in permafrost-underlain lowland sites in the Zackenberg Valley (NE Greenland, 74° N) and in the Adventdalen Valley (Svalbard, 78° N), both of which also feature automatic closed-chamber flux measurements during summertime.

In Zackenberg, wintertime fluxes were 1 to 2 orders of magnitude lower than summertime fluxes. CH_4 fluxes perennially resemble the same spatial pattern, which can be largely attributed to differences in summer soil wetness controlling substrate accumulation and microbial activity. The CH_4/CO_2 concentration ratios inside the snowpack showed no general trend as the gases diffuse upwards which renders significant gas sinks or sources inside the snowpack unlikely.

The isotopic signature of the CH_4 source in the soil was found to be largely the same during summer and wintertime.

In the polygonal tundra of Adventdalen the snowpack featured several ice layers, which suppressed the expected gas fluxes to the atmosphere, and conversely lead to snowpack gas accumulations of up to 86 ppmCH_4 and 3800 ppmCO_2 by late winter. The ratio of CH_4 to CO_2 indicated distinctly different source characteristics in the rampart of the ice-wedge polygons than on other parts of the measured transect, which we attribute to the soil thermal contraction cracking, which occurs when the polygons contract during winter cooling.

We argue that the identified processes can mediate interactions between summertime and wintertime, and may explain important dynamics of greenhouse gas exchanges in high Arctic tundra.

Quantifying the effect of lichen and bryophyte cover on permafrost soil within a global land surface model

Philipp Vincent Porada[1], Altug Ekici[2], & Christian Beer[1]

[1] *Stockholm University, Sweden*
[2] *University of Exeter, UK*

Near-surface vegetation at high latitudes, such as bryophytes and lichens, has an insulating effect on the ground. Consequently, it can protect permafrost soil by decreasing mean annual soil temperature. Warming due to climate change, however, may reduce the surface coverage of bryophytes and lichens. This can lead to permafrost thawing associated with a release of soil carbon to the atmosphere, resulting in a positive feedback on atmospheric CO_2 . Hence, it is crucial to estimate how the bryophyte and lichen cover at high latitudes will react to environmental change. Current global land surface models, however, contain mostly empirical approaches to represent the bryophyte and lichen cover. This makes it difficult to predict the future performance of bryophytes and lichens in a quantitative way. Therefore, we integrate a process-based model of bryophyte and lichen growth into the global land surface model JSBACH. We explicitly represent dynamic thermal properties of the bryophyte and lichen cover and their relation to climate. Subsequently, we compare simulations with and without bryophyte and lichen cover to quantify the insulating effect of near-surface vegetation.

We estimate an annual average cooling effect of the bryophyte and lichen cover of 2.7 K on topsoil temperature for the northern high latitudes under current climate. In some regions the cooling may reach 5.7 K. Furthermore, we show that neglecting dynamic properties of the bryophyte and lichen cover by using a simple, empirical scheme only results in an average cooling of around 0.5 K. This suggests that bryophytes and lichens significantly affect soil temperature at high latitudes and that it is also important to describe their thermal properties in a process-based way.

Constraining Arctic methane emissions through atmospheric methane signals at coastal sites

Friedemann Reum[1], Mathias Goeckede[1], Ute Karstens[2], Christoph Gerbig[1], Jošt Lavrič[1], Sergey A. Zimov[3], Nikita Zimov[3], Olaf Kolle[1], Frank-Thomas Koch[1], & Martin Heimann[1]

[1] *Max Planck Institute for Biogeochemistry, Germany*
[2] *ICOS Carbon Portal, Lund University, Sweden*
[3] *Northeast Science Station, Russia*

Methane budgets in the Arctic are highly uncertain at regional scales. We work towards reducing these uncertainties using measurements of atmospheric methane mixing ratios that we link to surface fluxes through atmospheric transport simulations, allowing to optimize fluxes through inverse modeling approaches. We present results based on the first year of data from a new observation site for atmospheric traces gases, located at the coast of the East Siberian Arctic Shelf in Ambarchik (69.6N, 162.3E). Inflowing air masses are influenced by adjacent wetlands and the Arctic Ocean, which are both potentially strong methane emitters [Shakhova et al., 2010, McGuire et al., 2012]. We use a regional atmospheric transport model (STILT) to map estimates of wetland methane emissions (WETCHIMP, Melton et al. [2013]) to methane concentrations in Ambarchik and other sites bordering the shelf, Tiksi (RU) and Pt. Barrow (AK, USA). We find larger variability in the observed than in the modeled concentrations and explore how scaling of the WETCHIMP prior flux fields as well as incorporating estimates of methane emissions from the East Siberian Arctic Shelf into the model reduces this discrepancy.

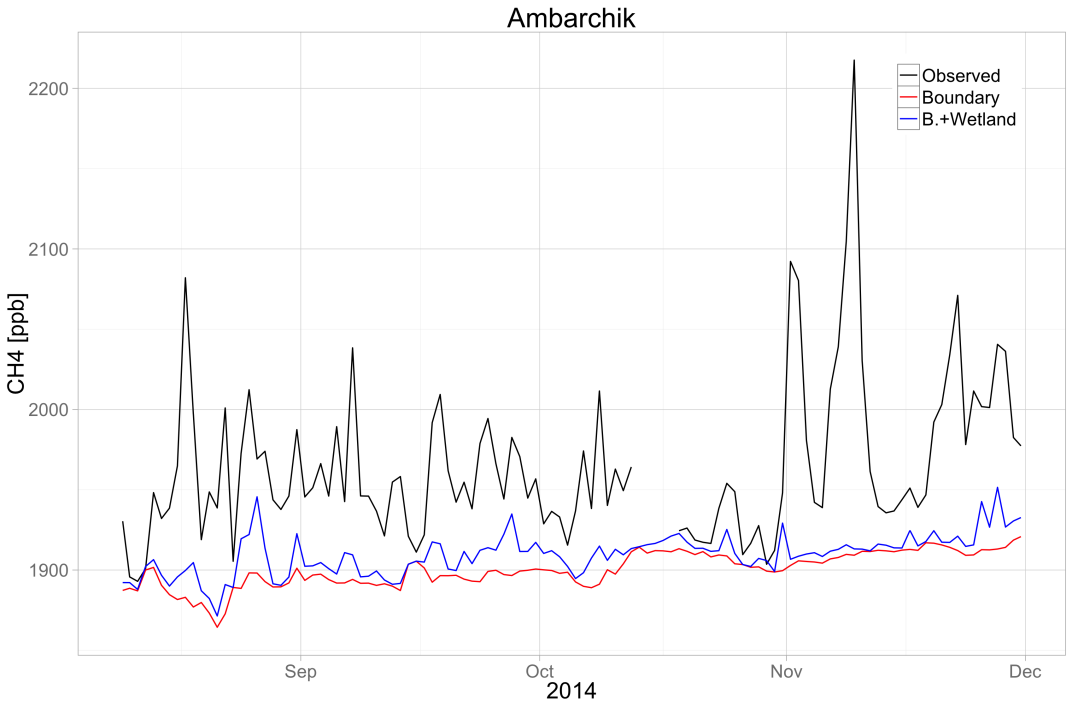

Figure 1: Observed and modeled methane mixing ratios in Ambarchik. Wetland fluxes are from the LPJ-Bern contribution to WETCHIMP (year 2004). Boundary conditions are from the Jena Inversion System (year 2011, adjusted for mean annual increase).

References

McGuire, A. D.; Christensen, T. R.; Hayes, D.; Heroult, A.; Euskirchen, E.; Kimball, J. S.; Koven, C.; Lafleur, P.; Miller, P. A.; Oechel, W.; Peylin, P.; Williams, M. and Yi, Y. [2012]: An assessment of the carbon balance of arctic tundra: comparisons among observations, process models, and atmospheric inversions. *Biogeosciences*, 9(8):3185–3204, doi:10.5194/bg-9-3185-2012.

Melton, J. R.; Wania, R.; Hodson, E. L.; Poulter, B.; Ringeval, B.; Spahni, R.; Bohn, T.; Avis, C. A.; Beerling, D. J.; Chen, G.; Eliseev, A. V.; Denisov, S. N.; Hopcroft, P. O.; Lettenmaier, D. P.; Riley, W. J.; Singarayer, J. S.; Subin, Z. M.; Tian, H.; Zürcher, S.; Brovkin, V.; van Bodegom, P. M.; Kleinen, T.; Yu, Z. C. and Kaplan, J. O. [2013]: Present state of global wetland extent and wetland methane modelling: conclusions from a model intercomparison project (WETCHIMP). *Biogeosciences*, 10(2):753–788, doi:10.5194/bg-10-753-2013.

Shakhova, Natalia; Semiletov, Igor; Salyuk, Anatoly; Yusupov, Vladimir; Kosmach, Denis and Gustafsson, örjan. [2010]: Extensive Methane Venting to the Atmosphere from Sediments of the East Siberian Arctic Shelf. *Science*, 327(5970):1246–1250, doi:10.1126/science.1182221.

Spatio-temporal variability of CH_4 fluxes and environmental drivers on a modern flood plain of the Siberian Lena River Delta

Norman Rößger, Christian Wille, Lutz Beckebanze, & Lars Kutzbach

Hamburg University, Germany

In the course of climate change in the Arctic, methane emissions may considerably increase due to more suitable production conditions comprising enhanced temperatures, greater abundance of moisture and increased availability of the carbon stock to microorganisms. These processes affect various arctic tundra ecosystems; thus, regional assessments of the altering carbon turnover are of vital importance for a precise estimation of the global carbon budget. However, assessments on the regional scale require at first comprehensive information on local carbon cycle processes and their site-specific spatio-temporal variability.

We address these problems on the modern flood plain of Samoylov Island in the Lena River Delta (72°22'N, 126°28'E). Flood plains constitute approximately 40 % of the soil-covered area of the Lena River Delta which likely holds more than half of the entire soil organic carbon mass stored in the seven major deltas in the northern permafrost regions (Zubrzycki et al., 2013). The climate is a dry, continental, arctic climate with a mean annual air temperatures of -14.7 °C [Sachs et al., 2010]. The area around the flux tower is characterised by annual flooding, a variety of non-cryoturbated permafrost-affected soils with different degrees of organic matter accumulation, a tundra vegetation dominated by dwarf shrub/sedges and a slightly undulating relief forming elevated, well drained areas und wet, partially inundated depressions [Boike et al., 2013].

Eddy covariance measurements ran between June 2014 and September 2015 including wintertime observations. The methane fluxes were determined using a LICOR 7700 open-path CH_4 analyser at a measurement height of 2.8 m. Despite this comparatively low height, all land types being characteristic for the flood plains and contributing to the carbon budget could be sensed. In order to explain the methane fluxes variability, a comprehensive data set of potential environmental controls has been acquired. Besides standard meteorological parameters, surface characteristics data have also been ascertained to account for the footprint's heterogeneity. This includes soil temperatures at multiple depths, ground water table depths, thaw depths, in-situ classification of vegetation, moss abundance and moisture levels as well as GIS-aided classification of the vegetation using a high-resolution orthophoto and a Landsat Scene respectively. Through footprint modelling, the relative contribution of each parameter class to every 30 min flux interval was determined allowing a comprehensive regression analysis.

Pulsed methane emissions in winter could be detec-

ted several times and where mostly associated with drops in air pressure. Snow depths of up to several tens of decimeters did not prevent these events. The main emissions occurred between June and September determined by spring thaw and refreezing in autumn. The highest methane emissions took place in early August reaching up to 0.03 μmol m^{-2} s^{-1}. Over the season the mean methane flux amounted to 0.012 μmol m^{-2} s^{-1}. This average is based on a large variability of methane fluxes which is to be attributed to the heterogeneity of the footprint. The methane sources are unevenly distributed; thus, the detection of methane fluxes is highly dependent upon the wind direction (see Fig. 1).

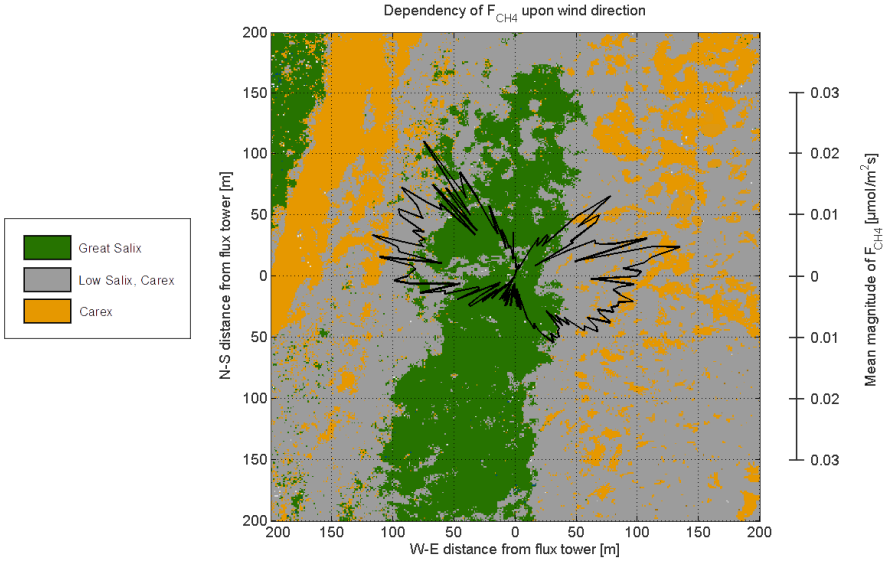

Figure 1: Dependency of methane fluxes (FCH_4) upon wind directions plotted on a classified vegetation map of the footprint. The flux tower is situated in the middle and captures higher methane emissions at easterly and northwesterly wind directions, i.e. when wind blows across *Carex*-dominated areas (sedges), which are characterised by a high abundance of wet and moist patches. The mean magnitude of the methane flux calculated for 2°wind direction bins is indicated by the distance from the black line to the tower.

Methane sources are known to be wet areas which exhibit a certain vegetation dominated by Cyperaceae (e.g. sedges and cotton grass) on the flood plain of Samoylov. Patches of this vegetation type could be identified through supervised classification; hence, wet areas likely to emit methane were localised and their relative contribution to the methane fluxes provides relevant information for the modelling of methane fluxes with respect of the heterogeneity of the footprint. Applying knowledge on the distribution of vegetation in the footprint increased the model fit dramatically and led to coefficients of determination around 0.7 depending on the modelled time scale and the model choice. Explaining the variability in methane fluxes is based on three approaches: deterministic modelling, step-wise regression and neural network. Using exponential relationships for flux drivers in the deterministic model with soil temperature and spatial information on the footprint as explanatory variables, all models yield similar fits. Eventually, the best-fit model will be utilised for the regionalisation of methane fluxes for the extensive flood plain areas of the Lena River Delta.

References

Boike, J.; Kattenstroth, B.; Abramova, K.; Bornemann, N.; Chetverova, A.; Fedorova, I.; Fröb, K.; Grigoriev, M.; Grüber, M.; Kutzbach, L.; Langer, M.; Minke, M.; Muster, S.; Piel, K.; Pfeiffer, E.-M.; Stoof, G.; Westermann, S.; Wischnewski, K.; Wille, C. and Hubberten, H.-W. [2013]: Baseline characteristics of climate, permafrost and land cover from a new permafrost observatory in the Lena River Delta, Siberia (1998-2011). *Biogeosciences*, 10(3): 2105–2128, doi:10.5194/bg-10-2105-2013.

Sachs, T.; Giebels, M.; Boike, J. and Kutzbach, L. [2010]: Environmental controls on CH_4 emission from polygonal tundra on the microsite scale in the Lena river delta, Siberia. *Global Change Biology*, 16(11):3096–3110, doi:10.1111/j.1365-2486.2010.02232.x.

Mobilization of organic carbon and nitrogen in a retrogressive thaw slump on Herschel Island, Yukon Territory, Western Canadian Arctic

Saskia Ruttor, George Tanski, & Hugues Lantuit

Alfred Wegener Institute Helmholtz Centre for Polar and Marine Research, Potsdam, Germany

Herschel Island, located in the southern Beaufort Sea, Western Canadian Arctic, shows a clear response to the global warming. Due to its ice-rich permafrost it is highly affected by environmental forcing and known for its high erosion rates and retrogressive thaw slump activity. Even though retrogressive thaw slumps have an effect on carbon and nitrogen cycling, until now there is not much known about the processes and carbon and nitrogen availability within a retrogressive thaw slump at a circumarctic scale. To provide new insides in this particular field, the retrogressive thaw slump "Slump D" on Herschel Island was divided into undisturbed (tundra zone, permafrost zone), and disturbed zones (mud pool zone, slump floor zone) and sampled via a fishnet grid. The tundra, mud pool and slump floor zones were sampled at 0 to 30 cm depth, for the permafrost zone permafrost profiles of up to 340 cm depth were sampled. In total 100 samples were analysed in their biogeochemical parameters (total organic carbon(TOC)-, total carbon(TC)-, total nitrogen(TN)-content) and stable isotope content (d13Corg). The organic carbon source was determined for all zones to illustrate eventual differences in the deposition milieu. To show the degree of decomposition and degradation during the slumping process TOC/TN-ratio and d13Corg were used as proxys. The results show that the tundra zone has the highest TC-, TOC- and TN-values follwed by the permafrost zone. The lowest values are determined for the slump floor and the mud pool zone. All of the zones show similar d13Corg-values of -26.9 ‰but obvious differences in the TOC/TN-ratio. From the results it is concluded that the tundra zone shows a higher degradation than the permafrost zone but less than the mud pool and slump floor zone. Based on high TOC/TN-values for the permafrost zone a vulnerable zone where carbon and nitrogen is available for decomposition during thawing processes is indicated. Due to the better quality of the organic matter within the permafrost zone labile carbon can be released right after thawing. The mud pool as well as the slump floor are highly degraded and store the more stable carbon which stays in the soil for several years. Within the slump floor zone no differences in degradation or composition are visible even though there is a mixture of old and new vegetated areas. With this findings the first step is made to understand the influence of degrading permafrost on carbon and nitrogen dynamics within a retrogressive thaw slump.

Low permafrost methane emissions from regional airborne flux measurements

Torsten Sachs[1], Andrei Serafimovich[1], Stefan Metzger[2], Katrin Kohnert[1], & Jörg Hartmann[3]

[1] *GFZ German Research Centre for Geosciences, Potsdam, Germany*
[2] *National Ecological Observatory Network, Boulder, Colorado, USA*
[3] *Alfred Wegener Institute Helmholtz Centre for Polar and Marine Research, Bremerhaven, Germany*

Large uncertainties still exist in the global methane budget with clear disagreements between bottom-up and top-down estimates, limiting confidence in climate projections. This is particularly true in the Arctic, which is warming rapidly while storing vast amounts of organic carbon that could potentially be released as carbon dioxide and methane, adding a new greenhouse gas source of unknown magnitude. Regional scale methane emission estimates and functional relationships between potential drivers and methane fluxes are currently unavailable.

The Airborne Measurements of Methane Fluxes (AIRMETH) campaigns are designed to quantitatively and spatially explicitly address this question. While ground-based eddy covariance (EC) measurements provide continuous in-situ observations of the surface-atmosphere exchange of energy and matter, they are rare in the Arctic permafrost zone and site selection is bound by logistical constraints among others. Consequently, these observations cover only small areas that are not necessarily representative of the region of interest. Airborne measurements can overcome this limitation by covering distances of hundreds of kilometers over time periods of a few hours.

During the AIRMETH-2012 campaign aboard the research aircraft POLAR 5 we measured turbulent exchange fluxes of energy and methane along thousands of kilometers covering the North Slope of Alaska. Time-frequency (wavelet) analysis, footprint modeling, and machine learning techniques are used to extract spatially resolved turbulence statistics and fluxes, spatially resolved contributions of land cover and biophysical surface properties to each flux observation, as well as regionally valid functional relationships between environmental drivers and observed fluxes that can explain spatial flux patterns and – if available in temporal resolution – allow for spatio-temporal scaling of the observations.

Here we present a 100 m resolution gridded methane flux map for the North Slope of Alaska, covering about 90.000 km^2. We show that surface properties like elevation, temperature, and NDVI along with meteorological drivers such as shortwave radiation, water vapor mixing ratio, and horizontal wind speed are sufficient to explain and project the measured fluxes. The median methane flux for the campaign period (end of June/beginning of July) was 19.4 mg m^{-2} d^{-1} after excluding all values with $\geq$ 30 % standard error. The largest fluxes were observed along the coast and in the Arctic coastal plain, decreasing towards the Brooks Range.

The new field laboratory at the Samoylov Island observatory – possibilities of controlled high precision instrumentation to obtain new insights in environmental conditions of the high arctic lowland tundra.

Peter Schreiber, Moritz Langer, Niko Bornemann, & Julia Boike

Alfred Wegener Institute Helmholtz Centre for Polar and Marine Research, Potsdam, Germany

Samoylov Island and its surrounding areas of the Lena River Delta serve as a baseline observatory for the validation and development of remote sensing products and climate models in the Arctic. The observatory is located in a typical high latitude lowland tundra landscape and hence represents one of the dominating and most important landscape types in the Arctic. The observatory is equipped with leading edge environmental monitoring systems which are used to observe changes in permafrost and soils, vegetation, boundary layer meteorology, soil/water biology, energy- and trace gas fluxes, geomorphology, and snow cover.

Samoylov Island is located in the Lena River Delta in North Siberia (72°22' N, 126°30 E), and features a surface area off about 5 km^2. The continuous permafrost in the area reaches depths of 500 to 600 m. The investigation area is mainly located on a Late Holocene river terrace. The landscape is characterized by wet polygonal tundra which is typical for circumpolar lowlands. The climate is characterized by an average temperature of -12.5 °C with mean temperatures of -33.1 °C in February and 10.5 °C in July. The surface temperature is respectively cold with a mean annual value of -10.1 °C and the average temperature of the active layer is -8.4 °C (at 0.03 m depth). In August the mean thaw depth reaches 0.5 m. Within the last 9 years a continuous warming of the permafrost is observed (about 2.3 °C in 10.75 m depth and 1 °C in 20.75 m depth). The average summertime rainfall is about 125 mm with strong interannual differences. Snow water equivalent adds app. 30 % to the total precipitation. The snow free period usually lasts from the beginning of June to the mid of September. The total vegetation is dominated by mosses and lichen covering about 95 % of the surface while vascular plants coverer about 30%.

Since 1998, the observatory delivers one of the most valuable databases for the implementation of permafrost processes into land surface schemes of IPCC global climate models. Furthermore, extensive validation studies on thermal remote sensing (MODIS LST), snow products (GlobSnow), land surface classification (Landsat), and SAR satellite products (ASCAT Soil Moisture, TerraSAR-X) were implemented successfully. For the first time, operational satellite-based permafrost monitoring was developed and tested at the Samoylov observatory.

The excellent infrastructure of the observatory now will be enhanced by the HGF road map project 'Advanced Remote Sensing – Ground-Truth Demo and Test Facilities' (ACROSS, http://across-project.de) which focuses on the establishment of state of the art monitoring stations for testing new satellite sensors, model schemes, and scaling techniques. With the focus to provide outstanding research possibilities we designed a field laboratory to run high precision scientific instruments in a controlled environment. Away from any influence of the nearby Artic Research station a streamlined igloo-shaped, temperature controlled and power backed up lab container will placed in the middle of the Samoylov Island next to various already installed automated environmental observatories. Already installed is a safeguarded power supply from the Arctic research station and a boardwalk to the undisturbed investigation area. Together with a new 10 meters high research tower with several instrumentation platforms this new field lab will run within an area of still ongoing long time observations of the permafrost environment. While the placement of the tower is scheduled for April 2016, the field laboratory is planned to be installed in July 2016. In the future the notably load-bearing tower will be equipped with high performance devices to measure several meteorological and micrometeorological parameters at different heights while the lab igloo will provide 15 m^3 of space to place various instruments in a professional rack-infrastructure.

Samoylov Island has great potential to become a leading edge, multi-disciplinary observatory for

the validation and development of remote sensing products and earth system models for terrestrial Arctic ecosystems. We will present the development status of the new field lab facilities and will discuss the future possibilities to raise new research projects there. To frame this we will provide an overview of the already achieved longtime measurement results from main meteorological, soil and snow observatories since 1998.

Airborne measurements of greenhouse gas and energy fluxes in the Lena River Delta

Andrei Serafimovich[1], Eric Larmanou[1], Stefan Metzger[2,3], & Torsten Sachs[1]

[1] *GFZ German Research Centre for Geosciences, Telegrafenberg, 14473 Potsdam, Germany*
[2] *National Ecological Observatory Network, 1685 38th Street, Boulder, CO 80301, USA*
[3] *University of Colorado, 1560 30th Street, Boulder, CO 80303, USA*

Due to a strong Arctic warming trend, potentially large greenhouse gas emissions from Arctic and sub-Arctic areas are of concern. The Lena River Delta located in north-east Siberia is the largest delta within the Arctic Circle, characterized by wetland ecosystems and wet polygonal tundra environments. These environments are currently thought to be sinks for carbon dioxide and sources of methane.

Tower-based eddy covariance is the most widely used direct method for quantifying exchanges of momentum, energy and trace gases between the surface and the atmosphere. However, they cover a relatively small footprint and constitute point measurements relative to the vast extend of tundra ecosystems. To improve spatial coverage and spatial representativeness of these direct flux measurements, airborne eddy covariance flux measurements across large areas are required. We used the helicopter-carried measurement system "Helipod" equipped with a turbulence probe, fast temperature and humidity sensors, and a fast response gas analyzer to measure turbulent fluxes of heat, carbon dioxide, and methane across the Lena River Delta in Russia in 2012 and 2014. The 2014 campaign covered several periods of the season from April to August 2014.

Wavelet transforms are used to improve spatial resolution of the flux measurements and footprint analysis is applied to find relations between surface fluxes and biophysically relevant land cover properties. Strong regional differences in trace gas fluxes were detected, indicating a non-uniform distribution of sources especially in wet sedge-, moist grass-, and moss-dominated tundra. In contrast, the sensible heat flux showed less variability across the investigation area. The obtained results are essential in understanding the role of Arctic ecosystems in the greenhouse gas budgets and to evaluate regional scale model simulations.

Variability of surface energy fluxes over high latitude permafrost wetlands

Andrei Serafimovich[1], Stefan Metzger[2,3], Jörg Hartmann[4], Sebastian Wieneke[5], & Torsten Sachs[1]

[1] *GFZ German Research Centre for Geosciences, Telegrafenberg, 14473 Potsdam, Germany*
[2] *National Ecological Observatory Network, 1685 38th Street, Boulder, CO 80301, USA*
[3] *University of Colorado, 1560 30th Street, Boulder, CO 80303, USA*
[4] *Alfred Wegener Institute Helmholtz Centre for Polar and Marine Research, Bremerhaven, Germany*
[5] *Institute of Geophysics and Meteorology, Cologne University, 50969 Cologne, Germany*

Arctic ecosystems are undergoing a very rapid change due to global warming and their response to climate change has important implications for the global energy budget. Therefore, it is crucial to understand how energy fluxes in the Arctic will respond to any changes in climate related parameters. Attribution of these responses, however, is challenging because measured fluxes are the sum of multiple processes that respond differently to environmental factors.

Ground-based measurements of surface fluxes provide continuous in-situ observations of the surface-atmosphere exchange. But these observations may be non-representative because of spatial and temporal heterogeneity, indicating that local observations cannot easily be extrapolated to represent global scales. Airborne eddy covariance measurements across large areas can reduce uncertainty and improve spatial coverage and spatial representativeness of flux estimates. Here, we present the potential of environmental response functions for quantitatively linking energy flux observations over high latitude permafrost wetlands to environmental drivers in the flux footprints. We used the research aircraft Polar 5 equipped with a turbulence probe as well as fast temperature and humidity sensors to measure turbulent energy fluxes across the Alaskan North Slope.

We used wavelet transforms of the original high-frequency data, which enable much improved spatial discretization of the flux observations, and determine biophysically relevant land cover properties in the flux footprint. A boosted regression trees technique is then employed to extract and quantify the functional relationships between energy fluxes and environmental drivers. Using the extracted environmental response functions and meteorological fields simulated by the Weather Research and Forecasting (WRF) model, the surface energy fluxes were then projected beyond the measurement footprints across the entire North Slope of Alaska.

Seida landscape heterogeneity and regional GHG modelling

Narasinha J. Shurpali, Christina Biasi, Yu Zhang, Maija Marushchak, Tarmo Virtanen, & Pertti Martikainen

University of Eastern Finland, Finland

Arctic tundra ecosystems are among the world's fastest warming biomes. These ecosystems, underlain by permafrost, are extremely vulnerable to the impacts of anthropogenic climate change [Koven et al., 2013]. They have been a huge store for organic C since last glaciation. The current warming arctic trend poses a threat to these ecosystems as their soil temperature is likely to rise above 0 °C leading subsequently to the thawing of the underlying permafrost. While the fact that these ecosystems are fast undergoing changes has been established with a fair degree of certainty based on field data [Romanovsky et al., 2010], how these ecosystems will respond to the future climate is still uncertain. Therefore, with a view to understanding the future ecosystem responses better, we have modelled CO_2 and CH_4 methane exchange from the Seida region in the northeast European Russia. This region is not yet well represented in the Arctic studies. For the purpose, we have validated NEST-DNDC, a biogeochemical and permafrost model [Zhang et al., 2012] with the field GHG flux data from all major land cover types in the region classed with a high resolution (2.4 m pixel size) land cover classification scheme [Marushchak et al., 2013]. This study synthesizes data from working groups involved in an EU funded CARBO-North project whose broad objective was to quantify the carbon budget in Northern Russia across temporal and spatial scales. The model results are extended to include the impact of future climate by the end of the 21^{st} century using the HIRHAM5 regional climate model outputs. We present here a few scenarios highlighting the most probable changes in the regional landscape associated with thawing of the permafrost and consequent feedbacks to climate.

References

Koven, C.D.; Riley, W.J. and Stern, A. [2013]: Analysis of Permafrost Thermal Dynamics and Response to Climate Change in the CMIP5 Earth System Models. *J Climate*, 26:1877–1900, doi:10.1175/JCLI-D-12-00228.1.

Marushchak, M. E.; Kiepe, I.; Biasi, C.; Elsakov, V.; Friborg, T.; Johansson, T.; Soegaard, H.; Virtanen, T. and Martikainen, P. J. [2013]: Carbon dioxide balance of subarctic tundra from plot to regional scales. *Biogeosciences*, 10(1):437–452, 2013. doi:10.5194/bg-10-437-2013.

Romanovsky, V.E.; Smith, S.L. and Christiansen, H.H. [2010]: Permafrost thermal state in the polar Northern Hemisphere during the International Polar Year 2007–2009: a synthesis. *Permafrost and Periglacial Processes*, 21(2):106–116, 2010. doi:10.1002/ppp.689.

Zhang, Y.; Sachs, T.; Li, C. and Boike, J. [2012]: Upscaling methane fluxes from closed chambers to eddy covariance based on a permafrost biogeochemistry integrated model. *Global Change Biology*, 18(4):1428–1440, doi:10.1111/j.1365-2486.2011.02587.x.

Monitoring a decade of change in Pan-Arctic CO_2 and CH_4 exchange through integrated satellite remote sensing

Jennifer D. Watts & John S. Kimball

The University of Montana, United States of America

The effects of climate change within terrestrial Arctic ecosystems are evident in a lengthening non-frozen season, a deepening of the permafrost active layer, and contrasting shifts in regional surface water inundation, soil wetness and patterns of vegetation greening and browning. These biophysical processes play a crucial role in greenhouse gas (CO_2, CH_4) exchange and the stability of carbon reservoirs in permafrost and wetland systems. Yet the synergistic regulation of carbon cycling by surface environmental constraints within Arctic wetlands remains poorly characterized given sparse in situ monitoring networks and large landscape heterogeneity in vegetation cover, surface moisture and temperature. Regional carbon budget assessments and observations of seasonal and year-to-year changes in vegetation productivity, soil decomposition and CO_2 and CH_4 emissions to the atmosphere rely heavily on combined in situ sampling and biophysical modeling. However, carbon model intercomparisons and validation studies continue to reveal considerable disagreement in the sign, magnitude and spatiotemporal patterns of predicted carbon sink/source strength within pan-Arctic systems. Much of this uncertainty reflects inadequate representation of driving processes (e.g. soil moisture and thermal controls on vegetation phenology, productivity and soil respiration) in the models and input datasets.

The Terrestrial Carbon Flux (TCF) model was developed to diagnose and reduce uncertainty in global carbon budgets, emphasizing the use of satellite remote sensing observations to define primary control factors affecting net ecosystem CO_2 exchange (NEE) and component carbon fluxes [Yi et al., 2013]. The satellite data driven TCF model framework provides a platform to quantify daily, seasonal and inter-annual variability in vegetation gross and net primary productivity (GPP; NPP), surface soil organic carbon storage and greenhouse gas emissions to the atmosphere from aerobic and anaerobic soil decomposition processes. The use of integrated multi-channel passive microwave remote sensing observations from AMSR-E and AMSR2 (on Terra and GCOM-W1 satellites), and new L-band retrievals from the NASA Soil Moisture Active Passive (SMAP) mission, provides a comprehensive assessment of daily changes in vegetation growth characteristics, surface water inundation, freeze/thaw state, and near-surface soil thermal and moisture conditions, with relative insensitivity to solar illumination constraints and signal attenuation from atmosphere contamination. These microwave based retrievals are used in conjunction with MODIS optical remote sensing and reanalysis data to estimate daily NEE, GPP, and ecosystem CO_2 loss through respiration (Reco). An anaerobic carbon cycling and CH_4 emissions component also allows the TCF model framework to effectively assess changes and regional contrasts in northern high latitude wetland ecosystem carbon budgets [Watts et al., 2014a].

The integrated TCF CO_2 and CH_4 model has been verified for boreal and tundra environments using tower eddy covariance records from sites in Alaska, Canada, Greenland, Sweden, Finland and Russia. The TCF model validations show favorable carbon flux accuracies of < 1.4 g C-CO_2 $m^{-2}d^{-1}$and < 0.02 g C-CH_4 m^{-2} d^{-1} (Root Mean Square Error) relative to eddy covariance observations when using relatively coarse input 1-km resolution MODIS (MCD15A3) FPAR and 0.5 degree NASA Global Modeling and Assimilation Office (GMAO) reanalysis meteorology. Model input satellite passive microwave (AMSR, SMAP) and ENVISAT Advanced Synthetic Aperture Radar (ASAR) retrievals provide multi-resolution characterization of fluctuating land surface soil moisture and inundation, including open water bodies and emergent vegetation, and high temporal regulation of anaerobic processes and CO_2 to CH_4 emission ratios [Watts et al., 2014b]. Regional TCF model simulations over the 2003 to 2014 period indicate that pan-Arctic CH_4 emissions can considerably reduce the net ecosystem carbon sink and may contribute to a positive net global warming potential. The TCF model simulations and satellite remote sensing records emphasize the importance of continued carbon flux monitoring to differentiate interannual climate variability and associated impacts on

Arctic carbon budgets from longer-term trends. The integrated TCF model framework provides the capability to monitor daily, pan-Arctic changes in carbon sources and sinks at a 1-km spatial resolution, improving our understanding of ecosystem vulnerability to carbon loss under a warming climate.

References

Watts, J. D.; Kimball, J. S.; Parmentier, F. J. W.; Sachs, T.; Rinne, J.; Zona, D.; Oechel, W.; Tagesson, T.; Jackowicz-Korczyński, M. and Aurela, M. [2014a]: A satellite data driven biophysical modeling approach for estimating northern peatland and tundra CO_2 and CH_4 fluxes. *Biogeosciences*, 11(7): 1961–1980, doi:10.5194/bg-11-1961-2014.

Watts, J.D.; Kimball, J.S.; Bartsch, A. and McDonald, K.C. [2014b]: Surface water inundation in the boreal Arctic: potential impacts on regional methane emissions. *Environmental Research Letters*, 9: 075001, doi:10.1088/1748-9326/9/7/075001.

Yi, Y.; Kimball, J.S.; Jones, L.A.; Reichle, R.H.; Nemani, R. and Margolis, H.A. [2013]: Recent climate and fire disturbance impacts on boreal and arctic ecosystem productivity estimated using a satellite-based terrestrial carbon flux model. *Journal of Geophysical Research: Biogeosciences*, 118(2):606–622, doi:10.1002/jgrg.20053.

Studies on carbon dioxide fluxes of alpine meadows at non-growing season in the continuous permafrost zone of the Qinghai-Tibet Plateau

Hanbo Yun, Qingbai Wu, Jing Luo, & Fujun Niu

Cold and Arid Regions Environmental and Engineering Research Institute (CAREERI) of the Chinese Academy of Sciences, People's Republic of China

As a sensitive region to global climate change and ecologically fragile region, Qinghai-Tibetan Plateau owns a large carbon pool, which plays an important role in global environmental changes. Land surface process in cold region had changed a lot with the climate change and the water-heat coupling of soil changed accordingly. This process will cause the reduction of soil organic matter input and damage of the protection layer, which gives rise to the increase of the soil organic matters decomposition rate and the positive feedback to the climate change.

The evaluation of the sink and source effect of CO_2 and the systematic analysis of its changing pattern and impact factors are important to the comprehensive understanding of the carbon cycle and mechanism of permafrost of the Qinghai-Tibetan Plateau. The magnitude, patterns and environmental controls of CO_2 emissions on different timescales, especially during the non-growing season, remain poorly understood, because of technical limitations and the harsh environments.

We conducted the first study on year-round CO_2 fluxes in an alpine meadow using the newly developed Li-cor 7500A open-path gas analyzer. Sites were located in continuous permafrost zone of the Qinghai-Tibet Plateau, China.

The results show that the total annual CO_2 emissions were -12.78 and -15.83 g/m^2 in 2012 and 2013, respectively. Non-growing season play an important role for CO_2 annual emissions, it accounted for 32.2–38.1 % of the annual emissions, highlighting an indispensable contribution that was often overlooked by previous studies. A two-peak seasonal variation in CO_2 fluxes was observed, with a small peak in the active layer thawing period and a large one in the growing season. Diurnal variation of CO_2 fluxes has a significant difference between the two seasons, growing season with two peaks and one peak in the non-growing season. The CO_2 fluxes during the growing season were well correlated with soil temperature, soil water content, net radiation and during the non-growing season were only highly correlated with soil temperature. Summer rainfall events may affect CO_2 flux, for example, CO_2 flux increased sharply following thundershower in August, but now we don't have a precisely quantification.

Additionally, our data suggest that active layer grazing and thawing significantly alters the CO_2 fluxes. However, more measurements of alpine meadow at permafrost sites are needed to assess active layer depth of freezing and thawing might affect the CO_2 fluxes at a larger regional or global scale.

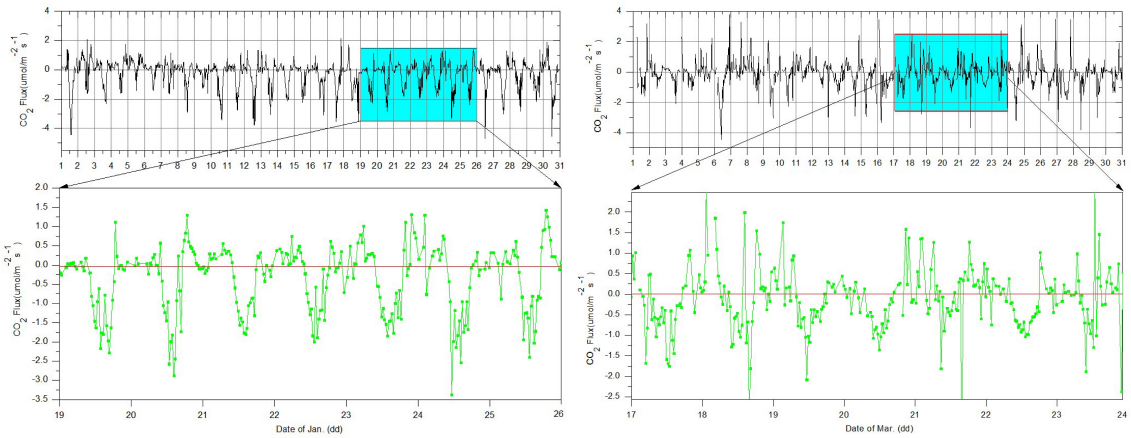

Figure 1: CO_2 fluxes

Variability of methane and carbon dioxide fluxes at permafrost peatland in the European Northeast

Svetlana Zagirova & Mikhail Miglovets

Institute Biology Komi Science Centre, Russian Federation

Bogs play an important role in preservation of soil carbon stocks in northern hemisphere. Increasing of GHG emission to atmosphere can be caused by climate warming and thawing of ice core in permafrost peatlands in the XXI century. Fluxes of methane and carbon dioxide is variability and can be effected by plant communities and weather that it is necessary to consider at estimation of emission GHG in peatland landscape in a whole.The study was carried out in May-September 2014 and 2015 years at palsa mire Kulitsanjur (65°54'10 N, 60°26'40" E) in Inta district of the Komi Republic, located on southern border of permafrost zone. Long-term frozen peat soils occupy about 11 % of the peatland area. Measurements of methane and carbon dioxide fluxes were made using of static dark chambers method and portable gas analyzer GGA-30p (Los Gatos Research, USA) on five sites with differen plant communities. Short-term strengthening of emissions of methane up to 0.9 mkg m^{-2} s^{-1} was observed in the end of May with the beginning of thawing of the upper peat horizon at palsa. Lichen communities absorbed methane from atmosphere in summer. Insignificant methane emission was observed from a peat spot surface.The most active emission of methane into atmosphere was noted at *Sphagnum-Ledum* and *Sphagnum-Eriophorum* communities on oligotrophic sites. Distinctions in weather conditions in 2014 and 2015 years have not affected intensity of methane emission at palsa, however it's variability was established for Sphagnum-Ledum and Sphagnum-Eriophorum communities on oligotrophic sites. The maximum values of carbon dioxide flux observed from a surface of lichen-shrubbery communities of palsa and *Sphagnum-Ledum* and *Sphagnum-Eriophorum* communities on oligotrophic sites (a median of 51 mkg m^{-2} s^{-1}). Using of a method Principal components analyses/PCA allows to establish that the temperature of air and peat describe more than 50 % of variability of GHG emission dispersion at palsa. Methane emission has been interfaced to peat temperature on depth of 20 sm (r^2=0.2, $p < 0.05$), at the same time change of carbon dioxide emission had weak communication with peat temperature (r^2=0.09/0.06, $p < 0.05$). It was assumed that with destruction of palsa mires and increasing of wetland areas emission of GHG into atmosphere will increase in the region.

SESSION 7

Reconstructing Past Permafrost: Spatial Distribution and Temporal Changes

Convener:

Marc Luetscher, *Austrian Academy of Sciences, Austria*

Susan Ivy-Ochs, *ETH-Zurich, Switzerland*

Josefine Lenz, *Alfred Wegener Institute Helmholtz Centre for Polar and Marine Research, Germany*

Understanding the long-term dynamics of permafrost is fundamental to quantify processes affecting the climate and landscape evolution. Whilst geomorphological features including ice-wedge pseudomorphs, cryoturbations and rock-glaciers are key for the identification of relict permafrost, chronological constraints are often difficult to achieve. Open questions include:

1. What was the maximum extent of permafrost during the last glacial cycle?
2. When did the last permafrost maximum occur regionally?
3. How did it respond to climate forcing?
4. Can the rate of permafrost thawing during the past be constrained?

This session invites contributions from observational and modelling studies.

The French Pleistocene permafrost database: GIS-based analysis and OSL dating of sand wedges

Eric Andrieux[1], Pascal Bertran[1,2], Mark Bateman[3]

[1] *PACEA, Université de Bordeaux, PACEA, France*
[2] *Inrap, Bègles, France*
[3] *University of Sheffield, Sheffield, UK*

GIS analysis of the French database of Pleistocene periglacial features allows an improved evaluation of the maximum extent of past permafrost. The distribution of typical ice-wedge pseudomorphs and composite wedges does not extend south of the Paris basin. The exclusive presence of sand wedges with primary infill between 45 and 47°N, mainly in the periphery of coversand areas, suggests that thermal contraction cracking of the ground occurred together with sand drifting in a context of deep seasonal frost or sporadic discontinuous permafrost, unfavourable for the growth of significant ground-ice bodies. The latitudinal variation of the wedge dimensions clearly shows that the sand wedges were located in the southern margin of the area affected by thermal contraction.

OSL dating of 14 sand wedges from southwest and central France provides an insight into the chronology of permafrost development. Because several contraction phases are recorded within a single sand wedge, single grain OSL dating of multiple samples for each wedge was used. The first results show that the peaks of thermal contraction fit with the Heinrich stadials which occurred during coversand deposition, i.e. HS3 to 1. Some wedges also provide evidence for renewed contraction during the Younger Dryas.

Permafrost and large ice wedge pseudomorphs in Last Glacial European loess series: a northern France perspective

Pierre Louis Antoine[1], Olivier Moine[1], Guérin Gilles[2]

[1] *UMR 8591 CNRS-Universités Paris I & UPEC. Laboratoire de Géographie Physique, Environnements quaternaires et actuels, Meudon, France*
[2] *Laboratoire des Sciences du Climat et de l'Environnement, IPSL, CEA-CNRS-UVSQ, Domaine du CNRS, Gif-sur-Yvette, France*

The great European Loess Belt is the most extensive continental archive of the Last Glacial period (Weichselian) in Europe. During the Last Glacial, this large area was ideally situated to record the impact of climatic fluctuations occurring in the North Atlantic region (Dansgaard-Oeschger cycles). Since a large part of Europe was affected by periglacial processes during the Last Glacial, permafrost studies and modelling aiming at reconstructing past fluctuations and associated impacts on landscape changes have generated an important research effort. Besides, in the frame of the investigations focusing on the most continuous loess-palaeosols records of this area (pedostratigraphy, dating, sedimentology, malacology), numerous evidences of periglacial features have been evidenced, especially ice-wedge pseudomorphs. By comparison with present-day high-latitude tundra environments, these features are considered as the best witnesses of permafrost conditions in northwest Europe. In the western part of the European Loess Belt, large networks of ice wedge pseudomorphs and thermokarst gullies and related infillings (TK features) have been studied and dated (OSL & ^{14}C) during the last 10 years. Recently, it is proposed that both features represent the two extreme states of Dansgaard-Oeschger cycles. In this presentation we

will focus only on the ice-wedges pseudomorphs from western European loess-palaeosols records. According to these researches ice-wedge pseudomorphs correspond to epigenetic ice-wedge forming large polygonal networks (10 – 20 m in diameter) identified as several successive levels separated by loess deposits within the Last Glacial sequences. Recent works lead in northern France, have allowed to start a new research effort allowing the evidencing of at least four distinct episodes of epigenetic ice-wedge pseudomorphs between ca. 45 and 23 – 22 ka. They are systematically connected with tundra gley horizons representing former permafrost active layers. According to malacology, sedimentology and dating tundra gleys are allocated to short interstadials of the NGRIP record. According to their distribution in Europe it is clear that these features are typical of the Western European loess domain where they are connected with relatively ice-rich permafrost environments. However, using accurate dating of the former loess infilling of the various ice-wedge casts, and detailed correlations with the Greenland reference records (NGRIP), it appears that ice-wedge networks have developed only during some (specific) stadials phases. These features thus typify original palaeoenvironmental and palaeoclimatic conditions that are still to be evidenced in the frame of a modelling approach involving sea-ice extent, Inlandsis dynamics, atmospheric circulation, and NGRIP temperature reconstructions.

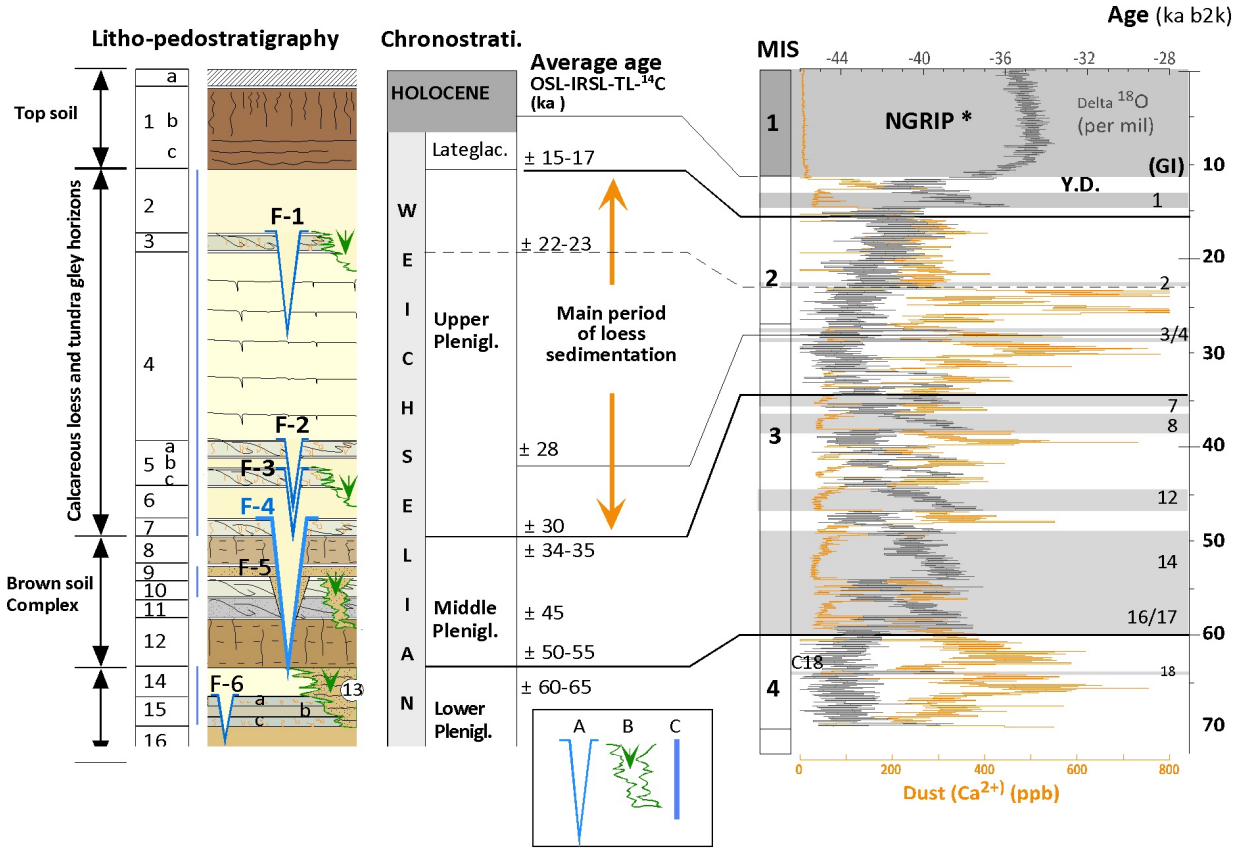

Figure 1: The main ice-wedge pseudomorph networks in the loess-palaeosols record of Northern France between and 23-22 ka (According to Antoine et al., 2014, modified).

Periglacial features and permafrost disappearance in the last glaciated area in N-Poland and NE-Germany

Andreas Börner[1] & Mirosław Błaszkiewicz[2]

[1] *State authority for Environment, Nature protection and Geology of Mecklenburg-Western Pomerania, Germany*
[2] *Polish Academy of Sciences, Institute of Geography and Spatial Organization*

At the time of the maximum Late Weichselian ice-sheet advance, very harsh climatic conditions prevailed. A large discussion, however, is raised by the issue of the permafrost existence in the Last Glaciation area. Recent studies of the areas covered by the last glaciation indicate that the disappearance of permafrost under the ice sheet was not complete, and even that it was limited only to the subglacial water circulation zones. More recently, in the last-glaciated area the possibility of partial preservation of permafrost under the ice sheet originating from the transgression period has been considered. An important argument in this discussion is the important role of permafrost under the ice sheet in the formation of subglacial drainage and subglacial channels [Piotrowski et al., 2009].

In the course of research in the Last Glaciation area some evidence pointing to encroachment of permafrost on the land released from the ice sheet were brought together. The most important include thermal contraction cracks, oriented kettle holes on outwash plains, permafrost-affected horizons in soil profiles, as well as the long-term preservation of buried dead ice blocks in depressions.

From the point of view of the appearance of lake deposits, three main lake generations were distinguished:

1. "early" pre-Allerød lakes,
2. lakes of the Bølling-Allerød complex and
3. "late" generation of lakes, generated during the Preboreal period.

In the context of the time of the final permafrost decay, the lakes of the youngest, Preboreal generation are particularly important, since the lakes age differentiator was the varied length of preservation of lake basins by buried dead ice blocks, which in turn was dependent primarily on the conditions of surface drainage network. The buried ice was preserved until the Preboreal period justifies the thesis about the preservation of permafrost patches. Under the permafrost conditions, full preservation of dead ice blocks took place when the mineral cover reached the thickness corresponding to the depth of the active layer. In this way, buried dead ice blocks became an essential element of the permafrost. Under thermokarst, at the places where dead ice blocks existed, quickly spreading taliks formed, which greatly hastened the process of permafrost degradation.

In the northern parts are some local evidences of periglacial features, like meso scaled ice wedges pseudomorphs and ball-and-pillow graviturbations, showing clearly the retreat of discontinious permafrost during Younger Dryas period.

This study is a contribution to the Virtual Institute of Integrated Climate and Landscape Evolution Analysis (ICLEA) of the Helmholtz Association.

References

Piotrowski, J.A.; Hermanowski, P. and Piechota, A.M. [2009]: Meltwater discharge through the subglacial bed and its land-forming consequences from numerical experiments in the Polish lowland during the last glaciation. *Earth Surface Processes and Landforms*, 34(4):481–492, doi:10.1002/esp.1728.

Active and fossil permafrost in the glacier-permafrost system. Storglaciären, Kebnekaise, Northern Sweden

Wojciech Dobiński & Michał Glazer

University of Silesia, Poland and Centre for Polar Studies KNOW (Leading National Research Centre) WNoZ UŚ

Introduction

Kebnekaise region of northern Sweden is a place where research on glacier and permafrost is conducted since 60. of the 20^{th} century [King and Seppälä, 1988]. Also in this area, on Tarfalaryggen (67°55'09"N, 18°38'29 " 1550 m a.s.l.) is located 100 m deep drillhole. Soil temperature monitoring is conducted in it since 20 March 2000. The extrapolated results of ground temperature measurements indicate that the maximum depth of permafrost located there can reach the depth ca. 350 meters below the ground surface [Isaksen et al., 2001]. The history of climate change shows that since the end of glaciation in the Tarfala valley favorable conditions for permafrost preservation always prevailed in this region in greater or lesser extent [Karlén, 1976]. The fluctuations of climate affect the evolution of permafrost occurring here as a result of the climate impact which change in a manner analogous to the change of air temperature. Those conditions led us to formulate hypothesis that permafrost currently occurring in this region may be associated both with the modern climate, as well as the early Holocene or past glacial period. Contemporary climatic conditions are responsible for existence of shallow located permafrost layer. It is possible however that permafrost from earlier geological periods may be located deeper in the ground.

Another aspect of the research is the relationship of permafrost with the retreating glacier. The recession of the Storglaciären takes place under conditions where the mean annual air temperature (MAAT) is about -4 °C. This means that despite the warming causing the recession of the glacier prevailing climatic conditions allow for permafrost aggradation on the forefield abandoned by the glacier. Polythermal nature of the glacier is also significant for the development of permafrost in its immediate vicinity.

Fieldwork research and results.

Extensive geophysical surveys were done both on the Storglaciären and in its immediate vicinity in order to verify the hypothesis accepted. Studies conducted on the glacier have to identify the boundary between warm and cold ice and the place in which the toe of the glacier is frozen to the glacier bed. To this aim a profiling using GPR with antennas 100 and 200 MHz were made. This ground-penetrating radar was used also in the forefield to identify the possible presence of dead ice blocks. The main aim of the study of glacial forefield, however, was to determine the depth of seasonal thawing (permafrost table) and the depth of permafrost (permafrost base). For this purpose, electroresistivity profiling method was used, with the device Terrameter LS.

About 3000 m GPR profiles were made showing the structure of the thermal structure of glacier both in longitudinal and transverse directions. In the forefield were made 5 ERT profiles with a length of 100 to 400 meters using electrodes minimal spacing 1 to 5 meters. The results obtained allowed to determine the course of cold-temperate transition surface (CTS) inside the glacier, and identify the place from which frozen to the ground part of the glacier begins. Where the ice freezes to the bedrock its temperature is lower than the temperature of the warm-ice with temperature equal to the pressure melting point. This condition allows permafrost for aggradation also under a glacier, beginning at the line where it starts freezing to the bed. It can be assumed that permafrost develops from this place, and not from the glacier margin. Permafrost aggrading in this way is also present further on the glacier forefield as a specific continuum in periglacial conditions. In order to detect the permafrost on the forefield the ERT profiling method was used. The use of different electrode spacings made possible to identify in the interpreted profiles the depth of the active layer as well as the permafrost base.

According to the accepted assumption consisting

the integral approach in description of the of cryospheric components, interpretation of results of geophysical research, within the scope of traditional approach of separate treatment glacier and permafrost was rejected [Dobiński, 2006]. Penetration of the cold wave which is an effect of the climate occurring during the winter season includes in a similar way both: glacier and its forefield. The same situation can be found in the summer when thawing of active layer is associated with warming of the climate. In the forefield, however, thickness of the thawed layer can be measured. In glacial environment – not. In the glacier active layer in it periglacial sense does not occur. It existence is not possible due to the melting of the ice layer in which the temperature rises above 0 °C. Here, the thickness of the seasonal thaw can be defined as the thickness of layer of which surface of the glacier decreasing during the summer season. The surface of the glacier at the end of ablation period can be compared to the permafrost table on the glacier forefield. The thickness of glacial permafrost and periglacial permafrost on the forefield is limited on the top by surface of 0 °C, which runs continuously as the surface of the glacier and then goes into the surface of permafrost table at 0 °C in glacier forefield (in periglacial conditions). Layer of cold-ice in glacier is limited in the bottom by the another surface which calls cold-temperate transition surface (CTS) [Pettersson et al., 2007], this surface on the forefield corresponds to 0 °C, surface which constitutes the lower limit of frozen soil - permafrost base (PB). Also this lower surface extends continuously from the glacial environment to periglacial one.

Conclusions

It can be concluded that the described surfaces of 0 °C that occur in the summer / ablation season on the glacier surface and in its forefield, as well as the CTS-PB surface constitute a specific environmental axis in relation to which ice and permafrost evolving as the elements of the same cryosphere. ERT research made on the forefield shows additional variations in the permafrost occurrence (Fig. 1). In this area not only the permafrost associated with currently existing climate was detected. Under the layer of shallow, contemporary permafrost much deeper layer of fossil permafrost is located, which was established much earlier and is probably a remnant of the earlier cold periods. It may be at least partly beyond the reach of modern seasonal climate changes. Without an accurate knowledge of the past climate evolution of the research area it is difficult to calculate its age but it is not excluded that, if even for a short period in the Holocene when MAAT temperatures in the study area was positive, the permafrost of the last glacial period could survive this warming. Such a conclusion also indirectly justifies the thickness of permafrost in the borehole at Tarfalaryggen. Permafrost with a thickness of 350 m is probably older than Holocene.

The CTS-PB surface can be seen as a specific axis in glacial / periglacial environments, which through termophysical process of freezing / thawing affect the physical properties of both of them. Examine the properties of this surface and its variability in time may allow a better understanding of the dynamic relationship present in the cryosphere also on a wider scale.

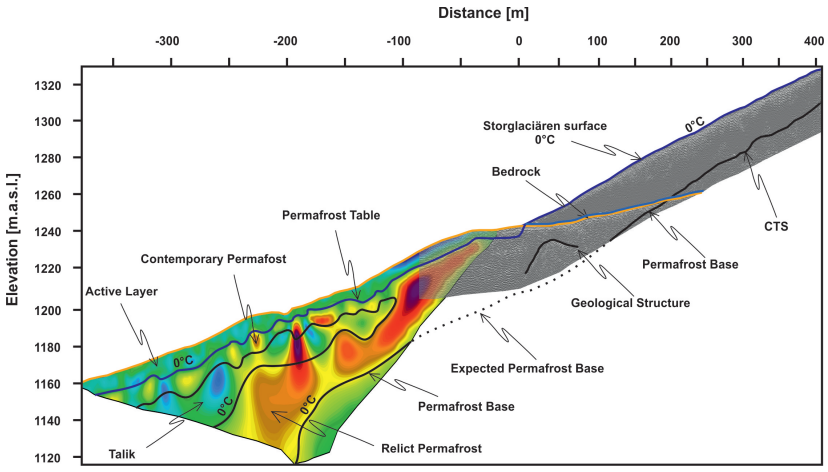

Figure 1: Results of the permafrost research in Storglaciaren and its forefield based on GPR and ERT methods

Acknowledgements

This research has been supported by the National Science Centre, Poland, grant no. DEC-2012/07/B/ST10/04268, and Centre for Polar Studies, Leading National Research Centre, KNOW, Poland. AMDG. The project has been also financed from the funds of the Leading National Research Centre (KNOW) received by the Centre for Polar Studies for the period 2014-2018.

References

Dobinski, W. [2006]: Ice and environment: A terminological discussion. *Earth-Science Reviews*, 79(3–4): 229 – 240, doi:10.1016/j.earscirev.2006.07.003.

Isaksen, K.; Holmlund, P.; Sollid, J. Ludvig and Harris, C. [2001]: Three deep Alpine-permafrost boreholes in Svalbard and Scandinavia. *Permafrost and Periglacial Processes*, 12(1):13–25, doi:10.1002/ppp.380.

Karlén, W. [1976]: Lacustrine sediments and tree-limit variations as indicators of Holocene climatic fluctuations in Lappland, northern Sweden. *Geografiska Annaler*, 58A(1–2):1–33.

King, L. and Seppälä, M. [1998]: Permafrost sites in Finnish Lappland and their environment. In *Proceedings of the Fifth International Conference on Permafrost*, volume 1, pages 183–188, Trondheim, Norway, August 2–5, 1988.

Pettersson, R.; Jansson, P.; Huwald, H. and Blatter, H. [2007]: Spatial pattern and stability of the cold surface layer of Storglaciären, Sweden. *Journal of Glaciology*, 53(180):99–109, doi:10.3189/172756507781833974.

Tracking the southern boundary of the Late Pleistocene permafrost in the Ural Mountains using cryogenic cave carbonates: a feasibility study

Yuri Dublyansky[1], Olga Kadebskaya[2], Mark Luetscher[1], Hai Cheng[3], Gabriella Koltai[1], & Christoph Spötl[1]

[1]*Leopold-Franzens-Universität, Institute of Geology, Innsbruck, Austria*
[2]*Mining Institute, the Ural Branch of the Russian Academy of Sciences, Perm, Russia*
[3]*Xi'an Jiaotong University, Institute of Global Environmental Change, China*

Cryogenic cave carbonates (CCCs) form by freezing-induced segregation and require the presence of both liquid water and freezing temperatures (i.e., the 0 °C isotherm). The latter situation occurs in conditions of degrading permafrost, when the active layer reaches the cave ceiling, whilst the permafrost persists at deeper levels of the cave. Because CCCs can be accurately dated using U/Th, they may be used to identify and date events of the (degrading) permafrost conditions during the past c. 600 ka.

In this study, CCCs were sampled in five caves, located along a 1000 km-long transect from the Northern (60.4° N) through the Central (58.5° N) to the Southern Ural (56.8°N). In addition, "common" speleothems, such as stalagmites and flowstone were sampled as markers of permafrost-free conditions. All studied caves are located between 240 to 340 m a.s.l. and, therefore, not affected by any altitudinal factors.

Five U/Th analyses of CCCs from three caves were reported by Chaikovskiy et al. (2014): 16.7±0.3 ka and 104.8±1.5 ka (Divja Cave, the Northern Ural); and 13.4±0.3 ka, 86.5±0.8 ka and 125.3±1.2 ka (Rossijskaya and Usvinskaya Caves, the Central Ural). In this study we obtained 12 additional U/Th ages from Rossijskaya Cave (between 129.4±0.5 ka and 661±100 ka). Further, we identified for the first time, and obtained five U/Th ages from CCCs in two caves in the Southern Ural: Shulgan-Tash and Victoria (between 33.3±0.1 ka, and 53.4±0.2 ka).

Ages older than ca. 450 ka have large analytical uncertainties and cannot be attributed to specific stages of the Pleistocene glaciations. Most of the ages <450 ka from the Northern and the Central Ural cluster near glacial Terminations V, II and I. Importantly, in this part of the Ural Mountains permafrost developed not only during major glaciations, including MIS 6 and MIS 2, but also in response to smaller-scale cooling episodes (MIS 5d and MIS 5b). In the Southern Ural permafrost was present in relatively shallow subsurface (30-50 m) during certain stages of MIS 3.

Chaykovskiy et al., 2014, Geochemistry International, 52, 4, 336–346.

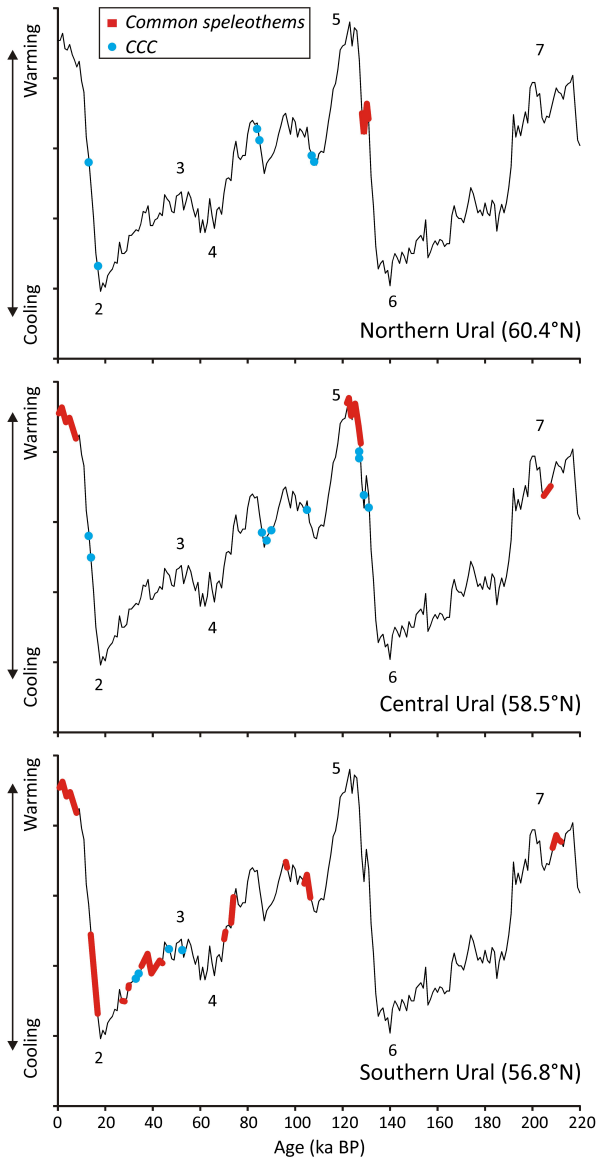

Figure 1: U/Th ages of cryogenic cave carbonates (CCC) and common speleothems from Northern, Central, and Southern Ural, compared to the paleoclimate curve based on benthic oxygen isotopes (LR-04). Numbers are Marine Isotope Stages (MIS).

On ice-age glaciers and permafrost in connection with radioactive waste repositories in northern Switzerland

Wilfried Haeberli[1], Denis Cohen[2], & Urs H. Fischer[3]

[1] *Geography Department, University of Zurich, Switzerland*
[2] *Department of Geological and Atmospheric Sciences, Iowa State University Ames, USA*
[3] *National Cooperative for the Disposal of Radioactive Waste, Nagra, Wettingen, Switzerland*

The long-term management of radioactive waste produced through the use of radioactive materials in power production, industry, research and medicine entails its containment and isolation within deep geological repositories over hundreds of thousands of years. Over such extended time periods, the performance of repositories in mid- and high-latitude regions can be affected by impacts from future ice-age conditions. Several countries have developed programs to investigate potential future ice-related environmental changes and their effects at depth [Fischer et al., 2014]. Primary aspects thereby concern deep erosion by glaciers or ice sheets, penetration of permafrost to great depth, changes in groundwater hydrology imposed through surface and subsurface ice as well as their complex interactions. Two main sources of information are being used:

a) qualitative and quantitative information about regional climate and ice conditions during past ice ages and especially the Last Glacial Maximum (LGM) as interpreted from paleoclimatic and paleo-ice proxies, and

b) numerical modelling of complex and strongly coupled ice/climate systems.

During the LGM, central Europe experienced extremely cold and dry conditions caused by the penetration of winter sea ice to low latitudes in the Atlantic Ocean and the corresponding closure of the primary humidity source north of the Alps. At this stage, flat and extended lobes of large piedmont glaciers spreading out over much of the Swiss Plateau were polythermal, characterized by low driving stresses (typically around 30 kPa) and surrounded by continuous periglacial permafrost [Haeberli et al., 1984] up to 150 m thick. Subsurface temperatures and groundwater flow conditions were strongly influenced by the presence of extended surface and subsurface ice. Glacial erosion in the ice-marginal zones with cold ice frozen to subglacial permafrost was probably limited due to strongly reduced basal sliding and melt-water flow. More humid conditions with higher flow velocities, increased basal sliding and stronger erosion by abrasion and melt-water effects must have prevailed during ice advance across the Swiss Plateau. Rapid down-wasting or even collapse (calving instability in lakes) is likely to have taken place during the retreat phase back into the Alpine valleys. It appears plausible to assume that similar cycles were characteristic for past ice ages in general and could also be characteristic for future ice-age conditions in northern Switzerland.

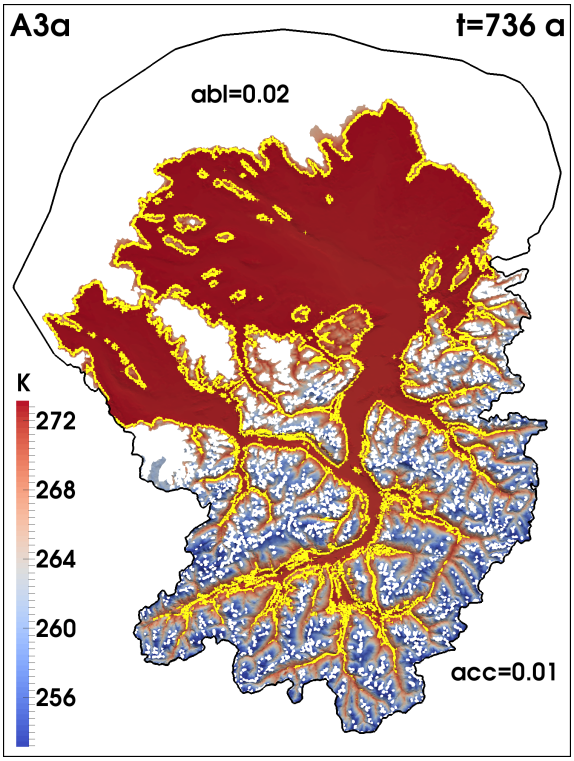

Figure 1: Modelled basal temperature of the Rhine glacier at the LGM. The yellow line outlines extent of temperate ice. Mass balance gradients used for the model run are 0.02 m per 100 m and year in the ablation area and 0.01m per 100m and year in the accumulation area.

Numerical simulations of the flow of the Rhine glacier at the LGM (Fig. 1) were carried out using Elmer, a finite element numerical model that solves the coupled three-dimensional heat, mass, and momentum equations for Stokes flow. The model is initialized using the reconstructed ice geometry. After adjusting this glacier geometry in order to eliminate unphysical velocity fields resulting from reconstruction artefacts a best fit with the geomorphological reconstructions (extent) was obtained with extremely low mass balance gradients [Cohen et al., 2015]. This result supports that climatic conditions of a cold desert must have existed during the LGM. Nevertheless, while the ice margins are cold and frozen to subglacial permafrost large parts of the modeled piedmont ice lobe are warm-based (Fig. 1). Because the proposed sites for the radioactive waste repositories are located in the marginal zones of ice-age glaciations, the involved glacier-permafrost interactions and their influence on deep groundwater hydrology must be considered. One key aspect thereby is the question whether permafrost is already in place when the ice margin advances over it. Such a development could lead to complex transient conditions of inverse heat flow from glacier parts near melting conditions into still frozen ground. In addition, the cold ice margin with subglacial permafrost represents an important hydraulic barrier to groundwater flow and may cause elevated water pressure in the transition zone from warm- to cold-based ice. This elevated water pressure increases basal sliding and, hence, erosion further up-flow beneath warm-based parts of the glacier.

References

Cohen, D.; Haeberli, W.; Fischer, U.H. and Machguth, H. [2015]: Mass balance reconstruction for the Rhine glacier, Swiss Alps, at the Last Glacial Maximum from three-dimensional thermo-mechanical modeling. In *Geophysical Research Abstracts 17, 2015 EGU General Assembly.*

Fischer, U.H.; Bebiolka, A.; Brandefelt, J.; Follin, S.; Hirschorn, S.; Jensen, M.; Keller, S.; Kennel, L.; Näslund, J.-O.; Normani, S.; Selroos, J.-O. and Vidstrand, R. [2014]: Radioactive waste under conditions of future ice ages. In *Snow and Ice-Related Hazards, Risks and Disasters*, pages 345–393. Elsevier.

Haeberli, W.; Rellstab, W. and Harrison, W.D. [1984]: Geothermal effects of 18ka BP ice conditions in the Swiss Plateau. *Annals of Gaciology*, 5:56–60.

Formation Chronology of Arsain Pingo, Darhad Basin, northern Mongolia

Mamoru Ishikawa[1] & Jambaljav Yamkhin[2]

[1] *Hokkaido University, Japan*
[2] *Institute of Geography and Geoecology, MAS, Mongolia*

Pingos are perennial frost mounds consisting of a core of massive ice, produced primarily by injection of water, and covered with soil and vegetation. They are prominent periglacial features in the Arctic and Subarctic, and a direct indicator of groundwater activity in permafrost environments. In areas of continuous permafrost, closed-system (hydrostatic) pingos may form after lakes underlain by a talik fully or partially drain, and the talik begins to refreeze. In zones of discontinuous permafrost, most open-system (hydraulic) pingos are found in areas of significant topographic relief, where conditions favor the development of hydraulic gradient and provide sub-permafrost or intra-permafrost aquifers for groundwater upwelling.

Pingos occur predominantly in pan-Arctic lowlands in continuous or discontinuous permafrost. Grosse and Jones [2011] identified more than 6,000 pingos in northern Russia. Information about pingos of the southerner regions, where permafrost distribute discontinuously, however, is still scarce. The aim of this study was to determine the formation chronology of pingos in Darhad basin, northern Mongolia, at the southern fringe of the north-eastern Eurasian permafrost zone.

Numerous pingos exist on the meander belt and alluvial fan around Arsain Gol River. In this environment, abundant water supply and inter-permafrost taliks may allow the development of artesian pressure that leads to groundwater upwelling. The Arsain pingo was drilled to a depth of 35m to determine the stratigraphy, and data were collected on ground-ice stable isotopic composition, electrical resistivity, ground temperature, and radiocarbon dating and interpreted in conjunction with the chronology of paleo-lake retreat in the basin (Fig. 1).

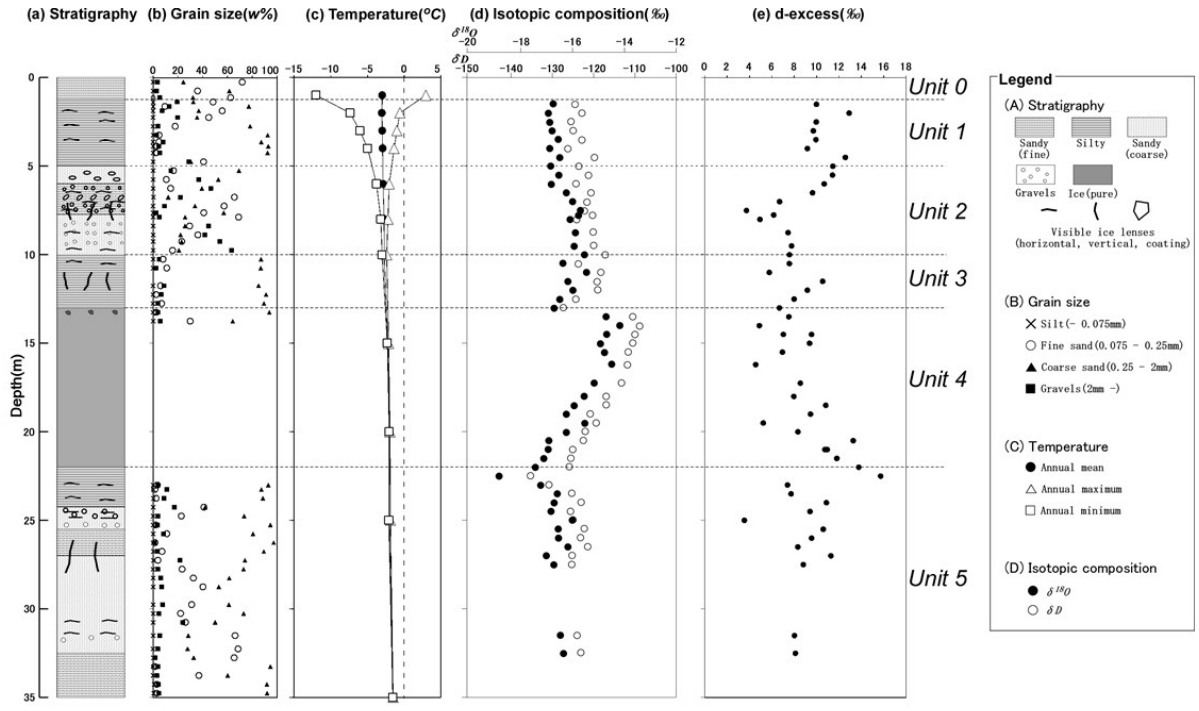

Figure 1: Results of drilling investigations on the top of the Arsain pingo.

A 10m thick ice core sandwiched between fine-grained lacustrine sediments was identified by drilling and electrical resistivity tomography. Stable isotope values of ice core samples indicated Rayleigh-type isotope fractionation during the freezing of liquid water. Consequently, closed-system freezing of artesian groundwater appears to be the driving mechanism of pingo formation. Near-surface, segregated ground ice formed from the open-system freezing of meteoric water, concurrent with pingo growth. Considering the history of paleo-lake shrinking reconstructed by Gillespie et al. [2008], which proposed that the lake coverage was extensive until about 10,000 yr BP, we concluded that the growth of the Arsain pingo began after 4500 yr BP, when the paleo-lake was completely drained. The pingo is not presently growing because of a limited groundwater supply to feed the ice core.

References

Gillespie, A.R.; Burke, R.M.; Komatsu, G. and Bayasgalan, A. [2008]: Late Pleistocene glaciers in Darhad Basin, northern Mongolia. *Quaternary Research*, 69(2):169 – 187, doi:10.1016/j.yqres.2008.01.001.

Grosse, G. and Jones, B. M. [2011]: Spatial distribution of pingos in northern Asia. *The Cryosphere*, 5 (1):13–33, doi:10.5194/tc-5-13-2011.

Extents of permafrost on the Qinghai-Tibet Plateau during the Last Glaciation Maximum (LGM) and Holocene Megathermal Period

Huijun Jin, Xiaoli Chang, & Ruixia He

State Key Laboratory of Frozen Soils Engineering, CAREERI, Chinese Academy of Sciences, People's Republic of China

On the basis of periglacial and permafrost evidence, and paleoclimatic-environmental records, permafrost development on the Qinghai-Tibet Plateau (QTP) was outlined for the Last Glaciation Maximum (LGM, 21±2 kya) and Holocene Megathermal Period (HMP, 6±2 kya). The peak summer monsoon was weakened during the LGM, which resulted in drier climate, reduced and salinized lakes, and stronger wind action. Under a very dry, cold climate, vegetation declined extensively. Sand and ice wedges developed extensively. The lower limit of permafrost (LLP) dropped by 1200-1400 m. Permafrost occupied 85 % of the unglaciated surface, with a cryospheric extent of 2.2 million square kilometer. During the HMP, temperatures were 2-3 °C warmer, and clearly wetter, than previously, resulting in extensive permafrost degradation. On the Chumar'he High Plain, permafrost thawed to depths of 14-16 m and became sporadic. Permafrost degradation was more intense on the eastern QTP, where permafrost vanished in regions lower than 4200 masl, thawed to depths of 15-25 m at elevations of 4200-4400 masl, resulting in buried (10-20 m) or doubled-decked permafrost. However, in the higher elevations of the Bayan Har and Anyemaqên mountains, patchy permafrost survived, with an LLP 300-400 m higher than, and permafrost extent 40-50 % of, today. The Last Permafrost Maximum (LPMax) and Minimum (LPMin) (jointly as LPMM) significantly differ between the LGM and HMP (i.e., the spatiotemporally asymmetrical buildup and decay of permafrost/glaciers). The LPMin could have antedated the LGM, and the LPMin behind the HMP. Much evidence for past permafrost activity needs clarification and integration. More updates need support from numerical modeling and reconstruction. However, to delineate the past permafrost extents in deserts would be challenging because of a lack of firm geochronogologies. The Action Group of the International Permafrost Association on the LPMM and LGM Permafrost, however, has been working on these topics.

Regional climatic significance of relict rock glaciers in the Eastern Alps

Olivia Carinda Kronig[1], Jürgen M. Reitner[2], Marcus Christl[1], & Susan Ivy-Ochs[1]

[1] *ETH Zürich, Switzerland*
[2] *Geological Survey of Austria, Vienna, Austria*

The Tandl rock glacier deposit is located in the province of Carinthia (Austria), at the western valley side of the Maltatal along the north facing flank of the Reisseck mountain range. It presents an outstanding and complex occurrence of series of very low-reaching relict rock glaciers. The rock glacier deposit covers a total area of approximately 0.9 km^2. Its lowest part reaches down to 1220 m above sea level (a.s.l.) and hence lies nearly 1300 m below modern permafrost limits, thus, representing the lowest relict rock glacier of the Eastern Alps (Reitner, 2007). This characteristic makes the Tandl rock glacier a good source for regional paleoclimatic reconstruction. The lower limit of intact rock glaciers can be used as a proxy for the lower limit of discontinuous permafrost on a regional scale. So the terminal position of relict rock glaciers will allows conclusions to be drawn about the discontinuous permafrost at the time when the rock glaciers were active. It has been shown that cosmogenic nuclides can be used to date how long since a rock glacier stabilized (end of a cold period), but have been only applied in few cases world-wide (Ivy-Ochs et al., 2009) . Based on modeling estimates in these areas (Avian & Kellerer-Pirklbauer, 2012) the formation of such features even prior to the Younger Dryas is plausible. First results of recently completed 10Be exposure dating of two gneiss boulders of the second lowest lobe of the rock glacier confirms these predictions. The lowest lobe may be even older. Therefore, in fall 2015 eleven more sample on different lobes were collected and will be prepared for 10Be exposure dating in 2016. The close proximity of the rock glaciers to likely Gschnitz stadial moraines provides an opportunity to combine rock glacier and moraine paleoclimate inferences. Furthermore, to assess the influence of the exposition of the rock glacier a second study area with the lowest southern facing rock glacier deposits of the Reisseck mountains (Reitner, 2007) will complete this study. In a side valley (Im Goassel) north of Mühldorf nine samples were collected at two small rock glaciers no further than 10 km south-west of the Tandl rock glacier deposit. One has its lowest limit around 1680 m a.s.l. and also consists of several rock glacier lobes. The other a comparable small one is on a western face and has its lowest lobe around1530 m a.s.l.. The detailed study, including field mapping as well as 10Be exposure dating on two sites with different geographical exposition, is an exceptional opportunity to elucidate regional paleoclimatic variations during the Lateglacial. Results will be compared with those from equilibrium line depression reconstructions from Lateglacial paleoglaciers and lake studies proxy data.

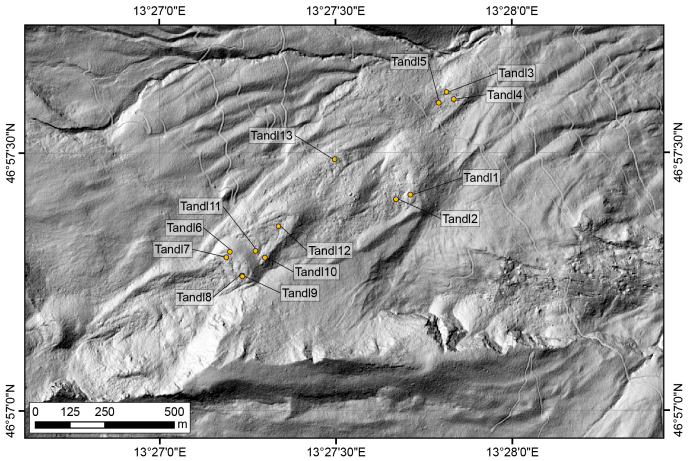

Figure 1: DEM (https://www.data.gv.at/katalog/dataset/land-ktn_gelandeschummerung-karnten) of the Tandl rockglacier showing the sampling locations.

Past permafrost and landscape dynamics in Central Beringia: Two case studies from drained thermokarst lake basin cores

Josefine Lenz[1,2], Sebastian Wetterich[1], Benjamin M. Jones[3], Katey Walter Anthony[4], Hanno Meyer[1], Anatoly Bobrov[5], Sabine Wulf[6,7,8], & Guido Grosse[1]

[1] *Alfred Wegener Institute Helmholtz Centre for Polar and Marine Research, Potsdam, Germany*
[2] *Institute for Earth and Environmental Sciences, University of Potsdam, Germany*
[3] *Alaska Science Center, US Geological Survey, AK, USA*
[4] *Water and Environmental Research Center, University of Alaska, Fairbanks, AK, USA*
[5] *Faculty of Soil Science, Lomonossov Moscow State University, Moscow, Russia*
[6] *Section 5.2 Climate Dynamics and Landscape Evolution, German Research Centre for Geosciences, Potsdam, Germany*
[7] *Senckenberg Research Institute and Natural History Museum, Frankfurt a.M., Germany*
[8] *Institute for Geosciences, University of Heidelberg, Heidelberg, Germany*

Thermokarst is a commonly observed process in the Arctic and an indicator of permafrost degradation. The formation of thermokarst landforms may indicate a localized disturbance to the ground thermal regime or be indicative of widespread permafrost degradation driven by climate-induced top-down permafrost thaw. Thermokarst lakes are one of the most prominent landforms that develop in ice-rich arctic and boreal lowlands. In our study, we investigate two drained thermokarst lake basins on the northern Seward Peninsula in Central Beringia to gain insights into site-specific landscape development and past permafrost dynamics during glacial and interglacial periods.

A 350 cm permafrost core (core ID: Kit-43) and a 400 cm permafrost core (core ID: Kit-64) were acquired from two drained lake basins that represent contrasting geological settings and cover a range of time periods (Mid-Wisconsin to Holocene). Kit-64 was a first generation lake in yedoma upland; Kit-43 was a later generation lake in a thermokarst-shaped lowland. The cores were analyzed using a multi-proxy approach including sedimentological (magnetic susceptibility, grain size), biogeochemical (TN, TC, TOC, $\delta^{13}C$), and micropaleontological methods (ostracods, testaceans), tephra analyses, radiocarbon dating on sediments, as well as isotope geochemical methods (δD and $\delta^{18}O$) on intra-sedimentary ground ice.

The Kit-64 core was acquired from a first generation lake basin on a yedoma upland that preserved a depositional environment of more than 45,000 years [Lenz et al., 2016] including:

1. Mid-Wisconsin yedoma accumulation,
2. intermediate wetland development between 41,500 and 44,500 yr BP,
3. South Killeak Maar tephra deposition that interrupted the wetland development,
4. continued terrestrial yedoma accumulation probably until the Late Glacial when a significant gap in the sedimentary record indicates formation of thermokarst lakes in the surroundings of this site that prevented further accumulation, and
5. finally a 300 cal yr BP thermokarst lake initiated and rapidly grew at the site which then drained in 2005 AD.

Modern permafrost aggradation is indicated in core Kit-64 however, unfrozen talik sediments were still present below a depth of 266 cm four years after drainage.

The Kit-43 core archived 12,100 cal yrs BP of predominately lacustrine deposition [Lenz et al., submitted] including:

1. Late Glacial thermokarst initiation and development of a deep thermokarst lake,
2. Early Holocene transition to a second, large and more dynamic lake generation by 9,500 cal yr BP with water level changes and intermediate wetland phases and tephra re-deposition from the catchment and
3. Late Holocene complete drainage at 1,060 cal yr BP with subsequent peatland development.

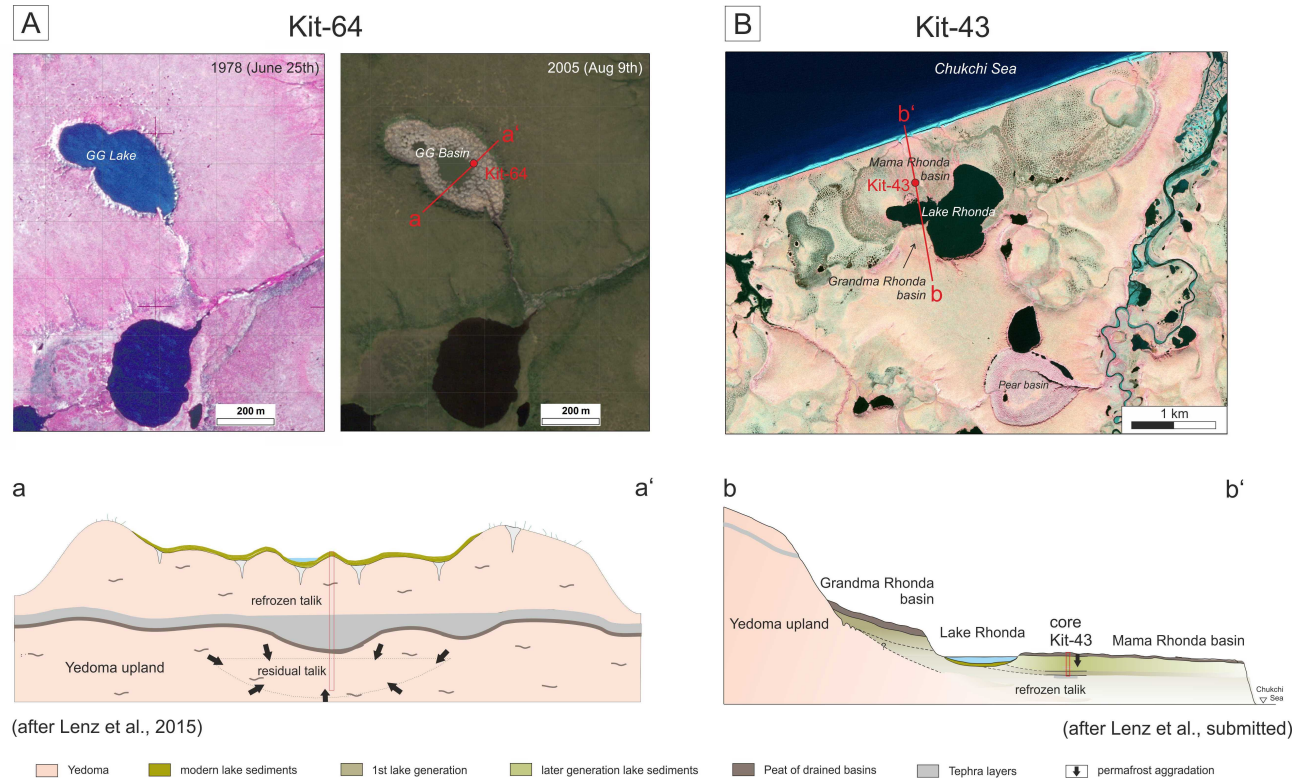

Figure 1: Contrasting case studies of permafrost dynamics: (A) core Kit-64 allows deeper insight into Mid-Wisconsin landscape evolution with a preserved talik, (B) core Kit-43 reveal multiple Holocene lake generations and re-aggradation. Schemes not to scale.

Interestingly, the isotopic composition of the intrasedimentary ice does not only capture the filling of the modern active layer by summer precipitation but also preserve similar patterns for the paleo-active layer 42–82 cm below modern surface, as well as permafrost aggradation in the refreezing paleo-lake talik from the surface down to 154 cm. The presence of an adjacent lake as a uniform water source presumably explains constant isotopic values below 154 cm. The presence of multiple lake cycles in the Kit-43 core, which was also corroborated from other basins by landscape-scale analysis of remote sensing images [Jones et al., 2012], emphasizes the complexity of organic carbon trajectories in thermokarst lake environments. Present TOC storage in lake sediments of the first lake generation of the Kit-43 basin during the Late Glacial period appears to be reduced due to originally lower organic matter inputs from late Pleistocene sediments being eroded at the shores as well as their long-term position within the talik of the following lake generation, allowing ongoing decomposition and release of carbon for several thousands of years. The later lake generation in turn had higher TOC contents most likely due to higher input from lake expansion into neighboring basins with peat cover. Hence, later generation lakes have high potential to sequester organic matter from erosion of organic-rich Holocene deposits.

These two case studies reveal the complex nature of Arctic landscapes that are affected by permafrost degradation and aggradation during a time when first humans migrated from Eurasia through North-America. They also highlight the interaction of global climate change, regional environmental dynamics, and local disturbance processes on different temporal scales. The maturation of landscapes by thermokarst dynamics on local level can have a significant influence on regional to global biogeochemical cycles.

References

Jones, M.C.; Grosse, G.; Jones, B.M. and Walter Anthony, K. [2012]: Peat accumulation in drained thermokarst lake basins in continuous, ice-rich permafrost, northern Seward Peninsula, Alaska. *Journal of Geophysical Research: Biogeosciences*, 117(G2), doi:10.1029/2011JG001766. G00M07.

Lenz, J.; Grosse, G.; Jones, B.M.; Walter Anthony, K.M.; A.and WulfBobrov, S. and Wetterich, S.

[2016]: Mid-Wisconsin to Holocene Permafrost and Landscape Dynamics based on a Drained Lake Basin Core from the Northern Seward Peninsula, Northwest Alaska *Permafrost and Periglacial Processes*, 27(1):56–75, doi:10.1002/ppp.1848.

Lenz, J.; Wetterich, S.; Jones, B.M.; Meyer, H.; Bobrov, A. and Grosse, G. Evidence of multiple thermokarst lake generations from a 12,100 years permafrost core on Northern Seward Peninsula, NW Alaska. submitted.

Reconstructing permafrost thaw events from alpine cave systems

Marc Luetscher[1,2], Dirk Hoffmann[3], Silvia Frisia[4], Birgit Sattler[5], & Christoph Spötl[1]

[1] *Austrian Academy of Sciences, Institute for Interdisciplinary Mountain Research (IGF)*
[2] *University of Innsbruck, Inst. Geology, A-6020 Innsbruck, Austria*
[3] *Max Planck Institute for Evolutionary Anthropology, D-04103 Leipzig*
[4] *The University of Newcastle, Environmental and Climate Change Research Group, Australia*
[3] *University of Innsbruck, Institute of Ecology, Technikerstrasse 25, A-6020 Innsbruck*

Understanding the long-term dynamics of mountain permafrost is fundamental to quantify processes affecting the alpine landscape evolution. Unfortunately, potential archives of past permafrost are rare, not the least because of erosion processes affecting surface sediments. Achieving a robust reconstruction of permafrost evolution through time is nonetheless critical to assess the long-term response of alpine environments to changing climate conditions and thus to delineate potential hazards associated with instable debris slopes and rock walls.

Cryogenic cave carbonates (CCCcoarse) recently emerged as one of the most promising archive for past water circulation in frozen karst systems [Žák et al., 2012]. These secondary calcites precipitate from the segregation of solutes during the progressive freezing of water pools at the surface of cave ice deposits. Accordingly, the occurrence of CCCcoarse reflects both, the local presence of permafrost and suitable conditions for sporadic water infiltration through the karst conduit network, most likely associated with extreme climate events.

Based on geomorphological criteria, 45 caves from seven high-altitude karst areas were selected as suitable for hosting Holocene cryogenic cave carbonates. Field investigations allowed identification of CCCcoarse at six sites located in a narrow altitudinal band ranging from 2500 to 2850 m a.s.l. Scanning electron microscopy suggests that the newly identified CCCcoarse belong to three distinct morphologic types:

1. polycrystalline aggregates;
2. fibrous-radial spherulites and
3. dendritic crystals.

Crystal fabrics suggest that supersaturation state with respect to calcite was variable as well as the Mg concentration, which, in the case of spherulites is high. Mg concentration appears to be crucial in determining the wide range of observed morphologies, in conjunction with microbially mediated nucleation and growth. Preliminary U-series ages indicate that CCCcoarse formation occurred during warm episodes in the Late Holocene [Luetscher et al., 2013]. Our data suggest that ages of CCCcoarse in alpine settings help constraining the onset and duration of warm phases in the Northern Hemisphere, thus contributing to a better understanding of the impact of climate forcing on the spatial and temporal distribution of past permafrost.

References

Luetscher, M.; Borreguero, M.; Moseley, G. E.; Spötl, C. and Edwards, R. L. [2013]: Alpine permafrost thawing during the medieval warm period identified from cryogenic cave carbonates. *The Cryosphere*, 7 (4):1073–1081, doi:10.5194/tc-7-1073-2013.

Žák, K.; Richter, D. K.; Filippi, M.; Živor, R.; Deininger, M.; Mangini, A. and Scholz, D. [2012]: Coarsely crystalline cryogenic cave carbonate – A new archive to estimate the Last Glacial Minimum permafrost depth in Central Europe. *Climate of the Past*, 8(6):1821–1837, doi:10.5194/cp-8-1821-2012.

Broken stalagmites may be an indicator of permafrost thawing

Lubica Luhová[1], Rastislav Milovský[1], Monika Orvošová[2], Stanislava Milovská[1], Juraj Šurka[1], Pavel Herich[3], Yu-Chen Chou[4], & Chuan-Chou Shen[4]

[1]*Earth Science Institute, Slovak Academy of Sciences, Dumbierska 1, Banská Bystrica, Slovak Republic*
[2]*Slovak Museum of Nature Protection and Speleology, Školská 4, Liptovský Mikuláš, Slovak Republic*
[3]*Slovak Caves Administration, Hodžova 11, Liptovský Mikuláš, Slovak Repubic*
[4]*High-Precision Mass Spectrometry and Environment Change Laboratory (HISPEC), Department of Geosciences, National Taiwan University, Taipei 10617, Taiwan ROC*

The cave precipitates (speleothemes) are outstanding records of paleoclimatic informations contained in time-series of their isotopic composition and trace-element ratios. Special types of cryogenically affected speleothems were recently recognized as a possible indicator of permafrost. They include mainly

1. cryogenic cave carbonates (CCC, Žák et al. [2004]), that precipitated from residual solution after freezing-out of large amount of dripwater, and

2. broken stalagmites or flowstones, that were fracturated by stresses in freezing ice or its later movements [Orvošová et al., 2012].

During the cold periods, the cave halls in zone of permafrost have negative temperature and their overburden is frozen, shielding the cave from water infiltration. When the overlying permafrost thaws in warm period, the water is released to the undercooled cave, where it freezes, causes precipitation of CCC, and destruction of speleothems. After thawing-out from ice, new stalagmites and flowstones continue to grow from restored drip, often discordantly on fallen speleothems. Such broken and overgrown stalagmites are object of our study, the aim is to verify whether or not the cryogenic events are pronounced in stable isotope and trace-element profiles.

As a model object for this research we chose cave Zlomiská, located at altitude 760 to 850 m a.s.l. on northern slopes of Nízke Tatry mountain ridge in central Slovakia. A motive for this choice is a widespread presence of dated and previously studied CCC populations in its halls [Orvošová et al., 2014], to which our results will be correlated. The cave is a 3D labyrinth of passages and halls in different levels below ground surface. Six samples of broken and overgrown stalagmites were documented in situ and collected near CCC occurences in cave halls situated in a perpendicular distance of 23 to > 100m from the surface.

The X-ray computer microtomography (V|tome|x L 240, GE) was used to obtain their 3D models to preserve informations about morphology and internal structure. Trace-element profiles were obtained using X-ray fluorescence microspectroscopy (μXRF – M4 TORNADO, Bruker) on cut and polished surfaces of both old stalagmite phase and new overgrowth. Stable C-O isotopes were measured on MAT253 mass spectrometer (Thermo) coupled to automated preparation device Gasbench II. Subsamples for isotope analysis were hand-drilled by a steel chisel of 0.8mm diameter at 1mm resolution along growth axes of stalagmite and further processed following the method of McCrea (1950) and analysed for isotope ratio of C and O. The U-Th ages were determined for start and end of growth for both old and new phase. On each sample, the start and end of growth of both old and new growth phase was dated by U-Th method, i.e. at least 4 dates per sample.

All the samples show similar stable isotope trends on both sides of the breaking boundaries. Before the break, we see a gradual rise of isotope values above their previous averages, of ca. 1 to 2 ‰and 4 to 6 ‰for $\delta^{13}C$ and $\delta^{18}O$, respectively, sometimes accompanied by synchronous drop in strontium concentration by cca 700 ppm. Assuming the constant Sr/Ca ratio of dripwater, drop in Sr concentration may be interpreted as temperature decrease based on temperature dependence of partition coeffcient of Sr between calcite and water. Increase in $\delta^{13}C$ may reflect supressed respiration in soil (production of light CO_2) and stronger influence of atmospheric and host-limestone carbon, i.e. either reduction of soil thickness or cease of respiration. Both may occur at turn towards cold climate.

In $\delta^{18}O$ trends, at least two factors may combine:

1. effect of temperature on fractionation by calcite precipitation,

2. parent rainwater composition.

Swings in a $\delta^{18}O$ at gradual $\delta^{13}C$ increase may reflect phase shift between these two processes, where effect of climate cooling is virtually instantaneous in soil respiration ($\delta^{13}C$), while rather delayed in global water cycle ($\delta^{18}O$).

These pilot results are showing systematic variations in environmental isotopes in intervals immediately preceding and following the cryofracturation. After thorough investigation of large set of similar samples, spatially connected with CCC and with precise U-Th series radiochronology, the phenomenon of cryogenically broken stalagmites may aspire to become a tool for estimating presence, age and thickness of permafrost in past.

Acknowledgements

This study was supported by a grant project VEGA 2-0193-15.

References

Orvošová, M.; Deininger, M. and Milovský, R. [2014]: Permafrost occurrence during the Last Permafrost Maximum in the Western Carpathian Mountains of Slovakia as inferred from cryogenic cave carbonate. *Boreas*, 43(3):750–758, doi:10.1111/bor.12042.

Orvošová, M.; Vlček, L.; Holúbek, P. and Orvoš, P. [2012]: Glacial-age cave ice and freezing in caves as a reason of speleothem destruction – examples from selected caves in Slovakia. *Slovenský kras*, 50 (2):97–112, in Slovak.

Žák, K.; Urban, J.; Cílek, V. and Hercman, H. [2004]: Cryogenic cave calcite from several Central European caves: age, carbon and oxygen isotopes and a genetic model. *Chemical Geology*, 206(1–2): 119–136, doi:10.1016/j.chemgeo.2004.01.012.

Heterochronous populations of cryogenic cave calcite may reflect depth of permafrost thawing events

Rastislav Milovský[1], Monika Orvošová[2], Stanislava Milovská[1], Juraj Šurka[1], Pavel Herich[3], Adrian Biroň[1], & Tomáš Mikuš[1]

[1]*Earth Science Institute, Slovak Academy of Sciences, Banská Bystrica, Slovakia*
[2]*Slovak Museum of Nature Protection and Speleology, Liptovský Mikuláš, Slovakia*
[3]*Slovak Caves Administration, Liptovský Mikuláš, Slovakia*

Cryogenic cave carbonates (CCC, Žák et al. [2004]) are becoming a powerful indicator of presence of permafrost, its thickness and age. Though they are generally regarded as being crystallized due to thawing of permafrost over the cave [Richter and Riechelmann, 2008], in our comprehensive set of radiometric datings they do not unequivocally fit with warming events. Our current research is largely focused to resolve this discrepancy in two ways: 1. understanding relationship of CCC with other cryogenic indicators, and 2. recognizing single/multiple successions in CCC populations in stable isotope and trace element trends, morphology and crystallography.

Field of study were several large cave systems in mountain ridges of Central Slovakia, with cave halls situated in different levels below ground, which predisposed them to develop many populations of CCC. 3D cave models were tied to surface polygons or LIDAR data to precisely measure perpendicular distance of studied halls from surface. The sampled cryogenic calcites were scanned on X-ray microCT (V|tome|x L 240, GE) with resolution of 1 micrometer to acquire 3D models of their morphology and internal structure. Stable C-O isotopes were measured on MAT253 mass spectrometer (Thermo) coupled to automated preparation devices Gasbench II and Kiel IV in samples of 20 to 80 micrograms. Vibrational spectra (micro-Raman spectrometer LabRamHR 800, Horiba Jobin-Yvon, micro FTIR spectrometer Nicolet iS50, Thermo) and X-ray diffraction patterns were measured to collect data on crystal structure. Trace-element distribution was studied in polished sections using X-ray fluorescence microspectroscopy (M4 TORNADO, Bruker) and field-emission electron microprobe JXA-8530F (JEOL).

We distinguish several morphological types of CCC, both as single monogenetic types and complicated overgrowths. Succession based on petrography of overgrowths correlates well with stable isotope composition. In earliest stages, single crystals with straight faces are prevailing, whether in compact or in skeletal growth forms. Later in succession, the crystal faces become bent and progressively twisted to form sferoids or hemisferoids, still with outlined vertices of a rhombohedron. Often the crystals appear to consist of microcrystallites agglutinated into final crystal shape in a fashion typical to mesocrystals. In latest stages, the evolution diverges into two morphotypes: rhombohedra with anomalous proportions, or spheroids of radial aragonite needles. Preliminary crystallochemical results show that these unusual morphologies are correlating with increasing concentrations of less compatible trace metals in CaCO3 lattice such as Mg and Sr, and stable isotope data confirm their crystallization from highly fractionated residual water after freezing-out of large amount of ice. Usually, the array of negatively correlating $\delta^{13}C/\delta^{18}O$ values is focused into narrow linear trends, typical for crystallization from freezing solution from one initial composition. But in some samples we distinguished parallel trends, suggesting a presence of several generations of cryogenic crystals. It is apparent that some cave halls were hit by thawing permafrost repeatedly, which is no surprise considering the frequency and intensity of Dansgaard-Oeschger events (most CCC ages in our caves fall into last glacial maximum, [Orvošová et al., 2014]. After systematic identification of heterochronous CCC populations, the U-Th radiometric dating will be employed to precise their ages and correlate them with known paleoclimatic events.

Acknowledgements

This study was supported by a grant project VEGA 2-0193-15.

References

Orvošová, M.; Deininger, M. and Milovský, R. [2014]: Permafrost occurrence during the Last Permafrost Maximum in the Western Carpathian Mountains of Slovakia as inferred from cryogenic cave carbonate. *Boreas*, 43(3):750–758, doi:10.1111/bor.12042.

Richter, D.K. and Riechelmann, D.F.Ch. [2008]: Late Pleistocene cryogenic calcite spherolites from the Malachitdom Cave (NE Rhenish Slate Mountains, Germany): origin, unusual internal structure and stable C-O isotope composition. *International Journal of Speleology*, 37(2):119–129.

Žák, K.; Urban, J.; Cílek, V. and Hercman, H. [2004]: Cryogenic cave calcite from several Central European caves: age, carbon and oxygen isotopes and a genetic model. *Chemical Geology*, 206(1–2): 119–136, doi:10.1016/j.chemgeo.2004.01.012.

Multi-proxy reconstruction of environmental changes and cryogenic processes in the Picos de Europa (Cantabrian Mountains, Northern Spain) since the Last Glaciation

Alexandre Nieuwendam[1], Jesús Ruiz-Fernández[2], Marc Oliva[1], Vera Lopes[3], Anabela Cruces[3], & Maria Conceição Freitas[3]

[1] *Centre for Geographical Studies/IGOT, Universidade de Lisboa, Portugal*
[2] *Department of Geography, University of Oviedo, Spain*
[3] *IDL, Faculty of Sciences, Universidade de Lisboa, Portugal*

The maximum ice expansion in the Western Massif of the Picos de Europa during the last glacial cycle occurred prior to the global Last Glacial Maximum. The spatial distribution of geomorphological landforms is indicative of the existence of several glacial phases over the last glacial cycle together with widespread periglacial processes. We retrieved a 5.4 m long sedimentary sequence from Belbín, a depression dammed by a moraine (Fig. 1). By combining the lithostratigraphic analysis of this section, grain-size measurements of the fine fraction and quartz grains analysis with geomorphological mapping we have reconstructed the environmental stages and intensity of cryogenic processes since the last glacial cycle until today.

The radiocarbon dating of the bottom sediments suggests that the maximum glacier advance occurred prior to 37.2 ka cal BP. Four different environmental stages were inferred based on the lithostratigraphic characteristics of this section:

1. 37.2-29 ka cal BP, intense periglacial processes with deposition of slope deposits;
2. 29-22 ka cal BP, progressive infilling of the depression;
3. 22-8 ka cal BP, presence of a paleolake;
4. since 8 ka, terrestrification of the paleolake with fire activity starting at 4.9 ka cal BP.

The micromophological features of the sediments evidence that persistent cryogenic conditions have prevailed in Belbín area since the last glacial cycle until present, with different degrees of intensity and type of weathering processes (Fig. 1). However, in some cases there are uncertainties about the time of climatic transition and geomorphic adjustment to changing climate conditions. When quartz grains become fragmented due to cryogenic cracking, the relation between silt production, quartz break-up and specific microfeatures, is more obvious in sedimentary archives. These descriptions provide data that can help to explain cryogenic processes from particular microfeatures and understand the successive events recorded in the sediments from previous climatic conditions.

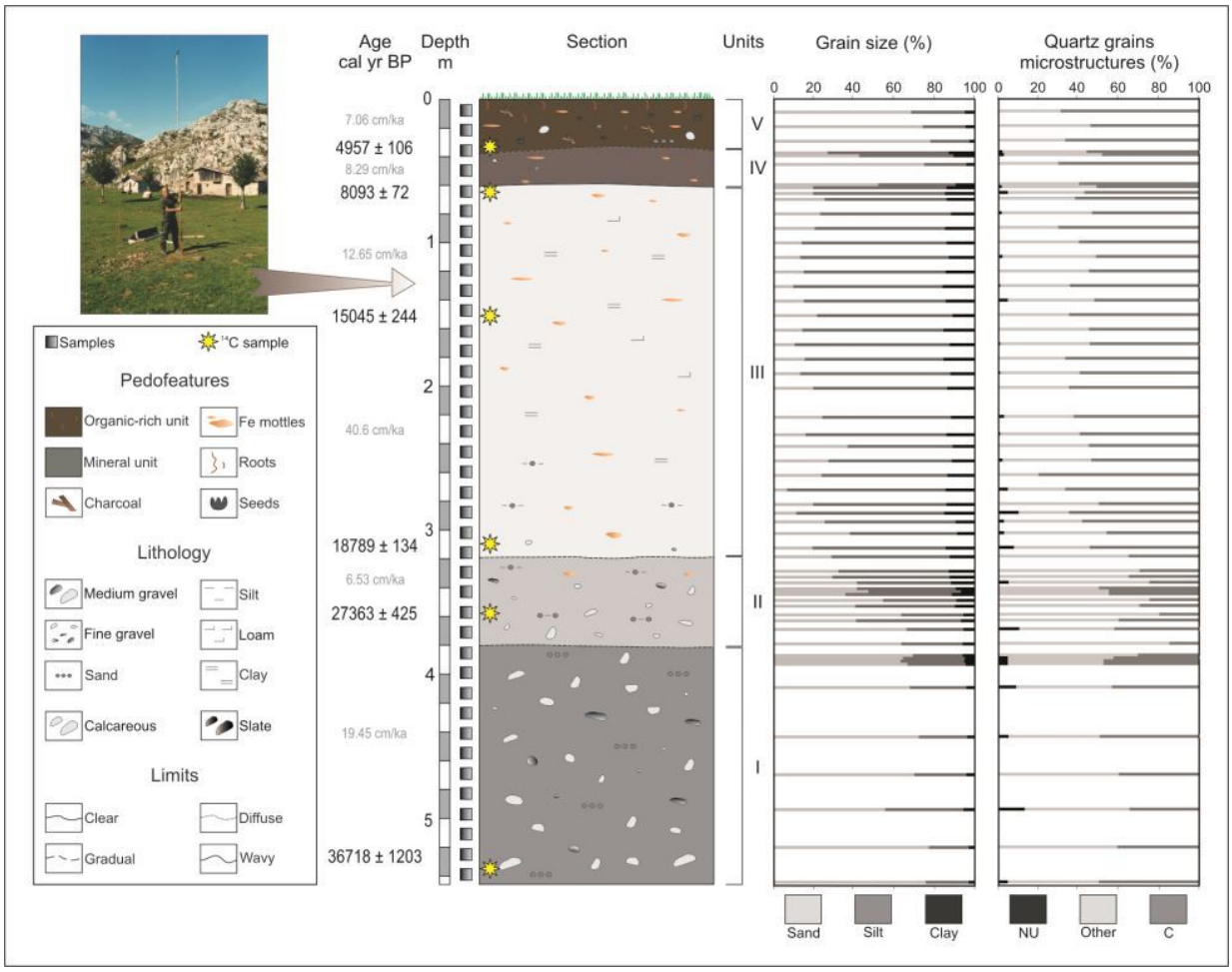

Figure 1: Lithostratigraphic units in the sediment core obtained from Belbín, showing ^{14}C AMS ages, grain size of the sediments and quartz grain microstructures. NU = Fresh and angular; Other = in-situ weathered; C = broken

Periglacially-induced versus earthquake-induced load structures - similarities and differences

Malgorzata (Gosia) Pisarska-Jamroży[1], Barbara Woronko[2], & A.J. (Tom) Van Loon[3]

[1] *Adam Mickiewicz University in Poznan, Poland, Poland*
[2] *University of Warsaw, Poland*
[3] *Geocom Consultants, Benitachell, Spain*

Soft-sediment deformation structures (SSDS) can be caused by a wide variety of processes, including glaciotectonics, gravity-induced sliding or slumping, permafrost-induced processes, cryoturbation, and fluidization or liquefaction due to instabilities resulting from reversed density gradients, to mention only the most common ones. The final morphology of SSDS resulting from liquefaction and fluidization (the processes that play the most important role during loadcasting) depend mainly on the initial sedimentary setting, the driving force and the duration of the deformable state, whereas the nature of the trigger mechanism seems to play a minor or negligible role. In other words, SSDS can have identical morphologies, independent of whether they were formed due to a seismic shock or under periglacial conditions. Loading is a widespread process facilitated by reversed density gradients.

As a consequence, it is commonly difficult to find out what caused the origination of a load structure, especially when the geological context does not provide a clue. This may easily result in incorrect interpretations. For instance, many periglacial structures and seismically-induced SSDS result from loading, but the trigger mechanisms are completely different. Moreover, one specific condition does not necessarily rule out other mechanisms: earthquakes may result in seismic shocks that cause loading of sediments in a periglacial environment, and thus detailed reconstruction of the deformational processes is required for a correct genetic interpretation.

In the periglacial environment, water in sediments can induce intense deformation during temperature changes around its freezing point. The freezing/thawing alternations during the Pleistocene glaciations affected many sediments, resulting in numerous SSDS. Some SSDS are considered by several authors (e.g. French [2007]) as characteristic of periglacial processes. Frost fissures, frost wedges and associated structures may, indeed, be a group (and probably the only group) that needs only periglacial processes. Cryoturbation (due to ice pressure and fluidisation of the sediment after ice melting) must, however, be considered as a result of typically periglacial processes in combination with much more common deformational processes such as loading and liquefaction. It is interesting in this context that even experienced researchers cannot always interpret without some doubt the periglacial origin of a specific SSDS.

Isostatic rebound can leave traces in the form of earthquake-induced SSDS. Earthquakes of sufficient intensity trigger liquefaction. Liquefaction of a sediment requires not only a water-saturated state, but it also needs a trigger. In the case of SSDS of a seismic origin, a loadcast can develop only if liquefaction takes place in the layer under the parent layer of the loadcast or its ultimate form, a pseudonodule [Moretti and Ronchi, 2011]. The type, size and complexity of SSDS in seismites are a function of the magnitude of the earthquakes [Guiraud and Plaziat, 1993]. The spatial distribution and lateral changes in the type, size and complexity of these SSDS can be used to locate the epicentre, which is sometimes a main active fault; in other cases it can locate the epicentre of a deep earthquake.

A fundamental question therefore now arises with the recently largely increased insight into the formation and characteristics of seismites: are all Pleistocene layers that contain abundant soft-sediment deformation structures and that were ascribed earlier to periglacial processes indeed due to periglacial processes, or were at least part of the deformations triggered by seismic shocks such as triggered by glacial rebound? We definitely come to the conclusion that a significant part of what were considered until now as periglacial SSDS are actually earthquake-induced soft-sediment deformation structures.

References

French, H.M. [2007]: *The Periglacial Environment*. John Wiley & Sons, Ltd, Chichester, 3rd edition, ISBN 978-0-470-86588-0.

Guiraud, M. and Plaziat, J.-C. [1993]: Seismites in the fluviatile Bima sandstones: identification of paleoseisms and discussion of their magnitudes in a Cretaceous synsedimentary strike-slip basin (Upper Benue, Nigeria). *Tectonophysics*, 225(4):493 – 522, doi:10.1016/0040-1951(93)90312-8.

Moretti, M. and Ronchi, A. [2011]: Liquefaction features interpreted as seismites in the Pleistocene fluvio-lacustrine deposits of the Neuquén Basin (Northern Patagonia). *Sedimentary Geology*, 235(3–4):200–209, doi:http://dx.doi.org/10.1016/j.sedgeo.2010.09.014.

Last Glacial palaeotemperatures in loess context from oxygen isotopes of earthworm calcite granules

Charlotte Prud'homme[1], Christophe Lécuyer[2], Pierre Antoine[1], Olivier Moine[1], Christine Hatté[3], François Fourel[2], François Martineau[2], & Denis-Didier Rousseau[4]

[1]*Laboratoire de Géographie Physique, Environnements Quaternaires et Actuels, UMR CNRS 8591, Université Paris I Panthéon-Sorbonne, France*
[2]*Laboratoire de Géologie de Lyon (LGL–TPE), UMR CNRS 5276, Université Claude Bernard Lyon 1, Villeurbanne, France*
[3]*Laboratoire des Sciences du Climat et de l'Environnement, UMR CEA-CNRS-UVSQ 8212, Gif sur Yvette, France*
[4]*Ecole Normale Supérieure, CERES-ERTI& LMD, Paris, France*

The Nussloch loess sequence (17-m-thick, profile P8) is considered as one of the most complete eolian record of the Last Glacial in western Europe. Its upper part, previously dated between 45 and 23 ka, is very dilated and is characterized by an alternation between loess (typical or laminated facies) and tundra gley horizons with the latter representing the active layer of a former permafrost. Fossil granules of calcite have been identified in this sequence. They are very abundant in tundra gley horizons and boreal brown soils. These granules produced by earthworms are composed of rhomboedric calcite crystals, organized in a radial crystalline structure. The oxygen isotopic composition ($\delta^{18}O$-VPDB) of these granules depends on soil temperature where earthworms lived and on the isotopic composition of the meteoric water. The aim of this study is to propose a new palaeothermometer for the Last Glacial loess deposits by using this new bio-indicator. 30 granules were extracted from 5-cm-thick samples taken from two boreal brown soils and from three tundra gley horizons. The isotopic composition has been measured on individual granules with an automated carbonate preparation system online with an isotopic ratio mass spectrometer. $\delta^{18}O$-VPDB values range from -14.8 to -0.9 ‰for tundra gley layers and from -10.7 ‰to -0.3 ‰for boreal brown soils. To generate quantitative climatic parameters from the granules $\delta^{18}O$-VPDB record, we first estimated the $\delta^{18}O$-VPDB of meteoric water from modern values corrected with palaeorecords data and we assumed that earthworms were inactive during the winter period (from October to April). We thus estimated the mean soil and air temperature for the warmest months, which are respectively 13±4 °C and 10±4 °C during tundra gleys formation and 15±4°C and 12±4 °C during boreal brown soils formation. These values are in agreement with the few other reconstruction generated from different proxies in western Europe (diatom assemblages, beetles, botanical remains). This original preliminary study highlights the potential of earthworm calcite granule $\delta^{18}O$-VPDB measurements as a new proxy for absolute mean soil and air temperature measurements during the warm season of Last Glacial interstadials in continental environments.

Dry valley dynamics in periglacial conditions (a case study from NE Poland)

Joanna Rychel[1], Barbara Woronko[2], Mirosław Tomasz Karasiewicz[3], Mirosława Kupryjanowicz[4], Magdalena Fiłoc[4], & Leszek Marks[1,2]

[1] *Polish Geological Institute-National Research Institute, Poland*
[2] *Faculty of Geology University of Warsaw, Poland*
[3] *Faculty of Earth Sciences Nicolaus Copernicus University, Poland*
[4] *Faculty of Biology and Chemistry, University of Bialystok, Poland*

A characteristic element in the morphology of areas from the extraglacial zone of the Last Glacial Termination (MIS 2) in Poland are flat-bottom dry valleys. Their formation is related with snowmelt erosion under cold-climate conditions [Kaltkowa, 1965, French, 2007, Kołodyńska-Gawrysiak, 2008]. They are commonly characterized by a well-developed network (presence of first- and second-order valleys according to the classification of Strahler, 1952) and the presence of small depressions, at present wetlands or water reservoirs, in the upper stretches of dry first-order valleys. In order to retrace the conditions of formation and development of such forms, sediments filling two dry valleys (5 km and 0.7 km long, respectively) from NE Poland were subject to sedimentological studies, pollen analysis and vertical electric sounding.

The obtained results evidence that the formation of the valleys was related to the deglaciation stage of the Saale ice sheet (MIS 6) and the activity of fluvioglacial waters. The areas released from under the ice were subsequently covered by permafrost. This stage of development of the dry valley should be linked with the formation of numerous small (several to over a dozen metres in diameter) and variably deep (2 to 10 m) depressions observed in the bottoms of first- and second-order valleys. Most probably most of them were formed as thaw (thermokarst) lakes in periglacial conditions. It is also possible that part of them were created by thawing pingos or by melting of dead-ice blocks. In the Eemian Interglacial (MIS 5e), the depressions functioned as lakes, which by the end of this period were transformed into peat bogs. The peat bogs existed till MIS 5b. By the end of the Early Vistulian (MIS 5a), the peat bogs were replaced by large water reservoirs. Lakes existed in the valley bottoms till MIS 4, when the dry valleys were incorporated into a concentrated flow. The LGM period (MIS 2) is recorded as slope (solifluction) processes under permafrost condition. They resulted in the shallowing of the dry valleys, levelling of most of the earlier depressions (lakes) and the change of the valley axes. The formation of ice wedges with a primary sandy infilling, pointing to the presence of permafrost and minor development of aeolian processes, is also linked with this period.

Acknowledgements

The studies were financed by the scientific project UMO-2013/09/B/ST10/02118.

References

French, H.M. [2007]: *The Periglacial Environment*. John Wiley & Sons, Ltd, Chichester, 3rd edition, ISBN 978-0-470-86588-0.

Kaltkowa, H. Vallons en berceau et vallées seches aux environs de łódź. *Acta Geographica Lodziensia*, 19: 124–142, 1965.

Kołodyńska-Gawrysiak, R. [2008]: Rola warunków lokalnych w ewolucji suchych dolin WyŻyny Lubelskiej podczas późnego vistulianu i holocenu. *Landform Analysis*, 9:37–40.

Paleo- permafrost and groundwater systems in the UK over the past 1 Million years

Johanna Scheidegger[1], Jonathan Busby[1], Christopher Jackson[1], Fiona McEvoy[1], & Simon Norris[2]

[1] *British Geological Survey, Nicker Hill, Keyworth, Nottingham, NG12 5GG, UK*
[2] *Radioactive Waste Management Limited, Didcot, Oxon, OX11 0RH, UK*

Over the last one million years Britain has undergone several glacial cycles, during which mean annual surface temperatures were below freezing. There is geological evidence that the East of England was glaciated during the Anglian Glaciation and during the Devensian glaciation, but during the other glacials there is no compelling evidence for ice coverage. In contrast, north-western parts of the British Isles were covered several times by the Scottish sector of the British Ice Sheet. Therefore, there were several cycles of permafrost formation during the past one million years. Evidence of past permafrost includes thermal contraction cracking and brecciation of the Chalk [Murton et al., 2015], and dating of paleowaters in the East Midlands Sherwood Sandstone aquifer suggest that recharge was limited between 20 ka and 10 ka BP, which has been attributed to permafrost coverage [Edmunds et al., 2001]. Groundwater recharge and discharge to and from the aquifer beneath permafrost during continuous permafrost coverage is limited because the pore spaces are filled with ice within the zone of saturation. Groundwater flow is then limited to the unfrozen zones, taliks, which perforate the permafrost.

This study aims to understand the processes governing the thickness and extent of permafrost for two different geological environments and what effects permafrost dynamics have on the groundwater flow system over the course of several glaciations. The first environment consists of a basement under sedimentary cover with permeable sedimentary rocks and is situated in north-western parts of the British Isles. The second environment is a sequence of Jurassic and Triassic sediments and is located in the East of England. This study includes the effects of permafrost dynamics, relative sea level change, and recharge from a subglacial meltwater source into the aquifers. In order to study the effect of different climate scenarios and geological environments on the thickness and distribution of permafrost within an idealised groundwater flow system, numerical modelling of coupled fluid flow and heat transport including latent heat is used.

The subsurface temperature distributions are calculated using the advection-diffusion equation, including the transient effects of latent heat of fusion to simulate freezing and thawing. Fluid flow is simulated using fully saturated fluid flow described by Darcy's Law.

Permafrost depth for one location is highly sensitive to the climate scenario used. The permafrost model is driven by ground-surface temperature series at the top of the model domain and a geothermal heat flux at the bottom of the model domain. The temperature time series is derived from a global $\delta^{18}O$ time series after Lisiecki and Raymo [2005] and scaled to different maximum temperature differences (ΔT) relative to present day temperatures. The maximum modelled permafrost thickness over the last one million years ranges from 50 m (ΔT = -10 °C) to 340 m (ΔT=-20 °C) for different temperature time series (Fig. 1a).

Modelled results for environment one of coupled heat and fluid flow suggest that when permafrost forms across the entire catchment, recharge and discharge decrease several orders of magnitudes and become near zero, and the groundwater flow magnitude decreases compared to unfrozen conditions. Under permafrost conditions the temperature distribution within the study site is conduction dominated.

During permafrost thaw of shallow permafrost heat advection becomes dominant underneath the permafrost where there is a large hydraulic gradient on the mountain slope. In contrast, when thick permafrost thaws then a suprapermafrost talik develops in the lowlands, in which heat advection becomes the dominant process thawing the permafrost (Fig. 1b). This difference in the importance of advective heat flow is caused by a weathered layer with a higher permeability than the underlying bedrock, enabling

higher advective heat transport than heat conduction in the weathered layer underneath shallow permafrost. For thicker permafrost exceeding the thickness of the weathered layer, heat conduction from the surface dominates thaw and forms a suprapermafrost talik, in which heat advection becomes dominant.

Recharge and discharge across the surface increase during permafrost thaw from the near zero conditions, and discharge is largest at the foot of the hill, near the permafrost boundary and where the hydraulic head gradient is largest.

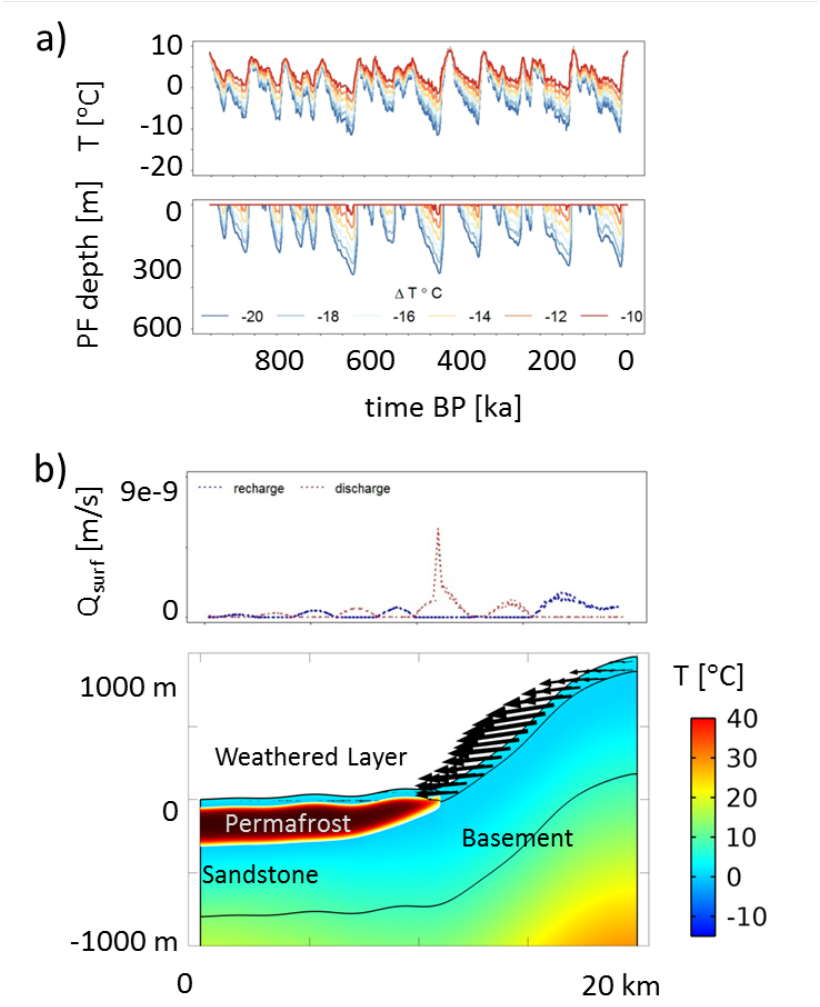

Figure 1: a) Scaled temperature time series after Lisiecki and Raymo [2005] for different minimum temperatures and modelled permafrost depths. b) Surface fluxes and permafrost/temperature distribution during a thawing event for sandstone overlying a basement.

Paleopedological cryotrassology: Tracers of former permafrost – the cases from the Late Pleistocene paleosol/sedimentary sequences of Europe and western Siberia

Vladimir Sheinkman[1], Sergey Sedov[2], Vladimir Melnikov[1], Birgit Terhost[3], & Aleksey Rusakov[4]

[1] *Tyumen State Gas and Oil University; Tyumen State University Earth Cryosphere Institute, Russian Federation*
[2] *Departamento de Edafología, Instituto de Geología, UNAM; Mexico;Tyumen State Gas and Oil University; Tyumen State University*
[3] *Institute of Geography and Geology, University of Würzburg, Germany*
[4] *Institute of Earth Sciences, Saint-Petersburg State University, Russia*

Identification and reliable interpretation of the witnesses of the past permafrost development (proposed as a special branch of geosciences – cryotrassology) is of major important for reconstructing past terrestrial environments of the former cold periods. Such indicators/tracers of those events as pseudomorphs after repeated ice wedges, cryoturbations in sedimentary layers, solifluction features, lenses of segregation ice etc. are reliable but not ubiquitous markers.

Therefore, we propose to use the cirtain indirect pedological indicators/tracers of past and former permafrost in order to complete the information about its spatial distribution and chronostratigraphic occurrence. The certain pedogenetic processes, also not necessarily linked to permafrost, are strongly influenced or modified in its presence. In particular icy permafrost layers could cause water saturation and thus switch on the hydromorphic soil forming processes: accumulation of peat and gleyzation in the mineral horizons, in the geomorphic positions and substrates where otherwise well-drained non-gleyic soils are formed.

We have interpreted some of Late Pleistocene gleyic soils as indirect tracers of ancient permafrost. Their characteristics consist in the next:

1). Recently well-developed paleosols formed during the late Marine Isotope Stage (MIS) 3 were discovered to the north from the Eurasian Loess Belt – in the Center-North area of European Russia (Upper Volga basin) (Fig. 1) [Rusakov and Sedov, 2012] and North-Western Siberia (Middle Ob basin) [Sheinkman et al., 2016].

The paleosols are developed within the Late Pleistocene alluvial and lacustrine sequences and produced radiocarbon dates from its organic materials within the time interval of 50 – 25 Ka BP. They represent hydromorphic profiles with Histic horizons or materials and gleyic colour pattern; in thin sections numerous specific ferruginous pedofeatures (concentric nodules, mottles, strypes). These paleosols demonstrate contrasting difference as well as from synchronous Cambisols and Chernozems formed within loess sequences to the south. Conspicuously they are developed in the well-drained geomorphic positions, where modern soils (Podzols and Luvisols) have only weak surficial redoximorphic features.

2). In the Late Pleistocene loessic sequences of Germany and Austria strongly gleyed soils (known as Tundragley or Naßboden) correspond to the strata, developed during MIS2 including MIS3/MIS2 transition [Terhorst et al., 2015]. Again, they are formed in the elevated landsurfaces providing good drainage on porous calcareous loess which hampers gleyzation. Indeed earlier (MIS3) and later (Holocene) soils of the same sequences are non-gleyic Cambisols and Luvisols. Additional evidences of permafrost in these soils are provided by morphological features of horizon fragmentation and mixing by cryoturbation and solifluction. Also in thin sections signs of cryogenic structuring, grainsize sorting, mixing of organic and mineral materials and deformation of plant debris and pedofeatures by frost processes are observed. As far as in both cases we attribute gleyzation to water-logging by permafrost, we classify these paleosols as Reductaquic Cryosols. From the described spatial/temporal occurrence of the cryogenic gleyic paleosols we deduce the shift of permafrost several hundreds of km to the southwest during the MIS3-MIS2 transition.

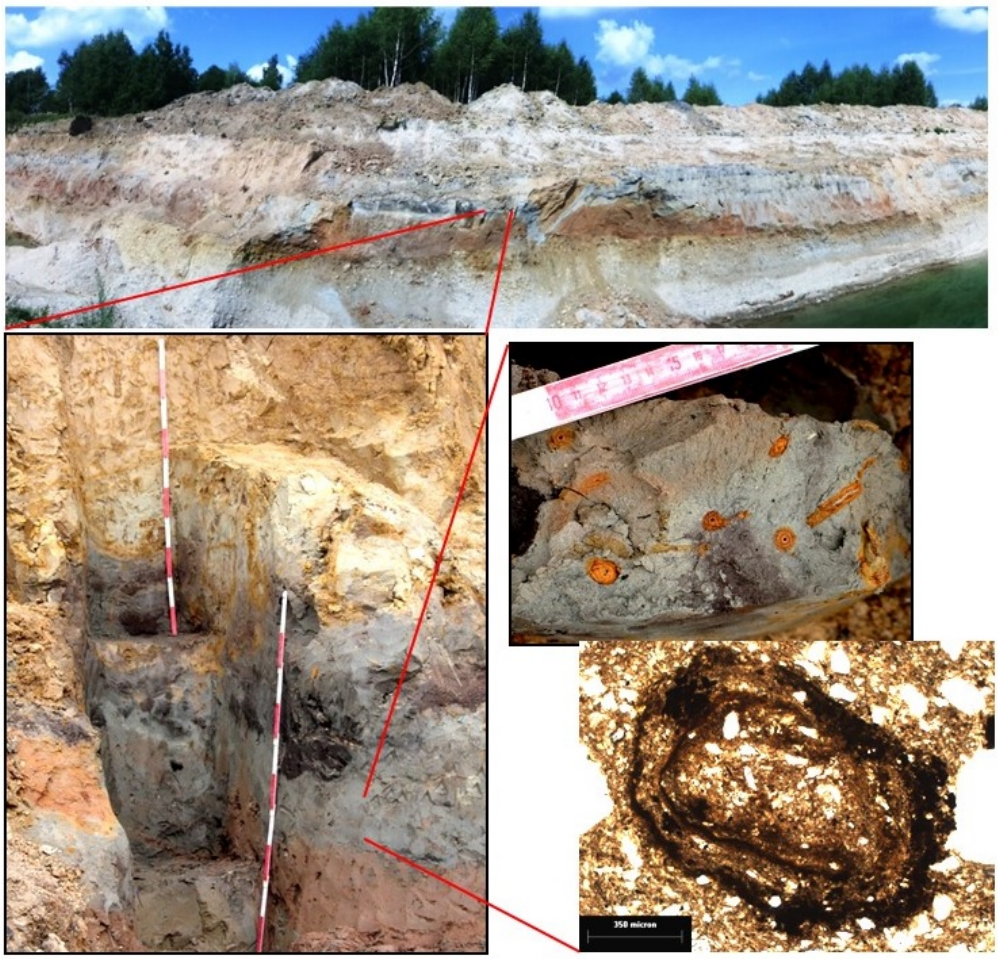

Figure 1: Gleyic cryogenic paleosols of the Upper Volga Basin: section Koskovo, paleosol macro-, meso- and micromorphology (photos by Alexey Rusakov)

References

Rusakov, A. and Sedov, S. [2012]: Late Quaternary pedogenesis in periglacial zone of northeastern Europe near ice margins since MIS 3: Timing, processes, and linkages to landscape evolution. *Quaternary International*, 265:126–141, doi:10.1016/j.quaint.2012.03.002. Special Issue: Paleosols in soilscapes of the past and present.

Sheinkman, V.; Sedov, S.; Shumilovskikh, L.; Korkina, E.; Korkin, S.; Zinovyev, E. and Golyeva, A. [2016]: First results from the Late Pleistocene paleosols in northern Western Siberia: Implications for pedogenesis and landscape evolution at the end of MIS3. *Quaternary International*, 418:132–146, doi:10.1016/j.quaint.2015.12.095. Special Issue: Paleosols, polygenetic soils and soil chronosequences as archives of landscape evolution.

Terhorst, B.; Sedov, S.; Sprafke, T.; Peticzka, R.; Meyer-Heintze, S.; Kühn, P. and Solleiro Rebolledo, E. [2015]: Austrian MIS 3/2 loess-palaeosol records-Key sites along a west-east transect. *Palaeogeography, Palaeoclimatology, Palaeoecology*, 418:43–56, doi:10.1016/j.palaeo.2014.10.020.

Permafrost as a background for development of ancient glaciation and the problem of bedded ice bodies in Northwestern Siberia

Vladimir Sheinkman & Vladimir Melnikov

Tyumen State Gas and Oil University; Tyumen State University, Earth Cryosphere Institute, RAS; Russia

Permafrost existed in Northwestern Siberia all over the Quaternary. Its extent fluctuated in size but permafrost always occupied a vast space here. Indicators of strong low-temperature freezing of the earth surface such as polygonal ice wedges occur in the north of Northwestern Siberia at present. Our research at the right-hand bank of the middle Ob' River revealed pseudomorphs after polygonal ice wedges, which demonstrated that similar environmental conditions have appeared during the Late Pleistocene even at a latitude of about 61° N, where today only high-temperature sporadic permafrost occurs . Ice wedge casts that formed during MIS 2 are most widespread in the study area, although more ancient wedges occur in places too. The ice wedge casts cover very large areas overall in Subarctic Northwestern Siberia and evidence that ice sheets have cannot existed at the time of their formation because the coeval occurrence of ice sheets and permafrost aggradation is inherently impossible. Nevertheless, some researchers suppose Pleistocene ice sheets extending all over Northwestern Siberia; and besides, they consider different ground ice bodies as relics of those ice sheets.

Ice sheets always transform their bed in any case. Even if preexisting ground ice persisted at the base of the glaciers, it would have been destroyed as a result of their geological work either partly, or completely. Long-lived ground bodies that are very sensible to any external influence have been however presented in a good appearance. On the other hand, there is not, however, today a clear explanation in order to unfold, from the positions of, The origin and development of ground ice in its observed variety cannot be explained based on current cryological knowledge, especially in the case when the appearance of the ground ice bodies is similar, in some features, to those of the ice bodies of glaciers. According to dependable data obtained in long-term research by the authors [Sheinkman, 2011, Sheinkman and Melnikov, 2014] from all glaciated areas of Siberia, neither ice sheets, nor any glaciers can be saved for a long time in a state of dead ice. It is impossible even in the Verkhoyansk region, the coldest area of the Northern Hemisphere, where the annual air temperatures are as low as −17 °C, and the absolute temperature minimum has been registered as of −67.8 °C.

The characteristic feature of Siberia's cold continental climate is a short, but at the same time hot summer season. In such a situation the coarse moraine material covering dead glaciers cannot preserve their ice bodies from melting. The moraine debris is not a good heat insulator, and active summer heat is able to penetrate deep through the debris into the dead glaciers by air and melt water. The longest time to save the buried ice blocks of dead glaciers under a moraine cover is 100-150 years only even in the coldest areas of Siberia. Even though some ice bodies of permafrost and, respectively, glaciers resemble each other, there is no reason to consider the currently inexplicable ice phenomena as relics of ancient glaciation. This point of view arose from the Alpine concept of glaciation defining high snow supply and ice transformation to form the glaciers which formed outside permafrost areas. Under initially high moisture, glaciations reached the form of ice sheets only during the geologically relatively short cryochrones of the Pleistocene. This model is suitable to explain the formation of past ice sheets in Northern Europe fed by Atlantic moisture. However such a model is not suitable in Siberia, including Northwestern Siberia, where cold and dry environments prevailed over the Quaternary as result of cryoaridization (gradual cooling at the background of increasing climatic continentality).

The traditional Alpine model of glaciation assumes active evaporation of moisture from the ocean, its transport to the continent over which it travels over relatively short distances, and the preservation of moisture deposited in solid phase by the glaciers (for a definite time). In this case, glaciers lie mostly on an unfrozen bed, and the main factor of glaciation is an intense metamorphism of snow at a background when ice melting is compensated by an intense supply of new portions of icy mass to the ablation zone, and heat input at the glaciers is largely expended to

overcome the threshold of ice melting, because ice, even it is predominantly in an isothermal state (at a temperature of 0 °C as in the given case) has been characterized by high heat of fusion.

With such an organization of matter and energy, the glaciers during global climate cooling were able to reach a final stage of development, the ice sheet. It was even at middle latitudes and under a geologically rapid change of thermochrones to cryochrones in the course of climatic rhythmic with such known interval as 20 Ka in Europe, for example. A change from thermochrones to cryochrones is accompanied by clearly pronounced humid phases of glaciation: first warm and then cold. Furthermore, with still abundant snow accumulation persisting during the early phase of cooling, a decrease in the period of ablation will lead to a rapid lowering of the firn line, entailing an active growth of the glaciers. The next cold humid phase will be changed by a cold dry phase with a deceleration of glacier growth; nevertheless, ice material sufficient to form the ice sheet will be already able to accumulate.

However, although the Alpine glaciation model is commonly used, it is not appropriate for Siberia with its continental climate conditions. This applies also for Northwestern Siberia, because the setting of cryoaridization remains constant throughout the Quaternary. Moisture is distributed and preserved differently here. Moisture arrives in Siberia mainly by the westerly transfer of Atlantic air masses, passing large distances and expending much of it en route. The Indian Ocean is not a relvant as moisture source for Siberia, since moisture has been blocked by high mountains of Southern Asia. Air masses from the Pacific don't reach much of Siberia because of the westerlies (Fig. 1). During the cryochrones of the Quaternary, a larger part of moisture is intercepted by the ice sheets in the north of Europe. Hence, the overall volume of moisture transferred to Siberia can never be large, neither today nor in the past, especially during the cryochrones of the Quaternary. It is also necessary to take into consideration that a significant portion of moisture in Siberia is conserved not only by glaciers but by ground ice and icings too.

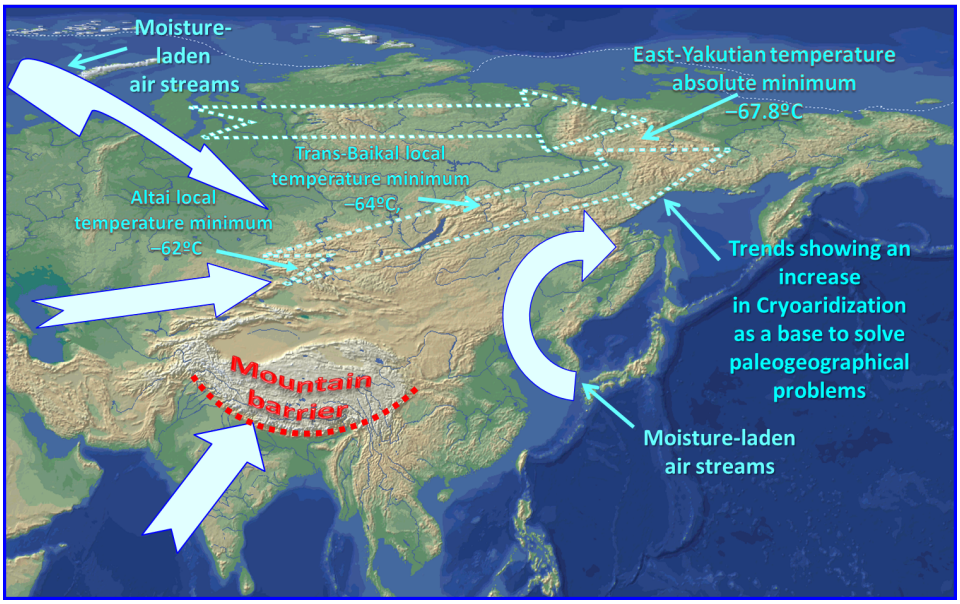

Figure 1: Factors determining continental climatic environments and conditions of cryoaridization in Siberia

During the cryochrones of the Quaternary, Siberia's glaciers responded differently to climate change. The amount of atmospheric precipitation is small in the mountains of Siberia; even at present it usually amounts 500–700 mm and very rarely exceeds this value. In the process of climatic cooling and, hence, cryoaridization, the precipitation amount is becoming even smaller, and an increasing part of moisture in the periglacial zone is preserved in icings and ground ice. Consequently, the glaciers will be growing slowly. Glaciers are, during short-lasting cryochrones of the Quaternary, only eventually able to reach the stage of valley glaciation. The climatic cyclicity of inland glaciations in Siberia synchronous to Marine Isotope Stages (MIS) is a matter of discussions based on evidence from different palaeogeographical records including deep ice and other cores (especially from the Baikal core, the most important in respect to Siberia). Ac-

cordingly, it was tempting to conclude that the course of glaciation in Siberia must be similar as recorded in the cores of the Atlantic marine, Greenland ice sheet, Baikal lake and other deep drilling .

However, the cryochrone–thermochrone rhythmicity in Siberia is not identical with the Glacial–Interglacial cyclicity in Europe. In Siberia, unlike Europe under the influence of the Atlantic, global climate cooling was able to cause primarily an enhancement in cryogenesis, and an expansion of the permafrost area. Only in special cases, when the mountains penetrated deep into the chionosphere ensuring the input of a sufficient amount of snow, there occurred a growth of mountain glaciers even under conditions of cryoaridization... In such a situation glacier formation was substantiated for Siberia's mountainous areas, including the mountains in the south of Western and Eastern Siberia. However, our later investigations showed that this also refers to Northwestern Siberia.

So, cryoaridization prevailed in Siberia beginning from its Northwestern area and depended on environments sufficient for the formation of glaciers, which differed from those considered as of the Alpine glaciation model and obtained properties more characteristic for permafrost objects. In spite of low snow supply and active ablation (an attribute of continental climate) during the cryochrones, the glaciers grew slowly due to additional ice feeding, when thawed water repeatedly freezes on their surface. Since they only gradually absorbed scanty moisture supply, glaciers reached only the valley form. Nevertheless, these properties did not favor the long-time preservation of the buried dead ice.

Cryoaridization can appear in Siberia either spatially or temporally. The magnitude of modern spatial environmental changes appears from the west to the east, and from the south-west to the north-east (see Fig. 1) similar to the changes which appeared temporally during the transition from cryochrones to thermocrones of the Pleistocene. Therefore the modern situation is a representative possibility to test models of environmental development in the Pleistocene.

On a whole, the obtained data allow to conclude that ice sheets have not been developed in Northwestern Siberia over all the Quaternary, and ground ice bodies are not relics of ancient ice sheets. Siberia's glaciers developed only valley forms interacting with permafrost. They formed in the permafrost area, their features are more characteristic for permafrost phenomena, and it is a reason to consider them as a component of permafrost.

References

Sheinkman, V.S. [2011]: Chapter 65 – Glaciation in the High Mountains of Siberia. In: Ehlers, J.; Gibbard, P.L. and Hughes, P.D.(eds.), *Quaternary Glaciations – Extent and Chronology – A Closer Look*, volume 15 of *Developments in Quaternary Sciences*, pages 883–907. Elsevier, doi:10.1016/B978-0-444-53447-7.00065-9.

Sheinkman, V.S. and Melnikov, V.P. [2014]: Siberian glaciers as a component of cryolithogenic-glacial geosystems. *Kriosfera Zemli (Earth's Cryosphere)*, 18(2):3–23, URL http://www.izdatgeo.ru/pdf/krio/2014-2/3.pdf. (in Russian).

The final disappearance of permafrost as a trigger for early Holocene landscape evolution in the southern Baltic lowlands

Michał Słowiński[1], Florian Ott[2], Agnieszka M. Noryśkiewicz[3], Nadine Dräger[2], Mateusz Kramkowski[2], Rik Tjallingii[2], Christoph Haas[2], Mirosław Błaszkiewicz[1], Jarosław Kordowski[1], Izabela Zawiska[4], Martin Theuerkauf[5], Elisabeth Dietze[2], Monika Rzodkiewicz[6], Markus J. Schwab[2], & Achim Brauer[2]

[1]*Institute of Geography and Spatial Organization Polish Academy of Sciences, Poland*
[2]*Helmholtz Centre Potsdam, GFZ German Research Centre for Geosciences, Section 5.2 – Climate Dynamics and Landscape Evolution, Telegrafenberg C, D-14473 Potsdam, Germany*
[3]*Institute of Archaeology, Nicolaus Copernicus University Torun, 44/48 Szosa Bydgoska, Torun 87-100, Poland*
[4]*Department of Geoecology and Climatology, Institute of Geography and Spatial Organization, Polish Academy of Sciences, Twarda 51/55, 00-818 Warsaw, Poland*
[5]*Institute for Geography and Geology, Ernst-Moritz-Arndt Universität Greifswald, Friedrich-Ludwig-Jahn-Str. 16, D-17487 Greifswald, Germany*
[6]*Adam Mickiewicz University, Department of Geology and Quaternary Paleogeography, Poznan, Poland*

This contribution will discuss possible impacts of the role of permafrost and dead ice melting on landscape evolution in the early Holocene (11.5 to 9.5 cal kyr BP) in the southern Baltic lowlands. This period is characterized by climatic instability and various and complex biotic and abiotic environmental responses at different time scales to the rapid warming within a few decades that marked the onset of our present interglacial period. Here, we present palaeoecology and geomorphological data from lake sediments from northern Poland, located on the outwash plain formed during the Pomeranian phase of the last (Vistulian) glaciation at approximately 16,000 ^{14}C yrs BP.

We reconstructed environmental changes using biotic (e.g. macrofossil, pollen, subfossil Cladocera, diatoms) and geochemical proxies as well as geomorphological investigations. Abrupt changes in lithology, sediment structures and biological proxy show distinct changes and threshold processes in environmental conditions between 11.5 - 9.5 cal kyr BP.

Our results confirm the existence of dead ice in this region even in the Holocene, which is clear evidence for remains of discontinuous permafrost at that time. This suggests an unstable landscape and a crucial role of permafrost melting for the regional landscape evolution including the vegetation succession and especially of the water distribution network. We document the occurrence of multi-aged lakes in the same channel which started to deposit lacustrine sediments after melting of dead ice during the early Holocene. In comparison with early Holocene lacustrine sedimentation at other lakes in a similar geomorphological setting in north-eastern Germany, our results might provide clues to Earth surface models, which should take into account factors such as permafrost thawing controlling landscape evolution in a warming scenario.

Acknowledgements

This research was supported by the National Science Centre Poland (grants No. NN 306085037 and NCN 2011/01/B/ST10/07367) and is a contribution to the Virtual Institute of Integrated Climate and Landscape Evolution (ICLEA) of the Helmholtz Association supported by TERENO infrastructure.

The late Pleistocene episodes of permafrost aggradation in the Wielkopolska region, Poland – palaeoclimatological and palaeogeographical implications

Robert Jan Sokołowski[1], Paweł Zieliński[2], Wojciech Wysota[3], Stanisław Fedorowicz[1], Krzysztof Przegiętka[3], & Anatoly Molodkov[4]

[1] *University od Gdańsk, Poland*
[2] *Maria Curie-Skłodowska University in Lublin*
[3] *Nicolaus Copernicus University in Toruń*
[4] *Institute of Geology, Tallinn University of Technology*

The occurrence of periglacial phenomena in the late Pleistocene deposits in the Wielkopolska region has been widely described [Kozarski, 1993, 1995, Bohncke et al., 1995, Sokołowski, 2007a,a, Ewertowski, 2009, Wysota et al., 2009, Zieliński et al., 2011]. The aggradation of periglacial structures is commonly associated with the main periods of cold climate during the middle-late Saalian and Weichselian Glaciation, particularly with the Last Glacial Maximum (ca. 20 ka). A smaller amount of data originates from the early and middle part of the Weichselian Glaciation.

The objective of the present investigations was to establish the number and chronology of periods of permafrost development in the Wielkopolska region during the late Pleistocene. The investigations were conducted at several key sites with well documented horizons of periglacial structures whose stratigraphic position was determined with luminescence dating (TL, OSL and IR-OSL). These were outcrops located in the areas covered by the LGM (Wapienno, Lubstów, Żabinko), in its marginal zone (Kaszczor) as well as the extraglacial zone (Postolin).

During the investigations, three or four generations of periglacial structures were documented: mainly sand wedges with primary infilling, ice-wedge pseudomorphs and small and large scale involutions. Deflation lags and initial soils are associated with these structures. Frost structures developed as epigenetic forms in fluvioglacial sandy gravels, glacial till and fluvial sands, and as syngenetic forms in fluvio-aeolian and fluvial silty sands. The deflation lag occurs at the top of glacial till and the gravel and sand sediments.

The results of the investigations show that the aggradation of periglacial structures began in the middle and late Saalian (ca. 200 ka). These were mainly ice-wedge casts and frost fissures in fluvial series (Wapienno) and ice-wedge pseudomorphs in gravel and sand sediments (Kaszczor).

The second period in the development of permafrost occurred in the early Weichselian (ca. 90-80 ka). Sand wedges with primary infilling developed in glacial till (Lubstów) and deflation lags indicating the development of aeolian processes in dry climate conditions (Kaszczor).

The third period in the development of permafrost occurred in the middle Weichselian during the Świecie Stadial (ca. 55-50 ka). Fluvial and fluvio-aeolian covers documented at the Wapienno, Lubstów and Kaszczor sites developed in that period. These covers contain ice-wedge pseudomorphs and deflation lag formed at their top. A complex of large load-cast structures found at the Wapienno site is probably a sign of the degradation of permafrost.

The fourth period in the development of permafrost began ca. 30 ka. It is well documented at the Wapienno site where a complex of polygonal structures developed at the top of older sediments (till from the Saalian Glaciation, covered in some places by fluvial sediments of the middle Weichselian). Polygonal structures comprise sand wedges with primary infilling. Ice-wedge pseudomorphs developed on gravel and sand covers. Deflation lag and initial soil also occur at the top of the periglacial structures at this level. Ice-wedges and deflation lag were also found at the Lubstów site. At both sites, periglacial structures are covered by glacial till from the LGM (Leszno Phase). At the Wapienno site, another level horizon of periglacial structures (sand wedges with primary infilling and deflation lag) covered by younger till of the main stadial (Poznań Phase) developed at the top of glacial till from the LGM. It should be concluded, however, that both horozins represent one period of permafrost aggradation.

The last period in the aggradation of periglacial

structures began ca. 16–17 ka and lasted until 12 ka. Structures dating back to that period were documented at the Wapienno (16-15 ka), Żabinko (16-12 ka) and Postolin sites (14-12 ka). These are primarily ice-wedge pseudomorphs and involutions. The older generation of the structures developed at the top of the youngest till of the main stadial (Wapienno) and in fluvial sediments (Żabinko and Postolin) while the younger generation occurs in fluvio-aeolian sediments (Żabinko and Postolin). Gleysol from the Bölling period was found to occur above the periglacial structures at the Żabinko site [Bohncke et al., 1995, Zieliński et al., 2011]. The discontinuity and relatively small dimensions of these structures as a whole seem to suggest that they formed as a result of periodic permafrost aggradation or strong seasonal freezing of the soil rather than continuous and lasting permafrost.

Summing up, the investigated complexes of periglacial structures document at least four periods of permafrost aggradation during the Saalian and Weichselian Glaciation interspersed by warmer periods during which permafrost was disappearing.

Acknowledgements

The investigations were financed by the grant 3P04D 037 23 and grant N N 306 197639 of the Ministry of Science and Higher Education.

References

Bohncke, S.; Kasse, C. and Vanderberghe, J. Climate induced environmental changes during the Vistulian Lateglacial at Żabinko, Poland. *Questiones Geographicae*, Special Issue 4:43–64, 1995.

Ewertowski, Marek. Ice-wedge pseudomorphs and frost-cracking structures in Weichselian sediments, central-west Poland. *Permafrost and Periglacial Processes*, 20(4):316–330, 2009. doi:10.1002/ppp.657.

Kozarski, S. Late Plenivistulian deglaciation and the expansion of the periglacial zone in NW Poland. *Geologie en Mijnbouw*, 72:143–157, 1993.

Kozarski, S. The periglacial impact on the deglaciated area of northern Poland after 20 kyr BP. *Biuletyn Peryglacjalny*, 34:143–157, 1995.

Sokołowski, R.J. *Stratygrafia i sedymentologia osadów plejstocenu w kamieniołomie "Wapienno", NE Wielkopolska*. PhD thesis, Uniwersytet Mikołaja Kopernika, Toruń, 2007a.

Sokołowski, R.J. Struktura i procesy sedymentacji osadów plejstoceńskich w Wapiennie. In: Molewski, P.; Wysota, W. and Weckwerth, P.(eds.), *Plejstocen Kujaw i dynamika lobu Wisły w czasie ostatniego zlodowacenia Ciechocinek, 3-7 września 2007*, pages 36–144. Torun, 2007b.

Wysota, W.; Molewski, P. and Sokołowski, R.J. Record of the Vistula ice lobe advances in the Late Weichselian glacial sequence in north-central Poland. *Quaternary International*, 207(1–2):26 – 41, 2009. doi:10.1016/j.quaint.2008.12.015.

P. andSokołowskiZieliński, R.J.; Fedorowicz, S. and Jankowski, M. Stratigraphic position of fluvial and aeolian deposits in the Żabinko site (W Poland) based on TL dating. *Geochronometria*, 38, 2011. doi:10.2478/s13386-011-0005-x.

Permafrost peatland succession in high latitudes: Regional trends in permafrost aggradation and thaw

Claire C. Treat[1] & Miriam C. Jones[2]

[1] *University of Alaska Fairbanks, United States of America*
[2] *U.S. Geological Survey, Reston, VA, USA*

Northern high-latitude peatlands accumulated more than 400 Gt of carbon over the Holocene. Vegetation changes, such as the succession from fen to bog species, are often clearly visible in peat profiles and can be caused by organic matter accumulation or by changes in regional climate. Most peatlands developed during the early Holocene as fens under a climate that was warmer than today and subsequently transitioned to bogs during the mid- to late-Holocene. Teasing out permafrost aggradation in peat cores remains a challenge, as they often resemble dry bogs. However, in many locations permafrost aggradation can be assumed especially if thermokarst is evident later in the peat record (i.e., an abrupt transition from dry bog or plateau peat to wet Sphagnum riparium or even fen peat). We use a combination of peat properties and plant macrofossils to identify the timing of permafrost aggradation in peatlands and to examine regional trends in permafrost aggradation that might be indicative of regional climate patterns rather than local, site-specific factors. Widespread permafrost aggradation, indicating a general cooling, began 7000 y BP in continuous permafrost regions and decreased C accumulation rates in Eurasia. Permafrost aggradation accelerates in both discontinuous and continuous permafrost regions after 1000 y BP, while permafrost thaw in peatlands becomes more common during the past 200 years. The overlaps and differences in timing of permafrost aggradation among regions suggest both widespread cooling as well as regional differences in permafrost formation processes.

Sedimentological evidence for stacked paleo-thaw (thermokarst) lake successions in Western Europe

Jacobus van Huissteden[1], Cinzia Berritella[1], & Jens M. Warnsloh[2]

[1] *VU University, Netherlands, Faculty of Earth and Life Sciences, De Boelelaan 1085, 1081HV Amsterdam*
[2] *J.M.W. Geo-consulting, Netherlands, Kierkegaardstraat 49, 1185 AH Amstelveen*

Sedimentary successions of Last Glacial age in Europe show evidence of episodic presence of permafrost, by a range of fossil permafrost phenomena such as ice wedge pseudomorphs and cryoturbation. Also lake deposits have been found that may have originated from permafrost thaw, in particular in basins and river valleys of the northwestern European plains along the North Sea and the Baltic. These deposits contain valuable information on the reaction of permafrost to past rapid changes in climate.

We present new data on a lacustrine succession near Hengelo (Netherlands), which has been investigated with cores and exposures. In this succession, evidence for at least four, and possibly five stacked thaw lake units has been found. The lacustrine sediment units are separated from each other by sands, loessic silts and peat with ice wedge pseudomorphs and large cryoturbations, indicating subaerial deposition. The lake sediments vary from almost purely clastic sediment (laminated silts) to organic sediment (gyttja). The underlying ice wedge pseudomorphs may have a partial infilling of lake sediment (see figure 1). Sandy lake shore benches with delta-like foresets indicate the repeated occurrence of periods of enhanced sediment supply to the lakes, from lake banks or from fluvial input.

We conclude that thaw lakes did occur repeatedly, in particular as a result of permafrost thaw during Marine Isotope Stage (MIS) 3 or Middle Weichselian. By contrast, the permafrost thaw during the Last Glacial Termination (MIS 2) in the same area did not cause widespread formation of thaw lakes; permafrost thaw occurred probably under rather dry conditions, evidenced by ubiquitous deflation horizons and eolian sand sheet and dune deposits of this age.

The sedimentological evidence at Hengelo is compared with other paleo-thaw lake deposits in northwestern Europe, and with thaw lake successions observed in Eastern Siberia, Alaska and Canada, to determine criteria for distinguishing thaw lake sediments in the geological record. This confirms a large variability of deposits, also seen in the paleorecord.

The interpretation of paleo-thaw lakes as indicators of climate change is not straightforward. The evidence on present-day thaw lake expansion is mixed, despite pronounced climate warming in the Arctic, and shows stability, net contraction or expansion of lake area in various regions. Widespread lake formation in present-day Arctic thaw lake regions did occur mainly during the Last Glacial Termination and early Holocene. By contrast, in Western Europe evidence of thaw lake formation as a result of permafrost thaw during the Last Glacial Termination is limited.

The paleo-thaw lake deposits in Western Europe appear to be associated with climate warming during the interstadials of the Middle Weichselian. We infer that thaw lake formation may have contributed to higher CH_4 emission during these interstadials, indicated by high CH_4 concentration in ice cores of this age.

Figure 1: Photo

Thermokarst evidences in the Paris Basin

Brigitte Van Vliet-Lanoe[1], Jacques Brulhet[2], Phillipe Combes[3], Cédric Duvail[3], Frederic Ego[2], Stéphane Baize[4], & Isabelle Cojan[5]

[1] *UMR 6538 Domaines Océaniques UBO-CNRS, IUEM, Pl.N.Copernic, 29280 Plouzané, France*
[2] *Service Géologie et Environnements de Surface, Andra-7, rue Jean-Monnet - 92298 Châtenay-Malabry cedex, France*
[3] *GEOTER SAS - FUGRO Group , Géologie Tectonique Environnement et Risques, 3, rue Jean Monnet 34830 Clapiers France*
[4] *IRSN, Seismic Hazard Division, BP 17 92262 Fontenay-aux-Roses Cedex*
[5] *MINES ParisTech, PSL - Research University Centre de géosciences 35 rue Saint-Honoré 77300 Fontainebleau, France*

Thermokarst is a collapse feature commonly described in former glaciated terrains or in present-day Arctic, especially with the Global Warming resulting from the thawing of ice-rich permafrost or of massive ice of various origins. This process is well observed and studied in Arctic. Little attention has been paid to the sedimentary fabric resulting from such collapse, outside glacitectonic. In Western Europe, two paleoforms are commonly studied: lithalsas, collapsed pingo or ice wedges, associated with the development of gullying and erosion. Very few papers compile present-day data and fossil ones.

Data collected from quarries in the eastern Paris Basin provide very nice records of such thermokarst collapses in alluvial calcareous sands and gravels. These deformations occur as well in drained and waterlogged situation resulting in specific pattern of deformations. They cover brittle to plastic comportment of sediments. They strictly resemble to passive glacitectonism, like in kettle holes. Normal and reverse faults, with offset increasing toward the surface are common and locally transpressive features may also be observed. Traces of segregation and reticulate ices are common.

Lithalsa, seasonal frost blister, spring frost blister, buried frozen oxbow lakes and perhaps pingo seem to have formed. Aerial photographs and high resolution DEM attest of the size, the density and the frequency of these commonly circular or elongated features on Fyb river terraces. Permafrost is also attested by the recurrent occurrence of metric pattern grounds at the surface of the chalk and of ice wedge casts.

The periods of development of ice bodies followed by thermokarst'events(s) are strictly constrained within a part of MIS 6, fossilized by the MIS5e pedogenesis. They fit the climatic evolution recognized in Western Europe for this period covering c.40 ka. A mapping on the scale of the Paris basin allows the reconstruction of permafrost extent at that time.

These thermokarst faults have been recurrently confused with neotectonic features triggered by paleo-earthquakes.Seeing the lack of seismic activity over the last 1.000 years and of valid elements (field, sismic, geophysic) to justify regional tectonic activity during Quaternary in the Eastern part of the Paris basin, our interpretation seems the most plausible to explain such faulting and other features of deformation. It seems likely that many other observations reported within the area of the paleo-permafrost extent and commonly attributed to neotectonic processes may result from similar confusions.

The reconstruction of past permafrost: recent results, present-day gaps and future challenges

Jef Vandenberghe

Vrije Universiteit Amsterdam, The Netherlands

The importance of palaeo-permafrost research includes, apart from reconstructing permafrost extent in the geological past, also an extrapolation to the future, identifying and quantifying factors that determine rates of permafrost aggradation and degradation, estimating the feedback of permafrost to climate and evaluating the role of permafrost in landscape shaping.

A first step to achieve these goals is to define extent and evolution of permafrost. By now, permafrost recognition through characteristic morphology and sedimentary deformations should pose no major problems anymore. Thus, the maximum permafrost extent of specific periods could be established (e.g. LPM; Vandenberghe et al. [2014]). However, improvements are always possible by new observations and methodologies [Lindgren et al., 2016]. In addition, a number of problems remain unsolved until now as, for instance, the survival of relict permafrost, regional differentiation of permafrost occurrence and the distinction between latitudinal and altitudinal permafrost.

In contrast to identification of permafrost, we are not far with quantifying the evolution of permafrost. Rate of growth and degradation of permafrost could until now only be estimated by reconstructions at specific time slices. However, such calculations require dating of permafrost. When permafrost has disappeared a direct dating is generally impossible, leaving no other way than the dating of permafrost indicators by interpolation between sediments which ages are derived from absolute dating or stratigraphical position. Fortunately, much progress is made nowadays by luminescence dating of last-ice age deposits.

In a next step, it is of principal interest to understand the causes and modalities of the reconstructed extent and evolution. Potential impacting factors are rather well known: for instance, vegetation, lithology, snow cover. However, quantification of each of them is still in its infancy.

This brings us from the state-of-the-art to present innovations and future perspectives for past-permafrost research. After many years of reconstruction it is clear that some of our goals and interests are impossible to reach solely by traditional field research. In the reconstruction of permafrost extent at specific times much progress may be expected from systematic inventories of well-dated permafrost indicators by the construction of databases. A modern example is the establishment of such an archive for France [Bertran et al., 2014]. It strongly asks for regional expansion and the set-up of similar initiatives. Furthermore, understanding and quantification of local environmental conditions and more general climatic impacting factors need theoretical physical approaches that can be achieved by model experiments. Some promising examples have been provided in recent special issues on palaeo-permafrost. From those examples it appeared also that permafrost models cannot be successful without field validation.

References

Bertran, P.; Andrieux, E.; Antoine, P.; Coutard, S.; Deschodt, L.; Gardère, P.; Hernandez, M.; Legentil, C.; Lenoble, A.; Liard, M.; Mercier, N.; Moine, O.; Sitzia, L. and Van Vliet-Lanoë, B. [2014]: Distribution and chronology of Pleistocene permafrost features in France: Database and first results. *Boreas*, 43(3):699–711, doi:10.1111/bor.12025.

Lindgren, A.; Hugelius, G.; Kuhry, P.; Christensen, T. R. and Vandenberghe, J. [2016]: GIS-based Maps and Area Estimates of Northern Hemisphere Permafrost Extent during the Last Glacial Maximum. *Permafrost and Periglacial Processes*, 27(1): 6–16, doi:10.1002/ppp.1851.

Vandenberghe, J.; French, H. M.; Gorbunov, A.; Marchenko, S.; Velichko, A. A.; Jin, H.; Cui, Z.; Zhang, T. and Wan, X. [2014]: The Last Permafrost Maximum (LPM) map of the Northern Hemisphere: permafrost extent and mean annual air temperatures, 25–17 ka BP. *Boreas*, 43(3):652–666, doi:10.1111/bor.12070.

Testing the accuracy of yedoma radiocarbon age

Alla Vasil'chuk & Yurij Vasil'chuk

Lomonosov Moscow State University, Russian Federation

It was supposed that the contamination with modern ^{14}C is the main factor for obtaining invalid ^{14}C ages. However, while this is correct for an open system, the array of syncryogenic permafrost sediments is not a true open system. Accumulation and simultaneous freezing of the sediments isolates the permafrost deposits surely. We suppose that contamination with old organic material in permafrost is of importance in aging of the ^{14}C dates. The main problem of radiocarbon dating within permafrost is the uncertain reliability of the ^{14}C ages. Syngenetic sediments contain allochthonous organic deposit that originated at a distance from its present position. To establish ice-wedge formation ages the strategy for the most authentic radiocarbon age selection for syngenetic sediments is considered on the base of a model of yedoma accumulation and distribution of reworked material related to the flood and aeolian transport. The re-deposition of organic material discussed in terms of cyclic syngenetic sedimentation of yedoma. Microcycles are associated with the seasonal periodicity of changes in the depth of an active layer and the accumulation of thin sediment layers. The duration of microcycles is estimated from several years to hundreds of years. The vertical scale of microcycles is several centimeters or tens of centimeters. Mesocycles are conditioned by the pulsing change of the water level of a reservoir, on the coast or shallows of which ice wedges are being formed. The duration of mesocycles is usually estimated from tens of hundreds to several thousand years. The vertical scale of mesocycles is several meters. For ^{14}C dating of ice, wedge complexes it is important to take into account the mesocycles due to the essential difference of the organic material re-deposition at the subaerial and subaqueous stages. For syngenetic ice wedges two stages can be distinguished mainly growth of ice (the subaerial stage), and mainly accumulation of sediments (the subaqueous stage). The growth of syngenetic ice wedges proceeds subaerially during the accumulation of peat or peaty sediments (Vasil'chuk, 2013). Periodically, when gravel, sand, sandy loam, loam, silt, and clay are deposited under subaqueous conditions, ice wedge growth decreases or stops. In real situation in permafrost during syngenetic accumulation at the subaqueous stage , the participation of old organic material may consist of 90-95 %. There are many examples of age reversal from peat from subaerial stage that is known to be autochthonous without any signs of re-deposition (Payette et al., 1986). Ancient methane bubbled from the bottom of thermokarst lakes, as shown by Zimov et al. (1997) and Walter et al. (2006) in the permafrost area. Therefore, methanotrophic bacteria, which provide Sphagnum mosses with carbon (Kip et al., 2010), could use ancient methane together with modern. Ancient soil carbon in permafrost soils may be metabolized upon thawing also. The radiocarbon ages of heterotrophically respired carbon ranged from less than 50 yr to 235 yr BP in July mineral soil samples and from 1,525 to 8,300 yr BP in August samples (Nowinski et al., 2010).

As syngenetic ice wedge is a closed system, microbial activity is excluded. The dating of organic microinclusions from ice wedges allows us to obtain the age of the ice wedge directly. However, results of the AMS ^{14}C dating of organic inclusions in ice wedges have demonstrated that the problem of an inhomogeneous concentrate also occurs.

The comparison of the ^{14}C ages of different fractions from the samples of organic material in the syngenetic ice wedges of a 24-meter terrace near the village of Seyaha demonstrates that the ages of the organic micro-inclusions (more than 200 μm) are the youngest. The concentrations of tritium in the ice were measured in order to evaluate the possibility of modern water participation in the ice wedge. It was shown that modern water did not penetrate into the ice. Micro-inclusions at a depth of 1.8 m are dated as 14,550 yr, and at a depth of 12 m as 14,720 yr BP. The ages of alkaline extracts from the same samples are respectively 19,920 yrs and 23,620 yr. Thus, the differences of 5 kyr and 9 kyr between the ages of the micro-inclusions and alkali extracts may be explained only by a very intensive process of ice wedge accumulation over about 14–15 kyr BP.

The advantages and the complications of dating of

ice wedges from ice wedges by the accelerator mass spectrometry (AMS) method are discussed applying to true age of dated material search. Radiocarbon ages of different organic materials from the same samples are compared, it is demonstrated that the difference between ages of the fractions from the ice wedges consist of about 9 ka in Seyaha ice-wedge complex in Yamal Peninsula and about 5 ka in Bison yedoma, Kolyma River valley. The principle of the choice of the youngest ^{14}C age from the set and from the layer is proposed for yedoma (Fig. 1).

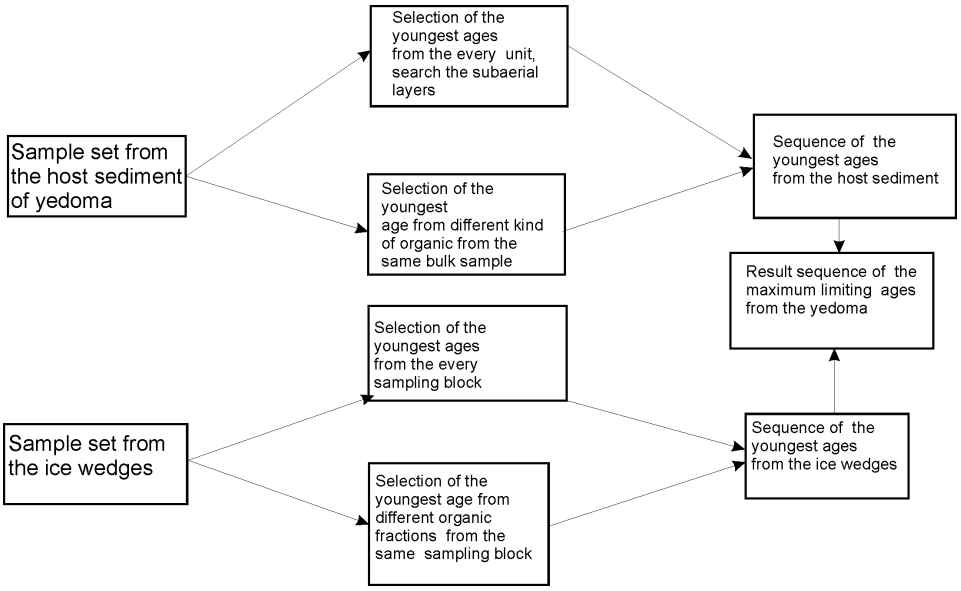

Figure 1: Principles of valid ^{14}C ages selection in yedoma

Approaches for the choice strategy are:

a) meso- and macro-cyclic model of thick syngenetic ice wedge formation (Yu.Vasil'chuk, 2006, 2013) taking into account;

b) modern re-deposition of organic material at subaqueous syngenetic conditions used as pattern for the past syngenetic accumulation of yedoma deposits;

c) possible re-working of organic material at syngenetic subaerial or subaerial accumulation,

d) comparison number of AMS ^{14}C ages of organic micro-inclusions, alkali extract and pollen concentrate in the ice wedges;

e) comparison of the ^{14}C ages from various materials from the same samples both in the ice wedges and in the host sediments.

The younger age of the yedoma from cross-sections of Duvanny Yar in Kolyma River valley (35–37 ka BP to 13–10 ka BP), Bison in Kolyma River valley (33.5 ka BP to 26 ka BP), Zelyony Mys in Kolyma River mouth (37 ka BP to 13.6 ka BP), Mamontova Gora in Aldan River valley (19 ka BP to 17 ka BP) etc. is substantiated due to the principle of the choice of the youngest ^{14}C from the set [Vasil'chuk and Vasil'chuk, 1997, 1998, 2014].

The ice wedges are considered as key subjects for ^{14}C dating of yedoma, as there are no any exchange processes between the environment and the ice wedges.

References

Vasil'chuk, Y. K. and Vasil'chuk, A. C. [1997]: Radiocarbon Dating and Oxygen Isotope Variations in Late Pleistocene Syngenetic Ice-Wedges, Northern Siberia. *Permafrost and Periglacial Processes*, 8(3):335–345, doi:10.1002/(SICI)1099-1530(199709)8:3<335::AID-PPP259>3.0.CO;2-V.

Vasil'chuk, Y. K. and Vasil'chuk, A. C. [2014]: Strategy of valid ^{14}C dates choice in syngenetic permafrost. *The Cryosphere Discussions*, 8:5589–5621, doi:10.5194/tcd-8-5589-2014.

Vasil'chuk, Y.K. and Vasil'chuk, A.C. [1998]: ^{14}C and ^{18}O in Siberian syngenetic ice wedge complexes. *Radiocarbon*, 40(2):883–893.

High temporal resolution winter air temperatures and permafrost maps at 40-12 ka BP using oxygen isotope data from Siberia yedoma

Yurij K. Vasil'chuk, & Alla Vasil'chuk

Lomonosov Moscow State University, Russian Federation

A methodology of yedoma study was developed more than 30 years ago [Vasil'chuk, 1982]; it includes detailed isotope horizontal and vertical sampling of large syngenetic ice wedges, and radiocarbon dating of surrounding sediments and of organic microinclusions directly in the wedges. The revision of the ratio of ^{18}O and winter temperature has been done using new data obtained over the past 20 years, including new 2015 ice wedge research data of A. Maslakov at Kotelny Island and Chukotka and J.Vasil'chuk at Yamal Peninsula. A good correspondence of the new data and previously derived relations is provided. Archive of the yedoma sections aged from 40 to 12 ka significantly supplemented with data obtained during Russian-German almost 20 years of research (Meyer et al, 2002, 2015; Schirrmeister, 2002, 2009, 2013; Opel et al., 2011) and Russian expeditions (Streletskaya et al., 2009-2015, Oblogov, 2015) and detailed work of international team at Duvanny Yar (Murton at al., 2015), and other works of the last decade.

Syngenetic ice wedges are a direct indicator of the existence of'cold'permafrost (French, 2012), with mean annual ground temperatures not above −1 to −3 °C [Vasil'chuk, 2013]. Winter air temperature is the main factor controlling the permafrost ground temperature in northern Eurasia. The duration of winters is about 8–10 months in these regions, summer duration is only 2–4 months; hence, even a two-or threefold increase in total summer temperatures would not significantly influence annual temperatures.

Large syngenetic ice wedges are widespread in the Russian permafrost zone. Syngenetic ice wedges accumulate in such a way that ice becomes vertically stratified. The most reliable information was obtained from uniformly thick ice-wedge systems, and from small buried ice wedges formed simultaneously. Although $\delta^{18}O$ data from large and small wedges tend to be similar, the larger wedges provide a more complete palaeoclimatic record. The main advantage of sampling small ice wedges is that their age is more accurately known; they are similar to, or slightly less than, the age of the host sediments. However, small ice wedges are rare, often located at the same depth, sometimes isolated within tiered ice-wedge systems. As such, they may have an anomalous $\delta^{18}O$ composition, reflecting the supply of stagnant bog water or water from other non-atmospheric sources [Vasil'chuk, 1992]. The $\delta^{18}O$ composition of ice-wedge ice is a function of the isotopic signatures of the contributing sources, the proportions contributed from each of them, and the isotopic changes (by mixing, evaporation, or fractionation) during either freezing or by diffusion after freezing. The parameter most strongly related to the $\delta^{18}O$ composition of ice-wedge ice is winter air temperature. In order to establish this relationship, the data on winter air temperature and the $\delta^{18}O$ composition have been compared with modern ice wedges <100 years old, each comprising 8–12 elementary ice veins, in different regions of the Eurasian permafrost zone (Vasil'chuk, 1990, 1992, 2006, 2013). The objectives is reconstruction of mean winter tempratures. Vertical sampling of ice wedges is favoured over horizontal sampling because with the latter it is impossible to establish the exact sequence of ice-wedge formation. Vertical sample spacing was typically 50–100 cm. This allows the oxygen isotope curves to be placed at a chronological scale.

The reconstruction of mean winter and January palaeotemperatures is based on the methodology and relationship established by Vasil'chuk [1992], and revised according to new isotope data in 2015. $\delta^{18}O$ values in modern syngenetic ice wedges ($\delta^{18}O$iw) show a strong empirical relationship with winter air temperatures. These relationships are expressed in the following simplified regression equation (Vasil'chuk 1990, 1992):

t_{mean} January = 1.5 $\delta^{18}O$iw (±3 °C).

where t_{mean} January is mean January temperature of the period of modern ice-wedge formation during last 60–100 years; $\delta^{18}O$ is oxygen isotope composition of ice-wedge ice formed during last 60–100 years

As re-deposition of organic material is common in permafrost [Vasil'chuk, 2013], ^{14}C dates should be carefully evaluated, especially those beyond the range

of radiocarbon dating; these usually correspond to re-worked organic material in yedoma. Therefore, the youngest ^{14}C date from the data set in a particular horizon is most likely the closest to the actual time of accumulation and freezing of the yedoma sediment. In arctic conditions wind-transported organic material may have an age that is clearly different from the time of formation of the wedge. Connecting the age of the surrounding sediment to the formation of an ice wedge is also far from straightforward. When dating is obtained from interpolation, the time window may not be so narrow (4 ka). As in Siberia today, the winter climatic conditions were stable for a long period 40-12 ka BP; therefore, the exact limits of the time window are not very significant for the accuracy of the palaeoreconstruction. Based on the principle of the choice of the youngest ^{14}C date, we selected for this paper 7 horizons (time duration 4 ka) formed approximately during 40-36, 36-32, 32-28, 28-24, 24-20, 20-16 and 16-12 ka BP in every yedoma outcrops.

References

Vasil'chuk, Y.K. [1982]: *Regularities of development of engineering geology conditions in the north of Western Siberia in the Holocene*. English summary (27 pp.) of phd dissertation in geology and mineralogy, Moscow State University, Nauka publ., Moscow (305 pp.).

Vasil'chuk, Y.K. [1992]: *Oxygen isotope composition of ground ice application to paleogeocryological reconstructions*. Volume 1, 420 pp., Volume 2, 264 pp. Theoretical Problems Department, Russian Academy of Sciences and Lomonosov's Moscow University Publications, Moscow (in Russian).

Vasil'chuk, Y.K. [20139 Syngenetic Ice Wedges: Cyclical Formation, Radiocarbon Age and Stable Isotope Records by Yurij K. Vasil'chuk, Moscow University Press, Moscow, 2006. 404 pp. ISBN 5-211-05212-9. *Permafrost and Periglacial Processes*, 24 (1):82–93, 2013. doi:10.1002/ppp.1764.

Micro-scale frost weathering of quartz sand grains

Barbara Woronko[1] & Małgorzata Pisarska-Jamroży[1]

[1] *University of Warsaw, Poland*
[2] *Adam Mickiewicz University, Poznan, Poland*

The most common result of frost weathering is fracturing. Clast-scale fractures (in the range of centimetres to metres) have been studied extensively, but frost weathering at the grain scale (in the range of microns to centimetres) and associated weathering mechanisms are still poorly understood [Matsuoka, 2001]. It is commonly believed that numerous freeze-thaw cycles leave traces on the surface of sand-sized quartz grains as a result of combined mechanical and chemical weathering [Hall and Lautridou, 1991].

Do microstructures resulting from frost weathering depend on the sedimentary environment, that is, what is the influence of previous transport conditions and the type of weathering on quartz surface structures and in which environments are quartz grains exposed to the most intense frost weathering?

Our present contribution examines the microstructures on the surface of sand-sized quartz grains (0.8–1.0 mm and 0.5–0.8 mm) resulting from frost weathering. The surface textures of almost 1,300 quartz grains in the 0.8–1.0 mm and 0.5–0.8 mm size fractions were studied in order to analyse the effects of frost weathering. Some grains had undergone periglacial processes in present-day active layers of Canada, Spitsbergen and Mongolia, whereas other grains were sampled from a former active layer in Poland. The microstructures were studied under a scanning electron microscope and the results were analysed statistically in order to distinguish characteristic microstructures resulting from frost weathering. The quartz grains with these microstructures were deposited during fluvial, aeolian and glacial processes and their characteristic microstructures are classified as primary microstructures. Microstructures that developed on the primary ones as a result of frost weathering are called secondary microstructures.

The most characteristic secondary microstructures are breakage blocks (>10 μm and <10 μm) and conchoidal fractures. Less common are crescentic gouges, curved grooves and scaling [Woronko and Pisarska-Jamroży, 2016]. Grains from every environment may be affected by frost weathering to the same degree, but grains that had been previously transported in, for example, aeolian, fluvial or beach environments are probably the most susceptible to frost weathering. Moreover, the better the rounding of the grains, the more susceptible they are to frost weathering. The primary microstructures that are most susceptible to frost weathering are the convex parts of grains (rounded edges), vertical microsteps (microcliffs) connected with crescentic gauges and big conchoidal fractures, and solution crevasses. Pre-existing microfaults, in-grain weakness zones and microcracks facilitate frost weathering [Woronko and Pisarska-Jamroży, 2016].

Acknowledgements

The work has been financially supported by a grant from the Polish Ministry of Science and Higher Education (research project N306 034 639).

References

Hall, K. and Lautridou, J.-P. [1991]: Introduction–Cryogenic weathering. *Permafrost and Periglacial Processes*, 2(4):269–270, doi:10.1002/ppp.3430020402.

Matsuoka, N. [2001]: Microgelivation versus macrogelivation: towards bridging the gap between laboratory and field frost weathering. *Permafrost and Periglacial Processes*, 12(3):299–313, doi:10.1002/ppp.393.

Woronko, B. and Pisarska-Jamroży, M. [2016]: Micro-Scale Frost Weathering of Sand-Sized Quartz Grains. *Permafrost and Periglacial Processes*, 27 (1):109–122, doi:10.1002/ppp.1855.

SESSION 8

Permafrost Mapping and Data

Convener/ Session Chairs:

Tingjun Zhang, *College of Earth and Environmental Sciences, Lanzhou University, China*

Philip P. Bonnaventure, *Department of Geography, Queen's University, Canada*

Hanne H. Christiansen, *Geology Department, The University Centre in Svalbard, UNIS*

Kirsten Elger, *GFZ German Research Centre for Geosciences, Germany*

Antonie Haas, *Alfred Wegener Institut Helmholtz Centre for Polar and Marine Research, Germany*

Permafrost is one of the least visible parts of the cryosphere. Therefore, there is a growing need to high resolution reliable permafrost maps, for verification of permafrost modelling, improved understanding of how permafrost landscapes might react to climatic changes and for geotechnical purposes. Although national and regional permafrost maps have been complied in the past several decades, the first Northern Hemisphere permafrost map was only published in 1998. Since then, progress has been made on permafrost mapping at national, regional, and/or global scales using a variety of methods. There has, however, not been any new attempt to compile all of the permafrost mapping information to develop new modern permafrost mapping tools.

The International Permafrost Association aims as one of its most important goals towards the development of an online permafrost mapping service. This service will include a collection of all existing permafrost maps at different scales, and potentially build on these to develop new circumpolar permafrost maps. So far no Southern Hemisphere permafrost map exist, and it will be necessary to review to which degree the existing Northern Hemisphere map need revision and updating or if a new map could and should be compiled based on increased permafrost extent and thermal state information.

For large mapping projects like this and especially for long-term permafrost and climate research open access data is becoming a more and more important resource for models and data compilations. This was triggered by the development of new sensor techniques and data storage capacities enabling the collection of high quantities of research data and the development of possibilities to make these data accessible via open international repositories (e.g. PANGAEA, ACADIS, NSIDC, ...) or data portals (e.g. GTN-P Database, NORPERM, maps.awi.de, Arctic Portal, expedition.awi.de, Nordicana D, Polar Data Catalogue, etc.).

In this session we therefore invite local, regional, national or circumpolar contributions to permafrost mapping using different approached such as modelling, remote sensing and direct field mapping or combinations of these and are also open for experiences in the reuse of published research data. Mapping can be of the permafrost extent, its landforms, ground temperatures, active layer thicknesses or other permafrost controlled conditions. We encourage presentations of new ways of performing and visualizing permafrost mapping at all scales. The aim of the session is to obtain a better overview of the state of permafrost mapping in all of the permafrost areas of the World, including in particular Asia and the Southern Hemisphere, from which traditional permafrost mapping has been less widespread.

Permafrost temperature and active-layer thickness of Yakutia with 0.5-degree spatial resolution for model evaluation

Christian Beer[1], Alexander N. Fedorov[2,3], & Yaroslav Torgovkin[2],

[1] *Department of Environmental Science and Analytical Chemistry, Bolin Centre for Climate Research, Stockholm University, Sweden*
[2] *Melnikov Permafrost Institute SB RAS, Yakutsk, Russia*
[3] *International Center BEST, North-Eastern Federal University, Yakutsk, Russia*

Based on the map of landscapes and permafrost conditions in Yakutia (Merzlotno-landshaftnaya karta Yakutskoi0 ASSR, Gosgeodeziya SSSR, 1991), rasterized maps of permafrost temperature and active-layer thickness of Yakutia, East Siberia at 0.5 degree pixel size were derived. The GIS data has been rasterized at 0.001-degree pixel size and then the mean and standard deviation at 0.5-degree grid cell size have been estimated by assigning a probability density function at 0.001-degree spatial resolution. The gridded datasets can be accessed at the PANGAEA repository doi:10.1594/PANGAEA.808240. Spatial pattern of both variables are dominated by a climatic gradient from north to south, and by mountains and the soil type distribution. Uncertainties are highest in mountains and in the sporadic permafrost zone in the south. The maps are suited for benchmarking permafrost-advanced global and regional biosphere models in addition to point observations because they already provide information at the spatial scale of interest.

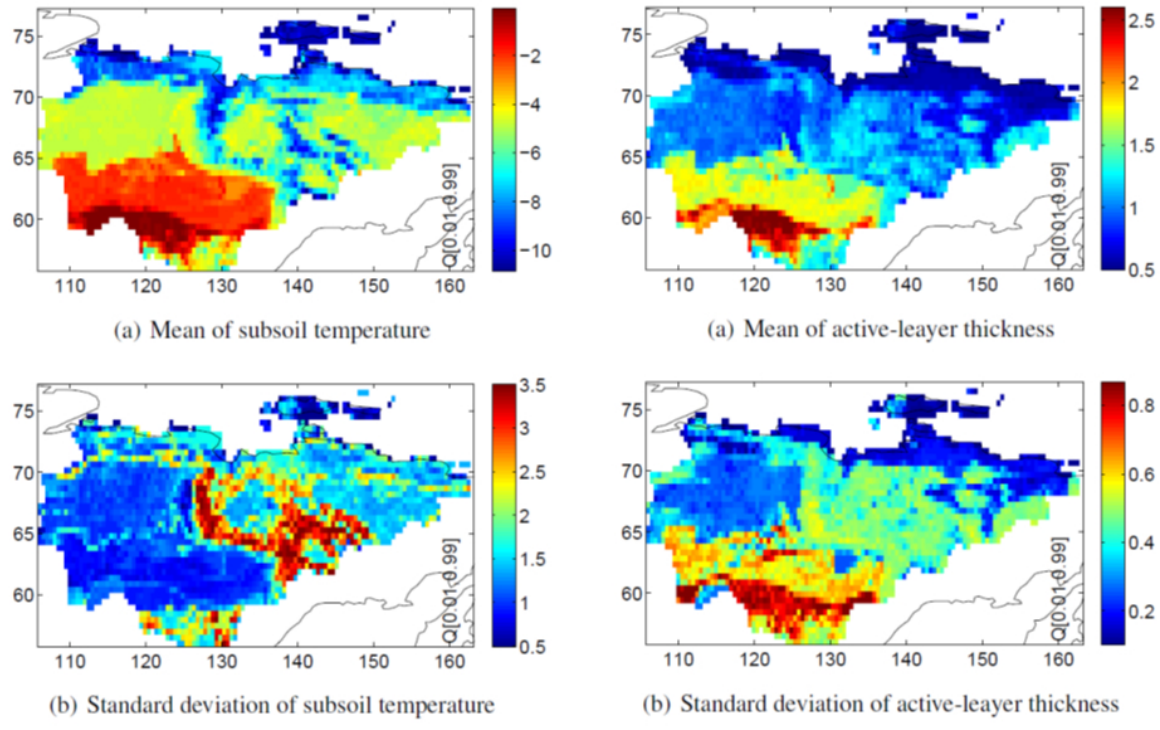

Figure 1: Subsoil temperature and active-layer thickness. Shown are (0.01,0.99)-quantile ranges of mean and standard deviation from several soil and permafrost types within a 0.5 degree grid cell.

Dependency of C- and Ku-band backscatter on snow height and air temperature in permafrost areas

Helena Bergstedt[1], Annett Bartsch[2], & Simon Zwieback[3]

[1] *University of Salzburg, Austria*
[2] *Zentralanstalt für Meteorologie und Geodynamik, Vienna, Austria*
[3] *ETH Zürich, Switzerland*

Microwave remote sensing is an important detection tool, used for a range of applications regarding monitoring of the land surface. The application of this technique in permafrost areas ranges from hydrological issues, soil moisture retrieval and the detection of freeze/thaw cycles to the investigation of questions related to snow and snow-melt events. Microwave remote sensing can provide information about changes in the snow cover relevant to permafrost and is not limited to cloud-free conditions as are optical sensors.

In this study, we assess the dependence of the backscatter signal acquired in C-and Ku-band on snow height and temperature in permafrost areas. To investigate and model this dependence, the analysis of covariance (ANCOVA) was applied. The analysis was done using a data set from the ASCAT Scatterometer on board the EUMETSAT MetOp- A satellite as well as a data set from the Sea Winds instrument on board the QuikSCAT satellite. The ASCAT satellite data has a spatial resolution of 25 km and a temporal resolution of 1-2 days. In addition reanalyses and in situ air temperature and snow data have been investigated. The air temperature data used here is the "CPC Global Summary of Day/Month Observations" data set, available in a daily resolution since 1979. The temperature data set was subset to the time period between 15^{th} of December until the temperature exceeds -1 °C or until the 1th of April for each year, in order to exclude situations of wet or refrozen snow and non-frozen ground. For purposes of mitigating the effect of autocorrelation, only every second day was taken into account. The snow data was obtained from the Russian Institute for Hydrometeorological Information and includes snow height measurements for different stations from 1966 onwards.

The snow height data was prepared similarly as described above concerning the temperature data. The resulting data set includes 20 stations where in situ temperature data and snow data are available and a decrease in the backscatter signal could be detected. The decrease in the backscatter signal indicates a change in the dielectric properties of the soil and points towards a freezing event of the upper soil. Seven stations were discarded due to problems with autocorrelation and/or irregularities in the data set concerning the normality of the residuals which was tested using the Durbin-Watson and the Jarque-Bera test. Furthermore, two stations were not considered due to their significant annual variations of the dependence of snow or temperature. These variations are likely to be caused by changes in vegetation, underlying ground structures or interannual changes in the snow structure (besides height). The final data set contains 11 stations.

Due to the limits of spatial coverage of the in situ data, the ERA-InterimReanalyses products were used to achieve a better spatial coverage, compared to the point analysis possible with the available stations, and temporal resolution of the results.

The snow data product used here represents the snow water equivalent instead of the snow height. To further investigate the influence of ground conditions, such as permafrost type and ground temperature, one site was chosen due to the availability of ground temperature measurements. The ground temperature was obtained from the gtnp-Database.

The results show a covariance of backscatter and instantaneous air temperature. Additionally, it is suggested that the dependence of the backscatter signal on snow height and air temperature depends on the underlying permafrost type as well as, to a smaller extent, on maximum snow storage and average winter temperature.

Comparing models for mountain and lowland permafrost in British Columbia, Canada

Alexandre R. Bevington[1], Marten Geertsema[1], Vanessa Foord[1], & Antoni G. Lewkowicz[2]

[1] *Government of British Columbia, Canada, Canada*
[2] *Department of Geography, University of Ottawa*

Permafrost is present in between approximately 5 and 10 % of the province of British Columbia, Canada. It exists mostly as mountain permafrost, though much of the northeastern region of the province experiences lowland ecosystem protected permafrost. Numerous modelling efforts have produced maps of permafrost probabilities or likelihoods in the region. Seasonal air temperature inversions, diverse snow pack characteristics, variable organic mats and sparsely mapped surficial geology all contribute to the varied results of these models. This study presents a synthesis of the results from ongoing permafrost modelling efforts in the province. New climate and ground thermal data will be also be presented from a large mountainous region with very little active data collection. Additionally, remote sensing measurements provide a valuable tool in such vast regions to investigate regional differences in climatology and topography.

Electronic edition of the permafrost map of Russia 1: 2 500 000

Anatoli Brouchkov & Arina Falaleeva

Lomonosov Moscow State University (MSU), Russian Federation

Significance of the permafrost studies including mapping is increasing due to the intensive development of the natural resources of the Northern Russia and climate change. Development of geoinformation systems (GIS), new methods of spatial analysis and computer modelling provide a great opportunity for a comprehensive and integrated analysis of the permafrost areas. Last paper version of the USSR permafrost map 1: 2 500 000 was published more than 20 years ago. Modern electronic permafrost map of Russia is needed as a basis for environmental assessment, monitoring of natural conditions, engineering projects and activities related to development of natural resources as well as for education purposes. The main purpose of the started work is updated electronic permafrost map 1: 2 500 000. The map gives a opportunity for modelling environmental changes. A few tasks are the part of the project:

1. To summarize published and other materials related the permafrost conditions of the Northern Russia and its current state;

2. To analyze data of the of weather stations network for the last 30 years, including the air annual mean and monthly temperatures, precipitation, density and thickness of snow and soil temperatures;

3. To produce electronic, updated and improved version of the permafrost map of Russia 1: 2 500 000 using analog version of permafrost map of USSR:

   a) to establish structure and content management rules;

   b) to analyze new geocryological, meteorological and remote sensing data (using Mosaic multispectral satellite images) and to compare with data of geocryological map of the USSR;

   c) to integrate the spatial data in the final electronic database for the permafrost map, as well as to produce additional raster layers (vegetation map, land cover map, landscape map) and vector layers (network of weather stations, ground temperature data);

   d) to model ground temperatures based on meteorological and environmental data reflecting the changes in the permafrost conditions of the Northern Russia;

   e) to produce the electronic geocryological map of Northern.

4. To analyze permafrost conditions and its change, to assess the reaction of permafrost to the climate change, to make short and long-term forecast and to visualize it on the map.

The permafrost map 1: 2 500 000 includes electronic topography map and geology maps produced by specialized national institutions. Space imaginary is an important part of the work. There are significant difficulties to integrate the data. A first edition of the electronic map is presented (Fig. 1).

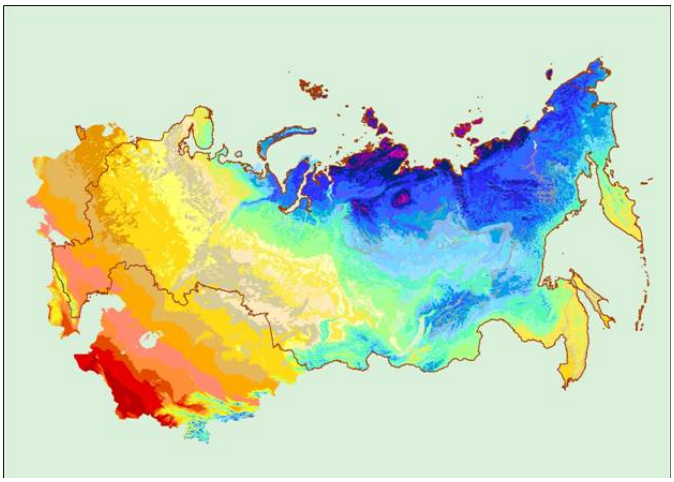

Figure 1: Electronic version of the permafrost map 1: 2 500 000 of Russia

HyLab: Alaska's in-state capability for airborne imaging spectroscopy – Applications for permafrost

Marcel Buchhorn[1,2], Anupma Prakash[2], Donald L. Hampton[2], Jordi Cristóbal-Rosselló[2,3], Christine F. Waigl[2], Martin Stuefer[2], Patrick Graham[2], & Donald A. Walker[1]

[1] *University of Alaska Fairbanks (UAF), Institute of Arctic Biology, United States of America*
[2] *University of Alaska Fairbanks (UAF), Geophysical Institute, United States of America*
[3] *University of Alaska Fairbanks (UAF), Institute of Northern Engineering, United States of America*

Though the impacts of climate change are being felt world-wide, they are far more significant in the Arctic region. The longer summer season and depleting sea ice along the Arctic coasts is posing new opportunities for access and for economic exploitation of the rich natural resources in the Arctic. For Alaska, the only US Arctic state, the need for mapping and monitoring its vastly unexplored terrain is heightened. Therefore, imaging spectroscopy provides a powerful tool to support resource exploration and ecological studies. One of the main ecological applications needed is the mapping and classification of near-surface permafrost. Although permafrost can not be directly detected by imaging spectroscopy, there is a documented correlation between vegetation and presence/absence of near-surface permafrost. Imaging spectroscopy can be used to improve vegetation composition mapping which is not possible with optical multi-spectral imaging. Panda et al. [2012] showed that black spruce in boreal forests can be associated with the presence of near-surface permafrost, whereas moist dwarf birch vegetation communities in tundra can be associated with watertracks and thermokarst prone areas (Fig. 1a).

Over the last decades, the University of Alaska Fairbanks (UAF) has become the research hub for high-latitude research. UAF's Hyperspectral Imaging Laboratory (HyLab), established in 2014 with a Major Research Instrumentation grant from NSF, provides much needed local airborne hyperspectral imaging capability using the HySpex sensor. The HySpex sensor consists of a VNIR-1800 camera (0.4 – 1.0 μm) and a SWIR-384 camera (1.0 – 2.5 μm) that are mounted on a versatile single-engine Aviat Husky A1-B airplane (Fig. 1b). This mobile and low-cost platform allows on–demand acquisition of high resolution hyperspectral data all over Alaska. The Hyspex system can also be configured for in-situ and field scanning by attaching it to a gimbal-mounted rotational stage on a robust tripod (Fig 1c). The HySpex data processing chain was developed by the German Space Agency (DLR) and guarantees the operational production of robust, geo-registered, surface radiance / reflectance products.

In 2014 and 2015, HyLab's HySpex camera system was used to acquire hyperspectral imagery in selected sites in Alaska, providing unique information on terrestrial and aquatic biogeochemical parameters, and diagnostic mineral properties in exposed outcrops. Processed imagery shows promise in mapping vegetation compositions, phytoplankton, and dissolved materials in inland water bodies. This poster shows HyLab's capabilities to support the permafrost community with state-of-the-art tools and algorithms for permafrost detection and mapping. Sample data and products are available on the University of Alaska Fairbanks Hyperspectral Imaging Laboratory (HyLab) website at `http://hyperspectral.alaska.edu`.

References

Panda, S.K.; Prakash, A.; Jorgenson, M.T. and Solie, D.N. [2012]: Near-Surface Permafrost Distribution Mapping Using Logistic Regression and Remote Sensing in Interior Alaska. *GIScience & Remote Sensing*, 49:346–363, doi:10.2747/1548-1603.49.3.346.

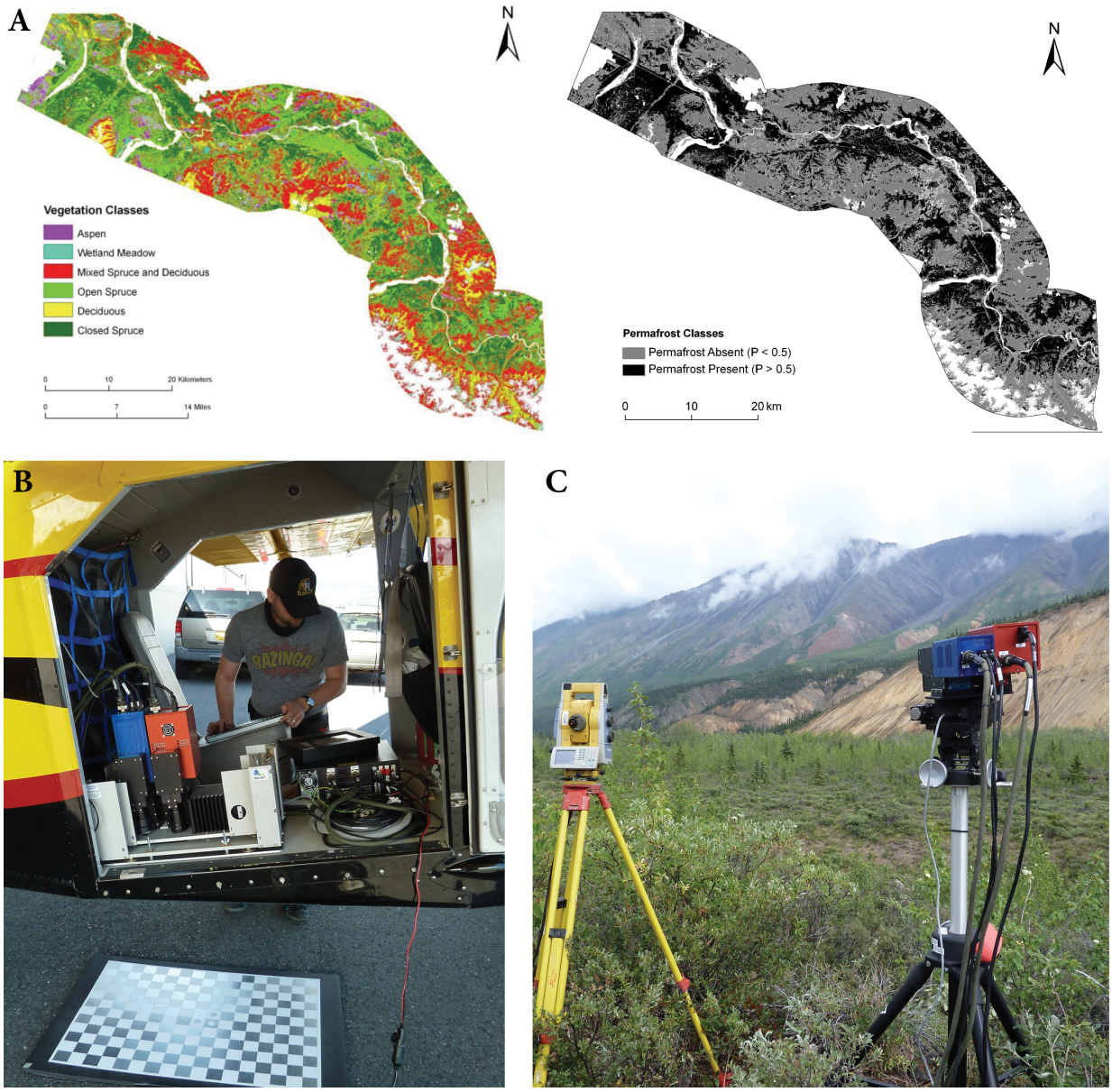

Figure 1: (a) Vegetation composition mapping using RS data and derived near-surface permafrost map (adapted from Panda et al. [2012]). (b) HyLab's HySpex camera system in airborne configuration. (c) HyLab's HySpex camera system in field configuration.

Assessment of permafrost areas using characteristics of rock glaciers in the Himachal Himalaya, North-west part of India

Pritam Chand[1], Sachin Kumar[2], & Milap Sharma[1]

[1] *Jawaharlal Nehru University, India*
[2] *Here Maps Pvt Ltd., Gurgaon, Haryana, India*

Rock glacier define as a creeping mass of ice-rich debris on mountain slopes; the presence of ground ice at depth is indicative of permafrost. The understanding of rock glaciers is relevant to the map the distribution of permafrost areas, the transport of sediment and debris, the evolution of landscapes and its impact on the regional hydrology. Himachal Himalaya is characterised by a distinct periglacial belt that contains many rock glaciers. To investigate the reason for their large size and variable occurrence, we analysed a representative subsample of the rock glaciers with respect to topographic and climatic variables. In addition, we provides first-order assessment of available permafrost maps by Gurber (2012) for the whole Himalayan region at basin scale by detailed mapping of rock glaciers and their characteristics in the Himachal Himalaya. Rock glaciers were mapped using high resolution (5 to 30 m) remote sensing datasets of Worldview, Corona and IRS-PAN with supplement from Google Earth, Bhuvan 2/3-D and field data.

A significant increase in the number of rock glaciers is seen from monsoon-influenced regions (e.g. Ravi, Beas, Satluj) to the dry westerly influenced regions (e.g. Chenab) with annual precipitation below 1000 mm and the lowermost elevation around 3800-4000 m a.s.l. A multi data integrate permafrost model indicates that the rock glaciers originate in the zone where permafrost occurrence is very likely and some large rock glaciers exists down to elevations where permafrost is unlikely to exist. Southward (SE, S, SW) facing slopes are the most suitable for rock glacier development and formation. More than 60 % area of rock glaciers in the inventory have developed on south-facing aspects (SE, S and SW), with SE being the predominant aspect (23.6 %). In addition, number of rock glaciers existence in the monsoon dominated basins (e.g. Ravi) indicate a shift towards more arid climate in the region. Besides, the youthfulness and active nature of the rock glaciers in this region are recorded by the advance over recent fluvial terraces and bottom of glaciated valley. These rock glaciers record recent and widespread ice retreat during late Holocene times, and likely since the Little Ice Age at the turn of this century as same reported by pervious studies for selected glaciers.

On a regional scale, rock glacier distribution is climatically controlled by precipitation and temperature, the latter dependent on elevation and aspect. Further analyses are under way and apart from climatic considerations, how the topographical factors, characteristics of debris covers, catchment morphology, intensive weathering and glacier hypsometry makes response on the distribution of rock glaciers and the permafrost area in the Himalayan region will be addressed.

The Barrow Area Information Database (BAID) and development of a wireless sensor network to provide near real-time climate data for the Barrow Peninsula area of Northern Alaska

Ryan Patrick Cody[1], Craig E. Tweedie[1], Stephen Escarzaga[1], Ari Kassin[1], Mauricio Barba[1] Allison Gaylord[2] William Manley[3] Florencia Mazza Ramsay[1] Sergio Vargas[1] Gabriela Tarin[1] Christine Laney[4] Leanne R. Lestak[3] Sandra Villarreal[1] Gesuri Ramirez[1] Qaiyaan Aiken[5] Julia Collins[6] Erika Green[5] & Lars Nelson[7]

[1] *University of Texas at El Paso, United States of America*; [2] *Nuna Technologies, Homer, AK, USA*
[3] *Institute of Arctic and Alpine Research, University of Colorado, Boulder, CO, USA*
[4] *National Ecological Observatory Network (NEON), Boulder, CO, USA*
[5] *UMIAQ, Barrow, AK, USA*; [6] *NSIDC, University of Colorado, Boulder, CO, USA*
[7] *Ukpeagvik Iñupiat Corporation, Anchorage, AK, USA*

The Barrow area of northern Alaska is one of the most intensely researched locations in the Arctic and the Barrow Area Information Database (BAID, www.barrowmapped.org) tracks and facilitates a gamut of research, management, and educational activities in the area. BAID is a cyberinfrastructure (CI) that details much of the historic and extant research undertaken within in the Barrow region in a suite of interactive web-based mapping and information portals (geobrowsers). The BAID user community and target audience for BAID is diverse and includes research scientists, science logisticians, land managers, educators, students, and the general public. BAID contains information on more than 12,000 research sites that extend back to the 1940's, and more than 640 remote sensing images and geospatial datasets. Recent additions and activities include information on more than 2000 new research sites, provision of differential global position system (dGPS) and high resolution aerial imagery support to visiting scientists, erosion surveys along ca. 120 km of coastline, bathymetric and seafloor habitat mapping of the nearshore environment, training of local GIS personal to aid decision making, and the development of a 5-node wireless micrometeorological sensor network. This presentation will present an overview of BAID efforts and specific detail on the development, deployment, web data visualization, and web data services for the wireless micrometeorological sensor network.

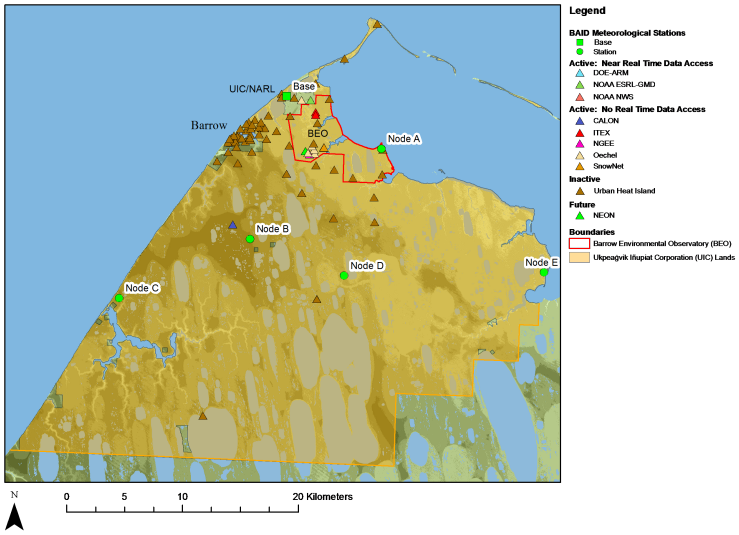

Figure 1: Sensor network station locations and other major monitoring efforts.

Characterization of sporadic discontinuous permafrost occurrences in Northeastern, British Columbia, Canada

Tara Lee Coultish, Geoff K. Claypool, & Lukas U. Arenson

BGC Engineering Inc., Canada

Since the mid 2000's, the Horn River Basin, located in northeastern British Columbia, Canada, has experienced a significant increase in the development of pipeline infrastructure to support development of natural gas deposits in this area. The area is located within the sporadic discontinuous zone of permafrost and primarily comprised of lowlands containing thick organic deposits. The permafrost within this area is highly sensitive to even small disturbances from the clearing of vegetation to permit pipeline construction and the operation of the pipelines at temperatures above freezing, which typically results in thawing of the permafrost. Due to the potential for settlement associated with this thaw and the further potential to induce strain on the pipeline, it is critical to identify and characterize permafrost occurrences along proposed routes to support pipeline design. Currently, minimal literature exists describing the permafrost characteristics in northeastern British Columbia. We present a detailed account of the permafrost identification and characterization program undertaken prior to construction of the pipeline.

A geotechnical assessment for a new pipeline project in the Horn River Basin was undertaken in 2009 and 2010. The project area is located approximately 70 km northeast of the town of Fort Nelson, British Columbia. The objectives of the geotechnical assessment program included identifying areas underlain by permafrost and characterizing the permafrost conditions through a combination of terrain mapping, geophysical investigation, subsurface investigation and thermistor installation along the approximately 74 km length of the proposed route.

Based on the results of the characterization program, approximately 5.4 km (non-continuous) of permafrost in 19 separate occurrences were identified along the pipeline route. The permafrost occurrences were found to range from 80 to 710 m in length along the route. Approximately 2.1 km (or approximately 40 %) of the identified permafrost occurrences were observed to be shallow and confined to the upper 3 m of the soil profile. The thickness of the permafrost was found to range from 2.1 to 7.6 m. Based on the characterization information, mitigation measures for select permafrost occurrences were implemented during construction.

Thermistor strings were installed in select permafrost occurrences in 2010, just prior to the construction of the pipeline. The temperature of the permafrost at the time of construction was measured to range from 0 to -1 °C. Ground temperature in areas where degradation was noted in the surface expression of permafrost areas, was at or near 0 °C +/- 0.2 °C. Thermistor readings taken post-construction in 2012 and 2013, indicated that sub-zero temperatures continued to persist below 1 m from ground surface. Monitoring of the ground temperatures in select permafrost occurrences is on-going for the purpose of determining when the permafrost has degraded.

Analysis and mapping of mountain permafrost data: spatial modelling using machine learning algorithms

Nicola Deluigi[1], Mikhail Kanevski[1], Reynald Delaloye[2], & Christophe Lambiel[1]

[1] *Institute of Earth Surface Dynamics, University of Lausanne, Switzerland*
[2] *Department of Geosciences, University of Fribourg, Switzerland*

It is commonly accepted that the distribution of mountain permafrost is extremely discontinuous. However, a clear representation on how the phenomenon is spatially distributed in sedimentary deposits is still difficult to obtain. Although physical models are able to efficiently simulate the ground thermal state at a single site (1D, e.g. borehole), they are not adapted to map mountain permafrost distribution (2D), because of the high number and high spatial variability of needed input data. Existing empirico-statistical models are more concerned with the prediction of the permafrost distribution rather than the description of the subsurface thermal state. They usually offer a good overview of the potential distribution at the local and regional scale. However, they are not always able to reproduce the high spatial discontinuity of mountain permafrost at the micro scale (scale of a specific landform; ten to several hundreds of meters) because they are generally thresholding the occurrence of permafrost on the basis of a restricted number of topographical and climatic parameters.

The objective of this research is to find an efficient alternative to both physical and empirico-statistical models. Machine learning (ML) algorithms are able to take into account a higher number of parameters compared to classic approaches, while producing high resolution maps with relative low computational times. With these techniques, the permafrost distribution can be modeled not only using topo-climatic parameters as a proxy, but also by including field permafrost evidences. Therefore, for this study, which deals with the analysis of mountain permafrost in the Western Valais Alps (Switzerland), machine learning algorithms were applied. The input dataset represents a high dimensional variable space (dimension = 20-25, spatial resolution = 10m), which was constructed using a digital elevation model, landcover maps, climate data, etc. Empirical data collected during field campaigns (mainly ERT and SRT profiles, apparent resistivity mapping lines and measured ground (surface) temperatures) and mapped active and inactive rock glaciers serve as training permafrost data. This information was then provided to ML algorithms with the purpose to estimate the class of unseen instances (pixels) using the model trained on known permafrost distribution data (positive and negative permafrost evidences). As we dispose of poor permafrost evidences available for rockwalls, we mainly focused our prediction in loose sediments.

With this approach, functional dependencies between permafrost and its explaining controlling factors are derived directly from data. Conversely to traditional models, these supervised learning techniques have the task of inferring a classification function from labelled training data (pixels of permafrost absence and presence) with the purpose of predicting the permafrost occurrence where the latter is unknown. In addition, ML techniques can be coupled with feature selection algorithms or have an embedded ability to provide measures of the variable importance. This allows the identification of the statistical contribution of each controlling factor and the refinement of the model by excluding non-relevant or redundant predictors (resulting in more robust and less uncertain prediction and reduced computational time).

We tested three different machine learning algorithms: Artificial neural networks (ANN), Support Vector Machines (SVM) and Random Forest (RF). ANN is a semiparametric nonlinear tool inspired by the way biological nervous systems process provides information (such as the brain). Neural networks are organized in layers (made of interconnected nodes) where the learning process is computed through a weighted connection system. Weights are iteratively processed and transformed by a function. This process is repeated until an output neuron is activated, providing a prediction. Differently, SVM try to classify a set of training data by constructing a decision (hyper-)plane directly in the multidimensional vari-

able space. The estimated (hyper-)plane allows the separation of the training examples with different labels (presence and absence of permafrost). The classification of unknown examples (pixels) is obtained by mapping them into that same space and estimating the side of the plane they fall on. Finally, RF is an ensemble learning method that operates by constructing a large collection of decorrelated classification trees, and then predicts the permafrost occurrence through a majority vote. Decision trees are able to capture complex structures in the data while keeping relative low bias.

The adopted machine learning algorithms have demonstrated to be efficient for permafrost distribution modelling with consistent results compared to the field reality. For instance, rock glaciers and limits between vegetation and mineral surfaces are correctly recognized and permafrost occurrence in talus slopes is predicted without recurring to altitude thresholds. The high resolution of the input dataset (10 meters) allows also elaborating maps at the micro scale with a modelled permafrost spatial distribution less optimistic than other classic spatial models. Moreover, machine learning is a non-deterministic approach, with a particular focus on uncertainties assessments. For this reason, we present retained permafrost models coupled with uncertainties maps providing information on the quality of our results.

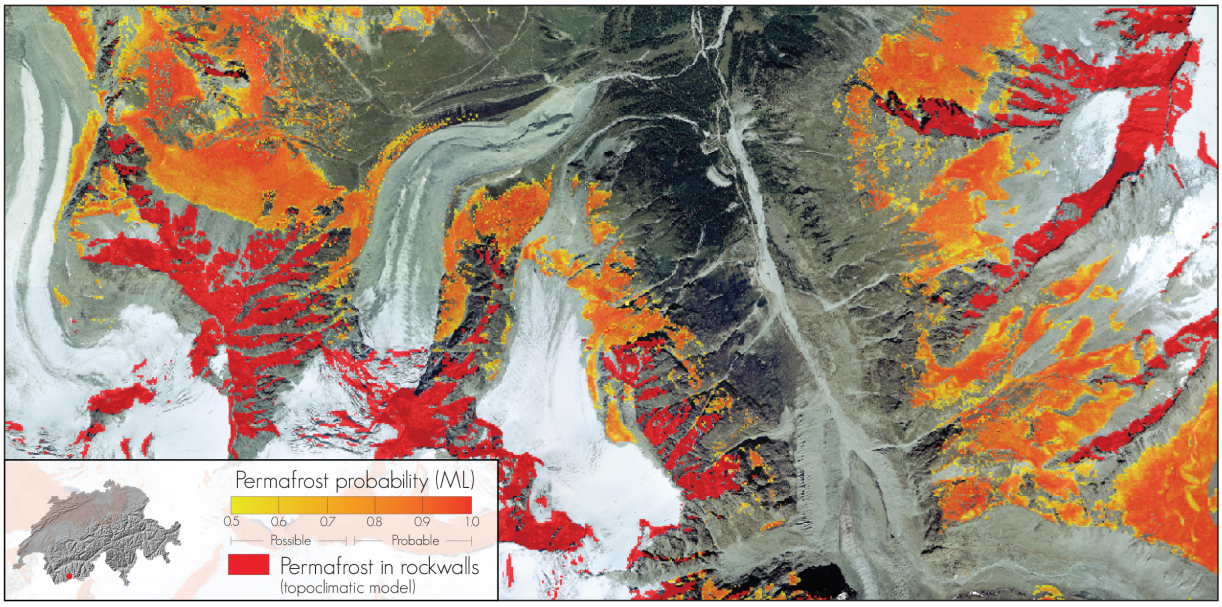

Figure 1: Potential permafrost distribution map using Random Forest for the Hérens Valley upper part (Arolla, Valais, Switzerland).

Feature selection algorithms for permafrost variable importance assessment: A support to efficient permafrost distribution mapping

Nicola Deluigi[1], Christophe Lambiel[1] Reynald Delaloye[2], & Mikhail Kanevski[1]

[1]*Institute of Earth Surface Dynamics, University of Lausanne, Switzerland*
[2]*Department of Geosciences, University of Fribourg, Switzerland*

Nowadays we observe constant improvements in terms of both spatial resolution and quality of geo-data, and as a consequence the size of datasets increases considerably. Spatial mountain permafrost models have experienced remarkable enhancements during the last two decades thanks to the availability of new geo-data. However, the extreme discontinuity of the permafrost distribution is still hard to map at

the micro scale (scale of a specific landform; ten to several hundreds of meters). High resolution maps are difficult to compute because of the necessary computational time and technical requirements, especially when dealing with physical models.

The main objective of this study is to present an alternative approach for mapping permafrost to both physical and statistical classic modelling techniques. Therefore, we mapped the distribution of mountain permafrost using machine learning (ML) classification algorithms. With this approach, functional dependencies between permafrost and its explaining controlling factors are derived directly from the data, and predictions of the permafrost occurrence can be made for sectors where the distribution is unknown. The used input dataset represents a so-called high dimensional variable space (dimension = 20-25, spatial resolution = 10m). It was constructed using a digital elevation model and derived variables (slope, orientation, potential solar radiation, etc.), landcover maps and climate data, and completed with permafrost evidences (field data and rock glacier inventories) that serve as training permafrost data. When dealing with such large set of high-dimensional data one of the major problems is the number of input features (variables) involved. The analysis of a large amount of raw data is not always an easy task in terms of computational difficulties. Applying classification algorithms to this large number of variables may lead to the risk of overfitting, with the consequence of a poor generalization of the new predicted data (permafrost occurrence for a given pixel). Feature selection (FS) techniques help to avoid these issues by simplifying the amount of factors required to the final modelling. As a consequence, raw data need to be analyzed and redundant variables to be removed from the dataset. On the one hand, this process lead to an improved knowledge on adopted features and their relation with the studied phenomenon. On the other hand, taking away irrelevant or redundant variables from the data may provide effectively an improvement to the ML modelling algorithms.

For this study, FS algorithms informed about variables that appeared less statistically important for permafrost presence/absence, allowing excluding useless predictors from the dataset in order to obtain an efficient model. All existing types of FS approaches were used in this context (filters, wrappers and embedded techniques). We compared three different algorithms: Information Gain (IG), Correlation-based Feature Selection (CFS) and Random Forest (RF). IG is a filter technique that evaluates the worth of a predictor by measuring the information gain with respect to the permafrost presence/absence. Conversely, CFS is a wrapper technique that evaluates the worth of a subset of predictors by considering the individual predictive ability of each variable along with the degree of redundancy between them. Finally, RF is a ML algorithm that performs FS as part of its overall operation. It operates by constructing a large collection of decorrelated classification trees, and then predicts the permafrost occurrence through a majority vote. With the so-called out-of-bag (OOB) error estimate, the classification of permafrost data can be validated as well as the contribution of each predictor can be assessed.

Exploited FS algorithms have proven to increase the performances of used ML permafrost distribution models, which were computed on an independent validation sets. The number of variables of the input dataset was reduced by removing irrelevant and redundant features, providing faster and more cost-effective predictors, and providing a better understanding of the underlying structures residing in permafrost data. Finally, permafrost predictors could be ranked not only based on their heuristic and subjective importance, but also based on their statistical relevance in relation of the permafrost distribution.

Data Publications – persistent and citable products of research

Kirsten Elger[1], Kerstin Lehnert[2], & Damian Ulbricht[1]

[1] *GFZ German Research Centre for Geosciences, Germany*
[2] *Interdisciplinary Earth Data Alliance, Lamont-Doherty Earth Observatory, Columbia University, USA*

During the past decade, the relevance of research data has been rising significantly and the free and open access not only to scientific results, but to research datasets has been identified as a key issue by the scientific community, funding agencies and the public. As a consequence, there is a dynamic co-evolution of national and international guidelines on management of and open access to research data (e.g. Berlin Declaration on Open Access to Knowledge in the Sciences and Humanities, G8 Open Data Charter, EU Horizon 2020 Guidelines, etc.) and the development of concepts to make data persistently accessible and citable products of research.

Especially in permafrost and climate research, long-term observatories and world-wide monitoring programmes are essential to understand the impact of, e.g., permafrost thaw on the Earth climate system and consequently of climate change. Many datasets are online available, via data portals or databases like, e.g. at the National Snow and Ice Datacentre, the GTN-P Database, NORPERM, Fluxnet, etc., but often without the possibility to give the data providers recognition and acknowledgement for contributing data to a global network.

During the past years, the publication of research datasets with assigned digital object identifier (DOI) has emerged as best practice for citable and persistent open access research data together with the deserved recognition of the data providers. An important step for the international acceptance and recognition of DOI-referenced data publication is the'Statement of Commitment'of the Coalition for Data Publication in the Earth and Space Sciences (COPDESS) that aims to promote joint policies and procedures for the publication and citation of data across Earth Science journals. Key commitments, signed by many publishers and data centres, are the acceptance of data citations within reference lists of research articles, the improvement of cross-references between journal articles and published datasets, and the strong recommendation to, whenever possible, store datasets in appropriate, theme-specific data repositories, in which data access and long-term preservation are guaranteed and datasets are accompanied by sufficient metadata to enable data reuse and discovery.

A comprehensive data description is essential for data reuse. Data publication is mostly known as supplementary material to scientific articles. Very often, however, the data description in the journal article is not sufficient for data reuse leading to many published dataset not being used as much as they could be. To improve this, many disciplines have developed and are developing "Data Journals" that aim to publish scientific articles with the detailed description of datasets, data portals or data collections that will be published along with the datasets. There are different formats for articles in data journals, but all have in common that they lack of any scientific interpretation of the described datasets. For standalone publication of datasets where neither format is an option, accompanying data reports are a convenient and flexible tool for enhanced data description.

Experiences of contributions to an international monitoring network from an institutional data repository

Joel Fiddes[1], Nataliya Kryvych[2], Charles Fierz[1], & Øystein Godøy[1]

[1] *WSL Institute for Snow and Avalanche Research SLF, Switzerland*
[2] *Ecole Polytechnique Féédérale de Lausanne, Switzerland*
[3] *Norwegian Meteorological Institute, Norway*

The Institute for Snow and Avalanche Research (SLF) in Switzerland has over the past several years been developing a research data platform that enables the management of multiple cryosphere based data-sources (mainly permafrost boreholes, snow measurements and meteorological stations) through real-time streaming, radio links, logger dumps etc. as well as providing an interface for data discovery, delivery and storage of related metadata.

Over the past year, as members of The Global Cryosphere Watch (GCW http://globalcryospherewatch.org/) and operating a GCW CryoNet Integrated site, we standardised metadata formats, delivery protocols as well as addressing issues of data publishing (DOI) and data access policies. We have benefited from a close collaboration with the Norwegian Meteorological Institute, who are leading the development of the GCW catalogue interface and interoperability tools. Our experience has covered a range of technological and political hurdles that represents the shift in both technological developments and data policies over the last decade.

Specifically, in this presentation we will:

1. Introduce and describe the interaction between an institutional data repository and international portal/ network, which possibly has a wider significance.

2. Describe the technology employed to transfer dynamic data-sources from sensor to data repository and enable metadata harvesting by external partners.

3. Discuss technical challenges of standardisation, interoperability and rapidly evolving technology/ standards.

4. Discuss political challenges faced by data policies and a groundswell in emerging data-platforms, networks and other data infrastructures.

This presentation aims to demonstrate a successful interface between an institutional repository and international network that draws on standard data/metadata formats, exchange protocols and other emerging forms of best practice in this young field. We hope the experience gained through this interface will be of broad interest to members of the community involved in similar models of data/metadata exchange.

A new permafrost map for the Scandinavian Peninsula

Kjersti Gisnås[1], Bernd Etzelmüller[1], Göran Alm[2], Hanne H. Christiansen[3], Jon Engström[4], Andrew Frampton[2], Jan Hjort[5], Ketil Isaksen[6], Peter Kuhry[2], Cristian Lussana[6], A. Britta K. Sannel[2], Sebastian Westermann[1], & Jonas Åkerman[7]

[1] *University of Oslo, Norway*
[2] *University of Stockholm, Sweden*
[3] *Arctic Geology Department, The University Centre in Svalbard, Norway*
[4] *Geological Survey of Finland, Finland*
[5] *University of Oulu, Finland*
[6] *Norwegian Meteorological Institute, Norway*
[7] *Lund University, Sweden*

Knowledge about the spatial distribution and temperatures of permafrost is crucial for several reasons, in particular as a baseline for validation of global and regional climate models and associated land surface models. It is also an important tool for planning of human activities. Permafrost is not necessarily visible on the ground surface as it is solely a thermally defined phenomenon. It is therefore important to establish a common, research-based understanding of the permafrost distribution at a sufficient spatial resolution to meet scientific and societal demands.

The "International Permafrost Association Circum-Arctic Map of Permafrost and Ground Ice Conditions" (the "IPA map") by Brown et al. [2001] is an example of such a map. This map was produced by gathering information from researchers working with permafrost all over the world, and acts as a baseline for validation today. It provides information on the spatial distribution of permafrost along with ground ice content, and is mainly based on experience and field observations. The scale of the map is coarse, and it has therefore only limited application in regional areas like the Scandinavian Peninsula. In this region, numerous field-based studies have been conducted since the 1980s, including the establishment of around 25 permafrost boreholes. The new knowledge draws a more differentiated image of the permafrost distribution, justifying a revision of the IPA map for the Scandinavian Peninsula.

The first priority for a new baseline map is to gain the trust of the researchers working with permafrost in the area. A new map should therefore also to a large degree be based on observations. For permafrost, this includes primarily all climate parameters such as air temperature and snow conditions, along with the distribution and type of surficial material. To achieve the desired spatial resolution, climate information must be transferred to soil temperatures, and thus permafrost distribution, applying a numerical model. A model used for this purpose should be robust enough to give trustworthy results, and simple enough to gain relevant input parameters over a larger area, preferably through field observations. In a second step, the resulting permafrost distribution must be validated in different areas, both quantitatively and qualitatively, to ensure that there is no spatial bias.

We present a new permafrost map for the Scandinavian Peninsula providing a more detailed and updated description of the permafrost distribution in this area. The map is obtained by applying a simple numerical equilibrium model, the CryoGRID1 [Gisnås et al., 2013], forced with 1 km^2 gridded data on daily air temperature and snow cover for the period 1981 – 2010. This gridded data set was recently developed by the Norwegian Meteorological Institute within the Nordic Framework For Climate Services (`http://blog.fmi.fi/nordmet/node/100`), based on the Norwegian Climate Database together with the ECA&D joint observation dataset [Klein Tank et al., 2002]. The permafrost model uses a very limited set of parameters, mainly to describe the temperature offsets between air, ground surface and deeper ground temperatures. These parameters were refined based on extensive field measurements for snow, mires and palsas. The model results are qualitatively evaluated by permafrost researchers with experience within the area, and against available ground thermal observations, BTS-mappings and geomorphological maps showing the location of permafrost landforms.

References

Brown, J.; Jr.Ferrians, O.J.; Heginbottom, J.A. and Melnikov, E.S. [2001]: Circum-Arctic map of permafrost and ground-ice conditions. International Permafrost Association, National Snow and Ice Data Center/World Data Center for Glaciology. Digital Media. Boulder CO, URL http://nsidc.org/data/ggd318.html.

Gisnås, K.; Etzelmüller, B.; Farbrot, H.; Schuler, T. V. and Westermann, S. [2013]: Cryogrid 1.0: CryoGRID 1.0: Permafrost Distribution in Norway estimated by a Spatial Numerical Model. *Permafrost and Periglacial Processes*, 24(1):2–19, doi:10.1002/ppp.1765.

Klein Tank, A. M. G.; Wijngaard, J. B.; Können, G. P.; Böhm, R.; Demarée, G.; Gocheva, A.; Mileta, M.; Pashiardis, S.; Hejkrlik, L.; Kern-Hansen, C.; Heino, R.; Bessemoulin, P.; Müller-Westermeier, G.; Tzanakou, M.; Szalai, S.; Pálsdóttir, T.; Fitzgerald, D.; Rubin, S.; Capaldo, M.; Maugeri, M.; Leitass, A.; Bukantis, A.; Aberfeld, R.; van Engelen, A. F. V.; Forland, E.; Mietus, M.; Coelho, F.; Mares, C.; Razuvaev, V.; Nieplova, E.; Cegnar, T.; Antonio López, J.; Dahlström, B.; Moberg, A.; Kirchhofer, W.; Ceylan, A.; Pachaliuk, O.; Alexander, L. V. and Petrovic, P. [2002]: Daily dataset of 20^{th}-century surface air temperature and precipitation series for the European Climate Assessment. *International Journal of Climatology*, 22(12):1441–1453, 2002. doi:10.1002/joc.773.

Measurement of subsurface ice content and temperature using broadband spectral induced polarization

Robert Grimm & David Stillman

Southwest Research Institute, United States of America

The electrical polarizabilities of unfrozen, interfacial water and protonic defects in ice cause large, diagnostic decreases in resistivity between 100 Hz and 100 kHz that can be exploited for permafrost mapping. We developed temperature-dependent relationships between ice volume fraction and resistivity frequency effect (the normalized resistivity difference in two frequencies spanning the decrease) for samples taken from the US Army Permafrost Tunnel (Fox, Alaska, USA) and applied them to field measurements along 16 m within the tunnel. We found a best-fitting temperature of -3 +/- 0.5 C and ice contents 45-95 % by volume. Both results agreed quantitatively with the bulk properties of the tunnel, and the ice-content image correlated qualitatively with major permafrost features. A follow-on set of surface surveys in Tok, Alaska, demonstrated that two widely-used, commercial, narrowband systems can recover the essential information much faster, especially if spot-calibrated by full broadband measurement. Broadband spectral induced polarization can also be applied to permanent surface-electrode installations to monitor subsurface temperature change (+/- 0.1 C) through the temperature dependence of the polarizability. These new geoelectrical methods can provide detailed images of permafrost properties beneath the active layer, without drilling.

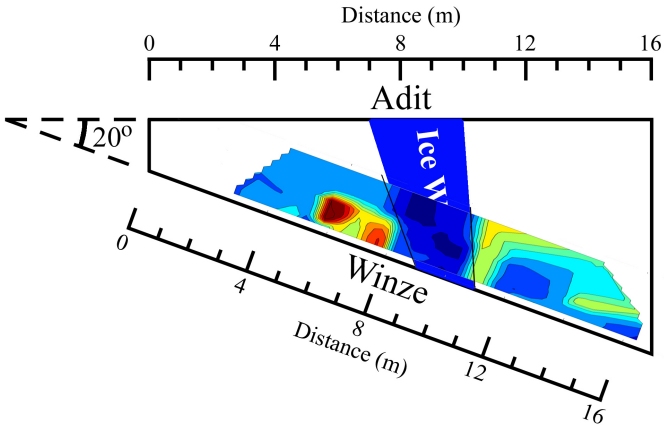

Figure 1: Ice content perpendicular to wall of Alaska Permafrost Tunnel

Continental and global scale permafrost mapping: Persistent challenges and new directions

Stephan Gruber

Carleton University, Canada

Permafrost usually cannot be directly observed at the land surface. Its detection and characterization are therefore difficult and costly, even when applied at one specific location, only. As a consequence, reliable permafrost data is sparse. For places and times without direct observations, we rely on models for predicting the existence or specific properties of permafrost based on observable or otherwise quantified variables. Because observations are rare, most of what we know about permafrost globally relies on models or one kind or another.

The continued expansion of human activity into cold regions together with concern about the effects of climate change have brought about a strong increase in the demand and ability to simulate permafrost. Simulations often produce spatial data or maps. On their basis, findings are aggregated to coarser scales or made accessible for further use. The confidence we have in such products – as well as the improvement of simulation tools – depend on our ability to quantify how well simulations agree with reality.

This presentation will review fundamental challenges in how we compare permafrost maps or spatial data with observations as well as avenues for addressing these challenges.

Permafrost-related research data - their accessibility, visualization, and publication using GIS and WebGIS technology

Antonie Haas[1], Birgit Heim[1], Sebastian Zubrzycki[2], Kirsten Elger[3], & Anne Morgenstern[1]

[1] *Alfred Wegener Institute Helmholtz Centre for Polar and Marine Research, Germany*
[2] *Universität Hamburg, Allende-Platz 2, 20146 Hamburg, Germany*
[3] *GFZ German Research Centre for Geosciences, Telegrafenberg, 14473 Potsdam, Germany*

Permafrost regions are highly sensitive to climate changes. To monitor key variables and to identify environmentally relevant-processes is of topmost importance in these environments. Beside data analysis and map creation capabilities, Geographical Information Systems (GIS) also comprise functionalities for mobile data acquisition in the field, data transfer, data monitoring, data description, as well as data sharing and publication of data as WebGIS Services (Web Map/Feature Services (WMS, WFS)). Due to their excellent usability GIS technology and services are very common in many scientific disciplines all over the world, and since most data formats are standardized data re-use and data interchangeability are guaranteed. We visualize field-derived and remote sensing-derived research data, collected within Russian and German cooperation projects in the Lena River Delta, Laptev Sea Region (Siberia) on a Web GIS Platform. We visualize the locations of long-term discharge measurements and of soil sampling for organic Carbon and Nutrients. Geormorphological feature classes derived from satellite data and publicly available environmental data layers (e.g. vegetation, soils, and digital elevation models) display the broader regional and thematic context. AWI offers WebGIS services published under http://maps.awi.de/awimaps/. The WebGIS core components are ArcGIS for Server 10.3 and PostgreSQL databases 9.3 including Spatial Database Engine (SDE).

The Arctic Permafrost Geospatial Centre (APGC): A new central platform for hosting and distributing geospatial permafrost datasets

Sebastian Laboor[1], Guido Grosse[1], Antonie Haas[2], Birgit Heim[1], & Ingmar Nitze[1]

[1] *Alfred Wegener Institute Helmholtz Centre for Polar and Marine Research, Potsdam, Germany*
[2] *Alfred Wegener Institute Helmholtz Centre for Polar and Marine Research, Bremerhaven, Germany*

The Arctic Permafrost Geospatial Centre (APGC) is currently being designed as a web interface showcasing high level projects producing geospatial datasets with permafrost focus and will provide an entry point for their geospatial product dissemination needs.

At the core of the APGC we are establishing two services for data discovery: an Open Access Data Catalogue and an Open Access WebGIS Application (Fig. 1). The APGC Data Catalogue will allow searching for project-specific geospatial data by tags, keywords, data type and format, licence type, or geographically, provides a data preview figure, localizes the dataset on a zoom- and pan-capable basemap, displays a variety of metadata, and links to a permanent DOI-based archival link at the PANGAEA data repository. The APGC Data Catalogue will be based on the open source CKAN data catalogue architecture, allowing geospatial data categorization associated with defined projects based on metadata standards. The Data Catalogue will contain all final products of projects that will be featured here, for example the ERC PETA-CARB project and the IPA Action Group on Yedoma ice-rich permafrost.

The WebGIS Application will rely on OGC-standardized Web Mapping Services (WMS) and Web Feature Service (WFS) technologies for data display and visualization. The WMS/WFS services are provided through the Data Catalogue. We are further evaluating the possibility to load external WMS/WFS services in the WebGIS Application. Legends will provide information on data attributes, and pop-up menus will provide information on metadata and a link to the archive location for a dataset. The WebGIS Application will provide a platform independent and visually interactive platform for displaying both raster and vector geospatial data from the project.

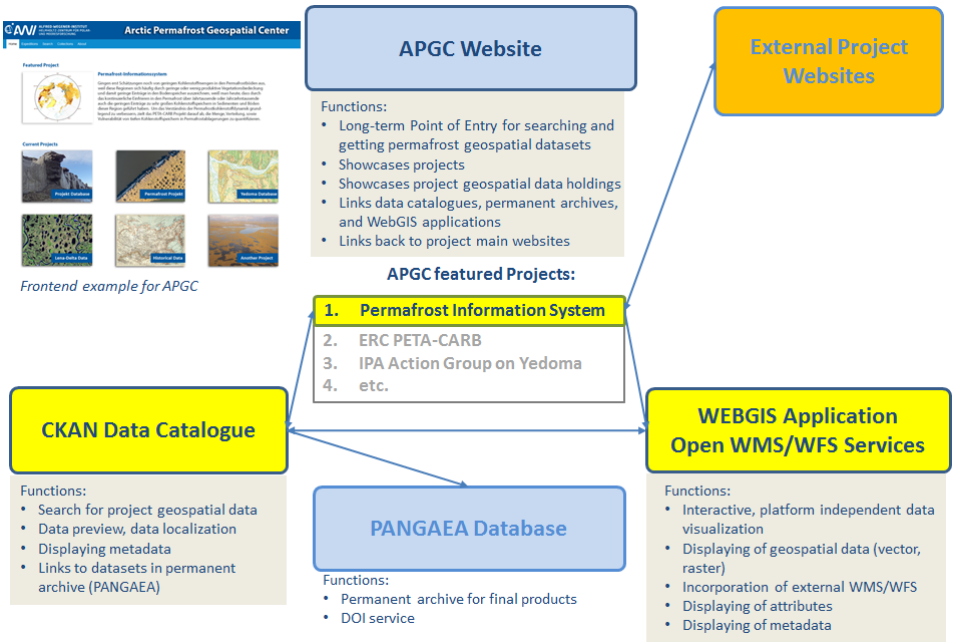

Figure 1: Conceptual structure, dependencies, and key functionalities of the Arctic Permafrost Geospatial Centre. Yellow: New Permafrost Information System including new Services; Blue: ERC PETA-CARB and AWI infrastructure; Orange: External project websites.

Mapping polygonal tundra geomorphology across the Arctic Coastal Plain of Alaska

Mark Jason Lara[1], Philip Martin[2], & Anthony David McGuire[1,3]

[1]*Institute of Arctic Biology, University of Alaska, Fairbanks, Alaska, USA*
[2]*Arctic Landscape Conservation Cooperative, U.S. Fish and Wildlife Service, Fairbanks, Alaska, USA*
[3]*U.S. Geological Survey, Alaska Cooperative Fish and Wildlife Research Unit, University of Alaska Fairbanks, Fairbanks, Alaska, USA*

The northern Alaskan Arctic Coastal Plain (ACP) represents approximately 60,000 km^2 of low relief, permafrost landscape, which is composed of a mosaic of low relief ice-wedge polygons, meadows, ponds, lakes, and rivers. Sub-surface ice aggradation and degradation related heaving and subsidence of the ground surface influences geomorphology and fine-scale surface microtopography, altering local hydrology, snow pack depth and density, plant community composition, soil organic carbon storage, land atmosphere CO_2 and CH_4 fluxes, and associated distribution of essential habitat for use by avian and mammalian wildlife. Despite the known importance of fine-scale tundra geomorphology on key ecosystem processes, the spatial distribution of these land cover types spanning large scales is largely unknown.

We use an object based image analysis, using LandSat 8–OLI satellite imagery and an array of ground based photography and field data to create the first polygonal tundra geomorphology map for the ACP of Alaska, at a spatial resolution of 30 × 30 meters. We map fourteen dominant land cover classes, including:

1. Coastal waters,
2. Lakes,
3. Ponds,
4. Rivers,
5. Meadows,
6. Coalescent low-center polygons,
7. Low-center polygons,
8. Flat-center polygons,
9. High-center polygons,
10. Drained slope,
11. Riverine barrens,
12. Sand dunes,
13. Ice, and
14. Urban (i.e. towns and roads).

Land cover classes correspond well with previous site-level geomorphic maps near Atqasuk, Prudhoe Bay, Barrow, and Fish Creek, Alaska. We find polygonal tundra distribution to be quite different across scales as topography, vegetation type, and soil type vary spanning the ACP (Fig. 1). Following Jorgenson et al. (2011), we divide this region into two primary subregions, the Arctic Peaty Lowlands and the Arctic Sandy Lowlands. Across the ACP we identify high and low-center polygons to be the most common geomorphic types, representing 34 and 18 %, respectively, while lakes, ponds, and rivers represent 12, 3, and 1 % of the land cover area, respectively. Though, high-center polygons are the dominant class of the region, most of this land cover type occurs within the Arctic Sandy Lowlands. This fine-scale polygonal tundra geomorphology map, characterizes arctic patterned ground across large scales, which may enable higher resolution characterization of important processes and parameters that control ecosystem structure and function over time and space, such as the patterns and distribution of surficial ground ice, soil carbon/nitrogen, vegetation, water bodies, wildlife habitat, and thermokarst features.

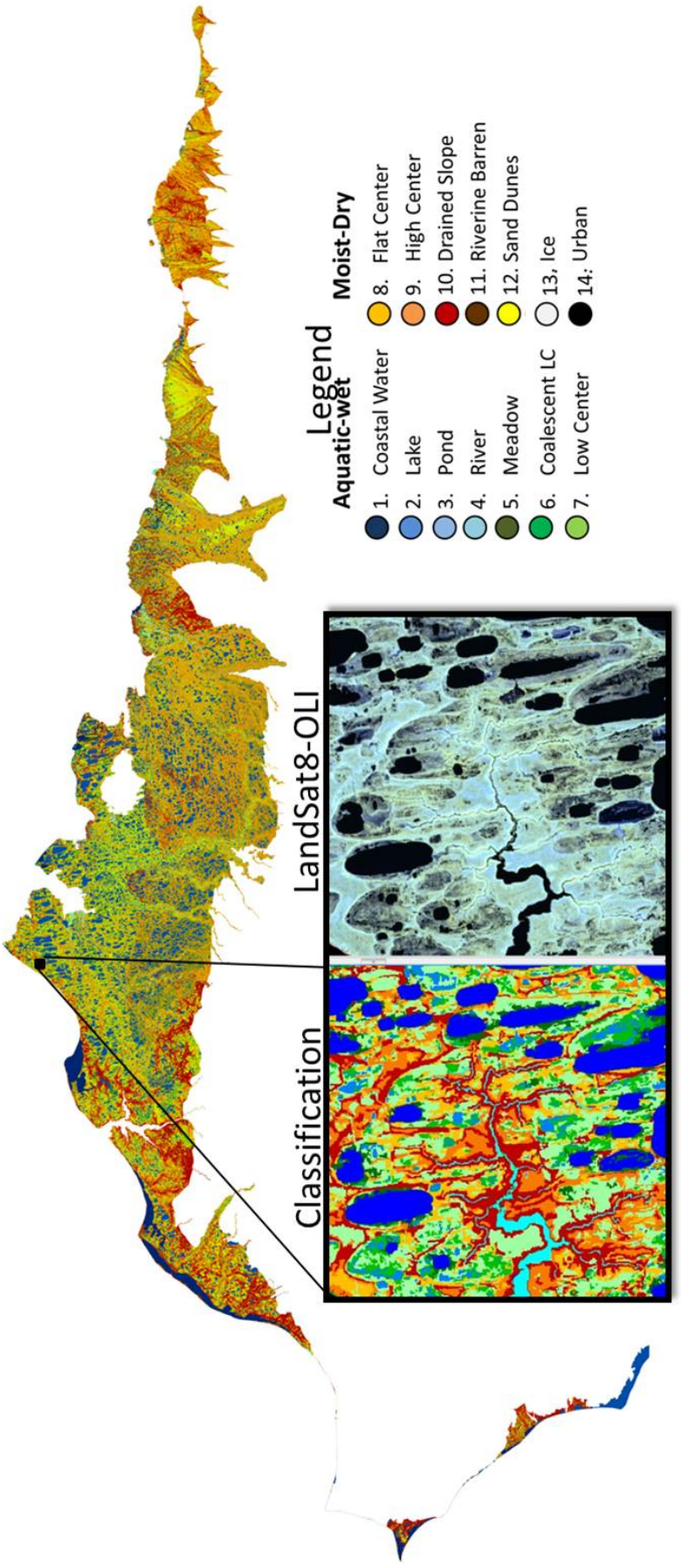

Figure 1: Polygonal tundra geomorphology map for the Arctic Coastal Plain of Alaska, mapped at 30 × 30 m spatial resolution.

Mapping permafrost distribution using the remote sensing techniques and geophysical measurements in a characteristic watershed on the Qinghai-Tibet Plateau, China

Dongliang Luo, Huijun Jin, Xinbin Wang, Shuhui Gao, & Lanzhi Lü

Cold and Arid Regions Environmental and Engineering Research Institute, Chinese Academy of Sciences, People's Republic of China

The controlling factors on permafrost are rather complex on the Qinghai-Tibet Plateau (QTP), where alpine permafrost mainly occurred in the world. The rugged microtopography and complicated hydrology could account for the spatial heterogeneity of permafrost. In this study, we retrieve the land surface temperature (LST) from the thermal infrared remote sensing data as collected from the Landsat 8 TIRS sensors in a rugged mountainous watershed in the Source Area of the Yellow River (SAYR), Northeastern QTP. And then correlate the LSTs with the digital elevation model (DEM) data derived from the ASTER GDEM products to obtain the lapse rates of LST in this specific watershed. The ERT techniques, detecting the sharp contrast between the frozen and unfrozen states within the sediments, were also employed at an experimental plot in this small watershed. The filed work was carried out in late August and early September in 2015, and the imaging interpretations were validated with ground temperature profiles collected at almost the same time. The explicit boundaries of permafrost base in the experimental plot were detected using specific dielectric properties. Then the spatial distribution of permafrost for the experimental plots were achieved. After the relationship between the LST and specific dielectric properties acquired through validation. Then the spatial distribution of permafrost is mapped. Preliminary results demonstrate that the thermal infrared remote sensing products and ERT measurements could be useful in detecting the permafrost distribution, even for the complex alpine permafrost regions at mid-latitudes.

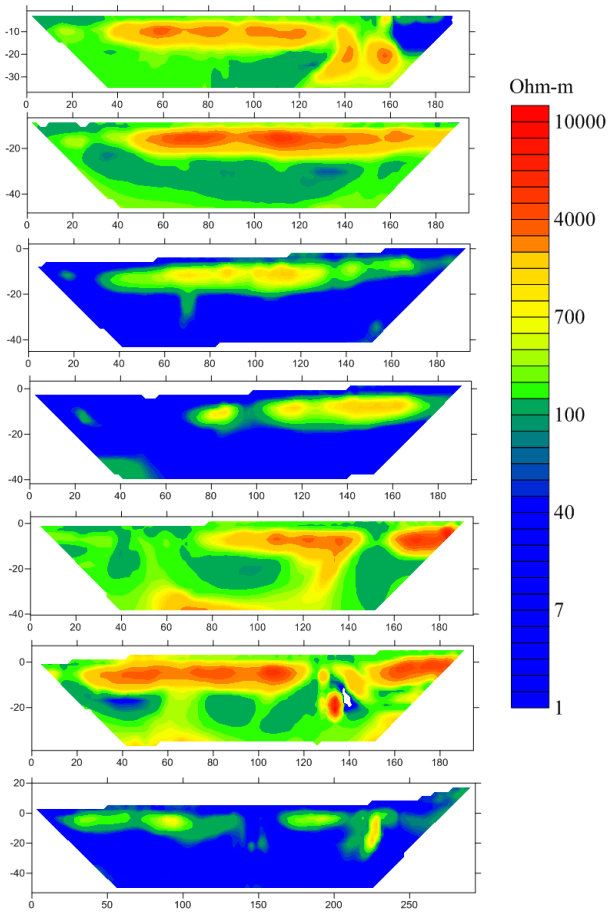

Figure 1

Permafrost map update for the Igarka region as a climate change and human impact tracking tool

Elizaveta Makarycheva[1,2], Nikita Tananaev[2,3], Dmitry Sergeev[1], & Andrey Litovko[2]

[1] *Sergeev Institute of Environmental Geoscience Russian Academy of Sciences (IEG RAS), Russian Federation*
[2] *P.I. Melnikov Permafrost Institute, SB RAS, Russian Federation*
[3] *Ugra Research Institute of Information Technologies, Russian Federation*

Igarka Geocryology Lab is one of the oldest geotechnical observatory in the Russian permafrost region. It was organized in 1930 to guide the construction and development of lumber industry in a newly built Igarka city (1929), a marine port 600 km to the south from the Arctic Ocean. Field observations on the distribution, vertical structure, and temperature regime of frozen grounds, as well as laboratory studies of their physical and mechanical properties, were the main research objectives during the Soviet period.

Permafrost mapping was also a research priority for the Igarka station. One of the first regional permafrost maps was created for the Yamal region by L.A. Meister (1953); later, in 1955, permafrost of the Igarka city area was mapped by N.S. Sheveleva at a 1:10,000 scale. Later, in early 1970s, larger part of the adjacent territory was mapped by the Igarka station staff.

Igarka is located in the discontinuous permafrost region, in the taiga-tundra transition zone, though the mean annual air temperature is close to -8 °C. Ground temperature data suggests a strong impact of the climate change on the permafrost conditions [Streletskiy et al., 2015]. Permafrost degradation trends, observed at the Igarka meteo station, may however differ depending on the landscape features; moreover, the land cover type at the meteo station may be deemed non-representative. We can assume, nevertheless, that the thermal state of frozen ground is, in general, affected by recent climatic shifts. Changes in spatial distribution of permafrost lead, in its turn, to the changes in the landscape structure of the territory. The permafrost ecosystems of the Igarka region are extremely vulnerable to ongoing changes, and are to disappear first if the global change will not slow its pace.

Updated permafrost map of the Igarka region may serve as an instrument to trace the recent changes in permafrost conditions in a retrospective and comparative study, as well as a'baseline'tool allowing to track future evolution of frozen grounds. Field-based landscape indication should allow the definition of the key landscapes and their relation to permafrost extent and thermal properties. Remote sensing data will be used further to up-scale the field observations, and subsequent 'ground-truthing' will provide verification and quality assessment of the final mapping product. The same principle may be applied to the tracing of technogenic transformation of permafrost conditions because of civil and industrial construction.

In the recent years, observations of the active layer depth at the CALM plot (R-40 Igarka), as well as ground temperature measurements in TSP boreholes are carried out. In 2015, three monitoring sites for the seasonal frost heave observation were organized. Due to significant transformation of permafrost conditions in the last decades, an important task is an assessment of the representativeness of landscapes selected for monitoring. Such assessment is necessary to conclude on the representativeness of the CALM & TSP monitoring sites, and to recommend the expansion or rearrangement of the existing monitoring network.

References

Streletskiy, D.A.; Tananaev, N.I.; Opel, T.; Shiklomanov, N.I.; Nyland, K.E.; Streletskaya, I.D.; Tokarev, I. and Shiklomanov, A.I. [2015]: Permafrost hydrology in changing climatic conditions: seasonal variability of stable isotope composition in rivers in discontinuous permafrost. *Environmental Research Letters*, 10(9):095003, doi:10.1088/1748-9326/10/9/095003.

Permafrost distribution in the French Alps: Statistical modelling using rock glacier inventory

Marco Marcer[1], Xavier Bodin[2], & Philippe Schoeneich[1]

[1] *Université de Grenoble Alpes, Institut de Géographie Alpine, France*
[2] *Université Savoie Mont Blanc, Laboratoire EDYTEM, France*

Along with a rising temperature trend registered in the past decades along the European Alps, several signals of permafrost degradation have been reported in the same region, e.g. rock glacier displacement acceleration and thickening of the active layer. Permafrost degradation is alarming due to its role in terrain destabilization and, in particular, ice-rich debris slopes are of great concern due to their proximity to inhabited areas. Therefore, in the past years increasing efforts have been made either by the scientific community and local authorities in understanding the processes and hazards linked to the alpine permafrost degradation.

The first step to manage the risk associated with permafrost degradation is to know its spatial extent. Since alpine permafrost does not manifest itself on the surface, exception made for rock glaciers, it is not suitable for automatic mapping. Therefore distribution models are required to infer permafrost occurrence. Traditionally, permafrost distribution models take advantage of rock glaciers as evidence of permafrost to extrapolate statistically its occurrence based on correlation with climate variables. Although several statistical models have been made at the whole alpine range scale, only one permafrost distribution map, calibrated on the Combeynot massif and validated on the Vanoise and Mercantour massifs, was designed specifically for the French Alps. However, permafrost statistical modeling using rock glacier inventories has been recognized to be biased depending on the data characteristics, making permafrost maps inaccurate at local scale when applied to specific areas. This is due to the fact that rock glaciers extents are not only influenced by climate, but also by their dynamics, a complex function of local topography, geology and ice content in the landform. Therefore, the validity of current models in the French Alps is, at least, questionable.

To address this issue, the service Restauration des Terrains en Montagne (RTM) in collaboration with the Institut de Géographie Alpine (IGA) realized the first complete rock glacier inventory of the French Alps. The inventory, which counts more than 2600 features, spacing from the Mont Blanc Massif to the Mediterranean Sea, represents an extremely valuable modeling dataset. The present study aims to exploit this inventory in order to assess permafrost distribution in the French Alps. As a first step, the performance of already existing models is evaluated. Rock glaciers are used as validation dataset and the models are tested for spatial bias, i.e. their performance is assessed in function of the area they are applied on.

Then, a statistical model is specifically developed for the French Alps. At first, the correlation between rock glaciers and geomorphological local parameters, as lithology and feeding area, is investigated by performing a statistical analysis. This allows to study and model climate control on rock glaciers activity and boundaries, avoiding biases introduced by topographic and geological local conditions. Climatic data include air temperature, solar radiation and precipitation. Due to the extent of area investigated, constant lapse rates are not applicable. In particular, geographical gradients in air temperature and precipitation are investigated and spatial interpolation of observations is performed.

Different modeling strategies are investigated, compared and discussed. The rock glacier inventory is partitioned to be used either as training and validation dataset. Other data, as BTS and GST, are used as validation where available. Finally, the model performing best on the validation set is selected. A land use map is used to select debris covered areas on the French Alps and permafrost occurrence is modeled. The resulting permafrost distribution map is expected to be a valuable decision support tool in permafrost degradation related issues.

Applicability of the ecosystem type approach to model permafrost and ground temperature dynamics across the Alaska North Slope

Dmitry Nicolsky, Vladimir Romanovsky, Santosh Panda, Reginald Muskett, & Sergei Marchenko

University of Alaska Fairbanks, United States of America

Permafrost is a central element of the cryospheric system. Its role in the climate system and more generally in the Earth System has become increasingly recognized by the public as well as in the scientific literature, especially in the most recent years. Changes in permafrost affect not only regional and possibly global climates, but also have a pronounced impact on local and regional ecosystems and infrastructure. Despite our current general understanding of how permafrost is changing and may change in the future, due to changes in climate, it is still very poorly understood how these changes will affect ecosystems and infrastructure on local and regional scales. The major hurdle in addressing this problem lies in our limited knowledge of local processes and consequences due to insufficient spatial and temporal resolution of models and projections of changing climate and resulting changes in other environmental characteristics, including permafrost.

Permafrost characteristics widely vary across the Arctic and within Alaska. Northern and especially north-west Alaskan communities are very susceptible to permafrost degradation because of generally high ice content in permafrost and because stable bedrock is often not near the surface. Recent assessments of permafrost demonstrate ongoing warming over large areas (Romanovsky et al., submitted), and local evidence of permafrost degradation is apparent in parts of Alaska, Russia and Canada. As a result of our prior research, a predictive permafrost model of moderate spatial resolution was developed for Alaska. The Alaskan 2 × 2 km resolution model (Jafarov et al., 2012) predicts substantial permafrost degradation in most of the Alaska. By the end of the 21^{st} Century permafrost will be relatively stable only in the Brooks Range and the North Slope. While the projected reductions in permafrost extent ranged from 10 % to as much as 40%, these projections are subject to three major caveats:

1. they are driven by output from coarse-resolution (300 km) GCMs of late-1990s vintage,
2. they do not capture fully the time lags between surface warming and the thaw of permafrost in areas of thick permafrost, and
3. the climate models suffer from systematic biases (some poorly known) partly caused by an incomplete treatment of snow and subsoil processes.

Nevertheless, even smaller changes in permafrost extent have serious implications for ecosystems, human activities (infrastructure and subsistence lifestyle) and feedbacks within the climate system (especially with respect to carbon and water fluxes). To address these problems, we develop a new technology for retrospective and predictive modeling of permafrost dynamics that includes the summarizing existing observational data, the use of remote sensing data, and GIS technology.

We employ the permafrost module of the Alaska Integrated Ecosystem Model and establish several high spatial resolution scenarios of changes in permafrost characteristics in the Alaskan Arctic in response to projected climate change. Properties of surface vegetation, soil type, layering and moisture content are up-scaled using the Landscape/Permafrost database and a 30 m-resolution unified ecological map by Jorgenson and Heiner (2003). Assimilation of the in-situ measured ground temperature at multiple sites across the Alaska North Slope allows us to parameterize ground thermal properties for each dominant ecosystem. Maps of the employed ecotypes and soil texture categories are shown in the top and bottom plots in figure 1, respectively. Totally, 51 different ecotypes-soil texture combinations are utilized to parameterize ground thermal properties for the 770x770 m computational grid cells. Soil temperature dynamics are simulated by solving the 1-D non-linear heat equation with phase change, while the snow temperature and thickness dynamics are simulated assuming the snow accumulation and compaction processes. To verify the developed model, we compare the modeled and observed active layer thickness at the Circumpolar Active Layer Monitoring (CALM) sites, as well

as the modeled and observed snow depth records at monitoring sites operated by the United States Geological Survey (USGS) and Geophysical Institute (GI), University of Alaska Fairbanks. The technology developed in this study will be relevant and applicable to many Alaskan and other Circum-Arctic locations.

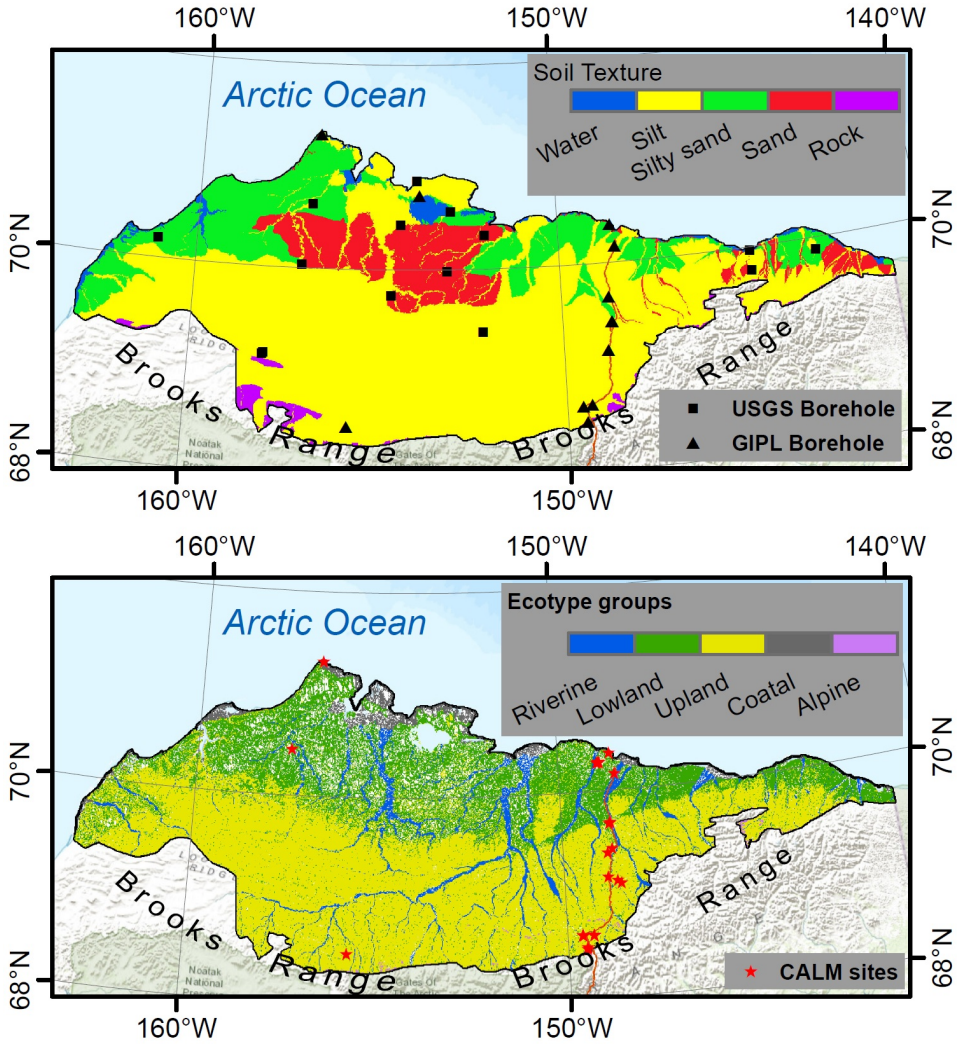

Figure 1: Map of the considered soil texture categories (top) and ecotypes groups (bottom). Temperature monitoring sites by GI and USGS are marked with black triangles and squares, respectively (top). Location of the CALM sites are marked by red stars (bottom).

Archeologically significant cold ice patches in southern Norway – an indicator of mountain permafrost

Rune Strand Ødegård[1], Atle Nesje[2], Ketil Isaksen[3], Liss M. Andreassen[4], & Trond Eiken[5]

[1]*Norwegian University of Science and Technology - NTNU, Norway*
[2]*University of Bergen, Bergen, Norway*
[3]*Norwegian Meteorological Institute, Oslo, Norway*
[4]*Norwegian Water Resources and Energy Directorate, Oslo, Norway*
[5]*Department of Geosciences, University of Oslo, Oslo*

Numerous archaeological finds at ice patches (i.e. perennial snowfields) have uncovered an urgent need for a better understanding of the physical characteristics of these features. There are about 3000 known artefact finds globally at ice patches; approximately 2000 of these finds are in in central southern Norway. A case study at the Juvfonne ice patch (1850-2000 m a.s.l., 61.676oN, 8.354oE) started in 2009. The objective of this case study is (1) to measure mass balance and thermal regime, (2) to make interpretations of ice stratigraphy and deformation on Holocene time scale and (3) to discuss processes relevant to artefact displacement and preservation. Juvfonne and the surrounding terrain is a well-preserved Iron Age hunting'station'documented by more than 600 registered wooden artefacts and 50 hunting blinds.

In 2009 Juvfonne had a maximum ice thickness of 17-19 m (width 500m, upslope length 350m, altitude range 150m). Juvfonne contains cold ice and is surrounded by permafrost; the 10-m depth ice temperature is -2 to -4 oC. The temperature observations strengthen the statement that perennial ice patches are an indicator of mountain permafrost. The ice temperatures is also expected to be quite representative for englacial 10m-temperatures in glacier ablation areas of the region. This implies that the glaciers of the region are polythermal rather than temperate with partially cold ablation areas.

A 5-year record of mass balance measurements indicates a complex coupling to climate. Winter balance is poorly correlated with winter precipitation during the period 2010-2014. In summer the measurements indicate that the mass balance depends on the spatial variability of the turbulent and latent heat fluxes. Local effects related to snow redistribution by wind in winter and turbulent fluxes in summer must be considered in future mass balance modelling of these features. Ice patches are, due to their existence, located in topographical settings that result in close to long-term zero mass balance. The extent of such small ice bodies is affected by shrinking and growing along the whole margin.

Two ice tunnels were excavated into Juvfonne, in 2010 and in 2012 respectively, which gave an excellent opportunity to collect samples of organic-rich layers embedded in the ice. Accelerator Mass Spectrometry (AMS) radiocarbon dating of thin (<5 cm), organic rich layers in the ice dates in chronological order from the base upwards (4711-4606 cal. yr Before Christ (BC) at the base). Polytrichum moss mats appeared along the margin of Juvfonne in the autumn of 2014. AMS radiocarbon dates show that the moss mats were covered (killed) by the expanding snowfield about 2000 years ago. Georadar soundings show that the near-surface reflection horizons are nearly parallel to the present surface (radiocarbon dating yielded modern age). At depth, curved reflection horizons are observed probably caused by deformation. The ice stratigraphy and radiocarbon dating suggest that the Juvfonne ice patch was small or absent during the Holocene thermal maximum (HTM), but existed continuously since ca. 6700 cal. yr Before Present (BP) without disappearing or developing into a glacier with basal sliding or strong internal ice deformation. The age of the oldest ice at the base can be interpreted as a minimum age of permafrost formation.

Surface processes (i.e. wind and melt water) and ice deformation may have caused significant displacement of artefacts from their original position. Thus, the dating and position of artefacts cannot be used directly to reconstruct previous ice patch extent.The existence of cold ice and permafrost is crucial in the preservation of artefacts.

Past, present and future permafrost distribution in national parks of Alaska: A high-resolution modeling investigation

Santosh Kumar Panda[1], Vladimir E. Romanovsky[1], Sergey S. Marchenko[1], & David K. Swanson[2]

[1] *University of Alaska Fairbanks, Fairbanks, Alaska 99775, United States of America*
[2] *National Park Service, 4175 Geist Road, Fairbanks, Alaska 99709, United States of America*

Permafrost underlies 70 % of all National Park Service administered land (i.e. 40 million acres) in Alaska and it provides a stable foundation to parks'ecosystems and wildlife habitats. However, this foundation is weakening as ground temperature is rising in response to climate warming. Consequently, thermokarst activities are on the rise and they are altering the parks' ecosystems and wildlife habitats. In order to effectively respond to these changes park management needs up-to-date knowledge of the permafrost distribution and temperature, and how they might evolve with changing climate in the future. To help park management understand and respond to the changing permafrost condition, we modeled near-surface permafrost dynamics—permafrost temperature, distribution, and active layer thickness—in eight national parks, preserves and monuments of Alaska at decadal time scale. Five of these parks, preserves and monuments are located in the Arctic: Gates of the Arctic National Park and Preserve, Noatak National Preserve, Kobuk Valley National Park, Cape Krusenstern National Monument, and Bering Land Bridge National Preserve; the remaining three parks and preserves are located in the sub-Arctic: Denali National Park and Preserve, Wrangell-St. Elias National Park and Preserve, and Yukon-Charley Rivers National Preserve.

We used Spatially Distributed Model of Permafrost Dynamics in Alaska (GIPL 1.0), the highest resolution (771 m) downscaled climate inputs available, and high-resolution (≈30 m) vegetation and soil landscape inputs. For climate inputs we used two downscaled climate data, Climatic Research Unit (1901-2009) and a composite of five IPCC Global Circulation Models under moderate emission scenario (2006-2099) that work best for Alaska (source: Scenario Network for Alaska and Arctic Planning [SNAP], University of Alaska Fairbanks). The 30 m resolution soil landscape and vegetation maps are derived from Landsat satellite images [Jorgenson et al., 2008, 2009]. We excluded areas underlain by glaciers and permanent ice-fields from modeling.

For the Arctic parks, our results suggest the distribution of near-surface permafrost (i.e. permafrost immediately below the active layer) will likely decrease from the current 99 % of the total park area (five parks combined) to 89% by 2050 and 36 % by 2100 (Fig. 1). Near-surface permafrost will likely continue to exist in the northern half of the Gates of the Arctic and Noatak parks by 2100, though its temperature will likely be up to 6 °C warmer than the present at certain places. Taliks or unfrozen ground will likely occupy the ground below the active layer in rest of the park areas. For the sub-Arctic parks, our results suggest substantial decrease in near-surface permafrost distribution by 2050s and almost complete disappearance by 2100 except on high elevation areas. For Denali National Park and Preserve, the decline in near-surface permafrost distribution will likely be from current 51 % to 6% by 2050 and 1% by 2100. For Wrangell-St. Elias National Park and Preserve, the decline will likely be from current 72 % to 42% by 2050 and 15 % by 2100 [Panda et al., 2014]. In sum, the near-surface permafrost will likely be degrading in most parts of Denali and Wrangell parks towards the end of the current century except at higher elevations where climate models continue to project cold temperatures. The comparison of model permafrost distribution with the field observations of permafrost presence/ absence at 1375 and 430 sites showed 86% and 95% agreement for Denali and Wrangell parks, respectively. In conclusion, the modeled high-resolution permafrost maps demonstrate the effect of changing climate on near-surface permafrost. These products fill an essential knowledge and data gap and complement research of other Arctic disciplines such as ecosystem modeling, hydrology and biology.

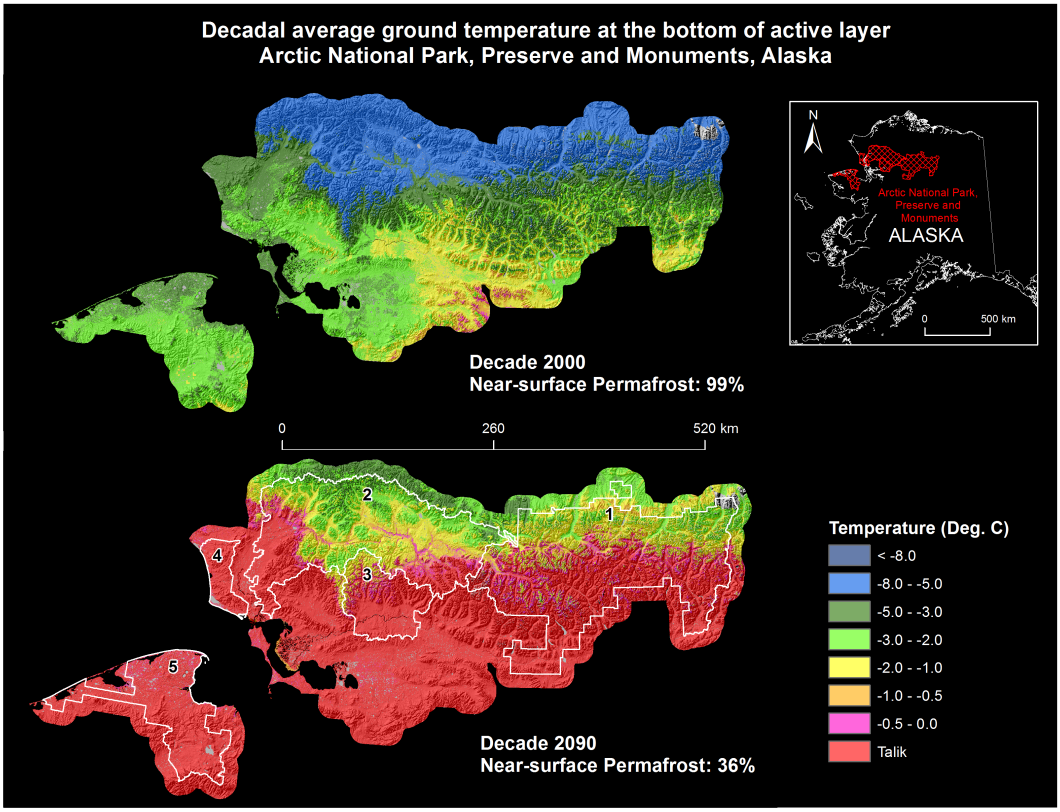

Figure 1: Modeled near-surface permafrost maps of Arctic national park, preserve and monuments at 28.5 m spatial resolution. The negative temperature values at the bottom of active layer suggest presence of near-surface permafrost i.e. permafrost immediately below the active layer. The red color indicates presence of Talik, unfrozen ground between active layer and permafrost. The temperature maps are draped over a hillshade model for 3D perspective. The outlines of 1) Gates of the Arctic National Park and Preserve, 2) Noatak National Preserve, 3) Kobuk Valley National Park, 4) Cape Krusenstern National Monument, and 5) Bering Land Bridge National Preserve are shown as white polygons on the bottom temperature map.

They offer decision makers a clear understanding of how near-surface permafrost distribution in the parks might change in the future, which was lacking up until now, to guide critical management decisions on use of park resources and public access, and to evaluate impacts of climate change on parks' infrastructure, ecosystems, and wildlife habitats.

References

Jorgenson, M.T.; Roth, J.E.; Loomis, P.F.; Pullman, E.R.; Cater, T.C.; Duffy, M.S.; Davis, W.A.; Macander, M.J. and Grunblatt, J. [2008]: An ecological and survey for landcover mapping of wrangell-st. elias national park and preserve. Natural resource technical report nps/wrst/nrtr-2008/094, National Park Service, Fort Collins, Colorado. d-100.

Jorgenson, M.T.; Roth, J.E.; Miller, P.F.; Macander, M.J.; Duffy, M.S.; Wells, A.F.; Frost, G.V. and Pullman, E.R. [2009]: An ecological and survey and landcover map of the arctic network. Technical report, National Park Service, Fort Collins, Colorado.

Panda, S.K.; Marchenko, S.S.; Romanovsky, V.E. and Swanson, D.K. [2014]: Modeling the effects of climate change on permafrost in national parks of Alaska: Will permafrost survive the climate change of 21^{st} century? In *American Geophysical Union Fall Meeting, 15-19 December 2014, San Francisco, California*, Abstract available online at https://agu.confex.com/agu/fm14/meetingapp.cgi/Paper/10814.

Permafrost distribution in the Aksu-Tarim Catchment (Central Tien Shan)

Juliane Peters[1] & Tobias Bolch[1,2]

[1] *TU Dresden, Institute for Cartography*
[2] *University of Zurich, Department of Geography*

Beside glaciers and snow permafrost is one of the key factors influencing discharge and water supply in the Tien Shan in Central Asia. However, information on the spatial distribution of permafrost is rare, mainly due to the "invisible" character of permafrost, which makes it difficult to investigate it in such remote and mountainous areas. Remote sensing methods have proven their suitability for supporting statistical modeling of permafrost occurrence. However, because of the coarse resolution of suitable input data the according model outputs exhibit a similarly coarse spatial resolution.

In this study, a statistical permafrost distribution model has been generated for a 42,157 km^2 area of the Aksu-Tarim Catchment in the Central Tien Shan incorporating remote sensing data and in situ measurements of mean annual ground temperatures (MAGT) and mean annual ground surface temperatures (MAGST). Field data of ground temperatures from two locations in the study region were available measured at depths between 2 cm and 1 m. Remote-sensing derived input data include MODIS landsurface temperature (LST) imagery, which were interpolated in the temporal dimension to account for missing data, as well as annual snow cover probability (SCP) data as a proxy for snow cover duration. Freezing and thawing degree days were calculated from MODIS LST. Additional parameters, that have been considered, are NDVI and potential incoming solar radiation (PISR). To overcome problems induced by the medium resolution of the satellite data – especially evident in a mountainous region like this – a downscaling approach has been developed for MODIS LST and SCP based on the elevation dependency of both parameters.

The final model has a spatial resolution of 90 m and provides information about the distribution of MAGT and MAGST, respectively, which have been linked to permafrost probabilities. Comparisons with borehole measurements and rock glaciers as a proxy for the occurrence of permafrost show a good agreement to the model results. First results indicate, that probably 40 % of the Aksu-Tarim Catchment are underlain by permafrost. Above an altitude of 3600 m a.s.l. permafrost can exists, above 4100 m a.s.l. permafrost occurrence is very likely.

Grounds thaw subsidence and spatial analysis of landscape transformation

Felix Rivkin[1], Yulia Vlasova[1], Sergey Marchenko[2], & Ivan Parmuzin[1]

[1] *Fundamentproject OJSC, Russian Federation*
[2] *Geophysical Institute of the University of Alaska, Fairbanks, USA*

Modern trends of climate dynamics in the Arctic and the consequent rise in temperature cause a change in geocryological environment. The frozen ground degradation is observed as a lowering of the permafrost table and development of the divided permafrost layers. If an upward trend in air temperature stays unchanged, the increase of divided permafrost will be causing substantial changes of frozen ground at the top of the cross-section by the end of the 21^{st} century. This trend will cause not only a change of temperature and conditions of the soil, but also a spatial transformation of the landscapes and permafrost distribution.

One of the major consequences of permafrost thawing is a present day grounds surface transformation as a result of frozen ground thaw subsidence.

The spatial grounds thaw subsidence non-uniformity, predetermined by spatial heterogeneity frozen grounds ice content, will significantly change the landscape conditions. First of all, this change will affect hydromorphic features of modern landscapes. Some landscapes which tend to decrease the relative surface will be turning into swamps, as opposed to others, tending to increase the relative surface. To predict the dynamics and scope of such transformation is extremely complex.

This paper presents the results of possible spatial transformation scenarios of surface conditions as a result of permafrost degradation. The research was carried out on the basis of detailed studies of permafrost test area within the project of THE EU 6FP CARBO-North project (Contract Nr. 036993).

The studies were conducted in the northwest of the European part of Russia on the left bank of the Sedyaha River. The area of the key site was approximately 4 km^2. The penetrated depth was 10 – 12 meters.

In geomorphological respect the survey area is located at the bottom of the Late Pleistocene lake marshy depression, 'slotted' by stream valleys and runoff stripes. The basin around the perimeter is framed by glacial Late Pleistocene ridges 120 – 130 m tall. The absolute level of the bottom surface makes 80 – 90m. Thus, the relative depth of the incision of the valley bottom is 30 – 60m. The relief area is polygonal with the raised blocks, which are covered with shrub-moss-lichen vegetation. The blocks are separated by runoff hollows, which are generally covered by thick bushes.

In the study area the permafrost spread mainly from the surface. Relatively elevated areas of small hollow spotted tundra and peat land permafrost are found directly under the active layer. The permafrost table is situated at a depth of 5 to 10 m thick in marshy depressions, runoff hollows, foot of the slopes, and on the gentle bushy slopes of the lake basin. The deep position of the permafrost table areas is observed in such areas between the active layer and permafrost table in the winter. Divided permafrost can be reduced during periods of cold weather, which is due to the increase in depth of seasonal freezing and formation of long-term soil freezing. This layer increases in the warm periods. This is both due to reducing the depth of the permafrost table and lowering of the roof as a result of frozen soil degradation.

Taliks of more than 10 m thick are located under the lakes and large marshy depressions, which are also observed in areas of open water.

The temperature of frozen ground ranges from minus 0.1 – 0.2 °C in swampy depressions and minus 2.1 °C on the tops of peat mounds.

Quantitative calculations of changes in permafrost conditions are made on the basis of permafrost degradation forecast under the influence of climate change. The scenario of air temperature within a given climate model looks overly aggressive, but it was adopted under the 6FP CARBO-North project. However, the use of this scenario allows evaluating the stability of permafrost conditions, and the main trends in the transformation of modern landscapes for the 21^{st} century.

Basic methodological stages of the study:

1. Development of modern spatial landscape geocryological model key site.

2. The provisions of permafrost roof forecast for the periods 2050 and 2099.

3. The forecast of surface sediment subsidence of modern landscape as a result of permafrost in 2050 and 2099.

Basic cartographic model of modern landscape and geological conditions was developed on the basis of the field and laboratory studies. Analysis of environmental factors that determine the formation of the modern geocryological environment was carried out in a matrix form [Rivkin, 2008].

The entire area of the key site occupies one level of glacial-fluvial lowland. Within that, there were allocated two geological genetic types: glacial and lacustrine-swamp sediments. The above-mentioned two sediment types that are found within the studied area are presented by the five typical cryolithological sections:

1. Loam with debris inclusions, thawed or frozen (ice-poor),

2. Peat (up to 0.5m thick), loams, covered by glacial sediments, thawed or frozen iciness (ice-poor),

3. Loams, occasionally covered with peat up to 0.4 m thick, sediments are thawed or frozen (with various ice content: ice-poor and iciness, up to ice-rich),

4. Peat 0.4–1 m thick, with underlying loams, sediments are frozen (iciness or ice-rich),

5. Peat up to 1–4.5 m thick, with underlying loams, sediments are frozen (with a various ice content: ice-poor and iciness, up to ice-rich).

Seven landscape zones are observed within the studied area based on analysis of topography, vegetation, groundwater depth, distribution and temperature of seasonal active layers:

a) Peatlands, flat, small-hummocky irregularly drained, herbaceous shrub/moss/lichen communities on mounds, moss/sedge in hollows. Discontinuous permafrost (occurs at 70 – 90 % of the area, at 10 – 30% of the area permafrost table is at 2 – 6 meter depth),

b) Small-hummocky, occasionally spot medallion herbaceous shrub/moss-lichen tundra, moderately drained. Discontinuous permafrost (occurs at 70 – 90 % of the area, at 10 – 30 % of the area permafrost table is at 2 – 6 meter depth),

c) Peatlands, hummocky, well eroded, well drained herbaceous shrub/moss/lichen tundra on mound, moss/sedge bogs in hollows Massive-island permafrost (occurs at 50% of the area, at 50 % of the area permafrost table is at 2 – 10 meter depth),

d) Moss/sedge bogs with remains of hummocky peatlands covered with herbaceous shrub/moss/lichen vegetation, hasyrey, Island permafrost (occurs at 20 – 30 % of the area, at 70 – 80 % of the area permafrost table is at 2 – 10 meter depth),

e) Middle/large-hummocky, shrub/moss/lichen tundra (shrubs up to 1.2 m high), irregularly drained, thawed grounds, permafrost table is at 2 – 6 meters depth,

f) Water lines with shrubs of varying density up to 2.5 m high, bogged depressions with herbs/sedges/mosses, poorly drained, thawed grounds (occurs at 70 – 80 % of the area, at 10 – 30 % of the area permafrost table is at 5 – 10 m depth),

g) Scattered shrubs with various density, thawed grounds.

The combination of selected landscape zones and typical cross-sections of the geological genetic sediment types allows selecting 35 potential typological areas, 15 of which were identified in the area of the key site as a result of field survey and analysis of high resolution satellite images. These typological areas represent the entire spectrum of the existing permafrost landscape conditions. Forecast permafrost changes (in particular, a temperature field of soil to a depth of 10 m), taking into account the climate change scenarios) are made for 2050 and 2099 years for the Seida key-site. According to the scenario, the average temperature for this period is minus 0.8 °C (in 2050), plus 1,2 °C towards the end of the century. As a result of such a temperature rise, partial permafrost degradation will be taking place (Tab. 1). For comparison, the modern average temperature is for the study area minus 5.41 °C. This temperature rise will inevitably be leading to an increase in temperature of frozen ground and its partial thawing.

Table 1: Results of a grounds thaw-subsidence forecast; * Temperature on the 10m depth, **(blue) – frozen areas, ***(yellow) – deep position permafrost table areas, ****(red) – taliks and (or) thawed areas.

index of a landscape zone	Lithology	August 2007		August 2050		August 2099	
		the permafrost table depth. m	ground temperature. °C *	permafrost table depth. m	ground temperature. °C *	permafrost table depth. m	ground temperature. °C*
1b	Loam with debris inclusions	1.8**	-1.7	6***	-0.2	>10****	>0
1e		2	-0.5	8	-0.1	>10	>0
1f		5	-0.2	10	0	>10	>0
1g		>10	>0	>10	>0	>10	>0
2b	Peat (up to 0.5 m thick), loams, covers glacial deposits	0.5	-1.7	1.7	-0.8	>10	>0
2e		2	-1	6	-0.2	>10	>0
2f		5	-0.2	7	-0.1	>10	>0
3b	Loams	1.7	-1	3.5	-0.9	>10	>0
	Loams, covered with peat up to 0.2 m thick	0.8	-1.7	1.7	-0.8	>10	>0
3e	Loams	5.2	-0.5	6	-0.2	>10	>0
3f	Loams, occasionally covered with peat up to 0.4 m thick	5	-0.2	10	0	>10	>0
4a	Peat 0.4-1 m thick, with underlying loams	0.4	-1.8	0.7	-1.2	9.5	-0.1
4c		0.5	-1.8	0.7	-1.2	9.5	-0.1
4d		0.4	-1	0.7	-1.2	9.5	-0.1
5a	Peat over 1-4.5 m thick, with underlying loams	0.5	-2.1	0.7	-1.7	0.8	-0.8
5c	Peat over 4.5 m thick, with underlying loams	0.5	-1.9	0.7	-1.7	0.8	-0.8
		0.4	-1.5	0.6	-1	0.7	-0.3

The simulation results show that, in general, a well predicted trend can be observed: correlation between the depth of a long-term thaw and landscape conditions and ice content of soil in the upper cross–section. The greatest depth of long-term thaw (i.e., the greatest reduction in the permafrost roof) by mid-century will be formed on the surface of clay ice–poor soil. This corresponds to a landscape with indices b, e, f, g and permafrost cross-sections with the indexes 1 and 2. That is, the highest thawing will be noted in areas 1b, 2b, 1e, 2e, 1f, 2f, 1g. The smallest changes in permafrost conditions will be observed at sites the upper part of which is composed of peat: 4a, 4c, 4d, 5a, 5c.

The peat thickness having a high ice content and, therefore, high heat capacity, is the controlling factor. By the end of the century all areas composed by peat up to 1 m thick will be completely thawed, and the areas where the peat is more than 1 m thick will be remaining in frozen condition, although the temperature of frozen ground in such areas will rise to critical values of 0.1: -0 2 °C. This corresponds to the temperature of freezing (thawing) soils. In the future, this will lead to the localization of the frozen ground under the peat areas and development of structures known as the «palsa», which are widespread in the northern part of Finland, Swedish Lapland and the north-eastern part of Norway.

References

Rivkin, F.M. [2008]: Release of methane from permafrost as a result of global warming and other disturbances. *Polar Geography*, 22(2):105–118, doi:10.1080/10889379809377640.

Method of assessing the significance of the factors contributing to the temporary temperature changes in the upper permafrost horizons using GIS tools

Yana Rumyantseva

Earth Cryosphere Institute SB RAS (ECI SB RAS), Tyumen, Russia, Russian Federation

The world community is puzzled over questions of global climate changes. The upper layers of the permafrost are unstable as a result of different climate changes. Researching and forecast of the permafrost temperature regime allows to choose the best solution for the designing and exploitation of the infrastructure.

The author proposes the assessing method of the factors contributing to the temporary permafrost changes over the years. The factors with the most significantly influence on the permafrost temperature regime has been chosen among the others factors. It is necessary to research the quantity and character of changes for each of the factors over the available period time based on the existing data in the studding area. The sources of such kind of the data could be permafrost regime observatories, the national meteorological stations, the different archives, the database collected by the organizations operating infrastructure. For all early chosen factors the GIS-database should be created. It coulds collect, represent, and allow to estimate each set of factors separately and in comparison over the researching period. The results could be displayed on the layers of the different scale electronic maps.

Comparison of the dynamics factors with the permafrost temperature changes rates allows to assess the impact of each of them in chosen region and defines the leading-one for each region, area, and landscape.

The theoretical basis of this approach was developed together with the developing of the V.A. Kudryavsev's permafrost observation methodic [Kudryavtsev, 1979]. The proposed author method includes the next steps of research:

1. The searching of the data sources for factors, describing the impact of the leading factors in the dynamics of permafrost temperature (there are no existing database, where are collected together all this data).
2. The choice of specific tools to visualize and analyze the data.
3. Selection of detail (scale) study, which depends, from the one hand, on the completeness of information and, from another hand, on the users requirements and purposes.

Available regional and global models allow to quantify the significance of permafrost dynamics factors and arrange them in order of priority.

The author hopes by the proposed method to evaluate changes in the role of continental climate over the past 40 years, and hold on scale researches of the significance factors of the temperature dynamic, which have been identified in the 70s years.

As part of the study area the regions of North Western Siberia were selected. This is a plain area that is dissected by rivers, where the permafrost is from continuous to isolated patchs extent and the average value of Tmagt is relatively low [Melnikov and Grechishchev, 2002].

The basis of used data was compiled from the half of a century of observations on the regime stations of the Earth Cryosphere Institute of the Russian Academy of Sciences. This stations were managed grace of employees and international projects), as well as new sites based on the international projects CALM and TSP and data of the leading operating organizations LSC "Gazprom".

References

Kudryavtsev, V.A.(ed.). [1979]: *Methodology of the permafrost observation*. MSU press: Moscow, 358 p.

Melnikov, E.S. and Grechishchev, S.E. on behalf of authors collective [2002]: Permafrost and development of petroleum provinces. In: E.S., Melnikov(ed.), *Western Siberia oil-gas provinces*, pages 43–100. GEOS, Moscow, in Russian.

Permafrost Information in the Engineering Geological Map of the Republic of Sakha (Yakutia), Scale 1:1 500 000

Alyona A. Shestakova[1], Vladimir B. Spektor[1], Yaroslav I. Torgovkin[1], & Valentin V. Spektor[1,2]

[1] *Melnikov Permafrost Institute Siberian Branch Russian Academy of Sciences, Russian Federation*
[2] *Ammosov North-Eastern Federal University in Yakutsk*

The Engineering Geological Map of the Republic of Sakha (Yakutia) covers about 3 million square km, or one-fifth of the land area of Russia. The information available (Modern Engineering Geological Map of Russia, Scale 1:2 500 000, 2010) and technological tools (GIS technologies) make it possible to summarize data on permafrost in Yakutia. Most of the area concerned lies within the continuous permafrost zone.

The map shows ground and geocryological conditions and active faults, while inset maps (scale 1:15 000 000) show hydrogeological and seismic conditions, as well as geotechnical hazards (Figure 1).

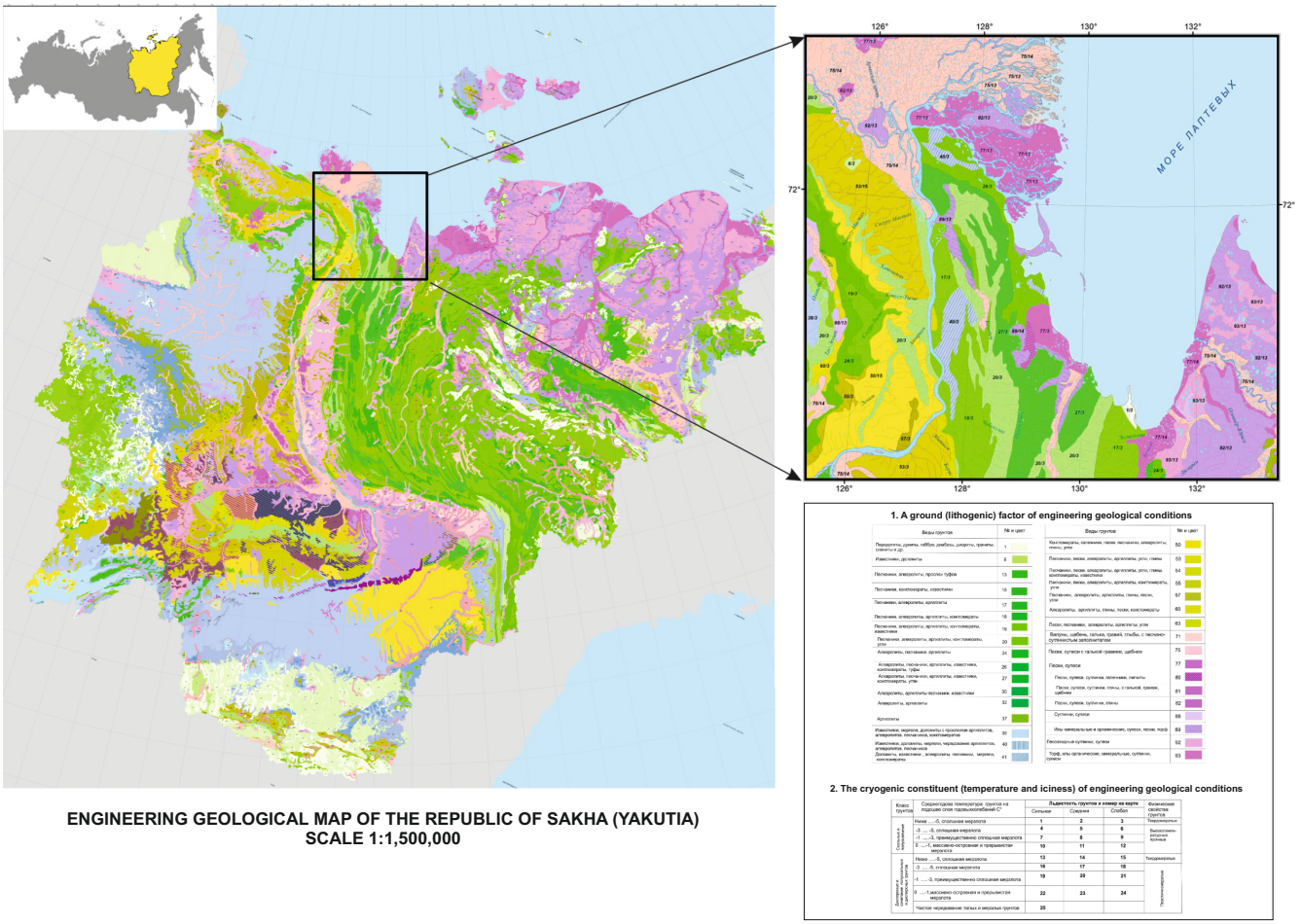

Figure 1: Engineering Geological Map of the Republic of Sakha (Yakutia), Scale 1:1,500,000.

The map is intended to provide information for large-scale construction and development projects and for environmental protection in the large Arctic region of Russia. Scientific purposes of the map include systemizing data according to distribution features of various natural factors and their interactions, as well as predicting environmental changes under construction and exploitation of engineering objects.

The main cartographic feature of the present map is a ground (lithogenic) factor of engineering geological conditions which is indicated by color and comprises the first section of the legend. The more stable ground varieties and their combinations are shown on the map by toned down and light shades while the most unstable ones are shown by toned up and heavy shades.

A distinguishing feature of the map is the indication of almost blanket distribution of the frozen ground class. Frozen ground in engineering geology is subdivided into the same taxons as thaw ground. Types of the frozen ground class are separated by lithology, while ground varieties are separated by temperature.

In comparison with traditionally separated groups of rocks, soft rocks and soils, the groups of combination of rocks and soft rocks as well as soft rocks and soils were separated. The "two-layer" structure wherein the upper part represents soils from 3 to 10 m thick while the lower part represents other classes and groups of ground is also separated into an individual group. In total, the legend includes 124 types and varieties of soils and rocks which can influence engineering geological properties.

The cryogenic constituent is provided in the second section of the legend. Numeration is used for designating the cryogenic constituent (temperature and iciness). The latter allows separating frozen ground varieties. Finally, the ground variety is shown on the map in fractional form. The numerator denotes the ground type and corresponds to the number of a sign in the Legend section "Ground Conditions". The denominator characterizes the ground variety and corresponds to the number of a sign in the Legend section "Geocryological Factors".

A temperature indicator is of great significance for our map because it influences the ground strength parameters. Frozen soils characterized by temperatures above -5 °C are termed plastic-frozen soil. The soil characterized by lower temperatures is termed hard-frozen soil.

The hydrogeological factor is portrayed on the map by speckle and is given in the third section of the legend. Within the map area, the most abundant type is fresh and ultra-fresh suprapermafrost water, which is subdivided into three subtypes: suprapermafrost perched water, water of the seasonal thaw layer, and suprapermafrost soil water [Shepelev, 2011]. The depth of this water is less than 3 m.

Modern active faults are shown on the map by red lines.

About 1.5 million square kilometers of Yakutia belongs to earthquake zone that is 30 % of the whole seismically active zone of Russia. The mapped area includes parts of two planetary seismic belts, the Arctic-Asian and the Baikalo-Stanovoi, that make engineering geological conditions more complicated.

The Engineering Geological Map of the Republic of Sakha (Yakutia) produced by the principles concluded above allowed us to describe the engineering geological conditions for the area, which is rather heterogeneous by its geological structure and natural conditions. Zoning of Yakutia was undertaken according to properties of engineering geological conditions taking into account regional factors under the principles stated by Trofimov and Krasilova [2007]. The following engineering geological regions are separated within Yakutia:

1. Plains and Plateau of Central Siberia;
2. Verkhoyansk-Kolyma Mountainous Area;
3. Area of Coastal Lowlands and Shelf;
4. Okhotsk-Chukotka Area;
5. Aldan-Stanovoi Area and 19 areas.

Analysis of the information presented on the map shows that least stable are the areas of ice-rich soils, termed the ice complex, which comprise the Coastal lowlands and Central Yakutia. Where cold (-5 °C or lower), hard-frozen soils are exposed, high rates of thermal abrasion (dozens of meters annually) are observed along the Arctic coasts and high rates of lateral erosion (up to 20 m/yr) occur along the river channels. Within the occurrence of this category of soils, thermokarst is active on the surface even at mean air temperatures of -15 to -20 °C.

Warmer frozen soils (-5 °C or higher) of the ice complex occur in Central Yakutia where they are subject to rapid degradation due to natural and human impacts. Engineering structures founded on these soils with no special measures to control their thermal regime are characterized by extremely low stability.

Other types of soils and rocks in Yakutia are characterized by greater stability and can be used as foundations, provided that their thermal regimes are controlled.

In terms of dynamic conditions (endogenic and exogenic processes), the least favorable for construction are the Verkhoyansk-Kolyma, Okhotsk-Chukotka, and Aldan-Stanovoi mountainous regions which are characterized by intensive slope processes and high seismicity.

An important consideration is that some areas of Yakutia are characterized by extremely low air temperatures in winter (below -40 °C) which cause thermal deformations in buildings and structures. These areas include Central Yakutia and the entire Verkhoyansk-Kolyma region.

All the areas mentioned above may be classified as unfavorable in terms of engineering geology. They comprise about 70 % of the total area of Yakutia.

References

Shepelev, V.V. [2011]: *Suprapermafrost Waters in the Cryolithozone*. Novosibirsk. Academic Publishing House "Geo", 169 pp.

Trofimov, V.T. and Krasilova, N.S. [2007]: *Engineering-Geological Maps: A Study Guide*. Moscow: KDU, 384 pp.

GlobPermafrost – how space supports understanding of permafrost?

Frank Martin Seifert[1], Annett Bartsch[2], Guido Grosse[3], Andreas Kääb[4], Sebastian Westermann[4], Tazio Strozzi[5], Andreas Wiesmann[5], & Claude Duguay[6]

[1] *European Space Agency, Italy*
[2] *Zentralanstalt fuür Meteorologie und Geodynamik, Austria*
[2] *Alfred Wegener Institute Helmholtz Centre for Polar and Marine Research, Potsdam, Germany*
[4] *University of Oslo, Norway*
[5] *Gamma Remote Sensing, Switzerland*
[6] *H_2O Geomatics, Canada*

ESA's GlobPermafrost project develops, validates and implements information products to support the research communities and related international organisations like IPA and CliC in their work on understanding permafrost better by integration of EO data.

Permafrost cannot be directly detected from space, but many surface features of permafrost terrains and typical periglacial landforms are observable with a variety of EO sensors ranging from very high to medium resolution in various wavelengths. Prototype cases will cover different aspects of permafrost by integrating in situ measurements of subsurface permafrost properties (active layer depth, active layer and permafrost temperatures, organic layer thickness, liquid water content in the active layer and permafrost), surface properties (vegetation cover, snow depth) and modelling to provide a better understanding of permafrost today. The techniques will extend point source process and permafrost monitoring to a broader spatial domain, to support permafrost distribution modelling and mapping techniques implemented in a GIS framework and will complement active layer and thermal observing networks.

Initial user requirements have been gathered at the DUE-IPA-GTNP-CliC workshop in Frascati in February 2014, which have been further consolidated within the Permafrost community during 2014 in request of the WMO Polar Space Task Group. A subset of these requirements will be demonstrated within GlobPermafrost and assessed by user organisations:

- Circumpolar permafrost extend
- Permafrost dedicated land cover class prototype
- Local cold spots
- Regional transects for 'hot spot' identification
- Mountain permafrost areas

Cartographic analysis of the damage, associated with geocryological processes

D. O. Sergeev[1], I. V. Chesnokova[2], A. V. Morozova[3], & A.S. Voytenko[1]

[1] *Sergeev Institute of Environmental Geoscience RAS (IEG RAS), Russian Federation*
[2] *Water Problems Institute, RAS*
[3] *Moscow State University*

The data base on unfavorable consequences of geocryological processes was prepared synthesizing materials of Russian and international conferences devoted to geocryological problems. The conferences were held in 2008-2014. The data have a spatial attachment. They characterize processes and their consequences, as well as expanded data on each recorded case.

While preparing the base of factual data, classifiers were elaborated for grouping the information and creating thematic cartographic coverings.

Major information data base fields are as follows: Type of a cartographic object, Geocryological process, Branch of economy, Element of the object (impact recipient). Stage of life cycle of the object, Month/ Season and Year of the damage recording, the period of the process development (during one year or many years), Geographic coordinates, Description of the damage, the Magnitude of the damage (money equivalent), Bibliographic reference. The applied structure secures the multidisciplinary character of accumulated information and its commonality.

The spatial attachment of data allowed preparation of thematic maps, which can be used for analysis of various aspects of the current and cumulative damage to economic facilities, caused by exogenic geological processes within the cryolithozone of Russia. The work demonstrates a wide geographical coverage of problems associated with the activity of geocryological processes, making evident that the climate warming is not the main cause of damage to the economy. It was found out that most problems are not associated with objects under construction but with those under operation.

The increasing need to develop methods of geocryological forecast, which could make it possible to assess the cost of protective and compensating measures in the process of operation of industrial object is also an original conclusion received during the work.

The authors plan further replenishment and development of the data base interconnected in time and space to secure systems of support of the managing decisions in all Arctic sectors. For this purpose it is suggested to use it together with spatial models of the geocryological forecast, similar to GIPL.

Acknowledgements

The work was supported by the Russian Foundation for Basic Research, 13-05-00462.

Using Random Forest to model permafrost distribution

Flavius Sirbu, Lucian Dragut, & Alexandru Onaca

West University of Timisoara, Romania

Modelling permafrost distribution at local scale can be a difficult task due to fine scale variations of the independent variables, and because the factors that are important in modelling at regional scales, such as the altitude, are less important on local scale models. Statistical models are used to relate documented occurrence of permafrost to topographic, land cover or climate data, ignoring the physical process that take place. While such models require less data than numerical models, they need to be locally calibrated to obtain good accuracies, therefore their transferability has been questioned.

We introduce a modelling approach based on the Random Forest (RF) algorithm [Breiman, 2001], with a twofold objective:

1. to assess its suitability in modelling permafrost distribution, and
2. to evaluate the transferability of a locally calibrated model to a similar area.

RF is an ensemble classifier that, put simply, learns all the characteristics of the independent variables at the training sites (for both presence and absence of permafrost) and searches for similar characteristics in the rest of the study area. It has several advantages compared to traditional statistical modelling (e.g. empiric-statistic, logistic regression etc.) among which the most important are:

i) the input data can be both continuous and discrete;

ii) there is no assumption regarding frequency distribution;

iii) robustness to outliers in the input data;

iv) handles a large number of variables.

The input data for the model consists in a number of sites where permafrost presence or absence was confirmed by in-situ measurements, using a combination of geophysical methods and thermal monitoring [Onaca et al., 2015]. From these areas, 469 samples for presence and 245 samples for absence were extracted as points. As independent variables, we used 21 land-surface variables derived from a 20 m Digital Elevation Model, plus a land cover map classified from a Landsat 8 satellite image.

The model produced three outputs: the permafrost distribution, the uncertainty associated with the permafrost distribution and the importance of the independent variables. The accuracy of the model was tested using the Area under the receiver operating curve (AUC), which returned a value of 0.95 for the locally calibrated model and a value of 0.73 for the same model transferred to another study area. These results show that

1. the RF model can compete with, and even outperform, the best statistical models, and
2. the RF model can be transferable to new areas with medium to good results.

Future work will focus on the sampling design, which is acknowledged to impact on the RF performance.

References

Breiman, L. [2001]: Random forests. *Machine Learning*, 45(1):5–32, doi:10.1023/A:1010933404324.

Onaca, A.; Ardelean, A.C.; Urdea, P.; Ardelean, F. and Sîrbu, F. [2015]: Detection of mountain permafrost by combining conventional geophysical methods and thermal monitoring in the Retezat Mountains, Romania. *Cold Regions Science and Technology*, 119:111–123, doi:10.1016/j.coldregions.2015.08.001.

Development and degradation of permafrost in the source region of the Datong River, Qilian Mountains

Shengting Wang, Sheng Yu, Jichun Wu, Jing Li, Xiaoying Hu, & Ziliang Feng

Chinese Academy of Sciences, People's Republic of China

The source region of the Datong River is located in the mid-east part of the Qilian Mountains, Qinghai Tibet Plateau with an area of about 4573 km^2. The region belongs to a typical alpine permafrost zone with an altitude range of 3443 to 5044 m asl. Alpine meadow is the typical vegetation type, and graze, coal mines and road construction are the main human activities in the region. Using borehole investigation and monitored permafrost temperature results, the development and distribution characteristics of permafrost in the region were analyzed. The lower limit of permafrost in the source region of Datong River is about 3650m, and the permafrost area accounts for about 66 % of the region. Most of the permafrost in the region is under an unstable or transition conditions. The observed permafrost temperature in the basin of the region is between -1.76 -0.02 °C. According to the recently measured data in 2014, the mean annual ground temperature (MAGT) appears a linear decrease with increasing altitude at a gradient of 3.82 °C km^{-1}. The MAGT is greatly affected by surface condition, especially swamp meadow shows a significant effect to benefit the development of permafrost. The permafrost thickness in the source region is also significantly dependent on altitude. With the elevation rising by 100 m, the thickness of permafrost increases about 10 m. In the plain areas, the observed thickness of permafrost ranges from 17 to 86 m. Active layer thickness, which is closely related to local factors, especially land cover condition, is about 0.9-5m in the regions. There is no clearly zonality relationship between active layer thickness and altitude. The thickness of active layer in swamp meadow condition is thinner than other land cover conditions. According to the land cover conditions, the average active layer thickness is in the line of swamp meadow, meadow and degraded meadow. Under the impact of global warming and human activities, permafrost in the source region is overall in the process of degradation. The degradation of permafrost is mainly expressed as rising permafrost temperature, appearance of talik. From southeast to northwest regions, the stability of permafrost increases gradually. Based on the measured permafrost temperature in recent years, most of the MAGT are increasing (Tab. 1), implying absorption of energy. The MAGT is increasing at a rate of about 0.0075 °C a^{-1}.

Table 1: Average annual ground temperature of some typical boreholes.

Boreholes	Altitude (m)	vegetation type	MAGT(℃)				
			2010	2011	2013	2014	2015
CD-7	3651	swamp meadow	- 0.66	-0.51	-	- 0.47	-0.59
CD-11	4119	bare land	-2.57	-2.52	-	-2.32	-2.26
CD-13	3685	meadow	-0.06	-0.05	-	-0.04	-
JC-24	3748	swamp meadow	-0.94	-0.91	-	-0.87	-0.83
JC-28	3756	swamp meadow	-0.33	-0.31	-0.31	-0.32	-0.27
JC-29	3756	swamp meadow	-1.00	-0.99	-1.00	-0.97	-
ML-10	4100	degraded meadow	-0.37	-0.37	-	-0.32	-0.29
ML-11	4103	swamp meadow	-0.88	-0.88	-	-0.85	-0.81

Field and model-based characterization of permafrost conditions in mountainous terrain in western Labrador

Robert G. Way & Antoni G. Lewkowicz

Department of Geography, University of Ottawa, Canada

The earliest maps of eastern Canada considered the inland region bordering Labrador and Quebec to be far south of the southern limits of permafrost (Brown, 1960). However, iron ore exploration in the interior of Labrador-Quebec revealed thick permafrost throughout upland tundra portions of the landscape in Schefferville with isolated patches of permafrost also found on mountaintops 100 km farther south near Labrador City (Ives, 1962). The observations of permafrost in the vicinity of Schefferville were studied in detail at the McGill Subarctic Research Centre for decades (Nicholson, 1979). However, to date no systematic assessment of permafrost along the Quebec-Labrador border has taken place south of Schefferville despite the presence of extensive mountainous terrain with alpine tundra. As part of the Labrador Permafrost Project, two alpine field sites approximately 100 km south of Schefferville near the Labrador-Quebec were selected for intensive summer and winter field investigations. Climate data collected from four monitoring stations indicate that cold permafrost (TTOP < -2.8 °C) is present on windswept hilltops at two sites, with inferred thicknesses of up to 80 m, but is absent at the monitoring stations below treeline. Basal temperature of snow surveys also suggest that permafrost is present in much of the upper alpine zones. Notably, permafrost is inferred to occur at locations where late-winter snow depths exceed the limiting criteria of 80 cm maximum thickness established 100 km farther north in Schefferville during permafrost mapping campaigns in the 1960s and 1970s (Nicholson, 1979).

BTS field data was used to validate a regional permafrost distribution map generated at a high spatial resolution (2 m) using the equilibrium temperature at the top of permafrost model (Smith and Riseborough, 2002; Riseborough, 2004). The model was developed using a high resolution vegetation dataset derived from semi-automated classification of Geoeye-2 satellite imagery (provided by the Geoeye Foundation) for assigning thawing n-factors. Freezing n-factors were derived using a wind exposure algorithm (Plattner et al., 2004) in combination with local field data for the estimation of average winter snow thickness, while snow density was estimated using snow climate classes partitioned using the Geoeye-2 satellite imagery. Spatial modelling of permafrost distribution using the TTOP model broadly agreed with field observations in terms of both ground temperatures and spatial and altitudinal limits of permafrost but underestimated the microscale variability in ground temperatures associated with local snow redistribution. The modelled distribution of permafrost in the region was elevation-dependent, largely due to altitudinal vegetation zones and their corresponding impacts on local snow cover (thickness and density). Permafrost was predicted to be almost absent below treeline (800 m a.s.l.) with less than 1 % probability below 725 m a.s.l. and less than 10 % probability between 725 m a.s.l. and 790 m a.s.l. At elevations between 790 m a.s.l. and 850 m a.s.l. permafrost was sporadically discontinuous ($> 10\%$ and $< 50\%$) with widespread permafrost ($> 50\%$) modelled to occur above 850 m a.s.l. Based on the results of the high resolution TTOP modelling, field data (BTS and ground loggers) and regional zonation, we conclude that permafrost is present beneath most of the higher elevation alpine tundra close to the Labrador-Québec border, with patches of permafrost found in wind-exposed sites at lower elevations down to treeline.

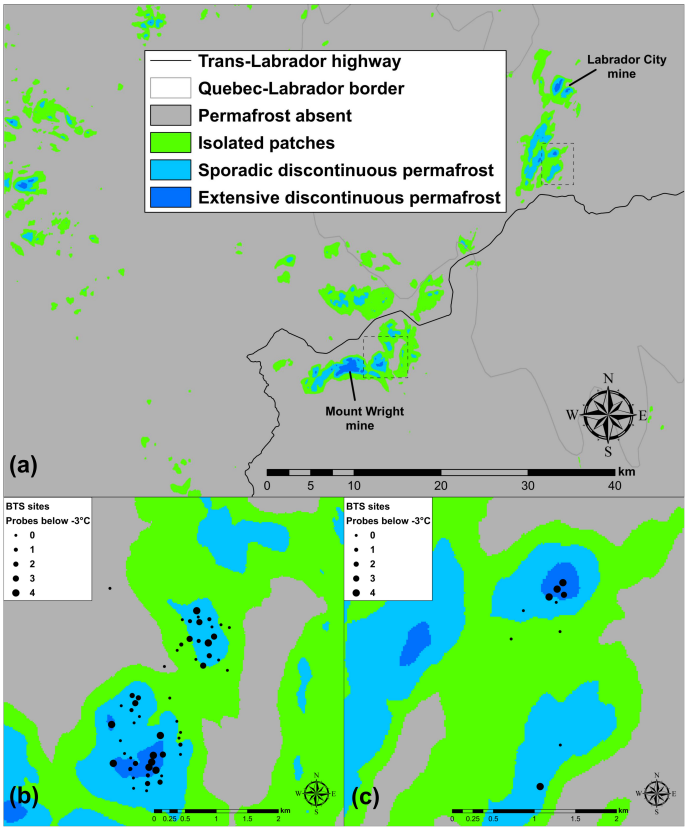

Figure 1: Modelled permafrost probability index reclassified according to elevation bands along (a) the southwestern Labrador-Québec border; (b) near the Mount Wright mine site; and (c) near the Labrador City mine site.

Mapping the thermal state of permafrost through modeling and remote sensing

Sebastian Westermann[1], Moritz Langer[2], Kristoffer Aalstad[1], Julia Boike[2], Kjersti Gisnås[1], Maria Peter[1,2], Thomas Schuler[1], Torbjørn Østby[1], & Bernd Etzelmüller[1]

[1] *University of Oslo, Norway*
[2] *Alfred Wegener Institute Helmholtz Centre for Polar and Marine Research, Potsdam, Germany*

With current remote sensing technologies, it is not possible to directly infer the thermal state of the ground from spaceborne platforms. We demonstrate that such limitations can be overcome by combining the information content of several remote sensing products in a data fusion approach: time series of remotely sensed land surface temperature, as well as snow cover and snow water equivalent, are employed to force ground thermal models which deliver ground temperatures and thaw depths.

First, we present a semi-empirical model approach based on remotely sensed land surface temperatures and reanalysis products from which mean annual ground temperatures (MAGT) can be estimated at a spatial resolution of 1 km at continental scales. The approach is tested for the unglacierized land areas in the North Atlantic region, an area of more than 5 million km^2. The results are compared to in-situ temperature measurements in more than 100 boreholes from which the accuracy of the scheme is estimated to approximately 2.5 °C.

Furthermore, we explore transient modeling of ground temperatures driven by remotely sensed land surface temperature, snow cover and snow water equivalent. The permafrost model CryoGrid 2 is applied to the Lena River Delta in NE Siberia (25000 km^2) at 1km spatial and weekly time resolution for the period 2000–2014. A comparison to in-situ measurements suggests a possible accuracy of around 1 °C for annual average ground temperatures, and around 0.1 m for thaw depth. However, information on subsurface stratigraphies including the distribution of ground ice is required to achieve this accuracy which is currently not available from remote sensing products alone.

Finally, we discuss the potential and limitations of schemes using a combination of remote sensing data and thermal permafrost models to assess the thermal state of the ground, and give a feasibility assessment for both mountain and lowland permafrost regions.

Application of logistic regression model and multi-criteria analysis methods to map permafrost distribution and assess its dynamics on the Qinghai-Tibetan Plateau

Tonghua Wu, Tianye Wang, Ren Li, & Yanhui Qin

Cold and Arid Regions Environmental and Engineering Research Institute, Chinese Academy of Sciences, People's Republic of China

The highest and most extensive mid-altitude permafrost on earth is located on the Qinghai-Tibet Plateau (QTP). During the last ten years, Chinese geocryologists and cold regions engineers have improved the permafrost monitoring network on the QTP by extending the Qinghai-Tibet highway (railway) corridor to the whole plateau. Some long-term and continuous permafrost monitoring sites have been established with the support of many projects. Long-term observations of permafrost on the QTP indicates that permafrost has been undergoing warming even extensive degradation on the plateau. The changes in permafrost thermal regimes on the QTP have affected local hydrology, ecology, and engineering infrastructure. In this study, we intended to apply logistic regression model (LRM) and multi-criteria analysis (MCA) methods for remapping permafrost distribution on the QTP and assessing its dynamics since 1960s. The in-situ investigation results for some typical permafrost regions have been used to validate the modeling results and to estimate the accuracy of the remapping results. The results showed that both LRM and MCA could mapping permafrost distribution on the QTP. LRM performed better than MCA in identifying the permafrost and seasonally frozen ground, while that MCA performed better than LRM in assessing permafrost dynamics under the scenario of climate warming on the QTP.

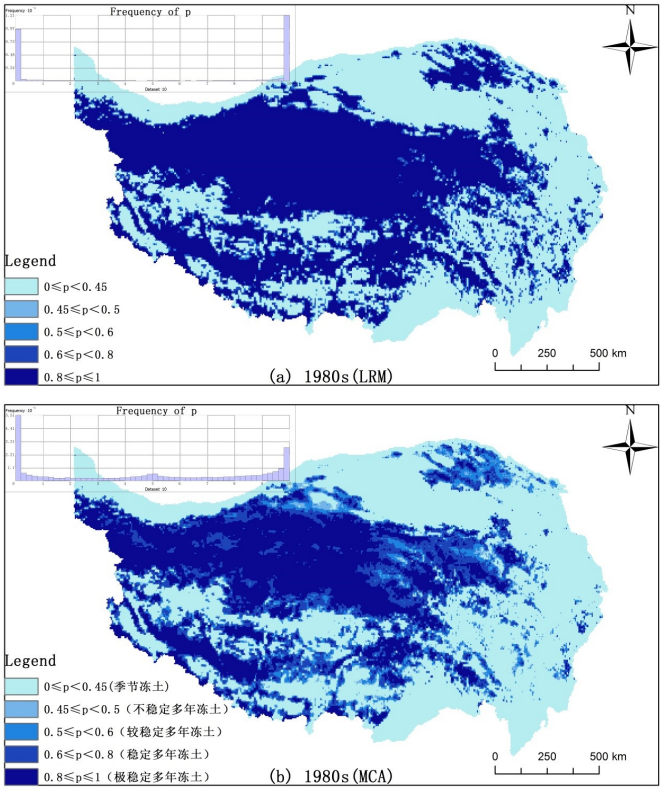

Figure 1: The remapping permafrost distribution on the QTP by using LRM and MCA methos

Reconstruction of MODIS LST data

Gansukh Yadamsuren, & Jambaljav Yamkhin

Institute of Geography and Geoecology, Mongolian Academy of Sciences, Mongolia

A one of main factors that govern the existence of any chemical, biological and physical processes and phenomena in near surface is surface temperature. Surface temperature trend in different land covers, including glacier and permafrost distributed area, is an important indicator of climate change

Therefore, high-resolution land surface temperature (LST) data from satellite sensor have been widely used in such climate change related studies. The LSTs derived from the Moderate Resolution Imaging Spectroradiometer (MODIS) sensor are available from NASA's official website (http://e4ftl01.cr.usgs.gov). The V5 level 3 MODIS LST (Terra-MOD11A1 and Aqua-MYD11A1) data is enormous (14600 maps have been generated for each MODIS map tile) and the data processing to be automated.

MODIS LST data, sometimes, does not contain value of temperature due to clouds, cirrus cloud, missing pixels, poor quality and other errors, and these obstacles interrupt to create fully reconstructed time series [Neteler, 2010]. In order to get over the problems and create reconstructed gap-free map areas, previous researchers have processed different approaches, for instance, Fourier transform, temporal average, 2D and 3D spline interpolations and multiple-regression [Metz et al., 2014]. Table 1 shows a summary of previous approaches to reconstruct LST time series.

Mongolia is located in East Asia from N40 – 50° of latitude to E84 – 123° of longitude, covering 4.7 million square kilometer including Altai high-mountain (4374 m.a.s.l.) in west and steppe lowland (560 m.a.s.l.) in east. The climate is extreme continental, winter mean temperature is -15 to -30 °C and summer mean temperature is 10 to 26.7 °C.

As surface temperature depends on location, altitude, exposition, solar radiation, land-cover, precipitation, and wind speed. Geographically, Mongolia is located between Siberian taiga in north and Gobi desert in south. Therefore, it is not possible to use the regression analysis and interpolation, because surface temperature changes in short distance. It depends predominantly on exposure in one area and depends on land cover in another areas.

We have used the difference between value of first day (001-Aqua-Day 13:30) and value of second day (002-Aqua-Day 13:30). If any values of these days (first day and second day) have missed, we used the values of previous days. If an LST grid does not contain any valid values, it is in our method reconstructed by using the temporally nearest reconstructed maps of the same time of day, only Aqua daytime values were used to estimate a missing Aqua daytime value [Hachem et al., 2009].

Here we present a method for reconstructing spatio-temporal gaps in remotely sensed land surface temperature (LST) time series at larger country scale. This approach takes a final product with 1000 m spatial resolution and four daily values per pixel position. We have processed an different reconstruction method, which we applied to larger Mongolia for all daily MODIS LST data available from 2004 to 2013.

Reconstructed LST data compared to ground based measurement data which air temperature at meteorological station (T_{air}) and permafrost ground surface temperature at at GTN-P sites of Mongolia (GST). Reconstructed LSTs have good fits with T_{air} during the cold season and with GST during warm season. We have found a following correlation between T_{air} and reconstructed LST. R = 0.89, mean difference (MD) = 0.2 °C, standard error 0.04 °C.

Table 1: List of previous approaches reconstruction of MODIS LST.

Authors	Method	Spatial Extent	Spatial Resolution	Temporal Extent	Temporal Resolution	Output
Scharlemann *et al.*, 2008	Temporal Fourier transform	Global	1000 m	2001–2005	2 maps/ 8 days	34 parameters describing LST temporal cycles
Neteler, 2010	Volumetric (3D) splines	Part of Northern Italy	200 m	2000–2008	4 maps/ day	Fully reconstructed time series
Crosson *et al.*, 2012	Seasonal mean	Contermin ous USA	1000 m	2003–2008	4 maps/ day	Partially reconstructed time series
Hengl *et al.*, 2011	Temporal average, 2D splines	Croatia	1000 m	2008	2 maps/ 8 days	Fully reconstructed time series
Benali *et al.*, 2012	Temporal aggregation	Portugal	1000 m	2000-2009	2 maps/ day	Partially reconstructed time series
Markus *et al.*, 2014	Temporal average, multiple regression, splines	Europe	250 м	2000-2013	4 maps/ day	Fully reconstructed time series
In this study	Temporal average	Mongolia	1000 m	2004-2013	4 maps/ day	Fully reconstructed time series

References

Hachem, S.; Allard, M. and Duguay, C. [2009]: Using the MODIS land surface temperature product for mapping permafrost: an application to northern Québec and Labrador, Canada. *Permafrost and Periglacial Processes*, 20(4):407–416, doi:10.1002/ppp.672.

Metz, M.; Rocchini, D. and Neteler, M. [2014]: Surface Temperatures at the Continental Scale: Tracking Changes with Remote Sensing at Unprecedented Detail. *Remote Sensing*, 6(5):3822, 2014. doi:10.3390/rs6053822.

Neteler, M. [2010]: Estimating Daily Land Surface Temperatures in Mountainous Environments by Reconstructed MODIS LST Data. *Remote Sensing*, 2 (1):333, doi:10.3390/rs1020333.

Temporal and spatial variation analysis on land surface temperature over Qinghai-Xizang Plateau

Chengsong Yang & Tao Che

Cold and Arid Regions Environmental and Engineering Research Institute, Chinese Academy of Sciences

The spatial distribution and multi-year change of land surface temperature over Qinghai-Xizang Plateau was analyzed using MODIS LST products. Firstly the null pixels were reconstructed by integrating temporal and spatial information. The validity ratio was showed to be over 97 % after LST recovery. A sine and linear piecewise function was utilized to fit the four instantaneous observations to mean daily LST. Ground observation of 0 cm soil temperature was employed to validate the fitting precision, which was proved to be within 1 K. At last a cosine function model was built to describe the seasonal fluctuation of LST. The mean annual LST, the amplitude and the peak LST date were subsequently extracted by this model. Results showed that the mean annul LST was highly correlated to attitude, latitude and the type of underlying surface. Amplitude was showed to rise from the southeast to northwest. The peak date of water was obviously delayed compared with other types. Slope analysis showed that the mean annual LST over Qinghai-Xizang Plateau was increasing with a velocity of 0.015 K per year. Amplitude was elevated by 0.076K per year, which indicated that the probability of extreme weather was larger than before, due to the greenhouse effect and climate change. The peak date of LST appeared earlier to some extent.

Building tools to bridge scales: Permafrost data integration for easier reuse

Lynn Yarmey[1], Kevin Schaefer[1], Elchin Jafarov[2], Halldór Jóhannsson[3], & Jean-Pierre Lanckman[3]

[1]*National Snow and Ice Data Center, United States of America*
[2]*University of Colorado Boulder, United States of America*; [3]*Arctic Portal*

Partnering permafrost and data management expertise, the US National Science Foundation-funded PermaData project led by the National Snow and Ice Data Center (NSIDC) has the goal of making existing permafrost data easier to access and use. PermaData has partnered with teams from the Global Terrestrial Network for Permafrost (GTN-P), and the Arctic Observing Viewer (AOV), the Arctic Data Committee, the Advanced Cooperative Arctic Data and Information Service (ACADIS), and others to ensure a widely useful approach that will support meaningful change to make permafrost data easy to use. PermaData aims to shorten the months-long time needed to find, aggregate, standardize, and use international in-situ permafrost data, especially in concert with remote sensing and modeling data, it is building a standardization process and tool using existing datasets from the Frozen Ground Data Center at NSIDC and the Advanced Cooperative Arctic Data and Information Service (ACADIS) as test cases. This Data Integration Tool is meant to easily understand and import diverse file formats, find key metadata and data fields, process data into standard form, and output files ready to ingest directly into the Global Terrestrial Network for Permafrost (GTN-P) for sharing and access. The Data Integration Tool will process 15 selected permafrost datasets into the standard GTNP format. All the processes permafrost data will then be available via the GTN-P portal. The Data Integration Tool will be made available through the GitHub. Over the course of the project thus far, the PermaData team has worked to standardize metadata and data approaches, and identify and mitigate inconsistencies in data practices across different communities over time. In addition, PermaData will complement other permafrost projects focusing on modeling and benchmarking starting up this year.

Geocryological Database of the Siberian Platform

Mikhail Zhelezniak, Vladimir Zhizhin, Denis Sivtsev, Ludmila Shipitsyna, & Leonid Gagarin

Melnikov Permafrost institute, Russian Federation

In permafrost regions, temperature is an important parameter indicating the state of ground. Permafrost temperature, distribution and thickness are controlled by a variety of environmental factors. Delineating occurrences of frozen ground and its characterization require that mapping indicators be identified and quantitatively estimated.

An objective knowledge of permafrost parameters and temperature characteristics can be obtained on the basis of detailed zonation and relationships among landforms, climate and ground thermal properties. If data available are few, they can be easily handled. If there are hundreds or thousands of measurements, this raises the issue of data processing, storage and analysis. The development of PC-based databases that provide a possibility to handle, process and analyze large volumes of data is the most appropriate tool in regional geocryology. Databases are also increasingly demanded by surveyors, design engineers, and geological engineering personnel of industrial and mining companies. Geocryological databases provide a foundation for assessing geotechnical conditions in mapping at regional, and often at local scales.

In 1995, the Melnikov Permafrost Institute began the development of a database for the Siberian Platform which contains geocryological data structured by tectonic units. The database was constructed in DELPHI which permits visual application development based on object-oriented programming. Besides, the DELPHI is one of the most used full-scale tools for DBMS development.

A significant advantage of applications developed in the Delphi environment is the availability of both relational and navigation programming for data manipulation. Relational methods enable manipulation with large data sets. Navigation methods provide the applications with fast access to the fields and records of database tables.

The world of databases tends to integration and therefore needs a standard language that could be used on all major platforms. The Structured Query Language (SQL) was selected as a standard language for interacting with other databases. It allows the user to create and manipulate relational databases, the collections of related data stored in tables. The Delphi special component TQUERY is designed to implement the queries. It has a series of features and methods that allow to use all advantages of SQL queries in operations with the data.

The Siberian Platform Geocryological Database (SPGD) is designed to store and organize a diverse set of geocryological, geothermal, thermophysical and other information available for the region. Basically, it is a compilation of technical information about boreholes and initial data on ground thermal regimes and thermophysical properties. From analysis of ground temperature data structured by geological structures and borehole sites, the users can develop a better understanding of permafrost distribution patterns. The SPGD also contains extreme and mean values for thermophysical properties. The SPGD consists of the following components:

1. a data set with information for sites and boreholes where geothermal investigations were conducted. It contains information on 35 parameters (borehole number, location and elevation, temperature measurement date, permafrost thickness, data source, etc.), including measured or estimated temperatures at selected depths;

2. a regional data set of ground thermal and physical characteristics (thermal conductivity, thermal diffusivity, specific heat, dry density, and gravimetric moisture content);

3. a set of borehole temperature measurement data.

The SPGD currently holds information describing 205 sites located within the Siberian Platform and 48 sites in adjacent areas. Measured temperature data sets are available for 1855 boreholes, 50 to 1800 m in depth. Tables on thermophysical properties contain data for 1425 core samples collected from different depths.

All geothermal measurement sites were plotted in ArcGIS into a tectonic map containing information about geological structures up to the fourth order. This allows the user to readily assess the availability of data for any geological structure and to obtain existing data on the temperature field and geocryological conditions for an area of interest.

Special-purpose maps characterizing the topography, geomorphology, landscape conditions and geology were added as basemap layers in ArcGIS. Information contained in these maps helps comprehensively analyze the geocryological data. It should be noted that the spatial coverage of geocryological research in the Siberian Platform is not uniform because of the different levels of industrial development across the region and inaccessibility of most areas. Central and southern areas of Yakutia have been studied in greater detail, while the Tunguska Basin and Anabar-Olenek High has received much less research. Our knowledge of permafrost thermal conditions in the region depends on the availability of boreholes for geothermal information.

The use of ArcGIS and Google Earth provides additional information about the borehole sites, and the possibility of viewing cartographic information by layers (geomorphology, landscapes, satellite and aerial imagery, etc.) helps improve the quality of data analysis and gain a better understanding of permafrost development at regional and local scales.

The SPGD is updated on a regular basis. It allows the user to view information in table and graphic forms, select relevant data, and conduct statistical or other mathematical processing. The SPGD can serve as a component of a regional or international database and as an independent system about the nature of the earth.

SESSION 9

Results from GTN-P: Thermal State of Permafrost (TSP) and Circumpolar Active Layer Monitoring (CALM)

Convener:

Sharon Lee Smith, *Natural Resources Canada, Geological Survey of Canada in Ottawa, Canada*

Dmitry A. Streletskiy, *Department of Geography, The George Washington University, USA*

Jeannette Noetzli, *WSL Institute for Snow and Avalanche Research SLF, Davos, Switzerland*

The focus of this session is reporting of the latest developments and results in permafrost and active layer temperature measurements in Earth's high latitude and altitude regions. The Global Terrestrial Network for Permafrost (GTN-P) will report on the development of the Data Management System for permafrost as an Essential Climate Variable including metadata statistics, quality control and data processing. All members of GTN-P, National Correspondents and potential new members are invited to contribute with findings on the thermal state of permafrost and active layer from local to global scale.

Characteristics of permafrost at local and regional scales: the Altai and Khentii Mountains, Mongolia

Dashtseren Avirmed[1], Ishikawa Mamoru[2], Iijima Yoshihiro[3], Jambaljav Yamkhin[1], Sharkhuu Natsagdorj[1], Yadamsuren Gansukh[1], Khurelbaatar Temuujin[1], Yondon Amarbayasgalan[1], Gansukh Tsogterdene[1], Tsogtbaatar Undrakhtsetseg[1]

[1] *Institute of Geography-Geoecology, Mongolian Academy of Science, Mongolia*
[2] *Graduate School of Environmental Science, Hokkaido University, Japan*
[3] *Research and Development Center for Global Change, Japan Agency for Marine-Earth Science and Technology, Japan*

In Mongolia, permafrost predominantly occurs in the Altai, Khuvsgul, Khangai, and Khentii Mountains and their surrounding areas where the southern boundary of the Siberian permafrost is roughly located. During the last several years numerous permafrost monitoring sites were established along these Mountains in order to measure the thermal properties of permafrost. The main objective of this article is to present basic characteristics of permafrost in local and regional scales in the case of the Altai and Khentii Mountains. Based on datasets from these boreholes we here present synoptically summarized results for the Altai and Khentii Mountains.

Altai Mountains: The Altai Mountains are located in western Mongolia (Fig. 1) and is comprised of the tallest mountains in the country. Currently there are 21 boreholes within the Altai and at varying depths (1-15 m). Of these 21 BH's, 3 have been re-drilled near older boreholes where soil temperature measurements were collected 30-33 years ago. The southernmost borehole (BH20) is located in a valley at 2415 m above the sea level (asl) where mean annual ground temperature (MAGT) at 8 m was -0.1 °C and active layer thickness (ALT) was more than 8 m for the last 5 years. However, the temperature at 8 m depth has been increased insignificantly by about 0.1 °C during last 30 years. This insignificant change in temperature is likely not intense enough to initiate a phase change. BH22 is in close proximity to BH20 however it is located on a gentle north-facing slope at 2025 m asl. At BH 20, the MAGT at depths of 1 m and 3 m was about 5.7 °C and 3 °C, respectively, likely indicating that there is permafrost absent. Similar results were found at BH 18 where MAGT was 6.7 °C at 1m depth. BH 72 with 2421 m asl and BH 73 with 2208 m asl are located on a north-facing slopes in the Khantaishir Mountains which lies between the Altai and Khangai Mountains. The distance between the sites is about 5 km and with similar slope inclinations and vegetation cover. At these sites, permafrost is present in BH 72 with more than 6 m ALT while permafrost is absent in BH 73, indicating that the elevation gradient is important for locally existing permafrost. BH 37 with 1714 m asl is located in a valley in the middle of the Altai Mountains, where MAGT at 10 m depth was -0.2 °C and ALT reached 3.5 m. Although elevations vary between BH20 and BH 37, the differences in MATG at both sites were small. These differences can be explained by variations in latitude at the sites.

In the northern Altai, permafrost is present in 13 out of 15. The two boreholes with no permafrost are located on south facing slopes. BH 29 experiences only thin permafrost between 8 m and 15 m where MAGT was -0.01 °C at 10 m. Interestingly BH 29 is located at the foot of a north-facing slope at 1995 m asl and similar vegetation cover compared with other sites. However, the MAGT decreases with increasing elevation along the north-facing slope. For instance, MAGTs at a depth of 10 m were -0.2 °C at BH 30 (2240 m asl), -2.2 °C at BH 31 (2358 m asl) and -3.3 °C at BH 32 (2500 m asl). The most northern boreholes in the Altai Mountains are BH 26 on the gently south-facing slopes and BH 27 on the gently north-facing slope and are separated by about 4 km. Yet, both boreholes possess similar elevation (2120 m asl), vegetation cover and soil textures. However, ALTs were 3.3 m at BH 26 and 3.9 m at BH 27, and MAGTs at 10 m were -0.76 °C and -0.40 °C, respectively. This indicate that topography has a strong effect on permafrost temperature at local scale. At BH 26, the MAGT at depth of 10m has increased by 0.4 °C during the last 30 years.

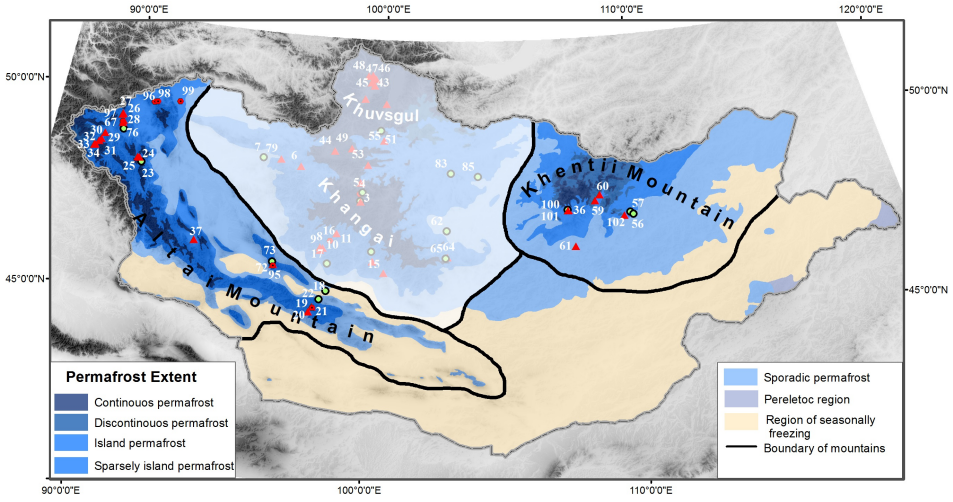

Figure 1: Permafrost distribution in Mongolia [Gravis et al., 1971], locations and numbers (BH); the monitoring sites in permafrost (red triangles) and without permafrost (green circles), and the ground surface temperature monitoring sites (red circles).

Khentii Mountains: The Khentii Mountains are approximately located in the transition zones between the Siberian boreal forests to wide steppe. This transition zone corresponds roughly to a change from Siberian continuous permafrost zone to the seasonally frozen ground zone. In the Khentii Mountains, nine boreholes are situated at different topographies, vegetation covers and elevations (Fig. 1). Automatic soil weather stations, including sensors of ground temperatures and moisture in boreholes, were installed at BH 100 on a south-facing slope covered be by steppe and BH 101 on a north-facing slope covered by forest, on permafrost. Both sites have almost the same elevation and slope inclinations of 11–12°), but are approximately 1.58 km apart. During the summer, the ground surface temperature was warmer at BH 100 than BH 101, due to the large amount of downward shortwave radiation received on the dry south-facing slope. But in the winter ground surface temperatures were warmer at BH101 due to more snow insulation effect. However, the MAGT was warmer at the BH100. Overall, the forests at the edges of boreal forests are an important factor in contributing to cooler ground temperatures and the existence of permafrost in this region, which occurs only beneath forested north-facing slope (see Ishikawa et al. [2012], Dashtseren et al. [2014]). The same MAGTs (-0.5 °C) were observed at the sites BH 59 and BH 60, where elevations were 1450 m and 1496 m, respectively.

The ground thermal dynamics in the southern boundary of the Siberian permafrost is altering. For example, permafrost has disappeared at both BH 57 and BH 56 over the last 30 years. In the BH 57, the soil temperature at 10 m was -0.1 °C in1984, however, it was 1.3 °C in 2014. The BH 61 is in a swampy bottom of a small depression, where MAGTs were -0.2 °C and -0.1 °C at the depths of 4.5 m of 9.5 m in 1978. Whereas, the MAGTs were -0.1 at 4 m, 0.3 °C at 6 m and 0.9 °C at 10 m in 2011, respectively.

References

Dashtseren, A.; Ishikawa, M.; Iijima, Y. and Jambaljav, Y. [2014]: Temperature Regimes of the Active Layer and Seasonally Frozen Ground under a Forest-Steppe Mosaic, Mongolia. *Permafrost and Periglacial Processes*, 25(4):295–306, doi:10.1002/ppp.1824.

Gravis, G.F.; Jamsran, C.; Zabolotnik, S.I.; Sukhodrovsky, V.L.; Sharkhuu, N.; Lisun, A.; Lonjid, H.; Luvsandagva, D. and Tumurbaatar, T. [1971]: Geocryology Map of Mongolia (1:1 500 000), 1971.

Ishikawa, M.; Sharkhuu, N.; Jambaljav, Y.; Davaa, D.; Yoshikawa, K. and Ohata, T. [2012]: Thermal state of Mongolian Permafrost. In: Hinkel, K.M.(ed.), *Proceedings of the Tenth International Conference on Permafrost*, Salekhard, Yamal-Nenets Autonomous District, Russia, 25–29 June 2012, volume 1: International Contributions, pages 173–178. The Northern Publisher: Salekhard. ISBN 978-5-905911-01-9. URL http://ipa.arcticportal.org/publications/conference-proceedings.

And it continues: A new borehole extends the longest mountain permafrost temperature record on rock glacier Murtèl, Swiss Alps

Alexander Bast[1], Jeannette Noetzli[1,2], Isabelle Gärtner-Roer[1], Martin Hoelzle[3], Christian Hauck[3], Daniel Vonder Mühll[4], Johann Müller[1], Marcia Phillips[2], Diego Wasser[1], & Andreas Vieli[1]

[1] *Universtity of Zurich, Department of Geography - 3G, Switzerland*
[2] *WSL Institute for Snow and Avalanche Research SLF, Switzerland*
[3] *University of Fribourg, Unit of Geography, Switzerland*
[4] *SystemsX.ch: The Swiss Initiative in Systems Biology, Switzerland*

The longest borehole temperature time series available in mountain permafrost is measured within the rock glacier Murtèl in the Corvatsch-Furtschellas area in the Upper Engadine, eastern Swiss Alps. The tongue-shaped landform is creeping with an average velocity of about 6-10 cm a^{-1}, spreading from 2750 m a.s.l. to 2600 m a.s.l. and covers an area of approximately 0.5 km^2. Scientific investigations started in the mid-1970s where an 11 m deep borehole was drilled to have access to the interior of mountain permafrost and of a rock glacier for the first time.

In early summer 1987, two boreholes of 21 and 58 m were drilled through the ice-rich frozen debris [Vonder Muehll and Haeberli, 1990] and thermistors and inclinometer tubes for the access with a hand-held inclinometer were installed in the deeper borehole. Continuous monitoring showed the uppermost 25 m rapidly warming between 1987 and 1994. Intensive cooling of the ground occurred in the following two winters due to late snow fall and a reduced snow cover thickness. Hence, permafrost temperatures then remained more or less at the same level until 2009. This is followed by a warming period since 2009 until today that can be detected at depths of 10 and 20 m. In addition, maximum active layer thickness has increased from about 3.5 m to more than 4 m in the past four years with a new record value of 4.4 m in the year 2015.

While the temperature measurements were conducted with only a few interruptions, considerable shearing at a depth of 28 m to 32 m stopped the hand-held inclinometer measurements in 1994 [Arenson et al., 2002]. In order to gain knowledge regarding the mechanical and geotechnical processes influencing deformation patterns of rock glaciers, two additional boreholes were drilled some 13 and 20 m up-slope from the 1987 boreholes in 2000 [Arenson et al., 2002].

Today, the Murtèl-Corvatsch site is one of the longest and best investigated mountain permafrost sites and is part of the Swiss Permafrost Monitoring Network (PERMOS) as one of its reference sites. The rock glacier Murtèl is a key component and a paramount example for a successful integration of research and long-term permafrost monitoring. The borehole measurements are complemented by a large variety of observations and methods, including a climate station, regular long-term terrestrial surveys and geophysical soundings.

The Swiss Federal Office for the Environment (FOEN) funded the drilling of a new borehole in the framework of the PERMOS network in 2015 in order to assure the continuation of the borehole temperature record in the case of an expected shearing-off of the installed temperature chains in the near future. In addition, this project allows the validation of the borehole temperature measurements performed with the 30-year old thermistors with the new installed ones in 2015, as well as the renewal of the deformation measurements stopped in 1994 due to shearing. A collected ice core permits the analyses of the ice using new dating methods.

The new borehole was drilled from September 14^{th} to September 22^{nd}, 2015 some 4 m apart of the 58 m borehole from 1987 (on the same ridge) and down to a depth of 60.5 m (Fig. 1). After 5 m of destruction drilling through the coarse blocky rock glacier surface and the first ice layers, the drilling process was changed to a Triplex drill, which permitted the extraction of drilling cores/ice cores down to approximately 32 m. Again, from 32 m down to 60.5 m destructive drilling was used after the shear horizon was penetrated. As in the drillings before [Arenson et al., 2002], three distinct layers appeared: An approximately 2.5 m thick surface layer consisting of

coarse blocky material covers an approximately 27 m thick layer of massive ice, whereas the content of rocks increases close to a depth of 30 m. Further down, the ice content decreases with depth and is present in the pores of the solid particles of sand and silt. Water was detected at a depth between 31.6 m and 32.4 m, which was presumably stored in a water pocket. Polyethylene (PE) tubes with an inside diameter of 110 mm were installed and sealed with a cap on the bottom to protect the measurement devices against water. Thermistors (YSI 46031, www.alpug.ch) were assembled in three chains down to 60 m with an increased resolution in the active layer (0–3 m) and the expected shearing zone (28-38 m). Furthermore, the three temperature chains overlap each other in 3 m, 5 m, 10 m, and 20 m depth to guarantee replication of measurements and redundancy in case of drift or loss of a thermistor at depths important for the long-term monitoring. An automatic inclinometer (SAAF, www.measurand.com) with a total length of 40 m and consisting of 80 segments having a length of 0.5 m each was additionally installed to automatically measure the rock glaciers internal deformation/displacement at regular time intervals.

Our contribution will focus on the planning, implementation and procedure of the drilling campaign, the measurement devices used in the project and will highlight the first results of the measurements of the 2015 drilling compared to the time series from 1987.

Figure 1: General overview of the installed drilling platform (a). A Muck Menzi walking excavator was holding and steering the drilling apparatus (b). Opening of a TRIPLEX drill string to remove the collected ice core (c). Storage of the ice cores in robust plastic

Acknowledgements

The authors would like to thank the Swiss Federal Office for the Environment (FOEN) for funding the project. Furthermore, we thank all the participants of the Murtèl workshop at the University of Zurich in May 2015, CrestaGeo (http://www.crestageo.ch) for a professional undertaking of the drilling, and Hansueli Gubler (http://www.alpug.ch) for technical support regarding the measurement devices.

References

Arenson, L.; M., Hoelzle and Springman, S. [2002]: Borehole deformation measurements and internal structure of some rock glaciers in Switzerland. *Permafrost and Periglacial Processes*, 13:117–135, doi:10.1002/ppp.414.

Vonder Muehll, D. and Haeberli, W. [1990]: Thermal characteristics of the permafrost within an active rock glacier (Murtèl/Corvatsch, Grisons, Swiss Alps). *Journal of Glaciology*, 36:151–158, 1990.

A global snapshot on the thermal state of permafrost and active layer thickness

Boris K. Biskaborn[1], Vladimir E. Romanovsky[2], Sharon L. Smith[3], Dmitry Streletskiy[4], Jeannette Nötzli[5], Gonçalo Vieira[6], Philippe Schoeneich[7], Jean-Pierre F. Lanckman[8], & Hugues Lantuit[1,9]

[1] *Alfred Wegener Institute Helmholtz Centre for Polar and Marine Research, Potsdam, Germany*
[2] *Geophysical Institute, University of Alaska Fairbanks, Fairbanks, USA*
[3] *Geological Survey of Canada, Natural Resources Canada, Ottawa, Canada*
[4] *George Washington University, Washington, USA*
[5] *WSL Institute for Snow and Avalanche Research SLF, Davos, Switzerland*
[6] *Instituto de Geografia e Ordenamento do Território, University of Lisbon, Lisbon, Portugal*
[7] *Institut de Géographie Alpine, Université de Grenoble Alpes, Grenoble, France*
[8] *Arctic Portal, Akureyri, Iceland*
[9] *University of Potsdam, Potsdam, Germany*

The Global Terrestrial Network for Permafrost (GTN-P, http://gtnp.org) is part of the Global Terrestrial Observing System (GTOS) of the Global Climate Observing System (GCOS). GCOS is a joint undertaking of the World Meteorological Organization (WMO), the Intergovernmental Oceanographic Commission (IOC) of the United Nations Educational Scientific and Cultural Organization (UNESCO), the United Nations Environment Programme (UNEP) and the International Council for Science (ICSU). GTN-P was established in 1999 by the International Permafrost Association (IPA) with the goal of systematic and long-term documentation of the distribution, variability and trends of permafrost (an Essential Climate Variable, ECV) based on a global network of field measurements. The two current cryospheric indicators are permafrost temperature and active layer thickness, throughout the Earth's permafrost regions. The network has been mainly operated by scientist and research institutions and programs.

GTN-P developed a Data Management System (http://gtnpdatabase.org) for the collection, processing (including standardisation) and dissemination of permafrost data and metadata. Recent data of ground temperature and active layer thickness are currently being compiled for a new global snapshot of the current permafrost state. The snapshot is intended for publication in 2016 and compared to the snapshot developed for the International Polar Year (IPY, 2007–2008).

Initial results indicate that permafrost temperature is generally following the trends in air temperature and continues to increase, especially in the arctic areas where permafrost is relatively cold. In the sub-arctic, where permafrost temperatures are relatively high, the warming trend is less pronounced and at many locations current permafrost temperature is similar to that of the IPY snapshot. In alpine permafrost areas, however, most measurement sites also show significant warming since 2009. Active layer thickness exhibits large interannual variability, mainly due to variations in snow-cover duration and thickness, but has generally increased since IPY in the majority of regions, especially in European Arctic sector where several sites experienced permafrost degradation. In several sites at northwest Antarctic Peninsula, active layer thickness has been stable or even decreased, with the controlling factors still being assessed.

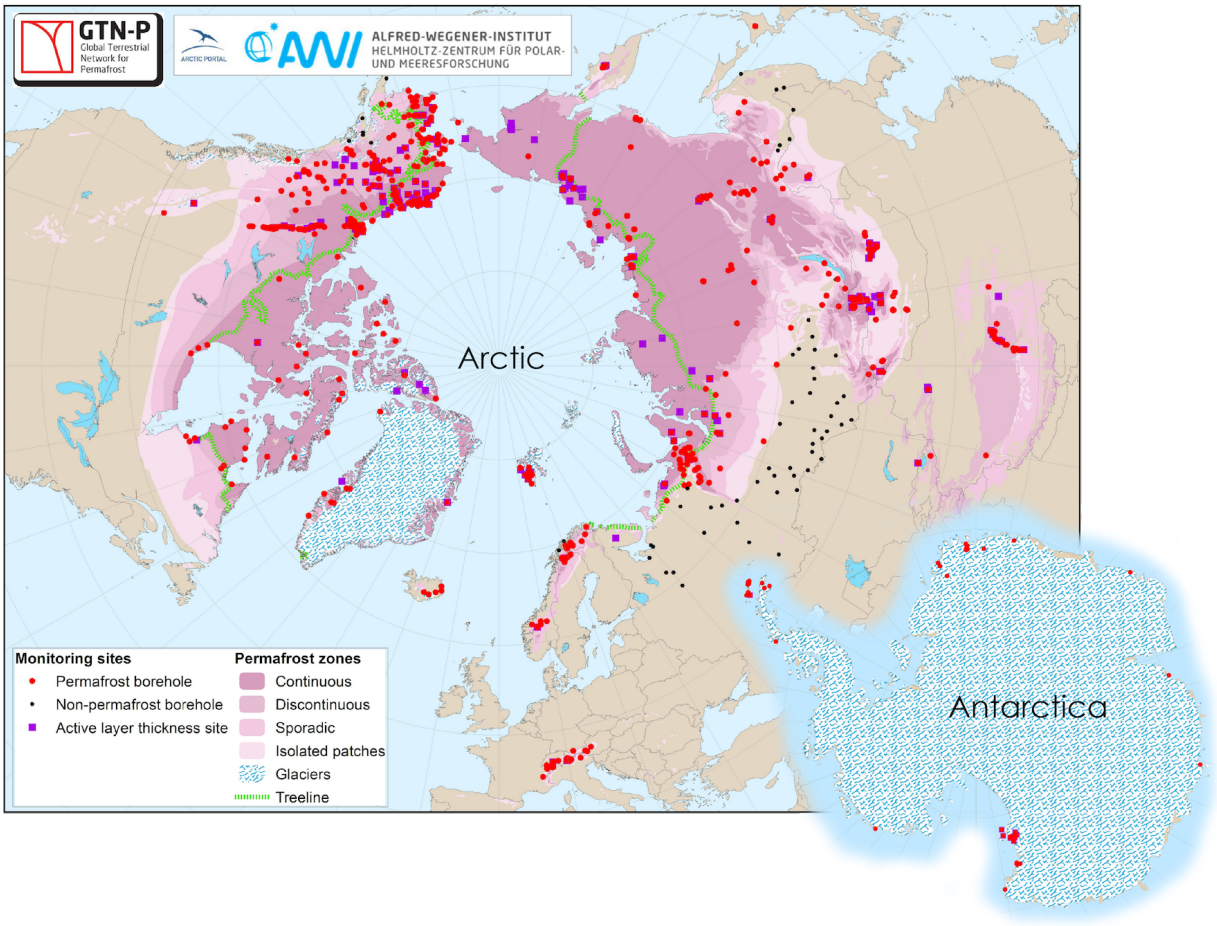

Figure 1: Map of permafrost zones in Arctic and Antarctic view, showing boreholes (n=1233) and active layer monitoring sites (n=248) in GTN-P.

Interactions between active layer thickness and soil properties of CALM sites in different permafrost zones (North West Siberia, Russia)

Anna Bobrik, Olga Goncharova, & Georgy Matyshak

Lomonosov Moscow State University, Russian Federation

The climatic record (North West Siberia) indicates a progressive warming of annual air temperatures of 2 °C over the last 18 years (an average of -6 °C to -4 °C), due to increase in both summer and winter temperatures [Goncharova et al., 2015]. It leads to a change in soils temperature regime, changing plant associations, gradual degradation of permafrost and changing landscape as a whole. We investigated the variability and interactions between active layer thickness and some soil parameters of CALM site R1 (Nadym Grid) in discontinuous permafrost zone and CALM site R50 (Urengoy grid) in continuous permafrost zone of Russian Arctic.

CALM site R1 (Nadym Grid, N65 °20', E72 °55', since 1997) is 1-ha (100m×100m) grid consists of a square array of permanent stakes separated by 10 m (121 data points per grid for all measurements). This site consists of 2 types of ecosystems: 1) frozen peatland, 2) bog. The average active layer thickness was 136±10 cm in Aug 2013, 164±8 in Aug 2014 and 163±8 in Aug 2015. The spatial variability of active layer thickness is determined by hypsometric levels (r=-0,30, p-level <0,05) and winter temperature of soil surface (r=0,38, p-level <0,05). Soil and vegetation cover of peatland have high complexity at fine scale [Bobrik et al., 2015]. Carbon dioxide efflux from soil is low and characterized by high variability (142 ±21 mg CO_2 m^{-2} h^{-1}, Aug 2013; 127 ±17 mg CO_2 m^{-2} h^{-1}, Aug 2014; Coef. Var. 63-85 %). The direct significant correlation between active layer thickness and carbon dioxide efflux was revealed (r=0,45, p-level <0,05). The values of microbial biomass are high, but permafrost and hydrothermal conditions inhibit all soil biological processes. Hypsometric level makes a major contribution to the spatial variability of the soil volumetric moisture and temperature of soil surface. This indirect influence is expressed in the redistribution of winter precipitation over the elements of the microrelief.

CALM site R50a (Urengoy Gas Field grid, N66 °31, E76 °91', since 2008) consist of 3 types of ecosystems: 1) frozen peatland, 2) shrub peatland, 3) forested mound. The average active layer thickness was 70±7 cm in Aug 2013, 76±7 in Aug 2014 and 85±10 in Aug 2015. The active layer thickness and soil parameters (CO_2 efflux, soil volumetric moisture, temperature of soil surface) are characterized by high spatial variability. Carbon dioxide efflux from soil is low and characterized by high variability (224 ±40 mg CO_2 m^{-2} h^{-1}, Aug 2015, Coef. Var. 78 %). Based on the regression analysis was revealed high and significant correlation of active layer thickness with carbon dioxide efflux from soil surface (r=0,53, p-level <0,05), soil volumetric moisture (r=-0,37, p-level <0,05) and soil surface temperature (r=0,56, p-level <0,05). So the main factor which determine the labile soil parameters (such us moisture content, temperature, carbon dioxide efflux) is the depth of permafrost table, it determines the type of ecosystem in such landscapes. Underestimation of the spatial variability of soil and permafrost cover in the region of continuous and discontinuous permafrost can lead to substantial distortion of estimates of the total greenhouse gases balance.

References

Bobrik, A.; Goncharova, O.; Matyshak, G.; Ryzhova, I.; Moskalenko, N. and Ponomareva, O. [2015]: Relationship of active layer thickness and landscape parameters of peatland in the North of West Siberia (Nadym station). *Earth's Cryosphere*, 19(4):31–38, URL http://www.izdatgeo.ru/pdf/earth_cryo/2015-4/29_eng.pdf.

Goncharova, O.; Matyshak, G.; Bobrik, A.; Ryzhova, I.; Moskalenko, N. and Ponomareva, O. [2015]: Temperature regimes of Northern taiga soils in the isolated permafrost zone of Western Siberia. *Eurasian Soil Science*, 48(12):1329–1340, doi:10.1134/S1064229315100038.

Influence of coastal proximity on ground thermal regime in a High Arctic environment, Eureka, Nunavut, Canada

Philip Bonnaventure[1], Antoni Lewkowicz[2], Sharon Smith[3], & Mark Ednie[3]

[1] *University of Lethbridge, Lethbridge, Canada*
[2] *University of Ottawa, Ottawa, Canada*
[3] *Geological Survey of Canada, Natural Resources Canada, Ottawa, Canada*

Introduction and objectives

The Geological Survey of Canada and the University of Ottawa collaboratively initiated a field project in July 2009 to examine and quantify the variability in ground thermal regime in the vicinity of Eureka (80° N, 86°W) on the Fosheim Peninsula of Ellesmere Island, Nunavut. The goal was to examine the impact of coastal proximity on ground temperatures in a High Arctic environment. The region is cold and dry with an average annual air temperature at the Eureka weather station of -18.8 °C and total yearly precipitation of 79 mm (1981-2010), about 60 % of which falls as snow (Environment Canada, 2015). Previous research showed that summer air temperatures inland can be as much 10 °C higher than in the immediate coastal zone on the Fosheim Peninsula due to the coastal effect [Atkinson and Gajewski, 2002]. The latter is mainly due to surface inversions resulting from cold, dense air over ice-covered waters forming a wedge that moves inland beneath warmer air heated by sensible heat transfer from the ground. In addition, coastal locations often have greater amounts of summer cloud cover. Without supporting data, Atkinson [2000] assumed that the distance to which coastal air impacts summer air temperatures inland becomes zero at 6 km. In winter, the impact of the coastal effect might reverse, with relatively warm ocean water beneath its ice cover potentially warming the air and the ground, but again, for an unknown distance inland. Most climate stations in the Canadian High Arctic are located at the coast so estimates of current ground temperatures based on their records could be inaccurate if there is a strong gradient inland, and in turn this would lead to inaccurate estimates of the impacts of future warming. Our objectives, therefore, were to examine the relative strengths of the seasonal influences of coastal proximity on air and ground temperatures and to establish the distance to which they penetrate inland.

Study Sites and Methods

Six shallow (5-10 m deep) boreholes were drilled by water-jet in the valley of Station Creek at sites with elevations of 10 to 75 m a.s.l. (EUK-1 – EUK-6). Surficial deposits at the boreholes were mainly ice-rich marine silts and clays with some sandy horizons and vegetation cover was less than 5 %. The sites were located at progressively greater distances from the coast of Slidre Fiord (100 m to 5 km) and at increasing distances from one another. Each borehole was instrumented with a multi-point thermistor cable and associated logger (RBR; accuracy better than ±0.1 °C). In addition, screen-height air and ground surface temperatures were measured at each site except EUK-1 using Hobo loggers (Onset; accuracy of ±0.2 °C) while snow depths were inferred from iButton temperature loggers (Thermochron; accuracy of ±1 °C) installed on a wooden stake at 5, 10, 20, 30, 40, 50, 60 and 80 cm above the ground surface.

Results and Discussion

Here we present the results of monitoring between 2009-2015 with a minimum of three years of record for each site. Seasonal and annual means were calculated from monthly averages, themselves compiled from all available complete months.

Air temperatures increased away from the coast on an annual as well as a seasonal basis. Mean annual air temperatures increased logarithmically inland by 1.6 °C from -17.2 °C to -15.6 °C (Fig. 1). The summer months (June, July, August) showed an increase of 2.7 °C, from 6.1 to 8.8 °C, while in the remainder of the year the average air temperature increased inland by 1.3 °C, from -25.0 to -23.7 °C. The annual temperature range (July mean temperature minus the mean temperature of the coldest month (January or February)) also increased inland, from 46.1 °C to 48.1 °C.

Mean ground surface temperatures varied from -13.3 °C to -14.3 °C and did not show a consistent trend inland on either an annual (Fig. 1) or a seasonal basis. Snow depths at the weather station, close to EUK-1 and 2, average about 10 cm from September to May (Environment Canada, 2015). Snow depths at all sites, inferred from the iButton data loggers, rarely covered even the lowermost logger at 5 cm above the ground. Annual surface offsets varied from 1.8 °C to 3.5 °C and showed no consistent trend, but summer surface offsets declined from 2.5 °C at EUK-2 to 0.5 °C at EUK-6. This suggests that near the coast, advection results in air warmed by solar heating being replaced by cold air moving in from the fiord whereas inland, air temperatures rise as a result of vertical sensible heat transfer to the air resulting in a smaller offset.

Mean ground temperatures at 0.5 m and 5 m depth increased inland from EUK-2 by up to 3 °C and 1.1 °C respectively (Fig. 1). EUK-2 is slightly colder than EUK-1 even though the latter is closer to the nearest shoreline. EUK-2, however, is on the delta of Station Creek which extends farther into the fiord than EUK-1 and this probably accounts for its lower temperatures. None of the boreholes reached the depth of zero annual amplitude with the temperature varying annually by about 2 °C at 10 m (EUK-3 and 4). The average temperature for the boreholes increased with depth for EUK- 1-4, and decreased with depth for EUK-5 and 6. Since the latter two were the warmest near the surface, coastal to inland differences in ground temperatures declined with depth.

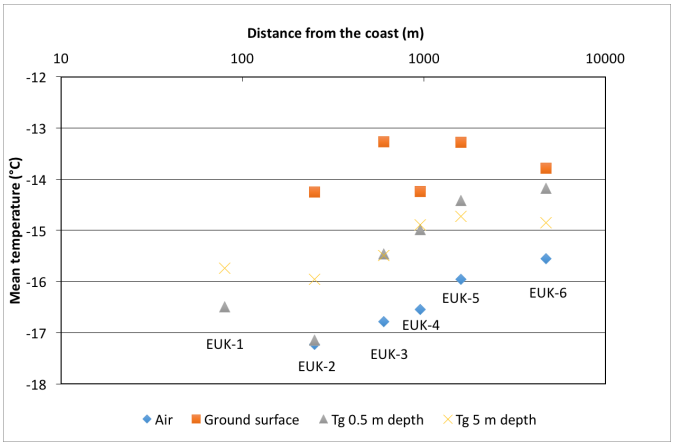

Figure 1: Mean air and ground temperatures at the six borehole sites in relation to distance from the shore of Slidre Fiord, Eureka, Nunavut. Note that distance is shown on a logarithmic scale.

Conclusion

We conclude that, in the Eureka area, both air and ground temperatures increase inland according to the logarithm of the distance from the coast for at least 5 km. The trends are clear for air and temperatures within the permafrost but not for ground surface temperatures. Air temperatures are warmer inland in summer, as expected, but are also warmer in winter for reasons that are not yet clear. Permafrost temperatures in the High Arctic are increasing faster than in many other parts of northern Canada and long-term monitoring of these sites will reveal if coastal and inland locations will warm at the same or different rates.

Acknowledgements

This project was supported by Natural Resources Canada, the University of Ottawa, the Federal Government's International Polar Year Program and Polar Continental Shelf Program. Additional logistical support was provided by Environment Canada. W. Pollard, M. Ward and A. Cassidy kindly assisted with data acquisition.

References

Atkinson, D.E. [2000]: Modelling July mean temperatures on Fosheim Peninsula, Ellesmere Island, Nunavut. *Geological Survey of Canada Bulletin*, 529:99–111.

Atkinson, D.E. and Gajewski, K.G. [2002]: High-Resolution Estimation of Summer Surface Air Temperature in the Canadian Arctic Archipelago. *Journal of Climate*, 15, doi:10.1175/1520-0442(2002)015<3601:HREOSS>2.0.CO;2.

Environment Canada. Climate normals for Eureka weather station (1981-2010), 2015. URL http://climate.weather.gc.ca/climate_normals. Accessed Nov 30, 2015.

Measured two-dimensional ice-wedge polygon thermal dynamics

William L. Cable[1], Vladimir E. Romanovsky[1], & Robert C. Busey[2]

[1] *Geophysical Institute, University of Alaska Fairbanks, USA*
[2] *International Arctic Research Center, University of Alaska Fairbanks, USA*

Ice-wedge polygons are perhaps the most dominant permafrost related features in the arctic landscape. Through frost driven deformation at the ice wedges, microtopography relief is typically created transforming these otherwise flat landscapes with rims and troughs between polygons, and low or high relief at their centers. As the climate warms and the ice wedges degrade, the soil above them settles and the relief becomes more pronounced. The microtopography of these features alters the local hydrology, as water tends to collect in the low areas and in the case of troughs, interconnected drainage pathways can also be formed. During winter, wind redistribution of snow leads to an increased snowpack in the low areas, while the slightly higher areas often have very thin snow cover, leading to differences across the landscape in vegetation communities, soil moisture and soil carbon content between these higher and lower areas. These differences in local surface conditions lead to spatial variability of the ground thermal regime in the different microtopographic areas and between different types of ice-wedge polygons. While many studies have focused on various aspects of ice-wedge polygons, relatively few of them have examined, in-depth, the ground thermal regime using in-situ measurements.

To study the thermal regime of these features we established temperature transects across four different types of ice-wedge polygons as part of the Department of Energy, Next Generation Ecosystem Experiment near Barrow, Alaska. The temperature transects were composed of five vertical array thermistor probes (VATP) beginning in the center of each polygon and extending through the trough to the rim of the adjacent polygon. Each VATP had 16 thermistors from the surface to a depth of 1.5 m. In addition to these 80 subsurface temperature measurement points per polygon, soil moisture, thermal conductivity, heat flux, and snow depth were all measured in multiple locations for each polygon. Above ground, a full suite of micrometeorological instrumentation was present at each polygon. Data from these sites has been collected continuously for the last three years.

We found snow cover, timing and depth, and active layer soil moisture to be the major controlling factors in the observed thermal regimes. In troughs and in the centers of low-center polygons, the combined effect of typically saturated soils and increased snow accumulation resulted in the highest mean annual ground temperatures (MAGT). Additionally, these areas were the last part of the polygon to refreeze during the winter. However, increased active layer thickness was not necessarily found in areas of higher MAGT. In fact, these wetter areas with higher MAGT often had shallower active layers, possibly due to thermal buffering as a result of the high (often saturated) soil moisture content. Active layer thickness does not appear to be correlated to mean annual air temperature but rather is a function of summer air temperature or thawing degree-days. While the refreezing of the active layer initiated at nearly the same time for all locations and polygons, we find differences in the proportion of top-down versus bottom-up freezing and the length of time required to complete the refreezing process. Examination of the daily temperature dynamics using interpolated two-dimensional temperature fields (like Fig. 1) reveal that during the summer, the predominate temperature gradient is vertical while horizontally the isotherms tend to follow the topography. However, as the active layer begins to refreeze and snow begins to accumulate, the thermal regime diverges. The fall shows an increased temperature gradient horizontally (Fig. 1) with landscape positions containing higher soil moisture and/or snow depth (low centers and troughs) cooling more slowly than the adjacent ground (rims and high centers). This two-dimensional effect is greatest as the active layer refreezes and persists until mid-winter, by which time the temperature gradients are again mostly vertical and the horizontal isotherms follow the topography. Our findings demonstrate the complexity and two-dimensionality of the temperature dynamics in these landscapes. The importance of these effects should be considered when measuring or modeling the thermal regime or conducting other research related to active layer or permafrost processes in these landscapes.

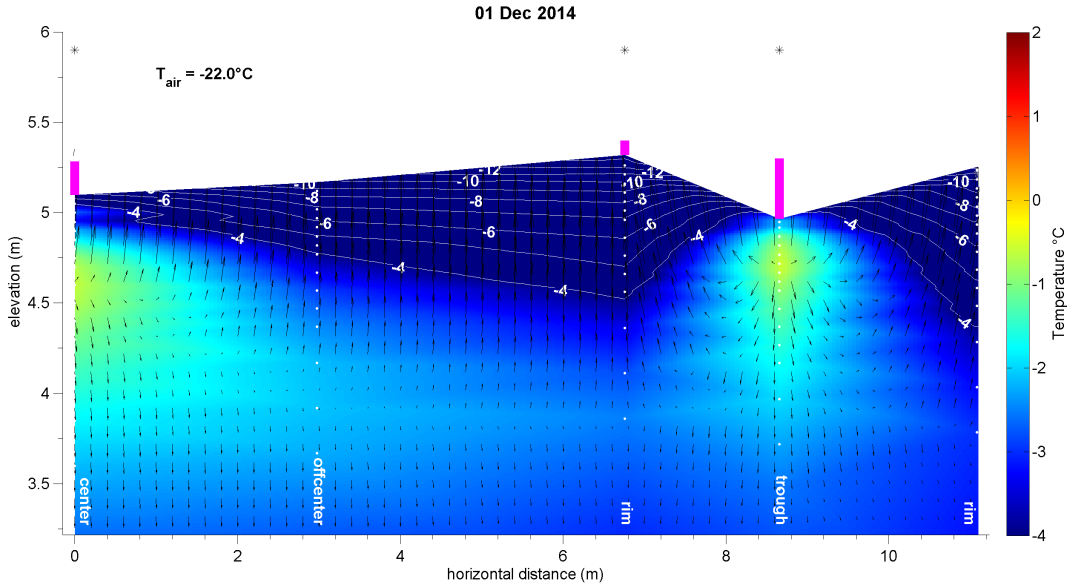

Figure 1: Daily average 2D temperature field from a low-centered polygon. Black arrows point in the direction of decreasing temperature and are proportional to the temperature gradient. Magenta bars are snow depth. VATP measurements, white dots and labels.

Best practices in permafrost temperature measurement

William L. Cable & Vladimir E. Romanovsky

Geophysical Institute, University of Alaska Fairbanks, USA

The definition of permafrost as any subsurface material that remains below 0 °C for two or more years is based solely on temperature and time. Thus, observing subsurface temperatures is the most valuable tool we have to determine the presence or absence and to monitor the thermal state of permafrost. When interest in permafrost temperatures began, around the time of the First International Polar Year (1882-1883), the technology available for temperature measurements was a glass thermometer. Collecting temperature readings in this way required lots of time, while the measurement resolution (and temporal and spatial resolution) was relatively low. Glass thermometers remained the dominant temperature measurement technology until the first commercially produced metal and semiconducting (thermistors) thermometers became available in the 1930's. With the advent of thermistors, came an improvement in measurement resolution, accuracy, and the ease at which measurements could be made. However, due to the complex measurement systems needed, specialized skills and knowledge were required to make these measurements. More recently, with the advent of modern data loggers, an array of data collection systems are available making temperature (and other parameters) easier to measure and record, and requiring little if any specialized knowledge. The decrease in cost and an increase in availability of sensors and data loggers for measuring temperature have led to a dramatic increase in the number of subsurface temperature measurements being made in permafrost regions. However, not all sensors and measurement systems are equal and it is important to have an understanding of the technology behind these sensors and systems to determine the quality of the data that will be collected. It is our aim to present some of the best practices when making subsurface temperature measurements in permafrost environments.

There are three major different sensor technologies in use today, thermistors, thermocouples, and integrated circuits. Thermistors, or thermally sensitive resistors, are inexpensive and offer accuracy and resolution of approximately 0.02 °C or better, depending on the measurement system used. Constructed from two dissimilar metals (wires), thermocouples, create a voltage proportional to temperature at their junction. However, while inexpensive and easy to construct, obtaining an accuracy better than ±1 °C from thermocouples is difficult due to material inconsistencies and measurement system errors. Integrated circuits can also be used to measure temperature and while they are easy to integrate into measurement systems (e.g. iButtons), they typically have a poor accuracy, approximately ±1 °C. A newer technology starting to receive some interest in the permafrost community, Distributed Temperature Sensing (DTS), uses fiber optics to measure temperature along a length of fiber optic cable. While DTS initially seems appealing for measuring a temperature profile in a borehole or along the ground surface, their accuracy of ±1 °C severely limits their application in permafrost research. There are also many different types of data collection systems, many of which have integrated or dedicated temperature sensors. These technologies all have advantages and disadvantages that should be understood and taken into account before a system is deployed for use in the field. Major considerations are measurement accuracy, measurement resolution, sensor stability, and operating temperature range, however frequently budgetary constraints are a limiting factor.

Sensor calibration is also an important consideration. Most sensors come pre-calibrated and with a stated accuracy and resolution when used with a particular measurement system. As permafrost researchers are interested in resolving temperatures at and near zero degrees Celsius, a proper ice-bath calibration should be, as a minimum, performed before putting a system or sensor into service. This not only serves as a critical system check but also ensures the accuracy of temperatures measured near the freezing point of water and makes sensors comparable with one another.

While there are a large assortment of preconfigured temperature sensors available, it is often desirable to construct your own sensor packages for specialized installations. We will also present methods for

constructing vertical array thermistor probes using readily available materials. These probes are robust and simple to construct. When paired with a data logger both high temporal and high vertical resolution temperature data can be collected within the active layer and permafrost to a depth of 1.5 meters. For depths beyond 1.5 meters, thermistor strings can be constructed and deployed in boreholes.

Although current technology makes it relatively inexpensive and easy to collect a large amount of subsurface temperature data, this does not necessarily mean the data collected is of good quality or accuracy. Thus, care must be exercised when selecting sensors and data loggers, and these systems properly calibrated, before field deployment. Additionally, when considering new technologies, such as DTS, it is important not to assume that newer or more expensive is better, before evaluating what improvements, if any, they deliver over older technology.

Constraining global permafrost thaw in the future using models and observations

Sarah Chadburn[1], Eleanor Burke[2], Peter Cox[3], & Pierre Friedlingstein[3]

[1] *University of Leeds, United Kingdom*
[2] *Met Office, UK*
[3] *University of Exeter, UK*

The rate of permafrost thaw in the future is of great importance. This is due, in a large part, to the potential release of stored soil carbon to the atmosphere, which may significantly impact the Earth's climate. Permafrost thaw also leads to changes in ecosystems, and in conditions and resources for human activity. Most of the frozen carbon in permafrost is found in the top 3 m of soils, and therefore large-scale modelling studies often consider 'near-surface' permafrost, defined as permafrost above 3m depth.

In the CMIP5 models, there is a large uncertainty regarding the future of near-surface permafrost. The present-day extent varies from 3 to 27 million km^2. The rate of loss of near-surface permafrost in the future varies from approximately 0.9 to 2.3 million km^2 per degree of high latitude warming. This has been highlighted in more than one study [Koven et al., 2013, Slater and Lawrence, 2013].

Here we show by further analysis of the CMIP5 results that a large amount of the variation in permafrost thaw rate can be explained by the relationship between air temperatures and the fraction of frozen/thawed ground in each model. This relationship remains approximately constant over time, so by knowing the relationship in the present day we can predict the near-surface permafrost under a given future climate. Thus the air temperatures alone explain large differences in the rate of permafrost loss between models.

The remaining variation is explained by factors such as the speed of the warming: Under a higher rate of warming, the near-surface permafrost does not have time to come to thermal equilibrium and therefore the rate of thaw 'lags' behind the rate of climate warming.

The relationship between air temperatures and frozen/thawed ground is calculated in such a way that it can also be obtained for the real world, using available observations. To give the best possible estimate of the observed relationship, data from several large-scale datasets is combined: The Russian historical soil temperatures, International Polar Year borehole data, new data from Global Terrestrial Network for Permafrost, and the Circumpolar Active Layer Monitoring observations. This relationship is then used to more tightly constrain the rate of permafrost loss under future climate warming.

References

Koven, C.D.; Riley, W.J. and Stern, A. Analysis of permafrost thermal dynamics and response to climate change in the CMIP5 earth system models. *Journal of Climate*, 26(6):1877–1900, 2013. doi:10.1175/JCLI-D-12-00228.1.

Slater, A.G. and Lawrence, D.M. Diagnosing present and future permafrost from climate models. *Journal of Climate*, 26(15):5608–5623, 2013. doi:10.1175/JCLI-D-12-00341.1.

Permafrost thermal state and active layer dynamics from various landforms in Svalbard

Hanne Hvidtfeldt Christiansen[1], Graham Lewis Gilbert[1,2], Sarah Marie Strand[1,3], & Ole Humlum[3,1]

[1] *The University Centre in Svalbard, UNIS, Norway*
[2] *Department of Earth Science, University of Bergen*
[3] *Departments of Geosciences, University of Oslo, Norway*

The permafrost thermal state and the thickness of the active layer are the most direct and important indicators of which changes the permafrost is undergoing. Since the IPY in 2008 continuous ground thermal observations have been going on in boreholes extending down through the layer of annual ground temperature variations in all the major periglacial landforms in central and western Svalbard. Since 2000 thaw progression data have been collected through the summers in the UNISCALM grid in central Svalbard. All the data is stored in the Norwegian Permafrost database (NORPERM), and selected datasets are also included into the Global Terrestrial Network on Permafrost (GTN-P). This collection of ground thermal data allow us to study how the individual periglacial landforms have responded to the meteorological interannual variations that characterize the maritime climate in Svalbard over a six year period. Just as the controls on active layer thaw progression can be studied in detail.

During this period the mean annual air temperature have varied from -4.1 °C in 2010 to -2.0 °C in 2012 at the Longyearbyen airport meteorological station. Due to the maritime setting particularly the winters have experienced very varied conditions with a February mean air temperature of only -1.7 °C in 2014, and a rather warm January 2012 of -3.4 °C and with 46.5 mm precipitation, some falling as rain. January 2010 was colder -7.2 °C, but with 68.7 mm precipitation, some of which also fell as rain. But also the summers have seen some variation in particular with a very wet August 2013, in which 59.2 mm of precipitation fell as rain. Very variable winters have occurred within this period, such as the winter 2010-2011, which had monthly air temperatures below -10 °C from November until April. And then followed by the winter 2011-2012, which had no monthly air temperature below -10 °C.

Since the active layer thickness thickness (ALT) observations started in 2000 in the UNISCALM grid, ALT has varied from a maximum of 110 cm in September 2008 to a minimum of 74 cm in September 2004. There is no correlation between mean annual air temperature and ALT. Also there is no correlation between the mean air temperatures in the period of thawing and ALT during this 15 year period. This means that other factors such as precipitation could affect the thaw depth. However, the UNISCALM site is located such that no drainage lead to this area and generally the active layer is rather dry. Also there is almost no vegetation in this site, and the snow depth is very limited.

Permafrost temperatures are recorded in the following periglacial landforms: solifluction sheets, fluvial terraces, ice-wedge polygons, pingos, rock glaciers, weathered bedrock plateau blockfields, exposed bedrock, strandflats and snowdrift sites. The depth of the annual temperature variations vary between these landforms. This variation reaches generally less than 10 m down in the relatively fine-grained sediments in the valleys, whereas there are still annual variations of up to almost 3 °C in the most coarse-grained rock glaciers. Also all coarse-grained landforms react quicker to the overall annual thermal variations, whereas the same size reaction in more fine-grained landforms, such as e.g. pingos, can be delayed with up to 5 months.

Permafrost temperature development in Norway and Iceland over the last decade

Bernd Etzelmüller[1], Christian Hauck[2], Christin Hilbich[2], Ketil Isaksen[3], & Sebastian Westermann[1]

[1] *University of Oslo, Norway*
[2] *University of Fribourg, Switzerland*
[3] *Norwegian Meteorological Institute*

Permafrost or ground thermal regime seems to be an important factor modulating geomorphological process rates and ultimately landscape development. The quantitative assessment of permafrost such as systematic temperature monitoring is a relatively young science, which is especially true for mountain permafrost. Therefore, for many fields of permafrost science and in many areas there are still knowledge gaps, which have to be addressed for the discussion of how permafrost will respond to climate change, and what consequences we can expect. As permafrost is thermally defined, climate is the factor governing where on earth permafrost can exist, which means along a longitudinal (Arctic permafrost) or an altitudinal gradient (mountain permafrost). The latter is known to by extremely heterogeneous and therefore difficult to address and especially to model in high spatial resolution. Scandinavia is situated precisely at the transition between areas where mountain permafrost dominates in the south, to more Arctic conditions towards Svalbard in the north. For Norway, the major permafrost areas are situated in this transition.

In Norway, since the 1980ies many studies have been carried out to evaluate the permafrost distribution and its dependence especially to climate and snow conditions. Some attention has also been given to the influence of the near-surface substrate, which ability to keep water/ice is an important modulator for the ground thermal dynamics. This knowledge has flown into numerical models, trying to calculated ground temperatures. However, these models, as elsewhere, are mainly driven by climate components (which are known), while the ground properties are poorly known and parameterised on various levels of simplicity.

Thus, for mountain permafrost areas such as in Scandinavia, there is an urgent need to improve the understanding of the ground property characteristics in relation to the permafrost distribution. There is a lack of understanding of the relative importance of climate forcing and modulation by ground properties, simply as they are poorly known for areas where mountain permafrost exists. This knowledge is of outmost importance when modelling permafrost response to climate change, not only for mountain areas like in Scandinavia, but also for Arctic Permafrost regimes.

At present Norway has an unique data set of bore holes where we measure temperatures along both altitudinal and latitudinal gradients. In addition at all sites geophysical soundings are available using seismic and ERT, partly multi-temporal. Finally, daily gridded data sets of meteorological parameters such as air temperature, precipitation and associated snow cover is available back to 1957, allowing the evaluation of climate-ground thermal regime relation along regional gradients. The analysis of these data allows us now to differentiate between climatic forcing and subsurface characteristics, emphasizing on our 10-13 years data series, which are already quite long in permafrost research.

This presentation present the unique combined data set from six major sites in Norway, wherein each site several localities exist. The results are discussed in the light of climate-permafrost-ground interaction and implication for quantitative climate change assessment on the ground thermal regime. This analysis is an important base line for present and future numerical modelling assessments of ground thermal regime under changing climate conditions, along with the evaluation of geomorphological processes and landscape Development.

Changes to permafrost active-layer temperature after tall shrub expansion in low Arctic tundra

Gerald V. Frost[1,2], Howard E. Epstein[2], Donald A. Walker[3], & Georgiy Matyshak[4]

[1] *Alaska Biological Research, Inc., USA*
[2] *Department of Environmental Sciences, University of Virginia, USA*
[3] *Alaska Geobotany Center, University of Alaska Fairbanks, USA*
[4] *Department of Soil Science, Moscow State University, Russia*

Arctic tundra ecosystems are undergoing a suite of interrelated changes to permafrost properties, vegetation, geomorphology, and hydrologic function due to a warming climate, with concomitant impacts to ecosystem services including the uptake and storage of atmospheric carbon. Vegetation, near-surface soil organic layers, and snow cover regulate energy exchange between the atmosphere and permafrost soils. Feedbacks between warming-induced changes in the stature and density of tundra vegetation, and the thermal state of underlying soils will fundamentally affect the properties and function of permafrost in a warmer world. The observational record and experimental studies indicate that expansion of deciduous shrubs is the most widespread and persistent form of ecosystem change that has accompanied recent climate warming in arctic tundra, and simulation modeling indicates high potential for future shrub increase. Current observations indicate a great deal of landscape heterogeneity, however, with development of canopy-forming tall shrublands concentrated on disturbed areas with mineral-rich soils. Here we present high-temporal resolution soil temperature data for a Low Arctic site near Kharp, northwest Siberia, with a known history of tall shrub expansion on abundant, cryoturbated microsites in patterned ground. We measured seasonal time-series of active-layer temperature at 5 cm and 20 cm depth, and physical properties of vegetation (Leaf Area Index, maximum shrub height) and soils (organic thickness, thaw depth/depth to rock) along a chronosequence of tall shrubland development: low-growing tundra lacking erect shrubs; newly-developed shrublands; mature, dense-canopied shrublands; and old, paludified shrublands with thick organic layers. The timing and extent of recent tall shrub expansion at the Kharp site were known based on previous analysis of high-resolution imagery from 1968 and 2010. Active-layer temperatures were measured at 4-hour intervals from 2 July 2012–8 June 2013 using a total of 146 iButton® thermochron dataloggers. Mean summer soil temperatures declined with increasing shrub cover and moss thickness, but winter soil temperatures increased with development of tall ($>$ 2-m height) alder shrubs. Mature shrub stands cooled summer soils by up to 8 °C (at 20 cm depth) relative to open tundra, yet warmed winter soils by $>$ 10 °C. However, the establishment of tall shrubs also attenuated differential frost-heave and cryoturbation, facilitating the establishment of mosses and the accumulation of a thick organic mat in late succession. Over time, paludification of soils in very old shrublands promoted cold summer active-layer temperatures, and winter soil temperatures declined to conditions comparable to colonization zones with scattered, small shrubs. Our results indicate that while tall shrub establishment does increase active-layer temperatures in winter, this warming may be transient as successional processes promote soil paludification and thinning of the tall shrub canopy over time. Current assessments of changes to soil thermal regime brought on by the development of tall shrubs tend to emphasize high-productivity shrublands and neglect successional processes and changes in soil environment that occur over decades following tall shrub development. Our detailed data for soils temperature, vegetation structure, and physical soil characteristics indicates that changes in soil thermal regime that accompany the establishment and succession of tall shrublands are non-linear and, in landscape positions that favor soil paludification, can ultimately promote soil cooling, organic accumulation, and aggradation of the permafrost table.

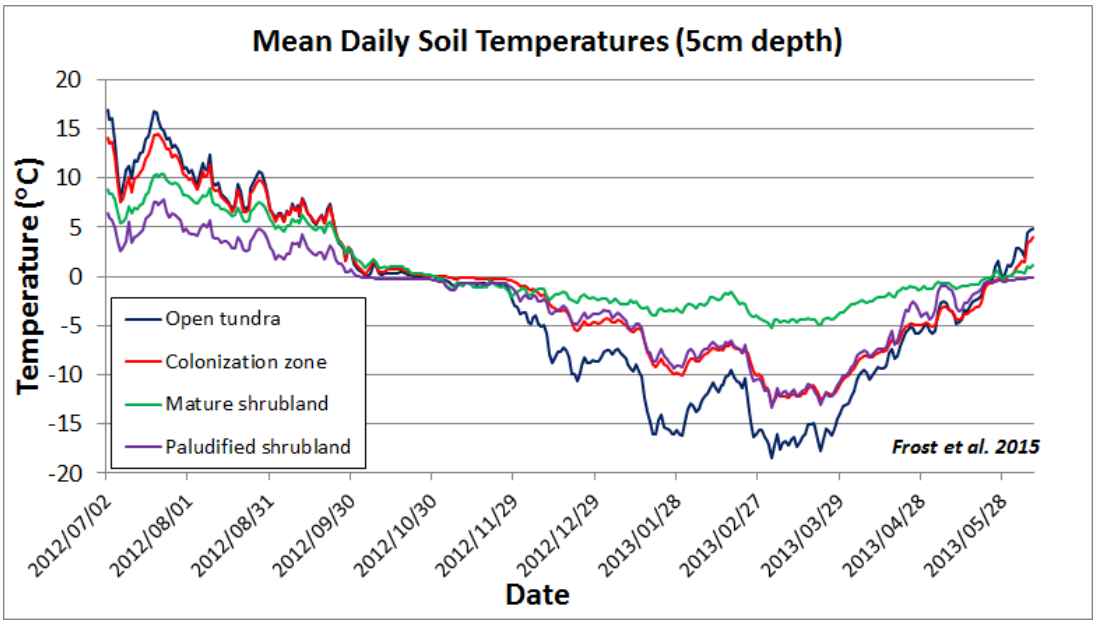

Figure 1: Mean 5-cm soil temperatures recorded in four stages of tall shrubland succession in arctic tundra.

Preliminary analysis of ground temperatures in north and northeast Greenland

Graham L. Gilbert[1,2] & Hanne H. Christiansen[1]

[1] *Arctic Geology Department, The University Centre in Svalbard, UNIS, P.O: Box 156, 9171 Longyearbyen, Norway*
[2] *Department of Earth Science, University of Bergen, Realfagbygget, Allegt. 41, 5007 Bergen, Norway*

Within the Northeast Greenland National Park, two ground temperature monitoring sites exist: Zackenberg (74°28' N, 20°34' W, 36 m a.s.l.) in northeast Greenland and Station Nord (81° 35' N, 16° 38' W, 43 m a.s.l.) in north Greenland. While the near-surface ground temperature record from Zackenberg extends back to the early 2000´s, the addition of two boreholes, each 20 m in depth, in 2012 permitted monitoring of ground temperatures at and below the depth of zero annual amplitude (DZAA). In 2014, two complimentary sites were installed at Station Nord, as part of the basic infrastructure for the newly expanded Villum Research Station.

Mean annual air temperatures are ca. -10.3 °C and -16.9 °C at Zackenberg and Station Nord, respectively. Despite this difference, ground temperatures at the DZAA vary by approximately 2 °C between these two locations. In the 2014-2015 hydrological year, ground temperatures at 20 m depth ranged between -5.8 and -6.6 °C at Zackenberg and -7.1 and -8.1 °C at Station Nord. Ground temperatures at Station Nord are particularly warm compared to other sites at this latitude. Warm temperatures are primarily attributed to the accumulation of a thick winter snow pack. In winter 2014-2015 maximum snow depth at Station Nord ranged between ca. 1.9 and 1.7 m at the two sites, compared to ca. 0.5 – 1.0 m at Zackenberg. Snowfall at Station Nord is feed by moist air generated over a polynya that forms off the northeast coast of Greenland

The purpose of this contribution is to present the first-year of ground temperatures from Station Nord and investigate and quantify differences between the ground thermal regimes at Station Nord and Zackenberg.

The influence of snow cover accumulation, snow fall intensity and air temperature on seasonal freezing and thawing depth

Vladimir Nikolaevich Golubev & Denis Maksimovich Frolov

Lomonosov Moscow State University, Russian Federation

Averaged periodicity of snowfall deposition, accumulation of snow cover thickness and seasonal variations of air temperature for the regions of European part of Russian North and Siberian North are generally well known. According to the data on these processes and on the base of construction norms the depth of freezing and placement of underground pipelines are determined.

However variations in the process of intraseasonal snowfall deposition, accumulation of snow cover and seasonal variations of air temperature in relation to mean values lead to variations of ground temperature, variations of ground freezing depth and hazards for underground pipelines.

According to Lawrence and Slater [2010], the change in snow cover thickness in north-eastern Siberia is responsible for 50 % or more of the change of ground temperature at the depth of 3.6 m. We continue our study of snow cover changes following previous work by Golubev et al. [2008] and investigate its impact on ground freezing depth.

The peculiarities of intraseasonal snowfall deposition, accumulation of snow cover thickness and seasonal variations of air temperature were considered for winter seasons 2006/07 - 2010/11 for meteorological stations of Naryan-Mar and Yakutsk. The role of these processes to peculiarities of ground freezing depth variations on these stations was established.

For example winter season of 2007/08 at Naryan-Mar was notable for extreme snow accumulation of snow. Maximal snow depth was more than 80 cm and there were abundant snow falls in the beginning of the season when snow accumulated on unfrozen ground. Resulting in maximal ground freezing depth of only 0.8 m. The winter season of 2009/10 in Naryan-Mar had on the contrary little amount of snow. Maximal snow cover depth reached 60 cm, main snow in the middle-end of the season and maximal ground freezing depth was more than 1.6 m.

In winter season of 2006/07 in Yakutsk there were many snowfall events occured in the beginning of winter season when snow accumulated on unfrozen ground and snow cower thickness was rather high – 50 cm. So in this year the active layer thickness was more than 3.2 m. In winter season of 2009/10 in Yakutsk snow thickness reached maximum of 20 cm only in the end of the season. So, thaw layer thickness that time was only 2.4 m.

So, variations in the process of intraseasonal snowfall deposition, accumulation of snow cover and seasonal variations of air temperature in relation to mean values plays drastic role in variations of ground freezing and thawing depth.

References

Golubev, V.N.; Petrushina, M.N. and Frolov, D.M. [2008]: Winter regime of temperature and precipitation as a factor of snow-cover distribution and its stratigraphy. *Annals of Glaciology*, 49:179–186.

Lawrence, D.M. and Slater, Andrew G. [2010]: The contribution of snow condition trends to future ground climate. *Climate Dynamics*, 34(7):969–981, doi:10.1007/s00382-009-0537-4.

The Eco-Grid of Ny Alesund: A multidisciplinary approach to investigate the Climate Change effects in the Arctic

Mauro Guglielmin[1], Stefano Ponti[1], Vito Vitale[2], & Nicoletta Cannone[1]

[1]*Insubria University, Italy*
[2]*Isac, CNR, Italy*

Since the mid-20th Century climate change (CC) has led to significant impacts in the Arctic, with increases in air and permafrost temperatures, snow cover decreases, and glacier retreat. The Arctic ecosystems play a key role in the global carbon cycle because northern permafrost soils account for approximately 50 % of the estimated global below-ground organic carbon pool. To monitor the effects of the CC at local scale, a new multidisciplinary approach has been started at Ny Alesund since 2014. Here, close to the Climatic Change Tower (CCT), a 30 m height tower designed to monitor the energy balance and fluxes, a grid of 50 × 50m at 55 m a.s.l. was equipped. The grid has 36 nodes with a span of 10 m. In each node a snow stake and a vegetation plot of 1 × 1 m are installed. The first is used to monitor the snow variability through a snow cam installed on the CCT. The second is used to monitor the vegetation changes as coverage, species richness and composition and structure through vegetation surveys every year. In addition, in each node the soil was characterized measuring surface grain size, the height of vegetation mats, organic horizon thickness and the grain size, water content, pH and organic matter content in the topsoil. In 12 of the 36 nodes a borehole with a depth ranging between 79 and 101 cm was equipped with 4 thermistors (0.2 °C of accuracy) placed at 2, 30, 60 cm and at the bottom of the borehole. Every thermistors is recording the mean ground temperature every 30 min. Active layer thickness is not measurable here with the classical frost probing because the sediments are too coarse. Finally, CO_2 fluxes measures with a IRGA system at the scale of the vegetation plot were carried out in the previous summer to select the plots for a systematic monitoring for the entire snow free season that will start from next season.

Despite of the relative morphological homogeneity of this almost flat area the ground surface and the vegetation show a quite strong spatial variability. The stonines on the surface is very variable at the vegetation plot scale from 5 to more than 80 %. The vegetation coverage in the same plots varies between 1-2 % to 100 % with its height ranging between 1 to 8 cm underlid by an organic litter variable from 0 to 3.5 cm of thickness. The underlying topsoil is characterized by a pH highly variable from acid (4.95 at the grasses plot) to neutral (7.1 in the barren soil). The soil water content is also strongly variable from 3 % to more than 50 % and also the thickness of the organic horizon A range between 0.4 to 7 cm. The medium-fine sand is the prevailing grain size of the soil although in some cases gravel and pebbles exceed the 80 % while silt+clay never reach the 30 %. In addition to the snow cam the snow variability was checked also through manual probing several times especially from the maximum accumulation to the melting. During the maximum accumulation in the winter 2014/15 snow height ranged between 115 and 65 cm while during the last week before the onset of the melting ranged between 98 and 42 cm. The snow melting period indicated by the zero curtain effect on the surface ended between the first week of June and the thrid week of June exceeding 20 days of difference among the 12 plots. The first data of ground surface temperature (GST) are related to the period 25 July 2014-17 July 2015 are very variable with an annual mean ranges between -0.7 to -3.6 °C. Vegetation type and snow characteristics seems the more effective factors in the GST differences. The active layer thickness (ALT) as the depth of 0 °C isotherm during the summer 2014 ranged between 117 and 194 cm. Despite of a good correlation between GST and ALT also the soil characteristics seem to be important in the ALT spatial variability.

Permafrost temperature measurements in the Okhotsk coastal area of the Verkhoyansk-Chukotka region

Sergeyy Aleksandrovich Gulyy[1], Mikhail Nikolaevich Zhelezniak[2]

[1] *North-Eastern Permafrost Station Melnikov Permafrost Institute, Russian Federation*
[2] *Melnikov Permafrost Institute, Russian Federation*

Introduction

The Verkhoyansk-Chukotka region occupies the northeastern part of Russia. Geomorphologically, the region comprises seven geomorphological provinces, ranging from folded mountains to lowlands. Two climate types are present in the region, highly continental and moderately continental (maritime). Mean annual air temperatures vary from -16.9 to -2.9 °C. Annual precipitation ranges from 200 to 700 mm; the maximum snow depth varies from 31 to 187 cm.

The coastal areas along the Sea of Okhotsk are distinctive in climatic, environmental and geocryological conditions. Unlike much of the Verkhoyansk-Chukotka region characterized by continuous permafrost 300 to 600 m in thickness, the coastal areas are within the sporadic and discontinuous permafrost zones.

In 1950-1990, a large volume of exploratory drilling was conducted in the Verkhoyansk-Chukotka region for geological, hydrogeological and engineering purposes. In some boreholes, ground temperature observations were made. In 2007, the Melnikov Permafrost Institute initiated a project to develop a geocryological information system and restore the observation network to monitor permafrost changes in the region. GTN-P program requirements are also taken into account. Based on research of 200 reports, information on 36 sites and 101 boreholes with records of prior observations were compiled into a geocryological database.

The next phase was to locate the abandoned boreholes in the field. Twelve boreholes were found near Magadan. In three boreholes, temperature measurements were taken immediately after inspection and data loggers were installed. Other boreholes found were useless for thermal observations. Of the rest 89 boreholes which location was only known from schemes and maps taken from the reports none was possible to use. They needed to be re-drilled.

The instrumentation included HOBO U12-008 Outdoor/Industrial 4 External Channels (HOBO U12-008) data loggers for year-round continuous (at 4 h intervals) recording of ground temperature at depths of 3, 5(7), 10, and 14.5 m; single-point one-channel HOBO Water Temp Pro and iBDL-L data loggers reading air and 0.6 m soil temperatures; and single thermistor sensors for periodical (annual) measurements in boreholes at depths of 20 m or more.

Results

Permafrost temperature time series have been obtained for the last eight years. Of particular interest are the ground temperature data from two boreholes where monitoring observations were conducted in the past (1989-1990). The boreholes are located on the watershed at the distance of 2.5 km from each other. They differ in elevation and surface conditions. The comparison of the data obtained in 2015 with those collected in the 1990s indicates that the ground temperature has increased by 0.47 °C at the depth of 14.5 m and by 0.22 °C at the depth of 20 m in borehole 1M where the surface is occupied by shrub vegetation. The borehole 4M is located in bare ground. During this period of observations the temperature in the borehole 4M has been increased at 0.67 °C and 0.44 °C respectively (Tab. 1).

Data recorded by the Magadan meteorological station also indicate a steady increase in mean annual air temperature from -5.1 °C in 1967 to -1.8 °C in 2014. Nevertheless, the main cause for colder ground temperatures and higher warming rates on the watershed divides is the difference in surface thermal conditions due to the presence or absence of snow cover. Annual snow depth observations have shown that snow is virtually absent on windward parts of the watershed divides (borehole 4M), while the areas covered by shrub vegetation may have snowcover as deep as 1.5 m (borehole 1M).

Table 1: Measured ground temperatures (°C) at several depths, Okhotsk coastal area

Borehole ID	Depth, m	Measurement date (September)									
		1990	2007	2008	2009	2010	2011	2012	2013	2014	2015
Borehole 1M	20.0	-0.48	-0.39	-0.39	-0.37	-0.35	-0.20	-0.31	-0.29	-0.28	-0.26
	14.5	-0.56	-0.39	-0.26	-0.23	-0.20	-0.17		-0.14	-0.12	-0.09
	10.0	-0.58	-0.22	-0.17	-0.12	0.44	0.38		0.66	0.88	0.83
Borehole 4M	20.0	-1.88		-1.53	-1.68	-1.60	-1.44	-1.52	-1.53	-1.50	-1.44
	14.5	-2.08		-1.62	-1.68	-1.64	-1.50	-1.76		-1.50	-1.41
	10.0	-2.38		-1.76	-1.64	-1.67	-1.44	-1.64		-1.50	-1.41

Conclusions

1. Analysis of the temperature data collected in the 1990s and recent measurements in boreholes re-established for thermal monitoring indicates a significant ground warming in the Okhotsk coastal areas. Ground temperatures at the depth of 20 m have increased by 0.22 to 0.44 °C over the last 18 years. The mean annual air temperature has increased by 1.1 °C over the same period.
2. The results of observations since 1990 to the present suggest that the rate of permafrost warming is 1.2 times higher at the snow-covered locations compared to the snow-free areas.

Thermal state of permafrost across the circumpolar permafrost regions – results from the latest assessment report, the SWIPA update

Ketil Isaksen[1], Vladimir Romanovsky[2], Sharon L. Smith[3], & Dmitry S. Drozdov[4]

[1]*Norwegian Meteorological Institute, Norway*
[2]*Geophysical Institute, University of Alaska Fairbanks, USA*
[3]*Geological Survey of Canada, Natural Resources Canada, Canada*
[4]*Earths Cryosphere Institute SB RAS, Russia*

In 2011 the Arctic Council directed the Senior Arctic Officials "to review the need for an integrated assessment of multiple drivers of Arctic change as a tool for Indigenous Peoples, Arctic residents, governments and industry to prepare for the future". This resulted in the project "Adaptation Actions for a Changing Arctic" (AACA; http://www.amap.no/adaptation-actions-for-a-changing-arctic-part-c). AACA is now moving rapidly. Input from the cryosphere and climate expert community is now needed on the current and future state of the Arctic. To ensure AACA uses the latest knowledge of the climate system there was a need to update selected aspects of the assessment report "Arctic Climate Issues 2011: Changes in Arctic Snow, Water, Ice and Permafrost" (SWIPA 2011; http://www.amap.no/swipa), which was published in 2012. The SWIPA update will be based on the latest state of knowledge and will lead to new stand-alone reports. One of these updates is on permafrost.

The SWIPA update on permafrost provides a synthesis of current knowledge across the circumpolar permafrost regions on

1. Thermal state of permafrost
2. Permafrost modeling and projections of future permafrost states,
3. Permafrost-related processes, coastal erosion, thermokarst and recent changes in thaw lake development, and finally on
4. Cumulative effects of infrastructure and climate change on permafrost and recent advances in understanding of permafrost-related geo-hazards.

Here we present the results from section 1: Thermal State of permafrost. During the International Polar Year (IPY) a snapshot of permafrost thermal state for 2007-09 was developed and provided a baseline against which future change can be measured. In Canada, Alaska, Russia and Nordic countries measurements of ground temperatures were made in over 575 boreholes representing the range in vegetation, geology and climate found in the permafrost regions of the Arctic and sub-Arctic [Christiansen et al., 2010, Romanovsky et al., 2010, Smith et al., 2010].

In this assessment we provide an updated picture of the current thermal state of permafrost that can be compared to measurements made during IPY to assess the change that has occurred since IPY. The analyses cover three pilot regions in the Arctic:

1. the Barents Region,
2. Baffin Bay/Davis Strait Region and
3. Bering/Beaufort/Chukchi Region.

The longer term records of permafrost temperatures (time series), more than three decades long for some sites, have also been extended which allows the changes since IPY to be placed within context of the longer record.

Since IPY, new record high ground temperatures are observed at many permafrost observatories across the Arctic. The greatest temperature increase since 2007-09 was more than 0.5 °C and was found in the colder permafrost of the Arctic and high Arctic. In warmer permafrost such as that in the southern and central Mackenzie Valley, in the Alaskan Interior, or in the discontinuous permafrost zone in Siberia and the Nordic region the temperature increase has been much smaller or not detectable. At a few locations permafrost temperature has even slightly decreased (typically by 0.1 °C).

References

Christiansen, H. H.; Etzelmüller, B.; Isaksen, K.; Juliussen, H.; Farbrot, H.; Humlum, O.; Johansson, M.; Ingeman-Nielsen, T.; Kristensen, L.; Hjort, J.;

Holmlund, P.; Sannel, A. B. K.; Sigsgaard, C.; Åkerman, H. J.; Foged, N.; Blikra, L. H.; Pernosky, M. A. and Ødegård, R. S. [2010]: The thermal state of permafrost in the nordic area during the international polar year 2007–2009. *Permafrost and Periglacial Processes*, 21(2):156–181, doi:10.1002/ppp.687.

Romanovsky, V.E.; Drozdov, D.S.; Oberman, N.G.; Malkova, G.V.; Kholodov, A.L.; Marchenko, S.S.; Moskalenko, N.G.; Sergeev, D.O.; Ukraintseva, N.G.; Abramov, A.A.; Gilichinsky, D.A. and Vasiliev, A.A. [2010]: Thermal state of permafrost in Russia. *Permafrost and Periglacial Processes*, 21 (2): 136–155, doi:10.1002/ppp.683.

Smith, S.L.; Romanovsky, V.E.; Lewkowicz, A.G.; Burn, C.R.; Allard, M.; Clow, G.D.; Yoshikawa, K. and Throop, J. [2010]: Thermal state of permafrost in North America: a contribution to the international polar year. *Permafrost and Periglacial Processes*, 21(2):117–135, doi:10.1002/ppp.690.

The influence of mountain climate, snow cover and vegetation on the ground surface temperature along environmental gradients in Norway

Ketil Isaksen[1], Rune S. Ødegård[2], Jarle I. Holten[3], & Atle Nesje[4]

[1] *Norwegian Meteorological Institute, Norway*
[2] *Gjøvik University College, Norway*
[3] *Terrestrial Ecology Research, Norway*
[4] *University of Bergen / Bjerknes Centre of Climate Research, Norway*

In 2001, an EU funded, Europewide project named GLORIA (Global Observation Research Initiative in Alpine Environments - http://gloria.ac.at), was launched as a pilot project for the establishment of a world-wide, long-term observation network for assessing and monitoring the effects of climate change on biodiversity in mountain environments. The GLORIA Norway project was initiated in 2007 in southern Norway. It following the 'GLORIA Mountain Slope Approach' and seeks to integrate biological and physical monitoring in order to detect effects of climate change on plant species richness and their altitudinal limits in Norwegian mountain areas. It is a long-term monitoring programme that links the mountain flora with climate parameters and especially soil temperatures and soil humidity.

In mountain areas, the high spatial variability of micro-climate (especially snow cover), topography, ground surface characteristics, vegetation and soil-specific factors results in highly variable ground thermal regimes at a local scale.

GLORIA Norway assess this by a gradient approach where the scientific activities are carried out in permanent plots (macro- and microplots, 10 × 10m and 1 × 1m respectively) located along three environmental gradients:

1. A regional coast – inland gradient,
2. A local elevation gradient along the mountain slopes and in different aspects and
3. A small-scale ridge - snow bed gradient.

In addition a latitudinal gradient were recently added by establishing new permanent plots in northern Norway.

The objective of the study presented here is to analyse and assess spatial and temporal variability in the ground surface temperature within the coast-inland gradient framework, at three of the GLORIA study sites in southern Norway: Stortussen/Snøtind (62.87°N, 7.51°E), Kaldfonna (62.63°N, 8.64°E) and Kolla (62.29°N, 9.50°E).

Results are presented based on a three to four-year dataset from about 120 miniature temperature dataloggers that were installed inside the macro plots near the soil surface in altitudinal belts and in different settings and aspects within the three study areas. The relations between topographic variables (elevation, aspect and slope), vegetation zones, land cover and ground surface temperatures are analysed - and finally, the influence of the mountain climate, seasonal snow cover, vegetation and soil type on the mountain permafrost and seasonal frost distribution at the three study sites is discussed.

Compilation of ground temperature records in the Northwest Territories, Canada

Kumari Karunaratne[1], Steven Kokelj[1], Peter Morse[2], Sharon Smith[2], Stephen A. Wolfe[2], Stephan Gruber[3], Michael Palmer[4], Ed Hoeve[5], & Trevor Lantz[6]

[1] *Northwest Territories Geological Survey, Government of the Northwest Territories, Yellowknife, NT, Canada*
[2] *Geological Survey of Canada, Natural Resources Canada, Ottawa, ON, Canada*
[3] *Department of Geography and Environmental Studies, Carleton University, Ottawa, ON, Canada*
[4] *Cumulative Impact Monitoring Program, Government of the Northwest Territories, Yellowknife, NT, Canada*
[5] *TetraTech EBA, Yellowknife, NT, Canada*
[6] *School of Environmental Studies, University of Victoria, Victoria, BC, Canada*

Knowledge of the ground thermal regime is an essential component of permafrost research, environmental monitoring, resource development projects, and infrastructure design and performance monitoring. In the Canadian North, these various needs drive the collection of ground temperature data including government and academic monitoring and research, regulatory monitoring, and industry-supported infrastructure related projects. Research and monitoring programs typically summarize the ground thermal regime in academic publications. Ground temperatures collected for infrastructure purposes are often summarized in design or maintenance reports. Regulatory monitoring data typically accompanies obligatory reporting to regulatory authorities. However, the actual temperature data used in research and monitoring, and contract reports usually reside with the research institute, government agency or private industry consultant that collected the data, and are typically not retained by institutions that are best suited to manage and archive temperature data and records, such as the Northwest Territories Geological Survey, or Geological Survey of Canada. As ground temperature data are expensive to collect, especially in remote areas, and because access to historical ground temperature data is of great value to the research community, project proponents and government, it is beneficial to organize and host these data so that it can be efficiently accessed for use in future projects for the Government of the Northwest Territories, the wider research community, industry and other users. This presentation describes our initiative to standardize and compile the metadata for the Northwest Territories' ground temperature records, so that this information can be made accessible to meet the diverse needs of potential users.

The first step towards compiling and housing ground temperature records in a database has been to establish a metadata reporting template so that information is described in a common format. Although the majority of ground temperature records are accompanied by some form of metadata, the nature of the documented supporting information varies widely depending on the purpose of data collection. Engineers and environmental scientists collecting permafrost ground temperature information may be interested in different metadata, and they may have different reporting standards and varying terminology because the information is collected for different purposes. For example, site vegetation descriptions can range from a few sentences for geotechnical investigations to detailed species inventories for research on climate-permafrost relations. The metadata standard that has been developed for the Northwest Territories builds on other initiatives such as the Global Terrestrial Network of Permafrost – GTN-P database [Biskaborn et al., 2015], and was revised based on feedback received from: permafrost researchers, thermal modellers, geotechnical engineers; public and private sector geologists; and civil servants (federal, territorial and municipal) involved with infrastructure performance monitoring. Our team has produced a metadata template that is divided into seven sections:

1. Project details;
2. Location of ground temperature measurements;

3. Installation of ground temperature cable;
4. Ground temperature record;
5. Site conditions;
6. Permafrost conditions; and
7. Related publications and data [Karunaratne et al., 2015].

Now that the metadata template is finalized, several tasks will be undertaken. First, a data management plan will be developed. Second, existing ground temperature datasets collected by the Northwest Territories Geological Survey and their collaborators will be published as NWT Open Reports so that this information can be readily accessed. Third, we will identify all historical and ongoing ground temperature data collections and archive the metadata for these records. Fourth, we will work with other departments in the Government of the Northwest Territories and northern agencies to develop strategies that leverage ground temperature data and make it accessible through this data management system. Finally, we will work with our research partners to produce an empirically-based map of ground temperatures for the Northwest Territories and synthesize patterns across a range of spatial and temporal scales.

The compilation of ground temperature records in the Northwest Territories will have multiple benefits. Evidence-based decision-making in the territory will be better supported because ground temperature data will be readily available to those involved with landuse planning and infrastructure development. Future permafrost monitoring initiatives will benefit from readily accessible information on where ground temperatures have been measured, the nature of the data (sensor depth, measurement frequency, and record duration) and its availability. International permafrost research will be enhanced as scientists will have access to NWT ground temperature data that will be made available to GTN-P. Finally, other jurisdictions, such as Nunavut, who are interested in organizing, managing and disseminating ground temperature data can modify this approach to meet their needs and circumstances.

References

Biskaborn, B. K.; Lanckman, J.-P.; Lantuit, H.; Elger, K.; Streletskiy, D. A.; Cable, W. L. and Romanovsky, V. E. [2015]: The new database of the Global Terrestrial Network for Permafrost (GTN-P). *Earth System Science Data*, 7(2):245–259, doi:10.5194/essd-7-245-2015.

Karunaratne, K.C.; Kokelj, S.V.; Palmer, M.J.; Wolfe, S.A. and Gruber, S. [2015]: Metadata template for ground temperature records in the northwest territories. In *GEOQuébec 2015: Challenges from North to South / 7th Canadian Conference on Permafrost*, 20-23 September 2015, Quebec City, QC.

Ground temperature and active layer monitoring at southern permafrost limit (Northeast European Russia)

Dmitry Kaverin & Alexander Pastukhov

Institute of Biology Komi SC RAS, Russian Federation

Active layer (AL) dynamics and soil temperature regimes have been studied in permafrost-affected soils at southern permafrost limit in the Northeast European Russia. Main soil types are Cryosols, Histosols, Stagnosols and Podsols. Monitoring studies are conducted at 2 AL monitoring sites, 23 shallow and 7 deep temperature boreholes.

At CALM R2 site, active layer thickness continuously increased during 1996-2007 period with site-averaged values from 67 to 88 cm. Then, in 2007-2015, a relative stabilization of AL thickness (in the range of averaged values from 87 to 91 cm) was observed. Dynamics of active layer thickness was synchronized with that of other two CALM sites located in the Northeast European Russia. AL thickness increase was statistically correlated with a rise of Degree Days Thaw (DDT). No significant correlation between AL thickness and other climatic variables (Freezing Degree Days (FDD), annual or summer precipitation, snow thickness) has been revealed. In mineral soils permafrost table retreat provoked soil surface subsidence, which rate was in proportional to the thickness and ice content of thawed upper permafrost. In turn, soil surface subsidence caused certain topographic changes all over the site.

It is revealed that permafrost is rather stable in Seida site, which represent a typical tundra peatland. Site-averaged AL thickness totaled 51 cm and have not increased significantly during the last five years. AL thickness is spatially differentiated on peat mounds, where is deeper under bare peat circles in comparison to vegetated sites.

In discontinuous permafrost subzone permafrost-affected soils, having rather different annual and winter temperature regimes. Diversity of soil winter temperature regimes resulted from spatial differentiation of snow accumulation, depending on tundra landscape pattern. “Cold” permafrost-affected soils, having severe winter temperature regime, occurred on peat and mineral mounds. At soil surface, FDD varied from -1036 to -2508 degree-days, mean annual soil temperatures (MAST) of active layer were in the range from 0.8 to -4.8 degrees C. “Warm” permafrost-affected soils are developed in flat sites and have MAST range from +1.1 to -1.9 degrees C in active layer and from -0.2 to -2.0 degrees C in permafrost.

Acknowledgements

The study was supported by CALM (Circumpolar Active Layer Monitoring) program, TSP (Thermal State of Permafrost) and UNDP/GEF ClimaEast 00059042 project.

Effect of vegetation and soil characteristics on thermal state of permafrost in Alaska

Alexander Kholodov[1], Vladimir Romanovsky[1], Susan Natali[2], Michael Loranty[3], & Katie Heard[2]

[1] *University of Alaska Fairbanks, United States of America*
[2] *Woods Hole Research Center*
[3] *Colgate University*

Significant declines in permafrost distribution are expected as the climate warms, but large uncertainties remain in determining the fate of permafrost under future climate scenarios. These uncertainties are driven, in large part, by changes in vegetation and ecosystem properties that modulate the effect of climate on permafrost temperatures. Long-term monitoring of permafrost temperatures demonstrates the importance of these local conditions especially in the zone of discontinuous permafrost distribution. Observations that have been conducted in Alaska since the beginning of 1980s show an increase of mean annual ground temperature from 1.5 to 3 °C northward of the Brooks Range and from 0.5 to 0.75 °C in Interior Alaska. At some locations this warming resulted in partial thawing of permafrost [Romanovsky, 2014].

Permafrost temperature is an integrated parameter and depends not only on air temperature, but also on the heat transfer conditions at the ground surface and on the thermal properties of soils. Surface conditions play especially important role in permafrost thermal state where ecosystem parameters can protect permafrost from thawing. Resilience of permafrost in areas close to its latitudinal boundaries is mostly determined by the ecosystem parameters such as vegetation composition, ecosystem productivity, and topography [Jorgenson et al., 2010].

Calculations of the components of the subsurface heat balance using the modified Kudryavtsev algorithm, which includes energy expenses on both sensible and latent heat within the active layer and underlying permafrost [Kudryavtsev et al., 1974], show that up to 80 % of incoming energy are spent on soil warming and moisture phase transitions within the active layer.

To understand the role of ecosystem parameters on ground temperature, we measured plant and soil properties at 24 locations across Alaska, where active layer and permafrost temperatures have been monitored for more than 20 years. These sites are located in boreal and tundra ecosystems and span a recent mean annual air temperature ranging from -3 to -12 °C. These ecosystem measurements were combined with an examination of temperature differences between the ground surface, active layer, and permafrost. Our approach was based on estimations of the differences between mean annual air and surface temperatures (dts) and surface and bottom of the active layer temperatures (dtal) at key stations. The first index (dts) will give us information about the influence of snow during the snow-covered period. During the growing season, comparison of dts in different ecosystems allows us to estimate insulation effect of canopy and surface vegetation and their input into the surface radiation balance. Combination of dtal with measurements of soil physical properties and thickness of organic layer as well as organic content in mineral soil provides the data for an estimation of the relationship between active layer temperature and soil organic content (Fig. 1).

Observed indices were compared with inventories of ecosystem vegetation and soil carbon stocks collected in summer of 2015. The following factors were determined to be most important in terms of their influence on surface energy balance: trees density, understory vegetation (shrubs, herbs and moss/lichens) biomass and soil carbon pool in active layer.

Results of our investigation show that highest gradient in system atmosphere – ground surface – permafrost corresponds to the above ground level (dts). Difference between mean annual air and ground surface temperatures ranges from 1.5 to 9 °C and is mostly caused by the warming impact of snow during winter season (dts winter) which consists of 3 to 13 °C. In the boreal forest zone the cooling effect of vegetation during the growing season (dts summer) due to shading effect and surface insulation can be as high as -5 °C, which is comparable in magnitude to snow influence.

It leads to lower values of mean annual dts in the boreal forest zone in comparison with tundra.

Processes of heat transfer within the active layer generate negative mean annual temperature gradient between the ground surface and the permafrost table for all investigated ecotypes. This difference value varies from -2.8 °C in boreal forest to -0.7 °C in tundra and has strong positive correlation with carbon content in the active layer soil. Besides the well-known insulating properties of organic horizon soil, organic matter in the mineral horizon (e.g., roots) also decreases thermal conductivity and increases soil moisture, both of which reduce heat transferred to permafrost.

In general increasing ecosystems productivity makes permafrost more resilient to the impacts of climate warming. Accurate forecasts of permafrost thaw under future climate scenarios will need to include the effects of changes on ecosystem productivity.

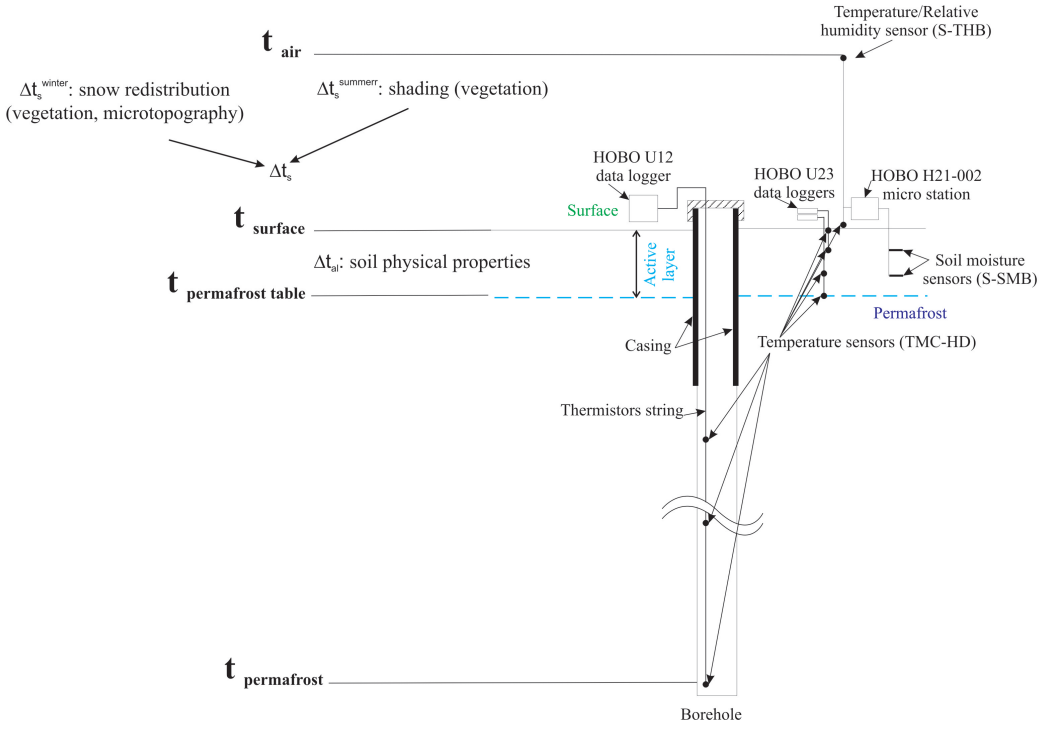

Figure 1: Scheme of sites instrumentation and temeprature gradients at different levels.

Acknowledgements

This research was supported by USA National Science Foundation projects ARC-0856864, ARC-1304271, and PLR-1417908.

References

Jorgenson, M.T.; Romanovsky, V.; Harden, J.; Shur, Y.; O'Donnell, J.; Schuur, E.A.G.; Kanevskiy, M. and Marchenko, S. [2010]: Resilience and vulnerability of permafrost to climate changeThis article is one of a selection of papers from The Dynamics of Change in Alaska's Boreal Forests: Resilience and Vulnerability in Response to Climate Warming. *Canadian Journal of Forest Research*, 40(7): 1219–1236, doi:10.1139/X10-060.

Kudryavtsev, V.A.; Garagula, L.S.; Kondrat'yeva, K.A. and Melamed, V.G. [1974]: *Osnovy merzlotnogo prognoza (in Russian)*. MGU, 431 pp. [CRREL Translation: V. A. Kudryavtsev et al., Fundamentals of Frost Forecasting in Geological Engineering Investigations, CRREL Draft Translation 606, 1977, 489 pp.].

Romanovsky, V. E. et al. [2014]: The Arctic Terrestrial Permafrost in "State of the Climate in 2013". *Bulletin of the American Meteorological Society*, 95 (7):S139–S141.

Comparison of measured air and soil-surface temperatures with satellite trends of increasing phytomass in northern Alaska

Anna E. Klene[1], Nikolay I. Shiklomanov[2], Frederick E. Nelson[3,4], Kelsey E. Nyland[4], Dimitry A. Streletskiy[2], & Qin Yu[2]

[1] *University of Montana, United States of America*
[2] *George Washington University, United States of America*
[3] *Northern Michigan University, United States of America*
[3] *Michigan State University, United States of America*

Multiple studies have presented evidence for widespread Arctic "greening". Most of these trends have been based upon long-term coarse satellite remote sensing datasets, but in situ vegetation studies have also found increasing shrub thickness and height in the region. This study presents long-term measurements of air and soil-surface temperatures at plots which were installed in 1995 to examine vegetation/permafrost interactions and potential fluxes of greenhouse gases along a latitudinal gradient in northern Alaska. The time-series of soil-surface temperatures and the difference between air and soil-surface temperatures over 20 years show increasing insulation of the soil surface which may be from increasing phytomass, such as measured from satellite-based NDVI.

Air and soil-surface temperatures have been measured continuously at nine 1-ha plots representative of a range of landscape types in the region established in 1995 as part of the US National Science Foundation's (NSF) Arctic System Science (ARCSS) Flux Study and continued under the Circumpolar Active Layer Monitoring (CALM) program. These plots were inventoried extensively for soils, vegetation, active-layer, ecological, and microclimatic characteristics. They are described in Walker and Bockheim [1995] and Klene et al. [2001] among others. Measurements were made using five two-channel dataloggers from Onset Computer Corporation. Nine soil-surface temperatures were measured by thermistors inserted at the base of the humic layer; air temperatures were measured at 2 m. Thermistors were installed in a range of microtopographic positions within each plot to capture the range of conditions present [Klene et al., 2001]. Instrumentation has been replaced several times, progressing from Stowaway™, to Hobo™, to HoboPro™, and currently HoboV2™ dataloggers. Data have been recorded hourly or bi-hourly over the period of record. Temperatures were processed into daily means and then mean July-August temperatures for each plot for this study to reflect growing season conditions.

Pinzon and Tucker [2014] have developed a global time-series of maximum Normalized Difference Vegetation Index (NDVI) values, using Advanced Very High Resolution Radiometer (AVHRR) and SeaWIFs satellite data known as NDVI 3g, building upon several previous datasets. A time-series of NDVI pixel values were extracted from the NDVI 3g dataset from 1982 to 2012 over each of the CALM Flux plots. In two instances, one 8 × 8 km pixel included neighboring plots which had similar climatic but contrasting land-cover types.

Comparison between the 30 year satellite dataset and 20 year temperature records from the CALM Flux plots revealed

a) small increasing trends in mean July-August air temperatures,

b) small decreasing trends in mean July-August soil-surface temperatures,

c) increasing differences between air and soil-surface temperatures, and increasing maximum seasonal NDVI3g values. Figure 1 shows these results for Flux Plot 6/ CALM Plot U12B at Toolik Lake.

Decreases in soil-surface temperatures could reflect several mechanisms, such as deeper burial of thermistors within an increasingly thick humic layer, increasing phytomass, and/or changes in moisture. Raynolds et al. [2012] measured phytomass at a nearby series of plots which correlated to increasing maximum NDVI3g values.

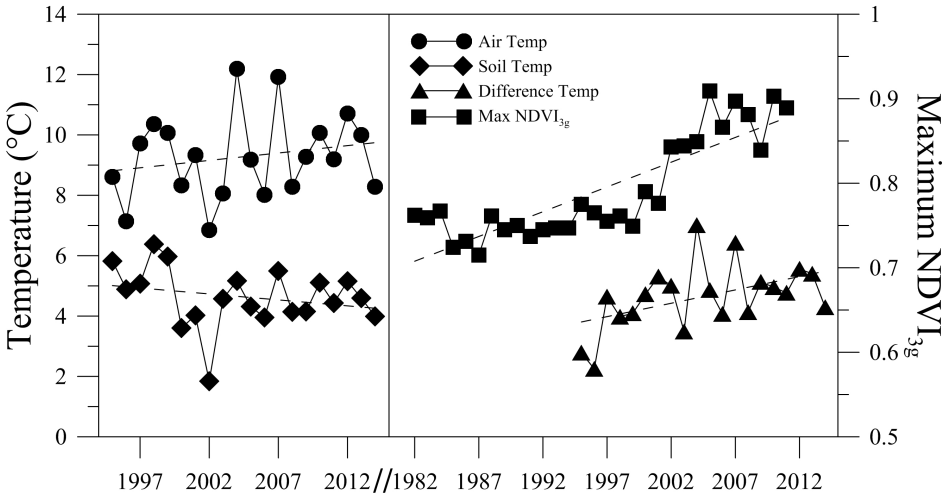

Figure 1: Graph showing (left) July-August air and mean soil-surface temperatures at Flux Plot 6 (CALM site U12B) at Toolik Lake, 1995–2014, and (right) the difference between the air and soil-surface temperatures and the maximum NDVI g3 data, 1982–2012.

Further research is needed to elucidate the complex feedbacks between changing temperature and moisture regimes, and responses of vegetation and soil components. These results illustrate the importance of long-term research to quantify changing landscape trends.

Acknowledgements

We thank the many people have assisted with the data collection over the years. This research was supported by the U.S. National Science Foundation (grants OPP-0095088, OPP-0352958, OPP-0856421, and OPP-1304555). Any opinions, findings, conclusions, or recommendations expressed in this study are those of the authors and do not necessarily reflect the views of the NSF. Mention of specific product names does not constitute endorsement by NSF.

References

Klene, A.E.; Nelson, F.E.; Shiklomanov, N.I. and Hinkel, K.M. [2001]: The n-factor in natural landscape: Variability of air and soil- surface temperatures, Kuparuk River basin, Alaska, USA. *Arctic, Antarctic, and Alpine Research*, 33(2):140–148.

Pinzon, J.E. and Tucker, J.C. [2014]: A non-stationary 1981–2012 AVHRR NDVI3g time series. *Remote Sensing*, 6(8), doi:10.3390/rs6086929.

Raynolds, M.K.; Walker, D.A.; Epstein, H.E.; Pinzon, J.E. and Tucker, C.J. [2012]: A new estimate of tundra-biome phytomass from trans-Arctic field data and AVHRR NDVI. *Remote Sensing Letters*, 3(5), doi:10.1080/01431161.2011.609188.

Walker, D.A. and Bockheim, J.G. [1995]: *Vegetation-Soil Characterization at the 12 Flux Tower Sites.* ARCSS/LAII/Flux Study. LAII Science Management Office, University of Alaska Fairbanks, Fairbanks, AK.

Surface temperature reconstructions in the Lena River Delta and in the Western Laptev Sea, Russia, from borehole data

Fabian Kneier[1], Mikhail N. Grigoriev[2], Moritz Langer[1], Julia Boike[1], & Paul P. Overduin[1]

[1] *Alfred Wegener Institute Helmholtz Centre for Polar and Marine Research, Potsdam, Germany*
[2] *Melnikov Permafrost Institute SB RAS, Russian Federation*

Palaeotemperature reconstructions play an important role as palaeoclimate records, for our understanding of the climate system behavior as such, as well as being the basis for models identifying the impact of these climate conditions on specific processes in the past and future. Temperature records reconstructed from borehole logs have a more direct relationship to the historic temperature history than other proxy-based reconstructions such as tree-rings, pollen or isotope ratios in ice cores, which can include influences from other independent factors on those proxies.

At larger depths borehole temperatures are dominated by the geothermal heat flux and a rather uniform geothermal gradient in the profile. At shallower levels temperature variations at the surface propagate as heat waves into the ground. The further down, the more the temperature reflects influences of longer periods of surface variations due to the Earth's damping higher angular frequency periods first.

This study uses two inversion optimization methods previously applied to ice core sites [Roberts et al., 2013] to reconstruct the local surface temperature history at two shallow (100m and 65m deep) permafrost borehole sites: Sardakh Island in the Lena-Delta and Cape Mamontov Klyk in the Western Laptev Sea, Russia (Fig. 1). We employed a flux-conserving finite volume numerical soil model to calculate temperature-depth-profiles from surface temperature histories. Thermal properties of the sites were retrieved from either the observed temperature field or the sediment composition analysis of the borehole. Two inversion schemes that employ the forward soil model to optimize surface temperature history in a least square sense were used in the reconstruction:

i) the least square QR (LSQR) method and

ii) the particle swarm optimization (PSO) method.

The latter resembles a Monte Carlo based approach [Ebbesen et al., 2012], the former is based on a generalized least-square solution of a linearized version of the problem as utilized by Orsi et al. [2012].

Recoverable time length for the surface temperature histories for the two borehole sites were found to be well above 400 years in both cases by frequency-dependent heat wave damping analysis.

The local surface soil temperature reconstructions for the two boreholes are discussed in comparison to other local as well as larger scale global temperature reconstructions to highlight important local and regional deviations.

Additionally, the reconstructions of both sites are compared on the basis that one (Mamontov Klyk) is situated away from any major river systems and the other (Sardakh) is situated in the Lena River Delta, possibly showing thermal influence by the river.

The local surface temperature history is important as a driving input factor in local permafrost models that assess the evolution, degradation and impact of permafrost in the high latitudes in the future climate system.

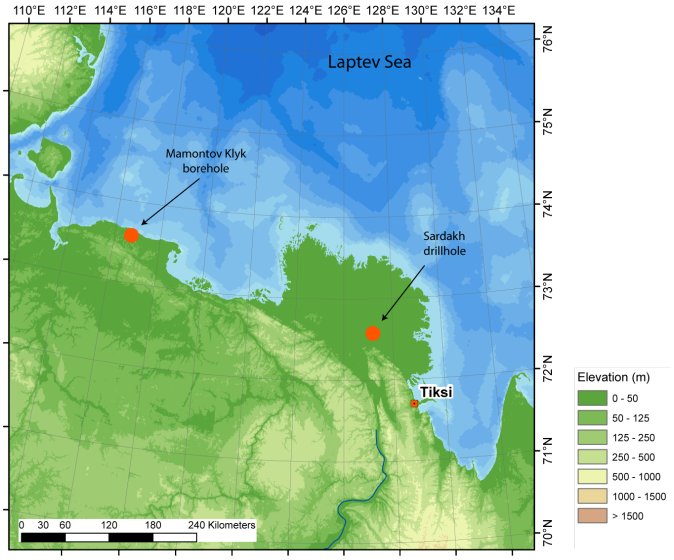

Figure 1: Location of shallow permafrost boreholes at Cape Mamontov Klyk and Sardakh Island.

References

Ebbesen, S.; Kiwitz, P. and Guzzella, L. [2012]: A generic particle swarm optimization Matlab function. In *American Control Conference*, pages 1519–1524.

Orsi, A.J.; Cornuelle, B.D. and Severinghaus, J.P. [2012]: Little Ice Age cold interval in West Antarctica: Evidence from borehole temperature at the West Antarctic Ice Sheet (WAIS) Divide. *Geophysical Research Letters*, 39(9), doi:10.1029/2012GL051260. L09710.

Roberts, J. L.; Moy, A. D.; van Ommen, T. D.; Curran, M. A. J.; Worby, A. P.; Goodwin, I. D. and Inoue, M. [2013]: Borehole temperatures reveal a changed energy budget at Mill Island, East Antarctica, over recent decades. *The Cryosphere*, 7(1): 263–273, doi:10.5194/tc-7-263-2013.

A 18-year record (1998-2016) of surface and ground temperature and water content from a high permafrost Arctic site (Bayelva, Spitsbergen): evaluation of land surface, permafrost and snowpack models and remote sensing data

Stephan Lange, Niko Bornemann, Sina Muster, & Julia Boike

Alfred Wegener Institute Helmholtz Centre for Polar and Marine Research, Potsdam, Germany

Since 1998 we record hourly data from the Bayelva site close to Ny-Alesund, on Spitsbergen Island in the Svalbard archipelago (78°551 N, 11°571 E), where continuous permafrost underlies the un- glaciated coastal areas. The West Spitsbergen Ocean Current, a branch of the North Atlantic Current, warms this area to an average air temperature of about -13 °C in January and +5 °C in July, and provides about 400 mm of precipitation annually, falling mostly as snow between September and May. Significant warming of air temperatures has been detected since 1960, which is generally attributed to changes in the radiation budget and in atmospheric circulation. This warming is also reflected in the permafrost temperatures, as recorded from boreholes as well as increased active layer thaw depths. The scientific goal is to establish a long term- permafrost observational site to investigate the observed warming of permafrost and potential causes. At the site, weather components (radiation components, temperature, humidity, wind speed and direction, snow) and soil temperature and moisture in the seasonally thawing surface layer. In 2007, additional instruments were added: an eddy covariance system and a 10 m permafrost temperature profile. In 2012, this site was equipped with a 220 V power supply and data transfer cables that are buried in the soil. Data are transferred hourly to Potsdam and loggers and sensors can be accessed and programmed remotely from AWI. Due to this major improvement, we obtained a data record without gaps since 2012. Thus, this site is included as validation site in satellite missions, for example in NASA's soil moisture active passive mission (SMAP).

We give an overview of the available data, as well as the processing and cleaning routines that are applied.

Variability in active layer dynamics associated with stand density in an arctic Siberian larch forest

Michael Loranty[1], Heather Alexander[2], Susan Natali[3], Alexander Kholodov[4], & Sergei Davydov[5]

[1] *Department of Geography, Colgate University*
[2] *Department of Forestry, Mississippi State University*
[3] *Woods Hole Research Center*
[4] *Geophysical Institute, University of Alaska Fairbanks*
[5] *North-East Scientific Station, Pacific Institute for Geography, Russian Academy of Sciences*

Permafrost responses to climate warming are variable in time and space, as evidenced by long-term monitoring of borehole temperatures and active layer depths. This observed decoupling of surface-air and subsurface substrate temperatures is most likely a consequence of ecosystem characteristics, hydrology, and snow distribution; the dominant controls on land surface and soil energy dynamics. Terrestrial ecosystems exert strong control on land surface energy dynamics via influences on energy partitioning. In areas underlain by permafrost this can modulate substrate temperatures across a range of spatial and temporal scales. Examples of such effects include decreases in soil temperatures beneath structurally complex tree and shrub canopies due to attenuation of solar radiation, and changes in soil thermal conductivity associated with variability in soil organic layer properties and moisture content. Despite this knowledge there is still uncertainty regarding the manner in which ecosystem properties influence substrate temperatures, especially where multiple mechanisms are involved.

Across the northern high latitude permafrost regions many of these ecosystem properties are changing with climate. Examples include changes in vegetation productivity, which has been linked to shrub expansion in tundra ecosystems, and also changing disturbance regimes. In the latter case wildfire is particularly important because it can lead to rapid short-term changes surface energy partitioning via combustion of vegetation and soils, and also long-term shifts in energy partitioning associated with post-fire vegetation regrowth. Here we examine the effects of ecosystem vegetation and soil properties on permafrost thaw depth and soil temperatures in the seasonally thawed active layer across a gradient of ecosystem properties within a single fire scar in northeast Siberian larch (*Larix cajanderi*) forest. The objective of our study is to identify differences in active layer properties and their underlying causes.

In this study we characterize variability in vegetation and soil properties within a single fire scar near Chersky, in northeastern Siberia (68.76N 161.45E). Within the burn scar we measured vegetation and soil carbon (C) stocks, canopy structural properties, understory vegetation composition, and active layer depth across nine stands. Form July 2014 through September 2015 we measured understory air temperature, relative humidity, photosynthetically active radiation (PAR), and soil temperature and moisture.

We find high variability in forest regrowth after fire, with aboveground larch biomass ranging from 500 – 2500 g C m^{-2}. High biomass stands exhibit reduced PAR, and air temperatures at 1m height associated with increased canopy closure. Low biomass stands have greater understory shrub biomass and lower moss cover in comparison high biomass stands. Consequently, soil temperatures and active layer depths decrease with increases in biomass. In these forests a combination of reduced radiation at the ground surface and lower thermal conductivity of near surface organic material buffer permafrost from changes in air temperature. The effects of moisture are less clear, as differences in soil moisture and relative humidity are not consistent across sites.

Our results demonstrate that variation of ecosystem structure and soil characteristics within a single ecosystem type can exert strong control on active layer dynamics. While numerous studies have examined how ecosystem characteristics influence active layer dynamics, many focus changes associated with shifts in ecosystem type. For example, several recent studies have demonstrated the likelihood of active layer soil temperature reductions with a shift from graminoid to shrub dominance in tundra ecosystems. We

demonstrate that structural changes affecting permafrost temperatures need not be characterized by shifts in vegetation communities. Additionally, our study highlights the important influence of disturbance, particularly wildfire, on ecosystem composition and active layer dynamics. In these larch forests fire can catalyze shifts in stand structure that occur much more rapidly than ecosystem responses to climate alone. Understanding these often bi-directional interactions between ecosystem properties, climate, disturbance will be crucial for predicting rates of permafrost thaw across arctic and boreal ecosystems.

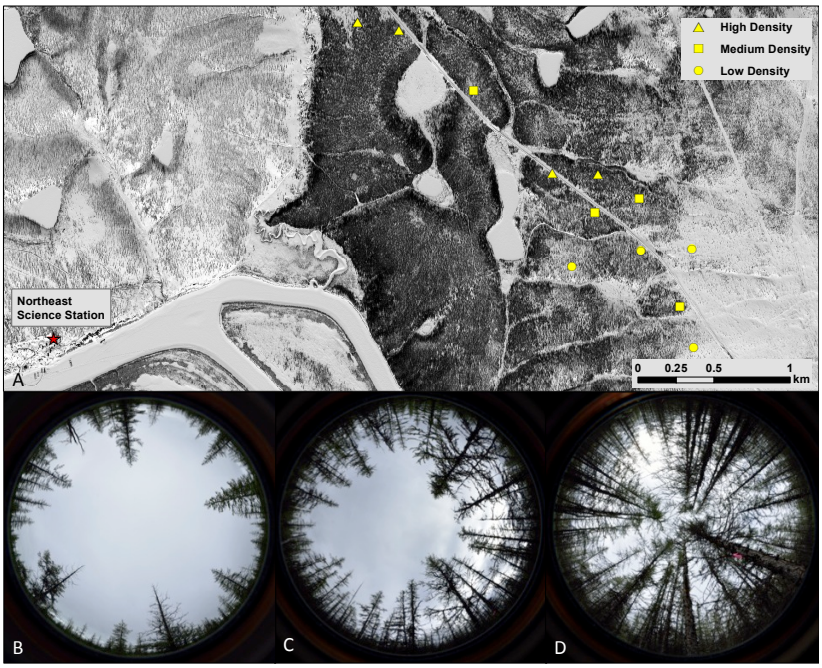

Figure 1: Map of the study site (a) and hemispherical photos of low (b), medium (c), and high density (d) larch stands.

Borehole temperature data processing and analysis using data from the SLF permafrost monitoring network

Rachel Luethi[1,2], Marcia Phillips[1],

[1] *WSL Institute for Snow and Avalanche Research SLF, Davos, Switzerland*
[2] *GEOTEST AG, Davos, Switzerland*

The SLF permafrost borehole temperature monitoring network comprises 25 boreholes at 12 sites in the Swiss Alps, nine of which are included in the Swiss Permafrost Monitoring Network (PERMOS). The boreholes are located at elevations above approximately 2400 m asl and cover different landforms like crests, rock walls, talus slopes and rock glaciers. The boreholes not included within PERMOS are presented here. They are up to 24 m deep and the longest measurement series was started in 1996. Borehole temperatures are measured with high precision thermistors (and at one location with UTL3 loggers) at various depths, in 2-hourly to daily resolution.

Within the IQUASAP-CCES (Competence Center Environment and Sustainability) project the data has been carefully quality checked and processed. Temperature data has been made available online via a GSN (global sensor networks) middleware and metadata via the Swiss Experiment platform.

Selected results are shown here, focusing on the discrimination between natural phenomena such as ground warming or local temperature contrasts, the effects of construction activity and sensor drift, all of which can have similar thermal effects and be difficult to distinguish correctly. The following phenomena will be shown:

i) Moisture-induced sensor drift leading to apparent warming was detected and corrected within the active layer in several boreholes. Temperature corrections to the order of 0.05-0.2 °C may reduce apparent active layer thicknesses by approximately 1 m – depending on the measurement setup and the temperature distribution in the profile.

ii) Apparent cooling, probably caused by mechanically strained cables was observed at one site.

iii) The influence of construction activity on ground temperature is discussed.

iv) Strongly contrasting ground temperatures over short distances measured at one site imply that even measurement redundancy with temperature measurements in neighboring boreholes is not always sufficient to detect sensor drift, due to the high variability of ground temperatures in mountainous terrain.

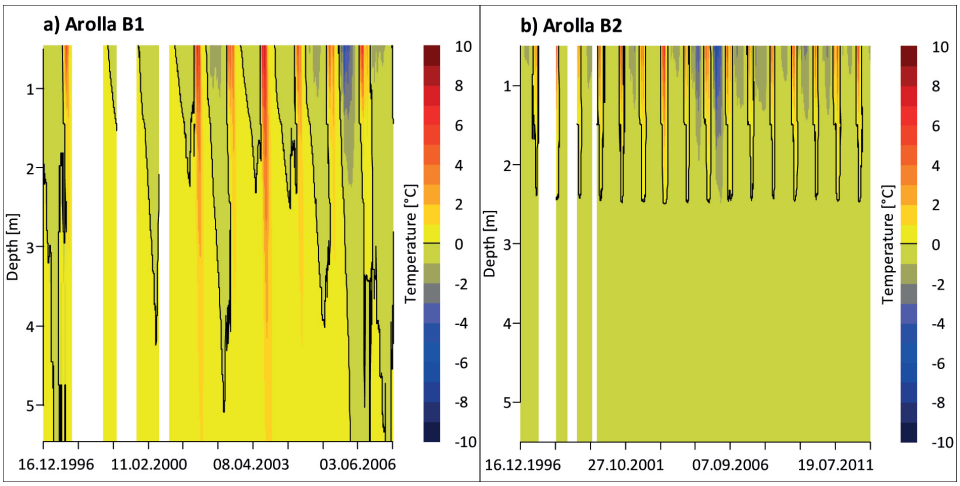

Figure 1: Contour plots of the ground temperatures in two boreholes at Mont Dolin (Arolla, Western Swiss Alps) showing contrasting ground temperatures over short distances.

Environmental and climatological monitoring at the Zackenberg Research Station, northeast Greenland

Magnus Lund[1], Kirstine Skov[2], & Jakob Abermann[3]

[1] *Aarhus University, Denmark*
[2] *University of Copenhagen, Denmark*
[3] *ASIAQ - Greenland Survey, Greenland*

Within the auspices of the Greenland Ecosystem Monitoring programme (www.g-e-m.dk), the GeoBasis and ClimateBasis monitoring programmes have since 1995 conducted environmental and climatological observations in the high Arctic Zackenberg valley (74.47°N, 20.55°W) within the Northeast Greenland National Park. Standard atmospheric parameters are collected redundantly on two masts in order to minimise data gaps and treat sensor biases consistently. Measurements of the active layer depth are performed on a bi-weekly basis during the snow free period in two CALM (Circumpolar Active Layer Monitoring) grids; one (ZEROCALM-1) located in an almost horizontal, well-drained Cassiope heath ecosystem consisting mainly of sandy sediments, and one (ZEROCALm-2) in a south-facing slope covering a seasonal snow-patch dominated by both sandy and silt-clay sediments.

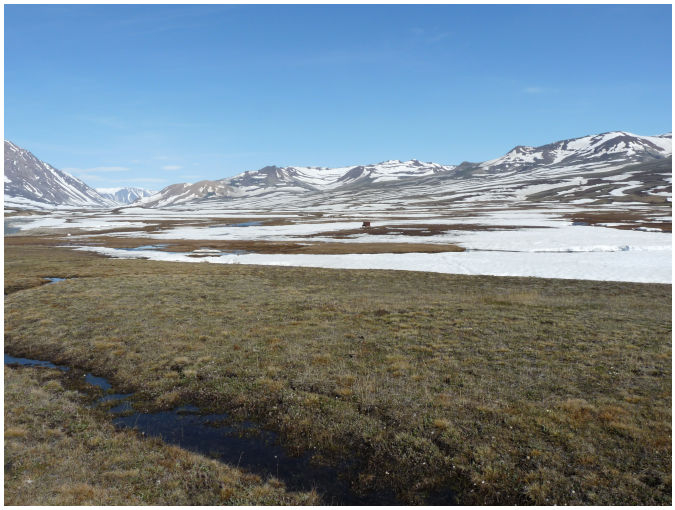

Figure 1: photograph

Furthermore, additional installations in the area include eddy covariance systems for assessing the exchange of CO_2, H_2O and sensible heat, complete surface energy balance stations, soil moisture, soil water chemistry, ground and permafrost temperature and NDVI measurements. Hydrology and water chemistry are continuously being monitored in the Zackenberg River. The width of the monitoring activities and the length of the existing time series thus make this area ideal for detailed biogeochemical modelling activities.

During 1996-2014, mean July air temperature has increased (0.12 K yr^{-1}, r^2=0.31, p=0.01) with associated increases in maximum thaw depth of approx. 1.1 cm yr^{-1} (p<0.001) in both CALM grids. Changes and feedback effects related to both the land-atmosphere exchange of carbon and energy has been observed [Lund et al., 2012, 2014], due to increased summertime temperature and active layer depths as well as decreased soil moisture content.

References

Lund, M.; Falk, J.M.; Friborg, T.; Mbufong, H.N.; Sigsgaard, C.; Soegaard, H. and Tamstorf, M.P. [2012]: Trends in CO_2 exchange in a high Arctic tundra heath, 2000–2010. *Journal of Geophysical Research: Biogeosciences*, 117(G2), doi:10.1029/2011JG001901. G02001.

Lund, M.; Hansen, B.U.; Pedersen, S.H.; Stiegler, C. and Tamstorf, M.P. [2014]: Characteristics of summer-time energy exchange in a high Arctic tundra heath 2000–2010. *Tellus B*, 66:21631, doi:10.3402/tellusb.v66.21631.

Thermal state of permafrost in disturbed and undisturbed cryogenic geosystems in the European North

Galina Malkova, Marat Sadurtdinov, Andry Skvortsov, & Andry Tsarev

Earth Cryosphere Institute, Russian Federation

Long-term monitoring of permafrost temperature is essential to assess the current state and tendencies of changes in cryogenic geosystems in the conditions of significant climate variations and technogenesis. During the last 20 years, the development of oil and gas fields in the European North has been progressing rapidly. However, the current data on the changes in permafrost conditions in disturbed and undisturbed landscapes have turned out to be insufficient for engineering needs. In this paper, the changes in permafrost that have occurred in the cryogenic geosystems during the last 30 years and their relation to observed climatic changes and technogenesis are analyzed. Field study of permafrost conditions included landscape description of transects and control points, drilling of boreholes and testing of soils, and application of geophysical methods for determination of permafrost table position, permafrost thickness, and boundaries of taliks.

The interannual dynamics of permafrost temperature and of the seasonal thawing depth has been studied. The correlation of temperature regime of permafrost in disturbed and undisturbed experimental sites was carried out. In the European North of Russia, the period from 1983 to 2015 is characterized by a significant increase in MAAT, equal to 0.08 °C/year. The thermal state of permafrost has some inertia, and an increase in MAPT under the natural conditions has been 2 to 8 times smaller than an increase in MAAT. Since 1983, the mean annual air temperature (MAAT) at the weather station Bolvansky increased by 3 °C, while the mean annual permafrost temperature (MAPT) in various landscapes increase only by 0.2 to 1.0 °C. An increase in MAPT is significantly lower that MAAT– from 0.01 to 0.04 °C/year (Fig. 1). The steepest trend of the MAPT is characteristic of the low temperature permafrost landscapes, and the lowest trend – of the high temperature landscapes [Romanovsky et al., 2010, Drozdov et al., 2012].

The temperature of the active layer reacts to changes in the air temperature much faster than underlying permafrost. In dominant landscapes, the mean annual active layer temperature has increased from –3.5 °C in 1980s to 0 °C in 2011-2012, which caused the lowering of the permafrost table and formation of closed taliks between the active layer and permafrost. The trends in increase of ground temperature (Tground) in various cryogenic geosystems lag behind trends in air temperature (Tair). The Tair trend for the 30-year period shows an increase of 0.08 °C/year; while for Tground it varies from 0.01 to 0.04 °C /year. In the last two years, the active layer thickness has reached its maximum value, and the closed taliks began to form at the hilltops underlain by ice-poor permafrost [Malkova, 2011].

In a disturbed cryogenic geosystems with the removal of vegetation and soil cover as a result of industrial development of the land occurs more intensive change: violated the heat balance of the surface, increases the amplitude of the temperature fluctuations at the surface and in the upper layers of permafrost, increasing the depth of the active layer and begins the permafrost degradation. It is established that due to the change of heat transfer on the surface of soil in disturbed sites of boreholes and pits began to form the closed taliks, and the permafrost table deepened to 4-12 m. To assess the impact of combined effects of climatic and anthropogenic changes in cryogenic landscapes, it is necessary to expand the monitoring network, use automated data collection, and widely apply remote sensing and geophysical methods to determine the of permafrost characteristics.

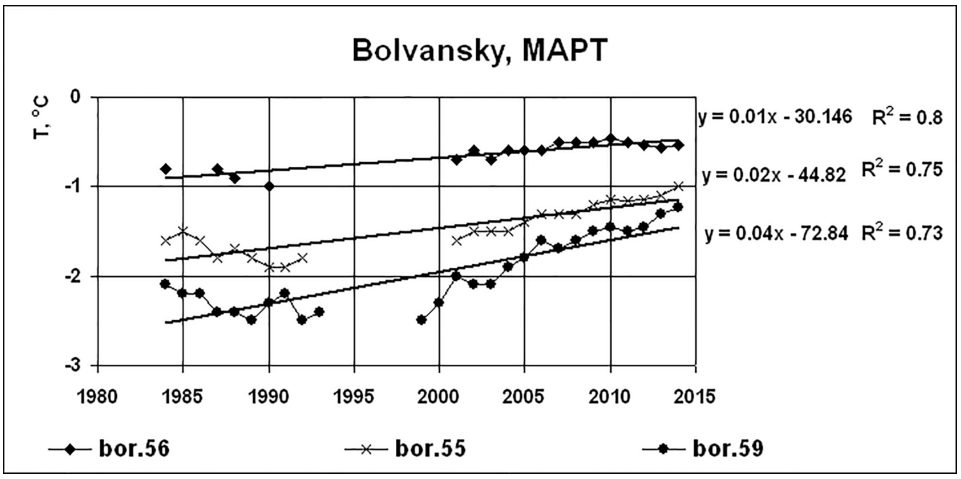

Figure 1: Mean annual permafrost temperature (MAPT) at the 10 m depth, Bolvansky station. Borehole 59 – the top of the hill, drained tundra; borehole 55 – polygonal peatland; borehole 56 – the edge of the terrace, slope, tundra.

Acknowledgements

The research was supported by international CALM and TSP programs, project ClimaEast (UNDP/GEF), integration program of the RAS Department, and the grant of the field support of SB RAS.

References

Drozdov, D.S.; Malkova, G.V.; Ukraintseva, N.G. and Korostelev, Y.B. [2012]: Monitoring of permafrost conditions in southern tundra landscapes of the European North and West Siberia. In *Proceedings of the Tenth International Conference on Permafrost: Resources and Risks of Permafrost Areas in a Changing World*, volume 3, pages 159–164. Salekhard, Yamal-Nenets Autonomous District, Russia, 25–29 June 2012, Ekaterinburg, Salekhard, Russia.

Malkova, G.V. [2011]: Monitoring of the permafrost temperature and seasonal thawing depth on the Bolvansky site in the Pechora river Delta. In *Proceedings of the 4th conference of geocryological Russia*, volume 2, pages 111–118, Moscow State University named after M. V. Lomonosov 7–9 June 2011, 2011. Moscow, publishing house of the University.

Romanovsky, V.E.; Drozdov, D.S.; Oberman, N.G.; Malkova, G.V.; Kholodov, A.L.; Marchenko, S.S.; Moskalenko, N.G.; Sergeev, D.O.; Ukraintseva, N.G.; Abramov, A.A.; Gilichinsky, D.A. and Vasiliev, A.A. [2010]: Thermal state of permafrost in Russia. *Permafrost and Periglacial Processes*, 21 (2): 136–155, doi:10.1002/ppp.683.

High resolution soil temperature and active layer dataset for estimating rates of permafrost degradation and their impact on ecosystems, infrastructure, CO_2 and CH_4 fluxes and net C storage following permafrost thaw in Alaska and Northwest Canada

Sergey Marchenko[1], Hélène Genet[2], Eugénie Euskirchen[2], David McGuire[3], Scott Rupp[4], W. Robert Bolton[5], Amy Breen[6], Mark Waldrop[7], Stephanie McAfee[8], Fengming Yuan[9], Yujin Zhang[2], Vladimir Romanovsky[1], John Walsh[5], Tom Kurkowski[6], Michael Lindgren[6], Alec Bennett[6], Matthew Leonawicz[6], Tobey Carman[2], Angie Floyd[6], & Kristin Timm[1]

[1] *Geophysical Institute, University of Alaska, Fairbanks, AK, United States of America*
[2] *Institute of Arctic Biology, University of Alaska, Fairbanks, AK, United States of America*
[3] *U.S. Geological Survey, Alaska Cooperative Fish and Wildlife Research Unit, University of Alaska Fairbanks, Fairbanks, AK, United States of America*
[4] *Alaska Climate Science Center, University of Alaska, Fairbanks, AK, United States of America*
[5] *International Arctic Research Center, University of Alaska, Fairbanks, AK, United States of America*
[6] *Scenarios Network for Alaska and Arctic Planning, University of Alaska, Fairbanks, AK, United States of America*
[7] *U.S. Geological Survey, United States of America*
[8] *University of Nevada Reno, NV, United States of America*
[9] *Oak Ridge National Laboratory, TN, United States of America*

Permafrost temperature has increased in most locations in the Arctic and Sub-Arctic during the past 30-40 years. The typical increase in permafrost temperature is 1 to 2 °C. Long-term permafrost thawing has already started at some locations in natural undisturbed conditions because of the degradation of ice-rich and carbon-rich permafrost.

The Soil Temperature and Active Layer Thickness (ALT) Gridded Database was developed to quantify the nature and rate of permafrost degradation and its impact on ecosystems, infrastructure, CO_2 and CH_4 fluxes and net C storage following permafrost thaw across Alaska and Northwest Canada. To develop this database, we used the process-based permafrost dynamics model GIPL2 developed in the Geophysical Institute Permafrost Lab, and which is the permafrost module of the Integrated Ecosystem Model for Alaska and Northwest Canada (IEM; Fig. 1). The IEM project is a multi-institutional and multi-disciplinary effort aimed at understanding potential landscape, habitat and ecosystem change in Alaska and Northwest Canada (https://csc.alaska.edu/projects/integrated-ecosystem-model-iem-alaska-and-northwest-canada). The climate forcing data for simulations were developed by the Scenarios Network for Alaska and Arctic Planning (SNAP) (http://www.snap.uaf.edu/). These data are based on the historical CRU3.1 data set for the retrospective analysis period (1901-2009) and the CMIP3 CCCMA-CGCM3.1 and MPI-ECHAM5/MPI-OM climate models for the future period (2009-2100). Both data sets were downscaled to a 1 km resolution, using a differencing methodology (i.e., a delta method) and the Parameter-elevation Regressions on Independent Slopes Model (PRISM) climatology. The two climate models were chosen from among the best performing climate models for Alaska, and each provided projections for three CO_2 emission scenarios. Additional input data (snow characteristics, soil thermal properties, water content, organic matter accumulation or its loss due to fire, etc.) came from the Terrestrial Ecosystem Model (TEM) and the ALFRESCO (ALaska FRame-based EcoSystem COde) model simulations.

We estimated the dynamics of permafrost temperature, active layer thickness, area occupied by permafrost, and volume of seasonally thawed soils within the 4.75 upper meters across the IEM domain. Simulations of future changes in permafrost indicate that, by the end of the 21^{st} century, late-Holocene permafrost in Alaska and Northwest Canada will be actively

thawing at all locations and that some Late Pleistocene carbon-rich peatlands underlain by permafrost will start to thaw at some locations. The modeling results also indicate how different types of ecosystems affect the thermal state of permafrost and its stability. Although the rate of soil warming and permafrost degradation in peatland areas are slower than other areas, a considerable volume of peat in Alaska and Northwest Canada will be thawed by the end of the current century. The release of carbon and the net effect of this thawing depends on the balance between increased productivity and respiration, which depend, in part, on soil moisture dynamics.

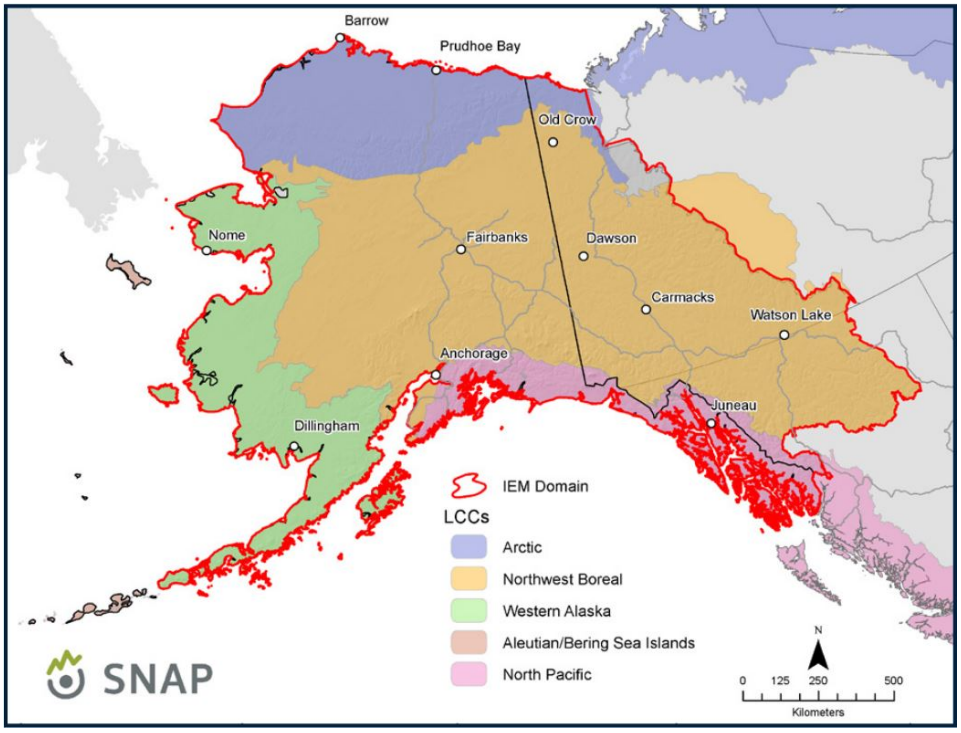

Figure 1: The Alaska and Northwest Canada geographic domain for the IEM and location of Landscape Conservation Cooperatives (LCCs)

Positive aspects of having GTN-P monitoring site in Eastern Chukotka

Alexey Maslakov[1], Vladimir Ruzanov[2], Oleg Tregubov[2], Gleb Kraev[3], & Dmitry Zamolodchikov[3]

[1] *Lomonosov Moscow State University, Moscow, Russia*
[2] *Laboratory of the integrated study of Chukotka, North-East Institute of Integrated Research, Anadyr, Russia*
[3] *Centre for Problems of Ecology and Productivity of Forests RAS, Moscow, Russia*

Although GTN-P's contribution to monitor Pan-Arctic permafrost changes had been recognized (IPCC, 2013) the GTN-P sites are distributed irregularly within the cryolithozone [Biskaborn et al., 2015]. The monitoring boreholes had been evenly distributed only in Alaska, however in Eurasia the data is very patchy, and hence biased. Chukotka is the part of Beringian Bridge, and the bridge is important for any network to check the consistency of variations of permafrost temperature change.

Chukotka is highly influenced by both the Arctic and the Pacific circulations [Zamolodchikov et al., 2008], and thus the tundra has very southern distribution (down to 63 N lat.). According to data from local weather stations (Uelen and Provideniya) there was a slight air temperature rise recently by 0.09–0.17 °C per decade during 1929–2009. The nearest GTN-P boreholes are Wales and Savoonga. These locations are separated from considered area by waters of Bering Sea. The only GTN-P monitoring site in Chukotka is Elgygytgyn, which was established in 2009 at the very specific location far from the sea shore.

Despite the remote location, 3 research groups are working on permafrost and environmental studies in Chukotka [Maslakov and Kraev, 2014, Zamolodchikov et al., 2004]. There is a number of active CALM sites in Eastern Chukotka (Fig. 1, upper): R-27 Lavrentia, R-41 Lorino, operated since 2000 and 2010 respectively. Since 2012 these sites equipped by data loggers measuring temperature at depths 0.05-1 meter. The monitoring plots are accessible all over the field season by car or ATV from the field station in Lavrentia, and by field helpers during winter, with the CH2M Hill Logistics provided. Another site is Anadyr area, where 4 CALM-sites equipped with boreholes and 3 boreholes with data loggers exist (Fig. 1, lower). There are also 9 boreholes known within this area (stationary Mt. Dionisiya) which are currently suspended. Operated boreholes organized in Anadyr Lowland are monitored repeatedly, not continuously. Operated boreholes are needed to include in GTN-P database and to be equipped with data loggers meeting the requirements of GTN-P standards.

Herewith we would like to show that the scientific basis the organized infrastructure and natural features of Chukotka could provide valuable supplement to gaining a holistic future view on the thermal state of permafrost by involvement into the GTN-P program.

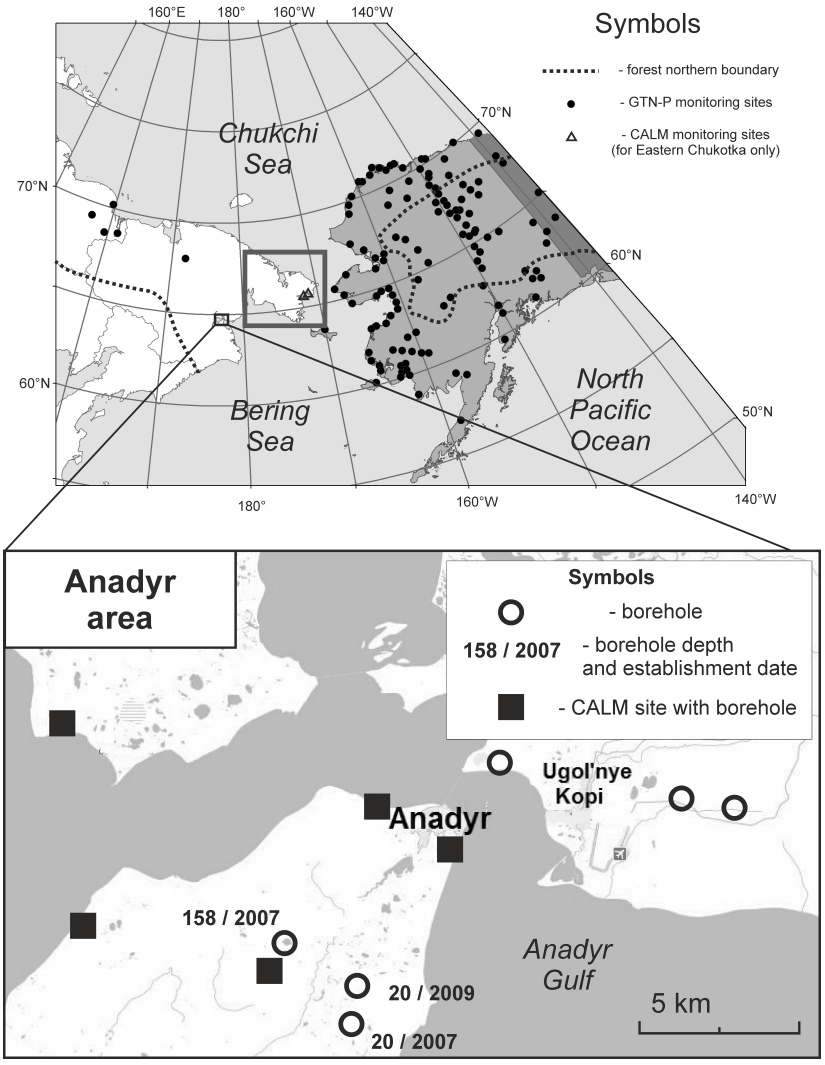

Figure 1: Schematic distribution of GTN-P and CALM monitoring sites across Bering Sea region.

References

Biskaborn, B. K.; Lanckman, J.-P.; Lantuit, H.; Elger, K.; Streletskiy, D. A.; Cable, W. L. and Romanovsky, V. E. [2015]: The new database of the Global Terrestrial Network for Permafrost (GTN-P). *Earth System Science Data*, 7(2):245–259, 2015. doi:10.5194/essd-7-245-2015.

Maslakov, A. and Kraev, G. [2014]: Coastal Hazards Within Indigenous Settlements of Chukchi Peninsula. In: Lollino, G.; Manconi, A.; Locat, J.; Huang, Y. and Canals Artigas, M.(eds.), *Marine and Coastal Processes*, volume 4 of *Engineering Geology for Society and Territory*, pages 33–36. Springer International Publishing, Cham, doi:10.1007/978-3-319-08660-6_6.

Zamolodchikov, D.; Kotov, A.; Karelin, D. and Razzhivin, V. [2008]: Recent Climate and Active Layer Changes in Northeast Russia: Regional Output of Circumpolar Active Layer Monitoring (CALM). In: Kane, D. and Hinkel, K. (ed.), *Proceedings of the Ninth International Conference on Permafrost*, Institute of Northern Engineering, University of Alaska Fairbanks, Fairbanks, USA, 29 June–3 July 2008, volume 2, pages 2021–2026. ISBN 978-0-9800179-3-9. URL http://ipa.arcticportal.org/publications/conference-proceedings.

Zamolodchikov, D.G.; Kotov, A.N.; Karelin, D.V. and Razzhivin, V.Y. [2004] Active-Layer Monitoring in Northeast Russia: Spatial, Seasonal, and Interannual Variability. *Polar Geography*, 28(4):286–307, 2004.

Russian contribution to the permafrost monitoring: Development of the State Geocryological Monitoring Research Sites

Vladimir Pavlovich Melnikov[1,2,3], Dmitry Stepanovich Drozdov[2,3,4], Vladimir Alexandrovich Dubrovin[6], Vladimir Evgenyevich Romanovsky[3,4,7], & Vadim Vladimirovich Pendin[5]

[1] *Tyumen Scientific Centre of Siberian Branch RAS, Tyumen, Russia*
[2] *Earth Cryosphere Institute SB RAS (ECI SB RAS), Tyumen, Moscow, Russia*
[3] *Tyumen State Oil and Gas University, Tyumen, Russia*
[4] *Tyumen State University, Tyumen, Russia*
[5] *Russian State Geological Prospecting University (MGRI-RSGPU), Moscow, Russia*
[6] *All-Russia Scientific and Research Institute of Hydrogeology and Engineering Geology (VSEGINGEO), Moscow, Russia*
[7] *Geophysical Institute, University of Alaska Fairbanks, Fairbanks, AK, USA*

The permafrost may cause numerous environmental problems in the Arctic and Sub-Arctic regions. In areas associated with intensive economic activities, natural geocryological processes may be exacerbated by numerous technogenic impacts. The extensive economic activities including expansion of oil and gas industry in the northern regions of Russia and the Arctic shelf require the development and implementation of long-term monitoring of permafrost and related environmental characteristics at locations representative to various geocryological conditions.

Permafrost covers two thirds of Russia, occupying its northern and northeastern regions, and has variable characteristics depending on location. Generally, continuous, discontinuous and sporadic permafrost zones replace each other from north to south. The relict Pleistocene permafrost located at tens to hundreds of meters below the surface and is separated from the Holocene permafrost by unfrozen soils. Besides continuity, other important characteristics of permafrost include thickness, temperature, ice content, lithology, salinity, and presence of cryopegs among others. Genesis of permafrost is equally important. For example, syngeneic permafrost may have ice content above 80 % by volume and present significant risk to economic development.

The risk of economic activities in the Arctic regions is controlled by the combined influence of two groups of factors:

1. climatic factors, and
2. technogenic factors.

The melting of ground ice due to changing climatic conditions may result in serious environmental problems, leading to changes in ecosystems and impacting infrastructure built on permafrost. Technogenic factors caused by economic activity may exacerbate these problems.

Large-scale development of the Russian Arctic entails greater number of breakdowns of engineering systems and higher risks of accidents. In order to decrease the risks associated with the development of Northern Regions on permafrost, the establishment of permafrost monitoring system in both natural and technogenic conditions (within urban areas) is critically important. The spatially distributed permafrost monitoring system will provide permafrost and other environmental observational data for a series of representative sites with high order of accuracy and reliability. The status of "State Research Sites" would insure long-term monitoring. The observational data from these sites will create a foundation for regional geographic assessments and permafrost forecast. The location of monitoring sites in the proposed State Program "RUSSIAN PERMAFROST" should be based on the appropriate zoning of Russian permafrost regions based on the characteristics discussed above. The map presents the results of such classification with a location of monitoring sites of state and local levels based on a hierarchical design and different levels of data aggregation (Fig. 1).

Hierarchical zoning of the Cryolithozone is performed sequentially in three steps. At first, the geological and tectonic characteristics were used (for the highest level of hierarchy). The morphostructural factor is involved at the second stage. Geocryological

and geomorphological characteristics were taken into account for the lowest level. Regions of the higher (state) level are sub-continental geological and tectonic structures (Roman numerals on the map); Regions of the mid-level are correlated with morphological structures (Arabic numbers on the map); regions of the lower (local) level associated with the types of frozen ground which is widespread at some geomorphological elements (river valleys, terranes, intermountain valleys, plateaus, mountain, etc. – color on the map).

Stations of the highest level (State Research Stations) should characterize the geographic sector and landscape province and collect all range of climatic, environmental and permafrost conditions. The Local Stations should collect primary information about changes of permafrost parameters. Currently the feasibility of connection of local permafrost stations with the existing network of weather stations in Russia and WMO is discussed under the umbrella of Global Cryosphere Watch (GCW) project.

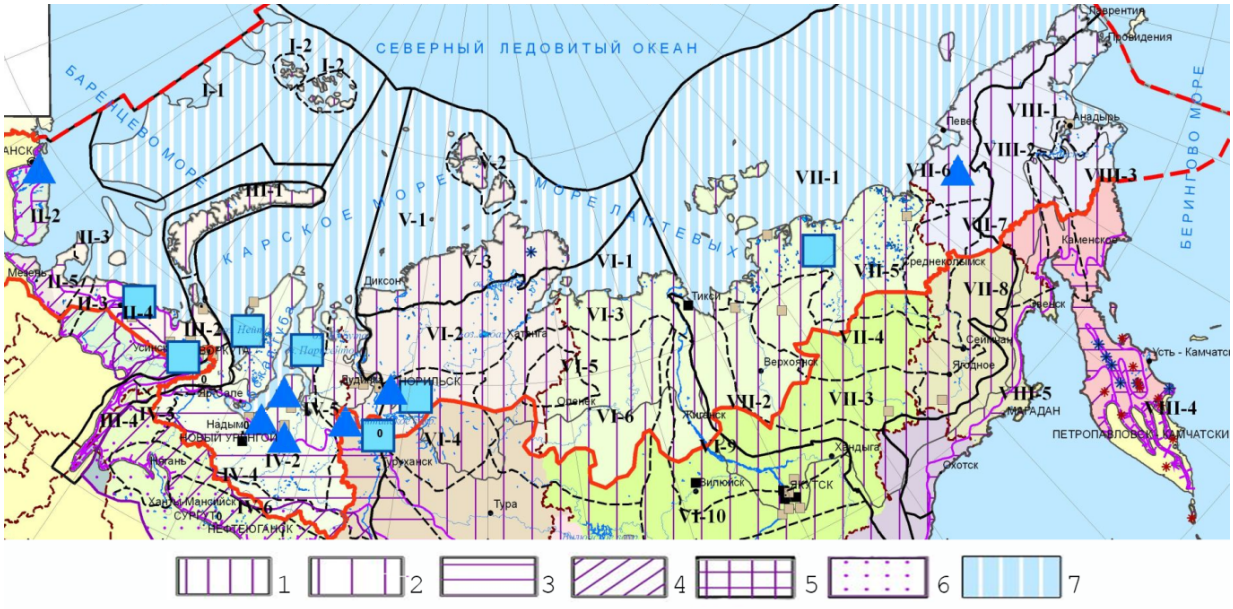

Figure 1: Zoning of Russian permafrost regions based on geo-structural characteristics. Red line is the official border of the Russian Arctic Zone; light-blue squares are proposed State Research Stations; blue triangles – the local stations and sites Permafrost characteristics (extent and temperature): 1 – continuous, t<5 °C; 2 – continuous, t= 1... 5 °C; 3 – discontinuous; 4 – sporadic; 5 – continuous and discontinuous in the mountains; 6 – deep frozen relics; 7 – sub-sea

Site-specific terrestrial model intercomparison of subsurface thermal regime in circum-Arctic region

Junko Mori[1,2], Kazuyuki Saito[2], Shin Miyazaki[3], Hirokazu Machiya[1,2], Yoshihiro Iijima[2], & Group GTMIP[2]

[1]*National Institute of Polar Research, Japan*; [2]*Japan Agency for Marine-Earth Science and Technology*
[3]*Sonic Corporation, Japan*

GRENE-TEA Model Intercomparison Project (GTMIP) is one of the modeling group's activities in "the terrestrial research project of the GRENE Arctic Climate Change Research Project" (GRENE-TEA), conducted in Japan. GTMIP stage 1, site simulations at GRENE-TEA observation sites using the common driving data elaborately combining reanalysis and site observation data, aims to assess the inter-model variations and the site-specific differences in energy, water and carbon budget and dynamics, to investigate the attributions of the implemented processes and their complexity of the models to those differences, and to propose possible improvements of physical and biogeochemical processes for the next generation modeling of the Arctic terrestrial (excl. glaciers and ice sheets).

Permafrost condition is one of the key elements in the circum-Arctic region, a hub to various physical and biogeochemical processes. Presence of permafrost controls soil moisture variability in time and space, modifying vegetation growth and carbon budget. In this study, we compared and evaluated the GTMIP output data with special attention to the subsurface thermal regime and relevant elements.

23 models participated in GTMIP, among which 11 models calculate explicitly ground thermal condition: physical land surface models (2LM, JULES, MATSIRO with 4 versions), a physical and biogeochemical soil dynamics model (PB-SDM), a terrestrial biogeochemical model (VISIT), a land surface model with carbon cycle (JULES-C), dynamic global vegetation models (SEIB-DGVM coupled with a land surface model (Noah-LSM)), and a coupled hydrological and biogeochemical model (CHANGE).

Driving and validation data were produced for the four GRENE-TEA observation sites: Fairbanks (USA), Kevo (Finland), Tiksi (Russia) and Yakutsk (Russia), which have different characteristics in terms of snow accumulation, ground freezing condition (seasonal freezing/permafrost), vegetation (taiga/tundra) and continentality.

The 34-year 30-minutes-interval forcing data (1980-2013) was created primarily from reanalysis data to compensate gaps and limitations in observation data. This dataset (level 0) was based on ERA-interim with local correction by CRU for air temperature and by GPCP for precipitation. Then, the site specific driving data (level 1) was created by fitting the level 0 data to the observations at the sites to inherit the site characteristics while securing enough temporal coverage.

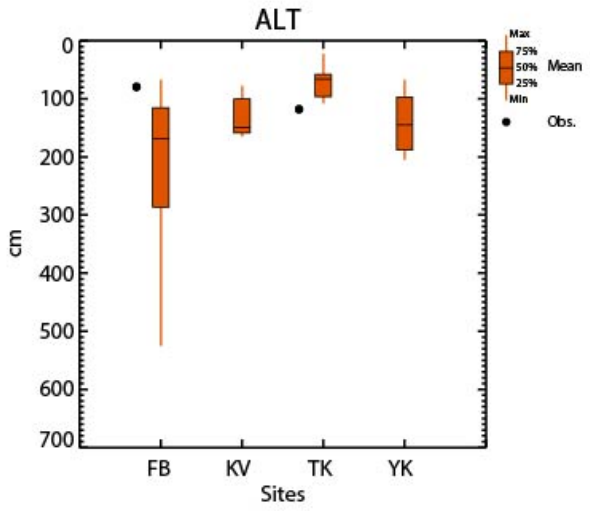

Figure 1: Boxplot showing the 34-year mean value of active layer thickness among the models. Black dots are the mean value of observation data for 19-years for Tiksi and 3-years for Fairbanks.

Fig. 1 shows box-whisker plot of the 34-year mean active layer thickness (ALT) among the models and observation. In Tiksi and Yakutsk, the two sites underlain by continuous permafrost, the calculated ALT values did not show large variation. For Kevo in seasonal frozen ground zone, however, 4 models calculated the existence of permafrost. For Fairbanks, locating in discontinuous permafrost zone, some models showed very deep ALT while other two models simulated no permafrost. In the margin of permafrost and seasonal frozen ground, the simulated ALT values exhibited high sensitivity to snow dynamics, and high variations among the models.

Connection of climatic agents with active layer depth dynamics on the Central Yamal

Damir R. Mullanurov, Yury A. Dvornikov, Artem Khomutov, & Andrey Polukhin

Earth Cryosphere Institute, Siberian Branch of Russian Academy of Sciences, Russian Federation

Active layer is one of the most variable components of permafrost study (Leibman, 2001). Research of this component is actual for the reason of global climate change [Konstantinov et al., 2006]. Dynamics of active layer depth on the Central Yamal in 1993-2000 is considered in [Leibman, 2001]. Main factors which influence active layer depth are determined. These parameters are air temperature, relief, vegetation cover, and substratum. Last three agents form persistent relation and this relation is unaltered for the short time period of 10 years. Air temperature and precipitation impact on the active layer depth is considered in this study for the period 1999-2015.

A period from September 1st to August 31st is referred to as rated year. The date of August 31st as the end of the rated year is considered as the nearest to the date of active-layer measurement day and corresponds to the date of maximum thawing depth.

Active layer depth records were obtained by annual field measurements (a gap in 2003). CALM site is a key site 100x100 m in size with 121 points through a 10 m-cell grid located on the Central Yamal, Vaskiny Dachi station. Key site is on the flat hilltop with sandy-silty composition and loamy slope underlain by clay.

Data from 99 gridnodes were used in calculations because the rest of the 22 points have unreliable data due to saline clay within the active layer. In table 1 data is presented for each rated year: mean, maximum and minimum active layer depth (ALD). Also average long-term data are presented in table 1.

The deepest thaw was observed in 2011-2013 and in 2014/2015 rated years. Mean active layer depth (for 99 points) in 2011/2012 is 102 cm (more than average long-term ALD of 91 cm, by 31 cm higher). At the same time, mean air temperature in 2011/2012 is almost twice higher than average long-term value (-6.7 °C and -3.4 °C respectively). Total annual precipitation in 2011/2012 (526 mm) exceeds average long-term value (425.9 mm) by 100 mm. In 2012/2013 ALD is 103 cm, but mean annual air temperature (-6.3 °C) is close to average long-term value (-6.7 °C) as is total precipitation (407.2 mm)

Mean annual air temperature and total precipitation dynamics do not reflect the active layer depth dynamics in full. Correlation coefficients of these parameters with active layer depth are given in table 1. The highest correlation is observed with freezing and thawing index. In the table 1 and discussion below these indexes in degree hours are divided by 1000. Average long-term thawing and freezing index are 18.2 °C/hour and -128.6 °C/hour respectively.

Correlation coefficient between ALD and thawing index is 0.69, between ALD and freezing index is 0.74. 2011/2012 is characterized by maximum thawing and freezing index: 25.5 °C/hour and -97.6 °C/hour. 2012/2013 are also characterized by high by absolute value (but less than in 2011/2012) freezing and thawing index: 20.5 °C/hour and -117.0 °C/hour, respectively. But ALD in 2012/2013 is higher than in 2011/2012 by 1 cm (103 versus 102 cm). The reason of such effect could be attributed to the effect of previous year when ground temperature in the active layer was so high.

In 2008/2009 minimum mean ALD was observed: 73 cm. This year is characterized by mean annual air temperature -6.3 °C. This value is very close to average long-term value (-6.7 °C). Also high total precipitation observed in this year: 520.2 mm. Thawing index is very close to average long term value 18.3 °C/hour, and freezing index is less by absolute value than average long-term value (-120.8 °C/hour).

A wide range of climatic controls results in a wide range of the active layer depth interannual dynamics. Maximum active layer depth in 1999-2015 for 99 points average is 103 cm, minimum – 73 cm. Variation coefficient of ALD is 8 %. Mean annual air temperature variation coefficient is 21 %, thawing and freezing index variation coefficient is 19 % and 10 % respectively. High value of total precipitation corresponds to the year with maximum ALD as well as to the year with minimum ALD. This fact argues that clear link between ALD and total precipitation is not observed.

Table 1: Main climatic parameters, active-layer depth range and their correlation (Tair – mean annual air temperature, Ti – thawing index, Fi – freezing index, R – total precipitation)

Year		Active layer depth			Tair	Ti/1000	Fi/1000	R
		Mean	Max	Min				
1999/2000		89	115	69	-5.8	15.8	-134.0	
2000/2001		90	117	70	-9.4	17.0	-146.8	
2001/2002		89	115	69	-7.0	17.2	-143.6	
2002/2003					-7.6	15.3	-129.4	
2003/2004		90	116	70	-7.4	21.3	-131.6	
2004/2005		93	121	71	-6.9	17.7	-126.2	
2005/2006		93	123	74	-6.4	21.1	-128.9	417.2
2006/2007		90	120	69	-6.4	18.9	-133.7	330.8
2007/2008		93	135	72	-5.2	21.1	-113.0	533.4
2008/2009		73	108	40	-6.3	18.3	-120.8	520.2
2009/2010		84	120	59	-8.9	14.6	-148.4	384.5
2010/2011		87	119	61	-6.1	14.5	-125.8	431.4
2011/2012		102	169	75	-3.4	25.5	-97.6	526.2
2012/2013		103	150	76	-6.3	20.5	-117.0	407.2
2013/2014		92	130	64	-7.7	12.2	-135.3	343.8
2014/2015		101	150	73	-6.0	21.1	-126.0	364.2
Average		**91.3**	**127.2**	**67.5**	**-6.7**	**18.3**	**-128.6**	**425.9**
Max		**103**	**169**	**76**	**-3.4**	**25.5**	**-97.6**	**533.4**
Min		**73**	**108**	**40**	**-9.4**	**12.2**	**-14.8**	**330.8**
Standard deviation		5.7	16.6	5.0	1.4	3.4	12.8	76.2
Variation coefficient		8%	13%	13%	21%	19%	10%	18%
Correlation coefficient with:	Tair	0.58	0.65	0.51				
	Ti	0.69	0.64	0.82				
	Fi	0.74	0.80	0.58				
	R	-0.15	0.17	-0.19				

Thus, dynamics of ALD is mainly defined by thawing and freezing index. Estimation of the impact degree is quite a difficult problem because of the wide range of parameters: maximum variation 19%. In addition, influence of precipitation and other factors (vegetation, relief) which do not have clear relations complicates this problem.

References

Konstantinov, P.Ya.; R.N., Argunov; E.Y., Gerasimov and I.S., Ugarov. [2006]: On the relationship between seasonal thaw depth and interannual variation of mean annual ground temperature. *Kriosfera Zemli (Earth Cryosphere)*, 10(3):15–22, 2006. URL http://www.izdatgeo.ru/pdf/krio/2006-3/15.pdf.

Leibman, M.O. [2001]: Active-layer dynamics and measurement technique at various landscapes of Central Yamal. *Earth Cryosphere*, 5(3):17–24, URL http://www.izdatgeo.ru/pdf/earth_cryo/2014-4/20_eng.pdf.

The contribution of the 2015 heat wave to mountain permafrost warming in Switzerland

Jeannette Nötzli[1], Reynald Delaloye[2], Isabelle Gärtner-Roer[3], Andreas Hasler[4], Christian Hauck[2], Christin Hilbich[2], Martin Hoelzle[2], Christophe Lambiel[5], Marcia Phillips[1], Cristian Scapozza[6], Sarah M. Springman[7], Benno Staub[2], & Daniel Vonder Mühll[7,8]

[1] *WSL Institute for Snow and Avalanche Research SLF, Davos, Switzerland*
[2] *Department of Geosciences, University of Fribourg, Switzerland*
[3] *Department of Geography, University of Zurich, Switzerland*
[4] *SensAlpin GmbH, Davos, Switzerland*
[5] *Institute of Earth Surface Dynamics, University of Lausanne, Switzerland*
[6] *Institute of Earth Sciences, University of Applied Sciences and Arts of Southern Switzerland, Canobbio, Switzerland*
[7] *Institute for Geotechnical Engineering, ETH Zurich, Zurich, Switzerland*
[8] *SystemsX.ch, Zurich, Switzerland*

Summer 2015 was the second warmest in Switzerland after the heat wave in summer 2003 and about 2.5 °C higher than the mean 1981–2010 (MeteoSwiss 2015). The year 2015 is likely to become (one of) the warmest ever recorded: annual mean air temperatures have been above average and show positive trends for nearly 30 years. This presentation provides an overview on the permafrost conditions measured in the framework of the Swiss Permafrost Monitoring Network (PERMOS) in the Alps during the extraordinary summers 2003 and 2015, and puts the results into perspective of the total available data series since the start of PERMOS in the year 2000.

Record values were reported in, or following, the year 2003 for nearly all sites and observation elements of the network: surface and subsurface temperature, active layer thickness, creep velocity and electrical resistivities (PERMOS 2007). In addition, an exceptionally large number of rock falls was reported in 2003 from high elevation areas that were possibly related to deepened active layers in bedrock permafrost (Gruber et al. 2004). The permafrost conditions were warmer than 2003 after the 2015 heat wave and a high number of rock falls has also been reported from permafrost areas during this summer. Most failures occurred at shallow depths that are influenced by seasonal temperature variations, with a peak of activity in the beginning of August. The largest incident registered occurred at 3400 m asl in the western flank of the Grande Dent de Veisivi (Valais), with an estimated volume of 80 000 m3. The events took place at all hours of the day and in all aspects, except South.

Summer heat waves typically lead to an increase of the mean annual ground surface temperature (MAGST) of ca. 0.5–1 °C. MAGST values (calculated as running annual average) in 2015 do not seem to exceed those in 2003, but show an accelerated increase. This can be explained mainly by the winter conditions, which are crucial for the ground thermal regime in snow covered areas. Winter 2002/2003 was one of the two warmest at the ground surface since the beginning of systematic measurements in the late 1990s and, hence, ground surface temperatures were at a very high level in spring already. Ground surface temperatures were lower in winter 2014/2015 because of a later onset of an insulating snow cover in autumn 2014 and a slightly longer lasting of the snow in summer 2015. MAGST were extreme in July 2015 and exceeded the previous record values from August 2003 at most of the observation sites. Mean summer GST (June–October) and the related ground surface thawing index did however not exceed the values measured in 2003.

In contrast, the active layer thickness (ALT) has reached new record values at most sites in 2015. Even very ice rich locations such as the rock glacier Murtèl-Corvatsch show recent changes in ALT, whereas no impact was observed in 2003: the ALT remained between 3.2 and 3.5 m since the start of measurements in 1987 and exceeded 4.0 m for the past four years. The maximum ALT is likely not to have been reached by the end of November 2015 for several

sites, although values are at record level already. At Schilthorn for example, ALT is currently at nearly 10 m (below 9 m in 2003) and the temperature at 9 m depth has been above the freezing point for the first time. The maximum ALT becomes deeper, with the timing shifted towards the end of the year.

The permafrost temperatures at depths of 10 m and more measured with thermistor chains in boreholes reveal a clear warming trend period since 2009 for most of the sites and are generally higher today than ever measured (Fig. 1). Winter ground temperatures have been remarkably high at a depth of 10 m during this period, especially for sites with temperatures only just below the melting point. This warming trend period is confirmed by the other elements observed within the monitoring network: Horizontal velocities of the observed rock glaciers have increased since 2006 and are at record level for most of the sites. Their temporal pattern seems to follow an exponential relationship to permafrost temperature and displacement rates of several m/year are becoming frequent. Further, geoelectrical monitoring reveals decreasing resistivities pointing to significant ice loss and increasing amount of unfrozen water, especially over the past seven years. This can be seen both, in the active layer and in the permafrost body.

These record values are not likely to be an effect of the 2015 heat wave alone, but a cumulative result of a series of very warm years. During the previous seven years, continuously warm to very warm permafrost conditions were recorded, compared to the entire measurement period of up to more than 20 years. This resulted in ground temperatures that were significantly higher before the 2015 heat wave than before the one in 2003. The response of permafrost substrates at depth below the uppermost meters will mainly be observed in 2016 due to the inertia of heat diffusion. Finally, the winter 2015/2016, and in particular the timing of the first thicker snow cover, will either redress or enhance the effects of summer 2015.

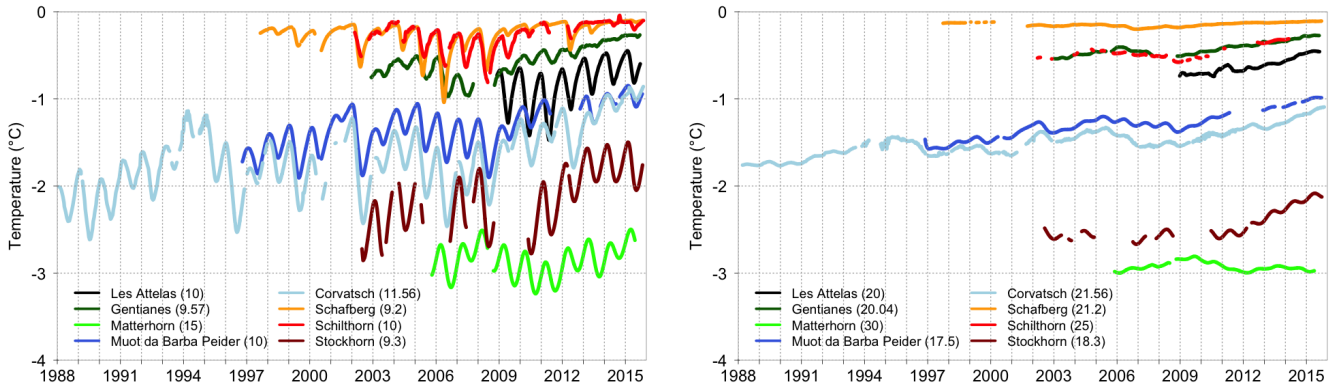

Figure 1: Borehole temperatures at ca. 10 m (left) and 20 m (right) depth for sites for which the 2015 data have already been obtained. The past seven years show a warming trend in all of the boreholes with particularly high winter ground temperatures.

Thermal conditions of permafrost on Peel Plateau, Northwest Territories, Canada

Brendan O'Neill[1], Chris Burn[1], & Steve Kokelj[2]

[1] *Carleton University, Canada*
[2] *Northwest Territories Geological Survey*

Peel Plateau is an extensive upland in Canada's western Arctic, covering nearly 60,000 km^2 of Northwest Territories and Yukon. In Northwest Territories, the plateau lies between the Richardson Mountains to the west, and the Peel Plain lowlands to the east. The Dempster Highway, the only all-season roadto Canada's western Arctic, traverses Peel Plateau on its route towards Fort McPherson, Tsiigehtchic, and Inuvik. The road passes through tundra at higher elevation near the top of the plateau, into forest at lower elevation. The continuous permafrost on Peel Plateau is characteristically ice rich in the near surface, and extensive massive ice is present at depth. Large retrogressive-thaw slumps are common [Lacelle et al., 2015], and the road has required heavy maintenance in recent years to address problems associated with the thaw of ice-rich permafrost [Burn et al., 2015]. The study area on Peel Plateau has a subarctic, continental climate, with a mean annual air temperature (1987-2006) of -7.0 °C recorded at Fort McPherson, the nearest meteorological station.

This presentation highlights distinct permafrost thermal regimes from three settings on Peel Plateau:

1. undisturbed dwarf-shrub tundra
2. disturbed tundra permafrost adjacent to the Dempster Highway, and
3. tundra water tracks, characterized by tall shrubs, saturated ground, and deep snow cover.

These observations are from a Ph.D. field campaign from 2011–15.

Annual mean ground temperatures in undisturbed tundra on Peel Plateau are relatively high for the continuous permafrost zone (commonly >-2.5 °C). This is partly due to strong winter air temperature inversions between Peel Plateau and Peel Plain that reduce the severity of the freezing season at higher elevations, and because of a deep snow cover. Snow depths on Peel Plateau, above elevational tree line, are greater than than in tundra north of latitudinal tree line near Inuvik [O'Neill et al., 2015], due to the structure of vegetation and greater snow fall.

Permafrost at the toe of the Dempster Highway embankment, where deep snow accumulates early in the freezing season, is presently degrading. Annual mean ground temperatures at four degrading sites were between -1.3 and 0.0 °C in 2012–15, and summer thaw is up to 5 m.

Near-surface ground temperatures in water tracks are elevated as at disturbed road sites, but their effect on deeper ground temperatures is limited due to the width of the features. Unlike at sites beside the road, deep snow and warm near-surface conditions in winter do not contribute to permafrost degradation in water tracks due to contrasting summer thermal regimes at these sites. Summer ground temperatures in water tracks are lower because of shading by shrub cover and organic matter accumulation.

These three settings on Peel Plateau will likely respond differently to future climate change. Disturbed road sites and water track sites will not readily respond to projected warming winter air temperatures due to thick snow cover, in contrast with undisturbed dwarf-shrub tundra. However, water tracks may be affected by thermal erosion if precipitation and runoff increases, and improvements in drainage management beside the road will be required.

References

Burn, C.R.; Moore, J.L.; O'Neill, H.B.; Hayley, D.W.; Trimble, J.R.; Calmels, F.; Orban, S.N. and Idrees, M. [2015]: Permafrost characterization of the Dempster Highway, Yukon and Northwest Territories. Paper 705. In *Proceedings, 68th Canadian Geotechnical Conference and 7th Canadian Permafrost Conference,* 21-23 September 2015, Quebec City, QC, Canadian Geotechnical Society, Richmond, BC, page 8,

Lacelle, D.; Brooker, A.; Fraser, R.H. and Kokelj, S.V. [2015]: Distribution and growth of thaw slumps in the Richardson Mountains–Peel Plateau region, northwestern Canada. *Geomorphology*, 235:40–51, doi:10.1016/j.geomorph.2015.01.024.

O'Neill, H. B.; Burn, C. R.; Kokelj, S. V. and Lantz, T. C. [2015]: 'Warm' Tundra: Atmospheric and Near-Surface Ground Temperature Inversions Across an Alpine Treeline in Continuous Permafrost, Western Arctic, Canada. *Permafrost and Periglacial Processes*, 26(2):103–118, doi:10.1002/ppp.1838.

Absence of permafrost conditions at the top of the Veleta Peak (Sierra Nevada, Spain)

Marc Oliva[1], Antonio Gómez-Ortiz[2], Ferran Salvador-Franch[2], Montserrat Salvà-Catarineu[2], David Palacios[3], Luis Miguel Tanarro[3], Miguel Ramos[4], Paulo Pereira[5], & Jesús Ruiz-Fernández[6]

[1]*Institute of Geography and Spatial Planning – CEG, Universidade de Lisboa, Portugal*
[2]*Department for Physical and Regional Geography, University of Barcelona*
[3]*Department for Regional and Physical Geography, Complutense University of Madrid*
[4]*Department of Physics, University of Alcalá*
[5]*Environmental Management Center, Mykolas Romeris University*
[6]*Department of Geography, University of Oviedo*

A 114.5 m deep drilling was carried out in the bedrock of the Veleta peak, at 3380 m in the massif of Sierra Nevada, Southern Spain. From September 2002 to August 2013, eleven thermal loggers have been recording soil temperatures at different levels along the first 60 m depth, together with air temperatures at the summit of the Veleta peak (Fig. 1).

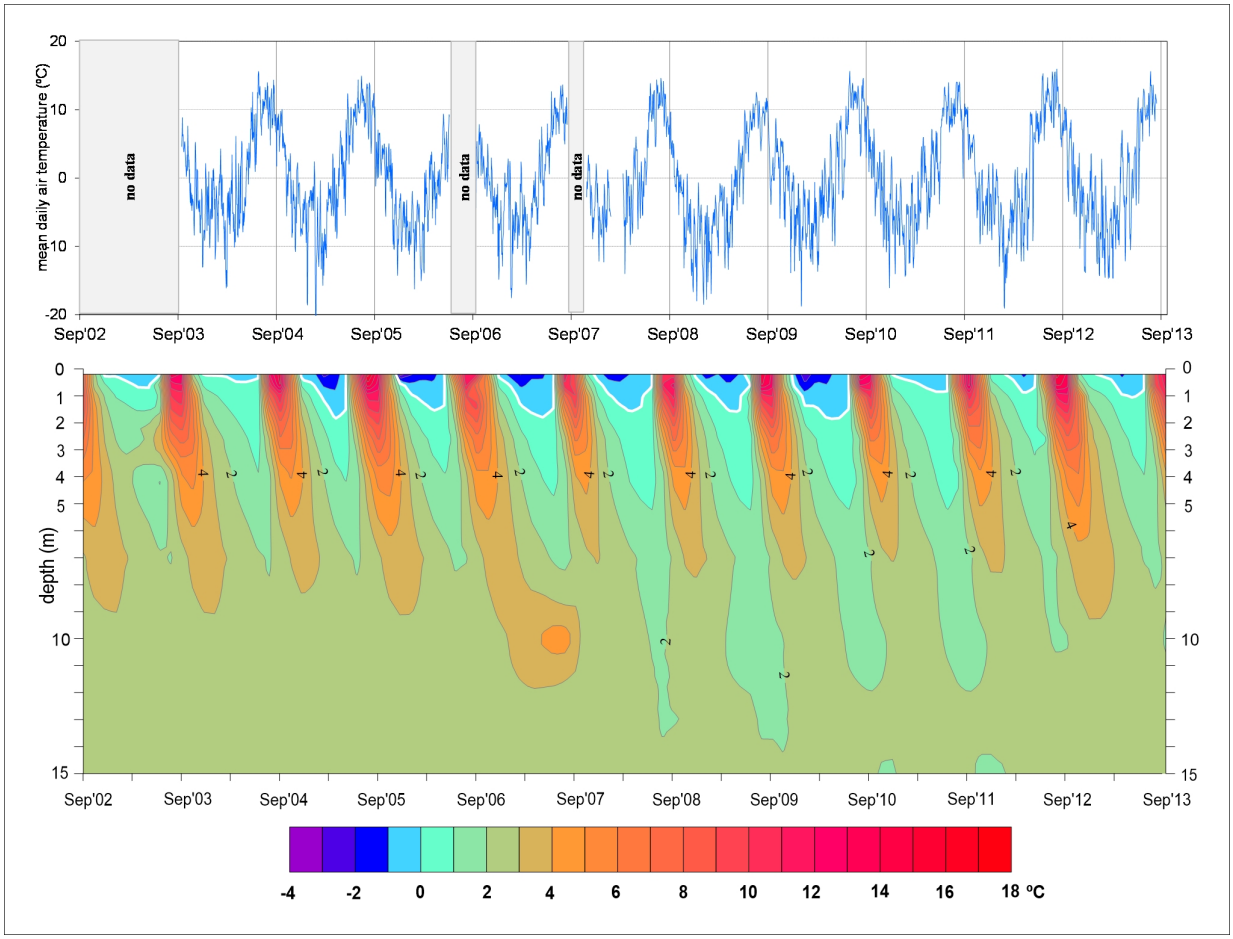

Figure 1: Evolution of the mean daily air and bedrock temperatures in the uppermost 15 m during the period 2002-2013.

Permanent negative temperatures have not been detected in the borehole, which indicates the absence of permafrost conditions nowadays in the summits of Sierra Nevada. Bedrock temperatures oscillated between 3.2 °C at 0.6 m depth and 2 °C at 20 m below the surface. The largest temperature ranges were recorded on the most surficial layers until 1.2 m depth, where values reached 22.3 °C. Seasonal temperature variations were significant until 10 m depth. The thickness of the seasonal frozen layer was highly variable (0.6-2 m) and dependent on annual climate conditions. The mean air temperature at the Veleta peak increased by 0.12 °C during the study period. Bedrock temperatures followed diverging trends: a drop of 0.3-0.4 °C down to 0.6 m depth, a decrease of up to 0.7 °C between 4 and 10 m, thermal stability at 20 m and a rise of 0.2 °C that occurred in 2009 at the deepest sensor at 60 m. The calculation of the thermal wave damping in the subsoil of the Veleta peak has allowed for quantifying the thermal diffusivity of the rock as 7.05 ± 0.03.10-7 m^2/s, which means that the external climate signal arrives with an 8.5-year lag to the sensor at 60 m deep. This allows to deduce a trend change in the climate of the area, moving from warmer conditions towards a trend of cooling from 2006 to 2007.

Model assessment of influences of snow depth on pan-Arctic permafrost temperature

Hotaek Park[1], Alexander N. Fedorov[2], & Pavel Y. Konstantinov[2]

[1] *JAMSTEC, Japan*
[2] *Melnikov Permafrost Institute, SB RAS, Yakutsk, Russia*

This study quantitatively evaluated how insulation by snow depth (SND) affected the soil thermal regime and permafrost degradation in the pan-Arctic area, and more generally defined the characteristics of soil temperature (TSOIL) and SND from 1901 to 2009. This was achieved through experiments performed with the land surface model CHANGE to assess sensitivity to winter precipitation as well as air temperature. Northernmost regions had snow that remained relatively stable and in a thicker state during the past four decades, generating greater increases in TSOIL. Changes in snow cover have led to changes in the thermal state of the underlying soil, which is strongly dependent on both the magnitude and the timing of changes in snowfall. Permafrost loss was greater when SND increased in autumn rather than in winter, due to insulation of the soil resulting from early cooling. Simulations revealed that TSOIL tended to increase over most of the pan-Arctic from 1901 to 2009, and that this increase was significant in northern regions, especially in northeastern Siberia where SND is responsible for 50 % or more of the changes in TSOIL at a depth of 3.6 m. In the same region, ALT also increased at a rate of approximately 2.3 cm per decade. The most sensitive response of ALT to changes in SND appeared in the southern boundary regions of permafrost, in contrast to permafrost temperatures within the 60° N–80°N region, which were more sensitive to changes in snow cover. Finally, our model suggests that snow cover contributes to the warming of permafrost in northern regions and could play a more important role under conditions of future Arctic warming.

Analysis of ground temperature and active layer thickness monitoring results in relation to a number of climatic controls at Vaskiny Dachi research station, Yamal, Russia

Andrey N. Polukhin[1], Yury A. Dvornikov[2], Artem V. Khomutov[2], Marina O. Leibman[2], Damir R. Mullanurov[2], & Dmitry D. Perednya[2]

[1] *Tyumen State Oil and Gas University, Tyumen, Russian Federation*
[2] *Earth Cryosphere Institute, Siberian Branch of Russian Academy of Sciences, Tyumen, Russian Federation*

Research is devoted to analysis of an impact of a number of climatic controls on interannual dynamics of the active layer thickness and temperature, monitored at Vaskiny Dachi research station in Central Yamal, Russia. Data of measurements in 1.5 m deep borehole and one adjacent grid point of the CALM site R5 were analyzed to exclude other climatic controls (vegetation, redistribution of snow). This grid point is on the hill top of the III-d alluvial-marine plain with sparse vegetation, sandy-silty deposits in the active layer, well drained and wind blowns snow. Monitoring data used are Marre-Sale weather station records, corrected after quality control and calculated as follows: mean annual air temperature for a calendar year, thaw index in degree days for a calendar summer, freeze index for a season (first half from the previous year and second half from the next year), summer (calendar) and winter (seasonal) precipitation, duration of the thaw and freeze periods. Monitoring data included active layer thickness for the period 2006-2015 and ground temperature at the depth of 1.5 m for 2009-2015. Monitoring data and weather station records were normalized by the average for the given period to better visualize correlation and trends.

For climatic parameters it was established that mean annual airtemperature and thaw index show slight cooling trend,while freeze index becomes slightly warmer, with high-amplitude fluctuations from year to year. Essential interannual fluctuations of atmospheric precipitation at the same time show negligible trend of winter precipitation and noticeable reduction of summer precipitation during the analyzed period.

Pairing correlation of normalized climatic parameters and both active layer thickness and ground temperature does not show satisfactory results. Active layer thickness correlation is quite low with the highest factors (0.50 and 0.49) for thaw index and freeze index respectively.

Mean annual ground temperature at the depth 1.5 m is expectedly best related to freeze index (0.85) and mean annual air temperature (0.80). There is negligible correlation between ground temperature and other factors. Little effect of snow is explained by wind redistribution, which depends on the wind speed rather than on total precipitation.

Parameters were also correlated to each other using R 3.2.2 statistical software (corrplot package, Fig. 1). As it was described above, the correlation of 0.5 was observed between ALT and freeze and thaw indexes (FI, TI). Lower correlation (0.41) was found between ALT and mean annual air temperature (MAAT). The same parameters showed the correlation with mean annual temperature at 1.5 meters (MTa). The correlation between MTa and FI, TI, MAAT was 0.85, 0.58 and 0.77 respectively. Based on this we conclude, that FI, TI, MAAT are the most important variables explaining the ALT and MTa variations, if the other controls like snow depth, landscape conditions are excluded.

Thus, ground-temperature trends for the period 2009-2015 are positive. The trend in active layer thickness for the period 2006-2015 trend is also positive. Variation in a single climatic parameter does not explain these trends. One reason is too a short period for real time-dependant statistics. Second, combination of various climatic controls is more important than pairing correlations.

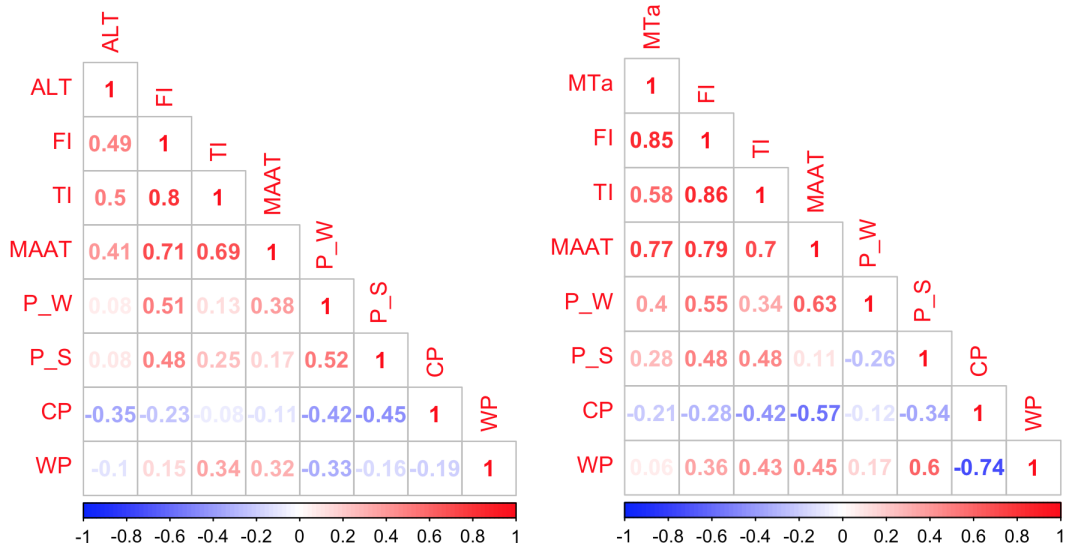

Figure 1: Correlation plots for ALT (left) and MTa (ground temperature, right): FI, freeze index; TI, thaw index; MAAT, mean annual air temperature; P_W, winter precipitation; P_S, summer precipitation; CP, length of the cold period; WP, length of the warm period

Hoher Sonnblick: A super site for monitoring the cryosphere

Claudia Riedl[1], Stefan Reisenhofer[1], Daniel Binder[2], Annett Bartsch[3], Adrian Flores-Orozco[2], Georg Heinrich[3], Wolfgang Schöner[3], Stefan Pfeiler[4], Robert Supper[4], & Ingo Hartmeyer[5]

[1] *ZAMG, Austria*
[2] *University of Vienna, Austria*
[3] *University of Graz, Austria*
[4] *Geological Survey, Austria*
[5] *University of Salzburg, Austria*

The Sonnblick Observatory at the summit of Hoher Sonnblick (3106 m a.s.l.), Austria, is an outstanding research station established in 1886. Since then ongoing research covers studies and monitoring of the atmosphere, the hydrosphere, the cryosphere, the lithosphere and the biosphere. The permafrost monitoring of the summit of Hoher Sonnblick was initially motivated because of the instability due to permafrost degradation that threatened local buildings and the associated stabilization work. The distribution of and changes in permafrost are under constant monitoring at the Sonnblick and on the adjacent hill slope Wintergasse since 2006. These measurements contribute to Cryonet - Sonnblick in one of the'integrated sites'within the Global Cryosphere Watch Program of the WMO.

In the Sonnblick area permafrost is probable above 2500 m in north faces and above 2750 m in south faces. An extensive observation network for ground surface, shallow and deep borehole temperatures, snow monitoring and geophysical measurements is established.

On the southern slope of Hoher Sonnblick continuous temperature measurements from three 20 m deep boreholes are available and can be viewed on the Web at www.sonnblick.net. Additionally, two Extensometer in 3 m and 5 m depth are installed in borehole 2 to survey permafrost-related crack movements. Close to this site in the investigation area Wintergasse measurements of 'Ground-Surface Temperature' (GST) and 'Bottom Temperatures of the Snow cover' (BTS) have been carried out since 2006. Additionally, since 2010 every year few shallow boreholes with depths between 40 and 140 cm have installed to determine near-surface temperature. Each of these boreholes is equipped with four temperature sensors with a spacing between 10 and 20 cm to reach a probable geothermal gradient.

In summer 2015 three-component geophones were installed in the topmost 20 m deep borehole and at the foot of the Sonnblick north face for the quantitative observation and understanding of high alpine seismicity and rockfall events. Terrestrial based LiDAR completes the rock fall activity monitoring and the seismic network. Surface status monitoring is currently implemented in addition based on the satellite data from Sentinel-1.

In cooperation with the Geological Survey of Austria a permanently installed ERT array was established in July 2015 in the upper summit area of Hoher Sonnblick, which supply continuous information on near-surface ground thermal conditions to a depth of approximately 10 m in a high spatial resolution. ERT results from the first year of prospection are shown.

According to active seismic measurements in the years 2008 and 2009 repetitive measurements were performed in the summer 2015. The evaluation of these results are presented. Furthermore, the results of the first electromagnetic survey are shown.

Past, present and future changes in permafrost temperatures in Alaska

Vladimir E. Romanovsky, Dmitry J. Nicolsky, Sergey S. Marchenko, William L. Cable, Alexander L. Kholodov, Santosh K. Panda, & Reginald R. Muskett

University of Alaska Fairbanks, United States of America

The impact of climate warming on permafrost and the potential of climate feedbacks resulting from permafrost thawing have recently received a great deal of attention. Ground temperatures are a primary indicator of permafrost stability. The monitoring network of the Thermal State of Permafrost (TSP) program was established during the Fourth International Polar Year. In Alaska, two major permafrost temperature measurement networks exist. One of them is operated by the U. S. Geological Survey predominantly within the North Slope of Alaska. The second network was established in the late-1970s and early-1980s by Professor Emeritus T. E. Osterkamp and has been supported since then by the Permafrost Lab at the Geophysical Institute, University of Alaska Fairbanks [Osterkamp, 2003]. Most of the research sites in our network are located along an Alaskan Permafrost-Ecological Transect. This transect spans all permafrost zones in Alaska from the southern limits of permafrost near Glennallen to the Arctic coast in the Prudhoe Bay region.

In this paper, the results of more than 30 years of the permafrost and active layer temperature observations along this transect will be presented. Most of the sites in Alaska show substantial warming of permafrost since the 1980s. The magnitude of warming has varied with location, but was typically from 0.5 to 3 °C. However, this warming was not linear in time and not spatially uniform (Fig. 1). While permafrost warming was more or less continuous on the North Slope of Alaska with a rate between 0.2 to 0.5 °C per decade, permafrost temperatures in the Alaskan Interior started to experience a slight cooling in the 2000s that has continued during the first half of the 2010s. There are some indications that the warming trend in the Alaskan Interior permafrost resumed during the last two years. In 2015, new record high temperatures, at 20 m depth, were measured at all permafrost observatories on the North Slope of Alaska.

Based on our observations, permafrost temperature obviously follows the changes in the mean annual ground temperature that, in turn, follows the changes in mean annual air temperature. The decadal time scale trend in permafrost temperature at our three northernmost sites (West Dock, Deadhorse, and Franklin Bluffs) is almost identical to the decadal trend in the air temperature at these sites. This may be an indication that there was no significant trend in the snow cover depth in this area of the Alaskan Arctic during the last 30 years. Only recently (during the last 5 years), it seems that the rate of change in near-surface permafrost temperatures have begun to exceed the rate of increase in the air temperature. This may indicate some increasing trend in snow cover depth during this period. The latest climate warming brought near-surface ground temperatures on the Alaskan North Slope to an unprecedented high level. While the mean annual temperatures at the ground and permafrost surfaces at Deadhorse in mid-1980s were near -8 °C, in 2014 the mean annual temperature at the ground surface was only -1.3 °C and -2.2 °C at the surface of permafrost. These temperatures were just slightly lower (-1.8 and -2.6 °C respectively) at the Franklin Bluffs site. This magnitude of ground surface and permafrost surface temperatures are more typical for the Alaskan Interior and indicate that permafrost in some areas of the North Slope is losing its thermal stability.

Analysis of the seasonality of changes in ground temperature shows that the warming is occurring in both summer and winter, but the major part of increase occurs during the cold season. As a result, the re-freezing of the active layer takes more and more time. While the complete freeze-up of the active layer in northern Alaska in the mid-1980s typically occurred in the first half of October, the typical freeze-up dates in the first half of the 2010s shifted to the middle of December. In the winter of 2013-2014, an unprecedented date of freeze-up (January 15) was observed at the Deadhorse site. This late freeze-up is more typical for the Fairbanks area. During the last 30 years, the average date of freeze-up increased by almost two months.

Higher permafrost surface temperatures supply a significant amount of heat to the deeper permafrost. This leads to substantial increase in permafrost temperatures not only at the surface but also at depth. Thus, the temperature of permafrost at 50 m depth at the West Dock and Deadhorse sites increased by almost 1 °C during the last 30 years. These data also indicate that the average long-term heat flux into the permafrost at these two sites was approximately 0.5 W/m^2 during the last 30 years.

The observed climate warming has triggered permafrost degradation in Alaska, especially in the north and at locations affected by human activities. Several climate change scenarios were used to make projections of possible changes in permafrost during the 21st century. A high resolution (770x770 m) stand-alone permafrost dynamics model [Nicolsky et al., 2007] was used to illustrate how changes in climate together with further industrial development of the North Slope of Alaska will impact permafrost and ecosystems in this region. Preliminary results of these modeling efforts will be also presented.

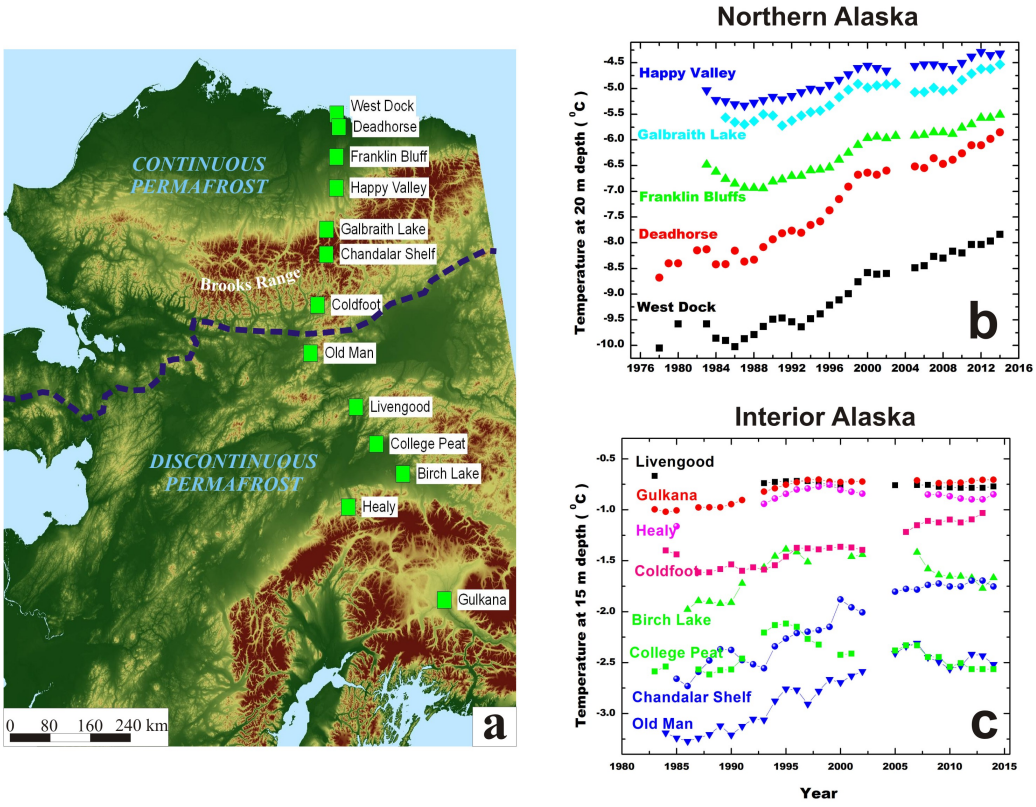

Figure 1: . (a) Continuous and discontinuous permafrost zones in Alaska (separated by the dashed blue line) and location of a north-south transect of permafrost temperature measurement sites; (b) and (c) time series of mean annual temperature at depths of 20 m and 15 m below the surface, respectively, at the measurement sites (updated from Romanovsky [2014].

References

Nicolsky, D. J.; Romanovsky, V. E. and Tipenko, G. S. [2007]: Using in-situ temperature measurements to estimate saturated soil thermal properties by solving a sequence of optimization problems. *The Cryosphere*, 1(1):41–58, doi:10.5194/tc-1-41-2007. URL http://www.the-cryosphere.net/1/41/2007/.

Osterkamp, T. E. [2003]: Establishing long-term permafrost observatories for active-layer and permafrost investigations in Alaska: 1977–2002. *Permafrost and Periglacial Processes*, 14(4):331–342, doi:10.1002/ppp.464.

Romanovsky, V. E. et al. [2014]: [The Arctic] Terrestrial Permafrost [in "State of the Climate in 2013"]. *Bull. Amer. Meteor. Soc.*, 95(7):S139–S141.

Active layer temperature variations in Ebba valley (central Spitsbergen) in the years 2009 – 2015

Krzysztof Grzegorz Rymer, & Grzegorz Rachlewicz

Institute of Geoecology and Geoinformation, Adam Mickiewicz University, Poland

The studies were conducted in order to identify the yearly state and dynamics of the permafrost active layer in Ebbadalen (Ebba valley) between July 2009 and September 2015. Study area was located in central Spitsbergen where climate is relatively more dry than in the other parts of Svalbard Archipelago.

Ground temperature monitoring was carried out in two different locations. Measuring points were located at dry and wet tundra surface. Measurements were conducted automatically with at least one hour interval (interval was variable in years). For automatic record TRIX-8 LogTag's temperature recorders and HOBO's Micro Station Data Loggers were used. Sensors were placed at depths of 5, 10, 20/25, 50, 75, 100 and 140/150 cm (except the wet surface where in the years 2009-2012 due to technical reasons it was placed only at 5 and 10 cm depths). Sediment samples were collected at all locations for laboratory analysis (standard grain size composition). In summer periods continuous meteorological observations were also made. In addition, using DGPS and surveying, topographical mapping and vegetation cover sketches were made at the all measuring points.

The sediments in the analysed locations were composed of poorly to moderately sorted sands and gravels. An increase of grain size with depth was also observed. Deposits genesis was connected mostly with marine and fluvial activity in Ebbadalen area. Vegetation depends on the terrain type and in lower and more humid parts of the area greater diversity of plant species was observed. Dryas octopetala, Equisetum arvense, Salix polaris, Carex rupestris, Cassiope tetragona, Saxifraga oppositifolia were mostly observed.

Changes in soil thermal structure show a significant dependence on air temperature (however, this impact is declining with depth), while in spatial variability of ground temperature the most important factors were: the presence of vegetation cover and sediment moisture (poor correlations with soil grain size composition, cloudiness and precipitation were found).

In addition, it has been observed that:

- greater and more frequent temperature variations occur closer to the surface,
- heat pulse reaches the low lying layers of soil with a well-defined delay,
- ground temperature is responding more quickly to increase of the air temperature than to the cooling,
- negative thermal gradient exist during summer periods,
- zero curtain effect occurs during freezing and thawing of soil,
- thermal gradient after total freeze-up (in cold season) keeps reversed: temperature rises with depth.

Acknowledgements

This study was supported by the Grants No. NCN 2011/03/B/ST10/06172 and NCN 2014/15/N/ST10/00825.

A Permafrost Benchmark System to evaluate permafrost models

Kevin Schaefer[1], Elchin Jafarov[2], Mark Piper[2], Christopher Schwalm[3], & Lynn Yarmey[1]

[1] *National Snow and Ice data Center, United States of America*
[2] *Institute of Arctic and Alpine Research, University of Colorado Boulder*
[3] *Woods Hole Research Center Inc., Woods Hole, Massachusetts*

The Permafrost Benchmark System (PBS) will evaluate simulated permafrost dynamics against observed permafrost conditions. A benchmark is an observational dataset to compare with model output to evaluate model performance. The project goals are 1) to develop a set of generic benchmarking tools capable of calculating performance statistics in multiple benchmarking efforts, and 2) develop benchmark datasets of permafrost dynamics based on available observations and 3) apply the PBS by evaluating multiple models. The PBS will provide an easily accessible, online tool to quickly evaluate model performance and guide model development without having to invest large resources into data preparation and organization. The ideal performance target is to match the observations within uncertainty, so the PBS benchmark datasets and evaluation metrics will account for observation uncertainty. The PBS will be a modular collection of tools built into the Community Surface Dynamics Modeling System (CSDMS) to leverage existing cyberinfrastructure and allow distribution of the benchmarking tools to the modeling community, including the International Land Model Benchmarking (ILAMB) project. The PBS fills a basic need of modeling teams to evaluate how well their models simulate permafrost dynamics, without a heavy investment in time and resources to organize the observations. Here we will present the current development status of the PBS as well as sample model-data comparisons for the chosen benchmark datasets of active layer thickness, permafrost temperature, and snow conditions.

Ground thermal regimes of seasonal frost in the French Alps

Philippe Schoeneich[1], Philippe Choler[2,3], Thomas Morin[1], & Darragh Kenny[1],

[1] *Université Grenoble Alpes, Institut de Géographie Alpine, France*
[2] *CNRS - Université Grenoble Alpes, Institut d'Ecologie Alpine, France*
[3] *LTER "Zone Atelier Alpes" , Grenoble, France*

Like other components of the cryosphere, seasonal frost will be affected by climate change. It was therefore defined by WMO as an Essential Climate Variable. Very few monitoring data are however available so far for the Alps. Several experimental measurement plots were installed in the area of Lautaret pass in the French Alps (45°03'10" N, 6°23'20" E), in a joint effort by the Station Alpine Joseph Fourier and the PermaFrance observing network, in order to explore the distribution and variability of seasonal frost. All measurement sites are situated on ecological observation plots. Seven profiles with sensors at 10, 30 and 50 cm depth were placed in 2011 in various conditions between ca 2300 and 2800 m a.s.l. Longer time series (longest since 2003) are available for over 50 other sites, with ground temperature measurement at 5 cm depth only, distributed between 1900 and 2800 m a.s.l. The poster will concentrate on the analysis of ground thermal regimes. Measurements are performed with autonomus sensors of two types (Hobo Pendant, TerraTransfer M-Log5w and Maxim I-buttons) with a resolution of 0.14 to 0.065 °C and a measurement interval of 1 to 4 hours, depending on the sensor. They are buried in an auger hole. Meteorological data are taken from the station intalled at the Lautaret pass, at 2070 m a.s.l. Snow cover data are taken from the nearby station of Monestier-les-Bains, and since 2012 from the Lautaret pass, and validated with local observations. Mean annual air temperature of the investigation area ranges from ca +3 °C at 2000 m a.s.l. to -2 °C at 2800 m a.s.l., and mean winter temperature (DJF) from ca -4.5 °C to -8.5 °C respectively. All observation sites are on vegetated alpine meadows.

First results show a dominant influence of the snow cover history on ground surface and subsurface temperatures, inducing both a temporal and a spatial variability. An early snow cover can prevent the ground from freezing during several months, even for the whole winter. On the contrary, a late onset of the snow cover allows a deep freezing of the ground. This induces very contrasted thermal regimes, in terms of frost occurrence, intensity and duration. The contrast between «cold » and «warm » years is much higher than on permafrost, measured at similar alitudes on the opposite slope at the Laurichard rockglacier: on permafrost, refreezing of the active layer occurs every year, even in case of early snow cover.

Seasonal frost shows also a very high spatial variability, due to local topographic and snow cover conditions. At similar altitudes, the frost intensity can vary drastically between wind blown and snow accumulation sites (Fig. 1). During snow melt and ground thawing, the onset of the zero curtain occurs in all cases simultaneously on the whole profile, possibly due to infiltration of melt water, but its duration depends on the amount of snow.

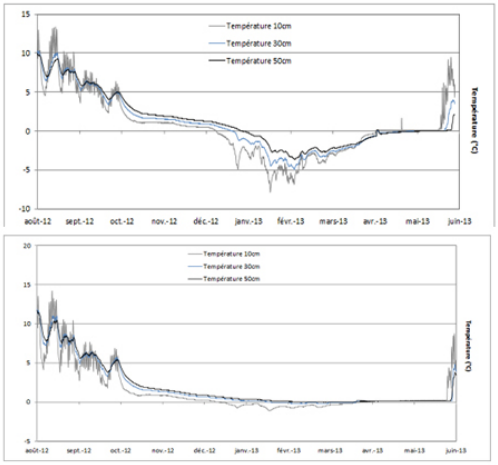

Figure 1: Thermal regimes of two sites at 2650 and 2690 m a.s.l. Above: wind blown site. Below: site with snow accumulation. The early onset fo the snow cover induces on both sites a moderate and progressive cooling of the ground.

These preliminary results show that the future evolution of seasonal frost will not depend only on the evolution of temperature but also on snow cover regimes. A later onset of the snow cover might lead to an increase of seasonal frost intensity and depth, at least in a first time. On the contrary, an increase of the snow cover, due to a possible increase of winter precitpitations, could insulate the ground and prevent it from freezing.

Soil moisture redistribution and its effect on active layer response to inter-annual temperature variations 2000-2014 in a dry loess terrace in Adventdalen, Svalbard

Carina Schuh[1], Andrew Frampton[1,2], & H. H. Christiansen[3]

[1] *Department of Physical Geography, Stockholm University, Sweden*
[2] *Bolin Centre for Climate Change, Stockholm University, Sweden*
[3] *Department of Arctic Geology, University Centre in Svalbard, Norway*

The active layer constitutes an important part of permafrost environments. Thermal and hydrological processes in the active layer determine local phenomena such as erosion, hydrological and ecosystem changes, and can have implications for the global carbon-climate feedback. Permafrost degradation usually starts with a deepening of the active layer, followed by the formation of a talik and the subsequent thawing of permafrost. Increasing active layer depths might thus be regarded as an indicator of permafrost degradation. The importance of hydrology for active layer processes is generally well acknowledged on a conceptual level, but the typically non-linear physical interdependencies between soil moisture, subsurface water and heat fluxes and active layer behavior are not fully understood. In this study, we used field measurements from the UNISCALM research site in Adventdalen, Svalbard, to investigate active layer dynamics in a loess-covered river terrace characterized by little to no summer infiltration and with unsaturated conditions in the active layer. Specifically, we tested

1. the importance of soil water retention properties for moisture and ground ice distribution in the active layer and the upper permafrost, and
2. their effect on active layer response to inter-annual ground surface temperature variations.

We used a physically-based numerical permafrost-hydrogeological model in conjunction with high resolution field data (ground temperature, soil moisture, and thaw depth) collected at the UNISCALM site during the period 2000-2014. To independently test the full range of soil water retention properties commonly reported for equivalent loess soils, a set of seven scenarios with varied van Genuchten parameters α and m was considered. Results showed that the soil water retention characteristics exhibit significant control over the moisture content and seasonal circulation within the active layer, which in turn lead to differences in active layer thickness. Regarding active layer development, we found that summer temperature is the major controlling factor for inter-annual variations in active layer depth, regardless of the soil water retention characteristics which is as expected for a dry site. Variations in winter temperature do not notably affect the subsequent summer thaw depths despite a general shallow snow depth. This again underlines the direct response of dry landforms to summer air temperature forcing. However, a tendency of increasing winter temperatures was found to cause a general warming of the subsurface down to 10 m depth (0.05-0.26 °C yr^{-1}, both observed and modeled) including active layer thickening (0.8 cm yr^{-1}, observed, and 0.3-0.8 cm yr^{-1}, modeled) during the 14-year study period.

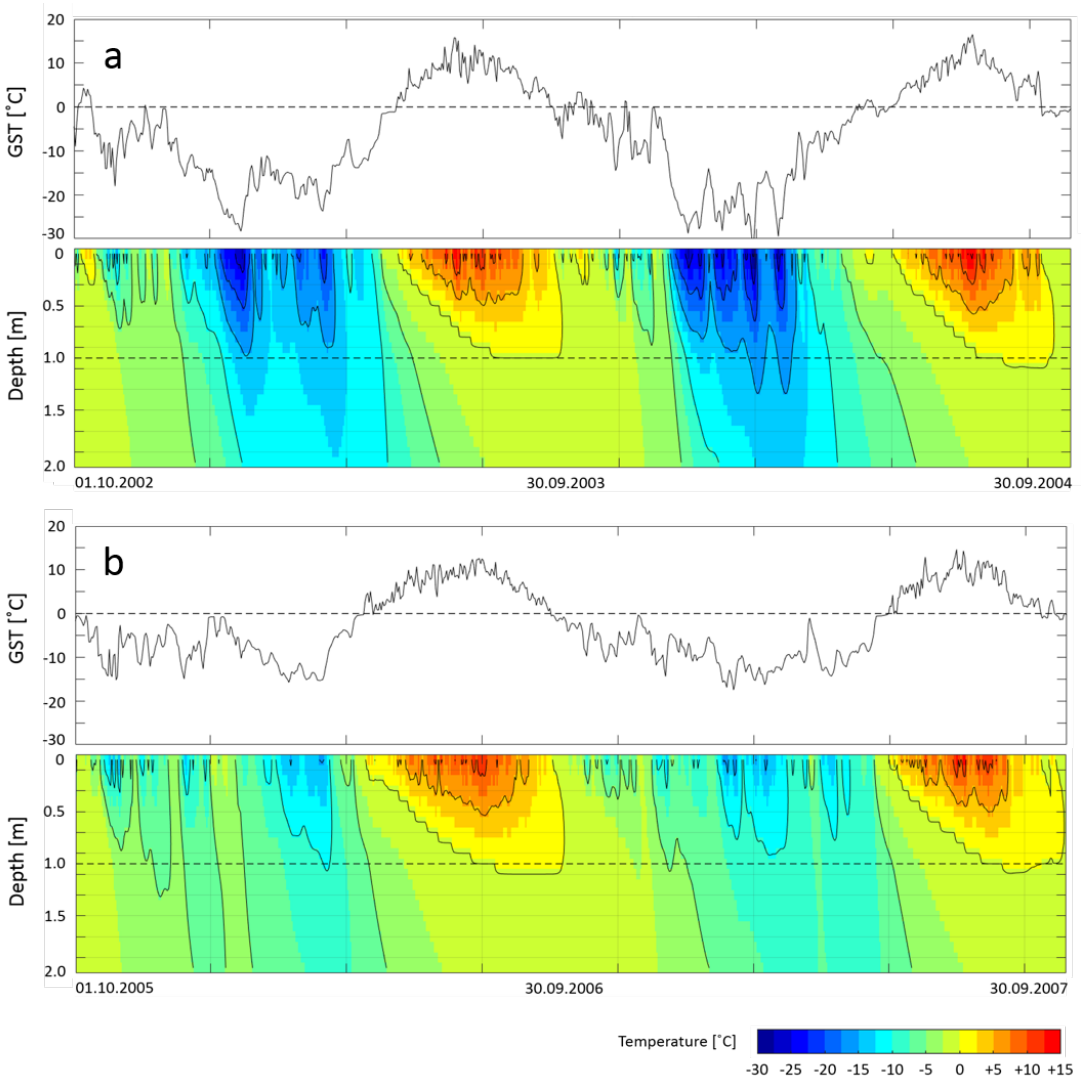

Figure 1: Modeled subsurface temperatures [°C] in the upper 2 m of the model domain as response to ground surface temperature (GST) input for a) particularly cold winters 2002/03 and 2003/04, and b) particularly warm winters 2005/06 and 2006/07.

Twenty years of active layer monitoring in Northern Alaska: Results and lessons learned

Nikolay Shiklomanov[1], Frederick E. Nelson[2,3], Anna E. Klene[4], Kelsey E. Nyland[2], & Dmitry A. Streletskiy[1]

[1]*Department of Geography,The George Washington University, USA*
[2]*Department of Geography, Michigan State University, USA*
[3]*Department of Earth, Environmental, and Geographical Sciences, Northern Michigan University, USA*
[4]*Department of Geography, University of Montana, USA*

The Circumpolar Active Layer Monitoring (CALM) network consists of more than 200 sites and represents the only coordinated and standardized program of observations designed to observe and detect decadal-scale changes in the dynamics of seasonal thawing in high-latitude soils. It provides long-term time series of active-layer thickness (ALT), ground temperature, and thaw settlement measurements at fixed locations across diverse terrain types and regions in order to establish trends, and validate models. The northern Alaska component of the CALM program presently consists of 25 active sites. The sites are located within the continuous permafrost zone, are distributed along the primary climatic gradient of northern Alaska, spanning the regional spectrum of vegetation and terrain conditions. The 16 sites featured in this analysis consists of seven surveyed and georeferenced 1 km^2 grids established to represent generalized conditions of the Coastal Plain and Arctic Foothills physiographic provinces, and nine 1 ha plots representing homogeneous examples of the typical landscape categories within these physiographic provinces. At each of the sites spatially-distributed ALT measurements have been conducted annually by mechanical probing since 1995. Air and soil-surface temperatures under natural surface covers (e.g. vegetation, snow) were monitored continuously over the 1995-2015 period at the nine 1 ha plots. Periodic, spatially oriented measurements of the elevational position of the ground surface were initiated in 2001 at three sites using a Differential Global Position System (DGPS) and an explicitly spatial sampling design.

In this Study we analyze data from 20 (1995-2015) years the field observations described briefly above to examine landscape-specific temporal and spatial active-layer variability and its relation to climatic forcing and heterogeneity in edaphic properties. Although no overall regional trend is evident from ALT observations, our analyses show pronounced landscape-specific differences in response to climatic forcing. The analysis of long-term temperature measurements demonstrates divergent trends in air and ground-surface temperatures during the snow-free period. These changes involve an overall increase in temperature differences between the air and soil surface and a corresponding decrease in summer n-factors. These results may indicate an increase in the thermal insulating properties of vegetation attributable to long-term climate-induced changes in biomass. Monitoring of the elevation of the ground surface indicates slow subsidence of the majority of the natural landscape underlined by ice-rich permafrost in response to a general warming of the climate, without initiation by localized anthropogenic or geomorphic disturbances. Twenty one years of observations in northern Alaska demonstrate a complex, non-linear responses of the active-layer/upper permafrost system to changes in climatic conditions. CALM's strategy of systematic long-term monitoring is necessary for detecting and quantifying changes involving multiple feedback mechanisms.

Investigations of effects of forest fires on the ground thermal regime and permafrost, Northwestern Canada

Sharon Lee Smith[1] & Philip Bonnaventure[2]

[1] *Geological Survey of Canada, Natural Resources Canada, Canada*
[2] *University of Lethbridge*

Introduction

Wildfires are a common occurrence in the boreal forest of northwestern Canada and can have significant impacts on the permafrost environments through their influence on the ground thermal regime. Increases in ground surface temperature due to microclimatic changes associated with organic layer removal or the loss of the coniferous tree cover, can result in increased thaw penetration, permafrost degradation and ground instability where soils are ice-rich. Understanding the long-term effects of environmental disturbance such as fire on permafrost environments is important for assessments of ecosystem change and for planning infrastructure in the context of a changing climate. The Geological Survey of Canada has maintained a number of field sites in the Mackenzie transportation/transmission corridor of the Northwest Territories and northern Alberta that have facilitated the characterization of thermal effects of fires on permafrost terrain up to two decades following initial fire events for sites underlain by warm permafrost in both mineral soils and peatlands.

Study Sites and Methods

The study sites are adjacent to the Norman Wells to Zama pipeline right-of-way which extends from the central Mackenzie Valley NWT to northern Alberta. This paper focusses on two sites. The first study site is a north facing slope located at kilometre post (KP) 182 (64.3° N, 124.5°W). The site is underlain by fine-grained soils (silt and clay). Permafrost is generally warm in this area with mean annual ground temperatures above -1 °C and underlain by ice-rich soils. The site was burned in 1994 but prior to the event the site was covered by a white spruce and white birch forest. Burning was more severe at the top of the slope with complete loss of the forest canopy and removal of the organic layer. Five instrumented boreholes, up to 1.9 m deep, were established at the site in 1995 to measure ground temperatures. Four of these were on the burnt area of the slope at the slope bottom (KP182B), mid-slope (KP182M), slope crest (KP182C) and top of the slope (KP182T). One borehole was also established in an unburnt area (KP182UB). Instrumentation was also installed to measure air temperature and near surface temperature (3-5 cm depth). A more detailed description of the site and instrumentation is provided in Smith et al. [2015].

The second study site is located on a peat plateau at KP783 (59.7°N 119.5°W) in northern Alberta. Two boreholes (20 m deep) were instrumented in 1984 to measure ground temperatures and instrumentation to measure air and ground surface temperature was installed in 1999. The forest cover at the site originally consisted of stunted black spruce and the site was underlain by thick (7 m) ice-rich frozen peat. Permafrost was 10 to 14 m thick and was at temperatures near 0 °C (-0.1 to -0.2 °C). The vegetation and peat surface at this site was severely burned in summer 2004. The instrumentation at the site allowed a comparison of thermal conditions before and after the fire. Earlier analysis of ground temperature data and additional information about the site can be found in Smith et al. [2008].

Results and Discussion

The near surface ground temperature data collected about one year following the 1994 fire at KP182 indicates that before the fire, annual mean surface temperatures were likely below 0 °C at the site. Following the fire, surface temperatures rose above 0 °C (Fig. 1) at the 4 burned sites with the highest temperatures found at the more severely burned sites in the upper part of the slope (KP182T, KP182C). The annual mean surface temperatures at burned sites were generally 1-2 °C warmer than at the unburnt site (KP182UB). At KP783 annual mean surface temperatures following the 2004 fire were generally higher than those recorded prior to the fire (Fig. 1).

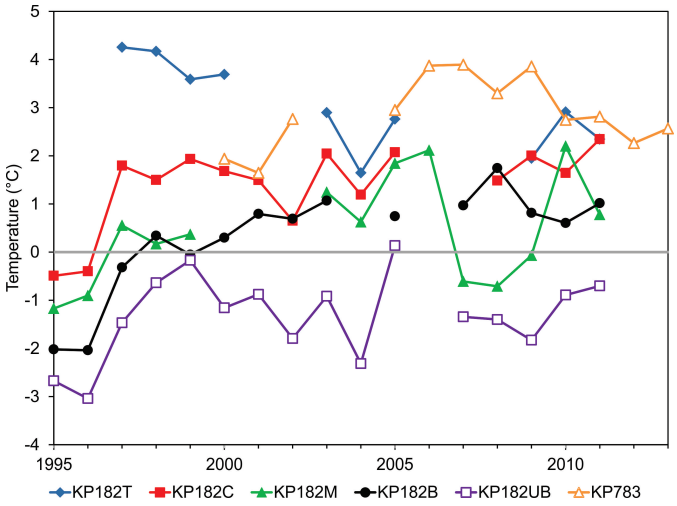

Figure 1: Annual mean near-surface temperature at KP182 after the 1994 fire and at KP783 before and after the 2004 fire (data for KP182 from Smith et al. [2015].

Decreases in surface temperature about 5 years after the fire at both KP182 and KP 783 were also observed which are assumed to be associated with regrowth of vegetation.

At KP182, shallow ground temperatures increased at all burned sites while the change in ground temperature at the unburnt site was relatively small. The ground warming at burned sites was accompanied by an increase in active layer thickness (determined from shallow temperature measurements) and in the upper portion of the slope where burning was more severe, thaw progressed to depths below 1.5 m shortly after the fire. At the top of the slope, permafrost is likely not sustainable as the ratio between frozen and unfrozen thermal conductivity in the upper portion of the soil is not sufficient to provide the required thermal offset [Smith et al., 2015]. Ground temperature data from other recovering burn sites in mineral soils in the central Mackenzie Valley also indicate that permafrost is degrading.

Although burning was severe at the KP783 site, warm permafrost still persists a decade after the fire with some increase in thaw depth following the fire which has been accompanied by surface settlement. The insulating effect of the peat likely reduces the impact of surface warming on the underlying permafrost. The large seasonal difference in thermal conductivity of the peat is able to maintain the thermal offset required to sustain permafrost at the site. There is also a high latent heat requirement for thawing the ice-rich peat.

Summary and Conclusion

The magnitude of the impact of forest fires on warm permafrost is associated with the severity of the fire and also the properties of the subsurface materials. Where severe burning occurred in areas underlain by mineral soils, degradation of permafrost is likely occurring. In contrast, at a severely burned peatland site, warm permafrost persists a decade after the fire with the thick peat reducing the impact of the higher surface temperatures. The loss of the surface buffer layer due to burning will also make the ground thermal regime additionally sensitive to increases in air temperature associated with a warming climate. Warming and thawing of ice-rich permafrost following fires can result in surface settlement and ground instability and these impacts need to be considered in planning and maintenance of infrastructure in a changing climate.

Acknowledgements

Field data collection has been supported by Natural Resources Canada and several other sources over the years including the Program for Energy Research and Development and the Northern Oil and Gas Science Research Initiative. The important contribution of our late colleague Dan Riseborough to the data analysis is also gratefully acknowledged.

References

Smith, Sharon L.; Riseborough, Daniel W. and Bonnaventure, Philip P. [2015]: EEighteen Year Record of Forest Fire Effects on Ground Thermal Regimes and Permafrost in the Central Mackenzie Valley, NWT, Canada. *Permafrost and Periglacial Processes*, 26(4):289–303, doi:10.1002/ppp.1849.

Smith, S.L.; Burgess, M.M. and Riseborough, D.W. [2008]: Ground temperature and thaw settlement in frozen peatlands along the Norman Wells pipeline corridor, NWT Canada: 22 years of monitoring. In: Kane, D.L. and Hinkel, K.M.(eds.), *Proceedings of the Ninth International Conference on Permafrost*, Institute of Northern Engineering, University of Alaska Fairbanks, Fairbanks, USA, 29 June–3 July 2008, volume 2: pages 1665–1670. ISBN 978-0-9800179-3-9. URL http://ipa.arcticportal.org/publications/conference-proceedings.

Spatial and temporal variability in permafrost thermal state and active layer thickness along the Mackenzie Valley transect, NWT Canada

Sharon Lee Smith[1], Caroline Duchesne[1], Mark Ednie[1], & Philip Bonnaventure[2]

[1] *Geological Survey of Canada, Natural Resources Canada, Canada*
[2] *University of Lethbridge*

Introduction

Permafrost is an important component of the landscape of the Mackenzie Valley Northwest Territories (NWT) that influences both natural and socio-economic environments. Changes in the ground thermal regime and active layer conditions in response to a changing climate can lead to alterations in drainage and ground stability, which has implications for environmental and infrastructure integrity. The active layer responds to shorter term fluctuations in climate compared to the thermal regime of deeper ground. Monitoring of two key cryospheric indicators (or essential climate variables), active layer thickness and permafrost thermal state, allows an assessment of both interannual variability and longer-term change in permafrost conditions.

The Geological Survey of Canada has maintained a permafrost monitoring network in the Mackenzie Valley (Fig. 1) since the mid 1980s that consists of a suite of sites representing the range of ecoclimatic conditions in the region. This paper describes the spatial variation in active layer thickness and permafrost thermal state and also documents the change that has occurred over time.

Study Sites and Instrumentation

The monitoring transect extends from the northern tundra environments of the Tuktoyaktuk peninsula to the boreal forest in the south. The terrain consists of lacustrine, moraine, fluvial and deltaic sediments. Extensive peatlands occur in the southern portion of the region where poor drainage has resulted in thick accumulations of peat. Ice-rich fine-grained sediments such as lacustrine clays are common. Permafrost is continuous and several hundred metres thick on the Beaufort Coastal Plain in the north and is sporadic and thin in the southern NWT.

Field sites (Fig. 1) were selected to be representative of the vegetation and terrain conditions in the region. The active layer monitoring network was initiated in 1991 and originally consisted of 66 sites with 45 still in operation. Thaw tubes are utilized to determine maximum summer thaw penetration as well as maximum heave and subsidence of the ground surface. Details on instrumentation and site descriptions are available in Smith et al. [2009]. To monitor permafrost thermal state, over 70 boreholes (up to 20 m deep) have been instrumented with thermistor cables connected to data loggers. Some sites have been operational since the 1980s, but many were established between 2006 and 2008, during the International Polar Year [Smith et al., 2010]. At many sites, instrumentation has also been installed to measure air and ground surface temperature. More information on the instrumented sites along with recent data collected can be found in Smith et al. [2015].

Current Conditions

Permafrost temperatures are above -2 °C throughout a large portion of the region, especially within the discontinuous zone. Colder conditions are found within the continuous permafrost zone but permafrost temperatures are highly variable ranging from -6 to -7 °C in the tundra uplands to higher than -2 °C in wet areas or where vegetation promotes snow accumulation. Active layer thickness (ALT) ranges from about 0.5 m in the north to greater than 1 m in the south with ALT generally being less above treeline compared to that below treeline. Considerable spatial variability in ALT is observed particularly below treeline where high shrubs dominate and influence snow accumulation.

Temporal Variability

Long-term records of permafrost temperature indicate that it has generally warmed in the Mackenzie Valley since the mid 1980s, consistent with increases in air temperatures [Smith et al., 2010]. Although this

warming of permafrost has continued over the last decade, it has generally been at a lower rate than that prior to 2000. Since 2007, when many of the sites were established, permafrost temperatures have increased at most sites. Between 2007 and 2014, increases in permafrost temperature ranged from less than 0.1 °C to 0.2 °C in the discontinuous zone and from 0.2 to 0.5 °C in the continuous zone [Smith et al., 2015]. At warmer permafrost sites, especially where ground temperatures are close to 0 °C and soils are ice-rich, latent heat effects associated with phase change result in ground temperatures being less responsive to changes in climate (Smith et al. 2010).

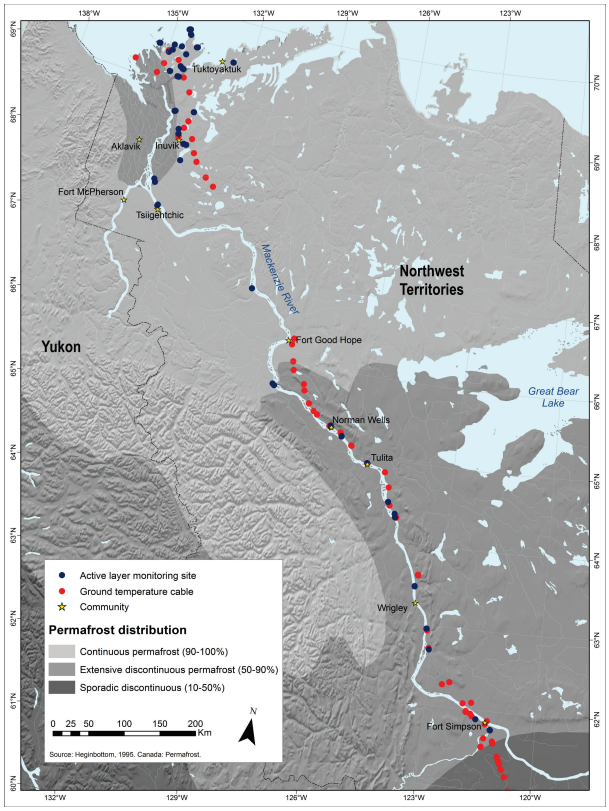

Figure 1: Location of active layer and ground temperature monitoring sites in the Mackenzie Valley, NWT.

Greater interannual variability is observed in active layer records compared to ground temperature records and there has been no pronounced trend in ALT over the 1991-2014 record. At many sites the maximum ALT occurred in 1998 which was one of the warmest years on record. ALT generally decreased following the 1998 peak, but there has been an increase in ALT at many sites since 2005 which seems to coincide with a period of higher summer air temperatures. Although active layer development is influenced by summer air temperatures, the surface freezing index has decreased recently at some sites and the observed increase in ALT may also be partly due to warmer winter conditions.

Summary

Data from the permafrost monitoring network has enabled characterization of spatial and temporal variability in active layer thickness and permafrost thermal state in the Mackenzie Valley. Recent increases in ALT and permafrost temperature have been observed but the magnitude and rate of change varies spatially. The monitoring network generates essential information on permafrost in an important transportation/transmission corridor, which can inform land management decisions, infrastructure planning and adaptation to a changing climate.

Acknowledgements

Field data collection has been supported by Natural Resources Canada and several other sources over the years including the Program for Energy Research and Development and the Northern Oil and Gas Science Research Initiative. Data management has been provided by J. Chartrand.

References

Smith, S.L.; Riseborough, D.W.; Nixon, F.M.; Chartrand, J.; Duchesne, C. and Ednie, M. [2009]: Data for Geological Survey of Canada active layer monitoring sites in the Mackenzie valley, N.W.T. Open file 6287, Geological Survey of Canada.

Smith, S.L.; Romanovsky, V.E.; Lewkowicz, A.G.; Burn, C.R.; Allard, M.; Clow, G.D.; Yoshikawa, K. and Throop, J. [2010]: Thermal state of permafrost in North America: a contribution to the International Polar Year. *Permafrost and Periglacial Processes*, 21(2):117–135, doi:10.1002/ppp.690.

Smith, S.L.; Chartrand, J.; Duchesne, C. and Ednie, M. [2015]: Report on 2014 field activities and collection of ground thermal and active layer data in the Mackenzie Corridor, Northwest Territories. Open file 7935, Geological Survey of Canada.

Varied response of near-surface ground temperatures in Spitsbergen to mid-winter warming events

Sarah Marie Strand[1,2] & Hanne Hvidtfeldt Christiansen[1]

[1] *The University Centre in Svalbard, Norway*
[2] *University of Oslo, Norway*

This study aims to explain the response of near-surface ground temperatures in Spitsbergen to mid-winter warming events, where the air temperature remains above 0 °C for multiple days in a row. The Svalbard archipelago is subject to significant winter air temperature fluctuations due to its maritime setting and position between the Icelandic low-pressure system and the Siberian high-pressure system. During the winter, a higher contrast between these air masses forces cold air from the north over Svalbard. However, when the difference between the Icelandic low and the Siberian high lessens, cyclones bring warm, wet air from the south, hitting Spitsbergen's west coast. A few of these warming events punctuate each winter in Svalbard, though their magnitude and moisture content is inconsistent. These mid-winter warming events are short-term phenomena, but they still have the potential to alter temperatures in both the active layer and upper permafrost.

When the warm air masses bring heavy rainfall, ice layers can form on the ground or within the snowpack. If enough water percolates through a pre-existing snowpack, the uppermost ground temperatures may subsequently warm as this water freezes into an ice layer, releasing latent heat. However, in areas with little or no snow, ice layer formation allows for greater ground cooling later in the winter, because ice has a much higher thermal conductivity compared to snow. Thus, the timing of winter rain events within the snow season influences their effect. The impact these meteorological events have on the ground is dependent on a number of other site-specific factors besides snow depth: elevation, slope angle, lithology, and landform type. The location of the permafrost boreholes selected for this study allows for the comparison of multiple periglacial landforms at varying elevations and distances to the coast. Though singular mid-winter warming events do not appear to impact the annual thermal regime, ground warming can be observed multiple meters into the ground, and can persist significantly longer than the event itself; this is particularly true for sites with fine-grained sediments. Generally, warm periods accompanied by substantial rainfall impact temperatures deeper in the ground than drier events, though neither of these event types cause complete thaw at the surface. A few publications have considered the thermal response of permafrost to rain-on-snow events, but the long-term meteorological and ground temperature data series available for Spitsbergen have never previously been used to compare distinct events and locality response.

Arctic permafrost thermal and active layer variability across an environmental gradient from continuous to sporadic permafrost

Sarah Marie Strand[1,2], Hanne Hvidtfeldt Christiansen[1], Julia Boike[3], Ko van Huissteden[4], Bo Elberling[5], Birger U. Hansen[5], Margareta Johansson[6], & Go Iwahana[7]

[1] *The University Centre in Svalbard, Norway*
[2] *University of Oslo, Norway*
[3] *Alfred Wegener Institute Helmholtz Centre for Polar and Marine Research, Potsdam, Germany*
[4] *University of Amsterdam, the Netherlands*
[5] *University of Copenhagen, Denmark*
[6] *Lund University, Sweden*
[7] *University of Alaska, Fairbanks, USA*

Permafrost thermal state and active layer thicknesses have been compared from five different Arctic field sites as part of the EU 7^{th} framework project PAGE21. Data has been compiled for the years 2012-2014 in the following locations: Samoylov and Kytalyk, both in Siberia, Russia, Zackenberg in northeast Greenland, Adventdalen in Svalbard, and Abisko in northern Sweden. These sites were chosen to exemplify the gradient between sporadic and continuous permafrost. The investigated ground thermal data all come from lowland sediment areas, primarily from ice-wedge polygonal landforms, except in the case of Abisko, where the permafrost only exits in palsas.

The two Siberian sites have the coldest permafrost, earliest active layer freeze-back periods, and significant annual thermal variation in the upper permafrost. These observations can be explained by the large annual air temperature amplitude in the region, high ground ice content, and limited snow cover. Permafrost temperatures in northeast Greenland are somewhat warmer than in Siberia, but are cooler than those of Svalbard. Seasonal air temperature variation is smaller in northeast Greenland than northern Russia, and this is reflected in the smaller variation in seasonal permafrost temperatures in the prior location. Svalbard permafrost has similar seasonal variability compared to northeast Greenland, but is warmer overall, showing the effect of mild winters. The warmest permafrost was measured at Abisko, where active layer thawing also occurs the earliest.

Active layer thickness (ALT) measurements from the five sites, collected via mechanical probing of CALM sites, reflect site meteorological variability in addition to differences in active layer material. In the past few years, only small scale changes in ALT have been observed (both thinning and thickening). However, examining the entire data series shows a general increase in ALT. The permafrost temperature and ALT data highlight climate as a main driver of regional permafrost conditions, but also demonstrate the influence of site specific factors which must be considered at the landscape scale.

Thermal state of permafrost and recent active layer dynamics in the South Shetlands, Antarctica

Gonçalo Vieira[1], Miguel Ramos[2], Miguel Angel de Pablo[2], Gabriel Goyanes[3], Marc Oliva[1], Carlos Schaefer[4], Alice Ferreira[1], Andrey Abramov[5], Antonio Correia[6], Alexandre Nieuwendam[1], & Carla Mora[1]

[1] *CEG/IGOT - Universidade de Lisboa, Portugal*
[2] *Universidad de Alcalá de Henares, Spain*
[3] *Instituto Antártico Argentino, Buenos Aires, Argentina*
[4] *Universidade Federal de Viçosa, Viçosa, Brazil*
[5] *Institute of Physicochemical and Biological Problems in Soil Science, Russian Academy of Sciences, Pushchino, Russia*
[6] *Instituto de Ciências da Terra, Universidade de évora, Portugal*

The Western Antarctic Peninsula has been one of the Earth's regions showing a faster warming rate since the 1950's, with an increase of over +2.5 °C in mean annual air temperatures since 1950. The South Shetland Islands, located some 100 km off its northwestern coast are near the climate limit of permafrost. Changing permafrost will influence the terrestrial ecosystems by modifications in the active layer thickness, ground freezing regime, hydrology, geomorphodynamics and possibly, by changes in biogeochemical fluxes.

Boreholes installed in Deception Island, Livingston island and King George Island aim at identifying regional controls on permafrost and the active layer, but also local and site-specific influences. For the former, we maintain 4 to 25 m depth boreholes with continuous logging of temperatures, as well as associated meteorological stations. For the later, we a number of very shallow boreholes with 0.8 to 2 m depth was installed at diverse settings in the vicinity of the main boreholes. The network is integrated in the Global Network for Permafrost (IPA/WMO/GCOS).

Permafrost temperatures across the South Shetlands are warm, between slightly below 0 and -1.5 °C and the ground thermal regime shows a strong dependence from varying snow conditions, as well as thermophysical properties and ice-content of the ground. Active layer thickness varies from 0.4 in the volcanic deposits of Deception Island, to several meters in high diffusivity bedrock. Active layer data since 2000 shows a large interannual variability in mean ground temperatures without any significant climatic trend. However, since 2008 active layer thickness has been decreasing and a general cooling has been observed at the South Shetlands sites, which are the only ones providing longer term data. The reasons for this ground cooling are related to a longer lasting snow cover during spring and summer, inhibiting ground heat gain.

The influence of increasing rainfall on permafrost on the Qinghai-Tibetan plateau

Zhi Wen, Mingli Zhang, & Mingli Zhang

Cold and Arid Environmental and Engineering Research Institute, Chinese Academy of Sciences, People's Republic of China

Rainfall on the Qinghai-Tibetan plateau has increased in the past decades. To better understand the influence of increasing rainfall on permafrost on the Tibetan Plateau, thermal-moisture dynamics of the active layer was measured and permafrost variation induced by increasing rainfall was evaluated. The observation data demonstrated that rainfall in summer led to the change of surface energy balance and caused subsurface soil cooling. The convective heat transfer from water infiltration reduced the temperature gradient with depth and changed near-surface heat fluxes. Our results suggest that the increase in rainfall mitigated permafrost degradation on the Tibetan Plateau. However, increasing rainfall tended to induce significant thermokarst processes and resulted in a thermokarst lake expansion in depth and area. Lake expansion due to thermokarst could be fairly rapid and depended on many factors including lake-bottom temperature and permafrost temperature. The development of the lake could significantly enhance the thermal effects on surrounding permafrost. Lake expansion caused a greater thermal disturbance to permafrost around and beneath them.

To evaluate the long-term effects of increasing rainfall, a coupled model for liquid water, water vapor and heat transport of saturated-unsaturated soil in cold regions was proposed. The model implemented a fully coupled simulation that includes water migration in both the vapor and liquid phases and heat transfer by means of conduction, convection, latent heat of vapor diffusion and phase change effects. The model was verified by the detailed field monitoring data. The comparison between simulated values and observed data showed that the numerical model was valid for calculating the coupled soil mass and energy budget. The role of water flow and vapor diffusion in the heat and mass transport of permafrost regions was analyzed. The results indicated that thermal conduction dominated the heat transport in the deeper layer (below 75 cm), but the impact of water movement on heat in summer was significant in shallow ground. Soil water was transported by both liquid water and water vapor and water vapor contributed more than 15 % of the water flux at all depths. Our results suggested that vapor and liquid water transport played an important role in soil mass and energy transfer, especially for the shallow ground. Increasing rainfall showed significant and long-term effects on permafrost.

Characteristics of permafrost at local and regional scales: The Khovsgol and Khangai Mountains, Mongolia

Jambaljav Yamkhin[1], Ishikawa Mamoru[2], Iijima Yoshihiro[3], Dashtseren Avirmed[1], Sharkhuu Natsagdorj[1], Gansukh Yadamsuren[1], Temuujin Khurelbaatar[1], Amarbayasgalan Yondon[1], Tsogt-Erdene Gansukh[1], & Undrakhtsetseg Tsogtbaatar[1]

[1] *Institute of Geography and Geoecology, Mongolian Academy of Sciences, Mongolia*
[2] *Graduate School of Environmental Science, Hokkaido University, Japan*
[3] *Research and Development Center for Global Change, Japan Agency for Marine-Earth Science and Technology, Japan*

Permafrost exists in 48 different countries, the top five by permafrost area are Russia, Canada, China, United States, and Mongolia, which together account for about 95 % of global terrestrial permafrost [Zhang et al., 2006]. Due to global climate warming, the changes in permafrost have been recorded everywhere with permafrost. Permafrost temperature increases in polar region [Romanovsky et al., 2010] and there were noted the active layer detachment, deepening of summer thaw, disappearing of shallow permafrost in the southern fringe of permafrost region. The permafrost with a temperature close to zero degrees has disappeared in the southern edge of Mongolian permafrost region [Jambaljav et al., 2013].

Recently there have been established national permafrost network with more than 120 boreholes in Mongolia within the framework of foreign and national programs and projects. Continuous records of temperatures in boreholes of permafrost network aren't not too long, however, some boreholes have temperature measurements once in 1960-1980s. Therefore, comparing the early measurements with recent records, the temperatures have changed with increasing trend in some depths of boreholes during the last 20–30 years.

In this study we present the results of permafrost monitoring and changes of permafrost temperature along transect from the northern Khovsgol Mountains to the southern Khangai Mountains of central Mongolia. In general permafrost degradation under the influence of climate warming in Mongolia has been more intense during the last 15-20 years than during the previous 15-20 years [Sharkhuu, 2011]. These recent increases in temperature have led to an increase in permafrost temperatures in northern Mongolia and the disappearance of permafrost in the southern fringe of the Mongolian permafrost region [Jambaljav et al., 2013].

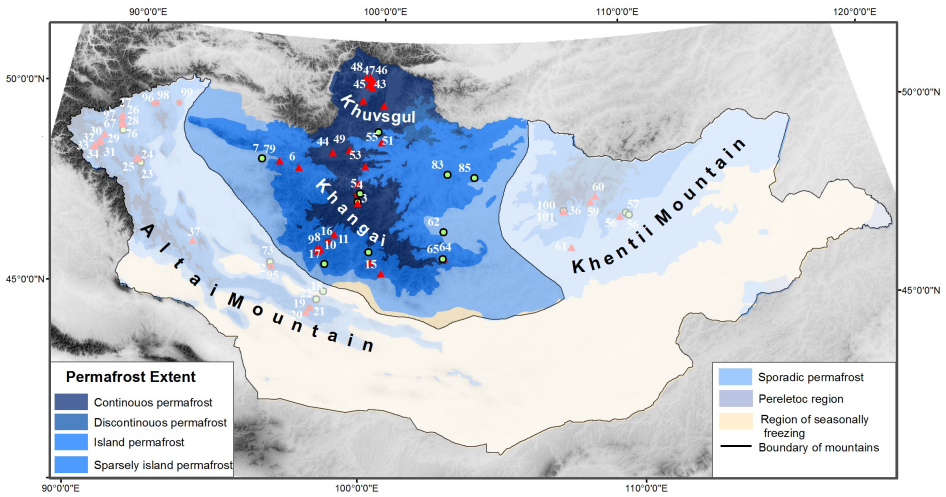

Figure 1: Permafrost distribution in Mongolia (Gravis et al,. 1971), locations and numbers (BH); the monitoring sites in permafrost (red triangles) and without permafrost (green circles), and the ground surface temperature monitoring sites (red circles).

Observations at boreholes No. 48 and No. 40 show permafrost temperatures have increased at the rate of 0.52 °C and 0.95 °C at depths of 10 m and 15 m respectively during the last 23-26 years in the Darhad depression (northern Mongolia) [Jambaljav et al., 2013]. Temperature at borehole No. 3 in the northern Khangai has warmed by 0.39 °C - 0.44 °C at depths of 10 m and 15 m over the last 24 years. Borehole No. 10 in the southern Khangai has shown an increase in temperature of 0.64 °C over the last 30 years at a depth of 10 m.

Depending on the geographical location and weather condition, the thickness of active layer and seasonally frozen ground is about 2-6 m in Mongolia. Due to global climate warming many observations indicate an increasing trend of active layer thickness and the depth of refreezing cannot reach the thawing depth of the previous summer. Measurements have revealed a talik in the southern fringe of Mongolian permafrost region. There is closed talik at a depth of 4 m near the Hoh Burd Lake in borehole No 15 [Jambaljav et al., 2013].

References

Jambaljav, Ya.; Vanchig, T.; Battogtokh, D.; Saruulzaya, A. and Dashtseren, A. [2013]: "Permafrost network over Mongolia". Scientific report, Institute of Geography, Mongolian Academy of Sciences, Mongolia.

Romanovsky, V.E.; Smith, S.L. and Christiansen, H.H. [2010]: Permafrost thermal state in the polar Northern Hemisphere during the International Polar Year 2007–2009: a synthesis. *Permafrost and Periglacial Processes*, 21(2):106–116, doi:10.1002/ppp.689.

Sharkhuu, N. [2011]: Long-term monitoring of permafrost in Mongolia. In *Extended Abstracts of Second International Symposium on Mountain and Arid Land Permafrost, 22-26 August, 2011, Ulaanbaatar, Mongolia.*

Zhang, T.; Parsons, M.A. and Barry, R.G. [2006]: Statistics of Global Permafrost Distribution. In *Abstracts of Asian Conference on Permafrost, August 7-9, 2006, Lanzhou, China.*

Estimating rainfall influence on the thermal regime of sandy soils

Aleksandr F. Zhirkov & Mikhail Zhelezniak

Melnikov Permafrost institute, Russian Federation

Temperature of any medium is a function of its thermal state which is governed by internal and external energy sources, as well as by material properties. Interior heat flow is virtually independent of surface conditions or rock composition and properties, and is stable in time. The heat flow density is determined by the amount of thermal energy generated in the Earth's interior. Incoming solar radiation is an external source of heat. It provides the main source of energy that drives the natural processes occurring on the ground surface and in the active layer, as well as in the atmosphere and hydrosphere. Even extremely cold areas with a mean annual air temperature of -6 °C or lower have locations with ground temperatures above 0 °C. To understand such phenomena, it is important to examine the relative roles of natural factors in controlling the ground temperature regime.

In the active layer of permafrost, the heat exchange processes are largely determined by surface air circulation, amount of precipitation, vegetation, and soil properties and characteristics. An important role in influencing the ground thermal regime is played by precipitation, both solid (snowfall) and liquid (rainfall).

With water movement in the active layer the processes of heat transfer require a detailed study and analysis of the relationship of heat exchange between liquid and solid components. In permafrost, heat transfer from the surface to the freeze-thaw boundary coincides with the direction of water movement. Therefore, heat conduction in the soil is accompanied by heat transferred from rainfall to sediment, which depends on its temperature at the surface.

To study the effect of rainfall infiltration on ground thermal regimes, an experiment was set up at a research site of the Melnikov Permafrost Institute, the Tuymaada site, located in Yakutsk. Two test plots were established in soils of similar lithology. The experiments were carried out in 2014 and 2015, from May 1 to September 30, and consisted of monitoring the soil temperature and moisture regimes at plots receiving different amounts of precipitation. The hydrothermal regime was monitored using data loggers which recorded soil moisture and temperature at 6-hour intervals. One plot received natural rainfall, while the other was additionally watered. The purpose of the experiment was to quantify the effect of rainfall infiltration on the ground thermal regime by comparing the ground temperature dynamics at two plots, taking into account condensation in the soil and evaporation from the soil surface.

The experiments and data analysis showed that the effect of precipitation at the Tuymaada site propagated to a depth of 5 m. Increasing the precipitation by three times increased ground temperatures by 0.2 to 2.3 °C.

As rainfall infiltrates into the soil, four zones can be identified which differ in the intensity of heat exchange between the water and the soil. The strongest thermal effect of rainfall infiltration is observed near the surface and is closely related to the hydraulic properties of the soils. The presence of the soils with different hydraulic properties within the profile significantly determines the character of rainfall-soil heat exchange and hence the penetration depth of rainfall effect.

Based on the review of published data and this experimental study, a model of the effect of rainfall on the ground thermal regime was developed, accounting for moist air condensation in soils and evapotranspiration.

SESSION 10

Palaeoenvironments in Permafrost Affected Areas

Convener:

Laura Epp, *Alfred Wegener Institute Helmholtz Centre for Polar und Marine Research, Germany*

Frank Kienast, *Senckenberg Research Institute and Natural History Museum, Research Station of Quaternary Palaeontology, Germany*

Permafrost is an excellent archive of ancient life, and permafrost affected areas provide ideal conditions for the long-term preservation of both fossil tissue and DNA. High latitude ecosystems are relatively pristine and simple, with low diversity of taxa, and therefore are extremely sensitive to environmental fluctuations. During Pleistocene cold stages, parts of the Arctic remained free of large ice sheets and were home to rich ecosystems. In Siberia, Alaska and Yukon, fossil bearing sediments were continuously deposited and synchronously incorporated into permafrost over tens of thousands of years providing a unique Quaternary fossil record. The recorded period also covers the time of the mammoth fauna extinction, human expansion and restructuring of arctic ecosystems at the dawn of the Holocene. In the proposed session, we intend to bring together specialists of all relevant fields to combine their expertise for the integrative reconstruction of Quaternary palaeoenvironments in permafrost affected areas of high latitudes and altitudes. The session Palaeoenvironments in permafrost affected areas at the International Conference on Permafrost is one of the few opportunities for a lively discussion with world leading scientists in palaeoecological disciplines as diverse as palaeontology, ancient DNA analysis, palynology, vegetation ecology, archaeology, isotope and biochemistry, and dating.

Special focus will be given on the young and innovative methodology of using ancient DNA from both organismal remains and sedimentary deposits for reconstructing the history of palaeoecosystems in permafrost environments.

We focus on novel methodological developments in the relevant fields and on stimulating the combination and integration of various proxies, approaches and methodologies to improve reconstructions of ancient ecosystems and their response to climate change, formation of migration routes and barriers, human occupation, and herbivore – vegetation interaction.

Environmental plant DNA (eDNA): To which degree does it represent the flora?

Inger Greve Alsos[1], Per Sjögren[1], Nigel Yoccoz[1], Mary E. Edwards[2], Ludovic Gielly[3], Eric Coissac[3], Marie K.F. Merkel[1], & Pierre Taberlet[3]

[1] *UiT – The Arctic University of Norway, Norway*
[2] *University of Southampton, UK*; [3] *University Grenoble Alpes, LECA, France*

Environmental DNA (eDNA) extracted from sediments has promise as a new proxy in studies of modern biodiversity and in palaeobiological reconstructions, particularly in the Arctic, where cold conditions contribute to good preservation of biological material in soil and sediments. Currently, little is known about how well this method represents flora and vegetation. We used the 'g' and 'h' universal plant primers to amplify DNA in samples from lake sediments and from soil with the aim of assessing how the recovered DNA represents the composition of surrounding vegetation. Better understanding of these relationships will aid rapid floristic surveys in remote areas and the interpretation of fossil data from lakes and terrestrial deposits (peat and yedoma) in permafrost regions. We collected lake sediment samples of different ages (modern, 100 – 200 years, and Holocene) from Svalbard, north Norway and Scotland. We compared the retrieved DNA with modern vegetation, pollen, and macrofossils, respectively, to evaluate the representation of different taxonomical groups, the geographical area likely to be represented, and the suitability of using eDNA compared with other proxies.

Our results show that eDNA of modern lake sediments represents about 50 % of the flora of the catchment area. Environmental DNA and pollen of 100 – 200-year-old lake sediments from regions where forest was planted in the mid-twentieth century showed that both proxies discern major vegetation change at the time of plantation, with similar quantitative changes. In a lake sediment core from the Arctic (Svalbard) dated to 8500 – 1200 cal. BP, all except two genera identified as macrofossils were also identified with eDNA (ancient DNA). Furthermore, eDNA identified six additional taxa and more species per sample. With one DNA extraction and one PCR per sample, we detect most common species independent of sample type or age. Increasing the number of extractions or PCR repeats increased the chances of detecting rare species. Thus, analyses of lake sediment DNA may have a higher and/or complementary taxonomic resolution and detection rate compared to analyses of pollen or macrofossils, and they may therefore be a useful method for reconstruction of past floras. However, the method needs further improvement for studies of modern biodiversity.

Analyses of soil samples from the Arctic showed that all taxa represented in the soil DNA grew within 3 m of the sampling point, most of them within 0.5 m. In modern arctic conditions, therefore, a soil sample (typically c. 100 cm^2) senses vegetation components immediately around the sampling site. This is likely to be a different picture of vegetation than that derived from pollen analysis and more similar to macrofossil analysis. This type of sample is typical of fossil samples analysed to date from yedoma deposits in Siberia and North America Willerslev et al. [2014].

We conclude that analysis of plant eDNA from sediments is a promising approach, but our results show that it is important to clarify the nature of the modern or ancient vegetation sampled, as this affects interpretation of the data.

References

Willerslev, E.; Davison, J.; Moora, M.; Zobel, M.; Coissac, E.; Edwards, M.E.; Lorenzen, E.D.; Vestergård, M.; Gussarova, G.; Haile, J.; Craine, J.; Gielly, L.; Boessenkool, S.; Epp, L.S.; Pearman, P.B.; Cheddadi, R.; Murray, D.; Bråthen, K.A.; Yoccoz, N.; Binney, H.; Cruaud, C.; Wincker, P.; Goslar, T.; Alsos, I.G.; Bellemain, E.; Brysting, A.K.; Elven, R.; Sønstebø, Jø.H.; Murton, J.; Sher, A.; Rasmussen, M.; Rønn, R.; Mourier, T.; Cooper, A.; Austin, J.; Möller, P.; Froese, D.; Zazula, G.; Pompanon, F.; Rioux, D.; Niderkorn, V.; Tikhonov, A.; Savvinov, G.; Roberts, R.G.; Macphee, R.D.E.; Gilbert, M.T.P.; Kjær, K.H.; Orlando, L.; Brochmann, C. and Taberlet, P. Fifty thousand years of Arctic vegetation and megafaunal diet. *Nature*, 506 (7486):47–51, 2014. doi:10.1038/nature12921.

Modern spatial variability of limnoecology and sedimentary processes in a mountain lake at the permafrost margin of southern Yakutia (Russia)

Boris K. Biskaborn[1], Bernhard Diekmann[1,2], Hanno Meyer[1,2], Bernhard Chapligin[1], Almut Dressler[1,2], Thomas Löffler[1,2] Laura Weniger[1,3] & Liudmila Pestryakova[4]

[1] *Alfred Wegener Institute Helmholtz Centre for Polar and Marine Research, Potsdam, Germany*
[2] *University of Potsdam, Potsdam, Germany*
[3] *Freie Universität Berlin, Berlin, Germany*
[3] *Yakutsk Federal University, Yakutsk, Russia*

The Northern hemisphere is strongly affected by on-going global warming since the late 18^{th} century. Recent climate warming and permafrost degradation is threatening both the residential areas of the local people and natural northern ecosystems. Especially lake ecosystems act as extremely sensitive sentinels of environmental changes. Lake Bolshoe Toko (56°15' N, 130°30' E, 903 m.a.s.l., length: 14 km, width: 7 km, maximum water depth: >70 m) is located at the marginal permafrost zone in southeastern Yakutia, Russia. The lake occupies a basin at the foot of the northern slope of the eastern Stanovoi mountain range, composed of Precambrian igneous rocks. At its northeastern margins the lake is bordered by moraines of three different glacial sub-periods. These geological boundary conditions give way to different depositional environments within the lake and hence cause spatial variability in habitat conditions for diatom species assemblages.

In our study, we analyse the sediment-geochemical properties (organic carbon, nitrogen, mineralogy and grain-size) from a set of 37 surface samples and compare them to the taxonomical diatom species distribution and the oxygen isotope signal measured from the diatom opal ($\delta^{18}O$ diat). Our initial results show significant within-lake variability of the species distribution, influenced by limnological parameters (water depth, habitat conditions, distance-to-shore) and differential catchment properties (i.e. nutrient supply). Short cores from selected locations were scanned for elemental composition, subsampled and $^{210}Pb/^{137}Cs$ dated. Currently, we analyse diatoms and sediment-geochemistry in a top-bottom approach to reveal the influence of the limnological and catchment properties as drivers of the biological and chemical lake development before and during recent climate change.

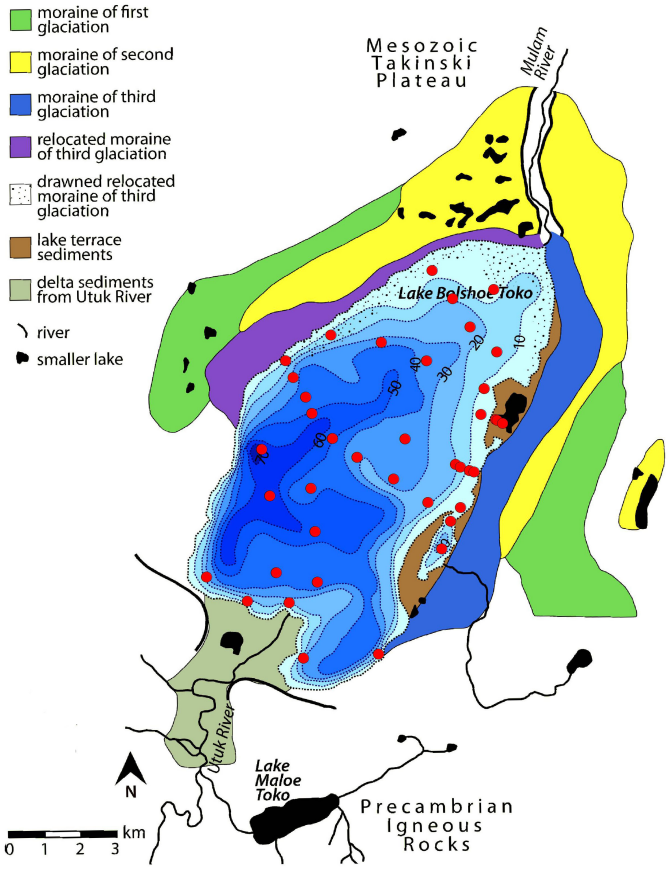

Figure 1: Geological setting and sample site distribution in Lake Bolshoe Toko, southeastern Yakutia (Russia)

Tree migration since the LGM in Siberia and the potential interaction with climate change and active layer depth development

Xianyong Cao[1] & Ulrike Herzschuh[1,2]

[1] *Alfred Wegener Institute Helmholtz Centre for Polar and Marine Research, Potsdam, Germany*
[2] *Institute of Earth and Environment Science, University of Potsdam, Germany*

High quality late Quaternary pollen spectra (ca. 150 sites) were collected from Siberia and surrounding regions with reliable chronologies. Following pollen percentage recalculations, taxonomic homogenization, and age-depth model revision, a taxonomically harmonized fossil pollen dataset was established covering the last 22 cal ka. Combined with our previous fossil pollen dataset from the eastern part of continental Asia, the spatial and temporal distributions of key arboreal taxa and their driving forces in northern part of continental Asia were investigated on the last glacial-interglacial time-scale by pollen abundance mapping. The invasion histories of trees are discussed before background information from proxy and modelling evidence on climate change and permafrost evolution.

Development and dynamics of ice-wedge polygons in NE Siberia revealed by interdisciplinary palaeoecological research

Pim de Klerk[1], Mariusz Gałka[2], & Hans Joosten[3]

[1] *State Museum of Natural Science Karlsruhe, Germany*
[2] *Adam Mickiewicz University Poznan*
[3] *Ernst Moritz Arndt University Greifswald*

Whereas classically ice-wedge polygons are considered rather stable landscape elements, recent research indicated that they are in fact highly dynamic systems. In order to reconstruct their development, we studied various peat sections from three different polygons in NE Siberia (Fig. 1) covering different microtopographic polygon elements, including depressions, ridges and troughs. Research included pollen -, macrofossil - and testate amoebae analysis, as well as geochemistry, which in combination provide a solid basis for palaeoecological reconstructions.

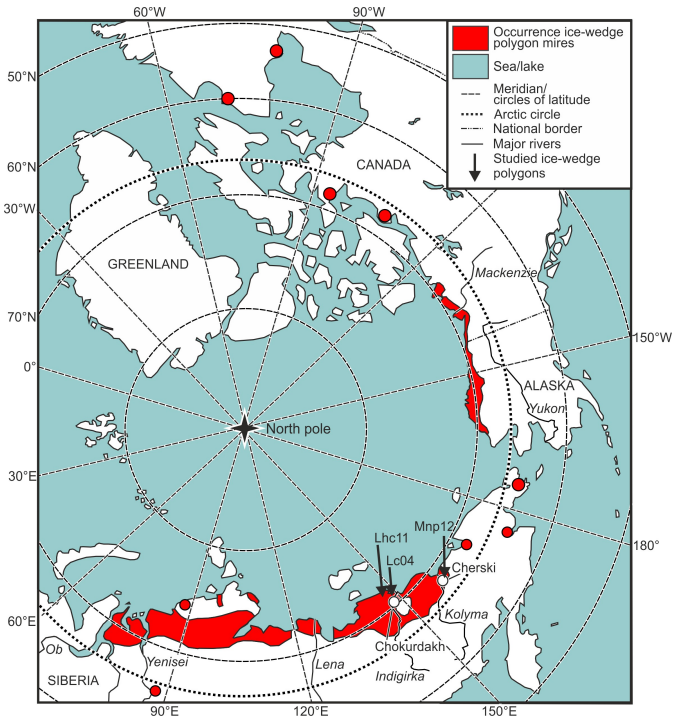

Figure 1: Worldwide distribution of ice-wedge polygon mires, and location of the studied polygons

In low-centred polygon Lc04 near Chokurdakh studies were carried out on a peat section from a ridge centre, a ridge-margin, a collapsed ridge, and the central depression [de Klerk et al., 2011]. Since the centre has been continuously wet, dry phases in the other profiles can be interpreted as phases of ridges carrying a drier vegetation. The polygon seems to have been present since 1400 CE. Around 1800 CE at least two ridges degraded. One of these regenerated after a century, the other remained in collapsed state. Surprisingly, formation of ridges connects to relatively warm climatic periods, whereas ridge degradation correlates to colder phases. This indicates that polygon formation is not ruled primarily by climate, but by indirect climate-dependent agents including e.g. precipitation, meltwater runoff and vegetational changes.

At polygon Lhc11 near Kytalyk - that represents an intermediate state between a low-centred and a high-centred polygon - in total seven profiles were analysed along a seven meter long transect covering the polygon depression, the margins and centre of a ridge, and a polygon trough [Teltewskoi et al., 2016]. The centre was continuously wet. The ridge seems to have existed since ca. 2000 years. The sections from the adjacent trough show that the ridge has in the past been wider, and that its marginal part has collapsed around after 1850-1900 CE or even later. Whereas peat formation at the ridge centre may have ceased already centuries ago, the trough has a rapid accumulation rate up to the present.

The third site Mnp12 consists of a complex of 6-8 former polygons of which the separating ridges have degraded to form a kind of "super-structure". Peat sections were retrieved from the large main depression, from two ridge-centres, and from nearby collapsed ridge-margins.

The comparison of these polygons allow a detailed reconstruction of development and dynamics of three distinctly different polygons, which contributes to a better understanding of ice-wedge polygon development as typical Arctic landscape elements.

References

de Klerk, P.; Donner, N.; Karpov, N.S.; Minke, M. and Joosten, H. [2011]: Short-term dy-

namics of a low-centred ice-wedge polygon near Chokurdakh (NE Yakutia, {NE} Siberia) and climate change during the last ca 1250 years . *Quaternary Science Reviews*, 30(21–22):3013–3031, doi:10.1016/j.quascirev.2011.06.016.

Teltewskoi, A.; Beermann, F.; Beil, I.; Bobrov, A.; De Klerk, P.; Lorenz, S.; Lüder, A.; Michaelis, D. and Joosten, H. [2016]: 4000 Years of Changing Wetness in a Permafrost Polygon Peatland (Kytalyk, NE Siberia): A Comparative High-Resolution Multi-Proxy Study. *Permafrost and Periglacial Processes*, 27(1):76–95, doi:10.1002/ppp.1869.

Patterns in vegetation and pollen deposition along surface sample transects in three ice wedge polygon

Pim de Klerk[1] & Hans Joosten[2]

[1] *State Museum of Natural Science Karlsruhe, Germany*
[2] *Ernst Moritz Arndt University Greifswald*

For a correct understanding of palynological data from ice-wedge polygons, it is crucial to understand the relationship between plants and pollen deposition in these landscape elements. In order to study this relationship, palynological surface samples were investigated along transects through three different ice-wedge polygons in NE Siberia: Lhc11 near Kytalyk [de Klerk et al., 2014], Lc04 near Chokurdakh [De Klerk et al., 2009] and MNP12 near Pokhodsk. Lc04 is a typical low-centred polygon, whereas Lhc11 seems to represent an intermediate stage between a low-centred and a high-centred polygon. MNP12 is a complex of 6-8 single polygons of which the separating ridges have collapsed to form a single "super-structure". Vegetation of these polygons was mapped in plots of 1 m2, and pollen surface samples were taken with a distance of 1 m (Fig. 1).

There is a clear connection between vegetation and microtopography, with wetliving plant taxa in the polygon depressions and –troughs (including e.g. *Carex chordorrhiza*, *Comarum palustre*, and *Utricularia*), and considerably drier vegetation on the polygon ridges (consisting of among others *Betula exilis*, *Rubus chamaemorus* and *Ericales*).

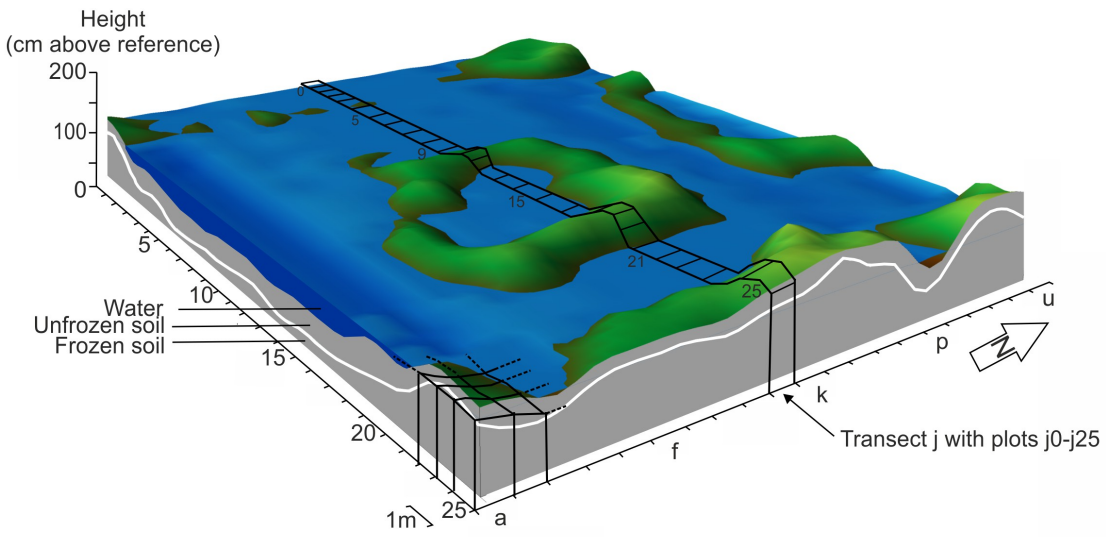

Figure 1: Research strategy of pollen surface sample research in ice-wedge polygons (example Lhc11): the polygon is divided into plots of 1m2 for vegetation relevees and measurement of abiotic parameter; surface samples are collected along one transect

High pollen/spore deposition normally occurs at only few plots within the total distribution range, which means that only one or few plant specimens obtain optimal flowering or pollen production. The distance to which enlarged deposition values (local and extralocal pollen deposition) occur are restricted to only one or two metres. Non-pollen-palynomorphs show a good relation with surface elevation: the *testate amoebae Assulina*, *Amphitrema* (*Archerella*) and *Arcella* occur at the higher polygon ridges, whereas algae of the *Zygnemataceae* family dwell in the wet polygon centres and troughs. These clear patterns indicate that past presence of various microtopographic polygon elements can be clearly identified in palaeoecological studies of peat sections, thus enabling reconstruction of polygon genesis and development [de Klerk et al., 2011].

The three sites show clear differences in their vegetation distribution connected to the different morphology of the polygons. Also pollen deposition patterns of various plant taxa differ greatly between the sites. This illustrates the complex relationship between plants, flowers and flowering, pollen production, pollen dispersal and pollen depositions, and polygon microtopography including depressions, ridges and throughs.

References

De Klerk, P.; Donner, N.; Joosten, H.; Karpov, N.S.; Minke, M.; Seifert, N. and Theuerkauf, M. [2009]: Vegetation patterns, recent pollen deposition and distribution of non-pollen palynomorphs in a polygon mire near Chokurdakh (NE Yakutia, NE Siberia). *Boreas*, 38(1):39–58, doi:10.1111/j.1502-3885.2008.00036.x.

de Klerk, P.; Donner, N.; Karpov, N.S.; Minke, M. and Joosten, H. [2011]: Short-term dynamics of a low-centred ice-wedge polygon near Chokurdakh (NE Yakutia, {NE} Siberia) and climate change during the last ca 1250 years . *Quaternary Science Reviews*, 30(21–22):3013–3031, doi:10.1016/j.quascirev.2011.06.016.

de Klerk, P.; Teltewskoi, A.; Theuerkauf, M. and Joosten, H. [2014]: Vegetation patterns, pollen deposition and distribution of non-pollen palynomorphs in an ice-wedge polygon near Kytalyk (NE Siberia), with some remarks on Arctic pollen morphology. *Polar Biology*, 37(10):1393–1412, doi:10.1007/s00300-014-1529-3.

Holocene vegetation change and turnovers of treeline forming species

Laura Saskia Epp[1], Stefan Kruse[1], Nadja J. Kath[1], Ludmila Pestryakova[2], & Ulrike Herzschuh[1]

[1] *Alfred Wegener Institute Helmholtz Centre for Polar and Marine Research, Potsdam, Germany*
[2] *Institute of Natural Sciences, North-Eastern Federal University of Yakutsk, Russia*

The prospected strong high-latitude warming is projected to cause a northward move of the arctic-boreal treeline. These changes will potentially have significant effects on climate, but their timing and mode are not well understood. Besides being governed directly by temperature increases, speed of treeline changes will also be influenced by the capacity of migration and establishment, and by competition between different treeline forming species. In Siberia, where about half of the global circum-arctic boreal treeline is located, the treeline is formed by monospecific stands of three species of larch, Larix sibirica, Larix gmelinii and Larix cajanderi. There is clear evidence for ecological separation, particularly between L. sibirica and the northeastern species, with only L. gmelinii and L. cajanderi being able to survive on permafrost with an active layer depth of less than 1-2 m, but L. sibirica being competitively superior at sites with low permafrost tables. Under a warming climate, the respective ranges of the treeline forming species are projected to shift to the Northeast, causing turnovers of forest tree species. The Siberian treeline has undergone several pronounced latitudinal fluctuations in the Holocene, and detailed analyses of the historical processes of vegetation change and competitive displacement would add to predictions for the projected future shift. We are using sedimentary ancient DNA to analyze lake sediment cores spanning most of the Holocene from the southern Taymyr peninsula, where the ranges of L. sibirica and L. gmelinii come together. Changes of the complete vegetation are revealed by DNA metabarcoding and pollen analyses, while diagnostic mitochondrial haplotypes trace the temporal dynamics in distribution of the two closely related larch species. We incorporated these two species into our larch population dynamics model LAVESI to understand the influence competition between these species might have on the speed and timing of treeline movement under changing climates. Simulations were forced with regional climate series at locations in the vicinity of the sampled lakes. These analyses offer a very high degree of resolution and shed light on the complicated ecological processes leading to a change in overall vegetation.

Resilience of plants communities to changes in climate, fire regime and carbon accumulation: Palaeoecological insights from arctic peatlands in Alaska

Mariusz Gałka[1], Graeme Swindles[2], Angela Gallego-Sala[3], Marta Szal[4], & Angelica Feurdean[5]

[1]*Department of Biogeography and Palaeoecology, Adam Mickiewicz Univeristy in Poznań, Poland*
[2]*School of Geography, University of Leeds, United Kingdom*
[3]*Department of Geography, University of Exeter, United Kingdom*
[4]*Institute of Biology, University in Białystok, Poland*
[5]*Biodiversity and Climate Research Centre (BiK-F), Frankfurt am Main, Germany*

High-latitude ecosystems have experienced higher-amplitude climate warming than other parts of the globe in recent decades, and are projected to continue to warm in the future, with consequences for vegetation communities, peat accumulation rates and carbon cycling [Yu, 2012, Kuhry et al., 2013]. Specifically, tundra vegetation communities are increasing in terms of cover and height, and fires are becoming more frequent [Myers-Smith et al., 2011]. These processes restrict the growth of other plant species by limiting light availability and increasing the frequency and intensity of fires. Most of the data concerning the response of plant communities (species, biomass phenology) to recent warming is based on current observational studies, with comparatively little research focusing on centennial to millennial scale changes. In addition, there are limitations in our understanding of fire regime dynamics and in particular of the tolerance of tundra plant species to increased fire frequencies. Therefore, studies that focus on long-term vegetation dynamics under varying environmental conditions are indispensable to our understanding of the contemporary changes in vegetation and the most likely long-term response to future climatic changes.

In this palaeoecological study, we use the fossil record (plant macroremains, testate amoebae, macro- and microcharcoal, carbon accumulation) and ^{210}Pb (for the last 150 years) and AMS ^{14}C measurements to determine the response of arctic plant communities to past climate warming in northern Alaska. Specific aims of our palaeoecological studies are:

i) to reconstruct local and regional vegetation changes during the last millennium; ii) to evaluate the influence of changes in climate and autogenous succession in the development of arctic plant communities; iii) to explore fire regime dynamics and vegetation feedback on fire activity; and iv) to determine shifts in carbon accumulation rates. We hypothesize that during warm climate episodes such as the Medieval Warm Period (MWP) or the more recent decades, moss-dominated vegetation communities become replaced by shrub-dominated communities and there are increased carbon accumulation rates in arctic peatlands.

To carry out our paleoecological studies, we selected eight peatland sites along a South-North transect, from the foothills of the Brooks Range, Toolik Field Station to Prudhoe Bay, along the road No. 11. In three of these peatlands, we additionally conducted replicated multi-proxy and high-resolution palaeoecological studies by analysing two cores. This replication improves the reliability of the paleoecological interpretations. The results from peatland sites in Alaska will allow for intercontinental comparison with both North America and European data of Arctic vegetation development, fire regime and carbon accumulation rates during the last millennium.

References

Kuhry, P.; Grosse, G.; Harden, J. W.; Hugelius, G.; Koven, C. D.; Ping, C-L.; Schirrmeister, L. and Tarnocai, C. [2013]: Characterisation of the Permafrost Carbon Pool. *Permafrost and Periglacial Processes*, 24(2):146–155, doi:10.1002/ppp.1782.

Myers-Smith, I.H.; Forbes, B.C. and Wilmking, M. et al. [2011]: Shrub expansion in tundra ecosystems: dynamics, impacts and research priorities. *Environmental Research Letters*, 6(4):045509, doi:10.1088/1748-9326/6/4/045509.

Yu, Z. C. Northern peatland carbon stocks and dynamics: a review. *Biogeosciences*, 9(10):4071–4085, doi:10.5194/bg-9-4071-2012.

Macrophyte (*Potamogeton sp.*) and ancient DNA analyses from Lake Sediments - Lake Karakul, Tajikistan

Liv Heinecke[1,2], Steffen Mischke[3], Maria Reschke[1,2], Laura Epp[1], Kathleen Stoof-Leichsenring[1], Ilhomjon Rajabov[4], & Ulrike Herzschuh[1,2]

[1] *Alfred Wegener Institute Helmholtz Centre for Polar and Marine Research, Potsdam, Germany*
[2] *University of Potsdam*
[3] *University of Iceland*
[3] *Climate Change Center*

Mountainous ecosystems in general and the high mountain areas of arid Central Asia in particular are very sensitive towards changes in moisture and temperature and therefore most likely to be affected by climate change. To be able to get a closer insight into the alpine system of the Pamir Mountains, a 11.25 m long core was retrieved from the eastern basin of Lake Karakul (3,929 m asl, 12 m water depth), Tajikistan. The brackish lake is located in a tectonic basin and the catchment is comprised of high alpine steppe to desert with partially snow-covered mountain peaks, up to 6,000 m asl, which are the main source of freshwater input into the lake. Annual precipitation averages at 82 mm and temperatures are approx. -3.8 °C in the annual mean. An age-depth model was constructed on 14 radiocarbon ages and an age of approximately 29 cal kyrs BP was determined for the core base.

In order to gain insights into palaeolimnological and hydrolocial changes we used two approaches. First, we investigated the nutrient content and paleo-productivity by means of biogeochemical analyses and second, we used an ancient DNA metabarcoding approach to identify changes in the submerged water-plant communities. In order to gain insights into changes in the paleo-productivity of Lake Karakul over the last 29 cal kyrs BP, we examined temporal gradients of elemental content (TOC, TN) and stable isotopes (δ^{13}C, δ^{15}N) of macrophyte remains (*Potamogeton sp.*) through the core. Thereby we made use of the ability of submerged macrophytes, such as Potamogeton, to use HCO3- for photosynthesis in times of CO_2 shortage and used the transferfunction published by Herzschuh et al. [2010] to reconstruct paleo-productivity. Furthermore we investigated temporal changes in the submerged plant community via ancient DNA metabarcoding analyses of 42 sediment samples. Biogeochemical analyses showed significant variations from core base until approximately 20 cal kyrs BP with $TOC_{Potamogeton}$ 25-45 %, $TN_{Potamogeton}$ 0.5% - 1.5%, δ^{13}C Potamogeton below -9 ‰ and $\delta^{15}N_{Potamogeton}$ of below 3.5 ‰ suggesting a cool climate and reflecting the Last Glacial Maximum at the bottom of the core. Sediments in

the upper 4.5 m (approx. 6.7 cal kyrs BP) were rich in macrophyte remains. Data retrieved from this part of the core revealed higher $TOC_{Potamogeton}$ and $TN_{Potamogeton}$ values. An enrichment of heavier isotopes with δ^{13}C Potamogeton up to -7 ‰ and $\delta^{15}N_{Potamogeton}$ up to 6 ‰ indicate a higher productivity within the lake due to more favourable conditions for macrophyte growth at the lake bottom. We assume shifts towards a warmer climate and

changes in lake level to be the dominating cause. No macrophyte remains were preserved in the investigated deposits from 20 to 7 cal kyrs BP. We suggest that this indicates either unfavourable conditions for plant growth at the coring site or a poor preservation environment during this time. We used a metabarcoding approach with subsequent Illumina sequencing focusing on chloroplast DNA with universal plant primers (g-h) after Taberlet et al. [2007]. The application of ancient sedimentary DNA analysis revealed 37 plant taxa within the core sediments, of which 35 are of terrestrial origin. However, the DNA sequences were dominated by two aquatic plant taxa (*Potamogeton sp.* and *Characeae*). The sequences of the identified aquatic taxa were used for a semi-quantitative evaluation of aquatic plant composition and showed a reversal in abundance between 20 and 13 cal kyrs BP. This is coherent with changes obtained by the biogeochemical analyses. The combination of biogeochemical and ancient DNA analyses demonstrated that both methods can complement and verify each other. We were able to detect shifts in the living

environment at the lake bottom from the LGM to the Late Holocene as well as from the surrounding vegetation / from the catchment area of the lake. Therefore, our results improved our understanding of ecological responses in the Pamir Mountains.

References

Herzschuh, U.; Mischke, S.; Meyer, H.; Plessen, B. and Zhang, C. [2010]: Lake nutrient variability inferred from elemental (C, N, S) and isotopic ($\delta^{13}C$, δ15N) analyses of aquatic plant macrofossils. *Quaternary Science Reviews*, 29(17–18):2161–2172, doi:10.1016/j.quascirev.2010.05.011.

Taberlet, P.; Coissac, E.; Pompanon, F.; Gielly, L.; Miquel, C.; Valentini, A.; Vermat, T.; Corthier, G.; Brochmann, C. and Willerslev, E. [2007]: Power and limitations of the chloroplast trnL (UAA) intron for plant DNA barcoding. *Nucleic Acids Research*, 35(3):e14, doi:10.1093/nar/gkl938.

The emergence of permafrost as vegetation driver in Siberia from the Plio-Pleistocene Transition onwards

Ulrike Herzschuh[1,2], John Birks[3,4], Andrei Andreev[5,6], Martin Melles[5], & Julie Brigham-Grette[7]

[1] *Alfred Wegener Institute Helmholtz Centre for Polar and Marine Research, Potsdam, Germany*
[2] *Institute of Earth and Environmental Sciences, University Potsdam, Potsdam, Germany*
[3] *Department of Biology, University of Bergen, and Bjerknes Centre for Climate Research, Bergen, Norway*
[4] *Environmental Change Research Centre, University College London, London, UK*
[5] *Institute of Geology and Mineralogy, University of Cologne, Cologne, Germany*
[6] *Institute of Geology and Petroleum Technologies, Kazan Federal University, Kazan, Russia*
[6] *Department of Geosciences, University of Massachusetts-Amherst, USA*

Vegetation change on all relevant temporal scales is assumed to be primarily driven by contemporary climate change. However, our results from multivariate analyses of pollen assemblages from Lake El´gygytgyn (NE Siberia) and other data covering the Mid-Pliocene-Warm-Period and the Plio-Pleistocene-Transition challenge this concept of broad-scale vegetation-climate equilibrium. Our results indicate that interglacial vegetation during the Plio-Pleistocene transition mainly reflects the condition of the preceding glacial instead of contemporary interglacial climate. We assume that the observed vegetation-climate disequilibrium, in particular the absence of pine and spruce in interglacials following strong glacial stages, originates from the combined effects of permafrost persistence, distant glacial refugia, and fire plus possible interactions. Our results imply that today's widespread larch ecosystem on permafrost is not in climate-equilibrium but rather represents a transient vegetation type which is still responding to the extreme glacial condition of the last glacial.

Last interglacial versus last cold stage: Palaeovegetation in North Yakutia's most continental part recorded in the Batagay permafrost sequence

Frank Kienast[1], Kseniia Ashastina[1], Natalia Rudaya[2], & Karsten Wesche[3]

[1]*Senckenberg Research Institute and Natural History Museum, Research Station of Quaternary Palaeontology, Weimar, Germany*
[2]*Centre of Cenozoic Geochronology (RAS SB), Institute of Archaeology & Ethnography Novosibirsk, Russia*
[3]*Senckenberg Museum for Natural History Görlitz*

Situated in the Yana-Highlands, the Batagay permafrost profile is the only active outcrop in interior Yakutia exposing an intact, more or less complete sequence of deposits of the Late Pleistocene and beyond. With Verkhoyansk recorded as place of the pole of cold, the Yana Highlands represent the region with the most severe climatic continentality in the northern hemisphere. Due to Quaternary sea level fluctuations, today's coastal lowlands in Yakutia were intermittently hit by tremendous coast line shifts. The Yana Highlands in contrast were always unaffected by maritime climate influence, which has been regarded as trigger of ecosystem restructuring in the lowlands at the dawn of the Holocene (Kienast 2013). Palaeoecological proxies preserved in the Batagay permafrost sequence thus presumably indicate the macroclimate evolution in NE-Siberia independently of regional maritime climate influence during phases of sea level high stands. Due to persisting continentality, interior Yakutia can be regarded one of the last stands of Pleistocene megafauna in Beringia. The outcrop thus represents a unique window into the evolution of terrestrial ecosystems in Beringia.

The modern vegetation around the outcrop is light coniferous forest composed of larch (*Larix gmelinii*) and Siberian dwarf pine (*Pinus pumila*) as well as, in the shrub layer, *Salix spp., Alnus fruticosa, Betula divaricata*, and *B. exilis*. Among dwarf shrubs, *Ledum palustre* and *Vaccinium vitis-idaea* are common. The ground is mostly wet and is densely covered with a thick layer of lichens and mosses allowing only few grasses and herbs to establish.

The Batagay outcrop formed as result of intense thermal degradation within about 30 years cutting 60 m deep into ice-rich permafrost deposits (Kunitsky et al. 2013). A 30 meter thick Ice Complex with characteristic, thick ice wedges constitutes a major part of the sequence. Overlaying a horizontally stratified silty-sand unit, an up to 2 m thick layer of plant material of presumably Eemian (Kazantsevo) origin is situated at the base of the Ice Complex. The plant material included large woody remains and was used for AMS radiocarbon dating (Poznan Radiocarbon Laboratory) with an indefinite result of >44.000 ^{14}C years BP.

The accessible upper part of the sequence (about 45 meters) was sampled from top to bottom in one meter steps. The samples were taken especially for plant macrofossil and other palaeoecological studies but also for sedimentological analyses. Characterized in general by a grain size signature typical for Ice Complex deposits, the Batagay profile is distinguished by a comparatively high fraction of fine sand over the whole recorded sequence, probably due to increased aeolian deposition from local sources.

Owing to the high fraction of sand, the preservation of fossil organism remains is in general relatively poor. This applies especially to pollen. We therefore focussed on material exceptionally rich in plant macrofossils. Based on two such plant fossil beds, we exemplarily contrasted the local palaeo-vegetation reconstructed for two major climate phases: the last (Zyryan) cold stage and the preceding (Kazantsevo) interglacial. The results are furthermore compared with modern vegetation in the area.

Fossil plant material, assigned to the last interglacial, was taken from the organic-rich layer beneath the base of the Ice Complex. It included numerous macroremains of plants characteristic for northern taiga forests as they occur today at the study site. Main components are larch (*Larix gmelinii*) as well as birches (*Betula spp.*) and alder (*Alnus fruticosa*).

Pinus pumila was not detected in the very rich and well preserved macrofossil assemblage indicating that this species was really absent. This is an important difference to the modern vegetation, where the

Siberian dwarf pine is very common at the site. Its absence during the last interglacial might indicate high wind exposure and a snow cover thickness of less than 40 cm, which is the minimum requirement of *Pinus pumila*. High amounts of charcoal in the sediment indicate fire events during the last interglacial. As a nitrophytic ruderal plant, *Urtica dioica* was found in high abundance. *Urtica* is an indicator of habitats eutrophic and disturbed may be as a result of zoogenic or fire action. Also, *Rubus idaeus* was common in the fossil assemblage. It also frequently occurs in forest glades after fires. *Sonchus arvensis* is another ruderal plant characteristic of highly disturbed ground.

Another contrast of last interglacial palaeovegetation to the modern plant cover at the site is the occurrence of open ground plants including grassland species such as *Poa sp.*, *Festuca sp.*, and *Puccinellia sp.* The latter is typical of meadows at places with fluctuating moisture, as they occur under arid conditions in continental regions. Xerophilous plants like *Papaver sp.* and the endemic species *Potentilla tollii* also indicate locally dry habitats existing in the area during the last interglacial.

The cold stage plant assemblage originates from material gathered by rodents in their burrow for winter storage. The rodent's nest was found within the Ice Complex sequence at a depth of about 460 cm below surface. On the basis of their droppings, the originators of the plant depot were identified as arctic ground squirrels (*Urocitellus parryii*, L. Maul, Senckenberg Weimar, personal communication). According to the results of our plant macrofossil analyses, the local vegetation during the last cold stage was composed almost exclusively of steppe plants such as *Alyssum obovatum, Artemisia sp., Agropyron cristatum, Festuca cf. lenensis., Koeleria cf. cristata, Phlox sibirica, Eremogone capillaris* and *Potentilla arenosa*. Also species characteristic of dry arctic/ alpine meadows (*Kobresietea*) like *Arnica sp.*, *Eritrichium villosum* and *Myosotis asiatica* could be identified. Two remains of *Larix* indicate the scattered presence of trees in the Yana highlands also during the last cold stage. The ground squirrels obviously harvested selectively, which is visible by the high proportion of nutritious inflorescences and fruits, e.g. from *Plantago canescens*, *Artemisia* and *Silene samojedorum* (*Lychnis sibirica*). P*lantago canescens* as a ruderal plant might also be a clue of frequent disturbances of vegetation due to grazing and trampling by herbivores.

In summary, the Last Interglacial plant macrofossil assemblage of the Batagay outcrop represents a mosaic of woody and open ground plant communities in a dry, herb-rich light-coniferous taiga that experienced wildfires. In the studied sample, pollen was nearly absent. Another sample, assumed to represent last interglacial deposits, was dominated by pollen of *Ericales*. High amounts of pollen from *Artemisia, Caryophyllaceae* and other herbs also indicate the presence of locally open ground and dry habitats. The plant macrofossil assemblage indicates that continentality was even higher than today. The absence of *Pinus pumila* is an argument for snow thickness less than today.

Figure 1: Pinus pumila is important constituent of modern vegetation (left photo) at the Batagay permafrost outcrop (right photo). But the species could not be recorded in plant macrofossil assemblages obtained from last interglacial permafrost deposits (inserted).

The presence of haline and xerophilous plants can be regarded as evidence for dry habitat conditions. Dry conditions absolutely prevailed during the subsequent cold stage, where almost exclusively steppe and dry alpine grassland plants could be proven by plant macrofossils. Only few larch remains indicate

the scattered occurrence of trees during that time. Palynological data from Ice Complex deposits 1m below the studied ground squirrel nest are dominated by spores of *Selaginella*, which is an indicator of dry exposed ground.

References

Kienast, F. [2013]: Plant macrofossil records – Arctic Eurasia. In: Elias, Scott A. and Mock, Cary(eds.), *Encyclopedia of Quaternary Science*, volume 3, pages 733–745. lsevier, 2nd Edition, ISBN: 9780444536433.

Kunitsky, V.V.; Syromyatnikov, I.I.; Schirrmeister, L.; Skatchkov, Yu. B.; Grosse, G.; Wetterich, S. and Grigoryev, M.N. [2013]: Ice-rich permafrost and thermal denudation in the Batagay area (Yana Upland, East Siberia). *Kryosfera Zemli (Earth's Cryosphere)*, 17(1):56–68, URL http://www.izdatgeo.ru/pdf/krio/2013-1/56.pdf.

Siberian treeline dynamics in a warming climate - results from larch population genetics and vegetation modelling

Stefan Kruse[1], Laura S. Epp[1], Kathleen Stoof-Leichsenring[1], Ludmila Pestryakova[2], & Ulrike Herzschuh[1]

[1] *Alfred Wegener Institute Helmholtz Centre for Polar and Marine Research, Potsdam, Germany*
[2] *Institute of Natural Sciences, North-Eastern Federal University of Yakutsk, Yakutsk, Russia*

A vegetation change from open tundra to dense taiga will fuel the global warming by positive feedback caused by albedo decreases. Yet, it is unclear how fast the arctic treeline, formed of *Larix* species, will advance north in the next decades. The most determinant factor of tree migration is the ability to disperse seeds (and pollen). Hence, to realistically forecast the migration of tree species in a dynamic vegetation model, it is crucial to incorporate reliable estimates of dispersal. Classical methods, for example counting seeds in seed traps, have been used to describe local dispersal abilities but are not applicable to give precise estimates on rare long-distance dispersal events. In this study we overcome this with the help of modern molecular techniques. By using a set of 16 nuclear microsatellites we inferred the cryptic signal of heritage among larch individuals to study the migration history among well-established tree stands and for different time-cohorts. We analyzed the genetic structure of larch populations for several latitudinal transects spanning north-to-south from tundra to open taiga forests in Siberia and additionally of several age cohorts which established throughout the last century in prevailing cold and warm periods. Finally, we present the results of simulations with our individual-based model LAVESI which was developed by us originally to study population dynamics of larch forest stands. Using downscaled global climate models and 'representative carbon pathway' (RCP) scenarios it is feasible to project the future treeline in Siberia.

Time-lagged response of siberian treeline forests revealed by individual-based modelling

Stefan Kruse[1], Mareike Wieczorek[1], Florian Jeltsch[2], & Ulrike Herzschuh[1]

[1] *Alfred Wegener Institute Helmholtz Centre for Polar and Marine Research, Potsdam, Germany*
[2] *Institute of Biochemistry and Biology, University of Potsdam, Potsdam, Germany*

Global warming allows Arctic vegetation, which is mainly limited by temperatures, to move north. A change from tundra to taiga will cause a decrease of albedo which further fuels the warming through positive feedback mechanisms. This raises several questions of which we want to address here:

1. Will trees move northwards and thereby change vast treeless tundra areas to taiga?

2. And if so, how long does this response lags behind the temperature changes?

To answer these questions we built an individual-based and spatially-explicit vegetation simulator model for larches in Siberia (LAVESI). We present the parametrization and validation of the model's incorporated processes which describe the full life-cycle of the simulated larch species *Larix gmelinii*. Furthermore, we share results of the first regional-scale simulations testing the model's performance at the Taymyr Peninsula, Russia, ranging from 64-80°N and 92-120°E. In a second experiment, we tested the influence of up to 6 °C warmer and cooler climates on simulated populations. Our results show that already the recent temperature rise will allow forests to expand farther north by roughly one degree, when no seed limitation hinders populations to migrate. Furthermore, climate warming caused populations to densify but with a time-lag of decades. We conclude that in the near future expanding taiga after its first establishment in the former tundra will rapidly form dense tree stands, thus ultimately fuelling the feedback loop of global warming. We show that simulation results of the newly-build vegetation model were reliable, and hence the model can be used as a tool to improve our knowledge about individual-based processes that are important to understand past and future treeline migration.

A biomarker-based paleoclimatic reconstruction of MIS1, MIS3 and MIS5e based on permafrost deposits from NE Siberia

Jannik Martens[1], Stephanie Kusch[1], Maria Winterfeld[2], Gesine Mollenhauer[2], Georg Schwamborn[3], Lutz Schirrmeister[3], Sebastian Wetterich[3], Pier Paul Overduin[3], & Janet Rethemeyer[1]

[1] *Institute of Geology and Mineralogy, University of Cologne, Cologne, Germany*
[2] *Alfred Wegener Institute Helmholtz Centre for Polar and Marine Research, Bremerhaven, Germany*
[3] *Alfred Wegener Institute Helmholtz Centre for Polar and Marine Research, Potsdam, Germany*

Understanding long-term environmental dynamics is crucial to elucidate recent and predict future feedback processes of permafrost in a changing environment. Northeastern Siberia is a key site to study organic matter (OM) that has been formed during the Pleistocene. This OM contains information about past vegetation, environment, and organismic communities, thus, offering the potential to understand environmental change of Arctic Russia on glacial and interglacial timescales.

We analyzed five permafrost cores from Bol'shoy Lyakhovsky Island and the Buor Khaya Peninsula to study the environmental history of Northeastern Siberia for the past 130 kyr (MIS1, MIS3, and MIS5e) using molecular and isotopic tools. We present a comprehensive biomarker data set including terrestrial vascular plant biomarkers such as n-alkanes, n-fatty acids, and lignin phenols. In addition, we analyzed bacterial and archaeal membrane lipids including branched and isoprenoid glycerol dialkyl glycerol tetraethers (brGDGTs and isoGDGTs) and bacteriohopanepolyols (BHPs) from which environmental properties including mean annual air temperatures (MAAT) and pH, and bacterial taxonomic information can be constrained. Initial results show that MAATs as determined using brGDGTs were on average higher during MIS3 than MIS1 on both Bol'shoy Lyakhovsky Island and the Buor Khaya Peninsula. Higher MAATs during MIS3 are accompanied by lower BIT indices (based on brGDGTs and isoGDGTs) indicating relatively higher in-situ archaeal production than during MIS1 when bacteria dominate and soil pH is lower. On Bol'shoy Lyakhovsky Island vascular plant-derived, high molecular weight (HMW) n-alkanes are also more abundant in the MIS1 deposits than the MIS3 deposits and co-vary with low pH and low MAAT while the opposite trend is observed for the Buor Khaya Peninsula deposits. HMW n-alkanes characteristic for Poaceae and Cyperaceae dominate the n-alkane assemblages during warm stages, while n-alkanes typical for the moss Hylocomium are less abundant indicating the pre-dominance of grass over moss during interstadials/interglacials. Moreover, n-alkane assemblages indicate that the grass community is dominated by Cyperaceae during all warm stages, but MIS1 is characterized by a stronger contribution of Poaceae in comparison to MIS3 in deposits from both Bol'shoy Lyakhovsky Island and the Buor Khaya Peninsula. HMW n-fatty acids inventories and assemblages show no pronounced difference for MIS1 and MIS3 deposits.

BHPs and lignin phenols are currently being analyzed as well as samples from Bol'shoy Lyakhovsky Island representing MIS5e. BHPs analysis will help to characterize bacterial communities and lignin phenols will contribute to disentangling vascular plant input from angiosperm and gymnosperm sources.

Climatic and environmental implications of millennial-scale phases of ice-rich permafrost active layer installation in western Europe between 35 and 20 ka evidenced by terrestrial mollusc fauna

Olivier Moine & Pierre Antoine

CNRS, France

On the continents, loess deposits are the main archive for the reconstruction of glacial palaeoenvironments in the periglacial domain. Indeed, during the Last Glacial, aeolian deposits covered most of the European lowlands between the ice caps and the Mediterranean domain. The most common traces of permafrost activity in loess deposits are tundra gley horizons. Absent from the Pannonian Basin and southeastern areas and only unsystematically present in Bohemia and Moravia, these hydromorphic soils are typical for loess sequences north of the Alps and the Carpathians from France to Ukraine, where they alternate with typical loess units. Loess units rarely show obvious glacial features owing to very dry conditions prevailing during their deposition. Also tundra gley horizons are not always cryoturbated and accompanied by ice-wedge casts. Loess-tundra gley alternations are not simply the result of binary climatic changes. Due to progresses in palaeoclimatology during the last decades, loess deposits have been studied more intensively using multi-proxy approaches. New proxies are regularly developed and proposed to understand the dynamics of sedimentary alternations and to reconstruct associated past environmental and climatic changes.

The first important resulting step was the development of a correlation scheme between the west-European reference loess sequence of the Nussloch (Rhine Valley, Germany) and the Greenland global climate records. Indeed, to elude the lack of precision and accuracy of luminescence dating methods, the main variations of two proxies of aeolian dynamics, i.e. the grain size index in loess and the dust concentration in ice, were used to correlate both types of records. Loess-tundra gley alternations then appeared to be linked with millennial-scale climatic changes known as stadial-interstadial, or Dansgaard-Oeschger, cycles. This correlation demonstrates that tundra gley horizons constitute periglacial palaeoenvironmental responses to global climatic changes and consequently are entities that can be correlated across the whole European Loess Belt.

The second important step was the characterisation of palaeoenvironmental changes associated with the development of tundra gley horizons based on high resolution multiproxy analyses including granulometry for aeolian dynamics, magnetic susceptibility for pedogenesis, total organic carbon content for vegetation density and malacology for vegetation diversity and edaphic factors. This combination resulted in a conceptual scheme depicting palaeoenvironmental changes in loessic context associated with the different phases of stadial-interstadial cycles.

The previous step highlighted the potential of one of the oldest loess palaeoenvironmental proxies – terrestrial molluscs – that have not yet been adequately investigated even by basic community analyses. Their study in European loess deposits dates back from the 19^{th} century and their spatial and temporal ubiquity compensates for the quasi-absence of pollen grains, which are poorly preserved in the porous carbonated sediments. A compilation of west-European terrestrial mollusc assemblages between 35 and 20 ka ago has thus been performed to depict palaeoenvironmental changes linked with loess-tundra gley alternations, which are particularly well-expressed from this time interval.

From a spatial point of view, the grouping of species according to their geographical distribution allowed to define several malaco-biogeographical domains characterised by increasing species richness from France to Germany. From a temporal point of view, the reconstruction of the environmental dynamics associated with loess-tundra gley alternations was not possible by these old data as most of the sites included only a few samples for the selected time interval. Only a few high resolution records were published in a pioneer work by Remy (1969), who, however, didn't consider the concept of millennial-scale climatic changes. The next contribution was the analysis of the Nussloch

loess sequence in 2003. Since then, other molluscan records from northern France allowed for comparisons with the Rhine Valley, each being in different malaco-biogeographical domains.

The comparison of the studied high resolution molluscan records throughout loess-tundra gley alternations highlights the following phases and changes:

1. deposition of typical loess units: low abundant molluscan fauna in both domains although there is a higher richness in the Upper Rhine Valley than in northern France;

2. tundra gley installation: successive quick and strong increases in abundances initially of dry- and then of wet-loving taxa in both domains, no or limited appearance of shade-loving taxa in northern France and in some places of the Middle Rhine Valley, disappearance of shade-loving taxa in other places of the Middle Rhine Valley and progressive disappearance of the most shade-loving taxa in the Upper Rhine Valley;

3. tundra gley thawing: highest molluscan abundances and highest proportions in hygrophilous taxa in both domains, no or slight disappearance in dry- or shade-loving taxa in northern France and Middle Rhine Valley, disappearance of shade-loving taxa in the Upper Rhine Valley;

4. tundra gley cryoturbation and loess deposition resuming: sudden and important decrease in molluscan abundances, no species appearance in northern France, disappearance of shade-loving species or slight appearance of dry- and shade loving species in the Middle Rhine Valley, reappearance of dry and shade loving species in Upper Rhine Valley.

As a chronological framework on the basis of correlations between loess sequences grain size index and ice-core dust concentration and oxygen isotope records, loess deposition phases

1. are linked with stadials, permafrost installation phases

2. are linked with stadial-interstadial transitions, tundra gley thawing phases

3. are linked with interstadial optimums, and tundra gley cryoturbation and loess resumption are linked with interstadial-stadial transitions.

Furthermore, several nested spatial consequences result from this conceptual scheme.

Summarised,

a) in the western domain, the molluscan faunas have always the same poor composition with a pool of 6-7 taxa; only abundances increase during interstadial phases;

b) in the intermediate domains, molluscan faunas are similar or tend to be similar to those of the western domain during stadial phases and interstadial optimums but may be richer during stadial-interstadial transitions;

c) at the Nussloch “hotspot”, molluscan faunas are the richest, especially during stadial phases, but tend to resemble those of the western domain during transitions from stadial to interstadial conditions.

As a result, changes in the terrestrial mollusc faunas highlight

1. that the increasing West-East richness gradient tends to be maximum during loess deposition phases and minimum during interstadial optimums, and

2. that in most sites, except the Nussloch hotspot, optimum phases with vegetation diversification occurred during stadial-interstadial transitions, whereas stadials were characterised by conditions too cold and too dry for molluscan faunas, and waterlogged environments prevailed during interstadial optimums.

The installation of an active layer in ice-rich permafrost, evidenced by the development of a tundra gley horizon, thus results from precipitation increases accompanied by longer and milder “warm seasons”. The absence of local moisture sources implies increasing precipitation and thus indicates a reorganisation of the atmospheric circulation also allowing for temperature increases and for the lengthening of the “growing season” as is deduced from the increase in the proportion of juvenile individuals in the thanatocoenoses. As a consequence on glacial palaeoenvironments, permafrost thawing generated moisture access that may benefit vegetation and molluscan fauna in the driest contexts as far as it does not result in waterlogged environment. In the most favourable contexts like Nussloch, biocenoses may impoverish as result of additional moisture supply. Besides, the persistent West-East increasing richness gradient in terrestrial molluscs, a

vegetation diversity gradient from a sparse vegetation cover to shrub tundra persisted too. Nowadays, polar deserts are characterised by longer but drier "growing seasons" than subarctic tundra, and summer precipitation is about one third higher in Heidelberg than in Amiens, and the time period with a monthly temperature average above 15 °C is there about 20 % longer. Thus, as far as modern and Last Glacial situations can be compared, differences in seasonality, as well as a flatter regional topography in northern France, offering potential refuges for more sensitive taxa than in the Rhine Valley, could have contributed to the persistence of this longitudinal vegetation and molluscan fauna richness gradient. In the same way, the trend to more homogeneous situations during the phases of development of an ice-rich permafrost active layer may also result from a reduction of such differences in seasonality at the scale of Western Europe.

Modern and ancient DNA in lacustrine sediments – Vegetation signals unraveled

Bastian Niemeyer[1,2], Laura Saskia Epp[1], Luidmila Pestryakova[3], & Ulrike Herzschuh[1,2]

[1] *Alfred Wegener Institute Helmholtz Centre for Polar and Marine Research, Potsdam, Germany*
[2] *Institute for Earth and Environmental Science of the University of Potsdam, Germany*
[3] *Department of Geography and Biology of Northeastern Federal University Yakutsk, Russia*

Current climatic changes, mostly triggered by global warming, influence broad parts of the northern latitudes all over the world, and reliable assessments of present and past vegetation are highly relevant to predict the future development of Arctic ecosystems. The northernmost Siberian arcto-boreal treeline areas in the Taymyr lowlands may be particularly affected by climatic changes, with latitudinal shifts of the treeline ecotone and resulting vegetation changes from tundra to taiga. Obtaining reliable information about present vegetation composition in such remote arctic locations is difficult, as vegetation surveys in the field can typically only be carried out during brief visits, and the flowering season is short. Although these techniques are time consuming, methods like vegetation assessment by ground surveys or palynological analyses are common tools to evaluate floral composition and provide valuable, complimentary information. While vegetation surveys mainly provide information about the status quo, pollen analyses also allow investigation of vegetation back in time. In recent years, sedimentary DNA has emerged as an additional and effective tool to improve knowledge about past vegetation. DNA metabarcoding of lake sediments and sediment cores has become more and more relevant as a tool for such research, but an explicit assessment of lake sediment DNA data in comparison to data obtained from pollen and vegetation surveys is still lacking. Here, we present a study comparing these three vegetation assessment methods for 31 lakes within a 300 km transect in arctic Siberia, reaching from Tundra, through the treeline area, to the light Taiga. Surface sediments of lakes were taken, subsampled for DNA and pollen analyses and processed in the respective laboratories. Together with six representative vegetation surveys, we present results of this comparative study. Our results show that taxa assigned by DNA sequence analyses are comparable to those found in the pollen and vegetation analyses. Overall, the DNA provides a higher taxonomical level of identification, while the pollen grains mainly identify to genus level. Compared to the vegetation survey, pollen and DNA provide more information, as they are able to track vegetation elements, which could not been surveyed at the time of the year the surveys were carried out. The results show that the combination and comparison of pollen, DNA and vegetation seems to serve as a calibration set for future investigations of such remote and highly dynamic ecosystems. Our investigation draws a multidisciplinary, comprehensive image of the current composition of the Siberian lowland vegetation by combining well established and promising, newly emerging methods.

West Beringia bison population dynamics during the late Pleistocene and early Holocene

Pavel Nikolskiy[1] & Vladimir Pitulko[2]

[1] *Geological Institute of the Russian Academy of Scienses, Russian Federation*
[2] *Institute for the History of Material Culture, Russian Academy of Sciences, Russian Federation*

Changes in numbers of radiocarbon dates over time may reflect the dynamics of animal population sizes during the Late Pleistocene and Early Holocene [Nikolskiy et al., 2011, Pitulko and Nikolskiy, 2012, Nikolskiy and Pitulko, 2013, Markova et al., 2015]. For a long time, a sufficient set of dates (hundreds) for such analysis was available only for the woolly mammoth from the Arctic regions of Siberia. In recent years, the number of finite ^{14}C dates from West Beringia bison increased from fifteen to about ninety, enabling analyses of the temporal dynamics and relative abundance of the steppe bison, which dominated the regional mammoth fauna during the Late Pleistocene and Early Holocene. The study suggests that the relative numbers of Western Beringian bison changed significantly over the past 50,000 years (Fig. 1). The general trend of the bison population change repeats the Milankovitch curve that is positively correlated with global temperature changes.

However, the small-scale fluctuations in the number of bison demonstrate an interesting peculiarity, especially when compared with the change in the population of mammoths in the area. Both bison and mammoth reached the maximum population numbers (in the radiocarbon range) 34,000-38,000 years ago. As shown previously [Nikolskiy et al., 2011], such fluctuations in mammoth number almost exactly repeat changes over time of the fraction of xerophytic beetles that composed the entomo-fauna. These xerophytic beetles indicate steppe vegetation in Pleistocene plant communities of Western Beringia. Fluctuations in the number of bison during the last 34,000 years appear as inverse of the mammoth population fluctuations. It is probable that the inverse relationship of the mammoth and bison numbers is related to the fact that both species are competitors for the same resources (steppe vegetation), which led to the mutual regulation of their populations. Obviously, in Western Beringia bison has successfully coexisted with humans while being one of the main food and material sources. Bison remains dominate the faunal material of the Yana archaeological site. However, human presence could have been fatal for bison about 9,500 radiocarbon years ago, at the same time and in the same way it was for the mammoth [Nikolskiy et al., 2011], in the period of significant decline of their population in response to the reduction of their habitat, ultimately due to significant environmental changes in the early Holocene.

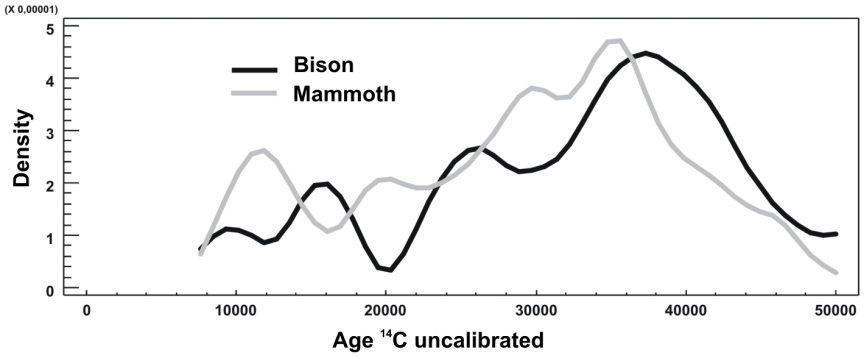

Figure 1: Comparative dynamics of the relative abundance of steppe bison and woolly mammoth at the end of the Pleistocene and Early Holocene in Western Beringia (by the temporal density of radiocarbon dates).

Faunal remains used for dating were collected over the years during expeditions in the New Siberian Islands and the northern regions of the Yana-Indigirka and Kolyma lowlands. The research is supported by the Rock Foundation (New York, USA), grants of the Presidium of the Russian Academy of Sciences and the Russian Foundation for Basic Research. A significant part of the dates at the final stage of the work were produced with the financial support of RFBR 13-06-12044 ofi-m.

References

Markova, A.K.; Puzachenko, A.Yu.; van Kolfschoten, T.; Kosintsev, P.A.; Kuznetsova, T.V.; Tikhonov, A.N.; Bachura, O.P.; Ponomarev, D.V.; van der Plicht, J. and Kuitems, M. [2015]: Changes in the Eurasian distribution of the musk ox (Ovibos moschatus) and the extinct bison (Bison priscus) during the last 50 ka BP. *Quaternary International*, 378:99–110, doi:10.1016/j.quaint.2015.01.020.

Nikolskiy, P.A.; Sulerzhitsky, L.D. and Pitulko, V.V. [2011]: Last straw versus Blitzkrieg overkill: Climate-driven changes in the Arctic Siberian mammoth population and the Late Pleistocene extinction problem. *Quaternary Science Reviews*, 30(17–18):2309–2328, doi:10.1016/j.quascirev.2010.10.017.

Nikolskiy, Pavel and Pitulko, Vladimir. [2013]: Evidence from the Yana Palaeolithic site, Arctic Siberia, yields clues to the riddle of mammoth hunting. *Journal of Archaeological Science*, 40(12):4189–4197, doi:10.1016/j.jas.2013.05.020.

Pitulko, V.V. and Nikolskiy, P.A. [2012]: Extinction of woolly mammoth in Northeastern Asia and the archaeological record. *World Archaeology*, 44(1): 21–42.

Impact of glacial climate on soil formation at the end of the Pleistocene, Ecuador

Sophie Opfergelt[1], Pierre Delmelle[1], Cédric Duhain[1], Aurélie de Potter d'Indoye[1], Ramon Vera[2], Qiuzhen Yin[1], & Alicia Guevara[2]

[1] *Université catholique de Louvain, Belgium*
[2] *Escuela Politécnica Nacional, Ecuador*

The contrasted climatic conditions between the Last Glacial Maximum (LGM) and the onset of the Holocene represent a key factor controlling water availability for chemical weathering and soil formation. Based on marine sedimentary records, it has been suggested that continental chemical weathering rate has increased since the LGM due to exposure of vast amounts of glacial flour. Given the important control that silicate weathering exerts on atmospheric CO_2 concentration and climate on geological timescale, it is of primary importance to better assess water availability for chemical weathering and soil formation at the LGM and at the onset of the Holocene.

Results from models which tested the influence of an ice sheet in the Northern Hemisphere (NH) and of changes in seasonality of insolation on the global climate at the LGM and the mid-Holocene are corroborated with observations on paleorecords from the NH. In the tropics, comparatively scarce information is available. Notably, the extent to which an ice sheet in the NH influenced rainfall and thereby, water availability for weathering, in the tropics during these periods is unclear.

Here we study a paleosequence of volcanic deposits and paleosols from the Ecuadorian Andes (Pifo, East Quito, 3000 m altitude) aimed at providing new insights into the impact of glacial climate on water availability for chemical weathering and soil formation in Quaternary paleoenvironments in the vicinity of glaciers at high altitude. The presence of glaciers down to 3500 m altitude at LGM in this region was established from pollen paleoreconstructions. The end of the Pleistocene in Ecuador is characterized by intense volcanic activity which led to sequences of thick volcanic ash deposits alternating with soil layers. Some of these volcanic Pleistocene deposits are indurated, known locally as "cangahua".

The study combines soil science, paleontology, quaternary geology, dating and climate modeling. The paleosequence is constituted by (from bottom to top): a volcanic pumice deposit (Pifo pumice, 170 kyr BP, before present), a paleosol/cangahua (31.4 kyr BP), a volcanic ash deposit (Chacana complex, 22 kyr BP), a paleosol and a paleosol/cangahua (22.5 kyr BP), a volcanic ash deposit (Pichincha volcano, 10 kyr BP), and the modern soil. The association of paleosol and cangahua is confirmed by the occurrence of fossil insect nests (Fig. 1a) and fossil traces of earth worm activity (Fig. 1b) in the cangahua. The fossil nests were formed by dung beetles which typically bury their nests in the soil surface. The nests indicate that the Ecuadorian Andes hosted an open grass-dominated habitat with large herbivores (part of the late Pleistocene megafauna) before and after 22 kyr BP.

The soil analyses show that both the clay and carbon contents are higher in the paleosol below 10 kyr than below 22 kyr. The paleosol below 10 kyr also exhibits well-differentiated horizons. These indicators of soil formation suggest a more advanced pedogenesis at 10 kyr than at 22 kyr which may have been driven by increased water availability for chemical weathering from the LGM to the onset of the Holocene. Climate models, e.g., the Paleoclimate Model Intercomparison Project Ocean-Atmosphere, were used to compare climatic conditions in the tropics at the LGM and at the onset of the Holocene. The models suggest cooler and drier annual conditions at the LGM, and warmer and wetter conditions in the tropics at Mid-Holocene 6 kyr and at 12 kyr, relative to the preindustrial situation. Our data provide direct measurements which support the conclusion from the models, i.e., the climatic conditions likely favored water availability for chemical weathering and soil formation at 10 kyr BP relative to 22 kyr BP.

In addition the climate model outputs suggest climate seasonality at the LGM in the Ecuadorian Andes characterized by drier winter (December, January,

February) and wetter summer (June, July, August). This is consistent with direct observations of Fe-Mn oxide nodules and secondary clay coating on mineral grains in the paleosol/cangahua deposit from the LGM. Occurrence of Fe-Mn oxide nodules can be attributed to redox processes, i.e., alternance of periods of water saturation and periods of reducing conditions. The formation of a clay coating (halloysite) on mineral grains in the porosity of the deposit (Fig 1c) may result from reorganization of the soil matrix. This requires wet conditions to allow particulate transport and/or chemical weathering alternating with drier conditions favoring clay deposition/precipitation. The observations of Fe-Mn oxide nodules and clay coatings in the paleosol/cangahua deposit corresponding to LGM both confirm alternating wet-dry conditions (climate seasonality) at this time. The origin of wet-dry conditions in this region at the LGM remains uncertain. This could be attributed to seasonal freeze-thaw of permafrost in a periglacial environment at high altitude.

This study contributes to improve our understanding of the impact of glacial climate on water availability for chemical weathering at high altitude in the vicinity of glaciers at the end of the Pleistocene. Our results provide field evidence for (i) contrasted soil formation in the Ecuadorian Andes between the LGM and the Holocene onset, and (ii) climate seasonality as controlling factor of water availability for chemical weathering at the LGM.

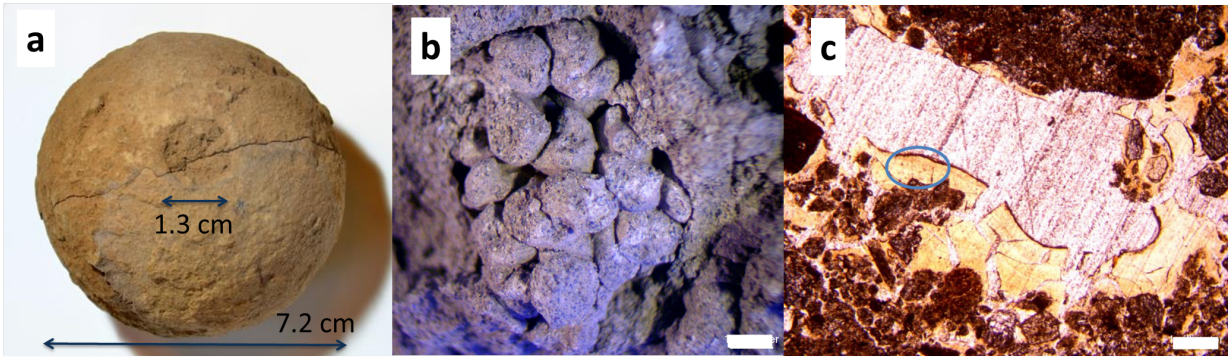

Figure 1: (a) Late Pleistocene fossil record of dung beetle nest. (b) Fossil record of earth worm casts in a paleosol/cangahua layer (22.5 kyr) (c) Thin section (natural light) of a clay coating (blue circle) on mineral grains in a paleosol/cangahua layer

Palaeoecology from permafrost deposits in Southwest Greenland - Inuit, Norse and their insect footprints

Eva Panagiotakopulu

School of GeoSciences, University of Edinburgh, United Kingdom

Using information from insects preserved by permafrost, this research examines existing and new data from hunting camps, farms and middens in Southwest Greenland during the Late Holocene and discusses the disappearance of the prehistoric Saqqaq culture in the Disko Bay region and the end of the Norse in the Western settlement. It attempts to find out whether there are evident patterns associated with the final phases of settlement and to understand possible triggers behind the sudden disappearance of peoples in the Greenland landscape. The assemblages from Qeqertasussuk in Disko bay, preserved in the permafrost, provide a unique insight into the palaeoeskimoes and their ecology, 2500-800 BC. Their activities, which centred on hunting and fishing, are accompanied with insect assemblages, primarily Diptera, which give indications of activity peaks and abandonment, before the final phase of settlement, after which the Saqqaq disappear. The faunas associated with the Norse farms provide equally interesting information. In particular, Coleoptera from Gården under Sandet, in the Western Settlement (10th to 14^{th} century AD), preserved in the frozen ground, give detailed evidence for the changes of the fauna during the several phases of the farm, including information of local extinctions. Species which are related to peat and woodland for example, disappear after Landnám as a result of landscape clearance and the faunas become strongly synanthropic with a range of introduced species becoming established for the duration of the Norse colonisation. There are similar results from Anavik, also in the Western settlement, where Iversen has claimed that the demise of the Norse farms was a result of caterpillars infesting the hayfields. It is unfortunate that the thawing of the permafrost has led to the destruction of preserved organic sediments and this perhaps improbable claim cannot be further examined.

Paleoenvironment and paleoclimate at the end of the late Pleistocene – Early Holocene in the western part of the Yana-Indigirka lowland (based on palaeobotanical data)

Elena Pavlova[1], Marina Dorozhkina[1], & Vladimir Pitulko[2]

[1] *Arctic and Antarctic Research Institute, Russian Federation*
[2] *Institute for the History of Material Culture, Russian Federation*

Paleoenvironmental and paleoclimatic changes at the transition from the Late Pleistocene to the Early Holocene in the western Yana-Indighirka lowlands were reconstructed based on^{14}C dating, pollen analyses, and plant macrofossils analyses of Quaternary deposits from the Northern Point locale of the Yana Paleolithic site (Yana RHS).

The cultural layer of the Yana RHS is confined to the middle part of the sediment profile exposed in the second terrace above the floodplain of the Yana River. The relative height of the second terrace is 16-18 m above water level (a.w.l.). Numerous 14C dates determined the age of the cultural layer as 28,500-27,000 years ago [Pitulko and Pavlova, 2010]. The terrace profile is composed of Ice Complex deposits, 14-16 m in thickness, represented by syncryogenic alluvial sediments with a developed network of two-generations of polygonal ice wedges. The Ice Complex sediments are overlain by a cover layer ranging from 0.6 to 2.5 m in thickness. Locally, in the upper part of the profile, there are Holocene peat bog deposits ranging from 1 to 2.5 m thickness, disturbed by Holocene ice wedges.

Detailed ^{14}C dating suggests that the deposits of the second terrace profile represent a nearly continuous record of paleogeographic events that took place 37,000-10,000 14C years ago.

For this time period, we reconstructed a sequence of changes in plant communities and main climatic indicators, such as the temperature of the warmest month (twm), the average annual temperature (tan) and the average annual precipitation (Pan). In addition, we constructed graphs of average minimum and maximum deviation of these parameters from modern values (δtwm, δtan, δPan), which indicate the range of possible values of climatic parameters for certain time slices.

During the time period studied here, the Karginsky interstadial (MIS 3) in the western Yana-Indighirka lowland was characterized by dry conditions with ΔPan = -60 – -70 mm/year with temperatures similar to modern or exceeding them by 2-4.7 °C for twm and 1-3 °C for tan. During the Karginsky thermochron interval studied, we observed two short-term cooling events, 34,000 and 30,500-29,500 years ago. In the final stages of the Karginsky warming, the warm and dry climate changed to a warm and wet one (Δtwm = -1,7 – +1.7 °C, Δtan = -1 – +1.5 °C with ΔP = -40 – +20 mm/year).The second half of the Karginsky interstadial was characterized by the development of hemicryophytic steppe landscapes, represented by grass-pink-sedge and forb-grass-sedge plant communities.

A sharp cooling occurred 25,000 years ago, marking the onset of the Sartan cryochron. In its initial stages, the climate was cold and relatively moist: Δtwm = -2.3 °C, Δtan = -2.5 – 0.5 °C and ΔPan reached +30 mm/year. At that time hemicryophytic steppe and tundra-steppe with forb-sedge-grass plant communities developed.

A climatic transition from cold and moist to cold and dry conditions occurred 21,000 years ago, when Δtwm amounted to -3.7 – -1 °C, Δtan= -1.5 – -0.5 °C and ΔPan was below today's values by 10-70 mm/year. The maximal cooling occurred at 21,000-19,000 years ago, when Δtwm amounted to -3.8 – -3.0 °C, Δtan = -1.5 – -0.5 °C and ΔPan reached -55 mm/year. The Sartan cryochron maximum was characterized by the development of a tundra-steppe with wormwood-sedge-grass, wormwood- pink -grass-sedge and forb-wormwood-grass-sedge communities.

Climate changes at the Late Ice Age-Holocene boundary proceeded very rapidly. A notable warming 12,600-12,100 years ago, corresponding to the Bølling warming in Europe, is reflected in the pollen sequences. In paleoclimate curves, it is indicated by a relative increase of twm by 1.5-2 °C compared with the previous period, while the average annual temperature and annual precipitation remained on the same level

(Δtan = -1.3 – -0.5 °C,ΔP = -50 – +15 mm/year). At that time, forb-grass-sedge vegetation developed.

The middle Dryas cooling around 12,100-11,900 years ago was short, but is reflected in the pollen spectra. The warming 11,900-11,000 years ago, corresponding to the European Allerød, was characterised by an increase in summer and average annual temperatures and an annual precipitation increase: Δtwm= +1.5 –+2.5 °C, Δtan= +3.5 – +5.5 °C, ΔPan = +70 –+125 mm/year.

The Younger Dryas cooling event at 11,000-10,500 years ago resulted in a brief return to climatic values which were, to certain degree, similar to that of the Sartan. Thus, estimated average annual temperatures (Δtan = -1.2 – -0.3 °C) and annual precipitation values (ΔPan = -50 – +20 mm/year) are very close to climatic conditions of Sartan time (see above), while reconstructed summer temperatures (Δtwm = +0.3 – +2.3 °C) appear to be exceeding the Sartan Δtwm values. Actually, this indicates severe winters.

At the turn of the Holocene, shrub-dwarf shrub-grass (sedge and forb) and shrub-dwarf shrub-grass-moss tundras formed. Environmental and climatic conditions during the period 37,000-10,000 years ago, including both MIS 3 and MIS 2, were suitable for human settlement and habitation in the Siberian Arctic.

References

Pitulko, V.V. and Pavlova, E.Y. [2010]: *Geoarchaeology and Radiocarbon Chronology of the Stone Age of the North-East Asia*. Saint Petersburg: Nauka.

Late Pleistocene – Early Holocene paleoenvironment proxy record from the Yana RHS site (low Yana river, Arctic Siberia)

Elena Pavlova[1], Evgeniy Zinovyev[2], Olga Korona[2], & Vladimir Pitulko[3]

[1]*Arctic and Antarctic Research Institute, Russian Federation*
[2]*Institute of Ecology of Plants and Animals, Russian Federation*
[3]*Institute for the History of Material Culture, Russian Federation*

Deposits that form the second above the floodplain (16-18 m thick) of Yana River contain unique paleoenvironmental information on the second half of MIS 3, MIS 2, and the Pleistocene-Holocene transition for the western part of the Yana-Indighirka lowland. The cultural layer of the Yana RHS site belongs to the middle part of the terrace body. It marks the oldest known human habitation in this area.

Samples for entomological and carpological analysis of the Northern Point locale of the Yana RHS site were chosen from the upper half of the profile from the level below cultural layer (CL) at the relative elevation range of 8-15.5 m above the water level (a.w.l.). With a 25-40 cm interval between samples along the entire deposit, a total of 19 samples were collected. The sampled portion of the profile was comprehensively dated by seven radiocarbon assays. Five resulting dates between 27,540 ± 180 yrs. BP (Beta-271405; CL level) and 16,710 ± 80 yrs. BP (Beta-271408) come from the Ice Complex (IC) deposits. The lowest portion of coating cover deposits (CCd) is dated to 12,660 ± 150 yrs. BP (LE-8914); the upper portion showed the age of 9,790 ± 110 yrs. BP (LE-8915).

The paleontological material includes more than 10,000 insect remains, belonging to 4,579 individuals, and 15,665 plant macrofossils, related to 86 taxa.

Species composition of insect faunas is typical for Pleistocene layers of northeastern Siberia. One of the peculiarities of studied insect complexes is the high concentration of pill beetle (*Morychus viridis*) fragments; this beetle is an important component of the Pleistocene tundra-steppe communities. Plant macrofossils reflect the cold and dry climatic conditions; in some samples the remains of woods (larch) and shrubs (birch) were found.

The bottom of this section (relative elevation of 8-12 m a.w.l.), dated by radiocarbon from 27.6 to 18.6 kya BP(uncalibrated), is characterized by xerophilous insect complexes with high amount of *Morychus viridis* (up to 90.7-91.9 % of individuals) along with tundra beetles and xerophilous steppe weevils of genus *Stephanocleonus* (*S. eruditus, S. foveifrons, S. cf. leucopterus*). Despite the significant differences between insect complexes within this part of the section,in general, the insect faunas reflect cold and dry climatic conditions, as indicated by the arctic, subarctic and *xerophilous* species, including include pill beetles M.viridis and steppe weevils of the genus *Stephanocleonus*. Most significantchanges in the insect complexes are observed with respect to the proportion of M. viridis: from 14.7 % of individuals insample ES2/5 to 91.2 % in sample EF1/7.

The analysis of plant macrofossils shows the existence of plant associations of the dry tundra type with mesoxerophytic communities; in some samples (EF1/10, EF1/3) we found larch (*Larix gmelini*) and dwarf birch (*Betula nana*) remains. In addition, in sample EF-1/10, megaspores of *Selaginella rupestris* (L.) Spring were found; this species inhabits south slopes of rocksand rocky-gravelly places in mountain tundras. The number of the pill beetle *M. viridis* reaches its maximum (91,2%) in sample EF-1/7. Plant macrofossils complex of the same sample show a co-existence of tundra and mesoxerophytic plant communities. In sample EF1/3 we observed ruderal species, which grow on disturbed lands (including gravelly, sandy slopes and scree): *Chenopodium prostratum*, *Potentilla cf. nivea* and *Rumex acetosella L.*; the same sample contained a relatively low proportion of pill beetle *M. viridis* (17.0 %).

Insect faunas from the upper part of IC deposits (relative elevation 12-13.5 m a.w.l., samples EF 2/15-2/5), radiocarbon dated to 16,710 80 yrs BP (from EF 2/15 sample), are characterized by the increasing contribution of tundra and xerophilous insects, such as *Harpalus spp.*, *Cymindisarctica*, and *C. binotata*. The amount of *M. viridis* in these samples ranges from 58.2% to 24.3 %.

Further decrease of the *M. viridis* proportion to 14.7% was observed in the bottom part of CCd layer – in sample EF2/5(relative elevation 13.8-14.1 m a.w.l., radiocarbon date 12,660 ± 150 yrs. BP [LE-8914]). Within this insect complex weobserved increasing proportion of dry tundra inhabitants (29.8 %) and xerophilous species (ground beetles of the genera *Harpalus* and *Cymindis*). This insect complex reflects a cold and dry climate, similar to that reconstructed for the paleoenvironment of sample EF2/4.

At the same time, plant macrofossils complex from the upper part of this section include a high amount of aquatic (Batrachium sp., Potamogeton sp.) and riparian (Ranunculus sp., Caltha cf. palustris, Eriophorum scheuchzeri, Eleocharis palustris, Sparganium hyperboreus) plant species. Mesoxerophytous and xerophytous plant species (Rumex acetosella, Potentilla cf. nivea, P. cf. stipularis) were found there too, corresponding to presence of xerophylous insect species in the same samples. Insect assemblage and plant macrofossils from sample NP/32 describe the Pleistocene-Holocene boundary conditions. This sample was collected from the bottom of a peat-bog layer in the upper part of the section (relative elevation 14.5 m a.w.l., radiocarbon dated to 11.9-11.6 kya). The insect complex may be characterized as a "mixed" type. This complex includes both xerophilous beetles (pill beetle *Morychus cf. viridis* (23.2% of individuals), *Stephanocleonus spp.*, *Poecilus (Derus) spp.* etc.), and aquatic and riparian beetles (*Hydroporus sp., Helophorus cf. splendidus* and others), as well as mesic tundra inhabitant *Dicheirotrichus mannerheimi*; the last one is typical for the Holocene sites from Northeastern Siberia [Pitulko et al., 2013]. Such peculiarities of this insect complex may be explained by the changing climatic conditions during the end of Pleistocene and beginning of the Holocene, which might cause the simultaneous existence of xerophilous habitats, moist tundras, and intrazonal biotopes.

The analysis of plant macrofossils showed the same tendency. The plant macrofossil complex of this sample did not contain any remains of tree vegetation. Shrubs represented the remnants of shrub birch, willow, and arcto-alpine species *Arctostaphylos uva ursi* and *Dryas sp.* Herbaceous plants are represented by aquatic, riparian and wet meadow species, some of them(*Thalictrum alpinum, Oenanthe cf. aquatica, Eriophorum gracilis, Eriophorum medium, Myriophyllum verticillatum, Comarum palustre*) were not found in the samples from underlying layers. The diversity of meso- xerophytic and xero-mesophyticspecies continues to exist. They are presented by *Kobresia myosuroides, Potentilla cf. nivea, Silene sp., Androsace sp., Astragalus sp.* Remains of mosses were represented in this part of the profile in small numbers.

The species composition of sample EF2/6 (top of this section, relative elevation 15.2-15.3 m a.w.l.., radiocarbon dated to 9,790 ± 110 yrs. BP [LE-8915]) differs from insect assemblages of underlying layers in the following aspects: 1) minor content of M. viridis (0.8% of individuals); 2) high amount of hygrophilous species (38.1 % of individuals); 3) presence of wood-dwelling insects, such as the bark beetle *Phoelotribus spinulosus*, trophically related to spruce and larch. This fauna might reflect the existence of moderately cold (cool) and moist climate. This complex is more comparable to Holocene insect assemblages of the Polar Urals and northern part of West Siberia than to Pleistocene insect faunas of northeastern Siberia. Similar characteristics are given to the plant macrofossils complex of this sample: we found numerous remains of trees and shrubs: larch (Larix) and birch (*Betula*), macrofossils of bilberry (*Vaccinium vitis-idaéa*) and crowberry (*Empetrum*). Remains of herbaceous plants are numerous and varied here; among this group, aquatic and riparian species dominate. A portion of the plant fragments represents wet meadow species. Larch (*Larix gmelini*) grows today at the forest-tundra boundary; perhaps the sampled flora reflects a similar humid climate and distribution of wood vegetation. Assemblages of modern insects collected in this area show the presence of arctic and subarctic species: *Pterostichus sublaevis, Amara torrida, Pterostichus (Cryobius) pinguedineus*, etc. At the same time, some xylophagous species are also found here: longhorn beetle *Monochamus galloprovincialis, buprestid beetle Trachyptedra acuminata*, and weevil *Hylobius albosparsus*. Thus, within the Yana-RHS section we can observe the dynamics of insect communities and plant associations, similar to those reconstructed from paleontological data. Most remarkable changes in sub-fossil insect faunas and plant macrofossils complexes were observed at the Late Pleistocene and Holocene boundary due to paleoenvironmental changes, i.e. increasing humidity in climate and formation of waterlogged forest-tundra communities.

References

Pitulko, V.V.; E.Y., Pavlova; S.A., Kuzmina; P.A., Nikolsky; A.E., Basilyan and M.A., Anisimov.

[2013]: Landscape-climatic changes in the vicinity of the Yana site (western part of the Yana-Indigirka lowland) in Late Pleistocene-Holocene. *Bulletin of the North-East Scientific Center, Russia Academy of Sciences Far East Branch*, 1:16–29.

Environmental changes and the archaeological record of arctic West Beringia within last 50,000 years

Vladimir Pitulko[1] & Elena Pavlova[2]

[1] *Institute for the History of Material Culture, Russian Federation*
[2] *Arctic and Antarctic Research Institute, Russian Federation*

From the very beginning, human habitation in Arctic Siberia was constantly driven by environmental changes whose effects on the human spatial distribution pattern, culture, and behavior are well-pronounced in the archaeological record. The open habitat created conditions for a number of revolutionary Upper Paleolithic technological innovations necessary to exist in a treeless, basically flat topography. For one, unlimited use of bone and ivory tools became the greatest innovation of the Upper Paleolithic, which is coeval to the time of the MIS 3, when mammoth steppe was widespread in northern Eurasia. As soon as humans were armed with this technology, which allowed successful protection and subsistence in open landscapes, they became capable to quickly colonize the mammoth steppe across northern Eurasia including the Arctic regions. A few lines of evidence indicate that it was anatomically modern humans who entered Arctic Siberia around 45,000 years ago, at the very end of early MIS 3.

The early occupants of Arctic Siberia were sparsely distributed, but their descendants presumably maintained successful survival throughout the middle MIS 3. By the end of MIS 3, they settled in the western part of Arctic Western Beringia inthe lower reaches of the modern Yana river valley. They were not exclusively restricted to mammoth hunting, as indicated by a lack of mammoth mass kill sites. Their subsistence was, instead, based mainly on bison, horse, and reindeer, while mammoth procurement was aimed largely at getting the tusks, an important raw material. Permanent shortage of wood, typical for treeless landscapes, stimulated wide use of ivory for tool making.

Early arrival of modern humans in the area close to the Bering land bridge and a long stay in this area would beadvantageous for humans entering the New World before the Last Glacial Maximum. Although there is currently to definitive evidence for this model, the possibility has to be taken into account.

Upper Paleolithic inhabitants continued living in Arctic Siberia during the LGM. At least at the beginning ofLGM, they occupied the Yana-Indighirka interfluve and possibly the Wrangel Island area. The evidence for these occupations is linked to mammoth artefacts in all cases, but currently lacks conclusive cultural attribution.

The decline of the mammoth population within Western Beringia during and after the LGM probably led to important cultural changes that are visible archaeologically. The dispersion of the Beringian Microblade tradition followed mammoth populations in a northerly direction when mammoth ranges shrinked. In the areas abandoned by mammoths, humans completely switched to the procurement of other herd species. Thus, mammoth extinction was a trigger for archaeologically visible technological changes. Notably, the oldest known microblades in Arctic Siberia date to 12,500 years BP.

The youngest pre-Holocene archaeological material in Arctic Siberia in all cases relates to mass accumulations of mammoth remains. Most of the sites suggest that people focused on mammoth hunting for meat towards the end ofthe “mammoth era”, while in the millennia before, they were more interested in the raw material this animal provided (ivory). Culturally, these sites reveal a stable trans-Beringian analogy - a Chindadn point.

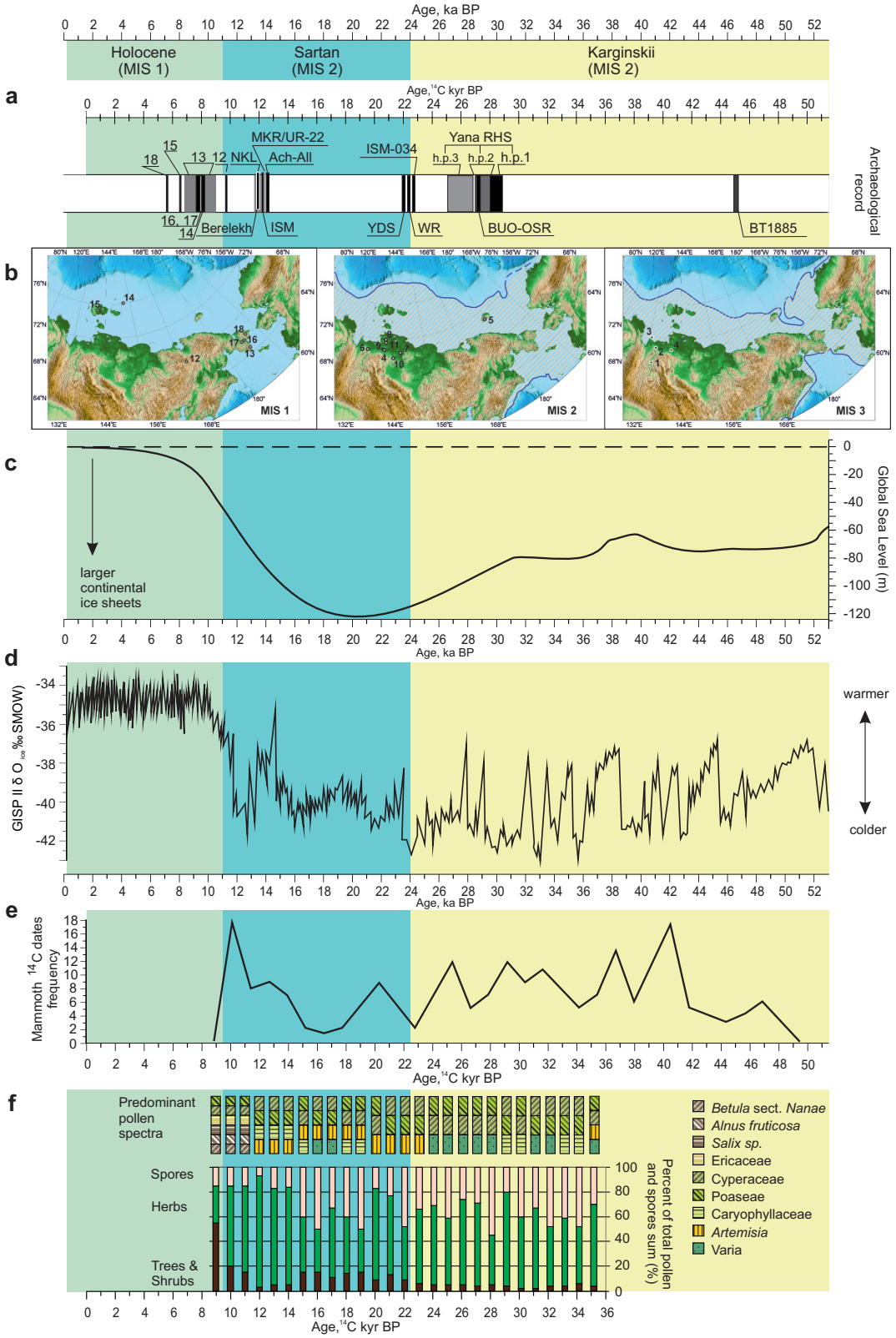

Figure 1: Environmental changes and human habitation record in the arctic Western Beringia in the Late Pleistocene and Early Holocene. Chronology (a) and location (b) of archaeological sites (Late Pleistocene: 1- Bunge-Toll 1885 site (BT-1885); 2 – Yana site complex (Yana RHS); 3 - Buor-Khaya/Orto-Stan site (Buo-OSR); Ilyn-Syalakh 034 (ISM-034); 5 – Wrangel island (WR); 6 – Diring-Aian site (YDS); 7 – Achchaghyi-Allaikha (Ach-All); 8 – Urez-22 (MKR/UR-22); 9 – Ilyn-Syalakh (ISM); 10 – Berelekh site (BEREL); 11 – Nikita lake site (NKL); Early Holocene: 12 – Tytylvaam site complex (T-vaam); 13 – Naivan (NN); 14 – Zhokhov site (Z); 15 – Tuguttakh (T-TAKH); 16 – Chelkun (CLK); 17 – Ananaiveem (A-VEEM); 18 – Koölen (KOL)); (c) global sea-level changes [Waelbroeck et al., 2002]; (d) GISP II oxygen-isotope curve [Stuiver and Grootes, 2000]; (e) relative changes in mammoth population numbers observed in ^{14}C dates frequencies [Nikolskiy et al., 2011]; (f) generalized changes in plant communities seen through the pollen spectra of the western Yana-Indigirka lowland.

The Chindadn connection is for now the only visible, and intriguing, cultural link between Eurasia and the New World, but it does not provide solid evidence that humans moved west to east. All such finds are related approximately to the same time, roughly corresponding to a transgression in the Bering land bridge area. In theory, these tools may have been linked to migrations from the central part of Beringia when it became inundated; reflecting a movement of people back to Arctic Siberia after the land bridge disappeared. The early Holocene human occupation record of Western Beringia in general is represented by a limited number of sitesknown mostly from Chukotka. In arctic Western Beringia, it is characterized by two sites only, both found in New Siberian Islands (the Zhokhov site, Zhokhov Island, and Tuguttakh site on Kotelnyi Island). The lack of more known early Holocene sites can probably be explained by taphonomic processes (denudation and erosion because of degradation of permafrost and development of thermocarst processes).

References

Nikolskiy, P.A.; Sulerzhitsky, L.D. and Pitulko, V.V. [2011]: Last straw versus Blitzkrieg overkill: Climate-driven changes in the Arctic Siberian mammoth population and the Late Pleistocene extinction problem. *Quaternary Science Reviews*, 30(17–18):2309–2328, doi:10.1016/j.quascirev.2010.10.017.

Stuiver, M. and Grootes, P.M. [2000]: GISP2 Oxygen Isotope Ratios. *Quaternary Research*, 53(3):277 – 284, 2000. doi:10.1006/qres.2000.2127.

Waelbroeck, C.; Labeyrie, L.; Michel, E.; Duplessy, J.C.; McManus, J.F.; Lambeck, K.; Balbon, E. and Labracherie, M. [2002]: Sea-level and deep water temperature changes derived from benthic foraminifera isotopic records. *Quaternary Science Reviews*, 21(1–3):295–305, doi:10.1016/S0277-3791(01)00101-9.

Metagenomic analyses of the late Pleistocene permafrost – additional tools for reconstruction of environmental conditions

Elizaveta Rivkina

Institute Physicochemical and Biological Problems in Soil Science, RAS, Russian Federation

A comparative analysis of the metagenomes from two 30,000 year-old permafrost samples, one of lake-alluvial origin and the other from late Pleistocene Ice Complex sediments (Yedoma), revealed significant differences within microbial communities. The late Pleistocene Ice Complex sediments (which have been characterized by the absence of methane with lower values of redox-potential and Fe2+ content) showed both a low abundance of methanogenic archaea and enzymes from the carbon, nitrogen and sulfur cycles.

The gDNA sequencing libraries were prepared using NEBNext® reagents (New England BioLabs Inc., USA), according to protocol recommended by the manufacturer, having an estimated peak insert size of 150 nt. Metagenome sequencing was performed at the CRG Genomics Core Facility (Centre for Genomic Regulation, Barcelona, Spain) on an Illumina HiSeq 2000™ machine using Flow Cell v3 with TruSeq SBS v3 reagents and a 2×100 cycle sequencing protocol. Raw sequencing data, i.e., 19.8 Gb representing 143.7 M sequences with an average length of 138 bp for IC4 and 19.7 Gb representing 131.7 M sequences with an average length of 150 bp for IC8, were uploaded to the MG-RAST server [Meyer et al., 2008] for gene calling and annotation under ID 4606864.3 for IC4 and 4606865.3 for IC8. A total of 6.6 % (IC4) and 3.4 % (IC8) sequences failed to pass the quality control (QC) pipeline, whereas 0.3 % of total sequences in both data sets were assigned to ribosomal RNA genes. For functional assignment, protein sequences of putative ORF were searched against the M5NR non-redundant protein database [Wilke et al., 2012] with an e-value threshold of $1e^{-5}$, minimum percentage identity of 60 %, and minimum alignment length of 15 aa. The taxonomic assignments of Illumina reads were performed against M5NR and M5RNA databases at default parameters. The best-hit classification method was used in both cases for match assessment.

In the current study, we performed a comparative analysis of the two permafrost samples isolated from lake sediments and Ice complex utilizing a metagenomic shotgun sequencing approach. The results show that the presence of methane in one sample and its absence in the second are associated with the prevalence of certain groups of microorganisms and their corresponding genes.

A possible scenario for the development of both Yedoma and lake sediments can be proposed on the basis of these findings. The metagenome analysis of IC4, a lake sediment sample, demonstrated the occurrence of many physicochemical reactions such as denitrification, iron reduction and sulfate reduction, which could reduce environmental redox potential and ultimately create favorable conditions for the development of a methanogenic community and methanogenesis. The composition of the IC8 metagenome reflects that the occurrence of such physicochemical reactions is sporadic, as no methanogenic activity and and no biogenic methane could be found in the late Pleistocene Ice complex on the Kolyma-Indigirka lowland.

The metagenomic and geochemical analyses described in the paper provide evidence that the formation of the sampled late Pleistocene Ice Complex sediments likely took place under much more aerobic conditions than lake-alluvial sediments.

The obtained results demonstrate that the metagenomic analysis of permafrost microbial communities can represent a valuable instrument for the reconstruction of paleo-conditions under which the permafrost sediments were formed.

Acknowledgements

This work was supported by grant from the Russian Science Foundation (14-14-01115)

References

Meyer, F.; Paarmann, D.; D'Souza, M.; Olson, R.; Glass, E.M.; Kubal, M.; Paczian, T.; Rodriguez, A.; Stevens, R.; Wilke, A.; Wilkening, J. and Edwards, R.A. [2008]: The metagenomics RAST server – A public resource for the automatic phylogenetic and functional analysis of metagenomes. *BMC Bioinformatics*, 9, 2008. doi:10.1186/1471-2105-9-386.

Wilke, A.; Harrison, T.; Wilkening, J.; Field, D.; Glass, E.M.; Kyrpides, N.; Mavrommatis, K. and Meyer, F. [2012]: The M5nr: A novel non-redundant database containing protein sequences and annotations from multiple sources and associated tool. *BMC Bioinformatics*, 13(1), doi:10.1186/1471-2105-13-141.

Simulated biome and permafrost distributions for the Late Quaternary Beringia

Kazuyuki Saito[1,2], Amy Hendricks[2], Nancy Bigelow[2], John Walsh[2], Sergey Marchenko[2], Vladimir Romanovsky[2], & Kenji Yoshikawa[2]

[1] *JAMSTEC, Japan*
[2] *UAF, USA*

We simulated Arctic biomes and frozen ground distributions in Beringia, across a region including Alaska and Eastern Russia, for selected eras in the Late Quaternary, using an equilibrium vegetation model and a statistical downscaling method, respectively. Through this we aim to illustrate geographical and temporal changes and to understand the dynamics behind the snow-permafrost-vegetation subsystem in the Arctic. Numerical simulation outputs from state-of-the-art global climate models (GCMs) or Earth System Models (ESMs) were utilized to represent the climate for four time periods, i.e., the Last Glacial Maximum (LGM; 21ka), the mid-Holocene Optimum (6ka), the pre-Industrial (0ka) to modern days, and the future (ca. the end of this century).

The BIOME4 biogeochemical and biogeographical vegetation model was employed to simulate the equilibrated vegetation distribution at a 0.5 degree spatial resolution . Forcing was taken from the Coupled Model Intercomparison Project phase 5 (CMIP5) models: CCSM4, GISS-E2-R, MIROC-ESM, MPI-ESM, and MRI-CGCM3. Present-day biome simulations were generally consistent with current vegetation observations in the study region, with much of the study area simulated to have evergreen and deciduous taiga and shrub tundras. Paleoclimatological simulations were compared with pollen samples taken throughout the study region. Simulations for the Last Glacial Maximum show the Bering Land Bridge covered almost entirely by cushion forb, lichen, and moss tundra, shrub tundra, and graminoid tundra (bottom Fig. 1). Three out of the five models' climate data produce evergreen and deciduous taiga in what is now southwestern Alaska. The distributions of cushion forb, lichen, and moss tundra and graminoid tundra differ noticeably between models, while shrub tundra distributions are generally in agreement. Simulations for the Mid-Holocene are in better agreement with pollen-based distributions of biomes. Shrub tundra is simulated along the Arctic coast, and in some cases along the eastern coast of Russia. Pre-Industrial biome simulations were very similar to Mid-Holocene simulations. Differences include more shrub tundra in both Russia and Alaska to the north, as well as less deciduous taiga in Alaska.

Future simulations exploring projected changes in climate conditions in the region under a RCP8.5 climate scenario show a northward shifting tree line while shrub tundra and graminoid tundra regions decrease significantly. Intrusions of cool mixed, deciduous, and coniferous forests above 60° N, especially in southwest Alaska, were notable. Across eastern Russia, deciduous taiga begins to overtake evergreen taiga, except along the coastal regions where evergreen taiga remains the favored biome. Frozen ground distribution was reconstructed using statistical classification using the freezing and thawing indices derived from the GCMs outputs for the horizontal resolution of 1 arc-minute (approximately 2 km in latitude) using a digital relief model, ETOPO1. On the Alaskan side, areas of seasonally frozen ground are found inside southeastern and southwestern Alaska (up to ca. 63° N) for the modern and 6ka reconstruction, while these were confined to the southernmost areas along the Alaskan bay and the Aleutian Islands for the LGM (top Fig. 1). The southern limit of continuous permafrost on the Bering Land Bridge for the same period was at 60° N. For Siberia, large areas were already underlain by permafrost, and simulated zones of seasonally frozen ground were found only in coastal areas of the Kamchatka Peninsula for the present simulations, whereas almost the entire region was underlain by permafrost for the LGM.

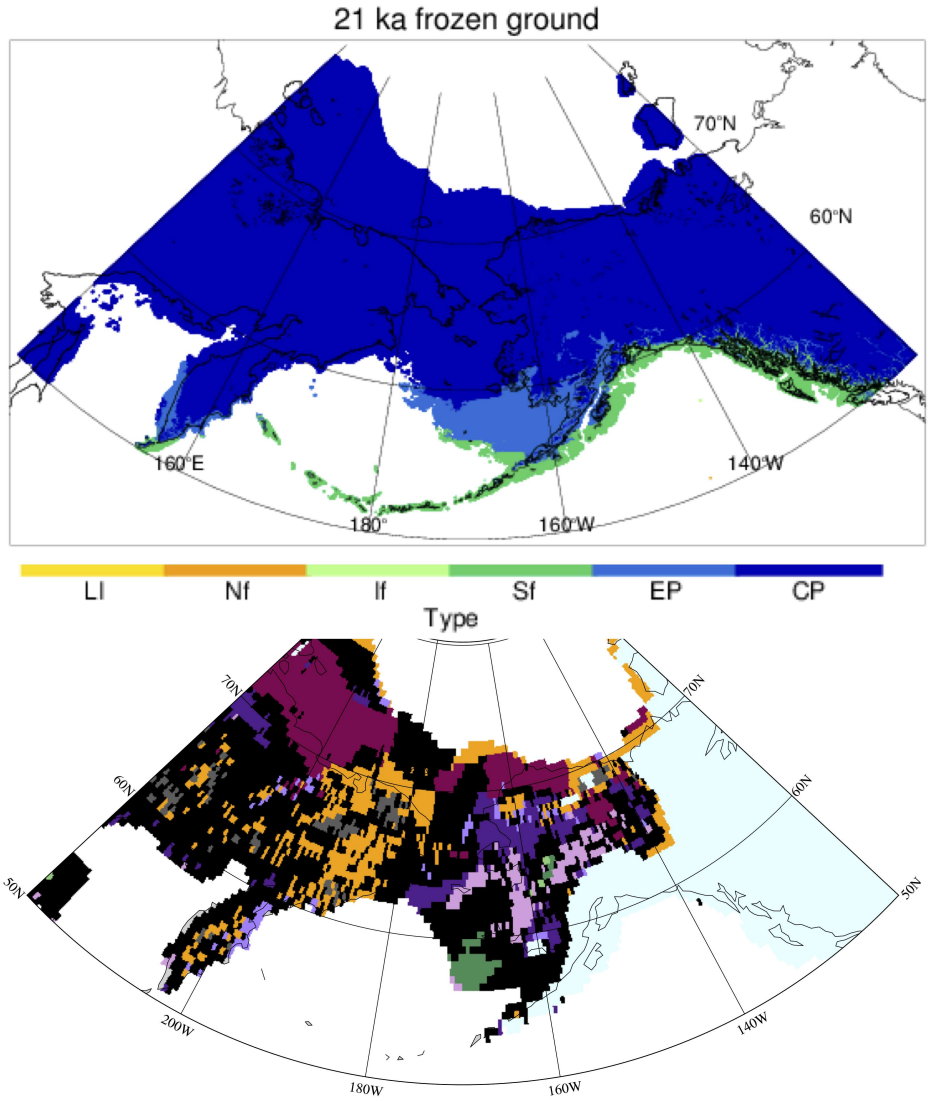

Figure 1: Reconstruced LGM biome and frozen ground distributions in Beringia

Glacial and interglacial sediment history on Bol'shoy Lyakhovsky, New Siberian Archipelago, from multiple permafrost cores

Georg Schwamborn[1], Lutz Schirrmeister[1], Sebastian Wetterich[1], Margret C. Fuchs[2], & Hanno Meyer[1]

[1] *Alfred Wegener Institute Helmholtz Centre for Polar and Marine Research, Potsdam, Germany*
[2] *Helmholtz-Zentrum Dresden-Rossendorf*

Bol'shoy Lyakhovsky, the southernmost island of the New Siberian Archipelago, holds the longest record of palaeoenvironmental history in the non-glaciated Siberian Arctic preserved in permafrost. It stretches back to 200 kyr before present and includes prominent last interglacial thermokarst and Yedoma (Ice Complex) sections. Yet, it is unknown, whether or not the depositional history of the site is affected by the deglaciation of the northern part of the New Siberian Archipelago. Potentially, it could give insight into the break-up of the proposed MIS 6 ice sheet located on the East Siberian Sea shelf [Jakobsson et al., 2014].

The lithostratigraphy of southern part of the island consists of palaeosols, floodplain and lake deposits, subaerial Yedoma and lacustrine to palustrine alas formations. Large ice wedges (partially up to several meters high and thick), segregation and pore ice record a syngenetic freezing of the Yedoma silts. Polymodal particle size distributions suggest that more than one transport mechanism drove sediment accumulation from more than one source. Recent papers conclude that the palaeoclimate record matches the general Late Quaternary climate history in northern Siberia [Andreev et al., 2011, Wetterich et al., 2014].

From a multi proxy data set we focus on (i) the mineral composition (63-125 μm fraction) to determine the provenance of the deposits and to identify possible changes of transport pathways. Complementary, we use (ii) pore ice hydrochemistry as a means to track changes of the soil solution that principally reflects the site's chemical weathering history preserved in permafrost. Presumably the two approaches complement each other, since the weathering solution should largely reflect the mineral matter composition.

The heavy mineral association suggests that most of the minerals derive from the underlying bedrock (Upper Jurassic-Lower Cretaceous sandstones and Upper Cretacous granites and diorites); among others it has high amounts of ilmenite and leucoxene, epidote, pyroxenes and amphiboles, along with garnet, tourmaline, apatite, and sphene. Ratios of stable versus unstable mineral associations show that the Late Quaternary strata overlying bedrock are enriched in more stable minerals (i.e. zircon, tourmaline, ilmenite), whereas more unstable minerals (i.e. amphiboles and pyroxenes) dominate the chronostratigraphically younger Quaternary strata. A remarkably high portion of weathered mica appears in MIS4 to MIS3 deposits and raises the question upon particular hydrodynamic conditions during that time, e.g. a floodplain environment that persisted for several thousands to ten thousands of years. It may have produced various impulses of flooding with floating particles that settle out quickly on the banks of the channel and on the leeward side (Fig. 1).

Overall pore ice chemistry shows that high electrical conductivity corresponds to low ice content (<20 wt. % of total sample weight) and vice versa; when ice content is high (>60 wt. %) the electrical conductivity is low. When compared with the average ion composition of tundra and taiga rivers, the whole core record is enriched in the sodium-potassium load, which partially even dominates over the combined calcium-magnesium load.

We preliminary conclude that the observed trends of heavy mineral and pore ice chemical variations in the Bol'shoy Lyakhovsky cores reflect short-distance material transport from weathered bedrock in the depositional area. The enrichment of mica in ice-rich deposits suggests floodplain hydrodynamics in the area during MIS 4 to MIS3. The fairly constant ionic proportions of the light soluble load in the ground ice confirm a local origin of the weathering solutes. High amounts of sodium-potassium are linked to the weathering of the granitic bedrock. Distinct concentration gradients in the downcore electrical conductivity are caused by postdepositional ionic migration from the bedrock weathering crust into the overlying Late Quaternary strata, by intensified weathering during the

Last Interglacial (MIS5e), and by stable surfaces that promoted effective (e.g. cryogenic) weathering during the last Glacial (MIS4 to MIS3).

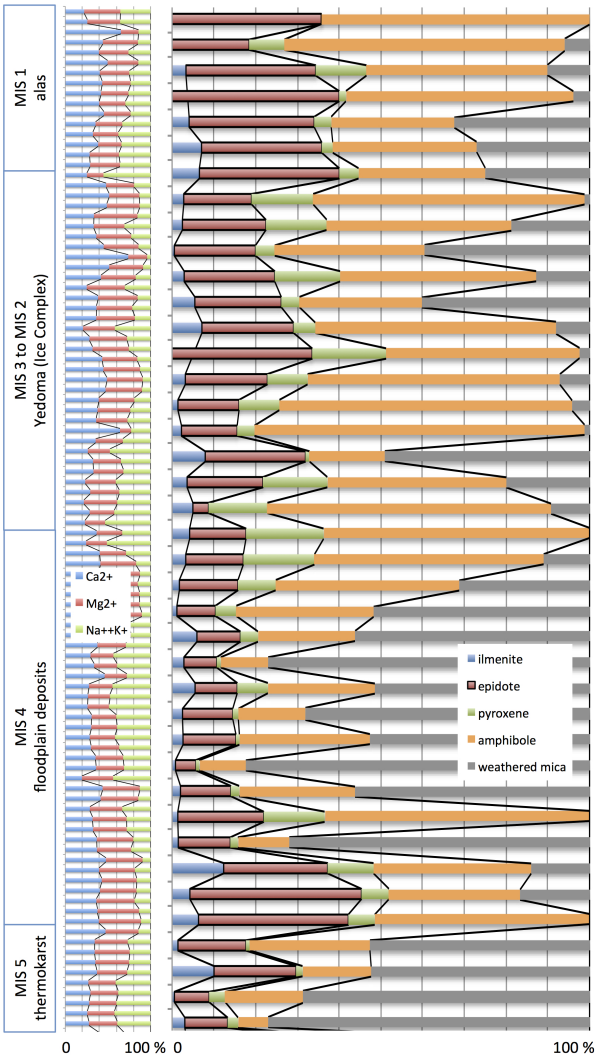

Figure 1: Changes of the main cation load (per cent of meq/l) and the heavy mineral composition (per cent of grains) of the Late Quaternary permafrost record from Bol'shoy Lyakhovsky, New Siberian Archipelago.

References

Andreev, A.A.; Schirrmeister, L.; Tarasov, P.E.; Ganopolski, A.; Brovkin, V.; Siegert, C.; Wetterich, S. and Hubberten, H.-W. Vegetation and climate history in the Laptev Sea region (Arctic Siberia) during Late Quaternary inferred from pollen records. *Quaternary Science Reviews*, 30(17–18):2182–2199, 2011. doi:10.1016/j.quascirev.2010.12.026.

Jakobsson, M.; Andreassen, K.; Bjarnadóttir, L.R.; Dove, D.; Dowdeswell, J.A.; England, J.H.; Funder, S.; Hogan, K.; Ingólfsson, O.; Jennings, A.; Larsen, N.K.; Kirchner, N.; Landvik, J.Y.; Mayer, L.; Mikkelsen, N.; Möller, P.; Niessen, F.; Nilsson, J.; O'Regan, M.; Polyak, L.; Nørgaard-Pedersen, N. and Stein, R.. Arctic Ocean glacial history . *Quaternary Science Reviews*, 92:40–67, 2014. doi:10.1016/j.quascirev.2013.07.033.

Wetterich, S.; Tumskoy, V.; Rudaya, N.; Andreev, A.A.; Opel, T.; Meyer, H.; Schirrmeister, L. and Hüls, M.. Ice complex formation in Arctic East Siberia during the {MIS3} interstadial. *Quaternary Science Reviews*, 84:39–55, 2014. ISSN 0277-3791. doi:10.1016/j.quascirev.2013.11.009.

Past genetic patterns of arctic freshwater diatoms - a study on ancient sedimentary DNA elucidates diatom diversification at the treeline ecotone

Kathleen Stoof-Leichsenring[1], Luidmila Pestryakova[2], & Ulrike Herzschuh[1,3]

[1] *Alfred Wegener Institute Helmholtz Centre for Polar and Marine Research, Potsdam, Germany*
[2] *North-Eastern Federal University of Yakutsk, Department for Geography and Biology, Yakutsk, Russia*
[3] *University of Potsdam, Institute of Earth and Environmental Science, Potsdam, Germany*

Arctic lake sediments are valuable archives for studying present and past changes of biodiversity. Diatoms, aquatic unicellular algae, are sensitive to environmental changes and their siliceous skeletons preserved in the sediment provide suitable indicators for lake history reconstruction by microscopic approaches. However, diatom diversity from sediments can be also tracked by metagenetic approaches, which can provide taxonomic determinations below the species level and genetic relatedness between diatom lineages, which is not possible when applying classical morphological methods. The treeline ecotone in Siberia, a region characterized by deep ice-rich permafrost, is defined by a gradual change from forest to tundra vegetation, which is a surrogate for related environmental changes across this area influencing also the embedded aquatic habitats. This study investigates the influence of temporal environmental changes on the diatom diversity and their relatedness patterns in order to understand the function of the treeline ecotone as a driver for diatom diversification. Therefore, we examine genetic diatom patterns from ancient sedimentary DNA, applying a short diatom diagnostic fragment of the protein coding rbcL gene used in a metagenetic approach coupled with next-generation Illumina amplicon sequencing. We analyzed two sediment cores from the treeline in North-Eastern Siberia (Khatanga, Krasnoyarsk region), one from recent tundra (11-Ch^{-1}2A) and a second from recent forest (11-CH-6D) vegetation. The core material was dated with the ^{14}C method and additionally the upper sediment slices were measured applying Pb-201 and Cs^{-1}37 radionuclide dating for sedimentation rate estimation. The tundra core revealed an age of about 7000 years and the forest core dated back to approximately 9000 years. Both cores showed periods of pronounced vegetation changes previously supported by pollen grain analyses. Until now, a preliminary analysis of the genetic data from both cores generally confirmed high genetic diatom diversity in most core samples. Further, we identified intra-specific temporal diversity shifts in the dominant diatom taxa Staurosira, Aulacoseira and Pinnularia and revealed selected lineage turnover within all the three diatom groups, which are coupled with non-synonymous nucleotide substitutions assuming putative functional variability. In particular, Staurosira lineages revealed a correlation between temporal variability and vegetation changes. A deeper data analysis will be performed in the next month and will further help to understand past diatom occurrences and relatedness patterns and its correspondence to environmental changes at the treeline ecotone. The obtained patterns of persistence and diversification of lineages might give a first insight into adaptive processes in diatoms across Holocene time scales.

The climate and permafrost evolution since 6 ka BP recorded by peat in the source area of the Yellow River, Northeastern Qinghai-Tibet Plateau

Qingfeng Wang[1], Huijun Jin[1], Qingbai Wu[1], Tingjun Zhang[2], Yadong Huang[1], Yuzhong Yang[1], & Min Liu[1]

[1] *State Key Laboratory of Frozen Soil Engineering, Cold and Arid Regions Environmental and Engineering Research Institute, Chinese Academy of Sciences (CAS), People's Republic of China*
[2] *College of Earth and Environmental Sciences, Lanzhou University, People's Republic of China*

The study of permafrost formation and evolution since the Holocene is critical for understanding the formation mechanism, changing processes, and long-term trends of changes in permafrost on the Qinghai-Tibet Plateau. As a key elevational permafrost region, the source area of the Yellow River (SAYR) on northeastern Qinghai-Tibet Plateau (QTP) has undergone dramatic changes since the onset of the Holocene. Based on the magnetic susceptibility, loss on ignition, and geochemical elements of the peat profile Wanlongwama, located in the Tangchama basin in the south of the Eling Lake, the climate and permafrost evolution since 6.0 ka BP in the SAYR is reconstructed. The results show that the climatic evolution since 6.0 ka BP in the SAYR can be divided into four stages. 1) It is the Holocene Megathermal Period (HMP) in 6.0 2.1 ka BP, which could be divided into two sub-periods by 5.5 ka BP: much more warmer and wetter in 6 5.5 ka BP, and less warmer and wetter in 5.5 2.1 ka BP. The climate is 2) cold and dry in 2.1 1.4 ka BP, 3) relatively warm and wet in 1.4 0.6 ka BP, and tends to be 4) warm and wet since 0.6 ka BP. The abnormal changes of the above parameters in the past hundred years might be influenced by human activity. There are six cold events since 6.0 ka BP, including 0.4 ka BP, 1.5 ka BP, 1.9 ka BP, 2.7 ka BP, 4.5 ka BP, and 5.5 ka BP. And the remaining five cold events, except the 1.9 ka BP cold event, could correspond with the North Atlantic Holocene Cold Event 0 4 obviously. The weakened solar activity might be the main reason for the cold event in middle and late Holocene, but the internal oscillations of the climate system may also affect it. From the perspective of the system theory, the peat swamp and permafrost is symbiotic, and then peat accumulation and freeze should be formed simultaneously in the geological sense. Different from other permafrost soils, the peat permafrost, with the effect of the semiconductor properties of peat, doesn't show the general historical process of degradation in the HMP and epigenetic freeze from ground surface downwards in the late Holocene. The program aims at providing key support and validation for the modeling, reconstruction, and prediction of climate and environment changes, and permafrost degradation, as well as the studies on the evolutionary mechanisms on northeastern QTP.

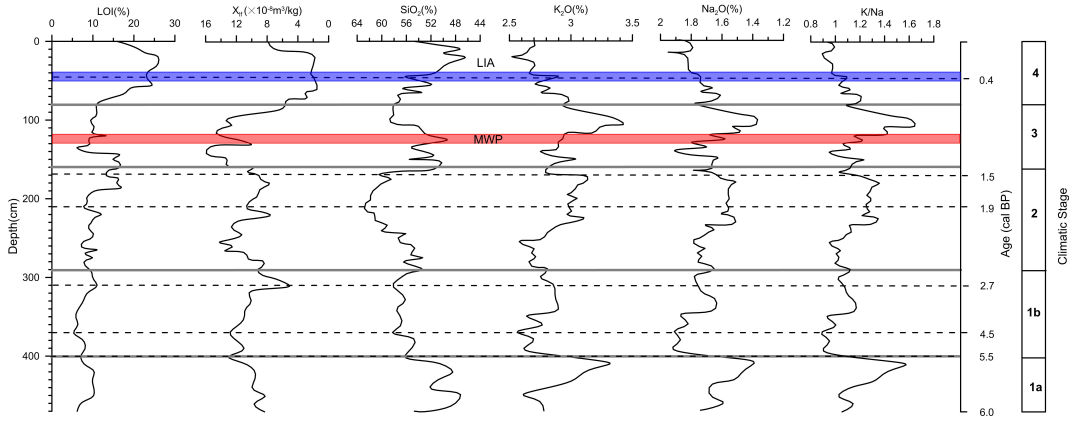

Figure 1: Changes of the magnetic susceptibility, loss on ignition, and geochemical elements of the peat profile Wanlongwama and climate periods divisions since 6 ka BP in the source area of the Yellow River, NE QTP

Development of polygonal peatlands on the Yukon Coastal Plain, Canada, during the past 5000 years

Juliane Wolter[1,2], Hugues Lantuit[1,2], Michael Fritz[1], & Ulrike Herzschuh[1,2]

[1] *Alfred Wegener Institute Helmholtz Centre for Polar and Marine Research, Potsdam, Germany*
[2] *University of Potsdam, Germany*

The Yukon Coastal Plain was partly glaciated during the Late Wisconsin. Landscape development following deglaciation was subject to periglacial processes, most notably permafrost aggradation, with intermittent periods of permafrost degradation, and the development of peatlands and thaw lakes.

The timing and dynamics of polygonal peatland formation and development on the Yukon Coastal Plain and Herschel Island, Canada, during the mid to late Holocene is not well understood. Drained thaw lake basins in the eastern parts of the coastal plain provide conditions suitable for the development of low-centred polygons. High-centred polygons are especially numerous where the proximity of eroding coastal cliffs or raised terrain inland cause drainage of polygon fields. The hypothesis that high-centred polygons are always degradation stages of low-centred polygons implies that there should be evidence for the presence of low-centred polygons beneath existing high-centred polygons. Such developments/degradation could be linear processes happening at long time-scales or rapid switches caused by erosional events or rapid warming. Little is known about the timing and causes of such development on the Yukon Coastal Plain. The subject of this study is the development of ice-wedge polygon peatlands and the timing and triggers of possible tipping points between polygon types.

We analyzed 10 cores from the active layer of two low-centred and two high-centred polygons along the Yukon Coastal Plain and on Herschel Island, Yukon Territory, Canada. We subsampled the cores in 1 cm increments and analyzed grain size distribution, total and organic carbon contents, nitrogen contents and stable carbon isotopes for each sample. We obtained 25 (including Herschel) radiocarbon dates from selected depths along seven of these cores. Plant macrofossils were identified for selected samples.

AMS radiocarbon dates indicated a mid Holocene (between 6000 and 5000 yrs BP) age for the base of the cores. The two high-centred polygons each showed a large hiatus between about 4500 yrs BP and 100 yrs BP. These hiatus were found in cores from the margins of the now raised parts of the polygons and were not mirrored in polygon centres. Organic carbon contents ranged between 7.5 wt. % in the oldest central parts of one polygon and 45 wt. % in the same polygon in the transition between ridge and centre (7.5 – 45.5 wt. %, median 32.8, SD = 11.2 wt. %). The gravimetric ratio of organic carbon to nitrogen showed similarly wide ranges, with elevated values on elevated surfaces in high-centred polygons and on the ridges of low-centred polygons (4.8-70.2, median 18.6, SD 10.7). Stable carbon isotopes, however, showed a narrow range (-30.9 to -26.3 ‰, median -28.2 ‰, SD = 0.77 ‰). Grain size distribution showed silty to sandy textures, with more fine grained material in the easternmost, unglaciated polygon and fine sand dominating in the western, formerly glaciated polygons. We found a general trend towards more fine-grained material downcore. Plant macrofossil analyses indicate shifts from aquatic vegetation (e.g. *Potamogeton*, *Batrachium*, *Menyanthes trifoliata*, *Charophytes*) to wetland vegetation (e.g. *Betula glandulosa*, *Ledum decumbens*, *Eriophorum vaginatum*) in the studied polygons.

We found signs of significant past disturbance in the two high-centred polygons indicated by grain size distribution, organic carbon contents and the hiatus in age depth relationships. The low-centred polygons show continuous peat accumulation. The development of polygon centres deviates significantly from that of polygon rims or margins from the same polygon. In our study, polygon centres seem to be more stable than polygon margins. This deviation needs to be taken into account in palaeoecological studies of peat sections in ice-wedge polygons.

These are the first results of a broader study on landscape development on the Yukon Coastal Plain. They indicate that large-scale processes of erosion and/or permafrost degradation could have caused

simultaneous events such as drainage of large lakes and increased thaw which shaped the landscape for the coming centuries to millennia. Low-centred polygons have been relatively stable over several millennia, while the establishment of high-centred polygons seems to be linked to disturbance, which could have caused the regime change.

Late Quaternary vegetation history of North-Eastern Siberia inferred from ancient DNA analyses of permafrost sediment cores

Heike Zimmermann, Laura Epp, Paul Overduin, Georg Schwamborn, Lutz Schirrmeister, & Ulrike Herzschuh

Alfred Wegener Institute Helmholtz Centre for Polar and Marine Research, Potsdam, Germany

Paleoenvironmental reconstructions help us to track vegetation responses to climatic changes, and can also tell us about the origin of plant organic matter stored in permafrost soils. Siberian permafrost soils are natural archives that preserve DNA over thousands of years owing to long-term cold conditions. This makes them particularly suitable for ancient DNA analyses, which we use to reconstruct past flora at high temporal detail, even for poorly preserved or meager plant macrofossils.

We reconstructed Late Quaternary vegetation history from permafrost sediments at the western coast of the Bour Khaya peninsula, previously part of Western Beringia, using sedimentary ancient DNA. Bour Khaya is located within the Late Pleistocene Ice Complex, where fine-grained, ice-rich deposits can be found (Yedoma). Analyses were conducted on an 18.9 m long core drilled from the top of a Yedoma hill (71.420°N, 132.111°E) in April 2012. The core was divided into two parts by a Late Pleistocene ice-wedge, whereby the top of the core included the transition from the Late Pleistocene to the Early Holocene and the part below the ice-wedge was deposited more than 46 thousand years ago, before the Last Glacial Maximum (LGM). Plant remains were sparsely distributed through the core and mainly composed of fine rootlets, small woody pieces and very few seeds and fruits. We isolated total DNA of 54 frozen sediment samples (excluding the ice-wedge) and obtained data on past plant assemblages by DNA metabarcoding.

The paleogenetic approach allowed us to detect at least 150 taxa. More than 35 taxa were identified to species level, including graminoids, shrubs, herbs and cryptogams. More than 55 taxa were assigned to genus level and at least 40 taxa were assigned to a level between genus and family. The two parts of the core exhibited several plant community changes through time. Holocene and Late Glacial deposits were dominated by taxa typically present in subarctic moist dwarf-shrub tundra, such as *Eriophorum*, *Ranunculus*, *Salix* and *Betula*. Deposits dated to the pre-LGM were characterized by the complete absence of Betula and could be subdivided into two parts. The major part below the ice-wedge was dominated by aquatic and wetland taxa such as *Potamogetonaceae*, *Caltha palustris* and *Eriophorum*, but still exhibited a high floristic diversity with the occurrence of *Rumex*, *Pedicularis* and *Castilleja*, a hemiparasitic plant. The deepest parts of the core were dominated by *Festuca*, *Plantago*, *Potentilla* and *Puccinellia* while aquatic and wetland taxa were almost completely absent.

Our results suggest that changes in Western Beringian flora occurred during the Late Glacial leading to a large reduction of the flora but also to the arrival of several subarctic taxa. Ancient DNA metabarcoding proved to be an appropriate tool to investigate Late Quaternary vegetation history, especially when plant macrofossils are rare.

SESSION 11

Microbial Ecology of Permafrost Ecosystems

Convener:

Susanne Liebner, *GFZ German Research Center for Geosciences, Germany*

Alexander Tøsdal Tveit, *UiT The Arctic University of Norway, Norway*

Marcus A. Horn, *Department of Ecological Microbiology, University of Bayreuth, Germany*

Research on microbial life exposed to permanent freeze or seasonal freeze-thaw has led to astonishing findings about microbial versatility, adaptation, and diversity in permafrost ecosystems. Microorganisms thrive in cold habitats and new sequencing techniques have produced large amounts of genomic, metagenomic, and metatranscriptomic data that allow insights into the fascinating microbial ecology at low temperatures. Moreover, permafrost soil ecosystems constitute major global carbon and nitrogen storages and are sources of the greenhouse gases methane (CH_4) and nitrous oxide (N_2O). Abiotic and biotic factors shape microbial communities and their huge genetic potential. Microbial communities ultimately influence reaction patterns of permafrost-affected soils towards global change. Altered patterns of seasonal temperature fluctuations and precipitation are expected in the Arctic and will affect the microbial turnover of soil organic carbon (SOC). Activation of nutrients by thawing and increased active layer thickness as well as erosion renders nutrient stocks accessible to microbial activities. However, the effects of these changes on the microbial mechanisms that determine greenhouse gas emissions are still poorly understood. In this context, the functional resilience of microbial communities in Arctic permafrost soils is of major interest. Particularly important is the ability of microorganisms and microbial communities to respond to changes in their surroundings by intracellular regulation and population shifts within functional niches, respectively. We ask whether environmental changes is met by a flexible microbial community retaining its function, or if the altered conditions also renders the community in a state of altered properties that affect the carbon cycle.

This session brings together research on different spatial scales and levels of complexity, spanning from ecosystem level to pure culture studies of model microbes in the laboratory. It aims to attract microbiologists, microbial ecologists and biogeochemists working with the effect of climate change and/or low temperatures on microbial nutrient cycling and communities, functions and cultivars under laboratory or in-situ conditions. We encourage submissions from research on terrestrial, marine and freshwater ecosystems in Arctic, Antarctic and alpine regions.

The impact of transcriptionally active microbial communities on soil greenhouse gas emissions in the Canadian High Arctic

Ianina Altshuler[1], Jen Ronholm[1], Tullis Onstott[2], Charles Greer[1,3], & Lyle Whyte[1]

[1] *McGill University*
[2] *Princeton University*
[3] *National Research Council of Canada*

Arctic permafrost is believed to harbour ≈50 % of global soil organic carbon stores. Climate warming and subsequent permafrost degradation releases these carbon stores for metabolism by microbial communities. This results in a positive feedback loop of greenhouse gas (GHG) soil emissions. Studying nitrous oxide (N_2O) and methane (CH_4) soil flux alongside carbon dioxide emissions can help us better understand this positive feedback loop.

Our objectives were to determine whether the Arctic ice-wedge polygon soils act as a source or sink of these gases, and to characterize the active microbial communities that explain this phenomenon. Metatranscriptome RNA sequencing was performed on surface soils overlaying permafrost at 5 cm depth to identify the functional microbes currently present in three soil types: the polygon interior, the wedge, and the polygon interior under vegetation.

The relative abundance of 16S rRNA genes of methanotrophs was greater compared to methanogens (≈0.156 % vs. 0.0013 %). Type II methanotrophs dominated the methanotrophic community in all soils. The methanogenic *Methanomicrobia* dominated the community in wedge soil whereas *Methanococci* dominated the polygon interior samples. Furthermore, we detected denitrification pathway genes (NosZ and NirK), as well as genes involved in methane oxidation (pmoA, B, and C) through both soil metatranscriptomics and qPCR. In situ gas flux measurements of the polygon interior and wedge soils indicate an overall negative CH_4 flux and a positive N_2O flux. Overall, our data demonstrates that the microbial community in the Arctic ice-wedge polygon soil is potentially capable of acting as a methane sink and a nitrous oxide source.

Methanotrophic population and methane oxidation around the Lena Delta, Siberia, Russia

Ingeborg Bussmann[1], Steffen Hackbusch[2], Patrick Schaal[1], & Antje Wichels[1]

[1] *Alfred Wegener Institute Helmholtz Centre for Polar and Marine Research, Germany*
[2] *Technical University Hamburg-Harburg, Germany*

The Lena River is one of the biggest Russian rivers draining into the Laptev Sea. Due to predicted increasing temperatures the permafrost areas surrounding the Lena will melt at increasing rates. With this melting high amounts of carbon, either organic or as methane will reach the waters of the Lena and the adjacent Laptev Sea. As methane is an important green house gas its further fate in the Lena Delta is of uttermost importance. Methane oxidation by methanotrophic bacteria is the only biological way to reduce methane concentrations. However, the polar estuary of the Lena River is a challenging environment, with strong fluctuations in salinity and temperature.

We determined the activity and abundance of aerobic methanotrophic bacteria (MOB), as well as their population structure. Activity was determined with 3H-CH_4 as radioactive tracer, abundance was determined with quantitative PCR and the population structure was characterized by a fingerprinting method (MISA).

Methane concentrations were rather low (41 $\pm$ 44 nM), as well as methane oxidation rates (1.1 $\pm$ 1.6 nM/d). In polar water (cold and saline) highest activities were found, whereas the highest abundance of MOB was in surface waters. The relation between methane turnover and abiotic factors will be used to characterize the eco-physiology of these polar and estuarine methanotrophs.

Changing chemistry and aquatic microbial functioning of streams draining sub-arctic landscapes impacted by permafrost thaw

Samuel Cottingham[1], Reiner Giesler[2], Ryan, A. Sponseller[2], François Guillemette[3], Robert, G. Spencer[3], Jorien, E. Vonk[4], David, A. Pearce[1], John Woodward[1], & Paul, J. Mann[1]

[1] *Northumbria University, UK*
[2] *Umeå University, Sweden*
[3] *Florida State University, US*
[4] *Utrecht University, Netherlands*

On-going permafrost degradation across sub-arctic systems is changing land-cover properties as peatland palsas collapse and transition into bog and fen stages, causing changes to terrestrial microbial processes and their associated greenhouse gas emissions. However, shifts in the composition of DOM exported to streams from catchments undergoing varying stages of permafrost thaw are poorly understood. Furthermore, little is known about how changes in terrestrial DOM supply, both in terms of quantity and quality, may influence aquatic microbial communities and their functional responses. Here, we measured DOM concentration and composition alongside indicators of microbial function (as potential C, N& P acquiring extracellular enzyme activities) across a chronosequence of streams impacted by warming in sub-arctic Sweden during July 2015. Maximum active-layer depths have been progressively deepening across this region (as determined by CALM records) corresponding to accelerated climate warming. We hypothesised that: 1) DOM composition varies across the streams reflecting differences in dominant land-cover type and the amount of permafrost thaw present across catchments, and 2) microbial function will vary in response to changes in stream DOM composition. We found that the composition of DOM varied significantly across the chronosequence as evidenced by DOM optical measurements (chromophoric CDOM and fluorescent FDOM), and high-resolution mass spectrometry (FTICR-MS). Extracellular enzyme activty analyses (EEAs) showed distinct variations in microbial functioning across the gradient, with higher potential DOC-normalised EEAs in streams draining tundra catchments than peatland or boreal forests. A positive relationship was also observed between the proportion of terrestrial humic-like DOM components and microbial C/N acquiring enzyme activities. Our results highlight the connectivity between terrestrial and aquatic systems and demonstrate that as landscapes transition with different stages of thaw, the changing composition of DOM exported to freshwaters can cause subsequent shifts in microbial function.

Linking microbial community activities to carbon turnover in Siberian subarctic permafrost-affected soils

Svetlana Evgrafova[1], Liudmila Mukhortova[1], Dirk Wagner[2], & Georg Guggenberger[3]

[1] *V.N. Sukachev Institute of Forest, Krasnoyarsk,Russian Federation*
[2] *GFZ German Research Centre for Geosciences, Helmholtz Centre Potsdam,Germany*
[3] *Institute of Soil Science Leibniz Universität Hannover, Germany*

Introduction

Northern ecosystems are characterized by extreme climatic conditions and low productivity during the short growing seasons. Deep soil temperature regimes and partially water saturation of large areas give rise to low microbial activity and long turnover time for organic materials. As a result, accumulation of organic matter is favored in cold climate soils (Rodionow et al., 2006). Knowledge of linking microbial community features and SOM quality as a substrate for decomposing organisms is necessary to predict the magnitude and the time-scale at which C will get mobilized in permafrost soils at climate change (Khvorostyanov et al., 2008).

Site description and methods

The study site is located in the homogeneous larch forests of the Central Evenkia (N 64°, E 100°). The investigated area is situated in the continuous permafrost zone, with a permafrost thickness up to 300 m and with the permafrost temperature of -3.5 °C. Soil cover is presented by Cryosols. Climate is highly continental with mean annual temperature of -8.9 °C (mean temperature in January, -36 °C; mean temperature in July, +16 °C) and a mean annual precipitation of 370 mm.

Labile organic matter was extracted using serial daily extractions of a soil sample by distilled water and 0.1N NaOH solution, without preliminary decalcifying. The content of stable soil organic matter was determined by a difference between the content of the total organic carbon and carbon of the labile organic matter.

Microbial biomass was assessed by rehydration method and using substrate-induced respiration (SIR). Basal (heterotrophic) soil respiration was estimated from CO_2 emission rate from soil samples incubated at 23 °C and 60 % moisture content. Quantitative PCR was used for analysing abundance of the 16S rRNA genes of bacteria.

Results

The total organic carbon stock in the active soil layer on the north-facing and south-facing slopes was 5.4 and 2.1 kg C m^{-2}, respectively, in spite of the thickness of the active layer on the south-facing slope, which was 1.3 times deeper thawed compared to the north-facing slope. The upper 0-20 cm soil layer of north-facing slope contained 2.3 times more carbon than soils on the south-facing slope. At both slopes, soil organic carbon concentrations decreased gradually with soil depth down to the permafrost table.

The main part of accumulation of soil organic matter stocks on both slopes was stable humus (Cstab). Cstab accumulation in the soil of the north-facing slope took place down to the permafrost table, while at the south-facing slope the accumulation occurred mostly within the top 0-30 cm of the mineral soil. Labile carbon (Clab) had larger contents in soils of north-facing slope. We assume that higher moisture conditions of a north-facing slope favored the migration of dissolved organic matter to the lower part of the active layer, where it accumulated in both fractions, as labile and stable organic matter.

Basal respiration rate as well as heterotrophic microbial biomass within the active layer of soil profiles at both slopes decreased with depth and were strongly correlated with the organic carbon content. The number of bacterial 16S rRNA gene copies in the soil of the south-facing slope decreased down on a profile with sharp increase in close to the permafrost table, while the number of gene copies in the soil of the north-facing slope was rather evenly distributed within active layer profile, with a tendency to decrease close to the permafrost table. Possibly, such distinction is bound to various soil moisture and its flushing regime on slopes. Also the pattern of biomass

of the heterotrophic microorganisms with soil depth was similar to that of the number of gene copies, indicating that the majority of the microorganisms in these soils were heterotrophs. However, the heterotrophic respiration in the deeper soil horizons was extremely low, thus showing that heterotrophic respiration is influenced by decreasing soil temperatures with depth.

Conclusion

The heterotrophic activity in the investigated permafrost soils is closely correlated to the labile fraction of soil organic matter while microbial biomass depends on total organic carbon content.

Acknowledgements

This work was supported by the Russian Government Megagrant (Project 14.B25.31.0031), the German—Russian project CARBOPERM, financed by the Federal Ministry of Education and Research (BMBF; 03G0836D)

What kills permafrost microbes during Marssimulations? More new questions than answers

Kai Waldemar Finster, Bente Aagaard Lomstein, Per Nørnberg, Jonathan Merrison, Aviaja Anna Hansen, & Lars Liengaard

Aarhus University, Denmark

Bacteria and biomolecules (DNA and proteins) in Arctic permafrost were exposed to simulated Martian conditions. The exposure time corresponded to 80 days on Mars as calculated from the respective accumulated UV dose. The treatment included the following effects: UV radiation, freeze-thaw cycles, atmospheric gas composition and pressure. The effect of the treatment was evaluated by determining the concentration of biomolecules, the number of dead and alive microbial cells and the number of culturable microbes at the end of the exposure as a function of distance from the UV exposed surface. While a significant reduction in the concentration of DNA and proteins was only observed in the upper 3 mm of the permafrost core the number culturable cells and viability of cells was reduced down to 15 mm. We observed a reduction in the number of culturable aerobic bacteria down to 6 mm while the community structure of culturable anaerobes was only effected to a minor extend. We suggest three causing factors to explain our observations:

i) direct UV radiation, which is restricted to the uppermost layer of the samples,

ii) UV generated reactive oxygen species (ROS) that may penetrate deeper into the samples and cause damaging effects on the cells and biomolecules and

iii) consecutive cycles of freezing and thawing that may effect the cells in the deeper strata.

Currently, the proposed production of ROS is only hypothetical and requires future investigations. Interestingly, we observe a significant destruction of DNA and not only a fragmentation and dimerization. We are not aware of a mechanism that can account for that effect. We have currently no explanation for our observation. Our simulation demonstrates and confirms that organic material and cells are rapidly destroyed at the surface and that a relatively thin layer of soil would provide sufficient protection against the extreme conditions at the surface. On the other hand our study also makes it clear that mixing of the surface layer by wind driven processes and thus exposing deeper well protected layers would lead to rapid destruction of biological signatures both on the molecule and on the cell level.In our opinion permafrost soil is an excellent analogue for Mars and icy Moons and we emphasize the need for studying the response of complex communities in stead of pure cultures in the astrobiological context.

Denitrifiers limited by available organic carbon drive nitrous oxide production in peat circles of the arctic Tundra despite their capability for nitrous oxide consumption

Stefanie Hetz & Marcus A. Horn

University of Bayreuth, Germany

Pristine permafrost-affected acidic peat circles (pH approximates 4) in the Eastern European Tundra have recently been discovered to harbor up to 2 mM of pore water nitrate (NO_3) and emit significant amounts of nitrous oxide (N_2O) in the range of heavily fertilized agricultural fields. N_2O is a greenhouse gas and ozone depleting substance. Thus, processes releasing and consuming N_2O are of major concern. Under anoxic conditions, N_2O is primarily produced by denitrification, which is the sequential reduction of nitrate via nitrite, nitric oxide, and N_2O to dinitrogen gas (N_2) in the absence of oxygen. Denitrification can act as both source and sink of N_2O. Denitrifiers are facultative aerobes that respire N-oxides rather than oxygen when oxygen becomes limited. Diverse new denitrifiers are associated with the N_2O production of peat circles. Microbially available organic carbon to nitrate ratios and pH regulate denitrification and the N_2O/N_2 ratio. High nitrate and pH-values lower than 6.5 increase the N_2O/N_2 ratio. Indeed, the assembly of a functional N_2O-reductase of neutrophilic model denitrifiers is blocked at acidic pH.

It is hypothesized that (i) peat circle denitrifiers are adapted to low pH and capable of complete denitrification to N_2, and (ii) high nitrate pore water concentrations in and N_2O fluxes of peat circles are due to denitrifiers operating under substrate (i. e., microbially easily degradable organic carbon) limited conditions. Anoxic slurry incubations with peat circle soil were conducted at in situ near pH 4 and under more neutral conditions at pH 6. Soil slurries were supplemented with and without nitrate- in the presence or absence of acetylene (inhibitor of the N_2O-reduction to N_2). Supplemental nitrate was quickly consumed and N_2O produced in the absence of oxygen at both pH-values. In treatments with acetylene, almost 100 % of supplemented nitrate-N was recovered in N_2O-N. N_2O was essentially not detected in the absence of acetylene. Ammonium, ferrous iron, sulfate and methane remained stable throughout the incubation or were below the detection limit, indicating that dissimilatory nitrate reduction to ammonium, iron and sulfate reduction as well as methanogenesis were marginal. Thus, the denitrifier communities present in peat circles are capable of complete denitrification at low pH.

In a second set of incubations, the effect of [^{13}C]- and [^{12}C]- acetate on denitrification was tested in anoxic soil slurries at pH4 with and without nitrate and in the presence of acetylene. Substrates were supplemented in pulses. Acetate was consumed without appreciable delay with nitrate and stimulated denitrification by 150% relative to nitrate only treatments. Nitrate stimulated acetate consumption and CO_2 production rates by 200% relative to acetate only treatments. Recovery of [^{13}C]-acetate carbon in [^{13}C]O_2 in nitrate and acetate supplemented slurries approximated 30-40%. [^{13}C]-labeled organic acids were insignificant, suggesting a substantial assimilation of acetate carbon by peat circle microbes. Recovery of nitrate-N in N_2O-N approximated 50%, likewise indicating assimilation. 65 % of the total CO_2 was [^{13}C]O_2, suggesting that acetate carbon was preferentially dissimilated relative to peat derived organic carbon. In the absence of acetylene, results were similar to incubations in the presence of acetylene with the exception that N_2O was not detectable, suggesting complete denitrification. Experiments are ongoing to identify the denitrifying key players in peat circles by stable isotope probing.

The combined data indicate that peat circle denitrifiers are substrate limited, thus producing large amounts of nitrate derived N_2O despite their remarkable capability to reduce N_2O and complete denitrification at pH4.

Diverse acid-tolerant denitrifier communities in arctic peatlands control nitrous oxide fluxes

Marcus A. Horn[1], Katharina Palmer[1,2], Nico Roßbach[1], & Stefanie Hetz[1]

[1] *University of Bayreuth, Germany*
[2] *Current affiliation: Water Resources and Environmental Engineering Research Group, University of Oulu, Oulu, Finland*

Unvegetated tundra peat circles (PC) are nitrate-rich'hot spots'of N_2O emissions, while adjacent vegetated tundra areas (VT), and moderately vegetated palsa peats (PP) emit only minor amounts of N2O. Soil pH approximated 4 for all sites. N_2O emission potentials of unsupplemented anoxic peat soil slurries and apparent maximal nitrate-dependent maximal reaction velocities were highest for PC, intermediate for PP, and lowest for VT. Stimulation of N_2O production by nitrate-, nitrite-, and/or acetylene suggested denitrification as major source of N_2O in all soils. $N_2O/(N_2+N_2O)$ ratios were 30, 55, and 100 % for PC, PP, and VT, respectively, when 10 μM of nitrate were supplied. Such dissimilar physiological responses suggested dissimilar denitrifier communities in the soils. Barcoded amplicon pyrosequencing of narG, nirK, nirS, and nosZ (encoding nitrate, nitrite, and N_2O reductases, respectively) revealed diverse denitrifiers including hitherto unknown species, and likewise suggested that denitrifier diversity differed between the soils. Sequences affiliated with Actino-, Alpha- and Betaproteobacteria as well as environmental sequences. Quantitative PCR of narG, nirK, nirS, and nosZ indicated that detected nirS outnumbered nirK in all soils. Detected narG and nirK were most abundant in PC. Most probable numbers of N_2O producers decreased with depth, and were 10-100×higher in PC than VT. N_2O was produced by PC from 2-45 °C with an optimum at 30-40 °C. N_2O production was highest at pH 4-5. Thus, denitrifiers were enriched and isolated at 5 and 30 °C, pH 5. Diverse isolates from high dilutions of PC and VT included known and unknown gram positive and negative species of the genera *Paenibacillus*, *Bacillus*, *Ralstonia*, and *Dyella*. The collective data indicates that

1. Proteobacterial nirS-type rather than nirK-type denitrifiers are abundant in acidic permafrost soils,
2. permafrost soil harbors psychrotolerant to mesophilic denitrifiers,
3. that hitherto overlooked denitrifiers of the Firmicutes might contribute to the N_2O emissions, and
4. the contrasting N_2O emission patterns are associated with contrasting denitrifier communities.

Distinct depth profile of bacterial and archaeal communities between four Alaskan soil cores

Mincheol Kim[1], Eunji Byun[2], Yongwon Kim[3], Jinho Ahn[2], Ji-Woong Yang[2], & Yoo K. Lee[1]

[1]*Korea Polar Research Institute, Korea, Republic of (South Korea)*
[2]*Seoul National University, Korea, Republic of (South Korea)*
[3]*International Arctic Research Center (IARC), University of Alaska Fairbanks (UAF), Fairbanks, USA*

Microbial response to permafrost thaw driven by climate warming varies by sites. Although a great deal of environmental heterogeneity is found across permafrost regions, vertical variation of microbial communities in permafrost affected soils is not well understood. Here, we sampled soil cores at four different sites including both continuous and discontinuous permafrost regions in Alaska. Abundance and community structure of soil bacteria and archaea were compared between cores at different depths using MiSeq sequencing and quantitative PCR targeting 16S rRNA gene. Abundance of bacteria and archaea overall changed in a similar way but did not show any directional pattern across depth. Both bacteria and archaeal communities were primarily structured by site difference, followed by depth and soil chemical properties. Interestingly, there were dramatic shifts in bacterial phyla dominance around permafrost table in two permafrost affected soils. Relative abundance of Chloroflexi was reduced to a great extent, while Caldiserica and Firmicutes markedly increased below 58 cm depth in a tussock tundra site. In a Sphagnum-dominated bog site, Verrcomicrobia and Planctomycetes almost disappeared, while Chloroflexi and candidate phylum AD3 dominated below 72 cm depth. These site-specific vertical variations of microbial community structure will be an important resource to predict how soil microbes respond to permafrost thaw.

Bacterial community shifts along the chronosequence in the Austre Lovénbreen glacier foreland, Svalbard

Yoo Kyung Lee, Ji Young Jung, & Mincheol Kim

Korea Polar Research Institute, Korea, Republic of (South Korea)

Primary succession after glacier retreat has been widely studied in plant communities, but bacterial succession is still poorly understood. Here, we sampled surface soils along a 140-year old chronosequence in Austre Lovénbreen glacier foreland on Svalbard. Soil bacterial community was investigated via 16S rRNA gene sequencing and environmental variables which best explain community variation were determined. Bacterial diversity increased dramatically at an early stage, kept increasing moderately at an intermediate stage, and the higher level of diversity was maintained to the late stage. It suggests high rates of bacterial species turnover occured over a short period of time. Bacterial community structure overall shifted from early to later stage of glacier retreat. However, highly mosaic patterns of community assembly were observed in the intermediate stage, indicating deterministic process driven by environmental variability plays an important role in community assembly at this stage. Time after glacier retreat and soil temperature were key determinants which best explained the community variation. Other edaphic factors such as soil organic carbon and pH also accounted for a large proportion of community structure. These findings suggest overall bacterial succession occurs along the glacial chronosequence but bacterial community structures are shaped largely by environmental heterogeneity in the course of succession.

Development of cell numbers and microbial community composition along a natural temperature gradient in subsea permafrost

Julia Magritz[1], Matthias Winkel[1], Linda Mahler[1], Fabian Horn[1], Pier P. Overduin[2], Monique Thiele[1], Christian Knoblauch[3], Dirk Wagner[1], & Susanne Liebner[1]

[1] *GFZ German Research Centre for Geosciences, Helmholtz Centre Potsdam, Section Geomicrobiology, Potsdam, Germany*
[2] *Alfred Wegener Institute Helmholtz Centre for Polar and Marine Research, Potsdam, Germany*
[3] *Institute of Soil Science, University of Hamburg, Hamburg, Germany*

Subsea permafrost is a natural laboratory for the impact of global change on microbial communities. Since it is a source of organic carbon thawing arctic permafrost and its effect on the activity of microbial communities and on their role in carbon turnover in turn is associated with a positive feedback on global change. In the northern hemisphere, permafrost underlies about 25 % of the land and large areas of the coastal sea shelves. The subsea permafrost and the coastal area of the Siberian Laptev Sea shelf were formed during the Holocene marine transgression. Following transgression, frozen terrestrial sediments were warmed by overlying sea water so that they reached thermal equilibrium. We expect that this warming of subsea permafrost stimulated microbial growth and altered microbial community composition. In our study we tracked microbial cell numbers and community composition in permafrost samples along a gradient of marine inundation and temperature and aimed at uncovering the underlying environmental controls.

Sediment cores from two different locations in the western and central Laptev Sea were retrieved. Within a transect of 12 km north of Cape Mamontov Klyk, western Laptev Sea, five sediment cores were drilled. They include one core onshore (C1, 60 m deep) and four cores offshore (C5, 31 m; C4, 30 m; C3, 29 m; C2, 71 m deep) with different periods of marine transgression and permafrost warming. Core 'C1' contained exclusively frozen terrestrial permafrost unaffected by transgression or erosion, while the offshore cores 'C2' to 'C4' were characterized by ice-bonded sediments overlain by unfrozen deposits. The core located furthest from the coastline (C2, 11.5 km) has been flooded about 2500 years ago and frozen terrestrial material was encountered at a depth of approximately 30 meters below sea floor (m bsf). At a second location about 800 m offshore to the west of the Buor Khaya Peninsula, central Laptev Sea, an additional core 'BK2' was retrieved (47.5 m deep). 'BK2' has been flooded 540 years ago. Ice-bonded sediment was encountered at 24.75 m bsf.

Sediment temperatures of 'BK2', 'C2' and 'C3' are similar and range between -2 to +1 °C suggesting that the thermal equilibrium state in a milieu of saline, ocean water is reached[1,2]. With decreasing distance towards the shore temperatures decrease notably. In the cores 'C4' and C5' temperatures range from 7 to 3 °C and -12 to -6 °C, respectively, while terrestrial permafrost temperatures of 'C1' vary from -18 to -12 °C. In the cores with unfrozen material highest temperatures were measured from just below the sea floor down to the permafrost table. In general, temperatures decrease with depth.

Various biogeochemical parameters for all sediment cores including methane concentrations and 13C isotope values of methane of 'BK2' and 'C2' were determined and were correlated to molecular microbial data. Total microbial cell counts (TCC) along the sediment cores were quantified by SybrGreen staining and varied by more than three orders of magnitude ranging from 1.6×104 to 4.6×107 cells g^{-1}1 sediment. Highest TCC were found in the unfrozen sediments. They decreased with depth, hence with decreasing temperature. On average, the microbial abundance in the sediment core 'C2' was one to two orders of magnitude higher than in 'BK2'. This may be due to a longer period of marine influence and permafrost warming being supportive for the resident community in 'C2'. Further analyses of the overall archaeal and bacterial community composition via 16S rRNA Illumina amplicon sequencing and TCC along the Cape Mamontov Klyk transect will help to evaluate changes in microbial abundance and community structure due

to permafrost warming.

References

Junker, R.; Grigoriev, M.N. and Kaul, N. [2008]: Non-contact infrared temperature measurements in dry permafrost boreholes. *Journal of Geophysical Research: Solid Earth*, 113(B4), doi:10.1029/2007JB004946. B04102.

Overduin, P.P; Liebner, S.; Knoblauch, C.; Günther, F.; Wetterich, S.; Schirrmeister, L.; Hubberten, H.-W. and Grigoriev, M.N. [2015]: Methane oxidation following submarine permafrost degradation: Measurements from a central Laptev Sea shelf borehole. *Journal of Geophysical Research: Biogeosciences*, 120(5):965–978, doi:10.1002/2014JG002862. 2014JG002862.

Frozen in time? Microbial strategies for survival and carbon metabolism over geologic time in a Pleistocene permafrost chronosequence

Rachel Mackelprang

California State University Northridge, United States of America

Permafrost is gaining interest as a model for exobiology. Since six of the other eight planets in our solar system, as well as their moons, asteroids, and comets are permanently frozen, life on these celestial bodies is most likely to be found in a subzero environment. On Earth, life can exist in permafrost for millennia and may act as an analogue reflecting potential inhabitants on extraterrestrial cryogenic bodies. Active microbial life exits in even the most ancient permafrost, but we know little about the strategies utilized by permafrost microbes that enable survival over geologic time. Here we describe a 16S rRNA gene and shotgun metagenomic study targeting a chronosequence (12kyr – 35kyr) of Pleistocene aged permafrost. 16S rRNA sequencing and analysis showed decreasing microbial diversity and higher abundance of endospore-forming Firmicutes in increasingly older samples. 16S rRNA gene and metagenomic data showed significant age-based clustering. The youngest samples were enriched in genes involved in the degradation of complex polysaccharides whereas older samples had significantly greater abundance of genes involved in amino acid and recalcitrant carbon degradation. These data suggest increasing reliance on scavenging of detrital biomass in older permafrost. An abundance of conjugation genes in the oldest samples indicate the importance of rapidly acquiring new adaptive traits. The oldest samples were also enriched in chemotaxis, cell envelope synthesis, surface attachment, and stress resistance genes. We binned 30 draft genomes from metagenomic assemblies including several members of *Thaumarchaeota*. Together, these data increase understanding of how permafrost microbes transform organic matter over geologic time and identify adaptations enabling long-term survival with no influx of new energy or materials.

The Arctic 'enzymic latch': Regulation of organic matter decomposition by extracellular enzymes in peat-permafrost

Alexander S. Rose[1], Christian Dunn[1], Hojeong Kang[2], & Christopher Freeman[1]

[1] *Bangor University, United Kingdom*
[2] *Yonsei University, South Korea*

Scope

Permafrost-affected peat soils attract a large amount of scientific attention, especially regarding the carbon [C] balance and microbial processes of soil organic matter [SOM] degradation. Although plenty of research topics investigate a range of limiting factors for C decomposition in polar ecosystems, one that remains severely neglected is the study of extracellular enzymes with only a handful of publications on the topic [Vorobyova et al., 1996].

It is known that boreal and temperate peatlands experience slow rates of enzymic decomposition and that this can account for their ability to store large amounts of SOM, raising questions about the role of extracellular enzymes in Arctic soils that store globally significant amounts of carbon. Molecular oxygen [O_2] is generally absent from all but the uppermost layer of peatlands, a characteristic mirrored in the vertical structure of many cryosols with aerobic conditions in the upper active layer only.

Given that specific enzymes such as phenol oxidase rely on O_2 in order to function, their inactivity in anaerobic peatland soils results in the accumulation of phenolic compounds. These recalcitrant, high molecular-weight molecules are potent inhibitors of hydrolases - the workhorse decomposers of organic matter – thus illustrating an enzymic mechanism regulating the rate of C breakdown [Freeman et al., 2004].

Therefore, our study looks at whether these same principles governing turnover of C in low-latitude peatland systems apply to high-latitude permafrost-affected soils experiencing warming from climate change. Specifically:

Can low hydrolase activities in thawed permafrost be attributed to oxygen constraints on phenol oxidase?

Method

Very few studies have experimented with permafrost in the presence and absence of oxygen [Wagner et al., 2009] and even less have tackled questions of soil enzyme activity. This poster presents intermediary results after method development during the first year of a PhD project and methods detail current work.

The robust experimental design of Freeman et al. [2004] is open to adaptation by replacing peat with peat-permafrost in laboratory analyses. Field samples from a site in Nome, Alaska were obtained by our collaborator Prof. Hojeong Kang of Yonsei University, South Korea.

To assess the relative impact of O_2 on extracellular enzymes, homogenised thawed permafrost samples are exposed to aerobic or anaerobic conditions followed by enzyme activity assays using labeled model substrates; L-dihydroxy-phenylalanine [L-DOPA] for phenol oxidases and methylumbelliferyl [MUF] for hydrolases (β-glucosidase, phosphatase and sulphatase). The impact of phenol oxidases on phenolic concentrations in permafrost pore water is also measured.

To quantify the impact of phenolics on hydrolase activities, permafrost homogenates are treated with phenolic-rich solution and assayed with MUF markers. Finally, hydrolase activities are examined in permafrost homogenates enriched with phenol oxidase, in order to test whether abundance of this enzyme stimulates the activity of others.

Expectations

1. Increase in phenol oxidase activity will exceed an increase in hydrolase enzyme activity as oxygen abundance rises (O_2 is a reaction participant).
2. Addition of phenol oxidase will reduce phenolic concentrations from the soil pore waters.
3. Removal of phenolics will increase hydrolase activities.
4. Enhanced phenol oxidase activity will positively correlate with activity of a hydrolase enzyme that is relatively unaffected by oxygen.

Fulfilment of these hypotheses would confirm the existence of an Arctic 'enzymic latch' mechanism and suggest that presence of phenolic compounds under O_2-limiting conditions may have a role to play in slowing down C release from thawing permafrost in a changing climate.

Project growth

A major objective of this poster is to present a call for collaboration whilst discussing intermediary findings. To witness enzymic decomposition control of this nature in permafrost-affected peat soils would support evidence of similar patterns in other peatland systems, potentially opening up a new branch of Arctic research with significant implications for biogeochemical models of C cycling in polar soils.

References

Freeman, C.; Ostle, N.J.; Fenner, N. and Kang, H. [2004]: A regulatory role for phenol oxidase during decomposition in peatlands. *Soil Biology and Biochemistry*, 36(10):1663 – 1667, doi:10.1016/j.soilbio.2004.07.012.

Vorobyova, E.A.; Soina, V.S. and Mulukin, A.L. [1996]: Microorganisms and enzyme activity in permafrost after removal of long-term cold stress. *Advances in Space Research*, 18(12):103 – 108, doi:10.1016/0273-1177(96)00005-1.

Wagner, D.; Kobabe, S. and Liebner, S. [2009]: Bacterial community structure and carbon turnover in permafrost-affected soils of the Lena Delta, northeastern Siberia. *Canadian Journal of Microbiology*, 55, doi:10.1139/W08-121.

Combined assessment of Archaeal and Bacterial communities in soil samples from Hornsund, Spitsbergen using Illumina Mi-Seq

Edwin Sien Aun Sia[1], Nastassia Denis[1], Aazani Mujahid[2], Jing Zhang[3], Siti Aisyah Alias[4,5], Siti Hafizah Ali[4,5], Azizan Abu Samah[5], & Moritz Mueller[1]

[1]*Faculty of Engineering, Computing and Science, Swinburne University of Technology, Sarawak Campus, Jalan Simpang Tiga, 93350, Kuching, Sarawak, Malaysia*
[2]*Department of Aquatic Science, Faculty of Resource Science and Technology, University Malaysia Sarawak, 94300 Kota Samarahan, Sarawak Malaysia.*
[3]*State Key Laboratory of Estuarine and Coastal Research, East China Normal University, Zhongshan N. Road 3663,Shanghai 200062, China*
[4]*Institute of Biological Science, Faculty of Science, University Malaya, 50603 Kuala Lumpur, Malaysia*
[5]*National Antarctic Research Centre, IPS Building, University Malaya, 50603 Kuala Lumpur, Malaysia*

Hornsund is a fjord which lies on the southern-most tip of Spitsbergen Island. It harbours a wide range of landforms which is governed by marine influence due to it facing the Greenland Sea. While the diversity of microfungi within this area has been published, there are few studies of the reconstruction of the prokaryotic community, including whether the community resides within a copiotrophic or oligotrophic environment. The bacterial and archaeal communities were assessed from nine habitats around Hornsund, Spitsbergen in the High Arctic by extracting the DNA. Subsequent analyses were done by obtaining 16s rDNA utilizing Illumina Mi-seq universal bacterial and archaeal primers to assess the diversity of the prokaryotic communities within distinct biogeographic regions. The 16s rDNA sequences were then analyzed by using Mothur as well as MEGAN5 (MetaGenome ANalyzer) program for detailed analyses. From the analyses, total assigned reads were normalized using sub-sample counts and the relative abundance was compared and analyzed for probable function based on the community composition. The Taxonomy Cluster Analyses revealed that ornithogenic influence showed the highest degree of dissimilarity as compared with other biogeographic regions. Also, the dominance shown by Acidobacteria, Proteobacteria, Actinobacteria, Bacteroidetes and Verrumicrobia in the shared biome were in agreement with other literature on Arctic soils, with the exception of Bacteroidetes in which Gemmatimonadetes was found to be the most prominent in other literature. While other samples were dominated by other phyla, Acidobacteria was the most predominant in the ornithogenic tundra, contributing to the overall dominance as shown in the shared biome. However, it is compelling to note that only the aforementioned soil has bacteria from the phylum Nitrospirae, indicating its role in the cycling of nitrogen from feces of ornithogenic origin, in an otherwise oligotrophic tundra as exhibited by the other samples. In addition to that, six out of nine samples contains bacteria from the Chloroflexi phyla, even though the highest percentage in a sample was only 7.14 %. This indicates the potential role of photosynthesis for nitrogen-fixation during the Arctic summer in the oligotrophic environment. Lastly, archaeal reads from the phylum Crenarchaeota were found in only in moist moss tundra from Hyttevika (2.67 %), in which its function within the community remains yet to be determined due to the low presence. The results from this study show that the distinct habitats in the Hornsund region exhibit varying degree of variability in terms of its prokaryotic community composition. To our knowledge, this is the first comparison of prokaryotic communities within this region, thus providing a platform for further work involving temporal and diurnal studies.

The Arctic methane oxidizer *Methylobacter tundripaludum* responds to changing temperatures by global transcriptional shifts

Alexander Tøsdal Tveit, Alena Didriksen, Serina Lee Robinson, & Mette M. Svenning

UiT The Arctic University of Norway, Norway

Methanotrophs are adapted to highly fluctuating temperatures at the interfaces of oxic and anoxic zones in soils and sediments and are essential to the greenhouse gas budget, greatly reducing methane emissions from natural and anthropogenic environments to the atmosphere. However, it is unknown how methanotrophs regulate their metabolism to optimize growth at different temperatures and how this affects methane oxidation potential. *Methylobacter* is a methanotrophic genus that dominate many soil and aquatic environments that are rich in CH_4 (methane) and have a pH close to neutral. We aimed to determine how the CH_4 oxidation potential and growth of the Arctic methanotroph, *Methylobacter tundripaludum*, responds to temperature and how this relates to the transcriptional regulation of its metabolism.

We calculated CH_4 oxidation rates, growth rates, and sequenced the transcriptomes of M. tundripaludum at 8, 15, 21 and 27 °C. The growth and CH_4 oxidation rates were distinctly different at the different experimental temperatures. M. tundripaludum displayed the highest CH_4 oxidation rates at 15 °C, yet grew optimally at 21 °C. The higher growth and oxidation rate at 8 °C than at 27 °C confirmed that it is low temperature adapted. The altered growth and oxidation rates of *M. tundripaludum* at different temperatures coincided with massive shifts in the transcript abundances for metabolic processes such as CH_4 oxidation to CO_2, RuMP pathway of carbon assimilation, TCA cycle, respiration, protein, nucleoside and fatty acid metabolism. Interestingly, genes related to cell division, translation and transcription was upregulated at temperatures above and below the growth optimum, strongly suggesting a cellular response to counteract reduced enzyme efficiencies in core metabolisms directly related to growth and overall cellular activity. The expression of most genes were adjusted, but not shut on or off, indicative of adaptation to different substrate flows through the pathways, and/or altered enzyme kinetics. However, the expression of some genes were partly replaced by the expression of homologues or analogues, presumably with other (thermo)kinetic properties. We show that the temperature-transcript patterns of all these central metabolisms fall into a restricted number of co-expression units, suggesting a cellular economization of transcriptional regulation. Altogether, the data showed that M. tundripaludum adapts its metabolism to different temperatures by massive transcriptional regulation of enzyme systems.

Microbial activity in thermokarst soils: Mechanisms of carbon loss following permafrost thaw

Mark Waldrop[1], Miriam Jones[1], Kristen Manies[1], Jack McFarland[1], Steve Blazewicz[1], Monica Haw[1], Rebecca Neumann[2], & Jennifer Harden[1]

[1] *US Geological Survey, United States of America*
[2] *University of Washington, Civil and Environmental Engineering*

Soil microbial communities play a critical role in regulating the Earth's climate through the production and consumption of greenhouse gases. Warming, particularly of subarctic soils, is predicted to cause widespread permafrost thaw. The high carbon (C) content of these systems could release CH_4 and CO_2 to the atmosphere, transitioning them from a net sink to a net source of C to the atmosphere. We examined the impacts of permafrost degradation on C storage, greenhouse gas production, and microbial community composition and activity along a lowland chronosequence of collapse-scar bog development following a natural thaw event. Our study area is located within the Bonanza Creek Long Term Ecological Research site in interior Alaska. Using a mass balance approach, we show that peat C contained in the forest floor and permafrost is rapidly lost post thaw. We hypothesize that this loss could be the result of higher microbial activity early in bog development. In support of this argument, at the young bog site we have observed higher rates of CH_4 flux at the surface, as well as the potential for higher rates of CH_4 production within the deepest horizons. Higher rates of methanogenesis and methane flux in the young bog were correlated with both increased availability of labile C from dissolved organic matter and, a higher abundance of aerenchymatous sedges (e.g. *Carex sp*). We suspect that increased occurrence of *Carex sp.* in the young bog allows for more rapid transport of CH_4 from the deep within the peat profile thereby circumventing the potential for CH_4 oxidation. Preliminary modeling results, based upon porewater gas concentrations and isotopes, indicate that microbial activities are higher in the base layers of the youngest bogs summer and winter months. Moreover, variation in the composition of the microbial community is reflective of the processes and rates occurring at these sites. Our results highlight how variation in microbial activity, driven in part by temporal changes in C availability post-thaw, interact with plant-mediated transport processes to drive rapid C loss early in the transition from permafrost to bog environments.

Exploring the rare biosphere of methanogenic archaea in frozen ground affected soils of the Tibetan Plateau

Sizhong Yang[1,2], Dirk Wagner[1], Matthias Winkel[1], & Susanne Liebner[1]

[1] *GFZ German Research Centre for Geosciences, Helmholtz Centre Potsdam, Germany*
[2] *State Key Laboratory of Frozen Soils Engineering, Cold and Arid Regions Environmental and Engineering Research Institute, Chinese Academy of Sciences, China*

In microbial communities a small number of different species accounts for the majority of the microbial biomass while the main richness is contributed by the rare taxa [Pedros-Alio, 2012] referred to as the low-abundant microbial populations. In recent years, the rare population was effectively detected by high-throughput sequencing methods. The consistent detection of a wide range of rare taxa in soils, oceans, and our own bodies suggests that rarity is a conserved way of microbial life [Lynch and Neufeld, 2015] and may act as inoculum when environmental conditions change. While our current knowledge about the rare biosphere is centered on overall bacterial communities, insights into rare taxa of specific functional groups are sparse. Using mcrA as a functional gene of methanogenic archaea, we applied 454 pyrosequencing and successfully targeted the rare methanogens in different, frozen ground affected soils from the Tibetan Plateau. Our results show that similar to general bacterial communities rare methanogens contribute disproportionally to diversity (82 % of total OTU richness) but only 15 % to the total sequence counts. Among all rare taxa some taxa are conditionally rare, i.e. rare in some samples and abundant in others. Generally, rare methanogenic taxa contributed only marginally to the total β-diversity which is consistent to what is known for overall bacterial populations. Interestingly, similar dominant genera and environmental correlation were identified for both rare and abundant groups even at an arbitrary relative abundance threshold of 0.1 %, implying comparable structuring processes and environmental filtering of both groups. The prevalent taxa are thus suggested to exert a positive influence on the structure of the rare biosphere. For macro-organisms such as plants, species diversity is regularly observed as a major determinant of ecosystem productivity, stability, and nutrient dynamics. We encourage further work to explore the ecological relevance of the rare taxa both as inoculum for and as potential driver of methane production in the environment.

References

Lynch, M.D.J. and Neufeld, J.D. [2015]: Ecology and exploration of the rare biosphere. *Nature Reviews Microbiology*, 13:217–229, doi:10.1038/nrmicro3400.

Pedros-Alio, C. [2012]: The rare bacterial biosphere. *Annual Review of Marine Science*, 4:449–466, doi:10.1146/annurev-marine-120710-100948.

SESSION 12

Planetary Permafrost and Earth Analogues

Convener:

Antoine Séjourné, *Univ. Paris Sud - GEOPS, France*

Andreas Johnsson, *University of Gothenburg, Sweden*

Jan Raack, *Open University, United Kingdom*

Over the past decade, a multitude of high-resolution data sets from space missions have provided ever increasing evidence for dynamic processes involving ice and permafrost on Mars and the icy satellites.

This session aims to give an up-to-date insight of the study of ice and permafrost and resulting landforms on planetary bodies with an emphasis on the use of cold-climate environments on Earth as analogues for studying the other planets. Presentations will be encouraged to discuss planetary periglacial and glacial processes and/or present analogies between terrestrial and planetary permafrost environments and can include fieldwork, remote sensing and laboratory studies. Scientists who are new to planetary science are particularly welcome.

Rock glaciers as proxies for identifying terrestrial and analogous Martian permafrost

Anshuman Bhardwaj[1,2], Lydia Sam[2,3], & F. Javier Martín-Torres[1,4]

[1]*Division of Space Technology, Department of Computer Science, Electrical and Space Engineering, Luleå University of Technology, Kiruna, Sweden*
[2]*Department of Environmental Science, Sharda University, Greater Noida, India*
[3]*Defence Terrain Research Laboratory, New Delhi, India*
[4]*Instituto Andaluz de Ciencias de la Tierra (CSIC-UGR), Armilla, Granada, Spain*

Rock glaciers are lobate or tongue-shaped creeping masses of ice-rich debris on mountain slopes. Permafrost represents a thermal state and any lithospheric material (and not necessarily ice) that remains at mean annual air temperatures (MAAT) below 0 °C for at least two year. Past researches have established rock glaciers as a proxy for permafrost [Schmid et al., 2015]. These rock glaciers, both on Earth and Mars, can be delineated using freely available high-resolution images. In order to establish any analogy between terrestrial and planetary landforms, it is preferable to search for well-preserved and undisturbed terrestrial specimens. High Himalayan terrain is a good example, as it majorly encompasses landscapes that are well preserved and away from any anthropogenic interference. We have developed a research in this region that during a first stage consisted in the investigation of rock glaciers and related features in the Himachal Himalaya, India, using high-resolution remote sensing images. In a second stage, we performed field visits to observe the features marked on high resolution images for the presence of permafrost. As a final step, we tried to identify analogous cold-climate landforms on Mars.

Our scientific team has been spending three months (July-September) each year since 2013 on the mountains of Baspa river basin, performing various glacio-hydrological measurements. During this total 9-months period, we have performed and published several additional studies, utilizing our continuous presence there. The present study was conceptualized in 2014 after making an observation on a seasonal snow-free and cloud-free Quickbird image (of 25 August 2014) showing rock glaciers present in the river basin (Fig. 1a). We identified two adjacent rock glacier-type features presenting different spectral and structural characteristics (marked as features 1 and 2 in Fig. 1a). Within the boundary, feature 1 showed two different surface types while feature 2 showed a homogenous surface pattern throughout, however different from feature 1. The two different surface types are shown in Fig 1a: (1) dashed blue boundary encompassing dust debris mixed with ice, (2) dashed red curves showing lobate flow patterns formed on thick rock debris over ice. Fig 1b shows the elevation profiles for the two features along the middle transects. This analysis helped us to establish some hypotheses regarding the structural and spectral differences between the two expected rock glaciers. Absence of either lobate flowing patterns or ice mixed-dust debris on feature 2 prompted us to study its elevation distribution with respect to feature 1. Approximate lengths of the features 1 and 2 are 1.9 km and 1 km, respectively and elevation ranges are 5004-5370 m and 4974-5243 m, respectively. Elevation statistics generated using ASTER Global Digital Elevation Model (GDEM) V2 shows that the mean elevation for features 1 and 2 are 5,181 m and 5,052 m, respectively. Another noticeable characteristic in Fig 1b is their average slope: 19 % for feature 1 and 23.3 % for feature 2. Now, clearly the elevation ranges and average elevations for both these features are similar and considerable for supporting the existence of rock glaciers. However, the average slope of feature 2 is considerably higher and therefore indicative of a higher flow velocity. Still, the absence of lobate flow patterns and the relatively brighter surficial tone even in the season of permafrost defrosting in this region seemed inexplicable to us. The darker tone (due to increased moisture content) of feature 1 on the other hand, was an evidence of this seasonal thawing process. Thus, a preliminary conclusion was that feature 1 was a typical mountainous rock glacier harboring permafrost, while feature 2 still needed field

verifications. For feature 2, we could only establish that: (1) either, it was a rock glacier with extremely thick debris cover pertaining to the adjacacent steeper rocky slopes contributing debris and masking the permafrost thawing process, or; (2) it was remnant of a long gone glacier. Next step of the study was the field validations. In situ observations clearly suggested feature 1 to be a rock glacier and feature 2 to be heavily debris-covered. We installed several bamboo stakes (yellow dots in Figure 1a) on 20 September 2014 to monitor the yearly flow velocities (if any) of these features. The readings recorded on 20 September 2015 depicted an average flow velocity of nearly 3.5 m/year for rock glacier 1 while feature 2 showed absolutely no sign of movement, thus denying the possibility of it being a rock glacier. Feature 2 certainly looked like the remnant of a past glacier. Another fact to be established was that whether feature 2 was representing a debris-covered dead ice mound as permafrost or any subsurface ice was absent. This was easily settled by a minor excavation of debris that after a depth of nearly 1.5 m exposed the dead ice at an elevation of around 5,000 m. This debris layer was thick enough to suppress the optical remote sensor-observable dark tone signal of seasonal defrosting or thawing of ice. However, the extent of this sub-surface dead ice is still unknown and the absence of any movement in it indicates the possibility of its existence only in limited area of lower reaches of feature 2 with relatively gentler slope.

We were further interested in finding the Martian analogues to these rock glaciers and associated features. The left panel of Fig 1c shows the seasonal permafrost defrosting in case of Earth and Mars. The Earth analogue is the zoomed in view of blue-dashed region of rock glacier 1, shown in Fig 1a. The Mars analogue is a HiRISE/Mars Reconnaissance Orbiter picture in the southern hemisphere on 3 January 2013 at latitude (centered): -69.789°and longitude (East): 98.777°. The yellow ellipses highlight the thawing permafrost on the slopes of a crater. Intermittent icy pixels surrounded by dark toned pixels are observable in these images. Another analogy between the lobate flowing patterns on terrestrial rock glaciers and the lobate debris aprons can be observed in the right panel of Fig 1c.

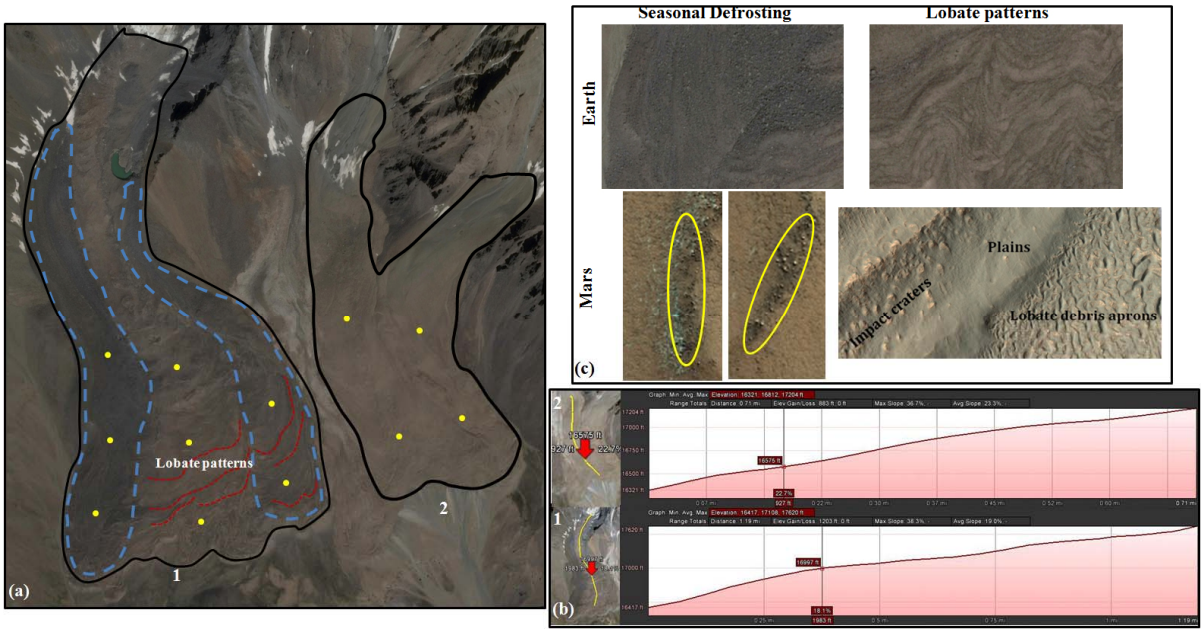

Figure 1: Terrestrial permafrost analogues on Mars. (a) High-resolution Quickbird image (25 August 2014) showing expected rock glaciers and related features in Baspa river basin, Himachal Pradesh, India. Black outline denotes the boundary. Dashed blue outline for glacier 1 denotes the different surface types within rock glacier boundary, showing defrosting permafrost towards the end of a mass balance year. Dashed red curves demarcate lobate patterns found in relatively fast creeping middle region of glacier 1. Yellow dots show the installed stakes for velocity measurements. (b) Elevation profiles for the expected rock glaciers. Yellow curve in left panel denotes the transects for drawing the elevation profiles. (c) Interplanetary analogy between permafrost-related landforms. The Martian landforms are seen on High Resolution Imaging Science Experiment (HiRISE) imagery (within yellow ellipses).

Colaprete and Jakosky [1998] are few of the early researchers who in detail discussed the ice flow characteristics and rock glaciers on Mars. They described the structure and properties of lobate debris aprons. They also reported these debris aprons to be of radial length, ranging from a few kilometers to over 15 km. Lobate debris aprons are very common in the fretted terrain separating the northern lowlands from the southern highlands between 280°and 250°longitude and almost all of them can be located between 50°and 80°latitudes [Squyres, 1989]. The lower right panel of Fig 1c shows these features in an autumn image captured by HiRISE on 26 November 2010 along the bottom of a hill in the Promethei Terra region of Mars. As it is already discovered using RADAR that such Martian features comprise of 100 % pure ice, it would be really interesting to automate the process of their detection using surface temperature images of Mars. The lobate structure can also get captured in high resolution Digital Terrain Models (DTMs).

This study is a preliminary effort to observe rock glaciers in high Himalaya using high-resolution remote sensing images and DEMs and in situ validation of the observations with respect to the presence of permafrost. We demonstrate a work-flow for conclusively identifying a rock glacier and distinguish it from the similar looking landforms. The study presently is at a local scale and inclusion of more rock glaciers in future and study of their surficial features can greatly improve our understanding of the feebly studied Himalayan rock glaciers and permafrost. The fact that these landforms in high Himalaya are still untouched and well-preserved, makes them perfect analogues to study the Martian landscapes and their evolutionary history.

References

Colaprete, Anthony and Jakosky, Bruce M. [1998]: Ice flow and rock glaciers on Mars. *Journal of Geophysical Research: Planets*, 103(E3):5897–5909, doi:10.1029/97JE03371.

Schmid, M.-O.; Baral, P.; Gruber, S.; Shahi, S.; Shrestha, T.; Stumm, D. and Wester, P. [2015]: Assessment of permafrost distribution maps in the Hindu Kush Himalayan region using rock glaciers mapped in Google Earth. *The Cryosphere*, 9(6): 2089–2099, doi:10.5194/tc-9-2089-2015.

Squyres, Steven W. [1989]: Urey prize lecture: Water on Mars. *Icarus*, 79(2): 229 – 288, doi:http://dx.doi.org/10.1016/0019-1035(89)90078-X.

Investigation of cryobot movement through frozen structures

Anton Butenko[1], Sergey Aksenov[1], & Olga Erokhina[1,2]

[1] *Space Research Institute, Russian Federation, Moscow State Institute of Electronics and Mathematics NRU HSE*
[2] *GeoForschungsZentrum, Potsdam, Germany*

Nowadays planetary bodies' studies are of the great interest. First of all, such space objects are the icy moons of the giant planets like Jupiter and Saturn: Europa, Ganymede, Enceladus. It's believed that they are the most likely places in Solar System for the detection of extraterrestrial life. One of the problems to solve is the problem of design of a special device capable to penetrate the frozen structure by in order to reach the internal ocean and make the in situ analysis of biological material embedded in or underneath frozen layers.

The approach is based on mathematical and computer simulation of the process in question. Studying of penetration process allows build the model of the movement that can be used in order to optimize the parameters of the probe in meaning of velocity maximization, minimizing energy consumption etc. A special feature of this process is significant impact of the properties of frozen structure. That's why it's necessary to explore the variation of the properties depending on different factors. Of course, melting probe or (cryobot) is supposed being tested on Earth and can be used for terrestrial explorations.

As long as driving forces of the penetration is gravity and melting a lot of questions arise: how the probe will move depending on gravity and pressure, how it's possible to perform in situ analysis inside a probe. Studying of penetration process allows build the model of the movement that can be used in order to optimize the parameters of the. In general the problem is supposed to be simulated as an iterative sequence of boundary problems for modified heat conduction equation in coordinate system attached to the probe. Besides mathematical and computer simulation, lab experiments and field tests under real conditions are indispensable sources of information for creation effective device for exploration and analysis.

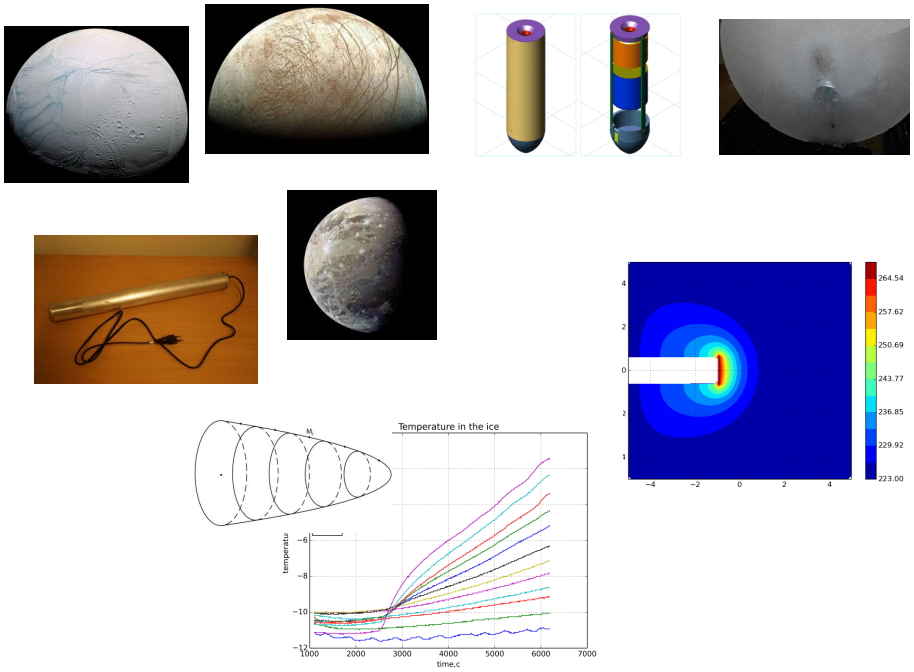

Figure 1

Mapping the northern plains of mars: origins, evolution and response to climate change – a new overview of recent ice-related landforms in Utopia Planitia on Mars

Francois Costard[1], Antoine Séjourné[1], Zuzanna M. Swirad[2], & Anna Losiak[3]

[1] *Univ Paris-Sud, CNRS, Laboratoire GEOPS, UMR8148, Orsay, France*
[2] *Department of Geography, Durham University, Durham, UK.*
[3] *Polish Academy of Sciences, Institute of Geological Sciences, Wroclaw, Poland*

Introduction

The northern plains of Mars, topographically lower than the "cratered highlands" of the southern hemisphere, comprise several large overlapping basins that are filled by sediments. The region has been proposed to have hosted an ancient ocean and currently contains near surface ground ice even at mid-latitudes, as demonstrated by observations of fresh craters, spectral measurements of hydrogen abundance, and direct observation at high latitude from the Phoenix Lander as well as many periglacial and glacial landforms.

However, no consensus about the nature of ground ice and formation of the planetary permafrost. The spatial distributions of ice-related landform at broad-scale and control by regional geology or climate is still not constrained. Improving the geological context of the northern plains will help constrain outstanding questions about martian geological evolution, environmental change and – if ice here was once liquid water – astrobiology.

An International Space Science Institute (ISSI) team project has been convened to study ice-related landforms in targeted areas in the northern plain of Mars: Acidalia Planitia, Arcadia Planitia, and Utopia Planitia. Here, we describe our mapping of western Utopia Planitia along a strip from 25°N to 75°N latitude of 250 km wide. The goals are to:

i) map the geographical distribution of the surface ice-related landforms;

ii) identify their association with subtly-expressed geological units and;

iii) discuss what the distribution tell us about the ice-content, sediment types and environmental evolution in UP.

Methods

Rather than traditional mapping with points, lines and polygons, we used a grid "tick box" approach to efficiently determine distribution of specific landforms by using grid of squares for each study area, each approximately 20×20 km. Over the region, ice-related landforms were identified and recorded as being either "present", "dominant", or "absent" in each sub-grid square displayed in a Cassini projection. The end result of the mapping is a "raster" showing the distribution of the various different types of landforms across the whole strip providing a digital geomorphological map.

Results

Our mapping shows that the scalloped depressions, pits and 100 m polygons occur over a broader area than previously shown (from 40°N to 65°N. Coalesced scalloped depressions of several km in diameter are concentrated near 50°N. Different impact craters are observed with glacial features (Concentric Crater Fills). We also observed that the thumbprint terrains, high-albedo mounds of different diameter and km-scale polygons are mostly seen in the southern UP (from 30°N to 40°N.

Based on their correlated distribution at regional scale but also at local scale where they are associated spatially, several assemblage of landforms can be defined. The scalloped depressions, pits and 100 m polygons are spatially associated at local scale because interrelated, pits cross-cut polygons that are degraded by scallops and at regional scale because same area between 40°N to 50°N. Scallops and pits being interpreted as due to sublimation of ground-ice and polygons due to thermal contraction, their distribution corresponds to an area where an ice-rich permafrost like on Earth.

Conclusion

Our knowledge of the distribution of ice-related landforms in UP was improved. Based on their spatial association, there are different assemblages of landforms. Their distribution is not only related to latitude but also on topography, geological context. Grid mapping provides an efficient and scalable approach to collecting data on large quantities of small landforms over large areas. The next step is to define unit : based on assemblage of landforms, albedo and/or crater counting. The differences/similarities of the key 3 regions in the northern plains reflect their complex geological history.

Acknowledgements

This work is a joint effort of an International Team sponsored by ISSI (International Space Science Institute).

Towards reconstructing the very recent climate on Mars: Insights from terrestrial analogues in the Arctic and Antarctica

Ernst Hauber[1], Jean-Pierre de Vera[1], Nicole Schmitz[1], Dennis Reiss[2], Andreas Johnsson[3], & Harald Hiesinger[2]

[1] *DLR, Germany*
[2] *Westfälische Wilhelms-Universität, Germany*
[3] *University of Gothenburg, Sweden*

Many very young landforms on Mars resemble terrestrial glacial and periglacial surface features in permafrost regions and show a latitude-dependent geographic distribution. These include surface mantling, viscous flow features, polygonally fractured ground, and gullies. Collectively, these landforms are hypothesized to represent the geomorphological surface record of Martian ice ages that were triggered by astronomical forcing and associated climate changes. It is debated, however, whether liquid water was generated in the geologically recent past – or even at present – through processes such as melting of snow and/or ice, or by the deliquescence of salts (e.g., Mg-perchlorates).

In previous field campaigns, we used permafrost landscapes on Svalbard as terrestrial analogues for morphologically similar surface features on Mars to develop formation hypotheses with and without liquid water. Most phenomena on Mars, but not Svalbard, can plausibly be explained by "dry" permafrost scenarios without the need to invoke freeze/thaw. Examples of such processes are the slow creep of ice-debris mixtures in permafrost, such as rock glaciers or debris-covered glaciers, or the aggradation and degradation of niveo-aeolian deposits. Other landforms could be explained with and without the availability of liquid water. Examples are thermal contraction polygons, which could form as ice-wedge polygons indicating thaw and liquid water, or, alternatively, as sand wedge or sublimation polygons. Former glaciers could have either been warm-based or cold-based, and therefore do not provide constraints on the history of liquid water. While geologically young gully-fan systems are morphologically similar to depositional systems on Earth which are formed by debris flows (i.e. mixtures of sediment and liquid water), present day gully modification might be linked to CO_2 condensation and defrosting.

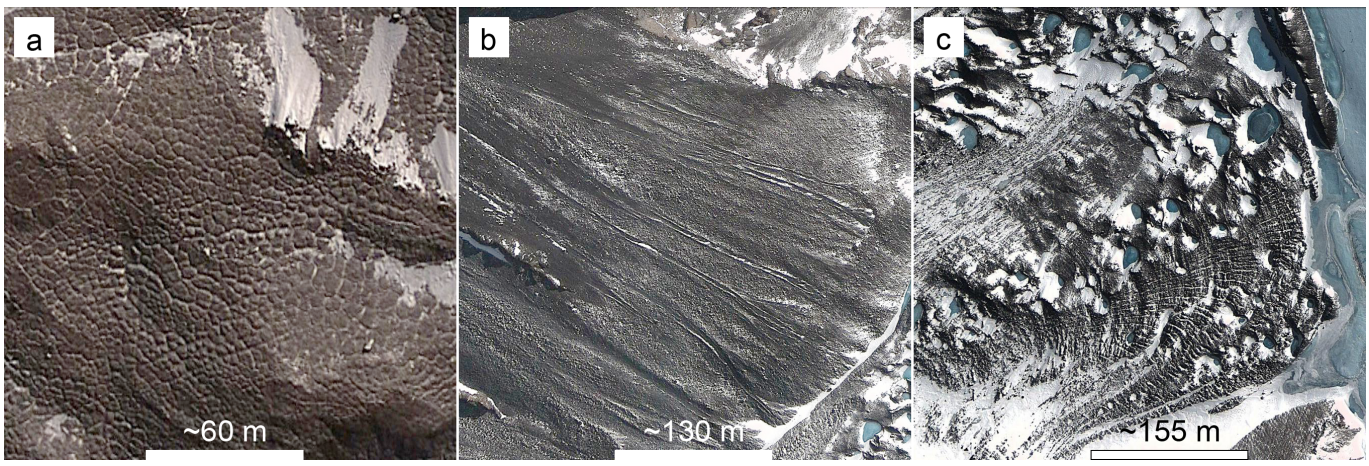

Figure 1: Mars-analogue landforms in Northern Victoria Land, Antarctica. (a) Patterned ground (71°36'22"S, 160°36'41"E); (b) Leveed channels (71°40'42"S, 162°05'50"E); (c) Viscous flow features (next to c). North is up. Credit: GoogleEarth/DigitalGlobe.

In contrast to Svalbard, continental Antarctica experiences colder and drier conditions that are more akin the current and/or past climatic environment on Mars. We present morphological observations from two field sites in Northern Victoria Land, Antarctica: A coastal site at the German research station "Gondwana" in Terra Nova Bay (74°38'S, 164°13'E), and a remote continental site/area in the Transantarctic Mountains in the Rennick Glacier/Usarp Mountains region (field camp in the Helliwell Hills, at about 71°55'S, 161°30'E). These sites display several landforms that resemble Martian mid-latitude surface features such as patterned ground, gullies with leveed channels, and ice-cored moraines (Fig. 1). At the time of writing, results are not yet available (field work will be conducted in January/February 2016). At the conference, we will present a comparative analysis of morphologically analogous landforms on Svalbard, in continental Antarctica, and on Mars, and we will discuss the evidence and the formation scenarios of liquid water in the Antarctic field sites, which in turn can inform the understanding of young cold-climate landforms on Mars.

Veiki-moraine-like landforms in Nereidum Montes on Mars: Insights from analogues in northern Sweden

Andreas Johnsson[1], Dennis Reiss[2], Ernst Hauber[3], Mark D. Johnson[1], Mats Olvmo[1], & Harald Hiesinger[2]

[1]*Department of Earth Sciences, University of Gothenburg, Sweden*
[2]*Institut für Planetologie, Westfälische Wilhelms-Universität, Münster, Germany*
[3]*Institut für Planetenforschung, Deutsches Zentrum für Luft- und Raumfahrt (DLR), Berlin, Germany*

Introduction

Mars is a cold hyper-arid planet where liquid water is extremely rare [McEwen et al., 2011]. Most water is instead locked in a number of frozen reservoirs such as the polar caps, ground ice and as glacier ice. Previously, numerous studies reported on glacier landforms such as viscous flow features and lobate debris aprons where water-ice is believed to exist under insulating debris cover [Milliken et al., 2003]. This notion was confirmed by SHARAD measurements [Holt et al., 2008]. However, very little is known about glacial landforms in which water is an important factor. Most studies have focused on moraine-like ridges that are associated to gully systems in crater environments [Arfstrom and Hartmann, 2005], glacier landforms at the equatorial volcanic province [Scanlon et al., 2015] and drop-moraines from CO_2 glaciers [Head and Mustard, 2006]. Here we report on unusual irregular ring-shaped landforms within a mountain complex in Nereidum Montes, Mars. These landforms are well-preserved and may suggest recent ablation of a debris-covered glacier. These martian ring-shaped landforms show a striking resemblance to the Veiki moraine in northern Sweden. Veiki moraines are believed to have formed at the lobate margins of a stagnant ice-sheet during the first Weichselian glaciation [Lagerbäck, 1988]. The Veiki moraine is characterized by ridged plateaus that are more or less circular and surrounded by a rim ridge. The newly acquired national LiDAR data over Sweden enable us studying these landforms in unprecedented detail. They also enable us exploring geomorphological similarities between Earth and Mars in large spatial contexts. This study aims to increase our understanding of glacial landforms on Mars by comparison to terrestrial analogues. Questions addressed are:

1. how morphological similar are the Martian landforms to the Veiki moraine of Sweden?
2. How does the ring-shaped landform relate to other well-preserved glacial landforms within the mountain complex?
3. Do the moraine-like landforms indicate the maximum extent?
4. Was any meltwater involved and are the preserved landforms ice-cored?

Data and Methods

For our study we use HiRISE (25 cm/pxl), CTX (6 m/pxl), MOLA topography and point data. CTX images have been processed using ISIS 3.0. The terrestrial analogues are covered by LiDAR. The LiDAR data have a point density between 0.5 to 1.0 points/m2, with a footprint of 0.5 m and a scan angle of 20°. Accuracy of the z-axis is typically better than 0.1 m on flat surfaces.

Observations

The martian ring-shaped landforms are located at the end of a valley that are open in the eastward direction. In plan form the overall morphology has a distinct lobe shape (Fig. 1A) and covers an area of approximately 80 km^2. Individual landforms form irregular open and enclosed ridges (Fig. 1B). By shadow measurements ridges are 10-15 m in height. Ridges show a high concentration of boulders and clasts (Fig 1C). The outer lobe border is mainly made up of fractured mounds. The Veiki moraines in northern Sweden show a similar irregularity of landforms forming ridged plateaus and enclosed depressions (Fig 1D).

Discussion

The ring-shaped landforms are located in close spatial proximity to other landforms such as pronival rampart-like glaciers and remnant cirque glaciers. The topography around the ring-shaped landforms shows

features that may be interpreted as roche moutonnées, bergschrunds (crevasses at the head of a glacier), arêtes, cols (saddle-like narrow depression formed by two head ward eroding cirques that reduce an arête) and cirques. If these interpretations are correct it shows an area with clear evidence of prolonged glacial activity and possibly the presence of preserved glacier ice. The floor of the valley, adjacent to the ring-shaped landforms shows a number of exhumed impact craters which probably represent the pre-glacial surface. The very few fresh looking impact craters point to a relatively young surface age post glacial recession.

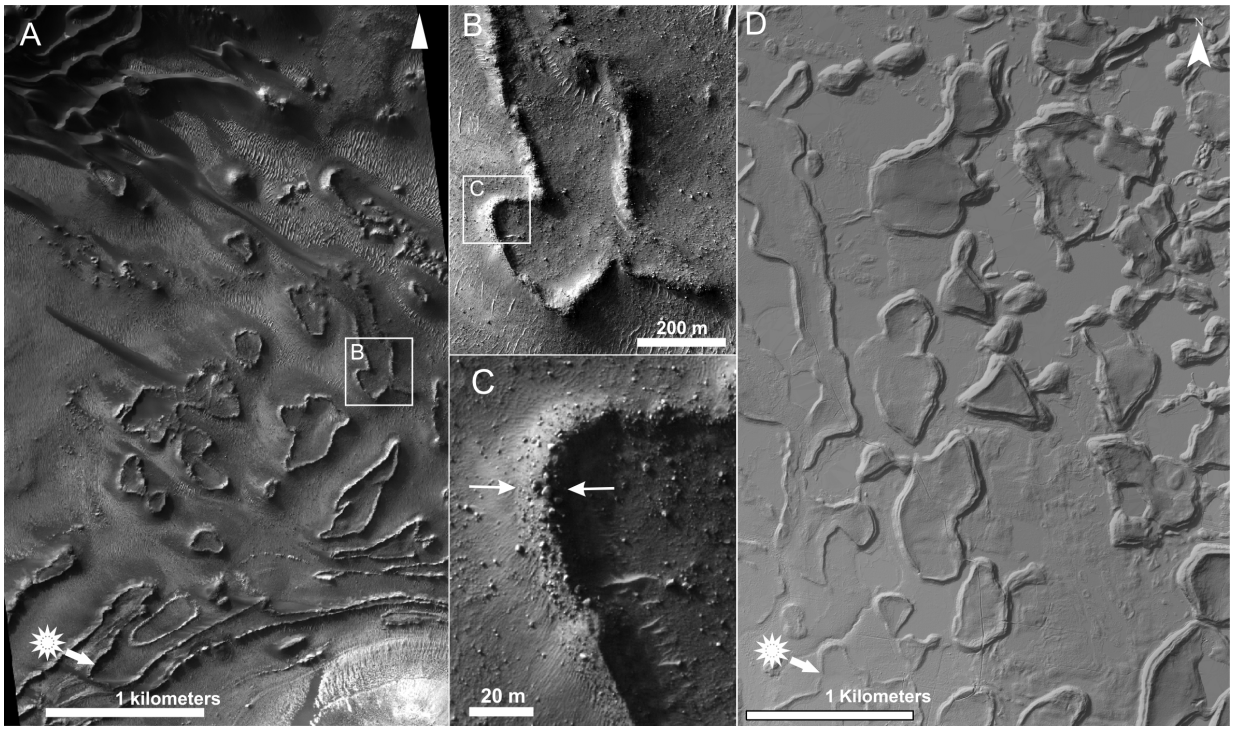

Figure 1: A) HiRISE image of multiple ring-shaped landforms forming a lobate pattern. B) Ridges form enclosed depressions with heights between 10-15 m. C) High clast concentrations at the ridges. D) LiDAR image of possible terrestrial analogues

Summary

We have identified an area in the Nereidum Montes region that shows clear evidence of glaciation, including possibly preserved glacier ice and glacial landforms. We have also found landforms strikingly similar to the Veiki moraines of northern Sweden. A better understanding of these features may provide important insight into Martian geologic and climatic history. This project is on-going and more work is needed to gain a better understanding of the sequential evolution of glacial landforms in this area.

Acknowledgements

This project has been financially supported by the Swedish National Space Board.

References

Arfstrom, J. and Hartmann, W.K. [2005]: Martian flow features, moraine-like ridges, and gullies: Terrestrial analogs and interrelationships. *Icarus*, 174: 321–335, doi:10.1016/j.icarus.2004.05.026.

Head, J.W. and Mustard, J.F. [2006]: Breccia dikes and crater-related faults in impact craters on Mars: Erosion and exposure on the floor of a crater 75 km in diameter at the dichotomy boundary. *Meteoritics and Planetary Science*, 41(10):1675–1690, doi:10.1111/j.1945-5100.2006.tb00444.x.

Holt, J.W.; Safaeinili, A.; Plaut, J.J.; Head, J.W.; Phillips, R.J.; Seu, R.; Kempf, S.D.; Choudhary, P.; Young, D.A.; Putzig, N.E.; Biccari, D. and Gim, Y. [2008]: Radar sounding evidence for buried glaciers

in the southern mid-latitudes of Mars. *Science*, 322 (5905):1235–1238, doi:10.1126/science.1164246.

Lagerbäck, R. [1988]: The Veiki moraines in northern Sweden – widespread evidence of an Early Weichselian deglaciation. *Boreas*, 17(4):469–486, doi:10.1111/j.1502-3885.1988.tb00562.x.

McEwen, A.S.; Ojha, L.; Dundas, C.M.; Mattson, S.S.; Byrne, S.; Wray, J.J.; Cull, S.C.; Murchie, S.L.; Thomas, N. and Gulick, V.C. [2011]: Seasonal flows on warm Martian slopes. *Science*, 333 (6043):740–743, doi:10.1126/science.1204816.

Milliken, R.E.; Mustard, J.F. and Goldsby, D.L. [2003]: Viscous flow features on the surface of Mars: Observations from high-resolution Mars Orbiter Camera (MOC) images. *Journal of Geophysical Research E: Planets*, 108(E6):11–1, doi:10.1029/2002JE002005.

Scanlon, K.E.; Head, J.W. and Marchant, D.R. [2015]: Remnant buried ice in the equatorial regions of Mars: Morphological indicators associated with the Arsia Mons tropical mountain glacier deposits. *Planetary and Space Science*, 111(1):144–154, doi:10.1016/j.pss.2015.03.024.

Surface temperatures and thermal inertia in Coogoon Valles Mars

Antonio Molina[1], Miguel ángel de Pablo[1], Iván López[2], Olga Prieto-Ballesteros[3], David Fernandez-Remolar[4], & Miguel Ramos[5]

[1] *Department of Geology, Geography and Environment. University of Alcalá, Madrid, Spain*
[2] *University Juan Carlos I. Madrid, Spain*
[3] *Department of Habitability and Planetology, Centro de Astrobiología. Torrejón de Ardoz. Madrid, Spain*
[4] *British Geological Survey*
[5] *Department of Physics and Mathematics. University of Alcalá, Madrid, Spain*

Permafrost on Earth is defined as any soil, rock or sediment layer at temperatures below the freezing point of water (273.15 K, 0 °C) for, at least, a continuous period of two years. Data collected in the last years evidence that, under the present Mars climate conditions, the day average surface temperature is below this point. To this regard, the surface of modern Mars occasionally exceeds 0 °C yearly in some areas during some time of the day, mainly in summer or spring. As a consequence, Mars permafrost can be considered hence to cover the full planetary extent. However, the absence of warm season temperatures and the exiguous amount of water available if any, impossibility the existence of a present freezing-thawing cycle and a proper active layer (Martian soils can share characteristics with dry permafrost on Earth, though). Anyhow, geomorphologic features characteristic of active layer processes (as polygonal grounds, pingos, gelifluction lobes, and even glacier-related) are abundant and ubiquitous on Mars. Those are likely to have formed in the geological past under different climate conditions. This planet has evolved from a warmer and wetter period (the Noachian), with a thicker atmosphere that allowed pluvial activity, to another much colder (the Hesperian). In this second period, large outflow channels caused by groundwater discharge may have created regional standing bodies, but the graduate decrease in planetary activity led to a loss of atmospheric pressure, which has finally evolved to arid conditions in modern times. This evolution has not been linear, and surface conditions are very conditioned to changes of planet obliquity (that is unstable and erratically oscillates among the history).

Mars surface is highly diverse, and the Highlands holds some of the best-preserved mineralogical and geomorphological signatures that date back from the Noachian and Hesperian ages. These changes are especially observable in Arabia Terra, where some of the oldest channels of the Highlands are located, being crucial to understanding the geological evolution of early Mars. We focus this work on one of such channels, Coogoon Valles, a Noachian outflow channel that terminates in a complex system of deltas/alluvial fans, where the primary candidate for the landing site of the ExoMars 2018 mission is located. Here we study the thermal infrared images that had been acquired for more than a decade, obtaining and analyzing the derived surface temperatures (ST) and thermal inertia (TI), and their temporal and spatial variation. They come from the data acquired by the Thermal Emission Spectrometer (THEMIS), an instrument that obtains multi-spectral thermal infrared images (100 m/pixel) in nine wavelengths centered from 6.8 to 14.9 µm and also visible/near-infrared images in another five bands. These wavelengths were specially selected to study surface mineralogy and physical properties of Mars. From Brightness Temperature Records (BTR), a specially calibrated product derived from the Band 9 (0.8 μm wide and centered at 12.57 μm), surface temperatures can be derived [Fergason et al., 2006]. The images were obtained from Planetary Data System (http://ode.rsl.wustl.edu/mars/), and the processing was performed with THMPROC (http://thmproc.mars.asu.edu/). Thermal inertia mosaics [Edwards et al., 2011] were recovered from the USGS Astrogeology Science Center web page (http://astrogeology.usgs.gov).

Fig. 1 shows daytime (14 to 16 hours in local time, A) and nighttime (4 to 6 hours in local time, B) surface temperature mosaics. The range in both images is of 20 degrees, but the difference between day and night temperatures is twice this amount, pointing to a larger temporal than the spatial difference in ST. On a surface with a very thin atmosphere with negligible moisture, and, therefore, limited specific

heat, direct insolation is the main variation factor for surface temperatures. The influence of topography on day temperatures is evident in Fig. 1-A; meanwhile surface temperatures during the night seem less conditioned to it. Crater interiors show relative increasing ST during the night and dropping during the night, as the contrary as in most of the surface at the central-eastern area. A similar thermal behavior as in the interior of craters was founded in the western lower side and an intriguing patch inside the central section of the channel.

If we plot average (points), as well as maximum and minimums (bars) surface temperatures (red are daytime and blue nighttime) of each available image for the study area, and whether this is plotted against the acquisition time (Fig 1-C), we obtain a sight of the thermal evolution in the area over the last 13 years. Whereas night ST remains roughly stable between 180 and 160 K (-80 to -100 °C), day ST are much more scattered and shows a very distinctive period, between 2010 and 2013, with a higher increase in ten degrees above temperatures that were observed in the period of 2002 to 2006. Following the 2010-2013 period, temperatures experience a significant decrease and gradual decline, which needs further observation.

Considering the Solar Longitude (Ls), instead Terrestrial acquisition day, a plot with the range of temperatures obtained during an average Martian year (687 Terrestrial days). The absence of data for the second half of the year avoid the observation of any clear annual trend but still allows to see which are the expected ST range that the upcoming mission would find shortly when it hopefully reaches the area.

The differences between day and night temperatures provide a hint of what is expected to found in thermal inertia. Thermal inertia provides information on the distribution of the materials that are exposed to the surface, and variation reflects diversity in composition and the range of states of consolidation. However, it also provides a way to probing the physical properties of shallow subsurface materials that may be obscured by thin coverings of dust and, therefore, revealing structures and textures that are indistinguishable on visible images. That is why IR information is not only useful to have a better understanding of the physical characteristic of a planetary surface leading to a greater knowledge of its geology through elaborating more accurate cartographies.

As THEMIS IR images were acquired at different local times, seasons, and years, and their features are quite diverse. As a consequence, it causes great uncertainness in calibration and calculation of the thermal inertia, which produces a high heterogeny in quantitative data. Fig 1-E shows the qualitative TI of the area. Quantitative data ranges from 130 to 1300 tiu (thermal inertia unit, J m^{-2} s^{-1}/2 K-1), with around 300 tiu in the inner patch of the channel, 300 to 400 tiu in the Western and nearly 1000 tiu in the interior of craters. The remaining areas display a tiu lower than 300. The interpretation of these results and a more extended analysis of the thermal data will be addressed in this work.

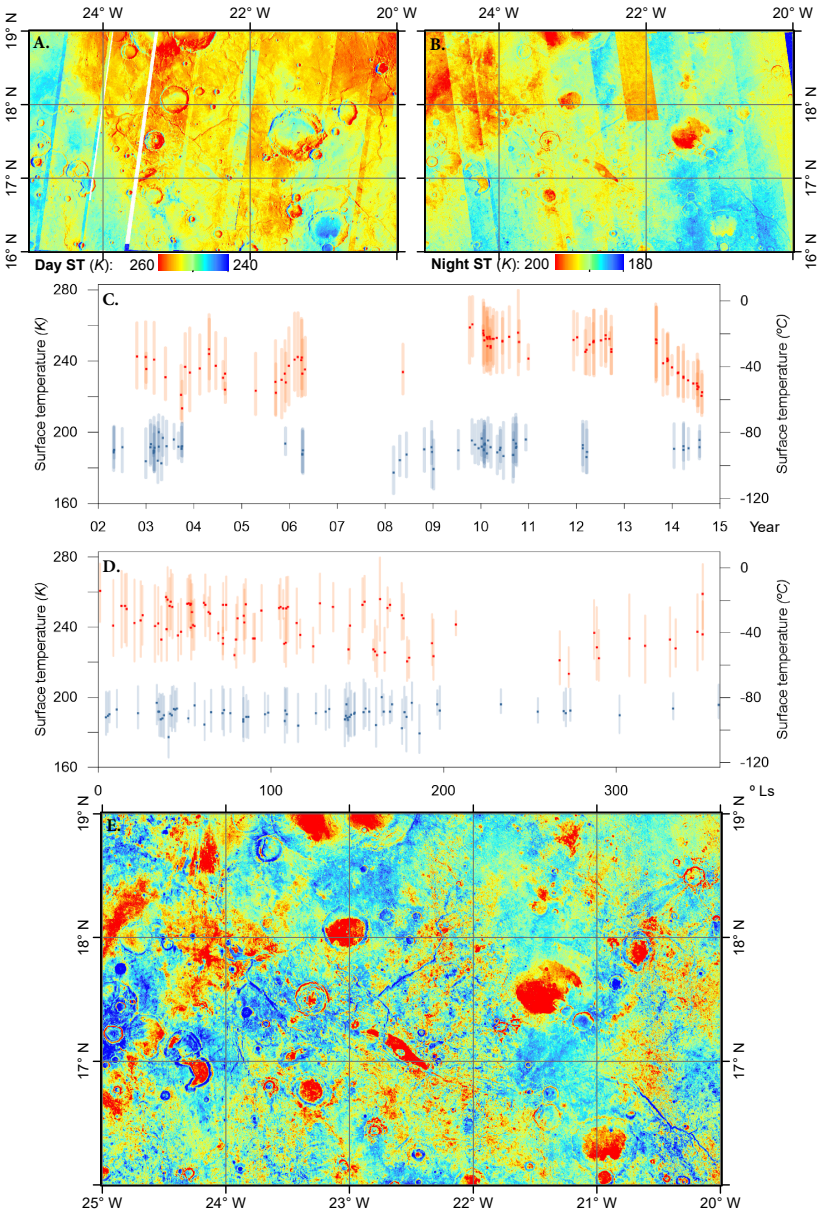

Figure 1: Daytime (A) and nighttime (B) surface temperature and thermal inertia (E) maps for Coogoon Valles area. Plots show surface temperatures (red, daytime; blue, nighttime) of each image available versus date (C) and Ls (D).

Acknowledgments

This work is supported by funds from the Ministry of Economy of the Government of Spain by the Polar Research Program (CTM2014-52021-R).

References

Edwards, C. S.; Nowicki, K. J.; Christensen, P. R.; Hill, J.; Gorelick, N. and Murray, K. [2011]: Mosaicking of global planetary image datasets: 1. Techniques and data processing for Thermal Emission Imaging System (THEMIS) multi-spectral data. *Journal of Geophysical Research: Planets*, 116(E10), doi:10.1029/2010JE003755. E10008.

Fergason, Robin L.; Christensen, Philip R. and Kieffer, Hugh H. [2006]: High-resolution thermal inertia derived from the Thermal Emission Imaging System (THEMIS): Thermal model and applications. *Journal of Geophysical Research: Planets*, 111(E12), doi:10.1029/2006JE002735. E12004.

Observed present-day seasonal gully activity within three Martian years in a south polar pit (Sisyphi Cavi) on Mars

Jan Raack[1], Dennis Reiss[2], Thomas Appéré[3], Mathieu Vincendon[4], Ottaviano Ruesch[5], & Harald Hiesinger[2]

[1]*Department of Physical Sciences, The Open University, Milton Keynes, MK7 6AA, UK*
[2]*Institut für Planetologie, Westfälische Wilhelms-Universität, Wilhelm-Klemm-Str. 10, 48149 Münster, Germany*
[3]*Institut de Planétologie et d'Astrophysique de Grenoble, Université Joseph Fourier, CNRS/INSU, Grenoble, France*
[4]*Institut d'Astrophysique Spatiale, Université Paris Sud, 91400 Orsay, France*
[5]*NASA Goddard Space Flight Center/Oak Ridge Associate Universites (ORAU), Greenbelt, MD, USA*

Introduction and Background

Seasonal activity of gullies under current climatic conditions on Mars was observed and described by several authors. Dundas et al. [2012] reviewed the present-day activity of classical gullies (including the gully presented in this work), dune gullies, and other mass wasting processes in the southern hemisphere on Mars. Recent polar gullies in Sisyphi Cavi were also analyzed by Hoffman [2002], who estimated ages of about 20 ka to 20 Ma for the gullies. According to Hoffman [2002], the formation process for the gullies are CO_2-gas lubricated flows.

In this study we focus on a single active gully in Sisyphi Cavi, located in the south polar region at 1.44°E and 68.54°S [Raack et al., 2015]. The gully occurs on the gullied equator-facing slope of an isolated polar pit within an infilled impact crater.

Results

With multi-temporal high-resolution images (High Resolution Imaging Science Experiment [HiRISE] with 0.25-1 m/pxl resolution) we identified clear modifications of a gully within a polar pit located at 68.5°S and 1.5°E in Martian Year (MY) 29 and 31 (Fig. 1). Dark material within the channel (Fig. 1b) leads to the formation of new dark deposits (Fig. 1c) between solar longitudes (LS) 209° and 226° (beginning of spring) in MY 29 flowing 70 m across the apron. The terminus of the gully channel is marked with a black arrow #1. At LS 247°, once surface ice has disappeared, deposition of material on the apron and within the channel shortens the channel by about 40 m (Fig. 1d; black arrow #2). The white arrow marks new deposition on the gully apron (small knob). Two martian years later in MY 31 at LS 215°, a dark flow-like feature on the apron is marked with a black arrow (Fig. 1e). The black horizontal lines represent the width of the gully apron. At LS 226°, a 130 m long dark flow-like feature at the western side of the gully apron is detectable (Fig. 1f). This is comparable to the dark flow-like feature presented in Fig. 1c, which occurred at the same season two martian years before (MY 29). At mid-spring (LS 236°), a new deposit at the western side of the gully is visible (black arrows; Fig. 1g). New material was deposited in the area where the dark flow-like feature occurred at LS 226°. The black horizontal lines illustrate a widening of the apron of approximately 7 m [Raack et al., 2015].

Topographic data, derived from a HiRISE Digital Terrain Model, show that the entire gullied slope is very homogeneous and showing consistent topography and slope angles of about 15°. Furthermore, the active gully and adjacent gullies show comparable morphologies [Raack et al., 2015]. In MY 31 about 300-600 m3 of material were deposited [Raack et al., 2015].

To identify possible mechanism(s) of the gully activity, maximum daytime surface temperatures of the study region were investigated with the Thermal Emission Spectrometer (TES), showing surface temperatures in autumn and winter of 150 K. In mid spring (LS 220°) temperatures increase rapidly due to solar insolation and ice sublimation. TES data show maximum surface temperatures up to 285 K in early summer between LS 270° and 310° [Raack et al., 2015].

To understand the temporal evolution of H_2O and CO_2, the band strengths of these volatiles (ices) in all available spectral datasets in the study region were analyzed. The investigations show that the gully is

active when temperatures begin to rise rapidly and volatiles begin to sublimate [Raack et al., 2015]. Spectral modeling shows that the dark flows are most likely formed by optically thick regolith flows superposed on an underlying CO_2 slab ice cover with inclusions of H_2O ice and dust [Raack et al., 2015].

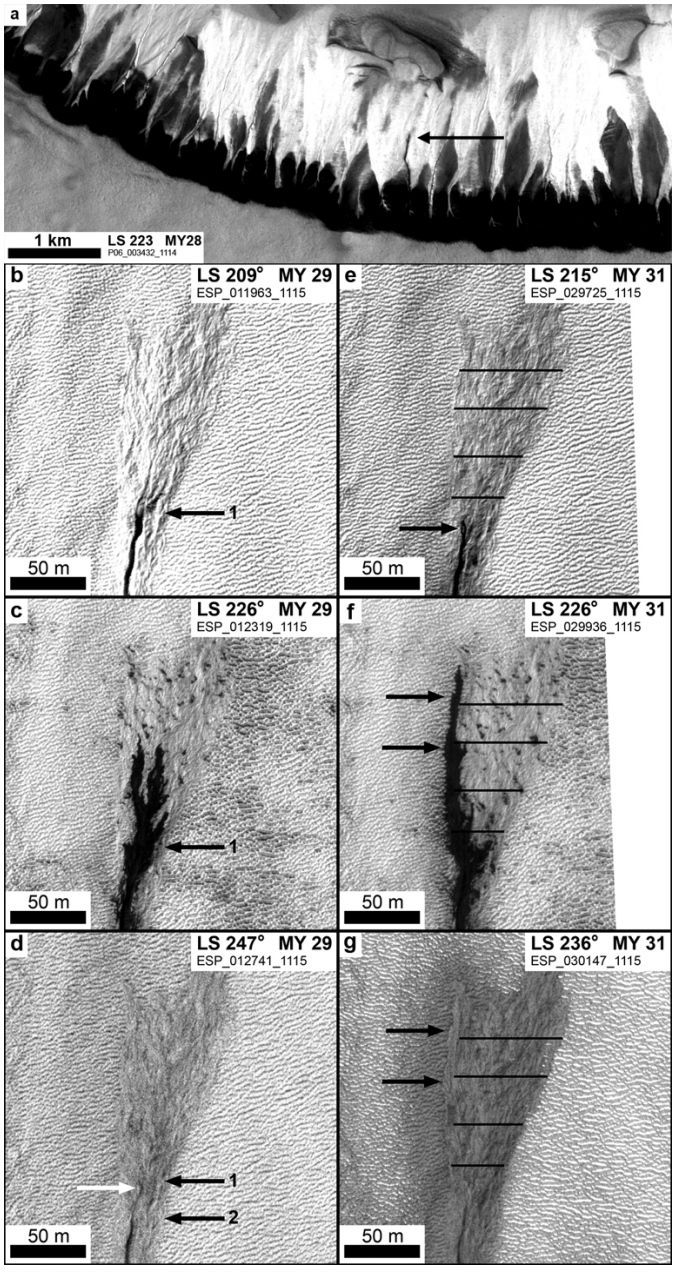

Figure 1: (a) One gully on the slope shows a dark flow like feature (black arrow). (b-g) Sequence of the seasonal changes in gully channel and apron morphology in martian years 29 and 31. Modified after [Raack et al., 2015].

Discussion and Conclusion

Three different scenarios were proposed to explain the identified dark flows, including

1. flows supported by liquid H_2O,
2. flows supported by CO_2 gas, and
3. dry flows [Raack et al., 2015].

On the basis of our study we find that scenario (1) is unlikely because of the very low temperatures during the active phase of the gully [Raack et al., 2015].

While scenario (2) is consistent with the observed beginning of CO_2 ice sublimation in the study area, it is unlikely because of the limitation of the activity to only one gully compared to surrounding gullies that share the same morphologies, slope angles, and volatile contents [Raack et al., 2015].

The temporal occurrence of morphologic changes of the gully linked to the maximum surface temperatures and to the seasonal behavior of volatiles compared to surrounding gullies implies that mass wasting is most likely related to dry flows. The material of the dry flows (sand) is possibly mobilized at the slopes of the gully channel and alcove during the sublimation process of the CO_2 ice cover. Furthermore, continued sublimation of CO_2 ice within the gully channel could support the mobilization of the dry material (observed dark flows) in the interior of the gully channel. Thus, we propose that a combination of scenario (2) and (3), dry flows possibly supported by the continued sublimation of CO_2 ice within the gully, is the most plausible scenario, when the observed active gully comprises different source material than the surrounding gullies, i.e., a higher content of probably sand-sized material from an outcrop located in the alcove [Raack et al., 2015].

References

Dundas, C.M.; Diniega, S.; Hansen, C.J.; Byrne, S. and McEwen, A.S. [2012]: Seasonal activity and morphological changes in martian gullies. *Icarus*, 220(1):124–143, doi:10.1016/j.icarus.2012.04.005.

Hoffman, N. [2002]: Active polar gullies on Mars and the role of carbon dioxide. *Astrobiology*, 2(3): 313–323, doi:10.1089/153110702762027899.

Raack, J.; Reiss, D.; Appéré, T.; Vincendon, M.; Ruesch, O. and Hiesinger, H. [2015]: Present-day seasonal gully activity in a south polar pit (Sisyphi Cavi) on Mars. *Icarus*, 251:226–243, doi:10.1016/j.icarus.2014.03.040.

Ice caves as a target location for the first Human Mission to Mars: The case for a Hebrus Valles Landing Site

Dirk Schulze-Makuch[1], Alfonso Davila[2], Alberto Fairen[3], Alexis Rodriguez[4], Jon Rask[5], & Jhony Zavaleta[5]

[1] *Technical University Berlin, Germany, Washington State University, USA*
[2] *SETI Institute, Mountain View, California, USA*; [3] *Centro de Astrobiologia, Madrid, Spain*
[4] *Planetary Science Institute, Tucson, Arizona, USA*; [5] *NASA Ames Research Center*

At NASA's First Human landing site close to 50 sites were suggested as possible landing sites and exploration zones for an anticipated human mission at about 2035 (http://www.nasa.gov/feature/mars-human-landing-site-workshop-presentations). Our research team suggested that the presence of "ice caves", which might contain significant amounts of perennial ice, would be a prime benefit for the anticipated mission, because they provide an opportunity to explore possible remnant water ice and protected subsurface environments, which are critical resources for the establishment of long-term human settlements, and present ideal targets for exobiological exploration [1].

Here we present the site, what is known about its geological setting, and why it is suitable for investigation by an anticipated human mission in the future. The suggested candidate landing site and exploration zone are located in the middle reaches of Hebrus Valles (Fig. 1, centered at 20°05' N, 126°38' E). An important fraction of the science and exploration efforts at this site would focus on the characterization of an extensive subsurface cavern network, and its scientific, engineering and in-situ resource utilization.

The proposed Exploration Zone (EZ) occurs within a broad outflow channel system in western Elysium Mons that dissects boundary plains materials along the southwest perimeter of the Utopia Impact basin. The lower reaches of the channels dissect into the Vastitas Borealis Formation (VBF), a possible remnant of a Late Hesperian ocean. This geologic formation exhibits widespread evidence for recent periglacial resurfacing, which along with fluvial bedforms, are not buried by aeolian mantles.

The VBF consists of a sedimentary deposit 30 to 170 m thick, formed during the Late Hesperian/Early Amazonian when sediment-laden water effluents of the outflow channels ponded in the northern lowlands, rapidly froze solid and sublimed [2,3].

Hebrus Valles is an intricate system of individual pits, pit chains, troughs and channels that extends for ≈500 km in a NW direction. The troughs and channels have been tentatively identified as outflow channels carved by large, catastrophic floods due to melting of subsurface ice [3]. At some locations within and around the EZ, features interpreted as mud volcanoes cluster into linear ridges, and are further indicators of liquid water activity at regional scales [4]. Hence, the EZ includes recently extruded water-rich sediments with geochemical signatures indicative of aqueous or groundwater/mineral interactions that could date back to the ocean's emplacement, freeze over and evaporation histories.

The lower reaches of Hebrus Valles consists of pits and trough interpreted as apertures that captured the catastrophic floods into networks of caverns [4]. The total extent of partially collapsed cavern sections in the Hebrus region include 2400 km of troughs, and 3600 km as indicated by the pattern of aligned sinkholes. Both the fluvial features with their associated sediments, the remnants of water ice, and the subsurface caverns have a high preservation potential for evidence of past habitability and fossil biosignatures.

A 900 m deep (15 km diameter) crater located in the eastern portion of the EZ would provide access to explore subsurface materials, likely composed of Hesperian deposits buried beneath the VBF sediments. The stratigraphic contact between these units can be used for relative age determinations.

The suggested landing site has also high engineering merit and is located in the middle of the EZ, between two large fluvial features (Fig. 1). Dissected near surface VBF materials in the EZ likely consist of desiccated permafrost and bouldery outwash materials (a few meters/tens of meters thick) overlying massive ice (tens/hundreds of meters thick). If confirmed, the presence of near surface massive ice would be a key resource for humans. Regionally, there are abundant, small and shallow craters that appear to be partially

infilled. Slope at the LS is <1° and surface materials have relatively low thermal inertia (<200 J m^{-2} K-1 sec-1/2), pointing to loose, fine surface dust and very few rocks. Practically no boulders larger than 1 m are observed near the landing site area in HIRISE images at 24 cm/pixel resolution, satisfying safety constrains for EDL operations.

The inferred magnitude of floodwater infiltration in the EZ points to the existence of structurally stable caverns that were largely evacuated of fluids and sediments prior to Hebrus Valles outflow channel activity [5]. The predicted typical mean annual surface temperature for the EZ investigated latitudes is -60 °C [6]. At these temperatures, permafrost could have a mechanical strength close to that of limestone [7, 8], which could have stabilized evacuated caverns. Chemical precipitation from circulating brines in terrestrial cold springs can produce cements along the periphery of feeder conduits, thereby enhancing their overall structural stability [9]. Cements developed in association with cold water circulation include calcite, aragonite, Fe-Mn oxides, sulfides and sulfates [10,11]. On Earth, caverns are known to occur in ice-welded sediments such as in association with networks of ice wedges in permafrost [12] and ice-welded moraine deposits [13]. Some glacier caverns are known to have remained stable over decades [14]. Subsurface caverns and steep walls in Hebrus Valles might represent natural terrain features that can be adapted for construction purposes. Hence, infrastructure could be emplaced or constructed at the suggested landing site.

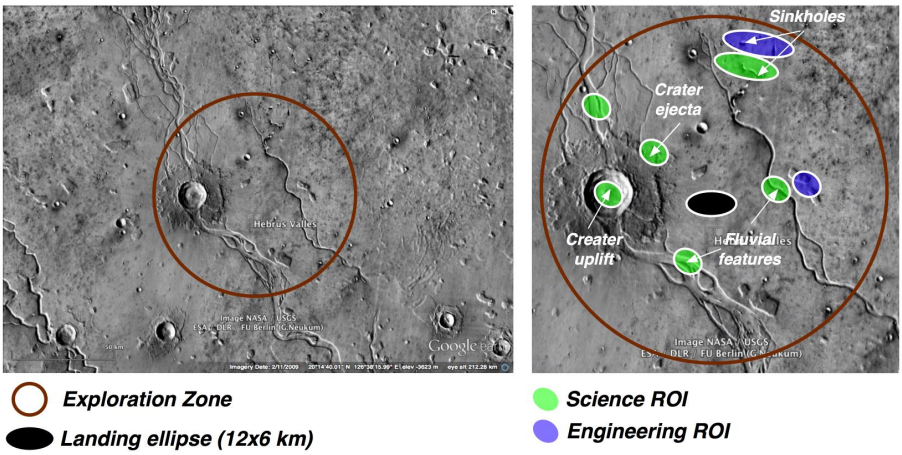

Figure 1: Proposed landing site, exploration zone, and region of interest in the Hebrus Valles region.

References

[1] Davila, A.F. et al. (2015) Abstract and Presentation at First Mars Human Landing Site Workshop, Houston, TX, Oct 26-30, 2015;

[2] Kreslavsky, M.A., Head, J.W. J. Geophys. Res., 107(E12), 5121;

[3] Tanaka et al (2005) U.S. Geological Survey Scientific Investigations Map 2888;

[4] Rodriguez, J. A. P., et al. (2012), Geophys. Res. Lett., 39, L22201;

[5] Carr, M.H., Malin, M.C. (2000), Icarus, 146(2), 366–386;

[6] Mellon, J.T. et al. (2004) Icarus, 169, 324–340;

[7] Kuribayashi, E. et al. (1985), Proceedings of the 4^{th} Internat. Symposium on Ground Freezing, 177–182, Balkema, Rotterdam, Netherlands;

[8] Ladyani, B. (2003), in Permafrost, edited by M. Phillips, S. M. Springman, and L. U. Arenson, pp. 621–626, Swets and Zeitlinger, Lisse, Netherlands.

[9] Pentecost, A. et al. (2003), Can. J. Earth Sci. 40(11), 1443–6;

[10] Jones, B. et al. (2007) Journal of the Geological Society, London, 164, 227-242;

[11] Guo, X., Chafetz, H.S. (2012) Sedimentology, doi: 10.1111/j.1365-3091.2011.01315.x;

[12] Costard, F. et al. (2012) Proc. Lunar Planet. Sci. Conf., 43^{rd}, Abstract 1822;

[13] Moorman, B. J. (2005) in Cryospheric Systems: Glaciers and Permafrost, vol. 242, edited by C. Harris and J. B. Murton, pp. 63–74, Geol. Soc., London;

[14] Halliday, W. R. (2007), J. Cave Karst Stud., 69(1), 103–113.

Constrain on the nature of polygons on Mars by studying thermokarst degradation in Utopia Planitia and comparison with Central Yakutia (Central Siberia)

Antoine Séjourné[1], Francois Costard[1], Julien Gargani[1], & Alexander Fedorov[2]

[1] *Univ Paris-Sud, CNRS, Laboratoire GEOPS, UMR8148, Orsay, France*
[2] *Melnikov Permafrost Institute, RAS, Yakutsk, Russian Federation*

Introduction

An assemblage of possible periglacial landforms dots the landscape of western Utopia Planitia in the northern mid-latitudes of Mars. The landforms comprise thermokarst scalloped depressions; spatially-associated thermal contraction polygons; and polygon-junction thermokarst pits. In the last few years, several works point to a thermokarst origin of the depressions and the pits, due to sublimation or melting of ground-ice. However, while the polygons have been interpreted to be thermal contraction in origin based on geomorphometric resemblance, the nature of the polygon wedge (ice, sand or composite wedge) is still unconstrained. Assessing their nature has implications for the climatic conditions of Mars during their formation.

Here, we study the thermokarst degradation of two types of polygons in Utopia Planitia, Mars in order to constrain the nature and dimension of the polygon wedge. In order to understand the processes of degradation, we compare these landforms with active thermokarst landforms occurring along thermokarst lakes in Central Yakutia (Siberia). Numerous high resolution images from the High Resolution Imaging Science and a HiRISE stereo Digital Elevation Model (DEM) (HiRISE, 50 cm/pixel) were used to study the landforms.

Results

Polygons (6-10 m in diam.) occurring inside scalloped depressions are particularly interesting because they show two distinct morphologies. Some polygons exhibit small ridges on their margins, giving them a low-centered morphology while others show a center higher than their sides, giving them a high-centered morphology (Fig. 1a) [Séjourné et al., 2011]. Semicircular hollows of 0.5-1 km in diameter are observed on the pole-facing slopes of scalloped depressions (Fig. 1b) [Séjourné et al., 2011]. The semicircular hollows are surrounded by degraded high-centered polygons (Fig 1b). Inside the semicircular hollows, no polygons or highly degraded polygons are observed. Associated with the hollows, cirque-shaped alcoves (10 m diam.) at polygonal troughs and failure cracks occur on the pole-facing scarp (Fig 1a).

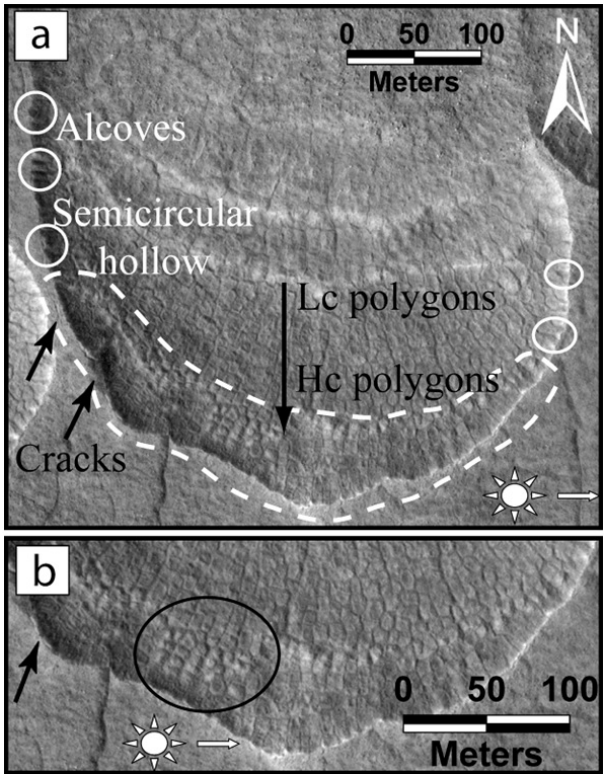

Figure 1: Semicircular hollows (dashed line) and cirque-shaped alcoves (circle) around high centered polygons on pole-facing slopes of scalloped depressions. NASA/Univ. Arizona

These landforms point to an important and localized thermokarst degradation of polygons. The semicircular hollows inside scalloped depressions are reminiscent of retrogressive thaw slumps occurring on the banks of thermokarst lakes on Earth. The high-centered polygons surrounded by cirque-shaped

alcoves on the scarp are similar to baydjarakhs of Siberia. The curved cracks associated with semicircular hollows indicate the subsidence and failures of the pole-facing scarps of depressions. The semicircular hollows formed through complete degradation of polygons and indicate a formation by downwearing and backwearing due to removal of ice.

From the comparison with terrestrial thermokarst, several geomorphologic differences arise. Inside semicircular hollows, no run-off features, mud-flows or fluvial-fan deposits are observed. The absence of thaw-related features point to a degradation of polygons by sublimation of ground-ice.

Inside scalloped depressions, the thermokarst degradation originates at the polygonal troughs on the pole-facing scarp (evolution from low- to high-centered polygons). Then, the polygons are successively degraded. From the observation of important degradation of polygons with no major deposits, we suggest that the polygons must have a substantial amount of ice and are potentially underlain by ice-wedges. The depth of the semicircular hollows being of 2 m, the depth of the wedge is approximately of 2 m.

Conclusion

Inside scalloped depressions, polygons are successively degraded by sublimation forming highly degraded high-centered polygons and then thermocirque-like hollows on their pole-facing slopes. The nearly complete degradation of the polygons argue for the presence of ice-wedge polygons inside the depressions.

References

Séjourné, A.; Costard, F.; Gargani, J.; Soare, R.J.; Fedorov, A. and Marmo, C. [2011]: Scalloped depressions and small-sized polygons in western Utopia Planitia, Mars: A new formation hypothesis. *Planetary and Space Science*, 59(5–6):412 – 422, doi:10.1016/j.pss.2011.01.007.

High resolution geomorphological mapping of glacial and periglacial landforms at the lower NW flank of the HecatesTholus volcano, Mars: A contribution to the paleoenvironmental reconstruction

Marcos Valcárcel[1], Jonathan F. Hall-Riaza[1], & Miguel ángel de Pablo[1]

[1] *Geografía, Universidade de Santiago de Compostela, Spain*
[2] *Geología, Geografía y Medio Ambiente, Universidad de Alcalá, Spain*

HecatesTholus is a volcanic edifice located at 32.1°N 150.2°E in the Elysium region of Mars, and the unique in the Elysium volcanic province showing glacial-related reliefs (de Pablo, 2015 and references therein). In a similar way than other Martian volcanos, glacial landforms are widely distributed on the NW flank of the edifice. In HecatesTholus, this flank is also characterized by nested depressions. One of them (the smaller one) has been proposed to be a lateral caldera of the volcano, probably formed 350 Ma ago [Neukum et al., 2004], meanwhile the origin of the other is still uncertain. Recently, a 1:100,000 in scale geomorphological map had been published [de Pablo and Centeno, 2012] based on the use of 6 m/pixel in resolution images acquired by the Context instrument on board of the Mars Reconnaissance Orbiter (MRO). This map, shows the distribution of both erosive and sedimentary glacial features, including moraine and other till deposits, glacial circus, crevasses, arêtes, or bergschrunds, among others.These features are widely distributed on the walls of the nested depressions as well as filling them. The geomorphological map, together with a detailed crater size-frequency analysis allowed to propose a reconstruction of the main glacial events along the 3.6 Ga long history of the edifice [de Pablo et al., 2013], including their relation to the last ice ages on Mars, matching the period of maximum obliquity of the ecliptic Mars.

Moreover, pingos had been also mapped in the area [de Pablo and Centeno, 2012], and they has been related to a more recent evolution of the ice below the regolith layer what could be covering the remnant ice of these glaciers [de Pablo, 2015]. However, the role of water and the periglacial conditions on the most recent period of evolution of this regions has not been previously studied. Since extremely high resolution (0.35 m/pixel) images acquired by HiRISE instrument from MRO mission are available of the NW flank of the HecatesTholus volcano, we used them to develop a more detailed geomorphological cartography of a sector of the main depression on this flank of the edifice. The aim is to provide more detailed observation about the glacial and periglacial landforms to be used to contribute to the previous paleoenvironmental reconstructions of the study area.Here we show the results of both, the geomorphological mapping and the paleoenviromental reconstructions.

References

de Pablo, M.A. [2015]: *Glacial geomorphology of the NW flank of the HecatesTholus Volcano, Mars*. Phd thesis, Faculty of Geological Sciences, Complutense University Madrid, Spain, pp.250.

de Pablo, M.A. and Centeno, J.D. [2012]: Geomorphological map of the lower NW flank of theHecatesTholus volcano, Mars. *Journal of Maps*, 8(3): 208–214, doi:10.1080/17445647.2012.703902.

de Pablo, M.A.; Michael, G.G. and Centeno, J.D. [2013]: Age and evolution of the lower {NW} flank of the Hecates Tholus volcano, Mars, based on crater size-frequency distribution on {CTX} images . *Icarus*, 226(1):455 – 469, doi:10.1016/j.icarus.2013.05.012.

Neukum, G.; Jaumann, R.; Hoffmann, H.; Hauber, E.; Head, J.W.; Basilevsky, A.T.; Ivanov, B.A.; Werner, S.C.; van Gasselt, S.; Murray, J.B.; McCord, T. and co-investigator team, The HRSC. [2004]: Recent and episodic volcanic and glacial activity on Mars revealed by the High Resolution Stereo Camera. *Nature*, 432:971–979.

Distribution and evolution of cold-climate landforms in a subpolar and hyperarid environment, Hellas Planitia, Mars

Martin Voelker, Ernst Hauber, & Ralf Jaumann

German Aerospace Center, Germany

Located in the mid-latitudes of the southern highlands of Mars, Hellas Planitia is the second-largest confirmed impact basin on the planet, having a diameter of 2,300 kilometers. The basin also contains the lowest elevated parts of Mars, and hence, the highest atmospheric pressure on the planet of up to 11 millibar. Temperatures vary by season from 150 to 300 K. Thus, this vast depression is one of the atmospherically most active regions of Mars. This is also shown by the seasonal dust storm activity in Hellas Planitia. More than 90 % of the basin's floor is covered with so-called Latitude-Dependent Mantling deposit (LDM); a several meters-thick layer draping the surface. It is believed to consist of a mixture of dust and ice falling out of the dusty atmosphere. It is unclear if this process is still active on Mars. However, according to crater-size frequencies, it deposited in geologically recent times (0.1 – 1 Ma). At certain environmental conditions LDM appears to get deformed or eroded into several morphologies, Layered Remnant Deposits in crater (LRD) or a scalloped terrain.

Results are based on a newly developed method for planetary mapping called grid-mapping [Ramsdale et al., 2015]. This is a useful method for analyzing the geospatial distribution of pre-defined landforms over a large area, by using high spatial resolution datasets. By using this method, the whole study area is separated into 20,000 grids, each with a size of 20×20 kilometers. Mapping has been carried out in a GIS environment on the basis of CTX images (Context Camera onboard the spacecraft Mars Reconnaissance Orbiter) at a scale of 1:30,000. Because of the huge size of the study area, only every second grid has been mapped (approx. 10,200 in total).

Our mapping results have shown that there is a significant elliptical gap of LDM in the NE part of Hellas, measuring 800×200 kilometers. The rest of the basin is covered by LDM. However, the more south the LDM is, the less it is textured and eroded, and appears to be young and smooth.

Scalloped terrain is referred to rimless and often axisymmetric depressions, formed by subsurficial loss of ice and/or volatiles; like it is assumed to be contained in the LDM. They always show a steep pole-facing rim at their northern side, and a gentle equator-facing rim at their southern side. It is assumed that their topography and development is linked to solar insolation and latitude. Although there is an almost completely closed LDM cover in Hellas, scalloped terrain only appears in scattered places south of 35°S. However, there is no other obvious distribution pattern recognizable.

North of 37°S there is an increased prevalence of LRD within smaller craters (0.1 – 3 kilometers in diameter). They usually occur on the southern parts of the crater interiors, and are hence exposed to the Sun. High-resolution images of the HiRISE camera (also on board of the Mars Reconnaissance Orbiter) have shown that LRD consists of a brittle material cracked into polygons.

We hypothesize that lack of LDM in NE Hellas may be the result of wind circulations within the basin. According to Howard et al. [2012], wind currents rotate clockwise in Hellas. Cold polar winds enter the basin at a gap in the rim in SW Hellas, draining down from the south polar highlands toward the north. When they reach the northern parts of Hellas at a latitude of 30°S they are likely to warm up, and begin to move south again. Thus, they may have either sublimed the LDM material in NE Hellas or prevented an atmospheric deposition as the winds have become too dry at that place. This observation supports theories of a high amount of volatiles within LDM.

The evolution of LRD remains much more enigmatic. We hypothesize three different scenarios.

1. Eolian processes might have caused sublimation. But wind does not explain the strict location of the CCF in the southern half of the crater bowls over such a huge area.

2. Volcanic ashes, transported over wide distances, like the Medusae Fossae Formation along some equatorial regions on Mars, are also a possibility. They can explain the uniform orientation of the

LRD's. However, there is no known volcanic feature northwest of Hellas. However, climate modeling by [Kerber et al., 2012] suggests that a dispersal of volcanic ashes is possible, but only originating from volcanoes northeast and southwest of Hellas.

3. Solar insolation, and hence thermal sublimation, could explain the uniform location of these remnants over a big area.

Moreover, this could explain the latitude-dependence of this landform, as they predominantly occur north of 37°. But this does not explain why the LRD-layers consistently "survived" in that part of craters that receives the most intense solar radiation. This theory would be conclusive if LRD's were located in the shaded northern half of a crater. However, we assume this scenario as the most likely. Because of Mars' permanently changing obliquity of up to 47°within the last 20 Ma, it is also possible that the northern parts of the crater interiors once received a high amount of solar insolation even at these latitudes. Thus, the volatile-rich material could have been removed there. If LRD is or was rich in volatiles, it is likely that it is composed of the same material like LDM. Another explanation for this paradoxical location might be that the LRD's are a result of an inverted relief.

Despite scalloped terrain is latitude-dependent, it does not appear continuously south of 35°S, although there is a complete LDM cover. A possible reason for this scattered pattern might be a varying amount of volatiles within the LDM blanket.

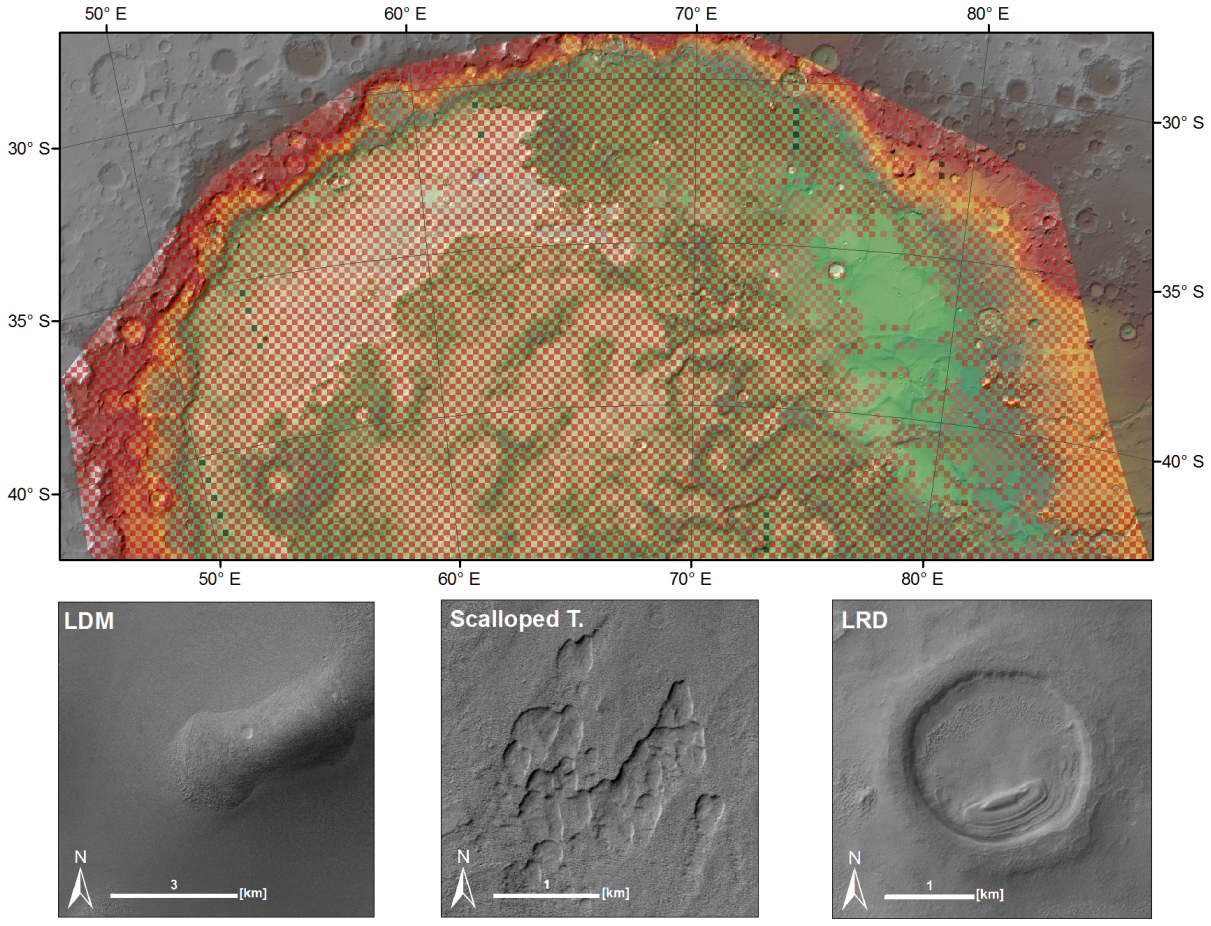

Figure 1: Map showing the distribution of LDM. Left: Smooth LDM unit draping a ridge (B19_016971_1346_XN_45S287W). Center: Scalloped Terrain within LDM unit (P13_006133_1394_XN_40S305W). Right: LDM and LRD within a crater (P18_008084_1461_XI_33S298W).

On basis of grid-mapping, it was possible to analyze the geospatial distribution of cold-climate landforms in Hellas. Thereby, an extensive elliptical gap of LDM in NE Hellas became apparent; probably caused by clockwise wind circulations within the impact basin, causing either prevention of LDM deposition or sublimation of a pre-existing LDM layer. The exact evolution of Layered Remnant Deposits (LRD) is still poorly understood. However, it appears likely that these deposits were eroded by a process controlled by solar insolation (i.e. sublimation), which means they contained, or still contain, certain amounts of volatiles like ice. Hence, our observations support existing theories of a volatile-rich layer in the Martian mid-latitudes, typically termed LDM. Detailed statistical evaluations of our grid map will test, i. a., if there is a correlation between landforms and their elevation, aspect, and slope. Thus, we will be able to derive further information about atmospheric conditions and layering within Hellas as well as the influence of obliquity cycles.

References

Howard, A.D.; Spiga, A. and Moore, J.M. [2012]: The Deepest Basin on Mars is Formed by Aeolian Erosion: Western Hellas. In *43rd Lunar and Planetary Science Conference, 19-23 March 2012*, number #1105.

Kerber, L.; Head, J.W.; Madeleine, J.B.; Forget, F. and Wilson, L. [2012]: The dispersal of pyroclasts from ancient explosive volcanoes on Mars: Implications for the friable layered deposits. *Icarus*, 219 (1):358 – 381, doi:10.1016/j.icarus.2012.03.016.

Ramsdale, J.D.; Balme, M.R.; Conway, S.J.; Costard, F.; Gallagher, C.; van Gasselt, S.; Hauber, E.; Johnsson, A.E.; Kereszturi, P.T.; Séjourné, A.; Skinner, J.A.jr.; Reiss, D.; Swirad, Z.; Orgel, C. and Losiak, A. [2015]: Mapping Mars' Northern Plains: Origins, Evolution and Response to Climate Change – An Overview of the Grid Mapping Method. In *46th Lunar and Planetary Science Conference, 16-20 March 2015, The Woodlands, USA*, number #1339.

SESSION 13

The Yedoma Region: Origin, Records and Future Projections in a Changing Arctic

Convener:

Aleksandra Veremeeva, *Institute of Physicochemical and Biological Problems in Soil Science, Russian Academy of Sciences, Russia*

Duane G. Froese, *University of Alberta, Department of Earth and Atmospheric Sciences, Canada*

Matthias Fuchs, *Alfred Wegener Institute, Helmholtz Centre for Polar and Marine Research, Germany*

Late Pleistocene Yedoma deposits, a suite of ice-rich silty sediments, accumulated in vast lowland areas of Beringia, extending from Siberia through north-western Canada. Interest in deposits of the Yedoma region, especially Yedoma and thermokarst (Alas) deposits, has been driven

1. by the exceptional preservation of past environmental records (e.g. stratigraphy, fossil bio-indicators, stable water isotopes, sediment parameters)
2. by the enormous ground ice content (massive syngenetic ice wedges and intrasedimentary ice) connected with a high vulnerability to surface subsidence, and
3. by the thaw-vulnerable frozen organic matter which has the potential to amplify the global warming through its release in a warming climate.

Despite the resurgence in Yedoma research, significant questions remain about the origins, processes and vulnerability of Yedoma to future climate change. Embracing the Yedoma in models has been slow to absent so far, a fact driven by the large uncertainties in its size, distribution, and thaw-vulnerability. As well, research is still challenged by significant regional differences in the interpretation of these records. Despite having a regional focus, the Yedoma region is of global significance. Thus, in this session we seek contributions about modelling, origin, cryostratigraphy, mapping, paleopedologie, paleobiology, biogeochemistry, climatic sensitivity and paleoclimatic significance of Yedoma region including its degradation forms (e.g. thermokarst depressions and thermoerosional valleys), summarizing the temporal and geographic range from Siberia, Alaska and north-western Canada.

The Batagai Outcrop – window into the past of North Yakutia's most continental part

Kseniia Ashastina[1], Lutz Schirrmeister[2], Bernhard Diekmann[2], & Frank Kienast[1]

[1] *Senckenberg Research Institute, Germany*
[2] *Alfred Wegener Institute Helmholtz Center for Polar and Marine Research, Potsdam, Germany*

Situated in the Yana-Highlands, the Batagai profile is one of the few inland permafrost outcrops in Yakutia and, for the time being, the biggest and most active thermoerosional cirque worldwide. With Yerkhoyansk recorded as place of the pole of cold, the Yana Highlands represent the region with the most severe climatic continentality in the northern hemisphere. In contrast to the numerous sequences in today's coastal lowlands, the Batagai sequence was always unaffected by maritime climate influence during its formation and thus better indicates the macro-climate evolution in NE-Siberia.

As result of intense thermal degradation, the outcrop formed within 40 years only and cut deep into ice-rich permafrost deposits [Kunitsky et al., 2013]. The 60 m deep outcrop is now about 850 m in diameter, but erosion rates as high as 15 m/year are changing the dimensions continuously. The Batagai profile thus represents a unique window into the past (and future) of ice-rich permafrost deposits in Yakutia.

Field based observations have shown that the permafrost sequence consists of 4 distinct units: below a thin Holocene surface cover, a 30 meter thick Ice Complex with characteristic thick ice wedges has formed. At the base of the Ice Complex, there is an up to 2 m thick layer of plant material including large woody remains. Subjacent to this organic layer of supposedly Eemian origin, there is a horizontally stratified unit composed of silty-sand and without thick syngenetic ice wedges presumably deposited during the Middle Pleistocene. At the very base of the sequence, there appears to emerge another unit including syngenetic ice wedges. This unit was not accessible for sampling.

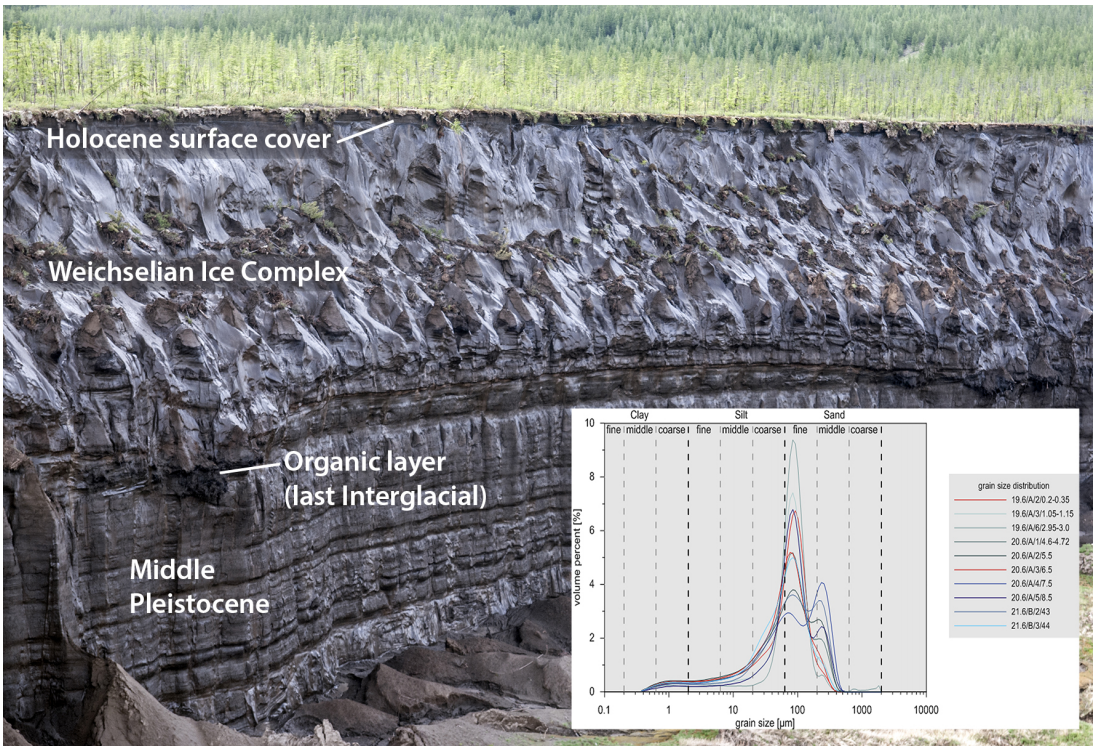

Figure 1: Batagai sequence

The accessible upper about 45 meter of the sequence were sampled from top to bottom in one meter steps using, due to the difficult accessibility of the permafrost wall, thermokarst mounds in the less steep part of the outcrop. The samples were taken for sedimentological analyses and especially for plant macrofossil and other palaeoecological studies. Whereas sediments give insight into the genesis of the sequence, fossil plant macroremains provide information on local vegetation patterns and habitats at the time of deposition; while palynological analyses reflect the regional vegetation and climate history. First palaeobotanical results will be represented in Session 10: "Palaeoenvironments in permafrost affected areas" by Kienast et al. on page 484.

The sedimentological analyses revealed that, despite clearly delimitable bedding units visible at the outcrop, there is no distinct litho-stratigraphical differentiation recognizable in the grain size distribution or other sedimentological parameters. Accordingly, the sequence is characterized by a grain size signature typical for Ice Complex deposits. In comparison to other Yakutian ice-rich permafrost sequences, e.g. in the coastal lowlands, the Batagai profile is however distinguished by a higher fraction of fine sand over the whole recorded sequence. This might be due to increased aeolian deposition from local sources, e.g. from barren ridges in the highlands uncovered by vegetation. The assumption that aeolian deposition played a substantial role in the formation of the sequence is also suggested by impressive dunes in the immediate vicinity of the profile at the boundary of Batagai city.

References

Kunitsky, V.V.; Syromyatnikov, I.I.; Schirrmeister, L.; Skatchkov, Yu. B.; Grosse, G.; Wetterich, S. and Grigoryev, M.N. [2013]: Ice-rich permafrost and thermal denudation in the Batagay area (Yana Upland, East Siberia). *Kryosfera Zemli (Earth's Cryosphere)*, 17(1):56–68, URL http://www.izdatgeo.ru/pdf/krio/2013-1/56.pdf.

A 10,000-year record of atmospheric mercury deposition in northern Yukon, Canada

Sasiri Bandara, Duane Froese, Colin Cooke, & Vincent St. Louis

University of Alberta, Canada

Lake sediments, peatlands, tree rings, and ice cores are often used to estimate the influence of recent human activities such as coal burning and climate change on the biogeochemical cycling of Hg. Over thousands of years, sub-arctic and arctic yedoma and peat permafrost sequestered atmospherically deposited Hg prior to human impacts. However, with continued climate warming, it is hypothesized that these northern cryosols will shift from stable carbon/Hg sinks to carbon/Hg sources through permafrost degradation. Accelerated loss of Hg from yedoma silts and peat bogs to adjacent aquatic environments may pose a threat to both wildlife and humans. Here, we reconstruct natural fluxes of atmospheric Hg deposition during the Holocene (last 10,000 years) through the drilling, recovery, and analysis of permafrost from peatlands along the Dempster Highway and the Old Crow and Bluefish basins in northern Yukon, Canada. Based on our analyses, we quantify the natural variability in atmospherically deposited Hg fluxes in light of millennial-scale climate as derived by pore-ice stable isotope ($\delta^{18}O$ and δD) trends over the last 10,000 years, from which we will be able to compare current rates of deposition due to human activities and quantify potential fluxes of Hg to downstream freshwater systems.

Methane as a paleopermafrost indicator of Yedoma accumulation in Yakutia

Maria Cherbunina[1] & Denis Shmelev[2]

[1] *Lomonosov Moscow State University, Russian Federation*
[2] *Institute for Physicochemical and Biological Problems in Soil Science, Russian Academy of Sciences*

Permafrost is a unique feature of Arctic and sub-Arctic landscapes. High-latitude landscapes underlain by permafrost are vulnerable to climate warming and may degrade in different ways, including active layer deepening and rapid-thawing of massive ground ice. Central and Northern Yakutia are covered by ice-rich silts that are penetrated by large ice wedges, resulting from syngenetic sedimentation and freezing in the Late Pleistocene (75 – 13 kyr BP). Yedoma deposits accumulated under periglacial weathering, transport, and deposition dynamics in non-glaciated regions during the Late Pleistocene (>60000 yrs BP) through the early Holocene (≈9,000 yrs BP). The deposits largely formed due to a combination of alluvial, colluvial, nival, and aeolian deposition together with syngenetic ground ice accumulation. The organic carbon is well-preserved and therefore available for decomposition after thaw in the Yedoma region [Strauss et al., 2013].

Yedoma deposits are one of the significant carbon pools in the Northern Hemisphere with estimates of ≈80 to 130 gigatonnes of organic carbon [Strauss et al., 2013]. The substantial volume of ground ice (up to 90 vol%) makes it highly vulnerable to potential thaw. The release of organic matter stored in deep Yedoma deposits is expected to affect modelled circumpolar methane fluxes. The methane pool of Yedoma in Northern Yakutia is estimated as trace levels [Rivkina et al., 2006], but Brouchkov and Fukuda [2002] report high methane concentrations in gas bubbles of ice wedges in central Yakutia in the Aldan river valley of eastern Siberia. The site, located 325 km upstream from the mouth of the River Lena is a result of recent river erosion up to ≈0.7 m per year with a Yedoma surface up to 50 m above river level.

The exposure has three main units: Late Pleistocene Yedoma ca. 40,000 to 15,000 years BP, overlying Middle and Early Pleistocene sands and clay (1 to 0.1 Ma frozen at the time of formation) and late Neogene (Miocene and Pliocene), mostly sands, likely frozen since the middle Pliocene, or perhaps Early Pleistocene [Brouchkov and Fukuda, 2002]. The Yedoma deposits are characterized by ice-rich, dark-grey and brown loam and silts penetrated by ice wedges with a total thickness of 7-10 m. The ground cryostructures variy from suspended at ice wedges to structureless, while organic detritus (wood) and turf inclusions are locally present.

In the studied deposits the methane distribution has been measured by "headspace" [Rivkina et al., 2006] and bubble degassing [Brouchkov and Fukuda, 2002]. Maximum concentrations were found in the Early Pleistocene alluvial sand (up to 0.2 ml/kg); at the same time, in Yedoma deposits methane (n=10) content does not exceed 0.001-0.006 ml/kg, in the ice wedges (n=5) – 0.001-0.016 ml/kg. Thus, we can speak about an absence of even trace amounts of methane in Yedoma. This result is in good agreement with data about methane distribution in Yedoma of Northern Yakutia [Rivkina et al., 2006], where methane is absent too. It should be noted, that our data conflict with previous investigations of the Central Yakutia which described high methane concentrations in ice wedge gas bubbles [Brouchkov and Fukuda, 2002]. The methane distribution through the vertical exposure does not show any systematic trend with depth that would suggest a deep subsurface source or penetration downward from the surface. In general, geological cross-sections of exposure methane-free units (Yedoma) appear to be sandwiched between methane-containing layers.

Despite a variety of Yedoma structures and properties, the lack of methane is a common paleo-indicator [Rivkina et al., 2006], which can be interpreted as evidence of common environmental conditions of sedimentation and freezing over vast areas of Yakutia. If we believe that the main origin of the methane in the upper permafrost is biogenic activity [Brouchkov and Fukuda, 2002, Rivkina et al., 2006], the methane absence suggests 1) a lack of Archaeal bacterial in the active layer at Yedoma accumulation in the Late Pleistocene or 2) the methane was released from deposits during Yedoma freezing in the Late Pleistocene. The first suggestion relates to aerial and oxidative conditions during Yedoma deposition such as dry

environmental and eolian accumulation, because Archaeal habitat requires anoxic conditions. Our second hypothesis does not conflict with the traditional alluvial or polygenetic concept of Yedoma origins [Strauss et al., 2013], because the methane could originate from the active layer during syncryogenic freezing. At the same time, Brouchkov and Fukuda [2002] reported methane conservation during refreezing of the active layer of wet landscapes in winter. Thus, only a comprehensive analysis of paleo bacterial diversity of Yedoma deposits (include 16S RNA gene sequencing and metagenomic analysis) can address the methane absence in Yedoma.

At first, our data reporting trace methane concentrations in Yedoma ice wedges is contrary to reported high methane concentrations (up to 3000 ppmv or 10 ml/kg) by Brouchkov and Fukuda [2002], but we think two significant differences may account for this. First, the methane content of the ice exceeds the methane concentration of the surrounding Yedoma silts by 2-8 times. Methane production is very local and can occur at separate points or sites. The aerial condition of the Yedoma surface during the Late Pleistocene, where ice wedge troughs held standing water, produced favourable conditions for biogenic methane production. Moreover, the methane storage in adjacent bubbles can differ at small spatial scales, while the distribution can be characterized as uniform. It is consistent with our hypothesis about the local scale of methane production. The second explanation of methane preservation in gas bubbles of ice wedges relates to the potential gas emissions from underlying methane into these units via deep frost cracks during formation. In the Mammoth Mountain exposure, Yedoma covers methane-rich Early and Middle Pleistocene sands. During syncryogenic ice wedge formation, the frost cracks could penetrate into this sand and provide an opportunity for methane degassing from the underlying sediments via the frost cracks. Further the methane bubbles were preserved in bogged frost cracks at freezing. Due to the insignificant thickness of the Yedoma strata (7-10 m) this process could occur throughout the Yedoma accumulation because of the exceptional depth of frost cracking during the severe cold conditions of the late Pleistocene.

The research has been supported by RFBR grant №16-35-00403

References

Brouchkov, A. and Fukuda, M. [2002]: Preliminary measurements on methane content in permafrost, Central Yakutia, and some experimental data. *Permafrost and Periglacial Processes*, 13(3):187–197, doi:10.1002/ppp.422.

Rivkina, E.M.; Kraev, G.N.; Krivushin, K.V.; Laurinavichus, K.S.; FyodorovDavydov, D.G.; Kholodov, A.L.; Shcherbakova, V.A. and Gilichinsky, D.A. [2006]: Methane in permafrost of Northeastern Arctic. *Kriosfera Zemli (Earth Cryosphere)*, 10 (3):23–41, URL http://www.izdatgeo.ru/pdf/krio/2006-3/23.pdf. in Russian.

Strauss, J.; Schirrmeister, L.; Grosse, G.; Wetterich, S.; Ulrich, M.; Herzschuh, U. and Hubberten, H.-W. [2013]: The deep permafrost carbon pool of the Yedoma region in Siberia and Alaska. *Geophysical Research Letters*, 40(23):6165–6170, doi:10.1002/2013GL058088. 2013GL058088.

Past and possible future evolution of the Yukon Flats southern upland yedoma region, Alaska

Mary Edwards[1,2], Benjamin Jones[3], Patricia McDowell[4], Guido Grosse[5], & Joshua Rose[6]

[1] *University of Southampton, United Kingdom*
[2] *University of Alaska, Fairbanks, USA*
[3] *US Geological Survey, USA*
[4] *University of Oregon, USA*
[5] *Alfred Wegener Institute Helmholtz Centre for Polar and Marine Research, Potsdam, Germany*
[6] *US Fish & Wildlife Service, USA*

The course of permafrost degradation depends on climate, vegetation, disturbance, and excess ground-ice content and distribution, which vary over time. The first three of these drivers are undergoing considerable change with arctic warming. Using combined lake-sediment records, field observations, aerial observations and LiDAR imagery, we reconstructed the late-Quaternary history of the marginal upland of the Yukon Flats, interior Alaska, a loess-mantled region with massive ground ice and numerous thermokarst lakes that is identified as yedoma. A switch to warmer, moister conditions during deglaciation triggered substantial thermal erosion and transport of silt, which washed into existing basins and formed widespread linear corrugations cutting across the uplands. Lakes began to form via thermokarst as early as 13,000 cal yr BP. Lakes intersect the corrugations, indicating lake formation followed initial landscape instability. Charcoal in basal sediments indicates fire may have influenced lake initiation. Small-scale surface topography revealed by LiDAR images includes deep gullies, features resembling lake drainage channels, and lowered lake shorelines. After ca 10,000 yr BP the region became colonized by dense evergreen conifer forest, which likely served to stabilize and insulate the ground surface, preventing the continuation of the high rates of permafrost degradation recorded in the earliest Holocene. Initial lake lowering and generation of steep local topography favouring drying of uplands, plus a summer water deficit, have also likely combined to shift the system to a more quiescent state through much of the Holocene. However, these changes have not prevented lake drainage events entirely. In 2013, several lakes drained or partially drained, possibly in response to fires and a high spring melt-water volume. The observed pattern of drainage is echoed in the older features preserved on the land surface. Based on the Holocene evolution of the region, increasing regional moisture and/or fire disturbance in the future could lead to an increase in permafrost degradation and lake drainage events.

Tracking the age of ice and the fate of carbon from yedoma thaw

Stephanie A. Ewing[1], Jonathan O'Donnell[3], James Paces[2], George Aiken[2], Mikhail Kanevskiy[4], Joshua Koch[2], & Robert Striegl[2]

[1] *Montana State University, United States of America*
[2] *United States Geological Survey*
[3] *United States National Park Service*
[4] *University of Alaska Fairbanks*

The residence time of ice in permafrost is an indicator of past climate history, and of the resilience and vulnerability of high-latitude ecosystems to global change. Development of geochemical indicators of ground-ice residence times in permafrost will advance understanding of the circumstances and evidence of permafrost formation, preservation, and thaw in response to climate warming and other disturbance. We used uranium isotopes to evaluate the residence time of segregated ground ice from yedoma permafrost cores in central Alaska, and the signal of permafrost thaw in neighboring streams. In the cores, characteristic ice morphologies, high segregated ice content, and wedge ice support an interpretation of syngenetic permafrost formation associated with loess deposition. Measured ($^{234}U/^{238}U$) values in ground ice showed an overall increase with depth in a series of five neighboring cores up to 21 m deep, consistent with increasing residence time of ice with depth as a result of accumulation of loess over time. A geometric model of ($^{234}U/^{238}U$) evolution suggests mean ages of up to 200 ky BP in the deepest core, with estimated uncertainties of up to an order of magnitude. We suggest that in this area of deep ice-rich loess permafrost, ice bodies have been preserved from the last glacial period (10-100 ky BP), despite subsequent fluctuations in climate, fire disturbance and vegetation. Radiocarbon (^{14}C) analysis of dissolved organic carbon (DOC) in thaw waters from cores supports ages greater than 40 ky BP below 10 m. DOC concentrations in thaw waters increased with depth to maxima of >100 mM, despite little change in ice content or cryostructures, suggesting a DOC production rate of 12 m mol DOC m^{-2} y-1 based on U model ages. Concentrations of low molecular weight organic acids in three cores were consistent and high, with acetate-C accounting for 24±1 % of DOC in all samples. This proportion suggests long-term anaerobiosis and is likely to influence thaw outcomes due to biolability of acetate upon release in many environments. The combination of uranium isotopes, ammonium concentrations, and calcium concentrations explained 86 % of the variation in thaw water DOC concentrations, suggesting that DOC production may be related to both reducing conditions and mineral dissolution over time. In regional streams, relationships between U and DOC suggest that U isotopes preserve the signal of yedoma thaw in select locations, while also integrating other flowpaths on the landscape that supply DOC to rivers.

The ancient cryosphere: diverse evidence for relict Middle Pleistocene permafrost from northwestern Canada

Duane Froese[1], Britta J. L. Jensen[1], Alberto V. Reyes[1], John A. Westgate[2], Hendrik Poinar[3], Beth Shapiro[4], & Grant Zazula[5]

[1]*Department of Earth and Atmospheric Sciences, University of Alberta, Canada*
[2]*Department of Earth Science, University of Toronto*
[3]*Department of Anthropology, McMaster University*
[4]*Department of Ecology and Evolution, University of California, Santa Cruz*
[5]*Department of Tourism and Culture, Government of Yukon*

Deep syngenetic permafrost of Beringia, or the deep Yedoma, hosts a reservoir of at least several hundred Pg of C that has survived through multiple interglaciations at least as warm or warmer than the present interglaciation. Relatively few sites are known across the northern hemisphere to estimate this reservoir, but based on known data, it appears that this reservoir is largely a feature of the Middle Pleistocene and may not pre-date the Early to Middle Pleistocene transition. Relict polygonal ice-wedge networks associated with syngenetic permafrost are present at four sites in the discontinuous permafrost zone of central Yukon and Alaska. They are stratigraphically associated with the Gold Run tephra (ca. 700 ka) and other Middle Pleistocene tephra beds, consistent with their normal magnetic polarity and vertebrate fossil assemblages. Soil organic matter content within these deposits is indistinguishable from Late Pleistocene and Holocene organic matter, with organic carbon ranging between 1 and 12 % reflecting the depositional context. Coupled with these records, water isotopes from relict pore and ice wedge ice indicates a repetition of depleted isotope values (-24 to -34 per mille) commonly preserved for cold stages, while warm stages show pore ice values closer to modern (ca. -19 to -24 per mille) for interstadial and interglacial stages. Plant and vertebrate communities show that the majority of this material accumulated in typical steppe-tundra ecosystems associated with Pleistocene cold stages, similar to late Pleistocene contexts. Where differences are more pronounced, however, is at the molecular scale. Ancient biomolecules show much greater rates of DNA damage reflected by decreases in the obtained plant and bacterial sequence diversity and elevated deamination of the 5 and 3' termini of DNA molecules, characteristic of ancient DNA extracts.

Soil organic carbon stocks along transects from Yedoma uplands into drained thaw lake basins on Sobo-Sise Island, Lena Delta, Siberia

Matthias Fuchs[1,2], Guido Grosse[1], & Frank Günther[1]

[1] *Alfred Wegener Institute Helmholtz Centre for Polar and Marine Research, Potsdam, Germany*
[2] *Institute of Earth and Environmental Science, University of Potsdam, Germany*

Late Pleistocene ice-rich syngenetic permafrost deposits called Yedoma store large amounts of organic carbon and are highly affected by climate warming and permafrost degradation. Permafrost thaw, ice-wedge melt, and thermokarst processes affect and expose these carbon-rich deposits to increased microbial activity. Therefore, organic carbon which has been protected by permafrost for thousands of years may partially be released to the atmosphere as greenhouse gases CO_2 and CH_4. However the fate of this low decomposed carbon and the amount and distribution of carbon stored in Yedoma uplands and deposits of thermokarst landforms is still discussed. Our study aims to present a detailed comparison of near-surface organic carbon and nitrogen stocks up to 3m depth in Yedoma uplands as well as thermokarst basins along two permafrost coring transects. The transects are located on Sobo-Sise Island (Fig. 1) in the eastern part of the Lena river delta (NE Siberia) and cover different stages of Yedoma degradation including adjacent deltaic deposits.

Sobo-Sise Island is characterized by Yedoma uplands (third Lena River Delta terrace) which are fragmented by thaw-induced erosion and thermokarst landforms. Inventarization of relief units revealed that about one quarter (86 km^2) of Sobo-Sise is covered by Yedoma and an additional 28 % (95 km^2) is covered by partially eroded Yedoma slopes between Yedoma and surrounding drained thaw lake basins or river channels. 11 % (38 km^2) are covered by lakes or rivers and the remaining area (117 km^2 or 35 %) is covered by drained thaw lake basins (DTLB).

Our approach is based on transect based soil sampling including sample locations on Yedoma uplands, slopes, and adjacent drained thaw lake basins of different generations as well as delta floodplains. Two transects were sampled which run from Yedoma uplands into thermokarst basins in equidistant intervals between the sampling points. In total 15 locations have been sampled with soil pits for the active layer portion and a SIPRE corer for the underlying permafrost. Total depths reached range from 45 cm to 318 cm. Prior to drilling with the corer, soil pits have been excavated down to the bottom of the active layer for a soil description and sampling of the active layer soils. As a result, for most sites the whole soil profile was sampled including active, transient and permafrost layer. Soil cores were subsampled and described in the field. Visual core description included sedimentology, plant macrofossils, and cryostratigraphy. Samples were transported frozen and analyzed in the laboratory for bulk density, total carbon (TC), total nitrogen (TN), total organic carbon (TOC), and grain size. 13 samples of plant macrofossils from both Yedoma uplands and drained thaw lake basin deposits were submitted for Accelerated Mass Spectrometry (AMS) radiocarbon dating to the Poznan Radiocarbon Laboratory, Poland. Mean soil organic carbon and nitrogen estimates were calculated based on the dry bulk density and % TOC and % TN respectively and added up to the reference depths of 30 cm and 100 cm. For an upscaling of the carbon content of the third terrace and whole Sobo-Sise Island, multispectral RapidEye satellite images at 5 m spatial resolution, Landsat satellite data at 30 m resolution and a GeoEye-1 based DEM with 2 m spatial resolution were included to establish a land cover classification.

Results show a mean soil organic carbon storage for the third terrace on Sobo-Sise of 13.20 kg/m^2 ±1.69 for 0 – 130 cm and 25.35 kg/m^2 ±8.99 for 0 – 100 cm of which 31% is stored in permanently frozen soil. The soil organic carbon mean values for drained thaw lake basins are slightly slower with 7.63 kg/m^2 ± 3.13 and 19.97 kg/m^2 ± 7.28 for 0 – 130 and 0 – 1100 cm respectively, of which 58% is stored in the permafrost layer in 0 – 1100 cm depth. However, this is only the first meter of soil. Taking into account deeper layers, significantly more organic carbon is stored in the permafrost layer.

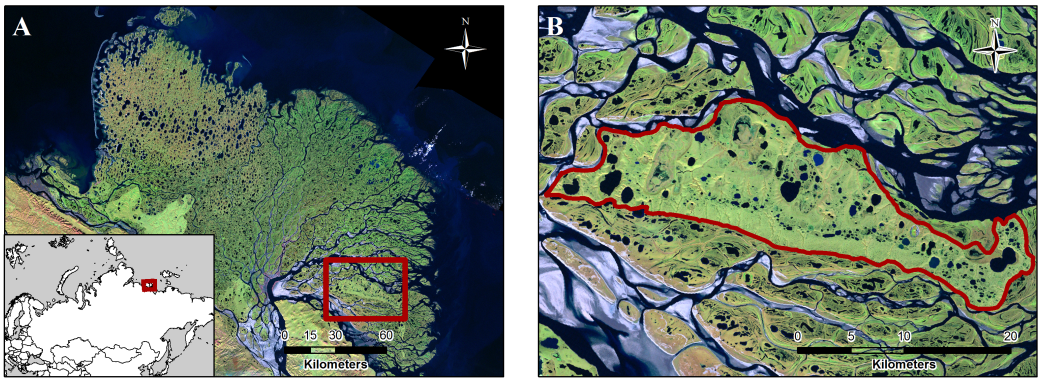

Figure 1: Study region Sobo-Sise Island, Lena River Delta, Siberia. A) Lena River Delta mosaic based on five Landsat 5TM scenes from 2009 and 2010. B) Red outline shows the study area Sobo-Sise Island (subset of the Landsat 5TM mosaic).

Mean TOC for Yedoma upland samples (n=80) is 3.74 wt % ± 2.33; for DTLB samples (n=114) 2.97 wt % ± 2.56. The TOC values for DTLB are therefore slightly lower, which is due to a sample site in one drained thaw lake basin that had very low organic carbon contents. Excluding this extreme outlier, the mean TOC value for DTLB samples is still lower than for Yedoma samples.

Mean nitrogen storage for Yedoma upland sites is 2.6 kg/m^2 for 0-100 cm and for DTLB samples 1.5 kg/m^2 for 0 – 1100 cm. In comparison to the 1.2 kg/m^2 ± 0.4 for the Holocene river terrace and 0.9 kg/m^2 ± 0.4 for the active floodplains found by Zubrzycki et al. [2013], these values are higher and accordingly also represent a substantial nitrogen pool. Overall, this indicates that sites in drained thaw lake basins on Sobo-Sise are more depleted in organic carbon and nitrogen than sites on the Yedoma uplands.

This study adds new data to and insights in the permafrost soil carbon storage estimate of the Lena river delta. Our study region on the third river terrace of Sobo-Sise Island has not been previously covered. A first total carbon pool estimation for Yedoma uplands and slopes representing the third terrace on Sobo-Sise Island (181 km^2) results in about 2 Tg organic carbon stored in the first meter of soil when taking into account a wedge-ice content of 46.3 volume % (proposed by Ulrich et al. [2014]) for Yedoma regions.

In this first assessment, we only cover the first meter of soil and therefore our Yedoma upland data can be considered a mix of modern active layer soils and Holocene cover deposits, while our radiocarbon dates indicate no presence of Late Pleistocene Yedoma in the first meter of soil. For 0 – 200 cm TOC for the third terrace on Sobo-Sise can be estimated to about 4 Tg; however, this estimate is based on only three sample sites. Our results are a contribution to a growing soil carbon database [Hugelius et al., 2014] and add top soil data for Yedoma environments where modern soils and Holocene cover deposits overlie Yedoma deposits.

More data will be processed in the future, in particular soil samples from three transects on the nearby Bykovksy Peninsula, to increase the significance of our findings and to investigate whether the rather low soil organic carbon storage in drained thaw lake basins of the western Lena Delta compared to Holocene cover deposits on Yedoma uplands on Sobo-Sise are exceptional or typical for the eastern Lena Delta region.

References

Hugelius, G.; Strauss, J.; S., Zubrzycki; Harden, J.W.; Schuur, E.A.G.; Ping, C.L.; Schirrmeister, L.; Grosse, G.; Michaelson, G.J.; Koven, C.; O'Donnell, J.; Elberling, B.; Mishra, U.; Camill, P.; Yu, Z.; Palmtag, J. and Kuhry, P. [2014]: Estimated stocks of circumpolar permafrost carbon with quantified uncertainty ranges and identified data gaps. *Biogeosciences*, 11, doi:10.5194/bg-11-6573-2014.

Ulrich, M.; Grosse, G.; Strauss, J. and Schirrmeister, L. [2014]: Quantifying Wedge-Ice Volumes in Yedoma and Thermokarst Basin Deposits. *Permafrost and Periglacial Processes*, 25(3):151–161, doi:10.1002/ppp.1810.

Zubrzycki, S.; Kutzbach, L.; Grosse, G.; Desyatkin, A. and Pfeiffer, E.-M. [2013]: Organic carbon and total nitrogen stocks in soils of the Lena River Delta. *Biogeosciences*, 10(6):3507–3524, doi:10.5194/bg-10-3507-2013.

Ice complex and Yedoma in Yakutia

Victor Kunitskiy

Melnikov Permafrost Institute SB RAS, Russian Federation

The terms "yedoma" and "ice complex" are often used in studies of ice-rich deposits in Yakutia and adjacent areas of the circumpolar region. Yet there is no consensus among researchers on the definition of these Russian terms.

The present author uses the term "yedoma" to mean a wetland plain with an irregular surface covered by various forms of thermal denudation. These surfaces have earlier been termed by some researchers as "mezhalasye", or inter-alas area.

The term "ice complex" was introduced by P.A. Soloviev to designate perennially frozen deposits of ice-rich silt, sandy silt and silty sand penetrated by ice wedges and comprising the inter-alases. However, this definition has not been used in the same way by all researchers. Some workers apply the term "ice complex" to any permafrost material that contains ice wedges. Others believe that several overlapping ice complexes may occur in the same permafrost section. Some also think that terrace ice complexes should be differentiated from slope (watershed) ice complexes. This opinion was clearly expressed in 1985 by E.M. Katasonov, V.A. Bazylev, E.A. Slagoda and P.A. Soloviev who distinguished valley-delta and watershed ice complexes in Central Yakutia.

Based on personal field observations, the present author compiled in 2007 a sketch map of ice-complex distribution in western and eastern Yakutia. This compilation delineates the areas of widespread, fragmentary and sporadic distribution of ice-complex deposits. A fragment of the map is shown in Fig. 1.

In this compilation, particular attention was given to the ice-complex deposits which comprise the watershed areas in the study area. This report will discuss some data on these deposits to evaluate the role of nivation, cryoplanation and thermal denudation in the development of Yedoma landscapes in the watershed between the Anabar and Olenek Rivers, north Central Siberian Plateau.

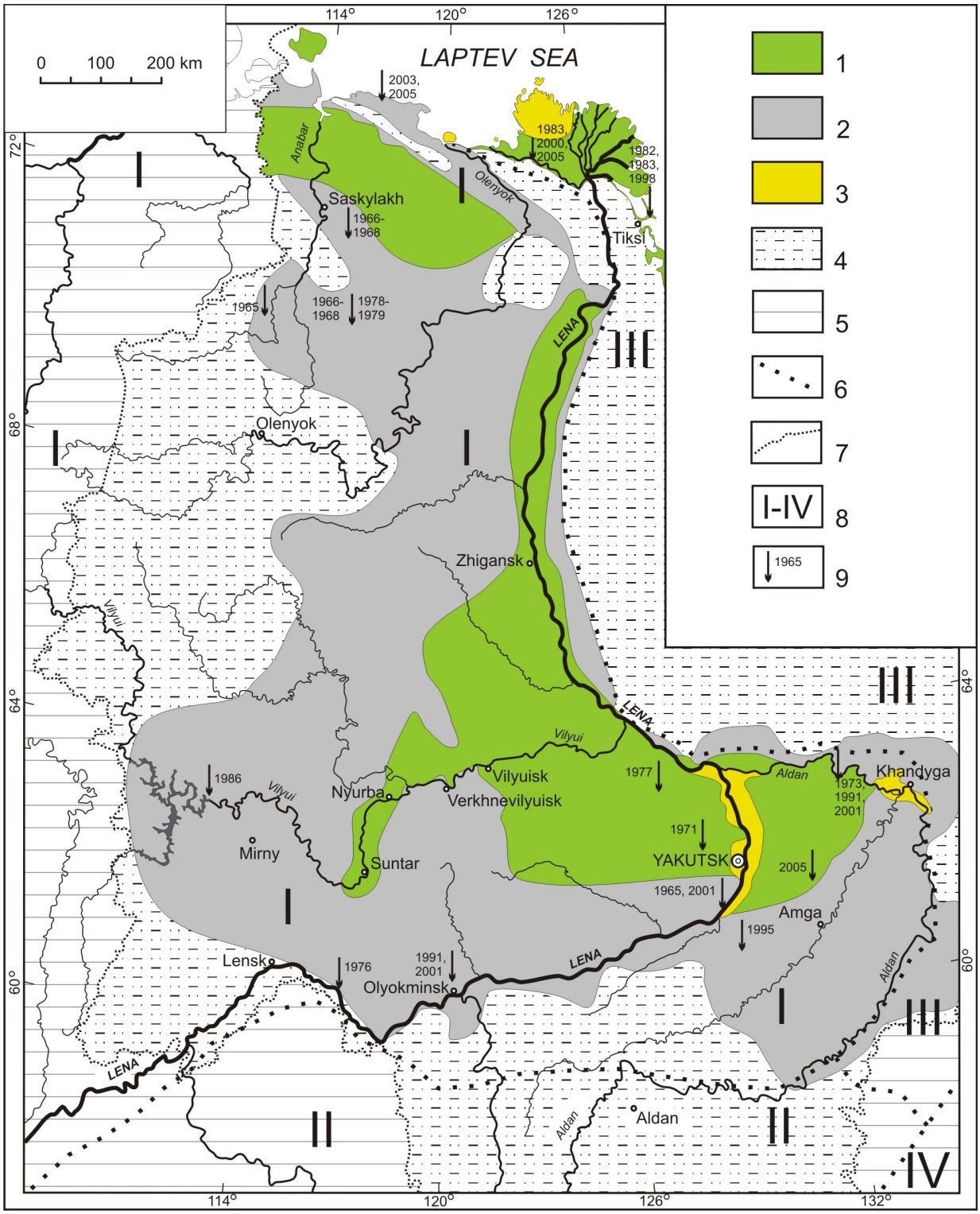

Figure 1: Sketch map showing the distribution of ice-complex deposits in western Yakutia: 1 – widespread; 2 – fragmentary; 3 – sporadic distribution of ice-complex deposits in lowlands; 4 – sporadic distribution of ice-complex deposits in plateaus and mountains; 5 – areas adjacent to Yakutia; 6 – geographical boundary; 7 – administrative boundary; 8 – physiographic provinces: Central Siberia (I); Pre-Baikal and Trans-Baikal Mountainous Region (II); Eastern Siberia (III); North Pacific Region (IV); 9 – location and year(s) of ice-rich permafrost studies conducted with participation of the author.

Late Quaternary palaeo-environmental history of Muostakh Island, Northern Siberia based on sedimentological and geocryological studies

Hanno Meyer[1], Thomas Opel[1], Alexander Yu. Dereviagin[2], Michael Fritz[1], Christoph Manthey[1], Christine Siegert[1], Lutz Schirrmeister[1], & Mikhail N. Grigoriev[3]

[1] *Alfred Wegener Institute Helmholtz Centre for Polar and Marine Research, Potsdam, Germany*
[2] *Lomonosov Moscow State University, Faculty of Geology, Moscow, Russia*
[3] *Melnikov Permafrost Institute, Yakutsk, Republic Sakha, Russia*

Muostakh Island (N 71°36'; E 129°57') is a spectacular site in the Siberian Arctic due to its very high coastal erosion rates of up to 20 m/year as well as substantial permafrost subsidence [Günther et al., 2015]. The island extends about 7.5 km in the N-S direction and up to 500m in E-W direction and has been connected to the mainland until a few thousand years ago. Sediments and ground ice of the Yedoma type (the so called Ice Complex; Schirrmeister et al. [2011] form up to 20 m high coastal cliffs on Muostakh Island. The main aim of this multi-proxy study is to cover the complete sedimentological and geocryological sequence for a detailed palaeoenvironmental interpretation of the island.

In general, the sedimentary sequence from Muostakh Island is divided into three stratigraphic units and consists of sediments of late Pleistocene to Holocene age. The lowermost unit A is approximately 8 m thick, rich in ground ice and comprises mostly sandy silt alternating with thin peat layers. At the top of this unit, a prominent 1 m thick peat layer is found in many sections on the island. In unit A, the ice wedges may reach widths of up to 5 m.

At ca. 10m a.s.l., a hiatus from ca. 41.6 kyr BP to ca. 19.7 kyr BP is indicated by an erosional plane sharply intersecting ice wedges and sedimentary structures as well as by geocryological observations, i.e. distinctly narrower ice wedges above the discordance.

Above this erosional plane, unit B, which is composed of 8-9 m of coarse-grained material, is indicative for fast and highly-energetic deposition, absent in many other sites of Ice Complex exposures in the Laptev Sea region (i.e. at nearby Mamontovy Khayata outcrop on Bykovsky Peninsula; Meyer et al. [2002].

The upper (and youngest) sedimentary unit C reaches a maximum thickness of about 4-5 m and is laterally discontinuous. About 10 m wide peaty patches of Holocene organic-rich and ice-rich sandy silts cover the underlying deposits. Peat patches are intersected by ice wedges of generally less than 1 m wide, but in exceptions also reaching 3-5 m in width, penetrating downwards into the older layers.

Here we present the complete sedimentological sequence of Muostakh Island including new AMS ^{14}C radiocarbon ages both from sediment and ice wedges. Sedimentological, geochemical and geocryological data include the coarse-grained layer for the first time, which highlights an episode of erosion and rapid deposition in Siberian Ice Complex during the Last Glacial Maximum. Stable isotope data from ice wedges complement this study with winter season paleoclimate information. This multidisciplinary study will re-evaluate the Late Quaternary depositional and palaeo-environmental history of the region.

References

Günther, F.; Overduin, P. P.; Yakshina, I. A.; Opel, T.; Baranskaya, A. V. and Grigoriev, M. N. [2015]: Observing Muostakh disappear: permafrost thaw subsidence and erosion of a ground-ice-rich island in response to arctic summer warming and sea ice reduction. *The Cryosphere*, 9(1):151–178, doi:10.5194/tc-9-151-2015.

Meyer, H.; Dereviagin, A.Yu.; Siegert, C. and Hubberten, H.-W. Paleoclimate Studies on Bykovsky Peninsula, North Siberia – Hydrogen and Oxygen Isotopes in Ground Ice. *Polarforschung*, 70: 37–51, 2002. URL http://epic.awi.de/5107/1/Mey2002a.pdf.

Schirrmeister, L.; Kunitsky, V.; Grosse, G.; Wetterich, S.; Meyer, H.; Schwamborn, G.; Babiy, O.; Derevyagin, A. and Siegert, C. [2011] Sedimentary characteristics and origin of the Late Pleistocene Ice Complex on north-east Siberian Arctic coastal lowlands and islands – A review. *Quaternary International*, 241:3–25, doi:10.1016/j.quaint.2010.04.004.

Reconnaissance palaeoenvironmental study of 90 m of permafrost deposits at Batagaika megaslump, Yana Uplands, northern Siberia

Julian Murton, Mary Edwards, Patricia Anderson, Marina Cherepanova, Tomasz Goslar, Stanislav Gubin, Julia Korzun, Anatoly Lozhkin, Alexei Lupachev, Grigoriy Savvinov, Alexei Tikhonov, & Oksana Zanina

University of Sussex, United Kingdom

The headwall of a megaslump at Batagaika, in the Yana Uplands of northern Yakutia, exposes a remarkable stratigraphic sequence that may provide a long or high-resolution record of Quaternary palaeoenvironmental change. The sequence of about 90 m of permafrost sediments ('ice complex') is dominated by fine sand and very fine sand, with small amounts of silt. The stratigraphy includes a banded unit containing about 16 organic layers beneath a unit of yedoma containing large syngenetic ice wedges. Between these units is a prominent black layer about 1 m thick, with an erosive base.

This presentation reports the results of a reconnaissance study of the Batagaika deposits that outlines their stratigraphy, age and potential palaeoenvironmental significance. Sampling of the basal sequence was performed in 2011 and of the main part of the sequence in 2013. Sediment samples were collected from different stratigraphic units to determine their sedimentological and palaeoecological properties, and four samples of wood and roots were ^{14}C dated to indicate, in outline, the age of the sequence. Analysis of sediment properties, pollen, spores, diatoms, phytoliths, vertebrate remains and plant macrofossils provides a palaeoenvironmental framework for interpreting the Quaternary history of the permafrost deposits.

We consider two palaeoenvironmental hypotheses. Hypothesis 1 interprets the prominent black layer as the Last Interglacial palaeosol/forest bed, similar to the Eva Forest Bed dated to about 125 ka in central Alaska [Péwé et al., 1997]. Hypothesis 2 interprets the organic layers in the underlying unit as the Karginsky Pedocomplex, in line with Haesaerts et al. [2005] reconstruction of 14 warm climatic episodes between 29,000 and 26,500 BP based on multiple palaeosols within loess at Kurtak in southern Siberia. Our preliminary results favour hypothesis 1 and provide tentative correlations between Batagaika and the loess-palaeosol stratigraphy of central Alaska.

References

Haesaerts, P.; Chekha, V.P.; Damblon, F.; Drozdov, N.I.; Orlova, L.A. and Van der Plicht, J. [2005]: The loess-palaeosol succession of Kurtak (Yenisei basin, Siberia): a reference record from the Karga Stage (MIS 3). *Quaternaire*, 16:3–24, doi:10.4000/quaternaire.171.

Péwé, T.L.; Berger, G.W.; Westgate, J.A.; Brown, P.M. and Leavitt, S.W. [1997]: Eva Interglaciation Forest Bed, unglaciated central Alaska: global warming 125,000 years ago. *Geological Society of America Special Paper 319*.

Characterization of organic matter stored in frozen Yedoma and thermokarst basin deposits on Sobo-Sise Island, Lena Delta

Darshan Neubauer[1], Jens Strauss[1], Kai Mangelsdorf[2], & Guido Grosse[1]

[1] *Alfred Wegener Institute Helmholtz Centre for Polar and Marine Research, Potsdam, Germany*
[2] *GFZ German Research Centre for Geosciences, Helmholtz Centre Potsdam, Germany*

The permafrost region approximately makes up one quarter of the land surface of the Northern Hemisphere. Its soil organic carbon pool is estimated to be about twice the size of carbon in the modern atmosphere [Hugelius et al., 2014]. In the context of climate warming, understanding the processes that are linked to permafrost thaw and its effects on the organic carbon pool is of major concern [Schuur et al., 2015]. In particular, permafrost carbon quality characteristics are of interest since they determine availability of carbon to microbial decomposition and may significantly influence the outcome of permafrost carbon feedbacks to climate.

We analyzed organic-matter quality of Late Pleistocene (Yedoma) and Holocene (thermokarst basin) permafrost deposits with regard to the degree of decomposition by applying a multi-proxy approach. Samples were taken from two exposures, one located in a thermokarst depression and the other on a Yedoma-to-thermokarst slope on Sobo-Sise Island in the Lena Delta (northeast Siberia). Additionally, a four meters long frozen core was taken from a baydzerakh hill on a Yedoma slope. In our approach, building on [Strauss et al., 2015], we used sedimentological (ice content, bulk density) and geochemical parameters (total organic carbon (TOC), dissolved organic carbon (DOC), stable isotopes ($\delta^{13}C$, $\delta^{18}O$), total organic carbon total nitrogen (C/N) ratios), as well as molecular biomarkers (n-alkanes, n-fatty acids, and biomarker indices, i.e., average chain length (ACL), carbon preference index (CPI), and higher-plant fatty-acid index (HPFA)).

Our results indicated higher concentrations of organic carbon in Yedoma when compared to thermokarst basin deposits. Concentrations of DOC were clearly higher for Yedoma, with values ranging from 200 mg/l to above 1000 mg/l, compared to DOC concentrations in thermokarst basin deposits of under 200 mg/l (Fig. 1 a). With values between 5-15 wt%, TOC was also higher for Yedoma, while in thermokarst basin deposits it only ranged from 4-6 wt% (Fig. 1 b). However, C/N ratio and δ13C showed no clear difference between data from Yedoma or thermokarst (Fig 1 b, c).

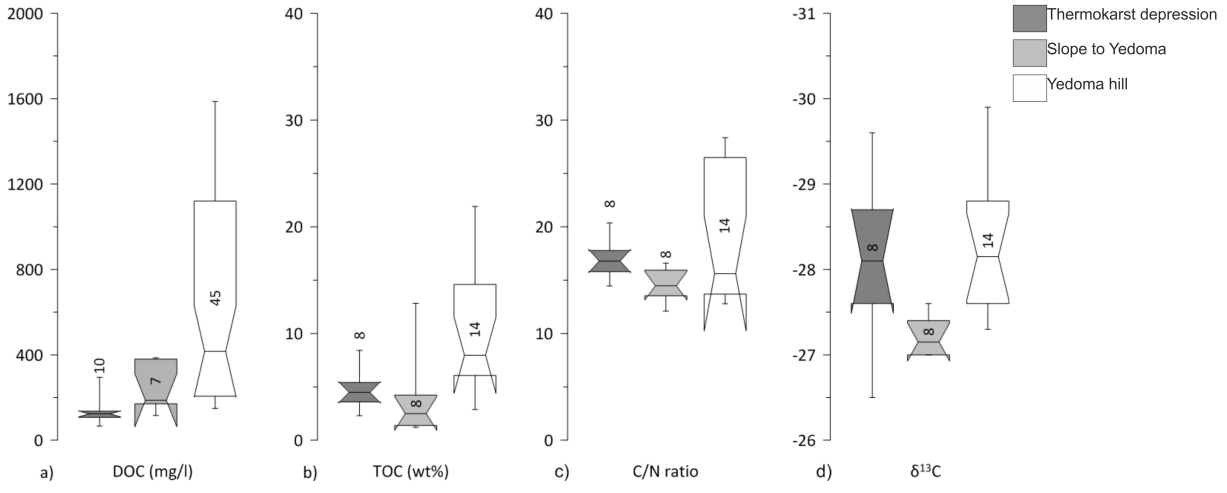

Figure 1: Boxplot-visualization of selected proxies for organic-matter degradation from the Yedoma core (white), the slope from a Yedoma hill into a thermokarst depression (light grey) and the thermokarst depression (dark grey). The numbers show the sample size.

TOC and DOC measured in this study suggest both less degradation of organic-matter stored in Yedoma deposits as in thermokarst. However, in Strauss et al. (2015) organic-matter from both Yedoma and thermokarst deposits showed no relation between degradation and depth, while C/N ratio and δ13C values suggested a better conservation of organic matter from thermokarst deposits compared to Yedoma deposits. Hence, Strauss et al. (2015) concluded that organic-matter vulnerability is heterogeneous and depends on different decomposition trajectories and previous decomposition and preservation history. Furthermore, biomarker data suggested that degradation rather occurs as a combination of degradation processes than a simple linear function of age or sediment facies. In this context, our study approach of combining lipid biomarkers and δ18O, together with our sedimentological and geochemical data, is promising to deliver valuable information about decomposition processes and trajectories of organic-matter in the Lena Delta.

References

Hugelius, G.; Strauss, J.; S., Zubrzycki; Harden, J.W.; Schuur, E.A.G.; Ping, C.L.; Schirrmeister, L.; Grosse, G.; Michaelson, G.J.; Koven, C.; O'Donnell, J.; Elberling, B.; Mishra, U.; Camill, P.; Yu, Z.; Palmtag, J. and Kuhry, P. [2014]: Estimated stocks of circumpolar permafrost carbon with quantified uncertainty ranges and identified data gaps. *Biogeosciences*, 11, doi:10.5194/bg-11-6573-2014.

Schuur, E. A. G.; McGuire, A. D.; Schadel, C.; Grosse, G.; Harden, J. W.; Hayes, D. J.; Hugelius, G.; Koven, C. D.; Kuhry, P.; Lawrence, D. M.; Natali, S. M.; Olefeldt, D.; Romanovsky, V. E.; Schaefer, K.; Turetsky, M. R.; Treat, C. C. and Vonk, J. E. [2015]: Climate change and the permafrost carbon feedback. *Nature*, 520(7546):171–179, doi:10.1038/nature14338.

Strauss, J.; Schirrmeister, L.; Mangelsdorf, K.; Eichhorn, L.; Wetterich, S. and Herzschuh, U. [2015]: Organic-matter quality of deep permafrost carbon – a study from Arctic Siberia. *Biogeosciences*, 12 (7):2227–2245, doi:10.5194/bg-12-2227-2015.

Holocene ice wedges in the Eurasian Arctic – review of stable-isotope based climate records

Thomas Opel[1], Hanno Meyer[1], Thomas Laepple[1], & Alexander Yu. Dereviagin[2]

[1] *Alfred Wegener Institute Helmholtz Centre for Polar and Marine Research, Potsdam, Germany*
[2] *Lomonosov Moscow State University, Faculty of Geology, Moscow, Russia*

The Arctic currently experiences a pronounced and unprecedented warming. This highly dynamic response on changes in climate forcing and the global impact of the Arctic water, carbon and energy balances make the Arctic a key region to study past, recent and future climate changes. Recent proxy-based Arctic-wide temperature reconstructions for the past two millennia [McKay and Kaufman, 2014] show a long-term cooling trend that has been reversed by the ongoing Arctic warming. Single Arctic proxy records and Northern Hemisphere temperature reconstructions (e.g. Sundqvist et al. [2014] indicate that the long-term cooling started already about 8 kyrs ago and is mainly related to a decrease in solar summer insolation. Climate model results on the other hand show no significant change or even a slight warming over this period. This model-proxy mismatch might be caused by the fact that most records used for temperature reconstructions are based on proxies that record summer information. As the reconstructions are, thus, expected to be seasonally biased towards the summer there is a strong need for past winter temperature information. Ice wedges may fill this gap and add substantial information for a comprehensive seasonal picture of Holocene Arctic climate variability [Meyer et al., 2015]. Polygonal ice wedges are a widespread permafrost feature in the Arctic tundra lowlands. Ice wedges form by the repeated filling of thermal contraction cracks with snow melt water, which quickly refreezes at negative ground temperatures and forms ice veins. As the seasonality of frost cracking and infill is generally related to winter and spring, respectively, the isotopic composition of wedge ice is indicative of past climate conditions during the cold season. $\delta^{18}O$ of ice is interpreted as proxy for surface air temperature in the region of precipitation (snow). Radiocarbon dating of organic remains in ice-wedge samples provides age information to generate chronologies for single ice wedges as well as regionally stacked records with an up to centennial resolution. In this contribution we seek to summarize Holocene ice-wedge stable-isotope based temperature reconstructions from the Eurasian Arctic. We strongly focus on own work in the Yedoma region around the Laptev Sea but consider as well literature data for study sites from Svalbard towards the East Siberian Sea region. We discuss the stable isotope data in terms of suitability for reconstruction of high-quality records. This includes also the consideration of different stratigraphic units of Holocene and modern ice wedges (e.g. river terraces, top of Ice Complex, thermokarst basin deposits) as well as ice-wedge dating and chronological approaches. The derived winter temperature trends for the Mid to Late Holocene are compared to other Arctic paleoclimate records, climate forcing factors as well as climate model results. We show that stable isotope records from ice wedges contribute significant seasonal information on past Arctic climate. However, the generation of high-quality reconstructions depends on careful selection of study sites and ice wedges, the availability of suitable organic matter for AMS ^{14}C dating, a high sampling resolution and suitable chronological approaches.

References

McKay, N.P. and Kaufman, D.S. [2014]: An extended Arctic proxy temperature database for the past 2,000 years. *Scientific Data*, 1, doi:10.1038/sdata.2014.26.

Meyer, H.; Opel, T.; Laepple, T.; Dereviagin, A.Yu.; Hoffmann, K. and Werner, M. [2015]: Long-term winter warming trend in the Siberian Arctic during the mid- to late Holocene. *Nature Geoscience*, 8, doi:10.1038/ngeo2349.

Sundqvist, H. S.; Kaufman, D. S. and McKay, N. P. et al.[2014]: Arctic Holocene proxy climate database – new approaches to assessing geochronological accuracy and encoding climate variables. *Climate of the Past*, 10(4):1605–1631, doi:10.5194/cp-10-1605-2014.

The last 50,000 years of hydroclimate change revealed by stable water isotopes of relict permafrost in the Klondike goldfields, Yukon, Canada

Trevor Porter[1,2], Duane Froese[2], & Matthew Mahony[2]

[1] *University of Toronto, Canada*
[2] *University of Alberta, Canada*

Precipitation stable isotope ratios (δD and $\delta^{18}O$) are sensitive air temperature proxies in the higher latitudes and are commonly measured in ice cores for paleothermometry. Similarly, relict ice in relict permafrost deposits record paleometeoric waters that could be used to fill spatial gaps in the paleotemperature field where ice cores are not available. Here we present a 50,000 year record of relict ice δD and $\delta^{18}O$ measurements from Late Pleistocene loessal silts and Late Holocene organic deposits from the Klondike goldfields, and use these data to constrain glacial-interglacial paleotemperatures. We examine wedge and pore ice which offer different seasonal blends of precipitation, and where they occur together in the sedimentary record they allow for a more nuanced interpretation of past hydroclimates. Wedge ice is the product of snowmelt, and this cold-season seasonality should be relatively constant over millennial timescales. Conversely, pore ice is the product of year-round precipitation, and the bulk isotopic composition reflects the relative contributions of precipitation throughout the year. In the modern period, the isotopic ratios integrated by Late Holocene wedge ice (δD = -187 ± 3 ‰, $\delta^{18}O$ = -24.5 ± 0.5 ‰) and pore ice (δD of -176 ± 5 ‰, $\delta^{18}O$ = -22.7 ± 0.6 ‰) are consistent with cold-season and mean annual precipitation, respectively, as confirmed by the nearby GNIP record at Mayo. Wedge ice from the transitional Marine Isotope Stage 3/2 is highly depleted with a mean δD of -227 ± 4 ‰ and a mean $\delta^{18}O$ of -29.3 ± 0.6 ‰. These isotopic ratios can be equated to an average cold-season temperature depression of ca. 14 ± 5 °C (1c.σ, compound error) below modern based on transfer functions calibrated for continental North America (δDprecip = 3.1 ‰ °C-1 × T – 155 ‰; $\delta^{18}O$precip = 0.41 ‰ °C-1 × T – 20.2 ‰; 1σ = ± 2.9 °C). MIS 3 wedges are slightly more enriched than the MIS 3/2 wedges, and the average cold-season depression is estimated to be ca. 9 ± 5 °C below modern. The ice wedge record lacks sufficient sample depth to warrant quantitative estimates during MIS 2 and the Early Holocene. Pore ice during MIS 3/2, bracketed by the wedge ice summarized above, has a mean δD of -222 ± 5 ‰and a mean $\delta^{18}O$ of -28.0 ± 1 ‰. These values are nearly as depleted as the MIS 3/2 wedge ice suggesting that the pore ice is mainly integrating cold-season precipitation, in contrast to the annual blend that is recorded in modern pore ice. This difference can be explained by a precipitation seasonality change. A ca. 70 % reduction of summer precipitation relative to modern is simulated by several PMIP3 models under full glacial boundary conditions, which corroborates the isotopic convergence of pore and wedge ice. This direction of precipitation seasonality change is opposite to coeval changes in the North Atlantic sector which are represented in Greenland ice cores, and may suggest a strong anti-phase coupling of the North Pacific and North Atlantic sectors during glacial times. The seasonality change complicates interpretation of the pore ice record during cold stages as a simple annual temperature proxy. However, the isotopic offset between modern and cold stage pore ice can be used as a maximum constraint on annual paleotemperatures. Based on the pore ice record, we estimate that annual paleotemperatures during MIS 3, 3/2 and 2 were depressed to a maximum of ca. 8, 16 and 21 °C ± 5 °C below modern, respectively. Early Holocene peak warmth is expressed in the pore ice record at ca. 10.5 cal. ka BP, with a mean δD of -158 ± 1 ‰and a mean $\delta^{18}O$ of -19.9 ± 0.1 ‰. We assume a similar-to-modern precipitation seasonality was in place by the Early Holocene (ca. 12-9 cal. ka BP), and estimate that mean annual temperatures at this time were ca. 4-5 °C (± 4 °C) warmer than present. This study provides new constraints on Late Pleistocene and Holocene temperatures in Eastern Beringia, and highlights the value of using multiple forms of relict ice to constrain past hydroclimatic change, which may be especially useful for studies of the major glacial-interglacial climate transitions of the Late Quaternary.

The polygenetic hypothesis of Yedoma origin - comparing grain-size distributions of Alaskan and Siberian Yedoma

Lutz Schirrmeister[1], Guido Grosse[1], Jens Strauss[1], Elisabeth Dietze[2], & Sebastian Wetterich[1]

[1] *Alfred Wegener Institute Helmholtz Centre for Polar and Marine Research, Potsdam, Germany*
[2] *German Research Centre for Geosciences GFZ, Section 5.2 Climate Dynamics and Landscape Evolution*

The formation of late Pleistocene Yedoma in western Beringia (Siberia) is still widely debated. Moreover, different geological and cryostratigraphical views on Yedoma exist between researchers focusing on western or eastern Beringia (Alaska and Northwest Canada). These differences largely concern the prominence of the role of eolian processes. In particular, previous studies on Yedoma in the Yukon Territories and Alaska interpret these deposits as being largely loess or re-transported loess (muck). In contrast, several hypotheses have emerged over decades of research in the extensive Siberian Yedoma region, including

1. alluvial genesis,
2. ice-sheet-dammed basin sediments,
3. deltaic formation,
4. proluvial and slope deposits,
5. cryogenic-aeolian deposits,
6. nival deposits, and
7. polygenetic origins.

Characteristics that most studies agree on include the dominance of large syngenetic ice wedges, mainly allochthonous silty to sandy sediment deposition in low-center polygons in combination with deposition of mainly autochthonous organic remnants from plants and animals, very harsh continental, glacial climate conditions. In terms of landscape and relief characteristics, various Yedoma types seem to exist across the extensive region where Yedoma does occur, ranging from spatially confined Yedoma valley fills including slopes to vast accumulation plains on Arctic lowlands and shelves. Accordingly, we here support the notion that Yedoma may have different depositional properties and genetic origins under a common frame of similar environmental and climatic conditions during the Late Pleistocene. This hypothesis is known as polygenetic formation of Yedoma.

An important aspect of Yedoma is the dominating presence of excess ground ice. Ice wedges and segregated intra-sedimentary ice constitute the majority of this deposit by volume (50–80 %) in most Yedoma regions and are thus one of the most critical factors in deposit genesis in contrast to accumulations of silty to sandy deposits in temperate regions.

The Yedoma Ice Complex formation includes cryogenic processes such as cryogenic weathering, ice segregation, syngenetic ice wedge formation and growth, secondary sediment deformation and reworking due to ground ice, and cryosol formation (including phases dominated by orthels, turbels, or histels). All these processes were promoted by long-lasting harsh continental climate conditions. Furthermore, the formation of large polygon ice-wedge nets and thick continuous sequences of frozen deposits is closely related to the persistence of stable, poorly drained, low topographic gradient accumulation areas.

A comprehensive cryolithogenic concept of polygenetic Yedoma formation combines cryogenic weathering, periglacial material transport and accumulation, and relief shaping under cold-arid climate conditions and considers two general formation processes: (1) the primary accumulation in low-centered ice-wedge polygons and (2) the syngenetic freezing and ice-wedge growth in non-glaciated Arctic lowlands under cold-arid climate of the late Pleistocene. Following this concept Yedoma represents a specific periglacial facies whose formation is controlled by the interaction of several climate, landscape and geological preconditions typical for non-glaciated Arctic and sub-Arctic lowlands and foothills.

In contrast to the pure aeolian (loess) or glacial hypotheses, the proposed cryolithogenic concept integrates several previous formation concepts and in particular takes the important role of ground ice in the deposit formation process into account. Generally, this corresponds to the polygenetic character of Yedoma formation. It also includes the potential for

several sediment sources, weathering processes, and pathways by which sediments in typical periglacial landscapes can build up the Ice Complex horizon.

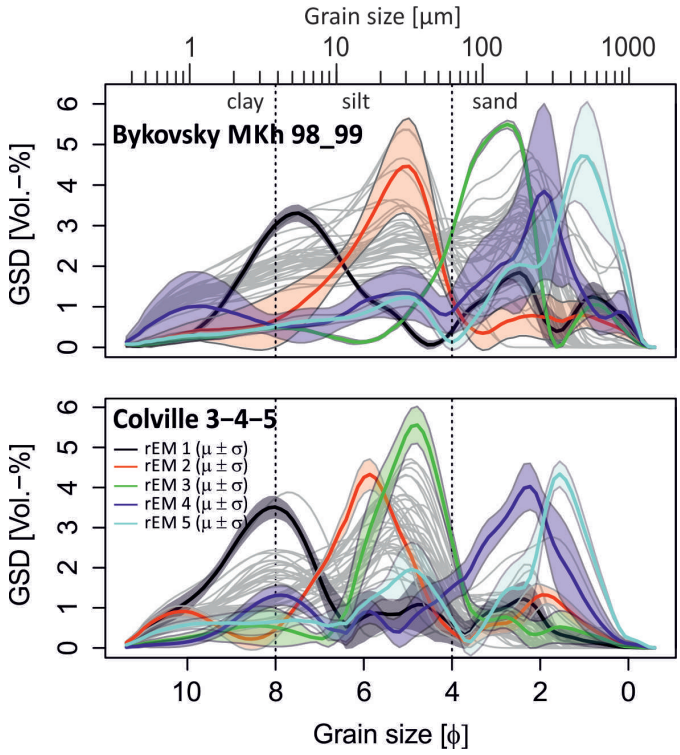

Figure 1: EMMA from two sites in Siberia and Alaska indicating that Yedoma is composed by sediments from multiple sources, transport and depositional processes. Original GSD are plotted in grey (for better comparability Bykovsky distributions were enlarged by 1.5).

Generally, Yedoma consists of often poorly sorted sediments with maxima in the silt and fine sand, but also coarse sand and gravels can be included. Grain-size characteristics differ with study sites and within horizons [Schirrmeister et al., 2011]. To understand the local characteristics as well as the regional variation in the sedimentology of the late Pleistocene Yedoma deposits, we analyzed the grain-size distribution (GSD) of hundreds of samples from dozens of Yedoma sites: The multi-modal GSD of two examples from the Bykovsky Peninsula (Siberia) and the Colville River (Alaska) already indicate a variety of sediment production, transport and depositional processes (Fig. 1). To disentangle these processes a robust end-member modeling analysis (EMMA) was performed on Yedoma sediments of the two sites following Dietze et al. [2012] and Dietze et al. [2014]. Multiple robust grain-size end-members (rEM) were unmixed (Fig. 1). The average robust model explains 85.6 % of the total grain-size variability in Colville and only 53.5 % of the Bykovsky Yedoma grain-size variability, the latter being indicative for very poor sorting and high heterogeneity of the Bykovsky sediments in contrast to Colville sediments. Both sites were composed of five robust end-members with modes at 4, 17, 36, 210 and 340 µm that explain 25, 28, 36, 8.2 and 2.8 % of the variance of Colville sediments. The Bykovsky rEM had modes at 5, 27, 120, 210 and 310 µm comparable to Colville rEMs, each of them explaining 8.9, 23, 22, 21 and 25 % of the grain-size fractions that can be explained by EMMA. The various grain-size end-members supports the hypothesis of polygenetic Yedoma origin involving multiple transport and depositional processes. Although both sites were dominated by silt-transporting and depositing processes, an important amount of finer fractions were deposited at Colville, whereas rather high amounts of coarse- to fine-sandy deposits composed the Bykovsky Yedoma.

Developing a site-specific interpretation of past depositional processes helps understanding the formation conditions of thaw susceptible Yedoma deposits in the terrestrial Arctic and could be crucial for understanding the future trajectories of this unique kind of permafrost in a warming Arctic.

References

Dietze, E.; Maussion, F.; Ahlborn, M.; Diekmann, B.; Hartmann, K.; Henkel, K.; Kasper, T.; Lockot, G.; Opitz, S. and Haberzettl, T. [2014]: Sediment transport processes across the Tibetan Plateau inferred from robust grain-size end members in lake sediments. *Climate of the Past*, 10(1):91–106, doi:10.5194/cp-10-91-2014.

Dietze, E.; Hartmann, K.; Diekmann, B.; IJmker, J.; Lehmkuhl, F.; Opitz, S.; Stauch, G.; Wünnemann, B. and Borchers, A. [2012]: An end-member algorithm for deciphering modern detrital processes from lake sediments of Lake Donggi Cona, {NE} Tibetan Plateau, China. *Sedimentary Geology*, 243–244:169 – 180, doi:10.1016/j.sedgeo.2011.09.014.

Schirrmeister, L.; Kunitsky, V.; Grosse, G.; Wetterich, S.; Meyer, H.; Schwamborn, G.; Babiy, O.; Derevyagin, A. and Siegert, C. [2011]: Sedimentary characteristics and origin of the Late Pleistocene Ice Complex on north-east Siberian Arctic coastal lowlands and islands – A review. *Quaternary International*, 241:3–25, doi:10.1016/j.quaint.2010.04.004.

Paleopermafrost conditions during Ice Complex accumulation, Kolyma Lowland, Dyvanny Yar exposure

Denis Shmelev[1], Mariya Cherbunina[2], Viktor Rogov[3], & Vyacheslav Konishchev[3]

[1]*Institute of Physicochemical and Biological Problems of Soil Science, Russian Academy of Sciences, Russian Federation*
[2]*Moscow State University, Geological faculty, Department of geocryology*
[3]*Moscow State University, Geography faculty, Department of cryolithology and glaciology*

Sediment transformation in deposits in the permafrost zone is accompanied by specific processes of cryogenesis, where the cryogenic weathering is a key factor for the composition and properties of the deposit during formation. The selective destruction of minerals caused by freeze-thaw cycles leads to specific grain size distribution, selective weathering of the main light minerals and their distribution by grain-size fractions. The development of greater concentrations of light minerals, more resistant to cryogenic weathering, occurs in the following order: quartz ⇒ amphibole ⇒ pyroxene ⇒ feldspars ⇒ mica. This allows the opportunity to quantify the rate of cryogenic deformation of deposits and freezing conditions using the Cryogenic Weathering Index (CWI) [Konishchev, 2013]. CWI is calculated as the ratio between quartz and feldspar grains in the silt (50-10 microns) and sand (50-100 microns) grain fractions. In general, CWI values >1 show evidence of active cryogenesis during sedimentation, with higher values reflecting more severe conditions.

The Late Pleistocene and Last Glacial Maximum (LGM, 22-14 kyr BP) is the coldest period in the Quaternary. According to the stable isotope content in ice wedges, winter temperatures were 10–15 °C cooler than modern and permafrost temperatures were 10-15 °C cooler [Schirrmeister et al., 2011, Konishchev, 2013]. There was also accumulation of Yedoma – Ice Complex deposits under periglacial conditions: tundra-steppe landscapes, cryogenic weathering, transport, and deposition dynamics in non-glaciated regions during the Late Pleistocene through the early Holocene [Schirrmeister et al., 2011, Murton et al., 2015]. The deposits were largely formed due to polygenetic deposition together with syngenetic frost cracking and ground ice accumulation. Yedoma generally can be divided into 2 main units: one formed during MIS 3 and 4 (with thick and infrequent ice wedges) and a second formed during MIS 2 (with thin and frequent ice wedges). Early Holocene warming and global landscape reorganization caused widespread degradation of the Yedoma by thermokarst development. The deep thawing of Yedoma ice wedges led to shallow lakes forming and permafrost subsidence. These sediments can be combined as an Alas Complex. The top of the Yedoma surfaces were reworked by Holocene thawing and refreezing and are characterized by a cover layer with a thickness of 2-3 m.

The Duvanny Yar site is one of the best known Quaternary exposures in western Beringia. It is located in the Kolyma Lowland (the eastern coastal plain of Yakutia). The exposure is located within a typical Yedoma landscape on the right bank of the Kolyma river. The outcrop is about 9 km long and up to 55 m high. Seven gentle domes of loess-like sediment (Yedoma hills) and four Holocene thermokarst lakes (alas depressions) can be distinguished. In summer 2013, field work focused on the 5^{th} and 7^{th} Yedoma domes on the Kolyma river (Fig. 1). At the first overview, we have selected three main stratigraphic units, which are named as Units A, B, and C in the following. Units A and B are different facies of Yedoma, while Unit C is the Holocene cover layer. Our separation of these units is based on the cryolithology of the deposits – a combination of lithology, cryostructures (segregation and pore ice) and ice wedge properties of each unit which reflects sedimentation and freezing conditions.

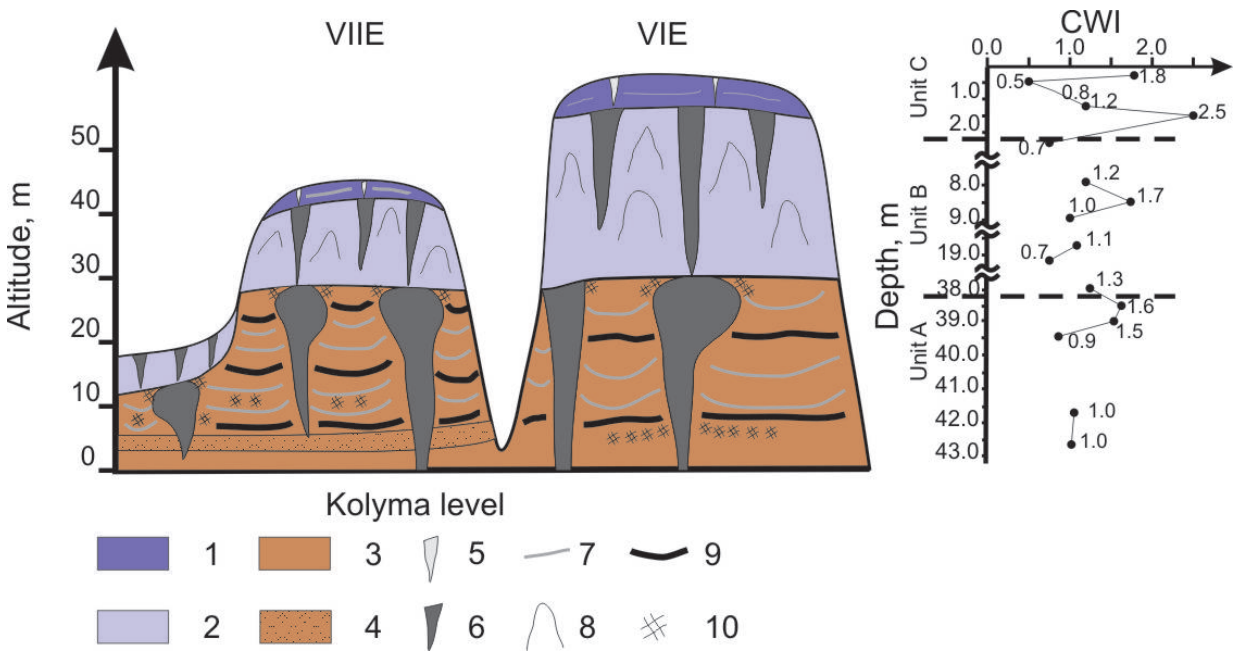

Figure 1: Right - The scheme of Duvanny Yar exposure according to field investigation and Murton et al., 2015. Left - CWI distribution in Pleistocene – Holocene deposits. 1 – Unit C, 2 – Unit B, 3 – Unit A, 4 – sandy layer in Unit A, 5 – milky ice wedges, 6 – brown and dark-brown ice wedges; 7 – ice schlier; 8 – baydzerakh; 9 – buried soil; 10 – peat or organic inclusion.

Unit A is located in the lower part of the exposure at elevations of 5-25 m above the Kolyma river. This layer is characterized by syncryogenic thick ice wedges with a visible width of 5-8 m and a separation of 10-15 m. The mineral part is represented by the dark-brown and black ice- and organic-rich dusty loam with peat layers and buried soils. The head of the ice wedges is surrounded by low-decomposed brown peat with woods and roots. Thus, the mineral part between ice wedges forms the so-called "polygon or wet bath". In the center of "the wet bath" of Unit A CWI values increase from 0.88 to 1.55 with maximum values in the upper part. At the ice wedges, CWI values are lower (0.77-1.11) than in the center of the mineral block, but there is an increase in the values to the top too. Thus, we can assume cryogenic weathering intensifies together with sedimentation.

In the overlying deposits of Unit B, at a height of 1 m above the contact, the CWI value is 1.32 in the mineral part and 0.78 at the ice wedge margins. On the basis of Scanning Electronic Microscopy (SEM) the dominant grain shape is moderately rounded with fresh surfaces and edges, medium relief and radial cracks. Unit B is found in the upper parts of 5th and 7th Yedoma domes at altitudes of more than 25 m above the Kolyma river. It should be noted, that Unit B is absent in many of the lower sections of the exposure. Unit B is distinguished from Unit A by the structure of ice wedges and the composition of the mineral part. In the upper facies, the thin (width is 1-2 m) and frequent (distance between them is 3-5 m) ice wedges dominate. Ice of wedges are dark-grey with inclusions of mineral grains, gas bubbles and vertical stratification. The tops of wedges are cut by milky white elementary hairline ice wedges. The inclined ice lenses are observed at the boundary between the ice wedge and mineral component. The mineral part is homogenous and represented by the grey and dark-grey dusty loam with structureless and lenticular cryostructures, and plant roots with a length of 1-10 cm. But despite the fact that Unit B is homogenous by its cryolithological composition, CWI distribution is heterogeneous. According to our samples CWI values vary between 0.66 and 1.70. It is interesting, that maximal values in Unit B are observed in samples located at ice wedges, and this the CWI of the mineral part is low and does not exceed 1.10. According to the SEM images, the dominant grain shape is rounded (more rounded than in Unit A) with unweathered surfaces, low relief and distinguished cracks.

Unit C, with a thickness of 2-3 m deposits in the top of Yedoma domes, overlies Unit B. Unit C formed in the Early Holocene due to deep thawing and subsequent freezing of the Yedoma top. Unit C contains rare thin milky ice wedges and is overlain by the modern active layer. The mineral part is closer to Unit

B, because it is the same deposit, but thawed and frozen during the Holocene. The main feature of Unit C is its cryostructural diversity: from structureless to suspended and pure ice layers. Moreover, these cryostructures can be combined into cycles which reflect the freezing conditions during the Holocene. The maximum CWI values have been recorded in Unit C, the CWI distribution could be associated with its cryostructural diversity. Thus, in the iceless layer, values typically range from 1.88-2.51, while in the ice-rich layers the CWI decreases to 0.52. From the SEM data, the grain shape variation ranges from well rounded to unrounded shapes with medium and low relief, edge rounding and high-frequency fractures.

The mineral composition of the Duvanny Yar deposits can be characterized as homogenous in all layers of the exposure. The heavy mineral fraction is composed of pyroxene, hornblende, pyrope and grains of pyrite, magnetite, apatite, goethite and siderite. The heavy mineral concentration is low and varies from 1.3 to 8.5 %. Comparing the Duvanny Yar deposits to modern alluvium and Yedoma located in the lower stream of Kolyma (Panteleikha mouth), there are significant differences in the mineral composition reflecting the changing sedimentary sources.

The age of the Duvanny Yar Yedoma has been discussed by many authors, but according to [Murton et al., 2015] the selected units can be related to MIS3 – MIS1. The "wet baths" of Unit A accumulated in MIS 3 (55-25 kyr BP), Unit B – in MIS2 (until 17-16 kyr BP) and Unit C is a result of thawing and freezing of Unit B in the early Holocene (12-6 kyr BP). Thus, we can analyze paleopermafrost dynamics based on the CWI distribution (Fig. 1). In the "wet bath" of Unit A the gradually drying of polygons was accompanied by the development of cryogenic weathering and permafrost conditions; but at this time, the permafrost above the ice wedges was soft, which is probably caused by seasonal streams in the active layer. Generally, this environment may be characterized as wet polygonal tundra. The stratigraphic boundary between Units A and B is distinct in terms of the cryolithology of the deposits. The accumulation of Unit B was accompanied by dry and severe conditions, the freezing of sediments moved from ice wedges, and this is reflected in the CWI distribution and cryostructures. The variation in the CWI for the mineral components reflects the high rates of freezing during syncryogenic sedimentation. The active layer depth was deeper than modern and in comparison to MIS3. Consequently, annual freezing was faster. The end of Yedoma accumulation (17-16 kyr BP) relates to Kolyma river migration and the development of the Alyoshkina terrace [Murton et al., 2015]. Unit C accumulated in the Early Holocene as a result of deep thawing and subsequent freezing at the top of the Yedoma deposits which formed in the LGM. The maximum CWI values can be explained by initial active cryogenic weathering of Yedoma during the LGM and re-freezing during the Holocene, but the rate of cryogenic weathering is dependent on the ice content and cryostructures.

Acknowledgments

The investigation has been supported by RF MK-9417.2016.5 grant.

References

Konishchev, V. N. [2013]: Nature of cyclic structure of Ice Complex, East Siberia. *Kriosfera Zemli (Earth' Cryosphere)*, 17(1):3–16, URL http://www.izdatgeo.ru/pdf/krio/2013-1/3.pdf. in Russian.

Murton, J.B.; Goslar, T.; Edwards, M.E.; Bateman, M.D.; Danilov, P.P.; Savvinov, G.N.; Gubin, S.V.; Ghaleb, B.; Haile, J.; Kanevskiy, M.; Lozhkin, A.V.; Lupachev, A.V.; Murton, D.K.; Shur, Y.; Tikhonov, A.; Vasil'chuk, A.C.; Vasil'chuk, Y.K. and Wolfe, S.A. [2015]: Palaeoenvironmental Interpretation of Yedoma Silt (Ice Complex) Deposition as Cold-Climate Loess, Duvanny Yar, Northeast Siberia. *Permafrost and Periglacial Processes*, 26(3):208–288, doi:10.1002/ppp.1843.

Schirrmeister, L.; Kunitsky, V.; Grosse, G.; Wetterich, S.; Meyer, H.; Schwamborn, G.; Babiy, O.; Derevyagin, A. and Siegert, C. [2011]: Sedimentary characteristics and origin of the Late Pleistocene Ice Complex on north-east Siberian Arctic coastal lowlands and islands – A review. *Quaternary International*, 241:3–25, doi:10.1016/j.quaint.2010.04.004.

The nitrogen inventory of the Yedoma permafrost region

Jens Strauss[1], Fabian Beermann[2], Christina Biasi[3], Claudia Fiencke[2], Guido Grosse[1], Lars Kutzbach[2], Tina Sanders[4], Lutz Schirrmeister[1], Thomas Schneider von Deimling[5], Sebastian Wetterich[1], & Sebastian Zubrzycki[2]

[1] *Alfred Wegener Institute Helmholtz Centre for Polar and Marine Reseach, Potsdam, Germany*
[2] *Universität Hamburg, Institute of Soil Science, Hamburg, Germany*
[3] *University of Eastern Finland, Department of Environmental Science, Kuopio, Finland*
[4] *Helmholtz Centre Geesthacht, Centre for Materials and Coastal Research, Geesthacht, Germany*
[5] *Max Planck Institute for Meteorology, Hamburg, Germany*

The biogeochemical composition of fossil organic matter stored in permafrost is an important subject in current climate change research. Multiple studies on the quality and quantity of permafrost organic carbon suggest that there is a high potential for carbon release into the active carbon turnover cycle through permafrost thaw in a warming Arctic. Other components of organic matter that are important for biogeochemical cycling, however, are less studied so far, including the amount and distribution of nitrogen [Keuper et al., 2012, Mack et al., 2004, Rustad et al., 2001]. Nitrogen from thawing permafrost could be a significant source of the greenhouse gas N_2O. Given its high global warming potential (about 300 times larger than CO_2 over 100 years), even small releases of N2O can affect the permafrost-climate feedback.

This study focuses on the abundance and distribution of nitrogen currently freeze-locked in the Yedoma region of Siberia and Alaska. Organic matter in permafrost deposits of the northern circumpolar region accumulated over tens of thousands of years during the last glacial and interglacial periods. A part of this permafrost region, the Yedoma region, is composed of thick ice-rich silts intersected by large ice wedges, resulting from sedimentation and syngenetic freezing accompanied by ice wedge growth in polygonal tundra, which was driven by certain climatic and environmental conditions during the late Pleistocene. These unique materials are called Yedoma deposits. They constitute a large organic carbon inventory of the (sub)Arctic but are also known to be nutrient-rich due to burial and freezing of plant remains. Besides carbon inventory estimates, detailed quantification of total nitrogen (TN) stocks is lacking. Based on the most comprehensive data set of TN content in permafrost to date, our study aims to estimate the present pool of nitrogen stored in the different stratigraphic units of the Yedoma region, which are

1. late Pleistocene Yedoma deposits;
2. in-situ thawed and diagenetically altered Yedoma deposits (taberite);
3. Holocene thermokarst deposits;
4. Holocene cover deposits on top of Yedoma and
5. the modern active layer of soils.

Nitrogen stock calculations are based on statistical bootstrapping techniques using resampled observed values. The total mean pool size estimate is derived for every of the 10,000 bootstrapping runs, resulting in an overall mean derived from 10,000 individual observation-based bootstrapping means. The conceptual formula for our nitrogen stock calculation is

$$m_{TN,tot} = \sum_{i=1}^{n} m_{TN,i} = \sum_{i=1}^{n} d_i \, (1 - f_{wedge,i}) \, \rho_{b,i} \, c_{TN,i} \, A_i$$

where
$m_{TN,tot}$: pool of total nitrogen in the included stratigraphical units of the Yedoma region,
$i = 1...n$: index numbers of the single stratigraphical unit considered for the nitrogen budgeting,
d_i: deposit thickness of stratigraphical unit i,
$f_{wedge,i}$: volume fraction of ice wedges in stratigraphical unit i,

$\rho_{b,i}$: bulk density of deposits of stratigraphical unit i,
$c_{TN,i}$: content of total nitrogen in deposits of stratigraphical unit i,
A_i: area stratigraphical unit i

We show that the deposits of the Yedoma region store a significant pool of TN. At least a portion of this nitrogen is expected to get mobilized after thaw, affecting biogeochemical budgets and cycles of thawing permafrost-affected ecosystems. Possible effects include mitigation of the current nitrogen limitation of Arctic tundra ecosystems or a contribution of additional greenhouse gases in the form of N2O. In both cases, the permafrost-climate feedback will be affected by the amount and availability of so far not accessible nitrogen.

Acknowledgements

This project is integrated into the Action Group "The Yedoma Region: A Synthesis of Circum-Arctic Distribution and Thickness" (funded by the International Permafrost Association (IPA) to J. Strauss). We acknowledge the support by the European Research Council (Starting Grant #338335), the German and Russian Science Foundations (DFG and RFBR "Polygon" project, DFG-HE 3622-16-1, and RFBR-11-04-91332-NNIO-a), the German Federal Ministry of Education and Research (Grant 01DM12011, and "CarboPerm" (03G0836A)), the Initiative and Networking Fund of the Helmholtz Association (#ERC-0013) and the German Federal Environment Agency (UBA, project UFOPLAN FKZ 3712 41 106).

References

Keuper, F.; van Bodegom, P.M.; Dorrepaal, E.; Weedon, J.T.; van Hal, J.; van Logtestijn, R.S.P. and Aerts, R. [2012]: A frozen feast: thawing permafrost increases plant-available nitrogen in subarctic peatlands. *Global Change Biology*, 18(6): 1998–2007, doi:10.1111/j.1365-2486.2012.02663.x.

Mack, M.C.; Schuur, E.A.G.; Bret-Harte, M.S.; Shaver, G.R. and Chapin, F.S. [2004]: Ecosystem carbon storage in arctic tundra reduced by long-term nutrient fertilization. *Nature*, 431(7007), doi:10.1038/nature02887.

Rustad, L.E.; Campbell, J.L.; Marion, G.M.; Norby, R.J.; Mitchell, M.J.; Hartley, A.E.; Cornelissen, J.H.C.; Gurevitch, J. and GCTE-NEWS [2001]: A Meta-Analysis of the Response of Soil Respiration, Net Nitrogen Mineralization, and Aboveground Plant Growth to Experimental Ecosystem Warming. *Oecologia*, doi:10.1007/s004420000544.

Ice-rich Yedoma permafrost: A synthesis of northern hemisphere distribution and thickness (IPA Action Group)

Jens Strauss[1], Alexander N. Fedorov[2], Daniel Fortier[3], Duane Froese[4], Matthias Fuchs[1], Guido Grosse[1], Frank Günther[1], Jennifer Harden[5], Gustaf Hugelius[6], Mikhail Kanevskiy[7], Alexander Kholodov[8], Viktor Kunitskiy[2], Gleb Kraev[9], Sebastian Laboor[1], Lyna Lapointe-Elmrabti[3], Anatoly Lozhkin[10], Elizaveta Rivkina[11], Joel Robinson[5], Lutz Schirrmeister[1], Denis Shmelev[11], Yuri Shur[7], Christine Siegert[1], Valentin Spektor[2], Mathias Ulrich[12], Sergey Vartanyan[10], Alexandra Veremeeva[11], Katey Walter Anthony[7], & Sergei A. Zimov[13]

[1] *Alfred Wegener Institute Helmholtz Centre for Polar and Marine Research, Potsdam, Germany*
[2] *Melnikov Permafrost Institute, Yakutsk, Russia*
[3] *Geography Department, Université de Montréal, Montréal, Canada*
[4] *Department of Earth and Atmospheric Sciences, University of Alberta, Edmonton, Canada*
[5] *United States Geological Survey, Menlo Park, USA*
[6] *Department of Physical Geography, Stockholm University, Stockholm, Sweden*
[7] *Institute of Northern Engineering, University of Alaska Fairbanks, Fairbanks, USA*
[8] *Geophysical Institute, University of Alaska Fairbanks, Fairbanks, USA*
[9] *Center of Ecology and Productivity of Forests, Moscow, Russia*
[10] *North-East Interdisciplinary Scientific Research Institute, Magadan, Russia*
[11] *Institute of Physicochemical and Biological Problems in Soil Science, Pushchino, Russia*
[12] *Leipzig University, Institute for Geography, Leipzig, Germany*
[13] *Northeast Science Station, Cherskii, Russia*

Vast portions of Arctic and sub-Arctic Siberia, Alaska and the Yukon Territory are covered by ice-rich silty to sandy deposits that are containing large ice wedges, resulting from syngenetic sedimentation and freezing. Accompanied by wedge-ice growth in polygonal landscapes, the sedimentation process was driven by cold continental climatic and environmental conditions in unglaciated regions during the late Pleistocene, inducing the accumulation of the unique Yedoma deposits up to >50 meters thick.

Because of fast incorporation of organic material into syngenetic permafrost during its formation, Yedoma deposits include well-preserved organic matter. Ice-rich deposits like Yedoma are especially prone to degradation triggered by climate changes or human activity. When Yedoma deposits degrade, large amounts of sequestered organic carbon as well as other nutrients are released and become part of active biogeochemical cycling. This could be of global significance for future climate warming as increased permafrost thaw is likely to lead to a positive feedback through enhanced greenhouse gas fluxes. Therefore, a detailed assessment of the current Yedoma deposit coverage and its volume is of importance to estimate its potential response to future climate changes. We synthesized the map of the coverage (see Fig. 1) and thickness estimation, which will provide critical data needed for further research. In particular, this preliminary Yedoma map is a great step forward to understand the spatial heterogeneity of Yedoma deposits and its regional coverage. There will be further applications in the context of reconstructing paleoenvironmental dynamics and past ecosystems like the mammoth-steppe-tundra, or ground ice distribution including future thermokarst vulnerability. Moreover, the map will be a crucial improvement of the data basis needed to refine the present-day Yedoma permafrost organic carbon inventory, which is assumed to be between 83±12 [Strauss et al., 2013] and 129±30 [Walter Anthony et al., 2014] gigatonnes (Gt) of organic carbon in perennially-frozen archives.

Hence, here we synthesize data on the circum-Arctic and sub-Arctic distribution and thickness of Yedoma for compiling a preliminary circum-polar Yedoma map (see Fig. 1).

Figure 1: Yedoma Northern Hemisphere Distribution and Thickness. This map is based on digitized geological maps (VSEGEI), the Alaska Permafrost map and published borehole/exposure data. Potential Yedoma paleo-extent on the shelves is illustrated by the 125m isobath

For compiling this map, we used

1. maps of the previous Yedoma coverage estimates,

2. included the digitized areas from Grosse et al. [2013] as well as extracted areas of potential Yedoma distribution from additional surface geological and Quaternary geological maps:

   a) 1:500,000: Q-51-V,G; P-51-A,B; P-52-A,B; Q-52-V,G; P-52-V,G; Q-51-A,B; R-51-V,G; R-52-V,G; R-52-A,B;

   b) 1:1,000,000: P-50-51; P-52-53; P-58-59; Q-42-43; Q-44-45; Q-50-51; Q-52-53; Q-54-55; Q-56-57; Q-58-59; Q-60; R-(40)-42; R-43-(45); R-(45)-47; R-48-(50); R-51; R-53-(55); R-(55)-57; R-58-(60); S-44-46; S-47-49; S-50-52; S-53-55;

   c) 1:2,500,000: Quaternary map of the territory of Russian Federation,

   d) Alaska Permafrost Map.

The digitalization was done using GIS techniques (ArcGIS) and vectorization of raster Images (Adobe Photoshop and Illustrator). Data on Yedoma thickness are obtained from boreholes and exposures reported in the scientific literature. The map and database are still preliminary and will have to undergo a technical and scientific vetting and review process. In their current form, we included a range of attributes for Yedoma area polygons based on lithological and stratigraphical information from the original source maps as well as a confidence level for our classification of an area as Yedoma (3 stages: confirmed, likely, or uncertain). In its current version, our database includes more than 365 boreholes and exposures and more than 2000 digitized Yedoma areas. We expect that the database will continue to grow. In this preliminary stage, we estimate the Northern Hemisphere Yedoma deposit area to cover approximately 625,000 km^2. We estimate that 53 % of the total Yedoma area today is located in the tundra zone, 47 % in the taiga zone. Separated from west to east, 29 % of the Yedoma area is found in North America and 71 % in North

Asia. The latter include 9 % in West Siberia, 11 % in Central Siberia, 44 % in East Siberia and 7 % in Far East Russia. Adding the recent maximum Yedoma region (including all Yedoma uplands, thermokarst lakes and basins, and river valleys) of 1.4 million km^2 (see Fig. 1 and Strauss et al. [2013]) and postulating that Yedoma occupied up to 80 % of the adjacent formerly exposed and now flooded Beringia shelves (1.9 million km^2, down to 125 m below modern sea level, between 105°E – 128°W and >68°N), we assume that the Last Glacial Maximum Yedoma region likely covered more than 3 million km^2 of Beringia.

Acknowledgements

This project is part of the Action Group "The Yedoma Region: A Synthesis of Circum-Arctic Distribution and Thickness" (funded by the International Permafrost Association (IPA) to J. Strauss) and is embedded into the Permafrost Carbon Network (working group Yedoma Carbon Stocks). We acknowledge the support by the European Research Council (Starting Grant #338335), the German Federal Ministry of Education and Research (Grant 01DM12011 and "CarboPerm"(03G0836A)), the Initiative and Networking Fund of the Helmholtz Association (#ERC-0013) and the German Federal Environment Agency (UBA, project UFOPLAN FKZ 3712 41 106).

References

Grosse, G.; Robinson, J.E.; Bryant, R.; Taylor, M.D.; Harper, W.; DeMasi, A.; Kyker-Snowman, E.; Veremeeva, A.; Schirrmeister, L. and Harden, J. [2013]: Distribution of late Pleistocene ice-rich syngenetic permafrost of the Yedoma Suite in east and central Siberia, Russia. US Geological Survey Open File Report 1078, U.S. Geological Survey Reston, Virginia, 37 pp.

Strauss, J.; Schirrmeister, L.; Grosse, G.; Wetterich, S.; Ulrich, M.; Herzschuh, U. and Hubberten, H.-W. [2013]: The deep permafrost carbon pool of the Yedoma region in Siberia and Alaska. *Geophysical Research Letters*, 40(23):6165–6170, doi:10.1002/2013GL058088. 2013GL058088.

Walter Anthony, K.M.; Zimov, S.A.; Grosse, G.; Jones, M.C.; Anthony, P.M.; Chapin III, F.S.; Finlay, J.C.; Mack, M.C.; Davydov, S.; Frenzel, P. and Frolking, S. [2014]: A shift of thermokarst lakes from carbon sources to sinks during the Holocene epoch. *Nature*, 511, doi:10.1038/nature13560.

Multi-proxy reconstruction of Holocene thermokarst dynamics in Central Yakutia

Mathias Ulrich[1], Johannes Schmidt[1], Natalia Rudaya[2], Sebastian Wetterich[3], Larisa Frolova[4], Luidmila Pestryakova[5], Christine Siegert[3], Birgit Schneider[1], Christoph Zielhofer[1], Peter Efremov[6], & Alexander N. Fedorov[6]

[1]*Leipzig University, Institute for Geography, Leipzig, Germany*
[2]*Institute of Archaeology& Ethnography SB RAS, Novosibirsk, Russia*
[3]*Alfred Wegener Institute Helmholtz Centre for Polar and Marine Research, Potsdam, Germany*
[4]*Kazan Federal University, Kazan, Russia*
[5]*North-Eastern Federal University, Yakutsk, Russia*
[6]*Melnikov Permafrost Institute, SB RAS, Yakutsk, Russia*

The study of past permafrost aggradation and degradation dynamics supports our understanding of contemporary thermokarst processes, and helps predicting future permafrost responses to climate change. Thermokarst processes in ice-rich terrain create basins, called alases, which are widespread in Central Yakutia, Eastern Siberia. Alas dimensions and geomorphic characteristics vary widely due to different cryolithological conditions. The history of Holocene thermokarst development is presumed to be dominantly climate-driven. How the Holocene alases of Central Yakutia formed and evolved is subject of contemporary research.

The overall aim of this study is the reconstruction of Holocene thermokarst (lake) and alas evolution, their influencing factors and environmental conditions in Central Yakutia. Sediment cores were drilled down to 3-4 m depth and sampled in summer 2013 from two alas basins on the eastside of the Lena River valley. Here, we focus on three sediment cores drilled within the alas Khara Bulgunnyakh (61.835215° N/130.647431° E). A multiproxy approach was applied to analyze the sedimentological and biogeochemical characteristics. One 4 m long core (KB7) drilled in a small pingo was additionally investigated for micropalaeontological proxies (pollen, ostracods, ephippia, diatoms) to determine Holocene environmental and thermokarst lake history and its contribution to alas evolution. Organic material and bulk sediment for selected samples were dated with the AMS method to determine ^{14}C ages for thermokarst deposits and age-depth modeling was done for the KB7 core.

The characteristics of the studied sediments point to small-scale varying depositional environments and predominantly lateral expansion in the edge region of rapidly growing small thermokarst lakes and basins by thermo-erosional processes during the Holocene. Their coalescence results finally in the development of the Khara Bulgunnyakh alas, which today cover an area of about 1.5 km^2. Clear evidence for long-lasting and stable lacustrine conditions was not obtained. The results of the 14C dating confirm an extensive deposition of reworked late Pleistocene sediments in peripheral basin zones during thermokarst lake extension, while the basin center is characterized by autochthonous thaw subsidence of Yedoma permafrost. Lacustrine fossil data of the KB7 core confirm lake presence between 6600 and 6300 cal yr BP that rapidly emerged and disappeared during the Holocene climatic optimum.

The presented study emphasize that alas and thermokarst lake evolution in the Central Yakutian Yedoma landscapes were not a constantly running process during the Holocene but rather limited to short-term phases of forcing climatic conditions that lead to very active thermokarst processes and rapid but locally variable landscape modification. Nowadays, similar processes are observed in the study region.

Landscapes and thermokarst lake area changes in Yedoma regions under modern climate conditions, Kolyma lowland tundra

Aleksandra Veremeeva[1], Nagezhda Glushkova[2], Frank Günther[3], Ingmar Nitze[3], & Guido Grosse[3]

[1]*Institute of Physical, Chemical and Biological Problems in Soil Science, Russian Academy of Sciences, Pushchino, Russia*
[2]*Institute of Geology and Mineralogy SB RAS, Novosibirsk, Russia*
[3]*Alfred Wegener Institute Helmholtz Centre for Polar and Marine Research, Potsdam, Germany*

Recent landscape changes in the Yedoma region are particularly pronounced in varying thermokarst lake areas reflecting the reaction of the land surface on modern climate changes. However, although thermokarst lake change detection is essential for the quantification of water body expansion and drainage within a region, remote sensing-derived surface reflection trends additionally provide valuable information about the general landscape development. The aim of this research is to reveal the regularities of landscape and thermokarst lakes area changes in the Kolyma lowland tundra in comparison with meteorological data and geological and geomorphological features.

The Kolyma lowland tundra occupies about 44500 km^2 and is located in Northeast Yakutia within the continuous permafrost zone. Mapping of Quaternary deposits using Landsat images shows that Yedoma (Last Pleistocene remnants formed by ice-rich silty to sandy syngenetic deposits with large polygonal ice wedges) occupies only 16 % of the entire region, while the largest part of it is occupied by alas complex (72 %), formed as a result of Yedoma thaw during the Holocene [Veremeeva and Glushkova, 2016].

For the analysis of the landscape and thermokarst lakes area changes of the last 15 years, the entire available Landsat archive from 1999 until 2015 was used for time-series analysis. For this purpose around 800 scenes were processed with an automated workflow, undergoing several necessary processing steps, such as masking, data distribution and calculation of multi-spectral indices. Multi-spectral indices (Landsat Tasseled Cap, NDVI, NDWI, NDMI) were calculated for each unobstructed (cloud-, shadow- and snow-free) observation within the summer months (June to September) between 1999 and 2015. A robust linear trend analysis has been applied to each pixel for the spatial representation of changes of different land surface properties over the observation period. This map shows the magnitude and direction of changes for each multi-spectral index, which are used as proxies for different land-surface properties. For single locations, the entire time-series can be further analyzed in more detail. For the period from 1999 till 2005 air temperatures and precipitation have been analysed for several weather stations that existed in the region. The Landsat time series analysis for the last 15 years shows that the northern part of the region became wetter over the last 5 – 6 years. The alases are particularly affected by the wetting trend. The analysis of the meteo-data shows a trend of increasing air temperature and especially precipitation during the summer from 2010. The wetness increase, particularly on the coastal zone, is supported by the fact that air temperature trends are the largest at near-coastal meteorological stations. This increase of air temperatures and precipitation is likely connected to the reduced sea ice cover [Bekryaev et al., 2010]. The strongest wetness increase were observed in the most northern part of the region within a 50 km wide zone along the East-Siberian sea shore between lowest stream of the Alazeya and Galgavaam rivers. This region is characterised by average terrain heights about 10-20 m, the yedoma and thermokarst lakes area here is about 10-20 %. There are less increase of wetness in the southern and eastern part of the coastal zone between Galgavaam and Bolshaya Chukochya rivers which is characterized by average heights of 0-10 m. The lakes area here is about 40 % and yedoma covers less then 10 % of the territory. Thus the strongest wetness trend for the northern coastal zone can be explained by the high degree of yedoma preservation and its thawing due to the coastal location and higher impact of the increasing temperatures and precipitation.

For the recent past from 1999 to 2015, thermokarst lake changes were analysed visually based on the

time series trend. For most thermokarst lakes of the Kolyma lowland tundra lake area was increasing from 1999 till 2015, however the trend is not significant. Some of the lakes partially or completely drained. Thermokarst lakes area coverage was quantified based on seven Landsat 8 images for the time period 2013–2014. In order to ensure consistency regarding surface moisture, only images acquired from August till September have been used. Atmospheric correction of each image was done for radiometric normalization across the dataset. An increase in ground resolution of the 30m multi-spectral data was achieved through resolution merge with the panchromatic channel to 15m pixel size. Subsequent mosaicking, classification and raster to vector conversion was done for the entire Kolyma lowland tundra. Thermokarst lakes cover about 12.9 % of the Kolyma lowland tundra. For the key investigation area located in the southern tundra around Lake Bolshoy Oler, which covers an area of 2800 km^2 , a comparison with lakes mapped in CORONA images from July 21, 1965 and lakes mapped in the 2014 Landsat mosaic was carried for analysis of changes over time during a period of up to 50 years. The overall thermokarst lake area for this region in 1965 and 2014 was 590 and 549 km^2 respectively. This corresponds to a limnicity decrease of 1.5 % within the study site from 21.1 to 19.6 %. About one third of this lake area decrease is due to partial drainage of big lakes with the area in 1965 and 2014 of 141.8 and 96.3 km^2, respectively. Analysis of the summer air temperature and precipitation trends from the 1965 till 2015 also shown the trend of their increasing. Therefore, despite the fact that many persistent thermokarst lakes in the Kolyma lowland tundra are increasing in area, modern climate conditions generally seem to favor further relief drainage development. Consequently, thermokarst lake drainage outpaces thermokarst lake growth. This heterogeneous pattern suggests that permafrost degradation and aggradation in the region proceed simultaneously close together.

Acknowledgements

This study was supported by the Russian Foundation for Basic Research grant 14-05-31368 and by the ERC grant 338335.

References

Bekryaev, R.V.; Polyakov, I.V. and Alexeev, V.A. [2010]: Role of polar amplification in temperature variations and modern Arctic warming. *Journal of Climate*, 23(14):3888–3906, doi:10.1175/2010JCLI3297.1.

Veremeeva, A.A. and Glushkova, N.V. [2016]: Relief formation in the regions of the Ice Complex deposit occurrence: remote sensing and GIS-studies in the Kolyma lowland tundra. *Kriosfera Zemli (Earth Cryosphere)*, 20(1):14–25, http://www.izdatgeo.ru/pdf/earth_cryo/2016-1/14_eng.pdf.

An isotopic tool to distinguish between Yedoma and topsoil organic carbon sources: compound-specific deuterium analysis

Jorien Elisabeth Vonk[1], Tommaso Tesi[2,3], Lisa Bröder[3], Gustaf Hugelius[4], Peter Kuhry[4], & örjan Gustafsson[3]

[1] *VU University, Faculty of Earth and Life Sciences, Amsterdam, The Netherlands*
[2] *ISMAR Institute of Marine Sciences, Bologna, Italy*
[3] *Stockholm University, Dept of Environmental Science and Analytical Chemistry, Stockholm, Sweden*
[4] *Stockholm University, Dept of Physical Geography and Quaternary Geology, Stockholm, Sweden*

Pleistocene Yedoma permafrost deposits contain roughly a quarter of the organic carbon (OC) stored in permafrost terrain. When permafrost thaws, its OC is remobilized into the environment where it is available for degradation, transport or burial. The fate of this OC is partly determined by the type of thaw processes: (i) abrupt thaw of Yedoma causing collapse and deep exposure, and (ii) gradual thaw of the surface active layer causing release of Holocene topsoil OC. The relative magnitude of each thaw pathway, along with the relative OC release from Yedoma versus topsoil, have earlier been distinguished and quantified through the use of dual carbon isotopes ($\delta^{13}C$ and $\delta^{14}C$) on bulk OC.

We here present compound-specific deuterium (δ^2H) analysis as an additional, more specific, tracing tool to distinguish between Pleistocene Yedoma OC release, primarily released through abrupt thaw, and Holocene topsoil OC release, primarily released through gradual active layer thaw. We analyzed δ^2H values of leaf waxes extracted from both Yedoma permafrost samples (n=9) and modern vegetation/O-horizon (topsoil) samples (n=9) from across northeast coastal Siberia. We analyzed both long-chain n-alkanes (chain lengths C25, C27, C29 and C31) as well as long-chain n-alkanoic acids (C22, C24, C26, C28).

Results show more depleted molecular values for the Yedoma samples (-264±33 and -280±6.5 ‰for average n-alkanes and n-alkanoic acids, respectively) than for the topsoil samples (-227±23 and -234±13 ‰, respectively). The variability in distribution and δ^2H signals for n-alkanoic acids and n-alkanes of topsoils is higher than in the Yedoma samples, that show more constant values, yet the isotopic distinction between the two sources is consistent. For n-alkanes, there is a clear decrease in δ^2H signal with chain length (from -201±32 to -247±23‰ for topsoil, and -221±26 to -297±15 ‰for Yedoma samples). These data suggest that δ^2H analysis on leaf wax lipids in environments receiving OC from permafrost thaw can be used to assess the relative input of Yedoma versus Holocene topsoil material. We will elaborate on the drawbacks and advantages of both isotopic tools ($\delta^{13}C$-$\Delta^{14}C$ on bulk OC vs. δ^2H on leaf waxes) in source-apportionment studies of Yedoma versus Holocene topsoil material.

Reconciling carbon-stock estimates for the Yedoma region

Katey Walter Anthony[1], Guido Grosse[2], Peter Anthony[1], Miriam Jones[3], Sergei Davydov[4], & Sergey A. Zimov[4]

[1] *University of Alaska Fairbanks*
[2] *Alfred Wegener Institute Helmholtz Centre for Polar and Marine Research, Potsdam, Germany*
[3] *United States Geological Survey*
[4] *Pacific Institute of Geography Russian Academy of Sciences*

Permafrost soil organic carbon (C) in the Yedoma region comprises a large fraction of the total circumpolar permafrost C pool, yet estimates based on different approaches during the past decade have led to disagreement in the size and composition of the Yedoma region permafrost C pool. This research aims to reconcile different approaches and show that after accounting for thermokarst and fluvial erosion processes of this interglacial period, the Yedoma region C pool (456 ± 45 Pg C) is the sum of 172 ± 19 Pg Holocene-aged C and 284 ± 40 Pg Pleistocene-aged C.

The size of the present-day Pleistocene-aged yedoma C pool was originally estimated to be 450 Pg based on a mean deposit thickness of 25 m, 1×10^6 km^2 areal extent, 2.6 % total organic C content, 1.65×10^3 kg m^{-3}dry bulk density, and 50 % volumetric ice wedge content [Zimov et al., 2006]. This estimate assumed that 17 % of the Last Glacial Maximum yedoma C stock was lost to greenhouse gas production and emission when 50 % of yedoma thawed beneath lakes during the Holocene. However, the regional scale yedoma C pool estimate of Zimov et al. [2006] did not include any Holocene C and assumed that all of the 450 Pg C was Pleistocene-aged.

In subsequent global permafrost C syntheses, soil organic C content (SOCC, kg C m^{-2}) data from the Northern Circumpolar Soil C Database (NCSCD) and Zimov et al. [2006] were used to estimate the soil organic C pool for the Yedoma region (450 Pg), assuming only Pleistocene-aged yedoma C from 3 to 25 m (407 Pg), and a mixture of C ages in the 0 to 3 m interval (43 Pg).

A more recent synthesis of Yedoma-region C stocks based on extensive sampling by Strauss et al. [2013] took into account lower C bulk density values of yedoma, higher organic C concentrations of yedoma, a larger landscape fraction of thermokarst (70 % of Yedoma region area), the larger C concentration of thermokarst, and remote-sensing based quantification of ice-wedge volumes. This synthesis produced lower mean- and median-based estimates of Yedoma-region C, 348+73 Pg and 211 +160/-153 Pg respectively. However, Strauss et al. [2013] focused on the remaining undisturbed yedoma and refrozen surface thermokarst deposits and thus did not include taberite deposits, which are the re-frozen remains of yedoma previously thawed beneath thermokarst lakes and still present in large quantities on the landscape.

In our study [Walter Anthony et al., 2014], we measured the dry bulk density directly on 89 yedoma and 311 thermokarst-basin samples, including taberites, collected in four yedoma subregions of the North Siberian Kolyma Lowlands. Multiplying the organic matter content of an individual sample by the same sample's measured bulk density yielded an organic C bulk density data set for yedoma samples that was normally distributed. Combining our subregion-specific organic C bulk density results with those of Strauss et al. [2013] for other yedoma subregions extending to the far western extent of Siberian yedoma, we determined a mean organic C bulk density of yedoma for the total Yedoma region (26 ± 1.5 kg C m^{-3}), which is similar to that previously suggested by Strauss et al. [2013] (27 kg C m-3 mean based approach; 16 kg C m^{-3} median based approach). Our estimate of the organic C pool size of undisturbed yedoma permafrost (129 ± 30 Pg Pleistocene C) in the 396,600 ± 39,700 km^2 area that has not been degraded by thermokarst since the Last Glacial Maximum (Tab. 1) is based on this regional-mean C bulk density value. Our calculation also assumes an average yedoma deposit thickness of 25 m and 50 % volumetric massive ice wedge content, as in previous estimates (Zimov et al. [2006], NCSCD; Tab. 1).

Table 1: Calculations of estimated C pool sizes and fluxes in the Yedoma region (a), their distribution on the landscape (b), and the significance of Pleistocene-aged C in taberites (c), based on Walter Anthony et al. [2014]. Cp,Pleistocene C; CH Holocene C.

a

		Area	Cumulative loss to atmosphere		Export to sea	
Land cover class	Fraction	(10^6 km^2)	(kg C_P m^{-2})	(Pg C_P)	(kg C_P m^{-2})	(Pg C_P)
Total yedoma region	100%	1.322 ± 0.132†		100 ± 34‖		45 ± 12**
Undisturbed yedoma	30%	0.397 ± 0.040†				
Thermokarst lakes/ alases	55%	0.727 ± 0.073†	131 ± 45‡	95 ± 34¶		
Thermoerosional gullies	15%	0.198 ± 0.020†	27 ± 9§	5 ± 2#	227 ± 49★	45 ± 12**

	Present-day stocks		Regional carbon pools			
Land cover class	(kg C_P m^{-2})	(kg C_H m^{-2})	(Pg C_P)	(Pg C_{H-lk})	(Pg C_H)	(Pg C_{total})
Total yedoma region			284 ± 40¶¶	159 ± 24¶¶	172 ± 19¶¶	456 ± 45¶¶
Undisturbed yedoma	325 ± 69††		129 ± 30		13 ± 1##	142 ± 30
Thermokarst lakes/ alases	194 ± 30‡‡	172 ± 19‖‖	141 ± 26	125 ± 19	125 ± 19	266 ± 32
Thermoerosional gullies	70 ± 9§§	172 ± 19‖‖	14 ± 2	34 ± 5	34 ± 5	48 ± 6

b

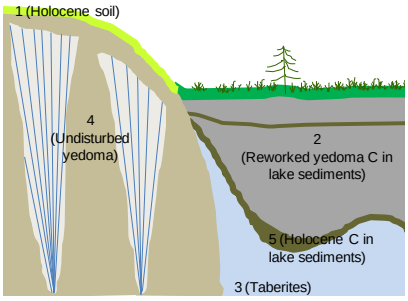

c

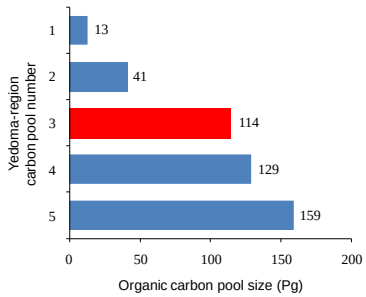

†The error term represents 10% uncertainty (Walter Anthony et al. 2014, SI 1.7.3).

‡131 ± 76 kg C_p m^{-2} [lost to the atmosphere from thermokarst lakes as methane (CH_4) and C dioxide (CO_2)] = 325 ± 69 kg C_p m^{-2} (yedoma C stock, see ††) - 194 ± 30 kg C_p m^{-2} (C_p remaining in lake basins, see ‡‡).

§27 ± 9 kg C_p m^{-2} (lost to the atmosphere from thermoerosional gullies as CH_4 and CO_2) = 325 ± 69 kg C_p m^{-2} (yedoma C stock, ††) - 70 ± 9 kg C_p m^{-2} (C_p remaining in lake basins, §§) - 227 ± 49 kg C_P m^{-2} (C_p exported to sea,); assumes 28 ± 12% of the remaining thawed yedoma organic C decomposed under anaerobic conditions in lacustrine facies F5 and F6, forming CH_4 and CO_2 that escaped to the atmosphere (see Table ED2 and SI 1.4 in Walter Anthony et al. 2014).

‖100 ± 56 Pg C_p (total Pleistocene yedoma C lost to the atmosphere as CH_4 and CO_2) = 95 ± 56 Pg C_p (loss from thermokarst lakes, ¶) + 5 ± 2 Pg C_p (loss from thermoerosional gullies, #)

¶95 ± 56 Pg (C_p lost to the atmosphere as CH_4 and CO_2 from thermokarst lakes) = 131 ± 76 kg C_p m^{-2} (‡) x 727,100 ± 72,700 km^2 (thermokarst lake/alas area, †).

#5 ± 2 (C_p lost to the atmosphere as CH_4 and CO_2 from thermoerosional gullies) = 27 ± 9 kg C_p m^{-2} (§) x 198,300 ± 19,800 km^2 (thermoerosional gully area, †).

227 ± 49 kg C_P m^{-2} (thawed Pleistocene yedoma C exported to the sea, including river deltas and continental shelves) = 0.7 (eroded fraction; SI 1.5) x 325 ± 69 kg C_p m^{-2} (yedoma C stock, ††).

45 ± 12 Pg (C_p exported to sea) = 227 ± 49 kg C_p m^{-2} ( ) x 198,300 ± 19,800 km^2 (thermoerosional gully area, †).

††325 ± 69 kg C_p m^{-2} (original, undisturbed yedoma C stock) = 25.98 ± 1.45 kg C_p m^{-3} x 25 ± 5 m yedoma deposit thickness x 50 ± 3% ice wedges.

‡‡194 ± 30 kg C_P m^{-2} (Pleistocene yedoma-derived C remaining in alases) = 29 ± 16 kg C_P m^{-2} (in facies F3) + 22 ± 4 kg C_P m^{-2} (in facies F5) + 143 ± 25 kg C_p m^{-2} (in facies F6); assumes. Assumes 28 ± 12% of original yedoma organic C decomposed under anaerobic conditions in F5 and F6, and 56 ± 24% under aerobic and anaerobic conditions in F3, forming CH_4 and CO_2 that escaped to the atmosphere (see Table ED2 and SI 1.4 in Walter Anthony et al. 2014). Calculation of the mineral fraction thickness of F3 and F5, based on dry bulk density mixing ratios, is summarized in Eq. 1 and Eq. 2 in Walter Anthony et al. 2014 (SI 1.4). We determined the mean thickness of F6 based on a conservation of mass of yedoma on the landscape, accounting for the difference in dry bulk density between frozen (F7) and thawed yedoma (F6).

§§70 ± 9 kg C_P m^{-2} (Pleistocene yedoma-derived C remaining in thermoerosional gullies) = 22 ± 4 kg C_P m^{-2} (in facies F5) + 48 ± 9 kg C_P m^{-2} (in facies F6). Assumes 28 ± 12% of original yedoma organic C decomposed under anaerobic conditions in F5 and F6, and 56 ± 24% under aerobic and anaerobic conditions in F3, forming CH_4 and CO_2 that escaped to the atmosphere (see Table ED2 and SI 1.4 in Walter Anthony et al. 2014).

‖‖172 ± 19 kg C_H m^{-2} is the area-weighted average (32% tundra, 68% boreal) of Holocene organic C stocks in tundra alases (122 ± 16 kg C m^{-2}, n = 18 sites) and boreal alases (196 ± 27 kg C m^{-2}, n = 10 sites) (Fig. 2e).

¶¶The regional C pools are the sum of the Pleistocene yedoma-derived and/or Holocene C pools in each of the land cover classes (undisturbed yedoma, thermokarst lakes/alases, and thermoerosional gullies). The C pools within each land cover class were calculated as the product of the associated C stocks and cover class areas.

##13 ± 1 kg C_H m^{-2} is the surface soil (0-100 cm) Holocene organic C pool overlying upland yedoma estimated from the distribution of histels, orthels and turbels in the Northern Circumpolar Soil C Database (NCSCD) (SI 3.5 in Walter Anthony et al. 2014). The error term is a minimum estimate, representing the 10% uncertainty in the yedoma region extent (this study, SI 1.7.3 in Walter Anthony et al. 2014).

Similar results found in the recent study of the Yedoma-region C inventory by Strauss et al. [2013] corroborate our estimate of the undisturbed yedoma C inventory. The size of the remaining yedoma C pool was estimated by Strauss et al. [2013] to be 112 Pg (vs. 129 Pg, this study) based on mean parameter values: organic C bulk density 27 kg C cm-3 (vs. 26.2 kg C cm-3 in this study), yedoma deposit thickness 19.4 m (vs. 25 m in this study), yedoma volumetric ice wedge content 48 % (vs. 50% in this study), and thermokarst extent (70% in both studies). The two studies took different approaches for estimating yedoma deposit thicknesses: Strauss et al. [2013] used 22 field sites from Siberia and Alaska with a mean thickness of 19.4 m; our calculations used a thickness value determined from Russian literature (25 ± 5m, references in Walter Anthony et al. [2014]). The mean derived from our limited (n=17) field sites was 38 m in the Kolyma region. The two studies further differ slightly in calculating Yedoma-region area: Strauss et al. [2013], which focused on still frozen deposits vulnerable to future thaw, did not include thawed deposits in present-day lakes, but did include deposits in known smaller yedoma occurrences outside the core Yedoma region such as valleys of NW Canada, Chukotka, and the Taymyr Peninsula. Our study focused on the extent of core-yedoma deposits as well as organic-C stored in present-day yedoma lake deposits. While differences in yedoma thickness and area values can impact upscaling calculations, efforts are underway by the Yedoma region synthesis IPA Action Group (Strauss and colleagues) to analyze more comprehensive data sets and better constrain the values.

Based on our approach that includes a differentiation of thermokarst-lake facies, we estimate that 155 Pg Pleistocene-aged organic C is stored in thermokarst-lake basins and thermoerosional gullies in the Yedoma region of Beringia [155 Pg is the sum of 114 Pg in taberite deposits and 41 Pg in various lacustrine facies]. This 155 Pg Pleistocene-aged C represents the remains of yedoma that thawed and partially decomposed beneath and in thermokarst lakes and streams. Altogether we estimate a total Pleistocene-C pool size of 284 ± 40 Pg for the Beringian Yedoma region in the present day as the sum of Pleistocene C in undisturbed yedoma (129 Pg) and in thermokarst basins (155 Pg, Tab. 1).

Separately, Holocene-aged organic C assimilated and sequestered in deglacial thermokarst basins in the Yedoma-region is 159 ± 24 Pg. Our upscaling is based on the mean C stocks of individual permafrost exposures (Fig. 2e in Walter Anthony et al. [2014]), which were normally distributed. To our knowledge, this is the first study to combine a geomorphologic classification of alas facies with C content, including the deeper lacustrine deposits, for the purpose of systematically upscaling to a regional alas C inventory.

We did not measure the C content of Holocene terrestrial soils overlying undisturbed yedoma permafrost; however, applying values from the NCSCD in Siberia for Histels (44.3 kg C m-2, 9 % of Yedoma region area), Orthels (26.0 kg C m-2, 17% of Yedoma region area) and Turbels (38.4 kg C m-2, 63 % of Yedoma region area) to the extent of 1-m surface deposits overlying the area of undisturbed yedoma permafrost (396,000 ± 39,600 km^2), results in 12.9 ± 1.3 Pg of Holocene C. This calculation assumes that the 70/30 ratio of thermokarst to undisturbed yedoma applies across the Histel, Orthel and Turbel cover classes.

Altogether, we estimate the Holocene and Pleistocene organic C pool size in the Yedoma region of Beringia as 456 ± 45 Pg (38% Holocene, 62 % Pleistocene) (Tab. 1). Despite the differences in approaches and locations of study sites, similarities in the mean-based estimates of the Yedoma-region organic C pool size between Strauss et al. [2013] and this study corroborate our findings. Not accounting for diagenetically altered organic C from yedoma thawed in situ beneath lakes (taberites), Strauss et al. [2013] estimated 348 Pg C for the regional pool size. Without taberite C, our estimate would be similar (342 Pg C). For our study, focusing on the C balance shifts from the Pleistocene to the end of the Holocene, we show that taberite deposits are an important component and need to be included in the budget as these deposits are a large C pool that represents diagenetically-altered organic C from yedoma thawed in situ beneath lakes (Tab. 1b). Our estimate of yedoma-derived taberite deposits underlying thermokarst basins (114 Pg C), would bring the Yedoma-region C pool estimate by Strauss et al. [2013] up to 462 Pg C, which is similar to our estimate of 456 Pg C.

In summary, the Yedoma-region organic C value (456 ± 45 Pg C, consisting of Pleistocene and Holocene C) determined by this study is similar to that calculated originally by Zimov et al. [2006] to represent only the Pleistocene yedoma C pool (450 Pg). Subsequently, the Pleistocene-aged yedoma C was considered to be 450 Pg C. Pleistocene-aged yedoma carbon was considered to be >90% of the regional pool

by the subsequent NCSCD syntheses for quantification of circumpolar permafrost carbon. The primary difference between the Yedoma-region C pool estimate presented here versus Zimov et al. [2006], which entered the NCSCD syntheses, is that in this study net C gains associated with a widespread thermokarst process are taken into account. The component of Pleistocene yedoma C was reduced in this study by 38% and a new Holocene-thermokarst C pool (159 Pg) was introduced. We lowered the Pleistocene-aged yedoma C pool based on larger, more recent data sets on yedoma's dry bulk density by this study and Strauss et al. [2013] and based on our more recent map-based analysis showing a 20% larger areal extent of deep thermokarst activity in the Yedoma region.

The major implications of this study pertain to the nature and fate of greenhouse gas emissions associated with permafrost thaw in the Yedoma region. Differentiation of the C pool in the Yedoma region (yedoma vs. thermokarst basins) is critical to understanding past and future C dynamics and climate feedbacks. Since a larger fraction of the yedoma landscape has already been degraded by thermokarst during the Holocene (70% instead of 50%), the size of the anaerobically-vulnerable yedoma C pool for the production of methane is 40% lower than that previously calculated. Second, there is concern that permafrost thaw will mobilize and release 'ancient' organic C to the atmosphere. Assuming average radiocarbon ages of Pleistocene-yedoma and Holocene deposits of 30 kya and 6.5 kya respectively, accounting for the new Holocene-aged thermokarst C pool (159 Pg C) lowers the average age of the current Yedoma-region C pool by about one third. This result is important to global C-cycle modeling since C isotope signatures provide valuable constraints in models. Finally, given differences in permafrost soil organic matter origins for the Pleistocene-aged steppe-tundra yedoma C pool [accumulated under aerobic conditions; froze within decades to centuries after burial; and remained frozen for tens of thousands of years] and the lacustrine Holocene-aged C pool [accumulated predominately under anaerobic conditions and remained thawed for centuries to millennia prior to freezing after lakes drained], it is likely that organic matter degradability differs substantially between these two pools. This has implications for differences in their vulnerability to decomposition and greenhouse gas production under scenarios of permafrost thaw in the future.

References

Strauss, J.; Schirrmeister, L.; Grosse, G.; Wetterich, S.; Ulrich, M.; Herzschuh, U. and Hubberten, H.-W. [2013]: The deep permafrost carbon pool of the Yedoma region in Siberia and Alaska. *Geophysical Research Letters*, 40(23):6165–6170, doi:10.1002/2013GL058088. 2013GL058088.

Walter Anthony, K.M.; Zimov, S.A.; Grosse, G.; Jones, M.C.; Anthony, P.M.; Chapin III, F.S.; Finlay, J.C.; Mack, M.C.; Davydov, S.; Frenzel, P. and Frolking, S. [2014]: A shift of thermokarst lakes from carbon sources to sinks during the Holocene epoch. *Nature*, 511, doi:10.1038/nature13560.

Zimov, S.A.; Schuur, E.A.G. and Chapin, F.S. [2006]: Permafrost and the Global Carbon Budget. *Science*, 312(5780):1612–1613, doi:10.1126/science.1128908.

Ice Complex chronologies and environments in western Beringia

Sebastian Wetterich[1], Vladimir Tumskoy[2], Natalia Rudaya[3], Andrei A. Andreev[4], Vladimir Kuznetsov[5], Margret C. Fuchs[6], Georg Schwamborn[1], Thomas Opel[1], Hanno Meyer[1], & Lutz Schirrmeister[1]

[1] *Alfred Wegener Institute Helmholtz Centre for Polar and Marine Research, Potsdam, Germany*
[2] *Moscow State University, Faculty of Geology, Moscow Russia*
[3] *Institute of Archaeology and Ethnography, SB RAS, Novosibirsk, Russia*
[4] *University of Cologne, Institute for Geology and Mineralogy, Germany*
[5] *St. Petersburg State University, Institute of Earth Sciences, Köppen Laboratory, Russia*
[6] *Helmholtz Centre Dresden-Rossendorf, Helmholtz-Institute Freiberg for Resource Technology, Freiberg, Germany*

Polygon tundra with tundra-steppe vegetation cover and growing syngenetic ice-wedge nets evolved during stadial and interstadial periods of the late Quaternary in non-glaciated Beringia. Remnants of such environments are called Ice Complex (IC; ледовый комплекс in Russian) in local and regional stratigraphic charts. The IC deposits preserve information of past periglacial landscape and climate conditions during the mid- and late Pleistocene. In western Beringia, IC of different ages and extent are studied in detail at certain locations. When using IC as archives of palaeo-environmental dynamics, changes of summer and winter conditions at millennial time scales are detectable. Commonly applied summer proxies are pollen, plant macrofossils, insect fossils and, most prominent, fossils of the Mammoth fauna. Geochemical and stable isotope properties of ground ice allow for insights into freezing (segregation ice) and winter conditions (ice wedges), while sediment properties reflect depositional processes.

IC chronologies remain challenging, because the formation and preservation of such ice-rich permafrost deposits vary with the local palaeo-relief (and related water availability for ice wedge growth) and with the intensity of thermokarst (and respective erosion). Both, palaeo-relief and erosion complicate the geochronological interpretation. The spatial variability in formation due to palaeo-relief cause consecutive late Quaternary deposits found at laterally different positions, and temporal shifts from permafrost aggradation to degradation result in gaps in studied permafrost sequences. Apart from those challenges for stratigraphic inferences, numerical dating may provide an absolute age control, but available approaches address different components of the IC. This includes radiocarbon (^{14}C) dating of organic material in sediments and ice wedges, infrared- and optically-stimulated luminescence (IRSL, OSL) dating on feldspar and quartz grains, radioisotope disequilibria of thorium-230 to uranium-234 (^{230}Th/U) dating of peat, and chlorine-36 to chloride ratios (^{36}Cl/Cl) of ground ice, in particular ice wedges. The combined application of various geochronological methods for the different substrate components (organic, mineral, ice) and different geochemical and physical properties allows unravelling the age intervals of certain IC deposits.

On the southern coast of Bol'shoy Lyakhovsky (New Siberian Archipelago) at least four distinct IC strata were recognised and dated (Tab. 1). Our paper discusses the current understanding of IC chronologies across the MIS7a (Yukagir IC), the MIS5 (Buchchagy IC), the MIS3 Yedoma (Molotkov IC) and the MIS2 Yedoma (Sartan IC). Geocryological and palaeo-environmental proxy data allow inferring the past periglacial landscape and depositional history and highlight distinct signals of past climate and ecological conditions in western Beringia.

Table 1 Ice Complex strata recognised at the southern coast of Bol'shoy Lyakhovsky Island

Local strata		Dating	Age [kyr BP]	Reference
Yedoma (Sartan) IC	MIS2	^{14}C	29 to 22	Wetterich et al. [2011]
Yedoma (Molotkov) IC	MIS2	^{14}C	>49 to 29	Wetterich et al. [2014]
Buchchagy IC	MIS5	^{230}Th/U	126 +16/-13 (117 +19/-14) to 98 ±5 (89 ±5)	Wetterich et al. [2015]
Yukagir IC	MIS7a	^{230}Th/U	200.9 ±3.4	Schirrmeister et al. [2002]

References

Schirrmeister, L; Oezen, D. and Geyh, M.A. [2002]: 230Th/U Dating of Frozen Peat, Bol'shoy Lyakhovsky Island (Northern Siberia). *Quaternary Research*, 57(2):253–258, doi:10.1006/qres.2001.2306.

Wetterich, S.; Rudaya, N.; Tumskoy, V.; Andreev, A.A.; Opel, T.; Schirrmeister, L. and Meyer, H. [2011]: Last Glacial Maximum records in permafrost of the East Siberian Arctic. *Quaternary Science Reviews*, 30(21–22):3139–3151, doi:10.1016/j.quascirev.2011.07.020.

Wetterich, S.; Tumskoy, V.; Rudaya, N.; Kuznetsov, V.; Maksimov, F.; Opel, T.; Meyer, H.; Andreev, A.A. and Schirrmeister, L. [2015]: Ice Complex permafrost of {MIS5} age in the Dmitry Laptev Strait coastal region (East Siberian Arctic). *Quaternary Science Reviews*, doi:http://dx.doi.org/10.1016/j.quascirev.2015.11.016.

Wetterich, Sebastian; Tumskoy, Vladimir; Rudaya, Natalia; Andreev, Andrei A.; Opel, Thomas; Meyer, Hanno; Schirrmeister, Lutz and Hüls, Matthias. Ice Complex formation in arctic East Siberia during the MIS3 Interstadial. *Quaternary Science Reviews*, 84:39–55, doi:10.1016/j.quascirev.2013.11.009.

SESSION 14

Permafrost Hydrology and Groundwater Systems

Convener:

Irina Fedorova, *Arctic and Antarctic Research Institute, St. Petersburg State University, Russia*

Huijun Jin, *State Key Lab. of Frozen Soils Eng. (SKLFSE), CAREERI, Chinese Academy of Sciences (CAS), China*

Lyudmila Lebedeva, *Melnikov Permafrost Institute, Russia*

Hydrological processes in permafrost-affected landscapes are highly variable, diverse and subject to rapid transformation under surface disturbance and/or changing climate conditions. The coupled water and heat fluxes control runoff generation, availability and connectivity of surface- and subsurface water storages as well as biogeochemical processes such as carbon and nitrogen regimes in aquatic and terrestrial environments. Including past, current and future states of the hydrological system, abstracts may include, but not be limited to, active layer and land-atmosphere hydrology, runoff from permafrost-affected basins, supra- and subpermafrost groundwater hydrology, and aquatic or subsurface hydrochemical, hydrobiological and biogeochemical processes as constrained by the water cycle and permafrost status. Results of field- and laboratory studies, modelling analyses, applications of remote sensing techniques and other research methods at the fine to pan-Arctic scales are invited to celebrate our current understanding as well as identified challenges in the science of permafrost hydrology.

Seasonal variability of groundwater discharge in a permafrost watershed, Ogilvie River, Yukon, Canada

Natalia Baranova & Ian Douglas Clark

University of Ottawa, Canada

Recent changes in the hydrological regime of the permafrost watersheds have been observed and variable trends identified include increasing or decreasing overall stream discharge, earlier timing of the spring freshet and in some cases increase in groundwater baseflow [Bawden et al., 2015, Walvoord and Striegl, 2007]. Study of these changing trends in the Arctic is difficult due to limited research on small and mid-sized watersheds necessary to form a baseline, limited hydrometric and meteorological data, and limited understanding of groundwater systems behaviour in the northern regions. The application of geochemical and isotopic tracers to the catchment hydrology has been applied to the southern watersheds and is also an important tool for the permafrost watersheds.

This study focuses on a mid-sized watershed of upper Ogilvie River in central Yukon (4,500 km^2) with the objective to correlate groundwater recharge and discharge with geological, cryological and meteorological controls, to understand the contribution of groundwater to discharge, and to examine potential groundwater recharge pathways. The annual hydrograph is analyzed by characterizing the flow components using geochemical tracers (anions, cations, dissolved organic and inorganic carbon), stable isotopes (δ^2H, $\delta^{18}O$, and $\delta^{13}C$) and radioactive isotopes (^{14}C and 3H) and then by further using mixing model approach to identify the composition of the watershed discharge. The field work was conducted over two seasons in 2014 and 2015. Samples of Ogilvie River water, surface runoff, rain precipitation, snowpack, groundwater and active layer water were collected in order to distinguish the geochemical and isotopic signatures of the hydrological system constituents. The two year record, focused on the spring freshet, allows for analysis of intra- and some inter-annual variations of the stream composition. Ogilvie River was successfully instrumented with water level logger prior to the 2015 snow melt which allows for quantification of the stream discharge using a historical rating curve. Stream flow data enables the analysis of the catchment exports in terms of flux.

Preliminary data shows that there are two groundwater components: shallow and deep and that both are recharged by an approximately equal mix of snow melt and rain. Both groundwaters undergo carbonate weathering under closed or partially closed conditions along their flow paths. The understanding of the groundwater contribution to the stream discharge can be used to estimate groundwater storage in the river basin and to evaluate the effect of potential changes of the hydrological regime on the river exports of carbon.

References

Bawden, A.J.; Burn, D. and Prowse, T.D. [2015]: Recent changes in patterns of western Canadian river flow and association with climatic drivers. *Hydrology Research*, 46(4):551–565.

Walvoord, M.A. and Striegl, R.G. [2007]: Increased groundwater to stream discharge from permafrost thawing in the Yukon River basin: Potential impacts on lateral export of carbon and nitrogen. *Geophysical Research Letters*, 34(12): doi:10.1029/2007GL030216. L12402.

Assessing agricultural vulnerability in a snow- glacier-fed watershed in central Chile

Antonio Bellisario , Jason Janke, & Sam Ng

MSU Denver, United States of America

Central Chile (32°-35°S) is the most important agricultural region for the country's food security. The region also holds the majority of the country's population and a large percentage of its economic activity; both are highly dependent on water supplied by snow- and permafrost-fed rivers originating in the high altitude of the Andes cordillera. This study assesses agricultural vulnerability under conditions of water deficit driven by drought and higher demand for water in the Aconcagua River Basin (32°S). The effects of decreasing precipitation, the associated reduction in streamflow, rising water demand, agricultural expansion, and land use and irrigation patterns are studied to assess the agricultural vulnerability of the Aconcagua River Basin. The water evaluation and planning (WEAP) model is used for this purpose. A critical assessment of government water planning and ongoing policies for the basin's water management is offered. A set of policies to increase water resilience and water management in the basin is also proposed. The Aconcagua River Basin concentrates most of the area of the Region of Valparaíso. It is located about 80 kms north of Santiago. It is an economically important basin due to the dynamism of its agricultural and mining sectors. The Aconcagua River flows westward for 190 kms to the Pacific Ocean from its headwaters in the high Andes cordillera at 5400-7000 m.a.s.l. Despite the relative aridity of the climate and its mountainous terrain, the Aconcagua basin holds ≈135,000 ha of first class agricultural land, of which about 50 % are irrigated. Due to its Mediterranean climate (marked by extremely low precipitation during the summers) the basin's agriculture depends almost exclusively on surface water for irrigation. Discharge during the growing agricultural season (October-April) in the Aconcagua River Basin is driven by snowmelt during spring months (which peaks in October-November) and glacier melt during the mid- to late-summer months (February-March). A glaciated area of 144 km^2 in the upper catchment of the Aconcagua contributes to about 50-90% of discharge in extreme dry years (La Ñina). The agricultural dependence on meltwater from the upper catchment becomes more significant in the Aconcagua, due to the absence of major reservoirs. Since 2010, central Chile has experienced a prolonged multi-year drought with abnormally low rainfall. The rise of the snowline and the current drought has caused less snow accumulation in the upper catchments. The amount of precipitation in the upper catchment is the most important factor controlling the variability of streamflow for snow- ice-fed watersheds in the central Andes. Average annual streamflow in the middle basin of the Aconcagua averages only 33 m3/s (1980-2010 average). During the current drought (2010-2015), streamflow has decreased by an average of 40% in the basin. This has caused extreme water scarcity in the water balance of the Aconcagua, where surface water availability is the main source for the population and economic activities. Moreover, in the last 15 years the irrigated land in the Aconcagua Basin has increased by 15 % and, from this total, the land surface planted with fruit trees has increased by 39 %– by crop reconversion or by expanding to marginal land on the slopes of the valley's hills. Fruit trees planted on higher slopes not only demand more water than traditional crops such as vegetables, but because of an increase in evapotranspiration with elevation, they have been found to require three times more water than the same crop planted at the bottom of the valley. The basin has experienced water stress due to the simultaneous rising demand and decreasing water availability. A deficient irrigation infrastructure and an inefficient management of the resource worsen the situation and has left the basin unable to meet the hydric needs of the population and those of economic activities. This study is important because climate change scenarios for central Chile predict increasing temperatures and decreasing precipitations. The study of the current multi-year drought could be used as the "canary in the mine shaft" to plan for the effects of climate change on water resources in the Aconcagua Basin and in central Chile in general. Glacier melt from permafrost landforms will be more

important as a contribution to surface runoff in a warmer and drier future climate on the watersheds of the central Andes. A reduction of the snowpack and an earlier spring melt might reduce water availability. Reduced streamflow will impose a substantive challenge to meet water needs. A new tool kit of policies needs to be implemented to improve the region's water resilience.

Towards an understanding of the impact of permafrost degradation on the hydrogeology of the Source Area of the Yellow River, Qinghai-Tibet Plateau, China

Victor Franciscus Bense[1,2], Huijun Jin[2], & Dongliang Luo[2]

[1] *Hydrology and Quantitative Management Group, Wageningen University and Research, Netherlands*
[2] *Cold & Arid Regions Environmental & Engineering Research Institute, Chinese Academy of Sciences, Lanzhou , China*

The groundwater flow conditions in the Source Area of the Yellow RIver (SAYR) are poorly known or understood. However, it is clear that the SAYR does contain substantial amounts of fresh groundwater hosted by extensive sedimentary aquifer systems present in deeply incised glacial valleys. A rudimentary water budget calculation for the SAYR suggests that groundwater recharge across the SAYR is probably very limited considering the low annual precipitation (300-400 mm/a) and high potential evaporation (1200-1500 mm/a). This would suggest that very little groundwater recharge takes place. Nevertheless, extensive wetland and lake systems occur across the area. Regional hydrogeological models on the other hand suggest that the SAYR can be regarded as an area of regional groundwater discharge, where regional down-welling of groundwater and up-welling are facilitated by faults acting as conduits for the regional transport of deep groundwater. This would imply the source of water in the SAYR is mainly from outside the hydrographic catchment area, and the aquifers are recharged from below. In this particular model, the presence of permafrost near the surface in the SAYR would hamper the discharge of groundwater, rather than preventing recharge.

If a forecast needs to be made of how the hydrogeological regime of the SAYR would change when the permafrost in the area degrades further and eventually disappears, it will be critical to understand to what extent either or a combination of these conceptual models applies to the SAYR.

Carbon outflow from the active layer of thermokarst lake catchments in the Lena River delta

Olga Bobrova[1], Irina Fedorova[2,1], Antonina Chetverova[1,2], Anne Morgenstern[3], & Antje Eulenburg[3]

[1] *Saint-Petersburg State University, Russian Federation*
[2] *Arctic and Antarctic Research Institute, Russian Federation*
[3] *Alfred Wegener Institute Helmholtz Centre for Polar and Marine Research, Potsdam, Germany*

Nowadays due to climate change the interest to the hydrological processes in the permafrost affected regions is growing. Permafrost soil is important carbon pool and thawing can cause the increase of carbon outflow from Arctic river basins.

During Russian-German expeditions Lena-2012 and 2013 some measurements were carried out on the catchment of the Fish Lake on Samoylovsky Island in the Lena River delta. Fish Lake is a thermokarst-polygonal lake, and the landscape of its catchment is typical for the Arctic polygonal tundra. These measurements were done in order to study the DOC income to the lake from an active layer of the catchment.

Measurements of the DOC concentration in the pore water and the depth of seasonal thawing were made at 21 points in the 1,52 sq km catchment. The points were selected in different parts of the polygons to consider the heterogeneity of the landscape. Samples for DOC were analyzed in the field using a Spectro::lyser probe and in the lab with a Shimadzu TOC-L probe.

In August the depth of the active layer was between 20 and 60 cm: 20-30 cm on the polygon rims, 30-60 cm in the polygon centers and near the lake. During the month when the measurements were made the depth increased by 10-15

For August the DOC concentration in the pore water of the active layer was 8-51 mg/l, for July – 5-30 mg/l, which correlates with the results of other researches in Arctic region. The changes in DOC concentration in pore water for the different thaw depth were examined. Maximum was observed on the depth 35-40 cm for July and 45-55 cm for August. So, for the same depth the variance in the concentration was the most significant.

The DOC flux to the Fish Lake was calculated using the mean measured concentration and water runoff from the catchment (Ogorodnikova, 2011). The DOC daily flux to the lake is evaluated as about 0,8 kg per day and the flow rate is 0,5 kg/ km^2*day, which is in ten time less than for the lake catchment of southern areas (Moore, 2003).

Prolongation of field measurements is necessary for reasons clarifying and for better understanding of DOC flux formation processes under different conditions including thawing increase.

Quantification of a full year water balance of a thermokarst lake in East Siberia based on field measurements

Niko Bornemann[1], Sascha Niemann[1,2], Samuel Stettner[1], Anne Morgenstern[1], Moritz Langer[1], & Julia Boike[1]

[1] *Alfred Wegener Institute Helmholtz Centre for Polar and Marine Research, Potsdam, Germany*
[2] *University of Potsdam, Germany*

Thermokarst lakes and basins are major components of the ice-rich permafrost landscapes in East Siberian coastal regions. One of the major control factors of thermokarst lake development is the local water balance. Variations in environmental and climate conditions due to climate change might have severe impacts on the water balance. Higher evapotranspiration and an increased active layer thickness could enhance the water flow and thus favor the thermal degradation of the tundra landscape.

In this study we quantified precipitation, evapotranspiration, runoff and storage of a thermokarst lake on Kurungnakh island. The island is located in the central part of the Lena River delta, northern Siberia and underlain by continuous, ice-rich permafrost to about 400-600m depth. The investigated lake has a surface area of approximately 1.2 km^2 with a maximum depth of about 8 m and a volume of about 4x106 m3. Field measurements of the water balance components were conducted in the period from August 2014 to end of July 2015. Precipitation was recorded by an automatic rain gauge, at a nearby site on Kurungnakh Island. The outflow of the lake was determined with an automatic sensor on a RBC-flume. The evaporation of the thermokarst lake was calculated by using water temperature of the lake, climate data from weather stations on Kurungnakh Island and the neighboring Samoylov Island. The lake water storage was measured using an automated water level sensor.

A previous study (Niemann, 2014) investigated only the summer balance (August 2013) of the lake and showed that evaporation dominated the water balance during this time period. Here we analyzed the seasonal and annual water balance components (precipitation, evaporation, runoff, change in storage) of the lake and the contribution of snow cover to the water storage.

Simulation and prediction of suprapermafrost groundwater level variation using Neural Networks model in permafrost response to climate change

Juan Chang[1] & Genxu Wang[2]

[1] *Lanzhou University*
[2] *Institute of Mountain Hazards and Environment, CAS, People's Republic of China*

The suprapermafrost groundwater has an important role in the hydrologic cycles. However, due to the harsh environment, the meager availability of field monitoring data of groundwater systems greatly limits the understanding of permafrost groundwater dynamics, and effective mathematical methods and theory for modeling and forecasting of the variations in permafrost groundwater dynamics. Two Artificial Neural Network (ANN) models are developed to simulate and predict the site-specific suprapermafrost groundwater table at slope scale. One of them has three input variables (antecedent groundwater level, air temperature and precipitation) and second one has two input variables – air temperature and precipitation only. The objectives of this research are:

1. to construct the suprapermafrost groundwater table model by using ANN framework and examine the validity of the models, and;

2. to investigate the impacts of variations in air temperature and precipitation on suprapermafrost groundwater dynamics and its spatial differentiations on the hill-slopes.

The results indicate that the ANN model with three input variables has better real-time, site-specific prediction capability, and produces good performance in simulating and forecasting of the variations in the suprapermafrost groundwater table in the study area in the Zuomaoxikong Qü (River) Watershed of the Fenghuo Mountains on the Qinghai-Tibet Plateau. However, if field observations of the suprapermafrost groundwater table are not available, the ANN model developed using only two input variables also has reasonable accuracy and high validity in simulating and forecasting the suprapermafrost groundwater table. Under the air temperature increase scenario of 0.5-1.0 °C per decade, the suprapermafrost groundwater table is predicted to rise by 1.2-1.4 %, and by 2.5 %-2.6 % per year with the precipitation increase scenario of 10-20 %, respectively. There were spatial variations in the responses of the suprapermafrost groundwater table to climate change at a slope scale. When the air temperature is increased by 0.5℃, the forecasted suprapermafrost groundwater table rose by an average of 1.15 cm (1.24%) at the down slope site and 0.88 cm (1.06%) at the upper slope site, and the air temperature increased by 1.0 °C, the forecasted suprapermafrost groundwater table rose by an average of 2.24 cm at the down slope site and 1.62 cm at the upper slope site, respectively. The amount and amplitude of changes in the suprapermafrost groundwater table at the lower slopes are larger than those at the upper slopes under a warming climate. Therefore, vulnerability and spatial variability of the suprapermafrost groundwater to climate change will impose pronounced effects on water cycles and alpine ecosystems in permafrost regions as evidenced by the Fenghuoshan area in the Interior of the Qinghai-Tibet Plateau.

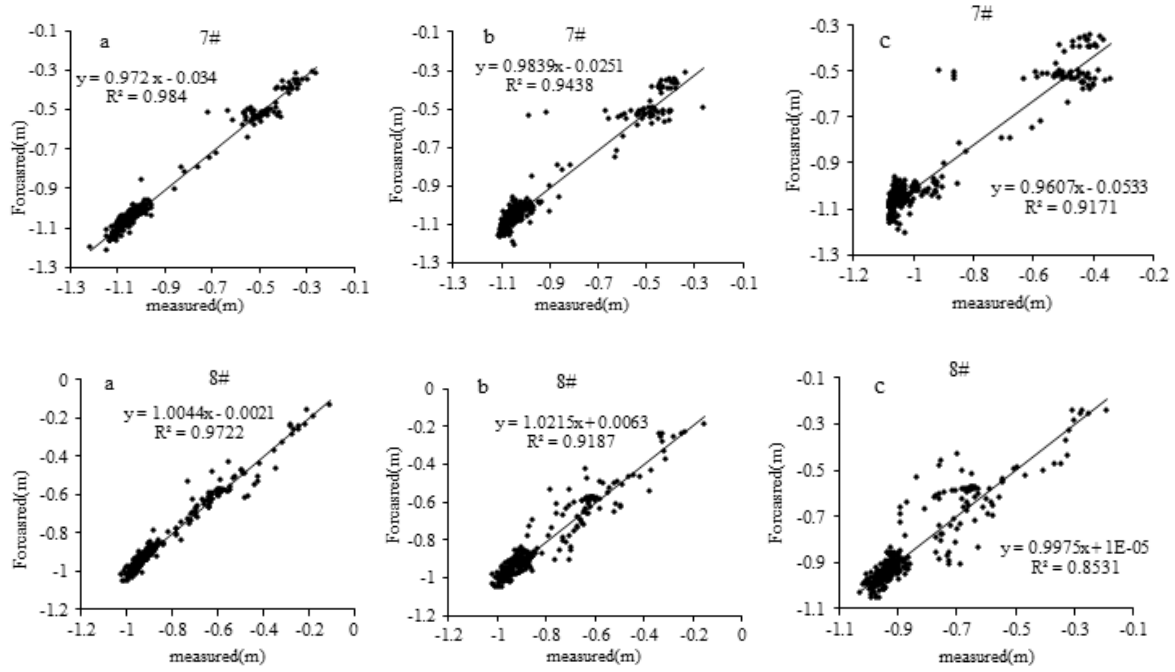

Figure 1: Comparison of the suprapermafrost groundwater values measured and1-days, 3-days and 5-days (corresponding to a, b, and c, respectively) ahead forecasted by the ANN model

Appendix

ANN (Artificial Neural Network) is a large parallelly distributed information processing system that has certain performance characteristics resembling biological neural networks of the human brain (Haykin, 1999). A neural network is characterized by its architecture that represents the pattern of connection between nodes, its method of determining the connection weights and the activation function. Unlike physically based numerical models, ANNs do not require explicit characterization and quantification of physical properties and conditions of the system under investigation. ANNs learn the system's behavior from representative data. The ability to learn and generalize from sufficient data pairs makes it possible for ANNs to solve large-scale complex problems (ASCE 2000a; Haykin, 1999). The most commonly used neural network structure is the feed-forward hierarchical architecture. A typical three-layered feed-forward neural network is comprised of a multiple elements also called nodes, and connection pathways that link them (Haykin, 1999). A neuron receives an input signal, processes it, and transmits an output signal to other interconnected neurons. The output of a node in a layer is only dependent on the input it receives from previous layers and corresponding weights. Figure 1 shows the feed-forward network for the current study having one hidden layer with several nodes in input and output layer. Information passes from the input to the output side. The nodes in one layer are connected to those in the next, but not to those in the same layer.

Assessing groundwater dynamics in a discontinuous permafrost environment using hydrogeochemical tracers

Marion Cochand[1,2], John Molson[1,2], Jean-Michel Lemieux[1,2], Johannes A.C Barth[3], Robert van Geldern[3], Richard Fortier[1,2], & René Therrien[1,2]

[1] *Centre d'étude nordique, Université Laval, Canada*
[2] *Département de géologie et génie géologique, Université Laval, Canada*
[3] *Friedrich-Alexander-Universität, Erlangen-Nürnberg, Germany*

In the current context of global warming, the influence of permafrost degradation on groundwater resources is still largely unknown, although it is expected that increased groundwater recharge and changing flow dynamics will lead to improved groundwater availability. Increased groundwater monitoring in permafrost regions is therefore needed to assess these changes, including the rate at which they will occur.

A detailed field study on groundwater dynamics in a discontinuous permafrost environment is being conducted in a small 2- km^2 watershed close to the Inuit village of Umiujaq (northern Québec, Canada) on the eastern shore of Hudson Bay. The study relies on a groundwater monitoring network belonging to the Québec Ministry of Environment, which was designed to assess the impacts of climate change on groundwater. The main aim of this study is to evaluate the potential of groundwater as a drinking water resource for the local communities. Groundwater origin and evolution, as well as flow dynamics and residence times within the watershed are being investigated using hydrogeochemical tracers such as major ions, stable water isotopes ($\delta^{18}OH_2O$ and $\delta 2HH_2O$), carbon phases (DIC, DOC, POC) and their stable carbon isotopes ($\delta^{13}C$), and dating tools (radiocarbon and tritium-helium methods).

The catchment is located in the Tasiapik valley, which is mainly filled with glacial-fluvial and Quaternary marine sediments. The area became de-glaciated about 7500 years ago, and permafrost mounds have formed within marine silts. The valley has two aquifers: an unconfined shallow sandy aquifer located in the upper part of the valley, and a deeper confined aquifer in sands & gravels located below the permafrost mounds.

Nine monitoring wells are being used to monitor groundwater levels and temperatures in both aquifers within a longitudinal transect along the valley. Moreover, 15 piezometers have been installed in the unconfined aquifer, 11 of which are being used to study groundwater flow at the metre-scale around a permafrost mound. Four field campaigns have been conducted in the summers of 2013, 2014 and 2015, and in November 2014, to sample precipitation, thermokarst lakes and stream waters, as well as permafrost ice lenses and groundwater in both aquifers.

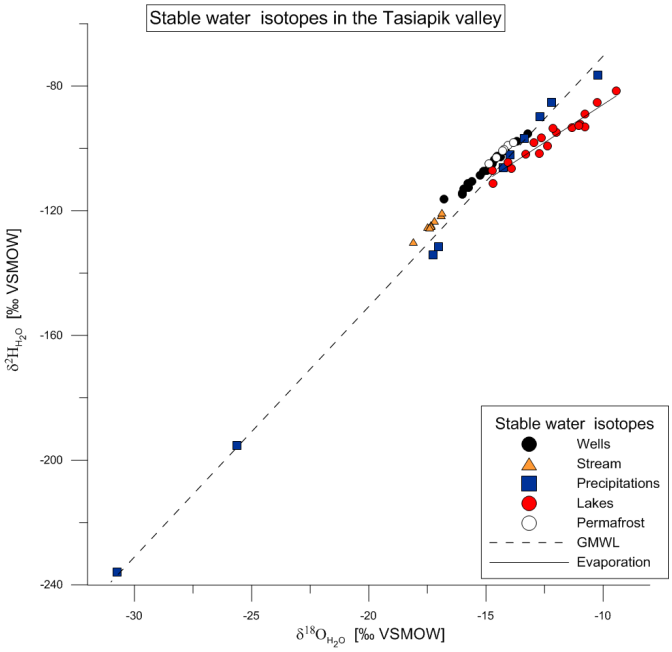

Figure 1: Water isotopes from a variety of water sources in the Tasiapik Valley, Umiujaq, Quebec, Canada.

Groundwater types mainly fall into the Ca-HCO3 field. Sample mineralisation (total dissolved solids) is close to the composition of rain and snow, and is likely linked to limited bedrock weathering caused by low levels of dissolved CO_2 in groundwater. These are in turn due to suppressed biological activity in the catchment. Stream-water samples at the watershed outlet had similar hydrochemical composition when compared to groundwaters. Preliminary δ18OH2O

and $\delta 2HH_2O$ results suggest that ice lenses within the top four meters of permafrost are under the influence of modern water as the isotopic signature here is similar to the groundwater signature (Fig. 1). Moreover, stream water sampled in July appears to be influenced by a snowmelt signature whereas water isotope ratios from thermokarst lakes show an influence of evaporation.

Combined with further hydrogeochemical data analyses and numerical modelling, these results will help provide insight into the groundwater flow dynamics and thermal regime in this watershed of degrading discontinuous permafrost. This will enable assessment of groundwater availability, including for use as a drinking water resource in northern communities.

Changing runoff pathways due to permafrost thaw in discontinuous permafrost terrains

Ryan Frederick Connon & William L. Quinton

Wilfird Laurier University, Canada

In the wetland-dominated basins that characterise the southern margin of permafrost, permafrost thaw and disappearance and resulting land-cover change, is occurring at an unprecedented rate. Permafrost thaw has the potential to fundamentally alter the processes giving rise to streamflow in this region by altering the physical structure, type and relative proportions of biophysical terrains. Field studies were conducted at the Scotty Creek Research Basin, a 152 km^2 watershed, located about 50 km south of Fort Simpson, Northwest Territories, Canada. Scotty Creek is typical of other basins in the region and is underlain by discontinuous permafrost. There are three major land-cover types in the basin, each exhibiting a distinct hydrological function. Channel fens convey water to the basin outlet, flat bogs can either store water or transmit water to the fen via ephemeral channels, and permafrost plateaus are runoff generators. As permafrost in this region thaws, the wetlands (i.e. fens and bogs) grow at the expense of the plateaus and are increasing both hydrological connectivity and runoff contributing area. At the study site, the annual ground heat flux (QG) is positive, indicating a net loss of permafrost and allowing for the development of taliks. The formation of a talik serves two purposes: 1) it allows for the year-round lateral transmission of water and energy between wetlands on either side of a plateau; and 2) it creates unstable thermal conditions for the underlying permafrost, as the temperature of the talik is always above 0 °C. Extensive frost table mapping was conducted in 2011 and 2015 to determine the depth to the frost table and the date when the active layer thawed through to a talik. 10 transects were completed across peat plateau-wetland interfaces to map both lateral and vertical changes in permafrost extent. Meteorological stations were installed in both wetland and plateau environments to determine differences in total energy input between the years. It was found that lateral thaw was most prevalent along the interface of peat plateaus and channel fens, where energy is advected due to flowing water. The depth of the permafrost table below the ground surface increased from 66.5 cm in 2011 to 86.2 cm in 2015 (n: 153). In 2015, frost was no longer detectable (using a 2m probe) at 18 points and a new talik had developed at 9 points. We hypothesize that increased ground thaw resulting in the formation of taliks is increasing the subsurface hydrologic connectivity between wetlands. The increased presence of taliks provides new routes for the transmission of moisture from bogs to fens; this moisture would have been previously unavailable to the fen network and retained as storage in the bog. This study will work towards incorporating the lateral transmission of subsurface water through taliks in conceptual and numerical models to create an improved understanding of the storage and flux of water in this region.

Laboratory simulation of river talik

Francois Costard[1], Nicolas Roux[1,2], & Christophe Grenier[2]

[1] *UMR 8148 GEOPS, CNRS-Université Paris Sud, Orsay, France*
[2] *UMR 8212 LSCE, CNRS-CEA-UVSQ, Gif-sur-Yvette, France*

Here, we address questions concerning the influence of meltwater on permafrost in Central Yakutia (eastern Siberia) using laboratory simulation. For most streams and rivers, annually, the flows of water during the spring and summer seasons interact with permafrost resulting in the formation of an unfrozen zone (talik). The preferential surface water run-off and accumulation of water in spring induce thawing line propagation and a thermal-erosion which promotes the subsidence of the ground, forming ponds at the junctions of polygons. The thermal erosion of permafrost by surface water runoff can initiate an unfrozen layer underneath the river, leading to the rapid development of an underground drainage system during the spring and summer season. The objective of this study is to understand the dynamics of river's talik within a continuous permafrost zone. More precisely, we propose to analyze the impact of flood on the degradation of a permafrost area – in Yakutia - by means of hydro-climatic data and modeling (physical and numerical).

During ice breakup, most rivers involve a thawing line propagation within the permafrost with formation of a talik (temperature > 0 °C). Interactions between hydrodynamics (break up period), fluvial processes (water temperature, discharge ...), specific periglacial processes (thermal erosion on the banks) and permafrost evolution is proposed.

Talik remains undocumented and anyway publications are restricted to specific areas of Yakutia and Alaska (Afanasenko, 1973; Ling and Zhang, 2003; Walker, 1983). Detailed observations and measurements about taliks in Central Siberia (Yakutia) remain sparse. Only a few studies report on the formation and evolution of taliks in Siberia (Anisimova and Pavlova, 2008; Milanovskiy et al., 2008). In particular, there is a general lack of data and detailed records about the impact of taliks for most small Siberian rivers. One of the main reasons is the difficulty in obtaining observations and measurements in such area. Just a few detailed observations of talik interactions with rivers exist (Shcheglov and Dmitriyev, 1973; Rivkin, 1998, Zayzev and Tshalov, 1989; Efimov, 1964) and many questions remain open like the exact characteristics of the taliks and the inter-annual variability of the talik.

To further test the formation of a talik along the river, we performed a more detailed analysis of the main parameters affecting the talik formation or degradation by means of a laboratory experiment. Here, we propose to test our theoretical talik model (see Grenier et al. this volume on page 659) with an experimental hydraulic channel flume of 2.5 m long and 50 cm width within our cold room facility at GEOPS-Orsay.

Several experiments of river talik evolution were performed in a cold room where a hydraulic flume full of frozen saturated porous material is overflown by a temperature and discharge-controlled stream. The schematic description of the experimental setup for the talik experience is illustrated in Figure 1. The permafrost is prepared inside the channel and frozen with a cooling coil at the bottom of the channel. To obtain these conditions, the upstream comes from a water thermostated tank. A pump insures the recycling of the water. The water flows over the permafrost with formation of a thermal gradient within the permafrost evolving with time. We used different Re regimes and the channel geometry has been calculated to be enough to produce various regime (from laminar to turbulent). Temperature measurements are registered with regularly spaced calibrated thermocouples at various depths. A data acquisition system allows the information acquisition and the control of the experiment. The hydraulic channel is located in the freezer hall facility in view to conduct the experiment under controlled conditions (mean air temperature: about +5 °C). Several experiments were performed for a wide range of Re, permafrost temperature (from -1 °C to -15 °C), water temperature (from 0,5 °C to 15 °C) and ice content (from 10 % to 80 %). Experiments run with various soils (fine sand, silt) analog to those in Yakutia (Siberia).

The purpose of the experimental study is to meas-

ure the propagation of the thawing line within the permafrost and the talik formation. The flow rates and water temperatures as well as initial permafrost temperature are varied to study the controlling parameters of the system. A hierarchy of parameters (Reynolds number, water and ground ice temperatures) is proposed to explain the formation of talik under periglacial rivers.

First results show the importance of water temperature and water flow velocities on the formation of a river talik [Roux et al., 2015]. Experimental results show that the sensitivity of the thawing front propagation with water temperature variations was much higher than with water velocity. These results are coherent with some previous experimental approach of heat exchange between water and permafrost (Randriamazaoro et al., 2007; Dupeyrat et al., 2011) that did an ablation study for the erosion of frozen blocks.

Our modeling can be viewed as a first stage of representing processes of heat transfer between a river and permafrost at a larger (kilometric) scale. We will consider in a further study an adaptation of this method to field conditions at a monitoring site in Syrdakh, Yakutia (see companion paper by Roux et al. in this ICOP volume on page 688). A parallel work between experiment and modeling was carried out to identify the proper river-soil boundary conditions and validate the code (see Grenier et al. ICOP this volume on page 659) on the experimental results. The same approach will be conducted on the field to study the applicability of the code for field natural complexity. It will assess the robustness of the experiments as well.

Figure 1: Experimental set up in the cold room

References

Grenier, C.; Roux, N.; Mouche, E.; Chanzy, Q. and Costard, F. wo benchmark cases for coupled thermo-hydrological numerical simulations in cold region environments. *in prep.*

Grenier, C.; Régnier, D.; Mouche, E.; Benabderrahmane, H.; Costard, F. and Davy, P. [2013]: Impact of permafrost development on groundwater flow patterns: a numerical study considering freezing cycles on a two-dimensional vertical cut through a generic river-plain system. *Hydrogeology Journal*, 21(1):257–270, doi:10.1007/s10040-012-0909-4.

Roux, N.; Costard, F. and Grenier, C. [2015]: Laboratory and numerical simulation of river talik evolution. *Permafrost and Periglacial Processes*, Accepted.

Thermal algorithms in the water balance simulation model

Ronald Daanen, Jörg Schulla, & Anna Liljedahl

DGGS, United States of America

Introduction

The water balance simulation model (WaSiM) is a well-known hydrological model in primarily European temperate and alpine catchments. Starting in 2013, University of Alaska Fairbanks began implanting a heat transfer module to adapt WaSiM to permafrost hydrology. This module enables WaSiM to simulate ground temperature, thaw depth and water movement in accordance with a dynamic active layer. In this presentation we will present the details of the thermal model and show preliminary results of multiple simulations, including the Fish Creek Watershed, Arctic Coastal Plain, Alaska. Other relevant modules currently included in WaSiM are a dynamic glacier module, an advanced snow accumulation module and various snowmelt routines that are flexible to data availability. WaSiM has strong and efficient hydrological simulation capabilities due to direct coupling in 2 1/2 D of groundwater and vadose zone water movement and now it also simulates the ground thermal regime.

Thermal Algorithm

The heat transfer module solves Fourier's Law for heat conduction. Heat capacity and thermal diffusion are calculated based on typical soil properties in the unfrozen and frozen states. Phase changes is accounted for by calculating the change in liquid water content with the change in temperature. However therefore the unfrozen water characteristic curve needs to be known. The freezing characteristic curve as it is also known, shows the relation between the quantity of liquid water in a soil and the freezing temperature. This curve is created by utilizing the soil moisture characteristic curve already available in WaSiM to solve Richard's equation. The moisture content is a function of the liquid water pressure head above the water table, also known as a suction, and on the pore size distribution of the soil. In WaSiM the soil moisture characteristic curve is based on Mualem's equation described by Van Genuchten. We generate the freezing characteristic curve from the moisture characteristic curve by combining it with the generalized Clapeyron equation to couple soil temperature to the local liquid water pressure head through a constant conversion factor. From theoretical calculation the value of this constant should be 122 m/ °C, however we leave it up to the user to decide what constant value fits their observations. We recommend users to maintain the Van Genuchten parameters from the soil moisture characteristic curve and fit the freezing curve using the Clapeyron conversion factor. The apparent heat capacity for the soil is corrected for the latent heat of fusion by adding the derivative of the freezing characteristic curve multiplied by the latent heat of fusion and the density of water. Depending on the soil type the apparent heat capacity curve spikes smoothly just below 0 °C. Unsaturated conditions are directly corrected in the freezing algorithm. No freezing occurs when a soil is unsaturated until the soil is cold enough for the soil liquid water pressure head to be higher than the freezing temperature pressure head. The implemented apparent heat capacity curve is smooth to avoid any numerical instabilities.

Thermal conductivity is calculated based on the amount of water and ice present in dry soil. The hydraulic conductivity is the same as the unsaturated hydraulic conductivity, which is automatically corrected for the amount of ice blocking the pores. The saturation for the Richards equation is the total water saturation, which is in contrast to the saturation based on the freezing temperature that is based only on the liquid water portion. Currently the model does not account for pore volume change during freezing or thawing and the digital elevation model (topography) is fixed. Currently, the upper boundary is controlled by the air temperature and n-factors, but an energy balance module is under development. The lower boundary can be a fixed temperature or a fixed heat flux, variable in space. The thermal model is solved for the vertical conductive and convective flows.

WaSiM is versatile in the simulation of the watershed scale water balance. Various approaches can be used to simulate hydrological components that are of interest to the user. Advanced meteorological data

distribution, snowmelt though surface energy balance, avalanches and dynamic glacier configuration, make WaSiM currently a state of the art model for high elevation watersheds. The addition of the thermal algorithms for freezing and thawing make WaSiM an ideal choice for simulating effects of climate change on hydrological processes and future stability of permafrost. Active layer dynamics strongly impacts storage and base flow during the summer months. Implementation of additional physically based hydro-thermal processes in the near future related to the surface energy balance, snowpack, water bodies and surface runoff will give WaSiM more capabilities to accurately simulate small scale processes in cold environments. The processes include, but are not limited to, snow melt timing through refined representation of liquid water storage in snow, aufeis formation, talik related groundwater movement and thermal effects of rivers on permafrost. We are also brainstorming inclusion of dynamic thermokarst processes especially related to ice wedge degradation, which changes the topography and drainage pattern of the landscape.

Model implementation

The model is multi-processor capable in MPI as well as OpenMP. Its performance scales well with millions of cells on large super computers or it can be used on your laptop using multi core technology. The physics applied can resolve centimeter to kilometer scale processes, with various amounts of available input data. The minimum forcing data that is required is air temperature and precipitation. The solution of Richards's equation simultaneously with the thermal simulation automatically corrects for shifting thermal properties associated with soil moisture change. This can make a dramatic difference in permafrost temperatures, especially in peat-rich areas, because dry peat is a strong insulator.

Preliminary Results

WaSiM is used successfully in a variety of projects where thermal processes need to be simulated. Observed soil temperatures mostly match modeled temperatures well. Proper permafrost temperature simulations affects the active layer dynamics, which in turn affects the hydrology. Thaw depths simulations also match observations well. Results from simulations spanning high resolution ice wedge polygons near Barrow, Alaska to low resolution alpine catchments in the Alaska Range.

Preliminary results for one simulation is present in this abstract, Fish Creek Watershed, North Slope, Alaska, the simulated thaw depths are slightly overestimated (≈30 %) for the terrestrial part and a slightly underestimated (≈30 %) for the lake taliks, while the depth to the groundwater table is slightly underestimated (≈50 %) these data are for August of 2009. Further development of the model through n-factor adjustments, and improved active layer hydraulic conductivity will resolve these problems (Fig. 1).

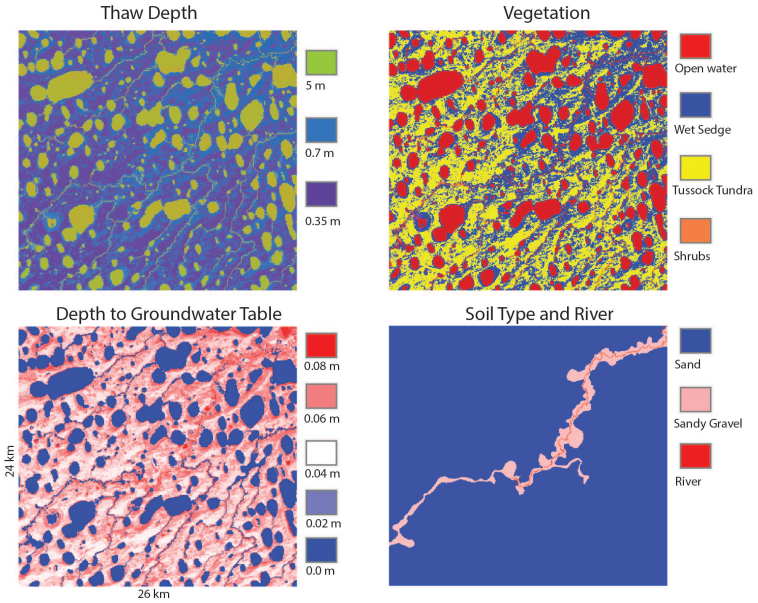

Figure 1: Fish Creek Watershed simulated data for Thaw Depth (August 2009), Depth to Groundwater Table, and input data for Vegetation and Soil Type.

River discharge for Fish Creek is currently simulated well except that the snow melt peak is modeled too early and base flow needs to be increased. Results in figure 1 are reported as an average for the month of July 2009 and at a resolution of 60 m. The figure has only a subset of the entire watershed to make it easier to read, the total watershed is 4852 km^2. The model has 1.3 million cells in the horizontal direction and the soil is represented by 25 layers. This domain is simulated using a 120 core high capacity computer and a 5 year simulation takes approximately 3 days.

Evaluation of the continental biosphere model (ORCHIDEE) over Siberia with remote sensing products

Sarah Dantec-Nédélec[1], Catherine Ottlé[1], Fabienne Maignan[1], & Nicolas Delbart[2]

[1]*Laboratoire des Sciences du Climat et de l'Environnement, CEA-CNRS-UVSQ, Gif-sur-Yvette, France*
[2]*PRODIG (UMR 8586), Université Paris Diderot (Paris 7), Paris, France*

Climate modeling is essential to better understand the surface-atmosphere interactions and their future evolution. In the high latitudes where the climate models predict the largest warming, one of the major challenges is to simulate the interactions between vegetation, snow and permafrost. The land surface model ORCHIDEE (Organizing Carbon and Hydrology in Dynamic Ecosystems), part of the IPSL Earth system model is a good tool for that purpose because it allows to represent the main cryospheric processes like soil thermodynamics in relation with hydrology.

In this paper, we present an evaluation of the ORCHIDEE land surface model over high latitudes. The evaluation has been performed on various datasets including remote sensing products developed in the framework of the PAGE21 European program. Surface temperature, soil moisture, leaf area index and vegetation phenology, snowmass, soil freezing and evapotranspiration were compared to regional products at 0.5°scale and on the last 30 years period 1979-2009 River discharges were also used to evaluate the routing model. The comparisons of the ORCHIDEE simulations with all these datasets permitted us to show the improvements brought by the recent developments focused on snow, soil freezing and vegetation mapping, Once validated on present time, the model allows to perform future climate simulations. The impacts of global warming on the surface variables and fluxes, and on the streamflows will be presented.

Modeling of pollutant transport in streams with riverbeds deformed due to thawing permafrost

Elena Debolskaya, Oksana Maslikova, Ilja Gritsuk, & Dmitri Ionov

Water problems Institute of the Russian Academy of Sciences, Russian Federation

A common problem for the Arctic region is the pollution with persistent organic compounds and other substances that have accumulated over the years in these areas. With increasing temperature, these substances can go from snow, ice, permafrost in the human environment. With climate warming and permafrost degradation the risk of toxic substances entering from places of burial of chemical and radioactive waste increases. Elements of facilities for the disposal of garbage and pollutants were often calculated on an impermeable layer structure of permafrost, and melting in these areas can lead to significant pollution of water resources. Therefore the problem of the effect of permafrost melting due to climate change and human impact caused by increasing levels of production and transportation of minerals on pollution of water bodies located in the permafrost zone is becoming increasingly important. The task of pollution distribution calculate is complicated by the need to consider the deformation of riverbeds composed of thawing rocks. The critical change occurring in the Arctic related to thawing permafrost is expected to increase erosion rates along the river beds. Laboratory experiments and field observations have shown that thermoerosion plays an important and sometimes more important than mechanical erosion during deformation riverbeds in permafrost zone. One of the most accessible methods of investigation of these processes is the mathematical modeling.

A mathematical model of the pollutant propagation in the rivers under conditions of riverbed deformations in permafrost areas is presented. The deformations are due to by thawing of the river banks under increasing of the ambient temperature. The model system consists of an hydrodynamic module, a thermal module, a riverbed deformation module and a pollutant transport module. The hydrodynamic module is based on the two-dimensional shallow water equations. The riverbed deformations module is based on the sediment mass balance conditions. The thermal module is based on the Stefan equation, which defines the "water-ice" boundary movement. As a modeling result, the three-dimensional distribution of flow velocities, pollutant concentration and changes in the relief of riverbed were obtained. The model was verified in the hydraulic tray. We compared the model predictions with the laboratory dates and obtained a good agreement.

As a result of numerical experiments the interesting conclusions about the features of pollution propagation in the deformed riverbeds were obtained. One of the important findings is that a cross sectional shape of the channel plays the most significant role in the accumulation of impurities.

Acknowledgements

The work was supported by the Russian Foundation for Basic Research (project 15-05-00342 A)

Modeling permafrost and its impacts on subarctic watersheds hydrology using distributed hydrological model WaSiM

Matvey Debolskiy[1], Regine Hock[2], Vladimir Romanovsky[2], Vladimir Alexeev[3], Dmitry Nicolsky[2], & Jörg Shulla[4]

[1] *University of Alaska Fairbanks, United States*
[2] *Geophysical Institute, University of Alaska Fairbanks, United States*
[3] *International Arctic Research Center, University of Alaska Fairbanks, United States*
[4] *Hydrology Software Consulting, Zürich, Switzerland*

Permafrost acts as an almost impermeable barrier for groundwater movement resulting in reduced aquifer recharge and/or exfiltration into rivers. Thawing of permafrost is expected to alter the interaction between the surficial fluvial network and deeper aquifer as well as aquifer capacity. Anticipated arctic climate warming and associated changes in the thermal state of permafrost pose a challenge for hydrological models. Here we aim to investigate how heat transfer dynamics in soils affects the hydrologic regime of sub-Arctic watersheds in Alaska. The specific objectives are to a) validate and explore the limitations of a 1-dimensional heat-transfer model embedded in a hydrological model, and b) to quantify the effects of permafrost on runoff of a meso-scale catchment in Alaska under current climate conditions using a hydrological model which can simulate permafrost behavior.

We use the distributed, deterministic, physically based Water Flow and Balance Simulation Model (WaSiM). The heat transfer module is validated using long-term ground temperature and soil moisture datasets from boreholes in both both continuous (Barrow) and discontinuous permafrost (Fairbanks) as well as analytical solutions of the Stefan problem and results from other, previously validated, heat-transfer models. After validation of the heat transfer model we apply WaSiM to Jarvis Creek, a sub-Arctic watershed on the northern slope of the Alaska range (630 km^2, 300-3000 m a.s.l.). About 4 % percent of the watershed area is glacierized. Discontinuous ecosystem-driven permafrost within the catchment influences stream-aquifer interactions. Jarvis Creek is an influent stream losing water to aquifer recharge. WaSiM is forced with daily air temperature and precipitation obtained from downscaling of NCEP-NCAR reanalysis with Weather Research and Forecasting (WRF) mesoscale model on a 150x150 km domain with 1 km cell size.

WaSiM is able to reproduce aquifer recharge from Jarvis Creek stream which results in lower discharge values downstream. Preliminary results show that it is important to account for wind induced snow redistribution to achieve a better fit with snow observations, eespecially in the mountainous part of the watershed. Including snow redistribution in the model greatly affects modeled soil temperatures. This indicates that adequate modeling of the redistribution of snow is important to make an accurate estimate of sub-permafrost aquifer capacity and associated lateral groundwater flux.

Improved parametrization of a meso-scale hydrologic model in a discontinuous permafrost, boreal forest ecosystem

Abraham Melesse Endalamaw[1], W. Robert Bolton[1], Jessica M. Young[2], Don Morton[3], & Larry D. Hinzman[1]

[1] *University of Alaska Fairbanks, International Arctic Research Center, United States of America*
[2] *United States Geological Survey, Anchorage, United States of America*
[3] *University of Alaska Fairbanks, Fairbanks, Alaska, United States of America*

Meso-scale hydrological modeling in the boreal forest/discontinuous permafrost ecosystem is very difficult due to the inadequate representation of important small-scale landscape features that are difficult to derive from large-scale data products. Permafrost and vegetation cover are among these small-scale features that mainly control the hydrology and ecosystem composition of the basins. Due to the presence or absence and spatial distribution of permafrost, watersheds in this region host sharply contrasting ecosystems which vary over short horizontal spatial scales. The distribution of permafrost is also controlled by climatic, geologic, topographic factors. However, topography is the primary contro that modifies the local climate through its effect on direct solar radiation. In general, north-facing slopes and valley bottoms are underlain with permafrost while south-facing slopes are generally permafrost free. To accurately simulate the hydrology of the region at any desired spatial and temporal scale, it is necessary to implement these generalized relationships among permafrost, vegetation and topography into process-based distributed hydrological models.

The objective of this study is to improve the parameterization of mesoscale hydrological modeling through fine-scale observation and modeling. Aspect, derived from 30 m Digital Elevation Model (DEM), is used as a proxy for permafrost distribution and vegetation composition parameterization. Small-scale parameterizations were conducted at the two contrasting sub-basins of the Caribou-Poker Creeks Research Watershed (CPCRW) using the Variable Infiltration Capacity (VIC) mesoscale hydrological model. The small-scale parameterization study in the CPCRW improves stream flow simulation in both permafrost dominated (5.7 km^2) and permafrost-free (5.2 km^2) sub-watersheds. In order to test the extent to which these small-scale parameterizations are valid at large scale, stream flow was simulated at the Chena River Basin (area ≈5,478 km^2), located in Interior Alaska, using the small-scale parameterizations results of CPCRW. Both results suggest that aspect based parameterization of the mesoscale hydrological modeling in the region improve prediction of stream flow.

Spatial-temporal coherence of different scale hydrological processes in the Lena River delta

Irina Fedorova[1,2], Antonina Chetverova[2,1], Olga Bobrova[2], Tatyana Skorospekhova[1], Gulnara Nigamatzyanova[3], Natalia Shumskaya[1], Alexandra Shadrina[2,1], Anne Morgenstern[4], & Vasiliy Dmitriev[2]

[1] *Arctic and Antarctic Research Insitute, Russian Federation*
[2] *Saint Petersburg State University, Russian Federation*
[3] *Kazan Federal University, Russian Federation*
[4] *Alfred Wegener Institute Helmholtz Centre for Polar and Marine Research, Potsdam, Gemany*

The Lena River delta is one of the hydrologically entertaining objects. Hundreds channels and thousands lakes as well as thawing ice complex and permafrost active layer dynamic allow to investigate spatial-temporal coherence of different scale hydrological processes. During 15 years Russian-German scientific collaboration on hydrological, hydrochemical and hydrobiological studies have been operated on different water objects for cause-effect relation of large and specific micro processes indication.

Transient liquid-frozen water phase change is significant not only for active layer runoff forming but also for hydrochemical and biological specific. Thus, maximum of DOC is in the overlaying soil layer than permafrost border [Bobrova et al., 2013]. It could be used for modeling of runoff forming and biological activity estimation. Measured temperature of lacustrine bottom sediment of one thermokarst lake on Samoylov Island shows maximal volume 3,7 °C on 1,75 cm beneath water-sediment border [Skorospekhova, 2015]. It is also can be interpreted as biological processes activity, for example, organic material destruction with additional heating. It could be observed more detail and can be used for modeling of a lake thermic regime.

Hydrobiological specificity shows similarity of species in the channels and lakes, poorness of biodiversity, especially in big channel; only stagnant in summer season Bulkurskaya channel has more zooplankton species in four times than the main river channel [Nigamatzyanova et al., 2015]. Decline of water turbidity from the delta top to channel edges is about 5-8 times [Charkin et al., 2009]. Considerable turbidity increase is formed according to permafrost thawing and can reach 500 g l-1 including high concentration of carbon and biogenic elements. Thermokarst lake degradation [Morgenstern et al., 2011] plays also an important role for permafrost hydrology in the delta. Outflow from an ice complex forms a high local suspended supply in adjacent river branches and influences on biological processes consequently [Dubinenkov et al., 2015].

Underestimated effect of water and sediment discharge increase in the middle part of river branches had been marked [Fedorova et al., 2015]. Head flux of the large Lena River forms taliks under channels with more sophisticated affect in the shoreline zone of the Laptev Sea due to aquifer dynamic and mixing of fresh and salt water. Talik effect on hydrology and sedimentation (and suspended material transformation) in the central part of the delta is currently carried out according to geophysical and hydrogeological methods. First field measurements are planned to be done in April 2016 and results will be presented in the ICOP 2016.

The studies have been done with support of RFBR grant 14-05-00787 and 15-35-50949, in the framework of Russian-German projects “ CarboPerm” and “Scientific station “Samoylov Island”. The project for both SPBU and DFG funding had also applied for field and scientific investigation as well.

References

Bobrova, O.; Fedorova, I.; Chetverova, A.; Runkle, B. and Potapova, T. Input of Dissolved Organic Carbon for Typical Lakes in Tundra Based on Field Data of the Expedition Lena–2012. In *Proceedings of the 19th International Northern Research Basins Symposium and Workshop, Southcentral Alaska, USA – August 11–17, 2013*, 2013.

Charkin, A.N.; Dudarev, O.V.; Semiletov, I.P.; Fedorova, I.; Chetverova, A.A.; J., Vonk; Sanchez-Garcia, L.; Gustafsson, ö. and Andersson, P. edi-

mentation in the System of the Delta Lena River - the South Western Part of Buor-Haya Gulf (the Laptev Sea). In *The 16th International Symposium on Polar Sciences. Incheon, Korea. 2009*, 2009.

Dubinenkov, I.; Flerus, R.; Schmitt-Kopplin, P.; Kattner, G. and Koch, B.P. [2015]: Origin-specific molecular signatures of dissolved organic matter in the Lena Delta. *Biogeochemistry*, 123(1):1–14, doi:10.1007/s10533-014-0049-0.

Fedorova, I.; Chetverova, A.; Bolshiyanov, D.; Makarov, A.; Boike, J.; Heim, B.; Morgenstern, A.; Overduin, P. P.; Wegner, C.; Kashina, V.; Eulenburg, A.; Dobrotina, E. and Sidorina, I. [2015]: Lena delta hydrology and geochemistry: long-term hydrological data and recent field observations. *Biogeosciences*, 12(2):345–363, doi:10.5194/bg-12-345-2015.

Morgenstern, A.; Grosse, G.; Günther, F.; Fedorova, I. and Schirrmeister, L. [2011]: Spatial analyses of thermokarst lakes and basins in Yedoma landscapes of the Lena Delta. *The Cryosphere*, 5(4):849–867, doi:10.5194/tc-5-849-2011.

Nigamatzyanova, G.; Frolova, L.; Chetverova, A. and Fedorova, I. Hydrobiological investigation of branches of the Lena River edge zone. In *Uchenye Zapiski Kazanskogo Universiteta, Seriya Estestvennye Nauki*. 2015. in Russian.

Skorospekhova, T. *Report of a spring campaign of the expedition "Lena 2015"*. AARI's library stock, 2015.

Permafrost contribution to streamflow under drought conditions in a river watershed of the extra tropical western Andes in central Chile

Francisco José Ferrando Acuña & A. Bellisario

University of Chile, Chile

An investigation of the effects of the ongoing mega drought (2010-2015), which is affecting central and southern Chile, on the streamflow of the Putaendo River Basin (a watershed of the Aconcagua River Basin - 32° S) was conducted. The significant reduction of precipitation and snow accumulation during the drought has impacted the streamflow of many rivers of this country. Rock glaciers, recently recognized in 40 watersheds, have been able to maintain river runoff, although reduced, during the dry semester of the southern hemisphere hydrological year. A comparative analysis of precipitation and streamflow between the present drought and the previous period (1940-2009) is used to illustrate the function of permafrost in maintaining streamflow under conditions of extreme drought.

The Putaendo River was selected because rock glaciers dominate its glaciated upper Andean section; unlike the rest of the Aconcagua River Basin, there are no white glaciers in the Putaendo watershed. This allows for an research of the contribution of water supplied by rock glacier sources to the water balance of this important sub-basin of the Aconcagua River Basin, under extreme drought conditions. This study corroborates previous analyses that in the Aconcagua River Basin, sporadic permafrost is found between 3000-3500 m.a.s.l., and discontinuous permafrost (represented by abundant active rock glaciers) exists between 3500-4250 m.a.s.l. (See Fig. 1).

In the central Andes, precipitation normally occurs part in autumn but mainly during the austral winter, and rivers discharge shows two peaks: winter and spring. The melt of the snowpack during the spring months generate the higher run-off peak. The depletion of the snow reserves in the high summits, and also the less run-off, takes place in late Summer (March) and early Fall (April). Into this context, the Aconcagua River basins has experienced a rise in the seasonal snowline of about 400 m (it is currently at 2000 m), which has reduced the area for snowpack accumulation and thus less river discharge.

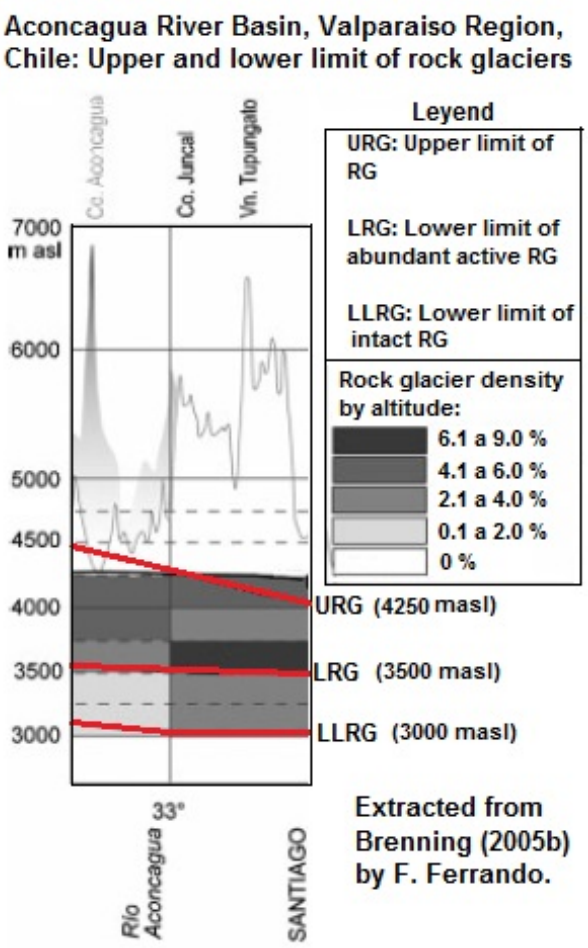

Figure 1: Aconcagua river basin, Valparaiso Region, Chile: Upper and lower limit of rock glaciers

Droughts are a progressive process of depletion of water in hydrogeological reserves. During the current mega drought (2010-2015) the sub-basin of the Rio Putaendo has registered very low rainfall, but discharge has been maintained above expectations, especially in the dry semester of the hydrological year (November-April). Rock glaciers and permafrost-associated landforms have been the main contributors to maintain runoff, also the agricultural activities of this valley.

This finding highlights the importance of enacting legislation to protect the Andean permafrost as a

water resource, especially from mining interventions, which have already caused serious destruction in some areas. This is even more important considering the effects of climate change in the Andes mountains, which have already been experiencing rising temperatures of 1 °C/40 years (Río Yeso meteorological station).

References

Azócar, G. F. and Brenning, A. [2010]: Hydrological and geomorphological significance of rock glaciers in the dry Andes, Chile (27°–33°S). *Permafrost and Periglacial Processes*, 21(1):42–53, doi:10.1002/ppp.669.

Brenning, A. [2005]: Geomorphological, hydrological and climatic significance of rock glaciers in the Andes of Central Chile (33–35°S). *Permafrost and Periglacial Processes*, 16(3):231–240, doi:10.1002/ppp.528.

Ferrando, F. [2014]: Glaciar Pirámide: Glaciar rocoso subtipo cubierto y efectos del calentamiento en la Cordillera de Los Andes de Chile Central. In: Gómez, O.A.; F. OlivaSalvador Franch, F.M. and Salvá, C.M.(eds.), *Avances, métodos y técnicas en el estudio del periglaciarismo*. Publicacions i edicions de la Universitat de Barcelona, Barcelona, ISBN 978-84-475-3830-0.

Mechanisms governing solute transport in the active layer of coupled permafrost-hydrogeological systems

Andrew Frampton[1,2], Romain Pannetier[1,2], & Georgia Destouni[1,2]

[1] *Stockholm University, Department of Physical Geography, SE-106 91 Stockholm, Sweden*
[2] *Bolin Centre for Climate Research, SE-106 91 Stockholm, Sweden*

The permafrost active layer is highly dynamic with seasonal variability and changes in temperature, moisture, heat and water fluxes, all of which affect transport of inert and reactive waterborne substances. Here there is a need for improved understanding of the mechanisms controlling subsurface solute transport in the active layer in order to better understand permafrost-hydrological-carbon feedbacks, in particular with regards to how dissolved carbon is transported in coupled surface and subsurface terrestrial arctic water systems under climate change. Studying solute transport in arctic systems is also relevant in the context of anthropogenic pollution which may increase due to increased activity in cold region environments [Elberling et al., 2010].

In this contribution subsurface solute transport under surface warming and degrading permafrost conditions is studied using a physically based model of coupled cryotic and hydrogeological flow processes combined with a particle tracking method [Frampton and Destouni, 2015]. Changes in subsurface water flows and solute transport travel times are analysed for different modelled geological configurations during a 100-year warming period (Fig. 1). Results show that for all simulated cases, the minimum and mean travel times increase non-linearly with warming irrespective of geological configuration and heterogeneity structure. The timing of the start of increase in travel time depends on heterogeneity structure, combined with the rate of permafrost degradation that also depends on material thermal and hydrogeological properties.

These travel time changes are shown to depend on combined warming effects of increase in pathway length due to deepening of the active layer, reduced transport velocities due to a shift from horizontal saturated groundwater flow near the surface to vertical water percolation deeper into the subsurface, and pathway length increase and temporary immobilization caused by cryosuction-induced seasonal freeze cycles.

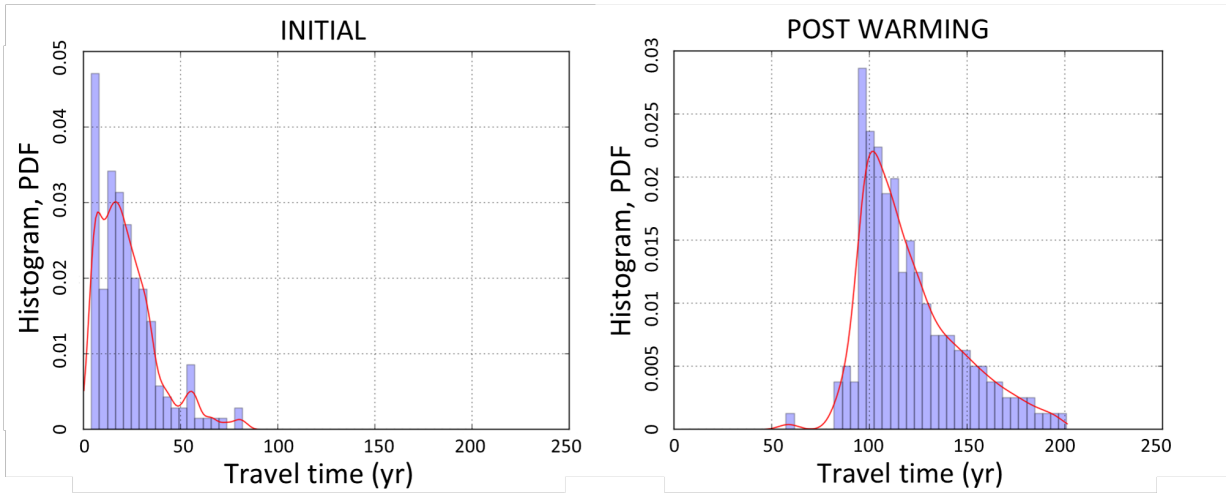

Figure 1: Groundwater travel times before (left) and after (right) an imposed 100-year warming period in a coupled groundwater-permafrost model. Both the peak and mean travel times are delayed, and the variance is increased as the system undergoes warming.

The impact these change mechanisms have on solute and dissolved substance transport is further analysed by integrating pathway analysis with a Lagrangian approach, incorporating considerations for both dissolved organic and inorganic carbon releases [Jantze et al., 2013]. Further model development challenges are also highlighted and discussed, including coupling between subsurface and surface runoff, soil deformations, as well as site applications and larger system scales.

References

Elberling, B.; Christiansen, H.H. and Hansen, B.U. [2010]: High nitrous oxide production from thawing permafrost. *Nature Geosciences*, 3, doi:10.1038/ngeo803.

Frampton, A. and Destouni, G. [2015]: Impact of degrading permafrost on subsurface solute transport pathways and travel times. *Water Resources Research*, 51(9):7680–7701, doi:10.1002/2014WR016689.

Jantze, E. J.; Lyon, S. W. and Destouni, G. [2013]: Subsurface release and transport of dissolved carbon in a discontinuous permafrost region. *Hydrology and Earth System Sciences*, 17(10):3827–3839, doi:10.5194/hess-17-3827-2013. URL http://www.hydrol-earth-syst-sci.net/17/3827/2013/.

Processed-based hydrological modeling of a continuous permafrost catchment on the Arctic Coastal Plain, Alaska to evaluate how climate change will affect surface water runoff and connectivity

Anne Gädeke[1], Anna Liljedahl[1], Christopher Arp[1], Ronald Daanen[2], Benjamin Jones[3], Vladimir Alexeev[4], & Lei Cai[4]

[1] *Water and Environmental Reserach Center, University of Alaska Fairbanks, United States of America*
[2] *Alaska Division of Geological and Geophysical Surveys, Department of Natural Resources, Fairbanks, United States of America*
[3] *United States Geological Survey, Alaska Science Center, Anchorage, United States of America*
[4] *International Arctic Research Center, University of Alaska Fairbanks, United States of America*

A changing climate is leading to rapid transformations of hydrological processes in Arctic environments. For example, lake ice regimes are shifting from bedfast to floating ice due to changes in winter ice growth and late summer precipitation. This regime shift has consequences for lake water balance and downstream runoff generation. Active-layer deepening and ice-wedge degradation are changing flowpaths and may be affecting subsurface and surface storage, respectively.

The aim of this study is to gain a deeper understanding of the climate-hydrology-permafrost system in a low-gradient Arctic Coastal Plain landscape where drained thermokarst lake basins are abundant. We focus on the Crea Creek watershed (30 km^2), which is located in the National Petroleum Reserve-Alaska (NPR-A), because of its varying permafrost landforms (bedfast and floating ice lakes, high and low centered polygons), existing observational data, and changing land-use. Crea Creek itself is a beaded stream with continuous flow from June to September. Measurements of discharge, snow depth, and meteorological variables have been collected since 2009. More recently, the entire watershed was mapped with airborne LiDAR to produce a digital elevation model of 0.25 m horizontal resolution, which allows representation of micro-topographic landscape features at the watershed scale. Oil development is also scheduled to begin in this area starting in 2017 with the construction of a permanent road and drilling pad.

The field measurements collected as well as the LiDAR digital elevation model serve as input data for the process-based, spatially distributed hydrological model WaSiM. Model calibration and validation is based on discharge, lake water level, soil temperatures and snow depth measurements. All aspects of the water cycle are simulated in WaSiM as well as permafrost and seasonal soil freeze and thaw. Our preliminary results demonstrate that the model reliably reproduces seasonal freezing and thawing of the ground, snow accumulation, snow melt peak runoff and the large seasonal variability in surface water extent during summer.

The model will be used to assess the impact of climate change on permafrost hydrology that affect lake ice regimes and spatiotemporal variation of surface water connectivity. Our results will provide regional stakeholders with information on the impacts of climate and land use change on surface water connectivity that affects aquatic ecosystems, especially fish movement and overwintering habitat. These finding will also benefit local communities that rely on these systems for subsistence and the petroleum industry in the mitigation of environmental impacts to permafrost landscapes within the NPR-A and elsewhere.

Assessing watershed-scale linkages between glaciers, permafrost and hydrology in sub-arctic Interior Alaska using field observations and a process-based hydrological model

Anne Gädeke[1], Anna Liljedahl[1], Tiffany Gatesman[1,2], Thomas Douglas[2], & Jing Zhang[3]

[1] *Water and Environmental Research Center, University of Alaska Fairbanks, United States of America*
[2] *Cold Regions Research and Engineering Laboratory (CRREL), US Army Corps of Engineers*
[3] *Department of Physics and Energy& Environmental Studies, NOAA-ISET Center, North Carolina Agriculture and Technical State University*

Hydrological processes in watersheds characterized by the presence of glaciers and permafrost are highly variable seasonally and spatially and are subject to rapid transformation during a changing climate. Here we combine field measurements and hydrological modeling to gain a deeper understanding of the linkages between glaciers, permafrost and hydrology at the watershed scale. Jarvis Creek watershed (630 km^2), a headwater basin of the Tanana River (12,000 km^2) in semi-arid Interior Alaska serves as our study area. The watershed is characterized by glaciers, till sediments of low hydraulic conductivity and, in the lower part of the watershed, glacier outwash fans and floodplains with thick gravel deposits of high hydraulic conductivity. Field measurements of differential runoff, glacier mass balance, end-of-winter snow depths, soil temperature, water geochemistry, and meteorology reflect an elevation gradient from north (lowland) to south (mountain). The process-based, spatially distributed hydrological model WaSiM was utilized to simulate all aspects of the water cycle, including glacier melt and dynamic glacier coverage as well as permafrost and seasonal soil freeze and thaw.

Our field observations show that Jarvis Creek basin glacier coverage, which is currently about 3 % of the total land area, has been reduced by about 34 % (1950-2010). The long-term reduction in glacier area coincides with a significant increase mean annual air temperature (+1.9 °C) and summer warmth index (+6.5 °C, 1947-2014 Delta Junction), which is the sum of all mean monthly air temperature above 0 °C. Solid precipitation has decreased on the northern side of the Alaska Range since 2000. Our measurements show that glacier melt provides about 27 % (2015) of total runoff at our upstream runoff measurement site. Differential discharge measurements show Jarvis Creek is a losing stream. In 2015, at least 30 % of streamflow was lost in the lowland region between our upstream and downstream runoff measurement sites. The seasonal variation in lowland groundwater levels reached nearly 15 m near the outlet of the watershed (2015). The groundwater levels steadily decrease during the mid- to late winter months, which suggests a continuous loss of warm groundwater (6.5 °C) to the lowland Tanana River.

Our field measurements suggest reduced glacier coverage, via increased aquifer recharge, is the primary cause of the observed increase in late winter baseflow of the Tanana River (+23%, 1974-2006, Fairbanks). The WaSiM simulations, which are driven and validated by our field measurements and downscaled climate simulations, serves as the tool to assess the processes linking the climate, glacier, permafrost and hydrology systems, where glaciers may not only be important for sustaining streamflow in headwater basins during summer but also in controlling the larger scale hydrological regime and permafrost distribution of subarctic watersheds.

Investigating features of permafrost and talik in the peripheries of the Wanlong Worma Lake using electrical resistivity tomography (ERT) in the source area of the Yellow River (SAYR), NE Qinghai-Tibet Plateau, China

Shuhui Gao, Huijun Jin, Xinbing Wang, Dongliang Luo, & Lanzhi Lü

State Key Laboratory of Frozen Soils Engineering, Cold and Arid Regions Environmental and Engineering Research Institute, Chinese Academy of Sciences, Lanzhou, China

Characterization of permafrost distribution is still a major challenge, but it may be improved by employing noninvasive and tomographic geophysical methods. Electrical resistivity tomography (ERT) offers several advantages:

1. it is not intrusive,
2. it exhibits spatial patterns at a decametric or hectometric scale, and
3. it provides information on both soil resistivity and soil depth.

In this study, ERT was employed to investigate the features of permafrost and talik in the peripheries of a thermokarst lake underlain saturated and unsaturated soil in the Source Area of the Yellow River (SAYR), NE Qinghai-Tibet Plateau, China.

Nine ERT profiles are laid out around the lake, five of them were made parallel to the axis of the lake, another four profiles were measured perpendicular to the lake axis with the same spacing. The inverted resistivity results of the ERT surveys show that permafrost is continuous on the Northeast of the lake, with a coverage of 90 % continuous permafrost distributed, the permafrost thickness is about 15 m, the active layer thickness is 2 m and taliks are embedded in the permafrost. On the Southeast of the lake, permafrost is sporadic and the thickness is about 10 m, with a 40 % coverage. 80–100 m away from the lakeside are basically melted region. On the Northwest of the lake, permafrost is sporadic with a coverage of 10 %, the thickness is no more than 5 m, and the surface is given priority to with characteristics of the black soil. There are scarcely any permafrost contained on the West area of the lake, and on the South area of the lake, discontinuous permafrost exists, with the permafrost thickness of about 10 m and 30 % coverage. Under a warming climate, more attention is concentrated on the permafrost degradation. The study does some simulations on the evolution of the shallow groundwater and permafrost development and the simulation results preliminary shows that the permafrost distribution decrease with the water level growth because of the changes in the hydrothermal regimes of permafrost and talik around the lake.

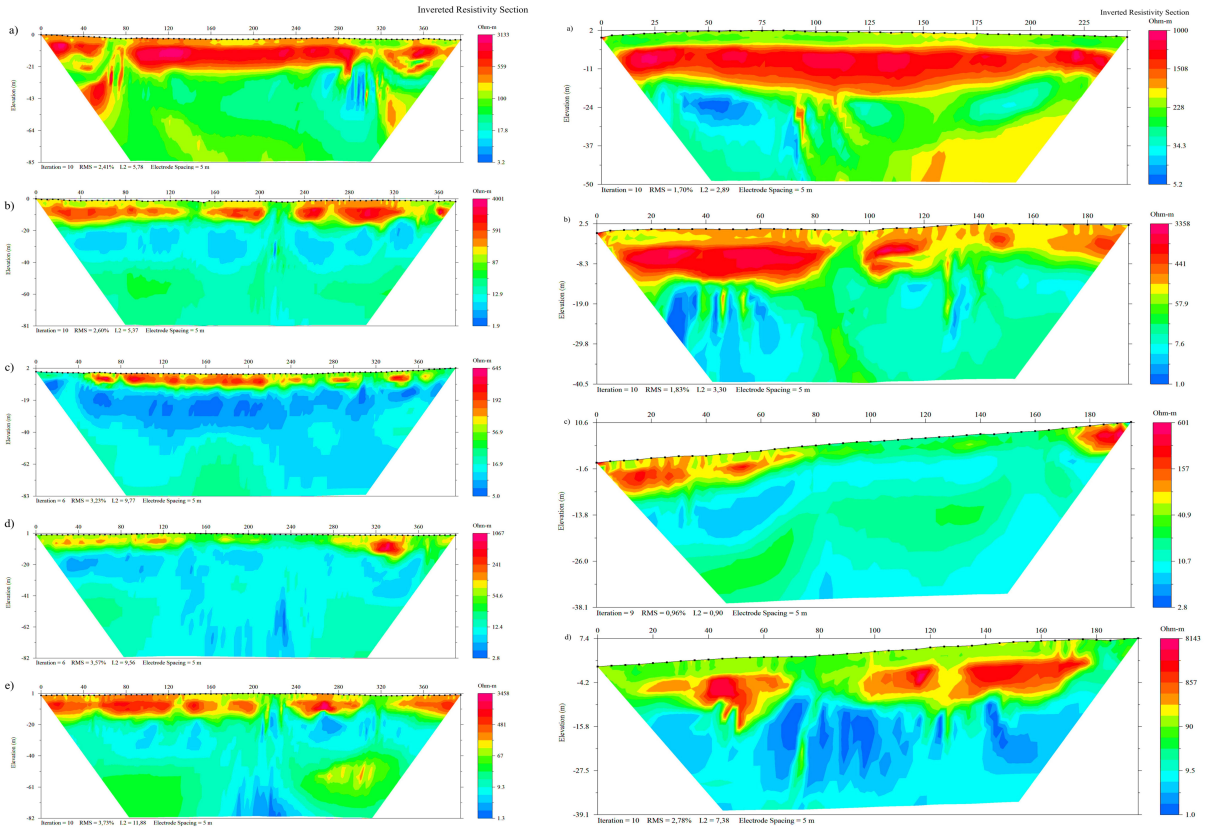

Figure 1: The inverted resistivity of the soil profile

Going with the flow: bank erosion versus floods on the Middle Lena River (Siberia)

Emmanuele Gautier[1], Clement Virmoux[1], François Costard[2], Alexander Fedorov[3], & Pavel Konstantinov[3]

[1] *University Paris 1 Panthéon-Sorbonne& CNRS Lab. Physical Geography, France*
[2] *University Paris-Sud XI, CNRS, GEOPS, UMR 8148, Orsay, France*
[3] *Permafrost Institute, RAS Siberian branch, Yakutsk, Russia*

Extreme hydrologic events represent a major threat for society (CRED, 2015). Fluvial infrastructures, navigation, flood risk management and water resources depend on a good understanding of hydrologic hazards. That is particularly true for the Central and Northern Siberia where social activities and industries are mainly associated to rivers. The first objective of the present paper is to detect of a potential evolution of floods in terms of intensity, duration and date, on the middle Lena River, near Yakutsk. The second objective is the evaluation of flood impact of morphologic and sedimentary evolution of the fluvial forms.

Water discharge data were compiled for 76 years at Tabaga gauging site, near Yakutsk (Siberia; Sakha Republic). With longer time series (1936 – 2012) than the previous studies [Yang et al., 2002, Shiklomanov et al., 2007], the present study can analyze long-term evolutions and can focus on very recent changes.

The hydrograph of the Central Lena is very representative of a periglacial and high-latitude continental area, where permafrost plays a major part. With a low mean annual discharge at Tabaga (around 7 200 $m^3\ s^{-1}$), the Lena River has a weak specific discharge: 7 – 8 $l\ s^{-1}\ km^{-2}$. From October to the end of April, the river shows a long period of low water stage, covered by an ice cap during 200 – 250 days. The hydrologic functioning is dominated by the spectacular break up occurring around May 15^{th} in the area of Yakutsk. The rising limb is very steep; the flood wave coming from the upper part of the basin located in the Prebaïkal Mountains propagates across floodplain and active channel that are still frozen. Two main discharge thresholds are determined for the middle Lena River: the first level represents the beginning of the overbank flow (around 30 000 $m^3\ s^{-1}$) and the second one is considered as a major flood (40 000 $m^3\ s^{-1}$).

Firstly, when examining floods at Tabaga gauging site since 1937, two periods of high frequency are identified: 1957 – 1966 and since 2006. Furthermore, the "wet" decade (1957 – 1966) is marked by long flooding durations, but the longest durations are registered since 1983 and increasingly, since 2004. Local population was inundated more than one month in 2006, 2007 and 2012. The frequency and duration of the highest floods (exceeding 40 000 $m^3\ s^{-1}$) is also increasing. Whatever is the water level considered (30 or 40 000 $m^3\ s^{-1}$), the last ten years seem to be subjected to an increasing intensity and duration of flood events. A change is also observed on the date of flooding. For the two last decades, "early"floods (at the beginning of May) and "late" floods (June) are more frequent, whereas before 1987, the great majority of events began between May 20^{th} and May 30^{th}.

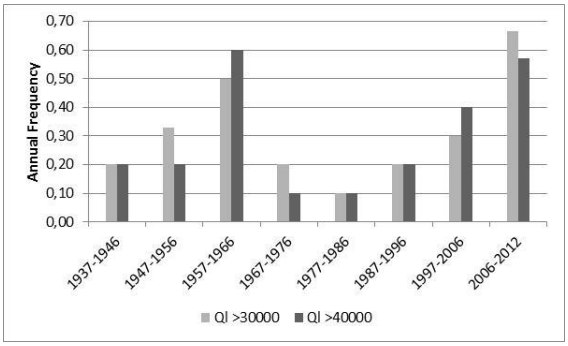

Figure 1: Annual frequency for two flood discharge thresholds: 30 000 m^3/s and 40 000 m^3/s (Lena River at Tabaga gauging station)

Secondly, we have determined interactions between flood intensity and duration, water temperature, ice-jam, alluvial vegetation and erosion/deposition processes. The Lena riverbanks are sensitive to mechanical and thermal erosion because of the permafrost. More precisely, the head of the fluvial islands are subjected to an active erosion, greater than the channel bank erosion: island head retreat can reach 40 m per

year [Costard et al., 2007]. We can make the assumption that the observed hydrologic variations induce a possible change of the fluvial dynamics in terms of erosion and sedimentation. The impact of hydrologic changes is examined at a pluri-decadal scale (since 1967) and an annual scale (2008 – 2013). The recent hydrologic change of floods certainly explains the increase by 30 – 40 % of the island head erosion since 2002. Two mains causes can be underlined. First, the flooding duration plays a major part on bank erosion, the longer is the overbank discharge, the higher is the bank retreat. Second, the "late" flood peaks enhance bank retreat, mainly on island heads. Late flooding accelerates thermal erosion of the frozen banks, certainly because of warmer water.

References

Costard, F.; Gautier, E.; Brunstein, D.; Hammadi, J.; Fedorov, A.; Yang, D. and Dupeyrat, L. [2007]: Impact of the global warming on the fluvial thermal erosion over the Lena River in Central Siberia. *Geophysical Research Letters*, 34(14), doi:10.1029/2007GL030212.

Jantze, E. J.; Lyon, S. W. and Destouni, G. [2013]: Subsurface release and transport of dissolved carbon in a discontinuous permafrost region. *Hydrology and Earth System Sciences*, 17(10):3827–3839, doi:10.5194/hess-17-3827-2013. URL http://www.hydrol-earth-syst-sci.net/17/3827/2013/.

Shiklomanov, A. I.; Lammers, R. B.; Rawlins, M. A.; Smith, L. C. and Pavelsky, T. M. [2007]: Temporal and spatial variations in maximum river discharge from a new Russian data set. *Journal of Geophysical Research: Biogeosciences*, 112(G4):n/a–n/a, doi:10.1029/2006JG000352. G04S53.

Yang, D.; Kane, D.L.; Hinzman, L.D.; Zhang, X.; Zhang, T. and Ye, H. [2002]: Siberian Lena River hydrologic regime and recent change. *Journal of Geophysical Research: Atmospheres*, 107(D23):ACL 14–1–ACL 14–10, doi:10.1029/2002JD002542. 4694.

The InterFrost benchmark of Thermo-Hydraulic codes for cold regions hydrology – first inter-comparison phase results

Christophe Grenier[1], Hauke Anbergen[2], Victor Bense[3], Ethan Coon[4], Nathaniel Collier[5], Francois Costard[6], Michel Ferry[7], Andrew Frampton[8], Jennifer Frederick[9], Johan Holmen[10], Anne Jost[11], Samuel Kokh[12], Barret Kurylyk[13], Jeffrey McKenzie[14], John Molson[15], Laurent Orgogozo[16], Romain Pannetier[8], Agnes Riviere[17], Nicolas Roux[1,6], Wolfram Rühaak[18], Johanna Scheidegger[19], Jan-Olof Selroos[20], Renë Therrien[15], Patrik Vidstrand[20], & Clifford Voss[21]

[1] *LSCE, UMR 8212 CNRS-CEA-UVSQ, Orme des merisiers, 91191 Gif-sur-Yvette Cedex, France*
[2] *APS Antriebs-, Prüf- und Steuertechnik GmbH, Götzenbreite 12, 37124 Rosdorf*
[3] *Department of Environmental Sciences. Wageningen University, Netherland*
[4] *Los Alamos National Laboratories, P.O. Box 166. Los Alamos, NM 87545*
[5] *ORNL Climate Change Science Institute, One Bethel Valley Road, PO BOX 2800, MS-6301, Oak Ridge, TN 37831-6301*
[6] *GEOPS, UMR 8148 CNRS – Université Paris Sud, 91405 Orsay Cedex, France*
[7] *MFRDC, 6 rue de la Perche 44700 Orvault, France*
[8] *Department of Physical Geography, Stockholm University, Stockholm, Sweden*
[9] *Desert Research Institute, Division of Hydrologic Sciences, 2215 Raggio Parkway Reno, NV 89512*
[10] *Golder Associates Kapellgränd 7, 11625 Stockholm, Sweden*
[11] *METIS, UMR 7619, Sorbonne Universités, UPMC Univ. Paris 6, 75005 Paris, France*
[12] *Maison de la Simulation USR 3441, Bâtiment 565 - Digiteo - PC 190, CEA Saclay, 91191 Gif-sur-Yvette cedex, France*
[13] *Department of Geoscience, University of Calgary, 2500 University Drive NW, Calgary, AB, T2N 1N4, Canada*
[14] *Department of Earth and Planetary Sciences, McGill University, 3450 University Street, Montreal, PQ, Canada H3A 0E8*
[15] *Département de géologie et de génie géologique, Université Laval, 1065 avenue de la Médecine, Québec, Canada, G1V 0A6*
[16] *GET, UMR 5563 CNRS-IRD-UPS, Université Toulouse, 14 avenue Edouard Belin, 31400 Toulouse, France*
[17] *MINES ParisTech - Centre de Géosciences, 35 rue Saint Honoré 77305 Fontainebleau, France*
[18] *Darmstadt Graduate School of Excellence Energy Science and Engineering, Technische Universität Darmstadt, Germany*
[19] *British Geological Survey. Nicker Hill, Keyworth, Nottingham, NG12 5GG, UK*
[20] *Swedish Nuclear Fuel and Waste Management Company, Box 250, 101 24 Stockholm, Sweden*
[21] *United States Geological Survey. 345 Middlefield Road. Menlo Park, CA 94025*

Climate change impacts in permafrost regions have received considerable attention recently due to the pronounced warming trends experienced in recent decades and which have been projected into the future. Large portions of these permafrost regions are characterized by surface water bodies (lakes, rivers) that interact with the surrounding permafrost. For example, the thermal state of the surrounding soil influences the energy and water budget of the surface water bodies. Also, these water bodies often generate taliks (unfrozen zones) within the permafrost that allow for hydrologic interactions between the surface water bodies and underlying aquifers and thus influence the hydrologic response of a landscape to climate change.

Recent field studies and modeling exercises indicate that a fully coupled 2D or 3D Thermo-Hydraulic (TH) approach is required to understand and model past and future evolution of landscapes, rivers, lakes and associated groundwater systems in a changing climate

[Kurylyk et al., 2014a]. However, there is presently a paucity of 3D numerical studies of permafrost thaw and associated hydrological changes, which can be partly attributed to the difficulty in verifying multi-dimensional results produced by numerical models.

Numerical approaches can only be validated against analytical solutions for a purely thermic 1D equation with phase change (e.g. Neumann, Lunardini). When it comes to the coupled TH system (coupling two highly non-linear equations with phase change introduces steep fronts), the only possible approaches are to compare the results from different codes to provide test cases and/or to have controlled experiments for validation. Such inter-code comparisons can provide the impetus to improve code performance.

A benchmark exercise was initialized at the end of 2014. Participants convened from USA, Canada, Germany, Sweden, Great Britain, The Netherlands and France, representing 13 simulation codes. The benchmark exercises consist of several test cases inspired by existing literature (e.g. McKenzie et al. [2007] as well as new ones [Kurylyk et al., 2014b, Rühaak et al., 2015]. They range from simpler, purely thermal 1D cases to more complex, coupled 2D TH cases (benchmarks TH1, TH2, and TH3). Some experimental cases conducted in a cold room complement the validation approach. A web site hosted by LSCE (Laboratoire des Sciences du Climat et de l' Environnement) is an interaction platform for the participants and hosts the test case databases at the following address: `https://wiki.lsce.ipsl.fr/interfrost`.

The results of the first stage of the benchmark exercise will be presented. We will mainly focus on the inter-comparison of participant results for the coupled cases TH2 & TH3. Both cases are essentially theoretical but include the full complexity of the coupled non-linear set of equations (heat transfer with conduction, advection, phase change and Darcian flow). TH2 considers an initially frozen square inclusion within a warmer domain. The initial inclusion progressively warms up due to conduction and heat exchange by water advection. TH3 considers a domain with two conflicting effects associated with imposed negative temperatures on the top and bottom while the input of warm water from the left side provides heat to the system. This system exhibits a threshold response to the flow velocity: the central talik closes for lower velocities and opens for higher velocities.

A series of Performance Measures (PMs) was introduced to provide easy and tractable comparisons. These include thermal and hydrological variables or their associated fluxes in the form of point values or values averaged over a surface area or volume. In the first approach, the time evolution of all PMs are plotted for each contributing code. A PM example is provided in the figure 1 below for TH2. These data represent the evolution of the temperature field minimum for a hydraulic gradient of 3 % (low velocity).

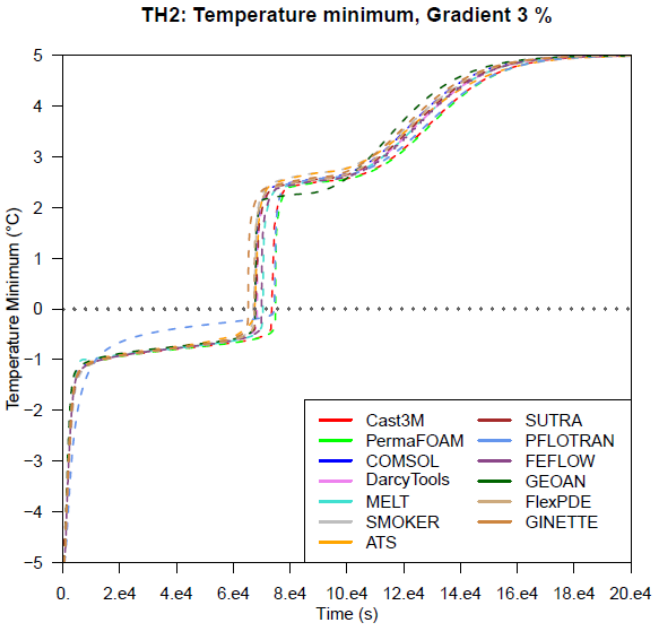

Figure 1: Evolution of the minimum of the temperature field (PM1) associated with Test Case TH2 and a head gradient of 3%

The complete set of inter-comparison results shows that the participating codes all produce simulations which are quantitatively similar and correspond to physical intuition. From a quantitative perspective, they agree well over the whole set of performance measures. However, discrepancies exist resulting from

1. differences in the set of simulated equations or characteristic curves (some participants were not able to run the test cases with identical conditions) and

2. precision issues resulting from spatial and temporal discretization and convergence (e.g. imprecise initial conditions due to non-dedicated meshing especially for TH3, temporal discretization strategies and convergence criteria for non-linear loops or other algorithms).

The differences among the simulation results will be discussed in more depth throughout the test cases and PMs, especially for the identification of the threshold times for each system as these exhibited the least

agreement. However, the results suggest that in spite of the difficulties associated with the resolution of the set of TH equations (coupled and non-linear structure with phase change providing steep slopes), the developed codes provide robust results with a qualitatively reasonable representation of the processes and offer a quantitatively realistic basis.

These test case results, as well as the associated overview of the numerical approaches used, will hopefully propel future code development, improvements, and application.

Further perspectives of the exercise will also be presented. Extensions to more complex physical conditions (e.g. unsaturated conditions and geometrical deformations) are contemplated. In addition, 1D vertical cases of interest to the climate modeling community, as well as comparisons to observed laboratory and field site data will be proposed during the year to come.

Acknowledgements

The InterFrost project is most thankful to the International Permafrost Association for the 2016-2017 IPA Action Group funding.

References

Kurylyk, Barret L.; MacQuarrie, Kerry T.B. and McKenzie, Jeffrey M. [2014a]: Climate change impacts on groundwater and soil temperatures in cold and temperate regions: Implications, mathematical theory, and emerging simulation tools. *Earth-Science Reviews*, 138:313 – 334, doi:10.1016/j.earscirev.2014.06.006.

Kurylyk, B.L.; McKenzie, J.M.; MacQuarrie, K.T.B. and Voss, C.I. [2014b]: Analytical solutions for benchmarking cold regions subsurface water flow and energy transport models: One-dimensional soil thaw with conduction and advection. *Advances in Water Resources*, 70:172 – 184, doi:10.1016/j.advwatres.2014.05.005.

McKenzie, J.M.; Voss, C.I. and Siegel, D.I. [2007]: Groundwater flow with energy transport and water–ice phase change: Numerical simulations, benchmarks, and application to freezing in peat bogs. *Advances in Water Resources*, 30(4):966 – 983, doi:10.1016/j.advwatres.2006.08.008.

Rühaak, W; Anbergen, H.; Grenier, C.; McKenzie, J.; Kurylyk, B.L.; Molson, J.; Roux, N. and Sass, I. [2015]: European Geosciences Union General Assembly 2015 - Division Energy, Resources and Environment, EGU 2015 Benchmarking Numerical Freeze/Thaw Models. *Energy Procedia*, 76:301 – 310, doi:10.1016/j.egypro.2015.07.866.

Hydrology of arctic regions. Synergy of modelling and remote sensing

Marilen Haver[1], Elena A. Zakharova[1], Alexei Kouraev[1], & Inna Krylenko[2]

[1] *Observatoire Midi-Pyrénées (OMP), France*
[2] *Moscow State University Russia*

The high latitudes of the Northern Hemisphere are particularly sensitive to climate change. Major changes in environmental and geotechnical conditions are expected as a consequence of melting permafrost. The degradation of the frozen ground will bring changes in hydrology and ecosystem dynamics as well as an acceleration of subsidence and erosion processes. In order to predict future functioning of hydrological systems and associated risks, it is crucial to be able to model the hydrological regime of soils and runoff processes in permafrost-affected catchments.

The objective of this study is to evaluate the benefit of using water storage remotely-sensed data in hydrological models dealing with permafrost environments. The distributed hydrological model WATFLOOD simulates water outflow and watershed water balance in five different watershed classes. We compare the anomalies of integrated water storage simulated by the model with those of the GRACE space gravimetry mission and with the snow water equivalent (GLOBSNOW product) and we aim to improve the simulations of the surface pool water storage using a prototype product of the future NASA-CNES Surface Water and Ocean Topography mission (SWOT).

This research has been done in the framework of the SWOT-TOSCA CNES, IDEX Transversalitë 2013 InHERA, OMP-AST "Arctique" and ANR "CLASSIQUE" projects, as well as by GDRI "CARWET-SIB II" and French-Siberian Centre for Education and Research.

The hydrological impact of rock glaciers in the Aconcagua river basin, Chile

Jason Janke, Antonio Bellisario, & Sam Ng

Metropolitan State University of Denver, United States of America

An inventory of firn fields, glaciers, debris-covered glaciers, and rock glaciers was conducted in order to assess water resources in the Aconcagua river basin of the semi-arid Andes of central Chile. A total of 916 landforms were identified, of which, rock glaciers were the most abundant (669) and occupied the most total area. Glaciers and debris-covered are less numerous, but are larger in comparison. The total area occupied by glaciers and debris-covered glaciers is roughly equivalent to the total area of rock glaciers. Rock glaciers accounted for 20 % of the area above snowline (2,000 m) and had the lowest mean elevation at 3,766 m compared to the other cryosphere landforms analyzed. Mean slope was roughly 20 for rock glaciers and debris-covered glaciers, whereas glaciers and firn occupied steeper mean slopes (27). Glaciers and firn fields were found predominantly on southern slopes; debris-covered glaciers on western slopes, and rock glaciers on southwestern slopes. Debris-covered glaciers and rock glaciers were subcategorized into 6 classes based on their ice content through interpretation of surface morphology on high-resolution satellite imagery. Extensive coring data allowed empirical formulas to be developed that associate the size of the landforms to water storage estimates. Minimum and maximum water storage was calculated based on a range of debris to ice content ratios for debris-covered glaciers and rock glaciers. In the Aconcagua basin, rock glaciers accounted for 48-64 % of the water stored within the landforms analyzed; glaciers accounted for 15-25 %; debris-covered glaciers were estimated at 15-19 %; firn fields contained only about 5-8 % of the water stored. Agricultural expansion is creating an increased water demand in the Aconcagua basin, which currently does not contain any constructed reservoirs. According to an NDVI analysis, irrigated agriculture has expanded 4% (292.5 km^2) from 1989 to 2010. The majority of this expansion has occurred in the foothills of the valley in less fertile soils. Exported fruit crops such as avocados and walnuts have significant economic value for large agri-farms or firms, but also require more water compared to traditional crops. Agricultural expansion has increased erosion on exposed slopes causing increase silting on rivers and has produced changes in coastal morphology. The valley has experience a reduction in winter precipitation of about 30-40% because of ENSO events (La Niña), which has produced a mega-drought since the year 2000. In sum, agricultural expansion and the current drought have put pressure on glacier melt water resources during the summer. Over the last 15 years, snowline in the basin has risen about 400 m. By mid-summer, less than 10% snow cover typically exists within the basin, suggesting that snowpack is a seasonal, temporary water resource. The water stored within rock glaciers provide a significant late season addition to stream flow to support irrigation during drought. However, these landforms are being removed for exploitation of mineral resources such copper. Their classification as glaciers is constantly been challenged by mining companies. In order to develop long-term, sustainable solutions, the importance of the water stored in rock glaciers or other alpine permafrost landforms such as talus slopes must be weighed against the economic value of mineral resources.

Hydrological and thermal modeling of Imnavait Cr. basin, Alaska, using WaSiM

Maria Kaiser[1], Anna Liljedahl[2], Ronald Daanen[3], Anne Gädeke[2], & Wolfgang Rieger[1]

[1] *Technische Universität München, Germany*
[2] *Water and Environmental Research Center, University of Alaska Fairbanks, USA*
[3] *Alaska Division of Geological and Geophysical Surveys, Department of Natural Resources, Fairbanks, USA*

Snowmelt and permafrost largely control the hydrology of Arctic basins. Here we calibrated and applied the physically based watershed model WaSiM to the Imnavait Cr. basin (2.1 km^2), which is located in the foothills of the Brooks Range, northern Alaska. Imnavait basin offers a unique long-term and intensive hydrological and meteorological field measurement record, which makes the watershed a prime candidate for testing a hydrological model. About one-third of the average annual precipitation (334 mm) falls as snow, which accumulates in a similar spatial pattern from year to year. The subsurface hydrological processes are limited to the active layer (25 to 100 cm) due to the continuous permafrost underlying the catchment. WaSiM was applied to the Imnavait Cr. basin for two consecutive years (2012-2013). The simulations were forced with air temperature, relative humidity, wind speed, incoming solar radiation and precipitation, and an extensive end-of-winter snow measurement campaign, which was used to derive the snow water equivalent storage prior the onset of melt. Ablation was calculated following two methods, the temperature index and energy balance approach. The seasonal freezing and thawing of the soil was modeled using the newly implemented heat transfer module. Simulated ablation, runoff, evapotranspiration and soil temperatures were calibrated (yr 2012) and validated (yr 2013) against field measurements. For simplicity, the groundwater module (lateral subsurface flow) was not activated in these simulations.

The energy balance method for snowmelt produced more effective results of snowmelt runoff compared to the temperature index method (NSE of 0.73 and 0.54, respectively). Simulated snowmelt runoff was overestimated using both ablation methods, although the energy balance method produced a relatively lower overestimate (14 % compared to 20 %). It proved difficult to effectively model the onset of the snowmelt runoff with the simulated runoff occurring too early. Mean monthly simulated soil temperature profiles were compared to a nearby deep borehole. Results show that WaSiM performs quantitatively and qualitatively well. The modeling of snowmelt runoff could be improved by incorporating a physical routine for melt water storage in the snow pack as well as by activating the existing physically-based two-dimensional groundwater module.

Altered stream discharge, chemistry, ecosystem productivity, and fish habitat related to climate change and permafrost thaw at the boreal-arctic transition in Alaska

Joshua C. Koch[1], Michael Carey[1], Jon O'Donnell[2], Chris E. Zimmerman[1], & George Aiken[1]

[1] *United States Geological Survey, United States of America*
[2] *National Park Service*

The boreal-arctic transition zone of Alaska is likely to experience drastic changes in the near future related to climate warming, permafrost thaw, and vegetation dynamics. These changes will impact stream discharge, chemistry, and temperature, and subsequently ecosystem productivity and fish habitat. Many fish species in this region are at their physiological limits due to cold water temperatures and limited food and habitat, and therefore warming temperatures and greater input of allochthonous carbon (C), nitrogen (N), and phosphorus (P) to streams will likely impact fish habitat and productivity. Quantifying the impacts of permafrost thaw on aquatic ecosystems is a challenge given the complex three-dimensional nature of thaw, subsurface hydrology, and lateral transfer of solutes from soils to streams.

To examine the effects of permafrost and other watershed characteristics on hydrology and stream chemistry, we sampled streams along a gradient reflecting spatial variation in permafrost thermal state (north- vs. south-facing aspects), vegetation (tundra vs. boreal forest), and elevation. Our study sites were established in Noatak National Preserve in northwest Alaska, which is situated in the discontinuous permafrost zone and spans the boreal-arctic transition zone. We hypothesized that spatial variation in permafrost extent and/or thaw depth would alter subsurface flow pathways, and subsequently stream hydrographs and chemistry. These factors in turn will affect fish habitat and food resources. We calculated hydrograph recession coefficients to evaluate spatial and seasonal patterns in watershed storage and runoff following storms and in relation to thawing of active layer soils. We observed large differences between catchments, with larger and south-facing catchments displaying significant decreases in storm recessions as the summer progressed, while many other catchments displayed no trends. Dissolved organic C (DOC) and dissolved inorganic N (DIN) concentrations were generally low (DOC < 5 mg C L^{-1} and DIN < 0.12 mg N L^{-1}), but sensitive to stream discharge, with large flushes of C and N during storms and seasonal patterns due to leaching and/or cycling of nutrients in deeper thawed soils at base flow. Spatial differences in DOC, nutrients, and other solutes reflect different water sources and biogeochemical cycling across streams, as mediated by permafrost extent and vegetation. These hydrologic and chemical differences suggest greater storage over the summer as seasonally frozen ground thaws. Together, these observations indicate a mosaic of stream productivity and fish habitat across the watershed, allowing us to rank streams in terms of potential climate effects and implications for fish performance. These results provide a first glimpse at the magnitude and speed with which climate warming and permafrost thaw can create ecosystems and habitat, and have relevance for predicting future ecosystem development under a warming climate.

Permafrost and hydrological conditions of the Baikal Lake basin under the impacts of climate and land use changes

Victoriia Kurovskaia[1], Olga Semenova[1,2], & Tatyana Vinogradova[1]

[1] *Saint-Petersburg State University, Russian Federation*
[2] *Gidrotehproekt Ltd, St. Petersburg, Russia*

Baikal is the deepest lake in the world and the unique ecosystem. The aim of this research is to assess the impact of climate and land use change on the characteristics of permafrost of different types and corresponding hydrological processes. The analysis of the long-term variability of characteristics of river inflow and permafrost conditions using the historical data was conducted as well possible changes were projected based on hydrological modelling.

The basin of the Lake Baikal has area about 545 000 km^2, half of which is situated in Russia. It is characterized by different types of continuous and discontinuous permafrost, various climate and landscape conditions and annual flow depth varying from 30 to more than 600 mm within the studied area. Land use changes (fires, for example) and climate variations have a strong impact on the permafrost conditions and the regime of rivers inflow to the Lake. The watersheds response caused by environmental non-stationarity can be variable and unpredictable. Therefore adequate hydrological models with accounting for permafrost and robust parametrization are required for future projections.

Several small and middle-size representative watersheds in different parts of the Lake basin with area from 151 to 7800 km^2 with various permafrost conditions and different types of hydrological regime were chosen for the study.The data base for modelling was developed which included the information about landscapes, soils, permafrost characteristics and dominant hydrological processes. The hydrological model parameters for different types of permafrost conditions and dominant landscapes were estimated based on that information.

We applied distributed process-based hydrological model Hydrograph [Vinogradov et al., 2011, Semenova et al., 2013]. It describes all essential processes of land hydrological cycle including detailed algorithm of water and heat dynamics in soil accounting for water phase change [Semenova et al., 2014].

The Hydrograph model was validated for the historical period and then used in projection mode with the conceptual scenarios of climate and land use change. The results of modelling projections were explored and the conclusions about possible changes of river inflow to the Lake Baikal were drawn. We propose that the Hydrograph model can be applied as the tool to estimate riverine inputs into the lake's systems in permafrost environment. The example of such approach is demonstrated here.

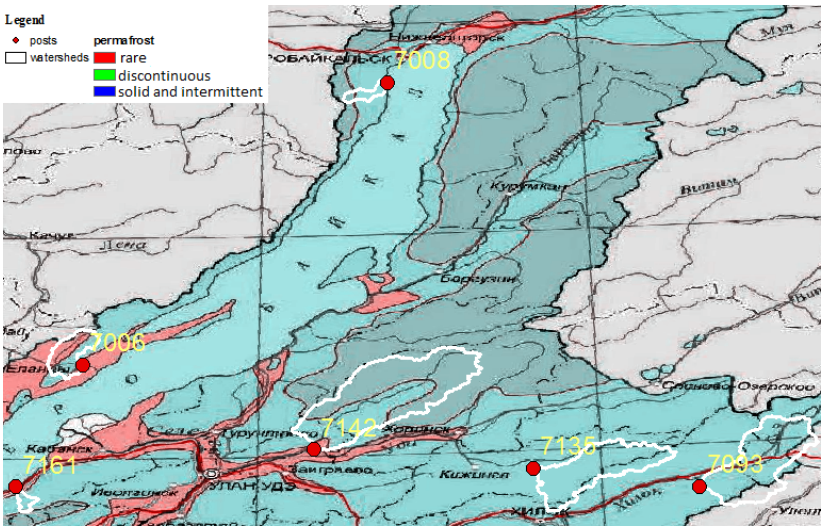

Figure 1: Permafrost regionalization of the Baikal Lake.

Acknowledgements

The study was partially supported by Russian Foundation for Basic Research (project 15-35-21146 mol_a).

References

Semenova, O.; Lebedeva, L. and Vinogradov, Y. [2013]: Simulation of subsurface heat and water dynamics, and runoff generation in mountainous permafrost conditions, in the Upper Kolyma River basin, Russia. *Hydrogeology Journal*, 21(1):107–119, doi:10.1007/s10040-012-0936-1.

Semenova, O.; Vinogradov, Y.; Vinogradova, T. and Lebedeva, L. [2014]: Simulation of Soil Profile Heat Dynamics and their Integration into Hydrologic Modelling in a Permafrost Zone. *Permafrost and Periglacial Processes*, 25(4):257–269, doi:10.1002/ppp.1820.

Vinogradov, Yu. B.; Semenova, O. M. and Vinogradova, T. A. [2011]: An approach to the scaling problem in hydrological modelling: the deterministic modelling hydrological system. *Hydrological Processes*, 25(7):1055–1073, doi:10.1002/hyp.7901.

Deciphering the impact of permafrost change and disturbance on catchment water quality

Scott F. Lamoureux & Melissa J. Lafreniere

Queen's University, Canada

Communities and Arctic development depend on knowledge to support safe communities and maintain water security. Projected climate change in the Arctic is expected to have substantial impacts on permafrost through increased seasonal thaw and these changes will likely result in changing water availability and alter hydrological processes that control water quality. Predicting these impacts is an important need for sustainable development and maintaining ecosystem health in Arctic regions.

We have investigated these processes through a long term integrated watershed program at the Cape Bounty Arctic Watershed Observatory (CBAWO) in the Canadian Arctic. Surface water discharge and quality has been assessed since 2005 and in particular, through a period of record summer temperatures that began in 2007. Exceptionally warm summer conditions resulted in deep active layer thaw and resulted in widespread localized slope and channel disturbances. Our research has documented the impact of these permafrost changes and tracked the recovery for seven years. In particular, we have demonstrated several key linkages between landscape disturbance, changing hydrological conditions and altered downstream water quality.

Deeper active layer thaw appears to alter subsurface flow paths, resulting sustained, multi-year changes to solute and nutrient fluxes and likely occur over most of the landscape. By contrast, physical disturbance due to localized permafrost slope failures (active layer detachments) generate impacts ranging from minimal to locally-significant increases in downstream sediment and solute transport. We note that this strong contrast between what we term "thermal" and "physical" perturbation represents a key impact of permafrost change in these settings. Deciphering the catchment-scale impact of permafrost changes requires determining the relative roles of these distinctive responses to improve our understanding and predictive capacity regarding hydrological change in the Arctic.

Interaction of permafrost and hydrological processes at a sandy permafrost hillslope in Central Yakutia: the observations and modelling results

Liudmila Lebedeva[1], Olga Semenova[2,3], Alexander Kolesnikov[1], & Vasiliy Ogonerov[1]

[1] *Melnikov Permafrost Institute SB RAS, Russian Federation*
[2] *Gidrotehproekt Ltd., Russian Federation*; [3] *St. Petersburg State University, Russian Federation*

Ground freezing/thawing and water fluxes are coupled in permafrost environments. The aim of the research is to simulate hillslope-scale permafrost and hydrological processes at well-studied sandy slope covered by sparse pine forest in Central Yakutia.

The studied hillslope is located within the Shestakovka river basin, the tributary of the Lena River, 20 km south from Yakutsk. The slope located next to the Malaya Chabyda lake is covered by sandy deposits. The permafrost thickness is 400 m. The dominant vegetation is sparse pine forest with thin bearberry cover. Although the climate is harsh continental with mean annual air temperature -9.4 °C (1951-2012), closed suprapermafrost talik was found at the slope.The talik depth is about 4-5 m. The lower part of the thawed zone is fully saturated all year round.

In 1970-1980s extensive observations of ground thaw depth, groundwater level, ground temperature, soil moisture, surface and subsurface flow were carried out at the talik and frozen part of the slope. Based on the observations the annual water balance components of the slope were assessed as the following: precipitation – 240 mm, evapotranspiration – 140-160 mm, groundwater flow – 80-100 mm. There are two mainhypotheses about possible mechanisms of the talik formation in harsh climateof Central Yakutia. According to one of them the talik was formed after the forest fire 50-60 years ago and it is now gradually shrinking along with the forest development. Another hypothesis suggests that ground thaws deeper and quicker in summer because sandy deposits in upper 1-2 m are wetter in summerthan during the winter.

The process-based Hydrograph model was applied with two objective:

i) to simulate slope-scale hydrological processes using observed data of ground thawing/freezing, ground temperature and soil moisture

ii) to test two hypotheses of talik formation mechanisms.

The Hydrograph model is a process-based distributed model that describes processes of land hydrological cycle at any scale from elementary slope to large river basin [Vinogradov et al., 2011]. Since it has algorithms that simulate heat and water dynamics in soil profile accounting for phase change and thermal properties change due to variable ice and water content the model could be applied in the permafrost environment [Semenova et al., 2014]. The parameters relate to observable ground and vegetation properties [Lebedeva et al., 2014].

The results of the simulations of ground thawing and freezing, soil moisture, ground temperature, surface and subsurface flow will be presented for 1977-1985. Two scenarios of possible talik formation mechanisms will be performed.

We assume that the model algorithms and developed parameter sets being tested at the detailed data at slope-scale have potential to adequately represent hydrological processes at larger basins in similar conditions and be robust modelling tools in changing climates and landscapes.

Acknowledgements

The study was partially supported by Russian Foundation for Basic Research (project 15-35-21146 mol_a).

References

Lebedeva, L.; Semenova, O. and Vinogradova, T. [2014]: Simulation of Active Layer Dynamics, Upper Kolyma, Russia, using the Hydrograph Hydrological Model. *Permafrost and Periglacial Processes*, 25(4):270–280, doi:10.1002/ppp.1821.

Semenova, O.; Vinogradov, Y.; Vinogradova, T. and Lebedeva, L. [2014]: Simulation of Soil Profile Heat Dynamics and their Integration into Hydrologic Modelling in a Permafrost Zone. *Permafrost and Periglacial Processes*, 25(4):257–269, 2014. doi:10.1002/ppp.1820.

Vinogradov, Yu. B.; Semenova, O. M. and Vinogradova, T. A. [2011]: An approach to the scaling problem in hydrological modelling: the deterministic modelling hydrological system. *Hydrological Processes*, 25(7):1055–1073, doi:10.1002/hyp.7901.

Distribution of organic matter in sub-channel permafrost deposit within the Lena River Delta

Georgii T. Maksimov[1], Mikhail N. Grigoriev[1], Sebastian E. Zubrzycki[2], Tamara V. Khodzher[3], & Tatiana V. Pogodaeva[3]

[1] *Melnikov Permafrost Institute SB RAS, Russian Federation*
[2] *Institute of Soil Science, Universität Hamburg, Germany*
[3] *Limnological Institute SB RAS, Russian Federation*

The Lena Delta is the largest arctic delta with an area of about 30,000 sq.km. It has numerous distributary channels which comprise, with channel bars, approximately 7,500 sq. km, or about a quarter of the delta area.

In contrast to the main river channel, the delta distributaries are very shallow as they spread over a large area. Shallow channels, with depths ranging to 2-2.5 m, freeze to the bottom in winter, promoting relatively deep freezing beneath the channel bed.

Field studies on Bolshaya Tumatskaya Channel have shown that permafrost is widespread beneath its bed, underlying half, and frequently more of the channel. A perennial talik only develops under the relatively narrow fairwater. The temperature of bottom sediments between the fairwater and banks was as low as -12 °C in April.

Borehole profiles indicate that the upper 10 m of sediments have a very high content of organic material consisting largely of wood debris. The high C/N ratios (25-50), i.e. high organic carbon and very low organic nitrogen levels, are likely to be due to the high presence of undecomposed organic matter, plant remains in the form of wood debris. The carbon-to-nitrogen (C/N) ratio in these sediments may reach 80 or higher. The C/N ratio is an indicator of the ways of organic matter transformation. At high C/N ratios, immobilization of nitrogen and degradation of organic matter occur in river taliks. As the organic matter is transformed, it is enriched with nitrogen and the C/N ratio decreases. At C/N ratios of 20-25, microbial processes of humufication are intensified.

With rapidly shifting and re-forming channels, organic matter begins to degrade in thawing sub-channel sediments. Organic matter transformation in bottom sediments within the delta of large arctic rivers can result in increased CO_2 emissions into the atmosphere.

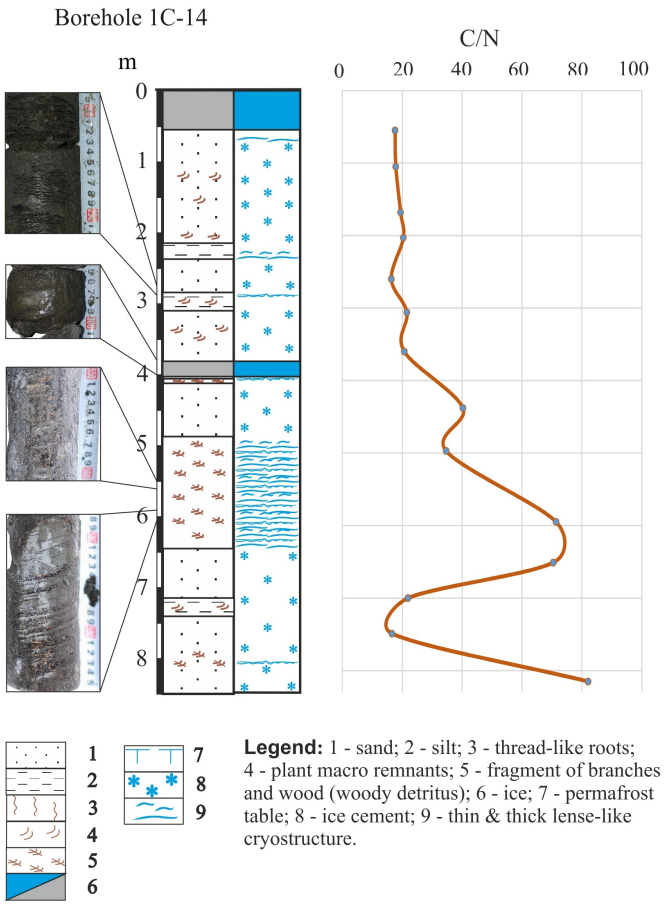

Figure 1: Section Bh 1c-14

Influence of seasonal conditions on the deformation of coastal slopes, occuring in the permafrost zone

Oksana Maslikova, Elena Debolskaya, Ilja Gritsuk, & Dmitri Ionov

Russian Academy of Sciences, Russian Federation, Institute of Water Problems

Problem and purpose: Global climate changes in recent decades inevitably lead to more frequent catastrophic events. Their negative effects on rivers located the permafrost zone, may be exacerbated by significant changes in channel deformations that are caused not only the influence of water flow, but significant changes of the channel due to the influence of increasing water and air temperatures on the structure of its constituent materials.

So far there are no methods that can link the climate, permafrost-geological, morphological and dynamic characteristics of the "atmosphere - channel flow - coastal permafrost" system. The investigation of the dynamics of ice shores are mainly related to the study of the shores of the Arctic seas. In the our paper we attempt to solve this problem for the river.

Figure 1 illustrates a distribution of liquid flows in the annual thawed layer located in the permafrost zone. It is obvious that during the process of thawing the fluid is redistributed in each block: the part of the melting flow is increased, the soil conductivity is changing and, accordingly, - the maximum possible amount of moisture for this type of soil is changing also. As a result, there is possible the changes capacity of infiltration and, as a consequence, the proportion of the flow of current on the slope changes over time. At the end of the thawing process the movement of the soil moisture in the slope is stabilized, and the proportion of the flow of current on the slope will depend on rainfall, which, in turn, is a function of the seasonal and diurnal temperatures and solar radiation.

Method: the laboratory study of the interaction of river flow with frozen soils under the thermal (warming) and mechanical (impact of rain) external influences were conducted. We studied the time of thawing of soil, infiltration in soil, sediment transport under the influence of thawing of frozen soils and rainfall.

We have considered a set of interrelated factors that have a significant impact on deformations of the coastal slopes in the permafrost zone under conditions of seasonal changes in the environment. The model consists of several blocks: the thawing of frozen soil and the occurrence of melt flow, the division of the precipitation on the infiltration and the catchment (surface fluxes) and the seasonal melting of snow as a type of the incoming rainfall, the impact of surface runoff erosion to the coastal slope of river.

Atmospheric precipitation that arriving at the soil surface (while the soil is thawing) consist of melting snow and/or rain. Snow melting occurs when the temperature at the snow surface becomes equal to 0 °C. Snow melting is classified as either convectional (thermal) melting, or radiation melting. The convectional snow melting occurs in dreary weather conditions, and is caused by the inflow of warm air masses. The radiation melting implies that the sun rays penetrating into the snow cause its melting both on the surface, and within a top layer 20-40 cm thick. We are using the law which states that the intensity of incoming solar radiation decreases with the depth (the Burger-Lambert Law) and take into account the snow albedo change during the melting.

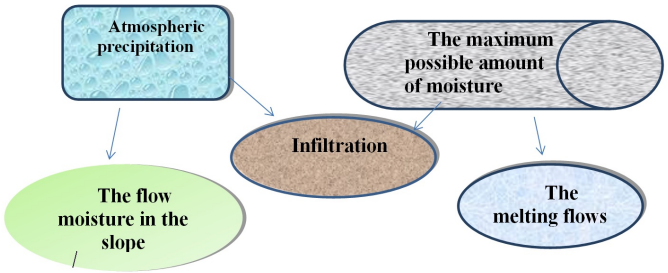

Figure 1: Distribution of fluid flows in annual thawed layer of water body coast

If the intensity of atmospheric precipitation, namely, of seasonal rainfalls or of melting snow (or, in many cases, of both) does not exceed the infiltration rate, then all moisture is spent for soil saturation, and no surface erosion occurs.

If the intensity of melting exceeds the infiltration rate, then the excess thawed water goes to runoff and causes erosion of the surface of the river slope.

In the laboratory for testing of some blocks we used the mechanism for the simulating of the rain with varying intensity that can measure the rate of flow during infiltration of the thawing soil and the amount of lateral flow. The effect of solar radiation (ultraviolet and infrared parts of the spectrum) was investigated also.

The presented mathematical model completely describes the erosion of seasonal thawed layer of coastal slopes of river that located in the permafrost zone, in conditions where the seasonal changes of environmental temperatures occur, and under exposure to atmospheric precipitation. Laboratory examination showed good agreement with theory.

Acknowledgements

The work was supported by the Russian Foundation for Basic Research (projects 15-05-00342 A, 16-08-00595)

Runoff modelling in the zone of frost mound bogs by the example of small watersheds of the Muravlenkovsky research station

Anna Stepanova Mysina[1] & Olga Mikhailovna Semenova[1,2]

[1] *Saint-Petersburg state university, Russian Federation*
[2] *Gidrotehproekt Ltd, Saint Petersburg, Russia*

The research aim was to assess the parameters of hydrological model Hydrograph for the zone of frost mound bogs. We used the data of hydrological, meteorological and thermal balance studies conducted by the West-Siberian Expedition of the State Hydrological Institute (SHI) located in the continuous permafrost zone of Western Siberia. The West-Siberian Expedition of SHI has conducted an extensive research in order to study the hydrometeorological regime of wetlands in Western Siberia from 1965 to 1993. The typology of wetlands, peat deposits structure, thermal and hydrophysical properties of active layer of peat deposits were studied as well [Novikov, 2009]). At the Muravlenkovsky station the observations of heat transfer in the active layer, temperature, freezing and thawing peat deposit, evaporation from wetlands, wetland water level, runoff and meteorological parameters were conducted during the period from 1983 to 1992. This unique data still have not been processed and never used for hydrological modelling.

The study objects are located at the research station Muravlenkovsky within the basin of the Pur river: the river Halmer-Jaha and the Bazovyj brook. The watersheds of Halmer-Jaha river with the area 124 km^2 and its tributary, the Bazovyj brook, area 52,8 km^2, are covered by wetlands (90 and 66 %, respectively). The bogs of basins are mainly frozen with domination of flat-mounds micro landscapes group (80 %), which is typical for large territory within the areas of northern taiga and forest-tundra [Novikov, 2009].

The Hydrograph model is a process-based model with distributed parameters [Vinogradov et al., 2011]. Input data includes standard meteorological information. The model parameters have a physical meaning and may be assessed on the base of observation data. The model has the block of calculation the dynamics of heat and moisture in the soil column which allow simulations of freezing and thawing processes in soil [Semenova et al., 2014]. The algorithm was verified in the conditions of mountainous areas of Eastern Siberia [Vinogradov et al., 2011]. The novelty of current work is to test the model for watersheds of wetland area of Western Siberia in the conditions of permanent water stagnation in upper layers of soil and active layer of peat deposit.

There are two types of microlandscapes, namely mounds and fens, which have specific features of active layer development and runoff formation processes at local scale in frost mound bogs. Fens are the subject to much deeper soil thaw than mounds and runoff water moves through them into streams. Based on the data of field studies the conceptualization of four runoff formation regimes reflecting the interaction between mounds and fens during different periods of the year was developed (Fig. 1A). Schematic soil-vegetation profiles for mounds and fens were elaborated. The combinations of three types of soil horizons identified as moss-lichen cover, peat layer and sand layer are applied to conceptualize typical soil profiles for each microlandscape type. Assessed physical properties are used as the Hydrograph model parameters to simulate thaw/freeze processes in microlandscapes and streamflow in studied watersheds for 1984-1992 period. The simulation results are in a satisfactory agreement with the observations (Fig. 1B) and will be presented at the conference.

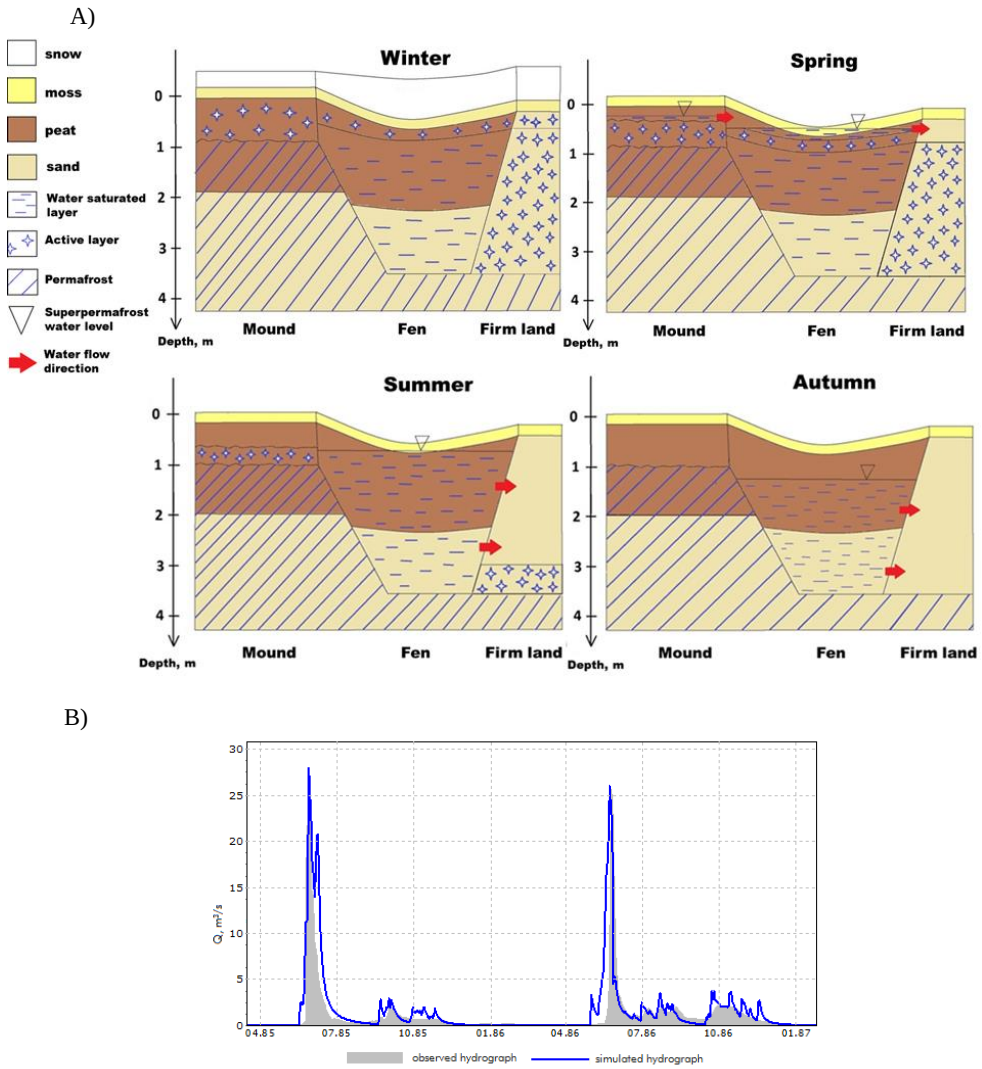

Figure 1: A – The schemes of runoff formation regimes reflecting the interaction between mounds and fens during the year; B – the example of simulated hydrograph for the river Halmer-Jaha for 1985 and 1986.

Acknowledgements

This work is the first stage of runoff modeling for wetlands of Western Siberia and supported by Russian Foundation for Basic Research (project 15-35-21146 mol_a).

References

Novikov, S.M.(ed.). [2009]: *Hydrology of frost wetlands of Western Siberia*. Saint Petersburg, VVM.

Semenova, O.; Vinogradov, Y.; Vinogradova, T. and Lebedeva, L. [2014]: Simulation of Soil Profile Heat Dynamics and their Integration into Hydrologic Modelling in a Permafrost Zone. *Permafrost and Periglacial Processes*, 25(4):257–269, doi:10.1002/ppp.1820.

Vinogradov, Yu. B.; Semenova, O. M. and Vinogradova, T. A. [2011]: An approach to the scaling problem in hydrological modelling: the deterministic modelling hydrological system. *Hydrological Processes*, 25(7):1055–1073, doi:10.1002/hyp.7901.

Hydrological processes at the Suntar-Hayata ridge (Eastern Siberia): Analysis of historical data and modelling

Nataliia Nesterova[1], Olga Semenova[1,2], & Lyudmila Lebedeva[3]

[1] *St. Petersburg State University, Russian Federation*
[2] *Gidrotehproekt Ltd., St. Petersburg, Russian Federation*
[3] *Melnikov Permafrost Institute, Russian Federation*

The detailed studies of permafrost, hydrological and glaciological processes at the Suntar-Hayata Ridge were conducted in 1957-1964 within the Program of International Geophysical Year (1957-1958) and following Geophysical Decade. The Suntar-Hayta Ridge (with highest mountain reaching 2959 m) is situated in Eastern Siberia and divides the Lena, Indigirka and the Okhotsk sea rivers basins. It is characterized by original combination of climate, geological and glaciological conditions.

In 2015 our research group got the access to the reports of High-Mountain Glaciological and Geocriological Suntar-Hayata station which were stored in the archives of Melnikov Permafrost Institute in Yakutsk, Russia [Grave et al., 1964]. We used revealed data for the assessment of factors governing runoff formation processes in remote high-elevation permafrost area, and estimated the parameters of hydrological model based on those findings.

Two watersheds of different scale were selected as the objects of our studies – the Suntar river (7680 km^2) (Fig. 1A) and the Sakharyniya River (84.4 km^2).

The Hydrograph model [Semenova et al., 2013] was used in the study as it explicitly describes hydrological processes in different permafrost environments including the dynamics of ground thaw/freeze (ex., Lebedeva et al. [2014]). In the Hydrograph model the processes have a physical basis and certain strategic conceptual simplifications. Main model parameters refer to observable soil and vegetation properties. The level of model complexity is suitable for a remote, sparsely gauged region such as Eastern Siberia as it allows for a priori estimation of the model parameters.

Based on the observations (meteorological data, ground temperature at different depth, soil profile descriptions, characteristics of vegetation, snow measurements, etc.) the model parameters were verified for four main landscapes of the studied watersheds (bare rocks and glacial, mountain tundra, sparse larch forest and river valleys - riparian forest at swamped soils) (Fig. 1A, B). The properties of typical soil-vegetation cover corresponding to these four landscapes were generalized resulting in development of soil-vegetation schemes assumed to be typical for each landscape.

At the first stage the simulations of individual processes, such as the modelling of snow formation and melting, soil thaw/freeze and evaporation for the Suntar-Hayata site were conducted. The results of this stage were considered satisfactory. For example, calculated values of temperature of the soil at various depths closely matched observed data with the largest discrepancies not exceeding 5 °C (Fig 1C).

At the second stage we conducted runoff modelling with initially assessed parameters for the period of maximum available meteorological information (1957-1964) for both studied watersheds (Fig 1D). Lastly, the simulation of runoff processes were conducted for the period 1965-2013 and for the future climates based on conceptual scenarios. Detailed results of runoff simulations for current and future climates are explored.

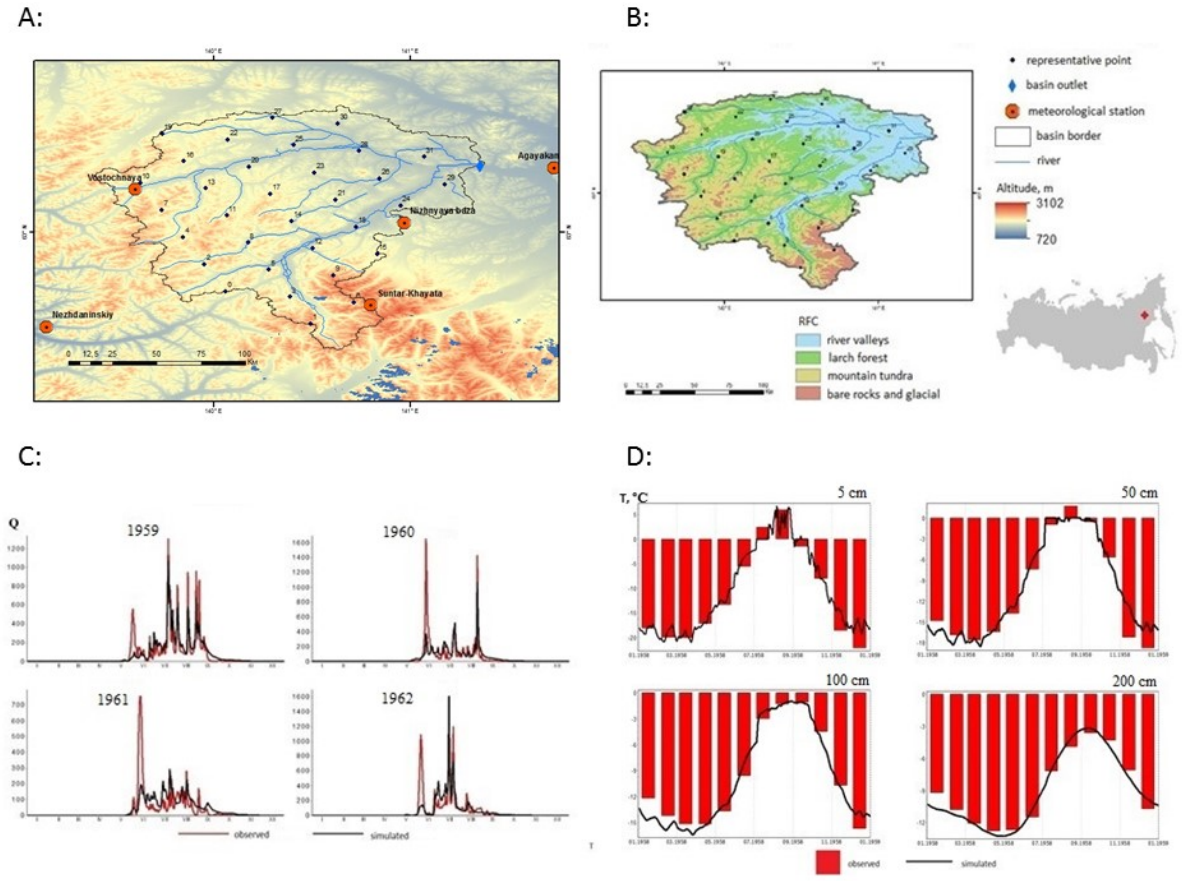

Figure 1: The study basin (A), its schematization (B), the results of modelling of runoff (C) and soil temperature (D). The Suntar-Hayata Ridge, Eastern Siberia

For vast regions of the world with sparse monitoring networks like much of Russia, detailed catchment data only exist in small-scale research basins. Process based model parameterizations that are confirmed and refined in such basins have the potential to be applied in hydrologically similar regions.

Acknowledgements

The study is supported by Russian Foundation for Basic Research (project 15-35-21146 mol_a).

References

Grave, N.; Gavrilova, M.; Gravis, G.; Katasonov, E.; Klyukin, N.; Koreysha, G.; Kornilov, B. and Chistotinov, L. [1964]: *The freezing of the earth's surface and glaciation on the ridge Suntar-Hayata (Eastern Yakutia)*. Nauka, Moscow.

Lebedeva, L.; Semenova, O. and Vinogradova, T. [2014]: Simulation of Active Layer Dynamics, Upper Kolyma, Russia, using the Hydrograph Hydrological Model. *Permafrost and Periglacial Processes*, 25(4):270–280, doi:10.1002/ppp.1821.

Semenova, O.; Lebedeva, L. and Vinogradov, Y. [2013]: Simulation of subsurface heat and water dynamics, and runoff generation in mountainous permafrost conditions, in the Upper Kolyma River basin, Russia. *Hydrogeology Journal*, 21(1):107–119, doi:10.1007/s10040-012-0936-1.

River routing over "Glass Surface" in permafrost regions

Maria E. Norman, Matthias Brakebusch, & Christian Beer

Stockholm University, Sweden

The Arctic is an important pool of soil carbon, since around 44 % of the Earth's near surface carbon is stored in the Artic [AMAP, 2012]. Thawing of permafrost would result in an increased release of carbon to the atmosphere. However, warming of the land surface may also result in increasing vegetation, and hence larger uptake of carbon. Fresh water in permafrost regions plays an important role in the carbon cycle since lakes and rivers have the capability to store, process, emit, and transport carbon. To simulate the effects of future climate change in permafrost areas, it is important to have an accurate representation of processing and transport of carbon in lakes and rivers in Terrestrial Earth System models. However, these processes are rarely included in current large-scale models.

This study is part of a project to add biogeochemistry in lakes in order to include freshwater carbon cycle in large-scale modelling. The aim of this study is to introduce river water transport in a hydrological model which will further be used also for transport of carbon and state variables. The model is a restructured version of Variable Infiltration Capacity (VIC) macroscale hydrologic model [Liang et al., 1994]. VIC is a grid based model which fully solves the water- and energy balance. There is sub-grid variability in land surface vegetation classes. The model includes a lake-wetland algorithm as well as snow and frozen soil algorithm. The new structure of the model allows interaction between grid cells, such as lateral transport of state variables.

The first application with the restructured model version is for a case with "glass surface", where different methods of estimating the river flow travel time is investigated. In the "glass surface" case it is assumed that the ground is frozen, and therefore there is no percolation into the soil. As a first step, the lakes are also assumed to be frozen. Therefore, all of the precipitation and snow melt in a grid cell is surface runoff to the river. There is inflow from upstream grid cells, and outflow to a neighbor downstream grid cell. River discharge during snowmelt season in two catchments, a semi-permafrost and a permafrost region, is modeled and compared to measured data.

References

Arctic Monitoring and Assessment Programme (AMAP), Oslo. *Arctic Climate Issues 2011: Changes in Arctic Snow, Water, Ice and Permafrost.* 2012. xi + 97pp.

Liang, X.; Lettenmaier, D.P.; Wood, E.F. and Burges, S.J. [1994]: A simple hydrologically based model of land surface water and energy fluxes for general circulation models. *Journal of Geophysical Research: Atmospheres*, 99(D7):14415–14428, doi:10.1029/94JD00483.

Preliminary studies of water, snow and ice in the Quebrada del Medio, Hans Stepanek rock glacier, Mendoza, Argentina

Michael Thomas OConnor[1], M. Bayani Cardenas[1], Bethany T. Neilson[2], Matthew H. Kaufman[1], & George W. Kling[3]

[1] *Department of Geological Sciences, The University of Texas at Austin, Austin, TX, USA*
[2] *Civil and Environmental Engineering, Utah Water Research Laboratory, Utah State University, Logan, UT, USA*
[3] *Department of Ecology and Evolutionary Biology, University of Michigan, Ann Arbor, MI, USA*

Vast reservoirs of organic carbon become accessible each summer when arctic soils thaw. The carbon leaches into shallow groundwater flowing through the thawed soil. Groundwater transports this dissolved organic carbon (DOC) into streams, where it can be further processed. However, we know little about how groundwater moves through the soil during progressive, seasonal thaw. Questions remain regarding the importance of liquid water as a mechanism for heat advection, and how that heat advection might augment active layer thaw, deepening flowpaths and prolonging groundwater residence times. Further understanding of these flowpaths is required to accurately understand the arctic terrestrial carbon budget.

Here we present findings from both field observations and coupled multiphysics numerical models that help discern where and how flowpaths develop in thawing soils. We monitored water table elevations, temperature, specific conductance, soil hydraulic conductivity, and thaw within an arctic active layer during summer 2015. We used these observations to inform the development of a coupled numerical model incorporating heat transport, groundwater flow, permafrost thaw, and DOC transport. Our field campaign captured a low-precipitation year, and thus allowed us to inform our model with baseline groundwater observations in an attempt to isolate the contribution to watershed DOC export.

Head and thaw observations showed groundwater flow paths and volumes to be scale-dependent. Groundwater flow paths are a subdued version of topography at the hillslope scale, however, they are an exaggerated version of microtopographic features, such as hummocks and hollows, at a more localized scale. The saturated thickness of these flowpaths also varied locally. This varying scale dependency significantly impacts groundwater export volumes and residence times in low-gradient areas. Local topographic exaggeration highlights the importance of advective heat transfer via groundwater flow in active layer and flowpath development. It suggests that the feedback between groundwater flow and heat transport affects flowpath development in the riparian zone, deepening flowpaths where groundwater is concentrated, which significantly increases groundwater residence times. This would allow for more leaching, storage, and ultimate transport of DOC. Furthermore, it implies that this process may be controlled by microtopography.

The observations and model results will help develop our understanding of arctic groundwater hydrology and its role in chemical transport. With a robust conceptual model of these systems, we will be better able to predict and quantify terrestrially-sourced arctic DOC.

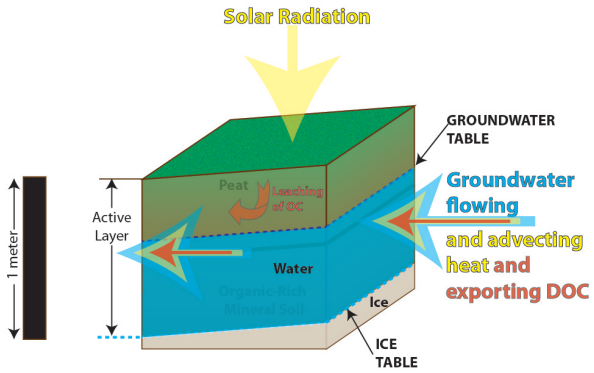

Figure 1: Conceptual model of the dominant groundwater flow, heat transport, and carbon transport processes in a generalized permafrost domain.

Transfers along slopes in a permafrost-dominated watershed of Central Siberia: A mechanistic 2D coupled thermo-hydrological modelling study

Laurent Orgogozo[1], Anatoly S. Prokushkin[2], Oleg S. Pokrovsky[1], Yves Goddéris[1], Christophe Grenier[3], Michel Quintard[4], Jérôme Viers[1], David Labat[1], & Stéphane Audry[1]

[1] *GET, UMR 5563 CNRS-IRD-UPS, 14 avenue Edouard Belin, Toulouse, France.*
[2] *V.N. Sukachev Institute of Forest, SB RAS, Krasnoyarsk, Russian Federation.*
[3] *LSCE, UMR 8212 CNRS-CEA-UVSQ, Orme des merisiers, Gif-sur-Yvette, France.*
[4] *IMFT, UMR 5502 CNRS-INPT-UPS, 2 Allée du Professeur Camille Soula, Toulouse, France*

This work presents a numerical study of water and energy transfers within a permafrost dominated experimental watershed of Central Siberia, the Kulingdakan catchment (e.g.: Viers et al. [2015]). This watershed has been studied for years in order to characterize and quantify the elementary transfers from the slopes to the stream along the seasonal cycles, and in the context of climate change. The water fluxes, strongly coupled with the thermal fluxes due to the presence of permafrost, are the main vectors of these matter transfers. In this study we aim to build a mechanistic model of the water and energy fluxes that may produce rigorous thermal and hydrological background for modellings the geochemical transfers from the slopes to the stream.

The use of a mechanistic approach consists in resolving numerically the governing equations of the considered physical phenomena, established in the framework of continuum mechanics. The tool we used to produce a mechanistic model of the thermo-hydrological transfers in soils is permaFoam [Orgogozo et al., 2015], a solver for the coupled equations that describe unsaturated water transfers (with evapotranspiration) and thermal transfers (with freeze/thaw), implemented in the framework of OpenFOAM®, a well-known open source tool box for computational fluid dynamics. The main interest of using OpenFOAM® lays in its good performances in massively parallel computing (e.g.: Orgogozo et al. [2014]). Indeed, due to the strong couplings and the strong non-linearities that are encountered in such physical problems, the use of high performance computing methods is needed to deal with the fine spatial and temporal discretizations required for the numerical resolutions. This is especially true when large scales are involved as is the case for the experimental watershed scale (here, Kulingdakan watershed, about 41 km^2 of surface).

The Kulingdakan watershed is dominated by continuous permafrost, with larch forests growing on soils produced from weathering of basaltic rocks. The main variability of the landscape is related to the aspect of the slope translated to the amount of solar radiation received, which in turn controls the thermal status of the soil. Specifically, the aspect of the slopes may be either south aspected (higher solar energy input) or north aspected (lower solar energy input). With permaFoam two 2D vertical sections are build up to represent both south and north aspected slopes, with heterogeneous soils (taking into account the presence of a moss layer and of an organic (mor) layer overlaying the mineral soil). The topography and the spatial scales of these 2D models are derived from a simple Gravelius rectangle approach, which lead to modelling domains of 2.5 km of width, with slopes of about 20 %. We produce a quantitative modelling of the seasonal cycle of the active layer dynamics, based on monthly soil temperatures and meteorological forcings obtained by multiannual averaging of data acquired in the watershed (observations done between 2006 and 2012). A representative behavior of the active layer dynamics in present conditions is modelled in this way.

The numerical results and the field data are in reasonable agreement. The model is capable of reproducing the variability of the thermo-hydrological dynamics between slopes of north and south aspects, as well as the variability of thermo-hydrological conditions along the slopes.

Finally, we discuss numerous perspectives related to this numerical development for the modelling of present and future geochemical fluxes under climate change scenarios.

References

Orgogozo, L.; Renon, N.; Soulaine, C.; Hénon, F.; Tomer, S.K.; Labat, D.; Pokrovsky, O.S.; Sekhar, M.; Ababou, R. and Quintard, M. [2014]: An open source massively parallel solver for Richards equation: Mechanistic modelling of water fluxes at the watershed scale . *Computer Physics Communications*, 185(12):3358 – 3371, doi:10.1016/j.cpc.2014.08.004.

Orgogozo, L.; Pokrovsky, O.S.; Goddéris, Y.; Grenier, C.; Viers, J.; Labat, D.; Audry, S. and Prokushkin, A. [2014]: Thermo-hydrologic modelling of permafrost with OpenFOAM®: perspectives of applications to the study of weathering in boreal areas. In *Geophysical Research Abstracts*, number EGU2015-9775-1, EGU General Assembly 2015.

Viers, J.; Prokushkin, A.S.; Pokrovsky, Oleg S.; Kirdyanov, A.V.; Zouiten, C.; Chmeleff, J.; Meheut, M.; Chabaux, F.; Oliva, P. and Dupré, B. [2015]: Zn isotope fractionation in a pristine larch forest on permafrost-dominated soils in Central Siberia. *Geochemical Transactions*, 16(1):1–15, doi:10.1186/s12932-015-0018-0.

Process-rich projections of permafrost integrated surface/subsurface thermal hydrology in a warming climate

Scott L. Painter[1], Ethan T. Coon[2], Adam Atchley[2], & Ahmad Jan[1]

[1] *Climate Change Science Institute and Environmental Sciences Division, Oak Ridge National Laboratory, USA*
[2] *Computational Earth Sciences Group, Earth and Environmental Sciences Division, Los Alamos National Laboratory, USA*

The need to understand potential climate impacts and feedbacks in Arctic regions has prompted interest in developing more detailed representations of permafrost hydrology for use in fine-scale, topography-resolving modeling studies. Fine-scale 100-year projections of the integrated permafrost thermal hydrological system in polygonal tundra near Barrow, Alaska will be presented. The new modeling capability [Painter et al., 2016] combines a surface energy balance model with recently developed three-dimensional subsurface thermal hydrology models [Painter and Karra, 2014, Karra et al., 2014] and new models for nonisothermal surface water flows and snow distribution in the microtopography. The diffusion wave equation is extended to include energy transport and phase change of ponded water to model the surface flow system. Variation of snow depth in the microtopography is also modeled heuristically with a diffusion wave equation. Representations of the multiple surface and subsurface processes are solved simultaneously on three-dimensional unstructured meshes by leveraging highly parallel community software [Moulton et al., 2012]. Simulations exploring microtopographic controls on permafrost hydrology in warming climate show significant differences in thermal conditions among the centers, rims, and troughs of ice-wedge polygons during the spring and fall seasons, but those differences are largely equilibrated by lateral heat transport during the summer. The results of the fine-scale simulations suggest an approximate representation for use at larger scales. In that intermediate-scale representation, individual ice-wedge polygons are used to define the horizontal discretization of the landscape. The mutually independent subsurface columns resulting from that discretization are then coupled indirectly through an overland flow system.

Acknowledgements

This work was supported by the Los Alamos National Laboratory, Laboratory Direction Research and Development project LDRD201200068DR, the Next Generation Ecosystem Experiment (NGEE-Arctic) project, and the Interoperable Design of Extreme-scale Application Software (IDEAS) Project. NGEE-Arctic is supported by the Office of Biological and Environmental Research in the DOE Office of Science.

References

Karra, S.; Painter, S. L. and Lichtner, P. C. [2014]: Three-phase numerical model for subsurface hydrology in permafrost-affected regions (PFLOTRAN-ICE v1.0). *The Cryosphere*, 8(5):1935–1950, doi:10.5194/tc-8-1935-2014.

Moulton, J. D.; Berndt, M.; Garimella, R.; Prichett-Sheats, L.; Hammond, G.; Day, M. and Meza, J. C. [2012]: *High-level design of Amanzi, the multi-process high performance computing simulatorRep.* ASCEM-HPC-2011-03-1, Office of Environmental Management, United States Department of Energy, Washington DC.

Painter, S. L. and Karra, S. [2014]: Constitutive Model for Unfrozen Water Content in Subfreezing Unsaturated Soils. *Vadose Zone J*, 13, doi:10.2136/vzj2013.04.0071.

Painter, S.L.; Coon, E.T.; Atchley, A.L.; Berndt, M.; Garimella, R.; Moulton, J.D.; Svyatskiy, D. and Wilson, C.J. [2016]: Integrated surface/subsurface permafrost thermal hydrology: Model formulation and proof-of-concept simulations. *Water Resources Research*, 52(8):6062–6077, doi:10.1002/2015WR018427.

The seasonal dynamics of a hydrohalite tufa associated with a perennial hyper-saline spring in the Canadian high Arctic

Wayne H. Pollard & Melissa K. Ward

McGill University, Canada

A series of unique salt formations resembling travertines and tufas occur in association with two hyper-saline perennial springs on Axel Heiberg Island in the Canadian High Arctic. Travertines and tufas are common spring deposits occurring in non-permafrost areas where they are produced by the surface accumulation of precipitated carbonate minerals and display a variety of morphologies (e.g. conical mounds, stalactites, stalagmites, spheres, terraces and steps). Perennial springs are rare in areas of cold, deep continuous permafrost; despite permafrost depths on the order of 500 m the combination of evaporite bedrock and numerous piercement structures (salt domes) create conditions conducive for the occurrence of perennial springs [Pollard et al., 1999]. Saline discharge during the winter is responsible for a range of icing and frost mound features as well as and mineral precipitates [Omelon et al., 2006, Pollard, 2005]. Hyper-saline springs at Strand Fiord and Whitsunday Bay are unique in that the features formed are comprised mainly of salt. At Whitsunday Bay a winter discharge forms series of large pool and barrage structures that resemble travertines and tufas. In this paper we document features formed almost entirely of sodium chloride (salt) and sodium chloride dihydrate (hydrohalite). Hydrohalite is a hydrous salt mineral that forms under cold conditions and is stable only at temperatures below -1 °C. Solute concentrations are near saturation for NaCl resulting in freezing depression; with eutectic freeze crystallization occurring as water temperatures approach -21 °C. During winter the formation of hydrohalite, halite and ice create an impermeable veneer forcing discharge to flow at the surface where it forms a series of pools that cascade down a narrow valley for roughly 800m. As warmer temperatures develop during the spring the hydrohalite begins to melt incongruently allowing the pools to drain. Such melting is readily accomplished by raising the temperature of sodium chloride dihydrate above about 1°C. Above this temperature, the dihydrate reverts to anhydrous sodium chloride crystals and saturated sodium chloride brine. Under warmer conditions the flow dissolves tunnels under the salt deposit washing out many of the barrage structures and collapsing pools. By midsummer much of the pool and barrage structure is destroyed leaving a more massive salt (NaCl) deposit.

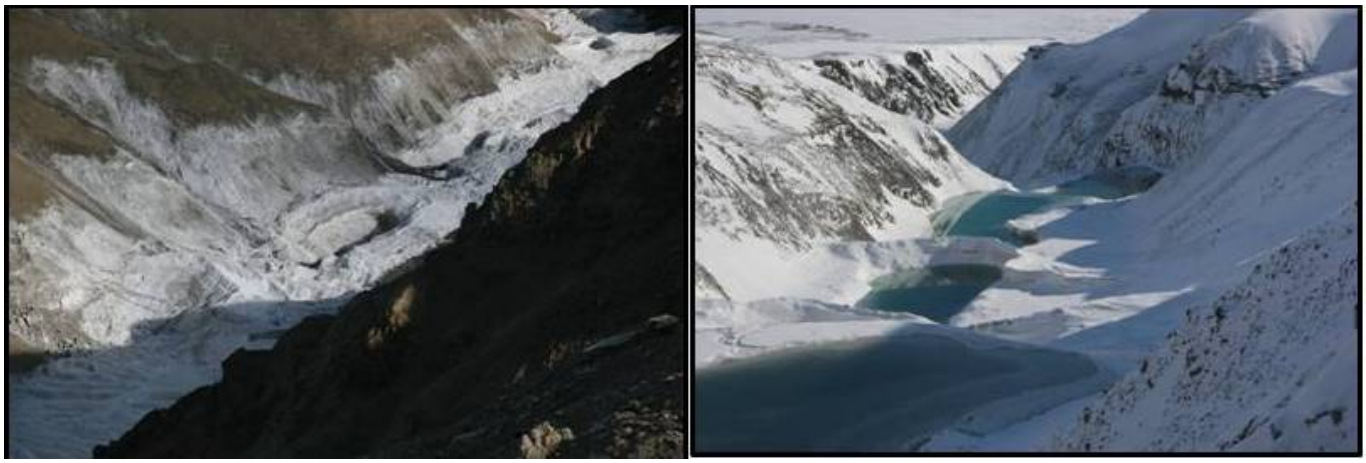

Figure 1: A salt deposit associated with hyper-saline spring discharge near Whitsunday Bay, Axel Heiberg Island showing both summer (left) and winter (right) conditions.

In this presentation we focus on the Whitsunday Bay spring located adjacent to Stolz diaper at 79°04'30" N; 87°04'30" W on the eastern side Axel Heiberg Island. At this site a tongue of salt staircases down a narrow valley for approximately 800m. At the mouth of the valley, discharge forms a large salt pan within the Whitsunday River floodplain. Perennial spring discharge flows into the Whitsunday Bay via the Whitsunday River. We use data loggers and time-lapse cameras to document the filling and draining of pools. NaCl, $NaCl.2H_2O$ and $Na_2SO_4.10H_2O$ were identified by XRD and VNIR spectral analyses. This study documents a unique winter dominated system of freeze crystallization of salt minerals that could be applicable to other geomorphic systems dominated by extreme cold and saline groundwater.

References

Omelon, C.R.; Pollard, W.H. and Andersen, D.T. [2006]: A geochemical evaluation of perennial spring activity and associated mineral precipitates at Expedition Fjord, Axel Heiberg Island, Canadian High Arctic. *Applied Geochemistry*, 21(1):1 – 15, doi:10.1016/j.apgeochem.2005.08.004.

Pollard, W. H. [2005]: Icing processes associated with high Arctic perennial springs, Axel Heiberg Island, Nunavut, Canada. *Permafrost and Periglacial Processes*, 16(1):51–68, doi:10.1002/ppp.515.

Pollard, W.H.; Omelon, C.; Andersen, D. and McKay, C. [1999]: Perennial spring occurrence in the Expedition Fiord area, Axel Heiberg Island. *Canadian Journal of Earth Sciences*, 36:105–120.

Mathematical Modeling of Climate - Permafrost - Groundwater Dynamics: A Study of Bestyakh Terrace, Lena River, Siberia

N. N. Romanovskii[1], G. S. Tipenko[2], S. N. Buldovich[1], D. O. Sergeev[2], A. V. Gavrilov[1], V. E. Romanovsky[3], N. S. Duxbury[4], & K. Yoshikawa[5]

[1] *Moscow State University, Geological Faculty, Russia*
[2] *Institute of Environmental Geoscience, Russian Academy of Sciences*
[3] *Geophysical Institute, University of Alaska, Faibanks, USA.*
[4] *George Mason University, USA.*
[5] *Water and Environmental Research Center, University of Alaska, Faibanks, USA*

In general, the dynamics of large taliks (subsurface thawed zones) can affect the annual river discharge structure. We have considered a typical case of the middle part of the Lena River in Siberia. Here the taliks were formed in the sand massifs of Bestyakh Terrace, and also in the lower part of the Viluy River stream. The Bestyakh Terrace (which is the fourth terrace from the river bed) occupies a hundred square kilometers and has a frontal bench of 20 – 45 m high. The absolute altitude of the terrace's surface is 130 – 160 m. The geological units are composed of fine-grained sands 20 – 90 m deep. These alluvial deposits lie on the Cambrian carbonate rocks or on the Jurassic sandstones.

The taliks are supporting year-round springs that are discharging to the bottom of the terraces. We have developed detailed physical and mathematical models of the coupled climate - permafrost dynamics (2-dimensional time-dependent temperature fields with multiple freeze-thaw phase transition fronts) and the water flow in porous media of the taliks under the Bestyakh terrace. Based on the results of our numerical experiments, we have developed methodological recommendations for hydro-geothermal surveying such as the number and location of boreholes, the optimal distance between them, and also the location and the type of sensors.

The developed mathematical model can be applied to a planetary cryolithosphere, e.g., to the Martian subsurface. Moreover, this is made possible with the recent discovery of the current flowing water on Mars (by the HiRISE camera on the Mars Reconnaissance Orbiter) and the more precise determination of the zero meridian [Duxbury et al., 2014].

References

Duxbury, T. C.; Christensen, P.; Smith, D. E.; Neumann, G. A.; Kirk, R. L.; Caplinger, M. A.; Albee, A. A.; Seregina, N. V.; Neukum, G. and Archinal, B. A. [2014]: The location of Airy-0, the Mars prime meridian reference, from stereo photogrammetric processing of THEMIS IR imaging and digital elevation data. *Journal of Geophysical Research: Planets*, 119(12):2471–2486, doi:10.1002/2014JE004678.

Thermal impact of a small alas-valley river in a continuous permafrost area - insights from field monitoring in Syrdakh (Central Yakutia) and 1D numerical analysis

Nicolas Roux[1,2], Christophe Grenier[1], Alexander Fedorov[3], Pavel Konstantinov[3], Antoine Sejourne[2], & Francois Costard[2]

[1] *UMR 8212 LSCE, CNRS-CEA-UVSQ, Gif-sur-Yvette, France*
[2] *UMR 8148 GEOPS, CNRS-UPSUD, Orsay, France*
[3] *Melnikov Permafrost Institute, RAS-SA, Yakutsk, Russia*

Lakes are probably the most prominent surface water bodies in continuous permafrost areas. As a consequence, they are also the most studied features in these regions (e.g. Fedorov et al. 2014). They are indeed of great interest, not only for local populations that use the water resource they represent both in winter and summer, but also from a climatic point of view as they can be a specific source of green-house gases due to the relatively warmer environment they create, especially associated with their taliks (thawed zone surrounded by permafrost located beneath large enough lakes). From a hydrogeological perspective, such taliks can form complex groundwater networks, thus possibly connecting sub-permafrost groundwater with surface water in the present context of climate change.

On the other hand, rivers, another important feature of permafrost landscapes providing similar challenges, have drawn less attention so that only a few studies focus on river interactions with permafrost (e.g. Costard et al. [2014], Grenier et al. [2013]. However, the processes of heat transfer at stake between river and permafrost strongly differ from lake systems for several reasons. The geometries differ, the river water flow and thermal regimes and interactions with the lateral slopes (valley) are specific. Of particular importance is the fact that the water, in the case of rivers, is in motion leading to specific heat exchange phenomena between water and soil.

Roux et al. [2015] addressed this issue recently by means of an experimental study in a cold room and associated numerical simulations (see Costard et al. on page 639). A river was created on a permafrost porous medium (sand, silty loam) with thermal monitoring of the progression of the warming up associated with the river water temperature. The controlled experimental conditions were varied to identify the dominant importance of river temperatures as opposed to flow rates in the propagation of heat. Numerical simulations were successful in reproducing the monitored temperatures provided ad hoc boundary conditions between river and porous medium were chosen and associated parameters calibrated.

The present study focuses on a real river-permafrost system with its full natural complexity. A small alas-valley in the vicinity of Yakutsk (Central Yakutia, Siberia) was chosen. Monitoring was started in October 2012 to study the thermal and hydrological interactions between a river and its underground in this continuous permafrost environment. This new study site is introduced here and the major results associated with the first two monitoring years are presented. These observations were also further analyzed using 1D vertical numerical simulation to identify the main processes and properties at stake.

Thermal sensors were installed inside the river, in the atmosphere and into boreholes in the permafrost, at different locations and various distances from the river and the upstream lake. Hydrological information was collected as well (e.g. water temperature, electrical conductivity, pH and isotopic profiles; river flow rates). Soil properties were studied in pits (e.g. thermal conductivity, soil humidity and temperature measurements).

The influence of the river and the upstream lake is visible in Fig. 1 providing the monitored temperatures at 2m depth at 4 locations during the two years Sept. 2012 – Sept. 2014. Results show a large inter-annual variability, typical of Central Yakutia. These curves are as well typical of the influence of water masses: the winter cooling of the soil is reduced in its vicinity due to latent heat effects; the overall temperature annual signal amplitude is buffered.

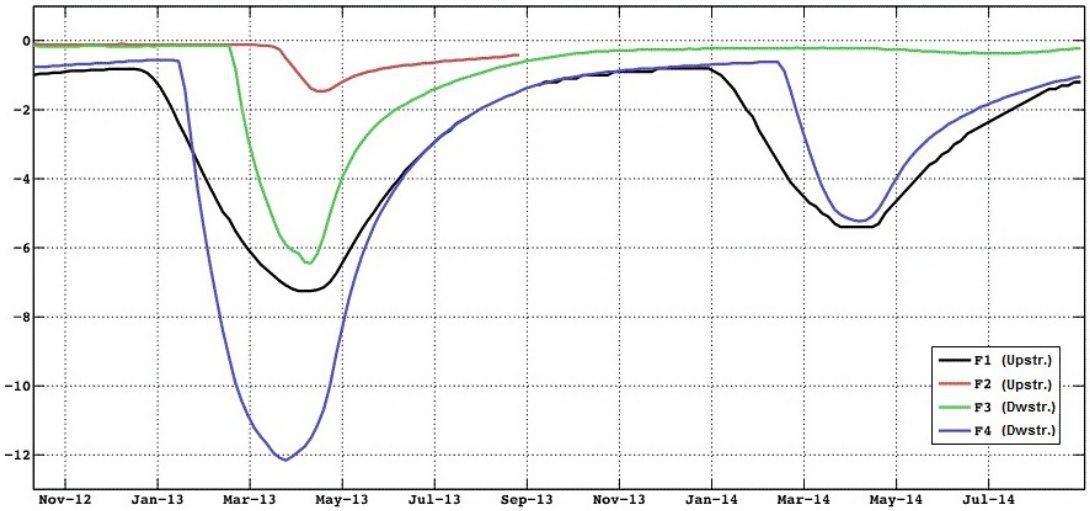

Figure 1: Temperature evolution at 2m depth for 4 locations (F1: Site close to the upstream lake, location far from river; F2: Site close to the upstream lake, location close to river; F3: Site far from lake, location close to river; F4: Site far from lake

Moreover, a closer analysis of the results showed that the inter-annual variability within the monitored permafrost temperatures is higher than the one associated with air and water temperatures. We suggest that this most probably results from the large water content variability at the start of the freezing period of the soils in the close vicinity of the river. This analysis is supported by a 1D numerical study considering warming and freezing with variable soil moisture levels. The specific shapes of the observed temperature signals are well matched with large levels of soil moisture.

The major conclusion is thus that the river lateral thermal influence is at least partly linked with its hydrological range of influence: the wetter zones in the vicinity of the river have a buffering effect on the autumn heat propagation due to phase change of such larger volumes of water. These zones are consequently warmer than the surrounding non river-(hydraulically) influenced zones.

The further perspective of the study is to simulate the hydrological and underground thermal evolutions in the future, raising questions of river underground thermal bulb evolution. All monitoring means were thus recently reoriented to study the thermal evolution of the river-permafrost system along a river transect. This will provide the opportunity to address the other important processes of river lateral heat conduction. This will later be confronted with 2D simulations of this transect and supported by geophysical surveys.

References

Costard, F.; Gautier, E.; Fedorov, A.; Konstantinov, P. and Dupeyrat, L. [2014]: An Assessment of the Erosion Potential of the Fluvial Thermal Process during Ice Breakups of the Lena River (Siberia). *Permafrost and Periglacial Processes*, 25(3):162–171, ISSN 1099-1530. doi:10.1002/ppp.1812.

Fedorov, A.N.; Gavriliev, P.P.; Konstantinov, P.Y.; Hiyama, T.; Iijima, Y. and Iwahana, G. [2014]: Estimating the water balance of a thermokarst lake in the middle of the Lena River basin, eastern Siberia. *Ecohydrology*, 7(2):188–196, ISSN 1936-0584.

Grenier, C.; Régnier, D.; Mouche, E.; Benabderrahmane, H.; Costard, F. and Davy, P. [2013]: Impact of permafrost development on groundwater flow patterns: a numerical study considering freezing cycles on a two-dimensional vertical cut through a generic river-plain system. *Hydrogeology Journal*, 21(1):257–270, doi:10.1007/s10040-012-0909-4.

Roux, N.; Costard, F. and Grenier, C. [2015]: Laboratory and numerical simulation of river talik evolution. *Permafrost and Periglacial Processes*. Accepted.

Watershed-scale hydrogeochemical impacts caused by permafrost thermal perturbation and physical disturbance, eastern Banks Island, NT, Canada

Ashley C. A. Rudy[1], Scott F. Lamoureux[1], Steve V. Kokelj[2], Melissa J. Lafrenière[1], & Rod Smith[3]

[1]*Department of Geography and Planning, Queen's University, Canada*
[2]*Northwest Territories Geological Survey, Government of Northwest Territories, Canada*
[3]*Geological Survey of Canada, Natural Resources Canada*

Regional climate models for the western Canadian Arctic project increases in precipitation and temperature. Warmer temperatures will result in deeper thaw, potentially leading to increased development of thermokarst and slope disturbances such as retrogressive thaw slumps (RTS). Intensive thermokarst in conjunction with deeper active layer thaw will alter subsurface pathways generating ion-rich runoff derived from the erosion of sediment and ice. Our study is on ice-cored glacigenic deposits in the high Arctic where we examine the hydrogeochemical impacts from both thermal perturbation and physical permafrost disturbance with an emphasis on how the impact on water quality varies across different watershed scales. Results from this study are placed in the context of research conducted at sites south and north of Banks Island to provide insight into the contributions of thermal perturbation and physical disturbance of permafrost on water quality at regional scales.

This study was undertaken in a polar desert, continuous permafrost environment at Johnson Point, eastern Banks Island, Canada. The study area is representative of the ice cored terrain which comprises a large ice marginal land-system along the eastern side of Banks Island called the Jesse Moraine. A comparison of 2015 satellite imagery with 2008/09 images reveals that there has been a substantial increase in the number and size of RTS in this area. This change and linkages between the slope-stream sediment cascade is indicated by the prominent sediment plume now entering the ocean from the study's main river channel that began in 2012. Synoptic water samples were collected from 2nd and 3^{rd} order streams and strategically along the main channel on July 8, 2015 and were analyzed for dissolved chemical constituents including major ions and metals, total dissolved solids (TDS), total suspended sediment (TSS), and water stable isotopes. The impact of physical disturbance is clear: impacted watersheds have mean TSS values that are four magnitudes greater than unimpacted watersheds (90,000 vs. 10 mg/L) and TDS values that are twice as high (500 vs. 250 mg/L). Increasing watershed order minimally diminishes the impact of physical disturbance with TSS and TDS values at the outlet of the river (6^{th} order, 230 km^2) reduced to 3030 and 320 mg/L, respectively.

Massive ground ice collected from within the headwalls of four RTS, and rain water were used as end members in a two-component isotope mixing model to separate river water samples into putative ground ice and rain components. At the time of sampling, RTS-impacted watersheds have a higher ground ice influence than unimpacted watersheds where the water is largely representative of rainfall. However, there are exceptions; a small number of unimpacted watersheds had high ground ice signals (>90 %) interpreted to indicate the thawing of near-surface permafrost. These watersheds are highly polygonised and show evidence of permafrost degradation distinguished by thermokarst ponding. Notably, melting ground ice from either thaw slumping (physical disturbance resulting in a surface exposure of ground ice), or thermal perturbation (increase in active layer thaw without any failure of overlying sediments) contributed to a large portion of the total catchment runoff. Isotopically, 2nd order streams average 50 % ground ice derived, but range from 25 % to 96 % reflecting individual catchments with and without RTS. Third order streams have increased ground ice proportions (70 %), and through dilution, the main river indicates c. 35 % ground ice contribution. While the proportion of ground ice meltwater in the main river is diminished it demonstrates widespread permafrost degradation throughout the study area.

Fluvial regimes across a range of watershed scales are impacted by physical disturbance and thermal perturbations to permafrost. Although the impact

of local disturbance is generally found to diminish as drainage area increases, the effects are still pronounced. Water quality impacts at this location are indicative of widespread permafrost degradation, an observation that is noted at a number of locations across the western Canadian Arctic. However, in polar desert environments where summer rainfall is historically low, it is important to note that warming induced ground ice melt may contribute significantly to baseflow, augmenting and changing summer runoff regimes. Furthering our understanding of the sedimentological and geochemical effects of physical disturbance and thermal perturbations on water quality and possibly quantity, is necessary for understanding the present state of the hydrological system, and predicting the potential impact of further change.

Runoff generation on hillslopes underlain by continuous permafrost

Caitlin Rushlow[1], Sarah E. Godsey[1], Clifford Voss[2], & Audrey Sawyer[3]

[1] *Idaho State University, USA*
[2] *U.S. Geological Survey, USA*
[3] *The Ohio State University, USA*

Through the runoff generation process, hillslopes and climate couple to determine the timing and amount of water delivery to aquatic systems. Predicting hillslope runoff behavior is necessary to effectively manage resources and infrastructure that depend on surface water bodies, particularly in Arctic regions where dramatic climate changes are expected and already underway. Hydrologic events this past year in Arctic Alaska demonstrate the importance of understanding the controls on runoff generation processes, as first ice break-up flooding in the spring shut down the Dalton Highway for an unprecedented 18 days at a reconstruction cost alone of more than $15 million dollars, and then low summer rainfall caused streams to dry up completely in the same watershed. Runoff generation in more temperature regions is found to often exhibit threshold behavior, where runoff increases dramatically , with inicreased precipitation intensity and/or antecedent water storage after a critical threshold [Ali et al., 2013].

The first section of this research asks whether a similar runoff generation threshold exists for hillslopes in regions of continuous permafrost, and if so, what underlying processes control threshold runoff behavior. To investigate these questions, six hillslope watersheds of the Upper Kuparuk River in north-central Alaska were instrumented in summers 2013 and 2014 to monitor rainfall, runoff, and water table fluctuations at hourly intervals, along with biweekly frost probe surveys of active layer thaw. The runoff amount for a given rainfall event has a threshold relationship with rainfall amount and antecedent water table depth, but no relationship with seasonal active layer thaw. The degree to which runoff depends on rainfall and antecedent water table depth varies between the six hillslopes. These results suggest that runoff from permafrost hillslopes is currently more sensitive to seasonal precipitation regime than to seasonal temperature regime.

To investigate sensitivity of runoff to hillslope structure and climate, we are simulating coupled heat and water transport for finite element models analogous to the hillslope field sites using SUTRA-ICE [McKenzie et al., 2007]. Runoff sensitivity to subsurface structure will be examined by changing the slope and curvature of hillslope surface, and by varying the thickness of an upper highly permeable layer of the model, which represents peat. An annual air temperature cyle will be applied to a thermal boundary layer at the top of the model [McKenzie and Voss, 2013], and sensitivity to climate will be examined by 1) increasing mean annual temperature through time and 2) manipulating the duration of snow cover via the thermal conductance of the thermal boundary layer.

References

Ali, G.; Oswald, C.J.; Spence, C.; Cammeraat, E.L.H.; McGuire, K.J.; Meixner, T. and Reaney, S.M. [2013]: Towards a unified threshold-based hydrological theory: necessary components and recurring challenges. *Hydrological Processes*, 27(2):313–318, doi:10.1002/hyp.9560.

McKenzie, J.M. and Voss, C.I. [2013]: Permafrost thaw in a nested groundwater-flow system. *Hydrogeology Journal*, 21(1):299–316, doi:10.1007/s10040-012-0942-3.

McKenzie, J.M.; Voss, C.I. and Siegel, D.I. [2007]: Groundwater flow with energy transport and water–ice phase change: Numerical simulations, benchmarks, and application to freezing in peat bogs. *Advances in Water Resources*, 30(4):966 – 983, doi:10.1016/j.advwatres.2006.08.008.

Recent changes of runoff characteristics in permafrost basins of Eastern Siberia

Olga Semenova[1], Nikita Tananaev[2,3,4], Luidmila Lebedeva[2], & Natalia Nesterova[1]

[1] *St. Petersburg State University, Russian Federation*
[2] *Melnikov Permafrost Institute, Russian Federation*
[3] *Ugra Research Institute of Information Technologies, Khanty-Mansiysk, Russia*
[4] *ECOLAB, Université de Toulouse, CNRS, INPT, UPS, France*

There are many speculations about possible impact of climate change at hydrological regime of Northern Eurasia, and permafrost basins in particular. Though the changes of flow of large rivers are relatively well described, the trends for small and middle-size watersheds are unknown. After the papers by Shiklomanov et al. (2007) and Smith et al. (2007) examining the variations of maximum and minimum flow in Northern Russia by 2001 there was no much update in this issue.

In this study we compiled the database of continuous daily runoff for more than 140 gauges within the Lena, Yana, Indigirka and Kolyma rivers basins with the order of basin area from 101 to 105 km^2. All currently functioning flow gauges with continuous observations not less than 30 years were selected for the database which contains the data up to 2013.

For chosen gauges the parameters of row-correlation, cyclic recurrence and the stationarity of main runoff characteristics (mean, maximum and minimum flow) were estimated. The conclusions are drawn about the evidence of unsteadiness and/or internal correlation in runoff series; the robust indicators of the intensity of detected changes are evaluated; the duration of water cycles and evaluation the spatial correlation between water cycles are explored.

The study is partially supported by Russian Foundation for Basic Research (project 15-35-21146 mol_a).

Study of river runoff generation in continuous permafrost zone based on new field data from Cherskiy, Russian Arctic

Alexander Shiklomanov[1,2], Igor Tokarev[3], Sergey Davydov[4], Anna Davydova[4], & Dmitry Streletskiy[5]

[1] *University of New Hampshire, United States of America*
[2] *Arctic and Antarctic Research Institute, Russia*
[3] *Resource Center "Geomodel", Research Park of Saint-Petersburg State University, Russia*
[4] *Northeast Science Station, Cherskii, Russia*
[5] *George Washington University, Department of Geography*

Stream flow integrates signal of numerous environmental processes and their changes aggregated over the large areas. To determine the contributions of various water sources to river runoff generation in streams located in continuous permafrost zone the extensive field data campaign has been carried near North East Science Station in the vicinity of the town of Cherskiy. The study area is located on the right bank of Kolyma River about 130 km south from the Arctic Ocean and is focused on two small experimental watersheds. Samples of precipitation, river flow and ground ice were collected during 2013-2015 period. Analysis of stable isotope composition of atmospheric precipitation, surface and ground water/ice along with hydrometeorological and hydrochemical data was conducted. The analysis of new isotopic data (2013 – 2015) on atmospheric precipitation with previously collected one (2005 – 2009) showed a pronounced seasonal pattern of the precipitation isotopic composition with a general trend towards heavier winter precipitation, attributed mainly to the observed increases in winter air temperature. The samples of water/ground ice from several boreholes have shown that isotopic compositions of water from the active layer, transient layer and permafrost are significantly different. Thus, stable isotopes can be used to assess contributions of different soil layers to stream flow generation. The increases in streamflow of small test watersheds were observed in the end of summer, beginning of fall. These increases were associated with considerable depletion of stable isotope composition. The additional release of water due to thawing of transient layer and possibly the upper layer of permafrost is a main cause of these increases. Significant negative correlation ($R^2 = 0.8$) between runoff and water temperature and low correlation ($R^2 = 0.22$) between runoff and air temperature during this period also confirms importance of permafrost and ground water in runoff generation. To quantitatively assess the contribution of various water sources to the river runoff we will use the field data along with physically based hydrological model as end member mixing model cannot provide reliable results due to significant variations of isotopic data for precipitation and ground water/ice.

Preliminary studies of water, snow and ice in the Quebrada del Medio, Hans Stepanek rock glacier, Mendoza, Argentina

Noelia R. Sileo[1], Dario Trombotto Liaudat[2], Cristina Dapeña[3], Xavier Bodin[4], Ivanna P. Marcosig[2], & Nicolas A. Taboada[1]

[1] *Comisión Nacional de Energía Atómica, Argentine Republic*
[2] *Instituto Argentino de Nivología, Glaciología y Ciencias Ambientales, CCT CONICET Mendoza, Argentine Republic*
[3] *INGEIS, CONICET-UBA, Argentine Republic*
[4] *Laboratoire EDYTEM, UMR 5204 CNRS / Université de Savoie, Le Bourget-du-Lac, France*

This paper intends to give some insights into the hydro-geochemical behavior of groundwater and surface water related to glaciers, covered glaciers and rock glaciers in the Vallecitos River basin. The goal of our study is to characterize different water origins and their hydrogeochemical composition in a typical cryogenic environment. The basin includes permafrost in situ as well as temporary and perennial snow patches. It also aims at understanding the dynamics of water within the cryogenic system, in particular inside the rock glaciers, in order to determine potential reservoirs of fresh water for the local population.

The study area is located between 69 °22' and 69 °25' W and 32 °56' and 32 °58' S, in the Cordón del Plata range, Cordillera Frontal, Mendoza, Argentina. The highest peaks in this region reach more than 6000 m asl. The Quebrada del Medio valley belongs to the Vallecitos River sub-basin, and lies at altitudes ranging from 3300 m at its lowest point to almost 5200 m asl at the summit of Cerro Rincón.

A network of surface water sampling has been set up with the main points corresponding to springs, streams and the Vallecitos River, together with sampling points for seasonal snow patches and ice (Fig. 1). A rain collector for isotope samples recording of any event has been installed, in order to generate a local meteoric water register. The first results reveal several differences between the three main sub- basins of the Vallecitos River basin. Different water sources and circulation patterns can be identified which are reflected in the hydrogeochemical and isotopic results [Sileo et al., 2015].

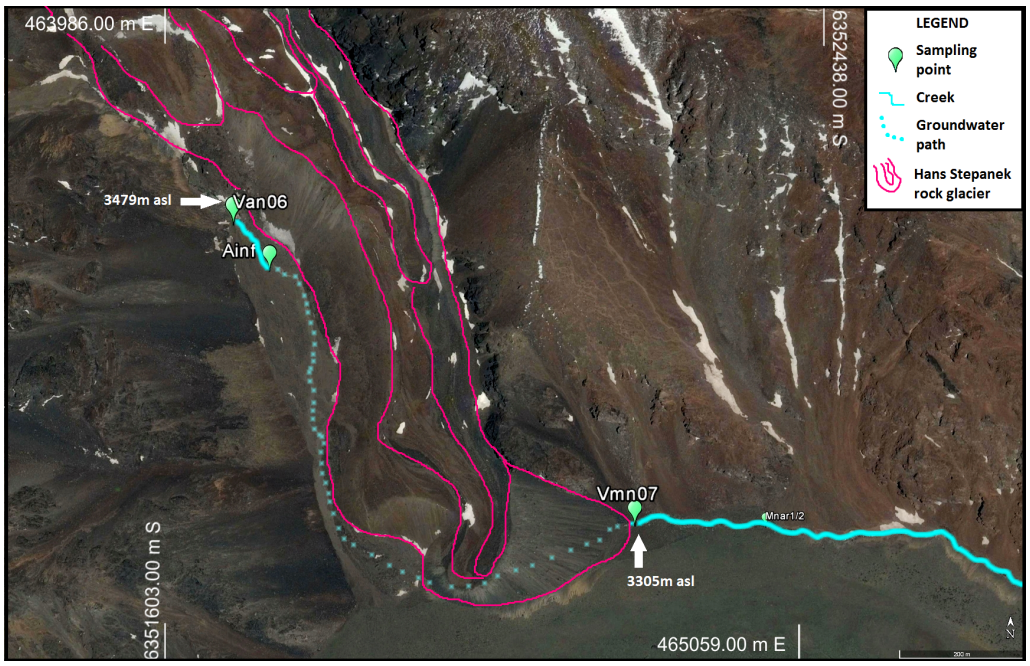

Figure 1: Quebrada del Medio stream and sampling points

Among the studied sampling points (Van06 and Vmn07) in this region, a temperature drop from 5 to 2.6 °C, a pH rise from 5.5 to 7.5, and variations in the concentrations of Zn, Cd, Ni, Mn and Si in relation to different altitudes are observed. Between the mentioned two points there is a horizontal distance of 800 m, where the stream flows underground, flowing (apparently) through the active rock glacier nose and changing its physical and chemical properties (Fig. 1). The decline of the toxic values of Ni at Vmn07, in comparison to higher values at higher altitude, found at the bottom of the cryoform gives it a special significance in terms of hydrochemical periglacial processes associated to some particular chemical elements, because something occurs for the retention of elements in its internal sedimentary structure.

Furthermore, other underground water inputs from other sources, such as sub-superficial melting water of parts of the rock glacier can explain physico- chemical phenomena at lower altitudes and they should not be discarded. In 2015, geodetic GPS measurements and terrestrial photogrammetric survey detected movements of the active layer, which appear to express internal changes of its cryogenic structure [Bodin and Trombotto Liaudat, 2015].

References

Bodin, X. and Trombotto Liaudat, D. [2015]: Evaluación de los aportes de la fotogrametría terrestre para el estudio de geoformas de alta montaña (Cordón del Plata, Mendoza, Argentina). *Acta Geológica Lilloana*, San Miguel de Tucumán, 27(2):87–96, http://lillo.org.ar/revis/geo/2015-27-2/03.pdf.

Sileo, N.; Trombotto Liaudat, D. and Dapeña, C. [2015]: Estudios preliminares del agua, nieve y hielo en la cuenca del río Vallecitos, Mendoza, Argentina. *Acta Geológica Lilloana*, San Miguel de Tucumán, 27(2):130–145, http://lillo.org.ar/revis/geo/2015-27-2/07.pdf.

Small-scale evapotranspiration in the polygonal tundra of the Lena River Delta, northeastern Siberia

Gillian Simpson[1], Tim Eckhardt[1], Benjamin Runkle[2], & Lars Kutzbach[1]

[1]*Institute of Soil Science, Center for Earth System Research and Sustainability, University of Hamburg, Germany*
[2]*Department of Biological and Agricultural Engineering, University of Arkansas, Fayetteville, USA*

Climatic warming is having pronounced effects on the Arctic region, impacting the energy, water and carbon cycles. These are tightly coupled in high-latitude wetland environments such as the polygonal tundra of the Lena River Delta, where evapotranspiration (ET, used interchangeably with latent heat flux) constitutes the main energy sink. Furthermore, by being a dominant flux in the water balance, ET also determines the water level and is hereby known to have a large impact on greenhouse gas emissions to the atmosphere [Billings et al., 1982, Peterson et al., 1984]. Arctic wetlands display strong spatial heterogeneity, with polygons of 5–20 m in size dominating the landscape creating a pronounced microtopography. This has a large impact on hydrology; however it is an aspect which is often neglected in large-scale modelling studies. This work examines estimates of ET across two spatial scales by comparing measurements made at the ecosystem scale using eddy covariance techniques with those made at the individual polygon scale by employing the closed chamber method. In doing so, it aims to determine the relative importance and impact of small-scale processes on ecosystem scale measurements.

Transparent chamber measurements were conducted in summer 2014 and 2015 across a single low-centered polygon on Samoylov Island, Lena River Delta (72°22'N, 126°28'E). Substantial differences were found in the ET fluxes at the two microsites; with average ET at the polygon center found to be around twice that measured at the polygon rim (e.g. 9,070 μg $m^{-2}s^{-1}$and 4,890 μg $m^{-2}s^{-1}$ in 2014 respectively). Flux results also show large temporal variability, with fluxes measured in 2015 being only around 10 % that of 2014. This difference is likely due the meteorological conditions; with a combination of lower temperature, higher humidity and lower insolation experienced over the second campaign period. Flux results from the chamber measurements will be used as calibration data for the Penman-Monteith combination equation, which will allow for continuous estimates of ET to be made from wet (polygon center) and dry tundra (polygon rim) based on meteorological data.

Results from the fitted Penman Monteith model will be upscaled in order to compare them to eddy covariance estimates of ET using a high resolution land cover classification map [Muster et al., 2012]. Flux estimates from the two methods will then be analysed and compared. To our knowledge this is the first study of this kind, and it will be of specific interest to see if there are any systematic differences between the two methods, and whether eddy covariance systems accurately capture processes happening at the microsite scale. This work will hence both

i) enhance understanding of present controls on ET at the individual polygon scale, which is of key importance to gas exchange with the atmosphere and

ii) provide a comparison of the two methods.

References

Billings, W.D.; Luken, J.O.; Mortensen, D.A. and Peterson, K.M. [1982]: Arctic tundra: a source or sink for atmospheric carbon dioxide in a changing environment? *Oecologia*, 53(1):7–11.

Muster, S.; Langer, M.; Heim, B.; Westermann, S. and Boike, J. [2012]: Subpixel heterogeneity of ice-wedge polygonal tundra: a multi-scale analysis of land cover and evapotranspiration in the Lena River Delta, Siberia. *Tellus B*, 64(0), doi:10.3402/tellusb.v64i0.17301.

Peterson, K.M.; Billings, W.D. and Reynolds, D.N. [1984]: Influence of water table and atmospheric CO_2 concentration on the carbon balance of arctic tundra. *Arctic and Alpine Research*, pages 331–335.

Implications of ignoring permafrost in glacio-hydrological models in high mountains

Shaktiman Singh[1], Anshuman Bhardwaj[1,2], & Rajesh Kumar[1]

[1] *Dept. of Environmental Science, School of Basic Sciences and Research, Sharda University, Greater Noida, India*
[2] *Division of Space Technology, Department of Computer Science, Luleå University of Technology, Kiruna, Sweden*

The seasonal snow cover, glaciers, permafrost and wetlands of the Himalaya are important source of freshwater supply in the densely populated areas downstream. These sources are mainly controlled by two meteorological parameters, namely, temperature and precipitation. The past studies carried out in the Himalaya suggest changes in temperature and precipitation patterns along with varying spatio-temporal trend. The effect of changes in these parameters is already evident on the glaciers and streamflow of the glacierised catchments and is predicted to change further. Due to difficult terrain and harsh weather conditions, the availability of observed data is scarce and fragmented. In this regard, the glacio-hydrological models based on either energy balance or degree-day factor have served as important tool to estimate streamflow. These models have been widely used to estimate changes in glaciers and streamflow in data scarce Himalayan region. However, the contribution of permafrost in the discharge and changes in it has been grossly ignored in the glacio-hydrological models used in the past studies. Permafrost is any lithospheric material that has remained at or below 0 °C for a minimum of two years. Since temperature is the dominant factor in determining the distribution of permafrost, observed warming in Himalaya will have apparent effects on it, ultimately affecting the streamflow. But limited studies with local records on permafrost are available for the region. A recent study attempted to map rock glacier as proxy of existence of permafrost within defines sample perimeters [Schmid et al., 2015]. There are no records of temporal changes in permafrost area for the region and therefore the implications of it on the hydrological regime of the region. In addition, the expected input of permafrost-melt in the total streamflow still needs inclusion within glacio-hydrological models used for the region. For example, a recent study by Immerzeel et al. [2015] attempted to inversely estimate the precipitation in upper Indus basin using glacier mass balance and concluded that the precipitation being recorded at valley stations or gridded precipitation datasets is significantly lower than what it should be to sustain the large glacier systems in the region. However, in discussing the results and inferring the conclusions, the authors overlook two important aspects which should have significant effects on the glacio-hydrology of such glacierised catchments:

a) the transient groundwater which can significantly affect storage capacity and cause delay in streamflow, and

b) the permafrost-melt which can significantly affect the discharge as well as the groundwater.

Although, the delay caused by groundwater does not have significant effect on net loss or gain at multiple year scale, the thawing of permafrost can significantly change the streamflow and may cause decrease in river runoff at basin outlet [Qui, 2012]. The regional analysis of change in in the permafrost area needs to be done to explain the discrepancy observed in the storage capacity of glacierised catchments in the Himalaya.

The present study analyses role of the permafrost hydrology in runoff from the glacierised Baspa basin (Fig. 1) in the western Himalaya. A degree-day factor-based glacio-hydrological model is used to estimate the discharge from the catchment for the period 2001–2008 and is compared with the observed discharge at basin outlet, at monthly scale. The temperature and precipitation and degree-day factors for different land cover (snow, debris free ice and debris covered ice) observed at daily resolution in the valley have been used as model inputs.

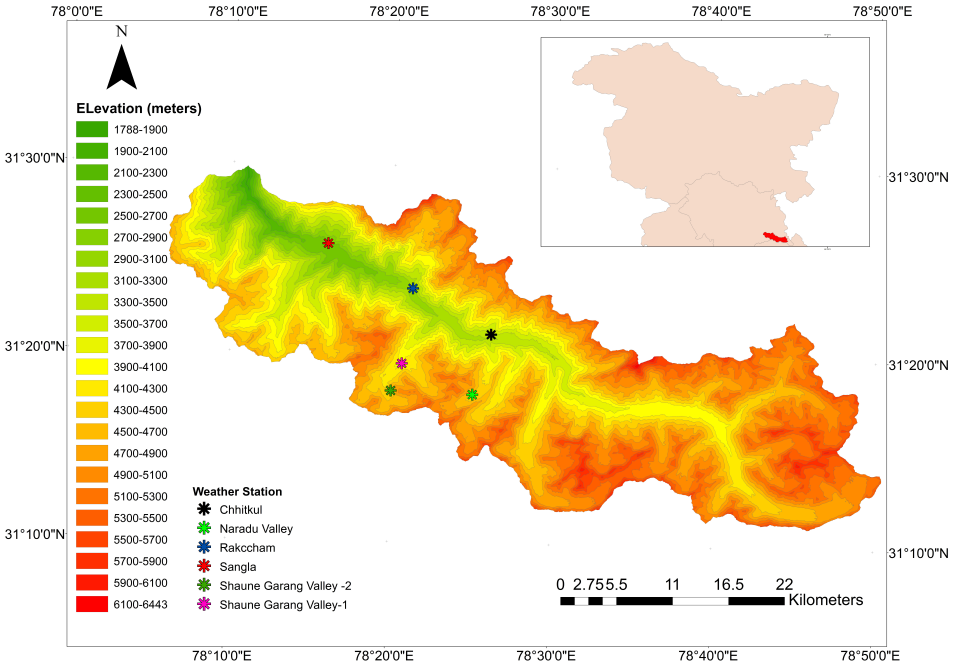

Figure 1: Location map of Baspa basin. The elevation zones and location of weather stations in the valley has been also shown in the figure

The area covered by rock glaciers was mapped using methods suggested by Schmid et al. [2015], in order to better model the permafrost within the basin. The permafrost area and melt is separately considered within the model. The modelled discharge after considering permafrost area and without considering it is compared with the observed discharge in the basin. The model results show significant changes after considering the area covered by the permafrost. The model output improves significantly after inclusion of permafrost component and shows a better correlation with observed discharge in comparison to the model output without considering the permafrost area and melt.

References

Immerzeel, W. W.; Wanders, N.; Lutz, A. F.; Shea, J. M. and Bierkens, M. F. P. [2015]: Reconciling high-altitude precipitation in the upper indus basin with glacier mass balances and runoff. *Hydrology and Earth System Sciences*, 19(11):4673–4687, doi:10.5194/hess-19-4673-2015.

Qui, J. [2012]: Thawing permafrost reduces river runoff. *Nature*, doi:10.1038/nature.2012.9749.

Schmid, M.-O.; Baral, P.; Gruber, S.; Shahi, S.; Shrestha, T.; Stumm, D. and Wester, P. [2015]: Assessment of permafrost distribution maps in the Hindu Kush Himalayan region using rock glaciers mapped in Google Earth. *The Cryosphere*, 9(6): 2089–2099, doi:10.5194/tc-9-2089-2015.

Impact from groundwater flow on ground temperature dynamics – Observations and numerical simulations for a sporadic permafrost peatland environment

Ylva Sjöberg[1], Ethan Coon[2], Britta Sannel[1], Romain Pannetier[1], Dylan Harp[2], Andrew Frampton[1], Scott L. Painter[3], & Steve Lyon[1]

[1] *Stockholm University, Department of Physical Geography, Bolin Center for Climate Research*
[2] *Los Alamos National Laboratory, Computational Earth Sciences*
[3] *Oak Ridge National Laboratory, Climate Change Science Institute and Environmental Sciences Division*

Sporadic permafrost peatland environments are illustrative of the complexity in heat flows that control freeze and thaw dynamics in natural landscapes. While representations of purely vertical heat flows by diffusion are often sufficient to model ground thermal dynamics for many continuous permafrost settings, in sporadic permafrost environments, lateral heat flows and groundwater-carried heat has the potential to more strongly influence freeze-thaw and permafrost dynamics. Still there is much uncertainty regarding the importance of these processes for permafrost dynamics in natural landscapes. We present observations and simulations of impacts from groundwater flow on ground temperatures and freezing in a sporadic permafrost peatland environment in northern Sweden.

We observed groundwater levels for one summer and ground temperatures (down to 2 m depth) for one full year to test the influence of groundwater flow rates on ground temperature fluctuations. For mechanistic understanding we complemented these observations with numerical simulations of coupled heat and groundwater flow, using the observed data to constrain the model. Two 2D simulation scenarios were used: one with no lateral groundwater flow across the domain, and another with a constant lateral groundwater flow. This allowed us to analyze the impact of lateral groundwater flow on ground temperatures and freeze-thaw dynamics.

Our observations suggest that lateral groundwater flows significantly affect ground temperatures. The numerical simulations, however, show only small differences in temperatures for the scenarios with and without groundwater flow for most of the simulated year. But for the early summer season, strong lateral temperature gradients in the observed data used to drive the simulations resulted in a rapid melt of seasonal ground ice in the scenario with groundwater flow. In this scenario, this seasonal ice melted 1 month faster as compared to the scenario with no groundwater flow, due to lateral transport of heat from the right side boundary into the domain by groundwater.

Based on these results we conclude that groundwater flows might have a small impact on ground thermal dynamics in sporadic permafrost peatlands for most of the year. There is, however, a need to more thoroughly investigate the role of high flow events, such as the snowmelt season, as these have the potential to considerably impact freeze-thaw dynamics.

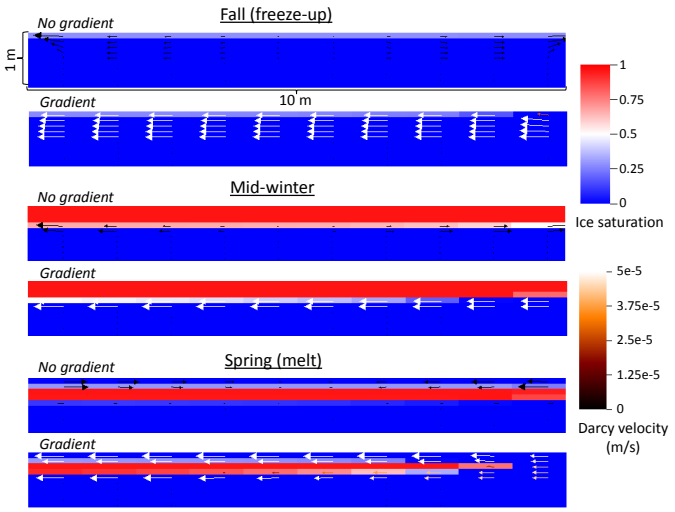

Figure 1: Ice saturation (color) and Darcy velocity (arrows) in the top 1 m of the domain for the two simulated 2D scenarios and for 3 time slices.

Relationships between colored dissolved organic matter (CDOM), dissolved organic carbon (DOC) and dissolved mineral substances in different surface waters of the Lena River Delta

Tatyana Skorospekhova[1], Irina Fedorova[2,1], Birgit Heim[3], Antonina Chetverova[2,1], Anne Morgenstern[3], Olga Bobrova[2], Antje Eulenburg[3], & Yury Dvornikov[4]

[1] *AARI, Russian Federation*
[2] *SPbSU*
[3] *Alfred Wegener Institute Helmholtz Centre for Polar and Marine Research, Potsdam, Germany*
[4] *Earth Cryosphere Institute, Siberian Branch, Russian Academy of Science*

In order to understand the influence of surrounding catchment characteristics on the CDOM concentration different types of surface waters in the Lena river delta region were investigated regarding their geochemical composition. The Lena River Delta consists of three geomorphological main terraces that differ in their relief, hydrological and cryolithological characteristics, which possibly influences the content of dissolved substances in their associated water bodies and in the neighboring river branches.

During summer seasons of 2013-2014 water samples were collected from river branches as well as from lakes and melt-water streams on the first and the third main terraces and analyzed them for concentrations of colored dissolved organic matter (CDOM), dissolved organic carbon (DOC), and main and trace elements (Na, K, Mg, Ca, HCO3, F, Cl, SO_4, Fe, Si, Sr). This type of research was carried out for surface waters in the Lena delta region for the first time. Statistical analysis revealed several correlations between CDOM, DOC and mineral ions. For example, R-squared (the coefficient of determination) for CDOM and Cl and for CDOM and Na in Lena River branches were 0.52 and 0.51, respectively. Correlation between CDOM and F was also found for melt-water streams from the Ice Complex (third terrace) (R-squared = 0.5).

Analysis of the relationship between CDOM and DOC showed strong correlation of these parameters for lakes (R-squared = 0.98) and lower correlation for river branches (R- squared = 0.48). In streams formed by the thawing of Ice Complex deposits on the third terrace was found the highest values of CDOM and DOC, but a correlation between them was not observed. A clear dependency was found out between CDOM and DOC correlation and the location of lakes on different terraces with specific permafrost conditions. A stronger correlation was observed for the lakes located on the third terrace (Ice Complex) compared to lakes located on the first terrace (Samoylov Island). Usually, lakes on the first terrace get flooded by river waters during spring, whereas lakes of the third terrace are not affected by river water inflow and have more stable conditions. The Lena delta branches are influenced by differing surrounding conditions, therefore CDOM and DOC concentrations change during summer season and did not show strong correlations.

Snowmelt water balance for a permafrost watershed: Case study from Alaska Arctic

Svetlana Stuefer, Douglas Kane, & Robert Gieck

Department of Civil and Environmental Engineering, Water and Environmental Research Center, University of Alaska Fairbanks, United States of America

Seasonal winter storage of precipitation and subsequent snowmelt provide large volumes of water to the drainage networks of Arctic watersheds. In this case study, snowmelt water balance computations are summarized for the relatively small Putuligayuk River watershed (471 km^2) located in a region of continuous permafrost on the Alaska Arctic coastal plain between the Kuparuk and Sagavanirktok Rivers. Low growing vegetation, flat terrain, and an abundance of lakes, ponds and wetlands are typical landscape features for this watershed. Observational hydrological program in Putuligayuk River watershed has been maintained from 1999 to the present by Water and Environmental Research Center/University of Alaska Fairbanks research personnel through support from state and federal agencies. Observed snowmelt runoff ranged by more than a factor of three during this period – from 51 mm in 1999 to 179 mm in 2014.

The objective of this study is to investigate what controls this range of variability in snowmelt runoff. It is hypothesized that storage plays a significant role in the runoff response of snowmelt in this region [Bowling et al., 2003]. Like most areas, precipitation (both solid and liquid), evapotranspiration and runoff are major fluxes in the water balance of these catchments. But storage, both surface storage in lakes, ponds and wetlands and subsurface storage in the active layer is an integral part of the hydrologic cycle. Because of the shallow active layer, subsurface storage is limited. However, surface storage is pervasive in these catchments. A direct measurement of this surface storage is still challenging [Kane et al., 2008].

The water balance approach is applied to the snowmelt period to evaluate the relative contribution of precipitation, evapotranspiration (ET) and surface storage to the snowmelt runoff from 1999 to 2008. Water balance computations are limited to the years of 2008 and before because net radiation measurements (used to estimate ET) at the nearby lake and wetland sites were discontinued after 2008. The Putuligayuk River streamflow was estimated at the Spine Road in the middle of the Prudhoe Bay oilfield using continuous stage records, periodic discharge measurements and site specific rating curve developed from the stage and discharge measurements. This stream does not have any flow in winter. Snowmelt runoff (R) was calculated as the cumulative discharge during the snowmelt period divided by the watershed area. Hydrograph analysis was applied to separate the spring flood recession from the summer baseflow to identify the last day of the snowmelt runoff period. The snowmelt period lasted for 14 to 39 days, usually ending in mid- to late June (Fig. 1B). Solid precipitation accumulating on the ground during the cold season was measured as snow water equivalent (SWE) at the end-of-winter at several sites in the catchment. Meteorological data was available from several stations in the area. Rainfall was recorded with the tipping bucket rain gauge, equipped with the Alter shield. Evapotranspiration was calculated by the Priestley-Taylor method, using net radiation data measured at the wetland, lake and the upland sites. The residual of the snowmelt water balance accounted for the combined change in surface and subsurface storage (δS) as well as errors (η) associated with the estimates of precipitation, evapotranspiration and runoff. The water balance equation was applied as (SWE + Rainfall) – (ET + R) = δS + η, with all components summed during the snowmelt period and converted to mm over the watershed area (Fig. 1A).

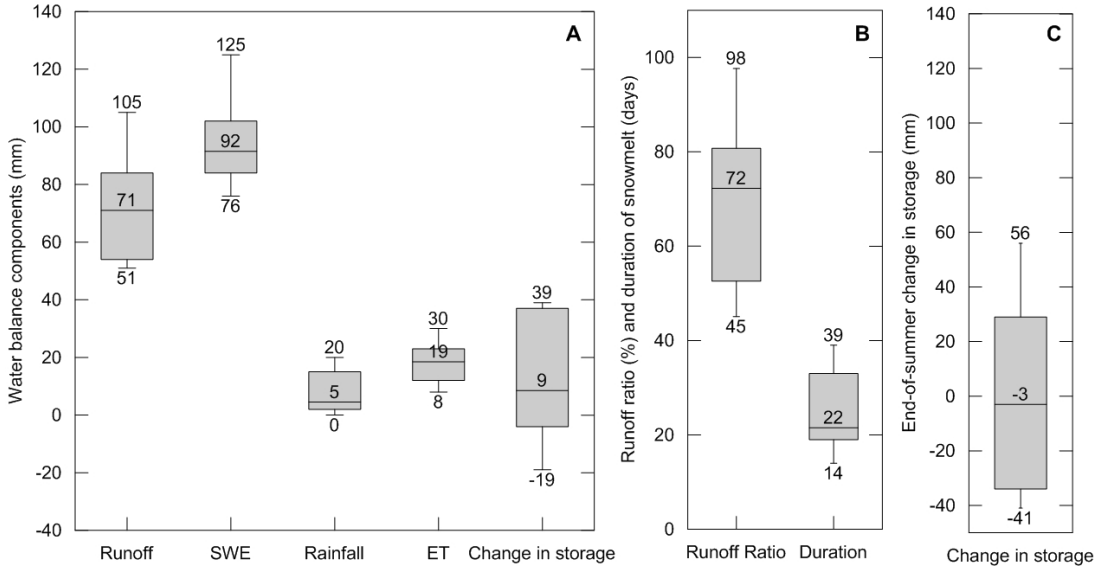

Figure 1: Box-whisker plots for snowmelt water balance components (A), duration of snowmelt runoff and runoff ratio (B), and change in storage in the end of summer (C).The median is printed in each box. The max and min values are shown by whiskers.

Results show that the contribution from snowmelt alone constitutes 45 – 98 % of snowmelt runoff from 1999 to 2008 (Fig. 1B). Winters with high snow accumulation tend to produce higher snowmelt runoff, however this is not always the case. For example, SWE accumulation in spring 2000 was 106 mm with 97 mm snowmelt runoff, whereas SWE accumulation in spring 2006 was 102 mm with only 55 mm snowmelt runoff. The input terms of water balance during both years become be the same (122 mm), when rainfall during the snowmelt period is added to the SWE. However, snowmelt runoff in 2006 is only 57 % of the snowmelt runoff in 2000. This contradiction is explained by the difference in surface and subsurface storage conditions that prevailed during the previous year. Watershed storage at the end of the summer 1999 was at its maximum (+56 mm) for the 10-year period, whereas storage at the end of summer 2005 was at -21 mm. Observed change in storage by the end-of-summer ranged from a maximum of +56 mm to a minimum of -41 mm relative to the 10-year average (Fig. 1C). It is suggested that this additional inflow to the channel network during snowmelt is likely to be supplied by the lakes and ponds (plus somewhat due to measurement error). The repository influence of the lakes and ponds is likely to be controlled by both the lake volumes prior to freezing the previous fall, and the lake ice cover conditions and snow damming during the snowmelt period.

References

Bowling, Laura C.; Kane, Douglas L.; Gieck, Robert E.; Hinzman, Larry D. and Lettenmaier, Dennis P. [2003]: The role of surface storage in a low-gradient Arctic watershed. *Water Resources Research*, 39(4), 2003. doi:10.1029/2002WR001466. 1087.

Kane, D.L.; Gieck, R.E. and Hinzman, L.D. [2008]: Water balance for a low gradient watershed in Northern Alaska. In: Kane, D.L. and Hinkel, K.M.(eds.), *Proceedings of the Ninth International Conference on Permafrost*, Institute of Northern Engineering, University of Alaska Fairbanks, Fairbanks, USA, 29 June–3 July 2008, volume 1, pages 883–888. ISBN 978-0-9800179-2-2. URL http://ipa.arcticportal.org/publications/conference-proceedings.

The role of paraglacial and paraperiglacial cryoforms on the water balance of a changing watershed in the Chilean and Argentinean Andes

Pablo A. Wainstein, Lukas U. Arenson, & Juan Umerez

BGC Engineering, Canada

Understanding the hydrological contributions from the glacial and periglacial belt on the runoff and water availability for downstream users under climate change conditions has become increasingly important in particular for dry areas, such as the Chilean and Argentinean Andes. This has become more acute by the initiation of glacier protection laws that determines the protection level of a certain landscape and cryoform based on its hydrological contribution and its significance.

While the periglacial environment often dominates the glacial one, very little scientific data are available on the contribution of permafrost degradation and associated ground ice thaw on the total annual runoff and on the general role of the active layer in the hydrographs of watershed outlet points. The lack of data is even more pronounced in the cases where the glacial environment is rapidly degrading and evolving into paraglacial and paraperiglacial environments [Slaymaker, 2011]. Despite the lack of data and understanding as to the role of various periglacial cryoforms, in particular rock glaciers within the hydrological cycle, some legislations have recently been implemented to protect them from any human induced impact. This is further complicated by the fact that these regulations erroneously include rock glaciers as part of the glacial environment. The combination of lack of data, poor understanding of the complexity that exists in rapidly changing mountain environments under changing climatic conditions and conceptually challenged regulations, pose a dare need for better assessing mountain permafrost hydrology, with particular focus on rock glaciers. However, it is fundamental to not just focus on a single cryoform, but to take a holistic approach respecting the entire watershed including all its components under its changing paraglacial conditions.

In this contribution we present a summary of a literature review on mountain permafrost hydrology, identify research needs and present a first approach on how hydrological role of mountain permafrost, including some of the dominant cryoforms, can be holistically assessed. The assessment is based on theoretical models supported by recent investigations in two watersheds, Rio Choapa and Rio Elqui, located in the Chilean Andes of the Coquimbo Region.

References

Slaymaker, O. [2011]: Criteria to Distinguish Between Periglacial, Proglacial and Paraglacial Environments. *Quaestiones Geographicae*, 30(1), doi:10.2478/v10117-011-0008-y.

Soil temperature-threshold based runoff generation processes in a permafrost catchment

Genxu Wang[1], Tianxu Mao[1], & Juan Chang[2]

[1] *Institute of Mountain Hazards and Environment, CAS, People's Republic of China*
[2] *Lanzhou University*

The contributing-area concept was the universal approach in rainfall-runoff processes modelling. However, it is unclear of the role of permafrost in controlling runoff generation processes. The areas that contribute to runoff generation are complex, variable and difficult to determine in permafrost catchments, and thus, there is no suitable quantitative approach for the simulation of runoff generating dynamics. To understand how thaw-freezing cycle in permafrost catchment effect the runoff generation processes, a typical catchment of continuous permafrost on the Tibetan Plateau was measured, and the spring and autumn season when runoff generation obviously differs from non-permafrost regions were focused on in this study. By introducing soil temperature threshold functions for surface saturation excess runoff generation and subsurface groundwater discharge, two dominant runoff generation types for permafrost catchments in different seasons are analysed, and corresponding simple quantitative approach related to the thawing and freezing periods are presented. The results show that the new approach can exactly identify the runoff generation dynamics of spring thawing and autumn freezing processes. In the permafrost headwater catchments of alpine meadows, the surface soil temperature or thawed depth threshold for variable runoff generation area depend on the zero thawing isotherms, which reach a depth of 40 cm. The subsurface groundwater discharge, which is controlled by soil temperature, contributes more than 85 % of the total river discharge in the autumn freezing period. The crucial variable for the spatial-temporal variation of runoff contributing area in the permafrost catchment is the soil temperature rather than soil moisture.

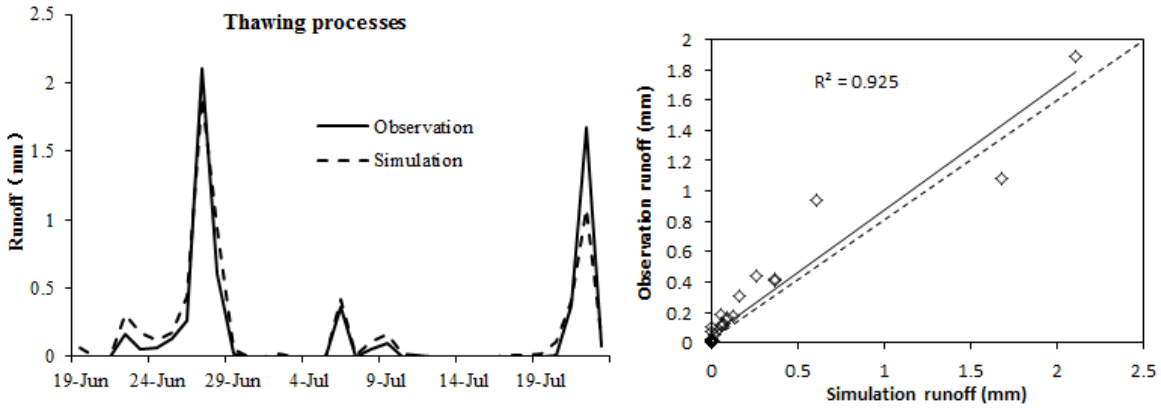

Figure 1: Modelled runoff generation compared with field observed runoff during the spring thawing period in a permafrost catchment. The left (a) referred runoff hydrograph comparison, while the right (b) is the simple scatter of statistical analysis.

Climate change, permafrost decline and its hydrological impact in the Sheldrake catchment (Québec, Canada)

Lingxiao Wang[1], Ralf Ludwig[1], & Monique Bernier[2]

[1] *Ludwig-Maximilians-Universität München (LMU), Germany*
[2] *Centre Eau, Terre& Environnement, Institut National de la Recherche Scientifique, Québec, Canada*

The dynamics of permafrost, a main cryosphere component in northern regions, influences hydrological processes, energy exchanges, natural hazards and carbon budgets. Climatic changes are particularly intense in the Arctic, and numerous evidences show that permafrost is degrading rapidly. The research studies the effects on seasonal flow brought by active layer thickening and associated landscape changes by aid of model simulation, thus to better understand the alterations of the hydro-thermal regime accompanied with permafrost decline.

The study is performed at Sheldrake river catchment near the Inuit village of Umiujaq (56°32' N, 76°31' W), at the eastern shore of the Hudson Bay in northern Quebec, Canada. It is located in the discontinuous permafrost zone, landscape in the study area is very heterogeneous. A mosaic of rock outcrops, lichen tundra patches, shrub thickets and forest stands spread in a small region. Mean annual air temperatures increased two degrees in the past two decades, which lead to 21 % of the existing permafrost in 1957 had disappeared in 2009.

Hydrological model WaSiM with one-dimensional transient heat transfer module is adopted to describe hydro-thermal processes in watershed at 30m resolution from 1980 to 2013. Reanalysis dataset ERA-Interim combined with Canada-Wide interpolated spatial models of daily precipitation were served as climate inputs. Spatial input datasets were developed based on satellite image interpolation, existed maps and in-site observations. Model results are calibrated and validated through discharge from gauging station in the outlet of catchment from 2009 to 2013, along with measured active-layer thickness and temperature profiles.

First findings show that the model is capable to describe hydro-thermal processes in the catchment of a discontinuous permafrost region. Model results show thawing process differs with soil texture and land cover conditions. After 1996, with temperature arise, maximum thawing depth increased correspondently.

Permafrost's influence on hydrological process is quantitatively analyzed utilizing two comparative model simulations. One is permafrost distribution in reality and one is hypothetically permafrost free. Permafrost's freeze and thaw process functions differs on the stream flow. In thawing season, larger runoff peaks brought by permafrost's distribution compared to permafrost-free simulation because surface permafrost acts as impermeable layer; in the freezing season, less water flow compared to permafrost-free simulation.

Permafrost degradation does not significantly affect water runoff curve in the test site, which is mainly decided by climate conditions, because of the small size of catchment and permafrost coverage is low (less than 25 % percentage of whole catchment area), however, changes brought by permafrost degradation are still visible. Though analyzing modeled monthly mean runoff data, it was inferred that with permafrost degradation, summer runoff are reduced and higher fall-winter flow appeared.

The influence of local factors on the seasonal freeze-thaw processes of the active layer in the alpine permafrost regions in the upper reaches of the Heihe River, in Qilian Mountains

Qingfeng Wang[1], Huijun Jin[1], Tingjun Zhang[2], Qingbai Wu[1], Bin Cao[2], Xiaoqing Peng[2], & Kang Wang[2]

[1]*State Key Laboratory of Frozen Soil Engineering, Cold and Arid Regions Environmental and Engineering Research Institute, Chinese Academy of Sciences (CAS), People's Republic of China*
[2]*College of Earth and Environmental Sciences, People's Republic of China*

The soil seasonal freeze-thaw processes and the hydrothermal dynamics of the active layer in the permafrost regions have profound influence on the terrestrial ecosystems, hydrological processes, water and heat budgets and carbon cycle between land and atmosphere, climate systems, and cold regions engineering constructions, etc. Based on the multilayer soil temperature and water content observation data of the active layer from 2013 to 2014 at the EB and AL7 observation sites at a close elevation, laid in the peatland on the north slope of Ebo Mountains in the east branch of the Heihe River and in the alluvial plain in the west branch in the alpine continuous permafrost regions in the upper reaches of the Heihe River (URHHR) in Qilian Mountains, the influence of the local factors on the soil seasonal freeze-thaw processes and the hydrothermal dynamics of the active layer are analyzed. The results show that, mainly due to the influence of the heat semi-conductivity properties of the peat soil, and the overlay of the impact of other local factors, such as snow, vegetation, topography, geomorphology, water, soil water content, and winter temperature inversion, the soil seasonal freeze-thaw processes and the hydrothermal dynamics of the active layer are significantly different on the north slope of Ebo Mountains and in the alluvial plain in the west branch. From the perspective of soil temperature, the soil seasonal freeze-thaw processes can be divided into the seasonal thaw process, the seasonal freeze process, and the completely frozen season process; while from the perspective of the soil water content, it can be divided into the thaw-rising stage, the relatively entirely thawed stage, the freeze-fall stage, and the completely frozen stage. The annual surface temperature range (ASTR), ground temperature at the bottom of the active layer (TTOP), and mean annual ground temperature (MAGT) are lower at the EB site on the north slope of Ebo Mountains, with the values of 19.6 °C, -1.1 °C and -0.8 °C, respectively; while they are bigger at the AL7 site, with the value of 28.4 °C, -0.4 °C and -0.1 °C, respectively. The characteristics of the soil seasonal freeze-thaw processes at the EB site are below:

1. With the earlier onset date of soil thaw and the later date reaching the maximum thaw depth, the duration and the rate of the seasonal thaw process is longer and lower, respectively;

2. Accordingly, with the later onset date of soil freeze from the ground surface downward, the duration and the rate of the seasonal freeze process is longer and lower, respectively; and

3. The duration of the completely frozen stage is longer.

The rate of change of the soil water content at the thaw-rising stage and the freeze-fall stage at the EB site is both significantly bigger than that at the AL7 site. The research on the influence of the local factors on the soil freeze-thaw processes and the hydrothermal dynamics of the active layer above can provide basic data and verification for the identification, simulation and prediction of the hydrological effects of the changes in the active layer and permafrost in the Heihe River Basin.

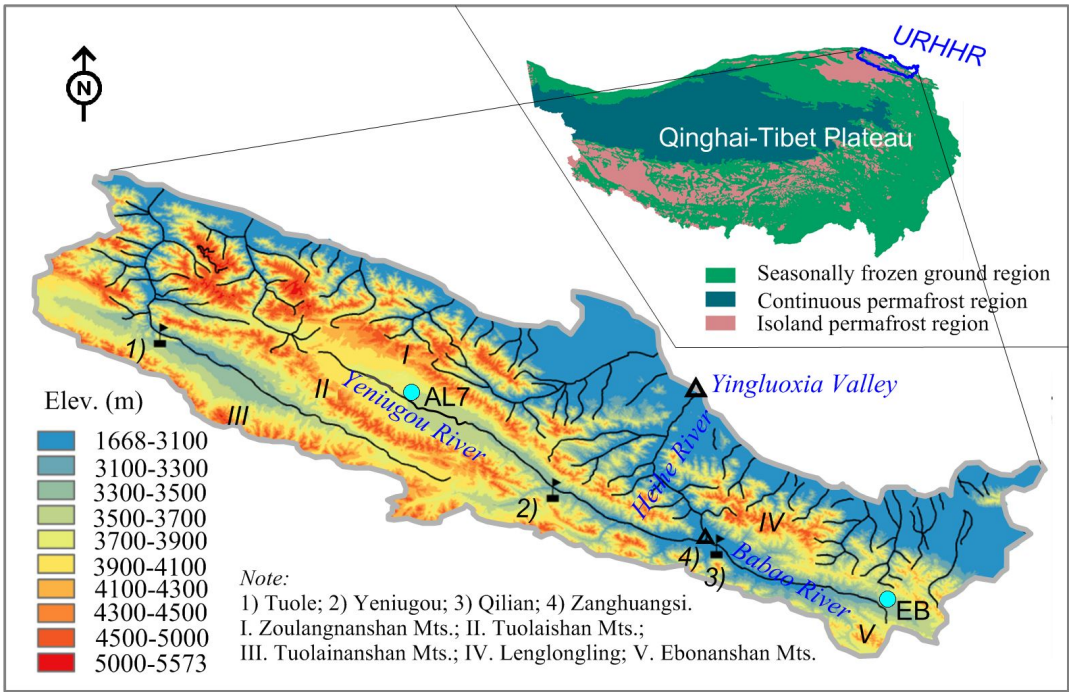

Figure 1: The alpine continuous permafrost regions in the upper reaches of the Heihe River (URHHR); Qilian Mountains

Simulating the impacts of surface hyper-saline spring activity on thermal regimes of underlying permafrost on Axel Heiberg Island, Nunavut

Melissa K. Ward & Wayne H. Pollard

McGill University, Canada

On Axel Heiberg Island in the Canadian high Arctic, a number of low temperature perennial saline springs occur despite being subjected to a cold polar desert climate with a mean annual air temperature of -18 °C. The region is characterized by very thick (≈600 m) continuous permafrost [Pollard, 2005]. Two of these hyper-saline springs form large salt pans produced by the accumulation of salt from migrating stream channels downstream of the spring outlets. The first site is located at Stolz Diapir (79°04'30" N; 87°04'30" W) and historical air photos from 1959 show that the location of the salt pan has shifted and grown in size. The second site is Wolf Diapir (79°07'23" N; 90°14'39" W) and the size, extent, and location of this salt pan has changed little since 1959. This study hypothesizes that salt accumulation at the ground surface mineralizes the active layer and causes it to deepen overtime by producing a hydrochemical talik-like effect. This study will use model simulations to determine how salt accumulation at the ground surface resulting from spring flow is changing the thermal regime of the underlying permafrost. Various scenarios (shifted and stationary salt pans) will be carried out to represent observed processes. This research represents preliminary findings, while model inputs such as spring water chemistry have been determined from previous field seasons [Ward and Pollard, 2015]. In addition, this research will be further complimented and validated by field observations scheduled for summer 2016.

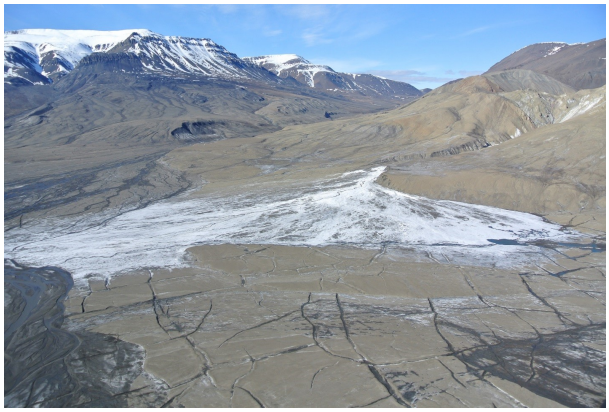

Figure 1: Salt pan produced by the hyper-saline spring at Stolz Diapir, Axel Heiberg Island, Nunavut.

References

Pollard, W. H. [2005]: Icing processes associated with high Arctic perennial springs, Axel Heiberg Island, Nunavut, Canada. *Permafrost and Periglacial Processes*, 16(1):51–68, doi:10.1002/ppp.515.

Ward, M. K. and Pollard, W. H. [2015]: Hyper-saline spring dynamics and salt deposits on Axel Heiberg Island, Nunavut. In *GeoQuebec 2015 – the 68th Canadian Geotechnical Conference and the 7th Canadian Permafrost Conference Proceedings.*

Isotope-tracing studies on impacts of degrading permafrost on hydraulic connections in the Source Area of Yellow River on SE Qinghai Plateau, SW China

Peng Yi[1,2], Huijun Jin[1], Victor Bense[1,3], & Yuzhong Yang[1]

[1] *State Key Laboratory of Frozen Soils Engineering, Cold and Arid Regions Environmental and Engineering Research Institute, Chinese Academy of Sciences, Lanzhou, Gansu, China*
[2] *State Key Laboratory of Hydrology-Water Resources and Hydraulic Engineering, College of Water Resources and Hydrology, Hohai University, Nanjing, Jiangsu, China*
[3] *Hydrology and Quantitative Water Management Group, Department of Environmental Sciences, Wageningen University, Wageningen, Netherlands*

Degrading permafrost significantly impacts hydraulic connections in the Source Area of the Yellow River (SAYR). A deepening active layer has led to reduced near-surface water resources, leading to deepened flow paths. As a result, runoff generation duration is increased as evidenced by the prolonged winter base flow and reduced summer peak flow. At present, however, there is only a limited understanding on the impact mechanisms of permafrost degradation leading to changes in hydraulic connections. This program aims at quantifying the nature of the mechanisms linking the permafrost degradation to changes in hydraulic connections. Drilling, geophysical sounding and investigations has proved an extensive presence of the supra- and sub-permafrost water in the taliks under and around medium and large lakes and rivers. Permafrost has been monitored for ground-truthing surface geophysical observations. Boreholes have provided access to the sub-permafrost aquifer system and groundwater age-dating for elucidating regional hydrogeology. Analyses of stable (Deuterium, or D and Oxygen-18) and radioactive (Tritium, or T) isotopes of different waters are applied for investigating changes in hydrologic connections. Four SAYR-scale water samplings have been deployed for understanding isotope distribution. Hydrological monitoring has been conducted at the small experimental watershed at the Shuangchagou Valley in south-central SAYR. A record of tritium in historical precipitation from 1956 to 2003 in the SAYR has been reconstructed, which implies a pre-1956 age for groundwater with tritium concentration less than 3.05 TU. Radon-222 river system model is established and used for studying the hydraulic connections, and in spring and autumn in particular. There are close hydraulic connections between surface and subsurface waters, and groundwater supplies about 10-36 % of stream flows. The spring water could be recognized as former years precipitation and had around 10 years ages while the ages of well water in Madoi Town reflect recent precipitation. The results suggest that:

1. The Yellow River and its tributaries are mainly recharged by shallow groundwater again fed on precipitation and melt-water in continuous permafrost areas, and with frequent transitions between surface and subsurface waters, and water cycling period is 2 years;

2. In discontinuous permafrost regions, streamflows are fed on active layer water, water surface evaporation is strong, and groundwater recharges lakes and rivers with open taliks, and they serve as flow paths for recharging deeper aquifers; water cycles every 10 years, and;

3. In regions of seasonally frozen ground with intense water surface evaporation, surface waters recharge groundwater; water cycles every 30 years.

Permafrost distribution and flow regime along a hill slope in West Greenland

Sebastian F. Zastruzny[1], Karsten Høgh Jensen[1], Bo Elberling[2], & Lars Nielsen[1]

[1] *Department of Geosciences and Natural Resource Management, University of Copenhagen*
[2] *Department of Geosciences and Natural Resource Management, Center for Permafrost (CENPERM), University of Copenhagen, Øster Voldgade 10, DK-1350 Copenhagen K. Denmark*

The observed climate warming will lead to substantial permafrost degradation and mobilization of formerly freeze-locked water and matter. Recent findings [Elberling et al., 2010] show that substantial amounts of inorganic nitrogen (mainly as ammonium) are stored in the perennially frozen ground of arctic ecosystems. Thus, future permafrost thaw can release significant amounts of bioavailable inorganic N, possibly mitigating the current N limitation of arctic tundra ecosystems. Therefore we have studied the distribution and movement of water in the active layer and top permafrost along a hill slope at a study site on Disko Island (West Greenland). The objective of this combined field and model study is to simulate water flow in the active layer and the associated transfer of dissolved matter.

The study site is a slope of a moraine in a glacial valley on Disko Island, where an 80 m long transect was investigated. Fieldwork was carried out during August 2015 and included a vegetation survey along the profile and measuring the active layer thickness using an auger. Soil thermal properties (thermal conductivity, specific heat capacity, thermal diffusivity and thermal resistivity) were measured at ten cm depth increments at eleven locations along the transect. A total of 24 volumetric and six mass soil samples were collected at different vegetation forms along the transect. The top and bottom of the profile were instrumented with eight sensors (Decagon Devices 5TE) at two depth levels in two locations to monitor ground temperatures, the soil water content and electrical conductivity. Additionally five of the same sensors were installed along one line in the middle of the profile to monitor a NaCl tracer experiment. 25 piezometers were installed in the active layer along the profile to capture water movement. At key locations water samples were collected from deeper and shallower piezometers. Snow melt water and samples from the uppermost permafrost were taken as reference samples. The extent of the permafrost was captured by DC-resistivity measurements along and perpendicular to the profile at the top, middle and bottom of the slope. Climate data is available from a nearby climate station (dist. 500 m). Water content, hydraulic conductivity, grain size distribution and carbon content were measured on soil samples and δO18 on water samples.

Preliminary results from the DC survey show continuous permafrost along the transect, with the active layer thickness ranging between 30-60 cm. At the top end permafrost could not be detected by the resistivity measurement, nor by auger probes to a depth of 120 cm. Perpendicular DC profiles showed a very heterogeneous distribution the permafrost. The laboratory analyses of the soil samples show a distinct separation of the active layer in an acrotelm (0-15 cm), with medium to high hydraulic conductivity (ca. 10-4 m/s) and extremely high porosity (ca. 90 %) and a catotelm (15-60 cm) with low to intermediate hydraulic conductivity (ca. 10-6 m/s) and medium porosity (ca. 50

The data gathered from field and laboratory analysis (soil properties and spatial distribution of soil type and permafrost) was implemented in a two-dimensional, cross sectional SUTRA model. Early model runs show that propagation of solute is unsteady and occurs after heavy rainfalls corresponding to observations in the field. The response of the high porous material towards wetting and drying processes thus occurs instantaneously. In the next stage calibration and validation will be done based on data from the installed sensors and the tracer experiment. With the knowledge gathered through this model setup it is anticipated to predict nitrogen transport along the slope as well as the response of the permafrost towards changing climate conditions.

References

Elberling, B.; Christiansen, H.H. and Hansen, B.U. [2010]: High nitrous oxide production from thawing permafrost. *Nature Geosciences*, 3, doi:10.1038/ngeo803.

SESSION 15

The Importance of Lakes and Ponds in Permafrost Regions

Convener:

Annett Bartsch, *Central Institute for Meteorology and Geodynamics, Austria*

Sina Muster, *Alfred Wegener Institute Helmholtz Centre for Polar and Marine Research, Germany*

Lakes and ponds are abundant in northern permafrost lowlands. Most are dependent on permafrost and all play a significant role in the local ground thermal regime, impact the radiation budget and carbon cycle. Their characterization across spatial and temporal scales is challenging but required for permafrost and climate modelling applications. What impact do lakes and ponds have on water, energy and carbon turnover in permafrost landscape on regional scales? Which lake and pond properties and parameters have to be considered to adequately represent their effect on landscape-scale processes?

This session invites contributions on lake characterisation across scales using in-situ measurements, remote sensing and/or modelling. On the one hand, lakes as single objects are of interest. Parameters include (but are not limited to) lake type (thaw lakes, polygonal ponds, etc.), the spatial and temporal variability of lake extent, lake depth, water level, water quality and ice cover across different landscape types. On the other hand, their interrelationship with the surrounding landscape needs to be considered. How and to what degree do lakes affect the hydrological, thermal and biogeochemical processes in Arctic landscapes? The session welcomes both local process studies that enhance our understanding of mechanisms and feedbacks as well as large-scale mapping and modelling efforts that aim to extrapolate and validate processes or parameters in space and time

Thermokarst lake changes between 1962 and 2008 in Mongolia

Saruulzaya Adiya[1], Ishikawa Mamoru[1], & Jambaljav Yamkhin[2]

[1] *Graduate School of Environmental Science, Hokkaido University, Sapporo, Hokkaidon, Japan*
[2] *Institute of Geography and Geoecology, Mongolian Academy of Sciences, Ulaanbaatar, Mongolia*

Thermokarst lakes are one of the most common features on the moist depressions and valleys with ice-rich permafrost regions of Mongolia, the southern boundary of Siberian permafrost regions. These lakes initiate when the ground subsides following thaw of ice-rich permafrost [van Everdingen, 2005]. After a thermokarst lake has formed, the lake size may change due to continued permafrost thaw, variations in air temperature, potential evapotranspiration and precipitation. Most of the previous studies investigated changes in thermokarst lakes across permafrost regions of the Siberia [Smith et al., 2005, Karlsson et al., 2014], however, the spatio-temporal changes of these lakes have not been observed in Mongolian permafrost regions. Therefore, quantifying changes in number and areal extent of thermokarst lakes is of importance for understanding the influences of permafrost degradation and climate warming on thermokarst lake changes in this region.

In this study, we used high resolution CORONA, and ALOS/AVNIR-2 satellite images from 1962 to 2008 and remote sensing techniques. The areas of a total of 1071 lakes were precisely outlined at eight sites on the continuous and isolated permafrost zones in Mongolia. We categorized the thermokarst lake areas into eight distinct classes in order to better understand the lake dynamics of individual lake size categories.

We found significant differences in the spatio-temporal dynamics of thermokarst lakes in the continuous and isolated permafrost zones. This difference concerns the lake size classification. The results indicated that total number and area of thermokarst lakes activity had increased in the continuous permafrost zone. In contrast, the isolated permafrost zone had a reduction in those lakes. Since the 1960s, the small lakes (<25 ha) increased by 163 ha in the continuous permafrost zone, while they decreased by 129 ha in the isolated permafrost zone, respectively. The lakes larger than 25 ha, on the other hand, remained almost stable in both the zones. Furthermore, a total of 91 new lakes (343 ha) were detected, especially in the continuous permafrost zone.

These changes observed for the lakes can be explained by climate variations and permafrost degradation. Even though no significant trend in summer precipitation was found in the last 50 years, despite, there was a significant increasing trend in potential evpotranspiration in the isolated permafrost zone rather than continuous permafrost zone. The mean annual air temperature increased significantly in the northern part of the country, while it increased only slightly in the southern parts. Due to ongoing atmospheric warming, patches of ice-rich subsurface, controlling the dynamics of small lakes, have thawed, and the area and number of small lakes (<25 ha) have accordingly increased in the continuous permafrost zone. Increasing potential evapotransipation and disappearing permafrost in the isolated permafrost zone likely caused the decrease in the area and number of such lakes. Small lakes (<25 ha) are especially sensitive to climatologic variations, thus they are useful indicators of permafrost degradation and disappearance in Mongolia.

References

Karlsson, J.M.; Steve, W.L. and Destouni, G. [2014]: Temporal Behavior of Lake Size-Distribution in a Thawing Permafrost Landscape in Northwestern Siberia. *Remote Sensing*, 6, doi:10.3390/rs6010621.

Smith, L.C.; Sheng, Y.; MacDonald, G.M. and Hinzman, L.D. [2005]: Disappearing Arctic Lakes. *Science*, 308:1429, doi:10.1126/science.1108142.

van Everdingen, R.(ed.). [2005]: *Multi-language glossary of permafrost and related ground-ice terms*. National Snow and Ice Data Center/World Data Center for Glaciology, Boulder.

Temporal variability of dissolved nutrients in lakes of Antarctic oases (Schirrmacher and Larsemann Hills)

Natalia Alekseeva[1,2], Natalia Lavinen[2], Irina Fedorova[2], Tatyana Skorospekhova[2], & Elena Dobrotina[2]

[1] *Federal State Budgetary Scientific Institution Trofimuk Institute of Petroleum Geology and Geophysics of Siberian Branch of Russian Academy of Sciences (IPGG SB RAS) and Arctic and Antarctic Research Institute (AARI), Russian Federation*

[2] *Arctic and Antarctic Research Institute(AARI), Russian Federation*

The Antarctic lakes are the result of melting of glaciers and snowfields, supplemented by precipitations and marine influence. The most part of Antarctic lakes located on Antarctic oases – areas of land naturally free from ice and snow, which are separated by continental ice sheet and ice shelf.

In the framework of Russian Antarctic Expedition hydrochemical study of lakes near Progress and Novolazarevskya Russian research stations in Larsemann Hills and Shirmacher oases respectively was carried out. Hydrochemical investigations of lakes in this region are unique due to the fact that the previous study of the lakes was carried out in in the 1970's. The results of previous studies gave us data about ionic composition, electrical conductivity and pH of lake waters. Antarctic lakes are unique and insufficiently explored water objects requiring careful consideration.

During three summer seasons (2009 – 2010, 2012 – 2013 and 2013 – 2014 yy) water samples from lakes near Progress and Novolazarevskya stations have been taken for dissolved nutrients content (silicates, phosphates, nitrites, ammonium nitrogen). The waters of the Antarctic lakes are well oxygenated (9 – 12 mg/l), pH is neutral (pH = 7), but during the summer period is changed to a pH of 8-9. The water of lakes are fresh and ultra fresh. Mineralization of lakes ranges 0,2 – 0,5 g/l. There are lakes exposed to influence of the sea. Results of sample analysis show that dissolved nutrients in the lakes are stable from year to year, except one parameter – silicates. The water of Antarctic oases lakes is characterized by very low concentrations of silicates, which ranges from 0.13 to 1.03 mg/l for Progress station lakes and from 0.34 to 1.49 mg/l for Novolazarevskaya station. Concentrations of phosphates and nitrites are $< 0{,}010$ mg/l and of ammonium nitrogen are $< 0{,}020$ mg/l. Our results show decreasing silicates concentration from 2009 to 2014. One of the main explanations of this decreasing dynamics is the weather conditions, the summer season of 2013 – 2014 was the coldest in comparison to 2009 – 2010. It should be noted that changes happened only with silicates and have not affected for other nutrients components.

TerraSAR-X backscatter and interferometric coherence of thermokarst lake ice in the Lena River Delta

Sofia Antonova[1], Claude Duguay[2], Andreas Kääb[3], Sebastian Westermann[3], Moritz Langer[1], Birgit Heim[1], & Julia Boike[1]

[1] *Alfred Wegener Institute Helmholtz Center for Polar and Marine Research, Potsdam, Germany*
[2] *University of Waterloo, Canada*
[3] *University of Oslo, Norway*

Thermokarst lakes and ponds are major elements of permafrost landscapes, occupying up to 40 % of land area in some vast thermokarst affected Arctic regions [Grosse et al., 2013]. These waterbodies contribute significantly to the exchange of energy and greenhouse gases (GHG) between the land surface and the atmosphere. Deeper lakes (> 2 m) remain typically unfrozen beneath floating ice during winter, leading to the formation of continuously thawed bottom sediments (talik) which facilitate microbial activity and GHG production throughout the year [Langer et al., 2015]. Shallower lakes (< 2 m) experience complete freezing down to the bottom which prevents talik formation and strongly limits the length of the GHG production period. Thus, distinguishing floating lake ice from grounded ice is crucial for evaluating the thermal and geobiochemical state of tundra landscapes. Radar remote sensing provides a powerful tool for accomplishing this task through the ability of radar signals to partially penetrate into or through the lake ice. Mostly, a method based on differences between backscatter signatures is used. In case of floating ice, radar signal backscatters from the ice-water interface and return is high in case of rough ice bottom, which is likely for lake ice [Atwood et al., 2015]. In case of grounded ice, radar signal penetrates through the ice layer and transmits to the frozen lake bottom due to insufficient dielectric contrast between ice and frozen sediments, resulting in low backscatter. Although the method has been known since 1970's, the potential of new generation satellite X-band radar imagery such as TerraSAR-X has yet to be evaluated. Interferometric coherence is a parameter which defines the degree of correlation between two radar signals and to a great extent depends on changes in backscattering surface occurred between two radar acquisitions. Interferometric coherence time series are used as a different approach for distinguishing floating lake ice from grounded ice. Coherence is low when the lake ice is growing, because backscattering surface (ice-water interface) changes with every acquisition. Coherence increases significantly when the ice reaches the lake bottom, creating permanent backscattering surface. Our study is based on TerraSAR-X data for the 2012-2013 and 2013-2014 winter seasons. We investigated the use of TerraSAR-X backscatter and interferometric coherence time series with high spatial (3 m) and temporal (11 days) resolution for the detection of grounded ice, for monitoring ice growth stages, for the detection of timing of ice grounding and furthermore, for the derivation of the ice thickness in the number of shallow and deep thermokarst lakes in the Lena River Delta. Ice thickness and water depth measurements obtained from these lakes during a field program in the spring of 2015 are used for ground validation.

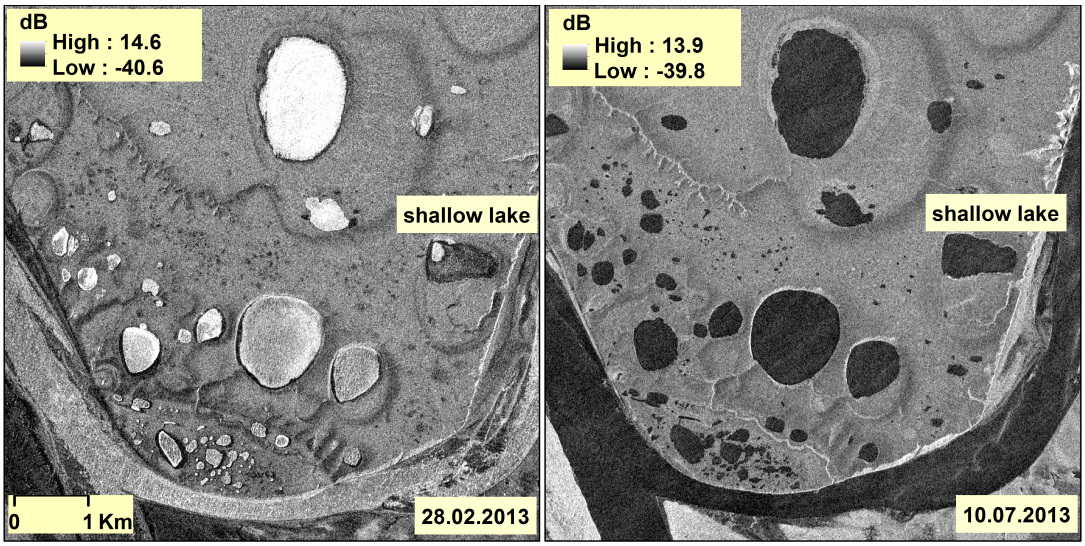

Figure 1: left: subset of backscatter intensity image taken on 28 February 2013, lake ice appears bright except of the shallow lake; right: subset of radar image taken on 10 July 2013, areas of open water appear dark.

References

Atwood, D.; Gunn, G.; Roussi, C.; Wu, J.; Duguay, C. and Sarabandi, K. [2015]: Microwave backscatter from Arctic lake ice and polarimetric implications. *IEEE Transactions on Geoscience and Remote Sensing*, 53(11), 2015. doi:10.1109/TGRS.2015.2429917.

Grosse, G.; Jones, B. and Arp, C. [2013]: Thermokarst lakes, drainage, and drained basins. In: Shroder, J.F.(ed.), *Treatise on Geomorphology*. Elsevier: Amsterdam.

Langer, M.; Westermann, S.; Walter Anthony, K.; Wischnewski, K. and Boike, J. [2015]: Frozen ponds: production and storage of methane during the Arctic winter in a lowland tundra landscape in northern Siberia, Lena River delta. *Biogeosciences*, 12(4): 977–990, doi:10.5194/bg-12-977-2015.

Extreme sensitivity of shallow lakes and sublake permafrost to Arctic climate change

Christopher Douglas Arp[1], Benjamin Jones[2], Allen Bondurant[1], Guido Grosse[3], Andrew David Parsekian[4], Vladimir Romanovsky[1], & Kenneth Hinkel[5]

[1] *University of Alaska Fairbanks, United States of America*
[2] *U.S. Geological Survey, United States of America*
[3] *Alfred Wegener Institute Helmholtz Center for Polar and Marine Research, Potsdam, Germany*
[4] *University of Wyoming, United States of America*
[5] *University of Cincinnati, United States of America*

The interaction and feedbacks between surface water and permafrost are fundamental processes shaping the surface of continuous permafrost landscapes. Lake-rich regions of Arctic lowlands, such as coastal plains of northern Alaska, Siberia, and Northwest Canada, where shallow thermokarst lakes often cover 20–40 % of the land surface are a pronounced example of these permafrost processes. In these same Arctic coastal regions, current rates of near-surface atmospheric warming are extremely high, 0.8 °C/ decade for example in Barrow, Alaska, primarily due to reductions in sea ice extent [Wendler et al., 2014]. The thermal response of permafrost over recent decades is also rapid, warming approximately 0.6 °C/ decade for example at Deadhorse, Alaska, yet this permafrost is still very cold, less than -6 °C [Romanovsky et al., 2015]. The temperature departure created by water in lakes set in permafrost is well recognized and where mean annual bed temperatures (MABT) are above 0 °C, a talik develops [Brewer, 1958]. The critical depth of water in lakes where taliks form is generally in excess of maximum ice thickness, which has historically been around 2 m in northern Alaska. Thus, lakes that are shallower than the maximum ice thickness, which are the majority of water bodies in many Arctic coastal lowlands, should maintain sublake permafrost and have a shallow active layer if MABT's are below freezing. Recent analysis, however, suggests a lake ice thinning trend of 0.15 m/ decade for lakes on the Barrow Peninsula, such that the maximum ice thickness has shifted to less than 1.5 m since the early 2000's. We hypothesized that the surface areas most sensitive to Arctic climate warming are below lakes with depths that are near or just below this critical maximum ice thickness threshold primarily because of changing winter climate and reduced ice growth. This hypothesis was tested using field observations of MABT, ice thickness, and water depth collected from lakes of varying depths and climatic zones on the coastal plain and foothills of northern Alaska. A model was developed to explain variation in lake MABT by partitioning the controlling processes between ice-covered and open-water periods. As expected, variation in air temperature explained a high amount of variation in bed temperature (72 %) and this was improved to 80 % by including lake depth in this model. Bed temperature during the much longer ice-covered period, however, was controlled by lake depth relative to regional maximum ice thickness, termed the Effective Depth Ratio (EDR). A piecewise linear regression model of EDR explained 96 % of the variation in bed temperature with key EDR breaks identified at 0.75 and 1.9. These breaks may be physically meaningful towards understanding the processes linking lake ice to bed temperatures and sublake permafrost thaw. For example if regional lake ice grows to 1.5 m thick, the first break is at lake depth of 1.1 m, which will freeze by mid-winter and may separate lakes with active-layers from lakes with shallow taliks. The second EDR break for the same ice thickness is at a lake depth of 2.9 m, which may represent the depth where winter thermal stratification becomes notable (greater than 1 °C) and possibly indicative of lakes that have well developed taliks that store and release more heat. We then combined these ice-covered and open-water models to evaluate the sensitivity of MABT to varying lake and climate forcing scenarios and hindcast longer-term patterns of lake bed warming. This analysis showed that MABT in shallow lakes were most sensitive to changes in ice thickness, whereas ice thickness had minimal impact on deeper lakes and variation in summer air temper-

ature had a very small impact on MABT across all lake depths. Using this model, forced with Barrow climate data, suggests that shallow lake beds (1-m depth) have warmed substantially over the last 30 years (0.8 °C/ decade) and more importantly now have an MABT that exceeds 0 °C. Deeper lake beds (3-m depth), however, are suggested to be warming at a much slower rate (0.3 °C/ decade), compared to both air temperature (0.8 °C/ decade) and permafrost (0.6 °C/ decade). This contrasting sensitivity and responses of lake thermal regimes relative to surrounding permafrost thermal regimes paint a dramatic and dynamic picture of an evolving Arctic land surface as climate change progresses (Fig. 1). We suggest that the most rapid areas of permafrost degradation in Arctic coastal lowlands are below shallow lakes and this response is driven primarily by changing winter conditions.

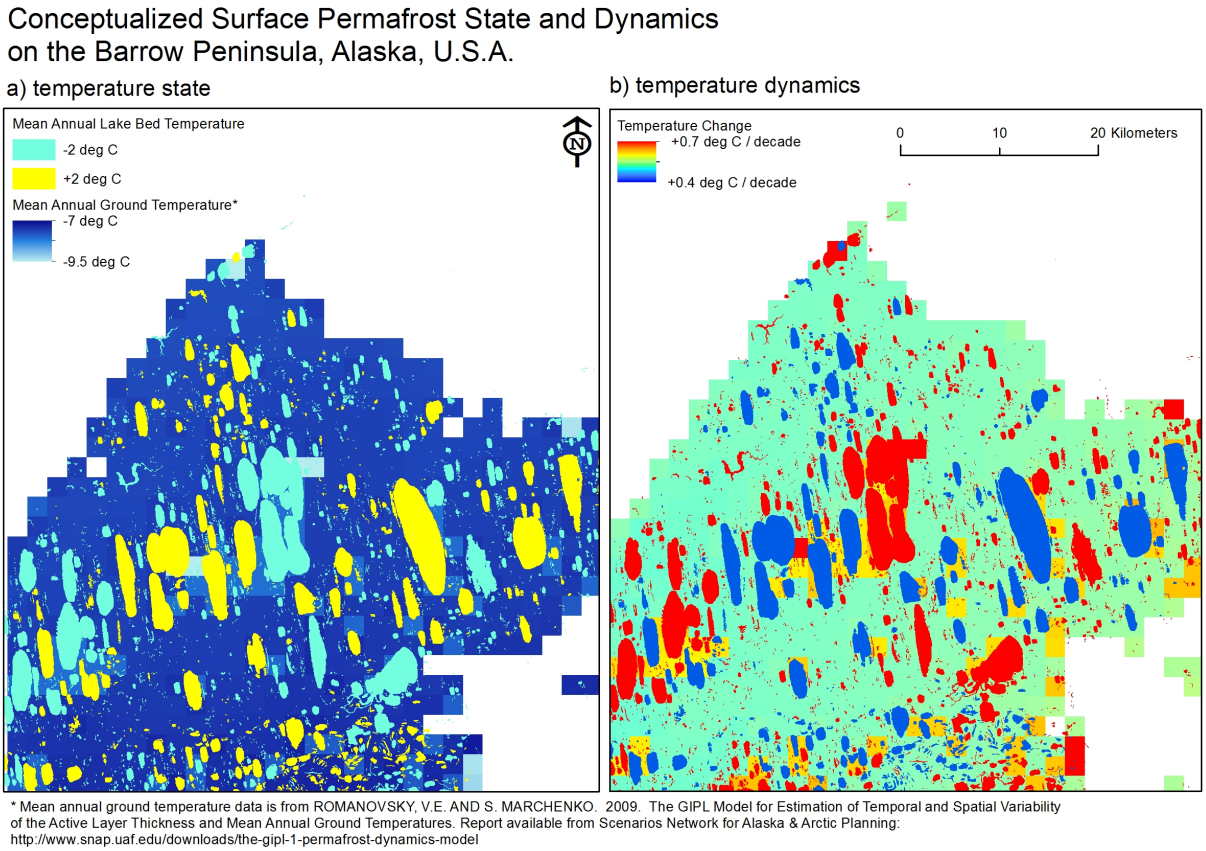

Figure 1: Conceptualized map of surface permafrost state and dynamics on the Barrow Peninsula, Alaska, U.S.A.

References

Atwood, D.; Gunn, G.; Roussi, C.; Wu, J.; Duguay, C. and Sarabandi, K. [2015]: Microwave backscatter from Arctic lake ice and polarimetric implications. *IEEE Transactions on Geoscience and Remote Sensing*, 53(11), doi:10.1109/TGRS.2015.2429917.

Brewer, M.C. [1958]: The thermal regime of an arctic lake. *Transactions of the American Geophysical Union*, 39:278–284.

Romanovsky, V. E.; Smith, S. L.; Christiansen, H. H.; Shiklomanov, N. I.; Streletskiy, D. A.; Drozdov, D. S.; Malkova, G. V.; Oberman, N. G.; Kholodov, A. L. and Marchenko, S. S. [2015]: The Arctic Terrestrial Permafrost in "State of the Climate in 2014". *Bulletin of the American Meteorological Society*, 2015.

Wendler, G.; Moore, B. and Galloway, K. [2014]: Strong temperature increase and shrinking sea ice in Arctic Alaska. *The Open Atmospheric Science Journal*, 8:7–15.

Stable isotope climate records from drained thermokarst lake basins in northern Yukon, Canada

Sasiri Bandara[1], Duane Froese[1], Trevor Porter[2], Fabrice Calmels[3], & Paul Sanborn[4]

[1] *University of Alberta, Canada*
[2] *University of Toronto Mississauga, Canada*
[3] *Yukon College, Canada*
[4] *University of Northern British Columbia, Canada*

Thermokarst lakes form following the thaw of ice-rich permafrost and typically drain after a few decades to millennia. Drained lake basins become epicentres for peat accumulation and, in many areas, ice-rich permafrost re-aggradation. This aggradation may be interrupted by subsequent thaw lake formation should disturbance occur. In this study, we investigate the history of lake basin dynamics through drilling and recovery of permafrost cores from drained thermokarst lake basins (DTLBs) in the Old Crow Flats, northern Yukon. Thermokarst lakes and drained thermokarst lake basins are ubiquitous (2700) in the Old Crow area, but little is known about their environmental dynamics over Holocene timescales, and whether these lakes follow the assumed "thaw lake cycle". Here, we establish the hydrology and drainage histories of seven DTLBs on the basis of cryostratigraphy, pore-ice stable isotope analyses and radiocarbon dating of associated plant macrofossils. Our results indicate that only one out of the seven lakes underwent multiple thermokarst cycles. Radiocarbon dates indicate that post-drainage peat accumulation rates are initially rapid, but decrease thereafter. Pore-ice stable isotope analyses suggest that four of the lakes became more depleted in $\delta^{18}O$ and δD over time, reflecting increased contributions from snowmelt, while one lake shows $\delta^{18}O$ enrichment likely as a result of partial drainage and evaporative enrichment of the remaining water. The two remaining lakes maintain relatively constant isotopic records, possibly due to largely unaltered physical dimensions of the DTLBs. These findings suggest variable post-drainage isotopic histories between different thermokarst lake basins as a result of spatially varying permafrost and hydrologic conditions. Based on our isotope results, including deuterium excess trends, we argue that syngenetic peat permafrost maintains relatively unaltered meteoric water archives while epigenetic lacustrine silts are inherently more variable. Consequently, syngenetic peat permafrost from northern DTLBs may be useful for millennial-scale paleoclimate investigations as we show through our reconstruction of Holocene climate change in northern Yukon.

Rates and mechanisms of expansion in thermokarst lakes with bedfast and floating ice regimes on the Arctic Coastal Plain of northern Alaska

Allen C. Bondurant[1], Chris Arp[1], Benjamin Jones[2], & Melanie Engram[1]

[1] *University of Alaska Fairbanks, United States of America*
[2] *US Geological Survey - Alaska Science Center, USA*

Thermokarst lakes form and expand through shoreline erosion of permafrost. This lateral expansion and eventual lake drainage is an important component of the thaw lake cycle. In the ice rich silt of the outer Arctic Coastal Plain (ACP) of northern Alaska, the dominant forms of shore erosion include thermo-erosional niche formation and subsequent block collapse, retrogressive thaw slumps and other thermally associated mass wasting processes including active layer detachments, mechanical erosion by wave action,

ice wedge degradation and associated thermal erosion, and spring ice shove. Understanding where and when such processes dominate is not well established. One important distinction between Arctic thermokarst lakes in general is the ice regime of a lake (i.e. bedfast ice or floating ice), particularly on the ACP. Previous analysis of 13 lakes located on the outer ACP has shown that whole-lake shoreline expansion rates average 0.9 m/yr for all lakes, above rates for thermokarst lakes in other regions, where expansion rates typically vary between 0.10 and 0.70 m/yr [Jones et al., 2011]. On the outer ACP, expansion rates range from below detection in bedfast ice lakes to 1.8 m/yr in floating ice lakes, and point specific rates can be even higher [Arp et al., 2011]. We hypothesize that this difference in ice regime is a major control on the mean annual bed temperature of the lake and ultimately on the thermal state of the permafrost underneath and adjacent to the lake. In floating ice lakes, the depth of thaw in soils beneath the lake can extend tens of meters deep or more, and the above freezing mean annual lake temperature warms the permafrost adjacent to the lake. In these floating ice lakes, shorelines are more susceptible to summertime thermal and mechanical erosional processes than their bedfast ice counterparts, where permafrost temperatures are colder in bluffs and there is no talik formation. Margins surrounding bedfast ice lakes take longer to thaw in the short Arctic summer and thus are more resistant to lake shore erosional processes. Temperatures in these margins are potentially an important contributing factor to the difference in shoreline expansion rates between ice regimes. Through analysis of modern and historical satellite and aerial imagery, this analysis will be expanded in both number of lakes analyzed and time series extent. Lake ice regime was determined through the analysis of multi-year time series synthetic aperture radar (SAR) imagery, where bedfast ice lakes have a lower magnitude radar backscatter return when compared to floating ice lakes. In a warming arctic climate, maximum ice thicknesses will likely decrease through time and bedfast ice lakes will potentially shift to a floating ice regime. Because up to 60 % of lakes on the ACP are near the approximately 1.5m depth [Jeffries et al., 1996] threshold for shifting ice regimes, they are among the most sensitive landscape features to climate change. The increased rates of expansion from lakes that had previously experienced bedfast ice conditions will have important landscape implications including degradation of sublake permafrost, increased lake surface area, and mobilization and release of stored carbon. The recognition of the potential for geomorphic change of lakes in a changing climate is important for future planning and development of resources in regions of continuous permafrost, such as the Arctic coastal plain. Understanding the rates and mechanisms of expanding lake shorelines is an important component to predicting lake dynamics under shifting climate conditions.

References

Arp, C. D.; Jones, B. M.; Urban, F. E. and Grosse, G. [2011]: Hydrogeomorphic processes of thermokarst lakes with grounded-ice and floating-ice regimes on the Arctic coastal plain, Alaska. *Hydrological Processes*, doi:10.1002/hyp.8019.

Jeffries, M.O.; Morris, K. and Liston, G.E. [1996]: A method to determine lake depth and water availability on the North Slope of Alaska with spaceborne imaging radar and numerical ice growth modeling. *Arctic*, 49(4), 1996.

Jones, B. M.; Grosse, G.; Arp, C. D.; Jones, M. C.; Walter Anthony, K. M. and Romanovsky, V. E. [2011]: Modern thermokarst lake dynamics in the continuous permafrost zone, northern Seward Peninsula, Alaska. *Journal of Geophysical Research: Biogeosciences*, 116:G00M03, doi:10.1029/2011JG001666.

Thermokarst and kettle lakes in the eastern Canadian Arctic: A paleolimnological perspective

Frédéric Bouchard[1,2,3], Isabelle Laurion[1,3], & Daniel Fortier[2,3]

[1] *Institut national de la recherche scientifique (INRS), Canada*
[2] *Université de Montréal, Canada*
[3] *Centre d'études nordiques (CEN - Centre for Northern Studies), Canada*

Lakes are widespread in permafrost regions and play a key role in large-scale biogeochemical cycles, including greenhouse gas emissions. Yet, little is known about the historical variability of these freshwater ecosystems, which limits our understanding of present day dynamics. Are these systems presently facing accelerated changes? Do such changes represent a progressive, gradual trend, or rather result from sudden threshold crossing? Investigating the temporal evolution of Arctic lakes based on sediment archives can provide baseline information to better anticipate their response to ongoing and future climate change. More specifically, we are interested in how future trajectories will influence water and carbon cycles at different spatial scales. Paleolimnological information retrieved from lake sediments, such as grain size distribution, organic and mineral contents, geochemical composition and sedimentary structures, generally requires destruction of the analyzed samples. Here we present an affordable, non-destructive approach for conducting qualitative and quantitative descriptions of lake sediment records in permafrost landscapes. This method is also useful to quickly target specific sediment layers/facies of interest for more detailed subsequent analyses (e.g., ^{14}C dating, thin sections). We collected sediment cores in two contrasted lakes located in a glacial valley on Bylot Island (Nunavut), in the eastern Canadian Arctic: a shallow (< 5 m) thermokarst lake and a deeper (> 10 m) kettle lake. Mineral (silt, sand, gravel) and organic (gyttja, peat) layers as well as sedimentary structures were observed and characterized using micro-computed tomography (CT). Two kinds of images were produced: 1) two-dimensional sections (longitudinal and transversal) allowing the volumetric measurement of the different mineral and organic fractions, and 2) virtual three-dimensional reconstructions of the entire core, which can be visualized as short movies. Combined with more classic paleolimnological tools, CT-scan images provide new insight on lake inception through thermokarst, glacial or other geomorphological processes, and on sedimentological processes such as organic and mineral matter erosion and deposition, as well as lake drainage.

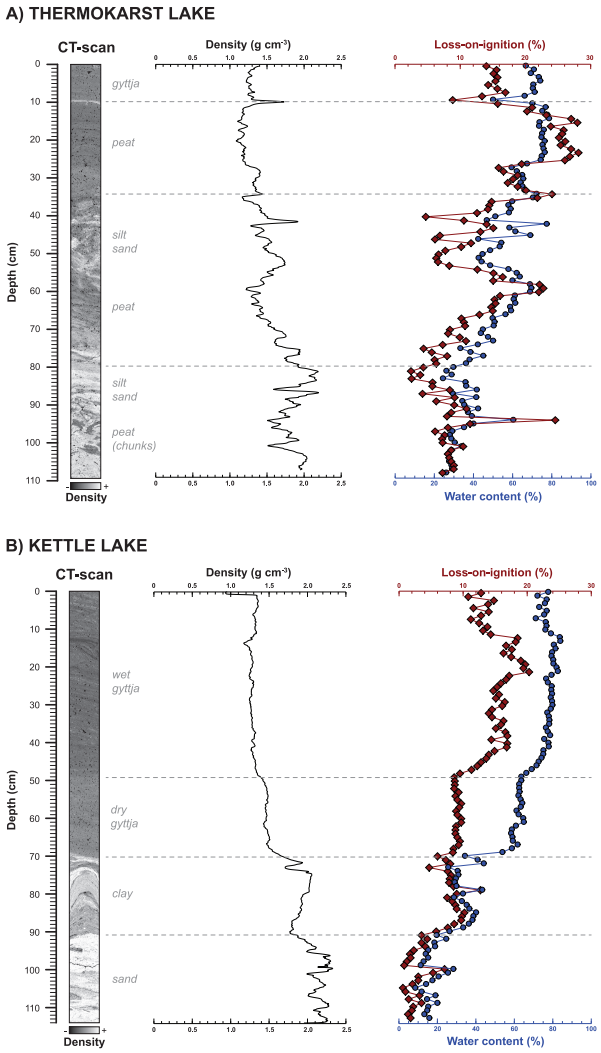

Figure 1: Sediment core properties from a thermokarst lake (A) and a kettle lake (B) on Bylot Island (Nunavut), eastern Canadian Arctic. From left to right: computed tomography (CT) images, mean density profiles, and loss-on-ignition (550 °C) and water content.

New compilation of formation dates, origins and fates for lakes within the Last Glacial/Permafrost Maximum domain of the Northern Hemisphere

Laura Brosius[1], Claire Treat[2], Josefine Lenz[3], Guido Grosse[3], Katey Walter Anthony[1], & Miriam Jones[2]

[1] *University of Alaska, United States of America*
[2] *United States Geological Survey, United States of America*
[3] *Alfred Wegener Institute Helmholtz Centre for Polar and Marine Research, Potsdam, Germany*

Global lake distribution datasets show that a vast majority of Earth's lakes by number and area are located in the high latitudes of the Northern Hemisphere. Lakes abundance in these regions has been linked to histories of glaciation, permafrost, and peatlands [Smith et al., 2007]. Although well-dated sedimentary lake records are regularly used for the reconstruction of paleoenvironmental conditions and landscape dynamics, so far no consistent panarctic database exists on the age and origin of northern high latitude lakes. Lake cores, peat cores and exposures detailed in primary literature sources often provide a complete picture of how and when lakes formed. Here, we compile an extensive dataset of 1154 unique lake basal and minimum ages from both past and extant lakes within the domain of glaciation and permafrost extent during the Last Glacial/Permafrost Maximum [Lindgren, 2015] collected primarily from detailed literature descriptions. We distinguish ten distinct classes of lake origin after [Vincent and Laybourn-Parry, 2008] and include information on the fates (both mechanism and timing) of non-extant lakes described in peat cores and exposures. Analysis of the dataset reveals an increase in rates of northern hemisphere lake formation beginning 14,500 cal. yr BP that was sustained, with a short lull during the Younger Dryas, until it began to generally decrease after 10,500 cal. yr BP. Peak lake formation in regions where ice sheets were present into the early and mid-Holocene occurred later. Formation frequencies for lakes of glacier-dependent origin (i.e. kettle, moraine-dammed, glacial scour) and glacier-independent origin (e.g. oxbow, thermokarst, coastal uplift) coincided, suggesting that climatic factors were driving processes such as glacial retreat and permafrost degradation responsible for lake formation simultaneously. The dataset also reveals a weak correlation ($R^2 = 0.26$) between the timing of lake drainage or terrestrialization and the timing of lake establishment. Although highly variable, the average length of lake persistence on the landscape determined from non-extant lake records was 5460 years.

References

Lindgren, A.; Hugelius, G.; Kuhry, P.; Christensen, T. R. and Vandenberghe, J. [2016]: GIS-based Maps and Area Estimates of Northern Hemisphere Permafrost Extent during the Last Glacial Maximum. *Permafrost and Periglacial Processes*, 27(1): 6–16, doi:10.1002/ppp.1851.

Smith, L.C.; Sheng, Y. and MacDonald, G.M. [2007]: A first pan-Arctic assessment of the influence of glaciation, permafrost, topography and peatlands on northern hemisphere lake distribution. *Permafrost and Periglacial Processes*, 18(2):201–208, doi:10.1002/ppp.581.

Vincent, W. F. and Laybourn-Parry, J.(eds.). [2008]: *Polar Lakes and Rivers*. New York, NY: Oxford University Press.

Lakes in the arctic carbon cycle: Long-term perspectives using a palaeolimnological approach

Mary Edwards[1], Suzanne McGowan[2], John Anderson[3], Peter Langdon[1], Vivienne Jones[4], Simon Turner[4], Maarten van Hardenbroek[1], Erika Whiteford[3], & Emma Wiik[5]

[1] *University of Southampton, United Kingdom*
[2] *University of Nottingham, United Kingdom*
[3] *Loughborough University, United Kingdom*
[4] *University College London, United Kingdom*
[5] *University of Regina, Canada*

Lakes are terrestrial carbon-processing hotspots. Globally, they receive 1.9 Pg of carbon (C) per year, of which 0.2 Pg are sequestered as sediment, ≈0.8 Pg are evaded as gas, and ≈0.9Pg end up in the ocean [Cole et al., 2007]. About 3,500,000 lakes with areas >0.0036 km^2 cover an area of ≈350,000 km^2 across the Arctic, which is about 6 % of the total land area. Most lakes lie in permafrost-affected regions.

The greatest projected warming over this century will be in the Arctic (IPCC 2014). The consequences of temperature increases are expected to be faster biological processing and increased productivity in a lake and its catchment, plus increasing catchment biomass, permafrost degradation and changes in the paludification regime. Warming is already changing the nature of arctic vegetation via shrub expansion (arctic greening), and changes to permafrost are occurring. These changes are likely to drive higher affect C-flux from the catchment to a lake and thus affect water quality. In turn, this will affect C-cycling in lakes and the balance between autotrophy and heterotrophy. Compared with the high Arctic, the boreal zone is characterized by relatively warm and moist conditions, high catchment productivity and C production, which tends to lead to lakes dominated by heterotrophy and net C emissions to the atmosphere. In the high Arctic, productivity and catchment C are relatively low, and lakes tend to draw down carbon from the atmosphere.

With warming and greening of the Arctic, the net balance of heterotrophy and autotrophy in lakes may change. However, such a transformation is difficult to observe in the contemporary landscape, as there are few long-term studies of lake status. Palaeolimnology can test lake responses under different conditions over the Holocene, e.g., past periods with warming and greening through analyses of dated sediments: C accumulation rate, the nature of sedimentary C (reflecting heterotrophy vs autotrophy), terrestrial vs lacustrine sources, dissolved organic carbon (DOC) levels, nitrogen levels, pollen and plant macrofossils reflecting catchment vegetation and aquatic macrophytes, etc. Based on this conceptual model of lake response to environmental change, we predicted the expected trajectories of lakes as Holocene environments changed. Our study regions were the Brooks Range of Alaska, north Norway and south-west Greenland, regions that span the northern boreal zone to the high Arctic.

At Ruppert Lake (Brooks Range), for example, late-glacial conditions (≈16,000 yr BP) were characterized by a relatively cool and dry climate and sparse vegetation. The pigment record, which reflects algal production and water clarity, indicates clear water, low DOC and high ultra-violet radiation penetration. A transition to shrub cover (≈12,500 yr BP), when conditions were relatively warm and slightly moister, is characterized by the highest autochthonous production of the record. The mid-Holocene expansion of boreal forest (≈8500 yr BP) coincides with a trend toward declining autotrophy and increased organic C input to the catchment. At this site, the trends in lake development conform to the model, and indicate that the lake shifted from net autotrophy to net heterotrophy, and thus from a net site of C sequestration to one of C release.

The results suggest that increases in catchment productivity, as are occurring with arctic greening, will lead to lakes across the Arctic shifting towards heterotrophy, and thus their contribution to the carbon cycle shifting towards C fluxes to the atmosphere. However, enhanced lacustrine productivity may also lead to greater rates of C storage. Further work is

focused on estimating rates of C sequestration over time.

References

Cole, J. J.; Prairie, Y. T.; Caraco, N. F.; McDowell, W. H.; Tranvik, L. J.; Striegl, R. G.; Duarte, C. M.; Kortelainen, P.; Downing, J. A.; Middelburg, J. J. and Melack, J. [2007]: Plumbing the Global Carbon Cycle: Integrating Inland Waters into the Terrestrial Carbon Budget. *Ecosystems*, 10 (1):172–185, doi:10.1007/s10021-006-9013-8.

Exchange of CO_2 and CH_4 between a Siberian thaw lake and the atmosphere

Daniela Franz[1], Eric Larmanou[1], Niko Bornemann[2], Moritz Langer[2], Julia Boike[2], & Torsten Sachs[1]

[1] *Helmholtz Centre Potsdam, GFZ German Research Centre for Geosciences, Germany*
[2] *Alfred Wegener Institute for Polar and Marine Research, Potsdam, Germany*

Freshwaters are an important component of the continental greenhouse gas (GHG) balance with emissions estimated to correspond to about 80 % of the land GHG sink [Bastviken et al., 2011]. Thaw lakes in permafrost landscapes and especially in Yedoma permafrost are considered to be strong processors of organic carbon and essential emitters of CH_4 [Walter et al., 2006]. As the Arctic experiences the recent global warming at a much faster rate than other regions of the world [AMAP, 2015], the importance of thaw lakes in the global GHG budget is expected to rapidly increase due to progressive permafrost degradation. However, especially arctic lakes are highly underrepresented in observational studies on lake-atmosphere GHG exchange. Only a few short-term studies exist, with a majority missing the ice break-up. This event is assumed to result in a spring emission peak that contributes considerably to the annual GHG emissions. In consequence, arctic freshwaters are not adequately represented in modelling approaches and scenarios of climate change.

Using a floating eddy covariance (EC) system, we investigate ecosystem CH_4 and CO_2 flux dynamics between the atmosphere and a Yedoma thaw lake in the Lena River Delta in northern Siberia. The compiled dataset covers the ice break-up and most of the ice-free period 2014. We chose the EC method as it allows direct, automatic and non-intrusive flux measurements in remote areas. The investigated lake is one of $>$ 500 lakes on Kurungnakh Island in the Lena River Delta. The study site lies within the zone of continuous permafrost and belongs to the arctic tundra zone. The lake covers an area of approximately 1.25 km^2 with a mean depth of eight meters. We will present first results of this study and discuss the importance of a spring emission peak during ice break-up in the annual GHG budget.

References

Arctic Monitoring and Assessment Programme (AMAP), Oslo. *Methane as an Arctic climate forcer*. 2015. 139 pp.

Bastviken, D.; Tranvik, L.J.; Downing, J.A.; Crill, P.M. and Enrich-Prast, A. [2011]: Freshwater methane emissions offset the continental carbon sink, *Science*, 331(6013):50–50, doi:10.1126/science.1196808.

Walter, K.M.; Zimov, S. A.; Chanton, J.P.; Verbyla, D. and Chapin, F.S. [2006]: Methane Bubbling from Siberian Thaw Lakes as a Positive Feedback to Climate Warming. *Nature*, 443(7107):71–75, 2006. doi:10.1038/nature05040.

'Lake colour' in permafrost landscapes of the central Lena River Delta and central Yamal - case studies of Coloured Dissolved Organic Matter (cDOM) and turbidity regimes

Birgit Heim[1], Annett Bartsch[2], & Yuri Dvornikov[3]

[1] *Alfred Wegener Institute Helmholtz Center for Polar and Marine Research, Potsdam, Germany*
[2] *Technical University of Vienna, Austria*
[3] *Earth Cryosphere Institute Moscow Russia*

We provide a first field-based & satellite-based inventory of optical lake types in the permafrost landscapes of the central Lena River Delta (Arctic Siberia) and central Yamal (Western Arctic Siberia) using field investigations and multi-sensor satellite data. Within the thematic network between our groups we seek to investigate:

- the water-leaving spectral signal of the lake water bodies: 'the lake colour'
- how to link lake colour to SAR-derived information
- geochemical and hydrodynamical in-situ measurements (cDOM, DOC, SPM)

We give an overview on different optical types of lakes in the thermokarst landscapes of central Yamal and the Lena River Delta. For several of the lakes in Yamal and fro some lakes in the central Lena River Delta we were able to sample for Dissolved Organic Carbon, DOC, and coloured dissolved organic matter, cDOM (the absorbing fraction of the DOC pool) and SPM. The cDOM regimes influence the transparency of the different lake types. We show simulations of cDOM influence on lake colour using the 'Water Colour Simulator' WASI©. However, turbidity seems to play the dominant role in providing the water-leaving colour of thermokarst lake types.

Remote sensing and quantitative statistic methods applied to different theories of thermokarst lake occurrence

Veronika N. Kapralova, A. S. Viktorov T. V. Orlov, O. N. Trapeznikova, M. V. Arkhipova, A. V. Zverev, E. G. Panchenko, & A. A. Sadkov

Sergeev Institute of Environmental Geoscience Russian Academy of Sciences, Russian Federation

One of the important questions, regarding the thermokarst development, is to find the principles of its distribution and dynamics with the purpose of forecasting environmental changes. Many researchers studied the thermokarst processes, but proper statistical methods regarding these are yet to be developed. In particular, the analysis of quantitative aspects of thermokarst is to be considered. Various researches attempted to determine the age of thermokarst lakes, as well as the time of their occurrence.

In this work we try to investigate and compare several models of the lake development by means of modeling and remotely sensed data. The first model is formulated on the basis of empirical data that were acquired from papers of Burn and Smith [1990], Shur and other authors. We attempted elaborating the model, when the growth rate of lakes is random and constant with time. If so, at the specific moment of time the average size of the lakes should be of normal distribution. The second model was formulated by Victorov [2006], and it implies that the growth rate of lakes is proportional to their size, and at the specific moment of time, lake diameters should be of lognormal distribution. Also, for each of the models we considered the situation of synchronous and asynchronous start of the thermokarst processes. As a result, we came up with four distributions and we also looked for conformity of theoretical and experimental data. We performed the model approval for several study areas, which are located in different Arctic regions of Russia, Canada, and of Alaska. We selected the study sites based on the morphological homogeneity of those and on the availability of the remotely sensed imagery. For the selected lakes we evaluated the relationship of empirical and theoretical distributions of the lake areas.

References

Burn, C.R. and Smith, M.W. [1990]: Development of thermokarst lakes during the holocene at sites near Mayo, Yukon territory. *Permafrost and Periglacial Processes*, 1(2):161–175, 1990. doi:10.1002/ppp.3430010207.

Victorov, A.S. [2006]: *General problems of the Mathematical morphology of landscape.* 252 p.

Regulation of methane fluxes from ponds of the northeast Siberian polygonal tundra

Christian Knoblauch[1], Oliver Spott[2], Svetlana Evgrafova[3], Lars Kutzbach[1], & Eva-Maria Pfeiffer[1]

[1]*Institute of Soil Science, Universität Hamburg, Germany*
[2]*Institute of Geography, Faculty of Physics and Earth Science, Leipzig University*
[3]*Sukachev Institute of Forest, Siberian Branch of the Russian Academy of Science*

The microbial degradation of organic matter in water-saturated soils and sediments is the most important source of the climate relevant trace gas methane (CH_4). Although ponds and lakes cover a substantial fraction of the permafrost affected landscape of northern Siberia, data on CH_4 fluxes from these water bodies and their regulation by microbial processes are very scarce. Therefore, we measured CH_4 production, oxidation and emission in ponds of the permafrost-affected polygonal tundra on Samoylov, a Holocene island in the northeast Siberian Lena River Delta. The studied ponds were characterized by open water areas without vascular plants in the centers of the ponds and vegetation dominated by *Carex spp.* and *Arctophila fulva* at the margins of the ponds. The bottom of the ponds was covered by a thick ($\geq$30 cm) layer of the brown moss *Scorpidium scorpioides*. Summer CH_4 fluxes were measured with closed chambers at the margins of ponds vegetated by vascular plants and in their centers without vascular plants. Furthermore, CH_4, carbon dioxide (CO_2), dissolved organic carbon (DOC) and oxygen concentration gradients, stable carbon isotope signatures of dissolved and emitted CH_4 as well as microbial CH_4 production and CH_4 oxidation were determined.

The depth profiles of oxygen showed saturation in the surface water, a strong depletion in the submerged moss layer and anoxic conditions in the bottom soil of the ponds. Methane concentrations were highest at the bottom of the active layer (0.6 to 1.5 mM CH_4) with significantly lower values in the rhizosphere of the pond margins. Above the soil surface, in the submerged moss layer, methane concentrations decreased by more than two orders of magnitude. Despite lower CH_4 concentrations, potential CH_4 production was significantly higher in the soils vegetated by vascular plants. Mean summer CH_4 fluxes (46.1 $\pm$15.4 mg CH_4 $m^{-2}d^{-1}$) were significantly higher at the margins of the ponds vegetated by vascular plants than at the open water centers without emerged vegetation (5.9 $\pm$8.2 mg CH_4 $m^{-2}d^{-1}$). CH_4 transport was dominated by diffusion in most open water sites, but substantial ebullitive fluxes (12.0 $\pm$8.1 mg CH_4 $m^{-2}d^{-1}$) were detected in one pond. Plant-mediated transport accounted for 70 to 90 % of total CH_4 fluxes above emerged vegetation. In the absence of vascular plants, 61 to 99 % of the CH_4 produced in the anoxic bottom soil was consumed in the submerged moss layer. The fraction of CH_4 oxidized was lower at sites with vascular plants since CH_4 was predominantly transported through their aerenchyma, thereby bypassing the CH_4 oxidation zone in the moss layer. These results are the first on CH_4 fluxes from small polygonal ponds of the Siberian Arctic emphasizing the importance of moss-associated CH_4 oxidation in water saturated soils. Low methane fluxes from the open water sites are due to efficient CH_4 oxidation below the water table, a process still neglected in most biogeochemical models simulating CH_4 emissions from wetlands.

Simulating the impact of water bodies on the thermal stability of permafrost using a coupled permafrost-lake model.

Moritz Langer[1,2], Sebastian Westermann[3], Julia Boike[1], Georgiy Kirillin[4], Guido Grosse[1], Shushi Peng[5], & Gerhard Krinner[2]

[1] *Alfred-Wegener-Institut, Helmholtz-Zentrum für Polar- und Meeresforschung, Germany*
[2] *Lab. de Glaciologie et Géophysique de l'Environnement, CNRS and Université Grenoble Alpes, France*
[3] *Department of Geography, University of Oslo, Norway*
[4] *Leibniz-Institute of Freshwater Ecology and Inland Fisheries (IGB), Germany*
[5] *Laboratoire des Sciences du Climat et de l'Environnement (LSCE CEA-CNRS-UVSQ), France*

Lakes and ponds are abundant in vast regions of the permafrost lowland landscapes in the Arctic. The areal fraction of open water surfaces can amount to more than 25 % in some lowland tundra landscapes. In some tundra landscapes, about 50 % of the total number of water bodies feature surface areas less than 10 m^2. Several studies emphasize that these water bodies strongly control fundamental ecosystem processes such as the carbon, heat, and water balance. So far, it is poorly understood how these ecosystems will respond to changing climate conditions. In particular, the presence of water bodies is strongly related to the stability of the surrounding permafrost soils. Permafrost is an effective water barrier that largely controls lake formation, drainage, and growth. In return, water bodies strongly affect the thermal state of the surrounding permafrost by modifying the surface energy balance and the subsurface heat transport and storage capabilities.

In order to gain a better understanding of the vulnerability of such landscapes the 1D transient permafrost model CryoGrid3 was coupled to the 1D lake model FLake. The development of the model was supported by a large observational dataset of water temperature profile measurements from lakes and ponds in northern Siberia. The coupled model was used for site level simulations for water bodies on Samoylov Island located in the Lena River Delta. Based on extensive Monte-Carlo sensitivity tests, we investigated the thermal impact of water bodies with different depths (0.2 – 5.0 m) on the thermal state of sediments underneath. Climate impact simulations until 2100 were performed considering a moderate and a strong climate warming scenario.

The preliminary results suggest that shallow water bodies (water depth < 1.5 m) can accelerate permafrost thaw by a factor of five. More importantly, the difference in permafrost thaw rate between moderate and strong climate warming vanish for water bodies deeper than 0.8 m. Furthermore, the results demonstrate that lateral heat fluxes play an important role for stabilizing permafrost underneath small water bodies.

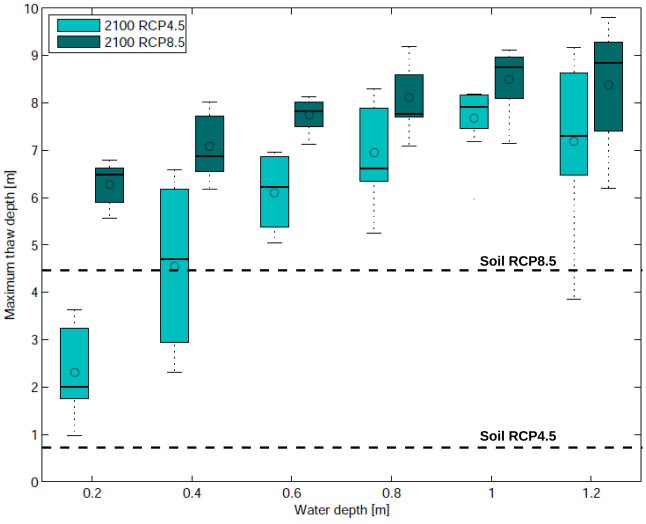

Figure 1: Simulated thaw depths underneath ponds of different water depth in the Lena River Delta following RCP4.5 and RCP8.5 climate warming scenarios. The thaw depths of pure tundra soils are indicated as dashed lines for comparison.

Landsat-based lake distribution and changes in Western Alaska Permafrost Regions between 1972 and 2014

Prajna Regmi Lindgren[1], Guido Grosse[2,1], & Vladimir Romanovsky[1]

[1] *Geophysical Institute, University of Alaska Fairbanks, USA*
[2] *Alfred Wegener Institute Helmholtz Centre for Polar and Marine Research, Potsdam, Germany*

Lakes are an important landscape and ecosystem component in the high northern latitudes and they are hotspots for biogeochemical processes in permafrost regions. In this study, we utilized Landsat MSS and OLI images from the 1970s and 2014 to assess broad-scale distribution and changes of lakes larger than 1 ha in 6 major lake districts from various permafrost zones (continuous, discontinuous, sporadic and isolated) located in western Alaska. The lake districts that we included are Beringia, Baldwin Peninsula, Kobuk Delta, Selawik, Central Seward Peninsula, and Yukon-Kuskokwim Delta covering a total area of 68,831.41 km^2 (Fig. 1). These regions encompass various types of lakes; thermokarst lakes are the most common type, while oxbow and delta lakes are also widely distributed in the river floodplains and delta regions. Additional lake types include maar lakes. The highest density of lakes is found in Yukon-Kuskokwim Delta with approximately 16 % of the mapped area covered with lakes. The least number of lakes are found in Baldwin Peninsula with only about 2.5 % of the mapped area covered with lakes. The lake districts in river deltas have the highest lake coverage (limnicity) with all three deltas (Kobuk Delta, Selawik and YK Delta) having above 10 % lake area.

For 3 study regions (Baldwin Peninsula, Kobuk, and Yukon-Kuskokwim Delta) an increase in total lake area by less than 4 % was observed, while the other 3 regions (Beringia, Central Seward Peninsula, and Selawik) showed lake area decrease ranging between ≈4 – 15 % (Fig. 1). The most significant change was noticed in Beringia and Central Seward Peninsula due to drainage of very large lakes. We found net lake area loss of about 15.3 % (6318.1 ha or 108.1 ha/100 km^2 net loss) and 12.4 % (6542.1 ha or 110.2 ha/100 km^2 net loss) since the 1970s in Beringia and Central Seward Peninsula, respectively. We noticed that 20 lakes larger than 100 ha drained in Beringia that contributed a total lake area loss of 4471.8 ha whereas 2 lakes larger than 100 ha drained in Central Seward Peninsula that contributed a total lake area loss of 6391.1 ha. Selawik experienced the highest number of drainage events but because most of the lakes that drained were small, the net lake area loss in Selawik is the smallest among all. Draining lakes in the 1-50 ha category in Selawik contributed an area loss of 5021.1 ha, which is about 81 % of the total drainage area (6171.2 ha) in the region. Additionally, we saw expansion of lakes larger than 100 ha in Selawik by 7 % (2812.3 ha) due to creation of water channels that coalesced multiple large lakes in the delta region. Hence, we observed a net lake area loss of 3.9 % (3358.9 ha or 52.9 ha/100 km^2 net loss) in Selawik.

In Baldwin Peninsula, there was a net increase in total lake surface area by 3.9 % (204 ha or 9.7 ha/100 km^2 net gain) due to expansion and coalescence of smaller lakes. In Kobuk, we observed formation of water channels fusing multiple large lakes in the delta region that contributed to a net lake area increase of 1.4 % (383 ha or 19.9 ha/100 km^2 net gain). Complex hydrological and landscape characteristics of the Yukon-Kuskokwim Delta region as well as shifting precipitation patterns could have played an important role influencing lake area change variability across this large lake district. Therefore, despite numerous large drainage events in Yukon-Kuskokwim Delta, we observed only a slight change in total lake area by 0.5 % (3922.8 ha or 8.4 ha/100 km^2 net gain).

Our assessment shows that lake drainage is widespread in the western Alaska study region. Overall, we found that a large number of lakes in the 10 – 100 ha size category drained with an estimated drainage rate of 11 lakes/year that contributed to an area loss of 304.6 ha/year. Not surprisingly, partial drainage of large lakes created numerous remnant pond and hence, lakes smaller than 10 ha increased at a rate of 115 lakes/year and 290 ha/year.

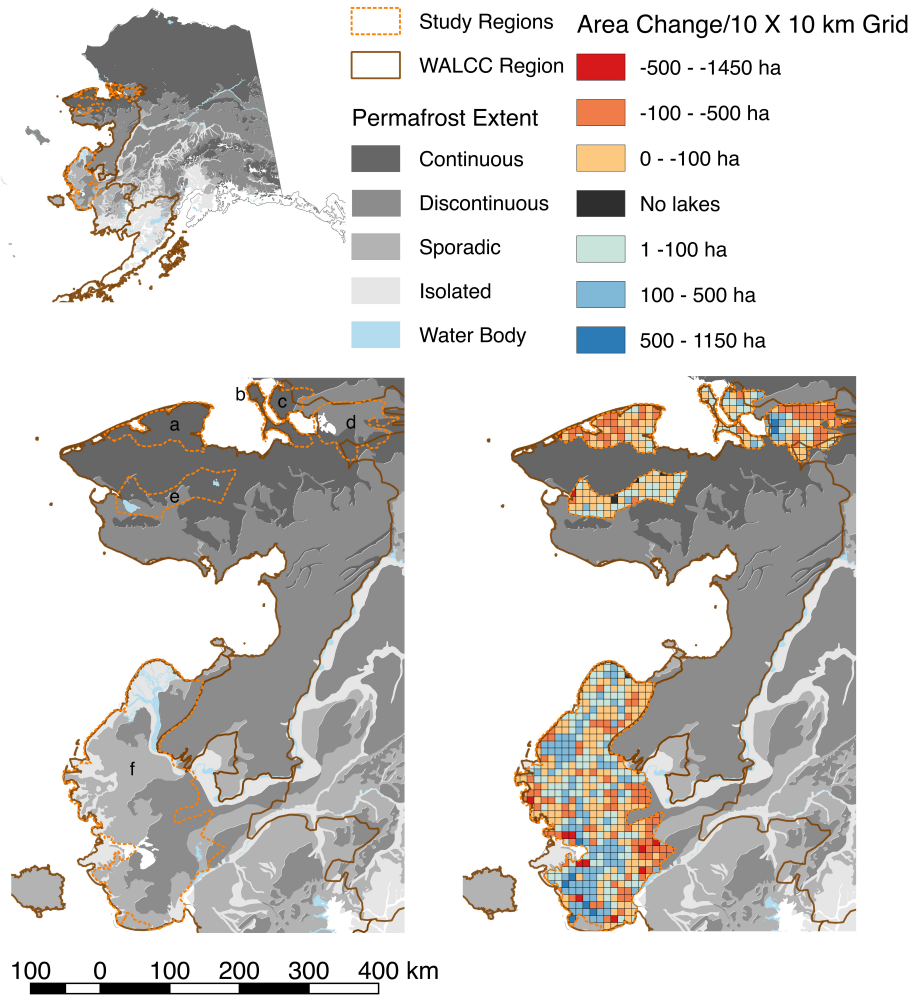

Figure 1: Maps showing study areas and lake area change in hectare per 10×10 km grid in each study site. Study sites are (a) Beringia, (b) Baldwin Peninsula, (c) Kobuk Delta, (d) Selawik, (e) Central Seward Peninsula, and (f) Yukon-Kuskokwim Delta. Permafrost extent overlaid on the maps is from [Jorgenson et al., 2008]

Regional permafrost ice content in the lake districts dictated lake change patterns even though there was no direct relationship between permafrost extent and direction of lake change. We observed that lake change patterns transitioned from net area gain due to lake expansion to net area loss in the ice-rich continuous permafrost region, whereas net lake area loss dominated most of the regions with non-continuous permafrost types. Thus, as climate gets warmer and permafrost continues to thaw, we expect increased numbers of drainage events in the continuous permafrost zone of the western Alaska study region. Additionally, as permafrost becomes less stable, influence of other factors such as surficial geology and landscape characteristics likely will magnify the variability of lake area change. Since high spatial and temporal resolution imageries are readily available, assessment of lake area change in high northern latitudes should be continued to quantify the feedbacks associated with lake changes in a warming climate as well as to assist in future planning and decision-making for land and resource management issues related to lakes.

References

Jorgenson, T. M.; Yoshikawa, K.; Kanevskiy, M.; Shur, Y. L.; Romanovsky, V.; Marchenko, S.; Grosse, G.; Brown, J. and Jones, B. [2008]: Permafrost characteristics of Alaska. In: Kane, D.L. and Hinkel, K.M.(eds.), *Proceedings of the Ninth International Conference on Permafrost*, Institute of Northern Engineering, University of Alaska Fairbanks, Fairbanks, USA, 29 June–3 July 2008, volume 1, pages 121–122. ISBN 978-0-9800179-2-2. URL http://ipa.arcticportal.org/publications/conference-proceedings.

Impact of thermokarst lake expansion rate on ground thermal regime and talik development beneath thermokarst lakes on the Qinghai-Tibet Plateau

Feng Ling

Zhaoqing University, People's Republic of China

Natural thermokarst lakes expand their basins by coupled heat conduction and thawing of permafrost and geomorphic processes such as slumps. The lake radiuses will increase by bank retreat. An accurate physically based model for describing permafrost thermal regime and talik development under the thermokarst lakes should account for lake initiation and lake expansion by permafrost thaw, and mass wasting. This study investigates numerically the impact of variations in the lake expansion rate on ground thermal regime and talik development under thermal lakes on the Qinghai-Tibet Plateau. The numerical model used is a two-dimensional unsteady finite element model for heat transfer with phase change under a cylindrical coordinate system. On the basis of previous studies on thermokarst lakes on the Qinghai-Tibet Plateau, a linear lake expansion rate of 0.7 m per year was chosen as the baseline of lake expansion rate, and the open talik formation time beneath the thermokarst lake and ground thermal regime at different years are obtained. Then four thermokarst lake expansion rates of 0.5 m/yr, 0.6 m/yr, 0.75 m/yr and 0.8 m/yr were used respectively, and the maximum permafrost thaw depth under the thermokarst lake and the mean permafrost thaw rate for each case were calculated.

Analysis of Sediment Cores and Methane Fluxes from Alaskan and Siberian Thermokarst Lakes

Ove Hanns Meisel

Vrije Universiteit Amsterdam, The Netherlands

The main focuses of this PhD project are the carbon balance and methane emissions of Arctic thermokarst lakes, based on the analysis of a set of sediment cores. During two separate field trips to Barrow, Alaska in November 2015 and Kytalyk, Siberia in April - May 2016 several sediment cores will be retrieved from at least three small-sized thermokarst lakes. The short sediment cores will not exceed a length of one meter and will be taken along transects across the lakes. This will allow for a detailed comparison and correlation of the sedimentary characteristics along lake profiles. At each coring site two cores will be recovered, one core will be used for a sedimentary analysis. The second core will provide pore water samples and will also be used for a long-term incubation experiment to evaluate the methane production of the uppermost lake sediments.

The pore water samples will be analyzed for DOC, DIC and their $\delta^{13}C$ signatures. During the incubation experiment the amount of escaping methane and its $\delta^{13}C$C signature will be analyzed, too. This experimental setup of the sediment cores will include different scenarios for "wet" conditions - representing a normal lake environment - and "dry" conditions - representing a drained lake scenario.

The sedimentary analysis will concentrate on parameters such as grain size, TOC-, TIC-, TC-, and density measurements of bulk sediment samples and non-destructive analysis like XRF- and X-ray-Scans and Magnetic Susceptibility measurements will be applied. As three to four cores along a transect will be available for analysis from each lake it might be possible to correlate different sedimentary layers or stratigraphic units across a lake profile. This correlation will be supported by simple bathymetric maps of the thermokarst lakes which do not exceed a depth of 6 meters. Additionally, radiocarbon ages will be taken from the base of the cores if reliable sources of dateable material can be found. The sum of these data might allow to make a statement about the expansion rate, development and methane production of these lakes throughout the last hundreds or thousands of years.

The outcome of this project will provide new data on the evolution of thermokarst lakes in the northern high latitudes and their potential for greenhouse gas emissions. Especially interesting will be the direct comparison of the data sets between Siberia with its yedoma- and ice-rich permafrost and the cores from Alaska with its more mineral-dominated subsoil. Also the location of the sites differ with regard to their distance to the Arctic shoreline with the Alaska lakes being located in close proximity to the ocean and the Siberian lakes with a distance of more than 100 km from the ocean. Thus, the influence of the marine climate in Alaska can be compared to a more continental setting in Siberia.

Hungry ponds in a thawing world: variations in subarctic pond runoff quality and quantity depend on peatland moisture and frost conditions

Matthew Morison[1], Merrin Macrae[1], Richard Petrone[1], & LeeAnn Fishback[2]

[1] *Department of Geography, University of Waterloo, Canada*
[2] *Churchill Northern Studies Centre, Manitoba, Canada*

In subarctic permafrost environments, ecological productivity is often nutrient-limited, both in terrestrial and aquatic vegetation. The subarctic is experiencing significant climatic change, including rapid warming and changing precipitation patterns, which may result in changes in nutrient dynamics within terrestrial and aquatic systems and hydrologic transport between them. It is unclear if changes in hydrologic connectivity throughout the ice-free season will also result in enhanced nutrient mobilization in the landscape, and/or if changes in seasonal dynamics will alter the speciation of those nutrients. The objective of this research was to characterize changes in runoff pathways, quantity and quality between peatlands and ponds over the snow-free summer season. Twenty-two ponds and five transects of piezometer nests along moisture gradients were instrumented to measure changes in hydrologic storage, frost table position, and water quality over three snow-free seasons in Churchill, Manitoba, within the Hudson Bay Lowlands. Differences in antecedent moisture conditions across landscape units, combined with frost table position (inhibiting infiltration and storage) produced non-linear, threshold responses in runoff generation. Greater inputs were required to exceed storage ('fill and spill') when a lower frost table permitted deeper infiltration. The snow-free (non-winter) hydrology of the site displayed three clear periods:

1. the post-melt wet period where runoff-generating threshold catchment storage was exceeded during rainfall events, and frost table development was rapid and consistent across space;

2. the mid-summer drying period in which ponds desiccated, threshold storage was not achieved in the catchment, resulting in hydrological disconnection between ponds and catchments. During this period, frost table development diverged within the catchment along a moisture gradient (most rapid development in wet soils and least on dry peat plateaus);

3. the autumnal wet-up period, where frost table development had slowed and/or progressed beneath the peat layer into underlying glacial till.

During this wet-up, antecedent wetness and catchment storage returned to the threshold conditions at which runoff was generated and catchments began to interact hydrologically with ponds again. Seasonal variations in groundwater chemistry were reflective of different layers of peat and mineral soil accessed at different times throughout the season, governed by frost table and water table positions. Varying thaw rates across landscape units (controlled by moisture and vegetation) resulted in changing groundwater pathways throughout the season, and, changing groundwater pathways combined with precipitation events throughout the season produced temporally variable nutrient concentrations in runoff and ponds. Although the decay of permafrost may expose nutrient-rich peat, this may not be reflected in future runoff chemistry or surface water bodies due to low hydraulic conductivities at those depths. Instead, hydrochemical contributions to ponds may be more reflective of extended drying period in early- to mid-summer and extended autumnal seasons with increased frequency and intensity of storms during a period of lesser evaporative demand with flow primarily through highly-conductive upper peat layers. This work has implications for how nutrient dynamics and exchange between terrestrial and aquatic systems in cold regions may evolve under a changing climate.

Temporal and seasonal variation in tundra pond seasonal biogeochemical trajectories in a permafrost landscape and implications for river export of solutes

Matthew Morison[1], Merrin Macrae[1], Richard Petrone[1], & LeeAnn Fishback[2]

[1] *Department of Geography, University of Waterloo, Canada*
[2] *Churchill Northern Studies Centre, Manitoba, Canada*

In peatland systems underlain by permafrost, shallow freshwater bodies have been the subject of interest due to their ubiquity in the landscape and capacity to store and exchange carbon. The intake of carbon is driven by primary productivity, which is frequently limited by bioavailable forms of phosphorus and nitrogen, although conditions of limitation may vary greatly over short spatial scales. Thus, there is scientific interest in characterizing nutrient dynamics in tundra ponds. This research characterizes spatial and temporal (seasonal, weather-driven) variability in water quality in a suite of 20 tundra ponds in the Hudson Bay Lowlands, and compares their biogeochemical patterns with observations of water chemistry in larger tributaries that flow towards the Hudson Bay. The study ponds span a range of biophysical properties including pond area, perimeter, basin morphology, hydrological connectedness, sediment composition (mineral/organic), and depth. Ponds were selected as they have been the subject of long-term study, and have been shown to be representative of other ponds in the region. In addition, three major tributaries flowing directly to the Hudson Bay were selected to determine how inland pond-peatland processes relate to hydrochemical export from larger rivers. Water samples were collected biweekly between May and October, 2014, and subsequently analysed for isotopic signatures (hydrogen and oxygen), nutrient speciation (dissolved forms of nitrogen and phosphorus) and major ions. Component-based statistical methods were used to determine major differences and similarities between seasonal pond chemistry trajectories within a season, across space, and between years. Previous work done in this region using mesocosm experiments has shown that benthic organisms in ponds rapidly consume bioavailable nutrient species added to ponds. The current project supports these experimental findings and demonstrates that it applies across a suite of ponds throughout the landscape. Hydrochemical trajectories of ponds and rivers were temporally coupled for parts of the snow-free season, but occasionally divergent under some conditions. Conditions and mechanisms of this variability are further discussed. Seasonal loading of nutrients was dominated by the hydrological weight of snowmelt, underscoring the importance of understanding within-snowpack ecological processes and the resulting snowmelt chemistry. Overall, this work demonstrates the importance of high temporal resolution in sampling design for biogeochemically active tundra ponds and rivers. Variation in pond chemistry of nutrient species during a single precipitation-runoff event can exceed the variability of the rest of the snow-free season. This work has important implications for the scaling of point measurements to larger regions and time periods.

Multi-year landscape-gradient assessment of thermokarst lake hydrology in Nunavik (Quebec, Canada) using water isotope tracers

Biljana Narancic[1], Reinhard Pienitz[1], & Brent Wolfe[2]

[1] *Université Laval, Canada*
[2] *Wilfrid Laurier, Canada*

A three-year landscape-gradient assessment of thermokarst lake hydrology provides baseline information on changes in hydrological processes associated with recent climate changes. Progressive and rapid degradation of permafrost since the mid-20^{th} century, followed by the development of thermokarst lakes and terrestrialization of peat-plateaus are all climate-driven changes with major consequences on regional landscape hydrology. Our study aims at assessing the influence of air temperature, precipitation, catchment vegetation and permafrost degradation on thermokarst lake hydrology. Our four main study areas are distributed across a latitudinal, vegetational, climatic and permafrost gradient between Whapmagoostui-Kuujjuarapik and Umiujaq, stretching from spruce-lichen woodland with sporadic permafrost in the south to shrub-tundra overlying discontinuous permafrost in the north. Lakes were sampled during mid-summer 2012-2014 and analyzed for water isotope composition ($\delta^{18}O$, δH^2) to provide a snapshot of lake hydrological conditions. An isotope-mass balance model was used to

1. infer lake-specific input water isotopic compositions (δI) that differentiate the relative roles of primary source waters (e.g., rainfall and snowmelt), and
2. calculate lake-specific evaporation-to-inflow (E/I) ratios to evaluate the influence of vapour loss (Fig. 1).

The lake water isotope data series defines two groups of lakes:

1. snowmelt-dominated lakes ($\delta I < \delta$p; δp is amount-weighted isotope composition of annual precipitation), and
2. rainfall-dominated lakes ($\delta I > \delta p$).

Snowmelt-dominated lakes are located within catchments with dense vegetation, whereas rainfall-dominated lakes tend to be more prevalent at sites with sparse vegetation. Lakes situated in the sporadic permafrost terrain to the south are more isotopically enriched, and thus experience greater evaporation, than those from discontinuous permafrost terrain to the north. Lakes overlying mineral-rich soils with scarce vegetation are also more isotopically enriched due to evaporation than lakes overlying organic-rich soils surrounded by forested vegetation (Fig. 1). This suggests that there is greater snow accumulation and meltwater input to lakes in the forested study areas. Lakes in close proximity to rivers are isotopically depleted likely due to river flooding.

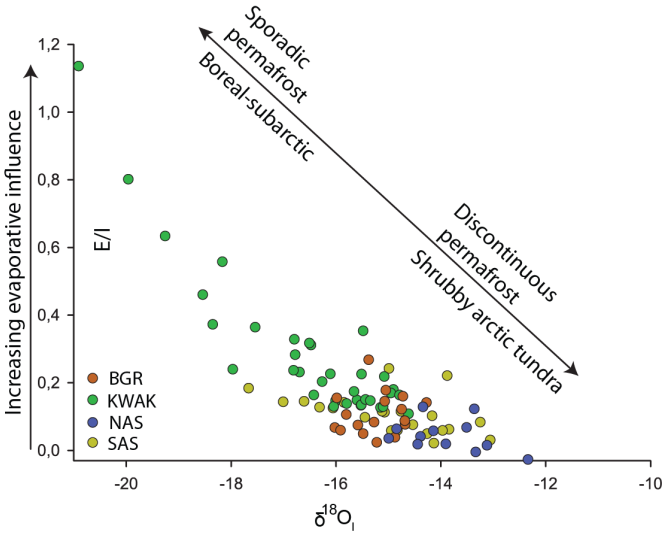

Figure 1: Comparative diagram illustrating evaporative influence between four study sites. Calculations are based on the data from 2013

Results from our three-year sampling campaign suggest that lake water balance reflects the latitudinal position of the lakes. Majority of the rainfall-dominated lakes are situated in the northern shrub-tundra terrain overlying discontinuous permafrost. Southern lakes that are in close proximity to the river and surrounded by forest-tundra have characteristics of isotopically depleted lakes probably related to spring river flooding and greater snowmelt input later in the ice-free season. Moreover, southern lakes that overly-

ing sporadic permafrost terrain experience greater evaporation compared to the lakes in northern discontinuous permafrost terrain. We speculate that thawing permafrost in discontinuous permafrost terrain offsets the effect of evaporation, whereas lakes in sporadic permafrost terrain are most vulnerable to becoming evaporation-dominated because permafrost thaw no longer provides a source of water.

A circumpolar dataset of bottom fast lake ice

Georg Pointner[1] & Annett Bartsch[1,2,3]

[1] *TU Wien, Austria*
[2] *Zentralanstalt für Meteorologie und Geodynamik, Austria*
[3] *Austrian Polar Research Institute, Austria*

Millions of lakes cover vast areas of the Arctic Tundra landscape and thus represent an important part of the hydrosphere and cryosphere. A large number of them are relatively shallow, with a maximum depth of a few meters only. Depending on their depths, they either freeze entirely to the bottom, or maintain areas of liquid water beneath the top ice layer in winter. There are numerous aspects that make it interesting to map these areas. Many of these lakes are major sources of Methane (CH_4) emissions and substantially contribute to the total global emissions. CH_4 is an important greenhouse gas and is considered to play a major role in global climate change. With warming of the Arctic regions and the accompanying thawing of the permafrost and expansion of the lakes, also the methane emissions are likely to increase. In areas where liquid water is present below the lake ice in winter, methane emissions occur all year. Thus it is of importance to identify areas, where the most liquid water is present. Many Arctic lakes are also important parts of ecosystems. Some of them provide overwintering habitats for a fish for example. Among other aspects, knowing the fresh water availability in certain areas during winter can be useful for ecological studies.

Synthetic aperture radars (SARs) provide day and night acquisitions that are independent of cloud cover and can observe large parts of the earth within a relatively short time period. 51 Envisat Advanced Synthetic Aperture Radar (ASAR) Wide Swath Mode (WSM) scenes acquired in April 2008 with circumpolar coverage were used to map the extent of areas of the lakes, where they completely freeze to the bottom and areas where water remains in liquid form under the top ice layer. The lake ice is nearly transparent for the C-Band radar signals of the ASAR instrument. The radiation can penetrate nearly undamped through the ice and is mainly scattered by the material beneath. Because of the distinct dielectric properties of water and soil, backscatter coming from water beneath the ice is in general significantly higher than the backscatter coming from soil beneath the ice. Based on this difference, lake areas were classified as "frozen to the bottom" or "not frozen to the bottom". Using samples for these two classes, a functional relationship between the incidence angle of the radar radiation and the backscatter coming from the lake areas was obtained. Based on this relationship a threshold for the classification was set in dependence of the incidence angle. The lake outlines were extracted from the high resolution GlobeLand30 dataset of the National Geomatics Center of China. River channels have been removed and only objects larger than 28.000 m^2 considered. For each of the lakes the percentage of lake area frozen to the bottom was calculated. The final results are features with 'percentage of frozen area to the bottom' and total 'frozen/unfrozen' areas as attributes. Additionally, statistics were computed for the area within the Circumpolar Arctic Coastline and Treeline Boundary as defined by the Circumpolar Arctic Vegetation Mapping Project and maps showing the spatial distribution of the two classes were created. More than 1.3 million lakes were considered in the classification. 68 % of the total lake area was classified as "not frozen to the bottom", which corresponds to an area of more than 250.000 km^2. The dataset is made available in Pangaea.

Carbon mobilization through the expansion of thermokarst lakes in polygonal tundra of Old Crow Flats, northern Yukon

Pascale Roy-Leveillee[1], Elyn. R. Humphreys[2], Christina Z. Braul[2], & Christopher R. Burn[2]

[1]*School of Northern Development, Laurentian University, Canada*
[2]*Department of Geography and Environmental Studies, Carleton University, Canada*

Arctic lakes are an important source of greenhouse gases to the atmosphere. In lakes that are expanding by thermokarst processes, carbon mineralization and emissions of methane and carbon dioxide are particularly active near receding shorelines. This is due to the input of organic material from eroding shore banks and to the anaerobic decomposition of this thawed material in the lake bottom. Methane production from thermokarst lakes is primarily controlled by the rates of lake expansion and by the amount of organic carbon contained in the surrounding permafrost [Kessler et al., 2012]. Such factors vary depending on local geomorphological history. The small number of observations from different types of thermokarst landscapes impedes our ability to assess the contribution of these landscapes to the global carbon cycle. This research contributes information from Old Crow Flats (OCF), a 5600 km^2 Arctic peatland located in one of Yukon's interior basins. OCF was not glaciated during the Wisconsinan Stage but was submerged beneath a 13,000 km^2 glacial lake that drained catastrophically 15,000 years ago [Zazula et al., 2004]. The area is underlain by continuous permafrost and includes thousands of thermokarst lakes.

Our goal was to examine rates of organic carbon input from bank erosion around a tundra lake and use this information to estimate rates of carbon input at the landscape scale. We measured bank heights and collected sediment cores to a maximum depth of 2.7 m from the tundra near the shores to estimate moisture, organic, and mineral fractions of sediments input to the lake. Samples were also incubated under aerobic and anaerobic conditions over a period of 100 days to assess the potential decomposability of the organic matter. We used aerial photographs and remotely sensed imagery to estimate rates of shore recession for the lake and surrounding water bodies ranging in size from less than 1 ha to more than 10 km^2, over a 55 year period.

Preliminary results indicate that bank height around the lake varied from 0.8 to 2.8 m with an average of 1.5 m. Rates of shore recession varied from 0 to 1.3 m a^{-1}, and were associated with rates of volumetric sediment input up to 1.3 m^3 a^{-1} per meter of shoreline around the lake. The peat layer in the polygonal tundra surrounding Lake 1 varied in thickness from 0.20 to 0.85 m (average: 0.6 m). Tundra surrounding the lakes contained an average of 78 kg C m^{-2} to a depth of 1.5 m. Rates of shore recession varied from 0 m a^{-1} to 2.9 m a^{-1} in surrounding thermokarst lakes, with an average of 0.4 m^2 a^{-1} of polygonal tundra lost to bank erosion for each meter of shoreline. This value increased exponentially with lake size due to the increased contribution of wave action to shore erosion with increasing fetch length. Assuming that conditions around Lake 1 are representative of this polygonal tundra landscape in OCF, we estimated an annual input of eroded bank sediment per meter of shoreline in thermokarst lakes of the area varying from 0.075 to 1.35 m^3 a^{-1}, depending on the size of the lake. This corresponds to an organic carbon input per meter of shoreline varying between 6 and 105 kg C m^{-1} a^{-1} from erosion of the lakeshore banks. Additional carbon is also released from thawing of permafrost beneath the bottom of expanding lakes.

Incubations under aerobic and saturated conditions at different temperatures suggest that the organic matter in the reworked glacio-lacustrine deposits has similar potential decomposability to the organic matter within the peat layer. Organic material from the peat layer that had fallen and accumulated at the bank foot had much higher decomposability than the peat material that was still within the bank. This may be due to the lake microbial community and the abrasive effect of silt-laden waves on the peat material.

References

Kessler, M. A.; Plug, L. J. and Walter Anthony, K. M. [2012]: Simulating the decadal- to millennial-scale dynamics of morphology and sequestered carbon mobilization of two thermokarst lakes in NW Alaska. *Journal of Geophysical Research: Biogeosciences*, 117(G2) doi:10.1029/2011JG001796. G00M06.

Zazula, G. D.; Duk-Rodkin, A.; Schweger, C. E. and Morlan, R. E. [2004]: Late pleistocene chronology of glacial lake old crow and the north-west margin of the laurentide ice sheet. In: Ehlers, J. and Gibbard, P.L.(eds.), *Quaternary Glaciations-Extent and ChronologyPart II: North America*, volume 2, Part B of *Developments in Quaternary Sciences*, pages 347 – 362. Elsevier, doi:10.1016/S1571-0866(04)80207-0.

Assessing the Contribution of Arctic Lakes to the Methane Budget via Upscaling and GOSAT Satellite Derived Flux Data

Kassandra Reuss-Schmidt, Jadu Dash, & Mary Edwards

University of Southampton, United Kingdom

The considerable contribution of northern lakes and wetlands to global methane emissions is likely to increase as the Arctic warms and carbon within permafrost becomes labile. However, large uncertainties are still present in baseline flux estimates. Satellite remote sensing promises a way to constrain fluxes at continental and hemispheric scales as it is spatially comprehensive and has, or promises, temporal depth. The GOSAT team (Japan) recently released the first global dataset of methane fluxes informed by satellite data. Here, for the Arctic (>66° N), we compare methane flux values from the GOSAT product with up-scaled flux values derived from field observations working in concert with pertinent GIS layers. Upscaling was done within the context of a novel geographic lake classification that recognizes regional differences in lake type and geomorphic history, which, in turn, reflect availability of organic carbon in the catchment/lake ecosystem. The up-scaled (bottom-up) approach yielded an annual flux of 3.89-13.0 Tg CH_4 yr -1, with 58-68 percent of the fluxes derived from lakes. This estimate flanks the remotely sensed (top-down) range of 5.36-7.15 Tg CH_4 yr -1. Furthermore, both estimates show similar spatial variation in fluxes. The convergence of results from these two independent methods underlines the potential of remotely-sensed methane observation as a new tool in estimating carbon budgets and the importance of regional variation in upscaling flux estimates. Though a first pass attempt at a spatially explicit pan-Arctic methane emission estimate, the results of this work are promising and could aid in closing the global methane budget.

Structure from Motion (SfM) orthoimage generation for characterizing methane ebullition features in thermokarst lake ice

Kerstin Schlobies[1,2], Guido Grosse[2], & Katey Walter Anthony[3]

[1] *Department of Physical Geography, Catholic University of Eichstätt-Ingolstadt, Germany*
[2] *Alfred Wegener Institute Helmholtz Center for Polar and Marine Research, Potsdam, Germany*
[3] *Water and Environmental Research Center, University of Alaska Fairbanks, USA*

Thermokarst lakes are characteristic landscape features in Arctic permafrost regions and are relevant emitters of the greenhouse gas methane [Walter et al., 2006]. A major pathway for methane emissions from these lakes is through bubbling (ebullition) from discrete seeps. An accurate assessment of the actual emission rates of CH_4 from thawed organic-rich talik sediments under thermokarst lakes is challenging due to poor accessibility and monitoring complexities concerning the spatially and temporally variable behavior of ebullition. In early winter, when lake surfaces start to freeze, or alternatively in late winter, the days before thawing sets in, a snow free ice cover reveals trapped gas-pockets and open hotspots of methane seeps. The detection and characterization of distinct ice-trapped CH_4 bubbles and bubble clusters, which depend on differing methane emission rates, is possible by field and remote sensing surveys of the lake ice cover during a short time window for image acquisition with ideal ice and snow conditions [Lindgren, 2015]. In this work we aim to generate spatially very high resolution orthophoto mosaics using low altitude aerial imagery from multiple years to provide a set of high quality baseline imagery for characterization of ebullition features in thermokarst lake ice cover in the Fairbanks region, Interior Alaska.

For our image processing, we relied on photogrammetric Structure-from-Motion (SfM) technology, which builds on image-based three-dimensional surface reconstruction algorithms. We applied this technique to large sets of overlapping aerial images using the workflow presented in Fig. 1 and the software Agisoft PhotoScan Professional™. In a first step, the software analyzes input photos and detects features that are stable under variable viewpoint and lighting conditions. As a result, a descriptor for each point based on its local neighborhood is obtained and serves for detecting identical tie points across photos. Automated feature detection and matching are then performed using software-internal algorithms comparable to the Scale-Invariant Feature Transform (SIFT) approach. Internal and external camera positions are estimated on basis of bundle- adjustment algorithms. For dense point cloud and mesh construction the software provides several processing methods depending on the final product (orthophoto, pointcloud, digital surface model – DSM), data size (number of photos and resolution), and image acquisition mode (terrestrial vs. airborne, horizontal vs. oblique). For texturing, the reconstructed surface is divided into fragments and blending is applied to generate a texture atlas.

We applied this full processing chain to a large set of 2601 images acquired during airborne flight campaigns with unmanned air vehicles (UAVs) and small aircrafts over several thermokarst lakes in the Fairbanks region in April 2012 and October of 2008, 2013 and 2014. In addition, aerial imagery of lakes in an abandoned gravel pit were gathered for comparison to thermokarst lakes and processed the same way. The 2601 aerial images were acquired at mean flight altitudes of 42 m.a.s.l. (UAV) and 327-606 m.a.s.l. (airplane). The images were grouped into seven regions covering sets of target lakes and provided the basis for 23 orthophoto mosaics. The number of images per mosaic ranged between 9 and 585. About 15 ground control points (GCPs) were equally distributed over the covered area for georeferencing. We achieved a ground resolution of 0.02 m/pixel to 0.12 m/pixel, a DSM resolution of 0.03 m/pixel to 0.24 m/pixel, and a point density of about 19 to 1849 points per m^2, depending strongly on actual flight height and photo resolution. Furthermore, the accuracy for surface reproduction is augmented by increasing image overlap with best results achieved when at least nine photos overlap. In one specific case, when image acquisition was conducted within a low flight altitude of 42 m.a.s.l. the SfM-method failed to align five

overlapping images in the center of a thermokarst lake (Goldstream Lake) due to the absence of detectable ice surface features (such as bubbles or cracks) underneath the ice cover. The placement of temporary markers in the misaligned images still did not result in a sufficient matching quality; hence these unaligned photos were not taken into account for further processing. Future field campaigns with UAVs at low flight altitudes over lake ice should therefore include installation of ground control points across very homogeneous surfaces. Inhomogeneous or changing illumination conditions during a flight campaign could also lead to poorer photo alignment due to false corner and edge detection. Orthomosaics consisting of images taken under changing illumination situations (e.g. sunrise, sunset) may result in irregular color parametrization.

The final orthomosaics are of high quality and can be used in further studies aiming at the identification, mapping, and quantification of methane ebullition features in the lake ice. In particular, the detection and characterization of different methane bubble cluster types is enhanced by the very high resolution of the orthophotos. In a further step, the estimation of whole-lake ebullition seep fluxes and the year-to-year development of ebullition seep features seem feasible. Additionally, it would be of major interest to test the practicability and accuracy of SfM generated high resolution repeat DSMs for detecting and quantifying thermoerosion at lake margins. For this, filtering vegetation, assigning an overlapping value to the point cloud, and evaluating the error of photogrammetric data is essential. Direct cloud-to-cloud or cloud-to-mesh distance measurements and horizontal displacement fields from tracking features could be applied for broader analysis.

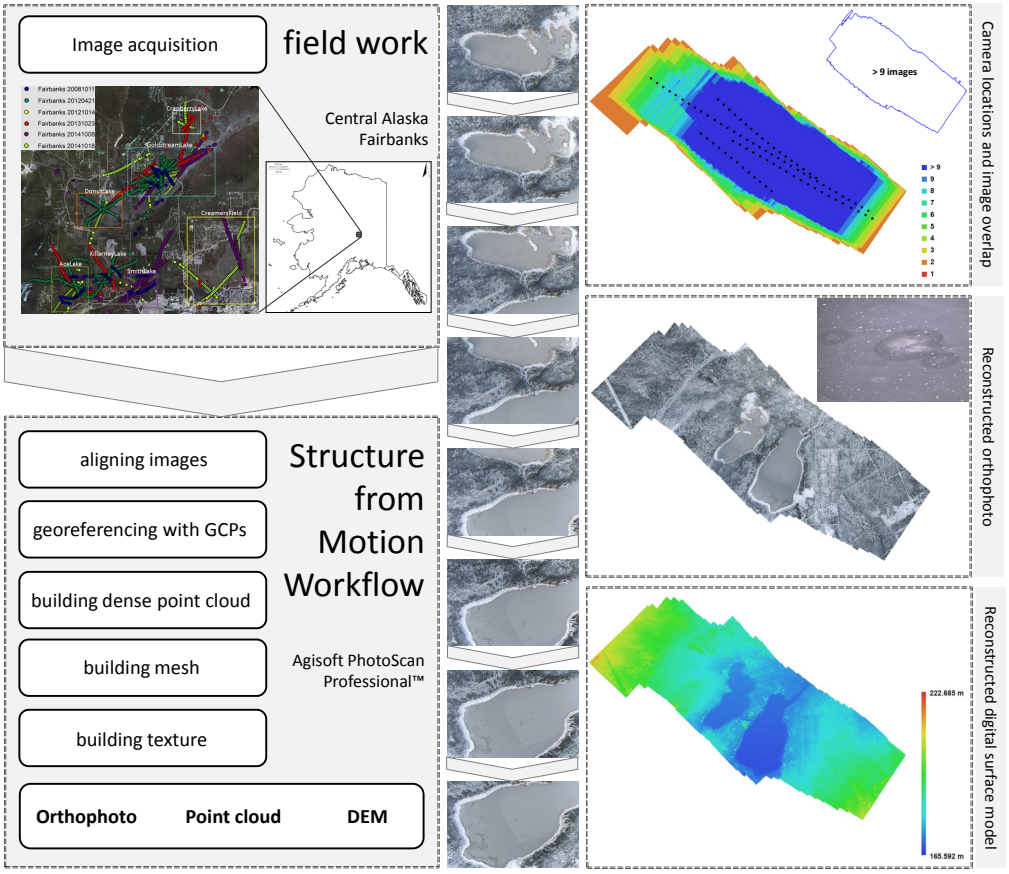

Figure 1: Applied workflow and final products

The presented investigations show, that using SfM within Agisoft PhotoScan Professional™ for processing aerial imagery is a suitable method to generate high resolution orthophoto mosaics that subsequently can be used to characterize ice-trapped ebullition bubbles and bubble clusters on thermokarst lake ice cover. The new dimension of information gain due to the very high resolution within centimeter range in orthophotos, point clouds, and DSMs using SfM offers new insights for better understanding biogeochemical and geomorphological processes in periglacial environments, in particular processes related to thermokarst dynamics such as lake methane ebullition or shore erosion.

References

Lindgren, P. R.; Grosse, G.; Walter Anthony, K. M. and Meyer, F. J. [2016]: Detection and spatiotemporal analysis of methane ebullition on thermokarst lake ice using high-resolution optical aerial imagery. *Biogeosciences*, 13(1):27–44, 2016. doi:10.5194/bg-13-27-2016.

Walter, K.M.; Zimov, S. A.; Chanton, J.P.; Verbyla, D. and Chapin, F.S. [2006]: Methane Bubbling from Siberian Thaw Lakes as a Positive Feedback to Climate Warming. *Nature*, 443(7107):71–75, doi:10.1038/nature05040.

Freshwater ostracods from ice-wedge polygon ponds in Adventdalen, Svalbard

Andrea Schneider[1], Sebastian Wetterich[2], Britta Sannel[3], & Lutz Schirrmeister[2]

[1] *Centre for Arctic Gas Hydrate, Environment, and Climate, UiT The Arctic University of Norway, Tromsö, Norway*
[2] *Alfred Wegener Institute Helmholtz Centre for Polar and Marine Research, Potsdam, Germany*
[3] *Department of Physical Geography, Stockholm University, Stockholm, Sweden*

Freshwater ostracods (*Crustacea, Ostracoda*) are of interest in modern biological studies, while fossil records of ostracod valves enable us to reconstruct past lacustrine environments. The about 1mm long crustaceans carry a calcite carapace that is biomineralized from dissolved components in the ambient water, and completely envelopes their body. Ostracods inhabit almost all aquatic environments, even shallow freshwater ponds in the vast circumartic permafrost areas. In high-latitude areas, ostracod species diversity, their modern ecological demands, and instrumental records of environmental parameters are only scarcely documented. Such reference information is the key to quantitatively reconstruct past environments from fossil ostracod assemblages. This gap in ostracod data limits their use as biological indicators in the Arctic, where the effects of future climate warming are expected to be strongest.

The objective of the study presented here was to extend the data set on arctic freshwater ostracods and environmental records by characterizing present-day habitat conditions, abundance and diversity of ostracod assemblages in periglacial freshwaters on Svalbard. The aims of this project were

1. to conduct an inventory of the abundance, diversity and ecological ranges of the freshwater ostracods living in polygon ponds in Adventdalen near Longyearbyen (78°11'11"N, 15°55'20"E),
2. to determine the present-day hydrochemical and sedimentary characteristics of ostracod habitats, and
3. to witness temporal variability in a polygon pond during the Arctic summer season 2013.

The study site was located near the University Centre on Svalbard (UNIS)-run monitoring site for thermal contraction cracking in ice-wedge polygons on a river terrace in outer Adventdalen [Christiansen, 2005]. Permafrost on Svalbard is estimated to be of late Holocene age with temperatures of -5.2 to -5.6 °C in boreholes in the Adventdalen area [Christiansen et al., 2010].

Ice-wedge polygons form in cold-climate environments under permafrost conditions and are the most common periglacial patterned ground features in the Arctic [Minke et al., 2007]. Since the permafrost table efficiently blocks drainage pathways, surface depressions hold ponding water during summer, and freeze solid in winter. Those shallow periglacial surface freshwaters, called polygon ponds, are hotspots of biological activity in the otherwise hostile tundra. They provide diverse habitats to aquatic communities including freshwater ostracods. For this study, we choose an area with polygon ponds that are known to persist during the summer season.

Our sampling scheme of 13 ponds in total comprised collecting freshwater ostracod individuals, pond water and sediment samples. One species, *Tonnacypris glacialis* (SARS, 1890), was found in only one of the sampled sites, the pond AD-01 (Fig. 1). Continuous water temperature records directly below the water surface in AD-01, and at the sediment surface in about 25cm water depth were collected between July 20 and September 25, 2013. We measured water and thaw depth in the pond centre and the thaw depth of the surrounding polygon rim. The last record at September 25, 2013 completed the observation season with the presence of 2-3cm lake ice.

Figure 1: Photograph of the monitored pond AD-01, taken at September 7, 2013. The red stick marks the position of the water temperature sensors.

Preliminary results suggest the pond water is well-oxygenated and dilute with slightly acidic pH. The hydrochemical fingerprint and sedimentary characteristics of inter- and intrapolygon ponds may allow a differentiation between the two subtypes for the first time, and are subject of ongoing work. Active-layer thickness was around 40-100 cmin polygon rims, we measured about 50-80 cm thaw depth under pond centres. A considerable increase in water surface area extend occurred in the monitored pond after a rain period. The records obtained from this and similar studies in the Siberian Arctic demonstrate that small and shallow periglacial surface waters are sensitive to local permafrost and climate variations.

References

Christiansen, H. H.; Etzelmüller, B.; Isaksen, K.; Juliussen, H.; Farbrot, H.; Humlum, O.; Johansson, M.; Ingeman-Nielsen, T.; Kristensen, L.; Hjort, J.; Holmlund, P.; Sannel, A. B. K.; Sigsgaard, C.; Åkerman, H. J.; Foged, N.; Blikra, L. H.; Pernosky, M. A. and Ødegård, R. S. [2010]: The thermal state of permafrost in the nordic area during the international polar year 2007–2009. *Permafrost and Periglacial Processes*, 21(2):156–181, doi:10.1002/ppp.687.

Christiansen, Hanne H. [2005]: Thermal regime of ice-wedge cracking in Adventdalen, Svalbard. *Permafrost and Periglacial Processes*, 16(1):87–98, doi:10.1002/ppp.523.

Minke, M.; Donner, N.; Karpov, N.; de Klerk, P and Joosten, H. [2007]: Distribution, diversity, development and dynamics of polygon mires: examples from Northeast Yakutia (NE Siberia). *Peatlands International*, 1:36–40.

Sediment-water interaction as an important factor of Arctic lake thermic regime

Aleksandra Shadrina[1,2], Irina Fedorova[2,1], Sergey Golosov[3], Julia Boike[4], Antonina Chetverova[1,2], & Tatyana Skorospekhova[2]

[1] *Saint Petersburg State University, Russian Federation*
[2] *Arctic and Antarctic Research Institute, Russian Federation*
[3] *Institute of Limnology of Russian Academy of Sciences, Russian Federation*
[4] *Alfred Wegener Institute Helmholtz Centre for Polar and Marine Research, Germany*

Research of polar lakes helps to obtain a new information about limnic process in Polar Regions. It is well known - that these areas are most sensitive to climate change, and therefore even a small shift of the important parameters in aquatic environments can play a huge role for water ecosystems.

The thermic regime of polar lakes has its own peculiarities. The water temperature variability in polar lakes usually ranges between 0 and 18 °C , the ice-cover thickness can reach up to 2 m. The freeze-up usually occurs in the first month of autumn, the breaking up of ice starts beginning of June.

Current studies present the particularities of the thermokarst lakes and their thermic regime. The thermal regime was modelled using the thermohydrodynamic model "Flake" developed by Russian – German research team (www.lakemodel.net). Input data for this model are meteorological characteristics as well as lake morphometric measurements.

Except climatic parameters what else is the thermic regime of lakes affected by? In our opinion, the heat turnover in the lacustrine sediments of the lake is one of the important processes that can give an additional thermic information. Lacustrine sediments represent a specific bottom "sediment chuck" between lake water body and a depression. Sediment properties such as thickness, humidity, grain-size, organic content and geochemical composition, significantly determine the physical characteristics that influence the lacustrine thermal regime. The thickness of the lacustrine bottom sediment is one of the important characteristics for lake thermal regime modeling,

especially in the lakes of the Arctic permafrost regions . This parameter is included in the aforementioned thermodynamic model. Numerical experiments were conducted to test the impact of sediment thickness on the thermal regime. Thickness of the lacustrine sediments were varied from 1 m to 5 m. Modeled results show that the dynamics of the thermic fluxes were similar for sediments with thicknesses of 3 m and 5 m. The maximum positive heat flux was calculated for a thickness of 3 m. The highest negative thermic flux was calculated for a sediment thickness of 1 m. In deep reservoirs, bottom sediments significantly slow down the freezing of the reservoir, since

heat accumulates during the summer period. Other physical characteristics of bottom sediments also affect the thermal regime of lakes. For example, wet bottom sediments warm slower because of their low heat capacity. The destruction of organic matter in the water also influences the thermal regime. Heat flow from the organic matter decomposition in sediments, can be quite significant. In the framework of this study, the mechanisms heat flow in lacustrine bottom sediments are analyzed and their parameterization in thermic modeling tested.

Acknowledgements

The study is realized under support of Department for young staff training at Arctic and Antarctic Research Institute and from the RFBR grant 14-05-00787.

Thermal Regime Caused by Difference of Freeze-Thaw processes between Lake and Permafrost Areas in Hovsgol Regions, Northern Mongolia

Akifumi Sugita[1], Kazuo Takeda[2], Masato Kimura[2], & Maximo L. Lopez Caceres[3]

[1] *The United Graduate School of Agricultural Sciences, Iwate University, Japan*
[2] *Obihiro University of Agriculture and Veterinary Medicine*
[3] *Faculty of Agriculture, Yamagata University*

To evaluate the effect of the lake on the seasonal climatic conditions in high latitudes [Scott and Huff, 1997], meteorological observations were obtained in Hovsgol Lake and Darhad Basin [Goulden et al., 2006], which are areas with similar topography, latitude, size, and altitude [Krivonogov et al., 2005] (Fig. 1).

According to the observation results, the maximum air temperatures in the lake and in the basin during the summer were 24.0 °C and 37.1 °C, respectively. It took five months for 1.14 m of the active layer to thaw, whereas it only took one to two months for the lake ice to thaw. On the other hand, the minimum air temperatures in the lake and in the basin during the winter reached -30.5 °C and -49.1 °C, respectively. Similarly, the active layer in the basin froze within one month in November, whereas it took 3.5 months for an ice layer of 1.18 m thickness to form on the lake.

To understand the difference of the mechanism of freezing and thawing process in Hovsgol Lake and Darhad Basin, we evaluated the total amount of latent heat at the surface using the data from our observations and references. In freezing process, the total amount of latent heat released from Hovsgol Lake and Darhad Basin was calculated to 361.2 MJ m^2 and 238.0 MJ m^2, respectively. Therefore, the latter amount became 66 % of the former.

Also, in order to clarify the features of freezing and thawing processes in Hovsgol Lake and Darhad Basin, the daily freezing and thawing rates of active layer in the basin or lake water were calculated using Stefan's equation so that the daily amounts of latent heat released and absorbed were estimated. During the thawing period, the amount latent heat of absorbed with thawing of ice in Hovsgol Lake was much larger than that with frozen soil in Darhad Basin. During freezing period, when the active layer in Darhad Basin was freezing, the latent heat was rapidly released.

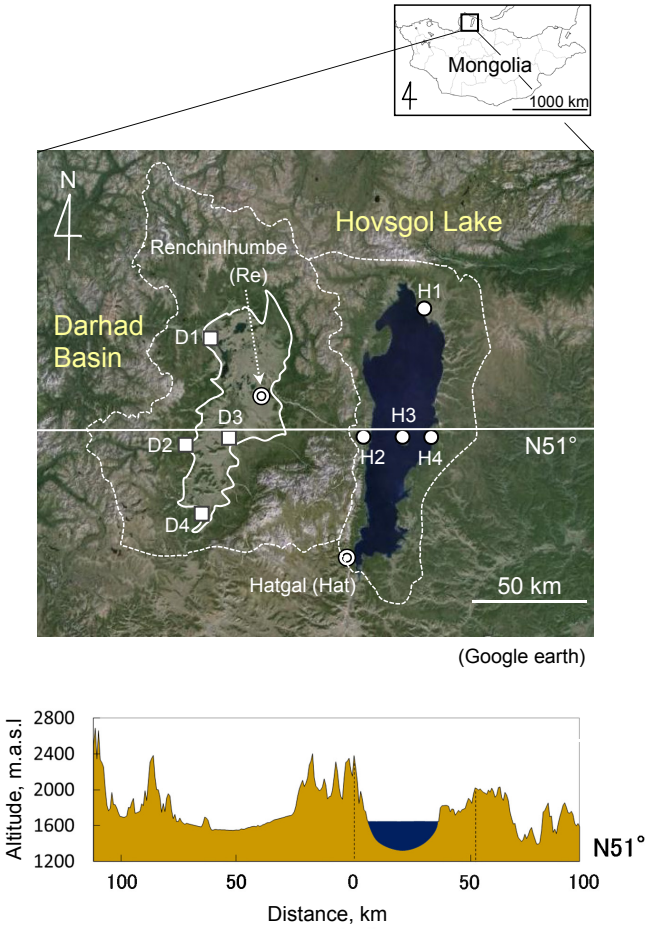

Figure 1: Observation points (circles: H1–H4, squares: D1–D4) and meteorological stations (double circles; Hat: Hatgal and Re: Renchinlhumbe) in the study area. Solid and dashed lines show the limits of each watershed.

After the freezing finished in Darhad Basin, the lake water in Hovsgol Lake froze releasing the latent heat for 3.5 months. Based on these findings, thermal analysis reveals that the latent-heat generation mechanism and its duration are quite different between the both areas. While the total amount of latent heat to

generate in the thawing process of lake ice is decided by the thickness of ice in the previous winter. That in the freezing process of active layer in the basin depends on the thickness of active layer formed in the previous summer. Namely, the total amounts of latent heat during thawing process of ice in the lake, in the freezing process of active layer in the permafrost area generate shifting each half year.

Assuming these areas to have the same net radiation, the difference in the latent heat causes to appear the difference in the sensible heat. As a result, in Darhad Basin in which the smaller latent heat generates, the rest of net radiation except the latent heat is used as the sensible heat for cooling of the frozen layer and atmosphere near the surface. That is the reason why the minimum air temperature in winter decrease to -50 °C in Darhad Basin while it was -35 °C in Hovsgol Lake so that the freezing index was always much larger. The difference of latent-heat in freeze-thaw processes characterizes the thermal regimes in high-latitude areas.

References

Goulden, C.E.; Sitnikova, T.; Gelhaus, J. and B., Boldgiv. [2006]: *The Geology, Biodiversity and Ecology of Lake Hovsgol (Mongolia)*. Backhuys Publishers, Kerkwerve.

Krivonogov, S.K.; Sheinkman, V.S. and Mistruykov, A.A. [2005]: Stages in the development of the Darhad dammed lake (Northern Mongolia) during the Late Pleistocene and Holocene. *Quaternary International*, 136(1):83 – 94, doi:10.1016/j.quaint.2004.11.010. Paleolimnological records from Asian lacustrine systems: archives of large scale seasonal atmospheric circulation changes in the northern hemisphere.

Scott, R.W. and Huff, F.A. [1997]: Lake effects on climatic conditions in the Great Lakes Basin. *Contr. Rep.*, 617.

Solar energy input determines methane emissions on timescales of days to seasons from shallow subarctic lakes

Brett F. Thornton, Martin Wik, & Patrick Crill

Stockholm University, Sweden

Although studies have strongly suggested that there is a positive relationship between temperatures in freshwater systems and methane production by Archaea, not all freshwater systems are alike. In permafrost regions of the Arctic and subarctic, small, very shallow lakes are a common feature. We hypothesize that such lakes'sediment temperatures (where methane production occurs) are particularly sensitive and responsive to solar shortwave flux (SW), because direct solar heating of the sediments can partly bypass the need for physical mixing of warm water downwards across stratifications in the water column (such mixing is necessary for heating the bottom sediments in deeper lakes).

Ebullition (bubble) fluxes of methane are far more varying, and may represent the additional methane production not being diffusively lost. Although bubble release triggering events such as air pressure changes are known to transiently produce bubbling, triggering events only release bubbles; such events do not produce bubbles.

We show a link to SW input on both shorter and longer timescales than previously demonstrated. However, it is difficult to separate SW-driven increases in autochthonous production leading to increased methane production from SW-driven temperature increases in sediment speeding methane production in the current dataset.

Using 6 years of summer-season data, we show that methane bubbling in a shallow (ca. 1 m deep) lake (Villasjön, in Stordalen Mire, Sweden), during summer (June-August) is closely tied to available SW input on timescales of a few days. For the study area in northern Sweden, the available SW also appears weakly linked to the phase of the North Atlantic Oscillation (NAO). Relationships between the winter NAO and snow cover, which impacts lake ice-out date, and available summer SW are also considered. Linking methane production in shallow lakes to the NAO may allow back-projections of methane production in the Stordalen region to the 1860s. We compare these back-projections to recently published back-projections based on lake ice-out dates for Stordalen dating back to 1916.

Finally, we utilize a long-term proxy for cumulative summer sunshine–stable carbon isotope ratios in tree rings—for the Stordalen area to produce estimates of methane bubbling for the past millennium.

UAV surveying of thaw lake areas for the characterization of geomorphology, vegetation and water colour (Whapmagoostui-Kuujjuarapik and Umiujaq, Quebec, Canada)

Gonçalo Vieira[1,2], Simone Girst[1], Vanessa Paulo[1], João Canário[2,3], Ana Padeiro[3], & Warwick Vincent[2]

[1] *CEG/IGOT - Universidade de Lisboa, Portugal*
[2] *Centre d'Etudes Nordiques, Université Laval, Canada*
[3] *CQE/IST - Universidade de Lisboa, Portugal*

Thaw lakes are frequent features in regions with degrading ice-rich permafrost. They show a strong biogeochemical dynamics and are significant for the carbon cycle. Arctic warming is accelerating thaw, affecting the whole landscape and influencing hydrology and soils, therefore generating new conditions for the vegetation communities. Significant changes affect the tundra-taiga boundary, with a marked increase in both tree and shrub formations. This project takes place in the Kuujjuarapik and Umiujaq areas and aims at analysing these processes, as well as geomorphological changes in thaw lake basins. This will be done by using historical aerial imagery, high resolution satellite imagery and very high resolution imagery obtained with a UAV. The spatial variability of the physico-chemical characteristics of the lakes will be analysed as a function of environmental conditioning factors.

We present the results from the field surveys that took place in Aug-Sept 2015 with a fixed-wing ebee UAV equipped with a RGB camera and a NIR camera. Aerial imagery was aquired at a resolution of 3 cm allowing to generate high resolution orthophotos produced, as well as Digital Surface Models. The preliminary results allow for a identification of the geomorphological controls on lake colour and also provide for significant advances in what concerns to the development of new spatial strategies for water sampling.

The following sites have been surveyed:

- SAS thaw lakes (55°13'N, 77°42'W), part of a permafrost peatland at a mean altitude of 110 m a.s.l.. The site is located in the sporadic permafrost zone, in the Sasapimakwananisikw River Valley. These lakes are associated to palsa collapse.

- The KWK thaw lakes (55°18'N, 77°30'W) are in a zone of isolated permafrost in the Kwakwatanikapistikw River valley, 110 m asl. These lakes span a wide range of colours and have derived from fully thawed lithalsas, with extensive tree and shrub development.

BGR ponds (56°37'N, 76°13'W) are in the Sheldrake River valley in the discontinuous permafrost zone. The ponds have formed in thawing permafrost mounds that are primarily organic (peat) or mineral from the thawing of lithalsas and are surrounded by shrubs (*Salix planifolia* and *Betula glandulosa*) and sparse trees.

Surface Water and Ocean Topography (SWOT) satellite mission prototype data for study the Arctic lakes seasonal dynamic and water storage

Elena A. Zakharova[1,2], Alexei V. Kouraev[1,2,3], Denis Blumstein[1], & Vladimir Elsakov[4]

[1] *LEGOS, Université de Toulouse, CNES, CNRS, IRD, UPS, Toulouse, France*
[2] *State Oceanography Institute, Russia*
[3] *Tomsk State University, Russia*
[4] *Biological Institute of Komi Scientific Center, Russia*

The Surface Water & Ocean Topography (SWOT) mission is a French-U.S. satellite that will be launched in 2020, and will carry a wide-swath Ka-band radar interferometer. It will be able to provide measurements of water level of lakes and rivers in 120-kilometer swath with ground resolution of 50 to 100 metres. The temporal coverage is estimated to be 3-8 days in high latitudes. The water level measurements associated with water mask retrieved from SWOT SAR antennas will make possible the estimation of the variability of water storage in lakes on the scale of whole river watershed.

Using a combination of ongoing/recent optical (Landsat 8) and altimetric (ENVISAT) satellite missions and JPL-CNES SWOT simulator we designed a prototype scene of SWOT measurements for 50 × 50 km^2 area covered by arctic lakes for June (high waters) and July (low waters) 2013. The water storage change in this area was then calculated from these two scenes.

The prototype scene is situated on the interfluvial area of Nadym and Pur Rivers in West Siberia. The results obtained on local scale were then extrapolated on whole watershed of Nadym River using July mask of lakes available from Landsat 7. The estimates of seasonal water storage due to thermokarst lakes in Nadym rivers is of 11 km^3.

Acknowledgements

This research has been done in the framework of the SWOT-TOSCA CNES, IDEX Transversalité 2013 INHERA and ANR "CLASSIQUE" projects, as well as by GDRI "CAR-WET-SIB II" and French-Siberian Centre for Education and Research.

SESSION 16

Where, when, and why will the Arctic become wetter or drier?

Convener:

Cathy Jean Wilson, *Los Alamos National Laboratory, USA*

Stan Wullschleger, *Oak Ridge National Laboratory, USA*

Ingmar Nitze, *Alfred Wegener Institute Helmholtz Centre for Polar and Marine Research, Germany*

Arctic landscapes are characterized by large expanses of saturated soils, wetlands, ice wedge polygon ponds and thermokarst ponds and lakes. The spatial and temporal dynamics of soil saturation and inundation drives subsurface and surface ecosystem responses, carbon and water cycles and local- to regional-scale energy balance. Earth System Models predict an overall drying of Arctic soils by the end of the 21^{st} century, but they are not able to represent the spatial and temporal heterogeneity in both increasing and decreasing lake, pond and wetland area observed over recent decades. We invite presentations using observations and models that aim to quantify and predict:

1. the spatial and temporal patterns of changes in soil moisture and inundation, and
2. the underlying controls (climate, meteorology, landscape structure, and permafrost, ecosystem and subsurface properties and processes) on shifts in landscape wetness in the past, present and future.

This session will aim to highlight a framework for improving our ability to predict where, when and why Arctic landscapes will become wetter or drier.

Satellite-derived changes in the permafrost landscape of central Yakutia, 2000 – 2011: Wetting, drying, and fires

Julia Boike[1], Thomas Grau[2], Birgit Heim[1], Günther Frank[1], Langer Moritz[1], Muster Sina[1], Gouttevin Isabelle[3], & Lange Stephan[1]

[1] *Alfred Wegener Institute Helmholtz Centre for Polar and Marine Research, Telegrafenberg A43, 14473 Potsdam, Germany*
[2] *Helmholtz Center for Environmental Research, Department Computational Hydrosystems, Permoserstraße 15, 04318 Leipzig, Germany*
[3] *RSTEA, Unité de Recherche Hydrologie-Hydraulique, 5 Rue de la Doua, CS 70077, 69626 Villeurbanne CEDEX, France*

The focus of this research has been on detecting changes in lake areas, vegetation, land surface temperatures, and the area covered by snow, using data from remote sensing. The study area covers the main (central) part of the Lena River catchment in the Yakutia region of Siberia (Russia), extending from east of Yakutsk to the central Siberian Plateau, and from the southern Lena River to north of the Vilyui River. Approximately 90 % of the area is underlain by continuous permafrost. Remote sensing products were used to analyze changes in water bodies, land surface temperature (LST), and leaf area index (LAI), as well as the occurrence and extent of forest fires, and the area and duration of snow cover. The remote sensing analyses (for LST, snow cover, LAI, and fire) were based on MODIS–derived NASA products for 2000 to 2011. Changes in water bodies were calculated from two mosaics of (USGS) Landsat high resolution (30 m) satellite images from 2002 and 2009. Within the study area's 315,000 km^2 the total area covered by lakes increased by 17.5 % between 2002 and 2009, but this increase varied in different parts of the study area, ranging between 11 % and 42 %. The land surface temperatures showed a consistent warming trend, with an average increase of about 0.12 °C/year.

The average rate of warming during the April-May transition period was 0.15 °C/year and 0.19 °C/year in the September-October period, but ranged up to 0.45 °C/year in some areas during April-May. Regional differences in the rates of land surface temperature change, and possible reasons for the temperature changes, are discussed with respect to changes in the land cover.

Our analysis of a broad spectrum of variables over the study area suggests that the spring warming trend is very likely to be due to changes in the area covered by snow. The warming trend observed in fall does not, however, appear to be directly related to any changes in the area of snow cover, or to the atmospheric conditions, or to the proportion of the land surface that is covered by water (i.e., to wetting and drying). These results suggest a complex interplay between different mechanisms affecting the land cover and land surface temperatures that warrants further investigation, possibly making use of higher resolution satellite data together with local and regional modeling, and taking into account the influence of lakes on the regional energy exchange.

Supplementary data (original data, digitized version of the maps, metadata) are archived under PANGAEA (doi:10.1594/PANGAEA.855124).

Dynamical downscaling products to facilitate climatic impact research on hydrology, permafrost, and ecosystems on the Alaskan North Slope

Lei Cai[1], Vladimir A. Alexeev[1], Christopher D. Arp[2], & Benjamin M. Jones[3]

[1] *International Arctic Research Center, University of Alaska Fairbanks*
[2] *Water and Environmental Research Center, University of Alaska Fairbanks*
[3] *United States Geological Survey*

Thermokarst lakes cover large portions of the Alaskan North Slope, are sensitive to climate, and their dynamics can create feedbacks with permafrost moisture and energy balance. In order to better understand the climate change impact on lakes, permafrost, and regional hydrology, a group of dynamical downscaling products have been created. These products are specifically designed to facilitate historical and projected high-resolution atmospheric background over the central Arctic Coastal Plain (Fish Creek Watershed) and the surrounding Alaskan North Slope region. ERA-interim reanalysis data-set and the Community Earth System Model (CESM) were applied as the forcing in the dynamical downscaling framework. The Weather Research & Forecast (WRF) model embedded with an optimization for the Arctic (Polar WRF) serves as the Regional Climate Model (RCM) in this framework. The downscaled output consists of multiple climatic variables for a 10 km grid spacing at 3-hour intervals covering the years from 1950 to 2100 at most. The modeling products have been carefully evaluated and calibrated via a bias-correction approach. As the result, ERA-interim forced WRF (ERA-WRF) produces reasonable climatic variables. It produces a more closely correlated temperature field than a precipitation field when comparing monthly climatology with its forcing and observational data. One of the reasons may be the lack of highly accurate precipitation data for the Arctic region rather than the performance of the model itself. A linear scaling method was then chosen to correct bias based on ERA-interim monthly climatology, and bias corrected ERA-WRF precipitation and temperature fields are then applied as the reference to the evaluation and bias correction of both the historical and the projected CESM forced WRF (CESM-WRF) products. CESM-WRF also recaptured the bias that CESM holds over the Alaskan North Slope, with a cold temperature bias during summer and a warm temperature bias during winter, as well as a wet bias for monthly-mean precipitation. Linear scaling helps correct these biases based on the linear-scaled ERA-WRF product, thus eventually producing more suitable high-resolution downscaling products for the Alaskan North Slope. These data sets were originally designed as the forcing for running hydrology models over the Fish Creek Watershed, but its capability is far more than that. Other climatic research that has been proposed based on these high-quality downscaling products with fine grids, include exploring historical and projected climatic extreme events and their possible connections to low-frequency sea-atmospheric oscillations as well as near-surface permafrost degradation.

Massive thermokarst lake area loss in continuous ice-rich permafrost of the northern Seward Peninsula, Northwestern Alaska, 1949 – 2015

Guido Grosse[1], Benjamin M. Jones[2], Ingmar Nitze[1], Prajna R. Lindgren[3], Katey M. Walter Anthony[4], & Vladimir E. Romanovsky[3]

[1] *Alfred Wegener Institute Helmholtz Centre for Polar and Marine Research, Germany*
[2] *Alaska Science Center, US Geological Survey, Anchorage, AK, USA*
[3] *Geophysical Institute, University of Alaska Fairbanks, USA*
[4] *Water and Environmental Research Center, University of Alaska Fairbanks, USA*

Thermokarst lakes are important factors for permafrost landscape dynamics and carbon cycling. Thermokarst lake cover is especially high in Arctic lowlands with ice-rich permafrost. In most of these regions, multiple lake generations have been identified that overlap each other in space and time, giving rise to the hypothesis of thermokarst lake cycling and its association with complex cryostratigraphical conditions where multiple lacustrine and palustrine sequences may follow on top of each other and talik and carbon cycle histories are complicated. In northwestern Alaska on the northern Seward Peninsula, ice-rich permafrost lowlands have strongly been affected by thermokarst during the Holocene and up to six generations of lake basins overlap spatially [Jones et al., 2012]. Modern thermokarst lakes are also abundant in this region and expand gradually by thermo-erosion along shores [Jones et al., 2011].

We here report on the analysis of multi-temporal remote sensing data for a 12,200 km^2 lowland area in the relatively warm continuous permafrost zone of the northern Seward Peninsula, demonstrating that thermokarst lake drainage in this region was occurring on a massive scale from 1949-2015. Contrary to most previous studies that suggest an increase in thermokarst lake area in continuous permafrost, we observed a significant net decrease in thermokarst lake area largely due to catastrophic lake drainage. Lateral lake expansion by thermo-erosion continued but did not offset the net area loss. Climate data analysis revealed a potential correlation with increased winter precipitation that may have resulted in a combination of high lake water levels, increased spring runoff with higher potential for drainage channel formation, and near-surface permafrost degradation, ultimately enhancing lake drainage. The observed magnitude of lake drainage implicates strong and lasting impacts on regional hydrology, biogeochemical cycling, surface energy budgets, state of the permafrost, ecosystem character, waterfowl and fish habitats, and subsistence lifestyles in the study region, portions of which belong to the Bering Land Bridge National Preserve. The datasets used in this analysis include a wide range of remote sensing images and topographic data available for this region, such as aerial photography, historic topographic maps, high resolution satellite images (Corona, Spot, Ikonos, Quickbird, Worldview, GeoEye), and the full Landsat archive. Field studies included reconnaissance flights targeting freshly drained lakes and ground based data collection such as lake basin coring.

Our findings suggest that a significant portion of lakes in this region has drained over the last decades and that in particular large lakes are vulnerable to disappearance. Initial analyses of relationships of lake drainages with permafrost distribution in the region suggest positive correlations between lake loss and permafrost degradation in much of the region. Our findings highlight that permafrost and lake-rich landscapes in Alaska are already changing rapidly and permanently in a warming world.

Acknowledgements

This set of studies was supported by funding from NASA Carbon Cycle Sciences, NSF Arctic System Sciences, the European Research Council, and the Western Alaska Landscape Conservation Cooperative.

References

Jones, B.M.; Grosse, G.; Arp, C.D.; Jones, M.C.; Walter Anthony, K.M. and Romanovsky, V.E. [2011]: Modern thermokarst lake dynamics

in the continuous permafrost zone, northern Seward Peninsula, Alaska. *Journal of Geophysical Research: Biogeosciences*, 116:G00M03, doi:10.1029/2011JG001666.

Jones, M.C.; Grosse, G.; Jones, B.M. and Walter Anthony, K. [2012]: Peat accumulation in drained thermokarst lake basins in continuous, ice-rich permafrost, northern Seward Peninsula, Alaska. *Journal of Geophysical Research: Biogeosciences*, 117(G2), G00M07, doi:10.1029/2011JG001766.

Can wet summers trigger permafrost collapse at a Siberian lowland tundra site?

Monique Heijmans[1], Ko v. Huissteden[2], Bingxi Li[1], Peng Wang[1], Juul Limpens[1], Trofim C. Maximov[3], & Frank Berendse[1]

[1] *Wageningen University, Netherlands, The*
[2] *VU University Amsterdam, the Netherlands*
[3] *Institute for Biological Problems of the Cryolithozone, Siberian Branch Russian Academy of Sciences, Yakutsk, Russia*

In recent decades, tundra shrub expansion has been observed in many places in response to Arctic climate warming. We question whether this shrub expansion is the only direction in which tundra landscapes will change. At our Siberian lowland tundra research site we observe both local shrub dominance and shrub drowning when conditions become too wet due to local permafrost collapse. In lowland tundra, which is poorly drained and underlain by ice-rich permafrost, shrub decline due to permafrost degradation could be a likely alternative for the widely assumed shrub expansion.

In 2007 we started a Betula nana shrub removal experiment at a Northeast-Siberian tundra site to investigate how shrub expansion would influence the summer thawing of permafrost. The removal of the shrub part of the vegetation initiated thawing of permafrost, resulting in collapse of the originally elevated shrub patches into waterlogged depression within five years [Nauta et al., 2015]. These results demonstrate the extreme sensitivity of these lowland tundra ecosystems to perturbations.

It was not only within our experiment plots that the permafrost collapsed. We observed many'natural'thaw ponds in the study area for which it often is unclear what caused the abrupt thawing. We think that wet summers, such as in 2011, could have been a trigger for the local permafrost collapse. Nine years of measurements in the unchanged control plots of the removal experiment showed that the thawing depth was not largest in the warmest summer, but in the wettest summer (2011), implying an important role for precipitation in this ecosystem. Using a novel application of dendrochronological methods to drowned shrubs, we assessed whether thaw pond development and associated shrub drowning can be traced back to recent climatic changes. Preliminary results indicate that most of the studied thaw ponds developed recently.

If a future warmer and wetter climate can more frequently trigger such local permafrost collapse, methane-emitting wetlands and thermokarst ponds would expand in the Siberian lowland tundra landscape, which contrasts with the widely assumed shrub expansion.

References

Nauta, A.L.; Heijmans, M.M.P.D.; Blok, D.; Limpens, J.; Elberling, B.; Gallagher, A.; Li, B.; Petrov, R.E.; Maximov, T.C.; van Huissteden, J. and Berendse, F. [2015]: Permafrost collapse after shrub removal shifts tundra ecosystem to a methane source. *Nature Clim. Change*, 5(1):67–70, doi:10.1038/nclimate2446.

Increasing impacts of summer precipitation on permafrost environmental change in eastern Siberia

Yoshihiro Iijima[1], Hotaek Park[1], Tetsu Nakamura[2], Yoshihiro Tachibana[3], & Alexander N. Fedorov[4,5]

[1]*Japan Agency for Marine-Earth Science and Technology, Japan*
[2]*National Institute of Polar Research, Japan*
[3]*Mie University, Japan*
[4]*Melnikov Permafrost Institute SB RAS, Russia*
[5]*North-Eastern Federal University, Russia*

Introduction

In the last decade, increases in both soil temperature and active layer thickness have been observed widely in eastern Siberia. The soil warming has been accompanied by corresponding increases in soil moisture within the active layer [Iijima et al., 2010]. These underground hydro-thermal changes were primarily due to perennially wet climate conditions rather than the atmospheric warming alone, resulted in abnormally large amounts of winter snow accumulation and rainfall during late summer (July, August and September). The present study aims to clarify the linkage between atmospheric and land surface variations in regions of continuous permafrost in eastern Siberia based on in situ observation and atmospheric climatic data analyses.

Data & Methods

Routine observational data was utilized in the identification of temporal and spatial variations in hydro-thermal conditions. The spatial extent of these variations was analyzed using data regarding soil temperature, soil moisture, and active layer thickness in the left and right banks of the Lena River, Yakutsk. In addition, we utilized output data from long-term simulation of hydro-thermal statuses of soil and the underlying permafrost. The simulation used a process-based land surface model (CHANGE; Park et al. [2011]) to calculate both water and carbon fluxes in the atmosphere-land system as well as the thermal and hydrologic status of soil, including an explicit treatment of soil freeze/thaw phase changes in the circum-Arctic region from 1901 to 2009.

The reanalysis dataset (NCEP2) was used to analyze large-scale atmospheric fields and determine storm activity. Based on the daily data, we calculated monthly mean values of transient storm activity in order to estimate interannual deviations in storm activity during late summer through early winter. A sea level pressure (SLP) and a water vapor flux (q) of 850 hPa of the NCEP2 reanalysis data were also used in analyses of storm activity.

Results & Discussions

The wet climatic conditions in 2004–2008 were corresponding to the enhancement of cyclonic pattern over the Arctic Ocean and eastward propagation of storm activity in northern Eurasia during late summer and early winter. Water vapor flux was widely converged in conjunction with the manifestation of precipitation in eastern Siberia. As a result, consecutive positive anomalies of rainfall in late summer (July to September) and snow in winter effectively humidified land surfaces in the permafrost region from 2005 onwards, which resulted in abrupt soil warming and wetting of both the active layer and the upper part of the permafrost.

According to composite analyses on the storm activities for the previous (before 1997) and recent (after 1998) wet years in eastern Siberia, Extensive positive anomalies were distributed throughout the whole of Siberia during the recent wet years, while positive anomalies of storm activity were confined in eastern Siberia. That is, anomalies occurring in both eastern Siberia and along the coast of the Arctic Ocean in Siberia were less intense during the previous wet years than those occurring during the recent wet years.

The running correlation between soil temperature and rainfall during late summer exhibited a long-term shift from a negative relationship observed before early 1980s, to a positive relationship after 1990s. The same relationship could be found in circum-Arctic simulation by CHANGE model; that is, the majority of

the simulated regions exhibited either negative or not significant correlations between rainfall in late summer and soil temperature during 1961–1980, whereas positive correlations were observed during 1990–2009. Consequently, the 2000s was the only period with both rainfall and snow significantly positive influences on soil temperature. The historically high air temperatures and torrential rainfall observed in late summer during the recent wet years were unanticipated indications of the hydro-climatic hazards associated with permafrost degradation in the circum-Arctic.

References

Iijima, Y.; Fedorov, A.N.; Park, H.; Suzuki, K.; Yabuki, H.; Maximov, T.C. and Ohata, T. [2010]: Abrupt increases in soil temperatures following increased precipitation in a permafrost region, central Lena River basin, Russia. *Permafrost and Periglacial Processes*, 21(1):30–41, doi:10.1002/ppp.662.

Park, H.; Iijima, Y.; Yabuki, H.; Ohta, T.; Walsh, J.; Kodama, Y. and Ohata, T. [2011]: The application of a coupled hydrological and biogeochemical model (CHANGE) for modeling of energy, water, and CO_2 exchanges over a larch forest in eastern Siberia. *Journal of Geophysical Research: Atmospheres*, 116: D15102, doi:10.1029/2010JD015386.

Quantifying lateral and subsurface flow potential on the Arctic Coastal Plain of Alaska

Joshua C. Koch[1], Joel A. Schmutz[1], M. Torre Jorgenson[2], Brian Uher-Koch[1], Kirsty E. Gurney[3], & Mark S. Wipfli[4]

[1] *United States Geological Survey, United States of America*
[2] *Alaska Ecoscience*
[3] *Environment Canada*
[4] *United States Geological Survey, Alaska Cooperative Fish and Wildlife Unit*

Lateral and subsurface water fluxes are not often considered or accurately quantified in Arctic Coastal studies for several reasons, including a focus on the spring freshet when soils are frozen, challenges in making accurate measurements, or the assumption that nearly flat topography and fine-grained soils limit subsurface flow potential. However, when considering the mid-summer period when the Arctic waters are thawed and ecosystems are active and productive, these fluxes may be critical and have the potential to affect soil moisture, nutrient movement, trace gas fluxes, plant growth, and fish and wildlife habitat. This study combines detailed measurements of soil properties and hydrologic models of pond and lake hydrology and biogeochemistry to test the hypothesis that lateral fluxes are critical to the movement of water and solutes on the Arctic Coastal Plain of Alaska (ACP), with implications for ecosystem structure and function.

Permeability, infiltration, and subsurface tracer tests were conducted at 21 locations near Prudhoe Bay and Admiralty Bay in Arctic Alaska. Permeability tests indicated that hydraulic conductivity varied from around 0.05 m d^{-1} in a pure silt soil, up to 1.2 m d^{-1} in organic material. Permeability was higher in sites with buried organic material, related to limnic processes in troughs and low-centered polygon ponds, as well as due to cryoturbation, and permafrost thaw. Infiltration and subsurface tracers indicated preferential flow through organic soil horizons near the surface and through plugs of buried organic material, as well as at the frozen boundary.

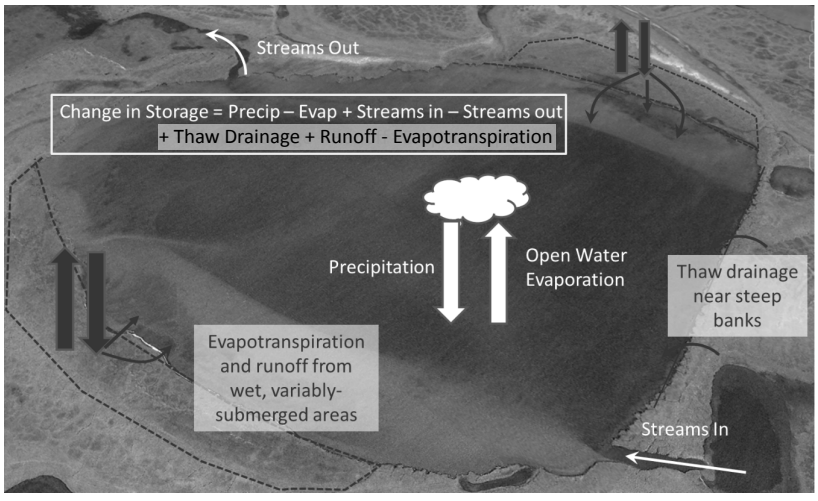

Figure 1: A conceptual model of the water budget of a partially-drained lake. White text indicates standard surface water fluxes. Dark text indicates additional lateral flows that were added to close the water balance.

We assessed the effect of these processes on the site and basin scales using solute and water budget and tracer studies in small ponds and large lakes. Results indicate that subsurface inflows provide critical nutrients to ponds, where ecosystem production appears to be limited by nutrients and low temperatures. At the basin scale, we assessed the effect of various mechanisms of lateral flow on water budgets for three lakes with different morphologies. A water budget focused on lake volume change and post snowmelt surface water fluxes (stream discharge, precipitation, and evaporation) could not close the budget for two of three lakes, even when input uncertainty was rigorously considered via a Monte Carlo approach. The water budget residual indicated that lateral inflows were entering the lakes and accounted for up to 70 % of mid-summer inflows. We modeled lateral flows based on three processes:

1. supra-permafrost subsurface inflows from basin-edge polygonal ground,
2. inflows due to runoff from drained lake margins during precipitation events, and
3. outflows from lakes due to drained lake margin evapotranspirative demand.

Measurements indicate that rapid subsurface flow could occur either along frozen boundaries and/or through highly conductive organic soils found near the surface and in organic plugs buried at depth. Drained lakes were hydrologically connected to marshy areas on the lake margins, receiving water from runoff following precipitation and losing up to 38 % of seasonal lake efflux to drained margin evapotranspiration. Lateral fluxes exerted a strong control on the overall lake water level, with implications for nutrient availability and cycling, ecosystem productivity and habitat. We conclude that lateral fluxes are an important component of the summer water budget that must be considered if we are to accurately predict future physical, biogeochemical, and ecosystem conditions on Arctic Coastal Plains.

Parameterizing permafrost thaw induced wetland dynamics and its effects on CH_4 dynamics in the Community Land Model (CLM)

Hanna Lee[1], Sean Swenson[2], & David Lawrence[2]

[1] *Uni Research Climate, Norway*
[2] *Climate and Global Dynamics Division, National Center for Atmospheric Research, Boulder, CO, USA*

Projecting permafrost carbon climate feedback largely depends on model representation of permafrost, permafrost thaw-associated local hydrological change, and the link between biogeophysics and biogeochemistry. Our previous work showed the effects of incorporating'excess ice'in the CLM and how excess ice and subsequent melting of excess ice under warming climate affects energy and hydrological cycles within the model. Here, we develop permafrost affected wetlands with melting of excess ice by using gridcell microtopography to better link permafrost thaw and subsequent CH_4 dynamics.

Production and oxidation of methane (CH_4) is a function of gridcell inundated fraction within the model. The functioning version of the CH_4 model parameterizes gridcell inundated fraction using water table depth and surface runoff. Unfortunately, this method contains problems in representing dynamic seasonality of the gridcell inundated fraction and is not compatible with some of the recent model developments to represent permafrost thaw related processes. The future model development plan is to parameterize inundated fraction based on precipitation and river channeling to capture seasonal dynamics of hydrological cycles. Here, we investigate how different model parameterization of inundated fraction affect Arctic hydrological cycles. In addition, we quantify the rate of CH_4 production and oxidation under changes in inundated fraction using different parameterization methods. We used CLM4.5BGC to understand the behavior of hydrology as well as CH_4 production and oxidation. The results show that using water table depth and surface runoff to parameterize inundated fraction result in unrealistic seasonality especially in the high latitude region. For instance, winter freezing, spring thaw, and summer increase in inundated fraction were not manifested using water table depth and surface runoff to parameterize inundated fraction. The two other methods simulated these processes more realistically throughout the season except that precipitation based parameterization underestimated and river channeling based parameterization overestimated the overall high latitude inundated fraction compared to satellite based estimation. Despite the large difference in inundated fraction estimation, total CH_4 production and oxidation simulated in the high latitude region were similar across the three different parameterization of inundated fraction.

These developments will allow more realistic simulations of permafrost thaw related processes within the Earth System Model by global scale simulations such as permafrost thaw, thermokarst formation, Arctic wetland formation and seasonal cycles, and CH_4 dynamics. Finally, the coupled framework of our model will provide a more accurate simulations of permafrost carbon-climate feedback cycles.

Active-layer soil moisture content regional variations in Alaska and Russia by ground-based and satellite-based methods, 2002 through 2014

Reginald R. Muskett[1], Vladimir E. Romanovsky[1,2], William L. Cable[1], & Alexander L. Kholodov[1]

[1] *Geophysical Institute Permafrost Laboratory University of Alaska Fairbanks, United States of America*
[2] *Tyumen State Oil and Gas University, Tyumen, Russia*

Soil moisture is a vital physical parameter of the active-layer in permafrost environments, and associated biological and geophysical processes operative at the microscopic to hemispheric spatial scales and at hourly to multidecadal time scales. While *in-situ* measurements can give the highest quality of information on a site-specific basis, the vast permafrost terrains of North America and Eurasia require space-based techniques for assessments of cause and effect and long-term changes and impacts from the changes of permafrost and the active-layer. Satellite-based 6.925 and 10.65 GHz sensor algorithmic retrievals of soil moisture by Advanced Microwave Scanning Radiometer – Earth Observation System (AMSR-E) onboard NASA-Aqua and follow-on AMSR2 onboard JAXA-Global Change Observation Mission – Water-1 are ongoing since July 2002. Accurate land-surface temperature and vegetation parameters are critical to the success of passive microwave algorithmic retrieval schemes. Strategically located soil moisture measurements are needed for spatial and temporal co-location evaluation and validation of the space-based algorithmic estimates. We compare on a daily basis ground-based (subsurface-probe) 50- and 70-MHz radio-frequency soil moisture measurements with NASA- and JAXA-algorithmic retrieval passive microwave retrievals. We find improvements in performance of the JAXA-algorithm (AMSR-E reprocessed and AMSR2 ongoing) relative to the earlier NASA-algorithm version. In the boreal forest regions accurate land-surface temperatures and vegetation parameters are still needed for algorithmic retrieval success. Over the period of AMSR-E retrievals we find evidence of at the high northern latitudes of growing terrestrial radio-frequency interference in the 10.65 GHz channel soil moisture content. This is an important error source for satellite-based active and passive microwave remote sensing soil moisture retrievals in Arctic regions that must be addressed.

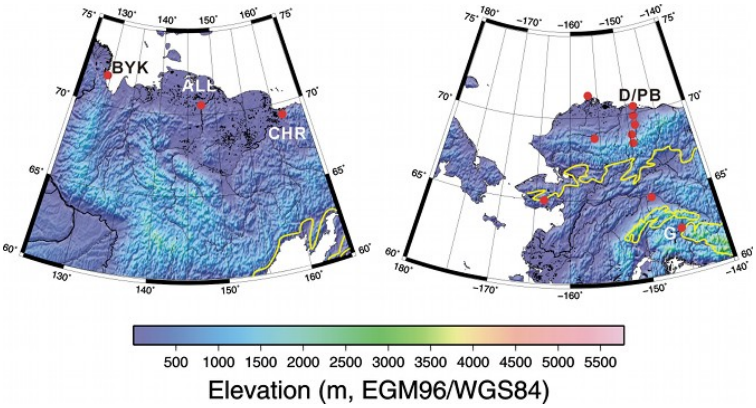

Figure 1: Regions of interest and active-layer soil moisture measurement stations (red dots) and those by abbreviation: Bykovsky (BYK), Allaiha (ALL) and Chersky (CHR) in Russia and Deadhorse/Prudhoe Bay (D/PB) and Gakona (G) in Alaska.

References

Muskett, R.; Romanovsky, V.; Cable, W. and Kholodov, A. [2015]: Active-Layer Soil Moisture Content Regional Variations in Alaska and Russia by Ground-Based and Satellite-Based Methods, 2002 through 2014. *International Journal of Geosciences*, 6, doi:10.4236/ijg.2015.61002.

Investigating patterns of pond and lake distributions to enhance the modeling of future Arctic surface inundation

Sina Muster[1], Kurt Roth[2], Moritz Langer[1], Fabio C. Aleina[3], William Riley[4], Charles Koven[4], Guido Grosse[1], Stephan Lange[1], & Julia Boike[1]

[1] *Alfred Wegener Institute for Polar and Marin Research*
[2] *University of Heidelberg*
[3] *Max Planck Institute for Meteorology*
[4] *Berkeley National Laboratory*

Permafrost acts as an impermeable subsurface in Arctic lowland landscapes. This hydrological barrier results in carbon-rich, water-saturated soils as well as many ponds and lakes. The rapidly warming Arctic climate very likely will affect the surface inundation in Arctic lowlands due to changes in precipitation, evapotranspiration, and permafrost degradation. Drying and wetting of the surface may occur in different regions and potentially alter the exchange of energy and carbon between the surface and the atmosphere. With increased permafrost thaw, for example, water may drain to deeper soil layers or drainage maybe enhanced due to newly forming drainage networks. Melting ground ice and subsequent inundation, on the other hand, may enhance formation of new ponds and wet areas. The current distribution of ponds and lakes in the Arctic is the result of complex interactions between climate, ground ice volume, topography, age and sediment characteristics. Because lake formation and growth processes occur at spatial scales orders of magnitude below those of the resolution for global or pan-arctic models land surface models, statistical representations of lake size distributions and other properties to inform such processes in future models are needed that can be related to macroscopic landcape properties. This study proposes basic observationally-constrained relationships to enhance the modeling of future Arctic surface inundation.

We mapped ponds and lakes in 21 circum-arctic sites representing different permafrost-soil landscapes, i.e., physiographic regions with similar surface geology, regional climate, and biomes. We used high-resolution optical and radar satellite imagery with spatial resolutions of 4 m or better to create detailed water body maps and derive representative probability density functions (PDF). PDFs of ponds and lakes vary little within the same ecoregion. Significant differences, however, do occur between landscapes. We used regional permafrost-soil landscape maps of Alaska, Canada, and Siberia to upscale the water body distributions to the circum-arctic. We here present regional distribution parameters, i.e. pond and lake fractions as well as PDF moments (mean surface area, standard deviation, and skewness) and their uncertainties. Younger landscapes, that developed in the early Holocene exhibit very skewed water body distributions. These landscapes are dominated by many ponds and feature only very few large lakes. Older landscapes, on the other hand, show more larger lakes but also a higher variability in pond and lake size. For lakes smaller than 5×10^5 m^2, PDFs change in a regular fashion across all sites: Relationships between mean surface area and standard deviation show a linear behaviour whereas the correlation between mean and skewness log-normal. We hypothesize that these relationships are an expression of pond and lake growth and/or lake formation in the landscapes and discuss the potential of the observed patterns to improve predictions of future distributions of Arctic ponds and lakes.

Monitoring Dynamic Changes in Pan-Arctic Land Surface Water Coverage

Jennifer D. Watts, John S. Kimball, Jinyang Du, & Youngwook Kim

The University of Montana, United States of America

Surface water inundation and soil wetness strongly regulate land-atmosphere energy and carbon exchange in northern environments and serve as important indicators of changing ecosystem conditions. However the dynamic nature of inundation and seasonal to interannual variability in near-surface soil water is not well quantified for Arctic-boreal landscapes, nor is the trajectory of regional change. Climate warming, a lengthening of the annual non-frozen season, shifts in precipitation patterns and evaporative demand, and increases in the frequency and severity of surface disturbances including fire will continue to alter hydrologic processes and surface water characteristics. The continuous, daily pan-Arctic monitoring of surface water through satellite remote sensing is necessary to evaluate the current state of wetland systems and to detect seasonal and longer-term fluctuations in surface hydrology in response to changing climate conditions and landscape disturbance.

Passive microwave remote sensing provides an effective method to monitor spatiotemporal changes in surface inundation and surface soil moisture, seasonal flooding events, and longer-term wetting or drying patterns across the pan-Arctic region [Watts et al., 2012]. Microwave remote sensing has advantages over optical-IR remote sensing by being insensitive to solar illumination and cloud, smoke and atmosphere aerosol contamination effects, enabling continuous daily observations over northern landscapes. Space-borne radars can provide relatively fine ($<$ 100-m) resolution characterization of wetland and open water lake bodies, but have more limited capabilities for global coverage and temporal frequency of observations than passive microwave sensors.

Here we apply a 12+ year (2003 to $>$ 2014) 25-km resolution global fractional open water (Fw) retrieval record derived from similar calibrated overlapping brightness temperature (Tb) records from the Advanced Microwave Scanning Radiometer for EOS (AMSR-E), FY3B-MWRI and AMSR-2 sensors. The AMSR Fw parameter represents the proportion of open water inundation within the sensor footprint, including contributions from lake, river and stream bodies, wetlands and flooded soils [Watts et al., 2012]. A newly developed Fw product obtained using higher frequency (89 GHz) AMSR Tb observations [Du et al., 2015] provides enhanced (6-km) resolution monitoring of open water bodies with 10 day temporal fidelity. The combined AMSR Fw products provide the means to better partition changes in lakes and rivers from shifts in the aerial extent of flooded vegetation across northern high latitude permafrost zones. Frozen surface controls on water extent are indicated by a corresponding classification of daily landscape freeze-thaw dynamics derived from AMSR 37 GHz V-polarized Tb observations [Kim et al., 2015].

The 2003-2014 AMSR Fw record indicates that approximately 6 % (1.3×10^6 km^2) of the pan-Arctic permafrost affected domain is inundated with surface water during the summer non-frozen season. The regional AMSR Fw inundation patterns are similar to those derived from finer resolution static water maps, including the 300-m ENVISAT Advanced Synthetic Aperture Radar Global Water Map (ASAR300), 250-m MODIS Global Water Mask (MOD44W), and 30-m Landsat based Global Land 2010 Water product (GLC30). The daily Fw retrievals reveal temporally dynamic fluctuations in surface water and seasonal pulses following precipitation events or snowmelt, and reductions in surface water bodies with mid-summer drying. Results from a non-parametric Mann-Kendall trend analysis indicate strong contrasts in ecosystem wetting and drying across the pan-Arctic domain (Fig. 1, left panel). Zones of significant ($p < 0.1$) multi-year wetting are observed in continuous permafrost areas across Siberia, northern Canada and Alaska (Figure 1, right panel). In contrast, severe surface drying occurs within portions of the Alaskan Seward Peninsula, the Canadian Shield, central Siberia and the Russian Kamchatka Peninsula. In total approximately 6 % of the pan-Arctic domain experienced significant drying over this period, while 9 % of the domain showed significant wetting with a slight 1-2 % increase relative to a prior 2003-2010 analysis [Watts et al., 2012]. We find these Fw patterns to correspond with thermokarst expansion, changes in precipitation, increasing non-frozen season length and landscape disturbances (e.g. fire and open pit mining).

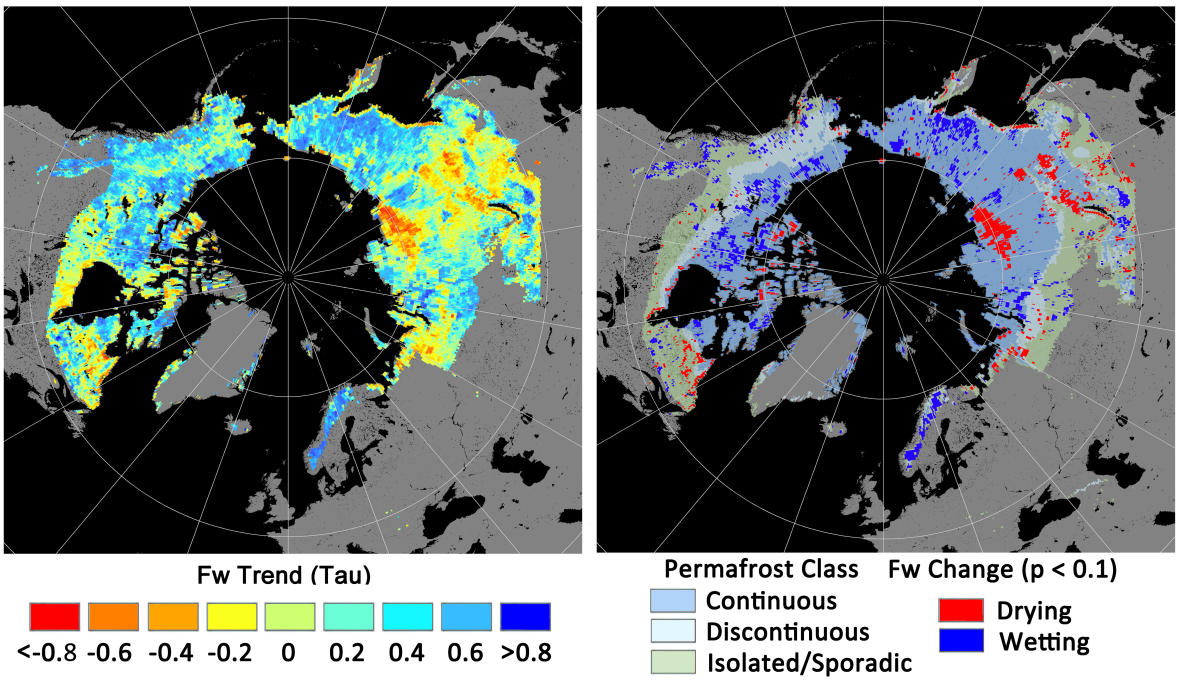

Figure 1: Regions of interest and active-layer soil moisture measurement stations (red dots) and those by abbreviation: Bykovsky (BYK), Allaiha (ALL) and Chersky (CHR) in Russia and Deadhorse/Prudhoe Bay (D/PB) and Gakona (G) in Alaska.

The continued monitoring of surface inundation and surface freeze/thaw dynamics supported by ongoing AMSR-2 operations, in conjunction with new soil moisture observations from the NASA Soil Moisture Active Passive (SMAP) mission and regional surveys using high spatial resolution optical-IR and radar remote sensing, will greatly improve understanding of long-term trends and variability in lakes, river networks and wetlands, and regional impacts to hydrology and biogeochemical processes under a changing climate.

References

Du, J.; Kimball, J.S.; Jones, L.A. and Watts, J.D. [2015]: Retrieval of land surface water inundation dynamics from satellite passive microwave observations at 89 GHz. *Remote Sensing of Environment*, (in review).

Kim, J.; Kimball, J.S.; Robinson, D.A. and Derksen, C. [2015]: New satellite climate data records indicate strong coupling between recent frozen season changes and snow cover over high northern latitudes. *Environmental Research Letters*, 10, doi:10.1088/1748-9326/10/8/084004.

Watts, J.D.; Kimball, J.S.; Jones, L.A.; Schroeder, R. and McDonald, K.C. [2012]: Satellite Microwave remote sensing of contrasting surface water inundation changes within the Arctic-Boreal Region. *Remote Sensing of Environment*, 127:223–236, 2012. doi:10.1016/j.rse.2012.09.003.

SESSION 17

Integrating Hydrology and Biogeochemistry along the Land-to-Ocean Continuum

Convener:

Paul James Mann, *Northumbria University, United Kingdom*

Jorien Elisabeth Vonk, *Utrecht University, The Netherlands*

Maria Winterfeld, *Alfred Wegener Institute for Polar and Marine Research, Germany*

As the Arctic permafrost regions warm, its large pool of organic matter becomes vulnerable to thaw and decomposition. Higher temperatures will intensify the coupling between the carbon and hydrological cycles and will introduce greater quantities of permafrost-derived carbon into inland and coastal systems. Hydrological processes play a crucial role in determining the rate and type of carbon released from thawing permafrost, affecting its biogeochemical role and eventual fate in aquatic systems.

In this session, we welcome contributions that aim to understand and integrate hydrological and biogeochemical processes, with the goal of shedding light on the fate of thawing permafrost matter released to inland or coastal waters. We invite submissions using various biogeochemical tracers such as bulk parameters (e.g., DIC, DOC, POC), terrestrial biomarkers, nutrients, major and trace elements, and isotopic compositions. Contributions can focus upon modeling or field-based studies, or be a combination of the two. Local and landscape-scale approaches are welcome, as are studies examining the complete land-to-ocean transport. Furthermore, we invite studies that present watershed budgets incorporating both terrestrial and aquatic organic matter fluxes.

Lateral and vertical fluxes of carbon and nitrogen from upland thermokarst

Benjamin W. Abbott[1,2], Jeremy B. J. Jr.[2], Julia R. Larouche[3], William B. Bowden[3], Sarah E. Godsey[4], & Andrew W. Balser[5]

[1] *Université de Rennes 1, OSUR, CNRS, ECOBIO, Rennes France*
[2] *Institute of Arctic Biology and Department of Biology& Wildlife, University of Alaska Fairbanks, Fairbanks, Alaska, USA*
[3] *The Rubenstein School of Environment and Natural Resources, University of Vermont, Burlington, Vermont, USA*
[4] *Department of Geosciences, Idaho State University, Pocatello, Idaho, USA*
[5] *Climate Change Science Institute, Oak Ridge National Laboratory, Oak Ridge, Tennessee, USA*

Release of greenhouse gases from thawing permafrost is potentially the largest terrestrial feedback to climate change and one of the most likely to occur; however, estimates of its magnitude vary by a factor of thirty. Some of this uncertainty stems from a suite of abrupt thaw processes loosely termed 'thermokarst' (mass-wasting due to ground ice melt), which alter controls on carbon and nitrogen cycling and expose organic matter from meters below the surface. While there is a general conceptual understanding of the influence of lowland thermokarst on landscape-level carbon balance, there is conflicting evidence about the importance of upland thermokarst to carbon and nitrogen release. Here we present results from three studies investigating particulate, gaseous, and hydrologic carbon and nitrogen flux from 90 upland thermokarst features on the North Slope of Alaska [Abbott and Jones, 2015, Abbott et al., 2014, 2015]. We synthesize these results with the quickly-growing upland thermokarst literature to assess the impact of upland thermokarst on carbon and nitrogen cycles at the site, landscape, and circumpolar scales.

We measured soil organic matter displacement, ecosystem respiration, soil gas concentrations, biodegradability of dissolved organic carbon (DOC), and hydrologic export of carbon and nitrogen from thermokarst features in various stages of development. Features included the three most common upland thermokarst morphologies: active-layer detachment slides, thermoerosion gullies, and retrogressive thaw slumps (Figure). We found that thermokarst morphology interacted with landscape characteristics to determine the initial displacement of organic matter and hydrologic flux as well as subsequent carbon and nitrogen cycling. The large proportion of ecosystem carbon exported off-site by slumps and slides resulted in decreased ecosystem respiration post-failure, whereas gullies removed a smaller portion of ecosystem carbon but increased ecosystem respiration and N_2O concentration in soils. Elevated N2O in gully soils persisted throughout most of the growing season, indicating sustained nitrification and denitrification in disturbed soils, representing a potential non-carbon permafrost climate feedback [Abbott and Jones, 2015]. Upland thermokarst caused substantial increases in dissolved organic carbon and other solute concentrations with a particularly large impact on inorganic nitrogen [Abbott et al., 2015]. DOC from upland thermokarst was some of the most biodegradable reported in natural systems [Abbott et al., 2014]. However, biodegradable DOC and most other solutes returned to undisturbed concentrations after feature stabilization. Lateral displacement of particulate and dissolved organic matter, primarily from the mineral soil, appears to be the dominant vector of carbon and nutrient loss from upland thermokarst.

Consistent differences between upland thermokarst types in regards to carbon and nitrogen export along with recent advances in upland thermokarst distribution represent a framework to incorporate this nonlinear process into projections of carbon and nitrogen release from degrading permafrost. However, accounting for fate of particulate and dissolved organic matter and nutrients delivered to downslope and downstream ecosystems remains a major challenge as does uncertainty about the duration of active feature growth for different upland thermokarst morphologies across regions. Because these feature form preferentially on river banks and lake shores and may affect 20 – 50 % of tundra uplands by the end of the century, upland thermokarst may be a dominant linkage transferring carbon and nutrients from terrestrial to aquatic ecosystems and eventually the atmosphere as the Arctic warms.

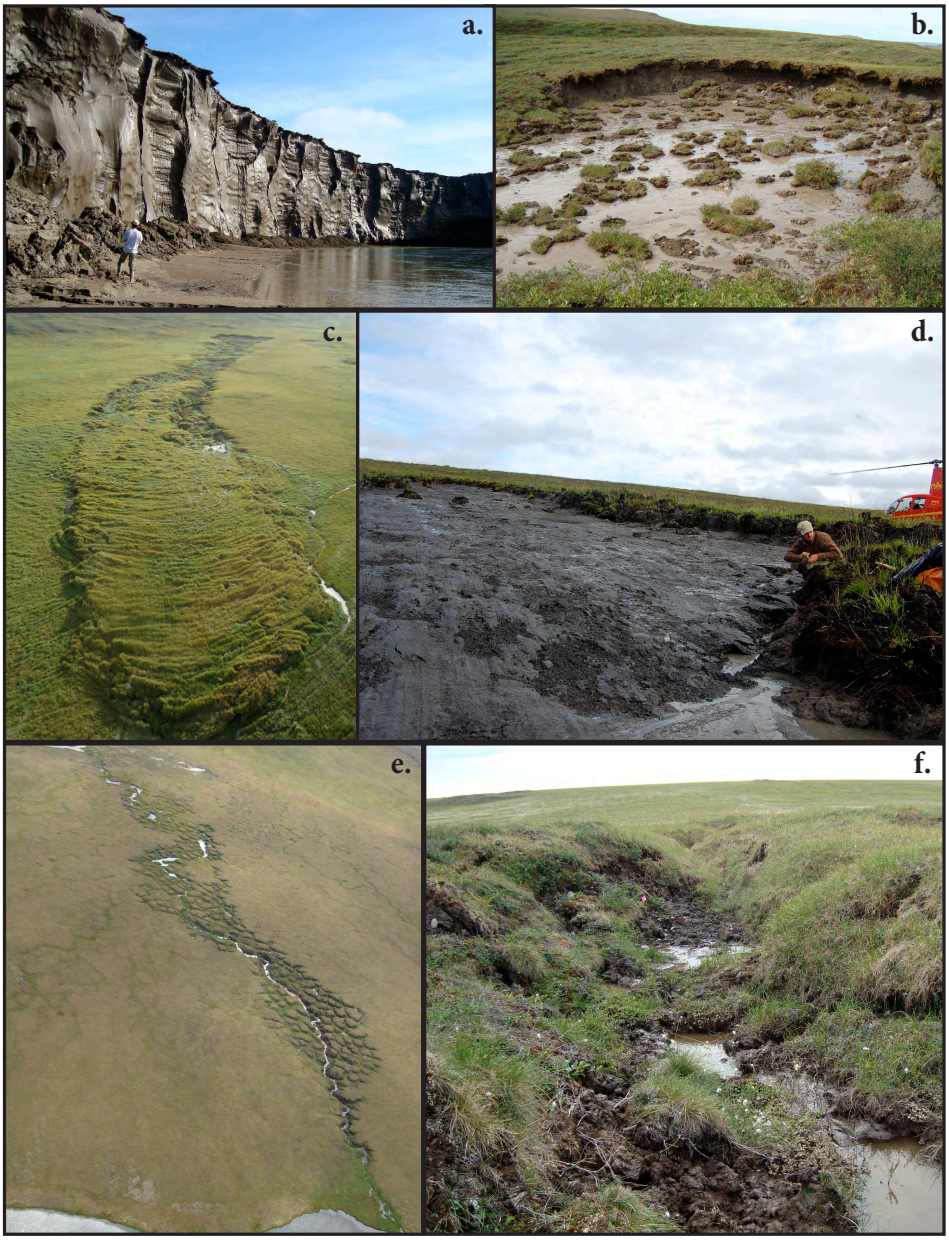

Figure. The three most common thermokarst morphologies in upland tundra: retrogressive thaw slumps (panels a, b), active-layer detachment slides (c, d), and thermo-erosion gullies (e, f)

References

Abbott, B.W. and Jones, J.B. [2015]: Permafrost collapse alters soil carbon stocks, respiration, CH_4, and N_2O in upland tundra. *Global Change Biology*, 21, 2015. doi:10.1111/gcb.13069.

Abbott, B.W.; Larouche, J.R.; Jones, J.B.; Bowden, W.B. and Balser, A.W. [2014]: Elevated dissolved organic carbon biodegradability from thawing and collapsing permafrost: Permafrost carbon biodegradability. *Journal of Geophysical Research: Biogeosciences*, 119. doi:10.1002/2014JG002678.

Abbott, B.W.; Jones, J.B.; Godsey, S.E.; Larouche, J.R. and Bowden, W.B. [2015]: Patterns and persistence of hydrologic carbon and nutrient export from collapsing upland permafrost. *Biogeosciences*, 12. doi:10.5194/bg-12-3725-2015.

A macro-scale biogeochemical model to simulate carbon emissions from high-latitude and permafrost lakes

Tina Karola Bayer[1], Matthias Brakebusch[1], Erik Gustafsson[2], & Christian Beer[1]

[1] *ACES, Stockholm University, Sweden*
[2] *Baltic Sea Centre, Stockholm University, Sweden*

Freshwaters are not only passive conductors of carbon from land to sea, but have been show to play an important role in global carbon cycling by processing, storing and releasing carbon to the atmosphere (e.g. Aufdenkampe et al. [2011]). For instance, lakes in permafrost are net emitters of carbon to the atmosphere, and their capacity to store, process and emit carbon is significant on a landscape scale, with a global flux of 8–103 Tg methane per year from lakes alone, i.e. 5 – 30 % of all natural methane emissions [Bastviken et al., 2011]. However, their contribution remains poorly qualified and is difficult to upscale due to the spatially and temporally highly localised character of freshwater methane emissions. In addition, current terrestrial Earth System Models rarely include lake and pond emissions or lateral carbon transport.

Thus, in order to model the present regional carbon release from lakes as well as their future response to changes in climatic drivers, we need to include biogeochemical cycling in freshwaters in large-scale modelling of the boundless carbon cycle. To achieve this objective we have combined an existing large-scale hydrological model (the Variable Infiltration Capacity Macroscale Hydrologic Model (VIC), [Liang et al., 1994] with elements of an aquatic biogeochemical model (BALTSEM, Savchuk et al. [2012], Gustafsson et al. [2014]) and developed a new methane module to simulate carbon dynamics in lakes, especially in permafrost. The resulting new process-based biogeochemical model is designed to model lake carbon emission on a regional (or even ultimately) global scale, and to perform well in permafrost environments. Our model includes carbon, oxygen and nutrient cycling in lake water and sediments, including primary production and methanogenesis (See figure 1). Here we present results of the application of the model to a semi-permafrost and a permafrost catchment with thermokast.

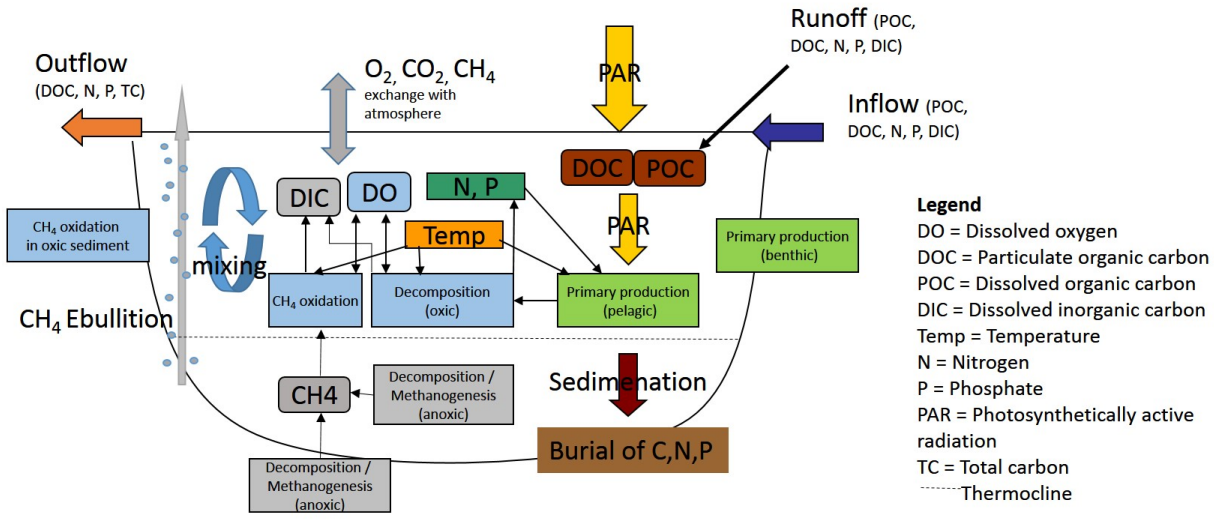

Figure 1: Schematic of biogeochemical cycling in lakes and processes included in our model

References

Aufdenkampe, A.K; Mayorga, E.; Raymond, P.A.; Melack, J.M.; Doney, S.C.; Alin, S.R.; Aalto, R.E. and Yoo, K. [2011]: Riverine coupling of biogeochemical cycles between land, oceans, and atmosphere. *Frontiers in Ecology and the Environment*, 9(1):53–60, doi:10.1890/100014.

Bastviken, D.; Tranvik, L.J.; Downing, J.A.; Crill, P.M. and Enrich-Prast, A. [2011]: Freshwater Methane Emissions Offset the Continental Carbon Sink. *Science*, 331(6013):50–50, doi:10.1126/science.1196808.

Gustafsson, E.; Deutsch, B.; Gustafsson, B.G.; Humborg, C. and Mörth, C.-M. [2014]: Carbon cycling in the Baltic Sea – The fate of allochthonous organic carbon and its impact on air-sea CO_2 exchange. *Journal of Marine Systems*, 129:289–302, ISSN 0924-7963. doi:10.1016/j.jmarsys.2013.07.005.

Liang, X.; Lettenmaier, D.P.; Wood, E.F. and Burges, S.J. [1994]: A simple hydrologically based model of land surface water and energy fluxes for general circulation models. *Journal of Geophysical Research: Atmospheres*, 99(D7):14415–14428, doi:10.1029/94JD00483.

Savchuk, O.P.; Gustafsson, B.G. and Müller-Karulis, B. [2012]: BALTSEM - a marine model for the decision support within the Baltic Sea Region (Technical Report No. 7). Technical report, BNI Technical Report Series.

Fate of permafrost-released organic matter in the Laptev Sea: What is its lateral transport time from the Lena delta area to the deep sea of the Arctic interior?

Lisa Bröder[1,2], Tommaso Tesi[3], Igor Semiletov[4,5,6], Oleg Dudarev[5,6], & örjan Gustafsson[1,2]

[1] *Stockholm University, Sweden*
[2] *Bolin Centre of Climate Research, Stockholm, Sweden*
[3] *CNR-National Research Council of Italy, ISMAR-Marine Sciences Institute, Bologna, Italy*
[4] *International Arctic Research Center, University Alaska Fairbanks, Fairbanks*
[5] *Pacific Oceanological Institute, Russian Academy of Sciences, Vladivostok, Russia*
[6] *Tomsk National Research Politechnical University, Tomsk, Russia*

Potentially increasing amounts of permafrost-derived organic carbon discharge both through rivers and coastal erosion to the Arctic shelves. The fate of this material in the marine environment is still unclear: it can be degraded to CO_2 and then outgassed, deposited in sediments or transported to the deep sea. In this study we assessed processes occurring during the cross-shelf transport and after burial for terrestrial organic carbon (TerrOC) on the Siberian Arctic Shelf by exploring how it changes in concentration, composition and degradation status both spatially and over time. We analyzed a suite of terrestrial biomarkers as well as source-diagnostic bulk carbon isotopes ($\delta^{13}C$, $\delta^{14}C$) in sediments from the wide Siberian Arctic Shelf and found contrasting trends for different carbon pools.

TerrOC concentrations and degradation status change noticeably more during cross-shelf transport than after burial. The concentrations of lignin phenols, cutin acids and high-molecular weight (HMW) wax lipids (tracers of vascular plants, i.e. terrestrial material) do not display clear trends over time after sediment accumulation, while they decrease significantly with increasing distance from the coast. Molecular-based degradation proxies for TerrOC (e.g., CPI of HMW lipids, the HMW acids/alkanes ratio and the acid/aldehyde ratio of lignin phenols) do not suggest extensive down-core mineralization, but there appears to be a trend to more degraded TerrOC along the transect. We infer that the degree of degradation of permafrost-derived TerrOC is a function of the time spent under oxic conditions (oxygen exposure time, OET). Specifically, protracted OETs during cross-shelf transport compared to rather short in situ OETs after burial would explain the observed patterns. To test this hypothesis we estimate lateral transport times using compound-specific radiocarbon analysis for terrestrial OC biomarkers (HMW fatty acids) and compare them with in situ OETs calculated from measured oxygen penetration depths and ^{210}Pb-derived sedimentation rates. Preliminary results suggest cross-shelf transport times of several millennia, while in situ OETs for the shelf are a few decades at most.

Permafrost draining rivers in the Canadian Arctic Archipelago: Biogeochemical properties and carbon export potential

Kristina A. Brown[1], Bill Williams[2], Eddy Carmack[2], Donald McLennan[3], Angulalik Pedersen[3], Adrian Schimnowski[4], Greg Fiske[5], Roger Francois[6], Valier Galy[1], Zhaohui A. Wang[1] & Bernhard Peucker-Ehrenbrink[1]

[1] *Woods Hole Oceanographic Institution, United States of America*
[2] *Institute of Ocean Sciences, Fisheries and Oceans Canada, Sidney, Canada*
[3] *Polar Knowledge Canada - Canadian High Arctic Research Station, Cambridge Bay, Canada*
[4] *Arctic Research Foundation, Winnipeg, Canada*
[5] *Woods Hole Research Center, Falmouth, USA*
[6] *University of British Columbia, Vancouver, Canada*

Increased precipitation, river runoff, and permafrost thaw have been observed across the pan-Arctic region, resulting in an increased flux of freshwater and land-derived materials to the coastal ocean (e.g., Carmack et al. [2016]). As a watershed-scale integrator, observations of river geochemistry provide an indirect view of the state of the terrestrial system and a direct indication of changing pressures on the nearshore marine environment. In this study we quantify the biogeochemical characteristics of 26 permafrost-draining rivers with a range of geomorphologic characteristics throughout the continuous permafrost zone of the Canadian Arctic Archipelago (CAA), north of 64°N. By focusing on smaller drainage basins, we endeavour to tie specific characteristics of each watershed (permafrost cover, soil organic carbon content, net primary productivity, bedrock geology) to the riverine carbon inventory at its outlet to the coastal ocean.

Over the 2014 and 2015 summer seasons we visited CAA rivers throughout the Northwest Passage, from Lancaster Sound in the east to Coronation Gulf in the west (Fig. 1).

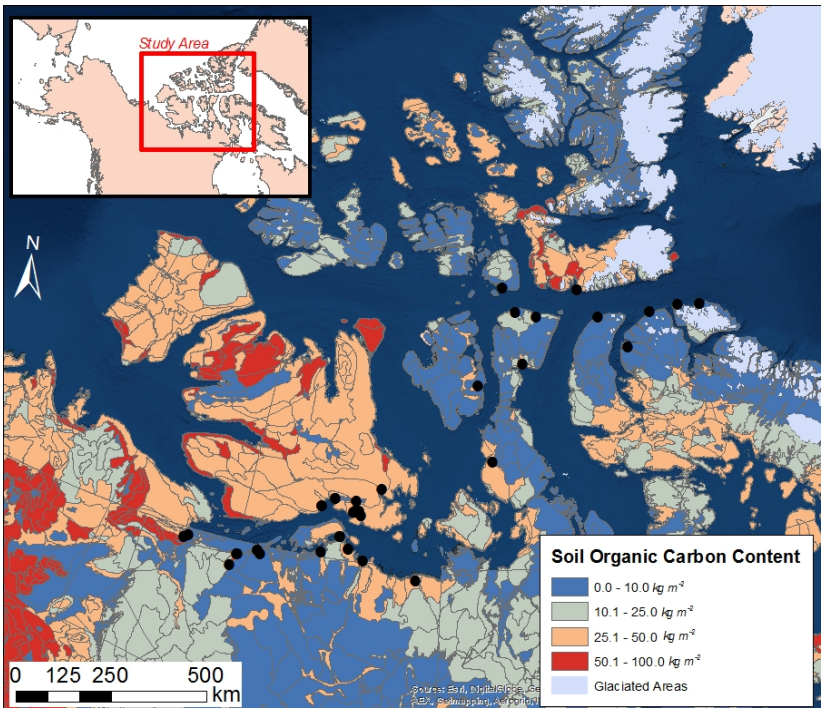

Figure 1: Permafrost organic carbon inventory (in kg m^{-2}) in the upper 100 cm of soils of the Canadian Arctic, as calculated by Hugelius et al. [2013]. Black circles indicate sampling locations visited for this study in 2014 and 2015.

We observed significant differences in the distributions of biogeochemical parameters across the study region. Rivers in the southern CAA were characterized by low concentrations of inorganic carbon (Dissolved Inorganic Carbon, DIC, and Total Alkalinity, TA) and relatively high concentrations of organic carbon (Dissolved Organic Carbon, DOC), likely reflecting higher organic carbon content of soils and higher Net Primary Productivity (NPP) within the watershed. Rivers in the central CAA, on the other hand, were characterized by high concentrations of DIC and TA, close to that of seawater, and much lower concentrations of DOC. The geochemistry of these rivers is expected to reflect low-productivity watersheds, predominantly underlain by sedimentary, likely carbonate-rich, bedrock. Major ion concentrations further indicate the importance of mineral weathering to river geochemistry in the CAA, with samples from the majority of the rivers falling on a mixing line between the composition of runoff from pure carbonate and pure silicate (granitic) end members. We discuss the impact of these observations to the delivery of terrestrial carbon to the shallow marine straits of the CAA.

Our present understanding of how permafrost draining watersheds will respond to the changing Arctic climate, however, remains limited, as previous studies have focused on the largest Arctic river systems that drain latitudes well south of the continuous permafrost zone. This work will permit the determination of important end-member states of continuous permafrost systems that are not accessible by studying large river basins that contain some permafrost. This study presents a unique characterization of river biogeochemistry across a gradient of the continuous permafrost zone of the CAA, from just south of the Arctic Circle to 75°N, and begins the important process of developing a baseline geochemical data set for this region. Working with local community partners we have also carried out time-series studies of two rivers draining into the CAA, Freshwater Creek (Cambridge Bay, NU) and the Coppermine River (Kugluktuk, NU). Observations from these sites illustrate the seasonal range of an Arctic river's geochemical properties and underscore the need for comprehensive geochemical measurements covering the entire flow cycle of CAA rivers. Collaboration with a network of northern partners (community organizations, NGOs, and academic research) has been essential to carrying out this work. A major outcome of this project will be to establish a framework for community-based observations of local river systems and develop long-term data sets from which to assess future environmental change.

References

Carmack, E. C.; Yamamoto-Kawai, M.; Haine, T. W. N.; Bacon, S.; Bluhm, B. A.; Lique, C.; Melling, H.; Polyakov, I. V.; Straneo, F.; Timmermans, M.-L. and Williams, W. J. [2016]: Freshwater and its role in the Arctic Marine System: Sources, disposition, storage, export, and physical and biogeochemical consequences in the Arctic and global oceans. *Journal of Geophysical Research: Biogeosciences*, 121(3):675–717, doi:10.1002/2015JG003140. 2015JG003140.

Hugelius, G.; Tarnocai, C.; Broll, G.; Canadell, J.G.; Kuhry, P. and Swanson, D.K. [2013]: The Northern Circumpolar Soil Carbon Database: spatially distributed datasets of soil coverage and soil carbon storage in the northern permafrost regions. *Earth System Science Data*, 5(1):3–13, doi:10.5194/essd-5-3-2013.

Trace element cycles in permafrost thaw lakes

João Canário[1], Ana Padeiro[1], Leandro Castanheira[1], Margarida C. Santos[1], Maria F. Araújo[2], Teresa Duarte[1], Maria C. Oliveira[1], José Ascenso[1], Teresa G. Nunes[1], Susana S. Gomes[2], Maria J. Ferreira[1], Gonçalo Vieira[3], & Warwick F. Vincent[4]

[1] *Centro de Química Estrutural, Instituto Superior Técnico, Universidade de Lisboa, Av. Rovisco Pais 1, Lisboa, Portugal*
[2] *Centro de Ciências e Tecnologias Nucleares, Instituto Superior Técnico, Universidade de Lisboa, Bobadela, Portugal*
[3] *IGOT, Centro de Estudos Geográficos, Universidade de Lisboa, Lisboa, Portugal*
[4] *Centre d'études nordiques& Dépt de biologie, Laval University, Québec City, Québec, Canada*

Rising temperatures are rapidly thawing Arctic permafrost, and this may cause the release of trace elements (TEs), organic carbon and greenhouse gases into water and atmosphere. These inputs could have serious consequences for aquatic biota and may further accelerate global warming. Several studies have evaluated the concentrations of carbon compounds and trace elements in thaw lakes, and have examined some of the biogeochemical processes responsible for the partitioning, speciation and fate of certain elements on these lakes. However the biogeochemical processes involved are still poorly understood.

In order to contribute to the understanding of trace element cycles in thaw lakes, field campaigns were undertaken in the Canadian subarctic region of Whapmagoostui-Kuujjuarapik (W-K) and Umiujaq (Quebec) in July 2014 and August 2015 as part of the Canadian ADAPT and the Portuguese PERMACHEM projects. Six thaw lakes and two rock basin reference lakes were sampled. Water samples were collected at different depths and analysed for labile and total dissolved metals using the DGT method and ICP-MS. Duplicates were sampled for 1H and 13C NMR (1D and 2D) as well as for mass spectrometry (GC-MS and HPLC-TOF). Lake sediments and nearby soils were also sampled and analysed using the equivalent techniques for solids and also by X-ray diffraction both in powder and single crystal analysis.

Results showed that in Umiujaq thaw lakes (lithalsa permafrost soils) the total concentrations of all the analysed trace elements (As, Cd, Cu, Cr, Ni and Pb) were in general higher than in W-K lakes (palsa permafrost soils). However, in both sites the dissolved organic matter (DOM) appears to be the main source of those elements that are remobilized during the DOM microbial degradation.

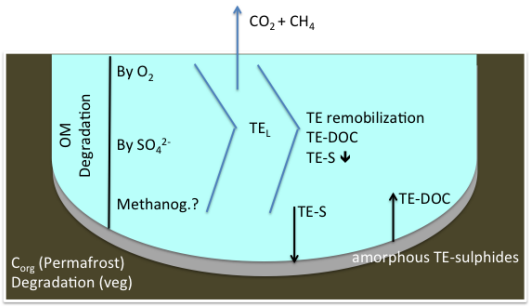

Figure 1: Conceptual model of trace element cycles in permafrost thaw lakes

In all sampled lakes the concentrations of the analysed TEs varied with depth, in general increasing towards the bottom. The proportion of labile (% of the total) elements also varied, being related with the anoxia of the water (assessed with a Hydrolab profiler) and the concentrations of dissolved organic carbon (DOC) and dissolved sulphide. Processes of co-precipitation/precipitation (with sulphide) and complexation (with DOC) were identified changing the TE- partitioning and availability in the water column. As an example, TE-sulphide precipitation/co-precipitation appears to play an important role for the removal of TE from the water. This hypothesis was supported by the analysis of the TE composition in surface sediments from the lake, which showed that up to 60 % (min 10 %) of the TE are in the form of sulphides. These results pointed to the importance of permafrost soils as a source of trace elements into thaw lakes and that.in a thaw lake drainage scenario these waters may impact downstream aquatic ecosystems including the coastal ocean.

This work was funded by Fundação para a Ciência e Tecnologia (Portuguese Polar Program and Projects Ref[a] UID/QUI/0010/2013 and UID/Multi/04349/2013) and by the Canadian NSERC Discovery Frontiers project ADAPT.

Sulphur biogeochemistry in permafrost thaw lakes

João Canário[1,3], Ana Padeiro[1,3], Leandro Castanheira[1], Margarida C. Santos[1], Gonçalo Vieira[2,3], & Warwick F. Vincent[3]

[1] *Centro de Química Estrutural - Instituto Superior Técnico - Universidade de Lisboa, Portugal*
[2] *IGOT, Centro de Estudos Geográficos, Universidade de Lisboa, Lisboa, Portugal*
[3] *Centre d'études nordiques& Dépt de biologie, Laval University, Québec City, Québec, Canada*

Rising temperatures are contributing to the rapid thaw of Arctic permafrost, and this may be a driving factor for the release of trace elements, organic carbon and greenhouse gases into water and air. These inputs could have serious consequences for aquatic biota and may further accelerate global warming.

Several studies have evaluated the concentrations of carbon compounds and some trace elements in thaw lakes, and have examined specific biogeochemical processes in these lakes. However little attention has been given to sulphur and their compounds in these abundant freshwater ecosystems. The chemistry of this element is of environmental importance because it plays a key role in the degradation of natural organic matter and also influences the partitioning, speciation and fate of trace elements.

In order to understand the role of sulphur in biogeochemical processes in thaw lakes, field campaigns were undertaken in the Canadian subarctic region of Kuujjuarapik-Whapmagoostui and Umiujaq (QC) in July 2014 and August 2015 as a part of the Canadian ADAPT and the Portuguese PERMACHEM projects. Six thaw lakes and two rock basin reference lakes were sampled. Water samples were collected at different depths and analysed for dissolved sulphur compounds (sulphide and sulphate). Lake sediments and nearby soils were also sampled and analysed for particulate sulphides, pyrite and elemental sulphur by voltammetry as well as organic sulphur compounds using 33SssNMR. X-ray diffraction both in powder and single crystal analysis were performed to identify crystalline sulphides. Finally, subsamples of soils, sediments and water were analysed for total particulate and dissolved organic carbon.

The results showed that the lake sulphur composition depends largely on the origin of permafrost soils. In lakes originated from organic-rich palsa permafrost soils, the proportion of organic sulphur (% of the total) is higher than 50 %, while in mineral lithalsa lakes the opposite was found. In both lakes the origin of sulphur was mainly from plant organic matter degradation, however we cannot exclude sulphur deposition in the form of sulphates.

Interestingly, the sulphur chemistry in the water column was independent of permafrost soil type. In all lakes, sulphate was identified as an important electron acceptor in the degradation of dissolved organic matter with the consequent formation of sulphides. These sulphides in the deepest waters promoted the precipitation of other trace elements, resulting in a sediment surficial layer enriched in trace element amorphous sulphides.

These preliminary results pointed to the importance of the sulphur biogeochemistry in permafrost thaw lakes and its strong linkage to lake origin, thus signalling the need for a full regional assessment of sulphur related processes, based on a large and detailed survey of thaw lake origin.

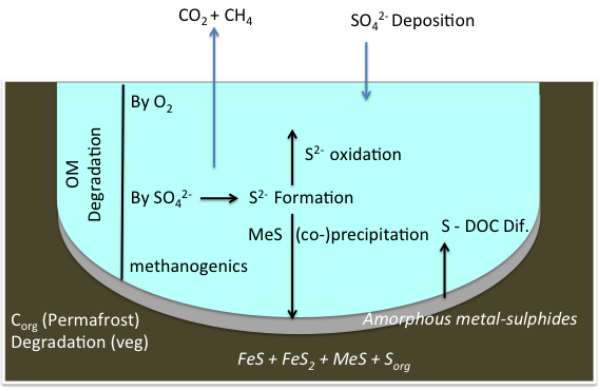

Figure 1: Conceptual model of the sulphur cycle in permafrost thaw lakes

Acknowledgements

This work was funded by Fundação para a Ciência e Tecnologia (Portuguese Polar Program and Projects Ref[a] UID/QUI/0010/2013 and UID/Multi/04349/2013) and by the Canadian NSERC Discovery Frontiers project ADAPT.

Hydro-geochemical characteristics and transformation processes of the Lena River Delta branches

Antonina Chetverova[1,2], Irina Fedorova[2,1], Anne Morgenstern[3], Olga Bobrova[1], Tatyana Skorospekhova[2], & Stepan Romanov[1]

[1] *Saint-Petersburg State University, Institute of Earth Science, Russian Federation*
[2] *Arctic and Antarctic Research Institute, Russian Federation*
[3] *Alfred Wegener Institute Helmholtz Centre for Polar and Marine Research, Germany*

Previous studies have shown that arctic river delta systems are areas of accumulation of geochemical substances at the sea-river mixing zone. In the Lena River Delta our previous work shows the tendencies of water runoff redistribution changes and heterogeneity of suspended supply distribution along the delta branches, accumulation and erosion zone in the different parts of the delta. Nevertheless, the processes of geochemical flow transformation in the subaerial deltas are so far underestimated. In order to close this gap, we sampled water, suspended and bottom sediments in the Lena River Delta in the summer seasons of 2010 and 2014. Most of the sampling points were tight to the profiles of hydrological measurements held in the delta and highlighted in Fedorova et al. [2015].

The results show that geochemical transformation of the Lena River runoff is taking place in the delta. The most active time for the transformation is the summer season due to the activity of sediment accumulation and biogeochemical processes. Hydrological conditions in the delta affect also its hydrogeochemical characteristics. Furcation of the delta branches affects the hydrodynamic conditions of different delta areas.

The factors influencing the geochemical characteristics of the delta were identified on the base of geochemical indexes approach applied to sediments and statistical factor analysis.

Based on geochemical indexes (Al/Na, Si/Al, Fe/Mn and Fe/Al ratios) similar conditions were determined for the main branch of the Lena, the upstream parts of Bykovskaya and Tumatskaya branches and in Olenekskaya branch near Chay-Tumus. Despite of high runoff the branches are characterized by element accumulation, which can be explained by decreasing of flow turbulence and specificity redox conditions in these areas. Bottom sediments are one of the most important indicators of geochemical transformation processes.

The results of statistical factor analysis show three main factors for formation of the these geochemical conditions in the delta:

1. the general water flow of the Lena River, which is influenced by the lithogenous base of the river catchment,
2. the cryogenic condition of the Lena Delta (permafrost degradation processes and cryogenic weathering) and
3. biogeochemical transformation during redistribution of chemical water components , suspended matter and bottom sediments.

Acknowledgements

The research was supported by grant № 14-05-00787 A of Russian Foundation for Basic Research

References

Fedorova, I.; Chetverova, A.; Bolshiyanov, D.; Makarov, A.; Boike, J.; Heim, B.; Morgenstern, A.; Overduin, P. P.; Wegner, C.; Kashina, V.; Eulenburg, A.; Dobrotina, E. and Sidorina, I. [2015]: Lena Delta hydrology and geochemistry: long-term hydrological data and recent field observations. *Biogeosciences*, 12(2):345–363, doi:10.5194/bg-12-345-2015.

Investigating hydrology and related nutrient dynamics on Herschel Island, Yukon Territory, Canada

Caroline Coch[1], Isabell Eischeid[1], Michael Fritz[1], Scott Lamoureux[2], & Hugues Lantuit[1]

[1] *Alfred Wegener Institute Helmholtz Center for Polar and Marine Research, Potsdam, Germany*
[2] *Department of Geography and Planning, Queen's University, Canada*

Coastal ecosystems in the Arctic are changing rapidly due to climate change. These changes lead to permafrost degradation, to a shifting hydrological regime and to the subsequent release of organic matter and nutrients to the atmosphere and/or to the Arctic Ocean. While the impacts of climate change on the hydrological regime of large rivers have been the focus of many investigations, the hydrological dynamics of small catchments, and in particular its interrelation with the degrading permafrost landscape have often been overlooked. Small catchments could yet contribute large amounts of sediment to the section of the coastal zone and induce localized but large effects on the Arctic Ocean's nearshore zone, in particular in relation to water quality and nutrient availability. This project is addressing this issue by investigating hydrology and transportation of sediment and nutrients of two small adjacent catchments on Herschel Island in the western Canadian Arctic.

This project will rely on existing datasets stemming from monitoring platforms installed in the catchment as well as retrieve data on the ground using methods in meteorology, hydrology, soil science and biogeochemistry. Data mining and remote sensing will also be utilized for a comprehensive assessment of the changing ecosystem. In the previous years, data of vegetation cover, discharge, active layer depth, soil organic carbon and nitrogen, soil temperature and soil moisture had been collected. The monitoring will be extended including the installation of meteorological stations in each catchment to identify microclimatic variations. Snow water equivalent estimations will be derived from snow probing along transects and from acoustic sensors at the weather stations. The hydrological stations at the outflow of each catchment will measure water height, temperature, turbidity and conductivity. Thaw dynamics are going to be investigated by active layer probing and continuous measurements of soil moisture and temperature. To analyze sediment and nutrient dynamics, turbidity values will be linked to suspended sediment concentration. Further, manual probing and laboratory analyses are going to reveal concentrations of carbon, nitrogen and dissolved solids. Mapping of vegetation and permafrost disturbances using remote sensing data and DGPS will complete geomorphological information derived from digital elevation models. The overall aim is to determine relevant factors that control sediment and nutrient dynamics.

In this presentation, we present an overview of the data collected over the past years and highlight some of the outstanding issues stemming from the analysis of the data. These include changing decoupling and coupling of the hydrological regime with snow, depending on the time in the season, but also on the abrupt changes in solute contents during rain events and the great spatial variability of the reservoirs of organic matter in the catchments.

Age and source of fluvial DOC, CO_2 and CH_4 in a carbon-rich landscape in the western Canadian Arctic

Joshua F. Dean[1,2], Michael F. Billett[1], Mark H. Garnett[3], Ype v. d. Velde[2], Robert Baxter[4], Kerry J. Dinsmore[5], Jason S. Lessels[6], Lorna E. Street[7], Jens-Arne Subke[1], Ian Washbourne[1,5], & Philip A. Wookey[7]

[1]*Biological and Environment Science Department, University of Stirling, Stirling FK9 4LA, UK*
[2]*Earth Sciences Department, Vrije Universiteit, 1081 HV Amsterdam, the Netherlands*
[3]*NERC Radiocarbon Facility, East Kilbride G75 0QF, UK*
[4]*School of Biological and Biomedical Sciences, University of Durham, Durham DH1 3LE, UK*
[5]*Centre for Ecology and Hydrology, Bush Estate, Penicuik EH26 0QB, UK*
[6]*Northern Rivers Institute, School of Geosciences, University of Aberdeen, Aberdeen AB24 3UF, UK*
[7]*Environmental Sciences, School of Life Sciences, Heriot-Watt University, Edinburgh EH14 4AS, UK*

Soils underlain by permafrost are estimated to contain 1,700 Pg of organic carbon (OC), much of which currently remains frozen beneath the active layer. Under projected warming scenarios Arctic permafrost soils are expected to become increasingly vulnerable to thaw, releasing ancient OC, which may be wholly or partly mineralised to CO_2 and CH_4 in the near-surface environment. Water flowing through the active layer then delivers dissolved and particulate OC (DOC and POC, respectively), CO_2 and CH_4 to inland waters. This leads to consistent oversaturation of CO_2 and CH_4 in Arctic freshwaters, with an additional contribution from mineralisation of OC in the water column.

Although radiocarbon dating (^{14}C) of DOC in Arctic freshwaters has been used as a key tool in detecting mobilised ancient C as evidence of recent permafrost thaw, the dissolved OC age (DO^{14}C) of major Arctic rivers is usually less than 1000 years BP. Recent work has indicated that we may be missing a component of old C in the major Arctic rivers due to the rapid mineralisation of DOC to CO_2 and/or CH_4 in headwater regions. New methods for the rapid collection of both CO_2 and CH_4 from inland waters have provided the opportunity to collect and analyse gaseous ^{14}C in freshwater environments (e.g. Garnett et al. [2016]). This allows a comparison of DO^{14}C with the age of gaseous C ($^{14}CO_2$ and $^{14}CH_4$), and therefore the ability to detect increased aquatic mobilisation of different forms of C from carbon-rich landscapes.

Here we present the first such results, comparing ^{14}C in DOC, CO_2 and CH_4 from a headwater stream, polygonal pools and lake systems underlain by continuous permafrost in the western Canadian Arctic. The ca. 14 km^2 study area (68°44' 54.5" N, 133°29' 41.7" W) is located east of the Mackenzie River Delta and north of the shrub-tundra transition zone. Sampling took place during the 2014 snow-free season, with samples collected in June through September in the Siksik headwater catchment (including polygonal pools) of Trail Valley Creek, and across a series of nearby lakes in August. Previous work on surface water chemistry indicated that the study site was not showing obvious signs of seasonally enhanced permafrost thaw or substantial thermokarst activity. In the current study, this is reflected in predominantly "modern" conventional radiocarbon ages of aquatic C (i.e. $\geq$ 100 % modern, meaning aged AD1955 or younger, which corresponds to 0 years BP; 68 out of 75 samples); DOC and CO_2 ranged from 97 to 110 % modern (233 to 0 years BP) and 98 to 109 % modern (160 to 0 years BP), respectively. CH_4 concentrations were generally low throughout the sampling season and only two dates were obtained, one 74 % modern (c. 2400 years BP), the other 101 % modern (0 years BP).

Using an age distribution model based on the atmospheric ^{14}C records prior to and since the ^{14}C bomb peak in the 1950's (modified from Evans et al. [2014]), we estimated the age of aquatic C that would otherwise be assumed to be "modern" using conventional radiocarbon dating. The results showed a close link between the age of aquatic CO_2 and DOC; DOC was between 4 and 346 years old (before sampling date), while CO_2 was between 3 and 312 years old.

Our results indicate that the age and source of DOC and CO_2 in headwater catchments in this area of the Arctic were similar and primarily derived from the

young, upper organic soil layers. There was, however, no indication of preferential mineralisation of older C in the aquatic phase, possibly due to the lack of an extremely ancient OC source, such as yedoma deposits, in the study region.

References

Evans, C.D.; Page, S.E.; Jones, T.; Moore, S.; Gauci, V.; Laiho, R.; Hruška, J.; Allott, T.E.H.; Billett, M.F.; Tipping, E.; Freeman, C. and Garnett, M.H. [2014]: Contrasting vulnerability of drained tropical and high-latitude peatlands to fluvial loss of stored carbon. *Global Biogeochemical Cycles*, 28 (11):1215–1234, doi:10.1002/2013GB004782.

Garnett, M.H.; Gulliver, P. and Billett, M.F. [2016]: A rapid method to collect methane from peatland streams for radiocarbon analysis. *Ecohydrology*, 9(1):113–121, doi:10.1002/eco.1617. ECO-14-0129.R1.

Modern and Holocene fluxes of sediment and organic matter into the Arctic Ocean

Michael Fritz[1,2] & Hugues Lantuit[1,3]

[1] *Alfred Wegener Institute, Helmholtz Centre for Polar and Marine Research, Potsdam, Germany*
[2] *Utrecht University, Department of Earth Sciences, Utrecht, The Netherlands*
[3] *University of Potsdam, Institute for Earth and Environmental Science, Potsdam, Germany*

Warming in the Arctic is expected to be roughly twice as high as the global mean. Sea ice extent is declining dramatically over the last years and favors accelerating coastal erosion. With erosion rates as high as 25 m yr^{-1}, the release of organic carbon and nutrients from permafrost coasts has dramatic impacts on the global carbon cycle, on nearshore food webs and local communities which are still relying on marine biological resources for food security.

During the Holocene, the delivery of sediments, nutrients, particulate organic carbon (POC) and dissolved organic carbon (DOC) varied in response to temperature and relative sea level changes. Phases of increased material input could serve as an analogue for future erosion scenarios. In the past, changing inputs of sediments, carbon, and nutrients may have altered the biogeochemical setting on the upper arctic shelves and may have impacted the global carbon cycle.

Recent flux estimates of sediment and POC from coastal erosion into the Arctic Ocean are 430 Tg yr−1 sediment and 4.9-14 Tg yr−1 POC, which is comparable to if not higher than riverine fluxes [Wegner et al., 2015]. However, the fate of sediments and organic carbon once eroded from the cliff remains largely unknown [Stein, 2004] and the release of DOC from melting ground ice in permafrost cliffs has not been considered yet [Fritz et al., 2015].

Material supply over the Holocene is difficult to quantify as it depends on erosion of a coastline whose original configuration is unknown. For example, large parts of the circum-arctic shelves were subaerially exposed during the last glacial maximum (LGM) and became flooded rapidly. Consequently, erosion of coastal permafrost deposits was probably stronger in the early Holocene than today and released more sediments, nutrients and carbon. In the middle Holocene sediment fluxes in the Laptev Sea for example were more variable than today, partly due to rising sea level, spatially and temporally variable flooding of bathymetric features, and coastline adjustments. With coastline retreat, the depocenters moved further southward and thereby successively reducing accumulation rates in the distal shelf areas. In other parts of the Arctic, however, glacio-isostatic rebound was significant so that global transgression was outpaced and therefore reduced shoreline retreat. Even after the modern sea-level highstand was approached around 5,000 cal BP, there is evidence that the depositional system on the shelves took time to stabilize [Bauch et al., 2001].

There are almost infinite possibilities to combine external factors determining the long-term pace of coastal erosion (e.g. climate variation, relative sea-level changes) with internal factors determining the vulnerability to coastal erosion (e.g. morphology, ground-ice content). Only a few of them can be directly measured or reconstructed throughout the Holocene. For the other factors, we need a conceptual model to start with. It is still unclear how much of the formerly dry shelf areas became subject to cliff and shoreface erosion or if they were simply flooded. The most reasonable assumption, though not quantitatively differentiated, is a combination of both processes. One the one hand, erosional discordances between late glacial terrestrial deposits and Holocene marine sediments indicate erosion. One the other hand, submarine permafrost from the LGM, which has not been eroded, is widespread too, and thus indicates preservation of terrestrial Pleistocene deposits after flooding.

In summary, quantitative estimates of erosion rates along Arctic coasts throughout the Holocene are still sparse and need substantial improvement to clarify the fate of terrigenous material in the Arctic Ocean. This is urgently needed to predict the potential impact of increasing erosion on the global climate, on regional ecosystem services and on local communities.

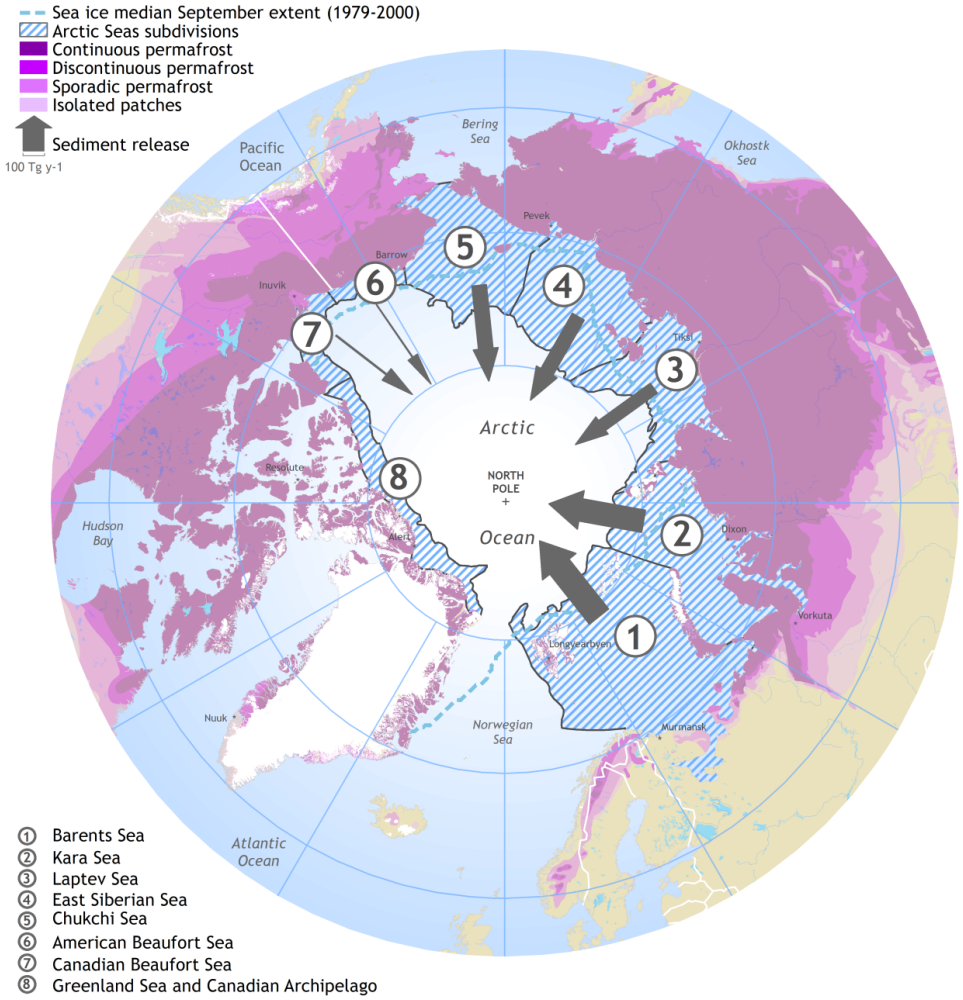

Figure 1: Modern sediment contribution (Tg y-1) from coastal erosion into the Arctic Ocean divided by marginal sea areas (Wegner et al., 2016)

References

Bauch, H.A.; Kassens, H.; Naidina, O.D.; Kunz-Pirrung, M. and Thiede, J. [2001]: Composition and Flux of Holocene Sediments on the Eastern Laptev Sea Shelf, Arctic Siberia. *Quaternary Research*, 55(3):344–351, ISSN 0033-5894. doi:10.1006/qres.2000.2223.

Fritz, M.; Opel, T.; Tanski, G.; Herzschuh, U.; Meyer, H.; Eulenburg, A. and Lantuit, H. [2015]: Dissolved organic carbon (DOC) in Arctic ground ice. *The Cryosphere*, 9(2):737–752, 2015. doi:10.5194/tc-9-737-2015.

R. & MacdonaldStein, R.W. [2004]: Organic carbon budget: Arctic Ocean vs. global ocean. In: R. & MacdonaldStein, R.W.(ed.), *The Organic Carbon Cycle in the Arctic Ocean*, pages 315–322. Springer. Berlin.

Wegner, C.; Bennett, K.E.; de Vernal, A.; Forwick, M.; Fritz, M.; Heikkilä, M.; łacka, M.; Lantuit, H.; Laska, M.; Moskalik, M.; O'Regan, M.; Pawłowska, J.; Promińska, A.; Rachold, V.; Vonk, J.E. and Werner, K. [2015]: Variability in transport of terrigenous material on the shelves and the deep Arctic Ocean during the Holocene. *Polar Research*, 34(0), ISSN 1751-8369. doi:10.3402/polar.v34.24964.

Dissolved organic matter properties in arctic coastal waters are strongly influenced by fluxes from permafrost coasts and by local meteorology

Michael Fritz[1,2], George Tanski[1,3], & Hugues Lantuit[1,3]

[1] *Alfred Wegener Institute, Helmholtz Centre for Polar and Marine Research, Potsdam, Germany*
[2] *Utrecht University, Department of Earth Sciences, Utrecht, The Netherlands*
[3] *University of Potsdam, Institute for Earth and Environmental Science, Potsdam, Germany*

Under future climate change scenarios, Arctic coastal waters are believed to receive higher terrestrial organic matter (OM) fluxes. Permafrost carbon is increasingly mobilized upon thaw from rivers draining permafrost terrain and from eroding permafrost coasts. Once received, the coastal waters are the transformation zone for terrestrial OM, although quantities, especially those of dissolved organic matter (DOM) released by coastal erosion, are largely unknown. This nearshore zone plays a crucial role in Arctic biogeochemical cycling, as here the released material is destined to be

1. mineralized into greenhouse gases,
2. incorporated into marine primary production,
3. buried in nearshore sediments or
4. transported offshore.

In this presentation, we show data on DOM quantities in surface water in the nearshore zone of the southern Beaufort Sea from two consecutive summer seasons under different meteorological conditions. Colored dissolved organic matter (cDOM) properties help to differentiate the terrestrial from the marine DOM component. Figure 1 shows DOC concentrations and salinities for 23 and 24 days in the summer seasons of 2013 and 2014, respectively. DOC concentrations in the nearshore zone of the southern Beaufort Sea vary between about 1.5 and 5 mg C L^{-1}. In the Lena River Delta, bay water, river water, and permafrost meltwater creeks yielded similar values between 5.8 and 5.9 mg C L^{-1} [Dubinenkov et al., 2015]. Similarly, Fritz et al. [2015] found DOC concentrations in ice wedges between 1.6 and 28.6 mg C L^{-1}.

In 2013, the first half of July was characterized by low salinity between 8 and 15 psu and high DOC concentrations of 3.5 to 5 mg C L^{-1}. Then, a sudden change in water properties occurred after a major storm which lasted for at least 2 days. This storm led to strongly decreased DOC (1.5 to 2.5 mg C L^{-1}) concentration and increasing salinity (14 to 28 psu) in surface water, probably due to upwelling In 2014, a more stable situation in both salinity and DOC prevailed, with relatively high salinity (23 to 29 psu) and low DOC concentration (1.5 to 2.5 mg C L^{-1}). This pattern was due to rather windy and wavy conditions throughout the whole season. The water column in 2014 was likely well-mixed and DOC-poor because saline waters have probably been transported from the offshore to the nearshore.

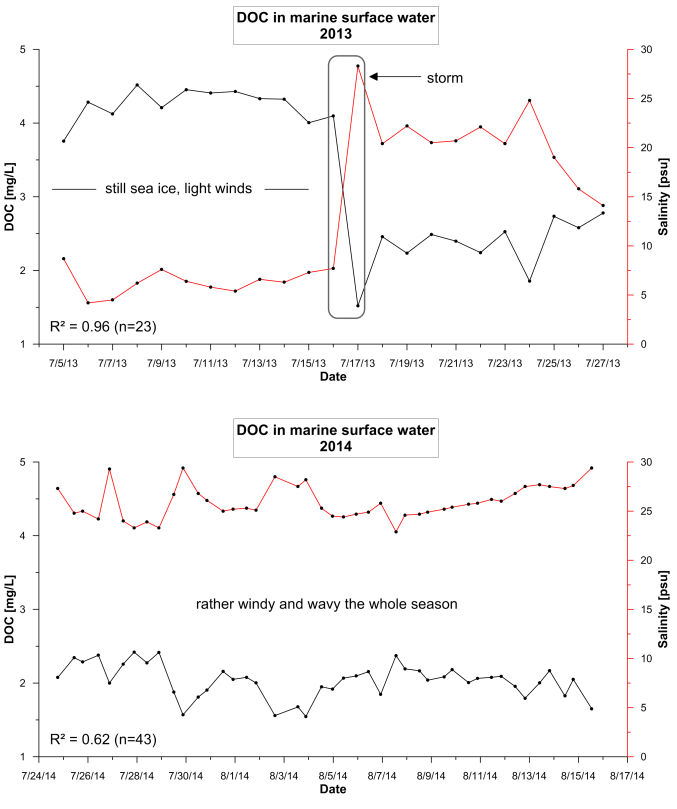

Figure 1: Dissolved organic carbon (DOC) and salinity of marine surface water in the southern Beaufort Sea (Canada) in 2013 and 2014. Correlation coefficient shows the relation between DOC and salinity. Major meteorological conditions are indicated.

We recognized a significant negative correlation

between DOC and salinity, independent from varying meteorological conditions. In general, this suggests a conservative mixing between DOC derived from terrestrial/permafrost runoff and marine DOC. The low salinity in July 2013 was probably due to prolonged sea-ice presence in the sampled area. This leads to the assumption that DOC also originates from melting sea ice. Quantitatively more important will be terrestrial runoff which is relatively rich in DOC. A stable stratification in the nearshore zone and calm weather conditions will increase the influence of terrestrial-derived DOM. The strength of the terrestrial influence can be estimated by salinity measures as they directly correlate with DOC concentrations; the lower the salinity the stronger the terrestrial influence.

We conclude that the terrestrial imprint of coastal erosion on DOM concentrations in the nearshore zone is significant. We see that DOC concentrations are significantly elevated also compared to riverine input in front of river mouths and deltas. Meteorological conditions play a major role for the strength of the terrestrial DOM signal, which can vary on short timescales. Our approach is different from ship-based oceanography because we study DOM that is directly derived from thawing permafrost coasts, explicitly excluding rivers. When qualifying DOM origin from permafrost landscapes apart from rivers we have to take into consideration the different DOM mobilization pathways.

1. Surface runoff and near-surface groundwater flow mainly drain and flush the active layer.
2. Melting ground ice releases DOM.
3. Ground ice meltwater leaches DOM from sedimentary OM upon permafrost thaw on land.
4. DOM is leached from sedimentary OM upon contact with sea water.

The latter three will mobilize old OM which is believed to be highly bioavailable (see Vonk et al. [2013a,b]).

References

Dubinenkov, I.; Flerus, R.; Schmitt-Kopplin, P.; Kattner, G. and Koch, B.P. [2015]: Origin-specific molecular signatures of dissolved organic matter in the Lena Delta. *Biogeochemistry*, 123(1):1–14, doi:10.1007/s10533-014-0049-0.

Fritz, M.; Opel, T.; Tanski, G.; Herzschuh, U.; Meyer, H.; Eulenburg, A. and Lantuit, H. [2015]: Dissolved organic carbon (DOC) in Arctic ground ice. *The Cryosphere*, 9(2):737–752, doi:10.5194/tc-9-737-2015. URL http://www.the-cryosphere.net/9/737/2015/.

Vonk, J.E.; Mann, P.J.; Davydov, S.; Davydova, A.; Spencer, R.G.M.; Schade, J.; Sobczak, W.V.; Zimov, N.; Zimov, S.; Bulygina, E.; Eglinton, T.I. and Holmes, R.M. [2013a]: High biolability of ancient permafrost carbon upon thaw. *Geophysical Research Letters*, 40(11):2689–2693, ISSN 1944-8007. doi:10.1002/grl.50348.

Vonk, J.E.; Mann, P.J.; Dowdy, K.L.; Davydova, A.; Davydov, S.P.; Zimov, N.; Spencer, R.G.M.; Bulygina, E.B.; Eglinton, T.I. and Holmes, R.M. [2013b]: Dissolved organic carbon loss from Yedoma permafrost amplified by ice wedge thaw. *Environmental Research Letters*, 8(3):035023, doi:10.1088/1748-9326/8/3/035023.

Dissolved organic matter export from forest-tundra ecotone of Siberia under discontinuous permafrost. Insights from high frequency acquisition in situ fluorescence of dissolved organic matter (fDOM)

Laure Gandois[1], Roman Teisserenc[1], Théo Ledantec[1], Anatoly Prokushkin[2], Stephane Binet[1], & Nikita Tananaev[3,4]

[1] *ECOLAB, Université de Toulouse, CNRS, INPT, UPS, France*
[2] *V.N. Sukachev Institute of Forest, SB RAS, Krasnoyarsk, Russia*
[3] *Melnikov Permafrost Institute, Siberian Branch, Russian Academy of Sciences, Yakutsk, Russia*
[4] *Ugra Research Institute of Information Technologies, Khanty-Mansiysk, Russian Federation*

Permafrost influenced watershed store half of the worldwide organic carbon stocks of soils. Dissolved organic matter (DOM) concentrations in rivers draining these watershed are high, and large amounts of organic carbon are exported by Arctic rivers to the Arctic Ocean [Amon et al., 2012]. In the context of permafrost alteration, understanding water and DOM origin at the outlet of these watersheds is critical. Indeed, DOM export originating from vegetation, soils, lake or groundwater from thawing permafrost have different implications in the perspective of establishing carbon budget for northern watersheds.

In permafrost influenced watersheds, DOM concentration and quality varies seasonally [Carey, 2003, Prokushkin et al., 2011]. This variability is related to different soils type contribution, different hydrological phases and changes in active layer depth. Classical surveys of DOM export in Arctic watershed imply monthly, weekly and in best cases daily analysis of DOM concentrations at the outlet of watersheds. However, processes controlling DOM export happen at finer timescales, including hours. Dissolved organic matter, composed of weak acids, holding aromatic functions presents natural fluorescence that can be measured in situ. Using these properties, it is therefore possible to survey with a high frequency DOM dynamic.

The study site is the catchment of Graviyka (323 km^2), a tributary of the Ienisei, in the surrounding of Igarka. The catchment is located in the transition zone between continuous and discontinuous permafrost and includes a variety of permafrost processes, with thermokarst and glacier lakes and palsas.

In 2015, it has been instrumented with a mutiparameter probe (including water level, temperature, dissolved oxygen, pH, turbidity, and fDOM (fluorescence of dissolved organic matter) at the outlet, acquiring data at an hourly time step. In order to evaluate watershed lakes contribution to the river, water level loggers have been installed in lakes of different geomorphological origin: one glacier Lake on the North bank and a thermokarst lake on the South bank.

Water level in lakes show contrasting trends. The glacier lake do not seem to be connected to the river. On the contrary, the thermokarst lake, part of a large peatland and thermokarst lake complex show a similar dynamic to the one recorded at the outlet of the Graviyka, revealing potential contribution to the Gravyjka River. Distinct temporal dynamics are observed for the different measured parameters. Temperature, pH and dissolved oxygen are governed by a diurnal cycle, whereas conductivity, turbidity and fDOM vary in relation with water level changes in the river.

A strong response of fDOM signal to water level rise in relation to rain events is observed. For example, in July, a sharp increase of fDOM (26 % in one day) is recorded following the rise of the water table. A slow (10 days) decrease follows, suggesting lateral inputs from soils and peatlands of the catchment. In addition, between June and the end of August, a strong increase of the baseline fDOM values is noticed, corresponding to DOC concentration increase from 11 to 19 mg L^{-1}.

The combined analysis of fDOM and other water parameters is critical to understand water and therefore carbon origin. In one hand, fDOM peaks induced by storm events are coupled with decreasing values of conductivity, indicating dilution and peatlands water contribution. On the other hand, the seasonal increase of baseline fDOM is coupled with a strong increase of

conductivity. This reveals the contribution of other water sources, potentially ground water originating from permafrost.

The high frequency and multiparameter acquisition of water quality at the outlet at the Graviyka catchment is building a novel dataset. It will contribute to the quantification of DOM fluxes and the understanding of DOM export controlling factors in permafrost affected watersheds.

References

Amon, R.M.W.; Rinehart, A.J.; Duan, S.; Louchouarn, P.; Prokushkin, A.; Guggenberger, G.; Bauch, D.; Stedmon, C.; Raymond, P.A.; Holmes, R.M.; McClelland, J.W.; Peterson, B.J.; Walker, S.A. and Zhulidov, A.V. [2012]: Dissolved organic matter sources in large Arctic rivers. *Geochimica et Cosmochimica Acta*, 94:217–237, doi:10.1016/j.gca.2012.07.015.

Carey, S.K. [2003]: Dissolved Organic Carbon Fluxes in a Discontinuous Permafrost Subarctic Alpine Catchment. *Permafrost and Periglacial Processes*, 14(2):161–171, doi:10.1002/ppp.444.

Prokushkin, A.S.; Pokrovsky, O.S.; Shirokova, L.S.; Korets, M.A.; Viers, J.; Prokushkin, S.G.; Amon, R. M.W.; Guggenberger, G. and McDowell, W.H. [2011]: Sources and the flux pattern of dissolved carbon in rivers of the Yenisey basin draining the Central Siberian Plateau. *Environmental Research Letters*, 6(4):045212, 2011. doi:10.1088/1748-9326/6/4/045212.

Dissolved Organic Matter export from forest-tundra ecotone of Siberia under discontinuous permafrost. Insights from high frequency acquisition in situ fluorescence of dissolved organic matter (fDOM)The formation of iron particles in the Lena River: Insights from iron isotopes (δ^{56}Fe), electron microscopy and X-ray spectroscopy

Catherine Hirst[1,2], Liselott Kutscher[1,2], Sam Shaw[3], Ian. T. Burke[4], Trofim Maximov[5], Melissa Murphy[6], Melanie Schmidtt[1], Carl-Magnus Mörth[2], Per. S. Andersson[1], & Don Porcelli[6]

[1] *Naturhistoriska Riksmuseet, Stockholm*
[2] *Department of Geological Sciences, Stockholm University*
[3] *Atmospheric and Environmental Sciences, University of Manchester*
[4] *School of Earth and Environment, University of Leeds*
[5] *International Center for BioGeoScience Education and Scientific Training (BEST) of North-Eastern Federal University*
[6] *Department of Earth Sciences, University of Oxford*

Boreal River iron particles are a crucial transport link between continent and ocean. In both systems, iron particles play a key role in i) electron transfer in biological processing, ii) trace elements (TE) and organic carbon (OC) transport. The bioavailability and transport of Fe particles is determined by their composition, particle size and associated phases. In this study we investigated the origin and transport of iron particles in the Lena River system, NE Russia. The catchment is dominated by continous permafrost containing cryotrubated mineral soils and Yedoma. We have analysed the

i size distribution,

ii mineralogy

iii chemical composition and

iv iron isotope composition of iron particles.

Samples were taken from major tributaries (draining the Central Siberian Plateau, Verkhoyansk Moutain Range, and South Aldan Shield) and the main channel in July 2012 and June 2013, following the spring flood.

Geochemical analysis of the particulate (>0.22 μm) and colloidal (<0.22 μm) fraction showed that >55 % of iron occurs in the particulate fraction. In contrast, >50 % of DOC occurs in the truly dissolved (<1 kDa) fraction. Transmission Electron Microscopy (TEM) was used to identify the composition of these Fe-rich particles and their associated phases on 10 samples. The following iron phases were identified in the particulate (>0.22 μm) fraction:

i poorly crystalline ferrihydrite;

ii crystalline heamatite,

iii Fe in clay minerals.

Transmission X-Ray Spectroscopy (STXM) was used to identify the association between Fe particles and OC. Ferrihydrite is observed to attach to the surface of primary produced (diatom tests, organic fibrils) particulate organic carbon (POC) in the central plateau. Whereas, ferrihydrite is trapped within an amorphous network of POC, in the tributaries draining mountain areas. In the main channel, ferrihydrite is mainly assocaiting with with clay minerals. Ferrihydrite was the only identified Fe particle in the colloidal (<0.22 μm) fraction and is not observed to complex with OC.

Ferrihydrite is the ubiquitous secondary mineral Fe phase in the Lena River main channel and major tributaries. The ferrihydrite is evident in the particulate and colloidal fraction. Hence, the particulate fraction from 36 sample stations was was leached to separate iron in the secondary minerals from the clay- bound iron and detrital iron oxides.

Iron isotope analysis was performed on the

i bulk particulate,

ii ferrihydrite,

iii detrital mineral,

iv colloidal fractions.

Tribuitaries draining mountain areas with low DOC concentrations show the lowest concentrations of particulate and colloidal ferrihydrite,. The ferrihydrite in these tributaries show positive δ^{56}Fe. In contrast, tributaries draining the central plateau which is dominated by wetlands, forest and high DOC, contain the highest concentrations of particulate and colloidal ferrihydrite. In these areas the ferrihydrite show negative δ^{56}Fe. The ferrihydrite concentrations and isotope composition in the Lena River main channel lie intermediate between these two end member regions.

We propose that ferrihydrite has two main origins in the Lena River catchment area: abiotic precipitation in tributaries draining mountainous terrain and biologically mediated precipitation in tributaries draining the low lying wetlands and forest.

Contrasting sources of dissolved and particulate organic matter along 62N – 72N in the Lena River

Emma S. Karlsson

Stockholm University, Bolin Centre of Climate Research, SE

The Lena River transports large amounts of sediment and dissolved organic matter to the shallow Laptev Sea, potentially releasing long-frozen organic carbon (OC) into the modern carbon cycle. We studied organic matter collected along a 1450 km section of the Lena River, from near 62° N to the deltaic region at 72° N, to better understand in-river processing of the terrestrial particulate and dissolved fractions in the river surface water. Carbon isotopes ($\delta^{13}C$ and $\delta^{14}C$) and plant wax lipid markers combine to reveal two distinct OC pools with different behavior in the river. The molar OC/total nitrogen (TN) ratios for particulate OC (POC) were low, suggesting contribution from (freshwater) plankton, but most of the POC was of old age (770-4500 ^{14}C years) which rather suggests a pre-aged origin - perhaps from erosion of riverbank permafrost material. Much in contrast, colloidal OC (COC) was young (20-440 ^{14}C years) and displayed a high OC/TN composition (23-56) with a steady $\delta^{13}C$ signal along the river course (-26.7 to -27.7).

There was an apparent absence of ice complex deposit permafrost (mineral soil/yedoma OC) in the COC fraction, and only small contributions to POC. The COC signal suggests contributions from contemporary plant detritus/surface soil OC. It seems as if pre-aged permafrost OC, potentially from riverbank erosion, partitions into the particulate pool and almost not at all to the dissolved OC (DOC) + COC pool. Degradation biomarkers indicate a highly degraded COC lipid pool and a less degraded POC.

DOC/COC and POC have clearly different terrestrial sources and different fates on their way to the shelf waters. Previously freeze-locked old permafrost OC remobilizes into the Lena River in particulate form which (at least temporarily) escapes degradation as it follows the river course seawards in a less degraded state.

Application of high resolution remotely sensed channel geometry to quantify lateral inflow gains through an arctic watershed

Tyler V. King, Bethany Neilson, Austin Jensen, Alfonso Torres-Rua, & Mitchell Rasmussen

Utah State University, United States of America

In high gradient portions of Arctic rivers surface heat fluxes and flow contributions from hillslopes compete for control of river temperature, a balance dictated in part by channel geometry and hillslope hydrology. A technique by which both channel geometry and lateral inflows (surface runoff and suprapermafrost subsurface flow) from adjacent hillslopes were evaluated through repeat, low cost high resolution remote sensing was developed. First, dry channel topography was extracted for a 35 km section of the Kuparuk River, AK through standard photogrammetric methods from aerial photography collected under low flow conditions. Subsequent flights provided spatially distributed estimates of wetted width that were used to estimate channel hydraulic properties (e.g., cross-sectional area, wetted perimeter, and water surface slope) over a range of flows. Discharge was then estimated at discrete locations over time using these extracted properties and standard hydraulic relationships. Estimated flows at these "synthetic" gaging stations were compared against four active gaging stations to determine accuracy of the procedure at discrete locations. Finally, based on differences in estimated flow longitudinally, lateral inflows were estimated at different spatial resolutions under a range of hydrologic conditions. From these data, we identified morphological features within the study reach that were suitable for use as synthetic gaging locations. Based on these findings and relationships, spatial and temporal understanding of changes in hydrologic responses in arctic basins can be extracted using only width estimates from imagery. This approach is most appropriate for arctic rivers due to highly dynamic flows and the remote nature of the landscape that impedes ground surveys.

Large spatial variations in export and sources of organic carbon in the Lena River basin, Siberia

Liselott M. Kutscher[1,2], Per S. Andersson[2], Carl-Magnus Mörth[1], Don Porcelli[3], Catherine Hirst[1,2], & Trofim Maximov[4]

[1] *Department of Geological Sciences, Stockholm University, 10691 Stockholm, Sweden*
[2] *Swedish Museum of Natural History, Department of Geosciences, Stockholm, Sweden*
[3] *Department of Earth Sciences, University of Oxford, Oxford, UK*
[4] *International Center for BioGeoScience Education and Scientific Training of North-East Federal University, Yakutsk, Republic of Sakha (Yakutia), Russia*

Permafrost areas are expected to experience large changes in export of riverine natural organic matter (NOM) due to climate warming. The Lena River basin, which is one of the largest contributor of organic carbon (OC) to the Arctic Ocean, is mainly underlain by continuous permafrost. This area is vulnerable to climate driven permaforst thawing, with possible future changes in OC fluxes. Previous research of NOM in the Lena River basin has mainly focused on the main channel of the Lena River or the delta.

Here we present a spatial dataset on annual export and fluxes of total organic carbon (TOC), as well as the main sources of dissolved organic matter (DOM) and particulate organic matter (POM) collected in the main channel of the Lena River and 40 different tributaries within the Lena River basin.

The annual export and fluxes, based on concentration data of DOC and POC and long term discharge data, showed large geographical variations related to differences in precipitation and catchment topography.

Stable carbon isotopes and C/N ratios showed that the primary sources of DOM were terrestrial plant debris and soil organic matter (SOM), while POM was a mixture between SOM and aquatic primary produced material. The sources of DOM indicated differences in water flow paths, with permfrost probably restricting water flow paths to topsoils in the samples collected earlier in the summer, while allowing deeper infiltration in late summer.

This study shows that the export, fluxes and sources of NOM are spatially variable within the Lena River basin. These results could influence current and future interpretations of the regional carbon cycle.

Dissolved organic matter flux, characterization and dynamic in the Yenisei river

Théo Aurélien Le Dantec[1,2], Roman Teisserenc[1,2], Allison Myers-Pigg[3], Patrick Louchouarn[3,4], Nikita Tananaev[5], Laure Gandois[1,2], & Jean-Luc Probst[1,2]

[1] *Université de Toulouse, INP, UPS, EcoLab (Laboratoire Ecologie Fonctionnelle et Environnement), ENSAT, Avenue de l'Agrobiopole, 31326 Castanet Tolosan, France*
[2] *CNRS , EcoLab , 31326 Castanet Tolosan, France*
[3] *Texas A& M University, Department of Oceanography, College Station, Texas USA*
[4] *Texas A& M University at Galveston, Department of Marine Sciences, Galveston, Texas USA*
[5] *Russian Academy of Science- Siberian Branch, Melnikov Permafrost Institute, Igarka Geocryology Laboratory, Igarka, Krasnoyarsk Krai, Russia*

High latitude ecosystems comprise the largest organic carbon pool on earth. The main stock is estimated around 1700 Pg in soils and represents about half of the global soil organic carbon. Most of this carbon is currently trapped in permafrost soils, however Arctic regions are experiencing high warming rates compared to other regions. Changes in temperature and moisture conditions may impact the fate of organic matter by influencing biomass production, permafrost stability (Active layer depth and extent), peat formation and decomposition, and the frequency of wild fires. Arctic rivers drain this immense carbon reservoir and deliver from 25 to 36 Tg-C yr^{-1}in the form of dissolved organic carbon (DOC) to the Arctic Ocean. This ocean receives, on a volume basis, the most important terrestrial organic matter input. How the riverine export of terrestrial organic matter will respond to climate change is still highly uncertain. Eurasian watersheds cover the most part of the Arctic (more than 76 %) and dominate the organic carbon exports but few data exist about DOC fluxes especially in the large Siberian rivers. Further, information concerning the quality of the DOC exported by Arctic Rivers is very scarce.

Our work focuses on the Yenisei river basin, the largest Arctic watershed ($2{,}54 \times 10^6$ km^2), which includes 36 to 55 % of permafrost and vegetation ranging from tundra, mixed taiga and pine forest from north to south. Intensive sampling (from daily to fortnightly basis) of the Yenisei river water has been performed in 2014 and 2015 close to the river outlet. This location provides an integrated and global signal of the organic carbon exported. A special attention has been given to capture the spring freshet. This specific period is key for Arctic river basins and is known to be crucial for organic matter export from terrestrial to aquatic and marine ecosystems (up to 70 % of the annual export). Huge volumes (100L) of water have been collected and processed by tangential flow filtration (0.45 μm) combined to reverse osmosis to concentrate the DOC fraction (around tenfold). The samples obtained were then freeze-dried. This process allows us to recover enough material (hundreds of mg) to conduct molecular, isotopic and nuclear magnetic resonance analysis to infer potential sources and degradation state of the organic carbon.

Until now, very few studies captured the spring flood at a high temporal resolution, thus sampling effort on this period is particularly valuable to refine flux estimates and our understanding of DOC dynamic. We evaluate the DOC flux in 2014 from the Yenisei watershed around 5,30 Tg yr^{-1}, slightly superior to previous estimates of 4,69 Tg yr^{-1} [Raymond et al., 2007, Holmes et al., 2012] and 5,08 Tg yr^{-1} [Amon et al., 2012]. The only period of May/June (freshet) contributed to 70 % of the total DOC export in 2014, with an increase of DOC concentration of more than sixfold between low and peak flow. Lignin export reached 55 Gg yr^{-1}, with more than 90 % of the total flux exported during may and june 2014 and a tenfold increase between low and peak flow. We recorded significant variations in organic matter quality during the freshet with an increase of fresh and low decomposed matter exported during the highest discharge (based on lignin oxidation product biomarkers). Low Syringyl/Vanillyl and Cinnamyl/Vanillyl ratios indicate that gymnosperm wood is the main source for lignin during the spring flood of the Yenisei,

reflecting the dominant vegetation of the watershed.

References

Amon, R.M.W.; Rinehart, A.J.; Duan, S.; Louchouarn, P.; Prokushkin, A.; Guggenberger, G.; Bauch, D.; Stedmon, C.; Raymond, P.A.; Holmes, R.M.; McClelland, J.W.; Peterson, B.J.; Walker, S.A. and Zhulidov, A.V. [2012]: Dissolved organic matter sources in large Arctic rivers. *Geochimica et Cosmochimica Acta*, 94:217–237, doi:10.1016/j.gca.2012.07.015.

Holmes, R.M.; McClelland, J.W.; Peterson, B.J.; Tank, S.E.; Bulygina, E.; Eglinton, T.I.; Gordeev, V.V.; Gurtovaya, T.Y.; Raymond, P.A.; Repeta, D.J.; Staples, R.; Striegl, R.G.; Zhulidov, A.V. and Zimov, S.A. [2012]: Seasonal and Annual Fluxes of Nutrients and Organic Matter from Large Rivers to the Arctic Ocean and Surrounding Seas. *Estuaries and Coasts*, 35(2):369–382, doi:10.1007/s12237-011-9386-6.

Raymond, P.A.; McClelland, J.W.; Holmes, R.M.; Zhulidov, A.V.; Mull, K.; Peterson, B.J.; Striegl, R.G.; Aiken, G.R. and Gurtovaya, T.Y. [2007]: Flux and age of dissolved organic carbon exported to the Arctic Ocean: A carbon isotopic study of the five largest arctic rivers. *Global Biogeochemical Cycles*, 21(4), doi:10.1029/2007GB002934.

Arctic river organic carbon export through the ice-free season: isotopic and compositional analyses of DOM and POM collected in the Lena Delta between May and August 2014

Gesine Mollenhauer[1,2], Maria Winterfeld[1], Luca Bodenstab[2], Carl-Magnus Mörth[3], Boris Koch[1], Birgit Heim[1], Jens Hefter[1], Anatoly Prokushkin[4], & Janet Rethemeyer[5]

[1] *Alfred-Wegener-Institute, Germany*
[2] *University of Bremen, Germany*
[3] *Stockholm University, Sweden*
[4] *Sukachev Institute of Forest, Russia*
[5] *University of Cologne, Germany*

Arctic rivers are known to export large quantities of carbon by discharge of dissolved and particulate organic matter, and in a warming and progressively moister Arctic, these exports may increase resulting in a reduction of continental carbon stocks in the region. In particular, mobilization of fossil carbon from terrestrial reservoirs, stored predominantly in Yedoma deposits, will result in a net carbon loss. Therefore, the radiocarbon (^{14}C) contents of carbon exported via rivers are of great interest to understand the on-going processes.

Recent work has shown that both particulate and dissolved organic matter exported by the Lena, one of the great rivers draining Siberian permafrost regions into the Laptev Sea, consists of a complex mixture of material derived from multiple sources (e.g., Winterfeld et al. [2015], Dubinenkov et al. [2015]). Organic matter derived from the different sources likely differs in its reactivity once released from the frozen deposits into the river waters. For example, it has been shown that ancient carbon is very rapidly respired, leading to predominantly modern ^{14}C signatures of dissolved organic carbon (DOC) in Arctic river waters discharged to the ocean [Mann et al., 2015].

Arctic rivers are characterized by highly variable discharge rates with a pronounced maximum during the spring freshet associated with highest concentrations of DOC and particulate organic carbon (POC). Most studies investigating the isotopic composition and quality of carbon exported by Arctic rivers, however, rely on samples taken in summer during base flow, which is due to the logistical challenges associated with sampling in the remote Siberian permafrost regions. Here we present a record of $\delta^{13}C$ and $\Delta^{14}C$ of DOC and POC collected between late May during the freshet and late August 2014 in the Lena Delta, and compare them with δ13C and $\Delta^{14}C$ of DOC and POC sampled in central Siberia. The latter represent the hinterland of the large rivers, while the Lena Delta data are considered to contain an integrated signal of the watershed. The central Siberian POC is generally younger than the Lena Delta POC in spring. Throughout spring and summer, POC becomes progressively older in central Siberia, while an initial trend towards older values in the spring samples from the Lena Delta is reversed in summer, associated with a shift towards more depleted δ13C values. We interpret these aging trends as reflecting progressive thawing throughout the ice-free season, resulting in mobilization of progressively older carbon from deeper thawed layers. The summer reversal indicates admixture of fresh organic matter.

We furthermore analysed the biomarker composition of Lena Delta particulate organic matter collected in spring and summer. From spring to summer, we observe trends in abundance of individual leaf-wax derived biomarkers indicating higher abundance of algal biomass in the summer particles. Trends in biomarkers associated with soil microbes suggest a shift in sources through the ice-free season. Our data illustrate that considering the seasonal evolution of carbon discharge from Arctic rivers will be required to understand the underlying mechanisms and to predict future changes.

References

Dubinenkov, I.; Flerus, R.; Schmitt-Kopplin, P.; Kattner, G. and Koch, B.P. [2015]: Origin-specific molecular signatures of dissolved organic matter

in the Lena Delta. *Biogeochemistry*, 123(1):1–14, doi:10.1007/s10533-014-0049-0.

Mann, P.J.; Eglinton, T.I.; McIntyre, C.P.; Zimov, N.; Davydova, A.; Vonk, J.E.; Holmes, R.M. and Spencer, R.G.M. [2015]: Utilization of ancient permafrost carbon in headwaters of Arctic fluvial networks. *Nature Communications*, 6, URL 10.1038/ncomms8856.

Winterfeld, M.; Goñi, M. A.; Just, J.; Hefter, J. and Mollenhauer, G. [2015]: Characterization of particulate organic matter in the Lena River delta and adjacent nearshore zone, NE Siberia – Part 2: Lignin-derived phenol compositions. *Biogeosciences*, 12(7):2261–2283, doi:10.5194/bg-12-2261-2015.

Hydrochemical assessment of water quality characteristics in frost mound bogs impacted by gas industry

Anna S. Mysina & Tatiana M. Potapova

Saint-Petersburg state university, Russian Federation

The aim of this study was the to analyze observational data on water quality of streams for the areas of gas deposits in permafrost area of Western Siberia for period of open channel flow over a longer period of time (2003 - 2014 years) on the example of the Medvezhe deposit.

The hydrochemical assessment of the Medvezhe deposit was conducted on the basis of statistical analysis of data by main indicators of a chemical composition of river and lake waters (pH, total mineralization, main ions, weighed substances, dissolved oxygen, chemical oxyden demand, biochemical oxygen demand over a 5-day period (BOD5), nutrients, heavy metals, mineral oil, synthetic surfactant and phenols). The modern anthropogenically modified range of background chemical components for rivers and lakes for the deposit for the ice-free period of the year was estimated.

The obtained data on the chemical composition of the waters indicate the tension of the modern hydrochemical background of rivers and lakes at the Medvezhe deposit, which is determined by their reduced natural ability to cleanse itself.

All identified features of the chemical composition of river waters draining the studied bogs, should be the basis for the development of conservation measures for all deposits located in continuous permafrost area of Western Siberia.

Contribution of permafrost degradation landforms to summer export of DOC from Yedoma-type Ice Complex to rivers, Lena Delta, Siberia

Anne Morgenstern[1], Lydia Polakowski[1,2], Antonina Chetverova[3,4], Antje Eulenburg[1], Irina Fedorova[4,3], Tatyana Skorospekhova[4], Olga Bobrova[3], Birgit Heim[1], Julia Boike[1], & Paul Overduin[1]

[1] *Alfred Wegener Institute Helmholtz Centre for Polar and Marine Research, Germany*
[2] *University of Potsdam, Institute of Earth and Environmental Science, Potsdam, Germany*
[3] *Saint Petersburg State University, Russia*
[4] *Arctic and Antarctic Research Institute, St. Petersburg, Russia*

Thermo-erosional landforms (valleys, gullies) and their associated streams are the main connecting pathways between inland permafrost areas and rivers and coasts. Surface and ground waters are routed along these streams, which transport particulate and dissolved matter from the catchments to the rivers and coastal waters. Regions of ice-rich permafrost, such as the Yedoma-type Ice Complex, are not only characterized by a high abundance of thermo-erosional landforms, which formed during the Holocene, but are subject to extensive degradation under current arctic warming by processes such as thermal erosion, thermokarst, and active layer deepening. In the Siberian Lena River Delta Yedoma-type Ice Complex deposits occur on insular remnants of a Late-Pleistocene accumulation plain that has been dissected by Lena River branches and degraded by thermal erosion and thermokarst during the Holocene. This region serves as suitable exemplary study area for estimating the contribution of 1) different permafrost degradation landforms to the export of water and dissolved matter from Yedoma-type Ice Complex to the river and 2) active degradation of old permafrost versus seasonal runoff from the surface and active layer. In the summers of 2013 and 2014 we sampled surface and soil waters from streams and their watersheds in Yedoma-type Ice Complex landscapes of the Lena River Delta and analyzed them for a range of hydrogeochemical parameters including electrical conductivity (EC), dissolved organic carbon (DOC) and stable isotopic composition. The sampling sites were spread over an E-W-extent of about 150 km and are characterized by very diverse geomorphological and hydrological situations in terms of distance to the river branches, catchment size, discharge, degree of thermo-erosional activity, and connection to other permafrost degradation landforms (thermokarst lakes and basins). Three key sites were sampled three and four times from June to September 2013 and 2014, respectively, in order to analyze intra-seasonal changes.

The results show large variances in EC (25 to 1205 μS/cm), DOC concentrations (2.9 to 119.0 mg/l), $\delta^{18}O$ (-29.8 to -14.6 ‰ vs. SMOW), and δD (-228.9 to -117.9 ‰ vs. SMOW) over the whole dataset, with distinct characteristics in the parameter combination for different degradation landform and water types. The temporal variability at the repeatedly sampled sites is low, which implies that there is not much change in the processes that determine the water composition throughout the summer season. By comparing differences in surface water chemistry between flow path systems that tap into varying amounts of source water (precipitation, surface and ground water, ground ice) and have differing residence times and extents, we explore the effect of future changes in thermokarst and thermo-erosional intensity and resulting changes in flow path hydrogeochemistry for thermo-erosional features draining ice-rich permafrost.

Summer surface water chemistry dynamics in different landscape units from Yedoma Ice Complex to the Lena River

Lydia Polakowski[1,2], Anne Morgenstern[1], Julia Boike[1], Niko Bornemann[1], & Paul Overduin[1]

[1] *Alfred Wegener Institute Helmholtz Center for Polar and Marine Research, Potsdam, Germany*
[2] *University of Potsdam, Institute of Earth and Environmental Science, Potsdam, Germany*

The effect of climate warming on the degradation of permafrost in Arctic coastal lowlands and associated hydrological and biogeochemical processes varies between different types of permafrost deposits. The Lena River Delta consists of three geomorphological main terraces that differ in their genesis and stratigraphic, cryological, geomorphological and hydrological characteristics. The third terrace was formed during the late Pleistocene and consists mainly of Yedoma-type Ice Complex deposits, whereas the first terrace has formed during the Holocene by deltaic processes. Permafrost degradation on both terraces releases dissolved organic carbon (DOC) to thermokarst lakes and via streams DOC gets transported to the Lena River channels and the Arctic Ocean. This presentation shows

1. differences in the surface water chemistry between the first terrace and the Yedoma Ice Complex and their landforms,
2. analyses of the temporal variability of DOC during the summer, and
3. an estimation of summer DOC flux for the considered catchment of about 6.45 km^2.

Between June and September 2013 and 2014, respectively summer surface water and soil water samples were collected in a small catchment in the south of Kurungnakh Island in the central Lena River Delta. This catchment covers the first terrace as well as the Yedoma Ice Complex and is characterized by thermokarst lakes and streams on both terraces. Two weirs were installed in the main stream along the drainage flow path to continuously measure discharge during summer 2013. We divided the study area into landscape units and compared pH, electrical conductivity, stable isotopic composition and DOC concentrations between units and between terraces. The considered landscape units are streams and thermokarst lakes on Yedoma Ice Complex and on the first terrace, Yedoma uplands, streams, which are fed by the Ice Complex, a relict lake on the first terrace and the Olenyokskaya Channel, a main branch of the Lena River.

DOC concentrations in the landscape units on Yedoma Ice Complex ranged between 3.5 mg L-1 (streams) and 52.5 mg L^{-1} (soilwater of Yedoma uplands) and on the first terrace between 2.8 mg L^{-1} (streams) and 15.6 mg L^{-1} (relict lake). The electrical conductivity on Yedoma Ice Complex ranged between 35 µS cm-1 (soilwater of Yedoma uplands) and 151 μS cm^{-1} (streams) and on the first terrace between 54 μS cm^{-1} (streams and relict lake) and 140 µS cm^{-1} (streams). $\delta^{18}O$ values on Yedoma Ice Complex and first terrace ranged between -22.4 ‰ (soilwater of Yedoma uplands) and -16.4 ‰ (streams) and between -20.4 ‰and -14.7 ‰ (streams), respectively. δD ranged between -165.6 ‰ (soilwater of Yedoma uplands) and 125.5 ‰ (streams, which are fed by the Ice Complex) and between -160.8 ‰ and -119.4 ‰ (streams). Source waters on the Yedoma Ice Complex had higher DOC concentrations and lower electrical conductivity than Yedoma Ice Complex thermokarst lakes and the drainage flow path. This suggests that more labile organic carbon, perhaps derived from permafrost degradation on the Yedoma Ice Complex, enriches the lake but is removed from the lake, for example, by mineralization in the water column. Along the drainage flow path no further decrease of DOC concentration was observed, despite increasing discharge from weir 1 at the beginning of the flow path to almost two and a half times at weir 2 at the end of the flow path, and despite decreasing discharge during the measuring period from 1814 m^3 d^{-1} in the end of July to 199 m^3 d^{-1} in the end of August for weir 1 and from 2819 m3 d^{-1} in the end of July to 567 m^3 d^{-1} in the end of August for weir 2.

The temporal variability of DOC concentration during the sampling periods was low. In 2013 one sample site of soil water collection fluctuated slightly in Au-

gust between 10.5 mg L^{-1} and 13.3 mg L^{-1}, whereas the remaining landscape units showed no temporal variability. In 2014 the DOC concentration of the relict lake on the first terrace decreased from July (13.5 mg L^{-1}) to September (11.1 mg L^{-1}). Otherwise there were no changes in DOC concentration in the remaining landscape units. DOC measurements of the Olenyokskaya Channel show a decrease in DOC concentration from 12.4 mg L^{-1} in June to 7.6 mg L^{-1} in September.

Using discharge data of 2013 a summer DOC flux of about 220 kg in 29 days for the study site above weir 2 with an area of 6.45 km^2 was calculated.

Contribution of retrogressive thaw slumps to the near shore carbon budget along the Yukon Coast, Canada

Justine L. Ramage[1,2], Anna M. Konopczak[1,2], Anne Morgenstern[1], & Hugues Lantuit[1,2]

[1] *Alfred Wegener Institute Helmholtz Centre for Polar and Marine Research, Potsdam, Germany*
[2] *University of Potsdam, Institute of Earth and Environmental Science, Potsdam, Germany*

The mechanism of carbon dioxide and methane release to the atmosphere in permafrost regions is not solely restricted to the progressive thawing of the upper part of the ground by warmer air temperatures. Organic carbon and nutrients are released to streams, rivers or coasts by abrupt processes such as thermokarst, thermal erosion and simply river bank or coastal erosion.

Thermo-erosion, as a mechanism of rapid permafrost thaw, reshapes Arctic coasts and has a clear impact on the mobilization and distribution of carbon and nitrogen in permafrost terrains. Retrogressive thaw slumps are one specific and highly dynamic landform, which results from thermo-erosion of ice-rich permafrost and leads to the displacement of large volumes of sediments. Studies reporting on the occurrence and evolution of retrogressive thaw slumps over the Arctic show that in varied Arctic areas, slumps have increased over the last decades. While the processes responsible for the initiation of retrogressive thaw slumps are well defined, little research has been done on a regional scale to define the terrains on which they occur, and to measure the volumes of sediments eroded through their development. There are currently no estimates of the contribution of these permafrost degradation landforms to the carbon budget, therefore thermo-erosional features are not yet accounted in the carbon models. With this study, we highlight the important contribution of retrogressive thaw slumps to the nearshore carbon cycle in the eastern part of the Beaufort Sea by

1. measuring their dynamics on a ca. 105 km coastline along the Yukon Coast over the last 60 years (1952-2011);
2. determining the prevailing factors accounting for their distribution and driving their expansion; and
3. estimating the amounts of carbon mobilized by measuring the eroded volumes of sediment associated with retrogressive thaw slump development.

We used a large set of high-resolution multispectral satellite images from 2011 (GeoEye and WorldView) for geocoding aerial photographs from the 1950s and the 1970s, using the software OrthoEngine (PCI Geomatica). This dataset was the basis for manually digitizing and classifying retrogressive thaw slumps according to morphological characteristics. We gathered additional observations during fieldwork in July and August 2015 on the current development stage of retrogressive thaw slumps and classified them (active and eroded; active and partially vegetated or stabilized). Based on remote sensing, we calculated and compared the surface area occupied by slumps in the 1950s, the 1970s and in 2011. We used principal component analyses to highlight the main environmental factors involved in the development of those landforms. Based on a simple model, we computed the volume of eroded sediments and estimated the amounts of mobilized particulate organic carbon and nitrogen. This model allowed us to measure the contribution of retrogressive thaw slumps to the near shore carbon budget in the area.

Hydrological fluxes of carbon within the Yenisei River basin: A multi-scale study

Anatoly S. Prokushkin[1], Rainer M. Amon[2], Mikhail A. Korets[1], Gesine Mollenhauer[3], Maria Winterfeld[3], Marina P. Prokushkina[4], Roman Teisserenc[5], Laure Gandois[5], William H. McDowell[6], Lyudmila S. Shirokova[7], Jan Karlsson[8], Oleg S. Pokrovsky[7], & Martin Heimann[9]

[1] *VN Sukachev Institute of Forest SB RAS, Russian Federation*
[2] *TAMUG, Texas 77553, USA*
[3] *AWI, D-27570 Bremerhaven, Germany*
[4] *Siberian Federal University, Krasnoyarsk 660041, Russia*
[5] *EcoLab, Observatoire Midi-Pyrenees, 31400 Toulouse, France*
[6] *University of New Hampshire, NH 03824 USA*
[7] *GET, Observatoire Midi-Pyrenees, 31400 Toulouse, France*
[8] *Umeå University, Abisko SE-981 07, Sweden*
[9] *MPI-BGC, 07745 Jena, Germany*

The Yenisei River drainage basin is the second largest and most diverse Arctic River watershed in terms of tributary watershed characteristics. It has the largest annual water discharge and total carbon export among all Arctic rivers. The documented increase in water discharge over the last decades along with observed positive relationships between discharge and carbon export suggest increasing carbon fluxes with an intensifying hydrological cycle in these high latitude watersheds. However, the understanding of processes involved in carbon mobilization and their response to climate warming within the Yenisei River catchment is highly complicated because its diverse subwatersheds vary with respect to climate, permafrost distribution, topography, soil types and vegetation.

Our research program combines seasonal observations of water and C fluxes in watersheds and tributaries (north of 58°N) representing most vulnerable zones within the Yenisei basin with an analysis of C flux evolution in the Yenisei River main channel as well as quantitative and qualitative estimates of carbon exported to the Arctic Ocean. The overarching goal of our study is to better understand how climatic, geological, pedogenic and biological processes interact to control C losses from terrestrial ecosystems to the aquatic environment. Specifically, we address the following questions:

1. what are the spatial and temporal variations of C export among tributaries within the Yenisei River catchment,
2. how do seasonal changes in flow paths and sources control C species yield,
3. how do climatic variables and permafrost affect C species export, and
4. what are the most important factors affecting the net hydrologic export of C species from the Yenisei River catchment.

Characterization of riverine C fluxes focuses on quantification of different C species, including dissolved organic (DOC) and inorganic carbon (DIC), particulate organic carbon (POC), dissolved carbon dioxide and methane and their respective isotopic, elemental, optical and molecular level composition, where appropriate.

As with all boreal rivers, the dominant portion of annual runoff in the Yenisey basin occurs during freshet when the accumulated snow pack melts in a relatively short period. Along with highest discharges there is a considerable enrichment of river waters with dissolved and particulate organic matter and, thus, the freshet constitutes up to 70 % of the annual C fluxes. However, there is a large spatial variation of C concentrations (e.g. 6-35 mg DOC/L) among tributaries draining landscapes with distinct hydrologic flow paths and water retention times. In particular, the highest concentrations of dissolved and particulate organic carbon are observed within permafrost terrains of the Central Siberian Plateau where only a small portion of snowmelt water may infiltrate the frozen

ground and rivers receive surface runoff that solely interacted with C-rich organic layers. Similarly, highest intra-seasonal fluctuations of C fluxes during summer-fall season occur within the permafrost-dominated area and are induced by rainstorm events. During summer drought/lowflow conditions substantial release of C is only observed in tributary watersheds with extensive peatland areas with a predominance of dissolved organic matter.

Headwaters of major tributaries show the highest concentrations of DOC, but DOC concentrations tend to decrease towards the mouths supporting the idea of significant carbon processing in water bodies during transport. However, another important complicating factor for decreased DOC concentrations in large Siberian rivers is a dilution with low-DOC waters originating from watersheds recently affected by wild-fires. The role of fires in modulating and partitioning of riverine C fluxes is substantial, as about 1 % of the watershed area is affected by wild-fires annually.

Our data indicate the important role of landscape properties and regional climate for carbon accumulation and export fluxes. Precipitation and water residence time, which is largely modulated by permafrost cover, control the lateral carbon export as well as the extent of respiratory carbon losses between carbon mobilization from the watersheds and discharge to the Arctic Ocean. However, the complex interactions involved in production, mobilization, transport and degradation of C in riverine systems require further multi-scale studies, including the gaseous C species (CO_2 and CH_4) and integrated modelling studies to understand and predict future changes to the boreal and Arctic carbon cycle.

Riverine carbon flux in permafrost terrains of Central Siberian Plateau

Irina V. Tokareva[1], Anatoly S. Prokushkin[1], Roman A. Kolosov[1], Sergey V. Titov[1], Lyudmila S. Shirokova[2], Oleg S. Pokrovsky[2], & Amon M. Rainer[3]

[1] *V.N. Sukachev Institute of Forest, Russian Federation*
[2] *GET, Observatoire Midi-Pyrenees,14, avenue Edouard Belin, 31400 Toulouse, France*
[3] *TAMUG, 1001 Texas Clipper Road, Galveston, Texas 77553, USA*

The role of Siberian watersheds underlain by permafrost in global element cycling is becoming increasingly important as permafrost degrades at high latitudes. In the present study, we examined variations in concentrations, fluxes and partitioning of C species in rivers of the Central Siberian Plateau, whose watersheds are characterized by different extent of continuous permafrost distribution, temperatures and vegetation types. The objectives of the study were to use continuous measurements of river water C concentrations and hydrology to trace major processes controlling losses of dissolved organic carbon (DOC), dissolved inorganic carbon (DIC) and particulate organic carbon (POC) from terrestrial ecosystems in this peculiar environment. Further we have analyzed 8 largest rivers draining northern and southern portions of the Central Siberian Plateau aiming to analyze climatic influences on C fluxes as selected basins are relatively monolithologic (flood basalts and tuffs). Like for other rivers of the pan-arctic region, relatively short snowmelt dominated annual fluxes of C (64-82 %). In contrast to the major Arctic rivers, DOC was the dominant component of terrestrial C released to rivers on the annual basis. Spatial analysis of riverine C behavior demonstrated steady decrease of both DOC and DIC concentrations with the decreased mean annual air temperature (MAAT) averaged for entire basins. The increasing coverage of conifer forests on the river watersheds within the Central Siberian Plateau is leading to increased dissolved OC flux to rivers. Particularly correlation between dissolved lignin concentrations and DOC as well as the dominance of vanillyl derivatives (lignin of conifers) in rivers of Central Siberia point out the importance of larch taiga biome in production and export of DOC to the Arctic Ocean. Annual dissolved carbon fluxes (sum of DOC and DIC) in the analyzed rivers of the Central Siberian Plateau varied from 3.0 to 9.9 gC/m2/year and tended to increase southward. Our findings suggest the growth of both DOC and DIC concentrations in the northernmost basins of Central Siberia with northward shift of the tree-line, increasing Net ecosystem productivity and weathering rates.

Permafrost carbon degradation and transport pathways at thermokarst coasts in the Arctic

George Tanski[1,2], Saskia Ruttor[1,2], Hugues Lantuit[1,2], Christian Knoblauch[3], Boris Radosavljevic[1,2], Justine Ramage[1,2], Gesine Mollenhauer[4], Jens Strauss[1], & Michael Fritz[1]

[1] *Alfred Wegener Institute Helmholtz Centre for Polar and Marine Research, Potsdam, Germany*
[2] *Potsdam University, Institute of Earth and Environmental Sciences, Potsdam, Germany*
[3] *University of Hamburg, Institute of Soil Science, Hamburg, Germany*
[4] *Alfred Wegener Institute Helmholtz Centre for Polar and Marine Research, Bremerhaven, Germany*

Climate change has a strong impact on permafrost coasts in the Arctic. With increasing air and water temperatures, ice-rich permafrost coasts will thaw, which will lead to enhanced thermokarst and erosion. Upon erosion, large amounts of organic carbon previously stored for thousands of years are remobilized and either emitted as greenhouse gases to the atmosphere, redeposited within the landward nearshore zone, or released into the ocean. Yet, little is known about carbon degradation before the organic matter enters the nearshore zone of the ocean. The objective of this study was to investigate these processes at ice-rich thermokarst coasts, by focusing on retrogressive thaw slumps. The study aimed at determining the quantity of organic carbon and nitrogen in undisturbed and non-disturbed (thermokarst affected) coastal stretches, to detect its degradation and accumulation pattern after thawing, as well as its fate in the nearshore of the ocean.

A retrogressive thaw slump located on Herschel Island (Yukon Territory, Canada) was sampled systematically along transects from the undisturbed parts (tundra, permafrost headwall) to disturbed parts (mudpool and slump floor) and the nearshore zone (marine sediments). These thermokarst landforms are ideal study sites as they spatially expose different transport and accumulation stages of thawed permafrost sediments before entering the ocean.

Total and dissolved organic carbon (TOC and DOC) as well as total and dissolved nitrogen (TN and DN) were analyzed to quantify carbon and nitrogen loss. C/N-ratios, stable carbon isotope concentrations ($\delta^{13}C$-TOC and δ13C-DOC), nutrient concentrations (ammonium, nitrite, nitrate), and lipid biomarkers were analyzed to estimate degradation, carbon metabolization, as well as nitrification and plant assimilation processes. Furthermore, dating of lead isotopes (Pb-210) in nearshore sediments and conductivity-temperature-depth (CTD) profiles of the sea water in front of the slump were analyzed to assess the possible fate of the organic material in the nearshore zone.

Our results show a general decrease of TOC and DOC as well as TN and DN contents from undisturbed to disturbed zones. TOC/TN-ratios are lower in disturbed zones, especially when comparing to permafrost sediments only. DOC/DN-ratios are highest in the tundra and slump floor but in general lower in disturbed zones. Stable carbon isotopes differ only slightly with lower values in disturbed zones, especially when comparing disturbed areas with permafrost only. Nitrate and nitrite concentrations are highest in disturbed areas, while ammonium concentrations are highest in permafrost and mudpool sediments. In the marine sediment core, Pb-210 values hinted towards a well-mixed environment and non-continuous accumulation. CTD surveys showed frequent brackish and mixed water column conditions.

These results lead to the assumption that sediments released through thermokarst activity are subject to strong degradation, which is supported by lower quantities of TOC and DOC as well as lower C/N-ratios in the disturbed zone. However, slightly lower values of stable carbon isotopes indicate that carbon is less degraded in the disturbed zone. High ammonium values in permafrost and mudpool sediments reflect an increasing activity of bacteria metabolizing organic material. No nitrate and nitrite was found in undisturbed parts, whereas detectable concentrations were found in disturbed parts, leading to the assumption that organic material has been subject to metabolization by bacteria. Lower DN-values in the slump floor reflected the nitrogen fixation by plants that recolonize the disturbed zones.

We suggest that before entering the nearshore zone

permafrost organic carbon and nitrogen is subject to substantial degradation and metabolization. Within the nearshore zone, the accumulated sediments are remobilized frequently and transported either along the shore or further offshore.

Erosion of ice-rich permafrost coasts and the release of dissolved organic carbon into the Arctic Ocean

George Tanski[1,2], Nicole Couture[3], Hugues Lantuit[1,2], Antje Eulenburg[1], & Michael Fritz[1]

[1] *Alfred Wegener Institute Helmholtz Centre for Polar and Marine Research, Germany*
[2] *Potsdam University, Institute of Earth and Environmental Sciences, Potsdam, Germany*
[3] *Geological Survey of Canada, Natural Resources Canada, Ottawa, Canada*

Ice-rich permafrost coasts in the Arctic are highly sensitive to climate warming and erode at a pace that exceeds the global average. Permafrost coasts deliver vast amounts of organic carbon into the nearshore zone of the Arctic Ocean. Numbers on flux exist for particulate and total soil organic carbon (POC and TOC). However, they do not exist for dissolved organic carbon (DOC), which is known to be highly labile. This study aims to estimate DOC stocks in coastal permafrost as well as the annual flux into the ocean. DOC concentrations in ground ice were analyzed along the ice-rich Yukon coast (YC) in the western Canadian Arctic. The annual DOC flux was estimated using available numbers for coast length, cliff height, annual erosion rate, and volumetric ice content in different stratigraphic horizons. Our results showed that DOC concentrations in ground ice range between 0.3 and 347.0 mg L-1 with an estimated stock of 13.55 g m^{-3}along the YC. An annual DOC flux of 54.9 Mg $yr^{-1}$was computed. These DOC fluxes are low compared to POC fluxes from coastal erosion or POC and DOC fluxes from Arctic rivers. We conclude that DOC fluxes from permafrost coasts play a minor role in the Arctic carbon budget. However, this DOC is assumed to be highly labile. We hypothesize that DOC from coastal erosion is important for ecosystems in the Arctic nearshore zones, particularly in summer when river discharge is low, and in areas where rivers are absent.

A lignin phenol-based assessment of the provenance of organic matter discharged from a large permafrost affected watershed (Lena River, Siberia)

Sara Trojahn[1], Maria Winterfeld[1,2], Jens Hefter[2], Sebastian Zubrzycki[3], & Gesine Mollenhauer[1,2]

[1]*Department of Geoscience, University of Bremen, Germany*
[2]*Alfred Wegener Institute, Helmholtz Centre for Polar and Marine Research, Bremerhaven, Germany*
[3]*Soil Science Institute, University of Hamburg, Germany*

Particulate organic matter (POM) discharged by rivers and deposited close to their mouth can be used to reconstruct paleoenvironmental conditions, as it is commonly assumed to record an integrated signal from the watershed. However, the particulate riverine load might be trapped in flood plains and the lower reaches of the rivers especially in large river systems with low topographic gradients. As a result, transport of POM, specifically from the distal parts of the watershed, may be inefficient and regionally biased. Furthermore, the POM likely undergoes degradation during its transport from source to sink. Therefore, investigating the different organic matter (OM) sources within a watershed will improve our understanding of OM transport in large river systems.

The Lena River is one of these large river systems. The catchment stretches from near Lake Baikal at 53° N to 71° N where the Lena discharges into the Laptev Sea. The permafrost soils within this vast and climatically diverse catchment, which store huge amounts of OM, will most likely respond differently to climate warming and remobilize previously frozen OM with distinct properties specific for the source vegetation and soil. The watershed can be broadly subdivided into two different biomes, arctic tundra and taiga [Amon et al., 2012]. The relative contribution of these biomes to the total OM load of the river and its discharge to the ocean is not well understood.

Lignin is the rigidifying component of terrestrial higher plants, and it consists of different phenolic units. Its most important components are vanillic, syringic, and cinnamic units distributed in specific different proportions among the gymnosperm and angiosperm plant tissues. The Cinnamyl/Vanillyl (C/V) and syringyl/vanillyl (S/V) ratios allow to distinguish different vegetation sources, such as woody and non-woody tissues as well as gymnosperm and angiosperm tissues [Hedges et al., 1982].

Previous analyses of surface sediments and suspended particulate matter samples collected in the tundra zone have shown that the C/V and S/V ratios clearly depict the catchment vegetation characteristics of the Lena River [Winterfeld et al., 2015]. However, suspended particulate matter of surface water samples, taken in highly dynamic systems like the Lena river delta, can only provide very local snapshots of the suspended matter properties. Furthermore, it has been shown that substantial amounts of sedimentary organic matter in the Buor Khaya Bay originates from Lena River catchment.

In this study we present the lignin phenol composition in different grain size fractions (bulk, $<63\mu$m and 63 μm^{-2} mm) of six soil samples from a latitudinal transect along the river (68° N to 72° N) plus one sample near the city of Yakutsk (63° N), and five marine surface sediments (71° N to 73° N) collected off the Bykovskaya and the Sardaksho-Trofimovskaya channel systems of the Lena delta. Estimating the relative OM contributions from tundra and taiga vegetation to the coastal sediments will be improved based on the latitudinal transect of soil samples refining the end-member values for the respective biomes. Assuming differential transport and, as a result, degradation during transport of the different grain size classes, the grain-size-fraction-specific lignin phenol compositions can be used to understand which of these fractions is reflected in the marine sediments, and if and how the lignin phenol composition changes from source to sink.

References

Amon, R.M.W.; Rinehart, A.J.; Duan, S.; Louchouarn, P.; Prokushkin, A.; Guggenberger, G.; Bauch, D.; Stedmon, C.; Raymond, P.A.; Holmes, R.M.; McClelland, J.W.; Peterson, B.J.; Walker, S.A. and Zhulidov, A.V. [2012]: Dissolved organic matter sources in large Arctic rivers.

Geochimica et Cosmochimica Acta, 94:217–237, doi:10.1016/j.gca.2012.07.015.

Hedges, J.I.; Ertel, J.R. and Leopold, E.B. [1982]: Lignin geochemistry of a Late Quaternary sediment core from Lake Washington. *Geochimica et Cosmochimica Acta*, 46(10):1869–1877, doi:10.1016/0016-7037(82)90125-9.

Winterfeld, M.; Goñi, M. A.; Just, J.; Hefter, J. and Mollenhauer, G. [2015]: Characterization of particulate organic matter in the Lena River delta and adjacent nearshore zone, NE Siberia – Part 2: Lignin-derived phenol compositions. *Biogeosciences*, 12(7):2261–2283, doi:10.5194/bg-12-2261-2015.

Connecting aquatic biogeochemical spatial and temporal heterogeneity to hydrological processes and active layer dynamics within the Yukon River Basin

Ryan C. Toohey[1], Edda Mutter[2], Nicole Herman-Mercer[1], & Paul Schuster[1]

[1] *US Geological Survey, United States of America*
[2] *Yukon River Inter-Tribal Watershed Council*

Several important studies have discovered that the Yukon River appears to be changing due to permafrost degradation. Permafrost degradation may be causing changes in discharge, groundwater contribution, carbon and other biogeochemical parameters. Several newer studies have documented hydrological processes within permafrost soils and their associated biogeochemistry. In this presentation, we combine both of these approaches by investigating additional long term and spatially diverse heterogeneity of the Yukon River's biogeochemical signature. Leveraging data collected by the USGS and the Yukon River Inter-Tribal Watershed Council, results suggest long term increases in several important soluable consituents related to weathering and permafrost degradation. Spatial heterogeneity appears to be greatly influenced by the sub-basin surficial and geologic characteristics of major tributaries. In addition, temporal variability of different constituents (C, cations and anions) is reflected by peak concentrations and loads at different times throughout the open water season suggesting corresponding different hydrological flowpaths. Changes in the biogeochemical signature also correspond to certain soil moisture patterns throughout the watershed suggesting a strong link between active layer soil moisture dynamics and the biogeochemical signature of the Yukon River and its tributaries.

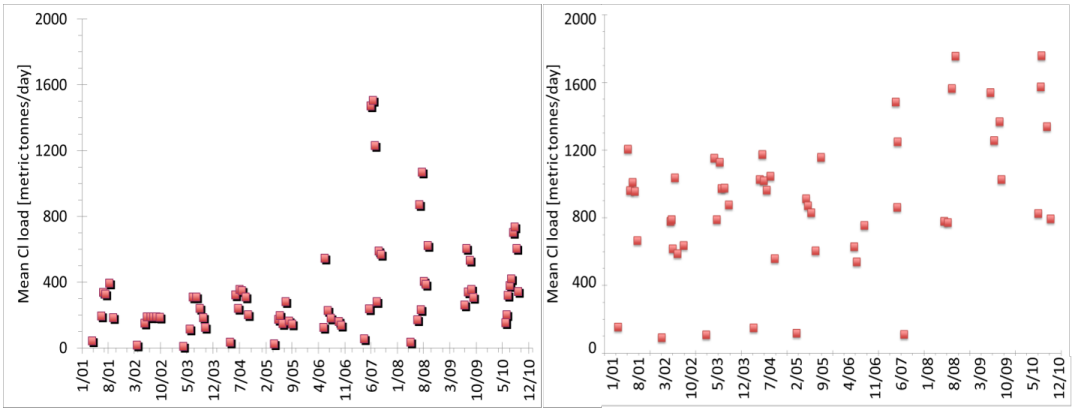

Figure 1: Chloride loads at Eagle, AK (left) and Pilot Station (right).

Current and future thawing dynamics in a mega retrogressive thaw slump and resulting fresh water, sediment and carbon release to the nearshore zone on Herschel Island, Yukon Coast Territory, Canada

Stefanie Weege[1,2] & Hugues Lantuit[1,2]

[1] *Alfred Wegener Institute Helmholtz Centre for Polar and Marine Research, Potsdam, Germany*
[2] *Institute of Earth and Environmental Science, University of Potsdam, Potsdam, Germany*

Retrogressive thaw slumps are backward retreating thermal erosion features initiated by thawing of exposed ice-rich permafrost on steep slopes and removal of debris by down sliding mudflows, wave erosion along coasts or fluvial erosion along lake shores or river banks. They are currently increasing in frequency, leading to heightened release of large quantities of organic carbon and nutrients to the environment [Lantz and Kokelj, 2008, Lantuit and Pollard, 2005, 2008]. Climatic factors such as solar radiation, air temperature, rain, wind speed, debris and snow cover affect the ablation of the headwall [Lewkowicz, 1986, 1987]. The complex geomorphology of these landforms, deposition processes in the slump floor and seasonal and/or daily variations in drivers affect the output [Kokelj et al., 2013, Lantuit et al., 2012]. Their current and future contribution to the arctic coastal zone sediment budget as well as their link to climatic drivers is poorly known.

In August 2012 and July 2013, a mega retrogressive thaw slump on Herschel Island (Yukon Coast, Canada) was surveyed and instrumented to better understand the climate-induced thawing dynamics and to quantify the release of discharge. The retrogressive thaw slump measured more than 450 m in width and had a headwall retreat of 9 m per year. Thawed sediment-meltwater from the ice-rich permafrost headwall eroded via outflow channels into the near-shore zone. A cut-throat flume was installed into an outflow channel to quantify the discharge volume. Two weather stations were installed, one above the headwall of the retrogressive thaw slump, on the undisturbed tundra and one within the retrogressive thaw slump in close vicinity to the 16 m high headwall. Incoming solar radiation, surface air temperature, wind speed and rainfall were recorded to determine the relationship between meteorological drivers and discharge volume. Each field season discharge was quantified and sampled over almost 18 days. Sediment-meltwater of the upper northern headwall was sampled with an automatic water sampler up to once an hour in the middle outflow just after passing the discharge station and 50 m before entering the near-shore zone.

We observed that sediment-meltwater discharge is influenced by incoming solar radiation, surface air temperature as well as rainfall, and is characterized by strong inter- and intra-diurnal fluctuations. The effect of wind speed, however, is insignificant. Discharge varied between a minimum of 324 m^3 and a maximum of 2212 m^3 sediment-meltwater volume per day. In the late thawing season of August 2012 little snow remained and a discharge of 15600 m^3 was recorded. In the early thawing season of July 2013 large snowbanks were present along the headwall and a discharge of 25000 m^3 was measured.

In total 81 sediment-meltwater samples were taken in August 2012 and 82 sediment-meltwater samples in July 2013. All samples were analyzed for discharge content. The total sediment eroding into the near-shore zone in August 2012 was recorded as 187 g l^{-1}, summing up to 2917 tons. While in July 2013 even though the sediment concentration was almost half (74 g l^{-1}), discharge was much higher (1850 tons). Sediment included total (in-) organic carbon and total nitrogen. Total organic carbon was 2.816 g l^{-1} (August 2012) and 0.846 g l^{-1} (July 2013), or effectively 44 tons of organic carbon during the first field season and 21 tons in the second field season. The total inorganic carbon released in the sediment released in August 2012 was 25 tons (1.589 g l^{-1}) and with 19 tons (0.775 g l^{-1}) in July 2013. In August 2012 total nitrogen was 0.294 g l^{-1} and added up to an erosion of 4586 kg. In July the total nitrogen concentration was 0.099 g l^{-1} and released 2475 kg total nitrogen into the near-shore zone.

In August 2012 the water volume was 93 %. In the following year, the headwall was covered with snowbanks and water volumes increased to 97 %. This

resulted in a total discharge of water of 14500 m^3 (August 2012) and 24250 m^3 (July 2013) over almost 18 days. The eroding water volumes also contained dissolved (in-) organic carbon. In August 2012 concentrations of 18 mg l-1and in July 2013 of 9 mg l^{-1} of dissolved organic carbon were observed. Concentrations of dissolved inorganic carbon in August 2012 of 35 mg l^{-1} and in July of 25 mg l^{-1} were released into the near-shore zone in front of the retrogressive thaw slump.

Since 1900 mean annual surface air temperature on Herschel Island has increased by 3.8 °C, and prolonged thawing seasons have been recorded, extending from 100 to 121 days, leading to potential increasing discharge. We estimate that a future increase of summer surface air temperatures by 2.0 °C would lead to a rise in discharge of retrogressive thaw slumps of 109 % (and 6 °C of 127 %) leading to an increasing release of fresh water, sediment, carbon and nitrogen into the near-shore zone.

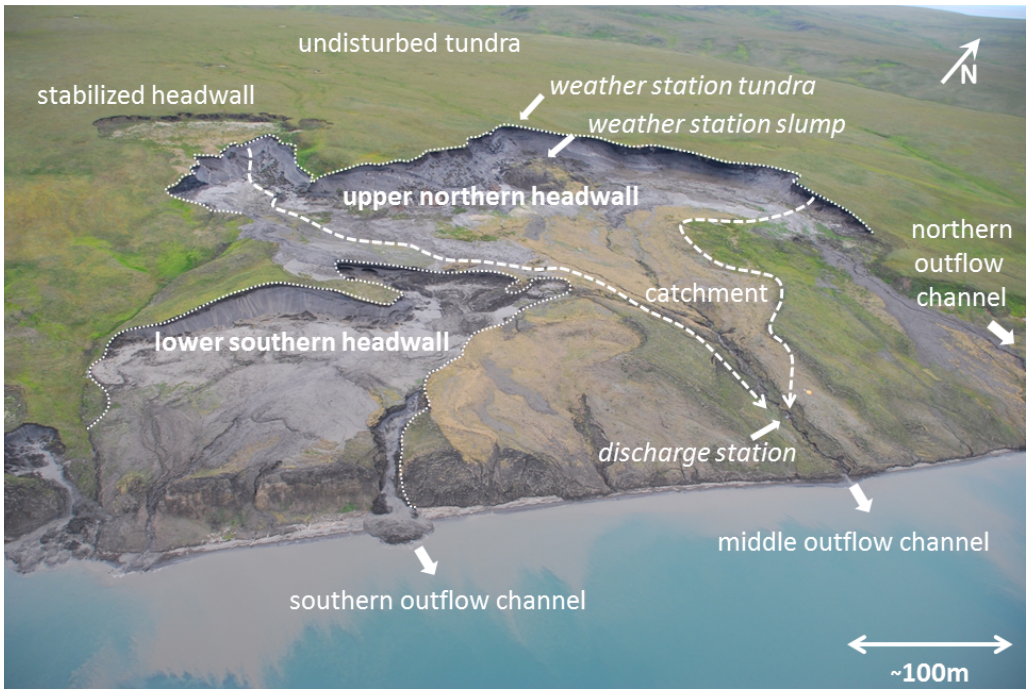

Figure 1: The retrogressive thaw slump is over 450 m wide. The upper northern headwall is located about 470 m inland from the shoreline. A second retrogressive thaw slump is reactivating polycyclically in the floor of the main slump. Its headwall is labelled

References

Kokelj, S.V.; Lacelle, D.; Lantz, T.C.; Tunnicliffe, J.; Malone, L.; Clark, I.D. and Chin, K.S. [2013]: Thawing of massive ground ice in mega slumps drives increases in stream sediment and solute flux across a range of watershed scales. *Journal of Geophysical Research: Earth Surface*, 118:681–692, doi:10.1002/jgrf.20063.

Lantuit, H. and Pollard, W. H. [2005]: Temporal stereophotogrammetric analysis of retrogressive thaw slumps on Herschel Island, Yukon Territory. *Natural Hazards and Earth System Sciences*, 5(3):413–423, doi:10.5194/nhess-5-413-2005.

Lantuit, H. and Pollard, W.H. [2008]: Fifty years of coastal erosion and retrogressive thaw slump activity on Herschel Island, southern Beaufort Sea, Yukon Territory, Canada. *Geomorphology*, 95(1): 84–102, 2008. doi:10.1016/j.geomorph.2006.07.040.

Lantuit, H.; Pollard, W. H.; Couture, N.; Fritz, M.; Schirrmeister, L.; Meyer, H. and Hubberten, H.-W. [2012]: Modern and Late Holocene Retrogressive Thaw Slump Activity on the Yukon Coastal Plain and Herschel Island, Yukon Territory, Canada. *Permafrost and Periglacial Processes*, 23(1):39–51, doi:10.1002/ppp.1731.

Lantz, T.C. and Kokelj, S.V. [2008]: Increasing rates of retrogressive thaw slump activity in the Mackenzie Delta region, N.W.T., Canada. *Geophysical Research Letters*, 35(6): L06502, doi:10.1029/2007GL032433.

Lewkowicz, A.G. [1986]: Rate of short-term ablation of exposed ground ice, Banks Island, Northwest Territories, Canada. *Journal of Glaciology*, 32(112): 511–519.

Lewkowicz, A.G. [1986]: Headwall retreat of ground-ice failures, Banks Island, North-west Territories. *Canadian Journal of Earth Sciences*, 24(6):1077–1085, doi:10.1139/e87-105.

Organic matter deposition and preservation off the Lena Delta during the last 140 years

Maria Winterfeld[1,2], Daniela Pittauer[3,4], Pai Han[2], Janet Rethemeyer[5], & Gesine Mollenhauer[1,2]

[1] *Alfred Wegener Institute Helmholtz Centre for Polar and Marine Research, Potsdam, Germany*
[2] *Institute of Earth and Environmental Science, University of Potsdam, Potsdam, Germany*

Over the last century amplified Arctic warming has lead to deeper thawing and enhanced degradation of permafrost soils. As a result, pre-aged organic carbon is respired, remobilized, and exported to the ocean via rivers and through coastal erosion. These processes are ongoing and intensifying, and will likely affect the regional and global carbon cycling.

Large Artic river catchments like the Lena River basin cover different climatic zones, which are likely affected differently by increasing temperatures and permafrost degradation. These environmental changes - including increasing thaw depth, variability in erosion in certain sub-basins of the catchment, and changes in hydrology - are expected to affect the amount and average composition of terrigenous particulate organic matter (POM) transported by the river and buried in marine sediments off the river mouth. Whether the anticipated increased discharge of the permafrost-derived terrestrial POM from the hinterland can already be recorded in these sediments remains largely unknown. While sediment records of the Colville River, Alaska, seem to record increased input from terrestrial POM over the last 50 years [Zhang et al., 2015], two records from the East Siberian Sea, one close to the Kolyma River, do not record any changes in sediment mass accumulation rates over the last century [Bröder et al., 2016].

Here we present biomarker and carbon isotopic ($\delta^{13}C$, $\Delta^{14}C$) composition data from two short sediment cores off the Lena Delta. The cores T4-1303 (73.03°N, 130.48°E) and T1-1304 (71.90°N, 130.69°E) were taken in water depths of 16 and 15 m off the main discharge channels of the delta, i.e. off the Sardakh-Trofimovskaya and Bykovskaya channels, respectively. ^{210}Pb and ^{137}Cs analyses were used to develop age models for each core. Core T4-1303 covers the last 80 years and core T1-1304 the last 140 years, and mean sedimentation rates range from 0.1 to 0.4 cm/year. The sediment accumulation at the core locations seems to be dominated by material delivered by the Lena River. Therefore, the biomarker composition, degradation indices, and ages are interpreted to reflect changes in the Lena hinterland as well as changes in riverine discharge over time.

References

Bröder, L.; Tesi, T.; Andersson, A.; Eglinton, T.I.; Semiletov, I.P.; Dudarev, O.V.; Roos, P. and Gustafsson, Ö. [2016]: Historical records of organic matter supply and degradation status in the East Siberian Sea. *Organic Geochemistry*, 91:16–30, 2016. doi:10.1016/j.orggeochem.2015.10.008.

Zhang, X.; Bianchi, T.S. and Allison, M.A. [2015]: Sources of organic matter in sediments of the Colville River delta, Alaska: A multi-proxy approach. *Organic Geochemistry*, 87:96–106, ISSN 0146-6380. doi:10.1016/j.orggeochem.2015.07.002.

SESSION 18

SSubmarine Permafrost, Arctic Gas Hydrate Deposits, and Greenhouse Gases in Arctic Coastal Waters

Convener:

Jennifer M. Frederick, *Desert Research Institute, USA*

Paul Overduin, *Alfred Wegener Institute Helmholtz Centre for Polar and Marine Research, Germany*

Dmitry J. Nicolsky, *Geophysical Institute, University of Alaska, Fairbanks, AK, USA*

Over the duration of the last glacial period in the Arctic, a thick, continuous permafrost layer formed within large regions of the terrestrial coastal plain. Ocean transgression during the Holocene has since inundated the coastal plain together with the permafrost, transforming it into the modern circum-Arctic continental shelf. Submarine permafrost- and gas hydrate-bearing sediments have been responding to the warming as a result of ocean transgression for the last ≈18 ka. Submarine permafrost is thought to be an important component in the global climate system. The permafrost layer presumably acts as a seal to subsea fluid and gas flow, allowing it to trap large amounts of greenhouse gases in the sediments. Submarine permafrost also thermodynamically stabilizes gas hydrate deposits on the continental shelf over interglacial periods because its latent heat sink can buffer surface warming. Moreover, the state of submarine permafrost is important for offshore drilling and pipeline infrastructure, resource exploration, and coastal stability. Several advances have been made in our understanding of the evolution of submarine permafrost and gas hydrate deposits on the circum-Arctic shelf, however, models of its spatial distribution differ widely, and direct observations are sparsely and unevenly distributed. Recently published modeling studies and field observations of submarine permafrost and greenhouse gas distribution in the shallow Arctic waters suggest that our understanding of submarine permafrost degradation is incomplete. This session seeks contributions that advance our understanding of the evolution of relict submarine permafrost, Arctic gas hydrate deposits, and greenhouse gases in the shallow Arctic coastal waters. We solicit work that spans the entire range of approaches, including but not limited to development of numerical models and their parameterization; observations using remote sensing, shallow geophysical techniques, or drilling; measurements and observations of gas concentrations or fluxes; seabed morphology; paleoclimatic studies; and climatic projections based on submarine permafrost degradation.

Is submarine groundwater discharge a gas hydrate formation mechanism on the Circum-Arctic Shelf?

Jennifer M. Frederick[1] & Bruce A. Buffett[2]

[1] *Sandia National Laboratory, United States of America*
[2] *University of California, Berkeley, United States of America*

Methane hydrate is an ice-like solid that can sequester large quantities of methane gas in marine sediments along most continental margins where thermodynamic conditions permit its formation. Along the circum-Arctic shelf, relict permafrost-associated methane hydrate deposits formed when non-glaciated portions of the shelf experienced subaerial exposure during ocean transgressions. Gas hydrate stability and the permeability of circum-Arctic shelf sediments to gas migration is closely linked with relict submarine permafrost. Heat flow observations on the Alaskan North Slope and Canadian Beaufort Shelf suggest the movement of groundwater offshore, but direct observations of groundwater flow do not exist. Submarine groundwater discharge (SGD), an offshore flow of fresh, terrestrial groundwater, can affect the temperature and salinity field in shelf sediments, and may be an important factor in submarine permafrost and gas hydrate evolution on the Arctic continental shelf. If SGD occurs within the permafrost-bearing sediments of the circum-Arctic shelf, such fluid circulation may transport large amounts of dissolved methane to the circum-Arctic shelf, aiding the formation of permafrost-associated gas hydrate. We investigate the feasibility of this new permafrost-associated gas hydrate formation mechanism with a benchmarked multi-phase fluid flow model, using the Canadian Beaufort Shelf as an example. The two-dimensional numerical model is based on the finite volume method for two-phase flow of pore fluid and methane gas within Arctic shelf sediments. The model tracks the evolution of the pressure, temperature, salinity, methane gas, methane hydrate, and permafrost fields given imposed boundary conditions, with latent heat of water ice and hydrate formation included. The permeability structure of the sediments is coupled to changes in the permafrost and gas hydrate deposits. The numerical model includes freeze/thaw permafrost processes and predicts the unsteady, 2D methane solubility field for hydrate inventory calculations. Model development and preliminary results will be presented.

Model results show that wide-spread, low-saturation hydrate deposits accumulate within and below submarine permafrost, even if offshore-flowing groundwater is under-saturated in methane gas. While intra-permafrost hydrate inventory varies widely depending on permafrost extent, sub-permafrost hydrate stability remains largely intact across consecutive glacial cycles, allowing widespread sub-permafrost accumulation over time. Methane gas escape to the sediment surface (atmosphere) is predicted along the seaward permafrost boundary during the early to middle years of each glacial epoch; however, if free gas is trapped within the forming permafrost layer instead, venting may be delayed until ocean transgression deepens the permafrost table during interglacial periods, and may be related to the spatial distribution of observed pingo-like features (PLFs) on the Canadian Beaufort Shelf. Shallow, gas charged sediments are predicted above the gas hydrate stability zone at the mid-shelf to shelf edge and the upper slope, where a gap in hydrate stability allows free gas to accumulate and numerous PLFs have been observed.

Lithogenetic types of offshore deposits of the Kara Sea

Olga Kalashnicova, Anna Kurchatova, Elena Slagoda, & Yana Tikhonravova

Earth Cryosphere Institute SB RAS, Russian Federation

In order to investigate the composition of the Kara Sea sediments a large number of samples were selected out during the expedition VNIIOceangeologia in 2007 [Slagoda et al., 2009]. The deposits of this area are interesting due to the oil and gas fields at the Arctic offshore, to construct the geotechnical facilities it is necessary to know the characteristics of sediments. In addition, the Arctic offshore is a key to understand the Late Quaternary history of the territory.

The grain size analysis of 33 samples using a laser diffraction particle size analyzer Mastersizer 3000 (Malvern) was made at the Institute of Earth Cryosphere SB RAS. All samples have a high content (50 to 74 %) of silt fraction (0.005-0.05 mm) therefore sediments are presented by various species of aleurite (Fig. 1(1)). The content of clay fraction (< 0.005 mm) is on average 21 %, the minimum amount of clay particles (15-16 %) are found in samples taken at the more shallow sites near the shore where the water depth is about 20-27 m, the maximum content (40 %) was observed in a single sample taken at a depth of 50 cm below the surface of the floor with the sea depth. The content of the sand fraction (> 0.05 mm) is varies in a wide range (from 0 to 36 %). Sandy layers are located in the sites with the shallow sea depth. The coefficient sorting of all the samples did not exceed 0.5 that indicates the well sorted sediments. Similar results were obtained by other researchers who studied deposits of the Kara Sea [Krylov, 2008, Levitan et al., 2004] but the clay fraction was prevailed in the composition of deposits because studies were carried out into deeper water.

The various diagrams describing lithogenetic features have been built to analyze the data. The diagram of dinamogenetic facies is based on the ratio of asymmetry – excess (Gostintsev, 1989) which reflects the mechanical differentiation of clastic particles. Two-thirds (20 of 33) of the samples were assigned to areas of active wave action, currents and tidal phenomena; 7 samples lie in the areas of weak currents, stagnant zones; 5 samples characterized as shallow water marine facies; and one sample belongs to the field of rivers and floodplains (Fig. 1(2)).

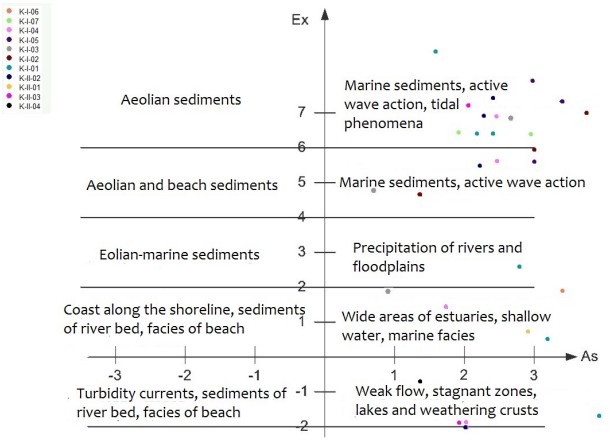

Fig. 1. The triangular diagram of granulometric composition

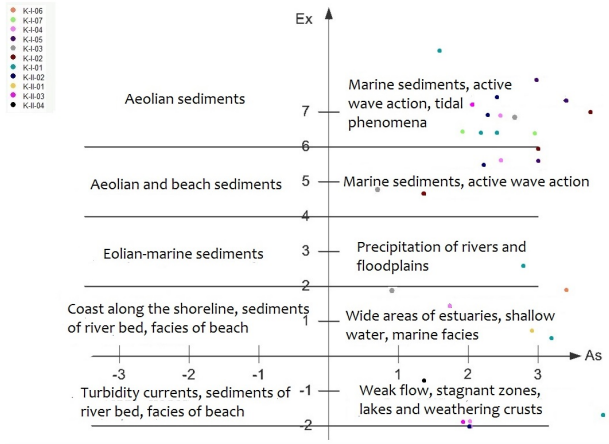

Fig. 2. The diagram of dinamogenetic facies (Gostintsev, 1989)

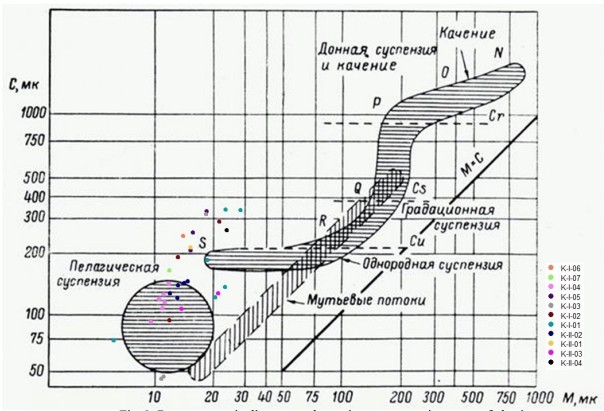

Fig. 3. Passega genetic diagram to determine transportation ways of clastic particles in aqueous environment.

Figure 1

Other chart is Passega genetic diagram to determine transportation ways of clastic particles in aqueous environment. According to the analysis, all samples

were assigned to the pelagic sediments and suspensions, most of them characterized as deposits of 'calm waters' (Fig. 1(3)). Thus, based on the results obtained by determining the origin according to granulometric analysis, it is possible to conclude:

1. In general, the granulometric characteristics of the sediments are monotonous, sandy-pelitic aleurite predominate. Deposits were become more clayey with increasing the water depth when sandy content was reduced. The sorting coefficient is showed the stable accumulation of well-sorted sediments.

2. Sediments are characterized as marine deposits of the zone of active excitement and stagnant zones with weak currents. Sedimentation sludge occurred in calm conditions which correspond to the marine genesis.

References

Krylov, A.A. et al. [2008]: The clay minerals as an indicator of conditions of accumulation of the top-Quaternary sediments Chutes St. Anne (the Kara Sea). *Oceanology*, 48(1):91–100, 2008.

Levitan, M. A.; Bourtman, M. V.; Demina, L. L.; Krupskaya, V. V.; Sedykh, E. M. and Chudetsky, M. Yu. [2004]: History of Holocene Sedimentation in the Southern Kara Sea. *Lithology and Mineral Resources*, 39(6):566–579, doi:10.1023/B:LIMI.0000046959.42527.71.

Slagoda, E.A.; Weinstein, B.G. and Leibman, M.O. [2009]: Cryogenic formation in the sediments at the bottom of the Kara Sea. In: Kontorovich, A.E. et al.(ed.), *Fundamental problems of the Quaternary: results of the study and the main directions for further research of the VI All-Russian Conference on Quaternary Research*, pages 551–554. Novosibirsk.

Impact of glacial isostatic adjustment on shoreline migration and sea-level evolution in the Laptev Sea and the East Siberian Sea during the last glacial cycle

Volker Klemann[1], Birgit Heim[2], Henning A. Bauch[3,4], Thomas Opel[2], & Sebastian Wetterich[2]

[1] *Helmholtz Centre Potsdam, German Research Centre for Geosciences GFZ, Germany*
[2] *Alfred Wegener Institute Helmholtz Centre for Polar and Marine Research, Potsdam, Germany*
[3] *GEOMAR Helmholtz Centre for Ocean Research, Kiel, Germany*
[3] *Academy of Mainz, Mainz, Germany*

The Laptev Sea and East Siberian Sea are extended shallow shelf seas which were largely land fallen during glaciated periods when the global mean sea level was more than 100 m below its present value. To understand the evolution of the large offshore (submarine) permafrost complexes in this region, a reconstruction of the sea-level variation and shoreline migration is demanded. In general, the eustatic sea-level curve, which approximates the global mean sea level change with time, is applied to consider sea level variations during the last glacial cycle on the evolution of the submarine permafrost.

The Laptev Sea and East Siberian Sea are located between the Laurentian and the Fennoscandian ice sheet. The vicinity to the regions where the Northern Hemisphere glaciation took place demands to discuss the impact of glacial isostatic adjustment (GIA). This process describes the vertical displacement of the solid earth as the respective sea level variations in response to the ice load of the waxing and waning ice sheets during the glacial cycle (glacial isostasy) and to the water load due to the accompanying sea level variations, which origin from eustatic sea level change as from the deformation of the solid earth (hydro isostasy).

Motivated as a sensitivity study, we consider GIA induced sea-level variations during the last glacial cycle and apply an earth-model ensemble which covers the range of reasonable rheological parametrisations for the lithospheric structure in this region. The geodynamically consistent sea-level reconstructions are used to predict the shoreline retreat in the Laptev Sea and East Siberian Sea. In Klemann et al. [2015], it was validated, that the application of the eustatic sea level curve for reconstructing the shore-line position since LGM is a sufficient first-order approximation. But, this approximation fails to predict the actual sea level height away from the shoreline. Here, the influence of GIA has to be considered; the predicted sea level height depends on the solid earth structure and on the respective glaciation history. During the early phase of the last glaciation, the impact of GIA was even larger as the Eurasian ice sheets extended further to the east into the Barents Sea and into the Kara Sea (e.g. Möller et al. [2015]).

References

Klemann, V.; Heim, B.; Bauch, H.A.; Wetterich, S. and Opel, T. [2015]: Sea-level evolution of the Laptev Sea and the East Siberian Sea since the last glacial maximum. *arktos*, 1(1):1, doi:10.1007/s41063-015-0004-x.

Möller, P.; Alexanderson, H.; Funder, S. and Hjort, C. [2015]: The Taimyr Peninsula and the Severnaya Zemlya archipelago, Arctic Russia: A synthesis of glacial history and palaeoenvironmental change during the Last Glacial cycle (MIS 5e-2). *Quaternary Science Reviews*, 107:149–181, 2015. doi:10.1016/j.quascirev.2014.10.018.

Non-equilibrium simulation of hydrate formation and dissociation from CO_2 in the aqueous phase

Khadijeh Qorbani Nashaqi & Bjørn Kvamme

University of Bergen, Norway

Storage of CO_2 in aquifers is one of several options for reducing the emissions of CO_2 to the atmosphere. Whether hydrate formation can provide long term additional sealing still remains unverified in view of all co-existing phases that affect hydrate stability. Yet another storage option for CO_2 is in the form of hydrate through exchange of in situ CH_4 hydrate.

Hydrates in nature come from various hydrate formers. Even when stable over the pressure and temperature domain, hydrate can generally not reach thermodynamic equilibrium due to Gibbs' phase rule and the combined first and second laws of thermodynamics. Reservoir simulations are one possible method for investigation of possible scenarios related to injection of CO_2 into underground aquifers.

The RetrasoCodeBright (RCB) simulator package was modified to enable formation (dissociation) of CO_2 hydrate from (to) CO_2 gas and water through injection of pure CO_2 gas [Vafaei et al., 2014]. In this work, the RCB hydrate simulator has been extended to account for hydrate formation and dissociation toward CO_2 in the aqueous phase, as well as in the water phase, using classical nucleation theory. Phase transitions are treated as non-equilibrium processes under local constraint of mass and heat fluxes. CO_2 hydrate formation and dissociation is resolved by looking at super-saturation and under-saturation with respect to thermodynamics variables (CO_2 mole-fraction, pressure and temperature). Competing hydrate phase transitions were determined by investigating Gibbs free energy differences between hydrate and parent phases and energy differences were calculated from variations in chemical potentials, which were estimated using non-equilibrium thermodynamic approach. We have used our simulations to study pressure and temperature and concentration dependencies of CO_2 hydrate formation and dissociation inside underground aquifers.

Results from this simulation shows that sealing effect of hydrate formation inside the stable areas might help in long term storage of CO_2 and impede leakage of gas.

Acknowledgements

Research Council of Norway, STATOIL

References

Vafaei, M.T.; Kvamme, B.; Chejara, A. and Jemai, K. [2014]: A new reservoir simulator for studying hydrate dynamics in reservoir. *International Journal of Greenhouse Gas Control*, 23:12–21, doi:10.1016/j.ijggc.2014.02.001.

Submarine permafrost map (SuPerMAP): a circum-arctic model of submarine permafrost distribution and state

Paul Overduin[1], Thomas Schneider von Deimling[2,3], Mikhail N. Grigoriev[4], & Sebastian Westermann[5]

[1] *Alfred Wegener Institute Helmholtz Centre for Polar and Marine Research, Potsdam, Germany*
[2] *Max Planck Institute for Meteorology*
[3] *Climate Analytics GmbH*
[3] *Melnikov Permafrost Institute, Siberian Branch, Russian Academy of Sciences, Yakutsk, Russia*
[3] *Department of Geosciences, University of Oslo*

Submarine permafrost has been mapped based on ice extent at the Last Glacial Maximum (LGM), global sea level history and modern bathymetry. In doing so, it was recognized that the first two of these factors, that is, regression and transgression histories, are primary determinants of relict submarine permafrost distribution at the circumpolar spatial scale. Cartographic represention of submarine permafrost by presence/absence reflects the probable distribution of cryotic sediments based on current oceanography, and not necessarily the distribution of frozen, relict, terrestrial permafrost. The latter, however, is of central interest in terms of permafrost's functions in the global climate system (energy and carbon cycle fluxes) and for infrastructure.

We model submarine permafrost development for up to the past 450 ka using distributed datasets of air temperature and ice sheet dynamics reconstructions from the CLIMBER 2 model and mapped geothermal heat fluxes, combined with modern bathymetry and topography for elevations between -150 and +50 m relative to sea level (m rsl). Sea level reconstructions and resulting sedimentation history also contribute to drive surface temperature histories. Initial assumptions of the relative rates of glacial, marine and terrestrial sedimentation provide the basis for shelf stratigraphy, ignoring the influence of coastal erosion, isostasy and neotectonics. Freezing characteristic curves of saline sediments are calculated by including an osmotic potential term.

We examine the evolution of permafrost along six transects in the Laptev, East Siberian, Beaufort and Barents seas, and in the Canadian Arctic Archipelago. The circum-arctic maps generated include the traditional map of the extent of cryotic sediment, including its thickness below the land or seabed, but focus on more important parameters such as pore space ice saturation (which controls gas permeability and the thermal inertia of permafrost). Future extensions of the model will focus on those processes to which modelled submarine permafrost state and distribution are most sensitive, including sediment composition and accumulation rates and permafrost ice content.

Sub-sea permafrost modelling based on idealised laboratory experiment

Matteo Puglini, Victor Brovkin, & Dirk Notz

Max-Planck-Institut für Meteorologie, DE

Submarine relic permafrost is gaining more and more interest in recent time due to the large amount of organic carbon that is thought to be stored in there (~1400 PgC) and consequently to the role it may play in the global climate system if that carbon were released. Subsea permafrost is also important since can stabilise clathrates.

In this work we aim at modelling thermochemical properties of submarine permafrost. To do so we carry out idealised laboratory experiments whose results are used to modify the permafrost model implemented into the land-surface model JSBACH (within MPI-ESM) [Ekici et al., 2014]. So far, JSBACH only accounts for terrestrial permafrost soil, and does not include any physics related to salt presence. We use the climate forcing from the last glacial cycle as simulated by the CLIMBER-2 model [Ganopolski and Calov, 2011] to spin up a permafrost soil which is later flooded and degraded, taking into account the change in bathymetry due to ice-complex disintegration [Nicolsky et al., 2012]. In order to test the model, we will limit it to a 1-D vertical setup with the stratigraphy prescribed from individual field measurements.

Because of the rare and sparse in situ measurements, the study of submarine permafrost has been mainly based on modeling whose results cannot be well evaluated due to missing data. In order to assess our model, simplified experimental setups in controlled environments have been performed and in this poster comparative results of a thawing permafrost/melting ice model in comparison to measurements are reported.

In the experimental setup, we first overlayed a freshwater ice sample with salty water and examined if the temperature and salinity evolution agree with model results. After this ancillary comparison, a setup was shaped to reproduce more faithfully a flooded ice-bonded soil. For this purpose, beads of different sizes have been used to simulate soil as a porous medium. They have been submerged with freshwater, then frozen and salty water at a temperature comparable with the one measured at the seabottom (-1.5 °C) has then been poured on top. Comparisons between salinity and temperature profile have been drawn, too.

References

Ekici, A.; Beer, C.; Hagemann, S.; Boike, J.; Langer, M. and Hauck, C. Simulating high-latitude permafrost regions by the JSBACH terrestrial ecosystem model. *Geoscientific Model Development*, 7(2):631–647, 2014. doi:10.5194/gmd-7-631-2014.

Ganopolski, A. and Calov, R. The role of orbital forcing, carbon dioxide and regolith in 100 kyr glacial cycles. *Climate of the Past*, 7(4):1415–1425, 2011. doi:10.5194/cp-7-1415-2011.

Nicolsky, D.J.; Romanovsky, V.E.; Romanovskii, N.N.; Kholodov, A.L.; Shakhova, N.E. and Semiletov, I.P. Modeling sub-sea permafrost in the East Siberian Arctic Shelf: The Laptev Sea region. *Journal of Geophysical Research: Earth Surface*, 117(F3): F03028, 2012. doi:10.1029/2012JF002358.

Laboratory-based simulations of the microbial influence on permafrost-associated methane gas hydrate formation

Judith Maria Schicks, Manja Luzi-Helbing, Susanne Liebner, Erik Spangenberg, Dirk Wagner, & Thomas Wiersberg

Helmholtz Centre Potsdam GFZ German Research Centre for Geosciences, Germany

Gas hydrates are ice-like crystalline solids composed of a three-dimensional network of hydrogen-bonded water molecules that confines gas molecules in well-defined cavities of different sizes. Since gas hydrates form under elevated pressure conditions at low temperatures they often occur in permafrost regions when sufficient amounts of water and gas are present. In this natural setting the gas is predominantly methane of microbial or thermogenic origin. In different field studies the occurrence of microbial methane in and below the permafrost could be proved: Collett and Dallimore [1999] report on intra-permafrost microbial methane in drill cores from the 92GSCTAGLU, the 92GSCKUMAK and the 92GSCUNIPKAT wells, situated close to a potential future scientific drilling target (NWT, Canada). The occurrence of intra-permafrost microbial methane has also been observed during drilling of the Mallik 4L-38 and 5L-38 wells (NWT, Canada). In submarine permafrost microbial methane occurrences could be detected in cores from the Siberian Arctic Shelf [Koch et al., 2009]. Noteworthy, the noble gas abundance data from Mallik imply that the source of gases were gas hydrates.

The relationship between gas hydrates, microorganisms and the surrounding sediment is extremely complex: Microorganisms producing methane provide the prerequisite for gas hydrate formation. However, as a result of microbial activity not only methane will be provided for hydrate formation but gas hydrates are surrounded by a great variety of organic compounds. These organic compounds are not incorporated into the hydrate structure but may influence the formation or degradation process. To understand the influence of microbial activity on the methane hydrate formation process and the stability conditions of the resulting hydrate phase we perform laboratory studies. Thereby, we mimic gas hydrate formation in the presence and absence of methanogenic archaea (e.g. Methanosarcina soligelidi) and other psychrophilic bacteria isolated from permafrost environments of the Arctic and Antarctic. Our results may contribute to understand and predict the occurrences and behavior of potential gas hydrates within or adjacent to the permafrost.

References

Collett, T.S. and Dallimore, S.R. [1999]: Hydrocarbon gases associated with permafrost in the Mackenzie Delta, Northwest Territories, Canada. *Applied Geochemistry*, 14(5):607–620, doi:10.1016/S0883-2927(98)00087-0.

Koch, K.; Knoblauch, C. and Wagner, D. [2009]: Methanogenic community composition and anaerobic carbon turnover in submarine permafrost sediments of the Siberian Laptev Sea. *Environmental Microbiology*, 11(3):657–668, doi:10.1111/j.1462-2920.2008.01836.x.

Present and future gas release from degrading submarine permafrost regions

Thomas Schneider von Deimling[1,2], Sebastian Westermann[3], & Pier Paul Overduin[2],

[1] *Max Planck Institute for Meteorology, Hamburg, Germany*
[2] *Alfred Wegener Institute Helmholtz Centre for Polar and Marine Research, Potsdam, Germany*
[3] *University of Oslo, Department of Geosciences, Norway*

A key feature of Arctic shelf regions is the large-scale existence of subsea permafrost. Glacial sea-level lowstands favoured the penetration of cold surface air temperatures into sediments that are located below sea level today. Given the long-term memory of frozen ground, permafrost extent and thickness is an expression of past climatic variations from glacial/interglacial cycles (i.e. varying histories of surface air temperature, inundation, and ice sheet coverage).

Ice in sediment pore volumes is a barrier to gas migration from the deeper ground to the shelf sea water column and atmosphere. Therefore, subsea permafrost thawing is often considered a positive feedback to global warming given the potential release, triggered by warming, of the potent greenhouse gas methane, which otherwise would be trapped in cryogenic structures when cold ground temperatures prevail. The lack of observational data which document the extent to which Arctic shelf sediments are perennially frozen today hinders current estimates of the potential of gas release from those regions. In our study we used a one-dimensional heat diffusion model (Cryogrid, Westermann et al. [2012]) to track the thermal state of submarine permafrost along various transects from the continent to the shelf edge with differing histories of past climatic conditions, such as air temperature, inundation and ice sheet coverage, over four glacial cycles. The lower model boundary condition is described by spatially resolved geothermal heat flux data. As we model the build-up of saline marine and fresh terrestrial sediments, we generate a model sedimentology of differing freeze characteristics and therefore different temperature sensitivities to thaw.

We illustrate the imprint of warming exerted by ocean bottom waters and assumed basal ice temperatures on the upper and lower permafrost boundaries. Our simulations suggest that sites with long durations of inundation or ice sheet coverage reveal rather shallow permafrost thicknesses of a few tens of meters. In contrast, our results support the existence of rather extensive permafrost build-up, down to many hundreds of meters, in shallow shelf regions. By running the model for enhanced surface temperatures over centuries into the future, we show the extent to which new pathways of gas migration from depth might arise in a warmer world. We discuss the implications for methane release resulting from our inferred layered structure of subsequent frozen and unfrozen sediment layers.

References

Westermann, S.; Langer, M. and Boike, J. [2012]: Systematic bias of average winter-time land surface temperatures inferred from MODIS at a site on Svalbard, Norway. *Remote Sensing of Environment*, 118:162–167, doi:10.1016/j.rse.2011.10.025.

How permanent is East Siberian Arctic Shelf permafrost?

Martin Stendel[1], Christian Rodehacke[1], Vladimir E. Romanovsky[2], Dmitri Nicolski[2], Sergei Marchenko[2] Jens Hesselbjerg Christensen[1], Ruth Mottram[1], & Martin Olesen[1],

[1] *Danish Meteorological Institute, Copenhagen, Denmark*
[2] *Permafrost Laboratory, Geophysical Institute, University of Alaska Fairbanks, USA*

Observations taken during recent expeditions indicate that the East Siberian Arctic Shelf (ESAS) is a source of methane in the global climate system. This methane is found in vast amounts in shallow hydrate seabed reservoirs and is under present climate conditions trapped under subsea permafrost which underlies most of the ESAS. As the release of only a small part of the total amount of carbon within the ESAS could have major implications for the global climate through the release of greenhouse gases, it is important to model the future fate of subsea permafrost with regard to changing atmospheric and oceanic circulation. Up to now only a few attempts to model subsea permafrost have been made and most of them have focused on the evolution of permafrost since the Late Pleistocene ocean transgression, approximately 14000 years ago and thus do not take into account the very long spinup time, which is in the order of 100000 years.

In contrast to land permafrost modeling, any attempt to model the future fate of subsea permafrost needs to consider several additional factors, in particular the dependence of freezing temperature on water depth and salt content, the differences in ground heat flux depending on the seabed properties and the amount of unfrozen water in the sediment. Previous research has also revealed that the initial temperature of the ocean at the beginning of the spinup period plays a crucial role. Using a system of coupled ocean, atmosphere and permafrost models allows us to capture the complexity of the different parts of the system and evaluate the relative importance of different processes.

Here we present results of coupling a dedicated permafrost model to a regional climate model for a region covering the Laptev Sea region in East Siberia and compare them to the limited observational data which is available using a cross section of the four-dimensional parameter subspace given by temperature, geothermal heat flux and soil salinity versus time. We find that ocean warming leads to thawing on the order of several hundreds of years, in good agreement with GCM results. However, subsea permafrost in the Laptev Sea region will not completely disappear within the next few thousand years.

Controls on permafrost distribution within the near-shore zone of the Mackenzie Delta, Canada

Christopher Stevens[1] & Brian Moorman[2]

[1] *SRK Consulting*
[2] *Universtiy of Calgary*

Permafrost presents a significant challenge to oil and gas development in nearshore environments due to its influence on the stability of foundation conditions for linear infrastructure. Environmentally safe and economically sustainable development of this environment requires an understanding of the spatial variability of ground temperatures and the response of permafrost to natural and human-induced changes of the environment.

Multi-year research conducted by the University of Calgary, the Geological Survey of Canada, and SRK Consulting has investigated the controls on permafrost beneath shallow-water environments seaward of the Mackenzie Delta, Northwest Territories, Canada. The findings of this work indicate that ground temperatures are mainly controlled by the presence of liquid water or ice at the sediment bed. Where ice freezes to the sediment bed surface (i.e. becomes bottom-fast) conductive transfer between cold air temperatures and relatively warmer underlying sediments leads to heat loss throughout the winter. Major controls on ground temperatures include the timing of bottom-fast ice which is influenced by the rate of ice growth and local changes to water depth cause by sediment deposition and erosion. Thermal modeling results indicate that the critical ice contact time for sustaining permafrost beneath near-shore zones of bottom-fast ice is about 140 days under current climate in the region. This finding was integrated with a time-series of synthetic aperture radar images, which define the timing of BFI across the near-shore zone to produce the first map of shallow-water permafrost for the outer Mackenzie Delta. Permafrost was mapped beneath 393.8 km^2. These locations typically represent areas where sediment supply exceeds present-day sea level rise. Monitoring permafrost beneath shallow water and ice will continue to be critical to the planning of Arctic resource development in dynamic nearshore environments.

Methane in tabular massive ground ice as a proxy of Late Pleistocene environmental conditions in western sector of Russian Arctic

Irina D. Streletskaya[1], Aleksandr A. Vasiliev[2], Gleb E. Oblogov[2], & Boris G. Vanshtein[3]

[1]*Lomonosov Moscow State University, Russian Federation*
[2]*Earth Cryosphere Institute SB RAS*
[3]*FSUE "VNIIOkeangeologia named after I.S.Gramberg"*

Methane emission triggered by permafrost degradation are important consideration in climate change debate in the Arctic making studies of origin and distribution of methane in permafrost of a considerable interest. Study of methane origin and content was performed at the Marre-Sale key site (N 69°43' E 66°49') at the western coast of Yamal Peninsula.

The study area is in the continuous permafrost zone with low ground temperatures. Geological section of the base of the coastal bluff is represented by lower saline silty clay unit of marine and coastal-marine origin and presumably associated with Marine Isotope Stage (MIS) 5. The eroded surface of marine and coastal-marine clayey sediments is overlaid by continental non-saline silts and sands formed during MIS 3 - MIS 1. Tabular massive ground ice (TMGI) bodies are represented by two types. The first type TMGI (3-10 m thick) was detected at the boundary between the marine and continental units. The ice contains uniformly distributed silt and sand inclusions. This type of TMGI can be described as ice-soil mix with layers of clear ice. The second type of TMGI (more than 10 m thick) was detected within the saline clayey unit of marine origin.

We collected 42 1-kg samples of TMGI and frozen soils for methane concentration analysis. The samples were disintegrated to a particle size of less than 0.25 mm with RETSCH mill at temperatures below freezing. Degassing of disintegrated ice was performed with SUOK-DG apparatus using a dynamic method of degassing. This method is based on diffusion of water containing gas to sub-micron level simultaneously with creation of high vacuum in diffusion zone. The gas volume obtained from 200 to 300 g of ice reached 10 to 33 ml depending on gas saturation of samples. Gas composition was determined by a method of gas chromatography using apparatus with plasma ionization detector SHIMADZU 2014.

For the samples with a high methane concentration, content of $\delta^{13}C(CH_4)$ isotopes (eight analyses) was determined in the Vernadskiy Institute of Geochemistry and Analytical Chemistry RAS (Moscow, Russia) using isotopic mass-spectrometer (GC-C-IRMS configuration). Content of the Hydrogen isotope in methane D vs. SMOW was determined for air bubbles obtained from six ice samples in the laboratory ISOLAB B.V. (The Netherlands). The highest level of methane saturation was typical of the samples of TMGI (6197 ppmv), while the lowest gas content was typical of frozen continental sands (115 ppmv) [Vasiliev et al., 2015].

Analysis of isotope composition of methane in the TMGI samples showed that according to ratio between $\delta^{13}C(CH_4)$ and D vs. SMOW, methane was produced by activity of anaerobic bacteria (Fig. 1).

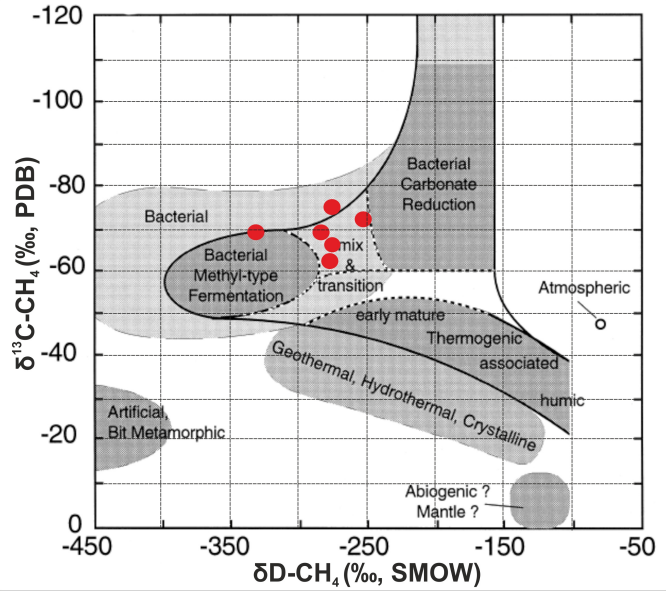

Figure 1: The red dots - the value of carbon isotope composition of methane (^{13}C, ‰) and deuterium methane (D, ‰) of gas bubbles in TMGI and the diagram the ratio of the isotopic composition of methane, depending on the genesis of gas by Whiticar [1999].

Results show that isotope composition of methane

in ground ice and frozen soils is substantially different than that of atmospheric methane and methane from gas bearing strata of Senomanian and Neokomian age in West Siberia used in gas production. The isotopic values of ^{13}C in methane in TMGI are close to the values of the carbon isotopes of methane in permafrost at depths of 46-52 and 114-120 m in the Bovanenkovo gas field, West Yamal, and characterized of isotope composition of methane (^{13}C, ‰) -70.4 to -76.8 ‰ [Chuvilin, 2007].

The high methane content in TMGI is a result of methane migration from the adjacent soils and accumulation inside ice bodies. Extremely high methane concentration in TMGI is a strong evidence of its intrasedimental and not atmospheric origin. It is difficult to select potential sources of gas bubbles trapped in TMGI. This heterogeneous medium, rich in organic matter, might have favored the anaerobic micro-environment necessary to explain the abnormally high methane content. Marshy coasts near shallow seas may have contributed to such conditions. The isotopic content of marsh gas in TMGI excludes the glacial origin of this ice.

References

Chuvilin, E.M.(ed.) [2007]: *Structure and properties of the south of the Bovanenkovo gas condensate field permafrost*. Moscow, GEOS, 137 p.

Vasiliev, A.A.; Streletskaya, I.D.; Melnikov, V.P. and Oblogov, G.E. [2015]: Methane in underground ice and frozen Quaternary deposits of Western Yamal. *Doklady Earth Sciences*, 465(2):1289–1292, doi:10.1134/S1028334X15120168.

Whiticar, M.J. [1999]: Carbon and hydrogen isotope systematics of bacterial formation and oxidation of methane. *Chemical Geology*, 161(1–3):291–314, doi:10.1016/S0009-2541(99)00092-3.

Methane isotopologues and eddy covariance fluxes above the mid and outer Laptev and East Siberian Seas during SWERUS-C3

Brett F Thornton[1], Patrick M Crill[1], Kristian Andersson[1], Martin Wik[1], Cèlia Sapart[2], John Prytherch[3], Ian M Brooks[3], Dominic Salisbury[3], & Michael Tjernström[1]

[1] *Stockholm University, Sweden*
[2] *Université Libre de Bruxelles, Brussels, Belgium*
[3] *University of Leeds, United Kingdom*

The Laptev, East Siberian, and Chukchi seas (Siberian Shelf seas) are wide (2.1 million square km), relatively shallow (ca. 50 m average depth) seas. Large emissions of CH_4 from the sea to the atmosphere have been reported in this area.

To better understand the scale and possible sources of these emissions, we made atmospheric measurements of $^{13}CH_4$, CH3D, $^{12}CH_4$, and CO_2 across the Siberian shelf seas during the SWERUS/C3 project in July and August 2014.

Continuous measurements were made using two LGR CRDS laser spectrometers (CH_4 and CO_2), and an Aerodyne TDLS laser absorption spectrometer (CH_4 isotopologues) from inlets along a 9–35 m height gradient above the sea surface to allow for gradient studies. We present an extensive set of atmospheric methane concentration and isotopologue observations during the SWERUS-C3 cruise in July and August 2014 in the Laptev and East Siberian seas. One CRDS spectrometer was dedicated to eddy covariance flux measurements of the CH_4 sea-air flux.

This unprecedented dataset of atmospheric methane across the outer Russian Arctic continental shelf seas may help us to make top-down estimations of methane sources from the Laptev and East Siberian Seas to the atmosphere.

Microbial activity mitigates the release of methane from degrading subsea permafrost

Matthias Winkel[1], Julia Magritz[1], Fabian Horn[1], Paul Overduin[2], Christian Knoblauch[3], Dirk Wagner[1], & Susanne Liebner[1]

[1] *GFZ German Research Centre for Geosciences, Helmholtz Centre Potsdam, Section of Geomicrobiology, Germany*
[2] *Alfred Wegener Institute Helmholtz Centre for Polar and Marine Research, Potsdam, Germany*
[3] *Universität Hamburg, Institute of Soil Science, Germany*

Thawing arctic subsea permafrost is a source of organic carbon in deep sediment layers. The permafrost that is at its thermal equilibrium releases biologically produced methane and a deep sulfate-methane transition zone (SMTZ) is formed due to sulfate-rich overlaying marine sediment layers. The process of anaerobic methane oxidation (AOM) in this environment has been suggested [Overduin et al., 2015] but AOM associated microbial communities remain to be identified. We aimed at providing evidence for anaerobic methanotrophic (ANME) archaeal communities at the deep SMTZ of the north-east Siberian Laptev Sea shelf.

Two sediment cores were retrieved (77 m and 47.4 m deep) from the coastal shelf north of Cape Mamontov Klyk 'C2' (11.5 km offshore) and west to the Buor Khaya Peninsula 'BK2' (800 m offshore), respectively. Methane and sulfate concentrations as well as ^{13}C isotope values of CH_4 were measured and correlated with molecular analysis of microbial communities along the thaw front. At the thaw front of BK2, at 23.7 meters below sea floor (mbsf) biologically produced methane (^{13}C= -70‰ VPDB) gets oxidized (^{13}C= -29.8‰ VPDB) [Overduin et al., 2015]. At the same depth, we found an increase in functional genes of methanogenic archaea (mcrA) and sulfate reducing bacteria (dsrB) analysed by quantitative PCR. Massive parallel tag-sequencing of the 16S rRNA gene showed an increase of ANME-2a/2b and ANME-2d sequences towards the thaw front in both cores. At the thaw front of the BK2 core, typical ANME-2 partners of the Desulfobacterales [Schreiber et al., 2010] were found to dominate the sulfate reducing bacterial community, whereas Desulfobacca sequences dominate in all samples of the C2 core. Theoretical methane oxidation rates (0.4–6 nmol cm^{-3} d^{-1}) [Overduin et al., 2015] based on estimated methane fluxes showed higher values than typically found in subsurface sediments and are more similar to rates of margin SMTZs [Knittel and Boetius, 2009]. Our data point at active anaerobic methane oxidizer communities at the thaw front of subsea permafrost that prevent methane from being released into the water column and subsequently to the atmosphere. Further analyses on lipid biomarkers and ^{14}C-CH_4 isotopic rate measurements will determine how active these communities are in situ.

References

Knittel, K. and Boetius, A. [2009]: Anaerobic Oxidation of Methane: Progress with an Unknown Process. *Annual Review of Microbiology*, 63:311–334, 2009. doi:10.1146/annurev.micro.61.080706.093130.

Overduin, PP.P; Liebner, S.; Knoblauch, C.; Günther, F.; Wetterich, S.; Schirrmeister, L.; Hubberten, H.-W. and Grigoriev, M.N. [2015]: Methane oxidation following submarine permafrost degradation: Measurements from a central Laptev Sea shelf borehole. *Journal of Geophysical Research: Biogeosciences*, 120(5):965–978, doi:10.1002/2014JG002862.

Schreiber, L.; Holler, T.; Knittel, K.; Meyerdierks, A. and Amann, R. [2010]: Identification of the dominant sulfate-reducing bacterial partner of anaerobic methanotrophs of the ANME-2 clade. *Environmental Microbiology*, 12(8):2327–2340, 2010. doi:10.1111/j.1462-2920.2010.02275.x.

Methane emission from the coastal retreat in the Western Yamal

Nataliia Zadorozhnaia[1], Vladimir Fedin[1], Gleb Oblogov[2], Alexandre A. Vasiliev[2], & Irina Streletskaya[1]

[1] *Lomonosov Moscow State University, Russia*
[2] *Earth Cryosphere Institute SB RAS, Tyumen, Russia*

The large amount of methane is withdrawn from turnover of the Earth and preserved in permafrost. Methane is emitted in the atmosphere during the permafrost degradation on the shelf, the continent and the melting of the subsurface ice. In recent decades great attention is given to analysis of the methane content inasmuch as, according to the relevance, methane is the second greenhouse gas after the carbon dioxide, its increase in the atmosphere has a significant impact on the climate as a whole. Since the second half of the XX century, the concentration of methane in the atmosphere has been increasing annually by 1 %.

Data on methane concentration in air inclusions into ground ice and permafrost exposed in a cliff near the Marre Sale polar station, the western Yamal (69°43'N/66°49'E) has been obtained for the first time.

Complex of quaternary deposits containing various generations of syngenetic ice wedges and two types of massive ice composed the section of the cliff near the station. Long-term regular observations of the sea coast retreat since 1978 showed a speed of about 1.7 meters per year [Vasiliev et al., 2006]. Total of 247 samples of gas from permafrost and ice were collected. CH_4 concentration was measured by headspace-equilibration, using KhPM-4 (Russia) gas chromatograph with flame ionization detector and hydrogen used as a carrier gas (Pushchino, Russia). The methane concentration in massive ice sheet was abnormally high. It reached 21.5 ml kg^{-1} in the ice, which exceeded by an order of magnitude the concentration found for other sediments composing the coastal section. Methane is practically absent in the Holocene sands and the ice of syngenetic ice-wedges. Given the coastal retreat rate, we assessed the annual flux of the methane buried in permafrost due to erosion of 100 m long coastal section near Marre-Sale. With the destruction of costal bluff near Marre-Sale that consists of sand and ice-wedge polygons, the atmosphere there receives 0.235 g of methane per 1 m2 in a single year, whereas melting of tabular massive ground ice liberated 19.7 g/a per 1 m^2 from permafrost.

Such variations of methane concentrations across sediment types correlated with permafrost genesis. Formation of syngenetic permafrost was shown to be unfavorable for methane accumulation on the contrary to epigenetic permafrost [Vasiliev et al., 2015]. The amount of methane released from permafrost due to erosion was estimated for 100 m of the coast and for the full length of 4.5 km long coastal section was estimated. It was found, that each year the destruction of 100 m of the sea coast in the research area causes 10300 g of methane to be released into the atmosphere and around 463500 g is released around a 4.5 km-long coastline.

Fluxes of methane buried in permafrost due to coastal erosion were dominated by methane from marine clays and loams, as shown on figure 1.

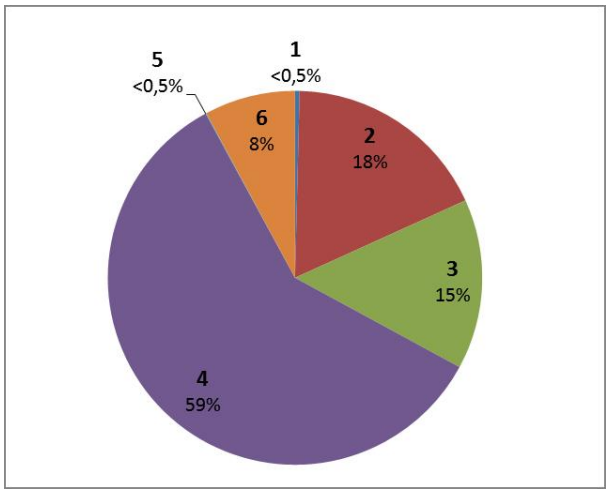

Figure 1: Annual contribution of methane fluxes from erosion of sediments and ice to the total emission of methane from the 100 m coastal section. (Key: 1 – alluvial sand (MIS 1 age); 2 – lacustrine silt and sand (MIS 2 age); 3 – lacustrine silt and sand (MIS 3-MIS 4 age); 4 – marine clay and loam (MIS 5 age); 5 – syngenetic ice wedges; 6 – tabular massive ground ice).

The comparison between the amount of methane released into the atmosphere from the surface of tundra wetland ecosystems of the north of Western Siberia and the amount of methane released into the atmosphere as a result of the destruction of the sea coast near the polar station Marre-Sale showed, that the

amount of methane coming from the 1 m2 section of the coast amounted to 5.01 g per year. Average methane emission from tundra wetland ecosystems was 1.17 g/a per 100 m2 [Kazantsev, 2013]. The value of methane emissions in the destruction of frozen sea shore with underground ice is high enough and comparable to the emission of methane from wetland ecosystems.

References

Kazantsev, V.S. [2013]: *Methane emission from swamp ecosystems of Western Siberia northern part.* Dissertation cand. biol. sciences, Moscow: Moscow State University, 26 p.

Vasiliev, A.A.; Streletskaya, I.D.; Cherkashev, G.A. and Vanshtein, B.G. [2006]: Coastal dynamics of the Kara Sea. *Kriosfera Zemli*, 10(2):56–67, URL http://www.izdatgeo.ru/pdf/krio/2006-2/56.pdf.

Vasiliev, A.A.; Streletskaya, I.D.; Melnikov, V.P. and Oblogov, G.E. [2015]: Methane in underground ice and frozen Quaternary deposits of Western Yamal. *Doklady Earth Sciences*, 465(2):1289–1292, doi:10.1134/S1028334X15120168.

SESSION 19

Polar Coastlines in Transition

Convener:

Louise Farquharson, *University of Alaska Fairbanks, USA*

Matt Strzelecki, *Wroclaw University, Poland*

Boris Radosavljevic, *Alfred Wegener Institute Helmholtz Centre for Polar and Marine Research, Germany*

Polar coastlines make up 34 % of the global total and are among the most dynamic in the world. In light of climate change, polar coastlines are becoming increasingly vulnerable to rapid change.

In the arctic sea ice extent and thickness has been declining by more than 10 % per decade since satellite observations began in 1981. This decrease in sea ice extent is lengthening the period in which arctic coastlines are vulnerable to storms and thermal erosion, potentially increasing rates of coastal change. These changes are expected to impact coastal morphology, causing increased rates of erosion, extensively modifying near shore sediment and organic carbon mobilization and transport, and potentially pushing coastal systems across critical geomorphological and ecological thresholds. In the Antarctic and parts of the Arctic, accelerated deglaciation has led to the exposure of new coastline. The evolution of those recently deglaciated coastal systems is controlled by permafrost-related processes and fluxes of sediments from paraglacially transformed glacial landforms.

To make accurate predictions of the trajectory of polar coastal evolution, erosion, and aggradation during the coming centuries a better understanding of what processes drive shifts in coastal dynamics is necessary. Currently most polar coastlines remain either un- or understudied.

This session invites submissions that will improve our understanding of polar (Arctic and Antarctic) coastal dynamics on local and regional scales. We encourage submissions focusing on both sub-aerial and sub-aqueous processes driving changes to coastal morphology, corresponding rates of change and consequences of these changes to polar coasts. We are especially interested in submissions focusing on issues related to extreme coastal processes and rapid coastal changes including accelerated permafrost thermoerosion, increased delivery of glacial sediments from retreating glaciers and ice-streams, coastal storm induced flood events, and polar tsunamis.

Analysis of coastal dynamics and permafrost conditions of the Yamal Peninsula using GIS

Alisa Vladislavovna Baranskaya[1], Stanislav A. Ogorodov[1], Nataliya G. Belova[1], Alexey P. Vergun[1], Natalya N. Shabanova[1], Dmitriy E. Kuznetsov[1], Olivier Gosmant[2], Eric Cauquil[2], Annie Audibert-Hayet[2], Pascal Dauboin[2], & Jean-Baptiste Geldof[2]

[1] *Lomonosov Moscow State University, Moscow, Russian Federation*
[2] *Total E&P Recherche Develoment, Paris, France*

Determining the features of coastal dynamics and the rates of coastal processes can be a difficult task for any region of the world. In the Arctic, knowing the main trends of the development of coastal processes and their expression in the morphology of coastal landforms, is of vital importance. Most of the settlements, transport corridors and areas of industrial development in the Russian Arctic are situated within the coastal zone. Polar coastal regions are important for subsistence hunting and fishing as well as for mineral resource exploration. Therefore, knowledge about Arctic coastal dynamics is necessary for local, regional and state government land management, as well as local subsistence users and mining companies.

In the Arctic, the movements of coastlines result not only from the direct action of wave abrasion and accumulation, but are highly dependent on permafrost factors which are absent in the temperate and tropical regions. To better understand coastal dynamics, coastal morphology and evolution should be observed together. The state of permafrost should also be considered, including its properties, Quaternary history, sediment composition and ice content. The presence of permafrost results in very specific processes of thermal coastal erosion. Despite the short dynamically active period (ice-free period) when the waves can affect the coasts, morpholithodynamic processes in the coastal zone of the Arctic seas are characterized by significant rates, determined by low stability of coastal forms composed by permafrost. About half of the length of the Eurasian Arctic coast is affected by thermal abrasion and retreats with average rates from 1 to 5 m/year [Ogorodov, 2008].

One more specific feature of the Arctic coasts is the action of sea ice on the coasts and bottom of seas. The length of the ice-free period influences the rates of thermal abrasion, while the wave energy coming to the coasts depends on the distance of the wave fetch. Therefore, the Arctic coastal dynamics should be analysed with connection to sea ice features in the region as well. Another important component is the meteorological factor, as the Arctic coasts composed by permafrost are the most vulnerable to the quick ongoing climatic changes.

For the investigations of coastal dynamics on a local scale, a regional study was made for Yamal Peninsula, Russia, by MSU and Zubov State Oceanographic Institute in collaboration with Total oil and gas company. Yamal is the centre of the Russian Arctic and one of the key areas of the North. In the last years, due to active oil and gas exploration, the industrial infrastructure is moving further and further towards the north. The main objects are situated in the coastal zone, as it is the most accessible location (by water transport). Integrative analysis of coastal morphology and dynamics, types of coasts, in connection with permafrost and Quaternary geology, sea ice impact and climate change will be a basis for decision-making connected with, on the one hand, designing and building separate industrial objects, and, on the other hand, planning a long-term strategy of development for the region.

To perform such comprehensive analysis, an integrative GIS-system was created. It includes layers on permafrost properties: Quarternary geology, sediment composition, depth of permafrost, temperature of permafrost, ground ice, active layer properties, etc. Information on sea ice impact is presented for the south-western part of the Kara Sea, for the Gulf of Ob and Baydaratskaya Bay. Layers on coastal morphology and dynamics include maps of types of coasts for Yamal Penisula in the scale of 1:1000000, together with maps of coastal resistance to wave erosion (with all other conditions being equal). For key areas, detailed maps of coastal dynamics are provided, including geomorphological maps, and maps of coastal

retreat with the indication of coastal retreat rates derived from multitemporal satellite imagery analysis. The difference of the maps of types of coasts from the existing ones (in particular, the integrative global map of types of coasts created in the framework of the ACD project [ACD, 2008] is that the present study focuses on the local scale, with Yamal Peninsula being the main object of investigations. A separate part of the GIS system is dedicated to sea bottom morphology and sediments including bathymetric, geomorphologic and other maps of the south-western part of the Kara Sea, Gulf of Ob and Baydaratskaya Bay. Meteorological data of the existing stations is also provided within the GIS.

The comprehensive analysis of such GIS system allows to determine the most dangerous areas of Yamal Peninsula which can be affected by the most intensive coastal erosion in the nearest future. Due to the integrative processing of permafrost, geomorphological, meteorological and other data, it can be suggested, which factors will be the most important for the development of a certain segment of the coastline.

A comprehensive study of coastal dynamics has been made for Yamal Peninsula using GIS in the framework of a joint project between Total and Zubov State Oceanographic Institute. Data on geomorphology, dynamics and permafrost features of the coasts have been combined. As a result, we have been able to analse the distribution of the coastal sections which are the most vulnerable in the future. Such investigations can help with planning and design of coastal infrastructure, as well as for global regional decision-making

References

Ogorodov, S.A. [2008]: The influence of climate change and sea ice extent of the Arctic seas on coastal dynamics of Eurasia. *Problemy Arktiki i Antarktiki*, 78(1):123–128, 2008.

ACD [2008]: Arctic Coastal Dynamics Project. URL www.arctic-coastal-dynamics.org.

Massive ice contribution to the coastal dynamics at Oyuyacha River mouth, west coast of Baydaratskaya Bay, Kara Sea

Nataliya G. Belova, Dmitry E. Kuznetsov, Aleksey P. Vergun, & Stanislav A. Ogorodov

Lomonosov Moscow State University, Russian Federation

The cryolithological composition and in particular the presence of massive ice in coastal bluffs influences significantly the morphology and evolution of the Arctic coasts. Study area is located on the western coast of Baydaratskaya Bay, Kara Sea, at the coastal section between Torasovey and Levdiev islands. Coastal erosion rates were obtained based on field observations at coastal dynamics monitoring network (1988-2012 yrs) and also as a result of multitemporal aerospace imagery analysis (1964-2005) [Kamalov et al., 2006, Ogorodov et al., 2011, Belova, 2014]. Data on coastal bluff retreat rate were compared with cryolithological parameters and height of the bluff.

Coasts of the study area are represented by the Late Pleistocene-Holocene lake-alluvial plain with altitudes up to 25 m a.s.l. The studied coastal section is characterized by relatively strong longshore wave energy flux. The unidirectional flow of the wave energy begins at the southern end of the Torasovey Island and gradually increases to the southeast. The coast is open for wave and ice impacts from the Kara Sea. On the west coast of Baidaratskaya Bay near the Oyuyacha River mouth the highest mean annual rate of coastal erosion is confined to the coastal section with massive ice deposits. The coastal bluff average retreat rate is 0.8-0.9 m/year (data on 41-year period 1964-2005). Coastal retreat rate increases up to 2.1 m/year (1964-2005) at the sections with massive ice beds outcrops, .i.e. here the erosion rate is 2.4 times higher than the average along the coast. In some decades similar coastal retreat rates (2.2-2.5 m/yr for 25 years period 1988-2012) have been recorded at low laida with ice wedges network. Sections of the coast with massive ice beds outcrops should be classified as unstable as for in some years the retreat rates increase dramatically after new exposure arisen.

Acknowledgements

The work has been supported by RFBR project N 16-35-60099 mol_a_dk.

References

Belova, N.G. [2014]: *Massive ice beds of the south-western coast of the Kara Sea*. MAKS Press, Moscow, (in Russian).

Kamalov, A.M.; Ogorodov, S.A.; Birukov, V.Yu.; Sovershaeva, G.D.; Tsvetsinsky, A.S.; Arkhipov, V.V.; Belova, N.G.; Noskov, A.I. and Solomatin, V.I. [2006]: Coastal and seabed morpholithodynamics of the Baydaratskaya Bay at the route of gas pipeline crossing. *Kriosfera Zemli (Earth's Cryosphere)*, 10(3):3–14, URL http://www.izdatgeo.ru/pdf/krio/2006-3/3.pdf. (in Russian).

Ogorodov, S.A.; Belova, N.G.; Kuznetsov, D.E. and Noskov, A.I. [2011]: Using multi-temporal aerospace imagery for coastal dynamics investigations at Kara Sea. *Zemlya iz Kosmosa (Earth from Space)*, 10:66–70, URL http://istina.msu.ru/media/publications/article/01e/ad3/594901/zik_ogor.pdf. (in Russian).

Human-induced relief and permafrost dynamics at Yamal Coast of Baydaratskaya Bay, Kara Sea

Nataliya G. Belova, Stanislav A. Ogorodov, & Olga S. Shilova

Lomonosov Moscow State University, Russian Federation

Coastal dynamics monitoring took place at the West Yamal, near the place where 'Yamal-Europe' gas pipeline network crosses Baydaratskaya Bay, 20 years before the beginning of construction (since 1988). Lithological, geomorphological and geological structures of the 20 kilometer section around the proposed pipeline alignment were studied simultaneously. Monitoring of landscape dynamics in this area continued during the construction period. A considerable amount of data was accumulated both before and during pipeline contstruction. This can be used to assess the sensitivity of the coastal landscape to anthropogenic influences. In addition, climate changes which practically coincided with the beginning of the construction, has become an important factor affecting coastal dynamics in the last decade. These changes expressed in air temperature increase, ice coverage reduction, prolongation of dynamically active period and storm activity growth. As a result the trigger mechanism was launched leading to irreversible changes of coastal landscapes which require urgent intervention to protect the newly constructed facilities of oil and gas infrastructure.

The coast in the study area is represented by the Late Pleistocene-Holocene lake-alluvial poorly dissected plain with altitudes up to 20 m a.s.l. In some places the plain is significantly lowered by aeolian and thermokarst processes (up to 4-10 m a.s.l.). Merging thermokarst basins of different generations are numerous within the plain; ice wedge polygons are forming on their humid bottoms. An extensive section of laida separated from the sea by modern barrier beach is situated directly within the pipeline landfall. This section is presented by a low (up to 3 m) wetland with lots of lakes, being under the influence of tides and storm surges. In areas where high surfaces meet the coastline the coast is abrasional with pronounced coastal bluff composed mostly by frozen sands with low or medium ice content. Retreat rate of such coasts does not usually exceed 0.4-0.6 m [Kamalov et al., 2006]. The barrier beach is located in the center of study area; it separates lagoon and laida from the sea. It represents a typical full profile beach – a very stable accumulative form ideal for wave energy dissipation. It was chosen for the exit site of the underwater pipeline crossing construction through Baydaratskaya Bay. The geological structure of the coast is studied by drilling, including drilling from fast ice in the shallow waters (Fig. 1).

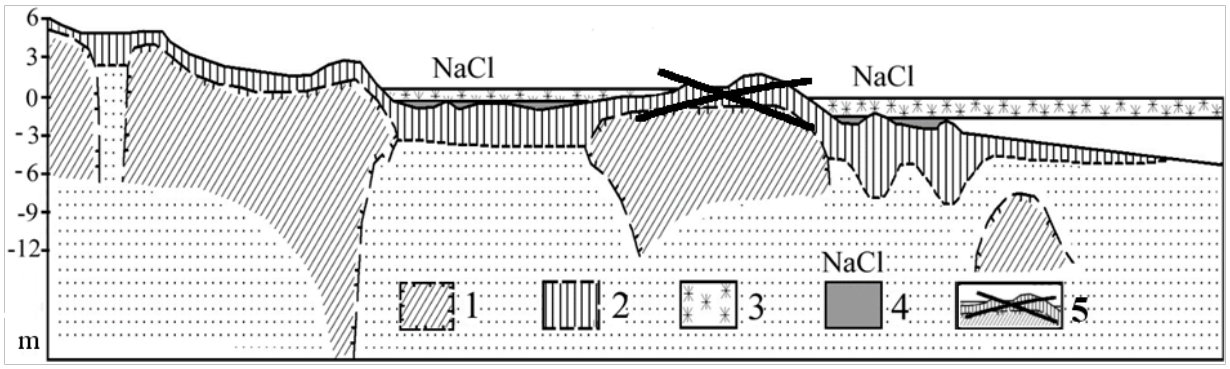

Figure 1: Geocryological crossection of Yamal coast of Baydaratskaya Bay, Kara Sea: 1 – permafrost; 2 – seasonally frozen (thawed) sediments; 3 – sea ice, 4 – cryopeg, 5 – seasonally thawed layer removal.

Permafrost is developed under the slope of high surfaces and under the barrier beach, while the sediments between them (under the lagoon and laida) are in unfrozen state, with permafrost cap both from the side of high surface and barrier beach. Relict permafrost block was found in shallow waters at a depth of about 2 m. In winter the cap of seasonally frozen sediments is formed within the underwater slope and lagoon up to the depth of about 3 m. The maximum seasonal freezing in shallow waters is marked under the longshore bars, as here sea ice in winter reaches the bottom. During the same period when the water exchange with the open sea is deteriorating in the depressions between the longshore bars and in the lagoon an increase of salt concentration as a result of ice formation takes place. It creates the conditions for the formation of saline soils and cryopegs. During summer and autumn the active layer becomes thawed; within the barrier beach its depth is 1.5 m.

Construction of the gas pipeline system began in 2007 and has significantly changed the appearance of the coastal zone. Sandy material composing the seasonally thawing layer on the surface of the barrier beach was almost completely removed for construction purposes. Barrier beach was formerly a natural and reliable protection from high storm surges. In the first year of construction the workers' settlement located on the laida right behind the barrier beach has been flooded as a result of storm surge 1.5 meter height typical (non-extreme) for October. Based on the altitude of the driftwood line within the laida the height of extreme surges here is at least 2.5-3.0 m a.s.l. Dredging in the river estuary south of the barrier beach led to a shortage of sediments in the estuary and partial interception of sediment flow coming from the south. As a result, abrasion accelerated on the adjacent parts of the coast and on the underwater slope, including the area of the pipelines alignment. Pipeline constructors were forced to proceed with the coast protection.

The surface of the barrier beach was artificially lowered and frozen sediments under the barrier beach were subjected to thawing. The dam made of coarse material with concrete block revetment was built directly on the barrier beach surface. As planned by the constructors, the dam was to protect the construction area from storm surges and coastal erosion. However, due to the removal of sandy material from the barrier beach the seasonally thawed layer shifted down the section, leading in permafrost thawing. As a result, coast protection construction simply 'failed' into the thawed permafrost. It should be noted that a similar technology was previously used on the Shishmaref settlement in Alaska, where it has proved to be completely unsuitable for the permafrost zone conditions [Mason et al., 2012].

Coastal processes activation on the Yamal Peninsula was caused by the construction of the pipeline excluding the existing norms and rules of work in the permafrost zone. It once again reminds us of the need for competent, evidence-based approach to environmental management in the Arctic at all stages of design, construction and operation of oil and gas facilities.

Acknowledgements

The work was supported by RFBR projects No 14-05-00408-a and 16-36-60099-mol_a_dk.

References

Kamalov, A.M.; Ogorodov, S.A.; Birukov, V.Yu.; Sovershaeva, G.D.; Tsvetsinsky, A.S.; Arkhipov, V.V.; Belova, N.G.; Noskov, A.I. and Solomatin, V.I. [2006]: Coastal and seabed morpholithodynamics of the Baydaratskaya Bay at the route of gas pipeline crossing. *Kriosfera Zemli (Earth's Cryosphere)*, 10(3):3–14, URL http://www.izdatgeo.ru/pdf/krio/2006-3/3.pdf. (in Russian).

Mason, O.K.; Jordan, J.W.; Lestak, L. and Manley, W.F. [2012]: Narratives of shoreline erosion and protection at Shishmaref, Alaska: The anecdotal and the analytic. In: Cooper, J.A.G. and Pilkey, O.H.(eds.), *Pitfalls of Shoreline Stabilization: Selected 73 Case Studies, Coastal Research Library 3*, pages 73–92. Dordrecht: Springer Science+Business Media.

Arctic beach ridge morphology and Holocene sea-level fluctuations

Mette Bendixen & Aart Kroon

CENPERM, Denmark

Beach ridges are formed at the waterline by wave-related processes of bores and swash. The height of beach ridges over a reference level is a proxy of the sea-level at time of formation. Beach ridges are found throughout large parts of Greenland and are often coupled to draining rivers, where sediment supply is abundant. In this study, we investigate beach-ridge morphology at Tuapaat along the Disko Bay in central west Greenland. We quantify the height, width, and volume of beach ridges at several levels over the present mean sea level, and relate this to existing sea-level curves of the area (e.g., [Rasch and Nielsen, 1995, Long et al., 2010]. At Disko Island, sea-level fell rapidly in early Holocene due to the isostatic uplift caused by the melting ice caps. During late Holocene the isostatic rebound was less pronounced and sea-level fall ceased. The first results of our study indicate that beach ridges are relatively narrow, low, and have a relatively small volume of sediment during rapid sea-level fall, while beach ridges are wider, taller, and have a large volume of sediment during a decreasing sea-level fall. We look at the intensity and duration of generating beach ridge processes at specific levels and couple this to the dimensions of the observed ridges. Simple statistics indicate that the forming processes do not have sufficient time to build large ridges when sea level falls rapidly. On the contrary, waves have longer time to build up larger ridges when sea level falls slowly or is stagnant.

References

Long, A.J.; Woodroffe, S.A.; Milne, G.A.; Bryant, C.L. and Wake, L.M. [2010]: Relative sea level change in west Greenland during the last millennium . *Quaternary Science Reviews*, 29(3–4):367–383, doi:10.1016/j.quascirev.2009.09.010.

Rasch, M. and Nielsen, N. [1995]: Coastal morpho-stratigraphy and Holocene relative sea level changes at Tuapaat, southeastern Disko Island, central West Greenland. *Polar Research*, 14(3):277–290, doi:10.1111/j.1751-8369.1995.tb00715.x.

Geomorphological features associated with coastal permafrost along an emerging coastline: Nunavik (Quebec), Canada

Antoine Boisson & Michel Allard

Centre for Northern Studies, Laval University, CA

Coastal classification and the dynamics of coastal permafrost in Nunavik (Quebec), Canada

As most of Nunavik shores along Hudson Bay, Hudson Strait and Ungava Bay are affected by post-glacial land uplift that is taking place at regionally variable rates, long stretches of coastline are evolving under a trend of falling relative sea level while others may be having a transitionally stable sea level and others even be in submergence, all depending on the rate of global sea level rise. As well, wave reworking of emerging rock outcrops, glacial till, moraines, glacio-fluvial sand and gravel and post-glacial marine sediments creates a labyrinthine coastline where new permafrost can aggrade under recently formed beaches and tidal flats. Along submerging or exposed thaw sensitive sectors, permafrost can be eroded, leading to accelerated coastal retreat. This highly dynamic geophysical context for coastal permafrost dynamics is further complicated by the current climate warming that can delay the freezing of soils newly exposed by emergence in prograding sectors or accelerate thawing in retreating ones. Through detailed mapping, segmentation and characterization of that ~10,000 km long coastline, one of our key objectives is to understand the dynamics of coastal permafrost by making local and regional interpretations of shifting permafrost features along the coastline such as frost cracks in beaches and flats, tundra polygons on actual and low elevation raised beaches, micro-cliffs, frost mounds, frost blisters, permafrost mounds, frost boils, thaw lakes and cliff erosion. Of particular interest is also the delineation of the boundary of shoreline permafrost within the tidal zone and under shore ice-covered beaches and flats, where the ground thermal regime is affected by tidal submersions and frozen-to-the bottom shore ice. The survey methodology makes use of geotagged videography and photography and a GIS application to classify the coastline into segments, as in the ACD project. Ancillary local data include aerial photographs, available satellite imagery and LiDAR data. In 2015, 4,500 km of shoreline, from Kuujjuarapik to Deception Bay (about 40 % of the total shoreline) was filmed and the rest will be surveyed in 2016. Quantitative measurements of coastal retreats or advances are being made wherever possible by comparisons with previous air photos and with published studies. Areas underscored by prograding or retreating permafrost are being mapped. Two thermistor cables installed in the coastal zone and reaching depths of several meters below sea level were monitored since 2005; they provide unique data about the rate of permafrost aggradation in newly emerged sediments and the thermal regime at the land's edge.

Delta progradation and offshore sedimentary lobes in Kongsfjorden (western Spitsbergen, Svalbard)

Marine Bourriquen[1], Agnès Baltzer[1], Denis Mercier[2], Jerome Fournier[3], Laurent Perez[4], Sylvain Haquin[4], Eric Bernard[5], & Maria Jensen[6]

[1] *University of Nantes, France*
[2] *University of Sorbonne, Paris, France*
[3] *MNHN BOREA-UMR, Dinard, France*
[4] *University of Caen, France*
[5] *CNRS, University of Franche Comté, France*
[6] *University Centre in Svalbard, Longyearbyen*

In the current context of climate change, high-latitude areas are the most vulnerable, with a warming rate twice as fast as the rest of the world, and temperature increases particularly during winter. Since the end of the Little Ice Age (LIA), high-latitude glaciers have undergone a net retreat in response to changing meteorological conditions. Located between 76° N and 80° N, western Spitsbergen has seen a climatic transition from a periglacial to a paraglacial system. On the northern shore of the Brøgger Peninsula (North West Spitsbergen), the average temperature increased by 3 °C from 1965 to 2015. Moreover, in accordance with [Førland and Hanssen-Bauer, 2000] and Quenet (2014), the precipitation total has been increasing from 1961 to nowadays, with a mean per year of 0.385 m from 1961 to 1990 and a value of 0.578 m/y for 2014. The share of liquid precipitation increased from 2010 to 2014, by 0.234 m/y to 0.410 m/y. This climatic change affects the alpine glaciers of Brøgger Peninsula. From 1995 to 2001, from east to west, Austre Lovenbreen retreated to 1000 m, Midtre Lovenbreen retreated to 850 m and Austre Brøggerbreen to 1200 m.

The glacier melt and the sediment transported by the subglacial rivers directly supply coastal zone, with development of deltas and coastal progradation. Thus, the coastal progradation is controlled by the increased runoff and sediment load from the rivers. With the retreat of glaciers, the drainage pattern is shifting at different time scales. Glacier outlet deltas which are drained by the rivers and are fed by transported sediment have registered a coastal progradation [Mercier and Laffly, 2005]. Those who lose rivers alimentation registered a coastal retreat. In the study area, the Kongsfjorden, the data set reveals that shoreline advance could have reached around 5 m/y from 1966 to 1990 for the most energetic outlet delta of Austre Lovenbreen, and around 4 m/y from 2011 to 2014 for the most energetic outlet delta of Midtre Lovenbreen. Three offshore sedimentary lobes were identified in the sub littoral area, in the prolongation of glacier outlet deltas. These lobes registered a net growth from 2009 to 2012. The biggest, located in the prolongation of outlet delta of Austre Lovenbreen, measured 1033 m length in 2009 and 1180 m length in 2012, and 153 m width in 2009 and 170 m width in 2012. This rapid coastal progradation and growth of offshore sedimentary lobes would continue, while the subglacial rivers sediment load is being supplied by the glaciers.

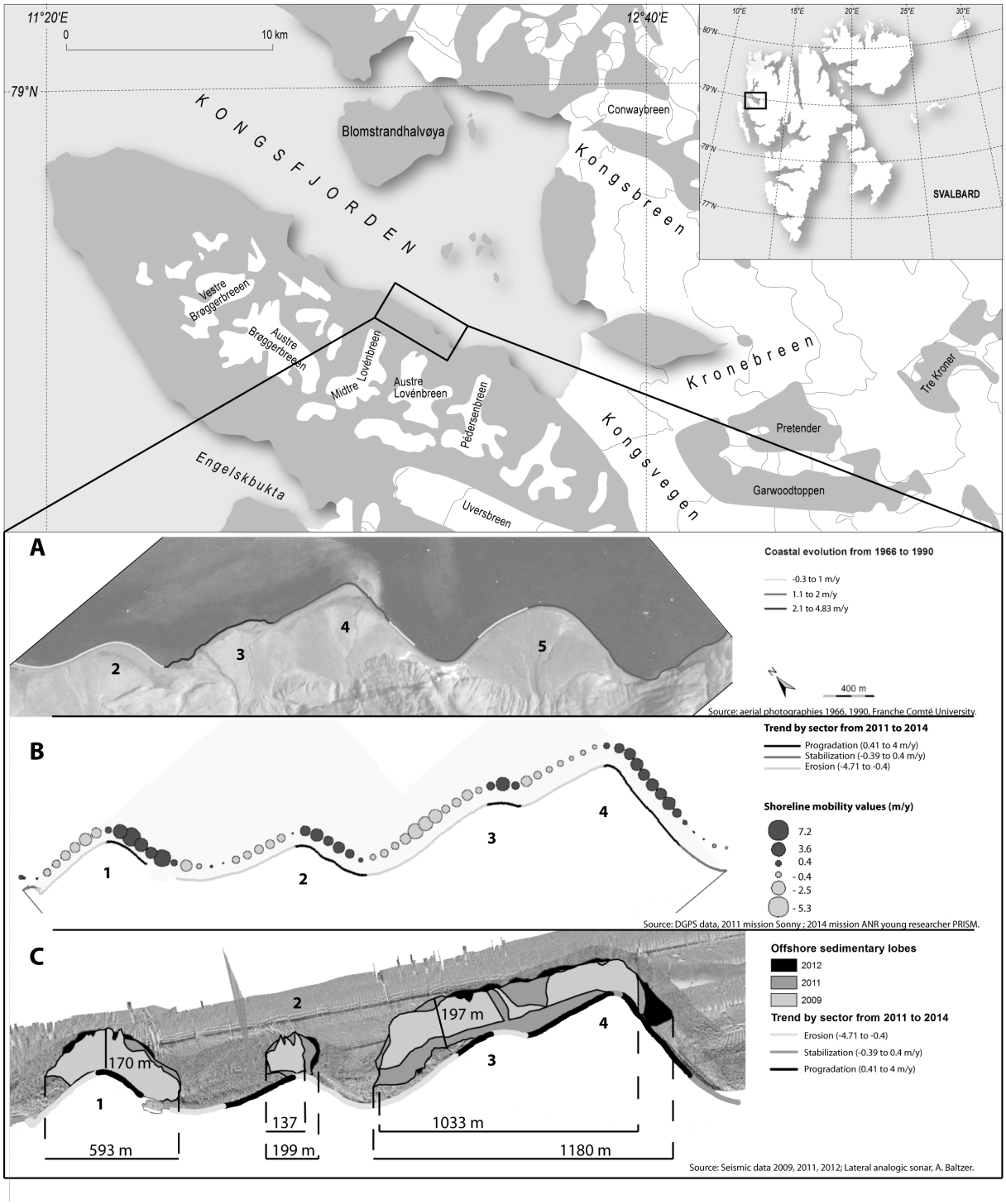

Figure 1: A. Historic coastal evolution in m/y by sector identified from 1966 to 1990. B. Current coastal evolution in trend by sector and in shoreline mobility values in m/y from 2011 to 2014. C. Offshore sedimentary lobes evolution from 2009 to 2012.

References

Førland, E.J. and Hanssen-Bauer, I. [2000]: Increased precipitation in the Norwegian Arctic: True or false? *Climatic Change*, 46(4):485–509, doi:10.1023/A:1005613304674.

Mercier, D. and Laffly, D. [2005]: Actual paraglacial progradation of the coastal zone in the Kongsfjorden area, western Spitsbergen (Svalbard). *Geological Society Special Publication*, 242:111–117, doi:10.1144/GSL.SP.2005.242.01.10.

Applying a coastal erosion model at Tuktoyaktuk, Northwest Territories, Canada.

Nicole Couture[1], Gavin Manson[2], & Dustin Whalen[2]

[1] *Geological Survey of Canada - Northern, Natural Resources Canada, Canada*
[2] *Geological Survey of Canada - Atlantic, Natural Resources Canada, Canada*

In the Arctic, coastal erosion is both a mechanical and a thermal process, and the presence of permafrost and ground ice results in rates of erosion that are up to three times greater than in more temperate regions. The hamlet of Tuktoyaktuk lies on the shore of the Beaufort Sea in Canada's Northwest Territories and is vulnerable to large storm surges which result in overtopping of the coastal spits and bluffs, flooding, and erosion of the shoreline. The erosion is exacerbated by the fact that the coastal sediments are ice-rich and often contain bodies of massive ice. Long-term rates of coastal retreat are on the order of 2 m/year [Solomon, 2005], however short-term rates can be much higher, with up to 15 m of shoreline erosion observed during a single storm. With future reductions in the sea ice cover, changes in storminess, and rising temperatures, erosion rates are likely to increase over the next several decades and pose a threat to coastal and nearshore infrastructure. Modelling future erosion will assist stakeholders in coastal management planning and development.

We use a morphodynamic model adapted for permafrost coasts [Leont'yev, 2004] to investigate coastal profile evolution and coastal erosion at Tuktoyaktuk. The model operates at two time scales, examining morphological changes due to storm events (i.e. the short-term or event scale), as well as coastal evolution over several years or decades (i.e., the long-term or engineering scale). Using a wind and wave re-analysis from the Meteorological Service of Canada, we established past wave climates and extracted storm parameters. The amount of sediment available for transport depends on cliff height and the volume of ground ice in the cliffs. Cliff heights were extracted from differential GPS ground-based surveys as well as digital elevation models derived from LiDAR and satellite imagery; they range from 1.7 to 9.0 m. Ground ice was quantified using a morphological model that accounts for different ground ice types (including pore ice and thin lenses, ice wedges, and large bodies of massive ice) and the stratigraphic relationships between them. Total ice volumes for the different terrain units range from 21 to 90 % by volume. Beach and nearshore slopes were established from topographic and bathymetric surveys carried out by the Geological Survey of Canada. A hydrodynamic model (Delft 3D) was used to simulate currents and wave-driven sediment transport in both the across- and along-shore directions. Variations in relative sea level were obtained from the Canadian Hydrographic Service tide gauge at Tuktoyaktuk. The erosion model was used to hindcast past coastal erosion in the Tuktoyaktuk region and the results are compared with historical shoreline recession to assess accuracy. Future erosion is assessed using predictions of changing environmental parameters for the southern Beaufort Sea and sea level rise projections.

References

Leont'yev, I. O. [2004]: Coastal profile modeling along the Russian Arctic coast. *Coastal Engineering*, 51(8-9):779–794, doi:10.1016/j.coastaleng.2004.07.009.

Solomon, S. M. [2005]: Spatial and temporal variability of shoreline change in the Beaufort-Mackenzie region, northwest territories, Canada. *Geo-Marine Letters*, 25:127–137, doi:10.1007/s00367-004-0194-x.

Comparing coastal dynamics between two geomorphologically distinct permafrost-affected coastlines in NW Alaska

Louise M. Farquharson[1], Daniel H. Mann[1], Guido Grosse[2], Benjamin M. Jones[3], David K. Swanson[4], & Vladimir Romanovsky[5]

[1] *University of Alaska Fairbanks, USA*
[2] *Alfred Wegener Institute Helmholtz Centre for Polar and Marine Research, Potsdam, Germany*
[3] *U.S. Geological Survey, Anchorage, Alaska, USA*
[4] *U.S. National Park Service, Fairbanks, Alaska, USA*
[5] *Geophysical Institute, University of Alaska Fairbanks, USA*

Arctic clastic coastlines are some of the most dynamic in the world and have a large impact on cultural and natural resources. Sea ice plays an important role in the erosion and accretion dynamics of these coastlines, and sea ice cover is currently declining at >10 % per decade. As a result of declining sea ice cover and an increase in the duration of open water days in the Arctic Ocean, we need to know more about coastal processes in polar seas, specifically how sea ice decline changes coastal processes, the rate at which such coastal changes can occur, and how the effects of declining sea ice interacts with local coastline characteristics including wave fetch, bathymetry, permafrost properties onshore, and pre-existing coastal geomorphology.

To assess the influence of sea ice decline on permafrost coastal dynamics we selected two segments of the coastline in NW Alaska with contrasting geography, surficial geology and geomorphology. Study site A, Cape Krusenstern National Monument (CAKR), has a wave-dominated, west- to south-west facing, coarse-clastic shoreline. Accreted beach ridges, barrier-closed lagoons, permafrost bluffs, longshore gravel bars, and gravelly beaches characterize coastal geomorphology. Study site B, the Bering Land Bridge National Park and Preserve (BELA), has a north-facing coastline with a shoreline characterized by yedoma and thermokarst basin permafrost bluffs, aggrading spits, sandy barrier islands, and open lagoons.

To establish rates of coastal change and identify key geomorphological processes, we digitally mapped the shoreline of both study areas using aerial photographs (1-meter resolution or better) and sub-meter resolution WorldView-2 satellite imagery from 2003 and 2014, respectively. We compared our data to the results of previous studies based on imagery taken between 1950 and 2003 [Lestak et al., 2010]. To better understand the relationship between geomorphology and rates of change, we established geomorphological landform classes for both study areas. We mapped coastal changes within a subset of each study area, using sub meter resolution imagery, over annual time steps to help us better quantify variations in the rate of event driven coastline change.

Mapping results for the period 2003 to 2014 suggest a change in erosion rates within both study sites. Erosion rates for the period 1950 to 2003 in BELA and CAKR were -0.12 m/yr and -0.98 m/yr respectively, where the negative signs indicate shoreline retreat [Gorokhovich and Leiserowiz, 2011]. These rates, for the period between 2003 and 2014, increased in CAKR to -0.86 and decreased in BELA to -0.69 m/yr. Rates of erosion were found to vary according to geomorphology, with overwash fans in BELA exhibiting the highest rates of change at -1.3 m/yr. Significant changes in geomorphology were observed for this time period including the development of a 200-meter long spit in CAKR, degradation of ice wedges on upland yedoma bluffs in BELA, and the infilling of numerous barrier island ponds due to overwash events in BELA. Our results illustrate the complexity of coastal responses along Arctic coastlines even within close proximity. To ensure robust projections of future coastal change, further mapping and analysis at intra-annual and sub-meter spatial resolution is necessary to firmly tie together cause and effect of arctic coastal processes with a changing climate.

References

Gorokhovich, Y. and Leiserowiz, A. [2011]: Historical and Future Coastal Changes in Northwest

Alaska. *Journal of Coastal Research*, pages 174–186, doi:10.2112/JCOASTRES-D-11-00031.1.

Lestak, L.R.; Manley, W.F. and Parrish, E.G. [2010]: *Digital Shoreline Analysis of Coastal Change in Bering Land Bridge NP (BELA) and Cape Krusenstern NM (CAKR), Northwest Alaska: Fairbanks.* AK: National Park Service, Arctic Network I&M Program, Geospatial Dataset-2184176.

Impact of storms on Arctic shorelines: Cases study

Emilie Guegan[1], Anatoly Sinitsyn[2], & Hanne Christiansen[3]

[1] *Norwegian University of Science and Technology - NTNU, Norway*
[2] *SINTEF Byggforsk - Trondheim,Norway*
[3] *The University center in Svalbard - UNIS, Norway*

Arctic storms occurring in fall are known to have dramatic short-term erosive impacts on coastal profiles [Hequette and Barnes, 1990]. While storms are sporadic episodic events, they can drastically accelerate coastal change. Hume and Schalk [1967] studied the sediment movement along a segment of the Alaska coast west of Point Barrow between 1948 and 1962, and reported that a single storm event, occurring October 1963, moved an amount of sediment equivalent to 20 years of normal transport. Storms, inducing storm waves reaching the coasts with length, strength and direction different than during fairweather conditions can also generate storm surge (leading to coastal flooding). These two natural processes can cause important damage on coastal settlements. Measures and protective infrastructures have to be considered for managing impact of coastal erosion. However, for designing these protectives structures, additional knowledge are needed on site-specific storm history (frequency), as well as the morphodynamic response of coastlines of various lithology and cryostratigraphy, in term of recession rates and failure mechanisms. The impact of a storm is not only dependent of the storm characteristics, it also varies with coastal topography, specially elevation. While low-lying tundra plain coasts are obviously very sensitive to storm surge and flooding, we present change of topography in coastal bluff areas. For this purpose, two examples are presented:

1. The change of coastal geomorphology in Bjørndalen and Vestpynten in Svalbard, related to the october 2015 storm and its consequences on local infrastructures, and
2. the dramatic coastal recession observed by remote sensing occurring in Varandey area (Northern Russia) in 2010.

In a current climate change, where the frequency and magnitude of storms event is predicted to increase, a better understanding of their effect on Arctic coasts could allow for elaboration of better coastal protection technics.

References

Hequette, A. and Barnes, P.W. [1990]: Coastal retreat and shoreface profile variations in the Canadian Beaufort Sea. *Marine Geology*, 91(1–2):113–132, doi:10.1016/0025-3227(90)90136-8.

Hume, J.D. and Schalk, M. [1967]: Shoreline processes near Barrow, Alaska: A comparison of the normal and the catastrophic. *Arctic*, 20(2): 86–103, URL http://pubs.aina.ucalgary.ca/arctic/Arctic20-2-86.pdf.

Permafrost coastal dynamics, a case study: Evaluating the coastal bluff in the Medynskiy sector (Varandey area), Barents Sea 2010 – 2015

Lucy C. Hyam[1,2], Anatoly Sinitsyn[2], Phil Hwang[1], & Emilie Guegan[3]

[1]*SAMS (Scottish Association for Marine Science), United Kingdom*
[2]*UNIS (The University Centre of Svalbard), Norway*
[3]*NTNU (Norwegian University of Science and Technology), Norway*

The coastal zone of the Varandey area, Eastern Barents Sea, is composed of unlithified perennially frozen sediments, and affected by coastal erosion processes. Knowledge of erosion rates is of primary importance for society in general and for industry in particular. Previous studies showed that the long-term erosion rates in the area are approximately 2 m/yr between 1961–2013, measurements were taken during ice free periods. However the short term rates were of much higher magnitudes.

In this study we focus our research only on one part of the Varandey area – the Medynskiy sector, where short-term erosion rates are assessed for 2010–2014. Estimates are based on analysis of satellite images and field-based observation. Hydrological parameters such as sea state, ice conditions, temperature for the ground, air and ocean (summer and winter), in order to determine the main drivers responsible for the observed changes in the corresponding years. Distribution of thermokarst lakes and ice wedges was studied, as well as the geological features that have impact erosion rates in the area. The results show a correlation extremely high erosion rates were caused by the catastrophic storm event in July 2010, followed by much lower rates typical for fair-weather conditions.

The laboratory simulation of the deformation of the coastal slope under the wave action in the permafrost zone

Dmitrii Ionov, Yelena Debolskaya, Vladimir Debolsky, & Ilya Gritsuk

Russian Academy of Sciences, Russian Federation

Extreme wave action on a natural or artificial underwater obstacles leads to loss of their stability and destruction. In the permafrost zone these processes and study of them are complicated due to the frozen ground conditions.

The work is devoted to research of sediment transport by wave action on the bed channel slopes and sea banks composed of frozen ground. The experiments were carried out in a laboratory model constructed in an open tray in the Russian Peoples' Friendship University.

Natural sand with grain size d50 = 0,20 mm was used as the material of the model. Above-water part of the model coastal slope was kept in a freezer at -18 °C for 24 hours, and other parameters were assigned according to the diagram below (Fig. 1).

The tray of circulation type with rectangular cross section is able to change a slope of the bottom, and is equipped with a programmable wavemaker. Its length is 16.0 m, width is 0.3 m, height of walls is 0.4 m.

The model has a slope angle 27°. Its dimensions: height is 27 cm, length of the base is 100 cm, width is 30 cm. The water depth over the model is 16 cm. For experiments with frozen ground the upper part of the model (12 cm from its total height) was kept in a freezer for 24 hours at -18 °C. For the experiments with soils having a positive temperature, model was formed from moist soil on the entire height (27 cm) directly in the tray.

In the first phase of research over 40 experiments

were conducted to determine the optimal wave and model parameters, as well as the experimental procedure as a whole. As a result of analyzing of the results of preliminary experiments the most suitable wave characteristics were determined for research purposes, based on which the finishing experiments performed. It should be noted that the repeatability of the experiment is high enough and the difference between the readings experiments performed under identical wave model parameters and ranges from 1 to 4 %.

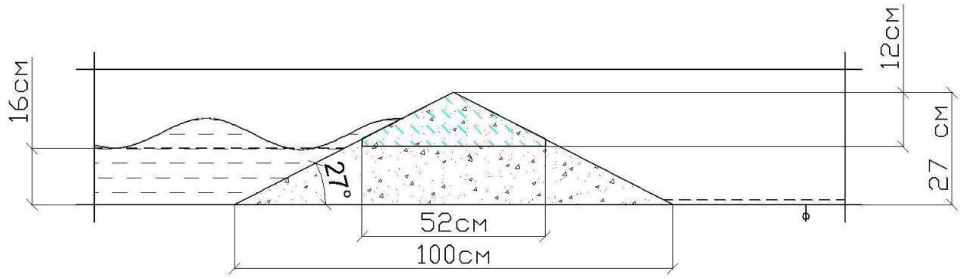

Figure 1: Scheme of the hydraulic model.

Results

1. Laboratory experiments showed that erosion of the slope composed of frozen soil under wave action is more intense than of the slope composed of sand with positive temperature *ceteris paribus*.

2. The volume of the deformation of frozen model, on average, 27 % higher than the volume of deformation of the model composed of sand with positive temperature.

3. The experiments showed that the laboratory modeling of wave processes and of deformation describe the natural processes of transformation of the coastal slope and sediment transport with a high degree of reliability.

4. The results of the research make it possible to develop physical and mathematical model of the transformation of the coastal slopes under the influence of wave processes.

5. The results can be widely used in the design, construction and operation of offshore structures, waterworks transport and energy sectors.

Acknowledgements

The work was supported by the Russian Foundation for Basic Research (project 13-05-41095 and 15-05-00342)

Dependencies of western Baydara Bay (Kara sea) coast retreat rate on lithology and height of coastal deposits

Vladislav Isaev[1], Sergey Buldovich[1], Andrey Koshurnikov[1], Ruslan Amangurov[2], Daria Aleksyutina[1], Nikita Onischenko[3], Oleg Podchasov[1], Ekaterina Grishakina[1], Ivan Sokolov[4], & Alexey Usov[1]

[1]*Moscow State University, Russian Federation*
[2]*JSC MSU-Geophysic, Russian Federation*
[3]*Schlumberger, USA*
[4]*Geoinzservice LLP Fugro Group, Russian Federation*

The retreat of the coastal line is occurred due to thermal denudation and thermal abrasion of coastal deposits. Thermal abrasion intensity depends from several main factors in the permafrost area, i.e.: ice regime, properties and composition of the seashore rocks, tidal activity of the sea level as well as water temperature and its salinity. Thermal denudation depends from radiation-heat transfer to the surface of slope, mechanical properties of grounds, ice content in ground and lithology of deposits.

Ice activity of the sea have the significant influence on the retreat of the seashore [Are, 1980, Zachar, 1982, Dallimore et al., 1996, Jones et al., 2009, Arp et al., 2011]. On the other hand, the most important phenomena are ice cover duration and ice coverage during the summer season. The easiest to erode are silty clay, sand and loam clays. These sediments are typical for genetic types of Quaternary permafrost sediments on Kara seacoast. They often have high ice content represented by ice layers, ice wedges and massive ice texture of frozen ground (Romanovsky, 1993).

Very important role in thermal abrasion is played by remove and ebbing work of the sea. It is not clear the role of sea level rising due to glaciers thawing. Besides that factor, it was found that seawater temperature and salinity do influence on the seashore erosion rate [Are, 1980].

Thermal denudation is spreading for shore composed by frozen rocks with rich ice content [Günther et al., 2013]. It include some exogenesis cryogenic gravitational processes (slumping, sliding, solifluction, erosion etc.) which develop in course of rock thawing as well as nivation (snow bank processes) which induces seashore destruction and material migration to the lower areas (beach). Thermal denudation impact on the above-water part of the littoral zone results in scarp flattening with their stability also affected by abrasion (Romanovsky, 1993). Development of thermal denudation processes acquires some specific features in massive ice areas since on such areas these processes turn to be very intensive. Thermal cirques and thermal terraces are confining to massive ice exposure areas with rate of their back land retreat much higher than rate of thermal abrasion-inspired scarp retreat in the neighboring areas.

For evaluation of rate of seashore retreat, Are et al. [2005] suggested and implemented the method based on thermal terrace dimensions and their lifetime data. Thermal denudation resulting from snow melting and summer rains is more active in the areas without any vegetation. Vegetative ground cover induces block caving in the top of thermal cirques. Often they are large blocks, which are delineate by frost fissures that caves down [Khomutov and Leibman, 2008].

In accordance, the above-mentioned method the complex scientific research of the coastal retreat carried out on the western coast of Baydara Bay of Kara Sea. That works focused on detailed study of cryogenic destruction of seashore permafrost. That includes different programs of works: geocryological, geodetic surveying, drilling, thermometric and laboratory researches and study of hydro physical, mechanical, thermophysical and other properties of the rocks in both samples and in-situ. The purpose of research carried out in the Kara sea coast are complex study and investigation of seashore to illuminate the dependence between the lithology of the coastal deposits and height of the coast and the retreat rate for this sites. It based on 2013–2015 season observations.

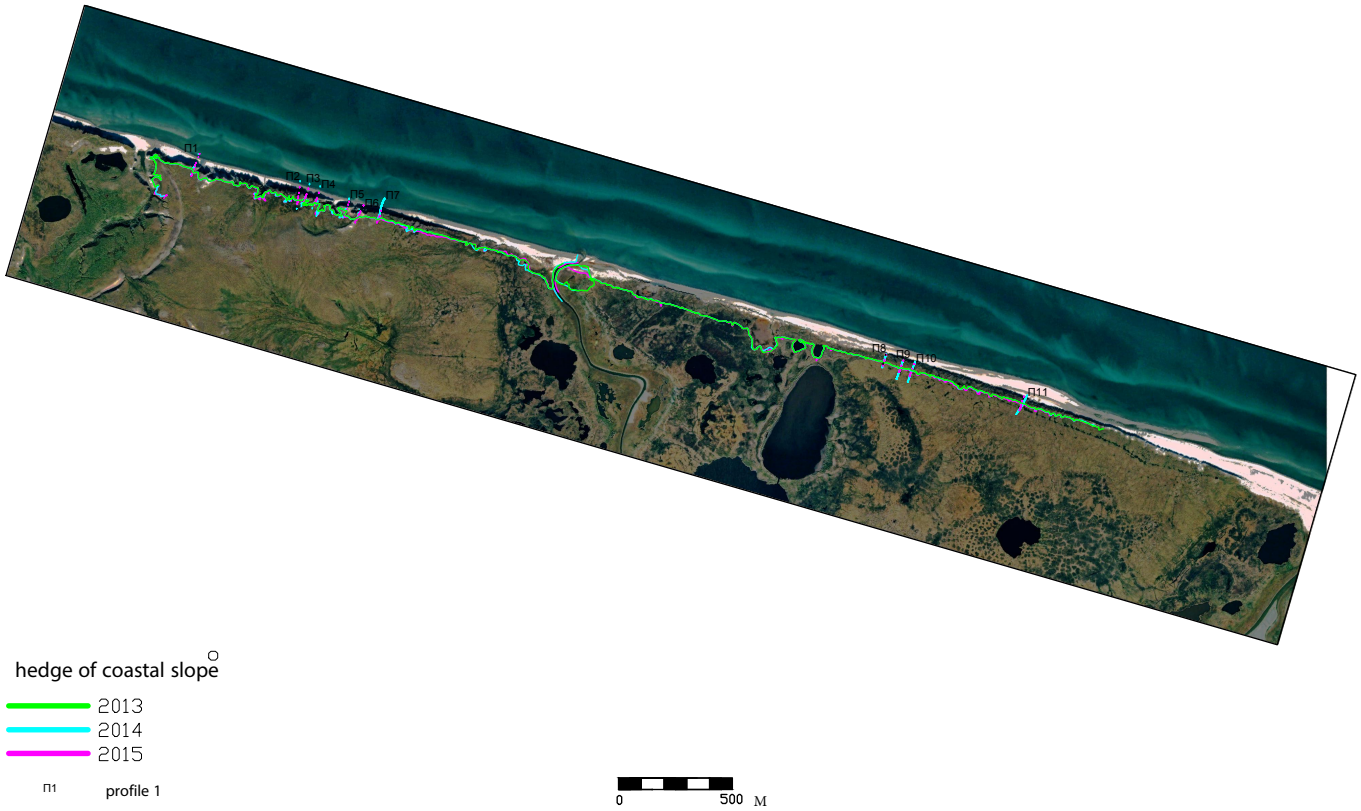

Figure 1: The interpolation of coastal line of Baydara gulf west coast from 2013 to 2015 year

References

Are, F.E. [1980]: *Termoabraziya morskikh beregov (thermal abrasion of sea coasts)*. Moscow, Nauka, 158 pp.

Are, F.E.; Grigoriev, M.N.; Hubberten, H.-W. and Rachold, V. [2005]: Using thermoterrace dimensions to calculate the coastal erosion rate. *Geo-Marine Letters*, 25:121–126, doi:10.1007/s00367-004-0193-y.

Arp, C.D.; Jones, B.M.; Urban, F.E. and Grosse, G. [2011]: Hydrogeomorphic processes of thermokarst lakes with grounded-ice and floating-ice regimes on the Arctic coastal plain, Alaska. *Hydrological Processes*, doi:10.1002/hyp.8019.

Dallimore, S.R.; Wolfe, S.A. and Solomon, S.M. [1996]: Influence of ground ice and permafrost on coastal evolution, Richards Island, Beaufort Sea coast, N.W.T. *Canadian Journal of Earth Sciences*, 33: 664–675, 1996. doi:10.1139/e96-050.

Günther, F.; Overduin, P.P.; Sandakov, A.V.; Grosse, G. and Grigoriev, M.N. [2013]: Short- and long-term thermo-erosion of ice-rich permafrost coasts in the Laptev Sea region. *Biogeosciences*, 10(6): 4297–4318, doi:10.5194/bg-10-4297-2013.

Jones, B.M.; Arp, C.D.; Jorgenson, M.T.; Hinkel, K.M.; Schmutz, J.A. and Flint, P.L. [2009]: Increase in the rate and uniformity of coastline erosion in Arctic Alaska. *Geophysical Research Letters*, 36 (3):L03503, doi:10.1029/2008GL036205.

Khomutov, A.V. and Leibman, M.O. [2008]: Landscape controls of thermodenudation rate change on Yugorsky Peninsula coast. *Kriosfera Zemli (Earth's Cryosphere)*, 12(4):24–35, URL http://www.izdatgeo.ru/pdf/krio/2008-4/24.pdf. in Russian.

Zachar, D. [1982]: *Soil erosion*, volume 10 of *Developments in Soil Science*. Amsterdam: Elsevier Scientific, 547 pp.

Controls of shoreline changes in Calypsostranda (Bellsund, Svalbard) over 1990 – 2015 period

Kamila Jarosz[1], Piotr Zagórski[1], Lukasz Pawłowski[2], Paulina Lewińska[3], Mateusz Czesław Strzelecki[2], & Marek Jaskólski[2]

[1] *Maria Curie-Sklodowska University, Lublin, Poland*
[2] *Uniwersity of Wrocław, Poland*
[3] *AGH-UST University of Science and Technology, Kraków, Poland*

The functioning of Arctic coasts reflects the exceptionally dynamic changes occurring in Arctic regions conditioned directly and indirectly by climate change. In Svalbard, the evolution of coastal zone depends to a large degree on the changes in glacial systems. Retreating glaciers expose new terrains and deliver large amounts of sediments to the coastal zone that in turn support the formation of new coasts. The state of the coast is also influenced by sea-ice conditions and permafrost related processes. Southern Bellsund is characterized by one of the most diverse coastal geomorphology on Svalbard in general. Coastal environments include vast tidal flats, wide gravel-dominated beaches, lagoons, migrating spits, and both rocky and ice cliffs. In this paper we summarise the geomorphological investigations along Calypsostranda between 1990 and 2015, focusing on the interplay of geological, geomorphological and climatic process controlling the coastal morphodynamics on annual timescales.

We applied a combination of methods including remote sensing mapping, field-based mapping using DGPS, terrestrial laser scanning, and GIS analyses (Digital Shoreline Analysis Tool).

The present-day state of the shores of the Calypsostranda is controlled by the operation of several processes:

1. glacial processes that supply sediments;
2. fluvioglacial and fluvial processes responsible for the transport of sediments towards the coast
3. ice processes (including sea and shore ice cover)
4. marine processes (waves, tides, longshore drifts).

Main tendencies in shoreline development were identified by comparing shoreline positions among various time steps (1990–2000, 2000–2005, 2005–2010, 2010–2015). Three time periods exhibited shoreline retreat (1990–2000, 2005–2010, 2010–2015). Shoreline advance was recoded in only one period (2000–2005). Significant coastal changes were also caused by extreme events, particularly in beach systems. This refers both to the exceptionally severe storms and the associated delivery of swash zone sediments (e.g. autumn of 1994, or beginning of August 2002), and extensive shore ice cover (spring/summer of 1993, 2005). Marine processes consisted of adapting the shoreline to 'optimum conditions', i.e. distributing surplus material along the shore and compensating for the losses. In many cases, the effects of such extreme events can control the development of coastal zone for decades. The other type of wave action, i.e. swell, led to significant changes in shoreline geometry in the period from 2000 to 2005, particularly in the Calypsobyen area.

Currently, Calypsostranda shoreline is adjusting to changes in sediment supply from rapidly retreating glaciers (Scottbreen and Renardbreen).

Acknowledgments

The fieldwork and data collection was financed by National Science Centre projects: No. NN 306 703840 'MORCOAST' and No. 2013/09/B/ST10/04141

Application of electrical resistivity tomography for monitoring of the state of coastal permafrost, SW Spitsbergen

Marek Kasprzak[1], Mateusz C. Strzelecki[1], Krzysztof Migała[1], Michael Lim[2], Marek Jaskólski[1], & Lukasz Pawłowski[1]

[1] *University of Wroclaw, Poland*; [2] *Northumbria University, UK*

Electrical resistivity tomography (ERT) is a widely used geophysical method in permafrost researches. ERT studies are based on clear assumption that ice or frozen ground are characterized by very low electrical conductivity (and a high resistivity), which distinguishes them from remaining unfrozen parts of the ground.

In recent years we have applied ERT surveys to determine the shape and spatial distribution of permafrost along the rocky coastal zone of SW Spitsbergen. Our study has also provided new arguments of a strong impact of warm and salty seawaters on the state of coastal permafrost. Over the seasons we have documented that seawaters influence the bottom of coastal permafrost and form a second,'bottom' active layer of permafrost. Seasonal variations in regular active layer and 'bottom' active layer of permafrost were detected using a relatively high resolution electrical imaging (narrow space between electrodes:1–1.5 m in each measurement profiles).

In our paper we describe a concept of geophysical monitoring of the permafrost active layers. We present results of two ERT test profiles located at Säterdalsneset cape (77°2.83'N, 15°8.18'E), perpendicular to the shoreline, carried out over three summer seasons 2012, 2014 and 2015. The ERT tests were also complemented by analyses of meteorological data from a nearby Polish Polar Station in Hornsund. Obtained inversion models gave an information about varying degrees of active layer development as well as different degrees of impact of a heat flux from the sea on the bottom part of coastal permafrost body. Comparison of ERT profiles carried out in August with those conducted in July showed the progress (rate) of seasonal thawing of upper and bottom layers of permafrost. The comparison of ERT profiles taken in July 2012, 2014 and 2015 shows a strong correlation between active layer thawing and seasonal weather (thermal) conditions.

This paper is a contribution to the National Science Centre in Poland OPUS project UMO_2013/11/B/ST10/00283: 'POROCO – Mechanisms controlling the evolution and geomorphology of rock coasts in polar climates'.

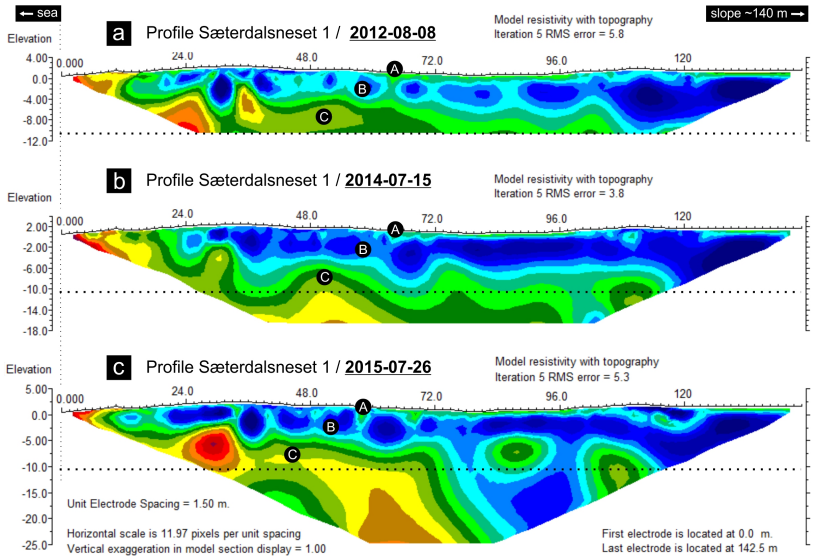

Figure 1: An example of permafrost changes imaged by electrical resistivity tomography; A - active layer, B - permafrost body, C - unfrozen ground.

Modern rates of thermal denudation and thermal abrasion on western Kolguev Island

Alexander Ivanovich Kizyakov[1], Mikhail Viktorovich Zimin[1,2], Anton Vladimirovich Sonyushkin[2], Marina Oskarovna Leibman[3], Natalia Vitalievna Pravikova[4], & Frank Günther[5]

[1] *Lomonosov Moscow State University, Faculty of Geography, Moscow, Russian Federation*
[2] *ScanEx Research and Development Center, Moscow, Russian Federation*
[3] *Earth Cryosphere Institute SB RAS, Tyumen, Russian Federation*
[4] *Lomonosov Moscow State University, Faculty of Geology, Moscow, Russian Federation*
[5] *Alfred Wegener Institute Helmholtz Centre for Polar and Marine Research, Potsdam, Germany*

Destruction mechanisms and dynamics of the Arctic coast, also in the western sector of the Russian Arctic, are studied in detail, including the use of remote sensing data. However, data on thermal abrasion and thermo denudation of Kolguev island is quite limited. Some estimates were presented in article of Velikotsky [1998]. Estimation of thermo denudation rates near the Sauchiha river mouth for the period 1948–2002 years was done by the authors earlier [Kizyakov and Perednya, 2003].

To obtain data about the modern (after 2002) shoreline retreat rates and growth of thermal cirque a high resolution remote sensing data were involved in our research (Fig. 1).

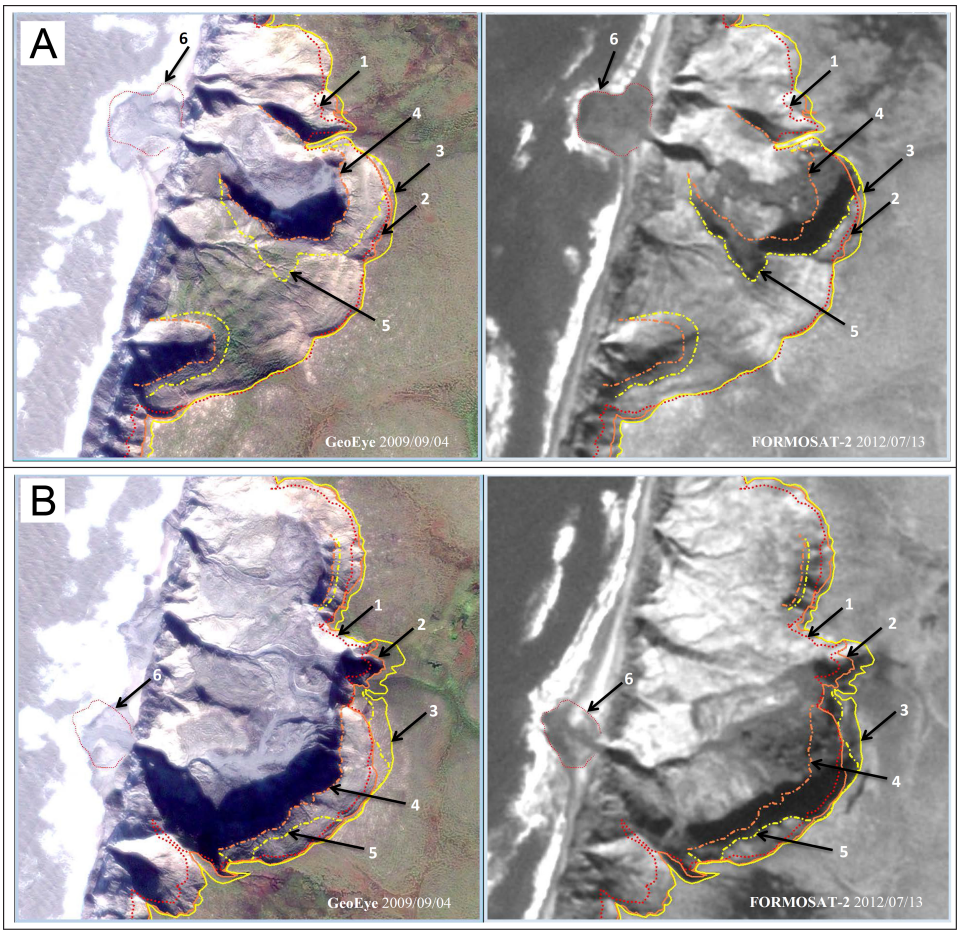

Figure 1: The scheme of thermal cirques edges retreat in 2002, 2009, 2012. A – Central; B – Southern thermo-cirque. Edges: 1 – in 2002, 2 – in 2009, 3 – in 2012, 4 – lower edge in 2009, 5 - lower edge in 2012, 6 - proluvial cones in 2012

Part of the western coast of Kolguev Island was inspected during field work conducted in 2002 by ECI SB RAS, together with VNIIOkeangeologia. The object of research was the coastal part with a group of three coastal thermal cirques, located 3.5 km south of the Sauchiha river mouth. In 2012, within the framework of the project 'Geoportal of MSU' operational satellite images have been acquired for Kolguev Island by FORMOSAT-2. This high resolution satellite imagery provides ample opportunities for visual interpretation of coastal landforms. Therefore, aerial photographs (1948 and 1968), surveying materials (2002), and high-resolution satellite images (2009 and 2012) provide the basis to study the dynamics of the coast and thermal cirques in the key investigation area south of the Sauchiha river mouth. Here we calculated:

- retreat rates of the edge of the coastal terraces and thermal cirques for the periods 1948 – 1968, 1968 – 2002, 2002 – 2009, 2009 – 2012;
- retreat rates of the foot of the coastal terrace for the periods 2002 – 2009, 2009 – 2012;
- volume of the material which enters the coastal zone by the thermal abrasion for one linear km of coastline [Kizyakov et al., 2013].

Average long-term retreat rates of the coastal terrace during 1948 – 2012 varied from 0.7 to 2.4 m/year; during 2002 – 2012 rates varied from 1.7 to 2.4 m/year. Identified rates are distinctive for the part of coast from the mouth of Krivaya river to the curve of coastline near the mouth of the Gusinaya river with a total coastline length of 60.5 km. These rates are 1.1 – 1.5 times lower than average rates of retreat of thermal cirque edges which are connected with melting of massive ice deposits.

The average growth rate of the thermal cirques during 1948 – 2002 was 2.4 m/year; during 2002 – 2012 it was 2.6 m/year. The maximum growth rate on some sections during 2009 – 2012 were 14.5 – 15.1 m/year. These are the highest rates that have been ever recorded in the western sector of the Russian Arctic. Causes for these abnormally high rates are related to an increase of the annual amount of positive air temperatures, which have been 1.4 – 1.5 times higher during 2011 – 2012 than the long-term average.

The determined rates of the development of thermal cirque can be extended to the north from the key area (near the Sauchiha river mouth) to the Gusinaya river mouth with total length of 32.3 km.

The next plans on studying the coastal dynamics on Kolguev Island - using additional satellite images for the purposes of:

- detailization of interannual dynamics through the analysis of more short time span series of satellite images,
- definition of variations of the coastal destruction rates on the Western and Northern coasts.

References

Kizyakov, A.I. and Perednya, D.D. [2003]: Destruction of coasts on the Yugorsky Peninsula and on Kolguev Island (Russia). In: Phillips, M.; Springman, S.M. and Arenson, L.U.(eds.), *Permafrost: Proceedings of the 8th International Conference on Permafrost, Zürich, Switzerland, 21 – 25 July 2003*, pages 79–80. The Netherlands: AA Balkema Publishers.

Kizyakov, A.I.; Zimin, M.V.; Leibman, M.O. and Pravikova, N.V. [2013]: Monitoring the rate of thermal denudation and thermal abrasion on the western coast of Kolguev Island, using high resolution satellite images. *Kriosfera Zemli (Earth's Cryosphere)*, 17(4):36–47, URL http://www.izdatgeo.ru/pdf/krio/2013-4/36.pdf.

Velikotsky, M.A. [1998]: Modern shore dynamics of Kolguev Island. In: Solomatin, V.I.; Sovershaev, V.A. and Mazur, I.I.(eds.), *Dynamics of Russian Arctic Shores*, pages 93–101. Moscow: MSU publishing house, ISBN 5-89575-007-9, in Russian.

Coastal erosion and resulting impacts along the ice-rich permafrost coast of the Ivvavik National Park, Yukon Territory, Canada

Anna Maria Konopczak[1,2], Hugues Lantuit[1,2], & Gavin Manson[3]

[1] *Alfred Wegener Institute for Polar and Marine Research, Germany*
[2] *Institute of Earth and Environmental Science, University of Potsdam, Germany*
[3] *Geological Survey of Canada-Atlantic, Dartmouth, Canada*

Due to its fine grained and very ice-rich sediments, the coast of the Yukon Coastal Plain forms a very dynamic landscape. Changing climatic conditions add to this by lengthening open water periods and increasing permafrost temperature, which contributes to an increase of coastal erosion. Even though the Yukon Territory has no permanent settlements along its Beaufort coast, this region is of exceptional value as it serves as a calving area for the Porcupine Caribou Herd and it comprises numerous archaeological sites which are rare remains of the rich human history of this region. The importance of this area is underpinned by the fact that about two third of the coast of the Yukon Territory is protected as part of the Ivvavik National Park, which in turn is a candidate for the UNESCO world heritage site status. Additionally, recurring plans to develop oil and gas-related infrastructure would dramatically change the nature of the coastal environment. Yet, no up-to-date information is available on the erosion of this long coastal stretch, which is detrimental to both environmental and industrial planning in the area.

Here, we present initial results of an assessment of shoreline dynamics and their influence on the coastal system in the Ivvavik National Park area. We first quantified shoreline changes of the approximately 150 km long coast by means of remote sensing data. We geocoded aerial photographs from the 1950s, the 1970s and the 1990s to a GeoEye scene from 2011 and digitized the respective shorelines. We then analyzed spatial and temporal shoreline dynamics by using the Esri ArcGIS extension DSAS (Digital Shoreline Analysis System). We coupled these results with a large range of ecological and cultural datasets, including ecological units, freshwater habitat extents and archaeological site positions, in order to determine the vulnerability of the coastal environment of the Ivvavik National Park. Our initial results show that coastal erosion is prevailing along most parts of the coast and only very limited coastal stretches experience accumulation. The analyses allow us to draw first conclusions about which habitats are most affected by arctic coastal changes and which archaeological sites are prone to get lost in the near future.

Polar beach-ridge systems: archives of a changing climate

Sebastian Lindhorst

University of Hamburg, CEN, Institute of Geology, Germany

The sedimentary architecture of polar gravel-beach ridges is presented and it is shown that ridge internal geometries reflect past wave-climate conditions. Raised beaches are common features on paraglacial coasts which experienced a net-uplift during the Holocene as the result of postglacial isostatic rebound. Consequently, elevated beach ridges play a major role in the reconstruction of Holocene sea-level variations.

Ground-penetrating radar (GPR) data obtained along the coasts of King George Island (South Shetland Islands, Western Antarctic Peninsula) show that beach ridges unconformably overlie seaward-dipping strata of the strand plain. Whereas strand-plain progradation is interpreted to result from swash sedimentation at the beach face under enduring calm conditions, ridge construction reflects enhanced wave action at the beach due to elevated storminess or reduced nearshore sea ice. The internal sedimentary architecture of individual beach ridges is interpreted to reflect maximum wave-runup height during the time of ridge construction. Ridges at sheltered parts of the coast exhibit either seaward-dipping beds, interpreted to result from swash deposition, or an aggradational stacking pattern being the result of wave overtopping. At exposed beaches, larger ridges develop composed of seaward- as well as landward-dipping beds. Development of individual beach ridges is seen to result from multiple storms rather than single events.

Gravel beach-ridge plains, composed of numerous ridges, result from the interplay of two distinct modes of sedimentation (Fig. 1). Mode 1 is characterized by the predominance of swash sedimentation and leads to net-progradation of the strand plain. This mode takes place under persistent calm conditions with a reduced frequency of storms. Shortening of the time intervals between consecutive storms switches the system to Mode 2 and results in the construction of a storm ridge, which becomes abandoned by the return to Mode 1 sedimentation or due to continued sea-level lowering.

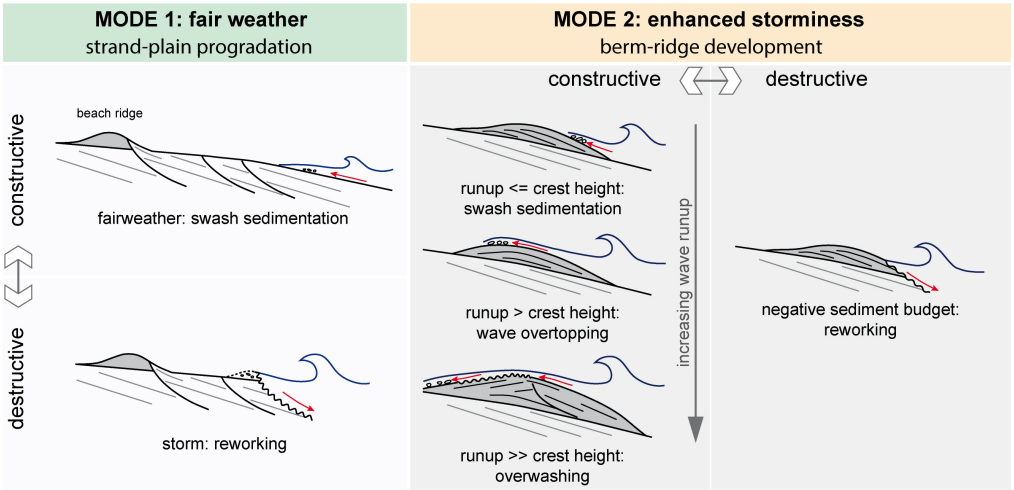

Figure 1: Distinct modes of sedimentation that lead to the formation of polar gravel beach-ridge plains

Sediments of the strand plain as well as the beach ridges are bound into packages by seaward-dipping erosional unconfomities. They indicate recurrent reworking of previous deposits and show that neither ridge construction nor strand-plain progradation is a continuous process. In consequence, polar beach-ridge systems have to be regarded as highly discontinuous sedimentary archives. Data presented in this study, however, indicate that beach ridges on sheltered segments of the coasts have less unconformities, i.e. provide a more complete sedimentary record than exposed ridges.

The number of individual ridges which are preserved from a given time interval varies along the coast depending on the morphodynamic setting: Sheltered coasts are characterized by numerous small ridges, whereas fewer but larger ridges develop on exposed beaches. In the study area, the frequency of ridge building ranges from decades in the low-energy settings up to 1600 years under high-energy conditions. In the study area, beach ridges cluster at 9.5, 7.5, 5.5, and below 3.5 m above the present-day storm beach. Based on radiocarbon data, this is interpreted to reflect distinct periods of increased storminess and/or shortened annual sea-ice coverage in the area of the South Shetland Islands for the times around 4.3, c. 3.1, 1.9 ka cal BP, and after 0.65 ka cal BP.

Data show that even ridges at higher elevations can be subject to later reactivation and reworking. This questions sea-level reconstructions based solely on morphology and dating of polar beach ridges and advise careful investigation of the stratigraphic architecture prior to sampling for dating purposes.

References

Lindhorst, S and Schutter, I. [2014]: Polar gravel beach-ridge systems: Sedimentary architecture, genesis, and implications for climate reconstructions (South Shetland Islands/Western Antarctic Peninsula). *Geomorphology*, 221:187–203, doi:10.1016/j.geomorph.2014.06.013.

Long-term local-scale study of coastal dynamics in Lorino, Chukotka

Alexey Maslakov[1] & Gleb Kraev[2]

[1] *Lomonosov Moscow State University, Russian Federation*
[2] *Centre for Problems of Ecology and Productivity of Forests, RAS, Russian Federation*

The large-scale drivers of coastal dynamic changes had already been established [Forbes, 2011] being the weather and marine changes induced by Arctic warming. However, the local-scale coastal retreat variance is more affected by the morphology and erosional features of the sediments composing coasts. We have studied the coastal retreat rate distribution, the permafrost features, lithology and morphology of the coastal bluff in Lorino settlement, located on the Bering Sea shore (Chukotka, Russia). The geodetical survey and remote sensing of 2012–14 and the archival engineering surveys available in the settlement since 1967 allowed examining of the composition, retreat rate dynamics, and mechanical properties of the permafrost composing the bluff. During the considered period (1967–2014) coast has retreated on 15.8 ±5.7 m (min. 7.4, max. 34.7) [Maslakov and Kraev, 2014]. Coastal retreat rate varied temporary in wide ranges: in 1967–2010 it was 0.25 ±0.1 m/a, in 2010–2014 it has increased to 1.41 ±1.6 m/a. In 2013-2014 coastal bluff has retreated by 2.53 m on average with the maximal rate of 8.61 m.

We have found the way to assess the erodibility through strength properties of soils: yield value of soil (R), long-time boundary cohesion of soil (C), porosity fraction (e). Erodibility considered in the study is the ability to disaggregate under thermal and mechanical impact of water flow. It was expressed as the erodibility coefficient Ke – volume of soil eroded by the unit of water flow (or wave) energy (m^3/J).

The erodibility coefficient (N) normalized for every cross-section of the studied coast given the soil types distribution across more than 30 sections under study had better correlation with the coastal retreat compared to the morphometry of the coastal bluff and beach (r = 0.782, Fig. 1).

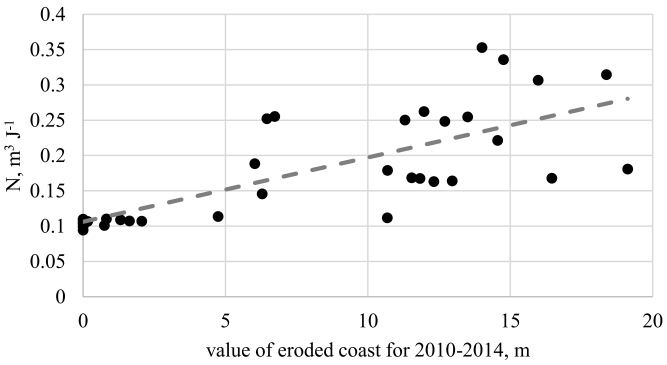

Figure 1: Correlation of the coastal retreat in 2010-2014 and the normalized strength erodibility coefficient.

The external factors like climate and wave activity set the regional background of coastal dynamics. The permafrost features of certain soil types on the local scale control the coastal retreat through different feedbacks to the regional background tendencies. The permafrost erosional features database might greatly improve forecasts of future coastal dynamics and the possibilities to improve it.

References

Forbes, D.L.(ed.). [2011]: *State of the Arctic Coast 2010 – Scientific Review and Outlook*. International Arctic Science Committee, Land-Ocean Interactions in the Coastal Zone, Arctic Monitoring and Assessment Programme, International Permafrost Association. Helmholtz-Zentrum, Geesthacht, Germany, URL http://arcticcoasts.org.

Maslakov, A. and Kraev, G. [2014]: Coastal Hazards Within Indigenous Settlements of Chukchi Peninsula. In: Lollino, G.; Manconi, A.; Locat, J.; Huang, Y. and Canals Artigas, M.(eds.), *Marine and Coastal Processes*, volume 4 of *Engineering Geology for Society and Territory*, pages 33–36. Springer International Publishing, Cham, doi:10.1007/978-3-319-08660-6_6.

The role of shore ice in shaping the Calypsostranda shore (W Spitsbergen) in 2014/15 season

Karolina Męsdrek, Jan Rodzik, & Piotr Zagórski

Maria Curie-Skłodowska University, Poland

All field works and data collection were conducted during the XXVII Polar Expedition organised by the Maria Curie-Skłodowska University in Lublin (UMCS). The scope of the field works included: the determination of topographic and structural features of shore ice, and photographic documentation of sediments covering it. Meteorological data were simultaneously collected. All of the works were performed along the Calypsostranda shore at the Bellsund Strait (west Spitsbergen) near the UMCS Calypsobyen Polar Base. The main topic of this study was the accumulation of shore material in Calypsostranda. Its substrate is made of tertiary sandstone susceptible to erosion and weathering. It is covered with glaciogenic deposits and gravel transported from the raised marine terraces. Shore deposits are mostly composed of gravel. The shore is shaped by wave action from the north and east sectors, as well as tides. The amplitude of tides is variable. During the maximum, it can reach up to 1.5 m, and during the minimum, it rarely reaches 0.5 m. Due to the openness of the bay, allowing for relatively high temperatures in coastal waters, solid ice in Calypsostranda rarely occurs. The common form of ice originating from the sea is known as shore naledi. Its forming process starts at the beginning of winter, and usually ends in June (Rodzik & Zagórski 2009).

The shore ice surveys were commenced on 8 June during high ablation. It was determined that shore naledi developed a berm with a width of several metres, and height of 0.5-1.5 m. Its surface was uneven, placed above the storm berm. It was usually located on the inner side of the shore terrace, and was confined by an ice cliff with overhangs. The inner part of the storm berm, with its cliff with a height of up to 1 m, was separated from the shore ice by a 1-3 m-wide depression. This small depression was either filled with snow or used by pronival drainage (Fig. 1).

This particular shore structure suggests its development during autumn storms before the shore ice ridge was formed. This was followed by the multiphase accumulation of shore naledi originating from initial forms of sea ice (frazile ice, grease ice, and shuga), and freezing water splashes. One to three gravel layers were found in the ice. They were probably made of off-shore material lifted during storms. Therefore, some of them contained seaweed. Also the surface of the shore naledi was covered with gravel of varied granulation and small size (0-3 cm).

Thirteen cross-sections were performed across shore ice alongside the 4 km-long part of the Calypsostranda shore. They were placed in locations specific to particular sections of the shore. Characteristic geometric elements were identified (such as waves range, swash zone, shore ice zone, backshore), and measured with a tape and a klinometer (width, height, and slope). Inside each of the cross-sections, photographic documentation of sedimentary material covering particular areas was prepared. Then, using Sedimetrics®Digital Gravelometer software, a detailed analysis of the sediments' grain structure was performed. Samples of sediments and ice with sedimentary material were also collected.

Figure 1: Fig. 1. Shore ice covered with thick gravel layer (on the left), small cliff storm berm. Picture was taken in the middle part of Calypsostranda (Photo J. Rodzik)

Due to its exposure to oceanic waves, in the northern part of Calypsostranda shore, its tide zone has

an inclination of more than 10°. The material covering the shore ice is mostly composed of 10-15 cm of gravel. The middle part of the studied coast is covered by material of variable grain structure due to small-sized sediments transferred to this area by the Scott River. The river's delta-shaped estuary stops the alongshore transport of coarser sediments in N-W direction. The material composing the right bank of the delta is dominated by coarse sand and fine gravel. The slope of the southern part of the shore is lower than in the northern part. The sediments are again composed of coarser gravel. The Old Renard Glacier outwash plane is subject to erosion in this part. In the inflow area, as well as in the ice throw area, and at the foot of the small cliff, some coarse-grained and flat gravel is mostly visible. It is sometimes sprinkled with fine aeolian sediments. This part shows the highest diversity of material of all of the cross-sections performed for this part of the shore.

GPS surveys were done multiple times. This permitted the assessment of the intensity of ice ablation in comparison to the structure and thickness of the gravel layer. The greatest loss of shore ice was caused by eastern winds permitting short steep waves to reach the shore at a 90° angle. Some loss was also observed during light rainfalls. The shore ice ridge was finally separated into smaller shore ice segments in the end of June. The dissections appeared near the "coves" in the ice cliff, and also where the ice ridge featured a local depression.

The final disintegration of individual gravel-covered small ice mounds occurred by 12 August. The ablation process in 2015 was therefore very long, lasting for more than two months. The process had started long before 6 June when the expedition reached Calypsobyen. The rate of ablation was slowed down by the 10-20 cm thick layer of gravel and good weather conditions. No heavy rainfalls or strong eastern winds (causing strong wave action) occurred. Moreover, the largest waves appeared during minimum tides.

Acknowledgments

Project of National Science Centre no. 2013/09/B/ST10/04141

References

Rodzik, J. and Zagórski, P. [2009]: Shore ice and its influence on development of the shores of southwestern Spitsbergen. *Oceanological and Hydrobiological Studies*, 38:163–180, URL http://meteo.umcs.lublin.pl/pz/publikacje/OandHS_Rodzik_Zagorski_2009.pdf.

Mass wasting and coastal erosion on Yukon Coast and Herschel Island

Jaroslav Obu[1], Hugues Lantuit[1], Frank Günther[1], Guido Grosse[1], Torsten Sachs[2], & Michael Fritz[1]

[1] *Alfred Wegener Institute Helmholtz Centre for Polar and Marine Research, Potsdam, Germany*
[2] *GFZ German Research Centre for Geosciences, Potsdam, Germany*

Erosion rates along permafrost coastlines are among the fastest in the world, despite the fact that they are only ice free for 3-4 months of the year. Yearly coastal erosion rates of up to 20 m were recorded along ice rich and unconsolidated coasts of the Beaufort and Laptev Sea. Coastal erosion can thus cause rapid land loss and release large amounts sediments, which can alter near-shore ecosystems. Mass-wasting processes such as active-layer detachments, retrogressive thaw slumping and block failures frequently occur along the coasts of Yukon Coastal Plain and Herschel Island. They can significantly impact coastal dynamics and sediment delivery on the shore.

In our study we use high resolution digital elevation models (DEMs) to observe short term coastal erosion along Yukon Coast and Herschel Island. DEMs were acquired from LIDAR surveys during the AIRMETH campaigns in 2012 and 2013. The DEMs were processed to obtain a horizontal resolution of 1 meter and compared to identify erosion and accumulation events.

Our results show that erosion behaviour is simple and relatively linear at low-elevation coasts (up to 10 m height), where we recorded yearly coastline retreat from 0 to 20 m. Coastal erosion behaviour becomes diverse and slower at higher-elevation coasts, where mass-wasting processes are more active. Among these mass-wasting processes, retrogressive thaw slumping is particularly important. Activated material can be accumulated at the slump outlets or can be transported along the coast by longshore drift. Such material accumulations caused up to 42 m of coastline progradation. Significant accumulation events were identified also due to block failures (up to 20 m of coastline progradation). Although they are generally short-lived features, they can occur frequently and can influence coastline digitalisations. Coastline observations are therefore not indicating the volume loss that is occurring due to mass wasting. We observe discrepancy between planimetric (coastline movement) and volumetric (recorded by DEMs) coastal erosion on Herschel Island. Exploring the relationship between both measures of coastal erosion would enable better estimates of released sediments from the coasts characterised by mass wasting.

The influence of climate change on the intensity of ice gouging at the Kara Sea bottom by hummocky formations

Stanislav A. Ogorodov, Vassiliy V. Arkhipov, & Osip V. Kokin

Lomonosov Moscow State University, Moscow, Russian Federation

Sea ice as a zonal factor is an important passive and active relief-forming agent in the coastal-shelf zone of the Arctic and other freezing seas [Ogorodov, 2003]. The passive influence of sea ice on the dynamics of the coasts and sea bottom lies in their protection from the impact of waves and tides by the fast and rifting ice. Blocking the coastal zone during most part of the year, the sea ice regulates the active hydrodynamic factors, reducing the time of their direct action and therefore determining the intensity of coastal and bottom erosion. The direct, or active, influence of sea ice is the ice gouging of the coasts and bottom, the sediment transport, executed by sea ice, the formation of frozen grounds in the zone of contact between the ice and the bottom and the local erosion around stamukhas and tidal cracks.

Among the kinds of direct ice impact mentioned above, ice gouging is the most dangerous towards underwater pipelines, cables and other hydrotechnical facilities. Ice gouging is the destructive mechanical action of ice on the bottom grounds, connected with the dynamics of the ice cover, hummocking and the formation of stamukhas under the impact of hydrometeorological factors and the relief of the coastal and shelf area.

Undervaluation of the intensity of ice gouging can lead to the damaging of engineering facilities; at the same time, excessive deepening of the infrastructure is expensive. Finding the optimal solution and therefore lowering the risk of emergency is the most relevant task of both fundamental and practical studies. This task becomes more complicated due to the global climate change, accompanying the current ongoing oil and gas infrastructure development in the coastal and shelf zone.

Within the territory of Russia, ice gouging processes are well studied within the Yamal shelf, Sakhalin shelf, as well as the northern Caspian. The most detailed investigations were conducted in the Baydaratskaya Bay, along the crossing of the main gas pipeline "Yamal-Europe" [Ogorodov et al., 2013], where the influence of climate change on ice gouging processes was investigated for the first time.

With all lithologic and geomorphologic conditions being equal, the intensity of the ice gouging on the bottom is mostly determined by the changing condition, area and thickness of the ice cover. These characteristics can be obtained based on the data of hydrometeorological stations and on satellite observations followed by the analysis of the results of the sounding of ice gouging microrelief for different years.

As a result of the warming, in autumn of 2007 and 2012, a historical minimum of sea ice area since the beginning of satellite observations in 1979 was reached in the Northern Hemisphere. The border of fast ice changes as well. With all other conditions being equal, the greater the sum of temperatures below zero is, the more stable and wide the fast ice can be. So, over the last decade only, the area of fast ice at the moment of its maximal extent decreased by 15 %. The ice-free period duration, in its turn, increased.

Under the conditions of climate warming, the character and intensity of ice gouging impact of ice formations on the coasts and bottom change considerably. Due to the decrease of the ice period duration and ice thickness, an activation of all the processes connected to sea ice occurs; ice hummocking increases. As a result, the width and stability of fast ice becomes lower; the action of sea ice on the coasts grows. At the same time, glaciers become more active as well: the rate of icebergs' calving increases; the probability of ice gouging by icebergs in deep water areas grows, as well as the probability of damaging of sea vessels and tankers.

During the last decades, along with the climate warming in the Arctic basin, not only a general decrease of the ice cover is observed, but also the circulation system of sea water and ice is changing, which leads to a redistribution of areas with thin young and thick perennial pack ice.

Among the first-year ice, clear anomalies of the ice cover thickness are observed in the last decade. A decrease of the ice thickness immediately leads to changes in the size of the hummocky ice formations,

the deepening of which directly depends on the ice thickness. These two parameters are directly connected. It is known from literature that in the Caspian Sea, where the ice thickness is 0,5 – 0,7 m, the maximal depth of stamukhas is 10 – 12 m; in the Pechora Sea, where the ice is 1,0 – 1,4 m thick, stamukhas form up to the depth of 18 m; in the Kara Sea and in the Laptev sea, with its ice thickness of 1,5 – 2,0 m, stamukhas form up to the depth of 26 – 28 m and of 24 m accordingly; and in the East Siberian Sea where the thickness of the first-year ice reaches 2,0 m, and the average thickness of perennial pack ice reaches 3 – 4 m, stamukhas can form at depths of up to 35 m.

Modeling of the ice hummocky formations' properties also shows direct physical dependence between these parameters. In this way, under the conditions of climate warming, the size of ice hummocks and stamukhas will decrease, together with the width of fast ice; as a result, the zone of the most intensive impact of ice formations on the bottom will move landwards, towards shallower water areas.

To assess the real intensity of the ice gouging impact during a given ice season, repeated sounding of the sea bottom microrelief is necessary, in order to select the ice gouges which were created in the period between the two consequent observations.

Field geophysical observations, including monitoring observations (made for the same profiles repeatedly), were made in the Baydaratskaya Bay of the Kara Sea and within the territory of the pipeline "Bovanenkovo-Ukhta" underwater crossing in the period from 2005 to 2012, corresponding to a significant climate warming and ice decrease in the Kara Sea.

During the last two decades, the duration of the ice period in the Baydaratskaya Bay decreased almost by 1,5 months; the fast ice often breaks and can be carried away during its formation (especially from the side of the Ural coast); the thickness of the ice cover decreased at least by 10 – 15 cm. In May 2007, an iceberg was documented by A.M. Kamalov in the clearing close to the Ural coast. The last time an iceberg was noticed in this area was in 1932, in a period which was also characterized by warming and ice cover decrease. The appearance of icebergs in this area is probably directly connected with warming. Under the conditions of temperature growth, the activation of glaciers at Novaya Zemlya leads to the increase in the number of icebergs calving into the Kara Sea. A system of constant currents and big clearings create conditions, suitable for the penetration of icebergs into the Baydaratskaya Bay.

Young ice gouges, which were formed after the construction of the Baydaratskaya Bay underwater pipeline crossing, are easy to detect above the recently filled trench on the bottom: fresh gouges leave traces on the ground deposited by the constructors, similar to a pencil leaving traces on a clean piece of paper (Fig. 1).

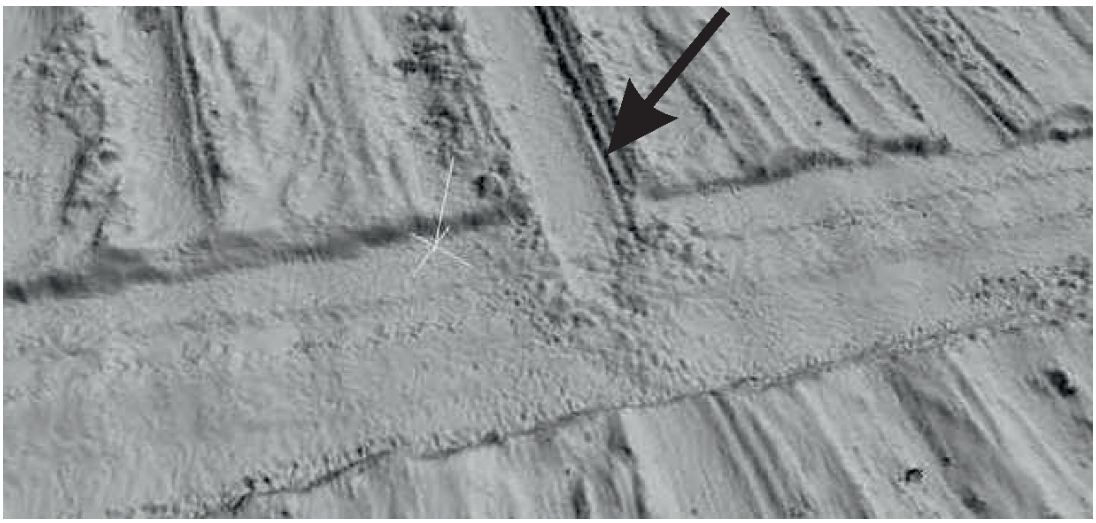

Figure 1: Example of the formation of a fresh ice gouge above the filled trench of the main gas pipeline

The executed observations prove that during the last years, a decrease of the ice cover thickness and the ice hummocks' size together with the fast ice width was observed. As a result, the area of the most intensive ice gouging impact moves to smaller water depths. If before, the maximum of the ice gouging impact (by the number and depth of ice gouges) was observed at depths from 17 to 20 m, at present, this zone has moved to 12 – 16 m. Ice gouges have stopped forming in the central, deep part of the bay. During the period of observations after the construction of the first pipeline, only once gouge formed at the depth of 20 m in winter of 2009. Its forming was possibly connected with the penetration of the iceberg into the Baydaratskaya Bay from the Kara Sea.

Based on the analysis of literature, modeling and field observations, it has been established that in the conditions of climate warming and ice cover decrease, the zone of the most intensive ice impact is moved landwards, to shallower water areas.

Acknowledgments

The work was executed with the financial support of the Russian Foundation for Basic Research (grant №14-05-00408a – "Sea ice effect on the dynamics of coastal and bottom topography under the condition of Arctic climate change").

References

Ogorodov, S.A. [2003]: The Role of Sea Ice in the Coastal Zone Dynamics of the Arctic Seas. *Water Resources*, 30(5):509–518, doi:10.1023/A:1025725113288.

Ogorodov, S.; Arkhipov, V.; Kokin, O.; Marchenko, A.; Overduin, P. and Forbes, D. [2013]: Ice Effect on Coast and Seabed in Baydaratskaya Bay, Kara Sea. *Geography, Environment, Sustainability*, 6(3): 21–37, URL http://epic.awi.de/34555/.

POROCO – Mechanisms controlling the geomorphology and evolution of rocky coasts in polar climate – preliminary results

Lukasz Pawłowski[1], Mateusz Czeslaw Strzelecki[1], Michael Lim[2], Piotr Migon[1], Marek Kasprzak[1], Zuzanna Swirad[3], Marek Wojciech Jaskolski[1], & Piotr Modzel[1]

[1] *University of Wroclaw, Poland*; [2] *Northumbria University, UK*; [3] *Durham University, UK*

A significant limit to current understanding of cold coast evolution is the paucity of field observations regarding development of rocky coastlines and, in particular, lack of precise recognition of mechanisms controlling rock coast geomorphology in polar climates.

Therefore the principle aim of our recently funded POROCO (Polar Rock Coasts) project is to quantify the processes controlling the evolution and behaviour of rock coasts in polar climates, based on representative examples from Svalbard (Arctic) and South Shetlands (Antarctic). POROCO aims to develop predictions of future rock coast change under scenarios of continued increases in air temperature, sea-level rise and the frequency and intensity of storms entering polar seas.

Our approach utilises a rigorous, coherent and novel suite of techniques to analyse the spatially and temporally diverse range of processes and responses controlling the polar rock coast environments

- Schmidt Hammer and Equotip tests of rock surface resistance
- micro-erosion meter measurements of rock surface downwearing rates
- observations of seasonal changes in the state of permafrost developed in solid rocks using electrical resistivity tomography (ERT)
- scanning of selected cliff faces and shore platform surfaces using Terrestrial Laser Scanner
- monitoring of thermal state of the rocky cliffs and platforms using network of thermistors
- monitoring of weather conditions and wave-activity using a system of portable weather stations, industrial cameras and tide gauges
- photogrammetric analysis of digital images of scanned cliffs and platforms and GIS processing of obtained data

In this paper we present the results of the first field campaign of the project carried out in summer 2015 in Hornsund, SW Spitsbergen that focused on:

- pilot survey of rock resistance using Schmidt Hammer Rock Tests (SHRT) and Equotip (EQ) across the modern and uplifted shore platforms formed in marbles and shales.
- pilot measurements of shore platform downwearing using the Traverse Micro-Erosion Meter (TMEM)

This lithological variability provided an excellent opportunity to examine the influence of rock resistance on the development of various coastal landforms in periglacial climate. SHRT, EQ and TMEM surveys along several morphologically different coast types demonstrated broad variety of interrelations between rock surface resistance and distance from present-day shoreline as well as thickness of sediment and snow covers. In general, rock cliff surfaces were the most resistant in their lower and middle zones which are thermally insulated by thick winter snowdrifts. Whereas the more exposed cliff tops were heavily fractured and weathered. The differences in rock resistance and downwearing rates observed along the shore platforms were highly dependent on thickness of sediment cover and shoreline configuration. These characteristics favoured stronger rock surfaces in areas exposed to the longest wave fetch, but also washing by meltwaters from decaying ice-foot. The results presented in this paper emphasize the richness of microrelief features and processes operating in polar coastal environments.

Acknowledgments

This paper is a contribution to the National Science Centre in Poland OPUS project UM$O_2$013/11/B/ST10/00283: 'POROCO – Mechanisms controlling the evolution and geomorphology of rock coasts in polar climates'.

Changes of High Arctic tidal flat systems as an indicator of climatic and sediment supply shifts in post-Little Ice Age period – examples from Svalbard

Lukasz Pawłowski, Mateusz Czeslaw Strzelecki, & Mariusz Szymanowski

University of Wroclaw, Poland

Recent rapid warming of the Arctic atmosphere has intensified the operation of the geomorphic processes that control coastal evolution, causing increased degradation of permafrost and prolonged periods of open-water conditions and wave activity. In High Arctic settings, such as Svalbard, a crucial role as a main sediment feeder to the coastal system is played by glaciers. Since the end of the Little Ice Age (beginning of the 20^{th} century) enhanced sediment supply from deglaciated catchments led to the formation of new landforms along coasts of Svalbard, which serve also as a last sediment storage system before the final deposition in fjords or shelf. Therefore, it is hard to believe but Svalbard tidal flat systems has never been studied in sufficient detail to assess their role in polar sediment cascade. Existing sediment budget studies in Svalbard have focused attention on quantifying the volumes of sediment transported by glacial rivers and derived from glacier erosion and reworking of fluvial catchment sediment. Little or no attention has been paid to the functioning of sediment storage and reworking systems within coastal zone, particularly in tidal flat systems developing in heads of numerous Svalbard fjords.

In this paper we summarise the pilot study of geomorphological changes that occurred in main tidal flat systems of Spitsbergen (main island of Svalbard Archipelago): Dicksonfjordnen, Billefjorden, Recherchefjorden and Van Mijenfjorden. We have analysed the collection aerial images taken by Norwegian Polar Institute in years 1936 – 2012 to map shifts in tidal creek and channels network and describe formation of new landforms such as lagoons, tidal islands and barriers. Presented study is a part of a PhD project that aims to improve our understanding of the role of tidal flats, alluvial fan deltas and proglacial lakes in High Arctic sediment cascade.

Acknowledgments

Ths paper is a contribution to the National Science Centre research project 'Model of the interaction of paraglacial and periglacial processes in the coastal zone and their influence on the development of Arctic littoral relief' (award no. 2013/08/S/ST10/00585)

Threats to coastal infrastructure from erosion and flooding: A case study from Herschel Island, Yukon Territory, Canada

Boris Radosavljevic[1,2], Hugues Lantuit[1,2], Wayne Pollard[3], Paul Overduin[1], Nicole Couture[4], Torsten Sachs[5], Veit Helm[6], & Michael Fritz[1]

[1] *Alfred Wegener Institute Helmholtz Centre for Polar and Marine Research, Potsdam, Germany*
[2] *Institute of Earth- and Environmental Science, University of Potsdam, Potsdam, Germany*
[3] *Dept. of Geography and Centre for Climate and Global Change Research, McGill University, Montreal, Canada*
[4] *Northern Canada Division, Geological Survey of Canada, Ottawa, Canada*
[5] *GFZ German Research Centre for Geosciences, Potsdam, Germany*
[6] *Alfred Wegener Institute Helmholtz Centre for Polar and Marine Research, Bremerhaven, Germany*

Arctic coastal infrastructure, cultural, and archeological sites are increasingly vulnerable to erosion and flooding due to amplified warming of the Arctic, sea level rise, lengthening of open water periods, and a predicted increase in frequency of major storms. Mitigating these hazards necessitates decision-making tools at an appropriate scale. The objectives of this study were to assess potential erosion and flood hazards at Herschel Island, a UNESCO World Heritage candidate site, and produce a map to be used as a decision making tool. The study focused on Simpson Point and the adjacent coastal sections, because of their archeological, historical, and cultural significance.

Shoreline movement was analyzed using the Digital Shoreline Analysis System (DSAS) after digitizing shorelines from 1952, 1970, 2000, and 2011. For purposes of this analysis, the coast was divided in seven coastal reaches (CRs) reflecting different morphologies and/or exposures. Using linear regression rates obtained from these data, projections of shoreline position were made for 20 and 50 years into the future. Flood hazard was assessed using a least cost-path analysis based on a high-resolution Light Detection and Ranging (LiDAR) dataset and current Intergovernmental Panel on Climate Change sea level estimates.

Widespread erosion characterizes the study area. The rate of shoreline movement in different periods of the study ranges from -5.5 to 2.7 m a^{-1} (mean -0.6 m a^{-1}). Mean coastal retreat decreased from -0.6 m a^{-1} to -0.5 m a^{-1}, for 1952-1970 and 1970-2000, respectively, and increased to -1.3 m a^{-1} in the period 2000-2011. Ice-rich coastal sections most exposed to wave attack exhibited the highest rates of coastal retreat. The geohazard map combines shoreline projections and flood hazard analyses to show that most of the spit area has extreme or very high flood hazard potential, and some buildings are vulnerable to coastal erosion.

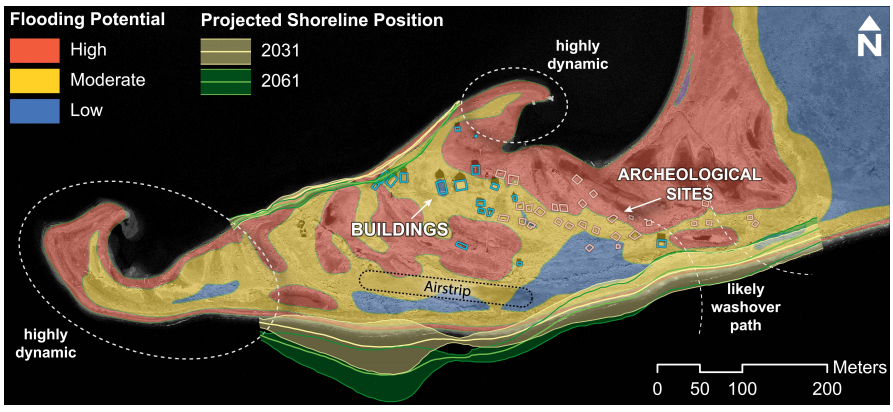

Figure 1: Coastal geohazard map indicating flooding potential, and projected shorelines, and dynamic areas with high hazard potential. These semi-transparent layers are superimposed on the 2011 image. Locations of buildings and archeological sites are highlighted.

Thermo-erosion processes on the Marre Sale coast, Western Yamal

Philippe Schoeneich[1] & Anna Kurchatova[2]

[1] *Université Grenoble Alpes, Institut de Géographie Alpine, France*
[2] *Tyumen Gas and Oil University, Russia*

On the Yamal Peninsula a very ice-rich permafrost developped in quaternary marine, lacustrine and alluvial sediments, and contains massive epigenetic and syngenetic ice bodies. Inland, the degradation of the permafrost induces numerous thermokarst lakes. On the Western Yamal coast, the ice bodies induce very active thermo-erosion processes, with high cliff regression rates.

The paper focusses on the Marre Sale coastline, in Western Yamal. In this area, two massive ice bodies can be encountered, a lower one at beach level, and an upper one in the upper half of the cliff, together with an extended network of wide ice-wedges. Depending on the presence or absence of one or the two ice bodies, cliff erosion processes show different sequences, from thermo-erosion to mud flows, fluvial erosion and transport, and final reworking and removal on the beach by wave action:

- in the absence of massive ice bodies, undercutting by wave action or thermo-abrasion is dominant, but seasonal accumulation of snow and ice cones protects the cliff base
- the upper massive ice body induces wide thermoerosion cirques, feeding mud flows, which build large mud cones on the beach
- thermoerosion of the lower ice body induces cliff collapses and large mudflows extending directly on the beach
- degradation of ice-wedges induces linear erosion, which cane volve into gully systems.

In all cases, the sediments are deposited first as mud-flow deposits or as mud or sand cones on the beach, and are then reworked and removed by mechanical wave action. The poster will present several type profiles in order to illustrate the various observed process chains.

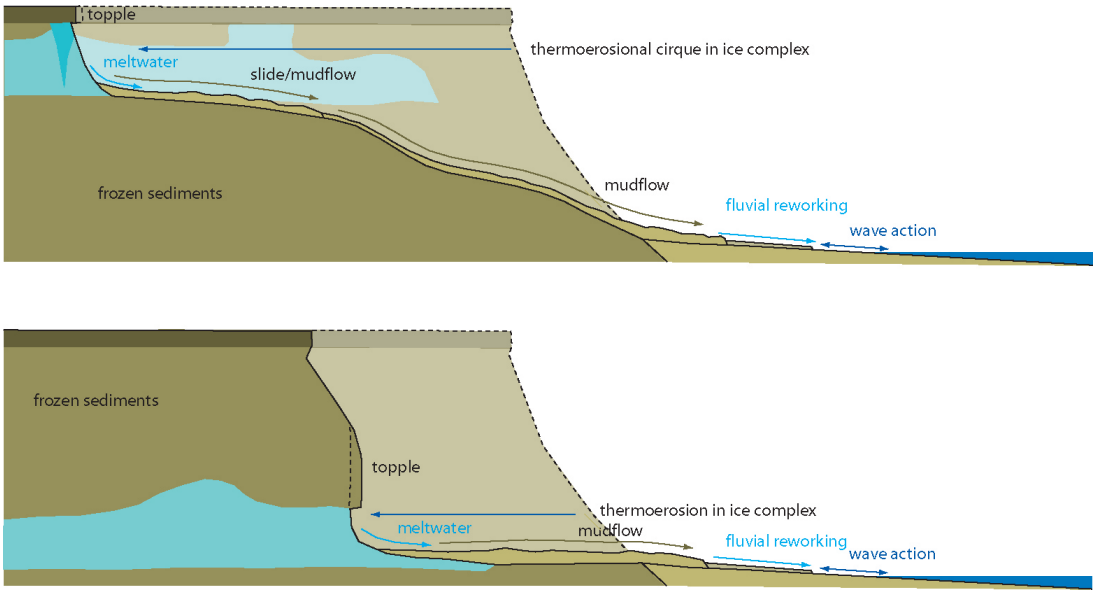

Figure 1: Thermo-erosion type profiles on the Marre Sale coastline, Western Yamal.

Holocene deglaciation, sea-level changes and shifts in sediment supply recorded in High Arctic paraglacial coastal systems – Bjonapynten case study, Tempelfjorden, Central Spitsbergen

Matt Strzelecki[1], Sebastian Lindhorst[2], Chris Hein[3], & Jessica Raff[3]

[1] *University of Wroclaw, Institute of Geography and Regional Devlopment, Poland*
[2] *University of Hamburg, Institute of Geology, Germany*
[3] *Virginia Institute of Marine Science, College of William and Mary, USA*

Understanding the High Arctic coastal zone evolution is crucial to decipher landscape changes and associated shifts in sediment fluxes triggered by climate change. The gravel-dominated paraglacial coastlines of the Svalbard Archipelago provide an excellent location to examine the processes that control High Arctic coastal change. Of special interest are the mechanisms by which coastal systems respond to enhanced landscape change following deglaciation. Existing sediment budget studies in Svalbard have focused attention on quantifying the volumes of sediment transported by glacial rivers and derived from glacier erosion and reworking of fluvial catchment sediment. Little attention has been paid to the functioning of sediment storage and reworking systems within coastal zone over various stages of the Holocene.

Our research aims to address this deficiency by improving our understanding of the mechanisms of Holocene adjustment of the High Arctic coastal zone to non-glacial conditions. In this paper, we summarize the results of a pilot study led by our research team along paraglacial coast at Bjonapynten, Tempelfjorden, central Spitsbergen. Our research was based on a combination of methods including aerial photogrammetric and GIS analyses, ground penetrating radar surveys, sedimentological tests of coastal deposits, novel approach in radiocarbon dating of uplifted beaches and field-based geomorphological mapping.

Our results document significant changes in rate of relative sea-level fall, sediment flux and coastal response (rate of coastal progradation, style of beach ridge formation) under intervals characterized by warming climate, retreating local ice masses, a shortened winter sea-ice season and thawing permafrost. We discuss our new data in the context of previously published RSL data and coastal evolution studies from Svalbard. The approach is potentially applicable elsewhere in Svalbard and the High Arctic to address questions of RSL change and beach ridge chronology, and hence wider questions regarding palaeoclimate and ice load history.

Acknowledgments

This paper is a contribution to the National Science Centre project 'Model of the interaction of paraglacial and periglacial processes in the coastal zone and their influence on the development of Arctic littoral relief' (award no. 2013/08/S/ST10/00585).

Hunting for Arctic tsunami - Impact of extreme waves on coastal evolution in western Greenland

Matt Strzelecki[1], Witek Szczucinski[2], Antony Long[3], Nick Rosser[3], Agata Buchwal[4], & Stuart Dunning[5]

[1] *University of Wroclaw, Institute of Geography and Regional Development, Poland*
[2] *Adam Mickiewicz University, Institute of Geology, Poland*
[3] *Durham University, Department of Geography, United Kingdom*
[4] *Adam Mickiewicz University, Cryosphere Research Department, Poland*
[5] *Newcastle University, School of Geography, Politcs and Sociology, United Kingdom*

Understanding the High Arctic coastal zone evolution is crucial to decipher landscape changes and associated shifts in sediment fluxes triggered by climate change. The gravel-dominated paraglacial coastlines of the Svalbard Archipelago provide an excellent location to examine the processes that control High Arctic coastal change. Of special interest are the mechanisms by which coastal systems respond to enhanced landscape change following deglaciation. Existing sediment budget studies in Svalbard have focused attention on quantifying the volumes of sediment transported by glacial rivers and derived from glacier erosion and reworking of fluvial catchment sediment. Little attention has been paid to the functioning of sediment storage and reworking systems within coastal zone over various stages of the Holocene.

Our research aims to address this deficiency by improving our understanding of the mechanisms of Holocene adjustment of the High Arctic coastal zone to non-glacial conditions. In this paper, we summarize the results of a pilot study led by our research team along paraglacial coast at Bjonapynten, Tempelfjorden, central Spitsbergen. Our research was based on a combination of methods including aerial photogrammetric and GIS analyses, ground penetrating radar surveys, sedimentological tests of coastal deposits, novel approach in radiocarbon dating of uplifted beaches and field-based geomorphological mapping.

Our results document significant changes in rate of relative sea-level fall, sediment flux and coastal response (rate of coastal progradation, style of beach ridge formation) under intervals characterized by warming climate, retreating local ice masses, a shortened winter sea-ice season and thawing permafrost. We discuss our new data in the context of previously published RSL data and coastal evolution studies from Svalbard. The approach is potentially applicable elsewhere in Svalbard and the High Arctic to address questions of RSL change and beach ridge chronology, and hence wider questions regarding palaeoclimate and ice load history.

Acknowledgments

This paper is a contribution to the National Science Centre project 'Model of the interaction of paraglacial and periglacial processes in the coastal zone and their influence on the development of Arctic littoral relief' (award no. 2013/08/S/ST10/00585).

Patterns and controls of erosion along the Elson Lagoon coastline, Barrow, Alaska (2002 – 2015)

Craig E. Tweedie[1], Stephen Escarzaga[1], Ryan P. Cody[1], Bill Manley[2], Allison Gaylord[3], Qaiyaan Aiken[4], & Jerry Brown[5]

[1] *University of Texas at El Paso, United States of America*
[2] *University of Colorado, United States of America*; [3] *Nuna Technologies, United States of America*
[4] *UMIAQ, United States of America*; [5] *Woods Hole, United States of America*

The International Conferences on Permafrost (ICOP) provide an ideal venue for documentation of long-term changes in permafrost environments. Our continuing observations of coastal erosion at Barrow, Alaska, is one such example. Starting with the Ninth ICOP in 2008 we presented results of the time series of erosion surveys made along 10.7 km of the Elson Lagoon on the Beaufort Sea coast of northern Alaska near Barrow [Aguirre et al., 2008]. We updated the annual observations through 2011 in the proceedings of the Tenth ICOP [Tweedie et al., 2012]. Both publications were a contribution to the Arctic Coastal Dynamics program under which the study was initiated. This extended abstract serves as our third ICOP update for the Elson Lagoon study site and includes sustained annual observations through summer 2015.

Seasonal erosion rates are measured in two ways and are facilitated by a network of automated cameras. Transects that are perpendicular to the coast were established as a contribution to the Arctic Coastal Dynamics program and are generally measured annually in early August (see table 1). Erosion rates are also calculated from repeat ground surveys of the 2-4 m high, coastal bluffs using a differential global positioning System (DGPS). Erosion rates are calculated using the USGS Digital Shoreline Analysis System. Erosion rates calculated from recent DGPS surveys (2002-2015) and long term analyses from aerial and satellite remote sensing (1948-2014) can be viewed through an interactive web mapping application designed with the intent of capacitating improved decision making and communication of scientific data (http://www.barrowmapped.org).

Repeat DGPS surveys show that rates of erosion generally averaged 1-4 meters per year from 2003-2015 for each of the four sections of coastline monitored, which is lower than other areas of the Beaufort Sea coast that lack protective barrier islands, but higher than historic decadal-scale change rates for this site. Since 2003, more than 20 ha of land eroded from the study site. Regression analyses indicate no significant change to the rate of erosion during the past 13 years.

Table 1: Change in ACD transect lengths along the Elson Lagoon coastline 2002-2015.

Transect	2002	2003	2004	2005	2006	2007	2008	2009	2010	2011	2012	2013	2014	2015	total loss (m)	m/yr
A1	92.2	89.2	88.1	86.2	76.0	75.0	68.7	68.7	66.0	66.0	X	58.7	52.4	50.3	41.9	3.2
A2	45.9	44.1	41.3	40.2	36.5	35.5	32.2	31.1	30.4	29.1	X	29.0	29.0	29.0	16.9	1.3
A3	110.4	109.1		107.3	105.0	103.9	104.0	103.8	103.8	102.5	X		101.4	97.0	13.4	1.0
A4	143.0	142.4		141.2	139.0	136.6	136.7	131.1	131.1	129.3	X	129.0	127.0	124.0	19.0	1.5
A5	56.0	55.0		53.6	53.2	50.8	49.5	49.3	47.1	45.3	X	45.0	44.6	40.0	16.0	1.2
B1	101.8			96.5	95.7	92.7	91.4	90.3	85.0	83.3	X	83.0		83.0	18.8	1.4
C1*		72.4	70.9		68.8	68.2	68.3	71.2			X				1.2	0.2
C2		37.7			29.3	28.6	31.0	29.5	30.1	30.0	X		25.0	25.0	12.7	1.1
C3		34.0	31.2		28.2	26.4	25.8	25.1	23.1	22.8	X		20.0	20.0	14.0	1.2
C4		97.3	95.6	91.9	88.0	80.8	79.4	78.5	77.5	75.3	X	75.0	74.0	73.0	24.3	2.0
C5	38.0	37.0	34.6	34.8		34.3		33.9	33.8		X				4.5	2.3
D1	52.0	49.0	41.6	34.5	16.7	14.3	11.2	8.6	5.4	Lagoon	X	Lagoon	Lagoon	Lagoon	52.0	5.8
D2	54.9	53.2	51.5	44.7	38.7	35.6	31.4	30.9	27.8	25.4	X	25.4	23.0	22.0	32.9	2.5
D3	64.5	59.7	57.1	49.3	34.6	26.3	11.8	7.8	3.3	Lagoon	X	Lagoon	Lagoon	Lagoon	64.5	7.2
* Site situated adjacent to a slough that drains to Elson Lagoon														Mean	23.7	2.28

Regionally, however, the study area shows some of the highest rates of erosion, and rates of aerial loss that are generally 2-3 times that recorded for the Chukchi Sea Coastline near Barrow. Analyses of our seasonal data indicate that rates of erosion are higher in summer survey periods when losses are normalized to the number of ice-free days. Analyses with the high-resolution vertical precision of DGPS also suggests that volumetric soil losses from erosion are higher than previously estimated for this section of coastline.

Regression tree analysis suggests that the biophysical controls of erosion differ between analyses run for aerial and volumetric losses [Aguirre, 2011]. These analyses also highlight key differences in controls between sampling periods with high/low wind-wave activity. In particular, analyses show the important influence of land cover type and landscape geomorphic history on erosion trends during periods of low storm activity.

References

Aguirre, A. [2011]: *Patterns and controls of erosion along the Barrow Environmental Observatory coastline, northern Alaska*. Master of science, University of Texas at El Paso, 73 pp.

Aguirre, A.; Tweedie, C.E.; Brown, J. and Gaylord, A. [2008]: Erosion of the Barrow Environmental Observatory Coastline 2003–2007, Northern Alaska. In: Kane, D.L. and Hinkel, K.M.(eds.), *Proceedings of the Ninth International Conference on Permafrost, Institute of Northern Engineering, University of Alaska Fairbanks, Fairbanks, USA, 29 June–3 July 2008*, volume 1, pages 7–12.

Tweedie, C.E.; Aguirre, A.; Cody, R.; Vargas, S. and Brown, J. [2012]: Spatial and Temporal Dynamics of Erosion along the Elson Lagoon Coastline near Barrow, Alaska (2002–2011). In: Hinkel, K.M.(ed.), *Proceedings of the Tenth International Conference on Permafrost*, Salekhard, Yamal-Nenets Autonomous District, Russia, 25–29 June 2012, volume 1: International Contributions, pages 425–430, The Northern Publisher: Salekhard. ISBN 978-5-905911-01-9. URL http://ipa.arcticportal.org/publications/conference-proceedings.

SESSION 20

Permafrost-related Land Surface Subsidence and Frost Heave

Convener:

Frank Günther, *Alfred Wegener Institute Helmholtz Centre for Polar and Marine Research, Germany*

Tazio Strozzi, *Gamma Remote Sensing, Switzerland*

Dmitry A. Streletskiy, *Geography Department, George Washington University, USA*

Due to its transitional function between permafrost and the atmosphere, dynamics of the active layer are of great importance. Active layer thickness changes are of relevance not only in terms of mobilization of previously frozen soil organic carbon pools, but especially for protecting underlying pure ground ice bodies and ground ice enriched soil horizons from thaw and subsequent disintegration and further landscape destabilization. The amplitude of vertical land surface movements associated with seasonal thaw settlement and frost heave after refreeze may differ depending on physical soil properties, landscape unit, and climatic variables. However, within areas of current and past permafrost degradation, or rather aggradation, such as thermokarst landforms (drained thaw lake basins, pingos etc.), these seasonal freeze-thaw mechanisms likely overlap with long-term geomorphic processes, and it is very difficult to differentiate between them.

Questions remain over whether the land elevation returns back to its initial state after a complete freeze-thaw cycle or if irreversible loss of permafrost occurred due to active layer deepening. Because of the wide spectrum of currently applied methodological approaches, it will become more difficult to draw a comprehensive picture of these phenomena and to compare results from different permafrost settings. This session aims to review state-of-the-art knowledge and to gather new research results about the general magnitudes and spatio-temporal patterns of permafrost-related land surface lowering and uplift. Of interest are contributions from process-oriented field studies, long-term monitoring perspectives from on-site instrumentations, geodetic monitoring efforts, mapping, and remote sensing based change detection studies. In particular, we encourage presentations in the field of Earth observation technologies.

The session generally offers a platform to present innovative methods using measurements from GNSS, interferometric SAR, photogrammetry, altimetry, laser scanning, theodolite, and measuring tape. Also, presentations from a practical or theoretical point of view dealing with the general topic are welcome.

PermaSAR – Improving TanDEM-X D-InSAR techniques for the detection of small-scale vertical movements in arctic permafrost regions

Inga Beck[1,3], Julia Boike[2], Sabrina Marx[2], Moritz Langer[1], & Bernhard Höfle[1,3]

[1] *Ruprecht-Karls Heidelberg University, Germany*
[2] *Alfred Wegener Institute Helmholtz Centre for Polar and Marine Research, Potsdam, Germany*
[3] *Heidelberg Centre of Environment*

Surface dynamics, such as subsidence and heave, as a result of permafrost thawing and freezing is a well-known phenomenon. Ground measurements are indicating that such movements exist and first attempts to use satellite data to detect these changes on a larger scale have been undertaken. In particular data from radar satellites have been used to generate differential interferograms (D-InSAR) in order to detect areas of movements. However there are still many uncertainties and limitations related to this method, such as the influence of vegetation and microtopography on the radar signal.

Within the PermaSAR project a multi-source approach, using TanDEM-X data, ground truth measurements (subsidence stations and RTK GNSS), but also highly precise terrestrial 3D LiDAR data shall help to identify influences of the captured surface characteristics on high-resolution D-InSAR. In a subsequent working step the identified influences will be quantified and a method developed in order to mask, reduce, or even eliminate, these effects.

For the study, a region in Northwest Canada, 50 km North of Inuvik has been chosen. The site, so-called Trail Valley Creek, lies in the continuous permafrost zone and the thickness of the permafrost is up to 370 m. The dominant vegetation in the basin are open tundra areas consist mostly of grasses, lichens and mosses. Research activities of the past reveal a potential of subsidence due to permafrost thawing in this region.

In 2015 two field campaigns in the region could be realized: One in early June, after the freezing period and one in late August at the end of the thawing period. During the first campaign 8 automated ground temperature loggers and manual 24 subsidence stations were installed. Active layer thaw depth, as well as subsidence was recorded at 12 sites manually. During both campaigns the high-performance terrestrial LiDAR system Riegl VZ-400 was used to survey at two different sites (40 × 50 m) the microtopography and vegetation in 3D. The used LiDAR has full-waveform recording, with each single 3D measurement having a range precision and accuracy of about 3-5 mm at 100 m. Both test sites have been scanned with a point spacing of 3 mm at a distance of 10 m from 7 different scan positions. Additionally the Leica GNSS RTK GS10/GS15 system was used to get exact information about ground height and coordinates of certain features.

First results indicate

i) a very good co-registration of the LiDAR data and RTK GNSS data of the two campaigns and

ii) a high correlation between the subsidence records of the LiDAR data, the RTK GNSS records and the subsidence stations.

The corresponding mean subsidence rates derived from the three independent sources (LiDAR, GNSS RTK and subsidence stations) range from -2.31 cm (LiDAR) to -2.72 cm (subsidence station) (std. deviations from 0.89 (LiDAR) to 1.01 (subsidence station)). First analysis of subsidence using the TanDEM-X data are shown and compared to our multi-source ground truth measurements.

Using PSInSAR to detect thermokarst-induced subsidence in Eboling Mountain, China

Jie Chen[1,2], Lin Liu[2], Hui Lin[1], Tingjun Zhang[3], & Bin Cao[3]

[1] *Institute of Space and Earth Information Science, The Chinese University of Hong Kong, Hong Kong, China*
[2] *Earth System Science Programme, Faculty of Science, The Chinese University of Hong Kong, Hong Kong, China*
[3] *College of Earth and Environmental Sciences, Lanzhou University, Lanzhou, China*

Thermokarst, a process that characterizes landforms caused by thawing of ice-rich permafrost, is a key indicator of permafrost degradation. Surface dynamics of thermokarst processes on Qinghai-Tibet Plateau (QTP) of China, is still poorly quantified or understood. It is also challenging to detect and measure surface subsidence due to loss of subsurface ice over a large area. The Persistent Scatterer Interferometric Synthetic Aperture Radar (PSInSAR) technique has the potential to detect local or regional thermokarst-induced surface subsidence with millimeter to centimeter accuracy [Ferretti et al., 2001].

Previous studies based on multi-baseline time series analysis have separated the seasonal and thermokarst-induced surface subsidence only using SAR images acquired during thaw seasons [Liu et al., 2015]. However, PSInSAR analysis using only thaw-season images, which is limited by the few number of data in deformation evolution, therefore is vulnerable to measurement noises and defects in thermokarst time series model. To improve the seasonal deformation model of Liu et al. [2015], we introduce frost heave during early freeze season and subsequent stable stage when the layer is completely frozen.

We identified 12 thermal gullies within the study area based on field investigations and high-resolution satellite images. It is difficult to detect surface deformation exactly located at these thermokarst landforms, which are narrower than 10 m, about the size of SAR image pixels. Thus we outlined a buffer zone around the thermal gullies to investigate their spatial patterns. The mean subsidence trend inside and outside our buffer zones reached to 1.2 cm/year and 0.5 cm/year, respectively. We found thermal gullies caused extended subsidence of up to 5 cm/year at its surroundings, using 17 L-band ALOS-1 PALSAR images taken from 2006 to 2011 (Fig. 1).

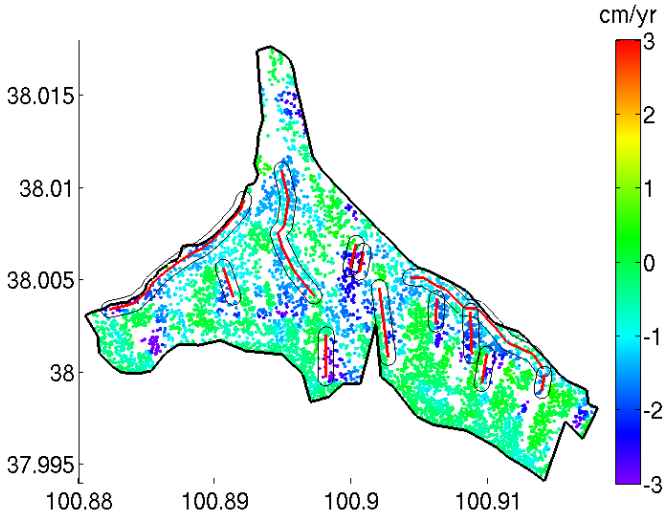

Figure 1: Map of thermokarst subsidence trend from 2006 to 2011. Negative values mean surface subsidence. The black polygon denotes the area of active thermokarst processes. The red lines denote the thermal gullies. Their encircling polygons mean the buff

Furthermore, to the northwest and northeast of the Eboling thermokarst area, there are several small areas with large subsidence trends, which are likely related to thermokarst processes.

This study promises a potential of using PSInSAR to identify thermokarst landforms, map and quantify surface subsidence due to permafrost degradation, and assess its impacts over large areas on the QTP.

References

Ferretti, A.; Prati, C. and Rocca, F. [2001]: Permanent scatterers in SAR interferometry. *IEEE Transactions on Geoscience and Remote Sensing*, 39(1):8–20, doi:10.1109/36.898661.

Liu, L.; Schaefer, K.M.; Chen, A.C.; Gusmeroli, A.; Zebker, H.A. and Zhang, T. [2015]: Remote sensing measurements of thermokarst subsidence using InSAR. *Journal of Geophysical Research: Earth Surface*, 120(9):1935–1948, 2015. doi:10.1002/2015JF003599.

Dynamic slopes – spatio-temporal patterns and signals in permafrost related geometry changes

Isabelle Gärtner-Roer, Samuel Weber, Johann Mueller, Vanessa Wirz, & Andreas Vieli

University of Zurich, Switzerland

Temperature-driven change in the state of permafrost has been widely documented in recent years and recognized as an indicator of global climate change [IPCC, 2014]. The influence of warming and vanishing permafrost has significant implications for subsurface conditions, such as ice content or the occurrence of aquifers. The related changes influence ongoing processes and often become visible by geometry changes at the landsurface. Thus, landsurface in this context is considered as the interface between lithosphere, atmosphere, hydrosphere and cryosphere and thus represents both controlling factor and result (form/shape) of processes acting on different scales. Geomorphological processes related to changing permafrost conditions influence bedrock as well as debris, and single landforms, complex slopes or entire regions. The movement of sediment along these (gravitational) trajectories may affect the ecosystem, the sediment budget, but also infrastructure or human beings. Especially in mountain regions it has been observed that instable landforms or slopes, which may cause damage to infrastructure or human beings, are becoming more frequent. In order to better understand high mountain geosystems, it is therefore important to investigate and monitor landform changes in the context of a changing cryosphere. As those changes occure at different spatial and temporal scales, it is further necessary to include investigations at different scales.

Our study aims at the combined analysis of movements in deep fractured rock slopes and in creeping talus/debris slopes (e.g., rockglaciers), as observed in the Swiss Alps. We use geodetic landform changes to capture ongoing environmental/climatic changes and assess possible related scales. With this approach we hope to contribute to a better process understanding.

The conceptual background of our study is given by the connection of the different parts of a slope, as represented in the coarse debris process chain: rock wall → rock fall → talus slope → permafrost creep → rockglacier [Barsch and Caine, 1984]. For the rock face system analysis, we provide recent data from the famous Matterhorn Hörnligrat, where relative changes are measured and processes in fissures and fractures are described and modeled. Here, a multisensor approach using crackmeter, acoustics/microseismics, but also terrestrial laser scanner (TLS), is performed. Fracture dynamic activity and partially resulting boulder fall events are mainly observed during summer and might be triggered by percolating meltwater. The talus slope and rockglacier systems are investigated by the application of terrestrial surveys (total station, differential Global Positioning System (dGPS)) and remote sensing techniques (mainly photogrammetry from different airborne sensors). Long-term monitoring is conducted on several landforms in the Swiss Alps by the application of total station surveys giving annual values on horizontal velocities of decimeters to several meters and vertical changes of centimeters to decimeters as depending on the properties and status of the individual landform (accuracy of 2 cm/a). Short-term variations are quantified by continuous differential GPS measurements for several fast moving landforms in the Valais and indicate mean annual velocities between 0.2 and 6.6 m/a (and an accuracy of around 0.4 mm/d), but with intra-annual variations between 6 % and up to 2000 %.

With the observed vertical changes and horizontal velocities we conclude on sediment transfer process and/or permafrost degradation on different spatial and temporal scales. While field observations provide essential high accuracy data, remote sensing offers a complementary and cost-effective tool that allows for the analysis on a more regional scale. In general we have to cope with the problem that despite the increasing number of (high resolution) data, the knowledge on internal processes in permafrost affected slopes is still limited. Therefore, we include also data on influencing factors such as topography and meteorological and snowpack factors (e.g., duration and thickness of snowcover) in our analysis.

For the comparison of the different slope systems, we describe and analyse movement patterns, such as

longterm/decadal trends, interannual changes, seasonal rythms or short-term peaks related to single events (e.g. to thunderstorms). We hope to see analogue or connected signals in the different systems, which will contribute to a better understanding of the process-interaction on permafrost affected slopes.

References

Barsch, D. and Caine, N. [1984]: The Nature of Mountain Geomorphology. *Mountain research and development*, 4(4):287–298, 1984.

IPCC Intergovernmental Panel on Climate Change [2014]: *Climate Change 2013 – The Physical Science Basis*. Cambridge University Press, Cambridge.

Modeling landscape vulnerability to thermokarst disturbance in boreal Alaska

Hélène Genet[1], Mark Lara[1], William Robert Bolton[1], Anthony David McGuire[1,2], Vladimir Romanovsky[1], & Merritt Turetsky[3]

[1] *University of Alaska Fairbanks, United States of America*
[2] *U.S. Geological Survey*
[3] *University of Guelph*

Estimation of the magnitude and consequences of permafrost degradation in high latitude regions is currently one of the most urgent research challenges related to climate change. Most studies to date have focused on permafrost degradation from top-down thaw that will vertically expose frozen soil layers to warming and subsequent thawing. This process will affect surficial frozen soil across large portions of the permafrost region. In addition to widespread active layer deepening and near-surface talik formation, ice rich permafrost can thaw laterally, often triggering abrupt thermokarst and subsidence of the ground surface [Jorgenson et al., 2013]. Wetlands or lakes quickly develop in thermokarst depressions, while surface water of the surrounding landscape may drain towards the depression. Furthermore, field measurements have documented large losses of deep, recently thawed organic carbon (OC) from thermokarst wetlands. Because of saturated conditions, these OC losses could involve substantial releases of methane. On the other hand, the accumulation of a new peat layer at the surface of these wetlands may partially offset permafrost C losses.

In boreal forest, thermokarst can lead to the development of collapse scar bogs, fens, or lakes. And recent studies in arctic and boreal regions have documented an acceleration of the rates of ice-rich permafrost degradation in peatlands [Baltzer et al., 2014, Lara et al., 2015]. However, although field studies have demonstrated the dramatic consequences of thermokarst formation on local ecosystem structure and function, the importance of thermokarst at the regional scale is still poorly understood, because of the limited spatial information about thermokarst distribution across Alaskan arctic and boreal forests.

To better understand the vulnerability of the landscape to thermokarst formation in boreal Alaska, we developed the Alaska Thermokarst Model (ATM), a state-and-transition model designed to simulate ecosystem transitions associated with thermokarst disturbance in Alaska and Northwestern Canada. In boreal regions, the model simulates transitions from permafrost plateau forest to thermokarst lake, bog or fen (Fig. 1), as a function of climate and fire dynamics, permafrost characteristics and physiographic information.

This model is designed and parameterized based on existing literature and new repeated imagery analysis that indicates an acceleration of permafrost plateau lateral degradation during the last 4 decades in one of the main wetland complex in boreal Alaska. This model is currently being run in dominant Alaskan boreal forest lowlands (i.e., Tanana Flats & Yukon Flats). We present simulations of thermokarst dynamics and associated land cover change from 2010 to 2100 for six climate scenarios associating 3 AR5 emission scenarios and two global circulation model simulations. This analysis has allowed us to assess the importance of thermokarst dynamics and landscape evolution associated with permafrost thaw in potentially vulnerable boreal forest regions during the 21st century and could be used as a baseline for managers to incorporate projected future changes in landscape and species composition in designing future land management strategies.

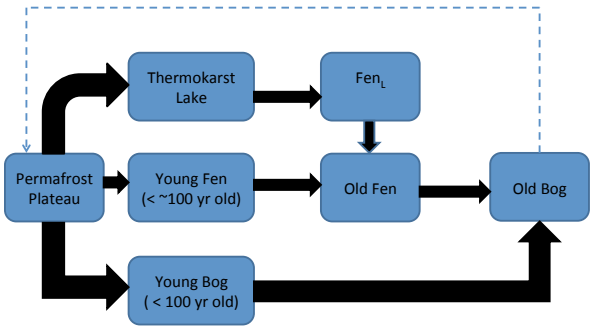

Figure 1: Diagram representing the state and transitions simulated in the Alaska Thermokarst Model for the boreal region.

References

Baltzer, J.L.; Veness, T.; Chasmer, L.E.; Sniderhan, A.E. and Quinton, W.L. [2014]: Forests on thawing permafrost: fragmentation, edge effects, and net forest loss. *Global Change Biology*, 20(3):824–834, doi:10.1111/gcb.12349.

Jorgenson, M.T.; ; Harden, J.; Kanevskiy, M.; O'Donnell, J.; Wickland, K.; Ewing, S.; Manies, K.; Zhuang, Q.; Shur, Y.; Striegl, R. and Koch, J. [2013]: Reorganization of vegetation, hydrology and soil carbon after permafrost degradation across heterogeneous boreal landscapes. *Environmental Research Letters*, 8(3):035017(13 pp.), doi:10.1088/1748-9326/8/3/035017.

Lara, M.J.; McGuire, A.D.; Euskirchen, E.S.; Tweedie, C.E.; Hinkel, K.M.; Skurikhin, A.N.; Romanovsky, V.E.; Grosse, G.; Bolton, W.R. and Genet, H. [2015]: Polygonal tundra geomorphological change in response to warming alters future CO_2 and CH_4 flux on the Barrow Peninsula. *Global Change Biology*, 21(4):1634–1651, doi:10.1111/gcb.12757.

Surface kinematics of periglacial sorted circles over 8 years using SfM close-range photogrammetry

Luc Girod[1], Andreas Kääb[1], & Ivar Berthling[2]

[1] *University of Oslo, Norway*
[2] *Norwegian University of Science and Technology, Trondheim, Norway*

Sorted soil circles are a form of periglacial patterned ground that is commonly noted for its striking geometric regularity. They consist of an inner fine domain bordered by gravel rings that rise some decimetres above the fine domain. Field measurements and numerical modelling suggest that these features develop from a convection-like circulation of soil in the active layer of permafrost. The related cyclic burial and exhumation of material is believed to play an important role in the soil carbon cycle of high latitudes. The connection of sorted circles to permafrost conditions and its changes over time make these ground forms potential palaeoclimatic indicators. In this study, we apply the photogrammetric structure-from-motion technology (SfM) to large sets of overlapping terrestrial photos taken in Augusts 2007, 2010 and 2015 over three sorted circles at Kvadehuksletta, western Spitsbergen. In 2015 we used a modified acquisition set-up and a new camera to push resolution and precision even further compared to the 2007 and 2010 data. We retrieve thus repeat digital elevation models (DEMs) and orthoimages with millimetre to sub-millimetre resolution and precision. Changes in microrelief over the 8 years are obtained from DEM differencing and horizontal displacement fields from tracking features between the orthoimages. In the fine domain, surface material moves radially outward at horizontal rates of up to 2 cm yr^{-1}. The coarse stones on the inner slopes of the gravel rings move radially inward at similar rates. A number of substantial deviations from this overall radial symmetry, both in horizontal displacements and in microrelief, shed new light on the spatio-temporal evolution of sorted soil circles, and potentially of periglacial patterned ground in general. The extension of our initial 2007-2010 period to a third epoch, 2015, enables us to draw first conclusions about the temporal variability of the sorted-circle kinematics obtained. Our results also demonstrate the large potential of SfM in general to investigate Earth surface processes at local scales with unprecedented precision and resolution – and with very limited effort.

Ponding vs. baydzherakh formation on Yedoma uplands: Implications for modern thermokarst development and thaw subsidence in North Yakutia

Frank Günther[1], Guido Grosse[1], Aleksandra Veremeeva[2], & Georgy Maksimov[3]

[1] *Alfred Wegener Institute Helmholtz Centre for Polar and Marine Research, Germany*
[2] *Institute of Physicochemical and Biological Problems in Soil Sciences, RAS, Pushchino, Russia*
[3] *Melnikov Permafrost Institute, Russian Academy of Sciences, Siberian Branch, Yakutsk, Russia*

Permafrost landscapes of Northern Yakutia recently experienced a widespread warming of mean annual air temperatures and mean positive daily air temperatures during the arctic summer [Fedorov et al., 2014]. Especially in the tundra zone this has led to increased active layer thickness (ALT) and suggests that thermokarst processes reactivate or intensify. However, particularly in the light of the enormous area underlain by ice and carbon-rich permafrost, still only few observations of permafrost-thaw related landscape dynamics exist. Permafrost degradation has consequences for local hydrology, ecosystems, biogeochemical cycling, and sometimes communities. For example, in East Siberian Arctic, widespread and irreversible thaw subsidence of up to 11 cm per year has been detected on Muostakh Island [Günther et al., 2015], where coastal erosion at average rates of 1.8 m/yr has not only reduced the island's area by 25 % over more than 60 years, but also provides a constant renewal of the erosional base. In this case, favorable drainage conditions provide the prerequisite for active layer thickness deepening during warm summers, when ground ice stability thresholds are exceeded and ground ice thaw and subsequent terrain lowering take place. Our combined approach of ground-based ALT measurements and remote sensing-derived observations of elevation change revealed an inverse connection of shallow seasonal thaw and strong long-term subsidence, which is related to the minimum depth where permafrost thaw encounters pure ground ice bodies.

In this study, we focus not only on monitoring thermokarst and subsidence of the land surface, but also aim to find commonalities and differences of change or no change on yedoma uplands, slopes, and thaw depressions on the landscape scale using multi-temporal digital elevation models (DEMs) from historical aerial photographies, modern satellite stereo imagery, and on-site repeat laser scanning campaigns. In this context, a best practice strategy for remote sensing data fusion combining 2D and 3D information from very high resolution imagery (GeoEye, WorldView, Kompsat, Alos Prism), complemented by local field measurements (meteorology, lake water and ground temperatures, and repeat geodetic surveys) on the Bykovsky Peninsula and Sobo-Sise in the Lena Delta, has been developed. In order to capture a large variety of sites across the Yedoma region, additional sites at Cape Mamontov Klyk in the Anabar-Olenyok Lowland, Bolshoy Lyakhovsky on the New Siberian Islands, and Cape Maliy Chukochiy in the Kolyma Lowland with less or no topographical ground control, were considered from the perspective of larger areal coverage.

Our high spatial resolution monitoring for the last decades and in comparison for the last years, shows that the current relief development in ice-rich permafrost enhances not only drainage of thermokarst lakes, but also drainage of the entire terrain, which leads to the formation of thermokarst mounds (baydzherakhs) on slopes of yedoma uplands. In contrast, simultaneous ponding on poorly drained massive Yedoma blocks in immediate proximity, suggests thermokarst development. However, formation of new thermokarst lakes on yedoma uplands is limited by topographical and stratigraphical constraints [Morgenstern et al., 2011]. Geomorphological mapping of Yedoma and Alas surfaces, baydzherakh fields and areas of newly formed ponds allows to differentiate and link observed topographical changes to specific processes of either thermokarst or denudation. First results show that widespread modern baydzherakh formation is indicative for large-scale permafrost thaw subsidence on yedoma uplands.

References

Fedorov, A.N.; Ivanova, R.N.; Park, H.; Hiyama, T. and Iijima, Y. [2014]: Recent air temperature changes in the permafrost landscapes of northeastern Eurasia. *Polar Science*, 8(2):114–128, doi:10.1016/j.polar.2014.02.001. Special Issue: The Third International Symposium on the Arctic Research (ISAR - 3).

Günther, F.; Overduin, P. P.; Yakshina, I. A.; Opel, T.; Baranskaya, A. V. and Grigoriev, M. N. [2015]: Observing Muostakh disappear: permafrost thaw subsidence and erosion of a ground-ice-rich island in response to arctic summer warming and sea ice reduction. *The Cryosphere*, 9(1):151–178, 2015. doi:10.5194/tc-9-151-2015.

Morgenstern, A.; Grosse, G.; Günther, F.; Fedorova, I. and Schirrmeister, L. [2011]: Spatial analyses of thermokarst lakes and basins in Yedoma landscapes of the Lena Delta. *The Cryosphere*, 5(4):849–867, doi:10.5194/tc-5-849-2011.

Analysis of summer subsidence in Barrow, Alaska, using InSAR and hyperspectral remote sensing

Mahmud Haghshenas Haghighi[1], Mahdi Motagh[1], Birgit Heim[2], Sabine Chabrillat[1], Dmitry Streletskiy[3], Guido Grosse[2], Torsten Sachs[1], & Katrin Kohnert[1]

[1] *Helmholtz Centre Potsdam, GFZ German Research Centre for Geosciences, Potsdam, Germany*
[2] *Alfred Wegener Institute Helmholtz Centre for Polar and Marine Research, Potsdam, Germany*
[3] *Department of Geography, The George Washington University, Washington, DC, USA*

In this study, gradual elevation change due to summer thawing of active layer in tundra permafrost landscape of Barrow, Alaska is investigated using SAR interferometry (InSAR) technique. We used a variety of SAR sensors including TerraSAR-X, ALOS, and Sentinel-1 images to assess elevation changes in summer season. Preliminary result, obtained by TerraSAR-X InSAR analysis, clearly delineates subsidence during the summer by identifying thousands of coherent pixels on the ground. InSAR time-series analysis from June to September 2013 show the progressive thaw-season subsidence on the Barrow coastal plain with maximum magnitude of 4 cm in satellite line of sight. The spatial pattern of InSAR elevation change reflects different thaw-related landscape features of permafrost. As a general pattern, detected elevation change is higher in wet thermokarst basins than tundra uplands. Barrow is one of the Global Terrestrial Network for Permafrost (GTN-P) sites. A lot of ancillary data that have been acquired in the last decades will help us in interpretation of InSAR results. We also use airborne hyperspectral data to derive characteristics like wetness and vegetation cover of the landscape to better understand the process and the link between estimated subsidence and landscape features.

First measurements of permafrost-related surface movements using ground based SAR interferometry: A case study in the Eboling Mountain on the Qinghai-Tibet Plateau

Liming Jiang[1], Lin Liu[1,2], Lin Liu[3], Binbin Gao[1,2], Yafei Sun[1,2], Hansheng Wang[1], & Tingjun Zhang[4]

[1] *State Key Laboratory of Geodesy and Earth's Dynamics, Institute of Geodesy and Geophysics, Chinese Academy of Sciences, Wuhan, China*
[2] *University of Chinese Academy of Sciences, Beijing, China*
[3] *Earth System Science Programme, Faculty of Science, The Chinese University of Hong Kong, Hong Kong, China*
[4] *College of Earth and Environmental Sciences, Lanzhou University, Lanzhou, China*

Objective

This paper aims to demonstrate measurements of surface movements over permafrost area in the Qinghai-Tibet Plateau, the very first of this kind by means of ground based SAR (GB-SAR) interferometry. A case study in the Eboling Mountain was carried out to measure permafrost-related surface movements with high precision (sub-mm) and at high spatial-temporal resolution.

Study area and data

Eboling Mountain is located in the upper reach of Heihe River basin in the eastern portion of the Qinghai-Tibet Plateau, with central coordinates 38°00' N and 100°55' E [Mu et al., 2013]. Thermokarst landforms, such as thaw slumps are well-developed within an area underlain by ice-rich permafrost [Mu et al., 2015]. In this study, we applied the IBIS (Image By Interferometric Survey) GB-SAR to take continuous SAR images and conduct time series interferometry analysis. The in-situ observations started on June 16, 2015 and lasted for about 66 hours. Overall, we acquired 632 SAR images with a spatial resolution of about 0.5 m.

Method and preliminary results

These continuous SAR images were processed by the SAR interferometry tool provided with the IBIS DV software. In particular, the errors caused by atmospheric distortions were corrected by the use of ground control points (GCPs) which are located at the relatively stable bed rocks. Finally, the derived surface movements were transformed from the SAR image coordinates into WGS84 coordinates. Fig. 1(a) illustrates the detailed surface displacements of the whole 66 hours over the study area in the Eboling Mountain generated by GB-SAR interferometry. In general, most of the area experienced relatively stable changes (between -1.5 mm and +1.5 mm), whereas larger surface movements (up to ~4.2 mm) were detected near the thermokarst landforms. Moreover, two corner reflectors (CR) (as indicated in figure 1(a)) were employed to detect temporal changes of surface displacements. It is shown in figure 1(b) that the ground surfaces at both CRs fluctuated diurnally, which was generally in agreement with the changes in air temperature.

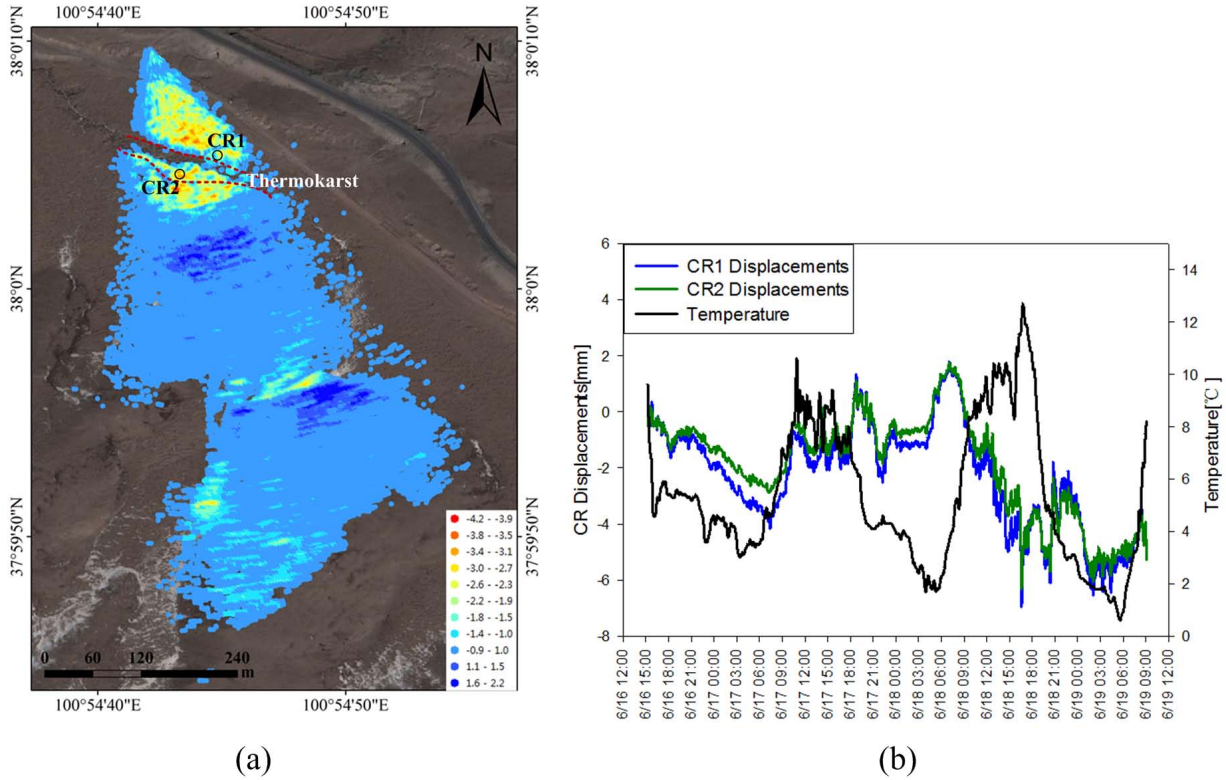

Figure 1: Fig.1. (a) Map of total surface displacements of the study area during the survey period of 66 hours and (b) time series of surface displacements at the two corner reflectors.

Conclusion

The surface displacements of permafrost region on the Eboling Mountain, Qinghai-Tibet Plateau were successfully observed with ground based SAR interferometry. The preliminary results demonstrated that the IBIS GB-SAR has a significant potential to measure the surface movements over permafrost-affected areas. Surface movements of the Eboling permafrost zone were found to be probably associated with the air temperature changes, for which exact mechanisms need to be further investigated.

References

Mu, C.; Zhang, T.; Cao, B.; Wan, X.; Peng, X. and Cheng, G. [2013]: Study of the Organic Carbon Storage in the Active Layer of Permafrost over the Eboling Mountain in the Upper Reaches of the Heihe River in the Eastern Qilian Mountains. *Journal of Glaciolgy and Geocryology*, 35(1):1–9, (in Chinese).

Mu, C.; Zhang, T.; Wu, Q.; Cao, B.; Zhang, X.; Peng, X.; Wan, X.; Zheng, L.; Wang, Q. and Cheng, G. [2015]: Carbon and Nitrogen Properties of Permafrost over the Eboling Mountain in the Upper Reach of Heihe River Basin, Northwestern China. *Arctic, Antarctic, and Alpine Research*, 47(2):203–211, doi:10.1657/AAAR00C-13-095.

Study of frost susceptibility of normally consolidated clay using NGI frost heave cell

Mehdi Kadivar[1], Gustav Grimstad[1], Seyed Ali Ghoreishian Amiri[1], Hans Petter Jostad[2], & Ellen Birkeland[2]

[1]*Norwegian University of Science and Technology (NTNU), Norway*
[2]*Norwegian Geotechnical Institute (NGI), Norway*

The Gibs free energy for ice is less than unfrozen water. Hence, wherever ice and unfrozen water coexist, there is a pressure difference between them, which is called cryogenic suction. Cryogenic suction depends on temperature and it causes ice to absorb water. In case of frozen soils, this phenomenon makes the pore ice crystals and therefore the soil mass to expand. The expansion of frozen soil due to absorption of water from unfrozen parts is called frost heave.

Frost heave happens if three conditions hold: 1-temperature is low enough 2-soil is frost susceptible and 3-enough unfrozen water is available to the frozen soil. Frost heave is a serious problem emerging damages into infrastructures in a large part of the world mainly in northern hemisphere. At low temperatures during wintertime, frozen soil absorb water and expands usually unevenly which makes bumps or cracks in road surfaces or it can break foundations of structures. On the other hand, melting frozen soil and releasing extra water in summer time can destroy road surfaces or even it can cause landslide.

In order to understand the behavior of soil during freezing and to measure the amount of frost heave, a frost heave cell device (Fig. 1) has been developed at Norwegian Geotechnical Institute (NGI). By using this device, it is possible to monitor the mechanical behavior of soil at different temperatures by time. The soil sample, either intact or reconstructed, is placed into the cell and adjustable temperature is applied from top, bottom and side of the sample. The freezing characteristics of soil that can be studied by this device are the location of freezing front, expansion of soil sample and amount of water intake from an external source, during test. Location of freezing front is obtained by checking the temperature at the sides of the sample in different time steps. The main purpose of this work is to study the frost susceptibility of normally consolidated clay with NGI frost cell device at different temperatures. First, the NGI frost cell is fully described. Then, the previous works with the device is shortly presented. Finally, the freezing behavior of a normally consolidated clay sample (a sample from Onsøy, a site near Oslo) is studied.

Figure 1: From right to left, three cooling devices, frost heave cell and external water source

Geophysical forecasting of the formation of thermal suffosion depressions in Central Yakutia

Ivan Ivanovich Khristoforov[1], Vladimir Vladimirovich Olenchenko[2], Leonid Gagarin[1], & Alexander Vasilievich Omelyanenko[1]

[1] *Melnikov Permafrost Institute of Siberian Branch Russian Academy of Sciences, Yakutsk, Russia*
[2] *Trofimuk Institute of Petroleum Geology and Geophysics of Siberian Branch Russian Academy of Sciences, Novosibirsk, Russia*

An unique groundwater spring Ulakhan-Taryn is located in Central Yakutia on the right bank of the Lena river, 50 km to the south from Yakutsk. The Ulakhan-Taryn spring discharge is high and constant over the year with long-term annual value of 240 l/s. Ulakhan-Taryn spring is located on the 4^{th} Lena river floodplain (Bestyakh) terrace. Its upper part is presented by eolian fine-grained sands covered by vegetation. Alluvial medium-grained sand with gravel and pebble-bed basis forms the lower part of the section. Base of terraces is represented by Middle Cambrian limestones, that are fractured from the top. Central Yakutia is located in continuous permafrost zone. Permafrost thickness reaches 600 m. However, on the Bestyakh terrace of the Lena river the permafrost thickness varies from 30 to 200 m. It increases up to 420 m in certain locations. Mean annual ground temperature at the base of the layer of seasonal thawing (0.4 – 3.5 m depth) varies from -0,2 °C on the flat areas with pine forest to -5 °C in the inter-ridge depressions and river valleys [Scryabin et al., 1998]. Another distinctive feature of the Bestyakh terrace is existence of the large interpermafrost aquifers. Numerous springs of interpermafrost water are confined mainly to the southern part of the terrace. The largest of them is Ulakhan-Taryn spring. Discharge of the confined groundwater is accompanied by the removal of a large amount of sandy material. Surface landform depressions are formed as a result of the thermal suffusion process (Figure 1(a)). It leads to the formation of gullies [Gagarin, 2013].

Ground Penetrating Radar (GPR) studies were conducted to identify and clarify the boundaries of zones of thermal suffosion ground decompression and taliks with high electrical conductivity, where there is a filtration of groundwater. Certified GPR "OKO-2" with a central frequency 50 MHz, 150 MHz, 300 MHz, 400 MHz and 600 MHz ("LogiS-Geotech") were used in the study. Data processing is carried out by means of the GeoScan_32 software. We conducted electrical resistivity tomography to obtain electrical ground properties. The measurements were carried out by multielectrode complex "Skala-48" developed at the Trofimuk Institute of Petroleum Geology and Geophysics. GPS Garmin 62S was used to position the survey profiles.

Permittivity parameter was set to 9. It was used to refer the measurement data to actual depth section. While GPR data processing it is necessary to take into the consideration the moisture of dispersed rocks, where the permittivity parameter can increase up to the value of 30 based on our practical experience [Scryabin et al., 1998].

GPR studies were performed at the "key" research site along the 6 parallel profiles with a length of 230-240 meters each. The first profile was located on the edge of the thermal erosion cirque. Other profiles were situated to the east from the first one. The average distance between the profiles was about 40 meters.

All types of antenna units were used for the measurements thus it allowed providing data up to 20 m depth from the surface. Electrical resistivity tomography survey was carried out to study distribution of the electrical resistance of rocks on each profile. To build a geoelectric section we selected scheme with two segments of cable with 24x electrodes each with distance of 5 meters from each other. Saline was used to improve the contact between the electrodes and the ground.

The data obtained by the low frequency GPR with central frequency of 50 MHz allow us identifying boundaries up to 20 m depth. There is a "dead zone" up to 3 m depth with no reflected signals. Monitoring of the active layer, as well as the dynamics of supra-permafrost groundwater is not possible to investigate at frequencies from 10 MHz to 75 MHz. Upper limit

of interpermafrost water could be detected. One of the drawbacks of low frequency GPR is a low depth resolution. In this case, only one boundary is identified at a depth of 3-4 meters, although there are two or three boundaries according to a high-frequency GPR data.

Figure 1(c) shows depth section of GPR profile with length of 235 m. It was obtained by double spectral GPR with central frequencies of 150 MHz and 400 MHz. This section was built by means of the procedure "layers on the profile". Permittivity was manually set as 5 for the frozen ground and 9 for thawing rocks. These values affect the depth scale. The exact values of permittivity will be received as a result of orientation drilling.

Measurements were conducted on the 13th of June. Thawing depth was a bit more than a meter at the beginning of the profile (in the range of 0 – 80 m) and increased up to 1.5 meters to its end (in the range 120 – 235 m). This is probably the effect of the vegetation and solar radiation. There is a seasonally frozen layer below with thickness about 1 m. It should be noted that its lower limit is quasi-horizontal and the depth of the upper one varies within a small range. We discovered the evenness of the lower limit of the seasonally frozen layer. The possible reasons are presence of the thawing layer below and unevenness of seasonally thawing layer. Thawing layer is traced below the depth of 2.5 meters. It is confirmed by a phase change of the reflected signal of the electromagnetic wave from the border. Phase change of the reflected signal from the border indicates phase transition of the water (ice to water). Complex reflector configuration with "depressions" to a depth of 8-9 m (Fig. 1 b) is an effect of the increased dielectric constant of water-saturated sands.

This profile is located 230 m to the east from the thermosuffosion cirque. It has no visible surface depressions. There are two areas with dispersed water-saturated rocks and presence of cavitation in the deep section. Additionally, the presence of internal zones with high water content is confirmed by the high-amplitude signals at the lower boundary.

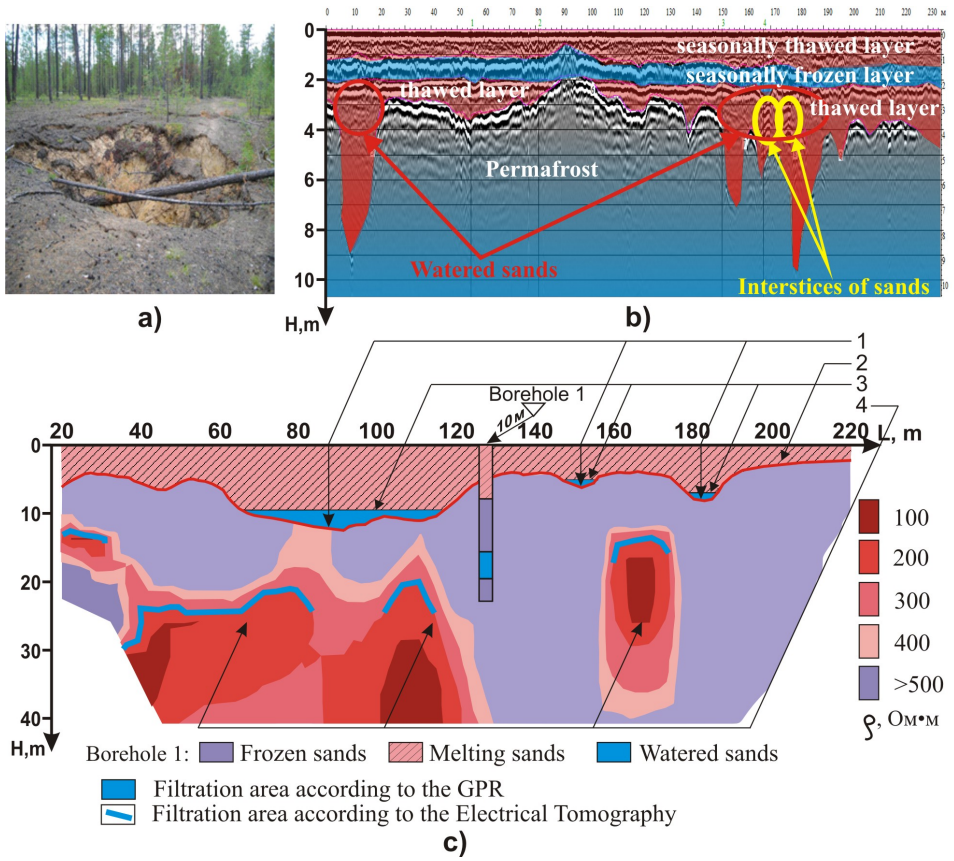

Figure 1: a) Thermal Suffosion Depression, b) Deep Interpretative Section with Identified Layers of GPR, c) Geophysical Interpretative Section of Ulakhan-Taryn

Radiograms received by high-frequency GPR with central frequency of 600 MHz, has high resolution that allows one to identify the freezing thawing layers with accuracy up to cm. Its significant drawback is that studied depth limited to 3 meters, that doesn't cover maximum seasonal freezing and thawing depth.

To improve the accuracy of the research we combined GPR and Electrical Resistivity Tomography methods. Figure 1 (c) shows the results of its combined usage. By means of the double spectral GPR method we identified areas of rocks decompression (1), determined talik zone (2), clarified the boundaries of groundwater filtration zone (3) from 5 to 12 meters depth. The spatial distribution of zones with high electrical conductivity (4) in the permafrost section was established by electrical resistivity tomography at the depth of 15 – 30 m. As a result presence of the two groundwater horizons could be suggested. Borehole 1 located 10 m away from the geophysical profile confirms the results of the interpretation. Electrical resistivity tomography and GPR methods complement since GPR perform well within the depths of 0.5 – 25 meters, and electrical resistivity tomography obtains data from 10 to 40 – 100 m depth.

We conclude that GPR with central frequencies from 100 to 400 MHz is an effective instrument for forecast of thermal suffosion processes in dispersed water-saturated frozen rocks. Combined application of GPR, electrical resistivity tomography and landscape classification allows establishing the geometry of suprapermafrost groundwater, locations of interpermafrost aquifers and identifying talik zones with high electrical conductivity, where there is a filtration of groundwater. Potential development of thermosuffosion processes could be detected by means of geophysical studies.

Further systematic studies on "key" site for a long period will be a basis for forecast of possible thermal suffosion depressions. The research results will be used to clarify the mechanism of such hazardous processes and to develop principles the potential depression formations.

Acknowledgements

The reported study was partly funded by RFBR research project No.15-45-05053r_vostok_a

References

Gagarin, L.A. [2013]: *Dynamics of Thermal Suffosion Processes on Permafrost Zone (Case Study of Central Yakutia)*. Yakutsk: Publishing House of Melnikov Permafrost Institute SB RAS, Abstract of Thesis, 22 pp.

Omelyanenko, A.V. and Khristoforov, I.I. [2013]: Double Spectral GPR Method for Sensing of Flooded Geological Environment. *Science and Education*, (1):33–38.

Scryabin, P.N.; Varlamov, S.P. and Skachkov, Yu.B. [1998]: Monitoring Studies of Soil Temperature in Central Yakutia. *Geography and Natural Resources*, (2):49–55.

ICESat GLAS elevation changes and ALOS PALSAR InSAR Line-Of-Sight changes on the continuous permafrost zone of the North Slope, Alaska

Reginald R. Muskett

Geophysical Institute, Permafrost Laboratory, University of Alaska Fairbanks, United States of America

Measuring centimeter-scale and smaller surface changes by satellite-based systems on the periglacial terrains and permafrost zones of the northern hemisphere is an ongoing challenge. We are investigating this challenge by using data from the NASA Ice, Cloud, and land Elevation Satellite Geoscience Laser Altimeter System (ICESat GLAS) and the JAXA Advanced Land Observing Satellite Phased Array type L-band Synthetic Aperture Radar (ALOS PALSAR) on the continuous permafrost zone of the North Slope, Alaska. Using the ICESat GLAS exact-repeat profiles in the analysis of ALOS PALSAR InSAR Line-Of-Sight (LOS) changes we find evidence of volume scattering over much of the tundra vegetation covered active-layer and surface scattering from river channel/banks (deposition and erosion), from rock outcropping bluffs and ridges. Pingos, ice-cored mounds common to permafrost terrains can be used as benchmarks for assessment of LOS changes. For successful InSAR processing, topographic and tropospheric phase cannot be assumed negligible and must be removed. The presence of significant troposphere phase in short-period repeat interferograms renders stacking ill suited for the task of deriving verifiable centimeter-scale surface deformation phase and reliable LOS changes.

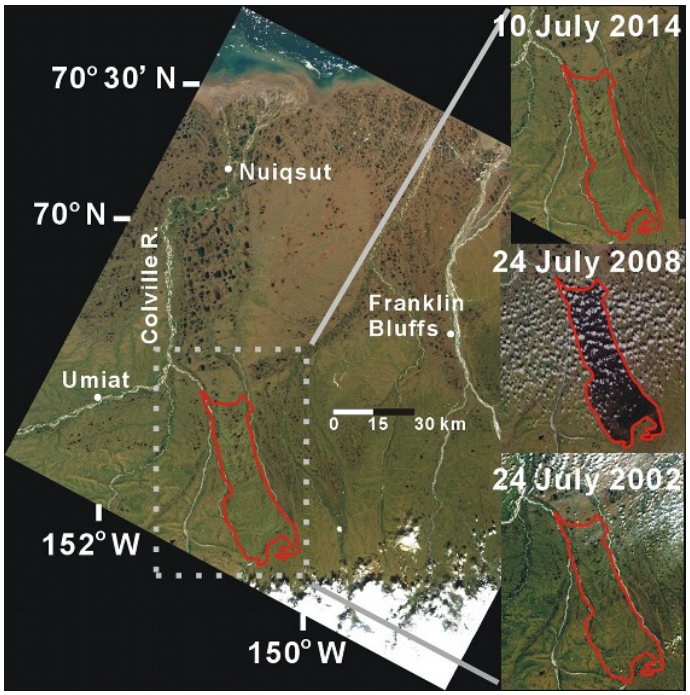

Figure 1: A region of interest on the North Slope, Alaska: The Anaktovuk Wildfire scar, as observed in LANDSAT7 and 8 images from 24 July 2002 (before the wildfire), 24 July 2008 (one year after the wildfire) and 10 July 2014 (showing vegetation recovery).

References

Muskett, R.R. [2014]: ICESat-Derived Elevation Changes on the Lena Delta and Laptev Sea, Siberia. *Open Journal of Modern Hydrology*, 4(1): 1–9, doi:10.4236/ojmh.2014.41001.

The potential of high resolution multi-scale monitoring of rockglacier kinematics using unmanned aerial vehicles (UAV) and terrestrial surveys

Johann Müller, Stamm Dominik, Isabelle Gärtner-Roer, Vanessa Wirz, & Andreas Vieli

University of Zurich, Switzerland

A whole range of remote sensing instruments is well suited for repeated and rapid observation in remote and inaccessible areas of high mountains. Mostly mono- and multitemporal digital elevation models derived from airborne and terrestrial platforms have repeatedly been used to describe geomorphological features and analyze related processes, such as rockglaciers in permafrost areas.

Terrestrial laserscanning (TLS), airborne photogrammetry and terrestrial surveys are established methods for the assessment of high mountain landform dynamics on different scales. Recent advances in UAV (Unmanned Aerial Vehicles) based photogrammetry facilitate the production of multitemporal digital elevations models (DEMs) of very high resolution in high mountain environments. Thus for many permafrost sites in the Swiss Alps, there is now a vast long-term data inventory of landform kinematics derived from different sensor systems. The question arises now about the potential and challenge of a combined data analysis. The data fusion and holistic assessment possibilities rely on the properties of each derived dataset such as resolution, precision and accuracy.

To introduce and discuss such a comprehensive dataset and its performance, we present multi-annual digital elevation data derived from terrestrial laserscanning and UAV-based photogrammetry and kinematic monitoring data from geodetic surveys and continuous differential GPS at the Muragl rockglacier in the Swiss Alps. The multitemporal TLS data (years 2013 to 2014) and UAV data (years 2014 to 2015) are used to derive annual flow velocities and surface dynamics. In addition they are compared to geodetic surveys (of single points on the rockglacier surface) of very high accuracy during the same time. Continuous singular dGPS measurements show the intra-annual variations which are not captured by the annual assessment during the same time span.

Since TLS and geodetic surveys have been applied frequently in rockglacier assessment and their characteristics are well known, we conduct an extensive accuracy assessment of UAV-based high resolution DEM which has not yet been systematically tested in such a complex environment.

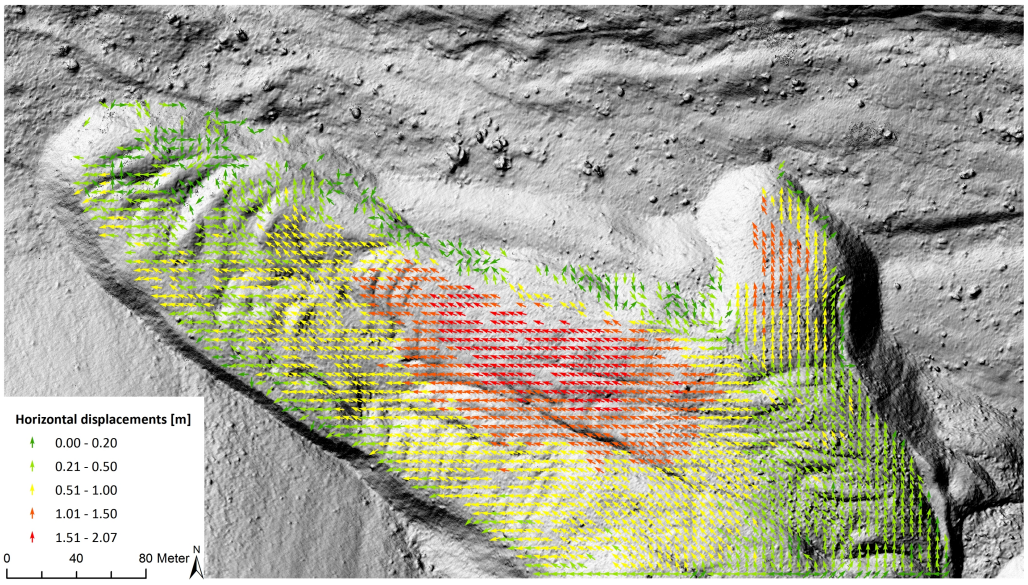

Figure 1: Annual horizontal displacements of the Muragl rockglacier derived from UAV DEMs.

The photogrammetrically derived UAV DEM is evaluated against geodetic field measurements and a terrestrial laser scan. Traditional global and local accuracy measures such as the root mean square error, standard deviation and absolute mean error are used to describe the vertical quality of the DEMs. The error distributions are additionally checked for normal distribution and robust statistical measures (Median, Normalized Median Absolute Deviation and several quantiles) are used to describe the accuracy of the DEM ideally.

The TLS-reference data focuses on the spatial characteristics of the UAV-DEM and the derived accuracy results are considered when conducting multisensoral analysis of rockglacier kinematics. The outcome of this study shows the level of detail to which UAV derived DEMs can be reliably used in geomorphological analysis of high mountain environments.

We present a comprehensive multisensoral data analysis to assess rockglacier kinematics where we focus on the role of accuracy properties of the fused data. Nevertheless the different datasets represent the characteristics of rockglacier kinematics on different spatial and temporal scales and therefore we elaborate on how they are complementary.

The main objectives of this study are:

- to present a multitemporal and multisensoral dataset on rockglacier kinematics in different spatial and temporal scales
- to assess the accuracy and applicability of UAV based photogrammetric DEMs in high mountain areas
- to show the benefits of a multisensoral monitoring approach for rockglacier kinematics and to elaborate on the advantages of each method/technique in a complementary way.

Stochastic model of thermokarst within disturbed areas and its empirical verfication using high resolution images

Timofey Orlov[1], Alexey Victorov[2], Sergey Sadkov[1], Evgeniy G. Panchenko[1], & Andrey Zverev[1]

[1]*Sergeev Institute of Environmental Geoscience RAS (IEG RAS), Russian Federation*
[2]*RAS Institute of Environmental Geoscience, Russian Federation*

Introduction

Nowadays there happens an expanding engineering activity across the entire permafrost zone. First of all, these are the linear structures such pipelines and road which are being constructed. Construction of the long-distance engineering objects is quite challenging due to the difficult geological conditions in permafrost regions. That requires an extensive investigation of how the dangerous geological processes affect the human built infrastructure. Given that, there is a significant demand for better understanding of such processes like thermokarst which is often massively activated, when constructing linear objects. An engineering activity planning in the permafrost regions apparently requires robust methods for the forecasting and assessment of the human-induced thermokarst.

The goal of the paper is the empirical verification of the stochastic model of a lacustrine thermokarst plain dynamics [Kapralova, 2007, Victorov et al., 2015]. The model we used is based on the scenario of the thermokarst synchronous start. It assumes the thermokarst depression growth to be proportional to the lake lateral surface heat loss. The framework of the model can be represented as the following:

1. The appearance of the initial thermokarst depressions took a short period (so called synchronous start). The process is stochastic and was happening independently within non-adjacent areas. The probability of the depression appearance within a study site depends exclusively on the site area (dS). For smaller sites, the appearance of a single depression is significantly higher, than that of the multiple ones, i.e.:

$$p1 = gdS + o(dS), pK = o(dS) k = 2,3...$$

2. The depression size growth is independent due to the thermoabrasive action. The growth is proportional the local heat accumulation and is inversely related to the depression lateral surface area. This specific type of growth we further name “logarithmic”.

The aforementioned assumptions allow concluding that the distribution of the depression number across a randomly selected site is conformed to the Poisson distribution [Victorov, 1998, 2006] i.e:

$$P(k,s) = \frac{(gS)^k}{k!} \times e^{gS}$$

where: g - average number of depressions per area unit, s - sample site area. The depression sizes are log normally distributed [Kapralova, 2007, Victorov et al., 2015]. This paper considers the initial depressions covered with water which appeared at the very start of the human-induced thermokarst [Perlshtein et al., 2005].

Data and methods

We selected two sample sites for testing the model. Central Yakut site has MAAT -7 °C, ground temperature -2 – -4 °C, mean annual precipitation 260 mm and the permafrost thickness up to 300-400 m. The site is located within a denudation plateau covered with eluvial deposits over Jurassic sandstones.

South Yakut site has MAAT -9.5 °C, ground temperature -1 °C, mean annual precipitation 570 mm and the sporadic permafrost thickness up to 30-150 m. The site is located within a tectonic-denudation plateau, covered with eluvial clay loams and scree.

The thermokarst initiation was registered within the areas clear cut of soil and vegetation as were prepared for the subsequent engineering works.

For the Central Yakut site we used the WorldView-2 images (0.5 m). These were acquired in a year after the soil and vegetation cover removal. The images depict the generation of the initial thermokarst depressions. The study area is 0.1 km^2.

For the South Yakut (Fig. 1a-b) site we used the aerial imagery (0.2 m) and the satellite images Pleiades (0.5m). Aerial imagery was acquired in a year after the pipeline construction started. The image depicts the initial stage of the thermokarst depression generation. The Pleiades image was acquired 4 years after the removal of the vegetation and soil cover. It shows the initial stage of the generation of the thermokarst depressions. The sample area used for the model testing was of a strip shape (50 m × 26 km). The testing area was uniformly segmented according to the thermokarst spatial density. Each segment is linearly uniform so its section is equal to that of any other segment. It is here necessary to employ the concept of the linear uniformity since the sample area contains the following linear objects: pipeline, power line, motor road.

It is important to mention there are thermokarst mitigation activities committed within the South Yakut site, so for the analysis we only selected the areas with the least mitigation activity implemented. For testing the model, we choose two parameters:

- distribution of the initial thermokarst depression sizes;
- distribution of the centroids derived from the initial depressions.

According to the model assumptions, the distribution of the depression sizes is expected to behave log normally. The distribution of the centroid numbers is expected to follow the Poisson law.

The sizes of the initial depression within the Central Yakut site appeared to be too small for the testing methodological framework; therefore, we only tested it for the distribution centroids.

Findings

We selected the most homogenous testing site within the Central Yakut site. The model empirical testing showed the consistency of the assumption on the Poisson behavior of the centroid number distribution. For the South Yakut site, we selected four testing areas with the initial thermokarst appearance. For three of these, the depression area distributions showed the log normal behavior. Two out of four testing areas revealed the Poisson following behavior of the distribution of the depression numbers projected to the pipeline axis.

Results

The research showed how the stochastic approach based on the landscape mathematical morphology can be employed for modeling the human-induced thermokarst dynamics along the linear engineering objects with the observation series of a short period.

Initially the model was designed for examining the cases of a long-term evolution of thermokarst. However, our research revealed the model can be reliably applied in a very short temporal analysis as well. The model application aims increasing the reliability of the thermokarst risk assessment.

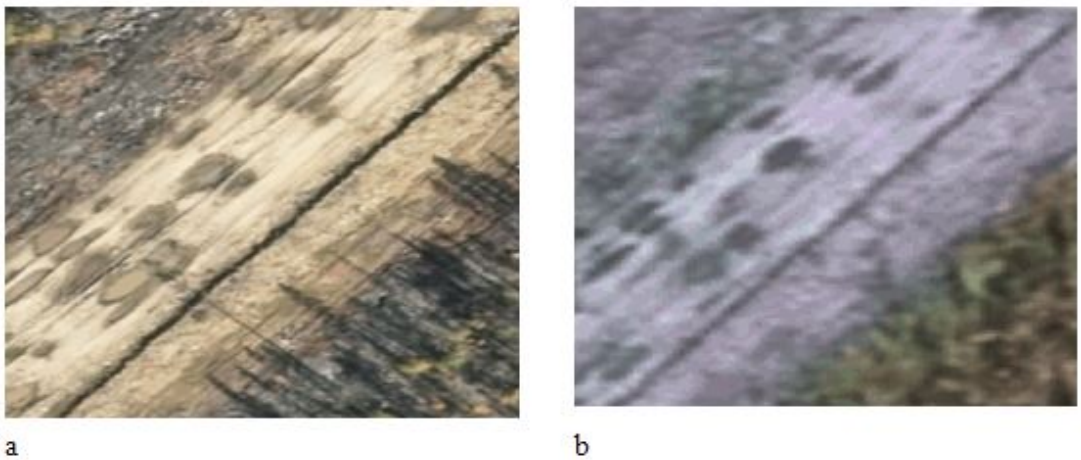

Figure 1: South Yakut site: a – aerial photo fragment, b – satellite image fragment.

Discussion

The model verification we present should be considered a primary test. The model requires a further validation for the areas with the human-induced thermokarst appearance. The authors keep elaborating the model related cases and look forward to receiving any help and support with ideas and data.

Acknowledgements

The research is funded by the Russian Scientific Foundation (project No 14-17-00357).

References

Kapralova, V. [2007]: Application of remote sensing and mathematical morphology of landscape for studying thermo-karst processes. *Landform Analysis*, 5:35–36, URL http://www.sgp.org.pl/la/lav05.htm.

Perlshtein, G.; Levashov, A. and Sergueev, D.O. [2005]: Analisis of the thermokarst's early stage with deterministic and probabilistic methods. In *Terra Nostra – 2nd European Conference on Permafrost, June 12-16, 2005, Potsdam , Germany, Programme and Abstracts*, pages 143–144, ISSN 0946-8978.

Victorov, A.; Kapralova, V.; Orlov, T.; Trapeznikova, O. and Archipova, M. [2015]: Patterns of distribution of thermokarst lakes. In *Proceedings of 15th International Multidisciplinary Scientific GeoConference SGEM 2015, June 18–24, 2015*, volume 2, pages 503–510, URL http://www.sgem.org, ISBN 978-619-7105-32-2 / ISSN 1314-2704.

Victorov, A.S. [1998]: *Mathematical morphology of landscape*. Moscow, Russia, (in Russian).

Victorov, A.S. [2006]: *General problems of the Mathematical morphology of landscape*. 252 p.

Realizing the full potential of Remotely Sensed Active Layer Thickness (ReSALT) Products

Kevin Schaefer[1], Albert Chen[2], Lin Liu[3], Andrew Parsekian[4], Elchin Jafarov[5], Santosh Panda[6], Tingjun Zhang[7], & Howard Zebker[8]

[1] *National Snow and Ice data Center, United States of America*
[2] *Jet Propulsion Laboratory*
[3] *Chinese University of Hong Kong*
[4] *University Of Wyoming*
[5] *Institute of Arctic and Alpine Research, University of Colorado Boulder*
[6] *University of Alaska, Fairbanks*
[7] *Lanzhou University*
[8] *Stanford University*

The Remotely Sensed Active Layer Thickness (ReSALT) product uses the Interferometric Synthetic Aperture Radar (InSAR) technique to measure ground subsidence, active layer thickness (ALT), and thermokarst activity in permafrost regions. ReSALT supports research for the Arctic-Boreal Vulnerability Experiment (ABoVE) field campaign in Alaska and northwest Canada and is a precursor for a potential Nasa-Isro Synthetic Aperture Radar (NISAR) product. ALT is a critical parameter for monitoring the status of permafrost and thermokarst activity is one of the key drivers of change in permafrost regions.

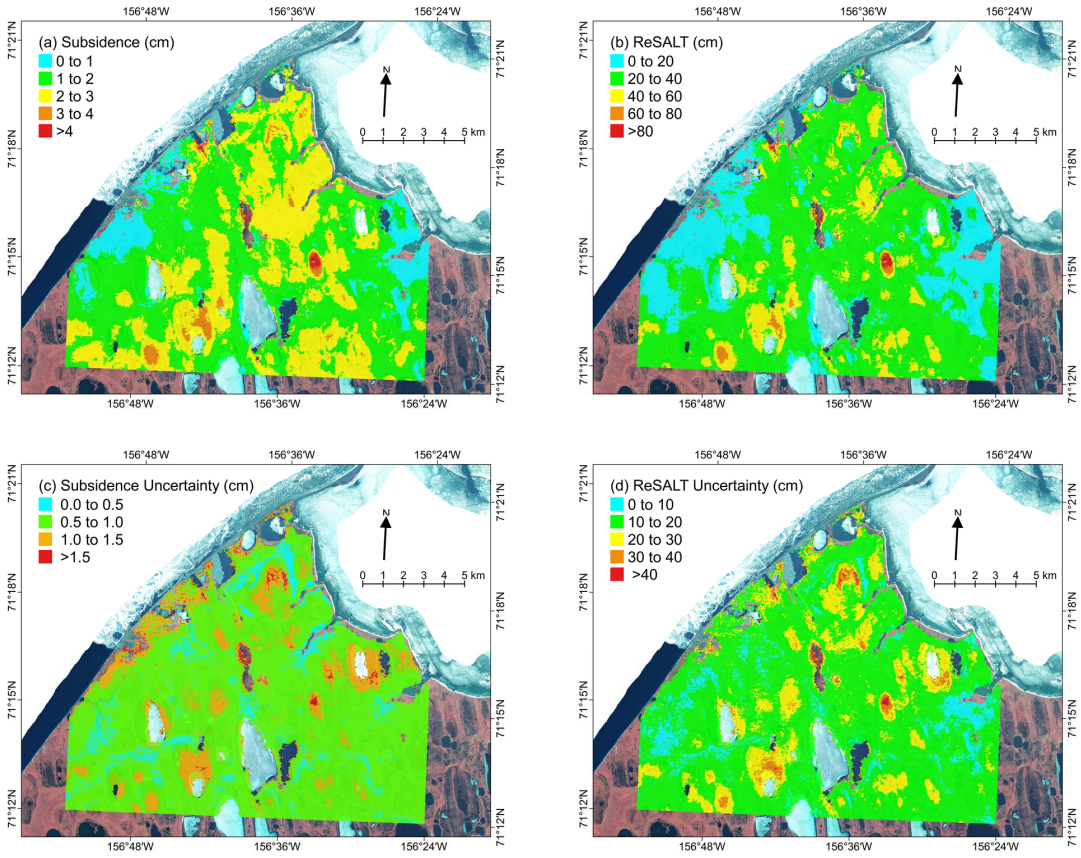

Figure 1: (a) The 2006–2010 average seasonal subsidence from Interferometric Synthetic Aperture Radar (InSAR). (b) The Remotely Sensed Active Layer thickness (ReSALT) and associated uncertainties (c,d). Locations with no coherent signal are left transparent.

The ReSALT product currently includes

1. long-term subsidence trends resulting from the melting and subsequent drainage of excess ground ice in permafrost-affected soils,

2. seasonal subsidence resulting from the expansion of soil water into ice as the active layer freezes and thaws, and

3. ALT estimated from the seasonal subsidence assuming a vertical profile of water within the soil column.

ReSALT includes uncertainties for all parameters and is validated against in situ measurements from the Circumpolar Active Layer Monitoring (CALM) network, Ground Penetrating Radar and mechanical probe measurements. We present high resolution ReSALT products on the North Slope of Alaska: Prudhoe Bay, Barrow, Toolik Lake, Happy Valley, and the Anaktuvuk fire zone. We believe that the ReSALT product could be expanded to include maps of individual thermokarst features identified as spatial anomalies in the subsidence trends, with quantified expansion rates. We illustrate the technique with multiple examples of thermokarst features on the North Slope of Alaska. Knowing the locations and expansion rates for individual features allows us to evaluate risks to human infrastructure. Our results highlight the untapped potential of the InSAR technique to remotely sense ALT and thermokarst dynamics over large areas of the Arctic.

Thaw subsidence in undisturbed landscapes, Barrow, Alaska, U.S.A.

Dmitry A. Streletskiy[1], Nikolay I. Shiklomanov[1], Frederick E. Nelson[2,3], Kelsey E. Nyland[3], Anna E. Klene[4], Jerry Brown[5], & Jonathon D. Little[6]

[1] *Department of Geography, The George Washington University, Washington, DC, USA*
[2] *Department of Geography, Michigan State University, East Lansing, MI, USA*
[3] *Dept. of Earth, Environmental, and Geographical Sciences, Northern Michigan University, Marquette, MI USA*
[4] *Department of Geography, University of Montana, Missoula, MT, USA*
[5] *Woods Hole, MA, USA*
[6] *Monroe Community College, Rochester, NY, USA*

Vertical movements of the ground surface due to frost heave and thaw subsidence are common phenomena in permafrost regions, and are extremely important periglacial geomorphic processes. On an annual scale, upward movement of the ground surface can be attributed to the migration of water to the freezing front and subsequent development of segregation ice. Meanwhile downward movement occurs due to sub-surface permafrost thaw during summer months. Domination of one of the processes at longer time scales can lead to changes in topography, such as the development of thermokarst terrain, flooding of coastal areas, and can result in changes in ecosystem properties, wildlife habitats, and emission of greenhouse gases from permafrost. To provide insight into the long-term behavior of the ground surface in undisturbed natural landscapes, periodic surveys of ground elevation accompanied by thaw depth measurements have being conducted near the Native Village of Barrow, Alaska.

The study area is located inside the Barrow Environmental Observatory, 5 km east of the village of Barrow at the northern edge of the Arctic Coastal Plain physiographic province. The primary landscape elements are drained lake basins and polygonized upland tundra divided by a gravelly beach ridge. Mean annual air temperature is -9.7 °C. The warmest month is July (4.5 °C) and the coldest is February (-26.4 °C). The average thawing period lasts for about 100 days/year. Permafrost temperature is -7 to -9 °C depending on landscape conditions and distance from the coast. Active layer thickness is from 20 to 40 cm in polygonized tundra and drained lake basin to greater than 50 cm in the less-vegetated beach ridge. Since the 1970s warming air temperature and an increase in precipitation have resulted in an increase of permafrost temperature, although ALT has not increased significantly over the same period.

The study area was the focus of permafrost investigations by the U.S. Army's Cold Regions Research and Engineering Laboratory (CRREL), beginning in the early 1960s [Brown et al., 2015]. CRREL established a series of 10×10 m plots along the 2.1 km transect in order to monitor a suite of botanical, soil, and geocryological parameters in representative landscape units [Brown and Johnson, 1965]. Measurements on these plots were made using a systematic sampling design to obtain 36 measurement points per plot. Active-layer measurements were conducted seasonally through most of the 1960s and the elevation of each plot point was determined using conventional optical leveling. Active-layer measurements on the CRREL plots were resumed in 1991 as part of the Circumpolar Active Layer Monitoring (CALM) program's first site (http://www.gwu.edu/~calm). Four of these plots, representing different elements of the polygonized tundra, were reoccupied in 2003 in order to continue monitoring of surface elevation. Initial elevation surveys during 2003-2006 were conducted at the beginning and end of the thaw period (mid-June and late August). Surveys were conducted once each year in the last week of August, when thaw depth is at its maximum, during the 2007-2014 period. Each plot was surveyed using the Rapid Static technique at five points marked with acrylite targets. Each target was surveyed for at least 10 min using Trimble 4700/5700/R7 Differential Global Positioning System (DGPS) units. To compare our geodetic data with the historical data survey, we surveyed the same control point used as a reference point during the 1962 survey. Monitoring of the vertical position of the ground surface at each point was accompanied by a probed

active-layer measurement using a graduated steel rod according to CALM's measurement protocol.

Comparison of the DGPS measurements from the Barrow plots with data from the historical survey indicates that the average elevation change between 1962 and 2003 was only 0.45 cm, as one plot heaved and one subsided and two remaining plots did not experience elevation change. The observations of ground surface taken at the end of the thawing period during 2003-2014, show subsidence trends at all four plots resulting with an average subsidence of 9 cm. Three plots with higher elevations (drier conditions) experienced net subsidence of 12-13 cm over the 12-year period, while the site with the lowest elevation (wet conditions) heaved by 1 cm over this period (Fig. 1). These subsidence values are similar to those at two other sites on the North Slope of Alaska where subsidence was monitored over the same period (Shiklomanov et al., 2013). As at those sites, we interpret the subsidence at Barrow to thaw penetration into the ice-rich transient layer immediately below the active layer.

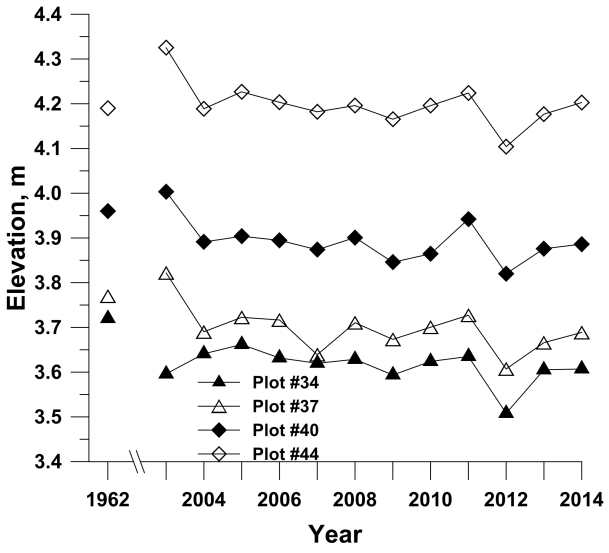

Figure 1: Changes in surface elevation of four CRREL plots.

To evaluate the integrated thermal response of permafrost landscapes at Barrow to climatic forcing, site-averaged annual thaw depth values were correlated with the square root of the cumulative seasonal degree days of thaw calculated from site-specific air temperature records and and surface elevation measurements. Incorporation of changes in surface elevation provided significant improvements in linear regressions of thaw depth on the thawing index. Moreover, accounting for thaw penetration into the ice-rich layer explains the apparent lack of active-layer thickening under warming climatic conditions at Barrow.

Differential subsidence initiated either by human-induced or natural disturbances is characterized by relatively rapid and substantial changes of surface elevation over relatively small areas. Natural landscapes underlain by ice-rich permafrost are subsiding slowly in response to warming of atmospheric climate, and without initiation by localized anthropogenic or geomorphic disturbances. This low magnitude, relatively slow subsidence has been referred to as isotropic subsidence [Shiklomanov et al., 2013] to distinguish it from the high magnitude differential subsidence associated with surface disturbances that commonly lead to development of thermokarst terrain. Integration of radar interferometry and ground based DGPS measurements of thaw subsidence in the future may provide assessment of isotropic thaw subsidence over large geographic areas [Haghshenas Haghighi et al., 2015].

References

Brown, J. and Johnson, P.L. [1965]: Pedo-ecological investigation, Barrow, Alaska. Technical report, U.S. Army CRREL Technical Report 159, URL http://www.dtic.mil/get-tr-doc/pdf?AD=AD0615998&Location=U2;doc=GetTRDoc.pdf.

Brown, J.; Nelson, F.E.; Romanovsky, V.E.; Seybold, C.; Hollister, R.D. and Tweedie, C.E. [2015]: Long-term observations of active layer thawing and freezing, Barrow, Alaska. In *68th Canadian Geotechnical Conference and 7th Canadian Conferences on Permafrost - GEOQuébec 2015, Québec, Canada, September 20-23, 2015*, #133.

Haghshenas Haghighi, M.; Motagh, M.; Heim, B.; Streletskiy, D.; Grosse, G. and Bartsch, A. [2015]: Evaluation of X-band InSAR technique for monitoring seasonal surface elevation change in a permafrost landscape, Barrow, Alaska. In *Advances in the Science and Applications of SAR Interferometry and Sentinel-1 InSAR Workshop*, 23–27 March 2015, Rome, Italy.

Shiklomanov, N.I.; Streletskiy, D.A.; Little, J.D. and Nelson, F.E. [2013]: Isotropic thaw subsidence in undisturbed permafrost landscapes. *Geophysical Research Letters*, pages 6356–6361, doi:10.1002/2013GL058295.

Differential interferometry for discontinuous permafrost monitoring with ALOS PALSAR data in Northern Quebec, Canada

Lingxiao Wang[1], Ralf Ludwig[1], Monique Bernier[2], & Philip Marzahn[1]

[1] *Ludwig-Maximilians-Universität München (LMU), Germany*
[2] *Centre Eau, Terre & Environnement, Institut National de la Recherche Scientifique*

In northern Quebec Canada, permafrost degradation is inevitable with climate warming. Permafrost evolution studies in subarctic Quebec showed continuous degradation of permafrost during the past 50 years. Permafrost degradation is seriously affecting the natural environment and has become problematic for the integrity of some transportation infrastructures.

The freezing-thawing cycle in the active layer, or the phase transition of ice-water cycle will result in movement at the ground surface. Some successful attempts have been made to use Differential InSAR (DInSAR) monitoring ground movements caused by permafrost activities. Almost all the studies of DInSAR technique application in permafrost region are limited in the continuous permafrost zone where landscape is normally homogeneous and vegetation distortion is very less. In discontinuous permafrost region, heterogeneous landscape and dense vegetation adds much difficulites in DInSAR application. Growing vegetation layer decreases coherence and same for the thawing caused saturated surfaces. Even though permafrost mounds themselves can keep acceptable coherence in same pairs, phase unwrapping errors are easily to occur due to disconnects between coherent regions.

In this study, we investigated whether DInSAR technique is also suitable for discontinuous permafrost environment monitoring using long wavelength L-band ALOS PALSAR data spanning from 2007 to 2010 with two orbits. Test site is near the Inuit village of Umiujaq (56°32' N, 76°31' W), at the eastern shore of the Hudson Bay in northern Quebec, Canada. The region is experiencing climate warming, mean annual air temperatures (MAAT) increased 2 degrees in the past two decades. Mineral permafrost mounds and peat-covered permafrost mounds with ice-rich cores are the dominant components of the periglacial landscape in the study area. The active layer is 1.5 – 3 m in the mineral permafrost mounds and is currently thickening. The landscape in the study area is very heterogeneous. A mosaic of rock outcrops, lichen tundra patches, shrub thickets and forest stands spread in a small region. Lichen is the dominant vegetation cover on mineral permafrost mounds. Between the mounds or on the edge of them, dense shrubs or spruces colonize.

L-band ALOS PALSAR shows great promise in monitoring ground displacement in the study area because of keeping good coherence. Inner-annual displacement signal is clear and strong, where inter-annual movements are still visible in several interferogram pairs. Referred to in-site daily thawing front depth and ground displacements from thaw/frost tube installed recently, we believe that DInSAR results from ALOS PALSAR are in the correct order of magnitude. From displacement results, thawing subsidence variation with space and time is manifested, which reflects the non-uniform internal thermal characteristics in permafrost mounds, even within a small area. However, limited by rough spatial resolution, signals over small permafrost mounds are neglected and more detailed difference within the large permafrost mounds can't be retrieved.

The displacements over permafrost areas were firstly mapped at several inner-year periods in the large area around Inuit village of Umiujaq. Thawing subsidence variations with space and time are analyzed combined with daily temperature, daily thawing front depth, soil texture profile and soil water content profile. Benefit from adequate data acquired in the year 2010, one displacement sequence in one year is given out. Displacements reached 10 cm at some places in the thawing season. In one interferogram of late summer from August 31 to October 16, around 2-3 cm (See Fig. 1) subsidence were detected which clearly revealed the thawing in the ice core or the deepening of active layer thickness because of high temperature in year 2010.

Sites with distinct thawing subsidence were visited

in the filed campaign of year 2015, which provided ground information and references for the DInSAR results. Spatial and magnitude of thawing subsidence information is also compared with serial optical remote sensing images from Landsat and RapidEye. It demonstrates that the places where showed strong thawing subsidence is usually combined with landscape changes such as thermokarst pond evolution and high dense vegetation colonise.

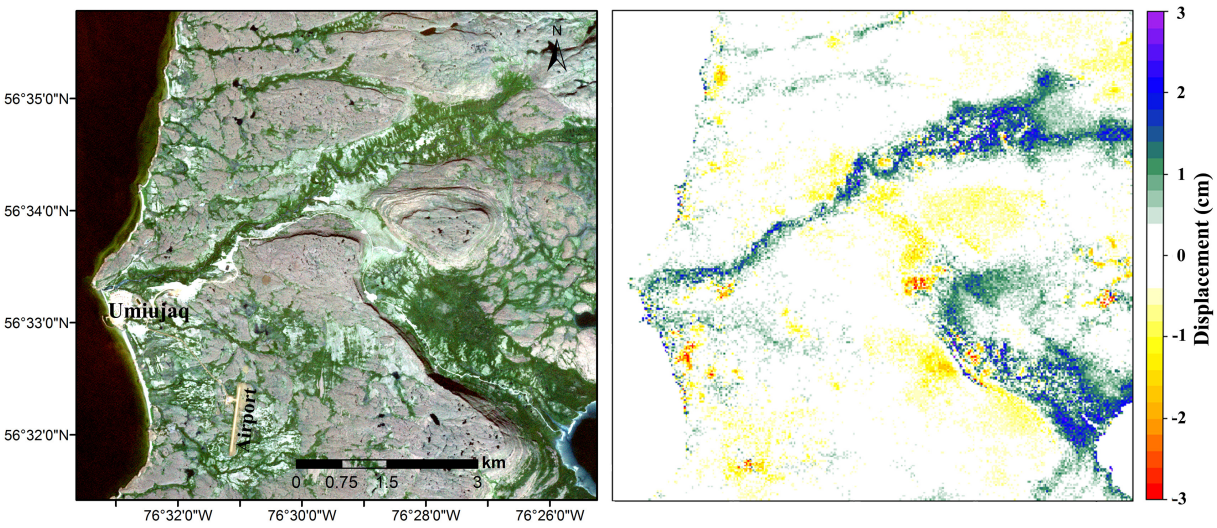

Figure 1: Thawing subsidence detected in late summer period of 2010-08-31 to 2010-10-16

SESSION 21

Integrating Field and Remotely Sensed Measurements of Thaw-Driven Landscape Change in Permafrost Regions

Convener:

Benjamin M. Jones, *U.S. Geological Survey, USA*

Gerald Frost, *Alaska Biological Research, USA*

Daniel J. Hayes, *School of Forest Resources, University of Maine, USA*

Thaw-driven landscape change in permafrost-influenced terrain has been widely documented in recent decades. These changes have significant implications for ecosystem function in Arctic and Boreal regions, particularly for hydrology, vegetation and soil structure, and biogeochemical cycling including carbon storage and fluxes. However, a key uncertainty in predicting how permafrost will respond to a projected warmer climate is identifying where and at what rates thaw-induced landscape change will occur. Permafrost degradation and thermokarst development occur across a variety of spatial and temporal scales and no one tool or method can adequately characterize these changes. Permafrost monitoring studies typically rely on field-level surveying, but this information needs spatial and temporal upscaling across large, remote and inaccessible high latitude regions. While field observations provide essential data for such upscaling efforts, remote sensing offers a complementary, cost-effective foundation from which to build spatially comprehensive and temporally consistent observation frameworks for mapping permafrost disturbance and associated landscape change. Recent remote sensing applications capitalizing on various sensors (e.g., optical, LiDAR, inSAR, hyperspectral, geophysical, etc.) from multi-scale platforms (i.e. ground, aircraft and satellites) have provided new insights into landscape change patterns, rates, and scales.

This session aims to highlight new and emerging research efforts focused on thaw-driven landscape change through the linkage of existing field-based research and monitoring with observations and data products from remote sensing. Of particular interest are studies focused on landscape change-detection for lakes, wetlands, vegetation, surface and subsurface hydrogeology, geomorphology, thermokarst, and subsidence processes, particularly where there are impacts to landscape structure, ecosystem services, and/or the carbon cycle. We invite contributions providing comments on the opportunities and challenges in using remote sensing information from various sensors and platforms to observe and quantify ecosystem dynamics in permafrost regions, and offer an improved understanding of the drivers and consequences of landscape change.

An ensemble-based snow data assimilation framework with applications to permafrost modeling

Kristoffer Aalstad[1], Sebastian Westermann[1], Julia Boike[2], Laurent Bertino[3], & Kjetil Schanke Aas[1]

[1]*Department of Geosciences, University of Oslo, Oslo, Norway*
[2]*Alfred Wegener Institute Helmholtz Center for Polar and Marine Research, Potsdam, Germany*
[3]*Nansen Environmental and Remote Sensing Center, Bergen, Norway*

Snow, with generally high albedo and low thermal conductivity, is a key control on the thermal state of near surface permafrost. At the same time, accurately estimating the seasonal snow cycle at the kilometre scale is a considerable hydrometeorological challenge. Consequently, snow represents a major source of uncertainty in permafrost models. To constrain this snow induced uncertainty we propose a new ensemble-based snow data assimilation framework (ESDA) for fine scale snow state estimation that fuses a simple subgrid snow model and fine scale satellite-based surface albedo retrievals using the ensemble Kalman filter (EnKF; reviewed in Evensen [2009]). The potential of ESDA is demonstrated for the Bayelva catchment near Ny Ålesund (Svalbard, Norway) where independent ground-based observations of snow cover and the near surface ground thermal state were available to perform validation.

On the modeling side of ESDA we adopt the subgrid snow distribution model (SSNOWD; see Liston [2004]) to estimate the snow water equivalent depth distribution, snow cover fraction and surface albedo at the grid scale (1 km). These model runs are forced by melt and net precipitation rates based on the energy and water balance derived from the meteorological fields provided by a (3 km resolution) Weather Research and Forecasting (WRF) model run. For observations our system makes combined use of two relatively new high level products: frequently available coarser scale (500 m) albedo retrievals from MODIS (MCD43A version 6) and intermittently available finer scale (30 m) albedos derived from Landsat8 surface reflectance retrievals. In the last step of the framework we apply the EnKF; a robust sequential data assimilation method that yields the optimal estimate of a system state based on the combined information from model results and observations, both of which are uncertain, provided a set of assumptions hold (see Evensen [2009]). The EnKF has been successfully implemented for a range of applications in numerous fields including oceanography, meteorology, hydrology, mining and reservoir geophysics, although to our knowledge this is the first time it is being applied directly to permafrost modeling. Simply stated an ensemble (a set) of model realizations, in this case capturing uncertainties in the meteorological forcing, are propagated forward in time and sequentially updated by the observations whenever these are available. The magnitude of the updates depends on the deviation of the model realizations from the observations as well as the respective uncertainties. Thereby, the result of the EnKF is expressed in terms of an ensemble of corrected model states, where the ensemble mean is interpreted as the most likely estimate and the ensemble spread is a measure of the uncertainty. Our results are promising; the evolution of the ensemble mean estimated snow cover using ESDA at Bayelva is shown to be much closer to the ground-truth, as observed by an independent automatic camera system, than that of the open-loop (no assimilation) estimate.

Finally, we incorporate ESDA into the recently developed CryoGrid3 surface energy-balance driven permafrost model described in Westermann et al. [2016]. The results, with and without ESDA, are compared to in situ measurements from an array of randomly distributed ground surface temperature measurements within the modeled grid cell. A significant improvement in the skill of the model at capturing the near-surface ground thermal state is demonstrated, particularly in the ablation season. Thus, ESDA provides improved estimates of the state of permafrost at Bayelva. Due to the cheap computational cost, the framework is also applicable to much larger model domains. Moreover, given the robustness, owing to the global span of the satellite retrievals and the option of running SSNOWD with reanalysis data (e.g. ERA-Interim), it is possible to apply this framework to most permafrost regions on the planet.

References

Evensen, G. [2009]: The ensemble kalman filter for combined state and parameter estimation. *IEEE Control Systems*, 29(3). doi:10.1109/MCS.2009.932223.

Liston, G.E. [2014]: Representing subgrid snow cover heterogeneities in regional and global models. *Journal of Climate*, 17(6):1381–1397. doi:10.1175/1520-0442(2004)017<1381:RSSCHI>2.0.CO;2.

Westermann, S.; Langer, M.; Boike, J.; Heikenfeld, M.; Peter, M.; Etzelmüller, B. and Krinner, G. [2016]: Simulating the thermal regime and thaw processes of ice-rich permafrost ground with the land-surface model cryogrid 3. *Geoscientific Model Development*, 9:523–546. doi:10.5194/gmd-9-523-2016.

Identifying the amount and rate of forest-wetland cover change over the southern Taiga Plains discontinuous permafrost region in Canada using remote sensing

Justin Adams[1], William Quinton[1], Aaron Berg[2], & Olivia Carpino[2]

[1] *Cold Regions Research Centre, Wilfrid Laurier University, Canada*
[2] *Department of Geography, University of Guelph, Canada*

In this presentation, we discuss results of a remote sensing change detection analysis over the southern Taiga Plains ecoregion, in Northwest Territories and British Columbia, Canada. This region extends to the southern boundary of the discontinuous permafrost zone (30-80 % aerial cover) and the landscape contains forested uplands and peat plateaus, or wetland dominated zones consisting of flat bogs and channel fens. Mean annual air temperature trends demonstrate that the climate of the southern Taiga Plains is rapidly warming. It has been widely shown that this warming climate correlates with dramatic changes to hydrologic processes and an altered landscape, especially due to loss of permafrost. In addition, intense industrial activities are occurring in some parts of this region relating to oil and natural gas exploration/extraction, which is compounding this issue. Consequently, it is important to understand these environmental changes for hydrological modelling and estimating future fresh-water availability. It has been shown that the geographic distribution of forest cover in this region is a reliable proxy indicator of permafrost (within metres). Tree covered (e.g. black-spruce (*Picea mariana*)) uplands and plateaus are at relatively higher topographic positions and are underlain by permafrost, whereas topographically lower wetland zones (flat bogs and channel fens) are not underlain by permafrost. Thawing creates thermokarst conditions and waterlogging of trees, which cannot be tolerated by most conifers. Therefore, several studies have exploited this proxy to estimate aerial loss of permafrost using historical change detection of forest to non-forest landscapes using optical remotely sensing. However, these previous analyses have generally only been conducted in several specific study areas and there is much less understanding on the extent and rate of permafrost loss regionally. The objective of this research is to generate a geographic sample of the percent aerial loss and rate of forest-wetland cover conversion over this region in the past four decades (1970s to present). Our analysis is conducted at 10 sample areas of interest (AOIs) within a study region approximately 250 km between Fort Simpson, Northwest Territories, to the north and Fort Nelson, British Columbia to the south. Each of the 10 AOIs has a 6 km^2 footprint. A historical (i.e. 1970s) grey-scale aerial photograph is visually analysed and digitized to produce a binary map of the percent forest and non-forest area in each image. The same procedure is completed for each AOI using a recent World View 2/3 panchromatic image to create a binary map of current forest/non-forest area. The proportions and rates obtained from each AOI are statistically compared to identify significant differences possibly attributed to geographic and climate factors. The two main implications of this study will be discussed. First, this research provides a regional assessment of permafrost loss, which is important for estimating thaw driven impacts to the hydrologic processes and ecology of this region. Second, this research is important for evaluating the representativeness of in-depth studies (hydrological modelling and field-studies) conducted at long-term research sites within the southern Taiga Plains.

Towards circumpolar assessment of thaw lake dynamics

Annett Bartsch[1,3,4], Georg Pointner[1,3], & Anna Maria Trofaier[2]

[1] *ZAMG, Austria*
[2] *ESA Climate Office, UK*
[3] *Vienna Universityof Technology, Austria*
[4] *Austrian Polar Research Institute*

Land surface hydrology related features in arctic and sub-arctic environments which can be detected with satellite data include open water, near surface soil water storage, snow and freeze/thaw state. The circumpolar spatial and temporal patterns of lakes are important for the understanding of land atmosphere exchange and changes in ground thermal properties. A large proportion is thaw lakes related to thermokarst phenomena. They are frequently investigated with satellite data for long-term changes with respect to climate change. Many lakes vary, however, seasonally in size. It has been shown in previous studies that inundation patterns (with respect to lakes) are not limited to spring time by use of synthetic aperture radar (SAR). In addition seasonal changes of aquatic vegetation extent needs to be considered. The aim of this study was to identify regions with seasonal patterns for the entire Arctic in order to support studies on long-term change. This contributes to the ESA GlobPermafrost project objectives.

Seasonal variations have been quantified in previous studies, over e.g. the Yamal region and a range of further sites (including PAGE21 sites, www.page21.eu) in Siberia based on ENVISAT advanced SAR (ASAR) which provides C-band data in ScanSAR mode. These data can be used for update of inundation status with 150 m spatial resolution at frequent intervals (several times per month depending on actual acquisitions). The wavelength is between 5–6 cm, which means that even moderate wind action on the water surface can impede the specular reflection. Longer wavelengths such as L-band (>20 cm) would be therefore preferable for this application but their availability is limited at present, as well as in the near future. A further problem related to the use of C-band radar is the very limited penetration of the signal through emerging vegetation, for example along lake shores. The ENVISAT archive provides nevertheless a unique opportunity for medium resolution inundation dynamics mapping. A freely available experimental dataset of inundation dynamics and saturated areas with 150 m resolution has been developed for the year 2007 within the ESA ALANIS project. It covers the majority of Russian lowlands north of 55° latitude. The temporary open water information is provided for 10-day periods. Data availability is however constrained for many regions. Additional information is therefore provided for the number of available acquisitions during the 10-day period and the number of days since last update. Several hotspots of seasonal changes could be identified by post-processing the ALANIS dataset.

An extension to other regions and years is impeded due to limited data availability. Also the currently available data from Sentinel-1 do not provide sufficient temporal sampling. Coarse resolution (25 km and larger) global inundation datasets can be used to identify the areas in general but don't give details on the type of water body (river flood plain, small or large lake etc.). Results from the ALANIS-dataset are therefore compared to further static but similar spatial resolution land-surface products which are available circumpolar. Relationships are quantified and used to predict regions of potential overlap of seasonal and long-term change.

Change of snow water equivalent in different arctic permafrost zones

Sabine Baumann

TUM, Germany

Permafrost is degrading and the active layer thickness is increasing as a result of climate change. Permafrost distribution and active layer development are primarily forced by mean annual air temperatures and snow cover characteristics. Permafrost degradation is primarily being forced by an increase in active layer thickness. Interactions between permafrost and snow cover are complex, because snow thickness, on- and offset of a consistent snow cover, and snow water equivalent (SWE) play an important role. In this study, SWE is assessed by different sources covering the last decade: microwave remote sensing data (e.g. Amsr-E), gravimetric satellite data (GRACE), and hydrological models (e.g. WGHM). All data have different resolutions and data formats. For the multi-ensemble approach, all datasets were converted to 1°grids and processed similar to GRACE data for comparison. Monthly data and trends are computed over several arctic large river basins. The data show the evolution of SWE in different areas (North America – Siberia) and permafrost zones (continuous, discontinuous zone). Together with data on active layer thickness from in-situ measurements and models, relations between SWE and active layer thickness in different permafrost zones are assessed.

Comparison of narrow, broad and visible band vegetation indices in a heterogeneous low Arctic ecosystem

Alison Leslie Beamish[1], Birgit Heim[1], N. Coops[2], & M. Buchhorn[3],

[1] *Alfred Wegener Institute Helmholtz Centre for Polar and Marine Research, Potsdam, Germany*
[2] *Faculty of Forestry, University of British Columbia, Canada*
[3] *Alaska Geobotany Center, University of Alaska Fairbanks, USA*

We evaluated how plot-based spectral data varied within and between heterogeneous vegetation communities at peak and late season in a central Alaskan low Arctic tundra ecosystem. Spectral data were collected with a handheld spectroradiometer and a consumer grade digital camera in four distinct vegetation communities. Three classes of vegetation indices were derived from the data; broadband, narrow-band and visible. We asked the following questions:

1. how do broadband, narrow-band and visible vegetation indices vary within and between heterogeneous low Arctic vegetation communities; and
2. what class of indices are best at distinguishing different vegetation communities.

We hypothesize that narrow band and colour indices will vary significantly between but not within communities while broadband indices will vary significantly between and within communities. Additionally, we hypothesize that the enhanced spectral resolution of narrow band indices will be optimal for differentiating the heterogeneous vegetation communities possible. Finally, we hypothesize that communities differentiation will be more significant with late season spectral data.

Conceptualization and application of the Alaska Thermokarst Model

W R. Bolton[1], Mark Lara[2], Hélène Genet[2], Vladimir Romanovsky[3], & A D. McGuire[2]

[1] *International Arctic Research Center, United States of America*
[2] *Institute of Arctic Biology, University of Alaska Fairbanks, United States of America*
[3] *Geophysical Institute, University of Alaska Fairbanks, United States of America*

Thermokarst topography forms whenever ice-rich permafrost thaws and the ground subsides due to the volume loss when ground ice transitions to water. The Alaska Thermokarst Model (ATM) is a large-scale, state-and-transition model designed to simulate transitions between landscape units affected by thermokarst disturbance. The ATM uses a frame-based methodology to track transitions and proportion of cohorts within a 1- km^2 grid cell. In the arctic tundra environment, the ATM tracks thermokarst-related transitions among wetland tundra, graminoid tundra, shrub tundra, and thermokarst lakes. In the boreal forest environment, the ATM tracks transitions among forested permafrost plateau, thermokarst lakes, collapse scar fens and bogs. The transition from one cohort to another due to thermokarst processes can take place if thaw reaches ice-rich ground layers either due to pulse disturbance (i.e. large precipitation event or fires), or due to gradual active layer deepening that eventually results in penetration of the protective layer. The protective layer buffers the ice-rich soils from the land surface and is critical to determine how susceptible an area is to thermokarst degradation. The initial landcover distribution is based upon analysis of compiled remote sensing data sets (SPOT-5, Inferometric Synthetic Aperture Radar, and LandSat8 OLI) at 30-m resolution. Remote sensing analysis and field measurements from previous and ongoing studies are used to determine the ice-content of the soil, the drainage efficiency (or the ability of the landscape to store or transport water), the cumulative probability of thermokarst initiation, distance from rivers, lake dynamics (increasing, decreasing, or stable), and other factors which help determine landscape transition rates. Tundra types are allowed to transition from one type to another (for example, wetland tundra to graminoid tundra) under favorable climatic conditions. In this study, we present our conceptualization and initial simulation results from in the arctic and boreal forest regions of Alaska.

Examining the ecosystem impacts of seismic lines in discontinuous permafrost from field and remotely sensed measurements

Michael Braverman, William L. Quinton, Justin Adams, Jennifer L. Baltzer, & Ryan F. Connon

Cold Regions Research Centre, Wilfrid Laurier University, Canada

Intensive seismic exploration in the Northwest Territories, Canada, began in the late 1960s. Since that time, the legacy of seismic surveys – i.e. straight lines cutting through boreal forest and tundra – has remained visible throughout northern Canada and Alaska. The removal of trees and compaction of the ground surface alter the thermophysical properties of the active (i.e. seasonally thawed) layer to such an extent that the underlying permafrost seriously degrades or even disappears completely. Such a transformation along linear corridors that cut indiscriminately across different terrain types with contrasting hydrological functions has potentially serious implications to the redistribution of water and energy within and among landscape units with feedbacks to permafrost thaw, land cover/ecosystem change and runoff generation. This talk characterizes the flow and storage of water and energy along an intensively studied seismic cut line in the high boreal zone of discontinuous permafrost in order to improve the understanding of these processes, their interactions and hydrological and ecological implications. We used ground-penetrating radar and multi-year ground temperatures and water levels along the line to derive the degree of permafrost degradation below it. The seismic line studied extends from a permafrost-free wetland (flat bog), over a permafrost body (peat plateau) and into another permafrost-free wetland (channel fen). It was found that once thaw had lowered the permafrost table below the ground surface elevation of the flat bog and channel fen, the seismic line forms a hydrological connection between them. It was also shown that during the permafrost thaw process, seismic lines develop a perennially thawed layer (talik) between the overlying active layer and underlying permafrost and that the talik conveys water as a conduit throughout the year. These intensive field studies were combined with an extensive study of the areal coverage of seismic lines throughout the southern Taiga Plains ecoregion, including an aerial archive of ecosystem changes arising from seismic networks. Using both intensive and extensive studies, we present a conceptual model for the hydrological, ecological and thermal impact of seismic lines in this sensitive region.

Airborne and field based measurements of thermokarst in pingos and adjacent collapse scar bogs in interior Alaska

Thomas A. Douglas[1] & Merritt R. Turetsky[2]

[1] *Cold Regions Research and Engineering Laboratory Alaska, United States of America*
[2] *University of Guelph*

A region of discontinuous permafrost approximately 50 kilometers southeast of Fairbanks, Alaska demonstrates multiple lines of evidence of rapid thermokarst and landscape change. This area, in interior Alaska, contains a dozen pingos (hydrolaccoliths). They are present as concentric features typically 100 meters across and 20 meters in elevation above the surrounding ground surface. All of the pingos have sunken craters in their centers, formed presumably through melting and subsequent collapse of the inner ice lens core. These collapsed pingos (ognips) may represent late stage autogenenic development that is typical of these features [Mackay, 1988] or they may be evidence of more recent change initiated by warming in the area. Adjacent to the pingos are areas of actively collapsing ice wedge polygons and sporadic collapse scar bogs in various states of formation. The pingos and collapse scar bogs are aligned along an arcuate pattern in a lowland region to the west of a set of small hills composed of bedrock and alluvium.

Permafrost in this part of interior Alaska is dominated by syngenetic ice-rich and carbon-rich permafrost within the yedoma belt stretching across Siberia, central Alaska, and northwest Canada. With a mean annual temperature of -1 degree C the area contains relatively warm ecosystem-protected permafrost that is highly vulnerable to thaw triggered by changes in temperature, precipitation, or vegetation [Jorgenson and Osterkamp, 2005]. Many of the pingos are surrounded by ice wedge terrain undergoing active thaw subsidence to polygons and thermokarst mounds (baydzherakhs). Some of the mounds are meters high and radiate away from the sides of the pingos. All of these dramatic geomorphologic features are easily discernible across the landscape from aerial imagery and ground level surveys.

In this study, our objectives are to:

1. identify whether the pingos and collapse scar bogs are actively forming,

2. identify how and where they may change in the future as a result of a projected warmer climate in the area, and

3. ascertain the ecological and biogeochemical consequences of thermokarst in these features.

We are combining historical records with field measurements to determine whether the pingos are experiencing ongoing degradation of their core ice lens and to identify where and at what rate the nearby collapse scar bogs are forming on the landscape.

To explore the historical state of permafrost and the ground thermal regime in the area we analyzed historical imagery, back to the 1970s, to track the water features in a subset of pingos. Sunken craters are evident in the 1970s imagery, which suggests the collapse of the ice cored centers are legacies of these pingo sites. We could not identify any pingos in our study region without some sign of collapse. However, the craters appear to have expanded over the past few decades, suggesting continued melting and collapse of the ice cored center. The pingo centers are filled with water or semi-aquatic vegetation that likely colonized open water over time. Collapse scar bogs in adjacent low-elevational terrain are roughly the same sizes as the pingos (Fig. 1A) but they have little vertical elevation gradient compared to the surrounding terrain and they are barely discernable in airborne LiDAR imagery (Fig. 1B). While we are currently quantifying the age and developmental history of the collapse scar features through peat core reconstructions, each collapse scar site shows signs of active thermokarst including drunken trees, flooding, and slumping soil.

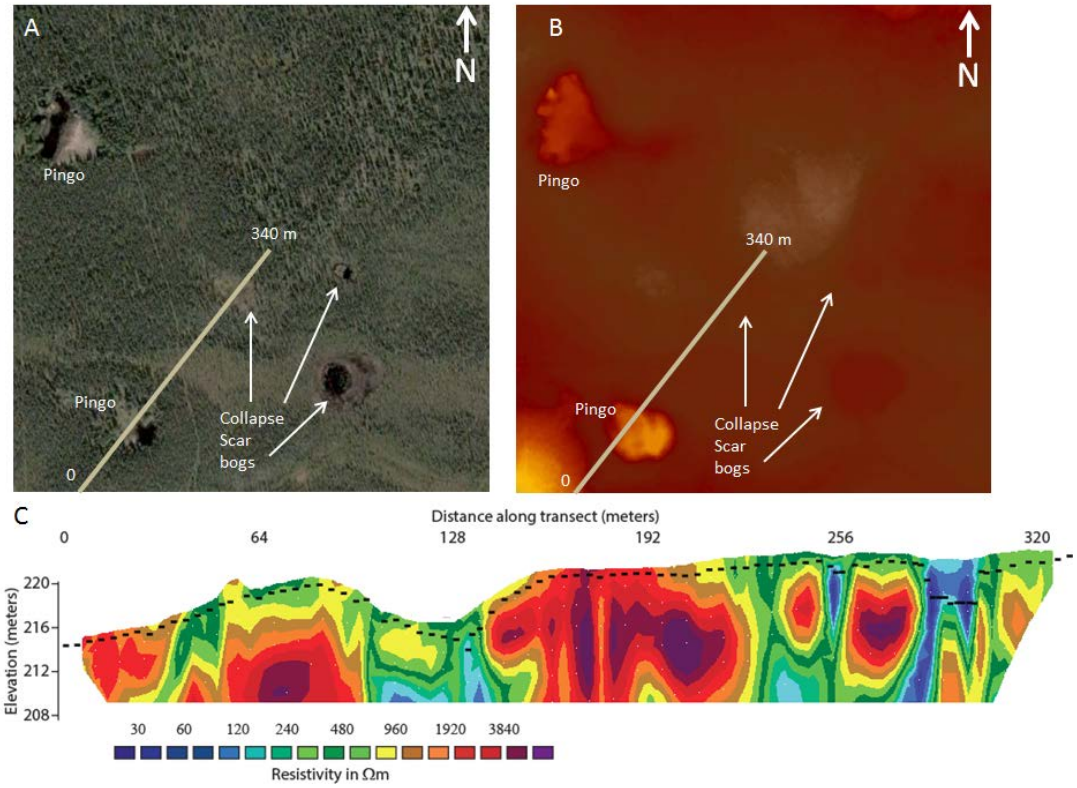

Figure 1: An aerial photo and LiDAR (top) and ERT and seasonal thaw measurements (bottom) from one of the pingos. A) An aerial photo of collapsed pingos and collapse scar bogs at our study site. One of three transects crossing a collapsed pingo is depicted as the tan line. B) Airborne LiDAR over the same region depicted in A. The elevation difference between high (red) and low (yellow) is 10 meters. C) An electrical resistivity tomography cross section through a 340 meter long transect across the pingo. Permafrost is present where resistivity values are 800 ohm-meters or greater. Dashes denote seasonal thaw depths.

Electrical resistivity tomography (ERT) measurements, high resolution GPS ground elevation surveys, and thaw depth probing were focused along three 400 meter transects across one pingo in the fall of 2015. This information is being used to identify the location of frozen ground in the subsurface and to identify relationships between ecological state and seasonal thaw. We have also collected SIPRE cores and installed thermistors into the permafrost to further explore the ice content and soil thermal regime across the pingo and collapse scar bog features. A large (40 meters across and 20 meters thick) lens shaped region of thawed permafrost is evident in the ERT results about 10 meters below the ground surface in the center of the pingo we surveyed (Fig. 1C). This is believed to be the original ice cored region of the pingo that has melted. A thin (1-5 meters thick) layer of permafrost is present above this thawed region while the rampart margins surrounding the pingo are underlain by thick (10-30 m) permafrost.

Overall, we argue these pingo features reside in a location where rapid permafrost thaw in response to warming or changing hydrology could provide a hot spot for landscape change, particularly given a projected climate warming of 5 degrees C over the next 80 years in the study region. As such, their future thermal, geomorphological, and ecological states may be a harbinger for how discontinuous permafrost in the region responds to projected climate warming.

References

Jorgenson, M.T. and Osterkamp, T.E. [2005]: Response of boreal ecosystems to varying modes of permafrost degradation. *Canadian Journal of Forest Research*, 35(9):2100–2111, doi:10.1139/x05-153.

Mackay, J.R. [1988]: Pingo collapse and paleoclimatic reconstruction. *Canadian Journal of Earth Sciences*, 25(4):495–511, doi:10.1139/e88-050.

Colored dissolved organic matter in thermokarst lakes of Yamal Peninsula: sources, annual variations and connection to lake and catchment properties

Yury Dvornikov[1], Marina Leibman[1], Birgit Heim[2], Annett Bartsch[3], Ulrike Herzschuh[2], Artem Khomutov[1], Barbara Widhalm[3], Tatiana Skorospekhova[4], & Maria Mikhaylova[5]

[1] *Earth Cryosphere Institute Siberian Branch, Russian Academy of Sciences, Russian Federation*
[2] *Alfred-Wegener-Institute for Polar and Marine Research, Germany*
[3] *Zentralanstalt für Meteorologie und Geodynamik, Austria*
[4] *Arctic and Antarctic Research Institute, Russian Federation*
[5] *Tyumen State Oil and Gas University, Russian Federation*

Ongoing Arctic warming changes arctic landscapes in various ways. It potentially alters the organic matter supply to lakes in the Arctic. Arctic warming may increase vegetation density in the catchments of lakes and thus increase of the organic matter supply to the lakes can be expected. Furthermore, warming may cause an increase of ground temperature and deepening of the active layer in permafrost soils, and thus activate various cryogenic processes including thermodenudation [Leibman et al., 2015]. We present results of study of colored dissolved organic matter (CDOM) in thermokarst lakes of the central Yamal peninsula (Western Siberia, Russia) and the interconnection of CDOM with lake and catchment characteristics. We used a complex approach including field observations, laboratory measurements, and high spatial resolution optical and synthetic aperture radar (SAR) remote sensing and geographical information system (GIS) data analysis. CDOM absorption and spectral slope values, and suspended particulate matter concentrations (SPM) in several thermokarst lakes were obtained during 2011 – 2015 field campaigns.

Availability of very high spatial resolution (GeoEye-1, WorldView-2) and high spatial resolution (SPOT5) optical satellite images as well as high resolution TanDEM-X DEM data, TSX and ALOS PALSAR SAR satellite images for the study area allowed to produce a large dataset of lake and catchment-related parameters (n=18). CDOM absorption at 440 nm in 363 lakes was retrieved from optical satellite images (correlation with in-situ data: R^2=0.68, n=24) using the band ratio method of Kutser et al. [2005]. We also detected that increased turbidity in some of the lakes due to wind events affect the accuracy of retrieved CDOM values. The statistical analysis "boosted regression tree" was applied in order to find the most important variables controlling the CDOM concentration in central Yamal thermokarst lakes. The results show the following most important variables: the lake area/lake catchment area ratio, the elevation of the lake (i.e., floodplain or non-floodplain lake), median value of the Normalized Difference Vegetation Index (NDVI) of the lake catchment, activity of thermodenudation (thermocirques above the shore line) and total snow water equivalent (SWE) in the lake catchment. In this analysis we used a representative data of approximately 350 square kilometers including all geomorphic terrace levels and the floodplains of Se-Yakha and Mordy-Yakha rivers.

Annual concentrations of CDOM in Yamal thermokarst lakes also differed. We found the clear relation of CDOM absorption values to climatic controls (summer T_{air} and precipitation) and recent activation of thermocirque in the study region. The enhanced erosion of the lake cliffs and enhanced atmospheric precipitation may increase the inflow of fresh terrestrial organic matter into the lakes from the surrounding catchments. Activation of thermocirques controls the additional input of SPM and CDOM into the lake water influencing also the lake color.

References

Kutser, T.; Pierson, D.C.; Kallio, K.Y; Reinart, A. and Sobek, S. [2005]: Mapping lake CDOM by satellite remote sensing. *Remote Sensing of Environment*, 94(4):535–540, doi:10.1016/j.rse.2004.11.009.

Leibman, M.O.; Khomutov, A.V.; A.A. DvornikovGubarkov, Y.A. and Mullanurov, D.R. [2015]: The research station "Vaskiny Dachi", Central Yamal, West Siberia, Russia – A review of 25 years of permafrost studies. *Fennia*, 193(1):3–30, doi:10.11143/45201.

Plant biomass, NDVI, and LAI along the Eurasian Arctic Transect

Howard E. Epstein[1], Donald A. Walker[2], Gerald V. Frost[3], Martha K. Raynolds[2], & Uma S. Bhatt[2]

[1] *University of Virginia, United States of America*
[2] *University of Alaska Fairbanks, United States of America*
[3] *ABR, Inc., Fairbanks, Alaska, United States of America*

The arctic tundra is an extensive biome that encompasses north-south spatial gradients of greater than 1500 kilometers and mean July temperature gradients of approximately 0-15 °C. Very few studies have examined comprehensively the properties of arctic tundra ecosystems along these latitudinal transects, yet this information on how tundra changes spatially with increasing temperatures provides crucial first-approximation data as to how these systems may respond to the dynamics of temperature over time. In addition, these data facilitate the development of maps and classifications of arctic tundra ecosystem properties (e.g. vegetation, soils, permafrost) throughout the entire circumpolar Arctic.

During the period 2007-2012, we conducted multiple field expeditions to five locations along a latitudinal transect in northwestern Siberia, Russia. Most of the locations were along the north-south oriented Yamal Peninsula; the southernmost sites were situated at the forest-tundra transition zone (Nadym), and the northernmost sites were on Hayes Island within the Franz Josef Land Archipelago. All five arctic tundra subzones (A-E representing north-south as identified in the Circumpolar Arctic Vegetation Map) were sampled in addition to the forest-tundra ecotone. At each of the locations, up to three sites were chosen, representative of different landscapes, with a primary focus of finding sites on both fine (loam) and coarse (sand) textured soils.

At each of the sites, we constructed a 50 × 50 m grid. Five 50-m transects were run across the length of the grid at 0, 12.5, 25, 37.5 and 50 m distances along one direction. In addition, five 5 × 5 m plots were uniformly situated within the grid. Along each of the five transects, we estimated the leaf area index (LAI) at 1-m intervals using a LICOR-2000 Plant Canopy Analyzer, as well as collected hyperspectral reflectances using an Analytical Spectral Devices PSII (also at 1m intervals); the hyperspectral data were also used to calculate the Normalized Difference Vegetation Index (NDVI). LAI and reflectance data (NDVI) were also captured for five uniform points within each of the 5 × 5 m plots. Vegetation species composition data were collected for the 5 × 5 m plots, using the Braun-Blanquet relevé approach. To estimate aboveground vegetation biomass, we harvested one 20 × 50 cm quadrat of vegetation material at the center of each of the 5 × 5 m plots. Vascular vegetation biomass was clipped at the top of the moss layer, and moss biomass was clipped at the top of the dead (brown) moss layer. Biomass components were separated into plant functional types (deciduous shrubs, evergreen shrubs, graminoids, forbs, mosses, and lichens), as well as into tissue types (foliar vs. woody, live vs. dead). Finally, we took soils samples in each of the 5 × 5 m plots and analyzed them for organic layer depth, as well as percent carbon and nitrogen.

To compare with the field data, we also collected NDVI data for the areas encompassing our field sites from both AVHRR and MODIS satellite sensors, and additionally we calculated the Summer Warmth Index (SWI – sum of mean monthly temperatures >0 °C) from Land Surface Temperatures derived from AVHRR. We used linear and non-linear regressions to analyze the different vegetation properties from the different sources of data along gradients of both latitude and SWI. We additionally examined the correlations among the various vegetation properties. Finally, we compared the relationships between fine and coarse textured soils.

Preliminary results indicate that both hand-held NDVI and AVHRR NDVI are strongly positively related to Summer Warmth Index (r^2 values = 0.81 and 0.69 respectively) along this Eurasian Arctic Transect (EAT), however, this relationship tends to saturate at NDVI values close to 0.60 and SWI values around 30 °C months. LAI increased exponentially with increasing SWI, and the relationship was very strong ($r^2 > 0.94$). NDVI was slightly greater (0.02) on fine textured soils compared to coarse textured soils, and LAI was also greater on fine textured soils with this difference being accentuated at warmer locations.

Total live biomass increased exponentially with SWI ($r^2 = 0.76$), ranging from < 50 g m^{-2}at the northernmost site to > 1000 g m^{-2} at the southernmost site. Despite an order of magnitude difference in aboveground live biomass along the EAT, mineral soil percent carbon essentially did not vary, with values ranging from 1.2 % to 2.5 %.

These results (and others to follow) provide important quantitative relationships between vegetation properties and environmental variables (temperature and soil texture) for the full latitudinal extent of the arctic tundra biome. This information can be using for mapping tundra ecosystem properties, as well as for modeling of ecosystem responses to climatic changes.

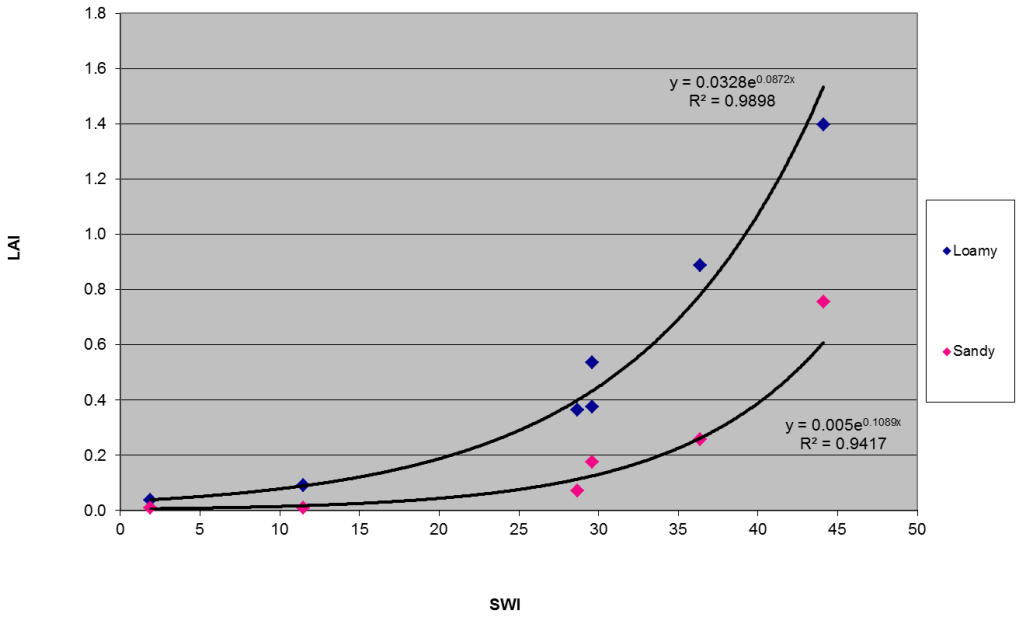

Figure 1: Leaf Area Index vs. Summer Warmth Index along the EAT for Loamy and Sandy Soils

Coupling soil field data with remote sensing to inventory permafrost soil carbon for two small Arctic river deltas, Alaska

Matthias Fuchs[1,2], Guido Grosse[1,2], Benjamin M. Jones[3], & Ingmar Nitze[1,4]

[1]*Alfred Wegener Institute Helmholtz Centre for Polar and Marine Research, Potsdam, Germany*
[2]*Institute of Earth and Environmental Science, University of Potsdam, Germany*
[3]*Alaska Science Center, US Geological Survey, Anchorage, Alaska, USA*
[4]*Institute of Geography, University of Potsdam, Germany*

Arctic river deltas are highly dynamic environments at the interface of land to ocean. Arctic deltas are underlain by permafrost deposits, which are highly vulnerable to a warming climate. The amount of soil carbon stored in these deltas and potentially vulnerable to mobilization due to permafrost thaw is poorly known and based on few data only. Previous soil carbon estimates (e.g. Hugelius et al. [2014], Tarnocai et al. [2009]) were based on data from three large deltas, and no data is so far available for small (<500 km^2) Arctic river deltas. In this study, we investigate the soil carbon pools of two small Arctic river deltas entering the Beaufort Sea on the Alaska North Slope, the Ikpikpuk and the Fish Creek river deltas. Our approach couples soil carbon information with remotely sensed data to estimate the total carbon stock in the upper 1 m for these environments. Both river deltas are located within the continuous permafrost zone and are characterized by typical fluvial-deltaic features and processes, such as river channels and islands, floodplains and mudflats, sand dunes, as well as episodic flooding, erosion, and deposition. In addition, permafrost processes are an important factor for thaw, erosion, transport, and accumulation dynamics within these deltas. As a result, features specific to permafrost-dominated deltas are widespread such as thermokarst lakes, drained thaw lake basins and ice wedge polygonal tundra. Under future climate warming projections, Arctic river deltas will be threatened due to thawing permafrost (including melting and settling of ice-rich deposits) and a rising sea level in combination with coastal erosion. To better estimate how much soil carbon may be vulnerable to mobilization under these projected changes and might be released as greenhouse gases, it is necessary to study the total soil carbon storage in Arctic river deltas.

This study presents the first carbon storage estimation in surface soils and sediments for two small Arctic deltas, which each cover each an area of about 100 km^2. Nine different soil cores between 54 and 215 cm depth, including both, non-permanently and permanently frozen deposits, were collected in April 2014 and July 2015, and were analyzed in the laboratory for total organic carbon (TOC), total carbon (TC), total nitrogen (TN), stable isotopes (δ^{13}C), grain size, and deposit age (^{14}C). The soil C parameters were upscaled to each delta based on landcover classifications derived from Landsat and Spot images in combination with high-resolution digital terrain models (DTM) from airborne LIDAR and IfSAR datasets. The upscaling of the total carbon storage was based on different approaches including the correlation of near surface soil carbon storage with various remotely sensed landcover indices. These indices, such as the Tasseled Cap or NDVI for the year 2014 were derived from linear trend analyses of Landsat data taking into account the full Landsat 5 – 8 archive from 1985 – 2014. For comparison, a supervised classification (maximum likelihood) with Landsat 8 and Spot 5 images was established based on training areas derived from field information from two field trips, very high resolution aerial and satellite images, and high resolution surface elevation information. The carbon content was finally upscaled based on mean carbon values for the different land cover classes.

The total organic carbon storage for the two deltas ranges between 1.5 and 2 teragrams (Tg) of carbon each for the first meter of soil (excluding all water areas), depending on the upscaling method and dataset used. The results compare favorably (comparing the mean carbon storage values per square meter) with what has been previously estimated for other, larger Arctic river deltas.

This study shows that remote sensing is a suitable tool to upscale soil carbon values in remote Arctic river deltas where only few soil data is available. We

are further working on extending our approach to other Arctic permafrost-influenced river deltas, such as the large Lena river delta, Siberia, where we and other colleagues have previously collected a substantial amount of soil carbon and landcover ground truth data.

References

Hugelius, G.; Strauss, J.; S., Zubrzycki; Harden, J.W.; Schuur, E.A.G.; Ping, C.L.; Schirrmeister, L.; Grosse, G.; Michaelson, G.J.; Koven, C.; O'Donnell, J.; Elberling, B.; Mishra, U.; Camill, P.; Yu, Z.; Palmtag, J. and Kuhry, P. [2014]: Estimated stocks of circumpolar permafrost carbon with quantified uncertainty ranges and identified data gaps. *Biogeosciences*, 11, doi:10.5194/bg-11-6573-2014.

Tarnocai, C.; Canadell, J.G.; Schuur, E.A.G.; Kuhry, P.; Mazhitova, G. and Zimov, S.A. [2009]: Soil organic carbon pools in the northern circumpolar permafrost region. *Global Biogeochemical Cycles*, doi:10.1029/2008GB003327.

User and Expert-supported Validation and Evaluation Experiments for high-latitude permafrost landscapes: ESA DUE PERMAFROST (2009-2012) and ongoing EnMAP, PAGE21, and HGF-EDA programs

Birgit Heim[1], Annett Bartsch[2], Alison Beamish[1], Samuel Stettner[1], Marcel Buchhorn[3], Claude Duguay[4], Hoegstroem Elin[5], Barbara Widhalm[2], Kirsten Elger[6], & Skip Walker[3]

[1] *Alfred Wegener Institute for Polar and Marine Research AWI, Germany*
[2] *Zentralanstalt fuer Meteorologie und Geodynamik, Vienna, Austria*
[3] *University Fairbanks, Alaska*
[4] *University Waterloo, Canada*
[5] *Technical University of Vienna, Austria*
[6] *GeoForschungsZentrum Potsdam, Germany*

The ESA Data User Element (DUE) Permafrost (2009-2012) created an Earth Observation service for permafrost-related applications with extensive involvement from the permafrost research community. The DUE Permafrost consortium produced time series on regional and circum-arctic scales of'Land Surface Temperature'(LST), 'Surface Soil Moisture' (SSM), 'Frozen/Thawed Surface Status' (Freeze/Thaw), and static products of 'Terrain', 'Land Cover' (LC), and 'Surface Waters'.

Most of the DUE Permafrost services are based on operationally available remote sensing products. However, permafrost landscapes are a challenge for qualitative and quantitative remote sensing. The land surface is highly heterogeneous characterized by patterned ground, disturbances, abundant small water bodies, and sharp moisture gradients. Only few error estimates or standard evaluation methods exist for remote sensing products from high-latitude terrestrial landscapes. An additional significant challenge in the evaluation of remote sensing products in high-latitude permafrost landscapes is the very sparse availability of ground data.

Ground-based evaluation of the operationally available remote sensing products is needed. International programs, such as the Global Terrestrial Network for Permafrost (GTN-P) initiated by the International Permafrost Association (IPA) as well as national programs such as the scientific preparation programs for two national satellite missions (hyperspectral EnMAP satellite mission, Tandem-L radar satellite mission (Helmholtz Alliance Remote Sensing and Earth System Dynamics HGF-EDA) provide ground data and evaluation experiments.

We will show examples of:

- Evaluation experiments of remote sensing products of 'Land surface temperature' (LST) and 'Frozen/ Thawed Surface Status' (Freeze/Thaw) using GTN-P data (ESA DUE Permafrost).
- Evaluation experiments of optical and microwave remote sensing products using the method of 'homogeneous measurement fields' (HGF-EDA, PAGE21, EnMAP).
- field-based spectral and BRDF measurements of vegetation at different scales collected in Alaska, Yamal (Western Siberia) and the Lena Delta (Arctic Siberia) (EnMAP).

Spatial characteristics of expanding water body and damaged boreal forest under permafrost degradation in central Yakutia by ALOS images

Yoshihiro Iijima[1], Konomi Abe[2], Hajime Ise[2], Tadashi Masuzawa[2], & Alexander N. Fedorov[3,4]

[1] *Japan Agency for Marine-Earth Science and Technology, Japan*
[2] *Regional Environmental Planning Inc., Japan*
[3] *Melnikov Permafrost Institute SB RAS, Russia*
[4] *North-Eastern Federal University, Russia*

Introduction

Large increase in precipitation in summer and winter had continuously occurred since 2004 winter in the central Yakutia. Soil moisture during subsequent years had been markedly increased as well, accompanying with thawing permafrost near the surface. The perennially waterlogged conditions furthermore exacerbated the boreal forest habitat, namely withered and dead trees widely extended in this region. According to field observations in boreal larch forest near Yakutsk, damaged trees was found along with saturated soil at flat terrain [Iwasaki et al., 2010] and transpiration by trees was significantly reduced [Iijima et al., 2014].

The present study examined the relationship between permafrost degradation and ecohydrological change in this region due to the extremely wet climate. We have attempted to extract the degraded boreal forest based on satellite remote sensing, along with expansion of the water surface area in relation to permafrost degradation in the central Yakutia.

Data & Methods

We used ALOS-PALSAR and AVNIR-2 images in both left and right bank of Lena River near in central Yakutia taken during late summer (August and September) from 2007 to 2010. We utilized the backscatter coefficient signals of PALSAR in multi-year to classify waterlogged and damaged vegetation area in associated with landscape classification by AVNIR-2 images of visible and infra-red bands. The backscatter signal by PALSAR shows significant difference not only between open water body, grassland and forest, but also between waterlogged conditions on vegetated surface. The classification produced the interannual changes in degraded boreal forest due to waterlogged conditions.

Results & Discussions

In the left bank area with underlying permafrost of sandy roam soil and less ground ice content, the forest degradation area with waterlogged surface in relation to deepening active layer shows banded pattern along the flat terrain and valley bottom. In the right bank with massive ice and high density of thermokarst depression (alas), the forest degradation was distributed in around-shaped pattern surrounding thermokarst lake. Field survey revealed that the gradient of wetting and deepening active layer corresponded to the area with forest degradation and enhanced thermokarst activity along the distance from thermokarst lakes. Both of increasing precipitation and thawing ice in permafrost might cause the degradation.

We extended the classification in Lena-Aldan interfluvial area of central Yakutia. Approximately 7 % of the whole analyzed area was classified as possible damaged forest with waterlogged surface. In brief, the method combining multi-year ALOS satellite images has possibility to detect permafrost and forest degradation caused by wet climate in boreal forest.

References

Iijima, Y.; Ohta, T.; Kotani, A.; Fedorov, A.N.; Kodama, Y. and Maximov, T.C. [2014]: Sap flow changes in relation to permafrost degradation under increasing precipitation in an eastern Siberian larch forest. *Ecohydrology*, 7:177–187, doi:10.1002/eco.1366.

Iwasaki, H.; Saito, H.; Kuwao, K.; Maximov, T. C. and Hasegawa, S. [2010]: Forest decline caused by high soil water conditions in a permafrost region. *Hydrology and Earth System Sciences*, 14(2): 301–307, doi:10.5194/hess-14-301-2010.

The presence and degradation of residual permafrost plateaus on the western Kenai Peninsula Lowlands, southcentral Alaska

Benjamin M. Jones[1], Carson A. Baughman[1], Vladimir E. Romanovsky[2], Andrew D. Parsekian[3], Miriam C. Jones[1], Guido Grosse[4], & Edward E. Berg[5]

[1] *U.S. Geological Survey, USA*
[2] *University of Alaska Fairbanks, USA*
[3] *University of Wyoming, USA*
[4] *Alfred Wegener Institute, Germany*
[5] *U.S. Fish and Wildlife Service (retired), USA*

Permafrost influences roughly 80 % of the Alaskan landscape [Jorgenson et al., 2008]. Permafrost presence is determined by a complex interaction of climatic, topographic, and ecological conditions operating over long time scales such that it may persist in regions with a mean annual air temperature (MAAT) that is currently above 0 °C [Jorgenson et al., 2010]. Ecosystem-protected permafrost may be found in these regions with present day climatic conditions that are no longer conducive to its formation [Shur and Jorgenson, 2007]. The perennial frozen deposits typically occur as isolated patches that are highly susceptible to degradation. Press disturbances associated with climate change and pulse disturbances, such as fire or human activities, can lead to immediate and irrevocable permafrost thaw and ecosystem modification in these regions.

In this study, we document the presence of residual permafrost plateaus on the western Kenai Peninsula lowlands of southcentral Alaska (Fig. 1a), a region with a MAAT of 1.5 ±1 °C (1981 to 2010). In September 2012, field studies conducted at a number of black spruce plateaus located within herbaceous wetland complexes (Fig. 1b) documented frozen ground extending from 1.4 to 6.1 m below the ground surface, with thaw depth measurements ranging from 0.49 to >1.00 m. Ground penetrating radar surveys conducted in the summer and the winter provided additional information on the geometry of the frozen ground below the forested plateaus. Continuous ground temperature measurements between September 2012 and September 2015, using thermistor strings calibrated at 0 °C in an ice bath before deployment, documented the presence of permafrost. The permafrost (1 m depth) on the Kenai Peninsula is extremely warm with mean annual ground temperatures that range from -0.05 to -0.11 °C (Fig. 1c).

To better understand decadal-scale changes in the residual permafrost plateaus on the Kenai Peninsula, we analyzed historic aerial photography and high-resolution satellite imagery from ca. 1950, ca. 1980, 1996, and ca. 2010 (Fig. 1d). Forested permafrost plateaus were mapped manually in the image time series based on our field observations of characteristic landforms with sharply defined scalloped edges, marginal thermokarst moats, and collapse-scar depressions on their summits. Our preliminary analysis of the image time series indicates that in 1950, permafrost plateaus covered ≈20% of the wetland complexes analyzed in the four change detection study areas (Fig. 1a), but during the past six decades there has been a ≈50 % reduction in permafrost plateau extent in the study area. The loss of permafrost has resulted in the transition of forested plateaus to herbaceous wetlands (Fig. 1b).

The degradation of ecosystem-protected permafrost on the Kenai Peninsula likely results from a combination of press and pulse disturbances. MAAT has increased by 0.4 °C/decade since 1950, which could be causing top down permafrost thaw in the region. Tectonic activity associated with the Great Alaska Earthquake of 1964 caused the western Kenai Peninsula to lower in elevation by 0.7 to 2.3 m [Plafker, 1969], potentially altering groundwater flow paths and influencing lateral as well as bottom up permafrost degradation. Wildfires have burned large portions of the Kenai Peninsula lowlands since 1940 and the rapid loss of permafrost at one site between 1996 and 2011 was in response to fires that occurred in 1996 and 2005. Better understanding the resilience and vulnerability of the Kenai Peninsula ecosystem-protected permafrost to degradation is of importance for mapping and predicting permafrost extent across colder permafrost regions that are currently warming.

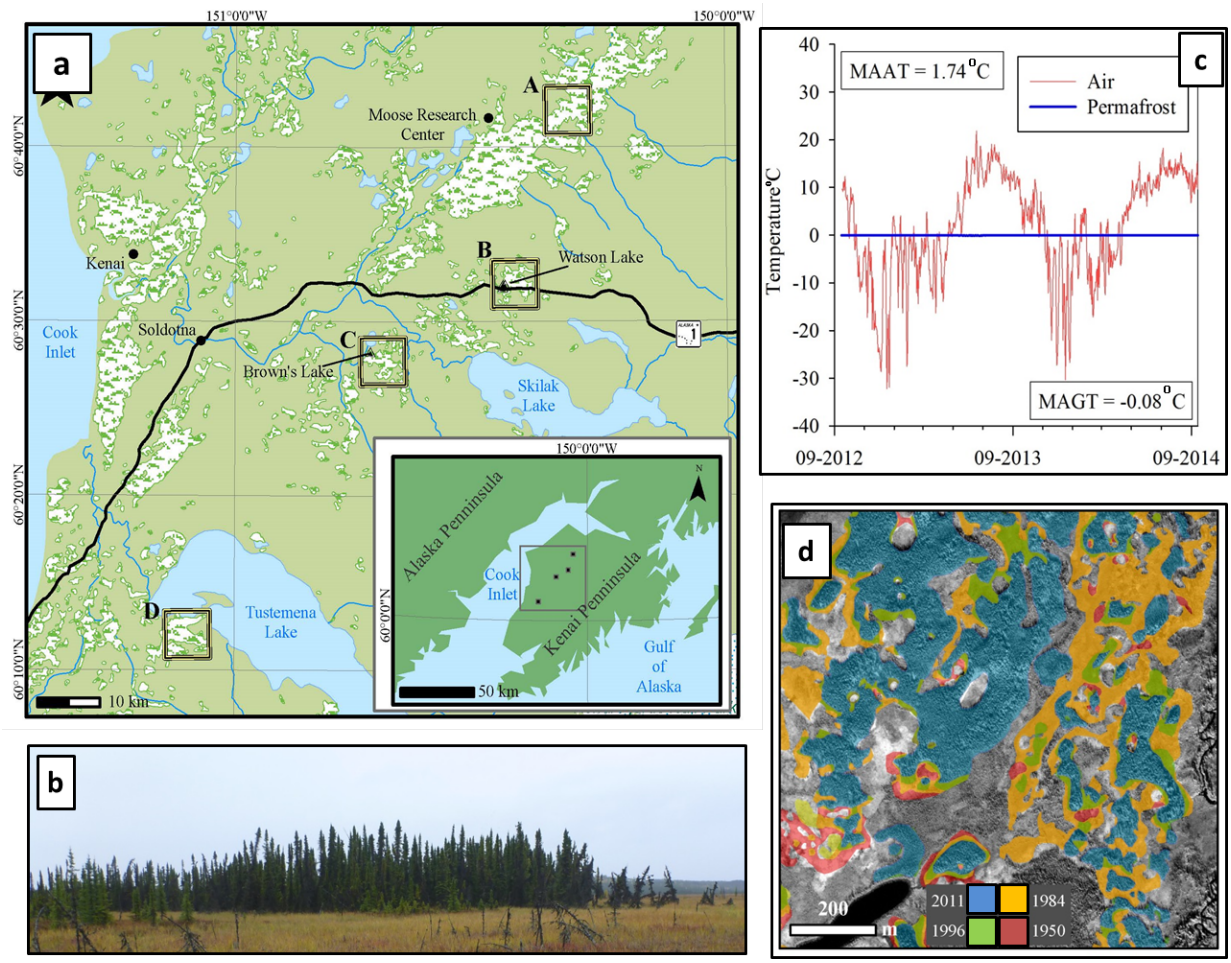

Figure 1: (a) The western Kenai Peninsula lowlands study region showing the location of ground temperature stations (Browns Lake and Watson Lake) and the four permafrost change detection study areas (A-D). (b) An ecosystem-protected permafrost deposit in the Browns Lake wetland complex. The residual permafrost plateau is surrounded by a thermokarst moat and the standing dead black spruce trees in the foreground and on the right side of the image indicate ongoing permafrost degradation. (c) Plot of air (Moose Research Center) and permafrost (1 m depth) temperature (Browns Lake wetland) between September 2012 and September 2014. (d) Change in residual permafrost plateau extent between 1950 and 2011 for a portion of the northerly change detection study area (A). Red shades indicate that permafrost disappeared between 1950 and 1984, orange between 1984 and 1996, and green between 1996 and 2011. The light blue shade indicates mounds mapped in 2011 imagery.

References

Jorgenson, M.T.; Romanovsky, V.; Harden, J.; Shur, Y.; O'Donnell, J.; Schuur, E.A.G.; Kanevskiy, M. and Marchenko, S. [2010]: Resilience and vulnerability of permafrost to climate changeThis article is one of a selection of papers from The Dynamics of Change in Alaska's Boreal Forests: Resilience and Vulnerability in Response to Climate Warming. *Canadian Journal of Forest Research*, 40(7): 1219–1236, doi:10.1139/X10-060.

Jorgenson, T. M.; Yoshikawa, K.; Kanevskiy, M.; Shur, Y. L.; Romanovsky, V.; Marchenko, S.; Grosse, G.; Brown, J. and Jones, B. [2008]: Permafrost characteristics of Alaska. In: Kane, D.L. and Hinkel, K.M.(eds.), *Proceedings of the Ninth International Conference on Permafrost*, Institute of Northern Engineering, University of Alaska Fairbanks, Fairbanks, USA, 29 June–3 July 2008, volume: Extended Abstracts, pages 121–122. URL http://ipa.arcticportal.org/publications/conference-proceedings.

Plafker, G. [1969]: Tectonics of the March 27, Alaska Earthquake. *US Geological Survey Professional Paper*, 74p., ISSN: 10449612.

Shur, Y.L. and Jorgenson, M.T. [2007]: Patterns of permafrost formation and degradation in relation to climate and ecosystems. *Permafrost and Periglacial Processes*, 18(1):7–19, doi:10.1002/ppp.582.

Investigating the dynamics of a rock glacier using terrestrial laser scanning, time-lapse photography, in-situ GPS measurements and satellite SAR interferometry: Ritigraben rock glacier, Switzerland.

Robert Kenner[1], Marcia Phillips[2], Jan Beutel[3], Philippe Limpach[4], Jessica Papke[5], Andreas Hasler[6], & Hugo Raetzo[7]

[1] *WSL Institute for Snow and Avalanche Research SLF, Switzerland*
[2] *WSL Institute for Snow and Avalanche Research SLF, Switzerland*
[3] *ETH Zürich, Computer Engineering and Networks Laboratory, Switzerland*
[4] *ETH Zürich, Institute of Geodesy and Photogrammetry, Switzerland*
[5] *Department of Geography, University of Leicester, United Kingdom*
[6] *SensAlpin GmbH, Switzerland*
[7] *Federal Office for the Environment FOEN, Switzerland*

Ritigraben rock glacier is located above Grächen in the southwestern Swiss Alps and it creeps into the top of the steep Ritigraben gully, where debris flows have been triggered in the past [Stoffel et al., 2005]. Borehole temperature measurements carried out since 2002 in this ice-rich permafrost feature show that an intra-permafrost seasonal talik has formed regularly since 2006 at a depth of 11-12 m, caused by snow melt and precipitation flowing through the ice-rich permafrost in summer [Zenklusen Mutter and Phillips, 2012].

We used terrestrial laser scanning, mono-plotting of time-lapse photography, an in-situ GPS device and satellite SAR interferometry (InSAR) to investigate the dynamics of the rock glacier and possible influences of the seasonal talik. These measurement systems complement one another in terms of temporal and spatial resolution, as well as accuracy.

Terrestrial laser scanning (TLS) provided high resolution and high accuracy 3D creep velocities on an annual basis for the whole rock glacier [Kenner et al., 2014], see right part of figure 1). This dataset is appropriate to determine the exact behaviour of this creeping permafrost feature at time scales relevant for long term monitoring and to draw conclusions for natural hazard safety or tourist infrastructure projects.

An L1 in-situ GPS sensor with integrated inclinometer [Wirz et al., 2013] provides data with a much higher temporal resolution exposing significant creep velocity variations albeit for a single point only. It provides information on the seasonal or even intra-seasonal creep behaviour and allows to determine whether rock glacier creep is coupled with environmental influences such as precipitation.

Time-lapse photography is less dependent on measurement redundancy than GPS and can therefore potentially provide even higher temporal resolutions, depending on the creep velocities. A 2D creep vector field in global coordinates has been generated by mono-plotting the creep rates obtained by time-lapse photography onto the TLS digital elevation model (left part of figure 1). Depending on the image geometry, the accuracy of the velocities obtained varies more strongly at the point scale than that obtained with GPS. However time-lapse photography mono-plotting provides area-wide information with a high temporal resolution. This is not only of interest for research purposes but also for practitioners, as short term local accelerations or rock falls from the rock glacier tongue can be captured and easily interpreted using the image information.

Satellite InSAR provides rock glacier surface velocity measurements during summer when the slopes are not snow covered. With TerraSAR-X satellite data the creep of the entire rock glacier can be mapped at a spatial resolution of about 10 metres and with a temporal resolution of 11 days, depending on data availability. The InSAR measurements complement the other velocity measurements and support the detection of monthly, seasonal and yearly creep velocity variations.

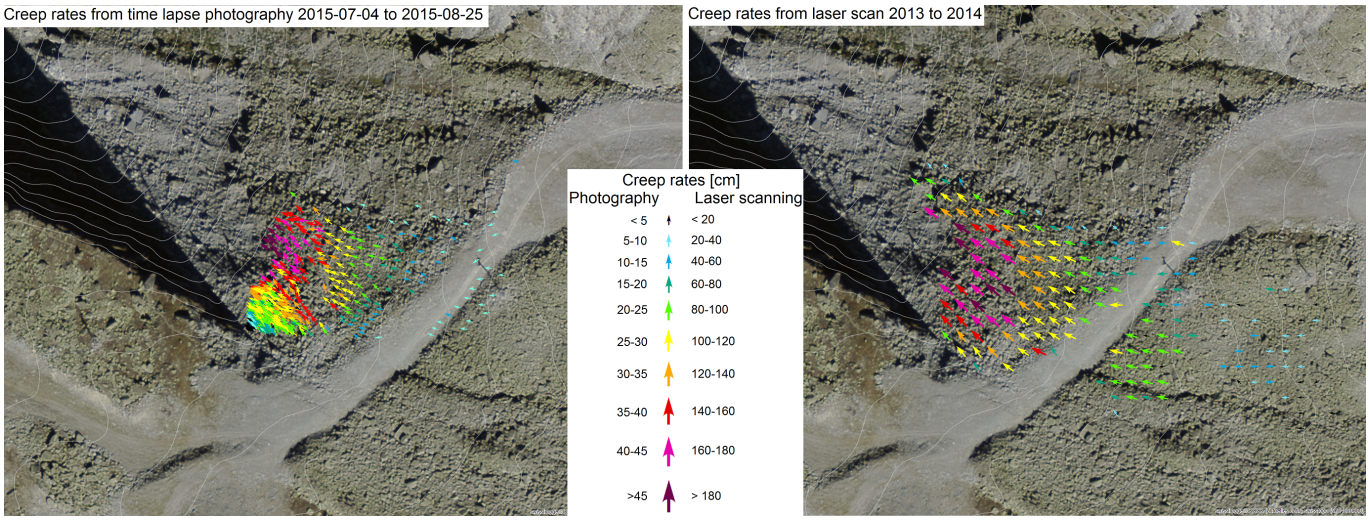

Figure 1: Creep rates of rock glacier Ritigraben calculated from time lapse photography (left) and laser scan (right).

References

Kenner, R.; Bühler, Y.; Delaloye, R.; Ginzler, C. and Phillips, M. [2014]: Monitoring of high alpine mass movements combining laser scanning with digital airborne photogrammetry. *Geomorphology*, 206: 492–504, doi:10.1016/j.geomorph.2013.10.020.

Stoffel, M.; Lièvre, I.; Conus, D.; Grichting, M.A.; Raetzo, H.; Gärtner, H.W. and Monbaron, M. [2005]: 400 Years of debris-flow activity and triggering weather conditions: Ritigraben, Valais, Switzerland. *Arctic, Antarctic, and Alpine Research*, 37(3):387–395, doi:10.1657/1523-0430(2005)037[0387:YODAAT]2.0.CO;2.

Wirz, V.; Beutel, J.; Buchli, B.; Gruber, S. and Limpach, P. [2013]: *Temporal Characteristics of Different Cryosphere-Related Slope Movements in High Mountains*, pages 383–390. Springer Berlin Heidelberg, ISBN 978-3-642-31337-0. doi:10.1007/978-3-642-31337-0_49.

Zenklusen Mutter, E. and Phillips, M. [2012]: Thermal evidence of recent talik formation in Ritigraben rock glacier: Swiss Alps. In: Hinkel, K.M.(ed.), *Proceedings of the Tenth International Conference on Permafrost*, Salekhard, Yamal-Nenets Autonomous District, Russia, 25–29 June 2012, volume 1: International Contributions, pages 479–483. The Northern Publisher: Salekhard, ISBN 978-5-905911-01-9. URL http://ipa.arcticportal.org/publications/conference-proceedings

The rates of thermocirque development and driving factors of their activation on Central Yamal, Russia

Artem V. Khomutov[1], Yury A. Dvornikov[1], Marina O. Leibman[1], Anatoly A. Gubarkov[2], & Damir R. Mullanurov[1]

[1] *Earth Cryosphere Institute, Siberian Branch of Russian Academy of Sciences, Tyumen, Russian Federation*
[2] *Tyumen State Oil and Gas University, Tyumen, Russian Federation*

Climatic fluctuations over the past few years significantly affected the increase of cryogenic processes activity in the tundra zone of the Yamal Peninsula. On Central Yamal, where there was a large-scale cryogenic landsliding in 1989 [Leibman and Kizyakov, 2007], cryogenic earth flows are actively developing since 2012 through tabular ground ice thawing. As a result, thermocirques form on lakeshores. The Vaskiny Dachi key site as a base for the cryogenic processes study [Leibman et al., 2015] extends from the Se-Yakha river floodplain in the north and north-east to the Mordy-Yakha river floodplain in the south and south-west on all geomorphic levels allocated in the area.

The paper focuses on «complex destruction» (the term proposed by Voskresenskiy [2001]), leading to the formation of specific landforms: thermocirques. They are resulting from a combined impact of several destructive relief-forming processes in tabular ground ice-bearing areas.

Key area during the period from 1989 to 2012 was characterized by a local occurrence of thermal denudation. By 2010, remote sensing data showed that this process in the study area was usually inactive and thermocirques looked stabilized, overgrown by vegetation.

Extremely warm summer of 2012 resulted in formation of new thermal denudation features, such as cryogenic translational landslides, cryogenic earth flows and furthermore, thermocirques, complex landforms resulting from ice wedges and tabular ground ice thaw. The 2012 warm season was characterized by a deeper active layer: at the end of the warm period deeper by 15 % than the average for the 1993-2011. Observed were indications of a high pore pressure in the active layer: effuse of liquefied clay in the tension cracks on many slopes. By 2013, according to the field and remote sensing data, there were more than 90 active thermal denudation landforms from 66 to 25700 m^2 in size on the territory of 345 km^2.

Monitoring of the thermocirque backwall retreat (Tab. 1), shows that at an initial stage of activation the rate of retreat is quite high and the annual increase in the area of thermocirques is about 20 % of their total area for typical thermocirques with tabular ground ice and up to 50 % of their total area for thermocirques formed by thawing of both tabular ground ice and ice wedges. Maximum retreat can reach up to 25-30 m/year, with average values of 15 m/year. The thermocirque backwall position on satellite image in the first half of the warm period of 2013 and the field data at the end of summer of 2012-2015 are compared. It shows that rate of the thermocirque area increase slows down as farther from process activation.

Table 1: Thermocirque backwall retreat on Vaskiny Dachi key site

Date of retreat measurement	Area of thermocirque, th.m^2 (area increase, %)
Thermocirque with tabular ground ice	
05.07.2013 (satellite image)	25.7 (0)
26.08.2013 (GPS survey)	30.8 (19.8)
27.08.2014 (GPS survey)	35.9 (16.5)
26.08.2015 (GPS survey)	40.8 (13.6)
Thermocirque with tabular ground ice and ice wedges	
05.09.2012 (GPS survey)	2.3 (0)
05.07.2013 (satellite image)	2.9 (26.9)
27.08.2013 (GPS survey)	4.2 (45.9)
30.08.2015 (GPS survey)	6.4 (50.2)

Thus, at the present time in the tundra of the Yamal Peninsula the predominance of the processes associated with tabular ground ice thawing (cryogenic earth flows) over the processes associated with the ice formation at the bottom of the active layer (cryogenic translational landslides) is observed. It is caused by both a periodic deepening of the active layer, and consecutive increase of ground temperature.

Activation of thermal denudation observed on the Yamal Peninsula last years is associated with extremely warm spring and summer of 2012. By the end of the warm season thawing of the top of icy permafrost and tabular ground ice on some slopes resulted in cryogenic landsliding and further thermocirque development.

Acknowledgements

The study is partially supported by RFBR, research project No. 13-05-91001-ANF_a; ASF No I 1401-N29; and The Presidential Council for grants, Science School Grant No. 3929.2014.5.

References

Leibman, M.O. and Kizyakov, A.I. [2007]: *Cryogenic landslides of the Yamal and Yugorsky peninsulas*. Melnikov, V.P.(ed.) Earth Cryosphere Institute, Russian Academy of Sciences, Siberian Branch, Moscow–Tyumen, 206p.

Leibman, M.O.; Khomutov, A.V.; A.A. DvornikovGubarkov, Y.A. and Mullanurov, D.R. [2015]: The research station "Vaskiny Dachi", Central Yamal, West Siberia, Russia – A review of 25 years of permafrost studies. *Fennia*, 193(1):3–30, doi:10.11143/45201.

Voskresenskiy, K.S. [2001]: *Modern relief-forming processes on plains of the Russia North*. Moscow University Press, Moscow, 262p., (In Russian).

Study of off-road vehicle trails impact on tundra landscapes by field and remote-sensing methods, Central Yamal, Russia

Artem V. Khomutov[1], Marina O. Leibman[1], Yury A. Dvornikov[1], & Olga V. Khitun[2]

[1] *Earth Cryosphere Institute, Siberian Branch of Russian Academy of Sciences, Tyumen, Russian Federation*
[2] *Komarov Botanical Institute of Russian Academy of Sciences, Saint Petersburg, Russian Federation*

Study of landscape changes caused by human impact are an important part of research in the Arctic. It was shown [Moskalenko, 2012] that moisture content and ground temperature were determinants of the landscape complex evolution in the island permafrost zone of West Siberia. However, northward, in treeless locations, distribution of low-temperature continuous permafrost and massive ground ice do not allow fully extrapolation of these results to the typical tundra subzone of Central Yamal. The study of technogenic impact including off-road vehicle trails was conducted by [Kumpula et al., 2011] for industrial zone of Bovanenkovo gas field where all terrain disturbed by gas industry (buildings and yards, roads, sand quarries, pipelines, etc.). It was established that 5.3 % of total 448 sq.km area of the gas field was disturbed by off-road vehicle trails.

Research station "Vaskiny Dachi" with long-term monitoring of permafrost and related environmental features including the dynamics of surfaces affected by off-road vehicles is a key area for the study of their technogenic impact on landscape complexes [Khomutov and Khitun, 2014]. In contradiction to Bovanenkovo, here off-road vehicle trails are the major disturbance of terrain.

Disturbance of landscapes with off-road vehicle trails is assessed for the period prior to railway Obskaya-Bovanenkovo construction (2010) in the study area. Visually determined are trails that were not used for a long time and those used recently. Disturbance is defined as an area of the trail versus area of the landscape unit. Trail area calculated from a satellite image is linear dimension multiplied by 5 m for abandoned or rarely used trails and 8 m for actively used ones. Fig. 1 shows the coverage of the territory by various landscape units (a) and disturbance by vehicle trails (b).

Field measurements combined with remote-sensing data showed the range of disturbance in the study territory between 0.7 and 13.5 % depending on the landscape properties (Fig. 1b). Subdivided 21 landscape units were aggregated in 4 groups with relatively narrow range of disturbance: low (<2.0 %), medium (2.0-4.9 %), high (5.0-10.0 %), and very high (<10 %) of trail area.

Main controls of degree of disturbance are complexity of topography and waterlogging in highly dissected rolling hills and flat-bottomed valleys and lake depressions, hindering cross-country driving. Less hindering are high shrubs often combined with complex topography of landslide affected slopes. Most favourable for driving and thus most disturbed are dry flat watersheds, well drained. At the same time, very highly disturbed are flat waterlogged landscape units because one cannot use the same trail for the second time and zone of the disturbance by trails in such units are extremely wide.

Several years after the main technogenic impact resulting from Bovanenkovo gas field development stopped and one year before railway embankment construction started when no further technogenic impact was applied, more than one-half of affected surfaces was consistently overgrowing. 10.3 % of such surfaces (0.11 sq.km) were characterized by high probability of wind-blown sands. Degradation and slow recovery of shrub cover were characteristic of 20.3 % (0.21 km^2) of surfaces affected by off-road vehicles. Increase of moisture content and swamping with higher risk of thermokarst were observed on 16.3% (0.17 km^2) of trails. The risk of thermal erosion and cryogenic landsliding due to technogenic impact increased by 4.8 % (0.05 km^2) of affected surfaces.

Thus, the total disturbance by vehicle trails on the area distant from Bovanenkovo gas field is almost the same as in Bovanenkovo itself (5.5 % against 5.3 %). Probably impact in Bovanenkovo was much higher at early stages of development but trails were partly covered by construction and drilling pads and embankments.

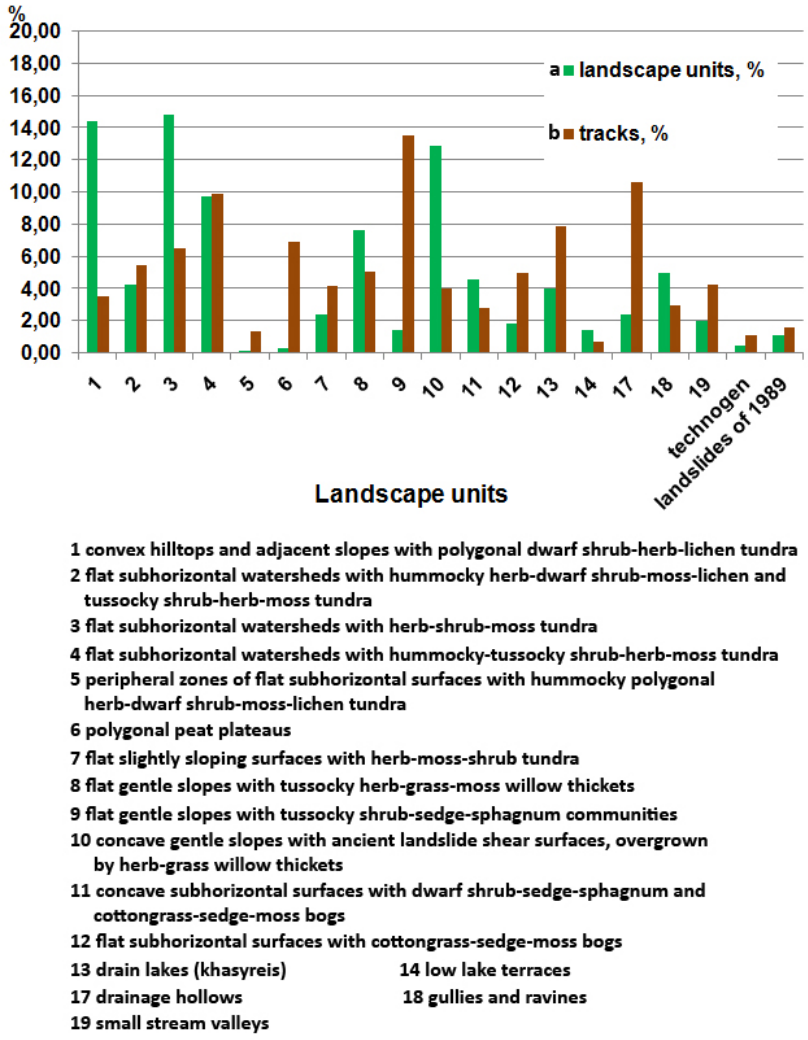

Figure 1: Percentage of (a) each landscape unit area in total study area; (b) trail area within each landscape unit.

Landscapes affected by vehicle trails in Vaskiny Dachi are characterized by different initial conditions of recovery of landscape components, or further technogenic activation of cryogenic processes. More than one half of affected surfaces is consistently overgrowing when no further technogenic impact is applied.

Acknowledgements

The study is partially supported by RFBR, research project No. 13-05-91001-ANF_a; ASF No I 1401-N29; and The Presidential Council for grants, Science School Grant No. 3929.2014.5.

References

Khomutov, A.V. and Khitun, O.V. [2014]: The dynamics of vegetation cover and the depth of seasonal thawing in the typical tundra of Central Yamal under technogenic impact. *Tyumen State University Herald*, 4:17–27, UDK: 581.524.34+551.345, (in Russian).

Kumpula, T.; Pajunen, A.; Kaarlejärvi, E.; Forbes, B.C. and Stammler, F. [2014]: Land use and land cover change in Arctic Russia: Ecological and social implications of industrial development. *Global Environmental Change*, 21(2):550–562, 2011. doi:10.1016/j.gloenvcha.2010.12.010. Special Issue on The Politics and Policy of Carbon Capture and Storage.

Moskalenko, N.G. [2012]: Cryogenic landscape changes in the West Siberian northern taiga in the conditions of climate change and human-induced disturbances. *Kriosfera Zemli (Earth's Cryosphere)*, 16(2):38–42, 2012. URL http://www.izdatgeo.ru/pdf/krio/2012-2/38.pdf. (in Russian).

Rapid palsa decay in Northern Finland interpreted from aerial photographs and RTK GPS field measurements

Timo Kumpula[1], Mariana Verdonen[1], Teemu Tahvanainen[2], & Alfred Colpaert[1]

[1] *Dept of Geographical and histrical studies, University of eastern finland, Finland*
[2] *Department of Environmental & Biological Sciences*

Palsa is a form of discontinuous permafrost in the circumpolar zone. Palsa are peat mounts with a core of permanently frozen peat, ice and mineral soil. The palsa can be from one to several meters high, dominating an otherwise flat mire area. There are several studies which indicate that palsa's are melting and decaying as a result of climatic warming. Weather conditions vary yearly and affect the depth of the active layer. The palsas under study are located in the Kilpisjärvi area, Finland, about 470 meters above sea level (lat 68°54' lon 20°58) (Laassaniemi and Peera).

Two palsa were measured using Real Time Kinematic (RTK) GPS with XYZ accuracy of one cm. A measurement grid with two meter interval was defined over each palsa, both have approximately 200 points. Measurements were carried out yearly in the last days of August (2007-2012). Active layer depth of each point was measured with an active layer probe. With ArcGIS we created 3-D models of palsa and yearly active layer surfaces. Weather data used is from the Kilpisjärvi climate station allocated about 15 km north of the study sites (1951-2011).

We also used a time serie of aerial photographs to detect the decay process of palsas (1959, 1985, and 2000. Both palsa's has experienced decay especially along the edges. The palsa in Laassaniemi has large collapsing side towards a thermokarst pond, here the core has collapsed more than one meter during the study period. In the 1959 image there are no signs of a thermokarst pond. Also a large Nierivuoma palsamire was examined with aerial images and between 1960 and 2010 53 % of palsas has disappeared and areal coverage (hectare) of palsas has declined 69 %.

Detailed RTK high accuracy GPS based palsa monitoring opens new aspects in palsa research. Combining historical aerial photographs the time span of the study can be stretched up to 50-60 years. Combining six years of detailed field data with 50 years of historical aerial photographs we can accurately follow the development of a palsa and its correlation to climatic factors. Both palsa's investigated and investigated palsa mire complex (Nierivuoma) were experiencing significant decay during the study period.

Thermokarst rates intensify due to climate change and forest fragmentation in an Alaskan boreal forest lowland

Mark J. Lara[1], Hélène Genet[1], A. D. McGuire[1,2], Eugénie S. Euskirchen[1], Yujin Zhang[1], Dana R. Brown[1], M.Torre Jorgenson[3], Vladimir Romanovsky[4], Amy Breen[5], & W. R. Bolton[6]

[1] *Institute of Arctic Biology, University of Alaska, Fairbanks, Alaska, USA*
[2] *U.S. Geological Survey, Alaska Cooperative Fish and Wildlife Research Unit, University of Alaska Fairbanks, Fairbanks, Alaska, USA*
[3] *Alaska Ecoscience, Fairbanks, Alaska, USA*
[4] *Geophysical Institute, University of Alaska Fairbanks, Fairbanks, Alaska, USA*
[5] *International Arctic Research Center, Scenarios Network for Alaska and Arctic Planning, University of Alaska Fairbanks, Fairbanks, Alaska, USA*
[6] *International Arctic Research Center, University of Alaska Fairbanks, Fairbanks, Alaska, USA*

Lowland boreal forest ecosystems in Alaska are dominated by wetlands comprised of a complex mosaic of fens, collapse scar-bogs, low shrub/scrub, and forests growing on elevated ice-rich permafrost soils. Thermokarst has affected the lowlands of the Tanana Flats in central Alaska (Fig. 1) for centuries, as thawing permafrost collapses forests that transition to wetlands. Located within the discontinuous permafrost zone, this region has significantly warmed over the past half-century, and much of these carbon-rich permafrost soils are now within ≈0.5 °C of thawing. Increased permafrost thaw in lowland boreal forests in response to warming may have consequences for the climate system. This study evaluates the trajectories and potential drivers of 60 years of forest change in a landscape subjected to permafrost thaw in unburned dominant forest types (paper birch and black spruce) associated with location on elevated permafrost plateau and across multiple time periods (1949, 1978, 1986, 1998 and 2009; Fig. 1) using historical and contemporary aerial and satellite images for change detection.

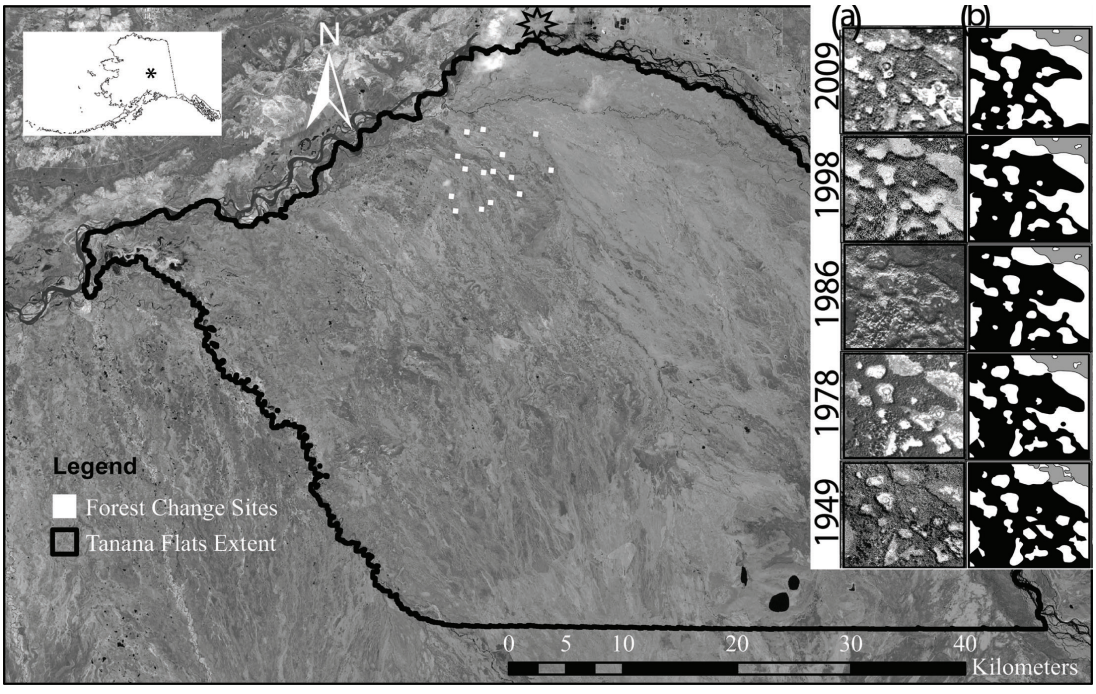

Figure 1: Study site located on the Tanana Flats (white outline), in interior Alaska. Fifteen 500 × 500 m windows were used in the land cover change assessment (see example, columns A & B), which delineated birch (black), spruce (grey), and wetlands (white).

Fifteen 500 × 500 m sites were randomly selected for use in the land cover change assessment (Fig. 1, columns A & B), where the extent of both forest types and wetlands were quantified each year. We developed

i) a deterministic statistical model to evaluate the potential climatic controls on forest change using gradient boosting and regression tree analysis, and

ii) a 30 × 30 m land cover map of the Tanana Flats to estimate the potential landscape-level losses of forest area due to thermokarst from 1949 to 2009.

Over the 60-year period, we observed a nonlinear loss of birch forests and a relatively continuous gain of spruce forest associated with thermokarst and forest succession, while gradient boosting/regression tree models identify precipitation and forest fragmentation as the primary factors controlling birch and spruce forest change, respectively. Between 1950–2009 landscape-level analysis estimates a transition of ≈15 km^2 or ≈7 % of birch forests to wetlands, where the greatest change followed warm periods. This work highlights that the vulnerability and resilience of lowland ice-rich permafrost ecosystems to climate changes depends on forest type.

Recent circum-Arctic ice-wedge degradation and its hydrological impacts

Anna K. Liljedahl[1], Julia Boike[2], Ronald P. Daanen[3], Alexander N. Fedorov[4], Gerald V. Frost[5], Guido Grosse[2], Larry D. Hinzman[1], Yoshihiro Iijima[6], Janet C. Jorgenson[7], Nadya Matveyeva[8], Marius Necsoiu[9], Martha K. Raynolds[1], Vladimir Romanovsky[1], Jörg Schulla[10], Ken D. Tape[1], Donald A. Walker[1], Cathy J. Wilson[11], & Hironori Yabuki[6]

[1] *University of Alaska Fairbanks, United States of America*
[2] *Alfred Wegener Institute Helmholtz Centre for Polar and Marine Research, Germany*
[3] *Department of Natural Resources, United States of America*
[4] *Melnikov Permafrost Institute, Russia*
[5] *ABR Inc. Environmental Research& Services, United States of America*
[6] *Japan Agency for Marine-Earth Science and Technology, Japan*
[7] *Arctic National Wildlife Refuge, United States of America*
[8] *Russian Academy of Sciences, Russia*
[9] *Southwest Research Institute, United States of America*
[10] *Hydrology Software Consulting, Switzerland*
[11] *Los Alamos National Laboratory, United States of America*

Ice-wedges are common permafrost features formed over hundreds to thousands of years of repeated frost cracking and ice vein growth. We used field and remote sensing observations to assess changes in areas dominated by ice-wedges, and we simulated the effects of those changes on snow accumulation and runoff. We show that top melting of ice-wedges and subsequent ground subsidence has occurred at multiple sites in the North American and Russian Arctic. At most sites, melting ice-wedges have initially resulted in increased wetness contrast across the landscape, evident as increased surface water in the ice-wedge polygon troughs and somewhat drier polygon centers. Most areas are becoming more heterogeneous with wetter troughs, more small ponds (themokarst pits forming initially at ice-wedge intersections and then spreading along the troughs) and drier polygon centers. Some areas with initial good drainage, such as near creeks, lake margins, and in hilly terrain, high-centered polygons form an overall landscape drying due to a drying of both polygon centers and troughs. Unlike the multi-decadal warming observed in permafrost temperatures, the ice-wedge melting that we observed appeared as a sub-decadal response, even at locations with low mean annual permafrost temperatures (down to -14 °C). Gradual long-term air and permafrost warming combined with anomalously warm summers or deep snow winters preceded the onset of the ice-wedge melting. To assess hydrological impacts of ice-wedge melting, we simulated tundra water balance before and after melting. Our coupled hydrological and thermal model experiments applied over hypothetical polygon surfaces suggest that

1. ice-wedge melting that produces a connected trough-network reduces inundation and increases runoff, and that
2. changing patterns of snow distribution due to differential ground subsidence has a major control on ice-wedge polygon tundra water balance despite an identical snow water equivalent at the landscape-scale.

These decimeter-scale geomorphic changes are expected to continue in permafrost regions dominated by ice-wedge polygons, with implications for land-atmosphere and land-ocean fluxes of water, carbon, and energy.

Multi-sensor investigations of thermokarst development in Eboling Mountain, Heihe River Basin

Lin Liu[1], Liming Jiang[2], Tingjun Zhang[3], Jie Chen[1], Binbin Gao[2], Jianguo Shang[3], Yanyun Nian[3], Yafei Sun[2,4], Bin Cao[3], & Lin Liu[2,4]

[1] *Earth System Science Programme, Faculty of Science, The Chinese University of Hong Kong, Hong Kong, China*
[2] *State Key Laboratory of Geodesy and Earth's Dynamics, Institute of Geodesy and Geophysics, Chinese Academy of Sciences, Wuhan, China*
[3] *College of Earth and Environmental Sciences, Lanzhou University, Lanzhou, China*
[4] *University of Chinese Academy of Sciences, Beijing, China*

Thermokarst landforms are common on the Qinghai-Tibet Plateau and high mountains of China, but their surface dynamics is still poorly quantified or understood, especially compared with their counterparts in the Arctic. In this study, our team carried out a variety of space-borne, air-borne, and ground-based measurements on thermal gullies within a valley at Eboling Mountain, near the upper stream of the Heihe River basin, aiming to investigate the spatial-temporal changes of these thermokarst landforms.

A comparison between historical aerial photos and modern high-resolution optical images acquired from satellites and unmanned aerial systems (UAS) reveals that the thermal gullies initiated between 1960 and 1990 and rapidly developed in the past 20 years, manifested as expansion in length towards higher elevations. By differentiating two digital elevation models, one obtained by the Shuttle Radar Topography Mission (SRTM) in 2000 and the other obtained using the X-band TanDEM images acquired in 2013, we observe cumulative subsidence of up to 1 m along the gullies. The Persistent Scatterer Interferometric Synthetic Aperture Radar (PSInSAR) technique is applied to L-band ALOS-1 PALSAR images to retrieve time series of surface subsidence from 2006 to 2011 at 46-day intervals with 30-m spatial resolution. We find linear subsidence trends of up to 8 cm/year with larger subsidence trends near but outside the gullies; and seasonal subsidence of 2 to 8 cm associated with the natural, seasonal thawing processes. We conducted a ground-based InSAR campaign in June 2015. Using the IBIS-FC equipment in Ku band, we were able to measure surface motion at 6-minute intervals with sub-mm accuracy and 0.5-m spatial resolution. Preliminary results show cumulative 4 mm surface motion during only 66 hours, with strong diurnal variations that are associated with air temperature changes.

By combining these multi-sensor measurements, we have obtained a comprehensive quantification of thermal gully development and associated surface motion at time scales ranging from minutes and hours to months, years, and decades. Yet the challenges lie in interpreting and reconciling these temporal changes corresponding to different time windows. The spatial changes observed from these sensors, however, are consistent in that they all reveal active surface subsidence within a short distance (of about 50 m) from the gullies. This suggests thermokarst processes, which are driven by thawing of ice-rich permafrost, are not restricted to where thermal gullies have developed but are more widely spread within the valley.

Quantifying the role of snow in soil thermal dynamics of the arctic terrestrial ecosystems

Zhou Lyu & Qianlai Zhuang

Purdue University, United States of America

This study introduces a snow model into an existing soil thermal model in a biogeochemistry modeling framework, the Terrestrial Ecosystem Model (TEM), to evaluate the effects of snow dynamics on soil thermal regimes in the Arctic for the period 2003-2010. Available satellite snow-cover data and site-level data are used to calibrate and evaluate the modeling system for the historical period. The study shows that the revised model well estimated the top-soil layers' thermal regime and freeze/thaw status for the region (Fig. 1) by comparing the simulations with satellite-based data over the region. The soil temperature estimates at depths 5 cm and 20 cm driven with satellite-based snow data are 5 °C warmer in winters compared to those using the previous version of the model without explicitly considering snow dynamics. There is a delay of soil cooling in early winter and a delay of soil warming in late spring considering the insulative snow effect. The frozen areas estimated by the revised model move slightly southward in late spring and slightly northward in early winter. This study shall help our future analysis of soil thermal and carbon dynamics of the terrestrial ecosystems under changing climate and snow covers in the Arctic.

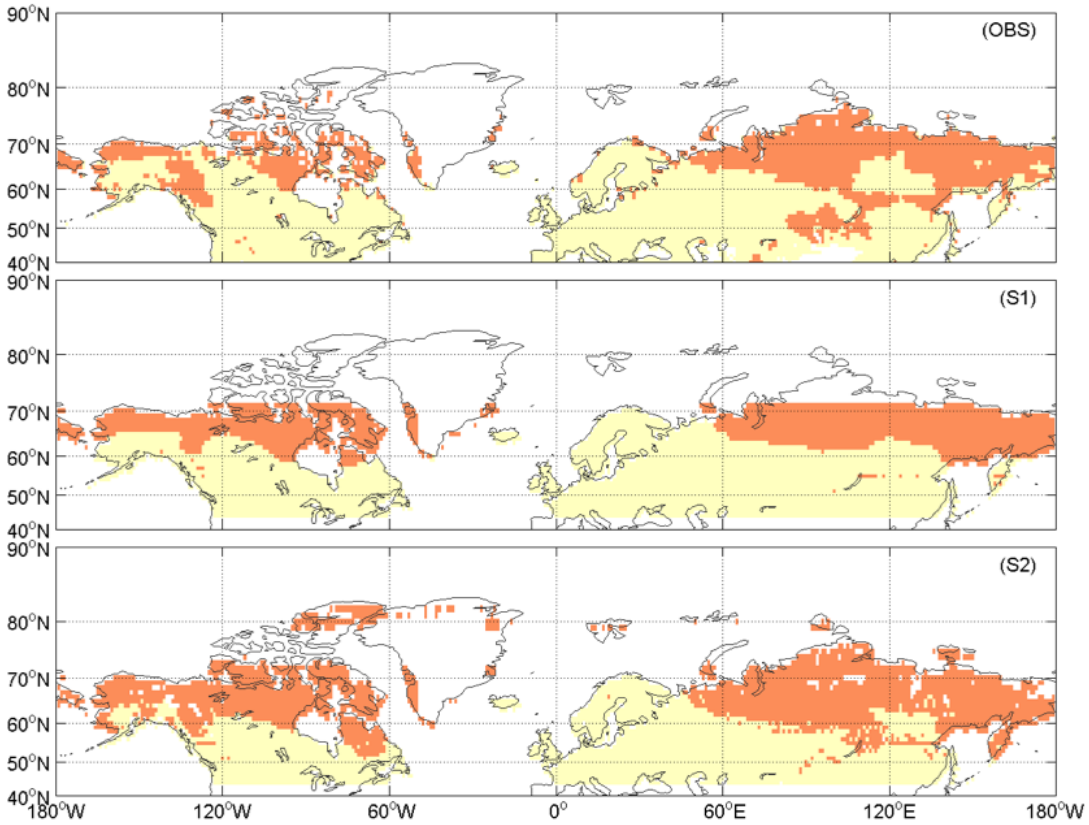

Figure 1: Freeze/thaw status in May, 2006 over the study area from (1) monthly averaged Global Record of Daily Landscape Freeze/Thaw Status, Version 3 product, (2) simulated freeze/thaw status from S1, and (3) S2

Analysis of regional formation regularities of thermokarst processes on the basis of ground-field and remote monitoring data

Elizaveta Makarycheva

Sergeev Institute of Environmental Geoscience, Russian Academy of Sciences, Russian Federation

Thermokarst phenomena along a 2500 km length oil pipeline in the South of the Eastern Siberia and the Far East was analyzed. This natural-technical system passes through different climatic, tectonic, landscape, and permafrost zones which require a variety of engineering geological and geodynamic conditions.

The study was done using the linkage between existing field-based research and data products from remote sensing. Based on a three-year monitoring survey (2010–2012) and geological surveys along the pipeline, 347 km with thermokarst phenomena were identified. The width of the survey area is one kilometer, therefore the phenomena were investigated not only in the pipeline affected zone, but also under natural conditions. Monitoring surveys along the pipeline showed significant transformation of landscapes in the zone of technogenic impact. A single technology was used during construction with the pipeline buried completely underground along the length of the pipeline. This enabled the estimation of the technogenic bearing on thermokarst processes in different geographical and geological conditions.

The analysis showed significant differences in phenomena distribution and morphological characteristics. All observed thermokarst phenomena were divided into 11 types based on their genetic and morphological characteristics (Fig. 1).

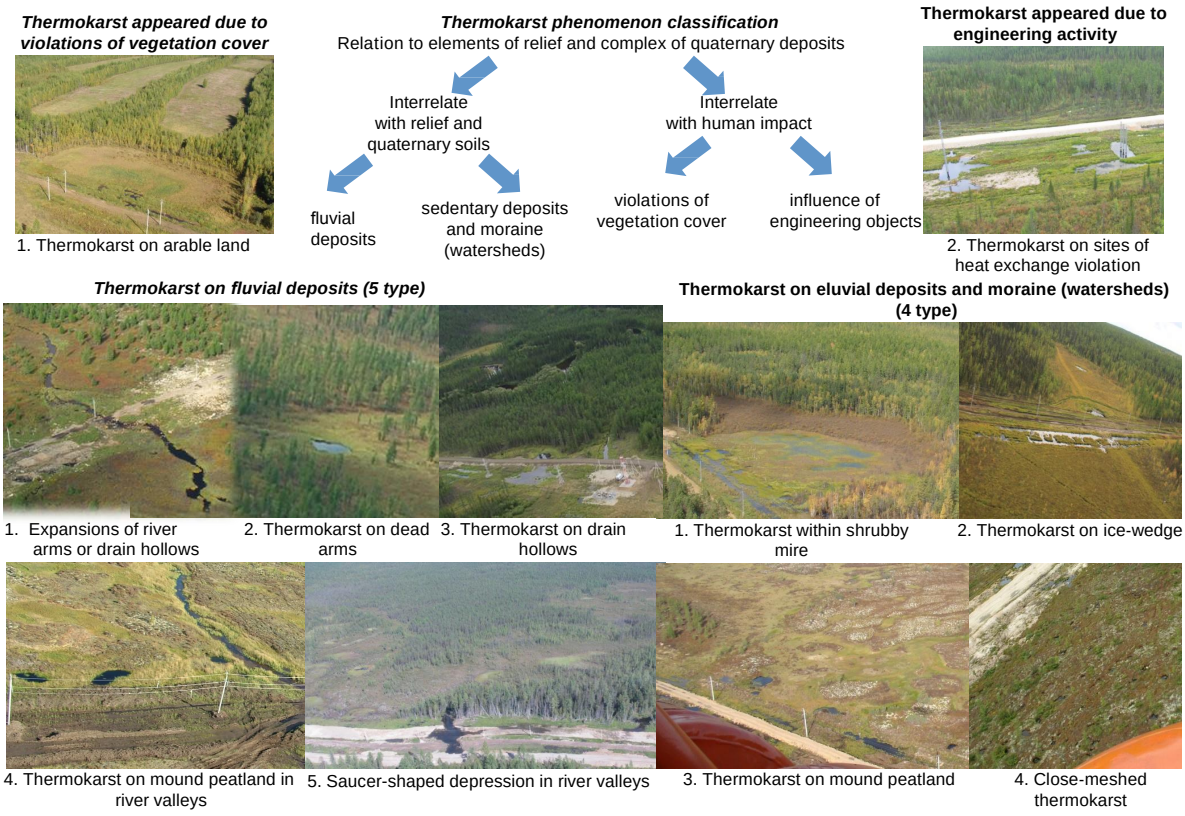

Figure 1: Thermokarst phenomenon classification by type near the southern border of the permafrost zone

The distribution of thermokarst phenomena allowed all the phenomena to be divided into two classes by their confinedness to relief elements. The first class, i.e. the phenomena having a natural genesis. The second class, i.e. the phenomena having a technogenic genesis. We also discovered natural phenomena that have been activated during operation of the pipeline. Identified thermokarst phenomena differ in degree of activity and stage of development.

We used large-scale maps of the pipeline area created by IEG RAS, as well as a series of small-scale maps of the territory. We also analyzed geological profiles along the length of pipeline, based on data obtained during engineering geological surveys. Average monthly changes in temperature and precipitation for the period from 2009 to 2012 were estimated according to data from 13 meteorological stations.

Using of independent criteria for mapping areas and phenomenon classification by type make it possible to apply a probabilistic assessment system. Natural factors and conditions impact on the formation of thermokarst processes was determined using a mathematical-statistical model.

Based on the comparison of the data available and data on the distribution of phenomenon, we determined the dependence of thermokarst processes on tectonic, permafrost, landscape, geomorphological, lithological and climatic conditions. The degree of the technogenic bearing on thermokarst processes in different landscape conditions was estimated.

These dependencies form the basis for a thermokarst formation map zoning based on the main factors and conditions.

The extent of the pipeline and variety of phenomena prohibit direct engineering studies of the possible impact of thermokarst processes on pipeline construction. Instead, estimates of the impacts are required. Due to the large number of phenomena identified in the monitoring work, it is complicated to estimate the impact of thermokarst processes on engineering construction. Current engineering projects employ a single evaluation criteria to assess construction hazards. However, a wide variety of process types with varying degrees of activity, stage of development and conditions of formation limits this approach. Zoning on the leading factors and conditions in the formation of thermokarst process will improve the existing system of hazard assessments, as well as enhance the effectiveness of protective measures.

Measuring permafrost ground motion with Unmanned Aerial Systems

Brian Moorman & Allison Cully

University of Calgary, Canada

One of the most ubiquitous aspects of permafrost terrain is the lack of stable ground. As a result of frost heave, ground ice deformation, differential settlement or subsurface ground shearing, it is very difficult to get an absolute measure of surface motion because all of the nearby ground is also moving, but not necessarily in the same direction or at the same speed. Attempts to get a stable datum included anchoring instruments or benchmarks in the permafrost, however, this has frequently proven unreliable [Tait et al., 2005]. Another method is to find an outcrop of bedrock and assume it is stationary. Unfortunately, bedrock is often not exposed at the surface where the study areas are located and sometimes bedrock has been shown to heave as well.

A more recent solution to this problem is the use of high-precision GPS. This is helpful, however there are limitations especially in high latitude regions where there is often poor satellite configuration. As well, GPS only provides point source positional data thus measuring motion fields across a large area is difficult and time consuming. Repeated traverses across the same area to make successive measurements can also result in the modification of the ground surface and impact the exact processes being measured.

Recent advancements in high-precision photogrammetry and LIDAR from Unmanned Aerial Systems (UASs) holds great promise of providing imagery, very accurate Digital Elevation Models (DEMs) and ground surface motion maps. Advantages of UASs include; high precision, low cost, repeat periods as frequent as you want, and no terrain disturbance in making the measurements.

For the last five years we have been testing different systems to measure the glacier and permafrost motion on Bylot Island in the Canadian Arctic. The resulting products are; georeferenced imagery with centimetre resolution, DEMs with decimetre resolution and surface motion maps where local velocity variations can be identified and accurately measured. As well, detailed work has been done on determining the actual uncertainty associated with this new type of data.

References

Tait, M.; Moorman, B. and Li, S. [2005]: The long-term stability of survey monuments in permafrost. *Engineering Geology*, 79(1–2):61–79, doi:10.1016/j.enggeo.2004.10.010.

A Landsat based monitoring framework for permafrost landscape dynamics

Ingmar Nitze[1,2], Guido Grosse[1], Benjamin M. Jones[3], & Daniel J. Hayes[4]

[1] *Alfred Wegener Institute, Germany*
[2] *University of Potsdam, Germany*
[3] *United States Geological Survey, USA*
[4] *University of Maine, USA*

Recent and projected future climate warming strongly affects permafrost stability over large parts of the terrestrial Arctic with local, regional and global scale consequences. The monitoring and quantification of permafrost and associated land surface changes in these areas is crucial for the analysis of hydrological and biogeochemical cycles as well as vegetation and ecosystem dynamics. It is also necessary for improved understanding of the consequences of climate change on past and present permafrost stability and potential future landscape conditions. Changes within vulnerable permafrost landscapes occur on different spatial and temporal scales and can result from both press (gradual) and pulse (event-driven) disturbances. Press disturbances that result from top down permafrost thaw have the potential to impact large expanses of the Arctic that will in turn change vegetation communities and hydrological conditions. Furthermore, destabilization of coastal regions has been identified as critical for the carbon cycle, but also for many Arctic communities built on permafrost terrain. Rapid thaw processes associated with land surface subsidence (thermokarst) and erosion in regions underlain by ice rich permafrost are a strong indicator of permafrost degradation. Typical thermokarst-related press disturbances include thaw slumps, detachment slides, degrading ice wedges, and thermokarst lake dynamics. Various stages of the thermokarst lake cycle that include thaw subsidence, ponding, lake formation, -expansion, and -drainage as well as vegetation succession affect vast stretches of coastal lowlands. In recent years, tundra fires have been recognized as an important disturbance which may trigger widespread permafrost degradation in severely burned areas.

Due to the size and remoteness of the Arctic, a large portion of potentially ecosystem-critical disturbance processes and landscape shifts remain undetected. Remote sensing methods are therefore important for understanding and quantifying these landscape dynamics. So far, most remote sensing studies of landscape change processes in the Arctic have been carried out at high spatial resolution for local scales or low to moderate spatial resolutions for regional scales. In most cases, the temporal resolution of high spatial resolution studies has been very limited, often including comparisons between a few snapshot datasets only. Dynamic assessments with repeat acquisitions over longer periods have so far largely relied on MODIS and AVHRR data at spatial resolutions of 250 to 1000 m. At this resolution, many characteristic disturbances, indicating initial landscape change, may remain unnoticed due to their small spatial extent. Therefore, detection and quantification of the abundance, distribution, and frequency of disturbances over large areas with a high spatial and temporal resolution has been very limited so far.

In this study, we present a methodology for monitoring landscape change in Alaska's northern and western tundra lowlands, across a 500,000 km^2 region, based on time-series analysis of the Landsat archive (TM, ETM+, and OLI) from 1985 to 2015. With a highly automated processing chain, we are able to analyze several thousand Landsat scenes, which allows for a multi-scaled spatio-temporal analysis at 30 meter spatial resolution. The processing system has been designed to handle nearly all working steps from data download to the final product with minimal user interaction. All necessary processing steps are carried out automatically, including data extraction, masking, reprojection, subsetting, data stacking, and calculation of multi-spectral indices. These indices, e.g. Landsat Tasseled Cap and NDVI among others, are used as proxies for land surface conditions, such as vegetation status, moisture or albedo. Finally, time-series analysis is applied to each multi-spectral index and each pixel over the entire observation period of around 30 years, from 1985 to 2015.

The resulting dataset consists of several information layers, e.g. linear trend parameters of each multi-spectral index, which allows for the detailed

analysis, but also visualization of land surface properties and processes over very large areas during the past three decades. Numerous processes, such as coastal and fluvial dynamics, lake area changes, fires, and also anthropogenic influences are detected. Numerous landscape changes were detected in northern and western Alaska that resulted from a myriad of disturbances such as thermokarst formation, coastal and lake bluff erosion, lake drainage, fires, and landscape wetting or drying, which have not been described in the appropriate spatial and temporal context before. With the high temporal density of the dataset it is even possible to determine the timing of initiation of pulse disturbances, such as lake drainage or tundra fires. Furthermore, the dataset allows for an assessment of post-disturbance successional trajectories across large permafrost, environmental, and climatic gradients.

Due to the high level of automation and the use of freely available Landsat data, the spatial extent of the analysis is transferable and scalable, which enables the comparison of different sites, across similar Arctic landscapes. With the presented processing chain and the resulting information, we envision enhancing the understanding of the response of permafrost landscapes to a warming climate as well as the quantification of changes in the frequency, magnitude, impact, and trajectory of various land surface disturbances in Arctic tundra regions. The combination of high temporal and spatial resolution in conjunction with freely available data and highly scalable tools provide a great opportunity for the analysis, monitoring and future projection of permafrost landscapes. With increasing computational capabilities and the launch and progress of further non-commercial earth-observation missions, such as Sentinel-2, we envision a pan-Arctic scale monitoring of rapidly changing permafrost regions

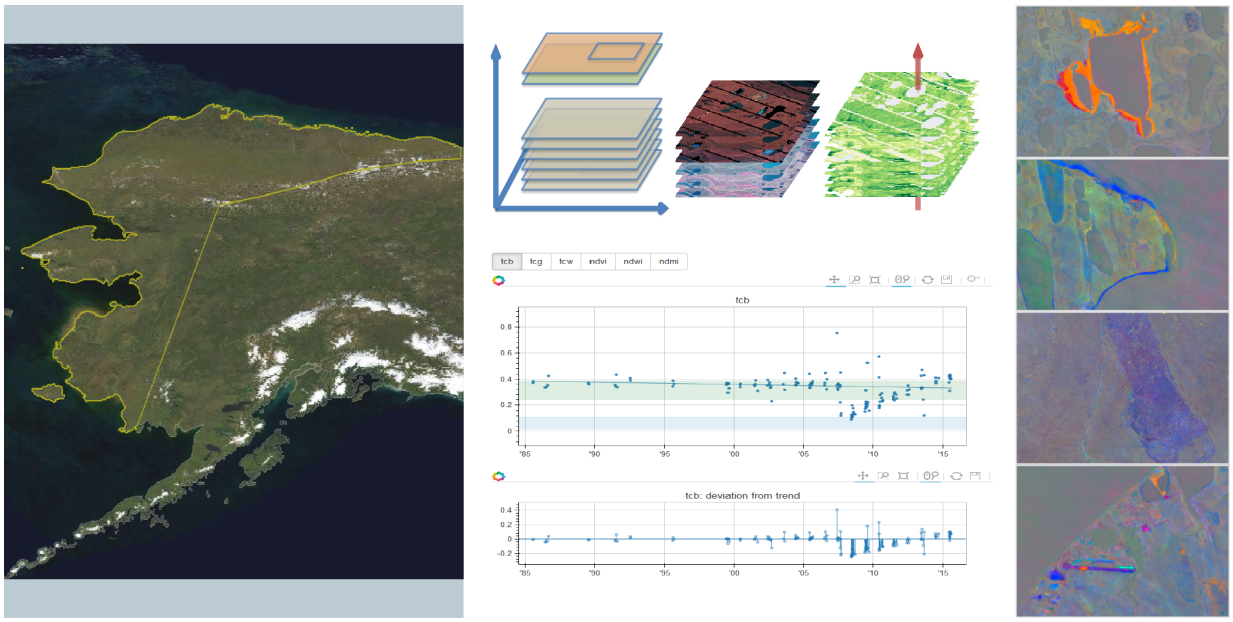

Figure 1: Left: Landsat time-series analysis study area. Top center: Schematic data stacking process. Bottom center: Multi-spectral time-series index of a severely burned tundra site. Right: Examples of (top-to-bottom): Lake drainage, coastal processes, fire event, and anthropogenic influence.

Distribution of thermokarst lakes and their area-frequency relations in Eastern Siberia

Hitoshi Saito[1], Yoshihiro Iijima[2], Mathias Ulrich[3], & Alexander N. Fedorov[4]

[1]*Kanto Gakuin University, Japan*
[2]*Japan Agency for Marin-Earth and Technology, Japan*
[3]*Leipzig University, Germany*
[4]*Melnikov Permafrost Institute, Yakutsk, Russia*

Eastern Siberia is characterized by widespread thawing of permafrost and subsequent thermokarst development. Dealing with predicted increases in precipitation and temperatures attributable to climate change requires quantitative knowledge about the spatial distribution and temporal changes of present and past thermokarst landscapes. This study specifically examined the spatial distribution of thermokarst lakes around Yakutsk. For the right and left banks of the Lena River Basin, the statistical relation between the lake area and frequency of changes was analyzed. After mapping thermokarst lakes and quantifying their areas using Landsat images from 2000–2013, we examined area–frequency distributions of these lake areas on different geomorphological terraces of ice-rich permafrost.

Results show inverse power-laws for the frequency distributions of lake areas. No significant difference was found in data related to the right and left banks of the Lena River. However, the spatial distribution of the lakes on the right bank was not uniform. Results show that that the area–frequency distributions in the higher terraces differ from those in the lower terraces. The lower terraces tended to have larger lakes of >105 m^2. Comparison of Landsat images taken during 2000–2013 demonstrated that lake areas expanded laterally, especially on the lower terraces. These results indicate that, for the distribution of the thermokarst lakes and their activity, their topography and surficial geology are important controlling factors. Additional studies must be conducted to verify the expansion of these lakes in terms of thermal and mechanical erosional processes.

Reconstruction of the development of retrogressive thaw slumps and controlling meteorological parameters in Central Yakutia (Central Siberia) using dendrochronology and remote-sensing

Antoine Séjourné[1], Armelle Decaulne[2], Francois Costard[1], & Alexander Fedorov[3]

[1] *Univ Paris-Sud, CNRS, Laboratoire GEOPS, UMR8148, Orsay, France*
[2] *CNRS UMR6554, Laboratoire de Littoral, Environnement, Télédétection, Géomatique, Nantes, France*
[3] *Melnikov Permafrost Institute, RAS, Yakutsk, Russian Federation*

Introduction

In the continuous permafrost area of Central Siberia, the Central Yakutia (CY; Central Siberia) shows an ice-rich permafrost of 70-80 % of ice by volume. As the mean annual air temperature at Yakutsk had increased by 3 °C since the 1960s and thermokarst processes seem to develop rapidly at different study sites in Central Yakutia since the early 1990s, this ice-rich permafrost is highly vulnerable and prone to extensive degradation. However, the correlation between thermokarst dynamics in the region and the increase in air temperature is not fully understood and thus has to be investigated.

Along the banks of thermokarst lakes, the deep thawing of permafrost induces retrogressive thaw slumping. We recently studied retrogressive thaw slumps (RTS) in CY 100 km from Yakutsk, using high resolution satellite images taken in 2011–2013 and conducting field studies [Séjourné et al., 2015]. The RTS expansion ranges from 0.5 and 3.16 m yr^{-1} in average. The occurrence and the rate of expansion are the most important on the southwest-facing banks of thermokarst lakes underlying a control by insolation. However, meteorological parameters initiating each summer the thaw slumping remain unconstrained.

In CY, the development of RTS on the forested banks of thermokarst lakes induces tilting and uprooting of trees (Fig. 1; Séjourné et al. [2015]). The patterns of tree rings reflect the growth disturbances which can be due to climate variations and/or cryogenic processes [Agafonov et al., 2004]. Tree-ring analyses have been used to reconstruct landslide and snow-avalanche occurrence [Speers, 2010] but it has been little used for thermokarst lake development and no literature has been found on tree-ring application for RTS studies. Investigations of RTS using tree-rings help studying the permafrost dynamics over a longer continuous period of time than isolated snapshots from aerial and satellite images or field studies.

Here, we reconstruct the development of RTS, their expansion rate and the controlling meteorological parameters on the banks of a thermokarst lake 100 km from Yakutsk during the last 100 years by analyzing larch (*Larix sibirica*) ring widths and remote sensing data.

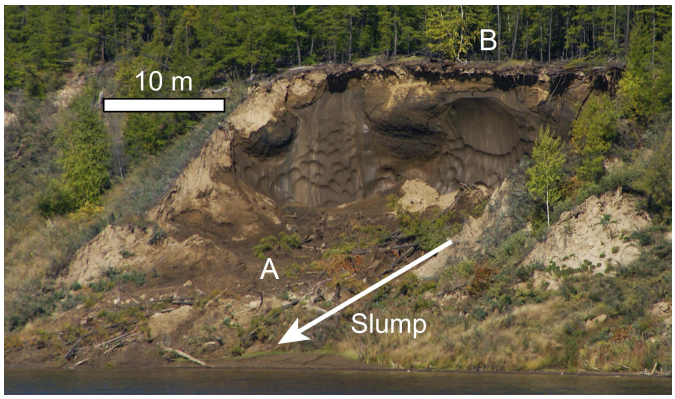

Figure 1: Retrogressive thaw slumping induces the destabilization and tilting of surrounding trees (tree 7 m high for scale).

Methods

Wood samples of living and dead Siberian larches (80 cross sections) were collected along transversal and longitudinal profiles throughout one RTS in September 2014 180 km east of Yakutsk (Fig. 1). Straight living trees were sampled for reference from a flat non-perturbed permafrost area close by. Preliminary analyses of sampled trees show that they have a living period from 80 to 200 years. In the laboratory, the wood samples were prepared and analyzed according to conventional tree-ring analysis methods [Speers, 2010]. Three radii were systematically measured for the reference stack (12 trees), while tree rings from

discs collected in the perturbed area were measured along the upslope and the downslope radii (69 trees).

All individual tree-ring chronologies were cross-dated first at the scale of the disc (tree scale) and compared with the reference stack (stand scale) for the purpose of detecting missing or fading rings. Asymmetrical tree-ring development is due to the formation of compression wood when a tree attempts to gain back its vertical position after tilting due to slumping. The onset of compression wood can be dated by dendrochronology, offering the date (with a seasonal accuracy) of tilting, i.e. root destabilization due to slump progression.

As the RTS seems to be active from June to August (Séjourné et al., 2015) and the vegetative season lasts at most from late May to early September, we compared the period of wood compression with changes in air temperature, precipitation and sunshine duration recorded at Yakutsk meteorological station for the June-August period from 1920 to 2014 (http://meteo.ru/).

Results

Preliminary results show that trees found into the RTS are tilted and developed compression wood, recording the expansion of RTS (Fig. 1). From tree-ring width analyses, we identified periods of compression wood in summer 1941, 1954, 1969, 1973, 1984 and finally 2000 (for instance living trees A in Fig. 1).

The compression wood periods correspond to deep seasonally thawed layer, when the root system loses the firm support of the permafrost (tilted trees B in Fig. 1). Consequently, the trees localized around the RTS cliff are progressively unbalanced due to RTS development, forcing them to produce compression wood to counter tilting. In contrast, trees from the reference stand do not develop compression wood during those periods, as they are not subjected to root unbalance. When the scar of the slump retrogresses towards the growing trees, the trunk fell into the RTS. The distance at which trees are affected by the progressive expansion of RTS is investigated.

The periods of intense compression wood formation, i.e. active slumping, seem to correlate with a rapid increase in air temperature rather than to an increase in precipitation or sunshine duration (vegetative period June-August). The increase in air temperature induces a deepening of the active layer causing melting of ground ice and slumping. From our preliminary results, the expansion of this RTS occurs by pulses of active but spatially limited development rather than a continuous progressive expansion.

Conclusion

Tree ring width analyses show that this RTS is expanding at least during the last 80 years and is caused by an increase in air temperature rather than in precipitation. Its development occur by pulses of active development rather than a progressive expansion. The study of the RTS development from tree-ring widths provides a better understanding of the current thermokarst dynamic in this region. In the context of recent air temperature increase in CY, the rate of thermocirque development may also increase in the future.

In the next months, all sampled trees will be analyzed and the history of development of RTS as well as the rate of thermokarst expansion will be calculated from the dates of its known positions and the distance of each tree from the contemporary RTS cliff. We will also compare the expansion periods to older remote sensing data such as Hexagon, Corona satellite or 1945 aerial data.

References

Agafonov, L.; Strunk, H. and Nuber, T. [2004]: Thermokarst dynamics in Western Siberia: insights from dendrochronological research. *Palaeogeography, Palaeoclimatology, Palaeoecology*, 209(1–4):183–196, 2004. doi:10.1016/j.palaeo.2004.02.024. High Latitude Eurasian Palaeoenvironments.

Séjourné, A.; Costard, F.; Fedorov, A.; Gargani, J.; Skorve, J.; Massé, M. and Mège, D. [2015]: Evolution of the banks of thermokarst lakes in Central Yakutia (Central Siberia) due to retrogressive thaw slump activity controlled by insolation. *Geomorphology*, 241:31–40, doi:10.1016/j.geomorph.2015.03.033.

Speers, J.H. [2010]: *Fundamentals of Tree Ring Research*. University of Arizona Press, 368 pp. (978-0-8165-2685-7).

Intra-annual dynamics of ice-rich riverbank erosion in the central Lena Delta

Samuel Stettner[1], Hugues Lantuit[1], Annett Bartsch[2,3], Birgit Heim[1], Guido Grosse[1], Achim Roth[4], & Barbara Widhalm[2,3]

[1] *Alfred Wegener Institute, Germany*
[2] *Central Institute of Meteorology& Geodynamics, Austria*
[3] *Department of Geodesy and Geoinformation, Vienna University of Technology, Austria*
[4] *Department Land Surface, German Aerospace Center, Germany*

Arctic warming accelerates the rapid degradation of ice- and organic-rich permafrost landscapes through thermokarst and thermal-erosion. These processes lead to the retreat of ice-rich coasts, riverbanks, lake shorelines, to surface subsidence and gullying. The subsequent reactivation of ancient carbon previously stored in the eroded ice- and organic-rich sediments could have tremendous impact on the carbon cycle from regional to global scale. Yet, information at high temporal and spatial resolution is often lacking to describe the rates and the timing of permafrost degradation. Synthetic aperture radar (SAR), which operates independently of atmospheric distortions, is particularly valuable to alleviate these issues because of its potential for high temporal resolution monitoring in a region where cloud cover often limits the use of optical satellite imagery.

In this study, we used SAR data to investigate the spatiotemporal dynamic of a rapidly degrading ice- and organic-rich up to 50-m-high and 2000-m long riverbank in the central Lena Delta. Our main objectives were to

1. assess the applicability of synthetic aperture radar (SAR) satellite data for high-temporal resolution monitoring of rapidly eroding riverbanks and

2. to identify the seasonal timing of ice-rich permafrost riverbank erosion.

We analyzed a unique time-series of high-spatial and temporal SAR images from the German TerraSAR-X (TSX) satellite, operating in X-band wavelength, as well as very high resolution optical satellite imagery and in-situ time-lapse data. We processed 77 HH-polarized SAR backscatter images with acquisition dates between August 2012 and October 2015. The imagery was first pre-processed using the Sentinel-1 toolbox from the European Space Agency. We then applied a thresholding to better identify the transition line from undisturbed tundra surface to the actively eroding cliff we refer to as cliff top line. We then calculated cliff top retreat rates and finally compared these with environmental baseline data to identify the main driving factors of riverbank retreat.

Visual interpretation of the TSX time-series showed that the cliff of the riverbank is only visible in the months June to October. Annual erosion rates were in the same range when comparing the optical reference with the SAR datasets. The in-situ time-lapse data for the summer of 2015 showed similar results for the intra-annual erosion compared to the SAR derived results. Based on the SAR dataset we detected mostly constant erosion rates at our test site throughout the thawing period for the years 2013, 2014 and 2015.

Our results show that the cliff-top at the test site retreats constantly over the thawing season rather than event driven (i.e. through the spring peak discharge only). The studied cliff top is protected from spring flood events by sandbanks in front of the riverbank. However, runoff caused by permafrost thaw, precipitation and flooding will degrade the protecting sand banks and consequently will lead to a reconnection of the cliff system to the Lena River System, even when water level is lower towards the end of the thawing season.

We conclude that x-band backscatter time-series are valuable for monitoring rapid permafrost degradation with high spatial and temporal resolution. Our results indicate that cliff top erosion of ice-rich riverbanks takes place constantly over the thawing period and is not event driven.

Quantifying thermokarst and alas lake changes and influencing factors during the last 70 years in Central Yakutia

Mathias Ulrich[1], Heidrun Matthes[2], Yoshihiro Iijima[3], Hotaek Park[3], Lutz Schirrmeister[4], Alexander N. Fedorov[5], & Juliane Schütze[6]

[1] *Leipzig University, Institute for Geography, Leipzig, Germany*
[2] *Alfred Wegener Institute, Atmospheric Circulations Section, Potsdam, Germany*
[3] *Japan Agency for Marine-Earth Science and Technology, Institute of Arctic Climate and Environment Research, Yokosuka, Japan*
[4] *Alfred Wegener Institute, Periglacial Research Section, Potsdam, Germany*
[5] *Melnikov Permafrost Institute, SB RAS, Yakutsk, Russia*
[6] *University of Applied Sciences Jena, Department of Fundamental Science, Jena, Germany*

The permafrost landscape of Central Yakutia is subject to rapid modifications due to intensive land use, extreme weather, and the current global warming. With regard to the predicted increase in precipitation and temperature as a result of climate change, quantitative knowledge of the small-scale variability of active thermokarst processes is required.

Here, we mapped the change of thermokarst and alas lakes (i.e. residual lakes in alas basins) for 11 times covering periods of 2 to 18 years between 1944 and 2014 at the Yukechi study site (61.761289° N/130.470602° E). Historical airborne, current satellite as well as field data were utilized in analyzing lake-area changes and thaw subsidence on local scale (Fig. 1). Additionally, a unique dataset of long-term climatic and ground-temperature data could be used in multivariate statistics to identify the climatological and/or general driving and inducing factors of thermokarst and alas-lake changes. On regional scale, size and distribution of lakes >0.1 ha were analyzed on different ice-rich permafrost terraces in the Lena-Aldan-Amga interfluve region east of Yakutsk on the basis of Landsat 8 data from July 2013.

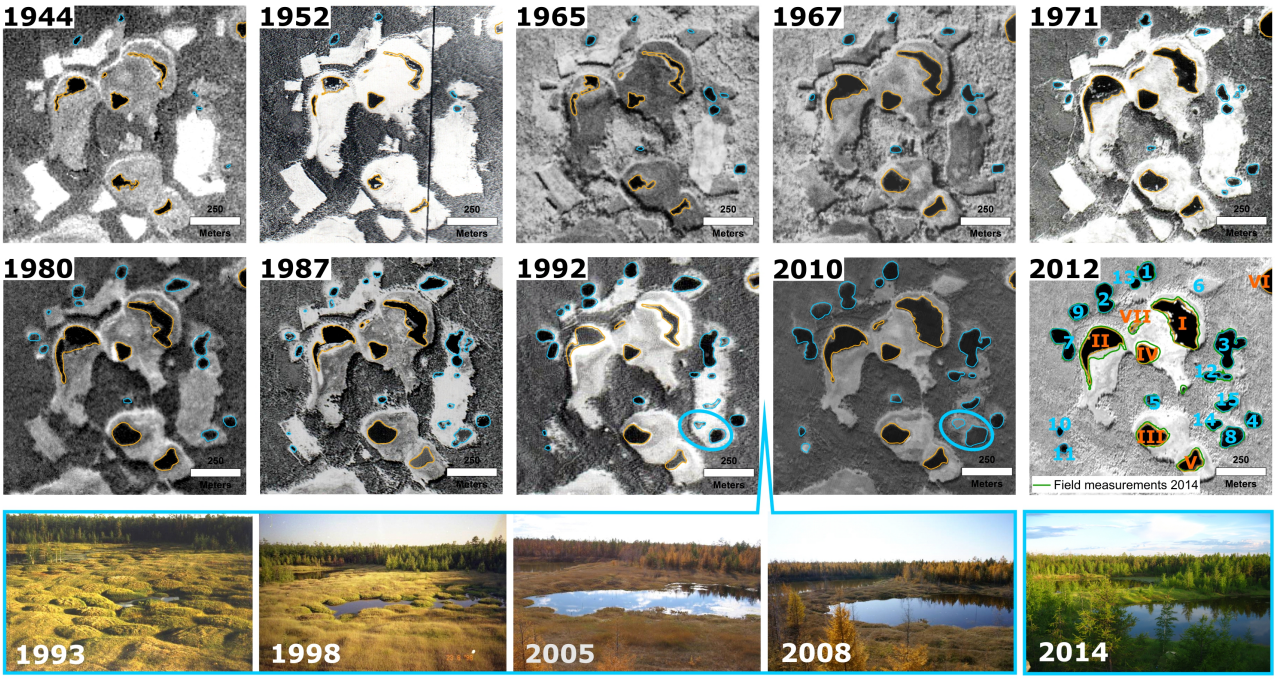

Figure 1: Annual temperature difference (ΔT) between calculated air temperature and measured rock face temperatures.

Regionally, larger lakes distributed in higher frequency are dominating lower terraces. Smaller lakes dominate higher terraces. In particular, smaller lakes are distributed in less density on older and more ice-rich terraces while highest lake densities and larger lakes characterize younger and less ice-rich terraces.

Remote sensing analyses at the Yukechi study site indicate that alas-lake levels are increasing strongly end of the 1960s and since the 1990s until present, but their area decrease in the 1940s, 1950s, 1970s, and 1980s. The mean rate of alas-lake-radius change for the 70 year time span account for 1.6 ±2.9 m/yr. In the meanwhile, extensive agricultural use in the postwar period on the Yedoma ice-rich permafrost deposits led to a rapid and sustained growth of young thermokarst lakes over the entire time span (Fig. 1). This is initiated by the strong disturbance of the thermal and hydrological balance of the permafrost. The mean rate of lake-radius change of all mapped thermokarst lakes is 1.2 ±1.0 m/yr. The mean thaw subsidence below the thermokarst lakes account for 6.2 ±1.4 cm/yr.

Our statistical analyses indicate that climatic parameters (i.e. precipitation, air and ground temperature, and evaporation) show higher correlations with thermokarst-lake changes than with alas-lake changes. In particular, the influence of annual air-temperature changes and evaporation is higher on thermokarst-lake level changes than on alas-lake level changes. However, the influence of precipitation, especially winter precipitation, is lower. Deeper ground-temperature changes (3.2 m depth) show higher correlation with thermokarst-lake changes, while the influence of ground temperatures in 1.6 m depth is similar. Multiple regression analyses reveal more complex interrelations of climatic and ground thermal conditions with thermokarst and alas lake changes but further study is needed to validate these results.

Our results show, however, that topography, geomorphology, and surficial cryolithology are important controlling factors on the regional distribution and size of the lakes. Furthermore, thermokarst activity is influenced by climatic parameters but it is accelerated and rapidly induced by disturbing factors such as land use. Climatic parameters are strongly affecting growing rates within certain time periods of thermokarst lakes but they do not lead to remarkable reductions or the disappearance of the lakes during the whole observation period. Alas lakes are increasing and decreasing. Distinguishing main controlling factors, however, are hampered probably due to larger catchment areas and subsurface hydrological conditions.

Stochastic models of lake thermokarst plain dynamics

Alexey Victorov & Veronika Kapralova

RAS Institute of Environmental Geoscience, Russian Federation

There is a significant number of the researches considering the issue of the dynamics of the lake thermokarst plains. Some of these are based on stationary observations of the thermokarst lake dynamics. C.R. Burn and M.W. Smith found out a uniform growth of lake diameters after monitoring some regions of the North America. In most investigations [Makarycheva Sergeev, Kapralova, Jin] thermokarst lakes are expected to appear during a relatively short period of time compared to that of the further development [Tumskoi, Kaplina]. Another point of view takes into account the long nascence period for the thermokarst lakes [Streletskaya, Turkina, Voskresenskii].

The aim of the work is to test different hypotheses of thermokarst lake origin and development, using mathematical modeling of a spatial morphological pattern. The mathematical morphology of landscape is the base for models being considered [Victorov]. The models are based in turn on the random processes theory.

Our studies resulted in the set of models, describing the morphological pattern development for the lake thermokarst plains in a uniform nature environment at a constant climate condition.

Each model is based on two simple assumptions 1 (or 1a) and 2 (or 2a).

1. Thermokarst depressions were appearing within a relatively short period (i.e. synchronous start). This stochastic process was running independently across the different non-adjacent landscapes. At the same time the probability of a new depression appearance within a sample plot was dependent exclusively on the plot area.

1a. Thermokarst depressions were constantly appearing (i.e. asynchronous start). This stochastic process was running independently for the non-adjacent areas during non-adjacent periods. There at the probability of the depressions to appear within a sample plot depends exclusively on the plot area and time.

2. Due to the thermoabrasive action, the size growth of lakes goes independently with a certain probabilistic distribution, depending on the density of heat loss through the side surface of a lake hole (so called “logarithm growth”).

2a. Due to the thermoabrasive action, the size growth of lakes goes independently and follows a constant probabilistic distribution (so called quasiuniform growth).

Thus, we got the set of four models of the spatial morphological pattern of thermokarst lakes as follows:

- 1.0 Development under logarithm growth and synchronous start;
- 2.0 Development under quasiuniform growth and synchronous start;
- 1.1 Development under logarithm growth and aynchronous start;
- 2.1 Development under quasiuniform growth and asynchronous start.

The mathematical analysis of the models showed the theoretical distribution of radii of thermokarst lakes at an observation moment varies, depending on the assumptions of the model. Thus we got different theoretical results of modeling after considerably long time from the start of the thermokarst process (Tab. 1). Hence, after comparison of the theoretical results with the empirical data on distribution of thermokarst lake diameters (and areas) we can make conclusions about the character of the thermokarst process within a study area such as the synchronous or asynchronous start, and the logarithmic or quasiuniform growth. At the same time distribution of the number of lakes at a random plot in each case similarly follows the Poisson distribution.

For the research we have selected 15 study sites in different regions, including the Yamal peninsula, the West Siberian lowland, the Kolyma lowland, and Alaska (Tab. 1). We used the following remote sensing data (RSD): archive of the survey Corona (3-12 meters per pixel, 1957-1976); current imagery mission data, such as IKONOS, QuickBird, Worldview 2, Geoeye-1, Pleiades, SPOT-5, SPOT-6, 0,5-2,5 (0,5-2,5 meters per pixel, June-August 2008-2014). We used both the commercial images and those which are openly available.

Table 1: Distribution of the thermokarst lake parameters under different lake thermokarst evolution scenarios

Thermokarst plain evolution scenario	Synchronous start	Asynchronous start
Lognormal growth of the lake radii	Model type 1.0 Lognormal distribution of the lake areas (radii)	Model type 1.1 "Logarithmic" distribution of the lake areas (radii)
Quasiuniform growth of the lake radii	Model type 2.0 Normal distribution of the lake areas (radii)	Model type 2.1 Uniform distribution of the lake areas (radii)

Processing algorithm included the choice of testing areas, digitizing and vectorizing thermokarst lakes, estimating areas and diameters of lakes. In order to find the most veracious variant of the model, the distribution fitting was tested for lake areas to lognormal and to "logarithm" distribution. Then for average lake diameters fitting to normal and uniform distribution.

To verify compliance of the empirical distributions with the theoretical ones, the strict conventional techniques (Pearson criteria) within a statistical software package were used. At first free parameters of the distribution were determined by the sample. Then Pearson criteria were found and compared with the critical one at 16 at the 0,95 and 0,99 confidence levels.

Sample sizes varied from 74 to 576 lakes. The statistical analysis showed, that the vast majority of sites are typical of the lognormal distribution (14 from 15 sites at 0,99 confidence level). Another distribution type ("Logarithmic") was defined for only one testing site in two of the three samples at the same confidence levels.

We consider the findings of the research as follows:

1. We designed the probabilistic models of the dynamics of lake thermokarst plains and then used those for testing four different hypotheses about the development of the plains.

2. Empirical testing of the thermokarst lake parameter distributions showed, that the observed area and radii distributions of thermokarst lakes obey the lognormal distribution at the vast majority of the study sites, and they do not correspond to other types of distributions in research.

3. Distribution of centers of thermokarst lakes obeys to the Poisson law.

4. Our research findings allow us supporting the following assumptions:

   - synchronous start for all areas of the thermokast lake origination process,
   - proportional rate of the thermokarst lake growth to the average density of the heat loss through the lake lateral surface.

Acknowledgements

The work is committed with the financial help of the Russian Science Foundation (project № 14-17-00357).

Eurasia Arctic Transect (Yamal Peninsula and Franz Josef Land, Russia): Relationships between climate, soil texture, vegetation, active-layer thickness, and spectral data

D. A. Walker[1], H.E. Epstein[2], M.O. Leibman[3], K. Ermokhina[3], A. Khomutov[3], N. Moskolenko[3], P. Orekhov[3], G. Matyshak[4], G.V. Frost[5], O. Khitubn[6], S. Chasnikova[7], J. Šibík[8], E. Kaärlejarvi[9], & J.P. Kuss[10]

[1] *University of Alaska Fairbanks, USA*; [2] *University of Virginia, USA*
[3] *Earth Cryosphere Institute, Russian Academy of Science, Tyumen, Russia*
[4] *Lomonosov Moscow State University, Russia*
[5] *Alaska Biological Research, Inc., Fairbanks, AK, USA*
[6] *Komarov Botanical Institute, Russian Academy of Science, St. Petersburg, Russia*
[7] *Institute of Landscape Ecology, Slovak Academy of Sciences, Bratislava, Slovak Republic*
[8] *Institute of Botany, Slovak Academy of Sciences, Bratislava, Slovak Republic*
[9] *Umeå University, Sweden*; [10] *University of Zurich, Switzerland*

The Eurasia Arctic Transect (EAT) stretches 1700 km from Nadym (65°19' N, 72°53' E) in the forest-tundra transition of northwest Siberia, to the extreme High Arctic, at the Krenkel hydro-meteorological station, Hayes Island, Franz Jozef Land (80°37' N, 58°03' E). The major reasons to establish the transect were to

1. develop a set of ground-based data from zonal sites in each bioclimate subzone along the Arctic bioclimate gradient that could be used to help interpret remote-sensing spectral data of the region;

2. examine the interactions between zonal climate, permafrost, vegetation and soils along a the bioclimate gradient; and

3. compare this transect to a similar transect in North America. The permafrost on the Yamal Peninsula is exceptionally sensitive to erosion by landslides.

Vegetation protects to varying degrees the permafrost from a warming climate and anthropogenic factors; so a primary interest was the relationship between summer temperature, aboveground biomass, active-layer thickness, vegetation composition, biomass, and soil texture. Here we present a synthesis of the vegetation information relevant to permafrost and remote-sensing studies along the EAT.

Plot samples were collected from Nadym (14 plots), Laborovaya (10 plots), Vaskiny Dachi (15 plots), Kharasavey (10 plots), Ostrov Belyy (20 plots) and Krenkel (10 plots). All locations had representative sites on zonal loamy soils and sandy soils except Nadym, where no loamy sites were sampled. All relevés were sampled according to Braun-Blanquet methodology. We also measured the active-layer thickness, height of the vegetation and numerous plant-canopy structure and spectral properties, including phytomass (by plant functional type), leaf-area index (LAI), and the normalized difference vegetation index (NDVI using a hand-held spectrometer). Soil pits were described and soil chemical and physical properties were analyzed in the top mineral horizon of each plot.

A detrended correspondence analysis ordination of the plots graphically displays their floristic similarity each other (Fig. 1). The plots are clearly separated along a complex latitude/summer-temperature/biomass gradient. The subzone A plots were most distant from the others, which reflects this locations isolation both geographically and floristically from the rest of the plots. Plots on the main part of the Yamal Peninsula (subzones E, D, C, and B), were less clearly separated along the latitude/temperature gradient. Within each cluster of plots in the same subzone (plots with the same color in Figure 1), there is clear floristic separation of plots according to soil texture (circles vs. squares). The strongest separation along the soil texture gradient occurs in subzone B and D, which also had the strongest textural differentiation of the soils. The weakest separation of loamy vs. sandy soils is in subzone A, where all soils are classed as either loamy sands or sands. In general the sandy plots within each subzone location are more

clearly separated along the temperature gradient than the loamy sites in the same subzones.

Active-layer thickness values are generally greater with warmer summer temperatures along the latitude gradient, but are generally thinner in cooler soils associated with the thicker vegetation carpets that occur on the more loamy soils. These trends are also reflected in the remote sensing data. Areas with higher biomass, associated with the warmer and more loamy soils also have higher LAI and NDVI values.

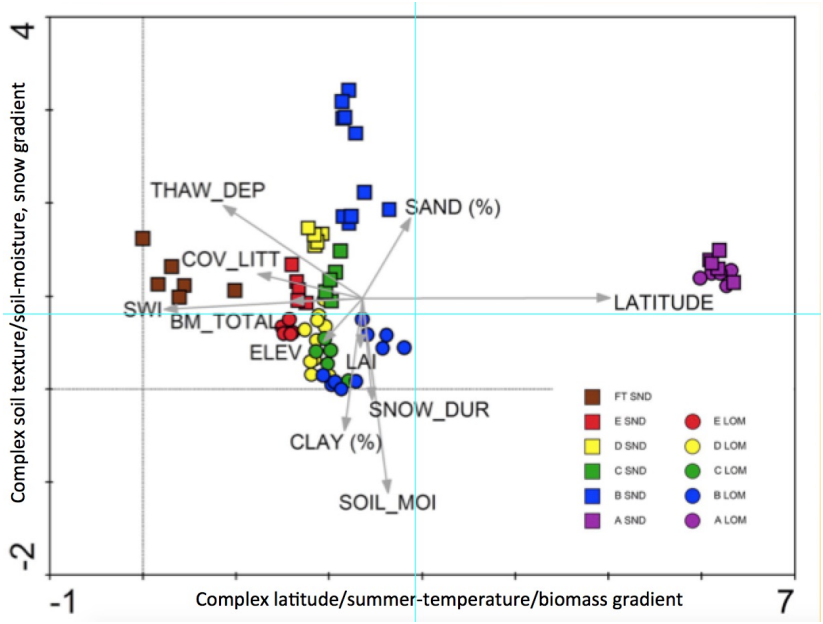

Figure 1: Detrended correspondence analysis ordination of 76 vegetation plots along the Eurasia Arctic Transect. Colors of the points represent Arctic bioclimate subzones according the Circumpolar Arctic Vegetation Map (subzone A = purple; B = blue; C = green; D = yellow; E = red) and the forest-tundra transition (FT, brown). Plots on sandy soils have square symbols, and those on loamy soils have circle symbols. Outlier plots (all wet plots) with no similarity to the others have been removed. Plots are positioned within the ordination space according to their floristic similarity, using Sorenson coefficient of similarity. The numeric units along the vertical and horizontal axis are sd units, where four sd units represent a complete turnover in species composition. The cluster of arrows in the central part of the diagram shows direction and strength of correlations for environmental and growth form variables. The labels on the horizontal and vertical axes indicate the complex of variables most closely associated with the axes of the diagram.

References

Leibman, M.O.; Epstein, H.E.; Khomutov, A.V.; Moskalenko, N.G. and Walker, D. A. [2008]: Relation of active layer depth to vegetation on the central Yamal Peninsula, Russia. In: Kane, D.L. and Hinkel, K.M.(eds.), *Proceedings of the Ninth International Conference on Permafrost*, Institute of Northern Engineering, University of Alaska Fairbanks, Fairbanks, USA, 29 June–3 July 2008, volume: Extended Abstracts, pages 177–178. URL http://ipa.arcticportal.org/publications/conference-proceedings.

Walker, D.A.; Epstein, H.E.; Raynolds, M.K.; Kuss, P.; Kopecky, M.A.; Frost, G.V.; Daniëls, F.J.A.; Leibman, M.O.; Moskalenko, N.G.; Matyshak, G.V.; Khitun, O.V.; Khomutov, A.V.; Forbes, B.C.; Bhatt, U.S.; Kade, A.N.; Vonlanthen, C.M. and Tichý, L. [2012]: Environment, vegetation and greenness (NDVI) along the North America and Eurasia Arctic transects. *Environmental Research Letters*, 7(1):015504, doi:10.1088/1748-9326/7/1/015504.

Walker, D.A.; Epstein, H.E.; Frost, G.V.; Chasníková, S.; Šibík, J.; Khitun, O.; Ermokhina, K.; Forbes, B.C.; Kaärlejarvi, ; Kuss, J.P.; Leibman, M.O.; Matyshak, G.; Moskalenko, N. and Orekhov, P. [2016 in prep.]: Zonal vegetation along the Eurasia Arctic Transect (Yamal Peninsula and Franz Josef Land, Russia): The effects climate, soil texture, and vegetation on active layer thickness, NDVI and LAI. *Phytocoenologia*.

Study on the method of building extraction based on the PolSAR images in permafrost regions

Wansheng Pei, Mingyi Zhang, Yuanming Lai, Shuangyang Li, Wei Zhai, & Xiyin Zhang

Cold and Arid Regions Environmental and Engineering Research Institute, Chinese Academy of Sciences, People's Republic of China

Synthetic Aperture Radar is an active remote sensing system working in the microwave spectrum. With the rapid development of synthetic aperture radar (SAR) system, numerous high resolution, multi-band and polarimetric SAR (PolSAR) data can be obtained. Those data could be widely employed in many fields, such as urban planning, land use investigation, hazards and risks assessment, and so on. SAR has become one of the significant methods of the earth observation and remote sensing. The building detection and outline extraction in permafrost regions is a key issue in cold regions engineering. Full PolSAR image contains not only the typical polarimetric features but also rich texture features of buildings, which seems to be more accurate for building detection and outline extraction. However, numerous details within the PolSAR image could cause the instability of building detection and extraction as well. Considering the abroad topography and sparse vegetation in permafrost regions, especially for the Tibet Plateau, the H/α/A-Wishart classification method is proposed to improve the accuracy and stability of building extraction in permafrost regions. The process of building extraction in permafrost regions mainly includes the following steps:

1. Extracting the H-α-A polarimetric features from the PolSAR imgae;
2. The Wishart unsupervised classification of the preprocessed data is carried out;
3. Based on the minimum dissimilarity, the classes are merged by the agglomerative hierarchincal clustering method;
4. The buildings are extracted from the merged classification results.

Based on the H/α/A-Wishart classification method, one PolSAR image (299×251) of Tibetan Autonomous Prefecture of Yushu, Qinghai Province in China, located in the hinterland of Tibet Plateau, was selected as experiment to validate the effectiveness of the building extraction algorithm in the paper. A reference image of the studied area from Google Earth, which has been registered with the PolSAR data, was taken to estimate the extraction accuracy. The overall accuracy could was nearly 82 %, the misclassification error for buildings was 19 %. This results show that the H/α/A-Wishart classification method based on the full PolSAR image is effective for building extraction in permafrost regions. In addition, the other PolSAR image of Xining, situated in the eastern of Qinghai Province in China, was taken as contrast experiment with the same method. However, the overall building extraction accuracy only reached 69 % and the misclassification error for buildings could reach 39.1 %. This difference reflects that the H/α/A-Wishart classification method based on PolSAR image could be effectively applied to the permafrost regions with abroad topography and sparse vegetation. However, for areas with variety kinds of constructions and diverse vegetation, this method has low accuracy for building extraction. The aim of the paper is to study method for building extraction in permafrost regions, especially on the Tibetan Plateau. Effective method is significant not only for the study of permafrost engineering hazards assessment, such as earthquake and land slip, but also for the planning of proposed engineering project.

Using a mix-methods approach to monitor thermokarst activity in the Eureka Sound Lowlands, Ellesmere Island, Nunavut

Melissa K. Ward & Wayne H. Pollard

McGill University, Canada

The Eureka Sound Lowlands are in an area underlain by approximately 600 m of ice-rich permafrost largely composed of massive ground ice and ice wedge polygons with a thin active layer of a mean thickness of 57 cm [Couture and Pollard, 2007]. The region has a polar desert climate, with a mean annual air temperature of -19 °C and approximately 67 mm of annual precipitation (falling mostly as snow). The Eureka Weather Station operated by Environment Canada (located at 79°59' N, 85°56' W) has been conducting daily meteorological measurements since it was founded in 1947. The area is sensitive to increasing summer temperatures as observed during 2012: as one of the warmest summers on record, there was a three-fold increase in thermokarst with the accelerated collapse of ice wedge polygon troughs and widespread development of retrogressive thaw slumps [Pollard et al., 2015]. This study will track historical thermokarst activity within the area using air photos from 1959, 1974 and 1982 and satellite imagery (WorldView2) from 2009 and 2012. Thermokarst activity between 2013 and 2015 has been monitored in the field using a differential GPS (Global Positioning System) to survey headwall locations of retrogressive thaw slumps. Using historical climate records, historic active layer thaw depths will be estimated using model simulations to determine historical active layer thermal regimes. The purpose of this study is to provide a detailed baseline of landscape processes to compare future landscape changes resulting from thermokarst in the area.

References

Couture, N.J. and Pollard, W.H. [2007]: Modelling geomorphic response to climatic change. *Climatic Change*, 85(3):407–431, doi:10.1007/s10584-007-9309-5.

Pollard, W.; Ward, M. and Becker, M. [2015]: The eureka sound lowlands: an ice-rich permafrost landscape in transition. In *68th Canadian Geotechnical Conference and 7th Canadian Conference on Permafrost - GEOQuébec 2015*, Québec, Canada, September 20-23, 2015.

Thermokarst-induced landscape change in the Yukon Kuskokwim (YK) Delta, Alaska

Matthew A. Whitley[1], Gerald V. Frost[2], Chris V. Maio[1], & M. T. Jorgenson[2]

[1] *University of Alaska Fairbanks, United States of America*
[2] *ABR, Inc.*

The YK Delta of Alaska is a dynamic region where permafrost and coastal processes drive the majority of landscape change. The YK Delta has relatively warm permafrost that is fragile to disturbance from storm surges and rising air temperatures [Terenzi et al., 2014]. While most of the YK is low and wet, ground ice raises the land surface in some areas, creating 'permafrost plateaus'. These plateaus have better drainage and are elevated above the level of saltwater influence; they support characteristic vegetation and soil conditions classified as a Lowland Moist Graminoid-Shrub Meadow ecotype (LMGSM) [Jorgenson and Ely, 2001]. Large storm surges in the region are known to drive up to 40 km inland due to the low elevation profile of the region [Terenzi et al., 2014]. These periodic surges set off thermokarst around the perimeters of permafrost plateaus, and the sea water kills salt-intolerant vegetation. With the decrease of fall sea ice in the Bering sea, and general eustatic sea-level rise, these storm surges are expected to increase in frequency and severity [Jones et al., 2009]. Thermokarst-induced slumping of the LMGSM reduces the vegetation's elevation, and exposes it to future flooding. This study utilizes satellite and aerial photography, as well as high resolution LiDAR digital elevation models of the region to map local scale changes in permafrost plateau extents from 1955 to the present. Aerial photography from 1955 and 1988, as well as Ikonos and World View 2 satellite composites from 2007/2008 and 2015 were used to programmatically map plateau extents and calculate rates of thermokarst. Comparison of historical and modern imagery show permafrost plateau retreat of 8-10 m in some areas over the course of 53 years. Future field work during the summer of 2016 in the area will supplement remote sensing analysis. Little prior work was been done mapping permafrost plateaus in the region, and results will contribute towards a better understanding of thermokarst in the region. The YK Delta is a dynamic landscape important to many migratory bird species, and is home to one of the largest indigenous human populations in the circumpolar arctic. Thermokarst rates in the region are expected to increase in the future, and should be monitored closely.

References

Jones, B.M.; Arp, C.D.; Jorgenson, M.T.; Hinkel, K.M.; Schmutz, J.A. and Flint, P.L. [2009]: Increase in the rate and uniformity of coastline erosion in Arctic Alaska. *Geophysical Research Letters*, 36 (3):L03503, doi:10.1029/2008GL036205.

Jorgenson, T. and Ely, C. [2001]: Topography and flooding of coastal ecosystems on the Yukon-Kuskokwim Delta, Alaska: implications for sea-level rise. *Journal of Coastal Research*, 17(1): 124–136, URL http://www.jstor.org/stable/4300157.

Terenzi, J.; Jorgenson, M.T. and Ely, C. [2014]: Storm-Surge Flooding on the Yukon-Kuskokwim Delta, Alaska. *Arctic*, 67(3), doi:10.14430/arctic4403.

Combining remote sensing and field studies for assessment of landform dynamics and permafrost state on Yamal

Barbara Widhalm[1,2], Annett Bartsch[1,2], Marina Leibman[3], Yury Dvornikov[3], & Birgit Heim[4]

[1] *ZAMG, Austria*
[2] *Austrian Polar Research Institute*
[3] *Earth Cryosphere Institute, Russian Academy of Sciences*
[4] *Alfred Wegener Institute, Germany*

The Yamal peninsula, northwestern Siberia, is a landscape in transition. Permafrost conditions are expected to change within this century due to climate warming. Human activities have increased in Western Siberia during recent decades due to gas and oil exploration.

Permafrost is a subsurface phenomenon which cannot be measured directly with remote sensing data. However, many parameters which influence the ground thermal regime and surface indicators can be captured with satellite data. Land surface dynamics including e.g. landslides and wetlands and their relation to the underlying permafrost are investigated within the COLD Yamal project which is an Austrian-Russian joint research project funded by the Austrian Science Fund and the Russian Foundation for Basic Research. The Earth Cryosphere Institute has been involved in longterm permafrost monitoring in this region for more than 25 years and has established a comprehensive geospatial database. Modern remote sensing technologies, specifically microwave remote sensing, are used to further develop monitoring schemes in this region.

Past investigations of this region with C-Band SAR have shown strong seasonal dynamics. Wetland dynamics were captured at 150 m resolution. More subtle changes and more detail can be captured with TerraSAR-X and ALOS PALSAR data. The advantages and disadvantages of different frequencies with respect to spatial resolution are discussed. The shorter wavelengths such as X-band provide information similar to conventional analyses with optical data. Longer wavelengths reveal additional detail. These differences have an impact on the quantification of longterm trends along with the seasonality which is so far unaccounted.

As a result of TerraSAR-X and ALOS Palsar data analysis geographical information system layers are created representing the expansion of high productive shrubs on the key area and time series of water body extents. These layers were used as a source for the developed geodatabase as well as for the further statistical analysis which aimed to understand the ongoing landscape processes in the “thermokarst lake – catchment” systems.

Mapping landscape level changes in plant communities and impacts on permafrost dynamics in Siberia

Qin Yu, Ryan Engstrom, Nikolay Shiklomanov, & Dmitry Streletskiy

George Washington University, United States of America

Arctic vegetation communities are changing across the Arctic due to amplified climate warming. Evidence of vegetation changes are generally reported either at the plot-scale through field survey [Elmendorf et al., 2012] or at the continental scale through coarse remote sensing mapping. However, little is known about the extent of plant community changes at the landscape scale (that is intrinsically correlated to permafrost dynamics due to a lack of applicable mapping methodologies that can estimate regional shifts in plant communities with high accuracy and efficiency. One recent study at this scale utilized pairs of very early satellite era remote sensing imagery and modern high spatial resolution imagery to quantify tall shrub and tree expansion in Russian Arctic since the 1960s across a number of scenes [Frost and Epstein, 2014]. While this is an accurate methodology, the techniques used are very labor-intensive and difficult to replicate over numerous scenes and large areas across heterogeneous Arctic landscape.

In this study, we aim to quantify the extent of plant community changes at the landscape level from the 1960s to today utilizing a consistent and efficient semi-automated contextual spatial feature based classification system on pairs of high spatial resolution satellite imagery. These changes will be used to assess the impacts of landscape scale, plant community changes to permafrost dynamics. Spatial features are image metrics that examine multiple groups of pixels at once to quantify the geometry, orientation, patterns, and spatial variability of objects within an image [Engstrom et al., 2015]. We selected a region with paired imagery (panchromatic high spatial resolution images) from 1960s and modern, multi-spectral commercial high spatial resolution imagery and ran spatial features on these images to test the applicability of this methodology. These spatial features are designed to be run on panchromatic imagery and include a rotation invariant Grey-Level Co-occurrence Matrix (GLCM) contrast texture, a Histogram of Oriented Gradients (HoG) feature that captures the distribution of structure orientations, Line Support Regions (LSR) which characterize lines and their orientation, Local Binary Patterns (LBP) a texture algorithm that examines pixel relationships around a center pixel, Hough transform which examines curves based on a set of given edge points by exploiting point/line duality, Fourier transform which examines the edges in the 2d frequency domain, and the local mean of each of the original band(s). We classified both images and quantified the changes in the extent of plant communities. For tall shrubs in particular, which impact permafrost temperature in summer by shading the soil and in winter by insulating the soil with trapped snow, our classification results matches 99.3 % of the classification in Frost et al. [2014]. When compared to classification based on Corona scene which currently seems to underestimate the tall shrub extent when compared to Frost et al. [2014], the preliminary results indicate that tall shrub has increased 17 % from 1968 to 2006 within the study area (Fig. 1).

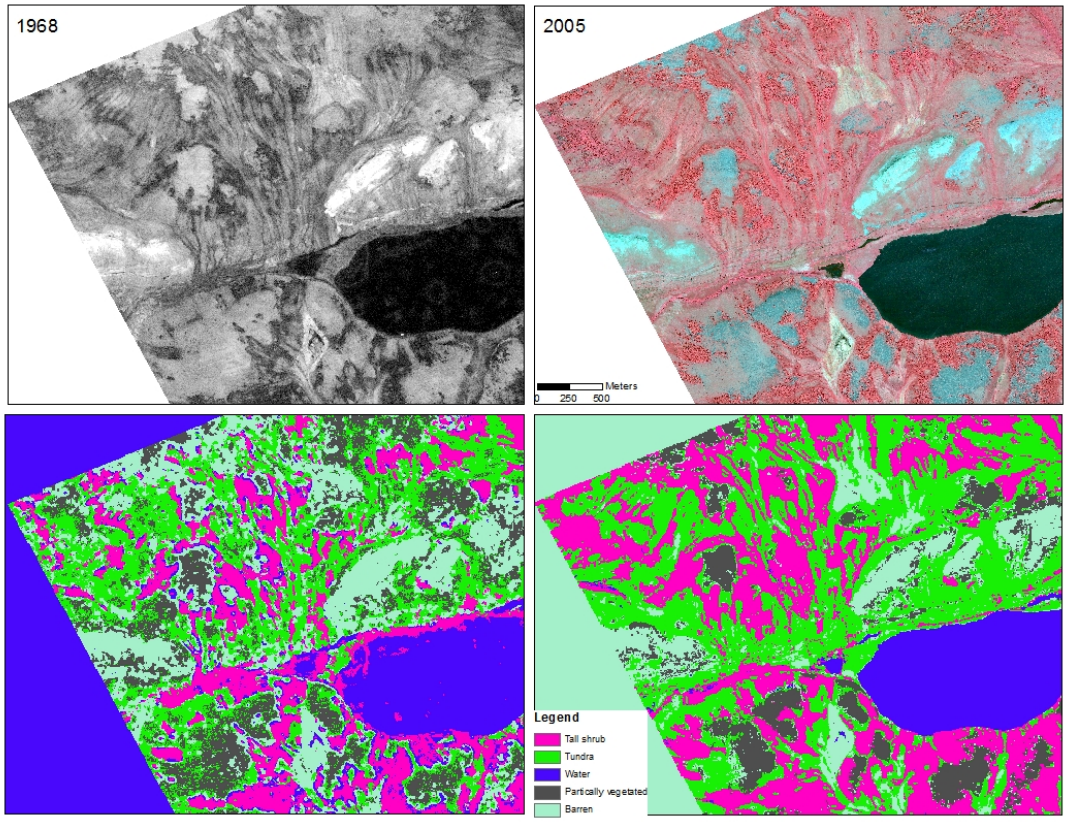

Figure 1: semi-automated remote sensing classification of high spatial resolution imagery based on spatial features.

References

Elmendorf, S.C.; Henry, G.H.R.; Hollister, R.D.; Björk, R.G.; Boulanger-Lapointe, N.; Cooper, E.J.; Cornelissen, J.H.C.; Day, T.A.; Dorrepaal, E.; Elumeeva, T.G.; Gill, M.; Gould, W.A.; Harte, J.; Hik, D.S.; Hofgaard, A.; Johnson, D.R.; Johnstone, J.F.; Jónsdóttir, I.S.; Jorgenson, J.C.; Klanderud, K.; Klein, J.A.; Koh, S.; Kudo, G.; Lara, M.; Lévesque, E.; Magnússon, B.; May, J.L.; Mercado-Díaz, J.A.; Michelsen, A.; Molau, U.; Myers-Smith, I.H.; Oberbauer, S.F.; Onipchenko, V.G.; Rixen, C.; Martin Schmidt, N.; Shaver, G.R.; Spasojevic, M.J.; Pórhallsdóttir, P.E.; Tolvanen, A.; Troxler, T.; Tweedie, C.E.; Villareal, S.; Wahren, C.-H.; Walker, X.; Webber, P.J.; Welker, J.M. and Wipf, S. [2012]: Plot-scale evidence of tundra vegetation change and links to recent summer warming. *Nature Climate Change*, 2(6):453–457, doi:10.1038/nclimate1465.

Engstrom, R.; Sandborn, A.; Yu, Q.; Burgdorfer, J.; Stow, D.; Weeks, J. and Graesser, J. [2015]: Mapping slums using spatial features in Accra, Ghana. doi:10.1109/JURSE.2015.7120494.

Frost, G.V. and Epstein, H.E. [2014]: Tall shrub and tree expansion in Siberian tundra ecotones since the 1960s. *Global Change Biology*, 20(4):1264–1277, doi:10.1111/gcb.12406.

Frost, G.V.; Epstein, H.E. and Walker, D.A. [2014]: Regional and landscape-scale variability of Landsat-observed vegetation dynamics in northwest Siberian tundra. *Environmental Research Letters*, 9(2): 025004, doi:10.1088/1748-9326/9/2/025004.

SESSION 22

Ground Based and Airborne Geophysical Applications in Permafrost

Convener:

Thomas A. Douglas, *U.S. Army Cold Regions Research and Engineering Laboratory, USA*

Paul Overduin, *Alfred Wegener Institute Helmholtz Centre for Polar and Marine Research, Germany*

Julia Stanilovskaya, *R &D, Total E&P Russie, Russia*

Airborne, water-borne and ground-based geophysical techniques, both electromagnetic and seismic, have been successfully used to detect permafrost and track permafrost-related processes. These measurements have shown great promise in investigating coastal erosion, thermokarst processes, and landscape change. Geophysical techniques so been used for facility life cycle assessments (from design to operation) to detect anomalies in permafrost and subsurface morphology. These methods, and their applications to permafrost terrains, have undergone significant recent developments. Since each technique has its strengths and limitations some methods are more suited for particular applications than others. Ground-truthing measurements of geophysical methods have also been expanded. These include surveys of elevation, soil composition, seasonal thaw depth, and terrain geomorphologic features. Boreholes and shallow cores provide critical information on cryostructure, ice content, soil composition, and mineralogy but they are expensive, time consuming, and are not feasible in remote locations or on unstable terrain. The goal of this session is to bring together field and airborne based geophysicists, geomorphologists, and remote sensors to explore how and where these broad interrogative tools can be used across heterogeneous permafrost environments. We also hope to foster exchange on the uses and new developments of these tools. Studies focused on developing airborne or satellite based geophysical techniques are encouraged as are studies that investigate the strengths and limitations of different techniques and simultaneous inversion methods. Our focus is on all permafrost types and localities in the Arctic and Antarctic including the discontinuous and continuous zones, coastal regions, and alpine permafrost.

Subsurface imaging with 3D ground-penetrating radar (GPR) in a permafrost landscape, Svalbard

Niklas Allroggen[1], Björn Heincke[2], Walter Wheeler[3]

[1] *Universität Potsdam, Institut für Erd- und Umweltwissenschaften, Germany*
[2] *Geological Survey of Denmark and Greenland, Department of Petrology and Economic Geology, Denmark*
[3] *Uni Research CIPR, Norway*

Ground-penetrating radar (GPR) is an established tool for the characterization the shallow subsurface. In electrically highly resistive materials, GPR is considered the geophysical technique providing the highest spatial resolution. As frozen soils typically show high electric resistivity, GPR is often applied to permafrost characterization. 2D GPR profiling has been deployed for permafrost studies such as salt-water intrusions, active layer depth, and imaging of ice wedges and polygons. However, elements of the permafrost, including the above, can include complex three dimensional structures, in which case the interpretation of 2D GPR surveys is misleading. In such settings, 3D GPR data acquisition and processing, can provide more-detailed and accurate information on the shape, structure and material properties of subsurface features.

In 2007 and 2008, we performed 2D and 3D GPR surveys on the Wordiekammen plateau in northern Billefjorden on Spitsbergen. The ≈500 m high, ≈3 km^2 plateau is composed of over 100 m thick layered, and gently-dipping regionally-extensive Carboniferous limestones. The plateau itself is covered by thick (>1 m) scree, but the bounding cliffs expose the layered limestones which are in places cut by tall pipe-like breccia bodies 20 to 100 m in width, some clearly reaching the plateau surface. In winter the scree was locally ice-filled and locally loose, whereas summer probing showed a ≈1 m thick typically well-drained active layer. The breccia pipes contain mostly unsorted limestone fragments (cm to meter size), with local layering indicating flow-related sorting or larger collapse events. The pipes typically have higher porosity and permeability than the surrounding host rock and consequently influence the local permafrost characteristics. The results of an electrical resistivity tomography survey support this interpretation by indicating lower (6 kΩm) resistivity values in brecciated areas compared to their surrounding (20 kΩm).

At the top of the plateau, numerous brecciated areas were identified using coarsely spaced (25 m) 2D GPR profiles, indicated by a change from layers to chaotic reflections. Cliff-side examples show the limestone surrounding the pipes to be heavily fractured and locally deformed, which complicates a detailed interpretation of the 2D GPR data. Two of the identified areas were studied in detail by 3D GPR using 50 MHz antennas attached to a pulseEKKO GPR acquisition unit. Precise mid-points for the 40 cm shot spacing were provided by post-processed local differential GPS and merged with the GPR data during the processing. After a 3D data processing, including a topographic migration scheme, our data (Fig. 1) reveal reflection events down to a depth of 30 to 40 m.

The base of the active layer is visible in the entire 3D data volume as a shallow reflection event at a depth of ≈1 to 2 m. It cuts the slightly dipping reflection events originating from the subsurface strata. The bodies of the breccia-pipes are identified by an interruption of the otherwise well layered and slightly dipping reflectors. Along selected reflectors, we apply a semi-automatic picking routine highlighting the main strata. The boundary between the host rock and breccia (pipe wall) is typically sub-vertical with local meter-scale vertical and horizontal roughness. The strata close to the pipes are locally offset by faults which we provisionally interpret as related to the collapse. The internal bodies of the breccia-pipes are characterized by mostly chaotic reflection patterns, which typically lack continuous reflections but locally show sparse, unconnected ≈5 to ≈10 m wide coherent events. In these areas an attribute-based interpretation promises to reveal additional information on the structures and processes inside the breccia pipe.

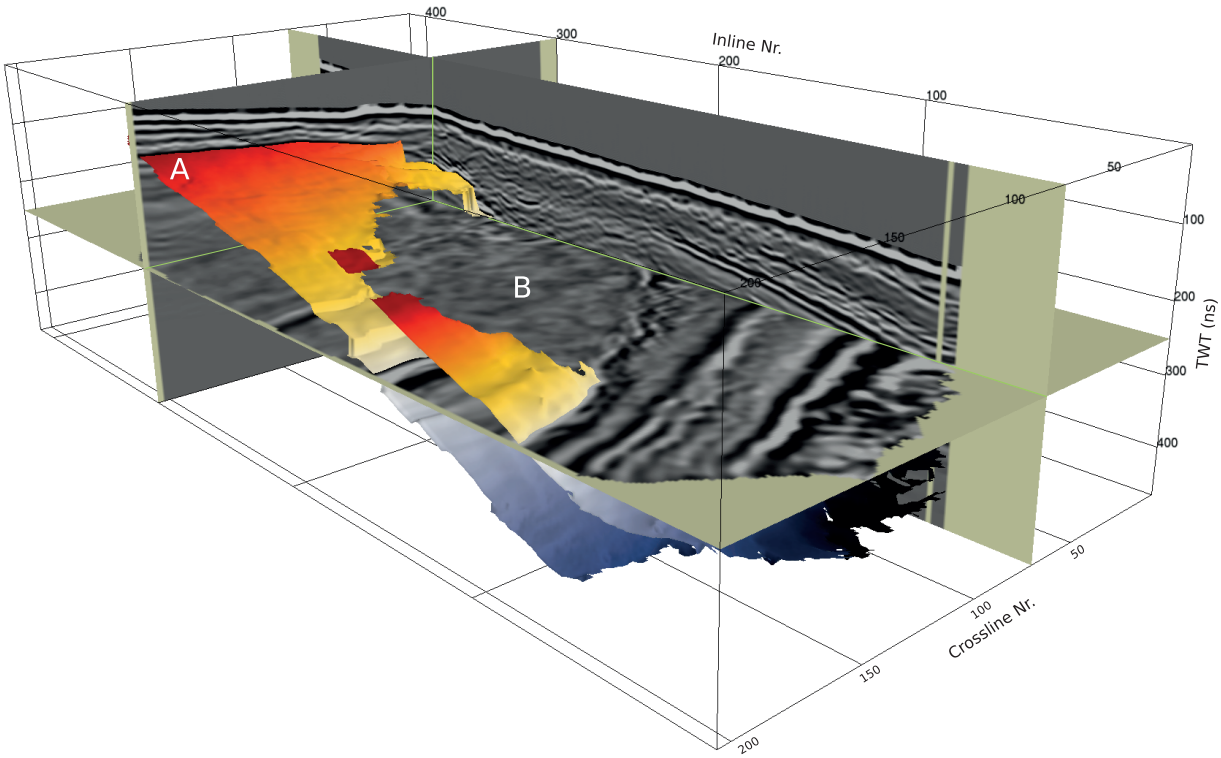

Figure 1: Oblique view of 3D GPR data cube and picked reflectors. The cube was collected where 2D profiles showed a local pipe-like breccia body. Colors corresponds to the depth of reflection events (A), which could not be traced in the brecciated area (B) due to t

In summary, our 3D analysis of the complex subsurface structure of a breccia-pipe provides a more detailed understanding of karst-related collapse structures, and provides a predictive basis for modelling permafrost morphology in such settings. Furthermore, this demonstrates the potential of 3D GPR for structural exploration of complex 3D subsurface targets, especially in permafrost environments.

Internal structure of a high arctic rock glacier based on quasi 3D electrical resistivity imaging and ground penetrating radar

Ivar Berthling[1], Alexander Bast[2,3], & Isabelle Gärtner-Roer[3]

[1] *Norwegian University of Science and Technology, Norway*
[2] *Swiss Federal Institute for Forest, Snow and Landscape Research WSL*
[3] *Department of Geography, University of Zürich*

The characterization of internal composition and structures of rock glaciers remain a difficult task, due to the costs and logistical challenges of coring and the often rough and dry surface conditions that inhibit survey speeds and ground coupling when using geophysical profiling methods.

To investigate the internal structure and dynamics of an arctic rock glacier we have attempted to obtain a quasi 3D image by using electrical resistivity tomography (ERT) in combination with ground penetrating radar (GPR) and Differential GNSS measurements. In addition, we distributed some temperature loggers to investigate the ground surface temperatures. The focus of the field work was on the performance of geophysical measurements. While two-dimensional soundings are the state-of-the art method in permafrost investigations, three-dimensional imaging is still in its opening stage within this field of investigation.

We chose the Brøggerbreen rock glacier (UTM33X E432600, N8761860) nearby Ny-Ålesund, Spitsbergen as our investigation site, due to earlier investigations [Berthling et al., 2000, Kääb et al., 2002]. The closeness of this rock glacier to the research facilities in Ny-Ålesund as well as its limited size and relative surface smoothness makes it ideal for the purpose. The Brøggerbreen rock glacier is lobe-shaped with a relatively simple surface geometry, lacking transverse furrows and ridges but with a marked reverse surface slope towards the front (Fig. 1a,b). On the southern side there is a very prominent lateral ridge that is partly mirrored on the northern side also (Fig. 1a). This causes longitudinal depressions to each side of the central part of the rock glacier that collects snow and act as traps for meltwater and subsurface runoff. A small pond is present in the northern depression Fig. 1c).

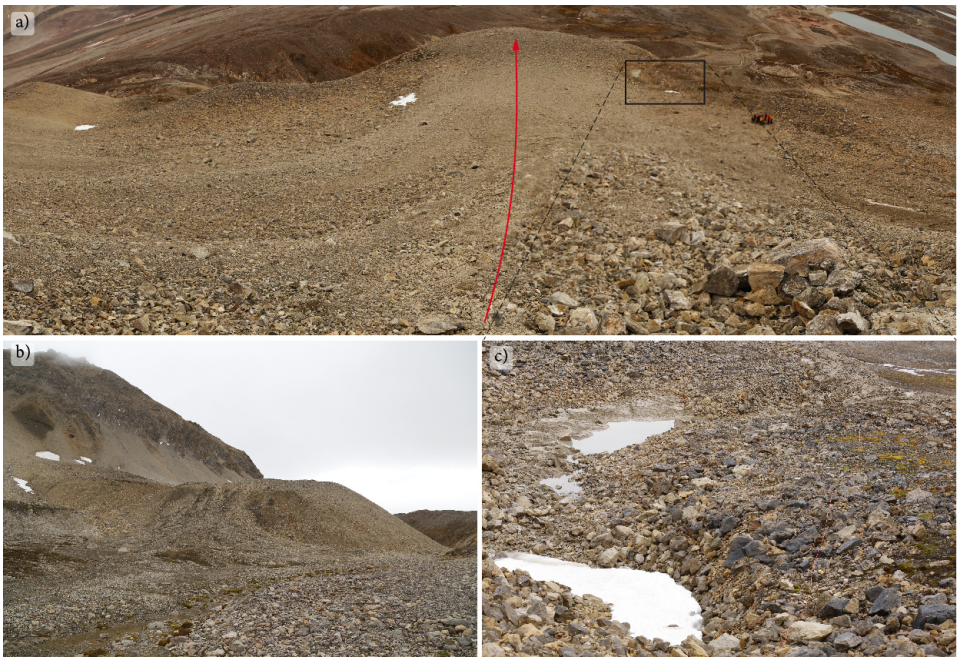

Figure 1: a) Overview of the rock glacier as seen from the talus slope, with central flow line (arrow), b) view from north, c) depression on northern side with pond

In total we performed 11 two-dimensional ERT surveys, each having a length of 200 m and an electrode spacing of 5 m. All ERT soundings were conducted with an ABEM Terrameter LS using the Schlumberger configuration since this array type is a reasonable compromise between acquisition time and resolution in periglacial environments. Each measured two-dimensional profile consists of 524 data points. Seven of the 11 ERT soundings were established parallel to an assumed rock glacier central flowline (x-direction, Fig. 1a). The distance between the survey lines is 10 m. Parallel to these ERT soundings in the center of the rock glacier, an additional profile was performed 35 m further northeast the marginal area of the rock glacier, outside the lateral ridge. The eight profiles along the x-direction expand from the talus slope from which the rock glacier originates, and to the top of the rock glaciers' frontal slope (to the lateral side of the front for the additional profile). Three perpendicular tie lines intersect the eight parallel profiles along the x-axes at 40 m, 120 m, and 200 m. Res2Dinv was used to invert the two-dimensional datasets and to check the quality of the resulting tomograms. Occurring bad data points were removed before the data were collated into a three-dimensional dataset. The robust inversion scheme of the Res3Dinv software was applied to create the quasi 3D subsurface image. Due to the grid design the center of the rock glacier shows the highest data density and hence, sensitivity.

The GPR profiles were measured along the same longitudinal profiles, but with 20 m profile distance, while the perpendicular profiles were measured for the central 100 meters only. We used a Malå GPR system, with 50 MHz antennae center frequency. Transmitter and receiver antennae were employed perpendicular to profile direction, with an antennae separation of 2 m, and a step size of 0.5 m achieved with the aid of non-metallic tapes that were rolled along the profile. Profiles where measured with DGNSS for terrain correction, and we also performed terrestrial laser scanning of the rock glacier and continued DGNSS measurements of surface displacements (going back to 1998) to be able to connect surface and subsurface characteristics.

References

Berthling, I.; Etzelmüller, B.; Isaksen, K. and Sollid, J. L. [2000]: Rock Glaciers on Prins Karls Forland. II: GPR Soundings and the Development of Internal Structures. *Permafrost and Periglacial Processes*, 11(4):357–369, doi:10.1002/1099-1530(200012)11:4<357::AID-PPP366>3.0.CO;2-6.

Kääb, A.; Isaksen, K.; Eiken, T. and Farbrot, H. [2002]: Geometry and dynamics of two lobe-shaped rock glaciers in the permafrost of Svalbard. *Norsk Geografisk Tidsskrift - Norwegian Journal of Geography*, 56(2):152–160, 2002. doi:10.1080/002919502760056486.

Ground penetrating radar detection of visible and "hidden" ice wedges in the Chara Depression (Eastern Siberia, Russia)

Svetlana Bricheva[1] & Julia Stanilovskaya[2]

[1]*Lomonosov Moscow State University, Faculty of Geology, Seismics and Geoacoustics Department, Moscow, Russian Federation*
[2]*Sergeev Institute of Environmental Geoscience of the Russian Academy of Sciences (IEG RAS), Moscow, Russian Federation*

There are several reasons why permafrost studies in large territories require special approaches. These studies often take place in hard conditions – in wetlands and in impassable areas like taiga with dense vegetation cover. Permafrost structure is very sensitive to various mechanical and thermal influences. Thus, methods of research in such conditions should be non-invasive, possibly remote, quick and effective. Geophysical research of frozen ground is sparing to environment and soils itself. Airborne research is a promising method, but the interpretation of images cannot give complete information about ground conditions of the study area. The complex of geological and geophysical works on the key sites should be carried out and further combined with images interpretation results. Such works allow extrapolating geophysical data from these specific sites to the nearest area and significantly increase the accuracy of satellite image interpretation.

A promising geophysical method in such conditions is ground penetrating radar (GPR). The high dielectric contrast between ice and water determines the possibility of identifying the boundaries between melt and frozen grounds on the GPR data (radargrams), as well as local objects such as ice wedges. The investigated medium can be represented as a layered model with constant electrical properties within a layer, and ice wedges – as the local objects within layers, with different properties.

The areas with clearly visible polygonal pattern ground are usually noted on satellite images. These polygonal grids indicate the frost cracking and ice wedge forming. The development stage estimation of ice wedges with different amounts of ground ice by satellite images can give only rough approximate results. Moreover, in the taiga zone there are relict deep buried ice wedges without visible polygonal grid. They are marked by fire places and not clearly marked in relief. Somewhere there are no indicators of ice wedges on the surface. At the same time on such sites there is ground ice visible in the river outcrops. Identification of such "hidden" ice wedges especially close to existing or prospective linear structures is an extremely important problem. We all know that the thawing of ice leads to disastrous consequences such as thermokarst.

The presence of ice in wedge may be determined by GPR. There are various features on the radargram that may be associated with ice [Arcone et al., 1982].

On the terrace of river Chara (Zabaykalsky Krai, Eastern Siberia, Russia) the staff of the IEG RAS (Sergeev Institute of Environmental Geoscience, Russian Academy of Sciences) have been studied syngenetic ice wedges for several years. Modern and relict ice wedges were observed in almost all parts of the Chara depression relief, though the most intensive growth occurs on the river terraces and floodplains [Vasil'chuk et al., 2010].

The results of experimental and methodic fieldwork carried out in Chara depression during expedition in August of 2015 are presented. The objectives of fieldwork were: the ice wedges depth determination; the evaluation of the shape and size of ice wedges and revealing ice wedges invisible on the surface. The research was carried out on non-disturbed areas and areas affected by anthropogenic influence (not paved roads, fire). We used GPR system ZONd-12e (Radar Systems Inc., Latvia); the central frequency of antenna was 300 MHz.

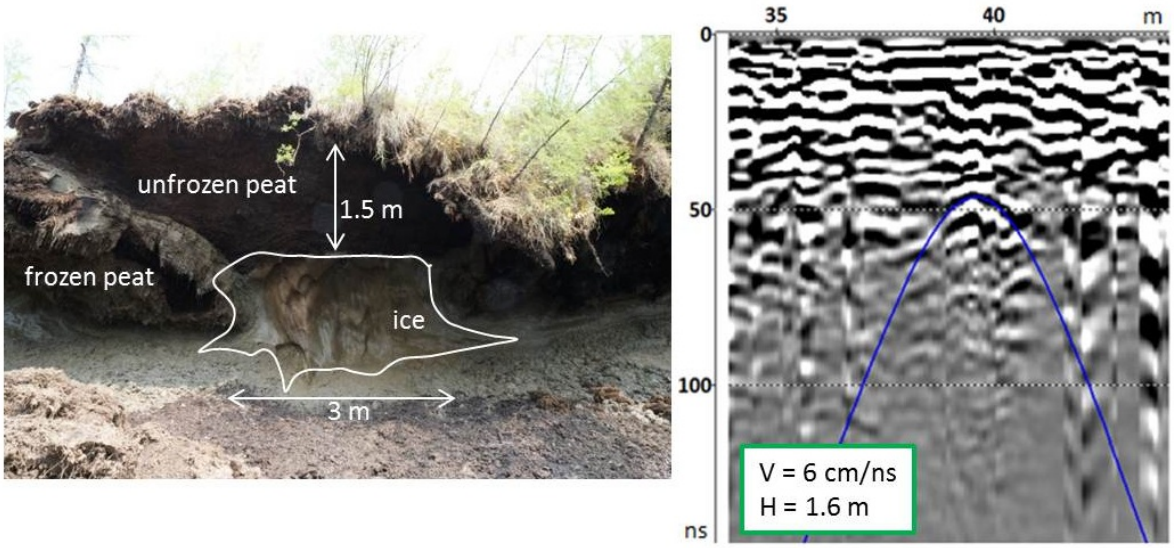

Figure 1: Ice wedge in Chara outcrop and GPR profile over it. The average velocity of the electromagnetic wave in a layer above the ice wedge and calculated depth to it are shown on the GPR profile.

Acknowledgements

The study was conducted using the funds of RFBR "My first grant" №14–05–31510.

References

Arcone, S.A.; Sellmann, P.V. and Delaney, A.J. [1982]: Radar detection of ice wedges in Alaska. CRREL Report, Hanover, N.H.: U.S. Army Corps of Engineers, Cold Regions Research & Engineering Laboratory, URL http://www.dtic.mil/cgi-bin/GetTRDoc?Location=U2&doc=GetTRDoc.pdf&AD=ADA124571. 82-43 pp.

Vasil'chuk, J.K.; Vasil'chuk, A.K. and Stanilovskaya, J.V. [2010]: Summer and winter air temperatures in the Northern Transbaikalia during the Holocene ice wedge formation. *Kriosfera Zemli (Earth's Cryosphere)*, 14(2):7–22, URL http://www.izdatgeo.ru/pdf/krio/2010-2/7.pdf. (in Russian).

Monitoring and quantifying soil processes and interaction with vegetation and landscape properties in Arctic tundra using above- and below-ground imaging

Baptiste Dafflon[1], Anh P. Tran[1], John Peterson[1], Rusen Oktem[2], Craig Ulrich[1], Haruko Wainwright[1], John B. Curtis[1], Margaret Torn[1], & Susan Hubbard[1]

[1] *Lawrence Berkeley National Laboratory, Berkeley (CA), USA*
[2] *University of California, Berkeley (CA), USA*

Quantifying surface and soil properties as well as their co-interactions at various spatial and temporal scales is crucial for terrestrial ecosystem understanding because near-surface soil hydrological, thermal and biogeochemical processes are generally influenced by both compartments. Also finding such co-interactions between sampled soil properties and remote sensing data is crucial to extrapolate soil characteristics at sufficiently high resolution over scales relevant for process-rich models that simulate feedbacks to a changing climate.

As part of the DOE Next-Generation Ecosystem Experiment (NGEE-Arctic), we are presenting advances in the characterization of complex Arctic ecosystems through

i) investigating the spatial distribution of soil properties and their linkages to landscape properties using point-scale, geophysical and low-altitude aerial imaging,

ii) novel autonomous aerial- and geophysical-based monitoring approaches that capture coincidently surface and subsurface dynamics in space and time, and

iii) both a data-driven statistical analysis as well as a novel coupled hydro-thermal-geophysical inverse modeling framework to investigate variability in key properties driving heat and water fluxes.

The investigation site is located in the Arctic tundra in Barrow, AK and covers a range of geomorphological conditions, including low- to high- centered polygons. Landscape characteristics are inferred from topographic and multi-spectral imaging measurements using either a kite-, pole- and tram- based platform at various temporal and spatial scales from continuous monitoring along a 35 m long transect to occasional campaigns along 500 × 40 m corridors. Surface properties are also monitored using a suite of above-ground measurements (e.g., precipitation, air temperature, wind speed, short-long wave radiation, canopy greenness). Soil properties are investigated using autonomous electrical resistivity tomography (ERT) and soil temperature/moisture sensors as well as soil core sample analysis and sporadic measurements of thaw and snow layer thickness.

The novel monitoring strategy enables us to image and quantify the freeze-thaw process in permafrost soil, and to identify spatiotemporal links between various soil and landscape properties (incl. vegetation, topography, thaw layer thickness, water content, temperature, electrical conductivity, and snow thickness). In particular, a strong relationship between changes in soil electrical conductivity, water content, thaw layer thickness and vegetation state exists, highlighting the covariance and time lag between permafrost thaw, soil moisture and vegetation growth as a function of geomorphology. Identifying such links is crucial to extrapolate strong knowledge from point-scale and core-based biogeochemical measurements at specific sites over larger scales and to improve parameterization of models simulating ecosystem feedbacks to climate. Furthermore, ERT shows to be particularly useful for spatiotemporal monitoring of changes in soil unfrozen water content, and when combined with soil core sample measurements to estimate soil properties (total water content, unfrozen water content and salinity) over larger spatial scales.

The novel coupled hydro-thermal-geophysical inverse modeling framework successfully simulates the land-surface energy balance and hydrological-thermal processes, as well as invert hydrological, thermal and geophysical data to estimate vertical profiles of thermal and hydraulic parameters that can be linked to mineral, organic, ice, water and air content. The results indicate that the inferred parameters can well

reproduce the spatiotemporal dynamics of the various datasets, and accurately predict the thaw layer thickness. In particular, results show the influence of the organic, mineral, air and water content on the freeze-thaw behavior, but also the role of the salinity, as well as the strong influence of surface properties affecting the energy balance. Finally, the hydrological and thermal dynamics are closely linked to the polygon types and polygon features.

Overall, this study effectively identifies spatiotemporal links between various soil and landscape properties and informs on the complementary nature of various ground- and aerial-based approaches and proxies to estimate soil properties at multiple spatial and temporal scales. The developed monitoring and inverse modeling strategy marks an important advance in understanding how complex, multi-compartment terrestrial ecosystems function and in providing estimates that can be used to initialize and parameterize models simulating ecosystem feedbacks to climate.

Geophysical surveying of the Dempster Highway, Yukon, Canada

Jane Dawson[1], Lekan Mitchell[2], & Jim Henderson[1]

[1] *DMT Geosciences, Canada*
[2] *Highways and Public Works, Government of Yukon*

Maintaining roads in the arctic is challenging (Kondratiev, 2010). Temperatures in Canada's north vary from -30 degrees Celsius in the winter up to 30 degrees Celsius in the summer and permafrost underlies most of the region. Civil engineers have long struggled with mitigating the effects of melting permafrost which occurs when the insulating layer is disturbed during construction of roads or buildings. With the increasing temperatures experienced in the north, road degradation is becoming even more severe as permafrost which had been stable, melts. Sinkholes created by melting of ice-rich permafrost, and subsequently failed drainage systems have become a major concern. The Dempster Highway is a 736 km year-round highway, beginning about 40 km east of Dawson City, Yukon on the Klondike Highway and ending in Inuvik, NT. The highway was constructed in the 1970's by advancing embankment fill over the natural organic cover of the land so as not to disturb the thermal stability of the permafrost during construction. However, despite efforts to minimize permafrost disturbance during construction, subsurface investigations have shown that the constructed highway embankment has altered permafrost conditions below and adjacent to the highway- usually within close proximity to drainage structures, streams and water bodies. Sinkhole development has been partially attributed to poor drainage along and through the highway, resulting in increases in convective processes leading to permafrost degradation as well as the subsurface erosion of thawing soils. In recent years, annual gravel surface restoration projects and culvert replacement projects have commanded increasingly larger portions of the highway operating and capital costs leading to more emphasis being placed on long term planning required to maintain the stability and safety of the highway.

The Yukon government has undertaken a number of surveys to assess the capability of geophysics to identify sinkholes and other hazards early in their development so as to mitigate damage. These projects have investigated a number of options: drones, ground resistivity, capacitively coupled resistivity (CCR), ground penetrating radar (GPR) and multichannel analysis of surface waves (MASW). Given the length of highway to be surveyed, a combination of CCR and GPR was identified as having high potential to identify potential problem areas efficiently.

In the summer of 2015, a geophysical survey was conducted to assess the condition of the permafrost beneath a section of the Dempster Highway, Yukon Territory (Km 35 to 36.5 and Km71.5 to km130). Ground Penetrating Radar (GPR) and CCR data were collected along one pass in both the north and southbound lanes of the areas of interest giving a total of 140km of data. From this data an additional seven targets were chosen to be investigated using Multichannel Analysis of Surface Waves (MASW). The region surveyed covered areas of discontinuous permafrost in the south and areas considered to be continuous permafrost in the north.

The CCR data showed great variability in resistivity along the Dempster Highway – from 30-ohm-m to in excess of 10,000 ohm-m. The resistivity data were interpreted to identify areas of potential higher ice content, active layer, and potential permafrost melt zones. An example of the data collected is shown in Figure 1. GPR overlain on the resistivity data provide further insight into the structures of the active layer and underlying permafrost. In the figure shown, GPR reflections show a regular pattern possibly related to ice-wedge polygons which have been observed in the area.

It has been shown by others [Hoekstra and Brabers, 1975, Angelopoulos et al., 2010] that resistivity is linked to temperature, ice content and composition. This makes interpretation challenging as there is overlap in the measured physical properties. Geotechnical drilling and temperature data have been used to compare the results of the geophysical survey with temperature gradients , ice content as well as sediment composition to gain insight into the best interpretation practices for surveys along linear transportation corridors.

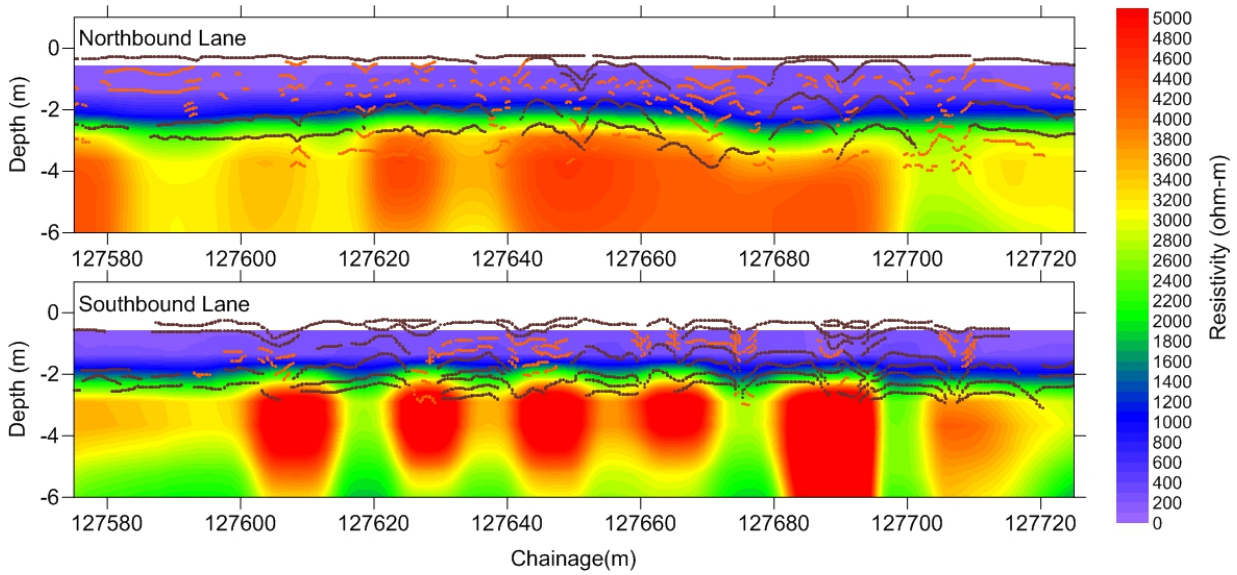

Figure 1: Example of CCR and GPR on the Dempster HIghway over possible ice-wedge polygons.

MASW surveys were conducted at 7 locations along the survey corridor to further investigate known areas of concern and anomalous areas identified from the combined CCR and GPR surveys. MASW results showed variations in stiffness which may indicate potential softening of the subsurface.

This work has shown that complementary geophysical surveys, such as those in this study are well suited to permafrost investigation. Techniques have been developed that may be used to monitor changes in the subsurface conditions of the highway and develop a better understanding of changing conditions so as to mitigate risk and decrease operating costs.

References

Angelopoulos, M.; Pollard, W.H. and Couture, N. [2010]: Integrated Geophysical Approach for the Detection and Assessment of Ground Ice at Parsons Lake, Northwest Territories . In *63rd Canadian Geotechnical Conference & 6th Canadian Permafrost Conference, GEO2010 in Calgary*, URL http://pubs.aina.ucalgary.ca/cpc/CPC6-1345.pdf.

Hoekstra, B. and Brabers, V.A.M. [1975]: Magnetocrystalline anisotropy and inversion degree of manganese-ferrous-ferrites. *Solid State Communications*, 17(3):249–253, doi:10.1016/0038-1098(75)90286-0.

Using electrical resistivity tomography, thermal and seasonal thaw depth measurements and airborne LiDAR to classify vegetation-geomorphology relationships in permafrost

Thomas A. Douglas[1], Christopher Hiemstra[1], Kevin Bjella[1], Stephen Newman[2], & John Anderson[3]

[1] *Cold Regions Research and Engineering Laboratory Alaska, USA*
[2] *Cold Regions Research and Engineering Laboratory New Hampshire, USA*
[3] *U.S. Army Geospatial Research Laboratory, Richmond, Virginia, USA*

Mean annual temperatures in interior Alaska, currently -1 °C, are projected to increase as much as 5 °C by 2100 [Chapman and Walsh, 2007]. Permafrost in the area is ice rich and carbon rich yedoma that is "ecosystem protected" against thaw by a cover of thick organic soils and mosses [Shur and Jorgenson, 2007]. The projected increase in mean annual temperatures is expected to degrade permafrost and alter hydrogeology, soils, vegetation, and microbial communities. Interactions between vegetation, permafrost ice content, and the snow pack and soil thermal regime are thus critical in maintaining permafrost in the area. We undertook this study to investigate how and where vegetation and soil surface characteristics can be used to identify subsurface permafrost composition. Of particular interest were potential relationships between permafrost ice content, the soils thermal regime, and vegetation. Our ultimate goal is to develop remote sensing and airborne sensors that can use vegetation spectral or physical measurements to assess permafrost extent and composition.

Our study was transect based and included a 400 m long transect through upland terrain above the CRREL Permafrost Tunnel in Fox, Alaska, a 500 m long transect in lowlands at the CRREL Farmer's Loop Permafrost Experimental Station, and a 500 m long the Creamer's Field migratory Refuge near Fairbanks. These sites represent a variety of ecotypes common in interior Alaska. There is evidence of ice wedge polygon structures at all of our sites (based on WorldView satellite and LiDAR analysis).

Airborne LiDAR imagery was collected from May 9-11, 2014 with a spatial resolution of 0.25 m. During the winters of 2013-2014 and 2014-2015 snow pack depths were made at roughly 1 m intervals along each transect using a snow depth datalogger coupled with a GPS. In late summer of 2014 and 2015 maximum seasonal thaw depths were determined at 4 m intervals along each transect. A Geoprobe 7822 Direct Push Technology track mounted drill rig was used to collect deeper (20 m) cores along the transects. Gravimetric ice content measurements and sediment identifications were made from these cores. Electrical resistance tomography measurements were made with an eight channel portable induced polarization galvanic earth resistivity meter. Permafrost resistivity values have been measured in the Fairbanks area in multiple studies. Resistivity values of 800 Ω-m are typically presumed to represent peramfrost [Douglas et al., in press].

The snow pack measurements show a clear relationship between vegetation cover and snow depth. Interception (and shallow snow depths) was evident in the birch and white spruce forests and where dense shrubs are present. The open tussock and intermittent shrub regions yield the greatest snow depths. Results from repeat seasonal thaw depth measurements also show a strong relationship with vegetation where mixed birch and spruce forest is associated with the deepest seasonal thaw. The tussock/shrub and spruce forest zones consistently exhibited the shallowest seasonal thaw. Roughly 60 % of the seasonal thaw along the transects occurred by mid-July and downward movement of the thaw front had mostly ceased by late August with little additional thaw between August 20 and early October.

All of our transects are underlain by permafrost across the entire transect but differences in ERT resistivity measurements were directly linked to changes in ice content which was, in turn, related to vegetation cover (Fig. 1). For example, at the Farmer's Loop transect the birch and white spruce forest and the black spruce forest are underlain by silts with minor peat and low ice contents of 30 to 100 g/g. These areas yielded ERT ρ values of 800 to 1,500 Ω-m.

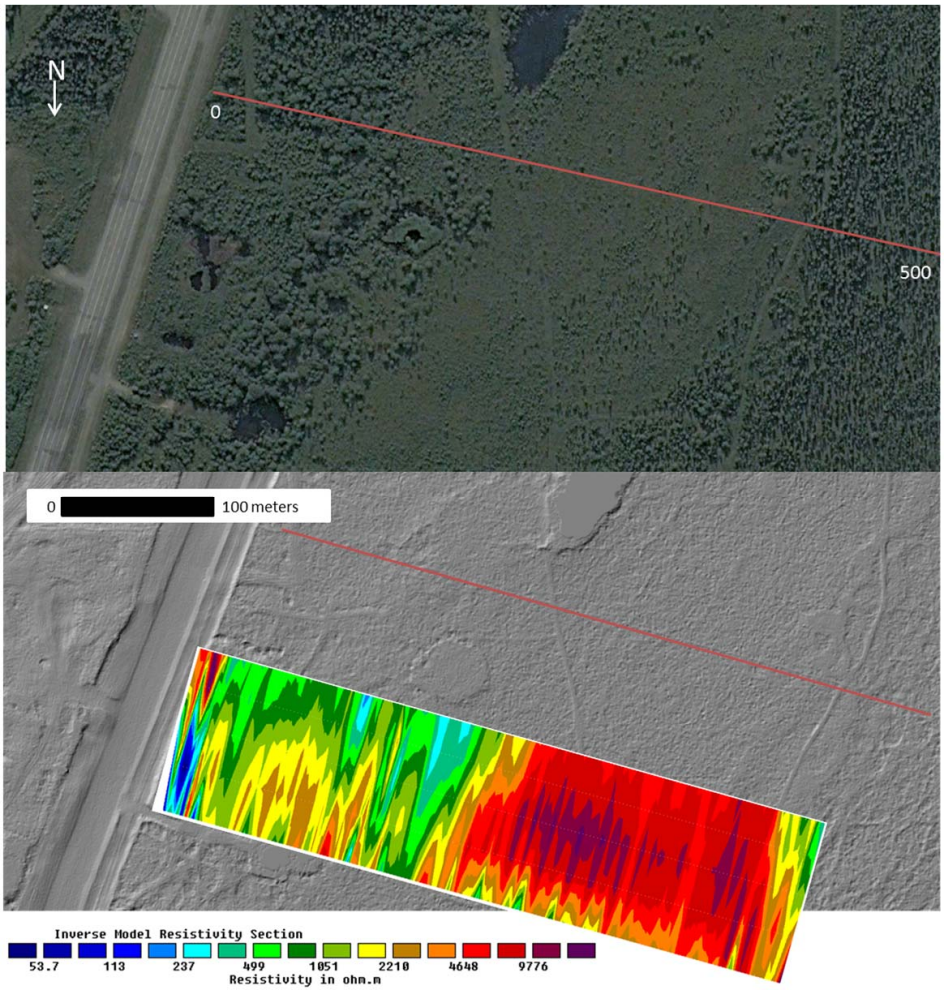

Figure 1: A Google Earth image (top) and airborne LiDAR and an electrical resistivity tomography cross section (bottom) from the Farmer's Loop site transect. The transect is 500 meters long.

There is a dramatic shift toward increased ρ values 210 m into the transect (>4,000 Ω-m) corresponding with the region of tussocks and shrub vegetation where ice rich peats are present in the subsurface.

Taken in total, the results from this study suggest there are clear relationships between the subsurface, surface, and aerial imagery measurements at our three field sites. These links between ecotype, permafrost composition, and seasonal thaw dynamics could be used to apply biophysical characteristics and standoff measurements like aerial imagery, hyperspectral measurements, and LiDAR, to ascertain the presence or absence of permafrost in similar terrains. Clearly a more broad set of measurements and applications must be made before being able to scale our measurements elsewhere but these initial results are promising. Our results also further confirm the application of ERT to map permafrost with clear relationships between frost probing, permafrost extent, and borehole cryostructural measurements.

References

Chapman, W.L. and Walsh, J.E. [2007]: Simulations of Arctic temperature and pressure by global coupled models. *Journal of Climate*, 20(4):609–632, doi:10.1175/JCLI4026.1.

Douglas, T.A.; Jorgenson, M.T.; Brown, D.R.N.; Campbell, S.W.; Hiemstra, C.A.; Saari, S.P.; Bjella, K. and Liljedahl, A.K. [in press]: Degrading permafrost mapped with electrical resistivity tomography, airborne imagery and lidar, and seasonal thaw measurements. *Geophysics*, in press.

Shur, Y.L. and Jorgenson, M.T. [2007]: Patterns of permafrost formation and degradation in relation to climate and ecosystems. *Permafrost and Periglacial Processes*, 18(1):7–19, doi:10.1002/ppp.582.

3D geoelectrical mapping of subarctic periglacial landforms

Adrian Emmert & Christof Kneisel

University of Wuerzburg, Germany

Alternating climatic conditions affect the formation or degradation of permafrost-related landforms. The magnitude of this response is determined by the sensitivity of the local subsurface conditions (e.g. subsurface layering, horizontal homogeneity of layers, varying ground ice content or frost table topography) which are key variables in the linkage between surface and subsurface processes. To enhance our understanding of the complex process system of landform development and their sensitivity to changing climatic conditions, a detailed knowledge of the internal structure of landforms is required, especially in areas of discontinuous or sporadic permafrost where subsurface conditions can show strong small-scale heterogeneities.

Electrical resistivity (ER) methods enable the detection of subsurface structures and are therefore commonly used in periglacial geomorphology. As an improvement of the conventionally used two-dimensional ER methods, the application of three-dimensional electrical resistivity imaging (ERI) approaches increased during the last years. These approaches not only enable a detection of the subsurface layering, but allow a multi-dimensional spatial mapping of underground conditions and hence to detect small-scale horizontal variations within the internal structure. Data can be collected either

i) by merging data points measured with parallel and/ or perpendicular 2D profile lines or

ii) by a rectangular-shaped electrode setup in the field.

While the first approach is suitable for surveying extensive areas, the second approach increases spatial data coverage by the measurement of diagonal quadripols.

In our contribution, we present results from multi-dimensional electrical resistivity imaging surveys which were performed on two periglacial landforms in central Iceland. To assure a high data coverage, all electrode setups were measured with different array types (Wenner-Schlumberger, Dipol-Dipol, Pole-Pole). At Orravatnsrústir palsa site (65.083°N, 18.535°W), one palsa (diameter c. 45m) was investigated with one 3D (approach ii) and one 2D survey. It shows a homogenous horizontal subsurface layering but strong contrasts in vertical resistivity distribution. The permafrost table is shaped rather even and could be detected in a depth of less than 1m. At the edge of the landform a probably unfrozen ring which is several meters broad indicates a degradation from the flanks. As a second landform, a field of patterned ground with small polygons (diameter c. 1 – 2 m) near Hofsjökull glacier (64.983°N, 18.850°W) was investigated intensively with three overlapping 3D surveys (approaches i and ii) and one 2D survey. The study area extends over 840m^2 and shows a heterogenic pattern of ground surface textures ranging from rather homogenous parts covered with fine-grained materials to parts which are covered with stones from a nearby lava flow. Polygons are visible in both kinds of surface cover, but not all over the study area. At the patterned ground site we observed strong variations in horizontal and in vertical direction. The depth of the permafrost table varies between 1m and 3m. A correlation between surface texture and resistivity distribution is obvious in horizontal direction.

Results show distinct interactions between surface and subsurface conditions and reflect the occurrence of small-scale heterogeneities in subarctic permafrost areas. The close relationship between surface and subsurface conditions indicates that the influence of lateral processes can be neglected for the presented small-scale investigations on the flat study sites. Nevertheless, it needs to be taken into account for the more extensive investigations. On a methodological view, our study shows the value and limitations of both 3D ERI approaches for resistivity mapping in two typical subarctic periglacial environments.

Evidence of subglacial permafrost revealed by an electromagnetic study on the Greenland ice sheet in Central West Greenland

Jon Engström[1], Timo Ruskeeniemi[1], Kimmo Korhonen[1], Heikki Vanhala[1], Jukka Lehtimäki[1], Anne Lehtinen[2], Lillemor C. Liljedahl[3], Jens-Ove Näslund[3], & Rickard Pettersson[4]

[1] *Geological Survey of Finland, Finland*
[2] *Posiva Oy, Finland*
[3] *Svensk Kärnbränslehantering AB, Sweden*
[4] *Uppsala University, Sweden*

The lateral and depth distribution of permafrost becomes an increasingly important factor when climate is changing resulting in a degrading permafrost that develop into a crucial environmental factor for the Arctic region. Permafrost has a major impact on the hydrology both at surface and in deep systems. The Greenland Analogue Project (GAP) has recently investigated hydrological, hydrogeological and geochemical processes during glacial conditions at continental-scale ice sheet in West Greenland [Harper et al., 2015]. A bedrock borehole drilled in bedrock at the ice margin in Kangerlussuaq area indicates 350 m thick permafrost at the edge of the ice sheet [Harper et al., 2015]. This raised the question whether there is subglacial permafrost far under the Greenland ice sheet. We applied a ground-based wide-band frequency-domain electromagnetic sounding system called SAMPO to investigate the question. The SAMPO sounding system was successfully used in Canada for permafrost investigations [Korhonen et al., 2009]. The electromagnetic properties of a rock differ depending on the thermal state of the water present in the rock pores and fractures. If the water is frozen or the rock is dry, the electrical resistivity is higher than in a wet rock. Thus, the key hypothesis we wanted to test was, whether a subglacial high-resistivity layer, indicative for frozen bedrock, exists underneath the Greenland ice sheet.

The electromagnetic SAMPO sounding system uses a transmitter loop to generate a magnetic primary field at 82 discrete frequencies between 2 Hz and 20 kHz. The primary field induces secondary magnetic fields in the subsurface conductors. The receiver coils are used to measure the radial, tangential and vertical components of the superposition of the primary and secondary magnetic fields (the total magnetic field) at a distance from the transmitter. For qualitative interpretation, the measured vertical-to-radial electromagnetic field component ratios are transformed into curves of apparent resistivity as a function of depth (ARD curves). The depth of investigation depends on the frequencies employed, on the electrical properties of the ground, and the distance between the receiver and transmitter. In favorable environments, the depth of investigation can be up to one kilometer or more. For modeling the data we used 1D layered earth inversion.

The area covered by the SAMPO soundings was 3×3 km^2 and the longest profiles (E–W orientation) extended about three kilometers inland from the ice sheet margin [Ruskeeniemi et al., 2016]. The reliability of the resistivity modeling of the EM measurements can be highly improved by site-specific information and in our case the ice thickness was measured with ground penetrating radar. The radar soundings showed that the range of ice thickness along the profiles was from 75 m in the west to up 350 m in the east. The EM modeling provided a consistent cryogenic structure for the sounding area. Four layers were distinguished from top to depth:

1. ice (high resistivity),
2. an unfrozen layer (low resistivity),
3. permafrost in bedrock (high resistivity), and
4. a low resistivity feature at depth.

The EM soundings show that subglacial permafrost is present at least 2 km east from the ice margin. This is too large spatial extent to be explained by lateral advance of proglacial permafrost underneath the ice sheet. Also, the ice thickness in the sounding area is large enough to ruling out the heat exchange at the atmosphere/ground boundary and consequently the

freezing of subglacial ground under present climate. Instead, it is likely that the subglacial permafrost originates from the cold period experienced 3400 – 2000 year BP and that it have been preserved until present in Central West Greenland.

References

Harper, J.; Hubbard, A.; Ruskeeniemi, T.; Claesson Liljedahl, L.; Lehtinen, A.; Bougamont, M.; Brown, J.; Dirkson, A.; Dow, C.; Doyle, S.; Drake, H.; Engström, J.; Fitzpatrick, A.; Follin, S.; Frape, S.; Graly, J.; Hansson, K.; Harrington, J.; Henkemans, E.; Humphrey, N.; Jansson, P.; Johnson, J.; Jones, G.; Kinnbom, P.; Klint, K.E.; Liimatainen, J.; Lindbäck, K.; Meierbachtol, T.; Pere, T.; Pettersson, R.; Tullborg, E.-L. and van As, D. [2015]: The Greenland Analogue Project: Data and Processes. SKB R-14-13, Svensk Kärnbränslehantering AB.

Korhonen, K.; Ruskeeniemi, T.; Paananen, M. and Lehtimäki, J. [2009]: Frequency domain electromagnetic soundings of Canadian deep permafrost. In *Proceedings of the Finnish National IPY Conference. Geophysica*, volume 45, pages 77–92.

Ruskeeniemi, T.; Engström, J.; Lehtimäki, J.; Vanhala, H.; Korhonen, K.; Lehtinen, A.; Claesson Liljedahl, L.; Pettersson, R. and Näslund, J.-O. [2016, in prep.]: Subglacial permafrost evidencing late–Holocene re-advance of the Greenland Ice Sheet over frozen ground at Kangerlussuaq, West Greenland. in prep.

Electrical resistivity tomography in Polar Regions, field data and high performance GPU-based 3D numerical modeling

Alexey Nikolaevich Fague, Denis Igorevich Fadeev, Igor Nikolaevich Yeltsov, Vladimir Arkadievich Kashirtsev, Dmitriy Evgenievich Ayunov, & Leonid Valerievich Tsibizov

IPGG SBRAS, Russian Federation

Electrical resistivity tomography (ERT) provides very accurate cross section at small depths: 1-40 meters, which is generally more than enough in Polar Regions. It is well known that active layer can reach only first meters and even deeper structures like taliks generally measure tens, rarely hundred of meters. Therefore, ERT is perfectly suited for Arctic surveys: high resolution allows for discovery of small subsurface features and relatively small equipment is very convenient because of transportation shortage.

Electrical resistivity tomography proved its usefulness for more than a hundred years now: 80+ years as a well-known Schlumberger vertical electrical sounding array (4 electrodes) and last 20-30 years as multiple electrode array (this is what we call ERT today). ERT is relatively light and compact in terms of equipment, adequately fast in terms of data acquisition speed and very good in terms of data informativity. By means or ERT it is possible to discriminate taliks from solid permafrost, determine preliminary sediments composition, roughly evaluate amount of ice in permafrost. All of the abovementioned can be accomplished in just few days. Therefore ERT could be quite useful for studies tied to permafrost degradation and related greenhouse gas efflux. However, there is a drawback: being a DC-based method, ERT is very sensitive to subsurface resistivity values. Extremely high resistivity (tens and hundreds kΩ-m) values result in very small incoming signal values, sometimes close to equipment sensitivity limits. Another problem is very high contrast: water saturated active layer in tundra sits alongside permafrost, which gives us resistivity difference values in the order of 3 to 6. In such conditions, even small surface features like puddles might dramatically affect long-line currents thus giving anomalies in interpreted data. To address this issue is especially important if we want to study active taliks by means of ERT. Many publications provide evidence based both on drilling and numerical modeling that active taliks under lakes and streams have quite predictable boundaries, usually not much exceeding its parent water line. In this situation, we have to place a part of our electrical survey line directly into the water, which, as mentioned previously, results in serious anomalies in interpreted data. These anomalies have to be separated from real data if possible. In worst-case scenario, it is important to decide if we are even able to see our object of interest through the noise raised by surface features.

Our proposed solution to the abovementioned problem is numerical modeling. It is a robust and time-honored way of verifying geophysical data. There is a drawback however: realistic description of a geological situation is only possible by means of three-dimensional (3D) setting. 3D solver requires substantial computational power: general size of a computational grid that provides physically correct simulation amounts hundreds of thousands (sometimes millions) nodes. The algorithm is highly parallel, thus it is possible to use cluster-based solutions to achieve comfortable modeling times. This, however, is not very convenient in terms of field operations. We decided to implement a 3D solver based on GPU-computing. This solution proved to be extremely fast comparing to CPU and allowed us to perform computations even on field notebooks. In this article, we would like to discuss the results of our field work during Lena delta expedition 2014 and 2015: acquired data, its interpretation and verification by means of 3D numerical modeling. We have managed to distinguish some geological features related to different types of permafrost and proved that ERT is a feasible method in Polar Regions if accompanied by solid verification instruments.

Geophysical investigation of aquifers in a degrading permafrost environment in Northern Quebec, Canada

Richard Fortier[1], David Banville[1], Jean-Michel Lemieux[1], Michel Ouellet[2], & René Therrien[1]

[1] *Centre d'études nordiques, Université Laval, Québec, Canada*
[2] *Ministère du développement durable, de l'environnement et de la lutte contre les changements climatiques, Québec, Canada*

A reliable and safe source of drinking water is a critical component of northern communities for their sustainable development. Among the fourteen Inuit communities in Northern Quebec, Canada, twelve municipalities rely on surface water to supply their inhabitants with drinking water while only two rely on groundwater in fractured bedrock [Lemieux et al., submitted]. Even if the rivers and lakes are abundant in Northern Quebec, they are vulnerable to contamination and drying up due to freezing in winter. Groundwater is recognized to be a more secure and sustainable source of water but, being stored as ice in permafrost or being in aquifers at depth with limited recharge due to low-permeability frozen ground above, its availability is somewhat limited in cold regions. However, as one of very few positive impacts of climate warming, the permafrost degradation can increase the availability of groundwater by releasing melt water in the ground and facilitating the recharge by surface water infiltration in permeable thawed layers [Lemieux et al., submitted].

In order to develop an expertise in cold regions hydrogeology, a small two square kilometre watershed located in the Tasiapik valley near the Inuit community of Umiujaq in Northern Quebec is currently studied (Fig. 1A). The objectives of this study are to monitor and assess the impacts of climate warming on permafrost and groundwater resource. The valley bottom is covered by a 30-m thick succession of glacial and marine sediments overlying the bedrock. Permafrost mounds are found in the frost-susceptible silty marine unit. A network of nine groundwater monitoring wells and three automated thermistor cables in seven sites not invaded by permafrost was installed in summer 2012 during a drilling campaign (Fig. 1B). This network is completed by several automated thermistor cables in the permafrost mounds, two meteorological stations including a pluvio-niveometer, and a gauging station at the watershed outlet (Fig. 1B). The numerical modelling of the coupled physical processes of groundwater flow and heat exchange for the assessment of the impacts of climate warming is a challenging task since a realistic 3D cryohydrogeological model is needed (Fig. 1B). To build this model, a geophysical investigation using induced polarization (IP) tomography was undertaken. The survey lines in the watershed are located in figure 1B. An example of electrical resistivity and chargeability models found from the inversion of IP tomography is given in figure 1C. An objective interpretation of these models based on a forward modelling-inversion approach and the identification of resistivity gradient maxima was used to identify the stratigraphic contacts and permafrost boundaries [Banville et al., submitted]. From the interpretation of these models taking into account the borehole logs and a map of Quaternary deposits, a 3D cryohydrogeological model was constructed in GoCAD (Fig. 1B). This model will be used for the numerical modelling of the dynamics of groundwater flow and permafrost according to different scenarios of climate change.

The current and anticipated permafrost degradation should enhance the groundwater availability and provide an opportunity for the use of this resource by northern communities for drinking water.

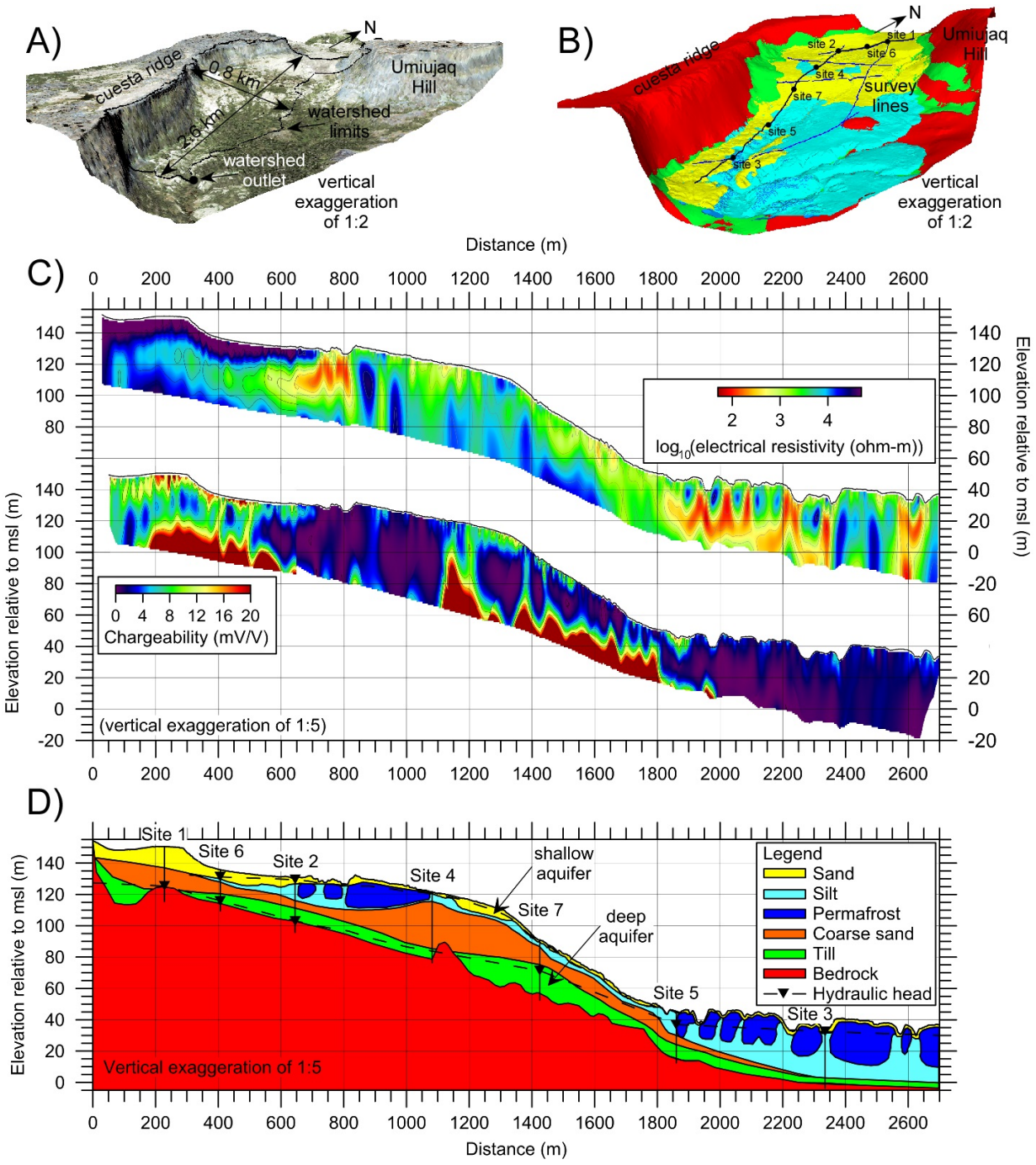

Figure 1: A) Tasiapik valley near Umiujaq. B) 3D cryohydrogeological model of the studied watershed. C) Resistivity and chargeability models along the black survey line in B. D) Cryohydrogeological cross-section assessed from the models in C.

References

Banville, D.; Fortier, R. and Dupuis, C. Interpretation of electrical resistivity and induced polarization tomography using a quantitative approach for a periglacial environment. *Journal of Applied Geophysics*, submitted.

Lemieux, J.-M.; Fortier, R.; Talbot-Poulin, M.-C.; Molson, J.; Therrien, R.; Ouellet, M.; Banville, D.; Cochand, M. and Murray, R. Groundwater occurrence in cold environments: Examples from Nunavik, Canada. *Hydrogeology Journal*, submitted.

Resolution capacity of hydrological processes in ice-rich permafrost – results from geophysical monitoring and synthetic modelling

Christin Hilbich[1], Benjamin Mewes[2], Reynald Delaloye[1], & Christian Hauck[1]

[1] *University of Fribourg, Switzerland*
[2] *University of Bochum, Germany*

Geophysical methods are frequently applied for the investigation of mountain permafrost. Among the most popular methods are electrical resistivity tomography (ERT) and refraction seismic tomography (RST), as these methods are particularly suited to differentiate between frozen and unfrozen conditions. ERT and RST monitoring allows to resolve phase changes between liquid water and ice as well as saturated and unsaturated conditions, and is thus well suited for the investigation of permafrost degradation.

In the context of the acceleration of creep velocities of many rock glaciers in the European Alps in recent years, a current research focus is the investigation of the role of liquid water for the kinematics of rock glaciers. The thermal and hydro-mechanical effects of water infiltration are assumed to play an important role for the seasonal and - if existing - short-time pattern of creep velocities, e.g. by the reduction of shear resistance by infiltrated melt water.

In this contribution we present results from the Becs-de-Bosson rock glacier in the Val de Réchy, Valais, Switzerland, where repeated ERT and RST measurements have been conducted during the last years to investigate the distribution of ground ice and the role of ice and liquid water content changes for rock glacier kinematics. The aim of this study is to analyze the qualitative and quantitative resolution potential of repeated geophysical measurements (ERT/RST) regarding processes related to snow melt infiltration and ice degradation.

After qualitative interpretation, the resulting tomograms were used as input for a quantitative modelling approach (4-phase model, 4PM) to estimate volumetric fractions of ice, water and air in the subsurface. In a second step, synthetic data with idealised scenarios of water infiltration and permafrost degradation were analysed regarding the resolution capacity of both methods in general for the relevant processes in coarse blocky alpine permafrost terrain. We compare the results from these synthetic scenarios with real field data from the Bec-de-Bosson rock glacier and discuss the feasibility of detecting preferential flow paths or ice loss at different depths and the performance of the 4PM.

Repeated ERT surveys to detect forest fire impacts on discontinuous permafrost, southwestern NWT, Canada

Jean Elizabeth Holloway & Antoni Lewkowicz

University of Ottawa, Canada

Forest fire is rarely taken into account in large-area predictive modelling of climate change impacts on permafrost even though it is a potential accelerant for permafrost loss. Moreover, the frequency and magnitude of fires is increasing as the climate warms [Wotton et al., 2010]. Wildfire is especially relevant in the zone of discontinuous permafrost where permafrost is buffered by forest vegetation from rising air temperatures. This ecosystem-protected permafrost covers millions of square kilometres in the subarctic and is particularly sensitive to climate and environmental change as it is just below 0 °C, thin, and discontinuous. Our research goal is to examine transformations of discontinuous permafrost following forest fire over a range of environmental conditions, with the purpose of improving forecasts to change. The extensive fires of 2014 in the southwestern NWT provide an experimental framework to examine how permafrost responds to natural surface disturbance in the sporadic and extensive discontinuous zones. This work is being carried out with an inter-university team of ecologists studying post-fire ecological succession and the carbon cycling in the region.

Burnt and unburnt sites covering the regional range of climatic, ecological and permafrost conditions were established in spring 2015 along a 300 km latitudinal transect. Stratified random sampling was used to select areas in seven burns representing a range of vegetation types, fire severity and fire history (repeated burns). The fires themselves were stratified by two coarse ecological units, the taiga plains and taiga shield ecozones. Within each burn, geospatial data was used to define a domain for sampling, generally within 1km of an all-season road, or of a lake shore accessible by boat or floatplane, with a few interior locations accessible by helicopter. Accessible locations were stratified, and a number of random locations were selected from each stratum. Further selection occurred in the field such that the first of three feasibly accessible locations within each stratum were surveyed. From these random locations, we chose sites for detailed investigation based on the presence or absence of a frost table and whether there were conditions where permafrost was expected. Unburnt control sites were chosen at the northern and southern end of the transect to determine the baseline impacts of climate change in the region. Air and ground temperature monitoring, repeat direct current electrical resistivity tomography (ERT) along permanent electrode arrays, as well as low-altitude aerial photographs taken from an unmanned aerial vehicle (UAV) were initiated to track and explain permafrost evolution. A total of 17 sites were set up in 2015, and a further three sites are planned for 2016.

The initial ERT surveys in June 2015 indicated that there are five sites with thin permafrost (5 m), two sites with isolated patches of thin permafrost, one site with 5 m of permafrost but a thick active layer developed due to severe burning, two sites with 10 m of permafrost and potential thermokarst and talik development, and three sites with 25+ m of permafrost including two ice-rich lithalsas (Fig. 1). We hypothesize that the permafrost at these sites will follow one of three disturbance pathways that will depend on pre-existing ground temperatures and burn severity:

1. complete degradation;
2. development of a supra-permafrost talik over permafrost preserved at depth that will eventually re-aggrade;
3. preservation of permafrost with a deepened active layer.

Results from ERT resurveys in August 2015 show the development of a thicker thawed layer in the near-surface and the possible loss of frozen ground from short sections of particular ERT profiles. Continued monitoring of the sites using ERT and ground temperature measurements is expected to reveal if incomplete active layer freeze-back occurs which would be the first sign of permafrost degradation. ERT surveys will also be undertaken at historic fire sites of differing ages and one-dimensional numerical modeling

will be used to predict long-term change, with fire as a primary source of disturbance to permafrost and employing the field data as inputs. The significance of this project is that it will elucidate how forest fire may combine with climate warming to influence permafrost loss in the discontinuous zones, while helping to verify the existence of positive-feedbacks in this region, and quantify their impacts, notably the release of carbon as permafrost thaws.

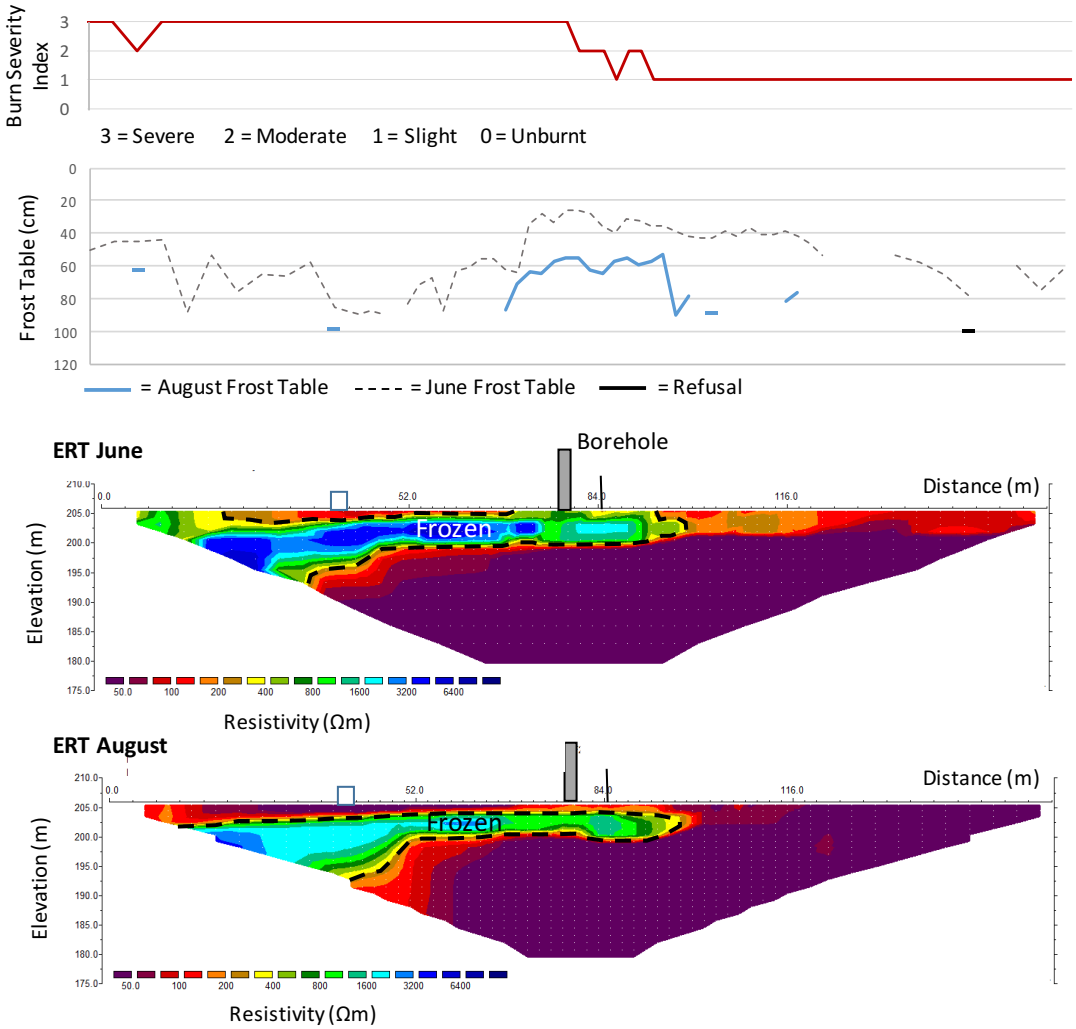

Figure 1: Burn severity, frost table measurements (gaps in data indicates measurements greater than 120cm probe), and resistivity for June and August at a burnt site in the southwestern NWT, Canada.

Acknowledgments

Funding for this project was provided by NSERC, the University of Ottawa, the Northern Scientific Training Program and the Government of the NWT. We gratefully acknowledge ongoing collaboration with Jennifer Baltzer, Steve Cumming, Jill Johnstone, Merritt Turetsky, Michelle Mack, and Stephen Wolfe, and the assistance of the numerous individuals who helped in the field, especially Xanthe Walker and Nicola Day.

References

Wotton, B.M.; Nock, C.A. and Flannigan, M.D. [2010]: Forest fire occurrence and climate change in Canada. *International Journal of Wildland Fire*, 19(3):253–271, doi:10.1071/WF09002.

Change in discontinuous permafrost in the Alaska Highway corridor examined by repeated electrical resistivity tomography and ground temperature monitoring, northwest Canada

Antoni G. Lewkowicz[1], Olivier Bellehumeur-Génier[1], Christina Miceli[1], & Sharon L. Smith[2]

[1] *University of Ottawa, Canada*
[2] *Natural Resources Canada*

Introduction and objectives

Ground temperatures within permafrost generally become less sensitive to net positive surface heat fluxes as they approach 0 °C because of the requirement to satisfy latent heat due to phase change. Repeated Electrical Resistivity Tomography (ERT) is an alternative method to monitor permafrost change at temperatures close to the point of thaw. ERT can, in theory, detect increases in the unfrozen moisture content of cryotic soils from both seasonal temperature cycling and long-term change (e.g. Hilbich et al. [2009]). Moreover, ERT provides a two-dimensional image of change, as opposed to the single point measurement location associated with a borehole.

Here we report on the first five years of a long-term study of ten sites located in the Alaska Highway corridor in northern British Columbia and southern Yukon. These sites all had permafrost when first examined by Roger Brown in 1964 [Brown, 1967] and permafrost persisted until re-examined during 2007-2008 [James et al., 2013]. With one exception, the permafrost at the sites is less than 25 m thick and close to 0 °C.

Methods

Each site is equipped with a permanent electrode array in a Wenner configuration with a minimum spacing of 1 m, and either 40 m or 80 m in length, which provides a profile extending to depths of 6 m or 12 m, respectively. Measurements are made in August close to the end of the thaw season using an ABEM Terrameter LS and frost probing is undertaken at the same time. In 2010-2011, additional measurements were made to examine the annual cycle in March (minimum near-surface ground temperatures), May, June and July, but equipment problems precluded measurements in August. Four of the sites have shallow boreholes with thermistor strings and data-loggers for monitoring ground temperatures dating from 2008, 2010 or 2012. All sites have climate stations measuring air temperature, ground surface and active layer temperatures and iButton stakes to infer snow depths.

Results

Ground temperatures at or below the depth of zero annual amplitude (3-5 m at the study sites) range from -0.2 to -0.05 °C and show very little change over the past 6 hydrological years. The longest series from the borehole at MP825 indicates a temperature decrease of 0.002 °C at 4 m from 2009-10 to 2011-12, followed by an increase of 0.006 °C up to 2014-15 (Fig. 1 upper panel). However, these apparent changes must be treated cautiously as they are much smaller than the expected accuracy of the measurement system. Apparent changes of similar magnitude occurred at the other monitored sites. The borehole data from MP825 indicate the presence of a supra-permafrost talik at 1.0 to 1.75 m depths from 2009-2010 onwards but the 1 m level refroze in the winter of 2014-15. At MP186, a talik developed at a depth of 1 m in 2013-14 and has persisted.

Average apparent resistivities at the sites vary from less than 100 Ωm to more than 1500 Ωm, with the value relating to the proportion of the profile that is frozen, the depth of permafrost, permafrost temperatures and ice content (Fig. 1 lower panel). Measurements during 2010-2011 showed a strong seasonal cycle as the active layer froze in winter and thawed in the following summer. Mean apparent resistivities for the sites increased by 1.2 to 6.2 times from August 2010 to March 2011 and then decreased to approach the previous year's values by July.

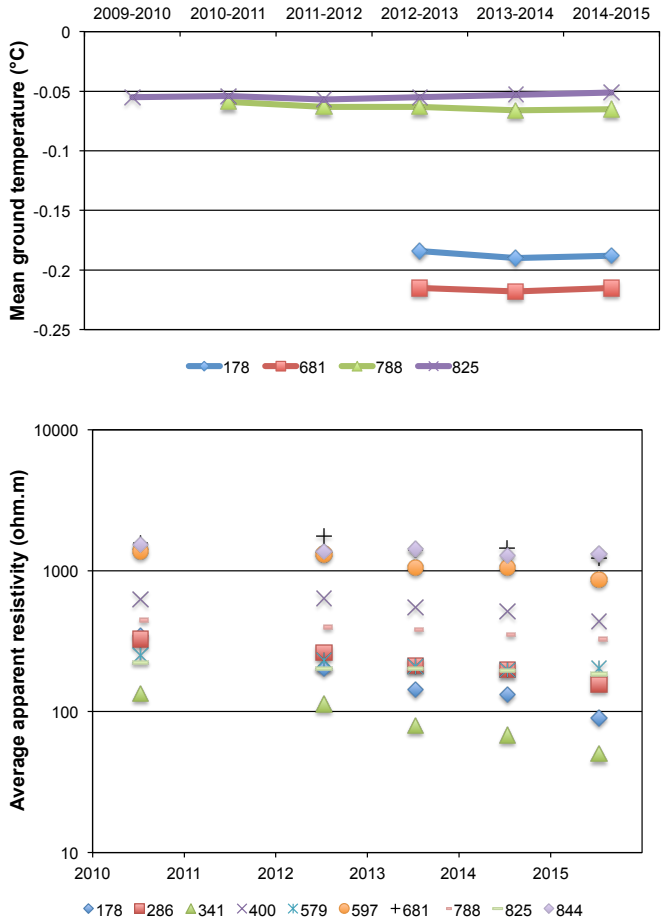

Figure 1: Time series of ground temperatures (3.75-5 m depths) and average apparent resistivity in August at the study sites in the Alaska Highway corridor.

End-of-summer mean apparent resistivity decreased by 14-74 % over the five-year period at the ten sites (Fig. 1 lower panel). For example, average values at MP597 fell from about 1400 Ωm to about 900 Ωm. This decline was generally progressive from 2010 onwards although two of the sites (MP400 and MP681) had their highest values in 2012. Since profiles at most sites extend below the thin permafrost to unfrozen sediments where resistivities remain almost constant, the changes in the permafrost layers are still greater and indicate a progressive increase in unfrozen moisture. Inverted ERT profiles at certain sites (e.g., MP341) show permafrost bodies that are apparently degrading laterally, and this is confirmed by frost table probing. These changes also affect the mean apparent resistivity of the profiles as a whole.

Conclusions

We conclude that the permafrost is degrading at most of the study sites. However, borehole temperatures alone have not provided a complete picture of the thermal state of permafrost because measurements are made at a single location which may not be representative of the entire permafrost body and inter-annual differences are very small at temperatures close to 0 °C. Annually repeated ERT profiling reveals progressive and readily detectable change and especially when combined with ground temperature measurements, has proven to be an effective way to monitor permafrost evolution during a phase of thaw.

Acknowledgments

This research was funded by NSERC, the University of Ottawa, the Northern Scientific Training Program, the Royal Canadian Geographical Society and Natural Resources Canada. We are grateful to Alex Bevington, Max Duguay, Graham Pope, Benoit Faucher, Zoé Kuntz, and Pavel Popov for their assistance in undertaking the field measurements.

References

Brown, R.J.E. [1967]: *Permafrost investigations in British Columbia and Yukon Territory*. Ottawa: National Research Council of Canada, Division of Building Research.

Hilbich, C.; Marescot, L.; Hauck, C.; Loke, M. H. and Mäusbacher, R. [2009]: Applicability of electrical resistivity tomography monitoring to coarse blocky and ice-rich permafrost landforms. *Permafrost and Periglacial Processes*, 20(3):269–284, doi:10.1002/ppp.652.

James, M.A.; Lewkowicz, A.G.; Smith, S.L. and Miceli, C. [2013]: Multi-decadal degradation and persistence of permafrost in the Alaska Highway corridor, northwest Canada. *Environmental Research Letters*, 8:045013, doi:10.1088/1748-9326/8/4/045013.

Occurrence of large massive ground ice bodies buried under glacio-fluvial deposits along the Alaska Highway, Dry Creek area, south-western Yukon, Canada

Benoit Loranger[1], Guy Doré[1], & Daniel Fortier[2]

[1] *Laval University, Canada*
[2] *Montreal University, Canada*

The Dry Creek study site (62°09'49"N and 140°40'55"W) is located along the Alaska Highway approximately 31 km south of the village of Beaver Creek, in a zone of discontinuous permafrost. Under an organic cover a few decimeters thick, the surficial deposit at the study is a glacio-fluvial gravel of varying thickness. A portion of this gravel layer has been removed by earthwork to provide fill material during reconstruction of the Alaska Highway in the mid-1990's. The bottom of the excavation was then levelled and a rest area was constructed at the site. Major settlement problems occurred after the rehabilitation of the highway in 1994-95; however, previous settlement problems have already been reported for the area prior to rehabilitation work. This highway section requires intensive maintenance due to the presence of linear subsidence and cracks in the road embankment shoulders. Surface disturbances due to organics and gravel removal, ground levelling and compaction resulted in the development of thermokarst lakes, large depressions, linear settlement crossing the road in several places and sinkholes. A $>$ 8.5 m deep and 30 m large depression was observed along the road embankment during the summer 2008 on the east side of the road. This led us to support the assumption that very ice-rich soils and most likely massive ground ice occurred at depth. All three electrical resistivity surveys conducted in 2013 and 2014 showed very high resistivity values at about 10 m depth. Micro-gravimetric surveys conducted in 2014 to evaluate the extent of massive ice the permafrost revealed strongly negative residual anomaly, especially for surveys conducted near a thermokarst lake and where depressions and sinkholes where reported [Loranger et al., submitted]. Drilling and coring operations conducted during the summer 2014 revealed a very complex cryostratigraphy with layers of both ice-poor and ice-rich silt, pure ice layers and the striking occurrence of massive beds of sediment-poor ice several meters thick. The latter was encountered in 4 out of 10 boreholes. One 13 m deep borehole showed cryofacies of massive sediment-poor ice over a thickness of 9 m (2-11m). The cryostructure of the ice is characterized by micro-aggregates of fine-grained sediments suspended in pure ice. Geocryological analysis of the massive ice is required to determine its origin.

References

Loranger, B.; Doré, G.; Fortier, D. and Lemieux, C. Massive Ice and Ice-Rich Soil detection by gravimetric surveying at Dry Creek, south-western Yukon Territory, Canada. submitted.

Using resistivity method to characterize water flow patterns in permafrost environment (Ilulissat, Greenland)

Julie Malenfant-Lepage[1], Guy Doré[1], Thomas Ingeman-Nielsen[2], & Fortier Daniel[3]

[1] *Laval University, Quebec City, Quebec, Canada*
[2] *Technical University of Denmark, Copenhagen, Denmark*
[3] *University of Montreal, Montreal, Quebec, Canada*

The construction of transport infrastructure in the north inevitably affects the hydrology of the watershed it overlaps by impeding water drainage on the land. Observations of events causing the rapid degradation of northern infrastructure suggest that liquid water transport and its thermal effects have been significantly underestimated in recent years in permafrost science and engineering. The consequences of convective heat transfers at the interface between flowing water and the ground, caused by concentration and channeling of runoff and groundwater around infrastructures, are poorly known. Electrical resistivity is one of the most effective geophysical methods used to map and characterize permafrost, as it is sensitive to the state (frozen/unfrozen) of the ground, its ice content and subzero temperatures. To study the extent of permafrost degradation caused by the redirecting of water flow, electrical resistivity surveys were conducted perpendicular to a stream draining a small watershed, south of the airport of Ilulissat in Greenland. Ilulissat is located on the west coast of Greenland, north of the 69°parallel in the continuous permafrost zone. The soil of the study site consists of marine clay and silt. Permafrost temperature is between -1 °C and -3.5 °C. The first 4 meters of permafrost is ice-rich and show high resistivity values while the soil below 4 meters depth is estimated to be unfrozen due to a high porewater salinity (Foged and Ingeman-Nielsen, 2009). The water flow patterns in the ice-rich zone are easily observable through lower resistivity values recorded due to permafrost warming at these locations. At this site, electrical resistivity profiles correlated with several permafrost properties such as: soil temperatures at different depths, active layer thickness, and water content of active layer and permafrost soils. Water discharge and water temperature in the stream were measured daily during the study period and implications for heat transfers are observed.

Reconstructing the last century evolution of the Dérochoir rock glacier using a multi-approach monitoring

Marco Marcer[1], Xavier Bodin[2], & Philippe Schoeneich[1]

[1] *Université de Grenoble Alpes, Institut de Géographie Alpine, France*
[2] *Université Savoie Mont Blanc, Laboratoire EDYTEM, France*

The Dérochoir is one of the very few active rock glacier located on the French side of the Mont Blanc massif. It extents from 2450 to 2700 m.s.l., on a gentle slope between the Rognes ridge and the steep "ravines" of the Arandellys stream.

Since 1887 several debris flows of significant magnitude occurred in the Arandellys basin, endangering the downstream village of Les Houches. The service Restauration des Terrains en Montagne (RTM) started to monitor the Derochoir, attributing to the landform the cause of the extraordinary gravitational activity. The reanalysis of archive documents permits to confirm an increased debris supply from the rock glacier front. In 1892 a subglacial lake in the nearby glacier of Tete Rousse outbroke, devastating the village of St. Gervais - Le Fayet, causing 172 causalities and rising the concerns about the Derochoir activity. However, since 1897 no extraordinary activity was recorded until nowadays, suggesting that the rock glacier activity suddenly decreased considerably.

Similarly to the 90's a general trend of increasing rock glaciers activity registered in the Alps, a preliminary study showed that the Dérochoir rock glacier almost doubled its average displacement speed from 0.1 m/y in the period 1895-1974 to 0.2 m/y 1974-2004, activating a monitoring campaign including differential GPS and Ground Surface Temperature measurements.

Annual DGPS and GST measurements are available since 2009, while a fixed GPS was installed and acquired data for an entire year in 2011. Additionally, in 2012 a Electric Resistivity Tomography campaign was performed on the site. Finally a time series of Digital Elevation Models is computed, taking advantage of the historical orthophoto dataset taken by the IGN for glacier monitoring, in order to better understand the dynamic evolution of the rock glacier to the present days.

The data indicate that the whole structure is accelerating considerably, with a registered averaged displacement speed of 0.5 m/y in 2009-2013 and of 0.8 m/y in 2013/2015. The ERT transects highlight the presence of temperate permafrost supersaturated in ice close to the melting point in the central part of the rock glacier, where the highest displacement rates are detected. GST measurement indicate a general trend of warming permafrost, in accordance with air temperature positive trend registered in the area. This context of highly degrading permafrost is responsible for the rock glacier rapid increase in activity that might become again a significant hazard for the downstream population and infrastructures in the near future as it used to be at the end of the XIX century.

Long-term electrical resistivity tomography (ERT) monitoring of mountain permafrost in Switzerland – comparison of different sites and relevance for thermal modelling

Coline Mollaret, Christin Hilbich, Samuel Python, & Christian Hauck

Department of Geosciences, University of Fribourg, Switzerland

Permanently frozen ground is a very sensitive climate change indicator in mountain terrain. A better understanding of mountain permafrost degradation implies a temporal and spatial permafrost distribution monitoring, which is of major importance regarding high mountain slope stability.

Electrical Resistivity Tomography (ERT) is broadly applied in the context of permafrost. Subsurface resistivity temporal variations depend on temperature, pore content (ice, water or air) and therefore also on soil moisture. Several orders of magnitude discriminate the electrical resistivity of ice and water, allowing a distinction between frozen and unfrozen ground.

We focus this study on the Schilthorn permafrost monitoring site (Swiss Alps), which includes a 17-year discontinuous resistivity dataset, the longest time series of ERT monitoring in mountain permafrost [Hilbich et al., 2008]. Both apparent and inverted specific resistivity are analysed in space and time. A special effort dedicates to comparing temporal resistivity changes between different depth levels: from shallow (active layer) to deeper levels (permanently frozen ground). The effects of the 2003 and 2015 summer heatwaves are investigated in detail in comparison with in-situ air and ground temperatures at several depths.

The results from Schilthorn are analysed in comparison with ERT monitoring data from other sites. These sites include additional 5 to 15-year discontinuous resistivity datasets, as well as meteorological and temperature ground truth data available from several boreholes for all sites. As the active layer is a critical parameter for frozen soil dynamics, we attempt to assess the spatial variability of active layer depth from resistivity data changes at specific depths. The subsurface ice content is finally quantitatively estimated for the different study sites using additional geophysical data. Finally, the obtained resistivity time series is used for calibration of the coupled heat and mass transfer model COUP [Jansson, 2012] which is currently used to project future permafrost evolution in mountainous areas. Standard modelling approaches use only ground temperature as calibration/validation (Cal/Val) variable. With the newly homogenised ERT datasets specific resistivity time series can be used as additional Cal/Val data for ground water content, which is an additional independent variable to the standardly used temperature data.

References

Hilbich, C.; Hauck, C.; Hoelzle, M.; Scherler, M.; Schudel, L.; Völksch, I.; Vonder Mühll, D. and Mäusbacher, R. [2008]: Monitoring mountain permafrost evolution using electrical resistivity tomography: A 7-year study of seasonal, annual, and long-term variations at Schilthorn, Swiss Alps. *Journal of Geophysical Research: Earth Surface*, 113(F1):F01S90, doi:10.1029/2007JF000799.

Jansson, P.-E. [2012]: Coupmodel: Model Use, Calibration, and Validation, *Transaction of the Asabe*, 55(4), 1335-1344, doi:10.13031/2013.42245.

Delineation of permafrost and ice-rich terrain within fine-grained sediments using electrical resistivity, Yellowknife, Northwest Territories

Greg Oldenborger, Stephen A. Wolfe, Peter D. Morse, & Andre Pugin

Geological Survey of Canada, Natural Resources Canada

The properties of frozen ground make electrical geophysics a potential tool for permafrost characterization. Permafrost can have a strong electrical signature where low temperatures reduce the mobility of charge-carrying ions and the freezing of water greatly reduces the availability and connectivity of pore fluid for electrolytic conduction. Electrical resistivity is typically observed to increase significantly for cryotic ground, and even more so for ice-rich permafrost. Consequently, in permafrost terrain, measurements of electrical resistivity provide valuable information for interpretation of some combination of the material type and the amount of ground ice (e.g., Oldenborger and LeBlanc [2015]). However, the relations between material type, thermo-physical state and electrical resistivity are non-unique and the imaging of the ground as typically achieved through inversion of geophysical data has resolution-dependant limitations. Qualitative interpretation or quantitative utilization of electrical resistivity images (ERI) should be done in the context of ERI uncertainty.

We utilize ERI results over a lithalsa (ice-rich permafrost mound) associated with a retrogressive thaw slump on an island in the Yellowknife River, Northwest Territories (Fig. 1A). The lithalsa has formed by permafrost aggradation within silty-clay of alluvial and lacustrine origins [Wolfe and Morse, 2015]. Observations along the headwall of the scarp reveal up to 70 % visible ice content within permafrost (Fig. 1A inset). ERI surveys were conducted to confirm the presence of ground ice at depth and to map the distribution of permafrost and ice-rich ground in the area. The geophysical results show distinct high relative resistivity anomalies consistent with occurrence of ice-rich ground (Fig. 1B). These anomalies occur in the context of relatively moderate resistive ground interpreted to represent ice-bonded permafrost, and also relatively conductive ground interpreted to represent unfrozen silt and clay within the active layer and taliks. The ERI results support the hypothesis of ice-cored terrain (lithalsa) and provide further insight into permafrost conditions including the near-shore extent of permafrost, potential locations of thin permafrost aggradation, and the presence of pond-related thaw bulbs and through-going taliks.

Additional data are used to further inform the interpretation of the ERI results. Several water jet-drilled boreholes provide observations on thaw depth, base of permafrost, and bedrock depth. Continuous water-borne single-channel seismic reflection data were acquired on the Yellowknife River adjacent to the island to provide additional estimates of bedrock topography and also information on underlying sediments. These data corroborate most ERI results, but also serve to identify limitations and regions of uncertainty or inconsistent data. In particular, the highly resistive ground associated with massive ice, combined with the highly conductive silty active layer result in limited depth of investigation despite very high quality data. Practically speaking, for ice-rich zones of this survey ERI may be limited to detection of resistive bodies as opposed to estimation of their actual resistivity. Furthermore, ERI may be unable to discriminate bedrock from massive ice, making estimates of potential heave or subsidence difficult based on these results alone. Similarly, the base of permafrost is observed here to be multi-valued in terms of electrical resistivity, demonstrating that the approach of using iso-resistivity surface for mapping thermo-physical transitions is flawed.

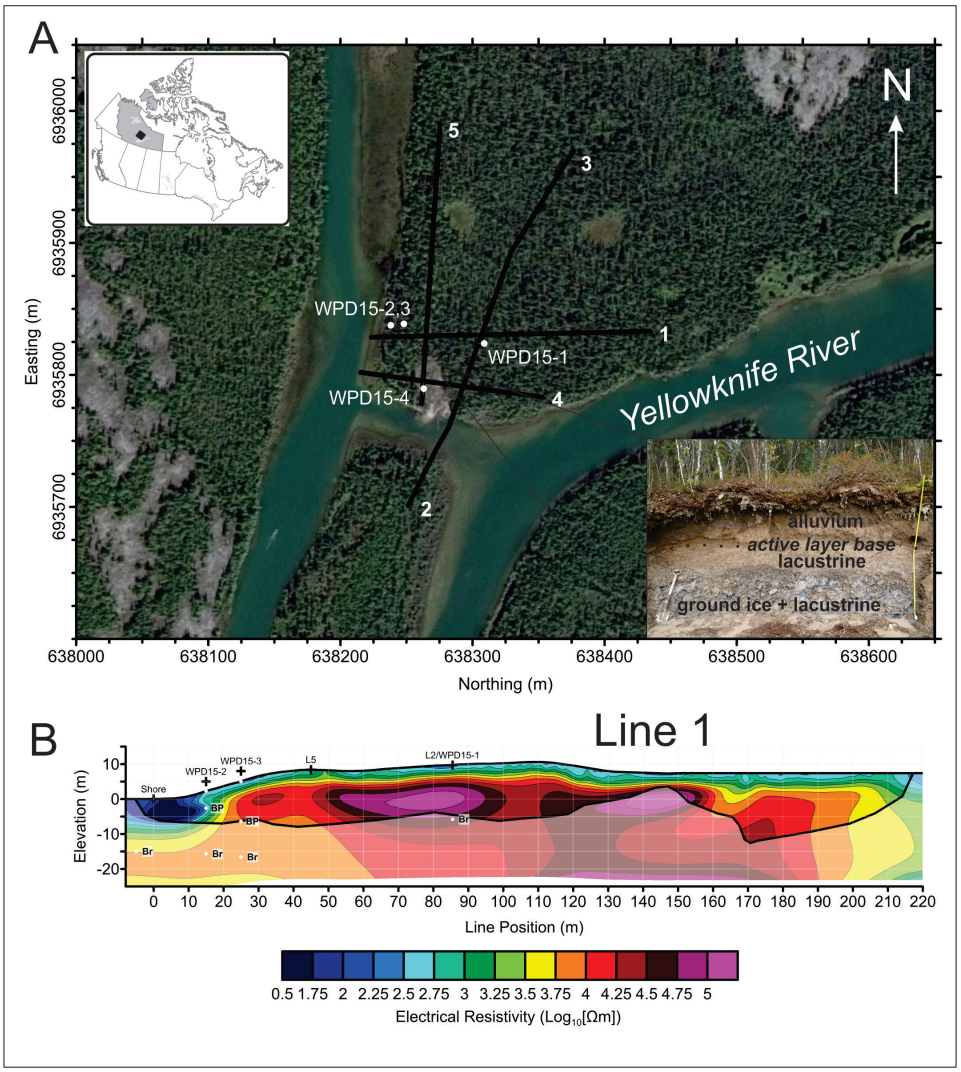

Figure 1: Electrical resistivity survey area and results. A) Delineation of surveys and boreholes (WPD15-1, 2, 3, 4) conducted within the vicinity of ice-bearing permafrost terrain (see inset) on an island adjacent to the Yellowknife River. Note WPD15-04

References

Oldenborger, G.A. and LeBlanc, A.-M. [2015]: Geophysical characterization of permafrost terrain at Iqaluit International Airport, Nunavut. *Journal of Applied Geophysics*, 123:36–49, doi:10.1016/j.jappgeo.2015.09.016.

Wolfe, S.A. and Morse, P.D. [2015]: Holocene lake-level recession, permafrost aggradation and lithalsa formation in the Yellowknife area, Great Slave Lowland. In *Proceedings of the Canadian Permafrost Conference*, # 236.

Geophysical evaluation of bedfast and floating ice lake talik, Alaska

Andrew Parsekian[1], Andrea Creighton[1], Christopher Arp[2], Ben Jones[3], Ronnie Dannen[4], Allen Bondurant[2], & Anne Gaedeke[2]

[1] *University of Wyoming, USA*
[2] *University of Alaska - Fairbanks, USA*
[3] *US Geological Survey - Alaska Science Center, USA*
[4] *Alaska Division of Geological & Geophysical Surveys, USA*

Thermokarst lake taliks have important relevance to the carbon and water cycles, however deep thaw and remote locations have resulted in few measurements of these permafrost subsurface features. The transition of these lakes between bedfast ice (frozen to the bottom in winter) and floating ice has important implications for talik initiation and development [Arp et al., 2012]. Several geophysical measurements have been demonstrated as effective for measuring talik dimensions including recent airborne electromagnetic mapping [Minsley et al., 2012]. Here we highlight surface nuclear magnetic resonance (NMR), a measurement with unambiguous sensitivity to liquid water to approximately 100 m depth [Parsekian et al., 2013]. Since we presume the talik is bounded vertically by open water (top) and permafrost (bottom), the contrast between thawed and frozen materials is an excellent geophysical target. We present the results of numerical and field experiments to resolve the vertical accuracy of surface NMR talik detection, as well as results from field exercises on the North Slope of Alaska to constrain the talik expansion rate and current geometry. Specifically, we target a range of lake ice regimes from drained lake basins, to shallow bedfast ice lakes, to deep floating ice lakes with the main question in mind: how does lake ice regime control talik depth? We find that these geophysical measurements resolve deep talik below floating ice lakes as well as variable talik associated with drained lakes and bedfast ice lakes. As expected, deep lakes are associated with taliks that extend several tens-of-meters below the water column. Bedfast ice lakes were variable, some supporting considerable volumes of unfrozen sediments, while others are mostly thaw-free. Unexpectedly, we also observed isolated taliks, potentially indicating partial refreeze after lake drainage. Combined with radiocarbon dating of material from sediment cores, and thermal modeling, we are able to evaluate talik formation over time below the drained lake basins.

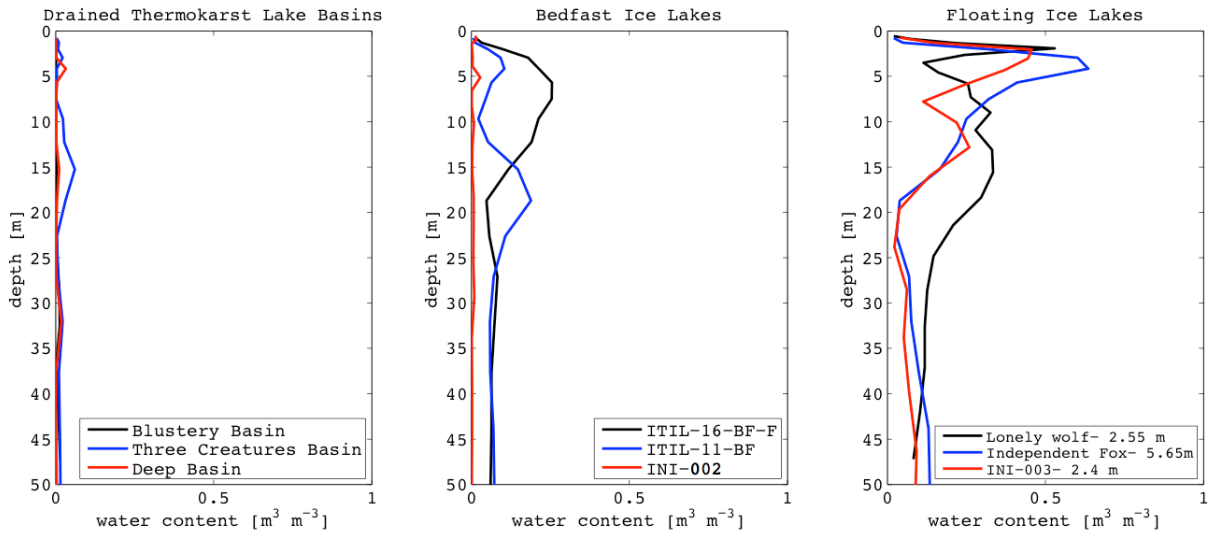

Figure 1: 1D surface nuclear magnetic resonance soundings of talik thaw.

References

Arp, C.D.; Jones, B.M.; Lu, Z. and Whitman, M.S. [2012]: Shifting balance of thermokarst lake ice regimes across the Arctic Coastal Plain of northern Alaska. *Geophysical Research Letters*, 39(16): L16503, doi:10.1029/2012GL052518.

Minsley, B.J.; Abraham, J.D.; Smith, B.D.; Cannia, J.C.; Voss, C.I.; Jorgenson, M.T.; Walvoord, M.A.; Wylie, B.K.; Anderson, L.; Ball, L.B.; Deszcz-Pan, M.; Wellman, T.P. and Ager, T.A. [2012]: Airborne electromagnetic imaging of discontinuous permafrost. *Geophysical Research Letters*, 39(2):L02503, doi:10.1029/2011GL050079.

Parsekian, A.D.; Grosse, G.; Walbrecker, J.O.; Müller-Petke, M.; Keating, K.; Liu, L.; Jones, B.M. and Knight, R. [2013]: Detecting unfrozen sediments below thermokarst lakes with surface nuclear magnetic resonance. *Geophysical Research Letters*, 40 (3):535–540, doi:10.1002/grl.50137.

Soil moisture data for the validation of permafrost models using direct and indirect measurement approaches at three alpine sites

Cécile Pellet, Christin Hilbich, Antoine Marmy, & Christian Hauck

Department of Geosciences, University of Fribourg, Switzerland

In regions affected by seasonal and permanently frozen conditions soil moisture influences the thermal regime of the ground as well as its ice content, which is one of the main factors controlling the sensitivity of mountain permafrost to climate changes. In this study, several well established soil moisture monitoring techniques were combined with data from geophysical measurements to assess the spatial distribution and temporal evolution of soil moisture at three high elevation sites with different ground properties and thermal regimes.

Within the framework of the SNSF-project SOMOMOUNT (Soil moisture in mountainous terrain and its influence on the thermal regime in seasonal and permanently frozen terrains), a network of six entirely automated soil moisture stations was installed in Switzerland along an altitudinal gradient ranging from 1'200 m. a.s.l. to 3'400 m. a.s.l. These stations were coupled (where possible) with already existing permafrost monitoring stations. The standard instrumentation of each soil moisture station comprises gravimetric soil sampling and the installation of Frequency Domain Reflectometry (FDR) and Time Domain Reflectometry (TDR) sensors for long term monitoring. Additionally, repeated geophysical surveys (Electrical Resistivity Tomography, ERT, and Refraction Seismic Tomography, RST) as well as spatial FDR (S-FDR) measurements are performed to assess the two dimensional spatial distribution of soil moisture in the ground.

Using this comprehensive dataset we develop a methodology to link the various methods and use the resulting dataset to calibrate and validate two types of model approaches, which are currently used in permafrost research:

1. the geophysically based four-phase model (4PM) [Hauck et al., 2011], that combines ERT and RST measurements to quantify the spatial variability of ice, water and air content in the near subsurface (down to 10-30m) and

2. the coupled heat and mass transfer model (COUP) [Jansson, 2012], that uses atmospheric forcing as input to reconstruct the entire energy and water balance for one soil column.

The results are then discussed with respect to the influence of spatio-temporal variability of subsurface ice and water content on the future permafrost evolution.

References

Hauck, C.; Böttcher, M. and Maurer, H. [2011]: A new model for estimating subsurface ice content based on combined electrical and seismic data sets. *The Cryosphere*, 5(2):453–468, doi:10.5194/tc-5-453-2011.

Jansson, P.-E. [2012]: Coupmodel: Model Use, Calibration, and Validation, *Transaction of the Asabe*, 55(4), 1335-1344, doi:10.13031/2013.42245.

Characterizing relict late Pleistocene permafrost valley fills along the Alaska Highway, southwest Yukon

Joel Pumple[1], Duane Froese[1], Fabrice Calmels[3], & Burke Minsley[2]

[1] *University of Alberta, Canada*
[2] *U.S. Geological Survey*
[3] *Yukon Research Centre*

The Alaska Highway through southwest Yukon is located in the Discontinuous Permafrost Zone with many areas of the highway corridor associated with degrading permafrost. Given the strategic value of the corridor, it is critical to have a clear understanding of permafrost characteristics and distribution, particularly in the context of a changing climate. In the Beaver Creek area, the Alaska Highway transverses both glaciated and non-glaciated terrain from the last glacial maximum. Permafrost characteristics are strongly influenced by regional glacial history including the distribution of relict Pleistocene syngenetic permafrost. In this study, we characterize relict Pleistocene permafrost valleys fills along the Alaska Highway between Beaver Creek and the Alaskan border using a multidisciplinary approach. Our surveys include electrical resistivity tomography (ERT), airborne electromagnetic (AEM) geophysical surveys, geomorphological mapping, permafrost drilling, cryostratigraphy, geochemical analyses, and environmental monitoring to define the boundaries and geometry of the valley fills. Using a combination of AEM and ERT data, we are able to map areas of syngenetic permafrost that are preserved beyond the glacial limit near hillslopes, from areas of predominantly epigenetic permafrost within the valley bottoms. Radiocarbon dating and stable isotope analyses of $\delta^{18}O$ and δ^{2}H combined with detailed cryostratigraphy confirm that much of the ground ice is relict from the late Pleistocene. The outcomes from this study will assist with development of future mitigation strategies and maintenance plans for the Highway.

Integration of seismic and GPR for study geocryological section in the floodplain of the Pechora river (the Nenets district, Russia)

Marat Sadurtdinov, Maria Sudakova, Galina Malkova, Andrey Skvortsov, & Andrey Tsarev

Earth Cryosphere Institute SB RAS, Russian Federation

One of the main tasks of research in permafrost zone is to determine depth and shape of permafrost's top. The task not always could be solved by direct research methods such as geoengineering and traditional permafrost studies.

In such cases using of geophysical methods could help. Seismic is one of effective geophysical methods, but it also one of the most consuming and expensive ones. GPR method is much cheaper and researcher can get significant amount of data over a short period of time. However, it has very strict limitations to use such as soils' high electrical conductivity.

The thesis is a case history of integration of seismic and GPR for permafrost studies application. Site of our investigations is in the floodplain of the Pechora river (the Nenets district, Russia). Nenets district is located in permafrost zone, both continuous and discontinuous. Pechora river has a significant warming impact on the permafrost state. In Pechora floodplain there is a big closed talik between active layer and permafrost. Nevertheless, there are local areas where permafrost is still preserved.

One of these areas occurs on island where is situated exploration drilling site of Kumzhinskoe deposit. The island had allocated vast areas of technological usage, include cross-country vehicle tracks, artificial caves, mounds etc. Geological cross-section on the island consist of are tight sands with thin layers of ferritization and oil contamination.

Before man-made intrusion on the altitude of the island within the tundra region permafrost deposits underlie everywhere. After destruction of vegetation cover depth of thawing began to gradually increase. At present time there is lowered permafrost roof at all areas of technological usage.

At the investigation area active layers' depth is more than 1.5m so it is impossible to estimate it by graduated steel rod. For this problem solving seismic and GPR were used. Seismic investigation was performed by refractive and reflective p- and sh-waves.

Seismic investigations were carried out on representative areas of the investigated site. The aim was to obtain information about nature and depth of main geological boundaries. By these studies using known seismic criteria the roof of permafrost and full water saturation zone boundary were identificated.

GPR research was performed using single-fold common-offset reflection survey. A Zond radar was used for the survey with 300MHz center frequency antenna. Sandy type of geological section at the site was favorable for GPR. To the other hand strong variability of surface conditions and sometimes absence of difracted waves made reliable determination of electromagnetic waves velocity impossible. So the depth of main reflecting boundaries was unknown for GPR. To define it seismic results were used. Taking seismic results into account it became possible to study structural features of the geological section in details using GPR data. By GPR data lithological boundaries in permafrost and layering of sands in thawed part of the section were defined. Besides that, was found boundary probably of oil polluted area in the sands.

The results showed that the permafrost's top depth varies from 1.5 to 3 meters at undisturbed areas. At technological usage areas active layer depth reaches 9 meters.

Main geological and physical boundaries depth and spatial location according to seismic and GPR data for virtually the same. This fact demonstrates the reliability of the obtained geophysical results.

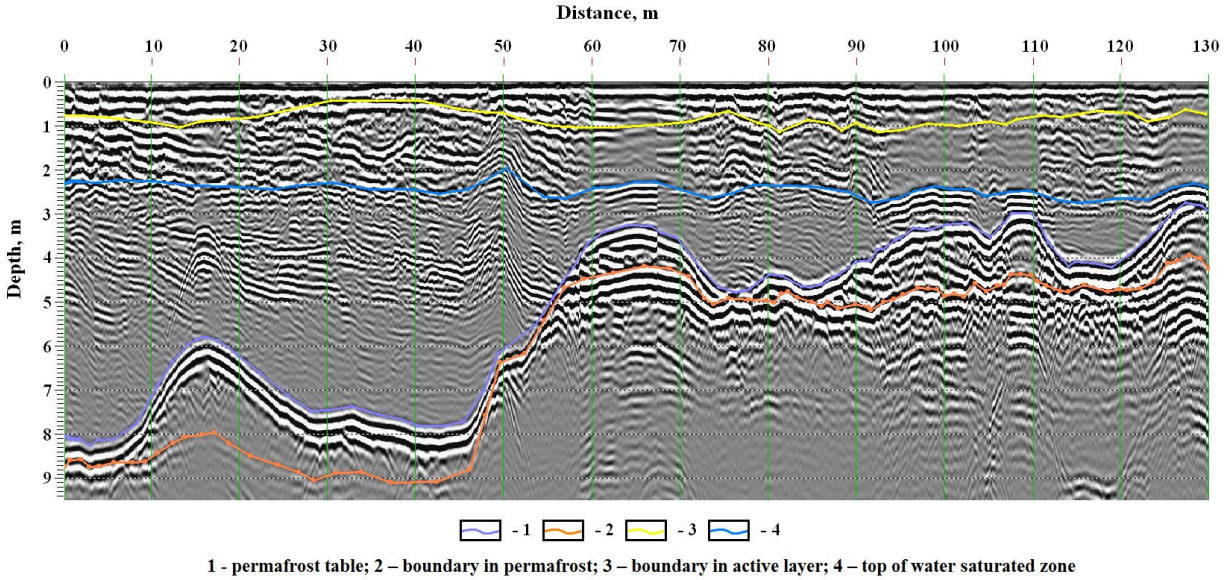

Figure 1: GPR cross section.

Conclusions

- Basic principles of the integrated use of seismic and GPR methods for permafrost problems solving were formulated and tested;
- By seismic studies the roof of permafrost and full water saturation zone boundary were identificated and their depth at representative areas was determined. It became basis for EM velocity determination for GPR geology cross-section.
- In a favorable type of deposits high-quality detailed GPR data was obtained up to the depth about 12 meters.
- The results have shown the high efficiency of the integrated use of seismic and GPR for the study of geological and permafrost cross-section and determination the nature of the geophysical boundaries.

The potential of ground-based 3D GPR imaging: 2D vs. 3D examples from the Yedoma region

Stephan Schennen[1], Jens Tronicke[1], Sebastian Wetterich[2], Niklas Allroggen[1], Georg Schwamborn[2], & Lutz Schirrmeister[2]

[1]*Institut für Erd- und Umweltwissenschaften, Universität Potsdam, Potsdam, Germany*
[2]*Alfred-Wegener-Institut, Helmholtz-Zentrum für Polar- und Meeresforschung, Potsdam, Germany*

Ground-penetrating radar (GPR) reflection imaging is a popular geophysical tool to explore subsurface structures in a non-invasive manner. In terms of GPR, reflective interfaces are defined by contrasts in dielectric permittivity, which result from, for example, variations in soil moisture or ice content. GPR is very suitable for electrically high resistive environments, such as frozen ground (typically $> 10{,}000$ Ωm). Here, GPR can be used to explore structural targets at depths up to tens of meters. Furthermore, GPR can be employed to explore more shallow environments where detailed information on the decimeter scale is required. In consequence, 2D GPR reflection profiling is used on different spatial scales in permafrost applications such as active layer characterization and imaging of pingos. However, a 3D strategy might be essential for obtaining a reliable image of subsurface structures, if the geometry of such targets is complex (e.g., structures vary in three dimensions). Additionally, 3D data allow to identify out-of-plane reflection events which might interfere with reflections from target structures. This advantage is especially interesting for the application of GPR in cold environments, where out-of-plane reflections are favored due to a broadened radiation characteristic of GPR antennas on frozen ground compared to unfrozen ground.

Here, we present a carefully designed 3D GPR acquisition and processing strategy [Schennen et al., 2016] and employ it to an exemplary data set. Our field site covers an area of approximately 20 × 70 m and is located on top of a Yedoma hill on Bol'shoy Lyakhovsky Island, Northern Siberia. Nearby borehole information provides cryostratigraphic details (up to a depth of approximately 30 m) interpreted in terms of three major stratigraphic units. These comprise two ice complex strata, which enclose a unit of floodplain deposits. Additional ground-truth is available from a 18 m high outcrop of the upper ice complex next to our survey area. Here, we observe large (up to 10 m wide) ice-wedges segmenting the ice- and organic-rich, loess-like sediments. In our unmigrated 3D GPR data, time slices show distinct circular diffraction features. As we move on to succeeding slices, we observe that these features originate from locations below thermokarst mounds, expand with a velocity of 0.17 m/ns, and interfere with each other at later traveltimes (Fig. 1a-d). They result in a complex 3D distribution of diffracted energy evident in the entire data cube. Thus, a 3D migration approach (e.g., Allroggen et al. [2014]) is essential to correctly image subsurface structures. Thereby we consider also topographic variations and possible subsurface velocity variations. In our migration result, we observe two distinct horizontal features at depths larger than 20 m. Taking borehole data into account, we interpret these features as the base of the upper ice complex unit and the underlying floodplain deposits, respectively. Furthermore, we are able to trace both interfaces in our data cube and compile our interpretation into a 3D cryostratigraphic model (Fig. 1e), which can be used to scale up borehole and outcrop information. In a concluding 2D vs. 3D comparison, we extract exemplary 2D profiles from our unprocessed 3D data to simulate a 2D GPR acquisition and processing strategy on the same field site. Thus, we are able to investigate the impact of data reduction on each processing step. Comparing results of our 2D and 3D processing strategies demonstrate, that a 3D GPR surveying and processing strategy is critical in complex permafrost settings.

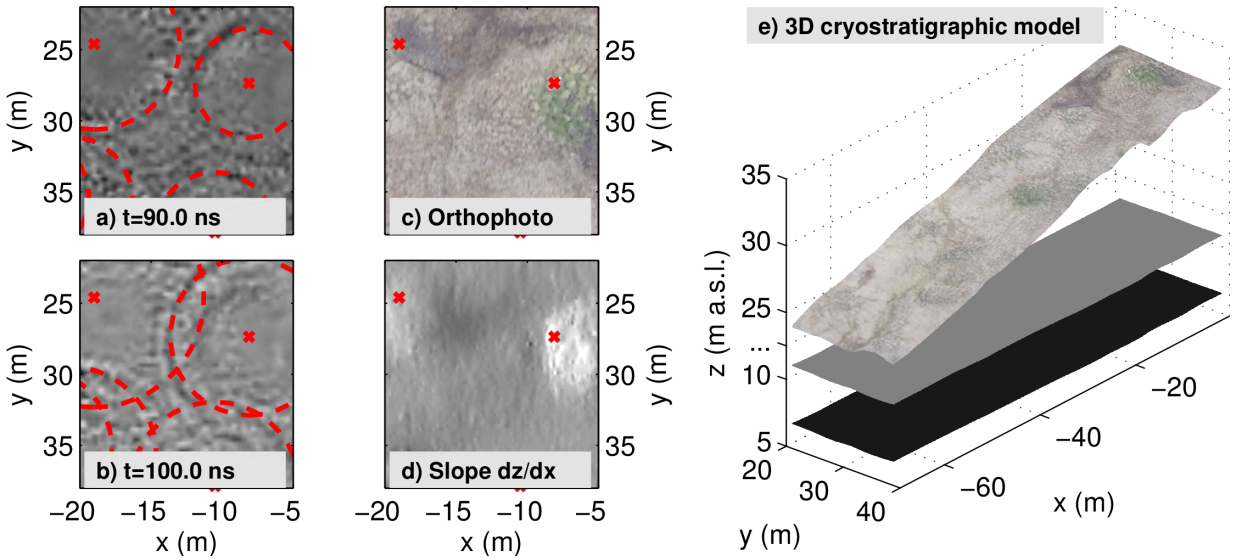

Figure 1: (a), (b) Two unmigrated time slices showing circular features originating from locations below thermokarst mounds, which are visible on (c), (d). (e) 3D model comprising the base of ice complex strata (grey) and floodplain deposits (black), respectively.

References

Allroggen, N.; Tronicke, J.; Delock, M. and Böniger, U. [2014]: Topographic migration of 2D and 3D ground-penetrating radar data considering variable velocities. *Near Surface Geophysics*, 13, doi:10.3997/1873-0604.2014037.

Schennen, S.; Tronicke, J.; Wetterich, S.; Allroggen, N.; Schwamborn, G. and L., Schirrmeister. [2016]: 3D GPR imaging of ice complex deposits in northern East Siberia. *Geophysics*, 81, doi:10.1190/GEO_2015-0129.1.

Optimizing electrode shapes for ERT monitoring in permafrost areas

Sonia Tomaskovicova[1], Thomas Ingeman-Nielsen[1], Anders V. Christiansen[2], Inooraq Brandt[3], Torleif Dahlin[4], & Bo Elberling[5]

[1] *Technical University of Denmark, Denmark*
[2] *Aarhus University, Denmark*
[3] *Orbicon, Greenland*
[4] *Lund University, Sweden*
[5] *University of Copenhagen, Denmark*

Very large and extreme variation in grounding resistances (GR) are some of the main challenges in the monitoring of permafrost and active layer processes with Electrical Resistivity Tomography in sedimentary deposits. The unfrozen, wet active layer typically results in low electrode grounding resistances in summer. In winter, however, when the active layer freezes, grounding resistances may increase many orders of magnitude, and hamper the acquisition of meaningfully long time series.

To investigate the factors conditioning the GR, we tested three stainless steel electrode types featuring increased size and surface area:

1. a rod electrode, with diameter 1 cm, length 8 cm and effective surface area: 27 cm^2
2. a square plate electrode, 10*10*0.1 cm (h*w*t), effective surface area: 204 cm^2
3. a wire mesh electrode, 10*10*0.6 cm (h*w*t), effective surface area: 985 cm^2

The electrodes were tested at three different localities in West Greenland: Qeqertarsuaq (69°15'N, 53°30'W, 30 m a.s.l.), Ilulissat (69°14'N, 51°3'W, 33 m a.s.l.) and Sisimiut site (66°56'N, 53°36'W, approx. 48 m a.s.l.). Each of these sites represents a different surface geology. The soil type at Ilulissat is a silty clay with little organic cover, at Sisimiut it is well drained fine sand likewise with very little organic cover, while at Qeqertarsuaq the surface deposits consists of a coarse sand with high organic content. Sisimiut and Qeqertarsuaq are located in the discontinuous permafrost zone, while Ilulissat has continuous permafrost.

At each site we installed three 10-electrode layouts (electrode separation 30 cm), each featuring a different electrode type. The grounding resistance of each individual electrode was measured using the focus-one protocol. The focus-one protocol, is essentially a two-electrode resistance measurement, where one electrode is connected to one terminal of the instrument, while all the other electrodes of the layout are connected in parallel to the other terminal, thereby effectively minimizing the contribution of their grounding resistances to the total measurement. Measurements were conducted at all three sites summer, fall and winter, to study also the effect of ground temperature.

The measured grounding resistances range from about 600 Ω to 1.2 MΩ (across seasons, electrode types and localities), and the effects of electrode type, locality (surficial geology) and ground temperature all tested statistically significant. Plate electrodes showed 28 to 69 % lower GR than rods during both thawed and frozen ground conditions at all sites. Mesh electrodes improved the GR by 29 to 37 % relative to plate electrodes in winter at the Ilulissat and Qeqertarssuaq sites. The increased effective surface area of the mesh electrodes seems to be an advantage when the electrodes are inserted or buried in fine grained mineral or organic soils with some cohesive properties, where the soil may fill the mesh openings. At the Sisimiut site, the coarser mineral soil results in no advantage of using mesh electrodes. Under thawed conditions, the plate and mesh electrodes did not test statistically different at any of the sites, indicating that the natural variation in soil and burial conditions is larger than the effect of the larger surface area.

An existing 64 electrode monitoring array installed at the Ilulissat site was used to further document the advantage of mesh electrodes over rod electrodes. Operating the monitoring setup, which was originally installed using rod electrodes, had been a challenge due to high grounding resistances in winter, effectively prohibiting the collection of measurements. Replacement of the rod electrodes with mesh electrodes

resulted in an immediate reduction of the average GR by 73 % from 1.5±0.9 to 0.4 ±0.1 kΩ (thawed conditions). Comparable winter grounding resistances were reduced from 64 ±32.1 to 25 ±11.4 kΩ, and following the replacement, measurements could be collected throughout the season.

We conclude that temperature, electrode shape and properties as well as lithology of the monitored site have significant impact on electrode grounding resistance and array performance, particularly in the cold/dry season. Thus, optimization of the electrode design should be a main consideration when planning a long-term monitoring project. Under the conditions we tested, the use of plate or mesh electrodes instead of rod electrodes were an advantage at all sites and all seasons. Mesh electrodes constitute an improvement only when the soil type allows to take advantage of the larger effective surface area (fine grained mineral or organic soils).

Automated long-term time lapse ERT monitoring of high-latitude permafrost – results of 3 years of monitoring and modeling study

Sonia Tomaskovicova & Thomas Ingeman-Nielsen

Technical University of Denmark, Denmark

The importance of long-term, continuous and relatively dense ERT timeseries for improved process analysis in permafrost is well established. However, due to remoteness of sites, logistical constraints and harsh environment, high latitude permafrost presents a particular challenge for long-term ERT monitoring. Furthermore, extremely high grounding resistances hamper acquisition of series of complete freeze-thaw cycles that are needed for comparison with climate observations. In this contribution, we share how we resolved some of the logistical and technical challenges inevitably linked to the ERT monitoring in the Arctic. We also show results of a comprehensive permafrost monitoring project, currently running successfully for more than 3 years.

Since August 2012, we have been operating an automated monitoring station for measuring ground resistivity, water content and temperature at a site near the airport in Ilulissat, West Greenland (69°14' N, 51°3' W, 33 m a.s.l.). The site has a long observation history, starting with geotechnical investigations in late 1970's. The site is located in continuous permafrost zone, with mean annual air temperature -5.1 °C (2003-2012). The active layer thickness at the site is approximately 80 cm, below which ice-rich permafrost is found. The sediment cover consists of postglacial silt and clay marine deposits. These deposits are fully leached in the upper part, with residual salinity increasing with depth. Consequently, deeper parts of the soil profile are technically unfrozen due to freezing point depression. Gneiss bedrock is encountered at 7 m depth [Ingeman-Nielsen et al., 2008].

The monitoring station consist of one ERT profile, measurements of unfrozen water content at two depths in the active layer, measurement of ground temperature in 2 deep boreholes (4 and 6 m) and one temperature probe (length 1.5 m, with 16 sensors every 10 cm) for detailed monitoring of temperature dynamics of the active layer. Additional environmental observations include air temperature, approximate snow depth (using temperature sensors above ground) and ground thermal conductivity.

The ERT profile consists of 64 stainless steel, mesh-shaped electrodes, with spacing of 0.5 m. The mesh electrode shape is result of extensive field and laboratory testing study aiming to optimize the electrode design for long-term ERT monitoring. Automated ERT measurement system consists of a terrameter SAS1000 with electrode selector ES10-64 and an on-site mini computer. The computer controls daily acquisition of grounding resistances for each electrode of the array and a protocol of total 1625 datapoints of Schlumberger and Gradient array. The data are uploaded daily to a server at The Technical University of Denmark via GSM network.

The unfrozen water content is measured at 30 cm and 55 cm depth in the active layer by sensors using frequency domain reflectometry method. A soil-specific calibration equation is used to convert the measured permittivity into volumetric water content.

Comparison of results of joint resistivity, temperature and soil moisture monitoring evidences that changes of subsurface ground resistivity follow closely temperature and water dynamics in the ground. In the frozen period of the year (ca December to June), water content is consistently at its minimum, at 20 %. During this time, however, even relatively small temperature oscillations well below 0 °C produce noticeable changes in ground apparent resistivity. This suggests that notable phase change happens at temperatures as low as -5 to -10 °C and it points to high sensitivity of the ERT to track these changes. During the thawed season, the changes in resistivity are driven mainly by the changes of water content due to water movement in the active layer. After the initial ground thawing throughout the month of June, the ground reaches full saturation at up to 76 %. The thawing is reflected in sharp decrease of ground resistivity throughout the profile. Initial steep increase in soil moisture is followed by a period of drying out, or water runoff, during which the water content declines down to 40 % (while ground temperatures remain positive).

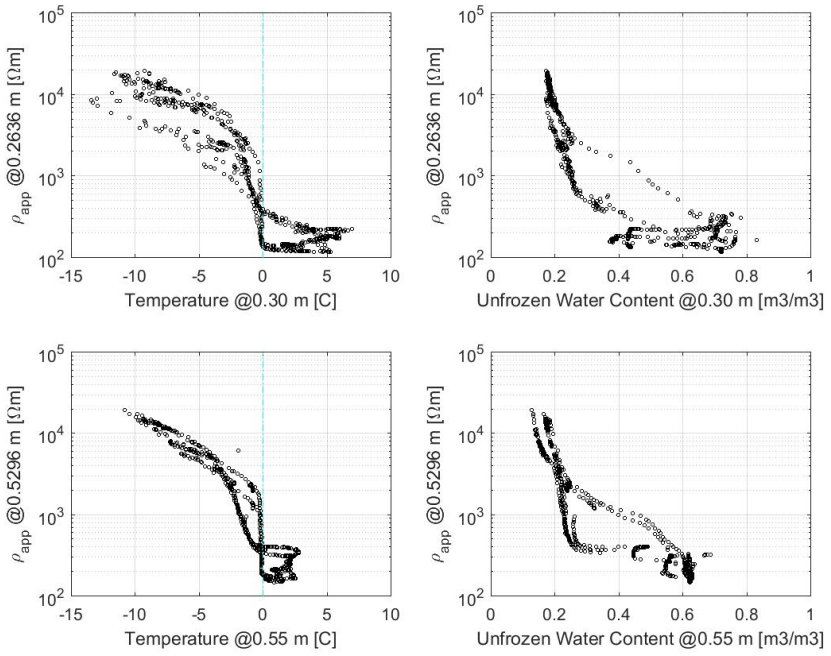

Figure 1: Scatter plots of the apparent resistivity against temperatureand water content at two depth levels in the active layer. Daily average values for 3 years.

This induces increase in resistivity at the top of the active layer, while the resistivity in the deeper portion of the profile steadily decreases as result of propagation of heat wave from ground thawing. The ground then reaches full saturation again during the relatively most humid months of August and September. It is only at this point that the ground resistivity reaches its yearly minimal values.

The ground surface temperature measurements have been successfully used in modeling of ground temperatures throughout the depth of the monitored profile. The 1D-heat model is able to reproduce the measured ground temperatures with mean deviation $\pm 0.2°$. While the full saturation condition at the site is valid (throughout the year except from July to mid-August), the unfrozen water content in the ground can be successfully modeled from ground temperatures (measured or modeled) using soil-specific freezing curve coefficients [Lovell, 1957]. As the changes in ground resistivity are intrinsically linked to the changes in the water content, this kind of integrated observation and modeling may pave the way for modeling of ground temperatures using exclusively surface observations (ground surface temperature and ground resistivity).

This ongoing monitoring project demonstrates feasibility and potential of long-term integrated high-latitude permafrost monitoring with focus on electrical and thermal properties of the ground. We present details of the permanent measurement setup and propose improvements to monitoring station design that mitigate the effects of extreme grounding resistances on acquisition of continuous resistivity timeseries. Results of 3 years of daily measurements of ground resistivity, temperature and water content provide insight into processes governing permafrost evolution and allow for modeling of important environmental parameters for which direct observations are difficult to acquire or missing.

References

Ingeman-Nielsen, T.; Foged, N.; Butzbach, R. and Stuhr Jørgensen, A. [2008]: Geophysical Investigation of Saline Permafrost at Ilulissat, Greenland. In: Kane, D.L. and Hinkel, K.M.(eds.), *Proceedings of the Ninth International Conference on Permafrost*, Institute of Northern Engineering, University of Alaska Fairbanks, Fairbanks, USA, 29 June–3 July 2008, volume 1, pages 773–778. ISBN 978-0-9800179-2-2. URL http://ipa.arcticportal.org/publications/conference-proceedings.

Lovell, C.W. Temperature effects on phase composition and strength of partially-frozen soil. *Highway Research Board Bulletin*, 168:74–95, 1957.

Magnetic studies in Lena river delta: the results of 2014-2015 fieldworks and future plans

Leonid Tsibizov[1,2], Dmitry Ayunov[1], Nikolay Semakov[1,2], Petr Dyadkov[1,2], & Daria Pavlova[1,2]

[1] *Trofimuk Institute of Petroleum Geology and Geophysics of Siberian Branch of Russian Academy of Sciences (IPGG SB RAS), Russian Federation*
[2] *Novosibirsk State University (NSU), Russian Federation*

Magnetic studies in Lena river delta in 2014 and 2015 were made both as a part of integrated geophysics and as an independent research effort and allowed to clarify a number of different-scale features in the region.

Magnetic measurement in permafrost zone can be a useful method to discriminate different types of permafrost due to the small difference in permafrost magnetic susceptibility because of its structure and composition. Pilot magnetic survey using proton magnetometer was made on the well-characterized thawed structure ("alas"), the measured value of magnetic anomalies are as high as 10 nT. The magnetic susceptibility of core samples from the borehole (17 m depth) in the centre of alas was measured (range from 0.0001 to 0.001 SI). Obtained data shows features in the alas subsurface structure like presumable zone of higher annual sedimentation and pieces of dry and wet permafrost. Short-term plans in this field are to research the detailed structure of upper permafrost section using high-precision square magnetic survey and to clarify the origin of such anomalies and the possibility of their accurate interpretation.

Another well-known application of magnetic survey is determination of geologic objects like faults and intrusive bodies, which can have an influence on the permafrost degradation being the conductor of endogenous thermal heat and gas emanations. Besides that, the information about basement structure heterogeneities can be important for the geological reconstruction of the area of the river delta evolution. During the 2014-2015 fieldwork period several basement features were located on Sardakh and Kurungnakh islands and along the Trofimovskaya channel using ground and river magnetic survey respectively, also magnetic properties of soil and rock samples from outcrops were measured. Based on interpretation of the obtained data some of these anomalies were explained: presumable block boundaries on Trofimovskaya channel near the main Lena delta fault were located; basalt stockwork between Amerika-Haia and Ortho-Haia barrows on the Kurungnakh island were found. The typical magnetic anomalies of such objects are up to 60 nT. We conducted our survey on two levels: 1 and 2 meters high from the ground to estimate the depth to an object of interest.

All these and further magnetic studies are complicated by the fact that Lena delta is in polar region where the magnetic field is greatly disturbed due to the proximity of the magnetic pole. We performed a number of studies in magnetic variation non-identities, placed a set of temporary base magnetic stations for the duration of field works. Data obtained from these stations showed that total magnetic field non-identities can reach several nT in magnetic-quiet periods and up to 50 nT in magnetic-disturbed periods. This fact should be taken into consideration in the process of most magnetic surveys.

It is well-known that the magnetic pole is moving to the North Siberia in the direction of Taimyr, giving another important application of such measurements: to determine the morphologic parameters of the magnetic field in polar region and to trace it's evolution. At present time there are very few magnetic observatories in the region, and the first step to change this is to establish a network of secular variation observation sites (SVOS) for annual vector measurements, that can supplement the observatory data. In 2015 several SVOS were founded in Lena delta and the first results allowed to clarify the data of Tiksi observatory. The short-term plans are to install such observation points on the northern coast between Lena delta and Taimyr. These investigations may have a significance in terms of probably relations between geomagnetic field and climate. In this case, geomagnetic field changes are to be taken into account in the permafrost degradation prognosis.

Geophysical identification of hydrologic flow paths on arctic hillslopes

Emily B. Voytek[1], Caitlin R. Rushlow[2], Sarah E. Godsey[2], & Kamini Singha[1]

[1] *Colorado School of Mines, USA*
[2] *Idaho State University, USA*

Shallow subsurface flow is a dominant process controlling hillslope runoff generation, soil development, and solute reaction and transport. Despite their importance, the location and geometry of flow paths are difficult to determine. In arctic environments, shallow subsurface flow paths are limited to a thin zone of seasonal thaw above continuous permafrost, which is traditionally assumed to mimic to surface topography. Here we use a combined geophysical approach of electrical resistivity tomography (ERT) and self-potential measurements (SP) to map shallow subsurface flow paths in and around water tracks, drainage features common to arctic hillslopes. ERT measurements delineate thawed zones in the subsurface that control flow paths, while SP is sensitive to groundwater flow. Frost probe and ERT data compared well in the areas of moist acidic tundra on the hillslope outside the water tracks, but in the water tracks, zones of lower electric resistivity extend deeper than the frost probe measurements. This finding suggests that traditional techniques may underestimate active layer thaw and the extent of the flow path network on arctic hillslopes. SP measurements identify complex 3-D flow paths in the thawed zone. Our results lay the groundwork for investigations into the seasonal dynamics, hydrologic connectivity, and climate sensitivity of spatially distributed flow path networks on arctic hillslopes.

SESSION 23

Hazards and Risks related to Changing Mountain, Low-Land and Coastal Permafrost

Convener:

Christian Huggel, *University of Zurich, Switzerland*

Fujun Niu, *State Key Laboratory of Frozen Soil Engineering, Cold and Arid Regions Environmental and Engineering Research Institute, Chinese Academy of Sciences, China*

Katy Barnhart, *University of Colorado Boulder, USA*

Environmental changes, including climate change, affect permafrost in various and complex ways. Changing permafrost, in turn, can alter hazards and risks. The physical processes that control changes of hazards related to permafrost are often insufficiently understood, and their characteristics depend on the region and type of environment. Risk, defined as a function of hazard, exposure and vulnerability, can also change although so far changes in exposure and vulnerability are typically more influential than the climatic component. This session aims at generating a synthesis perspective of the current state of knowledge in hazards and risks related to permafrost. Contributions from mountain, lowland and coastal areas are highly welcome. Contributions may focus on physical aspects related to hazards, and/or include other components of risk. They may cover various timescales, from past to present and future.

GIS of the gas-emission crater area (Yamal Peninsula, Russia)

Ksenia Ermokhina[1], Alexandr Kizyakov[2], Marina Leibman[1], & Artem Khomutov[1]

[1] *Earth Cryosphere Institute, Siberian Branch of Russian Academy of Sciences, Tyumen, Russian Federation*
[2] *Lomonosov Moscow State University, Faculty of Geography, Russian Federation*

GIS of the area was developed in order to study a phenomenon of the gas-emission crater in the Central Yamal. Formation of gas-emission craters is a newly discovered cryological phenomenon which may pose a hazard for economic facilities in permafrost zone.

GIS methods which were used enabled to collect, visualize and analyze spatial data. Development of the GIS is intended for

1. systematization and organization of existing information on geocryological, geomorphological and landscape structure of the area for joint analysis;
2. reveal of environmental conditions and estimation of the factors (or composition of factors) which led to gas-emission crater formation.

Fieldwork was carried out since 2014 [Leibman et al., 2014]. The most efforts were put on study of the exposed sections in the crater walls and thermocirque (which is located nearby), assessment of relief dynamics and investigation of landscape structure of the key site.

Mapping of relief and relief-forming processes, preliminary landscape mapping were carried out during the fieldwork. Field data was analyzed jointly with satellite images for estimation of relief features before and after the crater formation [Kizyakov et al., 2015]. A digital elevation model (DEM) of the relief was developed by processing of satellite image stereo pair (WorldView-1). This provided an opportunity to get quantitative specifications of the relief change. Joint processing of the field landscape descriptions and satellite data led to landscape typification which was used as a base for landscape mapping of larger than a key site territory (Fig. 1).

Narrow elongated watershed surfaces (42-48 m, evaluated by EGM96) dissected by erosion and thermokarst landforms are found in the north of the area. Those are supposed to be the surface of the Middle or Upper Pleistocene Marine plain. Polygonal microrelief could be found locally here as well.

Small lakes (diameter 80-230 m) are located in the upper parts of valleys which are dissecting watershed surface in all directions. Round shape of these valleys' openings (in plan view) is associated with lakes and drain lake depressions (khasyreis). Cryogenic landslides are widely distributed on slopes and lake shores. Gas-emission crater is situated to the south of a hill on the peripheral side of khasyrei formed in the upper section of erosion valley.

Along with relief, the other main GIS layer is vegetation which is the main land surface feature well seen on the images and rather well understood in environments of Yamal Peninsula.

Horizontal structure of vegetation cover reflects the main features of relief and geomorphological processes. Dwarf-shrub moss-lichen tundra occupies about 1/4 of study area (well-drained ecotopes) and is tightly associated with watershed surfaces. More than the half of the area (including significant sections of slopes and valleys) is covered by complex of willow- and shrub (willows+*Betula nana*) -grass-(moss) communities. Identifiable vegetation types are found on the khasyreis, low lake shores, wider sections of flood plains and relief depressions (in total about 9 % of the study area). In contrast to above-mentioned vegetation types these are more fragmented and occupy ecotopes of far lesser area. Shrub-(dwarf-shrub)-grass-(moss) hummock tundra is often developed on wet gentle slopes (5 % of the area). Complex of *Betula nana* communities (often dwarf shrub -moss-lichen) is associated with relatively dry ecotopes of hilltops (5 % of the area).

GIS of the area is an open system suitable for uploading new information sources of all types – raster, vector, tables and text.

Developed system of data accumulation, storage and processing of this unique cryological phenomenon serves as a basis for analysis of environmental conditions leading to its occurrence. The next planned step of the research is establishing ranking criteria (i.e. combination of natural settings) to predict the phenomenon. As a result, the methodological possibility for assessment of territory in connection to gas-emission craters hazard appears.

Plant communities	Main species	Horizontal structure (projective cover)
complex of wet meadows with sparse willows and sedge wetlands	*Salix glauca, Carex aquatilis, C. rotundata, C. rariflora, Eriophorum polystachion, E. scheuchzeri,* Sphagnum spp.	Total = 55-95% shrub layer < 5% dwarf shrubs and grasses layer = 45-95% moss-lichenous layer = 0-35%
dwarf-shrub moss-lichen tundra	*Vaccinium vitis-idaea subsp. minus, Salix nummularia, Carex arctisibirica, Poa arctica, Hierochloe alpina,* Alectoria nigricans, Cetraria islandica, Cladina arbuscula, Aulacomnium turgidum, Dicranum elongatum	Total = 90-100% shrub layer = 0% dwarf shrubs and grasses layer = 60-70% moss-lichenous layer = 90-100%
communities of khasyrei meadows and wet meadows of lake shores	*Arctophila fulva, Carex aquatilis, C. concolor, Eriophorum scheuchzeri, Calamagrostis neglecta, Dupontia fisheri, Comarum palustre, Nardosmia frigida, Saxifraga cernua,* Drepanocladus spp., Mnium spp.	Total = 80-100% shrub layer = 0% dwarf shrubs and grasses layer = 65-75% moss-lichenous layer = 0-90%
complex of valley communities (shrub and meadow communities)	*Salix lanata, S. glauca, Equisetum boreale, Carex concolor, Eriophorum scheuchzeri, Calamagrostis langsdorffii*	Total = 90-100% shrub layer = 0-40% dwarf shrubs and grasses layer = 50-100% moss-lichenous layer = 0-80%
shrub-(dwarf-shrub)-grass-(moss) hummock tundra	*Betula nana, Salix lanata, S. glauca, Carex arctisibirica, C. concolor, Rubus chamaemorus, Vaccinium vitis-idaea subsp. minus, Luzula multiflora,* Aulacomnium turgidum, A. palustre, Pleurozium schreberi, Sphagnum lenense	Total = 100% shrub layer = 50-60% dwarf shrubs and grasses layer = 30-50% moss-lichenous layer = 60-100%
complex of willow- and shrub (willows+Betula nana) -grass-(moss) communities	*Salix lanata, S. glauca, Betula nana, Carex concolor, Pedicularis lapponica, Nardosmia frigida, Polemonium acutiflorum, Ranunculus borealis, Equisetum boreale, Calamagrostis langsdorffii,* Hylocomnium splendens, Dicranum angustum, Sanionia uncinata	Total = 100% shrub layer = 40-100% dwarf shrubs and grasses layer = 30-70% moss-lichenous layer = 30-100%
complex of Betula nana communities (often dwarf shrub - moss-lichen)	*Betula nana, Empetrum subholarcticum, Ledum decumbens, Vaccinium vitis-idaea subsp. minus, Carex arctisibirica, Equisetum boreale, Calamagrostis lapponica,* Pleurozium schreberi, Dicranum spp., Flavocetraria cucullata, Cladina rangiferina, C. arbuscula, Ochrolechia frigida	Total = 90-100% shrub layer = 30-70% dwarf shrubs and grasses layer = 30-60% moss-lichenous layer = 60-100%

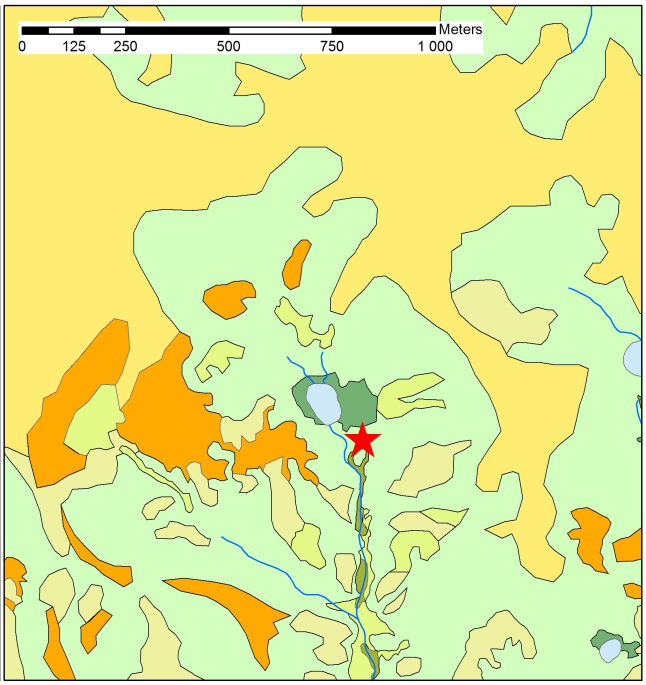

Figure 1: Vegetation map

References

Kizyakov, A.I.; Sonyushkin, A.V.; Leibman, M.O.; Zimin, M.V. and Khomutov, A.V. [2015]: Geomorphological conditions of the gas-emission crater and its dynamics in Central Yamal. *Earth's Cryosphere*, 19(2):13–22, URL http://www.izdatgeo.ru/pdf/earth_cryo/2015-2/13_eng.pdf.

Leibman, M.O.; Kizyakov, A.I.; Plekhanov, A.V. and Streletskaya, I.D. [2014]: New permafrost feature – Deep crater in Central Yamal (West Siberia, Russia) as a response to local climate fluctuations. *Geography Environment Sustainability*, 7(4):68–80, URL http://www.geogr.msu.ru/GESJournal/contents.php?iid=22&menupos=7.

Measuring and modelling permafrost at local and regional scales in the Kazbek region, Russian Caucasus

Regula Frauenfelder[1], Christian Huggel[2], Sonja Zgraggen-Oswald[3], Igor Galushkin[4], & Sergey Chernomorets[5]

[1]*Dept. of Geography, University of Zurich, Switzerland; now at Norwegian Geotechnical Institute Oslo, Norway*
[2]*Dept. of Geography, University of Zurich, Switzerland*
[3]*Dept. of Geography, University of Zurich, Switzerland; now at Amt für Tiefbau, Altdorf, Switzerland*
[4]*InfoTerra, Vladikavkaz, North Ossetia, Russia*
[5]*Lomonosov Moscow State University, Moscow, Russia*

Widespread melting of glaciers and rising permafrost temperatures provide an early indication of the environmental and societal significance of global warming. In both high-latitude and high-elevation mountain ranges, glaciers commonly interact with permafrost, leading to potentially hazardous geomorphological processes at the temporal and spatial interfaces between them. Glacier retreat and thawing permafrost affect the stability of steep slopes in alpine mountain ranges. Detachment of hanging glaciers as well as glacier retreat can change the stress distribution of a slope and may induce destabilization. Several combined avalanche/rockfall events in high mountain regions during the 20^{th} century are likely to have been connected to processes relating to glacier shrinkage and permafrost warming/thawing. With ongoing climate change, thermal conditions are becoming a critical aspect for slope stability in high mountains. Results from laboratory experiments and simulations have shown that the stability of ice-filled joints decreases with increasing ice-/bedrock temperature, with a presumed minimum stability between -1.5 and 0 °C. Phase transition from frozen to liquid water in rock fissures is therefore seen as an important factor influencing the slope stability.

A dramatic slope failure occurred on September 20th 2002, in the Kazbek massif of the Northern Caucasus (Republic of North Ossetia-Alania, Russia). After some precursory ice and rock avalanches on the Kolka glacier during the two months prior to the disaster, the main event started as a slope failure in the NNE face of Dzhimarai-khokh (4780 m a.s.l.) initially involving c. 10–20×106 m^3 of rock and ice from hanging glaciers. This mass fell onto the underlying Kolka glacier which was entrained to a major extent by disruption and liquidization. The resulting extremely large rock-ice avalanche, on the order of more than 100 × 106 m^3, devastated the valley for more than 30 km. The event caused the death of about 140 people and the resulting damage totalled nearly 20 million Euro. In May 2014, a similar, yet somewhat smaller event took place from the east face of Mount Kazbek where large amounts of ice and rock failed, transforming into a massive debris flow that travelled down the Devdorak glacier and valley and blocked the Terek River valley, which is the main connection between North Ossetia and Georgia [Chernomorets et al., 2007]. Similar mass flow events from Devdorak glacier are reported from the 18^{th} and 19^{th} century.

The Kolka-Karmadon case is one of the largest rock-ice avalanches to have been documented. Due to the implications for worldwide glacier and permafrost hazard assessments, it was important to systematically analyze the event. The permafrost study presented here was initiated within the context of the hazard assessment and disaster prevention carried out shortly after the event. Previous studies (e.g., Evans et al. [2009], Huggel et al. [2005]) have investigated the erosion and entrainment of Kolka glacier, the avalanche dynamics, possible trigger mechanisms and several post-disaster hazards. Publications emphasized the importance of the surface and sub-surface thermal conditions for the initial avalanche failure in the Dzhimarai-khokh NNE face but did not include in-situ observations or modelling. Based on data from a former weather station near the village of Karmadon, however, estimated a mean annual air temperature (MAAT) of -6 ±2 °C at the lower end and -11 ±3 °C at the upper end of the failure zone. Bedrock surface temperatures in the failure zone were thus estimated to be about -5 to -10 °C. The thermal conditions, however, were complicated by the exist-

ence of hanging glaciers in the Dzhimarai-khokh NNE wall. Such steep ice bodies can induce significant thermal anomalies within the underlying bedrock.

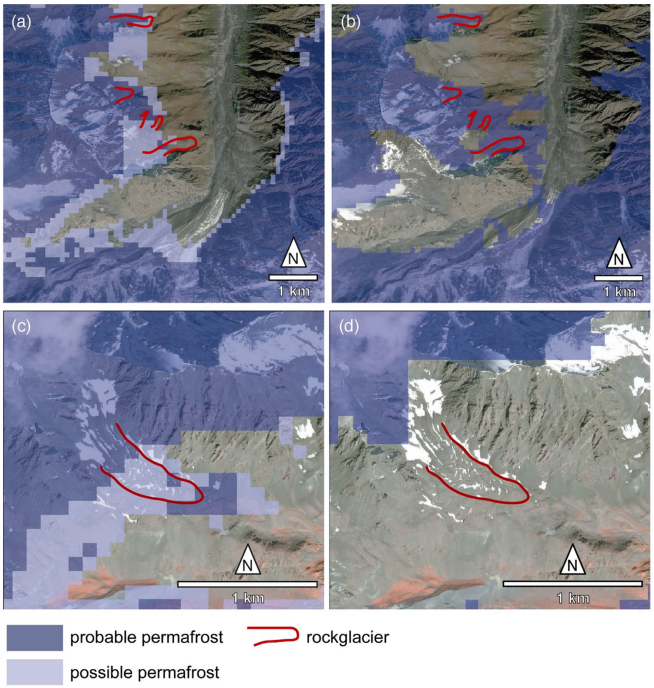

Figure 1: Permafrost distribution modelling results overlaid on a QuickBird satellite image of the Upper Genaldon valley (a and b) and the south-west face of Chach-khokh (c and d). Active rock glacier tongues are outlined in red.

In the present study, near-surface temperature rock-wall loggers were installed to gain a better understanding of temperature conditions near the rock-ice avalanche failure zone. These temperature data, along with rock glaciers, mapped from satellite imagery of the Advanced Spaceborne Thermal Emission and Reflection Radiometer (ASTER) and QuickBird, were used to validate spatial predictions undertaken with two existing permafrost models. The models were then applied to the mountainous terrain throughout North Ossetia-Alania, providing far greater detail on permafrost distribution in this part of the Caucusus than has been possible to date. The study represents an example of the level of permafrost assessment that can be achieved in a region with poor availability of climate data and ground information.

Our study provides an improved understanding of the permafrost distribution in the North Ossetian Caucasus in general, and in particular for the northern slopes of Dzhimarai-khokh and Mt. Kazbek. For the 2002 avalanche thermal conditions of glacier ice and frozen rock likely played an important role. For the 2014 Kazbek/Devdorak avalanche disaster the results of this study can represent an important basis for an improved understanding of the characteristics and triggers of the slope failure.

The modelling approach used could be applied despite the paucity of field data. The results show that the two permafrost models developed in a climatically similar region, can be adjusted based on regional climate data to provide first-order estimates of the permafrost distribution. The employment of rock temperature loggers in this setting was a challenge, but the resulting temperature data were important, both for model validation and more detailed on-site information of the Kolka rock-ice avalanche failure area. The permafrost map developed for the territory of the Republic of North Ossetia is considered to be a useful instrument for regional planning purposes and for guiding further detailed investigations at critical sites. Any local use would require more in-situ measurements such as geophysical soundings and more extensive temperature measurements. Finally, the study showed the potential and limitations for permafrost assessments in high-mountain regions worldwide, many of which have similar limited data availability.

References

Chernomorets, S.S.; Tutubalina, O.V.; Seinova, I.B.; Petrakov, D.A.; Nosov, K.N. and Zaporozhchenko, E.V. [2007]: Glacier and debris flow disasters around Mt. Kazbek, Russia/Georgia. In: Chen, C.-L. and Major, J.(eds.), *Debris-Flow Hazards Mitigation: Mechanics, Prediction, and Assessment*, pages 691–702. Rotterdam, Millpress.

Evans, S.G.; Tutubalina, O.V.; Drobyshev, V.N.; Chernomorets, S.S.; McDougall, S.; Petrakov, D.A. and Hungr, O. [2009]: Catastrophic detachment and high-velocity long-runout flow of Kolka Glacier, Caucasus Mountains, Russia in 2002. *Geomorphology*, 105(3–4):314–321, doi:10.1016/j.geomorph.2008.10.008.

Huggel, C.; Zgraggen-Oswald, S.; Haeberli, W.; Kääb, A.; Polkvoj, A.; Galushkin, I. and Evans, S.G. [2005]: The 2002 rock/ice avalanche at Kolka/Karmadon, Russian Caucasus: assessment of extraordinary avalanche formation and mobility, and application of QuickBird satellite imagery. *Natural Hazards and Earth System Sciences*, 5(2): 173–187, doi:10.5194/nhess-5-173-2005.

Ground thermal characteristics at a high-latitude rockslide site (Polvartinden, Northern Norway)

Regula Frauenfelder[1] & Ketil Isaksen[2]

[1]*Norwegian Geotechnical Institute, Oslo, Norway*
[2]*Norwegian Meteorological Institute, Oslo, Norway*

Introduction

In the morning of June 26th, 2008 a rock slide detached at approximately 595 m a.s.l. from the northeast facing slope of Polvartinden at 69°10'18"N/19°57'47"E, a 1275 m high mountain in Signaldalen, Troms county, Northern Norway. The rock slide endangered two farms and several recreation cabins, and it permanently destroyed a considerable amount of livestock pastures. Visible in situ ice was observed in the detachment zone just after the rock slide event. This observation led to the hypothesis that warming or degrading of permafrost could have played a role in the timing and the magnitude of the event. Therefore, a temporary temperature monitoring system was put in place and repeated surveying of the detachment zone and the adjacent slopes was carried out between 2009 and 2013.

Ground surface temperatures were measured with miniature temperature data loggers of the type M-Log5W (GeoPrecision GmbH, Germany), redesigned UTL-1 (University of Bern and University of Zurich, Switzerland) and UTL-3 (GEOTEST and WSL Institute for Snow and Avalanche Research SLF, Switzerland). The loggers were installed to measure temperatures at approximately 10 cm depth at several locations along the NNW-ridge of Polvartinden and in the valley ground. Measurements were ongoing from September 2009 to August 2013. Four temperature measurement series are continued beyond 2013. Nine temperature loggers (type M-Log5W and redesigned UTL-1) were installed in vertical or near vertical rock faces on rock outcrops and along small cliffs with different aspects, while five loggers (UTL-1, UTL-3) were placed directly into the soil material. One additional logger was installed in the valley floor in order to monitor air temperature.

Results

Regional climate data since 1948 and nearby borehole data suggest a general warming and that the highest mean near surface temperatures on record occurred some months before the Signaldalen rock slide detached. The correlation between the air temperature measurements (2009–2011) in the valley bottom and data covering the same period from a nearby official weather station in Skibotn is very high (R2 = 0.97). This allowed using the Skibotn data for modelling of the potential permafrost distribution and recent ground temperature changes in Signaldalen by coupling the in-situ surface temperature data with regional and large-scale climate data.

Our in situ rock temperature measurements show mean annual ground surface temperatures (MAGST) between -1.4 °C (coldest logger location R6) and -0.3 °C (warmest logger location R5) in 2009/2010, and between +0.4 °C (coldest) and +1.1 °C (warmest) in 2010/2011. Temperature recordings in all loggers were considerably higher during 2010/2011 than in 2009/2010. Interestingly, our first year measurements took place during the coldest period during the last 20 years.

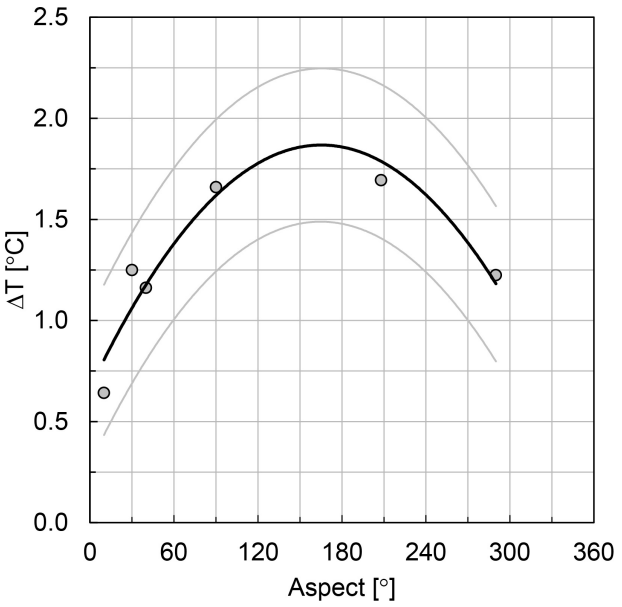

Figure 1: Annual temperature difference (ΔT) between calculated air temperature and measured rock face temperatures.

For the vertical rock face sites, the lowest MAGST was recorded at the north facing site in 2009/2010. The large inter-annual variability found between 2009/2010 and 2010/2011 is in congruence with general climate conditions in Troms and is confirmed by measurements in nearby mountain slopes [Isaksen et al., 2011].

The figure shows annual temperature difference (ΔT) between calculated air temperature and measured rock face temperatures showing the aspect dependency as derived from data. The points are the calculated mean values and the black line is the best polynomial fit to the data (R^2=0.90). The grey lines show the polynomial fit to the interquartile range of ΔT. Our results show that rockwall MAGST is aspect dependent also at this high latitude, but to a much lesser degree than in the Alps. We observe an altitudinal difference of MAGST of several tens of meters between northerly and southerly aspect, as compared to several hundred meters in, e.g., the Swiss Alps (cf. Gruber et al. [2004]). Due to our small sample size and since the southern orientation is missing there remains some uncertainty about the absolute values. Yet, Hipp et al. [2014] reported comparably small aspect dependencies of the lower permafrost limit for a location in Southern Norway (61°N).

References

Gruber, S.; Hoelzle, M. and Haeberli, W. [2004]: Rockwall temperatures in the Alps: modelling their topographic distribution and regional differences. *Permafrost and Periglacial Processes*, 15(3):299–307, doi:10.1002/ppp.501.

Hipp, T.; Etzelmüller, B. and Westermann, S. [2014]: Permafrost in Alpine Rock Faces from Jotunheimen and Hurrungane, Southern Norway. *Permafrost and Periglacial Processes*, 25(1):1–13, doi:10.1002/ppp.1799.

Isaksen, K.; Blikra, L.H. and Eiken, T. [2011]: The existence of warm permafrost in unstable rock slopes in western and northern norway. In *Geophysical Research Abstracts*, volume 13, EGU2011-10942, EGU General Assembly.

Root induced changes to soil hydrological properties and permafrost stability in Qinghai-Tibet Plateau, China

Zeyong Gao[1], Fujun Niu[1], Yibo Wang[2], Zhanju Lin[1], & Jing Luo[1]

[1] *State Key Laboratory of Frozen Soil Engineering, Cold and Arid Regions Environmental and Engineering Research Institute,Chinese Academy of Sciences, People's Republic of China*
[2] *College of Earth and Environment Sciences, Lanzhou University, People's Republic of China*

Root induced changes to soil hydrological properties (SHP) are an essential component in understanding the hydrology of an ecosystem, and the resilience of ecosystem to climate change. However, the research of alpine plant effect on SHP in Qinghai-Tibet Plateau is relatively small in the past few decades. In this study, field tests were carried out to investigate the alpine grassland root density (including alpine swamp meadow, alpine meadow, and alpine steppe), SHP (soil saturated hydraulic conductivity, soil infiltration processes and soil moisture content) and permafrost temperature. Soil physicochemical properties, soil water-holding capacity were also measured in laboratory. At last, we compared the difference of permafrost state under the several of psychrophyte roots density. The results showed that the plant roots have remarkable effects on SHP. When the root density decreases from 44.4kg m^{-3} at alpine swamp meadow to 5.78kg m^{-3} at alpine steppe, the soil saturated hydraulic conductivity increased from 46.08 cm d^{-1} to 361.44 cm^{-1}. However, soil water-holding capacity and soil moisture content decreased gradually with the decreasing of root density in active layer. The processes of plant roots effect on soil hydrological properties mainly including physical and chemical. On the one hand, the development of roots decreases the infiltration capacity of precipitation though blocking the soil porosity. On the other hand, plants roots are close related to soil chemical properties like organic matter, which is vital to form soil aggregation and act on soil moisture migration. Thereby the soil hydrological properties were all changed. Our results confirmed that peat soil layer played an important role in cooling permafrost and enhancing its stability, the each of three sites shows significant differences of annual mean ground temperature of 5-m depth, ranging from -1.58 °C (alpine swamp meadow) to -0.72 °C (alpine steppe). The less plant roots lead to an intense infiltration capacity of precipitation to deeper frozen soil.

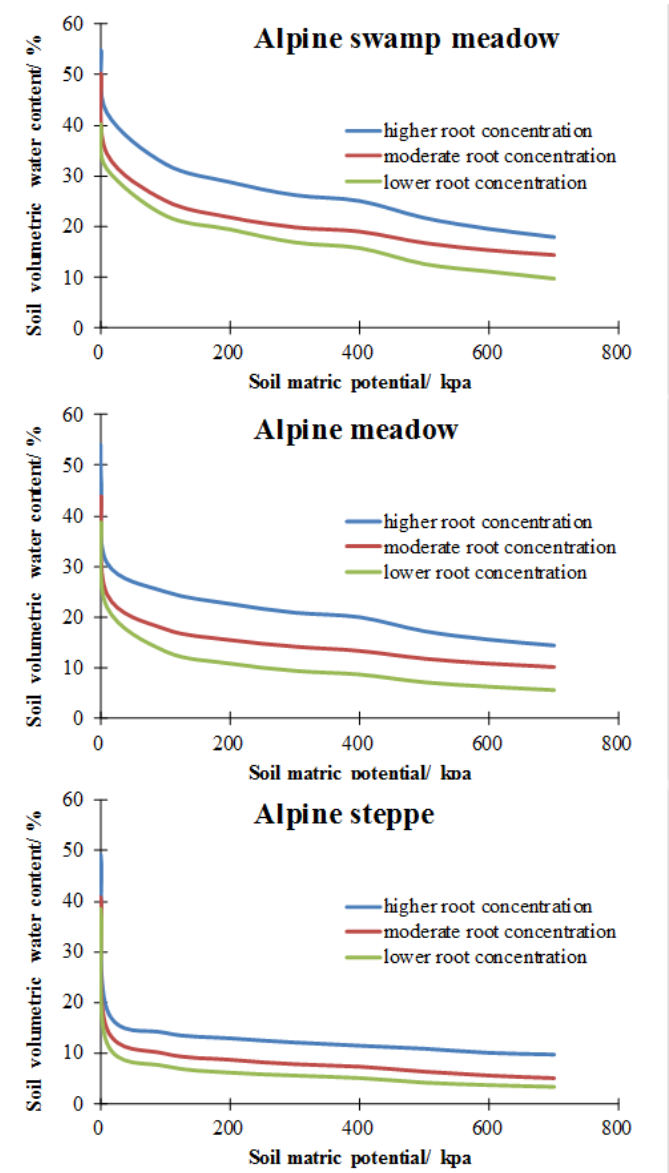

Figure 1: Root-induced changes of soil water-holding capacity

Consequently, the permafrost temperature was enhanced, and the permafrost stability was reduced. Results of the analysis showed that if the grasslands

are well protected under the impact of climate change and human activities, the alpine soil and permafrost stability will be improved in Qinghai-Tibet Plateau. Our results will be helpful for describing hydraulic parameters with the aim of modeling soil water flow more accurately in permafrost regions. Future work is required to modify the changes of SHP in the process of root growth, development and decompose. And to establish the model to describe the relationship among plant root, alpine soil and permafrost, which is essential to better understanding changes of ecological environment in the Qinghai-Tibet Plateau.

Historic movement analysis of frozen debris Lobes, Southern Brooks Range, Alaska

Nora L. Gyswyt[1], Margaret M. Darrow[1], & Ronald P. Daanen[2]

[1] *University of Alaska Fairbanks, USA*
[2] *Alaska Division of Geological& Geophysical Surveys, USA*

Introduction

We used historic imagery analysis to characterize the movement behavior of frozen debris lobes (FDLs), which are slow-moving landslides in permafrost areas. The eight FDLs presented here reside along the Dalton Highway in the southern Brooks Range between coordinates 67°58'47" N - 67°43'1" N, and 149°51'8" W - 149°42'54" W. It is their proximity to the Dalton Highway and the Trans Alaska Pipeline System that classifies them as geohazards. The Dalton Highway is Alaska's most economically important highway with respect to the energy resource industries it supplies. FDL research within this corridor began in 2008, including field observations and a preliminary analysis of historic rates using remote sensing data [Daanen et al., 2012]. Current research includes multiple years of field work to track surface movement rates of these lesser-known landforms through differential GPS (DGPS) measurements [Darrow et al., 2015]. Currently, FDL-A is the closest to the highway. As of August 2015, it was 39.2 m from the embankment and moving at a rate of 5.2 m yr^{-1}as determined from the DGPS measurements.

Field measurements provide high resolution data, but are intensive, costly, and focused within a narrow time scale, compared to the minimal costs of temporal remote sensing data acquisition. Long-term average movement rates can be calculated from historic imagery to provide predictions of future movement rates, which help to identify the risk FDLs pose to important infrastructure.

Methods

We obtained aerial and satellite imagery, Light Detection And Ranging (LiDAR) data, and Interferometric Synthetic Aperture Radar (IfSAR) data over a temporal span from 1955 to 2014. A variety of data sources were used, including the U.S. Geological Survey, Alaska High-Altitude Photography, Quantum Spatial, DigitalGlobe WorldView, and Ikonos. Geospatial data experts from the Geographic Information Network of Alaska (GINA) produced orthorectified mosaics for each data set. Within a GIS environment, we used contour lines derived from digital elevation models (DEMs) and terrain analysis to define lobe and catchment extents. There were limitations in imagery coverage, as only imagery from 1955, 1970, 1993, 2011, and 2014 covered all eight FDLs. Some of the FDLs also were covered by imagery from 1978, 1979, 1981, 2007, and 2009.

Changes in FDL size and position for each data set from 1955 to 2014 were mapped (see Figure 1 for a compilation of all outlines for each FDL). The historic movement of each FDL was analyzed by measuring the progression of the toe of the lobe in each data set. Because the FDLs demonstrate downslope movement with only minor lateral spreading, longitudinal profile lines were oriented along the center of each lobe and served as a consistent reference to measure change. Absolute movement between each toe location for a given data set year was divided by the time interval between data years, resulting in average movement rates for the time interval. The rates were assigned to the latter year of the time interval.

Results

Based on the historic imagery analysis, the eight studied FDLs can be divided into two general groups: those with increasing movement rates (i.e., FDL-A, -B, -D, -4, -5, and -7) and those with decreasing movement rates (i.e., FDL-C and -11). For example, FDL-B moved at 0.2 m yr^{-1} in 1970, accelerating to 3.9 m yr^{-1} by 2014. Approximately 5 km to the south, FDL-D moved at 1.2 m yr^{-1} in 1970, reaching a peak average rate of 32.1 m yr^{-1} in 2011, and slowing to 30.1 m yr^{-1} in 2014. FDL-A, the largest and closest FDL to the Dalton Highway moved at 1.9 m yr^{-1} in 1970, reaching an average rate of 3.9 m yr^{-1} in 2014.

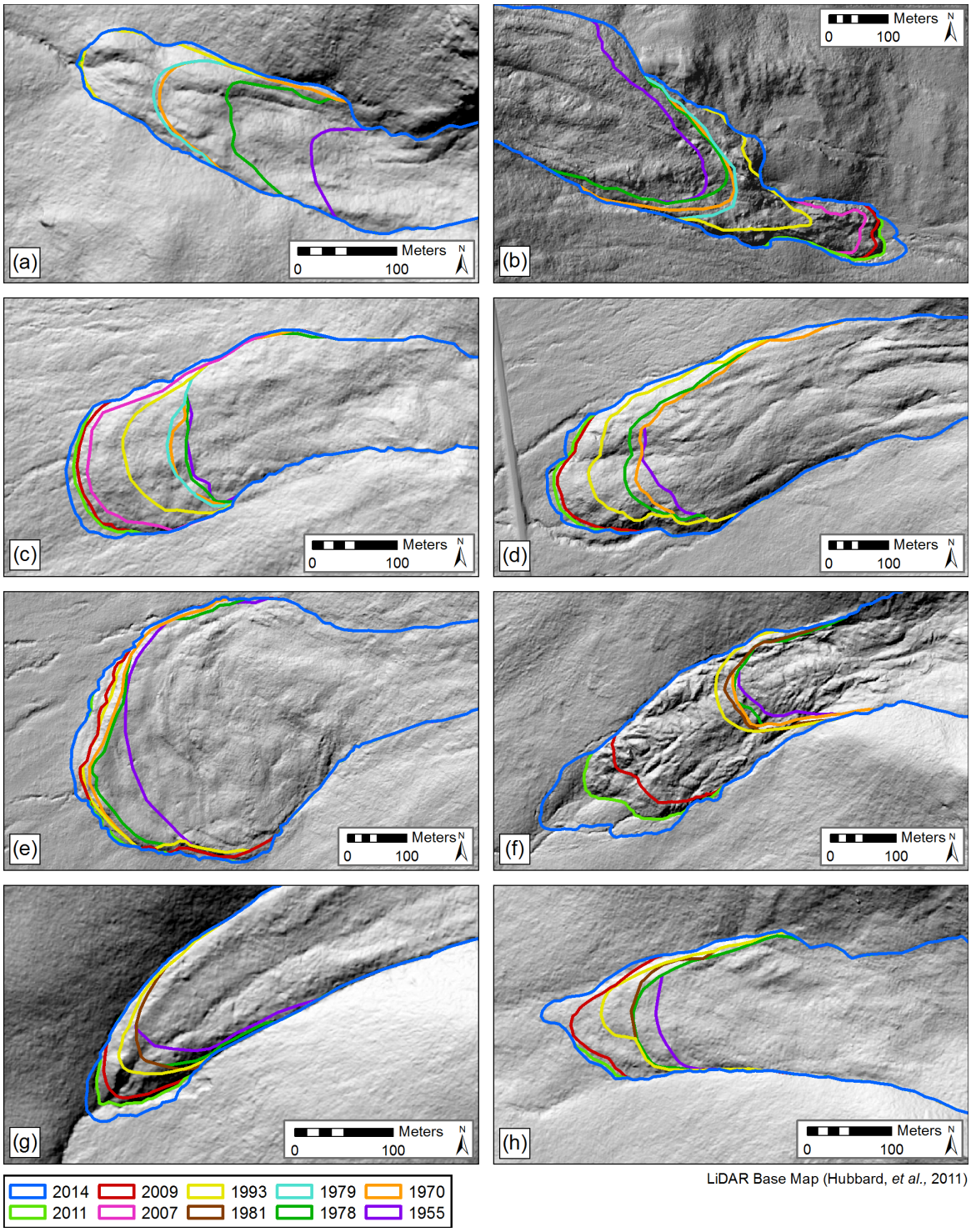

Figure 1: Compilation of FDL toe progression based on historic imagery analysis. The FDLs are presented from north to south: (a) FDL-11; (b) FDL-7; (c) FDL-B; (d) FDL-A; (e) FDL-C; (f) FDL-D; (g) FDL-5; and (h) FDL-4.

In contrast to these values, FDL-11 experienced a peak movement rate in 1978 at 9.4 m yr^{-1}. Its rate has been decreasing since then, with no significant change in the toe position from 2011 to 2014.

Conclusion

Historic imagery analysis can be used as an effective remote sensing tool to characterize FDL movement on a decadal scale. The analysis indicates asynchronous movement of these features, despite their close proximity to each other. A limitation to this research is the lack of suitable aerial imagery for this area. A significant amount of available imagery was unusable because of cloud cover, shadowing, skewed image geometry, and/or wash out. Additional imagery sets over the time period would increase the temporal resolution and improve the accuracy of the long-term trends.

Despite this limitation, the analysis of movement gives us a greater understanding of these geohazards. Most notable is the movement of FDL-A, as the historic rates fit a linear trend with a coefficient of determination (R2) of 0.88, providing confidence in projected movement rates. Based on this analysis, FDL-A is steadily accelerating and will reach the current highway alignment by 2023. The Alaska Department of Transportation and Public Facilities has plans to reroute the highway to avoid the approaching FDL-A (Currey, pers. comm., Aug. 2015). While this will place more distance between the Dalton Highway and the approaching geohazard, a long-term solution is still needed.

Acknowledgements

The authors thank L. Wirth and M. Slife for their expertise in geospatial data and image management.

Disclaimer

This research was funded by the U.S. Department of Transportation, OASRTRS-14-H-UAF-Project B. The views, opinions, findings, and conclusions reflected herein are the responsibility of the authors only and do not represent the official policy or position of the USDOT/OST-R, or any State or other entity.

References

Daanen, R.P.; Grosse, G.; Darrow, M.M.; Hamilton, T.D. and Jones, B.M. [2012]: Rapid movement of frozen debris-lobes: implications for permafrost degradation and slope instability in the south-central Brooks Range, Alaska. *Natural Hazards and Earth System Sciences*, 12(5):1521–1537, doi:10.5194/nhess-12-1521-2012.

Darrow, M.M.; Simpson, J.M.; Daanen, R.P. and Hubbard, T. [2015]: *Characterizing a Frozen Debris Lobe, Dalton Highway, Alaska*, pages 57–67. doi:10.1061/9780784479315.006.

Hubbard, T.D.; Koehler, R.D. and Combellick, R.A. [2011]: *Lidar Data Sets of Alaska: High Resolution Lidar Data for Alaska Infrastructure Corridors*. laska Division of Geological and Geophysical Surveys: Raw Data File 2011-3, 291 p.

Evaluation of rock slope failures in steep permafrost slopes in Norway - first insights in the geological history of the Mannen unstable rock slope in Møre og Romsdal

Paula Hilger[1,2], Reginald L. Hermanns[1], John C. Gosse[3], Bernd Etzelmüller[2], Sebatian Westermann[2], & Michael Krautblatter[4]

[1] *Geological Survey of Norway, Trondheim, Norway*
[2] *Department of Geosciences, University of Oslo, Norway*
[3] *Department of Earth Sciences, Dalhousie University, Canada*
[4] *Chair of Landslide Research, Technische Universität München, Germany*

Due to its steep-sided valleys and fjords unstable rock slopes are very common in Norway. Since large parts of the country are influenced by altitudinal permafrost many of the instabilities are located around the (assumed) lower permafrost boundary. Although it is well known that changing permafrost conditions are driving factors for rock slope instabilities only individual studies high lightened on this relation in Fennoscandia [Blikra and Christiansen, 2014, Böhme et al., 2015]. The CryoWALL project addresses four main research topics:

1. the spatial and
2. temporal distribution of the ground thermal regime in permafrost rock walls in Norway,
3. it's potential impact on slope instabilities, and
4. the development of a national hazard index to identify infrastructure and inhabitants at risk.

One of the key study sites is the Mannen instability in Møre og Romsdal. Several deep clefts indicate past movement and the sliding of a 15-20 million m3 large rock mass created a ca. 20 m high back scarp at the edge of the 1295-m-highplateau. Currently the upper part of this block moves at a rate of 5-6 cm/yr [Kristensen and Blikra, 2013]. At the foot of that slope complex stratigraphic relations of quaternary deposits exists. The lowermost unit are terraces built up of rock avalanche material that in turn are overlain by glacio-fluvial deposits. Those are covered by at least two end moraines predominantly made up by material from rock slope failures. The youngest deposits are at least three generations of rock avalanche lobes. We will define both the temporal distribution of the rock slope failures and paleosliding velocities by terrestrial cosmogenic nuclide dating. Preliminary ages of the back scarp show a movement pattern with changing velocities. Sliding started ca. 8 kyr ago with slow rates Indistinguishable ages 8 m apart suggest fast sliding at ca. 3 kyr ago. The height of the back scarp indicates that slip rates slowed down since then until the recent acceleration to today's velocity.

References

Böhme, M.; Oppikofer, T.; Longva, O.; Jaboyedoff, M.; Hermanns, R.L. and Derron, M.-H. [2015]: Analyses of past and present rock slope instabilities in a fjord valley: Implications for hazard estimations. *Geomorphology*, 248:464–474, doi:10.1016/j.geomorph.2015.06.045.

Blikra, L.H. and Christiansen, H.H. [2014]: A field-based model of permafrost-controlled rockslide deformation in northern Norway. *Geomorphology*, 208: 34–49, 2014. doi:10.1016/j.geomorph.2013.11.014.

Kristensen, L. and Blikra, L.H. [2013]: *Monitoring Displacement on the Mannen Rockslide in Western Norway*, In: Margottini, C. and Canuti, P. and Sassa, K.(eds.): Landslide Science and Practice, Volume 2: Early Warning, Instrumentation and Monitoring, pages 251–256. Springer Berlin Heidelberg, Berlin, Heidelberg, 2013. ISBN 978-3-642-31445-2. doi:10.1007/978-3-642-31445-2_32.

Svalbard coastal hazards and their impact on scientific and community infrastructure

Marek Wojciech Jaskólski, Mateusz Czesław Strzelecki, & Lukasz Pawłowski

University of Wroclaw, Poland

A recent report on the state of the Arctic coast emphasizes the role of the coastal zone as the interface where severe environmental changes impact directly on Arctic communities [Forbes, 2011]. Arctic warming, which is occurring at twice the rate as the rest of planet (IPCC 2007), has accelerated geomorphic processes that directly affect the functioning of the coastal zone.

In this paper we report the results of recently completed research project 'Assessment of impact of coastal hazards on scientific and community infrastructure in polar regions using remote sensing, geoinformation and new geomorphological mapping methods' undertaken in HOMING PLUS Program funded by the Foundation for Polish Science. The scientific aim of the project was to apply state-of-the-art geoinformation and remote sensing techniques together with new field-based geomorphological mapping methods to examine the impact of coastal hazards on scientific and community infrastructure along the coasts of Svalbard Archipelago, High Arctic.

Svalbard is located at a key boundary between oceanic and climatic fronts in the European part of the Arctic and is ideally placed to study sensitivity of the Arctic coastal zone to climate changes. On the contrary to uninhabited parts of the Arctic region, Svalbard is an area of intensive human activity that led to the development of scientific, industrial, touristic and community infrastructure, mostly within its coastal zone.

Recent reports from Hornsund [Zagórski et al., 2012] and Sassenfjorden [Sessford, 2013] documented the rapid erosion of Svalbard coasts during the last decades of the 20^{th} century which led to the destruction of scientific infrastructure at Polish National Polar Station (PPS) in Isbjornhamna and national heritage sites at Fredheim. The abandonment of Piramiden town (Billefjorden) by Russian community at the end of the 20th century exposed huge amounts of insecure litter and port infrastructure to the operation of coastal processes what in consequence polluted surrounding beaches and threatened the state of fjord ecosystem. In Longyearbyen, the largest settlement and the administrative center of Svalbard, several housing and warehouse facility are built on the coast and threated by storm action.

Our research documented significant changes in coastal zone in the surroundings of majority of research stations and towns in Svalbard, associated with increased coastal erosion, paraglacial transformation of coastal landscape and increasing duration of ice-free period.

To our knowledge, we prepared the first application of CVI (coastal vulnerability index) and Leopold matrix to assess the potential effects of geomorphic processes on coastal zone and coastal infrastructure in High Arctic setting.

Our work highlights the need for a greater understanding of the controls on Svalbard coastal hazards, especially given the potential for accelerated warming and sea-level rise in the coming decades and centuries.

References

Forbes, D.L.(ed.). [2011]: *State of the Arctic Coast 2010 – Scientific Review and Outlook*. International Arctic Science Committee, Land-Ocean Interactions in the Coastal Zone, Arctic Monitoring and Assessment Programme, International Permafrost Association. Helmholtz-Zentrum, Geesthacht, Germany, URL http://arcticcoasts.org.

Sessford, E. [2013]: *Spatial and temporal analysis of Holocene coastal development: applications to erosion assessment and cultural heritage mitigation in Svalbard*. Master thesis, Department of Geosciences, Oslo University, 148 p.

Zagórski, P.; Malczewski, A. and Leczyśńki, L. [2012]: Shoreline changes of isbjornhamna (hornsund, svalbard) in years 1960-2011, Field report UMCS University, 34 pp.

Evaluation of risk of ice-wedge degradation, Prudhoe Bay Oilfield, AK

Mikhail Kanevskiy[1], Yuri Shur[1], Donald A. Walker[1], Marcel Buchhorn[1], Torre Jorgenson[2], Georgiy Matyshak[3], Martha K. Raynolds[1], Jana L. Peirce[1], & Lisa M. Wirth[1]

[1] *University of Alaska Fairbanks, USA*
[2] *Alaska Ecoscience, USA*
[3] *Moscow State University, Russia*

Widespread degradation of ice wedges has been observed in the Arctic Coastal Plain of Alaska during the last decades, including the area of the Prudhoe Bay Oilfield (PBO), where it strongly affects environment and infrastructure [Raynolds et al., 2014, Jorgenson et al., 2015]. The upper permafrost of PBO contains significant amounts of excess ground ice, including segregated ice and large epigenetic ice wedges (width up to 4 m; vertical extent up to 3.5 m). High ice content makes the study area extremely vulnerable to thermokarst and thermal erosion. In most cases, these processes are triggered by climatic changes or human activities. Road infrastructure in PBO affects the ice-wedge degradation by an increase in the active-layer thickness (ALT) triggered by flooding of large areas due to construction of road embankments; accumulation of dust, which kills vegetation and changes thermal properties of soil; and additional snow accumulation near the embankment.

Our studies show that degradation of ice wedges is a cyclic process, which includes five main stages: Undegraded wedges (UD) – Degradation-initial (DI) – Degradation-advanced (DA) – Stabilization-initial (SI) – Stabilization-advanced (SA) [Jorgenson et al., 2015]. The processes of ice-wedge degradation, stabilization and recovery are determined by interactions between the active layer and the underlying transition zone of the upper permafrost [Shur, 1988], which includes transient layer (TL) and intermediate layer (IL). Accumulation of organic matter in the troughs developing on top of degrading wedges eventually leads to decrease in ALT and formation of the ice-rich IL, protecting ice wedges from further degradation [Jorgenson et al., 2015].

The model of the active layer/upper permafrost system suggests that in order to estimate a risk of ice-wedge thermokarst we should obtain information on thickness and properties of protective soil layers overlying ice wedges, including active, transient, and intermediate layers (Fig. 1A). A thickness of the protective layer PL1 (or a total thickness of frozen soil above the ice wedge, including the frozen part of active layer, transient layer, and intermediate layer) is measured during the field study. PL2 includes transient and intermediate layers; its thickness is measured at the end of warm season. PL3 consists of the intermediate layer, which can be distinguished by its specific cryogenic structure: this layer is extremely ice-rich with predominantly ataxitic (suspended) cryostructure and numerous thick ice layers (belts). Degradation of the ice wedge begins when the thawed and subsided PL1 layer joins the active layer and a part of thermal resources during the remaining part of the warm season can be spent on thawing of massive ice. Especially important is the information on thickness of the intermediate layer (PL3), which provides a long-term stability of ice wedges.

The color-coded system of evaluation of the risk of ice-wedge degradation as a function of thickness of protective layers of frozen soil above wedges (PL1, PL2, and PL3) includes six risk levels from bright red (risk level 1, the highest) to dark green (risk level 6, the lowest) (Fig. 1B). Two highest risk levels are related to currently degrading wedges. The difference between them is determined by the activity of degradation: while the first risk level refers to active degradation with significant thawing of ice wedges, the second one is related to slow degradation, when the depth of seasonal thawing can reach the tops of ice wedges only at the end of warm season. The third risk level is related to ice wedges which are not currently degrading, but the protective layer is so thin that degradation can start very easily, and some parts of studied wedges may already experience degradation by the time of study. Levels of risk strongly depend on stages of ice-wedge degradation / stabilization: while ice wedges at UD and SA stages are relatively well protected by the intermediate layer (P3), most of wedges at DI and DA stages have no protection.

A

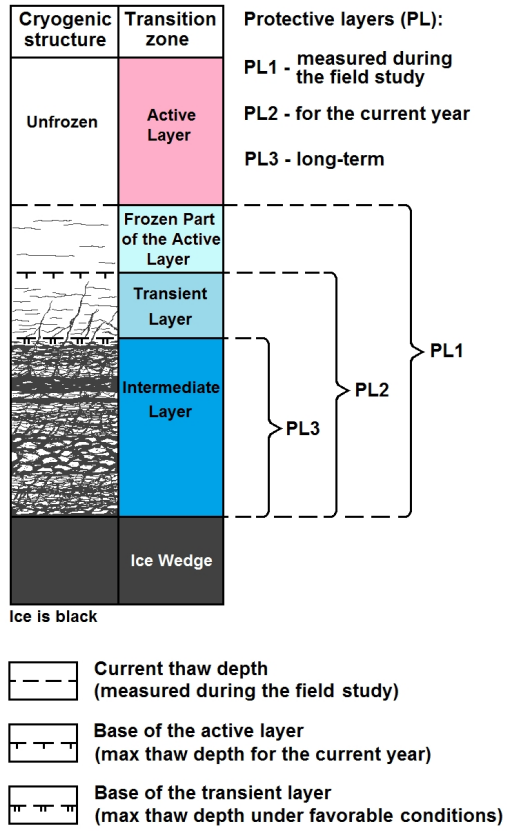

B

Risk level	Thickness of protective layers, cm			Notes
	PL1*	PL2**	PL3*	
1. Active degradation	0	0	0	No protective layers; the top part of the ice wedge is currently degrading; degradation of the ice wedge of up to 5 cm is expected by the end of warm season
2. Very high	1-5	0	0	Degradation of the top part of the ice wedge is expected by the end of warm season
	=PL3	0	1-5	Thin intermediate layer is currently degrading; degradation of the top part of the ice wedge is expected by the end of warm season
3. High	5-10	1-5	0	No intermediate layer, thin degrading transient layer; minor degradation of some parts of this ice wedge is possible by the end of warm season
	5-10	1-5	1-5	Partial degradation of the intermediate layer is expected by the end of warm season; minor degradation of some parts of this ice wedge is possible by the end of warm season
	=PL3	1-5	5-10	Intermediate layer is currently degrading; minor degradation of some parts of this ice wedge is possible by the end of warm season
4. Moderate	10-20	5-15	1-5	No significant degradation of the intermediate layer and no ice-wedge degradation are expected during the current year
	10-20	5-15	5-10	Partial degradation of the intermediate layer is possible by the end of warm season; no ice-wedge degradation is expected during the current year
	=PL3	5-15	10-20	Relatively thick intermediate layer is currently degrading; no ice-wedge degradation is expected during the current year
5. Low	20-30	15-25	5-10	No degradation of the intermediate layer is expected during the current year
	20-30	15-25	10-20	No significant degradation of the relatively thick intermediate layer is expected during the current year
	=PL3	>15	>20	Thick intermediate layer is currently degrading
6. Very low	>30, >PL3	>25, >PL3	>20	The ice wedge is well protected by thick and stable intermediate layer; ice-wedge degradation is possible only due to a strong impact on the surface (flooding, vegetation removal) or after accumulation of wedge ice within the intermediate layer

* Measured from late July to mid-August
** Measured from late August to mid-September (PL1=PL2)

Figure 1: Evaluation of risk of the ice-wedge degradation based on the thickness of protective layers. A – Protective layers of frozen soils preventing wedge ice from thawing; B – Evaluation of risk of the ice-wedge degradation for northern Alaska.

During 2-14 August 2014, 57 boreholes were drilled in ice-wedge polygon centers and troughs at the Colleen Site A (Lake Coleen area) along two 200-m-long transects (T1 and T2) established at the both sides of the Spine Road; 35 boreholes encountered ice wedges at various stages of degradation and recovery. At the time of drilling, a protective layer of frozen soil 1 to 27-cm thick (PL1) was observed above the majority of ice wedges. The ice-rich IL (PL3) up to 19-cm thick, which indicates relative stability of ice wedges, was encountered in 13 boreholes. Two ice wedges experienced thawing at the time of drilling, but calculations indicate that by the end of the thawing season six more wedges would be affected by thermokarst, and during exceptionally warm summers (the summer of 2014 was very cold) up to two thirds of wedges may experience partial melting. Thaw subsidence above degrading ice wedges during such summers can reach 8 cm/year. Average thicknesses of protective layers for T1 were 8.1 cm (PL1) and 1.2 cm (PL3), which correspond to high level of risk of ice-wedge degradation. For T2, average thicknesses were 11.1 cm (PL1) and 5.0 cm (PL3), which correspond to moderate level of risk of ice-wedge degradation. For comparison, at the adjacent Jorgenson's study area which was not affected by the road construction and heavy traffic [Jorgenson et al., 2015], the risk of ice-wedge degradation was also moderate but protective layers were thicker: PL1=17.7 cm and PL3=8.6 cm.

During 18-23 September 2015, when ALT reached its maximum values (PL1=PL2), 28 boreholes were drilled in ice-wedge polygon centers and troughs at the Airport Study Site along two 100-m-long transects (T3 and T5) established at the both sides of the Dalton Highway; 23 boreholes encountered ice wedges at various stages of degradation and recovery. At the time of drilling, a protective layer of frozen soil 0.5 to 15-cm-thick (PL2, which includes TL and/or IL) was observed above the majority of ice wedges. The ice-rich IL up to 14-cm thick was encountered in 10 boreholes. Seven ice wedges of 23 experienced thawing at the time of drilling. Average thicknesses of protective layers for T3 were 2.3 cm (PL2) and 2.0 cm (PL3), while for T5 they were 4.2 cm (PL2) and 2.6

cm (PL3). Such values correspond to high level of risk of ice-wedge degradation for both transects, though the risk of degradation is much higher at T3: along this transect, protective layers (of any thickness) were encountered only in 50 % of ice wedges (which means that a half of wedges were degrading by the end of summer), while at T5 more than 90 % of wedges had this layer, and most of them were protected by a thin intermediate layer.

Despite a strong influence of the infrastructure on the active layer and the upper permafrost stability through changes in hydrology and surface conditions, ice-wedge degradation in the study area is a reversible process. This was confirmed by our studies at the T2 transect. Initial degradation of ice wedges along T2 was probably related to the flooding of the southwest side of the Spine Road triggered by the road construction. Although thermokarst along T2 had been more active in previous years, our studies in 2014 showed that the ice wedges at this transect (even the wedges under the deep troughs filled with water) were more stable than the wedges along T1, which had not been affected by flooding. This may be explained by higher rates of accumulation of dust and organic matter in the ice-wedge troughs along T2.

Acknowledgements

This work was supported by the National Science Foundation (grants ArcSEES 1233854 and ARC 1023623). Any opinions, findings and conclusions or recommendations expressed in this material are those of the authors and do not necessarily reflect the views of the National Science Foundation.

References

Jorgenson, M.T.; Kanevskiy, M.; Shur, Y.; Moskalenko, N.; Brown, D.R.N.; Wickland, K.; Striegl, R. and Koch, J. [2015]: Role of ground ice dynamics and ecological feedbacks in recent ice wedge degradation and stabilization. *Journal of Geophysical Research: Earth Surface*, 120(11):2280–2297, doi:10.1002/2015JF003602. 2015JF003602.

Raynolds, M.K.; Walker, D.A.; Ambrosius, K.J.; Brown, J.; Everett, K.R.; Kanevskiy, M.; Kofinas, G.P.; Romanovsky, V.E.; Shur, Y. and Webber, P.J. [2014]: Cumulative geoecological effects of 62 years of infrastructure and climate change in ice-rich permafrost landscapes, Prudhoe Bay Oilfield, Alaska. *Global Change Biology*, 20(4):1211–1224, doi:10.1111/gcb.12500.

Shur, Y.L. [1988]: The upper horizon of permafrost soils. In: Kaare, S.(ed.), *Proceedings of the Fifth International Conference on Permafrost, Trondheim, Norway, August 2–5, 1988*, volume 1, pages 867–871. Tapir Publishers: Trondheim. ISBN 82-5 19-0863-9. URL http://ipa.arcticportal.org/publications/conference-proceedings.

Gas-emission crater, geomorphological characteristics and relief dynamics on Yamal Peninsula, Russia

Alexander Ivanovich Kizyakov[1], Marina Oskarovna Leibman[2], Anton Vladimirovich Sonyushkin[3], Mikhail Viktorovich Zimin[1,3], & Artem Valerievich Khomutov[2]

[1] *Lomonosov Moscow State University, Faculty of Geography, Russian Federation*
[2] *Earth Cryosphere Institute SB RAS, Russian Federation*
[3] *ScanEx Research and Development Center, Russian Federation*

Study is focused on a new permafrost feature - a gas-emission crater in central part of Yamal Peninsula. This feature after it was first discovered caused serious concern due to its possible danger to the infrastructure objects in the Arctic. Its hazardous nature is related to its formation in the form of an outburst, removal of a large amount of frozen rocks from the interior to the surface, and catastrophic in nature change of local topography. Characteristics of the relief within the area of crater formation were obtained based on the analysis of remote sensing data, including very high resolution stereo-pair data as well as field observations.

Landsat 8 and SPOT 5 satellite images for various time spans were interpreted to determine the time of crater formation. Time interval of the crater formation was defined as late fall 2013 [Leibman et al., 2014].

The relatively narrow, deep crater is surrounded by a parapet of thrown out silt, loam, clay and turf blocks. Parapet height changes along the rim from 0.5 to 4.0 m. Blocks of the clay and fragments of turf mat were thrown as far as up to 120 m from the crater. The farther from the crater, the smaller are the blocks, from 1 m close to the parapet to several centimeters farthest from the crater. Fragments of turf mat 50-100 cm in size are found up to 60 m away from the crater [Leibman et al., 2014].

To determine the relief morphology of the study area before and after the crater formation, digital elevation models (DEM) were derived from two stereo-pairs of WorldView-1 satellite images in the vicinity of the crater [Kizyakov et al., 2015].

Gas-emission crater was formed in a tundra zone of Central Yamal on a small relatively flat portion of the erosion valley. Closest to the crater site is a partly drained lake depression (khasyrei) 160×240 m in size with a remnant lake 95×115 m. Grassy meadow vegetation covers the bottom of the khasyrei. Shrubs cover hill slopes and part of the valley bottom.

WorldView-1 images of 09.06.2013 and derived DEM documented the existence of the bulge with base diameter 45-58 m and a height of about 5-6 m in the place of the crater. Hypsometric profiles across the landform are presented on Figure 1. The top of the bulge was covered by a tussocky grassy vegetation with willow shrubs on slopes and foot.

Interpretation of WorldView-1 images of 15.06.2014 and derived DEM allowed obtaining data on the size and structure of the crater closest to the time of its formation. Allocated were: upper part (funnel) comprising sloping walls, turning through a sharp bend into a cylinder with close to vertical sides. Diameter of the cylinder was 15-16 m, diameter of the vegetated rim 25-29 m.

Measurements of November 2014 showed that sharp bend was at the depth of 8 m below the rim. Upper funnel was built of highly icy sub-vertically stratified ice-loam interbedding. Below the bend, in the vertical, sometimes overhung walls tabular ground ice body was exposed, with rare, vertically oriented, lining the walls thin interlayers of silt. In June-July 2014 in the lower part of the north-eastern wall a grotto was seen, extending deep into the wall by about 5–8 m.

An analysis of multi-temporal DEM of 2013 and 2014 allowed calculating the volume of the crater inside, and the parapet formed around it. The volume of discharged material was 11200 m^3, the volume of material in the parapet was 1940 m^3 which is 6 times less than the void of the crater. The difference was due to a significant amount of ice exposed in the walls of the crater and probably ejected outside. This ice melted in early summer 2014.

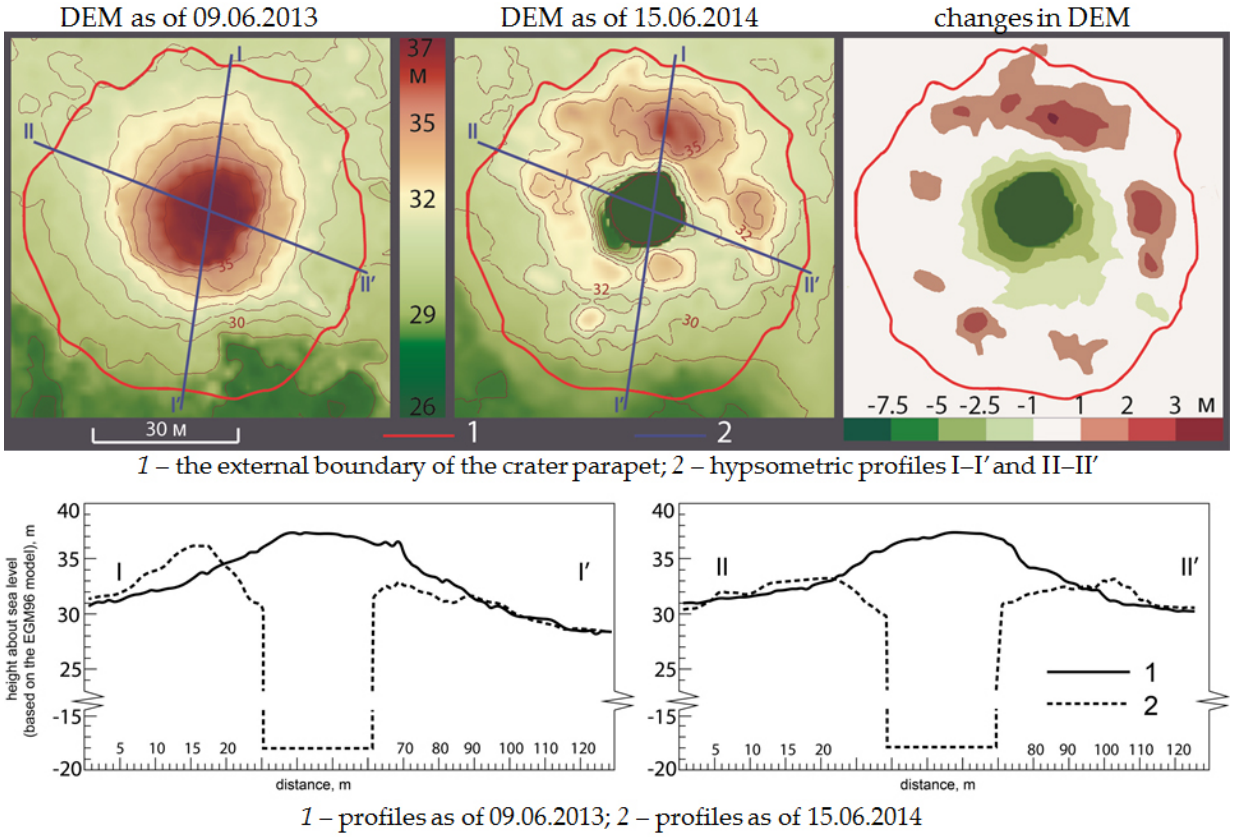

Figure 1: Fragments of study-site DEM and hypsometric profiles derived from satellite stereo pairs

Parapet material was irregularly distributed around the crater. Maximum area and thickness up to 3.2 m were noted north of the crater rim. Southern and western portions of parapet were fragmentary and its thickness up to 1 m above the surface existing in 2013 which is within the accuracy of the DEM. Difference in parapet morphology may be caused by parallax or inclination of the emission axis against the bulge top.

Joint analysis of the field and remote-sensing data allowed comparison of the time slices for crater evolution. Based on this outline, the rate of crater development: retreat of the walls and filling it in by water and sediment, was determined. By the time of initial observation in July 2014, water was found at the depth exceeding 50 m below the rim, in November 2014 this depth was 26 m. By September 2015 almost all the crater was inundated, with water surface about 5 m below the rim.

By the end of summer, 2015 the lateral dimensions of the crater increased dramatically. According to the very high resolution image of 15.07.2014 compared to field measurements of 31.08.2015 crater diameter at the rim level changed from 25-29 to 47-54 m, respectively. Sloping walls of the upper funnel turned into almost vertical walls. The rate of the wall retreat from June until November 2014) reached 3.5 m through the warm period. This rate is close to lowest rates of thermodenudation known for this area. In 2015, expansion of both the funnel and cylindrical parts was accompanied by the crater inundation. We consider the rise of the water level to result from the melt of snow, which filled the crater in winter, rainwater, thawing of massive and constitutional ground ice, collapse of the covering ice deposits and turf, as well as parapet material.

Study undertaken gives evidence of a very short life cycle of this landform. It took two warm seasons to almost entirely fill in the crater. Remaining ice-bearing walls continue to retreat causing failure of the remaining parapet. We suppose that during the next 1-2 years parapet will be entirely destroyed, and as a result the crater will look like an ordinary tundra lake.

Acknowledgements

This research is partially supported by RFBR grant 16-05-00612.

References

Kizyakov, A.I.; Sonyushkin, A.V.; Leibman, M.O.; Zimin, M.V. and Khomutov, A.V. [2015]: Geomorphological conditions of the gas-emission crater and its dynamics in Central Yamal. *Earth's Cryosphere*, 19(2):13–22, URL http://www.izdatgeo.ru/pdf/earth_cryo/2015-2/13_eng.pdf.

Leibman, M.O.; Kizyakov, A.I.; Plekhanov, A.V. and Streletskaya, I.D. [2014]: New permafrost feature – Deep crater in Central Yamal (West Siberia, Russia) as a response to local climate fluctuations. *Geography Environment Sustainability*, 7(4):68–80, URL http://www.geogr.msu.ru/GESJournal/contents.php?iid=22&menupos=7.

Complex study of gas-emission crater in Central Yamal, Russia

Marina O. Leibman[1], Alexandr I. Kizyakov[2], Irina D. Streletskaya[2], Artem V. Khomutov[1], Yuri A. Dvornikov[1], Ksenia A. Ermokhina[1], & Anatoly A. Gubarkov[3]

[1] *Earth Cryosphere Institute, Russian Academy of Sciences, Siberian Branch, Tyumen, Russia*
[2] *Lomonosov Moscow State University, Faculty of Geography, Moscow, Russia*
[3] *Tyumen State Oil and Gas University, Tyumen, Russia*

Study of the gas-emission crater in Central Yamal, first described in (Leibman et al., 2014) involved field and remote-sensing methods and resulted in compilation of GIS for the area adjacent to the crater. GIS systematizes results of cryolithological, geomorphic, geobotanical and environmental properties of the area and are considered as indicators of crater formation risks.

Field studies consisted of mapping landscape and geocryological features, sampling geological sections in the crater walls and thermocirque exposures with main attention paid to the ground ice. Environmental and specifically vegetation types were observed in field photographed and described later in the office. Few ground temperature measurements were performed as well. During four field campaigns crater proportions were measured to follow its evolution after the initial ejection (Fig. 1). Survey of water depth in the inner lake provided ideas on crater filling in with deposits and water, as well as freezing up.

Figure 1: Evolution of the crater: A, on July 16, 2014; B, on Aug 25, 2014; C, on Nov 9, 2014; D, on Sep 1, 2015.

Remote-sensing data were used to create a digital elevation model (DEM) of the area, obtain initial size of the crater, and determine the date range for its formation. Also landscape units were subdivided through interpretation of the satellite images based on field descriptions and the all the data arranged in the GIS-based geodatabase. Main environmental features of the area are high-elevated poorly drained marine plain, with narrow flat valleys and relatively rare small shallow lakes. Long gentle slopes, their foots and hill-top periphery are covered with dense willow and dwarf-birch shrubs, hilltops and valley bottoms are tussocky moss-grass tundras. Cryogenic processes and landforms observed include drain lakes (khasyreis), landslides, erosion gullies, frost-heave mounds and thermocirques with tabular ground ice exposures.

Description of the crater walls from date to date differs depending on the wall retreat through time. As followed from very high resolution satellite images and earlier field observations, a mound had preceded the crater formation. Its shape ("bulge") differed from that known for pingo. Therefore, we doubt that the reason for this mound formation can be referred to as freezing of a sub-lake talik. Anyway, there was heave which resulted in deformation of the stratified sediment consequence.

Earlier field observations (July-August 2014) described the sediments as silty-clayey highly icy deposits with deformed lenses of bubbly ice, covered in the uppermost portion of the section by stratified organic-rich loam. Later observations met the near-bottom layers inundated and descriptions dealt with the upper half of the section. On the other hand, crater walls retreated and the section changed dramatically. The walls then were built of almost pure ice, with vertical concentric stratification, accentuated by silt-rich interbeds. The latest observation (in September 2015) was possible only for the uppermost 5 m of exposed walls other parts being inundated by an inner lake. Due to significant wall retreat, the section lost all the indications of vertical deformations and looked much like the exposures described elsewhere in the area, specifically in the backwall of the active thermocirque exposing the surface of the IV^{th} or V^{th} Marine plain where tabular ground ice layers were overlain by clays. The upper portion of the crater walls differed from those in thermocirques showing rather stratified organic-rich lacustrine deposits covering clayey ones. This sequence was interpreted as formation of the mound at the periphery of the hasyrei and thus involvement of the lacustrine deposits in the vertical deformation. Deformed ice lenses seen at the earlier exposures of the crater walls were interpreted as projection of irregular near-vertical ice layers on the practically cylindrically shaped crater walls.

Sampling of the ice was undertaken to compare its geochemical properties with other ice bodies known from better understood Yamal exposures. It was found that both ionic concentration and stable isotope composition (^{18}O and D) were close to that obtained from the tabular ground ice samples from Marre-Sale and Bovanenkovo [Streletskaya et al., 2013].

Arguments in favor of authors'hypothesis of crater formation are:

1. high concentration of methane inside the crater, measured before it was inundated,
2. existence of a "bulge"in place of the crater prior to its formation,
3. traces of highly energetic emission which resulted in scattering of sand-clay-peat fragments as far as 120 m from the crater rim,
4. highly icy deposits with thick layer of tabular ground ice noted in the crater walls and in adjacent exposures, which are impermeable to gas diffusion and protect gas hydrates from decomposition until the temperature rise above critical values.

All of the above allows the authors suggest that the crater formation can be attributed to the air temperature warming trend along with the extreme of 2012. The increased ground temperature and amount of unfrozen water in the permafrost, formation of a pingo-like mound and its outburst due to high pressure produced by gas hydrate decomposition within permafrost are the main controls.

References

Streletskaya, I.D.; Vasiliev, A.A.; Oblogov, G.E. and A.G., Matyukhin. [2013]: Isotopic composition on ground ice in Western Yamal (Marre-Sale). *Ice and Snow*, 53(2), doi:10.15356/2076-6734-2013-2-83-92. (in Russian).

Temperature at bottom of thermokarst lakes and the relationship with lake depth along the Qinghai-Tibet Engineering Corridor

Zhanju Lin, Fujun Niu, & Jing Luo

Chinese Academy of Sciences, China, People's Republic of

Thermokarst lakes have greatly influenced landscapes in cold regions, and the thermal erosion of their lakeshores may induce ground instability that affects infrastructure. Our study area includes three sub-regions where thermokarst lakes have obviously extended: the Chumaerhe High Plateau, Wudaoliang Basin, and Beiluhe Basin. Based on continual monitoring of four lakes, and sporadic observations of lake-bottom temperatures of many lakes using HOBO Sensors in 2009-2010, the thermal regime of lake bottoms and the relation between lake-bottom temperature and water depth were examined. The results show that in January, when ice cover was present, the lake-bottom temperatures at 90 % of the lakes in Chumarhe High Plateau were below 0 °C. This is likely because of shallow depths and high salinity of lakes in the region. However, the lake-bottom temperature of most lakes in Wudaoliang and Beiluhe Basins were above 0 °C, except in some lakes shallower than the maximum ice thickness. In general, lake-bottom temperature in the three sub-regions increased with water depth during this period. When lakes were free of ice between June and October, the lake-bottom temperatures in the three sub-regions were all warm and the highest temperature was near 18 °C. The seasonal increase in lake-bottom temperature in summer is more rapid in shallower lakes, and the temperatures were inversely related to water depth. The annual variation in lake-bottom temperature approximates a sinusoidal curve, with the coldest temperature occurring in January to February and the warmest in July to August.

Characteristics of thaw-induced slope failures in permafrost regions of the Qinghai-Tibet Engineering Corridor, China

Jing Luo, Fujun Niu, & Zhanju Lin

State Key Laboratory of Frozen Soil Engineering, Cold and Arid Regions Environmental and Engineering Research Institute, Chinese Academy of Sciences, China, People's Republic of

The permafrost in the Qinghai-Tibet Engineering Corridor (QTEC) has been degrading at a rapid rate under the combined influences of persistent climatic warming and steadily increasing human activities. As a result, a series of the thawing hazards occurred frequently, especially the thaw-induced slope failures, which had posed a potential threat to the engineering constructions and environment in the corridor. Thaw slumps and active layer detachments are the mostly typical hazards of them. On the one hand, its development would result in the environmental deterioration and degradation of permafrost, including the thawing of massive ground-ice, rising of ground temperature, and destruction of ecological environment; on the other hand, if these slope failures locate nearly along the railway and highway, they would cause some troubles to the engineering construction and maintenance. Based on satellite image and field investigation, all of thaw slumps and active layer developed in the QTEC were identified within a 10-km wide corridor along the Qinghai-Tibet Highway from Xidatan to Anduo. The distribution of these slope failures was strongly associated with permafrost ice content, slope gradient, and ground temperature: 94 % of slope failures existed in regions with ice-rich permafrost, 88 % were in regions with slopes between 6 and 10°, and 40 % occurred where the mean annual ground temperature was higher than -0.5 °C. At the same time, these two types of slope failures are all arc-shaped and with long axis orientation in the NW direction. Thaw slumps may initiate due to artificial cutting or river water erosion at the toe of slopes. These features are usually 20-90 m in width and 40-150 m in length. Active layer detachments (landslides) may be caused by the thaw of permafrost, a rise in the ground water table, or earthquakes, and are generally 80-160 m in width and 120-280 m in length. Field investigation of an active layer detachment indicate that the occurrence of this slope failure had greatly modified the heat exchange between the air and ground surface and influenced the thermal regime of the underlying permafrost, which result in ground temperatures in the recently disturbed area and the scar area were significantly lower than in the undisturbed ground. In addition, due to the lateral heat flux near the headwall, the ground temperature in the undisturbed area close to the headwall was higher than that in the undisturbed ground.

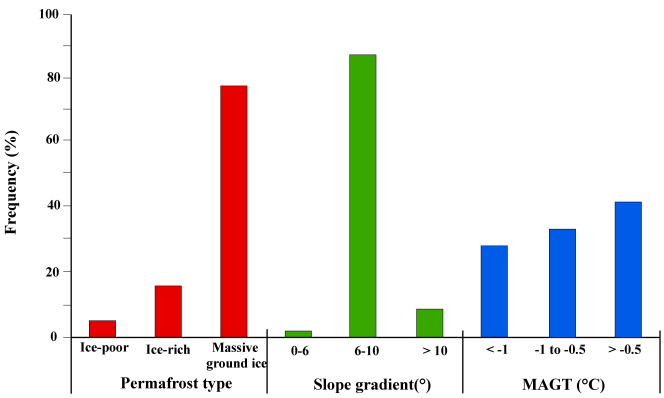

Figure 1: Statistical relations between the distribution of slope failures and the ice content, slope gradient, and MAGT

The effect of ground-ice on the mobility and behaviour of landslides: A case study in northern Iceland

Costanza Morino[1], Susan J. Conway[2], Þorsteinn Sæmundsson[3], Matthew R. Balme[4], Jón Kristinn Helgason[5], John Hillier[6], Colm Jordan[7], & Tom Argles[1]

[1]*Department of Environment, Earth& Ecosystems, Open University, Milton Keynes MK7 6AA, UK*
[2]*Laboratoire de Planétologie et Géodynamique de Nantes UMR-CNRS 6112, 2, rue de la Houssinière, BP 92208, 44322 NANTES Cedex 3, France*
[3]*Department of Geography and Tourism, University of Iceland, Askja, Sturlugata 7, Is-1 Reykjavík, Iceland*
[4]*Department of Physical Science, Open University, Milton Keynes MK7 6AA, UK*
[5]*Icelandic Meteorological Office, Avalanche Centre, Sudurgata 12, Isafjordur, Iceland*
[6]*Department of Geography, Loughborough University, Loughborough LE11 3TU, UK*
[7]*British Geological Survey, Environmental Science Centre, Keyworth, Nottingham NG12 5GG, UK*

Rapid mass movements can seriously endanger settlements in Iceland. After two catastrophic snow avalanches in 1995, the Icelandic government has drastically revised its policy regarding the risk assessment of rapid mass movements. The hazard from landslides and snow avalanches in Iceland is now better understood, and efforts have been made to comprehend their dynamics and their triggers, which are principally heavy rainfall/snowfall and snowmelt. However, the trend of increasing atmospheric temperatures in Iceland over the last decade has caused degradation of mountain permafrost, an additional "invisible" phenomenon that can affect slope stability [Sæmundsson et al., 2014]. The possible role of ground-ice in the behaviour and mobility of mass movements in Iceland is poorly understood. Our study aims to fill this gap, focussing on the different effects that ground-ice can have on the motion of landslides compared to "traditional" saturation-triggered landslides.

On 20th September 2012, a landslide occurred on the northwest-facing flank of Móafellshyrna Mountain (Trüllaskagi peninsula, northern Iceland), mobilising 500,000 m^3 of debris. Immediately after the failure, large blocks of ice-rich sediments and frozen deposits were observed, along with boulders and sediments derived from weathered bedrock. The landslide originated at 840 m elevation, and the main source of material was perched ice-rich talus deposits on a topographic bench. The elevation of the failed mass corresponds to the modelled elevation limits of the discontinuous permafrost in northern Iceland, which has been indicated above c. 800-900 m a.s.l. [Etzelmüller et al., 2007], with a decrease to about c. 400 m a.s.l. near the coast [Lilleøren et al., 2013]. The failure happened after an unusually warm and dry summer (up to 14 °C during the day of the event), followed by months of heavy precipitation (440 mm during the month before the event) and earthquake activity (two events recorded in Siglufjörður and ólafsfjörður in the morning of 20^{th} September all above 3 M on the Richter scale).

We will present the results of the morphological analysis of this unusual landslide. In summer 2015, we collected ground-based data, including differential GPS, Ground Penetrating Radar and colour photographic images for Structure from Motion (SfM) to aid the morphological and volumetric characterisation of the slide's features. Furthermore, in September 2015 the U.K. Natural Environment Research Council's Airborne Research and Survey Facility (NERC ARSF) collected air photography and LiDAR topography data for Móafellshyrna Mountain. We will compare and integrate the field data with the airborne data to identify and analyse the landforms, volumes and processes involved during the failure. We aim to quantify the volumes eroded, transported and deposited along the flow, therefore better characterising the mobility of the landslide.

Our preliminary analyses to-date have revealed that

i) the landslide' s motion was of complex-nature, beginning with a sliding motion, followed by a rock-debris fall - with failures of blocks of ice-rich sediments, boulders and frozen deposits - and evolving into a mobile large-scale debris flow/slide;

ii) ground-ice was cementing the talus before the event, hence leading the debris to behave like blocks during the initial failure, rather than being transported like loose material;

iii) water from ground-ice thaw combined with that from rainfall to over-saturate the landslide material, causing it to evolve into a debris flow.

These initial results show that ground-ice had a major role in the complex development of the landslide, not just promoting the failure and contributing to the transport with the thaw process, but also affecting the mechanical behaviour of the debris. Therefore, understanding the mobility and volumes (of rocks, debris, ground-ice and water) of such large slope failures is essential for mitigating the hazard in the case of similar events in inhabited regions.

References

Etzelmüller, B.; Farbrot, H.; Guðmundsson, Á.; Humlum, O.; Tveito, O.E. and Björnsson, H. [2007]: The regional distribution of mountain permafrost in Iceland. *Permafrost and Periglacial Processes*, 18(2):185–199, doi:10.1002/ppp.583.

Lilleøren, K.S.; Etzelmüller, B.; Gärtner-Roer, I.; Kääb, A.; Westermann, S. and Guðmundsson, Á. [2013]: The Distribution, Thermal Characteristics and Dynamics of Permafrost in Tröllaskagi, Northern Iceland, as Inferred from the Distribution of Rock Glaciers and Ice-Cored Moraines. *Permafrost and Periglacial Processes*, 24(4):322–335, doi:10.1002/ppp.1792.

Sæmundsson, T.; Helgason, J.K. and Pétursson, H.G. [2014]: ecline of mountain permafrost and the occurrence of recent large debris slides in Iceland. In *In EGU General Assembly Conference Abstracts, 27 April – 02 May 2014, Vienna, Austria*, volume 16, page 12930.

700 documented rockfalls in the Mont Blanc massif since 2003 validate the role of the permafrost warming in triggering

Ludovic Ravanel, Florence Magnin, & Philip Deline

Laboratoire EDYTEM, Université de Savoie, CNRS, Le Bourget-du-Lac, France

Rockfall is one of the main natural hazards in high mountain regions and its frequency is growing, especially since two or three decades. Collapses at high elevation are with an increasing certainty assumed to be a consequence of the climate change through the warming permafrost. In the Mont Blanc massif, data on present rockfalls (occurrence time when possible, accurate location, topographical and geological settings, volume, weather and snow conditions) were acquired for 2003 and for the period 2007-2015 thanks to a satellite image of the massif and a network of observers in the central part of the massif, respectively. The study of the 700 so-documented rockfalls shows a strong correlation at the year scale between air temperature and rockfall.

Along with this data acquisition, a statistical model of the Mean Annual Rock Surface Temperature (MARST) for the 1961-1990 period has been implemented on a 4-m-resolution DEM of the Mont Blanc massif. The model runs with Potential Incoming Solar radiation (PISR) calculated with GIS tools and air temperature parameters computed from Chamonix Météo France records.

Figure 1: Rockfall in the East face of the Tour Ronde (3792 m a.s.l.), Mont Blanc massif, August 27, 2015.

45 to 79 % of the 86 km^2 of steep rock faces $\geq$40° would be underlain by permafrost. It would be present from 1900 m a.s.l. in north faces and 2600 m in south faces in case of favourable local structural settings. Its presence would be more continuous from 2600 m and 3000 m, respectively, but it would occupy the totality of the rock walls, in any aspect from 3600 m a.s.l. We cross here the data on rockfalls with the permafrost distribution model to show that:

i) rockfall occurs mainly over modelled negative MARST (context of permafrost);

ii) simulated warm permafrost areas (> -2 °C) are the most affected by instabilities which is consistent with several laboratory studies that show the lesser strength of the ice under these temperatures;

iii) as the 1961-1990 period is supposed to be representative of the conditions at depth that are not affected by the climate warming during the two last decades, the latest results are mainly valuable for rockfalls related to pluri-decadal signal; and

iv) the higher (close to 0 °C) the MARST, the deeper the detachment (possibly related to the deepening of the permafrost active layer).

These results and field observations confirm that warming permafrost corresponds to the main required configuration for rockfall triggering at high elevation. In addition, we show that rockfalls for which ice observed in their scar indicates the presence of permafrost can be used to validate the permafrost distribution model.

Landscape hazards mapping for climate change adaptation planning in the Yukon

Louis-Philippe Roy[1], Bronwyn Benkert[1], Kristen Kennedy[2], Daniel Fortier[3], & Antoni Lewkowicz[4]

[1] *Northern Climate ExChange, Yukon Research Centre, Yukon College, YT, Canada*
[2] *Yukon Geological Survey, Whitehorse, YT, Canada*
[3] *Geocryolab, Département de Géographie, Université de Montréal, QC, Canada*
[4] *Department of Geography, University of Ottawa, ON, Canada*

Climate change represents a major challenge for northern regions, and its impacts are already being observed in many communities. In some areas, the thawing of permafrost caused by rising air temperature and disturbance can lead to ground subsidence, increased landslide risks and reduced bearing capacity of the soil. These effects increase considerably the complexity of community planning and are of particular concern in the Yukon, where there is a high prevalence of warm permafrost and permafrost degradation is already taking place. Risk assessments associated with permafrost degradation and its impact on contemporary landscapes have been performed in multiple Yukon communities for the past years by the Northern Climate ExChange (Yukon College, Canada), in order to help guide the planning efforts of the communities. The hazard mapping approach incorporated field investigations (soil and core samplings), geophysics (ground penetrating radar, electrical resistivity tomography) and geotechnical laboratory analyses (grain-size, ice content, thaw-settlement analyses, etc.) to assess the potential stability of landscape units. The data are integrated to produce ranked hazard risk maps of study communities. In turn, northern communities, First Nation governments, environmental assessment boards and private consultants are using these maps to develop adaptation strategies and reduce and mitigate risk.

The resulting hazards maps (Fig. 1)created through these projects are therefore highly valuable tools used to identify and plan potential future trajectories of change, reduce risk, and increase the resilience of Yukon communities. Different case studies from six Yukon communities will demonstrate the use of hazard mapping and the importance of implementation measures to better adjust to the negative impact of climate change in northern communities.

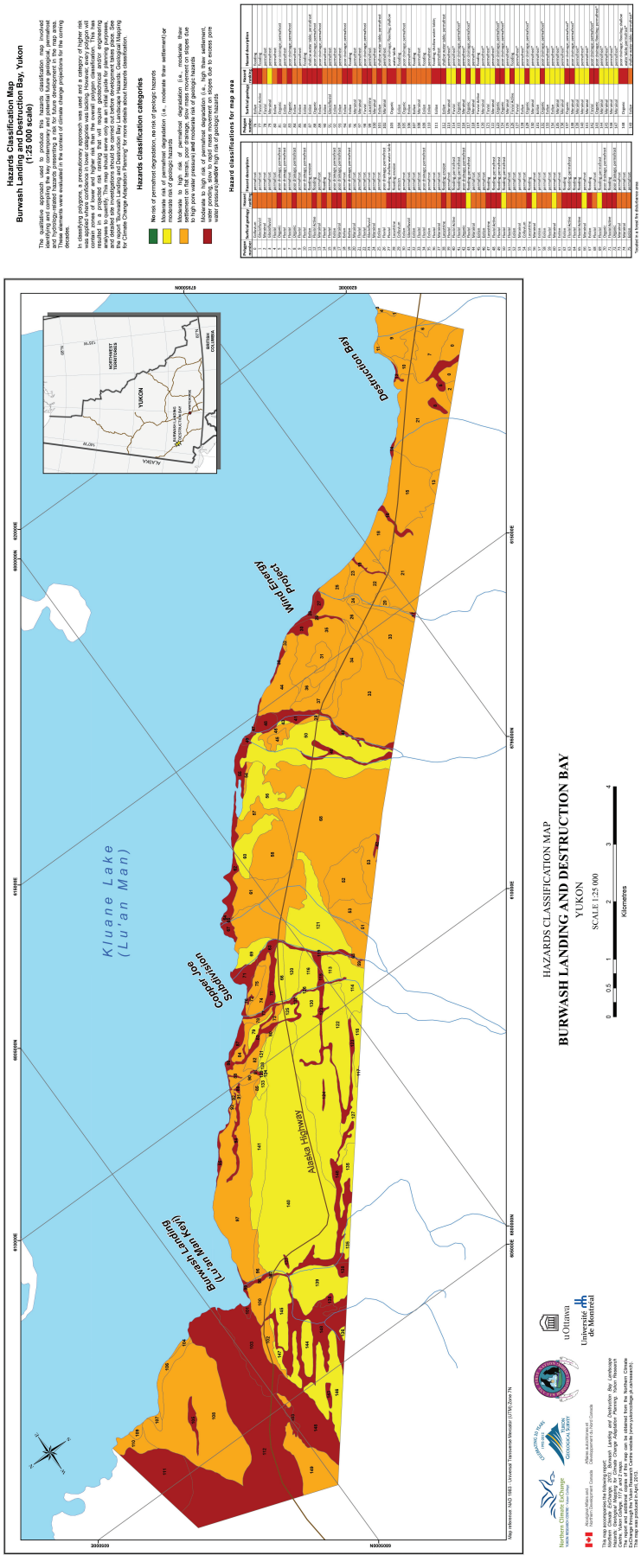

Figure 1: Hazards Classification Map, Burwash Landing and Destruction Bay, Yukon (1:25 000 scale)

Yamal Craters: State of knowledge and wished in-situ investigations

Dimitrii O. Sergeev[1], A. Khimenkov[1], G. Tipenko[1], A. Vlasov[1], E. Cauquil[2], E. Green[2], P. Dauboin[3], J. Stanilovskaya[3], & M. Mnushkin[1]

[1] *Sergeev Institute of Environmental Geoscience RAS (IEG RAS), Russian Federation*
[2] *Total, France*
[3] *Total E&P Russie*

A unified compilation of the existing facts relating to the formation of "Yamal Craters" as well as a generalized description of the existing hypotheses of their creation is presented. At least 6 craters have been observed in or close to Yamal peninsula, located in permafrost areas. Almost all craters are located near gas and gas-condensate fields. Main morphological, spatial and geological features of "Yamal Craters" are analyzed and. published hypotheses of crater formation in the Arctic are clustered in three major groups:

1. The phenomena are formed by the external direct influence.
2. The phenomena are formed by the explosion of perennial frost mounds (bulgunnyakhs, pingos, hydrolaccoliths) formed due to freezing of paleo-taliks.
3. The phenomena are formed by the decomposition of gas hydrates, including the cases of the thermal effects from the top and from the bottom.

The following hypotheses evaluation criteria are used:

1. Hypothesis completeness
2. Confirmation by in-situ observation data or experiments
3. Self-consistency and amount of unsolved problems
4. The principal technical possibility to verify the hypothesis (accessibility of the objects, instrumentation and laboratory facilities)
5. The availability of ready-to-use physical and mathematical models in place describing the assumed driving process (fundamental knowledge of the process).

The considered hypotheses are founded at selected major process of crater formation. Most likely, all of them can be real in part and form the geological consequence. In the first stage the gas hydrate partial decomposition forms the horizon with gas bubbles at the depths 60 and 100 meters. In the second stage the heating from underwater taliks leads to bubbles' growing and the moving of its to the surface. The drainage of the lake converts the taliks to closed system with pressure growing.

Authors present a preliminary computation of stress and deformation with possible temperature regime to create such craters through overpressure and explosive process. The mechanical model takes into account the elliptical shape of the cave at 30 m depth with consequent pressure growing. The insignificant influence of climate change as a result of thermal field modeling was obtained.

Then, authors developed the field study program using remote and in-situ methods to assess the areal distribution and a possible danger of "Yamal Craters" for the oil and gas infrastructure and the environment. In practical terms, this study sheds more light on the regularities in the interaction of gases with surrounding permafrost and cold soils and also on the evolution of reservoir properties of deposits.

Permafrost-related causes and consequences of the Sagavanirktok River flooding in spring 2015

Yuri Shur[1], Mikhail Kanevskiy[1], Donald A. Walker[1], Torre Jorgenson[2], Marcel Buchhorn[1], Martha K. Raynolds[1], & Horacio Toniolo[1]

[1] *University of Alaska Fairbanks, USA*
[2] *Alaska Ecoscience, USA*

In the first part of March 2015, a huge icing (aufeis) began to develop in the delta of the Sagavanirktok (Sag) River on the Beaufort Sea Coastal Plain of Alaska - an area with severe arctic climate and thick continuous permafrost. Icing is a mass of surface ice formed during the winter by successive freezing of sheets of water seeping from a river, groundwater or a spring. River icings develop when further winter flow in the river under ice is obstructed causing overflows. Icings occur in many cold regions but the permafrost region is the most susceptible to their formation. The 2015 icing in the Sag River Delta occurred next to the Dalton Highway, the only road in northern Alaska that provides access to major Alaska oilfields and is parallel to the Trans-Alaska Oil Pipeline. The overflow water raised to several meters above the normal winter level and flooded about 25 km of the Dalton Highway to a height of about one meter. It occurred during cold weather and caused rapid development of the huge icing, which became in reality an ice dam. This event led to the closure of the Dalton Highway from March 30 to April 2 and from April 5 to April 12.

In mid-May, higher than usual air temperature in the upper Sag River watershed caused fast melting of snow and high floodwater, which was obstructed in the Sag River Delta by the extensive ice dam. The floodwater ran over the highway, washed out several stretches of it, and reached the Deadhorse Airport. The highway was closed again and reopened on June 5, after a 18-day-long closure. Media in Alaska, nationwide and even abroad covered the Dalton Highway flooding and some of them characterized it as “epic” and extreme flooding.

The Alaska governor Bill Walker twice (in April and May) issued Declarations of Disaster Emergency due to the unprecedented flooding. The declarations acknowledged the severe impact and damage to highway infrastructure, including the road surface, embankments, and drainage structures; restricted or prohibited travel that caused economic hardship to local, regional, and international business; an urgent need for immediate road repairs and flow diversion efforts to alleviate future threats to that infrastructure. According to the declarations, the flooding and emergency work disrupted normal commercial and private traffic along the Dalton Highway, including critical fuel shipments to petroleum production and distribution facilities in Prudhoe Bay.

Causes of the severe Dalton Highway flooding were widely attributed to high precipitations in the previous summer, cold winter, and to warm spring. Surprisingly, the causes of formation of the huge icing, which ultimately functioned as a large ice dam, were not discussed. From a permafrost science point of view, formation of a gigantic (according to Russian classification) icing should be a starting point in any forensic study of the March to May 2015 severe and unusual flooding events on the Dalton Highway. Why was the under-ice flow obstructed, enhancing the overflow above the river ice? The main cause of icing formation is usually a deep freezing of the river and sediments beneath it. It can be natural or triggered by human activity. Under natural conditions, deep freezing may be caused by a severe winter and low snowfall. Comparison of temperatures for the cold period preceding overflow and icing formation during the winter of 2014-2015 and for the similar period of the previous winter did not show any significant difference. Snowfall in the winter of 2014-2015 was 86.3 cm (October to March), which is practically two times greater than for the similar period of the previous winter. It means that freezing in the winter of 2014-2015 should be smaller than in the previous winter.

Due to a lack of a strong climatic driver, we evaluated potential human-induced causes. We found that an Landsat image from April 2015 showed a wide swath of the delta containing the tracks of vehicles

from multiple crossings of the Sag River Delta that were part of a 3-D seismic exploration. Numerous trails of winter movement perpendicular to the delta are seen on the satellite image. Such activity over the delta is one of well-known causes of icing formations. In Russia, with its numerous arctic rivers, scientists and engineers know that deltas are very susceptible to icing formation associated with winter roads. Russian official requirements for design, construction, and maintenance of winter roads in Siberia [VSN, 1991] identify that winter roads in deltas pose a risk for triggering icing formation. This document states that winter roads should not cross deltas and that they be laid out only along a deep channel. Some other sources specify that even a single crossing by a tractor can lead to icing formation. Other studies also advise that river should be crossed at sites where the channels are straight and it is necessary to avoid crossings in areas with riffles, sand bars, islands, and especially in deltas.

Unfortunately, the Sag River Delta falls in this situation. Numerous winter crossings of the delta associated with seismic exploration compacted snow and, therefore, facilitated more rapid winter heat loss from the water and ground beneath the river. Thus, the most likely cause of the enhanced icing and severe flooding was deep freezing of water and shallow taliks under braided channels that blocked water flow under the ice, which was triggered by seismic exploration in the area. To prevent similar events in the future, we informed the Alaska Department of Transportation and the Department of Natural Resources about our evaluation of causes of the icing formation in the Sag River Delta that led to the severe flooding in spring 2015.

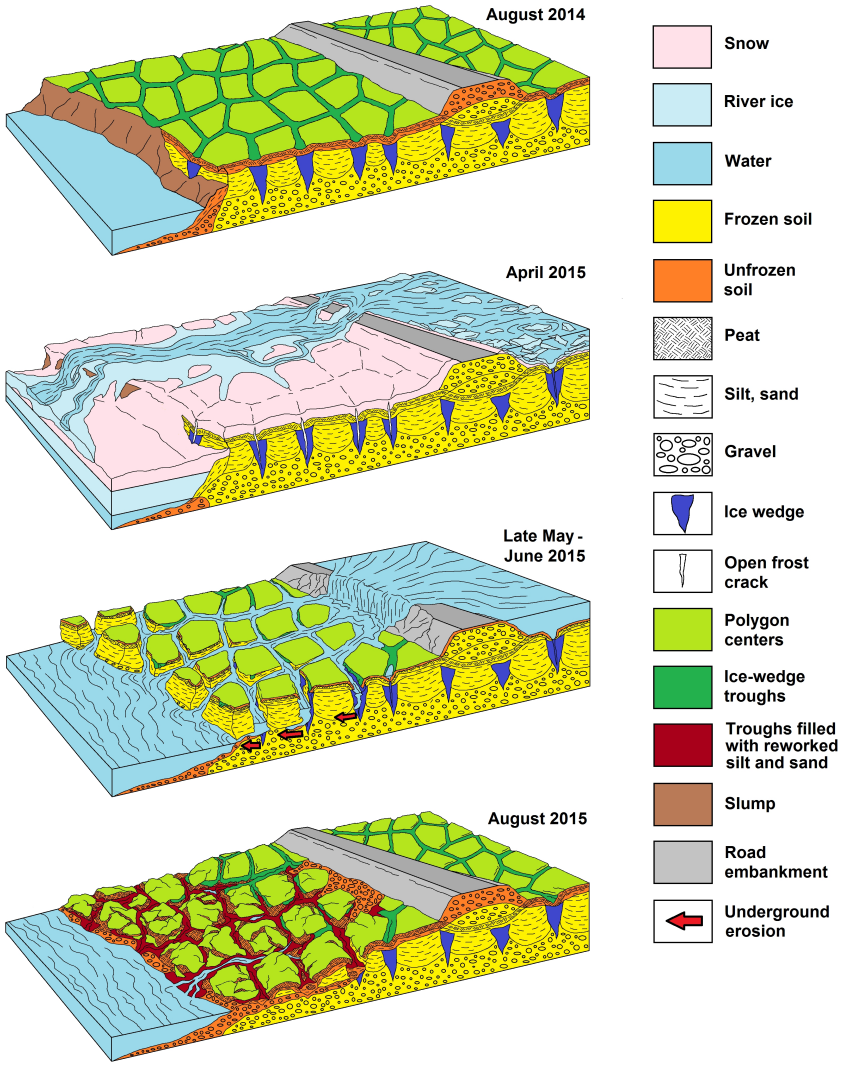

Figure 1: Erosional transformation of high-centered ice-wedge polygons on the floodplain affected by catastrophic flooding and underground erosion, Sag River Delta, spring 2015

The flooding event led to active underground erosion of the ice-rich permafrost. During our field work in the vicinity of Deadhorse in previous years, we observed areas of polygonal ground with a thin (< 1 m) layer of peat and fine-grained soil over river gravel. It was similar to the polygonal surface of the adjacent flood plain, but lower in elevation in about 2-3 m and without ice wedges. The observed features were located next to a stream created by water flow through two big culverts installed under the Dalton Highway. Severe flooding of the Sag River in spring 2015 and its impact on surrounding tundra revealed the process leading to formation of such a feature.

In May 2015, flooding overflowed the Dalton Highway and surrounding tundra. Running water was channelized by temporal culverts installed during the emergency response and at some places was subsequently distributed by the system of troughs of high-centered polygons. Water ran into open thermal cracks at the bottom of troughs and reached the gravel layer creating underground flow pathways through gravel toward the river (Fig. 1). The process of underground thermal erosion was described by Fortier et al. [2007] and Shur et al. [2012]. Running through the gravel, water eroded ice wedges and extremely ice-rich floodplain deposits from below and from the sides, which caused significant settlement of the polygonal surface. The organic-rich active layer was the most resistant to thermal erosion because it was strengthened by roots of grasses and shrubs. This thin resistant layer created the base of the low residual polygonal ground that formed as a result of transformation of the floodplain with high-centered ice-wedge polygons (Fig. 1).

Comprehensive studies of similar events in Arctic should always include the permafrost component.

Acknowledgements

This work was supported by the National Science Foundation (grants ArcSEES 1233854 and ARC 1023623). Any opinions, findings and conclusions or recommendations expressed in this material are those of the authors and do not necessarily reflect the views of the National Science Foundation.

References

Fortier, D.; Allard, M. and Shur, Y. [2007]: Observation of rapid drainage system development by thermal erosion of ice wedges on Bylot Island, Canadian Arctic Archipelago. *Permafrost and Periglacial Processes*, 18(3):229–243, ISSN 1099-1530. doi:10.1002/ppp.595.

Shur, Y.; Kanevskiy, M.; Jorgenson, T.; Dillon, M.; Stephani, E. and Bray, M. [2012]: Permafrost degradation and thaw settlement under lakes in yedoma environment. In: Hinkel, K.M.(ed.), *Proceedings of the Tenth International Conference on Permafrost*, Salekhard, Yamal-Nenets Autonomous District, Russia, 25–29 June 2012, volume 1: International Contributions, pages 383–388. The Northern Publisher: Salekhard. ISBN 978-5-905911-01-9. URL http://ipa.arcticportal.org/publications/conference-proceedings.

VSN [1991]: *Design, construction, and maintenance of winter roads in Siberia and North Eastern part of the USSR (VSN 137-89)*. MDesign, construction, and maintenance of winter roads in Siberia and North Eastern part of the USSR (VSN 137-89), (in Russian).

SESSION 24

New Frontiers in Mountain Permafrost Research

Convener:

Nadine Salzmann, *Department of Geosciences, University of Fribourg, Switzerland*

Dario Trombotto Liaudat, *Geocryology, IANIGLA, Argentina*

Ingo Hartmeyer, *Department of Geography and Geology, University of Salzburg, Austria*

The existence and changes of permafrost conditions in mountain regions can significantly modify landforms and ecosystems, and where people are living in these periglacial environments, they are confronted with hazards of destabilized steep slopes and impacts on infrastructure when permafrost thaws. In most mountain regions worldwide, the elevation-bands of periglacial environments are often only sparsely populated. As a result, scientific and political awareness of the (invisible) permafrost is often low, and has mostly only been raised in densely populated mountain ranges such as the European Alps. Nevertheless, permafrost occurrence is a very widespread temperature phenomena. For instance in the Andes some estimations hold that it would cover an area of approximately 140.000 km^2, which is larger than the known Southern Hemisphere permafrost in the Antarctica. Paleopermafrost also seems to have affected a major area there and today's estimations are that it covered approximately 600.000 km^2, 21 ka ago, during the Last Glacial Maximum. The currently observed and projected increase in air temperature and decrease in the duration and extent of seasonal snow cover (IPCC, 2013), will potentially lead to substantial changes in periglacial areas of many mountain regions worldwide at an unprecedented rate and also affect people living in these and adjacent environments.

This session invites contributions from all mountain regions worldwide, where permafrost research is still in an initial and developing stage, or existing research gained so far comparably little attention internationally. All aspects related to mountain permafrost, including geomorphology, geocryology, permafrost mapping and modelling, process studies, rock glaciers and other slope movements, monitoring activities (permafrost as an Essential Climate Variable) and impact assessments connected to natural hazards or water resources are equally welcomed. As a whole, the session aims at providing a platform to discuss mountain-permafrost related challenges in areas with so far reduced international awareness and knowledge of the phenomena.

Permafrost in the Indian Himalaya: A pilot Indo-Swiss study in Himachal Pradesh building new knowledge and scientific capacity

Simon Keith Allen[1,2], Joel Fiddes[1,3], Andreas Linsbauer[1,4], Surjeet Singh Randhawa[5], Brijesh Saklani[6], & Nadine Salzmann[4]

[1] *Department of Geography, University of Zurich, Switzerland*
[2] *Institute for Environmental Sciences, University of Geneva, Switzerland*
[3] *WSL Institute for Snow and Avalanche Research SLF, Davos Dorf, Switzerland*
[4] *Department of Geosciences, University of Fribourg, Switzerland*
[5] *State Centre on Climate Change, Himachal Pradesh, India*
[6] *Aryabhatta Geo-informatics & Space Application Centre, Department of Environment, Science & Technology, Shimla, India*

Little is known about permafrost occurrence in the Himalaya due to absent local investigations. Identifying where mountain slopes are expected to contain permafrost is an important first step which provides a scientific basis for assessing current and future impacts associated with warming and thawing of frozen ground. Therefore, under the Indian Himalayas Climate Adaptation Programme (IHCAP), Indian and Swiss scientists have joined forces to generate model-derived estimates of the spatial distribution of permafrost in mountain areas of Kullu district, Himachal Pradesh, while strengthening local scientific capacity to ensure methodologies can be outscaled to the larger Indian Himalayan Region (IHR). Here we briefly introduce the main components of the permafrost pilot study in Kullu, highlight some first results, and reflect on new experiences gained.

Our methodological approach was developed around three core components:

- Modelling of possible permafrost distribution,
- Initial evaluation based on mapped permafrost indicators (rock glaciers), and
- Assessment of permafrost terrain and related hazards.

As a new area of research in India, we deliberately began by implementing some fundamental concepts emphasizing mean annual air temperature (MAAT) and slope topography as key factors governing permafrost distribution. As a first step, the local elevation of the 0 °C MAAT isotherm was calculated from station data (see locations in figure 1). Simple empirically derived rules then provided a broad estimate of where permafrost is likely to occur based on topographic influences on solar radiation at the ground surface and snow accumulation. Based on studies largely conducted in the European Alps, it is known that permafrost is most likely to be found at elevations some hundreds of metres above the 0 °C isotherm (particularly on slopes with high insolation), but more rarely, permafrost can also be found at considerably lower elevations in the most topographically favourable situations. While such basic rules defining permafrost limits should not be simply transferred from the Alps to the Himalayan setting, this simple approach provided a useful starting point for introducing and discussing topographic controls on ground temperature, and thereby, set the stage for the use of physically based numerical models that explicitly capture these driving processes.

Physically based numerical modelling of Mean Annual Ground Surface Temperature (MAGST) provides a proxy for permafrost conditions where MAGST is below 0 °C. Our approach implemented in Kullu uses state of the art numerical methods driven by downscaled atmospheric datasets (ERA-Interim) (see Fiddes and Gruber [2012, 2014]), enabling large area simulations of the surface/subsurface at high spatial resolutions (ASTER 30 m DEM). The methods are optimised for remote, data-poor mountain regions, and thus suitable for outscaling to larger spatial scales. A basic evaluation of downscaled air temperature using a new network of automatic weather stations was completed as well as a comparison of modelled snow covered area (SCA) against remotely sensed SCA (from the MODIS sensor). These evaluation methods have the advantage of targeting different stages of the model chain.

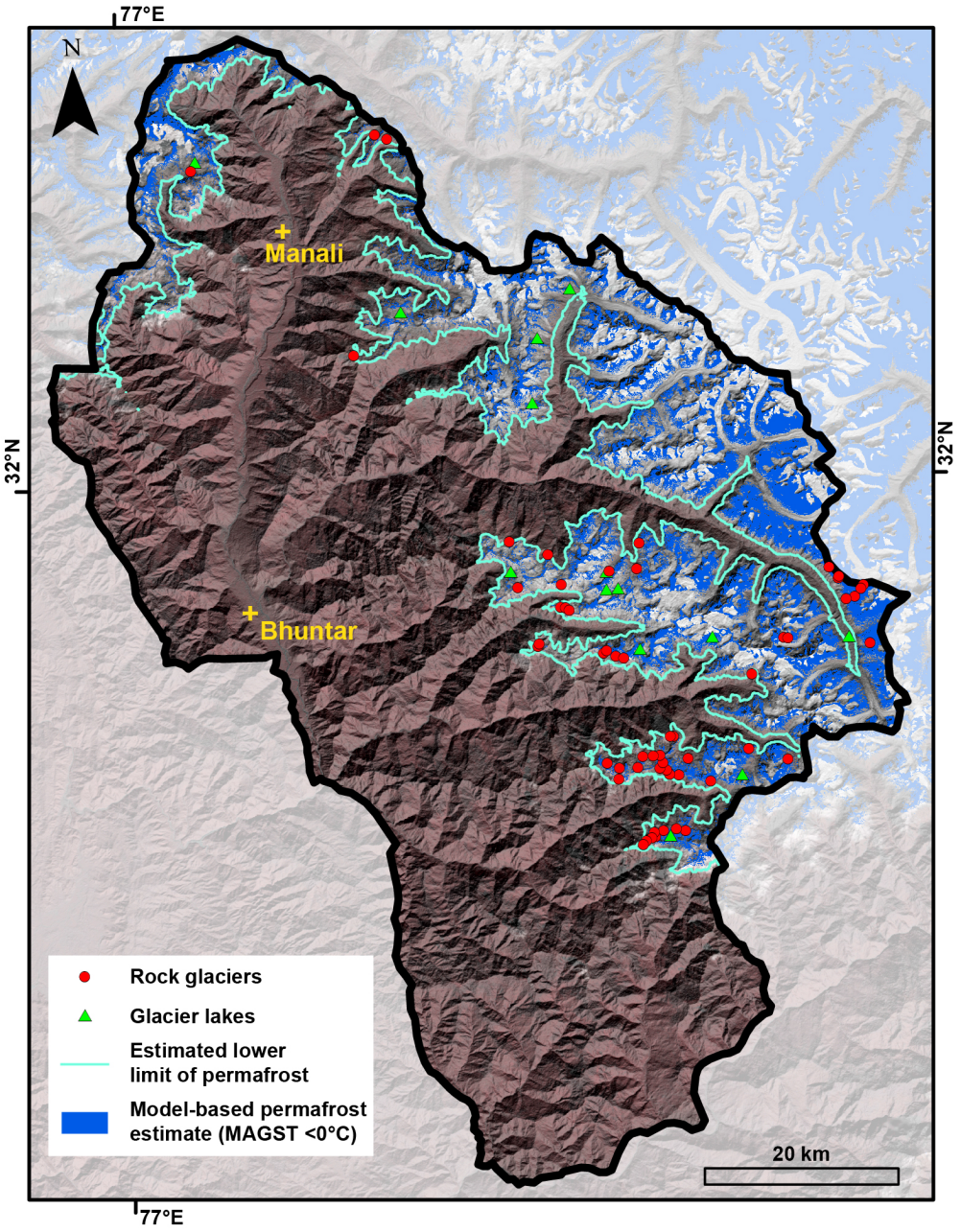

Figure 1: Mapped rock glaciers across the Kullu district are compared with a model-based estimated permafrost distribution. Also indicated is an empirically-derived estimated lower limit of permafrost in Kullu district, where permafrost might be expected

Using high resolution satellite imagery from Google Earth and the Indian National Remote Sensing Agency, rock glaciers have been mapped across all mountainous areas of Kullu district, and provide a first-order, qualitative evaluation of the validity of the model-based estimate of permafrost distribution. Our initial results suggest permafrost may extend down to 4200 m a.s.l in isolated instances, which compares favourably with the observed lower elevation limit from the ca. 60 mapped rock glaciers (interquartile range of 4280 – 4560 m a.s.l), and approximate lower limits to permafrost distribution established in relation to the local 0 °C MAAT isotherm (Fig. 1). This general consistency is promising, and encourages further field-based validation efforts that will ultimately enable outscaling of our methodology to other areas. Based on these initial results, around 9 % (420 km^2) of the modelled land area in Kullu district (excluding glaciers) is classified as permafrost. This new information on permafrost distribution in Kullu district is

yet to be integrated within a complete hazard and risk assessment. Nonetheless, an updated inventory of glacial lakes in the district shows that all lakes are formed either directly within, or immediately beneath permafrost terrain. Hence further consideration is to be given to possible thawing of permafrost in lake dam and outlet areas, and possible impacts from permafrost-related rockfall or debris flows entering into these lakes – factors not considered in previous GLOF hazard assessment schemes in the IHR.

As a pilot project under IHCAP, significant emphasis was directed towards ensuring local research capacities were strengthened through joint Indo-Swiss scientific collaboration, exchange, and training. Progress has largely been focused within two successful research exchanges, both in India and Switzerland, where educational seminars, practical exercises, and field excursions were combined with desk-based work towards the completion of the mapping and modelling components of the study. Targeting the next generation of leading Indian scientists, the IHCAP capacity building programme on Himalayan glaciology, hosted at Jawaharlal Nehru University (Delhi), brought together young graduate level Indian scientists for an intensive series of lectures and exercises taught by experienced Swiss and Indian researchers over the course of several weeks. Recognizing its importance as a new emerging area of Himalayan research, sessions were specifically devoted to the fundamentals of permafrost science, in addition to broader sessions on glacier and permafrost related hazards. In a practical exercise, the young scientists were tasked with implementing basic topographic, geomorphic, and climatic understanding to establish their best estimate of permafrost distribution in a region of the Indian Himalaya, thus, closely linking the training program with the research activities in Kullu district.

The Kullu pilot study has provided some first preliminary understanding of the possible extent and relevance of permafrost in this area of the Indian Himalaya, while strengthening local research capacities to ensure further measurement and monitoring projects can be initiated, and methodologies eventually expanded to larger areas. Field-based validation efforts (e.g., temperature measurements, geophysical monitoring, terrain deformation monitoring) are now needed to improve confidence in the modelling approaches, and will ideally be established with a view towards long term monitoring. Permafrost is clearly of broad importance, and potential exists to integrate the approaches and experiences of the Kullu pilot study within larger regional programs.

References

Fiddes, J. and Gruber, S. [2012]: TopoSUB: a tool for efficient large area numerical modelling in complex topography at sub-grid scales. *Geoscientific Model Development*, 5(5):1245–1257, doi:10.5194/gmd-5-1245-2012.

Fiddes, J. and Gruber, S. [2014]: TopoSCALE v.1.0: downscaling gridded climate data in complex terrain. *Geoscientific Model Development*, 7(1):387–405, doi:10.5194/gmd-7-387-2014.

Permafrost distribution modeling in the semi-arid Chilean Andes

Guillermo F. Azócar[1], Alexander Brenning[1,2], & Xavier Bodin[3]

[1] *Department of Geography and Environmental Management, University of Waterloo, Canada*
[2] *Department of Geography, Friedrich Schiller University Jena, Germany*
[3] *Laboratoire EDYTEM, Université de Savoie, CNRS, Le Bourget-du-Lac, France*

Mountain permafrost and rock glaciers in the Andes are of growing interest due to the increase in human activities in this remote area and new environmental regulations. Empirical models of mountain permafrost distribution based on the spatial analysis of intact and relict rock glaciers and Mean Annual Air Temperature (MAAT) have been established as a tool for regional-scale assessments of permafrost favorability across entire mountain ranges. In this approach, bias adjustments are made to account for differences in permafrost presence within rock glaciers and in general debris-covered high-mountain terrain [Boeckli et al., 2012,b]. This method allows for a rapid initial assessment of favorability for the presence of mountain permafrost in data-scarce vast mountain regions.

In the present study, this methodology is applied to map a Permafrost Favorability Index (PFI) throughout the semi-arid Andes of central Chile (29°S – 32°S), excluding areas of exposed bedrock (Fig. 1). For this purpose, an inventory of relict and intact rock glaciers was compiled for the study region, MAAT was regionalized based on scarce meteorological data available in the study region, especially for high altitude area, and permafrost favorability was spatially modeled empirically based on MAAT and potential incoming solar radiation (PISR).

The compiled inventory includes 3575 rock glaciers in the, Huasco, Elqui, Limarí and Choapa watersheds in Central Chile (total area: 38651 km^2, including low elevation areas), 1664 of which were classified as relict and therefore as indicative of permafrost absence; 51 rock glaciers were removed before modeling due to their exceptional locations. Glaciers in the study region are limited to the highest parts of the Elqui and Huasco catchments. The estimated total ice volume of rock glaciers in the study region is about 2.5 times as large as the total glacier ice volume [Azócar and Brenning, 2010]. MAAT for the 1981-2010 period was regionalized based on 116 station-years of annual air temperatures at 11 weather stations located between 2150 and 4000 m a.s.l. Due to the heterogeneity of time periods covered, a linear mixed-effects model with elevation and latitude as fixed-effects predictors and year as a random effect was used to account for spatial trends and for year-to-year variations, and MAAT was predicted from this model by averaging over the random effects.

A Generalized Additive Model (GAM) was built to model the activity status of 3524 rock glaciers based on the (nonlinear) interaction term of regionalized MAAT and PISR derived from the DEM. A Permafrost Favorability Index (PFI: ranges from 0 to 1) was obtained by adjusting model predictions. A temperature offset was applied to correct overestimation of permafrost related to downward creep of rock glaciers and their delayed response to climate change. The model's goodness of fit was found to be acceptable with an AUROC of 0.76. Conditions highly favorable to permafrost presence (PFI $>$ 0.75) were predicted for 1051 km^2 of mountain terrain, or 2.7 % of the study area. Favorable conditions were expected to occur in 2636 km^2, or 6.8 % of the area. Especially the Elqui and Huasco watersheds in the northern half of the study area include substantial portions (11.8 % each) that are considered to be favorable for permafrost presence, while predicted favorable areas in the southern Limarí and Choapa watersheds are mostly limited to specific sub-watersheds.

While the present results underline the importance not only of rock glacier distribution but also of expected mountain permafrost presence in the Chilean semi-arid Andes [Azócar and Brenning, 2010], in the future local ground-truth observations will be required to confirm permafrost presence in favorable areas, and to monitor permafrost evolution under the influence of climate change effects.

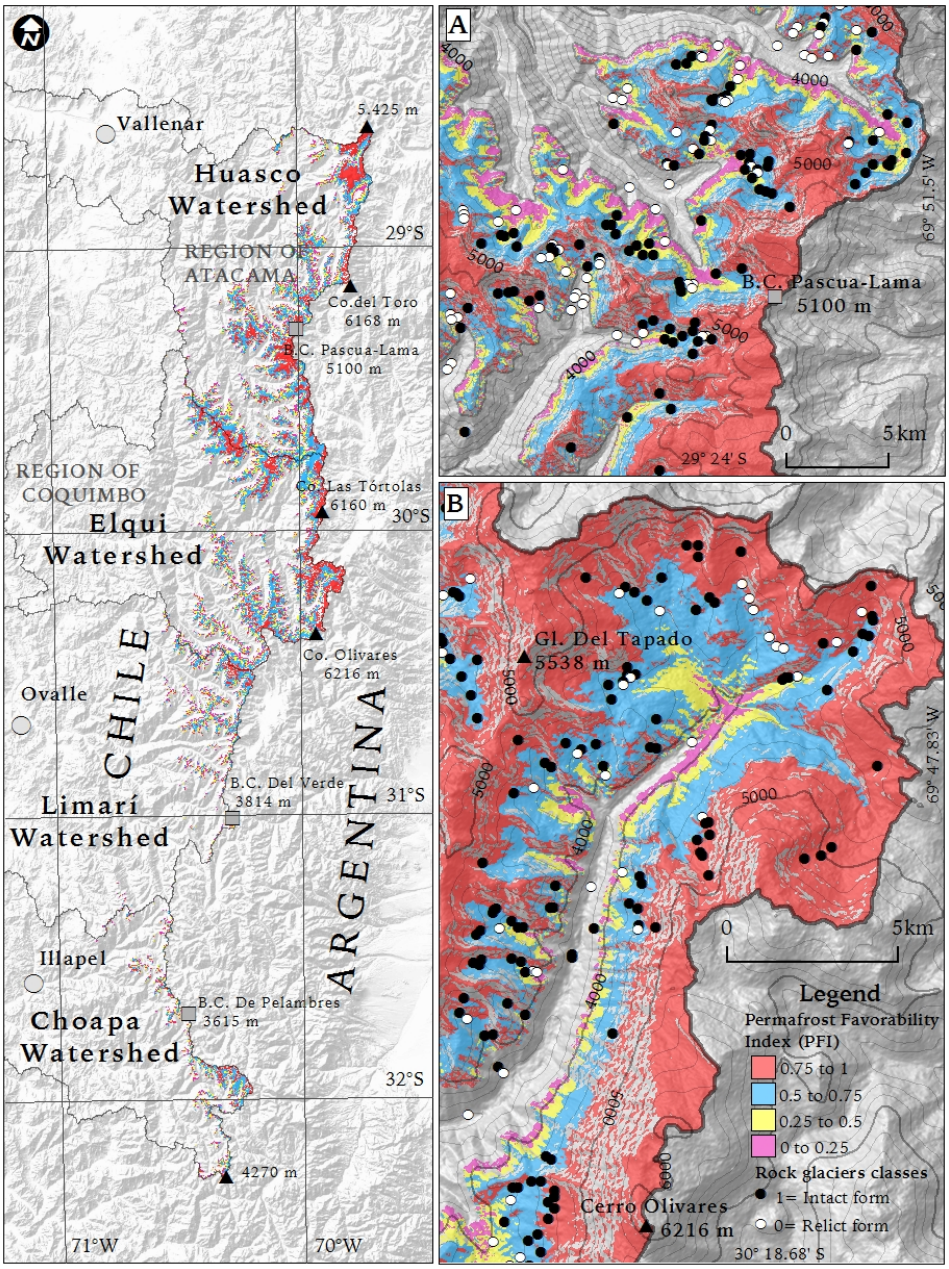

Figure 1: Permafrost favorability index (PFI) in the semi-arid Chilean Andes based on the permafrost distribution model for debris areas

References

Azócar, G. F. and Brenning, A. [2010]: Hydrological and geomorphological significance of rock glaciers in the dry Andes, Chile (27°–33°S). *Permafrost and Periglacial Processes*, 21(1):42–53, 2010. doi:10.1002/ppp.669.

Boeckli, L.; Brenning, A.; Gruber, S. and Noetzli, J. [2012a]: Permafrost distribution in the European Alps: calculation and evaluation of an index map and summary statistics. *The Cryosphere*, 6(4):807–820, doi:10.5194/tc-6-807-2012.

Boeckli, L.; Brenning, A.; Gruber, S. and Noetzli, J. [2012b]: A statistical approach to modelling permafrost distribution in the European Alps or similar mountain ranges. *The Cryosphere*, 6(1):125–140, doi:10.5194/tc-6-125-2012.

The PermaSense Mountain Lab – Technology and infrastructure for an open permafrost data repository

Jan Beutel[1], Samuel Weber[2], & Tonio Gsell[1]

[1] *ETH Zurich, Switzerland*
[2] *University of Zurich*

Starting in 2006 as a single research project PermaSense has pioneered experimental permafrost research in alpine environments using spatially distributed online wireless sensors. Conceived as a focused investigation to understand the utility of many miniature battery powered wireless sensors to be used in high-alpine permafrost research has since developed into a full-fledged multi-site research infrastructure spanning across the western part of the European Alps. This distributed sensing infrastructure is today serving both campaign-based experimental permafrost research as well as long-term monitoring and natural hazard warning needs. Driven by the main property of the core building blocks, namely miniature, battery powered wireless sensors, online and open data access was part of the concept from day one. The focus on a powerful, standardized and open data infrastructure has proven to be very successful enabling a multitude of data access needs simultaneously based on one common data infrastructure. A web frontend allows users to access both primary sensor data as well as data products incorporating metadata or value conversions, i.e. from machine to SI units as well as processed data products. All data on the PermaSense data repository can be accessed in real-time streaming formats as well as using full historic data digests. It was initially suggested that the data analysis would benefit significantly from low-latency online stream processing. This vision has however only been exploited once in the case of post-processing of RAW L1-GPS in the form of a research-grade prototype real-time kinematic processing. The other parts of the data collected by our online sensor systems is today still analyzed using traditional batch data processing. A benefit that the data streaming interface on a publicly accessible web platform does provide is that all interested parties can observe the evolution of a specific experiment in real-time and at their own pace without subscribing to and waiting for e.g. monthly data digests. Therefor this kind of online and open access experimentation facilitates to plan ahead, discuss actions and intervene at a much earlier time than with traditional data logging or closed data gathering systems.

The core functionality is wireless access to all sensors. This wireless access can be either realized using custom, ultra-low power wireless sensors for e.g. thermistors and crackmeters or commodity solutions like 802.11x Wireless LAN that can transfer much higher data rates e.g. from webcams or InSAR radar. We have gained very good experience using Wireless LAN as a high throughput data backbone on a valley scale and serving multiple field sites across the Mattertal Valley in Switzerland or the Aig. Du Midi, Chamonix, France. However, connectivity can fail intermittently and without notice. Additionally, explicit duty-cycling of devices, e.g. the wireless radio, while the sensor is kept operating is a common means for the reduction of power consumption. Therefore, all wireless devices require a storage layer to deal with disconnected operation, handle and synchronize delayed data. On the server side a scalable data management solution is required that on the one hand meticulously preserves all primary data in its original state and on the other hand allows to grow according to the user's needs and/or the evolution of new technologies and analysis methods. We have therefore partitioned the data management into an instance termed "private" acting as data ingress point and holding all incoming primary data in an original, unmodified state. A successive instance termed "public" is a structurally identically system with the added functionality of metadata mapping, value conversion. While the "private" server can be operated in a protected, firewalled environment ensuring long-term data consistency the "public" server also serves a public web frontend and data warehouse for different data aggregates. Upon incorporation of a new data analysis or the change of a data conversion function, metadata etc. data on the "public" server can be replayed, meaning data is deleted, fetched again from the "private" server and the updated data are computed and stored again on the "public" instance.

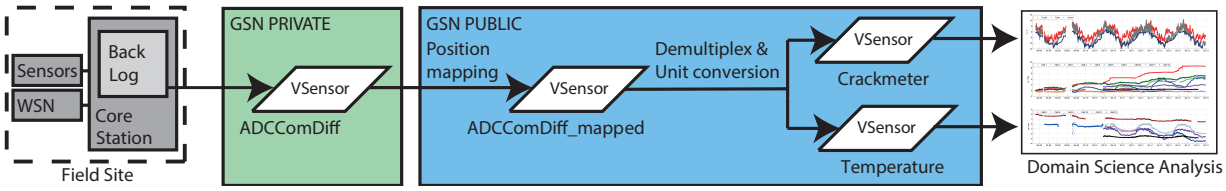

Figure 1: Data from the field sites is stored in unmodified form in the primary instance of the GSN data management server. After mapping of metadata and value conversion it is stored as secondary data in the public instance of GSN from where it is accessible by various tools.

We have gathered and maintained over 5,835,038,653 of data amounting to 1,352.6 GB of data and originating from over 8 field sites over the past ten years. The main users of the data are scientists although there is an increase of users from the government, local authorities, businesses and contractors w.r.t. natural hazard mitigation. While the science users are often searching for the unknown, frequently developing an analysis method while doing so and as such require frequent full access to all data, natural hazard experts prefer consolidated views and reports with a clear structure, low-latency and high update frequency. Hiding complexity on the one side while exposing all possibilities on the other is not possible. Therefore, the frontend data services provided are in a gradual but constant process of change, addition and refinement while the core of the data management system is remaining largely stable. The PermaSense data repository is accessible at http://data.permasense.ch.

References

Beutel, J.; Gruber, S.; Hasler, A.; Lim, R.; Meier, A.; Plessl, C.; Talzi, I.; Thiele, L.; Tschudin, C.; Woehrle, M. and Yuecel, M. [2009]: PermaDAQ: A Scientific Instrument for Precision Sensing and Data Recovery under Extreme Conditions. In *Proceedings of the 8th International Conference on Information Processing in Sensor Networks (IPSN)*, pages 265–276, April 2009.

Hasler, A.; Talzi, I.; Beutel, J.; Tschudin, C. and Gruber, S. [2008]: Wireless Sensor Networks in Permafrost Research – Concept, Requirements, Implementation and Challenges. In: Kane, D.L. and Hinkel, K.M.(eds.), *Proceedings of the Ninth International Conference on Permafrost*, Institute of Northern Engineering, University of Alaska Fairbanks, Fairbanks, USA, 29 June–3 July 2008, volume 1, pages 669–674. ISBN 978-0-9800179-2-2. URL http://ipa.arcticportal.org/publications/conference-proceedings.

Keller, M.; Beutel, J.; Saukh, O. and Thiele, L. [2012]: Visualizing Large Sensor Network Data Sets in Space and Time with Vizzly. In *roceedings of the Seventh IEEE International Workshop on Practical Issues in Building Sensor Network Applications (SenseApp 2012), Clearwater, FL, USA*, pages 963–971, October 2012.

Multi-temporal mapping of rock glacier displacements: insights from SfM, ALS and TLS high-resolution datasets on the Laurichard rock glacier, French Alps

Xavier Bodin[1], Olivier Sanchez[2], Stéphane Jaillet[2], Antoine Rabatel[2], & Emmanuel Thibert[3]

[1]*EDYTEM, CNRS/Université Savoie Mont-Blanc, France*
[2]*LGGE, CNRS/OSUG/Université Grenoble Alpes, France*
[3]*ETNA, IRSTEA Grenoble, France*

The deformation of rock glaciers is a climate-dependent process which affects many mountain debris slopes underlain with ice-rich permafrost [Haeberli et al., 2006]. Under temperate conditions, like in the Alps, the typical magnitude of movement is in the order of a few dm/a to 1-2 m/a [Barsch, 1996]. However, recent measurements of accelerating rock glaciers show that velocity can increase up to several m/a [Delaloye et al., 2012]. This kinematics variability can locally lead to slope instabilities and trigger hazardous phenomena: in France, the collapse of the Bérard rock glacier in 2006 [Bodin et al., 2016] and the debris-flow that started at the Lou rock glacier in 2015 [Pauhle, 2015] can be considered as two events that exemplify the possible impacts of permafrost degradation for human societies living in mountain territories.

At the limit between the Northern and the Southern -more Mediterranean-influenced- French Alps, the Laurichard rock glacier benefits from a long-term monitoring since the early 80's [Francou and Reynaud, 1992]. Using 30-year long annual geodetic surveys of blocks, we detected inter-annual fluctuations of velocity [Bodin et al., 2009], which synchronicity with many series on other surveyed rock glaciers in the Alps suggests that the atmospheric warming, modulated by the nivological conditions, is controlling the rock glacier deformation rates [Delaloye et al., 2012]. Nevertheless the knowledge on the processes that govern such behavior is still lacking physical basis: a better understanding requires to model the geomechanics of rock glacier, and for that accurate multi-temporal maps of surface displacements are fundamental.

For that purpose, we produced very high-resolution 3D models of the Laurichard rock glacier, acquired either by terrestrial laserscanning (TLS) in 2005, 2006, 2011 and 2013, airborne laserscanning (ALS) in 2012 and terrestrial photogrammetry (or structure-from-motion, SfM) in 2013 and 2015. The density of the generated point clouds we generated varies from 2 to 20 pt/m^2 and the accuracy of the coordinates after co-registration between the different datasets (2012 ALS dataset chosen as the reference) is in the order of 12-15 cm (standard error computed on stable areas). The main challenges for correct topographic mapping arose from the multi-scale variability: microtopographic features like plurimetric ridges and furrows shield some areas from the laser, whereas surface roughness of the pluri-decimetric coarse blocky cover may be difficult to cope with when comparing point-clouds between each other's.

We employed 3D point-cloud processing and image correlation tools to compare high resolution hill-shaded digital elevation models together and to extract various spatially-distributed measurements of surface movements. Both amplitude and direction of the displacements computed by images correlation were validated from comparison to in situ high precision geodetic (milimetric accuracy) measurements: at the various considered time scales and for 8 measured points, the mean difference between TLS/ALS/SfM-derived measurements and geodetics measurements is lower than 5 cm/a, for velocity that range between 25 and 150 cm/a. The spatially-distributed information provides rich insights into the deformation mechanisms of rock glaciers and open new challenging opportunities to move further into rheological laws and physical models. The ongoing next step of this work will consist in extracting 3D point-clouds from two fixed cameras surveying the Laurichard rock glacier, which will soon give access to higher resolutions, in both space and time dimensions.

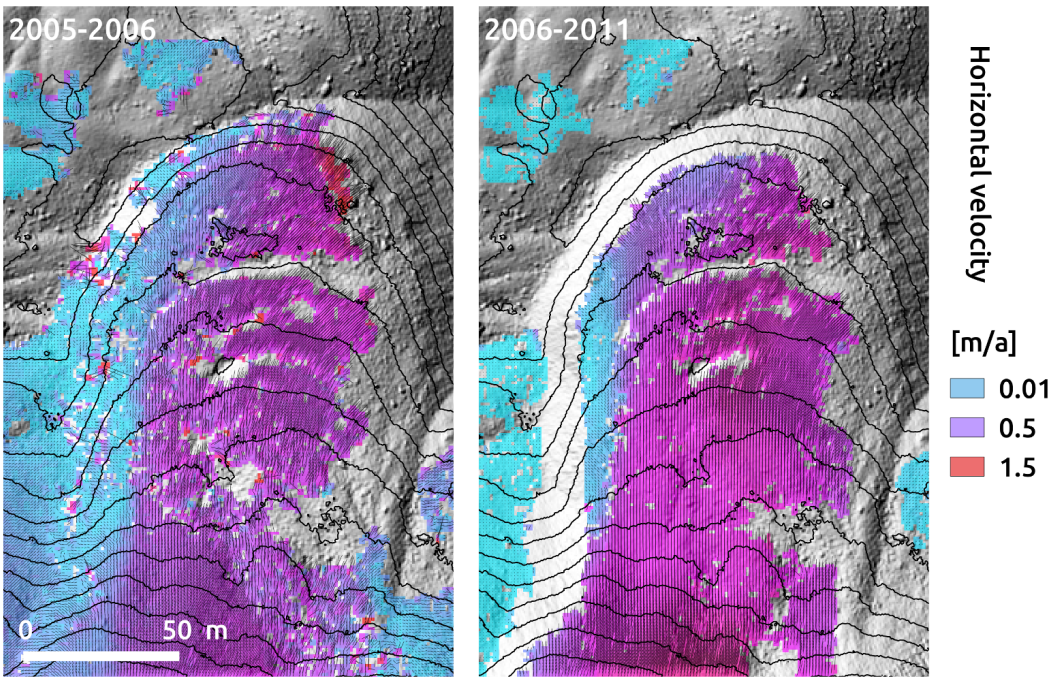

Figure 1: Displacement fields of the Laurichard rock glacier frontal part between 2005 and 2006 (left) and 2006 and 2011 (right), quantified by image correlation of 10-cm hillshaded DEMs from TLS (displayed on ALS-derived 50-cm hillshaded DEM)

References

Barsch, D. [1996]: *Rockglaciers : Indicators for the Present and Former Geoecology in High Mountain Environments*, volume 16 of *Springer Series in Physical Environment*. Springer-Verlag Berlin Heidelberg, doi:10.1007/978-3-642-80093-1. ISBN: 978-3-642-80095-5.

Bodin, X.; Thibert, E.; Fabre, D.; Ribolini, A.; Schoeneich, P.; Francou, B.; Reynaud, L. and Fort, M. [2009]: Two decades of responses (1986–2006) to climate by the Laurichard rock glacier, French Alps. *Permafrost and Periglacial Processes*, 20(4): 331–344, doi:10.1002/ppp.665.

Bodin, X.; Krysiecki, J.-M.; Schoeneich, P.; Le Roux, O.; Lorier, L.; Echelard, T.; Peyron, M. and Walpersdorf, A. [2016]: The 2006 Collapse of the Bérard Rock Glacier (Southern French Alps). *Permafrost and Periglacial Processes*, doi:10.1002/ppp.1887.

Delaloye, R.; Morard, S.; Barboux, C.; Abbet, D.; Gruber, V.; Riedo, M. and Gachet, S. [2012]: Rapidly moving rock glaciers in Matterthal. In: Graf, C.(ed.), *Mattertal – ein Tal in Bewegung. Publikation zur Jahrestagung der Schweizerischen Geomorphologischen Gesellschaft*, pages 21–31. 29. Juni–1. Juli 2011, St. Niklaus. Eidg. Forschungsanstalt WSL.

Francou, B. and Reynaud, L. [1992]: 10 years of surficial velocities on a rock glacier (Laurichard, French Alps). *Permafrost and Periglacial Processes*, 3:209–213, doi:10.1002/ppp.3430030306.

Haeberli, W.; Hallet, B.; Arenson, L.; Elconin, R.; Humlum, O.; Kääb, A.; Kaufmann, V.; Ladanyi, B.; Matsuoka, N.; Springman, S. and Vonder Mühll, D. [2006]: Permafrost creep and rock glacier dynamics. *Permafrost and Periglacial Processes*, 17 (3):189–214, doi:10.1002/ppp.561.

Pauhle, R. [2015]: Visite du glacier rocheux du col du Lou. Technical report, 25/08/2015. RTM 73 report, Chambéry, 2015.

Rock glacier activity and distribution in the semi-arid Andes of Chile and Argentina detected from dInSAR

Xavier Bodin[1], Echelard Thomas[2], Dario Trombotto Liaudat[3], Sebastián Vivero[4], & Pierre Pitte[3]

[1]*EDYTEM, CNRS/Université Savoie Mont-Blanc, France*
[2]*PACTE, CNRS/Université Grenoble-Alpes, France*
[3]*IANIGLA, CONICET/CCT Mendoza, Argentina; 4: CEAZA, La Serena, Chile*
[4]*CEAZA, La Serena, Chile*

Rock glaciers in the semi-arid Central Andes of Chile and Argentina (approx. 28-34° S) are widespread elements of the high mountain landscape but they still need to be studied more thoroughly. The presence and activity of this type of ice-rich and creeping permafrost has potential consequences for the hydrological functioning of the watersheds as well as for the stability of the debris slopes [Trombotto et al., 1997, Trombotto Liaudat and Buk, 1999]. Indeed, some cases of rock glacier destabilization observed in this region [Iribarren Anacona, 2010, Bodin et al., 2012] suggest that the geomorphological processes related to rock glacier dynamics may be changing because of warming conditions into the ground [Trombotto and Borzotta, 2009]. Nevertheless, up to now, knowledge on rock glacier kinematics in the Central Andes was restricted to a few sites [Apaloo et al., 2012, UGP-UC, 2011, Arenson et al., 2010] where study and monitoring efforts took place since generally less than 10 years. On the other side, ongoing human activities in high altitude areas, like mining, are increasingly impacting rock glaciers [Brenning, 2008, Brenning and Azócar, 2010], which has led to substantial efforts from public authorities to evaluate the cryospheric resources in their respective territories. For that purpose, in both Chile and Argentina, inventories of rock glaciers have recently been released [UGP-UC, 2011, IANIGLA, 2010] based on aerial and satellite imagery. Morphological features indicatives of the presence of ice-rich permafrost, mainly rock glaciers, have therefore been mapped. The assessment of the activity status of those landforms, which is of crucial importance for further studying their sensitivity to climate- and human-induced impacts, is generally done thanks to expert knowledge. Based on visual interpretation of optical imagery, sometimes combined with in situ observations, this approach induces subjectivity-related biases and a limited reliability of the analysis.

To overcome those limitations, and under certain conditions (e.g. orbital geometry, weather conditions, slopes orientation), the space-borne imagery method called differential radar interferometry (d-InSAR) can be used to produce raster maps of surface changes over large areas and for periods covering a few days to some months. In our work, we used 17 TerraSAR-X images acquired between April 2014 and January 2015 over two zones of the Central Andes (Cordón del Plata: 33°S; El Tapado: 30°S) to generate 15 interferograms (8 in descending mode and 7 in ascending mode) with a pixel size of 10 m, at 11, 22 and 33-day intervals and a baseline of the SAR pairs ranging from a few meters to some hundreds of meters. The topographic fringes were removed using the 90-m SRTM global DEM and a smoothing filter has been applied to the generated interferometric signal. The d-InSAR dataset has been locally validated thanks to in situ dGPS measurements (Tapado rock glacier site) performed between 2010 and 2014. We were able to evidence several areas of distinct velocity patterns, depending on the glacio-geomorphological activity (glacier/debris-covered glacier/rock glacier) for which a clear d-InSAR signal could be associated, as also observed in other high mountain sites in the Alps where such approach has been previously used.

The dataset covers a surface of almost 5100 km^2, with a median elevation of 4120 m asl (25-75 % quantiles = 3464-4606 m asl) and several hundreds of fresh rock glaciers inventoried. We present here a synthetic overview of the regional rock glacier's activity based on the interpretation of the TSX interferograms. The kinematic characteristics of some interesting rock glaciers is further presented and discussed, especially in terms of the correspondence between geomorphological observations and d-InSAR signal, as well as future research directions.

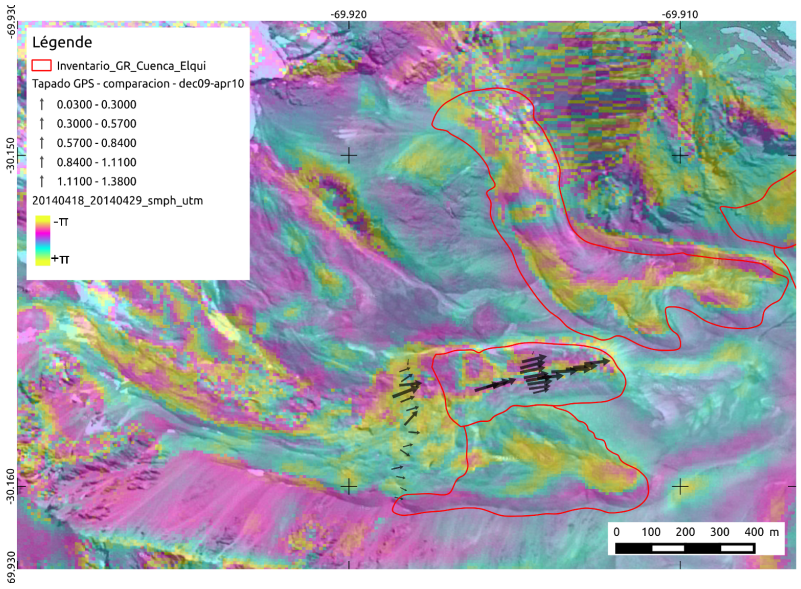

Figure 1: Interferometric phase from two TSX with a 11-day interval in the Tapado area (Chile). Direction and amount of horizontal displacements measured at DGPS-surveyed blocks are also displayed (dates of measurements : 15-12-2009 & 10-04-2010, unpublished data).

References

Apaloo, J.; Brenning, A. and Bodin, X. [2012]: Interactions between Seasonal Snow Cover, Ground Surface Temperature and Topography (Andes of Santiago, Chile, 33.5°S). *Permafrost and Periglacial Processes*, 23(4):277–291, doi:10.1002/ppp.1753.

Arenson, L.U.; Pastore, S.; Trombotto, D.; Bolling, S.; Quiroz, M.A. and Ochoa, X.L. [2010]: Characteristics of two Rock Glaciers in the Dry Argentinean Andes Based on Initial Surface Investigations. In *GEO2010 in the New West*, pages 1501–1508. Vol Calgary.

Bodin, X.; Krysiecki, J.-M. and Iribarren Anacona, P. [2012]: Recent collapse of rock glaciers: two study cases in the Alps and in the Andes. In: Koboltschnig, G.; Hübl, J. and Braun, J.(eds.), *Proceedings of the 12th Congress INTERPRAEVENT*. Vol Grenoble: International Research Society INTERPRAEVENT.

Brenning, A. [2008]: The Impact of Mining on Rock Glaciers and Glaciers. In: Orlove, B.S.; Wiegandt, E. and Luckman, B.H.(eds.), *Darkening Peaks: Glacier Retreat, Science and Society*, pages 196–205. Vol University of California Press, Berkeley.

Brenning, A. and Azócar, G. [2010]: Minería y glaciares rocosos : impactos ambientales, antecedentes políticos y legales, y perspectivas futuras. *Rev Geogr del Norte Gd.*, 158(1):143–158, 2010.

IANIGLA [2010]: *Inventario Nacional de Glaciares Y Ambiente Periglacial: Fundamentos Y Cronograma de Ejecución*. Mendoza.

Iribarren Anacona, P.R. [2010]: Análisis del movimiento en masa de la Quebrada Blanca: implicancias en la dinámica geomorfológica y criogénica. Cuenca superior del río Elqui. *Investig Geográfica*, 43:3–18.

Trombotto, D. and Borzotta, E. [2009]: Indicators of present global warming through changes in active layer-thickness, estimation of thermal diffusivity and geomorphological observations in the Morenas Coloradas rockglacier, Central Andes of Mendoza, Argentina. *Cold Regions Science and Technology*, 55 (3):321–330, doi:10.1016/j.coldregions.2008.08.009.

Trombotto, D.; Buk, E. and Hernández, J. [1997]: Monitoring of Mountain Permafrost in the Central Andes, Cordon del Plata, Mendoza, Argentina. *Permafrost and Periglacial Processes*, 8(1):123–129, doi:10.1002/(SICI)1099-1530(199701)8:1<123::AID-PPP242>3.0.CO;2-M.

Trombotto Liaudat, D. and Buk, E. [1999]: Rock glaciers in the Southern Central Andes (appr. 33° S.L.), Mendoza, Argentina: a review. In *Bamberger Geographische Schriften*, pages 145–173. Selbstverlag des Faches Geographie an der Universität Bamberg.

UGP-UC [2011]: *Dinámica de Glaciares Rocosos En El Chile Semiárido*. Unidad de glaciología y nieves, DGA/MOP, Santiago.

Geomorphological characteristics, internal structures and hydrological importance of moraine–rock glacier landforms in Ak-Shiirak Range (Inner Tien Shan, Kyrgyzstan)

Tobias Bolch[1,2], Nico Rohrbach[1], & Azamat Osmonov[3]

[1] *Universität Zürich, Switzerland*
[2] *Technische Universität Dresden, Germany*
[3] *Central Asian Institute for Aplied Geosciences, Bishkek, Kyrgyz Republic*

Rock glaciers are common landforms in semi-arid mountain ranges like the Tien Shan, where glaciers are typically polythermal or even cold and surrounded by permafrost. There, several glaciers terminate into large moraine complexes which show geomorphological indicators of ice content such as thermo-karst like depressions, and further downvalley ridges and furrows and a fresh, steep rock front which are typical indicators for permafrost creep ("rock glacier"). Hence, glaciers and permafrost co-exist in this region and their interactions are important to consider, e.g. for the understanding of glacial and periglacial processes. However, these relatively large moraine-rock glacier landforms are comparatively little investigated and their development, internal structure and ice content is poorly known.

In this study, we mapped all moraine-rock glacier landforms of the Ak-Shiirak-Range, located in Inner Tien Shan, Kyrgyzstan, based on satellite images and investigated two typical glacier-moraine-rock glacier complexes (area > 1 km^2) using ground penetrating radar (GPR) devices (frequencies: 20 and 25 MHz). Artificial curves were fitted to apparent diffraction hyperbolas to estimate the mean subsurface velocity and, hence, get some information about the subsurface material and ice content. In addition, surface elevation changes were calculated using digital elevation models derived from 1964 Corona and 2015 Pleiades data and the geomorphology mapped in the field and based on the 2015 high resolution satellite image.

The structure of the moraine-rock glacier landform is in general heterogeneous but can be subdivided for both landforms into a "glacier-affected" part and a periglacial part and consist of several geomorphological units. Larger areas of the glacier-affected part consist of dead-ice bodies covered by partially thick debris. These parts show significant surface lowering during the last decades identified by the differencing of the DEMs. Existence of massive ice is proven by the GPR measurements. The periglacial part is characterised by moraine-derived rock glaciers with different stages of activities. Slanting reflecting layers which reach depths of up to 40 m were measured by GPR where ridges and furrows are characterise the surface. Almost surface parallel layers are characteristic for the rock glacier parts with a smoother surface. In these rock glaciers, we could measure some massive ice lenses but the largest parts are likely characterised by rock-ice layers of different thickness and ice contents. We estimate, that the ice content decrease with towards the rock glacier with >80 % in the debris-covered dead-ice bodies to less than 20 % in the lowest parts of the ice-debris landforms. The overall area of the ice-debris landforms in the Ak-Shirak Range is 9 km^2 which is about 2.5 % of the glacierized area. These permafrost related landforms contain significant amount of ice and are of hydrological importance which will probably increase in the future with continuing glacier recession.

Preliminary modelling of mountain permafrost on La Ramada Range. Central Andes, San Juan, Argentina

Ana Paula Forte[1], Pierre Pitte[2], & Cristian Daniel Villarroel[3]

[1] *CONICET - CIGEOGIO,San Juan National University, Argentina*
[2] *CONICET - IANIGLA, CCT Mendoza. Argentina*
[3] *CONICET - FCEFN. San Juan National University, Argentina*

The altitudinal and spatial distribution of mountain permafrost is strongly influenced by the Potential Incoming Solar Radiation [Funk and Hoelzle, 1992] and the geomorphological features are considered one of the factors with less uncertainty for the modeling of the permafrost distribution [Etzelmüller et al., 2001]. Potential Incoming Solar Radiation is a morphometric parameter often used to estimate Mountain Permafrost (Oke, 1998; Wilson and Gallant, 2000; Boehner, 2009).

The Ramada Mountain Range, among the highest locations in South America, is part of the Central Andes region in the Province of San Juan, northwestern Argentina. The steep topography, the unstable slopes and the rock characteristics favor the availability of loose materials and the development of large glacier moraines, which is usually related to development of periglacial geoforms. Additionally, the study area has a large number of glaciers, debris-covered glaciers and perennial snow patches. The current developing of glacial environment is very important in the study area with a large number of glaciers, debris-covered glaciers and snow patches.

The goal of this paper is to develop an initial estimate of the areas of possible mountain permafrost in La Ramada Range based on the active rock glacier hypsometry and the potential solar radiation. This is a low cost methodology that can be carried out within a short time frame providing initial estimates for more specific future studies.

We used the lowest elevation of the active rock glacier as approximation to the lowest limit of possible permafrost [UNEP, 2007], and the medium height of the active rock glacier as an approximation to the lowest limit of probable permafrost. Then we combined this information with the potential incoming solar radiation on the area.

We also aim to understand altitudinal and spatial distribution of the glacial and periglacial geoforms present in the study area, its relationship with some climatic and morphometric parameters.

The study region encompasses an area of 2.085 km^2 and consists of different basins and sectors bordering the highest peaks of La Ramada Mountain Range, with an altitudinal distribution between 2.000 to 6.700 meters. The topography causes great variability in local climate, snow cover and surface processes like erosion, transport and deposition. Therefore the permafrost zone is not limited to height and orientation of hillside, but rather has a more complex distribution, unevenly and asymmetric in the valleys.

We used a three step methodology: First, we use satellite imagery and field information to catalog and delineate glacial and periglacial geoforms. Secondly, we use Digital Elevation Models (DEM) to derive slope, aspect, curvature and roughness. The processing takes into account latitude, topography and the sun elevation and azimuth. We also obtained other composite variables such as sky view factor, heliophany and potential incoming solar radiation. Finally, we analyzed the correlation between the geoforms distribution and the morphometric parameters to produce a permafrost likelihood model [Trombotto Liaudat et al., 2014].

We inventoried 61 glaciers, 69 covered glaciers, 168 snow patches, 104 cryogenic active rock glaciers, 8 glacigenic active rock glaciers, 95 inactive cryogenic rock glaciers and 17 fossil rock glaciers. We also identified 192 protalus ramparts and protalus lobes. We mapped creeping areas superimposed over older deposits, such as glacial moraines or landslides, in hillside and other solifluction areas (Fig. 1).

Glaciers occupy an altitudinal range between 4.065 and 6.365 m.a.s.l (average: 5.120 m.a.s.l), debris-covered glaciers 3.770 -5.935 (average: 4.550 m.a.s.l.), snow patches 3.980–6.680 m.a.s.l. (average: 5.100 m.a.s.l.), cryogenic active rock glaciers 3.670–5.010 m.a.s.l. (average 4215 m.a.s.l) and glacigenic active

rock glaciers 3830–5000 (average: 4270 m.a.s.l.).The altitude of active rock glaciers (cryogenic and glaciogenic) occupies a range between 3.670 to 5.010 m above sea level, and an average height of 4215 m.a.s.l. Considering only the minimum and average height of active rock glaciers we found that the area of probable Permafrost (high likelihood) is 530 km^2 and the area of possible permafrost (medium likelihood) is 620 km^2. This represents 25.4 % and 29.7 % respectively of the total study area (2.085 km^2).

In addition, we used the 1000 kWh/m^2 threshold to separate possible from probable permafrost. The potential direct insolation shows a minimum of 0 kWh/m^2 and a maximum of 2580 Kwh/m^2, while the average values on active rock glaciers are 260–1025 kWh/m^2.This method has provided better estimates because the areal distribution of the permafrost is irregular and well correlated with potential solar radiation. This is clear in south facing slopes, lower lying terrain and areas of shade casting which allow glaciers to develop at lower elevations. Low heliophany and potential solar radiation, associated with many hours of cast shadows, are key parameters for the development of glaciers down to 4000 m.a.s.l. and glacial environment to 3700 m.a.s.l., which is well below the regional average for Argentina´s Central Andes.

With this information we corrected our possible permafrost (medium likelihood) extent to 512 km^2 (above 3.600 m.a.s.l., annual potential solar radiation $\leq$1.000 kWh/m^2 and above 4.200 m.a.s.l., annual potential solar radiation $\geq$1.000 kWh/m^2). The probable area was corrected to 515 km^2 (above 4200 m.a.s.l., potential annual solar radiation $\leq$ 1000 kWh/m^2). This represents 24.5 % and 24.7 % respectively of the total study area (2.085 km^2).

The permafrost distribution in mountain regions is irregular due to the complex spatial distribution of surface temperatures, insolation and snow cover. Our results contribute to growing evidence that the potential solar radiation has a greater degree of influence on the surface temperature than other variables.

References

Etzelmüller, B.; Ødegård, R.S.; Berthling, I. and Sollid, J.L. [2001]: Terrain parameters and remote sensing data in the analysis of permafrost distribution and periglacial processes: principles and examples from southern Norway. *Permafrost and Periglacial Processes*, 12(1):79–92, doi:10.1002/ppp.384.

Funk, M. and Hoelzle, M. [1992]: Application of a Potencial Direct Solar radiation model for investigating ocurrences of mountain permafrost. *Permafrost and Periglacial Processes*, 3(2):139–142.

Trombotto Liaudat, D.; Wainstein, P. and Arenson, L.U. [2014]: *"Guía Terminológica de la Geocriología Sudamericana" / "Terminological Guide of the South American Geocryology"*.

UNEP [2007]: *Global outlook for ice and snow*. Nairobi, UNEP.

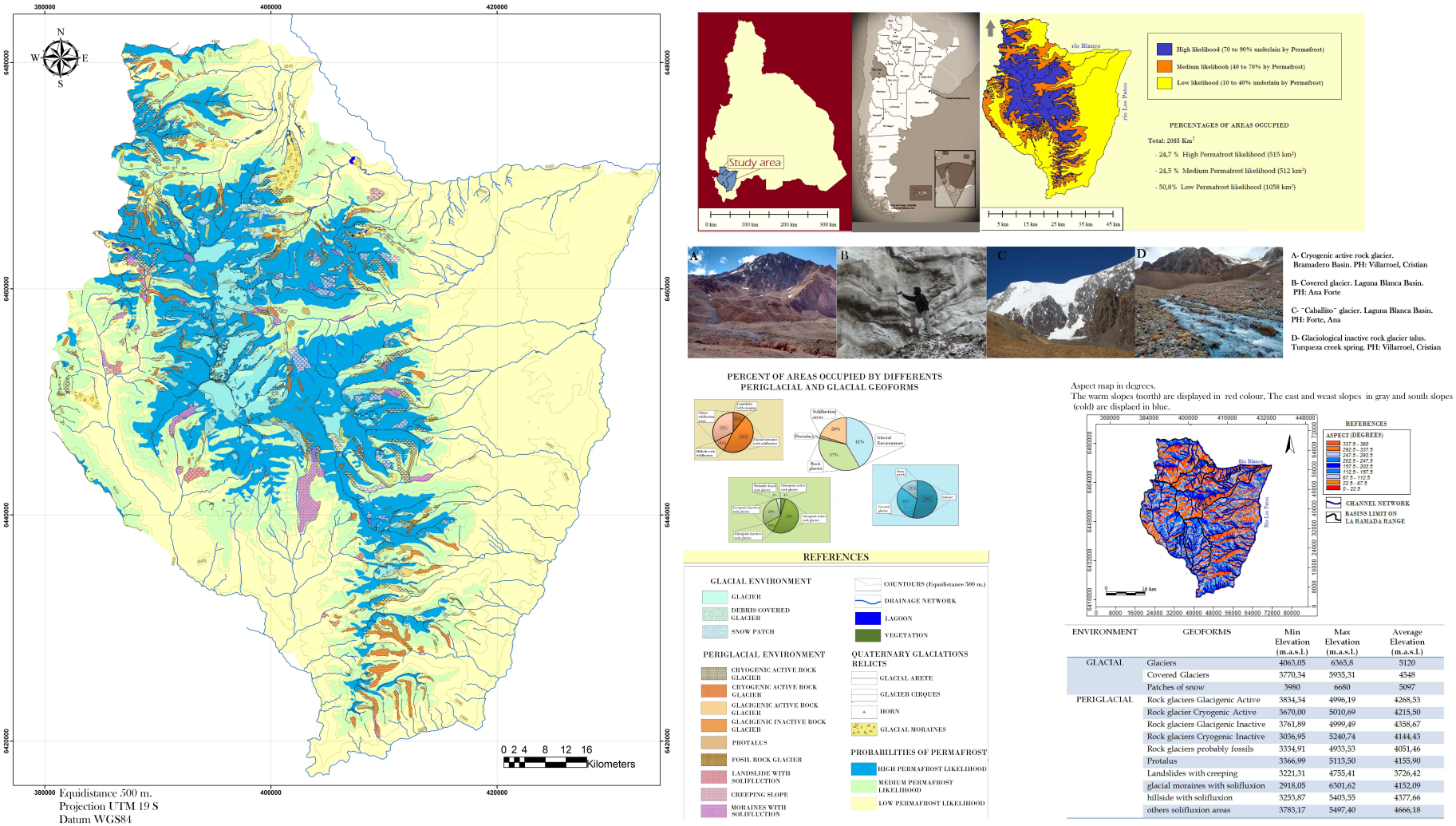

ENVIRONMENT	GEOFORMS	Min Elevation (m.a.s.l.)	Max Elevation (m.a.s.l.)	Average Elevation (m.a.s.l.)
GLACIAL	Glaciers	4063,05	6365,8	5120
	Covered Glaciers	3770,34	5935,31	4548
	Patches of snow	3980	6680	5097
PERIGLACIAL	Rock glaciers Glacigenic Active	3834,34	4996,19	4268,53
	Rock glacier Cryogenic Active	3670,00	5010,69	4215,50
	Rock glaciers Glacigenic Inactive	3761,89	4999,49	4358,67
	Rock glaciers Cryogenic Inactive	3036,95	5240,74	4144,43
	Rock glaciers probably fossils	3334,91	4933,53	4051,46
	Protalus	3366,99	5113,50	4155,90
	Landslides with creeping	3221,31	4755,41	3726,42
	glacial moraines with solifluxion	2918,05	6301,62	4152,09
	hillside with solifluxion	3253,87	5403,55	4377,66
	others solifluxion areas	3783,17	5497,40	4666,18

Figure 1: Geomorphological map and terrain modeling for the estimation of mountain permafrost distribution on La Ramada Range, San Juan, Argentina.

Morphometric characterization of cryogenic surfaces (Glacier Wedge) in the NW of the Iberian Peninsula and Argentinian Andes: applying a developed methology

Jonathan F. Hall-Riaza[1], Marcos Valcárcel[1], Ramón Blanco-Chao[1], & Raúl Mikkan[2]

[1] *Departamento de Geografìa, Universidad Santiago de Compostela, Spain*
[2] *Departamento de Geografìa, Universidad Nacional de Cuyo, Argentina*

The Glacier Wedge (Glaciar en Cuña, Breitböden) is the glacial erosion shape that we will be describing, this shape belongs to the category of wall or slope glaciers. This glacier appear under cold and dry continental conditions, proper from continuous permafrost, in high mountain (Asia and South America) and in medium mountain (Europe). This kind of glacier have a marked triangular shape, and the margins are usually incised by grooves, generated by the superficial ablation water. These glaciers were described for first time as an inherited shape by Höverman [1974], in the mountains of Hartz (Niedersachsen) (under the name of Breitböden), associating them to a dome of würm ice that covered almost the totality of the range. In the 90's Lehmkuhl [1991] described these shapes in active state (naming them Breitbodengletscher) in the ranges of Quilian Shan and Kunlun Shan (interior of China) where these glacier shapes are easily found because they are usually placed at the top of the mountains covered by ice, from where short and wide glacier tongues escape that descend smoothly with a predominant North orientation. This type of glacier form, popular in both ranges, usually represents a transition between upland escape glacier tongues and mountain glaciers. Recently this glacier shape has been described as a inherited shape by Schröder and Schmidt [2000] at Llullaillaco volcano, associating them to permafrost processes at the Andes region.

The study area is formed by three mountain areas situated in NW of the Peninsula Ibérica and a sector of the Andes range. The group of mountain ranges of the NW of the Peninsula Ibérica is formed by Xistral (with heights over 1000 m), Teleno and Montes Aquilanos (both of them with heights over 2000 m). In this study area we find around 50 glacier wedges in their inherited form. The recently added study area is a central sector of the Argentinean Andes (with heights over 5000 m), where we find active and inherited glacier wedges. All of these regions are and were climatically different.

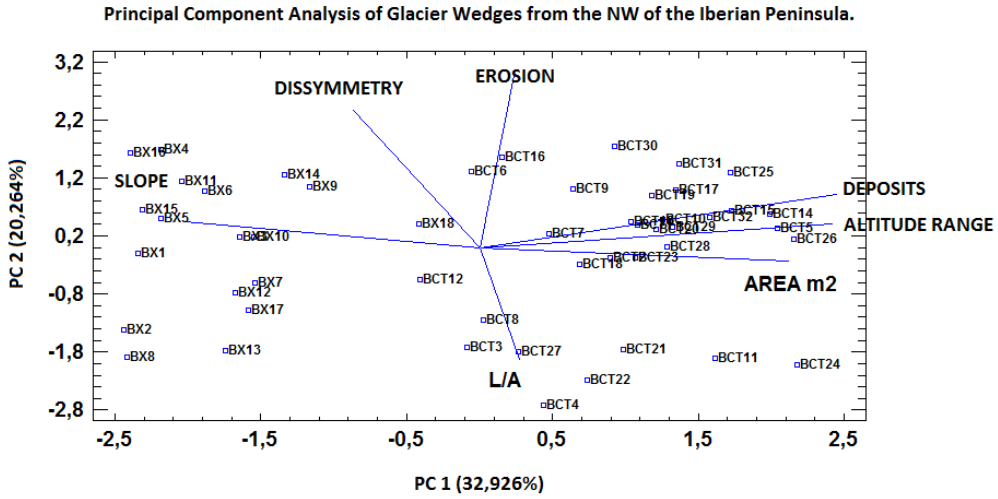

Figure 1: PCA analysis of Glaciar Wedges at the NW of the Iberian Peninsula

To perform this study we digitalised the glacier wedges, using topographic criteria, photointerpretation and field data. Afterwards morfometric parameters were extracted by 3D analysis of TDM of different resolutions. The parameters used included altitude, slope, aspect and geometry. With these parameters we made a statistic analysis with the objective of characterize the defining ranks of these shapes.

Glacier wedges are considered a marginal evidence in the glacier context, it's true that cohabitates with other glacial evidences like rocky glaciers or tongue glaciers. They do generate a very characteristic morphology without leaving great marks over the relief. The results of our statistical analysis gives us a geographic segregation but not a typologyc one.

References

Höverman, J. [1974]: Neue Befunde zur pleistozänen Harz-Vergletscherung. *Abhandlungen der Braunschweigischen Wissenschaftlichen Gesellschaft*, Band 24, URL http://www.digibib.tu-bs.de/?docid=00051839.

Lehmkuhl, J. [1991]: Breitböden als glaziale Erosionsformen – Ein Bericht über Vergletscherungstypen mi Qilian Shan und mi Kunlun Shan (VR China). *Zeitschrift für Gletscherkunde und Glazialgeologie*, 17/28:51–62, ISSN 0044-2836.

Schröder, H. and Schmidt, D. [2000]: Morfología climática y morfogénesis del Volcán Llullaillaco (Chile/Argentina). *Revista de Geografía Norte Grande*, 27:69–92, URL http://revistanortegrande.cl/archivos/27/08_27_2000.pdf.

Recent speed-up of an Alpine rock glacier: An updated chronology of the kinematics of Outer Hochebenkar rock glacier based on geodetic measurements

Lea Hartl[1], Andrea Fischer[1], Jakob Abermann[2], & Martin Stocker-Waldhuber[1]

[1]*Institute for Interdisciplinary Mountain Research, Austrian Academy of Sciences. Technikerstr. 21a, ICT Building, 6020 Innsbruck, Austria*
[2]*Asiaq – Greenland Survey. P.O. Box 1003, Qatserisut 8, 3900 Nuuk, Greenland*

Surface velocities have been regularly monitored at the rock glacier in Outer Hochebenkar, ötztal Alps, Austria, since the early 1950s. This study provides an update to previously published surface velocity time series Schneider and Schneider [2001], Nickus et al. [2015], showing mean profile velocities of four cross profiles since the beginning of the measurements (1951,1954, 1997; depending on the profile), as well as single block displacements from 1998 to 2015. Profiles P1, P2 and P3 have moved between 42 and 90 meters, at mean velocities between 0.70 to 1.48 m/a, since they were first established in the early 1950s (1951/54). Profile P0, established in 1997, has since moved 13 m or 0.75 m/a. An acceleration can be observed at all profiles since the late 1990s, with a particularly sharp velocity increase since 2010. All profiles reached a new maximum velocity in 2015, with 1.98 m/a at the slowest profile (P0) and 6.37 m/a at the fastest profile (P1). Year-to-year variations in profile velocities cannot be clearly attributed to inter-annual variations of climatic parameters like MAAT, summer temperature, positive degree days, or precipitation. However, there is evidence pointing to a correlation between velocities and cumulative anomalies of air temperature (MAAT and positive degree days) and summer precipitation. The lower profiles (P0, P1) show more pronounced year-to-year variations than the upper profiles (P2, P3). It is considered likely that processes other than climatic forcing (e.g. sliding, topography) contribute to the different velocity patterns at the 4 profiles.

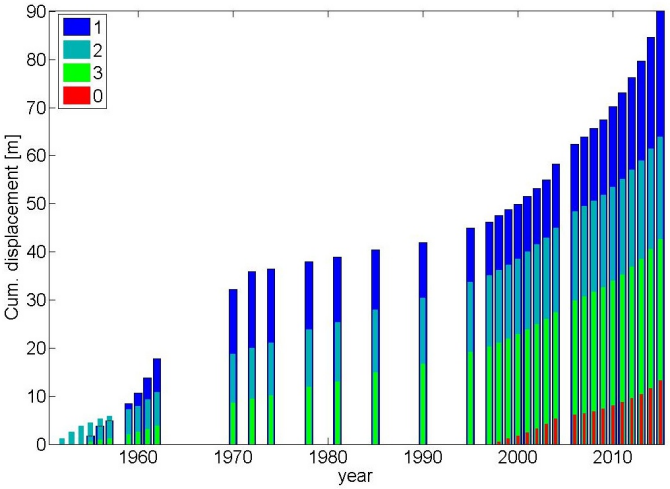

Figure 1: Cumulative displacement of the 4 block profiles used to measure movement at Hochebenkar rock glacier since the beginning of the measurements.

References

Nickus, U.; Abermann, J.; Fischer, A.; Krainer, K.; Schneider, H.; Span, N. and Thies, H. [2015]: Rock Glacier äußeres Hochebenkar (Austria) – Recent results of a monitoring network. *Zeitschrift für Gletscherkunde und Glazialgeologie*, 47:43–62.

Schneider, B. and Schneider, H. [2001]: Zur 60 jährigen Messreihe der kurzfristigen Geschwindigkeitsmessungen am Blockgletscher im äußeren Hochebenkar, ötztaler Alpen Tirol. *Zeitschrift für Gletscherkunde und Glazialgeologie*, 31:1–33.

Assessing future water contents in permafrost soils by calibrating permafrost models with temperature and electrical resistivity monitoring data

Chistian Hauck, Christin Hilbich, Antoine Marmy, Coline Mollaret, Cécile Pellet, & Samuel Python

University of Fribourg, Switzerland

Mountain permafrost is currently undergoing substantial changes due to climate change as a whole and especially due to the observed and projected air temperature increase. Current observational evidences suggest that the variable water/ice content in the near subsurface plays a major role, not only regarding the energy and water budget of the ground, but also regarding permafrost degradation and stability issues on sloping mountainous terrain. Hereby the relevance of different water related processes differ significantly at different elevation bands and for different substrates.

At very high elevations these processes have not yet been analysed in detail, and current state-of-the-art climate and climate impact simulations are neither calibrated nor validated regarding water content in the subsurface, mostly due to missing in-situ data of water or ice contents. Nevertheless, the hemispheric, regional or local permafrost evolution regarding subsurface temperatures or active layer depth is currently assessed in many modelling studies (e.g. Marmy et al. [2015]). These models are calibrated and validated only regarding ground temperature. In this study we introduce a novel methodological approach to assess the validity of especially ice and water content in these simulations and their temporal evolution. Besides analysing the importance of water and ice content for the dynamics of permafrost evolution, this approach also improves the modelling of the thermal regime and therefore projections of the future permafrost evolution.

For this we use a coupled geophysical-thermal approach by including electrical resistivity monitoring data in the calibration/validation (Cal/Val) procedure of the soil model COUP. Electrical resistivity can be related to water content via well-established petrophysical relationships, which are then used as additional calibration variable in COUP. Observed soil moisture data from the new network SOMOMOUNT [Pellet et al., 2016] can then be used as independent validation variable. This approach is tested for the Swiss mountain permafrost field sites at Schilthorn (where continuous resistivity monitoring is installed, Hilbich et al. [2011]) and Stockhorn, but could be easily transferred to other field sites where geophysical monitoring data is available.

References

Hilbich, C.; Fuss, C. and Hauck, C. [2011]: Automated Time-lapse ERT for Improved Process Analysis and Monitoring of Frozen Ground. *Permafrost and Periglacial Processes*, 22(4):306–319, doi:10.1002/ppp.732.

Marmy, A.; Rajczak, J.; Delaloye, R.; Hilbich, C.; Hoelzle, M.; Kotlarski, S.; Lambiel, C.; Noetzli, J.; Phillips, M.; Salzmann, N.; Staub, B. and Hauck, C. [2015]: Semi-automated calibration method for modelling of mountain permafrost evolution in Switzerland. *The Cryosphere Discussions*, 9:4787–4843, doi:10.5194/tcd-9-4787-2015.

Pellet, C.; Hilbich, C.; Marmy, A. and Hauck, C. [2016]: Soil Moisture Data for the Validation of Permafrost Models Using Direct and Indirect Measurement Approaches at Three Alpine Sites. *Frontiers in Earth Science*, 3:91, doi:10.3389/feart.2015.00091.

Groundwater storage and flow pathways in a rock glacier complex in the Canadian Rockies

Masaki Hayashi, Jordan Harrington, Alexsandra Mozil, & Laurence R. Bentley

University of Calgary, Canada

Hydrological functions of alpine glaciers and their responses to the warming climate have received much attention by hydrologists working in alpine catchments around the world. As alpine glaciers retreat, they commonly leave debris-covered ice or ice-cored moraine behind, which can remain frozen in ground for many decades or centuries. In many alpine catchments, characteristic landforms indicating rock glaciers or their relicts are found in locations where glaciers do not exist under the current climate. These landscape features associated with mountain permafrost are ubiquitous in alpine catchments, but their hydrological functions have not received much attention. Do rock glaciers and other mountain-permafrost features contribute significantly to the storage of snowmelt water and its delayed release, which sustains baseflow in the critical alpine stream habitats? How are these storage functions responding to the climate warming? In order to answer these questions, we initiated a hydrological study of rock glaciers in an alpine catchment in the Canadian Rockies in 2014. We will present preliminary results of our study using geophysical imaging techniques, hydro-meteorological monitoring, and groundwater tracing using various environmental tracers. Key findings are:

1. substantial amount of permafrost exists in the rock glacier which is inactive (i.e. no active motion) under the present climate,
2. spatial distribution of permafrost is controlled by both meteorological and geological factors,
3. the rock glacier complex contributes 30-50 % of summer stream flow even though they occupy less than 5 % of the catchment area, and
4. the low temperature (< 2 °C) of groundwater discharging at the toe of rock glacier plays a significant role in regulating the temperature of stream, which hosts a population of trout species that is listed as "threatened" in the list of the status of endangered wildlife in Canada.

Ground ice distribution and volumetric content in rock glaciers in the Chilean Andes – a comparison of geophysical data and ground truth from boreholes

Christin Hilbich[1], Coline Mollaret[1], Joaquim Perrenoud[1], Adrian Wicki[1], Jonas Wicky[1], Christian Hauck[1], Lukas Arenson[2], & Pablo Wainstein[2]

[1] *University of Fribourg, Switzerland*
[2] *BGC Engineering Inc., Vancouver, Canada*

Rock glaciers are a widespread phenomenon in the periglacial belt of the South American Andes. Within the context of the projected water shortage in the arid mountain regions as a consequence of continued climate change, the significance of these rock glaciers for the hydrological cycle is currently being discussed in a controversial way. Given the lack of comprehensive field measurements and quantitative data on the local variability of rock glacier internal structure, ice content and their hydrological contribution, an extensive site investigation campaign and periglacial monitoring program was initiated in the basin of Rio Choapa, located in Chilean Andes of the Coquimbo Region. The overall objective of this initiative is to assess runoff from the permafrost, in particular from the rock glaciers in the basin. Therefore it is critical to evaluate the ground ice content and its spatial distribution, which includes important parameters such as overall permafrost thicknesses, active layer thicknesses and volumetric ice contents. Rock glaciers and protalus ramparts are of special focus as they are considered being the main pool of ground ice in the basin. However, additional areas are investigated in order to evaluate the hypothesis.

Geoelectric and refraction seismic tomography was conducted to map and describe the structure of the ground ice of the rock glaciers and other areas of the basin. Further, both geophysical methods were combined in a quantitative approach to model the volumetric ice content and its spatial variability using the so-called 4-phase model. The resulting data are discussed in comparison with qualitative and quantitative ground truth data on structure and volumetric ice content from nine boreholes with undisturbed frozen core extraction and various test pits drilled and excavated at the same sites. These results will be used in a following step to better assess future runoff evolution from degrading permafrost in rock glaciers under ongoing climate change.

Long-term energy balance measurements at three different mountain permafrost sites in the Swiss Alps

Martin Hoelzle & Christian Hauck

University of Fribourg, Switzerland

In the framework of the PERMOS permafrost monitoring program, meteorological data is collected at several high altitude sites in the Swiss Alps since the late 1990s. From these stations, three were selected, which all are equipped with standard meteorological sensors such as a four component radiation sensor, air temperature, humidity, wind speed and direction as well as ground temperatures and snow height [Hoelzle and Gruber, 2008]. The energy balance constitutes one of the most important input parameter for the ground heat flux regime, and it is therefore crucial to understand the influence of the individual fluxes. As the individual measurements and the different approaches to calculate the energy balance show large uncertainties, a special focus is laid on the quantification of the uncertainty range of each flux. All three sites differ considerably by their ground material composition. The rock glacier Murtèl-Corvatsch site is located in the Engadine, Eastern Swiss Alps and consists mainly on coarse blocky debris in the active layer followed by an ice supersaturated layer of around 25 m thickness. The bedrock site Schilthorn is located at the Northern slope of a mountain summit in the Berner Oberland, Northern Swiss Alps, and is composed of deeply weathered micaceous shales, which are covered by fine grained debris of sandy and silty material. The bedrock site Stockhorn is located on a small plateau slightly inclined to the south in the Southern Valais Alps close to Zermatt, the bedrock consists on Albit-Muskovit schists and shows at some places the development of patterned ground, especially at the site where the station is located. Based on geophysical soundings the ice content at Schilthorn and Stockhorn are estimated to be much lesscompared to the Murtèl-Corvatsch site.

First results show that the mean surface temperature at Murtèl-Corvatsch (1997-2013) and Schilthorn (1999-2013) sites are quite similar with -3.23 °C and -3.56 °C, respectively, whereas surface temperatures at the Stockhorn (2002-2013) site are much colder with a mean of -8.98 °C. The corresponding mean ground temperatures measured in the PERMOS boreholes for the same investigation period are for Murtèl-Corvatsch (0.55 m depth) -0.24 °C, Schilthorn (0.2 m depth) -0.07 °C and Stockhorn (0.3 m depth) -0.42 °C. The measured net radiation is the most important energy input for the surface at each site and shows for Murtèl-Corvatsch 27.31 W m^{-2}, Schilthorn 32.52 W m^{-2} and Stockhorn 22.91 W m^{-2}. The calculated turbulent fluxes based on measurements of wind speed, air temperature and relative humidity using two different approaches (Bowen ratio and bulk methods) show for all sites values of around 8 to 10 W m^{-2} for the Bowen ratio method and 4 to 15 W m^{-2} for the bulk method. Large differences are observed in the energy which is used for melting the snow cover at the different sites. At Schilthorn a value of 22.86 W m^{-2} at Murtèl-Corvatsch 11.26 W m^{-2} and at Stockhorn 6.06 W m^{-2} is measured reflecting the different amount of snow height at these sites. The overall deviations of the energy balance were estimated to be 10.58 W m^{-2} at Murtèl-Corvatsch, 5.57 W m^{-2} at Schilthorn and 0.06 W m^{-2} at Stockhorn reflecting also that especially at the Murtèl-Corvatsch site not all fluxes are detected which confirms recent results by Scherler et al. [2014]. The high temporal variability of the individual fluxes and the additional large uncertainties in the determination of the turbulent heat fluxes caused by

i) lacking accurate input conditions of soil moisture contents at the surface and

ii) reasonable values for the surface roughness, does currently not allow a more precise determination of the whole energy balance.

However, the long-term measurement series of the individual fluxes at these sites areunique and serve as prerequisite for detailed modeling studies using these data as validation or as calibration measures.

References

Hoelzle, M. and Gruber, S. [2008]: Borehole and ground surface temperatures and their relationship

to meteorological conditions in the Swiss Alps. In Kane, D.L. and Hinkel, K.M. (eds.) *Proceedings of the 9th International Conference on Permafrost*, Fairbanks, Alaska, June 29–July 3, 2008, volume 1, pages 723–728, http://ipa.arcticportal.org/publications/conference-proceedings.

Scherler, M.; Schneider, S.; Hoelzle, M. and Hauck, C. A two-sided approach to estimate heat transfer processes within the active layer of the Murtèl-Corvatsch rock glacier. *Earth Surface Dynamics*, 2 (1):141–154, 2014. doi:10.5194/esurf-2-141-2014.

Variations in rockglacier speed in the Tien Shan and their significance

Andreas Kääb[1], Tazio Strozzi[2], Annina Sorg[3], & Markus Stoffel[3]

[1] *University of Oslo, Norway*
[2] *GAMMA Remote Sensing, Switzerland*
[3] *University of Berne, University of Geneva, Switzerland*

Theoretical considerations, laboratory and numerical modelling work, and observational series all suggest that a primary reaction of rockglaciers to increases in ground temperatures could be a long-term increase in deformation speed, probably due to a decrease in ice-core viscosity and the influence of percolating liquid water [Kääb et al., 2007]. As most of the observations available to investigate such rockglacier response stem from the European Alps, questions arise how rockglaciers in other mountains behave under the current atmospheric warming. Here, we investigate changes in rockglacier speed in the Kungei Alatau, a range of the Tien Shan between lake Issyk Kul (Kyrgyzstan) and Almaty (Kazakhstan). Based on an unprecedented combination of remote sensing data and methods we develop regional-scale time series of up to 70 years long. Up to about the year 2000 rockglacier surface velocities are mainly derived from Soviet-era air photos (from the 1940s and 1950s on) and Corona spy satellite images (1970s) using image correlation techniques. More recent velocities are obtained from correlating metre to sub-metre resolution optical satellite images from the Digital Globe constellation and radar interferometry based on among others on ALOS PALSAR and Sentinel-1 data. We also demonstrate for the first time the suitability of repeat Landsat and Sentinel-2 data for deriving regional-scale rockglacier velocities. In addition, we compare our results to dendrochronological data sampled on several of the rockglaciers that reflect their degree of activity over approximately the last century [Sorg et al., 2015]. Many of the rockglaciers investigated show comparably high surface speeds of up to several metres per year. This finding and the assumed warm permafrost conditions over the study region let already expect that these rockglaciers react particularly sensitive to changes in air and ground temperatures. While we find significant variations of rockglacier speed over multi-decadal timescales, these are quite contrasting over the area, with rockglaciers increasing their speed, more-or-less constant speed, or decreasing speed. Such contrasting behaviour is even found within rockglacier systems consisting of several individual rockglaciers in close horizontal or vertical proximity. We attribute these differences to the rockglaciers being in different states of activity and deactivation, among others probably related to their ice content, its depth, its thermal conditions, or water content. Thus, we interpret the rockglaciers investigated as an example for rockglacier response to atmospheric warming under warm mountain permafrost conditions where the general impact of increasing ground temperatures is modulated by the highly individual conditions of single rockglaciers. We discuss our findings related to their climatic significance and their implications, both for the study region and in general for rockglacier monitoring.

References

Kääb, A.; Frauenfelder, R. and Roer, I. [2007]: On the response of rockglacier creep to surface temperature increase. *Global and Planetary Change*, 56 (1–2):172–187, doi:10.1016/j.gloplacha.2006.07.005.

Sorg, A.; Kääb, A.; Roesch, A.; Bigler, C. and Stoffel, M. [2015]: Contrasting responses of Central Asian rock glaciers to global warming. *Scientific Reports*, 5:8228, doi:10.1038/srep08228.

A regional signal of significant recent ground surface temperature warming in the periglacial environment of Central Austria

Andreas Kellerer-Pirklbauer

University of Graz, Austria

Long-term data series of ground temperature from the periglacial environment of polar and alpine regions are essential to understand the effects of present global change on the distribution and the thermal characteristics of seasonal and perennial frost-affected areas. Such data series aid to quantify not only the "mean" thermal condition but also outliers and trends at a given monitoring site.

In this contribution up to eleven years of field data from nine different study areas in Austria are presented and discussed. All areas are located in the highest mountain range in Austria, the Tauern Range (max. elevation 3798 m a.s.l.) with its subunits Niedere and Hohe Tauern covering c.9000 km^2 of the national territory (Fig. 1a). The nine study areas are located between latitude 46°55' to 47°22' and longitude 12°44' to 14°41' (Fig. 1a). Altogether 57 ground temperature monitoring sites have been installed in 2006 and 2007 at the nine study areas using one- (at 23 sites) and three-channel (at 34 sites) miniature temperature dataloggers (all manufactured by GeoPrecision, Germany). These monitoring sites range from 1922 to 3002 m a.s.l., consider flat terrain as well as step rock walls, different substrates (coarse debris, fine-grained sediments and bedrock), and include all slope aspect classes adequately. Therefore, this monitoring network with its data series is presently the most comprehensive one in Austria [Kellerer-Pirklbauer, 2014].

Research questions addressed here are related to

a) general ground thermal conditions,

b) potential permafrost occurrence,

c) trends in thermal conditions during the observation period, and

d) regional pattern.

The data analysis focused on quantifying mean thermal conditions as well as statistical significant trends regarding a series of ground temperature derived parameters; i.e. mean annual ground surface temperature (MAGST), maximum surface temperature (MAX), minimum surface temperature (MIN), cumulative sum of freezing degree days (FDD), cumulative sum of thawing degree days (TDD), the surface frost number (F+; cf. Nelson and Outcalt [1987]), days with freeze-thaw cycles (FTC), days with positive temperatures (DPT), ice days (ID) and days with a seasonal snow cover (SCD). Annual, seasonal and monthly values for the above mentioned parameters were quantified. Statistical significant correlations between the temperature derived parameters and number of monitoring years, seasons (DJF, MAM, JJA, SON), and individual months have been tested. Regarding annual mean values, two types of annual data were computed; hydrological years (HY/01.10.-30.09.) and "monitoring years" (MY/01.08.-31.07.). The second annual period was chosen to account for the typical field-work month August, where the temperature data are commonly retrieved from the loggers.

The deviations from the mean annual values (MAGST) of the whole monitoring period at four selected monitoring sites (partly in permafrost, partly in seasonal frost) are exemplarily presented in Fig. 1b-e. These graphs also indicate, respectively, elevation, the MAGST value, and correlation coefficient as well as statistical significance of linear trends. Noteworthy is the following observation depicted in b, c and d. The deviation values and pattern of warmer/colder years compared to the mean are similar with negative deviations during the first 4-5 years of data and positive deviations in the subsequent 3-4 years. All three monitoring sites reveal statistical significant warming during the 8-year observation period 2007/08 to 2014/15. The exception is the monitoring site REI-SUM shown in Fig. 1e, where data series are longer and therefore also include the exceptional warm winter 2006/07. The unusually warm monitoring year 2006/07significantly influenced the linear trend for the entire monitoring period.

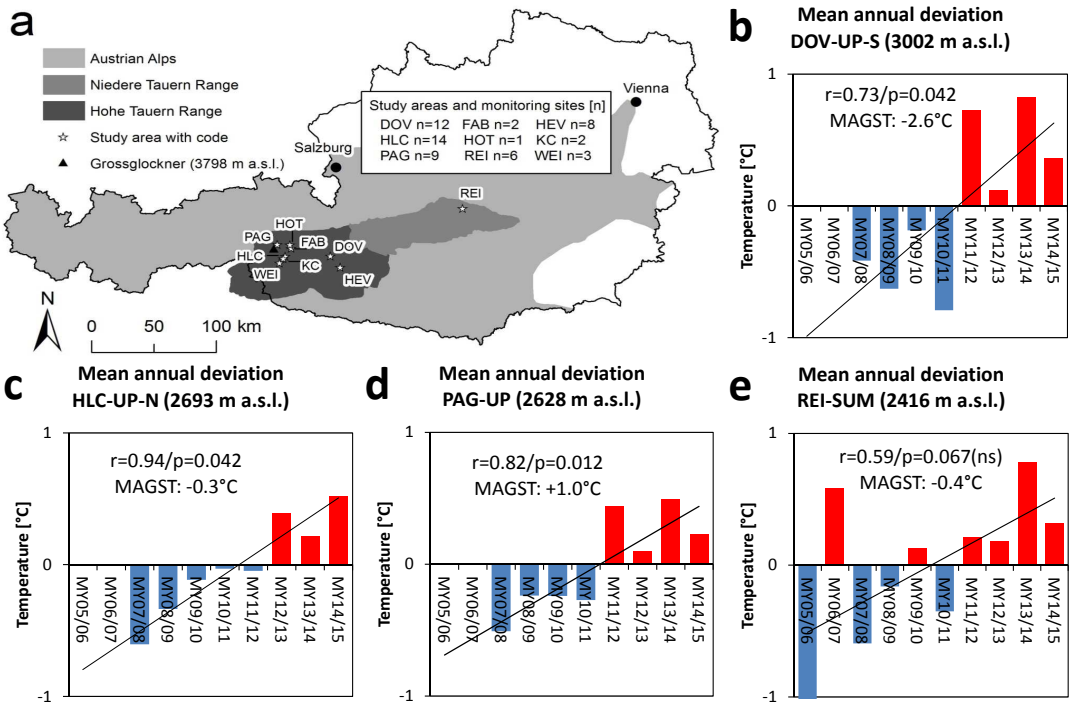

Figure 1: Study areas and selected results: (a) Location of the nine study areas in Austria with number of study sites; (b-e) Temperature deviation from the mean value during the monitoring period based on annual values (MY; 01.08.-31.07) at four sites.

For the site REI-SUM some more in-depth results are presented here. At this site, maximum temperatures (MAX) statistically increased and the surface frost number (F+) statistically decreased during the last years based on annual data. Regarding changes in the different seasons, no significant trends were revealed for spring (MAM) and autumn (SON). However, during summer (JJA) warming is confirmed by significant increases in MAGST, TDD, DPT whereas by a decrease in FDD. On a monthly basis, no statistical significant changes were revealed for JAN, FEB, APR, SEP and OCT. The remaining months show significant changes. Particularly in August several ground temperature derived parameters indicate substantial warming (MEAN, MAX, MIN, TDD, FTC, and DPT).

Based on the available long-term ground temperature data series presented in extracts in this contribution, it was possible to reveal that significant warming of seasonal and perennial frost areas in the central Austria occurred during the last decade. However, exceptional warm weather periods (e.g. warm winter 2006/07) or variations in the seasonal snow cover (onset, duration, thickness, melt-out data) might strongly influence the long-term ground temperature signal. The observations described here highlight the importance of long-term permafrost but also seasonal frost monitoring, an effort which is currently augmented in Austria within the framework of a national permafrost monitoring network (permAT) currently under development [Kellerer-Pirklbauer et al., 2015].

References

Kellerer-Pirklbauer, A. [2014]: Permafrost. In: Stowasser, R. and Köhler, M.(eds.), *Global Climate Observing System – Report Austria*, pages 58–59. Vienna, Wien. (in German).

Kellerer-Pirklbauer, A.; Bartsch, A.; Gitschthaler, C.; Reisenhofer, S.; Weyss, G.; Riedl, C. and Avian, M. [2015]: permAT - Langzeitmonitoring von Permafrost und periglazialen Prozessen und ihre Bedeutung für die Prävention von Naturgefahren: Mögliche Strategien für österreich. Endbericht von StartClim2014. In *StartClim2014: Anpassung an den Klimawandel in österreich - Beiträge zur Umsetzung der österreichischen Anpassungsstrategie*. Auftraggeber: BMLFUW, BMWF, öBf, Land Oberösterreich. (in German).

Nelson, F.E. and Outcalt, S.I. [1987]: A computational method for prediction and regionalization of permafrost. *Arctic and Alpine Research*, 19:279–288, doi:10.2307/1551363.

Relations between vegetation and mountain permafrost along elevation gradients, Yukon Territory, Canada

Zoé Marie Claude Ouellette Kuntz & Antoni Lewkowicz

University of Ottawa, Canada

Air temperature is the main driver for permafrost occurrence regionally. It is also one of the limiting factors for vegetation growth at high latitudes and high elevations. In turn, vegetation cover affects energy exchange between the air and the ground surface [Brown, 1966] and thus the probability of permafrost being present. At high elevations in northern regions where tundra dominates, permafrost may be continuous, but as one descends, air temperatures generally increase enabling shrubs and then trees to grow. Permafrost begins to break down spatially to the point that it may be present only in isolated patches. This study seeks to better understand the relationship between permafrost, elevation and vegetation cover, and to test the hypothesis that changes in mountain permafrost distribution and characteristics occur at vegetation type boundaries, as they do in latitudinal permafrost.

Electrical resistivity tomography (ERT) profiles were completed at vegetation transitions on selected Yukon slopes in July 2015 near Whitehorse and Dawson. An ABEM terrameter LS was used with electrodes spaced at 2 m in 160-280 m long Wenner arrays. Organic layer thickness and vegetative species composition were recorded along each profile. Ground-truthing via frost probing, pit digging, and ground temperature data from past and present weather stations aided in the analysis of ERT profiles.

Here we present five of the ERT profiles, located within or near the Wolf Creek Research Basin close to Whitehorse. Permafrost distribution is elevation controlled in the area, and models show the entire range of permafrost conditions occurring there from continuous to isolated patches [Lewkowicz and Ednie, 2004]. Altitudinal treeline elevation, consistently reported at 1300 m a.s.l., is often used in the demarcation of differences in permafrost-related processes such as active layer thaw and surface lapse rates [Lewkowicz et al., 2012]. In order to sample vegetation and permafrost transitions, the five profiles included segments of slopes with differing aspects, between 1210 and 1500 m a.s.l., with varying vegetation covers (Fig. 1).

Several different patterns in resistivity values are present along the profiles and appear to correspond to changes in surficial geology, organic mat thickness, shrub height or slope gradient. These patterns indicate the presence of permafrost along most of the slopes sampled (Figure 1B). The ERT profile at site 1, which is the highest site, is interpreted as showing deep permafrost with a possible talik where the profile crosses a 14 m wide depression which is likely a snowmelt and water flow channel. Permafrost is interpreted as present through most of site 2 (Fig. 1A). This site runs from an active debris flow fan up a moderately steep slope and changes from primarily shrub vegetation to scattered trees at higher elevations. The lower parts of the profile are subject to cold air drainage resulting in a slight warming of the air temperature with elevation. However, ground surface temperatures and temperatures close to the top of permafrost decrease with elevation. No changes in permafrost distribution and characteristics occur specifically at the lower treeline boundary (Fig. 1).

Site 3 is located on a south-facing slope with a mixed forest. It is the only site where permafrost was not interpreted to be present. Sites 4 and 5 are on the same slope, spaced about 400 m apart, but gave differing results. A thin layer of near-surface permafrost is interpreted almost continuously along the profile at site 4. Permafrost was confirmed to be present within a pit excavated in the forest at this site, and may even be thicker and colder there than in other unforested parts of the slope. In contrast, permafrost is interpreted as absent within most of the forested portion of the site 5 profile. The thicker colder permafrost bodies are interpreted upslope of the forest, in areas with denser, taller shrubs and with important changes in slope gradient.

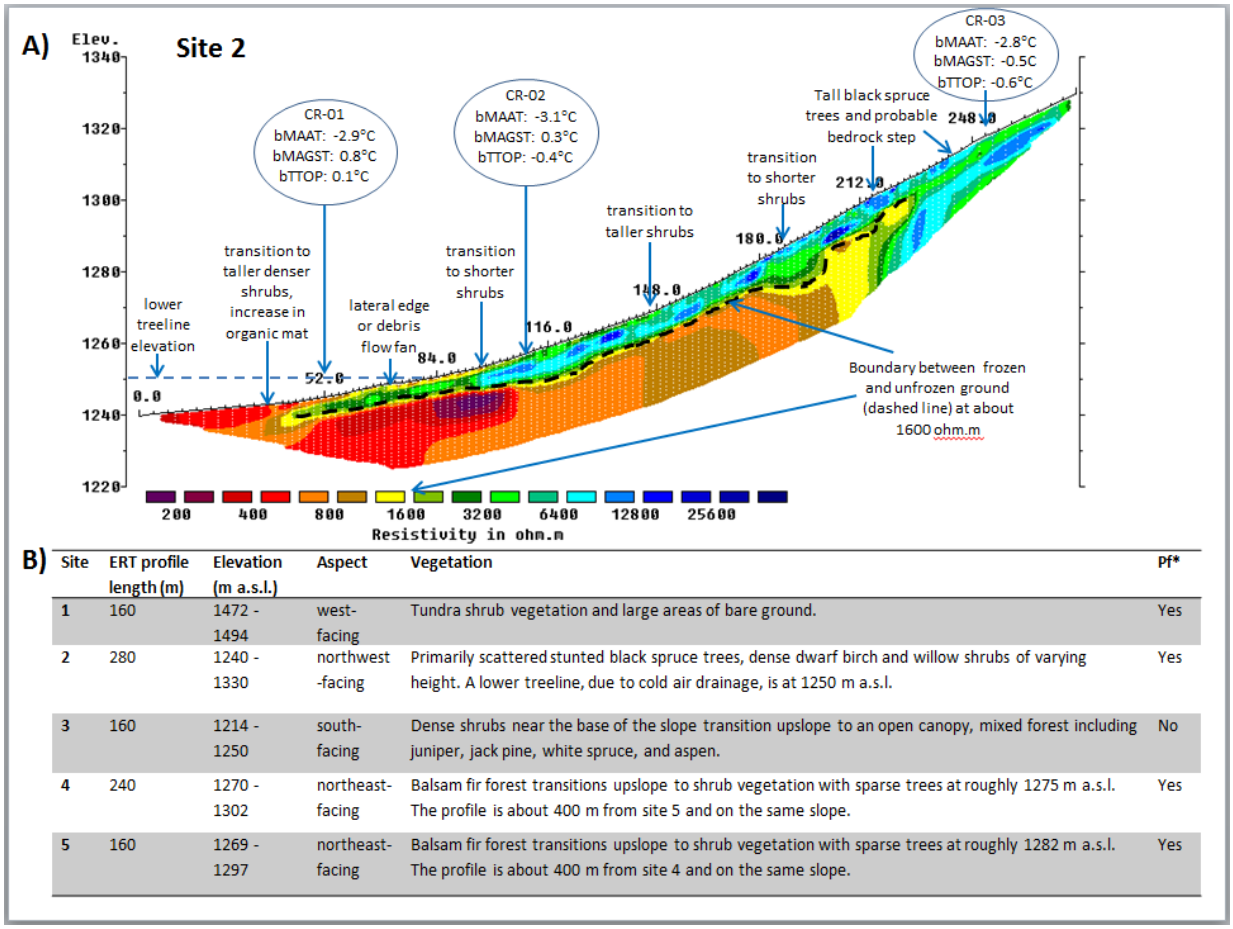

B)

Site	ERT profile length (m)	Elevation (m a.s.l.)	Aspect	Vegetation	Pf*
1	160	1472 - 1494	west-facing	Tundra shrub vegetation and large areas of bare ground.	Yes
2	280	1240 - 1330	northwest-facing	Primarily scattered stunted black spruce trees, dense dwarf birch and willow shrubs of varying height. A lower treeline, due to cold air drainage, is at 1250 m a.s.l.	Yes
3	160	1214 - 1250	south-facing	Dense shrubs near the base of the slope transition upslope to an open canopy, mixed forest including juniper, jack pine, white spruce, and aspen.	No
4	240	1270 - 1302	northeast-facing	Balsam fir forest transitions upslope to shrub vegetation with sparse trees at roughly 1275 m a.s.l. The profile is about 400 m from site 5 and on the same slope.	Yes
5	160	1269 - 1297	northeast-facing	Balsam fir forest transitions upslope to shrub vegetation with sparse trees at roughly 1282 m a.s.l. The profile is about 400 m from site 4 and on the same slope.	Yes

Figure 1: (A) Site 2 modelled resistivity profile with vegetation changes and blended-year statistics for air (bMAT), ground surface (bMAGST) and top of permafrost (bTTOP) temperatures. (B) Summary site descriptions. *Pf, Permafrost presence inferred.

Several difficulties arose in profile interpretation. Clasts were often present so that frozen ground presence could not be conclusively proved by probing. Furthermore, the likelihood of encountering highly resistive but unfrozen materials, such as coarse, dry soils, sandy, clast-rich till or near-surface bedrock, is greater on steep mountain slopes. The difficulty of ground-truthing and the inherent ambiguity of ERT inversion processes made interpretation of frozen ground conditions particularly challenging for some of the sites.

Our results indicate that changes in permafrost distribution and characteristics do not consistently occur at vegetation type boundaries. Rather, small scale changes in microtopography and shrub patch distribution, potentially creating protected hollows favouring snow accumulation, may be of greater importance to permafrost distribution and characteristics than the transition from one vegetation type to another.

References

Brown, R.J.E. [1966] Influence of vegetation on permafrost. In *Proceedings of the 1st International Conference on Permafrost*, 11–15 November 1963, Lafayette, Indiana, Building Research Advisory Board, National Academy of Sciences-National Research Council: Washington, pages 20–25, URL http://ipa.arcticportal.org/publications/conference-proceedings.

Lewkowicz, A.G. and Ednie, M. [2004]: Probability mapping of mountain permafrost using the BTS method, Wolf Creek, Yukon Territory, Canada. *Permafrost and Periglacial Processes*, 15(1):67–80, doi:10.1002/ppp.480.

Lewkowicz, A.G.; Bonnaventure, P.P.; Smith, S.L. and Kuntz, Z. [2012]: Spatial and Thermal Characteristics of Mountain Permafrost, Northwest Canada. *Geografiska Annaler: Series A, Physical Geography*, 94(2):195–213, doi:10.1111/j.1468-0459.2012.00462.x.

Importance of the multidisciplinary approach in volcanic areas

Elena Kuznetsova

Norwegian University of Science and Technology, Norway

The distribution of tephra (i.e. volcanic ejecta) from a particular volcanic eruption depends on its force and the dominant wind direction at the time. Before being deposited fine-grained tephra may travel hundreds of kilometers. It has been demonstrated that volcanic gases and particles from the eruptions produced by high-latitude volcanoes may encompass the poles faster due to the shorter pathway and higher wind speed. Thus, volcanic emissions from Mt. Hudson and Puyehue-Cordon Caulle, Chile, or Kasatochi, Alaska, were transported around the pole within 10-14 days (Barton et al., 1992; Schoeberl et al., 1993; Langmann, 2014).

Despite active volcanism, permafrost and glaciers often exist on slopes of high-elevation or high-latitude volcanoes (Kellerer-Pirklbauer et al., 2007) in places such as Hawaii (Woodcock 1974), Iceland (Etzelmüller et al., 2007), Kamchatka (Demidov and Gilichinsky, 2009), Mexico (Palacios et al., 2007), Peru (Rabatel et al., 2013), North America (Denton and Karlén, 1977; Dyke,1990), and Antarctica (Marchant et al., 1996).

Volcanic eruptions are one of the major causes of the burial of ice and snow in volcanic areas. This has been demonstrated on volcanoes in Iceland, USA and Chile, where the combination of a permafrost-favorable climate and a thin layer of tephra (with low thermal conductivity) is sufficient to reduce the sub-tephra layer snow ablation substantially, even to zero, causing ground ice formation and permafrost aggradation (Driedger, 1981; Major and Newhall, 1989; Kirkbride and Dugmore, 2003; Kellerer-Pirklbauer et al., 2007; Reid and Brock, 2010).

Properties of volcanic ash and pumice, as well as volcanic soils have been widely investigated due to their unique properties. Paleoscientists and tephrochronologists use volcanic ash as a tool for linking and dating geological, paleoecological, paleoclimatic, and archaeological sequences or events (Lowe, 2010; Lowe, 2011; Ponomareva et al., 2007; Marchant et al., 1996). Soil scientists are concerned with the unique physical, chemical and mineralogical properties of the soils formed on the volcanic ash (or Andisols) in respect to their high permeability, organic matter, secondary minerals, high surface area etc. (Nanzyo, 2002). In the cold environment volcanic ash is (1) an important factor in process-based studies that are investigating the influence of permafrost aggradation and degradation upon carbon and peat accumulation, and (2) as a marker in studies of rock glaciers and glacial moraines, as well as glacier fluctuations, moraine development and the chronology of glacial/glaciofluvial deposition ((Denton and Karlén, 1977; Dyke, 1990; Robinson and Moore, 2000; Bäumler, 2003; Froese et al., 2008). Glaciologists and permafrost researchers have investigated the influence of tephra on snow and ice ablation, permafrost aggradation, and the energy balance at the glacier–atmosphere interface (Pellicciotti et al., 2009; Brock et al., 2007; Kellerer-Pirklbauer et al., 2007; Hock, 2005; Greuell and Oerlemans, 1986). Terrestrial volcanoes in permafrost areas are being studied in order to establish volcanic permafrost models for Mars (Arvidson et al., 2004; Squyres et al., 2006; Demidov and Gilichinsky, 2009).

The paper discusses the application of multidisciplinary research on volcanic material covering permafrost and glaciers in volcanic areas. In cold environments, volcanic ash is widely used in different science disciplines in process-based studies examining paleoclimate reconstruction; the influence of permafrost aggradation and degradation; influence of tephra on snow and ice ablation; glacier fluctuations, deposition and moraine development; volcanic glass weathering and new minerals formation (e.g. allophane, palagonite).

The special properties of volcanic ash are critically reviewed particularly in relation to recent research in Kamchatka in the far east of Russia. Of particular importance are the thermal properties and the unfrozen water contents of ash layers and the rate at which the weathering of volcanic glass takes place. The weathering of volcanic glass results in the development of amorphous clay minerals (e.g. allophane, opal) but this takes place much slower in cold than under warmer climate conditions.

A rock glacier inventory of the Western and High Tatra Mountains, Western Carpathians

Peter Mida & Tomáš Uxa

Charles University in Prague, Czech Republic

Rock glaciers are lobate or tongue-shaped landforms resulting from creeping of ice-rich debris in mountain areas under permafrost conditions. If the topography and material supply are favourable and the time to develop is sufficient, active rock glaciers move downslope and their termini can indicate the lower limit of mountain permafrost zone on a regional scale. Similarly, the termini of relict rock glaciers can be used to delineate this boundary at the time when they were active. Therefore, rock glaciers are frequently used to map mountain permafrost distribution or to calibrate and validate permafrost distribution models and maps. Consequently, a large number of rock glacier inventories have been recently published from the European high-mountain areas (the Alps or the Scandinavian Mts.).

The Western and the High Tatra Mts. are the northernmost part of the Carpathians located on the border between Slovakia and Poland and reach maximum elevation of 2655 m asl. The lower limit of regional permafrost occurrence was suggested to be at 1930 ± 150–200 m asl [Dobiński, 2005]. Despite the rock glaciers are widespread in these mountain ranges, their distribution and morphology remains poorly investigated. Until now, the most extensive inventory was provided by Nemčok and Mahr [1974], who identified a total of 13 and 18 locations with rock glacier occurrence in the Slovak part of the Western and the High Tatra Mts., respectively. Another 14 rock glacier formations were identified by Kotarba [1986] in the Polish part of the mountains. However, mapping of these authors is not complete and does not contain the information about the exact number of rock glaciers and their altitudinal distribution and morphology is described rather superficially. Several other works have been published on rock glaciers in the Tatra Mts., but these are either too general or represent case studies on a local to medium scale. It is believed that the last phase of rock glacier activity took place during the Younger Dryas and they were suggested to be inactive or relict under present-day climate conditions.

Here, we provide the most comprehensive detailed rock glacier inventory for the Western and the High Tatra Mts. and we analyze their distribution and morphology. Rock glaciers were manually mapped and digitized based on aerial photographs with 0.1, 0.25, 0.5 and 1 m resolution, supported by field validation. Rock glaciers were classified according to their plan shape as lobate-, transient and tongue-shaped. The morphometric characteristics were derived from digital elevation model with 10 m resolution.

We delineated a total of 379 rock glaciers, which are almost evenly distributed between the Western (48 %) and the High (52 %) Tatra Mts. Most rock glacier termini are located within an altitudinal range of 1400–2200 m asl with an average altitude of 1731 m asl, however the altitude varies with aspect. Northern aspects dominate the rock glacier occurrence over the other sectors. Rock glaciers with northern aspects (NW, N, NE) are located at about 150 m lower mean elevations than rock glaciers on southern slopes (SE, S, SW). Rock glaciers in the High Tatra Mts. are located at significantly higher elevations compared to rock glaciers in the Western Tatra Mts. Average length of rock glaciers in both mountain ranges is 221 m, but it can reach up to 1550 m for the longest features. More numerous tongue-shaped rock glaciers in the Western Tatra Mts. are larger in area and longer (but not significantly) than predominantly lobate-shaped rock glaciers in the High Tatra Mts.

References

Dobiński, W. [2005]: Permafrost of the Carpathian and Balkan Mountains, eastern and southeastern Europe. *Permafrost and Periglacial Processes*, 16 (4):395–398, doi:10.1002/ppp.524.

Kotarba, A. [1986]: Lodowce gruzowe w Tatrach. *Wszechświat*, 87:97–99.

Nemčok, A. and Mahr, T. [1974]: Kamenné ľadovce v Tatrách. *Geografický časopis*, 26:359–374.

The effect of temporal variability of soil moisture on mountain permafrost: A combined model and monitoring approach

Cécile Pellet[1], Christian Hauck[1], & Manfred Stähli[2]

[1]*Department of Geosciences, University of Fribourg, Switzerland*
[2]*Swiss Federal Research Institute WSL, Birmensdorf, Switzerland*

Soil moisture is a key factor controlling the energy and mass exchange processes at the soil-atmosphere interface. In permanently frozen ground it strongly affects the thermal behaviour of the ground by influencing its physical properties such as ice content, thermal conductivity and heat capacity. It also influences other processes like evaporation, infiltration, refreezing rate and runoff and modifies the electrical and electromagnetic properties such as electrical conductivity and permittivity that are used in indirect geophysical and remote sensing methods.

In a first attempt to quantify the role of water content, a soil moisture network along an altitudinal gradient in middle and high mountain areas in Switzerland has been initiated, and first results confirm the importance of different water related processes that are dominant at different elevation bands.

At very high elevations, in permafrost regions, these processes have not yet been analysed in detail, and current state-of-the-art climate and climate impact simulations are neither calibrated nor validated regarding water content in the subsurface, mostly due to missing data. Using the data from the new soil moisture network in combination with measured in-situ ground temperatures and meteorological parameters (air temperature, global radiation, and wind speed), we calibrated the one dimensional heat and mass transfer model COUP [Jansson, 2012] at all locations. This model was then used to analyse the water balance and more precisely the specific repartition of precipitations into runoff, evaporation and change in moisture content. Finally, we analysed the relations between infiltrating water from the snow cover, phase changes and latent heat release and its influence on subsurface temperature in frozen terrains.

References

Jansson, P.-E. [2012]: Coupmodel: Model Use, Calibration and Validation. *Transaction of the Asabe*, 55(4):1335–1344, URL http://elibrary.asabe.org/abstract.asp?aid=42245&t=3.

Multi-disciplinary monitoring of rock glacier dynamic: the case study of Gran Sommetta (Valle d'Aosta, Italy)

Paolo Pogliotti[1], Umberto Morra di Cella[1], Fabrizio Diotri[1], Cécile Pellet[2], Reynald Delaloye[2], & Christian Hauck[2]

[1]*Environmental Protection Agency of Valle d'Aosta, Italy*
[2]*Department of Geosciences, University of Fribourg, Switzerland*

During the last years several steps forward have been made in the comprehension of rock glacier dynamics mainly for their potential evolution into rapid mass movements phenomena. Monitoring the surface movement of creeping mountain permafrost as well as its internal structure and thermal regime is important for understanding the potential effect of ongoing climate change on such landforms.

In this study we present the multi-disciplinary monitoring of surface velocities, internal structure and temperatures of a rock glacier located within a popular ski resort and directly overhanging on a ski track. The study area is located in the Western European Alps, at the head of the Valtournenche Valley (Valle d'Aosta, Italy), south of the main Alpine crest and facing toward the Mediterranean Sea. The upper half of the rock glacier, namely its morphological rooting zone, was thermally and mechanically disturbed during the Little Ice Age by the local development of a glacier which has today completely disappeared. As consequences permafrost is currently lacking in most of the area formerly covered by the glacier and creep processes do not occur. The downward part of the rock glacier is active and composed by two lobes spanning an elevation range between 2600 and 2750 m and is hence since more than a century fully disconnected from any sediment source.

The monitoring methods include

i) the reconstruction of surface movements and DSM (digital surface model) changes over the years 2012-2015 obtained by multi-temporal analysis of UAV (unmanned aerial vehicle) images and GNSS campaigns,

ii) the internal temperature regime measured within two 15 m deep boreholes since December 2014 and

iii) the internal structure of the rock glacier obtained by repeated ERT (electrical resistivity tomography) and RST (refraction seismic tomography) campaigns since July 2014.

The movement rates obtained by UAV-photogrammetry are combined to those obtained by the repeated campaign of differential GNSS on almost fifty points distributed on the rock glacier. Results reveal a high spatial variability of the surface velocities, with the orographic left lobe showing much higher velocities (up to 2 m/year) than the right lobe (less than 0.8 m/year). Surface velocities are then interpreted on the basis of internal structure and temperature which reveal the presence of thick ice-rich bodies in both lobes, with internal temperatures very close to the melting point. The influence of varying dominant lithology and bed topography is also considered to partially explain the different velocities of the two lobes. The significant increase in surface velocity which has been detected on most active sections of the rock glacier after three years of survey is concomitant to rates of acceleration observed for rock glaciers monitored on the neighboring but opposite northern side of the Alps.

Permafrost - Glacier interaction at the lower limit of mountain permafrost: A case study from Western Alps (Petit-Grapillon, Valle d'Aosta, Italy)

Paolo Pogliotti, Umberto Morra di Cella, Michel Isabellon, & Edoardo Cremonese

Environmental Protection Agency of Valle d'Aosta, Italy

The elevation of the lower limit of mountain permafrost in the European Alps is highly variable and depends essentially on topography and ground cover conditions. Moreover the recent glacial melt induced by global warming is clearing large areas at high elevation where new permafrost can possibly develop.

In this study we present ground temperatures measured in two 20 m deep boreholes, drilled in bare bedrock in the fore-field of the Petit-Grapillon glacier (Mont Blanc) at 3000 m a.s.l. The boreholes are 90 meters apart and have been drilled along a longitudinal transect at increasing distance from the present position of the glacial front: the upper borehole is free from glacier since 2005 while the lower is free since 1950 approximately.

The temperature monitoring started in September 2013 and revealed the absence of permafrost in both boreholes even at depth. The bedrock is warmer at the lower borehole, with deep temperatures around 1.5 °C and absence of seasonal freezing at the surface while, in the upper borehole, the deep temperatures are around 0.3 °C with a seasonal freezing that can penetrate beyond 5 meters of depth.

This differences detected in the sub-surface thermal regime are analyzed and discussed in spite of the recent glacial fluctuations and the lateral variability of temperatures due to site-specific snow cover conditions. Moreover the lower limit of mountain permafrost is considered and compared to the potential permafrost distribution provided by the Alpine Permafrost Index Map [Boeckli et al., 2012].

References

Boeckli, L.; Brenning, A.; Gruber, S. and Noetzli, J. [2012]: Permafrost distribution in the European Alps: calculation and evaluation of an index map and summary statistics. *The Cryosphere*, 6(4):807–820, doi:10.5194/tc-6-807-2012.

Permafrost occurrence in the Himalayas - first results from an empirical model approach for area-wide estimates

Marc-Olivier Schmid, Nadine Salzmann, Andreas Linsbauer, & Andreas Hasler

University of Fribourg, Switzerland

The Himalayas have probably the most widespread occurrence of permafrost outside the Arctic. Nevertheless, scientific and societal interest in alpine permafrost in this region has been widely neglected. Only in recent years, with growing evidence of climate change and associated impacts on glaciers and snow in the Himalayas, also permafrost related issues came into the spotlight. So far very few ground based studies have been conducted and the course-resolution global permafrost zonation index from Gruber [2012] is the only reasonable estimate of the permafrost distribution for this area.

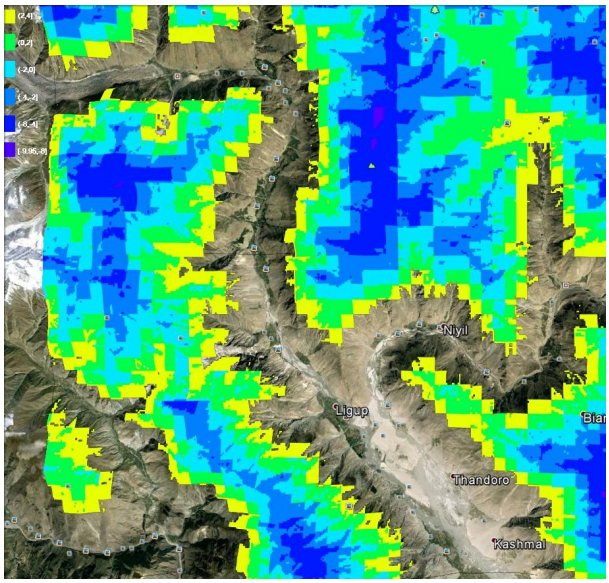

Figure 1: Example of modelled MAGST in the Himalaya shown in Google Earth. Yellow and green represent slightly positive MAGST and increasingly darker blues represent a stronger negative MAGST.

For regions where local ground data are missing, simple empirical permafrost models based on topoclimatic parameters can be applied over a whole mountain range to assess permafrost distribution. Here, such type of a model Boeckli et al. [2012] based on empirical relations as found in the European Alps and further generalized for the Rocky mountains in British Columbia, Canada, is tested for the Himalayas. The model calculates mean annual ground surface temperature (MAGST) based on air temperature and potential incoming solar radiation. We used the mean annual air temperature based on the Worldclim dataset and the SRTM DEM version 4.1 from CGIAR at a spatial resolution of 90 m for the calculation of the potential incoming solar radiation.

Preliminary results show a plausible estimate of the permafrost distribution. A negative MAGST and thus a high likelihood for the presence of permafrost was found for an area of approx. 140 000 km^2 which equals to one third of the area above 3000m a.s.l. For this preliminary result, areas covered by glaciers have not yet been subtracted. Comparing the modelled MAGST with the mapped rock glaciers from Schmid et al. [2015] shows that about two thirds of all rock glaciers reach areas with a positive MAGST. First results also indicate that the model predictions are in general agreement with the permafrost zonation index from Gruber [2012].

References

Boeckli, L.; Brenning, A.; Gruber, S. and Noetzli, J. [2012]: A statistical approach to modelling permafrost distribution in the European Alps or similar mountain ranges. *The Cryosphere*, 6(1):125–140, doi:10.5194/tc-6-125-2012.

Gruber, S. [2012]: Derivation and analysis of a high-resolution estimate of global permafrost zonation. *The Cryosphere*, 6(1):221–233, doi:10.5194/tc-6-221-2012.

Schmid, M.-O.; Baral, P.; Gruber, S.; Shahi, S.; Shrestha, T.; Stumm, D. and Wester, P. [2015]: Assessment of permafrost distribution maps in the Hindu Kush Himalayan region using rock glaciers mapped in Google Earth. *The Cryosphere*, 9(6): 2089–2099, doi:10.5194/tc-9-2089-2015.

New frontiers in detecting and quantifying mountain permafrost creep from radar interferometry

Tazio Strozzi[1], Rafael Caduff[1], Urs Wegmüller[1], Charles Werner[1], Chloé Barboux[2], Reynald Delaloye[2], & Hugo Raetzo[3]

[1] *Gamma Remote Sensing, Gümligen, Switzerland*
[2] *Department of Geosciences - Geography, University of Fribourg, Switzerland*
[3] *Federal Office for the Environment, Bern, Switzerland*

The best visual expression of mountain permafrost is represented by rockglaciers, which, in contrast to the permafrost itself, can be mapped and monitored directly using remotely sensed data. Changes in rockglacier motion are believed to be the most indicative short- to medium-term response of rockglaciers to environmental changes [Kääb et al., 2007] and thus an indicator of mountain permafrost conditions in general. Repeat-pass Interferometric Synthetic Aperture Radar (InSAR) is a powerful technique for mapping land surface deformation from space at fine spatial resolution over large areas [Strozzi et al., 2004]. Major advantages of this technique are the wide area coverage, the high sensitivity to surface displacement (centimetres to millimetres), and the availability since 1991 of a large archive of satellite acquisitions. Despite limitations due to vegetation cover, the special SAR viewing geometry, repeat-cycles on the order of one month, atmospheric artefacts, and snow cover, short-baseline interferograms are successfully applied in alpine areas for the mapping and monitoring of rockglacier's motion.

Besides satellite sensors, terrestrial instruments are in use for a variety of remote-sensing geoscientific applications. A terrestrial radar interferometer (TRI) compliments satellite SAR data in time and space, allowing the measurement of additional displacement vectors and velocity classes. The GAMMA Portable Radar Interferometer (GPRI) was developed and manufactured in-house by GAMMA Remote Sensing. The GPRI can operate over distances up to about 10 km and scans can be taken in less than one minute to allow for near real-time monitoring [Werner et al., 2012]. The basic principles used to determine displacements with TRI are the same as for satellite InSAR and similarly there is the potential to measure displacements with millimetre accuracy.

In the Oberwallis region in Switzerland we are studying since many years the motion of rockglaciers using various satellite SAR data along with the GPRI. Our area of interest encompasses numerous active rockglaciers with deformation rates ranging typically between 0.1 and 2.0 m/yr, recently destabilized (or "surging") rockglaciers showing morphological indices of landslide-like mass wasting (e.g. development of transversal cracks, surface subsidence of the upper section, rapid advance of the front position) and with rates of motion well above 5.0 m/yr, and many other much more slowly moving permafrost landforms. Differential interferometry was first performed using the high-resolution satellite SAR data (spatial resolution on the order of 20 m) of the ERS-1/2 SAR and JERS-1 sensors during the 1990's with acquisition time intervals from 1 day to several years to compile an inventory of slope movements. Since then, new SAR sensors, advanced processing techniques, and very-high resolution Digital Elevation Models (DEM) to more accurately compensate for the topography related phase have become available. In the last 7 years, very-high resolution SAR data with spatial resolution on the order of 3 m from the TerraSAR-X and Cosmo-SkyMed missions were used complementing the investigations performed with the high-resolution data of the ENVISAT, Radarsat-2 and ALOS PALSAR-1 sensors and permitting to partially overcome some of the limitations of the technique. Nowadays, the Sentinel-1 mission represents the newest approach to SAR mission design with acquisitions regularly available over nearly all mountainous areas worldwide every 12 days. Nevertheless, the spatial resolution of Sentinel-1 is lower than that of other current missions (TerraSAR-X, Cosmo-SkyMed, Radarsat-2) which represents a challenge in the case of surface motion affecting small areas. Starting from the end of the snow season in late spring 2015 we are using Sentinel-1 data for a systematic monitoring of known mass wast-

ing phenomena in Switzerland. In our presentation we will show selected results obtained with the various satellite and terrestrial radar interferometric sensors on well known permafrost landforms in the Matter and Saas valleys in Switzerland, make a comparison to products obtained with past and current satellite sensors of different spatial resolution and acquisition time intervals, and highlight the complementarity of satellite and terrestrial radar interferometry.

References

Barboux, C.; Strozzi, T.; Delaloye, R.; Wegmüller, U. and Collet, C. [2015]: Mapping slope movements in Alpine environments using TerraSAR-X interferometric methods. *ISPRS Journal of Photogrammetry and Remote Sensing*, 109, doi:10.1016/j.isprsjprs.2015.09.010.

Kääb, A.; Frauenfelder, R. and Roer, I. [2007]: On the response of rockglacier creep to surface temperature increase. *Global and Planetary Change*, 56 (1–2):172–187, doi:10.1016/j.gloplacha.2006.07.005. Climate Change Impacts on Mountain Glaciers and Permafrost.

Strozzi, T.; Kääb, A. and Frauenfelder, R. [2004]: Detecting and quantifying mountain permafrost creep from in situ inventory, space-borne radar interferometry and airborne digital photogrammetry. *International Journal of Remote Sensing*, 25(15): 2919–2931, doi:10.1080/0143116042000192330.

Werner, C.; Wiesmann, A.; Strozzi, T.; Kos, A. and Wegmüller, U. [2012]: The GPRI Multi-mode Differential Interferometric Radar for Ground-based Observations. In *Proceedings of EUSAR 2012, Nuremberg, Germany, 24-26 April 2012*.

Permafrost observation strategy in the Hindu Kush Himalayan region: A Proposal

Dorothea Stumm[1], Stephan Gruber[2], Christian Hauck[3], Rijan Kayastha[4], Muhammad Asif Khan[5], Moti Lal Rijal[6], Nadine Salzmann[3], Renoj J. Thayyen[7], & Philippus Wester[1,8]

[1] *International Centre for Integrated Mountain Development (ICIMOD), Nepal*
[2] *Carleton University, Canada*
[3] *University of Fribourg, Switzerland*
[4] *Kathmandu University, Nepal*
[5] *Karakoram International University, Pakistan*
[6] *Tribhuvan University, Nepal*
[7] *National Institute of Hydrology, India*
[8] *Wageningen University, The Netherlands*

As permafrost conditions are closely linked to atmospheric processes and the climate, borehole temperatures and active-layer thickness have been defined as essential climate variables (ECV) by the Global Climate Observing System (GCOS), and are recommended parameters for long-term monitoring. Permafrost thaw can impact hydrological and ecological systems, hazards and livelihoods. In the Hindu Kush Himalayan (HKH) region, many people live near or below areas with permafrost occurrences and are thus potentially affected by changes in permafrost conditions. However, knowledge and data on mountain permafrost occurrence and conditions in the HKH region is sparse, and no observation strategy exists.

In other parts of the world, such as in Canada or in the European Alps, mountain permafrost research has been conducted for several decades. Experiences have been gained, and comprehensive observation strategies have been developed and set in place. The goals of such observation strategies are to monitor mountain permafrost systematically, assess the state and future changes and to increase the understanding and knowledge on permafrost processes. Important criteria for a comprehensive and long-term observation strategy are that the observations are scientifically relevant, technically and economically feasible, and cost-effective.

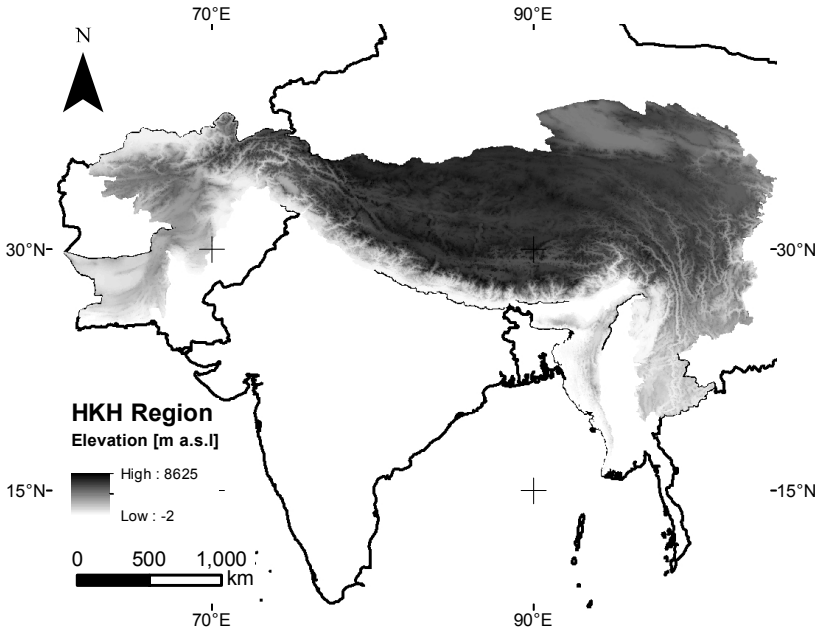

Figure 1: HKH Region

Here, we present a proposal for a comprehensive mountain permafrost observation strategy for the HKH region, based on the learnings and experiences from the Alps and Canada. Key observational aims of this strategy are borehole and near-surface temperatures, subsurface ice, active layer thickness, unfrozen water content, permafrost creep kinematics, and fast mass movements from permafrost areas. Borehole temperatures can be measured at strategically selected places in the HKH region, likely near mountain passes where existing infrastructure makes borehole drilling feasible. Near-surface temperature measurements complement the borehole temperatures and help in understanding the spatial distribution and the effect of different surface covers.

To confirm the presence of permafrost in a spatial context and to better understand the dynamics and processes of the permafrost and active layer regarding ground ice and unfrozen water content, electrical resistivity tomography observations and other geophysical methods are used. Permafrost kinematics such as rock glacier movement and ground subsidence are measured with geodetic surveys, photogrammetry or radar. Fast mass movements from permafrost areas such as rock fall events are important to understand the impact of permafrost thaw on the hazard potential. For a comprehensive approach, selected super sites with multi-level observations in representative climatic regions are proposed, together with a catchment research. At such research sites, meteorological and snow cover observations should also be integrated with permafrost measurements. The establishment of a permafrost observation database, including inventories of permafrost features (e.g. rock glaciers, ice faces) will assure a systematic documentation.

Modelling of mean annual air temperature (1979-2010) for the study of mountain permafrost in the SW of San Juan

Carla Cintia Tapia Baldis[1], Dario Trombotto Liaudat[1], Cristian Villarroel[2], & Federico Otero[1]

[1] *Instituto Argentino de Nivología, Glaciología y Ciencias Ambientales, Conicet, Argentine Republic*
[2] *UNSJ-FCEFyN, Departamento de Geología, Conicet, Argentine Republic*

It is the aim of the present study to estimate and statistically model the mean annual air temperature (MAAT) for the southwestern part of the Andes in the province of San Juan, Argentina (31°S to 33°S and 71°W to 69°W), an area with hardly any register of instrumental data. At a large scale the MAAT may provide a good approximation of permafrost distribution. The Argentine Central Andes have a mean altitude of 3500 m asl with several peaks of 6000 m asl and higher. The "reanalysis data" indicate a MAAT of 0.88 °C between 1979 and 2010 at a height of 3685 m asl.

The method of Gruber [2005], based on the correlation between MAAT and permafrost, in order to calculate the extension of permafrost (PE) and its derivation for the calculation of a global index of permafrost zones (PZI) was used. The extension of large areas of permafrost is obtained by extrapolating the MAAT isotherms that indicate its limits.

The set up MAAT model is based on the values of the data set from the National Center for Environmental Prediction (NCEP) Climate Forecast System Reanalysis (CFSR) [Saha, 2010] available on the website: cs.ncep.noaa.gov/cfsr/. The used period of reference in order to figure the MAAT in the present study comprises 01.01.1979 to 01.01.2011. The chosen NCEP-CFSR grid resolution is 0.5°×0.5°and MAAT data were calculated at 3685 m asl. The heights were taken from the digital elevation model of the Argentine Republic (MDE-AR) with a spatial resolution of 45 m (`http://www.ign.gob.ar/`).

The MAAT grid was readjusted to the topographical MDE-AR grid, obtaining a grid layer with the spatial MAAT distribution in function of topography , that is to say of 30 arc seconds of spatial resolution (see figure 1).

The lack of meteorological stations in the high mountains of the studied area complicates the validation of the interpolated MAAT values. Only two registers of meteorological stations could be compared to the MAAT model: 'Portezuelo de la Guardia' and 'Campamento Pachón' (see Arenson et al. [2010]).

Portezuelo de la Guardia in the surroundings of the Bramadero river basin at 31°53' S and 70°11' W recorded a MAAT of -2.15 °C between 2009-2014 at a height of 4019 m asl, whereas the value estimated by the model for this height is -0.93 °C. The nivo-meteorological station of the camp of the Pachón project (Glencore-Xstrata) at 31°34' S and 70°2' W indicated a MAAT of 1.3 °C in the year 2010 at 3600 m asl. The value estimated by the model for the same site is 2.28 °C.

In the study area (see Fig. 1) cryogenic belts with possible permafrost between 3700 and 4500 m asl and likely permafrost above 4500 m asl were previously established. The average height of the 0 °C isotherm (ca. 3900 m asl) indicates geomorphologically quite precisely the mean lower permafrost limit of sedimentary cryogenic debris slopes, which may contain ice in their matrix, while the limit of cryoforms with more specific creeping (rock glaciers, protalus lobes and protalus ramparts) locally lower the permafrost limit down to 3600-3700 m asl, where it is possible for permafrost to persist even under slightly positive MAAT temperatures (0.5 to 1 °C).

Thus considering the 0 °C isotherm as lower permafrost limit in situ, the surface covered by permafrost in the studied area is of 5546 km^2 approximately.

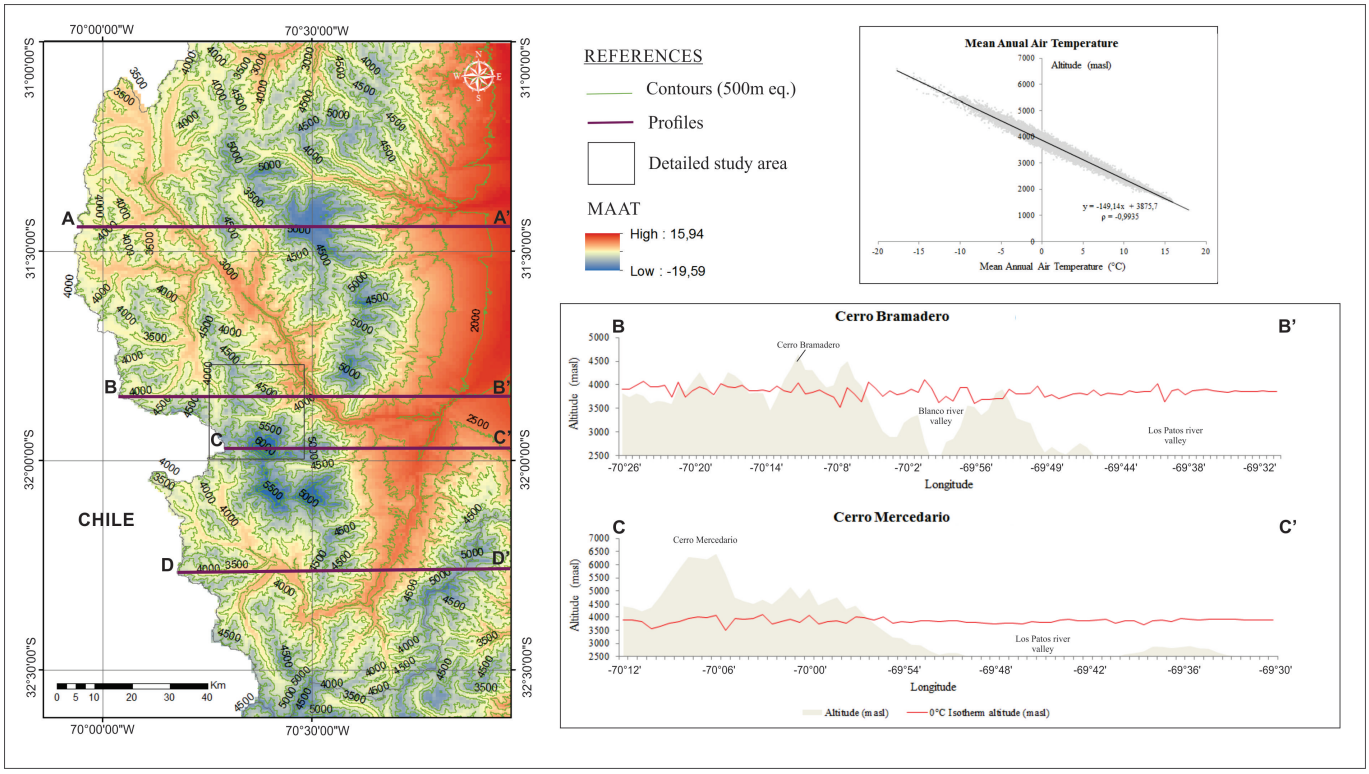

Figure 1: Modelled MAAT for the SW of San Juan between 31°and 32°S. Top right corner: regression function for MAAT versus altitude. Bottom right: topographic profiles showing the position of 0 °C isotherm at different latitudes.

References

Arenson, L.U.; Pastore, S.; Trombotto, D.; Bolling, S.; Quiroz, M.A. and Ochoa, X.L. [2010]: Characteristics of two Rock Glaciers in the Dry Argentinean Andes Based on Initial Surface Investigations. In *GEO2010 in the New West*, pages 1501–1508. Vol Calgary.

Gruber, S. [2005]: *Mountain permafrost: Transient spatial modelling, model verification and the use of remote sensing*. PhD thesis, Universität Zürich, Zürich.

Saha, S. et al. [2010]: NCEP Climate Forecast System Reanalysis (CFSR) 6-hourly Products, January 1979 to December 2010. Research Data Archive at the National Center for Atmospheric Research, Computational and Information Systems Laboratory.

Inventory of landslides at the Santa Cruz river basin (San Juan, Argentina) and its relationship with the Andean cryogenic environment

Carla Cintia Tapia Baldis & Dario Trombotto Liaudat

Instituto Argentino de Nivología, Glaciología y Ciencias Ambientales, Conicet, Argentine Republic

In mountainous areas as the Andes it is common to see mass removal processes produced at different scales, levels of activity and speed. Several authors have also reported that in regions underlain by permafrost there is the development of a special type related to the active layer which can occur when there is loss of shear strength, this process is called active layer failure.

The objective of this work is to identify and characterize the different types of landslides in the upper stretch of the Santa Cruz River basin in the Central Andes in the province of San Juan, Argentina on the assumption that they have a trigger mechanism linked to cryogenic processes.

The Santa Cruz River basin of 432 km^2 is located between 31°44' to 31°55' S and 70°11' and 70°28' W in the province of San Juan, Argentina. In the region there are abundant periglacial landforms and processes, as well as indicators of landslide processes. Seismic events related to those indicators are discarded because most of those events have their hypocenter more than 100 km of distance from the studied region and from 1985 to the present, no data related to removal processes are recorded as mass triggered by earthquakes [Penna et al., 2013].

Based on the digital analysis of high-resolution images, 39 rock- and / or debris slides, translational, rotational movements and composite bodies were identified. Extraction of topographic parameters from a digital elevation model also allowed the quantification of topographic determinants for each of them. It was found that the average height of the crown is 3900 m and 3500 m was the altitude at the foot. The average slope of the detachment is 23° and in the sector of the resulting body it is 17°. The total length measured between the crown and the foot varies between 165 and 2850 m while the detachment scar is between 18 and 240 m. The displaced masses are between 30-4150 m wide and 120-2700 m long. The total area involved in the landslide represents 4.3 % of the surface of the basin.

The identified bodies also show a major lithological and geometric control, since they occur mainly in continental environment with sedimentary lithologies or on very weathered igneous rocks, on slopes with unfavorable orientations. Fundamentally, the landslides zones as well as the deposits are located on slopes facing W, W-SW and W-NW. These orientations represent the most vulnerable hillsides, unprotected by the surrounding relief itself and receive a higher rate of global solar radiation throughout the year. Although there are no chronological datings of the studied deposits, based on geomorphological criteria they can be classified as inactive deposits and their estimated age can range from 100 to 5000 years (BP).

It is to add that the average altitude of the failure crowns is closely similar to the average altitude of the annual isotherm 0 °C and the lower limit of mountain permafrost in situ (without creeping). An important effect of permafrost is to stabilize slopes, increasing the resistance to the shear angle; however, an increase in the amount of moisture in the active layer or supra permafrost layer can contribute to reducing the resistance of the granulometric sedimentary material and trigger detachments. Haeberli [1992] indicated that an increase in air temperature produces not only degradation of permafrost but also slope instability in glacial and periglacial regions. This work proposes the degradation of Andean permafrost in San Juan linked to the increase of temperature within the climatic variability of the Holocene as a possible trigger for landslides.

References

Haeberli, W. [1992]: Construction, environmental problems and natural hazards in periglacial mountain belts. *Permafrost and Periglacial Processes*, 3 (2):111–124, doi:10.1002/ppp.3430030208.

Penna, I.M.; Derron, M.-H.; Volpi, M. and Jaboyedoff, M. [2013]: Analysis of past and future dam formation and failure in the Santa Cruz River (San Juan province, Argentina). *Geomorphology*, 186: 28–38, doi:10.1016/j.geomorph.2012.12.011.

Data and permafrost frontiers in South America

Dario Trombotto Liaudat[1], Kazuyuki Saito[2], & Ivanna P. Marcosig[1]

[1] *Argentine National Research Council, IANIGLA, CCT CONICET Mendoza, Argentina*
[2] *Japan Agency for Marine-Earth Science and Technology, Yokohama, Kanagawa, Japan*

Some authors distinguish between present maritime or tropical South American permafrost and continental permafrost of the Central Andes. Global warming processes enhance degradation of permafrost in different cryoforms in the Andes. Understanding how permafrost degradation relates to the changing climatic conditions is of great importance; for a hydrological necessity in the dry section of the Central Andes, and for overall understanding of the present landscape in the Southern Andes. In this sense, mountain permafrost is closely connected with human activities and socioeconomy, such as mining, engineering, use of water resources, etc. and it requires an ecological treatment.

Andean permafrost is still very poorly appreciated in scientific circles of Earth Sciences in the Northern Hemisphere. Some estimations hold that permafrost may extend according to a new estimate using the state-of-the-art "Global Climatic Models" (hereafter, GCM 2015), possibly to approximately 140,000 km^2 [Saito et al., 2016] which would be larger than the known extent of permafrost in the Antarctica (Fig. 1).

Figure 1: A = GCM 2015. Present permafrost in the Central Andes (in blue). B = GCM 2015. Past permafrost in Patagonia (deep seasonal frost in green). Orange, no freezing

Geomorphological analyses of cold environments in the Andes show interesting and remarkable geoforms, periglacial cryoforms of different spatial scales such as rock glaciers, cryoplanation surfaces, solifluction forms, cryogenic sedimentary slopes, either sorted or cryoturbated structures and patterned ground. This is mountain permafrost that the GCM 2015 could not properly capture, e.g. the location of the rock glaciers rich in ice which is lower than the altitude of the lower permafrost level. On this matter it is still necessary to also identify these rock glaciers and to find out how much ice they may contain and what could be their role if the 0 °C isotherm ascended because of global warming.

In terms of natural hazards and disasters in periglacial areas, more information and understanding about the frozen zones is needed. For example, in the areas of active volcanoes active along the Andean Cordillera, slope stability is modified by seismicity, and data need to be backed by geological information. Further, global warming produces important debris flows which ought to be studied more thoroughly.

Paleopermafrost also seems to have affected a major area during the LGM according to the CGM 2015. Downscaled distribution estimates the potential coverage (i.e., if not covered by glaciers or ice sheets) of approximately 435,000 km^2 in South America, about 21 thousand years ago. In this case it must be analyzed that mountain permafrost joined latitudinal permafrost in Patagonia during the ice ages. One factor to be taken into account is that the Patagonian climate is and was very dry and it is quite different from the numerous permafrost samples of the Arctic and Subarctic areas.

While paleopermafrost of the LGM in Patagonia and according to the mentioned model covered an approximate area of 110,000 km^2, present permafrost covers only 12,000 km^2 , an important part of which is glacier ice. It strikes the eye that the new CGM 2015 shows permafrost field evidence in the deep seasonal frost during the LGM (see Fig. 1).

The same model does not reveal traces of present permafrost for some sites, in Chubut for example, although rock glaciers and other cryogenic small processes occur and are corroborated by fieldwork and satellite images above the trimline. The issue remains how to validate and improve numerical models.

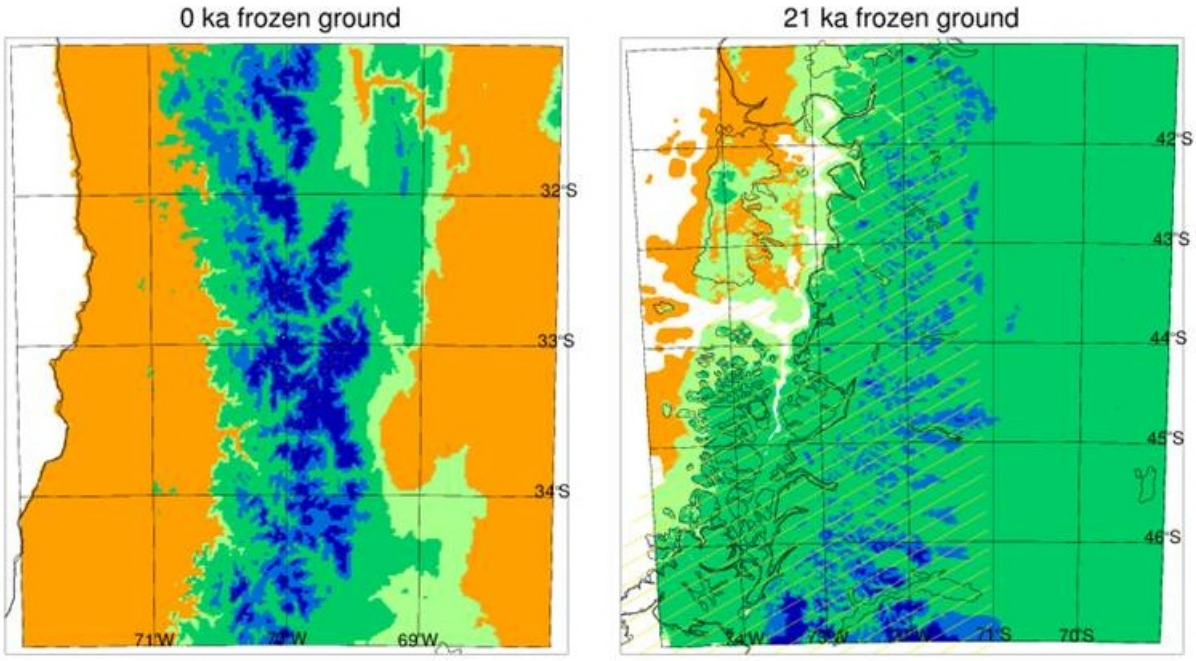

Figure 1: A = GCM 2015. Present permafrost in the Central Andes (in blue). B = GCM 2015. Past permafrost in Patagonia (deep seasonal frost in green). Orange, no freezing

Until now permafrost occurrence in Patagonia has been temporally associated to the glaciations (Cf Trombotto [2002]). However, there could have been a desynchronization of a large number of cryogenic events, variability in the maximum expansion of Andean ice in certain part of the Patagonian Andes due to other reasons than the general temperature descent during the LGM or other cryomeres. The poleward shift of the southern westerlies and the Pacific anticyclone [Boex et al., 2013] for example, might have provided more humidity, and helped to form ice in some parts of Central Patagonia, enhanced cryogenic activity at larger distance from the glaciations between 45 °30'and 47 °S in the extra Andean dry Patagonia.

Paleopermafrost has been relatively little studied together with the South American Geology. Hence, its role in the formation of quaternary landscapes and the interaction with the paleo-human cultures is unclear. Its participation in the distribution and extinction of species is also totally unknown until now.

References

Boex, J.; Fogwill, C.; Harrison, S.; Glasser, N. F.; Hein, A.; Schnabel, C. and Xu, S. [2013]: Rapid thinning of the late Pleistocene Patagonian Ice Sheet followed migration of the Southern Westerlies. *Scientific Reports*, 3:2118, doi:10.1038/srep02118.

Saito, K.; Trombotto Liaudat, D.; Yoshikawa, K.; Mori, J.; Sone, T.; Marchenko, S.; Romanovsky, V.; Walsh, J.; Hendricks, A. and Bottegal, E. [2016]: Late Quaternary Permafrost Distributions Downscaled for South America: Examinations of GCM-based Maps with Observations. *Permafrost and Periglacial Processes*, 27(1):43–55, doi:10.1002/ppp.1863.

Trombotto, D. [2002]: Inventory of fossil cryogenic forms and structures in Patagonia and the mountains of Argentina beyond the Andes. *South African Journal of Science*, 98: 171–180, URL http://personal.cricyt.edu.ar/dtrombot/south_african_journal2002.pdf. Review Articles, Pretoria, South Africa.

First results from thermal investigations of rock glaciers in the Slovak High Tatra Mountains, Western Carpathians

Tomáš Uxa & Kjetil Schanke Aas

Department of Physical Geography and Geoecology, Charles University in Prague, Czech Republic

Rock glaciers are prominent periglacial landforms commonly found in cold mountain areas and they are closely related to permafrost conditions. Because coarse openwork debris cover on a rock glacier surface favours ground cooling, active rock glaciers may locally extend well below the regional permafrost limit. Accordingly, inactive rock glaciers often represent places of the lowermost permafrost occurrence in marginal permafrost areas or in regions with degrading permafrost.

Despite the intense permafrost research in the High Tatra Mountains, particularly in the past twenty years, and widespread occurrence of rock glaciers, little data are available on their thermal regime. There are scattered short-term ground surface temperature (GST) and bottom temperature of snow cover (BTS) data from three rock glaciers located in the Dolinka Buczynowa, Świstowka Roztocka and Mengusovská dolina valleys suggesting presence of permafrost inside the investigated landforms [Kędzia, 2015]. However, data acquired by different methods are either contradictory or inconclusive and more comprehensive study on the topic is still lacking. In this contribution, we try to fill this gap and we present the first results from thermal investigations of seven rock glaciers located in the Slavkovská dolina and Veľká Studená dolina valleys. Studied accumulations lie between 1846 and 2077 m asl and mean annual air temperature based on climate station data from 1981-2010 is estimated to range between +0.3 and +1.8 °C.

GSTs were recorded every 1 or 3 hours between October 2014 and August 2015 using nine Minikin Tie (EMS Brno Inc.) and iButton DS1922L (Maxim Integrated Inc.) loggers with an accuracy of ±0.2 and ±0.5 °C, respectively, and the readings were indirectly calibrated at 0 °C using the zero curtain periods. The loggers were placed into voids between boulders just below the rock glacier surface to avoid direct exposure to solar radiation. We also mapped temperature distribution at snow-ground interface on the rock glaciers and in their immediate surroundings. 179 BTS measurements were made before the onset of spring snowmelt in 2015 using Greisinger GMH 3710 thermometer (Greisinger Electronic GmbH) and a 3 m long temperature probe with an accuracy of 0.1 °C.

While mean air temperatures for the whole observation period range between +1.6 and +2.6 °C (estimated from nearby Lomnický štít station using a lapse rate of 6.5 °C/km), mean values of GSTs are between -1.7 and +1.7 °C with an average of +0.4 °C. Three of the seven rock glaciers have average GST < 0 °C and one rock glacier has average GST < +0.5 °C. All investigated rock glaciers show negative surface offset up to 3.6 °C. GSTs recorded during the BTS window have an average of -4.2 °C and range between -6.4 and -2.6 °C, suggesting probable and possible permafrost occurrence (sensu Haeberli [1973]) at six and one of the rock glaciers, respectively. BTS values measured during the field campaign have an average of -3.3 °C and indicate probable and possible permafrost at three and four rock glaciers, respectively. However, considerable spatial heterogeneity of BTS values, ranging between -8.3 and -0. °C, exists over the rock glacier surfaces with the lowest BTS values occurring at the foot of talus slopes and along the most distinct furrows. Generally, rock glacier areas show significantly cooler conditions compared to nearby vegetated locations, where average BTS value is -0.6 °C.

Based on the preliminary results of the thermal investigations we infer that permafrost is likely to occur within all the studied rock glaciers. Given a relatively narrow altitudinal gradient, GSTs and BTS have no clear relationship to altitude, but local-scale variations in potential incoming solar radiation, snow cover thickness, topography, debris size, land cover and/or possible ventilation effects are the dominant factors. Rock glaciers show significant negative thermal anomaly, which may favour presence of permafrost at other rock glacier bodies or scree slopes situated below the lower limit of suggested regional permafrost occurrence (1930 ± 150–200 m asl; Dobiński [2005]). Further long-term data are, however, needed to validate and/or refine the above conclusions.

References

Dobiński, W. [2005]: Permafrost of the Carpathian and Balkan Mountains, eastern and southeastern Europe. *Permafrost and Periglacial Processes*, 16 (4):395–398, doi:10.1002/ppp.524.

Haeberli, W. [1973]: Die Basis-Temperatur der winterlichen Schneedecke als möglicher Indikator für die Verbreitung von Permafrost in den Alpen. *Zeitschrift für Gletscherkunde und Glazialgeologie*, 9: 221–227.

Kędzia, S. [2015]: Are There Any Active Rock Glaciers in the Tatra Mountains? *Studia Geomorphologica Carpatho-Balcanica*, 48:5–16, doi:10.1515/sgcb-2015-0001.

Permafrost detection through the use of geophysical methods in the Blanco River Basin, San Juan, Argentinia

Cristian Daniel Villarroel[1], Ana Paula Forte[2], & Carla Tapia Baldis[3]

[1] *Department of Geology-Faculty of Exact, Physical and Natural Sciences, Argentine Republic*
[2] *National University of San Juan. Research Center of the geosphere and the biosphere, Argentine*
[3] *Instituto Argentino de Nivologia, Glaciologia y Ciencias Ambientales, CCT CONICET Mendoza, Argentina*

Geophysical prospection is an indirect method which aims to determine the presence, depth and geometry of the base and top of the permafrost, in particular, for mountain areas where the permafrost pattern is often very complex [Vonder Müehll et al., 2001, Hausmann et al., 2007]. It is an important technique that can also aid to establish the degree of activity of the rock glaciers.

In this work, we describe geophysical surveys in five rock glaciers which have been conducted in the Santa Cruz River and Frio River watersheds located in the south west of San Juan province, which are part of Blanco river basin along the Central Andes of Argentina. This watershed has a total area of 4,860 sq. km and a large number of periglacial environment landforms (about 1000, among active and inactive rock glaciers and protalus).

We conducted between 7 to 3 geophysical 2-D surveys in five rock glaciers (El Colorado, El Negro, El Amarillo, El Pelado and Los Patos Norte) when the active layer shows greater development (March - April). We used 2-D seismic tomography in longitudinal and transverse traces. We estimated rock glacier activity based on satellite imagery. And we registered Vertical Electrical Sounding (VES) in two of the five rock glaciers.

We found that El Colorado rock glacier has a permafrost thickness of 14 m, with sectors up to 18 m thickness and mean p-wave velocity of 2500 m/s. VES performed on the central area of this body showed an active layer's depth of 2.67 m (142 Ωm resistivity) and permafrost thickness of 8.39 m (23.6 KΩ m resistivity).

El Negro rock glacier has an active layer with an average thickness of 3 m and mean p-wave velocity of 500 m/s. In particular, El Negro rock glacier permafrost has an average thickness of 7 m with local thickness up to 20 m and mean p-wave velocity of 2500 m/s.

El Amarillo rock glacier has an active layer with an average thickness of 1.5 to 5 m, with mean p-wave value of about 600 m/s. The greatest thicknesses coincide with collapse structures. Permafrost thickness is about 15 m, with sectors of up to 35 m in thickness with p-wave velocities vary between 1000 and 2800 m/s (Fig. 1).

Los Patos Norte rock glacier has an average active layer thickness of 2 m and p-wave velocity of about 400 m/s. Permafrost average thickness is about 10 m with sectors of up to 20 m thick. Average p-wave velocity is about 2800 m/s.

In El Negro rock glacier our results are consistent with the ones measured by [Arenson et al., 2010]. In addition we found that El Negro rock glacier also has termokarst features, which indicates certain disequilibrium with the current climatic conditions.

We also found signs of permafrost degradation inferred from seismic profile at the front slope in El Amarillo rock glacier.

We found that El Pelado rock glacier is inactive, that is consistent with morphological analysis.

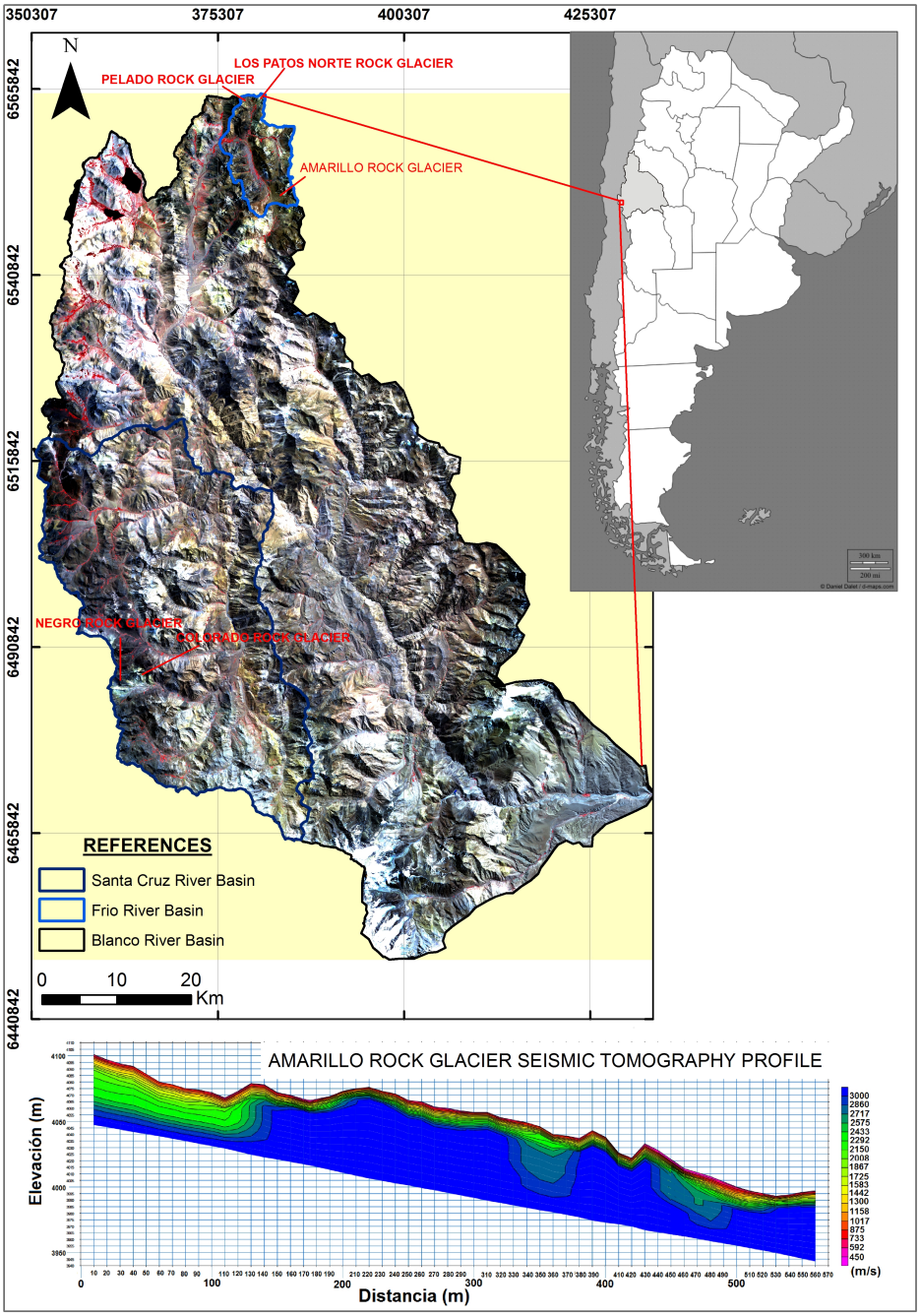

Figure 1: Location of the five rock glaciers in Santa Cruz and Frio river subbasin. Integrated seismic profile in Amarillo rock glacier

References

Arenson, L.U.; Pastore, S.; Trombotto, D.; Bolling, S.; Quiroz, M.A. and Ochoa, X.L. [2010]: Characteristics of two Rock Glaciers in the Dry Argentinean Andes Based on Initial Surface Investigations. In *GEO2010 in the New West*, pages 1501–1508. Vol Calgary.

Hausmann, H.; Krainer, K.; Brückl, E. and Mostler, W. [2007]: Internal structure and ice content of Reichenkar rock glacier (Stubai Alps, Austria) assessed by geophysical investigations. *Permafrost and Periglacial Processes*, 18(4):351–367, doi:10.1002/ppp.601.

Vonder Müehll, D.; Hauck, C.; Gubler, H.; McDonald, R. and Russill, N. [2001]: New geophysical methods of investigating the nature and distribution of mountain permafrost with special reference to radiometry techniques. *Permafrost and Periglacial Processes*, 12(1):27–38, doi:10.1002/ppp.382.

Soil moisture impacts on the thermal regime of mountain permafrost

Adrian Wicki, Christian Hauck, Cécile Pellet, & Christin Hilbich

University of Fribourg, Switzerland

Soil moisture may considerably impact the thermal regime of permafrost soils. In mountain regions it has been shown to largely influence the active layer dynamics, including recent degradation, by determining the ice content and the amount of latent heat which is needed to freeze/thaw the active layer each year. Due to slope effects liquid water will not necessarily stay in the active layer and complex interactions with the snow cover can be observed. At Schilthorn (2970 m asl, Swiss Alps), soil moisture has been identified to be a major contributor to the thermal differences between two borehole locations which are located 10 m apart [Scherler et al., 2010, Hilbich et al., 2011]. In this study, the spatial distribution and temporal variability of soil moisture at Schilthorn were assessed during the summer 2014 and compared to the thermal behaviour at the boreholes. Finally, the contrasting years 2014 (wet, cold) and 2015 (extreme heat wave) were compared.

Electrical resistivity tomography (ERT) was used to assess the spatial variability of soil moisture. A small electrode spacing (0.8 m) and a time-lapse inversion scheme were used to detect small scale hydrological processes under variable snow and weather conditions as well as in different geological contexts. Additional ERT data of an automated profile line provided daily measurements at a coarser resolution (2 m spacing). The resistivity changes were compared to soil moisture conditions measured by soil moisture monitoring sensors. Infiltration events were identified and related to snow melt and precipitation events using air temperature, precipitation and snow depth data. Finally, the hydrological regimes were compared to the ground temperatures measured at the boreholes to identify its thermal impact.

This complete methodology allowed for new insights into the thermal impact of soil moisture on alpine permafrost. Soil moisture conditions are spatially highly variable, particularly during the time of snow melt. At Schilthorn, infiltration is mainly limited by the thaw depth and bedrock topography, however even under frozen conditions, some infiltration takes place and evidence for preferential flow was found. The thermal impact of soil moisture was found to vary greatly depending on soil texture, geological setting and hillslope water flow. In general, latent heat fluxes are dominant in both frozen and unfrozen conditions through freezing and evaporation of soil water, respectively. Sensible heat fluxes are restricted to rainwater infiltration events and negligible. According to our findings, the change of ground thermal properties with depth (thermal conductivity and diffusivity) is a major contributor to the different thermal behaviour at the boreholes. The cold and wet summer 2014 resulted in shallow thaw depths as opposed to the large thaw depths recorded during the warm and dry summer 2015. High soil moisture is thus thought to precondition active layer thickening, whereas heat conduction is the dominant process of heat transport in the subsurface.

References

Hilbich, C.; Fuss, C. and Hauck, C. [2011]: Automated Time-lapse ERT for Improved Process Analysis and Monitoring of Frozen Ground. *Permafrost and Periglacial Processes*, 22(4):306–319, doi:10.1002/ppp.732.

Scherler, M.; Hauck, C.; Hoelzle, M.; Stähli, M. and Völksch, I. [2010]: Meltwater infiltration into the frozen active layer at an alpine permafrost site. *Permafrost and Periglacial Processes*, 21(4):325–334, doi:10.1002/ppp.694.

Short-term variability of rock glacier surface velocities in the Swiss Alps revealed by continuous GPS

Vanessa Wirz[1], Jan Beutel[2], Reynald Delaloye[3], Tonio Gsell[2], Stephan Gruber[4], Isabelle Gärtner-Roer[1], Andreas Hasler[5], Robert Kenner[6], Philipp Limpach[2], Johann Müller[1], Marcia Phillips[6], Hugo Raetzo[7], Cristian Scapozza[8], Andreas Vieli[1], & Samuel Weber[1]

[1] *University of Zurich, Switzerland*; [2] *ETH Zurich, Switzerland*
[3] *University of Fribourg, Switzerland*; [4] *Carleton University, Canada*
[5] *SensAlpin GmbH, Switzerland*; [6] *WSL – Institute for snow and avalanche research SLF, Switzerland*
[7] *Federal Office for the Environment FOEN, Switzerland*
[8] *Scuola universitaria professionale della Svizzera italiana (SUPSI), Switzerland*

In recent years, strong variations in the kinematics of rock glaciers have been detected, raising questions about the governing processes and hazard potential in a changing climate. Continuous differential L1-GPS measurements on permafrost slope movements have proved to be a suitable tool to study the intra-annual (short-term) variability of slope movements of rock glaciers [Wirz et al., 2016]. Measurements with a high temporal resolution (daily) allow to identify controlling factors on short-term velocity fluctuations, thus contributing to an improved process understanding of rock glacier movement and changes over time. Furthermore, continuous observations have the potential to detect relations between changes in the movement velocity observed and meteorological or snowpack factors.

We present continuous time series over three to five years of surface velocities of eleven GPS stations located on eight rock glaciers in different regions of the Swiss Alps. Each mobile GPS station consists of a low-cost single-frequency GPS receiver (u-blox LEA-6T) with active antenna (Trimble Bullet III) and a two-axis inclinometer (VTI SCA830-D07) allowing to detect the tilt of the GPS antenna mounted atop a boulder situated on each rock glacier [Wirz et al., 2013]. In cases of multiple measurement points closely co-located on either the same or on adjacent rock glaciers, data is collected using a low-latency low-power wireless sensor network [Beutel et al., 2011]. In the case of such online data the resulting data products are available in near real time, e.g. the daily positions and velocities used in this study are available every morning for each preceding day. For locations with offline data logging, data are collected annually and post-processed in batch mode. Where available, a local GPS reference mounted on a stable position adjacent to the rock glacier is used for differential processing of GPS data. The short baseline distance allows to reduce the position error considerably compared to the use of long baseline GPS reference data, e.g. from a national GNSS network.

Originating in an interdisciplinary research project [Wirz et al., 2013] the GPS sensor technology [Beutel et al., 2011] has been recently made available to partners on a national scale in the form of a pilot study of the Swiss Permafrost Monitoring Network (PERMOS) where further rock glaciers have been equipped with GPS-based continuous kinematic monitoring. To date the installed inventory includes the Dirruhorn, Steintälli, Grabengufer, Bielzug, Distelhorn, Ritigraben, Gruben, Jäggi (all Canton Valais, Switzerland), Schafberg, Muragl (both Canton Graubünden, Switzerland) and Largario (Canton Tessin, Switzerland) rock glaciers. The data obtained is accessible at http://data.permasense.ch. In the current study the signal-to-noise-thresholding method (SNRT, Wirz et al. [2014]) is applied to obtain reliable velocity estimates based on daily GPS positions for the rock glacier inventory. Similarities and differences between the individual rock glaciers are qualitatively investigated in the following.

Average velocities between 0.2 and 6.6 m/a were observed (Fig. 1a). Most stations (eight stations) had average velocities between 0.3 and 2 m/a. Three stations moved at velocities exceeding 3.4 m/a. The observed amplitude of intra-annual variability at all stations ranged from 6 to more than 2000 % (Fig. 1b). For most stations it ranged between 30 and 90 %. The continuous measurements with high temporal resolution revealed that all rock glaciers experience clear intra-annual variations in movement where the

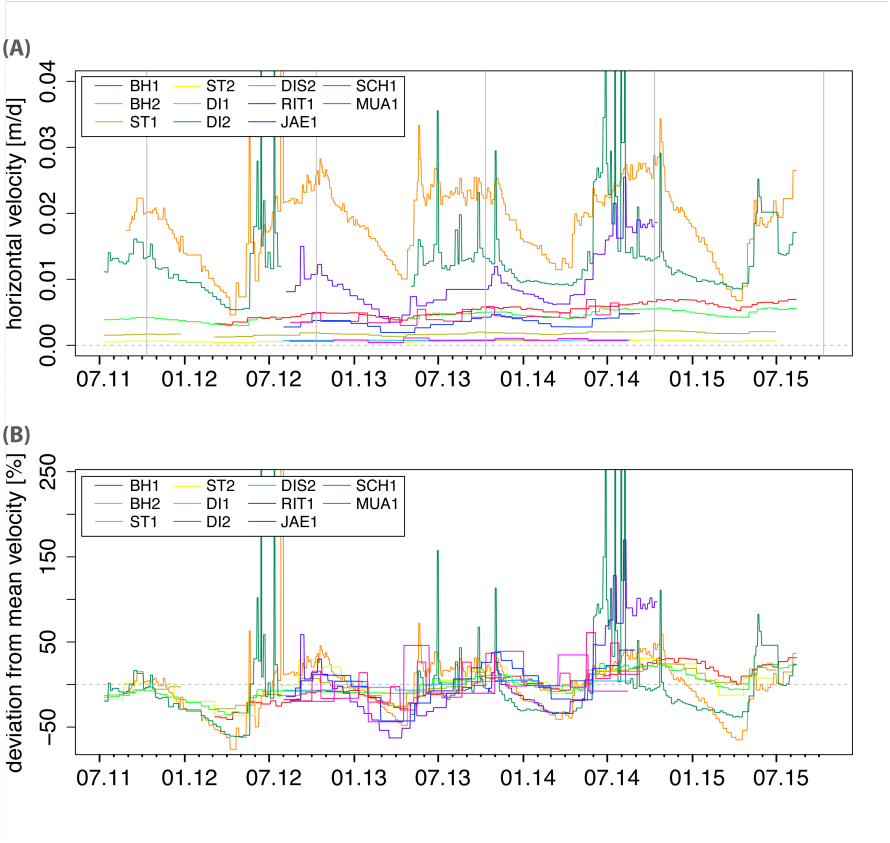

Figure 1: a) (top): Horizontal surface velocities of various rock glaciers in the Swiss Alps. Velocities were estimated based on daily GPS positions applying the SNRT method (with a threshold SNR-t of 40, Wirz et al., 2014). b) (bottom): Intra-annual variability of horizontal velocities, expressed as deviation from the corresponding average velocity. Vertical grey lines indicate individual hydrological years.

timing and the amplitude are rather similar between individual years (Fig. 1b).

Where a seasonal cycle exists, seasonal maximum in velocities occurred between September and January, minimum in velocities between March and May. Despite these similarities also differences exists. For example, at three stations (DI2, BH2, JAE1) with velocities above 3 m/a, in addition to the seasonal cycle short-term peaks in velocity were observed. In the near future, the continuous GPS data will be compared to distributed velocity fields (with much coarser temporal resolution) as derived from remote sensing methods. Further, we will investigate the impacts of a) the geomorphological and topographical setting and of) the meteorological and snowpack factors on the observed kinematic variations.

References

Beutel, J.; Buchli, B.; Ferrari, F.; Keller, M.; Thiele, L. and Zimmerling, M. [2011]: X-sense: sensing in extreme environments. In *Proceedings of Design, Automation and Test in Europe, 2011, 1–6, IEEE, Grenoble, France*, pages 1460–1465.

Wirz, V.; Beutel, J.; Buchli, B.; Gruber, S. and Limpach, P. [2013]: *Temporal Characteristics of Different Cryosphere-Related Slope Movements in High Mountains*, pages 383–390. Springer Berlin Heidelberg, Berlin, Heidelberg. ISBN 978-3-642-31337-0. doi:10.1007/978-3-642-31337-0_49.

Wirz, V.; Beutel, J.; Gruber, S.; Gubler, S. and Purves, R. S. [2014]: Estimating velocity from noisy GPS data for investigating the temporal variability of slope movements. *Natural Hazards and Earth System Sciences*, 14(9):2503–2520, doi:10.5194/nhess-14-2503-2014.

Wirz, V.; Geertsema, M.; Gruber, S. and Purves, R.S. [2016]: Temporal variability of diverse mountain permafrost slope movements derived from multi-year daily GPS data, Mattertal, Switzerland. *Landslides*, 13(1):67–83, doi:10.1007/s10346-014-0544-3.

Isotope tracking of water sources and growth patterns of ground ice at the Kunlun Mountain Pass on northern Qinghai-Tibet Plateau

Yuzhong Yang, Qingbai Wu, & Huijun Jin

Key Laboratory of frozen soil engineering, Cold and Arid Regions Environmental and Engineering Institute, Chinese Academy of Sciences, China, People's Republic of

Ground ice extensively occurs in permafrost on the Qinghai-Tibet Plateau (QTP). It provides one of the most convenient ways of evaluating permafrost development and hydrological processes. Here, ground ice from two deep boreholes (KL-2 (91.3 m), and KL-3 (65 m)) at the Kunlun Mountain Pass along the Qinghai-Tibet Highway on the QTP were investigated. Totally, 27 and 88 ground ice samples were collected from the KL-2 and KL-3 boreholes, respectively. The tracing method using stable isotopes was employed for assessing the growth patterns of ground ice and to unravel their origins at different depths. Study results primarily present the record of stable isotopic composition through a complete sequence of ground ice, and five different isotopic stratification characteristics were identified in two boreholes. The isotopic contents and the freezing line of ground ice in different depths showed significant deviations from regional precipitation and surface water, indicating the discrepancies in replenishment source water and the climatic conditions during ground ice formation periods: the subsurface ground ice (0-3 m) was mainly recharged by modern-age precipitation, and the growth of deep-layer ground ice (below 3 m) is related to the source water and freezing conditions during ice formation. The negative correlations between δD and d-excess suggested that ground ice at those depths formed from closed-system segregation freezing of liquid water. After compared the ground ice of two boreholes, it indicates that the isotopic variations against depth between 0-10 m is significantly different due to the topographic difference, vegetation cover induced moisture deviations which changed the freezing conditions. Below 10 m, the isotopes nearly stabled in a narrow range, which can be inferred to be the similar ice formation conditions in the two boreholes. Additionally, a stable freezing front at the depth of 9.6 m and a paleo-permafrost table at 91.3 m were established in Borehole KL-2 via isotopic variations and ground ice growth patterns. The current findings produce the stable isotopic stratification characteristics of deep borehole ground ice in permafrost regions on the QTP for the first time, providing a logical explanation regarding the complex origin of deep-layer ground ice and may supply further information for studying the evolution of permafrost on the QTP.

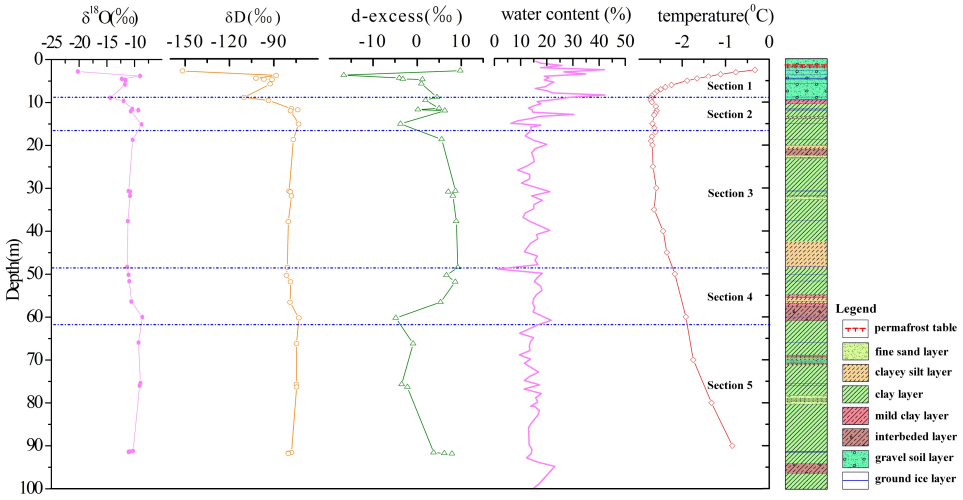

Figure 1: $\delta^{18}O$, δD and D-excess profiles of ground ice, ground temperature and water content against depth and strata description in the Kunlun Mountain Pass

SESSION 25

Changing Permafrost and its Impacts across High Asia

Convener:

Lin Zhao, *Cold and Arid Regions Environmental and Engineering Research Institute, Chinese Academy of Sciences, China*

Sergey Marchenko, *Geophysical Institute, University of Alaska Fairbanks, USA*

Tonghua Wu, *Cold and Arid Regions Environmental and Engineering Research Institute, Chinese Academy of Sciences, China*

High-elevated Asian regions (High Asia) are of the World's largest area of altitudinal permafrost. The Tien Shan, Pamir, Altay, Himalaya, Karakorum mountains and Qinghai-Tibet plateau hold a great concentration of glacier and permafrost ice at elevations over 3000 m, the melt water from which supplies roughly more than half of the total river runoff. Permafrost and associated periglacial landforms are extensively present in mountains of High Asia (HA) and can store large quantities of fresh water in form of ice. Recent permafrost studies show strong short-term changes as well as changes over longer periods such as the Holocene. Alpine ecological systems and hydrology are strongly depending on permafrost and glacier conditions, which also directly influence human activities. At the same time, permafrost is one of the physical elements in the landscape most sensitive to climatic changes. Therefore, study of the interactions between permafrost and other components of the mountain system (climate, hydrology, ground ice, biogeochemistry, vegetation), especially during a period of possible climatic warming, is one of the most important aspects of polar and alpine research.

Atmospheric warming was predicted to be greater in Polar Regions than at lower latitudes and more pronounced at high altitudes than in lowlands. The ongoing climate warming has already affected the surface and ground ice of these mountain ecosystems. The long-term series on permafrost temperature and active layer thermal regime and thickness in the High Asia were collected during the past few decades. Additional large quantity of boreholes were drilled across HA since 2000 in order to conduct permafrost research.

In this section, we will focus on the mountains and plateaus in High Asia, the impact of climate change on mountain ecosystems and society, regional variability, and changes in particular permafrost with respect to the feedback mechanisms between permafrost and other components of the cryosphere in mountain areas of Asia and how can we detect, quantify, and model these interactions. We invite contributions across the interdisciplinary teams using ground-based and space borne techniques and methods, modelling tools advancing the monitoring of regional changes in the High Asia.

Multi-time scale characteristics of climatic factors and its effects on permafrost in the Qinghai-Xizang Plateau

Siru Gao, Qingbai Wu, & Zhongqiong Zhang

State Key Laboratory of Frozen Soil Engineering, Cold and Arid Regions Environmental and Engineering Research Institute, Chinese Academy of Sciences

The Qinghai-Xizang Plateau (QXP), known as the "Roof of the World" and "Earth's third pole", has the most widely distributed high-elevation permafrost on Earth, with an average elevation exceeding 4000 m. It is well known that climate change is the main factor controlling the formation and existence of permafrost. Meanwhile, permafrost change is a sensitive indicator of climate change. In the context of climate warming, rises in permafrost temperature and active layer thickness have caused permafrost degradation on the QXP. However, most studies about effects of various climatic factors on permafrost were focus on the time domain, and neglected important information in the frequency domain. A combined time-frequency analysis provides a more profound understanding of the impacts of various climatic factors on permafrost. In this study, five climatic factors (air temperature, precipitation, wind speed, downward longwave radiation and downward shortwave radiation) and permafrost temperature data over the interval from 1996 to 2010 on the QXP were selected for analysis. Mult-time scale characteristics of five climatic factors were analyzed using Morlet wavelet transformation in the time-frequency domain. Air temperature has an 18 months period, precipitation had periods of 9, 18, 68 and 138 months, wind speed had periods of 9, 18, 28, 58, 122 and 178 months (Fig. 1a), downward longwave radiation had periods of 9, 18, 142 and 176 months, downward shortwave radiation had periods of 9, 18, 122 and 174 months. Permafrost temperature, under the effects of all climatic factors, has also multi-period characteristics; periods of 9, 18, 41, 110 and 176 months at in the shallow soil and periods of 9, 18, 68-71, 120 and 169-173 months in deep permafrost (Fig. 1b) were observed.

To evaluate the relationship between multi-period of climate change and permafrost temperature, their correlation coefficients were calculated; a significant positive correlation was showed between the two, which indicated multi-time scale in permafrost temperature were mainly controlled by multi-time scale in climate change. Here, mult-time scale of climate change was generated by stacking mult-time scale of all five climatic factors. Furthermore, which climatic factors among these five factors had greatest effect on the multi-period of the permafrost temperature was determined via grey incidence analysis. The multi-period of air temperature had the greatest effect on multi-period of soil temperatures in the shallow soil, while that of downward longwave radiation had the greatest effect on multi-period of permafrost temperatures in deep permafrost.

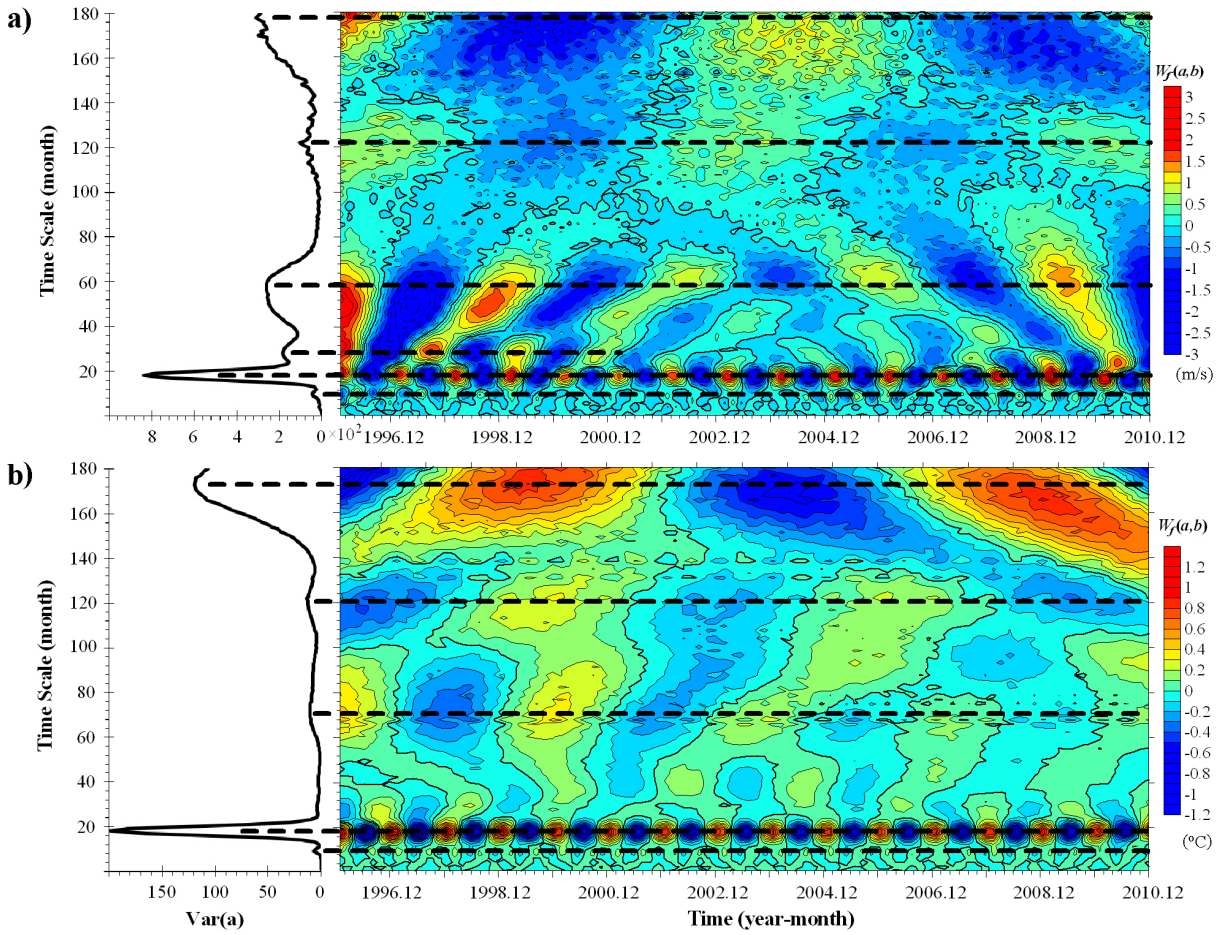

Figure 1: Wavelet variance (left panels) and time-frequency structure of real wavelet transformation coefficients (right panels) of wind speed (a) and permafrost temperature (b).

Differences of the heat-moisture process in active layer among different ecosystems in Beiluehe basin of the Qinghai-Tibet Plateau, China

Guanli Jiang, Qingbai Wu, & Zhongqiong Zhang

Cold and Arid Regions Environmental and Engineering Research Institute, Chinese Academy of Sciences, People's Republic of China

The heat-moisture process in active layer over permafrost has significant impacts on surface energy balance, carbon cycle, ecosystem and hydrological cycle. From 2010 to 2014, four monitoring sites were established in the Beiluhe Basin located in the heart of Qinghai-Tibet Plateau for soil temperature and moisture measurements in different ecosystems. We have investigated the differences of heat-moisture process in active layer among different ecosystems including alpine swamp, alpine meadow, desert grassland and barren. Data reveal that there are significant differences in some aspects, such as freezing and thawing processes, moisture distribution and active layer thickness among different ecosystems. For example, in thawing process, the moisture enriches only in the bottom of active layer for desert grassland; but for alpine meadow, the moisture enriches both in the bottom and the subsurface of active layer; and for alpine swamp, the whole active layer is fully enriched by moisture. Data collected at our monitoring sites also indicate that the surface conditions, especially the soil property, affect the moisture distribution in active layer, which affects the development of the ecosystems reciprocally. This finding suggests the mutual impact between active layer and the ecosystems, and the alpine swamp will degrade in sequences to alpine meadow, desert grassland and barren because of the heat-moisture changes in active layer. The mutual impact between active layer and the ecosystems shows the direct effect of climate change on the permafrost which adjusts the response patterns of active layer, and implies the degradation route of ecosystems in the Qinghai-Tibet Plateau.

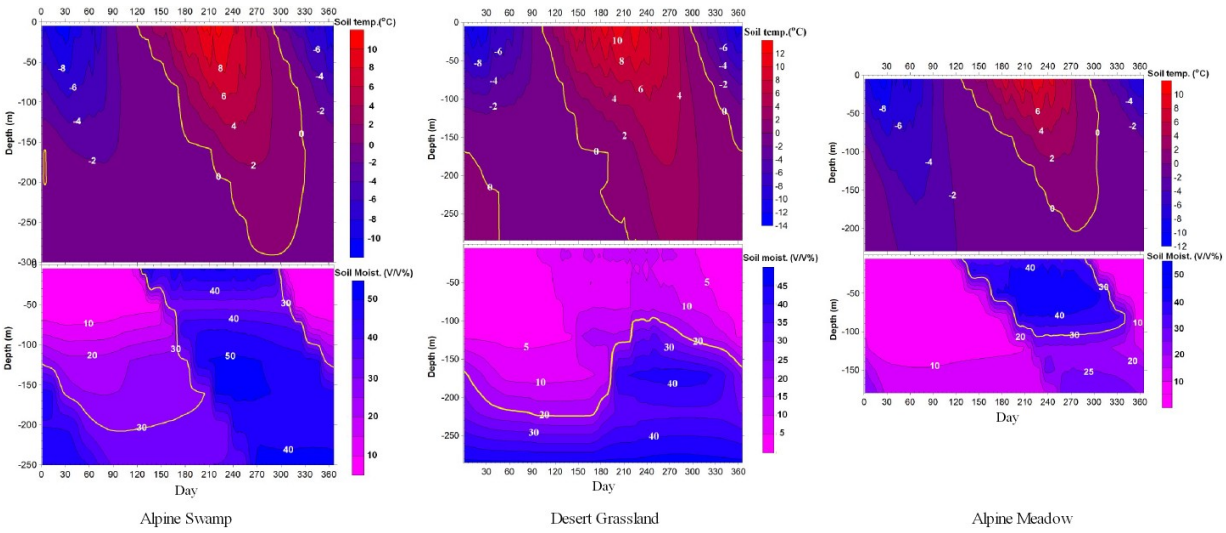

Figure 1: soil temperature and moisture distrubution of active layer in different ecosystems

Permafrost-related Characteristics of vegetation in an inland watershed of the Qilian Mountains, northwestern China

Jing Li[1], Yu Sheng[1], Jichun Wu[1], Xiumin Zhang[2], Ziliang Feng[1], & Shengting Wang[1]

[1] *Cold and Arid Regions Environmental and Engineering Research Insititue, Chinese Academy of Sciences, China*
[2] *Shaanxi Regional Electric PowerGroup Company Limited, Xi'an, Shaanxi, China*

The source area of Datong River (SADR) is located in the northeastern part of the Qilian Mountains, northwestern China, where permafrost was widely distributed above 3500m as the result of high-cold climate and the well developed vegetation cover on the ground surface. Vegetation cover had an important role in retaining permafrost degradation. The Datong River is the main water body flowing in northwest-southeast direction in the SADR. Reshui, Jiangcang and Muli are the main settlements. A railway from Reshui to Muli parallels to the river, and was one of main transportation lines.

Data collection and processing

Field investigations were carried out to find out vegetation communities characteristics in different permafrost areas. The investigation sites were located at different landform positions, such as the mountain top, hill slope, fluvial fan plain, river terrace and flood plain. At each site, a 50 m-long line was firstly set up along the topographic varying direction. And then, the line was equally segmented into four parts. Vegetation communities were quantitatively investigated in quadrats with a size of 1 × 1m at five nodes (including the starting point and the ending point). The investigations included species recognition, species composition, and the coverages of individual species and total community. In addition, the information of geographical locations such as latitude and longitude were recorded using a handheld GPS receiver (GARMIN 62sc).

Indoors, the dominate species and the vegetation type can be determined at each node on the basis of the measurements. For the investigated site, the vegetation type was determined using the frequency statistics method. That is taking the species with the highest occurrence from all the samples collected at five nodes as the dominant species to determine vegetation type. Three indices, the Shannon-Wiener diversity index (SWDI), the community evenness index (EI) and the richness index (RI) were calculated to describe the species composition characteristics at each site. Elevations at each site were derived from the Shuttle Radar Topography Mission (SRTM) DEM data with 90-m resolution using the ArcGIS software (ArcMap version 10.0).

Results

A total of 199 sites were investigated, which were divided into five types of vegetation, alpine meadow community (in amounts of 93), alpine swamp meadow (84), alpine shrub community (9) and alpine sparse vegetation (12) and alpine steppe (1) (Fig. 1). The dominant species of alpine meadow community was the mesic *Kobresia pygmaea* and the main accompanying species included *K. humilis, Potentilla nivea, Leontooinmnanum, Carex moorcroftii, Potentilla multifida*, and *Saussurea pulchra*. Structurally, it was characteristics with plentiful species compositions, low height, simple structure and unclear levelization. The alpine swamp meadow community was dominated by hygric *K. Tibetica*, and the main accompanying species included *K. humilis, Carex moorcroftii, Glaux maritime, Coluria longifolia, Gentiana straminea* and *Ranunculus longicaulis*. The *cyperaceous* and *gramineous* species occupied more than 85 % in composition. Vegetation coverage usually exceeded 80 %. Alpine shrub community was mostly located in the south-facing slope and in the river valley with drier soils. *Dasiphora fruticosa* and *Salix oritrepha* were the main dominant species. The plant height of this kind of vegetation community was generally greater than that of any other types. The alpine sparse vegetation community was mainly composed of xeric and mesoxerophytes cushion-like species with sparsely coverage. This kind of vegetation community was usually distributed on the mountain top. *Androsace tapete, Rhodiola rosea spp.* and *Cremanthodium humile* were

the common species (Fig. 1).

The calculation results of three indices, SWDI, EI and RI, indicated that alpine meadow had the highest calculated values, and that alpine sparse vegetation had the lowest calculated values, and that alpine swamp meadow had the medium calculated values (Tab. 1). As far as the vegetation coverage was concerned, the one-way ANOVA analysis the Least Square Differtence (LSD) method was used to realise a multipple comparison between the four vegetation communities. It was indicated that the alpine sparse vegetation had the lowest coverage (25.74 %), and alpine swamp meadow and alpine meadow had the highest coverage (78.21 % and 79.43 %), and alpine shrub had the medium coverage (72.96 %). There was no significant different between the four vegetation communities.

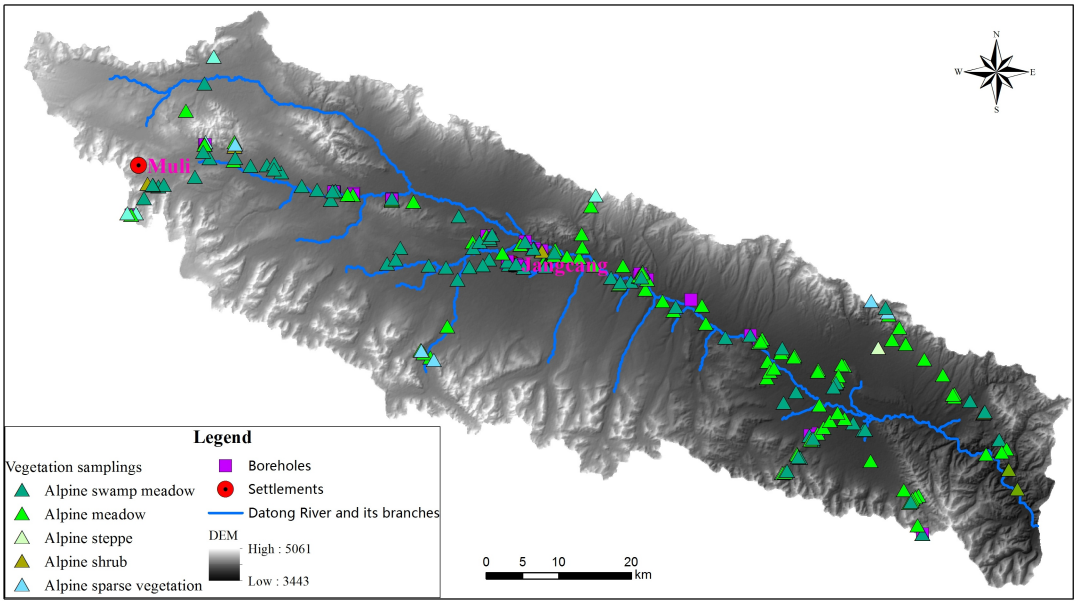

Figure 1: The sketch map of sampling sites, in which the base map was DEM with shadow effect.

The calculated indices of different vegetation communities in the source area of Datong River, Vegetation community RI SWDI EI:

- Alpine swamp meadow 11.1 ±3.72b 1.32±0.34b 0.56 ±0.09b
- Alpine meadow 12.5 ±3.99a 1.63±0.30a 0.62 ±0.08a
- Alpine shrub 14.8 ±3.46a 1.49±0.26ab 0.56 ±0.11ab
- Alpine sparse vegetation 7.8 ±3.88c 0.70 ±0.29c 0.35±0.09c

The lower-case symbol in the table represented a remarkable difference ($p<0.05$).

Permafrost was divided into different zones taking 0.5 °C as the interval. Variations in species compositions, coverages of vegetation communities in different permafrost zones indicated that the spatial changes of vegetation communities could indicated the changes of permafrost underlain. Within low-temperatures permafrost zones with ground temperatures lower than -1.5 °C, vegetation communities experienced the spatial changes from alpine sparse vegetation to alpine meadow and to alpine swamp meadow with the increase of permafrost temperatures. Within high-temperatures permafrost zones with ground temperatures higher than -1.0 °C, vegetation communities changed from alpine swamp meadow to alpine meadow with the increase of permafrost temperatures. Furthermore, alpine swamp meadow vegetation disappeared in high-temperatures permafrost zones. More results would be obtained with deep analysis of filed investigation.

The soil thermal conductivity regime within active layer at different land surfaces in the northern Qinghai-Tibetan Plateau, China

Ren Li, Lin Zhao, Tonghua Wu, Changwei Xie, Yao Xiao, Guokie Hu, & Yizhen Du

State Key Laboratory of Cryospheric Science, Cold and Arid Regions Environmental and Engineering Research Institute, Chinese Academy of Sciences, People's Republic of China

Soil thermal conductivity (STC) is one of important thermal parameters reflecting the ability of heat exchange at the ground surface or of the penetration amplitude and effects of the daily and seasonal temperature fluctuation. In this study, the STCs within the top soil of the active layer were investigated by using the in-situ measured data from September 2003 to December 2013 at Kekexili (KKXL), Beiluhe (BLH), Kaixinling (KXL), and Tongtianhe (TTH) sites in the northern Qinghai-Tibetan Plateau (QTP). The results showed that the STC within the topsoil of the active layer at all sites exhibited clear seasonal fluctuation. The STC was low during the cold season while high in the warm season. On average, the STC in those sites ranged from 0.752 to 1.291 $Wm^{-2}.K^{-1}$, with a mean value of 1.094 $Wm^{-2}.K^{-1}$. In the frozen state (FS), STC was 0.941 $W.m^{-2}.K^{-1}$ while in the unfrozen state (UFS), the STC was 1.241 $W.m^{-2}.K^{-1}$. Averagely, the STC in UFS was about 1.32 times larger than that in FS at those four sites. It was found that in the arid and semi-arid regions fine-grained soil with low unfrozen water content and a low saturation degree resulted in low STC in the cold season.

During a complete freeze-thaw cycle, there were two jumps in STC. One occurred in the transition from the frozen to the thawed state. The other occurred in the transition from thawed state to frozen state. Additionally, the land surface type had significant influence on the STC. STC increased with increasing soil bulk density but decreased with increasing vegetation cover. The STC of alpine frost meadow soil was greater than that of alpine frost steppe soil.

Moreover, an empirically derived model was proposed for estimating monthly average STC over the northern QTP. The monthly mean STC can be well expressed as a function of conventional meteorological data. Independent data collected in situ at Tanggula district from January 2011 to December 2013 were also used for the validation purpose. The statistical results showed that the mean absolute error (MAE) and mean relative error (MRE) were 0.062 $Wm^{-2}.K^{-1}$ and 7.2 %, respectively. The predicted STC values agreed well with the measured STC values. Such verification results further confirmed that the proposed model accurately predicts monthly STC values in the regions with similar conditions. The STC in the hinterland of the northern QTP has decreased at a rate of 0.003 $Wm^{-2}.K^{-1}$ per decade from 1981 to 2014.

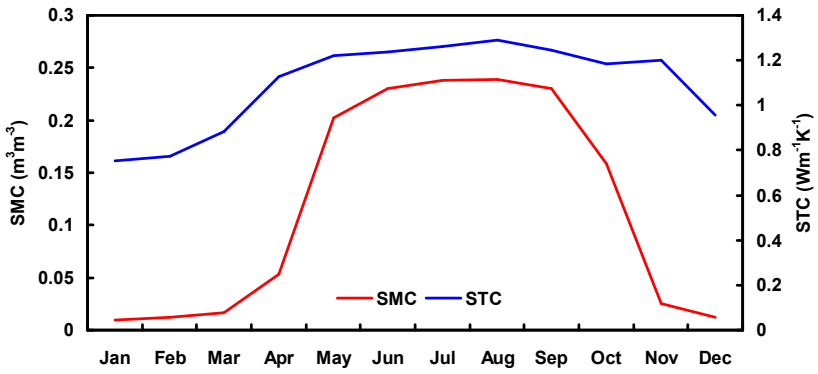

Figure 1: Variations in soil moisture content (SMC) and soil thermal conductivity (STC) at investigation sites during the time period from September 2003 to December 2014

Distribution characteristics of the depth of zero annual amplitude in permafrost regions on the Qinghai-Tibetan Plateau

Guangyue Liu, Lin Zhao, Changwei Xie, Tonghua Wu, Qiangqiang Pang, & Yongping Qiao

Cryosphere Research Station on Qinghai-Xizang Plateau, State Key Laboratory of Cryospheric Sciences, Cold and Arid Regions Environmental and Engineering Research Institute, Chinese Academy of Sciences, People's Republic of China

The depth of zero annual amplitude (ZAA) is an important parameter to the estimation of permafrost evolution, and also influences the effect of simulation in the climate models, land surface models or hydrological models.

16 boreholes were drilled on the Qinghai-Tibetan Plateau. Based on the analysis on ground temperatures observed in these boreholes, the primary distribution characteristics of ZAA are revealed. The results show that: The ZAA decreases firstly and increases afterward with the rising of permafrost temperature, and the turning point of ZAA appears when the permafrost temperature is close to the phase change temperature (near 0 °C); There is a more close relationship between ZAA and annual temperature amplitude at permafrost table than that between ZAA and annul amplitude at 0.5 m depth, due to the hydro-thermal dynamic and the freezing and thawing process of active layer; The differences of thermo-physical parameters among boreholes at different regions are the main cause of significant regional variation of ZAA.

A case study in Xidatan area is also conducted. The Xidatan area is located near the north boundary of permafrost region on the Qinghai-Tibetan Plateau. The observation show that the ZAA decreased over the recent 10 years when the annul temperature amplitude in the active layer increased. This indicates that the change in ZAA is predominantly controlled by the change in the thermo-physical parameters, rather than the change in the superficial annul temperature amplitude. Because the ground texture and the total water content of permafrost in depth cannot vary substantially, the change in thermal diffusivity of permafrost mainly depends on the change in unfrozen-water content which is mainly influenced by the ground temperature.

In some years, seasonal snow covers occurred occasionally and varied the ZAA. Thick snow cover can decrease the ZAA obviously, because it lifts the interface between ground surface and atmosphere, and changes the land surface conditions and the heat transfer process from atmosphere to the deep stratum.

Temporal, Altitudinal and Spatial Variability of Permafrost in the Tian Shan Mountains during the Holocene

Sergey Marchenko[1], Aldar P. Gorbunov[2], & Vladimir Romanovsky[1]

[1] *Geophysical Institute, University of Alaska, Fairbanks, USA*
[2] *Melnikov Permafrost Institute, Russian Academy of Science, Russia*

During the Late Holocene, there were numerous periods of warming and cooling in the Tian Shan Mountains Central Asia. The evolution of air and ground surface temperature in Tian Shan at altitudes of 2,500 and 3,300 m a.s.l. during the last millennium has been obtained by correlating the data from radiocarbon dates, tree-rings indexes, lichenometric, limnological, archeological and historical data. In the last millennium, the most significant periods of cooling occurred during 1150-1350 and 1600-1850.

Ground temperatures across the Tien Shan permafrost domain have been subject to repeated fluctuations during the Holocene brought about by the general planetary changes in climate. The altitudinal oscillations of the 0 °C mean annual air temperature (MAAT) isotherm had a range of about 500 m during the Holocene. Approximately, between 9,000 and 7,000 years ago, the most unfavorable time for the existence of alpine permafrost in the Tien Shan during the Holocene was observed [Marchenko and Gorbunov, 1997]. At that time, the mean annual ground temperatures were by 1.5-2.0 °C higher than those at present time. It was a period of permafrost degradation in the Tien Shan Mountains. A Middle Holocene (5-3 Ka B.P.) cooling was replaced by a short phase of warming in the Late Holocene, after which ground temperatures again significantly decreased. During the Little Ice Age (1600-1850), there was a downward shift of the lower boundary of permafrost distribution by 200-300 m of altitude. Since the second part of the nineteen century, permafrost in the Tien Shan Mountains has been experiencing a warming period, which continues up to the present.

The contemporary thermal state of permafrost in Tian Shan reflects climatic processes during the twentieth century when the average rise in mean annual air temperature was 0.01-0.03 °C per year for the different parts of the Tian Shan Mountains. Geothermal observations during the last 30-40 years documented an increase in permafrost temperatures by 0.3 - 0.6 °C. At the same time, the average active-layer thickness increased by 23 % in comparison to the early 1970s. The long-term records of air temperature and snow cover from the Tien Shan's high-mountain weather stations allow reconstruction of the thermal state of permafrost dynamics since the end of the Little Ice Age (ca. 19850). The modeling estimation shows that the altitudinal lower boundary of permafrost distribution has shifted by about 150-200 m upward during the last 125-150 years. During the same period, the area of permafrost distribution within two river basins in the Northern Tien Shan decreased approximately by 18 % [Marchenko et al., 2007]. Both geothermal observations and modeling results indicate that more favorable conditions for permafrost occurrences and preservation exist in the coarse blocky material, where the ice-rich permafrost could still be stable even when the mean annual air temperatures exceeds 0 °C (Fig. 1).

At the lower boundary of permafrost distribution the soil temperature now are close to 0 °C and at many locations the permafrost degradation has already started. Analysis of measured active layer and permafrost temperature coupled with numerical thermal modeling (permafrost temperature reanalysis) shows that most of the recently thawed permafrost had formed during the Little Ice Age. Since the second part of the nineteenth century, permafrost in the Tian Shan Mountains is experiencing a warming period, which continues up to present. The temperature observations and performed modeling indicate that in the Tian Shan Mountains more favorable conditions of permafrost occurrences and preservation exist in the coarse blocky material (Figure 1) where the mean annual temperature are typically 2.5-4.0 °C colder than the mean annual air temperature.

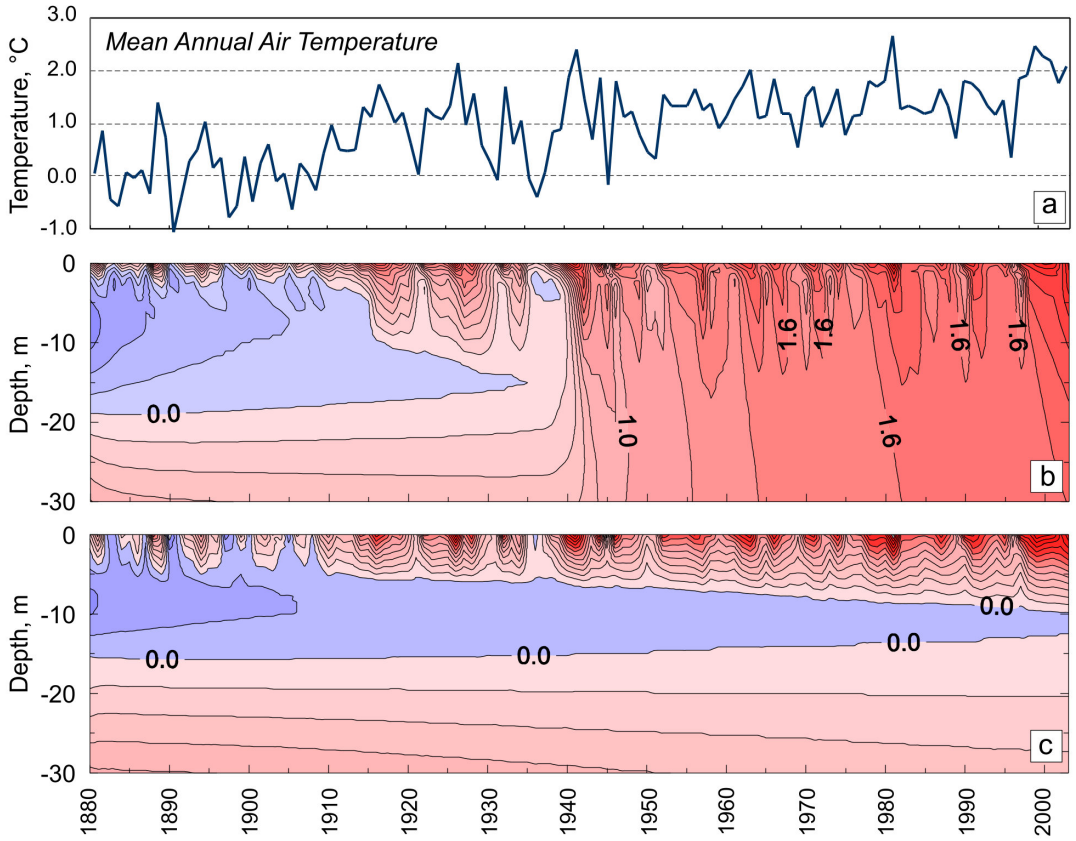

Figure 1: Observed mean annual air temperature (a) and simulated permafrost dynamics within fine-grained soils (b) and beneath the blocky materials (c) since 1880, at the altitudinal lower boundary of permafrost distribution (ca. 2500 m a.s.l) in the northern Tian

References

Marchenko, S.S. and Gorbunov, A.P. [1997]: Permafrost changes in the northern Tien Shan during the Holocene. *Permafrost and Periglacial Processes*, 8(4):427–435, doi:10.1002/(SICI)1099-1530(199710/12)8:4<427::AID-PPP262>3.0.CO;2-V.

Marchenko, S.S.; Gorbunov, A.P. and Romanovsky, V.E. [2007]: Permafrost warming in the Tien Shan Mountains, Central Asia. *Global and Planetary Change*, 56(3–4):311–327, doi:10.1016/j.gloplacha.2006.07.023. Northern Eurasia Regional Climate and Environmental Change.

Effects of stratified active layers on the high-altitude permafrost warming: A case study on the Qinghai-Tibet Plateau

Xicai Pan[1], Yanping Li[1], Qihao Yu[2], Xiaogang Shi[3], Daqing Yang[4], & Kurt Roth[5]

[1] *University of Saskachewan, Canada*
[2] *Laboratory of Frozen Soils Engineering, Cold and Arid Regions Environmental and Engineering Research Institute, Chinese Academy of Sciences, China*
[3] *CSIRO Land and Water, Christian Laboratory, Australia*
[4] *National Hydrology Research Centre, Environment Canada, Canada*
[5] *Institute of Environmental Physics, Heidelberg University, Germany*

Seasonally variable thermal conductivity in active layers is one important factor that controls the thermal state of permafrost. The common assumption is that this conductivity is considerably smaller in the thawed than in the frozen state, $\lambda t/\lambda f < 1$. Using a 9-year dataset from the Qinghai-Tibet Plateau (QTP) in conjunction with the GEOtop model, we demonstrate that the ratio $\lambda t/\lambda f$ may approach or even exceed 1.

Observations from the soil-weather monitoring site demonstrate that, given a unique weather of rainfall-dominated precipitation and occasional thin snow cover in winter, the permafrost in the studied area is characterized by a thick stratified active layer with strong seasonal liquid water content changes. This leads to a high ratio $\lambda t/\lambda f$ as well as a reverse thermal offset, namely a positive difference between the mean annual soil temperature at permafrost table and ground surface. This hypothesis is further consolidated by modeling. The simulated thermal offset is consistent with the observed one and it decreases to negative along with climate warming. Given such a weather pattern and hydraulic and thermal pattern in the stratified active layer, the effects of stratified active layers on high-altitude permafrost warming are evaluated with a variety of ideal simulations. Results suggest the thick stratified active layer strengthens permafrost warming apart from the controlling factors such as thermal conductivity of soil matrix and climate. These findings suggest that, given the increase in air temperature and precipitation, soil hydraulic properties, particularly soil architecture in those thick active layers must be taken into account properly in permafrost models.

Recent change in ground temperature in the east part of Qinghai-Tibet Plateau

Yu Sheng[1], Jichun Wu[1], Ji Chen[1], Jing Li[1], Ziliang Feng[1,2], Xiaoying Hu[1,2], & Shengting Wang[1,2]

[1] *State Key Laboratory of Frozen Soil Engineering, Cold and Arid Regions Environmental and Engineering Research Institute Chinese Academy of Sciences,Lanzhou 730000, China*
[2] *University of Chinese Academy of Science, Beijing, 100000, China*

Permafrost temperature is an indicative of thermal regime of permafrost at an observing site. The change of permafrost temperature is usually a direct response of permafrost conditions to climate change. Depending on the differences in lithology, water content, surface cover etc., permafrost temperature may appear different responses.

In the eastern part of Qinghai-Tibet Plateau, where permafrost with high ground temperatures is widely developing, we set up several permafrost boreholes with temperature cable installed to monitor permafrost temperatures along a national highway (G214) from 2002. Most of the boreholes have a depth of over 15meters, which is considered to be the depth of zero annual amplitude (ZAA). The permafrost temperature at the depth of ZAA is used as the representatives to analyze the recent change of permafrost temperature. The observed data indicated that the permafrost temperatures at all sites showed a successive increase, but had different increasing rates within a range from 0.035 to 0.231 °C/10a (Tab. 1). The maximum increasing rate, 0.231 °C/100a, appeared at the K417+970, where permafrost did not exist. Minimum increasing rates, 0.035 °C/100a, appeared at the K421+820, where the ground temperature was close to 0 °C, and had a very rich ice content in permafrost.

According to the observed data in the Madoi meteorological station, which is located around K480 of G214, the air temperature showed an obvious increasing trend after 1984. The average increasing rate of air temperature is about 0.85 °C/10a from 1984 to 2014, and 0.38 °C/10a from 2002 to 2014. The increasing rate of air temperature is much greater than that of permafrost temperature. Part of the reason is attributed to the attenuating ability of ground layer reflecting to the surface energy change. Also, the thawing of ice in permafrost should be another reason. Permafrost with the near freezing point temperature and rich ice content, consumes more heat for the thawing of ice, resulting in a weak response of the permafrost temperature to air temperature change. This characteristics indicates that permafrost, with high ground temperature and rich ice content, may perform a retarded degradation process to respond a warming climate.

Table 1: Average ground temperature and their increasing rate

Site position	Ice content in permafrost	Ground temperature /℃	Increasing rate /℃/100a
K354+800	poor	-0.63	1.34
K369+860	rich	-0.76	1.24
K391+085	mid	-0.85	0.89
K414+580	rich	-0.22	0.64
K416+300	rich	-0.43	1.63
K417+970	/	1.84	2.31
K421+820	very rich	-0.34	0.35
K426+260	very rich	-0.86	0.7

Seasonal variations of soil properties in a relic permafrost region on the eastern Qinghai-Tibet Plateau

Liming Tian[1,2,3], Lin Zhao[1], Xiaodong Wu[1], & Changwei Xie[1]

[1] *Cold and Arid Regions Environmental and Engineering Research Institute, Chinese Academy of Sciences, People's Republic of China*
[2] *University of Chinese Academy of Sciences*
[3] *College of Earth Environmental Sciences, Lanzhou University*

Climate change is the leading factor in the dynamic variation of permafrost, which has led to permafrost degradation. Together with grassland degradation, permafrost degradation could inevitably bring about the changing of soil nutrients. Therefore, under the scenario of climate change and permafrost degradation, the seasonal and dynamic variations of soil nutrients in permafrost regions, especially on the QTP, and its implication for climate change are crucial for the carbon cycle. However, these processes remain poorly understood. The soils were sampled at different depth (interval of 10cm) from 7 sites along a cross-profile in a relic permafrost region. This region is located at the Maxianshan Mountain, an intersection zone between the QTP and the Loess Plateau (LP), with an average elevation of 3,600 m above sea level. Every sample was collected to analyze the concentration of soil organic carbon (SOC), total nitrogen (TN), soil moisture, pH, and electrical conductivity (EC). Soil pH and EC were determined using a glass electrode with a soil/water ratio of 1:2.5 and 1:5, respectively. Soil moisture was confirmed by oven drying the samples at 105 °C on average. SOC and TN concentration was measured using the Walkley-Black dichromate oxidation procedure and the Semi-Micro Macro Kjeldahl approach, respectively.

The vertical distribution and seasonal variation of SOC, TN and soil moisture showed a similar pattern and tendency. The three indexes decreased with soil depth at four sites (MH02, MH03, MH06, and MH13), but fluctuated at two sites (MH04 and MH10) and increased at a site (MH08). As for the dynamic of these indexes, they declined first and then increased with time at the depth of 0-10cm, rose slightly at the depth of 10-20cm, 20-30cm, 30-40cm, and 40-50cm at the site of MH02, MH03, MH06, and MH13. However, at the site of MH04 and MH10, they went up significantly with time at the depth of 0-10cm and 10-20cm, and then reduced small of the surplus depths. Moreover, they stabilized with time at the depth of 0-10cm, then increased significantly at the depth of 10-20cm and 20-30cm, and finally decreased slightly at the last two depths. Conversely, the vertical distribution of soil pH increased with depth at four sites (MH02, MH03, MH06, and MH13) but decreased at the other sites, whereas the perpendicular allocation of EC reduced with depth at all sites. Meanwhile, correlation and linear regression analyses indicated that SOC, TN, and soil moisture were not related to pH at the seven sites, but SOC and TN were significantly related to soil moisture with the correlation coefficient of 0.77 ($P<0.01$) and 0.79 ($p<0.01$), respectively. Additionally, SOC correlated to TN strongly ($R2=0.89$, $P<0.01$). This suggested that soil moisture was the key factor for the dynamic of SOC and TN.

Thus, these results imply that the response of soil properties in alpine permafrost soils to climate change and permafrost degradation mainly rely on different underlying surface situations (e.g. vegetation types), and the large variation in soil properties at plot scale should be considered when estimating global SOC storage.

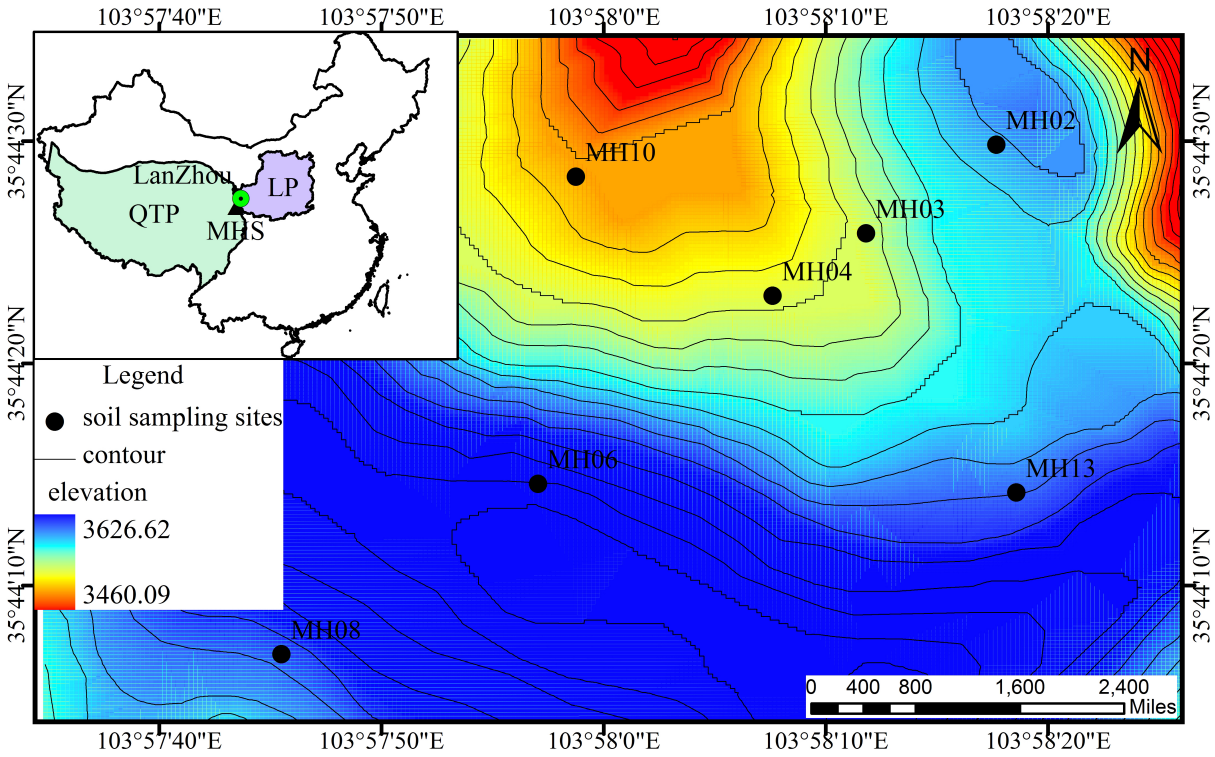

Figure 1: Spatial distribution of soil sampling sites on the top of the Maxianshan mountain, eastern QTP (note: QTP represents Qinghai-Tibet Plateau, LP stands for Loess Plateau, and MHS means Maxianshan Mountain)

References

Mulder, V.L.; Lacoste, M.; Martin, M.P.; Richer-de Forges, A. and Arrouays, D. [2015]: Understanding large-extent controls of soil organic carbon storage in relation to soil depth and soil-landscape systems. *Global Biogeochemical Cycles*, 29(8):1210–1229, doi:10.1002/2015GB005178. 2015GB005178.

Schuur, E. A. G.; McGuire, A. D.; Schadel, C.; Grosse, G.; Harden, J. W.; Hayes, D. J.; Hugelius, G.; Koven, C. D.; Kuhry, P.; Lawrence, D. M.; Natali, S. M.; Olefeldt, D.; Romanovsky, V. E.; Schaefer, K.; Turetsky, M. R.; Treat, C. C. and Vonk, J. E. [2015]: Climate change and the permafrost carbon feedback. *Nature*, 520(7546):171–179, doi:10.1038/nature14338.

Zhao, L.; Wu, Q.; Marchenko, S.S. and Sharkhuu, N. [2010]: Thermal state of permafrost and active layer in Central Asia during the international polar year. *Permafrost and Periglacial Processes*, 21(2): 198–207, doi:10.1002/ppp.688.

Initial result of permafrost assess in Mongolia

Undrakhtsetseg Tsogtbaatar, Jambaljav Yamkhin, Dashtseren Avirmed, & Temuujin Khurelbaatar

Permafrost department, Institute of Geography and Geoecology, Mongolian Academy of Science, Mongolia

Mining exploration is developing immediately in Mongolia during last few years. This mining operation occupies the permafrost region of Mongolia, especially in Hangai and Hentii mountain regions, where permafrost distributes from continuous in high elevation to sporadic in valley bottom and in center of depression. Due to mining operation in Mongolia the permafrost is degrading rapidly, because Mongolian permafrost has a temperature closely to 0 °C and is very sensitive to any changes. Also, Mongolian permafrost delineates the Siberian permafrost region and it is southern limit of Siberian permafrost region. North and high altitude of Mongolia have permafrost and south has no permafrost.

The permafrost, affecting the heat and water circle, plays more important role for ecosystem functionality, especially in arid and semiarid regions such as Mongolia (Jambaljav, 2011). Furthermore, all altitudinal permafrost zones bend round each of the three largest mountain systems of Mongolia: Hentii, Hangai and Mongolian Altai [Gravis, 2001].

Altai, Hangai, Hentii and Hovsgol mountains are the towers of pure water in Mongolia. 70 % of pure water is manufactured in these high altitudes of Mongolia (Davaa, 2002).

The permafrost is degraded and melts up during or before exploration of mining in these mountainous regions. It is one of serious issues of sustainable usage of ecosystem and it degrades the permafrost more rapidly than global warming. As permafrost is an important factor for sustainability of environment, it is needed to assess the permafrost especially in arid and semiarid region.

Main criterions of environmental assess are underground materials (some ore) forest, water (surface and underground), plants, and wildlife in Mongolia. As permafrost includes itself some ice and water, we are trying to assess it by ice and water contains as water.

Mongolia divides into twelve basins of underground water for environmental assessment. Each basin has an own cost of water with size of one cube meter. This cost estimation was derived from foreign countries.

For this study we have used the results of water contains in core samples from one of engineering permafrost investigation in Nalaikh, near Ulaanbaatar, to south-east from Ulaanbaatar. The thickness of active layer was 5.5 m and we sampled every one meter for ice and water contains. Ground materials are mostly gravel and sand with silt. Ice has a texture as massive and veins. Ice contain is different to depth from 9.4 – 43.7 %. For example, moisture contain was 16.0 % at depth of 5.5 m, 43.7 % at depth of 9.2 m, 19.5 % at depth of 18 m, respectively. Total average moisture contain is 17 % and it means that 1 cube meter ground contains 0.17 cube meter water. If the permafrost with 1 m thickness has been degraded and ice in which is melt up in area with 1 ha due to mining operation and it will be release 1700 cube meter water. Cost of 1 cube meter water is USD 0.8 in central Mongolia. Total cost of this permafrost is USD 1376.8 in central Mongolia based on assessment of water and ice contain.

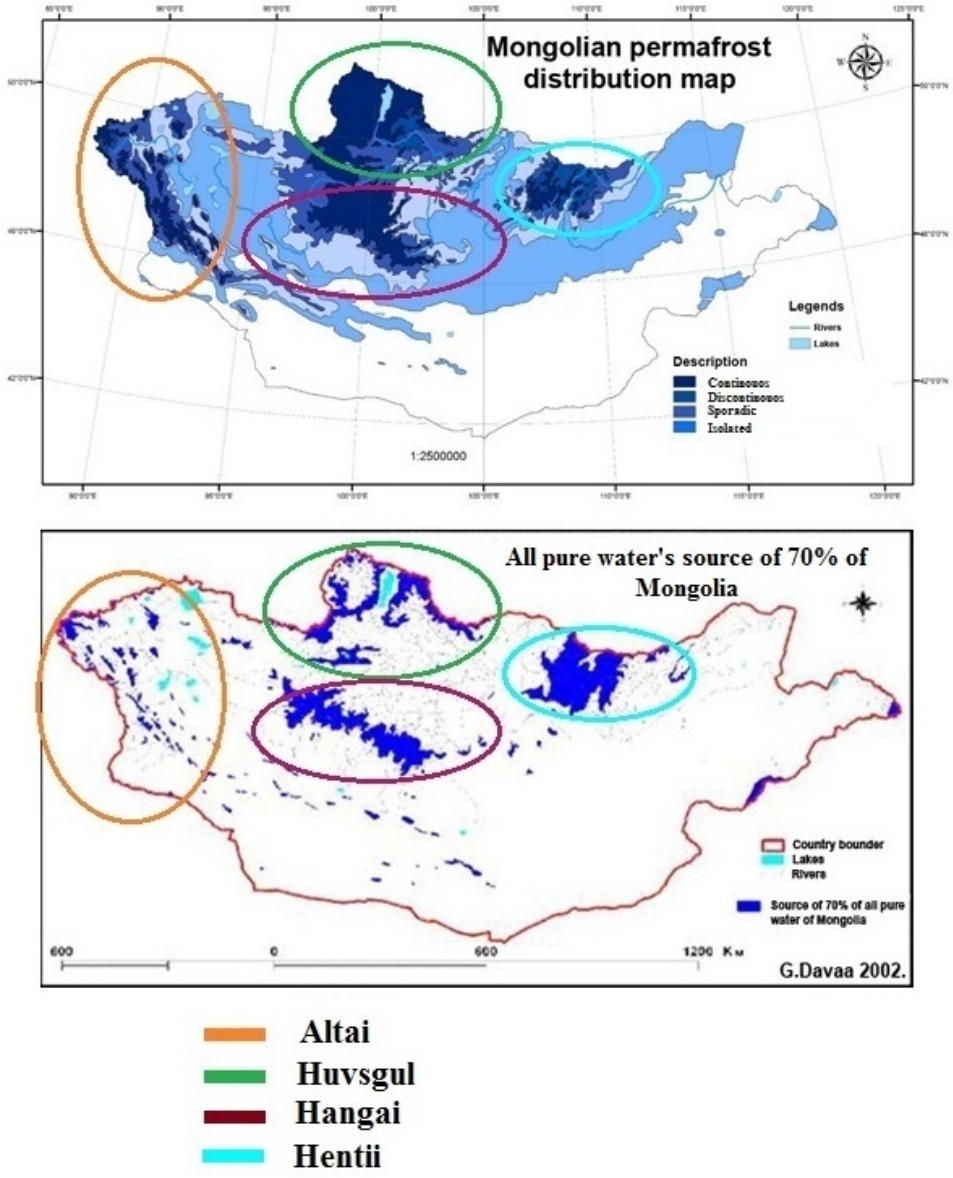

Figure 1: Dependence of Mongolian permafrost and water

References

Gravis, G.F. [2001]: Permafrost distribution and some indicators of its past changes in Mongolia. In *International symposium on mountain and arid land permafrost*.

Ministry of Environment [2010]: *Green development and Tourism of Mongolia*. Ministry of Environment, Methodology of Natural Resource Damage Assessment of Mongolia.

Sharkhuu, N. [2003]: Recent changes in the permafrost of Mongolia. In: Phillips, M.; Springman, S.M. and Arenson, L.U.(eds.), *Permafrost: Proceedings of the 8th International Conference on Permafrost, Zürich, Switzerland, 21 – 25 July 2003*, pages 1029–1034. The Netherlands: AA Balkema Publishers, 2003. URL http://research.iarc.uaf.edu/NICOP/DVD/ICOP%202003%20Permafrost/Pdf/Chapter_180.pdf.

Sukhodrovsky, V.L. [2001]: Geomorphologic indicators of permafrost occurrence and degradation in Mongolia. In *International symposium on mountain and arid land permafrost*.

Mapping and inventorying active rock glaciers in northern Tien Shan (China) using satellite SAR interferometry

Xiaowen Wang[1,2], Lin Liu[1], Tonghua Wu[2], Lin Zhao[3], Zhongqin Li[3], & Guoxiang Liu[2]

[1] *Earth System Science Programme, Faculty of Science, The Chinese University of Hong Kong, Hong Kong, China*
[2] *Department of Remote Sensing and Geospatial Information Engineering, Southwest Jiaotong University, Chengdu, China*
[3] *Cold and Arid Regions Environmental and Engineering Research Institute, Chines Academy of Sciences, Lanzhou, China*

Rock glaciers (RGs) are creeping permafrost landforms consisting of mixtures of unconsolidated rock debris and ice. Monitoring the dynamic of RGs is valuable for inferring the distribution of mountain permafrost and understanding the potential effects of ongoing climate changes on such a landform. RGs are widely distributed in high mountains in western China (e.g., Tien Shan, Tibet Plateau, Himalaya). However, little is known about their current activities as they have been ignored for more than 20 years with only a limited number of geomorphologic studies conducted in the 1980s and early 1990s.

Based on ALOS-1 PALSAR images acquired between 2006 and 2011 and the Sentinel-1A images acquired in summer of 2015, we investigated the active RGs in northern Tien Shan in Xinjiang province (China) using the interferometric synthetic aperture radar (InSAR) technique. The PALSAR and Sentinel-1A image series have a shortest temporal span of 46 days and 24 days, respectively, which maintain good interferometric coherence for detecting periglacial slope movements. We stacked interferograms to reduce the effects of topography errors and tropospheric delay.

Based on the InSAR-measured surface displacements, we identified and delineated active RGs with a validation using the optical images from Google Earth. We compiled an inventory of the active RGs with the study area of about 350 km by 90 km (42.75°44.35°N and 83.02°86.87°E). We have found more than 50 active RGs in the eastern part of the study area, which are located between 3070 m and 3760 m, with a mean elevation of about 3494 m. Most of the identified active RGs are tongue-shaped, with a mean length of 892 m and mean width of 239 m. Our results show that the annual motion speed of the active RGs ranges from 10 to 90 cm/year.

Our study demonstrates the use of the satellite SAR interferometry to investigate the dynamics of the RGs, which contributes a good data source for understanding the kinematics, evolution of the RGs at the lower boundary of permafrost distribution. We will also report the time series of surface motion on some typical RGs, obtained using the small baseline subset (SBAS) inversion method. We will use of climate data (e.g., ground and air temperature, precipitation), to interpret the temporal changes of RGs and to assess the relationships of RGs flow with regional climate and local conditions.

Diagnostic and model dependent uncertainty of simulated Tibetan permafrost area

Wenli Wang[1], Annette Rinke[1,2], John C. Moore[1], Xuefeng Cui[1], Duoying Ji[1], Qian Li[3], Ningning Zhang[3], Chenghai Wang[4], Shiqiang Zhang[5], David M. Lawrence[6], A. David McGuire[7], Wenxin Zhang[8], Christine Delire[9], Charles Koven[10], Kazuyuki Saito[11], Andrew MacDougall[12], Eleanor Burke[13], & Bertrand Decharme[9]

[1] *Beijing Normal University, China*
[2] *Alfred Wegener Institute Helmholtz Centre for Polar and Marine Research, Potsdam, Germany*
[3] *Institute of Atmospheric Physics, Chinese Academy of Sciences, Beijing, China*
[4] *School of Atmospheric Sciences, Lanzhou University, Lanzhou, China*
[5] *College of Urban and Environmental Sciences, Northwest University, Xi' an, China*
[6] *NCAR, Boulder, USA*
[7] *U.S. Geological Survey, Alaska Cooperative Fish and Wildlife Research Unit, University of Alaska, Fairbanks, USA*
[8] *Department of Physical Geography and Ecosystem Science, Lund University, Lund, Sweden*
[9] *GAME, Unité mixte de recherche CNRS/Meteo-France, Toulouse cedex, France*
[10] *Lawrence Berkeley National Laboratory, Berkeley, CA, USA*
[11] *Research Institute for Global Change, Japan Agency for Marine-Earth Science and Technology, Yokohama, Kanagawa, Japan*
[12] *School of Earth and Ocean Sciences, University of Victoria, Victoria, BC, Canada*
[13] *Met Office Hadley Centre, Exeter, UK*

We perform a land surface model intercomparison to investigate how the simulation of permafrost area on the Tibetan Plateau (TP) varies among six modern stand-alone land surface models (CLM4.5, CoLM, ISBA, JULES, LPJ-GUESS, UVic) [Wang et al., 2016]. We also examine the variability in the simulated permafrost area and distribution introduced by five different methods of diagnosing permafrost (from modeled monthly ground temperature, mean annual ground and air temperatures, air and surface frost indexes). There is a good agreement (99 to 135×10^4 km^2) between the derived permafrost areas from the two air temperature based diagnostic methods which are also consistent with the observation-based estimate (101×10^4 km^2; figure 1; Wang et al. [2006]). However the uncertainty (1 to 128×10^4 km^2) using the three methods that require the simulation of ground temperature is much greater. Moreover, the simulated permafrost distribution on TP is generally only fair to poor for these three methods (diagnosis of permafrost from monthly, and mean annual ground temperature, and surface frost index), while permafrost distribution using air temperature based methods is generally good. We used the most commonly applied threshold of each method, based on the empirical findings from previous studies, but changing the thresholds does not change the conclusions.

Model evaluation at field sites highlights specific problems in process simulations likely related to soil texture specification, vegetation and snow cover. Both the type and coverage of simulated vegetation differs greatly from the field sites. The most noticeable ground temperature discrepancies among the six models are the underestimation of soil temperature by LPJ-GUESS and the overestimation of soil temperature by UVic, which lead to the largest biases in simulated permafrost area. To help elucidate the causes of ground temperature discrepancies associated with soil processes we also inspect snow depth and vertical ground temperature gradients. The soil in LPJ-GUESS tends to have a high water retention capacity probably due to the clay-like soil texture specified for the TP as for the Arctic, producing a larger soil thermal conductivity in winter and greatly underestimating soil temperature in summer. A strong sublimation removes the snow in UVic and the subsequent large absorption of short wave radiation due to low albedo greatly increases the simulated ground temperature, leading to the absence of permafrost on TP. In addition, we point out the difference in

the simulated snow insulation effect for thinner and thicker snow. E.g., ISBA and JULES generally show the cooling effect of snow thinner than 4 cm in contrast to the warming effect of thicker snow. As the snow is generally rather thin on TP, the weak snow insulation effect is a unique feature and captured by the models but with different strength.

Models are particularly poor at simulating permafrost distribution using the definition that soil temperature remains at or below 0 °C for 24 consecutive months, which requires reliable simulation of both mean annual ground temperatures and seasonal cycle, and hence is relatively demanding. Although models can produce better permafrost maps using mean annual ground temperature and surface frost index, analysis of simulated soil temperature profiles reveals substantial biases. The current generation of land surface models need to reduce biases in the simulated soil temperature profiles before reliable contemporary permafrost maps and predictions of changes in permafrost distribution can be made for the Tibetan Plateau.

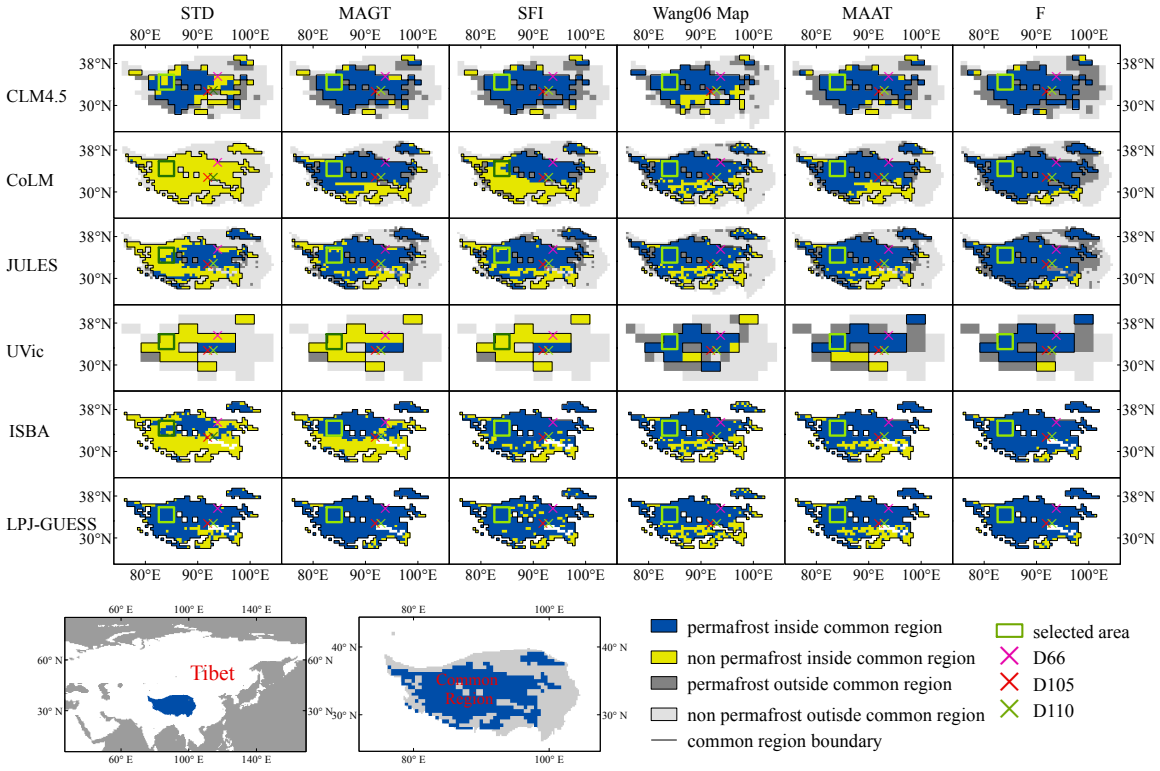

Figure 1: Permafrost maps derived from different diagnostic methods and models compared with Wang06 map.

References

Wang, T.; Wang, N.L. and Li, S.X. [2006]: Map of the glaciers, frozen ground and desert in China. 1: 4,000,000 (in Chinese), Chinese Map Press, Beijing, China.

Wang, W.; Rinke, A.; Moore, J. C.; Cui, X.; Ji, D.; Li, Q.; Zhang, N.; Wang, C.; Zhang, S.; Lawrence, D. M.; McGuire, A. D.; Zhang, W.; Delire, C.; Koven, C.; Saito, K.; MacDougall, A.; Burke, E. and Decharme, B. [2016]: Diagnostic and model dependent uncertainty of simulated Tibetan permafrost area. *The Cryosphere*, 10(1):287–306, doi:10.5194/tc-10-287-2016.

Comparison of climate and permafrost relations during recent years in mid-latitude alpine regions

Tonghua Wu, Lin Zhao, Ren Li, & Changwei Xie

Cold and Arid Regions Environmental and Engineering Research Institute, Chinese Academy of Sciences, People's Republic of China

The links between climate and permafrost were well documented in lots of previous literature. However, the responding mechanism of permafrost to climate change and the feedback of permafrost changes on the climate system were still kept poorly understood until now, especially in the mid-latitude alpine regions such as the Qinghai-Tibet Plateau, the Loess Plateau in China, and the Mongolian Plateau. Three typical permafrost sites in above-mentioned three plateaus were selected to perform the comparison analysis. The related meteorological elements and ground temperatures at different levels were continuously measured over the period 2008-2013. The difference of the impacts of climate on the permafrost was demonstrated in details in this study. The surface offset, the thermal offset, and the air and ground surface freezing/thawing indices were calculated according to the observation data. The possible impacting mechanism of climate conditions on the ground thermal regimes were quantified and compared. This study will enhance our understanding on the response of permafrost to recent climate changes across the mid-latitude alpine regions. The strengthened observations at those sites were suggested in the following work.

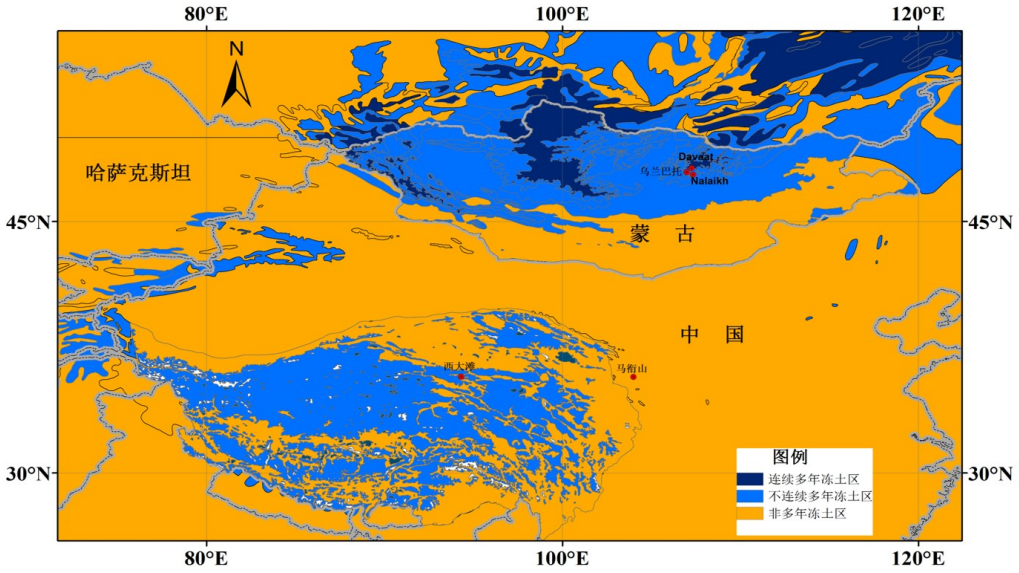

Figure 1: The location of the three study sites in mid-latitude alpine regions

Evolutionary history and environmental information of permafrost on Mahan Mountain, Chinese Loess Plateau

Changwei Xie

Cold and Arid Regions Environmental and Engineering Research Institute (CAREERI) of the Chinese Academy of Sciences (CAS, People's Republic of China

Mahan Mountain is located approximately 40 km south of Lanzhou City and is the highest point on the Chinese Loess Plateau. The climate of Mahan Mountain is sub-humid and cold despite being located in the expansive, arid Chinese Loess Plateau. Since May 2009, meteorological data on Mahan Mountain have been collected continuously by automatic meteorological stations, which record an average air temperature of -1.4 °C, and the area experienced negative temperatures for up to 7 months of the year. The mean ground surface temperature was 0.2 °C for the period from 26 May 2009 to 26 May 2011, and the annual precipitation was approximately 510-550 mm. The monitoring data indicate that approximately two months (from mid-June to mid-August) lack snowfall and the total annual snowfall is approximately 60-80 mm (water equivalent).

The Mt. Mahan is the only region in China's Loess Plateau where permafrost still exists. In 1985, permafrost on Mahan Mountain was first discovered in fractured bedrock in a stone mining area. From 1991 to 1993, permafrost was found in six locations, and the permafrost remains in a very fragile and sensitive state. In August 2008, two boreholes were drilled in Xiaohutan. Borehole #1 (28.5 m deep, orifice elevation 3565 m a.s.l) is located close to an old borehole drilled in 1992. Borehole #2 (16 m deep, orifice elevation 3564 m a.s.l.) is located on the edge of the permafrost area. Ice-rich permafrost was found in both boreholes at a depth of approximately 1.1-1.2 m, beneath the peat layer and the fine-grained soil. The ice is mainly located at a depth of 1.2-3.5 m below the surface, and the ice volume changes significantly with depth. The ice concentration exceeds 70 % between the depths of 1.2 and 1.9 m and contains ice lenses of 5.0-10.0 cm thickness. Gray silty particles were apparent in suspension within these ice lenses, approximately 3-7 % by volume. Ice-rich interbedded clayey gravel was found below 1.9 m and extending to 3.5 m, and the ice volume for this layer is approximately 30 % ice concentration with 0.2-2.0 cm ice lenses. The ice concentration decreases with depth and there are no visible ice lenses in the permafrost at depths lower than 9.5 m. Since December 2008, hydrothermal conditions of the active layer, ground temperature (since 26 May 2009) were continuously monitored. The lowest ground temperature of the permafrost is only -0.2 °C t the depths between 10 m and 16 m, increasing upward and downward with a gradient about ±0.01 °C/ m.

Based on the permafrost features and radiocarbon dating results of peat material, this study indicates that permafrost on Mountain Mahan has experienced several warm periods since it was formed at 3.0 ka BP, including some warming periods that are comparable to the modern warm period. The present conditions and evolutionary history of permafrost on Mountain Mahan indicates that given the current and projected environmental conditions, sensitive high-temperature permafrost will not disappear as quickly as expected. This discovery also indicates that permafrost degradation is a complex process and our understanding of this process is incomplete.

Figure 1: Surface morphology of the permafrost regions and mornitoring instruments.

Monitoring and modeling the thermal state of permafrost on the Tibetan Plateau

Lin Zhao, Yu Sheng, Qiangqiang Pang, Changwei Xie, Tonghua Wu, & Yongping Qiao

Cold and Arid Regions Environmental and Engineering Research Institute, China, People's Republic of

Permafrost occupies more than half the territory of the Tibetan Plateau (TP). To evaluate the status and changes of permafrost and its influences on water cycles, ecosystems, climate and infrastructures on TP, monitoring networks on permafrost and its influencing factors have been gradually established since 1960s, and were greatly improved after 2000. It includes more than 140 ground temperatures (GTs) monitoring boreholes equipped with thermistors chains to measure GTs once a year manually, and part of them connected with dataloggers to record GTs at 2-hour interval, more than 19 active layer profiles equipped with thermistor chains, moisture content sensors and soil heat flux plates connected to dataloggers, 10 automatic meteorological stations equipped with sensors of air temperature and humidity, wind speed and direction, both downward and upward radiation of short and longwave, precipitation, etc. The monitoring sites were set up along 3 main trans-sections from north to south along 3 main highways going across the hinter highland of TP. The monitoring network covers the whole main highland of the permafrost regions in TP. A new map on the thermal state of permafrost in TP were compiled based on the monitoring data. It showed that the thermal state of permafrost was well correlated with elevation, and regulated by annual precipitation, local geological, geomorphological and hydrological conditions through heat exchanges between ground and atmosphere. Generally, permafrost is well developed, and GTs is relatively lower in regions with higher precipitation, wetter surface layer soils as these regions are located at the same elevation and/or are with the same air temperatures. Depths of zero annual amplitude (DZAAs) were well correlated with GTs. Higher in GTs, shallower in DZAAs in permafrost regions, but deeper in non-permafrost regions. It means that the influencing depths of seasonal air temperature variation are smaller in permafrost regions with higher GTs, but higher in non-permafrost regions. Modeling results revealed that the penetrating depth of surface soil heat flux was shallower in regions with higher permafrost temperatures, but was becoming deeper in permafrost-free regions as GTs increasing. It was said that the buffer layer effect of the ground from ground surface to DZAAs to protect permafrost temperature increasing might become more effective accompanied with air temperature increasing, and the upwards ground heat flux below permafrost base might play more significant role in permafrost temperature increasing in warm permafrost regions.

SESSION 26

Frozen Ground Engineering

Convener:

Ma Wei, *State Key Laboratory of Frozen Soil Engineering, Cold and Arid Regions Environmental and Engineering Research Institute, Chinese Academy of Sciences, China*

Guy Dore, *Laval University, Canada*

Yanhu Mu, *State Key Laboratory of Frozen Soil Engineering, Cold and Arid Regions Environmental and Engineering Research Institute, Chinese Academy of Sciences, China*

In recent decades, socio-economic development has brought extensive man-made infrastructure expansion (residential, commercial and municipal buildings, roads, airfields, oil and gas pipelines and power transmission line networks) within vast areas of permafrost and seasonally frozen ground. Engineering design, construction and maintenance in areas impacted by frozen ground are beset with unique problems not encountered in temperate areas. How to cost-effectively and environmentally-friendly design, construct and maintain engineered infrastructures in and/or on frozen ground is a great challenge, in particular in the actual context of climate warming. Adaptive solutions and engineering methods have to be applied with increase care and meticulous planning.

In recent years, some major transportation networks, for instance, the Qinghai-Tibet Railway crossing large areas of high-altitude permafrost, and the Harbin-Dalian High-Speed Railway crossing large areas of deep seasonally frozen ground in Northeast China, have greatly promoted the research and practice of frozen ground engineering. Experiences and lessons learned from these engineering projects will be of great value for other similar engineering practices in areas of permafrost and seasonally frozen ground. In the near future, there are still lots of proposed major engineering projects located in and/or crossing these areas, such as the proposed railway from Moscow to Beijing, expressway crossing the Qinghai-Tibet Plateau, and the pending Xinjiang-Pakistan fast transportation corridor. Also, there will be lots of engineering construction in the Arctic and Subarctic regions such as the Denali Project (Arctic Gas Line) and China-Russia oil and gas pipelines, and infrastructure expansion and maintenance for northern communities. With the update of engineering grade, what we need to do on frozen ground engineering become more complicated and time- and cost-constrained.

In this session, we intend to invite contributions related to engineering behaviors of frozen soils (e.g., strength, creep, frost heave and thaw consolidation), hydrothermal interactions between the engineered infrastructures and permafrost environment, design and construction methods, engineering problems and hazards, adaptation strategy and solutions, and computer modeling and prediction of both thermal and mechanical performances of frozen ground engineering. Case studies are particular welcomed and encouraged.

Improving the methodology for characterizing permafrost terrain for engineering

Kevin Bjella[1], Jerry Johnson[2], Yuri Shur[2], Mikhail Kanevskiy[2], John Best[2], Paul Duvoy[2], & Ken Hinkel[3]

[1] *Cold Regions Research and Engineering Laboratory - Fairbanks, Alaska, USA*
[2] *University of Alaska – Fairbanks, USA*
[3] *University of Cincinnati, USA*

Ground ice content and lithology are key parameters governing the construction of vertical and horizontal infrastructure on permafrost terrain. A detailed knowledge of the spatial distribution of ground ice is especially crucial in determining initial design parameters, sensitivity to thawing, the amount of thaw-settlement likely to occur, and the vulnerability to climate warming. Drilling is the standard for permafrost characterization as it allows for the unambiguous identification of ground ice, the detailed measurement of the moisture content, and the assessment of soil bearing strength. However it is costly, where for government projects in Alaska, USA, drilling costs between 3000 and 5000 USD per borehole. Geophysical techniques have been used to survey permafrost terrain for many decades. Methods such as earth resistivity tomography (ERT) and ground penetrating radar (GPR), are particularly useful for mapping ice-rich vs. ice-poor, frozen vs. thawed, and for imaging ice saturated horizons [Kneisel et al., 2008]. Unfortunately these techniques are underutilized within the context of a frozen ground engineering characterization, therefore the benefits of an optimized geophysical survey in concert with the drilling campaign, are not fully realized, resulting in overly conservative designs. We will report on work being conducted to optimize the frozen ground engineering characterization process, with the goal of increasing the resolution of the ground ice heterogeneity, increasing the information available to promote the next generation of permafrost foundation methodology, decrease the costs of constructing on these terrains, and promote foundation designs which are cost effectively robust in light of current climate warming.

One particular aspect of this study is the appropriate borehole spacing and vertical sampling frequency. The objective is to determine the level of drilling effort and geophysical surveys required to adequately, yet efficiently, characterize the permafrost engineering properties of a proposed infrastructure site. To accomplish this we drilled and acquired ERT over two transects in very different Interior Alaska, warm permafrost terrains. The first transect, located on University of Alaska-Fairbanks property and adjacent to the Cold Climate Housing Research Center (CCHRC), we drilled every 3 m over 100 m, and vertically sampled every 30 cm. The sediments are primarily sands to silty-sands, with peaty slough deposits and Holocene ice wedges. These overlay sandy gravel at an average depth of 6 m to 8 m. The preliminary results of this transect provided guidance for the second transect, located at the Cold Regions Research and Engineering Laboratory (CRREL) Permafrost Tunnel facility, where we drilled every 6 m over 100 m, and vertically sampled every 30 cm. The sediments at the second location are primarily Holocene ice-poor silts overlying ice-rich Pleistocene silts with massive wedge ice (yedoma).

Using the borehole core analysis, we optimize the use of borehole data with a Bayesian Gaussian Process model. Bayesian analysis is a branch of statistics that is based on Bayes' Rule, a theorem of probability, allowing for the integration of prior information about the probability of an event into a statistical analysis. A Gaussian process is a semi-parametric model for fitting a surface (or curve) to data [Gelman et al., 2014]. This type of model fits a Gaussian (normal) distribution to every point along the surface. The overall shape of the surface is not restricted in this model, and so is primarily informed by the data, including points that we don't have direct covariate measurements for (that is, observations of discrete or continuous predictor variables), allowing it to be used for prediction. In this case, we use the spatial dependence of the variation of conditions between measured points to predict new locations. We expect that points that are close together will be more similar than those farther apart.

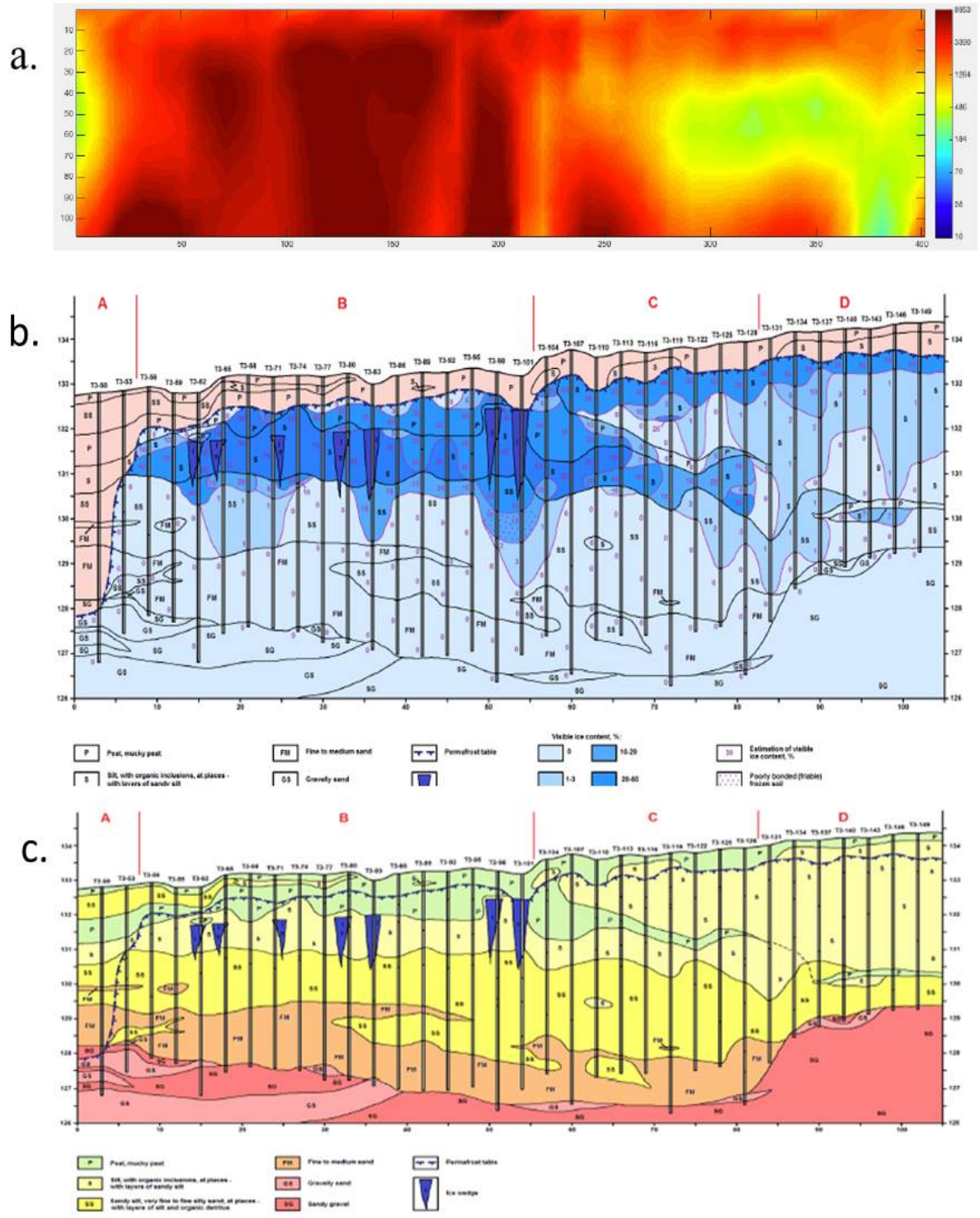

Figure 1: CCHRC intensive drilling transect. (a) resistivity profile along the track of borehole locations (b) borehole core analysis derived subsurface permafrost map and (c) soil conditions from interpretation of borehole core analysis.

In order to predict soil types (a categorical variable), we fit a surface representing the log-odds of a given soil type being present at any given location. Log odds are the logarithm of the ratio of the probability that an event occurs to the probability that an event does not occur. For example, the log odds of an event B is:

$$logit(P(B)) = log(P(B)/(1 - P(B)))$$

Log odds are a way of expressing probabilities that makes it easier to incorporate new data. The borehole

core analysis data provides the physical information about ground ice conditions and is used to improve the correlation between ground resistivity and subsurface conditions at the specific location of interest.

To perform the optimal site characterization, coarse resolution information about a site is initially obtained by expert opinion, both site-specific surface inferences and more generally from the literature. This information is input together with the first level geophysical survey(s). Initial borehole drilling locations are keyed to the highlights of the geophysical surveys, such as locations to verify inferred ice-rich vs. ice-poor vs. thawed conditions, and also at locations to verify suspected lithological changes and possible cryo-feature locations. The correlation then between the measured data of the permafrost and the ground resistivity is an additional Bayesian inference used to define the systematic borehole spacing and sampling depth for the remaining drilling which will adequately characterize the site and fully inform the design phase of the project. Further geophysical surveys may also be warranted based on the size and complexity of the site, and the size and use of the infrastructure.

References

Gelman, A.; Carlin, J.B.; Stern, H.S.; Dunson, D.B.; Vehtari, A. and Rubin, D.B. [2014]: Gaussian Process Models. In *Bayesian Data Analysis 3rd Edition*, chapter 21. CRC Press, ISBN 9781439840955.

Kneisel, C.; Hauck, C.; Fortier, R. and Moorman, B. [2008]: Advances in geophysical methods for permafrost investigations. *Permafrost and Periglacial Processes*, 19(2):157–178, 2008. doi:10.1002/ppp.616.

An experimental investigation of the mechanical behavior of frozen loess

Cong Cai

State Key Laboratory of Frozen Soil Engineering, Cold and Arid Regions Environmental and Engineering Research Institute, Chinese Academy of Sciences, People's Republic of China

Frozen soil consists of four phases, i.e., solid particles, ice, unfrozen water and air. It is extremely important to understand the strength and deformation properties of frozen soil under different stress paths for cold region engineering construction and maintenance. Previous research achievements show that the change mechanism of strength and deformation of frozen soil are more complicate than the thawed soil due to the complexity of the fabric. On one hand, frozen soil is sensitive to strain rate owing to the presence of ice. On the other hand, the development of strength, stiffness and deformation of frozen soil is affected by crushing and pressure melting of the ice under loading. Scholars have made great achievements on strength and deformation of frozen soil through the results of mechanical experiments of frozen soil under different test conditions, including temperature, pressure, stress level and strain rates. However, most of these studies are based on simple uniaxial compression or triaxial shear tests, and comparisons between test results under different stress paths are few. In order to investigate the mechanical characteristics of frozen Lanzhou loess, three kinds of laboratory tests were carried out at -6 °C namely, constant-confining pressure triaxial compression tests, isotropic compression tests, and constant-slope stress path tests. Further, experiments under different strain rates (10-6 10-2/s) and different confining pressure (0 2MPa) were also performed. Experimental results illustrate that the frozen Lanzhou loess exhibit a positive strain rate sensitivity and reinforcing effect under low confining pressure and the volumetric strain of frozen loess follows the law of first contraction and then dilatancy. In addition, this article studied the mechanical properties of frozen Lanzhou loess under different stress paths, strain rate and confining pressure systematically. Multivariable empirical formulas of stress-strain-time were proposed, which will provide important test parameters for establishing the rate-dependent constitutive model of frozen Lanzhou loess.

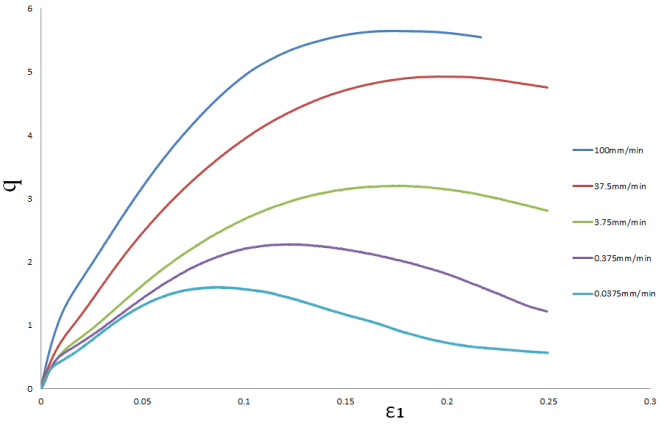

Figure 1

Influence of precipitation on the permafrost in the Fenghuo Mountain Region of Qinghai-Tibet Plateau

Hancheng Cai[1,2], ZhiWen Xiong[1,2], Lan Jin[1,2], Yong Li[1,2], Fen Li[1,2], Longwu Han[1,2], & Lu Rong[1,3]

[1]*Northwest Research Institute Co., Ltd of China Railway Engineering Corporation, The People's Republic of China*
[2]*Qinghai Province Key Laboratory of Permafrost and Environmental Engineering, The People's Republic of China*
[3]*School of Civil Engineering, Lanzhou Jiaotong University, The People's Republic of China*

The annual precipitation (AP) on the Qinghai-Tibet Plateau(QTP) is 482.8mm/a, most of which is concentrated in the warm seasons (from May to October) and there is little in the cold seasons. The stable snow cover is hard to form all year around. From the 1990s, the AP from the four weather stations in the permafrost region of QTP shows a significant increase. The average value of AP is 296.9mm/a from 1976 to 1980, while from 1996 to 2010, it climbs up to 373.5mm/a. Precipitation is one of the important factors that influences the permafrost condition for its characteristics and variation make a huge difference. This research is based on the data of the mean annual air temperature (MAAT), the mean annual ground surface temperature (MAST), AP and the permafrost temperature from 1976 to 2014 collected at Fenghuo Mountain Permafrost Observational Station (N34'43,E52'92,4765m asl,AMAT-6.1 °C. We smooth the curves of MAAT, MAST and AP by the Savitzky-Golay method, and we obtain a binary linear regression equation of the relationship among MAAT and AP and MAST using the Binary Linear Regression Analysis. Based on work above, we analysis the changing regularity and the interaction among MAAT, MAST, MAP and permafrost temperature, it turns out that: (1) In the Fenghuo Mountain region of the QTP, the precipitation during the cold seasons has a relatively weak insulation effect on the permafrost; while in warm seasons, it has a relatively strong cooling effect. In general, the precipitation cools the permafrost thus it acts as a protection. (2) Under the influence of the rising MAAT and MAST, the temperature of permafrost in the Fenghuo Mountain region of the QTP is increasing accordingly, thus the permafrost is degrading. But the increase of the precipitation can lower the surface temperature and reduce the heat transmitting to the underlying permafrost, which helps to slow down the increasing rate of the permafrost temperature, so that it serves as a remission of the permafrost degradation.

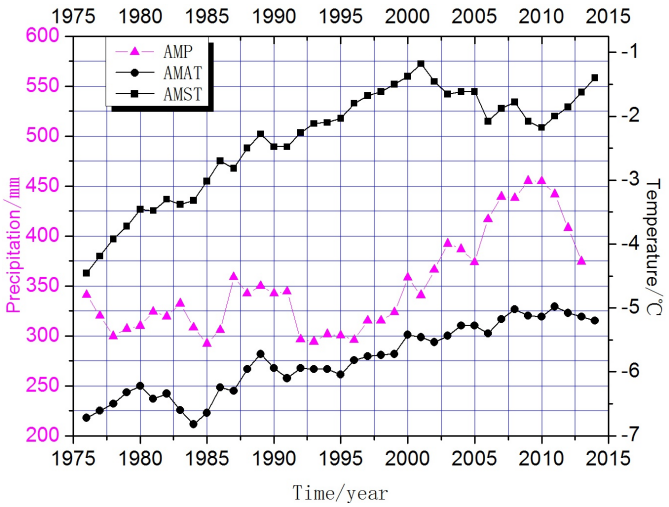

Figure 1: Curves of annual mean air temperature, annual mean land surface temperature and annual mean precipitation in FengHuo Mountain region of Tibetan plateau processed by the Savitzky-Golay method (1976-2014)

Large-scale direct shear testing of compacted frozen soil under freezing conditions

Earl Marvin De Guzman[1], Marolo Alfaro[1], Lukas Arenson[2], & Guy Doré[3]

[1] *University of Manitoba, Canada*
[2] *BGC Engineering Inc.*
[3] *Université Laval*

Embankments in the Arctic are usually constructed during winter conditions to preserve the permafrost foundation and minimize environmental impacts; however, there is limited understanding as to how frozen soils compacted during winter conditions behave and how it impacts the overall performance of the embankment. The fill material of such embankments is dominated by fine till that includes ground ice. Fills are very difficult to compact at sub-zero temperatures when ice is present. They are relatively strong while they remain frozen but they become soft and compressible after thawing. A series of direct shear tests were conducted on laboratory-prepared frozen soil to determine its shear strength properties using a large-scale direct shear equipment. The direct shear box has a diameter of 590 mm and height of 600 mm. Soil used for the testing program was taken from a borrow source for the embankment fill material of the Inuvik-Tuktoyaktuk Highway, Northwest Territories, Canada. Compaction testing was done for frozen soils prepared in the laboratory at different moisture contents to determine the optimum dry density. Dry soil was prepared passing 3/4" sieve size and matched with the gradation of soil samples taken from the embankment during construction of the highway. Frozen soils were compacted at -10 C and showed that the dry density linearly decreases with increased moisture contents. The optimum dry density commonly observed for compaction at normal room conditions was not observed for the compaction tests at -10 C. The workability during compaction also decreases as the water content of the frozen soil increases. Water content selected for soils prepared in the laboratory was taken from the average water content recorded from samples obtained in the field. The density of the soil considering the dry density and water content from the compaction curve at -10 °C was used to determine the amount of frozen soil required to fill the volume of the direct shear box. Normal pressures of 25, 50, and 100 kPa were selected corresponding to the pressures expected in the field. Tests were conducted in an environmental chamber at a constant temperature of -10 °C. Test temperature was selected based on the ground temperatures recorded from the field. Horizontal and vertical displacements, applied normal pressures, and horizontal loads were recorded throughout the duration of tests. Figure 1 shows a typical set-up for the direct shear test in an environmental chamber. This paper presents the preliminary results of a testing program to understand the behaviour of embankments with frozen soils compacted under freezing conditions. Properties obtained from different testing conditions will ultimately be used in numerical modelling to assess the behaviour of embankments constructed in Arctic regions and to develop mitigation strategies.

Figure 1: Typical direct shear test set-up in an environmental chamber

Framework for the prediction of the hydraulic conductivity and of the compressibility of the fine-grained thawed permafrost

Simon Dumais & Jean-Marie Konrad

Department of civil engineering, Université Laval, Canada

Consolidation of thawing fine-grained permafrost is mainly controlled by the hydraulic conductivity (kT) and by the compressibility of the thawed soil. As the thawing of ice-rich permafrost is a typical large-strain consolidation problem, the properties of the thawing soil are drastically changing throughout the thaw consolidation process. Both the hydraulic conductivity and the compressibility are dependent on the void ratio (e). While constant values can be used in simple thaw consolidation analyses, void ratio dependent hydraulic conductivity and compressibility relationships can yield more precise modelling of the thaw consolidation process when the void ratio variation is important.

The proposed framework is based on a large number of values found in the literature from oedometer testing during which the hydraulic conductivity of the soil was measured at different values of void ratio. This important compendium of literature values constitutes the first contribution of this proposal. The materials tested include intact and reconstituted permafrost and non-permafrost fine-grained soils.

In the proposed framework, the compressibility of the soil is characterized by a linear e-logσ'v relationship with a slope defined as the compressibility index of the thawed soil (CcT), with σ'v being the vertical effective stress. It is demonstrated that the compressibility index can be predicted from the liquid limit (wL) of the thawed soil. The hydraulic conductivity of the thawed soil is characterized by a linear e-logkT relationship. This relationship can be predicted from the grain size distribution of the soil. The proposed framework is unified in a combined logσ'v- e- log kT representation. The unified framework is defined with respect to a reference value of hydraulic conductivity defined at a reference void ratio for a reference value of effective stress. While the main focus and contribution of the framework is to provide input data for thaw consolidation analyses, the proposed relationships can also be used in other permafrost related studies such as seepage analysis, consolidation of dredged materials and slope stability analysis.

From the proposed logσ'v- e- logkT prediction framework, values of coefficient of consolidation (Cv) are also derived. The coefficient of consolidation is the primary input in Terzaghi's theory of consolidation and a key parameter in Morgenstern and Nixon's theory of thaw consolidation. This last contribution represents an innovative and efficient alternative to complex laboratory testing required in most thaw consolidation analysis.

Computer simulation of permafrost soil thermal regime under the thermal influence of engineering constructions

Vladimir Gordiychuk & Igor Gishkeluk

Simmakers Ltd., Belarus

The problem of permafrost soil stability under thermal influence of various constructions is well known. Various basement/foundation deformations are the result of land surface subsidence and heave due to the respective thawing and freezing of underlying moist permafrost soils. These processes could cause serious damage to constructions. In order to predict basement/foundation deformations computer simulation can be applied.

Computer simulation of permafrost thermal regime requires numerical solution of heat equation considering phase transition ("ice-water"). There is a number of numerical methods available for solving the nonlinear heat equation, however, they have some limitations. Simulation of thermal interaction between the construction and permafrost ground is complicated with the fact, that in order to achieve required accuracy it is necessary to perform discretization of computational domain with the fine mesh. The large quantity of cells (multi-million) in the computational domain is necessary because of:

1. large-scale computational domain requires a large quantity of cells to provide accurate discretization;
2. cell size increasing is restricted due to small size of the objects that are presented in the computational domain;
3. a dynamic phase front requires a more refined mesh around the phase transition boundary, otherwise severe error increase will take place.

Solving a nonlinear heat equation for large sites (computational meshes) is a difficult memory- and time-consuming computational problem. As a result, existing thermal simulation methods require an unaffordable amount of time (such models would take some days or moths to process on common PCs).

A new numerical method, satisfying all the above requirements, for solving Stefan problem in permafrost soils was developed and has a high degree of parallelization. This method is implemented in Frost 3D Universal software package, which can be used for computer simulation of permafrost soil thermal regimes under the thermal influence of pipelines, production wells, hydraulic constructions etc., taking into account the thermal stabilization of the ground. The key advantage of Frost 3D Universal is the ability of three-dimensional computer simulation of large-scale problems (regions with linear sizes of kilometers, multi-million cell mesh) and non-liner thermal processes for long time periods (many years) spending a reasonable computation time (about several hours) on a common personal computers.

Thermal state dynamics of permafrost basement on engineering objects in cryolithozone of Russia

Valery I. Grebenets[1], Dmitry A. Streletskiy[2], Nikolai I. Shiklomanov[2], Aliguoshad G. Kerimov[3], Ekaterina A. Ostroumova[1], Yury V. Konovalov[1], & Fyodor D. Andruschenko[1]

[1] *Lomonosov Moscow State University, Moscow, Russian Federation*
[2] *George Washington University, Washington, USA*
[3] *Engineering Scientific Company "Ecofoundations", Norilsk, Russia*

Large industrial centers on permafrost are characterized by a set of geocryological conditions different from natural environment. Thermal state of foundations on permafrost in areas of economic development depends on climate trends and upon technogenic impacts, such as type of impact, area of facility, permafrost temperature and duration of the technogenic pressure. Technogenic degradation of permafrost is evident in most urban centers on permafrost leading to deterioration of geotechnical environment and particularly foundations of buildings and structures. This situation is exacerbated by climate warming in such cities as Vorkuta, Chita, Nerungry, Salekhard and others where temperature rises at a rate of 0.4 – 1.2 °C/decade over the last 40 years. Using the method of spatial modeling, we calculated [Streletskiy et al., 2012] changes in bearing capacity of typical piles in the northern part of Western Siberia for the foundations of structures built based on the principle I with the conservation of the frozen state of the ground during construction for the entire period of the operation. Calculations showed that warmer climate of 1990–2010, in comparison with the 1960–1990 climatic norm, led to a decrease in the bearing capacity of the foundations of buildings and structures by 17 % in the region on average and in some areas – by up to 45 %.

To evaluate impact of climate change and technogenic factors on permafrost temperature regime and foundation bearing capacity we compared several objects in Norilsk, the largest city on permafrost. The facilities were selected to represent different parts of the town, different ages of built-up environment and were located in different permafrost and lithological conditions. We found a leading role of technogenic factors relative to climatic ones in dynamics of thermal state of permafrost in urban environment. Climate warming in Norilsk (0.15 °C/decade) was a small contributor, but gave an additional input to deterioration of geotechnical environment on permafrost. Analysis of many representative thermal regimes, formed in various frozen ground in urbanized areas, showed the following: almost 70 % of basements are exposed to degradational tendencies, 20 % – to permafrost aggradation, 10 % preserve frozen conditions which already existed before construction (status-quo). At the same time, implementation of engineering solutions of permafrost temperature cooling (such as cold ventilated cellar – the most widespread method of preserving permafrost on basement in cryolithozone) result in lowering of permafrost temperature. Field surveys in Yamburg showed that under some facilities permafrost temperature decreased by 1-1.5 °C over the last 15 years despite pronounced in the region climate warming of 0.5 °C/decade. However, their operation is often associated with various violations: absence of solid water barrier and water removal ducts, leaks in sewage network, lack of vents, and low position in relief, which leads to waterlogging. For example, about 85 % of the surveyed buildings in Dudinka had serious operational violations of ventilated crawl spaces [Grebenets, 2008]. This contributes to the degradation of permafrost soils manifested in the formation of local talik sand zones of soil heating. In addition, under the buildings, the formation of vertically discontinuous permafrost profile often occurs.

Calculations showed that in severe continental climate conditions (for example, in Verkhoyansk, Sakha Republic) even effectively functioning cellars do not maintain permafrost temperature in the course of time (Fig. 1).

Field surveys carried out in northern Siberia during the last 30-40 years showed that the efficiency of steam liquid thermosyphon (seasonal cooling systems – SCS, thermopile is one of the most widespread methods

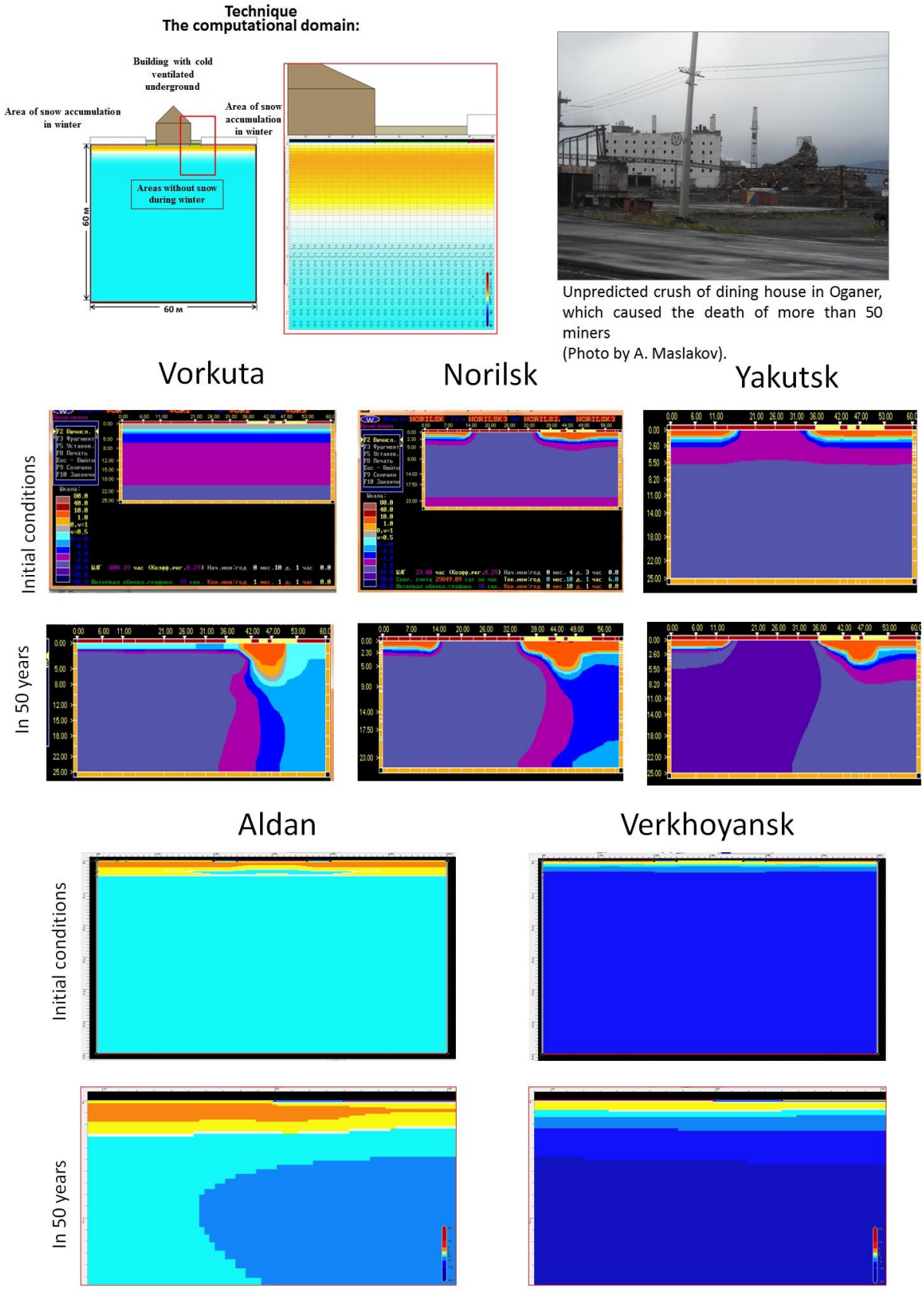

Figure 1: Prognosis of the thermal state of Permafrost in 5 different settlements on permafrost area in 50 years

of base ground freezing and refrigeration) functioning mostly depends on natural permafrost conditions, landscape conditions, climate change and technogenic objects. For example, steamliquid SCS proved to be highly efficient on hydroengineering objects in the Norilsk region, where after application of the method temperature of frozen impervious screen on dams decreased to minus 4-6 °C (due to positive values during construction). In addition, massive pile abutments of car-railway bridge over the Norilskaya river, that thawed in 20 years exploitation, were frozen by deep steam liquid thermosyphon to a frozen bank. As a result, bridge reliability was ensured. At the same time, in the northern part of Western Siberia thousands supports of powerful main pipelines do not ensure the stability of geotechnical systems, although steam liquid SCS are located close to the supports. The reason for it is that cooling systems are located either along the stream flow, or on artificially created during the construction watercourses, or on poorly drainable wetland areas. During the winter season operation of the SCS actually focuses on freezing of flowing surface water, as well as small lakes that appeared close to the supports. Foundation soil do not virtually cool down.

This shows that despite deterioration of permafrost conditions in the most Arctic regions due to technogenic pressure and climate warming, implementation of adequate engineering solutions allows stabilization of permafrost thermal regime.

Acknowledgements

The paper was financed by grant “Leading scientific schools” # NSH-335.2014.5 and Circumpolar Active Layer Monitoring U.S. National Science Foundation grant OPP-0352957.

References

Grebenets, V.I. [2008]: Technocryogenesis controls on the permafrost and geotechnical factors in towns of the permafrost zone. In: Kane, D. and Hinkel, K.(eds.), *Proceedings of the Ninth International Conference on Permafrost*, Institute of Northern Engineering, University of Alaska Fairbanks, Fairbanks, USA, 29 June–3 July 2008, volume 1, pages 541–543. ISBN 978-0-9800179-2-2. URL http://ipa.arcticportal.org/publications/conference-proceedings.

Streletskiy, D.A.; Shiklomanov, N.I. and Grebenets, V.I. [2012]: Change in the bearing capacity of permafrost due to global warming in the North of Western Siberia. *Kriosfera Zemli (Earth Cryosphere)*, 16(1):22–32, (In Russian), URL http://www.izdatgeo.ru/pdf/krio/2012-1/22.pdf.

Towards accurate measurement of soil freezing characteristic curves

Stephan Gruber, Andy Adler, & Hervé Gagnon

Carleton University, Canada

The Freezing Characteristic Curve (FCC) relates the proportion of liquid water in thawing or freezing soil to temperature. Knowledge of FCCs is important for the simulation of frozen soils because it is the basis for expressing apparent heat capacity and hydraulic permeability as a function of temperature. It can be important for the monitoring of infrastructure as it allows interpreting highly accurate temperature measurements within and underneath structures in terms of changing proportions of ice and water in the soil.

The FCC is controlled by the pore size distribution, specific surface area, and the chemical characteristics of particle surfaces and solutes. In the absence of reliable data, FCC parameterizations based on soil water retention curves are often used. The experimental testing of these parameterizations, however, is currently week and a number of open questions remain. It is debated, for instance, whether the liquid water content below 0°C is independent of the saturation level of the soil. Furthermore, it is striking that laboratory measurements of FCCs show stronger hysteretic behavior than measurements in natural conditions, pointing to possible problems with sample thermal equilibration during measurements or to the importance of incorporating hysteretic behavior in simulation tools.

Determining accurate FCCs requires a number of challenges to be addressed. The sample volume needs to large enough to capture the macroscopic behavior of soils and, at the same time, it needs to be small enough to allow fast temperature equilibration. Furthermore, the sample holder needs to accommodate density changes as the measured soil undergoes phase transition.

This poster will show progress in the characterization of a cylindrical sample cell designed to measure dielectric spectra of freezing and thawing, remolded soil while submerged in a temperature-controlled glycol bath.

Crack problems and causes of pavement and embankment in Qinghai-Tibet Plateau Permafrost Regions

Da Hu[1,2], Xin Li[1,2], Fenglei Han[1,2], Weibo Liu[1,2], Yan Lu[1,2], & Wenbing Yu[1]

[1] *State Key Laboratory of Frozen Soil Engineering, Cold and Arid Regions Environmental Research Institute, CAS, Lanzhou 730000, China*
[2] *University of Chinese Academy of Sciences, Beijing 100049, China*

Crack problems of pavement and embankment of Qinghai-Tibet highway are increasingly serious, which has a direct effect on the safety operation of highway. With the sustained and rapid development of modernization, the demand for keeping normal operation of the highway is urgent. Cracks will accelerate rainfall infiltration and exacerbate rates of permafrost thaw beneath the embankment, and eventually lead to thaw settlement. This in turn makes the cracks widen. The Qinghai-Tibet highway (from Golmud to Lhasa) is about 1161 km long and about 960 km of it is located at an altitude above 4000 m. The highest elevation along the highway route is about 5231 m at the Tanggula Pass. 550km of the route overlies continuous permafrost and 82 km is built on island permafrost. The permafrost table is at 0.8-4.8 m depth, although the anthropogenically disturbed permafrost table is much deeper at 2.8-10.0 m under the asphalt pavement.

Through field investigations and measurement, including mileage, embankment heights, road strike, climatic condition, at the typical damage sections, this paper summarize the distribution characteristics of cracks of pavement and embankment in the permafrost regions of Qinghai-Tibet Highway. The field investigations covered from K2968-600 to K3368+500. We measured the width of the cracks in different mileages, and drew the spatial distribution of cracks. Nearly 20 typical sections are measured in total. Field water injection tests of crack infiltration were conducted in the field to investigate the vertical penetrativity of cracks. At the mileage K2980+500 water infiltrates rapidly at a speed of 16.7 ml/s. The biggest crack width reaches to 37 cm at the mileage of K3330 in Tanggula area. The results indicate that most of the longitudinal cracks are located at the south-facing side, near to road shoulder and the running lane of south facing side, and few are in the central line of the embankment. Water infiltrates very fast in the cracks and all the longitudinal cracks are deep, which can stated that the longitudinal cracks are due to the thawing of permafrost foundation at the sections where the embankment height is lower than 3.0 m. Where the height is higher, the longitudinal crack is mainly caused by the instability of slope. Few longitudinal crack distributed at the north-facing side, which mainly caused by the water pond at the foot of slope, formed due to the early dig construction. Most of the transverse cracks and meshy cracks are shallow and just distributed in the asphalt layer. Water infiltration is very slow. Fatigue of materials due to severe temperature changing and heavy traffic load leads to the shallow cracks.

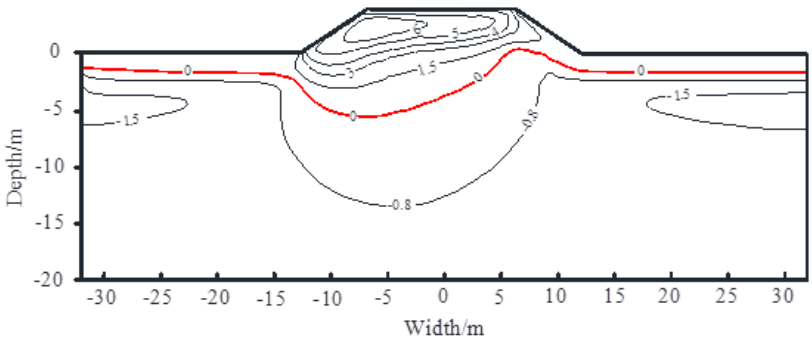

Figure 1: Simulated thermal regime of embankment of Qinghai-Tibet Highway, considering north-facing and south-facing slope effects

In addition, numerical simulations were conducted to analysis the thermal regimes of embankment, considering the effects of north facing and south facing slope. The geometric model of embankment, the strata and boundary conditions are based on the field measurements and drilling at Tibet Plateau. The strike of road is near to N8o E. It has a significant difference of solar radiation. The thermal regime shows a big difference of permafrost table on the north facing slope and the south facing slope. The south face facing slope has warmer temperature and deeper thaw depth, which leads to a difference of bear capacity of the foundation and tensile stress in soil. That is why most of the longitude cracks are near to the south facing side of the embankment.

In practice, heat pipe is adopted to mitigate the longitude cracks near the south facing slope of Qinghai-Tibet Highway. But the effect is not satisfied. Based on results obtained from the research, the following suggestions can be made to mitigate the crack problems of Qinghai-Tibet Highway.

1. To reduce the ground temperature of the south facing slope. Crushed rock revetment is better than heat pipe;
2. to enhance drainage of surface water. Digging near the road foot is strictly prohibited;
3. to improve the pavement materials and control overload of truck.

The thermal influence analysis of The different distances between parallel pipelines on the foundation in permafrost region

Xiaoying Hu[1,2], Yu Sheng[1], Jichun Wu[1], & Jing Li[1]

[1] *State Key Laboratory of Frozen Soil Engineering, Cold and Arid Regions Environmental and Engineering Research Institute Chinese Academy of Sciences, Lanzhou 730000, China*
[2] *University of Chinese Academy of Science, Beijing, 100000, China*

The area amount of permafrost is about 23 % in the word, and distribution area of permafrost accounts for about 21.5 % of China which is the third permafrost owner country. Lots of engineering buildings used permafrost as their foundation in China. And permafrost is a kind of complex and multiphase system composed with solid, ice, unfrozen water and gas, which also will become instability if the temperature increases to make the ice melt, so the stability of these engineering buildings relays on the thermal state of the permafrost underlying.

As a kind of typical permafrost engineering, the operation of oil pipelines with high oil temperature will induce the permafrost temperature to increase and the permafrost to thaw in permafrost regions, result in the bearing capacity and stability of foundation decrease, and even make the pipelines deformation failure. The parallel pipelines are amount to more thermal source considering the extra thermal superposition between the parallel pipelines. So the operation of parallel pipelines will aggravate the thermal effect above. This paper makes the Second Oil Pipeline between Mohe and Daqing in the Northeast of China as background and uses numerical calculation method to simulate the operation of parallel pipelines for 50 years with different distances such as 5m, 10m, 15m and 20m to make analysis of the thermal influences of different distances between parallel pipelines on the permafrost under different calculation circumstances with ice content being 35 % (according to the reconnaissance report). Take into account the complicated geographical environment of this permafrost region and poor engineering geological condition.

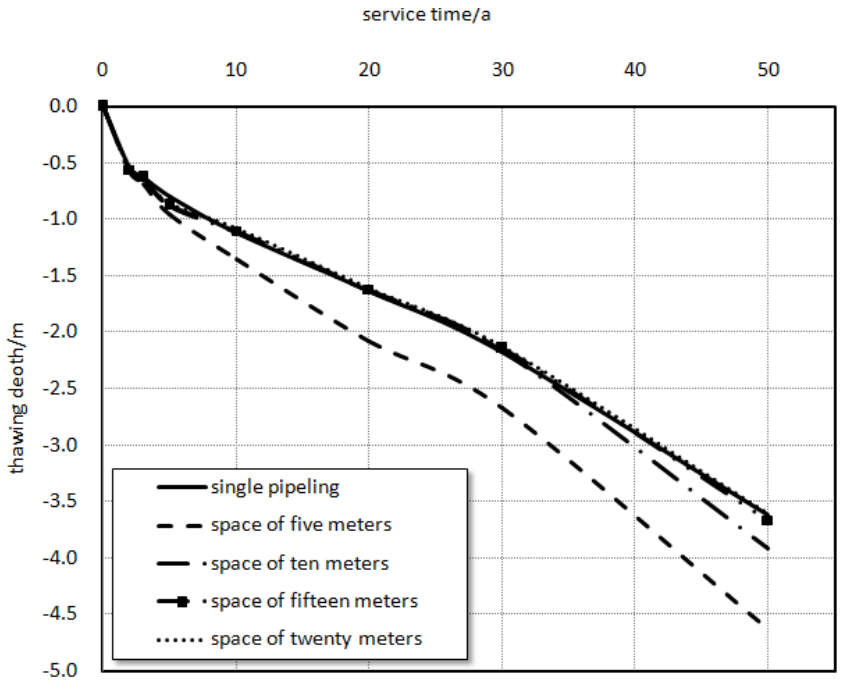

Figure 1: The compare of deferent thawing depths in the permafrost with ice content 35 % of under pipelines with insulation

The process of numerical calculation not only considers the superimposed thermal effects of parallel pipelines but also other different factors such as oil temperature (two different oil sinusoidal variation temperature according to the date measured), the thickness of insulation (three different thickness 0.5 cm, 0.8 cm and 1.2 cm) and average ground temperature (-0.3 °C and -1.2 °C according to the reconnaissance report), at last gets the relationship between the different distances and thermal effects.

Compare the maximum thaw depth under pipelines and the development of thaw cycles between different distances of parallel pipelines and the single pipeline to get some results. The results show that the extent of thermal effect which oil temperature makes on the permafrost is directly influenced by distances of parallel pipelines and values of oil temperature, and the differences of thermal influence are larger as the oil temperature becomes higher and distances decrease. Because higher oil temperature can bring more extra thermal superposition between parallel pipelines and larger distance can separate this thermal effect effectively, moreover, thermal insulation of large distance decreases as time passes. Figure 1 describes the maximum thaw depth under single pipeline and parallel with different distances during the operation time. It shows the insulation material can insulate the thermal effect available, and the thermal influence is inversely proportional to thickness of insulation. In other words, the insulation material is equivalent to decreasing the heat conduction of pipelines. Furthermore, the thermal effect from parallel pipelines increases with the average ground temperature increases. Therefore, the thermal effect of parallel pipelines in cold permafrost is smaller than warm permafrost in which the extra thermal superposition between the parallel pipelines deserves more attention. These regulations above may provide design reference to the route selection of the upcoming Second Oil Pipeline Project in the Northeast of China.

Mitigation techniques to preserve permafrost under transportation infrastructures: Study case of the Alaska Highway, Yukon

Xiangbing Kong[1], Guy Doré[1], Fabrice Calmels[2], & Chantal Lemieux[1]

[1] *Université Laval, Quebec, QC, Canada*
[2] *Northern Climate ExChange, Yukon Research Center – Yukon College, Whitehorse, Yukon, Canada*

Climate records show that climate in Canada is warming, especially in western and north-western Canada. In addition to climate changes, the construction and maintenance of linear infrastructure affect the thermal equilibrium of underlying permafrost, and lead to various negative impacts, especially in ice-rich, warm permafrost regions. Permafrost degradation results in many failures, such as differential settlements, sinkholes and longitudinal cracks, which are often observed along northern roads and airstrip, like the Alaska Highway in Yukon. Degradations are reducing the infrastructure serviceability while increasing risks for users. To maintain the stability of embankment, different mitigation methods have been developed, and several techniques have proved to be effective in cooling permafrost underneath embankment. However, there is a need to develop a decision tool taking into account the context of a specific site in the choice of mitigation technique to be applied in permafrost regions.

The goal of this research project is to determine the field of application for each technique developed, and produce a decision-tree to help select the best method considering the local context and needs. Many factors, such as soil type, mean annual ground temperature, total water content, climate warming, surface features, water seepage, embankment geometry and dimensions, snow cover, meteorological conditions, construction problems, costs of construction and maintenance, will be considered for the selection of mitigation techniques in cold regions. The decision tool will also have to take into account the availability of material and expertise in the selection of a mitigation technique. Based on above factors, but not limited to these, different mitigation techniques will be compared and classified to guide the selection of the most cost-effective method to be applied on specific sites.

To achieve the project goal, the following basic steps will be done:

1. improve the theoretical knowledge of different mitigation techniques;
2. identify the appropriate application conditions for each mitigation technique;
3. optimize the design of selected mitigation technique, using modelling to compare cooling effects of different mitigation techniques;
4. conduct combined feasibility study and cost-effectiveness analysis.

A two-dimensional finite element thermal model will be used to simulate the temperature distribution in the cross section of the road embankment and foundation.

Field sites have been selected to apply mitigation techniques on thaw-sensitive section along Alaska Highway in Yukon. The selected sites have different contexts, but all have discontinuous permafrost with high excess ice contents. These sites all are thaw-sensitive, and some already have shown recurrent settlement, longitudinal cracking and other problems. Preliminary designs for the best cost-effective remediation and mitigation techniques, based on local conditions, have been proposed for each site. Yukon Highways and Public Works is planning to build these large scale application of protection methods. The sites will be instrumented to monitor ground thermal behaviour within and underneath the embankment in order to assess the effectiveness of the method. The proposed presentation will summarize site investigation and the design of the protection techniques.

Evaluation of the Norwegian gradation based regulations for frost susceptibility of aggregates in roads and railways

Elena Kuznetsova[1], Kjell Arne Skoglund[2], Jostein Aksnes[3], Karlis Rieksts[1], & Inge Hoff[1]

[1]*Norwegian University of Science and Technology, Norway*
[2]*SINTEF, Norway*
[3]*Norwegian Public Road Administration, Norway*

Moisture fluctuations in soil and aggregate materials affect the pavement performance in all regions of the world, regardless of climatic conditions. The main difference between building roads and railways in cold and warmer regions is winter freeze-thaw cycles and expansion of the trapped water within the construction material. When pavements are constructed over moist and/or frost susceptible soils in cold and humid environments, granular layers becomes a very important part of the road system. According the Norwegian pavement design guidelines; N200 (2014), for the material to be non-frost susceptible and non-moisture-sensitive, the mass percentage of the material <0.063 mm must not be more that 7 % and of the material <0.02 mm – not more than 3 %, both for the fraction of the material less than 22.4 mm. Based on this the frost susceptibility criteria are divided into four categories T1 to T4, where T1 is non-frost-susceptible. Ballast, base and subbase layers should be non-frost-susceptible (T1); frost protection layers can be slightly frost susceptible (T2). According new regulations for the frost protection layer in road foundations, fines content (<0.063 mm) should be maximum 15 % of the material less than 22.4 mm.

Norwegian road and railway construction practice has changed significantly during the last 40 years due to the replacement of natural gravel by crushed rock materials in the granular layers of the pavements. As a result, the materials in use nowadays are generally coarser than natural gravels. However, the frost susceptibility criteria have not evolved correspondingly. There are several circumstances that need attention:

1. The traditional limitation of not taking into account the material content larger than 22.4 mm still applies. As before, the frost susceptibility is generally calculated on the basis of the content of material less than 0.020 mm from the fraction less than 22.4 mm. For coarse graded material layers in roads and railways this rule is not considered adequate as at least 80 % of the material is normally above 22.4 mm in size. Consequently, coarse graded materials with very small total contents of fines may be rejected. Little evidence has been found to substantiate this regulation; actually, the existing literature points out in the opposite direction. The reasons for only evaluating the fraction less than 22.4 mm have practical basis: limiting the maximum size makes both sampling and analyses easier, with smaller samples and smaller grain sizes.

2. When using the same frost susceptible criteria for new and coarser materials, we cannot be sure anymore that the different frost susceptibility categories (T1-T4) describe the same type and degree of frost problems for the whole range of materials. The new materials may give different problems since these materials were not included when the criterions were made. Specifically, it may be expected that coarse graded T2 materials can cause less frost problems, e.g. in terms of frost heave and thaw weakening, than finer graded T2 materials. The likely reason for this is that a coarse graded T2 material will have less total content of fines than a fine graded T2 material.

The paper will give an overview of main challenges with existing regulations and examples of few case studies for roads and railways. Main goal of the paper is to indicate the challenges with current regulations and indicate the directions, which we should choose to improve current regulations.

Study on the influence of pavement types to temperature transmission characteristics in permafrost regions

Jin-Ping Li

CCCC First Highway Consultants Co., LTD, Xi'an, Shaan Xi, People's Republic of China

In allusion to the problem that thermal stability of subgrade affected by heat absorptivity of black asphalt concrete pavement in plateau permafrost regions, the temperature transmission characteristics of asphalt concrete pavement and cement concrete pavement are discussed by analysis of the observed data and numerical simulation. First, the temperature differences at the upper and lower of pavement structure layer both in asphalt concrete pavement and cement concrete pavement are analyzed based on the temperature monitoring data of pavement structure layer in Qinghai-Tibet plateau permafrost regions. The thermal regime of subgrade under pavement is also analyzed by numerical simulation. The results show that the temperatures conducted to subgrade through asphalt pavement layer are obviously higher than that through cement pavement layer in the same condition, especially in summer. The maximum temperature difference is up to 5 6 °C. The thermal stability of subgrade under two type pavements is obviously different. Especially in high-temperature permafrost regions, the time of forming the thawed core in soil profile under the asphalt pavement is earlier than that under cement pavement.

Effects of using straw mulching as frost damage prevention measure for HSR under construction in deep seasonally frozen soil area in winter time

Zhenping Li[1], Yonghong Niu[2], & Qingsong Mu[1]

[1] *Lanzhou University, People's Republic of China*
[2] *State Key Laboratory of Frozen Soil Engineering, Cold and Arid Regions Environmental and Engineering Research Institute, Chinese Academy of Sciences, Lanzhou 730000, China*

The subgrade preparation for high speed railway construction in deep seasonally frozen soil area, if under given design, the maximum frost-free depth can be ensured by not reaching the water- rich and frost-susceptible natural soil situated below. However, due to various reasons, the subgrade construction may not be completed before winter comes. In the case without any preventive measures, the said frost-susceptible soil will be in frozen status that may cause those completed subgrade portion in deformation or lowered compact level and finally affects the quality of construction work. To prevent the soil beneath the subgrade from frozen, considering local available resources, paving corn stover onto subgrade is an economical and practical measures. This article is to provide engineering parameters on corn stover coverage, by studying the thermal state of the subgrade and use of commercial software.

According to the monitoring data obtained from test section of the Harbin-Dalian high-speed rail, a 2-D numerical calculation model of the completed subgrade thermal field is built by Geo-Studio software, and analyzed by finite element method. Then the feasibility of the model and selected parameters will be verified by comparison with the data obtained. The results proved the temperature from the center line of the subgrade agreed to the data obtained but with deviation for both side edges of the subgrade, which is the results of the snow effect not considered in model but actually bigger thickness of snow on the sewer section. It proves that the selected model and the corresponding parameters can be used to analyze the temperature field of the subgrade under straw mulching condition.

Using the selected model and the corresponding parameters, the thermal conditions of the stover covered subgrade with different filler thickness are calculated and analyzed . It found that, for the subgrade filled with less than 2/3 of design thickness in absence of straw mulch, the maximum frozen depth are likely to enter the natural soil with lower high water content, high rate of frost heave. The next step is to calculate the temperature conditions of the different thickness of straw mulch in the case of the subgrade filled with different filler thickness. Based on the numerical results, it offers the minimum thickness of straw mulch corresponding to different filler thickness. This result has a certain reference value to the practical engineering design.

The performance of direct driven piles in cold permafrost

Torsten Mayrberger[1], Sean Baginski[1], Matt Fenwick[2], & John Cologgi[3]

[1] *PND Engineers, Inc., USA*
[2] *American Piledriving Equipment, Inc., USA*
[3] *ConocoPhillips Alaska, Inc., USA*

The installation of foundation piles in the permafrost soils of Alaska's Arctic has favored using the drill-set-slurry (DSS) method. The DSS process requires drilling an oversized hole, placing and aligning the pile, and backfilling the pile annulus with an imported sand-water slurry. The pile capacity is developed through the frozen adfreeze bond at the pile-slurry interface. The process is labor- and equipment-intensive, requiring multiple personnel and equipment spreads, a slurry plant, and, for cross-country pipelines, the construction of an ice road to support heavy equipment. While direct-driven piles (DDP) are driven through an undersized predrilled pilot-hole and do not utilize a back-fill slurry. The work or energy applied to the in-situ permafrost soil during the driving process causes the soil to thaw at the soil-pile interface. The adfreeze bond or pile capacity is developed as this thawed interface refreezes. Direct-driven pile installation requires less equipment and support. Installation rates are potentially two to three times faster than DSS piles and may only require one equipment and personnel spread. Direct-driven piles can support service loads after 24 hours, while DSS piles may require weeks before service loads can be applied.

Tradition, uncertainty, and the lack of refined driving equipment have perhaps limited the wide range implementation of direct driven piles. However, new equipment and methods have been developed that may provide superior installation efficiency and reduced installation costs. This paper describes two different direct-driven methods:

1. A vibratory method utilizing a vibratory ram driven from a mast mounted rack on an excavator chassis. The energy of the vibrating pile thaws the frozen ground surrounding the pile as it is driven to its design elevation;

2. A rotary-drive method utilizing an excavator-mounted rotary driver. Friction at the pile-native soil interface was developed through rotation and cutting action. The friction developed sufficient heat to cause thaw of the native permafrost soils surrounding the embedded pile surface.

Two separate in-situ testing programs were performed to determine whether, despite great benefits in installation efficiency, the direct-driven piles would perform adequately. The objective of the testing programs was to characterize the long- and short-term adfreeze performance of the direct-driven piles installed into native frozen soils.

Fourteen 32.4 cm (12.75 in.) diameter steel pipe piles were installed in permafrost in the Alaskan Arctic; 8 piles were installed in ice rich sandy silt, 4 piles were installed in a frozen gravel soil, and 2 piles were installed in a layered peat and gravel substrate. Piles were loaded in tension for different durations ranging from 5 days to 7 months at loads varying from 16 metric tons to 68 metric tons. At the completion of long-term testing the test piles were unloaded, rested, and then loaded to failure to characterize the adfreeze short-term strength.

Data was collected continuously using electronic displacement and load transducers, thermistors, and RTDs (resistance temperature detectors). RTDs were mounted into the pile walls to measure installation temperature development and long-term adfreeze temperatures. Testing loads were supplied by compressed bottled nitrogen that delivered pressure to ram-less Freysinett jacks, a bleed-free system requiring no long-term maintenance. Data was analyzed to develop normalized long-term pile velocities and short-term strength as a function of stress and adfreeze temperature. Experimental results were statistically compared to theoretical and empirical performance.

It was shown that both short-term and long-term capacities compared well with drill-set-slurry pile methods and that long-term creep rates were comparable to predicted theoretical creep rates. This same theoretical behavior is used to describe and analyze drill-set-slurry pile behavior. By implication, it could be said that direct-driven piles could perform well and parallel slurry pile behavior.

Design challenges of North America's first major bridge north of the Arctic Circle

Torsten Mayrberger[1], Kenton Braun[1], Jim Brodie[2], & Mike Fitzpatrick[2]

[1] *PND Engineers, Inc., USA*; [2] *ConocoPhillips Alaska, Inc., USA*

The Colville River rises in the remote western Brooks Mountain Range in Alaska's Arctic and empties into the Beaufort Sea, a marginal sea of the Arctic Ocean. The river, which is frozen for more than six months each year and floods in spring, is approximately 560 kilometers long and is one of the northernmost major rivers in North America. The river separates the established oil and gas fields of the eastern Alaskan North Slope from the undeveloped National Petroleum Reserve to the west. In the early 2000s ConocoPhillips Alaska, Inc. sought to develop its holdings in the National Petroleum Reserve west of the Colville River. PND Engineers, Inc. was contracted as the prime civil and structural design engineer to design a series of four permanent bridges to allow ConocoPhillips all-season access to lands west of the Colville. This paper describes PND's engineering design of the largest of the bridges, the Nigliq Bridge, which spans the Nechelik Channel, the largest distributary of the Colville River.

The Nigliq Bridge, after years of planning and design, was completed in winter 2015. The bridge spans approximately 430 meters over the Nechelik Channel with eight spans and seven pier groupings. Each pier grouping consists of five piles – three bridge piles and two ice breaker piles. The ice breaker structure protects the bridge piles from the massive lateral loadings caused by ice floes during spring break-up. Ice floes as large as 2 meters thick and 30 meters in diameter continuously batter the ice breaker structures during the spring break-up. The design lateral ice loads were well in excess of 100 metric tons. The bridge was designed for year-round use to allow passage of heavy oil and gas well service equipment. The design bridge load was approximately 160 metric tons. Installed bridge pier piles were 122 centimeters in diameter and were embedded up to approximately 30 meters below the surface. The bridge is located in an extreme environment and remote location; as such, heavy constraints were put on constructability and the construction timeline. The constructability of the bridge was as influential a design factor as the physical constraints of the permafrost foundation soils, ice floes, and other physical criteria. The design would have to allow the bridge to be constructed during two three-month-long winter construction seasons. The beginning of the construction window was constrained by the need to build an ice road leading out to the project site, as well as time to allow for thickening of the river ice. The river ice required a thickness of over three meters to be able to support construction equipment and processes. At the time of bridge construction no permanent roads led to the project site. All work and equipment transport was dependent on ice roads. The end of the construction window was defined by the beginning of the river break-up in spring. Furthermore, the construction window was constrained by possible weather shutdown. In a location which can experience ambient temperatures down to -50 °C and wind chill factors down to -74 °C, the probability of prolonged work shutdown was expected.

The subsurface foundation environment proved to be even more challenging than the construction requirements. The project was faced with three primary geotechnical challenges: variable thermal regimes, variations in soil and ice characterizations, and a wide range in soil salinity. The bridge spanned over three different subsurface soil thermal regimes: the thaw bulb below the river, warm permafrost temperatures adjacent to the thaw bulb, and cold permafrost temperatures. Soil types ranged from very weak ice-rich silts and lean clays to ice-poor coarse gravels. The third geotechnical challenge was soil salinity in both bonded permafrost and frozen unbonded brine pockets; soil salinities ranged to approximately 90 grams/liter. The variable conditions required different pile types and different methods to develop capacity, including: adfreeze piles, end-bearing piles set in hard bonded ice-poor gravel layers, unique end-bearing piles in thawed zones, and the use of thermosyphons to develop adfreeze capacity. This paper describes the state-of-the-practice engineering, designs, and construction methods implemented to overcome these challenging conditions.

Impacts of permafrost degradation on roadway engineering along the Qinghai-Tibet Engineering Corridor

Wei Ma, Yanhu Mu, Qingbai Wu, Fujun Niu, & Guoyu Li

Chinese Academy of Sciences, People's Republic of China

The Qinghai-Tibet Engineering Corridor (QTEC) has a total length of 1120 km, and of which permafrost impacts about 550 km. Under a warming climate, roadway engineering within the QTEC were severely affected by geothechnical problems related to permafrost degradation. Based on field monitoring and investigation, permafrost-related problems to roadway engineering were analyzed along a highway and a railway within the QTEC. The results indicated that, for the highway, permafrost thawing and talik development were serious due to climate warming and heat absorption of the asphalt pavement. As a result, 80 percent of embankment hazards were caused by (differential) thaw subsidence. And local subsidence, longitudinal and transverse cracks widely developed on the pavement. While for the railway, the main geotechnical problems were considerable settlements at traditional sand gravel embankment without any cooling measures and uneven settlements at embankment-bridge transition sections. These settlements were resulted from permafrost creep and thaw consolidation, and the magnitude of which were closely related to the ice content of subgrade.

Geotechnical hazards of embankments on sloping terrains in permafrost regions along the Qinghai-Tibet Railway

Yanhu Mu, Wei Ma, Fujun Niu, & Guoyu Li

Chinese Academy of Sciences, People's Republic of China

The Qinghai-Tibet Railway, crossing about 550 km lavational permafrost areas on the interior Qinghai-Tibet Plateau, is the main terrestrial link between interior China and Tibet. Due to unreasonable layout of drainage ditch, uneven settlement at embankment-bridge sections on sloping terrains became more and more serious. Groundwater flow under the railway proceeds along preferential flow paths located within thawed embankment body. It is suggested that water flow under the railway resulted in underlying permafrost degradation through convective and conductive heat transfer processes. As a result, considerable settlement occurred to the embankment and already affected the railway safe operation. In the present paper, a typical embankment-bridge section on sloping terrain along the railway were introduced, including the terrain features, embankment hazards and mitigation methods used at present.

Impact of permanent and seasonal thermal insulation in a ventilated crawl space on permafrost temperature under buildings

Paul Vincent Perreault & Yuri Shur

University of Alaska, USA

Many engineers and scientists express concerns for climate change impacts on existing infrastructure built on permafrost. Some studies predict widespread collapse of the existing buildings. Adapting structures in the permafrost region to climate change is an important contemporary issue. With thermal modeling, we analyzed the impacts of using surface permanent versus seasonal thermal insulation on permafrost temperatures under heated buildings. In addition, we provide field results from a thaw-sensitive site in Fairbanks, Alaska. An analysis of the available data and our finite element models show that permanent thermal insulation increases the permafrost temperature in soils exposed to seasonal air temperature variations with mean annual soil surface temperatures below 0 °C. With permanent insulation, the amount of permafrost warming increases with a decrease of the permafrost temperature. Distinguish that permanent thermal insulation has different impacts on active layer thickness from the impacts on permafrost temperature. Using permanent thermal insulation decreases the thickness of the active layer and can reduce frost heave actions; while also increasing the permafrost temperature and decreasing its bearing capacity.

We studied the effects of summer seasonal insulation on permafrost temperature under buildings. The seasonal thermal insulation is applied in spring and removed in autumn; thereby restricting heat flow into the ground during summer. Absence of insulation in winter promoted soil cooling. We performed numerous two-dimensional thermal analyses for buildings on piles with an open crawl space for Fairbanks, Kotzebue, and Barrow, Alaska. All of them show sufficient decrease in the permafrost temperature. The seasonal thermal insulation effects are more significant in warm discontinuous permafrost than in cold continuous permafrost. The results show the effectiveness of using seasonal thermal insulation to promote permafrost cooling – even when faced with climate warming.

Summer seasonal thermal insulation, placed on the soil surface in a ventilated crawl space, decreases permafrost temperature and can be a valuable method for increasing foundation integrity in a warming climate. The impact from using seasonal insulation to decrease permafrost temperatures is especially valuable in those southern permafrost areas with a high Thawing Index. Seasonal insulation applies to thaw-sensitive permafrost within the discontinuous permafrost zone where the permafrost bearing capacity and adfreeze strength are sensitive to minor changes in soil temperature.

Using seasonal insulation is suitable for new and existing buildings with an open crawl space pile foundation system. The method is adaptive and flexible, and the initial cost is low, all of which are important considerations given the uncertainties of climate warming. The thermal value of the insulation applied may be increased or decreased, in response to actual soil temperatures measured at specific sites. Using seasonal insulation provides a suitable method for existing buildings on a pile or post foundations with an open crawl space beneath. Using seasonal insulation permits an incremental response to actual climate warming conditions.

Overview of trunk pipeline practice in Russian permafrost

Julia Stanilovskaya[1], Denis Shmelev[1], Erik Green[2], & Pascal Dauboin[1]

[1] *TOTAL E&P Russie, Russian Federation*
[2] *TOTAL E&P - DSO/TEC/GEO, France*

The main regions of fossil fuel reserves in Russia are located in the permafrost zone – north of European Russia, the Yamal peninsula, Western and Eastern Siberia, Southern Yakutia. A boom in trunk pipeline construction occurred after sharp price rises of oil and gas since 2000. 12 000 km of oil and 23 000 km of gas new trunk pipelines were commissioned [Lisin and Soschenko, 2013] between 2000 and 2013, including several notable new projects in permafrost: the "Eastern Siberia – Pacific Ocean" – 1, 2 (ESPO), the "Vankor – Purpe", the "Bovavenkovo – Ukhta", the "Power of Siberia", the "Zapolyarye – Purpe", and the "Kuyumba - Taishet".

Russian experience in the Cold Regions shows that interaction between permafrost and pipeline is complex and depends on various parameters of frozen strata themselves (ground temperature, active layer depth, ice content, cryogenic processes, soil type and geological origin, landscapes and soil-vegetation cover) and the anthropogenic impact of the pipeline on the environment. Inadequate appreciation of these characteristics during surveys, construction or operation stage leads to disturbance of normal operation, increased repairs and greater risk of accidents.

Analysis of Russian pipeline practice based on the new mega pipeline projects exemplifies the main new tendencies in pipeline practice, which have been combined in the following topics:

1. The development of a regulation-standard basis for engineering-geological survey, design and operation of pipeline. The Russian Building Code SP36.13330.2012 [2012] "Trunk pipelines" addresses design, construction and operation

2. Intensive application and developing of pipeline experience in the new pipeline projects - the evolution of Russian pipeline practice in permafrost. Thus, the "Zapolyarye – Purpe" pipeline is based on the design and construction of the "Vankor – Purpe" pipeline; the "Kuyumba – Taishet" and the Power of Siberia trunk pipelines are continuation of the practice on the ESPO-1, 2

3. The active application of thermo-hydro-mechanical modeling in pipeline practice at pre-investment, survey and operation stage. The goals of this modeling vary from estimation of artificial ground cooling and oil and gas temperature in the pipe to evaluation of economical efficiency of technical developments application [SP25.13330.2012, 2012]

4. The increasing importance of pipeline strain monitoring at the operation stage as a basis for efficient repair works.

The intensive development of Russian pipeline practice is based on new technical developments in pipeline construction. Russian practice of recent years demonstrates the feasibility of pipeline construction in severe natural conditions: from northern tundra to the southern permafrost boundary. The construction of a new pipeline in permafrost zone occurs in a relatively short time, for example, 6 years for ESPO-1 (from first discussion to pipeline commissioning). A few main design and technology developments are presented:

1. The main pipeline laying out way in permafrost is buried: the ESPO – 1, 2 and the Power of Siberia, the "Ukhta-Bovanenkovo" and the "Taishet – Kuymba" trunk pipelines were buried. The pipe-bridge way with thermal heat pipes has been implemented only for the "Vankor – Purpe" and the "Zapolyarye – Purpe" trunk pipelines on areas with continuous distribution of ice-rich permafrost. The widespread application of buried pipelines has lead to the development of compensators for pipe couplings

2. For buried gas pipelines various ballasting and anchorage methods have been developed in order to provide pipeline stability and ensure uplift prevention

3. Development of pipe insulation technology, including heat insulation and corrosion protection is an alternative to thermal heat pipes and thermosyphons. A totally new design is thermal insulation screen, installed under buried pipelines on bottom of trench in ice-rich permafrost area. The three main aims of pipe insulation evolution are: protection from mechanical impacts, protection from corrosion and chemical-biological weathering and protection from heat exchange between pipeline and permafrost. Development of pipe insulation, especially thermal insulation, is gradually decreasing the role of artificial ground cooling by thermosyphons

4. Development of construction technology of water transition of pipeline in permafrost. Today the main way for water transition is microtunelling; pipelining in the trench on the basin bottom is not implemented in new pipeline project. The sea crossing of the "Bovavenkovo – Ukhta" pipeline through Baydara Bay is a unique project of sea gas pipeline in the Arctic Ocean on shallow permafrost. The main method of pipeline laying out is an aboveground pipelining with concrete solidification of pipes. The blasting of pipes by concrete solidification allows protecting of pipeline from mechanical damages by storms, landslides, iceberg gouging and uplifting.

Despite the rapid development of pipeline technology, Russian pipelining practice is facing some issues. These difficulties are caused by different factors: from absence of law-regulation base to violations at construction and operation stages. The main cause of the problems at each stage (survey, design, construction and operation) is underestimation of initial permafrost properties and triggering of cryogenic processes development due to disturbance of natural conditions after construction.

References

SP. 25.13330.2012. *Foundations on permafrost.* Ministry of regional development of Russian Federation, 2012. 142 p.

SP 36.13330.2012. *Trunk pipelines.* Gosstroy of Russia, 2012. 146 p.

Lisin, Yu.V. and Soschenko, A.E. [2013]: *Technologies of Russian crude oil main pipelines.* Moscow, 421 p.

Effects of warm, discontinuous permafrost on site response spectra at a site near Fairbanks, Alaska

John Thornley[1] & Joey Yang[2]

[1] *Golder Associates Inc.*
[2] *University of Alaska Anchorage, USA*

Fairbanks is a city located within the central portion of the state of Alaska in the United States of America and is on the margins of the zone of continuous permafrost to the north. The Fairbanks area is known to have zones of discontinuous permafrost where remnant permafrost has slowly degraded. However, there are areas where the permafrost is on the order of several meters thick to greater than 60 meters thick. The permafrost is underlain by deep thawed soil deposits and bedrock below that. Frozen soils have been observed to have a substantial increase the shear wave velocity when compared to thawed soils. It is also known that higher velocity layers overlying lower velocity soil layers tend to amplify and modify measured responses at the ground surface. At a site near the Tanana River outside of Fairbanks, the permafrost is estimated to be approximately 35 to 45 meters thick and is underlain by approximately 200 meters of saturated sands and gravels to bedrock. Vertical shear wave velocity profiling was performed at this -1.5 °C warm permafrost site to develop the site-specific VS30. In order to evaluate the effects of the lower velocity structure (thawed sands and gravels) below the higher velocity permafrost layer, a one-dimensional equivalent linear model was developed. The permafrost layer over the thawed layer modified the spectral response at the ground surface when compared to a fully thawed site. These findings are significant because the changes in site response due to permafrost may likely affect the way that earthquake engineers consider site specific response spectra in these regions of discontinuous permafrost in the future. This is especially true in regions experiencing permafrost degradation due to climate change. These impacts on regional and local seismicity and ground response should be evaluated as infrastructure is being designed in permafrost regions.

Dynamics of the seasonal thawing of frozen ground at the disturbed area, Alexandra Land, Franz-Joseph Land Archipelago

Yana Tikhonravova

Earth Cryosphere Institute SB RAS, Russian Federation

In 2014 the expedition of the "Russian Arctic" National Park visited the Franz-Joseph Land archipelago. The geocryological studies included the assessing of the technogenic impact on the seasonal thawing of frozen ground at Alexandra Land.

The study of the dynamics of the seasonally thawed layer was performed at two sites 40 × 70 m in size of the polar desert at Alexandra Land at 80°38'38" N, 46°49'49" E (Fig. 1-a). The first site was presented by natural conditions with mosses and lichens. The second one was covered by the consumer waste of the past dump, fuel barrels and there was a part of the road as well. The island had been cleaned out of the wastes by 2014. Patches of fuel were removed by bulldozer, but black lenses were seen at the pit profile at depths of 2-5 cm.

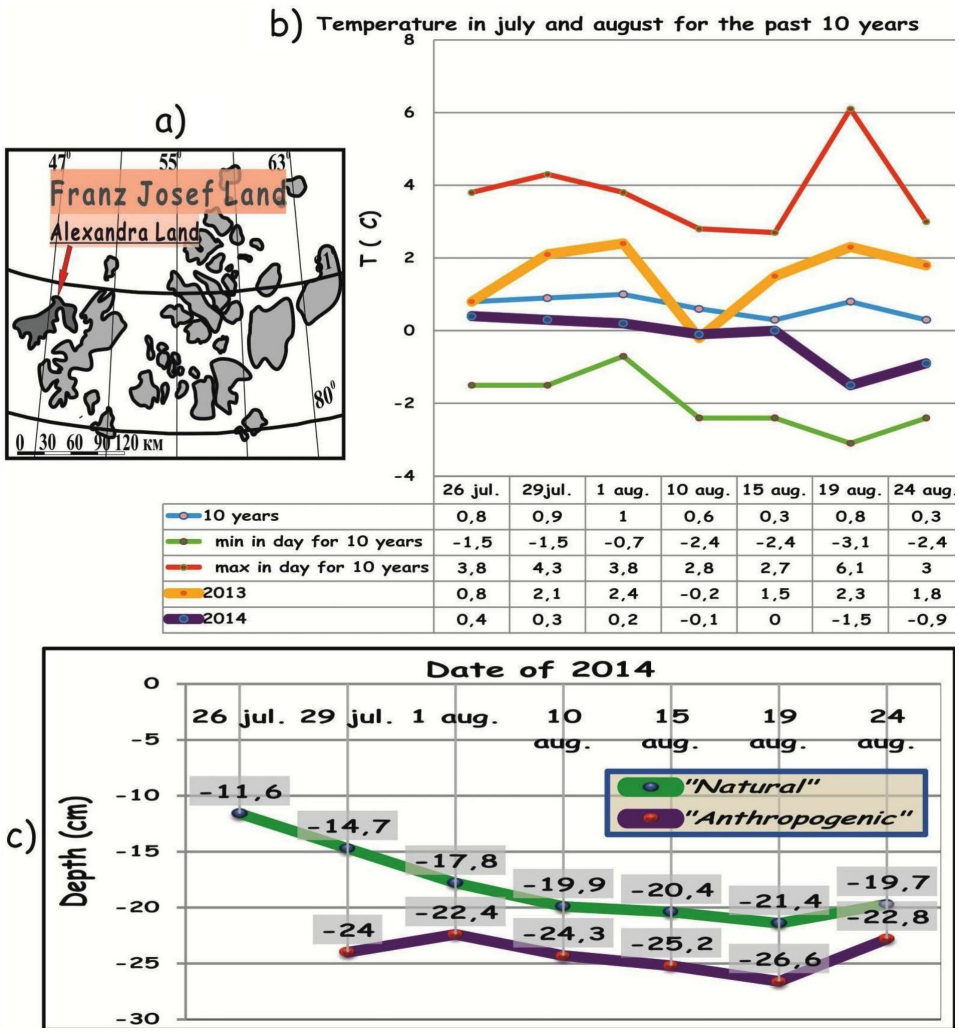

Figure 1: a) Location of the Franz Josef Land; b) Temperature in July and August for past 10 years; c) The depths of thaws on the natural and technogenetic sites in 2014, Alexandra Land, Franz Josef Land

The traditional method of active-layer thickness measuring by probing the bottom of the active layer with a graduated rod could not be used because of numerous large stones. The active-layer thickness was measuring during one month (26 July – 24 August) at test pits located on a grid with a step of 5 m. The repeated measurements were made at 5 points on the boundaries and in the center of the sites, the distance between the repeated pits was less than 0,5 m. The total water content was determined by point method [Ershov, 1985], samples were taken at the base of active-layer at the beginning and in the middle of the observation period.

The summer of 2014 was extremely cold at the archipelago; the area of sea ice cover was 30 % more than the area of conventional cover for the past 40 years according to the data of the 'Russian Arctic' National Park. The snow didn't melt completely at the island. According to the Ernst Krenkel Observatory [http://www.Rp5.ru], the air temperature was 1 °C below than the average temperatures of July-August for 10 years and it was 2 °C below than temperatures of 2013 for the same period (Fig. 1-b).

The dynamics of the active layer thickness at the sites is shown at the (Fig. 1-c). At the end of July the average depths of thawing were 14.7 cm at the natural site and 24 cm at the technogenic site. At the end of August, the differences of the thawing depth decreased and reached 21,4 cm at the natural site and 26,6 cm at the technogenetic site. Minimum depth of thawing was 7 cm, maximum depth of thawing was 33 cm during the research. The sub-zero air temperature was registered at August 16 and the upward freezing began from August 19 (Fig. 1-c).

The total water content was 20 % at the natural and 32 % at the technogenic site on July 29. It was 24 % at the natural site and 27 % at the technogenic site by August 10 [Tikhonravova, 2014].

The depths difference of permafrost roof at the natural and technogenetic sites is probably associated with the absence of vegetation cover.

The surface of technogenic site depressed because of continuous dump influence, it was lowered by cleaning up. Over the observation period, the dynamic of active-layer thawing was slower for the technogenic site because of higher total water content in compare with natural site.

At the beginning of summer thawing rate at the technogenic site was higher, but over time it decreased because of the total water content increasing with depth. The study began when active-layer thickness had already reached 11 cm at the natural site and 24 cm at the technogenic site. Perhaps, the lenses of oil and bitumen distort the dynamics of thawing through the shifting of heat exchange within the soil.

The data on active-layer thickness was obtained as a result of field studies under disturbed and natural conditions on the Alexandra Land.

Acknowledgements

Research has been supported by the Russian Science Foundation grant № 14-17-00131.

Experimental study on mechanical properties of coarse-grained soil in cold regions

Tian-liang Wang, Zu-run Yue, Tie-cheng Sun, & Hong-fang Song

Shijiazhuang Tiedao University, People's Republic of China

For the promotion and application of coarse-grained soil fillings in the railway subgrade in frozen regions, the shear strength properties of coarse-grained soil under freeze-thaw cycles and fines content are directly related to the subgrade stability. So that, the influencing rules of freeze-thaw cycles, fines content and confining pressure on the shear strength properties of coarse-grained soil are thoroughly studied and analyzed in laboratory tests. The results show that, with the increasing increment of fines content, the stress-strain curve of coarse-grained soil changes from strain-softening before freeze-thaw cycles to strain-hardening after freeze-thaw cycles. With the increasing increment of fines content, the cohesion function of fines effectively enhances the shear strength of coarse-grained soil before freeze-thaw cycles, but the frost heave properties of fines decreases the shear strength of coarse-grained soil after freeze-thaw cycles. The shear strength indexes of coarse-grained soil decrease and then are steady after 6 freeze-thaw cycles. The confining pressure effectively enhances the shear strength of coarse-grained soil. Finally, the reasonable fines content of 5 % is recommended for the railway subgrade coarse-grained soil fillings in frozen regions, and the mechanical indexes of 6^{th} freeze-thaw cycle are suggested for the engineering design values.

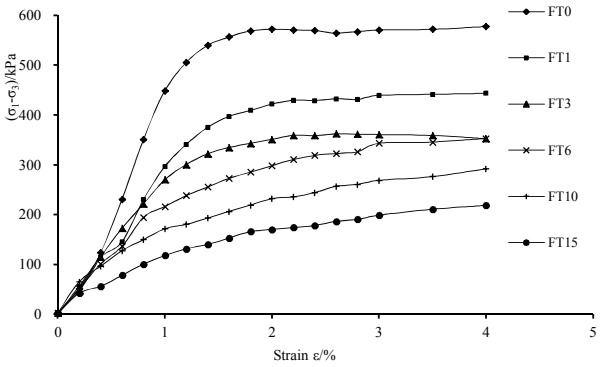

Figure 1

Theoretical creep models of frozen soils

Xiaoliang Yao[1], Wei Ma[1], Jilin Qi[2], & Fan Yu[1]

[1] *Cold and Arid Regions Environmental and Engineering Institute, Chinese Academy of Sciences, People's Republic of China*
[2] *School of Civil and Transportation Engineering, Beijing University of Architecture and Civil Engineering*

In this paper, the predicting performances of three creep models were evaluated based on a series of uniaxial creep test results. It was indicated that hypoplastic creep model can describe the three creep stage (i.e., primary, secondary and tertiary stages) reasonably; for the elementary rheological creep model, the primary and secondary can only be simulated, which was caused by the linear term used for calculating plastic strain; as for the soft soil creep model, the progressive conversion process from the primary to secondary and tertiary stages cannot be captured. This is caused by the constant strength parameter employed in this model. During the process of creep of frozen soil, the strength attenuates with time. Considering the parameters in soft soil creep model can all be obtained from conventional soil mechanical tests and the clear physical meaning of which, a frozen soil creep model was proposed by considering strength attenuation based on the model. It was verified that the frozen soil creep model can reasonably describe the feature of progressively developing process between different creep stages.

Challenges and countermeasures of a power transmission line in permafrost regions – the Qinghai-Tibet Power Transmission Line

Qihao Yu[1], Yanli Xie[2], Yanhui You[1], Lei Guo[1], & Xinbin Wang[1]

[1] *Cold and Arid Regions Environmental and Engineering Research Institute, Chinese Academy of Sciences, People's Republic of China*
[2] *Test Electric Power Research Institute of State Grid Qinghai Electric Power Company*

Infrastructures in permafrost regions frequently suffered engineering diseases, since the construction and operation of engineering constructions have thermal disturbance to the underlying permafrost. Power transmission lines construction on the Qinghai-Tibet Plateau(QTP) faced greater challenges as the permafrost on the QTP is warm and ice-rich and under the background of global warming . The Qinghai-Tibet Power Transmission Line (QTPTL), a project of the ±400kV direct current power transmission line from Golmud in Qinghai Province to Lhasa in Tibet autonomous Regions, China, was constructed in October 2011. The QTPTL is another milestone project following the Qinghai-Tibet Railway.

As the frost heave of the tower foundations are the major types of diseases, some new types of foundations, including cast-in-place spread footings, modular pre-cast footings, cast-in-place conical footings and cast-in-place piles were developed and used in the QTPTL. Considering the ground water, solar radiation during the pits excavation warm or thaw the surrounding permafrost, the construction was scheduled in later winter, and adequate preparation, quick excavation, fast pouring and timely backfill were required during the construction.

For assessing the stability and studying the potential engineering diseases, we established long term monitoring system along the QTPTL, in which the ground temperature, soil water content around tower foundations and deformation of tower foundations were monitored after the construction. The monitored data in the first several years showed that the ground temperature near the tower foundations decreased for the majority of the tower foundations. After the first freezing period, soils surrounding foundations all became frozen, then after warm season, soils underneath foundations kept freezing, which ensured tower-erection and wire-installation can be implemented. However, the water infiltration in summer results in the warm of foundation soil. The application of thermosyphons around tower foundations was crucial for the cooling of the foundation soils and ensure the stability of tower foundations.

The experience in the construction of the QTPTL may be beneficial to understanding the interactions between tower foundations and permafrost. That may also provide valuable insights for the design, construction and maintenance of power transmission lines, and similar engineering in permafrost regions.

Investigation on the pore water pressures during soil freezing and thawing

Lianhai Zhang, Wei Ma, & Chengsong Yang

Cold and Arid Regions Environmental and Engineering Research Institute, Chinese Academy of Science, People's Republic of China

Investigation of pore water pressure during soil freezing and thawing is essential for exploring frost heave mechanisms such as water migration and the initiation of ice lenses. In this article, a new pore water pressure gauge was designed and applied to sub-zero temperature environment in laboratory, and thus pore water pressure changes were observed when soils subjected to varied of temperature conditions such as freeze-thaw cycles, supercoiling and ice nucleation. The pore water pressure experienced a periodical change during the freeze-thaw cycles, decreased during freezing and increased during thawing. However, the pore water pressure remained almost constant during the supercoiling stage but increasing slightly during ice nucleation. Based on previous studies and our test results, the change mode of pore water pressure, herein, is suggested and discussed, and then the frozen fringe process is analyzed, which involves the consolidation in unfrozen zone, initial conditions of ice lens, water migration, the applicability of the generalized Clausius-Clapeyron equation (GCCE) and others.

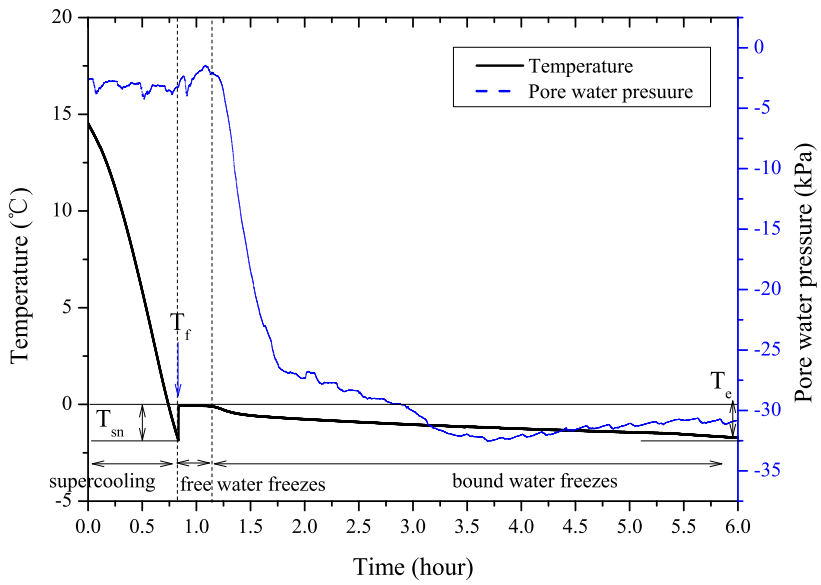

Figure 1: The changes of temperature and pore water pressure during the freezing point testing of sample CN1. Tsn: the temperature of spontaneous nucleation; Tf: the initial freezing temperature of free water; Te: the temperature of most of bound water frozen.

Numerical analysis of the thermal characteristics and seismic response of bridges in permafrost regions

Xiyin Zhang, Mingyi Zhang, Shuangyang Li, & Wansheng Pei

Cold and Arid Regions Environmental and Engineering Research Institute, Chinese Academy of Science, People's Republic of China

The Qinghai-Tibet Railway (QTR)project have been used a series of proactive measures to lower the temperature of the permafrost and to keep the stability of the permafrost, of which one is the dry bridges widely constructed instead of embankment as foundation of the QTR, especially in areas of warm and ice-rich permafrost. Meanwhile, the Qinghai-Tibet Plateau is regularly shaken by earthquakes, the dynamic performance and response of the bridges under seismic action are more complicated and readily to be destroyed compared to embankment. Therefore, in order to evaluate the anti-seismic performance of the bridges in service period in the future, it is very necessary to study the seismic response of bridges under basic and rare earthquake intensity in permafrost regions. This study established a numerical model to investigate the thermal characteristics and the seismic response of bridges in the QTR. The numerical results indicates that the bridge has a positive cooling effect on the permafrost due to the shading effect of the superstructure and transfer of cold energy on the ground under bridges. Based on the temperature characteristics, the free vibration characteristics and dynamic responses of the bridge-soil-pile system in different temperature conditions were analyzed respectively. Analysis results and their comparisons shows there are significant differences in the lateral displacement, maximum shear forces and bending moment between the warm and cold seasons. The frozen soil layer reduced the maximum lateral displacement of bridge piles and shifted the location of the zero and peak value of shear and bending moment, all of which could have significant impact on seismic performance of the bridge-soil-pile system. So, what is certain is that the bearing capacity of the bridge pile can not meet the seismic requirements if only one of the temperature condition is used in the design and construction.

Relative vertical displacement of pile-soil under the freeze-thaw action

Ze Zhang, Wei Ma, & Wenjie Feng

Cold and Arid Regions Environmental and Engineering Research Institute, Chinese Academy of Science, People's Republic of China

Vertical displacements of soil and piles occur at the same time under the freeze-thaw action, making it difficult to determine the frost heave and thaw subsidence of pile. To solve this problem, we monitored the vertical displacement of pile and soil simultaneously and found that pile soil interaction is different depending on the differences in backfill density, with a ultimate trend toward "pile-soil" system modification synchronization. Vertical displacement of the pile foundation needs to determine the relative displacement of pile and soil. Experimental results show that there is an optimal degree of soil compaction, in which vertical displacement change of pile is minimal.

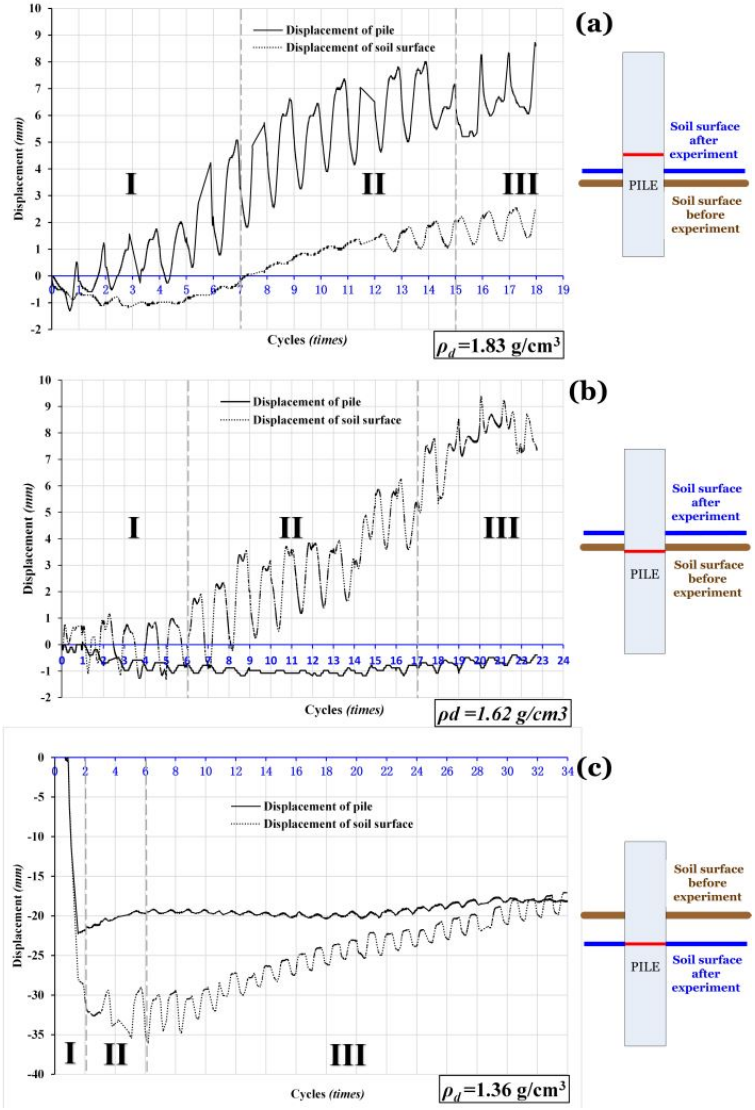

Figure 1: Vertical displacement changes of pile-soil with different soil compactness in freezing and thawing process: (a -1.83 g/cm^3, b -1.63 g/cm^3, c -1.36 g/cm^3).

SESSION 27

Infrastructure Stability in Permafrost Terrain

Convener:

Julie Malenfant-Lepage, *Université Laval, Canada*

Lukas Arenson, *BGC Engineering Inc., Canada*

Christopher Stevens, *SRK Consulting (U.S.) Inc., USA*

The stability of infrastructure on thaw-sensitive permafrost is of great importance for the socio-economic development of Subarctic and Arctic regions. However, there are many challenges to the construction and maintenance of sustainable infrastructure in permafrost environments. Infrastructure construction causes changes to the ground thermal regime, often resulting in decreased bearing capacity, increased creep deformation and thaw-consolidation. Adapted design and construction practices are required to limit disturbance to the ground thermal regime to preserve the mechanical stability of permafrost. This requires a better understanding of the factors contributing to permafrost degradation, improvement in investigation techniques to identify unstable soils, and the development of adaptive strategies as well as engineering tools to support infrastructure design. Climate change adds an additional level of uncertainty to infrastructure performance in permafrost terrain, which needs to be carefully considered in engineering practice to develop reliable infrastructure. This session intends to collect current knowledge and experience on infrastructure design, construction and management in permafrost environments and to promote discussions and idea sharing on these issues. The session should contribute to more durable and reliable infrastructure in permafrost regions

The decreasing of frozen foundations bearing capacity of Norilsk region buildings and structures associated with temperature changes

Fedor Andriushchenko & Valeri I. Grebenets

Lomonosov Moscow State University, Moscow, Russian Federation

Large settlements on permafrost have a significant impact on the natural geological conditions. The first feature that affects development on permafrost is soil temperature change, which defines the bearing capacity of frozen foundations and therefore the stability of engineering facilities. Temperature regime depends on both climatic trends and anthropogenic effects, their duration, intensity and the area of impact. Permafrost degradation within built-up areas is typical not only for Norilsk region, but also for many other large settlements in the Russian Arctic. Uunlike the other cities where temperature rising generally driven by climate change (e. g. Salekhard, Chita, etc.), Norilsk has made the most significant contribution to the development and use of the territory. We analyzed the temperature measured in boreholes within microdistricts of the city with different permafrost conditions. Measurement periods ranged from 2 to 70 years. We built temperature curves and profiles of soils under buildings for different periods of time, which shows the examples of both temporal and spatial changes.

Three main trends in soil temperature regime were revealed: a decrease in temperature, growth and invariability. The most typical was the most dangerous trend – a serious warming of soils foundation (almost 45 % of all buildings). Since the majority of the buildings in Norilsk built on pile foundations, which bearing capacity is provided by freezing of piles with frozen ground, the increase in temperature leads to a reduction in bearing capacity and, often, to the failure of the base. The reasons are climate warming trends as well as disturbances during buildings construction and exploitation. However, the leading reason is violation of cold ventilated cellars use (engineering solutions of maintaining of a low substrate temperature): flooding from the unregulated sewage, littering and obstruction of ventilation. This trend observed at bases of both old and modern buildings. At the same time, the facilities with a tendency to a lowering of soil temperature also occupy a significant proportion of the city total area. This trend provided by correct constructions exploitation as well as installation of heat pipe termosyphones, which compensates climate-warming trend. The temperature stability observed frequently that underlines the dynamical response of permafrost to external interference.

The dynamics of temperature regime creates a mosaic and inhomogeneous structure of permafrost conditions, which undoubtedly complicates the ongoing development of the Norilsk area. The studies of temperature changes reasons help to find solutions to the buildings deformability problems and structures associated with the loss of bearing capacity and potentially facilitate the development of the permafrost zone.

PIEVC vulnerability assessment for three airports in the Canadian North

Lukas Arenson[1], Midori Telles-Langdon[1], Jack Seto[1], Janice Festa[2], Jenna Craig[2]

[1] *BGC Engineering Inc., Canada*
[2] *Transport Canada, Canada*

In August 2005, Engineers Canada, the business name of the Canadian Council of Professional Engineers, established a national committee known as the Public Infrastructure Engineering Vulnerability Committee (PIEVC). The purpose of the committee is to oversee the planning and execution of a broad-based national engineering assessment of the vulnerability of Canadian public infrastructure to climate change. This is a continuing priority for the engineering profession because of the uncertainties caused by a changing climate that may jeopardize the validity of climatic design parameters, which are generally based on historic climate data. The PIEVC has developed a generalized step-by-step protocol for the assessment of infrastructure to climate change and provides a general framework that can be used for any infrastructure [Engineers Canada, 2012].

In March 2014, Transport Canada initiated the assessment of three airports in northern Canada that were experiencing infrastructure deformations due to permafrost thaw and frost heave, namely in Inuvik, Northwest Territories; Cambridge Bay, Nunavut; and Churchill, Manitoba. The focus of the vulnerability assessment lay on the evaluation of key elements required for safe air traffic operation, and included runways (gravel and asphalt), taxiways and aprons in at all three airports in addition to major buildings at Churchill.

We introduce the protocol and present the 5 key steps used to assess the three airports (Figure 1). While only few elements were identified to be at high risk, the systematic approach helps to identify infrastructure components for which it had not been clear before the assessment that they may be vulnerable to changes in climate parameters. The systematic assessment further helped identifying elements for which no immediate action is required, but additional measures are suggested to better monitor future performance. Since the assessment relies on projections about future climate it is recommended to continue monitoring relevant climate parameters and monitor structural elements that are currently identified with medium risk. The results of the protocol are useful in identifying those elements of airport infrastructure that are vulnerable to specific aspects of climate change and can therefore also be used as a planning and management tool.

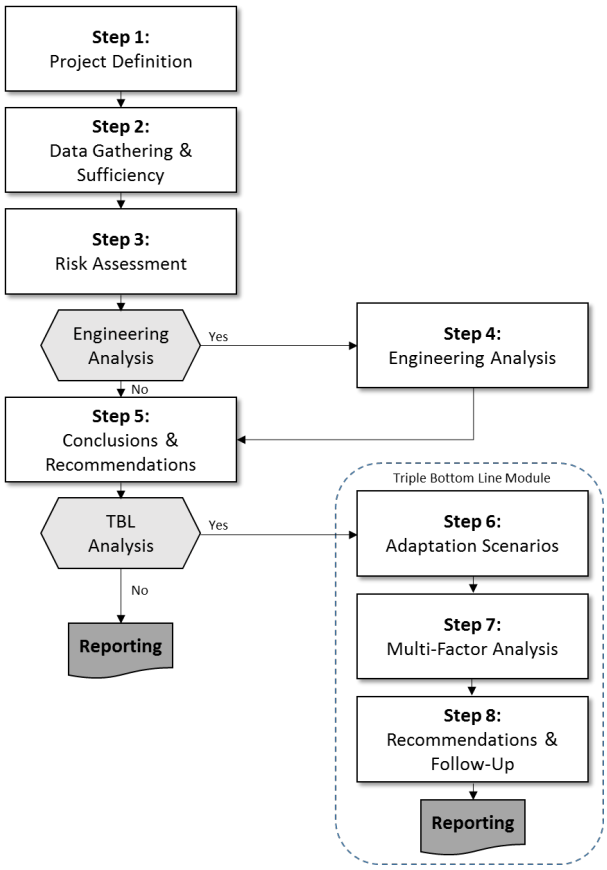

Figure 1: Overview of the Protocol (after Engineers Canada, 2012)

References

Engineers Canada [2012]: *PIEVC Engineering Protocol: For Infrastructure Vulnerability Assessment and Adaptation to a Changing Climate - PRINCIPLES and GUIDELINES*. Revision PG-10, May 2012, 153 p.

Assessment of embankments stability on the thawing base soil

Evgeny Ashpiz & Tatyana Vavrinyu

Moscow State University of Railway engineering, Russian Federation

The research describes the ways providing stability of the embankments which are constructed in the regions with the permanently frozen soil.

The objective of the work is to evaluate the embankment stability of different facilities on the thawing collapsing soil of the subgrade. The great importance is given to the simultaneous studying and recording of the process of subgrade soil consolidation and the thermophysical effect that changes the initial temperature pattern of the subgrade while blading fill materials.

It is known that the construction under the complicated engineering and permafrost conditions demands special actions to achieve strength and stability of the roadbed. Today we have revealed a complicated mechanism of the interaction between the roadbed and the permanently frozen soils with account of a large number of factors effecting on the work of the earth construction on the thawing subgrade and its deformation growth. It explains why there are great problems in accurate evaluation and forecasting of stress and stability of constructions done by traditional calculation methods.

Due to the existing Russian standards base, all calculations are conducted according to limit states and this process does not take into account the thawing speed of a construction and the speed of soil consolidation as well as its nonlinear deformation. That is why a new approach is to be introduced to evaluate the stability of the subgrade on the thawing soil. The new approach suggests that time should become the leading criterion for the calculations of the roadbed design.

Based on the results of the laboratory tests, the authors make a hypothesis that the thawing process of permafrost can lead to the formation of a layer with unconsolidated thawing soil under the roadbed. This layer possesses minor characteristics of strength and stress and can change principally the strain-stress state of the subgrade and the construction stability. On the basis of this hypothesis, a new three-layer model of the thawing subgrade has been worked out.

As a criterion for the layer formation of the unconsolidated soil (applied to the proposed three-layer model) in the thawing subgrade we offer to accept the ratio of thawing speed to soil consolidation speed. The ratio of thawing speed to soil consolidation speed (V_{th}/V_{cons}) allows to determine the characteristics which are needed for the thawing subgrade model design – thickness and time of consolidation of the weak unconsolidated layer – and to design a three-layer model of the subgrade for the further calculations with the application of the numerical experiment.

Quantifying probability of thaw settlement occurrence and vulnerability to climate warming – Iqaluit Airport, Nunavut

Heather M. Brooks, Guy Doré, Michel Allard, Ariane Locat, & Chantal Lemieux

Université Laval, Canada

Risk analysis tools, qualitative or quantitative, are used to select engineering designs and allocate funds for, linear infrastructure on permafrost. However, with changing climactic conditions and increasing infrastructure demands, infrastructure owners, operators and planners must possess tools to objectively aid their decisions on climate change adaptation and infrastructure maintenance. To this end, this presentation presents a review of quantitative risk analysis methods with specific focus on their application to permafrost regions. In order to conduct a risk analysis, two factors must be calculated or assigned for quantitative and qualitative risk assessments, respectively:

1. the probability of occurrence of a hazard, and
2. the consequence associated with the hazard's occurrence.

The presentation will review Monte Carlo Simulation methods, and their application to determining variability of thaw depth and the probability of thaw settlement occurrence beyond a threshold. The change in the probability of occurrence, due to variations in mean annual air temperature, is the vulnerability of the hazard to a changing climate. As an example, the calculation method is applied to soil and climate conditions at the Iqaluit Airport, in Iqaluit, Nunavut.

Experience in the assessment of long-term social-economic damage caused by the development of geocryological processes (Chara-China railway example)

Irina Chesnokova[1], Dmitriy Sergeev[2], Olga Borsukova[1], & Aleksandra Morozova[3]

[1] *Water Problems Institute Russian Academy of Sciences, Russian Federation*
[2] *Institute of Environmental Geoscience Russian Academy of Sciences, Russian Federation*
[3] *Moscow State University, Geography Department, Russian Federation*

Nearly any change in geocryological conditions leads to the activation of geocryological processes. The relative warming is favorable for thermokarst development, while cooling activates heave processes. The economic damage arising during the construction and operation of commercial facilities in the territory with widespread permafrost rocks may be associated with exogenic processes occurring in areas of permafrost rocks. Processes are: waterlogging, desertification, deflation, floods, mudflows, and landslides.

Geocryological processes are a source of immediate threat to engineering structures (thermokarst, cryogenic heaving and cracking, icing, thermoerosion). The danger lies in the direct dynamic influence on elements of technological constructions. Simultaneously, a consequential damage occurs from the formation of geocryological phenomena that change the condition of the water drainage and other characteristics of the landscape, which determine favorable conditions of economy management and operation of the object. All this will ultimately bring about economic damage, the annual amount of which may increase or decline, depending changes of the geocryological conditions.

Transport infrastructure is one of most vulnerable components of the national economy, as due to their extension transport facilities (roads and railways, pipelines, power lines) had to cross diverse landscapes, including geocryologically unfavorable, which react differently to climate changes. Climate changes lead to changing geocryological conditions, and the object may appear in conditions not envisaged by the project. Various segments of extended transport systems are characterized by different: records of system operation, climate changes in the region, and dynamics in the development of hazardous natural processes. Local problems in the operation of the transport system bring about changes in the conditions of their sustainable development. This in turn leads to an increase of risk recipients. Unplanned loss and profit shortfall threatens not only the firms operating the transport system, but also to the people, living in its vicinity, to the territorial and state budget and so on.

The report presents an analysis of a unique data set, which demonstrate total influence of geocryological processes on the 75 km Chara-China route (Northern Transbaikal). The originality of these investigations is that the influence of natural processes on the road was studied in the absence of any repair works, protective and compensating measures for a long period of time (13 years). This allowed to assess the real damage caused to the railroad.

The original techniques used in the work are based on zoning of railroad tracks by complexes of geocryological processes, features of relief, water runoff in the area, geological structure, history of geocryological development, technical features of the road and modern dynamics of technogenesis and climate. We calculated sums of maximum damage for each focus in the process development, as well as the specific damage for each area, corresponding to taxon of engineering geology zoning of the rail track.

Zoning of the area enabled us to estimate the role of different factors regulating the intensity of the overall (maximum or finite) impact on the technogenic object during the considered period of time. In particular, the role of relief, hydrological regime, severity of geocryological conditions, and paragenetic combination of geocryological processes were analyzed. The obtained information is recommended to be used as a methodical basis for extrapolation to other kinds of analogous objects situated in similar mountain regions with continental cool climate.

A geographic information system (GIS) has been elaborated for recording and assessing the economic damage to extended linear object, caused by exogenic geological processes under permafrost conditions.

Acknowledgements

The work was supported by Russian Foundation for Basic Research, project 13-05-00462.

Performance of a reinforced highway embankment along the Inuvik-Tuktoyaktuk Highway, Northwest Territories, Canada

Earl Marvin De Guzman[1], Aron Piamsalee[1], Lukas Arenson[2], Marolo Alfaro[1], & Guy Doré[3]

[1] *University of Manitoba, Canada*
[2] *BGC Engineering Inc., Canada*
[3] *Laval University, Canada*

A reinforced highway embankment test section was constructed along the Inuvik-Tuktoyaktuk Highway, Northwest Territories and its performance is continuously being monitored. The embankment was constructed under frozen conditions for logistical and environmental reasons; however, there is limited understanding on the mechanical behaviour of embankments that were initially compacted with frozen fill and then experienced natural thawing and settlements during the spring and summer season following winter construction. Embankments are constructed during the winter to minimize the disturbance of the permafrost foundation. The fill material of the embankment is dominated by fine till that includes ground ice. Fills are very difficult to compact at sub-zero temperatures when ice is present. They are relatively strong while they remain frozen but they become soft and compressible after thawing. Side-slope sloughing and fill cracking are caused by localize thaw-settlements under the shoulders and side-slopes of the embankment created by the rising of the permafrost table into the embankment fill in combination with the depression of the permafrost table at the toe of the embankment. The reinforced test section has layers of wicking geotextiles on its side slopes to provide reinforcement and drainage path for the water during the thawing season. The reinforced test section is instrumented with thermistors for temperature readings in the embankment fill and foundation soil, ShapeAccelArrays (SAAs) for the vertical and lateral displacements, vibrating wire piezometers for pore water pressures, and thermal conductivity sensors for suctions. Strain gauges were also installed at different locations along the length of the geotextile at different layers of the reinforced embankment. A control test section (unreinforced) with the same instrumentation was also constructed beside the reinforced test section to evaluate its performance. This paper presents the results of the continuous monitoring of the test sections from its completion until the end of the first thawing season. Recorded readings indicate that the thermistors closest to the ground surface are responding quickly to the warming air temperatures. The vertical SAAs are recording lateral movements closest to the ground surface, while the horizontal SAAs are showing maximum settlements near the centerline of the embankment. The lateral displacements recorded in the reinforced section are less than that of the control section. No significant change of readings from piezometers, thermal conductivity sensors, and strain gauges were recorded because the embankment fill core and foundation soil are still frozen as evidenced by the thermistor readings. Figure 1 shows the two test sections along the highway, with cracks noticeable in the unreinforced sections.

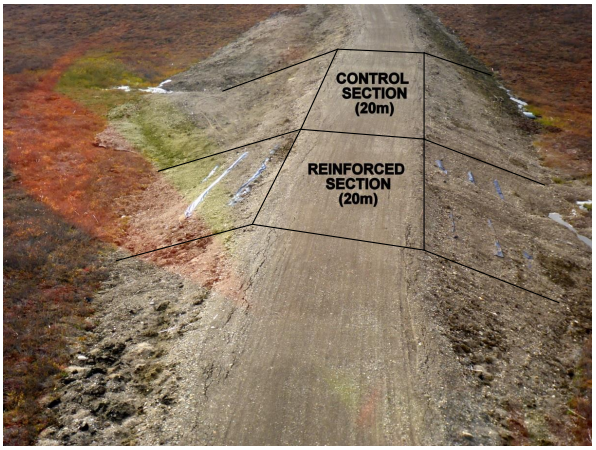

Figure 1: Reinforced and control test sections along the Inuvik-Tuktoyaktuk Highway, Northwest Territories, Canada

The construction of Kangerlussuaq Airport - A case story from West Greenland

Thomas Ingeman-Nielsen & Niels Foged

Department of Civil Engineering, Technical University of Denmark, Denmark

Kangerlussuaq Airport (Latitude 67.01° N and Longitude 51.69° W) is the main international airport hub of Greenland. Most international travellers arrive at Kangerlussuaq and are transferred to their final destinations by a network of local fixed-wing and helicopter flights. The future fate of the Kangerlussuaq airport has been the target of much political and media debate in Greenland in recent years, due to plans by the Greenland Government to restructure the airport infrastructure. Permafrost conditions at the airport has often been brought up in the debate without much factual evidence – which has prompted us to study and summarize the constructional history of the airport and on that basis evaluate the likelihood and extent of future damages due to permafrost degradation.

Kangerlussuaq Airport was established by the U.S. Army Air Force in October 1941 under the code name Bluie West 8 (BW-8) in order to provide an alternative runway to the base at Narsarsuaq (Bluie West 1), and was used as hub and refueling station for transatlantic flights during World War II. A harbor (Camp Lloyd) was established approx. 10 km south west of the airport at the eastern end of the 175 km Sondre Stromfjord (Kangerlussuaq:'the great fjord'). From 1954, regular civilian flights to Kangerlussuaq were operated as part of the route from Copenhagen to Los Angeles, and Kangerlussuaq thus became also a civilian airport and the main gateway for air traffic to Greenland. The U.S. Air Force operated the base until 1992 except a short period under Danish authority (1951-1952), after which the base reverted to the U.S. Air Force under a new defense agreement in light of Cold War fears (Jensen et al., 2013). It served as a Distant Early Warning (DEW) line base and supply station for other such facilities in Greenland. In 1992, after the fall of the Soviet Union, the U.S. Air Force abandoned the airport as a military base and handed over all facilities to the Greenlandic Government for civilian use, but retain priority military access at short notice. In recent decades, Kangerlussuaq has developed a local tourism industry benefitting from easy access to the Greenland Ice Sheet and serving as a hub for cruise ships.

The airport and supporting settlement (see figure 1) is situated in the rather complex geological setting of a marine delta in the valley system east of the head of the Kangerlussuaq fjord. The delta deposits formed during ice marginal retreat from the area approx. 7-8 ka BP, in a period of rapid sea level fall, and range from fine grained marine silt and clay deposits to coarse grained (sand, gravel and stones) river deposits. The combination of a relatively narrow valley confinement and rapid sea level fall, resulted in successive periods of fast depositional infill and subsequent erosion, leaving a system of distinct river terraces [Storms et al., 2012]. The major part of the Kangerlussuaq village, airport structures and runway are located on one such river terrace at an elevation of approximately +50 m.a.s.l., however, the western part of the runway extends onto a slightly sloping plateau of fine grained sediments (clays and silts) of marine origin at an elevation of +30 to +20 m.a.s.l. and dated around 6000 yr BP. Younger eolian deposits in the silt and fine sand fraction are wide spread in the area.

Due to the inland location and proximity of the Ice sheet, the airport experiences a stable dry subarctic climate with a mean annual air temperature of -3.3 °C (2004-2014). Winter temperatures range down to approx. -45 °C and summer temperatures up to 25 °C [Menne et al., 2012]. The area has continuous permafrost, the thickness of which has been estimated at 130 m at the airport location [Van Tatenhove and Olesen, 1994] and measured to 335 m by the ice sheet margin, 25 km inland at 450 m surface elevation [Harper et al., 2011]. Permafrost temperature measurements show an Active Layer Thickness (ALT) of about 2 m under natural conditions, while Ground Penetrating Radar measurements indicate an ALT of approximately 4 m below paved surfaces (Jørgensen & Ingeman-Nielsen, 2007). Perenially frozen fine grained marine and eolian deposits in the area are typically ice rich, however, in certain areas the marine sediments

Figure 1: Aerial view of the Kangerlussuaq airport and surrounding settlement situated on a river terrace in a marine delta at the head of the Kangerlussuaq fjord.

contain considerable residual salinity which suppresses the freezing point and leave the sediments technically unfrozen (although still cryotic). Coarser deposits typically range from well bonded to friable, with limited excess ice (e.g. of Engineers [1957]). Massive ground ice features such as ice-wedge polygons and pingos have been reported although not from the vicinity of the airport and settlement locality.

Runway construction commenced in autumn 1941 and was operational in spring 1942. 1700 m long and 46 m wide, the runway was constructed with a sand base course and asphaltic macadam pavement placed directly on the old river plateau at elevation +45 to +48 m.a.s.l. During the period of 1957-1960 the runway was extended to 3000 m length and widened to 61 m and the southern parking area was expanded. Areas adjacent to the existing runway were excavated, and frost susceptible and ice rich soils were replaced down to 3 m.b.s. by non-frost-susceptible (NFS) materials obtained from sand and gravel pits along the adjacent Watson River. The area of the original runway was not reconstructed, although the construction was reinforced by an additional sand-gravel base course and new pavement surface on top of the original construction. The western-most part of the new runway extended on to a lower plateau of marine fine-grained and very ice rich sediments. A thick embankment of NFS materials was constructed to protect the thermal regime of the underlying thaw-sensitive permafrost.

There have always been load restrictions on the runway in the summer time. These restrictions are related to the fact that the oldest part of the runway was constructed without replacement of weak surficial deposits. There are no restrictions in the wintertime, when the active layer is frozen, ensuring a high bearing capacity. Recently, a notam was issued on the westernmost 250 m of the runway, due to development of settlements and cracking of the pavement. It is presently unknown whether these settlements are related to insufficient compaction of the thick embankment or to thermal degradation of the ice-rich permafrost below or beside the embankment.

Other parts of the runway seem to experience no permafrost related issues due to a low ice content in the underlying sediments, but suffer from a deteriorating pavement. Thermal cracking is a severe problem due to the more than 60 °C surface temperature variation experienced over the course of a year. Crack sealing is performed yearly, but with the different thermal properties of original asphalt and sealant, cracking redevelops and worsen over time. As the runway has not been repaved since 1987, the typically applied 20-year runway repavement cycle is long overdue.

Thaw settlements do occur locally on the southern apron and taxiway. A preconstruction ravine filled with fine grained ice rich material has caused differential settlements of up to 45 cm, and a few other areas are affected by local settlements as well. The northern apron was originally designed for DC8 aircrafts, and the current use of the much heavier Airbus 330 and intensive traffic with domestic Dash 8 flights cause fatigue cracks and viscous deformation of the asphalt in the summer. Some of these issues have been ad-

dressed by painting the asphalt in a light color to reduce surface temperature, and the construction of concrete slabs at certain parking locations.

Generally the runway and main aprons are not expected to experience significant damage related to future permafrost degradation, due to thaw stable subgrade materials or thick protective embankments. Local thaw-settlements may continue to develop in areas with remaining ice-rich eolian deposits. The duration of active settlements will be limited by the relatively small thickness of ice-rich deposits (typically up to 2 m), and settlements should thus be manageable. However, the surrounding infrastructure, especially the road system, will continue to suffer locally from thaw degradation, which is expected to accelerate due to future warming and severe drainage problems which are presently not properly addressed.

References

Harper, J.; Hubbard, A.; Ruskeeniemi, T.; Liljedahl, L.C.; Lehtinen, A.; Booth, A. and Pedersen, K. [2011]: *The Greenland Analogue Project – Yearly Report 2010*. Svensk Kärnbränslehantering AB. Report R-11–23.

Menne, M.J.; Durre, I.; Vose, R.S.; Gleason, B.E. and Houston, T.G. [2012]: An overview of the Global Historical Climatology Network-Daily Database. *Journal of Atmospheric and Oceanic Technology*, doi:10.1175/JTECH-d-11-00103.1.

U.S. Army Corps of Engineers [1957]: BW-8 Sondre Stromfjord Airfield Paving – Runway Widening & Extension. Technical report, Drawing number AF 86-04-02 sheet 8.1 [Technical drawing]. Retrieved from Mittarfeqafiit.

Storms, J.E.A.; de Winter, I.L.; Overeem, I.; Drijkoningen, G.G. and Lykke-Andersen, H. [2012]: The Holocene sedimentary history of the Kangerlussuaq Fjord-valley fill, West Greenland. *Quaternary Science Reviews*, 35:29–50, doi:10.1016/j.quascirev.2011.12.014.

Van Tatenhove, F.G.M. and Olesen, O.B. [1994]: Ground temperature and related permafrost characteristics in west Greenland. *Permafrost and Periglacial Processes*, 5(4):199–215, doi:10.1002/ppp.3430050402.

Longyearbyen port development - soil conditions and geotechnical challenges

Arne Instanes

INSTANES POLAR AS / UNIS, Norway

The Port of Longyearbyen is located in Longyearbyen, Svalbard (N78°14' E15°36'). It is the main logistic point for the cruise industry and for important and export of cargo to and from Svalbard. The port consists of Bykaia and Gamle Bykaia, quays operated by the local council (Lokalstyre) and a coal quay at Hotellneset, operated by Store Norske Spitsbergen Grubekompani, the local coal company, see Figure 1. The coal quay is used for export of coal from the coalmine at Gruve 7 outside Longyearbyen. The total area of the port is approximately 104 000 m^2.

During the last 5 years, plans have been made to meet the demand for larger quays, due to increased traffic by larger ships, especially cruise vessels and large coal and cargo vessels. The port area has been expanded during the last 50 years by land reclamation through rock fill dumping in the nearshore area. The quality of the rock fill is varying and consists of river deposits from the Longyear River, waste rock from coal mining and also layers of fill material of uncertain origin.

In the area between Bykaia and Gamle Bykaia, the seabed slope angle is between 15°and 22° from 5 meters water depth to 20 meters water depth. From approximately 30 meters water depth, the slope angle is gentler, in general less than 10°. The undisturbed seabed consists of normally consolidated clay with undrained shear strength in the top layer of approximately 20 kPa. Slope stability analysis shows that continuous rock fill dumping on top of the slope may lead to instability of the quay area.

At the coal quay at Hotellneset, the seabed slope angle is approximately 30° from 5 meters water depth to 30 meters water depth. From 35 to 40 meters water depth, the slope angle is gentler, less than 10°. The soil conditions are different to the areas closer to Longyearbyen. The seabed consists of uniform loose sand with internal friction angle of 25 to 32°. Geotechnical investigations carried out in 1961 concluded that the seabed was unstable and the location was not suitable for quay construction.

This presentation gives the results from soil investigations in the area during the period 1961 to 2013. Geotechnical challenges and solutions related to the planning of the expansion of new areas in the Bykaia area and the design and construction of a new coal quay at Hotellneset are discussed.

Figure 1: Port area of Longyearbyen (photo from Google Earth, 2015)

Impact of the stationary thermal field on cryogenic processes in road embankments

Vladimir A. Isakov & Valery I. Grebenets

Moscow State University, Russian Federation

Currently there are more than several thousands of kilometers of roads constructed within the cryolithosphere. Many of these undergo deformations, which are the output to the cryogenic processes, happening in the embankment and underneath. Cryogenic processes become more active during the construction and service life of roads. The key reason to that are the changes in the stationary thermal field of the embankment and in that of the natural grounds underneath it. The thermal changes could be both seasonal or long-standing.

Quantitative modeling for 11 study sites, located within Russian cryolithozone [Isakov, 2015], showed the thermal field in the embankments and underneath it undergoes the transformations, resulting in the formation of the four types of the quasi stationary thermal field states: stable, transitory low temperature, transitory high temperature, non-stable (Fig. 1). The quasi stationary thermal field state (QSTF) here means the steady long term thermal state of frozen grounds without accounting for seasonal fluctuations.

Thermal conditions underneath the road embankment result from the long term dynamics (50 years as in the model). They shape significantly the dynamics of cryogenic processes which might get problematic to the engineering stability of the embankment. Among the key hazardous processes are thermokarst, frost heave, ground flows, and frost cracking. Below we consider how the cryogenic process dynamics differ from one QSTF type to another.

Thermokarst. The stable QSTF type implies there is no ground temperature increase so the thermokarst does not appear. For the two transitory types of QSTF we observe the temperature increase over 0°what makes the thermokarst appearance highly probable. Non-stable type of QSTF implies the active layer goes deeper than 5 m underneath the road embankment so the thermokarst would be practically inevitable.

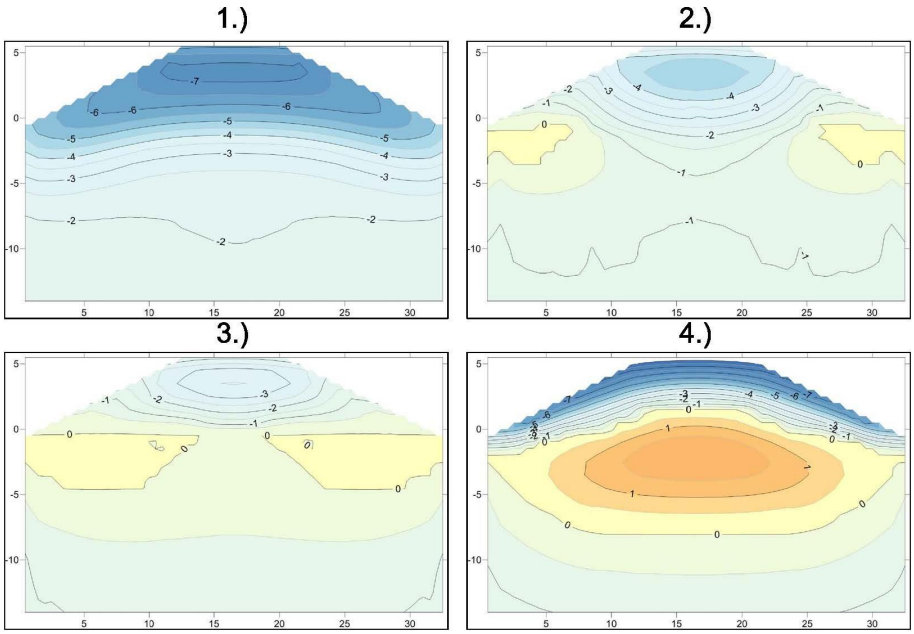

Figure 1: Types of the quasi stationary thermal field state in road embankment and underneath: 1) stable (Amderma); 2) transitory low temperature (Vorkuta); 3) transitory high temperature (Salekhard); 4) non-stable (Chita). Temperature values are given for the end

Frost heave. The stable QSTF types would have a limited potential for the frost heave development since there would be no significant moisture migration happening. The transitory QSTF types are featured with the increased frost heave action in the embankment top. The non-stable QSTF type would be featured with the increased frost heave action all over the embankment body.

Ground flows appear when the pressure on the embankment body exceeds the cohesive resistance of the frozen grounds, constituting the embankment body. The cohesive resistances of the frozen grounds depend on the ground temperatures. The stable QSTF type would keep the low potential for grounds to start flowing. The most intense ground flows would appear for the transitory high temperature QSTF.

Frost cracking damages road pavement and promotes the increased moisture flows into the embankment, hence causing the ice wedge formation. The frost cracking would appear for all the QSTF types. However, these are the stable and low temperature QSTF types, which would have the ice wedges to stay in the embankment.

Generally speaking, each type of the quasi stationary thermal field state (QSTF) is featured with the specific cryogenic dynamics. The intensity and the characteristics of the cryogenic dynamics depend on the QSTF type, which would be featured with specific deformations, appearing in the road embankment.

Thermokarst activation in the embankment basements causes subsidence in the upper filled grounds. The transitional QSTF types are typical of the subsidence at the embankment slopes, while the unstable type would express the subsidence at the subgrade [Isakov, 2012].

Cryogenic heaving in case of the stable QSTF appears as restricted to some small heaves. The transitional QSTFs are featured with the embankment slope deformations and bond-failure crack formations. The unstable QSTF would result in the seasonal heaving all over the embankment.

Plastic deformations of the frozen grounds would result in the uneven subsidence of the top of subgrade, where the pressure on the underlying fill grounds is at maximum.

Frost cracking would cause the road pavement break, the erosion on slopes and uneven subsidence of the subgrade. That is typical of the stable and transitional QSTFs.

Accounting for the type of quasi stationary thermal field state (QSTF) at the road embankment basement allows minimizing deformations by localizing road design solutions to each particular QSTF specific.

References

Isakov, V.A. [2012]: Main types and causes of deformations on railways and roads in the Norilsk industrial district. In: Melnikov, V.P.; Drozdov, D.D. and Romanovsky, V.E.(eds.), *Proceedings of the Tenth International Conference on Permafrost, "Resources and Risks of Permafrost Areas in a Changing World"*, Salekhard, Yamal-Nenets Autonomous District, Russia, 25–29 June 2012, volume 2: Translations of Russian Contributions, pages 133–136. ISBN 978-5-905911-02-6. URL http://ipa.arcticportal.org/publications/conference-proceedings.

Isakov, V.A. [2015]: Temperature state of road embankments in the cryolithozone. *MSU Vestnik*, Series 5: Geography(3):25–34.

Design procedure taking into account accumulation of snow along embankment built on permafrost

Florence Lanouette[1,3], Guy Doré[1,3], & Daniel Fortier[2,3]

[1] *Department of Civil Engineering, Université Laval, Québec, QC, Canada*
[2] *Department of Geography, Université de Montréal, Montréal, QC, Canada*
[3] *Center for Northern Studies, Université Laval, Québec, QC, Canada*

In northern regions, transportation infrastructures are vital for the subsistence, the economic development and the guarantee of a good quality of life of communities. As an example, in northern Quebec, communities are only reachable thanks to their airport for most part of the year. However, the building of linear infrastructures as airstrips induces temperature disturbance at the surface of the ground. Combined with climate changes, this thermal equilibrium modification causes the degradation of permafrost underlying. Then, the bearing capacity of the subgrade is affected and significant settlements can cause substantial damages to infrastructures. After their building, roads and airstrips stand in the way of the wind favouring accumulation of snow along the embankment according to the prevailing winds direction. Maintenance of roadways in winter also contributes to increase the thickness of snow at the toe of the embankment. This thickening of the snow cover raises heat retention in the ground because of the insulated properties of the snow. In winter, the ground cannot cool down as much as before and, with time, the permafrost will degrade.

The objective of this research is to elaborate a design procedure taking into account the impact of snow accumulation along embankments constructed on thaw-sensitive permafrost.

To achieve this goal, during the winter of 2014-2015, the thermal regime through the snowpack and the ground underlying were monitored at two study sites in Canada. One test site is along the Tasiujaq airstrip in northern Quebec and the other is along the Alaska Highway near Beaver Creek in Yukon. The data collected shows that the ground surface temperature reduction is more important for the first centimeters of snow, then progressively diminishes as the snowpack get thicker and denser. The relationship between the n-factor and the snow thickness that can be explain by a logarithmic equation. Also those data were used to develop and calibrate a 2D geothermal model using the modeling software TEMP/W. The goal of this modelization is to represent the heat transfer through the snow, the embankment and the ground underlying. Then, different simulations allowed to quantify the impact of embankment height and slope angle on the thermal regime in the ground and consequently, the mechanical behaviour of embankments.

Challenges emerging from climate change and urbanization in permafrost regions of Northeastern China

Yan Lu[1,2], Wenbing Yu[1], Fenglei Han[1,2], Xin Yi[1,2], Lin Chen[3], & Weibo Liu[1,2]

[1] *Cold and Arid Regions Environmental and Engineering Research Institute, Chinese Academy of Sciences, People's Republic of China*
[2] *University of Chinese Academy of Sciences, Beijing 100049, China*
[3] *Geography Department University of Montreal 520, ch. Côte Ste-Catherine Montreal, Qc, Canada*

In China, about 22.3 % of land area is underlain by permafrost. It is widespread in high-elevation and high-latitude areas. High-elevation permafrost is mainly located in the Tibet plateau. High-latitude permafrost is in northeast China. The researches on permafrost of Tibet Plateau are numerous. But in the past few decades, the research on permafrost in Northeast China is relatively small. Northeastern China is the second largest permafrost area in China. It is located in the southeastern edge of the Eurasian permafrost zone. It is characterized by snowy, high vegetation coverage. This is different from the drought and the extremely low vegetation coverage characteristics in Tibetan permafrost zone.

With the economic transformation and urbanization in this region, the environment and engineering challenges related to permafrost and climate change are beginning to be concerned by researchers. This presentation concludes and analyses the important issues facing Mohe communities in northernmost China by five years field investigations and measurements. We address the broad questions concerning the stability of foundation of buildings, infrastructures such as airports and roads, and the environment changes of a coal mine in Mohe County. Mohe County, occupies an area of 18 367 km^2 with 110 000 residents in 2010, is one of the densely populated areas in permafrost regions. The area of Xilinji town has increased from 5.74 km^2 in 1987 to 8.74 km^2 after the reconstructing by 1988. The urban population has grown from about 25 000 residents in 1992 to more than 41 000 in 2011. The local economic development is undergoing a transformation from forestry to tourism and ecological economy. In 2012, the tourists reached to 1.3 million and the tourism income was 1.19 billion Yuan. The year-on-year growth is 36.4 % and 53.3 %, respectively. In 2012, tourism revenue to GDP contribution rate reached to 30.6 %.

The mean annual air temperature data from 1959 to 2014 at Mohe County were analyzed. It shows a sure warming trend in this area. The five year moving average trend line shows that the climate warming tendency rate at Mohe County is 0.34 degree celsius per decade during the past 56 years. The average climate warming tendency of four meteorological stations in Daxinganling Mountain area is 0.32 degree celsius per decade in the same period. The annual fluctuation of snowfall and precipitation is relatively large. There is no a significant trend of increasing or decreasing during the past years.

Cumulative impact of climate warming and economy development caused serious numerous environmental and engineering challenges. Five roads, 886 km in total, were investigated in Daxinganling area. Thaw settlement and crack problems of roadway are substantial in each road, which has seriously affected the traffic safety. Thaw settlement and cracks happens in the new constructed highway which is paved with concrete in two years after the construction. It turned to be serious in the next 2 years.

The lowest permafrost table beneath the embankment reached to 9.8 m and a 5.3 m thick residual thawed layer exists in the embankment, which weakens the foundation and causes instability of embankment. The biggest subsidence reached to 70 cm in five years at the road S207, which is paved with asphalt. It can be seen that heavy thaw settlement happens both in light color pavement and black pavement in this area. Subsidence of building foundation is another serious issue in this area. Both old building and new building foundations have thaw settlement problems in Mohe County.

Serious thaw degradation of permafrost foundation has caused several buildings abandoned. Ground temperature profile shows that the permafrost depth near the destructive building goes down to about 15 m.

Cumulative impacts of housing heating, heat island effect of urban, climate warming and unreasonable foundation design lead to this problem. In addition, resource mining caused serious environmental problem. The Moon lake at Gulian coal mine gone dry due to the permafrost thawing at the lake bottom in 2013, which caused a harp decrease in the number of tourists, and then restaurants shut down. This is a typical case of the loss of social and economic development due to permafrost environmental changes in China.

The growing understanding of permafrost changes could be used to advise communities and governments on housing expansion, urban development, and the maintenance and future construction of infrastructures such as airports, roads, buildings, pipelines and mines in this region.

Effects in the active layer and permafrost of the spanish antarctic station "Gabriel De Castilla" (Deception Island)

Antonio Molina[1], Miguel ángel de Pablo[1], Miguel Ramos[2], Cayetana Blitz[3], M.á. Ropero[4], Gabriel Goyanes[5], & Manuel Prieto[6]

[1]*Department of Geology, Geography and Environment, University of Alcalá, Madrid, Spain*
[2]*Department of Physics and Mathematics, University of Alcalá, Madrid, Spain*
[3]*Department of Numerical Simulation in Science and Engineering (GSNCI), Polytechnic University of Madrid, Madrid, Spain*
[4]*Army Engineers Laboratory General Marvá - INTA (National Institute for Aerospace Technology), Madrid, Spain*
[5]*Instituto Antártico Argentino – Dirección Nacional del Antártico, San Martín, Provincia de Buenos Aires, Argentina*
[6]*Department of Automatics, University of Alcalá, Madrid, Spain*

Deception Island is an active volcano located in the South Shetland Islands archipelago, at the western sector of the Antarctic Peninsula. Due to its latitudinal location, the cold climate conditions allow the existence of permafrost, that is being monitored by Spanish and Portuguese research teams at the Crater Lake and Irizar CALM sites and at seven boreholes, that are included in the GTN-P network. Only less than a fifty percent of the island is free of ice, and its surface is characterized by the different type of volcanic materials, including basaltic lava flows, pyroclastic materials, and volcaniclastic deposits. These low-cemented surficial pyroclastic and volcaniclastic deposits reflect the effects of slope, fluvial and periglacial processes, resulting in a wide variety of landforms, such as thermokarsts, slumps, or patterned grounds, among many others. The periglacial landforms reveal the presence of an active layer what is measured at the CALM and GTN-P sites in about 50 cm on top of a permafrost layer, variable in thickness, ranging between 4 and 6 meters at 80 m a.s.l. in the Crater Lake CALM site.

The island is ring-shaped, with an interior sea (Port Foster) connected to the Brandsfiel Sea by a narrow straight (named Neptune Bellows). Near the western shore of this inner sea, at about 5 m a.s.l., it is located the Spanish Antarctic Station “Gabriel de Castilla” (62°58’38”s, 60°40’21”W). When it was established in early 1989, it was a simple shelter formed by a joined group of 3 conditioned shipping containers. The continuous growing of the scientific community interested in the geology, biology, and permafrost of the island required the corresponding growing of the Antarctic station to allow a higher capacity. Today, it is formed by a dozen of shipping containers and a pre-made modular facility, which is the main building of the station containing the essential services (dorms, toilets, kitchen, living room and the communications center). This one-floor building is 18.5 m long and 6.5 m wide. It does not hold directly on the ground since it is elevated on its frontal side up to 70 cm by metallic columns; meanwhile most of back side of the building is at ground level. A half of the building (containing the kitchen, the living room, and the communication center nowadays) was assembled in 2001. Meanwhile, the other half (containing the dorms, toilets and showers on present day) was extended in 2009. At least since 2009, the terrain at the front of the main building of the station, formed by up to seven meters thick pyroclastic deposits, is being eroded by surficial runoff processes. Those form rills and gullies at the nearest coastal scarp located only 25-30 meters from the building. Those rills were more abundant at the front of the older part the main building of the station (kitchen, living and communications side). This increase in the erosion rate was observed to be qualitatively higher than in the station surroundings, what could have significant effects on the inherent stability of the station. For this reason, research on the state of the active layer and the permafrost at the station location started in 2012. The erosive rate increased since then, mainly in December 2014 when the rills and gullies excavated the terrain in from of the station, exposing the buried septic tank.

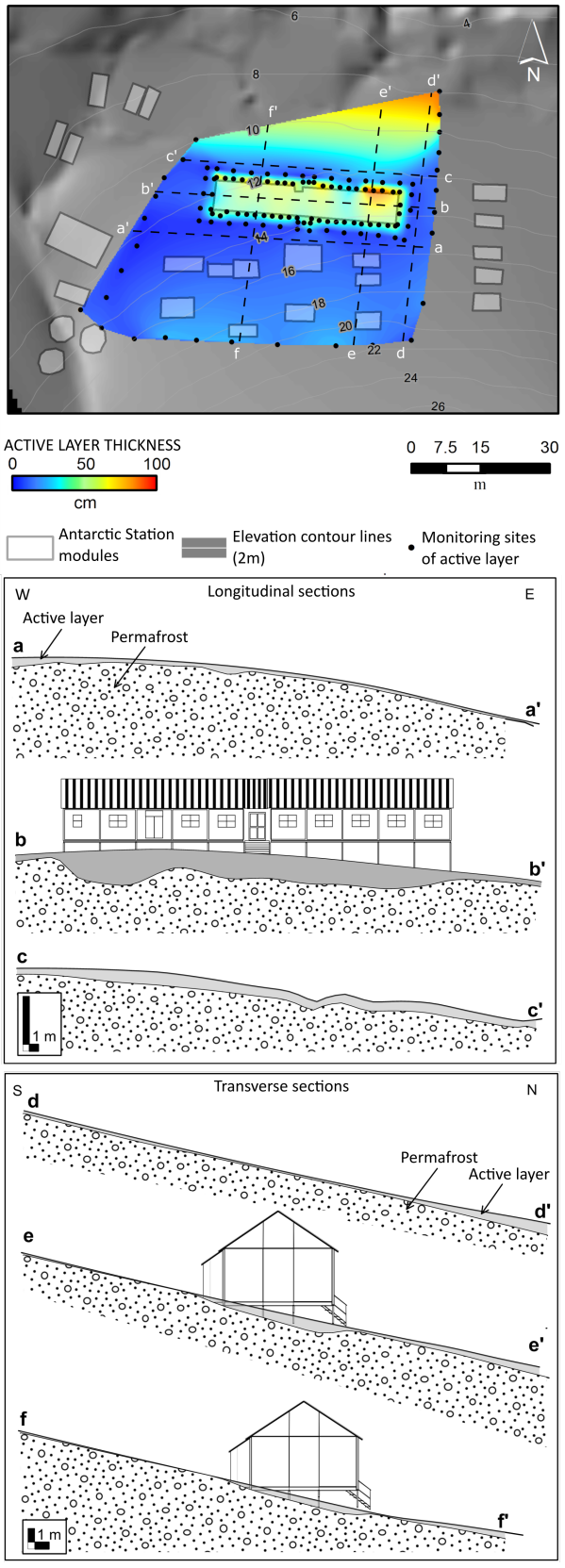

Figure 1: Shaded relief map of the study area showing the nearest neighborhoods interpolation of active layer thickness measured in February 2012 (black dots). Dashed lines mark the location of different longitudinal and transverse sections, showed below.

In February 2012, we drilled a borehole 70 cm deep close to the backside of the station in order to install an array of temperature sensors (DS1922L iButtons model from Maxim) to monitor ground temperatures. We have continuous data from them from 2012 to 2015. Also in February 2012 we measured active layer thickness by mechanical probing in the perimeter of the station as well as in its surroundings (Fig. 1) to detect any spatial variability related to the presence of the station main building. We were not able to measure active layer thickness again in the next years due to logistic problems or the presence of a thick snow cover (that allowed the ground to remain frozen during our stay in the Antarctic Station). In January 2015, we conducted temperature measurement for 10-days (employing iButtons miniature temperature loggers) at different sites inside and outside below the main building of the station, to study the isolation effect of the infrastructure and to deduce the possible impact on the active layer and permafrost.

Although we only have continuous data of the temperature at the shallow borehole, we present here some preliminary results that point to the negative effects of the main building on the permafrost stability. On the first hand, temperature data at the borehole shows that the active layer thickness is about 50 cm at the back side of the station. This data agrees with the active layer thickness measurement by mechanical probing made in early 2012. However, the measured active layer at the building perimeter varies significantly to reach more than one meter at the station front, related to the kitchen, living room and the communications center room (Fig. 1). This increase in the active layer clearly does not follow the local trend of the active layer, which increase toward the nearest coast to the north, as shows the resulting active layer thickness map interpolated from the measurements made in 2012. Then, although the station is elevated on the front side, the active layer is clearly higher than at the back side where the station rests directly on ground level. Different sections (Fig. 1) show the significant change in the active layer thickness from the station back to front sides, as well as along the edifice.

The analysis of indoor and outdoor temperatures measured in 2015 revealed that exist a delay on the outdoor temperatures. They approximately follow the behavior in the indoor temperatures, identifying the period of activity at the different parts of the station in the temperatures measured at the ground below the station, particularly in the living room and the

communications center.

All those results, although preliminary, allow to conclude that the main building of the Antarctic station is not enough thermally isolated. Despite the edifice is elevated from the ground, the temperatures on the ground reflect in some way the temperatures inside the station. This heat transfer increase of the active layer thickness, especially in the spots with higher indoor temperatures. Due to the shield effect of the building respect the air temperatures, during the winter, the active layer could do not reach as lower temperatures as other sites around the station, resulting in a continuous degradation of the permafrost and an increase of the active layer. The thawing of the permafrost has indirect effects, such as to facilitate the erosion of the not consolidated pyroclastic materials that constitute the terrain where the station is located. This erosion is caused by the natural runoff during the Antarctic summer when the snow melts and the active layer thaw.

Consequently, although a natural degradation of permafrost seems to be occurring on the island, at the station site this process could be increased because the shield effect of the building, and accelerated by a not enough thermal isolation of the station. Due to the severe problems it could produce, such as the mentioned erosion of the ground to expose the septic tank or the possible failure of the station supports, a more detailed and systematic monitoring research should be done.

Acknowledgements

This work has been supported by funds from the Ministry of Economy of the Government of Spain by the Polar Research Program (CTM2009-10165-E; CTM2011-15565-E; CTM2014-52021-R) and an arrangement between the University of Alcalá, the Spanish Institute of Geology and Mining, and the Spanish Polar Committee for the maintenance of the monitoring stations in Deception and Livingston Islands.

Available flow rate for culverts built on permafrost and influence of the water source on thermal stability

Loriane Périer & Guy Doré

Laval University, Center of Northern Studies, Canada

It is well known that water is a major cause of degradation in permafrost areas. Poor water management around an embankment exacerbates soil instabilities and similarly, water circulation through a culvert will likely affect the thermal regime of underlying permafrost and cause significant damage. Therefore it is important to pay particular attention on the design for drainage systems. A master's project was carried out to quantify the effect of water temperature and flow rate, through a culvert, on permafrost stability. Two test sites located on the Alaska Highway in Yukon (Canada) were used for this research.

The data collection at the first location, Beaver Creek, allowed the development of a 2D model in TEMP/W representing thermal conditions of soil under and around the culvert. The data of both sites, Beaver Creek and Border Culvert, were used to develop and validate an empirical model, based on the physical processes involved, relating heat flux underneath the culvert with water temperature and flow rate. By using the thermal and the mathematical models, various water temperatures, flow rates, and design parameters were applied. The proposed presentation will highlight the results of a sensitivity analysis done using the models developed. The analysis was based on assumed acceptable thaw depth for the Beaver Creek test site and a variation of heat flux imposed to the 2D model until acceptable thaw depth was reached. An allowable flow rate can then be derived using the mathematical model from the resulting heat flux. The results of the study are likely to provide a basis for the design of the drainage system using an allowable flow criterion in order to limit the impact to permafrost stability.

The mathematical model is also highly sensitive to water temperature. The heat flux values tend to increase considerably with water temperature increase. Consequently, water temperature has a significant impact on the thermal regime under the culvert. Water temperature, depending on the environmental context, should be taken into account when analyzing the effect of water flow in culverts. Therefore, it is necessary to characterize the source of the water. In other words, determine if the water comes from active layer melting, a watershed, from a mountain creek, or if it is stagnant. In this study, each site has a different water source. At the Beaver Creek test site, the water is stagnant before entering in the culvert due to the presence of a ditch intersected by a weir. At the Border Culvert test site, water comes from mountain and active layer thawing. The water flow context may cause the water temperature to increase by several degrees. The influence of these contexts will be analyzed and conclusions will be drawn in order to know and quantify the impact on the ground thermal regime under culverts.

Cone penetration testing for railways on permafrost

Ivan Sokolov[1], Nikolay Volkov[2], & Vladislav Isaev[3]

[1] *Geoinzservice LLP Fugro Group, Russian Federation*
[2] *Fugro Consultants, Inc, Houston USA*
[3] *Moscow State University, Russian Federation*

The Vorkuta railroad is experiencing continuous deformation due to permafrost thaw settlement. The railroad was built in early 1940's. Today the railroad is loaded to only 30 % of its capacity to serve coal and passenger traffic. The low traffic capacity is caused by continuing deformation of the railroad tracks, which are relevelled each year. The railroad connects Vorkuta, Labytnangy and Bovanenkovo with the European part of Russia. If the railroad extends to Sabetta port on Yamal peninsula, the railroad capacity must be increased up to 100 % of its capacity to satisfy growing traffic demand. Thus, continuing deformation of the railroad tracks must be fixed. Many sections of the studied railroad have deformed due to permafrost thawing and differential settlement. One of the sections, called "101^{st} km", is discussed to describe a possible technique for the problem detection. The railway embankment varies from 2 meters up to 6 meters high above the local ground surface. Thermokarst lakes are located on both sides of the railroad. Surface and groundwater flows through the railway embankment, particularly near the pipe culvert. The profile near the culvert pipe at the distance of 5 meters from the railway tracks is as follows: 1.5 meters of crushed rocks, then 1 meter of sand mix with native soils and construction waste; native soil – grey-brown soft clay – found below 2.5 meters. Permafrost table was found at the depth of 1.5-1.7 meters at a distance from the pipe culvert. Technologically, it was impossible to detect permafrost table right under the pipe culvert. Geotechnical borehole drilling is not practical on a railway in operation. Ground penetrating radar did not detect permafrost table, only showing thawed soils down to 4 meters. Geodetic survey showed that the differential settlement of the railway embankment was 62 cm. Periodic leveling of the railway embankment was performed to maintain the railway in operating condition. The task from the railway engineers was to find a new technique which is able to diagnose and/or confirm the problem, precisely describe the extent of the problem and provide enough information to find a feasible technical solution. The main restrictions for the technique include the following: demand for non-disruptive or low-disruptive testing, test time limit for 3 hours. Cone Penetration Testing (CPT) is a method used to determine the mechanical properties of soils and stratigraphy. CPT is one of the most common methods used and accepted for soil investigation worldwide. For permafrost soil investigation, CPT is now standardized in the updated Russian code 25.13330.2012 "Bases and Foundations on Permafrost Soils", Appendix Л "Determination of mechanical properties and pile bearing capacity of permafrost soils on CPT results". Based on CPT results, it is possible to estimate Deformation Modulus (Ef, MPa), Equivalent Cohesion (Ceq, kPa) (i.e. soil strength) and Pile Bearing Capacity (Fu, kN). The applied method consists of pushing an instrumented cone, with the tip facing down, into the ground at a controlled rate of about 2 cm/s. The cone is instrumented with a typical cone tip having a cross-sectional area of 15 cm^2, which corresponds to the cone diameter of 4.4 cm. The friction sleeve is also installed to quantify the sleeve friction and estimate soil cohesive strength. The cone tip measured cone resistance qcv. The shear sleeve measured sleeve friction fsv. In addition to them, at the cone tip the temperature sensor is installed to measure soil temperature. The accuracy of the temperature sensor is 0.01 textdegree C. The total penetration was reach at the depth of 12 meters. Two soil units were identified which correlates to the borehole data obtained several years before by a separate operator. For each element mechanical properties were estimated according to SP 25.13330.2012, which are Ef = 42 MPa and Ceq = 480 kPa for the first element (sand mix) and Ef = 22 MPa and Ceq = 84 kPa for the second element (native soils). CPT profile showed that permafrost is located from 4 meters down to 12 meters and lower. Six temperature measurements with thermal dissipation were performed which showed subzero values between -0.1 textdegree C and -0.7 textdegree C. Thus at the

tested location, the permafrost remained frozen and had not thawed as it was expected. However, the railway track differential settlement is a strong evidence of permafrost degradation which should be investigated in more details. The results of the test clearly showed that the reason of the thaw settlement is not connected to only thermal-radiation regime alteration caused by the railway embankment. Talik zone should be investigated in more details to indentify the true reason of permafrost degradation and to develop a technical solution to fully seize the deformation of the embankment. The trial CPT test on Vorkuta proved its applicability for permafrost investigations. Moreover, this example clearly presents the benefits of CPT compared to geotechnical borehole drilling in the view of time, cost, information content, etc.

In 2016 geotechnical campaign will continue CPT application for more detailed investigation of the deformed sections of the Vorkuta railway embankment.

Figure 1: Differential Thaw Settlement of Railways on Permafrost Terrain

Investigation and management of permafrost and groundwater conditions at mining sites: Case studies in continuous permafrost of Alaska and Canada

Eva Stephani[1], Michael Angelopouloss[3], Mark Musial[2], Steve Anderson[2], Patrick Gince[3], & Mayana Kissiova[3]

[1] *University of Alaska Fairbanks, Fairbanks, Alaska, USA*
[2] *Golder Associates, Anchorage, Alaska, USA*
[3] *Golder Associés, Montreal, Quebec, Canada*

Development of mining sites in permafrost areas often implies that new infrastructures are built and pits are excavated in remote areas where the frozen ground was previously unaffected by anthropogenic activities. Mining development changes the surface and subsurface conditions, such as the surface albedo, vegetation cover, hydrology and hydrogeology; ultimately changing the thermal conditions of permafrost that was previously protected from thawing. Mining activities also typically generate an abundance of surface water that must be managed and stored on site, both during the mine lifetime and reclamation phase. Although, the natural ground is generally cold in continuous permafrost areas, changes in subsurface and terrain conditions can initiate permafrost degradation as the ground thermal stability is sensitive. This is especially critical considering that permafrost in Alaska has been substantially warming since the 1980s and it is expected that the future changes in ground temperatures will closely follow the climate changes [Romanovsky et al., 2015]. Once initiated, permafrost degradation can increase furthermore due to a series of positive feedback effects. For instance, groundwater flow paths can develop in areas where permafrost has degraded and, consequently, permafrost degrades even further, such as observed under road embankments [de Grandpré et al., 2012].

Local permafrost degradation at mine sites yields to the reduction of the soils mechanical strength, such as decreased bearing capacity and increased thaw-consolidation. As a result, permafrost degradation can threaten the structural integrity of the mining infrastructures and open pits. This raises safety, environmental and economic concerns, which are particularly significant considering that these mining sites are generally located in remote areas where assistance is complex and costly.

Assessment of permafrost degradation at mining sites can be done using a series of complementary methods, such as drilling, soil and rock sampling, laboratory testing, geophysical surveying, and instrumentation installation for monitoring ground temperatures, groundwater levels, and surface displacements. Mitigation techniques and management plans can be recommended upon the investigation findings. This approach can be effective at solving permafrost degradation related issues, although in some cases the problems are solved only for short-term purposes and/or can be costly. A proactive approach to reduce permafrost degradation at mining sites, and therefore reduce upfront the safety, environmental and economic concerns, is to adapt the design and managements strategies at the development phase of the infrastructures and/or open pits (i.e. before initiating severe permafrost degradation issues). Elaboration of this proactive approach can greatly benefit from shared experiences across permafrost regions, including the types of permafrost degradation processes encountered, investigation methods, management plans, and implemented mitigation techniques. In this context, the presentation aims to summarize two case studies where permafrost degradation was investigated at two mining sites located in continuous permafrost areas of Alaska and Canada.

At Site 1, the development of a material site has led to multiple pits separated by natural berms, including a pit in reclamation that filled with water draining from adjacent terrain. The reclamation concept relied on the cold frozen ground to prevent hydraulic connections between the pit filled with water and any adjacent pits that are actively mined. However, the presence of a new water body that does not freeze trigger changes in the thermal regime and field observations suggested that groundwater flow paths possibly developed between these pits [Stephani et al., 2015]. At Site 2, a berm has been constructed to retain surface water produced by mining activities. Movements and longitudinal tension cracks along the berm sug-

gested that the cold underlying frozen ground was degrading.

Investigations to assess the permafrost and groundwater conditions included drilling, sampling, and geotechnical laboratory testing. Piezometers and temperature acquisition cables were installed for measuring groundwater levels and ground temperatures. At Site 1, electrical resistivity surveying was conducted along the borehole alignment and in extended areas. This allowed for correlation of the electrical resistivity surveying results with the drilling data to map subsurface materials in two dimensions. The elevation of the surface water level was also surveyed. At Site 2, a snow survey was also conducted to assess the snow cover variability along the infrastructure and potential impact on the local ground thermal regime.

Preliminary results at Site 1 indicated a distinct two-layer system; the upper part was characterized by lower resistivity values while the lower part had higher resistivity values, except in one area where lower resistivity values extended to greater depths under the pit separation berm. Ground temperatures at depth were generally well below 0 degrees Celsius (°C), except in the lower resistivity value zones extending at depth where ground temperatures were slightly above 0 °C. In the lower resistivity values area, groundwater was measured and the level was at the same elevation as the water level in the pit in reclamation. The preliminary results at Site 2 indicated that there are groundwater flow paths developed at depths under the berm and possibly other zones opened for groundwater flow in the upper parts of the berm. Therefore, raising the water level in the pit in reclamation increases the risk for groundwater flow into the active pit and refilling operations should be suspended to allow thermal conditions to stabilize and potentially refreeze the pit separation berm [Stephani et al., 2015]. Continued monitoring of ground temperatures indicated that the isothermal conditions persisted at least for over a year while no additional permafrost degradation was observed in the areas monitored under the berm.

Results at Site 2 indicated that ground temperatures at depths on the upstream side of the berm were only slightly below 0°C while they were colder by about 1 °C on the downstream side of the berm. The active layer on the upstream side of the berm had penetrated the soil layer under the berm and reached the top of bedrock. On the downstream side of the berm, the active layer was about one fifth the depth than on the upstream side. Groundwater was observed on both sides of the berm during drilling operations. Snow accumulation was significantly thicker where the downstream berm slopes were steeper and higher, while no snow accumulated on the flat wind-exposed surfaces of the berm crest. The overall results suggest that a significant thaw settlement below the upstream side of the berm should be limited in the future, as the maximum thaw depth has reached the top of bedrock. On the downstream side of the berm, the maximum thaw depth is located within the soil layer; therefore, thaw-settlement in the future could occur if ice-rich permafrost degrades. Although thick snow accumulation locally affected the underlying thermal regime, the presence of a large surface water body on the upstream side of the berm appeared to trigger the greatest changes in the thermal regime at Site 2.

These two case studies suggest that storage of surface water, groundwater flow, and thick snow accumulation are three significant factors that can trigger and exacerbate permafrost degradation under mining infrastructure and open pits and, as a result, threaten their structural integrity. Therefore, infrastructure design and management strategies should be developed to limit the accumulation of snow and surface water, and, hence, limit the risk of potential groundwater flow that further exacerbates permafrost degradation. The data collected from the monitoring programs will help guide future management strategies, including reclamation activities.

References

de Grandpré, I.; Fortier, D. and Stephani, E. [2012]: Degradation of permafrost beneath a road embankment enhanced by heat advected in groundwater. *Canadian Journal of Earth Sciences*, 49(8):953–962, doi:10.1139/e2012-018.

Romanovsky, V.; Cable, W.; Kholodov, A.; Nicolsky, D.; Marchenko, S.; Santosh, P. and Muskett, R. [2015]: Detecting and forecasting permafrost degradation in a warming climate. In *American Geophysical Union Annual Fall Meeting, 14-18 December 2015, San Francisco,* B31D-0576.

Stephani, E.; Musial, M. and Anderson, S. [2015]: Reclamation of material sites in continuous permafrost of Alaska: an example of groundwater flow between pits. In *Joint 68th Canadian Geotechnical Conference& 7th Canadian Permafrost Conference, Quebec, Canada.*

Management strategies of slope stability geohazards near developments in permafrost areas – Current state-of-the-art

Eva Stephani[1], Guy Doré[2], & Margaret Darrow[1]

[1] *University of Alaska Fairbanks, Fairbanks, Alaska, USA*
[2] *Laval University, Québec, Québec, Canada*

Common slope failure features and processes observed in Canada and Alaska include thaw slumps [Brooker et al., 2014], active layer detachment slides [Blais-Stevens et al., 2015], frozen debris lobes [Simpson et al., 2015], solifluction lobes, and creep. Many of the existing slope failures in permafrost soils do not pose a significant risk for anthropogenic activities, as they are often in undeveloped and remote northern areas; however, intensification of northern development, such as natural resource extraction, community infrastructure, and governments exercising sovereignty in the Arctic, will increase the number of engineered structures and other anthropogenic development activities that are at risk. Northern development also implies a greater amount of manmade slopes, such as road cuts and mining pit walls. These manmade slopes modify the natural terrain and subsurface conditions, such as the vegetation cover, ground thermal regime, cryostratigraphy, hydrology, and hydrogeology. In many cases, the permafrost thermal equilibrium is sensitive; thus, changes in terrain and subsurface conditions initiate permafrost degradation and can result in slope failures. Potential change in local climate and terrain conditions due to climate change also may exacerbate permafrost degradation and related failures of natural and manmade slopes.

Damage to engineered structures and anthropogenic development activities in permafrost regions from failure of natural and manmade slopes creates significant safety, environmental, and economic concerns, especially in these remote areas where assistance is complex and costly. For instance, on the North Slope of Alaska, several oil fields, including the Prudhoe Bay oil field that ranks in the first three most important oil fields of the nation, rely on one road access (e.g., the Dalton Highway) to support their economic activities. The Trans-Alaska Pipeline also travels along the same general road alignment. Among the various slope failure processes and features observed along the route, in the southern Brooks Range a frozen debris lobe (FDL-A), which is a slow-moving landslide in permafrost, is currently located less than 40 meters from the Dalton Highway and is moving toward the road at an average rate of 0.012 meter per day [Simpson et al., 2015]. It is unknown how FDL-A will react to climate change, but a temperature increase will result in melting of massive ice and thawing of ice-rich soil, which will increase pore water pressure and decrease soil strength (Simpson et al., in press), potentially yielding a faster movement rate or, ultimately, a catastrophic failure. Potential damage to this vital infrastructure from FDL-A or other slope failure processes and features can greatly impact the economic activities out of Prudhoe Bay, as well as trigger significant environmental disaster.

Given the hypothesis that slope stability geohazards in permafrost areas can be addressed for long-term purposes by implementing adapted stabilization practices and other mitigation techniques, we propose to develop a proactive management strategy for natural and manmade slope stability in permafrost areas of North America, which will include:

1. identifying potential failure types in given areas,
2. characterizing and quantifying the processes involved, and
3. delineating the spatial distribution of slope failures in extended areas.

Based upon these findings, the management strategy will propose locally-adapted slope stabilization practices and other mitigation techniques. This presentation will summarize the current state-of-the-art for managing slope stability geohazards in permafrost areas of Alaska and Canada, and will introduce the project to develop a proactive management strategy for natural and manmade slope stability in these regions.

References

Blais-Stevens, A.; Kremer, M.; Bonnaventure, P.P.; Smith, S.L.; Lipovsky, P. and Lewkowicz, A.G. [2015]: *Active Layer Detachment Slides and Retrogressive Thaw Slumps Susceptibility Mapping for Current and Future Permafrost Distribution, Yukon Alaska Highway Corridor*, pages 449–453. Springer International Publishing, Cham, ISBN 978-3-319-09300-0. doi:10.1007/978-3-319-09300-0_86.

Brooker, A.; Fraser, R.H.; Olthof, I.; Kokelj, S.V. and Lacelle, D. [2014]: Mapping the Activity and Evolution of Retrogressive Thaw Slumps by Tasselled Cap Trend Analysis of a Landsat Satellite Image Stack. *Permafrost and Periglacial Processes*, 25(4): 243–256, doi:10.1002/ppp.1819.

Simpson, J.M.; Darrow, M.M.; Huang, S.L.; Daanen, R.P. and Hubbard, T.D. [2015]: Investigating movement and characteristics of a frozen debris lobe, south-central Brooks Range, Alaska. *Environmental & Engineering Geoscience*, doi:10.2113/EEG-1728.

Cumulative economic damages in permafrost based on an example of a linear infrastructure (Railway Khanovey – Pesets)

Alina Sergeevna Voytenko & Dmitry Olegovich Sergeev

Institute of geoecology of a name E. M. Sergeyev Russian Academy of Sciences, Russian Federation

In permafrost zones, the deformations of railroad tracks is typically initiated during the construction processes and largely depends on the specific construction method used and the permafrost conditions encountered. The construction of a railway line modifies the heat transfer conditions at the surface. The change in the thermal state of the foundation caused by the construction further results in a modification of the physical characteristics and the mechanical properties of the soil and rock. However, settlements of the railroad embankment and tracks may also occur naturally in response to climate change. To prevent unwanted railroad deformations, foundation conditions must be known for the engineering design and for an accurate implementation of engineering solutions.

Vertical settlements are the dominant type of deformation of the roadbed that has been observed on the railway line between Khanovey and Pesets in Russia. Settlements begin to be appear during late summer, but do mainly occur in September and October. The settlements are believed to be associated with permafrost degradation and gradual lowering of the permafrost table. The areas of settlement occur where the seasonal frost no longer reaches the permafrost table and a layer of continuously thawed ground form. Where large taliks are present and in areas where the seasonal frost depth equals or exceeds the thaw depth in summer (active layer), generally, settlements do not occur.

The main reason for the permafrost degradation is the change in the thermal regime initiated by the construction of the railway. The construction of a railway in permafrost area affects the natural conditions of and the location of the permafrost table. Permafrost degradation can further be accelerated by using inadequate methods and procedures during the construction of the railroad bed, such as removal of peat. Drilling confirmed that the vegetation layer was removed during construction of the embankment.

These settlements may result in significant economic losses, which include, direct loss of material, structural damage to railroad infrastructure and indirect economic losses due to the interruption of railroad services. As highlighted, the permafrost in the area is affected by changes in seasonal freezing and thawing as well as human impacts. The standard depth of seasonal frost, according to the Building Regulations 2.01.01-82, for the soils encountered in the area is up to 2.5 m. Further, following the Manual for Designing Foundations of Buildings and Structures p.2.135., t39, the soil is classified as having a strong frost heaving potential. We present research that assessed the accumulated economic costs of long-term operation under a changing climate along the Khanovey - Pesets rail line.

Cooling effects of highly porous media embankments constructed with ventilation ducts in permafrost regions

Mingyi Zhang, Wansheng Pei, Xiyin Zhang, Zhiqiang Wu, & Zhi Wen

State Key Laboratory of Frozen Soil Engineering, Cold and Arid Regions Environmental and Engineering Research Institute, Chinese Academy of Sciences, Lanzhou 730000, China

Cooling methods and technologies have been applied to embankments to ensure the thermal stability of the important highway/railway engineering projects in permafrost regions, e.g. the Qinghai-Tibet Railway and Qinghai-Tibet Highway in China, the Alaska Highway in the USA and the Baikal-Amur Railway in Russia. The cooling effects of highly porous media embankments made from crushed rocks or concrete cinderblocks have been evaluated previously using numerical simulation, laboratory tests and in-situ observation. However, the single highly porous media embankment cannot effectively ensure the thermal stability of a permafrost expressway with a wide and high-temperature upper surface in the Qinghai-Tibet Plateau under global warming. Therefore, novel highly porous media embankments with ventilated ducts are developed, e.g. crushed-rock interlayer embankment with perforated ventilated ducts and concrete-cinderblock interlayer embankment combined with unperforated ventilated ducts. The thermal behaviors of the composite embankments are numerically simulated in permafrost regions of the Qinghai-Tibet Plateau under global warming. The numerical results show that the composite embankments have good cooling effects on the underlying permafrost and can improve the stability of permafrost expressways in the Qinghai-Tibet Plateau; and especially when the ventilated ducts are perforated or the crushed-rock interlayer embedded in the embankment is replaced with concrete-cinderblock layer, the cooling capacity of the highly porous media embankment with ventilated ducts can be greatly improved. The methods and technologies can provide a scientific guide for new permafrost expressway embankment design and construction in the Qinghai-Tibet Plateau.

SESSION 28

Permafrost Engineering in Mountainous Terrain

Convener:

Lukas Arenson, *BGC Engineering Inc., Canada*

Marcia Phillips, *WSL Institute for Snow and Avalanche Research SLF, Switzerland*

Antóin O'Sullivan, *University of Sussex, UK*

Large areas in mountain regions of the world are situated in permafrost, where the ground remains frozen throughout the year and may contain significant amounts of ground ice. The presence of ground ice and the effect of mountain topography brings unique challenges to engineering projects in mountainous terrain. These can generally be categorized into direct and indirect ones. While direct impacts are related to the behavior of the foundation, such as deformation due to ice creep or consolidation settlement, indirect ones are related to geohazards triggered within the permafrost terrain located upslope of an engineered structure. The latter range from simple rock fall caused by permafrost degradation to a complex chain of events such as a rock slide in the periglacial belt transforming into a debris flow, entering a lake and causing a displacement wave, and finally a flood. Climate change adds an additional level of uncertainty to the engineering design because changes in air temperature affect the permafrost in an unprecedented way. Therefore historic events cannot simply be used to predict future behaviour. The geotechnical properties of the substrate must be investigated carefully, the effect of future climate scenarios taken into account and specially adapted construction methods and materials must be used for engineering projects in mountainous permafrost terrain.

The purpose of this session is to showcase practical examples of engineering design and construction in mountainous terrain, where permafrost has had a significant role, direct or indirect, in the design or the performance of the structure.

Sonic drill for frozen core extraction in mountain permafrost in the dry Andes

Lukas Arenson, Pablo Wainstein, Juan Umarez, & Daniela Welkner

BGC Engineering Inc., Canada

Extracting and assessing undisturbed cores from geotechnical boreholes is the only method to reliably and accurately measure the physical parameters of the ground that are needed for a detailed geotechnical characterization [Andersland and Ladanyi, 2003, BNQ, 2016]. In a permafrost environment the extraction of high quality, undisturbed samples is further the sole way to determine the ground ice contents and its properties as it changes with depth. A detailed understanding of ice contents with depth in mountain permafrost is relevant for assessing the stability as well as the hydrological role of frozen slopes. However, drilling and extracting undisturbed samples is costly and therefore very few boreholes have been drilled especially in mountain permafrost environments. The heat generated during conventional drilling is the major challenge when extracting undisturbed samples. In particular, drilling through coarse frozen soils using diamond drill bits can result in major thermal disturbances if the temperature of the flushing fluid, which can be chilled air or brine, is not properly controlled. While drilling with chilled brine has several advantages over air and is very common in the Arctic, in mountains environments there are potential environmental as well as logistical challenges associated with this method. Those challenges include the loss of brine in porous layers below the permafrost base or the limited access to water at sites with difficult access.

Nine boreholes with depth of up to 90 m had to be drilled in the Chilean Andes to better understand the spatial distributions of ground ice contents in various rock glaciers and protalus ramparts with the ultimate goal of understanding the hydrological significance of the permafrost in a particular watershed. For the first time a Sonic drill was used to drill through a rock glacier and collect undisturbed, frozen samples. In addition to the physical characterisation, the ice of the undisturbed samples were chemically analyzed, which required the minimization of any cross contamination from drilling fluid. In contrast to conventional drilling, the Sonic drill does not require any drilling fluid when drilling and coring through the ice-rich permafrost of the rock glaciers. While the concept of the technology used for the Sonic drill was born nearly 100 years ago, the use of this technology in conventional geotechnical site investigations has only become increasingly popular over the last 20 years. Most recently the technology has demonstrated its functionality for frozen soil in some projects in the Arctic but never in mountain permafrost to those depths.

This presentation introduces the Sonic drill technology and presents the benefits as well as challenges associated in using this coring methodology for a series of nine boreholes in a complex permafrost environment of Chile where the hydrological and stability assessment of these cryoforms are the focus of the assessment carried out.

References

Andersland, O.B. and Ladanyi, B. [2003]: *Frozen Ground Engineering. 2nd Edition.* American Society of Civil Engineers and John Wiley and Sons Inc., 384 p., ISBN: 978-0-471-61549-1.

Bureau de normalisation du Québec [2016]: *Geotechnical Site Investigations for Building Foundations in Permafrost.* Standard CAN/BNQ 2501-500. In preparation.

Risk assessment of infrastructure destabilization due to global warming in high mountain in the French Alps

Pierre-Allain Duvillard[1,2], Ludovic Ravanel[1], & Philip Deline[1]

[1] *Laboratoire EDYTEM, Université de Savoie, CNRS, Le Bourget-du-Lac, France*
[2] *IMSRN, Parc Pré Millet - 680 Rue Aristide Bergès, 38330 Montbonnot, France*

Due to global warming, high alpine environments are affected by significant environmental changes. Alpine permafrost degradation (warming of permanently frozen ground) and glacial retreat cause geomorphological instabilities in rock walls or superficial deposits, which may lead to processes such as rock falls (volume > 100 m^3), boulder falls (volume < 100 m^3), landslides or subsidence. These processes generate a hazard of direct destabilization for high mountain infrastructures (huts, cable-cars, etc.). An increasing amount of damage to infrastructures is deplored, and sometimes carries heavy social and economic implications. For example, the destabilisation of the Cosmiques hut (Chamonix, France) in 1998 by a large rock fall required reinforcement work at the foundation. Another example is the subsidence of the Bellecombe chairlift arrival station (Les Deux Alpes, France), built on a rock glacier, which had to be raised during summer 2013. To help prevent these risks, an inventory of all high mountain infrastructures in the French Alps was carried out with a Geographic Information System. It uses several data layers, among which are the Alpine Permafrost Index Map and the inventories of the glaciers since the end of the Little Ice Age. 1,769 infrastructures have been identified in areas likely characterized by permafrost and/or possibly affected by glacier shrinkage. An index of destabilization risk has been built to identify and rank infrastructures at risk. This theoretical risk index includes a characterization of hazards and a diagnosis of the vulnerability. Infrastructures were classified according to their degree of risk ranging from low (159 infrastructures) to high (185), or very high (0, currently). A first validation of the index based on inventories of damage and observations was undertaken. The realisation of new inventories of damage will determine whether the index underestimates or overestimates the risk.

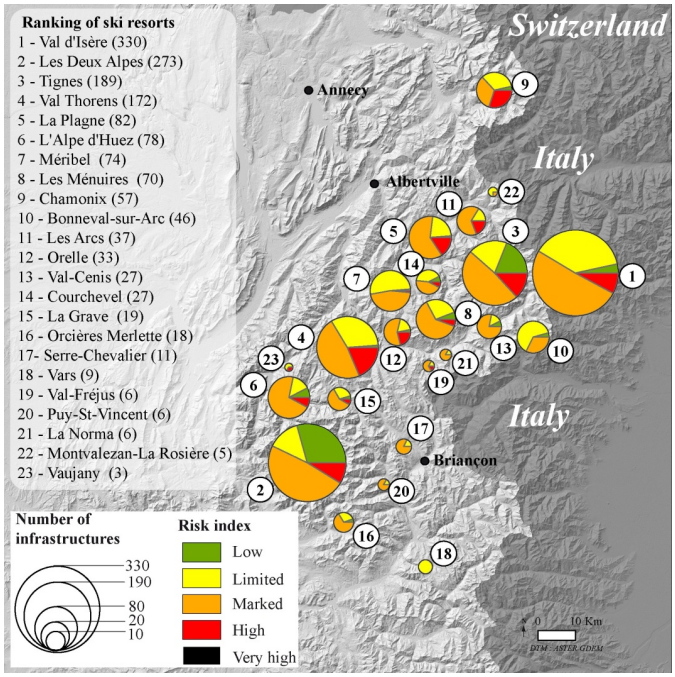

Figure 1: Distribution of the infrastructures at risk in the French Alps ski resorts (Duvillard et al., 2015)

References

Duvillard, P.-A.; Ravanel, L. and Deline, P. [2015]: Risk assessment of infrastructure destabilisation due to global warming in the high French Alps. *Journal of Alpine Research*, 103(2), doi:10.4000/rga.2896.

Ravanel, L.; Deline, P. and Lambiel, C. [2012]: Instability of a highly vulnerable high alpine rock ridge: the lower Arête des Cosmiques (Mont Blanc massif, France). *Geografiska Annaler: Series A, Physical Geography*, 95(1):51–66, doi:10.1111/geoa.12000.

Thermal monitoring of pipe and permafrost beneath the China-Russia Crude Oil Pipeline

Guoyu Li[1], Wei Ma[1], Huijun Jin[1], Yongping Wang[1], Yanhu Mu[1], Shanzhi Fan[1], & Fei Wang[1]

[1]*State key laboratory of frozen soil engineering, People's Republic of China*

The 813-mm-diameter China-Russia Crude Oil Pipeline (CRCOP) is 1,030 km long, beginning at Skovorodino, Russia, entering the Chinese territory at Lianyin, Mo'he County, Heilongjiang Province, and finally reaching Daqing City, Heilongjiang Province (Mo'he to Daqing Line, or MDL). The MDL is 953 km long passing 441 km of discontinuous, sporadic and isolated permafrost terrains, and 512 km of seasonally frozen ground. The MDL was built in the winter of 2009-2010, and began to operate officially in January 2011. The monitored monthly average oil temperatures at three pump stations on permafrost are all higher than 0 ºC (0.42 ºC – 17.86 ºC during the period from May 2011 to October 2015). The year-round operation at positive oil temperatures warmed and thawed the permafrost beneath the pipe, causing rapid permafrost degradation which likely buckled and distorted pipe. A geotechnical and geophysical investigation was initiated including drilling boreholes for installing thermistor cables and thermosyphons, ground-penetration radar (GPR) profiling to survey the active layer thickness and ground stratigraphy, and ground and oil temperature monitoring to evaluate the thermal regimes of permafrost and pipeline.

The latest oil temperatures show that monthly average maximum, minimum and mean annual oil temperatures rose year by year. For instance, the mean annual oil temperatures increased from 8.09 ºC in 2012 to 10.14 ºC in 2014 at Mo'he first station, from 5.65 ºC in 2012 to 6.45 ºC in 2014 at Jagdaqi station. The warming oil accelerated permafrost thaw. The monitored ground temperatures revealed the permafrost beneath the pipe gradually thawed and the ground surface settlement in the trench was ongoing. For example, at kilometer post (KP) 391, the active layer thickness (ATL) under the pipe without thermosyphons increased from 6 m of 2014 (October 14) to 7 m of 2015 (October 28), which was larger than 2 m in the undisturbed site. Some thermosyphons were installed near the pipe at KP 391 to cool the underlying permafrost and prevent thawing. The monitored ground temperatures in the 2-m-away borehole from the center of pipe and in the natural undisturbed site are illustrated in Figure 1. The ground temperatures near the pipe were much higher than those in the natural site. Since October of 2015, the ground temperatures near the thermosyphons began to decline, meaning the thermosyphons worked in the winter of 2015, absorbing heat in the deep ground and discharging it into the atmosphere and gradually cooling the permafrost.

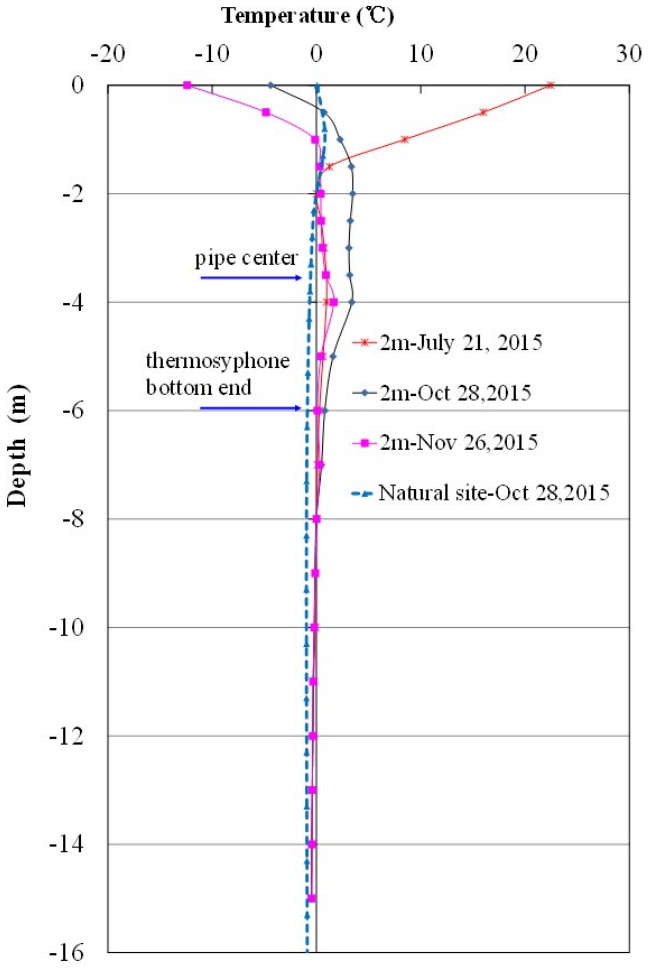

Figure 1: Ground temperature profile 2-m-away from the pipe center with thermosyphons at KP 391

Stability characteristics of a U-shaped crushed-rock embankment of the Qinghai-Tibet Railway in a warm permafrost region

Fujun Niu[1], Minghao Liu[2], & Jingchang Wang[3]

[1] *Cold and Arid Regions Environmental and Engineering Research Institute, Chinese Academy of Sciences, People's Republic of China*
[2] *Cold and Arid Regions Environmental and Engineering Research Institute, Chinese Academy of Sciences, People's Republic of China*
[3] *Qinghai-Tibet Railway Company, Xining, Qinghai,People's Republic of China*

The U-shaped crushed-rock embankment (UCRE) is a combination of crushed-rock sloped embankment and crushed-rock basement embankment, and is applied as a strengthening measure on the Qinghai-Tibet Railway (QTR). Its long-term cooling effect in warm permafrost regions is of interest. The cooling process, cooling mechanism and the deformation characteristics of a UCRE were analyzed, based on long-term in-situ monitoring data from the QTR in Chuma'er High Plain, where the permafrost is warm. The results indicate that the UCRE showed continual and steady cooling. The permafrost table beneath the UCRE rose quickly before reaching a stable state. Temperatures near the artificial permafrost table decreased. Thermal differences between the top and bottom boundaries of the crushed rock layers differed in cold and warm seasons, indicating that air convection occurred within the layer on the shaded side between December and April. Conversely, a 2 week lag in the convection period was observed on the sunny side. A weak warming caused by thermal disturbances from the initial construction of the embankment occurred in the deep permafrost, however this was quickly offset by the subsequent significant cooling. The settlement of the UCRE was small, and it has been stable since 2009. Deformation of the UCRE can be explained by compressional deformation, resulting from a short-term rise in ground temperature due to thermal disturbances associated with construction In general, UCRE proved to be effective at both inducing cooling and reducing deformation in warm permafrost regions, hence ensuring stability.

Modelling internal deformation and slope stability of a protalus rampart: 'Estrecho B' at Pascua Lama in the high Andes of Chile

Antóin M. O'Sullivan[1], Lukas U. Arenson[2], & Julian B. Murton[3]

[1] *University of New Brunswick*
[2] *BGC Engineering Inc.*
[3] *University of Sussex*

During the 1990s the global mining sector experienced a major shift in investment patterns due to changes in the national regulatory framework of over 90 countries worldwide. As a result, South America's mining industry experienced a period of rapid growth, with particularly large growth in Chile, Peru, Argentina and Mexico. One example of the many projects initiated is the Pascua-Lama open pit gold mining project, straddling the border between Argentina and Chile. Our presentation sets out to examine the effects of loading a protalus rampart named Estrecho B with waste rock. Pascua-Lama rests on a large mineralised belt and has been developed for ore extraction by the Canadian company Barrick Gold Corporation. The area is located in the high Andes and surrounded by glaciers and periglacial landforms such as rock glaciers, protalus lobes, protalus ramparts, scree deposits and moraines.

The objectives of the presentation are to quantify changes in Estrecho B's creep rate (currently about 25 cm yr^{-1}) when loaded with a waste rock pile 150 m thick and to evaluate changes in the slope stability due to different loading regimes. The creep analysis was carried out using a one-dimensional creep model. Due to the lack of available intrusive ground investigation at the site, model parameters were assumed using published literature and professional judgement; e.g., Arenson and Springman [2005] shearing angle model was applied to determine the geoform's angle of friction. The reference stress for the geoform was back calculated using the annual creep rate and temperature measurements from the site. The slope stability analysis was conducted using Geostudio's Slope/W numerical programme and applied Morgenstern-Price's Limit Equilibrium Method. The model simulated in-situ conditions and four loading regimes for an unengineered slope and an engineered slope that included a berm. Figure 1 compares the results from each simulation.

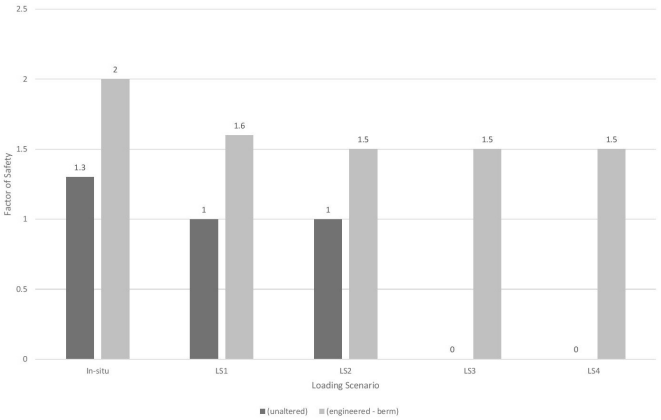

Figure 1: where LS1 = waste rock layer averaging 48 m in depth, LS2 = waste rock layer averaging 88 m in depth and LS3 and LS4 are waste rock layers averaging 123 m and 166 m in depth, respectively (LS3 and LS4 are not considered for the unaltered scenario

Results using the Andersland and Ladanyi [2003] model suggest an increase in annual creep rate from 0.25 m^{-1} to about 8.6 m^{-1} when Estrecho B is loaded with waste rock. Although large, this increase is reasonable because the deformation of rock glaciers (or protalus ramparts) is influenced by ice content, the size and distribution of the soil particles, confining pressure and the ground temperature. The model is limited by the assumptions applied to it; for example the geoform is considered to be homogeneous, whereas it is actually highly heterogeneous. Thus, creep rates will vary from the surface to the basal surface. The slope stability analysis indicated clear benefits when constructing a 2:1 sloped berm at the toe of Estrecho B. However, similar to the creep model, the slope stability analysis included several assumptions and limitations, such as the model is considered as a dry slope and does not consider the geoform to be in a state of steady-state creep. Additionally, both models fail to acknowledge the possibility of a 'chimney effect' phenomenon [Wakonigg, 1996], which may lead to cooling and permafrost aggradation, thereby further stabilising the geoform. The authors further noted

the possibility of solifluction occurring at the end of the talus debris deposit where Estrecho B rests, which may affect its stability.

The initial stability assessment of Estrecho B following loading by waste rock showed that creep rates would likely increase and that a toe berm would significantly increase the overall slope stability. Our assessment further illustrates the potentially complex interaction between the permafrost and the engineered structure, in terms of its thermal as well as mechanical response. Were the project to move ahead, detailed site investigations and stability assessment should be carried out in order to reduce the uncertainties introduced by the assumptions and limitations used in our preliminary analysis.

References

Andersland, O.B. and Ladanyi, B. [2003]: *Frozen Ground Engineering. 2nd Edition*. American Society of Civil Engineers and John Wiley and Sons Inc., 384 p., ISBN: 978-0-471-61549-1.

Arenson, L.U. and Springman, S.M. [2005]: Mathematical descriptions for the behaviour of ice-rich frozen soils at temperatures close to 0 °c. *Canadian Geotechnical Journal*, 42(2):431–442, doi:10.1139/t04-109. URL http://dx.doi.org/10.1139/t04-109.

Wakonigg, H. [1996]: Unterkühlte Schutthalden. *Beiträge zur Permafrostforschung in österreich, Arbeiten aus dem Institut für Geography, Karl-Franzens-Universität Graz*, 33:209–223.

Challenges in construction of Europe highest cable car station at Klein Matterhorn (Switzerland)

Daniel Tobler, Kaspar Graf & Pierre Dalban Canassy

GEOTEST AG, Switzerland

The Klein Matterhorn (3883 m a.s.l.) lies within the touristic Matterhorn-Paradise and its summit is connected by cable cars with the village of Zermatt at the valley bottom. The four-sided pyramidal peak of Klein Matterhorn is stretched along the North-South direction with two predominant, ice-free faces west-east oriented. Since 1979 a double cabins cable-car provides easy access to the summit for skiers, mountaineers and pedestrians throughout the entire year, making this place the highest point in the Alps reachable with a cable-car. This unrivalled situation has led to a continuously growing number of visitors. In order to increase the current transport capacity of 600 persons/hour up to 2600 persons/hour, the construction of an additional modern cable-car was decided by the Zermatt Bergbahnen AG in 2010.

In this perspective, geological and technical preliminary studies were performed since 2011. A route parallel to the existing facility was retained for the establishment of the departure station and supporting pylons. On the contrary, the limited space on the summit ridge of Klein Matterhorn prevented any additional construction. An alternative site for the new arrival station was therefore chosen at 3821 m a.s.l. in the 50-70 degree steep west face, at the exit of an existing gallery (Fig. 1, left). A proper geological and geotechnical analysis of the construction site combined with permafrost related investigations are the basis for a successful foundation concept.

The west face of Klein Matterhorn consists of strongly foliated serpentine. The pronounced downslope main foliation intersects a secondary ENE-WSW layering, leading to highly undulated terrain. Superficial material, up to 1 m deep, is composed of loose rock likely to break-off into small 1m long unstable slabs, while the underlying rock appears compact and only marginally faulted. Extensive laboratory tests have been conducted to define the major rock parameters.

The whole summit of Klein Matterhorn lies within the permafrost zone. Bedrock temperatures as low as –12 °C have been reported during the construction of the original funicular [Keusen and Häberli, 1983]. In the meantime bedrock temperatures have risen to −3 to −2 °C at several localities. This is due to heating and to the heat brought into the tunnel by the more than 500'000 visitors per year. In light of the considerable temperature rise in the bedrock at construction level, temperatures have been monitored since 1998 at ten places in order to take countermeasures if necessary. These measurements build an important basis for the foundation concept of the new cable car station and especially its implementation.

Figure 1: Visualization of the new cable car station at the top of Klein Matterhorn (left) and hotwater drillings in the steep summit flank (right).

In the vicinity of the new arrival station the bedrock is partly covered with snow and ice. To retrieve data about the bedrock topography hot water drillings have been carried out in different places (Fig. 1, right). Prior to the main construction work, starting in spring 2016, the construction site will be protected from rockfall processes. Therefore the installation of an integral rockfall and snow avalanche protection system has been implemented during winter 2015/2016.

The project represents a unique challenge – both in terms of technical requirement as well as installation conditions.

References

Keusen, H.R. and Häberli, W. [1983]: Site investigation and foundation design aspects of cable car construction in Alpine permafrost at the «Chli Matterhorn», Wallis, Swiss Alps. In *Proceedings of the 4th International Conference on Permafrost*, University of Alaska and National Academy of Sciences, Fairbanks, 17–22 July 1983, pages 601–605, URL http://ipa.arcticportal.org/publications/conference-proceedings.

SESSION 29

Permafrost Problems in Mineral, Oil and Gas Exploration and Production

Convener:

Pavel Talalay, *Polar Research Center at Jilin University, China*

Andrew Clennel Palmer, *Dept. of Civil and Environmental Engineering, National University of Singapore, Singapore*

Lorna Linch, *University of Brighton, UK*

The Arctic is endowed with petroleum and minerals that increasingly attract the interest and mobilize the purchasing power of the emerging economies. The Arctic contains 13 % of the world undiscovered oil resources and 30 % of gas resources, making Arctic oil and gas an important economic and geopolitical issue. In addition to hydrocarbon deposits, the Arctic is also home to nickel, iron ore, and other rare earth minerals. Although the full extent of these resources is not yet known, each of the different Arctic countries has made efforts to cultivate these resources. One of the main features of Arctic mineral, oil and gas exploration and production is that the upper portions of the Earth's surface contain permafrost which thickness, depending on location, can be as deep as 500 m in the continuous permafrost zone. The deepest permafrost zone is extended down to 1370 m depth in the upper reaches of the Viluy River in Yakutia, Russia.

The nature of permafrost creates certain problems in mineral, oil and gas exploration and production, for example, thawing of permafrost by drilling fluid; freezing of the drilling fluid in the hole when the drilling process is interrupted; crater-shaped thaw-subsidence of the surface near wellhead; freezing of cement slurry and casing collapse while the hole fluids are freezing in the annulus between casing and borehole wall. Solving of these and some of other problems are planned to discuss in this session.

Application problems and potential for utilization of industrial outage of liquid natural gas cooling capacity for foundation soil thermostabilization as in the case of freezing of lenses of cryopegs with different salt content rage

Dina Bek & Komarov Ilyas

Lomonosov Moscow State University, Moscow, Russian Federation

In the permafrost propagation areas thermal interaction between constructions and foundation soil leads to the thawing of soil and, therefore, to the loss of soil bearing capacity. One way to solve this problem and to minimize such negative influence is to use facilities for foundation soil thermostabilization: the seasonal cooling devices working during period of air temperatures below zero; machine methods of cooling with compulsory ventilation of coolant.

Liquefaction of natural gas is important and even priority technology of gas import and usage. At the stages of designing and operation of gas-condensate fields infrastructure the problem of thermostabilization of foundation soils appears. Thus, one of the perspective decisions could be potential possibility of partial utilization of the liquefied natural gas cooling or some others liquid hydrocarbons such as ethane, propane etc.

Technological norm of liquid natural gas (LNG) storage is estimated by value of liquefied gas in the tank storage daily evaporability, which is approximately 0.1 % of the mass of the liquefied gas in one tank. It is possible to use these technological outages with low freezing temperature for foundation soil thermostabilization, using for this purpose recuperative heat-exchanging facilities. In that way, in line with ensuring competence of constructions foundation, this technology allows to utilize these outages of gas effectively.

In contrast with usually applied seasonal thermostabilizers (TS), use of cooling capacity of the LNG complex allows: to provide reliable operation of a construction all the year round and irrespective of climatic conditions; to utilize selected gas for cooling of the foundation soil; to provide much higher rate of the soil frost penetration; to minimize effect of the frost heaving (the high rate of frost penetration provides minimization of volume of water migrating to the freezing front); to freeze cryopegs with various degree of a mineralization.

Besides obvious advantages of LNG utilization as a refrigerant liquid for soil thermostabilization it can lead to appearance of negative processes, such as frost cracking caused by emergence of big gradients of temperature near the wall of thermostabilizer tube. For that matter, it is required to pay special attention to the determination of optimum value of LNG-inlet temperature and the constructive solution of TS, for the purpose of prevention (minimization) of process of frost cracking.

The task description and software products used for mathematical modeling are given in this article, and also results of calculations of frost penetration process of surrounding soil with various grain size compositions and salinity degree, and cryopegs with different mineralization are presented. The estimates of tension arising during the rapid frost penetration which allow us to find optimum values of LNG-inlet temperature and constructive solutions of TS, for the matter of minimization of process of frost cracking are given.

Study on recovery of permafrost and ecological environments after a strip-pit backfilling –A case study in the Da Xing'anling Mountains in Northeast China

Ruixia He, Huijun Jin, Lanzhi Lu, & Shaoling Wang

State Key Laboratory of Frozen Soils Engineering, Cold and Arid Regions Environmental and Engineering Research Institute, Chinese Academy of Sciences, People's Republic of China

In cold regions, strip mines greatly and adversely impact permafrost and ecological environment. Advance stripping and mining pits clear up surface vegetation and partially remove permafrost layers. These mining activities can substantially alter the land-atmospheric heat exchange and hydrothermal processes in the active layer and permafrost, leading to grave damage to permafrost, water and ecological environments. This paper is based on the study of a coalmine strip pit in the Da Xing'anling Mountains backfilled in summer and autumn 2007. Three segments representative of surface conditions after backfilling, Sites/Borehole CK4 and CK3 respectively at the center and on the margin of the backfilled strip-pit, and undisturbed site (Borehole CK2), were chosen for studying the recovery of the hydrothermal state, nutrient conditions and vegetation restoration seven years after refilling using the methods of vegetation survey, drilling and ground temperature measurement. The investigations indicate a backfill soil temperature of more than 20 °C in warm season in 2007. Drilling and ground measurements in 2014 indicate that after 7 years, ground temperatures have not yet recovered to those of natural (undisturbed) state. In particular, at the Borehole CK4 with a backfilled layer of more than 20 m, temperatures of soil layers deeper than 10 m still have annual averages of 3-5 °C and the permafrost has been thawing under the backfill. A new type of talik, or backfill strip-pit talik, has been forming. At the Site CK4, new permafrost layers have been developed in the backfilled layer and layers shallower than 10 m because of the thin (2.6 m) backfilling, and the active layer and the new permafrost is becoming attached with the underlying permafrost. Temperatures of the backfilled soils and surface vegetation recovery have close relationships with backfilling season, moisture and temperatures of backfilling soils, and soil types and nutrients. It is evident that a timely refilling of strip pit is the most effective approach for restoring permafrost environments after mining, and the key is to successful rebuild the soil horizons for re-vegetation and plant growth. This study is the first on ecological environment after the refilling of a strip coalmine in permafrost regions in China, and the rehabilitation methods, mitigative measures and construction techniques can provide technical support for restoration of ecological environments in strip mines.

Changes of the engineering geocryogical conditions in the Yamburg settlement (Taz Peninsula)

Anna Tolstogan[1], Valery Grebenets[1], Vladimir Pavlunin[2], & Oleg Kislov[2]

[1] *Lomonosov Moscow State University, Russian Federation*
[2] *"Gazprom Dobycha Yamburg" Engineer Technical Center "Yamburg permafrost laboratory"*

Yamburg gas condensate field (YGCF) is one of the largest in the world. It is located on the Taz Peninsula in the Yamalo-Nenets Autonomous District (Russia). The development of the gas condensate field was initiated in 1986. The proven initial gas reserves are estimated to be 6.9 trillion cubic meters. It ranks YGCF the fifth in the world. The local natural conditions are featured with the subarctic climate, typical of tundra landscapes on sandy, fine-grained and medium-grained sediments. YGCF is located in the area of continuous permafrost, it is featured with the widespread development of thermal erosion, thermokarst, cryogenic heaving, and frost cracking. The average values of ground temperatures vary spatially from 0 °C (for floodplains, under bushes) to -5 ... -7 °C (for peat bogs) due to the changes in landscape conditions. During the rapid and intense development 25-30 years ago, permafrost conditions have been affected by various engineering constructions (buildings and infrastructure). The technogenic impact resulted in changes of the ground temperatures as well as in the radical changes of the physical, chemical, and mechanical properties of those. The technogenesis induced geocryological changes is a leading factor, causing the reduction of the bearing capacity of engineering structures, and they lead to the development of deformation, buckling of the supports of linear objects and to the development of taliks. In order to assess the impact of the engineering structures on the environment, we identified and evaluated the following parameters: influence on the underlying surface, the intensity of the impact of buildings on the ground, the area of contact and the duration of exposure. The research findings show, that the permafrost feedback due to the impacts of various engineering objects showed an uneven spatial distribution.

The analysis of the geotechnical safety was carried out in several directions. The study of the local anthropogenic changes was based on the analysis of various climatic, permafrost, lithological data up to 2015, including the reported data of earlier on-ground measurements committed in 1980s. The study showed that the anthropogenic impact could lead to the degradation of permafrost, but the permafrost aggradation may also happen locally, where a proper maintenance of engineering structures is promoted (Fig. 1). One of the study results was the division of the YGCF area into seven natural-technogenic permafrost complexes. Among these:

1. Modern urban infrastructure with an optimum combination of techniques to preserve permafrost (Yamburg settlement);
2. 'Starofinsky' district, where the oldest buildings at YGCF are found and have not been regularly provided with a proper permafrost conservation maintenance;
3. Zones of utility-production services;
4. Linear structures (pipelines, etc.);
5. Municipal waste dumpsites;
6. Abandoned villages;
7. Unaffected natural landscapes.

Via the field and laboratory based works, we collected the data on the current conditions of permafrost, foundation structures and cryogenic processes in the area. We also conceptualized the forecast map of cryogenic hazards. Having done the aforementioned, we provide recommendations on the arrangement of the permafrost stabilization for foundations and engineering structures.

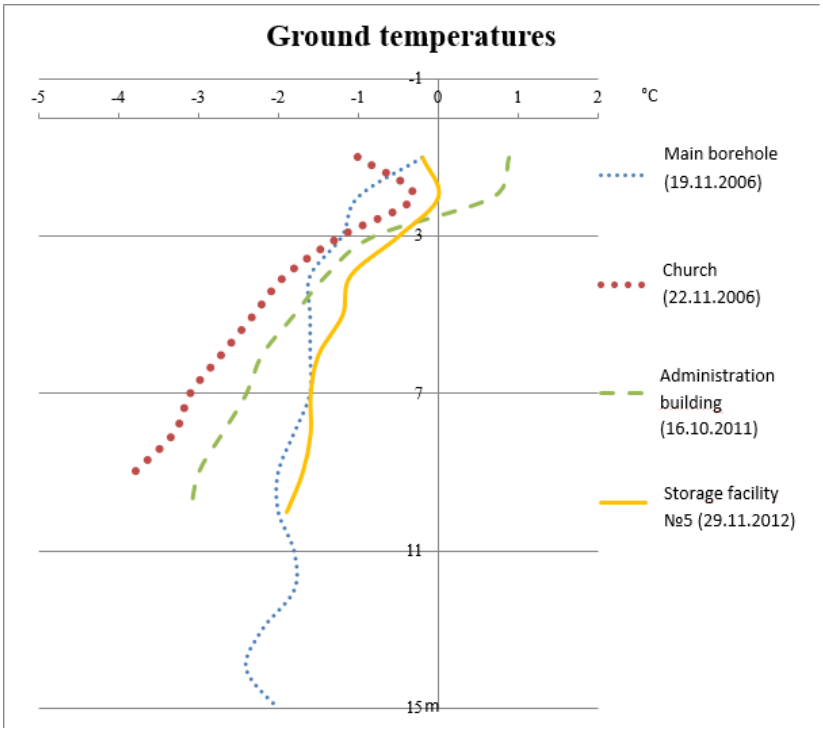

Figure 1: Ground temperatures under different conditions

The most significant changes were detected at the zones of utility-production services on Yamburg oil depository, one of the largest oil depositories in the Arctic. Due to multiple oil discharges, there happened the technogenic salinization of soils down to the depth of piles in permafrost. However, permafrost was generally detected to be stable at the areas of the modern development and under gas plants. Measurement, taken at the crude oil storage in 20 years after it was constructed, revealed negative ground temperature values in the zone of laying piles (-2.5 ... -4 °C) in non-frozen and plastic-frozen grounds. Besides, at the depth of 2-3 m organic pollutants in those were detected to have concentration u 10 -12 g/ l. It means the grounds have almost lost their bearing capacity. Excessive concentrations of organic pollutants in the soil caused its transition to the salted state.

Integrated geophysical monitoring as a basis for effective assessment of the influence of geocryological processes on slope stability in open pit mines

Sergei Velikin, Dmitrii Shesternev, Iuliia Marchenko, & Artem Yakimov

Melnikov Permafrost Institute, SB RAS, Russian Federation

The construction and operation of open pit mines in permafrost cause significant changes in engineering-geocryological conditions that determine the stability of pits and surrounding environment. These changes may lead to permafrost degradation and rapid development of cryogenic processes. In this case, hazards may develop associated with ground instability in pit bottoms and slopes (Fig. 1). It is therefore important to identify and control changes in geocryological conditions caused by mining activities. These issues, as well as problems of the prevention and management of transformation of the geocryological environment in the development of mineral deposits have been dealt with the organization and carrying out of complex geophysical monitoring. The monitoring program established at the Nyurba open pit diamond mine included electrical resistivity tomography, radio-frequency electromagnetic imaging, natural-gamma logging, ground penetrating radar and vertical seismic profiling. Geocryological and engineering-geological methods complemented the geophysical studies.

In seismic surveys, the Summit Compact multi-channel seismograph from DMT (Germany) was employed. Seismic sections were acquired for the eastern slope of the Nyurba mine. Several linear zones of sub-meridional strike were identified on the seismic time slice maps of Vs/Vp and Poisson's ratio. The presence of sub-meridional zones with alternating values of Vs/Vp and Poisson's ratio can be interpreted as a reflection of the separation mechanism of the landslide body when it is displaced towards the pit slope. These zones correlate well with the deeper (up to 50 m) structure of the geoelectrical sections derived from electrical survey data. The electrical resistivity tomography was carried out using a Syscal-Pro multi-channel, multi-electrode resistivity system (Iris Instruments, France). The processed electrical tomography data indicate that the geological material at the study site consists of a high-resistivity upper part and a relatively low-resistivity lower part. Over the entire depth interval, however, there are lateral variations in resistivity. For ground radar surveying, the GSS SIRSystem-2000 with a 200 MHz antenna was used. Twenty five profiles were collected along the eastern slope of the Nyurba mine in order to assess the condition in the near-surface sediments.

Figure 1: Slope failure of an open-pit mine in frozen ground.

These and other studies have shown that:

- the main causes of pit slope movements are the geocryological structure of the area and the mining activities promoting permafrost degradation, while the triggering mechanism has been provided by exogenous geological processes resulting from the neglect of permafrost properties in mining operations;
- electrical resistivity tomography is the most useful geophysical method in detecting and monitoring ground displacements in the vicinity of the open-pit mine; in combination with radio-frequency electromagnetic imaging, natural-gamma logging and thermometry it can provide detection and control of dynamic surface permafrost-related processes.

Geophysical monitoring offers the opportunity to:

- identify the areas at risk of slope slides and other massive failures at the early stage of changes in the permafrost medium;
- develop controlling actions on the permafrost medium for development of structural and ground improvement measures to maintain effective mining operations.

SESSION 30

Frozen Ground Properties: Field and Laboratory Testing

Convener:

Jiankun Liu, *Research Institue of Subgrade and Foundation Engineering, Beijing Jiaotong University, School of Civil Engineering, China*

Lidiya Roman, *Moscow State University, Faculty of Geology, Department of Geocryology, Russia*

Erika Grechishcheva, *OJSC Fundamentproekt, Russia*

Frozen ground is a multicomponent system with many different physical and chemical processes taking place. Construction and engineering activities in the permafrost areas have a significant influence on soils-foundation. Influence can be mechanical or thermal. In such a situation, it becomes necessary to create models of interaction of buildings and structures with the soils-foundation, as well as the opportunity to forecast the temperature regime of soils and development of negative geocryological processes.

Currently, there are many models and programs for this prediction. However, the basis of any model (thermal or mechanical), except formulas, is the primary data about soil properties. There are two important fundamental problems: the research of the influence of various factors on soils properties, (for understanding the significance of factors when creating a model) and obtaining high quality primary data on soil properties. The importance of these studies is due to the fact that the results of modelling depend essentially of the primary data.

The session discusses issues concerning soils properties and the influence of various factors on the mechanical, thermal and geophysical on the soils' properties. Besides, the problems of methods for properties determining, possible errors and methods to improve data quality are considered. Particular attention is paid to comparison of field and laboratory research, comparison of the data obtained by different methods in different conditions.

Effects of adsorbed cations and temperature on zeta potential of clay soils

Heni Amanda Barnes & Margaret M. Darrow

University of Alaska Fairbanks, USA

Introduction

The mass and mobility of unfrozen water in frozen soils is of paramount importance. It influences the soil's strength, affecting foundation design and slope stability in cold regions, and its movement to the freezing front is essential in the frost heave process. The amount of unfrozen water within a frozen soil at sub-freezing temperatures can be measured using various techniques, such as nuclear magnetic resonance (NMR), time-domain reflectometry (TDR), or differential scanning calorimetry (DSC); however, its mobility is harder to quantify.

The clay-mineral fraction of a heterogeneous soil has the biggest effect on unfrozen water. The behavior of a clay particle is affected by its surface charge, which is influenced by the adsorbed cations at the surface. Measuring the zeta potential is one way to characterize the effects of adsorbed cations on the electrokinetic potential at a distance from the mineral surface. Zeta potential is defined as the electrokinetic potential at the shearing plane, which marks the boundary between the bulk water in solution and the adsorbed and diffuse swarm of hydrated ions that travel with the clay particle. Changing the adsorbed cations at the mineral surface significantly affects the zeta potential [Aydin et al., 2004]. The zeta potential also partly describes how micro-aggregates form in the soils [Lambe, 1953]. Clay particles with low zeta potential can approach one another and aggregate, while clay particles with high zeta potential repel one another, creating a dispersed soil fabric. The resulting soil structure will impact the soil permeability and mobility of unfrozen water.

We present some preliminary results from a multi-faceted research project that explores the mass and mobility of unfrozen water in frozen soil. Elements of this project include measuring the unfrozen water content of cation-treated clays using the NMR method and investigating the cation-treated soil structure using X-ray diffraction. Here, we present the soil preparation procedures and the zeta potential measurement results for one cation-treated clay at a suite of above-freezing temperatures.

Soil preparation and testing

We prepared Mg^{2+}, Ca^{2+}, Na^{+}, and K^{+} cation treatments of five standard clays (kaolinite, montmorillonite, illite, illite/smectite, and chlorite, all obtained from the Source Clays Repository), and one heterogeneous soil (Copper River clay sampled from the Copper River Basin, Alaska). All of the original untreated samples were soaked, gently crushed using a mortar and pestle, and then processed through a ball mill and a micronizer to separate pre-existing aggregates. We then collected the minus 2 μm fraction of each cation-treated sample using a standing water column.

The particle size and zeta potential measurements were conducted using a Brookhaven ZetaPlus Zeta Analyzer, which measures the velocity and direction of movement of the soil particles using electrophoresis and a laser. For each cation treatment, we prepared a 1 mMol solution using the same cation as in the treated soil (e.g., NaCl was used for Na^{+}-treated samples, $MgCl_2$ was used for Mg^{2+}-treated samples, etc.). The 1 mMol solution is necessary for measurements because a higher solution concentration suppresses the diffuse double layer and allows for better understanding of individual particle properties. Each cation-treated clay sample was suspended in a 1 mMol solution at a 0.1 mg/mL concentration. Once prepared, the samples remained stationary for 12 hours to allow any dust particles to settle. After the 12-hour period, we measured particle size for each cation-treated sample at 22 °C. The particle size values were used as an input parameter to calculate the zeta potential, which was measured at 20 °C, 15 °C, 10 °C, and 6 °C.

Results and Discussion

Figure 1 contains the results of the particle size and zeta potential measurements for the cation-treated illite/smectite samples. The divalent cation-treated samples had similar particle sizes, which were larger than the monovalent cation-treated samples (Fig. 1a). The divalent cation-treated clays demonstrated less negative zeta potentials (between -9 and -13 mV),

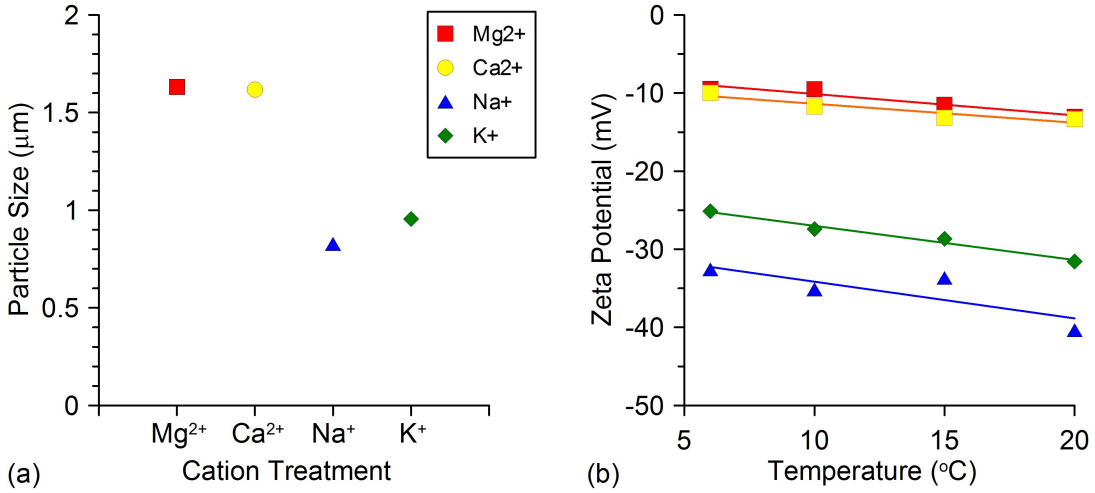

Figure 1: Effects of cation treatment on illite/smectite (a) particle size and (b) zeta potential at above-freezing temperatures.

while the monovalent samples demonstrated much lower zeta potentials (between -22 and -40 mV; see figure 1b). This indicates that the divalent cations neutralized the surface charge more effectively, lowering the zeta potential and allowing the clay particles to approach each other and to aggregate, resulting in larger particle sizes [Grim, 1958]. Conversely, the monovalent cation-treated samples demonstrated a greater negative charge, causing the particles to repel each other resulting in a more dispersed condition and smaller particle sizes. For all of the cation-treated samples, the zeta potential increased (i.e., became less negative) as temperature decreased. Each suite of temperature measurements fit a linear trend with coefficients of correlation (R2) ranging from 0.68 to 0.98.

Conclusion

These results indicate that there are clear relationships among the dominant adsorbed cation on the clay mineral surface, the zeta potential, and the tendency for the particles to aggregate or disperse. While interesting, these results were obtained at a suite of above-freezing temperatures, and thus do not apply directly to frozen soils. To the best of our knowledge, zeta potential has not been measured at sub-freezing temperatures. We are currently developing a procedure for testing zeta potential at -2 °C. We anticipate that the results will yield insight into how electrolyte concentrations affect viscosity, thus affecting unfrozen water mobility. Additional tests include measuring zeta potential versus pH to determine the variable charge characteristics for each suite of cation-treatments for each soil type.

Acknowledgements

The authors thank Dr. T. Trainor for his valuable insight and for the use of his laboratory. We also thank T. Nick, Y. Miao, and R. Sinnok for their many hours spent preparing soil samples for testing and for vetting the testing procedures. This research was supported by the National Science Foundation under Grant Number 1147806. The views, opinions, findings, and conclusions reflected in this abstract are the responsibility of the authors only and do not represent the official policy or position of the NSF, or other entity.

References

Aydin, M.; Yano, T. and Kilic, S. [2004]: Dependence of zeta potential and soil hydraulic conductivity on adsorbed cation and aqueous phase properties. *Soil Science Society of America Journal*, 68:450–459.

Grim, R.E. [1958]: Organization of water on clay mineral surfaces and its implications for the properties of clay-water systems. *National Research Council, Highway Research Board*, 40:17–23, 1958.

Lambe, T.W. [1953]: *Cold Room Studies, Third Interim Report of Investigations.* App. D – Mineral and Chemical Studies. Arctic Construction and Frost Effects Laboratory, Boston.

The new test device for determining the frozen pressure and the strength of silty soils below the low temperature

Adil Binal

Hacettepe University, Faculty of Engineering, Department of Geological Engineering, Turkey

The new test device was developed to determine the frozen pressure and the strength of silty soils. This device composes of freezing unit and compartment. The system is capable of cooling up to -22 °C with liquid coolant as well as it includes three cooling apparatus for the top, bottom and ambient cooling. Also, cartridge heaters were used at the bottom for simulating earth temperature. Four soil samples obtained from Palandöken, Erciyes, Ilgaz and Kaçkar mountains areas of Anatolia were tested at the -4 °C. The minimum frozen pressure was 20 kPa, and the maximum value of it was 30 kPa. The lowest strength of the soil samples was 3.39 MPa, and the highest value of it was 5.35 MPa.

Design and development of a test system for measuring ultrasonic wave of frozen soil

Hui Bing, Yuxia Du, & Xing Huang

Cold and Arid Regions Environmental and Engineering Research Institute,CAS, People's Republic of China

The ultrasonic detecting technique is highly efficient, handy and non-destructive, and reflects the physical properties of the tested object, which is widely used in geotechnical engineering testing. A little work has been done particularly on the techniques and methods of obtaining the ultrasonic velocity of frozen soil, and the current testing work is unable to meet the testing accuracy. So based on the mainframe of ultrasonic detecting (RSM –SY5(T) made in Wuhan Sinorock Technology Ltd., its operating temperature is -5 °C ≈+40 °C), a test system for measuring ultrasonic wave velocity of frozen soil has been designed and developed sufficiently considering the frozen soil properties that it is sensitive to the temperature, the mass of energy transduce to the test object and the coupling between the testing object and the energy transduces. The system which can used to test the ultrasonic wave of the frozen soil with various sizes includes a constant temperature oven and the support for the energy transduces. The constant temperature oven offer the measurement environment with the temperature range from -30 °C to +30 °C,and the support for the energy transduces can be put into the oven during testing. To avoid the influence of the energy transduce mass on the test in vertical measuring, the support offers the horizontal testing platform, and a strain gage have been placed to monitor the coupling extent between the energy transduces and the testing objects to improve the testing accuracy. The testing results of the frozen soil with various temperatures using the system indicate the feasibility of the test system.

The physical properties of permafrost soils of some mountain areas of Turkey

Adil Binal, Orkun Karamut, Bertan Base, & Parisa Adeli Ghareh Viran

Hacettepe University, Department of Geological Engineering, Beytepe Campus, Turkey

The permafrost soils of three mountain areas located in the middle and north-east Anatolia were investigated regarding physical properties in this study. The altitudes of soil sampling areas have changed between 2700 m and 3300 m. The natural moisture contents of the permafrost soil samples of Palandöken (Erzurum city), Erciyes (Kayseri city) and Kaçkar Mountains (Rize city), respectively, were 21.47 %, 6.82 %, and 29.38 %. The values of specific gravity were ranging from 2.52 and 2.6. In Atterberg limit tests, the fine part of soils samples of Palandöken and Kaçkar Mountains showed plastic behaviour but Erciyes Mountain's sample was not. As to the Unified Soil Classification System (USCS), Palandöken Mountain soil sample was classified as silty gravel (GM), Erciyes Mountain sample was categorised as well-graded gravel (GW) and Kaçkar Mountain's soil was grouped as silty sand (SM).

Normalized stress-strain behavior of silty sand under the influence of freeze-thaw cycles

Dan Chang[1], Jiankun Liu[1], & Xu Li[1,2]

[1] *Beijing Jiaotong University, China*
[2] *Transportation Industry Laboratory of Highway Construction and Maintenance Technology in Permafrost Regions-Qinghai Research Observation Base, Qinghai Research Institute of Transportation, Xining, Qinghai 810000, China*

In order to study the stress-strain relationship properties of silty sand after freeze-thaw cycles, the unconsolidated undrained tri-axial shear tests (UU tests) of unfrozen silty sand as well as the one experiencing various numbers of freeze-thaw cycles are conducted. Based on the test results, the unfrozen silty sand exhibits weak strain softening phenomenon under low confining pressure. Silty sand experiencing the first few freeze-thaw cycles also appears to be weak strain softening, and then shows strain hardening afterwards when the confining pressure is low. The stress-strain relation is strain hardening when the confining pressure is higher. The stress-strain curves of silty sand are almost the typical hyperbola pattern. The normalization of the stress-strain relationship is vital to study the stress-strain properties. In this paper, four kinds of common normalization factors accounting for the influence of confining pressure, as well as the corresponding normalized conditions, are introduced. These four normalization factors are widely applied for unfrozen soil to study stress-strain properties. Based on the normalization factors above, a new normalized factor is proposed to analyze the stress-strain relation for soils under freeze-thaw cycles and the normalized conditions are defined. The new normalized stress-strain relationship based on the proposed normalized factor is established to predict the stress-strain curve of silty sand after different numbers of freeze-thaw cycles. Comparison of the prediction and test results shows that the established predict model can consider the influences of freeze-thaw cycles well and has high fitting and prediction accuracy.

Comparison of methods to estimate methane content in permafrost

Maria Cherbunina[1], Anatoliy Brouchkov[1], Denis Shmelev[2], & Vladimir Kazancev[3]

[1] *Lomonosov Moscow State University, Russian Federation*
[2] *Institute for Physicochemical and Biological Problems in Soil Science, Russian Academy of Sciences, Russian Federation*
[3] *A.M. Obukhov Institute of Atmospheric Physics of Russian Academy of Sciences, Russian Federation*

Estimation of methane storage and emission in Arctic landscapes has become actual in the last decade. One of the big issues is to evaluate correctly this amount because of releasing from thawing frozen grounds due to climate change .

For methane content measurements a few approach is used. To determine the content of methane in the permafrost the most commonly used method is "headspace". A small sample (about 50 grams) of frozen soil is degased by placing it in a syringe and saturates with a known volume of a concentrated solution of NaCl [Alperin and Reeburgh, 1985]. After thawing, the syringe is shaken intensively and the gas goes into solution from the sample and into the atmosphere inside the syringe with a known concentration of the gas. The gas mixture transferred through the syringe needle to the 30-50 mL flask filled with a concentrated solution of NaCl. Next, volume of the solution is displaced by injected gas through the compensation needle. For the second method over-saturated salt water was used for the collection of air bubbles from ice and frozen soil so as to avoid additional air entry to the sample holder, which is placed on the top of a funnel in hot water. Frozen samples are melted under a plastic funnel in a saturated solution of NaCl. The funnel is connected by a gum tube with a special gas container; tube container is also full with the solution. The bubbles discharging while the ice melts displace the liquid from the container, which is closed hermetically, being full of gas [Arkhangelov and Novgorodova, 1991]. The main advantage of the first method is the ability to hold a large number of measurements in a short time and it's usability. The main disadvantage of the method is impossible to identify the gas volume in the sample and to consider methane from the air. As for the second method the main advantage is to have the concentration in air bubbles and to get the hole volume of the gas sample, but it can be problem to obtain a frozen monolith of sufficient quantity of gas(10 cm^3). It is laborious and time-consuming

Experiments were conducted to determine the scale effect on the measurement results. In general, the scale effect is called the dependence of the properties of soils to their volume. For this purpose there were taken the 20 samples of ice and frozen soils from Mammoth Mountain (Central Yakutia) and Larsemann Hills (Antarctic Oasis). The deposits are presented by Early and Late Pleistocene coarse and medium sand, sandy silts (Larsemann Hills), fine sand, loam (Mammoth Mount) and ice of ice wedges (Mammoth Mount) and ice-rich ground (Larsemann Hills). This deposit diversity allow to research sediment with different methane content: from null value in Late Pleistocene Ice Complex (loams and ice wedges) to high value in the sand of Mammoth Mount. Thus, we can compare accuracy and sensitivity of each method in different deposits with different content,

As the result there is some correlation between these methods. Usually, the concentration measured by "headspace" method is higher than using the second one. For example, according to "headspace" the methane content of ice wedges from Mammoth Mount is 2-16 mkl/kg, by bubbles discharging is 1-7 mkl/kg. Methane content of Late Pleistocene loam is 1-6 mkl/kg and 1.4-2.6 mkl/kg according to "headspace" and bubbles discharging. General methane content according to "headspace" is double according to bubbles discharging. In the Early Pleistocene sands methane content can reach up to 200 mkl/kg by "headspace" and 40 mkl/kg. General, "headspace" method determines methane content in 2 time bigger, than according to bubbles discharging.

We believe, that this difference between approaches to methane measuring can be explained by the few reasons. In first time in the "headspace" method about 88-90 % of the gas out of the sample after extraction. In second time, general bubbles discharging is increased syringe in "headspace", but inaccuracy can be explained by:

1. the method is cumbersome and requires large volume of degassed deposit and more time for full gas realizing;

2. part of gases can dissolve in the water, in result the total amount of the emitted gas is inaccuracy.

As we can see each method has its pros and cons. The main advantage of "headspace" method is a easy, little volume of sample for analyze and statistics. At the same time bubbles discharging apply to estimate the total amount of gas in the deposits and get large volume of methane, that can be used for further analyze.

Acknowledgements

The research has been supported by RFBR grant № 16-35-00403.

References

Alperin, M.J. and Reeburgh, W.S. [1985]: Inhibition experiments on anaerobic methane oxidation. *Applied and Environmental Microbiology*, 50(4):940–945.

Arkhangelov, A.A. and Novgorodova, E.V. [1991]: Genesis of massive ice at "Ice Mountain", Yenesei River, Western Siberia, according to results of gas analyses. *Permafrost and Periglacial Processes*, 2 (2):167–170, 1991. doi:10.1002/ppp.3430020210.

Thermal conductivity variations of gas bearing soils in permafrost during different conditions of hydrate accumulation

Evgeny Mikhailovich Chuvilin[1,2] & Boris Alexandrovich Bukhanov[2]

[1] *Lomonosov Moscow State University, Russian Federation*
[2] *Skolkovo Institute of Science and Technology (Skoltech), Russian Federation*

There are two types of gas hydrate deposits in cryolithizone. They are inter-permafrost and under-permafrost. To date, a large amount of data of under-permafrost hydrates are collected (Malik, the northern slope of Alaska, Tibet and other). For inter-permafrost gas hydrate deposits there are few reliable data. Today, it is extremely difficult to mark and single out hydrate bearing horizons in permafrost using traditional main geophysical methods (mainly seismic). This is due to values similarity of most physical parameters for hydrate and ice component. However, there are parameters that have a distinct difference for hydrate and ice. In particular, it is thermal conductivity. Thus, the thermal conductivity of hydrate and ice are almost four times different (0,6 and 2,23 W/(m·K), respectively) and similar for water and hydrate (0,55-0,65 and 0,6 W/(m·K), respectively). So there is a prospect of using thermal conductivity data to identify hydrate bearing layers in permafrost.

Special experimental investigations allow us to trace the influence of gas hydrate accumulation processes on thermal conductivity of gas saturated sediments. The experiments were performed on a special installation with integrated system for measuring the thermal conductivity of hydrate-saturated sediment samples under pressure of hydrate-forming gas [Chuvilin et al., 2015]. The method of steady-state thermal regime is at the basis of determining thermal conductivity of dispersion media. Accuracy of thermal conductivity measurements was found to fit the range of 5-7 % with a confidence level of 0,95. In this case, the random error of measurement of thermal parameters does not exceed 4 %. To control and maintain desired accuracy during calibration, we used reference materials with values of thermal conductivity in the range of 0,3 to 2,2 W/(m·K). Model sediments and natural soil with destroyed structure were used as the object of investigations. The model sediments were presented by fine sand (mJ3) and sandy-clay mixture (fine sand + 14 % kaolinite clay (eP2)). Natural soils were presented by different sands, which were selected from permafrost horizons and the Laptev's sea shelf cryolithozone. Experimental data shown that the thermal conductivity of sediments can increase or decrease depending on conditions of porous hydrate formation [Chuvilin and Bukhanov, 2014].

During hydrate accumulation in frozen sediments recorded decrease thermal conductivity associated with different conductivity of hydrate and ice. In natural conditions, this corresponds to formation of gas hydrates in permafrost at negative temperatures. This mechanism can be realized by forming a cargo pockets in freezing soils, and thus the occurrence of high pressures due to pore water of crystallization (crystallization factor), as well as by the action of external load (baric factor) centered on a result of the freezing gas accumulations in the permafrost. At the same time when hydrate formation in the field of positive temperatures ($t > 0$ °C) thermal conductivity of gas-saturated saturated are practically unchanged, a slight increasing of thermal conductivity (up to 13 %) recorded only at high value of hydrate saturation (Sh more 0,4) in pore space. During freezing of hydrate-bearing sediments under gas pressure above the equilibrium, we observed decreasing of thermal conductivity due to additional hydrate accumulation despite the appearance of pore ice. By reducing the pressure under equilibrium, in frozen hydrate containing sediments were revealed increasing of thermal conductivity associated with the partial dissociation of porous hydrate and increase of the content of pore ice. Additional hydrate accumulation was recorded during thawing of frozen hydrate containing sediments, and was accompanied with thermal conductivity decreasing.

Thus, experimental investigations allow us to trace thermal conductivity variations of gas-saturated sediments in permafrost at different mechanisms of hydrate accumulation.

References

Chuvilin, E.; Bukhanov, B. and Brovka, G. [2015]: Method of determining the thermal conductivity of dispersed gas-saturated sediments under conditions of hydrate and ice formation. In *Joint 68th 7th Canadian Permafrost Conference*, Quebec City, Canada, ABS_305.

Chuvilin, E.M. and Bukhanov, B.A. [2014]: Thermal conductivity variations of gas-saturated sediments during hydrate formation and freezing–melting. Part 2. Results. *Earth's Cryosphere*, 18(2):51–57, URLhttp://www.izdatgeo.ru/pdf/earth_cryo/2014-2/51_eng.pdf

Change of gas permeability of frozen sandy soils during thawing

Evgeny Mikhailovich Chuvilin[1,2], Sergey Igorevich Grebenkin[1], & Michel Sacleux[3]

[1] *Moscow State University, Russian Federation*
[2] *Skolkovo Institute of Science and Technology (Skoltech), Russian Federation*
[3] *Total EP exploration*

Study of the gas permeability of frozen and thawed sediments is of great interest considering the emissions of natural gas in the Arctic. It is also important when analyzing results of the geochemical surveys in the permafrost regions for hydrocarbon exploration. In this regard, experimental studies were conducted to assess the permeability of sandy rocks with different moisture content in frozen state and after thawing, the results of which are presented in this paper.

To study the permeability of frozen and thawed soils used a special technique [Chuvilin and Grebenkin, 2015]. Equipment, developed by "Ecogeosprom" Ltd., allowing the evaluation of the gas permeability of the soil wet samples with a diameter of 3 cm and a length of 3-5 cm at various temperature and pressure conditions. The object of research were sand samples selected in the permafrost sediment of marine origin (mQ3) from the South Tambey gas condensate field in the Yamal Peninsula. The samples in natural condition (samples with water content 16-18 %), and samples in disturbed condition (samples with water content 0-14 %) prepared from the frozen core was used in the experiments.

During experimental studies to assess the permeability of sandy rocks data on the effect of moisture content on gas permeability of sandy soils in the frozen and thawed states were obtained. It revealed that for the frozen sandy soils with increasing power of pore filling by ice from 0 to 40 % the permeability was reduced by an order. At increasing ice saturation of sand samples from 40 to 50 % decrease of permeability was several orders of magnitude. At ice saturation of samples about 50 % the gas permeability were not more than a few mD. With further increase of ice saturation (60 %) permeability measurements decreased below the limit of the experimental setup (0.01 mD) (Fig. 1).

It was presented experimentally that during thawing permeability of sand increases. This difference in the gas permeability increases with increasing power of pore filling. For the studied sands at a power of pore filling up to 40 % difference permeability values for frozen and thawed samples less than 1 order at a power of pore filling more than 40 % difference is several orders of magnitude (3-5).

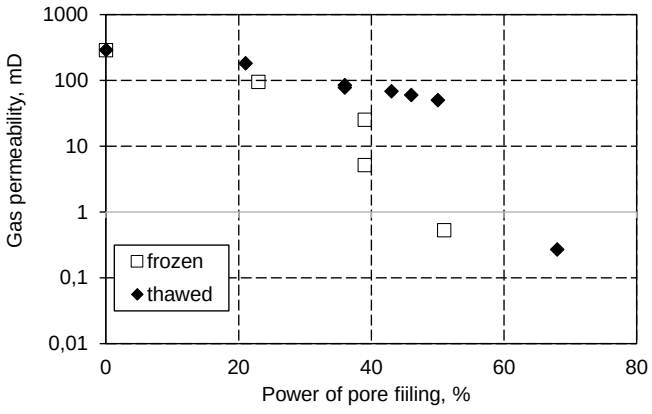

Figure 1: Dependence of the permeability of frozen and thawed samples of fine sand from the power of pore filling by ice and water.

The nature of the changes permeability of sandy rocks from the power of pore filling by water is largely due to their structural features, and above all the dependence of type ice-cement from the water content.

At low ice saturation of sample (30 %) ice-cement is the contact that located in the contact region of the particles blocking only a few channels, but pores mostly remain open. With the predominance of contact type ice-cement of sand sample with increasing ice saturation occurs logarithmic decrease gas permeability, while the gas permeability is not reduced by more than an order of magnitude. With further increase of the ice saturation it appears a film ice-cement, while in the fine pores may be present already as pore ice-cement. A sharp bend in the permeability graphic occurs at ice saturation over 45 %, when the starts to predominate pore ice-cement including large pores. Wherein the share of ice-film cement is significantly reduced. As a result, film and porous ice-cement block most channels and significantly reduce the volume of open pores. With further increase in the proportion of pore ice-cement and the appearance of basal ice-cement the gas component in the pores become isolated not able to filtration gas.

Acknowledgements

The authors express their gratitude to the company Total for the financial support given experimental research.

References

Chuvilin, E.M. and Grebenkin, S.I. [2015]: Gas permeability variations in gas-filled soils upon hydrate formation and freezing: An experimental study. *Kriosfera Zemli (Earth Cryosphere)*, 19 (2):59–64, URL http://www.izdatgeo.ru/pdf/krio/2015-2/67.pdf.

Oil contamination influence on water phase composition and thermal conductivity of frozen soils

Erika Stanislavovna Grechishcheva[1] & Rimma Grigorievna Motenko[2]

[1] *OJSC Fundamentproject, Russian Federation*
[2] *MSU, Russian Federation*

Oil and gas deposits are situated mainly in the northern regions, and most of them – in the permafrost area. A significant part of the permafrost zone is occupied by saline permafrost.

Soil contamination with oil can occur in various ways: the development of deposits, during storage it in the fields and processing plants, as well as there is a danger of leakage during the transportation of oil and petroleum products. In the process of oil extraction both contamination and salinization of the soil can happen. The sources of salts in this case are the reservoir of liquid waste produced, water content of barns and other geochemically active substances used for extraction and oil desalting. In addition, co-salinization and contamination could occur with leakage of on saline soils, where are the way of oil transportation.

Forecast of soil temperature, seasonal thawing and freezing, development of permafrost negative processes and design of buildings and structures in the permafrost zone is impossible without knowledge of soil properties. Obtaining high-quality data on the thermal properties and phase composition of moisture in the soil has a great importance for the calculation of thermal fields in the ground and assessing the impact of thermal influence on the soil-foundations.

The authors worked on the experimental procedures and assess their applicability to the saline and oil-contaminated soil in the process of freezing and thawing [Grechishcheva and Motenko, 2010]. Experimental study of joint influence of salinization and oil pollution on freezing and unfrozen water content. An experimental investigation of thermal properties and water phase composition was conducted for soils with different particle size distribution and different values of oil pollution and salinity. The characteristics of the soil were investigated, such as the freezing point, unfrozen water content, thermal conductivity, specific heat, thermal diffusivity. The changes of these parameters were obtained in the dependence of temperature, salinity and oil pollution. The authors used contact and cryoscopic methods for research [Motenko and Grechishcheva, 2013]. Different types of equipment were used for investigation of thawing temperature and water phase composition. The article considers the advantages and disadvantages of each type of equipment. Thermal properties. Thermal properties were also investigated using several experimental methods and plants. Their advantages, disadvantages and the range of applications are also discussed in the article.

The results were obtained for samples of pure, saline, polluted and joint saline and polluted soil. The role of oil pollution in the formation of thermal properties and water phase composition of saline soil (in the range of salinity and oil pollution) was established (Fig. 1). The dominant influence of salinity is revealed for the freezing point and water phase composition. The mechanism of the joint effect of salinity and oil pollution on the thermal properties is more complex and depends of many other factors.

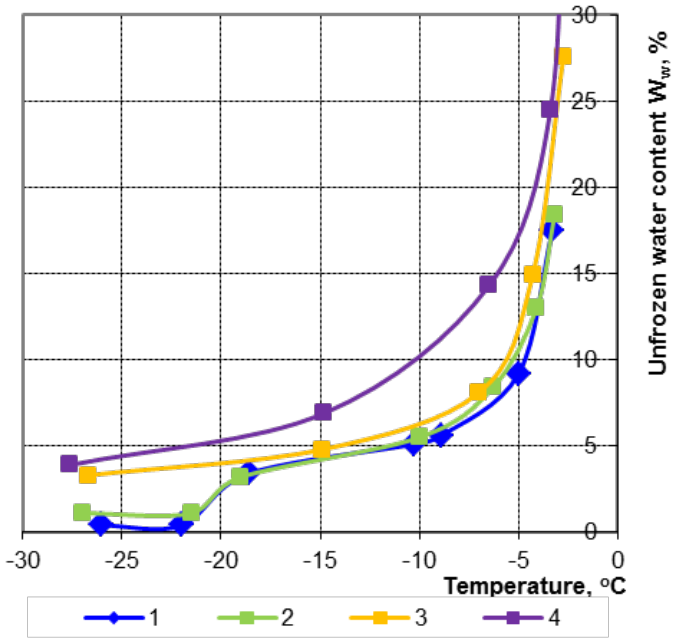

Figure 1: Unfrozen water content for saline (D_{sal}=1 %) oil-polluted (z=8 %) soils: 1 – sand, 2 – silt, 3 – silty clay, 4 - clay

References

Grechishcheva, E.S. and Motenko, R.G. [2010]: Experimental study of joint influence of salinization and oil pollution on freezing and unfrozen water content. In *9th International Symposium on Cold Regions Developement, Yakutsk, Russia.*

Motenko, R.G. and Grechishcheva, E.S. [2013]: Oil contamination influence on water phase composition of frozen sand. In *International Conference "Earth Cryology: XXI Century ", Pushchino, Russia, 29 September–3 October 2013*, Program and Conference materials, page 44, URL http://cryosol.ru/attachments/article/59/52_Abstracts.pdf. ISBN: 978-5-9905029-1-8.

Strength of frozen and unfrozen artificial rock joints depending on material porosity

Friederike Katharina Günzel

University of Brighton, United Kingdom

This contribution investigates the relationship of the uniaxial compressive strength and shear strength of frozen and unfrozen synthetic samples. Synthetic samples were used to be able to carry out multiple tests with the same material and surface characteristics; the materials were Ordinary Portland Cement (OPC) mortar and two types of plaster, Fine Casting Plus (FCP) and Herculite No. 2 (H2). OPC mortar and plaster were chosen as a large range of compressive strengths and porosities can be achieved with these materials.

Uniaxial compressive tests were carried out on small cylindrical samples (38mm diameter, 80mm height) and direct shear tests were carried out on samples with a surface area of 60mm×60mm; the surface is a smooth undulating surface, created by 3D scanning of a siltstone bedding plane.

Barton [1976] relates shear strength of rock joints to compressive strength and joint roughness coefficient with the equation

$$\tau p = \sigma tan(JRC \times log(JCS/\sigma) + \varphi R)$$

where τp is the peak shear strength, σ' is the effective normal stress, JRC is the joint roughness coefficient, JCS is the joint wall compressive strength (equal to the uniaxial compressive strength for unweathered material) and ΦR is the residual friction angle.

Porous materials show an increase of compressive strength when frozen as the ice in the pore space gives additional strength to the material [Krautblatter et al., 2013]. This increase strongly depends on the porosity of the material: in the experiments, the increase of compressive strength between saturated frozen and unfrozen material ranged from 21 % for an OPC mortar (porosity = 17 %) to 230 % for FCP (porosity = 36 %). It has to be noted that OPC mortar and plaster have different behaviour: while the compressive strength of OPC mortar only changes very little with moisture content, the strength of plaster is strongly dependent on the moisture content. Saturated plaster is very weak (compressive strength as low as 4MPa for FCP), and is considered too dissimilar to rock material in Alpine permafrost regions. Therefore the shear tests were carried out with dry unfrozen and saturated frozen plaster samples which have very similar compressive strength.

If Barton's relationship is valid for frozen samples an increased shear strength is expected in the direct shear tests with concrete samples and the same shear strength is expected for plaster samples. However, the direct shear tests did not show this behaviour. For the unfrozen samples both peak and residual strength were lower for the OPC mortar samples than the plaster samples.

Shear tests with frozen samples were conducted at -4 °C. Care was taken that the sample surfaces were free of ice prior to each test to avoid sliding on ice surfaces. The tests were carried out without allowing any adfreezing of the two sample surfaces. All frozen samples showed lower peak shear strength compared to the dry samples of the same material (see Fig. 1 left). This reduction increased with increasing porosity of the sample material. The same pattern is even more apparent for the residual strength (Fig. 1 right) of the samples where φR for FCP is as low as 10°. These results may be explained by the low friction of the ice-filled pores: as the two parts of the sample slide against each other, solid grains will be in contact with ice thus reducing the shear resistance.

It can be concluded that Barton's equation has to be used with extreme caution for frozen materials as the large reduction of the residual angle of friction (φR) reverses any strength gain due to increased compressive strength.

These laboratory results may be used to assess the stability of rock slopes in a warming permafrost environment. As soon as ice bridges across a rock joint are broken, e.g. by ingress of melt water, the shear strength of a rock joint will be greatly reduced if the rock on either side of a joint remains frozen. This will potentially lead to instability of frozen rock slopes.

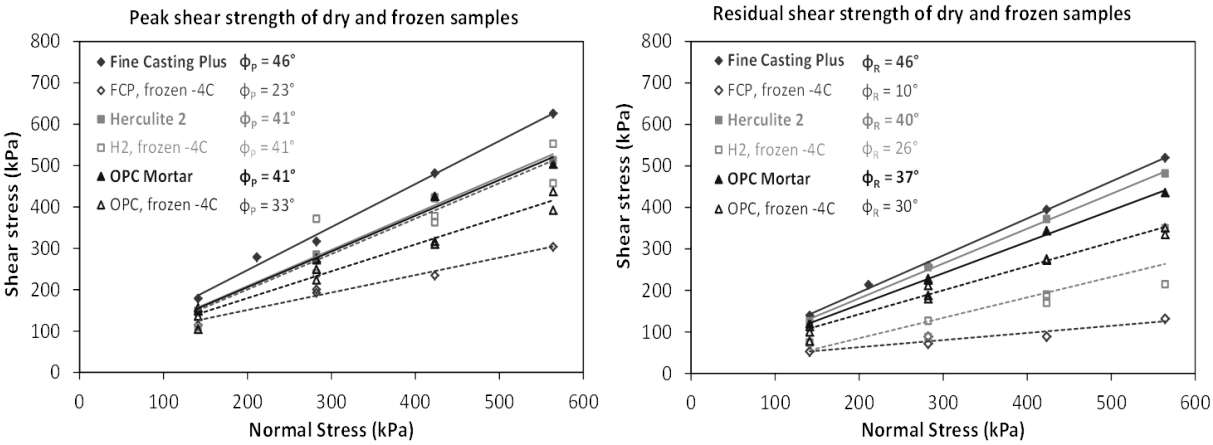

Figure 1: Peak shear strength (left) and residual shear strength (right) of three different materials, frozen and unfrozen

References

Barton, N. [1976]: The shear strength of rock and rock joints. *International Journal of Rock Mechanics and Mining Sciences & Geomechanics Abstracts*, 13(9):255–279, doi:10.1016/0148-9062(76)90003-6.

Krautblatter, M.; Funk, D. and Günzel, F.K. [2013]: Why permafrost rocks become unstable: a rock-ice-mechanical model in time and space. *Earth Surface Processes and Landforms*, 38:876–887, 2013.

Express method for unfrozen water content in soils by using water potential

Vladimir Aleksandrovich Istomin[1,2], Evgeny Mikhailovich Chuvilin[2,3], & Boris Aleksandrovich Bukhanov[2]

[1] *Scientific Research Institute of Gazprom (VNIIGAZ JSC), Russian Federation*
[2] *Skolkovo Institute of Science and Technology (Skoltech), Russian Federation*
[3] *Department of Geology, Moscow State University (MSU), Russian Federation*

Different technique were proposed for experimental determining of the unfrozen water content in frozen soils: calorimetry, differential scanning calorimetry, nuclear magnetic resonance, time domain reflectometry, as well as cryoscopic, adsorption and contact methods. This paper present a practical applications of a new method [Istomin et al., 2015] for determination of unfrozen water content in the soils at negative temperatures by using express water potential measurement at positive temperatures. Two types of soils were used for testing the method: kaolinite and polymineral clays. The comparison of proposed method with contact method is presented. So, the unfrozen water (W_{unf}, %) in frozen soils is in equilibrium with bulk ice phase.

In soil physics the water potential Y (MPa) is widely used for description of the thermodynamic properties of pore water. The water potential determination at porous sample with water content W is realized in serial devices. One of such devices for rapid measuring of water potential is WP4 T by Decagon Devices (USA) [Campbell et al., 2007]. If experimental data of pore water potential Y=Y(T,W) or pore water activity a=a(T,W) are experimentally determined at two or three positive temperatures (for example +15, +20 and +25 °C), we may extrapolate Y and a to negative temperatures (up to -15 °C). If measurements are made only at the room temperature at first approximation it may be neglected the temperature dependence of Y and a.

The unfrozen water content (W_{unf}, %) via temperature T in frozen soil may be determinate by using the followings procedure. At first we obtain experimental dependence of pore water activity on moisture content (W, %) of the dispersed sample at several positive temperatures. The initial value of moisture content of sediment sample is set equal to maximum molecular moisture capacity and after water potential measuring the sample is stepwise dried (not less 6-7 stages) in air. The moisture content of the sample is determined at each stage of drying and measuring of water potential until dry state (until moisture content of maximum hygroscopic). Control of the moisture content of the sample is carried out both before and after determination of water potential. Then using experimental data of pore water activity at different moisture content, we calculate the equilibrium temperature (Teq, %) by the formula

$$T_{eq} = 99.27 ln a - 3.113(1 - a)$$

,where the value of temperature (T_{eq}< 0 °C) is corresponded to the equilibrium between porous water in the sample and bulk ice.

As a result, we obtain a functional connection between the temperature (Teq) and the equilibrium content of the liquid phase in the sediment sample, i.e. unfrozen water content (W_{unf}). Then we get the inverse relationship, i.e dependence of unfrozen water content from the negative Celsius temperatures W_{unf}=W_{unf}(T).

Using the proposed method, the content of unfrozen water for clay soils were calculated and were compared with experimental data obtained by the contact method. Good agreement was obtained.

It is important to note that the developed method for determination unfrozen water content in frozen sediments can be considered as a express-method. Because the experimental determination of porous water activity in soils takes time less than one hour and significantly faster than other experimental techniques. Thus, it is enough for 5-6 hours to get unfrozen water contact values in the frozen sediments at 6-7 constant temperatures (up to -15 °C).

References

Campbell, G.S.; Smith, D.M. and Teare, B.L. [2007]: *Application of a Dew Point Method to Obtain the Soil Water Characteristic*, pages 71–77. Springer Berlin Heidelberg, doi:10.1007/3-540-69873-6_7, ISBN 978-3-540-69873-9.

Istomin, V.A.; Chuvilin, E.M.; Bukhanov, B.A. and Uchida, T. [2015]: A method for determination of water content in real and model porous media in equilibrium with bulk ice or gas hydrate. In *68th Canadian Geotechnical Conference and 7th Canadian Conference on Permafrost - GEOQuébec 2015*, Québec, Canada, September 20-23, 2015, ABS_658.

Regularities of cryogenic metamorphism of cryopegs with marine and continental quality of salinity

Nadezhda Vladimirovna Kiyashko & Ilya Arkadievich Komarov

MSU, Russian Federation

The paper considers regularities of transformation of chemical and phase composition of cryopegs in progress of cryogenic metamorphism. Under study cryopegs have marine and continental quality of salinity. The object of the study, we used data on the composition of 60 cryopegs of Yamal Peninsula and saline soil solutions of Yakutia. Indication of regularities of cryogenic metamorphism was realized by use of thermodynamic simulation. This simulation differs from earlier data based on freezing of sea water in possibility to take into account specify of chemical composition and value of total ionic solution concentration. It also is capable of reveal four indicative stages of cryogenic metamorphism process in the range of negative temperatures and to reveal limit concentration of solution when the process of cryogenic metamorphism occurs in absence of freezing due to redistribution of the liquid and solid phases.

Forecasting technique of changing of phase and chemical composition for cryopegs in the act of changing of thermobaric conditions

Ilya Arkadievich Komarov[1], Michael Victorovich Mironenko[2], & Nadezhda Vladimirovna Kiyashko[1]

[1] *MSU, Russian Federation*
[2] *Vernadsky Institute im.V.I. Vernadsky*

The paper considers forecasting technique of changing of the freezing temperature, phase and chemical composition, density and pH, thermophysical properties of cryopegs for two cases. First case - when there is information about ion composition of water sample and software program: software program is used to estimate characteristics. Second case - when there is information only about total salt content of water sample, software program is absence: express methods determination is used to estimate characteristics.

Express methods determination developed based on result of thermodynamic simulation, statistical processing of literature data and obtained experimental results. Express methods determination are offered in the form of analytical dependences.

Refinement of pulse nuclear magnetic resonance (P-NMR) techniques for accurate determination of unfrozen water content in frozen soils

Aaron Kruse[1], Margaret Darrow[1], & Satoshi Akagawa[2]

[1] *University of Alaska Fairbanks, USA*
[2] *Cryosphere Engineering Laboratory, Japan*

Introduction

The determination of unfrozen water content within frozen soils by means of pulse nuclear magnetic resonance (P-NMR) was established by individuals such as Tice et al. [1978]; since then, unfrozen water content has been calculated using the first return values of the free induction decay (FID) data. This is the signal generated after a 90° pulse. To prevent damage to the coil that acts both as a transmitter and a receiver within the P-NMR instrument, a dead time is used after the pulse generation before the coil begins to receive the FID signal; the dead time may be instrument-dependent but is typically on the order of 10 μs. The first return value is the largest signal intensity (SI) of the FID after the coil begins to receive the signal. It is commonly assumed that the FID signal is produced only from liquid unfrozen water, since the FID of ice is very fast; however, Watanabe and Wake [2009] indicated the FID signal of ice can extend to 50 μs, based on P-NMR theory.

Akagawa et al. [2012] presented an alternative means of calculating the unfrozen water content, which we call the normalization method. This method is based on the requirement that the ratio between the FID SI at any sub-freezing temperature and the SI at an above-freezing reference temperature must be constant. In this method, all FID curves are normalized to the reference-temperature FID curve. The SI at the point where the normalized FID curves are horizontally parallel is used to calculate the unfrozen water content; this time is later (e.g., 80 μs) than the typical first return signal.

Here we present the results of research designed to address two objectives. First, we compare the unfrozen water content results obtained using two different P-NMR instruments, with one system located at the University of Alaska Fairbanks (UAF) and the other located at Hokkaido University. Secondly, we explore the differences in the unfrozen water content results obtained using the traditional first return data and the normalization method.

Procedures and Results

The P-NMR instrument at the UAF is housed within a modified refrigerator that maintains a set point of 2 °C ±0.07 °C. Modifications include secondary Plexiglas doors with dry-box gloves that allow manipulation of samples without opening the doors and compromising the thermally stable environment. The P-NMR device is a Maran Ultra 23MHz instrument with a variable temperature (VT) probe. For an NMR instrument to operate correctly, the magnet must be at 40 °C to be tuned to the probe. This warm temperature is obviously not suitable for the measurement of soil at negative temperatures. To address this temperature dilemma, many researchers have chosen to disconnect the P-NMR heater and run the magnet at cooler temperatures, an action that may lead to errors d % to temperature fluctuations and the eventual detuning of the probe. The combination of the P-NMR with VT probe and the temperature-controlled chamber at the UAF overcomes this complication. The temperature of the VT probe is controlled by a refrigerated bath filled with a 60:40 ethylene glycol-water mixture. This arrangement demonstrates excellent temperature control, varying ±0.02 °C from the set point. A second refrigerated bath controls the temperature of an additional remote bath located adjacent to the P-NMR instrument in the temperature-controlled chamber; the soil samples are stored in the additional bath during testing.

The tested soil was kaolinite (KGA-1b obtained from the Source Clays Repository). The soil was mixed to a gravimetric water content of 100 % using distilled, deionized water and stored to equilibrate for two days. Three samples were made from the soil slurry: an unconsolidated sample, and two samples consolidated at 27 and 87 kPa, respectively. Once prepared, each sample was flash-frozen using liquid nitrogen, and placed into a Teflon test tube sealed

with a plastic stopper. The samples were stored in a freezer at -20 °C until testing.

Testing was conducted over a suite of temperatures ranging from -20 °C to -0.5 °C. Samples were equilibrated at each temperature for two hours before testing. Each sample within the test tube was taken from the bath, quickly wiped dry, and placed into the probe and tested. This procedure took approximately 30 s to complete, with samples demonstrating negligible warming (<0.06 °C). After the FID signals were obtained for the suite of sub-freezing temperatures, the samples were thawed and FID curves were obtained for 5 °C and 10 °C. This suite of UAF test data is referred to herein as Study A. The same soil prepared the same way was tested at Hokkaido University in Japan also using a Maran Ultra P-NMR instrument, but without the VT probe. The Japanese study is referred to as Study B.

Using the normalization method, we determined that a time of 60 μs was the earliest at which the FID SI curves were horizontally parallel to each other, thus indicating unfrozen water content and not ice. Unfrozen water content then was calculated from FID signal intensity at 60 μs using the gravimetric water content obtained from the samples after testing. A similar procedure was conducted using the SI at 80 μs. The final unfrozen water content curves produced using the 60 and 80 μs FID signals from Studies A and B were compared to each other (Fig. 1). The unfrozen water contents determined using the normalization method at 60 and 80 μs from Studies A and B are within 0.3 % of each other at temperatures lower than -3 °C for all loading conditions (Fig.1a, b, c). The difference between values from Studies A and B increases to 2.6 % at the near-freezing temperatures; this is attributed to differences in the initial water contents of the samples during preparation.

Figures1d, e, and f illustrate the unfrozen water contents measured for the different loading conditions using the normalization method and the traditional first return data from the FID. The unfrozen water content calculated from the 60 and 80 μs data differ by less than 1.4 %, while the first return data indicates unfrozen water contents up to 3.3 times greater for a given temperature.

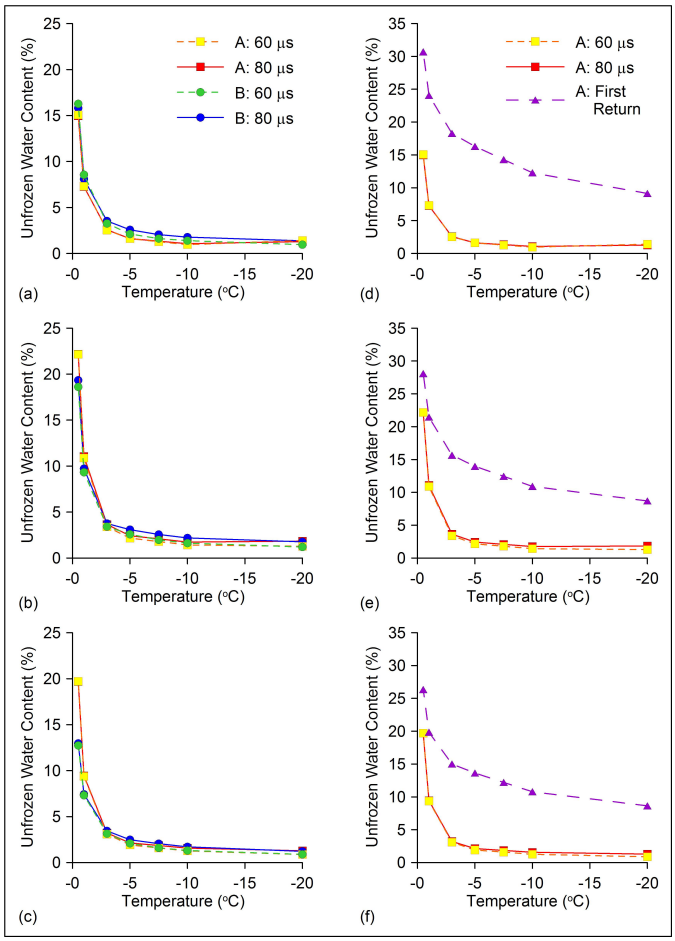

Figure 1: Comparison of unfrozen water content curves from Studies A and B (a, b, c) and using the first return data versus the normalization method (d, e, f). Results are shown for an unconsolidated sample (a and d), and samples consolidated at 27 kPa

Discussion and Conclusions

These results demonstrate repeatability of the P-NMR method using two different instruments. The results also indicate that the amount of unfrozen water in a frozen soil for a given sub-freezing temperature varies dramatically, depending on what time after the 90° pulse is chosen for the calculations. The first return data, which has been used traditionally for these calculations and may be instrument-dependent, also may include the signal from ice yielding an overestimate of unfrozen water content. The normalization method suggested by Akagawa et al. [2012] yields consistent results using FID signal intensity from 60 and 80 μs. Based on this data, we recommend choosing a consistent time after the 90° pulse (such as 80 μs) to perform the normalization method to calculate unfrozen water content. This eliminates any variation that may be specific to the dead time required for

a certain P-NMR instrument, and also removes the risk of inadvertently reading the FID signal from ice within the soil pore space. Because the difference in unfrozen water content determined from the traditional first return method and the normalization method is significant, we recommend further investigation, such as comparing these P-NMR results to those obtained using other methods, such as time domain reflectometry (TDR) or differential scanning calorimetry (DSC).

Acknowledgements

The authors thank Y. Miao for his many hours spent working on the temperature stability of the P-NMR system. This research was supported by the National Science Foundation under Grant Number 1147806. The views, opinions, findings, and conclusions reflected in this abstract are the responsibility of the authors only and do not represent the official policy or position of the NSF, or other entity.

References

Akagawa, S.; Iwahana, G.; Watanabe, K.; Chuvilin, E.M. and Istomin, V.A. [2012]: Improvement of Pulse NMR Technology for Determination of Unfrozen Water Content in Frozen Soils. In: Hinkel, K.M.(ed.), *Proceedings of the Tenth International Conference on Permafrost, Salekhard, Yamal-Nenets Autonomous District, Russia, 25–29 June 2012*, volume 1, International Contributions, pages 21–25, URL http://ipa.arcticportal.org/publications/conference-proceedings.

Tice, A.R.; Burrous, C.M. and Anderson, D.M. [1978]: Determination of Unfrozen Water in Frozen Soil by Pulsed Nuclear Magnetic Resonance. In *Proceedings of the Third International Conference on Permafrost, 10-13 July 1978, Edmonton, Alberta, Canada*, volume 1, pages 149–155, ISBN 0-660-1735-0. URL http://ipa.arcticportal.org/publications/conference-proceedings

Watanabe, K. and Wake, T. [2009]: Measurement of unfrozen water content and relative permittivity of frozen unsaturated soil using {NMR} and {TDR}. *Cold Regions Science and Technology*, 59(1):34–41, doi:10.1016/j.coldregions.2009.05.011.

Experimental research on acoustic wave propagation properties of frozen silt after freeze-thaw cycles

Dongqing Li[1], Xing Huang[2], Feng Ming[1], Yu Zhang[1], & Hui Bing[1]

[1] *SKLFSE, Cold and Arid Regions Environmental and Engineering Research Institute, Chinese Academy of Sciences, Lanzhou 730000, China*
[2] *College of Architecture and Urban-Rural Planning, Sichuan Agricultural University, Du Jiangyan, Sichuan 611830, China*

Ultrasonic P-wave tests of frozen silt was conducted under different negative temperatures after freeze-thaw cycles by using RSM-SY5(T) nonmetal ultrasonic test meter to study the velocity characters of P-wave. The experimental results indicate that: The P-wave velocity is affected by freeze-thaw cycles and temperatures, increase with a decrease of temperature and increases at first and then decreases with freeze-thaw cycles. The characteristic parameters of acoustic wave can reflect the mechanical properties of frozen soils after freeze-thaw cycles to some extent. This research gives a better understanding of changes in engineering properties of frozen soils.

Frost heave property of saturated silty clay under one side freezing

Hongyan Ma, Feng Zhang, Decheng Feng, & Bo Lin

Harbin Institute of Technology, China

This paper investigates the frost heave property of saturated silty clay in seasonally frozen region under different testing conditions, which different cooling temperature, different overburden pressure and different compactness. The silty clay used in this study is the subgrade material for the highway of Harbin downtown in China. The physical properties of silty clay from Harbin are: specific gravity 2.75, liquid limit 36.98 %, plastic limit 25.19 %, plasticity index 11.79, maximum dry density 1.74g/cm^3, optimum water content 17.4 %. As shown in the grain size distribution curve of the silty clay, that the particles with size smaller than 0.075 mm account for 94.7 %. The frost heave test system was designed to investigate the frost susceptibility of the porous materials. The cooling temperature, warming temperature, overburden pressure and water supply condition are conducted by testing design simulating conditions in the field. The freezing testing specimen was 100 mm in diameter and 150 mm in height. The temperature and frost heave of freezing soil under one side freezing condition were real-time collected in laboratory. After frost heave testing the moisture content of frozen soil was obtain in layers by drying method. The curves of temperature and frost heave with freezing time are plotted, respectively. The water content of frozen soil with height of specimen curve is plotted. In addition, the relation between freezing rate (and frost heave rate) and temperature gradient was analysis, with based on measure results of temperature and frost heave with freezing time. The frost heave properties of saturated silty clay under on side freezing and results of this study are as follows: In the freezing process, the temperature of specimen is temporal variations. The freezing front is fixedly, when the temperature is stability. But the frost heave of specimen is continuous increase in beginning of thermal stabilized. The frost heave is maximums in frost heave stability condition. After frost heave test, the water content of frozen soil in middle region more than in the both ends. And the water content near freezing font is maximums. Further analysis clearly shows that significant positive correlations between the freezing rate (and frost heave rate) and temperature gradient in frozen fringe of saturated silty clay under one side freezing condition.

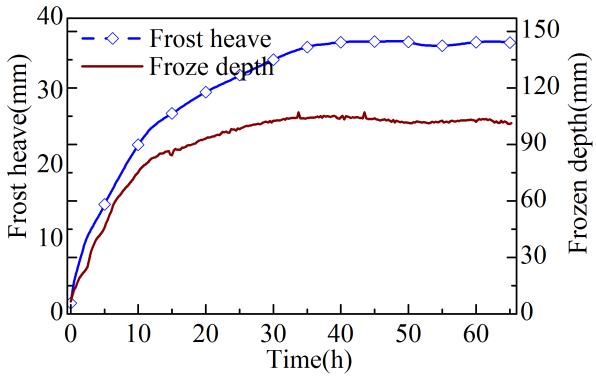

Figure 1: frost heave and frozen depth with time of 5# sample

Frost heave caused by formation of ice lenses in porous media

Feng Ming & Dongqing Li

Cold and Arid Regions Environmental and Engineering Research Institute, Chinese Academy of Sciences, People's Republic of China

Frost action has caused damage to structures with footings placed in frost susceptible soils above frozen depth. This is mainly due to water migration and formed ice lens. In this paper, a model is developed to describe the growth of ice lens during the freezing in a saturated soil. Movement of unfrozen water content in frozen soil are analyzed by use of the thermodynamic theory for the liquid layer near a substratum. for a simplify, water transfer in the frozen fringe and unfrozen zone is dealt with as Darcy flows. A new model of coupled moisture and heat transfer is constructed based on it. Also. the mechanism of ice lens growth process is investigated, a new ice lens is allowed to form when the neutral strength exceeds the sum of overburden pressure and tensile strength. A typical process of water migrates in a deformable, saturated freezing soil column, including the formation of ice lens, is simulated by COMSOL Multiphysics software. Finally, the model is verified by experimental data.

The predicted ice lenses distribution at different times is shown in figure 1. The black and white sections denote the soil and ice lenses, respectively. Ice lenses are distributed discontinuously layer by layer. Similar ice lenses distribution was also found in other papers. When an ice lens begins to form, more ice lenses are formed and then grow to increase the frost heave. At the top of the sample, due to a high temperature gradient close to the cold end, there is not sufficient time for water transfer. Thus, the ice lenses in the top are invisible, although ice lens are initialed. Many multilayered ice lenses exist in the numerical results. This can be explained that with the lens temperature decreasing, as the frozen fringe thickens and the water migrates toward colder temperatures, the pore space can become sufficiently filled with ice that a new lens initiates at a warmer temperature so that periodic lensing results.

Results show that the temperature curve can be divided into the fast freezing section, the transitional section and the stable section. Ice lens formed different cryogenic structure in different sections due to the limitation of water supply. The amount of frost heave is influenced by the overburden pressure. Water intake flow is constantly changing with the elapsed time and has a peak value. The water intake rate increases with freezing time to a peak value, and then decreases with time. As pore water pressure is lost, soil in unfrozen zone is consolidated. The amount of frost heave almost increases linearly with elapsed time. The results of simulation are in a good agreement with experiment.

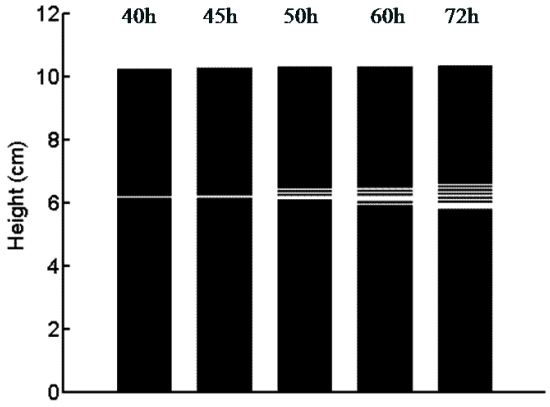

Figure 1: The predicted ice lenses distribution at different times

Changes of moisture in soil freezing, Central Russia

Vladislav S. Norkov[1], Valery I. Grebenets[1], Aleksey A. Maslakov[1], Vasiliy A. Tolmanov[1], & Dmitry A. Streletskiy[2]

[1] *Lomonosov Moscow State University, Russian Federation*
[2] *George Washington University, USA*

Seasonal freezing (active) layer is a phenomenon which affecting natural and anthropogenic environment. Winter coldness, landscape variability, different conditions of snow accumulation and lithological composition determines active layer dynamic. Soil moisture (W_{tot}) is an important factor which depends on either regional or local conditions and determines active layer depth [Maslakov et al., 2012]. Considered studies have been conducting in center of East European Plain (Moscow region) for several last years and have two stages:

1. at first decade of December when soil conditions in the beginning of active layer formation were described and measured and sampling of pre-winter moisture, grain size distribution, micro-landscape conditions were carried out;

2. at last decade of February, when active layer is almost formed, the description of the cryogenic textures and determining seasonal freezing depth (df) were accomplished.

The thermometric control on the surface and through the soil profile was put through by Hobo data loggers. For the representativeness of studies the measurements sites were put on sectors with different (and most typical for the region) soil and landscape conditions.

The main factor which determines df is cold period temperature regime. For example, depending on cumulative number of degree-days below 0 °C (so-called «index of cold»- DF) an average df for Moscow region was:

a) in forest at the 1st river terrace at DF=896 °C × days (2005-2006) df = 28 cm, at DF = 493 °C × days (2013-2014) df = 13 cm;

b) at the 3^{rd} river terrace it was 60 and 15 cm respectively for the same seasons.

Values of W_{tot} in active layer varies widely: from 0.05 to 0.5. It depends on grain size amount of humus and peat in soil. The average moisture content of loamy sands and loams within active layer in different years is 0.15-0.2 (maximum 0.5-0.6). Significant inter-annual differentiation depends on several factors. Pre-winter moisture (as a result of autumn precipitations) has an important role; generally, after relatively dry autumn soils are dryer and at other things being equal active layer is thicker. Soil freezing thickness distribution is associated with moist related primary filtration features of deposits and drain conditions. For example, in the beginning of December 2014, W_{tot} at 10-cm depth (loams) was 0.12 (slope, good drainage) and W_{tot} = 0.2 (swamped sector of watershed).

Moisture variation with depth related with ground and landscape conditions, snow accumulation and freezing rates. Equal values of W_{tot} in December and February in the upper horizon of the soil profile (Fig. 1-A) associated with its rapid freezing in the beginning of winter. Empty pores in upper soil layers formed by decomposed plant roots and physical deformations contributes accelerated cold penetration; pore cryostructures often formed in these places (Fig. 1-D1.). During rapid and relatively deep freezing in sands and loamy sands moisture, experiencing pressure of growing ice crystals, pressed down and continues to drain (see Fig. 1A). In this case active layer usually forms a massive cryostructure (Fig. 1-D2). At slow freezing under relatively thick snow cover in loamy sands and loams, moisture pulls up to the front office segregation (Fig. 1-B). In general there are layered, reticulate or lens type (Fig. 1-D4) cryostructures forms. Such effect in silty and clayey soils is associated with the depletion of liquid water cover around the particles exposed to negative temperatures and covered with ice crystals. As a result, there is a lack of liquid moisture at freezing front occurs and it begins to catch up from the lower horizons. This cryogenic redistribution of moisture in the seasonally frozen layer is well illustrated in figure 1

1-C the pre-winter moisture W_{tot} = 0.18-0.2; at the end of the freezing W_{tot} = 0.25-0.5. Redistribution of moisture and formation of cryogenic structures are significantly influenced by local landscape conditions. At wetlands or flooded areas, needle ice is often noticed (Fig. 1-D3);on forest roads and trails the soil is compacted, therefore seasonal freezing forms massive cryostructure and typically has the highest depth values (at DF = 896 °C × days, df = 98 cm; at DF = 586 °C × days, df = 60 cm). Changes in moisture conditions during soil seasonal freezing affects anthropogenic objects (enhanced frost heaving of foundations and pavements), changing the particle size distribution (increase the number of dust particles due to aggregation of clay and dispersion of sand particles), flooding conditions (ice-ground prevents drainage of melt water into the ground), the development of ravine systems (periods of thaw increased solifluction), on the life of soil-moving animals. Many of the revealed patterns are spread in active layer of permafrost.

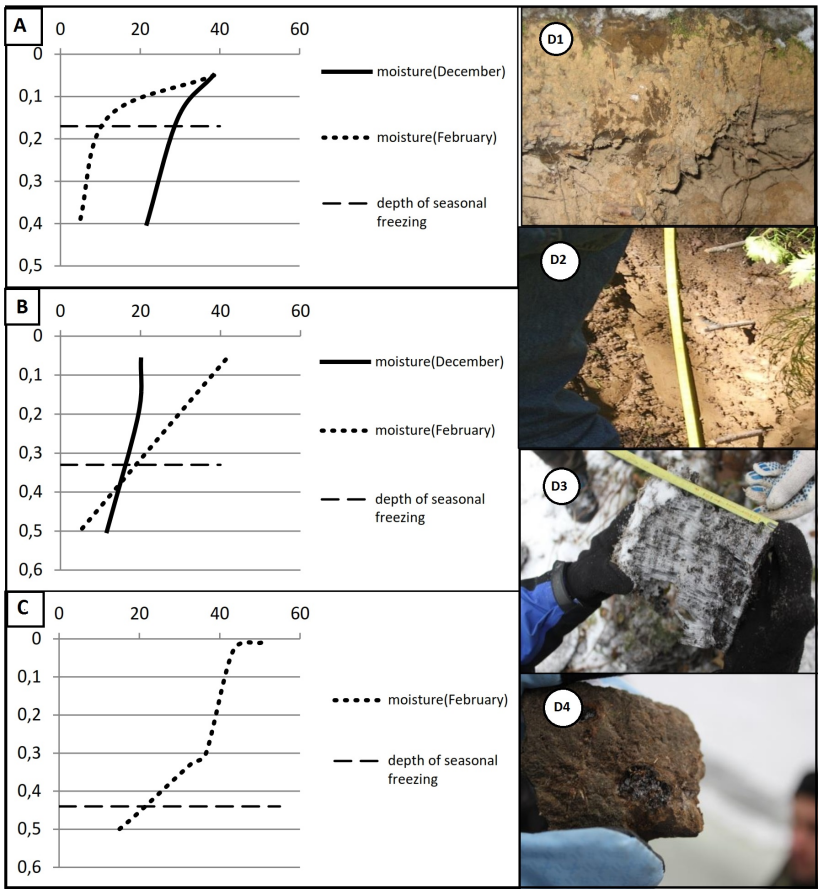

Figure 1: Moisture distribution in freezing soils, Central Russia A – slope of the 3rd river terrace (watershed), mixed forest; B - 3rd river terrace (watershed), waterlogged surface with shrubs and young trees; C - 1st river terrace, spruce forest; D - formation

Acknowledgements

The paper was financed by grant "Leading scientific schools" # NSH-335.2014.5 and Circumpolar Active Layer Monitoring U.S. National Science Foundation grant OPP-0352957

References

Maslakov, A.; Grebenets, V.; Ablyazina, D.; Shmelev, D.; Radosteva, A.; Pastukhov, V.; Antonov, V.; Bykovskiy, A.; Gavrilov, G.; Gorbatyuk, A.; Mandzhiev, D.; Melnik, P.; Saveleva, A.; Smirnov, A.; Khmelnitskiy, G.; Shpuntova, A.; Kraev, G. and Streletskiy, D.A. [2012]: The Dynamics of Seasonal Soil Freezing in Central Russia. In: Melnikov, V.P.; Drozdov, D.D. and Romanovsky, V.E.(eds.), *Proceedings of the Tenth International Conference on Permafrost*, Salekhard, Yamal-Nenets Autonomous District, Russia, 25–29 June 2012, volume 2: Translations of Russian Contributions, pages 253–259. The Northern Publisher: Salekhard. ISBN 978-5-905911-02-6. URL http://ipa.arcticportal.org/publications/conference-proceedings.

Laboratory investigations of thermal properties of crushed rock materials

Karlis Rieksts[1], Elena Kuznetsova[1], Jean Cote[2], & Inge Hoff[1]

[1] *Norwegian University of Science and Technology, Norway*
[2] *Laval University, Quebec City, Canada*

During the last decades, Norwegian road construction practice has changed considerably. Due to limitations of available natural materials like sand and gravel, they were substituted by crushed aggregates. In addition, in recent years, there has been increased interest in use of local materials for construction purposes. Nowadays, Norway is one of the European countries with the highest percentage of crushed aggregates used in construction. Yet, petrology of the rocks can vary significantly in different regions within the country. There are some data available on the thermal conductivity of Norwegian solid rocks. However, data for crushed rock materials are very limited. Therefore, evaluation of thermal conductivity of these diverse crushed rock materials is important.

For engineering purposes, empirical models are widely used to assess the thermal conductivity. Most of the widely accepted models are based on soil properties (e.g. water content, density). However, it is observed that thermal conductivity of crushed aggregates can vary significantly due to their particle's shape and size, porosity, mineralogy, quartz content and density. Therefore, using these models might lead to false results.

In a frost design method, the required parameter values of crushed rock aggregates are thermal conductivity, density and water content. The heat transfer during the freezing of natural soils is assumed proportional to thermal conductivity of the material. In the current calculations used by Norwegian Public Road Administration, thermal conductivity of granular layers is considered as 1 W/mK at 5 % water content. Experiments conducted by [Côté and Konrad, 2005a] for several types of crushed rocks (granite, limestone, quartzite, syenite) show that in dry state thermal conductivity can range from 0.5 to 1.5 W/mK. While in wet conditions, thermal conductivity might vary between 1.1 and 3.7 W/mK in unfrozen state and between 1.2 and 4.4 W/mK in frozen state, when water content values are around 5 or 6 %.

The main objectives of our investigations are:

i) to measure thermal conductivity of crushed aggregates with various mineralogy and grain size distribution,

ii) to evaluate the influence of different parameters (e.g. water content, density, porosity, fine content) on it, and

iii) to use the obtained data to validate existing empirical models.

The paper presents laboratory results of thermal conductivity measurements of crushed rock materials collected from different quarries around Norway. The thermal conductivity cell is based on experimental setup previously developed by Côté and Konrad [2005a]. This method implies testing material with maximum particle size of 20 mm under constant temperature gradient in frozen and unfrozen states. Sample is placed between two heat flux meters that are borosilicate glass discs with constant thermal conductivity. In order to assess the various thermal conductivities, the influence of porosity, water content, particle size gradation and mineralogy is investigated. Obtained laboratory data is further analyzed and compared with the existing empirical model presented by Côté and Konrad [2005b] to validate or adapt it for Norway's crushed materials.

References

Côté, J. and Konrad, J.-M. [2005a]: Thermal conductivity of base-course materials. *Canadian Geotechnical Journal*, 42(1):61–78, doi:10.1139/t04-081.

Côté, J. and Konrad, J.-M. [2005b]: A generalized thermal conductivity model for soils and construction materials. *Canadian Geotechnical Journal*, 42 (2):443–458, doi:10.1139/t04-106.

Using attribute of Electromagnetic wave to determine the water content and frost table in the permafrost area

Yupeng Shen, Yahu Tian, & Jiankun Liu

Beijing Jiaotong University, China

Seasonal melting permafrost generates damage on the sub ground Qinghai-Tibet Plateau highway. Using ground penetrating radar (GPR) technology, the maximum permafrost melt interface can be effectively divided and imaged. Permafrost region shows a clear hierarchical feature on the imaging profile OF GPR data. The complete ablation zone and part of the ablation zone display obvious. In addition, the details of subsurface layer can be effectively characterized by GPR attribute analysis technology. Using attribute calculation and filter, the instantaneous amplitude, instantaneous frequency and relative wave impedance can be more efficient to divide complete ablation zone, part of the ablation and non-ablation interface. The Comprehensive GPR attribute analysis can obtain the relative distribution of water content in Seasonal thawing permafrost region.

A coupled model for water, heat and solute transport in frozen soil: Evaluation with laboratory experiments

Mousong Wu[1,2], Jiesheng Huang[1], Jingwei Wu[1], & Xiao Tan[1]

[1] *State Key Laboratory of Water Resources and Hydropower Engineering Science, Wuhan University, China*
[2] *Royal Institute of Technology, Sweden*

To study the coupled transport of water, heat and solute in frozen soil, a mathematical model was setup in COMSOL 5.0 considering the effects of solutes on water and heat transport. Evaporation from frozen soil was taken into consideration with detailed descriptions of vapor flow in frozen soil. Mathematical relationships for soil freezing characteristic curves as well as soil thermal properties accounting for solute effects were incorporated into the model based on laboratory and field experiments. Two groups of laboratory freezing experiments with different lower boundary conditions were conducted simultaneously to test the model in simulations of water, heat and solute dynamics in frozen soil: one experiment with 60 cm soil in height and without water recharge, while the other with stable water table at 60 cm depth from the soil surface. Soil temperature and liquid water content were detected during experiments. Results showed that water and salt moved upward during freezing and accumulated at the freezing front with shallow water table. The movement of water and salt carries heat to the frozen soil, which can result to the redistribution of heat in soil column and slow down the advance of freezing front. The coupled model was shown to have the ability in detecting dynamics of water, heat and solute transport in frozen soil, and further verification of the model with field experiments will be of high interest.

Experimental study on anti-frost-heaving performance of screw pile foundations of photovoltaic stents in seasonal frozen soil region

Tengfei Wang[1], Jiankun Liu[1], Yalong Shang[2], & Huagang Zhao[1]

[1] *Beijing Jiaotong University, People's Republic of China*
[2] *North China Power Engineering CO., LTD of China Power Engineering Consulting Group, China*

Brief introduction, methodology and key results

China is a vast country, 53.5 % of which is covered by seasonal frozen soil. Under the influence of negative temperature during winter, on one hand, pore water in top soil layer freezes accompanied by volume expansion, on the other hand, water transfers to the top layer and freezes, causing even greater frost heaving. The total frost heaving amount can be as much as 10-30 cm, or even 40 cm. Structures can barely endure such great deformation. Solar photovoltaic power generation is a new green energy industry, and lights-rich regions it requires are widely distributed in seasonal frozen regions. So it's of great significance to study photovoltaic foundation. Although research on pile foundation in seasonal region has been carried out for many years, it's limited to deep-pile foundations bearing heavy load. The results can't be applied to photovoltaic piles for that it bears low load and has shorter length. We choose screw pile foundation out of the consideration that it's easy to construct, environmentally-friendly and convenient to recycle. Our tests are based on these to find out the optimal pile which has greatest anti-frost-heaving performance through parameter optimization.

We picked site soils (sample A) to conduct experiments and Tibetan plateau clay (sample B) in contrast. The piles we chose were listed as: large-double-blade screw pile, small-double-blade screw pile, large half-bladed screw pile, small half-bladed screw pile, all-bladed screw pile and smooth pile. The tests were divided into 8 groups: the first 6 groups were carried out using 6 different types of piles in soil sample A; In contrast, the last 2 groups were conducted in soil sample B. Based on actual conditions and similarity principle, we set test conditions as: cooling bath was -15 °C, froze 3 similar piles at the same time for 7 days. Temperature sensors and stress sensors were placed around the piles to monitor temperature and stress. Dial indicators were put on the top to detect displacement.

Figure 1 below shows that frost heaving amounts of 3 piles varying with time. These 3 piles showed same trend for the similar situation they were in.There were no frost heaving during initial period, then it began to frost heave gradually. After 144h, when it reached the third stage, the frost heaving amount grew rapidly, with average value reaching 0.352 mm.

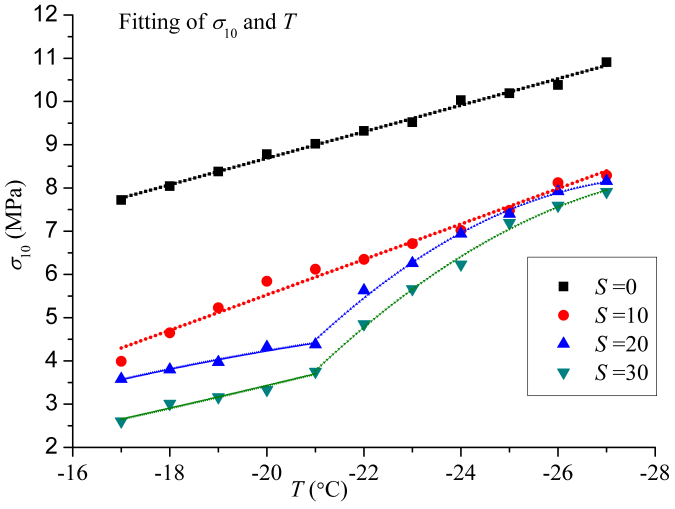

Figure 1: Frost heaving amount of small half-bladed screw pile vs. time

These screw piles differ in width and interval of blades and so on, which also leads to different performances in anti-frost–heaving. The numbers of blades in unfrozen region and frozen region respectively will also play a part. In the series of experiments, large-double-blade screw pile shows the best anti-frost-heaving performance.

Conclusions

1. According to the results, the average value of frost heaving of screw piles were less than that of smooth pile, which indicated that screw piles performed better than smooth pile, regardless of soil samples.

2. The frost heaving amounts were listed as below: large-double-blade screw pile < large half-bladed screw pile < small half-bladed screw pile < small-double-blade screw pile < all-bladed screw pile. For large-blade screw pile: Partial blades of half-bladed screw pile were in frozen region, and they would generate great uplift force to pile in the process of freezing, which turned into larger frost heaving amount than double-blade screw pile (both blades in unfrozen region). However this effect wasn't significant in small-blade screw pile, leading to result that half-bladed screw pile performed better than double-blade screw pile. In all, large-double-blade screw pile shows the best anti-frost-heaving performance.

References

Chen, X.; Liu, J. and Liu, H. [2006]: *Frost action of soil and foundation engineering.* 208-250, 390-434.

Dong, X.; Li, L.; Wang, W. and Wang, M. [2008]: Experimental Analysis on the Lamina-soils Interaction in Pullout Screw pile Foundation. *Engineering Mechanics*, 28(11):150–155.

Model test on pore water pressure of soils subjected to freeze-thaw cycles

Donghui Xiao, Wei Ma, Shuping Zhao, & Ze Zhang

Cold and Arid Regions Environmental and Engineering Research Institute, Chinese Academy of Science, People's Republic of China

In seasonal frozen regions, freeze-thaw actions change the physical and mechanical properties of soils. In this study, two groups of model tests on soils with freeze-thaw cycles were carried out: one group was conducted without any load and the other was with a static load. During the test, the pore water pressures (PWP) within the soil layers were measured and the data were collected by a data logger. The results showed that the PWP of soils decreased during the freezing process but increased during the thawing process under both no load and static load conditions. With an increasing number of freeze-thaw cycles, the PWP had an increasing trend under both two conditions. In addition, under the static load condition, the PWP distributed more regular within the soil layers with an increasing number of freeze-thaw cycles. And there were three concentrated areas of PWP from the longitudinal section: one was directly below the loading position, and the other two were located between the edge of loading area and the test chamber. What's more, the concentration area of PWP below the loading area is nearer to the soil surface than that between the edge of loading area and the test chamber. Under the static load, the distribution of PWP resembled to the stress field which calculated by corner-points method. It was considered that the present of these concentrated areas was related to the stress field of soils produced by the static load.

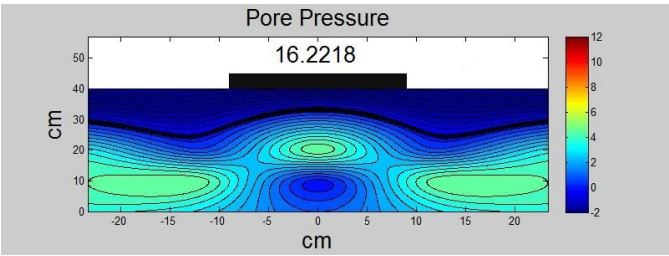

Figure 1: Pore pressure

Thermal, Electrical and Mechanical Properties of Permafrost from the North Slope, Alaska

Zhaohui Yang[1], Feng Zhang[2], Benjamin Still[1], Jiahui Wang[2], Haipeng Li[3], & Hannele Zubeck[1]

[1] *University of Alaska Anchorage, USA*
[2] *Harbin Institute of Technology, Harbin, China*
[3] *China University of Mining & Technology, Xuzhou, China*

The thermal, electrical and mechanical properties of permafrost are of great importance for the energy exploration and extraction in the arctic region. Laboratory test data obtained from undisturbed permafrost samples is limited. This paper present the results from a comprehensive test program aiming to study the physical properties of permafrost obtained from a deep boring program. Large samples were acquired by sonic drilling from the North Slope, Alaska and transported to laboratory with minimal thermal disturbance. A lathe was used to machine the sample into right cylindrical specimens of appropriate size and care was taken to minimize the thermal and mechanical disturbance to the frozen soil [Still et al., 2013]. The bulk density, dry density, ice content, and salinity are obtained. A series of tests were carried out in a cold room to investigate the physical properties of permafrost specimens at temperatures changing from -10 °C to -2 °C at an interval of 2 °C. A portable thermal conductivity analyzer utilizing the transient line heat source method was used to measure the thermal conductivity and heat capacity of the permafrost. A RC circuit with known capacity was used to measure the electrical resistivity. Mechanical properties including shear modulus, and Young's modulus were measured by shear- and pressure-wave velocity method [Park and Lee, 2014]. Specifically, bender elements and piezo disk element pairs were used to measure the shear- and pressure-wave traveling velocity in the permafrost specimen. Poisson's ratio was evaluated based on shear modulus and Young's modulus. The thermal, electrical and physical properties were analyzed in terms of temperature, ice content, and dry density. The results show that the thermal, electrical and mechanical properties are greatly affected by temperature, ice content, and salinity. The elastic moduli including shear and Young's modulus exhibit strong anisotropy. Empirical formulas are proposed based on the test results for correlation of thermal, electrical and mechanical properties of permafrost.

References

Park, J.-H. and Lee, J.-S. [2014]: Characteristics of elastic waves in sand-silt mixtures due to freezing. *Cold Regions Science and Technology*, 99:1–11, doi:10.1016/j.coldregions.2013.11.002.

Still, B.; Yang, Z. and Ge, X. [2013]: Sampling, machining, and testing of naturally frozen soils. *ASTM Special Technical Publication*, volume 1568 STP, pages 49–61, doi:10.1520/STP156820130003.

A review of physical and mechanical properties of saline frozen soil

Yuanming Lai[1,3], Zean Xiao[1,2], Daoyong Wu[1,2], Mengke Liao[1,2], & Xusheng Wan[4]

[1]*State Key Laboratory of Frozen Soil Engineering, Cold and Arid Regions Environmental and Engineering Research Institute, Chinese Academy of Sciences, Lanzhou 730000, China*
[2]*University of Chinese Academy of Sciences, Beijing 100049, China*
[3]*School of Civil Engineering, Lanzhou Jiaotong University, Lanzhou, Gansu 730070, China*
[4]*School of Civil Engineering and Architecture, Southwest Petroleum University, Chengdu Sichuan 610513, China*

Saline soil is widely distributed in cold regions of China. The water freezes and salt crystallizes in response to seasonal temperature variations. Detrimental frost heave and salt expansion may occur in the freezing process, which have significant implications on constructions. This interest has led to an increase in studying the effects of salt on the physical and mechanical properties of saline frozen soil. Herein, a general review is presented with a discussion including the effect of salt on unfrozen water content, soil freezing temperature depression, the change of mechanical strength with salt content, and water and solute transfer mechanism in unidirectional freezing experiments. The differences and similarities of phase change between pore solution and free solution are discussed. It is confirmed that non-uniform pore size is the main cause resulting in the differences. The temperature of phase change in soil deviates from that of free solution, and this deviation increases with unsaturated degree increasing. Apart from the phase change sequence, the relation between the soil freezing temperature and the radius of the ice crystallization is obtained. Moreover, the influencing factors of soil freezing temperature are analyzed. Based on Pitzer model, the formula of soil freezing temperature is derived and used to explore the factors including salt content, water content, salt type, and salt crystallization. Soil freezing temperature test illustrates that the freezing temperature of soil is lower than that of the corresponding solution which is controlled by water activity. When the pore solution is unsaturated, soil freezing temperature decreases with salt content increasing and water content decreasing. If the concentration of pore solution is saturated or supersaturated, salt crystallization begins to influence the soil freezing temperature, this may be due to the liquid water content of soil decreasing and the content of large pores reducing with crystalline salt (e.g. $Na_2SO_4.10H_2O$, $Na_2CO_3.10H_2O$) formation. In addition, the change of sodium sulfate sand strength with different salt contents of 0.0, 0.5, 1.5, and 2.5 % under confining pressures from 0 MPa to 16 MPa at -6 °C is investigated. As the content of sodium sulfate increases, the strength of frozen sand firstly increases and then decreases. Triaxial shear test suggests that the critical state line of saline frozen sand in p-q plane is a curve that doesn't pass through the origin. Soil particle has an initial anisotropy rotation angle and a characteristic of stress induced anisotropy rotation in loading process. Shear dilatancy occurs instead of shrinkage as the confining pressures are low (Smaller than 6 MPa). When the confining pressures are larger than 6 MPa, the shrinkage of strain is gradually strengthened. Finally, the water and solute transfer mechanism is investigated by a series of unidirectional freezing experiments, and the mechanism of salt and ice crystal nucleation and growth is also discussed. The review not only confirms the effect of salt on the physical and mechanical properties of the soil, but also provides a theoretical basis for further enriching solute transport theory and studying the damage mechanism of saline soils in cold regions.

Use of mercury intrusion porosity for microstructural investigation of silty clay with different contents of sodium sulfate

Zhemin You, Yuanming Lai Mengke Liao, & Qinguo Ma

Cold and Arid Regions Environmental and Engineering Research Institute, CAS, People's Republic of China

Salt crystallization changes the inner pore structure of materials. Mercury Intrusion Porosity (MIP) tests of saline silty clay with different mass contents of sodium sulfate were performed. The changes of porosity, pore size distribution and pore shape (ink-bottle type pores) were investigated by performing intrusion-extrusion cycles. There exists hysteresis between intrusion and extrusion.The results show that the cumulative volumes of pores increases with the increase of salt contents until the largest with 1.5 %, and then decreases. It is in coincidence with the freezing temperature test that it decreases with the increase of salt content until 1.5 % and then the opposite change trend. The distribution of log-differential volume is shown for a diameter range from 3 nm to 0.35 mm. All these can be explained by the crystallization kinetics of salt phase change and the content change of unfrozen water. The comprehensive approach allows to investigate the transport processes together with the related phenomena and asses the durability of porous materials.

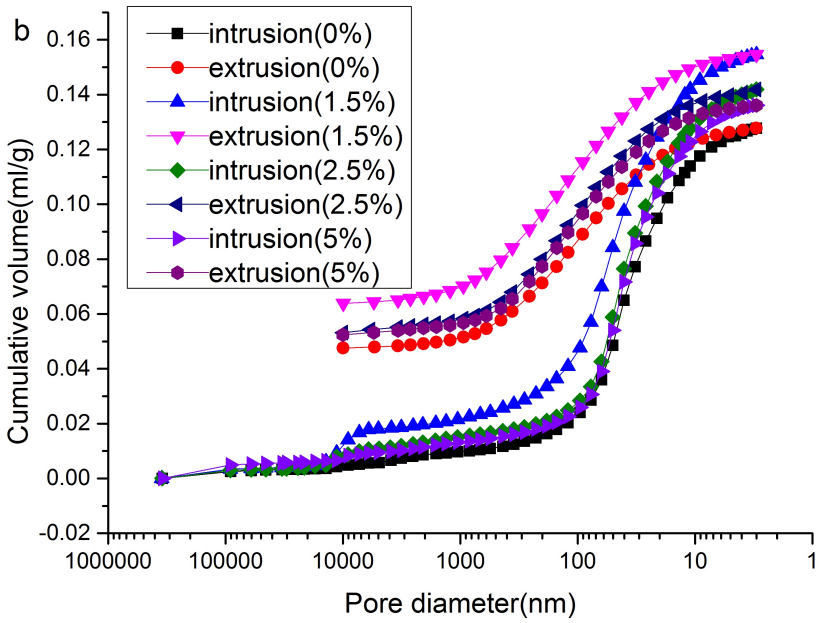

Figure 1: cumulative volume-Pressure

Experimental investigation on creep characteristics of artificial warm and ice-rich frozen sandy silt

Feng Zhang[1], Decheng Feng[1], Hongyan Ma[1], & Leizhou Cai[1,2]

[1] *Harbin Institute of Technology, People's Republic of China*
[2] *Research Institute of Highway Ministry of Transport, People's Republic of China*

Creep characteristics of warm ice-rich frozen soil causes a significant permanent deformation, it affects the long-term stability of infrastructures built in the permafrost regions. In this paper, the disturbed sandy silt was sampled from Huashixia-Dawu Highway, China, and the artificial warm and ice-rich frozen specimens were prepared in cold room. Then, a series of closed-system tri-axial creep tests were carried out to investigate the creep behaviors of artificial warm and ice-rich frozen soil. During the tests, five different experimental conditions were considered as follows: the ice content (60 %, 80 % and 100 %), the consolidation stress (25kPa, 50kPa and 75kPa), the consolidation temperature (-1.5 °C, -1.0 °C and -0.5 °C), the load stress (100kPa, 125kPa and 150kPa) and the temperature when applied the load (-1.5 °C, -1.0 °C and -0.5 °C). The experimental results showed that the creep deformation of frozen sandy silt increases with the increasing of the ice content, and effects greatly by the load stress and temperature. However, the consolidation stress and consolidation temperature play a little role on the creep characteristics.

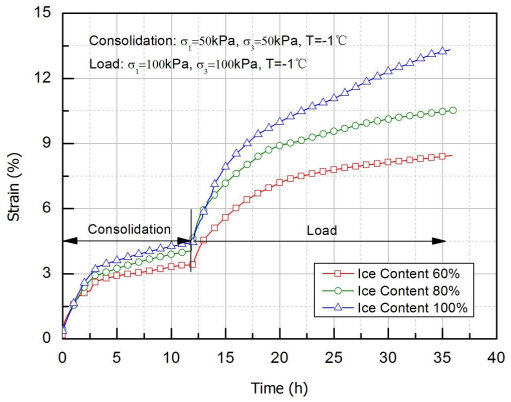

Fig. 1 Effects of ice content on the creep behavior of frozen sandy silt

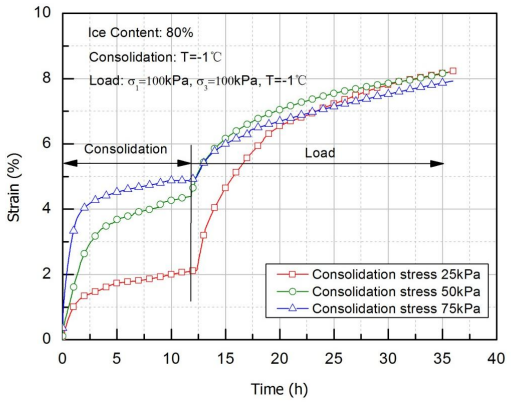

Fig. 2 Effects of consolidation stress on the creep behavior of frozen sandy silt

Figure 1: Effects of test conditions on creep behaviours

SESSION 31

Permafrost in History and Culture

Convener/ Session Chairs:

Mathias Ulrich, *University of Leipzig, Institute for Geography, Germany*

J. Otto Habeck, *University of Hamburg, Institute for Social Anthropology, Germany*

Pey-Yi Chu, *Pomona College, USA*

Alexander N. Fedorov, *Melnikov Permafrost Institute, Russia*

Frederick E. Nelson, *Michigan State University, USA*

Nikolay Shiklomanov, *The George Washington University, USA*

Permafrost has been a key factor in ongoing human-environment interactions in Arctic, Subarctic, and high-altitude regions. Investigating permafrost therefore encompasses not only bio-geo-physical systems but also political, social, and cultural dynamics. What has been the role of permafrost in human culture, past and present? This session integrates two often disconnected scholarly approaches: geo-scientific and environmental research on the one hand, and research into human activities, behaviors, experiences, and perceptions on the other. It aspires to develop a better understanding of human involvement in permafrost landscapes at different times and places. We welcome contributions from all fields of science analyzing the historical, political, and cultural aspects of permafrost, including the development of knowledge about permafrost, land use in permafrost regions, and local adaptations to environmental change. In an age of global warming, understanding's people's connections to and engagement with permafrost is more important than ever. Ultimately, we seek to enlarge the thematic scope of future research in diverse permafrost landscapes. This session is affiliated with the International Permafrost Association (IPA) action group, 'Permafrost and Culture' (PaC).

Urban livelihoods in past, present and future permafrost environments: Contrasting public perception of changes and instrumental data

Oleg Anisimov[1], Yuri Zhegusov[2], Yelena Ziltcova[1], & Vasily Kokorev[1]

[1] *State Hydrological Institute, Russian Federation*
[2] *International Biogeochemical Educational and Training Center, Yakutsk, Russian Federation*

For centuries, humans lived in the Arctic in relatively small, self-sustained communities in harmony with the harsh local climate and permafrost environment. In contrast to that earlier period, the modern Russian Arctic is characterized by intensive urban development, including cities whose populations exceed more than 100,000 people. Arctic urban sustainability depends on the complex interplay of multiple factors, including governance and economic development, demography and migration, environmental changes and land use, changes in the ecosystems and their services, permafrost and climate change. While the latter can be seen as a factor that exacerbates the existing vulnerabilities to other stressors, changes in temperature, precipitation, snow, river and lake ice, and the hydrological regime also have direct implications for the cities in the North. Climate change leads to reduced demand for heating energy, on one hand, and heightened concerns about the fate of the infrastructure built upon thawing permafrost, on the other. Changes in snowfall are particularly important and have direct implications for the urban economy, as together with heating costs, expenses for snow removal from streets, airport runways, roofs and ventilation corridors underneath buildings erected on pile foundations on permafrost constitute the bulk of the city's maintenance budget. Many cities are located in river valleys and are prone to flooding that leads to enormous economic losses and casualties, including human deaths. Climate could thus be viewed as an inexhaustible public resource that creates opportunities for sustainable urban development. Long-term trends show that climate as a resource is becoming more readily available in the Russian North, notwithstanding the general perception that globally climate change is one of the challenges facing humanity in the 21^{st} century.

In this study we compare the observational data on climate and permafrost changes from Russian weather stations and permafrost observational sites with the results of the public survey conducted in Yakutia in the period 2012-2015. The survey involved more than 1600 respondents in 3 cities (Yakutsk, Aldan, Nerungri) and 2 villages (Ust-Maja, Saskhulakh) representing distinctly different economical, sociological, permafrost, vegetation, and climatic conditions. We developed the system of numerical indexes that could be used to quantitatively characterize the objective changes in the state of the environment and compare those with the public perception of such changes. Metrics of the public perception of changes include the Environmental State Index, Environmental Degradation index, Climate Change perception index. These metrics are compared with the information about the state of the permafrost and climate derived from instrumental observations and modelling.

Results of the study indicate that the public perception of the permafrost, climatic, and environmental changes do not always coincide with the observational data and is often affected by factors other than long term trends of the key variables. Low probability extreme events, such as unusual weather patterns or abrupt landscape changes (permafrost thaw) may have greater effect on the modifications of the conventional lifestyle of the Arctic citizens than the objective changes in the baseline climatic conditions. This finding has important implication for developing strategies of adaptation to ongoing changes in permafrost environment. To be effective, such strategies should combine knowledge coming from instrumental- and model-based analysis of environmental changes with the public perception of such changes.

A database of participants attending the International Conferences on Permafrost (1963 – 2012)

Jerry Brown[1], M. McGraw[2], & Julia Stanilovskaya[3]

[1] *Self, United States of America*
[2] *Southeastern Louisiana University, Hammond, LA 70402, USA*
[3] *Sergeev Institute of Environmental Geoscience, Moscow, Russia*

More than 3200 individuals from 39 countries have participated in the ten International Conferences on Permafrost (ICOP). The vast majority of participants have been from the USA, Canada and Russia/ USSR. These numbers reflect the fact that each of the three countries have hosted at least two conferences and that permafrost conditions dominate social, economic and environmental concerns in their northern regions. Chinese and European participation in the conferences have increased in recent decades.

During the Ninth International Conference on Permafrost (NICOP) in 2008 in Fairbanks, Alaska, a publication was presented in celebration of the first 25 years of the International Permafrost Association (1983- 2008). It documented activities of the nine conference and presented statistics on participation and publications. Several more recent reports provide summaries of the Tenth International Conference on Permafrost (TICOP) [May et al., 2012, Stanilovskaya, 2012]. In commemoration of the 50^{th} anniversary of the First ICOP at Purdue University, Brown [2013] presented a summary and statistics for all ten conferences.

As part of that NICOP celebration, the two senior authors of this abstract prepared a photographic 'Honor Roll' in PowerPoint of participants in the first eight conferences. Approximately 175 photographs of individuals who attended two or more conferences were included as well as a selection of non-attending honorary scientists and engineers. The presentation was updated for the 2012 conference in Salekhard, Russia, with a total of 239 photographic entries. Both presentations were available on either CD or DVD. We plan another update for this XI ICOP. However, it is not feasible for the 2016 Honor Roll presentation to obtain many additional photographs, particularly for those attending only one conferences; a task perhaps left to the Permafrost Young Research Network (PYRN). The 'Honor Roll' is derived directly from the database of ICOP participants as described in this report. It is organized by number of conferences an individual attended. No one individual has attended all ten conferences and only three attended nine conferences. A total of 246 individuals have attended three or more conferences. Unfortunately, at least 41 of those are known to be deceased.

Table 1 present summaries of information contained in the database. Since the US hosted three conferences, two in Alaska with many participants from private sector, government agencies and universities and the first ICOP at Purdue University in Indiana, its participation totals about 40 % of all ICOP attendees (1215). Second in number of participants is Russia (628), again having large industrial and academic interests. Canada ranks third (583) and China fourth (201) with its total not including additional unrecorded participants. Germany, Switzerland, Norway, Japan and the UK had between 50 and 100 participants. Individuals from four of the thirty-nine participating countries attended only one conference. In addition to tabulating the number of participants, we can also tabulate the larger number of total registrants (4283 *vs.* 3203 individuals), since many participants attended multiple conferences.

The updated compilation of ICOP participants, including more than 500 TICOP attendees, represents a valuable historical database for both present and future use. This Excel database, organized by country, now includes information on some of the deceased participants (year of birth and death) and identifies young participants who received financial assistance for the last two conferences. For NICOP, 80 grants were awarded to young researchers from 18 countries. For TICOP, 150 PYRN grants were available to individuals from 16 countries.

Table 1: Number of participants by countries in the ten International Conferences on Permafrost.

	1963	1973	1978	1983	1988	1993	1998	2003	2008	2012	Individuals
Country	USA	USSR	CAN	USA	NOR	China	CAN	SWITZ	USA	RUS	
Argentina	1		2	1			2	1	1	2	6
Australia				1		1					1
Austria				1			2	7	4	7	17
Belgium		1		3	1	1	2	3	2	1	6
Canada	47	39	246	137	61	28	114	37	98	22	583
Chile				1							1
China			9	21	27	122	9	22	15	25	201
Czechoslovakia		2		1							3
Denmark		2	1	5	7	3		3	9	7	26
Estonia							1		1		2
Finland				7	10		5	7	9	2	30
France		3	2	2	3	3	2	6	7	3	17
Gambia								1			1
Georgia								1			1
Germany	1		6	17	10	4	7	20	31	36	96
Greenland									1	1	1
Hungary		2							1		3
Iceland				1				1			2
India				1							1
Israel					1	2					2
Italy				4	6	2	2	7	12	1	24
Japan		2	12	5	12	6	9	18	16	7	56
Kazakhstan		1	1			1					1
Mongolia		3				1	1	1	2		5
Nepal									1		1
Netherlands			1	3	6	2	1	3	3	3	12
New Zealand							1	4	4	3	6
Norway		1	3	4	36	4	7	18	18	12	68
Poland	1	5		1	3	1	1	3	1	1	12
Portugal								2	1	4	4
Romania						1	1		1	3	3
Russia/USSR	5	279	27	6	10	33	9	54	49	286	628
South Africa				1		1					2
South Korea						1					1
Spain									7	2	8
Sweden	4		2	5	11	2	2	2	8	4	29
Switzerland			1	8	4	4	13	42	18	10	73
United Kingdom		2	1	16	14	1	8	9	11	2	55
United States	224	54	136	614	90	52	54	56	273	72	1215
Attendees	283	396	450	866	312	276	253	328	604	516	**3203***

*total individuals vs total registrations of 4283

Although financial assistance was provided for earlier conferences that information is not readily available for this report or the current version of the database. The database also identifies additional PYRN members (membership as of 2014) who have attended recent conferences. With additional effort it would be possible to identify authors of papers and extended abstracts and possibly link them to the conference publication, all of which are available electronically.

The future of the database and resulting 'Honor Roll' is uncertain. Certainly names of participants in the XI ICOP can be added. Perhaps a voluntary process can be developed for editing and adding information to the database. The U.S. Permafrost Association maintains a wiki site for all of its internal paper work. The site is password protected and accessible to members of the USPA governing board. Initially the USPA might host this ICOP database and corrections and additions updated through the USPA Secretary or designee.

It is most likely that errors exist in some entries, since the sources of information have varied from conference to conference. Some inadvertent omissions are also likely. We apologize in advance for omissions and existing errors.

Acknowledgements

We thank Mandy Pickering who assisted Molly McGraw in preparing the updated spreadsheet. Anna Kurchatova, Tyumen University, assisted with identifying and editing of names of Russian participants in the 2012 conference. Irina Streletskaya, Moscow State University, provided dates for deceased Russian geocryologists, many of whom attended the 1973 conference in Yakutsk. Boris Radosavljevic, Alfred Wegener Institute Helmholtz Centre for Polar and Marine Research, provided the PYRN membership list.

References

Brown, J. [2013]: Guest Editorial: The 50th Anniversary of the First International Conference on Permafrost and Beyond. *Permafrost and Periglacial Processes*, 24(4):263–267, doi:10.1002/ppp.1788.

May, I.; Hubberten, H.-W. and Lewkowicz, A.G. [2012]: Report from the International Permafrost Association: Tenth International Conference on Permafrost (TICOP) in Salekhard. *Permafrost and Periglacial Processes*, 23(4):342–345, doi:10.1002/ppp.1757.

Stanilovskaya, J. [2012]: X International Conference on Permafrost. *Oil & Oil Products Pipeline Transportation: Science & Technologies*, 3(7):31, URL http://en.pipeline-science.ru/archive/.

Effects of 45 years of heavy road traffic and climate change on the thermal regime of permafrost and tundra at Prudhoe Bay, Alaska

Marcel Buchhorn[1,2], Martha K. Raynolds[1], Mikhail Kanevskiy[3], Gosha Matyshak[4], Yuri Shur[3], Michael D. Willis[1], Jana L. Peirce[1], Lisa M. Wirth[2], & Donald A. Walker[1]

[1] *University of Alaska Fairbanks, Institute of Arctic Biology, USA*
[2] *University of Alaska Fairbanks, Geophysical Institute, USA*
[3] *University of Alaska Fairbanks, Department of Civil & Environmental Engineering, USA*
[4] *Moscow State University, Department of Soil Science, Moscow, Russian Federation*

The upper permafrost of the Prudhoe Bay Oilfield contains significant amounts of excess ground ice including large ice wedges which form high- and low-centered polygons. An increase in infrastructure development and road traffic since the initial development of the Prudhoe Bay Oilfield in 1968 has resulted in extensive flooding, accumulation of road dust, and roadside snowbanks, all of which alter the thermal properties, hydrology, surficial geomorpholopgy, soils, vegetation, and spectral properties [Walker et al., 2014].

We established four transects in 2014 and 2015 to document the long-term effects of natural climate change, road construction, and heavy road traffic on adjacent tundra [Walker et al., 2015]. Two transects were established perpendicular to the Spine Road north of Lake Colleen (Colleen Site A) and three perpendicular to the Dalton Highway next to the Deadhorse airstrip (Airport Site) (Fig. 1a). We conducted a time-series analysis of aerial photographs from 1949 to 2014 at Colleen Site A, and measured several geoecological factors along the transects at both sites. The transect studies included detailed topography, active-layer-thickness, soil and air temperatures, vegetation and soil surveys, field spectroscopy, and permafrost coring, We also installed 129 Maxim Thermochron® iButton® devices along the two transects at Colleen Site A in 2014, which logged temperature data every 4 hours for 1 year. Air temperature loggers were set up at 0, 0.1, 0.2, 0.5, 1.0, and 1.5 m height and soil temperature loggers were set up at 0, -0.20, and -0.40 m depth at polygon centers and polygon troughs spaced at 5, 10, 25, 50, 100 and 200 m distance from the road (Fig. 1c). In August 2015, we retrieved the iButtons and found that 15 of the 72 soil temperature loggers failed, probably because their protective plastic bags leaked and the iButton devices are not waterproof. After that, 260 iButtons were installed over the four transects for the 2015 to 2016 measurement period, with increased moisture protection in order to reduce the failure rate.

Prior to infrastructure development in 1949, rather homogeneous networks of low-centered polygons with less than 30 cm of trough-rim elevation contrast covered both locations [Walker, 1985] (Fig. 1b). The time-series of air photos from Colleen Site A and climate record from the nearby Deadhorse station, indicate that thermokarst was virtually unchanged during the period from 1949 to 1985 with only relatively minor increases road-side thermokarst. In 1989, 1995, 1999, and 2013 corresponding to unusually warm summers, region-wide themokarst increased and has continued to expand (Fig. 1b, c).

Since then, thawing of the top of the ice wedges had converted some of the low-centered polygons to high-centered polygons with deep (> 50 cm) troughs, in many cases filled with water. Direct effects of road traffic and infrastructure development such as flooding, road dust, and snow drifts have led to increase in soil temperatures and active-layer thickness near the road. Dust from the road has produced thick mineral horizons that lie on top of the original organic soil surface horizons. This is noticeable in the 1-year record of soil temperatures for Colleen Site A. Differences in the soil-temperature regime are also noticeable between the south-side transect (T2) and the north-side transect (T1). One of the reasons is that the >1-m tall road embankment blocks all drainage between the two sides of the road. The historical aerial photos show that this artificial blockage increased ice-wedge melting on the south side of the road, leading to subsidence in the ice-wedge polygon troughs. Today, the south-side transect is hydrologically connected to Lake Colleen, the north-side transect is not.

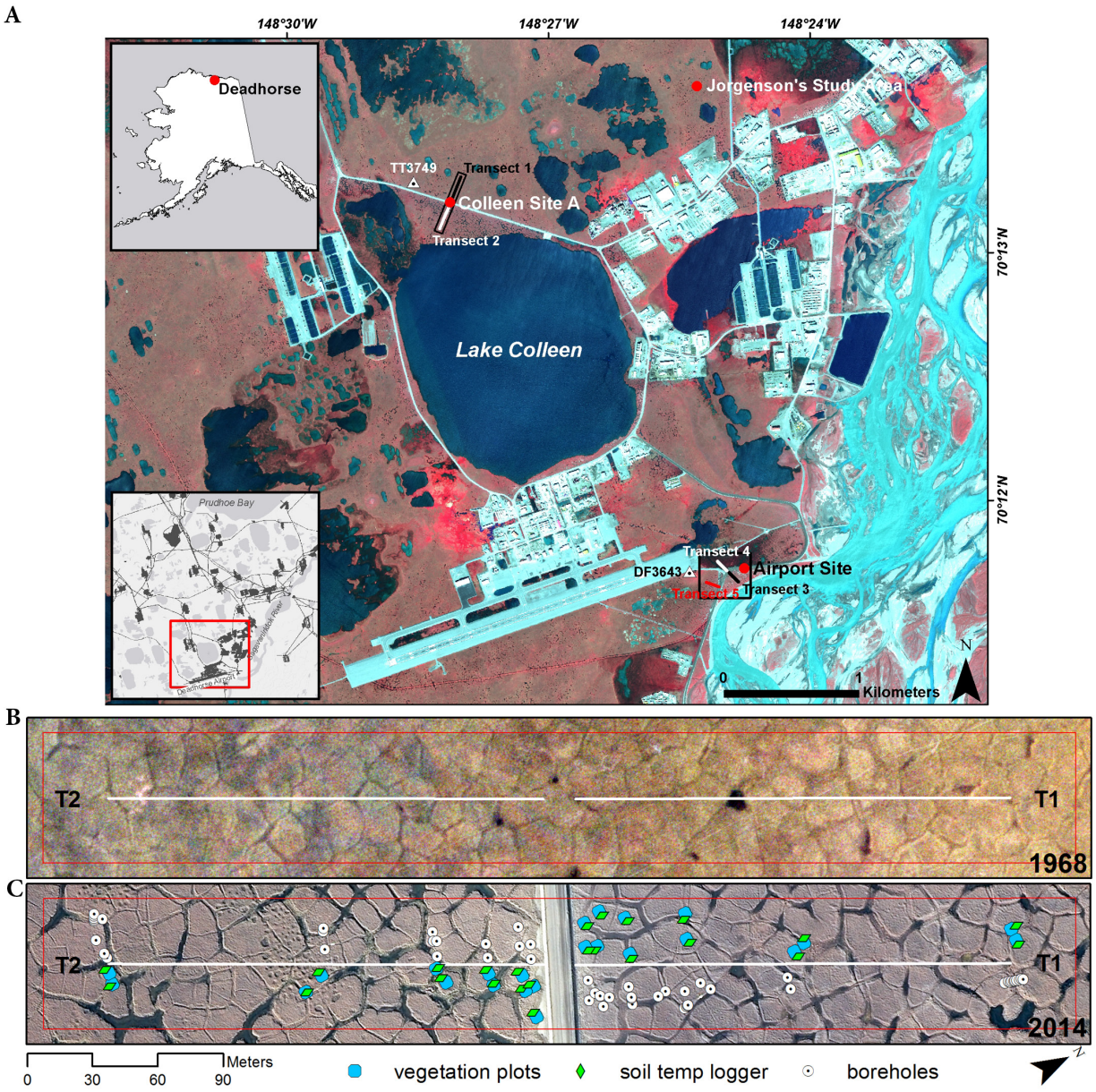

Figure 1: (a) The Lake Colleen region including both study areas. (b) Aerial image of Colleen Site A before the Spine road was constructed (1968). (c) Aerial image of Colleen Site A from 2014 including positions of field installations.

The wetter troughs along T2 have grown lush vegetation, attracting geese and other herbivores, increasing the nutrient regime, and forming thick organic layers in the troughs, insulating the surface and protecting remaining wedge ice in the troughs from further thawing.

These factors have all contributed in different ways to alteration of the ground temperatures, surface geomorphology, and plant canopy, which altered in turn the surface albedo. Our analysis demonstrates the cumulative effects of infrastructure-related and climate-related factors on the thermal regime of these arctic landscapes underlain by the ice-rich permafrost.

References

Walker, D.A. [1985]: *Vegetation and Environmental Gradients of the Prudhoe Bay Region, Alaska*, volume 85 of *CRREL Report*. Hanover, NH: US Army Corps of Engineers, Cold Regions Research & Engineering Laboratory, URL http://www.geobotany.org/library/reports/WalkerDA1985_crrel_85-14.pdf.

Walker, D.A.; Raynolds, M.K.; Shur, Y.L.; Kanevskiy, M.; Ambrosius, K.J.; Romanovsky, V.E.; Kofinas, G.P.; Brwon, J.; Everett, K.R.; Webber, P.J.; Buchhorn, M.; Matyshak, G.V. and Wirth, L.M. [2014]: In: Walker, D.A. and Raynolds, M.K. and Buchhorn, M. and Peirce, J.L.(eds.) *Landscape and Permafrost Changes in the Prudhoe Bay Oilfield, Alaska.* Alaska Geobotany Center Publication. Fairbanks, AK, 2014. URL http://www.geobotany.uaf.edu/library/pubs/WalkerDA2014_agc14-01.pdf. AGC 14-01.

Walker, D.A.; Buchhorn, M.; Kanevskiy, M.; Matyshak, G.V.; Raynolds, M.K.; Shur, Y.L. and Wirth, L.M. [2014]: In: Walker, D.A. and Raynolds, M.K. and M. Buchhorn and Peirce, J.L.(eds.) *Infrastructure-Thermokarst-Soil-Vegetation Interactions at Lake Colleen Site a, Prudhoe Bay, Alaska.* Alaska Geobotany Center Data Report. Fairbanks, AK, 2015. URL http://www.geobotany.uaf.edu/library/pubs/WalkerDA2015_agc15-01_datarpt.pdf AGC 15-01.

Translation and contestation: Researching permafrost in the early cold war

Pey-Yi Chu

Pomona College, USA

This paper explores the transfer of Soviet ideas about frozen earth to North America during the 1940s and 1950s. In 1943, the US Army Corps of Engineers published a report entitled "Permafrost, or Permanently Frozen Ground, and Related Engineering Problems". The author, Siemon Muller, was a geology professor at Stanford University who had been born in Russia but emigrated after the Bolshevik Revolution. Drawing upon the research of a pioneering generation of permafrost scientists in the Soviet Union, Muller coined the word "permafrost" based on his translation of vechnaia merzlota, the expression for frozen earth adopted in the USSR.

The term "permafrost", however, generated controversy. In a 1953 memorandum for the United States Geological Survey, geologist Inna Poiré wrote that "permafrost has been considered a translation of the Russian vechnaia merzlota". But whereas, she wrote, "vechnaia means – continuous (in time), or long lasting, or usual", nevertheless "it does not mean fixed, or unchangeable, i.e. it does not mean permanent". She asserted that "merzlota, in general, is one of the least permanent phenomena in nature". Therefore, "all terms derived from permafrost, such as: permafrostology, permafrozen, permafrost process do not comply with the actuality, for freezing is not permanent under the present conditions on the earth, known to us". Like Muller, Poiré was a native speaker of Russian, a trained geologist, and an émigré to the US. If she did not consider "permafrost" to be an appropriate word for the phenomenon, then how did the term enter English scientific and popular language?

I approach this question by focusing on the history of permafrost science during the Cold War. First, I explore the reasons for US interest in Soviet encounters with frozen earth. Thanks to geographical accident, extensive stretches of the territory of the USSR were underlain by frozen earth. Moreover, the imperative of socialist industrialization during the 1920s and 1930s made understanding and adapting to frozen earth essential. As a result, scientists and engineers developed experience operating in frozen earth environments earlier in the USSR than elsewhere. They began to build a discipline centered on the study of frozen earth, establishing working groups, research stations, periodic conferences, and a journal dedicated to the phenomenon. When the US embarked on large-scale construction projects in the Arctic and sub-Arctic beginning in World War II, it looked to Soviet precedents for guidance.

Second, I examine initiatives for and barriers to exchanging information about frozen earth. Soviet and US scientists expressed the need to translate research by their foreign counterparts, but both sides struggled with a shortage of individuals with the technical and linguistic competence to undertake such work. Furthermore, in the USSR, permafrost scientists who cultivated foreign connections and sent articles abroad fell under suspicion during the anti-Western and anti-cosmopolitan campaigns of late Stalinism.

Finally, I analyze the scientific and linguistic difficulties of translation. Part of the problem of trans-

lating vechnaia merzlota into permafrost was ongoing debate about the nature of frozen earth. Within the Soviet Union, a younger generation of scientists attempted to do away entirely with the term vechnaia merzlota. In the US, researchers put forth alternative nomenclature for describing frozen earth. Due to language and political barriers, however, these conversations took place largely in isolation from each other. The combination of intensifying Cold War competition and the need for rapid progress in applied research about frozen earth meant that the skepticism of some American scientists gained little traction. At the same time, cultural and diplomatic divisions prevented the heated debates of Soviet scientists in the 1950s from becoming known outside the Eastern bloc.

The story of permafrost science offers an intriguing case for illuminating the globalization of Soviet scientific knowledge. My goal is not simply to credit Soviet contributions but to probe the accidents, crossed moments, and varied understandings that characterize the transnational movement of ideas. I argue that the intellectual history of permafrost as a concept, including the cultural contexts, scientific debates, and political contingencies that influenced its evolution and popularization, belongs as much to understandings of the natural phenomenon as do investigations into the material reality of frozen earth. In the twentieth century, the Soviet project played a crucial role in shaping what is not only a scientific and environmental but also a historical object.

This paper is based upon archival research using unpublished documents in repositories such as the Russian State Archive of the Economy, the Archive of the Russian Academy of Sciences, and the National Archives at College Park, Maryland.

The cautionary tales of the Alaska Highway and the Trans-Alaska Pipeline System

Margaret Hope Cysewski & Yuri Shur

Department of Civil and Environmental Engineering, University of Alaska Fairbanks, USA

Introduction

When thinking about permafrost engineering in Alaska, the two most iconic projects are the Alaska Highway and the Trans-Alaska Pipeline System. The Alaska Highway is the iconic cautionary tale of building on permafrost, while on the opposite side the Trans-Alaska Pipeline System is the iconic success story of building on permafrost. What key elements make one story a success and the other a failure?

Alaska Highway

The Alaska Highway is a 2300-kilometer (1400-mile) road that was built in the summer of 1942 to bring supplies from the continental U.S. to Alaska through Canada during WWII (McFadden and Bennett 1991). The road is remembered as being built by 10,607 U.S. Army soldiers in the summer of 1942 (March to November). While cutting a road of this length was a feat, this initial road was only a rough survey road. The Public Roads Administration with a staff of 1,800 along with a civilian workforce of 14,100 continued to work on the highway through the next year. Their improvements were what brought it up to tote road standards by end of 1943 [Cysewski, 2013].

The Alaska Highway is remembered in history due to the national news on the struggle the U.S. Army Corps of Engineers had with permafrost. When the Army's bulldozers charged in side-by-side pushing all of the trees and moss aside, the permafrost quickly turned into soupy-mud in the hot sun. Through laborious trial and error the crews eventually stumbled on what they thought was a new technique to build on permafrost. They hand cleared the trees and brush and laid them across the roadway, keeping the moss intact and the permafrost frozen. Then bulldozers covered the logs and branches with a meter (few feet) of unfrozen dirt and gravel. This method has been used for four thousand years, and is called the corduroy road. Decades before the Alaska Highway, gold miners used this technique on permafrost in Alaska. The Army basically created something that already existed instead of consulting these gold miners or even the seasoned Alaska Road Commission. But political pressure to get the road completed led the builders to rush into the project with little planning and no knowledge that permafrost even existed [Cysewski, 2013].

Trans-Alaska Pipeline System

The Trans-Alaska Pipeline System (TAPS) is a 1,300-kilometer (800-mile) pipeline built from Prudhoe Bay to Valdez, Alaska from 1974 to 1977. Even with the cautionary tale of the Alaska Highway, TAPS almost followed the same mistake. In 1969, the joint venture between three oil companies (later the Alyeska Pipeline Service Company) were ready to charge in and build the pipeline in the conventional buried method [Borneman, 2003]. However, a 60-degree Celsius (145-degree Fahrenheit) hot oil pipeline buried in permafrost "would slice through ice-rich permafrost like a hot knife through butter"(McFadden and Bennett [1991], 42). When the oil companies made their announcement to build in 1969 and started getting their permits in order, the process was abruptly stopped. Both the National Environmental Policy Act (which created the Environmental Protection Agency (EPA)) and the Alaska Native Claims Settlement Act were in the works, and political officials as well as lawsuits prevented construction. A big push to conduct an extensive environmental impact statement led to a pipeline redesign, a comprehensive site analysis, and even a change in alignment. Finally five years later, Alyeska got the federal permits to start construction [Borneman, 2003].

The success of TAPS is due to utilizing the expertise from several permafrost scientists and engineers in different fields for its extensive redesign to achieve federal approval. Several advanced techniques were applied to develop a detailed, comprehensive solution to building a pipeline on permafrost. Site selection became crucial in avoiding ice-rich permafrost as much

as possible. Aerial photos were used in landform analysis. Soil and terrain types could be delineated on the aerial photos, then tested with borehole analysis to create a fairly reliable map of permafrost conditions. Through the design phase, Alyeska drilled 3,000 boreholes and analyzed 30,000 core samples. The final pipeline design for ice-rich permafrost conditions was an elevated pipeline to prevent the permafrost from thawing, with roughly half of TAPS elevated. With the pipeline constructed north to south, the southern portion of TAPS is in "warm" permafrost, or permafrost near thawing temperatures, and additional measures were needed. Heat pipes or thermosyphons are used within the vertical support members of the elevated pipeline. These heat pipes contain anhydrous ammonia that has an evaporation temperature lower than the natural permafrost temperature. So during the winter, the ammonia that is near the bottom of the heat pipe will evaporate and the vapor will move to the top. At the top of the pipe, the cold winter air removes the heat from the ammonia with the help of radiator fins, which causes the ammonia to condense and the liquid to drain to the bottom of the pipe. Then the cycle continues as the ground heats the ammonia causing it to evaporate. This process passively runs all winter, then stops when the air temperatures become too warm. These heat pipes work by making the permafrost much colder than it is naturally, creating a cold storage to last through the summer [McFadden and Bennett, 1991]. All of these techniques were used in this sophisticated solution for building a pipeline on permafrost, but did come with a high price tag of $8 billion ($31 billion today) [Borneman, 2003].

Conclusions

The biggest take away is that inexperience and being naive can lead to serious ramifications. Political pressure is what caused poor planning and bad outcomes in the 1942 construction of the Alaska Highway. But then with TAPS in 1969, it was political pressure that prevented history from repeating itself and forced a redesign with comprehensive planning that led to a successful outcome. Both projects are really a cautionary tale for politicians and engineers alike. Large projects like the potential gas pipeline in Alaska, or even smaller projects like roads or houses, need experienced, seasoned permafrost engineers to lead a project to success.

References

Borneman, W.R. [2003]: *Alaska: Saga of a Bold land.* HarperCollins: New York.

Cysewski, M. [2013]: *Initial Permafrost Engineering Research in Alaska.* Ms thesis, College of Engineering and Mines University of Alaska Fairbanks.

McFadden, T.T. and Bennett, F. L. [1991]: *Construction in Cold Regions: A Guide for Planners, Engineers, Contractors, and Managers.* John Wiley& Sons: New York.

Alas landscapes of Central Yakutia: Towards a periodization of land use and permafrost degradation

Roman V. Desyatkin[1], Joachim Otto Habeck[2], & Aytal I. Yakovlev[3]

[1] *Inst. Biol. Probl. Cryolithozone, Russian Academy of Sciences, Yakutsk, Russian Federation*
[2] *Universität Hamburg, Germany*
[3] *North-Eastern Federal University Yakutsk, Russian Federation*

The interplay of socio-economic factors and landscape development in permafrost regions has rarely been discussed. Trying to address this deficiency, the authors present a periodization of landscape development and resource use in the central part of the Republic of Sakha (Yakutia). Special attention is given to alas development. In earlier millennia, land use (hunting, fishing, gathering) impacted on the natural landscape development only to a negligible extent. The emergence of pastoralists in the region (approx. 800 years ago) marked the beginning of extensive human interaction with the natural landscape in certain areas. Sakha/Yakut pastoral economy came to utilize the thermokarst depressions locally known as alas; simultaneously, pastoralists exerted some palpable influence on permafrost dynamics. From the mid 17^{th} century to the early 20^{th} century, resource use in Central Yakutia intensified, due to increased hunting for fur animals, growing numbers of settlers, and – albeit on a small scale – crop cultivation. The early Soviet period (late 1920s onward) was characterized by collectivization and mechanization of agriculture enhanced by industrialization. Crop cultivation was extended significantly. Additionally, many hitherto unused alas areas were opened up for animal husbandry. Smaller settlements were amalgamated into larger ones, leading to higher population density at some locations. All this was accompanied by intensive modifications of the alas landscapes, including human-induced permafrost degradation. The last 25 years have seen significant changes in land and resource use, with locally divergent trends towards extensification or intensification, which in turn will lead to divergent changes in alas and ajacent areas. The aim of the paper is not only to sketch out a regional history of land use and landscape development, but also to assess the main drivers of future permafrost landscape development.

Permafrost in synthetic view of glacial and periglacial domain: New terms and definitions

Wojciech Dobiński

University of Silesia, Poland and Centre for Polar Studies KNOW (Leading National Research Centre) WNoZ UŚ

Introduction

The definition of permafrost was formulated about 70 years ago, and the terminology used in the studies on permafrost and periglacial environment only found its full expression at the end of the 20th century [van Everdingen, 1998, revised May 2005].

Almost from the very beginning the study of permafrost was placed separately to the study of glaciers [Waller et al., 2012]. Especially in the tradition of Russian research, permanent freezing was called underground glaciation as opposed to surface glaciation [Danilov, 1990]. The development of research, however, facilitated bringing both disciplines – glaciology and permafrost science, significantly closer. Their interdependence began to be recognized (e.g. Harris and Murton [2005]).

This results in turning back to the common roots of the two disciplines, for which the cryosphere as an area of research and cryology as a scientific discipline are a common reference point. The awareness of the overlapping of glaciology and 'periglaciology' makes the permafrost science more and more widely recognized. This makes necessary to revise the understanding of the definition of permafrost, and add others, which, although in a conventional way have been already functioning in the works of permafrost science, have been neither ultimately nor sufficiently defined.

Revision of certain definitions is also a need for a holistic approach in research on the cryosphere on Earth and in space (e.g. Mars). This paper is a proposition of improvement of permafrost definition, and the introduction of new term: "glacial permafrost" necessary for holistic understanding permafrost which can be present in both the glacial and periglacial environments [Dobiński, 2011, forthcoming].

Definition of permafrost

In the IPA glossary [van Everdingen, 1998, revised May 2005], permafrost is defined as follows: "Ground (soil or rock and included ice and organic material) that remains at or below 0 °C for at least two consecutive years" (Definition no 390, p.55). The added note clarifies the definition: "Permafrost is synonymous with perennially cryotic ground: it is defined on the basis of temperature. It is not necessarily frozen, because the freezing point of the included water may be depressed several degrees below 0 °C; moisture in the form of water or ice may or may not be present. In other words, whereas all perennially frozen ground is permafrost, not all permafrost is perennially frozen. Permafrost should not be regarded as permanent, because natural or man-made changes in the climate or terrain may cause the temperature of the ground to rise above 0 °C. Permafrost includes perennial ground ice, but not glacier ice or icings, or bodies of surface water with temperatures perennially below 0 °C (...)" [van Everdingen, 1998, revised May 2005], Definition no. 390, comment, p. 55-56). The phrase in the commentary to the definition – "Permafrost includes perennial ground ice, but not glacier ice or icings, or bodies of surface water with temperatures perennially below 0 °C" ; I believe should be changed as follows: Permafrost as a (geo) physical state of the litosphere: its temperature, does not have a material manifestation and in the places of its occurrence it encompass the lithosphere. Permafrost encompass also perennial ground ice, surface ice e.g.: snow patches, glaciers and glacial ice-shelves as a parts of the litosphere.

Substantiation

In recent years permafrost has been commonly associated with the physical state of the ground – its temperature, and duration for at least two consecutive years. Sometimes, however, it is still identified with the underground ice, especially of not glacial origin

that meets the criterion of time. Such understanding of permafrost is incorrect, in particular when the cryotic state is treated as the synonym for permafrost. Freezing understood as a solid state of water (in soil) is not a prerequisite for its being named 'permafrost', or more correctly: 'encompassed by permafrost'. According to the commentary on the definition of 118, Multilanguage Glossary of Permafrost and Related Ground-Ice Terms [van Everdingen, 1998, revised May 2005]: "The term >cryotic< and >noncryotic< were introduced to solve a major semantic problem (...) namely the lack of specific separate terms to designate >above 0 °C< and >below 0 °C < as opposed to >unfrozen< (not containing ice) and >frozen< (containing ice). Cryotic and noncryotic refer solely to the temperature of the material described, independent of its water or ice content. Perennially cryotic ground refers to ground that remains at or below 0 °C continuously for two or more years and is therefore synonymous with permafrost".

These statements are consistent with the establishments generally accepted in permafrost science. A number of specialists claim similarly. "Agreement will surely be given to the fact that permafrost is a condition of the ground and not, of itself, a material. The name is used to describe that condition of the ground when its perennial mean temperature is always less than 0 °C". [Legget, 1963]. Black [1954] writes that "permafrost is defined on the basis of temperature and thus may consist of any type of natural or artificial material, whether consolidated by ice or not". In 1976, the same author claims that "The definition is based exclusively on temperature, irrespective of texture, degree of induration, water content, or lithologic character"[Black, 1976]. H.M. French [2007] writes: "Permafrost is defined on the basis of temperature: it is ground (i.e. soil and/or rock) that remains at or below 0 °C for at least two consecutive years. (...) Furthermore, permafrost may not necessarily be frozen since the freezing point of included water may be depressed several degrees below 0 °C" . Haeberli et al. [2006] argue that permafrost is a "specific ground thermal condition". Harris et al. [2009] begin their article with the statement: "Permafrost (...) is thermally defined as ground that remains below 0 °C for at least two years".

Glacial permafrost

Term which is absent in the IPA dictionary is 'glacial permafrost'. This type of permafrost in the earlier period of study was present in the permafrost science. This consistency is also important because of the fact that the Earth Sciences, including glaciology and permafrost sciences, are applied to space exploration (e.g. Prockter and Pappalardo [2000], Patterson et al. [2006]). The definition of glacial permafrost may be as follows:

Glacial permafrost: permafrost encompassing a glacier, ice sheet or a shelf glacier.

Substantiation

Constitutive issue for the substantiation of the existence of glacial permafrost is the answers to the following questions:

1. whether ice is rock (part of the lithosphere) and
2. whether it may freeze for more than two years.

An active layer does appear in glacial permafrost, as ice during warm period of the year turns into another state by melting, and it is removed from the surface of the glacier gravitationaly. In the Earth Sciences such as petrography and mineralogy, ice is treated as a mineral, and the same should be applied to other areas of the Earth Sciences in order to preserve the unity of science. Ice possesses all the characteristics of a mineral, hence its accumulation may be called 'rock'. It used to be treated as rock at the outset of cryology, and the conventional classification [Shumskiy, 1955, Dobiński, 2006] distinguishes ice as a sedimentary, metamorphic, magmatic rock. It is worth recalling this classification, especially when the ice tested on other celestial bodies is widely considered as the icy-lithosphere (e.g. Prockter and Pappalardo [2000]). In a glacier, a number of geological processes can be identified, such as: sedimentation, folding, faulting, metamorphism, karst and many others. Therefore it should be excluded from the hydrosphere and transferred to the lithosphere, wherein it belongs in fact.

A.L. Washburn allows the presence of permafrost in glaciers when writing in 1973: "Glaciers whose temperature does not reach 0 °C are permafrost by either definition but they are frequently omitted from discussion of permafrost and treated separately". Embleton and King [1975] argue, in turn, that "Cold glaciers are 'permafrost' by Muller's definition, but they are conventionally excluded from the term". Mackay and Black [1973] claim that "... permafrost may have persisted for many millennia, first as part of glacier". Pettersson et al. [2003] who claim that: "The cold

surface layer is comparable to ground permafrost and is a result of the energy balance at the glacier surface and advection of temperate ice through glacier flow". The concept of permafrost with respect to glacial ice has been also discussed in more detail in chapter 4.5 of the article Dobiński [2006], and further in another work [Dobiński, 2012] where he divides glacial permafrost into 'A' type – including cold ice, and 'B' type including temperate ice. The perception of permafrost in glaciers help to solve the problem of the glacier - permafrost relationship, which is studied recently [Harris and Murton, 2005, Waller et al., 2012].

Conclusions

Both the glacial and periglacial domains are present in the Earth's and extraterrestial environments. Gaining knowledge about them and researching into them should be based on the principle of non-contradiction: they should be treated alike, by analogy. The proposals of the aforementioned definitions address this need. Their adoption allows clarification of ambiguities and maintaining the unity of the Earth Sciences both in relation to the Earth's cryosphere, and in the extraterrestial environment. They also facilitate bringing together separated nowadays scientific disciplines: glaciology and permafrost science.

Acknowledgements

This research has been supported by the National Science Centre, Poland, grant no. DEC-2012/07/B/ST10/04268, and Centre for Polar Studies, Leading National Research Centre, KNOW, Poland. AMDG. The project has been also financed from the funds of the Leading National Research Centre (KNOW) received by the Centre for Polar Studies for the period 2014-2018.

References

Black, R.F. [1954]: Permafrost: A Review. *Geological Society of America Bulletin*, 65(9):839–856, doi:10.1130/0016-7606(1954)65[839:PR]2.0.CO;2.

Black, R.F. [1976]: Features Indicative of Permafrost. *Annual Review of Earth and Planetary Sciences*, 4(1):75–94, doi:10.1146/annurev.ea.04.050176.000451.

Danilov, I.D. [1990]: *Podzemnyje l'dy*. Moskwa, Nerda.. (in Russian).

Dobiński, W. [2006]: Ice and environment: A terminological discussion. *Earth-Science Reviews*, 79(3–4): 229–240, doi:10.1016/j.earscirev.2006.07.003.

Dobiński, W. [2011]: Permafrost. *Earth-Science Reviews*, 108(3–4):158–169, doi:10.1016/j.earscirev.2011.06.007.

Dobiński, W. [2012]: The cryosphere and glacial permafrost as its integral component. *Central European Journal of Geosciences*, 4(4):623–640, doi:10.2478/s13533-012-0109-8.

Dobiński, W. [Forthcoming]: Permafrost – definition and extent. In *The International Encyclopedia of Geography*. Malden, Oxford: John Wiley and Sons, Ltd.

Embleton, C. and King, C.A.M. [1975]: *Periglacial Geomorphology*. London: Edward Arnold.

French, H.M. [2007]: *The Periglacial Environment*. John Wiley & Sons, Ltd, Chichester, 3rd edition, ISBN 978-0-470-86588-0.

Haeberli, W.; Hallet, B.; Arenson, L.; Elconin, R.; Humlum, O.; Kääb, A.; Kaufmann, V.; Ladanyi, B.; Matsuoka, N.; Springman, S. and Vonder Müehll, D. [2006]: Permafrost creep and rock glacier dynamics. *Permafrost and Periglacial Processes*, 17 (3):189–214, doi:10.1002/ppp.561.

Harris, C. and Murton, J.B.(eds.). [2005]: *Cryospheric Systems: Glaciers and Permafrost*. Geological Society, London, Special Publications, 242, http://sp.lyellcollection.org/content/242/1

Harris, C.; Arenson, L.U.; Christiansen, H.H.; Etzelmüller, B.; Frauenfelder, R.; Gruber, S.; Haeberli, W.; Hauck, C.; Hölzle, M.; Humlum, O.; Isaksen, K.; Kääb, A.; Kern-Lütschg, M.A.; Lehning, M.; Matsuoka, N.; Murton, J.B.; Nötzli, J.; Phillips, M.; Ross, N.; Seppälä, M.; Springmann, S.M. and Vonder Mühll, D. [2009]: Permafrost and climate in Europe: Monitoring and modelling thermal, geomorphological and geotechnical responses. *Earth-Science Reviews*, 92(3–4):117–171, doi:10.1016/j.earscirev.2008.12.002.

Legget, R.F. [1963]: Permafrost in North America. In *Proceedings of the International Conference on Permafrost, Lafayette, Indiana, USA, 11–15 November 1963*, publication no.

1287, pages 2–7. National Academy of Sciences – National Research Council, Washington D.C., URL http://ipa.arcticportal.org/publications/conference-proceedings.

Mackay, J.R. and Black, R.F. [1973]: Origin, composition, and structure of perennially frozen ground and ground ice: a review. In *Proceedings of the Second International Conference on Permafrost*, 13–28 July 1973, Yakutsk, USSR. volume: North American Contribution, pages 185–192. National Academy of Sciences, Washington, D.C., ISBN 0-309-02115-4 URL http://ipa.arcticportal.org/publications/conference-proceedings.

Patterson, G.W.; Head, J.W. and Pappalardo, R.T. [2006]: Plate motion on Europa and nonrigid behavior of the Icy lithosphere: The Castalia Macula region. *Journal of Structural Geology*, 28(12):2237–2258, doi:10.1016/j.jsg.2006.03.032.

Pettersson, R.; Jansson, P. and Holmlund, P. [2003]: Cold surface layer thinning on Storglaciären, Sweden, observed by repeated ground penetrating radar surveys. *Journal of Geophysical Research: Earth Surface*, 108(F1):6004, 2003. doi:10.1029/2003JF000024.

Prockter, L.M. and Pappalardo, R.T. [2000]: Folds on Europa: Implications for Crustal Cycling and Accommodation of Extension. *Science*, 289(5481): 941–943, 2000. doi:10.1126/science.289.5481.941.

Shumskiy, P.A. [1955]: *Osnovy strukturalnogo l'edovedeniya*. Akademiya Nauk SSSR, Izdatel'stvo Akademii Nauk SSSR.

van Everdingen, R.O.(ed.). [1998 (revised May 2005)]: *Multi-language glossary of permafrost and related ground-ice terms*. Boulder, CO: National Snow and Ice Data Center/World Data Center for Glaciology, URL http://nsidc.org/fgdc/glossary/english.html.

Waller, R.I.; Murton, J.B. and Kristensen, L. [2012]: Glacier–permafrost interactions: Processes, products and glaciological implications. *Sedimentary Geology*, 255–256:1–28, doi:10.1016/j.sedgeo.2012.02.005.

Washburn, A.L. [1973]: *Periglacial processes and environments*. London: Edward Arnold.

Climate warming- and human-induced thermokarst activity in Central Yakutia and its social response

Aleksandr Nikolaevich Fedorov[1], Pavel Konstantinov[1], Nikolay Basharin[1], Roman Desyatkin[2], Yoshihiro Iijima[3], Hotaek Park[3], Mathias Ulrich[4], Antoine Sejourne[5], Francois Costard[5], Christophe Grenier[5], Tetsuya Hiyama[6], & Go Iwahana[7]

[1]*Melnikov Permafrost Institute, Russian Federation*; [2]*Institute of Biological Problems of Cryolithozone, Russian Federation*; [3]*JAMSTEC, Japan*; [4]*Leipzig University, Germany*; [5]*University Paris Sud 11, France*; [6]*Nagoya University, Japan*; [7]*IARC, University of Alaska, USA*;

Central Yakutia, one of the most populated regions within the permafrost zone, is currently facing serious problems associated with the response of permafrost landscapes to climate warming. The presence of ice-rich permafrost deposits (i.e. ice complex), an increasing population, changing technologies, and expanding human activities make the Central Yakutian landscapes sensitive to disturbance. In human-disturbed or modified permafrost landscapes a self-preservation mechanism is lacking, because the shielding layer between the top of massive ice bodies and the active layer has been lost in these areas. This is the result of climatic changes over the last three to four decades.

The land cultivation on the ice complex has a long history of several centuries. Using these areas agriculturally was introduced to the aboriginal population after Yakutia was connected to Russia. Alases, that were traditionally used by the local population have been deemed unsuitable for crop production because of high soil salinity within these thermokarst basins. Therefore, deforestation on the ice-complex uplands around the alases became a common practice to make the land available for cultivation.

Croplands in deforested areas have been widely used until 1990. However, the climate warming and the overall economic collapse after the political changes in Russia have caused a significant reduction of crop acreage. During the period from 1990 to 2013, the total area of cropland has decreased by 2.5 times. One of the main reasons was the land degradation due to thermokarst development. Our observations indicate that thermokarst processes have intensified in response to the warming of the subsurface. This is causing an increase of the seasonal thaw depth and the widespread development of initial thermokarst landforms. The strongest response of the ice-rich landscapes to these processes occurred in the 1990s to 2000s. During this period, surface subsidence was observed in large areas. This was caused by the downward melting of ice wedges and resulted in hummocky polygonal landforms. Rates of surface subsidence were quite high and ranges from 1.0 to-1.5 m between 1990 and 2015. At the same sites of intensive permafrost degradation, the area of thawing lakes expanded by 2-4 times. In some locations, the expansion of these lakes now influences the areas of alases that were formed during the Holocene optimum.

Significant effects on the permafrost landscapes have also been exerted by forest fires and outbreaks of the Siberian silk moth. These also led to changes to the ground-thermal regime and in ground settlements. In some places, these disturbed areas already turned into thermokarst lakes.

Thermokarst and permafrost degradation is also enhancing in and around rural communities. The ice complex has generally lost its shielding layer and surface subsidence is now a common process in these areas. The shifting from the traditional dispersed form of settlement in alases to a concentrated settlement pattern has imposed a serious burden on the permafrost landscapes. The growing population within the communities requires expansion to new areas. People have to build their homes on unstable ground where surface subsidence is already an ongoing problem.

It is thus evident that permafrost landscapes in Central Yakutia are experiencing significant pressure from current changes in climate and increasing human activities. The reduction of areas suitable for agriculture and homestead development, as well as the changes in water balance of the landscapes induced by forest fires, deforestation, and the outbreaks of forest defoliators are leading to social problems. Our goal is to inform the public about processes currently occurring in permafrost landscapes to find solutions for a sustainable development of the society in permafrost regions.

A methodological framework for the evaluation of climate change adaptation projects: A pilot study using the'Terrain Analysis in Nunavut'project in Arviat, Canada

Melanie Jade Flynn[1], James D. Ford[2], & Jolène Labbé[2]

[1] *United Nations University- Institute for Environment and Human Security and Universität Bonn, Germany*
[2] *Department of Geography, McGill University, Montreal, Québec, Canada*

Subject matter

This research provides "An evaluation of climate change adaptation in a permafrost environment: A pilot study using the 'Terrain Analysis in Nunavut' project in Arviat, Canada". The work aims to create a flexible methodological framework for use in the evaluation of climate change adaptation projects in the Arctic and empirically apply this framework to the 'Terrain Analysis in Nunavut' (TAN) project to provide insight into community adaptation in permafrost environments and to pilot the performance of the framework.

Methods of analysis

The research involved four weeks of fieldwork in Arviat, Nunavut, an area currently believed to be underlain by continuous permafrost. The work used a case study approach and produced a critical analysis of the maps and technical data using a literature review; a logic model [AUSAID, 2005]; magnitude coding of semi-structured interviews (n=19) with key project stakeholders to capture the different perspectives and viewpoints to provide meaningful feedback; and an application of the Adaptation Readiness Framework [Ford and King, 2015]. The framework rated the project using indicators to determine linkages and barriers for effective adaptation at a governance and policy level (Fig. 1).

Findings

The TAN project is still in its fourth year and as a consequence final project outcomes could not be evaluated, however the project is on track to achieving desired outcomes. The project has created a large scale development suitability map which is expected to aid climatic considerations in urban development decisions within the community. Stakeholder interviews highlighted key strengths in the TAN project, particularly; the combination of community engagement with the map production which facilitated communication of results, collaboration between groups and creating a cohesive narrative for permafrost research in Arviat. This is something which was highlighted as missing in a systematic review of hazard mapping projects in the Canadian North.

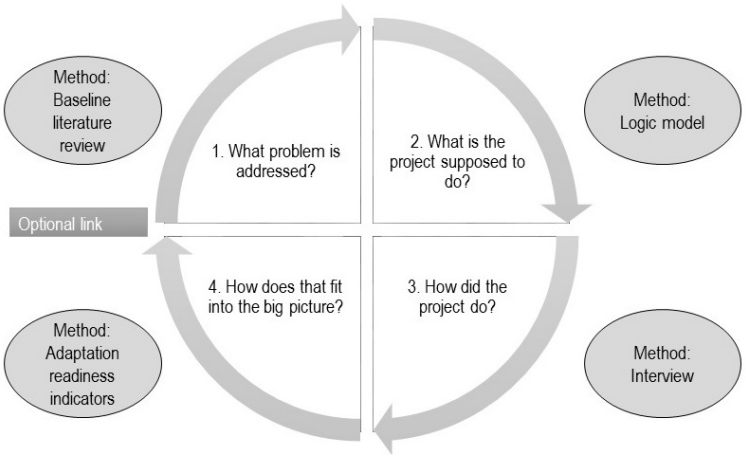

Figure 1: A methodological framework for evaluating climate change adaptation projects at the community level

Feedback suggested that there is room for improvement in the incorporation of stakeholder input at the local level. The project was rated on eight factors which influence the ability to 'do' adaptation: Each factor was scored out of 4. The project is performing well in institutional organisation (4 points) and public support (3 points). But has room for improvement on usable science, funding and resources, stakeholder engagement, leadership, Inuit Qaujimajatuqangit (IQ) (2 points), and decision making (1 point).

Wider applicability of the research

The evaluation framework created was found to be appropriate for evaluating adaption projects in an Arctic setting (Fig. 1). Framework sub-questions and research tools allow a flexible application that would fit with most climate change adaptation projects and would address the current deficit of project evaluation currently observed.

The use of magnitude coding in semi-structured interviews was found to provide helpful context-specific feedback for project creators. Which was particularly effective in aiding learning through evaluation, a key objective of evaluation in climate change adaptation which can help to minimise the risk from maladaptation [Bours et al., 2014].

Adaptation projects do not take place in a vacuum and are therefore influenced by the governance and policy environment in which they take place. The application of the adaptation readiness indicators and scoring, provides insight into key governance issues which influence the likelihood of adaptation occurring.

References

AUSAID [2005]: *AusGuidelines: The Logical Framework Approach*. Australia: Australian Government.

Bours, D.; McGinn, C. and Pringle, P. [2014]: *Selecting indicators for climate change adaptation programming*. Phenom Penh and Oxford: SEA Change CoP and UKCIP.

Ford, J. D. and King, D. [2015]: A framework for examining adaptation readiness. *Mitigation Adaptation Strategy Global Change*, 20:505–526.

Early investigations of permafrost in Siberia by Baltic-German and German scientists

Diedrich Fritzsche[1] & Erki Tammiksaar[2]

[1] *Alfred Wegener Institute Helmholtz Center for Polar and Marine Research, Potsdam, Germany*
[2] *University of Tartu, Faculty of Science and Technology, Estonia*

In the 18th and 19th century several German and Baltic-German scientists investigated almost unknown territories of the Russian Empire. Many of them were invited by the Russian Imperators and some became academicians of the St. Petersburg Academy of Sciences, and later had considerable influence on the development of science in Russia in general and on the organization of expeditions to the Far East and Siberia in particular. German naturalists like Georg Wilhelm Steller (1709-1746), Johann Georg Gmelin (1709-1755), Peter Simon Pallas (1741-1811), Karl Ernst von Baer (1792-1876), Ferdinand von Wrangell (1797-1870) and Alexander Theodor von Middendorff (1815-1894) traveled through Siberia collecting information about flora, fauna, geology, climate, ethnology, history and economy of the Far East of Russia. Their results were published in Russian, German and French, mostly in journals of the Russian Geographical Society (St. Petersburg), in travelogues or in separate monographs and book-chapters. Results of investigations of the Russian Empire became available in Europe by special scientific journals edited e.g. by P.S. Pallas, J.G. Georgi, Th. Fr. Ehrmann, A. Erman, K.E. v. Baer and G. v. Helmersen.

The western world was first informed about frozen ground in Siberia by J. G. Gmelin, who reported finding the phenomenon in Yakutsk, but Leopold von Buch (1774-1853) doubted his report and argued that plants were growing in this region, which considered impossible on permanently frozen ground. As a result, he demanded that Gmelin's data be removed from scientific textbooks [Buch, 1828]. On behalf of a merchant of the Russian-American Company, Fedor Shergin, a shaft was dug in Yakutsk to get drinking water. To Shergi's surprise he was unable to reach liquid water, but the governor of the Russian- American Company, Ferdinand von Wrangell, requested him to continue digging at the expense of the Company, for studies of the frozen ground underneath Yakutsk. The sinking of the well, starting in 1828, has been continued until 1837 reaching an end depth of 382 English feet (about 116.5 m), without reaching unfrozen soil [Helmersen, 1838]. The shaft developed great importance for further geocryological studies. First measurements of soil temperature were carried out therein in April 1829 by the German physicist Adolph Erman (1806-1877). Down to the bottom depth of 46 Paris feet (about 15 m) at that time he recorded continuously -6 °R (-7.5 °C) in all deeper parts of the well, which corresponded very well with the mean annual temperature of Yakutsk of – 5.9 °R. This result can be credited as a first finding of the permafrost depth of "Zero Annual Amplitude". Assuming a geothermal gradient of 1 °R/100 feet, Erman expected liquid water in a depth of 600 feet (about 190 m) [Erman, 1838] but Shergin's measurements published in 1838 indicated temperatures of -0.5 °R at the end bottom of the shaft (116.5 m) [Helmersen, 1838]. Several scientists were doubtful about Shergin's data [Erman, 1838].

Between 1838 and 1843 Karl Ernst von Baer compiled all data available on frozen ground in Siberia, from sources either published or from Russian archives. He wrote a special permafrost study including the first classification of permafrost and made suggestions for regular observations in Shergin's shaft. Baer and the commission responsible formulated instructions for an expedition to eastern Siberia initiated by Baer and led by Alexander Theodor von Middendorff with the focus to investigate the region north of Turukhansk to the Chatanga River and to investigate permafrost, especially its thickness, temperature and distribution [Baer et al., 1843]. Baer also drew the first map of permafrost distribution (Fig. 1). Unfortunately his permafrost study and this permafrost map were not published before 2000 [Bér, 2000]. Baer also suggested that investigations of air and soil temperatures be carried out in British North America [Baer, 2001].

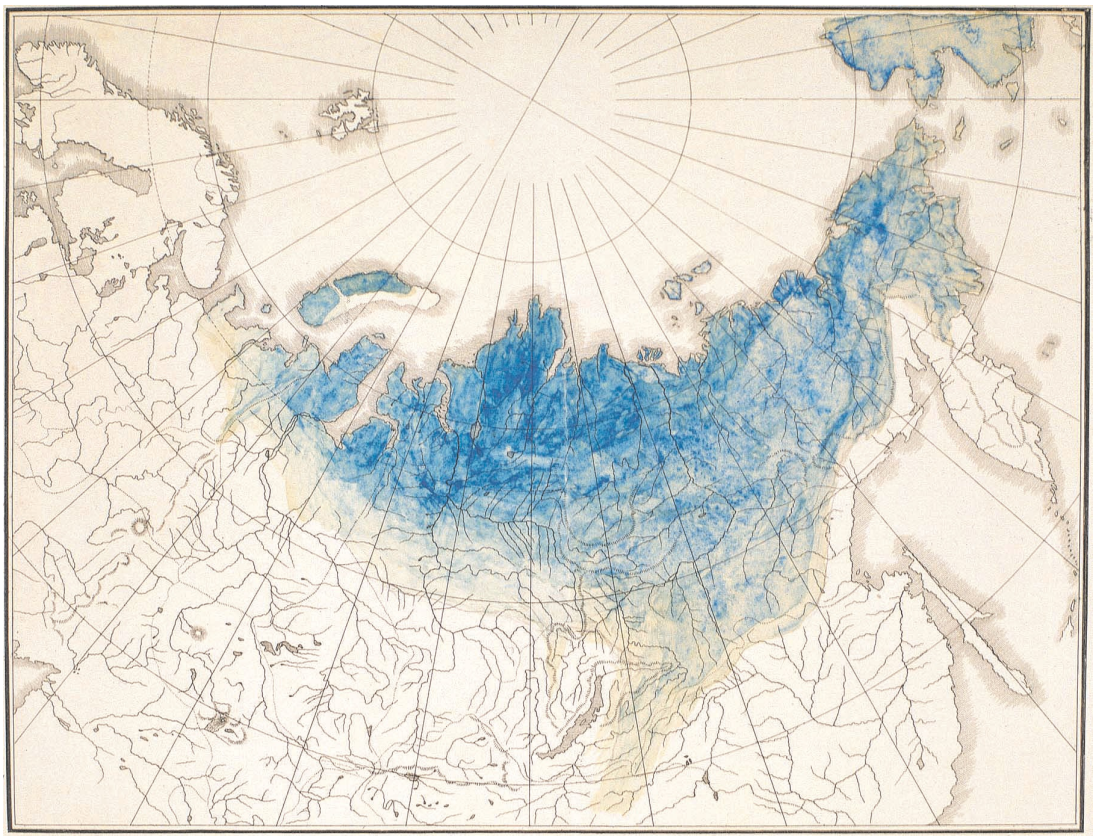

Figure 1: Baer's map of permafrost in Siberia (1843), the first ever produced [Baer, 1843]

According to Baer's guide in 1843-1845, Middendorff carried out soil temperature measurements at Turukhansk and other Siberian places. In the Shergin shaft in Yakutsk, regular measurements, started by him in 1844, had been continued until 1846 by local observers. Middendorff reported a bottom temperature in the shaft of -2.4 °R. He published his geothermal investigations in great detail, including data on the thermal conductivity of soils, which were a result of the geothermic measurements in Shergin's shaft [Middendorff, 1848].

As Erman had also earlier assumed, he supposed a permafrost depth of 600 feet beneath Yakutsk. Baer began a long discussion with him about his conclusions and the geothermal gradient he reported [Baer, 1850] (cf. also [Shiklomanov, 2005]). Middendorff's collection of permafrost observations in Siberia and his conclusions for the geographical distribution and thickness of permafrost provided the foundation for a generation of geocryologists.

Temperature measurements in the active layer were carried out within the framework of the International Polar Year 1882-1883 at Sagastyr Station in the Lena River delta and on Novaya Zemlya. Soil temperature observations had been included in the meteorological program and were carried out regularly at 0.4 m, 0.8 m and 1.6 m depths [Wood and Streletskiy, 2008]. The medical doctor Alexander von Bunge (1851-1930) was a participant of this expedition. He described the place on Bykovsky Peninsula where Adams found the first mammoth carcass in 1799 and reported on other mammoth carcasses found in the Lena Delta, and on permafrost soils, polygonal structures and ice wedges that he observed. He published a hypothesis on the genesis of ground ice by thermal contraction [Bunge, 1902]. In 1885-1886 Bunge was the leader of the expedition of the St. Petersburg Academy of Sciences to the New Siberian Islands during which he and his companion Eduard von Toll (1858-1902) found mammoth relicts and studied the ground ice formations on Great Lyakhovsky Island. European scientists were deeply impressed by the first photographs of huge ground ice wedges published by Toll. He speculated that these formations were relicts of glaciers and introduced terms like "fossil ice"and "ice rock"(Steineis) into geocryology [Toll, 1897].

References

Baer, K.E.v. [1843a]: *South boundary of permafrost in Siberia*, f. 129, op.1, No. 759, I.1. St. Petersburg: Department of the Archives of the Academy of Sciences of Russia.

Baer, K.E.v. [1850]: Ueber nothwendig scheinende Ergänzungen der Beobachtungen über die Boden-Temperatur in Sibirien. *Bulletin de la Classe physico-mathematique de l'Académie Impériale des Sciences de Saint-Pétersbourg*, T.VIII(No. 14):209–224.

Baer, K.E.v. [2001]: Materialien zur Kenntniss des unvergänglichen Boden-Eises in Sibirien. *Berichte und Arbeiten aus der Universitätsbibliothek und dem Universitätsarchiv Giessen*, Bd. 51, Unpublished manuscript; commented by Erki Tammiksaar; edited by Lorenz King.

Baer, K.E.v.; Brandt, F.; Lenz, E. and Meyer, C. [1843]: Instructions donnees a M. le docteur de Middendorff, pour son voyage en Siberie. *Bulletin de la Classe physico-mathematique de l'Académie Impériale des Sciences de St.-Pétersbourg*, T.1:177–185.

Bér, K.M. [2000]: *Materialy k poznaniju netajuscego pocvennogo l'da v Sibiri.* Jakutsk, Institut merzlotovedenija SO RAN. (in Russian).

Buch, L.v. [1828]: Einige Bemerkungen über Quellen-Temperatur. *bhandlungen der Königlichen Akademie der Wissenschaften zu Berlin aus dem Jahre 1825*, pages 93–105.

Bunge, A.v. [1902]: Einige Worte zur Bodeneisfrage. *Rus. K. Min. Gesell. Verh.*, 2. Ser., V.40:203–209.

Erman, A. [1838]: Extract from a letter dated Berlin March 5, 1838. *The Journal of the Royal Geographical Society of London*, 8:212–213.

Helmersen, G.v. [1838]: Notiz über einen in der Stadt Jakutsk angelegten Brunnen. *Bulletin scientifique publié par l'Academie Impériale des Sciences de St.-Pétersbourg*, H.13:193–198.

Middendorff, A.T.v. [1848]: Geothermische Beobachtungen. In *Reise in den äussersten Norden und Osten Sibiriens: Einleitung, Klimatologie, Geognosie. St. Petersburg*, Bd. 1. Taf. XII-XIV.

Shiklomanov, N.I. [2005]: From exploration to systematic investigation: development of geocryology in the 19^{th}- and early-20^{th}-century Russia. *Physical Geography*, 26(4):249–263, doi:10.2747/0272-3646.26.4.249.

Toll, E.v. [1897]: Iskopaemye ledniki Novo-Sibirskikh ostrovov, ikh otnoshenie k trupam mamontov i k lednikovomu periodu (Ancient glaciers of New Siberian Islands, their relation to mammoth corpses and the Glacial period). *Zapiski Imperatorskogo Russkogo Geograficheskogo obshestva po obshei geografii (Notes of the Russian Imperial Geographical Society)*, 32:1–137, (in Russian).

Wood, K.R. and Streletskiy, D.A. [2008]: Soil and permafrost temperature data obtained during the First International Polar Year 1882–1883. In: Kane, D.L. and Hinkel, K.M.(eds.), *Proceedings of the Ninth International Conference on Permafrost*, Institute of Northern Engineering, University of Alaska Fairbanks, Fairbanks, USA, 29 June–3 July 2008, volume 2, pages 1957–1962. ISBN 978-0-9800179-3-9. URL http://ipa.arcticportal.org/publications/conference-proceedings.

Changing permafrost-landscape conditions in an Arctic city experiencing urban decline (Igarka, Russia)

Afanasy S. Gubanov[1], Valery I. Grebenets[1], Kelsey E. Nyland[2], & Andrey V. Litovko[3]

[1]*Lomonosov State University, Moscow, Russia, Russian Federation*
[2]*Departement of Geography, Michigan State University, East Lansing, MI, USA*
[3]*Igarkageocryological laboratory, Institute on Permafrost, Igarka, Russian Federation*

The city of Igarka is located in Arctic Siberia, in Krasnoyarsk region, Russia. The city is situated near the southern boundary of continuous permafrost, in forest tundra. Landscape conditions, warming influence from the nearby Yenisei River and local climatic conditions through the Pleistocene-Holocene resulted in the formation of the underlying discontinuous permafrost. The discontinuous permafrost zone is characterized by the presence of tundra spaces with permafrost and forested areas without permafrost. The thermal regime under natural conditions outside city, range from -0,5 to -1 °C in the forest-tundra, up to -1,5 °C tundra parts (peat mounds). Permafrost in this region can reach up to 300 m thick. In loamy deposits, according to our observations, small ice lenses thickness is 5-7 cm occur. The natural landscape is characterized by two main cryogenic processes: frost heaving of grounds and thermokarst.

The city if Igarka grew and developed both size and population until the collapse of the Soviet Union, followed by a crisis in all areas of city life. The port went into decline, the timber processing plant closed and the old areas of the city demolished or burned. Population has also undergone rapidly, including massive out migration, following the collapse of the Soviet Union to today: in 1931 - 3000 people; 1967 – 18000 p.; 1989 - 18820 (max.) p.; 1996 – 14900 p.; 2005 – 8000 p.; 2015 – 5117 peoples. Continued severe decline in population was contributed by decision of local government to close the city. The remaining buildings have significant geotechnical problems: the deformation of structures under differential settlement of frozen pile foundations, destruction of underground utilities, subsidence and frost-heaving on roads and sidewalks, collapsing bridges and others. As long as the city was developing, the timber plant processing, the port was active and the local Permafrost Laboratory operating, dangerous cryogenic processes in the built-up area were being monitored, the necessary engineering and permafrost geotechnical solutions were implemented to stabilized and maintained situation. After the city fell into decline, permafrost-ecological conditions also deteriorated. There is no apparent recovery of permafrost at the site of the demolished districts,it has re vegetated primarily as forest vegetation- indicator of taliks. When the historical section of the city was still populated there was regular snow removing and water drainage (precipitation 550 mm / year, of which 300 mm falls as snow), protecting underlying frozen ground. Nowadays, the ground is insulated by snow cover in the abandoned parts and there is some increase in water infiltration into the ground. These changes have triggered thermokarst processes causing increases surface water logging in the old quarter in Igarka central parts, have resulted in increased of deformation of the remaining buildings. Succession of non-tundra vegetation does not promote the conservation and restoration of permafrost (Fig. 1): the actively overgrown by *parvifolia* shrubs (increasing snow accumulation, minimized the influx of winter cold into the ground), tundra landscapes and natural pine forests are not reversed.

Approximately 40 % of the built-up area consisting of an abandoned sawdust storage area (they stretch 5 km along the Yenisei river), where the chemical decomposition of waste is going. In fact, if the city were to be revived, these areas cannot be used for a perspective development. It will be necessary to explore new territory for development.

Is there any chance of revitalizing the city of Igarka as the base city with the development of oil and gas fields? How will local permafrost behave after the city was razed? What can be done to help quickly restore the 'fragile' natural forest tundra and typical tundra landscapes? To investigate these questions have been carried out field observations and surveys, route works, full-scale study of permafrost in the Igarka permafrost museum and examination of archival materials. These annual field studies were complimented by remote sensing and repeated photography.

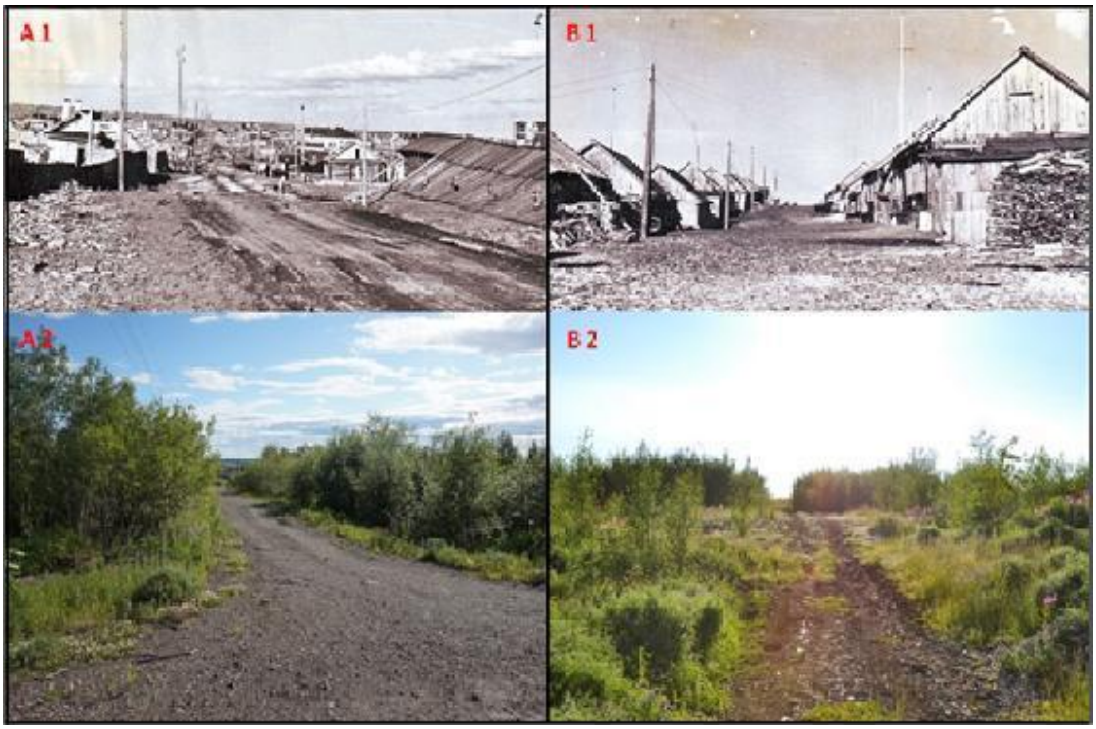

Figure 1: Changing landscape conditions in the razed historic district of Igarka. Taimyrskaya St.(A1–1964, A2–2015); Sovetskaya St. (B1–1964, B2–2015)

This comprehensive evaluation of the socio-economic and environmental changes that have occurred in Igarka affords valuable perspective on a common situation facing a number of urban areas in the Russian Arctic.

Acknowledgements

The paper was financed by grant "Leading scientific schools" # NSH-335.2014.5 and Circumpolar Active Layer Monitoring U.S. National Science Foundation grant OPP-0352957

Permafrost landscapes as objects of scientific tourism

Rozaliia Ivanova & Alexander Fedorov

Melnikov Permafrost Institute, Russian Federation

Science and culture affect the basic motivations of the travel of people. The main objectives of tourism are entertainment, recreational and educational purposes. Currently we are witnessing a new phenomenon – conference tourism and the use of scientific expeditions and stations included in the orbit of tourism. Basically, their potential is directed to finding new, unused itineraries in the nature, supporting and developing national parks and protected areas, rehabilitating water resources, restoring the fisheries, fauna and flora, and strengthening the environmental perspective of tourism. From this perspective, we would like to discuss the possibility of using permafrost landscapes for scientific tourism.

Permafrost landscapes are those developing on permafrost and are dominated by periglacial processes, including frost action, thermokarst, thermal contraction cracking, frost heave, thermal erosion, solifluction, and others. These processes result in characteristic landforms, such as alas, tympy, dyuedya and bylar produced by the process of thermokarst, polygonal ground resulting from thermal contraction cracking, terrace-like features produced by solifluction, frost mounds created by heaving, and many other forms.

In the Republic of Sakha (Yakutia), most of the region is dominated by taiga and tundra landscapes. Within these landscape types are distinguished various types of forests and meadows, alases, thermokarst lakes, bogs, steppes, icings (taryns), tukulans (sand dunes) and others. Each of these landscape types is unique and develops only under certain, geographical, climatic, geological, biological conditions. Let us consider some of them in more detail:

The Arctic desert lies north of 74°N on the New Siberian Islands archipelago, except for Bolshoy Lyakhovsky Island. The tundra occupies the Arctic islands and coasts (about 10 percent of Yakutia). The forest tundra is characterized by a patchy distribution of forest stands and scattered trees between the taiga and the tundra. The taiga is a natural zone characterized by coniferous forests, consisting mostly of larch. Meadow landscapes are common throughout Yakutia, occurring on alases, floodplains, river terraces, and gentle hillslopes.

Swampy sparse larch forests (mari) occur in poorly drained areas, commonly in gentle depressions on watersheds. Tukulans are deltaic sands of ancient rivers formed during ancient glaciation. Steppes are found along the Lena, Vilyui and Amga valleys, on south-facing alas slopes, and on south-facing valley flanks in the middle Yana and Indigirka Rivers.

Thermokarst lakes are lakes whose formation and evolution are related to melting of ground ice. Rudimentary bylar, bylar, dyuedya and tympy are the successive stages in thermokarst lake development.

Alases are considered to be the final stage of thermokarst lake development. They are produced by melting of ground ice and represent a gentle-sided, flat- bottomed depression with thermokarst lake remnants and meadow-steppe vegetation. Freezing of lake taliks in the alases result in perennial frost mounds with an ice core, termed 'bulgunniakh' or 'hydrolaccolith'.

An icing is a mass of ice formed in winter on the river or lake ice cover due to pressure discharge of surface and ground water upon freezing of river channels or aquifers.

Spasskaya Pad, Neleger, Yukechi and other research stations and monitoring sites of the Institute of Biological Problems of Cryolithozone SB RAS and Melnikov Permafrost Institute SB RAS are unique sites for scientific tourism, with special instrumentation and equipment. These facilities have no analogues in northeast Russia in terms of their economic, technical and human components. Over the years, these stations and sites have been visited by hundreds of scientists from Russia and foreign countries. International conferences on climate change-related dynamics of permafrost ecosystems are held periodically on their base.

It would be interesting to use the potential of the stations mentioned above in the development of scientific tourism in the Republic of Sakha (Yakutia). Economically, it is important that tourists take on a significant share of scientific and expedition costs, and in return, join scientists in their expeditions for learning purposes. This is, in fact, scientific outreach activities with the help of tourists.

Landscape and climate changes and their impacts to nenets reindeer herding in Yamal peninsula, Russia

Timo Kumpula[1], Marc Macias-Fauria[3], Anna Skarin[4], Mariana Verdonen[1], Tatiana Mikhailova[2], & Bruce C. Forbes[5]

[1]*Department of Geographical and historical studies, University of Eastern Finland, Finland*
[2]*School of Geography and the Environment, University of Oxford*
[3]*Swedish University of Agricultural Sciences, Sweden*
[4]*Earth Cryosphere Institute Siberian Branch of Russian Academy of Science, Russian Federation*
[5]*Arctic Centre, University of Lapland, Finland*

The traditional landuse in the Yamal is reindeer herding practiced by nomadic Nenets herders. The hydrocarbon industry is presently the source of most ecological changes in the Yamal peninsula and socio-economic impacts experienced by migratory Nenets herders who move annually between winter pastures at treeline and the coastal summer pastures by the Kara Sea.

In central Yamal peninsula which is permafrost area both natural and anthropogenic changes have occurred during the past 40 years. Mega size Bovanenkovo Gas Field (BGF) was discovered in 1972. The large scale building of infrastructure started already in mid 1980's. Gas field was finally opened in production and in October 2012. We have studied gas field development and natural changes like increases in shrub growth, cryogenic landslides, drying lakes in the region and these impacts to Nenets reindeer herding.

Employing a variety of high- to very high-resolution aerial photographs and satellite-based sensors (Corona, KH-9, Landsat, SPOT, ASTER Terra VNIR, Quickbird-2, Worldview-2, MODIS), we have followed the establishment and spread of Bovanenkovo. Extensive onsite field observations and measurements of land use and land cover changes since 1985 have been combined with intensive participant observation in all seasons among indigenous Nenets reindeer herders and long-term gas field workers during 2004–2007 and 2010–2014.

Another focus of the study has been to cryogenic landslides. With CORONA image (1969) we were able to build 46 year time serie and investigate cryogenic landslide occurance and peaks of larger landslide events. KH-9 image from 1976 reveal landslide peak from early 1970's which magnitude and scale was unknown before this study. Landsat TM images from 1988 and 1990 reveals clearly main landslide event in 1989. Reindeer tends to use fresh barren landslides as an area of insect relief and after few years landslides began to grow grasses that reindeer graze. Later landslides are occupied by willows (*Salix*) eg. increase of shrub growth. Totally in the study area there were about 400 landslides in early 1970's and about 800 landslides in late 1980's. Another important change in the landscape for reindeer herders is draining of lakes, some larger lakes have drained and herders have lost important fishing lakes but on the contrary old lake bottoms have turned into good pasture land.

Nenets managing collective and privately owned herds of reindeer have proven adapt in responding to a broad range of intensifying industrial impacts at the same time as they have been dealing with symptoms of a warming climate and thawing permafrost phenomena. Here we detail both the spatial extent of gas field growth, landslides drying lakes, shrub increase and the dynamic relationship between Nenets nomads and their rapidly evolving social-ecological system.

Permafrost Research Priorities, a roadmap for the future of permafrost research

Hugues Lantuit[1,2], Michel Allard[3], Mauro Guglielmin[4], Margareta Johansson[5], Gleb Kraev[6], Michael Kraublatter[7], Gerhard Krinner[8], Edward Schuur[9], Ylva Sjöberg[10], Jenny Baeseman[11], & Karina Schollän[1,12]

[1] *Alfred Wegener Institute Helmholtz Center for Polar and Marine Research, Potsdam, Germany*
[2] *University of Potsdam, Germany*
[3] *Université Laval, Québec, Canada*
[4] *Insubria University, Varese, Italy*
[5] *Lund University, Lund, Sweden*
[6] *Centre for Forest Ecology and Productivity, Russian Federation*
[7] *Technical University of Munich, Munich, Germany*
[8] *LGGE, Grenoble, France*
[9] *Northern Arizona University, Flagstaff, USA*
[10] *Stockholm University, Sweden*
[11] *Scientific Committee for Antarctic Research, Cambridge, UK*
[12] *International Permafrost Association, Potsdam, Germany*

At present, no consensus document ("white paper" or "strategy") exists at the international level to identify forwardlooking priorities in permafrost research. CliC has partnered with the International Permafrost Association (IPA) to seize the opportunity offered by the upcoming International Conference on Arctic Research Planning III (ICARP III) and the SCAR Horizon Scan to frame a consultative process that will result in the formulation of such permafrost priorities. Entitled "Permafrost Research Priorities: A Roadmap for the Future", it focuses on all permafrost regions, from the Arctic to the Antarctic and mountain permafrost around the globe in order to accurately represent the level of overlap in scientific challenges in all three domains. The product stemming from the effort will consist of a high level, but short publication (ca. 2–3 pages) in a high-profile journal listing and putting into context permafrost research priorities. The document aims to become the benchmark against which permafrost research should be gauged starting in 2016. Here we present the results stemming from this effort and the lessons drawn from the process in terms of consultation, community engagement and evaluation.

Geocryological investigations in Louise Arner Boyd's 1933 and 1937 American Geographical Society Expeditions to East Greenland

Frederick E. Nelson[1], & Robert D. Lukens[2]

[1] *Department of Geography, Michigan State University and American Geographical Society Library and Department of Geography, University of Wisconsin, Milwaukee, USA*
[2] *Chester County Historical Society, USA*

Although nineteenth and early twentieth century polar exploration has been characterized as a "cult of masculinity", counter examples existed. Unlike many societies and clubs concerned with exploration and field research, the American Geographical Society (AGS) welcomed women into its ranks, from its inception in the early 1850s. Perhaps the most extraordinary woman of long-standing AGS affiliation was Louise Arner Boyd, described by the historian of geography J.K. Wright as "the world's most enterprising woman explorer."Boyd contributed substantially to scientific knowledge about the Arctic through her seven expeditions to the Arctic, most of them under AGS sponsorship (Boyd 1950). Several geographical features in East Greenland were named for her, including "Miss Boyd Land", "Cape Louise", "Louise Boyd Bank", and "Louise Glacier". "Geographical Society Land" was so-named because of Boyd's work in the area under the auspices of the AGS.

Boyd's extensive correspondence in the AGS Archives and elsewhere leaves no doubt about her ability to exercise authority over well-credentialed male scientists. Her expeditions employed scientists who eventually became highly influential in their respective fields. Among others, Boyd employed the renowned earth scientists J Harlan Bretz, Richard Foster Flint, A. Lincoln Washburn, and Noel Odell. Also on Boyd's expeditions were AGS staffers O.M. Miller and W.A. Wood, who developed and applied innovative ground-based survey and photogrammetric techniques. Permafrost and periglacial features formed an important part of the investigations on Boyd's expeditions to East Greenland in 1933 and 1937 (Fig. 1). Documented features included talus slopes, ice-wedge polygons, nivation hollows, protalus ramparts, rock glaciers, frost mounds, and sorted patterned ground.

Figure 1: Boyd photographing in NE Greenland with her Fairchild Aro K 6 tripod-mounted aerial camera. Photo courtesy of American Geographical Society Library, University of Wisconsin-Milwaukee.

Washburn, who later became the first Director of the Arctic Institute of North America, received his introduction to Arctic work on the 1937 expedition, on which he served as Flint's graduate-student research assistant. He returned to the fiord region of East Greenland in the 1950s to conduct an award-winning program of research on periglacial weathering and mass wasting, published in Meddelelser om Grønland.

Boyd's expeditions to East Greenland in the 1930s were predictive of the type of collaborative campaign that after World War II would characterize government-sponsored and international scientific efforts.

"Planned as a unit", Boyd's expeditions were thoroughly integrated scientific enterprises that investigated a wide variety of natural phenomena within representative areas. The volumes resulting from this work, published as AGS Special Publications (Boyd, 1935, 1948), contain large-scale hydrographic and topographic maps, high-resolution glacier maps, extended treatments of East Greenland's geology, glacial history, botany, hydrology, and a wealth of Boyd's own stunning photographic work.

In 1955, Boyd became the first woman to fly over the North Pole. She was the first woman to serve as an AGS Councilor, was a signer of the Society's Fliers' and Explorers' Globe, and received the Society's Cullum Geographical Medal in 1938.

Boyd, an accomplished photographer, was responsible for the majority of the photographic documentation of her expeditions. Thousands of images, never used in publications, are in the AGS Archives in Milwaukee. This presentation is one of the first public displays of Boyd's images of periglacial features, and documents the historic geocryological investigations of Bretz, Odell, Flint, and Washburn.

References

Boyd, A. The Louise A. Boyd seven Arctic expeditions. *Photogrammetric Engineering*, 16:651–657, 1950.

Boyd, LA. *The Fiord Region of East Greenland*, volume 18. American Geographical Society Special Publication, 1935. 369 pp.

Boyd, LA. *The Coast of Northeast Greenland*, volume 30. American Geographical Society Special Publication, 1948. 339 pp.

Traditional and urban-industrial impacts on permafrost change

Kelsey E. Nyland[1], Nikolay I. Shiklomanov[2], Frederick E. Nelson[1,3], Anna E. Klene[4], & Dmitry A. Streletskiy[2]

[1] *Michigan State University, USA*
[2] *The George Washington University, USA*
[3] *Northern Michigan University, USA*
[4] *University of Montana, USA*

The amplified climate warming occurring in the Arctic has resulted in significant body of documentation about thawing permafrost and other changes throughout the circumarctic region. Climate warming impacts the human environment with direct, immediate implications for land use, the economy, and subsistence life. Recent decades also show marked social, economic, and institutional change across the Arctic. Some of these changes are applying additional pressure to already stressed permafrost environments. This study provides examples of interactions between changes in permafrost conditions, traditional indigenous livelihoods and nontraditional industrial activities. Specifically, we examine

1. the state of traditional ice cellars in Barrow on Alaska's North Slope;
2. the state of urban infrastructure built on permafrost in the City of Noril'sk, Russia; and
3. impacts of urban heat islands and industrial pollution on permafrost conditions in Central Siberia.

Permafrost and traditional indigenous livelihoods: Ice Cellars in Barrow, Alaska

Ice cellars are a form of natural refrigeration for whale and other game harvested for subsidence by the indigenous Iñupiat people of the coastal Alaskan Arctic. An ice cellar consists of a shaft leading down to a room excavated into the permafrost. This method of food storage has been employed by the Iñupiat for at least a millennium and continues to be an essential part of the Iñupiat life style as it provides inexpensive, accessible, year-round frozen storage. Over the past few decades there have been reports from Barrow and other indigenous communities documenting ice cellars are "failing". This includes instances when cellars have flooded, had collapsing or sloughing walls, become extremely moldy, or the shaft has collapsed in on the excavated room beneath. Substantial publicity has attributed these catastrophic failures to climate change. When ice cellars fail, large industrial chest freezers are one of the few alternative replacements. However, these provide significantly less storage, incur costs for purchase and electricity, do not allow the meat to age in the same way, and represent the loss of a cultural practice. Five ice cellars have been continuously thermally monitored in Barrow, Alaska since 2005. A survey of all the ice cellars in Barrow was also conducted in order to map their distribution. The large number of cellars observed in Barrow illustrates the magnitude of the potential loss to this village and others like it. Though the five cellars monitored in Barrow appear thermally stable and functioning (remain consistently freezing), despite evidence of sloughing and mold. Other impacts on ice cellars from development in Barrow and other potentially influencing factors warrant further investigation as these structures are inherently linked to permafrost conditions and provide an important economic and cultural resource to these traditional subsistence communities.

Permafrost and Urban Infrastructure: Noril'sk under Changing Socio-Economic and Climatic Conditions

Noril'sk, with a population of 178,000 is one of the largest cities built on permafrost. The most of Noril'sk's urban landscape consists of brick or mass-produced concrete buildings constructed on piling foundations during the 1960 and 1970s. The stability of these structures greatly depends on the consistency of the permafrost thermal regime. The collapse of the Soviet Union, diminished government support, and mass migration out of Noril'sk and the surrounding region in the 1990s contributed to the neglect of the urban infrastructure. These changes have coincided with climate-induced warming and permafrost degradation, resulting in widespread deterioration,

deformation, and in some instances, collapse of structures throughout the city. To maintain Noril'sk as a prominent regional urban center, significant efforts have been made in recent years to address the problem of crumbling infrastructure by developing innovative and economically viable approaches to revitalize the areas affected by human- and climate-induced changes in structural stability of buildings.

Impacts of Industrial development on the Permafrost System

Land cover changes in sensitive Arctic Environments are already being influenced by the warming atmosphere. These changes are then compounded by localized human influences, including the intensified heat and air pollution produced by industrialized areas found in the Russian Arctic. Representative of the different tracks that these remote urban areas have taken after the collapse of the Soviet Union are three cities found on the Yenisei River in Central Siberia indicative of their socio-economic situations, including continued population and infrastructure decline (Igarka), a relatively stable community (Dudinka), and a community receiving local reinvestment (Noril'sk). Pollution, in close proximity to heavy industrial activity, caused a secondary plant succession process. The urban heat island was also analyzed for the Noril'sk industrial district. Land cover changes induced by the urban industrial complexes along with the heat island cause localized permafrost degradation.

Evaluation of anthropogenic impacts on the thermal state of landscapes in Central Yakutia

Pavel Nikolaevich Skryabin, Stepan Prokopievich Varlamov & Aleksandr Nikolaevich Fedorov,

Melnikov Permafrost Institute, Russian Federation

The results of long-term permafrost investigations conducted during geotechnical exploration, design, construction, and temporary operation of the Tommot-Yakutsk Railway are presented. Any disturbance to the environment (forest cutting, fires, surface stripping, embankment placement, etc.) inevitably causes changes in permafrost conditions.

The study area is situated on the west and east sides of the Lena River at the latitude of Yakutsk and is characterized by complicated geocryological conditions, such as continuous permafrost, supra- and intrapermafrost water-bearing taliks, and widespread ground ice at shallow depth. Investigations are carried out in eight terrain types: floodplain, low terrace, sand ridge, inter-ridge depression, alas, inter-alas, small valley, and interfluve. The objective of the on-going study is to evaluate anthropogenic impacts on the thermal dynamics of the active layer and upper permafrost. The study employs the method of geothermal monitoring based on long-term field observations. The observation network covers the geotechnical system consisting of the railway embankment and the adjacent areas subject to various degrees of anthropogenic disturbance. Field observations include repeated surveys of the disturbed landscapes and the embankment, as well as measurements of snow depth, snow density, soil properties, thaw depth, and ground temperature. The primary focus is on active layer thickness and permafrost temperatures above the level of zero amplitude, which are indicators of alterations to the ground thermal state.

The last decade in the observation period was characterized by warmer than normal mean annual air temperatures with significant interannual variations in winter snowfall. However, the ground thermal regime in undisturbed areas showed little response to these variations in meteorological conditions.

Significant increases in mean annual temperature of the upper permafrost layers, as well as in seasonal thaw depth were observed following tree removal, ground surface stripping and post-fire clearing. Soil thaw depths on the railway right-of-way showed a distinct increase from year to year, in places reaching the top of ice wedges and causing permafrost degradation. Observations indicate the development of hazardous cryogenic processes (ground subsidence, erosion, thermokarst, etc.) due to the environmental disturbance in ice-rich permafrost areas. Quantitative estimates are given for the dynamics of mean annual ground temperatures on selective, gradual and clear cuts, as well as on old and recent burns in relation to plant succession stages. Long-term dynamics of the ground thermal state in disturbed landscapes illustrates relatively high stability in the sand-ridge terrain type and low stability in the inter-alas terrain type.

Experimental studies of the ground thermal regime in and beneath the embankments of different designs incorporating thermosyphons and insulation materials have shown that the annual cooling effect of higher embankments is less than that of lower embankments. Winter placement of embankment material resulted in rising of the permafrost table. The placement of a zero embankment with removal of the active layer resulted in a perennial thaw bulb. Degradation of ice-rich permafrost was observed on the cut slopes and ditches in the cut sections. Thermosyphons and Penoplex insulation have proved to be beneficial in reducing ground temperatures in and beneath the embankments and in rising the permafrost table.

The results of this study were used in the design and construction of the northern section of the Tommot-Yakutsk Railway. Engineering and biological reclamation measures were proposed to maintain the stability of disturbed landscapes. The experimental data can be further used in mathematical modeling and prediction of the thermal dynamics of geotechnical systems for rational land management in northern Asia.

A study of the bottom variety of the cultural layer in urban landscapes of Yakutsk

Igor Innokentevich Syromyatnikov, & Victor Victorovich Kunitskiy

Melnikov Permafrost Institute SB RAS, Russian Federation

The term 'cultural layer' is one of the basic terms in archaeology, but it is used in other sciences as well. It refers to a layer of earth on sites of human habitation containing traces or remains of man's activities over a relatively continuous time [Martynov, 2005].

The geotechnical implications of a cultural layer in permafrost areas have been evaluated differently by various authors. Saltykov [1946], for example, attributes "harmful" properties to the cultural layer and believes that its development provides a more severe temperature regime in permafrost and reduces the active layer thickness. He also notes that the development of a cultural layer which is represented by seasonally freezing ground results in increased soil moisture contents and greater frost-susceptibility, as well as in the appearance of saline suprapermafrost water in this layer.

Melnikov [1950] gives a different view on the role of a cultural layer in permafrost. In his opinion, high moisture contents of this layer impede thawing in summer and promote greater cooling during the winter. Melnikov thinks, however, that the cultural layer is not a single factor controlling thaw depth variations from site to site within the urban area. In his work, Melnikov reports on sites with shallow thaw depths where the cultural layer is absent or very thin. He negates the claim that the cultural layer tends to depress permafrost temperatures.

In this study, we continue the research on the cultural layer initiated by P.I. Melnikov and N.I. Saltykov. However, in contrast to previous investigations which aimed at subaerial deposits, we focus on subaqueous deposits within the cultural layer.

To study the bottom type of the cultural layer we investigated sections from surface water bodies. Consideration was given to the ice regime, as well as to the uneven distribution of the water bodies in the study area.

The uptown parts of Yakutsk are characterized by a large number of surface water bodies. In all, the water bodies occupy an area of about 10 sq. km, comprising approximately 12 % of the total land area.

Sediments comprising the bottom variety of the cultural layer within the limits of Yakutsk were studied on cores from boreholes drilled in 2009–2011 as part of a permafrost monitoring program. Bottom sediments were recovered from six drill holes located in different landscape settings and extending to various depths (up to 32 m). All boreholes are within the urban part of Yakutsk.

The site of borehole 21 is interpreted as an aquatic cryogenic landscape developed with active human participation. The section differs in that sediments of the seasonally freezing layer are deposited on a newly formed layer of wet cryotic ground. Similar sections with cryopegs of anthropogenic origin are known to exist elsewhere in the study area.

The borehole 24 site was identified as an aquatic paracryogenic landscape produced by human activity. It substrate consists of a seasonally freezing layer which develops over a hydrogenic talik. The profile of borehole 25 also implies a paracryogenic landscape.

The aquatic landscape on a hydrogenic talik, which has probably developed not without human interference, was characterized in the Ytyk-Kyel Lake basin on a core from borehole 1. The sites of boreholes 61 and 62 are also interpreted as being of the same type of landscape.

The results of this study suggest that cryolithogenic deposits comprising the bottom variety of the cultural layer are an integral and significant component in the structure of water ecosystems, which account for over 12 % of the total area of Yakutsk.

The development of the cultural layer represented by a bottom variety of cryolithogenic deposits leads to notable changes in the geocryological conditions. New natural-territorial complexes develop which can be interpreted as cryogenic and paracryogenic landscapes produced with human participation.

References

Martynov, A.I. [2005]: *Archeology*. Vysshaya Shkola: Moscow, 447 pp.

Melnikov, P.I. [1950]: Permafrost in the Yakutsk area. In *Permafrost Studies in the Yakutian Republic*, vol. 2, pages 53–70. Izdatelstvo AN SSSR: Moscow.

Saltykov, N.I. [1946]: About building foundations at Yakutsk. In *Transactions of the Obruchev Institute of Permafrost Studies*, vol.1, Residential and Small-scale Industrial Construction in Permafrost Areas, pages 102–136. Izdatelstvo AN SSSR: Moscow-Leningrad.

Alexander Theodor von Middendorff and permafrost study in the Russian empire in the second half of the 19^{th} century

Erki Tammiksaar

University of Tartu, Estonian University of Life Sciences, Estonia

The expedition to North and East Siberia of the St Petersburg Academy of Sciences took place under the conduct of the Baltic German Alexander Theodor von Middendorff in 1842–1845. One of the main purposes of the expedition was to establish the extent, thickness and temperature of permafrost in different regions of Siberia. In those days it could be called a "hot topic" which many naturalists were interested in [Tammiksaar, 2001]. After the expedition, von Middendorff published the results of the observations on the thickness of permafrost in Yakutsk and its geothermal gradient in the first volume of his travel monograph under the title "Reise in den äussersten Norden und Osten Sibiriens während der Jahre 1843 und 1844" (1848). The reaction to this publication was favourable as in Europe as well as in Russia. But there also were critics, the most loud-sounding among them was Karl Ernst von Baer, the mentor of von Middendorff and the initiator of the Siberian expedition [Tammiksaar, 2002, Tammiksaar and Stone, 2007].

The publishing period of the four-volume travel monograph by von Middendorff was very long – 1847–1875. That also had a positive aspect. By the beginning of the 1860s, when von Middendorff began to sum up his observation results on the Siberian climate, several other expeditions to Siberia had taken place (in the 1850s) under the leadership of Ernst Hofmann Alexander von Schrenck, Carl von Ditmar, Richard Maack, Nikolai von Agthe, Friedrich Schmidt and Leopold Schwarz who, using as an example the investigations started by von Middendorff, collected new data on the climate of Siberia, the extent of permafrost depending on it and the structure of permafrost. Like in the case of von Middendorff, the publication of their data was also delayed. Von Middendorff had personal contacts with all the above-mentioned explorers. That provided him an opportunity to analyse and draw generalizations on the basis of his own data on permafrost and, in addition, of those of Hofmann, Schrenck, Ditmar, Maack, Agthe, Schmidt and Schwarz. The results were published in the monograph appearing in 1861, volume 4. The third part of it (over 200 pages!) was devoted to the climate of Siberia [Middendorff [1861]; cf. Sukhova and Tammiksaar [2015]: 217–233].

In his work, von Middendorff analysed temperatures in different regions of Siberia, the freezing of rivers and lakes in the area of permafrost and also land(scape) forms coming into being as a result of permafrost. Von Middendorff was especially interested in the origin and genesis of such a formation as Aufeis, which were heatedly disputed about until the end of the 19^{th} century [Tammiksaar [2013]: 257–259].

In my report, I would like to analyse the importance of the publications of Middendorff for further studies of permafrost in Siberia in the second half of the 19^{th} century and the beginning of the 20^{th} century. In my opinion, the study of the Siberian climate by von Middendorff, published in 1861, was the most outstanding publication on permafrost in the 19^{th} century.

References

Middendorff, A.Th.v. [1861]: Das Klima Sibiriens. In *Reise in den äussersten Norden und Osten Sibiriens während der Jahre 1843 und 1844 mit Allerhöchster Genehmigung auf Veranstaltung der Kaiserlichen Akademie der Wissenschaften zu St. Petersburg ausgeführt und in Verbindung mit vielen Gelehrten herausgegeben von Dr. A. Th. v. Middendorff*. St. Pbg.: Kaiselriche Akademie der Wissenschaften, Bd. IV, Th. 1, Lief. 3.

Sukhova, N.G. and Tammiksaar, E. [2015]: Александр Федорович Миддендорф. К двухсотлетию со дня рождения. Переработанное и дополненное издание. С-Петербург: Нестор-История.

Tammiksaar, E. [2001]: «Materialien zur Kenntniss des unvergänglichen Boden-Eises in Sibirien»Die erste «Dauerfrostbodenkunde» von Karl Ernst von Baer. In *Baer, K.E.v. Materialien zur Kenntniss des unvergänglichen Boden-Eises in Sibirien.* Unveröffentliches Typoskript von 1843 und erste

Dauerfrostbodenkunde. King, L. (Hrsg.). Giessen: Universitätsbibliothek. S. I–XLIV.

Tammiksaar, E. [2002]: The contributions of Karl Ernst von Baer to the investigation of the physical geography of the Arctic in the 1830s–1840s. *Polar Record*, 38(205):121–140, doi:10.1017/S0032247400017514.

Tammiksaar, E. [2013]: Gerhard Baron von Maydell (1835–1894) und die Bedeutung seiner Forschungen in Nordost-Sibirien. In *Reisen an den Rand des Russischen Reiches. Die wissenschaftliche Erschliessung der nordpazifischen Küstengebiete im 18. und 19. Jahrhundert*, pages 243–267. Fürstenberg/Havel: Verlag der Kulturstiftung Sibierien, SEC Publications, URL http://www.siberian-studies.org/publications/PDF/rrrtammiksaar3.pdf.

Tammiksaar, E. and Stone, I.R. [2007]: Alexander von Middendorff and his expedition to Siberia (1842–1845). *Polar Record*, doi:10.1017/S0032247407006407.

Rapid Arctic Transitions due to Infrastructure and Climate (RATIC): An ICARP III initiative focusing on the cumulative effects of Arctic infrastructure and climate change

D.A. Walker[1], J. Peirce[1], T. Kumpula[2], M.O. Leibman[3], G. Matyshak[4], D. Streletskiy[5], M.K. Raynolds[1], Y.S. Shur[1], M. Kanevskiy[1], M. Buchhorn[1], G. Kofinas[1], K. Ambrosius[6], H.E. Epstein[7], V.E. Romanovsky[1], B.C. Forbes[8], A. Khomutov[3], O. Khitun[9], N Shiklomanov[5], V. Grebenets[5], M. Lemay[10], M. Allard[10], W. Vincent[10], S. Lamoureux[11], T. Bell[12], D. Forbes[13], G. Fondahl[14], E. Kuznetsova[15], L.-P. Roy[16], A. Petrov[17], & P. Schweitzer[18]

[1] *University of Alaska Fairbanks, USA*
[2] *University of Eastern Finland, Joensuu, Finland*
[3] *Earth Cryosphere Institute, Siberia Branch, Russian Academy of Science, Tyumen, Russian Federation*
[4] *Lomonosov Moscow State University, Moscow, Russian Federation*
[5] *The George Washington University, USA*
[6] *Quantum Spatial Inc., Anchorage, Alaska, USA*
[7] *University of Virginia, Charlottesville,VA, USA*
[8] *Arctic Centre, Rovaniemi, Finland*
[9] *Komarov Botanical Institute, Russian Academy of Science, St. Petersburg, Russian Federation*
[10] *Université Laval, Center for Northern Studies, Québec, Canada*
[11] *Queens University, Kingston, Ontario, Canada*
[12] *Memorial University, St. John's, Newfoundland, Canada*
[13] *Geological Survey of Canada, Retired, Dartmouth, Nova Scotia, Canada*
[14] *University of Northern British Columbia, Prince George, British Columbia, Canada*
[15] *Norwegian University of Science and Technology, Trondheim, Norway*
[16] *Northern Climate ExChange, Yukon Research Centre, Whitehorse, Yukon, Canada*
[17] *University of Northern Iowa, Cedar Falls, Iowa, USA*
[18] *University of Vienna, Vienna, Austria*

The Rapid Arctic Transitions due to Infrastructure and Climate (RATIC) initiative is a forum for developing and sharing new ideas and methods to facilitate the best practices for assessing, responding to, and adaptively managing the cumulative effects of Arctic infrastructure and climate change. Arctic Science Summit Week 2015 in Toyama, Japan (23–30 April) brought together nearly 700 international scientists, students, policy makers, research managers, Indigenous Peoples and others interested in developing, prioritizing and coordinating plans for future Arctic research (http://www.assw2015.org). Members and Fellows of the IASC Cryosphere Working Group, Social & Human Working Group, and the Terrestrial Working Group produced and IASC white paper [Walker and Peirce, 2015] that summarizes the activities of two RATIC workshops at the Arctic Change 2014 Conference in Ottawa, Canada and the 2015 Third International Conference on Arctic Research Planning (ICARP III) meeting in Toyama, Japan. In this poster we will summarize five case studies with conclusions and recommendations presented at these conferences.

The major conclusions from workshops were:

- There is a pressing need to examine the cumulative effects of infrastructure in the context of Arctic social-ecological systems (Fig. 1). Each case study had a unique set of social, economic, political, ecological, technological, and climatic "drivers of change" that require regionally appropriate adaptive management approaches to mitigate adverse changes.
- Permafrost thawing and its associated impacts on natural and built environments were clearly identified as priority issues at all locations. The specific issues related to permafrost differed in each region and require detailed ground-level

knowledge for predicting change and planning purposes.

- The indirect effects of infrastructure exceed the direct effects of the planned footprints. Fragmentation of large intact ecosystems is a major impact that is inadequately addressed in Russia and North America. Assessments of infrastructure must address effects on the adjacent ecosystems, local communities, regions, and areas outside the Arctic.
- New GIS and remote-sensing tools are needed to assess regional changes over large areas now affected by infrastructure and climate change. The spatial resolution of current global scale remote-sensing databases is inadequate to detect changes to fine-scale patterned ground features and to monitor details of infrastructure change. High-resolution imagery is great but is costly and not available for all areas, but can be used for hierarchical analysis of smaller regions.
- The cumulative interactions between infrastructure and climate change are not adequately addressed by any national or international-level Arctic science plan. NASA LCLUC is providing examples of scientific approaches to the issue of cumulative effects of infrastructure development in Russia and North America. Other examples are available from industry and other Arctic governments.

The RATIC workshop participants agreed that science plans emerging from ICARP III need to explicitly address rapidly expanding infrastructure networks. Recent studies indicate that combinations of industrial development and climate change have resulted in major changes to local ecosystems, including the permafrost, hydrology, vegetation, wildlife, and local people. The effects are both positive and negative with respect to biological resources and the local communities and economies. The effects of resource development and fragmentation of large intact ecosystems by extensive networks of roads, railroads, and pipelines are apparent and keenly felt by the indigenous people of the Arctic. The effects on broader regions are currently difficult to assess, but require more attention because of the cumulative effects beyond the areas of immediate impact.

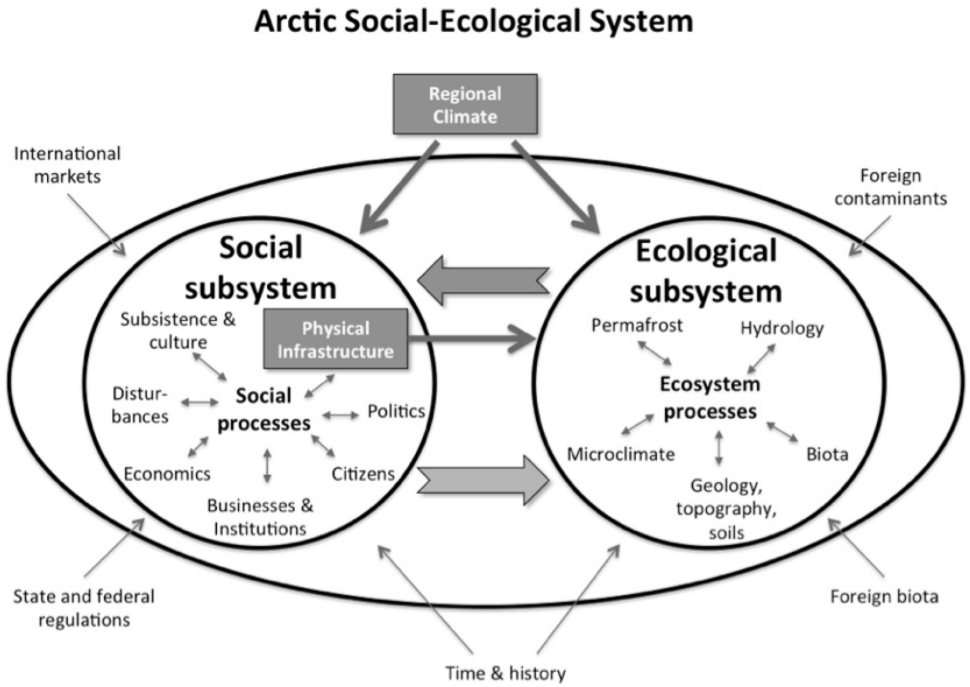

Figure 1: The Arctic social-ecological system (SES) emphasizing the roles of climate and physical infrastructure, and the feedback to the social subsystem from the ecological subsystem.

This topic is internationally important because mineral and hydrocarbon exploration have transnational effects that are broadly occurring across the circumpolar Arctic. The social, economic, regulatory, and political drivers of development vary across the Arctic. The national and international programs supporting research described in the case studies are examples that need to be built on for the next decade.

The scope of the challenge includes:

1. examining the drivers of Arctic infrastructure in widely different Arctic cultures, economic systems, political environments, and ecological systems;
2. monitoring and understanding the vulnerabilities, resilience and full cumulative effects of Arctic infrastructure on the diverse group of Arctic social-ecological systems that are currently undergoing change;
3. planning, managing, and shaping future Arctic infrastructure, and
4. involving the Association of Polar Early Career Scientists (APECS) in the process to provide new energy and new ideas and assure continuity of the effort through the next decade of Arctic research.

Future planning needs to include consideration of the widely divergent political systems, economies, cultures, communities and landscapes present in the Arctic, fragmentation of presently intact natural landscapes by large networks of roads and pipelines, Arctic urban infrastructure, engineering of subarctic infrastructure, and Arctic off-shore infrastructure.

As first steps, the RATIC group recommends that the combined IASC Cryosphere, Human and Social, and Terrestrial Working Groups work together to:

1. Finish the RATIC white paper and post it on the ICARP III website as a product of the ICARP III planning process;
2. publish a summary of the white paper and follow-up synthesis activities in an appropriate peer-reviewed journal;
3. develop an IASC interdisciplinary Infrastructure Action Group that includes participation by members of all IASC working groups and APECS;
4. incorporate infrastructure-related issues more explicitly in the IASC working groups'research priorities;
5. promote regular infrastructure workshops at international scientific meetings;
6. emphasize the need for social-ecological-system studies in relationship to infrastructure; and
7. promote infrastructure-related themes in future international research initiatives.

References

Walker, D.A. and Peirce, J.L.(eds.). [2015]: *Rapid Arctic Transitions due to Infrastructure and Climate (RATIC): A contribution to ICARP III.* Alaska Geobotany Center publication (No. AGC-15-02) U. of Alaska Fairbanks, URL http://www.geobotany.uaf.edu/library/pubs/WalkerDAed2015-RATICWhitePaper-ICARPIII.pdf. 51 pp.

SESSION 32

Permafrost Education and Outreach: Students, Communities, and the World

Convener:

Anna E. Klene, *Department of Geography, University of Montana, USA*

Inga Beck, *Alfred Wegener Institute Helmholtz Centre for Polar and Marine Research, Germany*

Ylva Sjöberg, *Department of Physical Geography and Quaternary Geology, Stockholm University, Sweden*

Education and Outreach are an integral part of modern science and the necessity for such activities continues to grow. The International Permafrost Association (IPA) has been very active in developing a series of products and initiatives to meet this need. The International University Courses on Permafrost (IUCP) database and the Permafrost Young Researchers Network (PYRN) are good examples of the IPA's recent efforts. The IPA established a Standing Committee on Education and Outreach in 2010 to systematically support and help to coordinate activities supporting permafrost education and outreach.

This session will provide a forum for the exchange of information and ideas for past and future permafrost Education and Outreach activities. Contributions will focus on outreach materials designed for distribution through websites targeted to the general public. Others may describe classroom-based lessons or well-established national programs of permafrost educations within the K-12 school system. Yet others will describe successful field courses allowing undergraduate and graduate students to participate in the full scientific process from making their own permafrost field observations, through analysis, modeling, and presentation. We encourage contributions which are targeted to a wide range of ages: from K-12, undergraduate and graduate students, the general public, to elders. Participation in this session is not limited to permafrost scientists but we invite contributions from individuals from polar and educational organizations such as local schools, communities, APECS, UArctic, etc.

As awareness of permafrost continues to grow within the research community and the general public, it is critical to support education and outreach as central activities of the IPA.

A Frozen-Ground Cartoon: Explaining international permafrost research using comic strips

Frédéric Bouchard[1,2,3], Bethany Deshpande[3,4], Michael Fritz[5], Julie Malenfant-Lepage[2,3,6], Alexandre Nieuwendam[7], Michel Paquette[2,3], Ashley Rudy[8], Matthias Siewert[9], Ylva Sjöberg[9], Audrey Veillette[2,3], & Jon Harbor[10]

[1] *Centre Eau Terre Environnement, Institut national de la recherche scientifique (INRS), Canada*
[2] *Department of Geography, Université de Montréal, Canada*
[3] *Centre d'études nordiques (CEN - Centre for Northern Studies), Université Laval, Canada*
[4] *Department of Biology, Université Laval, Canada*
[5] *Department of Periglacial Research, Alfred Wegener Institute Helmholtz Centre for Polar and Marine Research (AWI), Germany*
[6] *Department of Civil and Water Engineering, Université Laval, Canada*
[7] *Centro de Estudos Geográficos& IGOT, Universidade de Lisboa, Portugal*
[8] *Department of Geography and Planning, Queen's University, Canada*
[9] *Department of Physical Geography, Stockholms Universitet, Sweden*
[10] *Department of Earth, Atmospheric, and Planetary Sciences, Purdue University, USA*

Apart from people in cold region communities and a small – although steadily growing – scientific community, the general public knows very little about permafrost properties, its dynamics in response to climate change, and the research going on in the field. We are addressing this by making permafrost science accessible to children, youth, their parents, and teachers. We are producing a 100 % outreach-related project that aims at 'Fostering permafrost research to the ends of the Earth' (http://ipa.arcticportal.org), but with a casual approach via a series of comic strips. Cartoons are excellent ways to communicate messages in today's media landscape: they are graphic, funny and direct, and can be rapidly shared via social media to reach many people. Our outreach project targets the general public, focusing on young students who have to choose career paths at the high school or college levels. By introducing them to permafrost research activities, particularly fieldwork, our 'Frozen-Ground Cartoon' will enhance the dissemination of permafrost knowledge and broaden the international community of permafrost 'lovers'. This new project is coordinated by a core group of permafrost early career researchers from Canada, Germany, Sweden and Portugal (in collaboration with an 'external senior advisor'), and is endorsed by the International Permafrost Association (IPA) as a targeted 'Action Group' (http://ipa.arcticportal.org/activities/action-groups). Here we present an overview of our Action Group, including main objectives, significance, and potential future outcomes.

Hot times in cold places: Taking permafrost educational programs on the road

Margaret Hope Cysewski[1], Matthew Sturm[1], Laura Carsten-Conner[1,2], Victoria Coats[3], & Angela Larson[4]

[1] *Geophysical Institute, University of Alaska Fairbanks, USA*
[2] *College of Natural Science and Mathematics, University of Alaska Fairbanks, USA*
[3] *Oregon Museum of Science and Industry, Portland, Oregon, USA*
[4] *Goldstream Group, Fairbanks, Alaska, USA*

Introduction

The Permafrost Tunnel in Fox, Alaska is known from its dozens of publications on permafrost research, but it is also equally valuable for education and outreach on permafrost and climate change. The tunnel has provided an immersive experience that is novel and memorable for thousands of visitors, from children and teachers to world leaders. The massive ice, syngenetic cryostructures, Pleistocene bones, and plant matter are real, tangible, and life-size. The rare experience of seeing and being "in" the permafrost may shift visitor's perceptions of its climate change impacts from something that is hidden underground and confusing to something that is tangible and has visible consequences. Unfortunately, access to the tunnel is limited, so how can we bring the same experience to the broader public?

This has been the subject of a new project sponsored by the National Science Foundation. Teams from the University of Alaska Fairbanks (UAF), the Oregon Museum of Science and Industry (OMSI), and the Goldstream Group are using a four-prong approach to broaden the reach of the tunnel, with the target audience being families with children ages 9-14. First, we are improving the exhibits and signage at the Permafrost Tunnel. Second, we are developing educational products that we will travel with to 27 rural Alaskan villages for community science programs. Third, we are creating a national traveling museum exhibition on permafrost and climate change, which will be the first of its kind. Fourth, we are conducting research on the importance and value of real objects (versus replicated and/or virtual) in informal science learning.

Background

The Permafrost Tunnel is operated by the U.S. Army Cold Regions Research and Engineering Laboratory (CRREL). The tunnel fortuitously contains an abundance of Pleistocene bones and ice features. Thousands of visitors have experienced the highly atmospheric tunnel, where they are surrounded with real climate-sensitive materials. Visitors can feel the cold surroundings, touch the ice, and see the true size of a large ice wedge. They also can smell and see "carbon in the permafrost" with frozen-in-time plant matter. They can grasp the age of permafrost by seeing and touching Pleistocene bones frozen into the walls. The tunnel is a perfect inspiration point for our project in developing unique ways to educate the public concerning permafrost and climate change.

Concept Goals

The key concepts of our project are: timescales of change, tipping points and irreversible effects, and feedback cycles between regional and global climate. Timescales include the concept of geologic time with respect to the formation of permafrost (thousands years), compared to the short period of time in which modern climate change can affect permafrost (several years). Tipping points can be easily seen when comparing the structured ice and soil of frozen permafrost against the soupy-mud of thawed permafrost. The pungent smell of the organic matter within the tunnel is a memorable experience, and can provide educators with a starting point for exploring carbon feedback cycles.

Real Objects

During tunnel tours, visitors are invariably fascinated with the realness of the ice and bones that are tens of thousands years old. We have observed that taking

permafrost samples to educational events also gains the same response when you explain that the ice is 30,000 years old. Would the same response come from a replicated permafrost sample?

The concept of using real objects versus replicated or virtual objects has been previously studied in the relation to informal science learning in museums. Leinhardt and Crowley (2002) suggest that objects, real or simulated, have four features that make them "unique nodes for ideas and their elaboration". 1) Resolution and density of information: Real objects are rich with information. Virtual or replicated objects are representations of originals and usually contain less information. For instance, they may lose texture, smell, or even a three-dimensional nature if the representation is just a photo. 2) Scale: Real objects are at their actual scale, while virtual objects or representations may or may not be. Inherent in this construct is the idea that large objects have power in part because of their scale. 3) Authenticity: In this construct, authenticity refers to original objects, but arises in part from the significance that humans impart to the object. 4) Value: The value construct refers to an object's uniqueness and/or monetary value. Data gathered from our research will help inform us about what is most impactful and meaningful about real objects, such as those found in the tunnel.

Alaskan Outreach

For our informal science learning programs in rural Alaskan villages, we have developed educational products that use real objects from the tunnel, as well as replicated or virtual products related to permafrost. In developing these products, we realized that in addition to the key concepts there are some additional concepts we wanted to convey that deal with living with permafrost.

In the first 15 months of the four year project, we have visited seven rural Alaskan communities. During these visits, we utilize real permafrost samples along with other real cryospheric ice samples (glacier ice, sea ice, and aufeis ice) for comparison. The University of Alaska Museum of the North has loaned us several large Pleistocene bones from mammoths, steppe bison, and Pleistocene horses. In addition, we have a jar of organic-rich silt from the tunnel to demonstrate the decay smell of permafrost. To allow children to identify and feel like a scientist, we let participants wear clothes commonly worn in the tunnel during research, including a hard hat, bunny boots, and military parka that smells like the tunnel.

In addition to the real objects, we have created several replicated or virtual products to convey permafrost-related concepts.

1. University of Alaska Museum of the North filmed a 360-degree video tour of the Permafrost Tunnel (attached photo) that is displayed in an inflatable planetarium, a 4-meter hemispheric dome, on loan from UAF Geophysical Institute Education Outreach group. This experience is immersive and engaging, as well as allows viewers to see ice features in life-size.

2. We have created three physical models of permafrost features, including

   a) micro-lenticular ice,

   b) ice wedge polygons, and

   c) discontinuous permafrost landscape with climate change impacts of forest fires and thermokarst terrain.

3. We have created a permafrost soil profile within a Plexiglas box, with frozen ice-rich soil and topped with thick moss cover. The participants get to try frost probing the permafrost then explore the soil profile that is common for Alaska.

4. We have created a small metal house that we place on a piece of permafrost to aid in explaining how Alaskan structures can impact permafrost. We heat the metal house with a propane torch, resulting in the house slowly sinking, often lopsided, into the permafrost.

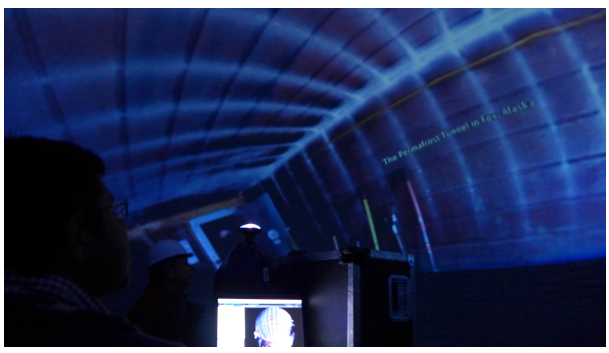

Figure 1: 360-degree video of a Permafrost Tunnel tour shown inside an inflatable planetarium

Front-End Evaluation Results

The consulting firm Goldstream Group led the front-end evaluation at the Permafrost Tunnel to give formative feedback about what aspects of the tunnel attracted people, what prior knowledge visitors came with, and information about visitors' interests. For one day, families with children ages 9-14 were invited to the tunnel. Interviews and surveys were conducted along with audio recording and visual tracking as the families moved through the tunnel on their own, with experts on hand to answer questions. The results showed that participants strongly valued the tunnel environment as a learning tool, compared to learning about permafrost in a setting outside of the tunnel. Navigating the tunnel along with seeing in-situ features and research tools (thermometers) were effective in engaging children to wonder what scientists do or to take on a scientist persona. The bones and ice wedges were given the most attention, because they are the most accessible both physically and conceptually. The evaluation exposed a common misconception about geologic time, specifically that dinosaurs co-existed with mammoths during the last Ice Age. Participants did not make personal connections to permafrost while inside the tunnel. However, they did make these connections when reflecting about their tunnel experience during their post-interviews. These Alaskan participants were more interested in how to adapt and prepare for the future effects of climate change in Alaska, rather than how to prevent or mitigate climate change or the thawing of permafrost [Goldstream Group, 2015a].

There was a similar study at OMSI, where interviews were conducted with image cards related to the Arctic, the Ice Age, permafrost, and climate change. It was found that while participants only had some prior knowledge of the concepts and minimal prior knowledge of permafrost, they still expressed interest in learning more about the concepts. Even with limited knowledge of Arctic-related details, the participants expressed "the importance of the Arctic as a litmus test for climate change globally" (Goldstream Group [2015b], 22).The misconception of dinosaurs during the last Ice Age was also seen at OMSI, along with misconception that the Arctic is barren and uninhabitable. In sharp contrast with the Alaskan participants, the OMSI participants had a "strong belief in the possibility of mitigating change through scientific research and related actions" (Goldstream Group 2015b, 22). They also expressed they lacked of confidence in their understanding of climate change details [Goldstream Group, 2015b].

Further research conducted by UAF researchers along with the Goldstream Group will look at real versus replicated and/or virtual objects as the project progresses. Data will be collected during our village visits and will provide us with formative evaluation to improve our educational products and program. Once the museum exhibition has been installed at OMSI, research into the concept of real versus replicated and/or virtual will continue in collaboration with the OMSI Evaluation and Visitors Studies Team.

Summary and Further Research

At the time of writing, we are only 15 months into our four year project in developing educational products for informal science learning programs for families with children ages 9-14. With the partnership between UAF and OMSI, we are

1. developing new displays for the Permafrost Tunnel,

2. developing educational products and hosting science outreach events in rural, Alaskans communities, and

3. developing a national traveling museum exhibition on permafrost and climate change.

With the aid of the Goldstream Group, we are planning on researching the importance of real versus replicated and/or virtual geologic materials in informal science learning.

We have completed our front-end evaluation, which has focused our efforts in certain areas. The development of the national traveling museum exhibition is progressing and OMSI will be developing exhibit prototypes and conducting formative evaluation with museum visitors. The content for the new Permafrost Tunnel displays has been identified, and development and production of the displays are underway.

We are still developing educational products for the rural Alaskan village outreach events. The educational products that have been developed have been focused on real objects and permafrost education in general. Going forward, we will be developing products that focus on our key concepts of timelines, tipping points, and feedback cycles.

Acknowledgements

The UAF team also consists of Jessica Garron, leading the Alaskan outreach programs, Santosh Panda, one of our permafrost educators, and Suzanne Perin, a post-doc researcher studying the importance of real objects. We appreciate the U.S. Army Cold Regions Research and Engineering Laboratory (CRREL) for allowing us to use the Permafrost Tunnel facility, as well as using the tunnel as a muse for our educational programs. The Pleistocene bones on loan from the University of Alaska Museum of the North have been crucial in engaging participants in our programs. The 360-degree Permafrost Tunnel video filmed by the University of Alaska Museum of the North and shown in the UAF Geophysical Institute Education Outreach group's planetarium is a center piece of our programs. This material is based upon work supported by the National Science Foundation under Grant No. 1423550

References

Goldstream Group [2015a]: *Hot times in cold places, front-end report: tunnel day and outreach, internal report.* Goldstream Group: Fairbanks, Alaska.

Goldstream Group [2015b]: *Hot times in cold places, front-end report: OMSI, internal report.* Goldstream Group: Fairbanks, Alaska..

Leinhardt, G. and Crowley, K. Objects of learning, objects of talk: Changing minds in museums. In: Paris, S.G.(ed.), *Perspectives on Object-Centered Learning in Museums.* Lawrence Erlbaum Associates: Mahwah, New Jersey, 2002.

Secrets in ice: Interdisciplinary summer permafrost science education for middle school and high school students

Rebecca Anne Finger[1] & Margaret Cysewski[2]

[1] *Dartmouth College, USA*; [2] *University of Alaska Fairbanks, USA*

Permafrost is a great interdisciplinary education tool which can span a wide range of Science, Technology, Engineering, and Math (STEM) fields. Students studied and explored permafrost dynamics and distribution and developed inquiry-based independent projects in two summer STEM programs. The 2015 Alaska Summer Research Academy (ASRA) at the University of Alaska Fairbanks (UAF) worked with middle school students, while the 2015 Joint Science Education Program (JSEP) run by Dartmouth College out of Kangerlussuaq, Greenland worked with high school students. Throughout the ASRA and JSEP programs, instructors provided hands-on learning opportunities for students including: soil science, global carbon cycling, paleontology, engineering, ground heat flux, forest fire science, long-term ecological monitoring, and polar climate change.

During the two-week middle school ASRA module, students started with an immersive two day exploration of the Cold Regions Research and Engineering Laboratory (CRREL) Permafrost Tunnel, outside of Fairbanks, AK USA, in order to learn about permafrost features and their formation. While at the tunnel, students also drilled permafrost cores, and sifted through debris piles in search of bones and other relics of the Pleistocene. Collected specimens from the tunnel were then brought to the UAF Museum of the North for identification. ASRA students also visited active research sites, including Carbon in Permafrost Experimental Heating Research (CiPEHR) project near Healy, AK USA, in order to participate in ongoing research linking changes in permafrost stability to global carbon cycles, plant growth, and changes to the local landscape. Student also visited forest fire burn scars and met with local fire fighters to draw linkages between forest fire severity and permafrost stability. In addition to exploring the geographical, geological, and biological history of permafrost, students also explored the challenges of building and engineering on permafrost, by building model foundations and visiting engineering successes and failures around the Fairbanks area. Throughout the module, the student worked on educational videos on permafrost and climate change concepts.

JSEP students learned about permafrost as a part of a three week science education program that is jointly supported by the government of Greenland and the National Science Foundation's Division of Polar Programs. While in Kangerlussuaq, Greenland, students from the USA, Denmark, and Greenland learned about permafrost distribution across the Arctic and explored the surrounding tundra for signs of permafrost. Students dug soil pits, measured vegetation, and mapped the landscape in order to answer their own research questions regarding active layer depths, vegetation height, and spatial distribution of permafrost between the Greenland Ice Sheet and the town of Kangerlussuaq. Students were also responsible for developing their own outreach materials, which included an educational video of their research project and a poster of their study area that was displayed at the Kangerlussuaq airport.

For both of these summer research academies, positive student feedback was received by program administrators. Students felt engaged, challenged, and empowered by inquiry-based science exploration. Here we demonstrate that permafrost education can serve as a unique and useful tool for educators to teach interdisciplinary science curriculum and engage students in polar science.

Figure 1: Middle school students exploring the CRREL Permafrost Tunnel located outside of Fairbanks, AK USA

The experience of the international field student courses on permafrost in northern Siberia

Valery I. Grebenets[1], Dmitry A. Streletsky[2], Nikolai I. Shiklomanov[2], Kelsey E. Nyland[3], Anna N. Kurchatova[4], Alexandr V. Boycov[5], Eva-Maria Pfeiffer[6], Anne E. Klene[7], & Aliguoshad G. Kerimov[8]

[1] *Lomonosov State University, Moscow, Russia, Russian Federation*
[2] *George Washington University, USA*
[3] *Departament of Geography, Michigan State University, East Lansing, MI, USA*
[4] *Earth Cryosphere Institute, Siberian Branch, Russian Academy of Sciences, Tyumen, Russia*
[5] *Tyumen State Oil and Gas University, Tyumen, Russia*
[6] *University of Hamburg, Hamburg, Germany*
[7] *University of Montana, Missoula,Montana, USA*
[8] *Engineering Scientific Company " Ecofoundations", Norilsk, Russia*

Since 2007, the Department of Cryolithology and Glaciology, in the Geography Faculty of Moscow State University, together with a number of Russian and international universities, inspired by the International Permafrost Association and in time for the International Polar Year, have been conducting international field courses on permafrost in northern Siberia. From 2007 to 2009 these field schools were conducted in western Siberia (near Novy Urengoi and Yamburg), in 2012 (in the Polar Urals and Yamburg), and in 2011, 2013, 2014, and 2015 in the lower Yenisei area (near Igarka, Dudinka, and Norilsk). In total, approximately 150 students from various universities in Russia, Austria, China, England, France, Germany, Norway, and the US have participated in the course.

Topics each year include: the origin and development of permafrost, regional features of cryolithozone, cryogenic processes and phenomena, tundra and forest-tundra landscapes, ecology of the northern regions, and engineering geocryology.

During the international field course, students experience Siberian taiga, tundra, and mountain landscapes, with a focus on relationships between biogeographic communities, and their role as indicators of permafrost conditions, and their influence upon the development of micro-relief and northern taiga, forest tundra, and tundra soils. Students get to examine a range of lithogenetic conditions and periglacial geomorphology in Pleistocene-Holocene sediments (peat mounds, pingos, wetlands, exposures of massive ice beds and ice wedges, various thermokarst stages, and slope processes in cryolithozone (solifluction, cryogenic landslide flows, and slides). In Igarka or Yamburg, access to underground laboratories allows the structure and properties of permafrost (cryostructure, lithogenetic complexes, etc.) to be readily visible.

At a range of sites, students participate in hands-on data collection and detailed field work (Fig. 1). Digging pits allows measurements of the physical, mechanical, and thermal characteristics (desiccation, thixotropy, plasticity, etc.), of frozen and thawing soils, and collecting photographs and sketches of landscape-permafrost gradients.

Figure 1: Piece of field students' courses on permafrost, Northern Siberia

Field measurements of the depth of active layer in different landscape and lithogenetic conditions are collected following Circumpolar Active Layer Monitoring (CALM) protocols, which are then compared to results from previous seasons. This contributes to discussions on differences in the depth of seasonal thawing due to lithological and landscape conditions. Techniques for monitoring soil temperatures are also discussed. Further, transects revealing the impact of local conditions (drainage, vegetation, snow accumulation, the activity of slope processes, etc.) are conducted. In some years, laboratory resources are available and laboratory determination of moisture content, density, and grain-size distribution can be done from soil samples.

Engineering challenges and impacts are stressed throughout the course. Methods and technologies for construction on permafrost (the types of foundations, etc.) are discussed. Soil temperatures in natural landscapes and urban areas and factors affecting permafrost temperature, including technological systems to stabilize these temperatures (cold-ventilated cellars, steam liquid thermosyphons, bedding, etc.) are key topics. Methodologies to analyze and minimize the potential impacts of intensive anthropogenic development on northern biota for engineering and environmental purposes are discussed and many examples are available.

Depending upon the location, a variety of social, economic, and geographical issues of northern development and Arctic urbanization have been included each year. Tours of a variety of facilities have been available, for instance, of the metallurgy plant in Norilsk and a processing plant in northwestern Siberia which prepares natural gas for pipeline transportation. Museums and memorial complexes are included as well. Applied projects such as the development of an ecological and landscape-permafrost schematic map around Norilsk, and an assessment of a role of the GULAG in development and creation of industry in northern Russian, broaden the student's experience.

Throughout the course a variety of lectures are presented by the professors and students. Almost daily, data collection and field work are carried out, computer processing of various measurements, creation of databases, etc., are undertaken so that each student can compile a series of reports and presentations of their results by the end of the class.

Acknowledgements

We acknowledge the support of PLC «Gazprom», «Norilsk Nickel», «ConocoPhillips », the Institute on Permafrost's Igarka Geocryological Laboratory, and the Russian Ministry of Emergencies Arctic Center.

Frost depth outreach program in Japan

Koichiro Harada[1], Kenji Yoshikawa[2], Go Iwahana[2], Julia Stanilovskaya[3], & Yuki Sawada[4]

[1] *Miyagi University, Japan*
[2] *University of Alaska Fairbanks, USA*
[3] *Sergeev Institute of Environmental Geoscience, Russian Academy of Sciences, Russia*
[4] *Fukuyama City University, Japan*

In order to emphasis their interest for earth sciences, an outreach program through measurements of frost depth is conducting in Japan since 2011. This program is made at elementary, junior high and high schools in Hokkaido, northern part of Japan where seasonal ground freezing occurs in winter. At schools, a lecture was made and a frost tube was set at schoolyard, as the same tube and protocol as UAF's Permafrost Outreach Program, using clear tube with blue-colored water. Frost depth was measured directly once a week at each school by students during ground freezing under no snow-removal condition. In 2011 season, we started this program at three schools, and the number of participated school is extended to 29 schools in 2014 winter season, 23 elementary schools, 5 junior high schools and one high school. We visited schools summer time and just before frost season to talk about the method of measurement, and did measurements with students. After the end of measured period, we also visited schools to explain measured results by each school and the other schools in Japan, or Alaska, Canada and Russia. The measured frost depths in Hokkaido ranged widely, from only a few centimeter to more than 50 cm. However, some schools had no frost depth due to heavy snow. We confirmed that the frost depth strongly depends on air temperature and snow depth. We discussed with student why the frost depth ranged widely and explained the effect of snow by using the example of igloo. In order to validate the effect of snow and to compare frost depths, we tried to measure frost depths under snow-removal and no snow-removal conditions at the same elementary school. At the end of December, depths had no significant difference between these conditions, and the difference went to ^{14}Cm after one month, with about 30 cm of snow depth. After these measurements and lectures, students noticed snow has a role as insulator and affects the frost depth. The network of this program will be expected to expand, finally more than a hundred schools.

PermaModel new online tool on permafrost modeling

Elchin Jafarov[1], Kevin Schaefer[2], & Lynn Yarmey[2]

[1] *INSTAAR, University of Colorado Boulder, USA*
[2] *NSIDC, University of Colorado Boulder, USA*

Permafrost data and products are critically important for scientists, engineers, policy makers, indigenous communities, and the general public. There is a need to study permafrost dynamics via modeling. However, the availability of such models to the community of permafrost scientists are quite limited. PermaModel project enables the broader use of permafrost models by creating the Integrated Modeling Toolbox (IMT) consisting of several permafrost models representing a range of capability and complexity. The IMT provides easy online access to students, stakeholders, and scientists who want to use permafrost models, but lack the expertise and resources to develop them. The IMT includes multiple sets of sample inputs representing a variety of conditions and locations to enable immediate use of any permafrost model in the IMT. The IMT is built on the Community Surface Dynamics Modeling System (CSDMS) Modeling Framework platform. CSDMS provides an on-line environment where users can link and run models from multiple Earth science disciplines. The simple user interfaces, easy online access, open source models, and quick visualization tools can make permafrost models accessible to a broad audience well beyond the permafrost research community. These new easy-to-use modeling tools are especially useful to wide-range of users beyond the research community, such as educators, students, and policy-makers. The IMT applications target the needs of specific user communities and demonstrate the full potential of this new cyberinfrastructure, advancing and broadening the practical use of permafrost models and laying the foundation for future interdisciplinary research of permafrost dynamics.

Tandems 2 win

Monika Kallfelz

Pfalzmuseum für Naturkunde, Bad Dürkheim, Germany

The new project "schule@polarforschung" of the polar teachers' working team in the German federation of polar science connects teachers and scientists in an unbureaucratic way. Both, teacher and scientist together prepare their mutual project. They reach an agreement in regard to the topic, the goal or product, the character and the number of meetings and the time period. By this way scientists bring their research projects into classrooms and teachers use the authentic research project to improve teaching.

There are already some good practice examples to be presented in order to give some orientation.

For example: We had

- cooperations to create parts of an exhibition, (observation of marine mammals, photosynthesis of antarctic soil crusts, ice drilling cores and climate history, salinity and ocean currents, diatoms in the southern ocean, sediment analyses)
- cooperations to develop and publish classroom materials
- punctual cooperations in teachers trainings, where scientists presented their research
- scientists, presenting their research in a dialog in classrooms
- scientists or their institution provided materials like a survival box, polar clothes or trash of Polarstern
- last but not least the most important and most sustainable kind of cooperation, the attendance of teachers on expeditions. Teachers watch or do research and communicate as much as possible with students during the expedition.

We are a small group of people working on these different projects. We know each other and we would be happy to motivate more teachers and more scientists to get involved in such projects. We are working with our networks, the established newsletter of the polar teachers´ working team, with conferences like this in Potsdam to inform teachers and scientists and with a short questionnaire to find adaquate partners.

Hopefully, in Potsdam some interested scientists and teachers come together and start a project on permafrost. We really would like to bring you together. Please let us know if you are interested.

Permafrost as a topic in German schools

Rainer Lehmann

FWS Hannover-Bothfeld, Germany

30 years ago permafrost was not a topic in German schools. Even at university it was exceptional and studied only as a matter of particular interest in geography. Permafrost was relevant when working as a geomorphologist in polar, subpolar or high mountain regions. There was no reason to teach it in German schools.

Since climate change and natural hazards research became of interest in the science community and also to the public during the past 20 years, permafrost was recognized as one important component of the system. But for teachers and students permafrost is still not a topic.

Why should permafrost be an issue at school?

In school curricula the subjects climate change and natural hazards may be found. But permafrost is not a key issue. However, the students need to deal with permafrost to understand relationships and processes related to the mentioned subjects. Important curricula topics connected to permafrost are therefore carbon cycle and catastrophic mass movements due to thawing of permafrost, for example in high mountains like the Alps. Relevant geography and biology curricula will be shown for different states of Germany. On that basis examples to integrate permafrost topics into curricula will be shown for the German state Niedersachsen: biology 12th grade "carbon cycle" and geography 11th grade "polar regions".

What should students know about permafrost?

One main objective should be the phenomenon of frozen ground. What does permanently frozen mean? How thick and how old is it? For a better understanding it is important to know the differences between loose soil and solid ground such as bedrock, both of which can have temperatures below zero and a certain content of ice. Therefore the definition has to be explained using exemplifying drawings, photographs and diagrams of temperature changes with depth. To understand surface processes and the formation of frost forms, for example polygons, sorted stone circles or solifluction lobes, active layer and frost changes are important factors which should be kept in mind. The distribution of permafrost in a vertical and horizontal sense can be shown by diagrams and maps. One should differentiate between continuous/discontinuous/patchy permafrost and polar/alpine permafrost. Rock glaciers as an alpine permafrost form and their role in the formation of mudflows or landslides due to thawing permafrost are of special interest in the Alps. And in addition, ski lifts, mountain huts and other infrastructure are threatened by thawing permafrost. These methods and topics are suggestions and have to be discussed and developed in detail. The students involved should be older than 15 years, in order to understand interactions and processes.

Methods to communicate permafrost to the students are implemented in Germany only by few examples for dedicated and interested educators. One educational book offers information and an experiment which convey the results of melting permafrost due to global warming to the students. The students create two different frozen models with great enthusiasm and discuss the observed thawing process when the models are heated. They transfer the outcome to arctic permafrost zones and are concerned about the effects on buildings such as houses, roads or oil pipelines as well as on plants and animals.

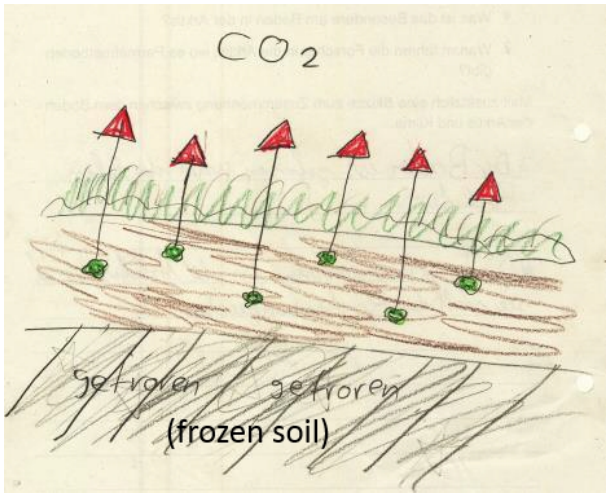

Figure 1: Students conception of permafrost (Wiebke Kaiser 2014)

The future of permafrost research: A contribution from early career researchers to ICARP III and beyond

Anne Morgenstern[1], Michael Fritz[1,2], Bethany Deshpande[3,4], Frederic Bouchard[4,5,6], Elin Högström[7,8], Julie Malenfant-Lepage[4,5,9], Alexandre Nieuwendam[10], Marc Oliva[10], Michel Paquette[4,5], Ashley Rudy[11], Matthias Siewert[12,13], Ylva Sjoberg[12,13], & Stefanie Weege [1,14]

[1] *Alfred Wegener Institute Helmholtz Center for Polar and Marine Research, Potsdam, Germany*
[2] *Utrecht University, Department of Earth Sciences, Utrecht, The Netherlands*
[3] *Université Laval, Department of Biology, Quebec City, Quebec, Canada*
[4] *Université Laval, Centre for Northern Studies (CEN), Quebec City, Quebec, Canada*
[5] *Université de Montréal, Department of Geography, Montreal, Quebec, Canada*
[6] *Centre Eau Terre Environnement, Institut national de la recherche scientifique (INRS), Quebec City, Quebec, Canada*
[7] *Vienna University of Technology (TUW), Dept. of Geodesy and Geoinformation (GEO), Vienna, Austria*
[8] *Vienna University, Austrian Polar Research Institute, Vienna, Austria*
[9] *Department of Civil and Water Engineering, Université Laval, Quebec, QC G1V 0A6, Canada*
[10] *Universidade de Lisboa, Center for Geographical Studies, Institute of Geography and Spatial Planning, Lisbon, Portugal*
[11] *Queen's University, Department of Geography, Kingston, Ontario, Canada*
[12] *Stockholm University, Department of Physical Geography, Stockholm, Sweden*
[13] *Stockholm University, The Bolin Centre for Climate Research, Stockholm, Sweden*
[14] *University of Potsdam, Institute for Earth and Environmental Science, Potsdam, Germany*

Over the past two decades, the International Arctic Science Committee (IASC) and the Scientific Committee on Antarctic Research (SCAR) have organized activities focused on international and interdisciplinary perspectives for advancing Arctic and Antarctic research cooperation and knowledge dissemination in many areas (e.g. Kennicutt II et al. [2014]). For permafrost science, however, no consensus document exists at the international level to identify future research priorities, although the International Permafrost Association (IPA) highlighted the need for such a document during the 10^{th} International Conference on Permafrost in 2012. Four years later, this presentation, which is based on the results obtained by Fritz et al. [2015], outlines the outcome of an international and interdisciplinary effort conducted by early career researchers (ECRs). This effort was designed as a contribution to the Third International Conference on Arctic Research Planning (ICARP III). In June 2014, 88 ERCs convened during the Fourth European Conference on Permafrost to identify future priorities for permafrost research. We aimed to meet our goals of hosting an effective large group dialogue by means of online question development followed by a "World Café" conversational process. An overview of the process is provided in figure 1. This activity was organized by the two major early career researcher associations Permafrost Young Researchers' Network (PYRN) and the Association of Polar Early career Scientists (APECS), as well as the regional research projects PAGE21 (EU) and ADAPT (Canada). Participants were provided with live instructions including criteria regarding what makes a research question [Sutherland et al., 2011]. The top five questions that emerged from this process are:

1. How does permafrost degradation affect landscape dynamics at different spatial and temporal scales?

2. How can ground thermal models be improved to better reflect permafrost dynamics at high spatial resolution?

3. How can traditional environmental knowledge be integrated in permafrost research?

4. What is the spatial distribution of different ground-ice types and how susceptible is ice-rich permafrost to future environmental change?

5. What is the influence of infrastructures on the thermal regime and stability of permafrost in different environmental settings?

As the next generation of permafrost researchers, we see the need and the opportunity to participate in framing the future research priorities. Across the polar sciences, ECRs have built powerful networks, such as the Association of Polar Early Career Scientists (APECS) and the Permafrost Young Researchers Network (PYRN), which have enabled us to efficiently consult with the community. Many participants of this community-input exercise will be involved in and also affected by the Arctic science priorities during the next decade.

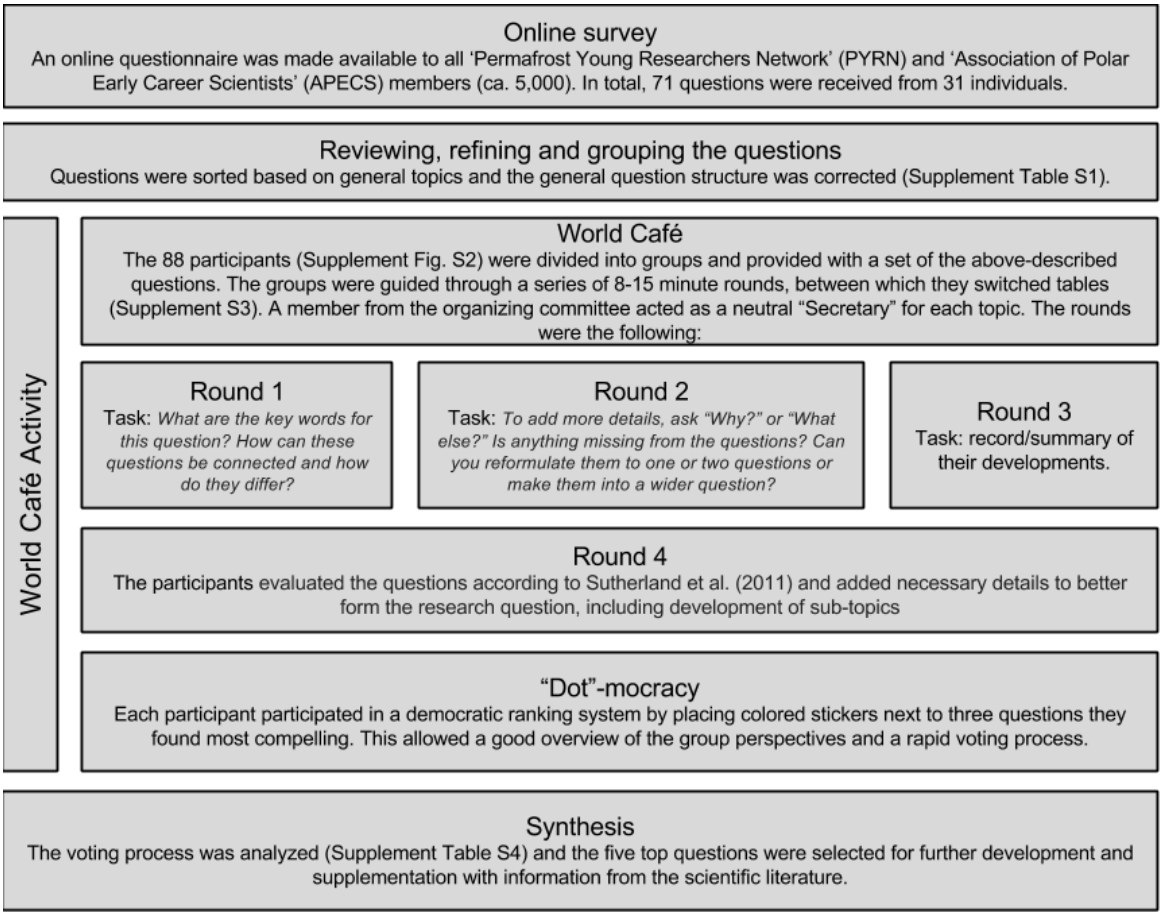

Figure 1: Flowchart of the process used to develop and refine future research questions for permafrost science. Based on community votes, five questions were selected for further development and dissemination (after Fritz et al. [2015]).

Therefore, we need to

i) contribute our insights into larger efforts of the community such as the Permafrost Research Priorities initiative by the Climate and Cryosphere (CliC) project together with the IPA and

ii) help identify relevant gaps and a suitable roadmap for the future of Arctic research.

Critical evaluation of the progress made since ICARP II and revisiting the science plans and recommendations will be crucial. IASC and the IPA, together with SCAR on bipolar activities, should coordinate the research agendas in a proactive manner engaging all partners, including funding agencies, policy makers, and local communities. Communicating our main findings to society in a dialogue between researchers and the public is a priority. Special attention must be given to indigenous peoples living on permafrost, where knowledge exchange creates a mutual benefit for science and local communities. The ICARP III process is an opportunity to better communicate the global importance of permafrost to policy makers and the public.

References

Fritz, M.; Deshpande, B. N.; Bouchard, F.; Högström, E.; Malenfant-Lepage, J.; Morgenstern, A.; Nieuwendam, A.; Oliva, M.; Paquette, M.; Rudy, A. C. A.; Siewert, M. B.; Sjöberg, Y. and Weege, S. [2015]: Brief Communication: Future avenues for permafrost science from the perspective of early career researchers. *The Cryosphere*, 9(4):1715–1720, doi:10.5194/tc-9-1715-2015.

Kennicutt II, M.C.; Chown, S.L.; Cassano, J.J.; Liggett, D.; Massom, R.; Peck, L.S.; Rintoul, S.R.; Storey, J.W.V.; Vaughan, D.G.; Wilson, T.J. and Sutherland, W.J. [2014]: COMMNENT: Six priorities for Antarctic science. *Nature*, 512, doi:10.1038/512023a.

Sutherland, W.J.; Fleishman, E.; Mascia, M.B.; Pretty, J. and Rudd, M.A. [2011]: Methods for collaboratively identifying research priorities and emerging issues in science and policy. *Methods in Ecology and Evolution*, 2:238–247, doi:10.1111/j.2041-210X.2010.00083.x.

The International Permafrost Association: Current initiatives for cryospheric research

Karina Schollaen[1,2], Antoni G. Lewkowicz[2,3], Hanne H. Christiansen[2,4], Vladimir E. Romanovsky[2,5], Hugues Lantuit[1,2,6], Lothar Schrott[2,7], Dimitry Sergeev[2,8], & Ma Wei[2,9]

[1] *Alfred Wegener Institute Helmholtz Center for Polar and Marine Research, Potsdam, Germany*
[2] *International Permafrost Association, Potsdam, Germany*
[3] *University of Ottawa, Canada*
[4] *The University Centre in Svalbard, UNIS, NO*
[5] *Geophysical Institute, University of Alaska Fairbanks, USA*
[6] *University of Potsdam, Germany*
[7] *University of Bonn, Germany*
[8] *Institute of Environmental Geoscience Russian Academy of Sciences, Russian Federation*
[9] *Chinese Academy of Sciences, China, People's Republic of China*

The International Permafrost Association (IPA), founded in 1983, has as its objectives to foster the dissemination of knowledge concerning permafrost and to promote cooperation among persons and national or international organizations engaged in scientific investigation and engineering work on permafrost. The IPA's primary responsibilities are convening International Permafrost Conferences, undertaking special projects such as preparing databases, maps, bibliographies, and glossaries, and coordinating international field programs and networks. Membership is through adhering national or multinational organizations or as individuals. The IPA is governed by its Executive Committee and a Council consisting of representatives from 26 Adhering Bodies having interests in some aspect of theoretical, basic and applied frozen ground research, including permafrost, seasonal frost, artificial freezing and periglacial phenomena.

This presentation details the IPA core products, achievements and activities as well as current projects in cryospheric research. One of the most important core products is the circumpolar permafrost map. The IPA also fosters and supports the activities of the Global Terrestrial Network on Permafrost (GTN-P) sponsored by the Global Terrestrial Observing System, GTOS, and the Global Climate Observing System, GCOS, whose long-term goal is to obtain a comprehensive view of the spatial structure, trends, and variability of changes in the active layer thickness and permafrost temperature. The IPA also organizes International Conferences on Permafrost (ICOP) every four years and Regional Conferences on Permafrost (RCOP) two years after the International Conference. Given the growing interest in permafrost, RCOPs are planned to occur in all years without an International Conference starting in 2017, although Council will continue to meet only at the RCOP mid-way between ICOPs.

A further important initiative of the IPA are the biannually competitively-funded Action Groups which work towards the production of well-defined products over a period of two years. Current IPA Action Groups are working on highly topical and interdisciplinary issues, such as the synthesis of circum-arctic distribution and thickness of Yedoma permafrost, an arctic coastal web implementation, the integration of multidisciplinary knowledge about the use of thermokarst and permafrost landscapes, and defining permafrost research priorities - a roadmap for the future. The latter project is a joint effort with the Climate and Cryosphere initiative (CliC) and a contribution to the International Conference on Arctic Research Planning III (ICARP III). The product stemming from the effort will consist of a journal publication listing permafrost research priorities and putting them into context.

In all of these activities, the IPA emphasizes the involvement of young researchers (especially through the Permafrost Young Researchers Network and APECS) as well as its collaboration with international partner organizations such as IASC, SCAR, CliC, IACS, IUGS and WMO.

Field education in discontinuous permafrost region, Igarka Geocryology Lab

Nikita Tananaev[1,2], Elizaveta Makarycheva[3], Andrey Litovko[1], & Dmitry Sergeev[3]

[1] *P.I. Melnikov Permafrost Institute, SB RAS, Russian Federation*
[2] *Ugra Research Institute of Information Technologies, Russian Federation*
[3] *Sergeev Institute of Environmental Geoscience, RAS, Russian Federation*

More than 60 long-term monitoring sites were operated in Soviet Union permafrost areas since the 1920s. The majority of those was closed or suspended owing to the lack of funding and general interest on the topic in the 1990s. Only a few research stations from this extensive network had managed to maintain a certain level of activities, e.g., Vorkuta, cape Bolvansky, Marre-Sale, Nadym, Igarka, Chernyshevsky, Magadan, to name but a few. In recent years, certain efforts are put to revive the interdisciplinary research programmes in the Russian permafrost regions, accounting for the experience of the existing research stations.

Igarka Geocryology Lab is the second oldest in Russia (1930), after the famous Skovorodino research station (1927). Igarka station was organized by 'Severstroy', an enterprise responsible for the construction of the city of Igarka, and Nikolay Bykov, former director of the Skovorodino station, was appointed as a lead scientist. In 1935, Igarka station was handled to the Soviet Academy of Sciences, and since 1960, it became a regional branch of Permafrost Institute. The best Soviet experts on permafrost, including P.I. Melnikov, A.M. Pchelintsev, N.F. Grigoriev, based their research in Igarka. Field and laboratory data accumulated for over 85 years allow to support a wide range of interdisciplinary research projects.

Igarka is located in the discontinuous permafrost region, at the taiga-tundra frontier, though the mean annual air temperature is close to -8 °C. Ground temperature data suggests a strong impact of the climate change on the permafrost conditions, the lowering of the permafrost table and the decrease in the depth of seasonal freezing have together promoted development of the residual thaw layer above the permafrost in late 1980s [Streletskiy et al., 2015]. The related changes in landcover are observed, including an increase in taiga-occupied areas, and intensive thermokarst in the peat plateau regions. The permafrost ecosystems of the Igarka region are extremely vulnerable to ongoing changes, and are to disappear first if the global change will not slow its pace.

Igarka Lab is a unique field base with a capacity for year-round observations, offering its facilities and logistic support for visiting researchers. Major objectives of the lab activity are a) to sustain year-round observations of basic natural variables (ground temperatures in various landscapes, active layer thicknesses, water stages and basic chemistry) across the region, and b) provide local knowledge and advise, as well as data sharing and field support, for visiting research groups. Data from CALM plot (R-40 Igarka), several TSP boreholes, as well as from several stream gauges in the vicinity of Igarka, are available. This allows the researchers to concentrate on their research priorities, and provide opportunities for building-up new projects backed with basic data and the results from previous studies.

Ongoing projects already have an educational component, since several PhD students are constantly involved in the current studies. Moreover, since 2010, Igarka Lab hosts International Field Courses in Geocryology for students, organized by Moscow State University. Since 2015, as a part of strengthening of the international interdisciplinary collaboration through the development and promotion of educational activities. Within the framework of the Lower Yenisei Observation Network, Igarka Geocryology Lab plans inviting young researchers either to enroll in existing projects or to develop their own research objectives.

Lower Yenisei Observation Network (LYON), as a concept, emerged following the discussions during the conference held in Igarka in July 2015. This concept, still in its development phase, assumes the creation of a regional network of research stations and associated laboratories, jointly supporting research efforts in the Northern Yenisei region. Several teams from Russia, Europe and U.S. agreed to promote data sharing and coordination of research efforts in the region. These goals would become more achievable under the auspices of EU-funded INTERACT 2 programme and its Transnational Access support.

In July 2017, Second LYON Workshop will be held in Krasnoyarsk and Igarka, summarizing the advance of the regional research around the Northern Yenisei basin. This workshop will accommodate a summer field school for students. During the workshop, students will benefit from exchange with researchers having regional experience in the area. In Igarka, after the workshop, summer school will continue with field trips to the key study sites in the region. The poster presentation at ICOP will introduce the most attractive key sites in the vicinity of Igarka, and the ongoing projects. The students will have a possibility to communicate their research objectives and findings to the community of Igarka.

References

Streletskiy, D.A.; Tananaev, N.I.; Opel, T.; Shiklomanov, N.I.; Nyland, K.E.; Streletskaya, I.D.; Tokarev, I. and Shiklomanov, A.I. [2015]: Permafrost hydrology in changing climatic conditions: seasonal variability of stable isotope composition in rivers in discontinuous permafrost. *Environmental Research Letters*, 10(9):095003, doi:10.1088/1748-9326/10/9/095003.

New approaches in climate science communication: an example from the field of permafrost research

Renate Treffeisen[1], Jan Borm[2], Klaus Grosfeld[1], Peter Lemke[1], & Rolf Teigler[3]

[1] *Alfred Wegener Institute Helmholtz Center for Polar and Marine Research, Germany*
[2] *Institut des études culturelles et internationales (IECI) Membre du laboratoire DYPAC, EA 2449, Université de Versailles Saint-Quentin-en-Yvelines (UVSQ), France*
[3] *DEKRA Hochschule für Medien, Berlin, Germany*

Communicating and interacting with the public and society about research outcomes is challenging but at the same time it is of vital importance. The increasing interest of society in taking advantage of research results leads to the pressure, putting research to use, and interacting with users of research as there is a big agreement that citizens get easy access to the results of research they have paid tax for. Policies and measures that mobilize these intellectual assets for use through broader access can accelerate scientific breakthroughs, increase innovation, and promote economic growth. That's why it is of growing importance to ensure that results of public-funded scientific research are made available to and useful for the public, industry, and the scientific community [Scott, 2000].

The Climate Office for Polar Regions and Sea Level Rise has furthered this important communication and dialogue processes from the scientific community to the society and its groups through various projects since nine years. Some examples of specific activities around the theme of permafrost will be presented which is part of the outreach activities of the Helmholtz Climate Initiative REKLIM (Regionale Klimaänderungen/Regional climate change).

This involves presenting the process and results of a school art project performed with the Wilhelmsburg comprehensive school in Hamburg in context of a long-term cooperation project"Maritime Centre Elbe Islands" (MZE). About 200 pupils between grades 5 to 10 developed under the lead of their art teacher Guni Wiemer in the school year 2015/2016 an art project around the theme of permafrost under climate change. The project was realized during regular weekly working hours and during specific project days and several outcomes could be realized: a small installation with collage technique, two boards with abstract drawings about the kids see permafrost from their perspective, an animated cartoon as well as a small booklet.

Figure 1: Figure left: Cihad (left) and Tom (right) drawing permafrost in black and white . Figure right: Claudia drawing concentrated her permafrost project contribution. Pictures: Angela Dietz

There are many ways to channel information of scientific research results. Among these, the Internet plays a major role in contributing to improve public awareness [Breyer et al., 2007]. The advantage of web-based methods compared with conventional communications channels is a huge opportunity to share the outcomes of scientific research more extensively and quickly across the entire society. Thus, two further projects will be presented focusing on the internet as an important dialogue tool. One is the work with about 20 students of the DEKRA Hochschule für Medien Berlin for the ICOP 2016. They are responsible to serve all social media channels of the ICOP conference website. They have been trained during their studies about the theme permafrost and prepared for the work in courses. As well REKLIM, Institut des études culturelles et internationales (IECI)and the DEKRA Hochschule für Medien Berlin are initiating an interdisciplinary social media project, focusing on permafrost degradation and societal impacts in the Yakutsk area, Russia.

The presentation will discuss approaches, how to overcome obstacles and describe learning processes of all partners during these projects.

References

Breyer, D.; Daubresse, P. and Sneyers, M. [2007]: Bringing scientists to the people – the Co-Extra website. *Biotechnology Journal*, 2(9):1081–1085, doi:10.1002/biot.200700115.

Scott, A. [2000]: *The dissemination of the results of environmental research.* Environmental issues series No 15, November, European Environment Agency, URL http://www.eea.europa.eu/publications/Environmental_issues_No_15/at_download/file ISBN: 92-9167-262-9.

Catching permafrost in the Zwickau classroom

Michael Weidlich[1], Lutz Schirrmeister[2], & Georg Schwamborn[2]

[1] *KOMPAKT-Schule mit Zukunft Zwickau, Germany*
[2] *Alfred Wegener Institute Helmholtz Center for Polar and Marine Research, Potsdam, Germany*

Earth's Polar Regions are not included in the school curriculum in Saxony, SE Germany. However, in the media their role in climate change is often emphasized. Understanding the related connections is difficult for the pupils and therefore has little influence on their climate relevant behavior. Climate change and the connection to the Polar Regions could be approached multidisciplinary as a comprehensive topic in various school subjects.

At the KOMPAKT School in Zwickau, twelve pupils of grade 6 were interested in permafrost as a subject and dedicated several weeks to the topic. The goals included understanding basic principles, build on those to gain specific knowledge and finally find possibilities to use this knowledge in school.

In the first part of the project, the students built a simplified model that allowed studying permafrost thaw and the related consequences. These studies were accompanied by observations of thawing and freezing of different soil and vegetation samples. The students reported their observations becoming familiar with keeping records of the setup and the experiments' outcome. They used their protocols to create a documentation of the experimental work.

The cooperation with the Alfred Wegener Institute in Potsdam then allowed the pupils to connect to scientists working on permafrost, to learn about the scientific questions those scientists address, and how and where they worked on. The pupils had the possibility to ask questions about fieldwork and follow up lab work during a visit at AWI in Potsdam.

An additional part of the project was the collection of information from permafrost related articles in newspapers and journals. The pupils are not used to long, scientific texts, the extraction of relevant content and relating this information to their own knowledge was very difficult. One key insight of this part of the project was that results of scientific research can lead to vastly different interpretations. Complete answers, as the pupils know them from class, are not provided. Rather, scientific research means to discuss results from different perspectives to struggle together for realistic explanations of nature phenomena.

In the final stage of the project, the pupils took part in an excursion to Westerwald around Dornburg, where phenomena related to freezing processes could be observed in- situ. The pupils were encouraged to find explanations for their observations themselves. Some theories were astonishingly accurate.

Figure 1: Activities of the cool permafrost class in Zwickau. Left: Experimental arrangement to study permafrost thaw; middle: Presenting first results at a project week in school; right: Description and weight measurements of thawed samples after the experiment

During the project, we always discussed the responsibility that each of us has towards the protection of nature. Do we have influence on nature at all? Are children and teenager also affected? This discussion is carried on beyond the project. All participating students are now encouraged to take part in the discussion with their new insights from the classroom exercises. They can also better relate to the public discussion of climate change. They learned new ways to pose questions and that at times, it can be difficult to obtain answers. They have worked on one specific subject during a long time and are now able to stimulate discussion in class whenever permafrost or Earth's climate are topics. They can resort to the results of their own model and experiments and their observations as well. They can give information to others and maybe intrigue them with the subject. From this point of view, the project was a complete success.

Author Index

Ødegård, R.S., **370***, 418
Østby, T., 386
Şerban, R.D., **87***
Åkerman, J., 359
Čapek, P., 251
Šantrůčková, H., 251
Šibík, J., 933

Aalstad, K., 386, **478***, **890***
Aas, K.S., 396, 478, 890, 1084
Abakumov, E., 175, 182, 260
Abbott, B.W., **184***, 227, **765***
Abe, K., 905
Abermann, J., 432, 1035
Abramov, A., **116***, 467
Abramova, A.S., **165***
Adamczyk, J., 53
Adams, J., **892***, 896
Adeli Ghareh Viran, P., 1171
Adiya, S., **713***
Adler, A., 1101
Ahn, J., 153, 190, 525
Aiken, G., 566, 665
Aiken, Q., 352, 859
Akagawa, S., 1183
Aksenov, S., 538
Aksnes, J., 1107
Aleina, F.C., 761
Alekseeva, N., **714***
Aleksyutina, D., 837
Alexander, H., 429
Alexeev, V., 645, 653, 752
Alfaro, M., 1095, 1130
Ali, S.H., 530
Alias, S.A., 530
Allard, M., 199, 200, 829, 1128, 1224, 1234
Allen, S.K., **1018***
Allroggen, N., **942***, 977
Alm, G., 359
Alsos, I.G., **473***
Altshuler, I., **517***
Alves, R.J.E., 251
Amangurov, R., 837
Amann, F., 80
Amarbayasgalan, Y., 394
Ambrosi, C., 39
Ambrosius, K., 1234
Amesbury, M., 256
Amiri, S.A.G., 873
Amon, R.M., 795
Amschwand, D., 30
Anbergen, H., 659
Anderson, J., 723, 952
Anderson, P., 604
Anderson, S., 1146
Andersson, K., 818
Andersson, P.S., 784, 787
Andreassen, L.M., 370
Andreev, A.A., 483, 627
Andreeva, V.V., 94
Andrieux, E., **302***
Andriushchenko, F.D., 1098, **1125***
Angelopoulos, M., **12***, 1146
Anisimov, O., **263***, **1199***
Antcibor, I., 230
Anthony, P., 249, 623
Antognini, M., 39
Antoine, P.L., **302***, 490
Antoniades, D., 79
Antonova, S., **715***
Appéré, T., 549
Araújo, M.F., 772
Ardelean, A.C., 100
Arenson, L., 353, 704, 1038, 1095, 1124, **1126***, 1130, 1151, **1152***, 1156
Argles, T., 1008
Arkhipov, V.V., 850
Arkhipova, M.V., 726
Arp, C.D., 653, **717***, 719, 752, 971
Ascenso, J., 772
Ashastina, K., 484, **560***
Ashpiz, E., **1127***
Atchley, A., 681
Audibert-Hayet, A., 823
Audry, S., 679
Aurela, M., 267, 274
Avirmed, D., **394***, 469, 1081
Ayunov, D.E., 957, 983
Azócar, G.F., **1021***

Böhme, L., 250
Börner, A., **304***
Bárta, J., 251
Babin, V., 49
Baeseman, J., 1224
Baginski, S., 1110
Baize, S., 337
Balks, M., 124, 137, 164, **166***
Balme, M.R., 1008
Balser, A., **149***, 765
Baltzer, A., 830
Baltzer, J.L., 896
Bandara, S., **562***, **719***
Bandeira, L., 82
Bange, U., 170
Banville, D., 958
Banyasz, I., 198
Baranova, N., **630***
Baranskaya, A.V., **14***, **823***
Barba, M., 352
Barboux, C., 1051
Bard, E., 214
Barnes, H.A., **1168***

Barnhart, K., 985
Barta, J., 215
Barth, J.A.C., 637
Barth, T., 62
Bartsch, A., 75, 346, 380, 452, 712, 725, 736, **893***, 899, 904, 928, 938
Bas, B., 1171
Basharin, N., 1214
Bast, A., **396***, 944
Bateman, M., 302
Bauch, H.A., 808
Baughman, C.A., 906
Baumann, S., **894***
Bavay, M., 42
Baxter, R., 776
Bayer, T.K., **767***
Beamish, A.L., **894***, 904
Beck, I., **862***, 1237
Beckebanze, L., 289
Beer, C., **185***, 208, 270, 271, 278, 283, 287, **345***, 677, 767
Beermann, F., 614
Bek, D., **1161***
Belelli Marchesini, L., **265***, **267***, 271, 274
Bell, T., 1234
Bellehumeur-Génier, O., 963
Bellisario, A., 649, 663
Bellisario, S., **631***
Belova, N.G., 148, 823, **825**, **826***
Bendixen, M., **828***
Benkert, B., 1011
Benmergui, J., 272
Bennett, A., 435
Bense, V.F., **632***, 659, 710
Bentley, L.R., 1037
Berendse, F., 754
Berg, A., 892
Berg, E.E., 906
Bergstedt, H., **346***
Bernard, E., 830
Bernier, M., 706, 887
Berninger, A., 269
Berritella, C., 336
Berry, T., 83
Berthling, I., 868, **944***
Bertino, L., 478, 890
Bertran, P., 302
Best, J., 1090
Beutel, J., 109, 908, **1023***, 1064
Bevington, A.R., **347***
Bhardwaj, A., **535***, 698
Bhatt, U.S., 900
Biasi, C., 245, 296, 614
Bigelow, N., 508
Billett, M.F., 776
Binal, A., **1170**, **1171***
Binder, D., 452
Binet, S., 782
Bing, H., **1170***, 1185
Biraud, S., 284
Birkeland, E., 873
Birks, J., 483
Biroň, A., 319
Biskaborn, B.K., **398***, **474***
Björk, R.G., 186, 187
Björkman, M.P., **186**, **187***, 227
Bjella, K., 952, **1090***
Blanco-Chao, R., 103, 1033
Blazewicz, S., 532
Blitz, C., 1140
Bloethe, J.H., 44
Blok, D., 215
Bloom, A., 284
Blumstein, D., 749
Bobrik, A., 177, **400***
Bobrov, A., 314
Bobrova, O., **633***, 647, 701, 774, 792
Bockheim, J.G., 226
Bodenstab, L., 790
Bodin, X., 367, 695, 967, 1021, **1025***, **1027***
Boeckx, P., 186
Bohn, T.J., 208
Boike, J., 78, 207, 236, 267, 271, 293, 386, 426, 428, 466, 478, 634, 715, 724, 728, 744, **751***, 761, 792, 793, 862, 890, 917
Boisson, A., **829***
Bolch, T., 373, **1029***
Bolton, W.R., 435, 646, 867, **895***, 915
Bondurant, A., 205, 717, **719***, 971
Bonnaventure, P., 344, **401***, 461, 463
Boreham, S., 83
Borm, J., 1256
Bornemann, N., 293, 428, **634***, 724, 793
Borsukova, O., 1129
Bouchard, F., 231, **721***, **1238***, 1250
Bourriquen, M., **830***
Bowden, W.B., 765
Boycov, A.V., 1244
Bröder, L., 622, **769***
Bracho, R., 221, 237
Braillard, L., 36, 54
Brakebusch, M., 677, 767
Branco, J., 82
Brandt, I., 979
Brauer, A., 332
Braul, C.Z., 737
Braun, K., 1111
Braverman, M., **896***
Breen, A., 435, 915
Brenning, A., 1021
Bricheva, S., **946***
Brigham-Grette, J., 483
Brodie, J., 1111
Bromfield, S.S., **16***
Brooks, H.M., **1128***
Brooks, I.M., 818
Brosius, L., **188***, 241, **722***
Brouchkov, A., **348***, 1172
Brovkin, V., 811
Brown, D.R., 915
Brown, J., 859, 885, **1200***
Brown, K.A., **770***
Brulhet, J., 337
Brutel-Vuilmet, C., 271
Buchhorn, M., **349***, 894, 904, 999, 1014, **1203***, 1234
Buchwal, A., 858
Budantseva, N.A., 160
Budishchev, A., 265
Budney, J., 284
Buffett, B.A., 805
Bukhanov, B.A., 1174, 1181
Buldovich, S., 687, 837
Bumby, A., 143
Burjack, I., **269***, 279
Burke, E., **189***, 196, 208, 224, 271, 407, 1084
Burke, I.T., 784
Burn, C.R., **150***, 446, 737
Busby, J., 325

Busey, R., 403
Bussmann, I., **518***
Butenko, A., **538***
Byun, E., 153, **190***, 525
Błaszkiewicz, M., 304, 332

Cable, S., **18***, 154
Cable, W.L., **403***, **405***, 453, 760
Caduff, R., 1051
Cai, C., **1093***
Cai, H., **1094***
Cai, L., 653, **752***, 1197
Calleja, J. F., 119
Calmels, F., 719, 974, 1106
Campos, N., 82
Canário, J., 748, **772**, **773***
Canassy, P.D., 1158
Cannone, N., **191***, 414
Cao, B., 707, 863, 918
Cao, X., **475***
Cardenas, M.B., 678
Cardoso, M., 82
Carey, M., 665
Carmack, E., 770
Carman, T., 435
Carpino, O., 892
Carrera, P., 82
Carsten-Conner, L., 1239
Cary, G., 116
Cassidy, A.E., **193***
Castanheira, L., 772, 773
Castro-Morales, K., **270***
Cauquil, E., 823, 1013
Celis, G., 221, 237
Chabrillat, S., 870
Chabudziński, L., 53
Chadburn, S., 189, 196, 208, **271***, **407***
Chand, P., **351***
Chang, D., **1171***
Chang, J., **635***, 705
Chang, R., **169***, 272, 284
Chang, X., 312
Chanton, J., 233, 249
Chao, W., 244
Chapin III, F.S., 184
Chapligin, B., 474
Charman, D., 256
Chasnikova, S., 933
Chazanoff, S., 284
Che, T., 390
Chen, A., 883
Chen, G., 208, 224
Chen, J., **863***, 918, 1078
Chen, L., 1138
Chen, X., 208
Cheng, H., 308
Cherbunina, M., 275, **563***, 611, **1172***
Cherepanova, M., 604
Chernomorets, S., 988
Chernyanskii, S.S., 165
Chesnokova, I., 381, **1129***
Chetverova, A., 633, 647, 701, 744, **774***, 792
Chizhova, J.N., 160
Choler, P., 457
Chou, Y.-C., 317
Christen, A., 193
Christensen, C., 267
Christensen, J.H., 814
Christensen, T., 191, 229, 286
Christiansen, A.V., 979
Christiansen, H.H., 18, 68, 108, 154, 162, 191, 286, 344, 359, **408***, 412, 458, 465, 466, 834, 1253
Christiansen, J.R., 212
Christl, M., 313
Christopherson, T.C., 32
Chu, P.-Y., 1198, **1205***
Chuvilin, E.M., **1174**, **1175***, 1181
Clark, I.D., 630
Claypool, G.K., 353
Clennel Palmer, A., 1160
Coats, V., 1239
Coch, C., **775***
Cochand, M., **637***
Cody, R.P., **352***, 859
Cohen, D., 309
Coissac, E., 473
Cojan, I., 337
Collier, N., 659
Collins, J., 352
Cologgi, J., 1110
Colpaert, A., 914
Combes, P., 337
Commane, R., 227, **272***, 284, 285
Connon, R.F., **638***, 896
Conway, S.J., 1008
Cooke, C., 562
Coon, E., 659, 681, 700
Cooper, E., 227
Cooper, W., 233
Coops, N., 894
Correia, A., **117***, 467
Costa-Casais, M., 103
Costard, F., **539***, 553, **639***, 657, 659, 688, 926, 1214
Cote, J., 1190
Cottingham, S., **519***
Coultish, T.L., **353***
Couture, N., 798, **832***, 855
Cox, P., 407
Craig, J., 1126
Creighton, A., 971
Cremonese, E., 1049
Cresto Aleina, F., **273***
Crill, P., 233, 747, 818
Cristóbal-Rosselló, J., 349
Cruces, A., 320
Crummer, K.G., 217
Cui, X., 1084
Cully, A., 922
Curtis, J.B., 247, 948
Cysewski, M.H., **1207***, **1239***, 1243
Czimczik, C.I., **194***, 197, 227, 259

D'Hondt, O., 145
Díaz-Puente, J., 137
Dąbski, M., **20***
Daanen, R., 249, **641***, 653, 664, 917, 994
Dafflon, B., 247, **948***
Dahlin, T., 979
Dalleske, R., 47
Daniel, F., 966
Dannen, R., 971
Dantec-Nédélec, S., **643***
Dapeña, C., 695
Darrow, M., 994, 1148, 1168, 1183
Dash, J., 738
Daube, B., 284
Dauboin, P., 823, 1013, 1114
David, A.S., 82
Davila, A., 134, 551
Davydov, S., 227, 429, 623, 694

Davydova, A., 227, 694
Dawson, J., **950***
De Guzman, E.M., **1095***, **1130***
de Klerk, P., **476***
de Pablo, M.á., **119***, **121***, 131, 133, 141, 142, 467, 546, 555, 1140
de Potter d'Indoye, A., 496
de Vera, J.-P., 541
Dean, J.F., **776***
Debolskaya, E., **644***, 671
Debolskaya, Y., 835
Debolskiy, M., **645***
Debolsky, V., 835
Decaulne, A., 926
Decharme, B., 225, 1084
Delaloye, R., **22***, 36, 39, 54, 57, 96, 354, 355, 444, 960, 1048, 1051, 1064
Delbart, N., 643
Deline, P., 61, 62, 1010, 1153
Delire, C., 225, 1084
Delmelle, P., 496
Deluigi, N., **354, 355***
Demidov, N., 146
Denis, N., 530
Dereviagin, A.Y., 155, 603, 607
Deshpande, B., 1238, 1250
Destouni, G., 651
Desyatkin, A., 260
Desyatkin, R.V., **1209***, 1214
Dethloff, K., 219
Didriksen, A., 531
Diekmann, B., 474, 560
Dietze, E., 332, 609
Dikau, R., 26
Dinardo, S., 285
Dinsmore, K.J., 776
Diotri, F., 1048
Dlugokencky, E., 285
Dmitriev, V., 647
Dobiński, W., **305***, **1210***
Dobrotina, E., 714
Dolman, H., 222, 265, 267
Domine, F., 225
Dominik, S., 878
Doré, G., 965, 966, 1089, 1095, 1106, 1128, 1130, 1137, 1143, 1148
Dorozhkina, M., 499
Douglas, T.A., 654, **897***, 941, **952***
Dräger, N., 332
Draebing, D., **24***, 26
Dragut, L., 382
Dressler, A., 474
Drozdov, D.S., 417, 439
Du, J., 762
Du, Y., 1073, 1170
Duarte, T., 772
Dublyansky, Y., **308***
Dubrovin, V.A., 439
Duchesne, C., 463
Dudarev, O., 769
Duguay, C., 380, 715, 904
Duhain, C., 496
Dumais, S., **1096***
Dummann, W., 254
Dunn, C., 528
Dunning, S., 858
Duvail, C., 337
Duvillard, P.-A., **1153***
Duvoy, P., 1090
Duxbury, N.S., 687
Dvornikov, Y.A., 75, 183, 442, 450, 701, 725, **899***, 910, 912, 938, 1004
Dyadkov, P., 983

Eckhardt, T., **195***, 697
Ednie, M., 401, 463
Edwards, M., 473, **565***, 604, **723***, 738
Efremov, P., 619
Ego, F., 337
Eichel, J., **26***
Eiken, T., 370
Eischeid, I., 775
Ekici, A., 189, **196***, 271, 287
Elberling, B., 18, 186, 187, 198, 215, 227, 271, 466, 711, 979
Elder, C.D., **197***
Elger, K., 344, **357***, 361, 904
Elin, H., 904
Elsakov, V., 749
Emmert, A., **954***
Endalamaw, A.M., **646***
Engel, Z., 119, 129, 135
Engram, M., 719
Engström, J., 359, **955***
Engstrom, R., 939
Enomoto, H., 157
Epp, L.S., 472, **480***, 482, 487, 493, 515
Epstein, H.E., 235, 410, **900***, 933, 1234
Ermokhina, K., 933, **986***, 1004
Erokhina, O., 538
Escarzaga, S., 352, 859
Etzelmüller, B., **28***, 359, 386, **409***, 997
Eulenburg, A., 633, 701, 792, 798
Euskirchen, E., 274, 435, 915
Evgrafova, A., **170***, 204
Evgrafova, S., **520***, 727
Ewing, S.A., **566***

Fadeev, D.I., 957
Fague, A.N., **957***
Faillettaz, J., 109
Fairen, A., 551
Falaleeva, A., 348
Fan, S., 1154
Fang, F., 284
Farquharson, L.M., 822, **833***
Faucherre, S., **198***, 215
Fedin, V., 820
Fedorov, A.N., 153, 345, 449, 553, 616, 619, 657, 688, 755, 905, 917, 925, 926, 929, 1198, **1214***, 1222, 1229
Fedorova, I., 629, 633, **647***, 701, 714, 744, 774, 792
Fedorowicz, S., 333
Feng, D., 1186, 1197
Feng, W., 1123
Feng, Z., 383, 1071, 1078
Fenwick, M., 1110
Fernández, J.M., 82
Fernández, S., 119
Fernandes, M.V., **29***, 59
Fernandez-Remolar, D., 546
Ferrando Acuña, F.J., **649***
Ferreira, A., 82, **123***, 467
Ferreira, M.J., 772
Ferry, M., 659
Festa, J., 1126
Feurdean, A., 481
Fiddes, J., **358***, 1018
Fiencke, C., 614
Fierz, C., 358

Finger, R.A., **1243***
Finster, K.W., **522***
Fischer, A., 1035
Fischer, U.H., 309
Fishback, L., 733, 734
Fisher, D., 134
Fiske, G., 770
Fitzpatrick, M., 1111
Fiłoc, M., 324
Flores-Orozco, A., 452
Floyd, A., 435
Flynn, M.J., **1215***
Foged, N., 1131
Fondahl, G., 1234
Foord, V., 347
Forbes, B.C., 1223, 1234
Forbes, D., 1234
Ford, J.D., 1215
Forte, A.P., 1061
Fortier, D., 148, 231, 616, 721, 965, 1011, 1137
Fortier, R., 637, **958***
Fourel, F., 323
Fournier, J., 830
Frampton, A., 359, 458, **651***, 659, 700
Francois, R., 770
Franz, D., **724***
Fraser, R., 52
Fratianni, S., 39
Frauenfelder, R., **988***, **990***
Frederick, J.M., 659, 804, **805***
Freeman, C., 528
Frehner, M., **30***
Freitas, M.C., 320
Friborg, T., 267
Friedlingstein, P., 196, 407
Frisia, S., 316
Fritz, M., 514, 603, 775, **778***, **780***, 797, 798, 849, 855, 1238, 1250
Fritzsche, D, **1217***
Froese, D., 559, 562, **598***, 608, 616, 719, 974
Frolking, S., 233
Frolov, D.M., 413
Frolova, L., 619
Frost, G.M., 933
Frost, G.V., **32***, **410***, 889, 900, 917, 937
Fuchs, M., 0, 559, **599***, 616, **902***
Fuchs, M.C., 155, 510, 627

Gädeke, A., **653, 654***, 664
Gärtner-Roer, I., **2***, 30, **34***, 73, 396, 444, **865***, 878, 944, 1064
Günther, F., **0***, 599, 616, 620, 751, 841, 849, 861, **869***
Günzel, F.K., **1179***
Gómez-Lende, M., 82, 88
Gómez-Ortiz, A., 79, 448
Gaedeke, A., 971
Gagarin, L., **33***, 391, 874
Gagnon, H., 1101
Gagnon, S., **199, 200***
Gajek, G., 53
Galeeva, E., **152***
Gallego-Sala, A., 256, 481
Gallinar, D., 82
Galushkin, I., 988
Galy, V., 770
Gandois, L., **201***, **782***, 788, 795
Gansukh, T.E., 469
Gansukh, Y., 394
Gao, B., 871, 918
Gao, S., 365, **655***, **1068***
Gao, Z., **992***
García-Hernández, C., 82
Gargani, J., 553
Garnett, M.H., 776
Gatesman, T., 654
Gautier, E., **657***
Gavrilov, A.V., 687
Gawrysiak, L., 53
Gaylord, A., 352, 859
Gałka, M., 476, **481***
Geertsema, M., 347
Geldof, J.-B., 823
Genet, H., **203***, 227, 435, **867***, 895, 915
Gentsch, N., 251
Gerbig, C., 288
Ghirlanda, A., **36***
Giaccone, E., **39***
Gibbard, P., 83
Gieck, R., 702
Gielly, L., 473
Giesler, R., 519
Gilbert, G.L., 18, **154***, 408, **412***
Gilles, G., 302
Gince, P., 1146
Girao, I., 82
Girod, L., **868***
Girst, S., 748
Gishkeluk, I., 1097
Gisnås, K., **359***, 386
Gittel, A., 251
Glazer, M., 305
Glushkova, N., 620
Goddéris, Y., 679
Godsey, S.E., 692, 765, 984
Godøy, Ø., 358
Goeckede, M., 217, 227, 262, 267, 269, 270, **274***, 278, 279, 288
Golosov, S., 744
Golubev, V.N., **413***
Golubyatnikov, L., **275***
Gomes, S.S., 772
Goncharova, O., 177, 400
González-Amuchastegui, M.J., 79
González-García, M., **41***, 82, 88
González-Trueba, J.J., 41, 88
Goossens, R., 49
Gorbunov, A.P., 1075
Gordiychuk, V., **1097***
Goslar, T., 604
Gosmant, O., 823
Gosse, J.C., 997
Goswami, S., 276
Gottlieb, E., 284
Gouttevin, I., 751
Goyanes, G., 82, 467, 1140
Graf, K., 1158
Graham, P., 349
Grau, T., 751
Grebenets, V.I., **1098***, 1125, 1135, 1163, 1188, 1220, 1234, **1244***
Grebenkin, S.I., 1175
Grechishcheva, E.S., 1167, **1177***
Green, E., 352, 1013, 1114
Greer, C., 517
Grenier, C., 639, **659***, 679, 688, 1214
Grigoriev, M.N., 426, 603, 670, 810
Grimm, R., **360***

Grimstad, G., 873
Grishakina, E., 837
Gritsuk, I., 644, 671, 835
Grosfeld, K., 1256
Grosse, G., 0, 188, 205, 236, 241, 249, 276, 314, 362, 380, 565, 599, 605, 609, 614, 616, 620, 623, 717, 722, 728, 729, 739, **753***, 761, 833, 849, 869, 870, 902, 906, 917, 923, 928
Gruber, S., **361***, 419, 1053, 1064, **1101***
Gsell, T., 1023, 1064
Gubanov, A.S., **1220***
Gubarkov, A.A., 910, 1004
Gubin, S., 176, 604
Guegan, E., **834***, 835
Guevara, A., 496
Guggenberger, G., 170, 204, 251, 520
Guglielmin, M., 115, **124***, 191, **414***, 1224
Guillaso, S., **126***, 145
Guillemette, F., 519
Gulyy, S.A., **415***
Guo, L., 1120
Gurney, K.E., 757
Gustafsson, ö., 622, 769
Gustafsson, E., 767
Gyswyt, N.L., **994***

Höfle, B., 862
Höfle, S., 226, 232
Högström, E., 1250
Haas, A., 344, **361***, 362
Haas, C., 332
Haas, F., 105
Haase, I.C., 170, **204***
Habeck, J.O., **3***, 1198, 1209
Haberkorn, A., 24, **42***
Hackbusch, S., 518
Haeberli, W., **309***
Haghshenas Haghighi, M., **870***
Hall Riaza, J.F., **46***, 82, 103, 555, **1033***
Halla, C., **44***
Hambrey, M.J., 106
Hampton, D.L., 349
Han, F., 1102, 1138
Han, L., 1094
Han, P., 803
Hansen, A.A., 522
Hansen, B.U., 466
Hansen, C.D., 115, **127, 128***, 138
Haquin, S., 830
Harada, K., **1246***
Harbor, J., 1238
Harden, J., 211, 532, 616
Hardman, S., 284
Harp, D., 700
Harrington, J., 1037
Hartery, S., 285
Hartl, L., **1035***
Hartmann, J., 280, 281, 292, 295
Hartmeyer, I., **47***, 452, 1017
Hasler, A., 109, 444, 908, 1050, 1064
Hatté, C., 201, 323
Hauber, E., **541***, 543, 556
Hauck, C., 111, 396, 409, 444, 960, 968, 973, **1036***, 1038, 1039, 1047, 1048, 1053, 1063
Haver, M., **662***
Haw, M., 532
Hayashi, M., **1037***
Hayes, D.J., 208, **276***, 889, 923
He, R., 312, **1162***
He, Y., 203
Heard, K., 422
Hefter, J., 254, 790, 799
Heijmans, M., **754***
Heim, B., 75, 361, 362, 701, 715, **725***, 751, 790, 792, 808, 870, 894, 899, **904***, 928, 938
Heimann, M., 217, 269, 279, 288, 795
Hein, C., 857
Heincke, B., 942
Heinecke, L., **482***
Heinrich, G., 452
Helgason, J.K., 1008
Helm, V., 855
Hempel, L., 234
Henderson, J., 272, 284, 950
Hendricks, A., 508
Hendrickx, H., **49***
Henry, G., 193
Herich, P., 317, 319
Herman-Mercer, N., 800
Hermanns, R.L., 997
Herzschuh, U., 475, 480, 482, **483***, 487, 488, 493, 512, 514, 515, 899
Heslop, J.K., **205, 206***
Hetz, S., **523***, 524
Hicks Pries, C., 217
Hidalgo, M.á., 119, 121
Hiemstra, C., 952
Hiesinger, H., 541, 543, 549
Hilbich, C., 409, 444, **960***, 968, 973, 1036, **1038***, 1063
Hilger, P., **997***
Hillier, J., 1008
Hinkel, K., 197, 717, 1090
Hinkel, M., 226
Hinzman, L.D., 646, 917
Hirst, C., **784***, 787
Hiyama, T., 1214
Hjort, J., 359
Hock, R., 645
Hodson, A., 210
Hoelzle, M, 42
Hoelzle, M., 444, **1039***
Hoeve, E., 419
Hoff, I., 1107, 1190
Hoffmann, D., 316
Holden, S.R., 194, 259
Holloway, J.E., **961***
Holmen, J., 659
Holten, J.I., 418
Horn, F., 526, 819
Horn, M.A., 516, 523, **524***
Horsfield, B., 239
Hoyt, A., 201
Hrbacek, F., 119, **129***, **131***, 135, 139
Hu, D., **1102***
Hu, G., 258, 1073
Hu, X., 383, 1078, **1104***
Huang, J., 1191
Huang, X., 1170, 1185
Huang, Y., 513
Hubbard, S.S., 247, 948
Hubberten, H.-W., 0, **207***
Hugelius, G., 198, **208***, 212, 215, 218, 228, 238, 251, 255, 271, 616, 622
Huggel, C., 985, 988
Huissteden, K.v., 222, 754

Humlum, O., 68, 408
Humphreys, E.R., 737
Huntingford, C., 196
Hutchings, J., 221
Huwiler, A., 80
Hwang, P., 835
Hyam, L.C., **835***
Høgh Jensen, K., 711

Iijima, Y., 441, **755***, **905***, 917, 925, 929, 1214
Ikeda, A., 68
Ilya, K., 1161
Ingeman-Nielsen, T., 966, 979, 981, **1131***
Instanes, A., **1134***
Ionov, D., 644, 671, **835***
Isabellon, M., 1049
Isaev, V., **837***, 1144
Isakov, V.A., **1135***
Isaksen, K., 359, 370, 409, **417**, **418***, 990
Ise, H., 905
Ishikawa, M., **311***
Istomin, V.A., **1181***
Ivanova, R., **1222***
Ivy-Ochs, S., 301, 313
Iwahana, G., 466, 1214, 1246

Jóhannsson, H., 390
Jørgensen, C.J., 198
Jackson, C., 325
Jafarov, E., 208, 224, 227, 390, 456, 883, **1247***
Jaillet, S., 1025
Jammet, M., 267
Jan, A., 681
Janke, J., 631, **663***
Jarosz, K., **839***
Jaskólski, M.W., 839, 840, 853, **998***
Jastrow, J., 227
Jaumann, R., 556
Jeltsch, F., 488
Jensen, A., 786
Jensen, B.J.L., 598
Jensen, M., 830
Jeong, S.-J., 284
Ji, D., 224, 1084
Jiang, G., **1070***
Jiang, L., **871***, 918
Jiao, K., 258
Jimenez, J., 119, 121, **133***, 141, 142
Jin, H., **312***, 365, 513, 629, 632, 655, 707, 710, 1066, 1154, 1162
Jin, L., 1094
Johansson, M., 271, 466, 1224
Johnson, J., 1090
Johnson, K., 203
Johnson, M.D., 543
Johnsson, A., 534, 541, **543***
Joly, D., 61
Jones, B.M., 314, 565, 653, 717, 719, 752, 753, 833, 889, 902, **906***, 923, 971
Jones, E.L., **210***
Jones, J.B., 149, 184, 765
Jones, M.C., 188, 205, **211***, 241, 335, 532, 623, 722, 906
Jones, V., 723
Joosten, H., 476
Jordan, C., 1008
Jorgenson, J.C., 917
Jorgenson, M.T., **4***, 149, 757, 915, 937, 999, 1014
Jost, A., 659
Jostad, H.P., 873
Jung, J.Y., 525
Jørgensen, C.J., **212***

Kääb, A., 380, 715, 868, **1040***
Köhler, P., **214***
Kühn, P., **172***, 204
Křížek, M., 101
Kaärlejarvi, E., 933
Kadebskaya, O., 308
Kadivar, M., **873***
Kaiser, C., 251
Kaiser, M., **664***
Kaiser, S., 270, **278***
Kalashnicova, O., **806***
Kallfelz, M., **1248***
Kane, D., 702
Kanevski, M., 354, 355
Kanevskiy, M., 566, 616, **999***, 1014, 1090, 1203, 1234
Kang, H., 528
Kao-Kniffin, J., 226
Kapralova, V.N., **726***, 931
Karaevskaya, E., 116, 146
Karamut, O., 1171
Karasiewicz, M.T., 324
Karion, A., 272, 284, 285
Karlsson, E.S., **785***
Karlsson, J., 795
Karstens, U., 288
Karunaratne, K., **419***
Kashirtsev, V.A., 957
Kasprzak, M., **840***, 853
Kassin, A., 352
Kath, N.J., 480
Kaufman, M.H., 678
Kavan, J., 139
Kaverin, D., 174, 230, **421***
Kayastha, R., 1053
Kazantsev, V., 275, 1172
Kellerer-Pirklbauer, A., **50***, **1041***
Kennedy, K., 1011
Kenner, R., 24, 42, 80, **908***, 1064
Kenny, D., 457
Kerimov, A.G., 1098, 1244
Kessler, A., 234
Keuschnig, M., 47
Khabibullina, F., 180
Khan, M.A., 1053
Khimenkov, A., 1013
Khitun, O.V., 912, 933, 1234
Khodzher, T.V., 670
Kholodov, A., **422***, 429, 453, 616, 760
Kholopov, Y., 174
Khomutov, A.V., 75, 442, 450, 899, **910***, **912***, 933, 986, 1002, 1004, 1234
Khristoforov, I.I., 33, **874***
Khurelbaatar, T., 469, 1081
Kienast, F., 472, **484***, 560
Kim, K., **153***
Kim, M., **525***, 525
Kim, Y., 190, 227, 525, 762
Kimball, J.S., 284, 297, 762
Kimura, M., 745
King, T.V., **786***
Kireev, R., 177
Kirillin, G., 728
Kislov, O., 1163
Kissiova, M., 1146
Kittler, F., **279***
Kiyashko, N.V., **1182***, 1182

Kizyakov, A.I., **841***, 986, **1002***, 1004
Kleemann, V., **808***
Kleinen, T., **213***, 270
Klemedtsson, K., 187
Klene, A.E., **424***, 460, 885, 1227, 1237, 1244
Kling, G.W., 678
Klingbeil, L., 26
Kloster, S., 283
Kneier, F., **426***
Kneisel, C., 954
Knoblauch, C., 183, 185, 195, 230, 250, 273, 526, **727***, 797, 819
Knoltsch, A., 251
Knorr, G., 214
Košutnik, J., 78
Koch, B., 790
Koch, F.-T., 288
Koch, J.C., 566, **665***, **757***
Koch, M., 126, 145
Kofinas, G., 1234
Kohnert, K., **280**, **281***, 292, 870
Kokelj, S., **52***, 112, 419, 446, 690
Kokh, S., 659
Kokin, O.V., 850
Kokorev, V., 1199
Kolesnikov, A., 669
Kolle, O., 288
Kolosov, R.A., 796
Koltai, G., 308
Komarov, I.A., **1182***, 1182
Kong, X., **1106***
Konishchev, V., 611
Konopczak, A.M., 85, 794, **843***
Konovalov, Y.V., 1098
Konrad, J.-M., 1096
Konstantinov, P., 449, 657, 688, 1214
Kooi, H., 162
Kordowski, J., 332
Korets, M.A., 795
Korhonen, K., 955
Korona, O., 501
Korzun, J., 604
Kos, A., 80
Koshurnikov, A., 837
Kotzé, C.., 138
Kouraev, A.V., 662, 749
Koven, C., 208, 224, 284, 761, 1084
Kołodyńska-Gawrysiak, R., **53***
Kraev, G., 437, 616, 846, 1224
Kramkowski, M., 332
Krautblatter, M., 12, 24, 64, 997, 1224
Krinner, G., 271, 728, 1224
Kronig, O.C., **313***
Kroon, A., 18, 828
Kruse, A., **1183***
Kruse, S., 480, **487**, **488***
Krylenko, I., 662
Kryvych, N., 358
Kuhlmann, H., 26
Kuhry, P., 198, **215***, 218, 228, 234, 238, 251, 255, 276, 359, 622
Kumar, R., 698
Kumar, S., 351
Kummert, M., 36, **54***
Kumpula, T., **914***, **1223***, 1234
Kunitskiy, V., **601***, 616, 1230
Kuntz, Z.M.C.O., **1043***
Kupryjanowicz, M., 324
Kurchatova, A.N., 99, 152, **216***, 806, 856, 1244
Kurkowski, T., 435
Kurosu, T., 284
Kurovskaia, V., **666***
Kurylyk, B., 659
Kusch, S., 232, 489
Kuss, J., 933
Kutscher, L.M., 784, **787***
Kutzbach, L., 182, 195, 260, 267, 271, 273, 274, **282***, 289, 614, 697, 727
Kuznetsov, D.E., 823, 825
Kuznetsov, V., 627
Kuznetsova, E., **1045***, **1107***, 1190, 1234
Kvamme, B., 809
Kwon, M.J., **217***

L'Hérault, E., 199
Löffler, T., 474
Löppmann, S., 226
Lü, L., 365, 655
Láska, K., 119, **135***, 139
Lécuyer, C., 323
López, I., 546
López-Martínez, J., 126, **137***, 145
Labat, D., 679
Labbé, J., 1215
Laboor, S., **362***, 616
Lacal, M., 137
Lacelle, D., 52, 134
Laepple, T., 607
Lafrenière, M.J., 668, 690
Lai, Y., 935, **1195***, 1196
Lambiel, C., 39, **57***, 96, 354, 355, 444
Lamoureux, S.F., 52, **668***, 690, 775, 1234
Lamprecht, R.E., 245
Lanckman, J.-P.F., 390, 398
Laney, C., 352
Langdon, P., 723
Lange, S., **428***, 751, 761
Langer, M., 271, 293, 386, 426, 634, 715, 724, **728***, 751, 761, 862
Lanouette, F., **1137***
Lantuit, H., 0, 12, 85, 207, 291, 398, 514, 775, 778, 780, 794, 797, 798, 801, 843, 849, 855, 928, **1224***, 1253
Lantz, T., 52, 419
Lapalme, C.M.L., **134***
Lapointe-Elmrabti, L., 616
Lapteva, E., **174***, 180
Lara, M.J., 227, **363***, 867, 895, **915***
Larmanou, E., 294, 724
Larose, C., 187
Larouche, J.R., 765
Larson, A., 1239
Lashchinskiy, N., 251
Laska, K., 129, 131
Lasslop, G., **283***
Laurila, T., 267
Laurion, I., 231, 721
Lavinen, N., 714
Lavrič, J., 288
Lawrence, D., 224, 284, 759, 1084
Le Dantec, T.A., 782, **788***
Lebedeva, L., 629, **669***, 675, 693
Ledman, J., 237
Lee, H., **759***
Lee, Y.K., **525***, 525

Lehmann, R., **1249***
Lehmkuhl, F., 49
Lehnert, K., 357
Lehning, M., 42
Lehtimäki, J., 955
Lehtinen, A., 955
Leibman, M.O., 75, 450, 841, 899, 910, 912, 933, 938, 986, 1002, **1004***, 1234
Lemay, M., 199, 1234
Lembke-Jene, L., 254
Lemieux, C., 1106, 1128
Lemieux, J.-M., 637, 958
Lemke, P., 1256
Lenz, J., 188, 301, **314***, 722
Leonawicz, M., 435
Lessels, J.S., 776
Lestak, L.R., 352
Lewińska, P., 839
Lewkowicz, A.G., 347, 384, 401, 961, **963***, 1011, 1043, 1253
Li, B., 754
Li, D., **1185***, 1187
Li, F., 1094
Li, G., 1112, **1154***
Li, H., 259, 1194
Li, J., 383, **1071***, 1078, 1104, **1108***
Li, Q., 1084
Li, R., 387, **1073***, 1086
Li, S., 935, 1122
Li, X., 1102, 1171
Li, Y., 1077, 1094
Li, Z., 1083, **1109***
Lian, O.B., 112
Liao, M., 1195, 1196
Liebner, S., 516, 526, 533, 812, 819
Liengaard, L., 522
Liljedahl, A.K., 32, 641, 653, 654, 664, **917***
Liljedahl, L.C., 955
Lim, M., 840, 853
Limpach, P., 908, 1064
Limpens, J., 754
Lin, B., 1186
Lin, H., 863
Lin, Z., 992, **1006***, 1007
Linch, L., 1160
Lindaas, J., 272, 285
Lindgren, A., **218***
Lindgren, M., 435
Lindgren, P.R., **729***, 753
Lindhorst, S., **844***, 857
Lindwall, F., 186
Ling, F., **731***
Linsbauer, A., 1018, 1050
Litovko, A., 366, 1220, 1254
Little, J.D., 885
Liu, G., **1074***, 1083
Liu, J., 1167, 1171, 1191, 1192
Liu, L., 871, 918
Liu, Lin, 863, 871, 883, **918***, 1083
Liu, M., 513, 1155
Liu, W., 1102, 1138
Locat, A., 1128
Lomstein, B.A., 522
Long, A., 858
Lopes, L.F., 29, **59***
Lopes, V., 320
Lopez Caceres, M.L., 745
Loranger, B., **965***
Loranty, M., 235, 422, **429***
Losiak, A., 539
Louchouarn, P., 788
Lousada, M., 82
Lozhkin, A., 604, 616
Lu, L., 1162
Lu, Y., 1102, **1138***
Ludwig, R., 706, 887
Luethi, R., 80, **431***
Luetscher, M., 301, 308, **316***
Luhová, L., **317***
Lukens, R.D., 1225
Lund, M., 225, 267, 286, **432***
Luo, D., **365***, 632, 655
Luo, J., 299, 992, 1006, **1007***
Lupachev, A., 164, **175**, **176***, 604
Lupascu, M., 227
Lussana, C., 359
Luus, K., 272, 274, 284
Luzi-Helbings, M., 812
Lyon, S., 700
Lyu, Z., **919***

Mörth, C., 784, 787, 790
Müller, C.W., **226***, 232
Müller, J., 34, **73***, 396, 865, **878***, 1064
Ma, H., **1186***, 1197
Ma, Q., 1196
Ma, W., **1112***, 1112, 1119, 1121, 1123, 1154, 1193
Macander, M.J., 32
MacDougall, A., 224, 1084
Machiya, H., 441
Macias-Fauria, M., 1223
Mackelprang, R., **527***
Macrae, M., 733, 734
Maestro, A., 145
Magnin, F., 11, **61**, **62***, 1010
Magritz, J., **526***, 819
Mahler, L., 526
Mahony, M., 608
Maignan, F., 643
Maio, C.V., 937
Maji, V., **63***
Makarycheva, E., **366***, **920***, 1254
Maksimov, G.T., 94, **670***, 869
Malenfant-Lepage, J., **966***, 1124, 1238, 1250
Malkova, G., **433***, 975
Mamoru, I., 394, 469, 713
Mamot, P., **64***
Mangelsdorf, K., 239, 605
Manies, K., 211, 532
Manley, W., 352, 859
Mann, D.H., 833
Mann, P.J., 519, 764
Manson, G., 832, 843
Manthey, C., 603
Mao, T., 705
Marcer, M., **367***, **967***
Marchenko, I., 1165
Marchenko, N.A., 165
Marchenko, S., 368, 371, 374, **435***, 453, 508, 814, 1067, **1075***
Marcosig, I.P., 695, 1058
Mari, S., 39
Mariager, T., 212
Marks, L., 324
Marmy, A., 973, 1036
Martín-Torres, F.J., 535
Martínez Cruz, K.C., 205
Martens, J., **489***
Martikainen, P., 245, 296
Martin, P., 363
Martineau, F., 323

Marushchak, M., 245, 296
Marx, S., 862
Marzahn, P., 887
Maslakov, A., **437***, **846***, 1188
Maslikova, O., 644, **671***
Mastepanov, M., 286
Masuzawa, T., 905
Matsuoka, N., **66***, **68***, 108
Matsuura, Y., 261
Matthes, H., **219***, 929
Matveyeva, N., 917
Matyshak, G., **177***, 400, 410, 933, 999, 1203, 1234
Mauritz, M., **221***, 237
Maximov, T., **222***, 265, 267, 754, 784, 787
Mayrberger, T., **1110**, **1111***
Mazza Ramsay, F., 352
McAfee, S., 435
McDonald, K., 284
McDowell, P., 565
McDowell, W.H., 795
McEvoy, F., 325
McFarland, J., 532
McGowan, S., 723
McGraw, M., 1200
McGuire, A.D., 203, 208, **224***, 242, 276, 363, 435, 867, 895, 915, 1084
McIntyre, C., 254
McKain, K., 284
McKay, C., 134
McKenzie, J., 659
McLennan, D., 770
Meiklejohn, K.I., 127, 128, **138***, 143
Meisel, O.H., **732***
Melles, M., 483
Melnikov, V.P., 90, 327, 329, **439***
Melton, J., **225***
Mercier, D., 830
Merino, A., 82
Merkel, M.K.F., 473
Merrison, J., 522
Metzger, S., 280, 281, 292, 294, 295
Mewes, B., 960
Meyer, H., 155, 314, 474, 510, **603***, 607, 627
Miceli, C., 963
Michalak, A., 284, 285
Mida, P., 101, **1046***
Migała, K., **70***, 840
Miglovets, M., 300
Migon, P., 853
Mikhailova, T., 1223
Mikhaylova, M., 899
Mikkan, R., 1033
Mikuš, T., 319
Mikutta, R., 251
Millán, R., 137
Miller, C., 272, **284***, 285
Miller, J., 284
Miller, S., 284, **285***
Milovská, S., 317, 319
Milovský, R., 317, **319***
Ming, F., 1185, **1187***
Mink, S., 126, 137, 145
Minsley, B., 974
Mironenko, M.V., 1182
Mischke, S., 482
Mitchell, L., 950
Miyazaki, S., 441
Mnushkin, M., 1013
Modzel, P., 853
Moine, O., 302, 323, **490***
Molina Gamez, M., 226
Molina, A., 82, 119, 121, 141, 142, **546***, **1140***
Mollaret, C., **968***, 1036, 1038
Mollenhauer, G., 254, 489, **790***, 795, 797, 799, 803
Molodkov, A., 333
Molson, J., 637, 659
Moore, J.C., 1084
Moorman, B.J., **72***, 106, 815, **922***
Mora, C., 119, 133, 467
Morawski, M., 86
Morel, X., **225***
Morgenstern, A., **0***, 75, 85, 105, 236, 361, 633, 634, 647, 701, 774, **792***, 793, 794, **1250***
Mori, J., **441***
Morin, T., 457
Morino, C., **1008***
Morison, M., **733**, **734***
Morozova, A.V., 381, 1129
Morra di Cella, U., 1048, 1049
Morse, P.D., 112, 419, 969
Morton, D., 646
Moskolenko, N., 933
Motagh, M., 870
Motenko, R.G., 1177
Mouteva, G., 284
Mozil, A., 1037
Mu, Q., 1109
Mu, Y., 1089, **1112***, 1112, 1154
Mueller, M., 530
Mujahid, A., 530
Mukhortova, L., 520
Mullanurov, D.R., **442***, 450, 910
Murphy, M., 784
Murton, J., 11, 63, **604***, 1156
Musial, M., 1146
Muskett, R.R., 368, 453, **760***, **877***
Muster, S., 428, 712, 751, **761***
Mutter, E., 800
Myers-Pigg, A., 788
Myhra, K.S., 28
Mylius, M.R., 286
Mysina, A.S., **673***, **791***
Męsdrek, K., **847***

Näslund, J., 955
Nötzli, J., 393, 396, 398, **444***
Nakamura, T., 755
Narancic, B., **735***
Nashaqi, K.Q., **809***
Natali, S., 221, **227***, 235, 422, 429
Natsagdorj, S., 394, 469
Necsoiu, M., 917
Neilson, B.T., 678, 786
Nel, W., 127
Nelson, F.E., 76, 424, 460, 885, 1198, **1225***, 1227
Nelson, L., 352
Nesje, A., 370, 418
Nesterova, N., **675***, 693
Neubauer, D., **605***
Neudorf, C.M., 112
Neumann, R., 532
Newman, S., 952
Ng, S., 631, 663
Nian, Y., 918
Nicolsky, D., 224, **368***, 453, 645, 804, 814
Nielsen, L., 711
Niemann, S., 634

Niemeyer, B., **493***
Nieto, A., 126, 145
Nieuwendam, A., 79, 82, **320***, 467, 1238, 1250
Nigamatzyanova, G., 647
Nikolskiy, P., **494***
Niro, Y., 162
Nitze, I., 0, 362, 620, 750, 753, 902, **923***
Niu, F., **5***, 299, 985, 992, 1006, 1007, 1112, **1155***
Niu, Y., 1109
Noerling, C., **75***
Norkov, V.S., **1188***
Norman, M.E., **677***
Norris, S., 325
Noryśkiewicz, A.M., 332
Noses Spinola, D., 172
Notz, D., 811
Nunes, T.G., 772
Nyland, K.E., **76***, 424, 460, 885, 1220, **1227***, 1244
Nyssen, J., 49
Nyvlt, D., 119, 129, 131, 135, 139
Nørnberg, P., 522

O'Donnell, J., 211, 566, 665
O'Neill, B., **446***
O'Neill, T., 126, 137, 166
O'Sullivan, A.M., 1151, **1156***
Oblogov, G.E., 816, 820
Obu, J., **78***, **849***
OConnor, M.T., **678***
Oechel, W., 227, 284
Ogonerov, V., 669
Ogorodov, S.A., 823, 825, 826, **850***
Ohta, T., 222
Oktem, R., 948
Oldenborger, G., **969***
Olefeldt, D., 242
Olenchenko, V.V., 874
Olesen, M., 814
Oliva, M., 29, 59, **79***, 117, 129, 131, 320, **448***, 467, 1250
Oliveira, M.C., 772
Olvmo, M., 543
Omelyanenko, A.V., 874
Onaca, A., 87, 100, 382
Ondruch, J., **139***
Onischenko, N., 837
Onstott, T., 259, 517
Opel, T., **155***, 603, **607***, 627, 808
Opfergelt, S., **496***
Orekhov, P., 933
Orgogozo, L., 659, **679***
Orlov, T.V., 726, **880***
Orvošová, M., 317, 319
Osmonov, A., 1029
Ostroumova, E.A., 1098
Otero, F., 1055
Ott, F., 332
Ottlé, C., 643
Otto, A., 170
Ouellet, M., 958
Overduin, P., 78, 426, 489, 515, 526, 792, 793, 804, **810***, 813, 819, 855, 941

Pérez-Alberti, A., 79
Périer, L., **1143***
Paces, J., 566
Padeiro, A., 748, 772, 773
Painter, S.L., **681***, 700
Palacios, D., 79, 448
Palmer, K., 524
Palmer, M., 419
Palmtag, J., **228***, 251, 255
Pan, X., **1077***
Panagiotakopulu, E., **498***
Panchenko, E.G., 726, 880
Panda, S.K., 368, **371***, 453, 883
Pang, Q., 1074, 1088
Pannetier, R., 651, 659, 700
Papke, J., 908
Paquette, M., 1238, 1250
Parazoo, N.C., 272, 284, **285***
Park, H., **449***, 755, 929, 1214
Parmentier, F.-J.W., 191, **229***, 265, 267
Parmuzin, I., 374
Parsekian, A., 717, 883, 906, **971***
Pastick, N., 203
Pastukhov, A., 174, **230***, 421
Paulo, V., 748
Pavlova, D., 983
Pavlova, E., **499***, **501***, 503
Pavlunin, V., 1163
Pawłowski, L., 839, 840, **853**, **854***, 998
Peón, J. J., 119
Pearce, D.A., 519
Pedersen, A., 770
Pedersen, S.L., 286
Pei, W., **935***, 1122, 1150
Peirce, J.C., 1234
Peirce, J.L., 999, 1203
Pelayo, M., 137
Pellet, C., **973***, 1036, **1047***, 1048, 1063
Pellitero, R., 82
Pellitero-Ondicol, R., 79
Pendin, V.V., 439
Peng, S., 208, 224, 728
Peng, X., 707
Perednya, D.D., 450
Pereira, P., 448
Perez, L., 830
Pergaud, J., 61
Perreault, P.V., **1113***
Perrenoud, J., 1038
Pestryakova, L., 474, 480, 487, 493, 512, 619
Peter, M., 386
Peters, J., **373***
Peterson, J.E., 247, 948
Petrone, R., 733, 734
Petrov, A., 1234
Petrzhik, N., 177
Pettersson, R., 955
Peucker-Ehrenbrink, B., 770
Pfeiffer, E.-M., **179***, 182, 185, 195, 230, 250, 260, 727, 1244
Pfeiler, S., 452
Phillips, M., 24, 42, **80***, 396, 431, 444, 908, 1064, 1151
Piamsalee, A., 1130
Pienitz, R., 735
Piilo, S., 256
Ping, C.-L., 249
Piper, M., 456
Pirk, N., 191, **286***
Pisabarro, A., **82***, 88
Pisarska-Jamroży, M., **322***, 343
Pittauer, D., 803
Pitte, P., 1027, **1030***
Pittman, J., 284
Pitulko, V., 494, 499, 501, **503***

Podchasov, O., 837
Podest, E., 284
Pogliotti, P., 62, **1048**, **1049***
Pogodaeva, T.V., 670
Pohl, B., 61
Poinar, H., 598
Pointner, G., **736***, 893
Pokrovsky, O.S., 679, 795, 796
Polakowski, L., 0, 792, **793***
Pollard, W.H., 12, 134, 148, **685***, 709, 855, 936
Polukhin, A.N., 442, **450***
Ponti, S., 191, 414
Popescu, M., 87
Porada, P.V., 271, 283, **287***
Porcelli, D., 784, 787
Porter, T., **608***, 719
Potapova, T.M., 791
Potter, C., 284
Poulter, B., 256
Prėskienis, V., **231***, 234
Prakash, A., 349
Pravikova, N.V., 841
Price, S.J., **83***
Prieto, M., 119, 121, 1140
Prieto, O., 546
Probst, J., 788
Prokushkin, A.S., 261, 679, 782, 790, **795***, 796
Prokushkina, M.P., 795
Prommer, J., 251
Prud'homme, C., **323***
Prytherch, J., 818
Przegiętka, K., 333
Pugin, A., 969
Puglini, M., **811***
Pumple, J., **974***
Python, S., 968, 1036

Qi, J., 1119
Qiao, Y., 258, 1074, 1088
Qin, Y., 387
Quintard, M., 679
Quinton, W.L., 638, 892, 896

Rößger, N., **289***
Rühaak, W., 659
Raack, J., 534, **549***
Rabatel, A., 1025
Rachlewicz, G., **84***, 455
Radosavljevic, B., 797, 822, **855***
Raetzo, H., 908, 1051, 1064
Raff, J., 857
Rainer, A.M., 796
Rajabov, I., 482
Ramage, J.L., **85***, **794***, 797
Ramirez, G., 352
Ramos, M., 119, 121, 123, 131, 133, **141**, **142***, 448, 467, 546, 1140
Randerson, J., 284
Randhawa, S.S., 1018
Rask, J., 551
Rasmussen, M., 786
Rautio, M., 231
Ravanel, L., 61, 62, **1010***, 1153
Raynolds, M.K., 900, 917, 999, 1014, 1203, 1234
Recondo, C., 119
Reisenhofer, S., 452
Reiss, D., 541, 543, 549
Reitner, J.M., 313
Rempel, A., 157
Reschke, M., 482
Rethemeyer, J., 186, 187, 226, **232***, 489, 790, 803
Reum, F., **288***
Reuss-Schmidt, K., **738***
Reyes, A.V., 598
Rezanezhad, F., 227
Rich, V.I., **233***
Richter, A., 215, 251
Riedl, C., **452***
Rieger, W., 664
Rieksts, K., 1107, **1190***
Rijal, M.L., 1053
Riley, W., 761
Rinke, A., 219, 1084
Risk, D., 227
Riviere, A., 659
Rivkin, F., **374***
Rivkina, E., 116, 146, **506***, 616
Robinson, J., 616
Robinson, S.L., 531
Rodehacke, C., 814
Rodríguez-Rastrero, M., 137
Rodriguez, A., 551
Rodzik, J., 847
Rogov, V.V., 152, 216, 611
Rohrbach, N., 1029
Romanov, S., 774
Romanovskii, N.N., **687***
Romanovsky, V.E., 1, 368, 371, 398, 403, 405, 417, 422, 435, 439, **453***, 508, 645, 687, 717, 729, 753, 760, 814, 833, 867, 895, 906, 915, 917, 1075, 1234, 1253
Rong, L., 1094
Ronholm, J., 517
Ropero, M.á., 1140
Rose, A.S., **528***
Rose, J., 565
Rosser, N., 858
Rotem, D., 162
Roth, A., 928
Roth, K., 761, 1077
Rousseau, D.-D., 323
Roux, N., 639, 659, **688***
Roy, L.-P., **1011***, 1234
Roy-Leveillee, P., **737***
Roßbach, N., 524
Rudaya, N., 484, 619, 627
Rudolph, E.M., **143***
Rudy, A.C.A., 52, **690***, 1238, 1250
Ruesch, O., 549
Ruiz-Fernández, J., 79, 82, 117, 131, 320, 448
Rumyantseva, Y., **377***
Runkle, B.R.K., 273, 282, 697
Rupp, S., 435
Rusakov, A., 327
Rushlow, C.R., **692***, 984
Ruskeeniemi, T., 955
Ruttor, S., **291***, 797
Ruzanov, V., 437
Rychel, J., **86***, **324***
Rymer, K.G., 84, **455***
Rzodkiewicz, M., 332

Séjourné, A., 534, 539, **553***, 688, **926***, 1214
Sachs, T., 262, 267, 274, 280, 281, 284, **292***, 294, 295, 724, 849, 855, 870
Sacleux, M., 1175
Sadkov, A.A., 726
Sadkov, S., 880
Sadurtdinov, M., 433, **975***
Saito, H., **925***
Saito, K., 441, **508***, 1058, 1084

Saklani, S., 1018
Saleska, S., 233
Salisbury, D., 818
Salmon, V., 221, 235
Salvà-Catarineu, M., 448
Salvador-Franch, F., 448
Salzmann, N., 1017, 1018, 1050, 1053
Sam, L., 535
Samah, A.A., 530
Sanborn, P., 719
Sanchez, O., 1025
Sanders, T., 614
Sanjosé, J.J., 88
Sannel, A.B.K., 49, **234***, 359, 700, 742
Santos, M.C., 772, 773
Santruckova, H., 215
Sapart, C., 818
Saruya, T., **157***
Sattler, B., 316
Sauheitl, L., 170, 204
Saulnier, G.-M., 62
Savvinov, G., 604
Sawada, Y., 1246
Sawyer, A., 692
Scandroglio, R., 64
Scapozza, C., 39, 444, 1064
Schädel, C., 183, **235***
Schöner, W., 452
Schütze, J., 929
Schaal, P., 518
Schaefer, C.E.C.G., 172, 467
Schaefer, K., 208, 390, **456***, **883***, 1247
Scheidegger, J., **325***, 659
Schennen, S., **977***
Schicks, J.M., **812***
Schimel, D., 284
Schimnowski, A., 770
Schirrmeister, L., 155, 236, 239, 489, 510, 515, 560, 603, **609***, 614, 616, 627, 742, 929, 977, 1258
Schleper, C., 251
Schlobies, K., **739***
Schmid, M.-O., **1050***
Schmid, T., 126, 137, **145***
Schmidt, J., 619
Schmidtlein, S., 26
Schmidtt, M., 784
Schmitz, N., 541
Schmutz, J.A., 757
Schnecker, J., 251
Schneider von Deimling, T., **236***, 249, 614, 810, **813***
Schneider, A., **742***
Schneider, B., 619
Schoeneich, K., **457***
Schoeneich, P., 367, 398, **856***, 967
Schollaen, K., 0, 1224, **1253***
Schreiber, P., **293***
Schrott, L., 11, 44, 47, 1253
Schuh, C., **458***
Schuler, T., 386
Schulla, J., 641, 917
Schulze-Makuch, D., **551***
Schuster, P., 800
Schuur, E., 184, 217, 221, **237***, 276, 1224
Schwab, M.J., 332
Schwalm, C., 456
Schwamborn, G., 489, **510***, 515, 627, 977, 1258
Schweitzer, P., 1234
Sedov, S., 327
Segal, R., 52
Seifert, F.M., **380***
Selbmann, A., 227
Selroos, J., 659
Semakov, N., 983
Semenchuk, P., 227
Semenova, O., 666, 669, 673, 675, **693***
Semiletov, I., 769
Sepulveda-Jauregui, A., 205
Serafimovich, A., 274, 280, 281, 292, **294**, **295***
Serban, R.D., 100
Sergeev, D., 366, **381***, 687, **1013***, 1129, 1149, 1253, 1254
Serrano, E., 41, 79, **88***, 126, 137, 145
Seto, J., 1126
Seybold, C., 124
Shabanova, N.N., 823
Shadrina, A., 647, **744***
Shamrikova, E., 174
Shang, J., 918
Shang, Y., 1192
Shapiro, B., 598
Sharma, M., 351
Shaw, S., 784
Sheinkman, V., **90***, **327***, **329***
Shen, C.-C., 317
Shen, Y., **1191***
Sheng, Y., 1071, **1078***, 1088, 1104
Shestakova, A.A., 94, **378***
Shesternev, D., 1165
Shi, X., 1077
Shibistova, O., 170, 204, 251
Shiklomanov, A., **694***
Shiklomanov, N., **6***, 424, **460***, 885, 939, 1098, 1198, 1227, 1234, 1244
Shilova, O.S., 826
Shipitsyna, L., 391
Shirokova, L.S., 795, 796
Shmelev, D., **146***, 563, **611***, 616, 1114, 1172
Shulla, J., 645
Shumskaya, N., 647
Shur, Y., 616, 999, **1014***, 1090, 1113, 1203, 1207, 1234
Shurpali, N.J., 267, **296***
Sia, E.S.A., **530***
Siegert, C., 603, 616, 619
Siekacz, L., **92***
Sierra, M.J., 137
Siewert, M., **238***, 1238, 1250
Sileo, N.R., **695***
Simpson, G., 195, **697***
Singh, S., **698***
Singha, K., 984
Sinitsyn, A., 834, 835
Sirbu, F., **382***
Sivtsev, D., 391
Sjögren, P., 473
Sjöberg, Y., **7***, **700***, 1224, 1237, 1238, 1250
Skarin, A., 1223
Skoglund, K.A., 1107
Skorospekhova, T., 647, **701***, 714, 744, 774, 792, 899
Skov, K., 432
Skryabin, P.N., **1229***
Skvortsov, A., 433, 975
Slagoda, E., 99, 152, 806
Slater, A., 284

Slater, G., 259
Smith, L., 247
Smith, R., 690
Smith, S.L., 393, 398, 401, 417, 419, **461***, **463***, 963
Sokolov, I., 837, **1144***
Sokołowski, R.J., **333***
Song, H., 1119
Sonyushkin, A.V., 841, 1002
Sorg, A., 1040
Spötl, C., 308, 316
Spangenberg, E., 812
Spektor, V., 616
Spektor, V.B., 94, 378
Spektor, V.V., **94***, 378
Spencer, R.G., 519
Spielvogel, S., 170, 204
Sponseller, R.A., 519
Spott, O., 727
Springman, S.M., 444
St. Louis, V., 562
Stähli, M., 1047
Stanilovskaya, J., 158, 941, 946, 1013, **1114***, 1200, 1246
Stapel, J.G., **239***
Staub, B., 22, 36, 54, **96***, 444
Steiner, N., 284
Stendel, M., **814***
Stephani, E., **1146***, **1148***
Stettner, S., 0, 634, 904, **928***
Stevens, C., **815***, 1124
Still, B., 1194
Stillman, D., 360
Stocker-Waldhuber, M., 1035
Stoffel, M., 1040
Stoof-Leichsenring, K., 482, 487, **512***
Strand, S.M., 408, **465**, **466***
Strauss, J., 236, 605, 609, **614***, **616***, 797
Street, L.E., 776
Streletskaya, I.D., **816***, 820, 1004
Streletskiy, D.A., 393, 398, 424, 460, 694, 861, 870, **885***, 939, 1098, 1188, 1227, 1234, 1244
Striegl, R., 566
Strozzi, T., 380, 861, 1040, **1051***
Strzelecki, M.C., 822, 839, 840, 853, 854, **857**, **858***, 998
Stuefer, M., 349
Stuefer, S., **702***
Stumm, D., **1053***
Sturm, M., 1239
Subke, J., 776
Sudakova, M., 975
Sueyoshi, T., 157
Sugimoto, A., 222
Sugita, A., **745***
Sukhova, D., 177
Sullivan, M., 233
Sun, T., 1119
Sun, Y., 871, 918
Supper, R., 452
Surka, J., 317, 319
Svenning, M.M., 531
Swanson, D.K., 371, 833
Sweeney, C., 272, 284, 285
Swenson, S., 759
Swindles, G., 481
Swirad, Z.M., 539, 853
Syromyatnikov, I.I., **1230***
Szal, M., 481
Szczucinski, W., 858
Szymanowski, M., 854
Słowiński, M., **332***

Taberlet, P., 473
Taboada, N.A., 695
Tachibana, Y., 755
Tahvanainen, T., 914
Takeda, K., 745
Takriti, M., 251
Talalay, P., 1160
Tammiksaar, E., 1217, **1232***
Tamstorf, M.P., 286
Tan, X., 1191
Tananaev, N., **98***, 170, 201, 204, 366, 693, 782, 788, **1254***
Tanarro, L.M., 448
Tanski, G., 291, 780, **797**, **798***
Tape, K.D., 917
Tapia Baldis, C.C., **1055***, **1057***, 1061
Taratunina, N., **99***
Tarin, G., 352
Tas, N., 247
Teigler, R., 1256
Teisserenc, R., 201, 782, 788, 795
Telles-Langdon, L., 1126
Temuujin, K., 394
Terhost, B., 327
Tesi, T., 622, 769
Thayyen, R.J., 1053
Therrien, R., 637, 659, 958
Theuerkauf, M., 332
Thibert, E., 1025
Thiel, C., 18
Thiele, M., 526
Thomas, E., 1027
Thornley, J., **1116***
Thornton, B.F., **747***, **818***
Tian, L., **1079***
Tian, Y., 1191
Tiedemann, R., 254
Tikhonov, A., 604
Tikhonravova, Y., 806, **1117***
Timm, K., 435
Tipenko, G.S., 687, 1013
Titov, S.V., 796
Tjallingii, R., 332
Tjernström, 818
Tobler, D., **1158***
Tokarev, I., 694
Tokareva, I.V., **796***
Tolmanov, V.A., 1188
Tolstogan, A., **1163***
Tomaskovicova, S., **979***, **981***
Toniolo, H., 1014
Toohey, R.C., **800***
Torgovkin, Y., 345
Torgovkin, Y.I., 94, 378
Torn, M., 247, 284, 948
Torres-Rua, A., 786
Torsvik, V.L., 251
Townsend Small, A., 197, 259
Traczyk, A., 70
Tran, A.P., 948
Trapeznikova, O.N., 726
Treat, C.C., 188, 211, 227, **241***, **335***, 722
Treffeisen, R., **1256***
Tregubov, O., 437
Trofaier, A.M., 893
Trojahn, S., **799***
Trombotto Liaudat, D., 695, 1017, 1027, 1055, 1057, **1058***
Tronicke, J., 977

Tsarev, A., 433, 975
Tsibizov, L., 957, **983***
Tsogtbaatar, U., 469, **1081***
Tsogterdene, G., 394
Tumskoy, V., 627
Tunnicliffe, J., 52
Turetsky, M.R., **8***, **242***, 867, 897
Turner, S., 723
Tveit, A.T., 516, **531***
Tweedie, C.E., 352, **859***
Tyson, G., 233

Uher-Koch, B., 757
Ulbricht, D., 357
Ulrich, C., 247, 948
Ulrich, M., 616, **619***, 925, **929***, 1198, 1214
Umarez, J., 704, 1152
Undrakhtsetseg, T., 394
Urdea, P., 87, **100***
Urich, T., 251
Usov, A., 837
Uxa, T., **101***, 1046, **1060***

Väliranta, M., 256
Valcárcel, M., 46, 79, **103***, **555***, 1033
van der Molen, M., 265
van Geldern, R., 637
van Hardenbroek, M., 723
van Huissteden, J., 265, 267, **336***
van Huissteden, K., 271, 274, 466
Van Loon, A.J., 322
Van Vliet-Lanoe, B., **337***
Vandenberghe, J., **338***
Vanhala, H., 955
Vanshtein, B.G., 816
Vargas, S., 352
Varlamov, S.P., 1229
Varner, R., 233
Vartanyan, S., 616
Vasil'chuk, A.C., **158***, 160, **339***, 341
Vasil'chuk, Y.K., 158, **160***, 339, **341***
Vasiliev, A.A., 816, 820
Vavrinyu, T., 1127
Veh, G., **105***
Veillette, A., 1238
Velde, Y.v.d., 776
Velikin, S., **1165***
Venevsky, S., **244***
Vera, R., 496
Veraverbeke, S., 284
Verdonen, M., 914, 1223
Veremeeva, A., 559, 616, **620***, 869
Vergun, A.P., 823, 825
Victorov, A., 880, **931***
Vidstrand, P., 659
Vieira, G., 79, 115, 119, 121, 123, 131, 133, 141, 142, 398, **467***, **748***, 772, 773
Vieli, A., 73, 109, 396, 865, 878, 1064
Viers, J., 679
Viitanen, L.-K., 207
Viktorov, A.S., 726
Villarreal, S., 352
Villarroel, C.D., 1030, 1055, **1061***
Vincendon, M., 549
Vincent, W.F., 748, 772, 773, 1234
Vinogradova, J., **180***
Vinogradova, T., 666
Virmoux, C., 657
Virtanen, T., 296
Vitale, V., 414
Vivero, S., 1027
Vlasov, A., 1013
Vlasova, Y., 374
Voelker, M., **556***
Voigt, C., **245***
Volkov, N., 1144
Vonder Mühll, D., 396, 444
Vonk, J.E., **9***, 519, **622***, 764
Voss, C., 659, 692
Voytek, E.B., **984***
Voytenko, A.S., 381, **1149***

Wachecka-Kotkowska, L., 86
Wagner, D., 239, 520, 526, 533, 812, 819
Waigl, C.F., 349
Wainstein, P.A., **704***, 1038, 1152
Wainwright, H.M., **247***, 948
Waldrop, M., 211, 227, 435, **532***
Walker, D.A., 32, 349, 410, 900, 904, 917, **933***, 999, 1014, 1203, **1234***
Waller, R.I., **106***
Walsh, J., 435, 508
Walter Anthony, K., 188, 197, 205, 206, 241, **249***, 314, 616, **623***, 722, 739, 753
Walz, J., **250***
Wan, X., 1195
Wang, C., 1084
Wang, F., 1154
Wang, G., 169, 635, **705***
Wang, H., 871
Wang, J., 1155, 1194
Wang, K., 707
Wang, L., **706***, **887***
Wang, P., 754
Wang, Q., **513***, **707***
Wang, S., **383***, 1071, 1078, 1162
Wang, T., 271, 387, **1119***, **1192***
Wang, W., **1084***
Wang, X., 365, 655, 1120
Wang, Xiaowen, **1083***
Wang, Y., 1154
Wang, Yi., 992
Wang, Z.A., 770
Ward, M.K., 685, **709***, **936***
Warnsloh, J.M., 336
Washbourne, I., 776
Wasser, D., 396
Watanabe, T., 68, **108***, 157
Watts, J.D., 262, 284, **297***, **762***
Watzka, M., 251
Way, R.G., **384***
Webb, E., 221
Weber, S., **109***, 865, 1023, 1064
Wecht, M., 50
Weege, S., **801***, 1250
Wegmüller, U., 1051
Wei, M., 1089, 1253
Weidlich, M., **1258***
Weinstein, Y., **162***
Weiss, N., 198, 215, **253***, 255
Welker, J.M., 194
Welkner, D., 1152
Wells, A.F., 32
Wen, Z., **468***, 1150
Weniger, L., 474

Werner, C., 1051
Wesche, K., 484
Wester, P., 1053
Westergaard-Nielsen, A., 18
Westermann, S., 28, 62, 271, 359, 380, **386***, 409, 478, 715, 728, 810, 813, 890, 997, 1030, 1060
Westgate, J.A., 598
Wetterich, S., 155, 314, 489, 510, 609, 614, 619, **627***, 742, 808, 977
Wever, N., 42
Whalen, D., 832
Wheeler, W., 942
Whiteford, E., 723
Whitley, M.A., **937***
Whyte, L., 259, 517
Wichels, A., 518
Wicki, A., 1038, **1063***
Wicky, J., **111***, 1038
Widhalm, B., 75, 899, 904, 928, **938***
Wieczorek, M., 488
Wieland, M., 26
Wieneke, S., 295
Wiersberg, T., 812
Wiesmann, A., 380
Wiggins, E., 284
Wiik, E., 723
Wik, M., 747, 818
Wild, B., **251***
Wille, C., 267, 282, 289
Willerslev, E., **10***
Williams, B., 770
Willis, M.D., 1203
Wilson, C.J., 750, 917
Wilson, G., 116
Winkel, M., 526, 533, **819***
Winkler, A.J., 273, 282
Winterfeld, M., **254***, 489, 764, 790, 795, 799, **803***
Wipfli, M.S., 757
Wirth, L.M., 999, 1203
Wirz, V., 865, 878, **1064***
Wofsy, S., 272, 284, 285
Wojcik, R., **255***
Wolfe, B., 735
Wolfe, S.A., **112***, 419, 969
Wolter, A., 80
Wolter, J., **514***
Wolter, S., 284
Woodward, J., 519
Wookey, P.A., 776
Woronko, B., 322, 324, **343***
Worthy, D., 284
Wu, D., 1195
Wu, J., 383, 1071, 1078, 1104
Wu, Jingwei, 1191
Wu, M., **1191***
Wu, Q., 299, 513, 707, 1066, 1068, 1070, 1112
Wu, T., **387***, 1067, 1073, 1074, 1083, **1086***, 1088
Wu, X., 1079
Wu, Y., 247
Wu, Z., 1150
Wulf, S., 314
Wullschleger, S., 750
Wylie, B., 203
Wysota, W., 333

Xiao, D., **1193***
Xiao, Y., 258, 1073
Xiao, Z., 1195
Xie, C., 1073, 1074, 1079, 1086, **1087***, 1088
Xie, Y., 1120
Xiong, Z., 1094
Xu, X., 197, 201

Yabuki, H., 917
Yadamsuren, G., **388***, 469
Yadav, V., 284
Yakimov, A., 1165
Yakovlev, A.I., 1209
Yamkhin, J., 311, 388, 394, **469***, 713, 1081
Yang, C., **390***, 1121
Yang, D., 1077
Yang, J., 1116
Yang, J.-W., 153, 190, 525
Yang, S., **533***
Yang, Y., 513, 710, **1066***
Yang, Yang, 244
Yang, Z., **1194***
Yao, X., **1119***
Yarmey, L., **390***, 456, 1247
Yechieli, J., 162
Yeltsov, I.N., 957
Yi, P., **710***
Yi, X., 1138
Yin, Q., 496
Yoccoz, N., 473
Yoiu, Z., **1196***
Yondon, A., 469
Yoon, H., 153
Yoshihiro, I., 394, 469
Yoshikawa, K., 508, 687, 1246
You, Y., 1120
Young, J.M., 646
Yu, F., 1119
Yu, Q., 1077, **1120***
Yu, Qin, 424, **939***
Yu, S., 383
Yu, W., 1102, 1138
Yuan, F., 435
Yue, G., 258
Yue, Z., 1119
Yun, H., **299***

Zadorozhnaia, N., **820***
Zaehle, S., 270
Zagirova, S., **300***
Zagórski, P., 839, 847
Zakharova, E.A., 662, **749***
Zamolodchikov, D., 437
Zanina, O., 604
Zastruzny, S.F., **711***
Zavaleta, J., 551
Zawiska, I., 332
Zazula, G., 598
Zebker, H., 883
Zgraggen-Oswald, S., 988
Zhai, W., 935
Zhang, F., 1186, 1194, **1197***
Zhang, H., **256***
Zhang, J., 530, 654
Zhang, L., **1121***
Zhang, Mingli, 468
Zhang, Mingli., 468
Zhang, Mingyi, 935, 1122, **1150***
Zhang, MMingchu, 206
Zhang, N., 1084
Zhang, S., 1084
Zhang, T., 344, 513, 707, 863, 871, 883, 918
Zhang, W., 1084
Zhang, Xiumin, 1071
Zhang, Xiyin, 935, **1122***, 1150
Zhang, Y., 435, 915
Zhang, Yu, 296, 1185
Zhang, Z., 1068, 1070

Zhang, Ze, **1123***, 1193
Zhang, Zhen, **256***
Zhao, H., 1192
Zhao, L., 258, 1067, 1073, 1074, 1079, 1083, 1086, **1088***
Zhao, S., 1193
Zhao, Y., **258***
Zhegusov, Y., 1199
Zhelezniak, M., **391***, 415, 471
Zhirkov, A.F., **471***
Zhizhin, V., 391
Zhu, Z., 203
Zhuang, Q., 203, 227, 919
Zielhofer, C., 619
Zieliński, P., 333
Ziltcova, Y., 263, 1199
Zimin, M.V., 841, 1002
Zimmerman, C.E., 665
Zimmermann, H., **515***
Zimmermann, N., 256
Zimov, N., 217, 279, 288
Zimov, S.A., 217, 279, 288, 616, 623
Zinovyev, E., 501
Ziolkowski, L.A., **259***
Zona, D., 227, 284
Zoor, L., 226
Zubeck, H., 1194
Zubrzycki, S., 164, 179, **182***, 226, **260***, 361, 614, 670, 799
Zverev, A.V., 726, 880
Zwieback, S., 78, 346
Zyrianov, V., **261***
Zyryanova, O., 261

www.icop2016.org